IJACSA
WHERE WISDOM SHARES

International Journal of Advanced Computer Science and Applications

Volume 12 Issue 7

July 2021

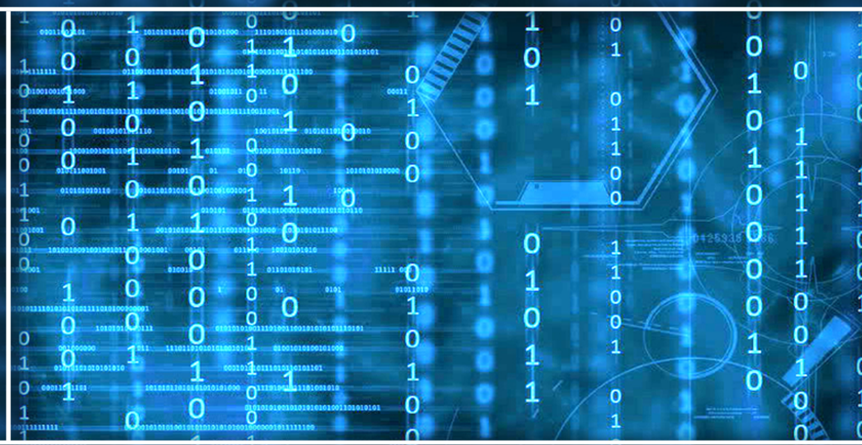

ISSN 2156-5570(Online)
ISSN 2158-107X(Print)

SAI

www.ijacsa.thesai.org

Editorial Preface

From the Desk of Managing Editor…

It may be difficult to imagine that almost half a century ago we used computers far less sophisticated than current home desktop computers to put a man on the moon. In that 50 year span, the field of computer science has exploded.

Computer science has opened new avenues for thought and experimentation. What began as a way to simplify the calculation process has given birth to technology once only imagined by the human mind. The ability to communicate and share ideas even though collaborators are half a world away and exploration of not just the stars above but the internal workings of the human genome are some of the ways that this field has moved at an exponential pace.

At the International Journal of Advanced Computer Science and Applications it is our mission to provide an outlet for quality research. We want to promote universal access and opportunities for the international scientific community to share and disseminate scientific and technical information.

We believe in spreading knowledge of computer science and its applications to all classes of audiences. That is why we deliver up-to-date, authoritative coverage and offer open access of all our articles. Our archives have served as a place to provoke philosophical, theoretical, and empirical ideas from some of the finest minds in the field.

We utilize the talents and experience of editor and reviewers working at Universities and Institutions from around the world. We would like to express our gratitude to all authors, whose research results have been published in our journal, as well as our referees for their in-depth evaluations. Our high standards are maintained through a double blind review process.

We hope that this edition of IJACSA inspires and entices you to submit your own contributions in upcoming issues. Thank you for sharing wisdom.

Thank you for Sharing Wisdom!

Kohei Arai
Editor-in-Chief
IJACSA
Volume 12 Issue 7 July 2021
ISSN 2156-5570 (Online)
ISSN 2158-107X (Print)

Editorial Board

CONTENTS

Edge-based Video Analytic for Smart Cities

Dipak Pudasaini[1], Abdolreza Abhari[2]
Department of Computer Science
Ryerson University
Toronto, Canada

***Abstract*—Video analytic is the important tool for smart city development. The video analytic application requires more memories and high processing devices. The problems of cloud-based approach for video analytic are high latency and more network bandwidth to transfer data into the cloud. To overcome these problems, we propose a model based on dividing the jobs into smaller sub-tasks with less processing requirements in a typical video analytics application for the development of smart city. The object detection, tracking and pattern recognition method to reduce the size of videos based on edge network will be proposed. We will design a video analytic model, and simulation is performed using iFogSim simulator. We will also propose Convolutional Neural Network (CNN) based object tracking model. The experimental verification shows that our tracking model is more than 96% accurate, and the proposed edge and cloud-based model is more than 80% effective than only cloud-based approach for video analytic applications.**

***Keywords*—Video analytic; cloud computing; smart city; object detection; object tracking; edge network**

I. Introduction

Smart city is a city that uses technologies to provide the sophisticated lifestyle for humans. It provides improvement in transportation, accessibility, social services, sustainability, and other services. The smart cities have several types of technologies such as Information and Communication Technology (ICT), connected physical devices using the Internet of Things (IoT), Geographical Information System (GIS), Video Analytic System (VAS) and more.

IoT plays the important roles for the development of smart cities. IoT is used to input and transmit large volumes of data such as video, audio, text, etc. The suitable infrastructures are needed for the processing of large volumes of data from IoT devices to the processing devices. Therefore, edge computing and cloud computing technologies are the important concepts for the development of smart cities to process video data.

Edge network is a networking environment that focuses on bringing computing closer to the data source. It is the local processing technique near the Internet of Things (IoT) devices. It is the emerging technology used in many fields such as video analytics, machine learning, robotics and more. Edge computing is a helpful technique to solve the challenges of high latency and bandwidth consumption.

The combination of fog/edge computing architecture with IoT devices and the cloud computing is a very important research area for smart cities to minimize the resources and providing optimization for the users' benefits. The extension of cloud computing towards the IoT devices is called fog/edge computing. It is the middle layer between cloud layer and IoT layer. The fog computing consists of low processing servers or terminals with small storage capacity. It has limited physical resources in terms of storage, memory, and processing power [1]. Cloud computing architecture is the centralized architecture to store and process a huge amount of data. Edge computing is an open platform to store and process data at the edge of the network. Video analytics applications are examples of applications that uses edge computing.

Video analytic is a kind of analytic system that can be used to process and analysis the video files. Video analytic can be used for motion detection, facial recognition, license plate reading and more. The video data are excessively available in social media, traffics, film industry etc. The powerful technology is needed to process these data. Therefore, the combination of edge computing and cloud computing technology is the more powerful technology to process video data. In this research, we will propose video analytic system to process video data for smart city development. The object detection, tracking and pattern recognition methods are more important phases of video analytic system. We will propose the framework of object detection, tracking and pattern recognition of videos using Convolutional Neural Network (CNN). We will also propose the CNN based object tracking model.

The rest of the paper is organized as follows: Section II presents problem statements and contributions. Section III presents the literature review. Section IV describes the details of our proposed approach. The experimental results and simulation are explained in Section V and Section VI. Finally, Section VII presents the conclusion of a paper.

II. Problem Statements and Contributions

In traditional video analytic system, video data from the data source is directly transferred into the cloud where video frames are extracted, and objects are detected and analyzed [2]. The traditional cloud based centralized approach has suffered from high latency and more network bandwidth when transfer data into the cloud. The bandwidth usage problem's solution is to develop models that integrate the IoT devices with edge and cloud devices. Another problem is more uses of network resources in the existing approach. Since addressing these problems in a real system is very expensive or sometimes impossible, the known methodology to examine these problems' solutions is the simulation. The sample framework of dividing video analytic into subtasks was presented in [3] but was not simulated. In this proposed work, we define the details about video analytic pipeline, prototyping model and parameter feed directly into the simulator. The video analytics jobs are huge applications referred to as edge computing killers [4]. We address this problem by assuming different tasks for a common video analytics application. The problem of video analytic application is that it requires more processing time and network bandwidth to transfer large files into the cloud. Therefore, the solution of this is to divide the video analytic system into more phases and reduce the size of video in the consecutive phases. We divide the video analytic into four phases which are motion detection, object detection, object tracking and pattern recognition. Then we propose the CNN method to reduce the video in consecutive phases based on edge computing architecture.

In a common video analytics application, there are many object tracking methods. Some of these are just tracking, and some are tracking by detection. Some of these methods are based on CNN, and some are not. The tracking methods without using CNN are faster but have low accuracy [5]. The CNN based tracking methods are more accurate, but the execution time is high [6]. In this research, we will modify the layers of the existing CNN model to decrease the execution time of the tracking model. We will also propose object detection, tracking and pattern recognition model using CNN based on Edge network.

The main contributions of this study are as follows:

- Dimensionality reduction: Proposing model for dividing video analytic application in different tasks by dimension reduction which means dividing them based on the processing requirement. The video analytic application consists of a number of phases such as motion detection, object detection, object tracking etc. We will purpose a model for dimensionality reduction in each consecutive phase of video analytic application.
- Object detection and tracking method: An object tracking module is a separate part of video analytics. There are the large number of object detection and tracking techniques for moving objects. We will use standard model for the detection of the objects, then modify the existing object tracking architecture using CNN to reduce the execution time of tracking.
- Verification of object Tracking method: We will experimentally verify our tracking method by using public video files and real time videos.
- Verification of model using iFogSim: The proposed model will be verified using iFogSim simulator. It will provide the effectiveness of using edge and cloud in our model in comparison with only the cloud-based architecture.

III. Related Work

The uses of fog computing in smart cities have been explained in [7]. The service oriented middle wire to reserve the issues of smart city development has proposed in [8]. It has presented the effective integration and utilization of Cloud of Things (CoT) and fog computing. Edge computing focuses on bringing the services and utilities of the cloud computing closer to the user for fast processing. The cost-effective technique for aerial surveillance in which large computation tasks are in the cloud and limited computation task in Unmanned Aerial Vehicle (UAV) devices using edge computing technique has been proposed [9]. The frames with normal behaviors are processed into edges and the frames with abnormal behaviors are passed into the cloud for abnormal behaviors detection. The simulation framework for the modelling of IoT and edge computing has been proposed [10]. It has extended the capacity of CloudSim to address the features of edge and IoT devices. The integration of edge and cloud computing with distributed deep learning for smart city IoT has been proposed [11]. It developed the hybrid model to optimize the system utility and bandwidth allocation.

The CNN-based framework for multi-object tracking has been proposed in [12]. It used RoI-pooling to obtain individual features for each target. In this method, spatial-temporal attention of the target is learned online to deal draft caused by occlusion. In [13], deep neural based appearance feature for multi-object tracking has been proposed. An algorithm for multi-object tracking was used for online and offline tracker. The real time object detection and tracking using deep learning OpenCV has been proposed [14]. It used Single Shot Detector (SSD) with mobile net framework for object detection and tracking. The fast vehicle detection based on evolving convolutional neural network has been proposed [15]. Tetris has proposed to provide maximum parallel processing of videos on a single GPU [16]. It has performed CPU-based tiling of active regions to combine the activities of video input. It ran the deep learning model and improved the GPU utilization.

In [17], the multiple objects tracking method with correlation filter has been proposed. In this method, the SSD was used for multi-object detector and CNN was used for tracking the objects. The real time object recognition model by using deep CNN to extract deep features has been proposed [18]. A multi-level three-dimensional convolutional neural network for the recognition of moving objects has been proposed [19].

IV. Methodology

A. Fog Computing Architecture for Smart Cities

Edge-cloud technology is a very important technology for wide geographical areas. The storage and processing of services in centralized based cloud approach provide more latency and bandwidth. We will use IoT-Edge-Cloud technology to support mobility with minimal overhead cost. The IoT-Edge-Cloud architecture is defined in Fig. 1. It consists of three tiers. The end devices such as sensors are considered as first tire. The fog/edge devices near the source are considered as second tire. The cloud devices joined with fog devices and far from the IoT devices are considered as third tire. The combination of three tires provides IoT-Fog-Cloud technology.

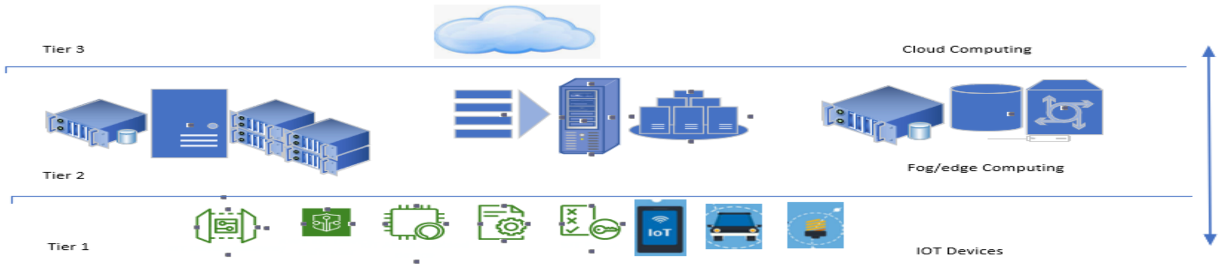

Fig. 1. Fog Computing Architecture for Smart Cities.

In the generic architecture, the IoT layer receives the input from the first tire. The fog layer consists of terminals, small servers, routers, access points, gateways and more [20]. This is an intermediate layer connected between IoT and the cloud. Cloud is the final layer in which data are transferred from fog layers. It has mass storage and processing capacity.

We propose a method for video analytic system to provide dimensionality reduction for object detection and tracking based on edge computing architecture. Edge devices are responsible to process the videos captured by cameras then object detection and tracking are taken place. Then the trajectories are sent to the cloud for pattern recognition. The testcase scenario of our proposed model is explained in section VI.

B. *Object Detection and Tracking Model for Video Analytic using CNN*

We will recommend the real video analytic application for object detection and tracking in this section. These real programs will be recommended in edge devices in our model. For the detection of the objects, we will use CNN-based object detection method YOLO. For the tracking of the objects, we will use deep sort and our own appearance model based on residual network. The trajectories created from tracking method are passed into the standard machine learning algorithms for pattern recognition.

1) Proposed object detection, tracking and pattern recognition model pipeline: The pipeline for this model consists of three stages: labelling stage, learning stage and prediction stage. In the labelling stage, the raw image data are annotated. Similarly, in the learning stage we fit different machine learning models on the data. And finally, we use the fitted Machine Learning (ML) model in the prediction stage. Since we will use two different models: Object Detection model and Appearance Model, in our prediction, we will apply labelling and learning stages separately for object detection and appearance model as illustrated in Fig. 2.

a) Labelling Stage: The labelling stage is the data annotation phase. Human annotators take in the raw data and annotate the data for the specific tasks. Since we have two models: object detection model and appearance model, we have two labelling stages where data gets annotated separately. For the detection model, human annotators take in the raw images and annotate the bounding boxes for the objects present and the corresponding categories of the objects. As a result, we get object detection annotation files. Similarly, for the appearance model, the human annotators take in frames from raw video data and annotate for object re-identification. They associate the objects with the same identities with a common id. This results in our annotated re-identification files.

b) Learning Stage: In the learning stage, a data pipeline gets created which takes in labelled images and the annotation files and creates datasets for the corresponding tasks. These datasets are then augmented randomly to increase robustness of the models and reduce overfitting. Then, different machine learning models with different architectures with varying numbers of parameters are learnt and validated by feeding in the data pipeline. The models which perform well on the validation sets are dumped to the disks. As a result, we have models with varying architectures and varying numbers of parameters which have different computational requirements. Based on the problem criterion, we choose the best model and mark it as the selected model for the prediction phase.

c) Prediction Stage: The prediction stage is the final stage. Here, we feed in the video frames and generate the final tracking results. First, we pass the video frames to a detector model, which we have learned from the learning stage. Then, we take in the predictions from the object detector to an association and tracking model. This appearance model performs deep association by using the appearance model we've learned earlier. Then the output from the tracking model is passed for pattern recognition.

In our proposed edge-based model, we will recommend using YOLO and updated deep Simple Online and Realtime Tracking (SORT) for object detection and tracking in edge levels. The architecture of this model is presented in Fig. 3. The frames of the video file are passed to YOLO method. We will use only vehicles class to reduce the timing of the detection method. Then YOLO provides classes and the bounding box. The bounding box is again passed to the deep association metric with residual network CNN architecture for object tracking. Finally, trajectory data are passed for pattern recognition. In this architecture, the dimensionality of the original data is reduced at each stage, which is another contribution of our model.

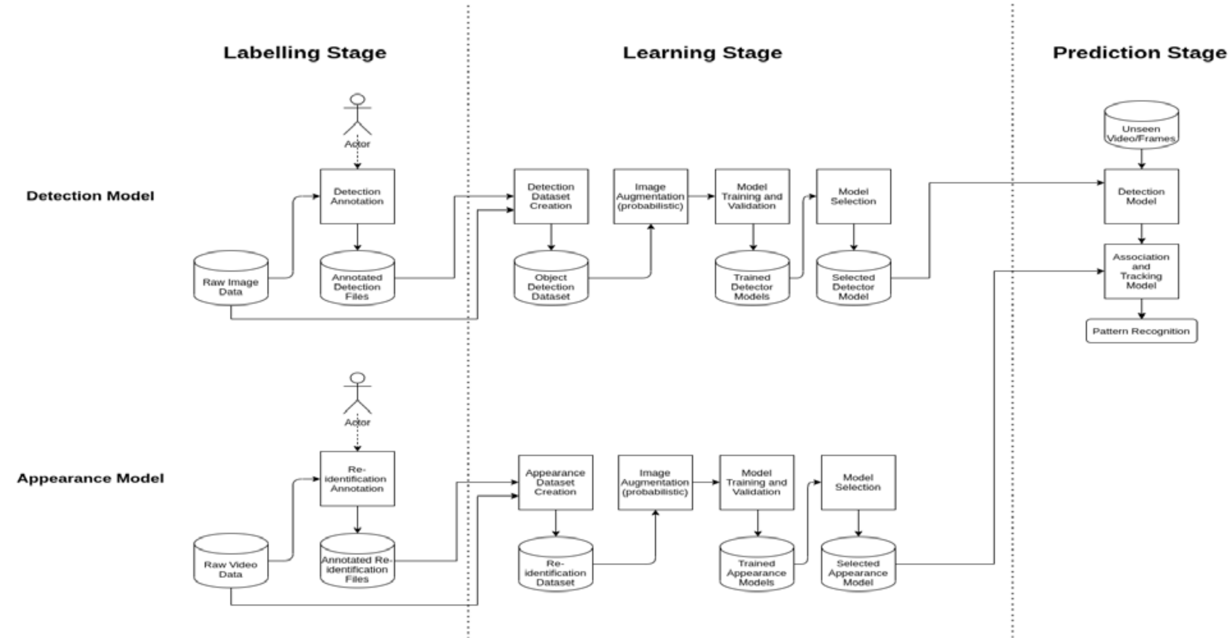

Fig. 2. Object Detection, Tracking and Pattern Recognition Model Pipeline.

2) Object detection model: YOLO is the object detection technique. The architecture of the YOLO is under the regression problem. In [21] [22], an image in the form of pixel values is the input of YOLO and the vector of bounding boxes with class predictions is the output. When the image inputs in the form of pixels, it passes through the neural network similar to CNN, then the vectors of bounding boxes and class predictions are in the form of output. The network uses the entire image to predict each bounding box. The image is divided into the SxS grid that grids are responsible for the detection of the objects. Each grid cell predicts *B* bounding boxes as well as *C* class probabilities. The bounding box prediction has 5 components: *(x, y, w, h, confidence)*, where *(x, y)* coordinates represent the centre of the bounding box, (w, h) represents the width and height of the bounding box. The confidence score is the score of predicting the object in a box. The YOLO is implemented in CNN using PASCAL VOC dataset. There are mainly two stages in YOLO. During the first stage, convolutional layers are used to extract the features from the image. During the second stage, the fully connected layers are responsible to provide the output probabilities and coordinates. It consists of 24 convolutional layers followed by 2 fully connected layers. The convolutional layers are pretrained in ImageNet dataset that used Darknet framework. The layers are presented in Table I.

The main strength of YOLO is speed. It is best object detection algorithm for fast detection. The weakness is more localization errors compared to faster R-CNN. The detection accuracy is less for very small objects. In this research, we are using object detection at edge level. It has light version and tiny version. Therefore, it is suitable for small processing edge devices. Another reason of using YOLO in this work is because of fast processing speed.

TABLE I. DARKNET-53 CONVOLUTIONAL NETWORK USED BY YOLOV3

	Type	Filters	Size	Output
	Convolutional	32	3x3	256x256
	Convolutional	64	3x3/2	128x128
1x	Convolutional	32	1x1	
	Convolutional	64	3x3	
	Residual			128x128
	Convolutional	128	3x3/2	64x64
2x	Convolutional	64	1x1	
	Convolutional	128	3x3	
	Residual			64x64
	Convolutional	256	3x3/2	32x32
8x	Convolutional	128	1x1	
	Convolutional	256	3x3	
	Residual			32x32
	Convolutional	512	3x3/2	16x16
8x	Convolutional	256	1x1	
	Convolutional	512	3x3	
	Residual			16x16
	Convolutional	1024	3x3/2	8x8
4x	Convolutional	512	1x1	
	Convolutional	1024	3x3	
	Residual			8x8
	Avgpool		Global	
	Connected		1000	
	Softmax			

We will use only vehicles classes to reduce the timing of the object detection model. We will use light version and standard version of the YOLO for the object detection. We will recommend light and standard YOLO depends upon the capacity of edge devices.

3) Object tracking using modified deep SORT: Deep SORT is a real time object tracking method [6]. It is an updated version of SORT. It integrates an appearance model which provides the deep appearance features for the detected objects in each frame. The method called the association of detected objects as a deep association metric. The inclusion of deep association metric allowed objects to be tracked in case of longer occlusions too and also the number of misclassifications were highly reduced. We use our modified version of deep SORT in this pipeline.

The pipeline for the deep SORT association is shown in Fig. 3. Video frames are fed into a robust object detector model. The object detector outputs the class categories and bounding boxes for the objects of interest in the video frames. Then, using the bounding boxes, the regions of interest in the frames are cropped and passed to the appearance model. The appearance model outputs the feature description for each detected object. The Deep SORT method leverages these feature descriptions for association of the detected objects with tracks in addition to the previous SORT based association, which uses the Kalman filter for predicting the location of the objects in the next timestamp.

The CNN architecture of our proposed architecture is shown in Table II. We use the residual network architecture as base line architecture [23]. In our proposed architecture, first two convolutional layers are used then pass into six residual blocks with same patch size and different stride. Then the outputs are passed into another convolutional layer. We employ a wide residual network with three convolutional layers and six residual blocks. In dense layer 11, the global feature map of dimensionality 128 is computed. This network is suited for online tracking.

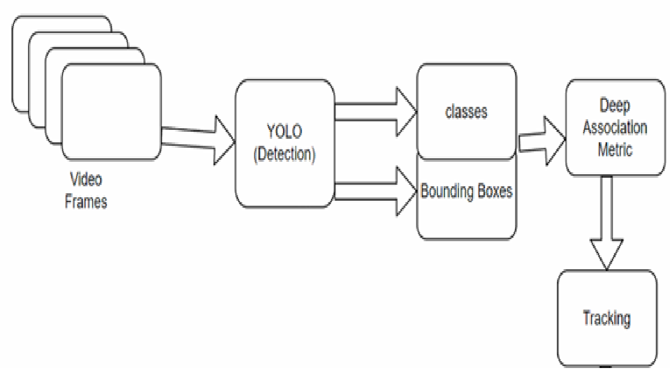

Fig. 3. Object Tracking Pipeline.

TABLE II. CNN ARCHITECTURE OF TRACKING

Name	Patch size/Stride	Output size
Conv 1	3 × 3/1	32 × 128 × 64
Conv 2	3 × 3/1	32 × 128 × 64
Max Pool 3	3 × 3/2	32 × 64 × 32
Residual 4	3 × 3/1	32 × 64 × 32
Residual 5	3 × 3/2	64 × 32 × 16
Residual 6	3 × 3/1	64 × 32 × 16
Residual 7	3 × 3/2	128 × 16 × 8
Residual 8	3 × 3/1	128 × 16 × 8
Conv 9	3 × 3/2	256 × 8 × 4
Flatten 10		8192
Dense 11		128
Batch and l2 normalization		128

4) Pattern recognition: The tracking model generates the trajectories of the moving objects. The large numbers of trajectories collected from tracking model are passed to machine learning algorithms for pattern recognition. The scalable pattern recognition of moving objects has been proposed in [5]. The supervised and unsupervised machine learning algorithms have been used for the pattern recognition of the trajectories.

V. OBJECT DETECTION AND TRACKING RESULTS

The object detection and tracking of our proposed model was implemented in a machine with an ubuntu operating system. It was implemented and tested on Intel Core I5-7300U CPU @2.6GHz with 16GB RAM. The programming platform for detection and tracking the objects was Python 3.7.6 and the OpenCV library. The Python with anaconda environment was used for its implementation. Other tools used in this research were Pytorch and TensorFlow.

1) Dataset: The model was trained using marketplace dataset for bounding box [24]. The Market-1501 dataset was collected with six cameras. The dataset contains 12937 images for training datasets and 19732 images for testing dataset. For the varification, it used any types of videos on of social media or stored in database or can create new videos. Mainly, the YouTube videos were collected, and tracking was done in real time to test this system.

The sample pictures of online tracking are shown in Fig. 4 and Fig. 5. Each figure shows the moving objects at a time and rectangle around objects shows travelling of motion of objects.

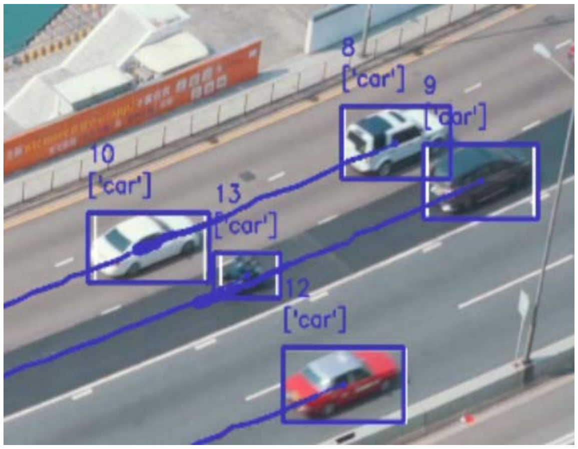

Fig. 4. Object Tracking Result Sample 1.

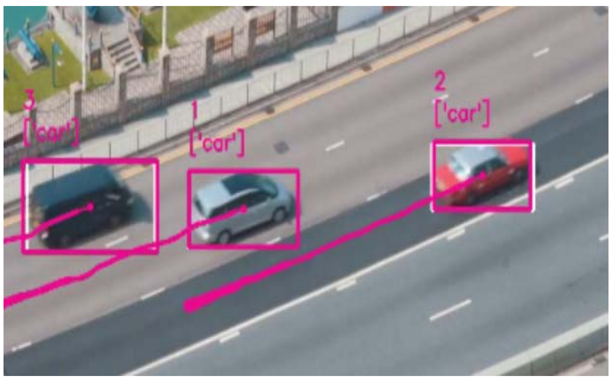

Fig. 5. Object Tracking Result Sample 2.

One objective of this research is the dimensionality reduction in each successive phase. The dimensionality of data in each phase is extremely reduced in our proposed model. The proof of dimensionality reduction has presented in Table I and Table II in methodology chapter. When the frames of the video are passed into proposed model then size of output data is reduced in each layer.

We also present the dimensionally reduction of input video in Table III. First input video is passed into YOLO method for object detection that produces the dimension reduced bounding box. The bounding box is passed into tracking method that produces the trajectories in the form of text data. In this experiment, we passed similar quality of video data.

TABLE III. DATA SIZE REDUCTION

Video number	Input size (kb)	No of frames	After detection	After tracking (kb)
Video1	526	122	Bounding boxes	12.3
Video2	720	140	Bounding boxes	16.8
Video3	655	131	Bounding boxes	15.0
Video4	912	185	Bounding boxes	25.1

TABLE IV. RECALL, PRECISION AND TRACKING ACCURACY OF DIFFERENT VIDEOS

Based on objects in videos	TP	FP	FN	Recall	Precision	Accuracy
Number of Vehicles in Highway	500	8	9	0.98	0.98	98
Number of Vehicles in city road	450	12	9	0.98	0.97	98

TABLE V. COMPARISON OF EXECUTION TIME OF PROPOSED TRACKING WITH YOLOV3 TINY AND YOLOV3

Type of YOLO	Average video size (KB)	Execution time (seconds)
YOLOv3	512	320
YOLOv3 tiny	512	80

TABLE VI. COMPARISONS OF EXECUTION TIME OF THE TRACKER

Tracking	Average video size (MB))	Execution time fps (frame per second)
POI [25]	1.8	0.18
Baseline Deep sort [6]	1.8	0.72
Improved Deep sort (Proposed Model)	1.8	0.75

The proposed model is trained by using marketplace data set and the performance is calculated on test data. We use two versions of YOLO that depends upon the size of edge devices which was defined on previous unit. The light YOLO goes to the small size edge device and the normal YOLO goes to the large size fog device. The execution time of the light YOLO is less than normal YOLO that is presented in Table V. The tracking accuracy of this model is around 98% which is explained in Table IV. The execution time of our proposed tracking model is faster than current deep sort model and Person of Interest (POI) model which is explained in Table VI.

VI. TEST SCENARIOS, SIMULATION AND COMPARISON OF RESULTS

A. Test Scenarios

In this research, we use video surveillance system of moving vehicles as test scenario for smart city. If we pass video files directly into the cloud, more memories are needed. In addition, centralized process takes more latency and uses more network bandwidth. Therefore, processing of videos in decentralized methods are more advisable methods nowadays. In our method, we will extremely reduce the size of video files, then pass to the cloud for further processing. We will recommend decentralized method for the processing of video files using edge computing architecture.

The overall performance of our proposed model will be measured by iFogSim simulator. We have four stages in the video analytic system: motion detection (s1), object detection (s2), object tracking (s3), and pattern recognition (s4) shown in Fig. 6.

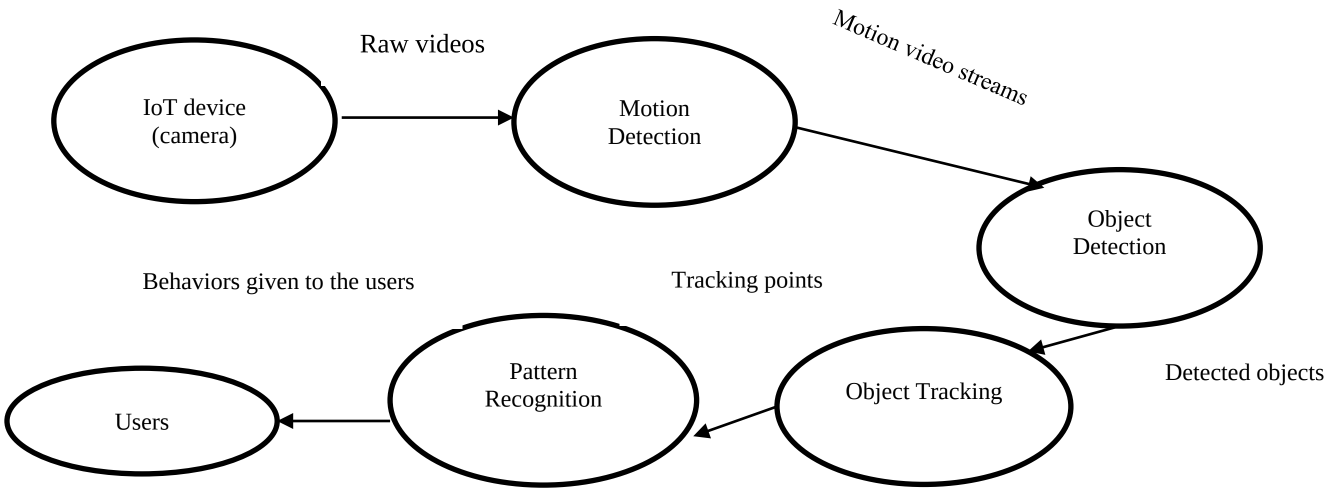

Fig. 6. Video Analytic Pipeline Scenario.

Motion detection (s1): The video camera continuously captures the raw video stream to detect the motion then forwarded to an object detection module.

Object detection (s2): The object detection module receives the video streams of detected motion from the motion detection module. This module is responsible to detect the objects then pass into the object tracking module.

Object tracking (s3): The object tracking module receives the results from object detection module. Then, the object tracking module tracks the path of moving objects and pass into pattern recognition module.

Pattern recognition (s4). It receives the tracking path from object tracking module. It is responsible to find the pattern of moving objects then recommend the patterns to the users.

The unique part of this work is to divide the video analytic into tasks which works as a pipeline. It is very close to real system because the output of one module is the input of another module such as the output of object detection is the input of object tracking.

CASE 1: In this case, edge and cloud are used for video processing. The motion detection (s1) from video camera goes to the edges for object detection (s2) and object tracking(s3). Finally goes to the cloud for pattern recognition (s4).

CASE 2: In this case, only edges are used for video processing. All the stages of video analytic application which are motion detection (s1), object detection (s2), object tracking (s3), and trajectory pattern recognition (s4) are performed on edge devices.

CASE 3: In this case, only cloud is used for video processing. The detected motion (s1) from video camera directly goes to cloud for object detection (s2), object tracking (s3), and pattern recognition (s4).

B. Simulation Tool and Physical Topology

The iFogSim simulator is used in this research. iFogSim [26] is a discrete event simulator for simulation and modelling of edge/fog computing environment. It is based on the CloudSim simulator. In this paper, new model is simulated in which each module is used for monitoring and its output results is the input of another module i.e. pipeline. The simulation has been achieved using a personal computer with Windows 10 operating system. It has simulated on Intel Core I5 CPU @2.3GHz with 8GB RAM. The programming language java with eclipse has been used for the implementation.

The physical topology consists of the cloud data center at the top of the network called first tire. The second tire is the proxy server which is connected between cloud and fog devices. The fog devices are called third tire containing fog nodes. The number of fog devices can be added in different places depending upon the demand of applications. The number of video cameras is connected to the fog devices for our proposed video analytic model for intelligent surveillance application. The physical topology is presented in Fig. 7.

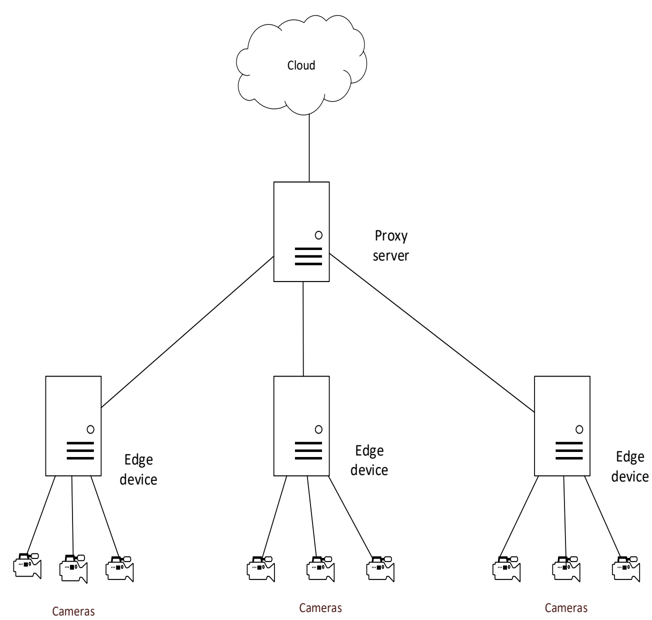

Fig. 7. Physical Experimental Set Up.

C. Defining Simulation Data

The video data is the input of video analytic system. The CNN-based object tracking method explained in previous chapter has video data as an input. For the simulation of video analytic model, we will input the video data similar to our CNN-based object tracking model into our simulator. The videos are not automatically read into iFogSim simulator. Therefore, in this simulation, moving vehicle video data first need to convert into pixel file. The data rate is bits per pixel i.e. bpp. This CSV file contains bpp of videos. There are 13 attributes which are tuple id, total number of pixels, dilation, x coordinate, y coordinate, z coordinate, frame difference, moving rate frame per second, motion ptz, contours, grey color, black color and final contours. There are 65535 rows of data on that file.

Based on the topology designed for the simulation, various fog devices are created and assigned on the nodes of the topology. The fog devices are represented as uniquely working nodes such as camera, edge device, proxy server and cloud. Each fog device has its own processing capacity and configuration like CPU, RAM, upload/download bandwidth, power consumption which setting is defined in Table IX. In this simulation, camera is the sensor that creates the tuples and passed into another device. The different application modules such as motion detection, object detection and so on are assigned to the fog devices according to their capacity. Following are the details about the device configuration parameters:

CPU (MIPS): It is the processing capacity of a CPU given on millions of instructions per second. Higher the processing capacity of a device, higher will be the task execution rate.

RAM: It is the temporary data storage medium where the processing data are stored while the device is online.

Up/Down Bandwidth: It is the speed of the device at which the data are uploaded and downloaded to and from the device.

Power Consumption: It is the electrical power in watt that a device consumes while operating.

The tuple CPU length is the size of data to be passed from one module to another module. The network length (bandwidth) is the rate of transfer of data from one module to another module. In case of object tracking module, after completed a tracking process, the size of data transferred into another module is tuple CPU length and transferred rate is network bandwidth which setting is defined in Table VII.

D. Parameter Settings and Network Configuration

The choice of configuration values is based on the minimum requirement of video surveillance in the real-world scenarios that is referred from the iFogSim Simulator. The Table VII below outlines the configuration of application module components in the video surveillance application. Table VIII presents the latencies configuration between the source and the destination nodes. It explains how the communication between the nodes is managed. Table IX describes the capacities of fog nodes and cloud. It presents the size of different devices in our physical topological structure.

TABLE VII. VALUES FOR MONITORING APPLICATION

Tuple types	**Tuple CPU length (MIPS)**	**Network length (Bandwidth)**
Raw video stream	1000	2000
Motion video stream	2000	2000
Detected objects	1000	100
Tracking points	1000	800

TABLE VIII. NETWORK LATENCIES CONFIGURATION

Between	**Latency (Milliseconds)**
Cloud to Proxy server	100
Proxy server to fog devices	50
Fog devices to camera	1

TABLE IX. CAPACITY OF FOG NODES

Device	**CPU (MIPS)**	**RAM (Bytes)**	**Up bandwidth (Mbps)**	**Down bandwidth (Mbps)**	**Power consumption (Watt)**
Cloud	40000	40000	1000	10000	450 (B) 250 (I)
Proxy server	2800	40000	10000	10000	200(B) 100 (I)
Fog device	2500	4000	1000	10000	100 (B) 83 (I)
Camera	500	1000	100	100	87(B) 82 (I)

E. Performance Evaluation

The evaluation of the performances in our proposed model is resource utilization, bandwidth, latency, and power consumption. These performances are measured in three test cases which was explained in the above section. Test cases are a) Using cloud and edges, b) Using only edges and c) Using only cloud. There are four configurations for simulation results. The number of areas and number of cameras in each place is varied on these configurations. The setting of the configuration is presented in Table X.

The network performance is calculated by the configuration of Table X. We test the results in three scenarios. The first scenario is testing our proposed model in the combination of fog devices and cloud. The second scenario is testing our proposed model in fog/edge devices only. The third scenario is testing our proposed model in cloud devices only. The four parameters of the performance matrix are measured. They are resource utilization, latency, bandwidth, and energy consumption. The resource utilization is the how much resources are utilized to process the data. The Latency/loop delay is the time taken for an application loop to execute. In the application, this loop starts with the camera sensors producing the video stream, goes through the motion detector, object detector, object tracking, and finally pattern recognition. The maximum amount of data which can be transmitted over the network on specific time is called bandwidth. Energy consumption refers to the amount of energy used to process in the system.

TABLE X. CONFIGURATION FOR SIMULATION

Configuration	Areas	Cameras
Config1	3	1
Config2	5	2
Config3	8	4
Config4	10	6

The results are explained in Fig. 8 to Fig. 11 in three scenarios cloud and edges, only edges, and only cloud. The Fig. 8 presents the comparison of network bandwidth. The edge and cloud architecture saved the network bandwidth by 81% in comparison with only cloud-based architecture. The Fig. 9 presents the comparison of resource utilization in these three scenarios. The edge and cloud architecture saved more resources which is around 88.3% in comparison with only cloud-based architecture. Fig. 10 describes the comparison of latency in these three scenarios. The edge and cloud architecture has less latency in comparison with only cloud-based approach; the latency has saved by 97.4%. Similarly, only fog-based approach is slightly better than the combination of cloud and fog devices. Fig. 11 presents the comparison of energy consumption in these three scenarios. The energy consumption in the system is around same for all scenarios.

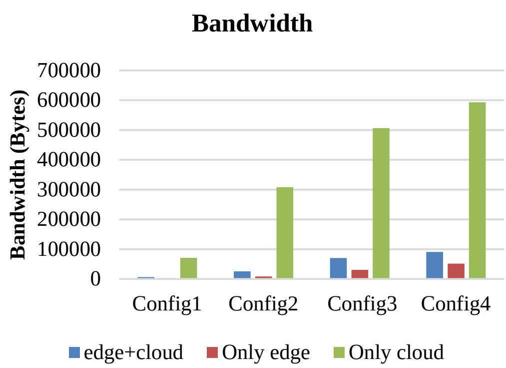

Fig. 8. Comparison of Bandwidth.

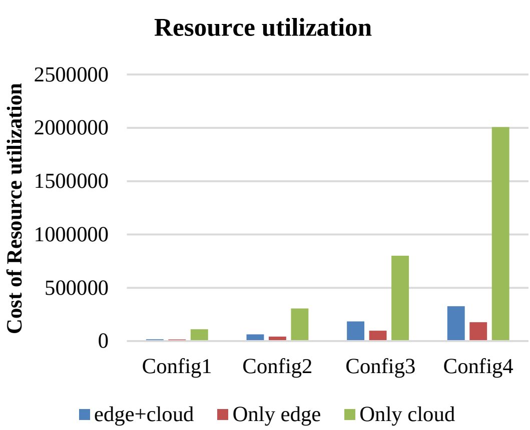

Fig. 9. Comparison of Resource Utilization.

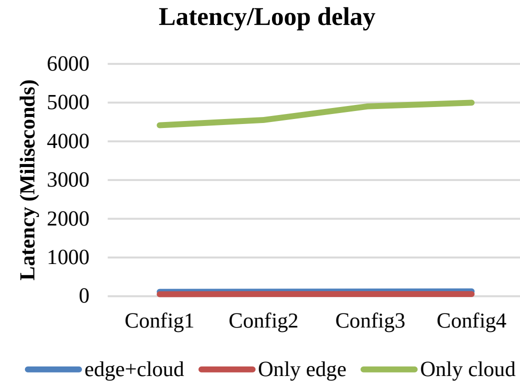

Fig. 10. Comparison of Latency.

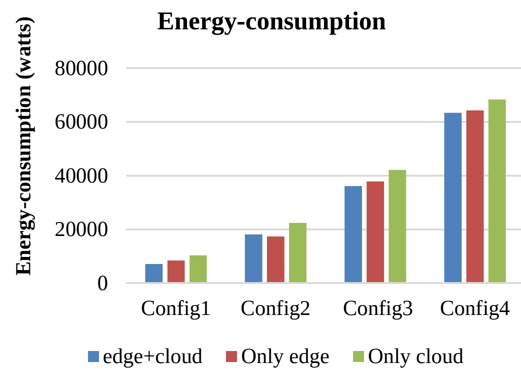

Fig. 11. Comparison of Energy Consumption.

VII. CONCLUSION AND FUTURE WORK

The combination of edge computing and the cloud computing is the main paradigm for video analytic system to build smart city application. In this paper, we developed the new approach for video analytic application to process the data in edge devices and the cloud for smart city in which modules are working as pipeline. We proposed the dimensionality reduction of data in the consecutive steps of video analytic application to increase the network performance. The proposed edge computing technique for video analytic will result in less traffic on the internet because only a small portion of the data will pass into the cloud. One contribution is separating the job into pipeline of sub-tasks and another contribution is implementing the sub-tasks by using deep learning methods. This research also proposed scalable object detection and tracking of moving objects based on CNN. The large numbers of moving vehicles can be tested by our prototype model. Dividing a video analytic job into pipeline of sub-tasks will help to process large number of videos with low latency and low network bandwidth and less cost of resource utilization. The experimental results show that proposed tracking by detection method is more than 96% accurate.

We simulated a proposed model using iFogSim, the result shows that latency, bandwidth, and resource utilization are 97.4%, 81% and 88.3% efficient than only the traditional cloud- based approach.

We simulated our model on large number of fog devices using iFogSim simulator, but we tested a smaller number of videos in CNN-based model. This is a limitation of this work.

The future work will improve the deep learning-based object detection and tracking method. We will improve the performance and compare with different Convolutional Neural Network architecture with large number of video files.

REFERENCES

[1] A. Yousefpour, G. Ishigaki, and J. P. Jue, “Fog Computing: Towards Minimizing Delay in the Internet of Things,” in *Proceedings of IEEE 1st International Conference on Edge Computing*, pp.68–73, 2017.

[2] A. Anjum, T. Abdullah, M. F. Tariq, Y. Baltaci, and N. Antonopoulos, "Video Stream Analysis in Clouds: An Object Detection and Classification Framework for High Performance Video Analytics," *IEEE Transactions on Cloud Computing*, vol. 7, no. 4, pp. 1152-1167, 2019.

[3] D. Pudasaini and A. Abhari, “Scalable Object Detection, Tracking and Pattern Recognition Model Using Edge Computing,” in *Proceedings of Spring Simulation Conference (SpringSim)*, pp. 1-11, 2020.

[4] G. Ananthanarayanan, P. Bahl, P. Bodik, K. Chintalapudi, M. Philipose, L. Ravindranath, and S. Sinha, “Real-Time Video Analytics: The Killer App for Edge Computing,” *IEEE*, vol. 50, no. 10, pp. 58-67, 2017.

[5] D. Pudasaini and A. Abhari, “Scalable Pattern Recognition and Real Time Tracking of Moving Object,” *Spring Simulation Conference (SpringSim)*, pp. 1-11, 2019.

[6] N. Wojke, A. Bewley, and D. Paulus, “Simple online and real-time tracking with a deep association metric,” in *Proceedings of IEEE International Conference on Image Processing*, pp. 3645-3649, 2017.

[7] G. Javadzadeh and A.M. Rahmani, “Fog Computing Applications in Smart Cities: A Systematic Survey,” *Wireless Networking*, vol. 26, pp. 1433–1457, 2019.

[8] N. Mohamed, J. Al-Jaroodi, I. Jawhar, S. Lazarova-Molnar, and S. Mahmoud, "SmartCityWare: A Service-Oriented Middleware for Cloud and Fog Enabled Smart City Services," *IEEE* , vol.. 5 pp. 17576-17588, 2017.

[9] M. S. Alam, B. V. Natesha, T. S. Ashwin, and R. M. Guddeti, “UAV based cost-effective real-time abnormal event detection using edge computing,” *Multimedia tools and Applications*, vol. 78, pp. 35119-35134, 2019.

[10] D. N. Jha, K. Alwasel, A. Alshoshan, X. Huang, R. K. Naha, S. K.Battula, et al., "IoTSim-Edge: A Simulation Framework for Modeling the Behaviour of IoT and Edge Computing Environments," *arXiv:1910.03026*, pp. 1-19, 2019.

[11] H. Wu, Z. Zhang, C. Guan, K. Wolter, and M. Xu, “Collaborate edge and cloud computing with distributed deep learning for smart city internet of things,” *IEEE Internet of Things Journal*, vol. 7, no. 9, pp. 8099-8110, 2020.

[12] C. Qi, W. Ouyang, H. Li, X. Wang, B. Liu, and N. Yu, “Online Multi-Object Tracking using CNN-Based Single Object Tracker with Spatial-Temporal Attention Mechanism,” *International Conference of Computer Vision*, pp. 4836-4845, 2017.

[13] Y. Fengwei, W. Li, Q. Li, Y. Liu, X. Shi, and J. Yan, “POI: Multiple Object Tracking with High Performance Detection and Appearance Feature,” *European conference of computer vision*, pp. 36-42, 2016.

[14] G. Chandan, A. Jain, H. Jain, and Mohana, “Real Time Object Detection and Tracking Using Deep Learning and OpenCV,” in *Proceedings of* IEEE *International Conference on Inventive Research in Computing Applications (ICIRCA)*, pp.1305-1308, 2018.

[15] F. Zhu, Y. Lu, N. Ying, and G. Giakos, “Fast vehicle detection based on evolving convolutional neural network,” *IEEE International Conference on Imaging Systems and Techniques (IST)*, pp. 1-4, 2017.

[16] T. Stone, N. Stone, P. Jain, Y. Jiang, K. Kim, and S. Nelakuditi, “Towards Scalable Video Analytics at the Edge,” *Annual IEEE International Conference on Sensing, Communication, and Networking*, pp. 1-9, 2019.

[17] D. Zhao, H. Fu, L. Xiao, T. Wu, B. Dai, “Multi-Object Tracking with Correlation Filter for Autonomous Vehicle,” *Sensors (Basel, Switzerland)*, vol. 18, no. 7, pp. 1-17, 2018.

[18] L. Yang, L. Wang, and S. Wu, “Real-time Object Recognition Algorithm Based on Deep Convolutional Neural Network,” in *Proceedings of the 3rd IEEE conference on cloud computing and big data analysis*, pp. 331- 335, 2018.

[19] T. He, H. Mao, and Z. Yi, “Moving Object Recognition using Multi-View Three-dimensional Convolutional Neural Networks,” *Neural Computing and Applications*, vol. 28 no. 12, pp. 3827-3835, 2017.

[20] L. M. Vaquero and L. Rodero-Merino, “Finding your Way in the Fog: Towards a Comprehensive Definition of Fog Computing,” *Computer Communication Review*, vol. 44, no. 5, pp. 27-32, 2014.

[21] J. Redmon and A. Farhad, “YOLOv3: An Incremental Improvement,” Retrieved from: https://pjreddie.com/media/files/papers/YOLOv3.pdf, 2018.

[22] J. Redmon, S. Divvala, R. Girshick, and A. Farhadi, “You Only Look Once: Unified, Real-Time Object Detection,” 2016, Retrieved from: https://arxiv.org/pdf/1506.02640.pdf.

[23] S. Zagoruyko and N. Komodakis, “Wide residual networks,” *BMVC*, pp. 1–12, 2016.

[24] Retrieved from: https://www.kaggle.com/pengcw1/market-1501.

[25] F. Yu, W. Li, Q. Li, Y. Liu, X. Shi, and J. Yan, "POI: Multiple Object Tracking with High Performance Detection and Appearance Feature," *arXiv:1610.06136*, 2016.

[26] H. Gupta, A. V. Dastjerdi, S. K. Ghosh, and R. Buyya, “iFogSim: A Toolkit for Modeling and Simulation of Resource Management Techniques in the Internet of Things, Edge and Fog Computing Environments,” *Software Practice & Experience*, vol. 47, no. 9, pp. 1275- 1296, 2016.

SmartTS: A Component-based and Model-Driven Approach to Software Testing in Robotic Software Ecosystem

Vineet Nagrath[1], Christian Schlegel[2]
Service Robotics Research Center
Technische Hochschule Ulm
89075 Ulm, Germany

***Abstract*—Validating the behaviour of commercial off-the-shelf components and of interactions between them is a complex, and often a manual task. Treated like any other software product, a software component for a robot system is often tested only by the component developer. Test sets and results are often not available to the system builder, who may need to verify functional and non-functional claims made by the component. Availability of test records is key in establishing compliance and thus selection of the most suitable components for system composition. To provide empirically verifiable test records consistent with a component's claims would greatly improve the overall safety and dependability of robotic software systems in open-ended environments. Additionally, a test and validation suite for a system built from the model package of that system empirically codifies its behavioural claims. In this paper, we present the "SmartTS methodology": A component-based and model-driven approach to generate model-bound test-suites for software components and systems. SmartTS methodology and tooling are not restricted to the robotics domain. The core contribution of SmartTS is support for test and validation suites derived from the model packages of components and systems. The test-suites in SmartTS are tightly bound to an application domain's data and service models as defined in the RobMoSys (EU H2020 project) compliant SmartMDSD toolchain. SmartTS does not break component encapsulation for system builders while providing them complete access to the way that component is tested and simulated.**

Keywords*—Model-Driven Engineering (MDE); Component-based Software Engineering (CBSE); Model-Driven Testing (MDT); Component-based Software Testing (CBST); Service Robotics; Software Quality; Automated Software Testing

I. Introduction

A software product may be difficult to understand and modify, it might be prone to misuse and difficult to use, it might not integrate well with another piece of software and it might work on only a particular machine and only under some very hard assumptions. Unless one looks under the hood to measure software on these parameters, the *quality* of the software can not be judged purely on the basis that it works and was delivered on time [1]–[3]. Fig. 1 shows key characteristics that can be used to evaluate the overall quality of a software product * [1]. A good software product can be qualified as testable if it performs well on the following quality parameters as suggested by Boehm et al. [1].

B1 **Accountability**: *Code*[2] allows for mechanisms to measure its usage, e.g. code instrumentation B1.

B2 **Accessibility**: Code allows selective usage of its parts and provides side entrances for test access B2.

B3 **Communicativeness**: Code allows specification of inputs and provides corresponding outputs in a usable form B3.

B4 **Self-descriptiveness**: Code provides enough information, e.g., a test model, for its *use*[3] and *verification*[4] B4.

B5 **Structured**: Code is organized into definite interdependent parts, i.e. the software system is composed of part-wise/component-based testable units B5.

In summary, *a testable code has an established verification criterion and supports performance evaluation*. Testing in the software industry is broadly categorised into *unit*, *integration* and *system testing* [4]–[7]. A fourth level, namely, *acceptance testing* may be added on some occasions (see Fig. 2).

L1 **Unit testing** as the name suggests tests individual *code components* L1.

L2 When different code modules are joined, the test of data flowing through the *interface* is **integration testing** L2.

L3 A system prepared by several code units is tested against *functional and non-functional system-level requirements* in **system testing** L3.

L4 An additional *enforcement* check performed against a contract, after the final delivery of the software product is **acceptance testing** L4.

High speed, repeatable, low effort and inexpensive testing improves the overall quality of the software product and its development workflow. A well-structured test and validation mechanism can be made cheaper when automated. Removing the human element from the testing and enforcement equation

[1] * Throughout this paper, Indicators like B1, L2, R3, A3S3, E8 & are internal connections between notions presented in the paper.

[2] *Code* in software engineering is short for *source code* unless stated otherwise.

[3] Component blocks, ports (required and provided services), connectors.

[4] Objectives, assumptions, constraints, revisions and usage history.

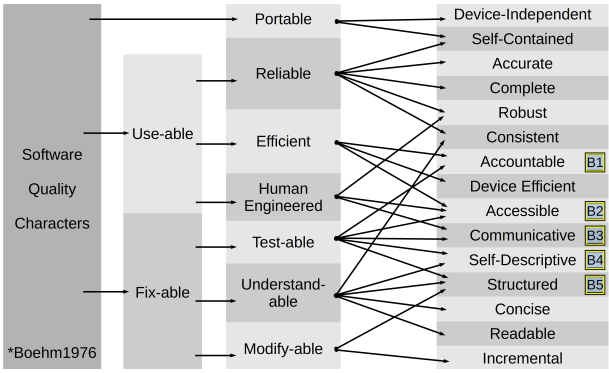

Fig. 1. Software Quality Characteristics Tree [1].

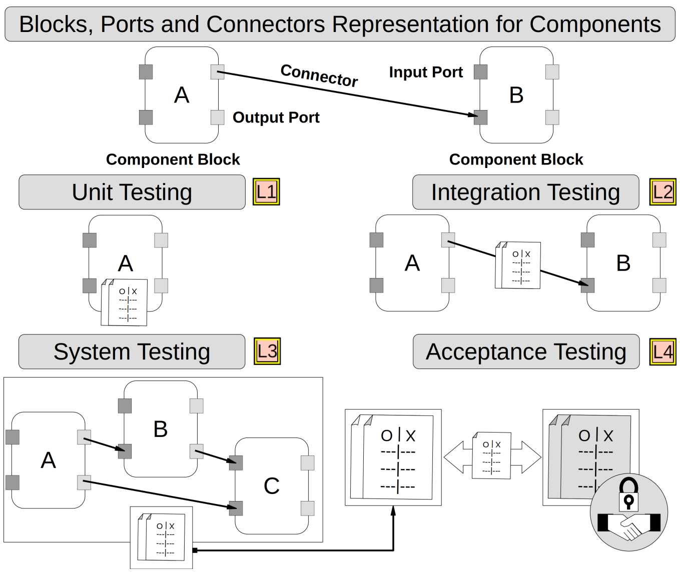

Fig. 2. Software Test Levels. *Blocks-ports-connectors* Representation for Software Code Modules.

is of great value for high complexity, incrementally growing software systems. Machine delivered tests allow for frequent regression checks on legacy systems in a long-term life cycle of a software product. The importance of automation in software testing was realized very early in the development of software development as an industrial process [8], [9]. A trade-off exists between the degree of automation in testing and the regularity by which those tests will be executed, which tilts heavily in favour of automation as a system grows more elaborate and mission-critical [10]. Thus, it will be safe to assume that any modern software development methodology will be incomplete without a comprehensive plan to automate testing in all test levels (L1-L4)@ and across all test quality parameters (B1-B5)@.

Testing robotic software differs from software testing in general for several reasons.

R1 *Robots interact with the* ***physical world*** with sensors and actuators which are inherently prone to noise and faulty execution [11] R1.

R2 **Environments**, where robots work, are often *open-ended* with very few assumptions [12]. There is a physical danger involved while working with robotic systems, especially during their testing R2.

R3 **Safety** concerns are high especially when *robots work near humans* R3.

R4 ***Robot cost*** is high and their availability for extensive testing is low R4.

R5 Robots, sensors mounted on those robots and the software driving the two are often *built by* **different vendors** with a wide scope of utilization in mind. Robust and verifiable hardware and software composition thus become ever more important for robotic systems [13] R5.

R6 Very few off-the-shelf software components fit real-world applications, a large portion of *code has to be* **custom made** for a particular robot R6.

R7 Robots are built using several **hardware** components like gears, wheels and consumables which *wear down, get damaged or replaced* over time. The challenge is to reuse, with confidence, the existing software against worn-out or some new, slightly different hardware [11], [14] R7.

R8 Difficult to specify what constitutes a **correct behaviour** for a robotic system [15] i.e. it is not always clear *what needs to be tested*. The challenge comes in particular from the open-ended world for which full coverage testing is not possible R8.

R9 *People from various domains* work on a robot, not all of them **are trained software engineers** R9.

R10 *Lack of* **communities** and uniform **standards** for the *robotic industry*. Standards for robotic hardware and software should be made abstract and encapsulated to hide the intellectual property of a business, while not compromising its usability and configurability for the end-user R10.

A recent extensive study on the challenges of testing robotic systems concluded with three important themes describing major challenges in testing robots. Following are the themes and suggested solutions reasoned in the study [16].

A1 **Real-world complexities**: A robot's interactions with the real world is a key difficulty in testing robotic software A1.

A1S1 Rapid development of *reliable simulators* with better Application Programming Interface (APIs) and User Interfaces (UI), leading to better automated simulation testing A1S1.

A1S2 Research on tools and techniques for *automated testing* of robotic software A1S2.

A2 **Communities and standards**: Community-driven standards promote product quality and incentivise member businesses A2.

A2S1 Developing a *robotic software ecosystem* with special emphasis on software quality standards A2S1.

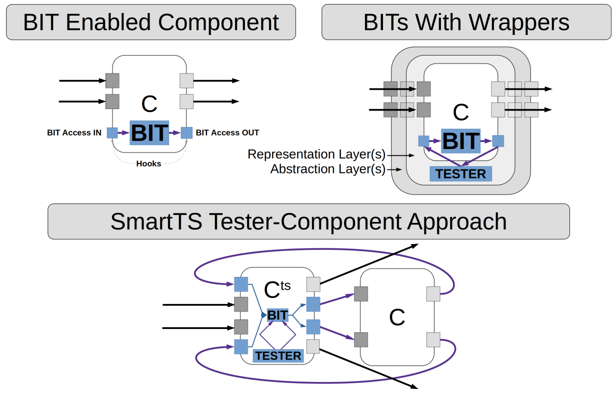

Fig. 3. SmartTS Approach in the Context of *BITs* and *Test Wrappers*.

A2S2 *Guidelines and tools* to promote healthy practices for the growth of the ecosystem A2S2.

A3 **Component integration**: Robotic software demands an integrated (hardware + software) approach to system testing A3.

A3S1 Better *availability of hardware* components for testing within the community A3S1.

A3S2 Promote tools like hardware-in-the-loop simulation borrowed from other industries A3S2.

A3S3 Develop better *test oracles*[5] to ensure that the testing apparatus knows with confidence the results of running a test A3S3.

In the past decade, there have been some application-specific proposals for systems for testing software for robots [17]–[27]. These approaches present tools and algorithms to address the above (A1-A3)@ concerns but they are either too specific for a particular robotic application [18]–[20] or are generic extensions of general software testing techniques and standards [21], [22] with little to no planning specifically for robotic software testing (R1-R10)@. In either case, none of these is community-driven or providing tools or standards for businesses to follow. A notable exception to this is the Robot Testing Framework (RTF) [23] which is the right step towards test automation by a plug-in based approach to testing that is independent of platform, middleware and programming language used for writing the test plug-ins. There are works focusing on improving simulation testing [24]–[26] and model-driven performance testing [27]. An idea borrowed from the computer hardware industry [28], the *built-in test enabled components* [29]–[31], is to have a functionally separate maintenance mode to provide access to **Built-In Tests (BITs)**. Using **test-wrappers** is another common approach that works along with the BIT approach to envelop the software component in a single or multi-layer software wrapper that is transparent to both the component being tested and its peers in the environment. These wrappers, when used with BITs, enable *testing without breaking component encapsulation*. The *RESOLVE* [32] approach is one such approach, it proposes a two-layer wrapper to achieve *automated black-box testing of software components*.

[5] *Test oracle* (or simply Oracle) is software engineering terminology for any mechanism by which a test scrip determines whether a test case has passed or not.

The *SmartTS* approach to component testing is to create a tester component whose model is derived from the model of the component being tested. *This tester component* ***implements the BITs for automated testing*** *of the component and its code is transparent (white-boxed) to the ecosystem, thus the* ***component encapsulation*** *is maintained (*black-boxed*) while no additional operational overload is attached to the component for implementation and execution of BITs in maintenance/test mode* (See Fig. 3).

According to our experience of working with robots in the *service robot industry, community-driven models* with a special focus on *Component-Based Software Development (CBSD)* works best for the development of the *robotic software component*. Although there exist several *Model-Based Engineering (MDE)* approaches for software development in general [31], [33]–[37], approaches with a special focus on the robotic industry are essential for the growth of the robotics industry (Multi-annual roadmap [38], the European SPARC Robotics [39] initiative). One such effort towards creating an ecosystem for model-driven and component-based development of robotic software is the EU H2020 *RobMoSys: Composable Models and Software for Robotics* [40], [41] project. *Meta-models* that promote *separation of concerns* [42], [43] along different roles such as robotic experts and application domain experts are highly desirable for the industry. MDE supports the separation of concerns and of roles since it provides operational modules dedicated to use by specific stakeholders. The *RobMoSys* approach has a special emphasis on a clear separation of concerns and roles and promotes community building for efficient collaboration between stakeholders. Other model-based efforts towards a *robotic software ecosystem* [44]–[47] are also taking separation of concerns and roles as an essential part of their working philosophy, which will be essential for their success [48].

In CBSD for *software-intensive service robotic systems*, validating the behaviour of a supplied component and its interactions with other components is a complex, and often a manual task. In *EU Robotics Strategic Research, Innovation and Deployment Agenda 2020 on AI, Data and Robotics Partnership* [49], ***trustworthiness*** was identified as one of the *core characteristics* that *robotics and AI systems* need to display. ***Trustworthiness*** **is a property of the** ***system derived from the trustworthiness of its constituents and their interactions***. Treated like any other software product, a software component for a robot system is tested by the *component developer* (and/or *component tester*) at the vendor's (*component supplier*) end. *Test-sets* and records of *test-results* are often not available to the *system builder*, who may need them to *verify functional and non-functional claims* made by the vendor about the component. Availability of test records is key in *establishing compliance* and thus *selection* of the most suitable component for *system composition*. To provide ***empirically verifiable test records consistent with a component's claims*** would greatly improve the overall safety and dependability of robotic software systems in open-ended environments. It is of added benefit that when a system is composed of several components, a part of the *system's test and validation suite* is *automatically generated* from the *test-suites of the constituent components*. This further helps

empirically codify a system's functional and non-functional behavioural claims. To the best of our knowledge, there is an absence of **a wholistic model-driven approach towards CBSD for robotic systems, that *integrates support for test and validation suites*[6] within the *model-package*[7] of a robotic software component or system**. Inclusion of test sets and expected results within the *model-package* in *model-driven component-based software development* enables the following modelling and transformational[8] functionalities.

E1 Meta-modelling framework to define and codify **component-test-model** E1.

E2 **Automated generation of user-editable component-level test-suites** from *component* and *domain model packages*. Automated **model to data transformations (M2D)** of user-ascribable *test-data sets* from *domain* and *user test documents*.

E3 **Automated testing** at vendor's side E3.

E4 Empirically verified **adequate component selection** during system composition E4.

E5 Meta-modelling framework to define and codify **system-test-model** E5.

E6 **Automated generation of system-level test-suites** from *component-level test suites* and *system-test-model packages* E6.

E7 **Does not break component encapsulation** E7.

E8 **Does not break system encapsulation** to *enforcement and verification* agents E8.

In this paper, we present the **"SmartTS methodology": A component-based and model-driven approach to generate model-bound test-suites for software components and systems**. The test-suites in *SmartTS* are tightly bound to an *application domain's data and service models* as defined in the ***RobMoSys** [40] (EU H2020 project) compliant **SmartMDSD** [50], [51] Toolchain*. *SmartTS* provides *automated generation, execution* and *transformation* of *test-suite models* and *test-suite results* across a *service domain*, *component* and *system models*, *enabling automated testing* and *verification* of *components* and *systems*. *Component test-suite results* are used for *selecting* an *appropriate component* for *composition*. *System test-suite results* are used for *documenting* or *sensing system behaviour* during *composition, acceptance testing, enforcement* or for *run-time diagnosis*. *SmartTS* does not break *component encapsulation* for *system builders* while providing them complete access to the way that a *component* is *tested* and *simulated* (Supporting *composition* and *separation of roles*).

The rest of the paper is organized as follows. Section titled **SmartTS Overview** introduces the intended *goals* and *contributions* of the *SmartTS toolchain*. It presents the *principles* and *methodologies* that have inspired *SmartTS*. Sections

[6]A *test and validation suite* is a set of testable statements about a software component or a multi-component system, which when true indicates the validity of a particular behavioural claim of the entity.

[7]A set of models that collectively define an entity.

[8]A model transformation in MDE is an automated mechanism of transforming one entity into another, where the entity could mean a model or text (including raw data or code written in a programming language).

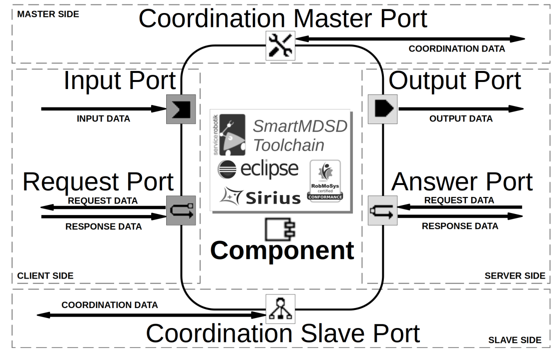

Fig. 4. Anatomy of a SmartMDSD Component.

SmartTS and the SmartMDSD Toolchain and **SmartTS in the Context of RobMoSys** present how *SmartTS integrates* with the existing *SmartMDSD toolchain* and the *RobMoSys ecosystem*. This paper puts the focus on **new** *meta-models*, *domain-specific languages* (DSLs), *roles, views, model-to-model* (MMT), *model-to-text* (M2T) and *model-to-data* (M2D) *transformations* that *SmartTS* introduces. Section **SmartTS in Action** presents a few use-cases for SmartTS to showcase its impact. An illustrative sketch of *SmartTS* tooling based on *Eclipse* features and plug-ins is provided without going into how it is implemented. Finally, Section **Conclusions and Future Works** draws some conclusions on the presented work and outline future research direction and works.

II. SmartTS Overview

The *core philosophy and contribution* of the *SmartTS methodology* is to embed models describing the tests for a component within the model package of the *component*. A *tester component* is then generated from the *model package* that without breaking *component encapsulation* implements *built-in tests* and drives *automated testing* for the *component*. The *tester component* generates *empirically verifiable test records* which are distributed with the *component* to support its *claims*. **Since the *trustworthiness* of a *system* is derived from its *components*, the *system-level test-suite* is partly derived from *tester components* and *models* of *components* that constitute the *system*.** *Model-driven* and *component-based software development* form the base on which the *SmartTS methodology* is placed. In this section, we will walk through the *methodology* and present the *mechanism* by which *SmartTS* proposes a *component-based* and *model-driven approach* to *software testing* in a *robotic software ecosystem*.

SmartTS is a member of the *RobMoSys/SmartMDSD ecosystem*. In this paper, we are presenting the *SmartTS methodology* in the *context* of its *core ecosystem* (*RobMoSys/SmartMDSD*). **The *principles* and *mechanisms* described here though can be *transported as-is* to any *component-based* and *model-driven software ecosystem*.** Fig. 4 shows the *anatomy* of a *typical SmartMDSD component*. It is typical in *CBSD* to represent *components* and *systems* using the *blocks ports connectors notation* (see Fig. 2). In this paper, we use a *custom blocks ports connectors notation* (Fig. 5) to present the *SmartTS methodology*. Note that *SmartMDSD components* can have any number of *input, output, request* or *answer ports* and exactly one *coordination* & *configuration*

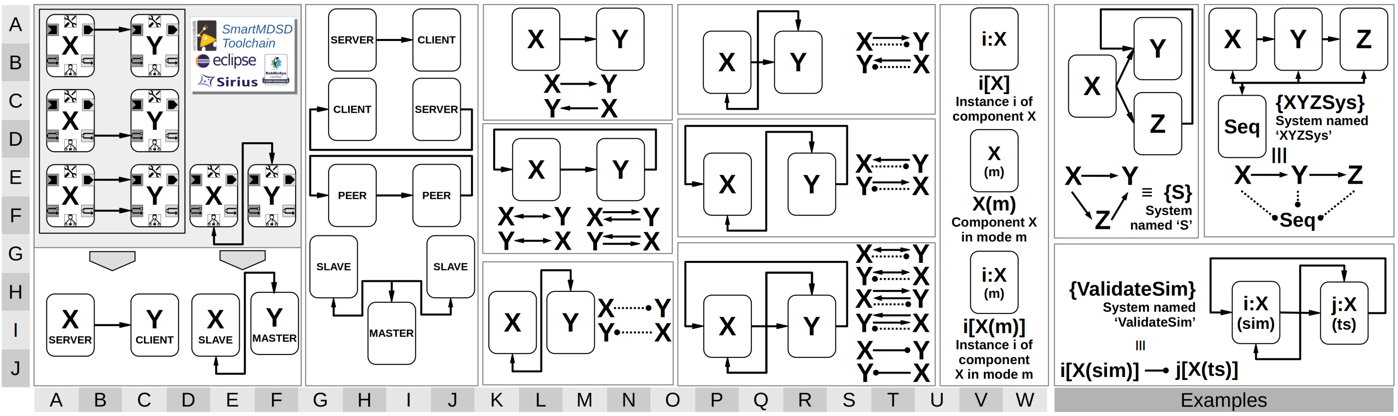

Fig. 5. Custom Blocks Ports Connectors Notation used in SmartMDSD::SmartTS Methodology.

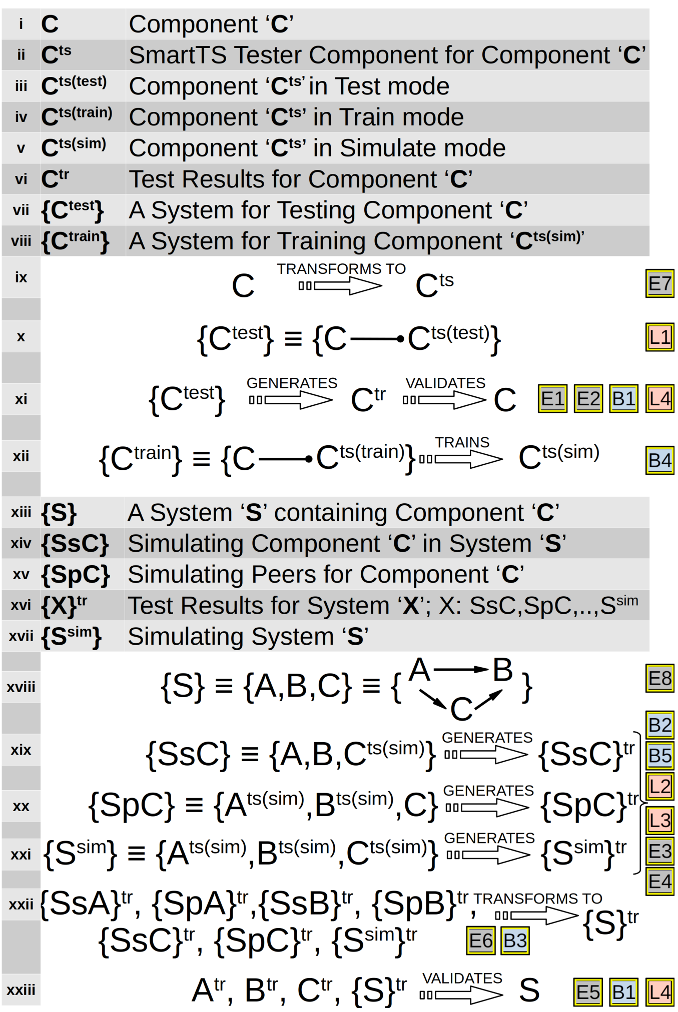

Fig. 6. SmartTS Transformations and Validation Mechanisms.

slave port unlike what one may infer from the simplified representation in Fig. 4. If a *component* has a *master* port of a *coordination* & *configuration interface* integrated then it can *coordinate* and *control* other *components*. Furthermore, the four-side arrangement of *ports* in Fig. 4 is only for representation and the *SmartMDSD toolchain* GUI doesn't tightly bound these *ports* to particular sides of a *component*. *SmartMDSD Services* [52] is an item being transported (*communication object* [53]) in a particular manner (*communication pattern* [54]). Depending on the *communication pattern*, the *SmartMDSD component* could possess an *input, output, request or answer port* (Fig. 4). The '*send*' *communication pattern* is *one-way* while a '*query*' *communication pattern* is for *two-way* communication of *communication objects*. A *publish/subscribe* mechanism is available for *one-to-many* communication using '*push*' (distribution) and '*event*' (asynchronous notification) *communication patterns*. *Coordination ports* are for a *two-way* exchange of '*coordination*' *patterns* ('*parameters*', '*states*', '*dynamic wiring*' and '*monitoring data*'). These '*coordination*' *patterns* are internally built on top of '*data*' *patterns* ('*send*', '*query*', '*push*' and '*event*'). A *system* built using the *SmartMDSD toolchain* has a *default coordination master* (e.g. a *sequencer*) with all *constituent components* as its *coordination clients*, in a configuration similar to the *system* XYZSys (examples)[9].

For the benefit of the *reader*, it is enough to retain that a ***SmartMDSD component* typically acts as a *service consumer* as well as a *service provider* at the same time. It is *coordinated* by a *global coordination master component* (*sequencer*) which in normal usage is hidden from the *user***. A *SmartTS tester component* to a *component* would thus become a *consumer* to every *service* provided by the *component* and *provider* to all *services* requested by the *component*. It will also act as a *coordination master* to the *component* and the *system* built using the *component* and its *tester component* would have a *configuration* similar to the one shown in (GO-JU)[9] between *component* X (HP[9]) and its *tester component* Y (HR[9]). In *shorthand notation*, this *system* would be written as IT[9]. The *reader* is advised to go through the *notation* given in Fig. 5. A *component* can have more than one *instance* in a *system* (CV[9]) and can have differently *named operating modes* (FV[9]). *Systems* are represented with their names in *curly brackets* (examples[9]). *Mapping* of *SmartMDSD component notation* (Fig. 4) to *SmartTS custom notation* is given in (AA-JF)[9].

Fig. 6 shows key *SmartTS transformations* and *validation mechanisms*. A *component* C (Fig. 6.i) is *transformed* to its

[9]See alphanumeric coordinates in Fig. 5

tester component C^{ts} (Fig. 6.ii, Fig. 6.ix). In *SmartMDSD*, the *component code* is *generated* from its *component model package*. The same *model package* is *transformed* into the *model package* for the *component* C^{ts}. This *tester component* provides an empty *code template* which is later filled to *implement BITs* for *component* C. Once *BITs* are *implemented* and *linked* to associated *test* and *validation data* (discussed later in the Section **SmartTS and the SmartMDSD Toolchain**), the *component* C^{ts} is *deployed* to *test component* C (Fig. 6.x). The *component* C^{ts} has three *principal operating modes* namely *test*, *train* and *simulate* (Fig. 6.iii-v). In *test mode*, the *component* C^{ts} is *deployed* with *component* C to form the *test system* $\{C^{test}\}$ for *component* C (Fig. 6.vii, x). The *test results* C^{tr} from the *system* $\{C^{test}\}$ are used to *validate* the *claims* made by the *component* (Fig. 6.vi, xi). The *component* C^{ts} is *deployed* in *train mode* to form the *training system* $\{C^{train}\}$ for *component* C (Fig. 6.viii, xii). This *training system* $\{C^{train}\}$ *trains* the *component* C^{ts} to work in the *simulated mode*. Note that the C^{ts} is *simulated* against *BITs* which may not match the *BITs implemented* for its *test mode*. The difference between these two sets of *BITs* is only in terms of the *motivation* behind their existence.

SmartTS Tester Component
SmartTS tester component for a *component* is a *consumer* to every *service* provided by the *component*, *provider* to all *services* requested by the *component* and it acts as a *coordination master* to the *component*.

SmartTS Test System
SmartTS test system is a *system* with a *component* and its *tester component deployed* to *execute* the *BITs implemented* by the *tester component* and *generate* corresponding *test results*.

SmartTS Trainer System
SmartTS trainer system is a *system* with a *component* and its *trainer component deployed* to *execute* the *BITs implemented* by the *trainer component* and *generate* a fully *trained simulator component*.

SmartTS Simulator Component
SmartTS simulator component is a *tester component operating* in the *simulate mode*. The *simulator component* can *reproduce* the *service* and *coordination behaviour* of the *component* for a specific set of *BITs*.

In Principal, once *trained*, the *component* C^{ts} in *simulate mode* can *reproduce* the *service* and *coordination behaviour* of *component* C for a specific set of *BITs*. This *simulated mode component* C^{ts} is then used in various *simulated variants* ($\{SsC\}$, $\{SpC\}$ and $\{S^{sim}\}$: Fig. 6.xiv, xv, xvii, xix-xxi) of a given *system* $\{S\}$ (Fig. 6.xiii, xviii). *Results* (Fig. 6.xvi, xix-xxii) from these *simulated variants* of the *system* are *transformed* to a single set of *simulation test results* $\{S\}^{tr}$ for the *system* $\{S\}$ (Fig. 6.xxii). ***Trustworthiness*** **(*Conformance* to *claims* and agreed upon *BITs*) is a *property* of the *System* ($\{S\}$) derived from the *trustworthiness* of its *constituents* (A^{tr}, B^{tr} and C^{tr}) and their *interactions* ($\{SsA\}^{tr}$, $\{SpA\}^{tr}$, $\{SsB\}^{tr}$, $\{SpB\}^{tr}$, $\{SsC\}^{tr}$, $\{SpC\}^{tr}$, $\{S^{sim}\}^{tr}$).** The *simulation test results* $\{S\}^{tr}$ for the *system* $\{S\}$ along with *test results* of its *constituents* (A^{tr}, B^{tr} and C^{tr}) are used to *validate* the *claims* made by the *system* (Fig. 6.xxiii).

III. SmartTS and the SmartMDSD Toolchain

SmartMDSD toolchain [50], [51] is a *RobMoSys* [40] compliant *model-driven* tooling for *component-based robotic software* development based on the *SMARTSOFT methodology* [55]. *SmartTS*: *Test-suite* extensions for *SmartMDSD toolchain*, presented for the first time through this paper is an addition to the existing *SmartMDSD toolchain* and provides constructs for modelling *built-in contract testing* in *systems* built using the *SmartMDSD toolchain*. *SmartTS* provides *models* to associate a *test* and *validation suite* with any of the existing *SmartMDSD models*. It also allows for the creation and usage of *data elements* associated with the *test* and *validation suites*. ***Eclipse features and plug-ins*** **for *SmartTS* are available for download** [56]. *Context* and *video tutorials* on the use of *SmartTS* **will soon be** available online at *SRRC wiki* web page [57]. Fig. 7 shows the key elements of the *SmartTS methodology*.

SmartMDSD and *SmartTS* elements span across two tiers (1-20, 20-50)[10] and involve four main actor-groups. *Domain experts* (2C,15N)[10], *component developers* (24D, 48L)[10], *system builders* (23D, 48R)[10] and *behaviour developers* (22C[10]). The two tiers in the *SmartTS methodology* correlate with *tier-2* and *tier-3* of *RobMoSys* (Section **SmartTS in the Context of RobMoSys**). *Component developers*, *system builders* and *behaviour developers* are *tier-3 ecosystem users* (22E, 25N, 25R)[10]. A *tier-3 ecosystem user exchanges content* (20P, 5K, 20T, 20V)[10] and *writes models* (28C, 36C, 48C, 33T)[10] that *conforms to* (20B, 31J)[10] *domain-specific models* (7C, 6G)[10] *defined* by the *domain experts* in *tier-2*. The *domain experts write* the *SmartMDSD domain model package* (7C[10]) which contains several *domain models* (9A-19D)[10] about *services* (19B[10]), *data* (12B[10]), *dependency* (15B-18B)[10], *modes* (13B[10]), *parameters* (9B[10]), *tasks* (10B, 11B)[10] and *documentation* (14B[10]). These *models* are later *implemented* or *imported* by *tier-3 users* (22E[10]) in *SmartMDSD component* (28C[10]), *system* (36C[10]) and *behaviour* (48C[10]) *models*. *SmartMDSD component model package* (28C[10]), *written* by *component developers* (24D[10]) consists of *component models* (30A-35D)[10] that describe a *component's parameters* (30B[10]), *code structure* (35B[10]), *ports* (35B[10]), *dependency objects* (34B, 35B)[10], *skills* (31B[10]) and *documentation* (33B[10]). *System builders* (23D[10]) *write* the *SmartMDSD system model package* (36C[10]) containing *models* (38A-46D)[10] that describe *structure* (39B, 46B)[10], *operations* (38B, 40B, 42B)[10], *dependency* (44B, 45B)[10] and *documentation* (43B[10]) for the *system*. *Behaviour developers* (22C[10]) write the *SmartMDSD behaviour model* (48C[10]) that specifies how *domain tasks* (11B[10]) are *realized* (50C[10]) in a particular *behaviour*. The *SmartTS models* (7F-18J, 34F-48J)[10] are *derived* (17F, 48F)[10] from the existing *SmartMDSD domain*, *component*, *system* and *behaviour models* [58].

[10]See alphanumeric coordinates in Fig. 7

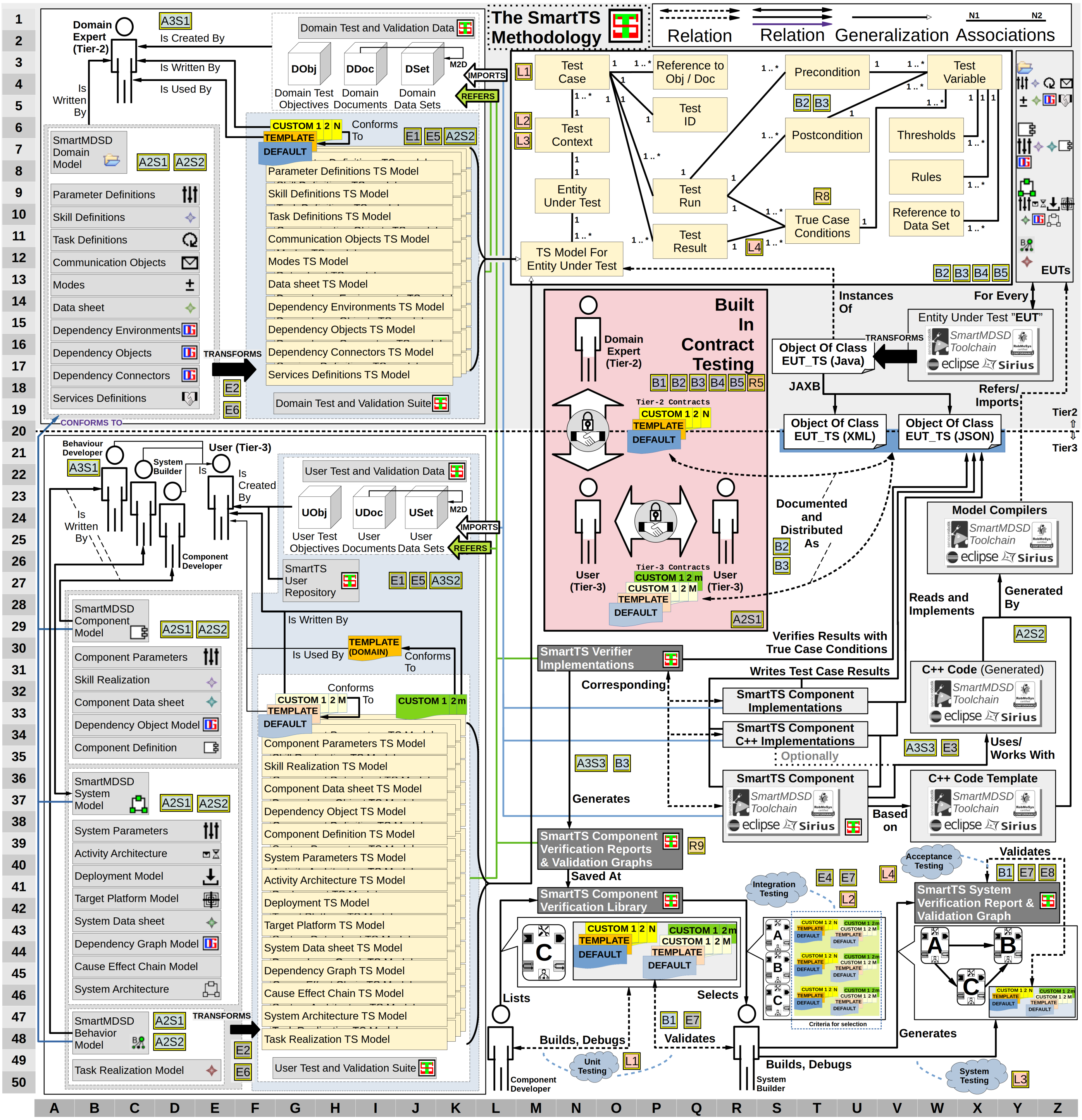

Fig. 7. The *SmartTS* Methodology.

Tier-2 SmartTS models (7F-18J)[10] are *packaged* together to form the *domain test and validation suite* (19G[10]). A *default* (6G[10]) *domain test and validation suite package* is *transformed* (17F[10]) from the existing *SmartMDSD domain model package*. For every *model* in the *SmartMDSD domain model package*, a corresponding *SmartTS model* is *generated*. The *transformation* also *produces* a *template* (6G[10]) to *write* any number of *custom* (6G[10]) *domain test and validation suite packages*. These *custom packages* are *written* by *domain experts* using the *template* (6G→4F→2C)[10]. Similarly, for *tier-3 SmartTS models* (34F-48J)[10] in *user test and validation suite* (49G[10]), the *default*, *template* and *custom* (33G[10]) *user test and validation suite packages* are *transformed* (48F[10]) and *written* (33G→26F→22E)[10]. Additionally, a *tier-3 user* (22E[10]) can *write* a *custom user package* (33T[10]) that *conforms* to any *template* from a *domain test and validation suite template*

(30I↔6G)[10].

Once *written* and *locked* (20N↔6G, 28P↔33G, 28P↔33T)[10], the *domain/user test and validation suite packages* (6G, 33G, 33T)[10] are provided to *tier-3 users* (25N, 25R)[10] and *establishes* the *foundation* for *built-in contract testing* (14M-29R)[10] in the *ecosystem*. *Domain test and validation suite packages* (20P↔6G)[10] *govern contract testing* between *tier-2 domain experts* (15N[10]) and *tier-3 ecosystem users* (25N[10]) as *conforming parties*. Similarly, *user test and validation suite packages* (28P↔(33G, 33T))[10] that *govern contract testing* amongst (25N↔25P↔25R)[10] any number of *different tier-3 ecosystem users* (25N, 25R)[10].

These *tier-3 contracts* (28P[10]) can be *written* for *claims* made by a *component developer*, *requirements* made by a *system builder*, *mutually* agreed upon *behaviour* or any other *contractual requirement* that any of the *models* from a *SmartMDSD model package* should *adhere* to. The *tier-3 contracts* (28P[10]) in *built-in contract testing* could also be *shared* between different *component developers* as *standard tests* that all *components* of a particular kind *should pass* or between *system builders* as *standard tests* for *quality assurance* or *enforcement-related requirements*. *Standard tests* for *domain requirements*, *quality assurance* and *enforcement* can be *distributed* as *tier-2 contracts* (20P[10]) between *domain experts* (15N[10]) and *ecosystem users* (25N[10]).

A *SmartTS model* (7F-18J, 34F-48J)[10] is required to define sets of *data* to be used in *tests*. This *data* is *modelled* as *domain/user test and validation data* (1G, 22G)[10] in *SmartMDSD domain repository* (1A-19K)[10] or *SmartTS user repository* (21F-50K)[10]. *SmartTS test and validation data package* contains *documentation* for *uniquely identifiable test objectives* (3G, 24G)[10] and *documents* (3I, 24I)[10]. *Domain/user data sets* (3J, 24J)[10] are *transformed* from respective *documents* (3I→3K→3J, 24I→24K→24J)[10]. These *model to data transformations* (*M2D*: 3K, 24K)[10] *compile* the *data range* mentioned in the *documents* to *create* the *data* for *uniquely identifiable data sets* mentioned in the *documents*. *SmartTS models* (7F-18J, 34F-48J)[10] *refers* (12L→5K, 41L→(25K, 5K))[10] to these *data sets*, which are later *imported* ((5K, 25K)→(33S,34S,38S))[10] during *test execution*.

Every *SmartTS model* (7F-18J, 34F-34J)[10] for an *entity under test* ((3Y-13Z)↔(9A-19D, 30A-35D, 38A-46D, 50C))[10] is a *generalization* (12L→12N, 41L→12N)[10] for a *common SmartTS model class* (12N[10]). The *SmartTS model class* for an *entity under test* is *structured* (3L-13Y)[10] to *encorporate context* (9N, 6N, 3P)[10], *runs* (3N, 5P, 9P, 11P, 10T)[10] and *conditions* (3T, 6T, 3X, 6V, 8V, 10V)[10] for *tests*. For every *entity under test* (15Y[10]) from the *SmartMDSD model package* (17X[10]) is *transformed* to *Java instances* of *SmartTS model class* (17V, 17T)[10] and *documented* and *distributed* (24T[10]) as *XML* and *JSON documents* (17T→18T→(20T, 20V))[10] to work as *contracts* (20P, 28P)[10] for *built-in contract testing* (14M-29R)[10].

The *SmartMDSD compilers* (24X[10]) *generate background C++ code* (33X[10]) and a *template* (38X[10]) based on which the *component developer* can create the *SmartTS component* (38S[10]). The *SmartTS component* works with the *background C++ code* (38S→35X→33X)[10] and *implements* the *contracts* (38S→27V→20W→(20T, 20V))[10]. It is also possible to *implement components created* without the use of *SmartMDSD toolchain* (33S, 34S)[10], and yet *adhere* to the *SmartTS contracts* ((33S, 34S)→27V→20W→(20T, 20V))[10]. Any *component implementing SmartTS contracts imports domain/user data sets* when they are *referred* to in the *SmartTS model* ((33S, 34S, 38S)→(5K, 25K))[10]. A *SmartTS verifier implementation* (30N[10]) *corresponding* to (33P[10]) the *SmartTS component implementation verifies* the *results generated* by *SmartTS components* against the *contracts* (30N→30V→20V→(20T, 20V))[10] and *generates SmartTS component verification reports* (model, text) and *validation graphs* (graphics) (39N, 33P→37N→39N→42N)[10].

These *verification reports* and *validation graphs* are listed in the *SmartTS component verification library* (39N→42N, 48L→46L→44M→42N)[10] after they are used by *component developers* for *debugging* (*unit-testing*: 50N)[10] the *component* (48L→48N→46P)[10]. *System builders* (48R[10]) *selects* (48R→46R→44S→42N)[10] and *validates* (48R→48Q→46P)[10] *components*, and *builts* a *system* (44W, 48R→50X→44W)[10] after *performing integration* (41S[10]) and *system* (50X[10]) *testing*. *System builder* also *generates system verification report* (model, text) and *validation graphs* (graphics) for the newly *composed system* (48R→48V→42W)[10]. *System contracts* (44V[10]) are a collection of *contracts* that exist between *tier-2* and *tier-3 parties associated* with the *system*. *System contracts* are *validated* against *system verification report* and *validation graphs* during *acceptance testing* (42W→40Y→44Y)[10].

The *SmartTS platform-independent model* (A-K)[10], based on *the SmartTS meta-model* (1L-20Z)[10] is thus *condensed* into *shareable documents* (20T, 20V)[10] to be *received* and later *implemented* (20L-40Z)[10] and *tested* (41L-50Z)[10] for *specific platforms*. Fig. 8 shows key *users*, *models*, *transformations* in the *SmartTS workflow* as explained in Sections **II** and **III**.

IV. SmartTS in the Context of RobMoSys

RobMoSys: *Composable models and software for robotics* [40], [41] is an *EU H2020* funded project (2017-2020, Grant number 732410) to create better *modelling standards* and *tooling* for *robotic systems*. *RobMoSys* has a *three-tier ecosystem* for *model-driven*, *component-based software development* for *robotic systems* (*RobMoSys*: *Wiki* [41]). Fig. 9 shows the *three tiers* of the *RobMoSys ecosystem* and the *roles* that participate in these *tiers*. *Members* of a *lower-tier conform* to *models* defined by *members* of a *higher-tier* in the *ecosystem*. *SmartMDSD toolchain* [50], [51] is a *RobMoSys conformant toolchain* that *enables ecosystem users* to *share components* and *compose systems* that are *according* to the *principles dictated* by *RobMoSys*. *SmartTS* is an addition to *SmartMDSD tooling* and provides a *model-based methodology* for *software testing* in the *RobMoSys ecosystem*.

V. SmartTS in Action

Fig. 10 shows some of the key features of *SmartTS* acting along with the *SmartMDSD toolchain*. *Tier-2 domain experts* and *Tier-3 users transform SmartMDSD models* to *contracts* (Fig. 10.a) and *documents* (Fig. 10.b). *SmartTS documents* are *transformed* into *data sets* (Fig. 10.c) which are *referred* to in

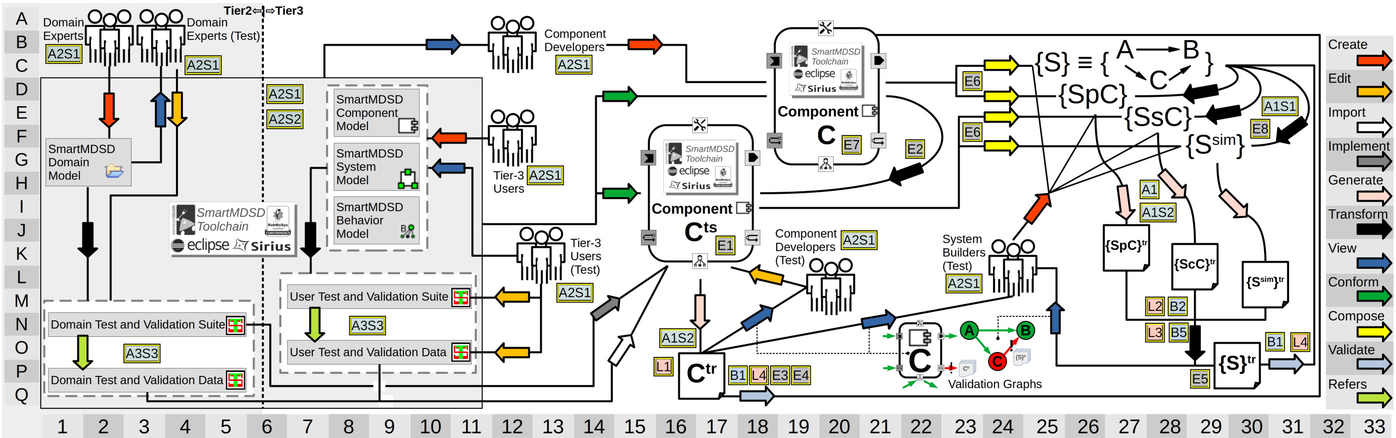

Fig. 8. Key users, Models, Transformations in the SmartMDSD::SmartTS Workflow.

SmartTS contracts. *Component models* are *transformed* to their *SmartTS tester component* (Fig. 10.(d,e,f)) which is used to *test* (Fig. 10.g) or *simulate* (Fig. 10.h) the *component*. ***SmartTS tooling* as it stands today is *functionally complete* for the *workflow* described in Fig. 8**. *Automation* and *visualization* of some *workflow elements* (e.g. *validation graphs*) is planned to further *improve user experience*. ***Eclipse features and plug-ins* for *SmartTS* are available for download** [56]. *Context* and *video tutorials* on the use of *SmartTS* **will soon be** available online at the *SRRC wiki* web page [57].

VI. Conclusions and Future Works

Validating the *behaviour* of *commercial off-the-shelf components* and *system interactions* is *enhanced* by the *availability* of *empirically verifiable test records consistent* with a *component's claims*. The ***trustworthiness of a system is derived from the trustworthiness of its constituents.*** *Test and validation suite* for a *system* can be *built* using *model-driven test and validation suites* of its *components*. In this paper, we presented the "**SmartTS methodology**: A **component-based** and **model-driven approach** to **generate** *model-bound test-suites* for *software components* and *systems*". The *test-suites* in *SmartTS* are *tightly bound* to an *application domain's data and service models* as *defined* in ***RobMoSys*** (EU H2020 project) compliant ***SmartMDSD toolchain***. *SmartTS* does not break *component encapsulation* for *system builders* while providing them complete access to the way that component is *tested* and *simulated*. At present, the *SmartTS functionality* is partially consolidated in the *SmartMDSD toolchain* (E1-E8). Plans to *automate* remaining *SmartTS transformations* are marked for *incorporation* in future releases of the *SmartMDSD toolchain* as *SmartDBE* (*Smart digital business ecosystem*) *features* and *plug-ins* [56].

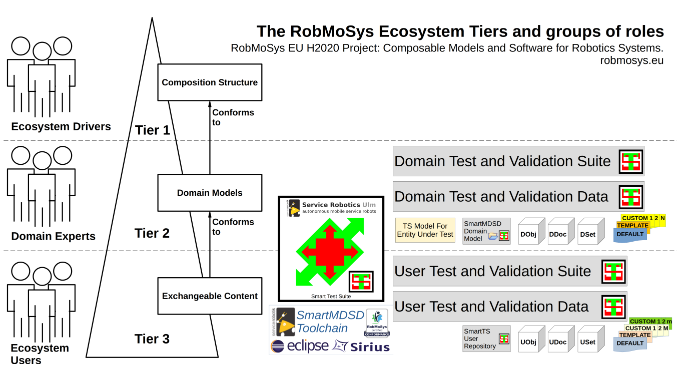

Fig. 9. SmartTS in RobMoSys Ecosystem.

Acknowledgment

This paper is supported by the German Federal Ministry for Economic Affairs and Energy (BMWi) in the programme "Development of Digital Technologies (PAiCE)" under grant agreement No. 01MA17003D, project *SeRoNet - Eine Plattform zur arbeitsteiligen Entwicklung von Serviceroboter-Lösungen* [59] and by the European Union's Horizon 2020 research and innovation programme under grant agreement No 732410, project *RobMoSys: Composable Models and Software for Robotics* [40]

References

[1] B. W. Boehm, J. R. Brown, and M. Lipow, "Quantitative evaluation of software quality," in *Proceedings of the 2nd International Conference on Software Engineering*, 1976, pp. 592–605.

[2] B. Kitchenham and S. L. Pfleeger, "Software quality: the elusive target [special issues section]," *IEEE Software*, vol. 13, no. 1, pp. 12–21, 1996.

[3] P. Ammann and J. Offutt, *Introduction to Software Testing*. Cambridge University Press, 2008.

[4] K. E. Wiegers, *Creating a software engineering culture*. Pearson Education, 1996.

[5] G. J. Myers, T. Badgett, and C. Sandler, *The Art of Software Testing : Module (Unit) Testing*. John Wiley and Sons, Ltd, 2012, ch. 5, pp. 85–111. [Online]. Available: https://onlinelibrary.wiley.com/doi/abs/10.1002/9781119202486.ch5

[6] ——, *The Art of Software Testing: Higher-Order Testing*. John Wiley and Sons, Ltd, 2012, ch. 6, pp. 113–142. [Online]. Available: https://onlinelibrary.wiley.com/doi/abs/10.1002/9781119202486.ch6

[7] ——, *The Art of Software Testing: Usability (User) Testing*. John Wiley and Sons, Ltd, 2012, ch. 7, pp. 143–155. [Online]. Available: https://onlinelibrary.wiley.com/doi/abs/10.1002/9781119202486.ch7

[8] R. W. Gray, "Automation versus Manual Testing," in *SAE Technical Paper*. SAE International, 02 1966. [Online]. Available: https://doi.org/10.4271/660694

[9] C. V. Ramamoorthy, S. . F. Ho, and W. T. Chen, "On the Automated Generation of Program Test Data," *IEEE Transactions on Software Engineering*, vol. SE-2, no. 4, pp. 293–300, 1976.

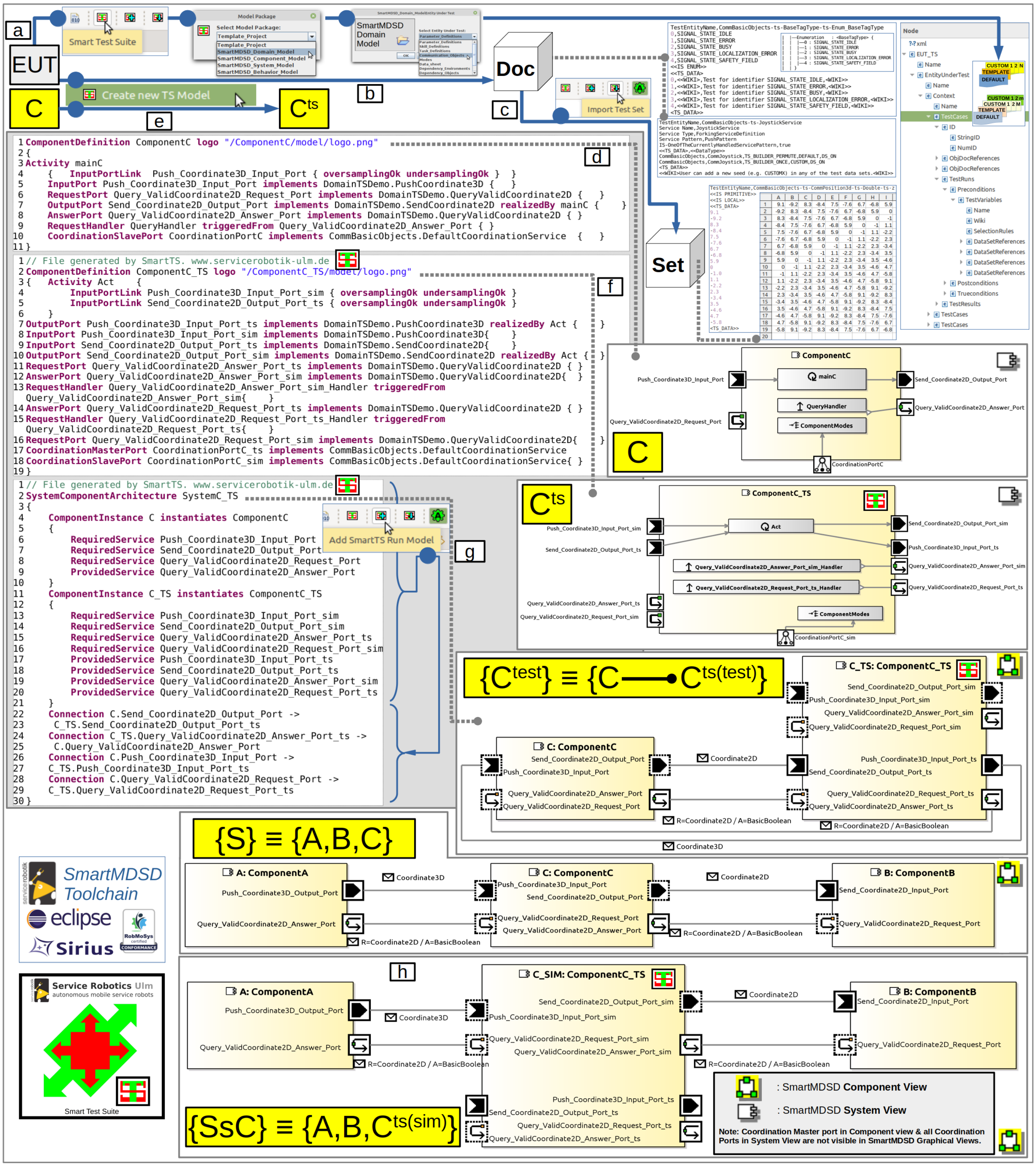

a: Entity under test (EUT) is transformed to domain/user contracts in form of a SmartTS model. EUT is any SmartMDSD model from domain, component, system or behaviour model package.
b: Entity under test (EUT) is transformed to domain/user documents in SmartTS domain/user repository (model to text transformation).
c: Domain/user documents in SmartTS domain/user repository is transformed to corresponding domain/user data sets in domain/user repository (model to data transformation).
d: SmartMDSD component-definition model for component named C.
e: SmartMDSD component-definition model for component named C is transformed to its SmartTS tester component named C_TS (model to model transformation).
f: SmartMDSD component-definition model for SmartTS tester component named C_TS for component C.
g: SmartMDSD System-component-architecture model for SystemC_TS (test) with one instance each of components C and C_TS. Connections are automatically made between components.
h: SmartMDSD System-component-architecture model for SystemSsC with component C_SIM simulating component C.

Fig. 10. SmartTS in Action. Creation of a SmartTS Contract for a Domain Communication Object and its Integration with the SmartTS Test Component.

[10] J. Chacón Montero, A. Jimenez Ramirez, and J. Gonzalez Enríquez, “Towards a Method for Automated Testing in Robotic Process Automation Projects,” in *2019 IEEE ACM 14th International Workshop on Automation of Software Test (AST)*, 2019, pp. 42–47.

[11] H. Li, *Communications for control in cyber physical systems: theory, design and applications in smart grids*. Morgan Kaufmann, 2016.

[12] L. Esterle and R. Grosu, “Cyber-physical systems: challenge of the 21st century,” *E & I Elektrotechnik und Informationstechnik*, vol. 133, no. 7, pp. 299–303, 2016.

[13] M. A. S. Brito, S. R. S. Souza, and P. S. L. Souza, “Integration testing for robotic systems,” *Software Quality Journal*, Nov 2020. [Online]. Available: https://doi.org/10.1007/s11219-020-09535-w

[14] C. Hutchison, M. Zizyte, P. E. Lanigan, D. Guttendorf, M. Wagner, C. Le Goues, and P. Koopman, “Robustness testing of autonomy software,” in *2018 IEEE ACM 40th International Conference on Software Engineering: Software Engineering in Practice Track (ICSE-SEIP)*. IEEE, 2018, pp. 276–285.

[15] D. Marijan, A. Gotlieb, and M. K. Ahuja, “Challenges of testing machine learning based systems,” in *2019 IEEE International Conference on Artificial Intelligence Testing (AITest)*. IEEE, 2019, pp. 101–102.

[16] A. Afzal, C. L. Goues, M. Hilton, and C. S. Timperley, “A Study on Challenges of Testing Robotic Systems,” in *2020 IEEE 13th International Conference on Software Testing, Validation and Verification (ICST)*, 2020, pp. 96–107.

[17] R. Pietrantuono and S. Russo, “Robotics software engineering and certification: Issues and challenges,” in *2018 IEEE International Symposium on Software Reliability Engineering Workshops (ISSREW)*. IEEE, 2018, pp. 308–312.

[18] T. Bretl and S. Lall, “Testing static equilibrium for legged robots,” *IEEE Transactions on Robotics*, vol. 24, no. 4, pp. 794–807, 2008.

[19] S. Sheng and N. Becker, “Challenges in standardizing ram testing for small unmanned robotic systems,” in *2013 Proceedings Annual Reliability and Maintainability Symposium (RAMS)*. IEEE, 2013, pp. 1–6.

[20] M. Farrell, R. C. Cardoso, L. A. Dennis, C. Dixon, M. Fisher, G. Kourtis, A. Lisitsa, M. Luckcuck, and M. Webster, “Modular verification of autonomous space robotics,” *arXiv preprint arXiv:1908.10738*, 2019.

[21] M. Mossige, A. Gotlieb, and H. Meling, “Testing robot controllers using constraint programming and continuous integration,” *Information and Software Technology*, vol. 57, pp. 169–185, 2015.

[22] Y. K. Chung and S.-M. Hwang, “Software testing for intelligent robots,” in *2007 International Conference on Control, Automation and Systems*. IEEE, 2007, pp. 2344–2349.

[23] A. Paikan, S. Traversaro, F. Nori, and L. Natale, “A generic testing framework for test driven development of robotic systems,” in *International Workshop on Modelling and Simulation for Autonomous Systems*. Springer, 2015, pp. 216–225.

[24] C. S. Timperley, A. Afzal, D. S. Katz, J. M. Hernandez, and C. Le Goues, “Crashing simulated planes is cheap: Can simulation detect robotics bugs early?” in *2018 IEEE 11th International Conference on Software Testing, Verification and Validation (ICST)*. IEEE, 2018, pp. 331–342.

[25] V. Mayoral-Vilches, N. García-Maestro, M. Towers, and E. Gil-Uriarte, “Devsecops in robotics,” *arXiv preprint arXiv:2003.10402*, 2020.

[26] A. Afzal, D. S. Katz, C. L. Goues, and C. S. Timperley, “A study on the challenges of using robotics simulators for testing,” *arXiv preprint arXiv:2004.07368*, 2020.

[27] J. Wienke, D. Wigand, N. Koster, and S. Wrede, “Model-Based Performance Testing for Robotics Software Components,” in *2018 Second IEEE International Conference on Robotic Computing (IRC)*, 2018, pp. 25–32.

[28] B. Konemann, G. Zwiehoff, and J. Mucha, “Built-in test for complex digital integrated circuits,” *IEEE Journal of Solid-State Circuits*, vol. 15, no. 3, pp. 315–319, 1980.

[29] R. Freedman, “Testability of software components,” *IEEE Transactions on Software Engineering*, vol. 17, no. 6, pp. 553–564, 1991.

[30] Y. Wang, G. King, and H. Wickburg, “A method for built-in tests in component-based software maintenance,” in *Proceedings of the Third European Conference on Software Maintenance and Reengineering (Cat. No. PR00090)*, 1999, pp. 186–189.

[31] H.-G. Gross, I. Schieferdecker, and G. Din, “Model-based built-in tests,” *Electr. Notes Theor. Comput. Sci.*, vol. 111, pp. 161–182, 01 2005.

[32] M. Sitariman and B. Weide, “Component-based software using RESOLVE,” *ACM SIGSOFT Software Engineering Notes*, vol. 19, pp. 21–22, 10 1994.

[33] H.-G. Gross, *Component-Based Software Testing with UML*. Springer-Verlag Berlin Heidelberg, 2005.

[34] P. Feiler, D. Gluch, and J. Hudak, “The Architecture Analysis and Design Language (AADL): An Introduction,” p. 145, 02 2006.

[35] MARTE, “A UML Profile for MARTE:modeling and analysis of real-time embedded systems.” http://www.omg.org/spec/MARTE/1.1/, 2011, accessed: 2021-03-15. [Online]. Available: http://www.omg.org/spec/MARTE/1.1/

[36] OMGSysML, “SysML: OMG Systems Modeling Language.” https://www.omg.org/, 2012, accessed: 2021-03-15. [Online]. Available: https://www.omg.org/

[37] Amalthea, “Amalthea: An open platform project for embedded multicore systems.” http://www.amalthea-project.org, 2013, accessed: 2021-03-15. [Online]. Available: http://www.amalthea-project.org

[38] SPARC, “Robotics 2020 Multi-Annual Roadmap: SPARC Partnership for Robotics in Europe, February 2015, call 2 ICT24 – Horizon 2020.” http://www.eu-robotics.net/cms/upload/Multi-Annual Roadmap2020 ICT-24 Rev B full.pdf, 2015, accessed: 2021-03-15. [Online]. Available: http://www.eu-robotics.net/cms/upload/Multi-AnnualRoadmap2020ICT-24RevBfull.pdf

[39] ——, “SPARC: European SPARC Robotics Initiative.” http://sparc-robotics.eu/, 2015, accessed: 2021-03-15. [Online]. Available: http://sparc-robotics.eu/

[40] RobMoSys, “RobMoSys EU H2020 Project (2017-2020): Composable models and software for robtics systems - towards an eu digital industrial platform for robotics.” http://robmosys.eu, 2017-2020, accessed: 2021-03-15. [Online]. Available: http://robmosys.eu

[41] RobMoSysWiki, “RobMoSys EU H2020 Project Wiki,” http://robmosys.eu/wiki, 2017-2020, accessed: 2021-03-15. [Online]. Available: http://robmosys.eu/wiki

[42] W. L. Hürsch and C. V. Lopes, “Separation of Concerns,” College of Computer Science, Northeastern University, Tech. Rep., 1995.

[43] V. Kulkarni and S. Reddy, “Separation of concerns in model-driven development,” *IEEE Software*, vol. 20, no. 5, pp. 64–69, 2003.

[44] D. Alonso, C. Vicente-Chicote, F. Ortiz, J.-A. Pastor Franco, and B. Alvarez-Torres, “V3CMM: A 3-view component meta-model for model-driven robotic software development,” vol. 1, 01 2010.

[45] S. Dhouib, S. Kchir, S. Stinckwich, T. Ziadi, and M. Ziane, “RobotML, a Domain-Specific Language to Design, Simulate and Deploy Robotic Applications,” in *SIMPAR*, 2012.

[46] H. Bruyninckx, M. Klotzbücher, N. Hochgeschwender, G. Kraetzschmar, L. Gherardi, and D. Brugali, “The BRICS component model: a model-based development paradigm for complex robotics software systems,” in *SAC ’13*, 2013.

[47] V. Nagrath, “Software Architectures for Cloud Robotics : The 5 View Hyperactive Transaction Meta-Model (HTM5),” Ph.D. dissertation, 2015, thèse de doctorat dirigée par Mériaudeau, Fabrice et Morel, Olivier Informatique Dijon 2015. [Online]. Available: http://www.theses.fr/2015DIJOS005

[48] A. Lotz, J. Inglés-Romero, D. Stampfer, M. Lutz, C. Vicente-Chicote, and C. Schlegel, “Towards a Stepwise Variability Management Process for Complex Systems – A Robotics Perspective,” *Int. Journal of Information System Modeling and Design (IJISMD)*, vol. 5, pp. 55–74, 11 2014.

[49] euRobotics, “EU Robotics Agenda 2020: EU Robotics Strategic Research, Innovation and Deployment Agenda 2020 on AI, Data and Robotics Partnership,” 2020, accessed: 2021-04-25. [Online]. Available: https://www.eu-robotics.net/cms/upload/downloads/ppp-documents/AI-Data-Robotics-Partnership-SRIDA-V3.0.pdf

[50] C. Schlegel, “Navigation and Execution for Mobile Robots in Dynamic Environments: An Integrated Approach,” Ph.D. dissertation, University of Ulm, 2004.

[51] D. Stampfer, A. Lotz, M. Lutz, and C. Schlegel, “The SmartMDSD Toolchain: An Integrated MDSD Workflow and Integrated Develop-

ment Environment (IDE) for Robotics Software," *Journal of Software Engineering for Robotics (JOSER)*, vol. 7, pp. 3–19, 08 2016.

[52] SRRC, "SmartMDSD Services," 2021, accessed: 2021-04-30. [Online]. Available: https://robmosys.eu/wiki/modeling:metamodels:service

[53] ——, "SmartMDSD Communication Objects," 2021, accessed: 2021-04-30. [Online]. Available: https://robmosys.eu/wiki/modeling:metamodels:commobject

[54] ——, "SmartMDSD Communication Patterns," 2021, accessed: 2021-04-30. [Online]. Available: https://robmosys.eu/wiki/modeling:metamodels:commpattern

[55] C. Schlegel, "SMARTSOFT: Components and Toolchain for Robotics." http://www.servicerobotik-ulm.de/, 2011, accessed: 2021-03-15. [Online]. Available: http://www.servicerobotik-ulm.de/

[56] V. Nagrath, "SmartDBE Git: Eclipse features and plugins pertaining to SmartDBE additions to SmartMDSD Toolchain." https://github.com/Servicerobotics-Ulm/SmartDBE, 2021, accessed: 2021-05-08. [Online]. Available: https://github.com/Servicerobotics-Ulm/SmartDBE

[57] SRRC, "Service Robotics Research Center Wiki," 2021, accessed: 2021-04-30. [Online]. Available: https://wiki.servicerobotik-ulm.de/tutorials:start

[58] ——, "SmartMDSD Collection of Applications, Software Components, (Domain) Models," 2021, accessed: 2021-04-30. [Online]. Available: https://wiki.servicerobotik-ulm.de/directory:collection

[59] SeRoNet, "SeRoNet: Eine Plattform zur arbeitsteiligen Entwicklung von Serviceroboter-Lösungen." https://www.seronet-projekt.de/, 2017-2021, accessed: 2021-03-15. [Online]. Available: https://www.seronet-projekt.de/

AUTHORS' PROFILE

Dr. Vineet Nagrath (M) is a researcher at the Service Robotics Research Centre, Ulm University of Applied Sciences (Technische Hochschule Ulm) in GERMANY. He received his dual doctoral degrees in 2015 from University de Bourgogne, FRANCE, and Universiti Teknologi Petronas, MALAYSIA in a Bi-national dual degree doctoral program (Software Architectures for Cloud Robotics - The 5 View Hyperactive Transaction Meta-Model for Agent-Oriented Cloud Robotic systems). He has earlier completed STIC MSc. in Computer Vision (MCV)(M1) and Erasmus Mundus Masters in Vision and Robotics (M2) from University de Bourgogne, FRANCE. His research focus is on Cloud-Connected Robots, Multi-Agent Systems, Model-Driven Software Engineering, and Machine Learning. Since 2017 he is contributing to the SmartMDSD Toolchain for BMWi PAiCE SeRoNet and EU H2020 RobMoSys projects. **vineetnagrath.com**

Prof. Dr. rer. nat. Christian Schlegel (M) is Professor for Real-Time and Autonomous Systems in the Computer Science Department of Technische Hochschule Ulm since 2004. He is Head of the Service Robotics Research Group. His research interests are in model-driven software and systems engineering for real-world cognitive systems such as service robotic and their application in industry 4.0. He is the technical lead of the EU H2020 RobMoSys project and the elected coordinator of the euRobotics Topic Group on Software Engineering, System Integration, System Engineering. **servicerobotik-ulm.de**

http://www.servicerobotik-ulm.de/

Vietnamese Short Text Classification via Distributed Computation

Hiep Xuan Huynh[1], Linh Xuan Dang[2], Nghia Duong-Trung[3], Cang Thuong Phan[4]
Can Tho University, Can Tho city, Vietnam[1,2,4]
Technische Universität Berlin, Berlin, Germany[3]

***Abstract*—Social networking has been growing rapidly in Vietnam. The sharing information is diverse and circulates in many forms. It requires user-friendly solutions such as topic sorting and perspectives analysis in analyzing community trends, advertisements or anticipating and monitoring the spread of bad news. Unfortunately, Vietnamese is highly different from other languages and little research has been conducted in the literature on messages classification. The implementation of machine learning models on Vietnamese has not been thoroughly investigated and these models' performance is unknown when applying in a different language. Vietnamese text is a serialization of syllables, hence, word boundary identification is not trivial. This research portrays our endeavor to construct an effective distributed framework for addressing the task of classification of short Vietnamese texts on social networks using the idea of probability categorization. The authors argue that addressing the task sharps the successful combination of machine learning, natural language processing, and ambient intelligence. The proposed framework is effective and enables fast calculation, suitable for implementation in Apache Spark, meeting the demand for dealing with large amounts of textual data on the current social networks. Our data has been collected from several online text sources of 12412 short messages classified into five different topics. The evaluation shows that our approach has achieved an average of 82.73% classification accuracy. Thoughtfully learning the literature, we could state that this is the first attempt to classify short Vietnamese messages under a distributed computation framework.**

Keywords*—Short text classification; Naïve Bayes; Apache Spark; Vietnamese; distributed computation

I. Introduction

Social networking, also called virtual social network is a service that connects members on the Internet with many different purposes regardless of space and time. The online social network is a representative of Web 2.0 to simulate real social relationships using Web technology to connect members and allow them to create and share information with each other through mechanisms such as making friends, chatting, liking, sharing, tagging photos, commenting, or subscribing to a blog, a channel. In Vietnam in particular and the world in general, Facebook is the most popular social network. A person who joins a social network will be able to post or comment on another person's post. A person's post can be thoughts of self-expression, feeling of subjects, commenting on a problem or simply announcing an event. These messages, if interested by many people, will be shared by people and continue to be commented and become hot topics. Innovative social networks completely change how netizens link together and become an inevitable part of every day for hundreds of millions of members around the world. These services have provided platform for the participants to find friends and partners: based on groups (such as school names or city names), based on personal information (such as e-mail addresses, phone numbers), based on personal interests (sports, movies, books, or music), areas of interest (business, sales). According to [1], up to four Southeast Asian countries are in the top ten countries with the most Facebook users. In particular, Vietnam ranks 7th with 64 million users, accounting for 3% of the total global Facebook accounts. Thailand is right behind Vietnam, at No. 8 with 57 million users. Indonesia and the Philippines rank No. 4 and No. 6 with 126 million and 69 million accounts respectively. Capturing the popularity of social networks in Vietnam, many business components including companies, small and medium enterprises and especially online business individuals have found many measures to take advantage of its promotion to meet its business purpose.

Social networks' success has drawn the mindfulness of research on natural language processing. Among the significant exploitation, text classification has been described as one of the most important tasks, becoming a major discipline of the information systems [2]. The message on a social network can be a message between two people, a status line, or a comment of a certain status line. The message needs to have certain content. A person who wants to post an article on a personal page usually knows the topic he is talking about. Social media posts often have content that is not too long and only shows emoticons on a topic. A user can post one or more posts at the same time. These posts are generated continuously and without quantity limits. The spread of these messages is also very fast and wide [3]. The theme of messages on social networks is almost the same as the topics of common types of documents such as Science, Business, Law, Health, Sports, Technology. The problem is that collecting sample data takes a lot of time and effort. But in the classification problem, the sample dataset plays a very important role. In addition, there is an ambiguity about the topics of social media posts, because the messages do not always present a clear purpose for their users. An article can sometimes belong to two or three different topics when placed in another context. The messages themselves are short documents, contain very little information. Most of the messages on social network have images or videos attached, which limit the content analysis. The documents accompanying with these videos or images are sometimes just an unknown introduction, the core content of the article is in the videos and images. The amount of articles that are too large requires building on a large data processing platform, towards real-time processing to meet the needs of huge data analysis. In Vietnam, there are not many research groups in the field of social network analysis. There are not many studies on the classification of published messages especially for Vietnamese so that it is difficult to compare results and evaluation.

Consequently, the need to classify the text-based messages electronically available has significantly grown. One can argue that automated text classification is one of the most crucial tasks in social media analytics [4]. Many research papers have been conducted to solve such problems as topic modeling [5], [6], [7], [8], geolocation [9], [10], and document classification [11]. Although many Vietnamese documents are electrically available, no one has been recently conducted on short Vietnamese messages classification. This research portrays our endeavor to construct an effective distributed framework for addressing the task of classification of short Vietnamese texts on social networks. We have collected a large amount of Vietnamese textual sources of 12412 messages and investigated message representation, word tokenization, and learning method that are suitable for the requirements of acceptable classification accuracy and distributed calculation.

The rest of this research paper is organized as follows. First, we discuss previous research on short Vietnamese text classification in Section (II). Next, we summarize fundamental materials and methodology in Section (III). The proposed framework for addressing the probabilistic classification of short Vietnamese messages is presented in Section (IV). In Section (V), the experiments are thoughtfully discussed. And finally, conclusion is stated in Section (VI).

II. Related Works

Text classification is a classic problem in data mining and machine learning [12]. The goal of the main classification problem is to find the appropriate topic in a set of predefined topics. Streams of text classification research has been done in several top-tier conference, journal and workshop. Criteria to select the appropriate topic for documents based on the similarity between them with the text in the training material semantically. Automatic sorting of text into a topic makes it easier to organize, store and query documents later. Besides, text classification is also used to assist in the process of searching, extracting information [13], [14].

Over the years, the research field of ambient intelligence has witnessed remarkable achievements. Scholars have raised the potential integration between natural language processing and ambient intelligence that can further generate cutting-edge research leading to substantial technological advances. A vibrant part of many information repositories is textual sources across various media, usually in the nonstructural form. One can conclude that the capacity to process and make use of nonstructural information can boost ambient intelligence systems to a much higher level of quality. Applying machine learning within the task of text classification involves transforming a variety of textual sources into structured knowledge. The authors argue that the combination of machine learning, natural language processing, and ambient intelligence opens up exciting research challenges [15].

A text classification task contains four different research disciplines: feature extraction, dimensionality reduction, classification algorithms, and evaluation. Texts are unstructured data, and we need to transform them in a feature space. Several common feature extraction techniques from basic to more advanced are TFIDF, Word2Vec [16], and Glove [17]. The most crucial step of completing a text classification task is to choose the best classifier, starting from non-parametric techniques, e.g., k-nearest neighbor, to simply logistic regression, to tree-based classifiers, to deep learning-based models. Recently, we have witnessed the success of deep learning approaches over previous classification models due to its excellent performance and capacity to address non-linear relationships within text data. However, regarding the feasibility characteristics, Naïve Bayes algorithm, which is a very computationally inexpensive and low amount of memory consumption, is one of the most generative model. These implementations have one characteristic in common: the classifier is trained on a simple machine, ranging from a regular personal computer to a dedicated server. The extend of training phase in case of handing a large amount of data can be broadcast to several machines in a cluster, which yields the idea of distribution computation [18], [19], [20], [21]. In the implementation, we deploy our distributed framework upon Apache Spark.

An early effort to address the task of Vietnamese text classification was conducted more than a decade ago [22]. In that paper, the authors solved the problem of automatically categorizing given textual sources into predefined categories. A comparison between statistical N-Gram language modeling and bag of words approaches has been investigated on their collected dataset. Although they achieved a good accuracy score, the implemented models were not efficient in term of computation time, e.g. only three documents/second comparing to 776 documents/second in our distributed framework. The task of automatic text categorization has been studied by comparing the performance of several term weighting schemes rather than analyzing the actual classification task [23]. Nevertheless, these approaches have investigated short messages in very different classification tasks. For the problem of classifying Vietnamese text, many research projects have been published but their work were done in an isolated environment [24], [25], [26]. Thoughtfully learning the literature, we could state that this is the first contribution to classify short Vietnamese messages under a distributed computation.

III. Materials and Methods

A. Problem Definition

Given a set of n input texts denoted as $D = \{d_1, d_2, \ldots, d_n\}$. By applying some processing techniques we will classify them into a set of m classes denoted as $C = \{c_1, c_2, \ldots, c_m\}$. An example of text classification is the arrangement of news in newspapers into corresponding categories such as Sports, Entertainment, and Society. This can be done manually by the editors but this method faces some of the following difficulties: (i) It takes a lot of time and effort. (ii) Manual classification is sometimes inaccurate because the decision depends on the understanding and motivation of the implementer. (iii) For some professional fields, experts (medical, legal, economic) are needed. The decision of several experts may be contradictable. And (iv) When the number of documents is relatively high, an expert might find it difficult to implement.

TABLE I. VIETNAMESE TEXT AFTER TOKENIZATION PROCESS BY VNTOKENIZER SOFTWARE. THE UNDERSCORE CHARACTER IS ADDED BETWEEN INDIVIDUAL WORDS TO FORM AN APPROPRIATE MEANINGFUL TOKEN. THE TRANSLATED PARTS ARE FOR EXPLANATION IN THIS PAPER ONLY

Message id	Message content
[00164]	Đúng là làm Manuel_Neuer không dễ Bài_học đau_lòng cho Iker_Casillas. *Translated:* It is true that Manuel Neuer is not easy to do. The painful lesson for Iker Casillas.
[00202]	Trong hàng triệu triệu cổ_động_viên hướng về đội_tuyển quốc_gia Việt_Nam ngày hôm_nay những_ai có_mặt tại sân_vận_động chứng_kiến trực_tiếp trận đấu có_lẽ là những người may_mắn nhất nhưng có_lẽ cũng là những người vất_vả nhất Thời_tiết ở thành_phố Thường_Châu những ngày này rất khắc_nghiệt với nhiệt_độ âm và tuyết đã rơi trắng đường Nhưng chẳng điều gì ngăn được bước chân của các cđv Việt_Nam. *Translated:* Millions of fans are heading to Vietnam national team today. Those presented at the stadium witnessing the match directly were probably the luckiest people, but perhaps also the hardest. The weather in Changzhou City these days is very harsh. The temperature drops to negative degrees Celsius and white snow has fallen. But nothing stops the footsteps of Vietnamese fans.
[03189]	Hè sắp đến rồi CÙNG GIẢI NHIỆT MÙA HÈ THÔI Hay lên kế_hoạch cho những chuyến vi_vu xả_hơi để tận_hưởng thắng_cảnh tại nước_ngoài hay các biển đảo mới được biết đến như Đảo_Nam_Du hoặc tận_hưởng ngắn ngày cho một chuyến du_lịch về vùng sông_nước hoà_mình với thiên_nhiên chưa Hãy cùng Du_Lịch_Việt chuẩn_bị cho một chuyến du_lịch cùng mùa. *Translated:* The summer is coming and LET'S ENJOY THE SUMMER SEASON. Have you planned for a relaxing trip to enjoy the sights in foreign countries or new islands known as Nam Du or enjoying a short trip to rivers, mix with nature yet? Let's travel with Vietnam Travel to prepare for a trip with the season.
[04037]	Chiều Về lại thị_trấn Dương_Đông Kết_thúc chuyến tham_quan. *Translated:* Back to Duong Dong town in the afternoon. End of the tour.
[06840]	Từ hôm_nay đến hết đi Easy_Taxi tại thủ_đô Hà_Nội và thành_phố Hồ_Chí_Minh để có ngay voucher mua_sắm trên ứng_dụng Lazada trị_giá Easy_Taxi là một lựa_chọn gọi taxi ở các quán bar khách_sạn, siêu_thị nhà_hàng hay bất_cứ nơi đâu trở_nên tuyệt_vời nhanh_chóng và an_toàn hơn bao_giờ hết Tải ngay ứng_dụng Easy_Taxi tại đây IOS bitly easytaxiios ANDROID bitly easytaxiandroid WINDOW PHONE bitly easytaxiwp Voucher sẽ được gửi qua email và có giá_trị_sử_dụng đến hết Dành cho đơn hàng trên và chỉ áp_dụng khi mua qua ứng_dụng Lazada trên điện_thoại. *Translated:* From today to the end, go with Easy Taxi in Hanoi and Ho Chi Minh City to receive your voucher on Lazada application right away. Easy Taxi is a great option for making taxi calls at hotel bars, restaurants or anywhere, easily and safely than ever. Download now Easy Taxi application at bitly_easytaxiiosm, ANDROID bitly_easytaxiandroid and WINDOW PHONE bitly_easytaxiwp. The voucher will be sent via email and will be valid for use on the above orders and only applicable when purchased via Lazada on the phone.
[07040]	Cấp_báo Cô Ba_Sài_Gòn đã có_mặt tại Lazada xinh quá Ad muốn ngất xĩu rồi_đây. *Translated:* The newspaper Ba Ba Saigon was present at beautiful Lazada so Ad wanted to faint.
[09677]	Dùng_Android mà bỏ_qua các mẹo này là hối_hận đó nhé. *Translated:* Using Android without skipping these tips is regretful.
[12364]	Nỗi lo rụng tóc khi hoá_trị ung_thư sẽ không còn nữa. *Translated:* The worry of hair loss when cancer chemotherapy is no longer available.

B. Text Pre-processing

Data pre-processing is the first important step of any data mining process. It makes data in its original form easier to observe and explore. For the problem of text classification, due to specific characteristics, each language has its own characteristics. The preprocessing process will help improve sorting efficiency and reduce the complexity of the training algorithm. Depending on the purpose of the classifier, we will have different preprocessing methods, such as

- Convert text to lowercase and correct spelling errors.
- Remove punctuation marks (if no sentence separation is performed).
- Remove special characters ([], [.], [,], [:], [”], [”], [;], [/], [[]], [~], [´], [!], [@], [#], [$], [%], [^], [&], [*], [(], [)]), digits.
- Separate of words by single word method (English) or compound words (Vietnamese).
- Remove the stopwords, e.g. the words that appear most in the text that are not meaningful when participating in text classification.
- Standardize the words, switch back from the original (usually applicable to English).
- Convert text into vectors as input for classification learning machine.

C. Text Transformation and Presentation

One of the first tasks in dealing with text classification is to choose an appropriate text representation model. A raw document (string form) needs to be transferred to another model to facilitate representation and calculation. Depending on the different classification algorithms, we have our own representation model. The vector space model is one of the simplest and most commonly used models in this task. A text source is represented in the form, with an n-dimensional vector to measure the value of the text element. A document is expressed as a collection of tokens and/or words, each token is considered an attribute or characteristic and the text corresponds to an attribute vector. After identifying the properties, we need to calculate the attribute value (or weighted keyword) for each text.

We discuss term frequency-inverse document frequency

(TFIDF) [27], one of the most fundamental techniques for retrieving relevant documents from a text source or from a collection of text sources. Although TFIDF is fundamental, it statically proves the effectiveness in text mining [28], [29]. Having gathered all the tokens from the tokenization step, all given messages are converted from bag-of-words representations of token counts into sparse vectors with TFIDF weights. TFIDF is an acronym of term frequency-inverse document frequency, and this score often used in text processing and information retrieval. The idea of TFIDF weight is to calculate a score that expresses the relative importance of words in the documents. The score is statistically measured by evaluating the significance a token gains in a document and in a collection. The importance of a word is proportionally judged by counting the number of times it exists in a document while compensating its appearance in the corpus. In this way, we discard grammar structure, words' order, and part-of-speech. It is intuitive that the frequency with which a token appears in a message could indicate the extent that the message pertains to that token. The TFIDF weight reflects how significant a token gets to a message. The more appearance a token exists in many messages, the more penalty it gets punished. The best characteristics of the tokens to the message is measured by the highest score of TFIDF.

TFIDF weight is expressed as

$$\mathit{TFIDF} = \mathit{TF} * \mathit{IDF} \ , \tag{1}$$

where *TF* is how many times a word appears in a document, and *IDF* is the logarithm score of the number documents in the whole corpus divided by how many documents that the specific word appears. More precisely, the *TF* is calculated as follows:

$$\text{TF}(w,d) = \frac{n^d(w)}{|d|} \ , \tag{2}$$

where the number of times a word w appears in a document d and the total number of words in d are $n^d(w)$ and $|d|$, respectively.

While the TF is calculated on a per-document basis, the IDF is computed on the basis of the entire corpus. Thus, the IDF is calculated as follows.

$$\text{IDF}(w) = \log \frac{|C|}{n^C(w)} \ , \tag{3}$$

where $|C|$ represents the number of documents in the corpus and $n^C(t)$ represents the number of documents that contains the word w.

TABLE II. STATISTICS OF DATA COLLECTION

Topic	Site	Likes / Followers	Raw messages	Filtered messages
Sport	banthethaovtv	135000 / 184000	2511	2386
News	thoisuvtv	616000 / 715000	2989	2278
Traveling	dulichviet	144000 / 144000	3344	2986
Sales	lazadavietnam	22 million /22 million	3039	2343
Technology	thegioididong	3 million / 3 million	3088	2419
Total			**14971**	**12412**

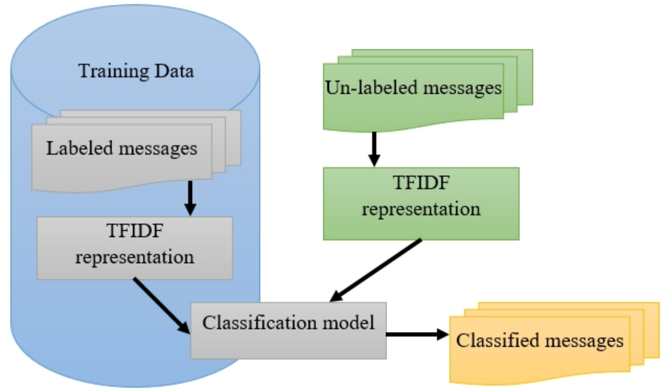

Figure 1. The Overall Architecture of a Textual Classification Model.

D. Naïve Bayes Classifier

Naïve Bayes is a popular machine learning model thanks to its great performance [30]. It merely meant as a machine learning approach that we utilize in the work. Readers may refer to mathematics or probabilities machine learning textbook [31] for advanced information.

Given an observation, model's parameters and a label represented by a vector **u**, a set of parameter ω and a target $t = c$ respectively, the generative model to classify **u** is defined as follows:

$$P(t=c|\mathbf{u},\omega) = \frac{P(t=c|\omega)P(\mathbf{u}|t=c,\omega)}{\sum_{c'} P(t=c'|\omega)P(\mathbf{u}|t=c',\omega)} \tag{4}$$

where $P(\mathbf{u}|t = c,\omega)$, $P(t = c|\mathbf{u})$, and $P(t = c)$ are the class-conditional density, the class posterior, and the class prior respectively. Proportionally, Equation (4) can be computed as in the following equation:

$$P(t=c|\mathbf{u},\omega) \propto P(t=c|\omega)P(\mathbf{u}|t=c,\omega). \tag{5}$$

Moreover, the class-conditional density $P(\mathbf{u}|t = c,\omega)$ in Equation (4) is calculated as follows:

$$P(\mathbf{u}|t=c,\omega) = \prod_{i=1}^{D} P(u_i|t=c,\omega_{ic}) \tag{6}$$

which we yield a Naïve Bayes classifier.

IV. Our Proposed Framework for Addressing Probabilistic Classification of Short Vietnamese Messages

A. Design Concept

In this research, we introduce a framework to explore and label topics for short Vietnamese messages according to the traditional text classification procedure which is presented in Fig. (1). Nevertheless, we employ the message classification via a distributed framework Apache Spark [32], [33]. The complete design of our proposed framework is presented in

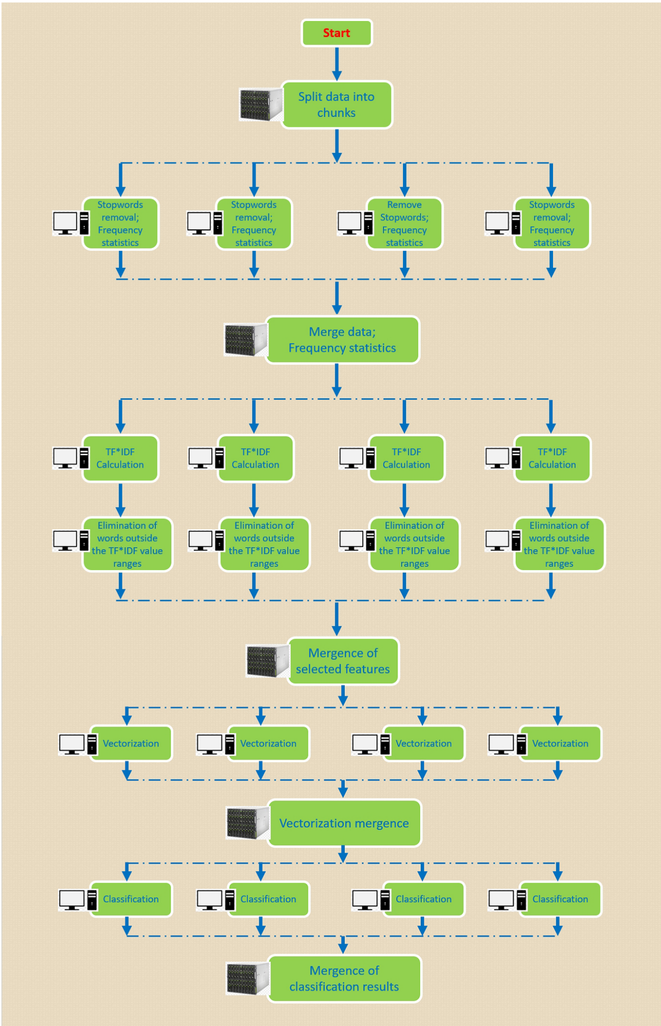

Figure 2. The Overall Architecture of our Proposed Distributed Framework.

Fig. (2). Consequently, heavy load, e.g. data pre-processing, vectorized representation, and classification, of a traditional machine learning task is effectively done in parallel.

B. Text Classification Pipeline

Depending on each specific case, the text classification problem will have different processes. Here are some basic steps: (1) Pre-processing data is a step to clean the data before starting to process in the next steps. It includes some concepts of natural language processing such as removing redundant characters, deleting stop words that don't make much sense, removing words that appear in most texts, spell checking. (2) Separation is an extremely important step, especially for Vietnamese. There are many ways to separate different words, we will learn more in the next section. (3) Document representation is the pipeline of transforming the input text data set into attributes compatible with the classification model in the next steps, facilitating easier problem-solving. (4) Characteristic extraction is the step to find the core characteristics from the original dataset or in other words, to choose a typical characteristic that is representative of the dataset as the basis for the algorithm. (5) Model training is the step in which we use machine learning algorithms to find the best model. Finally, classification (6) is the use of the trained model in the above step to conduct classification for the dataset in practice.

C. Distributed Computing Framework

Many people can agree that one of the most successful cluster computing platform is Apache Spark due to its great ability to compute fast and can be generally utilized in many research and business domains [33]. Hinging on the efficiency of supporting a broad variety of computations' types, Apache Spark can handle stream processing and queries by the extension of the well-known MapReduce model [34]. Moreover, a physical execution engine called the DAG scheduler gains great achievement in processing batch and streaming data. From the very first idea of design, Apache Spark executes computation directly in machine's memory which in turn boosting the computing speed significantly. Apache Spark provides multi-purposed APIs that support many modern programming languages, e.g. in Python, Scala, and Java. Spark Core is the main architecture of Spark consisting of components for fault recovery, memory management, optimization, task scheduling, and storage interaction. Apache Spark's main programming abstraction is resilient distributed datasets, or called RDDs in short, is a distributed collection of elements defined by Spark's main architecture. During computation, RDDs are distributed around a cluster of machines and can be performed in parallel effectively and transparently. A wide variety of machine learning functionalities are integrated into Spark's MLlib library [35]. Apache Spark can be deployed in a standalone machine or associated with Mesos [36]. The overall architecture of our distributed framework is illustrated in Fig. (2).

V. Experiments

A. Data Collection

We utilize a commercial tool called Facebook Fplus [37] developed by a domestic company FPLUS24H. Corresponding to each topic, we choose Facebook pages based on the number of likes and followers in the belief that these pages will focus on writing articles related to their main subject. For each topic, we select the Facebook pages with the most number of likes and followers compared with other similar pages. Our statistics of data collection is presented in Table (II). The process of filtering messages by topic is done through the following steps. First, we filter empty messages, or messages holding too little content leading to unclear meaning and unknown topics. Second, we remove messages embedding videos, images with accompanying texts that do not show the right content. Next, we filter wrong spelling messages, e.g. without Vietnamese accents. Fourth, we remove messages that the topics do not match with the contents. And finally, we split messages into separate files for easy storage and processing in Apache Spark.

B. Vietnamese Text Tokenization

For the tokenization task, we utilize vnTokenizer [38] in our research, see Table (I). The combination of tokenization accuracy among software is out of the main concern of this research paper. We utilize a list of 1942 Vietnamese stopwords [39] in our data processing.

C. Evaluation Metrics

Suppose we are solving a binary classification task with a labeled dataset $\mathcal{D} = \{\mathbf{x}_i, t_i\}$. Given a threshold parameter ϕ that guilds our decision rule $g(\mathbf{x})$ We also define m_+ the total of condition positives, m_- the total of condition negatives, $\hat{m}_+$ the total predicted condition positives, $\hat{m}_-$ the total predicted condition negatives, and m the total population.

We can compute the sensitivity, also known as true positive rate (TPR), probability of detection, or recall by using:

$$\text{TPR} = \frac{\text{TP}}{m_+} \approx P(\hat{t} = 1 | t = 1) \ . \tag{7}$$

Similarly, we can compute the fall-out, also known as false positive rate or probability of false alarm by using:

$$\text{FPR} = \frac{\text{FP}}{m_-} \approx P(\hat{t} = 1 | t = 0) \ . \tag{8}$$

The true negative rate (TNR) or specificity is defined as follows:

$$\text{TNR} = \frac{\text{TN}}{m_-} \approx P(\hat{t} = 0 | t = 0) \ . \tag{9}$$

The false negative rate (FNR) or miss rate is calculated as follows:

$$\text{FNR} = \frac{\text{FN}}{m_+} \approx P(\hat{t} = 0 | t = 1) \ . \tag{10}$$

If we work with a dataset for binary text classification when the number of negatives is very large or a dataset for multi-class text prediction when class imbalance exists, considering TPR, FPR, TNR and FNR themselves is not very informative. Before going further, we define positive predictive value (PPV) or precision as follows:

$$\text{PPV} = \frac{\text{TP}}{\hat{m}_+} \approx P(t = 1 | \hat{t} = 1) \ . \tag{11}$$

By combining Equation (7 and 11), we can compute F1-score as follows:

$$\text{F1-score} = 2\frac{\text{precision} \cdot \text{recall}}{\text{precision} + \text{recall}} \ , \tag{12}$$

which is widely used in information retrieval systems.

D. Implementation

The fundamental goal of machine learning models is to make accurate predictions on unseen observations. In order to estimate the strength of a particular learning model, practitioners usually split data into several proportions which serves for specific purposes in the machine learning pipeline. More specifically, the data is split into a training set containing samples to train the model and a test set consisting of instances to pretend an unbiased evaluation of the investigated learning model. We set up five different splitting schemes by tuning various split ratios. For each topic, we eventually examine how the proposed framework performs on these five dataset splitting schemes.

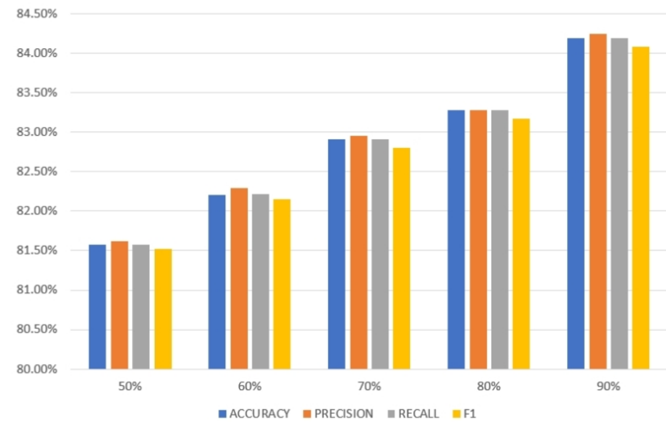

Figure 3. The Framework Performance on all Five Dataset Splitting Schemes

- Splitting scheme a. The percentage of the training and test parts is 50% and 50% respectively. We denote it as 50|50 and 50% hereafter.
- Splitting scheme b. The percentage of the training and test parts is 60% and 40% respectively. We denote it as 60|40 and 60% hereafter.
- Splitting scheme c. The percentage of the training and test parts is 70% and 30% respectively. We denote it as 70|30 and 70% hereafter.
- Splitting scheme d. The percentage of the training and test parts is 80% and 20% respectively. We denote it as 80|20 and 80% hereafter.
- Splitting scheme e. The percentage of the training and test parts is 90% and 10% respectively. We denote it as 90|10 and 90% hereafter.

All experiments have been conducted on a normal laptop including distributed computing infrastructure and virtual machines. The environment specifications are CPU Intel Core i7 MQ, 8GB of RAM, graphics card NVIDIA GT 740M, Apache Spark 2.2.0, IDE IntelliJ IDEA 2017 ver 2.6, Scala programming language.

E. Experimental Results

All experiments have been conducted five times to assure the performance stability of the system. The authors then reported average scores and their standard deviation, e.g., a measure of the amount of variation or dispersion of our five-times computation. A low standard deviation indicates that the scores tend to be close to the mean of 5 times, while a high standard deviation indicates that the scores are spread out over a broader range. The experimental process is split into two scenarios. First, we investigate the performance on each topic separately. We present the experimental results on five topics (see Table (III) for Sports, see Table (IV) for News, see Table (V) for Traveling, see Table (VI) for Sales, see Table (VII) for

Technology). Second, we investigate the performance on the complete dataset, see Table (VIII) and Fig. (3).

TABLE III. THE CLASSIFICATION PERFORMANCE ON THE SPORTS TOPIC

Sports			
Splitting scheme	# Test instances	# Accurate prediction	Percentage
50|50	1183.2 ± 9.7570	963.8 ± 10.2323	0.8145 ± 0.0051
60|40	916.2 ± 18.3084	762.8 ± 28.0303	0.8323 ± 0.0157
70|30	705 ± 27.3404	591.4 ± 18.4607	0.8391 ± 0.0168
80|20	465.6 ± 12.7590	389.4 ± 12.9537	0.8363 ± 0.0139
90|10	223 ± 48.0468	201.4 ± 16.1338	0.8281 ± 0.0313

TABLE IV. THE CLASSIFICATION PERFORMANCE ON THE NEWS TOPIC

News			
Splitting scheme	# Test instances	# Accurate prediction	Percentage
50|50	1169 ± 25.4263	992.8 ± 23.7002	0.8492 ± 0.0072
60|40	946.8 ± 16.6943	809.6 ± 10.5023	0.8552 ± 0.0118
70|30	711.4 ± 35.9277	614.6 ± 27.8980	0.8641 ± 0.0076
80|20	474.4 ± 34.5079	410.2 ± 32.5079	0.8646 ± 0.0233
90|10	256.2 ± 10.0598	221.2 ± 6.6858	0.8637 ± 0.0156

TABLE V. THE CLASSIFICATION PERFORMANCE ON THE TRAVELING TOPIC.

Traveling			
Splitting scheme	# Test instances	# Accurate prediction	Percentage
50|50	1497.8 ± 17.0792	1355.2 ± 17.5698	0.9047 ± 0.0047
60|40	1192 ± 41.2492	1094.6 ± 34.1291	0.9183 ± 0.0058
70|30	896 ± 22.0340	816.4 ± 20.6712	0.9111 ± 0.0083
80|20	593 ± 16.9558	538.4 ± 16.4103	0.9079 ± 0.0147
90|10	304.8 ± 13.9713	282.4 ± 15.0266	0.9263 ± 0.0125

TABLE VI. THE CLASSIFICATION PERFORMANCE ON THE SALES TOPIC

Sales			
Splitting scheme	# Test instances	# Accurate prediction	Percentage
50|50	1150 ± 17.2481	817.8 ± 29.1753	0.7109 ± 0.0167
60|40	905.4 ± 20.3297	649.6 ± 23.7339	0.7174 ± 0.0182
70|30	668 ± 27.0277	474.2 ± 16.4225	0.7102 ± 0.0198
80|20	460.2 ± 21.2179	338.8 ± 11.3666	0.7366 ± 0.0194
90|10	226 ± 12.2882	166.8 ± 10.3778	0.7380 ± 0.0220

TABLE VII. THE CLASSIFICATION PERFORMANCE ON THE TECHNOLOGY TOPIC

Technology			
Splitting scheme	# Test instances	# Accurate prediction	Percentage
50|50	1209.6 ± 25.0059	902.6 ± 27.4918	0.7461 ± 0.0166
60|40	969 ± 25.7099	732.4 ± 21.8929	0.7558 ± 0.0074
70|30	731.6 ± 28.6408	557.8 ± 33.4917	0.7619 ± 0.0182
80|20	484 ± 21.7715	374.2 ± 6.9426	0.7740 ± 0.0269
90|10	247.2 ± 15.7066	191.2 ± 14.5670	0.7730 ± 0.0175

F. Remark and Discussion

The average execution time of the system is calculated through two phases: Phase I: Filter characters, separate words, vectorize messages, and perform in vector space model for the dataset. The average execution time is 20 minutes 55 seconds. Phase II: Divide the data into two parts, train the machine learning model, and predict the test set, calculate the accuracy of each topic, and analyze the system's efficiency. The average execution time is 16 seconds, which proves the feasibility of Naïve Bayes classifier. It works well with text data and is fast in comparison to other classification algorithms. The advantages of Naïve Bayes the biased assumption about the shape of the data distribution. The model limits the prediction capacity to data scarcity and frequency of words in the whole text source.

With the highest accuracy of about 83.18% with a minimal value of standard deviation 0.93%, the experimental results have proved the feasibility and computation stability of our proposed system. The topic with the highest predictive rate is Traveling with 92.63%. Particularly, the Sales topic has the lowest rate, with 73.80%. It can be explained for this reason because the Lazada fan page specializes in selling goods online. The categories of goods are very diverse. The standard deviation of all experiments is quite low, which indicates the performance stability of the proposed system. Furthermore, the execution time of the system is also relatively short, especially the classification process. When the data set is large enough, the learning process only occurs once, and the classification process must be repeated over time.

TFIDF is one of the most popular term-weighting schemes today as 83% of text-based recommender systems in digital libraries use it [40]. It is widely supported in many machine learning libraries and can be applied as on-the-shelf effectively. Therefore, traditional TFIDF is applied in this paper. The pitfall of this text presentation is that it ignores the semantics and syntactic of the text. The calculation time also depends on how many unique words in all text corpora. The tuning might be considered to improve the shortcomings of the IFIDF algorithm regarding the classification accuracy of machine learning models used, ignoring the calculation efficiency in the classification process. How to improve the accuracy together with efficiency is the direction for further research in the future.

To get a confirmation on how our proposed solution performs, we have conducted several experiments by replacing Naïve Bayes classifier by logistic regression, decision trees, and random forests. The operating configuration is similar, except for the models themselves. The experimental results reported in Tables IX, X, and XI have proved the advancement of our proposed solution.

VI. CONCLUSION

The problem of discovering and identifying themes for social network messages is an urgent problem in the context of the current social network explosion. The topics explored from these messages in combination with analyzing the perspective will contribute to predicting the spread of the messages. It helps develop solutions to monitor and prevent bad information, causing serious impacts, spreads on social networks. The paper has proposed and built a distributed framework for addressing probabilistic classification using Apache Spark to meet the need to handle large amounts of data. The Naïve Bayes classification method is suitable to build on a large data processing platform. Initial results for an accuracy score of about 83% and can be further improved when collecting more amount of dataset. we have also built a set of social network messages including five topics for the process of analyzing and researching social networks. The paper contributes to solving the problem of classifying the topic of short messages that are appearing on social networks in Vietnam.

REFERENCES

[1] "Tnw: The heart of tech." [Online]. Available: http://www.thenextweb.com/

TABLE VIII. THE CLASSIFICATION PERFORMANCE ON THE COMPLETE FIVE TOPICS

The complete experimental dataset						
Splitting scheme	# Test instances	# Accurate prediction	Accuracy	Precision	Recall	F1 score
50|50	6193.6 ± 78.99	5051.2 ± 101.22	0.8155 ± 0.0087	0.8158 ± 0.0089	0.8155 ± 0.0087	0.8144 ± 0.0088
60|40	5003.8 ± 52.51	4104.2 ± 65.00	0.8201 ± 0.0044	0.8206 ± 0.0043	0.8201 ± 0.0044	0.8190 ± 0.0045
70|30	3710.8 ± 75.98	3052.8 ± 69.92	0.8226 ± 0.0055	0.8236 ± 0.0055	0.8226 ± 0.0055	0.8217 ± 0.0054
80|20	2510.8 ± 44.37	2073.4 ± 29.66	0.8258 ± 0.0056	0.8269 ± 0.0059	0.8258 ± 0.0056	0.8249 ± 0.0059
90|10	1248.4 ± 29.59	1039.4 ± 19.70	0.8326 ± 0.0077	0.8344 ± 0.0088	0.8326 ± 0.0077	0.8318 ± 0.0093

TABLE IX. THE CLASSIFICATION PERFORMANCE ON THE COMPLETE FIVE TOPICS. LOGISTIC REGRESSION MODEL IS USED

Splitting scheme	Accuracy	Precision	Recall	F1 score
50|50	0.7450 ± 0.0045	0.7465 ± 0.0038	0.7450 ± 0.0045	0.7444 ± 0.0041
60|40	0.7549 ± 0.0064	0.7572 ± 0.0066	0.7549 ± 0.0064	0.7549 ± 0.0067
70|30	0.7659 ± 0.0106	0.7674 ± 0.0105	0.7659 ± 0.0106	0.7659 ± 0.0107
80|20	0.7710 ± 0.0088	0.7722 ± 0.0081	0.7710 ± 0.0088	0.7707 ± 0.0084
90|10	0.7716 ± 0.0123	0.7733 ± 0.0120	0.7716 ± 0.0123	0.7718 ± 0.0120

TABLE X. THE CLASSIFICATION PERFORMANCE ON THE COMPLETE FIVE TOPICS. DECISION TREES MODEL IS USED

Splitting scheme	Accuracy	Precision	Recall	F1 score
50|50	0.6816 ± 0.0068	0.7514 ± 0.0110	0.6816 ± 0.0068	0.6643 ± 0.0084
60|40	0.6820 ± 0.0035	0.7532 ± 0.0029	0.6820 ± 0.0035	0.6649 ± 0.0039
70|30	0.6851 ± 0.0166	0.7517 ± 0.0112	0.6851 ± 0.0166	0.6680 ± 0.0183
80|20	0.6924 ± 0.0071	0.7621 ± 0.0099	0.6924 ± 0.0071	0.6763 ± 0.0085
90|10	0.6956 ± 0.0146	0.7560 ± 0.0139	0.6956 ± 0.0146	0.6811 ± 0.0170

TABLE XI. THE CLASSIFICATION PERFORMANCE ON THE COMPLETE FIVE TOPICS. RANDOM FOREST MODEL IS USED

Splitting scheme	Accuracy	Precision	Recall	F1 score
50|50	0.6325 ± 0.0074	0.7968 ± 0.0054	0.6325 ± 0.0074	0.6071 ± 0.0058
60|40	0.6209 ± 0.0080	0.7950 ± 0.0025	0.6209 ± 0.0080	0.5949 ± 0.0084
70|30	0.6253 ± 0.0160	0.7983 ± 0.0035	0.6253 ± 0.0160	0.6003 ± 0.0171
80|20	0.6266 ± 0.0201	0.7974 ± 0.0048	0.6266 ± 0.0201	0.6007 ± 0.0206
90|10	0.6180 ± 0.0199	0.8001 ± 0.0016	0.6180 ± 0.0199	0.5933 ± 0.0227

[2] V. Basile, C. Bosco, E. Fersini, N. Debora, V. Patti, F. M. R. Pardo, P. Rosso, M. Sanguinetti *et al.*, "Semeval-2019 task 5: Multilingual detection of hate speech against immigrants and women in twitter," in *13th International Workshop on Semantic Evaluation*. Association for Computational Linguistics, 2019, pp. 54–63.

[3] H. X. Huynh, B. U. Lai, N. Duong-Trung, H. T. Nguyen, and T.-C. Phan, "Modeling population dynamics for information dissemination through facebook," *Concurrency and Computation: Practice and Experience*, p. e6333, 2021.

[4] N. Duong-Trung, *Social Media Learning: Novel Text Analytics for Geolocation and Topic Modeling*. Cuvillier Verlag, 2017.

[5] T. T. Dao, T. D. Thanh, T. N. Hai, and V. H. Ngoc, "Building vietnamese topic modeling based on core terms and applying in text classification," in *2015 Fifth International Conference on Communication Systems and Network Technologies*. IEEE, 2015, pp. 1284–1288.

[6] N. Duong-Trung and L. Schmidt-Thieme, "On discovering the number of document topics via conceptual latent space," in *Proceedings of the 2017 ACM on Conference on Information and Knowledge Management*, 2017, pp. 2051–2054.

[7] N. Duong-Trung, N. Schilling, L. Drumond, and L. Schmidt-Thieme, "Matrix factorization for near real-time geolocation prediction in twitter stream." in *LWDA*, 2016, pp. 89–100.

[8] N. Duong-Trung, M.-H. Nguyen, and H. T. Nguyen, "Clustering stability via concept-based nonnegative matrix factorization," in *Proceedings of the 3rd International Conference on Machine Learning and Soft Computing*, 2019, pp. 49–54.

[9] N. Duong-Trung, N. Schilling, and L. Schmidt-Thieme, "Near real-time geolocation prediction in twitter streams via matrix factorization based regression," in *Proceedings of the 25th ACM international on conference on information and knowledge management*, 2016, pp. 1973–1976.

[10] N. Duong-Trung, N. Schilling, L. R. Drumond, and L. Schmidt-Thieme, "An effective approach for geolocation prediction in twitter streams using clustering based discretization," 2017.

[11] G.-S. Nguyen, X. Gao, and P. Andreae, "Vietnamese document representation and classification," in *Australasian Joint Conference on Artificial Intelligence*. Springer, 2009, pp. 577–586.

[12] K. Kowsari, K. Jafari Meimandi, M. Heidarysafa, S. Mendu, L. Barnes, and D. Brown, "Text classification algorithms: A survey," *Information*, vol. 10, no. 4, p. 150, 2019.

[13] M. M. Mirończuk and J. Protasiewicz, "A recent overview of the state-of-the-art elements of text classification," *Expert Systems with Applications*, vol. 106, pp. 36–54, 2018.

[14] V. B. Kobayashi, S. T. Mol, H. A. Berkers, G. Kismihok, and D. N. Den Hartog, "Text classification for organizational researchers: A tutorial," *Organizational research methods*, vol. 21, no. 3, pp. 766–799, 2018.

[15] S. Kumar and M. I. Nezhurina, "An ensemble classification approach for prediction of user's next location based on twitter data," *Journal of Ambient Intelligence and Humanized Computing*, vol. 10, no. 11, pp. 4503–4513, 2019.

[16] T. Mikolov, K. Chen, G. Corrado, and J. Dean, "Efficient estimation of word representations in vector space," *arXiv preprint arXiv:1301.3781*, 2013.

[17] J. Pennington, R. Socher, and C. D. Manning, "Glove: Global vectors for word representation," in *Proceedings of the 2014 conference on empirical methods in natural language processing (EMNLP)*, 2014, pp. 1532–1543.

[18] G. Aydin and I. R. Hallac, "Document classification using distributed machine learning," *arXiv preprint arXiv:1802.03597*, 2018.

[19] P. Semberecki and H. Maciejewski, "Distributed classification of text documents on apache spark platform," in *International Conference on Artificial Intelligence and Soft Computing*. Springer, 2016, pp. 621–630.

[20] J. Xin, Z. Wang, C. Chen, L. Ding, G. Wang, and Y. Zhao, "Elm: distributed extreme learning machine with mapreduce," *World Wide Web*, vol. 17, no. 5, pp. 1189–1204, 2014.

[21] H. X. Huynh, V. T. Nguyen, N. Duong-Trung, V.-H. Pham, and C. T. Phan, "Distributed framework for automating opinion discretization from text corpora on facebook," *IEEE Access*, vol. 7, pp. 78 675–78 684, 2019.

[22] V. C. D. Hoang, D. Dinh, N. Le Nguyen, and H. Q. Ngo, "A comparative study on vietnamese text classification methods," in *2007 IEEE International Conference on Research, Innovation and Vision for the Future*. IEEE, 2007, pp. 267–273.

[23] V. T. Nguyen, N. T. Hai, N. H. Nghia, and T. D. Le, "A term weighting scheme approach for vietnamese text classification," in *International Conference on Future Data and Security Engineering*. Springer, 2015, pp. 46–53.

[24] H. T. Huynh, N. Duong-Trung, Q. D. Truong, and H. X. Huynh, "Vietnamese Text Classification with TextRank and Jaccard Similarity Coefficient," *Advances in Science, Technology and Engineering Systems Journal*, vol. 5, no. 6, pp. 363–369, 2020.

[25] H. T. Huynh, N. Duong-Trung, X. S. Ha, N. Q. T. Tang, H. X. Huynh, and D. Q. Truong, "Automatic keywords-based classification of vietnamese texts," in *2020 RIVF International Conference on Computing and Communication Technologies (RIVF)*. IEEE, 2020, pp. 1–3.

[26] L.-D. Quach, N. Duong-Trung, A.-V. Vu, and C.-N. Nguyen, "Recommending the workflow of vietnamese sign language translation via a comparison of several classification algorithms," in *International Conference of the Pacific Association for Computational Linguistics*. Springer, 2019, pp. 134–141.

[27] C.-H. Chen, "Improved tfidf in big news retrieval: An empirical study," *Pattern Recognition Letters*, vol. 93, pp. 113–122, 2017.

[28] Z. Zhu, J. Liang, D. Li, H. Yu, and G. Liu, "Hot topic detection based on a refined tf-idf algorithm," *IEEE Access*, vol. 7, pp. 26 996–27 007, 2019.

[29] D. Kim, D. Seo, S. Cho, and P. Kang, "Multi-co-training for document classification using various document representations: Tf–idf, lda, and doc2vec," *Information Sciences*, vol. 477, pp. 15–29, 2019.

[30] M. Allahyari, S. Pouriyeh, M. Assefi, S. Safaei, E. D. Trippe, J. B. Gutierrez, and K. Kochut, "A brief survey of text mining: Classification, clustering and extraction techniques," *arXiv preprint arXiv:1707.02919*, 2017.

[31] W. M. Bolstad and J. M. Curran, *Introduction to Bayesian statistics*. John Wiley & Sons, 2016.

[32] A. G. Shoro and T. R. Soomro, "Big data analysis: Apache spark perspective," *Global Journal of Computer Science and Technology*, 2015.

[33] M. Zaharia, R. S. Xin, P. Wendell, T. Das, M. Armbrust, A. Dave, X. Meng, J. Rosen, S. Venkataraman, M. J. Franklin *et al.*, "Apache spark: a unified engine for big data processing," *Communications of the ACM*, vol. 59, no. 11, pp. 56–65, 2016.

[34] I. A. T. Hashem, N. B. Anuar, A. Gani, I. Yaqoob, F. Xia, and S. U. Khan, "Mapreduce: Review and open challenges," *Scientometrics*, vol. 109, no. 1, pp. 389–422, 2016.

[35] X. Meng, J. Bradley, B. Yavuz, E. Sparks, S. Venkataraman, D. Liu, J. Freeman, D. Tsai, M. Amde, S. Owen *et al.*, "Mllib: Machine learning in apache spark," *The Journal of Machine Learning Research*, vol. 17, no. 1, pp. 1235–1241, 2016.

[36] R. Ignazio, *Mesos in action*. Simon and Schuster, 2016.

[37] "Facebook fplus - instagram zalo shopee - advertisement." [Online]. Available: https://plus24h.com/

[38] N. T. M. Huyen, A. Roussanaly, H. T. Vinh *et al.*, "A hybrid approach to word segmentation of vietnamese texts," in *International Conference on Language and Automata Theory and Applications*. Springer, 2008, pp. 240–249.

[39] Stopwords, "stopwords/vietnamese-stopwords," Apr 2017. [Online]. Available: https://github.com/stopwords/vietnamese-stopwords/blob/master/vietnamese-stopwords.txt

[40] J. Beel, B. Gipp, S. Langer, and C. Breitinger, "Paper recommender systems: a literature survey," *International Journal on Digital Libraries*, vol. 17, no. 4, pp. 305–338, 2016.

Development of Intelligent Tools for Detecting Resource-intensive Database Queries

Salah M.M. Alghazali[1], Konstantin Polshchykov[2], Ahmad M. Hailan[3], Lyudmila Svoykina[4]
Department of Applied Informatics and Information Technology, Belgorod State University, Belgorod, Russia[1]
Institute of Engineering and Digital Technologies, Belgorod State University, Belgorod, Russia[2]
College of Computer Science and Mathematics, Thi-Qar University, Thi-Qar, Iraq[3]
Institute of Intercultural Communication and International Relations, Belgorod State University, Belgorod, Russia[4]

***Abstract*—The detection of resource-intensive queries which consume an excessive amount of time, processor, disk, and memory resources is one of the most popular vulnerabilities of Database Management Systems (DBMS). The tools for monitoring and optimizing queries typically used in modern DBMS were analyzed, and their shortcomings were identified. Subsequently, the relevance of new intelligent tools' development for timely and reliable detection of resource-intensive queries to databases was distinctly justified. The study concluded a set of analysis of an extended statistical parameter which indicated to be of interest for identifying resource-intensive queries. The initial set of queries' parameters reduced by two consecutive methods. Firstly, normalizing the set of indicators using a sigmoid function. Secondly, selecting a finite number of principal components based on the Cattell test. Whereas the clustering of a set of queries performed using self-organizing Kohonen maps. Suggestions for further studies in the classification algorithm context were indicated in lights of the study's conclusions.**

***Keywords*—Resource-intensive queries; database; detecting; self-organizing Kohonen maps; statistical parameters**

I. Introduction

A resource-intensive request to the database will be considered as such when a request uses an excessive amount of time, processor, disk, and memory resources to process that request. Search and conversion of resource-intensive queries is carried out by Data Base Administrators (DBAs) based on information from clients. The gradual decline in the performance of distributed clients' systems requires proactive optimization measures.

Queries to databases are programmed based on special tools which are part of the Structured Query Language (SQL) [1]. The existing methods currently used in system utilities for searching and identifying problematic queries do not always identify resource-intensive SQL statements. Correspondingly, there are instances where those queries would wrongfully not be classified as resource-intensive. This is due to the fact that utilities only exploit a limited number of performance parameters or incorrect analysis's algorithms based on simple ranking. Furthermore, the functional redundancy and high cost of such utilities are yet other drawbacks for the effects of those inefficient queries.

It is perceived that manual searches could provide correct detection of problematic SQL queries. Notwithstanding, the complexity and time-consuming processes of analyzing large amounts of information does not allow a person to process data at a reasonable speed. Manual searches involve continued time-wasting and require experience in Database Management Systems (DBMS). Especially the knowledge on the architecture, features of storing system information, the language of structured queries, data structures and models of application programs.

The identification of resource-intensive SQL queries entails the purchase of expensive tools. Likewise, it compels the involvement of highly qualified specialists with relevant knowledge and experience in writing unique scripts for the necessary data acquisition.

This article presents the results of research obtained by the authors on the analysis and development of intelligent tools designed for timely and reliable automatic detection of resource-intensive database queries.

II. Literature Review

There are many approaches is use today to either prevent or minimize the impact of inter-query interactions on a shared cluster. Despite these measures, performance issues due to concurrent executions of mixed workloads still prevail causing undue waiting times for queries [2]. The foundation of modern database query optimization is the collection of statistics describing the data to be processed, but when a database or Big Data computation is partially obscured by user-defined functions, good statistics are often unavailable [3]. H.Bodepudi [4] mentioned how the Relational DBMS reporting scripts performance can be improved by incorporating the Spark framework without changing the existing queries in the RDBMS. In paper [5] presents Intermittent Slow Query Anomaly Diagnoser, a framework that can diagnose the root causes of Intermittent Slow Queries with a loose requirement for human intervention. Intermittent Slow Queries are slow queries which might be more hazardous to database users than other slow queries.

Z.Miao [6] proposes a system designed to help users understand SQL query evaluation and debug SQL queries. The system lets users interactively "trace" the evaluation of complex SQL queries, including those with correlated subqueries.

B.G.Lekshmi [7] focuses on the hardware-conscious the query optimization in a relational DBMS using extended rules and cost models as well as on refining the optimization strategies for changes in the hardware state of execution.

Cost-based optimizer studied in paper [8] is adopted in almost all current database systems. A cost-based optimizer introduces a plan enumeration algorithm, and then uses a cost model to obtain the cost of that plan, and selects the plan with the lowest cost. In the cost model, cardinality, the number of tuples through an operator, plays a crucial role. The research [9] aims to provide approximate query processing as a middleware solution using query optimization for heterogeneous databases.

A large scale of resource requirements can be reduced by minimizing query execution time that maximizes resource utilization [10]. Recently, parallel DBMSs have significantly improved query processing performance [11].

Thus with the growing volume of data being analyzed, more and more advanced monitoring, preventive analysis, and proactive optimization tools are required to identify problematic SQL queries. The above reasons determine the relevance of developing new intelligent tools for timely and reliable resource-intensive database queries' detection.

III. Materials and Methods

During processing of the request, a plan for executing a SQL statement should be formed to get the information requested from the database more quickly and cost-effectively. Modern tools for monitoring and optimizing queries in Oracle DBMS, MS SQL Server, and DB2 sort and evaluate SQL statements based on the values of one, less often two, or three indicators that characterize the speed of query processing. Further, the use of these indicators could be used to assess the resources used for the processing of queries. These methods were found to be causing an erroneous diagnostics of the resource-intensive queries and beg the need for an optimized method.

Advanced data collection technologies for resource-intensive queries searching are implemented in the automatic workload storage of the Oracle DBMS [12]. These include the Advanced Workload Repository (AWR). This infrastructure provides services to Oracle DBMS components for collecting, maintaining, and using statistics for problem detection and self-tuning [13]. AWR makes it possible to collect various information about requests and the operation of the system. The statistics on executed SQL statements contained in the DBA_HIST_SQLSTAT table are best suited for searching and subsequent optimization of resource-intensive queries.

The main source of information useful for identifying problematic SQL statements is statistical data on the query execution period. Most often, a resource-intensive SQL query detection is performed using the following parameters:

1) for a large number of disk reads;

2) by the number of logical reads or buffer gets operations;

3) by the number of parse calls;

4) by the number of executions.

However, studies had shown that the extended set of parameters contained in Table I is of interest for identifying resource-intensive queries. The initial statistical analysis of the initial data on various test sets showed that almost all parameters have sharply asymmetric right-hand distributions with long thin tails. The asymmetry coefficients take values from 10 to 15, and the excesses take values from 150 to 400.

TABLE I. Extended Set of SQL Query Parameters

Parameter	***Name***
Executions	number of request executions
sharable_mem	the size of the sharable memory occupied by the child cursor (bytes)
loaded_versions	the number of child cursors for which memory is allocated
version_count	total number of child cursors
physical_read_bytes	the number of bytes physically read from the disk
physical_write_bytes	number of bytes written to disk
physical_read_requests	number of disk reads
physical_write_bytes	number of bytes written to disk
physical_read_requests	number of disk reads
physical_write_requests	number of operations to write information to disk
rows_processed	number of rows processed and returned
parse_calls	number of calls to the parsing procedure
px_servers_execs	the number of runs of auxiliary server processes for parallel execution of the request
end_of_fetch_count	the number of times the query returned a full set of data on successful completion
Fetches	the number of calls to the procedure for extracting rows with data from the cursor
buffer_gets	number of gets from the buffer cache (logical read)
Invalidations	the number of times the child cursor became invalid
Loads	number of memory downloads / reloads
Sorts	number of sorting operations
direct_writes	number of direct write operations to disk
cpu_time	processor time for parsing, executing, and fetching data for a given cursor (μs)
elapsed_time	total request duration time (μs)
javexec_time_delta	time elapsed in the execution of Java programs (μs)
plsexec_time_delta	PL/SQL code execution time (μs)
iowait	time spent waiting for user input / output (μs)
apwait	time spent waiting for the app (μs)
ccwait	time spent waiting for shared data and resources (μs)
clwait	time spent waiting for concurrency events to complete (μs)
io_interconnect_bytes	the number of bytes sent between the DBMS and the Exadata storage system
io_offload_elig_bytes	the number of bytes filtered for processing at the Exadata data store level
io_offload_return_bytes	number of bytes returned from the Exadata data store layer
cell_uncompressed_bytes	number of bytes received during data decompression on Exadata data storage nodes
optimized_physical_reads	number of optimized reads from the Exadata data store

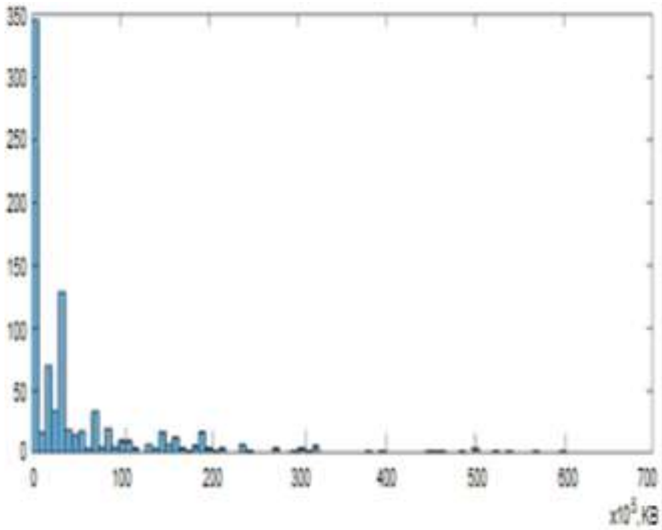

Fig. 1. Distributions of the Sharable_Mem Parameter.

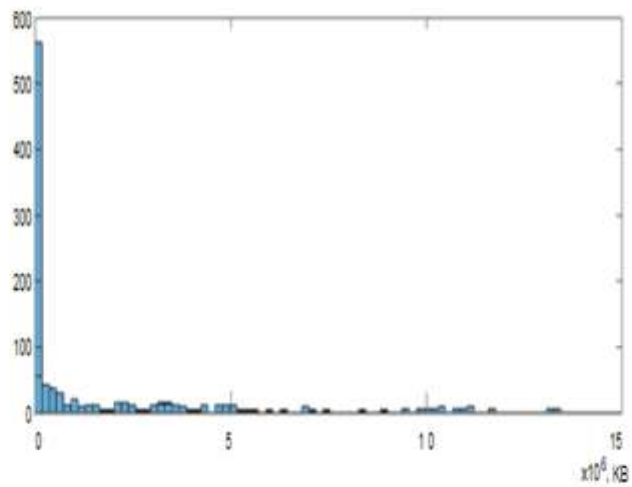

Fig. 2. Distributions of the Physical_Read_Bytes Parameter.

Fig. 1 depicts typical distributions of the sharable_mem parameter. Fig. 2 illustrate a typical distribution of the values of the physical_read_bytes parameter.

Visual histogram analysis outlines most of the SQL query parameter values which were found to be concentrated in the range of 1-2% of the entire diapason of possible values. The parameter values that are in the tails of the distributions indicate the presence of resource-intensive queries in the analyzed sets.

The extended set of parameters presented in Table I is redundant. To account for all these indicators in order to detect resource-intensive queries, algorithms with high computational complexity will be required, which is undesirable in the process of performing practical tasks. It is necessary to significantly reduce the number of analyzed parameters and leave the most informative ones.

The ranges of changes in statistical parameters differ by several orders of magnitude, so to reduce the number of these parameters, a preliminary normalization of the indicators set was carried out using a sigmoid function:

$$\tilde{x} = \text{sigmoid}\left(\frac{x - \bar{x}}{\sigma}\right) \quad (1)$$

where $\tilde{x}$ is the normalized value of the parameter; x is the initial value of the parameter; $\bar{x}$ is the average value of the parameter.

The value of the sigmoid function of the value a is calculated using the expression:

$$\text{sigmoid}\ (a) = \frac{1}{1 + e^{-ca}}. \quad (2)$$

where c is the extension coefficient of the sigmoid. For most parameters, the best value is c=8.

Further, in order to reduce the number of parameters that characterize SQL queries, the Principal Component Analysis (PCA) method was used to get the better analyze and make best decision based upon detect the relevant parameters [14].

The PCA implementation allowed us to construct a new space of parameters to reduce dimensions. In this case, the variance of the initial parameter space was first calculated. Then, eigenvectors were obtained that determine the directions of the principal components and the value of the variance associated with them. In order to reduce dimensionality, the variance value associated with each principal component was divided by the sum of the variances for all components. As a result, the proportion of variance associated with each component is obtained. At the final step, so many components were discarded so that the proportion of the variance of the remaining components reached 80%.

The results of applying the PCA method are presented in Table II. The second column shows the variances of the selected components. The third column shows the percentage of the total variance for each component. The first component explains 21% of the total variance, the second component explains 11.5% of the total variance, and so on. The fourth column contains the values of the accumulated variance. Each value shown in the fourth column is the sum of those values from the third column whose component numbers do not exceed the number of the calculated value of the accumulated variance. For example, the value of the accumulated variance in the fourth row of Table II was obtained by summing the values of the third column contained in rows 1, 2, 3, and 4.

The choice of a finite number of principal components was carried out on the basis of the Cattell criterion, which allows us to preserve from 65 to 80% of the information concentrated in the original set of significant features. The selection of the first main components based on the Cattell test is shown in Fig. 3. The number of principal components according to the Cattell criterion was determined by the inflection point on the graph of eigenvalues. In this case, the inflection point is the boundary between the interval of the sharp decline of the analyzed graph and the subsequent interval of the flat curve.

TABLE II. RESULTS OF THE PCA METHOD APPLICATION

Component number	*Component value*	*Explained variance proportion*	*Accumulated variance*
1	6.819	21.31	21.31
2	3.670	11.47	32.78
3	2.673	8.35	41.13
4	2.531	7.91	49.04
5	3.670	11.47	32.78
6	1.838	5.74	54.78
7	1.660	5.19	59.97
8	1.299	4.06	64.03
9	1.112	3.48	67.51
10	1.066	3.33	70.84
11	1.031	3.22	74.06
12	1,005	3.14	77.20
13	0.999	3.12	80.32
14	0.997	3.12	83.44
15	0.949	2.97	86.40
16	0.913	2.85	89.26
17	0.790	2.47	91.73
18	0.716	2.24	93.97
19	0.693	2.17	96.13
20	0.350	1.09	97.22
21	0.262	0.82	98.04
22	0.247	0.77	98.81
23	0.199	0.62	99.44
24	0.101	0.32	99.75
25	0.065	0.20	99.96
26	0.013	0.04	100.00
27	0.001	0.00	100,.0

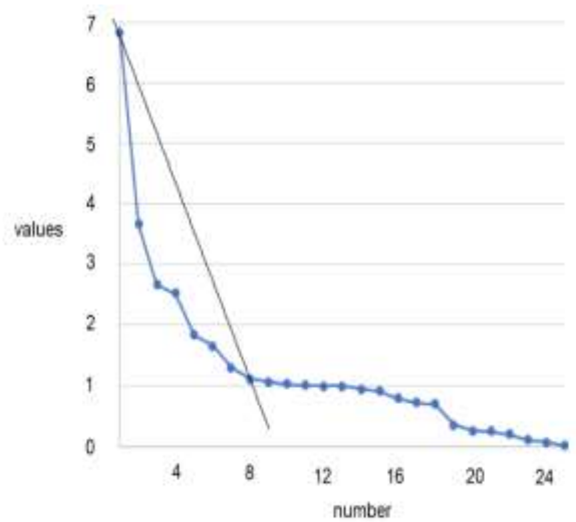

Fig. 3. The Selection of the First Main Components based on the Cattell Test.

The first eight components can be recognized as the main components. For the remaining components, there is a significant slowdown in the values decrease. The selected main eight components contain a fairly high percentage of the explained variance, approaching 70%. The selection of the main components using the PCA method and the Cattell test was performed for different sets of parameter values that characterize SQL queries. As a result, it was found that to detect problematic database queries, it is enough to use from four to nine significant parameters instead of the original thirty-two.

The set of all possible SQL queries must be divided into an unknown number of clusters. For this purpose, the device of Kohonen's Self-Organizing Maps (hereinafter SOM) is used [15, 16, 17]. The SOM training algorithm is developed, based on the use of a rational value of the winning neuron topological neighborhood width, which makes it possible to configure the neural network to prevent its overfitting. The implementation of neural network clustering using more than 200,000 instances of SQL statements processed in the past made it possible to form 4 main subsets of queries, of which two clusters can be classified as resource-intensive queries.

The further process of automating the search for problematic queries can be associated with the construction of a Bayesian classifier [18,19,20], which can be trained on a limited, independent, pre-researched and marked-up subset of SQL queries. The classifier can be trained to assign the studied elements to one of two classes (resource-intensive and non-resource-intensive queries). Further training and improvement of the classifier for subsequent use for operational and proactive optimization can be carried out on newly identified resource-intensive queries. Information about such requests can be received from DBA specialists in an interactive mode.

IV. CONCLUSION

Thus, in the process of detecting problematic SQL statements, it is proposed to use up to nine significant statistical parameters that characterize the speed of query processing, as well as the resources used for this purpose. The original set of thirty-two analyzed parameters contained in the DBA_HIST_SQLSTAT table of the Oracle DBMS workload storage was reduced by first normalizing the set of indicators using a sigmoid function and then selecting a finite number of principal components based on the Cattell criterion. Clustering a set of SQL statements based on SOM made it possible to form four main subsets of queries. At the same time, resource-intensive requests were concentrated in two clusters.

As a result of this study, the authors were able to substantiate the correctness of using a reduced set of statistical parameters to detect resource-intensive queries. This made it possible to successfully perform neural network clustering of the analyzed queries.

The subject of further research would be the development of a classification algorithm designed to determine the ratio of the analyzed SQL statement to one of the previously allocated clusters, which will automatically detect resource-intensive queries.

References

[1] C. Wang, A.Cheungc and R. Bodik,"Synthesizing highly expressive SQL queries from input-output examples," Proceedings of the 38th ACM SIGPLAN Conf. on Programming Language Design and Implementation, pp. 452-466, June 2017.

[2] P. Kalmegh, S. Babu and S. Roy, "Analyzing Query Performance and Attributing Blame for Contentions in a Cluster Computing Framework," arXiv:1708.08435v2, 2018.

[3] S. Sikdar and C. Jermaine, "MONSOON: Multi-Step Optimization and Execution of Queries with Partially Obscured Predicates", Proceedings of the 2020 ACM SIGMOD International Conference on Management of Data (SIGMOD '20). Association for Computing Machinery, New York, pp. 225–240, 2020.

[4] H. Bodepudi, "Faster The Slow Running RDBMS Queries With Spark Framework," International Journal of Scientific and Research Publications, volume 10(11), pp. 287-291, 2020.

[5] M. Ma, Z. Yin and S. Zhang et al. "Diagnosing Root Causes of Intermittent Slow Queries in Cloud Databases," PVLDB, vol. 13(8), pp. 1176-1189, 2020.

[6] Z. Miao, T. Chen, A. Bendeck, K. Day, S. Roy and J. Yang, "I-Rex: an interactive relational query explainer for SQL," Proc. VLDB Endow, vol 13, pp. 2997–3000, 2020.

[7] B.G. Lekshmi and K.Meyer-Wegener, "COPRAO: A Capability Aware Query Optimizer for Reconfigurable Near Data Processors," 2021 IEEE 37th International Conference on Data Engineering Workshops (ICDEW), pp. 54-59, 2021.

[8] H. Lan., Z. Bao and Y.A. Peng, "Survey on Advancing the DBMS Query Optimizer: Cardinality Estimation, Cost Model, and Plan Enumeration," Data Sci. Eng., vol 6, pp. 86–101, 2021.

[9] M. Muniswamaiah, T. Agerwala and C.C. Tappert, "Approximate Query Processing for Big Data in Heterogeneous Databases," 2020 IEEE International Conference on Big Data, pp. 5765-5767, 2020.

[10] A. Bachhav, V. Kharat and M. Shelar, "An Efficient Query Optimizer with Materialized Intermediate Views in Distributed and Cloud Environment," Tehnički glasnik, vol 15, pp. 105-111, 2021.

[11] X. Zhou and C. Ordonez, "Matrix Multiplication with SQL Queries for Graph Analytics," 2020 IEEE International Conference on Big Data (Big Data), pp. 5872-5873, 2020.

[12] I. Fernandez, "Beginning Oracle Database 12c Administration. From Novice to Professional," Apress, p. 384, 2015.

[13] S.M.A.Fattah, M.A. Mahmoud and L.A.E. Abd-Elmegid, "An Adaptive Hybrid Controller for DBMS Performance Tuning," (IJACSA) International Journal of Advanced Computer Science and Applications, vol. 5(5), 2014.

[14] S. Belattar, O. Abdoun and H. El khatir, "New Learning Approach for Unsupervised Neural Networks Model with Application to Agriculture Field," (IJACSA) International Journal of Advanced Computer Science and Applications, vol. 11(5), 2020.

[15] S. Sinha, T.N. Singh, V.K. Singh and A.K. Verma, "Epoch determination for neural network by self-organized map (SOM)," Computational Geosciences, vol. 14, pp. 199-206, 2010.

[16] M. Sakkari and M. Zaied, "A convolutional deep self-organizing map feature extraction for machine learning," Multimedia Tools and Applications, vol. 79, pp. 19451-19470, 2020.

[17] L.R.Clovis, C.A.Scapim, R.J.B. Pinto, M.Vivas, J.E.A. Filho and A.T.A. Júnior, "Yield stability analysis of maize hybrids using the self-organizing map of Kohonen," Euphytica, vol. 216, p. 161, 2020.

[18] J. Yu, M. Bai, G. Wang and X. Shi, "Fault diagnosis of Planetary Gearbox with incomplete information using assignment reduction and flexible naive bayesian classifier," Mechanical Science and Technology, vol. 32, pp. 37-47, 2018.

[19] S.R.B. Shree and H.S. Sheshadri, "Diagnosis of alzheimer's disease using naive bayesian classifier," Neural Computing and Applications, vol. 29, pp. 123-132 , 2018.

[20] W. Zhang, Z. Zhang, HC. Chao and FH. Tseng, "Kernel mixture model for probability density estimation in Bayesian classifiers," Data Mining and Knowledge Discovery, 2018, vol. 32, pp. 675-707.

A New Approach for Network Steganography Detection based on Deep Learning Techniques

Cho Do Xuan[1], Lai Van Duong[2]
Information Assurance Department
FPT University, Hanoi
Vietnam

***Abstract*—One of the techniques that current cyber-attack methods often use to steal and transmit data out is to hide secret data in packets. This is the network steganography technique. Because millions of packets are sent and received every hour in internet activity, so it is very difficult to detect the theft and transmission of system data out using this form. Recent approaches often seek ways to compute and extract abnormal behaviors of packets to detect a steganography protocol or technique. However, such methods have the difficult problem of not being able to detect abnormal packets when an attacker uses other steganography techniques. To solve the above problem, this paper proposes a network steganography detection method using deep learning techniques. The highlight of this study is some new proposed features based on different components of the packet. By combining these many components, this proposal will not only provide the ability to detect many steganography techniques in the network, but also improve the ability to accurately detect abnormal packets. Besides, this study proposes to use deep learning for the task of detecting normal and abnormal packets. The authors want to take advantage of the big data analysis and processing capabilities of deep learning models in order to improve the ability to analyze and detect network steganography techniques. The experimental results in Section IVD have proved the effectiveness of this proposed method compared with other approaches.**

***Keywords*—Network steganography; network steganography detection method; abnormal packets; deep learning techniques**

I. Introduction

A. The Problem

The study [1] listed 11 different techniques commonly used to hide information in the network. These techniques are generally divided into three main technique groups: packet modification, stream modification, and hybrid. The research [2] presented some main difficulties that make it very difficult to detect and prevent network steganography techniques. To fix the problems in the research [2], current approaches often use two main methods: i) technique-specific methods, comprises methods proposed as countermeasures for specific steganographic techniques. Methods in this category usually operate on low-level network data, require relatively much computation resources, and are not able to detect other steganographic techniques instead of the one or several for which they are designed; ii) generic methods, comprises methods that are not designed to detect one specific steganographic technique but offer a comprehensive approach to network anomaly detection and categorization of network traffic for potential steganographic utilization. Methods in this category may not provide detailed information on detected suspicious traffic but can label it for further investigation. Most generic methods fall into two subcategories that characterize their approach: statistical or machine learning. The studies [3, 4, 5, 6, 7, 8] presented several studies and proposals for detecting network steganography based on the abnormal behavior analysis technique and the ruleset database. However, noticed that these approaches have two problems [1, 2, 9, 10, 11, 12]: using the available dataset and focusing on detecting only one steganography technique. Therefore, although these studies brought very high efficiency on experimental datasets, when applied in reality, they did not bring the desired result. To solve the above problems, this paper proposes a new method based on a group of generic methods. Specifically, this proposal will seek a way to optimize two main problems: i) defining and proposing features and characteristics of abnormal behavior of network steganography techniques; ii) use deep learning techniques on the basis of big data analysis to detect and classify cyber-attack techniques based on their unusual behavior defined in the task (i). Details of abnormal behaviors and algorithms for classifying network steganography techniques are presented in Section III of the paper. The results of evaluating the effectiveness of the proposed method are presented in detail in Section IV of the paper. Evaluation, conclusion, and future development direction are presented in Section V of the paper.

B. Contributions of the Paper

The practical significance and scientificity of this paper include:

- Proposing some features and characteristics of the packet. The features proposed in the paper are new study, and are synthesized and extracted on many different components of the packet. The experimental results have proved these proposed features have brought many meanings.
- Proposing the use of deep learning models for the task of detecting network steganography. In the experimental section, this paper tunes the parameters in each deep learning model to provide the ability to choose for the systems to ensure a balance between the time and the efficiency of the detection method.

II. Related Work

In the study [13], Mike et al. proposed a method to detect network steganography using the IDS tool. Specifically, the authors used the rulesets built in the IDS tool to detect hidden information in the network based on data sections of packets. In the study [14], the authors proposed a method to detect steganography in VoIP using the Least Significant Bits technique. Taeshik Sohn et al. [15] proposed a network steganography detection method using the Support Vector Machine (SVM) algorithm for detecting hidden information in TCP/IP protocols. Similarly, research [16] proposed using the Naive Bayes algorithm to detect secret information hidden in TCP/IP header. Cho et al. [3] proposed a method of detecting storage-based network steganography using machine learning. Specifically, in their research, the authors used the Random Forests (RF) algorithm to classify abnormal behaviors on ICMP and TCP/IP packets. Smolarczyk [2] proposed a method to detect steganography in the network using the multi-layer analysis technique.

III. Proposing the Network Steganography Detection Method using Deep Learning

A. *Proposing the Method to Select and Extract Abnormal Behavior of Network Steganography Techniques*

As mentioned above, the purpose of this paper is to use deep learning algorithms to detect network steganography based on analyzing different components of the packet. Specifically, three network steganography techniques studied in this paper are:

- Size Modulation: The covert channel uses the size of a header element or of a PDU to encode the hidden data.
- Random Value: The covert channel embeds hidden data in a header element containing a random value
- Reserved/Unused: The covert channel encoded hidden data into a reserved or unused header/PDU element.

Based on these attack techniques, this study will find ways to collect and analyze packets to look for their abnormal behaviors. Table I present 38 features proposed to extract and chose to use.

TABLE I. Proposed Abnormal Features of the Packet

No.	Category	Feature	Description	Type
1	IP	ip.id	IP Identification	Integer
2		ip.flags	IP Flags	Integer
3		ip.frag_offset	IP Fragment Offset	Integer
4		ip.checksum	IP Header Checksum	Integer
5		ip.ttl	IP Time to live	Integer
6		ip.tos	IP Type of Service	Integer
7		ip.src	IP Source Address	String
8		ip.dst	IP Destination address	String
9		ip.num_option	IP Number of options	Integer
10	TCP	tcp.flags	TCP Flags	Integer
11		tcp.checksum	TCP Checksum	Integer
12		tcp.seq	TCP Sequence Number	Integer
13		tcp.flags.res	TCP Reserved	Boolean
14		tcp.urgent_pointer	TCP Urgent Pointer	Integer
15		tcp.ack	TCP Acknowledgment Number	Integer
16		tcp.srcport	TCP Source Port	Integer
17		tcp.dstport	TCP Destination Port	Integer
18	UDP	udp.srcport	UDP Source Port	Integer
19		udp.dstport	UDP Destination Port	Integer
20	ICMP	icmp.type	ICMP Type number	Integer
21		icmp.unused	ICMP Unused	Bytes
22		icmp.reserved	ICMP Reserved	Bytes
23		icmp.seq	ICMP Sequence number (BE)	Integer
24		icmp.seq_le	ICMP Sequence number (LE)	Integer
25		icmp.length	ICMP Length	Integer
26		icmp.ident	ICMP Identifier (BE)	Integer
27		icmp.checksum	ICMP Checksum	Integer
28	Frame	frame.number	Frame number	Inetger

29		frame.len	Frame length on the wire	Integer
30		frame.cap_len	Frame length stored into the capture file	Integer
31	Ethernet	eth.src	Source	String
32		eth.dst	Destination	String
33	IPv6	ipv6.nxt	Next Header	Integer
34		ipv6.src	Source Address	String
35		ipv6.dst	Destination Address	String
36	MQTT	mqtt.topic	Topic	String
37		mqtt.msgtype	Message Type	Integer
38		mqtt.client.id	Client ID	String

B. *The Detection Method*

Thus, based on features of anomalous behaviors of packets defined and extracted in Table I, this paper will propose a method to classify these packets. It can be seen that to detect network steganography, previous studies often used algorithms such as SVM [4, 15], RF [3]. To improve the efficiency of the network steganography detection method, this paper proposes to use some deep learning algorithms and models. Specifically, some deep learning algorithms and models proposed to use include: Multilayer Perceptron (MLP), Convolutional Neural Network (CNN), Long short term memory (LSTM). Regarding the MLP network, the study [17] presented in detail the architecture of an MLP network that is built by simulating the way neurons work in the human brain. MLP networks usually have 3 or more layers including 1 input layer, 1 output layer, and more than 1 hidden layer. Besides, the efficiency of the MLP network depends on the activation function. This paper will tune activation functions to evaluate the effectiveness and suitability of activation functions for the network intrusion detection task. The CNN network is defined as a set of basic layers including convolution layer + nonlinear layer, fully connected layer. The detailed structure of CNN as well as the terms (stride, padding, MaxPooling) are presented in detail in the paper [18]. In which, the activation function used is ReLU.

The study [19] introduced the LSTM and its ability to remember information for a long time. This is reflected in the structure of the gates in each memory cell. A memory cell consists of three main components: input gate, forget gate, and output gate. Firstly, the forget gate decides what information should be discarded in the cell state. Next, the input gate decides what information is updated into the cell state. Finally, the output gate performs computing the desired output. During this process, the cell state is propagated through and updated when it passes through all nodes.

IV. Experiments and Evaluation

A. *Description of Data Collection Method*

1) For normal dataset: The dataset of normal packets is collected at [20]. This dataset belongs to the "MAWI Working Group" and the "WIDE Project" which collected network traffic at ISP points in Japan. PCAP files are network traffic collected on April 30, 2021. Then 2,200,000 packets in these PCAP files are taken to conduct experiments. Table II shows the number of collected and extracted normal packets.

2) For stego dataset: This study proposes to use some network steganography tools to generate stego packets. Table III below describes the tools and the steganography type of these tools in detail.

After successfully installing the above tools, running those tools and use Wireshark to capture the network traffic generated by those tools. Network traffic generated by each tool is saved as separate files. For example, network traffic generated by ptunnel is saved as a separate PCAP file, network traffic generated by covert_tcp is also be saved as a separate PCAP file. Only packets generated by these tools are saved. Other unrelated packets such as ARP or system packets are deleted to ensure that the PCAP file contains only stego packets containing secret information. Table IV below presents the number of stego packets generated by the tools listed in Table III.

TABLE II. Support Tools for Generating Normal Packets

Name	**Generation tool**	**The number of packets**
Normal Packet	mawi.wide.jp	2,200,000

TABLE III. Support Tools for Generating Packets Containing Secret Information

Tool	**Protocol**	**Field**
Ptunnel	ICMP	Payload
pingtransfer	ICMP	Payload
dns2tcp	DNS/UDP	TXT record
covert_tcp	TCP/IP	IP Identification / TCP ISN
syn-file	TCP	TCN Syn Sequence number
netcat	TCP	Space in payload
hcovert	TCP	Segment data

TABLE IV. The Total Number of Generated Stego Packets

Name	**Generation tool**	**The number of packets**
Size Modulation	netcat	421,839
Random Value	covert_tcp, syn-file	1,703,306
Reversed/Unused	ptunnel, pingtransfer, dns2tcp	481,651
Others	hcovert	109,208
Total		**2,716,004**

3) Data synthesis: Based on the data collection method in Sections 1) and 2) above, obtaining an aggregated dataset for training and testing for detecting network steganography as shown in Table V.

TABLE V. THE TOTAL NUMBER OF COLLECTED PACKETS

Description	The number of packets
Normal packet	2,200,000
Stego packet	2,716,004
Total	**4,916,004**

B. Evaluation Criteria

The following measures will be used in this paper to evaluate the accuracy of models:

- Accuracy: The ratio between the number of samples classified correctly and total number of samples.

$$accuracy = \frac{TP+TN}{TP+TN+FP+FN} \times 100\% \quad (1)$$

In which: TP - True positive: The number of stego packets classified correctly; FN - False negative: The number of stego packets classified as normal; TN - True negative: The number of normal packets classified correctly; FP - False positive: The number of normal packets classified as stego.

- Precision: The ratio between the true positive value and total number of samples classified as positive. The higher value of precision, the more accurate in stego packet detection.

$$precision = \frac{TP}{TP+FP} \times 100\% \quad (2)$$

- Recall: The ratio between the true positive value and the total real stego packets. The higher value of recall, the lower rate of missing positive samples.

$$Recall = \frac{TP}{TP+FN} \times 100\% \quad (3)$$

- F1-score: The harmonic mean of precision and recall. The higher F1 score, the better the model is

$$F1\text{score} = \frac{2 \times precision \times \mathrm{Re}call}{precision + \mathrm{Re}call} \quad (4)$$

- TP: The same to Recall. This shows the ability to detect the true stego packet.
- FP: The ratio between false positive value and the false positive plus true negative. This shows the false alarm rate of stego packet.

C. Experimental Scenario

1) Scenario for experimental dataset: With the experimental dataset listed in Table V, the dataset is divided into different parts and then conduct experiments and evaluate the accuracy of the proposed models based on these experimental datasets. The whole process of dividing the experimental dataset into the scenarios will be chosen randomly in which 80% of the dataset is used in the training process, the remaining 20% is used in the testing process.

2) Evaluation scenarios: To see the effectiveness of the proposed method, this paper conducts two experimental scenarios as follows:

- Scenario 1: Compare and evaluate the effectiveness of deep learning methods. For this scenario, this study conducts the evaluation according to the following algorithms: MLP, CNN, LSTM. During the experiment process, the authors tune parameters to see the effectiveness of the deep learning models.
- Scenario 2: Compare and evaluate the deep learning model with some other approaches on the same dataset.

D. Experimental Results

1) Experimental results of scenario 1: Comment: From the experimental results in Tables VI, VII, VIII, noticed that:

- Regarding accuracy: Based on the classification results, found that the LSTM model yielded better performance than other deep learning models. Specifically, at the Accuracy measure, the LSTM model reached the absolute rate with two and three layers. This result is higher than that of CNN models by 1.5 % and MLP by 1.45%. Similarly, with the Recall measure, the LSTM model is higher than other models from 0.01 to 0.3%. In general, deep learning models brought high efficiency for the task of classifying normal and abnormal packets. The authors think the reason is that the packets are analyzed by us into different components, and then features are extracted from these components. This makes their abnormal behaviors are highlighted so it supports the classification process better. In addition, deep learning models, especially LSTM with the ability to remember features and hidden layers, have synthesized many important features. Therefore, it can be seen that this proposal is completely correct and reasonable.
- Regarding prediction time: Based on the experimental results, noticed that the LSTM model takes more time than other models for both training and testing processes. In particular, the training time of the LSTM model is about 2 times higher than the CNN model and 7 times higher than the MLP model. Regarding the detection time, the LSTM model is about 12 times higher than the CNN model and 4 times higher than the MLP model. From this result, seeing that although the LSTM model is more efficient than other models, they are many times more time-consuming than other models. Therefore, in reality, monitoring and detection systems need to choose the appropriate model to balance both detection time and efficiency.

TABLE VI. EXPERIMENTAL RESULTS OF DETECTING NETWORK STEGANOGRAPHY USING MLP

MLP	**1st**	**2nd**	**3rd**
Precision	1.00	1.00	1.00
Recall	0.97	0.97	0.97
F1- Score	0.98	0.98	0.98
Accuracy (%)	98.50	98.50	98.67
Training time(s)	263.28	377.65	465.67
Prediction time(s)	37.06	41.43	41.24

Deep Learning Model	**N. of layer**	**N. of nodes / Dimension of hidden state**
MLP	5	32-16-16-8-8-1
	5	64-32-16-8-1
	4	64-32-16-1

TABLE VII. EXPERIMENTAL RESULTS OF DETECTING NETWORK STEGANOGRAPHY USING THE CNN MODEL

CNN	**1st**	**2nd**	**3rd**
Precision	0.97	0.98	0.98
Recall	0.99	0.99	0.99
F1- Score	0.98	0.98	0.99
Accuracy (%)	98.1	98.3	98.5
Training time(s)	1163	1129.6	2557.5
Prediction time(s)	22.8	19.67	21.5

Deep Learning Model	**N. of layer**	**N. of nodes / Dimension of hidden state**
CNN	2	32 - 32
	2	64 - 64
	3	64 – 64-64

TABLE VIII. EXPERIMENTAL RESULTS OF DETECTING NETWORK STEGANOGRAPHY USING THE LSTM MODEL

LSTM	**1st**	**2nd**	**3rd**
Precision	0.99	1.00	1.00
Recall	1.00	1.00	1.00
F1- Score	0.99	0.99	0.99
Accuracy (%)	99.99	100	100
Training time(s)	29439.51	29812.13	30810.10
Prediction time(s)	53.69	136.12	175.51

Deep Learning Model	**N. of layer**	**N. of nodes / Dimension of hidden state**
LSTM	1	64
	2	64 - 128
	3	64 – 128 - 64

2) Experimental results of scenario 2: For this scenario, this paper will compare and evaluate the effectiveness of this proposed method with two other algorithms, RF and SVM, which were proposed in previous research. Table IX describes the experimental results of these algorithms.

TABLE IX. EXPERIMENTAL RESULTS OF DETECTING NETWORK STEGANOGRAPHY WITH SOME OTHER APPROACHES

Algorithm	**RF [3]**	**SVM [4, 15]**	**LSTM [This proposal]**
Precision	0.98	0.95	1
Recall	0.95	0.989	1
F1- Score	0.96	0.96	0.99
Accuracy (%)	0.972	0.962	1
Training time(s)	777.33	1430.5	29812
Prediction time(s)	15.71	27.61	136.12

The results in Table IX show that the LSTM model proposed in this study gave 2% to 5% better performance than other algorithms in the same approach. It can be seen that the result of this study is superior to other related studies. The reason is that this study has proposed new meaningful features, and the deep learning classification algorithm also developed the ability to synthesize and analyze features.

V. CONCLUSION

In this paper, with the purpose to propose a new method to improve the efficiency of the network steganography detection process, the study has accomplished two tasks: i) proposing features and characteristics of abnormal packets; ii) using deep learning models for the abnormal packet classification task. Regarding the problem of analyzing abnormal features and characteristics, based on different components of the packet, this study has extracted many important and meaningful features. This is a breakthrough proposal in the task of analyzing and extracting features of packets. Regarding proposing the deep learning model, this study has succeeded in training the models to support the classification process. The experimental results in section IV.D have proved that this approach not only has scientific meaning, but also has many practical meanings, because this proposal has yielded better results than other models on all metrics. In the future, to improve the ability to detect abnormal packets, based on the research results in this paper, the authors think that it is possible to consider improving and supplementing two main issues: i) abnormal features of packets; ii) classification methods using combined deep learning networks or Attention networks.

REFERENCES

[1] Steffen Wendzel , Sebastian Zander , Bernhard Fechner , Christian Herdin, “Pattern-Based Survey and Categorization of Network Covert Channel Techniques,” ACM Computing Surveys, vol. 47(3), pp. 1–26. https://doi.org/10.1145/2684195.

[2] Smolarczyk M., Szczypiorski K., Pawluk J., “Multilayer Detection of Network Steganography,” Electronics, vol. 9 (12), pp. 2128, 2020. https://doi.org/10.3390/electronics9122128.

[3] Cho D.X, Thuong D.T.H, Dung N.K, “A Method of Detecting Storage Based Network Steganography Using Machine Learning,” Procedia Computer Science, vol. 154, pp. 543-548, 2019.

[4] M. Chourib, “Detecting Selected Network Covert Channels Using Machine Learning,” 2019 International Conference on High Performance Computing & Simulation (HPCS), pp. 582-588, 2019. https://doi.org/10.1109/HPCS48598.2019.9188115.

[5] James Collins, Sos Agaian, “Trends toward real-time network data steganography.” arXiv, arXiv:1604.02778.

[6] S. Sayadi, T. Abbesm, A. Bouhoula, "Detection of Covert Channels Over ICMP Protocol," 2017 IEEE/ACS 14th International Conference on Computer Systems and Applications (AICCSA), pp. 1247-1252, 2017. https://doi.org/10.1109/AICCSA.2017.60.

[7] Murdoch S.J., Lewis S, "Embedding Covert Channels into TCP/IP," In: Information Hiding (IH 2005), Springer, vol 3727, 2005. https://doi.org/10.1007/11558859_19.

[8] Lubacz J., Mazurczyk W., Szczypiorski K., "Principles and overview of network steganography," IEEE Commun. Mag., vol. 52, pp. 225–229, 2014.

[9] Fraczek, W.; Mazurczyk, W.; Szczypiorski, K. Hiding information in a Stream Control Transmission Protocol. Comput. Commun. 2012, 35, 159–169.

[10] Bieniasz J., Stepkowska M., Janicki A., Szczypiorski K., "Mobile agents for detecting network attacks using timing covert channels," J. Univ. Comput. Sci., pp. 1109–1130, 2019.

[11] Lu S., Chen Z., Fu G., Li Q., "A Novel Timing-based Network Covert Channel Detection Method," J. Phys. Conf. Ser., 1325, 012050, 2019.

[12] Szczypiorski K., Tyl T, "MoveSteg: A Method of Network Steganography Detection," Int. J. Electron. Telecommun., vol. 62, pp. 335–341, 2016.

[13] Mike Sieffert, Rodney Forbes, Charles Green, Leonard Popyack, Thomas Blake, "Assured Information Security: Stego Intrusion Detection System," The Digital Forensic Research Conference, 2004.

[14] Dittmann J, Hesse D, Hillert R, "Steganography and steganalysis in voice-over IP scenarios: operational aspects and first experiences with a new steganalysis tool set," In: Proc SPIE, Security, Steganography, and Watermarking of Multimedia Contents VII, vol 5681, pp. 607–618, 2005.

[15] Taeshik Sohn, JungTaek Seo, Jongsub Moon, "A study on the covert channel detection of TCP/IP header using support vector machine," In Proceedings of the 5th international conference of information and community security, pp. 313–324, 2003.

[16] Ms. Apurva, N. Mahajan, Prof. I. R. Shaikh, "Detect Covert Channels in TCP/IP Header using Naive Bayes," International Journal of Computer Science and Mobile Computing, vol 4, pp. 881-886, 2015.

[17] Daniel Svozil, Vladimir Kvasnicka, Jiří Pospíchal, "Introduction to multi-layer feed-forward neural networks," Chemometrics and Intelligent Laboratory Systems, vol. 39(1), pp. 43-62, 1997.

[18] Keiron O'Shea, Ryan Nash, "An Introduction to Convolutional Neural Networks." arXiv, arXiv:1511.08458.

[19] Sepp Hochreiter, Jürgen Schmidhuber, "Long Short-Term Memory," Neural Computation, vol. 9(8), pp. 1735 - 1780, 1997.

[20] Packet traces from WIDE backbone. https://mawi.wide.ad.jp/mawi/.

Is Face Recognition with Masks Possible?

Yaaseen Muhammad Saib[1], Sameerchand Pudaruth[2]
ICT Department, FoICDT
University of Mauritius
Reduit, Mauritius

***Abstract*—With the recent outbreak of the COVID-19 pandemic, wearing face masks has become extremely important to protect us, and to reduce the spread of the virus. This measure has made many existing face recognition systems ineffective as they were trained to work with unmasked faces. In this paper, several methods have been proposed for masked face recognition. Two pre-trained deep learning architectures (VGG16, and MobileNetV2) and the Histogram of Gradients (HOG) technique were used to extract the relevant features from face images of celebrities. A SoftMax layer and Support Vector Machines (SVM) were used for classification. Five scenarios were devised to assess the different models and approaches. With an accuracy of 96.8%, the best model was obtained with MobileNetV2 with a SoftMax layer on the dataset consisting of a mixture of masked and unmasked images. Three different types of masks were also used in this study. The mean accuracy was 91.35% when the same type of mask is used for training and testing. However, the accuracy dropped by an average of 5.6% when a different type of mask is used for training and testing. A contactless attendance system using the best masked face recognition model has also been implemented.**

Keywords—Face detection; face recognition; face mask; deep learning; VGG16; MobileNetV2; HOG

I. Introduction

There are several biometric systems available that can be used to secure access to data but in this work, the focus is on face recognition systems. Symanovich defined face recognition as the process of using the face of an individual from a photo or video to verify their identity [1]. Klosowski explained how this technology is being used around the world for many purposes such as unlocking mobile phones and laptops, monitoring people's physical access to restricted areas such as high-tech laboratories or even taking attendance in lectures [2]. Blokdyk explained the main processes in the face recognition system: face detection, feature extraction and classification [3]. The process of taking an image and locating the region that contains the face only is known as face detection. This region is then stored as a set of coordinates representing a bounding box around the detected faces. This is a very challenging task since faces in different images have many variations with regards to facial expressions, pose, degree of occlusions and lighting conditions [4].

The world is suffering from the outbreak of COVID-19, a contagious virus spreading from person to person [5]. People can become infected by getting into contact with an infected patient or by touching contaminated surfaces. Traditional systems such as passwords and fingerprints require contact with a surface and are therefore not secure when it comes to the transmission of the coronavirus while face recognition does not require any physical contact and can therefore be considered a safer approach in the current context. The United States Centers for Disease Control and Prevention has stated that the best way to prevent spreading of the virus is to avoid social contact and to wear a face mask [6]. However, face masks have made many existing face recognition systems fail. Face recognition systems usually use the geometry of the whole face including the nose and mouth, but this is now covered with a mask and therefore this makes the process more challenging. Furthermore, it is unsafe if the users have to remove their masks each time to verify their identity. Existing face recognition technologies have an accuracy rate of 97.7% for unmasked faces whereas for masked faces, the accuracy drops to 50% and sometimes the algorithm fails completely which makes the existing technology very inefficient. Furthermore, different mask shapes and colours also affect the accuracy of the face recognition systems [7].

The prime objective of this work is to develop a system to allow masked faces to be recognized with a high degree of accuracy. Several methods have been devised and tested to find the most suitable one for this problem. A classroom attendance system based on the best model was also implemented. This attendance system can also be used in different places. This paper proceeds as follows. Section 2 provides an overview of related works on masked face recognition. The methods, algorithms and datasets are described in Section 3. Implementation details are provided in Section 4. The results and their evaluation are discussed in Section 5. Section 6 concludes the paper.

II. Literature Review

In this section, we provide an overview of works that have been done on unmasked and masked face detection. Ejaz and Islam developed a masked face recognition system using transfer learning [8]. They used the AR and IIIT-Delhi Disguise Face Database datasets on which data augmentation was performed. MTCNN was used to detect and align masked faces. The face regions were cropped and resized to 160*160 images. Google FaceNet model combined with a deep CNN was used to extract features to be classified with SVM. For training and testing purposes, they used a ratio of 0.7 and 0.3 respectively. The system was tested with multiple scenarios and the average test accuracy obtained was 82.5%.

Wang et al. devised a method to improve the performance of face recognition systems by re-training them to recognize masked faces [9]. They proposed three datasets: MFDD, RMFRD and SMFRD. MFDD contains 25000 masked faces downloaded from the internet. RMFRD consists of 525 subjects with 5000 masked images and 90000 unmasked images. The last one was a software generated dataset. They developed a mask simulation software that adds virtual masks to faces. It performs face detection and alignment using the 68 face landmarks shape predictor. This allows retraining of existing face recognition systems to recognize masked images achieving an accuracy of 95%.

Hariri developed a system that performs masked face recognition whereby occluded regions of the face are discarded [10]. Firstly, face detection is performed on the image followed by face alignment. The image is then resized to 240*240 pixels. The image is cropped to keep the eye region. Features are then extracted using VGG16 and passed to the MLP classifier. RMFRD dataset was used to test the system. The highest accuracy obtained was 91.3%.

Anwar and Raychowdhury developed a system to convert existing face datasets to masked face datasets by using MaskTheFace, an open-source tool [11]. This dataset was then used to retrain the existing face recognition systems. Facenet face recognition was used to test the effectiveness of their masked dataset. After implementation, they reported an increase of approximately 38% in the true positive rate. The same was also achieved when tested using the real-world dataset MFR2. To train the program, they used a subset from the VGGFace2 dataset and applied the MaskTheFace tool to add virtual masks to the images. The accuracy achieved varied between 86% and 93%.

Li et al. implemented a system that focused mainly on the upper half face [12]. To extract features, ResNet50 was used to assign more expressive weights to the region of the eyes and lower weights to the occluded regions. Furthermore, they cropped the face at different levels to find the optimal cropping that would provide better results. They first discarded the bottom 50%, 30% and 10% of the image. They concluded that dropping the bottom 30% provided the best accuracy of 82.5%. Tests were performed on several datasets: AR Dataset, Extend Yela B Dataset and LFW dataset and a recognition rate between 81.4% and 92.6% was achieved.

Alyuz et al. devised a method to allow face recognition systems to work with partially occluded faces [13]. A technique called masked projection was used that analysed the face for occlusions and excluded them from the image. The occlusions are detected on a face by comparing them to a threshold value of distances on a non-occluded face. An alignment process is also done by comparing the centre of the image to one of an aligned face. Any necessary pose corrections are performed by the ICP algorithm. For training purposes, there is an independent matrix for each non-occluded region of the face that represents a subspace. The software is trained for each of the subspaces and when a face is to be recognized, the same process is applied and is then compared against corresponding subspaces of non-occluded regions. A recognition rate of 90% was achieved.

A system to recognize partially occluded faces with different poses was developed by Bagchi et al. [14]. Weighted median filters were applied to the dataset to remove noise. The faces are converted to data using the ICP algorithm. Occluded regions are detected from the face by comparison to a normalized face and information about those regions are discarded. The occluded regions detected are then restored to obtain a full face. This process is done by taking data from a normalized face and using the necessary regions. Lastly, feature extraction is performed, and the images are classified. The highest accuracy achieved was 91.3% .

Shepley developed a face recognition system using deep learning [15]. For face detection, DCNN was used which outperformed Haar Cascades and LBPs due to the large databases available. Face alignment was performed followed by extraction of features used to train a DCNN. To recognize unknown faces alignment and feature extraction is performed again. The encodings are then used for similarity comparison between the gallery faces and the face to be recognized. DeepFace, FaceNet and VGG-Face datasets were used to test the program and the recognition rate varied between 75% and 99%.

Parkhi et al. designed a system using deep learning to detect and recognize single or multiple faces from images and videos [16]. As for the model, CNN was used consisting of 11 blocks each having a linear operator and max pooling layers. The last 3 layers consisted of filters to match the size of the data. Data for 2500 male and 2500 female was collected to train and test the program. To evaluate the system, LFW and YTF datasets were used and a recognition rate of 96.0% was achieved.

Ge et al. developed a face recognition system to detect masked and occluded faces [17]. 35806 masked faces and 30811 unmasked images were downloaded from the internet. To detect faces, two pre-trained CNNs were combined for the extraction of features from input images which were then converted to a similarity-based descriptor by making use of the LLE algorithm and a dictionary that contains data of masked faces and synthesized normal faces. This allows facial landmarks from occluded regions to be recovered. An improvement of 15.6% was achieved on state-of-the-art at that time. Chowdary et al. developed a system that performs face mask detection to identify individuals who were not wearing a mask with a very high accuracy [18]. Image augmentation was performed on the SMFD dataset to increase the size of the training data. DNN was used for the image classification process. The Inception-v3 deep learning architecture was used to enhance the performance of the neural network.

Rekha and Chethan developed a face recognition system to take attendance automatically using live video [19]. Viola and Jones algorithm was used for face detection. The face region is cropped, and a correlation technique is used to recognize the face by comparing it to trained images. Finally, the attendance registry is updated for the recognized faces. Several tests were performed with different scenarios and the average face recognition rate achieved was 90%. Varadhrajan et al. also designed a face recognition system to take attendance [20]. The faces in the image are detected and cropped separately. For recognition, the eigenvalue method was used. An accuracy of 93% and 87% was achieved for face detection and recognition, respectively.

A large number of works on masked and unmasked face detection and recognition have been reviewed. While the majority of works has been done on unmasked faces, there are also a number of works that had been done on masked faces and on faces with different types of occlusion. There has also been a gradual and consistent increase in the accuracy of these systems.

III. Methods

The main objective of this study is to perform face recognition on masked faces. In this section, a solution has been proposed to overcome the main challenge of performing face recognition on masked faces. After acquiring the dataset, hybrid sampling is used to bring equality among all the classes in the dataset. Face detection is performed on the dataset to keep the face region only and discard any unnecessary information. This new dataset contains unmasked faces. Several versions of this dataset are created. Machine learning and deep learning algorithms are then used for extracting the relevant features before recognition is performed. The model is evaluated using standard performance measures. This set of steps is shown graphically in Fig. 1.

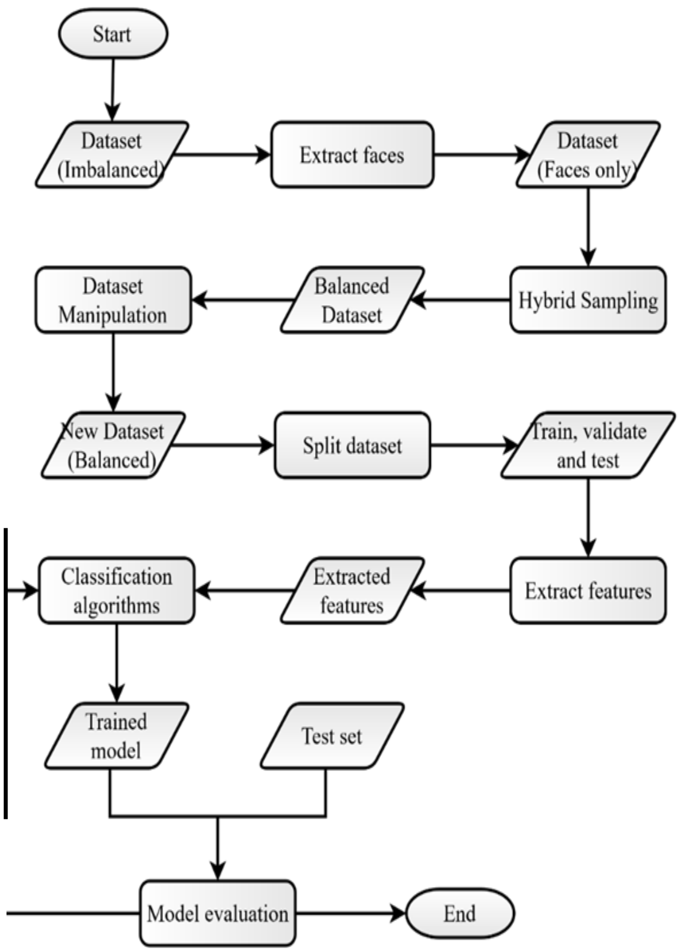

Fig. 1. Face Recognition with Masks.

Fig. 2. Sample Images from the Celebrity Dataset.

The Pins Face Recognition dataset was used in this study [21]. This dataset consists of 17,534 faces of 105 celebrities collected from Pinterest. The images are cropped to keep the face region only. There is an average of 150 unmasked images for each person. The images were taken in slightly different poses and different lighting conditions. This dataset was augmented with more celebrity images from the internet. Our final dataset consists of 170 persons with an average of 150 images per subject. Sample images from this unmasked celebrity dataset are shown in Fig. 2. For subjects with more than 150 images, undersampling was done by discarding the extra images and for subjects with less than 150 images, oversampling was done by adding slightly processed versions of existing images.

Four different variations of the original dataset were created. In the first one, a virtual mask is applied to all the images in the dataset using MaskTheFace [11], as shown in Fig. 3. In the second scenario as shown in Fig. 4, another variation of the dataset containing both masked and unmasked faces were created. In the third scenario, the images are cropped to keep the upper half of the face only i.e. the eyes and forehead regions only as shown in Fig. 5.

Fig. 3. Masked Faces.

Fig. 4. Mixture of Masked and Unmasked Faces.

Fig. 5. Eyes and Forehead Regions Only.

In the fourth scenario, firstly face detection is performed to keep the face region only. Then for each face image, the bottom half is replaced with the bottom half face of another person. The same bottom half face is used for all images as shown in Fig. 6.

Fig. 6. Face Bottom Half Face.

In this section, we have described all the different steps in the face recognition system. We also described the dataset that we have used and how it was manipulated to produce four other datasets. The next section will provide implementation details to shed more light on how the system was developed.

IV. Implementation

This section aims to describe the different components of the system, the hardware and software requirements and the additional tools and facilities that are required to find the best masked face recognition system and to implement the attendance system. The libraries and the tools used for the development of the system are shown in Table I.

TABLE I. TOOLS

Tools	**Description**
OpenCV	Open-source library for image processing and machine learning [22].
NumPy	Powerful library used to handle matrix and multi-dimensional arrays. Also used for scientific mathematical operations [23].
Tensorflow	Performs rapid numerical calculations and allows the development of machine learning and deep learning models [24].
Keras	API used for deep learning and multiple back end deep learning is also supported [25].
Scikit-Learn	Support for a variety of unsupervised and supervised learning algorithms [26].
Face_recognition	Performs face detection, encoding and recognition [27].
Pillow	Powerful library written in python offering a wide range of image processing techniques [28].
Notebook PC	Windows OS, Intel i7 CPU, 8G RAM, NVIDIA GeForce GTX850M
Google Colab Pro	Training, validating, and testing the deep learning models

Firstly, a pre-trained deep learning model such as VGG16 and MobileNetV2 is loaded using cv2.dnn.readNet (modelFile, configFile) from the OpenCV library. The image is loaded using cv2.imread and then passed through a blob that performs pre-processing and normalization tasks using cv2.dnn.blobFromImage (image, scalefactor = 1.0, size, mean) where *image* is the input image, *scalefactor* is the value through which the image will be scaled, *size* is the dimensions of the image and *mean* is the mean RGB value of the pixels. The blob is then passed through the network to obtain the relevant blobs using net.setInput(blob). For each blob, a probability is calculated and if it is less than a specified value, the blob is ignored. If the probability is higher or greater than the specified values, it is considered to form part of the face region. Face detection is performed on all images in the original dataset. Feature extraction is performed using HOG and deep learning (VGG16 and MobileNetV2) architectures. For classification, a SoftMax layer and SVM have been used. For SVM, a linear kernel was used. All the eight scenarios are shown in Table II.

TABLE II. SUMMARY OF MODELS

Feature Extraction	Trainable Layer	Classifier
MobileNetV2	True	SoftMax
	False	SoftMax
VGG16	True	SoftMax
	False	SoftMax
VGG16	True	SVM
	False	SVM
HOG	-	SoftMax
	-	SVM

The face recognition system has been used to implement an attendance system. This system consists of five modules: Register Student, Train Model, Modules, Take Attendance and Exit, as shown in Fig. 7.

Fig. 7. Homepage of the Attendance System.

The Student Register module is used to register a student either by uploading an image or capturing one image using a webcam, as shown in Fig. 8.

Fig. 8. Register Student Module.

The Train Model module is used to train the model based on the dataset, as shown in Fig. 9. The Modules management feature allows a user to add or delete courses for attendance purposes, as shown in Fig. 10. And the Take Attendance module is used to record attendance by uploading images or capturing one using a webcam, as shown in Fig. 11.

Fig. 9. Train Model Module.

Fig. 10. Module Management.

Fig. 11. Take Attendance Module.

V. RESULTS AND EVALUATION

In this section, all the models implemented are tested and evaluated with the five types of datasets to find the limitations of the models and ultimately determine the most suited model and type of dataset. The face recognition API is also tested and evaluated for applicable datasets. This section is divided into five parts, one for each type of dataset. The performance of each model is evaluated using classification accuracy. The dataset consists of 10,200 images, 170 subjects each having 60 images. Before training each model, the dataset was split into 2 sets, 0.9 for training and validation and 0.1 for testing. The training set was further split into two more sets, 0.8 for training and 0.2 for validation.

A. Unmasked Faces

After testing all the models with the unmasked dataset, the accuracy values obtained can be observed in Table III. The model performs better when features are extracted using transfer learning having trainable layers. The two best accuracy scores obtained were 93.82% and 95.59% with the VGG16 and MobileNetV2 models, respectively. Both the scores were obtained when the layers in the two models were set to trainable. For VGG16, there is a decrease of 3.06% in the accuracy score when the layers of the model were set to non-trainable. Furthermore, it can be observed that the accuracy decreases by 12.65% when HOG was used for feature extraction compared to the MobileNetV2 model. The SVM classifier results in a lower accuracy score compared to a SoftMax classification layer.

TABLE III. UNMASKED FACES

Model	Trainable Layer	Accuracy
VGG16 + SoftMax	True	0.9382
	False	0.9039
VGG16 + SVM	True	0.8833
	False	0.8833
MobileNetV2	True	0.9559
	False	0.7676
HOG + SoftMax	-	0.8294
HOG + SVM	-	0.8456

B. Masked Faces

All the accuracy scores obtained when testing all the models with the masked dataset are recorded in Table IV. The two best accuracy scores of 93.24% and 94.12% were obtained when VGG16 and MobileNetV2 were used. MobileNetV2 performed slightly better than VGG16. When HOG was used with and without SVM, an accuracy of 77.75% and 78.14% were obtained, respectively. When the SVM classifier was used to classify features obtained from the VGG16 model, the accuracy obtained was 85.25%, 7.99% less than the accuracy obtained when NN was used to classify the same features.

TABLE IV. MASKED FACES

Model	Trainable Layer	Accuracy
VGG16 + SoftMax	True	0.9324
	False	0.8480
VGG16 + SVM	True	0.8525
	False	0.8525
MobileNetV2	True	0.9412
	False	0.7745
HOG + SoftMax	-	0.7814
HOG + SVM	-	0.7775

C. Unmasked Faces and Masked Faces

The accuracy scores obtained with the different models when tested on the dataset consisting of an equal number of masked and unmasked faces are recorded in Table V. It can be observed that the two best accuracies obtained are 91.37% and 96.76% for the VGG16 and MobileNetV2 models, respectively. When the trainable layer in MobileNetV2 model is set to true, the accuracy drops to 79.51%. This is a significant difference of 17.25%. When the features were extracted using HOG and classified using SVM and SoftMax, the accuracies obtained are 90.83% and 85.10%, respectively. We observe that mixing the masked and unmasked dataset leads to a slightly higher accuracy than when using only the masked or unmasked datasets separately.

TABLE V. UNMASKED FACES AND MASKED FACES

Model	Trainable Layer	Accuracy
VGG16 + SoftMax	True	0.9137
	False	0.8814
VGG16 + SVM	True	0.9074
	False	0.9074
MobileNetV2	True	0.9676
	False	0.7951
HOG + SoftMax	-	0.8510
HOG + SVM	-	0.9083

D. Upper Half Face Only

The dataset consisting of the upper half face only is tested with all the models built and the accuracies are shown in Table VI. The two best accuracies achieved are 95.29% and 89.61% with the MobileNetV2 and VGG16 models, respectively. When the layers in the MobileNetV2 model were not set to trainable, the accuracy dropped to 75.49% which is 19.80% less than when the model has its layers set to trainable. The lowest accuracy of 71.08% was obtained when features were extracted using HOG and classified with a SoftMax layer. To conclude, the highest accuracy achieved with this dataset is 95.29% with the MobileNetV2 model whose layers were set to trainable during training. With this dataset, the model had fewer features to extract and classify compared to the unmasked dataset and the accuracy achieved is lower by only 0.30%.

TABLE VI. UPPER HALF FACE ONLY

Model	Trainable Layer	Accuracy
VGG16 + SoftMax	True	0.8961
	False	0.8206
VGG16 + SVM	True	0.8137
	False	0.8152
MobileNetV2	True	0.9529
	False	0.7549
HOG + SoftMax	-	0.7108
HOG + SVM	-	0.7456

E. Upper Half Face and Fake Lower Half Face

The dataset consisting of the original upper half face with a fake lower half face added to cover the masked region was tested with all the models and the accuracies achieved were recorded in Table VII. The best accuracy achieved is 93.33% and 93.04% with VGG16 and MobileNetV2, respectively, when both have their trainable layer set to true. For the VGG16 model, when the layers are set to non-trainable the accuracy dropped to 82.65, which is 10.68% less than when the trainable layer is set to true. When HOG is used, the accuracy dropped even further to 68.92%.

TABLE VII. UPPER HALF FACE AND FAKE LOWER HALF FACE

Model	Trainable Layer	Accuracy
VGG16 + SoftMax	True	0.9333
	False	0.8265
VGG16 + SVM	True	0.8294
	False	0.8294
MobileNetV2	True	0.9304
	False	0.6480
HOG + SoftMax	-	0.6892
HOG + SVM	-	0.7569

HOG feature extraction consistently resulted in lower performance and accuracy because it is a standard feature extractor, and it applies the same procedures to any given image. It determines the number of edges and their orientations region by region of the image and forms a collection of histograms of pixel orientations. When transfer learning such as VGG16 and MobileNetV2 are used, they extract features that are more specific and complex depending on the data on which they are training. Ultimately, they obtain the optimal feature space to achieve better performance [29].

A higher accuracy was achieved for all types of datasets when the layers of the pre-trained model were set to trainable since the features to be extracted from a face are more specific. Using pre-trained weights on face datasets does not give the best results since the model is trained on ImageNet dataset which is completely different and hence the need to retrain the model to optimize the feature space completely and adapt it specifically to this dataset. However, it takes more time to train the program since all the layers have to be updated but it achieves better performance [30].

In general, the SoftMax classifiers performed better than the SVM classifier. The average accuracy obtained with the SVM classifier was 83.23%. Luca explained why SoftMax generally performs better than SVM [31]. It can be observed that the MobileNetV2 model is robust as it consistently achieves the highest accuracy for each dataset except for the last dataset. The second most robust is the VGG16 model which has the second-best accuracy for each dataset. From Table V, it can be deduced that the dataset consisting of both masked and unmasked faces yielded the highest accuracy.

F. Mask Type

Different mask types are applied to faces in the testing set to observe whether the type of mask used affects the performance of the system. The different tests performed, and the results obtained are shown in Table VIII.

TABLE VIII. IMPACT OF MASK TYPE ON ACCURACY

Type of mask: Training	Type of mask: Testing	Accuracy
Surgical	Surgical	0.9412
	N95	0.8498
	Cloth	0.8756
N95	N95	0.9562
	Surgical	0.8726
	Cloth	0.9294
Cloth	Cloth	0.9531
	Surgical	0.9184
	N95	0.9194

G. Comparison with Existing Works

The dataset consisting of masked and unmasked faces yielded the highest accuracy. However, both the training and testing data had similar mask types. When tested with different types of masks, the accuracy decreases by approximately 5.6%. With an accuracy of 99.2% on unmasked faces, the Python face recognition API (face_recognition) outperforms all the implemented models. However, it cannot process half faces or masked faces, and therefore we added a fake bottom unmasked half face to the images. By doing this, we were able to make the API work and achieved an accuracy of 87.56% for masked face recognition.

Ejaz and Islam used CNN for feature extraction and SVM for feature classification and achieved an accuracy of 82.5% [8]. Wang et al. proposed a method whereby all existing face recognition systems have to be retrained by adding virtual masks to the faces in the existing datasets [9]. However, in this work, we saw that the accuracy drops by an average of 5.6% when face masks are used. Hariri developed a system whereby only the upper half face is used and the accuracy achieved was 91.3% using the RMFRD dataset which consists of 525 subjects [10]. Our proposed system was tested with the same type of dataset but consisting of only 170 subjects and the highest accuracy achieved was 95.3%. Hariri had used a VGG16 model while our best system requires MobileNetV2 [10]. The system developed by Anwar and Raychowdhury was tested using a dataset containing 42 images per person while our model was tested with 60 images per person [11]. They used the Inception-ResNet v1 architecture. The system was evaluated only on a dataset of masked images. This limits the system to perform well only with masked faces and is less effective with unmasked images. Our system performs equally well on both masked and unmasked faces.

VI. Conclusion

The COVID-19 pandemic has imposed the wearing of face masks in public places as well as in workplaces. This has created some difficulties for systems that were not trained to handle masked faces. Moreover, the wide varieties of face masks that are available make the face detection and recognition even more difficult. The objective of this work was to find out whether it is possible to recognise masked faces with a high degree of accuracy. Thus, five different variations of a celebrity dataset were created. Several feature extraction methods such as HOG and pre-trained deep learning models were used. The final classifications were made using a SoftMax function and SVM. The dataset consisting of the upper half face only may be deemed to be the more suitable one for practical applications since it has a reasonably high accuracy of 95.29% and it recognizes both masked and unmasked faces. Moreover, the type of masks used does not affect this system since the bottom half of the face is not taken into consideration. This system was further used to implement an attendance system. This face recognition system can be enhanced so that it can distinguish between real and fake faces in real-time. The attendance system can also be further developed so that it generates attendance reports automatically and send them to the required personnel via an email messaging system.

References

[1] Symanovich, S. (2019, February 8). How does facial recognition work? Retrieved May 28, 2021, from Norton: https://us.norton.com/internetsecurity-iot-how-facial-recognition-software-works.html.

[2] Klosowski, T. (2020, July 15). Facial Recognition Is Everywhere. Here's What We Can Do About It. Retrieved May 28, 2021, from New York Times: https://www.nytimes.com/wirecutter/blog/how-facial-recognition-works/.

[3] Blokdyk, G. (2018). Facial Recognition A Complete Guide. 5STARCooks.

[4] Dubey A. K. and Jain, V. (2019). A review of face recognition methods using deep learning network. Journal of Information and Optimization Sciences, vol. 40, pp. 547-558. https://doi.org/10.1080/02522667.2019.1582875.

[5] Sauer, L. (2021, May 19). What Is Coronavirus? Retrieved May 28, 2021, from John Hopkins Medicine: https://www.hopkinsmedicine.org/health/conditions-and-diseases/coronavirus.

[6] CDC. (2021, March 8). How to Protect Yourself & Others. Retrieved May 28, 2021, from Centers for Disease Control and prevention: https://www.cdc.gov/coronavirus/2019-ncov/prevent-getting-sick/prevention.html.

[7] NIST. (2020, July 27). NIST Launches Studies into Masks' Effect on Face Recognition Software. Retrieved October 15, 2020, from NIST: https://www.nist.gov/news-events/news/2020/07/nist-launches-studies-masks-effect-face-recognition-software.

[8] Ejaz, S., & Islam, R. (2019). Masked Face Recognition Using Convolutional Neural Network. In: Proceedings of the International Conference on Sustainable Technologies for Industry 4.0 (STI), 24-25 December, Dhaka, Bangladesh. https://doi.org/10.1109/STI47673.2019.9068044.

[9] Wang, Z. et al. (2020). Masked Face Recognition Dataset and Application. https://arxiv.org/abs/2003.09093.

[10] Hariri, W. (2021). Efficient Masked Face Recognition Method during the COVID-19 Pandemic. https://arxiv.org/abs/2105.03026.

[11] Anwar, A., & Raychowdhury, A. (2020). Masked Face Recognition for Secure Authentication. https://arxiv.org/abs/2008.11104.

[12] Li, Y., Guo, K., Lu, Y., & Liu, L. (2021). Cropping and attention based approach for masked face recognition. Applied Intelligence, vol. 51, pp. 3012-3025. https://doi.org/10.1007/s10489-020-02100-9.

[13] Alyuz, N., Gokberk, B., & Akarun, L. (2013). 3-D Face Recognition Under Occlusion Using Masked Projection. IEEE Transactions on Information Forensics and Security, vol. 8, no. 5, pp. 789-802.

[14] Bagchi, P., Bhattacharjee, D., & Nasipuri, M. (2014). Robust 3D face recognition in presence of pose and partial occlusions or missing parts. International Journal in Foundations of Computer Science & Technology, vol. 4, no. 4, pp. 21-35.

[15] Shepley, A. J. (2019). Deep Learning for Face Recognition: A Critical Analysis. https://arxiv.org/abs/1907.12739.

[16] Parkhi, O. M., Vedaldi, A., & Zisserman, A. (2015). Deep Face Recognition. In Xianghua Xie, Mark W. Jones, and Gary K. L. Tam, editors, Proceedings of the British Machine Vision Conference (BMVC), pp. 41.1-41.12. BMVA Press, September 2015.

[17] Ge, S., Li, J., Ye, Q., & Luo, Z. (2017). Detecting Masked Faces in the Wild with LLE-CNNs. In: Proceedings of the Conference on Computer Vision and Pattern Recognition (CVPR), 21-26 July, Honolulu, USA.

[18] Chowdary, J., Punn, N. S., Sonbhadra, S. K., & Agarwal, S. (2020). Face Mask Detection using Transfer Learning of InceptionV3. In: Bellatreche L., Goyal V., Fujita H., Mondal A., Reddy P.K. (eds) Big Data Analytics. BDA 2020. Lecture Notes in Computer Science, vol 12581. Springer, Cham. https://doi.org/10.1007/978-3-030-66665-1_6.

[19] Rekha, A. L., & Chethan, H. K. (2014). Automated attendance system using face recognition through video surveillance. International Journal For Technological Research In Engineering, vol. 1, no. 11, pp. 1327-1330.

[20] Varadharajan, E., Dharani, R., Jeevitha, S., Kavinmathi, B., & Hemalatha, S. (2016). Automatic Attendance management system using face detection. In: Proceedings of the Online International Conference on Green Engineering and Technologies (IC-GET), 19 November, Coimbatore, India. https://doi.org/10.1109/GET.2016.7916753.

[21] Burak. (2020). Pins Face Recognition. Retrieved October 30, 2020, from Kaggle: https://www.kaggle.com/hereisburak/pins-face-recognition.

[22] OpenCV. (2021). Open Source Computer Vision. Retrieved June 24, 2021, from OpenCV: https://docs.opencv.org/3.4/.

[23] NumPy. (2021, June 22). NumPy v1.21 Manual. Retrieved June 24, 2021, from NumPy: https://numpy.org/doc/stable/.

[24] TensorFlow. (2021). API DOcumentation. Retrieved June 24, 2021, from TensorFlow: https://www.tensorflow.org/api_docs.

[25] Keras. (2020). About Keras. Retrieved June 24, 2021, from Keras: https://keras.io/about/.

[26] Scikit-learn. (2021). Machine Learning in Python. Retrieved June 24, 2021, from Scikit learn: https://scikit-learn.org/stable/.

[27] Face_recognition. (2020, February 20). face-recognition 1.3.0. Retrieved June 24, 2021, from PyPi: https://pypi.org/project/face-recognition/.

[28] Pillow. (2021). Pillow. Retrieved June 24, 2021, from Pillow: https://pillow.readthedocs.io/en/stable/.

[29] Kibria, S. B., & Hasan, M. S. (2017). An Analysis of Feature Extraction and Classification Algorithms for Dangerous Object Detection. In: Proceedings of the 2nd International Conference on Electrical & Electronic Engineering (ICEEE), 27-29 December, Rajshahi, Bangladesh. https://doi.org/10.1109/CEEE.2017.8412846.

[30] Sagar, R. (2019, May 25). What Does Freezing A Layer Mean And How Does It Help In Fine Tuning Neural Networks. Retrieved May 23, 2021, from AnalyticsIndiaMag: https://analyticsindiamag.com/what-does-freezing-a-layer-mean-and-how-does-it-help-in-fine-tuning-neural-networks/.

[31] Luca, G. D. (2020, September 9). SVM vs Neural Network. Retrieved May 23, 2021 from Baeldung: https://www.baeldung.com/cs/svm-vs-neural-network.

Requirements Engineering: A State of Practice in Gulf Cooperation Countries

Dr Asaad Alzayed[1], Dr. Abdulwahed Khalfan[2]
Computer Science Department, Public Authority for Applied Education and Training (PAAET), Kuwait

Abstract—Requirement Engineering (RE) is one of the crucial elements for successful software development. Nevertheless, in terms of research discussing the failure or success of various products, little has been undertaken to examine this area as it pertains to the Gulf Cooperation Council (GCC) nations, i.e. Saudi Arabia (KSA), Kuwait, United Arab Emirates (UAE), Bahrain, Qatar, and Oman. The aim of this research is to present an analysis of the current ways in which software is developed in these nations. The researchers undertook a survey of practitioners in software development, asking questions regarding their recent work. The survey was based on an extensive survey that was adapted in view of contemporary software development practice. The research reports on requirement practices and how they relate to project sponsors/customers/users and project management. The respondents came from GCC nation companies, most of whom worked on developing software in-house. The outcomes demonstrate that the majority of IT companies in these nations do not employ the optimal methodologies for requirement engineering processes, using their own. In addition, project managers are often lacking in complete authority. Making comparisons between our findings and past research, requirements engineering practices is still inadequate in these nations. Thus the research results are particularly useful as the data is derived from countries where published research about software development practices is scant.

Keywords—Requirements engineering; project success; software development; requirements engineering practices; GCC countries

I. Introduction

Although a considerable amount of research has been undertaken with the aim of designing novel improved solutions to address software development (SD) difficulties [1-3], it is crucial to develop an understanding of contemporary software development methods and which of them offers optimal outcomes. Past research has demonstrated that accuracy and completeness in the requirements engineering (RE) practices of developers play a significant part in the success or failure [4-6].

Hall et al. [7] have stated that a significant number of difficulties with SD are a result of poor RE. Having to amend requirements in the final stages of a project is extremely expensive [8, 9]. Much research [10-12] has found that successful IT projects are comparatively rare, with approximately 20% being complete failures, with 50% either being delivered late, over budget, and/or without all requirements fulfilled. 44% of projects that fail do so as a result of inadequate RE. From the 1990s onwards, researchers have proposed that RE is a crucial and major reason for project failure [13, 14]. The high failure rate of software development projects and the way in which this correlates with RE has led to a greater focus on RE, both by practitioners and management. As a result, novel methodologies for both RE and SD have been developed that use incremental systems for dealing with requirements (e.g., continuous deployment/integration and agile processes).

Verner and Evanco undertook a survey of software developers in Chile, Australia, the USA, and Vietnam [15]. Their results found a clear correlation between good RE and successful projects. Although both academics and practitioners have noted globally that there are difficulties and issues with RE in many software development projects [6, 11, 14], there has been little focus on what difficulties and problems there are in this area in GCC nations. To develop an understanding of how software is developed in Kuwait and other GCC countries, authors employed an existing questionnaire [3] for collecting data from companies in this region regarding their recent software projects. Thus the aim of this research is to make a comparison of its outcomes with the outcomes found by Verner et al. [6, 15], in the research previously mentioned. Authors wish to reveal which RE practices lead on to successful projects in this region. The structure of the research paper takes the following pattern: Section 2 offers background information and a review of the literature, Section 3 details the research methodology, Section 4 details and discusses the findings, with Section 5 offering a conclusion.

II. Background and Literature Review

RE practices have been shown to be a crucial element of successful projects [4, 5, 16]. Research into software engineering has demonstrated that both clients and organizations involved in software development are lacking in knowledge about RE practices [17-20].

Successful software projects almost always have completeness and accuracy in RE [21]. Managing requirements is one of the initial phases of any SD project and can make a contribution to every phase of the project if the correct development methodologies are employed [22]. If organizations use RE effectively, they will generally accrue numerous benefits across the project's life-cycle. To improve the RE practices Pandey et al. [23] proposed a method for requirements gathering and management. This method is divided into four key phases: "requirements elicitation and development," "requirements documentation," "validation and verification of requirements", and "requirements management and planning". The method provides a high-level framework for the requirements engineering process. Additionally, good practice with RE can cut the economic costs of SD and produces better quality results [24, 25]. Whilst the demands of gathering requirements appear basic, this is frequently neglected despite its crucial influence on all SD projects [26]. RE are crucial in the definition, estimation, and management of all software projects [27]. Whether the methodology used for a requirements process is traditional or agile, there is still the same demand for good quality RE [28]. If every facet of quality RE is in place, including ownership, support from management, clear requirements, and stakeholder involvement, a project will begin with higher chances of succeeding [29]. However, if requirements are incomplete or change, if management is not supportive, and if stakeholders are not involved, costs will most likely increase and the project risks failing [29]. Research into 12 UK companies revealed that problems with RE represented 48% of all problems in SD [7]. Because of this, the industry has been seeking to develop reliable, effective RE frameworks. From the 1990s onwards, numerous methodologies have been created to attempt to address this need [30]. Nevertheless, no complete solution for the problems has yet been found. Siahaan and Irhammi demonstrated that 43% of failed projects were caused by the use of unsuitable RE [31]. It has been suggested that one way of avoiding failed projects is to switch from the traditional waterfall methodology to novel methodologies, e.g., agile development [32]. When employing agile methodologies, it is possible to split up the requirements of a project into smaller sections and address them in a gradual manner. This method removes the need to define all of the system requirements initially, and makes it easier to correct errors as they arise. Nevertheless, if a developer doesn't/can't have enough dialogue with the client to enable them to correctly define the requirements of the system, agile methods will often lead to a project stalling [33].

Up to now the position in GCC nations has not been sufficiently researched, with just a few works looking at RE in one country in the GCC, e.g. Kuwait or Saudi Arabia [34-36]. There has been no research examining RE practices across the GCC nations. For this reason, Authors undertook to survey software development companies in this region in order to gain an overview of the difficulties with RE and SD currently being experienced. The survey employed for this research is an adaptation of the one used by Verner and Evanco [3].

III. Methodology

The questionnaire, adapted from that created by Verner and Evanco [3], reveals certain issues with software engineering in relation to development teams, development processes, customers and users, and management. In the revised questionnaire, a four point Likert type scale (not at all/partially/somewhat/yes) was employed for the majority of questions. Certain questions were changed from a five point scale to a four point one, e.g. the (RE2) question. Employing a four point scale ensured that respondents could not give neutral answers. In addition, a new section dealing to global SD projects is being included, as this is becoming an important element of SD [16]. As there were four possible answers to each question, two positive and two negative, these were occasionally consolidated in reporting the results.

Responses to the questions were harvested using in-person interviews, phone calls, and email. Respondents were asked to answer the questions in relation to an SD project they had worked on recently. At the end of the questionnaire, respondents were asked whether they regarded the SD project to which they were referring to have been a success or failure (see Table I). In addition, respondents were asked whether a project was generally regarded as a success by their organization, giving us two perspectives on project success, that of the developer and that of the organization for which they worked. A predefined definition of success was not provided, instead allowing respondents to define it in their own words. This accord with contemporary practice, e.g., Osei-Kyei & Albert [37] suggested that success is perceived differently by different stakeholders, and that those undertaking research should not impose a general definition of what makes a successful project. The survey was sent to a number of SD companies across the GCC region, asking respondents to answer the questions with reference to a recent IT project on which they had worked.

IV. Result and Discussion

163 individuals responded to research questionnaire, 36 from UAE, 36 from Qatar, 6 from Oman, 12 from Kuwait, 36 from Saudi Arabia, and 37 from Bahrain; all of these individuals had worked on different projects. In terms of demographics, 5 respondents were MIS managers, 20 were customers, 28 were users, 37 were project managers, 47 were developers, and 26 were in some other form of management; the respondents were involved with developing software to be deployed inside their organizations. The organizations represented included banks, other financial institutions, and educational institutions situated in GCC nations. Authors feel that sampling over 163 separate projects is a suitable cohort for search into software engineering. 154 projects were seen as having been a success and 8 as failures (4 in Qatar and 4 in Saudi Arabia). 17% of the projects were substantial maintenance/enhancement projects (15% success), and 72% were development projects (69% success). Bahrain had the highest proportion of successful projects. It may be that either the organizations with which the respondents are involved enjoyed a high level of successful projects, or possibly the respondents found it preferable to refer to a successful project when responding. For the purposes of reporting and analysis, the four point Likert scale was sometimes consolidated to only two points of success or failure.

The questionnaire was divided into subsections which covered the whole SD process. This paper considers questions around RE/requirements management, as shown in Table I. The table illustrates the percentage of survey questions that elicited a "Yes" response.

Table II illustrates the significant correlations of questions with project success (>0.05) and how responses to selected questions were associated. The questions in these tables are divided into the following categories: RE (questions about requirements), PM (questions about how the development process was managed), UC (questions related to project sponsors, clients, and users). Requirements Questions.

On the basis of previous research [38], it was predicted that for all projects that the respondents regarded as successful would begin with full and accurate requirements that had been gathered using a specific methodology, having a clear definition of scope that was not changed across the course of the project. Bearing in mind such elements, the following questions were asked in relation to requirements.

A. Were Requirements Gathered Using a Particular Method? (RE1)

When organizations define requirements when commencing a project, it is expected that they would employ an RE methodology [39]. Nevertheless, the outcomes of the chi-square test did not have significance (p = 0.546), which suggests that there was no significant correlation between using a specific methodology for harvesting requirements and project success, either from the perspective of the respondents or their organizations. No successful project from Bahrain employed a specific methodology for harvesting requirements. 125 out of 163 (75%) respondents used no specific methodology, with just 38 projects doing so. Seven projects that did not use a specific methodology for harvesting requirements did not experience success as they were unaware of what methodology they should employ. This demonstrates that a number of organizations do not have experience with methodologies for harvesting requirements. In the successful projects that did employ a specific methodology, nine of them used meetings, six of them used interviews, two of them used workshops, two of them used brainstorming meetings, one of them used previous system analysis, four of them employed email, telephone calls, and online research, two of them used an agile methodology, two of them used ASAP, and one of them used a questionnaire. The only projects which had complete and accurate harvesting for requirements and where sufficient time was set aside to complete the harvesting were ones in which project managers had employed phone calls, online discussion, emails, interviews, and stakeholder meetings. Only one project employed a specific methodology: this was the method of their own devising and the project ended in failure. Closer investigation of this failed project shows that it failed due to the requirements methodology being changed across the life-cycle of the project, not enough time being set a time to harvest requirements, and developers being unaware of how the new methodology should be used.

TABLE I. PERCENTAGE OF "YES" RESPONSES TO QUESTIONS

Factor	Item	Failure, "yes"1		Success, "yes"2		Total, "yes"3	
		Count	Row N %	Count	Row N %	Count	Row N %
UC1	Were the other stakeholders committed and involved?	68	41.7%	95	58.3%	80	56.3%
UC2	Did senior management affect the project in any other way?	122	74.8%	41	25.2%	31	21.8%
UC3	What level of confidence did the customer/user have in the project manager/team members?	18	11.0%	145	89.0%	134	94.4%
UC4	Did you run into problems due to the large number of customers/users involved?	98	60.1%	65	39.9%	54	38.0%
RE1	Were requirements gathered by using a particular method?	125	76.7%	38	23.3%	35	24.6%
RE2	Were the requirements complete and accurate?	17	10.4%	146	89.6%	127	89.4%
RE3	Were the requirements completed adequately?	114	69.9%	49	30.1%	31	21.8%
RE4	Was the scope of the project well defined?	131	80.4%	32	19.6%	23	16.2%
RE5	Did the scope change during the project?	135	82.8%	28	17.2%	15	10.6%
RR6	Did the customers/users make adequate time available for requirements gathering?	33	20.2%	130	79.8%	110	77.5%
RE7	Did the size of the project negatively affect requirements elicitation?	112	68.7%	51	31.3%	41	28.9%
PM1	Was the delivery date decision made with appropriate requirements information?	39	23.9%	124	76.1%	119	83.8%
PM2	Was the project manager experienced in the application area?	19	14.2%	115	85.8%	105	87.5%
PM3	Was a defined development methodology (your own or another) used?	99	60.7%	64	39.3%	55	38.7%
PM4	Was the development methodology appropriate for the project?	108	66.3%	55	33.7%	54	38.0%

[1] This column represents the percentage of 'yes' answers to questions for failed projects.
[2] This column represents the percentage of 'yes' answers to questions for successful projects.
[3] This column represents the percentage of 'yes' answers to questions for all projects.

TABLE II. CORRELATION OF QUESTIONS TO PROJECT SUCCESS AND OTHER QUESTIONS

ID	Questions	The direction of Success Relationship	Significant Correlation with Project Success	Correlation with other Questions
UC1	Were the other stakeholders committed and involved?	+	0.003	UC2, UC4, RE1, RE3, RE5, RE7, PM3 & PM4
UC2	Did senior management affect the project in any other way?	+	0.014	UC1, UC4, RE3, RE5, RE7, PM1 (-), PM3 & PM4
UC3	What level of confidence did the customer/user have in the project manager/team members?	-	0.012	RE3, RE5 & RE6 (+)
UC4	Did you run into problems due to the large number of customers/users involved?	+	0.014	UC1, UC2, RE3 & RE5
RE1	Were requirements gathered by using a particular method?	+	0.017	UC1, RE2, RE5, PM1, PM3 & PM4
RE2	Were the requirements complete and accurate?	-	0.03	RE1 (+), RE3, RE6 & RE7
RE3	Were the requirements completed adequately?	+	0.0012	UC1, UC2, UC3 (-), UC4, RE2 (-), RE4, RE5, RE7 & PM1 (-)
RE4	Was the scope of the project well defined?	+	0.001	RE3 & RE5
RE5	Did the scope change during the project?	+	0.01	UC1, UC2, UC3 (-), UC4, RE1, RE3, RE4, RE7 & PM1 (-)
RE6	Did the customers/users make adequate time available for requirements gathering?	+	0.037	UC3 & RE2
RE7	Did the size of project negatively affect requirements elicitation?	+	0.004	UC1, UC2, RE2 (-), RE3, RE5 & PM3
PM1	Was the delivery date decision made with appropriate requirements information?	-	0.011	UC2, RE1 (+), RE3, RE5
PM2	Was the project manager experienced in the application area?	no Direction	not Significant	
PM3	Was a defined development methodology (your own or another) used?	+	0.001	UC1, UC2, RE1, RE7 & PM4
PM4	Was the development methodology appropriate for the project?	+	0.005	UC1, UC2, RE1, PM1 & PM3

The results of this research are comparable to those of Verner et al. [6] in that only four projects employing UML to document requirements experienced success. Verner and Evanco found that developers were either not familiar with UML or were using non-requirement notation to record requirements [3]. Additionally, there was a significant correlation between successful projects and the use of defined SD methodologies (PM3) and methodologies that were tailored to the specific project (PM4) identified in Verner and Evanco's research [15]. RE1 is the most effective predictor of successful companies in Saudi Arabia (KSA) when using univariate analysis variance. Only 2.6% of projects employed specific methodologies, and the chi-square outcomes for this result do not have a significant correlation with project success, either from the organizational or respondent perspective. This result is explainable by the fact that so few projects employed requirements methodologies, and the findings do not preclude the suggestion that requirement methodologies could be effective if they had been employed by more projects in the sample. Additionally, It was discovered that employing defined methodologies (PM3) did not have significance with the chi-square testing in terms of completeness and accuracy of requirements (RE2) when the results was divided into successful and unsuccessful projects. However, in terms of organizational management perspectives, there is significance to the chi-square test outcomes: organizational management was more likely to view a project as having been a success when specific methodologies were employed to eliciting requirements.

B. *Were the Requirements Complete and Accurate at the Start of the Project? (RE2)*

There was no surprise that the outcomes of the chi-square test of this variable against project success had significance ($p < 0.001$), which suggests that when there was completeness and accuracy regarding requirements, a project was more likely to experience success. Nevertheless, 31 projects were successful when they had only partially complete requirements, and just 8 failed. The outcomes demonstrated that 33% of the projects did not adequately harvest requirements, 50% only harvested then partially, and in all cases users and/or clients did not set aside sufficient time for the process. 20% of such projects ended in failure, and this creates significance with the chi-square test, which suggests that a project is more likely to fail if requirement harvesting is only partially complete as compared to a project where no requirement harvesting occurs. This is due to the fact that partially completed harvesting adds no new functions to the existing product, so if clients take a decision to halt development in particular areas or a complete product, or partially completed harvesting has been wasted [40]. Results of this research show that if requirements are only partially harvested, there are generally very low levels of user involvement. Additionally, it was discovered that the majority of projects with incomplete requirements used in-house approaches or none at all.

By regarding projects that were only part successful as being failures, it was estimated that 39% (15/38) of projects that only partially completed their requirement were failures. There is also significance in the organizational perspective for this variable.

C. *If Requirements were not Complete and Accurate at the Start, were they Completed Adequately? (RE3)*

The outcome of the chi-square test for this question had significance ($p < 0.001$), which suggests that there is a correlation between successful projects and completing requirement harvesting. The answer to this question was given as yes for just 25% of failed projects, whilst it was given as yes for 60% of successful projects, with a significance of 0.007. This element also had significance (0.002) when a four-point scale was employed regarding project size which showed that the majority of the large and small scale projects enjoyed success. This analysis also had significance from an organizational perspective. In 10 projects, the project was regarded as a success even though requirements had not been adequately completed. Examining these 10 projects more closely, it was shown that in the majority of the projects the project manager had complete or almost complete control and authority; only a small number of projects succeeded if the project manager possessed little authority. In addition, when delivery date decisions were taken using suitable requirements information (PM1), there was accurate estimation of the project length and requirements and sufficient staff were imported as required. Project managers played a significant part in respondents regarding a project as being a success, because project managers required clear vision for the project, understanding of user requirements, the ability to communicate well with staff, and the ability to create a working environment that suited developers. This concurs with the findings of Verner and Cerpa [15], who demonstrated that a project had a good chance of success if requirements had been completed at some point. In six of eight projects there was inadequate completion of requirements; in 33 of 52 projects (63%) the project enjoyed success even with partial or no completion of requirements. Chi-square testing demonstrates that on the whole this variable has no significance for the success of a project. RE3 had significance when the true success of a project was closely examined using a four point scale for level of success rather than conflating the scale into just successful or unsuccessful. Employing a univariate analysis of variance, the regression effect (B = 13.032; Sig = 0.012) demonstrated that RE3 is the most effective means of predicting project success.

D. *Was the Scope of the Project Well Defined? (RE4)*

Being well defined in scope means that a team knew what was required to complete a project and what the aims of the project [41]. Research findings with a chi-square test demonstrated significance ($p = 0.032$), which suggests a correlation between defined scope and project success (RE4). Haass and Neda found that a failure to define scope in the beginning phases of a project generally introduces problems in the process of implementing the project later [42]. Research findings demonstrate that around 50% of projects did not have a clearly defined scope for their project, although this is almost the same level as for successful projects. Nevertheless, in the majority of projects the project scope changed, although from the organizational perspective it was felt that two thirds of projects had no change in scope and that there was no significance from this perspective. It was found that 17/50 projects which had changing scope were regarded as failures, and this also did not have significance from the organizational perspective. Thus there was no correlation between a project failing and its scope being changed in the course of the project. This finding accords with those of Verner and Evanco [3] and Suchan [43]; these authors stated that projects will inevitably change and there must be a capacity for coping with this if it happens. Fabiola et al., [44] note that there may be a number of reasons why project scope could need changing, which includes internal influences as stakeholders get a better idea of the problem and external influences, e.g., changes in the market or government regulations. Nevertheless, research findings do not concur with those of Boehm [45] who argues that when a project changes scope this has a correlation with projects failing.

E. *Did the Customer/Users Make Adequate Time Available for Requirements Gathering? (RE6)*

The outcome for the chi-square testing of this variable against project success had significance ($p = 0.002$), which suggests that projects are more likely to succeed when customers/users make sufficient time for developers to gather requirements. Only 25% of failing projects returned a yes answer for this variable; where 60% of successful projects returned a yes answer with the chi-square having significance at 0.007. There was also significance (0.002) when a four-point scale was used in relation to project size; there is also significance from an organizational perspective. Organizations appear to be acutely aware of this characteristic. Research findings demonstrated that the correlations between RE6, UC3, and RE2 suggests that when customers/users have high levels of confidence in their project manager (UC3) they provide sufficient time for gathering of requirements (RE6) and this leads to adequate completion of requirement gathering (RE3).

F. *Did the Size of the Project Negatively Affect Requirements Elicitation? (RE7)*

The outcomes of the chi-square testing for this variable did not have significance in terms of project success ($p = 0.128$), which suggests that project success and project size are not correlated. The majority (74.5%) of successful projects was not influenced by the size of the project, and this was also true for 59% of somewhat successful projects and 54% of partially successful projects, while 50% of unsuccessful projects were influenced by size.

These outcomes suggest that as the size of the project increases there is a greater likelihood that this will influence the ability to elicit requirements, but the chi-square test does not show a significant correlation with project success. This element also does not have significance when size is viewed from the organizational perspective. These findings differ from those of Suchan, [43] who suggested that project size can have a negative correlation with requirement elicitation and can be the cause of a lack of clarity, instability, and incomplete requirements. Nevertheless, a comparison of research findings with those of other practitioners shows similarities with the findings of Verner and Evanco [3], who felt no negative correlation between project size and requirement gathering. It may be the case that developers, users, and managers have a greater awareness that problems may come up with larger projects and so are more prepared to address them.

G. Sponsor, Customer and User Questions

Researcher findings demonstrate a negative correlation for project success and UC3/RE6. This shows that projects fail even if users set aside sufficient time for collecting requirement (RE6) but did not have confidence with their project manager (UC3). Research has demonstrated that customer/user involvement across the development of a project (from collecting requirements to final acceptance) is crucial if a project is to succeed. The research of Glass [46] and Zhiwei [47] accords with this research result, agreeing that it is crucial for users to be involved in the requirement gathering process (RE6). The correlations of stakeholder commitment/involvement across the project (UC1) as well as adequate completion of requirements by developers (RE3) had a significant correlation with the influence of senior management right across the project. Thus support from management must be available at every phase of the project. These findings accord with those of Kitapici and Boehm [26], who found that the absence of support from management has now become the biggest reason for a project failing, replacing user involvement which was previously the primary cause. Employing univariate analysis of variance, UC for well shown to be the most effective predictor for questions for users, customers, and sponsors in successful projects in in UAE specifically and GCC region in general.

H. Project Manager (PM) Questions

Research findings demonstrate that the experience level of the project manager (PM2) did not have a significant correlation with the success of a project. This accords with the findings of Verner and Evanco [3] that indicated that project manager success is more likely to stem from their skills as a manager and interpersonal abilities, not technical knowledge [48,49]. The findings of this research additionally demonstrate that projects that have continual senior management support alongside involvement and commitment from stakeholders, as well as projects in which the project manager has selected a suitable means of collecting requirements, have the greatest likelihood of success. This accord with the research of Young and Jordan [50], which demonstrated that senior management support is the primary necessity for a successful project. Nevertheless, it is of greater importance that a project manager should be an effective communicator and have a healthy relationship with stakeholders than that they should have technical knowledge. This agrees with the research of Siahaan and Irhammi [31] and De Araujo and Pedron [51]. Projects for which the delivery date is created on the basis of suitable requirements information (PM1) are positively correlated with collecting requirements using a specific methodology (RE1). Nevertheless, there is a negative correlation between PM1 and successful projects. When the research findings are examined more thoroughly, it becomes clear that project managers frequently have no involvement over delivery date decisions and are not consulted in any meaningful way during the planning process. Research findings suggest that successful projects are those in which the project manager is involved with planning from the outset. Using univariate analysis variance, it was discovered that PM1 is the best predictor for KSA in particular and GCC nations in general.

V. Limitation and Validity of the Results

This study contains limitations that may affect the validity of its findings. This research was built by the authors after a thorough evaluation of the literature. Because there is a scarcity of material on RE practices in the GCC area, the authors relied on some older material as evidence. Furthermore, as a secondary piece of evidence, the authors examined some of the participants' software documentation, which they had collected during the interview. Only the perceptions of software engineers were reported in the survey. However, when conducting a survey, the authors relied on the information supplied by the respondents. There is a good chance that the software developers' perspectives will alter when the project is completed. It is also likely that respondents choose to choose only successful projects. Because software engineers were the only participants surveyed by the authors, the findings were limited to their views and opinions about the projects and teams in which they worked. The data gathered by the software engineers working in various positions and directly participating in the projects was used to generate the conclusions of this study; the views of the software engineers were studied without the author's influence. The questionnaire used by the authors had been used effectively in other studies [4], [6], [15].

A. Internal Validity

The authors applied exploratory research to investigate the issue of RE practices from the perspective of software engineers in the GCC area. They comprised project managers, users and clients, as well as programmers and developers, all of whom had varying perspectives on project success.

B. Construct Validity

The author's questionnaire, which was employed in this study, has been utilized effectively numerous times with other software engineers from other nations [6], [15]. As a result, because the questionnaire had been tested several times, the authors could utilize it as a valid tool to investigate the RE practices for software engineering in the GCC nations.

C. External Validity

Because this research sample is convenient rather than random, the authors does not believe the results are as trustworthy as a random survey. This is due to the fact that a convenient sample may be biased and entails inference. However, respondents took part in software development procedures in a variety of projects. Because this study was conducted in the GCC nations, which constitute a tiny portion of the globe, the findings cannot be generalized. The study is limited to the sample population size at the time the survey was completed.

VI. Conclusion and Future Work

This research is the first to discuss IT project success and failure in GCC countries. For the IT projects in this research sample, found that project success has a negative correlation with project manager's experience and that the best predictor of successful projects is that requirements should be complete and accurate. Comparing current research results with previous research conducted in 2005, reviewing projects in the US, Chile, Australia and Vietnam, current results show that requirements problems still exist in the GCC countries and not have been completely solved. Most of the projects in the current research dataset either used their own requirements-gathering methods or did not use a methodology for the software development process. Only a few projects used a well-known requirements-gathering methodology that fitted with development approaches, such as a waterfall method, or modern development methods, such as agile methodologies. Authors suggest that this situation is due to either the developers being inexperienced in using well-known methodologies or that they are using an inconsistent notation for the requirements. This study also finds that the most important factor in project success is that requirements should be completed adequately; this is followed by top management support and effective project planning. It is interesting to note that it is worse to have partially completed requirements than not completing the requirement process at all. The study also confirms that the project team, project manager, and a suitable requirements methodology are important for project success. However, project sponsor and stakeholder involvement from the project's start also contribute to project success. It was also found that altering the project scope during the project stages is not always associated with project failure. Furthermore, the findings of this study demonstrate that senior management support, as well as stakeholder engagement and involvement throughout the project, are critical for project success. Authors believe that the research results are especially interesting as the data comes from countries where there has been very little published about their software development practices.

Future work will include an in-depth analysis of the rest of the research survey dataset. Authors would be interested in applying the survey being used in Europe, the Asia/Pacific region, and the Americas to investigate the current state of practice of SD and whether these practices have changed significantly over the past 15 years.

Acknowledgments

Both Authors would like to thank the Public Authority of Applied Education and Training (PAAET) for their full support and understanding during the research work.

References

[1] M. Bianchi, G. Marzi, M. Guerini, "Agile, Stage-Gate and their combination: Exploring how they relate to performance in software development". Journal of Business Research. 2020, vol. 110, pp.538-553.

[2] A. Alzayed, A. Al-Hunaiyyan, "A Bird's Eye View of Natural Language Processing and Requirements Engineering" International Journal of Advanced Computer Science and Applications (IJACSA), vol. 12, no. 5, 2021. http://dx.doi.org/10.14569/IJACSA.2021.0120512.

[3] J. M. Verner, W. Evanco, "In-house software development: What software project management practices lead to success?" IEEE Software, vol. 22. 2005. pp. 86-93.

[4] S. Fricker, R. Grau, A. Zwingli, "Requirements engineering: best practice", In: S. Fricker, C. Thümmler, A. Gavras (eds), Requirements engineering for digital health, Springer, Cham, 2015.

[5] H. Hofmann, F. Lehner, "Requirements engineering as a success factor in software projects", IEEE Software vol. 18 no. 4, 2001, pp. 58-66.

[6] J. M. Verner, K. Cox, S. Bleistein, N. Cerpa, "Requirements engineering and software project success: an industrial survey in Australia and the USA", Australasian Journal of information systems, vol. 13, no. 1, Nov. 2005.

[7] T. Hall, S. Beecham, A. Rainer, "Requirements problems in twelve companies; an empirical analysis", IEEE Proceeding Software, Vol. 149, no. 5, 2002, pp. 153-160.

[8] D. Hughes, N. Rana, and A. Simintiras. "The changing landscape of IS project failure: an examination of the key factors." Journal of Enterprise Information Management, vol. 30, no.1, pp. 142-165, 2017.

[9] A. Davis, D. Zowghi, "Good requirements practices are neither necessary nor sufficient, in: Requirements Engineering", Springer, London, vol. 11, pp. 1-3, , 2006.

[10] The Standish Group, Chaos: A Recipe for Success, Standish Group International, 1999.

[11] The Standish Group, CHAOS Report, 2014; available online: http//www.versionone.com/assets/img/files/CHAOSManifesto,2013.pdf

[12] R. Stanley, L. Uden, "Why projects fail, from the perspective of service science", 7th International Conference on Knowledge Management in Organizations: Service and Cloud Computing, in: Advances in Intelligent Systems and Computing, Springer, Berlin, Germany, vol. 172, 2013, pp. 421-429.

[13] G. Stepanek, Software project secret, "why software projects fail," Apress, 2005.

[14] D. M. Fernández, S. Wagner, M . Kalinowski, "Naming the pain in requirements engineering." Empirical software engineering, vol. 22, no.5, 2017, pp. 2298-2338.

[15] J.M. Verner, N. Cerpa, "Australia software development: what software project requirement practices lead to success?", Proceeding of the 2005 Australian Software Engineering Conference, IEEE, 2005.

[16] M. Shafiq, Q. Zhang, M.A. Akbar, A.A. Khan, "Effect of project management in requirements engineering and requirements change management processes for global software development." IEEE Access. vol. 6, 2018, pp. 25747-25763.

[17] E. Klotins, M. Unterkalmsteiner, and T. Gorschek. "Software engineering in start-up companies: An analysis of 88 experience reports." Empirical Software Engineering vol. 24, no.1, 2019, pp. 68-102.

[18] N. M. Mohammed, M. Niazi, M. Alshayeb, "Exploring software security approaches in software development lifecycle: A systematic mapping study." Computer Standards & Interfaces. Vol. 50, 2017, pp. 107-115.

[19] G. Casale, C. Chesta, P. Deussen, E. Di. Nitto, "Current and future challenges of software engineering for services and applications," Procedia Computer Science. Vol. 97, 2016, pp. 34-42.

[20] T. Major, M.T.I. Trammell, A. Moulton, S.E. Madnick, Effects of funding fluctuations on software development: a system dynamics analysis, Engineering Management Journal, vol. 28, no. 2, 2016, pp. 71-85.

[21] K. Curcio, T. Navarro, A. Malucelli, S. Reinehr, "Requirements engineering: A systematic mapping study in agile software development." Journal of Systems and Software. Vol. 139, 2018, pp. 32-50.

[22] M. Watz, S. I. Hallstedt. "Profile model for management of sustainability integration in engineering design requirements." Journal of Cleaner Production. Vol. 247, 2020, pp. 119155.

[23] D. Pandey, U. Suman, and A. Ramani, "An effective requirement engineering process model for software development and requirements

management," in 2010 International Conference on Advances in Recent Technologies in Communication and Computing, 2010, pp. 287-291.

[24] K. El-Emam, N.H. Madhavji, “A field study of requirements engineering practices in information systems development,” in: Proceedings of the Second IEEE International Symposium on Requirements Engineering, 1995, pp. 68.

[25] H. Barki, S. Rivard, J. Talbot, “Toward an assessment of software development risk,” Journal of Management Information Systems. Vol. 10, 1993, pp. 203–225.

[26] H. Kitapci, B.W. Boehm, “Formalizing informal stakeholder decision,” Annual Hawaii International Conference on System Sciences, 2007.

[27] A. Bennaceur, T. T. Tun, Y. Yu, B. Nuseibeh, "Requirements Engineering." Handbook of Software Engineering. Springer, Cham, 2019. pp. 51-92.

[28] R. Raisinghani, R. Riggen, K. Ryan, “Adopting an agile methodology requirements-gathering and delivering,” Price Water House Coopers, 2014, available online: https://www.pwc.com/en_US/us/insurance/publications/assets/pwc-adopting-agile-methodology.pdf.

[29] E. Hull, K. Jackson, J. Dick, “Requirements engineering,” Springer Verlag, 2002.

[30] H. Liao, “Requirement elicitation of enterprise informationizion from view of VCA,” in: 6th International Conference on Networked Computing, Gyeongiu, South Korea, 2010, pp. 390-395.

[31] D. Siahaan, F. Irhammi, “Advanced technology for requirements engineering technique solution (AMRETS),” International Journal of Dvancement in Computing Technology. Vol. 4, no. 5, 2010, pp. 75-80.

[32] S. Alam, S. Nazir, S. Asim, D. Amr, "Impact and challenges of requirement engineering in agile methodologies: A systematic review." Int. J. Adv. Comput. Sci. Appl. Vol. 8, no. 4, 2017, pp. 411-420.

[33] E. Colonese, “Agile: the human factors as the weakest link in the chain,” in: Proceedings of 4th International Conference in Software Engineering for Defense Application (Advances in Intelligent Systems and Computing), 2016, pp. 59-73.

[34] I. Keshta, M. Niazi, and M. Alshayeb. "Towards implementation of requirements management specific practices (SP1. 3 and SP1. 4) for Saudi Arabian small and medium sized software development organizations." IEEE Access, vol. 5, 2017, pp. 24162-24183.

[35] Z. Azida, H. Al-Ahmadi, “An investigation of software requirements practices among software practitioners: a study in Jeddah, International Journal of Software Engineering & Application,” vol. 8, no. 3, 2017, pp. 1-14.

[36] K. Rouibah, S. Al-Rafee, “Requirement engineering elicitation methods: A Kuwaiti empirical study about familiarity, usage and perceived value,” Information Management & Computer Security, vol. 17, 2009, pp.192-217.

[37] R. Osei-Kyei, and APC. Chan. "Stakeholders’ perspectives on the success criteria for public-private partnership projects." International Journal of Strategic Property Management, vol. 22, no. 2, 2018, pp.131-142.

[38] J. D. Procaccino, J. M. Verner, S. P. Overmyer, M. Darter, “Case study: factors for early prediction of software development success,” Information and Software Technology, vol. 44, 2001, pp.53-62.

[39] J. M. Verner, W. M. Evanco, “An investigation into software process knowledge, in: Managing software engineering knowledge,” Springer, Berlin, Heidelbrg, 2003, pp. 29-47.

[40] C. Hibbs, S. Jewett, M. Sullivan, “The art of lean software development: a practical and incremental approach,” O’Reilly Media, Inc., 2009.

[41] M. Ajmal, M. Khan, and H. Al-Yafei. "Exploring factors behind project scope creep–stakeholders’ perspective." International Journal of Managing Projects in Business (2019).

[42] O. Haass, and N. Aziz, "Exploring the Challenges and Solutions for Knowledge Sharing: A Conceptual Framework." ECKM 2019 20th European Conference on Knowledge Management 2 VOLS. Academic Conferences and publishing limited, 2019.

[43] J. Suchan, “How to evaluate project change request,” Microsoft, Redmond WA, 2007.

[44] N. Fabiola, J. Shukla, E. Ndabaga, “Analysis of project scope change management as a tool for project success: case study of Akazi Kanoze projects,” European Journal of Business and Social Science, vol. 4, no. 3, 2015, pp. 29-41.

[45] B.W. Boehm, “Software risk management principles and practice,” IEEE Software, vol. 8, no. 1, 1991, pp. 32-41.

[46] R.L. Glass, “How not to prepare for a consulting assignment and other ugly consultancy truths,” Communication of the ACM, vol. 41, no. 12, 1998, pp. 11-13.

[47] S. Zhiwei, “User involvement in system development process,” in: Proceedings of the 2nd International Conference on Computer Science and Electronic Engineering, 2013.

[48] T. DeMarco, T. Lister, “Risk management during requirements,” IEEE Software, vol. 20, 2003, pp. 99-101.

[49] J. Jurison, “Software project management: the manager's view, Communications of the Association for Information Systems”, vol. 2, no. 17, 1999, pp.50.

[50] R. Young, E. Jordan, “Top management support: Marta or necessity?”, International Journal of Project Manager, vol. 26, no. 27, 2008, pp.713-725.

[51] C.C.S. De Araujo, D. Pedron, “IT project manager competencies and IT project success: a qualitative study,” Organizational Project Management, vol. 2, no. 1, 2015, pp. 53-72.

Structural Limitations with K Means Algorithms in Research in Perú

Javier Pedro Flores Arocutipa[1], Juan Luna Carpio[5]
Universidad Nacional de San Agustín
Arequipa, Perú

Julio César Lujan Minaya[3]
Universidad Nacional de Cañete
Cañete, Perú

Jorge Jinchuña Huallpa[2]
Universidad Nacional de Moquegua
Moquegua, Perú

Ruth Daysi Cohaila Quispe[4]
Gamaniel Carbajal Navarro[6]
Universidad José Carlos Mariátegui
Moquegua, Perú

***Abstract*—In the world of science there are high-level, moderate-level, and low-level emerging countries. The indicators are an investment in research and development (I&D), number of universities, investment, researchers, intellectual production, expenditure on education, gross domestic product (PBI), and quality of life (IDH). In Methodology, it is basic, explanatory, of conglomerates. There are 37 countries analyzed. The data comes from the FMI, datosmacro.com, UNESCO, URWU. There are 11 indicators. These are data taken in two stages, 2006 and 2019. The Results shows R2= 0.9887, which explains the behavior of the PBI by the investment in I&D. The positive and significant relationship between IDH and PBI per capita, which is 0.824, is transcendent. In conclusion, there are three clusters with clearly differentiated indicators. Peru's problem is structural in that it does not have a per capita PBI of $ 30,000 per person or more. Investment in I&D in Peru is low and PBI is also low. Therefore, countries with higher investments in science have high PBIs and better IDH.**

Keywords—Researchers; PBIpc; investment in I&D; exports; universities

I. Introduction

One thing that sets developed countries apart from non-developed countries in science and technology. This is what Francisco Sagasti, current president of Peru, reminds us [1] today, the production of vaccines against COVID 19 can only be produced by countries called "rich"? So should the long-term vision of Latin or African countries be rethought? The capacity of researchers? Resources for Research? And above all, the will of the state to achieve quality-of-life goals for its citizens? Underdevelopment and dependence are related [2] In the same way PBI and scientific production are related [3]. This document leads us to specify data and strategies to help us reflect on what needs to be done within the framework of social welfare.

The lack of vaccines shows the reality of the Peruvian state, the health crisis, the scientific infrastructure to confront the disease. The concept of a failed state was pointed out by the Ombudsman, who said, "the state is not up to the needs of Peruvian citizens" [4].

The experience of rapid testing revealed that not only was there no science, but strategic confusion to deal with evil. By failing to detect asymptomatic, rapid tests announced that only 2% of them had COVID [5].

Today there is a conviction that if there are no vaccines, the economy can't be reactivated. China demonstrates this growth in 2020 by 2%; the world has recessed by -4.5%. Some countries face quickly and effectively, as of April 7, 2021, the portal [6] notes that Israel has already vaccinated 61.18% of its population, Chile 37%, the United States 33%, Peru 2%.

Bill Gates, who has inside information, has said he should be surpassing COVID 19 by the end of 2022. Of course, he is thinking of developed countries. That phrase for Peru means 2024.

Our hypothesis is that emerging countries, such as Peru, have little chance of successfully dealing with any pandemic if they do not achieve a plan to achieve a per capita PBI over $30,000, a developed country IDH, that their exports be of differentiated products, where qualified researchers are one thousand per million, accredited by CONCYTEC and the resources for research exceed 1000 dollars per person.

II. Methodology

Since 1993, we have observed and accumulated information on research resources, for education, by country, making statistical relations between the variables of analysis.

Data have been collected for the year 2006 compared to 2019, although there are 13 years of difference to assess that the reality has changed very little [1]. The World Bank, datosmacro.com, [7], the National Council for Science and Technology (CONCYTEC) [8] has been used to observe levels of explanation of the number of researchers and investment in I&D, in addition to locating relationships between variables.

Variables have been grouped in annual PBI, in current terms, the number of universities by country, Human Development Index (IDH), PBI per capita, Per capita Expenditure Education, in dollars, Education Expenditure (millions), Exports (millions), Research (millions), research in science and technology per person (invCTporpers), Researchers per million inhabitants, indexed publications (Scopus) [8] per 100000 inhabitants.

How many researchers per million are there in Peru? Although in the CONCYTEC portal it can be read by March 31, 2021, that 5942 people have been qualified in the segments of Maria Rostorowski and Carlos Monge, and with that data, the location of Peru in the World Ranking is achieved. The Pearson correlation and determination coefficient is used.

III. Results

Stage 1. (2006): In 2006, four variables were analyzed: investment in I&D, PBI, exports, and the number of universities by macro-region of the world.

What was the situation in 2006 about the reality to be investigated? Gross domestic product per capita is vital for development. And it comes from the wealth generated by countries. Thus, North America had 47.5% of the world's wealth, followed by the Asia Pacific with 25.5%, in third place, Europe with 19.7%, Latin America with 5.9%, and Africa with 1.3% of the world's wealth. This means that Europe has a GDP of 4.5 trillion, North America 11 trillion, Asia Pacific 5.9 trillion, Latin America 1.37 trillion, Africa 0.3 trillion, with a world total of 23.2 trillion dollars.

In the world, in 2006, the region that achieved the best universities in the world was Europe. So of the first 500, she had 207, then there was North America with 189 universities, the Asia Pacific got the third place with 92 universities, Latin America only got 7, and finally Africa with 5 universities. It should be noted that, among the top 20 universities, North America had 17, or of the top 100 58 were from North America, so, when the top 200 universities were counted, North America had 95 universities. And in the first 400 and 500 Europe regains its first place. It should be noted that the best universities are concentrated in the United States.

In 2006 (Table I), which is based on [9] [10] [11], 7.5 trillion were exported in the world, and 36% were concentrated in Europe with 2.7 trillion, North America with 29% representing 2.2 trillion. The Asia Pacific had 28% with 2.1 trillion, Latin America with 5% with exports worth 375 billion, and Africa with 2% of total world exports.

It can be assumed that developed country exports differ from emerging country exports; while some export sophisticated products and others export raw materials [12]. And they are sophisticated products because there is a strong investment in research and development to achieve goods and services of high productivity and effectiveness with prices that allow selling volume with decreasing prices.

Over time, North America has achieved a higher percentage of investment in I&D. Thus in 1994 the investment in C&T represented 35.1% and in 2003 it was 41.9%. However, Europe decreased, from 30.6% to 28.2%, also the Asia Pacific regions from 31.3% to 27.3%, and Latin America from 1.6% to 1.3%, and Africa plus Oceania from 1.4% to 1.3%.

The results (Table II), the correlation coefficient of the variables analyzed indicates that, between the number of universities by region and the level of exports, is 0.94, meaning that the regions that have more universities than their exports are greater and vice versa.

TABLE I. List of Variables for 2006

Continents	**Univer (a)**	**Expor(b)**	**PBI Real(c)**	**InverI&D (d)**	**PBI EST (e)**
Europe	207	2701	4591	242	6511
North America	189	2178	11057	360	9549
Asía Pacific	92	2100	5932	234	6305
Latín America	7	375	1377	11	562
África	5	150	300	2	330

TABLE II. Correlation Coefficient

	Univer	**Expor**	**PBI**	**InverID**
Universities	1.00	0.94	0.78	0.91
Exports	0.94	1.00	0.74	0.91
PBI	0.78	0.74	1.00	0.95
I&D investment	0.91	0.91	0.95	1.00

On the other hand, there is a high and significant relationship between the number of universities per region and investment in I&D, which is 91%. It turns out that PBI is associated with 95% investment in research and development, which is high and determining since it informs us that the greater the investment in I&D the greater the PBI (wealth). Likewise, the regions that have greater exports are related to the regions that invest more in I&D, this is 0.95 or 95%. Countries that invest little in I&D then their exports are smaller. And they export raw materials or very little differentiation.

When it is assumed that the dependent variable is prestigious universities, understand by internationalized [13] as part of the world, with a global or global vision, this depends on the following three variables: world exports, global PBI, and the resources allocated for research and development. This is deduced because the Pearson correlation exceeds the 74% that is high.

The ratio of wealth generated to investment in research and development, by region in the world, is 90%. All this refers us to [14] which maintain that in A.L. despite the efforts of science in recent years has not given levels of satisfaction. There is no doubt that it could be improved, but for the time being, these are the results that can be observed.

In the Econometric Analysis 2006, based on the calculation in the Eviews Software, you will find the following model that explains the behavior: PBI = 278.955900199 + 25.7505541802*R&D investment. That informs us that the level of explanation or R squared is 0.906 that the investment beta has a p-value of 0.01 that makes it very significant. In addition, the DW is 2.57 which is on the margins of 2. It is a model that explains that the size of the wealth of regions depends up to 90% on investment in I&D. It indicates the relationship between the behavior between the historical series and that calculated by the equation, which will allow us to affirm that in history the levels of explanation of I&D, if it is related to the levels of wealth in the world (2006).

One question, what is the elasticity of investment in I&D, in PBI growth by region? The statistical evidence indicates, the impact is, if investment in I&D increases by 10%, then wealth grows by 6%; and in that way proportionally. The model is: Log (PBI)= 5.46+ 0.6047* log (I&D inversion) with the p-value for the coefficient of the variable is 0.0037 which signals that the coefficient is significant.

And with a Prob (F-statistic) of 0.0036 that indicates that the model is acceptable.

It is confirmed that the levels of economic growth should be higher than the growth of the SAP. With appropriate levels of technology and high productivity, it can enable improvements in the IDH [15] of citizens within a jurisdiction.

Therefore, economic growth is a good reason, as it happened in China, which, with rates between 7% and 11%, [16] has managed to raise its PBI per capita from 1000 (1999) to 10 thousand euros in 2019.

State policies, prioritizing production, education, research, exports of sophisticated goods, the optimization of resources, and maximum productivity, could aspire to the development of our country. The author Quinde [17] carried out the mathematical analysis of the relationship between PBI and expenditure in science in Latin America, between the years 1990-2015, it turns out that for A.L. there are no levels of explanation or relationship but if for the country of Ecuador. To perform the demonstration, it uses the Granger causality test, cointegration, and the unit root test.

How was 2019?

13 years later. The ranking of researchers by countries of the world is associated with the ranking of PBI generated, at the top are the developed countries. In the world, there are TOP-countries in research, those that carry out average research, and countries that do little and little research [3] translated into scientific articles, patents, and innovations.

This is a strong correlation between the number of researchers per million inhabitants (NIPMH) per country and the PBI per capita. The number of scientific articles produced per 100,000 inhabitants to (NIPMH) per country. In (Table III) it is observed that in the first column there are 37 countries, in the second column the number of universities per country in the first 1000 in the world. Then comes the pc PBI. All of the following values are measured in euros. Except for the IDH. Looking at the averages of the variables exposed, it is observed that the maximum data for Peru are well below the world average.

At the end of 2020, Peru had 181 researchers per million inhabitants [12]. Perhaps they should be a little overjoyed, given that below Peru, there are, for example, India with 137 per million, Colombia 126, Bolivia 120, Paraguay 71, and Ecuador 69 per million. But at the same time, it should be worrying, that Israel, according to [10], has 8250 researchers per million inhabitants, and Finland, Iceland, are above 7305 per million inhabitants. The case of Singapore, Denmark, Japan, Norway, Sweden, which are above 5200 researchers per million inhabitants, then the United States, the United Kingdom, Canada, Australia, which are above 4200 researchers per million inhabitants, would be Portugal, Germany, France, Switzerland, Belgium, Ireland with more than 3000 researchers per million and the block of Spain, Hungary, Poland, Italy, and China with more than 1000 researchers per million, also Argentina, Chile, Brazil, Cuba, Mexico, above 300 per million and then there would be Venezuela, Peru, India, Colombia, Bolivia, Paraguay, Ecuador above 69 per million but below 187 researchers per million.

Among the results, (Table IV) it can be noted that there is a positive relationship between wealth (PBI) of 37 countries and investment in (I&D) in 2019. In that sense, an R of 0.983 was found, a very valuable relationship, that if countries have greater wealth then they would allocate in absolute terms a greater portion of resources for research. And vice versa to lower PBI then investment in (I&D) will be lower. Another of the results (Table V) is the positive and very high relationship between the NIPMH and PBI pc (0.7); with per capita expenditure on education (0.74); with investment in (I&D) pc (0.828) and a positive relationship with publications per 100 thousand people in Scimago. In the same way, the scientific production measured by Scimago in the analyzed countries is related to their PBIpc (0.916) with the level of exports (0.642).

It is also imperative to note the number of universities per country is related and explains the investment in (C&T) per capita by country. Here the R2 is 0.904 and the R of Pearson is 0.951, the higher investment, the greater number of universities ranked within the first thousand in the world. Similarly, spending on education correlates with the size of wealth per country with a fairly significant Rho of 0.9934. Here, Wagner's law seems to be adhered to, that the larger the size of the economy, the greater the public spending on education.

Universities are innovation center's that interpret productivity as the ultimate goal for competitiveness, [18] in that sense it has been found that the number of universities per country is related to export levels per country. They are the patents and research in science and technology that allows greater exports or vice versa greater number of universities in the world. Here the Rho is 0.843 is significant.

Indeed, the number of universities within the first thousand in the world is related to their respective PBI of the country. The Pearson Rho is 0.969. It means that if the PBI is high then the number of universities will also be high. It has been stated that exports of raw materials and sophisticated goods are one thing. It should be understood that developed countries or countries with a PBI above 30,000 dollars' per capita export sophisticated goods unlike countries of the second or third world. In this sense, it should not be overlooked that exports by country are significantly related to education spending by country. The Rho is 0.825 quite high and direct. It could not be overlooked that I&D investment, research aims at differentiating products and services that make raising productivity improves competitiveness levels thus achieving a greater share (%) of the markets, the relation with exports is 0.8.

TABLE III. RESULTS PER UNIT

Countries	Univ	IDH	PBI pc	Expenditure pc Education	Exports pc	Rese-arch pc	Researchers per million	Scimago for 100000
Israel	7	0.919	39698	2070	5768	1928	8255	4451
Corea del Sur	32	0.916	28472	2748	18871	2755	7980	2315
Finlandia	8	0.938	43570	2864	11875	1206	7707	6508
Singapur	4	0.938	58934	2293	61194	1130	6088	5568
Austria	14	0.922	44780	2368	17929	1416	5733	4696
Dinamar-ca	6	0.94	53760	3658	16997	1644	5670	7314
Japón	40	0.919	35888	1069	4994	1173	5573	2293
Noruega	5	0.957	67730	5549	17088	1397	5468	6327
Suecia	14	0.945	46160	3567	13887	1534	5239	6817
EE.UU.	206	0.926	58485	2497	4475	1655	4663	3909
Reino Unido	65	0.932	37770	2138	6263	647	4269	5544
Canadá	28	0.929	42048	1895	10505	643	4260	4939
Australia	34	0.944	48969	2375	9495	902	4224	5837
Portugal	6	0.864	20740	898	5823	284	3799	3243
Alemania	49	0.947	41510	2048	15999	1282	3532	3875
Francia	30	0.901	35960	1935	7575	793	3496	3341
Suiza	14	0.955	76200	3853	32623	2559	3436	8880
Bélgica	8	0.931	41460	2653	34645	1166	3435	4945
Irlanda	5	0.955	72260	2358	30514	825	3090	4474
España	40	0.904	26430	1103	6303	326	2944	3147
Rusia	11	0.824	10346	343	2549	102	2784	819
Malasia	5	0.81	9380	418	6542	134	2397	999
Polonia	8	0.88	13870	662	6214	170	1623	1872
Italia	46	0.892	29660	1140	7978	420	1616	3155
Irán	12	0.783	4586	175	591	38	1475	698
Turquía	11	0.82	8230	345	1820	24	1379	769
Tailandia	4	0.777	6307	251	3159	61	1350	286
China	144	0.761	9180	348	1594	200	1307	471
Argentina	3	0.845	9028	505	1294	48	980	501
Chile	4	0.851	13457	714	3258	47	833	856
Brasil	22	0.765	7562	470	946	95	694	489
Egipto	5	0.707	2231	69	257	15	687	229
México	2	0.779	9090	373	3223	28	353	272
Pakistán	4	0.557	1326	40	100	3	336	85
Perú	0	0.777	5933	218	1310	8	181	91
India	15	0.645	1741	62	212	11	137	137
Colombia	1	0.767	5801	250	700	14	126	227

TABLE IV. CORRELATIONS

	Annual PIB	Universities	Education expenditure (millions)	Exports (million)	I&D Invest. (millions)
Annual PIB	1	0.969	0.993	0.843	0.983
Universities	0.969	1	0.973	0.843	0.951
IDH	0.04	0.134	0.074	0.095	0.123
PBI Per cápita	0.119	0.175	0.151	0.1	0.196
Per capita expenditure on education	-0.037	0.024	0.008	-0.062	0.032
Expenditure on education (million)	0.993	0.973	1	0.825	0.982
Exports (in millions)	0.843	0.843	0.825	1	0.8
Research (in millions)	0.983	0.951	0.982	0.8	1
Researchers per million inhabitants.	0.042	0.102	0.06	0.034	0.143
Documents Scimago per 100000	-0.044	0.052	-0.004	-0.027	0.02

TABLE V. CORRELATION OF PEARSON WITH 37 DATA

	University	PBI pc	Gasto pc education	Exportpc	Investigation I&D pc	Imvest por million hab	Scimago for 100000
Gasto pc education	.073	,899	1	,602	,826	,740	,904
Sig. (bilateral)	.668	.000		.000	.000	.000	.000
Export pc	-.137	,710	,602	1	,563	,487	,642
Sig. (bilateral)	.419	.000	.000		.000	.002	.000
Investig. (I&D) pc	.181	,784	,826	,563	1	,828	,759
Sig. (bilateral)	.284	.000	.000	.000		.000	.000
Imvest por million hab (NIPMH)	.102	,702	,740	,487	,828	1	,730
Sig. (bilateral)	.549	.000	.000	.002	.000		.000
Scimago for 100000	.052	,916	,904	,642	,759	,730	1
Sig. (bilateral)	.759	.000	.000	.000	.000	.000	

One IDH input is per capita PBI. And the latter is directly and highly related to per capita spending on education, which confirms that countries that have achieved levels of development allocate more budget for education in their respective countries. So Pearson's Rho is 0.879 confirms our hypothesis.

Models have been generated that allow us to understand, what depends on the number of researchers per million people, an explanation was found. The (NIPMH) depends on PBI and research investment as a percentage of PBI. Researchers per million = 1288.34537675 + 2.7812350751*I&D investment per person. R2= 0.6535, (0.0004) (0.0000) Dw (1.0298).

Now, what does the recorded scientific output in [8] per country depend on? The software has generated the following: Scientific production = 24.4+ 0.0544*PBIpc + 0.9968*GpcED. (R2= 0.8949, (0.9159) (0.0002) (0.0001) Dw (2.075951)) means that the articles published by 100 thousand in the world and accredited by [8] are explained by the PBI and per capita expenditure on education. And as you know these depend on the size of public spending that depends on the wealth of each country.

The next question has also been asked, what does investment in research and development depend on? And it was found, that it depends on the wealth by country (PBI) of the quality of life (IDH) and the of course sophisticated exports made by the country. I&D investment = -85005.2962607 + 0.0295136063527*PBI + 95633.8393054*IDH - 0.0266531438077*EXPOR. R2= 0.9779, (0.001) (0.000) (0.0013) Dw (2.1916).

And the last concern was, what does the size of a country's wealth depend on with the proposed 10 variables? It was determined that it depends on education spending, and levels of I&D investment. PBI = -2876.20676559 + 18.8401561792*GEDUCA + 8.02960074926*Inves (I&D). R2= 0.9887, (0.9458) (0.0000) (0.028) Dw (1.6097).

It means that the creation of wealth depends on the expenditure in education by country and the investment in I&D and explains it in 98.87%.

Algorithm analysis K means. When performing the algorithms (Fig. 1) it is observed that there are three groups with quasi-similar characteristics by the observation of data.

Fig. 1 shows the 37 countries analyzed. With the software, they were grouped into three clusters. So in the conglomerate, one country remained 16, in the two, 17 countries and in the three, four countries. It can be observed that group two includes Peru and most Latin countries, which are emerging countries.

This conglomerate includes Portugal, Russia, Malaysia, Poland, Iran, among others. It should be noted that in cluster one are developed countries and in group three are Norway, Switzerland, Ireland, and Singapore. (Table VI) This last conglomerate stands out for occupying the first places in PBI per capita, in the human development index, in exports per person, which means that there are respectable reasons to accept conglomerates. Similarly, the countries of the second cluster have similar indicators and are in the last places in the ranking. The number of countries per cluster is summarized in (Table VII).

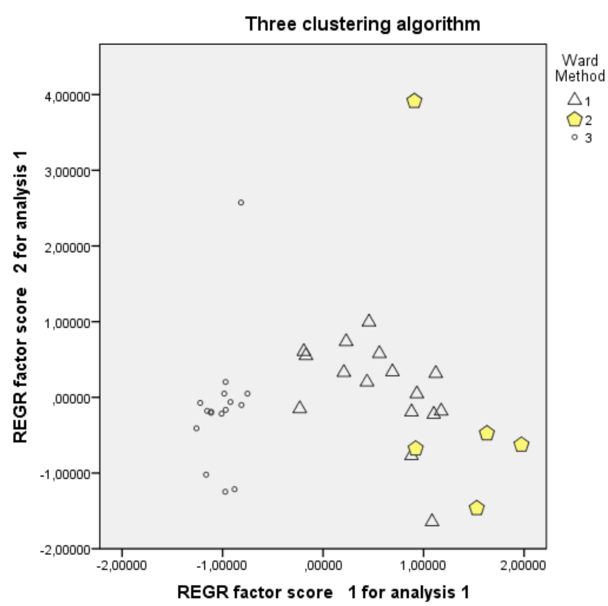

Fig. 1. Three Final Clusters.

TABLE VI. CLUSTER OF RELEVANCE

Case	Conglomerate clusters		
	Countries	*Cluster*	*Distance*
1	Israel	1	7298
2	Corea del Sur	1	14757
3	Finlandia	1	4364
4	Singapur	3	27735
5	Austria	1	7050
6	Dinamarca	1	14117
7	Japón	1	9096
8	Noruega	3	18434
9	Suecia	1	6140
10	Estados Unidos	1	19173
11	Reino Unido	1	6755
12	Canadá	1	2202
13	Australia	1	8594
14	Portugal	2	13558
15	Alemania	1	4244
16	Francia	1	6985
17	Suiza	3	8459
18	Bélgica	1	22609
19	Irlanda	3	6536
20	España	1	15855
21	Rusia	2	2705
22	Malasia	2	4555
23	Polonia	2	7019
24	Italia	1	12584
25	Irán	2	3993
26	Turquía	2	549
27	Tailandia	2	2087
28	China	2	1292
29	Argentina	2	1389
30	Chile	2	5399
31	Brasil	2	1611
32	Egipto	2	6332
33	México	2	1603
34	Pakistán	2	7279
35	Perú	2	2733
36	India	2	6878
37	Colombia	2	3106

TABLE VII. NUMBER OF CASES IN EACH CLUSTER

Cluster		
Clúster	1	16,000
Clúster	2	17,000
Clúster	3	4,000
Valid		37,000

IV. DISCUSSION

The results argue that it is essential to generate wealth (PBI), to have an impact on intense expenditure on education and research, and a human capital with an attitude to propose to carry out scientific research manifested in the records of [8], which allows for greater and better exports [19] with higher.

They argue that the provision of professionals and technicians with relevant training is the crux of making economic development and quality of life sustainable, [20] (P.4) which is one of the elements in the global era of science and technology. Similarly, the World Bank [21] in 1999 noted that development is related to knowledge-based on human capital.

Another of the works that encourage to point out is when the economic resources are vital for the production of knowledge whether laboratory, or not experimental, is the one that demonstrates [22] when it states that the adequate remunerations are related to the production of knowledge.

It was not for less, since, if there are financial resources, economic, equipment, laboratories it is possibly better and more research. The relationship with the acquisition of software is highlighted, demonstrating the importance of this input. (A: 0.999). Another aspect to be taken into account is when UNESCO demonstrates and highlights the role of the institutions, their speed, their vocation, their long-term perspective to improve the elaboration of knowledge. The author in [23] (P.1), one of the determinations assumed by the author [24] is the scientific gap between countries unequal in material wealth. For the author, economic inequality and institutional factors allow for a greater gap. Per capita support is far less than decent in countries with moderate and low wealth, and skilled human resources are still a critical mass in the making. In the case of Peru, the Renacyt researchers as of March 31, 2021, are 5942.

Inequality in Latin America is increasingly difficult. Those who have managed to concentrate wealth are a smaller percentage of the population; today you can say that they define media policies, norms, and long-term policies.

It has been said that the best way to measure this situation is with the Lorentz curve [25] that designs us that decile of society has the greatest percentage of national wealth.

Discounted investment due to depreciation should be considered higher in the next period to emphasize the growth of the economy and move towards a welfare state as supported by the Harrod Domar model. That is the ingredient that long-term policies must have, for investment, and when domestic savings are lacking, then external savings must be attracted. In Peru, in reality, the pandemic has, for the time being, weakened the possibility of achieving greater human capital and of ensuring that research spending is minimal, even painful. COVID 19 has exposed the reality of research in the so-called emerging countries, today the so-called developed countries demonstrate that they are in the capacity to create the vaccine, to do experimental research, and to finance it, while the vast majority, if not 193 of the 200 countries of the world, cannot produce it because they do not have the human capital, the necessary resources and the solvency that experience gives. In any case, technology decides the leading role that imposes conditions. The global economic structure points out those countries in the second and third world must wait for vaccines to arrive. It is proven that the production function is corroborated again and again in China, Singapore, Taiwan, North Korea, Israel, England, Germany, USA, which are examples of the technological progress that makes faster the cumulative process of capital that generates social benefit.

In this regard [26] supports how the University of Concepción (Chile) contributes with competitive human capital, in the creation of knowledge and contribution to regional development. Chile is coping better with the pandemic.

Another work that comments on the role of universities is that of [27] who shows that actions with a view to development objectives take effect. The number of actions or activities contributed between 2016 and 2020 was 3329. Then the new production of goods and services is enriched by the application of the scientific research method to give validity and/or contribute to science and technology.

Gary Becker, has analyzed different forms of investment in the professional working in the company, in training, training, workshops, specialization and has obtained different results, [28] but all positive. The difference is in impact. [29], argue that investment in assets generates externalities that drive the economy, so that all investment is important, which is very little applied in emerging countries, and what at one stage was not considered to be the most appropriate, corrects economist Robert Lucas when he ratifies the performance of investment to generate more production, in the long run, and to grow productivity [28] is a complicated but necessary issue.

The impact of investing in human capital (CH) and its effects on the economy was measured by economist Lucas [30], and he found that if investment in CH increased by 10%, then the output would grow by 4%. For this, developed countries inject immense resources into research and thus confirm the elasticity found is 0.4. Although the world power, U.S. with the experience they have, the state funds the impulse in education. There can be no better example than this for emerging countries when they should fund research and the preparation of scientific tables. Providing support to accredited researchers, they do not yet do so. The data in this document shows this. Another contribution that can be derived from this work is the positive externalities that the experienced human capital contributes.

In that same direction is the contribution of [31] when it finds that if it increases by ten percent in research and development then the product would increase by between 0.6 and one percent. This is confirmed by the investigator [32]. Another author is Solow, [33] who developed the theoretical basis for explaining the factors that contribute to economic growth. The contribution was based on the technological advance and that generates the so-called aliquot of Solow, that there is a part of the economic growth that only explains it the technological advance. [34]. Experience, education, technology per person. The equation [35] was generated in application to the period between 1909 and 1949 where there were differences between the incremental rates of PNB, man-hour, and the capital factor in the period.

Thus the so-called residue was obtained. It happens that in the period the product had grown by 100%, and that the capital per worker explained 12% of that difference while the remaining 88% was explained by the technological progress. This was confirmed by Denison when analyzing the variables mentioned in the period 1929 to 1982 [36], thus also showing that education contributes to the increase of goods and services. Another argument is when the training and training provided by the company allow productivity to increase per worker [29].

At the national level from this perspective, the renowned educator has spoken [37] who with their experience defines that research has a leading role in generating knowledge but at the same time promotes methodologies and patents for increasing productivity, In that understanding, the new university law of the year 2014 rectifies the delivery of the bachelor degree without thesis.

For the same reason that it allows the generation of researchers qualified by CONCYTEC [24], the proposal is to publish in journals with peer reviewers [38]. Does a strategic direction for the development of scientific production become necessary? Of course, yes. This has to do with financing, human capital, researchers, organizational design. [39] the only way to see results in the long term. Soria adds that they can be defined as state policies [40].

V. Conclusion

It is shown that investment in I&D has a positive relationship with higher PBI and this fulfills its cycle with greater scientific research, and vice versa.

The analysis of mean K determines three groups with dissimilar characteristics, based on per capita PBI, the human development index, per capita investment in research, and per capita exports. It is understood that group three countries, Switzerland, Singapore, Norway, and Ireland lead these indicators, group two being developing countries while cluster one being developed countries.

The long-term structure indicates that the circumstances have not changed in the two analysis periods, 2006 and 2019.

The educational model implemented in the conglomerate requires generating greater wealth (PBI) to guarantee the quality of life (IDH). It is necessary to implement expenditure on education and scientific research in absolute terms.

The largest number of universities per country are concentrated where there is higher spending on education, higher investment in I&D, where PBI is higher, where exports are differentiated products. The problem of Peru is structural and it is defined that it will be so, as long as the per capita is less than 30 thousand dollars.

VI. Future Work

Future work will focus on comparative analysis of the behavior of the first and second waves of covid-19, a proposed model with reviews software and 2020-2021 algorithms.

Effects of the COVID-19 coronavirus on employment, family income, and digital education in Peru, 2020 - 2021 using econometric models.

Algorithms that explain the effects of COVID 19 on tax collection, private and public investment in Peru 2021.

REFERENCES

[1] F. R. Sagasti, Tecnología, planificación y desarrollo autonomo, Primera. Lima: Instituto de estudios peruanos, 1977.

[2] S. Figueroa, G. Sánchez, and A. Vidales, La ciencia y tecnología en el desarrollo: una visión de América Latina, vol. 53, no. 9. Zacatecas: Universidad Autónoma de Zacatecas, 2009.

[3] [G. Flórez García, "Innovación en países desarrollados y subdesarrollados," p. 58, 2020, [Online]. Available: https://repository.ucc.edu.co/bitstream/20.500.12494/16629/4/2020_Florez_innovacion_paises_desarrollados_subdesarrollados.pdf.

[4] Audioplayer-RPP, "Defensor del Pueblo: Estado peruano ha tenido una pésima gestión frente a la pandemia - Entrevistas ADN - RPP Noticias," 2020. https://audioplayer.pe/podcast/entrevistas-adn/defensor-del-pueblo-estado-peruano-ha-tenido-una-pesima-gestion-frente-a-la-pandemia-6761) (accessed Apr. 17, 2021).

[5] Prensaregional, "Las pruebas rápidas no sirven… el tiempo nos da la razón | La Prensa Regional," 2020. https://prensaregional.pe/las-pruebas-rapidas-no-sirven-el-tiempo-nos-da-la-razon/ (accessed Apr. 17, 2021).

[6] H. Ritchie, "Coronavirus (COVID-19) Vaccinations - Statistics and Research - Our World in Data," 2021. https://ourworldindata.org/covid-vaccinations (accessed Apr. 17, 2021).

[7] worldmeter, "Deaths from the Coronavirus - Worldometer," 2021. https://www.worldometers.info/coronavirus/ (accessed Apr. 17, 2021).

[8] Scimago, "Scimago Journal & Country Rank," 2021. https://www.scimagojr.com/ (accessed Apr. 17, 2021).

[9] P. Salama, "UNA Globalización Comercial Acompañada DE UNA Nueva Distribución Cartográfica," Rev. Econ. Inst., vol. 14, no. 27, pp. 57–80, 2012, Accessed: Apr. 17, 2021. [Online]. Available: http://www.scielo.org.co/scielo.php?script=sci_arttext&pid=S0124-59962012000200003&lng=en&nrm=iso&tlng=es.

[10] UNESCO (UIS), "How much does your country invest in R&D?," 2020. http://uis.unesco.org/apps/visualisations/research-and-development-spending/ (accessed Apr. 17, 2021).

[11] ARWU, "ARWU World University Rankings 2020 | Academic Ranking of World Universities 2020 | Top 1000 universities | Shanghai Ranking - 2020," 2020. http://www.shanghairanking.com/ARWU2020.html (accessed Apr. 17, 2021).

[12] Datosmacro, "Estados Unidos - Gasto público 2019 | datosmacro.com," 2021. https://datosmacro.expansion.com/estado/gasto/usa (accessed Apr. 17, 2021).

[13] V. Sacoto-Castillo, N. Viña-Palomino, and J. Landívar-Vera, "El aporte de la internacionalización en el desarrollo de competencias profesionales en las Universidades ecuatorianas," Rev. Cienc. UNEMI, vol. 13, no. 33, pp. 96–107, 2020, [Online]. Available: http://ojs.unemi.edu.ec/index.php/cienciaunemi/article/view/1045/1097.

[14] J. J. Ibañez-Marti, "La Ciencia en Latinoamérica: Tendencias y patrones," Rev. la Fac. Ciencias, vol. 7, no. 1, pp. 23–39, 2018, doi: 10.15446/rev.fac.cienc.v7n1.69409.

[15] G. M. Tóala-tóala, A. A. Mendoza-briones, and R. Cevallos-Enriquez, "Desarrollo económico : ¿ la clave para el desarrollo sostenible ? Economic development : the key to sustainable development ? O desenvolvimento econômico : a chave para o desenvolvimento sustentável ? Resumen," Dominio las ciencias, vol. 2, pp. 432–447, 2016, [Online]. Available: ISSN 24778818.

[16] "Presión Fiscal 2020 | datosmacro.com," 2021. https://datosmacro.expansion.com/impuestos/presion-fiscal (accessed May 05, 2021).

[17] V. Quinde, R. Bucaram, M. Bucaram, and C. Silvera, "Relación entre el gasto en Ciencia y Tecnología y el Producto Interno Bruto . Un análisis empírico entre América Latina y el Caribe y el Ecuador," Espacios, vol. 40, no. 2008, 2019.

[18] C. Clemenza, J. Ferrer, R. Araujo, and S. Espina, "Fortalecimiento de la competitividad Institucional a través de la calidad en la educación: Caso Universidad del Zulia," Rev. Venez. Gerenc., vol. 11, no. 36, pp. 615–637, 2006, Accessed: Apr. 17, 2021. [Online]. Available: http://ve.scielo.org/scielo.php?script=sci_arttext&pid=S1315-99842006000400007&lng=es&nrm=iso&tlng=es.

[19] W. Toledo, "El rol de las exportaciones en el crecimiento económico: evidencia de una muestra de países de América Latina y el Caribe," Rev. Econ., vol. 34, no. 89, pp. 78–100, 2017, Accessed: Jul. 22, 2021. [Online]. Available: http://www.scielo.org.mx/scielo.php?script=sci_arttext&pid=S2395-87152017000200078&lng=es&nrm=iso&tlng=es.

[20] G. Yamada, J. F. Castro, and M. Rivera, "Educación Superior en el Perú: Retos para el Aseguramiento de la Calidad Estudio del SINEACE encargado a los especialistas," Sist. Nac. Evaluación, Acreditación y Certificación la Calid. Educ. SINEACE, vol. 32, no. 10, pp. 1365–1367, 2012.

[21] D. I. Pérez-Fuentes and J. L. Castillo-Loaiza, "Capital humano, teorías y métodos: importancia de la variable salud," Econ. Soc. y Territ., vol. 16, no. 52, pp. 651–673, 2016, Accessed: Apr. 17, 2021. [Online]. Available: http://www.scielo.org.mx/pdf/est/v16n52/2448-6183-est-16-52-00651.pdf.

[22] V. H. Moquillaza-Alcántara, "Producción científica asociada al gasto e inversión en investigación en universidades peruanas," An. la Fac. Med., vol. 80, no. 1, pp. 56–59, 2019, doi: 10.15381/anales.v80i1.15626.

[23] C. Cabezas Sánchez, "Rol de estado en la investigación científica en salud y transparencia en la información," Med. Exp., vol. 23, no. 4, pp. 275–283, 2006.

[24] L. Vela Meléndez, E. R. Acevedo Sánchez, P. Yesquen Zapata, and G. Venturra Carrillo, "Ciencia, tecnología e innovación en el Perú. Necesidad de una política pública descentralista, que institucionaliza las alianzas Academia-Empresa-Estado y Sociedad Civil," Geogr. Rev. Digit. para Estud. Geogr. y Ciencias Soc., vol. 9, pp. 138–157, 2018, doi: 10.14198/geogra2018.9.106.

[25] B. Moscoso Rojas, L. Huamán Angulo, M. Núñez Vergara, E. Llamosas Félix, and W. Pérez, "Inequidad en la distribución de recursos humanos en los establecimientos del Ministerio de Salud de cuatro regiones del Perú," An. la Fac. Med., vol. 76, p. 35, 2015, doi: 10.15381/anales.v76i1.10968.

[26] O. Barrientos, C. Zaror, and J. Hernández, "La Universidad de Concepción y su aporte al desarrollo de la región del Biobío y el país," Rev. Nupem, vol. 12, no. 27, pp. 180–199, 2020, doi: 10.33871/nupem.2020.12.27.180-199.

[27] C. Picado Madrigal and C. Azofeifa Ureña, Aportes de las universidades estatales costarricenses y el Conare para el logro de los Objetivos de Desarrollo Sostenible y Agenda 2030, no. 17. 2020.

[28] L. Serrano Martínez, "Indicadores de capital humano y productividad," Rev. Econ. Apl., vol. 4, no. 10, pp. 177–190, 1996.

[29] F. L. B and J. D. Sachs, "Macroeconomía en la economía global." p. 796, 2002.

[30] A. Rodríguez Arana, Crecimiento económico y capital humano: metodología para la simulación de una variante del Modelo de Lucas con aplicación a México, vol. 12, no. 2. Instituto Mexicano de Ejecutivos de Finanzas, A. C., 2017.

[31] Z. Griliches, "Productivity Puzzles and R&D: Another Nonexplanation," J. Econ. Perspect., vol. 2, no. 4, pp. 9–21, 1988, doi: 10.1257/jep.2.4.9.

[32] T. J. Sargent and C. A. Sims, "Empirical Macroeconomics," Indian Econ. J., vol. 59, no. 4, pp. 3–33, 2012, doi: 10.1177/0019466220120402.

[33] A. C. Chu, Advanced Macroeconomics. 2020.

[34] G. N. Mankiw, Macroeconomics. 2010.

[35] F. Jiménez, "Macroeconomía: Enfoques Y Modelos Nuevos Ejercicios Resueltos," PUCP, 2019.

[36] A. R. Peña Sánchez, "Human capital, investment on education and economic growth: A review and updating of regional economic asymmetry in Spain (1980-2012) | Capital humano, inversión educativa y crecimiento económico: Revisión y actualización de la asimetría económica regiona," Rev. Estud. Reg., no. 106, pp. 21–53, 2016, [Online]. Available: https://www.redalyc.org/pdf/755/75547651002.pdf.

[37] L. Piscoya Hermoza, "Los paradigmas psicológicos como soporte científico de las tecnologías de la educación," Rev. Investig. en Psicol., vol. 18, no. 1, p. 139, 2016, doi: 10.15381/rinvp.v18i1.11783.

[38] M. A. Bunge, "El planteamiento científico," Rev. Cuba. Salud Pública, vol. 43, no. 3, pp. 1–29, 2017.

[39] L. Pedraja-Rejas and E. Rodríguez-Ponce, "La relevancia del proyecto estratégico como determinante de la calidad en las universidades," Idesia (Arica), vol. 32, no. 4, pp. 101–103, Nov. 2014, doi: 10.4067/S0718-34292014000400013.

[40] O. Soria, "Descentralización Educativa Título : El dilema entre saber , poder y querer . ¿ Una nueva universidad para el siglo XXI ?," Rev. Iberoam. Educ., vol. 3, p. 14, 1994.

The Effects of Adaptive Feedback on Student's Learning Gains

Andrew Thomas Bimba[1], Norisma Idris[2]
Department of Artificial Intelligence,
University of Malaya
Kuala Lumpur, Malaysia

Ahmed Al-Hunaiyyan[3]
Computer & Information Systems Department,
College of Business Studies,
Public Authority for Applied Education and Training (PAAET), Kuwait

Salwa Ungku Ibrahim[4], Naharudin Mustafa[5], Izlina Supa'at[6], Norazlin Zainal[7], Mohd Yahya Ahmad[8]
Center of Science Foundation Studies, University of Malaya,
Kuala Lumpur, Malaysia

***Abstract*—There is an increase in the implementation of adaptive feedback models, which focus on the relationship between adaptive feedback and learning gains. These literatures suggest that the complex relationship between feedback, task complexity, pedagogical principles and student's characteristics affect the significance of feedback effects. However, current studies have shown insufficient research on the effect of adaptive feedback characteristics on student's learning gains. Thus, there is a need to investigate the effect of multiple adaptive feedback characteristics on student's learning gains. The adaptive feedback model proposed supports the retrieval of appropriate feedback for students based on established weights between related concepts. In comparing three experimental groups, students who were provided with adaptive feedback showed learning gains and normalized learning gains of 0.87 and 0.05 over the normal feedback group, with 0.97 and 0.07 over the non-feedback group. This research yielded better outcomes than previous similar studies.**

Keywords*—Authoring tools and methods; evaluation of CAL systems; intelligent tutoring systems; teaching/learning strategies; pedagogical issues

I. Introduction

With progressions in educational innovations, e-learning systems have advanced to deliver learning conditions to the privileged and under-privileged individuals so they can study at their own speed. The accomplishment of these frameworks depends on engaging experience, timely and precise feeedback to the students [1] . One of the key element in learning support is to provide distinctive feedback based on an individual's requirement [2]. Customizing feedback according to student's qualities and other external parameters is a promising method for executing adaptation in computer-based learning environment [3], [4]. Adaptive feedback unlike generic feedback is dynamic, as students work through instructions, different students will receive diverse information [5]. Tending to this need, numerous researchers have proposed different ways to deal with assisting students in learning [6]. As a result, they have identified gaps and have been developing various frameworks and educational systems that are able to analyze student learning and provide adaptive feedback. These literatures suggests that the complex relationship between feedback, task complexity, pedagogical principles and student's characteristics affect the significance of feedback effects. The detailed categorization of previous methods used in providing multiple adaptive feedback to students, has been presented in our earlier work [7]. However, in this section, we briefly review recent adaptive feedback implementations which are similar to our previous work [7], with an addition of student's learning gains.

The author in [8], developed an intelligent tutoring system (ITS), using natural language processing and dialog to assist students in comprehending Newtonian Physics. The tool *Auto-Tutor*, provides feedback which consists of hints, prompts, and assertions are provided in form of dialogs according to a student's knowledge level. The main objective of the feedback provided by *Auto-Tutor*, is to simulate the construction of knowledge based on the constructivist principle [8]. Experimental results, show a learning gain of 0.8 between a control and experimental group.

On the other hand, *Guru* is an ITS which supports conversation with students while solving exercises in high school biology [9]. Similar to *Auto-Tutor*, *Guru* provides feedback in form of a dialog based on the student's knowledge level. However, *Guru* does not provide feedback based on any pedagogical principle or learning theory [7]. While comparing the control and experimental groups in an experiment, the effect of this feedback strategy on student's learning gains was 0.72 .

Gerdes's tutor, is developed as an interactive functional programming tutor for Haskell programming language [10]. The feedback provided by *Gerdes's tutor*, does not involve any characteristics of the students, however, the hint provided is generated automatically from a syntax tree of the model solution [7]. The hints provided are in form of steps, from a less reviling hint to a more detailed description of the solution.

A multimedia based ITS known as *Wayang Outpost*, is aimed at assisting student's in solving mathematical problems [11]. It provides feedback in form of hints, which are based on the learner's cognitive profile. These hints are provided based on the modality, contiguity, and animation multimedia learning principles. The cognitive apprenticeship principle is also utilized with the aim of encouraging students to accomplish more difficult task. However, an experiment to determine the effect of this feedback strategy did not yield any significant results [7].

DeepTutor is another dialog-based intelligent tutoring system that uses scaffolding to improve student's knowledge during problem-solving [12]. *DeepTutor* utilizes the students' knowledge level in order to determine the type and frequency of feedback [12]. *DeepTutor* provides scaffolding and a sequence of progressive hints, based on the student's knowledge level as articulated in the student model [13], [12]. Experiments show a learning gain of 0.79 for students in the experimental group as compared to the control group.

The author in [14], developed a framework for generating a generic prompting principle and prompts with the ability to support learning and skill acquisition for novices solving ill-structured problems. The feedback provided by the framework is based on the different levels of problem difficulty. It utilizes meta-cognitive principles and scaffolding techniques to support learning in ill-structured problem-solving context [14]. However, this framework has not been evaluated to determine the effect of the proposed feedback strategy on student's learning gains.

The Paired Associate Deterministic Learning Task (PADL) was designed to determine if feedback information which is limited to positive and negative, is suitable in a deterministic learning process [15]. The feedback in PADL is provided based on the student's solution with motivational factor in the form of an expected monetary reward. Experiments indicate that the learning process is influenced by the type of feedback provided and the expected monetary reward. But, the feedback technique used was not evaluated for its effect on student's learning gains.

Computational Thinking using Simulation Modeling *CTSiM*, is a learning tool that assist in learning science and computational thinking in middle school [16]. The feedback provided by *CTSiM*, is based on the student's proficiency which is evaluated based on the measure of the student's effectiveness and coherence. The hints are provided based on the scaffolding strategy using a conceptualized conversational dialog [16]. Experiments indicates positive learning gains of 0.29 between the experimental and control groups.

In an attempt to assist students in problem-solving, Negotiation-based adaptive learning system *NALS* was implemented [17]. *NALS*, uses student's solution to provide 3 level of hints and worked-out examples. The self-regulated learning principle is used for providing feedback, in order foster independence and lead students to seek help only when it is needed. Experiments indicate that *NALS*, helps in regulating student's help-seeking behaviors [17]. However, there was no study on the effect of this adaptive feedback technique on student's learning gains.

ALICE:fractions is an interactive mathematics textbook for helping students understand fractions [18]. Feedback in this tool is provided based on the student's answers. The principle of self-regulated learning is used in providing task level feedback in *ALICE:fractions*. Mostly, in *ALICE:fractions*, feedback is provided in form of text or visualization. Similar to other implementations, *ALICE:fractions* did not evaluate the effect of the feedback provided on student's learning gains.

The author in [1] developed a technique which provides feedback to students based on their performance, collaborative learning behavior, engagement, and understanding of concepts. This technique was reported to significantly improve student's performance. However, the student's learning gains were not considered in evaluating the system developed. Additionally, the complex relationship between task complexity, pedagogical principle, and student characteristics was not taken into consideration.

Paraprofessionals focus on educating students with severe disabilities. The author in [19] focused on the techniques that make paraprofessionals more effective in providing feedback. In their study the demonstrated that delayed, video-based performance feedback is an effective and efficient means of providing feedback. Based on the student's performance, simultaneous prompting and least-to-most (LTM) prompting are provided as feedback.

The Life-Saving Instruction for Emergencies (LIFE) app was developed by [20] to provide health care providers with self-regulatory learning content which is independent of classroom tutoring. A simulated medical emergency is made available to health care providers using a smartphone-based game, through which their management skills is been assessed. An immediate feedback is provided at every wrong attempt. The effectiveness of the feedback was measured based on the learning gains of an experiment and controlled group. The experimental group which were provided with adaptive immediate feedback showed a learning gain of 0.09.

The author in [21] developed a learning analytic dashboard that provides visualized feedback and adaptive support for face-to-face collaborative argumentation (FCA). Students utilize the dashboard to monitor their FCA process and the instructors provide real-time immediate feedback based on the student's performance.

Table I shows a summary of adaptive feedback implementations, indicating the feedback characteristics and learning gains. Based on these current studies, there are insufficient researches on the positive effect of multiple adaptive feedback characteristics on student's learning gains. A reason for this could be the complex nature of representing multiple adaptive feedback characteristics. Thus, these research aims at investigating the effect of multiple adaptive feedback characteristics on student's learning gains. To achieve the aim of this research an adaptive feedback model and algorithm is proposed in Section 2. In Section 3, the evaluation methods and processes are discussed. While the results of the evaluation process is presented in Section 4, and discussed in Section 5. Finally, the findings, limitations of the research, and future works are presented in Section 6.

II. Proposed Adaptive Feedback Model

Information in a computer-based learning environment can be regarded as models. The three most imperative models are the pedagogical model, domain model, and the student model [7]. The pedagogical model represents information and ways of teaching. The particular knowledge represented in the pedagogical model is based on pedagogical principles or learning theories. This principle or theory decides the successful teaching methods, instructional methods, sequence of activities, feedback types, and assessments modeled by the

TABLE I. ADAPTIVE FEEDBACK IMPLEMENTATIONS

S/N	Feedback Implementation	Feedback Characteristics	Learning gains	Normalize learning gains
1	AutoTutor (2012) [8]	Student's knowledge level, hints, student's solution, prompts, constructivist principle, Sequence of feedback	0.8	N/A
2	Guru (2012) [9]	Student's knowledge level, Scaffolding and sequential hints (domain knowledge), Based on a constructivist scaffolding strategy, Levels of details, Active learner.	0.72	
3	Gerdes's,Tutor (2012) [10]	Local to global	N/A	N/A
4	Wayang Outpost (2014) [11]	Cognitive apprenticeship, Step-by-step hints	Not significant	N/A
5	DeepTutor (2015) [12]	Student's knowledge level, scaffolding and sequential hints, based on a constructivist scaffolding strategy, levels of details and active learner.	0.79	N/A
6	Smy (2016) [14]	prompts, meta-cognition, scaffolding, and problem's level of difficulty.	N/A	N/A
7	PADL (2017) [15]	Monetary reward, positive and negative feedback, and learner's solution	N/A	N/A
8	CTSiM (2017) [16]	Student's proficiency, incorrect solutions, scaffolding, and hints	0.29	N/A
9	NALS (2018) [17]	Student's solution, hints and prompts, worked example, levels of detail, and self-regulated learning.	N/A	N/A
10	ALICE:fractions (2018) [18]	Student's answer and self-regulated learning.	N/A	N/A
11	[1]	Performance, collaborative learning behavior, engagement, and understanding of concepts.	N/A	N/A
12	[19]	Performance, simultaneous prompting, and least-to-most (LTM) prompting.	N/A	N/A
13	LIFE [20]	Performance, immediate feedback, and incorrect attempt.	0.09	N/A
14	[21]	Immediate feedback and student's activities.	N/A	N/A

learning environment. In a different circumstances, the domain model, is an aspect of the pedagogical model, which represents the knowledge of the subject been learned. The domain model represents concepts, learning materials, facts, problems, solutions, feedback, rules equations, etc. Finally, the student model shows information about the student's knowledge of the domain, learning style, interactions with the system, response to feedback, emotional state, performance etc. These data decides the characteristics of the students while interacting with the domain and pedagogy.

In this research, we center on the cognitive apprenticeship pedagogical principle and the physics domain. The challenge, is to show the properties of the cognitive apprenticeship principle that influence the type, timing, goal, and sequence of feedback, relating it to the characteristics of the domain and student models. Fig. 1, shows the Pedagogy, Domain, and Learner (PDL) model which were introduced in our earlier work [22]. The representation of the characteristics of all 3 models relating to adaptive feedback is shown in Fig. 1. The knowledge shown in the proposed PDL model is based on the OAR model. The nodes of the concept network in Fig. 1, represents concepts in the pedagogy, domain and student model in a computer-based learning environment. The arcs represent the relationship between concepts and their traits.

A. Adaptive Feedback Algorithm

The purpose of the adaptive feedback algorithm is to determine the appropriate feedback for different students based on adaptive characteristics [23]. The input to the adaptive feedback algorithm is the partial problem solving state PS_s. PS_s consists of attributes from the domain and student model. As show in Eq. 1, the problem solving state involves the student's cognitive style, student's knowledge level,goal (expected performance and completion time) problem's level of difficulty, and domain topic.

$$PS_s = (S_{cs}, S_{kl}, P_s, P_t, C_p, D_c) \tag{1}$$

The similarity between the current problem solving state PS_s and existing problem solving states PS_si in the knowledge base is determined iteratively. All the states that are above a certain threshold are stored as a list. The problem solving state with the highest cumulative weight is selected and its influence on the student's performance which has been defined by the knowledge bonding algorithm (Algorithm 1) is the output.

Thus, during a learning season when the problem solving state is determined, an appropriate feedback is provided based on existing knowledge of the most similar state in the knowledge base. This approach utilizes the content-addressed

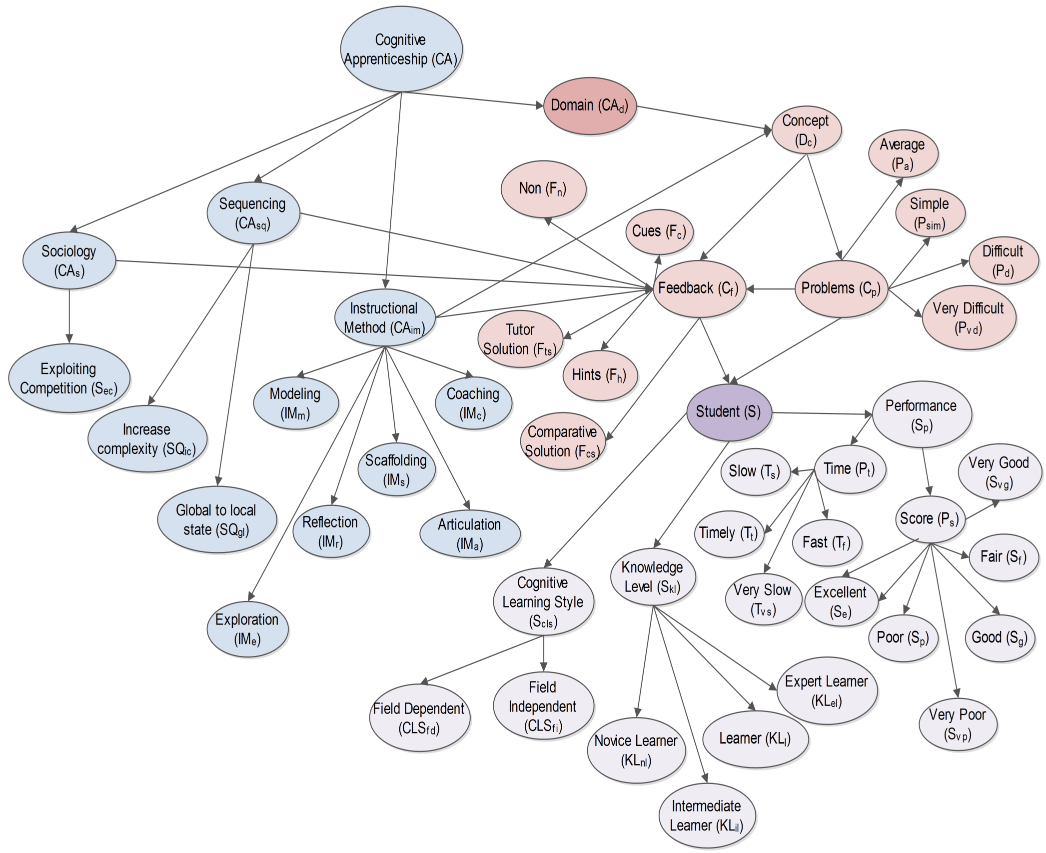

Fig. 1. PDL Model for Adaptive Feedback in Physics [22].

mechanism of a CKB for knowledge retrieval and manipulation which is enabled by the structural models.

III. Materials and Method

To establish the effectiveness of the PDL model in providing adaptive feedback, a group of pre-university (foundation studies) students are studied. The analysis is focused on the learning gains received by students receiving the PDL-based feedback as compared to traditional feedback and no feedback at all. The traditional feedback provides only feedback to the students without considering the adaptive characteristics of feedback.

A. Participants

The experimental process involves students distributed into three groups. The three groups consist of the traditional feedback group (Normal), no feedback (Non) group, and the experimental group (Adaptive). All students are allowed to take their regular classes. A pre-test before exposing students to the adaptive feedback tool is provided, followed by a problem-solving session with the adaptive feedback environment for four weeks, with each session lasting 30 minutes. After the experimental process, the students are provided with a post-test.

The pre-test and post-test comprise of 10 physics problems each in introductory mechanics with similar sub-topics and difficulty levels. While the problems provided by the PDL-based adaptive feedback system comprise of 160 problems. The students are required to solve 10 problems daily for the 4 weeks (5 days/week) period of the experiment. All the problems are provided by the physics experts.

The participants are 31 pre-university (foundation studies) students from Center of Foundation Studies of the University of Malaya taking physics course and are currently learning a topic on introductory mechanics. They are randomly categorised into three groups:

- The traditional feedback group (Normal) consist of students who solve problems with the adaptive feedback system, but are provided with the same type of feedback without considering the adaptive characteristics of feedback.
- The no feedback group (Non) involves students who undergo the problem-solving process with the adaptive feedback system with no feedback provided.

Algorithm 1: Adaptive Feedback Algorithm

Data: PS_s,time stamp
Result: R^{in}
read data;
create and initialize problem solving state list PS_{sL}
while PS_{si} *is available* **do**
  compute similarity $PS_s \sim PS_{si} = \left|\frac{A \cap A_i}{A \cup A_i}\right| = \begin{cases} 1 & PS_s = PS_{si} \\ (0,1) & PS_s \leftrightarrow PS_{si} \vee PS_s < PS_{si} \vee PS_s > PS_{si} \\ 0 & PS_s \neq PS_{si} \end{cases}$
  ;
  if $PS_s \sim PS_{si} > TH$; `/* TH is the similarity threshold */`
  then
    retrieve PS_{si};
    add to problem solving state list $PS_{sL} = PS_{sL} + PS_{si}$;
    current section becomes this one;
  else
    Create random $PS_s i$
determine highest PS_{si};
output the influence of related concepts of the highest PS_{si}, $R_i^{in} \subseteq \bigcup_{i=1}^{|R_i|} R_i^c$;

TABLE II. Participant's Demographics

S/N	Size	Total
Age		31
18 Years	31	
Gender		
Male	11	31
Female	20	
Others	0	
Major		
Physical Science	11	31
Life Science 1	11	
Life Science 2	9	

- The experimental group (Adaptive) comprises of students who undertake the problem-solving process while they are provided with adaptive feedback based on the PDL-model.

The 31 participants are all 18 years old with 64.52% female and 35.48% male as shown in Table II. The participants where taken from three majors of Physical Science, Life Science 1, and Life Science 2. The three classes of students are then assigned to the Adaptive, Normal, and Control groups as shown in Table IV

All participants are enrolled in the pre-university (foundation studies) program at the same time and are attending the same classes in introductory mechanics. The problems provided are from four main topics of Static, Linear Motion, Rotational Motion, and Gravitation in introductory physics. The problems are based on three levels of difficulty which includes easy, moderate, and difficult. The distribution of the problems based on the topics and difficulty level is shown in Table III.

B. Evaluation Method

Cross-disciplinary researches that involves artificial intelligence in education can be difficult to conduct due to the restrictions placed on research with human subjects. Experimental controls are restricted, and arbitrary sampling is difficult to achieve in a classic classroom setting. As computer scientists, we ought to have the expertise to construct valid, compelling studies of student's learning under the difficult conditions imposed by researches based on human subjects [24].

1) Learning Gains: Student's learning with a computer-based learning approach is usually evaluated using the relationship between a pre-test and a post-test scores to determine the learning gains and normalized learning gains [25]. The tests given prior to the provision of computer-based instructions or interventions are pre-tests, while the tests administered after the intervention are post-test [26]. In general, students who tend to perform well during a pre-test, do well in the post-test. The learning and normalized learning gains utilizes pre-test and post-test to evenly compare students' learning among experimental and control groups [27]. Equations 2 and 3 indicate that both the learning gains and normalized learning gains incorporate pre-tests (pre) and post-tests (post).

The normalized learning gains was introduced because, the learning gains provided an unfair advantage to groups with low pre-test scores. Most assessments involve problems with different levels of difficulty, and some information are easier to assimilate than others. Thus, a student with a low pre-test score has a wider scope of difficulty levels to learn than a student with high pre-test scores. The normalized learning gain was developed to rectify this uneven advantage [28].

2) Analysis of Covariance: In statistics and probability, there is a possibility that a trend is seen in several groups of data but later disappear when the data is combined, this phenomenon is called the Simpson's paradox. The paradox shows that a statistically significant relationship in a certain direction can result to an opposite direction when investigated with a covariant [29]. Since most investigations do not arbitrary assign students to experimental groups and the pre-test scores are usually related to the post-test scores, learning gains can show significant difference which favors a certain group but another group may be more effective when using the pre-test as a covariate. Analysis of Covariance (ANCOVA) eliminates the impact of a covariate to establish a fair comparison among different groups.

ANCOVA assesses whether the means of a dependent variable are equivalent throughout the dimensions of an independent variable, while statistically managing the impacts of continuous variables that are not essential, known as covariates [30]. As shown in Equation 4, an ANCOVA model expects a linear relationship between the dependent variable and the covariate.

$$y_{ij} = \mu + \tau_i + \mathrm{B}(x_{ij} - \overline{x}) + \epsilon_{ij}. \quad (4)$$

TABLE III. Distribution of Problems in Introductory Physics

S/N	Topic	Difficult	Intermediate	Easy	Total
1	Static	5	2	1	8
2	Linear Motion	26	32	26	84
3	Rotational Motion	10	12	16	38
4	Gravitation	10	10	10	30
5	Total	51	56	53	160

$$Learning\ gains\ lg = post - pre \tag{2}$$

$$Normalized\ learning\ gains\ nlg = \frac{learning\ gains}{possible\ learning\ gains} = \frac{(post - pre)}{(100\% - pre)} \tag{3}$$

TABLE IV. Distribution of Students Amongst Experimental Groups

S/N	Major	Adaptive	Normal	Non	Total
1	Physical Science	3	5	3	11
2	Life Science 1	5	4	2	11
3	Life Science 2	4	3	2	9
4	Total	12	12	7	31

TABLE V. Distribution of Student's Response to the Experiment

S/N	Group	Pre-test	Adaptive Tool	Post-test	All
1	Adaptive	18	12	12	12
2	Normal	16	12	12	12
3	Non	16	7	9	7
4	Total	50	31	33	31

In Equation 4,

- dependent variable y_{ij} is the j^{th} observation for the i^{th} group.
- covariate x_{ij} is the j^{th} observation of the covariate the i^{th} group.
- grand mean is μ
- global mean of covariant is x
- the effect of the i^{th} level of the independent variable is τ_i
- line slope is B
- associative non observed error for the j^{th} observation for the i^{th} group is ϵ_{ij}

In conducting an ANCOVA, there are some assumptions that are tested. First there is a need to determine that no outliers exists. Then, the observations in the dependent variable should be normally distributed for each level of the independent variable. This test is known as the assumption of normality. This assumption requires multiple conditional distributions of the dependent variable for every combination of the covariate to be normally distributed. If the population distributions are not normal and the sample sizes are small, the significant values obtained with ANCOVA may be invalid. Another assumption that is tested in ANCOVA, is the homogeneity of regression slopes. The regression lines for individual groups are assumed to be parallel, having the same slope. The failure to meet this assumptions implies that there is an interaction between the covariant and the independent variable. Usually this assumption is evaluated by the F-test, if the value is significant then the assumption of homogeneity of regression slopes is violated. The final assumption considered in this experiment is the homogeneity of variance. This test shows the relationship between the dependent variable and the covariate for the entire dataset, ignoring the various groups of the independent variable. Thus, if there is a positive relationship between the covariate and the independent variable of one group, then there should be a possible relationship for the rest of the groups.

IV. Analysis of Results

The pre-test and post-tests scores are rated on a 100-points scale, where 0 indicates a poor performance and 100 indicates an excellent performance. The rating is done by physics experts who provided the problems to be solved. The assessment focused on the workings towards a solution, identification of known, unknowns, equations and principles along with the correct answer. At the beginning of the experiment, 63 students were invited, 50 turned up for the pre-test and registered to use the adaptive learning environment. Then, out of the 50 students, 33 students turned up for the post-test. In the end, only 31 students did the pre-test, used the adaptive learning tool, and also participated in the post-test. Table V, show the detailed break-down of the students responses to the experiment according to the experimental groups.

1) Results of Student's Learning Gains: In order to determine the effect of proposed adaptive feedback model on student's learning gains, the results of the pre-test and the post-test of each group is collected as shown in Table VI. The pre-test and post-test scores are based on the average scores of the 10 problems solved by each student. The learning gains and normalized learning gains are calculated according to Equations 2 and 3. The average learning gains of each experimental group and a comparison between the average

TABLE VI. STUDENT'S PRE-TEST AND POST-TEST SCORES

S/N	Student ID	Major	Group	Pre-test Score	Post-test Score	Learning Gains	Normalized Learning Gains
1	0073	Life Science 2	Adaptive	0.00	9.90	9.90	0.10
2	0036	Physical Science	Adaptive	2.00	16.00	14.00	0.16
3	0057	Life Science 1	Adaptive	8.70	25.20	16.50	0.28
4	0041	Physical Science	Adaptive	2.00	20.40	18.40	0.21
5	0048	Life Science 1	Adaptive	5.50	28.00	22.50	0.30
6	0061	Life Science 2	Adaptive	1.00	13.70	12.70	0.14
7	0072	Life Science 2	Adaptive	3.00	24.50	21.50	0.25
8	0056	Life Science 1	Adaptive	6.50	32.40	25.90	0.35
9	0045	Life Science 1	Adaptive	7.80	20.90	13.10	0.23
10	0051	Life Science 1	Adaptive	0.70	17.70	17.00	0.18
11	0059	Life Science 2	Adaptive	4.00	21.50	17.50	0.22
12	0032	Physical Science	Adaptive	8.00	31.50	23.50	0.34
13	0037	Physical Science	Normal	3.00	10.00	7.00	0.10
14	0067	Life Science 2	Normal	1.00	7.60	6.60	0.08
15	0055	Life Science 1	Normal	10.40	10.00	-0.40	0.11
16	0074	Life Science 2	Normal	6.25	7.70	1.45	0.08
17	0031	Physical Science	Normal	9.00	17.70	8.70	0.19
18	0049	Life Science 1	Normal	12.50	10.50	-2.00	0.12
19	0054	Life Science 1	Normal	5.80	29.00	23.20	0.31
20	0047	Life Science 1	Normal	13.00	29.50	16.50	0.34
21	0044	Physical Science	Normal	3.50	9.50	6.00	0.10
22	0070	Life Science 2	Normal	0.00	2.40	2.40	0.02
23	0030	Physical Science	Normal	9.30	19.50	10.20	0.21
24	0043	Physical Science	Normal	6.00	11.90	5.90	0.13
25	0064	Life Science 2	Non	10.55	13.30	2.75	0.15
26	0046	Life Science 1	Non	5.50	13.5	8.00	0.14
27	0033	Physical Science	Non	6.50	10.00	3.50	0.11
28	0052	Life Science 1	Non	11.90	7.00	-4.90	0.08
29	0042	Physical Science	Non	6.30	11.80	5.50	0.13
30	0038	Physical Science	Non	6.50	20.40	13.90	0.22
31	0062	Life Science 2	Non	0.50	10.15	9.65	0.10

TABLE VII. COMPARISON OF STUDENT'S LEARNING GAINS

S/N	Group	Learning Gains	Normalized Learning Gains
1	Adaptive	16.24	0.21
2	Normal	7.98	0.16
3	Non	6.55	0.14
4	Adaptive Vs. Normal	8.72	0.05
5	Adaptive Vs. Non	9.69	0.07
6	Normal Vs. Non	1.43	0.02
7	Adaptive Vs. (Normal & Non)	8.98	0.06

learning gains are presented in Table VII. As expected, each experimental groups had a positive learning and normalized learning gains.

2) One-way ANCOVA Results: In this study, ANCOVA is used with a view to eliminate bias for a certain experimental group. The Statistical Package for the Social Science (SPSS) tool was used to analyze the student's pre-test and post-test scores shown in Table VI. The ANCOVA allows us to see if there is a difference in the dependent variable (post-test) by the levels of the independent variable (group) while controlling for the effect of the covariate (pre-test). The independent variable used is the experimental group (group), has three levels which are adaptive, normal, and non. The dependent variable is the post-test, which is measured at a continuous level, while the pre-test is the covariate, which is also measured at a continuous level.

Table VIII, shows a descriptive statistics of the post-test according to the three experimental groups. It provides a summarized description of the post-test, for each group by presenting the mean, median, variance, range, standard deviation, skewness, and kurtosis. The mean post-test score of the adaptive feedback group was higher than the normal and non feedback groups.

In respect to ANCOVA models, data must be scrutinized to evaluate the existence of outliers, and affirm that it meets fundamental assumptions of normality, homogeneity of regression

TABLE VIII. POST-TEST DESCRIPTIVE STATISTICS

	Group			Statistic	Std. Error
PostTest	Adaptive	Mean		21.8083	1.99292
		95% Confidence Interval for Mean	Lower Bound	17.4219	
			Upper Bound	26.1947	
		5% Trimmed Mean		21.8815	
		Median		21.2000	
		Variance		47.661	
		Std. Deviation		6.90368	
		Minimum		9.90	
		Maximum		32.40	
		Range		22.50	
		Interquartile Range		10.88	
		Skewness		-.032	.637
		Kurtosis		-.640	1.232
	Non	Mean		12.3071	1.59091
		95% Confidence Interval for Mean	Lower Bound	8.4143	
			Upper Bound	16.2000	
		5% Trimmed Mean		12.1524	
		Median		11.8000	
		Variance		17.717	
		Std. Deviation		4.20916	
		Minimum		7.00	
		Maximum		20.40	
		Range		13.40	
		Interquartile Range		3.50	
		Skewness		1.129	.794
		Kurtosis		2.236	1.587
	Normal	Mean		13.7750	2.45058
		95% Confidence Interval for Mean	Lower Bound	8.3813	
			Upper Bound	19.1687	
		5% Trimmed Mean		13.5333	
		Median		10.2500	
		Variance		72.064	
		Std. Deviation		8.48904	
		Minimum		2.40	
		Maximum		29.50	
		Range		27.10	
		Interquartile Range		10.90	
		Skewness		.982	.637
		Kurtosis		.112	1.232

and variance [31]. Fig. 2, shows a box plot showing the overall pattern of the post-test scores for the experimental groups. The result from the box plot indicates that the adaptive and normal feedback groups have varying post-test scores, while the non feedback group had similar post-test scores. However, one outlier was identified in the non feedback group as seen in Fig. 2.

The results of the normality test is shown in Table X. The observations from the Shapiro-Wilk test shows that the post-test is normally distributed for the adaptive, normal, and non feedback groups. Furthermore, Fig. 3, 4, and 5, presents the Quantile-Quantile (Q-Q) plots for the three experimental groups. The ideal dataset should have all points on the trend line, however, the results presented from the Q-Q plots are not ideal.

To further explore the data, the homogeneity of regression slopes assumption is tested. It is assumed that the regression lines for the adaptive, normal, and non feedback groups are parallel. Table X, displays the results of the test for homogeneity of regression slopes using the general linear model in SPSS. The p-value (0.106) of the interaction term is non-significant (for $\alpha = 0.05$) indicating a non-violation of the

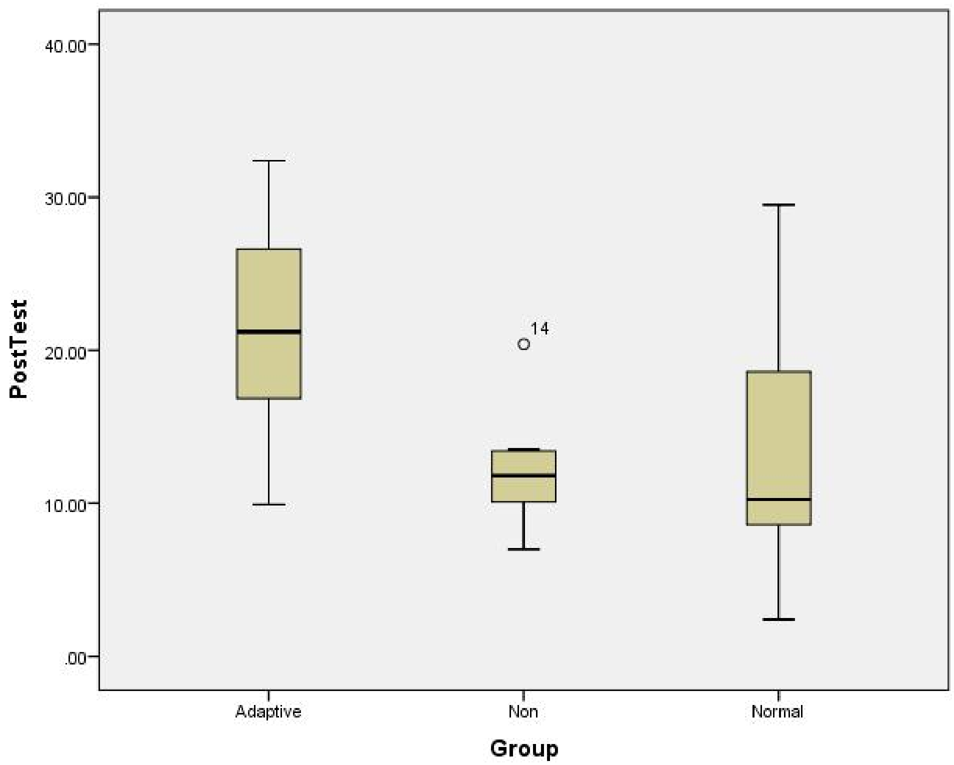

Fig. 2. Test for Outliers.

TABLE IX. TESTS OF NORMALITY

	Group	Shapiro-Wilk		
		Statistic	df	Sig.
PostTest	Adaptive	.978	12	.973
	Non	.914	7	.421
	Normal	.867	12	.060

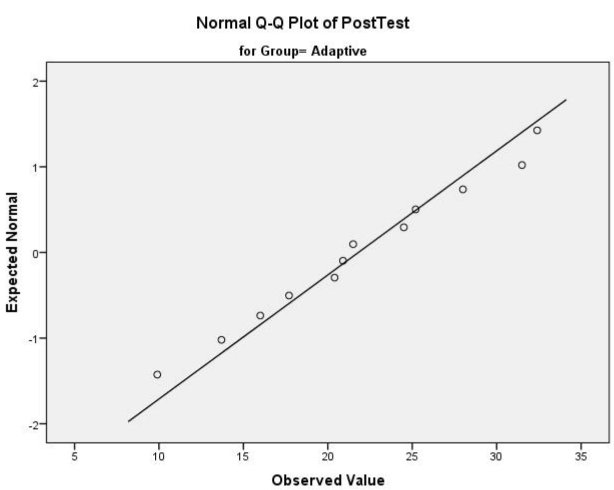

Fig. 3. Adaptive Feedback Q-Q Plot for Post-Test.

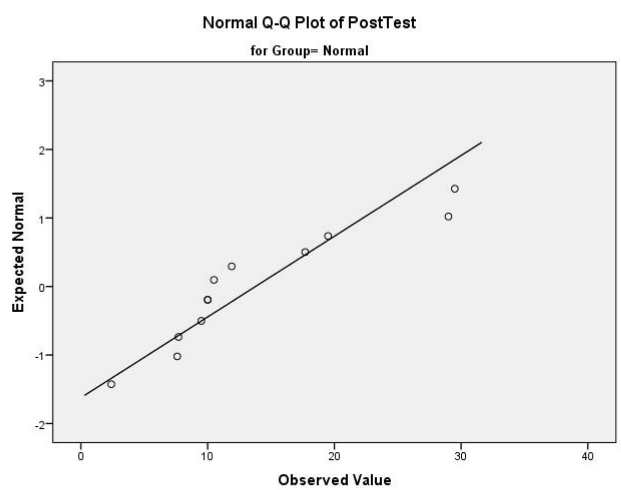

Fig. 4. Normal Feedback Q-Q Plot for Post-Test.

assumption of homogeneity of regression slopes. Thus, there is no interaction between the pre-test and the experimental groups.

In this study, the last assumption tested was the homogeneity of variance. The Levene's test of homogeneity of variance was carried out. As shown in Table XI, this assumption is satisfied because $p(0.773) > \alpha(0.05)$

For testing the main hypothesis, a One-way ANCOVA was conducted to determine a statistically significant difference

TABLE X. TEST OF HOMOGENEITY OF REGRESSION SLOPE

Tests of Between-Subjects Effects
Dependent Variable: PostTest

Source	Type III Sum of Squares	df	Mean Square	F	Sig.	Partial Eta Squared
Corrected Model	1111.712a	5	222.342	6.450	.001	.563
Intercept	952.967	1	952.967	27.645	.000	.525
Group * Pretest	169.187	2	84.594	2.454	.106	.164
Group	127.362	2	63.681	1.847	.179	.129
Pretest	268.347	1	268.347	7.785	.010	.237
Error	861.783	25	34.471			
Total	10467.783	31				
Corrected Total	1973.495	30				

R Squared = .563 (Adjusted R Squared = .476)

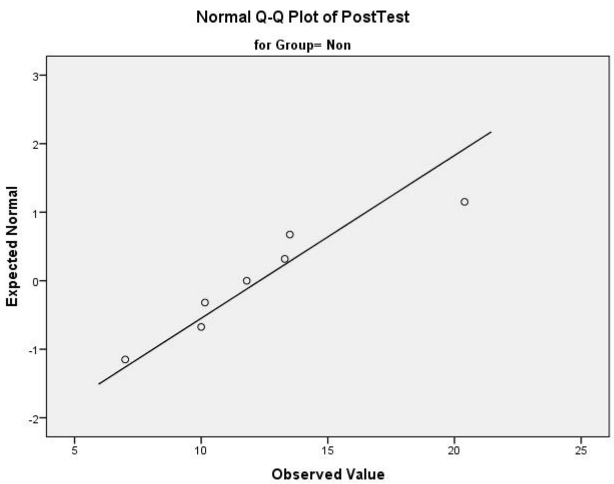

Fig. 5. No Feedback Q-Q Plot for Post-Test.

TABLE XI. TEST OF HOMOGENEITY OF VARIANCE

Levene's Test of Equality of Error Variances
Dependent Variable: PostTest

F	df1	df2	Sig.
.260	2	28	.773

Tests the null hypothesis that the error variance of the dependent variable is equal across groups.
Design: Intercept + Pretest + Group

between students provided with adaptive feedback, students provided with normal feedback and students with no feedback on a post-test controlling for pre-test. The results shown in Table XII, shows a significant effect ($p < 0.001$) of adaptive feedback on the post-test after controlling for the pre-test.

Considering the fact that a significant main effect was obtained and there are three levels of the independent variable, there is a need to conduct a post hoc to determine the significant pairwise differences. According to the results in Table XIII, there is a significant difference between adaptive and normal feedback groups ($p = 0.001$) and adaptive and non feedback groups ($p = 0.001$). However, there was no significant difference between the normal and non feedback groups ()$p = 1.000$).

V. DISCUSSION

The main aim of conducting this experiment is to determine the effect of adaptive feedback on student's learning gains. The three groups analyzed in this experiment are the adaptive, normal, and non feedback groups. To achieve a valid conclusion on the effect of adaptive feedback, two fundamental methods were used. First, the student's learning gains (LG) and normalized learning gains (NLG) were analyzed. Based on the results in Table VII, all the students in the three groups achieved positive learning gains and normalized learning gains after using the adaptive feedback tool. This is due to the interventions received by the students between the pre-test and post-test periods. However, despite the positive learning gains and normalized learning gains, the group which were provided with adaptive feedback ($LG = 16.24, NLG = 0.21$) had higher learning and normalized learning gains than those with the normal feedback ($LG = 7.98, NLG = 0.16$) and non feedback ($LG = 6.55, NLG = 0.14$). In comparing the three experimental groups, students who were provided with adaptive feedback showed learning gains and normalized learning gains of 8.72 and 0.05 over the normal feedback group, with 9.69 and 0.07 over the non feedback group. The results of this comparison shows that the student's who received adaptive feedback achieved superior learning gains than those who received normal and no feedback. In addition, student's who received normal feedback, had better learning gains than student who did not receive feedback. The results of this experiment implies that the adaptive feedback provided by the proposed PDL model has a positive effect on student's learning gains.

Previous researchers have conducted similar experiments to determine the effect of the feedback provided. Table XIV, shows the comparison of our results with the previous studies on a 10 point scale. The adaptive feedback provided by the proposed PDL model has more positive effect on student's learning gains than adaptive feedback models proposed in previous researches.

In view of eliminating any form of bias in our experimental results, a one-way ANCOVA was conducted to compare the effectiveness of the three feedback methods using the pre-test and post-test scores. The main hypothesis states that *the*

TABLE XII. Analysis of Covariance

Source	Type III Sum of Squares	df	Mean Square	F	Sig.	Partial Eta Squared
Corrected Model	942.525a	3	314.175	8.228	.000	.478
Intercept	831.111	1	831.111	21.766	.000	.446
Pretest	392.304	1	392.304	10.274	.003	.276
Group	827.258	2	413.629	10.832	.000	.445
Error	1030.970	27	38.184			
Total	10467.783	31				
Corrected Total	1973.495	30				

R Squared = .478 (Adjusted R Squared = .420)

TABLE XIII. Post-Hoc Analysis of Covariance

Pairwise Comparisons
Dependent Variable: PostTest

(I) Group	(J) Group	Mean Difference (I-J)	Std. Error	Sig.	95% Confidence Interval for Difference	
					Lower Bound	Upper Bound
Adaptive	Non	12.232*	3.060	.001	4.422	20.043
	Normal	10.588*	2.646	.001	3.835	17.341
Non	Adaptive	-12.232*	3.060	.001	-20.043	-4.422
	Normal	-1.644	2.939	1.000	-9.147	5.859
Normal	Adaptive	-10.588*	2.646	.001	-17.341	-3.835
	Non	1.644	2.939	1.000	-5.859	9.147

Based on estimated marginal means
* The mean difference is significant at the .05 level.
b Adjustment for multiple comparisons: Bonferroni.

TABLE XIV. Comparison of Proposed PDL Model and Previous Models

S/N	Feedback Tool (Year)	Learning Gains	Normalized Learning Gains
1	AutoTutor (2012) [8]	0.8	N/A
2	Guru (2012) [9]	0.72	N/A
3	Wayang Outpost (2014) [11]	not significant	N/A
4	DeepTutor (2015)[12]	0.79	N/A
5	CTSiM (2017) [16]	0.29	N/A
6	LIFE (2020) [20]	0.09	N/A
7	Proposed PDL Model	0.90	0.06

adaptive feedback group will perform better than the normal and no feedback group in a post-test after using the adaptive feedback tool. During the analysis of the data, one outlier was identified in the non feedback group. The outlier was not removed from the dataset because there was no significant difference in the overall analysis with its exclusion. The Shapiro-Wilk test for normality showed that the post-test is evenly distributed between the groups with a non-significant value of $p(0.973) > \alpha(0.05)$ for adaptive, $p(0.60) > \alpha(0.05)$ for normal, and $p(0.421) > \alpha(0.050$ for non. The test for homogeneity of regression was conducted and the assumption was made with a non-significant value of $p(0.106) > \alpha(0.05)$. Then, the Levene's test for homogeneity of variance was carried out and a non-significant value of $p(.773) > \alpha(0.05)$ was obtained. This indicates that the null hypothesis of the error variance of the post-test is equal across all experimental groups. Since non of the assumptions tested were violated, the results obtained from the main ANCOVA is valid.

From the results, it is found that there was a significant difference in the mean post-test scores ($[F(2, 27) = 10.832, p < 0.001]$) between adaptive, normal, and non feedback groups. The partial Eta Squared value of 0.445 indicates the effect size. Based on the Cohen' s guideline the effect size is small. This implies that the variance in the post-test to a small effect, is explained by the experimental groups. The post hoc test indicated a significant difference between the adaptive and normal feedback groups ($p(0.001) < \alpha(0.05)$), adaptive and non feedback groups ($p(0.001) < \alpha(0.05)$). This indicates that the adaptive feedback technique provided by proposed the PDL model has a significant effect in improving student's post-test scores than the normal and no feedback techniques. Comparing the normal and feedback groups showed no significant difference ($p(1.000) > \alpha(0.05)$).

VI. Conclusion

The main objective of this research is *to evaluate the effect of the adaptive feedback model, on student's learning gains*. The effect of the adaptive feedback provided based on the proposed model, was evaluated to determine its effect on student's learning gains. Overall, the experimental findings from calculating the students learning gains and a One-way ANCOVA, showed that the adaptive group who receive feedback based on the PDL model showed a statistically significant gain in learning outcomes as compared to the normal and non feedback groups. This suggests that adaptive feedback based on the PDL model can have a sustained positive impact on student's learning gains. Additional findings from the one-way ANCOVA showed that, there is no statistically significant difference in the post-test scores of students who are provided with normal feedback, as compared to those who had no feedback. However, the student's provided with normal feedback had better learning gains and normalized learning gains of 1.43 and 0.02, respectively, as compared to those without feedback. A comparison of the findings with other similar studies showed that the adaptive feedback provided by the PDL model is superior. As a conclusion, based on the aim of this case study, the provision of adaptive feedback using the PDL model is an effective tutoring strategy. Limitations of this study are moderate. First of all, a single case study design, of the effect of the adaptive feedback on students learning gains is not representative. In addition, more number of students might have been desirable, however, this was not possible due to the availability of the students. Besides the number of students, more interactions by the students with the adaptive learning tool is also desirable, but was not possible due to the nature of interaction with human subjects. This could be due to the difficulty in using the tool, as the student's are required to be familiar with writing equations in the latex format. Subsequently, from a science measurement perspective, while the adaptive feedback model fit reasonably well and indicated superior learning gains, additional characteristics of the pedagogy, domain, and student models need to be considered to determine the best fit. The proposed adaptive feedback model can be extended by adding additional characteristics of the student, domain and pedagogy. This new model can be evaluated to determine which characteristics has more effect to improve student's learning gains.

Acknowledgment

This work was supported by the University of Malaya Research Grant [RP040B-15AET, 2018].

References

[1] M. A. Hassan, U. Habiba, H. Khalid, M. Shoaib, and S. Arshad, "An adaptive feedback system to improve student performance based on collaborative behavior," *IEEE Access*, vol. 7, pp. 107 171–107 178, 2019.

[2] E. G. Advisors, "Learning to adapt: A case for accelerating adaptive learning in higher education," *Education Growth Advisors*, 2013.

[3] A. A. Al-Hunaiyyan, A. T. Bimba, and S. Alsharhan, "A cognitive knowledge-based model for an academic adaptive e-advising system," *Interdisciplinary Journal of Information, Knowledge, and Management*, vol. 15, pp. 247–263, 2020.

[4] S. Narciss, S. Sosnovsky, L. Schnaubert, E. Andres, A. Eichelmann, G. Goguadze, and E. Melis, "Exploring feedback and student characteristics relevant for personalizing feedback strategies," *Computers and Education*, vol. 71, pp. 56–76, feb 2014.

[5] N.-T. Le, "A Classification of Adaptive Feedback in Educational Systems for Programming," *Systems*, vol. 4, no. 2, p. 22, 2016.

[6] S. Farid, R. Ahmad, and M. Alam, "A hierarchical model for e-learning implementation challenges using ahp." *Malaysian Journal of Computer Science*, vol. 28, no. 3, 2015.

[7] A. T. Bimba, N. Idris, A. Al-Hunaiyyan, R. B. Mahmud, and N. L. B. M. Shuib, "Adaptive feedback in computer-based learning environments: a review," *Adaptive Behavior*, vol. 25, no. 5, pp. 217–234, 2017.

[8] S. D'mello and A. Graesser, "Autotutor and affective autotutor: Learning by talking with cognitively and emotionally intelligent computers that talk back," *ACM Transactions on Interactive Intelligent Systems (TiiS)*, vol. 2, no. 4, p. 23, 2012.

[9] A. Olney, S. D'Mello, N. Person, W. Cade, P. Hays, C. Williams, B. Lehman, and A. Graesser, "Guru: A computer tutor that models expert human tutors," in *Intelligent Tutoring Systems*. Springer, 2012, pp. 256–261.

[10] A. Gerdes, J. Jeuring, and B. Heeren, "An interactive functional programming tutor," in *Proceedings of the 17th ACM annual conference on Innovation and technology in computer science education*. ACM, 2012, pp. 250–255.

[11] I. Arroyo, B. P. Woolf, W. Burelson, K. Muldner, D. Rai, and M. Tai, "A multimedia adaptive tutoring system for mathematics that addresses cognition, metacognition and affect," *International Journal of Artificial Intelligence in Education*, vol. 24, no. 4, pp. 387–426, 2014.

[12] V. Rus, N. B. Niraula, and R. Banjade, "Deeptutor: An effective, online intelligent tutoring system that promotes deep learning." in *AAAI*, 2015, pp. 4294–4295.

[13] V. Rus, M. Conley, and A. Graesser, "The dendrogram model of instruction: On instructional strategies and their implementation in deeptutor," *Design Recommendations for Intelligent Tutoring Systems*, p. 311, 2014.

[14] V. Smy, M. Cahillane, and P. MacLean, "Sensemaking and metacognitive prompting in ill-structured problems," *The International Journal of Information and Learning Technology*, vol. 33, no. 3, pp. 186–199, 2016.

[15] M. Gawlowska, E. Beldzik, A. Domagalik, A. Gagol, T. Marek, and J. Mojsa-Kaja, "I don't want to miss a thing in learning dynamics and effects of feedback type and monetary incentive in a paired associate deterministic learning task," *Frontiers in psychology*, vol. 8, p. 935, 2017.

[16] S. Basu, G. Biswas, and J. S. Kinnebrew, "Learner modeling for adaptive scaffolding in a computational thinking-based science learning environment," *User Modeling and User-Adapted Interaction*, vol. 27, no. 1, pp. 5–53, 2017.

[17] C.-Y. Chou, K. R. Lai, P.-Y. Chao, S.-F. Tseng, and T.-Y. Liao, "A negotiation-based adaptive learning system for regulating help-seeking behaviors," *Computers & Education*, vol. 126, pp. 115–128, 2018.

[18] S. Hoch, F. Reinhold, B. Werner, J. Richter-Gebert, and K. Reiss, "Design and research potential of interactive textbooks: the case of fractions," *ZDM*, vol. 50, no. 5, pp. 839–848, 2018.

[19] M. E. Brock, M. A. Barczak, and S. A. Dueker, "Effects of delayed video-based feedback and observing feedback on paraprofessional implementation of evidence-based practices for students with severe disabilities," *Focus on Autism and Other Developmental Disabilities*, vol. 35, no. 3, pp. 153–164, 2020.

[20] T. Tuti, N. Winters, H. Edgcombe, N. Muinga, C. Wanyama, M. English, and C. Paton, "Evaluation of adaptive feedback in a smartphone-based game on health care providers' learning gain: Randomized controlled trial," *Journal of medical Internet research*, vol. 22, no. 7, p. e17100, 2020.

[21] J. Han, K. H. Kim, W. Rhee, and Y. H. Cho, "Learning analytics dashboards for adaptive support in face-to-face collaborative argumentation," *Computers & Education*, vol. 163, p. 104041, 2020.

[22] A. T. Bimba, N. Idris, A. A. Al-Hunaiyyan, R. B. Mahmud, and N. L. B. M. Shuib, "Design of an algebraic concept operator for adaptive feedback in physics," in *Conference on e-Business, e-Services and e-Society*. Springer, 2018, pp. 181–190.

[23] A. Al-Hunaiyyan, A. T. Bimba, N. Idris, and S. Al-Sharhan, "A cognitive knowledge-based framework for social and metacognitive support in mobile learning." *Interdisciplinary Journal of Information, Knowledge & Management*, vol. 12, 2017.

[24] L. Gatti, M. Ulrich, and P. Seele, "Education for sustainable development through business simulation games: An exploratory study of sustainability gamification and its effects on students' learning outcomes," *Journal of Cleaner Production*, vol. 207, pp. 667–678, 2019.

[25] J. A. Ruiperez-Valiente, P. J. Munoz-Merino, and C. Delgado Kloos, "Improving the prediction of learning outcomes in educational platforms including higher level interaction indicators," *Expert Systems*, p. e12298, 2018.

[26] N. P. Moreno, A. D. Newell, L. R. Zientek, K. Nimon, and G. L. Vogt, "Linking science education and hiv using viral biology, epidemiology and science practices," *Health Education Journal*, p. 0017896918783778, 2018.

[27] S. Sanhueza Haro, A. Bravo Escobar, C. Faundez Araya, and E. Utreras Cofre, "Icts as cognitive tools of inclusion in physics class for high school students," *GONDOLA-ENSENANZA Y APRENDIZAJE DE LAS CIENCIAS*, vol. 13, no. 2, pp. 306–324, 2018.

[28] L. Hsu, "Measuring the effectiveness of summer intensive physics courses for gifted students: A pilot study and agenda for research," *Gifted Child Quarterly*, vol. 47, no. 3, pp. 212–218, 2003.

[29] K. Hochberg, J. Kuhn, and A. Maeller, "Using smartphones as experimental tools - effects on interest, curiosity, and learning in physics education," *Journal of Science Education and Technology*, pp. 1–19, 2018.

[30] C. Saini and J. Abraham, "Implementing facebook-based instructional approach in pre-service teacher education: An empirical investigation," *Computers & Education*, vol. 128, pp. 243–255, 2019.

[31] T. R. Johnson, "Violation of the homogeneity of regression slopes assumption in ancova for two-group pre-post designs: Tutorial on a modified johnson-neyman procedure," *The Quantitative Methods for Psychology*, vol. 12, no. 3, pp. 253–263, 2016.

A Fuzzy MCDM Approach for Structured Comparison of the Health Literacy Level of Hospitals

Abed Saif Ahmed Alghawli[1]*
Department of Computer Science, College of Sciences and Humanities
Prince Sattam Bin Abdulaziz University, Aflaj, Kingdom of Saudi Arabia

Adel A. Nasser[2]
Department of Computer Science and Information Systems
Faculty of Science, Sa'adah University
Sa'adah, Yemen

Mijahed N. Aljober[3]
Department of Computer Science
Faculty of Science, Hajjah University
Hajjah, Yemen

***Abstract*—The primary objective of this study is to develop a hybrid multi-criteria decision-making (MCDM) model to evaluate and compare the organizational health literacy responsiveness (OHLR) level of hospitals. To achieve this goal, the health literacy performance indicators are selected, some potential uses of single and hybrid MCDM and qualitative approaches for structured comparison purposes are illustrated, one more common hybrid approach based on the Fuzzy Analytic Hierarchy Process and fuzzy Delphi method was chosen, developed, and applied. To compare the proposed model with its classical non fuzzy version (Qualitative – AHP), a case study example on the effect of their implementation on a structured comparison decisions is conceded, and the Bland Altman agreement method is applied to compare the results obtained by them. The results present the suitability of the application of both hybrid approaches for solving the problem. It also shows that the application of them leads to a distinctive outcomes. Robust Fuzzy based outcomes, and small agreement interval (< 0.0113) and little average change level in the rates of the hospitals (< 2.08 %) are observed between results acquired by the Fuzzy based approach and those which were defined by the other model. Based on these results, a fuzzy based model was recommended for structured comparison of the OHLR level of hospitals under uncertainty conditions. It supports sustainable planning practices, and helps with improvement and effectively distributes the necessary resources.**

Keywords*—Health literacy; the organizational health literacy standard; fuzzy analytic hierarchy process; fuzzy Delphi method; structured comparison

I. Introduction

Providing a healthy life for citizens, enhancing well-being for them, providing timely and reliable delivery of quality healthcare, granting access to quality essential healthcare services, reducing risk and cost of services, and improving health outcomes are considered some of the leading sustainable development targets of countries [1,2,3]. Corporate social responsibility is regarded as one way to achieve such targets [4]. To improve the sustainability status of organizations and to integrate the sustainability issues into the business of it, companies should plan their sustainable development, and corporate social responsibility practices based on the sustainability need of communities [5,6]. Measuring, prioritizing, and ranking healthcare practices are considered one way of achieving these goals [7-9]. However, the existence of unreasonable portions of citizens and patients with restricted health literacy in many developing societies and the adverse effects resulting from the increase and spread of this phenomenon negatively affects the use of healthcare, its costs, and output [10]. Additionally, it has adverse effects on health status and health service utilization [11]. This phenomenon is associated with increased transitional care needs [12], risk of death, and hospitalization [13]. So, the implication of low health literacy leads to an increase in the economic, social, and health burdens of individuals, societies, and countries, which negatively affects the implementation of a country's sustainable development plans in general and the health plans in particular. Studying and understanding the health literacy from a systemic perspective is based on an understanding of the inputs, processes, relationships, and outputs of many relevant components considered one of the recent research and application directions for developing solutions that limit the effects of this phenomenon [14,15]. The influential relationship between the individual's competencies, system's demands, and its complexities, where health literacy decisions and actions are taken, and the primary health literacy of an individual (health literacy abilities) in this system, is one of the fundamental justifications for this research and its applied directions [10, 16]. The health literacy concept is used as a tool to [10]: simplify and understand the health systems, which are often complicated,, improve the service provided; structure services in ways that maximize simplicity of systems and reduce challenges that limit access for services, ensure meeting the necessary health literacy requirements and preferences of all individuals that the healthcare organization serves; and improve patient outcomes and healthcare quality.

Assessments of the real status of the organizational health literacy of health facilities is an essential requirement for improving the organizational health literacy outcomes in a way that ensures community service and achieves its sustainable development goals as well as choosing, controlling, and adapting measures to improve it. Ranking and prioritization of the health literacy factors and a comparison of the actual level of health literacy practices in healthcare sector

*Corresponding Author

facilities is considered one of the most important steps for health services planning and for health-oriented sustainable development and corporate social responsibility planning processes.

A structured comparison of the organizational health literacy responsiveness (OHLR) level of a healthcare organization helps to determine the preferred health literacy development areas, the companies suggested for healthcare sustainable development planning, and the planning of the social responsibility directions of companies. Additionally, it helps decision makers fairly, equally, and effectively allocate their resources.

Conducting a structured comparison of the level of implementation, allows stakeholders to allocate, distribute and manage the related support resources in a way that contributes achieving the fair and sustainable distribution of resources, and supports meeting the ethical, economic, environmental and legal social responsibilities [1,3,4,5,6,10]. For example, the government wants to determine and rank the healthcare institutions that are most in need to support, determine how should government resources be fairly distributed among them according to their real application gaps in the application of health literacy practices, classify the application factors into different groups in terms of their sustainable importance, taking into account local economic conditions, and distribute resources between hospitals at different improvement stages so that the most important aspects are supported first; such questions become more important when the countries concerned are poor, and cannot provide sufficient support to fully address the health literacy situation simultaneously.

On the other hand, international organizations and local institutions offer different support programs in this regard, and most of them only focus on one sub-field or set of specific areas of application, in a way that serves the orientations and objectives of the institution. Such organizations are mostly seeking to find out how theirs support resources can be fairly divided among institutions according to the actual needs of those institutions, and taking into account their economic, and legal obligations .

There are four main practical aspects to help decision makers in solving these challenges; the first aspect lies in assessing the actual reality of the application, and identifying the application gap for each of the concerned institutions, the second lies in determining the relative importance of the health literacy sub-domains and their indicators on a sustainable basis, the third aspect consists in conducting merger operations between the outputs of the two previous processes to obtain weighted scored levels of application, while, the fourth is devoted to structurally compare the evaluation results between organizations.

In practice, the organizational health literacy responsiveness can be measured directly or indirectly. Regrettably, there is no unanimously accepted standard. To approximate an organizational health literacy responsiveness level in organizations, lists of metrics or indicators are used, and most of them are measured qualitatively with some quantitative measures available. The qualitative method is one of the common methods that were being used increasingly for evaluation purposes; and researchers rely on it in their studies in many fields [17- 19], and the field of study is no exception to that [10, 20, 21]. But, the qualitative approach is not always reliable, and the quantified version of metrics is still not as accurate as what humans perform in its development, and this can lead to possible impreciseness, errors in measurement process, and misinterpretations [22]. Furthermore, the specifics of the healthcare organizations, their business needs, priorities, and strategies all vary, and this means that the weights of the organizational health literacy responsiveness factors differed from one to another, and a structured comparison of the organizational health literacy responsiveness level metric between healthcare organizations, or between branches, is not possible without taking these variances into consideration. For deal with this case, Authors in [22] proposed an analytic hierarchy process-based approach for dealing with this problem as a MCDM problem and experimentally validated their approach using information security data. However, their approach is not ideal in this situation for two main reasons. The analytic hierarchy process method does not deal with the uncertainty involved in assessing the importance of the factors of an MCDM problem and the organizational health literacy responsiveness level of companies; additionally, their approach is used as a single qualitative preference point measurement scale for capturing the evaluation data, and this approach is sometimes not accurately expressed in the case being assessed [23-25]. Additionally, it does not deal with the vague assessment situation. The uncertainty problem occurred through the evaluation process because of a lack of information or imprecision related to the decision making values and judgments [24]. Fuzzy based MCDM approaches are accomplished of demonstrating this vagueness and dealing with its fuzzy situations [23-25].

In any case, analysis of worldwide and locally observational studies observed that studies that have addressed a structured comparison of the organizational health literacy responsiveness (OHLR) level of a healthcare organization and the comparative analysis of MCDM models to each other in health literacy applications do not exist; on the second hand, the available reviews provide a non-fuzzy model for structured comparison purposes [22], and as it was early explained, this model is not the suitable to solve the structured comparison problem under uncertainty conditions.

On the other hand, in addition to the fact that the qualitative methods proposed in that study are not ideal in evaluating the level of application, and the inability of the traditional qualitative – AHP integrated method to solve the problem of ambiguity related to evaluation, there is another problem, their model [22] in the last structured comparison step relied on a single scale to map the evaluation results of investigated alternatives to the relevant comparison scale for all objectives, and this of course generates inaccurate comparison results, especially if the differences in the evaluation scores between the alternatives are small.

Therefore, this study addresses to reduce this gap attempting to describe how to structurally compare the health literacy performance of healthcare organizations in a specific health sector (or sub-healthcare organization of a particular organization in the healthcare sector) under an uncertain environment and taking into account the sustainable priorities of this sector and the varying importance of the evaluation factors. It also aims to develop a fuzzy based framework to solve this problem.

The remainder of this paper is organized as follows. In Section 2 a brief overview of the related work was provided. Section 3 described our methodology. The results are shown in Section 4, followed by a discussion and conclusion in Section 5 and Section 6, respectively.

II. Related Work and Literature Review

A. *The Potential of Health Literacy to Address the Related UN Sustainable Development Goals*

Ensuring healthy lives and promoting well-being at all ages is the main health goal among the 2030 – sustainable development Goals [26]. The sustainable development G numbers 1, 2, 4, 8, and 10 are also allied to health and will contribute to the enhancement of the health of the overall population [27]. Knowledge and education, culture, gender roles, and quality, and cost of services effect the stakeholders to access services, engage with them and enact decisions that represent a group of healthcare engagement barriers [28, 29]. The knowledge of services; hazards; problems with services, availability, and quality; and health system responsiveness are of highly priority and considerable sustainable development goal targets for dealing with such challenges [29]. Making sound decisions about the health of the overall population and public health promotion is a basic requirement to improve and maintain the quality of life in society, and this requirement cannot be achieved without the availability of characteristics, skills, competence, and motivation among individuals who work in health information and services. The availability of these features, without the necessary support to access this information and these services, understand, and use them also hinders the achievement of these goals .These two factors are directly linked to health literacy, and the integration of these factors to achieve this requirement in the scope of one system summarizes the concept of health literacy [28] .Accordingly, health literacy is a pivotal determinant of discernment, reaching, and benefitting health data and services and strongly supports achieving the 2030 goals and targets. It is important that the health literacy needs of the community are directed and that measures for improving it are selected, adjusted, and implemented. To achieve this, the health literacy responsiveness should be considered, assessed, and improved [10, 28], and diagnosis of the actual status of health literacy is a basic step for achieving that [10].

B. *The Corporate Social Responsibility, Sustainable Development and Health Literacy*

Lately, the interaction between the conceptions of corporate social responsibility and sustainable development has consolidated, and sustainable development is considered an integrated community project. It works to achieve community security by focusing on the main components, which are environmental security, social security, and economic security, to protect society from environmental, social, and economic risks that threaten its security and stability [30, 31]. Therefore, all segments of society must participate in it. All governments, private sector companies, and institutions, and civil society organizations should participate and contribute to raising the level of societies by adopting social responsibility initiatives that are in line with development goals. Corporate responsibility and corporate sustainability can be used as synonyms (United Nations Global Compact, 2013). Both the corporate social responsibility and the sustainable development are based on the same dimensions that ultimately lead to achieving their goals in societies [31]. Both corporate social responsibility and sustainable development are highly contextual in terms of their temporal and societal setting. They are both subject to issue attention cycles in which events or findings give them urgency, and organizations respond and adapt [31]. Pesmatzoglou [32] estimates that there are absolutely no development goals that social responsibility cannot contribute to. Thus, the aforementioned social and health challenges and the consequences of economic problems that fall within the objectives of sustainable development, can be processed by addressing and increasing corporate social responsibility. However, to improve health literacy, corporate social responsibility decision makers should focus on [33]: (1) integrating health literacy initiatives into existing corporate social responsibility programs focused on health and well-being in the workplace; (2) engaging in an active dialogue with key healthcare stakeholders; and (3) developing a "Blueprint for Action in Health Literacy," based on best practices and case studies. Companies and programs that are moving toward enhancing their social role in society will be able to solve many problems by assessing the current organizational health literacy responsiveness situation of healthcare organizations, knowing and arranging the different areas and weaknesses of health literacy in organizations according to the sustainable development priorities of the health sector, and focusing on these points and creating partnerships between health institutions and the institutions. The most prominent is that the investment in dedicated resources will be distributed in accordance with sustainable health priorities, and the supported corporate social responsibility programs and services will differ from one region to another and from one health organization to another, in accordance to the actual needs of the citizens benefiting from its services. In turn, these conflicts with sustainable health goals will lead to poor health sustainable situation [33].

C. *The Fuzzy Analytic Hierarchy Process*

The Hierarchy Analysis Process (AHP) is the most common and widely used method to derive relative weights of criteria. The analytic hierarchy process was developed by Saaty [34]. In practice, the process of analytic hierarchy process implementation requires two main stages to structure problems and derive priorities and importance through two comparison processes. In the first stage, the complex problem is divided into a hierarchy, while the second step begins with the prioritization procedure to determine the relative importance of the criteria at each level. In the last step, the hierarchical assessment is based on an indirect comparison of the decision maker's preferences, and the relative weights of each matrix are determined and normalized [35, 36]. The main feature of this approach is to turn a complex multidimensional problem into a one-dimensional problem and provide mechanisms for calculating the final standardized solution for multiple evaluation experts (combine the final choices of a group to agree on a single outcome). This method is flexible and capable to test irregularities. Also, it provides mechanisms for computing the expert consensus.

However, according to [25, 37] the traditional Satty's analytic hierarchy process method does not deal with the uncertainty involved in assessing the importance of the criteria For this reason, a fuzzy version of it was selected. This approach performs analytic hierarchy process under uncertainty and ambiguity, has received increasing acceptance, and has been approved and implemented to solve decision-making problems in many fields.

D. Fuzzy Delphi based Assessment Method

Several methodologies have been proposed in literature. Dalkey and Helmer [38] developed the classic Delphi method for surveying and consulting with experts, which is widely used for this purpose in numerous surveys over the last three decades. However, applying this method is still accompanied by some problems [39]: misinterpretation of expert views because of ignorance of the fuzzy variables; the need to repeat the assessment process, leading to a loss of specialist interest in progress assessment data, which makes the study more costly and systematically changes the original views. Another uncertainty problem occurred through the evaluation process because of a lack of information or imprecision. The fuzzy version of the Delphi method was developed to avoid such dilemmas. Application of this method reduces costs and time during the assessment of each item in the questionnaire, reduces the number of survey tours, increases the rate of retrieval of questionnaires, allows experts to express their opinions using fuzzy numbers, represents discretionary categories whose problem with fuzzy assessment disappears when used, provides a mechanism for dealing with nonconsensual cases accompanying the assessment, improves the integrity and consistency of opinions, and enhances expert consensus without opposing the original expert views on changes that contribute to a more realistic assessment of relevant problems and indicators [39].

E. Assessment of the Organizational Health Literacy Responsiveness Level in Health Care Organizations

Numerous healthcare organizations utilize an organizational health literacy responsiveness level estimation of the indicators from international standards to get a dependable measurement. Using this tool in accordance with specific requirements and guidelines is enough to get a picture of the situation in any organization and enough to make necessary improvements upon it. On the contrary, getting this picture at the branch level of any multi-branch hospital, or at the institutional level of the public or private sector, is still not enough to make a correct comparison between their different health literacy states. This is because different branches or institutions have different sustainable objectives, environments, and priorities; consequently, the importance of evaluation areas and processes also varies. These comparisons are needed to ensure the economical investment of company resources as well as to ensure a sustainable distribution for government services and resources that support improving the situation as well as the resources for enterprises supporting the sustainability of the health status as a type of social responsibility. As equitable and sustainable distribution requires an answer on where and to whom economic resources should be distributed to achieve the maximum possible benefits, this could be determined by the structured comparison assessment through adapting suitable methods.

Several evaluation frameworks and tools have been developed, collected, and tested—most notably those presented in [10, 41-42]. In this paper, we will use the international assessment tool of the HPH and HLO Working Groups - 2019 [10] because this tool is shown to be mature, widespread, and globally recognized. It is suitable for application in institutions of different sizes, with different levels of application, even if these institutions do not have previous experience in this regard. The assessment tool is designed so that it can be adapted to suit different international contexts and can be used as a comprehensive evaluation tool or, partly, through the selection of a brief set of its criteria and indicators, to assess the aspects that suit particular environments. The adaptation of such a tool minimizes the additional effort for collecting the required metrics.

Despite the different methods and procedures used to measure the actual level of literacy requirements, and despite the different tools used, the reviewed and applied research can be classified in this regard into four types. The first type is focused on measuring the level of adherence to literacy practices according to specific factors for the purpose of identifying and improving weaknesses in a specific healthcare institution [43] or in a group of institutions [44-46]. The second type is focused on measuring the relative importance of the areas and indicators of applying literacy practices for the purpose of determining the most important or most appropriate factors for the institution or a specific health sector [47]. However, there is an applied research gap around the third and fourth types. The third framework is focused on merging the previous two types into a single evaluation framework with the aim of evaluating the actual level of practices and taking into account the importance of various evaluation indicators and factors. A number of studies have used this framework but in other application domains [25]. Additionally, the fourth type uses additional tools called ranking tools to make comparisons between different institutions in terms of their general or indicator level of application for certain applied practices [8, 9]. In any case, the comparison process in the fourth type requires the presence of two main inputs, the first input is the relative weight (relative importance) of the decision factors and indicators, and the second input is the result of the evaluation process. In practical terms, the applied study closest to our study is the one presented by Schmid [20], and it agrees in terms of the general objective and the methodological steps it followed, but it differs in other respects: (1) the field of application, Schmidt's study addressed the structured comparison of the information security maturity level of organizations, while this study focuses on the structured comparison of an organizational health literacy responsiveness Level in hospitals and (2) the method used to evaluate the importance of the criteria, Schmidt's study applied the analytic hierarchy process method, this technique is not ideal as explained in the introduction, for this reason the Fuzzy analytic hierarchy processes applied in this study and (3) the 5-point scoring qualitative method was applied for evaluation of the performance level in the Schmidt's study, this method is not deal with the foggy environmental problems of the evaluation, for this reason in this study the fuzzy Delphi method is used. Additionally, this study differs from the studies on literacy assessment in that we use tools to assess the actual reality of literacy practices based on fuzzy techniques that diminish the ambiguities and flaws of the first and second assessment types, which we referred to earlier in the introduction, by relying on the fuzzy Delphi and fuzzy analytic hierarchy process methods. It compares the relative importance of the organizational health literacy responsiveness indicators in terms of their relevance and appropriateness for achieving the sustainable objectives of health institutions.

Additionally, it also differs from all previous studies in that the proposed model does not use to measure the organizational health literacy responsiveness level of hospitals only, but, instead, uses to analyze and compare the cases of implementation between these hospitals according to each indicator and under the ambiguous conditions of the assessment. It also relied on multi-measurement scale to link the evaluation results with the structured comparison scale, in order to obtain more accurate comparative results.

III. Structured Comparison Application and Model Design

Based on the previously review of the dissimilar assessment tools and approaches, qualitative and quantitative assessment methods, and fuzzy and non-fuzzy weighting methods that have been presented in the literature, the model design implemented in this study is presented through the following stages:

- Defining the general requirements for the implementation of the proposed model.
- Process chart design for the model by integrating the requirements of the international assessment tool of the HPH and HLO Working Groups, fuzzy AHP, and fuzzy Delphi methods.
- Criteria selection which is used for pairwise comparison by the experts and matrices development.
- Different rules and procedures that are provided in the literature using MCDMs in order to practically implement the proposed model.

A. *Requirements of the Proposed Model*

This framework could be used in general or as a specific framework. The following are required: (1) To achieve a good picture of the importance of health literacy criteria from the sustainable perspective of the country, the healthcare sustainable conditions in its different areas and the role of the selected healthcare facility in achieving it should be considered; (2) The importance of the criteria is deferent by cities and healthcare facility types (hospital, unit, or center and public or private), and this deference should also be considered; (3) The investigated and compared healthcare organizations should be located at the same location, and have the same facility type; (4) The selected indicators should be applicable for use in the selected sector [10]; (5) The information gathering should be repeatable and stable, and the consistency test for the data gathered should use fuzzy analytic hierarchy process data, and an agreement test for the decision makers' opinions gathered using fuzzy Delphi should be performed; and (6) The framework should allow the healthcare sector or companies to visualize and explain the results of the evaluation, weighting, and comparison and, finally, allow a derivation of the areas where the government or companies could improve or where the business sector could help, serve, or plan its corporate social responsibility practices.

B. *Model Design*

In order to design the desired model taking into account the functional requirements of it and based on the procedural requirements of the international assessment tool of the HPH and HLO Working Groups, fuzzy AHP, and fuzzy Delphi methods, more than thirty articles using fuzzy hybrid methodologies were studied. Therefore, Fig. 1 is the process chart for design the model of this study, it uses for forming interrelationships between the structured comparison requirements, OHLR criteria and indicators, the calculation of the local and global weights of them, and the aggregation and testing the consistency of the fuzzy scores, and classification, ranking of criteria, and structurally comparing of hospitals, respectively. The detailed explanation of the model will be displayed in the next two sections.

C. *Criteria Selection which is used for Pairwise Comparison by the Experts and Matrices Development*

The SAT-OHL-Hos-v1.0-EN-international tool [10] is used to select criteria and sub criteria, which is divided into 8 standards, 23 sub standards, and 156 indicators. For simplicity, the fourth standard was selected as a case study example. The fourth standard of this tool is devoted to measuring the application level of organizational health literacy responsiveness in providing and supporting easy navigation and access to documents, materials, and services. Its sub standards are: (C4-1) the organization enables first contact via user-friendly website and phone; (C4-2) the organization provides the information necessary for patients and visitors to get to the organization; (C4-3) Support is available to help patients and visitors navigate to the hospital; and (C4-4) Health information for patients and visitors is easy-to-understand and available for free. Taking requirement number 4 into consideration, and by interviewing 10 experts, 22 indicators were selected as an applicable measurement indicator for organizational health literacy responsiveness assessment. Table I shows these indicators and their distribution, while the final decision tree of the problem is presented in Fig. 2.

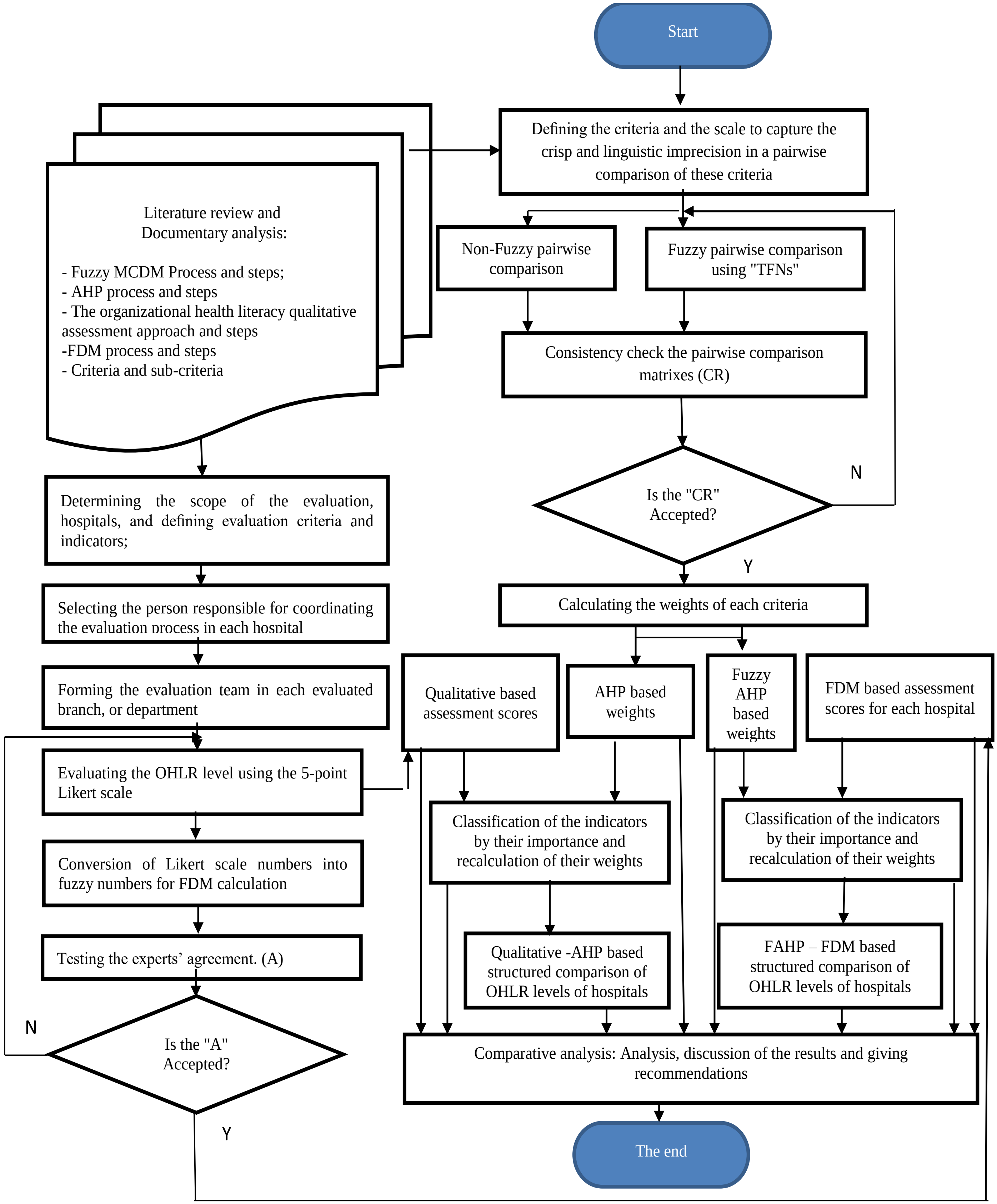

Fig. 1. Process Chart of the Model Design.

TABLE I. OHLR INDICATORS OF THE FOURTH HLO STANDARD

Indicator	Statement
C4-1-1	The organization can easily be reached by telephone 24 hours a day by an automated system and by a person.
C4-1-2	If there is an automated phone system, there is a clear option to repeat the menu items.
C4-1-3	People at a hotline or an information desk are qualified to adequately answer patient inquiries.
C4-1-4	Contact information, location, and arrival information is easy-to-find via Internet search engines.
C4-1-5	The website is easy-to-use for people with low digital HL and/or low HL.
C4-1-6	The website provides evidence-based information on frequent treatments and cites the scientific sources appropriately.
C4-2-1	The naming of locations on maps is consistent with the terms or wording used.
C4-2-2	The healthcare organization provides patients with easy-to-understand information about directions from the patient's home, including public and private transportation options.
C4-2-3	The healthcare organization negotiates with local transportation services to assist patients by displaying adequate signage, clear announcements, and location information at public transportation stations.
C4-2-4	Admission departments are clearly marked and visible.
C4-3-1	An information desk is available at all main entrances to support navigation.
C4-3-2	Printed maps are available for free to support navigation.
C4-3-3	Maps clearly indicate the individual's location through easy-to-understand symbols or "You are here" signage.
C4-3-4	The staff responsible for the admission of patients appropriately directs patients and visitors to their respective unit and staff.
C4-3-5	The signage design is based on the appropriate height, location, color, and font size.
C4-3-6	Consistent wording and use of symbols is applied to all locations and rooms within the organization.
C4-4-1	Patients are informed about deductibles or other costs for treatment or services in advance.
C4-4-2	Patients are informed about their patient rights.
C4-4-3	A physical or virtual patient information center comprising free health information is available.
C4-4-4	Various formats of easy-to-understand information regarding disease prevention are available.
C4-4-5	Various formats of easy-to-understand information regarding healthy lifestyles are available at multiple locations for free.
C4-4-6	Easy-to-understand menu information is available at bedside and in the cafeteria or canteen indicating nutrients and calories to support healthy choices.

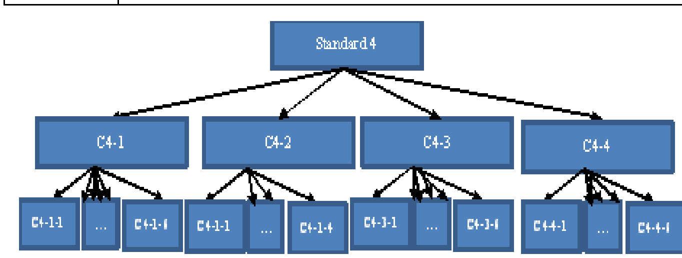

Fig. 2. The Decision Tree of the Problem.

IV. THE PROPOSED ALGORITHM AND ITS IMPLEMENTATION: DEMO APPLICATION

1) First Stage: Weighting criteria and indicators by the fuzzy analytic hierarchy process.

In this study, the fuzzy analytic hierarchy process steps will be used as follows:

a) Step 1—Defining the criteria (Section III.B).

b) Step 2—Defining the scale. This step captures the linguistic imprecision in a pairwise comparison of the criteria and indicators. Because the proposed framework considers the subjectivity, uncertainty, and ambiguity of experts' judgments, a fuzzy linguistic approach analog to the 9-point scale conceived by Saaty [34] should be used (Table II).

TABLE II. TRIANGULAR FUZZY CONVERSION SCALE

Level of Importance	Linguistic	The Scale of the Fuzzy Number
9	Absolute preference	(8, 9, 10)
8	Preference between very strong and absolute	(7, 8, 9)
7	Very strong preference	(6, 7, 8)
6	Preference between strong and very strong	(5, 6, 7)
5	Strong preference	(4, 5, 6)
4	Preference between moderate and strong	(3, 4, 5)
3	Moderate	(2, 3, 4)
2	Preference between the equal and moderate	(1, 2, 3)
1	Equal	(1, 1, 1)

c) Step 3—Building the fuzzy pairwise comparison matrix.

This step shows the preference of one criterion over the other for prioritization of all of the criteria and sub criteria. This represents the domain specific part of the fuzzy analytic hierarchy process calculations, and it only needs to be done once per substandard. The characteristics of the healthcare facility type (hospital, unit, or center and public or private) and their locations have a significant influence on the pairwise comparison when the individual indicators are compared. This is because the sustainability healthcare priorities in different locations of the country are not the same, and the sustainability, responsibility, and functionality role of different types of organizations in each location are not equivalent. However, taking the first three requirements of comparison into consideration, the decision maker must compare each criterion with its pair and denote which of the two criteria appears more important to him/her. This method of pairwise comparison allows the decision maker to elicit a very precise evaluation from the multitude of competing criteria. The comparisons must be carried out for one healthcare sector (e.g., public hospitals in Sana'a). In the case of our hierarchy based on the organizational health literacy responsiveness indicators, 4 pairwise comparisons have to be made by each decision maker for the main HL's sub-categories and twenty two for the indicators based on four decision trees, respectively. For this study a number of 50 pairwise comparison matrixes were generated, these matrixes are generated the taking into account the consistently check conditions presented below.

d) Step 4—Consistency check the fuzzy pairwise comparison matrix and calculate the consistency ratio (CR). During this step, the consistency of the aggregate judgment matrix of all of the pairwise comparisons is determined by its consistency ratio (CR). To ensure a certain quality level for a decision, we have to analyze the consistency of the evaluation. To test the value of consistency of the comparison matrix depended on n, the consistency rate (CR) has to be computed. The CR is defined in [37] as a ratio between the consistency of a consistency index (CI) and the consistency of a random consistency index (RI). Saaty suggests that the consistency of the matrix is acceptable only if CR < 0.10 [37]. When a matrix is inconsistent, then new pairwise comparison judgments are required. Once the consistency ratio is accepted, it is possible to calculate the weights of the criteria.

e) Step 5—Calculating the weights of each criterion if the CR is accepted, then apply the change's fuzzy analytic hierarchy process procedures [48]. In our case study example, the CR were calculated and accepted. Table III represents the calculated CR values and the overall consensus rate (CR%) for 10 decision makers (experts). While, Table IV represents the calculated weights and ranks of criteria based on F-AHP methods. It also represents the alternative calculated weights and ranks of criteria using the classical AHP method.

TABLE III. CR TESTING RESULTS

decision tree	**Expert**										**CR (%)**
	EX1	***EX2***	***EX3***	***EX4***	***EX5***	***EX6***	***EX7***	***EX8***	***EX9***	***EX10***	
C4	0.03	0.022	0.076	0.043	0.09	0.043	0.09	0.079	0.03	0.07	96.1
C4-1	0.02	0.086	0.08	0.031	0.073	0.061	0.08	0.09	0.05	0.03	97.8
C4-2	0.06	0.063	0.09	0.022	0.043	0.05	0.07	0.02	0.02	0.075	98
C4-3	0.026	0.084	0.08	0.08	0.081	0.063	0.08	0.09	0.091	0.06	96.9
C4-4	0.035	0.078	0.067	0.062	0.08	0.013	0.07	0.053	0.078	0.057	96.5

TABLE IV. THE ORGANIZATIONAL HEALTH LITERACY RESPONSIVENESS INDICATORS, THEIR WEIGHTS AND RANKS

		FAHP		**AHP**	
C-N	**Indicator**	**Global Weight**	**Rank**	**Global Weight**	**Rank**
C4-1	C4-1-1	0.029	13	0.034304	14
	C4-1-2	0.028	15	0.035584	12
	C4-1-3	0.030	12	0.043264	10
	C4-1-4	0.124	1	0.073472	3
	C4-1-5	0.044	11	0.040448	11
	C4-1-6	0.014	22	0.029184	17
C4-2	C4-2-1	0.047	10	0.043554	9
	C4-2-2	0.052	6	0.053074	8
	C4-2-3	0.017	21	0.03451	13
	C4-2-4	0.121	2	0.106862	1
C4-3	C4-3-1	0.026	17	0.027888	18
	C4-3-2	0.025	18	0.02772	19
	C4-3-3	0.022	19	0.022848	21
	C4-3-4	0.029	14	0.033768	15
	C4-3-5	0.028	16	0.030912	16
	C4-3-6	0.021	20	0.024696	20
C4-4	C4-4-1	0.062	5	0.070616	4
	C4-4-2	0.071	3	0.076824	2
	C4-4-3	0.047	8	0.05626	7
	C4-4-4	0.065	4	0.069064	5
	C4-4-5	0.048	7	0.05626	7
	C4-4-6	0.047	9	0.057424	6

2) Second stage: classification of the indicators by their importance and recalculation of their weights.

To compare the organizational health literacy responsiveness levels of the company for each importance category, the indicators should be classified into importance categories. In this study, four categories were defined and the importance of their indicators was recalculated. The weight of each indicator is calculated by the division of its global weight on the total weights of groups' indicators. Based on the results obtained from the first stage, four importance categories were defined (G1-G4), and the relative importance (LW) and the ranking order (NR) of their indicators were recalculated using FAHP and AHP as shown in Table V.

3) Third stage: Applying the organizational health literacy Assessment approach and the fuzzy Delphi method to determine the health literacy responsiveness level of the healthcare organization.

The methodology was used to measure the real situation according to this international standard, which can be summarized as follows [10]:

a) determining the scope of the evaluation and defining evaluation criteria and indicators;

b) selecting the person responsible for coordinating the evaluation process, having the ability to coordinate and manage the process;

c) forming the evaluation team in each evaluated branch, or department. Between 5 and 10 experts from the following areas should be involved: management; quality management; health promotion; human resource development; medicine; nursing; therapeutic professions, preferably from different departments; building services engineering or maintenance; patient-ombudsman or woman; self-help and patient representatives, communications, or spokesperson;

d) evaluating the OHLR level, to capture the results and compare them, the 5-point Likert scale (1 = very poor to 5 = very good) is suggested for this process; and.

e) discussing the results in the next meeting, focusing on which assessment best describes the overall situation.

In this step, to determine the values that describe the overall situation on each indicator in each organization, the fuzzy Delphi method should be applied as follows [39]:

- conversion of Likert scale numbers into fuzzy numbers;
- defuzzification of the fuzzy scores; and
- testing the experts' agreement.

TABLE V. CLASSIFICATION OF OHLR INDICATORS BY THEIR IMPORTANCE CATEGORY

	F-AHP					AHP					Indicator	FAHP		AHP	
G	Indicator	W	Rank	LW	LR	Indicator	W	Rank	LW	LR		Order	Class	Order	Class
G1	C4-1-4	0.099	1	0.24	1	C4-2-4	0.107	1	0.290	1	C4-1-4	1	1	3	1
	C4-2-4	0.121	2	0.29	2	C4-4-2	0.067	2	0.181	2	C4-2-4	2	1	1	1
	C4-4-2	0.071	3	0.17	3	C4-1-4	0.073	3	0.199	3	C4-4-2	3	1	2	1
	C4-4-4	0.065	4	0.15	4	C4-4-1	0.062	4	0.167	4	C4-4-4	4	1	5	1
	C4-4-1	0.062	5	0.15	5	C4-4-4	0.060	5	0.163	5	C4-4-1	5	1	4	1
G2	C4-2-2	0.052	6	0.22	1	C4-4-6	0.050	6	0.206	1	C4-2-2	6	2	8	2
	C4-4-5	0.048	7	0.2	2	C4-4-3	0.049	7	0.200	2	C4-4-5	7	2	7	2
	C4-4-3	0.047	8	0.2	3	C4-4-5	0.049	7	0.200	2	C4-4-3	8	2	7	2
	C4-4-6	0.047	9	0.19	4	C4-2-2	0.053	8	0.217	3	C4-4-6	9	2	6	2
	C4-2-1	0.047	10	0.19	5	C4-2-1	0.044	9	0.178	4	C4-2-1	10	2	9	2
G3	C4-1-5	0.044	11	0.2	1	C4-1-3	0.043	10	0.195	1	C4-1-5	11	3	11	3
	C4-1-3	0.054	12	0.25	2	C4-1-5	0.040	11	0.182	2	C4-1-3	12	3	10	3
	C4-1-1	0.029	13	0.14	3	C4-1-2	0.036	12	0.160	3	C4-1-1	13	3	14	3
	C4-3-4	0.029	14	0.13	4	C4-2-3	0.035	13	0.156	4	C4-3-4	14	3	15	3
	C4-1-2	0.032	15	0.15	5	C4-1-1	0.034	14	0.155	5	C4-1-2	15	3	12	3
	C4-3-5	0.028	16	0.13	6	C4-3-4	0.034	15	0.152	6	C4-3-5	16	3	16	4
G4	C4-3-1	0.026	17	0.21	1	C4-3-5	0.031	16	0.189	1	C4-3-1	17	4	18	4
	C4-3-2	0.025	18	0.2	2	C4-1-6	0.029	17	0.179	2	C4-3-2	18	4	19	4
	C4-3-3	0.022	19	0.18	3	C4-3-1	0.028	18	0.171	3	C4-3-3	19	4	21	4
	C4-3-6	0.021	20	0.17	4	C4-3-2	0.028	19	0.170	4	C4-3-6	20	4	20	4
	C4-2-3	0.017	21	0.14	5	C4-3-6	0.025	20	0.151	5	C4-2-3	21	4	13	3
	C4-1-6	0.014	22	0.11	6	C4-3-3	0.023	21	0.140	6	C4-1-6	22	4	17	4

The procedures in the last step should be repeated for each investigated indicator for each organization. The number of experts should be optimal and comply with the previous suggestions for the Delphi method implementation, which are between ten and fifty [49]. In this study, 10 evaluators were selected as an evaluation team in each organization, and this number is optimal and complied with both the Delphi [49] and organizational health literacy assessment tool requirement [10]. The triangular fuzzy numbers provided an opportunity for each recorded response made by an expert in the form of the Likert-scale scoring to be translated into fuzzy scoring (refer to Table VI. After that, the fuzzy scores should be averaged for the defuzzification process. This process is to identify the organizational health literacy responsiveness level of the organization on each indicator. In the last step, the experts' agreement (expert consensus) should be calculated and must be ≥ 75% [36/145]. If this condition is not achieved, the fourth and fifth evaluation processes should be repeated. Table VI was used for mapping the averaged fuzzy scores to their relevant organizational health literacy responsiveness levels. Section 4 describes the obtained results. In this study the experts' consensus equaled 100% for each indicator in all three virtual organizations of the case study example. The OHLR level of hospitals based on both qualitative-AHP based model and FDM _FAHP methods are presented in Table VII, and Table VIII, respectively. After that, to simplify the comparison process of the results, these score were represented in percentage form, and the practical gaps in the implementation of the OHLR practices for each alternative hospital were also calculated.

After that, the overall weighted evaluation scores of hospitals based on both models on each main original category (C4-1-C4-4), and on the whole (C4) standard were calculated, these values were also mapped into the percentage scale as well. Tables IX, and X represent the results. In addition, the overall weighted evaluation scores of hospitals based on both models on each importance category (G1-C4) were calculated. These values were also mapped into the percentage gap scale. Tables XI and XII represent the result.

TABLE VI. FUZZY DELPHI EVALUATION SCALES AND ASSESSMENT INDEX

Likert Scale	**Linguistic Variable**	**Fuzzy Scale**		
		n1	***n2***	***n3***
5	Very good (VG)	0.6	0.8	1
4	Good (G)	0.4	0.6	0.8
3	Fair (F)	0.2	0.4	0.6
2	Poor (P)	0	0.2	0.4
1	Very poor (VP)	0	0	0.2

TABLE VII. THE QUALITATIVE –AHP BASED EVALUATION RESULTS

	Indicator	**LW**	**local rank**	**ES**			**ES %**			**Gap**			
G				**H1**	**H2**	**H3**	**H1**	**H2**	**H3**	**H1**	**H2**	**H3**	**Max-Gap**
G1	C4-2-4	0.290	1	4.3	4.6	4.7	86	92	94	14	8	6	14
	C4-4-2	0.181	2	1.4	2.7	2.6	28	54	52	72	46	48	72
	C4-1-4	0.199	3	1.2	1.5	1.6	24	30	32	76	70	68	76
	C4-4-1	0.167	4	4.4	4.4	4.5	88	88	90	12	12	10	12
	C4-4-4	0.163	5	2.6	2.7	2.8	52	54	56	48	46	44	48
G2	C4-4-6	0.206	1	4.2	4.5	4.6	84	90	92	16	10	8	16
	C4-4-3	0.200	2	2.4	2.8	2.9	48	56	58	52	44	42	52
	C4-4-5	0.200	2	4.1	4.3	4.5	82	86	90	18	14	10	18
	C4-2-2	0.217	3	3.2	3.2	3.3	64	64	66	36	36	34	36
	C4-2-1	0.178	4	3.2	3.6	3.8	64	72	76	36	28	24	36
G3	C4-1-3	0.195	1	3.3	3.7	3.8	66	74	76	34	26	24	34
	C4-1-5	0.182	2	1	1.3	1.5	20	26	30	80	74	70	80
	C4-1-2	0.160	3	1	1.2	1.5	20	24	30	80	76	70	80
	C4-2-3	0.156	4	3.6	3.8	3.6	72	76	72	28	24	28	28
	C4-1-1	0.155	5	3.2	3.7	3.8	64	74	76	36	26	24	36
	C4-3-4	0.152	6	4.7	4.9	4.6	94	98	92	6	2	8	8
G4	C4-3-5	0.189	1	4.8	4.8	4.9	96	96	98	4	4	2	4
	C4-1-6	0.179	2	1	1	1.1	20	20	22	80	80	78	80
	C4-3-1	0.171	3	3.4	3.7	3.6	68	74	72	32	26	28	32
	C4-3-2	0.170	4	2.3	2.7	2.8	46	54	56	54	46	44	54
	C4-3-6	0.151	5	4.9	4.9	4.9	98	98	98	2	2	2	2
	C4-3-3	0.140	6	4.6	4.8	4.8	92	96	96	8	4	4	8

TABLE VIII. THE FDM-FAHP BASED EVALUATION SCORES

	Indicator	LW	LR	ES			ES %			Gap			
G				H1	H2	H3	H1	H2	H3	H1	H2	H3	Max-Gap
G1	C4-1-4	0.24	1	0.09	0.13	0.15	11.63	16.63	18.38	88.38	83.38	81.63	88.38
	C4-2-4	0.29	2	0.66	0.72	0.74	82.50	90.00	92.50	17.50	10.00	7.50	17.50
	C4-4-2	0.17	3	0.12	0.34	0.32	15.00	42.50	40.00	85.00	57.50	60.00	85.00
	C4-4-4	0.15	4	0.32	0.34	0.36	40.00	42.50	45.00	60.00	57.50	55.00	60.00
	C4-4-1	0.15	5	0.68	0.68	0.70	85.00	85.00	87.50	15.00	15.00	12.50	15.00
G2	C4-2-2	0.22	1	0.44	0.44	0.46	55.00	55.00	57.50	45.00	45.00	42.50	45.00
	C4-4-5	0.20	2	0.62	0.66	0.70	77.50	82.50	87.50	22.50	17.50	12.50	22.50
	C4-4-3	0.20	3	0.28	0.36	0.38	35.00	45.00	47.50	65.00	55.00	52.50	65.00
	C4-4-6	0.19	4	0.64	0.70	0.72	80.00	87.50	90.00	20.00	12.50	10.00	20.00
	C4-2-1	0.19	5	0.44	0.52	0.56	55.00	65.00	70.00	45.00	35.00	30.00	45.00
G3	C4-1-5	0.20	1	0.07	0.11	0.14	8.38	14.13	17.50	91.63	85.88	82.50	91.63
	C4-1-3	0.25	2	0.46	0.54	0.56	57.50	67.50	70.00	42.50	32.50	30.00	42.50
	C4-1-1	0.14	3	0.44	0.54	0.56	55.00	67.50	70.00	45.00	32.50	30.00	45.00
	C4-3-4	0.13	4	0.74	0.78	0.72	92.50	97.50	90.00	7.50	2.50	10.00	10.00
	C4-1-2	0.15	5	0.07	0.09	0.13	8.38	11.63	16.63	91.63	88.38	83.38	91.63
	C4-3-5	0.13	6	0.76	0.76	0.78	95.00	95.00	97.50	5.00	5.00	2.50	5.00
G4	C4-3-1	0.21	1	0.48	0.54	0.52	60.00	67.50	65.00	40.00	32.50	35.00	40.00
	C4-3-2	0.20	2	0.26	0.34	0.36	32.50	42.50	45.00	67.50	57.50	55.00	67.50
	C4-3-3	0.18	3	0.72	0.76	0.76	90.00	95.00	95.00	10.00	5.00	5.00	10.00
	C4-3-6	0.17	4	0.78	0.78	0.78	97.50	97.50	97.50	2.50	2.50	2.50	2.50
	C4-2-3	0.14	5	0.52	0.56	0.52	65.00	70.00	65.00	35.00	30.00	35.00	35.00
	C4-1-6	0.11	6	0.07	0.07	0.08	8.38	8.38	10.00	91.63	91.63	90.00	91.63

TABLE IX. THE OVERALL WEIGHTED EVALUATION SCORES OF HOSPITALS: QUALITATIVE – AHP MODEL

Category	W	R	Weighted ES			Weighted ES %			Gap			
			H1	H2	H3	H1	H2	H3	H1	H2	H3	Max-Gap
C4-1	0.256	3	3.148	3.499	3.565	62.950	69.982	71.308	37.050	30.018	28.692	37.050
C4-2	0.238	2	3.186	3.492	3.655	63.726	69.834	73.098	36.274	30.166	26.902	36.274
C4-3	0.168	4	3.030	3.257	3.281	60.590	65.146	65.614	39.410	34.854	34.386	39.410
C4-4	0.338	1	3.134	3.357	3.399	62.674	67.148	67.974	37.326	32.852	32.026	37.326
C4	1		3.132	3.409	3.483	62.645	68.176	69.651	37.355	31.824	30.349	37.355

TABLE X. THE OVERALL WEIGHTED EVALUATION SCORES OF HOSPITALS: FDM– FAHP MODEL

Category	W	R	Weighted ES			Weighted ES %			Gap			
			H1	H2	H3	H1	H2	H3	H1	H2	H3	Max-Gap
C4-1	0.273	3	0.195	0.246	0.267	24.314	30.769	33.387	75.686	69.231	66.613	75.686
C4-2	0.237	2	0.558	0.608	0.627	69.790	75.965	78.428	30.210	24.035	21.573	30.210
C4-3	0.149	4	0.623	0.660	0.652	77.835	82.480	81.475	22.165	17.520	18.525	22.165
C4-4	0.341	1	0.425	0.500	0.514	53.123	62.475	64.283	46.878	37.525	35.718	46.878
C4	1		0.423	0.480	0.494	52.890	59.997	61.762	47.110	40.003	38.238	47.110

TABLE XI. THE OVERALL WEIGHTED EVALUATION SCORES OF HOSPITALS ON IMPORTANCE GROUPS: QUALITATIVE– AHP MODEL

Category	W	R	Weighted ES			Weighted ES %			Gap			
			H1	H2	H3	H1	H2	H3	H1	H2	H3	Max-Gap
G1	0.368938	1	2.896	3.295	3.359	57.921	65.896	67.171	42.079	34.104	32.829	42.079
G2	0.24501	2	3.426	3.678	3.816	68.511	73.567	76.322	31.489	26.433	23.678	31.489
G3	0.221878	3	2.756	3.060	3.102	55.122	61.195	62.050	44.878	38.805	37.950	44.878
G4	0.163248	4	3.444	3.591	3.628	68.883	71.826	72.560	31.117	28.174	27.440	31.117

TABLE XII. THE OVERALL WEIGHTED EVALUATION SCORES OF HOSPITALS ON IMPORTANCE GROUPS: FDM– FAHP MODEL

Category	W	R	Weighted ES			Weighted ES %			Gap			
			H1	H2	H3	H1	H2	H3	H1	H2	H3	Max-Gap
G1	0.419178	1	0.384	0.452	0.463	48.025	56.443	57.915	51.975	43.557	42.085	51.975
G2	0.241367	2	0.483	0.534	0.562	60.429	66.795	70.279	39.571	33.205	29.721	39.571
G3	0.178825	3	0.387	0.429	0.436	48.343	53.658	54.504	51.657	46.342	45.496	51.657
G4	0.160506	4	0.475	0.529	0.537	59.368	66.164	67.135	40.632	33.836	32.865	40.632

4) Fourth Stage: Structured comparison of the OHLR levels of the hospitals using AHP.

In this stage, a structured comparison of the OHLR levels of hospitals, according to their overall weighted scores (C4), their overall weighted scores on each original category of indicators (C4-1, C4-2, C4-3, and C4-4), and their evaluation scores on each importance class (G1, G2, G3, and G4).

As all ambiguous and vague problems associated with the early implemented evaluation steps were solved using FAHP and FDM methods, there is no longer needed to use the fuzzy based technique to structurally compare the organizational health literacy responsiveness levels of hospitals. So, The AHP method will be used; the same analytic hierarchy process procedures should be applied to compare them. This stage is used for pairwise evaluation of the indicators' level of hospitals, so the alternatives of the MCDM problem are the indicators' and categories' health literacy responsiveness levels of three hospitals (H1, H2, and H3). The gap between the comparative organizational health literacy responsiveness levels of two hospitals' indicators will decide which hospital is doing worst, or need more financial support at a whole system, specific group of indicators.

In this study, the total comparison processes are nine; one process at the overall OHLR level, four processes at the original domain level, and four processes at the importance domain level, for each process need to map the gap scale (0-max gap value) to the 9-stage analytic hierarchy process score. The result is a table where each GAP interval represents an analytic hierarchy process score, which is verbally described the situation.

The proposed model used a dynamical table [Table XIII] for mapping the related implementation gaps of hospital to 9 point scale, with interval equals (max gap/9).

For example, if the evaluation scores of the three hospitals on the indicator 'C4' are (0.423, 0.480 and 0.494), the related implementation gaps of them are (47.110, 40.003, and 38.238), and the max gap is 47.110. This means the (0-47.110) gape scale should be mapped to 9 point scale, with interval equals 5.23; the first analytic hierarchy process score level (1) will be mapped to the (0-5.23), while the second level well be mapped to the (5.24-10.46),…., the last level (9) will be mapped to the (41.89-47.11). This also means that the first hospital is the worst one, and the implementation gap between it and the second hospital is 7.1. Then, the analytic hierarchy process score is—as it corresponds to the GAP interval 2—2 if the first hospital is compared with the second or third, and it is 1/2 if the second or third hospital is compared with the first. By the same way, the analytic hierarchy process score is 1, if the second and third hospitals compared with each other. This process was repeated 9 times and the results are presented in the following analysis section. This multi measurement scale was implemented instead of the suggested by [22] static mapping scheme; the static measurement scale is presented in Table XIV.

TABLE XIII. MAPPING BETWEEN THE ANALYTIC HIERARCHY PROCESS SCORE AND EVALUATION GAPS

AHP process Score		1	2	3	4	5	6	7	8	9
Dynamic Gap scale	C4	5.23	10.47	15.70	20.94	26.17	31.41	36.64	41.88	47.11
	C4-1	8.41	16.82	25.23	33.64	42.05	50.46	58.87	67.28	75.69
	C4-2	3.36	6.71	10.07	13.43	16.78	20.14	23.50	26.85	30.21
	C4-3	2.46	4.93	7.39	9.85	12.31	14.78	17.24	19.70	22.17
	C4-4	5.21	10.42	15.63	20.83	26.04	31.25	36.46	41.67	46.88
	G1	5.78	11.55	17.33	23.10	28.88	34.65	40.43	46.20	51.98
	G2	4.40	8.79	13.19	17.59	21.98	26.38	30.78	35.17	39.57
	G3	5.74	11.48	17.22	22.96	28.70	34.44	40.18	45.92	51.66

TABLE XIV. MAPPING BETWEEN THE ANALYTIC HIERARCHY PROCESS SCORE AND FIVE POINT EVALUATION GAPS [16]

AHP process Score	5-point scale	Persentage scale
9	4.44-5	88.89-100
8	3.89-4.44	77.78-88.89
7	3.33-3.89	66.67-77.78
6	2.78-3.33	55.56-66.67
5	2.22-2.78	44.44-55.56
4	1.67-2.22	33.33-44.44
3	1.11-1.67	22.22-33.33
2	0.56-1.11	11.11-22.22
1	0-0.56	0-11.11

V. STRUCTURED COMPARISON RESULTS AND ITS DISCUSSION

As it explained previously, the proposed model (A) depends on three different procedures that distinguish it from the model (B) that was proposed in study [22]; It relies on the fuzzy hierarchical analysis technique instead of the classical hierarchical analysis technique for the purpose of determining the weights of indicators and criteria; It depends on the fuzzy Delphi technique instead of the qualitative evaluation technique that depends on a five-point Likert scale for assessing literacy practices of hospitals. It also uses a multi-measurement scale, instead of the single one to link the evaluation results with the structured comparison scale, in order to obtain more accurate comparative results. on the overall weighted scores of implementation (C4 - level), the overall weighted scores on each sub category of indicators (SC-level: C4-1, C4-2, C4-3, and C4-4), and on each importance class (G-level: G1, G2, G3, and G4).

Table XV and Fig. 3 show, the structured comparison results of three models: (A, B, and C); the third model (C) is built based on the qualitative-AHP evaluation methods, which are used by the (B) model and it used a multi-measurement scale of the first model (A) for structured comparison purpose.

By analyzing the results of the study, the following were found:

It has become clear that the model (B) gives consistent comparative results for all nine comparison cases, and this means that the ratios that have been assigned to alternatives according to this model are not accurate as required. This result can be explained by the nature of the evaluation findings themselves; the convergence of evaluation results has been clearly observed, with very little variation in the application gap for alternatives; It is in a range of (0-0.56). This makes the results of the process of mapping these results to the levels used to study the comparison are limited to a single level, and corresponded to the first AHP - comparison assessment level (referred to Table XVI), and This in turn generates equal comparison rates for alternatives, 33 percent each (Fig. 3).

Although this model does not address the ambiguity associated with the evaluation process, it is appropriate for the purpose of study, if one condition is met. Only if the results of the application gap for alternatives are significantly different, and can be mapped to more than one comparison level. Unfortunately, in practice that cannot be guaranteed. This makes us stress the need to use multi-measurement scale to link the application gap of alternatives to the AHP comparison scale (Model C). Therefore, in the following sub section, the results of the proposed model (A) will be compared with those which were acquired by the model(C).

TABLE XV. THE STRUCTURED COMPARASION RESULTS OF ALL MODELS

L	Category	The proposed model (A)			The qualitative – AHP [22](B)			The qualitative – AHP (Dynamic mapping) (C)		
		H1	H2	H3	H1	H2	H3	H1	H2	H3
C4	C4	50.00%	25.00%	25.00%	33.33%	33.33%	33.33%	50.00%	25.00%	25.00%
SC	C4-1	41.26%	32.75%	25.99%	33.33%	33.33%	33.33%	54.99%	24.02%	20.98%
	C4-2	54.99%	24.02%	20.98%	33.33%	33.33%	33.33%	54.99%	24.02%	20.98%
	C4-3	50.00%	25.00%	25.00%	33.33%	33.33%	33.33%	50.00%	25.00%	25.00%
	C4-4	54.99%	24.02%	20.98%	33.33%	33.33%	33.33%	50.00%	25.00%	25.00%
G	G1	50.00%	25.00%	25.00%	33.33%	33.33%	33.33%	50.00%	25.00%	25.00%
	G2	54.99%	24.02%	20.98%	33.33%	33.33%	33.33%	54.99%	24.02%	20.98%
	G3	41.26%	32.75%	25.99%	33.33%	33.33%	33.33%	50.00%	25.00%	25.00%
	C4	50.00%	25.00%	25.00%	33.33%	33.33%	33.33%	41.26%	32.75%	25.99%

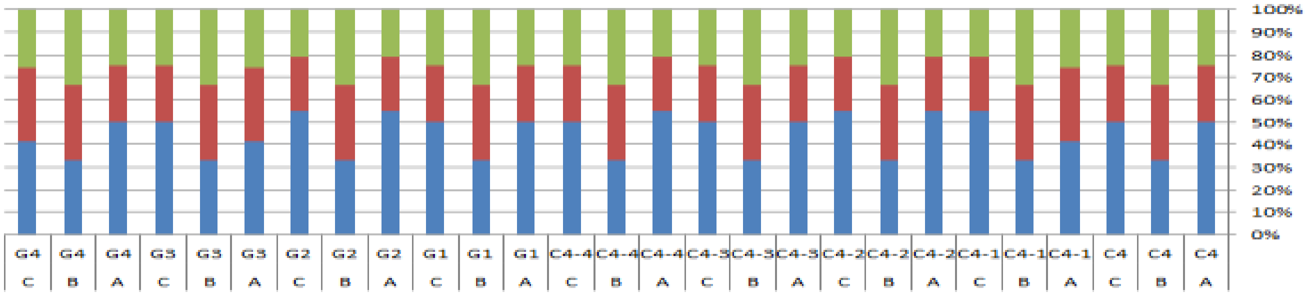

Fig. 3. The Structured Comparison Results of All Models.

TABLE XVI. The Single and Multi-measurment Scale

L	Category	ES			Gaps			The AHP mapped level of the gap level using single measurement scale (0-5)			The AHP mapped level of the gap level using multi - measurement scale		
		H1	**H2**	**H3**	**H1**	**H2**	**H3**	**H1vs H2**	**H1vs H2**	**H2vs H3**	**H1vs H2**	**H1vs H2**	**H2vs H3**
SC	C4-1	3.148	3.499	3.565	0.3516	0.4179	0.0663	1	1	1	2	3	1
	C4-2	3.186	3.492	3.655	0.3054	0.4686	0.1632	1	1	1	2	3	1
	C4-3	3.030	3.257	3.281	0.2278	0.2512	0.0234	1	1	1	2	2	1
	C4-4	3.134	3.357	3.399	0.2237	0.265	0.0413	1	1	1	2	2	1

The results of the comparison of the output of the two models (A and C) at the general level of health literacy showed that the first hospital was most in need for the financial support allocated for improving the level of health literacy. This result suggests that the first hospital have to get 50 per cent of the resources, whereas other hospitals have to get 25 per cent each.

Also, results of the comparison of their output at the sub-domain level of the fourth standard used in this study (SC-level) and at the sub-class level of indicators classified according to their importance (G-level) show that there are differences in the financial support rates that those hospitals have to get.

To compare results of these models, the average change in the output of two models, which are the values of the rates each hospital must have and the Bland-Atman agreement analysis between them were used.

The Bland-Atman agreement analysis is implemented using the following steps [50]: (1) calculate the average weights and differences in them, (2) determine the mean of differences (d), and (3) compute limits of agreement. With assumption that the differences are normally distributed, and prediction interval of 95% as suggested by [50, 51]; the limits of agreement were calculated as (d + 1.69 * Sd ; d - 1.69 * Sd), where Sd is the standard deviation of the differences.

The results of the analysis showed that the average change in the financial support ratios that the first hospital has to get was roughly 2.02%; and it were 2.08%, and 1.22 % in the case of the second and third hospitals. This is because there is no change in the rates assigned by these models for 0.55%, 0.55%, and 0.45% of the comparative processes, respectively.

It also presents that the proposed model (A) gives more accurate evaluation results in comparison with the other model; multiple levels of importance were assigned to indicators, and sub-domains that got one level in the other model. For example, Using the fuzzy based results (model A), For the first hospital case, two deferent values of importance 41.26 %, 54.9 % were assigned to the (C4-1, and C4-2) classes, while the same rate 54 % has been assigned to them when the Qualitative – AHP results were used. For the same reason the proposed model gave better results when comparing the results of hospitals on the (C4-3, and C4-4), and (G1, and G3) pairs. The similar findings have been obtained in the case of other hospitals.

In addition, in the case of hospital (1), the values of (-0.0048) and (0.033) were obtained, the first represents the mean of difference; the second describes the standard deviation of the differences for the investigated models. In addition, the value of (0.010) upper limit and (- 0.00079) lower limit of the confidence interval (0.0113) for the investigated pair were shown. This means that a 95 % of the differences in weights between models are possible to fall in the scope (0.010, – 0.00079). By the same way, a 95 % of the differences in weights of (H2) between the two investigated models are possible to fall in the scope (0.0084, – 0.0002), within an (0.0082) interval, and the same percentage of the differences of the third hospitals' weights between the two models are possible to fall in the scope (0.0025, – 0.0014), within an (0.0093).interval.

Finally, the analysis of the average change in the hospitals' rates of both models shows that the fuzzy based model (A) is better than its equivalent classical model (B) in that it gives non-convergent evaluation results, allowing for better arrangement of criteria, because of that the fuzzy algorithm modifies experts' opinions by using three-valued numbers as an alternative to the one valued numbers representing the AHP rating levels, and this considerably affects the final weight [52]. Also, the agreement results indicate that the limits of agreement between these models are small enough to be confident that the proposed model (A) can be used in place of the second one (C). Regarding this, the F_AHP-FDM based model for structured comparison of the OHLR level of hospitals will be recommended to use instead of the previously suggested Qualitative - AHP based model [22].

VI. Conclusion

The results of the first and second stages show that, with the pairwise comparison using FAHP, it is possible to obtain a priority for each individual indicator and classify them into different groups, and, thus, it is very granular in the overall context of the OHL – standartd4. The fuzzy approach with the pairwise comparison by fuzzy AHP meets all of the requirements of the methodology. The results of the third stage show that the OHLR evaluation process is an important step to determine the development and enhancement directions. Additionally, these results show that with the evaluation using the fuzzy Delphi method, it is possible to obtain an OHLR level for each individual indicator in each organization, and, thus, it is very granular in the overall context of the OHL – standartd4 for the hospital sector. The fuzzy Delphi method also meets all of the requirements of the methodology. Similarly, it is shown that the weighting of the pairwise comparisons of the OHLR level for the hospitals can be mapped granularly to the indicators of the OHL – fourth standard. Additionally, it was possible to derive the FAHP score from the OHLR levels automatically. This makes it easy to compare the rankings of the hospitals. The only effort that needs to be invested is the prioritization of the HL indicators. The results show that all hospitals need additional resources and actions to improve their status. Additionally, it shows which hospital must get the biggest share of the support budget (the first hospital in our example). The results suggest that the approach works in conjunction with the simulation data. However, it can be strongly assumed that the method is directly applicable to public hospitals with the same or similar results.

Also, the comparison results of the application of the proposed model with those obtained using the qualitative AHP based model suggest that the FDM-FAHP based model is well suited to define the organizational health literacy responsiveness level of different hospitals. The results of the pairwise comparison suggest that analytic hierarchy process based on the based on the multi-measurement scale is suited to compare the organizational health literacy responsiveness levels and to find the hospital with the worst health literacy responsiveness level within a public hospital sector. It has been proven that a comparison within some of the healthcare hospitals is possible using this integrated model. This proposed model has demonstrated how fuzzy analytic hierarchy process and fuzzy Delphi methods might be used together to assist decision makers with the evaluation and prioritization of organizational health literacy responsiveness factors in one sector, evaluation of the organizational health literacy responsiveness levels in each hospital in this sector, and rank of these hospitals by their actual organizational health literacy responsiveness level for future healthcare development, social responsibility, and sustainable planning objectives.

Acknowledgments

This research was supported by the Deanship of Scientific Research at Prince Sattam bin Abdulaziz University.

References

[1] V.A. Luyckx., M Tonelli and J W. Stanifer, “The global burden of kidney disease and the sustainable development goals ,” Bulletin of the World Health Organization 96(6), 2018, pp 414-422. https://doi.org/10.2471/blt.17.206441.

[2] E. A. Adeyemi, Y. A. Adebisi, and A. O. Babatunde,“Psychosocial Impacts of Chronic Kidney Disease and Dialysis Therapy," SciMedicine Journal, 3(2), 2021, pp 129-137. https://doi.org/10.28991/scimedj-2021-0302-5.

[3] F. Korançe,“The growing Relation between Environment and Public Health ,” SciMedicine Journal, 3(2), 2021,pp 100-115. https://doi.org/10.28991/scimedj-2021-0302-3.

[4] X, Cao, “Corporate Social Responsibility,” In Fair Development in China . Springer, Cham., 2017, pp. 119-134. https://doi.org/10.1007/978-3-319-43663-0_8.

[5] Mohammed M Said, Adel A Nasser and Abdualmajed A Alkhulaidi. , “ Prioritization of the Eco-hotels Performance Criteria in Yemen using Fuzzy Delphi Method,”. *International Journal of Applied Information Systems* 12(36):20-29, March 2021, https://doi.org.10.5120/ijais2020451900.

[6] T. Floričić, “Sustainable Solutions in the Hospitality Industry and Competitiveness Context of ‘Green Hotels,’” Civil Engineering Journal, vol. 6, no. 6, pp. 1104–1113, Jun. 2020. https://doi.org/10.28991/cej-2020-03091532.

[7] D. N. Jackson, N. Trivedi, and C. Baur , “ Re-prioritizing Digital Health and Health Literacy in Healthy People 2030 to Affect Health Equity ,” Health Communication, 2020, pp. 1-8. https://doi.org/10.1080/10410236.2020.1748828.

[8] A. A. Nasser, A. A. Alkhulaidi, M. N. Ali, M. Hankal, and Al-olofe M., “A Study on the impact of multiple methods of the data normalization on the result of SAW, WED and TOPSIS ordering in Healthcare Multi-attributtes Decision Making Systems based on EW, ENTROPY, CRITIC and SVP weighting approaches,” Indian Journal of Science and Technology, vol. 12, no. 4, pp. 1–21, Jan. 2019.. https://doi.org/10.17485/ijst/2019/v12i4/140756.

[9] A. A. Nasser, A. A. Alkhulaidi, M. N. Ali, M. Hankal, and Al-olofe M., “A Weighted Euclidean Distance - Statistical Variance Procedure based Approach for Improving The Healthcare Decision Making System In Yemen,” Indian Journal of Science and Technology, vol. 12, no. 3, pp. 1–15, Jan. 2019. https://doi.org/10.17485/ijst/2019/v12i3/140661.

[10] International Working Group Health Promoting Hospitals and Health Literate Healthcare Organizations (Working Group HPH and HLO): International Self-Assessment Tool Organizational Health Literacy (Responsiveness) for Hospitals - SAT-OHL-Hos-v1.0-ENinternational.Vienna:WHO Collaborating Centre for Health Promotion in Hospitals and Healthcare (CC-HPH), 2019. Availible at : https://www.hphnet.org/wp-content/uploads/2020/04/SAT-OHL-Hos-v1-0-EN-international_final.pdf, acceced March 2021.

[11] Y. Yu, A. He, S. Zheng, J. Jiang, J. Liang, B. Shrestha, and P. Wang, “How does health literacy affect the utilization of basic public health services in Chinese migrants?,” Health Promotion International, Apr. 2021. https://doi.org/10.1093/heapro/daab040.

[12] D. J. Chisolm, H. E. Keedy, L. C. Hart, L. J. Chavez, M. Dolce, J. Morack, C. Grannis, and K. Kelleher, “Exploring Health Literacy, Transition Readiness, and Healthcare Utilization in Medicaid Chronically Ill Youth,” Journal of Adolescent Health, May 2021. https://doi.org/10.1016/j.jadohealth.2021.03.023.

[13] E. Calero-Molina, E. Hidalgo, L. Rosenfeld, J. M. Verdú-Rotellar, J. Verdú-Soriano, A. Garay, L. Alcoberro, S. Jimenez-Marrero, P. Garcimartin, S. Yun, C. Guerrero, P. Moliner, C. Delso, L. Alcober, C. Enjuanes, and J. Comin-Colet, “The relationship between self-care, long-term mortality, and heart failure hospitalization: insights from a real-world cohort study,” European Journal of Cardiovascular Nursing, May 2021. https://doi.org/10.1093/eurjcn/zvab011.

[14] O. Lindly, M. Crossman, M. Eaves, L. Philpotts, and K. Kuhlthau, "Health Literacy and Health Outcomes Among Children With Developmental Disabilities: A Systematic Review," American Journal on Intellectual and Developmental Disabilities, vol. 125, no. 5, pp. 389–407, Sep. 2020. https://doi.org/10.1352/1944-7558-125.5.389.

[15] M. Fabbri, M. H. Murad, A. M. Wennberg, P. Turcano, P. J. Erwin, F. Alahdab, A. Berti, S. M. Manemann, K. J. Yost, L. J. Finney Rutten, and V. L. Roger, "Health Literacy and Outcomes Among Patients With Heart Failure," JACC: Heart Failure, vol. 8, no. 6, pp. 451–460, Jun. 2020. https://doi.org/10.1016/j.jchf.2019.11.007.

[16] D. Schillinger, R. Balyan, S. A. Crossley, D. S. McNamara, J. Y. Liu, and A. J. Karter, "Employing computational linguistics techniques to identify limited patient health literacy: Findings from the ECLIPPSE study," Health Services Research, vol. 56, no. 1, pp. 132–144, Sep. 2020. https://doi.org/10.1111/1475-6773.13560.

[17] Adel A. Nasser, Nada Kh. A. Al Ansi, Naif A. N. Al Sharabi, "On The Standardization Practices of the Information Security Operations in Banking Sector: Evidence from Yemen," International Journal of Scientific Research in Computer Science and Engineering, Vol.8, Issue.6, pp.8-18, 2020. https://www.isroset.org/pdf paper_view.php?paper_id=2166&2-ISROSET-IJSRCSE-05015.pdf.

[18] A. N. Al-Shameri, "Hierarchical Multilevel Information security gap analysis models based on ISO 27001: 2013," *International Journal of Scientific Research in Multidisciplinary Studies*, *3*(11),2017, 14-23. https://www.isroset.org/pub_paper/IJSRMS/3-IJSRMS-0588-24.pdf.

[19] A. Nasser, "Information security gap analysis based on ISO 27001: 2013 standard: A case study of the Yemeni Academy for Graduate Studies, Sana'a, Yeme,n'". *Int. J. Sci. Res. in Multidisciplinary Studies Vol*, *3*(11).2017. https://www.isroset.org/pub_paper/IJSRMS/2-IJSRMS-0573.pdf.

[20] H. Storms, N. Claes, B. Aertgeerts, and S. Van den Broucke, "Measuring health literacy among low literate people: an exploratory feasibility study with the HLS-EU questionnaire," BMC Public Health, vol. 17, no. 1, May 2017. https://doi.org/10.1186/s12889-017-4391-8.

[21] K. Sørensen, J. M. Pelikan, F. Röthlin, K. Ganahl, Z. Slonska, G. Doyle, J. Fullam, B. Kondilis, D. Agrafiotis, E. Uiters, M. Falcon, M. Mensing, K. Tchamov, S. van den Broucke, and H. Brand, "Health literacy in Europe: comparative results of the European health literacy survey (HLS-EU)," The European Journal of Public Health, vol. 25, no. 6, pp. 1053–1058, Apr. 2015. https://doi.org/10.1093/eurpub/ckv043.

[22] A. Schmid and S. Pape, "A Structured Comparison of the Corporate Information Security Maturity Level," IFIP Advances in Information and Communication Technology, pp. 223–237, 2019. https://doi.org/10.1007/978-3-030-22312-0_16.

[23] S. Greco, J. Figueira and M. Ehrgott , Multiple criteria decision analysis , New York: Springer., 2016. https://doi.org/10.1007/978-1-4939-3094-4.

[24] A. A. Afsordegan, "Contribution to multi-criteria decision making in sustainable energy management based on fuzzy and qualitative reasoning," Tesi doctoral, UPC, Departament de Projectes d'Enginyeria, 2015. Disponible a: http://hdl.handle.net/2117/96001.

[25] Adel A Nasser, Abdualmajed Al-Khulaidi and Mijahed N. Aljober, " Measuring the Information Security Maturity of Enterprises under Uncertainty Using Fuzzy AHP," International Journal of Information Technology and Computer Science(IJITCS), 2018; **10**, 10-25.DOI: https://doi.org/10.5815/ijitcs.2018.04.02.

[26] R. J. Andrews, J. V. Rosenfeld, and N. Crisp, "The Importance of Surgical Care to Achieve the United Nations Sustainable Development Goal for Healthy Lives by 2030," JAMA Health Forum, vol. 2, no. 6, p. e211213, Jun. 2021.https://doi.org/10.1001/jamahealthforum.2021.1213.

[27] M. C. Watson and J. Lloyd, "Creating health promoting schools will improve population health and help reduce inequalities," BMJ, p. n1290, May 2021.https://doi.org/10.1136/bmj.n1290.

[28] S.S. Budhathoki, P.K. Pokharel,S. Good, S. Limbu, M. Bhattachan, and R.H.Osborne , "The potential of health literacy to address the health related UN sustainable development goal 3 (SDG3) in Nepal: a rapid review ,"BMC health services research, 17(1), 2017, pp 1-13. https://doi.org/10.1186/s12913-017-2183-6.

[29] L. Mutea, S. Ontiri, F. Kadiri, K. Michielesen, and P. Gichangi, "Access to information and use of adolescent sexual reproductive health services: Qualitative exploration of barriers and facilitators in Kisumu and Kakamega, Kenya," PLOS ONE, vol. 15, no. 11, p. e0241985, Nov. 2020. https://doi.org/10.1371/journal.pone.0241985.

[30] Fasoulis and Rafet, "Embracing Sustainability in Shipping: Assessing Industry's Adaptations Incited by the, Newly, Introduced 'triple bottom line' Approach to Sustainable Maritime Development," Social Sciences, vol. 8, no. 7, p. 208, Jul. 2019. https://doi.org/10.3390/socsci8070208.

[31] L. Mishra, "Corporate social responsibility and sustainable development goals: A study of Indian companies," Journal of Public Affairs, vol. 21, no. 1, Apr. 2020. https://doi.org/10.1002/pa.2147.

[32] D. Pesmatzoglou, I.E. Nikolaou, K.I., Evangelinos, and S. Allan, "Extractive multinationals and corporate social responsibility: a commitment towards achieving the goals of sustainable development or only a management strategy? ," Journal of International Development, 26(2), 2014, pp.187-206. https://doi.org/10.1002/jid.2871.

[33] K. Sørensen, and H. Brand , "Health literacy—A strategic asset for corporate social responsibility in Europe ," Journal of health communication, 16(3), 2011, pp.322-327.https://doi.org/10.1080/10810730.2011.606072.

[34] T. L. Saaty, "Optimization by the Analytic Hierarchy Process," Jan. 1979. https://doi.org/10.21236/ada214804

[35] J. Franek and A. Kresta, "Judgment Scales and Consistency Measure in AHP," Procedia Economics and Finance, vol. 12, pp. 164–173, 2014. https://doi.org/10.1016/s2212-5671(14)00332-3.

[36] J. Y. Yap,C.C. Ho, and C.Y. Ting, "Aggregating Multiple Decision Makers' Judgement," In Intelligent and Interactive Computing . Springer, Singapore., 2019, pp. 13-21. https://doi.org/10.1007/978-981-13-6031-2_26.

[37] Kaya, B. Çiçekalan, and F. Çebi,"Location selection for WEEE recycling plant by using Pythagorean fuzzy AHP," Journal of Intelligent and Fuzzy Systems, 38(1), 2020, pp. 1097-1106 https://doi.org/10.3233/jifs-179471.

[38] N. Dalkey, and O. Helmer , "An experimental application of the Delphi method to the use of experts," Management Science, 9(3), 1963, pp. 458-467. https://doi.org/10.1287/mnsc.9.3.458.

[39] S.K. Manakandan, I. Rosnah, R.J. Mohd, and R. Priya, "Pesticide applicators questionnaire content validation: A fuzzy Delphi method," Med J Malaysia, 72(4), 2017, 228. https://pubmed.ncbi.nlm.nih.gov/28889134/.

[40] M. Stuit, "Implementing the Information Literacy Framework: A Practical Guide for Librarians," Public Services Quarterly, vol. 14, no. 4, pp. 348–349, Oct. 2018. https://doi.org/10.1080/15228959.2018.1537987.

[41] C. Pennell, "Implementing a New Literacy Program: Professional Learning and Coaching," Evaluating the K–12 Literacy Curriculum, pp. 133–136, Feb. 2020. https://doi.org/10.4324/9780429261107-12.

[42] A. G. Brega, M. A. G. Freedman, W. G. LeBlanc, J. Barnard, N. M. Mabachi, M. Cifuentes, K. Albright, B. D. Weiss, C. Brach, and D. R. West, "Using the Health Literacy Universal Precautions Toolkit to Improve the Quality of Patient Materials," Journal of Health Communication, vol. 20, no. sup2, pp. 69–76, Oct. 2015.https://doi.org/10.1080/10810730.2015.1081997.

[43] L.Y. Prince, , C. Schmidtke, J.K. Beck, and K.B. Hadden , "An assessment of organizational health literacy practices at an academic health center ," Quality management in health care, 27(2), 2018,pp.93-97. https://doi.org/10.1097/qmh.0000000000000162.

[44] N. Kružliaková, K. Porter, P. A. Ray, V. Hedrick, D. J. Brock, and J. Zoellner, "Understanding and Advancing Organizational Health Literacy Within a Public Health Setting," HLRP: Health Literacy Research and Practice, vol. 5, no. 1, Jan. 2021.https://doi.org/10.3928/24748307-20210114-01.

[45] C. A. Vamos, E. L. Thompson, S. B. Griner, L. G. Liggett, and E. M. Daley, "Applying Organizational Health Literacy to Maternal and Child Health," Maternal and Child Health Journal, vol. 23, no. 5, pp. 597–602, Jan. 2019 https://doi.org/10.1007/s10995-018-2687-7.

[46] H. KUCUKALI, O. ATAC, O. OZER, and O. HAYRAN, "Evaluation of individual health literacy among inpatients of different types of

hospitals in Istanbul," Marmara Medical Journal, May 2020. https://doi.org/10.5472/marumj.740539.

[47] H. Shekari , "Investigating and Prioritizing Factors Affecting Health Literacy in University Students of Yazd Using Artificial Neural Network Technique ," Journal of Community Health Research, 9(1),2019, pp 29-37. https://doi.org/10.18502/jchr.v8i1.559.

[48] D.Y. Chang, "Applications of the extent analysis method on fuzzy AHP," European journal of operational research, 95(3), 1996, pp. 649-655. https://doi.org/10.1016/0377-2217(95)00300-2.

[49] H.A. Linstone, and M. Turoff, "The Delphi method ," Reading, MA: Addison-Wesley., 1975. https://doi.org/10.2307/1268751.

[50] J M Bland, and G A Douglas , "Statistical methods for assessing agreement between two methods of clinical measurement. ," The lancet,1989;1:307-310, https://doi.org/10.1016/S0140-6736(86)90837-8.

[51] J M Bland, and G A Douglas, "Measuring agreement in method comparison studies ," Statistical Methods in Medical Research, 1999;8.2. https://doi.org/10.1177%2F096228029900800204.

[52] R. Mosadeghi, J. Warnken, R. Tomlinson, and H. Mirfenderesk, "Comparison of Fuzzy-AHP and AHP in a spatial multi-criteria decision making model for urban land-use planning," Computers, Environment and Urban Systems, vol. 49, pp. 54–65, Jan. 2015. https://doi.org/10.1016/j.compenvurbsys.2014.10.001.

WorkStealing Algorithm for Load Balancing in Grid Computing

Hadeer S.Hossam[1], Hala Abdel-Galil[2], Mohamed Belal[3]
Computer Science Department, Faculty of Computers and Artificial Intelligence, Helwan University, Egypt

***Abstract*—Grid computing is a computer network in which many resources and services are shared for performing a specific task. The term grid appeared in the mid-1990s and due to the computational capabilities, efficiency and scalability provided by the shared resources, it is used nowadays in many areas, including business, e-libraries, e-learning, military applications, medicine, physics, and genetics. In this paper, we propose WorkStealing-Grid Cost Dependency Matrix (WS-GCDM) which schedule DAG tasks according to their data transfer cost, dependency between tasks and load of the available resources. WS-GCDM algorithm is an enhanced version from GCDM algorithm. WS-GCDM algorithm balances load between all the available resources in grid system unlike GCDM which uses specific number of resources regardless how many resources are available. WS-GCDM introduces better makespan than GCDM algorithm and enhances system performance from 13% up to 17% when we experiment algorithms using DAG with dependent tasks.**

Keywords*—Grid computing; static scheduling; dynamic scheduling; load balancing; directed acyclic graph (DAG)

I. Introduction

Importance of grid computing comes from the need to access resources which are geographically distributed and cannot be moved or duplicated to the same location. Grid computing offer approaches to overcome these obstacles. By using a grid, distributed resources can be treated as if they are into single place [1,2]. Assigning tasks to processors /machines is an important issue as it improves the performance of the whole job so that our concern will be on scheduling resources in grid computing. Resources can be computers, storage space, instruments, software applications, and data, are all connected through the Internet and a middleware layer that provides basic services for security, monitoring, resource management, and so forth as shown in Fig. 1. This work concerned with the processing time efficiency. Resources available on grid are shared under policies that specify who is permitted to access resources, what are the resources that will be available for everyone, and under what conditions they will use these resources [3].

Nature of grid computing resources is dynamic; therefore achieving high performance is a challenge as new resource can be submitted to the grid or withdraw from the grid. There are number of factors, which can affect the grid application performance; load balancing is one of the most critical features of Grid infrastructure.

Scheduling tasks in grid computing is critical as it influences the execution of the whole application. The problem of mapping tasks in grid computing is to find proper assignment of tasks to the available processors in order to optimize system utilization and load balancing and to minimize execution time [4].

This paper is organized as follows. In Section 2, related works for the independent and dependent task scheduling algorithms are discussed. In Section 3, we clarified our problem statement. And, we describe our proposed algorithm and how the WS-GCDM balance task scheduling between the available resources. And, we discuss the experimental results under varying gridlets and number of resources between the GCDM and WS-GCDM algorithms. In Section 4, we provide our final conclusion and the detailed algorithm.

II. Related Work

Over the past few years, a lot of grid computing algorithms have been introduced. Such algorithms focused on arranging and allocating tasks to resources in a way that minimizes the execution time in order to enhance performance and data transfer cost between these resources. This section surveys previous work in scheduling tasks in grid computing.

After user submit an application, the scheduler divides this application into tasks. These tasks may be dependent on each other and need to be scheduled based on the precedence between tasks, or sometimes each task is stand-alone and can be scheduled without affecting other tasks. This categorized scheduling in grid computing according to task dependency.

As an example of independent task scheduling algorithms: Opportunistic Load Balancing (OLB) algorithm [5, 6], Minimum Execution Time (MET) algorithm [7], Minimum Completion Time (MCT) algorithm [8], Min-min algorithm [9], Max-min algorithm [10, 11, 12], Suffrage algorithm [13, 14].

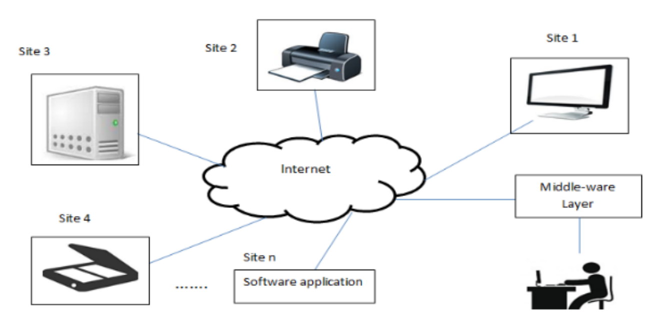

Fig. 1. Framework of Grid Computing.

Dependent task scheduling algorithms use the Directed Acyclic Graph (DAG) to represent dependency between tasks. Algorithms schedule dependent tasks such as Fully Decentralized P2P Grid scheduling (FDPGS) algorithm proposed by Piyush Chauhan and Nitin [15]. Sorted nodes in leveled DAG division (SNLDD) algorithm proposed in [16]. Grid costs and dependence matrix (GCDM) algorithm was proposed in [17]. CCF (Cluster ready Children First) algorithm proposed by Florin Pop and Valentin Cristea [18]. Communication inclusion generational scheduling (CIGS) algorithm proposed by Communication Inclusion Generational Scheduling (CIGS) algorithm [19], Dynamic Critical Path for Grid (DCP-G) and rescheduling DCP-G (Re-DCP-G) [20], and Grid Workflow Scheduling (GWS) algorithm [21].

This work is concerned with the task scheduling problem. We present application subtasks as a Directed Acyclic Graph (DAG) then these subtasks are mapped to the available processors. Moreover, we are trying to balance load across the available resources by using workstealing algorithm. WorkStealing algorithm (WS-GCDM) redistributes the initial scheduling work over idle processors, and as long as all processors have tasks to execute, no scheduling overhead occurs. This is the advantage of using receiver-initiated scheduling rather than sender-initiated scheduling as every resource maintains it as work queue and idle processors try to steel work from other resources.

III. Proposed Algorithm

Architecture of proposed WS-GCDM algorithm has two main components: Resource Discovery and Workflow Task Scheduling.

Resource Discovery component is responsible for discovering grid resources. It continuously collects information about which resources are available to the system. After finishing this task, it sends the collected information to the Grid Information Service (GIS) about the registered resources. The information includes number of processing elements (PEs), million instructions per seconds (MIPS), architecture and their operation systems.

Workflow Task scheduling component is responsible for scheduling workflow tasks. It receives Directed Acyclic Graph (DAG) from the user and based on the collected information about the registered resources from GIS it instantiates static scheduling phase. Ready tasks are then dispatched to the mapped resources based on their priority on the workflow. When resource becomes idle, it tries to steal tasks from the busy resources and the initial static scheduling change.

A. *Overview of WS-GCDM **A**lgorithm*

A WS-GCDM tries to minimize the execution time of the whole workflow application (makespan). The proposed WS-GCDM algorithm consists of three phases: Resource Discovery, Static Scheduling, and Rescheduling by WorkStealing phase.

Resource discovery phase is responsible for collecting information about the available resources. Then static scheduling phase tries to map DAG tasks to the appropriate resources based on the collected information stored in the GIS with the aim to reduce data cost transfer, which is the cost of transferring data from task to another task, and execution time of the whole application. The schedule is then submitted to Execution Manager (EM), which is responsible for getting ready tasks and executing these tasks to the scheduled resources. Final phase is the rescheduling by WorkStealing. This phase is responsible for monitoring the status of the available resources. When resource becomes idle it tries to find resource with tasks on its queue. Once it succeeded to finds this resource it tries to steal tasks from that resource which become a victim. We call idle resource which stole work from other resources stealer. Stealer resources try to steal tasks which can be finished as earlier as possible in order to search for other tasks to execute it.

B. *Static Task Scheduling*

Static task scheduling considers dependencies and data cost transfer between tasks in the workflow. Consider we have N tasks in the DAG workflow. Dependency (D) and data cost transfer (C) matrices (N*N) then created.

In this stage number of resources that will be used initially will be as the number input nodes in the DAG. Steps of static task scheduling are:

- Determine input nodes.
- Mapping input nodes.
- Mapping remaining nodes in the DAG.

1) Determine input nodes: In this step input nodes are determined considering D matrix. Input nodes are the nodes which did not depend on any other nodes. Also, sometimes, they are called entry nodes.

2) Mapping input nodes: After determining input nodes, number of resources that will be used initially is determined. In this step each input node is mapped to separate resource. If number of registered resources is less than number of input nodes, then we start mapping the outnumber tasks with the previously mapped tasks. Each processor now has its own set containing nodes that will be executed by this it.

3) Mapping remaining nodes in the DAG: In the step all the remaining tasks in the workflow DAG is mapped to the used resources in the previous step. DAG is divided into levels and nodes will be scheduled level by level in order to perceive priorities between nodes. Let us consider we have m levels in the DAG, this mean that node in level i ($0<=i<m$) have higher priority than nodes in level i+1. Considering C matrix and sets of each processor nodes in the next level can be determined, and then these nodes can be scheduled considering their parent nodes. There are two cases for each node while scheduling it:

- Node has only one parent. This node is not shared and scheduled to processor which has its parent on its set.
- Node has more than one parent. This node is shared between other parent nodes and will be scheduled according to the following rule:

a) If parent nodes are mapped to the same resource, then this node will be added to this processor set.

b) If parent nodes are mapped to different resources, then task will be added to the processor that are more transferring cost to its nodes.

4) Rescheduling by work stealing phase: Workflow scheduling should be balanced to the available resources. GCDM fail to balance load across the resources, as this algorithm did not consider all the available resources and use only specified number of resources which is equal to the input nodes. Therefore, we can find resources idle while other resources may be overloaded. This may influence the execution of the whole application makespan; which is the time when all jobs are completed.

WS-GCDM balance load across the available resources by using WorkStealing algorithm. Tasks are submitted to the mapped resources initially by using sender-initiated policy, which means scheduler is responsible for sending tasks to the resources. After this stage each resource will have its own queue containing ready tasks that will be executed by this resource. When execution of tasks begins on the mapped resources WorkStealing algorithm will be triggered. Idle resources, which are called stealer nodes, will try to find resources with tasks that can be stolen; these resources are called victim nodes. After succeeding to find this resource stealer node will steal Least Waiting Tasks (LWT) from victim and add this task to its own queue. LWT are tasks that have minimum waiting counter which represent number of tasks needed to be finished to start executing this task. We choose the LWT in order to make resource finish this task earlier than possible and try to steal another task from other victim nodes. Steal nodes become receiver initiated and by this utilization of idle resources are enhanced as it helps to make these resources as busy as possible.

5) WS-GCDM pseudo code: As in this heading, they should be Times New Roman 11-point boldface, initially capitalized, flush left.

This section describes the pseudo code of the WS-GCDM algorithm for scheduling workflow tasks which is shown in Algorithm 1.

Algorithm 1. Work Stealing Grid Cost Dependancy Matrix (WS-GCDM) algorithm

1.Input: Directed acyclic graph.
2.Construct dependency matrix
3.Construct data transmission cost matrix
4. Loop from i=0 to number of gridlets in dependency matrix
  If gridlet does not depend on any other node
    Add this gridlet to inputGridlets.
5. Number of resources= the number of gridlets in inputGridlets
6.Loop from i=0 to number of inputGridlets
  Schedule each gridlet to processor.
7.While there are gridlets in DAG not scheduled
  1.If gridlet is not shared between resources then:
    i. Assign task to the processor that the tasks dependent on before it in set.
  2.Else if gridlet is shared between resources then:
    If parent nodes are mapped to the same resource
    then
      Add task to the parents processor set.
    If parent nodes are mapped to different resources
    then
      Add task to the processor that are more t
        ransferring cost to its nodes.
8.Construct gridletResourceCharacteristics for each gridlet which contains
  Direct Parent list
  Waiting counter
  Direct children list
9.Construct gridletProcessor list for each processor.
10.Begin
  I. Loop from i=0 to number of gridlets on every gridletProcessor list
      If gridlet waiting counter=0
        Submit gridlet to its scheduled
    resource
        Add this gridlet to runningGridlets
  II. Loop from i=0 to runningGridlets
    Loop from i=0 to number of gridletProcessor
    While gridletProcessor.size==0
    Create random number from 0 to

number of processors

      Loop from i=0 to
      gridletProcessor[randomNumber].size()

    Get gridlet with minimum waiting counter

  III. Add this gridlet to gridletProcessor list of this resource
  IV. Get direct children of those runningGridlets
  V. Add direct children to waitingGridlets
  VI. Loop from gridlet=0 to number of waitingGridlets
    Send message to waitingGridlets to decrement their waiting counter.
    Get direct children of those waitingGridlets
    Add direct children to waitingGridlets
    Go to step vi
  VII. Go to step i

Initially the first phase of statically scheduling tasks to available resources.

Steps 1-3 take DAG and construct its data and cost matrix. Then Steps 4-6 determines input or entry nodes and assigns each input node to the specified number of resources. Step 7 schedules the remaining tasks in DAG to processors according to the previously described algorithm in section Static task scheduling. Step 8 adds parameters to gridlet beside its characteristics. Direct Parent list contains Parents which are directly connected to this gridlet. Waiting counter contains number of tasks needed to be executed to start executing this gridlet and is calculated by incrementing waiting counter of its direct parents waiting by one. Direct children list contains children of this gridlet which are directly connected with it. Step 9 construct waiting queue for each processor which contains tasks that will be executed by this processor.

Step 10 send gridlets with waiting counter =0 which means this gridlet become ready to be executed to running queue. After sending task to the running queue of the mapped processor, message from this task need to be sent to each child in the direct children list. This message is to inform the child that parent who sends message start executing and to be ready for executing. This means that this child needs to decrease its waiting counter by one. Also, this child needs to send message to each child in its direct children list to decrease its waiting counter and continue sending message from child to child until we reach the exit node. While there are tasks in the running queue idle resources search for victim nodes and try to steal work from it.

6) Implementation: In our work, we use GridSim toolkit simulator. The GridSim toolkit provides modeling and simulation of entities in distributed computing systems, users, resources, and resource brokers (schedulers) for design and evaluation of scheduling algorithms. It was originally conceived by Buyya [22].

There are five different entities used in the system:

- User.
- Gridlets.
- Resources.
- Grid Information Service (GIS).
- Grid Broker.

The makespan, resource busy time percentage, and system improvement are the used measure to compare the performance of GCDM and WS-GCDM algorithms.

Makespan is the total time elapsed between the start time of executing the first task in the DAG workflow to the completion time of last task.

Resource busy time percentage which is the percentage of time the resource is busy in executing tasks in its ready queue.

System improvement rate that specifies the performance improvement rate of WS-GCDM algorithm with respect to GCDM algorithm can be measured as the difference between GCDM makespan and WS-GCDM makespan over the makespan of WS-GCDM algorithm.

Table I shows the characteristics of all resources that will be used in our simulation environment. We have used a subset of resources of the World-Wide Grid (WWG) testbed, as used in [23].

TABLE I. THE WWG TESTBED RESOURCES

Resource ID	Resource Name	MIPS Rating	No of PEs	Operating System Architecture
5	Resource_0	515	4	OSF1 Compaq AlphaServer
9	Resource_1	377	4	Solaris Sun Ultra
13	Resource_2	377	4	Solaris Sun Ultra
17	Resource_3	377	2	Solaris Sun Ultra
21	Resource_4	380	2	Linux Intel Pentium/VC820
25	Resource_5	410	6	IRIX SGI Origin 3200
29	Resource_6	410	16	IRIX SGI Origin 3200
33	Resource_7	410	16	IRIX SGI Origin 3200
37	Resource_8	380	2	Linux Intel Pentium/VC820
41	Resource_9	410	4	IRIX SGI Origin 3200

The following subsections show six different experiments for evaluating the performance of WS-GCDM algorithm. DAG in each experiment is generated randomly. The gridlets in the generated DAG varying in their length and input file size. In addition, the first five experiments are done using only the first five resources from Table I and different number of gridlet (twenty gridlets, forty gridlets, sixty gridlets, eighty gridlets and one hundred gridlets).

Experiment six shows the performance of GCDM and WS-GCDM algorithms under different number of resources.

IV. EXPERIMENTS

A. Experiment One

We implement GCDM and WS-GCDM algorithms on random DAG with 20 tasks and two input tasks.

Fig. 2 and Fig. 3 indicate the busy time percentage of the available five resources for GCDM and WS-GCDM algorithms, respectively.

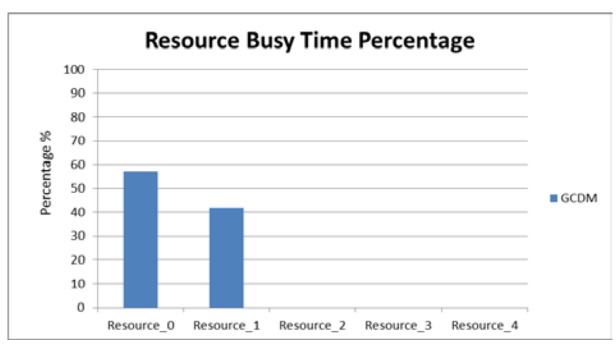

Fig. 2. Resource Busy Time Percentage for GCDM Algorithm on Random DAG with 20 Tasks.

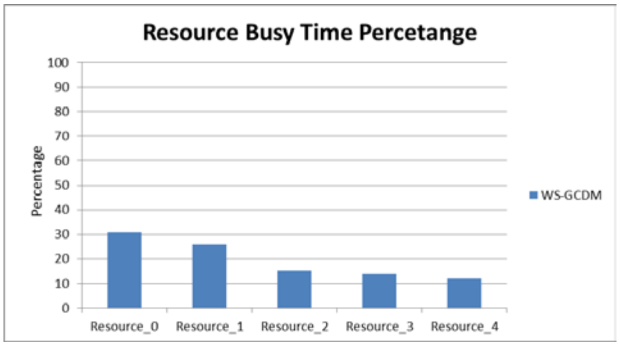

Fig. 3. Resource Busy Time Percentage for WS-GCDM Algorithm on Random DAG with 20 Tasks.

Makespan of GCDM=10563.763 sec, while makespan of WS-GCDM=9128.416 sec.

From the makespan results we can conclude that WS-GCDM improve performance rate with nearly 15%.

B. Experiment Two

We experiment GCDM and WS-GCDM algorithms on random DAG with 40 tasks and three input tasks.

Fig. 4 and Fig. 5 indicate the busy time percentage of the available five resources for GCDM and WS-GCDM algorithms, respectively.

Makespan of GCDM= 46630.65 sec, while makespan of WS-GCDM= 39797.880 sec.

From the makespan results we can conclude that WS-GCDM improve performance rate with nearly 17%.

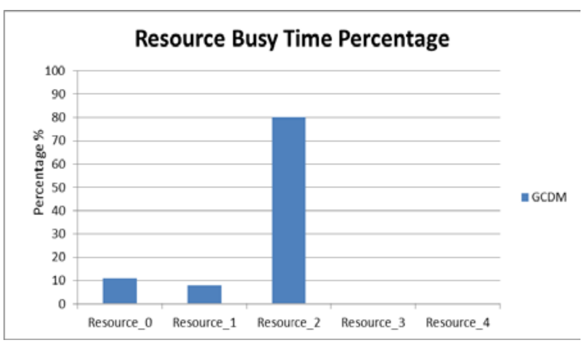

Fig. 4. Resource Busy Time Percentage for GCDM Algorithm on Random DAG with 40 Tasks.

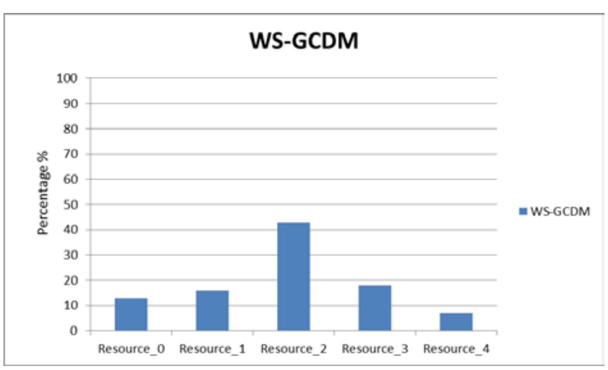

Fig. 5. Resource Busy Time Percentage for WS-GCDM Algorithm on Random DAG with 40 Tasks.

C. Experiment Three

We experiment GCDM and WS-GCDM algorithms on random DAG with 60 tasks and three input tasks.

Fig. 6 and Fig. 7 indicate the busy time percentage of the available five resources for GCDM and WS-GCDM algorithms, respectively.

Makespan of GCDM= 64844.101 sec, while makespan of WS-GCDM= 57213.422 sec.

From the makespan results we can conclude that WS-GCDM improve performance rate with nearly 13%.

D. Experiment Four

We experiment GCDM and WS-GCDM algorithms on random DAG with 80 tasks and four input tasks.

Fig. 8 and Fig. 9 indicate the busy time percentage of the available five resources for GCDM and WS-GCDM algorithms, respectively.

Makespan of GCDM= 75219.907 sec, while makespan of WS-GCDM= 65978.606 sec.

From the makespan results we can conclude that WS-GCDM improve performance rate with nearly 14%.

E. Experiment Five

We experiment GCDM and WS-GCDM algorithms on random DAG with 100 tasks and two input tasks.

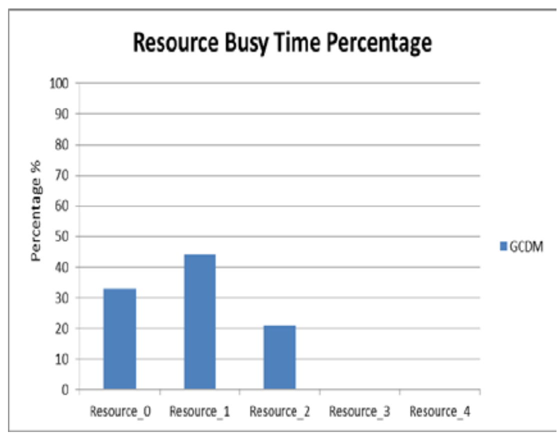

Fig. 6. Resource Busy Time Percentage for GCDM Algorithm on Random DAG with 60 Tasks.

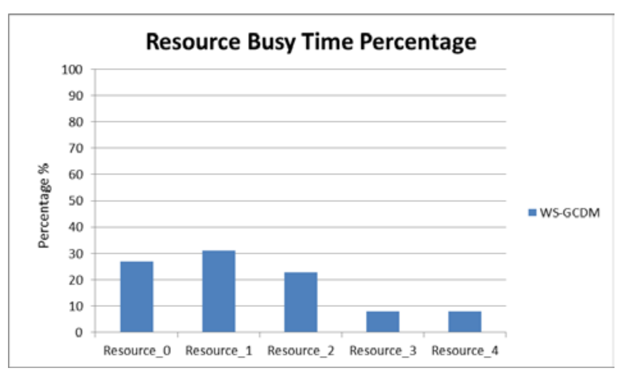

Fig. 7. Resource Busy Time Percentage for WS-GCDM Algorithm on Random DAG with 60 Tasks.

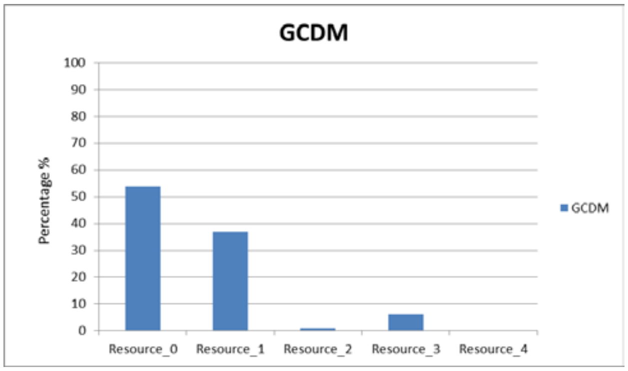

Fig. 8. Resource Busy Time Percentage for GCDM Algorithm on Random DAG with 80 Tasks.

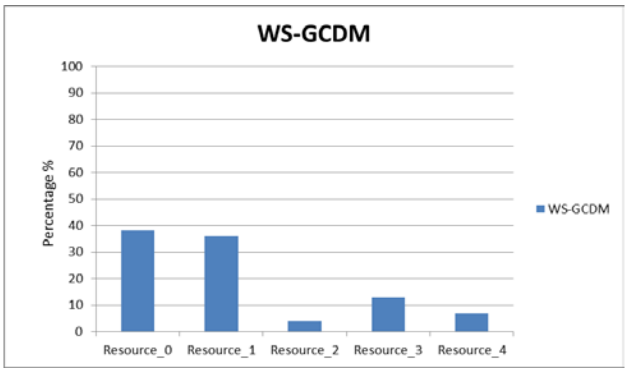

Fig. 9. Resource Busy Time Percentage for WS-GCDM Algorithm on Random DAG with 80 Tasks.

Fig. 10 and Fig. 11 indicate the busy time percentage of the available five resources for GCDM and WS-GCDM algorithms, respectively.

Makespan of GCDM= 87280.950 sec, while makespan of WS-GCDM= 76115.103 sec.

From the makespan results we can conclude that WS-GCDM improve performance rate with nearly 14%.

F. Experiment Six

In this experiment we compare load balance between resources and makespan of GCDM and WS-GCDM algorithms when number of resources varies. We make this evaluation using DAG with 100 tasks.

From Fig. 12, we can conclude that makespan of GCDM under different number of resources does not change a lot as it uses only limited number of resources considering number of input tasks in the DAG whereas makespan of WS-GCDM under different number of resources always are less than makespan of GCDM as all resources are busy and has gridlets to execute.

G. Experiment Seven

In this experiment we compare our proposed algorithm WS-GCDM with Adaptive Workflow Scheduling (AWS) algorithm [21]. We compare makespan of WS-GCDM and makespan of AWS under different number of tasks.

From Fig. 13, we can conclude that makespan of WS-GCDM is less than makespan of AWS.

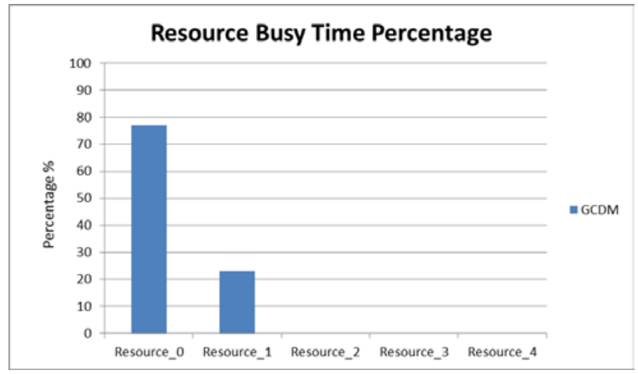

Fig. 10. Resource Busy Time Percentage for GCDM Algorithm on Random DAG with 100 Tasks.

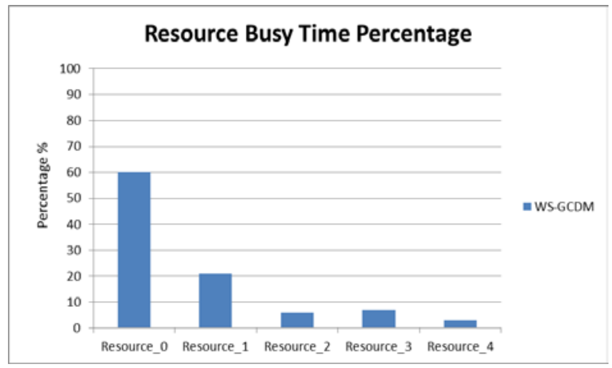

Fig. 11. Resource Busy Time Percentage for WS-GCDM Algorithm on Random DAG with 100 Tasks.

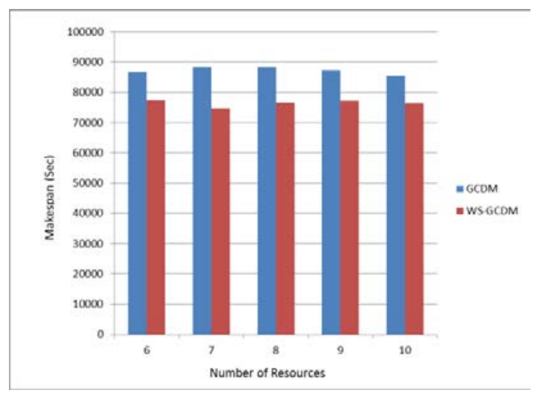

Fig. 12. Makespan of GCDM and WS-GCDM under different Number of Resources.

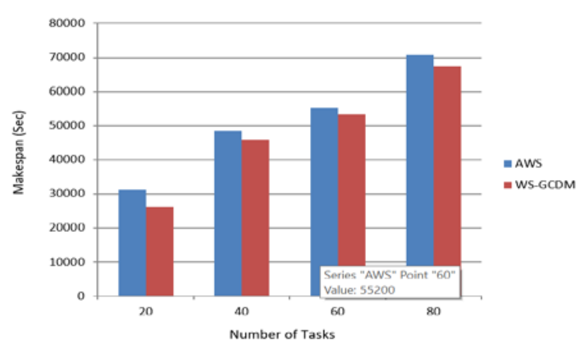

Fig. 13. Makespan of AWS and WS-GCDM under different Number of Resources.

V. Contributions

Load Balancing is one of most important features of Grid Middleware for efficient execution of intensive applications. The efficiency of load balancing of the algorithm decides the efficiency of grid middleware.

Our proposed algorithm WS-GCDM focus on balancing load among resources Work-Stealing Grid Cost Dependency Matrix (WS-GCDM) algorithm which is enhanced version from Grid Cost Dependency Matrix (GCDM) algorithm.

WS-GCDM and GCDM are implemented and compared using the same data. It is found that WS-GCDM improves performance of the GCDM and the makespan in case of using WS-GCDM is better than GCDM.

Also, we compared, this makespan of the proposed algorithm WS-GCDM with Adaptive Workflow Scheduling (AWS) algorithm and from the experiments results WS-GCDM introduces better load balancing and enhances the makespan than GCDM and AWS algorithms as all the available resources are utilized. It enhances system performance by nearly 15%, 17%, 13%, 14% and 14% when we experiment algorithms using DAG with 20,40,60,80 and 100 dependent tasks, respectively.

References

[1] Dr. K. S. Kanna, Dr. P. Devabalan, S.Hariharasitaraman and P. Deepa, Some Insights on Grid Computing-A Study Perspective, International Journal of Pure and Applied Mathematics Volume 118 No. 8 2018, 47-50.

[2] 7 things you should know about grid computing, Educause65 learning initiative, January 2006.

[3] Fangpeng Dong and Selim G. Akl, Scheduling Algorithms for Grid Computing: State of the Art and Open Problems, School of Computing, Queen's University Kingston, Ontario January 2006.

[4] I.I. Kurochkin and E.A. Gerk, Modeling of task scheduling in desktop grid systems at the initial stage of development, Proceedings of the VIII International Conference "Distributed Computing and Grid-technologies in Science and Education, 2018.

[5] George Amalarethinam. D.I, Vaaheedha Kfatheen .S, "Max-min Average Algorithm for Scheduling Tasks in Grid Computing Systems", (IJCSIT) International Journal of Computer Science and Information Technologies, Vol. 3 (2) , 2012.

[6] Naglaa M. Redaa, A. Tawfikb, Mohamed A. Marzokb, Soheir M. Khamis, "Sort-Mid tasks scheduling algorithm in grid computing1", Journal of Advanced Research Volume 6, Issue 6, November 2015.

[7] P. K. Suri, Sunita Rani, "GRID Distance and Execution Time based Scheduling Algorithm", International Journal of Computer Engineering and Technology (IJCET), ISSN 0976-6367(Print), ISSN 0976 - 6375(Online), Volume 5, Issue 7, July (2014).

[8] Adil Yousif, Sulaiman Mohd Nor, Abdul Hanan Abdualla, and Mohammed Bakri Bashir, "Job Scheduling Algorithms on Grid Computing: State-of- the Art", International Journal of Grid Distribution Computing Vol. 8, No.6, (2015).

[9] T. Kokilavani, Dr. D.I. George Amalarethinam, "Load Balanced Min-Min Algorithm for Static Meta-Task Scheduling in Grid Computing", International Journal of Computer Applications (0975 – 8887) Volume 20– No.2, April 2011.

[10] Navdeep Kaur, Khushdeep Kaur, "Improved Max-Min Scheduling Algorithm", IOSR Journal of Computer Engineering (IOSR-JCE) e-ISSN: 2278-0661, p-ISSN: 2278-8727, Volume 17, Issue 3, Ver. 1 (May – Jun. 2015).

[11] Zhongping Zhang, Yupeng Feng, Shan Zhang and Ying Sun, "Heuristic Grid Resource Scheduling Algorithm based on Group of Task and Secondary Distribution", International Journal of Security and Its Applications Vol.9, No.8 (2015).

[12] Salman Meraji and M. Reza Salehnamadi," A Batch Mode Scheduling Algorithm for Grid Computing", Journal of Basic and Applied Scientific Research, J. Basic. Appl. Sci. Res., 3(4)173-181, 2013.

[13] Naglaa M. Reda, "An Improved Sufferage Meta-Task Scheduling Algorithm in Grid Computing Systems International Journal of Advanced Research (2015), Volume 3, Issue 10, 123 -129.

[14] Nabeel Zanoon, Nashat Al Bdour and Evon Abu-Taieh, "Survey of Algorithm: Scheduling Systems and Distributed Resource Management in Grid", International Journal of Computer Applications (0975 – 8887) Volume 98– No.1, July 2014.

[15] Piyush Chauhan and Nitin, "Decentralized Scheduling Algorithm for DAG Based Tasks on P2P Grid", Hindawi Publishing Corporation Journal of Engineering Volume 2014, Article ID 202843,14 pages, January 2014.

[16] Nirmeen A. Bahnasawy, Magdy A. Koutb, Mervat Mosa and Fatma Omara, "A new algorithm for static task scheduling for heterogeneous distributed computing systems" African Journal of Mathematics and Computer Science Research Vol. 4(6), pp. 221- 234, June 2011.

[17] Amir M Bidgoli and Zahra Masoudi Nezad, "A new scheduling algorithm design for grid computing tasks", 5th SASTech 2011, Khavaran Higher- education Institute, Mashhad, Iran.

[18] Florin Pop andValentin Cristea, "Intelligent Strategies for Dag Scheduling Optimization in GRID Environments", 16th International Conference on Control Systems and Computer Science (CSCS16'07).

[19] Ian Foster, Carl Kesselman and Steven Tuecke, "The Anatomy of the Grid Enabling Scalable Virtual Organizations", To appear: Intl J. Supercomputer Applications, 2001.

[20] Mustafizur Rahman , Rafiul Hassan , Rajiv Ranjan , and Rajkumar Buyya , "Adaptive workflow scheduling for dynamic grid and cloud computing environment", Published online 4 March 2013 in Wiley Online Library (wileyonlinelibrary.com). DOI: 10.1002/cpe.3003.

[21] Ritu Garg and Awadhesh Kumar Singh, "Adaptive workflow scheduling in grid computing based on dynamic resource availability", Engineering Science and Technology, an International Journal (2015).

[22] Jia, Rajkumar Buyaa, "Workflow Scheduling Algorithms for Grid Computing", Technical Report, Grid Computing and Distributed Systems Laboratory, The University of Melbourne, Australia, May 31, 2007.

[23] Mustafizur Rahman , Rafiul Hassan , Rajiv Ranjan , and Rajkumar Buyya , "Adaptive workflow scheduling for dynamic grid and cloud computing environment", Published online 4 March 2013 in Wiley Online Library (wileyonlinelibrary.com). DOI:10.1002/cpe.3003.

Multi-parameter Coordinated Public School Admission Model by using Stable Marriage

Purba Daru Kusuma
Computer Engineering, Faculty of Electrical Engineering
Telkom University, Bandung, Indonesia

***Abstract*—School admission is a very important process in improving the education quality. Meanwhile, one problem in the school admission system is the mismatch. There are unassigned applicants and unallocated seats. In Indonesia, zone-based model is adopted in the public-school admission system. Students are assigned to their nearest school. Besides location, student's academic performance and economic level are also concerned. Based on it, this work proposes coordinated public school admission model that accommodates flexible number of the concerned parameters. It is built based on the stable marriage algorithm or the deferred-acceptance algorithm as its derivative. The proposed model is a combination between the mandatory approach and the school choice approach. The concerned parameters are school-home distance, student national exam score, school rank, applicant poor status, and applicant's preference. The simulation is conducted to investigate the performance of the proposed model compared with the previous models: the zone-based model and the two-step model. The prioritization of the concerned parameters is proven easily adjusted. The simulation result shows that in the over-demand condition, the proposed model creates higher average student national exam score and higher average school-home distance rather than the previous models. When the number of applicants is twice of the number of seats, the proposed model creates 6.6 percent higher in the average student national exam score and 71.4 percent higher in the average school-home distance. The simulation result also shows that the mismatch is solved.**

***Keywords*—School admission; school choice; stable marriage; deferred-acceptance; education**

I. Introduction

School admission system is an important system in the school management system [1]. The role of school admission system is allocating the available seats to the appropriate applicants. In the over-demand condition, the school admission plays as selection or sorting mechanism so that the preferred applicants are accepted while the others are rejected [2]. The problem becomes more complicated in the public-school admission system. The public-school admission system is usually coordinated by the local government due to its responsibility in managing them [1]. The most common problem in this admission system is the mismatch between the schools and the applicants. There is possibility where there are unallocated seats in several schools in one side, and unassigned applicants in another side.

There are several conditions that make this problem happens. First, some schools are more favourite rather than the others. The favourite schools usually receive more applicants so that they face over demand condition [3]. Hart and Figalo [4] found that in Florida, schools with “A” accreditation receive higher enrolment rather than schools with “B” or “C” accreditation. Hofflinger, Gelber, and Canas [5] found that parents with higher socioeconomic status prefer high performing schools in Chile. Erickson [6] noted that in the United States, parents value the school quality although it is not always the highest determinant. In the other side, the non-favourite schools receive less applicants so that they face over-supply condition [7]. Second, several schools are in the strategic location, for example in the city central or in the middle of residential area, while several other schools are in the non-strategic area. Schools that face over-demand condition will reject the less appropriate applicants so that there are unassigned applicants. In the other side, several schools that face over-supply condition will have unallocated seats.

In Indonesia, public-school admission system is coordinated by the local government. This system adopts zone-based system so that schools prioritize students who live in the same zone [8]. This concept has several goals. The first goal is to allocate students to attend the school near their residential location so that the school-home distance and the transportation cost can be minimized [7]. The second goal is to minimize segregation among public schools so that there is not any stigma between favourite and non-favourite schools [9]. This segregation among schools has been blamed for creating inequality among schools where the favourite schools can maintain their superiority in academic performance compared with the non- favourite schools [7]. In the previous era, admission in public schools in Indonesia was based on the students' academic performance, specifically based on the students' national final exam score. High performing students tend to achieve high national exam score and have higher probability to be accepted in the favourite schools [7]. The opposite condition occurred in the non-favourite schools. Less favourite schools are almost impossible to complete the favourite ones.

Meanwhile, implementation of the full zone-based system has been criticized by some stakeholders. A strict zone-based system makes students from the outer zone are difficult to be accepted [9]. Students do not have choice although the academic performance of their in-the-zone schools is low. Besides, full zone-based system is blamed for eliminating incentive for students with high academic achievement to be accepted in the favourite schools. So, parents that are unwilling to submit to the low performance in-the-zone public schools, will send their children to the high-performance private schools to avoid sacrificing their children education quality [8]. Several local governments respond this problem by opening several admission channels sequentially to accommodate the academic achievement and the national regulation about zone-based system [8]. Unfortunately, this policy still cannot solve the mismatch problem.

There is a popular algorithm that was used in the school admission system. It is stable marriage algorithm [10] or in other term is deferred-acceptance algorithm [11]. In its origin, this algorithm is illustrated in the matching process between equal number of men and women [10]. In practical, this algorithm is used in the matching process between colleges and students [12] and between hospitals and residents [13]. This algorithm also has been implemented in New York school admission system [14]. To date, this algorithm has been improved widely.

Unfortunately, to be implemented in public-schools admission system in Indonesia, this stable marriage model needs to be improved. In the previous work, parameters included in the admission mechanism are the applicant's preference list and school-home distance [14]. Meanwhile, in Indonesia, there are some unaccommodated parameters. The first is the student national exam score [1]. The second is the affirmative mechanism where there should be mandatory allocation for every public school to accept students with several disadvantages, for example is student from low-income background [1].

Based on the explanation above, it can be summarized as follows. First, the school choice approach and mandatory approach have advantages and disadvantages so that the combination between both approaches may produce better outcomes. Second, the stable marriage algorithm is potential to solve this problem. Third, existing studies or solutions in the school admission system that used stable marriage problem usually concern in one or few parameters. Fourth, to be complied with the regulation in Indonesia, the basic stable-marriage based solution should be improved.

Based on this problem, we propose coordinated student admission model for public schools. This work aims to develop school admission problem that accommodates both school choice approach and mandatory approach; and it complies with the requirements of school admission in Indonesia. This model is developed based on the stable marriage algorithm or deferred-acceptance algorithm.

Contribution of this work is as follows. Mainly, coordinated public school admission model is proposed based on the stable marriage algorithm with several advantages. First, this model guarantees that there will be no unassigned applicants in the over-supply or equal supply-demand condition. Second, this model accommodates parameters that are concerned by the stakeholders (school, family, and government): school-home distance, student national exam score, and affirmative scheme. Third, this model can be adjusted easily by every local government who is in charge in the public-schools admission process in its district. Fourth, this model simplifies the previous admission models process, both in the zone-based model [7] and the two-step model [14].

The remainder of this paper is organized as follows. In the second section, the previous literatures in the school admission, school choice, and stable marriage algorithm are explained. In the third section, the proposed model is explained. In the fourth section, the simulation work and simulation result are discussed. In the fifth section, the findings and the deeper analysis connecting the result with the previous works are discussed. In the sixth section, this work is concluded in answering the research purpose and the future research potentials are described.

II. Related Works

There are two models in the school admission system, especially in the public school. The first is mandatory model [14] and the second is school choice model [15]. These models are usually adopted in the elementary school to high school. In the mandatory model, students will be allocated to the public school which is near or the nearest to their home [1]. In the school choice model, students can choose schools that they prefer the most [16]. In some cases, hybrid model is implemented. In the first model, zone-based system is usually implemented. Schools prioritize the in-the-zone students [8]. If there are available seats, schools can accept students from the outer zones.

There are some supporting arguments to the mandatory model. First, schools must be attended by students which their house is near the school [17]. The goal is minimizing school-home distance. The short school-home distance offers some benefits. Students' travel time can be minimized so that their physical condition can be maintained to improve academic performance and risk or probability of the students for being late can be minimized too [17]. Short school-home distance also may reduce pollution and traffic congestion [17]. Second, there should be no selection to attend public schools. Schools are also forbidden to discriminate students based on their ability, for example student academic performance or family financial power [18].

In the other side, there are some supporting arguments to the school choice. The core reason is the market mechanism and competition. Competition among public schools can improve the school performance [19]. Schools are forced to improve their performance so that they are attracting enough to receive applications to fulfil their available seats [16]. In the school choice model, families are free to choose schools which are most preferred. In the common condition, schools with higher academic performance tend to receive large number of applicants so that in many cases, over-demand occurs [3]. In the over-demand situation, schools will implement selection process to accept their more preferred students and reject their less preferred ones [19]. In the other side, schools with less performance often meet over-supply condition which in the end of admission process, they still have unallocated seats. Several criteria that are often used in the selection process are student academic performance, siblings, and school-home distance.

Nowadays, public schools in Indonesia adopt zone-based system. This system is similar with the mandatory model. Schools prioritize students from the same zone in the acceptance process. The goal is also the same, which is allocating students to the school that is near them. The second goal is to eliminate segregation among public schools which discriminate public schools into two terms: favourite schools and non-favourite schools [7]. This goal is tried to be achieved by eliminating student's national exam score from the selection criteria. In the previous era, student's national exam score was the main criterion in the selection process [7]. Students with high national exam score competed to apply to the favourite schools. In the end, favourite schools were attended by the high performing students while non-favourite schools were attended by the low performing students [17]. It made competition occurs only among favourite schools. Based on their low intake, it was almost impossible for the non-favourite schools to compete [7].

Moreover, the exam-score based selection was also blamed in generating segregation among students based on the family income level [7]. Several studies showed that there is proportional relation between family income and student academic achievement. Students from high family income have more privilege and support to improve their academic achievement [3]. For example, they can take expensive additional academic course to support their performance at school. The opposite condition, although it is not always, happens to the students from the low family income. In the end, the students from the higher income family tend to achieve better national exam score compared with the students from the lower income family [17].

Based on this problem, government of Indonesia has announced policy for every public school to allocate certain minimum quota for poor students. This policy is called affirmative channel [1]. In many cases, in this channel, student national exam score and/or student school-home distance were excluded in the selection criteria. As far as these students can show legal poor family certificate, they can be accepted in any public schools, even in the favourite schools. Also in many cases, the quota of the affirmative channel can surpass the quota of the academic achievement channel. Moreover, in some cases, this policy triggers fraud where many applicants come with fake poor family certificate because the affirmative channel is easier than the regular zone-based channel or academic achievement channel in securing seat in the favourite school.

In Indonesia, the selection process occurs in several sessions [9]. The regular zone-based channel and affirmative channel usually occurs earlier. The academic achievement channel usually occurs last if there are some available seats. Students that are rejected from the previous channel can propose for the next channel. In several places, the zone-based system is interpreted as the applicants are sorted based on the school-home distance and the student national exam score are excluded. Different implementation of the zone-based system also occurs in the different districts. School-home distance is converted into several classes with discrete score [1]. Students are sorted based on the accumulation of the national exam score and the school-home distance score. Applicants can choose one or more schools. If they are rejected from their preferred schools, then they fail in attending public schools. This process may create mismatch.

The simpler mechanism is implemented for example in the New York city [14]. The selection or matching process adopts the deferred-acceptance algorithm [15]. Students can choose up to some schools as their preference. Then, the selection runs in two rounds. In the first round, system will try to allocate the applicants based on their choices [14]. The students' preference is then matched with the schools' preference. The students who are rejected in the first round then go to the second round. In the second round, the students will be allocated to the school as near as possible to their home [14]. This mechanism accommodates both school choice and zone-based models. This system also has advantage in minimizing the mismatch. In the over-supply or equal supply-demand condition, all applicants are guaranteed to be assigned.

This deferred-acceptance algorithm is a derivative of the stable marriage algorithm which was introduced by Gale and Shapley [11]. This algorithm is popular and widely implemented. This algorithm works to match between two groups. The first group acts as the proposal submitter and the second group acts as the proposal evaluator. In its origin, there are two groups: men and women. The process of the algorithm is as follows [10]:

1) In the beginning, every man submits proposal to his most preferred woman. Some women may receive some proposals while some women do not receive proposal.

2) Then, every woman who receives proposals will choose the man whom she prefers most. Other proposals will be declined. Every man whose proposal is accepted becomes engaged.

3) Every unengaged man then submits new proposal to his most preferred woman in the rank, but first, he must exclude women whom he has sent proposal to in the previous time from his list.

4) Every woman who receives proposal or proposals then selects the men, including whom she currently engages with. She accepts the most current preferred men and declines the others.

5) In the condition of equal number of men and women, the process ends after the last woman receives and accepts proposal. In other word, the process ends after there is no more rejection.

In the scenario where men become submitters, it is called as male-optimal solution [20]. It is because men have better opportunity to engage with his most preferred woman. The men's satisfaction decreases only when they are rejected so that they must submit to the other women. In the other side, women can improve their satisfaction only when they receive better proposal in the future rounds. This scenario is interchangeable so that it is called as female-optimal solution [20].

This one-to-one matching is easily transformed into many-to-one matching as it was conducted by Gale and Shapley [10] in the college admission or by Abdulkadiroglu [21] in the school admission. As a school or college has quota, then students who are submit to a school will be sorted based on the school's preference. Students who are inside the quota will be temporarily engaged while students who are outside the quota will be permanently unengaged to this school. In the scenario where the students submit the proposal then it is called as student-dominant scenario [21]. This condition is also interchangeable so that it is called as school-dominant scenario [21].

Based on this explanation, the stable marriage algorithm or deferred-acceptance algorithm is potential to be adopted in developing student selection model in Indonesia that meets the stakeholders' (student, family, and government) interest and eliminating the mismatch. Meanwhile, this algorithm must be improved first so that it can meet the requirement. Moreover, due to the autonomy in every district government, the proposed model must be easily adjusted because prioritization may be different among district governments.

III. Proposed Model

The proposed admission model consists of students and schools [10]. In this model, the students act as the proposal submitters so that this model is called as student-optimal model [21]. Meanwhile, the schools act as proposal evaluators so that schools can accept or reject the incoming proposals. Every school has their own quota [10]. There are some students' concerned parameters and schools concerned parameters. Similar with the previous work [14], every student can choose some preferred schools. It means, the school choice is accommodated in this model [16]. The prioritization among parameters can be different. Before we explain the proposed model further, first we explain that all notations that are used in the mathematical model are described in the nomenclature section.

There are several notations that are used in this proposed model. These notations are as follows:

i	student index
j	schools index
k	parameters index
n_a	number of applicants / students
n_s	number of schools
n_{pa}	number of school-concerned applicants' parameters
n_{ps}	number of applicant-concerned schools' parameters
q_j	quota of school j
$s_{a,k,i}$	applicant i's score for parameter k
$s_{s,k,j}$	school j's score for parameter k
$s_{amin,j,k}$	applicant minimum score for parameter k
$s_{amax,j,k}$	applicant maximum score for parameter k
$s_{smin,i,k}$	school minimum score for parameter k
$s_{smax,i,k}$	school maximum score for parameter k
$s_{an,i,j,k}$	applicant i's normalized score for parameter k
$s_{sn,i,j,k}$	school j's normalized score for parameter k
$s_{ta,i,j}$	applicant i's total score based on school j's perspective
$s_{ts,i,j}$	school j's total score based on applicant i's perspective
$S_{pr,j}(t)$	set of received proposals for school j until time t
$S_{pa,j}(t)$	set of accepted proposals for schools j until time t
$S_{ps,i}(t)$	set of submitted proposals by applicant i until time t
t	time index
$w_{a,k}$	weight of school-concerned applicant parameter
$w_{s,k}$	weight of applicant-concerned school parameter

Decision taken by both applicants and schools is determined based on the total score of the opponents. Selected school that the applicant will submit to at time t is determined by using (1). Meanwhile, set of applicants that are accepted until time t is determined by using (2). In (2), it is shown that the accepted applicants until time t is determined by sorting the received proposals from the highest to the lowest based on the applicants' total score and they are taken up to the school quota [10].

$$sel_{s,i}(t) = j, max\big(s_{ts,i,j}(t)\big) \wedge j \notin S_{ps,i}(t-1) \tag{1}$$

$$S_{pa,j}(t) = sort\_descending(S_{pr,j}(t), s_{ta,i,j}(t), q_j) \tag{2}$$

The total score, both in the applicant's score and the school's score, is the accumulation of the weighted scores. By augmenting the weight in every parameter score, it is easily to set which parameters are more important and which ones are less important. This weighing concept is similar with the previous work that accommodated multiple parameters [22]. More weight to be augmented in some parameters means more important these parameters are [22]. The applicant's total score is calculated by using (3) while the school's total score is calculated by using (4).

$$s_{ta,i,j}(t) = \sum_{k=1}^{n_{pa}} \big(w_{a,k}.\, s_{an,i,k}(t)\big) \tag{3}$$

$$s_{ts,i,j}(t) = \sum_{k=1}^{n_{ps}} \big(w_{s,k}.\, s_{sn,i,k}(t)\big) \tag{4}$$

Each score, before it is calculated with the weight, will be normalized first. In this work, the min-max normalization method is used [23]. It ranges from 0 to 1. The reason in normalizing this score is because every parameter uses its own metric. For example, applicant's national exam score ranges from 0 to 100. School-home distance is in meter or any other distance units. The applicant's poor status is 0 or 1. Based on it, normalized score is used so that all scores are comparable to each other. If the value of the parameters is proportional to the score, such as student poor status [1] or national exam score [7], then the applicant's normalized score is calculated by using (5) while the school's normalized score is calculated by using (6). In the other side, if the value of the parameters is inversely proportional to the score, such as school-home distance [17] or school rank, then the applicant's normalized score is calculated by using (7) while the school's normalized score is calculated by using (8). To determine the normalized score, the minimum and maximum scores in the set are used.

$$s_{an,i,j,k}(t) = \begin{cases} \frac{s_{a,k,i} - s_{amin,j,k}(t)}{s_{amax,jk}(t) - s_{amin,j,k}(t)}, s_{amax,j,k}(t) \neq s_{amin,j,k}(t) \\ 1, s_{amax,j,k}(t) = s_{amin,j,k}(t) \end{cases} \tag{5}$$

$$s_{sn,i,j,k}(t) = \begin{cases} \frac{s_{s,k,j} - s_{smin,i,k}(t)}{s_{smax,i,k}(t) - s_{smin,i,k}(t)}, s_{smax,i,k}(t) \neq s_{smin,i,k}(t) \\ 1, s_{smax,i,k}(t) = s_{smin,i,k}(t) \end{cases} \tag{6}$$

$$s_{an,i,jk}(t) = \begin{cases} 1 - \frac{s_{a,k,i} - s_{amin,j,k}(t)}{s_{amax,j,k}(t) - s_{amin,j,k}(t)}, s_{amax,j,k}(t) \neq s_{amin,j,k}(t) \\ 1, s_{amax,j,k}(t) = s_{amin,j,k}(t) \end{cases} \tag{7}$$

$$s_{sn,i,j,k}(t) = \begin{cases} 1 - \frac{s_{s,k,j} - s_{smin,i,k}(t)}{s_{smax,i,k}(t) - s_{smin,i,k}(t)}, s_{smax,i,k}(t) \neq s_{smin,i,k}(t) \\ 1, s_{smax,i,k}(t) = s_{smin,i,k}(t) \end{cases} \quad (8)$$

The minimum and maximum score is determined as follows. The applicant's minimum and maximum scores are compared among applicants that is submitting proposals to the school j plus applicants in the school j's quota. In the other side, the school's minimum and maximum scores are compared among schools that has not been submitted by the applicant i. The applicant minimum and maximum scores are determined by using (9) and (10). The school minimum and maximum scores are determined by using (11) and (12).

$$s_{amin,j,k}(t) = min(s_{a,i,k}) \wedge i \in S_{pr,j}(t) \quad (9)$$

$$s_{amax,j,k}(t) = min(s_{a,i,k}) \wedge i \in S_{pr,j}(t) \quad (10)$$

$$s_{smin,i,k} = min(s_{s,j,k}) \wedge j \notin S_{ps,i}(t-1) \quad (11)$$

$$s_{smax,i,k} = min(s_{s,j,k}) \wedge j \notin S_{ps,i}(t-1) \quad (12)$$

IV. Simulation Result

This proposed model is then implemented into the student admission simulation. This simulation is a coordinated school admission which consists of schools and applicants. The simulation is based on the senior high school admission system. The schools are public schools. The environment is Yogyakarta city in Indonesia. This city size is approximately 46 km^2. There are eleven public senior high schools in Yogyakarta. In this simulation, the quota of every school is assumed equal, which is 100 students so that the total quota is 1,100 students. In this work, the students' home location and schools' location are distributed uniformly in the city. The student's national exam score is distributed normally with the mean is 80 and standard deviation is 10.

There are some concerned parameters by the applicants and the schools. The applicant-concerned parameters are school rank, applicant's preference [1], and school-home distance [7]. Meanwhile, the school-concerned parameters are national exam score [1], school-home distance [7], and poor status [1]. In the default condition, weight of all these parameters is set 0.5. It means that all parameters are equally prioritized.

There are three simulations and three observed parameters. These three observed parameters are average student's school-home distance, average student's national exam score, and number of accepted applicants. The first and second parameters are observed in the first and second simulation. The third parameter is observed in the third simulation. The average student's school-home distance is observed because it is the important determinant in both the zone-based model [7] and in the school choice model, specifically in the two-step model [14]. The average student national exam score is observed because it is a relatively concerned parameter by the stakeholders who concern in competition. The number of accepted applicants is observed to evaluate whether there is mismatch in the admission process. These first two parameters are evaluated based on the accepted students. The first simulation is to observe the relation between the number of applicants and the first two observed parameters. The second simulation is to observe the relation between the national exam score-school rank and student national exam score weights; and the first two observed parameters. In the first simulation, the performance of the proposed model is compared with the previous works: the zone-based model [7] and the two-step model [14]. In the first simulation, the number of students ranges from 1,100 to 2,200 students. In the second simulation, the national exam score and school rank weights range from 0.1 to 0.9. In the second simulation, the number of applicants is 2,200 persons. In the third simulation, the number of applicants ranges from 220 to 2,200 students which represents from over-supply to over-demand condition.

Now, we will discuss the simulation result. The result of the first, second, and third simulations is shown in Fig. 1, Fig. 2, and Fig. 3, consecutively. In Fig. 1, zoning represents the zone-based model [7], two-step represents the two-step model [14], and SM represents the proposed stable marriage-based model.

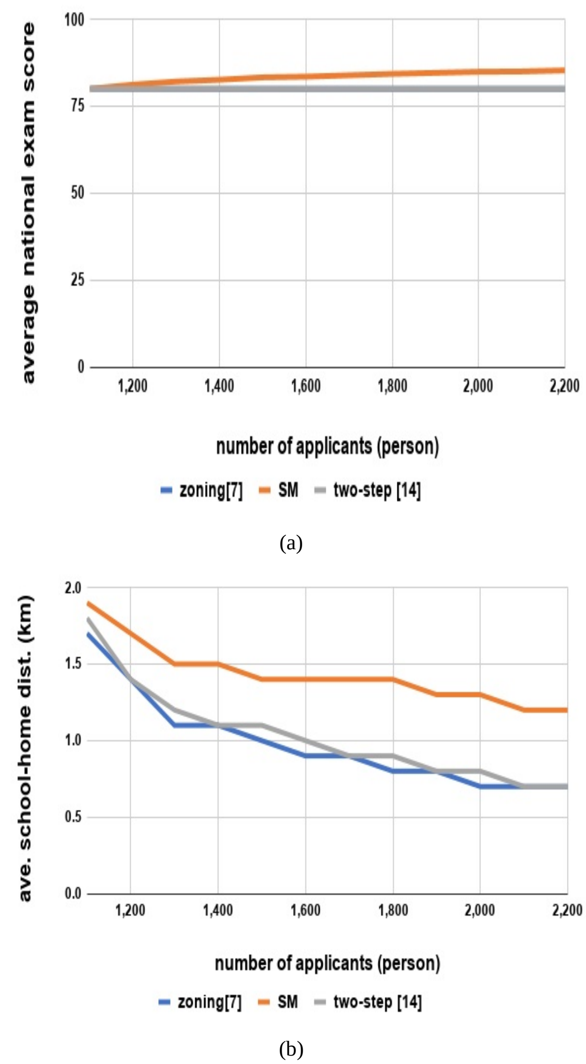

Fig. 1. Number of Applicants vs. Observed Parameters: (a) Average National Exam Score (b) Average School-Home Distance.

The explanation of the result in Fig. 1(a) is as follows. When the system implements zone-based model [7] or the two-step model [14], the increasing of the number of applicants does not affects the average national exam score of the accepted students. Meanwhile, when the system implements the stable marriage model, the increasing of the number or applicants makes the average national exam score increases. In the beginning, the inclination is high. Meanwhile, it goes lower due to the increasing of the number of applicants. In the beginning, in the equal supply-demand condition, all models perform equally. In the extreme over-demand condition, when the number of applicants is twice of the total quota, the average national exam score of the accepted students of the proposed model is 6.6 per cent higher than the previous models [7,14]. Based on this explanation, it is proven that this proposed model accommodates the academic competition among the applicants [16].

In Fig. 1(b), it is shown that the average school-home distance decreases due to the increasing of the number of applicants. It happens in all models. The average school-home distance of the previous models [7,14] tends to be equal. Meanwhile, the average school-home distance of the stable marriage model is the highest among models. In the beginning, due to equal supply-demand condition, the gap between the stable marriage model and the previous models is narrow. This gap becomes wider due to the increasing of the number of applicants. In the extreme over-demand condition, when the number of applicants is twice of the total quota, the average school-home distance of the stable marriage model is 71.4 per cent higher than the previous models. Based on this explanation, it is proven that this model accommodates the concern in reducing the school-home distance [17].

The explanation of the second simulation is as follows. Result in Fig. 2(a) shows that in the over-demand condition, when the school rank and student national exam score weights are low (0.1), the average national exam score of the accepted students is a little bit higher than the average national exam score of all applicants. In the other side, when these weights are set high (0.9), the average national exam score of the accepted applicants is 7.7 per cent higher than all applicants. The result in Fig. 2(b) shows that in the over-demand condition, the average school-home distance increases due to the increasing of these weights. When these weights are set low (0.1), the average school-home distance is 0.8 km and when these weights are set high (0.9), the average school-home distance is 1.7 km or 112.5 per cent higher.

In Fig. 3, it is shown that the proposed model has solved the mismatch problem in the admission process. When the number of applicants ranges from 220 persons to 1,100 persons, which is from over-supply to equal supply-demand condition, the number of the accepted applicants is equal to the number of applicants. It means that all applicants are accepted and there is no rejection. After that, when the number of applicants ranges from 2,320 persons to 2,200 persons, which is over-demand condition, the number of accepted applicants is still 1,100 persons or it is same as the total quota.

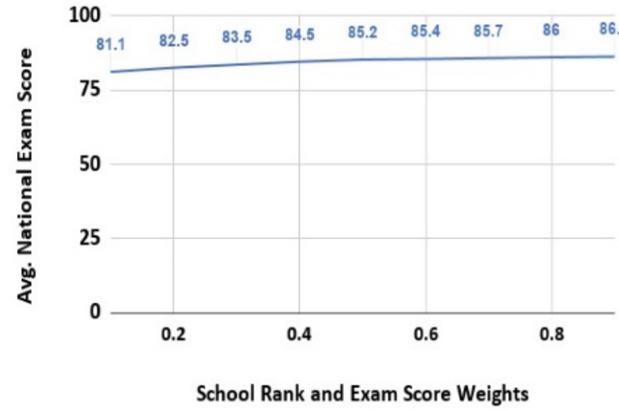

(a)

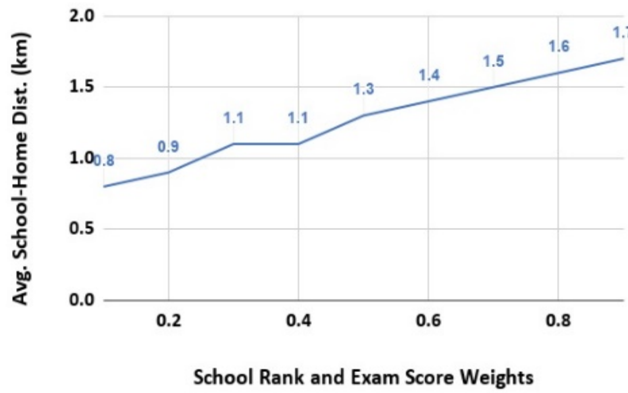

(b)

Fig. 2. School Rank and Exam Score Weights vs. Observed Parameters: (a) Average National Exam Score (b) Average School-Home Distance.

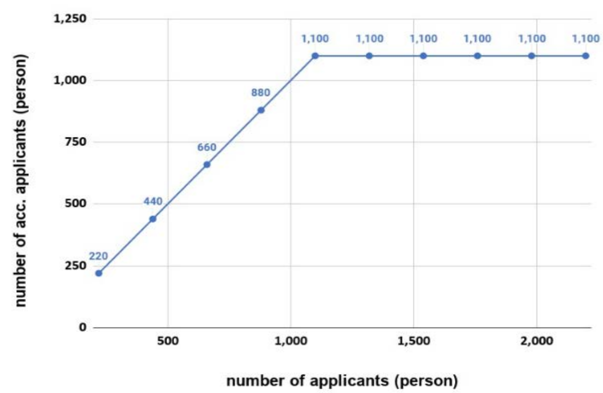

Fig. 3. Number of Applicants vs. Number of Accepted Applicants.

V. Discussion

There are several findings due to this simulation result. It is shown that, compared with the previous models, both the zone-based model [7] and the two-step model [14], the proposed model achieves the highest one in minimizing the school-home distance. This gap becomes wider in the over-demand condition. The reason is that the school-home distance is not the only concerned aspect in this model. It is different from the previous models which focus on the school-home distance. Fortunately, this proposed model performs as the best model in achieving the highest average student national exam score although the different is not high. Once again, it is because the student national exam score is also not the only concerned parameter in this proposed model.

Based on this explanation, it can be said that this model can compromise all concerned parameters (school-home distance [17], competition [19], equality [9], affirmative [1], and preference/choice [16]). It is also shown that by using this model, the process becomes simpler because all parameters are calculated together in a single process, and they are easily adjusted due to the stakeholders' interest. It is different from the previous models [7,14] where the process is divided into multiple sessions, and they run sequentially. It is also shown that the model guarantees that all applicants will be accepted when there are available seats in the system or in the over-supply to equal demand-supply condition. It means that the mismatch is eliminated.

VI. Conclusion

A coordinated stable marriage-based student admission model has been developed and it accommodates multi concerned parameters in both schools and applicants. This model has also been implemented in the student admission simulation so that its performance can be analysed and compared with the previous models (zone based and two-step models). Based on the observations of the simulation result, some concluding observations are given below.

- The proposed model is proven in solving the mismatch problem in the school admission process.
- In the over-supply to equal supply-demand condition, the average student national exam score of the proposed model is equal with the previous models. In the over-demand condition, the average student national exam score of the proposed model is higher than the previous model. In the condition where the number of applicants is twice of the number of seats, the average student national exam score of the proposed model is 6.6 per cent higher than the previous models.
- The average school-home distance of the proposed model is higher than the previous models. The gap of it is wider due to the increasing of the demand. When the number of applicants is twice of the number of seats, the average school-home distance of the proposed model is 71.4 per cent higher than the previous models.

The prioritization of the concerned parameters is proven easily adjusted by manipulating the weights. When the number of applicants is twice of the number of seats, the high school rank and student exam score weights (0.9) perform 7.7 per cent higher in the average student national exam score and 112.5 per cent higher in the average school-home distance compared with the low weights (0.1).

There are several future research potentials due to this work. This work has proposed the coordinated based model. This work can be modified to become autonomous or semi-autonomous model where each school has better independency. In this model, all parameters are treated parallelly. Meanwhile, in some regulation, some parameters become requirement for other parameters so that a decision-tree based model can be used to improve the model that is proposed in this work.

Acknowledgment

This work was supported by Telkom University, Indonesia.

References

[1] Sularto, Wahyudi, and Sukmawati, "The admission of the new students based on online system at SMAN 2 Singkawang", Journal of Education, Teaching, and Learning, vol. 3, no. 2, pp. 336-341, 2018.

[2] A. Abdulkadiroglu, Y. K. Che, and Y. Yasuda, "Expanding choice in school choice", American Economic Journal: Microeconomics, vol. 7, no. 1, pp. 1-42, 2015.

[3] D. Kessel, "School choice, school performance and school segregation", dissertation. Stockholm University, Stockholm, 2018.

[4] C. M. D. Hart and D. N. Figalo, "School accountability and school choice: effect on student selection across schools", National Tax Journal, vol. 68, no. 3S, pp. 875-900, 2015.

[5] A. Hofflinger, D. Gelber, and S. T. Canas, "School choice and parents' preferences for school attributes in Chile", Economics of Education Review, vol. 74, article ID: 101946, 2020.

[6] H. H. Erickson, "How do parents choose schools, and what schools do they choose? A literature review of private school schoice programs in the United States", Journal of School Choice, vol. 11, no. 4, pp. 491-506, 2017.

[7] Y. Sulistyosari, S. I. A. Dwiningrum, N. Q. A. Zummi, S. W. Tomo, and D. Indrahadi, "Examining the basic educational rights in the newly implemented school zoning policy in Indonesia", Proceedings of the 2nd International Conference on Social Science and Character Education (ICoSSCE), Yogyakarta, Indonesia, 2019.

[8] Suryanto and Komary, "The implementation of school zonation system in Yogyakarta", Proceedings of the 3rd International Conference on Sustainable Innovation 2019-Humanity, Education, and Social Science (IcoSIHESS), Yogyakarta, Indonesia, 2019.

[9] K. A. B. Bakar, Y. Supriyati, and I. Hanafi, "Evaluation of admission student policy based on zoning system for acceleration education quality in Indonesia", Journal of Management Info, vol. 6, no. 2, pp. 19-24, 2019.

[10] D. Gale, and L. Shapley, "College admissions and the stability of marriage", American Mathematical Monthly, vol. 69, no. 1, pp. 9-15, 1962.

[11] P. Dworczak, "Deferred acceptance with compensation chains", Operations Research, vol. 69, no. 2, pp. 456-468, 2020.

[12] A. F. M. S. Saif, M. Rashid, I. Z. Bhuiyan, M. W. S. Ifty, and M. R. Sarker, "Stable marriage algorithm for student-college matching with quota constraints", Proceedings of the International Conference on Computing Advancements (ICCA), Dhaka, Bangladesh, 2020.

[13] M. Mnich and I. Schlotter, "Stable matchings with covering constraints: a complete computational trichotomy", Algorithmica, vol. 82, pp. 1136-1188, 2020.

[14] A. Abdulkadiroglu, N. Agarwal, and P. A. Pathak, "The welfare effects of coordinated assignment: evidence from the New York City high school match", American Economic Review, vol. 107, no. 12, pp. 3635-3689, 2017.

[15] F. Klijn, J. Pais, and M. Vorsatz, "Improving schools through school choice: an experimental study of deferred-acceptance", Economic Letters, vol. 186, article ID: 108853, 2020.

[16] A. Abdulkadiroglu, P. A. Pathak, J. Schellenberg, and C. R. Walters, "Do parents value school effectiveness", working paper, Cambridge, 2019.

[17] Martifah, "Zoning system of education as a strategy for equalizing education quality in the disruptive era (legal aspect review)", Proceedings of the 1st International Conference on Education, Social Sciences, and Humanities (ICESSHum) 2019, Padang, Indonesia, 2019.

[18] M. Bertoni, S. Gibbons, and O. Silva, "School choice during a period of radical school reform: evidence from the academy programme", IZA discussion paper, no. 11162, 2017.

[19] P. Hennerdal, B. Malmberg, and E. K. Andersson, "Competition and school performance: Swedish school leavers from 1991-2012", Scandinavian Journal of Educational Research, vol. 64, no. 1, pp. 70-86, 2020.

[20] D. Zivkovic, "A note on the stable marriage problem", SN Computer Science, vol. 1, article ID: 115, pp. 1-4, 2020.

[21] A. Abdulkadiroglu and T. Sonmez, "Matching market: theory and practice", Advances in Economics and Econometrics: Tenth World Congress. Cambridge University Press. Cambridge, 2013.

[22] P. D. Kusuma and H. U. Mustakim, "Multi parameter high school student admission system", Journal of Engineering and Applied Sciences, vol. 14, no. 15, pp. 5258-5266, 2019.

[23] H. Benhar, A. Idri., and J. L. Fernandez-Aleman, "Data preprocessing for heart disease classification: a systematic literature review", Computer Methods and Programs in Biomedicine, vol. 195, article ID: 105635, 2020.

IoT-based Smart Greenhouse with Disease Prediction using Deep Learning

Neda Fatima[1]*, Salman Ahmad Siddiqui[2], Anwar Ahmad[3]
Department of Electronics and Communication Engineering
Jamia Millia Islamia, New Delhi, India

***Abstract*—Rapid industrialization and urbanization has led to decrease in agricultural land and productivity worldwide. This is combined with increasing demand of chemical free organic vegetables by the educated urban households, and thus, greenhouses are quickly catching trend for their specialized advantages especially in extreme weather countries. They provide an ideal environment for longer and efficient growing seasons and ensure profitable harvests. The present paper designs and demonstrates a comprehensive IoT based Smart Greenhouse system that implements a novel combination of monitoring, alerting, cloud storage, automation and disease prediction, viz. a readily deployable complete package. It continuously keeps track of ambient conditions like temperature, humidity and soil moisture conditions to ensure a higher yield of crop and immediate redressal in case of abnormal conditions. It also has a built-in automatic irrigation management system. Finally, it employs the most efficient deep learning model for disease identification with leaf images. Furthermore, with memory and storage optimization through cloud storage, an individual living in the city can also build a greenhouse and can monitor it from his home and take redressal methods as and when desired.**

***Keywords*—Cloud; deep learning; greenhouse; humidity; IoT; soil moisture; temperature**

I. Introduction

With increasing globalization and consequent urbanization, land under agriculture has been reducing. Furthermore, with excessive amount of fertilizers and pesticides, its natural productivity has also been depleting. Moreover, with the increasing awareness about the harmful effects of pesticides and fertilizers on human body and environment, demands have risen for organic plants and vegetables. Consequently, greenhouses have emerged to be highly beneficial gardening solutions especially in extreme weather condition countries.

Greenhouses offer a controlled environment which guarantees higher yields in a sustainable pattern. The controlled growing pattern with a longer growing season allows for round the year harvest with a diversity of crops, exotic plants in particular. The greenhouse structure shield plants from extreme weather protection such as strong, gusty winds or high intensity ultraviolet rays. The enclosed structure allows for diffused penetration of light and prevents pest attacks and damage of crops by stray animals thus reducing potential man-animal conflicts.

Easy portability and customization of the structures provide for better planting efficiency and higher yields with modern outlook. Thus, greenhouses offer viable cultivation and plantation in a sustainable manner with least damage to environment.

The present research and the development of Smart Greenhouse System that focuses on novel combination of monitoring, alerting, automation and data analysis aspects of the greenhouse. The system design architecture comprises of four parts i.e. firstly, automated monitoring system that is Temperature, humidity and soil moisture monitoring with data storage on cloud. Secondly, it sends alerts to the farmer in case the ambient conditions shift from the appropriate conditions to take remedial action. Thirdly, it provides for automatic switching of irrigation on the basis of sensor data. Finally, the system implements plant disease detection analysis through deep learning techniques.

II. Review of Literature

This section describes the different works in the current area of research. There are researches [1], [2] cited to understand the importance and pressing need of greenhouses in agriculture. It describes the sustainable advantages of greenhouses particularly with respect to climate change. It demonstrates their portability and customization that helps to make it easy to implement for modern farming practices. Since limited space is utilized, it leads to cost efficient solutions with improved yield and decreased effect of pests and erratic weather conditions.

Sincere efforts and earlier attempts have been made in the area of Smart greenhouses, however, the research has been restricted to only a few certain aspects and do not cover all the parameters that influence the system. For instance, in [3], a review paper has been presented to demonstrate different values of temperature and humidity for different types of crops that can be grown in a greenhouse. Furthermore, in [4], methods have been studied and demonstrated to improve crop yields in the system.

The author in [5] presents a demonstration of solar panels and sensors in greenhouses and limits its functioning to determine the stress conditions in the greenhouse. In [6], the paper focuses only on the automation aspect and presents an automatic irrigation system for the greenhouse that makes human interference minimal for running of greenhouse. Similarly in [7], using Raspberry Pi and Arduino, different parameters that impact the yield of crops like humidity, CO2 levels, light intensity, soil moisture, and temperature are being monitored, controlled and coordinated.

*Corresponding Author

Incorporating the use of sensors and IoT, the paper [8] develops a drip irrigation mechanism and a tube well controlled using a GSM Module. In [9], the paper presents an on field study in a tomato greenhouse located in Michurinsk, Russia's Tambov region with deployment of the Internet of Things (IoT) to identify the monitoring aspect of greenhouse and the growth rate of tomatoes. Similar application of the Internet of Things (IoT) in automation of greenhouse environment has been performed in the paper [10]. The paper [11] demonstrated an IoT system with a bot notification on tomato growing stages to provide smart farming solutions. In [12], the paper attempts to establish an automated greenhouse control system for speeding up the plant growth and increasing their production. In [13], a web application is developed to monitor and track the greenhouse's parameters and the plants' growth in a greenhouse.

Employing the aspect of machine learning, the paper [14] presents the idea of environmental monitoring and disease detection in green house for Bangladesh. The paper [15] reviews the applications of artificial neural networks (ANNs) in greenhouse technology and presents model development in adaptation of new technologies. The author in [16] presents a method for early detection of leaf diseases in plants based on feature extraction. The author in [17] specifically reviews deep learning and transfer learning algorithms in advanced technologies for agricultural disease image recognition. The author in [18] uses forest classifier algorithm with color histogram for plant disease detection using a set of images.

Similarly while in [19], the review research attempts to explore the application of IoT in arable farming, the author in [20] limits it to monitoring function of greenhouse using WSN.

The present paper addresses the shortcomings of the previous research like limited automation and inefficiencies in the predictive modeling by testing multiple deep learning models on an enlarged and varied dataset unlike its predecessors. The previous studies are incomplete and insufficient in one way or the other. The present paper demonstrates a novel comprehensive solution implementing an IoT based Smart Greenhouse that employs sensory data for continuous monitoring and automation as alerts are sent as soon as temperature, humidity fall below or rise above the ambient levels. It operates the automatic irrigation system as soil moisture levels rise or fall below the threshold. Furthermore, the paper tests multiple deep learning models and finally justifies the adoption of the most efficient model for the disease detection in the plant through leaf images and provides for early disease detection to prevent/reduce yield loss.

III. Methodology

This paper proposes an all-inclusive approach for implementing a Smart Greenhouse with aspects of monitoring, alerting, efficient memory utilization, irrigation automation and disease prediction of plants. It leverages the combination of sensor data to obtain input based on Temperature, Humidity and soil moisture sensors and images taken from camera placed in the greenhouse to evaluate three different deep learning models.

The microcontroller monitors the ambient parameters and alerts the farmer when the parameters drop/ rise from the normal. The continuous monitoring of parameters is stored at a cloud account promoting memory efficiency. The microcontroller is programmed to operate the irrigation motor based on the inputs from the sensors. Further, the image data set from internet and real time has been used to train and test the deep learning models that predict the disease. The workflow of the proposed methodology is shown in Fig. 1.

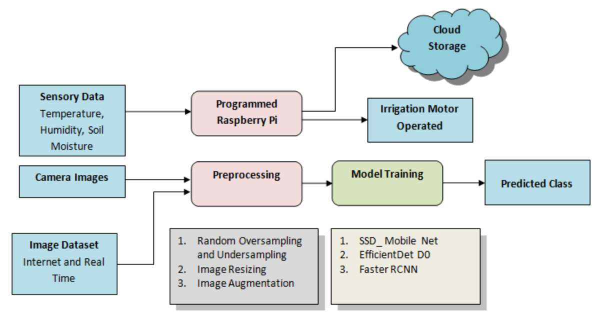

Fig. 1. System Overview.

The block illustration of the system depicting the components and their connections has been represented in Fig. 2. On the basis of this demarcation, the developed system is subdivided into three subsystems each with different functioning:

- Ambient Condition Monitoring and Alerting System.
- Automated Irrigation System.
- Disease Prediction System.

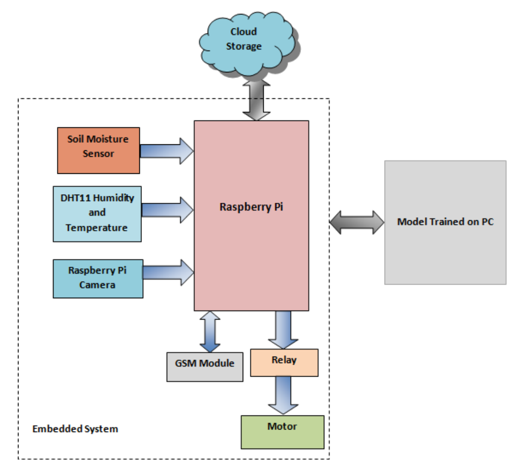

Fig. 2. Block Illustration.

A. Ambient Condition Monitoring and Alerting System

1) Temperature and Humidity Sensor data has been taken as Input from DHT 11 Humidity and Temperature sensor.

2) DHT 11 is a simple and ultra low-cost digital temperature and humidity sensor. A thermistor and a capacitive humidity sensor are used to test the ambient air quality and the outcome of the digital signal provided by the data pin. It is easy to use; however, in order to collect information, it takes a few seconds.

3) Thus, in this system, an ambient temperature threshold is set. An alert will be sent to the farmer's phone/email so as to increase or decrease the temperature as desired when there is a deviation of ±50°F from the set parameters.

4) Soil Moisture Sensor has been used that detects the ambient moisture content in the soil. Capacitance is used by the soil moisture sensor to obtain the dielectric permittivity of the surrounding medium.

5) Dielectric permittivity is a function of water content in the soil. The sensor generates a voltage that is proportional to the dielectric permittivity, and accordingly, to the soil water content. The water content is averaged over the whole length of the sensor.

6) It measures loss in soil moisture in due course of time because of reasons like evaporation and plant uptake. It also helps to assess optimum soil moisture content for different plant species and to monitor soil moisture content to control irrigation.

7) The inputs from the sensors are fed to Raspberry Pi. Raspberry Pi 3 is a development board in Pi series that can be considered a single board computer. It operates on LINUX Operating system. It has high processing speed making it suitable for advanced operations like disease detection and image processing. It uses Wireless LAN and Bluetooth facility and can set up WIFI Hotspot for internet connectivity. It has dedicated port for LCD Display and a dedicated camera port.

8) The data from the sensors are stored into ThingSpeak cloud via Raspberry Pi using write API of ThingSpeak thus promoting memory efficiency.

9) Using the data fed by the sensors, heat index is computed. These heat indexes measured can be then compared with the heat index of the plants and crops that are planted. The Heat Index (HI) is a thermodynamic value that combines air temperature and relative humidity to determine the equivalent temperature experienced by humans.

10) The heat index formula is expressed as,

$$HI=c_1+c_2T+c_3R+c_4TR+c_5T_2+c_6R_2+c_7T_2R+c_8TR_2+c_9T_2R_2 \quad (1)$$

In this formula,
HI = heat index in degrees Fahrenheit
R = Relative humidity
T = Temperature in ∘F
c_1 = -42.379; c_2= -2.04901523
c_3 = -10.14333127; c_4 = -0.22475541
c_5 = -6.83783 x 10^{-3}; c_6 = -5.481717 x 10^{-2}
c_7 = -1.22874 x 10^{-3}; c_8 = 8.5282 x 10^{-4}
c_9 = -1.99 x 10^{-6}

B. Automated Irrigation System

1) The information received by the temperature and humidity sensor and also the soil moisture sensor is continuously fed to the cloud via Raspberry Pi.

2) Raspberry Pi connected to Wi-Fi allows any device connected to that network to communicate with the module.

3) In this system, when the irrigation levels are too high or too low, an alert is sent to turn off/ on the water supply to inform about the ambient presence of soil moisture.

4) Based on input from this sensor, this farmer can control the on and off of motor through 5V Single Channel Relay Module mechanism by sending SMS to GSM module for changing the motor motion.

5) This Relay board module controls higher current loads from microcontroller development board. It can switch up to 7amps and it is safely driven by transistor bc547 which protects the input device from relay circuit. To further protect the microcontroller from relay kick back, a freewheeling diode is present.

C. Disease Prediction System

Three different deep learning models were trained with set parameters and results were obtained to identify the most efficient model. Following the comparison of models, the image dataset was taken from real time as well as internet and model was trained.

1) SSD mobile net model: The ssd_mobilenet_v1_coco model is a Single-Shot multi box Detection (SSD) network that is intended to perform object detection. It differs from mobilenet-ssd in the way that the latter can detect only faces whereas ssd_mobilenet_v1_coco model can detect objects.

SSD architecture is a single convolution network which learns to predict and classify bounding box locations in one pass. Thus, SSD is trained end to end. The SSD network comprises of base architecture (in our instance, MobileNet) and multiple convolution layers.

MobileNet employs an efficient CNN architecture designed for mobile and embedded vision application. In order to build lightweight deep neural networks, this architecture uses proven depth-wise separable convolutions.

- A feature layer is obtained after going through certain number of convolutions for feature extraction. To detect the location of bounding boxes, SSD operates on feature maps.
- For each feature map location, k bounding boxes are predicted. These k bounding boxes have different sizes and aspect ratios.
- For each of the bounding box, c class scores and 4 offsets relative to the original default bounding box shape are computed.

The shape of the box is not predicted by SSD instead it predicts its position. Each k bounding boxes have a predetermined shape which has been set prior to actual training.

2) EfficientDet D0 Model: Object detectors, in general, comprise of three major components: a backbone which performs feature extraction from the given image; a feature network which inputs multiple levels of features from the backbone and outputs a list of fused features which exhibit salient features of the image; and the final class/box network that uses the fused features to predict the class and location of each object.

EfficientDet is a type of object detection model, which uses EfficientNet as the backbone network**,** utilizes several optimization and backbone tweaks, such as the use of a BiFPN, and a compound scaling method that uniformly scales the resolution, depth and width for all backbones, feature networks and box/class prediction networks at the same time. EfficientNet has higher accuracy than previous ResNet networks.

3) Faster RCNN model: Faster RCNN (Region Based Convolutional Neural Networks) architecture comprises of two modules:

a) Region Proposal Network (RPN).

b) Fast R-CNN.

The RPN generates region proposals and applies the concept of attention in neural networks, so it guides the Fast R-CNN detection module to detect objects in the proposed regions.

The Faster RCNN is a two stage detector:

- In the first pass, input image is taken and output is generated as regions where objects may be detected (called as region proposals or regions of interest). This process can be carried out either by an external algorithm (Selective Search) or even by a neural network.
- In the second pass, a neural network identifies these regions of interest and classifies it into one of the target object classes. The extracted feature vectors are then classified using the Fast R-CNN. The class scores of the detected objects as well as to their bounding-boxes are returned as output.

Certain parameters were compared to be able to predict the most efficient model. Loss parameters constitute an important feature for efficient model determination. A loss function is used to optimize deep learning algorithms. Loss value determines the behavior of deep learning model after every iteration of optimization. The deviation of the predicted values from the actual values in the training data is determined by loss function. The loss is minimized by changing model weights.

Loss is the penalty for a bad prediction. If the model's prediction is perfect, the loss is zero; otherwise, the loss is greater. The loss is calculated on training and validation and its interpretation implies the correctness of model prediction. The loss comprises of two parts in the Tensorflow Object Detection API: the localization loss for bounding box offset prediction and the classification loss for conditional class probabilities. Both parts are calculated by the sum of squared errors. Unlike accuracy, a loss is not a percentage. The goal of training a model is to find a set of weights and biases that have low loss, on average, across all examples.

Another important parameter is Mean Average Precision. Mean Average Precision is a popular evaluation metric used for object detection (i.e. localisation and classification) in computer vision systems. Localization determines the location of an instance (e.g. bounding box coordinates) and classification demonstrates what it is (e.g. tomato leaf/corn leaf). The mAP or simply AP in coco models measures the performance of models for performing document/information retrieval and object detection tasks. It summarizes the precision-recall curve into a single value that represents the average of all precisions. Here, the difference between the current and next recalls is calculated and then multiplied by the current precision using a loop that scans all precisions/recalls. Alternatively, AP is the weighted sum of precisions at each threshold where weight is the increase in recall.

If higher precision implies more confidence in the model when it classifies a sample as Positive, then higher Recall connotes higher number of positive samples correctly identified as Positive by the model.

When a model has a high recall but a low precision, it accurately identifies the majority of positive samples but has a lot of false positives (i.e. classifies many Negative samples as Positive). On the contrary, if a model has high precision but low recall, then the model is accurate in identification of sample as Positive however, only some of the positive samples are classified as such.

4) Model training steps: The flowchart in Fig. 3 represents the training model methodology as implemented in the present system. The same sequence has been employed for SSD Mobile Net, EfficientDet D0 512*512 model and Faster RCNN Model as well.

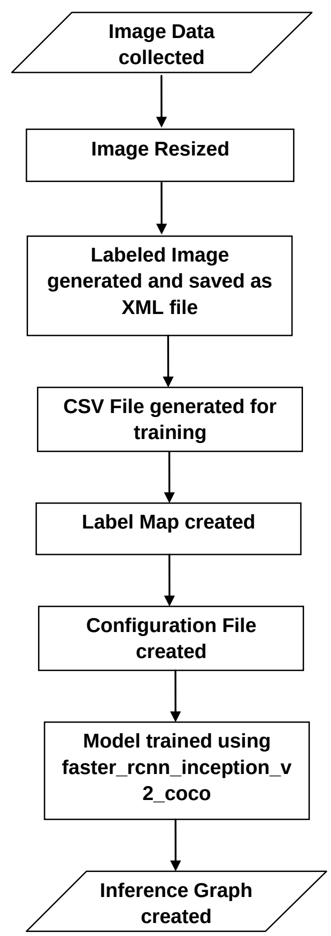

Fig. 3. Model Training Steps.

D. System Schematic

Fig. 4 represents the schematic diagram and the pin connections of the system.

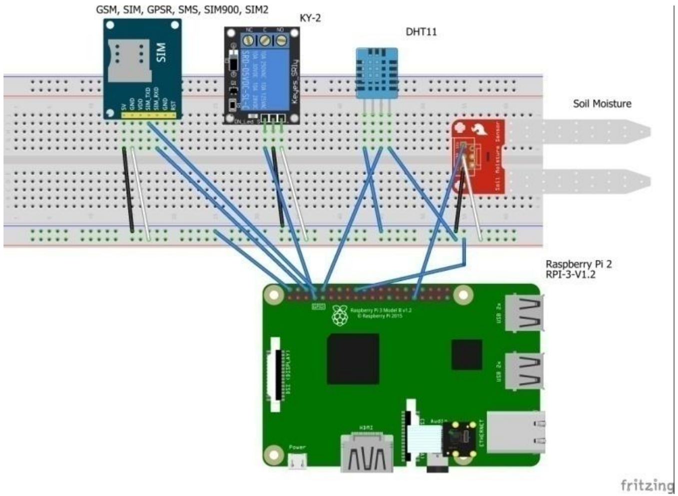

Fig. 4. System Schematic.

IV. Results

A. Ambient Condition Monitoring Results

1) Temperature and Humidity were monitored and stored on cloud account on ThingSpeak as shown in Fig. 5 and 6 that can be continuously monitored in real time even from a remote area.

2) Heat index can be calculated with the formula in Equation (1) and have been tabulated in Table I. Monitoring of heat index is depicted in Fig. 7.

3) Furthermore, to compute accuracy of measurement, measured temperatures by sensor (denoted by T_M) have been compared with a standard room thermometer (denoted by T_A) and Root mean square error has been computed.

4) Similarly, humidity measured by sensor (denoted by H_M) has been compared with a standard hygrometer (denoted by H_A) and Root mean square error has been computed.

5) Soil Moisture measured (denoted by SM_M) is also monitored in real time as shown in Fig. 8 and tabulated in Table I.

6) The Root Mean Square Error calculated for Temperature, denoted by $RMSE_T$=1.292788 and Root Mean Square error calculated for Humidity, denoted by $RMSE_H$=1.040833.

7) Alerts are sent when ambient conditions deviate from the threshold levels. Different threshold can be set according to seasons. For example, in summer months, the temperature limit is kept as 38°C and humidity limit as 55 RH. If there is a greater deviation during the day from these limits, planters will be informed.

8) The threshold value has been kept 500 in summer season and irrigation motor is switched ON if the 'dryness' rises to 500 and above and remains OFF below threshold value of 500.

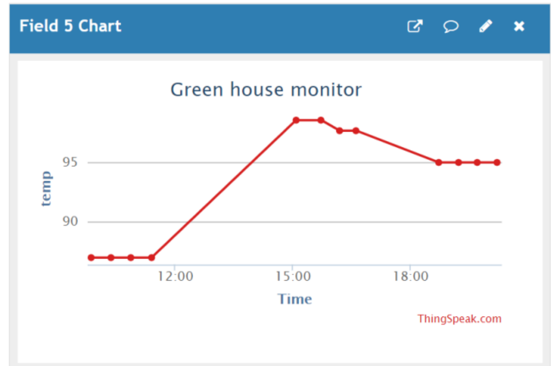

Fig. 5. Temperature Monitoring Results.

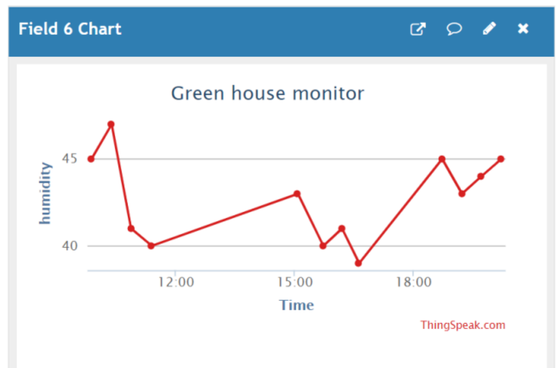

Fig. 6. Humidity Monitoring Results.

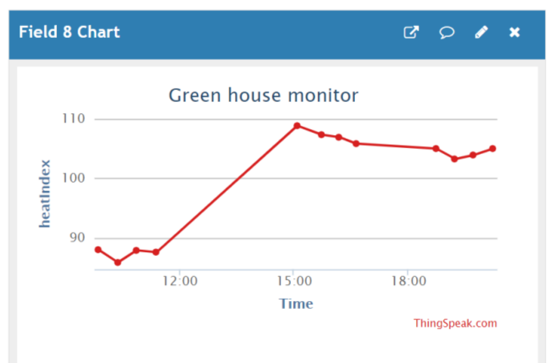

Fig. 7. Heat Index Monitoring Results.

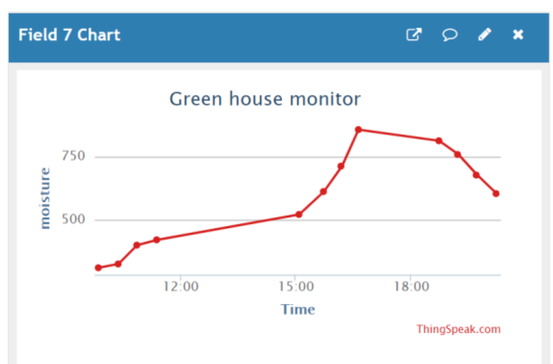

Fig. 8. Soil Moisture Monitoring Results.

TABLE I. MEASURED AND ACTUAL TEMPERATURE AND HUMIDITY READINGS AND SOIL MOISTURE READINGS

Time Duration	T_A (°F)	T_M (°F)	H_A (%)	H_M (%)	Heat Index (°F)	SM_M	Motor ON/OFF
Morning IST 0900-1100	86.9	87.08	45%	45.00	88.03	310	OFF
	86.9	85.10	46%	47.00	85.88	325	OFF
	89.6	87.80	41%	41.00	87.91	399	OFF
	89.6	87.62	40%	40.00	87.62	420	OFF
Afternoon IST 1500-1700	98.6	98.78	41%	43.00	108.86	520	ON
	98.6	99.14	41%	40.00	107.35	610	ON
	97.7	98.60	41%	41.00	106.92	710	ON
	97.7	98.78	41%	39.00	105.85	854	ON
Evening IST 1800-2000	95	96.44	44%	45.00	105.02	810	ON
	95	96.26	44%	43.00	103.27	756	ON
	95	96.26	44%	44.00	103.94	675	ON
	95	96.44	44%	45.00	105.02	602	ON

B. *Model Training Results*

1) Training time was an important determinant for predicting efficiency of deep learning models. Training took around 4 hours for SSD Mobile Net and 3 hours for EfficientDet D0 and less than 2 hours for Faster RCNN model.

2) Higher loss is the worse (bad prediction) for any model. Loss decrement including classification loss, localisation loss, clone loss as well as regularisation loss for the three models is demonstrated by the graphs in Fig. 9, 10, and 11.

3) The loss parameters obtained for the three models have been tabulated in Table II.

4) The mAP calculates a score by comparing the ground-truth bounding box to the detected box. A higher score implies a more precise model. mAP values can be compared for all three models. Table III depicts the mAP values for all models.

5) Mean Average Recall (mAR) values have been compared in Table III for the training models. It implies the maximum number of positives correctly identified as positives by the model.

6) Further, the model performance were further validated by changing the optimiser hyper parameter (such as Adam optimiser, momentum optimiser, RMSprop optimiser) in the configuration file of the models and Faster RCNN proved the most efficient in these as well.

7) As can be inferred from the speed parameters, loss values and mAP and mAR values, faster_rcnn_inception_v2 model performed better than EfficientDet D0 512*512 model and ssd_mobilenet_v1_coco_2018_01_28. This justifies its adoption for deployment in disease prediction algorithm.

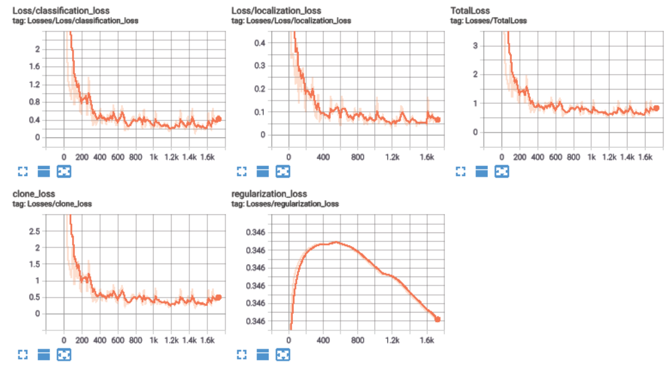

Fig. 9. Loss Parameters of SSD MobileNet.

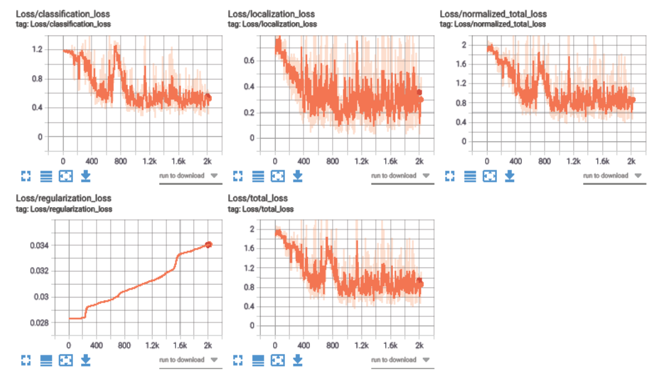

Fig. 10. Loss Parameters of EfficientDet D0.

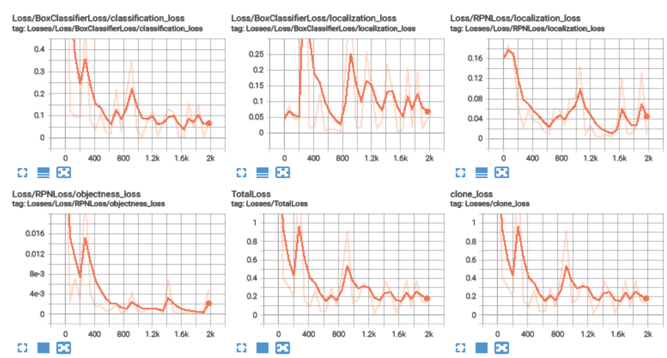

Fig. 11. Loss Parameters of Faster RCNN.

TABLE II. LOSS PARAMETER COMPARISON FOR THREE MODELS

Model	Min loss	Max loss	Avg loss
SSD Mobile Net	0.4601	26.232	3.75
EfficientDet D0	0.494	2.008	0.9972
Faster_RCNN	0.0207	1.7	0.4

TABLE III. mAPAND mAR PARAMETER COMPARISON FOR THREE MODELS

Models	**mAP IoU = 0.50:0.95**	**mAP IoU = 0.50**	**mAP IoU = 0.75**	**mAR (IoU@0.5:0.95) maxdet=100**
Faster_RCNN	0.414	0.804	0.39	0.601
EfficientDet D0	0.182	0.386	0.211	0.539
SSD_MobileNet	0.439	0.681	0.431	0.543

C. Disease Prediction Results

In view of the parameter comparisons from Tables II and III, Faster RCNN inception model was chosen to be deployed and its results on dataset images and real time images were obtained. In conducting the experiments and evaluation, Tensorflow version 2.4.0 has been used and Keras version 2.4.3.

1) The total dataset consists of 1000 images, with 80% of the images being used to train the models and the rest 20% being used for testing.

2) The hyper-parameters tuned are: learning rate, batch size, and optimizer used. The optimal parameters have been obtained through the grid search, i.e. a learning rate of 0.002, batch size of 16 images.

3) The total number of true positive values is divided by the entire object detector and multiplied by 100. Thus, the accuracy obtained is 80.4%.

4) Smaller percentage of data for testing datasets has been used because a bigger dataset has been implemented, and using this approach, a large amount of data can be leveraged for training purposes.

5) The images were taken at real time at a tomato farm field and corn farm field and some from internet. For the disease prediction, four varieties of leaf images are considered for testing the working of the proposed system, viz. healthy tomato, healthy corn, rust corn, bacterial tomato.

6) The result accuracy is more than 80% for live video testing as well. The results show accurate detection for every 8 out of 10 images. This is depicted in Fig. 12, 13, 14, 15, and 16.

7) Fig. 12, 13, and 14 show the detected output with supplied input of tomato and corn leaves.

8) Live video testing from tomato and corn fields as depicted was also performed. The process accurately determined the healthy and diseased leaves apart as shown in Fig. 15 and 16.

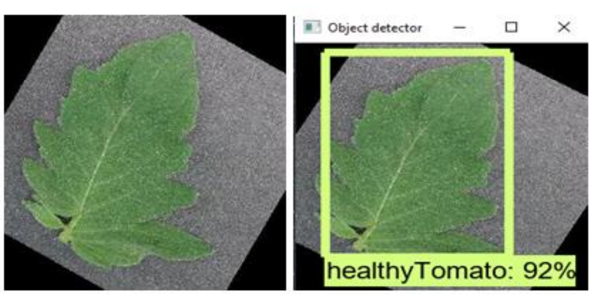

Fig. 12. Input Image and Detected Output of Healthy Tomato Leaf.

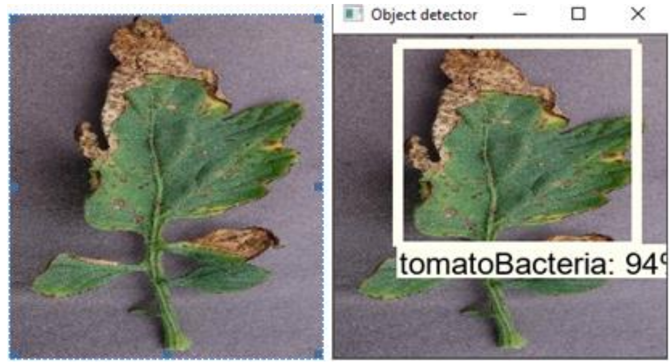

Fig. 13. Input Image and Detected Output of Bacterial Tomato Leaf.

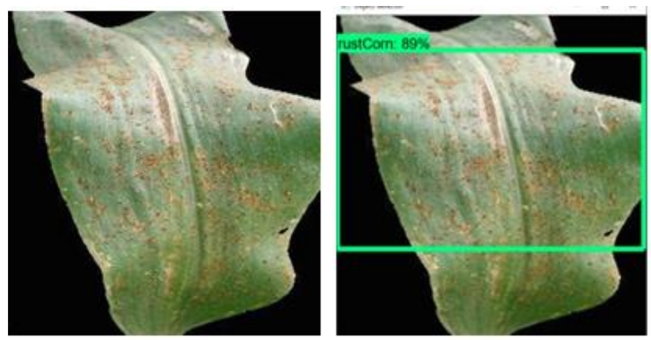

Fig. 14. Input Image and Detected Output of Rust Corn.

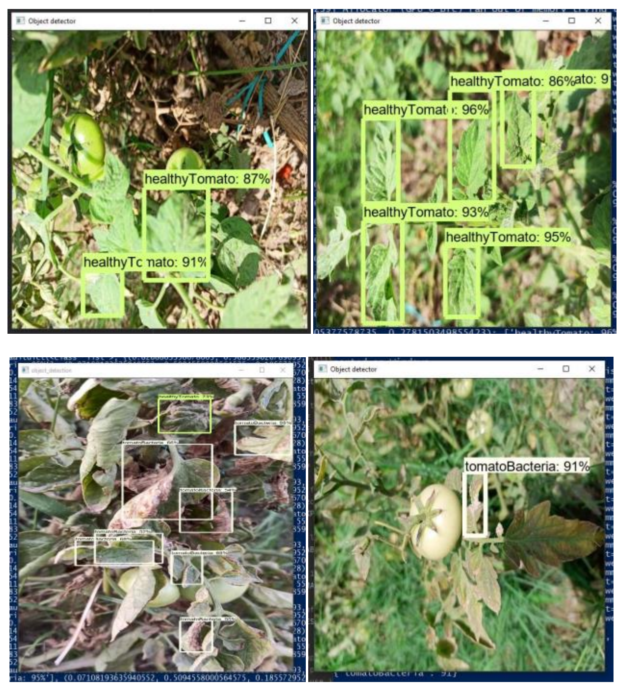

Fig. 15. Images from Real Time Video of Tomato Field.

9) If diseased leaves are identified by the system, SMS or email alerts are sent to the concerned person to apprise him of the situation so that he can take remedial measures.

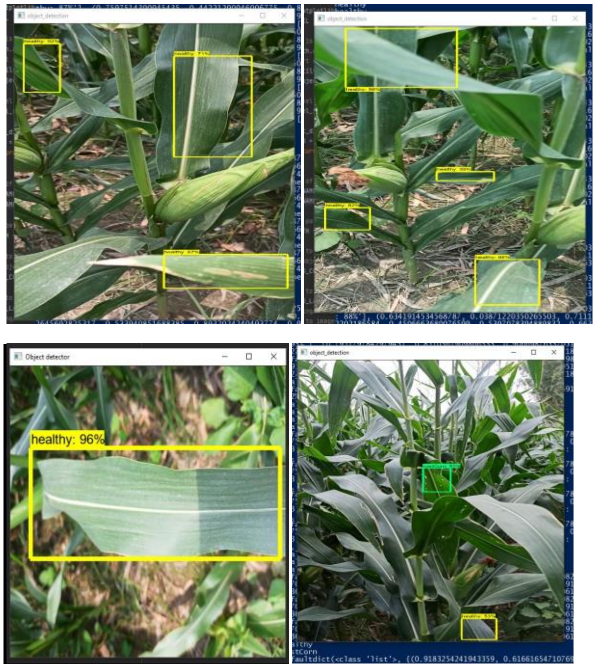

Fig. 16. Images from Real Time Video of Corn Field.

V. Discussion

The Smart Greenhouse System implemented offers a comprehensive, modern and inexpensive alternative to 24x7 manually monitored system even in remote areas. It presents a novel combination of multiple elements that is monitoring, alerting, cloud storage, efficient predictive modeling and accurate disease prediction and consequently implements a comprehensive IoT based Smart Greenhouse system that can be deployed on a large scale in greenhouses and farms alike. The paper constructs and implements a system that continuously monitors the ambient conditions and alerts if levels rise or fall below the threshold and switches off/on irrigation motor accordingly. The system employs the most efficient Deep Learning model after a thorough comparison of training and testing of three different models to implement disease detection at a nascent stage of disease outbreak ensuring that no other plants are harmed and farmers are able to undertake essential reforms at the appropriate moment. The system also implements efficient memory utilization by using secure cloud storage to overcome external storage and memory redundancy. Thus, it presents a scientific, improved and calibrated approach towards data analysis in agriculture that is largely dependent on manual workforce.

The system can be utilized both in small and large greenhouses. For smaller areas, a small compact kit is developed whereas for larger greenhouses, multiple Pi cameras in the same kit could suffice for accurate results. This system is adjustable and can be modified to utilize modern sensors to improve performance. Furthermore, enlarged datasets can also be used to improve results.

VI. Conclusion

The research paper has successfully implemented a comprehensive, complete package in the form of IoT based Smart Greenhouse employing a novel combination of Monitoring, Alerting and Automation and Disease Prediction using Deep Learning. The results developed, using both from internet and live testing, have high accuracy and employ memory efficiency. Future implementation of this system can be to include more number of sensors for improvement of data by including more parameters and installing multiple cameras at distinct points. This would generate a much wider database and would further aid in honing the results. However, there might be a possibility that its portability could be limited in that case. Further, with academic industry partnership this system can be made available to the farmers with small land holdings and encourage them to opt for greenhouses so that they don’t bear the brunt of pests, droughts and floods and can minimize their crop loss.

References

[1] R. Geneve and G. Niu, “Moving toward sustainability with alternative containers for greenhouse and nursery crop production: a review and research update,” no. April, 2015, doi: 10.21273/HORTTECH.25.1.8.

[2] J. A. Aznar-Sánchez, J. F. Velasco-Muñoz, B. López-Felices, and I. M. Román-Sánchez, “An analysis of global research trends on greenhouse technology: Towards a sustainable agriculture,” Int. J. Environ. Res. Public Health, vol. 17, no. 2, 2020, doi: 10.3390/ijerph17020664.

[3] C. V. Zabeltitz, “Integrated greenhouse systems for mild climates: climate conditions, design, construction, maintenance, climate control”, Berlin: Springer-Verlag, 2011.

[4] P. Dedeepya, U. S. A. Srinija, M. Gowtham Krishna, G. Sindhusha, and T. Gnanesh, “Smart greenhouse farming based on IoT” Proceedings of the 2nd International Conference on Electronics, Communication and Aerospace Technology, ICECA 2018, Iceca, 1890–1893. https://doi.org/10.1109/ICECA.2018.8474713.

[5] M. R. A. Azhar, M. Hamid, M. H. Irfan, M. Awais, U. S. Khan, and A. Zeb,“Automated greenhouse system” 2019 2nd International Conference on Communication, Computing and Digital Systems, C-CODE 2019, 215–219. https://doi.org/10.1109/C-CODE.2019.8681013, 2019.

[6] T. Bhuvaneswari, and J. T. H. Yao, “Automated greenhouse” 2014 IEEE International Symposium on Robotics and Manufacturing Automation, IEEE-ROMA2014, 194–199. https://doi.org/10.1109/ROMA.2014.7295887, 2015.

[7] H. Jaiswal, P. Karmali Radha, R. Singuluri, and S. A. Sampson, “IoT and machine learning based approach for fully automated greenhouse,” 2019 IEEE Bombay Sect. Signat. Conf. IBSSC 2019, vol. 2019January, 2019, doi: 10.1109/IBSSC47189.2019.8973086.

[8] T. C. J. Jeaunita, V. Sarasvathi, M. S. Harsha, B. M. Bhavani, and T. Kavyashree, “An automated greenhouse system using agricultural internet of things for better crop yield”, IET Conference Publications, 2018(CP747), 1–6. https://doi.org/10.1049/cp.2018.1388, 2018.

[9] P. Tripicchio, M. Satler, Gand Dabisias, E. Ruffaldi, “Towards smart farming and sustainable agriculture with drones”, Int. Conf. on Intelligent Environments (Prague), 2015.

[10] Fazeel Ahmed Khan, Adamu Abubakar Ibrahim and Akram M. Zeki, Environmental monitoring and disease detection of plants in smart greenhouse using internet of things, Journal of physics comm.

[11] N. Kitpo, Y. Kugai, M. Inoue, T. Yokemura, and S. Satomura, “Internet of things for greenhouse monitoring system using deep learning and bot notification services,” 2019 IEEE Int. Conf. Consum. Electron. ICCE 2019, pp. 14–17, 2019, doi: 10.1109/ICCE.2019.8661999.

[12] R. Osama, N. El-Huda Ashraf, A. Yasser, S. Abdelfatah, N. El Masry, and A. Abdelraouf, “Greenhouse plant growth supervision with the led lights using machine learning,” ACM Int. Conf. Proceeding Ser., pp. 169–173, 2020, doi: 10.1145/3436829.3436847.

[13] S. Fernando, R. Nethmi, A. Silva, A. Perera, R. De Silva, and P. K. W. Abeygunawardhana, “Intelligent disease detection system for greenhouse with a robotic monitoring system,” ICAC 2020 - 2nd Int. Conf. Adv. Comput. Proc., pp. 204209,2020,doi:10.1109/ICAC51239.2020.9357143.

[14] Shamse Tasnim Cynthia, Kazi Md. Shahrukh Hossain, Md. Nazmul Hasan, Md. Asaduzzaman, Amit Kumar Das, "Automated detection of plant diseases using image processing and faster r-cnn algorithm, International conference on sustainable technologies in Industry", 2019.

[15] A. Escamilla-García, G. M. Soto-Zarazúa, M. Toledano-Ayala, E. Rivas-Araiza, and A. Gastélum-Barrios, "Applications of artificial neural networks in greenhouse technology and overview for smart agriculture development," Appl. Sci., vol. 10, no. 11, 2020, doi: 10.3390/app10113835.

[16] C. Mattihalli, E. Gedefaye, F. Endalamaw, and A. Necho, "Real time automation of agriculture land, by automatically detecting plant leaf diseases and auto medicine," Proc. - 32nd IEEE Int. Conf. Adv. Inf. Netw. Appl. Work. WAINA 2018, vol. 2018-January, pp. 325–330, 2018, doi: 10.1109/WAINA.2018.00106.

[17] Y. Yuan, L. Chen, H. Wu, and L. Li, "Advanced agricultural disease image recognition technologies: A review," Inf. Process. Agric., no. xxxx, pp. 1–12, 2021, doi: 10.1016/j.inpa.2021.01.003.

[18] M. H. Jumat, M. S. Nazmudeen, and A. T. Wan, "Smart farm prototype for plant disease detection, diagnosis and treatment using IoT device in a greenhouse," IET Conf. Publ., vol. 2018, no. CP750, 2018, doi: 10.1049/cp.2018.154.

[19] R. K. Kodali, V. Jain, and S. Karagwal, "IoT based smart greenhouse" IEEE Region 10 Humanitarian Technology Conference 2016, R10-HTC 2016 - Proceedings. https://doi.org/10.1109/R10-HTC.2016.7906846, 2017.

[20] R. A. Li, X. Sha, and K. Lin,"Smart greenhouse: A real-time mobile intelligent monitoring system based on WSN", IWCMC 2014 - 10th International Wireless Communications and Mobile Computing Conference,1152–1156. https://doi.org/10.1109/IWCMC.2014.6906517, 2014.

Snapshot of Energy Optimization Techniques to Leverage Life of Wireless Sensor Network

Kavya A P[1]
Assistant Professor
Dept. of Electronics and Communication Engineering
Vidyavardhaka College of Engineering
Mysuru, Karnataka, India

Dr. D J Ravi[2]
Professor
Dept. of Electronics and Communication Engineering
Vidyavardhaka College of Engineering
Mysuru, Karnataka, India

***Abstract*—Energy Optimization in Wireless Sensor Network (WSN) deals with the techniques which targets higher degree of energy efficiency using resource-constraint sensor nodes with minimal inclusion of any different variants of resources. At present, there are various approaches and techniques towards addressing the problems of energy but not all the research implications can be considered as optimized approach. Therefore, this paper reviews all the existing energy optimization schemes, categorizes them, briefly discuss about their strength and weakness to offer a compact snapshot of existing energy optimization techniques in WSN. The paper also contributes towards exploring the updates research trends and highlights about the open-end research problems in WSN. It is anticipated that the study findings of this manuscript will offer a true picture of study effectiveness in dealing with energy challenges so that favorable direction of investigation towards evolving up optimized solution comes up with promising outcome.**

Keywords—Battery; energy efficiency; energy optimization; network lifetime; sensor node; wireless sensor network

I. Introduction

Wireless Sensor Network (WSN) has been used for long time towards remote sensing various attributes of physical environment [1]. One of the prime beneficial factors of relying on WSN is its capability to work in harsh environment which are inaccessible to humans. There are various applications in WSN and majority of them demands to have an extensive life time [2]-[5]. In this regard, optimizing the energy attribute has become one of the significant concerns among the researchers as well as users in the field of WSN. The primary reason for interest in energy optimization is because of limited lifetime of external batteries within this sensing device [6]. Usually, this external battery offers the direct power for all the internal and external operations to be carried out by a sensing device in WSN. After the battery is exhausted, they are usually discarded and the sensors are considered to be operationally dead. However, a recent concept of energy harvesting allows the node to harvest energy and achieve power from different sources which can recharge the battery [7][8]. Although this idea is impressive, but an energy harvester module will require obtaining power from external environment where there is no guarantee of its availability [9]. Hence, it is always a wise decision to focus on energy optimization principle rather than looking for other non-sustainable alternatives for energy conservation in WSN. The study towards energy problems is very old and various standard protocols as well as schemes has been already evolved out [10]-[14]; however, there is no such scheme which has offered a proof that there is a long lasting sensor. Basically, a sensor is a very miniature device characterized by external battery as well as its components is characterized by low processing capability too. Even if a potential solution towards energy efficiency is designed, it is essential that it should be operationally supported by the processing components of a sensing device. Existing approaches has discussion of various energy conservation techniques but they are highly symptomatic in nature which deals with one set of problem only. Hence, in spite of large archives of investigation work towards energy issues in WSN, the problem is yet an open-end problem by large. Apart from this, it is also known that a sensor node is an integral part of Internet-of-Things (IoT) which offers further magnified connectivity of sensors [15]. IoT connects all nodes with common platform of internet and certain operating devices like switches and gateways [16]. The amount of traffic on IoT is extensively more compared to WSN and existing standards of energy conservation techniques are not directly executed over an IoT platform leading to another set of incompatibility. This problem of offering a communication bridge by using a translation services is now possible by using gateway in IoT. However, the question still is left open: How to optimize the energy in sensor nodes when connected in form of network? The answer to this question would possibly lead us towards evolving a novel energy optimization principle in future.

Therefore, this paper contributes towards offering a compact snapshot of strength and weakness of existing schemes which is claimed for offering energy optimization in WSN. The idea is to assist the research community to make a practical decision and derive a conclusive remark about the existing picture of different variants of energy optimization schemes in WSN. The organization of the proposed manuscript is as follows: Section II discusses about the WSN energy optimization scheme in existing times followed by discussion of existing approaches of energy optimization in Section III. Section IV highlights about existing trends of research approaches followed by significant highlights of open-end research problems in Section V. Finally, study findings of this paper are presented in Conclusion under Section VI.

II. Insights on WSN Energy Optimization

This section discusses about all the necessary information associated with energy optimization in WSN. At present, there are three terms which looks more-or-less alike to each other with respect to energy e.g., energy efficiency, energy aware, and energy optimization. The first term energy efficiency is about implementation scheme which attempts to restore maximum amount of possible energy by adopting different methodologies. However, the final outcome of energy consumption could be still high, but this is the most practical plan and widely used. The second term energy aware is based on implementation techniques using budgeted amounts of resources in presence of test environment. Such techniques are good for assessing smaller scale of implementation or when the test environment is practically equivalent to real-environment of implementation. The third term energy optimization is associated with those techniques where the target is to reduce energy consumption without adding or utilizing more number of resources. There has been some number of studies towards energy optimization in WSN and still it is an ongoing arena of research in order to yet come out with some fail-proof solution. Prior to understanding the energy optimization, it is necessary to review various essential points associated with this. They are briefed as below:

A. Reason for Energy Depletion in WSN

A modern architecture of a sensor node basically consists of a power unit and power harvester [17]. There are various components within a power unit i.e., sensing units, computing units, communication unit, and power unit. All this units have different ranges of energy consumption. All the existing and ongoing research studies towards energy management system as well as optimization is carried out over the block of power management and energy prediction which resides within a computing unit of sensor hardware architecture as shown in Fig. 1.

It will mean that other units (power, sensing, and communication) are ignored while modelling existing solution. Hence, existing models are not found to consider the complete hardware perspective while modelling solution towards energy problems in WSN and hence the problems still exit todays.

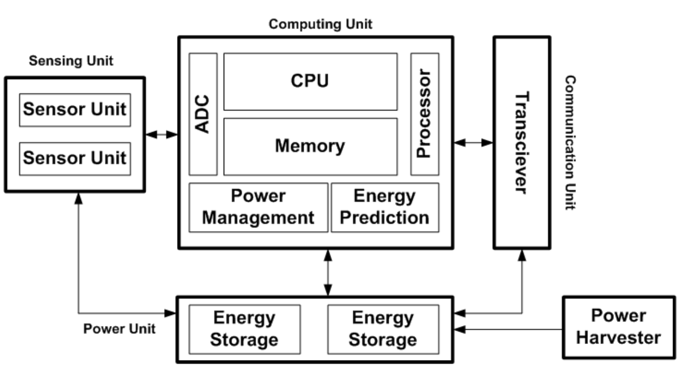

Fig. 1. Hardware Architecture of Sensor node in WSN [17].

However, the good news is that existing research work towards energy problems has made some potential discover towards exploring prominent reason for energy depletion in WSN as follows:

- Energy Conservation Problems: This problem is associated with predicting data, compressing higher ranges of aggregated data, reduction of data size, and optimizing the radio. The significant problem is that none of the above-mentioned attributes has been ever combinely studied for solving energy problems [17].

- Energy Transfers Problems: This kind of problem is mainly linked with power units of a sensor and therefore it is essential to consider. Various problems associated with charging techniques, energy transfer techniques, its associated tools, integrated data and energy transmission are essential attributes of an upcoming investigation in WSN, which is still under the roof of research and development [17].

- Energy Harvesting Problems: Currently, all the sensor node that is meant for deploying in critical environment are equipped with harvester node. At present, there are various ongoing and completed research in this perspective [17]; however, the addressed issues are still associated with source of energy to be harvested, energy storage, and performing neutral operation on energy.

- Addressing Routing Issues: At present, there are good number of research publication where routing [18] and clustering [19] has been used for achieving energy conservation in WSN. However, this scheme majorly doesn't consider the complete attributes that causes energy depletion. Hence, the effectiveness of such solution is only partially reasonable and applicable in real world environment.

B. Existing Studies on Energy Optimization

There are various studies that have been carried out towards energy optimization schemes by various means. Different non-linear optimization issues have been discussed by Asorey-Cacheda et al. [20] while multi-objective optimization schemes are reviewed by Fei et al. [21]. According to Cao et al. [22], there is a potential contribution of swarm intelligence-based optimization scheme applicable in case of involvement of mobility in sensor network. The work carried out by Diab et al. [23] discussed various data transmission scheme in WSN integrated with cognitive network emphasizing on energy constraints. The study carried out by Srinidhi et al. [24] have discussed about network optimization associated with IoT. The most recent study carried out by Khisa and Moh [25] has presented review of updated data transmission scheme towards energy efficiency associated with underwater WSN applications. Discussion presented by Williams et al. [26] has presented updated schemes of energy harvesting schemes in WSN. Therefore, there are various existing approaches towards addressing energy optimization under different methodologies. However, the extent of successful optimization associated with energy is yet not quantified till date.

III. Existing Approaches of Energy Optimization

This section briefs about different approaches targeting towards optimizing energy. The term optimization experimentally refers to accomplishing the target aim of controlling every factor and reason to reduce energy efficiency without inclusion of very large or significant number of resources involved in it. However, it is yet to investigate the degree of optimization used in the adopted approaches, its degree of solution associated with problems, its beneficial aspect as well as its limiting factor. The proposed investigation witnesses different methods towards an objective of solving energy problems in WSN and hence, they have been clustered into six different approaches as discussed below:

A. Game-based Approach

From the theoretical aspect, game theory is basically known to assists in making decision for a given number of confusing choices of strategies [27]. Owing to the potential of carrying out decision, game theory is used in carrying out decision towards data forwarding in WSN [28]. The sensor node can be assumed as a player in game theory who is required to opt for choosing a route for data transmission towards base station (in single hop) or to neighboring cluster head (in multi-hop). At present, there is a slowly increasing adoption towards using game theory; however, the target is again a scattered one. The work carried out by Chowdhury et al. [29] targets towards two problems i.e., energy depletion and congestion in WSN emphasizing over low-end sensor node deployment. The author has designed non-cooperative game in order to optimize the process of improving data forwarding rate with an idea of resisting bottleneck condition in WSN. Game theory is also witnessed to be used in improving clustering approach as seen in work of Lin et al. [30] where a game model is designed using Nash Equilibrium point selecting dual cluster heads. This work uses energy and distance to carry out the process of optimizing cluster head. Apart from this, it is also known that Software-Defined Network (SDN) significantly improves network performance of WSN. This fact is reported to be further improved upon by Peizhe et al. [31] where game theory is used by mapping the SDN and WSN. Different from all above-mentioned work, Shahrokhzadeh and Dehghan [32] has presented a unique study where coverage performance is improved for WSN with capability to sense visual signals. A unique distributed game model is constructed which bridges the gap between energy depletion and quality of network coverage of visual sensor node. Another unique approach of game modelling is carried out by Zayene et al. [33]. The solution is for addressing the problems associated with cooperative exchange of data. This model is constructed on the basis of consumed energy and completion time where a unique merge and split algorithm is constructed along with network coding which can perform instantaneous decoding capabilities. A coalition game model is developed emphasizing over achieving energy efficiency assessed over a test bed of WSN with mobility aspect being considered. Hence, game theory has offered some unique techniques in order to perform routing which directly or indirectly also controls energy efficiency in WSN.

B. Machine Learning Approach

The evolution of Machine Learning (ML) approaches dates back more than two decades old while its implementation witnesses a potential hike in various forms of applications and services. Powered by the potential of artificial intelligence, ML approach offers significant capability to solve complex problem without any instruction from humans [AR]. At present, ML approaches are widely used in networking in order to enhance its management, analytical operation, and security [AR]. Different numbers of computational models are used in order to embody ML approach. In the area of WSN, ML has been used for multiple purposes which directly or indirectly is linked with routing operation. Basically, ML approaches are classified into supervised approach and unsupervised learning approach (Fig. 2).

- Supervised Learning Approach: Supervised learning approach is further categorized as classification and regression-based approaches. From classification perspective, there are four variants viz. Support Vector Machine (SVM), discriminant analysis, naïve bayes, and nearest neighbor. In recent studies, SVM is reported to be used for improving the accuracy of the sensor readings in WSN (Jeong et al. [34]). The usage of SVM is also witnessed in work of Li et al. [35] where the idea is mainly to offer fault detection in WSN considering temperature and acceleration. The next role of classification approach is played by discriminant analysis where it is reported to be used for formulating dynamic adjustment policy toward monitoring multiple sinks in WSN for data aggregation (Chen et al. [36]). Another variant of classification scheme under supervised learning policy is Naïve Bayes which performs probability-based classification (Chu et al. [37]). The work carried out by Barnawi and Keshta [38] have carried out a study where Naïve Bayes is studied alongside with multi-layered perceptron and SVM. The outcome of this study is not in favor of Naïve Bayes as better form of classification existing in current times. Finally, the nearest neighboring approach is used in supervised learning approach in WSN. The work carried out by Fu et al. [39] have used nearest neighboring approach for performing query processing in WSN with an idea of optimizing latency and energy involved. The work carried out by Marchang and Tripathi [40] have focused on crowd sensing particularly on spatial and temporal perspective. From regression-based supervised learning approach, there are following approaches seen to be used in WSN i.e., Linear Regression (LR), Support Vector Regression (SVR), Ensemble method, Decision Trees, and Neural Network. The first form of the supervised regression scheme is Linear Regression scheme. The work carried out by Yilmaz et al. [41] has carried out study of WSN with respect to achieve the accuracy of target along with stopping criterion formulation. Upadhyay et al. [42] have implemented Gaussian Regression of non-linear form in order to form an effective clock synchronization. The scheme uses adaptive modelling with outcome of lower error rate in time synchronization. The next technique of regression is

Support Vector Regression (SVR) which is meant for performing analysis of data with respect to classification and regression. The work carried out by Shamshirband et al. [43] where SVR is combined with Kalman filtering in order to carry out data fusion in WSN. The study outcome shows that SVR performs well with Radial Basis Function better than other SVR approaches with polynomial kernel approach. The work carried out by Guo et al. [44] have used SVR for the purpose of predicting the energy required for forwarding data in WSN of distributed form. The outcome shows SVR performing better with random forest regression. The next method is Ensemble learning which is another frequently used mechanism in regression-based supervised learning scheme. This method makes use of different learning models in order to achieve its optimization target. Most recently, the work is being carried out by Alotaibi [45] have used this technique for detecting the mode of sensor-based transportation application. The study outcome shows different accuracy score for different dataset. Study towards optimizing sensory array was witnessed in work of Wijaya [46] where ensemble method is used for monitoring the quality of food. The next prominent process of regression in supervised learning method is decision tree. The study carried out by Rout et al. [47] and Zheng et al. [48] have used decision tree for addressing energy conservation problems and recognition problems in WSN. The final form of regression-based supervised learning scheme is neural network, which is also one of the most frequently deployed schemes in wireless networks. Neural network implementation has been seen in the study carried out by Lin et al. [49], Wu et al. [50], and Mukherjee et al. [51] addressing the problems associated with energy consumption, energy harvesting, and identification of cluster head respectively.

- Unsupervised Learning approach: This approach basically carries out clustering operation which are further classified into Fuzzy C-Means, Gaussian Mixture, Neural Network, and Hidden Markov Model. Fuzzy-C Means (FCM) clustering offers the benefit of more tangible unsupervised learning by offering more data points for analysis. The work of Cheng et al. [52] has used FCM approach towards location quantification using received signal strength indicator in WSN. Further usage of FCM was witnessed in study of Fei et al. [53] emphasizing over clustering operation towards energy efficiency. The second type of unsupervised learning scheme is Gaussian Mixture Model (GMM) which is a potential clustering algorithm. A unique usage of GMM was witnessed in work of Shi and Feng [54] where the target is to retain maximum signal in WSN. On the other hand, GMM was also witnessed in work of Eguchi et al. [55] which carry estimation of joint angle. Discussion of recent studies in neural network is carried out in previous approach. The final model of unsupervised clustering technique is Hidden Markov Model (HMM). The work carried out by Liu et al. [56] have used HMM for training occupancy sensing while the work of Xu & Wang [57] have used HMM for meteorology factor identification.

Fig. 2 highlights the taxonomies of existing ML approaches. Proliferated usage of ML approaches in WSN is seen in work of Kim et al. [58]. Apart from the above discussed frequently used ML approaches, there are various other approaches too viz. Deep reinforcement learning (Ashiquzzaman et al. [59], Ke et al. [60], Nguyen et al. [61]), deep neural network with sparse autoencoder (Ayinde [62]), opportunistic routing (Dinh et al. [63]), energy saving using simulated annealing (Kang et al. [64]), and energy harvesting using artificial neural network combined with linear regression (Kwan et al. [65]), Hence, it can be said that there are various dedicated research attempt towards using ML approach over WSN; however, not all the approaches are found to directly address energy problems in WSN.

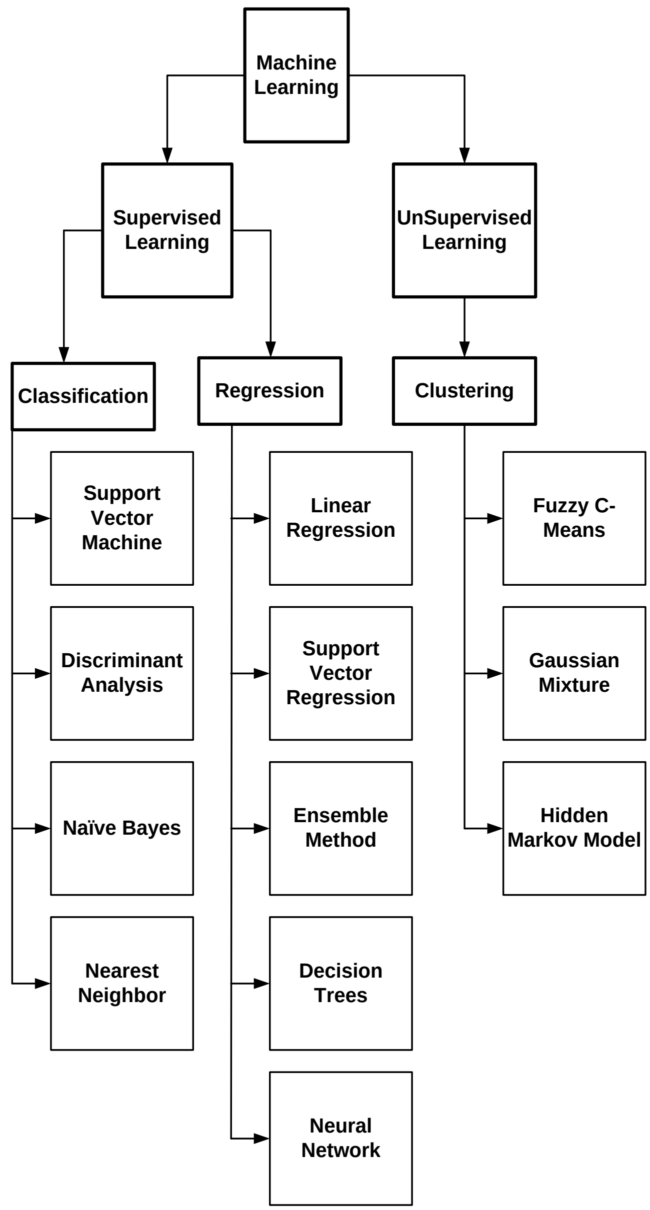

Fig. 2. Taxonomy of ML based Approach in WSN (Need Amendment).

C. Scheduling Approach

Scheduling based approaches mainly make use of making a proper routine along with provisioning of resources in order to ensure accomplishment of pre-defined target. Provisioning scheme assists in optimal deployment of sensor as witnessed in study of Du et al. [66]. Scheduling scheme is also reported to save energy depletion along with secure communication in WSN (Feng et al. [67]) using probability-based modelling. Scheduling approach is also applied for estimating the state of the remoteness on the basis of stochastic event considering the case study of WSN with cognitive radio networks (Huang et al. [68]). It was also noticed that there is a significant improvement in system performance when allocation of different attributes of resource is considered in scheduling process. Such direction of work is carried out by Li et al. [69] towards tracking multiple targets; however, it lacks optimization. Focus on optimizing the scheduling from temporal aspects is seen in work carried out by Liu et al. [70] which is basically meant for IoT networks by improving the power allocation ratio. A different form of study has been carried out by Shi et al. [71] in order to address the problems associated with convergecast scheduling. The idea of this work is mainly to increase the number of concurrent transmissions in WSN considering the constraints of integer programming. The work of Wan et al. [72] has presented discussion about sleep scheduling approach in WSN for conserving energy. The study has used fuzzy concept in order to perform organization of sensors along with aggregation of data on the basis of similarity matrix. Wang et al. [73] have carried out study towards deterministic scheduling for controlling an effective transmission delay. The study implements a scheduling rule on the basis of classified link conflict and initial reduced extent of conflict. The work carried out by Yang et al. [74] has presented a scheduling policy using unique power allocation scheme in WSN. Another scheduling scheme using distributed Multiple Input Multiple Output (MIMO) has been implemented by Zhang et al. [75] emphasizing over allocation of resource and scheduling of device for the purpose of detection and tracking in WSN.

D. Harvesting Approach

Energy harvesting technique is strongly linked with energy optimization scheme in WSN. Using varied sources of energy (magnetic, vibration, temperature, solar, etc.), a harvester node stores energy ensuring to deliver a satisfactory backup for the energy supply demanded by the specific sensor node. Hence, node using harvesting module should have better harvesting capabilities. At present, there are existing research studies towards energy harvesting techniques in WSN are i) using reinforcement learning (Aoudia et al. [76]), duty-cycle based modelling (Chew et al. [77]), opportunistic routing with cooperative charging (Hu et al. [78]), intra-vehicular communication based energy harvesting (Koca et al. [79]), energy aware interface design with vibration-based energy harvesting (Ruan et al. [80]), polynomial time-scheduling for solar energy harvesting (Wang et al. [81]), multi-objective optimization based hybrid energy harvesting (Xiong et al. [82]), and optimized data buffer scheme (Zhu et al. [83]).

E. Cross Layer Approach

From the viewpoint of protocol layer, both hierarchical and cross-layer approach is meant for incorporating optimized performance growth in WSN. However, hierarchical architectures suffer from issues e.g., signal fading, interference between users, access conflicts. However, proper maximization of the limited resources in protocol stack is not possible in hierarchical design, which is possible using cross-layer approach. By using cross-layer approach, it is possible for different layers to interact with each other for exchange of information. This phenomenon is utilized for solving different issues in WSN. From bottom to top, the protocol stack of WSN consists of IEEE 802.15.4 layer, which has data link layer and physical layer, network layer, transmission control layer, and application support layer. At present, there are various cross-layer based approach presented for improving performance on various aspects in WSN. However, there exists specifically only few approach associated with respect to energy aspect using following cross-layer based methodologies viz. routing reliability using time-based factor for energy (Abbasi et al. [84]), improved geographic routing for green efficiency in IoT with Markov queuing model (Hasan et al. [85]), maximizing network lifetime using cross layer (Hermann [86]), MAC scheduling with adaptiveness (Ngo et al. [87]), optimization of cross-layer for shortest and multipath routing (Shimly et al. [88]), optimizing data aggregation and choosing cluster head using particle swarm optimization using cross layer approach (Sun et al. [89]), optimizing energy-efficient routing for conventional LEACH protocol using cross layer (Zhang et al. [90]). Majority of the existing approaches of cross layer in WSN make use of network management layer which consist of physical layer, data link layer, network layer, and transmission control layer. They are meant for serving remote management, mobility control, network security, quality of service supportability, energy management, and topology control.

F. Swarm Intelligence Approach

This approach is designed on the basis of decentralized behaviour of self-organized system. Theoretically, swarm intelligence falls under the category of population-based search approach of metaheuristics method in optimization technique. It comes within approximated combinatorial method. They are designed on the basis of cognitive behaviour of certain biologically inspired entity e.g., ant, honeybee, firefly, frog, fish, cat, dolphin, etc. The studies that has used swarm intelligence linking with energy efficiency are as follows: Gray-wolf optimization (Arafat et al. [91]), Bat algorithm (Cao et al. [92]), flocking control scheme using swarm intelligence (Dai et al. [93]), firefly mating optimization (Faheem et al. [94]), fish algorithm with k-means clustering (Feng et al. [95]), multi-swarm optimization (Hasan et al.[96]), Harris' Hawk optimization (Houssein et al. [97]), particle swarm optimization (Mukherjee et al. [98]), Chicken swarm optimization (Osamy et al. [99]), reinforcement learning with swarm intelligence (Wei et al. [100]). However, different approaches have their own structure of working which is implemented on WSN on different targets of optimization towards energy efficiency. Table I summarizes the existing reviews.

TABLE I. SUMMARY OF EXISTING OPTIMIZATION APPROACHES IN WSN

Authors	Problems	Solution	Advantage	Limitation
Chowdhury et al. [29]	-energy depletion -congestion	Non-cooperative game, optimizing data transmission rate	Better energy and delay control	Not applicable for heterogeneous network
Lin et al. [30]	Optimizing clustering	Dual cluster head selection	Increase span of network lifetime	Doesn't deal with data complexity and not applicable for sparse network.
Peizhe et al. [31]	Energy completion	SDN with game model	A synced communication between controller and sensor node	Doesn't support dynamic environment
Shahrokhzadeh and Dehghan [32]	Improving coverage	Learning algorithm on the basis of pay-off.	Improve network lifetime	not applicable for large dynamic network.
Zayene et al. [33]	Energy depletion	Coalition game model	Improve scalability	Involves computational complexity owing to highly iterative operation.
Jeong et al. [34], Li et al. [35]	Assessing reading accuracy	Support Vector Machine	Satisfactory accuracy	Doesn't contribute towards energy efficiency directly.
Chen et al. [36]	Multi-sink monitoring	Discriminant Analysis	Good energy conservation	Unable to differentiate data acquisition process
Barnawi and Keshta [38]	Comparative study	Naïve Bayes	Simpler comparison	Naïve Bayes not found to be an effective
Chu et al. [37]	Classification of data fault	Naïve Bayes	Higher accuracy in fault detection	Dynamic faults not accessed in the study
Fu et al. [39], Marchang [40]	Query processing, crowd sensing	Nearest neighboring	Reduced resource consumption	Not applicable for heterogeneous network
Yilmaz et al. [41]	Sequential estimation, decentralized	Linear Regression	Effective stopping time	Doesn't emphasize on peak traffic condition
Upadhyay et al. [42]	Clock synchronization	Non-linear gaussian regression	Reduced error	Applicable on static environment only
Shamshirband et al. [43]	Comparison analysis of SVR	Kalman filtering + SVR	Higher precision	Doesn't evaluate energy efficiency
Guo et al. [44]	Energy prediction	SVR with random forest, gradient boosting regression	Higher precision	Doesn't evaluate energy efficiency
Alotaibi [45]	Detecting mode of transportation	Ensemble Learning	Satisfactory accuracy	Doesn't deal with scalability performance
Wijaya [46]	Optimizing sensor array	Ensemble Learning	Higher accuracy	Limited to static and low scale application
Rout et al. [47]	Finding optimal switching policy	Decision Tree, Markov	Satisfactory energy control	Absence of benchmarking
Zheng et al. [48]	Recognition of target	Decision Tree	Effective benchmarking outcomes	Not applicable for heterogeneous and massive data
Lin et al. [49]	Estimation of energy depletion	Neural Network (Radial basis, generalized regression)	Lower energy consumption	Lower scope of test evaluation
Wu et al. [50]	Energy harvesting	Neural Network	Higher learning efficiency	Doesn't evaluate energy efficiency
Mukherjee et al. [51]	Identification of cluster head	Neural Network (Back propagation)	Better control of energy consumption	Computational complexity not analyzed.
Cheng et al. [52]	Location Quantification	FCM	Simplified voting process	The study is carried out in low-end application environment.
Fei et al. [53]	Clustering	FCM	Energy efficient	Leads to computational complexity due to higher iteration.
Shi and Feng [54]	Signal restoration	GMM	High quality of signal preservation	Doesn't address energy optimization
Eguchi et al. [55]	Estimation of joint angle	GMM	Higher accuracy	Doesn't address energy optimization
Liu et al. [56]	Training for accuracy in Occupancy sensing	HMM	Improve sensing time	Not applicable for heterogeneous WSN
Xu et al. [57]	Quantification of fine particulate	HMM	Simplified operation	Absence of benchmarking
Du et al. [66]	Node placement	Scheduling using wireless energy transfer	Optimizes node deployment	Absence of benchmarking
Feng et al. [67]	Energy saving	Sleep scheduling	Energy saving performance is good	Not applicable for heterogeneous network
Huang et al. [68]	Estimating remote state	Open-close loop scheduling of stochastic events	Reduces communication rate	Doesn't discuss its impact on energy consumption
Li et al. [69]	Tracking multi target	Resource allocation, sensor scheduling	Effective resource saving	Involves computational overhead.

Liu et al. [70]	Increasing data transmission rate	Time scheduling	Effective analysis of outage probability	Complete power attributes for device not considered
Shi et al. [71]	Maximize concurrent transmission	Convergent scheduling	Reduces latency	Doesn't evaluate energy extensively
Wan et al. [72]	Energy efficiency	Sleep scheduling	Ensure data accuracy	Not assessed for scalability
Wang et al. [73]	Reduction of transmission delay	Scheduling based on classified link conflict	Low complexity	Low scale deployment
Yang et al. [74]	Distributed filtering	Power allocation, experimental	Improves estimation accuracy	Low scale deployment
Zhang et al. [75]	Detection and tracking of target	Allocation of resource, distributed MIMO	Lower computational burden	Iterative scheme leading to lowering of network lifetime in long round.
Aoudia et al. [76]	Energy harvesting	Reinforcement learning	Significant increase in average packet rate	Doesn't address bottleneck condition in traffic
Chew et al. [77]	Energy harvesting for TSCH nodes	Network joining using duty-cycle	Simplified design architecture	Absence of benchmarking
Hu et al. [78]	Environmental changes	Integrating energy transfer approach with energy harvesting, opportunistic routing	Enhanced network lifetime	Not applicable for dynamic and large-scale network
Koca et al. [79]	Feasibility analysis of energy harvesting in vehicles	Intra-vehicular communication	Effective transmission performance	Leads to computational complexity
Ruan et al. [80]	Energy harvesting	Harvesting using Vibration	Energy aware modelling	Doesn't ensure scalability
Wang et al. [81]	Wireless charging	Harvesting using Solar, polynomial time scheduling	Reduce energy consumption and cost of vehicle moving	Time of wireless charging not sufficient enough in case of large traffic scenario
Xiong et al. [82]	Energy harvesting	Bidirectional local search, particle swarm optimization with multiple objectives	Prolonged network lifetime	Not scalable for large traffic
Zhu et al. [83]	Maximize throughput during harvesting	Data buffer, super-frame optimization, stochastic modelling	Improved throughput	Specific to device with IEEE 802.15.4 standard only
Abbasi et al. [84]	Communication reliability	Cross-layer based routing	Better quality of service	Lacks optimization of resources
Hasan et al. [85]	Essential of cooperative demands in multihop communication	Cross-layer based queuing model, geographic switching	More green efficiency	Doesn't consider hardware-based factors for switching
Herrmann et al. [86]	Maximizing network lifetime	Lifetime optimization	Significant energy depletion control	Not scalable for large traffic
Ngo et al. [87]	Adaptive scheduling in body sensor network	Cross layer, MAC scheduling	Better quality of service	Absence of benchmarking
Shimly et al. [88]	Any-to-any routing	Cross layer optimization	Reduce retransmission	Possess overhead when exposed to dynamic traffic
Sun et al. [89]	Clustering	Cross-layer sensing	Optimize aggregation efficiency	Highly iterative process
Zhang et al. [90]	Clustering efficiency	Cross layer optimization of LEACH protocol	Reduce cluster computation	Not analyzed with dynamic traffic system
Arafat et al. [91]	Clustering, localization	Compressive sensing based on gray-wolf optimization	Efficient routing tree	Involves cost and complexity
Cao et al. [92]	Data fusion	Bat algorithm	Improve network lifetime	Cannot handle bottleneck condition
Dai et al. [93]	Decision making for autonomous vehicular movement	Swarm intelligence, experimental	Low energy consumption	Doesn't ensure data quality
Faheem et al. [94]	Energy-efficient routing	Firefly mating optimization	Ensure satisfactory quality of service	Residual energy could be optimized more
Feng et al. [95]	Optimizing Network Coverage	Fish swarm algorithm, K-means algorithm	Good energy saving	Tested over small network
Hasan et al. [96]	Meeting Quality of service for Industrial IoT	Particle Swarm Optimization	Satisfactory quality of service	Tested over small network
Houssein et al. [97]	Sink node placement	Harris Hawk Optimization	Reduced energy consumption	Throughput is dependent on node position
Mukherjee et al. [98]	Resource allocation	Adaptive Particle Swarm Optimization	Faster response time and reduced energy	Computationally complex process
Osamy et al. [99]	Clustering	Chicken Swarm Optimization	Enhanced network lifetime	Static fitness function design
Wei et al. [100]	Charging sensors	Firefly algorithm, Reinforcement learning	Better energy utilization	Dynamic energy consumption not evaluated.

IV. Current Research Trends

The previous section has discussed about taxonomies of all the existing approaches that are frequently used for solving energy problems in WSN. However, all the solutions evolved up till date cannot be termed as optimized problems. There are different categories of research-based solution towards this purpose by different names; therefore, this paper contributes towards forming up a standard name of this approach in order to understand the current research trends. Fig. 3 highlights the number of different publications towards different types of research-based solution for addressing energy problems in WSN.

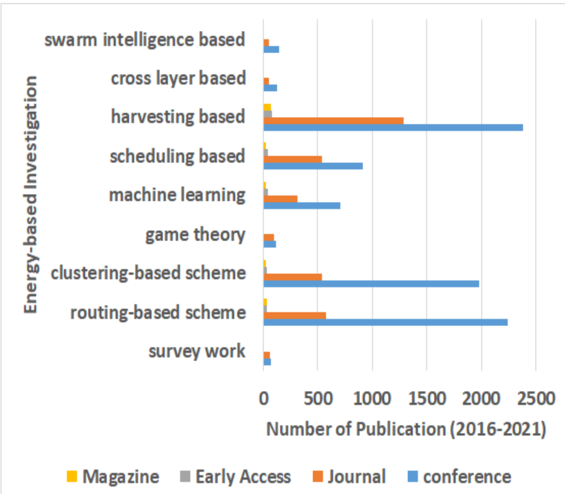

Fig. 3. Current Research Trend towards Energy in WSN.

Following are the findings of the research trends seen from the research-based manuscript published within the year of 2016-2021 as one of the contributions of proposed study being carried out:

- More insights towards research approaches are now evolving towards energy harvesting based approaches. Although, this is another level of future of using sensory application for network lifetime improvement but yet no robust standardization is yet obtained for harvesting models in WSN. It still has a long way to go.
- Routing-based and clustering-based approaches are the most frequently used approach that are being consistently adopted as core research problem since last decade. There are evolution of standard routing and clustering techniques known for energy efficiencies in WSN; but still, they do not encapsulate all the factors responsible for energy depletion.
- Scheduling-based and machine learning is next frequently adopted approach for energy efficiencies. Although, these approaches are proven fruitful towards energy conservation schemes in WSN but they are less inclined towards energy optimization.
- A unique observation is obtained from cross-layer based and game theory-based schemes as they are not yet found fruitful towards energy optimization. They are proven fruitful for solving other problems in WSN but not much in energy control and management.
- Adoption of swarm intelligence is still a novel approach towards energy optimization although they are proven effective for solving other problems in WSN. There is a need of more number of researches in order to consider this approach towards energy optimization.

V. Open Research Challenges

After reviewing the existing studies towards controlling energy problems in WSN, certain level of conclusive remarks has been formulated. The open research challenges associated with the achieving optimized energy in WSN are briefed as following:

- Mono-issue Modelling Practices: Majority of the discussed techniques is found to address a specific problem which is associated with energy. For an example, problems associated with routing and energy is considered without considering hardware inclusion or without considering clustering techniques. Such approaches cannot be considered as wholesome solution as other connected factors related to energy are often found ignored, irrespective of any techniques discussed in this study. Hence, majority of the modelling practices in current times considers addressing one problem of energy in WSN.
- Less Focus on Practical Modelling: It should be known that majority of the application of WSN is hypothetical and less practical from commercial and real-time aspect. Commercial practices in current times calls for using sensors in IoT or smart city development which has massive number of challenges and issues to be sorted out apart from energy problems. Apart from this, even if WSN domain is researched than there is a need to consider heterogeneity in protocol implementation, data quality, data complexities, environmental parameters affecting data transmission should be considered. Protocols of WSN are not applicable in IoT and protocols of IoT are not applicable in WSN. Hence gateway concept comes in features to bridge this incompatibility issues. This aspect of energy modelling is found extremely low in existing studies in WSN as well as in IoT towards energy challenges.
- Ambiguity in Defining Optimization: There are various manuscript with title or with discussing of using optimization principle to reduce energy. However, this is slightly far from reality as such papers are often found with a big gap between their theoretical implication and practical implication. The practical implication of optimization concept calls for an evidential proof of higher energy retention with lower involvement of resources (both hardware and software). It is also required to offer an evidence that optimized outcome is also scalable in nature for truly understanding its effectiveness. Further computational complexity is also required to be proven low, which is not found in existing.

- Absence of Benchmarking during Analysis: Adoption of analytical test bed which has universal acceptance towards performance parameters, test values, initialized values of simulation parameters, involvement of standard and reliable energy computational, and involvement of multiple test cases is very much required. Existing studies towards energy optimization, although they are few in relevancy of implementation, are not found to be benchmarked.

VI. Conclusion

Majority of existing as well as upcoming application of WSN demands a node to work for an extensive period of time unattended. This paper has discussed about various approaches which are found to address the problems associated with energy factor. There are large number of techniques in existing system towards energy problems in wireless sensor network, but there is a lack of compact study carried out towards discussion effectiveness of recent literatures. Hence, this paper contributes to review maximum number of significant implementation in energy problems in wireless sensor network and contributes to highlight the appropriate information associated with strength and weakness of existing studies. This findings will contribute towards research community to make a better decision towards evolving up with a necessary model to deal with identified problems and challenges in energy efficiency in sensory network. The contribution of this paper are in terms of essential findings as follows viz. i) unlike existing review studies or discussion paper, this paper makes a categorization of extensively used energy conservation approaches which are claimed to offer optimization; ii) there is highly scattered study towards addressing the challenges associated with energy optimization in WSN, in fact, there are extremely few existing approaches to offer evidence of energy optimization in WSN; iii) almost all the existing approaches are found to have limitations which is necessary to address in order to show practicality as well as adaptability of existing models; and iv) here is a need to evolve up with a novel mathematical model with multi-objective function and with less iterative scheme to offer benchmarked outcomes and cost effectively in data aggregation of WSN. Hence, developing an effective scheme for ensuring better lifetime in sensory application demands inclusion of various factors, e.g. states of nodes, types of links, scheduling scheme being used, inclusion of both hardware and software resources, as well as algorithm effectiveness. The lighter the algorithm operation, more is computational efficiency that will result in more extensive operation resulting in improved network lifetime.

Hence, the future work will be carried out in the direction of addressing the research gap discussed the proposed study. The future work should be initially designed to construct a formulation which considers all the practical constraints of WSN followed by developing a mathematical modelling of energy optimization. Essential check point should be given to ensure less iterative, faster computation, and higher data quality, and cost effectiveness along with scalability is ensured along with future modelling of energy optimization.

References

[1] J. Liu, Z. Zhao, J. Ji and M. Hu, "Research and application of wireless sensor network technology in power transmission and distribution system," in Intelligent and Converged Networks, vol. 1, no. 2, pp. 199-220, Sept. 2020, doi: 10.23919/ICN.2020.0016.

[2] S. Liao and Q. Zhang, "A Multiutility Framework With Application for Studying Tradeoff Between Utility and Lifetime in Wireless Sensor Networks," in IEEE Transactions on Vehicular Technology, vol. 64, no. 10, pp. 4701-4711, Oct. 2015, doi: 10.1109/TVT.2014.2372793.

[3] X. Yang, L. Wang and Z. Zhang, "Wireless Body Area Networks MAC Protocol For Energy Efficiency and Extending Lifetime," in IEEE Sensors Letters, vol. 2, no. 1, pp. 1-4, March 2018, Art no. 7500404, doi: 10.1109/LSENS.2018.2795566.

[4] J. Shi, M. Sha and Z. Yang, "Distributed Graph Routing and Scheduling for Industrial Wireless Sensor-Actuator Networks," in IEEE/ACM Transactions on Networking, vol. 27, no. 4, pp. 1669-1682, Aug. 2019, doi: 10.1109/TNET.2019.2925816.

[5] D. Sharma and A. P. Bhondekar, "Traffic and Energy Aware Routing for Heterogeneous Wireless Sensor Networks," in IEEE Communications Letters, vol. 22, no. 8, pp. 1608-1611, Aug. 2018, doi: 10.1109/LCOMM.2018.2841911.

[6] N. Aslam, K. Xia and M. U. Hadi, "Optimal Wireless Charging Inclusive of Intellectual Routing Based on SARSA Learning in Renewable Wireless Sensor Networks," in IEEE Sensors Journal, vol. 19, no. 18, pp. 8340-8351, 15 Sept.15, 2019, doi: 10.1109/JSEN.2019.2918865.

[7] H. Ko and S. Pack, "OB-DETA: Observation-based directional energy transmission algorithm in energy harvesting networks," in Journal of Communications and Networks, vol. 21, no. 2, pp. 168-176, April 2019, doi: 10.1109/JCN.2019.000015.

[8] T. Ruan, Z. J. Chew and M. Zhu, "Energy-Aware Approaches for Energy Harvesting Powered Wireless Sensor Nodes," in IEEE Sensors Journal, vol. 17, no. 7, pp. 2165-2173, 1 April1, 2017, doi: 10.1109/JSEN.2017.2665680.

[9] D. Newell and M. Duffy, "Review of Power Conversion and Energy Management for Low-Power, Low-Voltage Energy Harvesting Powered Wireless Sensors," in IEEE Transactions on Power Electronics, vol. 34, no. 10, pp. 9794-9805, Oct. 2019, doi: 10.1109/TPEL.2019.2894465.

[10] I. Khan, F. Belqasmi, R. Glitho, N. Crespi, M. Morrow and P. Polakos, "Wireless sensor network virtualization: A survey," in IEEE Communications Surveys & Tutorials, vol. 18, no. 1, pp. 553-576, Firstquarter 2016, doi: 10.1109/COMST.2015.2412971.

[11] P. Park, S. Coleri Ergen, C. Fischione, C. Lu and K. H. Johansson, "Wireless Network Design for Control Systems: A Survey," in IEEE Communications Surveys & Tutorials, vol. 20, no. 2, pp. 978-1013, Secondquarter 2018, doi: 10.1109/COMST.2017.2780114.

[12] S. H. R. Bukhari, M. H. Rehmani and S. Siraj, "A Survey of Channel Bonding for Wireless Networks and Guidelines of Channel Bonding for Futuristic Cognitive Radio Sensor Networks," in IEEE Communications Surveys & Tutorials, vol. 18, no. 2, pp. 924-948, Secondquarter 2016, doi: 10.1109/COMST.2015.2504408.

[13] S. Movassaghi, M. Abolhasan, J. Lipman, D. Smith and A. Jamalipour, "Wireless Body Area Networks: A Survey," in IEEE Communications Surveys & Tutorials, vol. 16, no. 3, pp. 1658-1686, Third Quarter 2014, doi: 10.1109/SURV.2013.121313.00064.

[14] S. Jayaprakasam, S. K. A. Rahim and C. Y. Leow, "Distributed and Collaborative Beamforming in Wireless Sensor Networks: Classifications, Trends, and Research Directions," in IEEE Communications Surveys & Tutorials, vol. 19, no. 4, pp. 2092-2116, Fourthquarter 2017, doi: 10.1109/COMST.2017.2720690.

[15] S. Ezdiani, I. S. Acharyya, S. Sivakumar and A. Al-Anbuky, "Wireless Sensor Network Softwarization: Towards WSN Adaptive QoS," in IEEE Internet of Things Journal, vol. 4, no. 5, pp. 1517-1527, Oct. 2017, doi: 10.1109/JIOT.2017.2740423.

[16] Z. Ma, M. Xiao, Y. Xiao, Z. Pang, H. V. Poor and B. Vucetic, "High-Reliability and Low-Latency Wireless Communication for Internet of Things: Challenges, Fundamentals, and Enabling Technologies," in IEEE Internet of Things Journal, vol. 6, no. 5, pp. 7946-7970, Oct. 2019, doi: 10.1109/JIOT.2019.2907245.

[17] F. Engmann, F. A. Katsriku, J-D Abdulai, K. S. Adu-Manu, and F. K. Banaseka, “Prolonging the Lifetime of Wireless Sensor Networks: A Review of Current Techniques”, Hindawi, Wireless Communications and Mobile Computing, 2018.

[18] X. Liu, "Atypical Hierarchical Routing Protocols for Wireless Sensor Networks: A Review," in IEEE Sensors Journal, vol. 15, no. 10, pp. 5372-5383, Oct. 2015, doi: 10.1109/JSEN.2015.2445796.

[19] D. N. Sandeep and V. Kumar, "Review on Clustering, Coverage and Connectivity in Underwater Wireless Sensor Networks: A Communication Techniques Perspective," in IEEE Access, vol. 5, pp. 11176-11199, 2017, doi: 10.1109/ACCESS.2017.2713640.

[20] R. Asorey-Cacheda, A.-J. Garcia-Sanchez, F. Garcia-Sanchez, J. Garcia-Haro, “A survey on non-linear optimization problems in wireless sensor networks”, Elsevier- Journal of Network and Computer Applications 82 (2017) 1–20.

[21] Z. Fei, B. Li, S. Yang, C. Xing, H. Chen and L. Hanzo, "A Survey of Multi-Objective Optimization in Wireless Sensor Networks: Metrics, Algorithms, and Open Problems," in IEEE Communications Surveys & Tutorials, vol. 19, no. 1, pp. 550-586, Firstquarter 2017, doi: 10.1109/COMST.2016.2610578.

[22] L. Cao, Y. Cai and Y. Yue, "Swarm Intelligence-Based Performance Optimization for Mobile Wireless Sensor Networks: Survey, Challenges, and Future Directions," in IEEE Access, vol. 7, pp. 161524-161553, 2019, doi: 10.1109/ACCESS.2019.2951370.

[23] R. A. Diab, N. Bastaki and A. Abdrabou, "A Survey on Routing Protocols for Delay and Energy-Constrained Cognitive Radio Networks," in IEEE Access, vol. 8, pp. 198779-198800, 2020, doi: 10.1109/ACCESS.2020.3035325.

[24] N.N. Srinidhi, S.M. Dilip Kumar, K.R. Venugopal, “Network optimizations in the Internet of Things: A review”, Elsevier- Engineering Science and Technology, an International Journal 22 (2019) 1–21.

[25] S. Khisa and S. Moh, "Survey on Recent Advancements in Energy-Efficient Routing Protocols for Underwater Wireless Sensor Networks," in IEEE Access, vol. 9, pp. 55045-55062, 2021, doi: 10.1109/ACCESS.2021.3071490.

[26] A. J. Williams, M. F. Torquato, I. M. Cameron, A. A. Fahmy and J. Sienz, "Survey of Energy Harvesting Technologies for Wireless Sensor Networks," in IEEE Access, vol. 9, pp. 77493-77510, 2021, doi: 10.1109/ACCESS.2021.3083697.

[27] J. He et al., "Application of Game Theory in Integrated Energy System Systems: A Review," in IEEE Access, vol. 8, pp. 93380-93397, 2020, doi: 10.1109/ACCESS.2020.2994133.

[28] M. A. Abd, S. F. M. Al-Rubeaai, B. K. Singh, K. E. Tepe and R. Benlamri, "Extending Wireless Sensor Network Lifetime With Global Energy Balance," in IEEE Sensors Journal, vol. 15, no. 9, pp. 5053-5063, Sept. 2015, doi: 10.1109/JSEN.2015.2432114.

[29] S. Chowdhury, A. Benslimane and C. Giri, "Noncooperative Gaming for Energy-Efficient Congestion Control in 6LoWPAN," in IEEE Internet of Things Journal, vol. 7, no. 6, pp. 4777-4788, June 2020, doi: 10.1109/JIOT.2020.2969272.

[30] D. Lin and Q. Wang, "An Energy-Efficient Clustering Algorithm Combined Game Theory and Dual-Cluster-Head Mechanism for WSNs," in IEEE Access, vol. 7, pp. 49894-49905, 2019, doi: 10.1109/ACCESS.2019.2911190.

[31] L. Peizhe, W. Muqing, L. Wenxing and Z. Min, "A Game-Theoretic and Energy-Efficient Algorithm in an Improved Software-Defined Wireless Sensor Network," in IEEE Access, vol. 5, pp. 13430-13445, 2017, doi: 10.1109/ACCESS.2017.2727139.

[32] B. Shahrokhzadeh and M. Dehghan, "A Distributed Game-Theoretic Approach for Target Coverage in Visual Sensor Networks," in IEEE Sensors Journal, vol. 17, no. 22, pp. 7542-7552, 15 Nov.15, 2017, doi: 10.1109/JSEN.2017.2739183.

[33] M. Zayene, O. Habachi, V. Meghdadi, T. Ezzedine and J. P. Cances, "A Coalitional Game-Theoretic Framework for Cooperative Data Exchange Using Instantly Decodable Network Coding," in IEEE Access, vol. 7, pp. 26752-26765, 2019, doi: 10.1109/ACCESS.2019.2900982.

[34] S. Jeong, M. M. Tentzeris and S. Kim, "Machine Learning Approach for Wirelessly Powered RFID-Based Backscattering Sensor System," in IEEE Journal of Radio Frequency Identification, vol. 4, no. 3, pp. 186-194, Sept. 2020, doi: 10.1109/JRFID.2020.3004035.

[35] W. Li et al., "Vibrational Triboelectric Nanogenerator-Based Multinode Self-Powered Sensor Network for Machine Fault Detection," in IEEE/ASME Transactions on Mechatronics, vol. 25, no. 5, pp. 2188-2196, Oct. 2020, doi: 10.1109/TMECH.2020.2993336.

[36] Suxia Chen, Quanzheng Huang , Yang Zhang and Xin Li, “Double sink energy hole avoidance strategy for wireless sensor network”, Eurasip Journal on Wireless Communication and Networking, 2020.

[37] Shu-Chuan Chu, Thi-Kien Dao, Jeng-Shyang Pan, and Trong-The Nguyen, “Identifying correctness data scheme for aggregating data in cluster heads of wireless sensor network based on naïve Bayes classification”, Eurasip Journal on Wireless Communication and Networking, 2020.

[38] Abdulaziz Y. Barnawi and Ismail M. Keshta, “Energy Management in Wireless Sensor Networks Based on Naive Bayes, MLP, and SVM Classifications: A Comparative Study”, Hindawi Publishing Corporation, Journal of Sensors, 2016.

[39] T. Fu, W. Peng and W. Lee, "Parallelizing Itinerary-Based KNN Query Processing in Wireless Sensor Networks," in IEEE Transactions on Knowledge and Data Engineering, vol. 22, no. 5, pp. 711-729, May 2010, doi: 10.1109/TKDE.2009.146.

[40] N. Marchang and R. Tripathi, "KNN-ST: Exploiting Spatio-Temporal Correlation for Missing Data Inference in Environmental Crowd Sensing," in IEEE Sensors Journal, vol. 21, no. 3, pp. 3429-3436, 1 Feb.1, 2021, doi: 10.1109/JSEN.2020.3024976.

[41] Y. Yilmaz, G. V. Moustakides and X. Wang, "Sequential and decentralized estimation of linear-regression parameters in wireless sensor networks," in IEEE Transactions on Aerospace and Electronic Systems, vol. 52, no. 1, pp. 288-306, February 2016, doi: 10.1109/TAES.2015.140665.

[42] D. Upadhyay, A. K. Dubey and P. S. Thilagam, "Application of Non-Linear Gaussian Regression-Based Adaptive Clock Synchronization Technique for Wireless Sensor Network in Agriculture," in IEEE Sensors Journal, vol. 18, no. 10, pp. 4328-4335, 15 May15, 2018, doi: 10.1109/JSEN.2018.2818302.

[43] S. Shamshirband, D. Petković, H. Javidnia and A. Gani, "Sensor Data Fusion by Support Vector Regression Methodology—A Comparative Study," in IEEE Sensors Journal, vol. 15, no. 2, pp. 850-854, Feb. 2015, doi: 10.1109/JSEN.2014.2356501.

[44] Ni Guo, Weifeng Gui, Wei Chen, Xin Tian, Weiguo Qiu, Zijian Tian and Xiangyang Zhang, “Using improved support vector regression to predict the transmitted energy consumption data by distributed wireless sensor network” Eurasip Journal on Wireless Communication and Networking, 2020.

[45] B. Alotaibi, "Transportation Mode Detection by Embedded Sensors Based on Ensemble Learning," in IEEE Access, vol. 8, pp. 145552-145563, 2020, doi: 10.1109/ACCESS.2020.3014901.

[46] D. R. Wijaya and F. Afianti, "Information-Theoretic Ensemble Feature Selection With Multi-Stage Aggregation for Sensor Array Optimization," in IEEE Sensors Journal, vol. 21, no. 1, pp. 476-489, 1 Jan.1, 2021, doi: 10.1109/JSEN.2020.3000756.

[47] R. R. Rout, M. S. Krishna and S. Gupta, "Markov Decision Process-Based Switching Algorithm for Sustainable Rechargeable Wireless Sensor Networks," in IEEE Sensors Journal, vol. 16, no. 8, pp. 2788-2797, April15, 2016, doi: 10.1109/JSEN.2016.2519399.

[48] J. Zheng, S. Yang, X. Wang, X. Xia, Y. Xiao and T. Li, "A Decision Tree Based Road Recognition Approach Using Roadside Fixed 3D LiDAR Sensors," in IEEE Access, vol. 7, pp. 53878-53890, 2019, doi: 10.1109/ACCESS.2019.2912581.

[49] C. Lin, Y. C. Yang, J. Wang and Y. Yang, "A Wearable Sensor Module With a Neural-Network-Based Activity Classification Algorithm for Daily Energy Expenditure Estimation," in IEEE Transactions on Information Technology in Biomedicine, vol. 16, no. 5, pp. 991-998, Sept. 2012, doi: 10.1109/TITB.2012.2206602.

[50] K. Wu, F. Li, C. Tellambura and H. Jiang, "Optimal Selective Transmission Policy for Energy-Harvesting Wireless Sensors via Monotone Neural Networks," in IEEE Internet of Things Journal, vol. 6, no. 6, pp. 9963-9978, Dec. 2019, doi: 10.1109/JIOT.2019.2933579.

[51] A. Mukherjee, D. K. Jain, P. Goswami, Q. Xin, L. Yang and J. J. P. C. Rodrigues, "Back Propagation Neural Network Based Cluster Head Identification in MIMO Sensor Networks for Intelligent Transportation Systems," in IEEE Access, vol. 8, pp. 28524-28532, 2020, doi: 10.1109/ACCESS.2020.2971969.

[52] L. Cheng, J. Hang, Y. Wang and Y. Bi, "A Fuzzy C-Means and Hierarchical Voting Based RSSI Quantify Localization Method for Wireless Sensor Network," in IEEE Access, vol. 7, pp. 47411-47422, 2019, doi: 10.1109/ACCESS.2019.2909974.

[53] W. Fei, B. Hexiang, L. Deyu and W. Jianjun, "Energy-Efficient Clustering Algorithm in Underwater Sensor Networks Based on Fuzzy C Means and Moth-Flame Optimization Method," in IEEE Access, vol. 8, pp. 97474-97484, 2020, doi: 10.1109/ACCESS.2020.2997066.

[54] M. Shi and L. Feng, "Plug-and-Play Prior Based on Gaussian Mixture Model Learning for Image Restoration in Sensor Network," in IEEE Access, vol. 6, pp. 78113-78122, 2018, doi: 10.1109/ACCESS.2018.2884795.

[55] R. Eguchi, B. Michael, M. Howard and M. Takahashi, "Shift-Adaptive Estimation of Joint Angle Using Instrumented Brace With Two Stretch Sensors Based on Gaussian Mixture Models," in IEEE Robotics and Automation Letters, vol. 5, no. 4, pp. 5881-5888, Oct. 2020, doi: 10.1109/LRA.2020.3010486.

[56] P. Liu, S. Nguang and A. Partridge, "Occupancy Inference Using Pyroelectric Infrared Sensors Through Hidden Markov Models," in IEEE Sensors Journal, vol. 16, no. 4, pp. 1062-1068, Feb.15, 2016, doi: 10.1109/JSEN.2015.2496154.

[57] M. Xu and Y. Wang, "Quantifying PM2.5 Concentrations From Multi-Weather Sensors Using Hidden Markov Models," in IEEE Sensors Journal, vol. 16, no. 1, pp. 22-23, Jan.1, 2016, doi: 10.1109/JSEN.2015.2485665.

[58] T. Kim, L. F. Vecchietti, K. Choi, S. Lee and D. Har, "Machine Learning for Advanced Wireless Sensor Networks: A Review," in IEEE Sensors Journal, vol. 21, no. 11, pp. 12379-12397, 1 June1, 2021, doi: 10.1109/JSEN.2020.3035846.

[59] A. Ashiquzzaman, H. Lee, T. Um and J. Kim, "Energy-Efficient IoT Sensor Calibration With Deep Reinforcement Learning," in IEEE Access, vol. 8, pp. 97045-97055, 2020, doi: 10.1109/ACCESS.2020.2992853.

[60] H. Ke, J. Wang, H. Wang and Y. Ge, "Joint Optimization of Data Offloading and Resource Allocation With Renewable Energy Aware for IoT Devices: A Deep Reinforcement Learning Approach," in IEEE Access, vol. 7, pp. 179349-179363, 2019, doi: 10.1109/ACCESS.2019.2959348.

[61] K. K. Nguyen, T. Q. Duong, N. A. Vien, N. -A. Le-Khac and M. -N. Nguyen, "Non-Cooperative Energy Efficient Power Allocation Game in D2D Communication: A Multi-Agent Deep Reinforcement Learning Approach," in IEEE Access, vol. 7, pp. 100480-100490, 2019, doi: 10.1109/ACCESS.2019.2930115.

[62] B. O. Ayinde and A. Y. Barnawi, "Energy Conservation in Wireless Sensor Networks Using Partly-Informed Sparse Autoencoder," in IEEE Access, vol. 7, pp. 63346-63360, 2019, doi: 10.1109/ACCESS.2019.2917322.

[63] N. Dinh, T. Gu and Y. Kim, "Rendezvous Cost-Aware Opportunistic Routing in Heterogeneous Duty-Cycled Wireless Sensor Networks," in IEEE Access, vol. 7, pp. 121825-121840, 2019, doi: 10.1109/ACCESS.2019.2937252.

[64] J. Kang, J. Kim, M. Kim and M. Sohn, "Machine Learning-Based Energy-Saving Framework for Environmental States-Adaptive Wireless Sensor Network," in IEEE Access, vol. 8, pp. 69359-69367, 2020, doi: 10.1109/ACCESS.2020.2986507.

[65] J. C. Kwan, J. M. Chaulk and A. O. Fapojuwo, "A Coordinated Ambient/Dedicated Radio Frequency Energy Harvesting Scheme Using Machine Learning," in IEEE Sensors Journal, vol. 20, no. 22, pp. 13808-13823, 15 Nov.15, 2020, doi: 10.1109/JSEN.2020.3003931.

[66] R. Du, M. Xiao and C. Fischione, "Optimal Node Deployment and Energy Provision for Wirelessly Powered Sensor Networks," in IEEE Journal on Selected Areas in Communications, vol. 37, no. 2, pp. 407-423, Feb. 2019, doi: 10.1109/JSAC.2018.2872380.

[67] W. Feng et al., "Joint Energy-Saving Scheduling and Secure Routing for Critical Event Reporting in Wireless Sensor Networks," in IEEE Access, vol. 8, pp. 53281-53292, 2020, doi: 10.1109/ACCESS.2020.2981115.

[68] L. Huang, J. Wang, E. Kung, Y. Mo, J. Wu and L. Shi, "Stochastic Event-Based Sensor Schedules for Remote State Estimation in Cognitive Radio Sensor Networks," in IEEE Transactions on Automatic Control, vol. 66, no. 5, pp. 2407-2414, May 2021, doi: 10.1109/TAC.2020.3007510.

[69] Z. Li, J. Xie, H. Zhang, H. Xiang and Z. Zhang, "Adaptive Sensor Scheduling and Resource Allocation in Netted Collocated MIMO Radar System for Multi-Target Tracking," in IEEE Access, vol. 8, pp. 109976-109988, 2020, doi: 10.1109/ACCESS.2020.3001358.

[70] X. Liu, Y. Gao and F. Hu, "Optimal Time Scheduling Scheme for Wireless Powered Ambient Backscatter Communications in IoT Networks," in IEEE Internet of Things Journal, vol. 6, no. 2, pp. 2264-2272, April 2019, doi: 10.1109/JIOT.2018.2889700.

[71] H. Shi, M. Zheng, W. Liang and J. Zhang, "Convergecast Scheduling for Industrial Wireless Sensor Networks With Local Available Channel Sets," in IEEE Sensors Journal, vol. 19, no. 22, pp. 10764-10772, 15 Nov.15, 2019, doi: 10.1109/JSEN.2019.2929672.

[72] Runze Wan, Naixue Xiong and Nguyen The Loc, “An energy-efficient sleep scheduling mechanism with similarity measure for wireless sensor networks”, Human-Centric Computing and Information Sciences, 2018

[73] H. Wang, S. Tan, Y. Zhu and M. Li, "Deterministic Scheduling With Optimization of Average Transmission Delays in Industrial Wireless Sensor Networks," in IEEE Access, vol. 8, pp. 18852-18862, 2020, doi: 10.1109/ACCESS.2020.2968491.

[74] W. Yang, Y. Zhang, C. Yang, Z. Zuo and X. Wang, "Online Power Scheduling for Distributed Filtering Over an Energy-Limited Sensor Network," in IEEE Transactions on Industrial Electronics, vol. 65, no. 5, pp. 4216-4226, May 2018, doi: 10.1109/TIE.2017.2756594.

[75] H. Zhang, J. Xie, J. Shi, Z. Zhang and X. Fu, "Sensor Scheduling and Resource Allocation in Distributed MIMO Radar for Joint Target Tracking and Detection," in IEEE Access, vol. 7, pp. 62387-62400, 2019, doi: 10.1109/ACCESS.2019.2916334.

[76] F. Ait Aoudia, M. Gautier and O. Berder, "RLMan: An Energy Manager Based on Reinforcement Learning for Energy Harvesting Wireless Sensor Networks," in IEEE Transactions on Green Communications and Networking, vol. 2, no. 2, pp. 408-417, June 2018, doi: 10.1109/TGCN.2018.2801725.

[77] Z. J. Chew, T. Ruan and M. Zhu, "Energy Savvy Network Joining Strategies for Energy Harvesting Powered TSCH Nodes," in IEEE Transactions on Industrial Informatics, vol. 17, no. 2, pp. 1505-1514, Feb. 2021, doi: 10.1109/TII.2020.3005196.

[78] J. Hu, J. Luo, Y. Zheng and K. Li, "Graphene-Grid Deployment in Energy Harvesting Cooperative Wireless Sensor Networks for Green IoT," in IEEE Transactions on Industrial Informatics, vol. 15, no. 3, pp. 1820-1829, March 2019, doi: 10.1109/TII.2018.2871183.

[79] M. Koca, G. Gurbilek, B. Soner and S. Coleri, "Empirical Feasibility Analysis for Energy Harvesting Intravehicular Wireless Sensor Networks," in IEEE Internet of Things Journal, vol. 8, no. 1, pp. 179-186, 1 Jan.1, 2021, doi: 10.1109/JIOT.2020.3001992.

[80] T. Ruan, Z. J. Chew and M. Zhu, "Energy-Aware Approaches for Energy Harvesting Powered Wireless Sensor Nodes," in IEEE Sensors Journal, vol. 17, no. 7, pp. 2165-2173, 1 April1, 2017, doi: 10.1109/JSEN.2017.2665680.

[81] C. Wang, J. Li, Y. Yang and F. Ye, "Combining Solar Energy Harvesting with Wireless Charging for Hybrid Wireless Sensor Networks," in IEEE Transactions on Mobile Computing, vol. 17, no. 3, pp. 560-576, 1 March 2018, doi: 10.1109/TMC.2017.2732979.

[82] Y. Xiong, G. Chen, M. Lu, X. Wan, M. Wu and J. She, "A Two-Phase Lifetime-Enhancing Method for Hybrid Energy-Harvesting Wireless Sensor Network," in IEEE Sensors Journal, vol. 20, no. 4, pp. 1934-1946, 15 Feb.15, 2020, doi: 10.1109/JSEN.2019.2948620.

[83] Y. -H. Zhu, S. Gong, K. Chi, Y. Li and Y. Fang, "Optimizing Superframe and Data Buffer to Achieve Maximum Throughput for 802.15.4-Based Energy Harvesting Wireless Sensor Networks," in IEEE Internet of Things Journal, vol. 8, no. 5, pp. 3689-3704, 1 March1, 2021, doi: 10.1109/JIOT.2020.3024615.

[84] U. F. Abbasi, N. Haider, A. Awang and K. S. Khan, "Cross-Layer MAC/Routing Protocol for Reliable Communication in Internet of Health Things," in IEEE Open Journal of the Communications Society, vol. 2, pp. 199-216, 2021, doi: 10.1109/OJCOMS.2020.3047888.

[85] M. Z. Hasan, F. Al-Turjman and H. Al-Rizzo, "Analysis of Cross-Layer Design of Quality-of-Service Forward Geographic Wireless Sensor Network Routing Strategies in Green Internet of Things," in IEEE Access, vol. 6, pp. 20371-20389, 2018, doi: 10.1109/ACCESS.2018.2822551.

[86] M. J. Herrmann and G. G. Messier, "Cross-Layer Lifetime Optimization for Practical Industrial Wireless Networks: A Petroleum Refinery Case Study," in IEEE Transactions on Industrial Informatics, vol. 14, no. 8, pp. 3559-3566, Aug. 2018, doi: 10.1109/TII.2018.2819678.

[87] M. V. Ngo, Q. D. La, D. Leong, T. Q. S. Quek and H. Shin, "User Behavior Driven MAC Scheduling for Body Sensor Networks: A Cross-Layer Approach," in IEEE Sensors Journal, vol. 19, no. 17, pp. 7755-7765, 1 Sept.1, 2019, doi: 10.1109/JSEN.2019.2915635.

[88] S. M. Shimly, D. B. Smith and S. Movassaghi, "Experimental Analysis of Cross-Layer Optimization for Distributed Wireless Body-to-Body Networks," in IEEE Sensors Journal, vol. 19, no. 24, pp. 12494-12509, 15 Dec.15, 2019, doi: 10.1109/JSEN.2019.2937356.

[89] Z. Sun et al., "An Energy-Efficient Cross-Layer-Sensing Clustering Method Based on Intelligent Fog Computing in WSNs," in IEEE Access, vol. 7, pp. 144165-144177, 2019, doi: 10.1109/ACCESS.2019.2944858.

[90] W. Zhang, X. Wei, G. Han and X. Tan, "An Energy-Efficient Ring Cross-Layer Optimization Algorithm for Wireless Sensor Networks," in IEEE Access, vol. 6, pp. 16588-16598, 2018, doi: 10.1109/ACCESS.2018.2809663.

[91] M. Y. Arafat and S. Moh, "Bio-Inspired Approaches for Energy-Efficient Localization and Clustering in UAV Networks for Monitoring Wildfires in Remote Areas," in IEEE Access, vol. 9, pp. 18649-18669, 2021, doi: 10.1109/ACCESS.2021.3053605.

[92] L. Cao, Y. Cai, Y. Yue, S. Cai and B. Hang, "A Novel Data Fusion Strategy Based on Extreme Learning Machine Optimized by Bat Algorithm for Mobile Heterogeneous Wireless Sensor Networks," in IEEE Access, vol. 8, pp. 16057-16072, 2020, doi: 10.1109/ACCESS.2020.2967118.

[93] F. Dai, M. Chen, X. Wei and H. Wang, "Swarm Intelligence-Inspired Autonomous Flocking Control in UAV Networks," in IEEE Access, vol. 7, pp. 61786-61796, 2019, doi: 10.1109/ACCESS.2019.2916004.

[94] M. Faheem et al., "FFRP: Dynamic Firefly Mating Optimization Inspired Energy Efficient Routing Protocol for Internet of Underwater Wireless Sensor Networks," in IEEE Access, vol. 8, pp. 39587-39604, 2020, doi: 10.1109/ACCESS.2020.2976105.

[95] Y. Feng, S. Zhao and H. Liu, "Analysis of Network Coverage Optimization Based on Feedback K-Means Clustering and Artificial Fish Swarm Algorithm," in IEEE Access, vol. 8, pp. 42864-42876, 2020, doi: 10.1109/ACCESS.2020.2970208.

[96] M. Z. Hasan and H. Al-Rizzo, "Optimization of Sensor Deployment for Industrial Internet of Things Using a Multiswarm Algorithm," in IEEE Internet of Things Journal, vol. 6, no. 6, pp. 10344-10362, Dec. 2019, doi: 10.1109/JIOT.2019.2938486.

[97] E. H. Houssein, M. R. Saad, K. Hussain, W. Zhu, H. Shaban and M. Hassaballah, "Optimal Sink Node Placement in Large Scale Wireless Sensor Networks Based on Harris' Hawk Optimization Algorithm," in IEEE Access, vol. 8, pp. 19381-19397, 2020, doi: 10.1109/ACCESS.2020.2968981.

[98] A. Mukherjee, P. Goswami, Z. Yan, L. Yang and J. J. P. C. Rodrigues, "ADAI and Adaptive PSO-Based Resource Allocation for Wireless Sensor Networks," in IEEE Access, vol. 7, pp. 131163-131171, 2019, doi: 10.1109/ACCESS.2019.2940821.

[99] W. Osamy, A. A. El-Sawy and A. Salim, "CSOCA: Chicken Swarm Optimization Based Clustering Algorithm for Wireless Sensor Networks," in IEEE Access, vol. 8, pp. 60676-60688, 2020, doi: 10.1109/ACCESS.2020.2983483.

[100] Z. Wei, M. Li, Z. Wei, L. Cheng, Z. Lyu and F. Liu, "A Novel On-Demand Charging Strategy Based on Swarm Reinforcement Learning in WRSNs," in IEEE Access, vol. 8, pp. 84258-84271, 2020, doi: 10.1109/ACCESS.2020.2992127.

Truck Scheduling Model in the Cross-docking Terminal by using Multi-agent System and Shortest Remaining Time Algorithm

Purba Daru Kusuma
Computer Engineering, Faculty of Electrical Engineering
Telkom University, Bandung, Indonesia

***Abstract*—One most important and critical problem in a cross-docking system is truck scheduling. Many studies in it assumed that the temporary storage is unlimited which is in the real world, the temporary storage is limited. Many studies focus on minimizing total completion time. Meanwhile, studies that focus on minimizing temporary storage are hard to find, although this aspect is very important. Due to its complexity, especially in the cross-docking system with multiproduct characteristics, manual scheduling is almost impossible to achieve its goals. Many studies used several techniques, such as genetic algorithm (GA) and mixed integer programming where these methods are computationally expensive. Based on this problem, in this work, we propose new truck scheduling model in a cross-docking terminal with limited temporary storage constraint. This model is developed by using multi-agent system. The main contribution of this work is proposing the multi-agent-based truck scheduling model with limited temporary storage capacity constraint and temporary truck changeover permit. In it, there are three agents: inbound-trucks scheduler agent, outbound-trucks scheduler agent, and material handler agent. The shortest remaining time (SRT) algorithm is adopted in every agent. Based on the simulation result, this proposed model is proven competitive compared with the existing FIFO based models and integer-programming based model. Compared with the integer-programming model, it creates 41.8 percent lower in maximum inventory level. Compared with the FIFO based model, it creates 52.1 to 55.1 percent lower in maximum inventory level. In total time aspect, it creates 0.2 to 2.2 percent lower than the FIFO based model. It creates 7.2 percent higher in total time compared with the integer-programming based model.**

***Keywords*—Truck scheduling; cross-docking system; multi agent system; shortest remaining time; intelligent supply chain**

I. Introduction

Cross-docking system is one popular supply chain management (SCM) system which is implemented in a distribution center [1,2]. This system is different from the conventional supply chain management system. In the conventional system, the arriving products are stored first in a big warehouse or storage area [1]. Then, these products are sorted and delivered to the customers [1]. Meanwhile, in the cross-docking system, the arriving products from the inbound vehicles will be transferred immediately to the outbound vehicles. The temporary storage is used as a sorting and consolidation area, and it is usually small [2]. In the conventional system, products can stay in the warehouse in days, weeks, or months. In the other side, in the cross-docking system, products are in the terminal usually in less than 24 hours [2].

Based on its characteristics, the cross-docking system has several advantages. The first advantage is improving service level [1] by reducing total completion time [1] in the terminal and delivery time [3,4] so that the products will be delivered to the customers faster. The second advantage is the cross-docking system can reduce the cost of warehousing [3], such as inventory-holding cost [3,4], handling cost [3], transportation cost [3,4], labor cost [3], storage space cost [3], and order picking cost [4]. The third advantage is the cross-docking system may reduce or avoid product quality degradation, or risk of product damage or obsolescence [3], especially for the perishable products due to its less time in a warehouse. Because of its advantages, the cross-docking system has been adopted by some largest chained retailers, such as Walmart, Target, COSTCO, and Auchan [5]. This system has also been adopted by some big shipping companies, such as FedEx, UPS, USPS, and DHL [5].

One important problem in the cross-docking system is the truck scheduling problem. Because the fast-processing time is achieved by transferring the products from the inbound vehicles to the outbound vehicles as immediately as possible, the accuracy of the truck scheduling must be high [1]. This scheduling model means matching the inbound trucks and the outbound trucks which are docked at the doors at the same time [1]. In the cross-docking system, although it usually consists of some doors in both inbound and outbound sides, the number of doors is still less than the number of vehicles [1]. Because of its complexity, many studies used computational solution to solve this problem because this problem is almost impossible to be solved manually. Many studies used integer programming method [5-7]. Other studies also used metaheuristic method [8], such as genetic algorithm [1,3] due to its characteristics as a combinatorial solution. Meanwhile, some other studies implemented FIFO method [4,7] in one side (inbound or outbound).

There are several problems due to these existing studies in modeling the truck scheduling in the cross-docking system. First, many studies assumed that the temporary storage is unlimited [1,9,10]. This assumption was taken because in these previous models, every vehicle (usually truck) will be docked at the door until it completes its process. For the inbound truck, completion means that all carried products have been unloaded. Meanwhile, for the outbound truck, completion means that all requested products have been loaded. By reducing temporary changeover potential during loading and unloading process, the total completion time can be minimized. Unfortunately, in the real world, the temporary storage has limited capacity. Second, implementing metaheuristic or integer programming methods is a resource consuming process because of its computationally expensive characteristics.

Based on these problems, this work aims to propose truck scheduling model in the cross-docking system with the constraint is a limited temporary storage capacity. In this work, the inbound and outbound vehicles are trucks with same size or identical. Due to this constraint, in our work, temporary truck changeover is permitted. The objective of our proposed model is minimizing the total time and the inventory level.

This model is developed by using multi-agent system. This method is adopted due to the characteristics of the truck scheduling in the cross-docking system consists of three sub systems: inbound trucks scheduling, material handling, and outbound trucks scheduling. In every sub system, the shortest remaining time algorithm is adopted rather than metaheuristic method so that this process is computationally light.

This work has several novelties. These novelties are as follows.

- The new multi agent-based truck scheduling is proposed where the inbound scheduling, outbound scheduling, and material handling processes are conducted autonomously.
- The limited temporary storage capacity is applied in this model.
- The temporary truck changeover is allowed. It means that the trucks can be shifted temporarily during its loading or unloading process when other trucks are more available.

This paper is organized as follows. In the first section, the background, problem, research purpose, novelty, and paper organization are explained. In the second section, the latest previous works in truck scheduling are explored. In the third section, the proposed model is described. In the fourth section, the simulation, result, and findings are discussed. In the fifth section, the main result of this work related to the research purpose is concluded.

II. Related Works

Cross-docking system is a supply chain system that is popular in a distribution center [1,2]. In it, the incoming products are directly transferred from the incoming vehicles to the outcoming vehicles without storing them [2]. This mechanism is different from the conventional or traditional distribution center. In the conventional one, the incoming products are stored in the warehouse first. Then, when there is request or order for these products, they are packed and then sent to the customers. In this conventional way, the activities include receiving, storing, order picking, and shipping [2]. These stages occur due to the mismatch in supply and demand which usually happens in the conventional system. Different from it, in the cross-docking system, precise synchronization of the inbound and outbound vehicles plays critical role [2]. Besides, although it is almost impossible to be achieved, perfect synchronization between supply and demand is very important. That is why there are many studies in the cross-docking system that assumed that supply and demand are equal [11].

The performance of the cross-docking system can be divided into two aspects: design aspect and operational aspect [1]. The design aspects include location, terminal layout, number of docks, and temporary storage capacity [1]. Meanwhile, the operational aspects include sorting, consolidation, and truck scheduling [1]. The structure of the cross-docking terminal can be I-shape, X-shape, L-shape, or T-shape [10]. The illustration of the cross-docking terminal is shown in Fig. 1.

The scenario of the cross-docking system is usually as follows [1]. The cross-docking terminal consists of multiple receiving (inbound) docks and multiple shipping (outbound) docks. Inside the terminal, there are sorting and consolidating facilities, and temporary storage. The inbound trucks arrive and then are assigned to any available (empty) inbound dock. If there is not any available inbound dock, then, this truck should wait until at least one inbound dock is available. When a truck arrives in an inbound dock, then it unloads all the products it carries. After the unloading process completes, this truck then leaves the dock as soon as possible so that this dock can be used by other trucks. In the sorting and consolidating facilities, the unloaded products are split and merged with other products that are carried by other trucks. Then, they are loaded to the designated outbound trucks. After the loading process completes, this outbound truck also leaves the area as soon as possible so that this outbound dock can be used by other outbound trucks.

In the cross-docking system, temporary storage is needed to store the unloaded products that are not needed by the current docked outbound trucks but will be loaded to the future outbound trucks. The unloaded products usually stay in the temporary storage no more than 24 hours [1,2]. If they stay longer than 24 hours, then the system cannot be called as cross-docking system [2].

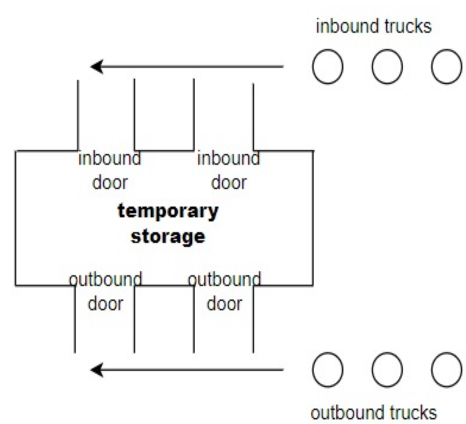

Fig. 1. Cross-docking Terminal.

There are many studies that are conducted in the truck scheduling in the cross-docking system. It is because truck scheduling plays important role to achieve the main goal of the cross-docking system. The objective of the most studies is minimizing the total time [8-10]. Besides, several other objectives are minimizing total cost [10,11], additional penalty [11] and delivery cost [7], flow time [12], processing time [12], tardiness of the outbound trucks [12], waiting time [10,13], completion time [1], inventory level [14], total product stay time [14], and total truck loading and unloading time [12]. Most of studies assumed that the temporary storage is unlimited [1,9,10] although it is impossible to be implemented in the real world. Several methods that were used are FIFO [4,7], integer programming [5-7], and genetic algorithm [1,3]. Most of studies conducted single inbound dock and single outbound dock [1,4]. Meanwhile, other studies conducted multiple inbound docks and multiple outbound docks.

Yu, Ha, and Park [1] used genetic algorithm in arranging the sequence of the inbound and outbound trucks. In their work, the goal is minimizing the maximum completion time. In it, the cross-docking terminal consists of multiple inbound docks and multiple outbound docks. The temporary storage was assumed unlimited. The simulation process consisted of 8 receiving docks, 8 shipping docks, 20 inbound trucks, 30 outbound trucks, 18 product types, 8,460 unit of products. The changeover time was assumed 75 time-units while the product moving times was assumed 100 time-units.

Issi, Linfati, and Escobar [2] used mixed-integer linear programming to solve this scheduling problem. This work aimed to minimize total time (makespan). This work used a multinational food company in Chile as a study case. In it, the products routing was excluded in the scheduling algorithm. Meanwhile, they proposed that warehouse tasks and vehicle routing problem should be included in the scheduling model for the future research potential.

Mohammadzadeh, Sahebjamnia, Fathollahi-Fard, and Hahiaghaei-Keshteli [8] focused on optimizing the total time in the truck scheduling in the cross-docking system. In this work, they used and compared three nature inspired metaheuristic models: red deer algorithm (RDA), virus colony search (VCS), and water wave optimization (WWO).

Lee, Lim, and Ko [11] used endosymbiotic evolutionary algorithm to solve the vehicle routing and truck scheduling problem in the cross-docking system. This work aimed to minimize the total cost. In it, the truck scheduling is integrated with the vehicle routing. This work implemented zero temporary storage. All vehicles are assumed identical. Tardiness or earliness is allowed with some penalty. The changeover time is fixed.

Fathollahi-Fard, Ranjbar-Bourani, Cheikhrouhou, and Hajiaghaei-Kesthteli [9] used social engineering optimizer algorithm to solve the truck scheduling problem in a cross-docking system. The cross-docking facility has I-shaped structure. The assumption was that all trucks are available at time zero. The changeover time is same for all vehicles. The temporary storage is unlimited.

Dulebenets [5] combined the diploid evolutionary algorithm with the mixed integer mathematical model to solve the truck scheduling in the cross-docking system. In this work, temporary storage was assumed unlimited. Rather than all trucks are available at time zero, in this work, each truck was expected arrives in certain time with zero arrival time.

Molavi, Shahmardan, and Sajadieh [7] used FIFO method in the loading mechanism in the truck scheduling in a cross-docking system. Meanwhile, the mixed-integer programming is used in the unloading mechanism. This work aimed to minimize the total cost due to the penalty and additional delivery cost because of the delayed shipment.

Larbi, Alpan, Baptiste, and Penz [4] used FIFO method in the truck scheduling in the cross-docking system. As FIFO is implemented strictly in the inbound side, the arrangement was conducted in the outbound side. This work aimed to minimize the total cost. This work implemented three scenarios. First, the system has complete and precise information about the order and the contents of the inbound trucks. Second, the system does not have the information of the incoming trucks but only knows the daily quantities of the products that must be shipped to every destination. Third, the inbound trucks sequence is known but the information of the content is only known after the inbound truck arrives to the receiving dock.

TABLE I. PREVIOUS WORKS SUMMARY

Authors	**Objective Parameters**	**Method**
Yu, Ha, and Park [1]	total completion time	genetic algorithm
Issi, Linfati, and Escobar [2]	total completion time	mixed integer programming
Mohammadzadeh, Sahebjamnia, Fathollahi-Fard, and Hahiaghaei-Keshteli [8]	total completion time	red deer algorithm. virus colony search algorithm
Lee, Lim, and Ko [11]	total completion time	evolutionary algorithm
Dulebenets [5]	total completion time	evolutionary algorithm
Molavi, Shahmardan, and Sajadieh [7]	total cost	first-in-first-out
Larbi, Alpan, Baptiste, and Penz [4]	total cost	first-in-first-out
Fathollahi-Fard, Ranjbar-Bourani, Cheikhrouhou, and Hajiaghaei-Keshteli [9]	total completion time	social engineering optimizer
Chargui, Bekrar, Reghioui, and Trentesaux [6]	energy consumption, total cost	simulated annealing, tabu search
Khorasani, Keshtzari, Islam, and Feizi [15]	delivery lead time	mixed integer linear programming
Ye, Li, Li, and Fu [16]	total completion time	particle swarm optimization

The summary of these previous works is shown in Table I. Based on this summary, it is shown that most of the studies in the truck scheduling in the cross-docking system focused on minimizing the total completion time. The other objective is minimizing total cost. Unfortunately, Research which their objective is maintaining the inventory level in the temporary storage is not popular although the temporary storage becomes important part in the cross-docking system. Based on it, this work, which focuses on minimizing the inventory level while maintaining low total time becomes very relevant.

III. Proposed Model

In this work, we propose a truck scheduling model that is implemented for the cross-docking terminal based on multi agent system. Its objective is to minimize the inventory level and the total completion time. It is developed by combining the multi-agent system and shortest remaining time algorithm. This cross-docking system implements single-inbound-single-outbound. Multiple products are handled in this system. There is temporary storage capacity constraint.

The detailed assumptions in the proposed model are as follows. The terminal has one inbound door for receiving and one outbound door for shipping [4]. The temporary storage has limited capacity [13]. This is a multiproduct logistic system so that it handles multiple products with various quantity [1]. The inbound trucks carry products from suppliers. The outbound trucks carry products to be delivered to customers. Each truck, either inbound or outbound, carries several products. All trucks have same capacity [11]. The inbound trucks carry less products, but the quantity of each product is higher. The outbound trucks carry more products, but the quantity of each product is less. As a just-in-time model, the total amount of the received products is equal to the shipped products in both product variation and quantity [11]. It is guaranteed that the temporary storage is empty in the end of scheduling process. In the beginning of the scheduling process, all inbound trucks and outbound trucks has been arriving in the cross-docking terminal [9].

This proposed model is developed by using multi agent system. Wooldridge defined an agent as a software or entity that can observe its environment, make decision, and perform actions that affect its environment and its own or other agents' internal states [17]. As a multi agent system, this model consists of three agents: inbound trucks scheduler agent, outbound trucks scheduler agent, and material handler agent. Every agent cannot be interfered or subordinated by other agent based on the autonomous concept of the multi agent system [18]. The role of the inbound-trucks scheduler is to conduct the inbound-trucks traffic flow in the cross-docking terminal. The role of the outbound-trucks scheduler is to conduct the outbound-trucks traffic flow in the cross-docking terminal. The role of the material handler is to organize the material flow among inbound truck, outbound truck, and temporary storage. This model is illustrated in Fig. 2. As an agent-based model, each agent has its own goal that must be achieved which is explained later. These three agents are developed as rule-based agents since they behave based on specific rules or mechanisms [19]. This rule-based concept is chosen due to its simplicity as a collection of conditional statements which is stored and selected based on the condition to achieve better performance [20].

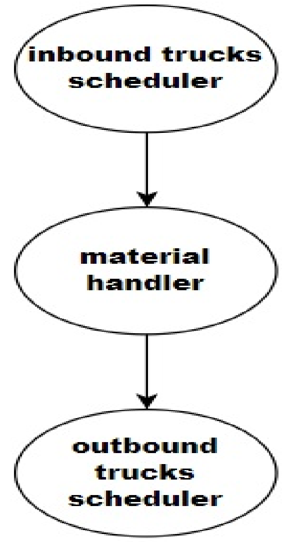

Fig. 2. Multi Agent Architecture in the Cross-docking System.

The explanation of Fig. 2 is as follows. The inbound trucks scheduler arranges the inbound truck sequence or traffic based on the temporary storage and outbound door condition. Then, the material handler has responsibility in managing product traffic among inbound door, outbound door, and temporary storage. Finally, the outbound trucks scheduler arranges the outbound truck sequence or traffic based on the temporary storage and inbound door condition. These three agents work autonomously but share information among them.

Before we explain further, the notations used in this model are as follows.

i	inbound truck index
j	outbound truck index
n_{pv}	product variety
p	product
P	set of products
q_{av}	available quantity
q_{re}	requested quantity
s	Status
s_{so}	inbound-outbound contribution status
s_{sw}	inbound-storage contribution status
t_i	inbound truck
t_{is}	selected inbound truck
t_o	outbound truck
t_{os}	selected outbound truck
w	temporary storage
Δ	gap

The mechanism of the inbound-trucks scheduler is as follows. When the inbound door is empty, the inbound-truck scheduler will check whether there exists inbound truck in the queue then determine this truck to go to the inbound door. When there are several inbound trucks in the queue, then the scheduler will decide which truck is assigned to the door for docking process. During the docking process, this inbound truck unloads its products sequentially. If this inbound truck cannot unload its products but still has products inside it, this truck will be assigned back to the queue. This policy is taken due to the limited capacity of the temporary storage. This concept is different from other previous studies about cross-docking where the inbound truck will stay at the outbound door until all the carried products are completely unloaded to the outbound trucks or the temporary storage [1]. When all the carried products have been unloaded, this truck will leave the inbound door immediately [1]. The activities of the inbound truck are illustrated in Fig. 3. Meanwhile this mechanism is formalized by using (1) to (6). This process can also be seen in algorithm 1.

algorithm 1: inbound trucks scheduler

```
while inbound queue > 0 do
  find the fittest inbound truck
  if unloading is possible then
  unloading
  else
  if truck payload > 0 then
   back to queue
  else
   leave the system
  end if
  end if
end while
```

$$s(t_i) = \begin{cases} 0, t_i \neq t_{is} \wedge q_{av}(t_i) > 0 \\ 1, t_i = t_{is} \\ 2, t_i \neq t_{is} \wedge q_{av}(t_i) = 0 \end{cases} \tag{1}$$

$$t_{is} = \begin{cases} min(\Delta(t_i, t_{os})), \exists t_{os} \\ max\left(n_{pv}(t_i, w)\right), \nexists t_{os} \end{cases} \tag{2}$$

$$\Delta(t_i, t_{os}) = \sum_{p \in P} \Delta\left(q_{av}(t_{i,p}), q_{re}(t_{os,p})\right) \tag{3}$$

$$\Delta\left(q_{av}(t_{i,p}), q_{re}(t_{os,p})\right) = \begin{cases} q_{re}(t_{os,p}) - q_{av,p}, q_{re}(t_{os,p}) > q_{av,p} \\ 0, else \end{cases} \tag{4}$$

$$q_{av,p} = q_{av}(t_i, p) + q_{av}(w_p) \tag{5}$$

$$n_p(t_i, w) = \sum_{p \in P} p, q_{av}(t_{i,p}) > 0 \wedge q_{av}(w_p) = 0 \tag{6}$$

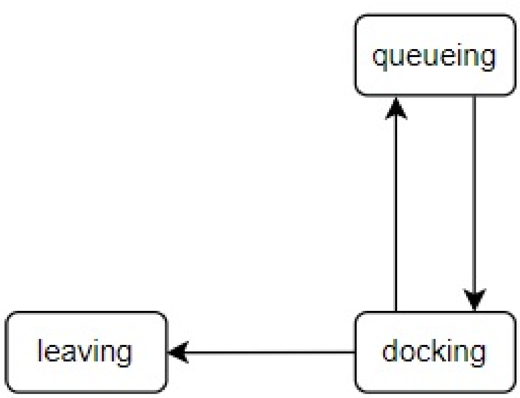

Fig. 3. Inbound Truck State Diagram.

Equation (1) shows that there are three possible values of the inbound truck status. Status 0 indicates the inbound truck is in the queue. Status 1 indicates that the inbound truck is at the inbound door. Status 2 indicates that the inbound truck leaves the cross-docking system.

Equation (2) shows that there are two options in determining the selected inbound truck. It depends on whether there exists outbound truck at the outbound dock. In case there exists an outbound truck at the outbound dock, the shortest remaining time scheduling is adopted so that the outbound truck can be served as fast as possible. The shortest remaining time scheduling method is chosen due to its characteristics that prioritize the fastest job that can be executed due to current condition [21]. It is done by choosing the most suit inbound truck that can provide the selected outbound truck. In case there does not exist an outbound truck at the outbound dock, the pre-emptive of the shortest remaining time is adopted. It is done by selecting the most suit inbound truck that can improve the product variety in the temporary storage. Higher product variety may improve product movement possibility [22].

The explanation of (3) to (6) is as follows. Equation (3) shows that the gap between the inbound truck and the selected outbound trucks is accumulation of all products. Eq. (4) shows that the gap is calculated only if the quantity of the requested products in the selected outbound truck is more than the quantity of the available product. Equation (5) shows that the available product is the accumulation of products in the inbound truck and the temporary storage. Equation (6) formalized the calculation of the number of product variation in the temporary storage that can be supported by the inbound truck. The result of (6) is used in (2).

The inbound truck still stays at the inbound door only if it can contribute to the cross-docking terminal. First, this truck still has product in its container. Empty truck cannot contribute so that it must leave the inbound door immediately. If there is selected outbound truck, this inbound truck must have product needed by the selected outbound truck. If there does not exist selected outbound truck, then the inbound truck still can contribute only if the temporary storage current capacity is still less than its maximum capacity. This mechanism is formalized by using (7) to (9).

$$s(t_{is}) = \begin{cases} 1, s_{so}(t_{is}) = 1 \vee s_{sw}(t_{is}) = 1 \\ 0, else \end{cases} \tag{7}$$

$$s_{so}(t_{is}) = \begin{cases} 1, \exists t_{os} \wedge \exists(q_{av}(t_{is}, p) > 0 \wedge q_{re}(t_{os}, p) > 0) \\ 0, else \end{cases} \tag{8}$$

$$s_{sw}(t_{is}) = \begin{cases} 1, \nexists t_{os} \wedge \exists\left(q_{av}(t_{is}, p)\right) \wedge q(w) < q_{max}(w) \\ 0, else \end{cases} \tag{9}$$

The explanation of (7) to (9) is as follows. Equation (7) formalizes the selected inbound truck status, whether it still can contribute or not. It depends on two aspects. The first aspect is whether it still can contribute to the selected outbound truck, which is formalized in (8). The second aspect is whether it still can contribute to the temporary storage which is formalized in (9).

The mechanism of the outbound-trucks scheduler is as follows. When the outbound door is empty, the outbound truck scheduler will check whether there exists an outbound truck in the queue so that it can move to the outbound door. If there are several outbound trucks in the queue, then selection process runs. The scheduler selects the most possible truck to be provided by the temporary storage without observing whether there exists an inbound truck at the inbound door. This flow is illustrated in Fig. 4 and algorithm 2.

algorithm 2: outbound trucks scheduler

```
while outbound queue > 0 do
  find the fittest outbound truck
  loading
  leave the system
end while
```

This concept is adopted based on the shortest remaining time scheduling [21]. Different from the inbound truck which can be transferred back to the queue, once the outbound truck is in the outbound door, it remains there until all its requested products are fulfilled [1]. Once all its requested products are fulfilled, this outbound truck then leaves the cross-docking system [1]. This mechanism is formalized by using (10) to (13).

$$s(t_o) = \begin{cases} 0, t_0 \neq t_{os} \wedge q_{re}(t_o) > 0 \\ 1, t_o = t_{os} \\ 2, t_o \neq t_{os} \wedge q_{re}(t_o) = 0 \end{cases} \quad (10)$$

$$t_{os} = t_o, min\big(\Delta(t_o, w)\big) \quad (11)$$

$$\Delta(t_o, w) = \sum_{p \in P}\big(q_{re}(t_{is,p}) - q_{av}(w_p)\big), q_{re}(t_{is,p}) > q_{av}(w_p) \quad (12)$$

$$s(t_{os}) = \begin{cases} 1, \exists q_{re}(t_{os}) > 0 \\ 0, else \end{cases} \quad (13)$$

The explanation of (10) to (13) is as follows. Equation (10) shows that there are three possible values of the outbound truck. Status 0 indicates that the outbound truck is in the queue. Status 1 indicates that the outbound truck is at the outbound door. Status 2 indicates that the outbound truck leaves the cross-docking system. Equation (11) and (12) indicate that the selected outbound truck is the outbound truck with the minimum gap between its requested products and the available products in the temporary storage. Equation (14) shows that the selected outbound truck is still active until its request is completely fulfilled.

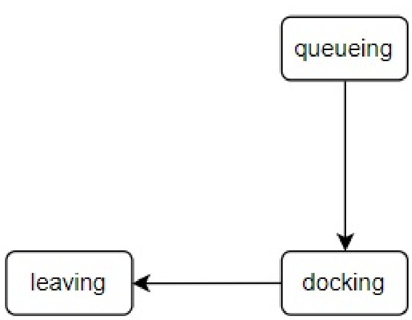

Fig. 4. Outbound Truck State Diagram.

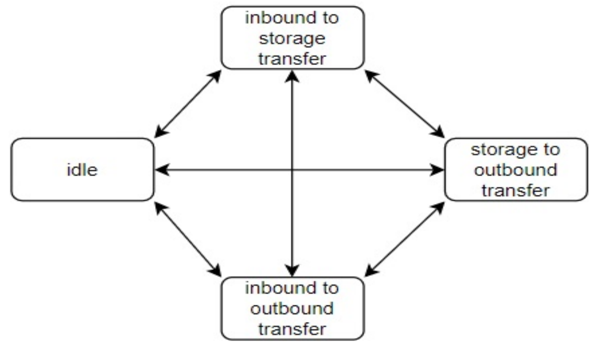

Fig. 5. Material Handling State Diagram.

The primary goal of the material handler agent is serving the selected outbound truck as fast as possible. Meanwhile, the secondary goal is transferring the products in the inbound truck container as fast as possible while maintaining low temporary storage or inventory level [14] so that it is not exceeded. It means that the material scheduler observes the existence of the selected outbound truck first before the selected inbound truck. Fig. 5 illustrates the product movement in the cross-docking terminal.

The material scheduler prioritizes to fulfill the outbound truck request from the inbound truck [2] rather than from the temporary storage so that the container of the inbound truck will be empty faster so that the waiting time in the inbound queue can be minimized [13]. The request is fulfilled by the temporary storage only if the request cannot be fulfilled by the inbound truck. If there does not exist an outbound truck in the outbound door, the product moves from the selected inbound truck to the temporary storage only if its current capacity is still less than its maximum capacity. This mechanism is formalized by using (15). This process is also formalized in algorithm 3.

algorithm 3: material handler

```
if inbound-to-outbound is possible then
  move product from inbound to outbound
else
  if storage-to-outbound is possible then
  move product from storage to outbound
  else
  if inbound-to-storage is possible then
   move product from inbound to storage
  else
   idle
  end if
  end if
end if
```

$$A(w) = \begin{cases} m(t_{is}, t_{os}), \exists t_{is} \wedge \exists t_{os}, \exists\big(q_{av}(t_{is,p}) > 0 \wedge q_{re}(t_{os,p}) > 0\big) \\ m(w, t_{os}), \nexists t_{is} \wedge \exists t_{os}, \exists\big(q_{av}(w_p) > 0 \wedge q_{re}(t_{os,p}) > 0\big) \\ m(t_{is}, w), \exists t_{is} \wedge \nexists t_{os} \wedge q(w) < q_{max}(w) \end{cases} \quad (15)$$

IV. Result and Discussion

This proposed model is then implemented into truck scheduling simulation so that its performance can be evaluated. In this simulation, there are two observed variables: total time and maximum inventory level. Total time is one of the most important operational parameters in the cross-docking system. It is also widely observed in many studies [2,8-10]. Maximum inventory level is observed due to one of the goals in implementing cross-docking system is reducing inventory level [14]. In this simulation, this proposed multi agent based (MAS) model is compared with three previous truck scheduling models: inbound FIFO (I-FIFO) model [4], outbound-FIFO-integer programming (O-FIFO-IP) model [7], and mixed-integer programming (MIP) model [2]. In this work, there are three simulations. The first simulation is conducted to observe the relation between the changeover time and the observed parameters. The second simulation is conducted to observe the relation between the maximum storage capacity and the total time. The third simulation is conducted to observe the relation between the number of trucks and the total time per truck.

In this simulation, there are several default variables. These default variables are applied in these three simulations. The number of products is 20 units. The average number of products carried by the inbound trucks is 5 units. The average number of products carried by the outbound trucks is 10 units. The products distribution in every truck follows normal distribution. The truck capacity is 50 units. The product moving time is 1 time-unit. In this work, the time-unit is used as unit for time related variables, such as total time and changeover time, to generalize the simulation.

In the first simulation, we observe the relation between changeover time and the observed variables. The reason is that the changeover time affects the total time so that in several studies, the truck stays at the dock until it completes its work [1,2]. In this simulation, the number of inbound trucks is 4 units. The number of outbound trucks is 4 units. The temporary storage capacity is 50 units. The changeover time ranges from 5 to 15 time-unit. The result is shown in Fig. 6 and Fig. 7.

Fig. 6 shows that the increasing of the changeover time makes the total time increases. This trend tends to be linear. This trend occurs in all models. Compared among models, the proposed model is competitive enough. The MIP model [2] performs as the best model in creating low total time. Compared with the MIP model, the proposed model performs 7.2 percent higher in total time. Meanwhile, compared with the I-FIFO [4] and the O-FIFO-IP [7] models, the proposed model performs better. Compared with the I-FIFO model [4], the proposed model performs 2.2 percent lower in total time. Compared with the O-FIFO-IP model, the proposed model performs 0.2 percent lower in total time.

The explanation of Fig. 7 is as follows. The increasing of the changeover time increases the maximum inventory level in all previous works [2,4,7]. Meanwhile, in the proposed model, the maximum inventory level does not change. Compared with the previous models, the proposed model performs as the best model in minimizing the maximum inventory level. Compared with the I-FIFO model [4], it performs 55.1 percent lower. Compared with the O-FIFO-IP model [7], it performs 52.1 percent lower. Compared with the MIP model [2], it performs 41.8 percent lower.

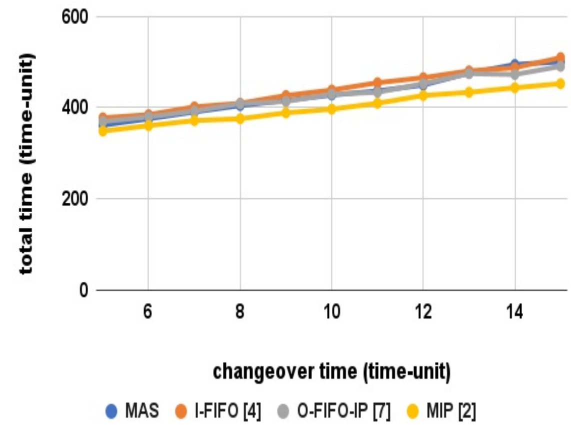

Fig. 6. Relation between Changeover Time and Total Time.

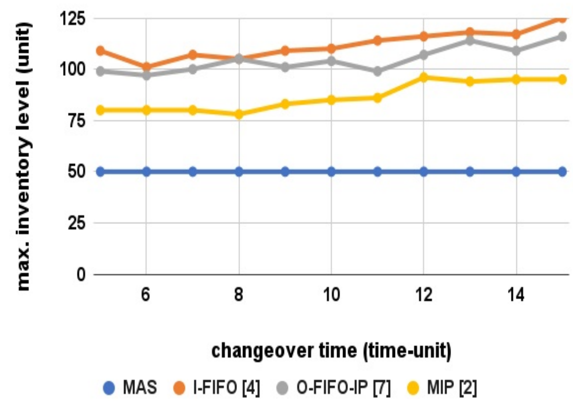

Fig. 7. Relation between Changeover Time and Maximum Inventory Level.

In the second simulation, we observe the relation between the temporary storage capacity and the observed variables. In this simulation, the number of inbound trucks is 4 units. The number of outbound trucks is 4 units. The changeover time is 5 time-unit. The temporary storage capacity ranges from 50 to 100 units. The result is shown in Fig. 8 and Fig. 9. This simulation occurs only for the proposed model because in the compared models [2,4,7], the temporary storages capacity does not become a constraint. The simulation result is then compared with the previous compared models.

Fig. 8 shows that in the proposed model, the increasing of the temporary storage capacity does not affect the total time. The total time tends to be stable. The total time ranges from 353 time-unit to 366 time-unit with the average value is 358.7 time-unit. Compared with the previous models, the proposed model is still worse than the MIP model [2] but better than the I-FIFO [4] and the O-FIFO-IP [7] models.

Fig. 9 shows that in the proposed model, the increasing of the temporary storage capacity makes the maximum inventory level increase too. When the temporary storage capacity ranges from 50 to 65 units, the maximum inventory level is equal to the temporary storage capacity. After that the maximum inventory level still increases but it is below the temporary storage capacity.

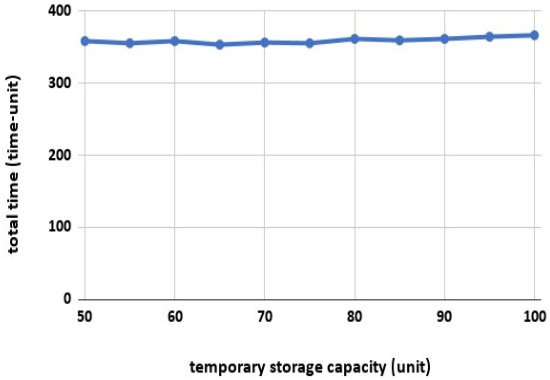

Fig. 8. Relation between Temporary Storage Capacity and Total Time.

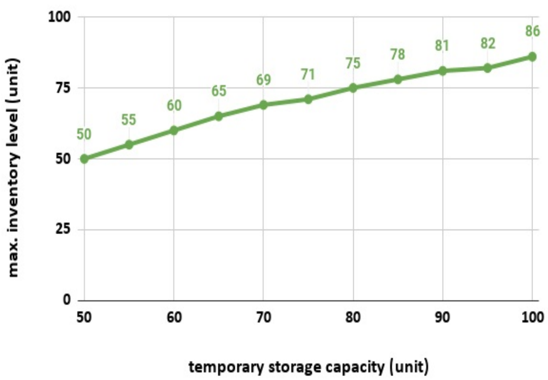

Fig. 9. Relation between Temporary Storage Capacity and Maximum Inventory Level.

Comparison between the proposed model and the previous models is as follows. Compared with the previous models [2,4,7], when the temporary storage capacity is high (100 units), the proposed model still performs as the best model in creating low maximum inventory level. Compared with the I-FIFO model [4], it performs 31.2 percent lower. Compared with the O-FIFO-IP model [7], it performs 25.8 percent lower. Compared with the MIP model [2], it performs 10.4 percent lower.

In the third simulation, we observe the relation between the number of trucks and the total time per truck. In this simulation, the changeover time is 5 time-unit. The temporary storage capacity is 50 units. The number of inbound or outbound trucks ranges from 5 to 15 units. The result is shown in Fig. 10.

Fig. 10 shows that the increasing of the number of trucks makes average total time per truck increase too. It is because the scheduling becomes more complicated. Fortunately, this increasing is not significant. When the number of inbound or outbound trucks increases 100 percent (from 5 units to 10 units), the total time per truck increases only 8.8 percent. Meanwhile, when the number of inbound and outbound trucks increases 200 percent (from 5 to 15 units), the total time per truck increases only 10.9 percent. It means that the waiting time also increases with low inclination due to the increasing of the number of inbound or outbound trucks.

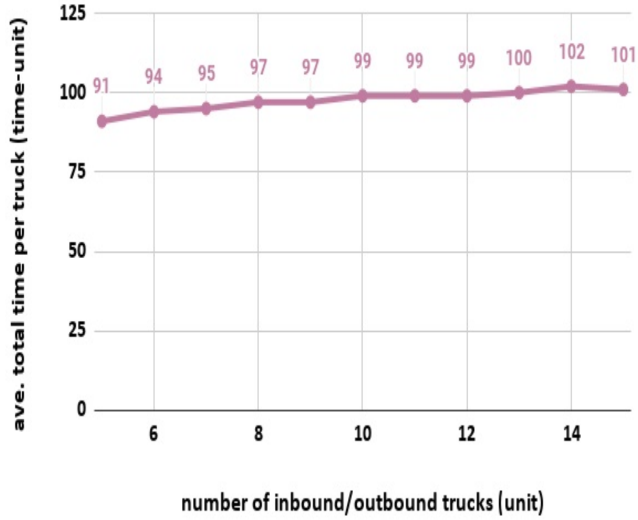

Fig. 10. Relation between Number of Inbound or Outbound Trucks and Average Total Time per Truck.

Based on the result, there are several findings due to this work. First, overall, our proposed model performs as the best model in creating low inventory level as it is one of goals in the cross-docking system [14]. Second, our proposed model is still competitive in creating low total time as it is the main goal of the cross-docking system in making efficient and fast processing mechanism [2,8-10]. The integer programming model still performs as the best model in finding optimal solution [23]. The problem in implementing the integer programming is its computationally expensive due to its polynomial time algorithm characteristic [23]. In the other side, the shortest remaining time algorithm that is adopted in our proposed model is a linear time algorithm so that our proposed model is computationally lighter than the integer programming-based truck scheduling model.

The third finding is that our proposed model still creates low waiting time due to the increasing of the number of trucks because the total time per truck increases but with low inclination. This condition also related with one of the goals of the cross-docking system in minimizing waiting time [10,13].

V. Conclusion

This work shows that the proposed model, which is developed by using multi-agent system and shortest remaining time algorithm, can solve the truck scheduling problem in the cross-docking system. It is proven competitive compared with the existing FIFO based model and integer-programming based model. This proposed model performs as the best model in creating low inventory level. Compared with the integer-programming model, it creates 41.8 percent lower in maximum inventory level. Compared with the FIFO based model, it creates 52.1 to 55.1 percent lower in maximum inventory level. In total time aspect, it creates 0.2 to 2.2 percent lower than the FIFO based model. Although this proposed model creates 7.2 percent higher in total time compared with the integer-programming based model, it is computationally lighter due to its complexity is linear time rather than the integer-programming based model that its complexity is polynomial time. In this proposed model, the waiting time increases with low inclination due to the increasing of the number of trucks.

This work has proposed new truck scheduling model in the cross-docking system by using multi-agent system. In the future, the multi-agent system can be implemented in the cross-docking system not only for the truck scheduling. Moreover, it can be implemented in the material handling and forklift management. Forklift management can be modeled as a swarm robot with collaborative approach. This work uses single-inbound-single-outbound scenario. In the future, it can also be expanded into multiple doors where each door is treated as an autonomous agent and there is collaboration among the doors.

ACKNOWLEDGMENT

This work was supported by Telkom University, Indonesia.

REFERENCES

[1] W. Yu, C. Ha, and S. Park, “A hybrid genetic algorithm for integrated truck scheduling and product routing on the cross-docking system with multiple receiving and shipping docks”, Mathematical Problems in Engineering, article ID: 2026834, pp. 1-17, 2021.

[2] G. C. Issi, R. Linfati, and J. W. Escobar, “Mathematical optimization model for truck scheduling in a distribution center with a mixed service-mode dock area”, Journal of Advanced Transportation, article ID: 8813372, pp. 1-13, 2020.

[3] R. K. Mavi, M. Goh, N. K. Mavi, F. Jie, K. Brown, S. Biermann, and A. A. Khanfar, “Cross-docking: a systematic literature review”, Sustainability, vol. 12, article ID: 4789, 2020.

[4] R. Larbi, G. Alpan, P. Baptiste, and B. Penz, “Scheduling cross docking operations under full, partial, and no information on inbound arrivals”, Computers & Operations Research, vol. 38, pp. 889-900, 2011.

[5] M. A. Dulebenets, “A diploid evolutionary algorithm for sustainable truck scheduling at a cross-docking facility”, Sustainability, vol. 10, article ID: 1333, 2018.

[6] T. Charqui, A. Bekrar, M. Reghioui, and D. Trentesaux, “Multi-objective sustainable truck scheduling in a rail-road physical internet cross-docking hub considering energy consumption”, Sustainability, vol. 11, article ID: 3127, 2019.

[7] D. Molavi, A. Shahmardan, M. S. Sajadieh, “Truck scheduling in a cross docking systems with fixed due dates and shipment sorting”, Computer & Industrial Engineering, vol. 117, pp. 29-40, 2018.

[8] H. Mohammadzadeh, N. Sahebjamnia, A. M. Fathollahi-Fard, and M. Hahiaghaei-Keshteli, “New approached in metaheuristics to solve the truck scheduling problem in a cross-docking center”, International Journal of Engineering-Transactions B: Applications, vol. 31, no. 8, pp. 1258-1266, 2018.

[9] A. M. Fathollahi-Fard, M. Ranjbar-Bourani, N. Cheikhrouhou, and M. Hajiaghaei-Keshteli, “Novel modifications of social engineering optimizer to solve a truck scheduling problem in a cross-docking system”, Computer & Industrial Engineering, vol. 137, article ID: 106103, 2019.

[10] O. Theophilus, M. A. Dubelenets, J. Pasha, O. F. Abioye, and M. Kavoosi, “Truck scheduling at cross-docking terminals: a follow-up state-of-the-art review”, Sustainability, vol. 11, article ID: 5245, 2019.

[11] K. Y. Lee, J. S. Lim, and S. S. Ko, “Endosymbiotic evolutionary algorithm for an integrated model of the vehicle routing and truck scheduling problem with a cross-docking system”, Informatica, vol. 30, no. 3, pp. 481-502, 2019.

[12] N. Boysen, “Truck scheduling at zero-inventory cross docking terminals”, Computer and Operations Research, vol. 37, no. 1, pp. 32-41, 2010.

[13] K. L. Choy, H. K. H. Chow, T. C. Poon, G. T. S. Ho, “Cross-dock job assignment problem in space-constrained industrial logistics distribution hubs with a single docking zone”, International Journal of Production Research, vol. 50, no. 9, pp. 2439-2450, 2012.

[14] A. L. Ladier and G. Alpan, “Cross-docking operations: current research versus industry practice”, Omega, vol. 62, pp. 145-162, 2016.

[15] S. T. Khorasani, M. Keshtzari, M. S. Islam, and R. Feizi, “Intravenous fluid delivery time improvement: application of cross-docking system”, International Journal of Health Care Quality Assurance, vol. 31, no. 8, pp. 1070-1081, 2018.

[16] Y. Ye, J. Li, K. Li, & H. Fu, “Cross-docking truck scheduling with product unloading/loading constraints based on an improved particle swarm optimisation algorithm”, International Journal of Production Research, Vol. 56, no. 16, pp. 5365-5385, 2018.

[17] M. Wooldridge, An Introduction to MultiAgent Systems, 2nd ed., John Wiley & Sons, 2009.

[18] K. M. Lhaksmana, Y. Murakami, and T. Ishida, “Role-based modeling for designing agent behavior in self-organizing multi-agent systems”, International Journal of Software Engineering and Knowledge Engineering, vol. 28, no. 1, pp. 79-96, 2018.

[19] J. Dietrich, A. Kozlenkov, M. Schroeder, and G. Wagner, “Rule-based agents for the semantic web”, Electronic Commerce Research and Applications, vol. 2, no. 4, pp. 323-338, 2003.

[20] Sugiyanto, G. Fernando, and W. K. Tai, “A rule-based AI method for an agent playing big two”, Applied Sciences, vol. 11, article ID: 4206, pp. 1-23, 2021.

[21] M. L. Pinedo, Scheduling: Theory, Algorithms, and Systems, 3rd ed., Springer, New York, 2008.

[22] T. J. van Kampen, D. P. van Donk, and D. J. van der Zee, “Safety stock or safety lead time: coping with unreliability in demand and supply”, International Journal of Production Research, vol. 48, no. 24, pp. 7463-7481, 2010.

[23] M. Conforti, G. Cornuejols, and G. Zambelli, Integer Programming, Springer, Switzerland, 2014.

A Note on Time and Space Complexity of RSA and ElGamal Cryptographic Algorithms

Adeniyi Abidemi Emmanuel[1], Okeyinka Aderemi E[2], Adebiyi Marion O[3], Asani Emmanuel O[4]
Department of Computer Science, College of Pure and Applied Sciences
Landmark University, Omu-Aran
Kwara State, Nigeria

***Abstract*—The computational complexity study of algorithms is highly germane to the design and development of high-speed computing devices. The whole essence of computation is principally influenced by efficiency of algorithms; this is more so the case with the algorithms whose solution space explodes exponentially. Cryptographic algorithms are good examples of such algorithms. The goal of this study is to compare the computational speeds of RSA and ElGamal cryptographic algorithms by carrying out a survey of works done so far by researchers. This study has therefore examined some of the results of the studies already done and highlighted which of the RSA and ElGamal algorithms performed better under given parameters. It is expected that this study would spur further investigation of the behaviour of cryptographic structures in order to ascertain their complexity and impact on the field of theoretical computer science. The experimental results of many of the papers reviewed showed that RSA cryptographic algorithm performs better as regards to energy usage, time complexity and space complexity of text, image and audio data during encryption process while some studies showed that ElGamal performs better in terms of time complexity during decryption process.**

Keywords*—RSA algorithm; ElGamal algorithm; time complexity; space complexity; data security

I. Introduction

Cryptography is the scientific technique of converting plain texts to non-readable form and back to plain text again. Born out of wartime exigencies, the idea of cryptography is to make texts unreadable to unauthorized or unintended users. This is done by deploying various cryptographic algorithms [1],[2]. Data sent in an encrypted state can only be decrypted by the targeted party using cypher keys. Thus, it hard or in many cases impossible to decode by an intruder who intercepts the encrypted files. Contemporary cryptosystem security is not focused on data secrecy but on the secrecy of a relatively small amount of knowledge, called a cypher key [2],[3]. There are five major functions of cryptography, viz. authentication, privacy, integrity, non-repudiation and service reliability. Authentication encompasses the processes of verification. Cryptography helps to verify authenticity of the data source, as well as that of the data, that is to ensure the data has not been modified. This is achieved through public key infrastructure (PKI), digital certificate and digital signature. Cryptography also ensures the privacy of the data being transferred. In order words, the data is protected against unauthorized user and attacks. Cryptography also ensures the integrity of the data that is to ensure the message has not been modified. Non-repudiation means that the sender and recipient cannot dispute they've had the message sent. Finally, cryptography ensures Reliability in service; this is to ensure that the users are provided with quality service since systems are prone to attack.

Cryptographic algorithms are generally classified either as private key cryptography or public key cryptography (see Fig. 1 for the cryptography classification tree).

Private key cryptography, also referred to as Secret key cryptography (SKC) algorithms or Symmetric cryptography are set of one key techniques in which the encryption and decryption process require one and the same key [4]. As shown in Fig. 2, the sender uses the key to scramble the plaintext (or any set of values) and send the cipher text to the receiver. The recipient uses the same key to decrypt the information and retrieve the plaintext. Since both functions have a single key, secret key cryptography is often called symmetric encryption.

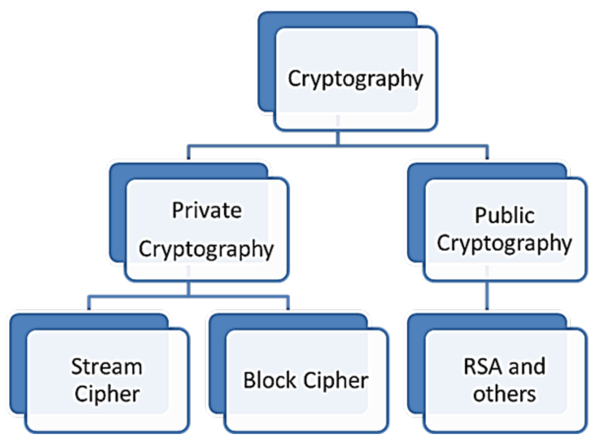

Fig. 1. Classification Tree of Cryptographic Algorithms.

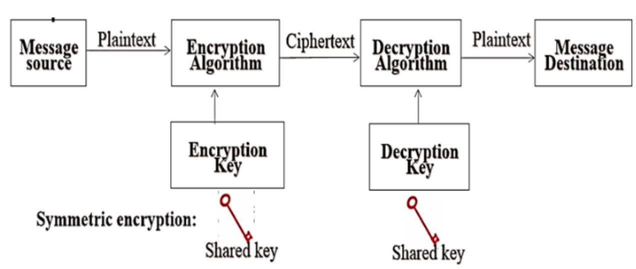

Fig. 2. Private Key Cryptographic Algorithm [5].

SKCs are further classified into Stream Buffers and Block Buffers. The Stream buffer encodes a message's characters a little at a time. Stream Cipher is used on a data stream by working on it in bits at one time. Block cipher accepts bits and then encrypts them as one entity [6]. If data is in blocked state, the data is encrypted / decrypted. Most commonly employed cryptographic secret key techniques include: Data Encryption Standard (DES), Triple Data Encryption Algorithm (3-DES), Advanced Encryption Standard (AES), BLOWFISH, and Rivest Cipher 4 among many others. The main hindrance to the practical application of a symmetric-key method is the need to share secret keys properly [7]. This has to be executed in a way to limit vulnerability or interception of the message. In the past, this will always have to be achieved by some sort of face-to - face interaction, which in certain situations appears very unrealistic when considering space and speed. If one believes that privacy is a concern, first of all the sharing of keys becomes more troublesome because of the need for a secure transferring of information. Some other concerns about the symmetric technique relates to secret key mismatch. All individual does have an equivalent secret key in the symmetric encryption. If the number of transaction participants rise, the probability of conflict or key mismatch increase drastically. Increasing new user requires more possible vulnerability point which an intruder might exploit. If such an attacker succeeds in obtaining control of just one of the secret keys, others will be totally compromised [8].

Public keys on the other hand are referred to as Asymmetric cryptography because the encoding key varies from the decoding key, which is private to the user only [9]. Asymmetric cryptography employs the use of mathematical techniques in the generation of keys without the possibility of being able to generate one key from the other. Anyone who may want to submit a message gets a public key readily accessible. A second key is kept private, so only the recipient is aware of it. Files that are encoded using the public key (text, binary files or documents) could not be decoded using the same method, but using the corresponding private key. Public key cryptographic algorithms are known to be slower during encryption process due to number of files generated. Nevertheless, they are more secure when it comes to security measures. Fig. 3 depicts the encryption and decryption processes of the Asymmetric cryptography.

Some of the commonly used public key cryptographic algorithms are: RSA, DIFFIE-HELLMAN, PAILLIER and Elgamal.

These cryptographic algorithms are combinatorial in nature; hence an evaluation of their complexities is sacrosanct to their design, development and deployment in high-speed computing devices. Therefore, the goal of this study is to review existing experimental works in literature with special focus on the complexities of the RSA and ElGamal cryptographic algorithms.

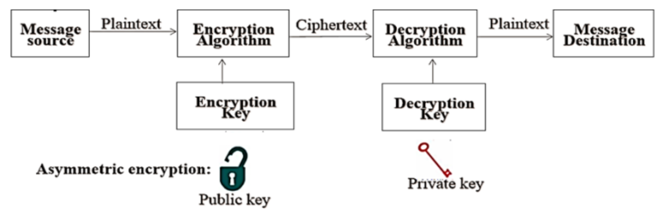

Fig. 3. Public Key Cryptography Algorithm [5].

II. The RSA Algorithm

RSA is a public-key cryptography technique which is centered mostly on purported complexity of factoring large prime numbers. An RSA user initiates and then presents, as their public key, the combination of two large prime numbers together with an auxiliary number. It is important to keep the prime numbers hidden. Anyone may use the public key to encode the data, conversely with current established approaches, if the public key is big enough, the message can only be decoded by someone who knows the prime numbers [10],[11]. The encryption and decryption procedure is described using the following pseudocode ().

Start
Generate two large and prime numbers $\boldsymbol{p}$ and $\boldsymbol{q}$, where $\boldsymbol{p} \cong \boldsymbol{q}$
Compute $\boldsymbol{n} = \boldsymbol{p} * \boldsymbol{q}$
Compute $\boldsymbol{\varphi}(\boldsymbol{n}) = (\boldsymbol{p} - \mathbf{1}) * (\boldsymbol{q} - \mathbf{1})$
Select $\boldsymbol{e}$ such that for $\mathbf{1} < \boldsymbol{e} < \boldsymbol{\varphi}(\boldsymbol{n})$, $\boldsymbol{e}$ and $\boldsymbol{n}$ are coprime.
Compute $\boldsymbol{d}$ such that $(\boldsymbol{d} * \boldsymbol{e})\ \boldsymbol{mod}\ \boldsymbol{\varphi}(\boldsymbol{n}) = \mathbf{1}$
stop

Key Generation
Public Key is $(\boldsymbol{e}, \boldsymbol{n})$
Private Key is $(\boldsymbol{d}, \boldsymbol{n})$
Encryption= $\boldsymbol{C} = \boldsymbol{M}^{\boldsymbol{e}} \boldsymbol{mod}\ \boldsymbol{n}$
Decryption= $\boldsymbol{M} = \boldsymbol{C}^{\boldsymbol{d}} \boldsymbol{mod}\ \boldsymbol{n}$

Users have to produce the pair of keys before encryption and decryption is completed and then those keys are used for encryption scheme.

The RSA offers a high security; thus, given the complexity and huge keys, an attacker should not be able to crack RSA by factoring. RSA is used for data encryption / decryption, which has the power to sign and/or validate digital data. RSA doesn't really need the use of a specific hash function, so the protection of the signatures and encryption depends in part on the preference of hashing algorithm used to measure the signatures [12]. The public key cryptography RSA is by far the most commonly used asymmetric cryptographic algorithm. It may be used in order to some anonymity and digital certificates and its protection is centered on the challenge of integral factorization being intractable.

III. The ElGamal Algorithm

The Elgamal algorithm was created by Taher Elgamal in the year 1984. It is an asymmetric cryptographic technique that is centered on key exchange. Elgamal encryption / decryption technique is based on the complexity of discrete logarithm where it is simple to lift digits to large powers however the inverse calculation of the discrete logarithm is far more complex to do. The dual important benefits of this approach are fast standardized security for long messages and data growth rate. ElGamal's biggest downside is its need for randomness and its slow process [13]. The encryption and decryption procedure of the ElGamal algorithm is described using the following pseudocode ().

Key Generation
Step 1: Start
Step 2: Generate big random prime p and θ of Z^*_p
Step 3: Select a random integer a, $1 \leq a \leq p-2$ and compute θ^a (mod p)
Step 4: Compute the public key as (p, θ, θ^a) and the private key as a.

Encryption
Step 5: Obtain the Receiver public key (p, θ, θ^a).
Step 6: Denote the message as an integer m in the range $\{0,1\ldots\ldots, p-1\}$
Step 7: Select a random integer k, $2 \leq k \leq p-2$
Step 8: Compute $y = \theta^k$ (mod p) and $d = m\,(\theta^a)k$ (mod p)
Step 9: Encrypt the message $c = (y, d)$

Decryption
Step 10: use private key a to compute $y^{p-1-a} (mod\ p)$
Step 11: Decrypt the message m with $y^a.d\ (mod\ p)$
Step 12: Stop

IV. Complexity of Cryptographic Algorithms

The study of the complexity of cryptographic algorithms is an important area of theoretical computing that helps to find or select the most efficient and effective algorithm to solve a combinatorial problem. The study on complexity of cryptographic algorithms improves on data security and privacy and also mode of data communication with the aim to understand the intrinsic difficulty of computational problems. The complexity of any cryptographic algorithm can be measured in terms of time, space or energy needed for it to encrypt and decrypt in a worst-case scenario. Thus, complexity describes the computational efforts needed for a crypto-system to encrypt and decrypt data. The algorithm's time complexity measures the amount of time the algorithm takes to execute as a function of the input length. The time complexity of cryptographic relies on factors such as hardware, operating system, processor among others. An algorithm's time complexity is commonly expressed through asymptotic notations: Big O which is denoted as O(n), Big Theta denoted as Θ(n) and Big Omega demoted as Ω(n). The time complexity analysis of an algorithm begins by trying to count the range of simple tasks to be performed while running the algorithm. Addition, subtraction, multiplication, division and compare are simple operations. The iteration below gives the description of operation of computing the time complexity of an algorithm.

```
for i : 1 to length of N
  if N[i] is equal to x
    return TRUE
  return FALSE
```

The total time of the algorithm depends on the length of the array N; if the length of the array increase the time of execution will also increase.

The space complexity of cryptographic algorithm is the measure of space (memory) it takes the algorithm to run as a function of its input-length. The complexity of space is determined by the size of any input. If for a given input size the complexity is taken as the maximum complexity over all inputs of that size, then the complexity is called the worst-case complexity. And if the complexity is taken as the average complexity over all inputs of a given size, then the complexity is called the expected complexity.

V. A Review of Existing Related Studies on the Complexity of RSA and ElGamal

Kayalvizhi et al [14] studied the energy complexity of RSA and ElGamal Algorithms for Wireless Sensor Networks. The study compared the performance of the RSA cryptographic algorithm with the ElGamal cryptographic algorithm by evaluating their energy efficiency and network lifetime. The study implemented both algorithms on a cluster network topology environment and compared the performance of the different network cluster. The computational experiments evaluated the complexity of RSA and ElGamal cryptographic algorithms in term of energy required and it was observed that the energy complexity of RSA was minimal when compared to ElGamal. Hence, RSA cryptographic algorithm requires less energy when it comes to protection of wireless communication. Therefore, RSA is said to be computationally efficient in terms of complexity of energy usage.

Qing and Yunfei [15] designed and implemented an efficient RSA variant with the aim to speed up RSA decryption process. In order to increase computational complexity, EAPRSA (Encrypt Assistant Multi-Power RSA) was introduced by moving some decryption arithmetic operations to encryption. Multi-Power RSA and RSA-S2 systems are integrated in the current new RSA variant. The multi-Power RSA used the N = p^2 q(b=3) formula modulus where p and q are n/3 bits respectively. The proposed technique reported that the space complexity of the decryption process of the proposed EAPRSA was a substantial improvement over the generic RSA.

Afolabi [16] performed a comparative performance assessment study on RSA cryptographic Algorithms. The study determined the complexity of the cryptographic algorithm in terms of Time, memory and output bytes. The study was conducted using a cryptographic technique on text file of different sizes. It was reported that RSA utilizes more time to encrypt and decrypt data and also uses more space while generating low output byte.

Chia et al., [17], studied time and space complexity of RSA and ElGamal cryptography algorithms. Encryption and decryption operations were achieved by modular exponentiation in RSA cryptographic algorithm. Also, fast modular exponentiation in RSA algorithms was considered of practical importance. By using the fast modular exponentiation of documenting the typical components in the folded sub strings, the performance of the binary algorithm could be improved and thus, reducing the computational complexity of modular exponentiation effectively.

In addition, Farah et al. [18], presented the implementation and comparative evaluation of techniques for variable text files: RSA, ElGamal, and Paillier; the encoding time, decoding time, encoded data rate and decoded data rate for each algorithm. The paper also identified and determined which algorithms perform better in terms of the time complexity. The experimental result showed that the time complexity of RSA during encryption process is computationally good and ElGamal did better with regard to decryption time complexity. Indeed, the overall complexity of RSA cryptographic algorithms in measure of the throughput was higher in the encryption process while ElGamal throughout complexity was higher during decryption process.

Vijayalakshmi and Bommanna [19] undertook a comparative analysis of RSA and ECC in Identity-Based Authenticated Modern Multiparty key Agreement scheme. The study implements two popular public key cryptographic algorithms and compared there performance by computing the processing time and memory size for the method of encryption and decryption. The study used different key sizes and variable text lengths to analyze the performance of both algorithms. The identity-based authenticated key agreement protocol showed that the protocol using ECC block cipher for user authentication offered significantly better performance in terms of memory complexity requirements and processing time complexity. Thus, their findings demonstrated ECC dominance over RSA in terms of time and memory complexities allocation for execution.

Furthermore, Annapoorna et al., [20] compared two asymmetric algorithms RSA and ElGamal for secure file transmission. The paper gave tabular reports of Key length value, algorithm sort, security threats, pace usability of the model, key usage, energy consumption and hardware / software implementation discrepancy between complexity of RSA and ElGamal cryptographic algorithms. The study analyzed the complexity of the cryptographic algorithm in terms of their security level. The study stated that ElGamal algorithm is more secure as compare to RSA cryptographic algorithm. Additionally, RSA algorithm was reported to perform poorly in terms of time complexity because it generates more than one public keys when encrypting and decrypting data.

Tin and Su [21], carried out a comparative Study of RSA and ElGamal on audio protection systems, based on the period of execution. The implemented encryption algorithms provide a secure communication over the internet and play a crucial role in efficient information security systems. The proposed system utilized two public key algorithms RSA and ElGamal algorithms to analyze their complexity of execution time on audio file. The study used audio (.mp3) file type with various file sizes to analyze the encryption and decryption of complexity time using C# programming language. The experimental results showed that RSA algorithm is faster than ElGamal algorithm in encrypting and decrypting audio file.

Andysah et al., [22], studied the Performance comparison of the public-key cryptographic algorithms RSA and ElGamal. RSA occured in the factorization of large primes whereas ElGamal occured in the computation of discrete logarithms. The study utilized public-key RSA and Elgamal encryption techniques for the encryption and decryption of a text file. The results of the experiments revealed that RSA algorithm outperformed the Elgamal algorithm in terms of time complexity.

More so, Kyaw, Kyaw and Nay [23], studied the time complexity of RSA public key encryption method and ElGamal public key encryption method. The study was concerned with the encryption process on text, image and audio data to obtain the encryption and decryption time of RSA and ElGamal cryptographic algorithms. The results of the experiment showed that RSA encryption and decryption time complexity was significantly better than those of the ElGamal cryptography algorithm.

Haval et al., [24], proposed and implemented a modified ElGamal cryptographic algorithm to increase the complexity of the algorithm in term of time, speed and reducing the expansion rate in the file size after encryption process. Some modification was performed on the traditional ElGamal cryptographic algorithm such as using addition operation instead of multiplication in the encryption process to decrease the file size. A comparative evaluation of the modified and traditional ElGamal was carried out on text data and the result showed that the time complexity performance of modified Elgamal was better than the traditional Elgamal.

VI. Conclusion

In this paper, survey of performance analysis of asymmetric cryptographic algorithms in particular RSA and ElGamal was carried out and analyzed. The experimental results of many of the papers reviewed showed that RSA cryptographic algorithm performs better as regards to energy usage, time complexity and space complexity of text, image and audio data during encryption process while some studies showed that ElGamal performs better in terms of time complexity during decryption process. This survey was limited to text, image and audio data. However, more performance metrics like video file and mixed data can be considered in further studies in order to widen the scope of this survey.

References

[1] M. Marwaha, R. Bedi, A. Singh, and T. Singh, “Comparative analysis of cryptographic algorithms”. Int J Adv Engg Tech/IV/III/July-Sept, 16, 18. 2013.

[2] S. Rani, and H. Kaur. “Technical review on symmetric and asymmetric cryptography algorithms”. International Journal of Advanced Research in Computer Science, 8(4). 2017.

[3] A. G. Walia. “Cryptography Algorithms: A Review.” International Journal of Engineering Development and Research. 2014.

[4] R. Sonia and K. Harpreet "Technical Review on symmetric and Asymmetric Cryptography Algorithms". International Journal of Advanced Research in Computer Science. www.ijarcs.info. 2017.

[5] F. Muhammad, J. Sapiee and H. Abdulkadir et. al., "A survey on Cryptographic Encryption Algorithms". International Journal of Advanced Computer Science and Applications, ol. 8, No. 11. pp 333-344. 2017.

[6] K. Howard. U.S. Patent No. 10,009,168. Washington, DC: U.S. Patent and Trademark Office. 2018.

[7] K. Sajay, S. Babu, and Y. Vijayalakshmi. "Enhancing the security of cloud data using hybrid encryption algorithm". Journal of Ambient Intelligence and Humanized Computing, 1-10. 2019.

[8] S. Ankush, A. Jyoti, D. Aarti and S. Pratibha. "Implementation & Analysis of RSA and ElGamal Algorithm". Asian J. of Adv. Basic Sci.: 2(3), 125-129. 2014. ISSN (Online): 2347 – 4114. www.ajabs.org.

[9] R. Sonia and K. Harpreet. "Technical Review on symmetric and Asymmetric Cryptography Algorithms". International Journal of Advanced Research in Computer Science. www.ijarcs.info. 2017.

[10] E. Arboleda, J. Balaba, and J. Espineli. "Chaotic rivest-shamir-adlerman algorithm with data encryption standard scheduling". Bulletin of Electrical Engineering and Informatics, 6(3), 219-227. 2017.

[11] N. Jayapandian, and A. Rahman. "Secure and efficient online data storage and sharing over cloud environment using probabilistic with homomorphic encryption". Cluster Computing, 20(2), 1561-1573. 2017.

[12] M. Baba-Ahmed, F. Benmansour, and A. Sedjelmaci. "A Cryptosystem Architecture and Design for Encrypted Data Transmissions". Electrotehnica, Electronica, Automatica, 67(2). 2019.

[13] M. Marwaha, R. Bedi, A. Singh, and T. Singh. "Comparative analysis of cryptographic algorithms". Int J Adv Engg Tech/IV/III/July-Sept, 16, 18. 2013.

[14] R. Kayalvizhi, M. Vijayalakshmi, and V. Vaidehi. "Energy Analysis of RSA and Elgamal Algorithms for Wireless sensor Networks". CNSA 2010. CCIS 89, pp. 172-180. 2010. Springer-Verlag Berlin Heidelberg.

[15] L. Qing, L. Yunfei, L. Hao. "On the Design and Implementation of an Efficient RSA Variant", Advanced Computer Theory and Engineering (ICACTE), 2010, pp.533-536.

[16] A. Afolabi, and O. Atanda. "Comparative analysis of some selected cryptographic algorithms". Computing Information Systems, Development Informatics and Allied Research Journal. Vol, 7, 41-52. 2016.

[17] L. Chia, and H. Chen. "Computational Complexity Theoretical Analyses on Cryptographic Algorithms for Computer Security Application", Innovations in Bio-Inspired computing and Applications(IBICA), 2012, pp. 307 – 311.

[18] S. Farah, Y. Javed, A. Shamim, and T. Nawaz. "An experimental study on performance evaluation of asymmetric encryption algorithms". In Recent Advances in Information Science, Proceeding of the 3rd European Conf. of Computer Science,(EECS-12). 2012. (pp. 121-124).

[19] P. Vijayalakshmi, and K. Bommanna. "Performance Analysis of RSA and ECC in Identity-Based Authenticated New Multiparty Key Agreement Protocol". International Conference on Computing, Communication and Applications (ICCCA), 22-24 Feb. 2012, pp 1-5.

[20] S. Annapoorna, S. Shravya, and K. Krithika. "A review on Asymmetric cryptography RSA and Elgamal Algorithms". International Journal of Innovation Research in Computer and Communication Engineering. Vol. 2, 2014. Special Issue 5.

[21] Z. Tin, and W. Su. "Performance Analysis of RSA and ElGamal for Audio Security". International Journal of Scientific Engineering and Technology Research. Volume.03, issue.11, June-2014, Pages: 2494-2498.

[22] P. Andysah, K. Elviwani and O. Boni. "Comparative Analysis of RSA and Elgamal Cryptographic Public-key Algorithms". 2018.

[23] M. Kyaw, S. Kyaw, and A. Nay. "Time Performance Analysis of RSA and Elgamal Public-Key Cryptosystems". International Journal of Trend in Scientific Research and Development (IJTSRD). Volume 3 Issue 6, October 2019 Available Online: www.ijtsrd.com e-ISSN: 2456 – 6470.

[24] I. Haval, W. Hussein and M. Abduallah. "An efficient ElGamal cryptosystem scheme". International Journal of Computers and Applications, 2019. DOI: 10.1080/1206212X.2019.1678799.

Anomaly Detection on Medical Images using Autoencoder and Convolutional Neural Network

Rashmi Siddalingappa[1], Sekar Kanagaraj[2]
Department of Computational and Data Science
Indian Institute of Science, C V Raman Road, Bangalore 560012, India

Abstract*—Detection of anomalies from the medical image dataset improves prognosis by discovering new facts hidden in the data. The present study aims to discuss anomaly detection using autoencoders and convolutional neural networks. The autoencoder identifies the imbalance between normal and abnormal samples. They create learning models flexible and accurate on training data. The problem is addressed in four stages: 1) training: an autoencoder is initialized with the hyper-parameters and trained on the lung cancer CT scan images, 2) test: the autoencoder reconstructs the input from the latent space representation with a slight variation from the original data, indicated by a reconstruction error as Mean Squared Error (MSE), 3) evaluate: the MSE value of the training and test dataset are compared. The MSE values of anomalous data are higher than a base threshold, detecting those as anomalies, 4) validate: the efficiency metrics such as accuracy and MSE scores are used at both training and validation phases. The dataset was further classified as benign and malignant. The accuracy reported for outlier detection and the classification task is 98% and 97.2%. Thus, the proposed autoencoder-based anomaly detection could positively isolate anomalies from the CT scan images of lung cancer.

Keywords—Anomalies; autoencoder; convolutional neural networks (CNN) (ConvNets); deep neural network architecture; regularization

I. Introduction

Outliers are the data that are not normal when compared to the rest of the information in any dataset. They indicate extreme values which usually diverge from the general model [1]. The occurrence of outliers in the dataset is possible for many reasons, such as a fault in the system, manual errors, fraudulent errors, equipment errors, and the data may vary for inexplicable reasons camouflaging a few unseen motifs. At times, these unusual patterns indicate hidden knowledge about the data. For instance, irregular Electrocardiography (ECG) data may suggest heart-related problems because it will be dissimilar from the ECG report of a healthy person. Thus, identifying outliers is an essential part of the knowledge discovery process [2]. Because of this reason, outlier detection has always been an exciting factor for researchers, scientists, and data analysts. Outlier detection is widely employed in nearly all subject areas such as medical, fraud detection, credit card analysis, financial sectors, social network analysis, and weather forecast analysis. Outliers are of different types: univariate, multivariate, point/global, context, and collective outliers [3]. The outlier detection approaches [4] are broadly classified into three categories; 1) Statistical method: this approach is used in a typical univariate environment where the data distribution is normal/ Gaussian-like. Here, approximately 68% of the data fall with the normal distribution anchored to the 1st standard deviation measure. About 98% of data distribution fall in the 2nd standard deviation and 99.7% of data value belong to the 3rd standard deviation. The approach yields faster results. The compact representation of the model facilitates anomaly detection even on large datasets. However, the statistical methods often fail in a multidimensional dataset environment, and also, they require prior knowledge about the anomaly pattern [5], 2) supervised method: The model is trained on the labeled features that differentiate between a normal and an abnormal data class. The unseen data is fed to the system, i.e., test data, and the model determines to which category the data point belongs. Interestingly, they do not rely on any prior knowledge of the anomaly pattern and it is easy to train the model. Again, this model fails in a high-dimensional space, further attributed with the local neighborhood problem [6], 3) unsupervised method: the anomalies are detected through a heuristic approach with certain assumptions of segregating the regular instances versus other data points that deviate from the cluster. K-means and DBSCAN are the prominent techniques here [7]. These methods are highly dependent on users' perception making the outlier detection task quite spontaneous. The main drawback of this approach is the binary nature of data separation, which is used for data grouping. Several algorithms have been proposed in the realm of anomaly detection however, they focus on arbitrary labels in the classification of datasets to distinguish between previously observed outlier samples. The protocols for feature selection are not indicated, making the model detect only the previously known anomalies. Moreover, the statistical methods will lead to high false negatives that may skip identifying the actual anomalies, and the rule-based models are highly dependent on user-set parameters, whereby changing these features will negatively impact the performance of the model [8]. Therefore, to fill the research gap of the existing methods, the present study uses a deep learning approach – autoencoder and convolution neural network (CNN). These methods have been doing miracles on a diverse range of datasets amidst any complexities in the structure. Thus, the main objective of the present study is to use an autoencoder with encoder and decoder arrangement to detect and eliminate outliers on lung cancer computerized tomography (CT) scan images [9]. During the training, the encoder will learn the latent representation of the normal data at the core layer. Thereon, the decoder will use the information present in the core layer to reconstruct the data. The normal and abnormal data's behavior is separated by using a Mean Squared Error (MSE) score. The MSE calculates the difference between the original input data and the data the model constructed at the output side. For a good model, the MSE scores should be small. In further steps, the images are subsequently classified into benign and malignant. The significant contributions of the proposed work are as follows:

- Image datasets are highly sparse with a complex structure. Thus, the study empirically demonstrates a deep neural architecture to detect the medical image outliers.
- The input data distribution is transformed into output distribution space with the least amount of feature loss (distortion).
- A reconstruction error is calculated for the training and test data for understanding the gap between normal and abnormal data samples. A base threshold is pivotal for this mapping function [10].
- The proposed method works on an unsupervised dataset without any labels, making the framework efficient enough to ascertain the unusual patterns in the underlying data.

The remainder of the paper is organized in the following sections. Section 2 discusses various works related to the present study. Section 3 introduces the autoencoder. The implementation details are shown in Section 4. Section 5 delivers results and analysis of the proposed model. Lastly, the paper culminates with Sections 6 and 7, highlighting the discussions, scope for future research, and conclusion.

II. Literature Study

The problems associated with anomaly detection are found abundantly in the literature. Various researchers have proposed various models and methods globally in the past two decades [11] [12]. In [13], LUNA16 dataset, CT scan images with label nodules are used by the authors to detect cancer using 3D-CNN. Initially, the raw images are preprocessed using a threshold approach, and later vanilla 3D NN architecture is used to classify the images into cancerous and non-cancerous. The model achieved 80% accuracy with 120-sec computational time. Though the results of this research work are better than the previous results, it uses a relatively small amount of dataset (~100 CT images). The same LUNA16 (lung nodule analysis 2016) datasets have been used by the authors Gritli, et al. in [14]. The aim was to classify the datasets into benign and malignant using 3D AlexNet architecture. Through 10-fold cross-validation, the proposed approach resulted in 97%, proving to be efficient than the existing methods even at low-dose CT scan images. However, the layers at the semantic network are tiny and light, making the class activation function not perform well. There was a significant amount of data lost in the process of maintaining the class equivalence. The lung cancer detection in CT scan images using CNN is proposed by Sharma, et al. in [15]. The researchers have performed preprocessing and segmentation. Later U-net model is used to classify the patients' nodules into cancerous or non-cancerous. The authors claim to obtain 77% accuracy but the proposed model suffers from data-imbalance problems, due to which the accuracy is dropped. Rasha, et al. [16] have worked on anomaly detection in lung cancer image datasets. The features have been selected through techniques such as local binary pattern (LBP), discrete wavelet transform (DWT), and histogram of oriented gradients (HOG). The firefly algorithm is used to optimize the selected features and later on support vector machine (SVM) is applied to classify the normal instance of the image. The authors have not shown the real-time datasets taken from Moulana hospital. The details of the preprocessing of the dataset are not discussed. When the training set contains a small fraction of outliers, it becomes extremely challenging to identify anomalies in the given image dataset. Thus Laura Beggel, et al. in [17] have proposed a unique anomaly detection using adversarial autoencoders that places anomaly patterns in low likelihood regions. The proposed model is performed on the MNIST image dataset. The model resulted in some overlap with reconstruction images making the task rely on a supervised training mode. The performance is not studied for a high-dimensional dataset. The 3D-National lung screening trial (NLST) datasets have been used to study anomaly detection using deep generative models in [18]. The model works on the fact that positive samples are available in scarce; thus, the likelihood of the unseen data is estimated without the implications of the negative samples, thereby identifying the samples as low likelihood datapoints. However, the applicability is not suited when the complexity of the data increases. The results of the 0.62 score under ROC results are still not good enough for determining anomalies at the nodule level. Mehdi, et al. [19] have proposed lung cancer detection using an autoencoder that is semi-automatically trained on datasets from the Lung Image Database Consortium image collection (LIDC-IDRI) database. The dataset of healthy patients is used for training, later the output was fed to a segmentation process, and the variation in a pattern other than healthy patients was removed. However, the segmentation network could fail while training on abnormalities of the diseased images.

III. Architecture Recurrent Outlier Detection using Deep Neural Architecture – Autoencoders

Autoencoders (AE), a multi-layered feed-forward neural network, is an unsupervised machine learning approach [20] used for dimensionality reduction in a multivariate data environment. However, on a univariate dataset, the autoencoders are similar to linear regression or a typical principal component analysis (PCA) problem [21]. Though PCA and other clustering algorithms perform reasonably well on multidimensional data, the autoencoder does a better job because of hyper-parameters [22]. A significant difference between a PCA and an AE is that the latter perform analysis on the data with a non-linear activation function on the hidden layers. Architecturally, an AE is a simple feed-forward network because the information is fed to the input layer, passed through a set of hidden layers. Each has a varied number of nodes/neurons to transform the input and arrives at the output. The nodes are extrapolated into different layers, each connected to all the nodes on the previous layers. The input and the output layers have the same number of nodes, 'n,' due to the symmetric arrangement of the autoencoder that intends to reconstruct input at the output side. The values predicted at each node through activation functions are passed into consecutive layers ahead. The general representation of AE is shown in Fig. 1. An AE consists of two main stages, an encoder and a decoder [23]. An encoder maps the given input into a compressed representation, and a decoder transforms the compressed data back into the original input. Alongside, an encoder wraps the original data by hidden layers into a squeezed vector representation.

$$x_n = \sum_{i=1}^{n} e_n(w_{en}x_0 + b_{en}) \tag{1}$$

Where, e_n is an encoding function of the hidden layer ranging between 1 and n, w_{en} and b_{en} are the weight and bias parameters at layer 'n' and x_0 is the original input vector from the input layer. Similarly, at the decoder side, the output will be the same as the input that the system received initially but with a difference that the output at encoder represents the input (x) as a reconstruction error for x_0.

$$x' = \sum_{i=1}^{n} d_n(w_{dn}x_n + b_{dn}) \tag{2}$$

Where, x' is a decoding function at nth decoding hidden layer with the weights and bias being represented for the corresponding nth decoding layer as w_{dn} and b_{dn}.

The AE extracts the crucial features and stuff in a latent space representation between an encoder and a decoder. Besides, this representation contains a low-dimensional version of the original input. Thereby, at the decoder, the AE reconstructs the input data as the output from the latent space features. This reconstruction is dependent on the training data, i.e., an AE cannot build a new representation of the input but only specific to what has been trained. Furthermore, the autoencoder calculates the reconstruction error through MSE. For a normal data sample, the reconstruction error is small. However, these numbers are usually large and above a certain base threshold for the anomalous data, typically set by the user.

The encoding section takes the input image; the autoencoder captures only the spatial features and converts them to a low dimensional image. Further, in the decoding section, the image is reconstructed.

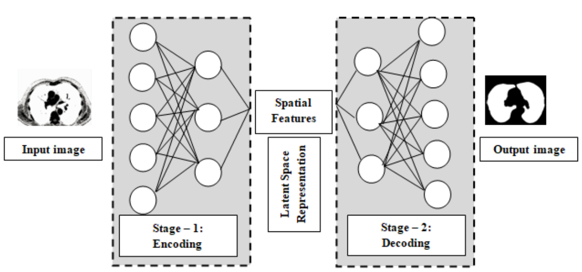

Fig. 1. A Diagrammatic view of an Autoencoder Network.

IV. AUTOENCODERS AND ITS COMPONENTS IN ANOMALY DETECTION

The fundamental role of an AE in anomaly detection is to determine how much the output data (reconstructed data) deviates from the input data. Thus, the AE is essentially trained on the theory of minimizing the reconstruction error. The following parameters are considered during the training process:

- The number of hidden layers – The decision boundary is observed to split the input data into several classes, and later these classes are expressed as a straight line [24]. The joining curve of these lines indicates the number of hidden layers, and the number of consecutive lines decides the number of neurons in these hidden layers. In an AE, the number of neurons in the input and the output layers are the same.
- Regularization – The main objective of using any machine learning approach is to make the model fit for both training and test data to avoid overfitting and underfitting. In both cases, the model will not generalize well. The regularization techniques are adopted to minimize the error rate on the test data at the cost of boosting the training error. Lasso regression (L1) and Ridge regression (L2) are the two popular regularization methods [25]. Here, L1 regularization [26] is used since this is particularly useful for the feature selection process on a wide range of input values. The loss function is given by;

Loss Function

$$= \sum_{i=1}^{n} (Z_i - \sum_{j=1}^{p} y_{ij}\alpha_j)^2 \tag{3}$$

Here, Zi is the input variable at some neuron layer 'i' (i ∈ 1 to 'n' inputs), and yij is the output layer obtained at some neuron layer 'j' corresponding to the input 'i'. The output has 'j' layers, the same as the input layer such that j ∈ 1 to 'p' outputs. αj is the reconstruction error. The entire component is squared to eliminate any negative value. The L1 regression defines an absolute value of the magnitude for a penalty term along with loss function [27], and it is given by;

Regularization Function (L1) =

$$\text{Loss Function} + \rho\sum_{j=1}^{p}|\alpha_j| \tag{4}$$

- Learning rate: Indicates the number of weights updated at every epoch. It tunes the algorithm to achieve minimum reconstruction error.
- Batch size: This refers to the number of training samples used at different iterations from which the model learns.
- Optimizer: An optimizer is used to combat the time complexity of the algorithm. Adam Optimization algorithm [28] is a replacement for a traditional stochastic gradient descent method to update the

training network's weights. The learning rate is calculated for various parameters and frequently preserved for individual network weights. These values are finally adopted as a learning process unfolds.

A. Training a Deep Neural Network through ConvNets

When an input image passed through a standard neural network, many of the temporal [29] (time-related: pictures that were taken at different time intervals) and spatial [30] (space-related: properties related to a single image such as coordinates, gradients, resolution and so on) features are lost. Convolutional Neural Network – ConvNet – CNN [31] model is used to overcome this problem. Spatial elements are essential to reconstruct the images as they describe each image's characteristics. An AE retains only spatial features, eliminating the images' temporal aspects. The encoder comprises three ConvNet layers with different dimensions. At the core, there is a hidden layer that is dense and fully connected autoencoder with neurons. Once the image is resized, a low-dimensional version of the input is stored in the latent space. The decoder comprising three deConvNets reconstructs the input image with limited features. Each image is 512x512 pixels. The first layer of ConvNet is a convolutional layer with 32 filters such that each filter is of size 5x5. Only one feature out of 32 will be considered at each evaluation step, indicated by 512x512x1. The second layer is pooling with a 3x3 pool size. The output size is 509x509 since pooling prunes 3x3 pixels from each side. Here, the image would be reduced to 169x169 (509/3 ~ 169) with 32 filters (a similar process is repeated for the 2nd and 3rd ConvNets). The flattening process induces the product of these numbers. The pooled features of the input image are mapped onto columnar representation. The fully connected layer in the core is then turned on with batch size = 128. The spatial features are juxtaposed to form many attributes sufficient to create the original input image. At the decoding side of DeConvNets, the same process is reversed by retaining the dimensions constant.

The architecture of a CNN model is shown in three stages, Fig. 2.

- Convolutional Layer: The feature space is created for an input image and preserves the relationship between the pixels through filtering. The filters' values are usually; 1, -1, and 0 – a positive value for feature brightness, a negative value for darkness, and 0 for a grey image. These values are placed indefinitely at different locations in the filters. When an original image passes through the filters, the filtered image features produce two types of high and low scores for a match and low for a no-match/mismatch. The filters here represent the number of features that the model can extract. However, with a more significant number of filters, the training process is prolonged. The filter values are 32, 64, 128, and so on.
- Activation Function: The activation function helps the model map the resulting feature values into a normalized value between 0 to 1 and -1 to +1. In the proposed system, two activation functions are Sigmoid and ReLu. The sigmoid function squashes the feature values between 0 and 1. The ReLu – Rectified Linear Unit – substitutes a negative value to zero [32].
- Pooling: This is used to reduce the size of filter vectors. For instance, in max-pooling, if the filter is 3X3, the highest value is chosen at every 3X3 matrix. Once the pooling is completed, the filtered images are stacked up to form a list.

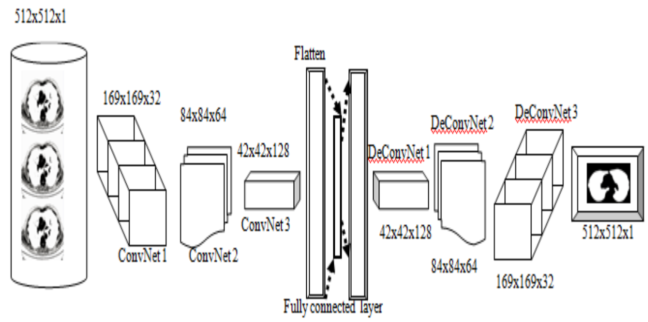

Fig. 2. The Encoding and Decoding Processes of an Autoencoder using ConvNets and DeConvNets, Respectively. The Encoding and Decoding Processing are Symmetric and have the Same Layers in each Section.

B. Training Algorithm for ConvNets-Autoencoders using Adam Optimization Technique

Adam optimizer is used to train a deep neural network using ConvNets. Here, the learning curve is estimated based on the lower-order moments with fewer memory requirements. Algorithm 1 illustrates the training process adopted for this research study.

Algorithm 1: Training algorithm for ConvNets using Adam Optimization Technique

Input: Training data split (d); the input vector (x_0); Adam's learning rate parameters $\beta = (e_n, w_{en}, b_{en})$; the number of hidden layers; the number of epochs; batch size; ρ is the regularization parameter;

Output: Trained model with decoding function (x') returns α_j as reconstruction error; fw,d(x)~ x

1: start
2: arrange the data required for the training model with the dataset (d)
3: initialize the parameters $\beta = (e_n, w_{en}, b_{en})$;
4: **for** P ∈ (1, 2, 3, 4… epochs)
5: **for** q∈ (1, 2, 3, 4… batch size)
6: **for** fw,d(x) ∀ x in d
7: transform the input layer vectors into their corresponding hidden layers in a series of encoder layers and compute output layer with decoding function [eq. 1 and eq. 2]
8: calculate the reconstruction error α_j by using eq. 4
9: update Adam's learning rate parameters $\beta = (e_n, w_{en}, b_{en})$; for each iteration
10: **end for**
12: **end for**
13: **end for**
14: train the model with the results of the above steps and return
15: stop

V. Implementation

A. Dataset Description

CT scan images of lung cancer are used as a dataset[1]. The dataset is a subset of the LUNA16 Grand Challenge[2]. The dataset is efficient enough to analyze the model because it contains the images exposed to a two-phase annotation process by four different radiologists. Thus, it makes the dataset suited for testing with an emphasis on identifying anomalies. Further, the images are adequately compressed, due to which no additional image compression techniques are used in the present study. A total of 297 images are separately marked for training and testing purposes. Convolutional autoencoders are implemented on the Spyder platform version 4.1.5 [3]by adopting a high-level neural network application package – Keras 2.3.0 [4] ,which runs on Tensorflow v2.4.1 [5] at the background. The code is written in python 3.8.8 [6]

B. Parameter Setting and Preprocessing

The details of the hyper-parameters used for the implementation are as follows: learning rate: 0.01, epochs: 40, batch size: 30, Adam optimizer parameters: alpha (learning rate) = 0.001, beta1 (exponential decay rate for the first estimate) = 0.9, beta2 (exponential decay rate for the second estimate) and epsilon (to overrule divide by zero error) = 10E-8, input images: 297, corresponding to 297 neurons in each hidden layer, sequential CNN model with kernel size = (3,3) at convolution layer and pool size = (2,2) at MaxPooling layer.

The images were preprocessed before the model is executed on the input. Those are; a function was called to load images from the folder onto an array variable. Further, images in the dataset had varying sizes. Thus, the height and width were rescaled to 512 pixels each to maintain uniformity throughout. The pixel values of the image (0 –black to 255 – white) are scaled between the ranges of 0 and 1 in the process called normalization (the ImageDataGenerator divides the pixel value by 255, for instance, 1/255 = 0.0039). This is performed because a neural network usually works with small weights used to update the neurons. If a large value is used, the network consumes a great deal of time, slowing down the learning process. With 40 epochs, the model attained an accuracy of 98% and an MSE value as low as 0.011. With every epoch, the model learns the features better with extra latent manifolds. The relevant features are then retained, and the characteristics that are not scalable for latent space representation are pruned.

C. Results

Out of 297 images, the dataset was split into three categories as training: 70% (207 images), validation: 10% (29 images), and test: 20% (61 images). The efficacy of the proposed system is measured at both the times – training and validation. The terms used are:

- Overall accuracy – accuracy is calculated at every epoch as, accuracy= images the system constructed correctly / the total number of images in each epoch (batch size).
- MSE – MSE defines an average square of the difference between the original input image and the image constructed by the model.

$$\text{MSE} = \frac{1}{B}\sum_{i=1}^{B}(X_i - \hat{X}_i)^2 \tag{5}$$

Here, 'B' indicates the batch size since the parameters are considered for individual batches. The error score of the original input image at the 'i' instance is given by X_i, and the error score of the reconstructed image at 'i' is provided by $\hat{X}_i$. MSE score of the anomalous data tends to be above the normal data threshold. The MSE scores for all samples are calculated to set the base threshold. The distribution of these MSE scores determines the threshold; 92% of the data was in the range of 0.011 to 0.6. The remaining 8% of the data had many variations in their MSE scores, such as 17.5, 2.5, 9.2, and 11.3, so on. Therefore, by looking at this distribution, the base threshold for anomaly detection was set as 0.7. The MSE score of the reconstructed images of the normal samples will be less than or equal to 0.7, and for abnormal images, the score will be greater than 0.7.

Of the 297 images, 23 images are identified as anomalies, with an MSE score greater than 0.7, and the 274 images are identified as normal samples, as demonstrated in Fig. 3(a). Initially, the accuracy was low even for a low MSE score; however, it is evident that, as the epoch progressed, the accuracy increased for normal data; however, the accuracy dropped as low as 11%, indicating a very high MSE score (17.5) for some data. Nevertheless, it is observed that the samples with high MSE scores have low accuracy values indicating the presence of the outliers. The accuracy achieved with low MSE scores was excelled, nearing 98%. The data with high MSE and low accuracy indicate the presence of the outliers, which were identified through the MSE scores.

- Val_loss: This is applied to the test data. val_loss is a good sign of how the model performs on the unseen data. Smaller val_loss indicates that there is no problem with overfitting. Consequently, if the model is trained heavily on the data, the val_loss increases as evidence of overfitting.
- Val_accuracy: The overall accuracy is an indicator of the classification performed on the training data. But for the test data, val_acc is crucial as it tests the accuracy of the unseen data. A neural network model is considered good when the val_loss starts decreasing, and the val_acc starts increasing [33], as shown in Fig. 3(b). Here, the number of examples used to calculate the loss/ error gradient is called a batch size or simply a batch. However, the training epoch indicates that the model has made learning for a randomly selected batch. As the validation loss is calculated in terms of samples, the term batch is used.

---

[1] https://www.kaggle.com/kmader/finding-lungs-in-ct-data
[2] https://luna16.grand-challenge.org/Data/
[3] https://www.spyder-ide.org/
[4] https://keras.io/
[5] https://www.tensorflow.org/
[6] https://www.python.org/

- Val_mse: The MSE score for the validation/test data

The overall evaluation of the proposed model is plotted in a line chart for the key terms explained so far. This is shown in Fig. 4. It must be noted that, as the epochs progress, the accuracy metrics increases, and the MSE values decreases. Additionally, val_loss is also reduced, indicating that the model is trained appropriately. Fig. 5 shows a set of images identified as anomalies and normal data. Once the outliers are removed, the image dataset is classified into either benign or malignant with simple neural network architecture [34].

The predicted output is put forward in the form of a confusion matrix in Fig. 6. Out of 297 input images, 259 images were correctly classified as benign (TP), and 22 out of 24 (actual number of malignant) images were classified as outliers (TN), 5 images that are non-benign (actual malignant) but are identified incorrectly as benign (FP) and 11 images were obtained incorrectly as malignant (FN). The ROC (Receiver-Operating-Curve) is plotted to determine the model performance based on predicting the probabilities of outcome (whether an image is an outlier or not) as illustrated in Fig. 7. The ROC is plotted against True Positive Rate (TPR) and False Positive Rate (FPR) for a wide range of threshold values. TPR – Recall – Sensitivity is given by, TPR = (TP) / (TP + FN) and FPR is given by, FPR = (FP) / (FP + TN). Area-Under-Curve (AUC) measures the degree of separation, which tells how capable the system is at distinguishing between the classes.

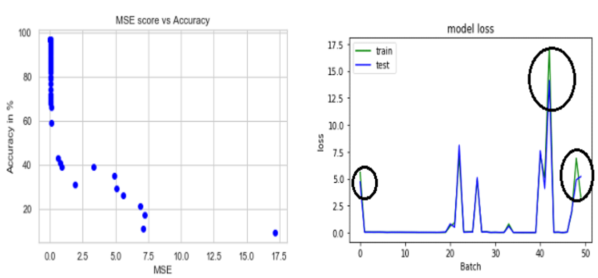

(a) (b)

Fig. 3. (a) A Graphical Representation of Variation in the Accuracy and the MSE Scores. The Accuracy Increased, and the MSE Value is Dropped to a Minimum towards the End of 40 Epochs, (b) A Graphical Representation of Variation in Training and Test v_loss. As Observed, the val_ loss of Test Data is Slightly Reduced at Encircled Points.

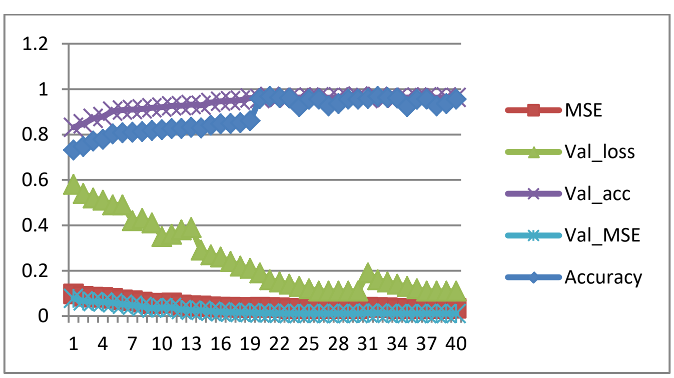

Fig. 4. The Evaluation Metrics Such as MSE, Val_loss, Val_acc, val_MSE, and Overall Accuracy Plotted across 40 Epochs.

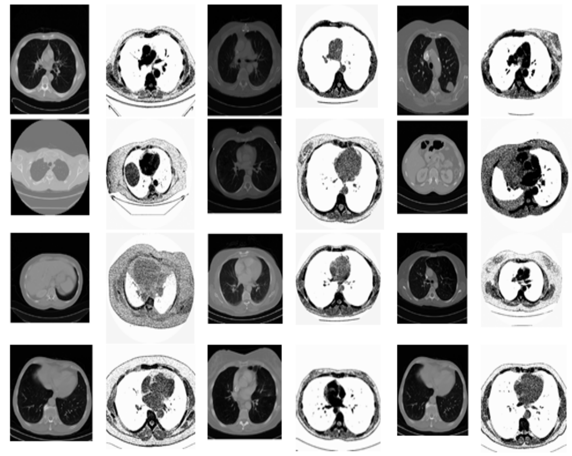

Fig. 5. A Series of Data for both Anomalous (Black Background) and Normal (White Background) as Identified by the Proposed Model.

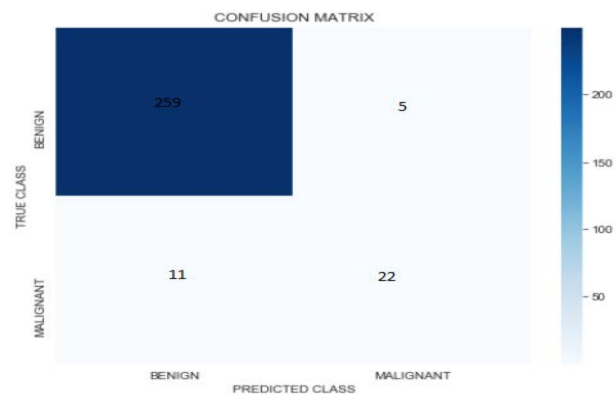

Fig. 6. A Confusion Matrix for the Two Classes – benign and Malignant Plotted against the True and Predicted Classes. Here, 259 Indicates TP, FP = 5, FN = 11 and TN = 22. The Ranking is shown for all the 297 Input Samples.

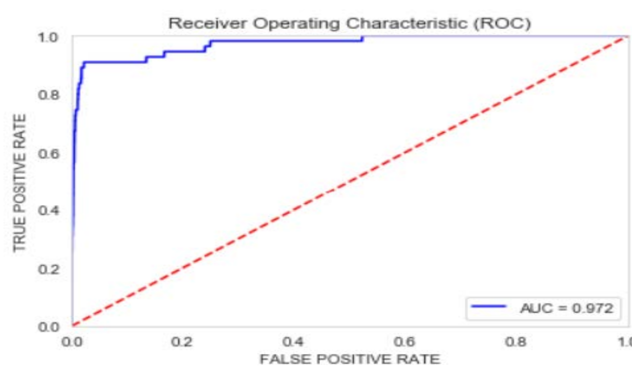

Fig. 7. ROC Curve for Cumulative Results of the Classification Task. The Value of AUC = 0.972 (97%) Reveals that the Model is Excellent in Distinguishing between the benign and Malignant Classes.

D. *Comparison of Various Outlier Detection Methods with the Proposed Model*

In this subsection, the proposed model is compared with the classical state-of-art systems. The result of this comparison is described in Table I. The proposed model outperformed the other conventional methods by achieving 98% accuracy. This indicates that the model can be well adapted even for distinct datasets with complex structures.

TABLE I. COMPARISON OF THE PROPOSED MODEL WITH THE OTHER STATE-OF-ART TRADITIONAL SYSTEMS IN TERMS OF ACCURACY

	Accuracy
Gritli. et.al in [14]. 3D AlexNet architecture.	97%
Sharma. et.al in [15]. CNN-based architecture	77%
Rasha. et.al [16]. Firefly algorithm with SVM	78%
Laura Beggel. et al. in [17]. Adversarial autoencoder-based	0.62 [Under 0.62]
AnoGAN deep convolution using adversarial network [35]	84%
Our proposed method	**98% - outlier detection** **97.2% - classification task**

VI. DISCUSSIONS

Like any other expert system, the proposed model also deals with some limitations. The model is highly dependent on the training data. As a result, when unseen data – a typical healthy heart image – was fed as an input, the system calls it an anomaly. This could be a potential problem mainly when the corpus is more generic than domain-specific. The proposed model considers only the spatial features, thereby removing the temporal characteristics of the image in the cleaning step. Thus, the edges and variations in the local binary pattern of the images are skipped, leading to misrepresentation of features sometimes. Interestingly, the global minimum MSE score is 0.01, and it cannot be reduced even with further training. This hypothesis helped to shorten the input size and exemplify the latent space representation. Additionally, a sparse hierarchical model is witnessed in most activations, mainly when the spatial features are selected. Further, the complex representation is brought down to lower dimensions in the encoder and later decoded into an original image. During this transformation, the model may memorize the data during the training process leading to overfitting. Therefore, the proposed method restricts the number of neurons in the core layer, usually half of the number of input variables in the network. This will ensure that the model is learning the key patterns, rules, and essential features from the input data. It is imperative to note that no training labels are used in the model, making it completely unsupervised. However, each neuron at the hidden layers is driven by the data on hand that makes the system data-reliant. Thus, when the input features change, the activation function triggers different neurons and results in a different output through the network. While the latent space representation stress enough on the encoding and decoding process, the regularization used in the network minimizes the error rate through the L1 regularization technique. Though the proposed model performs reasonably well, there is still room for improvement. For instance, the gradient-weighted activation mapping technique could be used to obtain visual explanations of the predictions made by the system, and using a larger dataset could further improve the performance.

The future direction of this research study is to identify the nodule location and size measurement using Deep NN techniques and later categorize it into different cancer stages. The present work could be implemented on different types of autoencoder for a complex dataset and study the performance. The hyper-parameters may be tweaked to refine the CNN model and check if the accuracy is improved. The outliers can be grouped into different clusters and analyze their behavior in each set. Alongside, the feature rules can be generated to highlight the anomaly score of each group to understand the depth of anomalies present in the data. The accuracy could be improved further by choosing a giant database such as LUNA16 or LIDC/IDRI. The results obtained will help clinicians detect cancer more accurately with an anomaly-free dataset.

VII. CONCLUSION

A study on outliers in medical data has been one of the leading research concerns over the past few years. By and large, the anomalies in the medical data are inevitable but impose complications if left unnoticed. Previously known anomaly detection approaches using PCA are equally efficient; however, PCA attempts to uncover the lower-level features of the input data, but autoencoders learn features from the data having higher dimensions with any complex and non-linear structures. With the help of an encoder and a decoder, clustered in multiple convolutional layers, the autoencoders efficiently remove the outliers without any training labels in the dataset. The encoder absorbs significant features of the images. The original image is reconstructed at the decoder side. Of the 297 images, 23 images are identified as anomalies, with an MSE score greater than 0.7, and the 274 images are identified as normal samples. With 40 epochs, the model attained an accuracy of 98% and an MSE value as low as 0.011. With every epoch, the model learns the features better with extra latent manifolds. The outputs are further classified into benign and malignant. The confusion matrix indicates a good classification of the two classes. Out of 297 input images, 259 images were correctly classified as benign, and 22 out of 24 images were classified as outliers, 5 images that are non-benign but are identified incorrectly as benign, and 11 images were obtained wrongly as malignant. The ROC-AUC curve showed 97.2% efficiency on the classification task. Thus, autoencoder could be a one-stop destination to remove the outliers from complex multivariate data.

ACKNOWLEDGMENTS

One of the authors (RS) acknowledges the Department of Science and Technology – Science and Engineering Research Board (DST-SERB), New Delhi, India, for providing a research grant and postdoctoral fellowship (NPDF, sanction order no PDF/2019/000254). The authors would like to thank the Department of Computational and Data Sciences, Indian Institute of Science, Bangalore, India, for providing complete support to execute this work.

AVAILABILITY OF DATA AND MATERIALS

For ease of use of the proposed methodologies for other researchers and academicians, the entire code and datasets with relevant results have been deposited in the GitHub repository, available (https://github.com/RashmiSKarthik/Outlier-Detection-Anomaly-Detection). The code can be used for other cancer datasets, and the model works efficiently on any Python platform. The researchers may reproduce any copyrighted material with appropriate citations of this work. The repository is for restricted use and in private access mode. However, one of the authors (RS) wishes to provide access to those who need the implementation model adopted in this research paper. Kindly write a mail to drrashmis64@gmail.com to obtain access to this repository.

Declaration of Conflicting Interests

The author(s) declare that there are no potential conflicts of interest concerning this current research, authorship, and/or publication of this work.

References

[1] Liu, H., Li, J., Wu, Y., & Fu, Y. (2018, January 5). Clustering with outlier removal. *ArXiv*. arXiv. https://doi.org/10.1109/tkde.2019.2954317.

[2] Yu, W., Ding, Z., Hu, C., & Liu, H. (2019). Knowledge Reused Outlier Detection. *IEEE Access*, *7*, 43763–43772. https://doi.org/10.1109/ACCESS.2019.2906644.

[3] Lodhia, Z., Rasool, A., & Hajela, G. (2017). A survey on machine learning and outlier detection techniques. *International Journal of Computer Science and Network Security*, *17*(5), 271–276.

[4] Almardeny, Y., Boujnah, N., & Cleary, F. (2020). A Novel Outlier Detection Method for Multivariate Data. *IEEE Transactions on Knowledge and Data Engineering*. https://doi.org/10.1109/TKDE.2020.3036524.

[5] Gribl, A., & Petrinovic, D. (2021). A Robust Method for Gaussian Profile Estimation in the Case of Overlapping Objects. *IEEE Access*, *9*, 21071–21084. https://doi.org/10.1109/ACCESS.2021.3055282.

[6] Bawono, A. H., & Bachtiar, F. A. (2019). Outlier Detection with Supervised Learning Method. In *Proceedings of 2019 4th International Conference on Sustainable Information Engineering and Technology, SIET 2019* (pp. 306–309). Institute of Electrical and Electronics Engineers Inc. https://doi.org/10.1109/SIET48054.2019.8986101.

[7] Wang, H., Bah, M. J., & Hammad, M. (2019). Progress in Outlier Detection Techniques: A Survey. *IEEE Access*, *7*, 107964–108000. https://doi.org/10.1109/ACCESS.2019.2932769.

[8] Ramchandran, A., & Sangaia, A. K. (2018). Unsupervised anomaly detection for high dimensional data-An exploratory analysis. In *Computational Intelligence for Multimedia Big Data on the Cloud with Engineering Applications* (pp. 233–251). Elsevier. https://doi.org/10.1016/B978-0-12-813314-9.00011-6.

[9] Legrand, A., Niepceron, B., Cournier, A., & Trannois, H. (2019). Study of Autoencoder Neural Networks for Anomaly Detection in Connected Buildings. In *2018 IEEE Global Conference on Internet of Things, GCIoT 2018*. Institute of Electrical and Electronics Engineers Inc. https://doi.org/10.1109/GCIoT.2018.8620158.

[10] Chang, S., Du, B., & Zhang, L. (2019). A Sparse Autoencoder Based Hyperspectral Anomaly Detection Algorihtm Using Residual of Reconstruction Error. In *International Geoscience and Remote Sensing Symposium (IGARSS)* (pp. 5488–5491). Institute of Electrical and Electronics Engineers Inc. https://doi.org/10.1109/IGARSS.2019.8898697.

[11] Cook, A. A., Misirli, G., & Fan, Z. (2020, July 1). Anomaly Detection for IoT Time-Series Data: A Survey. *IEEE Internet of Things Journal*. Institute of Electrical and Electronics Engineers Inc. https://doi.org/10.1109/JIOT.2019.2958185.

[12] Yao, D. (Daphne), Shu, X., Cheng, L., & Stolfo, S. J. (2017). Anomaly Detection as a Service: Challenges, Advances, and Opportunities. *Synthesis Lectures on Information Security, Privacy, and Trust*, *9*(3), 1–173. https://doi.org/10.2200/s00800ed1v01y201709spt022.

[13] Ahmed, T., Parvin, Mst. S., Haque, M. R., & Uddin, M. S. (2020). Lung Cancer Detection Using CT Image Based on 3D Convolutional Neural Network. *Journal of Computer and Communications*, *08*(03), 35–42. https://doi.org/10.4236/jcc.2020.83004.

[14] Neal Joshua, E. S., Bhattacharyya, D., Chakkravarthy, M., & Byun, Y. C. (2021). 3D CNN with Visual Insights for Early Detection of Lung Cancer Using Gradient-Weighted Class Activation. *Journal of Healthcare Engineering*, *2021*. https://doi.org/10.1155/2021/6695518.

[15] Sharma, S., Kaur, M., & Saini, D. (2019). Lung cancer detection using convolutional neural network. *International Journal of Engineering and Advanced Technology*, *8*(6), 3256–3262. https://doi.org/10.35940/ijeat.F8836.088619.

[16] Lung Anomaly Detection System (LADS) Using SVM based on Firefly Algorithm. (2017). *International Journal of Science and Research (IJSR)*, *6*(7), 540–544. https://doi.org/10.21275/art20175294.

[17] Beggel, L., Pfeiffer, M., & Bischl, B. (2020). Robust Anomaly Detection in Images Using Adversarial Autoencoders. In *Lecture Notes in Computer Science (including subseries Lecture Notes in Artificial Intelligence and Lecture Notes in Bioinformatics)* (Vol. 11906 LNAI, pp. 206–222). Springer. https://doi.org/10.1007/978-3-030-46150-8_13.

[18] Buitrago, N. R. S., Tonnaer, L., Menkovski, V., & Mavroeidis, D. (2018, November 2). Anomaly detection for imbalanced datasets with deep generative models. *ArXiv*. arXiv.

[19] Astaraki, M., Toma-Dasu, I., Smedby, Ö., & Wang, C. (2019). Normal Appearance Autoencoder for Lung Cancer Detection and Segmentation. In *Lecture Notes in Computer Science (including subseries Lecture Notes in Artificial Intelligence and Lecture Notes in Bioinformatics)* (Vol. 11769 LNCS, pp. 249–256). Springer. https://doi.org/10.1007/978-3-030-32226-7_28.

[20] Albahar, M. A., & Binsawad, M. (2020). Deep Autoencoders and Feedforward Networks Based on a New Regularization for Anomaly Detection. *Security and Communication Networks*, *2020*. https://doi.org/10.1155/2020/7086367.

[21] Albahar, M. A., & Binsawad, M. (2020). Deep Autoencoders and Feedforward Networks Based on a New Regularization for Anomaly Detection. *Security and Communication Networks*, *2020*. https://doi.org/10.1155/2020/7086367.

[22] Meng, Q., Catchpoole, D., Skillicom, D., & Kennedy, P. J. (2017). Relational autoencoder for feature extraction. In *Proceedings of the International Joint Conference on Neural Networks* (Vol. 2017-May, pp. 364–371). Institute of Electrical and Electronics Engineers Inc. https://doi.org/10.1109/IJCNN.2017.7965877.

[23] Tan, Y., Jin, B., Nettekoven, A., Chen, Y., Yue, Y., Topcu, U., & Sangiovanni-Vincentelli, A. (2019). An encoder-decoder based approach for anomaly detection with application in additive manufacturing. In *Proceedings - 18th IEEE International Conference on Machine Learning and Applications, ICMLA 2019* (pp. 1008–1015). Institute of Electrical and Electronics Engineers Inc. https://doi.org/10.1109/ICMLA.2019.00171.

[24] Cao, J., Su, Z., Yu, L., Chang, D., Li, X., & Ma, Z. (2019). Softmax Cross Entropy Loss with Unbiased Decision Boundary for Image Classification. In *Proceedings 2018 Chinese Automation Congress, CAC 2018* (pp. 2028–2032). Institute of Electrical and Electronics Engineers Inc. https://doi.org/10.1109/CAC.2018.8623242.

[25] Muthukrishnan, R., & Rohini, R. (2017). LASSO: A feature selection technique in predictive modeling for machine learning. In *2016 IEEE International Conference on Advances in Computer Applications, ICACA 2016* (pp. 18–20). Institute of Electrical and Electronics Engineers Inc. https://doi.org/10.1109/ICACA.2016.7887916.

[26] Sangari, A., & Sethares, W. (2016). Convergence Analysis of Two Loss Functions in Soft-Max Regression. *IEEE Transactions on Signal Processing*, *64*(5), 1280–1288. https://doi.org/10.1109/TSP.2015.2504348.

[27] Osman, H., Ghafari, M., & Nierstrasz, O. (2017). Automatic feature selection by regularization to improve bug prediction accuracy. In *MaLTeSQuE 2017 - IEEE International Workshop on Machine Learning Techniques for Software Quality Evaluation, co-located with SANER 2017* (pp. 27–32). Institute of Electrical and Electronics Engineers Inc. https://doi.org/10.1109/MALTESQUE.2017.7882013.

[28] Kingma, D. P., & Ba, J. L. (2015). Adam: A method for stochastic optimization. In *3rd International Conference on Learning Representations, ICLR 2015 - Conference Track Proceedings*. International Conference on Learning Representations, ICLR.

[29] Anusha, A., Rao, I. S., & Student, M. T. (2018). A Study on Outlier Detection for Temporal Data. *International Journal of Engineering Science and Computing*, *8*(3), 16354–16356. Retrieved from http://ijesc.org/.

[30] Karadayi, Y., Aydin, M. N., & Ögˇrenci, A. S. (2020). A hybrid deep learning framework for unsupervised anomaly detection in multivariate spatio-temporal data. *Applied Sciences (Switzerland)*, *10*(15). https://doi.org/10.3390/app10155191.

[31] Xin, M., & Wang, Y. (2019). Research on image classification model based on deep convolution neural network. *Eurasip Journal on Image and Video Processing*, *2019*(1). https://doi.org/10.1186/s13640-019-0417-8.

[32] Alrawashdeh, K., & Purdy, C. (2018). Fast Activation Function Approach for Deep Learning Based Online Anomaly Intrusion Detection. In *Proceedings - 4th IEEE International Conference on Big Data Security on Cloud, BigDataSecurity 2018, 4th IEEE International Conference on High Performance and Smart Computing, HPSC 2018 and 3rd IEEE International Conference on Intelligent Data and Security, IDS 2018* (pp. 5–13). Institute of Electrical and Electronics Engineers Inc. https://doi.org/10.1109/BDS/HPSC/IDS18.2018.00016.

[33] Sadaf, K., & Sultana, J. (2020). Intrusion detection based on autoencoder and isolation forest in fog computing. *IEEE Access*, *8*, 167059–167068. https://doi.org/10.1109/ACCESS.2020.3022855.

[34] Xin, M., & Wang, Y. (2019). Research on image classification model based on deep convolution neural network. *Eurasip Journal on Image and Video Processing*, *2019*(1). https://doi.org/10.1186/s13640-019-0417-8.

[35] T. Schlegl, P Seeböck, S.M.Waldstein, U.Schmidt, G. Langs, “Unsupervised Anomaly Detection with Generative Adversarial Networks to Guide Marker Discovery”, (2017).

A Comparative Study of Unimodal and Multimodal Interactions for Digital TV Remote Control Mobile Application among Elderly

Nor Azman Ismail[1]
Nur Haliza Abdul Wahab[3]
School of Computing, Faculty of Engineering, Universiti Teknologi Malaysia, Johor Bahru, Malaysia

Nurul Aiman Ab Majid[2]
User Experience (UX) Department
Software R&D Division
Sony EMCS (Malaysia) Sdn. Bhd

Farhan Mohamed[4]
Media and Games Innovation Centre of Excellence (MaGICX)
Universiti Teknologi Malaysia
Johor Bahru, Malaysia

***Abstract*—A research was conducted to study user interactions design for the TV remote control applications that are preferable among the elderly. Now-a-days smart home concept is widely accepted around the globe. Many applications were developed based on smart home concepts, such as smart remote-control applications for TVs and air conditioners. These applications were helpful in our daily life. However, the elderly tends not to use these applications because of the complexity of the processes and interaction design that is unfriendly. Therefore, this study was conducted to determine which interaction design is preferable for the elderly, enhancing the elderly experience in using the TV remote control application besides encouraging them to use one in daily life and keep up with new technologies. In this paper, the two types of new interaction designs – a touch-based only (unimodal) interaction and multimodal interaction prototypes and an existing TV Remote Control application were compared by conducting usability testing of these three applications on the elderly. Three parameters were considered to compare these three interaction designs: task completion time, error rate, and satisfaction. Also, using usability testing's data collection, statistical analysis was conducted to find out which type of interaction is preferable by the elderly. Ten elderlies participated in the usability testing carried out. The results show a significant difference in these three interactions designs regarding task completion time and satisfaction, but not error rate. After considering usability testing and analyses conducted, the elderly prefers a unimodal interaction design in the TV Remote Control application. Nevertheless, the unimodal interaction was not the typical "tapping buttons" user interface in existing applications. Instead, the favourable interaction design was the one that involved swiping gestures to replace several features that were implemented using buttons on existing TV remote control applications.**

***Keywords*—HCI; usability testing; unimodal; multimodal; elderly**

I. Introduction

Life is all about improvising and making things a lot better and easier than yesterday. Thus, since introducing the first desktop PC in the 1960s, people have developed different styles and ways to interact. Later, when smartphones were introduced to the public, the same thing happened. Nowadays, through the "Smart Home" concept, smartphones had become a powerful device that can control almost everything. One of the most common smartphone applications in the "Smart Home" domain is the remote-control application (app), such as the air-conditioner remote control app and TV remote control app. All the applications provided by this Smart Home remote-control apps make life easier, saving money and cost and save jobs time. However, besides all the superiority given, there is still a lack of Smart Home apps that can cater elderly's special needs, or in other words, elderly friendly. Research in Human-Computer Interaction (HCI) is meant for humans to find and study a better UI to enhance user experience [1].

All the above issues have motivated this study to determine which interaction design is preferable for the elderly in using the TV remote control application. This HCI research focused on enhancing elderly people's experience in using the TV remote control app on smartphones by testing out two types of a new set of interaction designs – touch-based only (unimodal) and multimodal interactions to simplify the user interaction and encourage the elderly to use the application. A usability study was then executed for each proposed solution and an existing system as the benchmark to determine which one was preferred by the elderly – the unimodal, gesture-based only interaction or its multimodal counterpart. Then, the collected data were analysed using statistical Analysis of Variance (ANOVA) tests and paired T-tests to find out where the significant difference arises between those three tested interaction designs.

The contribution of the work reported here is summarized as follows.

1) This study provides a possible solution to enhance the elderly's experience in using TV remote control applications with preferred user interaction design. This will further encourage them to use the latest technology and break down the social exclusion walls besides making their daily lives easier without the need to face the complicated user interface available on existing applications.

2) Proposing an elderly-friendly user interaction design for remote control applications will decrease the need for the elderly to rely on the physical remote control that has many reoccurring problems. Examples of these problems are cannot clearly see buttons on the remote control due to poor eyesight and confused which button on the remote control should be pressed to do some action as there are too many buttons on the remote control.

3) The outcome of this study can raise awareness of the importance of designing a specialized user interface for elderly people.

II. Related Works

According to United Nations (UN), elderly people are defined as people aged 60 and above. World Health Organization (WHO) also uses the 60 years old as a cut off for categorizing elderly or older persons, supporting the UN's definition [2]. In recent years, the percentage of the elderly people population has increased drastically worldwide [3]. Researchers in [4] stated that the European Union (EU) is now the world's oldest region, with 16% of its population comprised of people aged more than 64 years old. This fact is further proven in China, whereas China is the only nation with over 100 million ageing populations [5, 6]. In Malaysia, statistics from the Malaysian Communications and Multimedia Commission (MCMC) state that smartphone usage of people ranged between 60 to 64 years old had increased from 1.9 to 2.9% in 2012 until 2014, respectively [7].

Furthermore, Nielsen stated that today's elderly people tend to have a dynamic lifestyle and most of the time, they are interested in modern technology, including in smartphone usage [6]. Statement in [8] shows that around 30% of elderly own smartphones meet the 11-emerging discussion in [9] that commonly mentions that everyone in this world owns a smartphone. Thus, the rise in figures calls for a need to cater to elderly people's demand for a better user experience, especially in terms of the device itself and the interaction with the applications installed in it. This demand surfaced as elderly people have lower physical and mental capabilities than younger people [10]. Examples of these capabilities are sight, hearing, and motor abilities. These capabilities will go on degrading as people keep on getting older. As per all points stated above, a Mobile Application User Interface (UI) that seems "fit-for-all" is unsuitable for elderly people.

Mobile apps UI is graphical and usually touch-sensitivity on a device to permit communication and interaction between other devices. Mobile app UI, especially for the elderly, need to be designed to be user-friendly and easy to use to motivate the adoption of the technology [11].

Generally, the existing standard applications' UI is not user-friendly to elderly people in some ways. The author in [12] addressed that most smartphone UI is designed for youngsters and professional groups, which cause for elderly to struggle in learning and use their smartphones.

As the solution for these needs and requirements of the elderly, some previous studies found out that the elderly prefer applications with uncluttered, straightforward UI [13]. For instance, it is understandable that older people with poor vision might find it is challenging to read text displayed on the screen and recognize which button is for which action. Many types of research focused on this issue from various angles and managed to come out with several solutions on designing better user interaction for the elderly. Mobile design guidelines, UI principles, mobile health guidelines, inclusive design guidelines, and many others are referred to be summaries on to design the elements for the Mobile apps' UI [11].

The 4th Industrial Revolution (4IR) era has broad the Smart Home concept into a reality, though it is still a lack of friendly usage to the elderly [14]. The lack of elderly-friendly Smart Home applications hinders the elderly to keep up to date with the latest technology, thus widening the social gap with younger people. The cause of this problem may be due to the complexity of the features offered by the application itself to control smart devices effectively [15].

One of the most used Smart Home applications, remote control app, complexity arises from its features to support remote buttons. The need to support an extensive number of remote buttons leads to a complicated user interface and confuses elderly people [16]. Some of those buttons may not even be used by them. Also, most of these applications implemented a unimodal interaction design which involves tapping buttons as inputs. This type of interaction is indeed the simplest form of interaction. However, considering the vast number of remote buttons will confuse users, especially the elderly, on which button should be pressed for each feature. As a result, elderly people may opt not to use this application and still use traditional physical remote control. This too is a loss for the elderly as they need to keep on bearing typical problems when using the physical remote control, such as cannot see the remote buttons clearly due to degraded sight, misplacing the remote control.

Research by [17] combine voice commands, non-verbal behaviours, and gestures in their work. The result shows that natural interaction is more required if compared to remote control based on smartphones. The author in [18] provides a review and analysis of multimodal navigation solutions aimed at people with visual impairments. Both [17, 18] shows that it is important to understand how UI is suitable for the elderly. Thus, in this paper, a comparative study in Unimodal and Multimodal interactions for Digital TV Remote Control Mobile Application among the Elderly will be discussed.

III. Methodology

The evaluation of the proposed unimodal and multimodal interaction designs was conducted in three phases. The first phase was usability testing, where participants need to carry out a set of the same tasks on three different digital TV remote application interactions. One of the applications was the existing application, LG TV Remote, while the other two applications were the prototype built for each proposed interaction design, respectively. During the testing, the task error rate and time taken to complete each task for each participant was noted down. Besides, each participant was required to fill in the System Usability Survey (SUS) questionnaire for each interaction design tested and a Post-Test Questionnaire to compare participants' preferences between the two proposed interaction designs. Next, the second phase was User Preference Analysis. During this phase, the Post-Test Questionnaire results from all participants were analysed to know which participants and why they preferred interaction design. Finally, the Statistical Analysis using the Analysis of

Variance (ANOVA) was carried out to analyse the collected data during the usability testing.

A. Usability Testing

To carry out the usability testing, both independent variables and dependent variables need to be determined. Independent variables are conditions that this research manipulated to assess their effects on participants' behaviours and performance. In contrast, dependent variables are parameters that responded to the manipulation of independent variables. A total of ten participants were gathered for the usability testing experiment conducted. Despite the small sample size (N=10), it was comparable and in line with published studies that recommended a baseline of 5-10 participants for usability studies [19].

Most of the participants are elderly residents from Kampung Jalan Kebun, Shah Alam. Fig. 1 shows usability testing conducted on one of the participants of this testing.

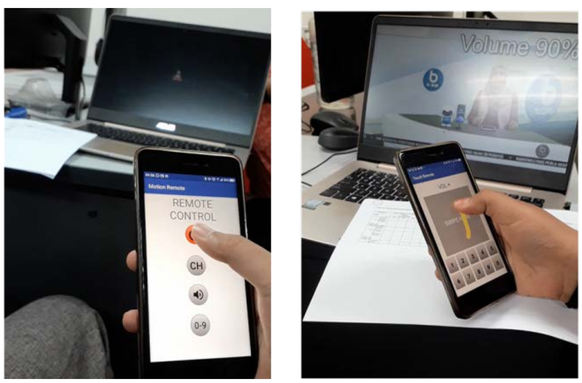

Fig. 1. Usability Testing.

1) Independent variables: There were three independent variables manipulated in this research that closely related to the proposed interaction designs for a TV remote control application. These three independent variables were:

a) Existing TV remote control application (shown in Fig. 2).

b) TV remote control prototype with the proposed touch gestures interaction (unimodal) only (shown in Fig. 3).

c) TV remote control application prototype with the proposed multimodal interaction (shown in Fig. 4).

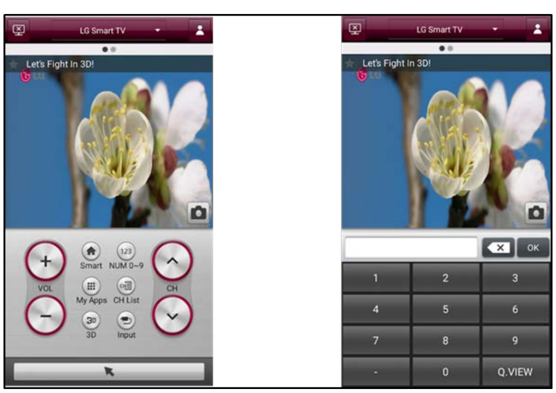

Fig. 2. LG TV Remote App user Interface. [13].

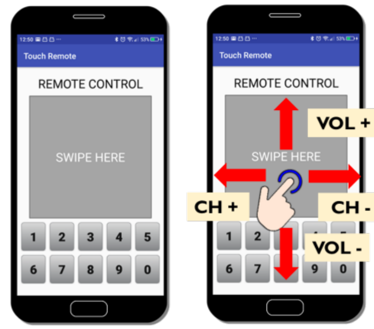

Fig. 3. Proposed unimodal (Solution 1) user Interface.

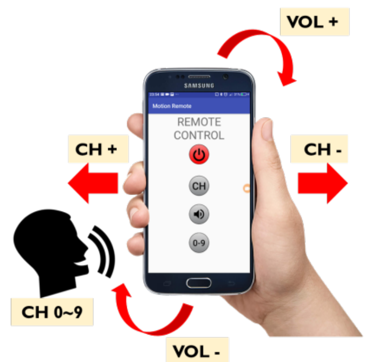

Fig. 4. Proposed Multimodal (Solution 2) user Interface.

2) Dependent variables: The dependent variables, also known as evaluation metrics, captured by this usability testing were effectiveness (error rate), efficiency (task completion time) and satisfaction.

According to [20], effectiveness is universally recognized as an essential usability metric. The participants' error rate measured the effectiveness metrics in this research. A user error was considered to happen when the participant made a mistake that diverted from the task assigned [20]. For example, a task was given to the participant to increase the volume of the TV. However, the participant mistakenly decreases the TV volume thus needed to redo the task assigned until completed. The error rate of participant j for task i can be calculated as the total of user error(s) made by participant j for task i, as shown in Equation 1 [21].

$$Error\ Rate,\ error_{ij} = \sum(user\ error\ made) \tag{1}$$

Next, to measure the efficiency of the task, the time taken for participants to complete the task need to be calculated [22]. Equation 2 below showed the formula to calculate the task completion time of participant j for task i, t_{ij}[23].

$$Task_i\ Completion\ Time,\ t_{ij} = End\ Time - Start\ Time \tag{2}$$

Finally, according to [24], satisfaction can be defined as user acceptance and contentment levels experienced by participants. The satisfaction metric in this research was measured using the System Usability Scale (SUS), a 10-question long survey aiming to quantify the usability of the developed TV remote control app prototypes with the proposed interaction designs.

The SUS score can be calculated using the formula depicted in Equation 3 [25]. In the equation, $\sum OddQ$ referred to the summation of points from odd-numbered questions while $\sum EvenQ$ referred summation of points from even-numbered questions.

$$SUS\ Score = \left((\sum OddQ - 5) + (25 - \sum EvenQ) \right) \times 2.5 \quad (3)$$

B. User Preference Analysis

The user preference analysis was conducted using a Post-Test Questionnaire to determine which interaction designs are more preferred by the elderly – touch gestures-only or multimodal approach and the reasons behind it. The Post-Test Questionnaire was given to participants after they completed the usability testing for both prototypes. This questionnaire consisted of nine questions, and its scoring was designed based on a 7-point Likert Scale to analyse the more favoured prototype by each participant, respectively. Table I shows the list of the Post-Test Questionnaire questions list.

C. Statistical Analysis using ANOVA

To compare the usability of the three different interaction designs, the data gathered during the usability testing needed to be analysed to confirm the relationship between the independent and dependent variables chosen. This analysis was conducted using the one-way Analysis of Variance (ANOVA) with repeated measures and an equal sample size. The ANOVA with repeated measures was applied to evaluate the effects of different conditions (independent variables): existing user interface, proposed touch-based only interaction, and proposed multimodal interaction, on efficiency (task completion time), effectiveness (error rate), and satisfaction.

For each ANOVA analysis carried out, a set of a null hypothesis and alternate hypothesis was established. Therefore, in total, there were three sets of hypotheses tested, as shown in Table II.

TABLE I. POST-TEST QUESTIONNAIRE'S QUESTION LIST

Question Number	Post-Test Questionnaire Question
1	Which interaction design will you prefer to use in the future?
2	Which interaction design did you find complex?
3	Which interaction design did your find easier to use?
4	Which interaction design would you need the help with to use?
5	Which interaction design did you find more intuitive to control a TV?
6	Which interaction design is most accurate?
7	Which interaction design do you think people would learn to use quicker?
8	Which interaction design did you find more cumbersome to use?
9	Which interaction design did you feel more confident using?

TABLE II. HYPOTHESES USED IN ANOVA ANALYSES

Metric	Hypothesis	Hypothesis Description
Time taken to complete (efficiency)	$H1_0$	There is no difference in the user's efficiency in controlling the TV using an application with the existing interface, proposed touch-based gestures interface and proposed multimodal interface.
	$H1_1$	There is a difference in user's efficiency in at least one of the interfaces tested.
Error rate	$H2_0$	There is no difference in the user's error rate in controlling the TV using an application with the existing interface, proposed touch-based gestures interface and proposed multimodal interface.
	$H2_1$	There is a difference in the user's error rate in at least one of the interfaces tested.
Satisfaction	$H3_0$	There is no difference in user's satisfaction in controlling the TV using an application with the existing interface, proposed touch-based gestures interface and proposed multimodal interface.
	$H3_1$	There is a difference in user's satisfaction in at least one of the interfaces tested.

IV. RESULTS AND ANALYSIS

This part focused on evaluating the usability of the two proposed interactions dialogue designed. The evaluation was carried out with the latest and most stable version of the prototypes, together with an existing application, LG Remote TV [13], to serve as a benchmark. Firstly, the collected data on ten participants aged at least 50 years old and above were analysed to understand their background and experiences. Next, the usability testing results were described, tabulated, and illustrated in graphs. Furthermore, analysis was conducted in two ways i) user preference analysis to study which proposed user interaction designs were preferable by elderly and, ii) the statistical analysis using ANOVA on three different metrics measured on three different interaction designs (existing application and the two proposed designs) to find out is there any significant difference between them.

A. Task Completion Time (Efficiency)

Table III shows the means and standard deviations of task completion times for all participants, and these data were described in Fig. 5. For each user interaction design, participants were required to complete a set of identical five tasks. Participants were requested to carry out tasks 1A to 5A on the existing application, tasks 1B to 5B on proposed Solution 1, and tasks 1C to 5C on proposed Solution 2.

Based on Table III and Fig. 2, it was deduced that for each user interaction design, the task that took the least average time to complete was task 1A, 5B, and 5C, respectively, which were tasks to turn on the TV (for existing application) and task to turn off the TV (for both proposed design). Overall, on average, participants took the shortest time to turn off the TV using proposed Solution 1, which took 1.6 seconds, followed by proposed Solution 2 with 1.7 seconds. On the other hand, the task that took the longest time to complete was task 2A, to change the channel to "TV3" using the existing application, with an average of 12.8 seconds. The same task carried out for the two proposed solutions 1, task 2B, managed to significantly reduce the average time taken by approximately one fifth to 2.2 seconds only.

On average, participants spent the longest time to complete the tasks list when using the existing application, LG TV Remote, with an average of 31.15 seconds. In contrast, the proposed Solution 1 interaction design allowed participants to complete all the tasks fastest with an average time of 15.74 seconds. The proposed multimodal interaction (Solution 2) came in second fasted with a total average of 22.96 seconds.

B. *Error Rate (Effectiveness)*

In this study, the error rate was calculated based on the number of errors participants made per task. The means and standard deviations for participants' error rate of each task for all participants (n=10) were shown in Table IV. At the same time, Fig. 6 illustrates the total number of errors made by all participants, categorized by the type of interaction design used.

TABLE III. MEANS & STANDARD DEVIATIONS FOR TASK COMPLETION TIME OF EACH TASK FOR ALL PARTICIPANTS

Task	Description	Mean, $\bar{x}$	Standard Deviation, σ
1A	Turn on the TV (Existing app)	2.5	1.714
2A	Change channel to "TV3"	12.8	4.368
3A	Turn up volume	5.6	2.383
4A	Change to next two channels	7.6	3.456
5A	Turn off the TV	2.7	0.465
1B	Turn on the TV (Solution 1)	2.3	1.217
2B	Change channel to "TV3"	2.2	0.660
3B	Turn up volume	2.9	1.119
4B	Change to next two channels	6.7	4.461
5B	Turn off the TV	1.6	0.663
1C	Turn on the TV (Solution 2)	2.5	1.852
2C	Change channel to "TV3"	5.1	2.110
3C	Turn up volume	4.8	2.114
4C	Change to next two channels	8.9	4.237
5C	Turn off the TV	1.7	0.962

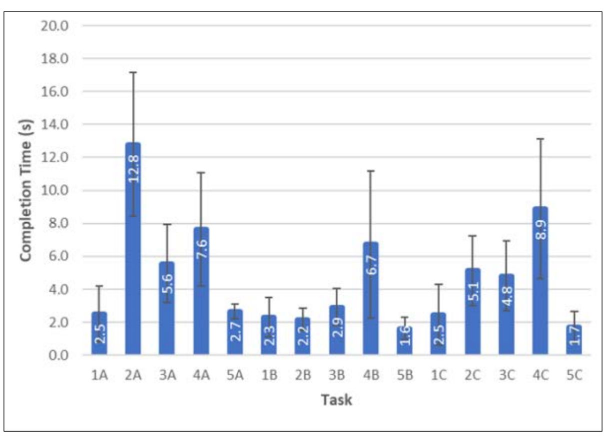

Fig. 5. Participants' Task Completion Time Average for each Task.

TABLE IV. MEANS & STANDARD DEVIATIONS FOR PARTICIPANTS' ERROR RATE OF EACH TASK

Task	Description	Mean, $\bar{x}$	Standard Deviation, σ
1A	Turn on the TV (Existing app)	0.0	0.000
2A	Change channel to "TV3"	0.7	1.059
3A	Turn up volume	0.2	0.422
4A	Change to next two channels	0.2	0.632
5A	Turn off the TV	0.2	0.422
1B	Turn on the TV (Solution 1)	0.0	0.000
2B	Change channel to "TV3"	0.1	0.316
3B	Turn up volume	0.0	0.000
4B	Change to next two channels	0.1	0.316
5B	Turn off the TV	0.3	0.675
1C	Turn on the TV (Solution 2)	0.0	0.000
2C	Change channel to "TV3"	0.0	0.000
3C	Turn up volume	0.5	0.707
4C	Change to next two channels	0.1	0.316
5C	Turn off the TV	0.0	0.000

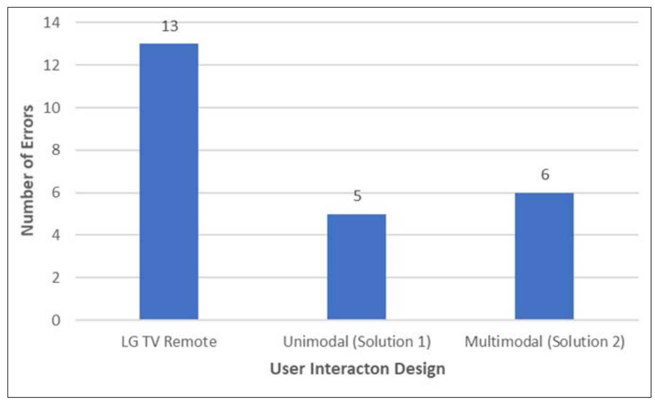

Fig. 6. The Total Number of Errors made for each Interaction Design.

A total of 13 errors were made by all participants when using the existing application, which was the most number among the three interaction designs. The least total number of errors made was from the proposed unimodal interaction design (unimodal). Five errors were made in total, which was more than half of the errors made when using the existing application. Next, followed closely in second, was the proposed multimodal interaction, with a total of six errors made.

C. *Satisfaction*

The satisfaction of participants was measured based on the SUS for each interaction design used in the usability testing. SUS is a 10-question survey to measure participants' satisfaction with the system, or in this case, interaction design tested. A higher total score equals higher satisfaction. An interaction design with good usability should score at least 70 and above [20]. Upon finishing a specific interaction design test, participants were requested to fill in the SUS for that interaction design. Thus, in total, each participant needed to fill in three SUS forms.

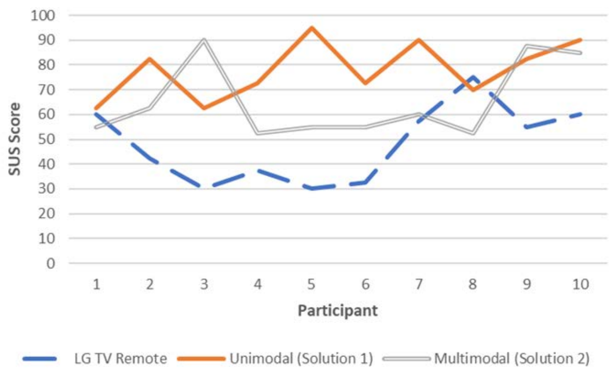

Fig. 7. Line chart of Participant Individual SUS Scoring for each Interaction Design.

Fig. 7 draws a line graph based on the individual SUS score for the three interaction designs of all participants. Based on Fig. 7, the lowest score, 30, was given by two participants for the existing system interaction design. On the other hand, a participant had given the highest SUS score in this research, 95, for the proposed unimodal interaction (Solution 1).

Most of the participants (n=7) preferred Solution 1 the most. Two out of three remaining participants (n=2) inclined towards multimodal interaction design (Solution 2), while the remaining one participant (n=1) opted for the existing system as her top choice.

Fig. 8 shows the average SUS score given by all participants (n=10) for each interaction design. The proposed unimodal interaction design (Solution 1) has the highest average SUS score, 78.0, compared to the other two. The second highest interaction design with an average SUS score of 65.5 was the proposed multimodal interaction design, followed by the existing LG TV Remote application with a 48.0 score. Based on these average scores, in general, it can be deduced that only the proposed unimodal interaction design (Solution 1) has good usability.

D. User Preference Analysis

After carrying out the designated set of tasks for all three interaction designs, participants need to answer a Post-Test Questionnaire to understand the reasons behind their preferences between the two proposed solutions. The Post-Test Questionnaire consisted of 9 questions, whereas participants need to score them between one and seven. The lower score given means that a particular participant favoured the proposed unimodal interaction design (Solution 1) more, while the higher score was given in favour of multimodal interaction design (Solution 2). A score in the middle range (i.e., four) means participants could not decide their inclination towards which interactions related to that question.

Fig. 9 illustrated the average score given by all participants for each questionnaire's question. Based on the average scores, the proposed unimodal interaction design was highly preferred by participants in terms of future usage (Question 1, $\bar{x}_{score} = 2.9$), easiness to use (Question 3, $\bar{x}_{score} = 2.8$), interaction design accuracy (Question 6, $\bar{x}_{score} = 2.5$), learnability (Question 7, $\bar{x}_{score} = 2.7$), and confidence in usage (Question 9, $\bar{x}_{score} = 2.8$).

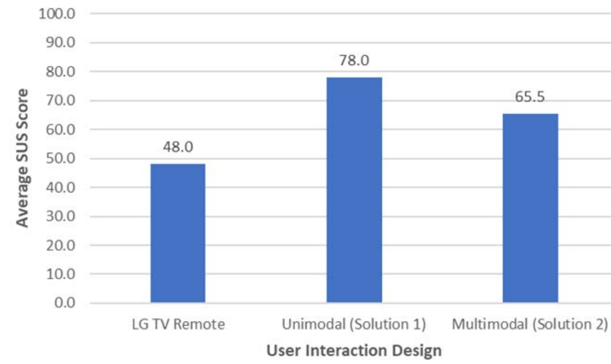

Fig. 8. Average SUS Scoring for each Interaction Design.

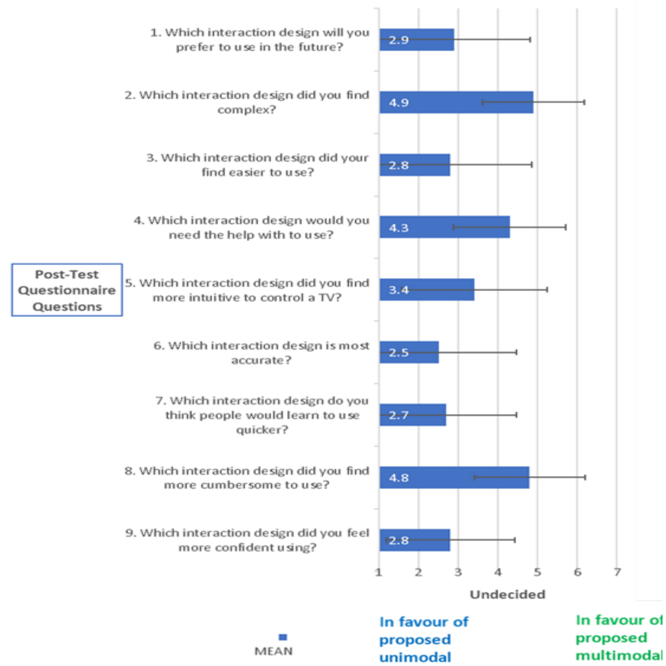

Fig. 9. Average Post-Test Questionnaire score given by All Participants.

E. Statistical Analysis using ANOVA

ANOVA statistical analyses with a confidence level of 95% were carried out to justify rejecting or accepting the previously defined set of hypotheses in part II [26]. ANOVA was used as the significance test needed to be carried out on three different TV Remote Control interaction designs – the existing application, the proposed unimodal interaction, and the proposed multimodal interaction. A total of three ANOVA analyses were conducted, each for task completion time (efficiency), error rate (effectiveness) and satisfaction.

If the null hypothesis for an ANOVA test conducted was rejected, a post hoc analysis was carried out to have in-depth perspectives on which interaction design(s) had a significant difference from other interaction design(s). In this case, the Bonferroni corrected alpha was used to compare against the p-values conducted on the post hoc analysis. This corrected alpha value was used to account for the error rate that may be increased when carrying out multiple t-tests. The formula for the Bonferroni corrected alpha, $\alpha_{corrected}$, was shown in

Equation 4 [24]. α in the below equation stands for the original alpha value used in this experiment which is equivalent to 0.05.

$$\alpha_{corrected} = \frac{\alpha}{number\ of\ tests\ performed} \quad (4)$$

1) Comparison between the different interaction designs in controlling TV efficiency: The ANOVA analysis was conducted to justify any significant difference in task completion time taken (efficiency) between the three different interaction designs. Table *V* showed the descriptive statistics of task completion time for each interaction design. On average, participants took the least time when using the proposed Solution 1 (15.74s), followed by Solution 2 (22.96s), and finally the existing application (31.15s). The variance of each value was then calculated and further down used to carry out the ANOVA analysis.

The ANOVA analysis conducted revealed that the p-value of this test was 4.745×10^{-5}. As the p-value is less than the alpha value used for this test ($\alpha = 0.05$), the null hypothesis, $H1_0$, “there is no difference in user’s efficiency in controlling the TV using an application with the existing interface, proposed touch-based gestures interface and proposed multimodal interface”, was rejected. Instead, the alternative hypothesis, $H1_1$, “there is a difference in user’s efficiency in at least one of the interfaces tested”, was accepted.

As the null hypothesis, $H1_0$ was rejected, a post hoc analysis was then carried out to determine which user interaction design has different efficiency. For this post hoc analysis, the $\alpha_{corrected}$ used was 0.0167 (α = 0.05 divided by 3 tests). Based on the T-tests conducted, there were significant differences in user’s efficiency between when using the existing application and using the proposed Solution 1 ($p-value = 6.380 \times 10^{-5} < \alpha_{corrected}$), and between using the proposed Solution 1 and using the proposed Solution 2 ($p-value = 0.0107 < \alpha_{corrected}$). However, there was no significant difference in user efficiency between using the existing application and using the proposed Solution 2 ($p-value = 0.0172 > \alpha_{corrected}$).

2) Comparison between the different interaction designs in controlling tv effectiveness: Next, ANOVA analysis was carried out to test the existence of significant differences in the mean of error rate (effectiveness) between the three interaction designs – existing application, proposed unimodal, touch-based only (Solution 1) and proposed multimodal interaction. The descriptive statistics of the error rate for these three interaction designs were tabulated in Table VI.

The results of the ANOVA test conducted showed that there was no significant difference in error rate (effectiveness) between these three interaction designs. The p-value for this test was 0.285, which was greater than the alpha value, 0.05 ($\mathrm{p-value} > \alpha$). Therefore, the null hypothesis for this test, $H2_0$, “there is no difference in user’s error rate in controlling the TV using an application with the existing interface, proposed touch-based gestures interface and proposed multimodal interface”, was accepted.

3) Comparison between the different interaction designs in controlling tv user’s satisfaction: Finally, statistical analysis using ANOVA was conducted to determine any significant difference in participants’ satisfaction when using three different user interaction designs of the TV Remote Control application. The descriptive statistics of participants’ satisfaction when using the three different user interaction designs were shown in Table VII.

The results of the ANOVA analysis were conducted for participants’ satisfaction with an existing application. Solution 1 and Solution 2 indicated a significant difference in participants’ satisfaction with the three different user interaction designs. The p-value of this ANOVA analysis was 0.000323, lesser than the alpha value, α , which was 0.05 ($\mathrm{p-value} < \alpha$). Therefore, the null hypothesis for this ANOVA testing, $H3_0$, “there is no difference in user’s satisfaction in controlling the TV using an application with the existing interface, proposed touch-based gestures interface and proposed multimodal interface”, was rejected. Instead, it was concluded that the alternative hypothesis, $H3_1$, “there is a difference in user’s satisfaction in at least one of the interfaces tested”, was accepted.

TABLE V. DESCRIPTIVE STATISTICS OF TASK COMPLETION TIME FOR EXISTING APP, SOLUTION 1 AND SOLUTION 2

Interaction Design	**n**	**Sum, Σ**	**Mean, $\bar{x}$**	**Variance, σ^2**
Existing app	10	311.5	31.15	57.689
Proposed touch-based, unimodal gestures (Solution 1)	10	157.4	15.74	24.967
Proposed multimodal gestures (Solution 2)	10	229.6	22.96	38.465

TABLE VI. DESCRIPTIVE STATISTICS OF ERROR RATE FOR EXISTING APP, SOLUTION 1 AND SOLUTION 2

Interaction Design	**n**	**Sum, Σ**	**Mean, $\bar{x}$**	**Variance, σ^2**
Existing app	10	13	1.30	2.900
Proposed touch-based, unimodal gestures (Solution 1)	10	5	0.50	0.944
Proposed multimodal gestures (Solution 2)	10	6	0.60	0.489

TABLE VII. DESCRIPTIVE STATISTICS OF SATISFACTION FOR EXISTING APP, SOLUTION 1 AND SOLUTION 2

Interaction Design	**n**	**Sum, Σ**	**Mean, $\bar{x}$**	**Variance, σ^2**
Existing app	10	480	48.00	242.778
Proposed touch-based, unimodal gestures (Solution 1)	10	780	78.00	135.833
Proposed multimodal gestures (Solution 2)	10	655	65.50	241.389

To further study the ANOVA testing results, a post hoc analysis was conducted to understand which user interaction design(s) significantly differed in user satisfaction compared to another interaction design.

All the p-values from the additional tests (three t-tests) carried out were compared against the Bonferroni corrected alpha value ($\alpha_{corrected} = 0.0167$). Based on the posthoc analysis conducted, it was indicated that the significant difference only existed between the existing application and the proposed unimodal interaction design (Solution 1), with p-value 0.000142, ($p - value = 0.000142 < \alpha_{corrected}$). However, there were no significant differences in user's satisfaction between the existing application and proposed Solution 2 ($p - value = 0.0216 > \alpha_{corrected}$), and between the proposed Solution 1 and proposed Solution 2 ($p - value = 0.0577 > \alpha_{corrected}$).

V. Discussion

The study observed three hypotheses of efficiency, error rate and satisfaction. Acceptance through the efficacy of the novel unimodal approach in H1 showed potential in improving elderly interaction requirements through new interaction designs, where at the same time, the H2 result showed that unimodal interaction is still the best solution in addressing elderly interaction requirements. While there is no significance found between unimodal and multimodal interaction in H3, further understanding of elderly cognitive load such as cognitive classification [27] could be further explored in designing multimodal interaction for the elderly.

VI. Conclusion

Based on the results and analysis conducted, it was proven that participants had the best efficiency (tasks completion time) when controlling the TV using the proposed unimodal, touch-based only interaction design (Solution 1) than when using the existing system and the proposed multimodal (Solution 2). It was also noted that participants were more satisfied when using the proposed unimodal (Solution 1) than the existing system. However, there was no significant difference in user satisfaction between the proposed Solution 1 and the proposed Solution 2.

On the other hand, there was no significant difference in effectiveness (error rate) when using different interaction designs. Most participants did not make any human error when executing the designated tasks on either interaction design.

Therefore, the new set of unimodal interaction designs (touch-based only) was better than the other two interaction designs in terms of efficiency and produced better satisfaction than when using the existing system. Nevertheless, the unimodal interaction was not the typical "tapping buttons" user interface in existing applications. Instead, the favourable interaction design was the one that involved swiping gestures to replace several features that were implemented using buttons on existing TV remote control applications.

A few suggestions can be carried out in the future. First, this research can include elderly people in the design process of interactive dialogue for controlling TV using the TV remote control application. Finally, more in-depth research can be conducted to study elderly interaction design preference for the TV Remote Control application based on their health conditions (i.e., healthy elderly versus elderly with mild cognitive impairments). This is to study whether the elderly's health conditions affect the interaction design preferred or not.

Acknowledgment

Special thanks to Pusat Aktiviti Warga Emas Johor Bahru (PAWEJB) and elderly residents of Kampung Jalan Kebun, Shah Alam, for participating in the interview session and usability testing experiment conducted for this research. The authors also wish to thank the Ministry of Higher Education, Malaysia, for funding this study under the Fundamental Research Grant Scheme (FRGS/1/2019/ICT04/UTM/02/8).

References

[1] Jiahao Wang, (2019). From Self-efficacy to Human-Computer Interaction Design, Journal of Physics: Conference Series 1168(3):032060, DOI: 10.1088/1742-6596/1168/3/032060.

[2] United Nations, Department of Economic and Social Affairs, Population Division (2019). World Population Ageing 2019: Highlights (ST/ESA/SER.A/430). The United Nations, ISBN: 978-92-1-148325-3, 2019.

[3] Xunjie Cheng,Yang Yang,David C. Schwebel,Zuyun Liu,Li Li,Peixia Cheng,Peishan Ning,Guoqing Hu, (2020). Population Ageing and Mortality During 1990-2017: A Global Decomposition Analysis. DOI: 10.1371/journal.pmed.1003138.

[4] Jonathan Cylus, Josep Figueras, Charles Normand, (2019). Will Population Ageing Spell The End of The Welfare State?: A review of evidence and policy options, World Health Organization (WHO).

[5] B. Jiang and D. Deng, (2016). The Research on Elderly-Adaptive Interface Design Based on Choice-Oriented Attention Theory, in Design, User Experience, and Usability: Design Thinking and Methods, vol. 1, pp. 293–303.

[6] Zhu, H., Lu, J., Zhang, Y. et al., (2019). Responses to Population Ageing in The New ERA: a national condition report from China", China population devision stud. 2, 272–283. DOI: 10.1007/s42379-018-0017-9.

[7] Aslina Baharum, Nurul Hidayah Mat Zain, Aryanto Taharudin, Rozita Hanapi, Azali Saudi and Rayner Alfred, (2017). "Guidelines of User Interface Design for Elderly Mobile Applications: A Preliminary Study", Asian Journal of Information Technology 16 (1) Medwell Journal: 38-44.

[8] Muath Alhussain Khawaji, (2017). Overcoming challenges in Smart Phone use Among Older Adults in Saudi Arabia, Graduate Theses and Dissertations, IOWA State University Digital Repository.

[9] Gladden, D'Juan, (2018). The Effects of Smartphones on Social Lives: How They Affect Our Social Interactions and Attitudes, OTS. Master's Level Projects & Papers. 586.

[10] McPhee, Jamie S et al. (2016). Physical activity in older age: perspectives for healthy ageing and frailty. Biogerontology vol. 17,3 (2016): 567-80. DOI:10.1007/s10522-016-9641-0.

[11] Khan Kalimullah, Donthula Sushmitha, (2017). "Influence of Design Elements in Mobile Applications on User Experience of Elderly People", The 7th International Conference on Current and Future Trends on Information and Communication Technologies in Healthcare, Procedia Computer Science 113, 352-359.

[12] Wong et. al., Rahimah Ibrahim, Tengku Aizan Hamid, Evi Indriasari Mansor, (2018). Mismatch between older adults' expectation and smartphone user interface, Malaysian Journal of Computing, 3(2): 138-153.

[13] Kapczynski, Adrian & Lawnik, Marcin. (2020). Initial survey on the interaction of elderly people with smartphones. Scientific Papers of Silesian University of Technology. Organization and Management Series. 303-313. DOI:10.29119/1641-3466.2020.149.26.

[14] Vaportzis, Eleftheria et al. (2017). Older Adults Perceptions of Technology and Barriers to Interacting with Tablet Computers: A Focus

Group Study. Frontiers in psychology vol. 8: 1687. DOI:10.3389/fpsyg.2017.01687.

[15] Punchoojit Lumpapun, Hongwarittorrn Nuttanont, (2017). Usability Studies on Mobile User Interface Design Patterns: A Systematic Literature Review, Journal Advances in Human-Computer Interaction, DOI:10.1155/2017/6787504.

[16] Mithun Ahamed, (2021). Theory of Usability Index (TOUI) For Improving The Usability of Human-Computer Interaction Design", Thesis for: PhD in Information and Communication Technology, DOI: 10.13140/RG.2.2.18750.41280.

[17] Chiara Cogerino, Giovanni Rosso, Ilaria Bosi, Antonella Frisiello, Marco Bazzani, (2017). Multi-modal input devices for Active and Healthy Ageing, The 25th International Conference on Software, Telecommunications and Computer Networks.

[18] Kuriakose, Bineeth, Raju Shrestha, and Frode E. Sandnes 2020. "Multimodal Navigation Systems for Users with Visual Impairments—A Review and Analysis" Multimodal Technologies and Interaction 4, no. 4: 73. DOI:10.3390/mti4040073.

[19] Macefield, R. (2009). How to specify the participant group size for usability studies: a practitioner's guide. Journal of Usability Studies, 5(1), 34-45.

[20] N. A. Ismail and Y. Y. Pang, (2015). A Multimodal Interaction for Map Navigation and Evaluation Study of its Usability, vol. 10, no. 23, pp. 17962–17970.

[21] Lee Son, T, Wesson, J., and Vogts, D., (2018). Designing a Natural User Interface to support information sharing among co-located mobile devices, South African Computer Journal 30(2), 44–71. DOI: 10.18489/sacj.v30i2.440.

[22] Jeff Sauro, James R. Lewis, (2016). Quantifying The User Experience: Practical Statistics For User Research, Elsevier Science & Technology, 2nd Edition.

[23] T. Lee Son, J. Wesson, and D. Vogts, (2018). Designing a Natural User Interface to Support Information Sharing among Co-Located Mobile Devices, South African Comput. J., vol. 30, no. 2, pp. 44–71.

[24] Rasmus Magnusson, (2020). High Confidence Network Predictions from Big Biological Data, PhD Thesis, Linkoping Studies in Science and Technology.

[25] Orfanou, K., Tselios, N., & Katsanos, C. (2015). Perceived usability evaluation of learning management systems: Empirical evaluation of the System Usability Scale. The International Review of Research in Open and Distributed Learning, 16(2). DOI:10.19173/irrodl.v16i2.1955.

[26] Department of Statistics and Data Sciences, (2016). ANOVA and Post Hoc 2016," 2016.

[27] Chirayus, K., & Nanthaamornphong, A. (2019). A systematic mapping review: Mobile user interface design guidelines for the elderly with cognitive impairments. In 2019 23rd International Computer Science and Engineering Conference (ICSEC) (pp. 35-42). IEEE.

Harnessing Emotive Features for Emotion Recognition from Text

Rutal Mahajan[1], Mukesh Zaveri[2]
Department of Computer Engineering
Sardar Vallabhbhai National Institute of Technology, Surat, Gujarat, India

***Abstract*—With the prevalence of affective computing, emotion recognition becomes vital in any work related to natural language understanding. The inspiration for this work is provided by supplying machines with complete emotional intelligence and integrating them into routine life to satisfy complex human desires and needs. The text being a common communication medium on social media even now, it is important to analyze the emotions expressed in the text which is challenging due to the absence of audio-visual cues. Additionally, the conversational text conveys many emotions through communication contexts. Emoticon serves the purpose of self-annotation of writer's emotion in text. Therefore, a machine learning-based text emotion recognition model using emotive features proposed and evaluated it on the SemEval-2019 dataset. The proposed work involves exploitation of different emotion-based features with classical machine learning classifiers like SVM, Multilayer perceptron, REPTree, and decision tree classifiers. The proposed system performs competitively well in terms of f-score 65.31% and accuracy 87.55%.**

Keywords—Emotion recognition; emotive features; natural language processing; affective computing

I. Introduction

A human newborn comes with primary settings for understanding and communicating basic feelings, as well as an immense ability to learn. A newborn baby can cry or stay calm, smell, and turn her head towards her mother. With the growing age, her neural network starts learning facial expression and gradually develops to read and express more emotions using different senses. The sense of recognizing and expressing emotion develops gradually from basic to complex linguistic if-then scenarios. To make computers understand and manage emotions as a human baby can do requires lots of work in that direction. How communication takes place is important in emotion recognition because it's not about what is being said, but about how it is being said. Expressions matter, as the sentiment behind each encounter and the emotions, are raised. Emotion is knotted with the literal meaning of words used. New research in artificial intelligence is giving machines, like software agents, computers, robotic pets, and any digital device, smart capabilities along with emotional intelligence Artificial intelligence is progressing towards emotional intelligence by implementing different tasks in real-time. Sentiment analysis is now considered the general task of natural language understanding. It is evolved as coarse-grained emotion recognition that is multiclass classification of sentiments.

Emotion recognition in the text is similar to many other problems in text classification and analysis. It is considered as a sub-task of sentiment analysis. Text is categorized into different 5 basic categories of emotions based on different emotion models that exist in psychology [1]. Currently, researchers have categorized the text into more than 20 complex emotion categories and applied to detect depression, joy, happiness index of the country, and many more application domains [2],[3]. Text Emotion recognizing has a variety of applications including identifying anxiety or depression of individuals and measuring the well-being or public mood of a community. Emotion recognition concerns extracting detail-level sentiment and associated emotion extraction from text. [4]. Sentiment analysis classifies the text into different polarities. Whereas, emotion classification can follow a detailed level of emotion categories belonging to particular polarity. Moreover, perceiving emotions from only text expressions is a difficult task due to the lack of audio and visual expressions. Thus gradually emoticons or emoji are evolved as substitutes for facial expressions during written commination over time. Emoticons are the pictorial simplified representation of facial expression conveying affective information in text communication. By using, emoticons, readers can understand the sender's emotional state without using many more words than simple text during textual communication. If the origin of any language is studied, they have evolved from ideographs, i.e. a graphical symbol representing an idea or concept regardless of specific language, words, and phrases[5]. Due to common communication features and evolving emoticon lexicons regardless of any language, emoticons become the universal language of communication [6],[7]. The deep learning models gain popularity with rise in the resources running these heavy models requiring large amount of training data [8], [9], [10], [11]. But these models are computationally costly and require resources affecting the environment [12], [13].

In this paper, to produce the human like prediction results for the emotion of the conversational text, simple machine learning based models is used with emoticon-based features. Emoticons are important entities conveying emotion expressed by a writer using tiny facial images. They evolved from a single smiley face to emoticons to images and complex emotion conveying stickers. Among all these, non-verbal emotion conveying parts of the text, images most widely use symbolic language during digital written communication [14]. Thus to capture the non-verbal emotional clues from the text, which are conveyed by the writer by use of emoji, sentiment information-related resources for emoji are utilized in our work. Moreover, emotions conveyed in the conversational text require contextual information to identify it. Thus other lexical resources to capture emotions conveyed in the text are also used here.

The rest of this paper is as follows. Section 2 explores the notions related to emotion, emotion representation models, work done in the field of emotion recognition. The details about the proposed work on emotion recognition in conversational text messages, features, and experimental setups are given in Section 3. In Section 4, an analysis and discussion on the results of the proposed work are carried out. Finally, a conclusion with possible future directions of this work is described in Section 5 followed by references.

II. Related Works

Emotion recognition in the text is gaining interest in the research community aiming to extract detail level emotions from personal opinions, reviews, or any kind of feeling expressed in text over various media [4]. Due to various ways to express emotion in text such as using a direct expression, indirect expression, using graphical emoji and many ways, from text with polarity, it is evolved to an interesting field of research these days. Different factors affecting emotion recognition in the text are the domain and scope of data, the language used in data, choice of emotion model for deciding emotion labels in output, and classifiers, or recognition models for predicting the output.

Wherever human communication involves, emotions come into the picture. Emotions appear in varieties of speakers depending on the formal communication style or informal communication style. Sarcasm and humor are such types of figures of speech that convey a variety of emotions very complex manner [15]. It can be observed in the text communications over various mediums like Twitter, emails, Facebook or any websites providing platform to share personal views of people with numerous topics of discussions. It can be observed in the text communications over various mediums like Twitter, emails, Facebook or any website providing platform to share personal views of people with numerous topics of discussion. Emotion can occur in different sizes of text segments ranging from words to paragraphs and long documents, and even collections of documents. This parameter is crucial to decide the scope of the recognition model. Emotion recognition at the word level can be used to build the emotional vocabulary resources by using its connected emotional words. Document or paragraph level emotion recognition can be useful to give an emotional abstract view of the topic [16]. Emotion recognition from a collection of documents, paragraphs, and such longer scopes can give insights about the view of people on a certain topic, event, and product. For example, extracting and analyzing YouTube comments for emotion detection can give insights into the reaction of people on a particular topic, product, or user. Understanding emotions in absence of audio-visual cue is a hard problem. For example, when you read, "Why are you ignoring me", it is difficult to decide whether it is conveying an angry or sad emotion? The context of this conversation should be known to recognize emotion. In this work, emotion recognition is carried out on such textual conversation data.

Most of the work on emotion recognition is done in the English language due to the easy availability of resources required for linguistic processing. Chinese [17] and Japanese [18] are other frequently studied languages in this field. Numerous multilingual systems are also present in the literature for the sentiment analysis task but left understudied for a detailed level categorization task, that is, emotion recognition. In this work, we focused on the English language conversation texts for the categorization of emotion beyond positive, negative, and neutral tags.

To recognize emotions from text, first text need to be represented formally using different emotion models. For emotion recognition from text, researchers used both dimensional and categorical models of emotions. 2-dimensional Valence-Arousal space [19], and 3-dimensional Pleasure-Arousal-Dominance model are most commonly chosen dimensional model in this area of research. The most commonly used categorical models are Ekman's [20] emotion model with the 6 basic emotions and Plutchik's [1] emotion model with 8 primary emotions. In this work, we use the categorical model with simply four basic categories of emotions: happy, sad, angry, and others.

Different emotion recognition approaches in the literature are studied in this work, which can broadly be categorized into three categories:

A. Non Machine Learning Methods

Many methods make use of keywords in a sentence and use their co-occurrence with other keywords with explicit emotional value [21]–[23]. For finding the emotional values of words, different lexical resources are used. Popular lexical resources developed for English language are WordNet-Affect [24] and SentiWordNet [25]. These methods are heavily dependent on handcrafted rules created by human experts and resources used.

B. Non-neural Machine Learning Methods

Unlike other text categorization tasks, emotion recognition, most machine learning methods work by extracting features such as the presence of frequent words, negation, punctuation, emoticons, and so on to create feature representation of the sentence [15]. This representation is used as input by various classifiers to predict the output [26]–[28]. These methods often require a good knowledge of feature engineering for better prediction.

C. Deep Learning Methods

Neural network-based approaches with deeper network architecture have become a popular choice in varied tasks in text, speech, and image domains due to ease of not worrying about feature engineering. Variants of Recurrent Neural Networks, such as LSTM [29] has been effective in modelling sequential information. Also, Convolutional Neural Networks [30] have been a popular choice. These methods require large quantities of data to be worked on properly. The summary of various works reported in literature in the field of text emotion recognition with recent consideration is given in Table I. The majority of the work is done using resource costly deep learning models with a popular choice of deep learning model being variants of LSTM.

TABLE I. SUMMARY OF RECENT EMOTION RECOGNITION WORK IN TEXT

Ref.	No. of Emotions	Approach	Language	Dataset	Performance	Remarks
[15]	2 (Humor, Not Humor)	Machine Learning based (Support Vector Machine, Naïve Bayes, Multilayer Perceptron)	English	Yelp Review Data (6000)	Precision:60.2% Recall:90.1% Fscore:72.2% Accuracy: Not given	Humor or Not Humor is predicted based on affect-based and user's writing style specific features (2020)
[8]	4 (Happy, Sad, Angry, Others)	Deep Learning (Transfer learning based model)	English	SemEval 2019 Task 3 (Train: 30160 Test: 6032)	Precision: Recall: Fscore: Accuracy: Not given	LSTM and BERT based emsemble model (2020)
[9]	4 (Happy, Sad, Angry, Others)	Deep Learning (Simplest Long short term memory network with fully connected neural network at output layer)	English	SemEval 2019 Task 3 (Train: 30160 Test: 6032)	Precision:50.21% Recall:71.04% Fscore:58.51% Accuracy: Not given	100 dimensional GloVe embedding, 128 dimensional representation of sentence,4 dimensional output representation, Baseline system of SemEval 2019 Task-3 (2019)
[10]	4 (Happy, Sad, Angry, Others)	Deep Learning (Fine-tuned BERT with hierarchical Long Short Term Memory Network)	English	SemEval 2019 Task 3 (Train: 30160 Test: 6032)	Precision:56% Recall:81.66% Fscore:77% Accuracy: Not given	Semantic and emotional content of text encoded via GloVe, ELMo and DeepMoji (2019)
[11]	4 (Happy, Sad, Angry, Others)	Deep Learning (Sentiment and Semnatic LSTM)	English	Text Conversation Dataset (Train: 30160 Test: 6032)	Precision:80.87% Recall:64.08% Fscore:79.34% Accuracy: Not given	LSTM based approach proposed to predict Happy , Sad or angry in text conversations (2017)
[31]	2 (positive, Negative)	Support Vector Machine, Naive Bayes. Semantic relatedness between aspect word and student's opinion sentence is calculated.	English	Tweets on Educational aspects (1728)	Precision:96.85% Recall:84.6% Fscore:89.95% Accuracy: Not given	Aspect based sentiment analysis. SentiWordnet used to categorize words into different polarity. (2017)
[32]	8 (joy, hate, love, expect, surprise, anxity, sorrow, anger)	Hierarchical Bayesian inference methods	Chinese	Blog articles (train:917, test: 230)	Precision:84.00% (documentl level) 46.68% (word-level) Recall: 83.24% (document-level) 36.06(word-level) Fscore: 53.06% (document –level) 45.11(word-level) Accuracy: Not given	Contextual information used, predicts emotion for word and document(2017)
[33]	2 (Happiness, Sadness) or (Positive, Negative)	Lexicon based backtracking approach for sentiment analysis	Bengali	301 Bengali Text sentences	Precision: Not given Recall: Not given Fscore: Not given Accuracy: 77.16%	Used lexical resources , experiment done on very limited data (2017)
[34]	4 (Happy, Sad, Angry, Others)	Machine Learning based method (Light-GBM tree)	English	SemEval 2019 Task 3 (Train: 30160 Test: 6032)	Precision: 76.8% Recall: 78.76% Fscore: 77.65% Accuracy: Not given	combination of lexical features such as word and character grams, along with additional signals like emotional intensity, valence-arousal-dominance scores (2019)

III. Proposed Emotion Recognition Model

In natural language understanding, emotion recognition is a hierarchical task carried out based on the indirect expression of feelings and emotions. Text communications are very common these days due to the prevalence of various digital communication media, and they may contain figurative language. So the novelty of this work is to implement the emotion recognition model for textual conversation data using classical machine learning algorithms along with minimalistic features. The set of various emotion features based on emoticon (emoji) sentiments and lexical emotion resources are proposed in this work for text emotion recognition.

Emotion recognition in text conversation is implemented as a classification task. Let U = $\{u_1, u_2\}$ be the users involved in 3-turn text conversation. C = $\{(c_1u_1, c_1u_2, c_1u_1), (c_2u_1, c_2u_2, c_2u_1) \ldots (c_nu_1, c_nu_2, c_nu_1)\}$ be the set of n 3-turn conversations between user u_1 and u_2. In this input conversation text, 3 conversation texts are provided. First is by user 1, second is its reply from user 2 and last is again the turn of user 1. E=$\{e_1,e_2,e_3,\ldots e_n\}$ be the corresponding set of emotion labels given to each conversation triplets where e ∈ {happy, sad, angry, other} indicates the corresponding output emotion conveyed in 3-turn conversation. The objective of the proposed model is to predict conditional label distribution P(e|c) from the text conversation dataset of SemEval-2019 [11] to assess the competitiveness of the proposed work globally. The proposed emotion recognition model works as shown in Fig. 1. The file containing 3-turn conversation text and emotion labels are given as input to the feature extractor where 20 different features related to emotions and emoticons are extracted. The classifier is trained using extracted features to classify the text conversation triplets into any of four emotion labels, namely, happy, sad, angry, and others. The detailed process is explained below:

A. Phase 1: Pre-processing

Before using the dataset on the proposed emotion recognition model, it is pre-processed to resolve inconsistencies.

1) Emoticons/emoji from text conversations are replaced with their corresponding description of conveyed emotion. The words in the emoticon description are used to extract the sentiment and emotion-related information using lexical resources. For replacing emoticon sentiments and related description details, the sentiment of emoji is used as a lexical resource [35].

2) Tokenization: short text conversation in each turn is divided into distinct words, punctuations across the white spaces. Emotion description is considered separately for processing by lexical resources as per emotive word presence in it.

B. Phase 2: Feature Extraction

To identify different emotions from the given text fragment, suitable features are extracted from the given text. These features act as determinants of different output emotion classes. Phase 1 replaces emoticons appearing in text with their short descriptions. Emotions in the text can be conveyed majorly by emoticons, if present, and by various linguistic units like specific emotive words and contexts used by writers. The Emotion-based and emoticon sentiment-based features are used as an emotion feature vector in the emotion recognition model. These features use various lexical resources like EmoLex [36], EmoSenticNet [37], and Emoji Sentiment Ranking [35]. 10 features are extracted using 2 EmoLex sentiments (positive and negative) and 8 different emotion labels, namely, Surprise, joy, anger, trust, anticipation, fear, disgust. Sadness. Similarly, from EmoSenticnet lexicon 6 features using different emotion labels, namely, anger, disgust, fear, joy, sadness, and surprise are extracted. Another emotive resource used in this work is related to the sentiment of emoticons, which is related to calculating the negative, positive, neutral, and overall sentiment score of the emoticon.

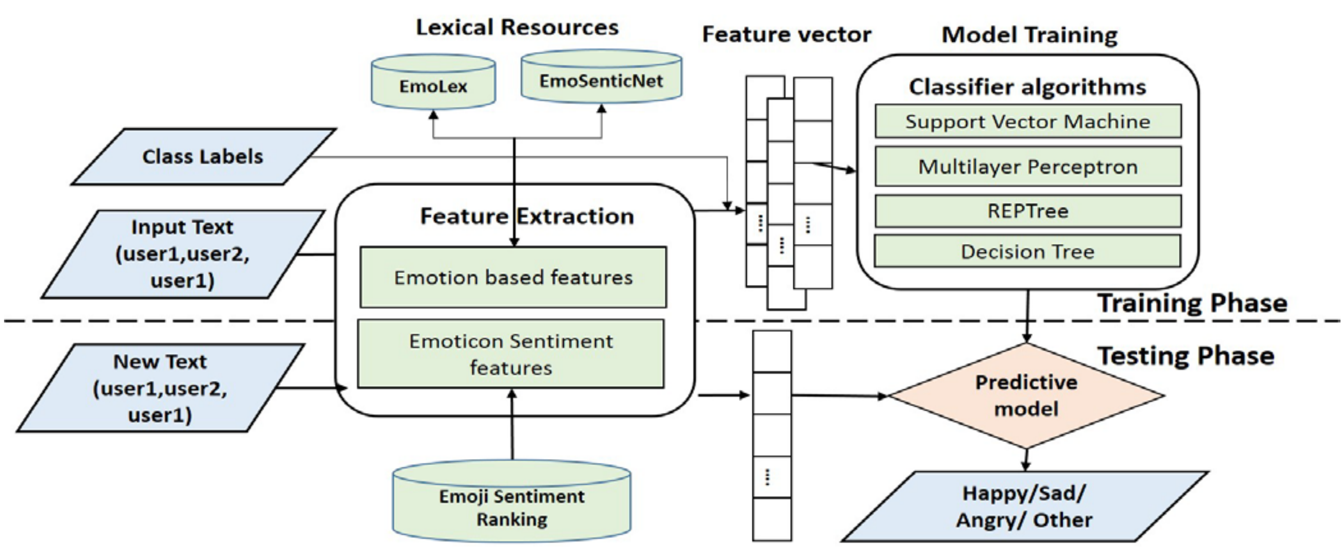

Fig. 1. Proposed Emotion Recognition Model using Emotion and Emoticon Sentiment-based Features.

C. Case 3: Classification

For classification of text conversations according to emotion, it exhibits, four different classifiers are tested on the dataset, namely support vector machine, multilayer perceptron, REP (reduced error pruning) Tree, and decision tree classifiers. These classifiers are chosen based on their performances in the literature on tasks related to emotion recognition [38], [39],[2]. We used the implementation of these algorithms as given in the experimental environment [40]. Support Vector Machine: SVM (Support Vector Machine) is a supervised algorithm working well for both classification and regression. We implemented sequential minimal optimization-based SVM here. Multilayer Perceptron is a simple yet effective neural classifier algorithm. REPTree is a fast decision tree algorithm for classification.

D. Dataset

The difficulty of emotion recognition increases when we need to recognize the emotion conveyed in the conversational text. Because as humans, on reading the text “You missed our 5th anniversary!!” It can be either interpreted as a sad or angry emotion and the same ambiguity exists for machines. So the performance of this work is evaluated on a 3-turn text conversation dataset released by SemEval 2019 [11]. One sample of the dataset contains conversations from Twitter in three turns, i.e. User 1’s tweet; User 2’s response to the tweet, user 1’s response to User 2’s response [41]. A total of 30160 samples are used in the training of the classifier, each sample labeled with Happy or Angry or sad or other. 2755 samples are used for validation and 6032 samples are used for testing of the model [11]. The details of emotion class label distribution for samples in the dataset are as given in Table II. As the distribution of data in various class labels in the training set impacts the classifier performance, Fig. 2 represents the data distribution in various emotion classes in the training set. 50% of samples are having other labels and 50% of samples are having emotion class labels from happy, sad, and angry. These emotion labels are distributed as 18% of samples in the dataset are having angry, 18% samples are having sad and 14% samples are having happy emotion labels.

The challenge of working with this dataset is the size of data in each conversation sample, which is relatively small, approximately 4 words in each user conversation. During pre-processing and feature extraction it becomes of utmost importance to ensure minimal loss of useful information with noise removal from each conversation samples.

TABLE II. DETAILS OF SEMEVAL 2019 TEXT CONVERSATION DATASET

	Train	Validation	Test
Happy	4243	142	803
Sad	5463	125	1114
Angry	5506	150	1121
Others	14948	2338	2994
Total Samples	30160	2755	6032

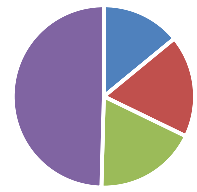

Fig. 2. Emotion Class Label Distribution in the Training Dataset.

IV. EXPERIMENTAL SETUP

A. Experiment Configuration

The experimental environment used for training of the proposed emotion recognition model is a CPU-based system having Intel 64-bit core i5 2.5 GHz processor with Windows 7 operating system and 4 GB RAM. For evaluation, we used different metrics as described in Section 4.2. In the experiment, we have evaluated our hypothesis for the effectiveness of emotion-based and emoticon-based features which we defined to explore its power for recognizing emotions in text.

Hypothesis: Does the proposed emotion recognition model benefit from emotion and emoticon-based features?

Experiment: To check the effectiveness of this hypothesis ,the emotion recognition model with implementations of simple state-of-the art classifiers from Weka such as support vector machine, different variants of multilayer perceptron, decision tree classifiers, and REP Tree classifier is trained with three variations: 1) individual set of emotion-based features, 2) emoticon-based features, and 3) emotion-based and emoticon-based features altogether. Comparative evaluation is done on the results of all classifiers with these three cases. We have not taken results on only emoticon-based features as most of the time any text in the dataset contains approximately 3 to 4 words and optional presence of emoticons.

B. Evaluation Measures

Considering emotion recognition as a task of classification, different measures used to evaluate the performance of classification model are precision, recall, f-score, accuracy, and Mathew’s Correlation Coefficient for evaluating the performance of most natural language understanding systems.

Precision is calculated by Eq. (1) as follows. The higher values of precision indicate not only more occurrences of correctly classified values but mainly fewer occurrences of False Positive (FP) values.

$$precision = \frac{TP}{TP + FP} \tag{1}$$

Recall is calculated by Eq. (2) as follows. The higher values of recall indicate not only more occurrences of correctly classified values but mainly fewer occurrences of False Negative (FN) values.

$$recall = \frac{TP}{TP + FN} \tag{2}$$

Precision and recall cannot be used independently to evaluate the performance of any classifier. System recall can be easily increased by labelling class values at the cost of precision and vice versa. Thus F-score is used which considers both the precision and recall to balance. It can be given by Eq. (3) as follows.

$$f - score = 2 * \frac{precision * recall}{precision + recall} \tag{3}$$

Accuracy is the proximity of measurement results to the true value. It can be given by Eq. (4) as follows.

$$Accuracy = \frac{TP + TN}{P + N} \tag{4}$$

Matthew's correlation coefficient is not much popular evaluation measure in classification tasks but it is promising than f-score and accuracy while evaluating qualitatively the performance of the classifier. It can be given by Eq. (5) as follows.

$$MCC = \frac{TP \times TN - FP \times FN}{\sqrt{(TN + FN)(FP + TP)(TN + FP)(FN + TP)}} \tag{5}$$

F-score ignores the count of true negatives (TN), whereas MCC considers all the entries of the confusion matrix for evaluating the performance of the classification model. This measure does well only when the classifier is doing well on both negative and positive elements. So F-score gets affected more when the minority class is labeled as negative. When the majority class is labeled as negative f-score can be considered as a good measure because in such cases rare items are of interesting samples for classification.

V. Result and Discussion

Higher average accuracy is considered as a good score, where the task is to predict the label of the emotion considering all the emotion class labels have an equal number of the sample distribution. Here as mentioned in the dataset description given in Table I, happy, sad, and angry emotion classes have almost equal proportion of samples but another 50% of samples belong to other emotion categories. So we evaluate the performance of our proposed model using f-score values for each classifier. Table III shows a summary of results with different classifiers on a different set of features.

From the results of the experiment, it is evident that the accuracy and f-score of REP Tree are higher in the cases of individual 16 emotion-based features and with all 20 emotion and emoticon-based features. Tree-based classifiers have performed better than other classifiers in the emotion recognition task. Moreover, from Fig. 2 and Fig. 3, the effect of the use of emotion-based features on the performance of classifiers can be observed. It is marked that after including emoticon-based features in the feature set for classification of emotion, a significant improvement is observed in the f-score as well as in accuracy.

In Fig. 3, f-score (20) represents all 20 features used for classification, and f-score (16) represents all emotion-based features used for classification. Similarly in Fig. 4, accuracy (20) represents all 20 features used for classification, and accuracy (16) represents all emoticon-based features used for classification. With the inclusion of 4 emoticon-based features in classification, SVM performance is improved by 1.91% accuracy and 0.89% f-score. In REPTree, it is improved by 2.08% accuracy and 0.7% f-score. With the inclusion of emoticon based features proposed emotion recognition model achieves the highest accuracy of 87.55% and f-score of 65.31% with the use of the REPTree classifier.

TABLE III. Performance of Proposed Emotion Recognition Model with Various Feature Sets on SemEval 2019 Dataset

	Classifier	SemEval 2019 Text Conversation Dataset			
		Precision	***Recall***	***F-Score***	***Accuracy***
Emotion Features (16)	SVM	56.15%	38.06%	45.37%	83.07%
	MLP	61.35%	48.74%	54.32%	84.86%
	MLP-3	51.34%	59.02%	54.92%	84.43%
	REPTree	62.29%	54.12%	57.92%	85.47%
	Decision Tree	65.46%	43.89%	52.55%	85.36%
Emotion (16) + Emoticon Sentiment Features(4)	SVM	61.95%	48.38%	54.33%	84.98%
	MLP	67.30%	57.09%	61.77%	86.95%
	MLP-3	61.09%	61.04%	61.06%	85.62%
	REPTree	**67.26%**	**63.46%**	**65.31%**	**87.55%**
	Decision Tree	69.52%	47.30%	56.30%	86.43%

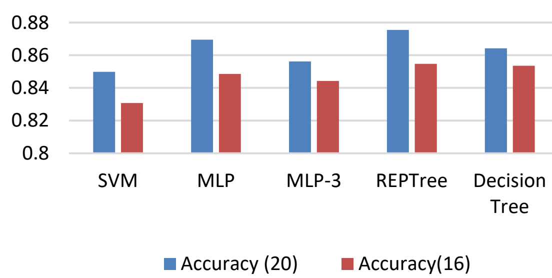

Fig. 3. Comparison of the Effectiveness of Features of Classifier Performance in Terms of Average f-score of all Emotion Classes.

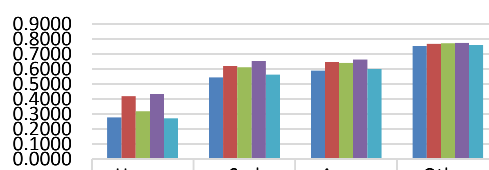

	Happy	Sad	Angry	Other
SVM	0.2777	0.5433	0.5891	0.7528
MLP	0.4183	0.6178	0.6478	0.7684
MLP-3	0.3185	0.6107	0.6420	0.7706
REP Tree	0.4337	0.6531	0.6629	0.7752
Decision Tree	0.2708	0.5630	0.6013	0.7600

SVM MLP MLP-3 REP Tree Decision Tree

Fig. 4. Comparison of the Effectiveness of Features on Classifier Performance in Term of Average Accuracy of all Emotion Classes.

The performance comparison of our model with different machine learning classifiers with other similar systems on SemEval 2019 text conversation dataset is summarized in Table IV. This global evaluation was carried out in the SemEval 2019 in task 3. Majority participant systems has implemented their emotion recognition module with LSTM / BiLSTMs with well-known word embedding like GloVe is used for input representation and BERT is used for transfer learning by most systems using deep learning. We proposed machine learning based solution to give results close to human performance on text based emotion prediction, which is less resource expensive in comparison with deep learning approaches. The best performing classifier in our model repots the f-score higher than the mean f-score of all participating teams in this evaluation, which are implemented using deep learning; the top few among them are represented here in summary Table IV. Another interesting fact to notice from the analysis is that our model with all chosen classifiers except SVM performed well in terms of higher f-score than the baseline provided for the global evaluation. The baseline system was also implemented using deep learning model with 100 dimensional GloVe embedding. Our model with 20 different emotion-based features performs well.

Class label distribution has a great effect on classifier performance, which can be observed very clearly in the performance of each classifier. Fig. 5 describes the emotion-wise performance of each classifier in terms of an f-score. The happy emotion class has not performed well with any of the classifiers used in the proposed model. The highest f-score value achieved on the happy emotion class is 43.47% by using the REPTree classifier. The evident reason found for the bad performance of all classifiers on the happy emotion class is that the happy class has the least sample distribution in the dataset. Another reason we observed that the statements in conversations conveying the happy emotion need context to understand them. Detailed analysis of each emotion class is carried out with best performing classifier REPTree in terms of correctly classified and misclassified samples in each emotion class. The confusion matrix is prepared as shown in Fig. 6 for each emotion class, namely, happy, sad, angry, and others. For each emotion class, Matthew's correlation coefficient (MCC) is calculated, which is useful to evaluate the classifier in terms of quality. This coefficient takes into account true positives and true negatives as well as false positives and false negatives. It is considered as a balanced measure that can be used even if the classes are of very different sizes and hence suitable for evaluating the performance of the proposed model. The REPTree classifier in the proposed model has achieved the highest average accuracy of 85.47% and 87.55% by considering all 16 emotion features and 20 emotion and emoticon-based features altogether respectively. This information does not exhibit the weaknesses of the classification process where the performance can be further improved. But from Fig. 6(a)-(e), it is evident that MCC gives information regarding the quality of classification for each emotion class. MCC of 0.4161 for the happy class depicts the number of misclassified samples are more in it, compared to other emotion classes. Total correctly classified samples using the REPTree classifier are 4225 samples (70.043%) and 1807 (29.95%) are incorrectly classified from a total of 6032 samples. From Fig. 6(a), it is clear that emotion class anger and others have major contributions is this average correctly classified samples by this classifier. In the case of the SVM classifier, the happy class has more misclassified samples. The misclassified happy class samples reversely affect the performance of classifiers which has comparatively performed better at classifying samples at other emotion classes. Among the total 6032 samples, SVM has classified 3929 (65.14%) samples correctly and 2103 (34.86%) samples incorrectly. In this total correct prediction of all emotion classes, the major share of correct samples is from emotion class other and angry.

TABLE IV. PERFORMANCE COMPARISON OF VARIOUS DEEP LEARNING AND MACHINE LEARNING MODELS ON SEMEVAL 2019 DATASET

	Precision	**Recall**	**F-Score**	**Accuracy**
Proposed Model (REPTRee)	67.26%	63.46%	65.31%	87.55%
Proposed Model (SVM)	61.95%	48.38%	54.33%	84.98%
Proposed Model (MLP)	67.30%	57.09%	61.77%	86.95%
Proposed Model (MLP-3)	61.09%	61.04%	61.06%	85.62%
Proposed Model (Decision Tree)	69.52%	47.30%	56.30%	86.43%
Baseline*	50.21%	71.04%	58.51%	-
SS-LSTM [11]	80.87%	64.08%	79.34%	-
BERT Based[8]	86.2%	86.4%	86.3%	-
Light-GBM Tree[34]	76.8%	78.76%	77.65%	-
BERT based Hierarchical LSTM[10]	56%	81.66%	77%	-

*It is Deep Learning based baseline –LSTM with 100-D GloVe embeddings

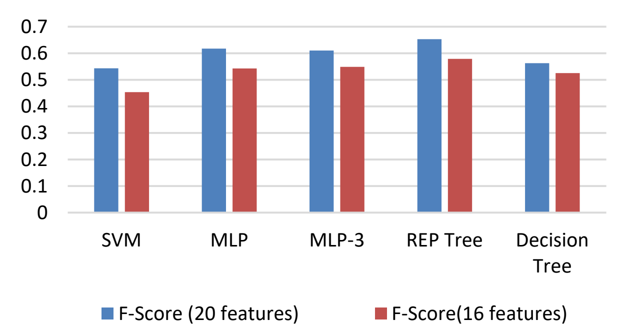

Fig. 5. Individual Emotion Class Wise Classifier Performance Comparison based on f-score Values.

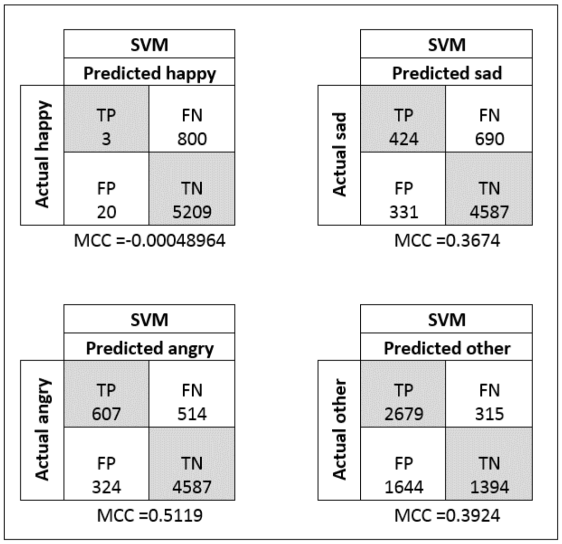

(a) Confusion Matrix for Individual Emotion-class (Happy, Sad, Angry, other) with SVM Classifier.

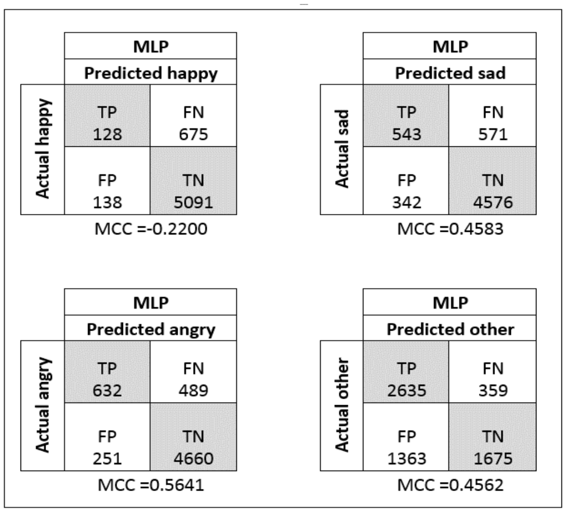

(b) Confusion Matrix for Individual Emotion-Class (Happy, Sad, Angry, other) with MLP Classifier.

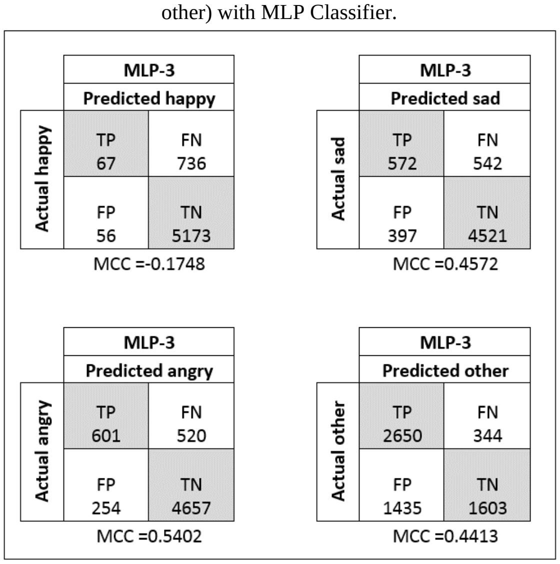

(c) Confusion Matrix for Individual Emotion-class (Happy, Sad, Angry, other) with MLP-3 Classifier.

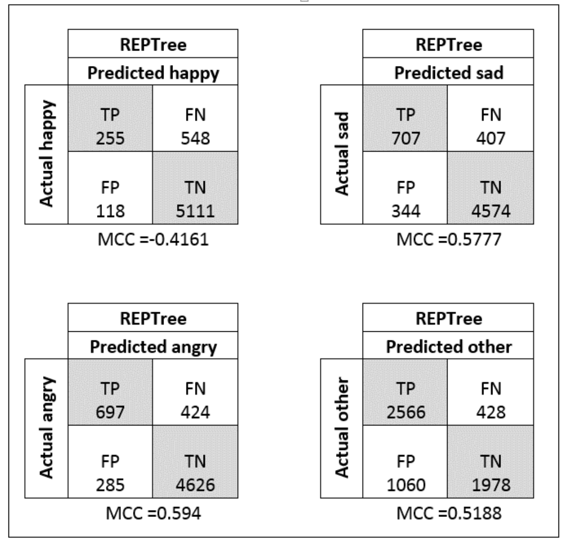

(d) Confusion Matrix for Individual Emotion-class (Happy, Sad, Angry, other) with REP Tree Classifier.

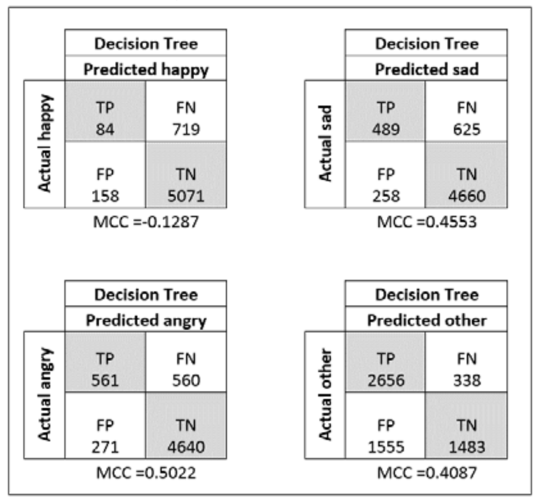

Fig. 6. (e) Confusion Matrix for Individual Emotion-class (Happy, Sad, Angry, other) with Decision Tree Classifier.

VI. Conclusion

In this work, we addressed the issue of recognizing emotions conveyed in text conversations using traditional machine learning approaches. This had explored the directions of research for the proposed emotion recognition model for text conversations. The emotion recognition model based on a set of emotion and emoticon sentiment related features are proposed and implemented, which has achieved competitive results with modern resource costly deep learning approaches used in the literature. On evaluating our contributions in this work by employing emoticon-based features with simplistic state-of-the-art machine learning classifiers competitive performance is observed. This finding may help apply emotion recognition with low cost resources with human like prediction results. Some cases are left by the classifier to identify correctly, which can be incorporated by exploiting rules in the future. The possible direction of research are identified based on this work are as 1) exploring and experimenting with hybrid machine learning based and rule-based approach to recognize the emotions from textual conversations. 2) Applicability of emotion recognition model to further understand the figurative language components in textual conversation. 3) Findings from the results of the multilayer perceptron say that there might be a significant improvement in performance if the sample size in the emotion class increases while using neural classifiers.

References

[1] R. Plutchik, "integration, differentiation, and derivatives of emotion," Evolution and cognition, vol. 7, no. 2, pp. 114–125, 2001.

[2] N. Alswaidan and M. E. B. Menai, "A survey of state-of-the-art approaches for emotion recognition in text," Knowledge and Information Systems, 2020, doi: 10.1007/s10115-020-01449-0.

[3] S. Baccianella, A. Esuli, and F. Sebastiani, "SENTIWORDNET 3.0: An enhanced lexical resource for sentiment analysis and opinion mining," 2010.

[4] B. Liu, "Sentiment analysis and opinion mining," Synthesis lectures on human language technologies, vol. 5, no. 1, pp. 1–167, 2012.

[5] G. Santamaría-Bonfil and O. Grabiel Toledano López, "Emoji as a Proxy of Emotional Communication," in Becoming Human with Humanoid - From Physical Interaction to Social Intelligence, 2020.

[6] F. Barbieri, G. Kruszewski, F. Ronzano, and H. Saggion, "How cosmopolitan are Emojis? Exploring Emojis usage and meaning over different languages with distributional semantics," in MM 2016 - Proceedings of the 2016 ACM Multimedia Conference, 2016, pp. 531–535, doi: 10.1145/2964284.2967278.

[7] B. Eisner, T. Rocktäschel, I. Augenstein, M. Bosnjak, and S. Riedel, "emoji2vec: Learning Emoji Representations from their Description," in Proceedings of The Fourth International Workshop on Natural Language Processing for Social Media, 2016, pp. 48–54, doi: 10.18653/v1/w16-6208.

[8] Z. Ahmad, R. Jindal, A. Ekbal, and P. Bhattachharyya, "Borrow from rich cousin: transfer learning for emotion detection using cross lingual embedding," Expert Systems with Applications, vol. 139, 2020, doi: 10.1016/j.eswa.2019.112851.

[9] A. Chatterjee, K. N. Narahari, M. Joshi, and P. Agrawal, "SemEval-2019 Task 3: EmoContext Contextual Emotion Detection in Text," 2019.

[10] A. Basile, M. Franco-Salvador, N. Pawar, S. Štajner, M. C. Rios, and Y. Benajiba, "SymantoResearch at SemEval-2019 Task 3: Combined Neural Models for Emotion Classification in Human-Chatbot Conversations," in Proceedings of the 13th International Workshop on Semantic Evaluation, 2019, pp. 330–334.

[11] U. Gupta, A. Chatterjee, R. Srikanth, and P. Agrawal, "A sentiment-and-semantics-based approach for emotion detection in textual conversations," arXiv preprint arXiv:1707.06996, 2017.

[12] L. Amarpuri, N. Yadav, G. Kumar, and S. Agrawal, "Prediction of CO2 emissions using deep learning hybrid approach: A Case Study in Indian Context," 2019, doi: 10.1109/IC3.2019.8844902.

[13] L. Lu and B. Lyu, "Reducing energy consumption of Neural Architecture Search: An inference latency prediction framework," Sustainable Cities and Society, vol. 67, 2021, doi: 10.1016/j.scs.2021.102747.

[14] Q. Bai, Q. Dan, Z. Mu, and M. Yang, "A Systematic Review of Emoji: Current Research and Future Perspectives," Frontiers in Psychology. 2019, doi: 10.3389/fpsyg.2019.02221.

[15] R. Mahajan and M. Zaveri, "Humor identification using affect based content in target text," Journal of Intelligent and Fuzzy Systems, vol. 39, no. 1, pp. 697–708, 2020, doi: 10.3233/JIFS-191648.

[16] V. Sintsova, "Advancing Fine-Grained Emotion Recognition in Short Text," 2016.

[17] C. Quan and F. Ren, "A blog emotion corpus for emotional expression analysis in Chinese," Computer Speech & Language, vol. 24, no. 4, pp. 726–749, 2010.

[18] K. Matsumoto, Y. Konishi, H. Sayama, and F. Ren, "Analysis of Wakamono Kotoba emotion corpus and its application in emotion estimation," International Journal of Advanced Intelligence, vol. 3, no. 1, pp. 1–24, 2011.

[19] J. A. Russell and A. Mehrabian, "Evidence for a three-factor theory of emotions," Journal of research in Personality, vol. 11, no. 3, pp. 273–294, 1977.

[20] P. Ekman, "An argument for basic emotions," Cognition and Emotion, vol. 6, no. 3–4, pp. 169–200, 1992, doi: 10.1080/02699939208411068.

[21] A. Balahur, J. M. Hermida, and A. Montoyo, "Detecting implicit expressions of sentiment in text based on commonsense knowledge," in Proceedings of the 2nd Workshop on Computational Approaches to Subjectivity and Sentiment Analysis, 2011, pp. 53–60.

[22] F.-R. Chaumartin, "UPAR7: A knowledge-based system for headline sentiment tagging," in Proceedings of the 4th International Workshop on Semantic Evaluations, 2007, pp. 422–425.

[23] Z. Kozareva, B. Navarro, S. Vázquez, and A. Montoyo, "UA-ZBSA: a headline emotion classification through web information," in Proceedings of the 4th international workshop on semantic evaluations, 2007, pp. 334–337.

[24] C. Strapparava, A. Valitutti, and others, "Wordnet affect: an affective extension of wordnet.," in Lrec, 2004, vol. 4, pp. 1083–1086.

[25] S. Baccianella, A. Esuli, and F. Sebastiani, "Sentiwordnet 3.0: an enhanced lexical resource for sentiment analysis and opinion mining.," in LREC, 2010, vol. 10, no. 2010, pp. 2200–2204.

[26] R. C. Balabantaray, M. Mohammad, and N. Sharma, "Multi-class twitter emotion classification: A new approach," International Journal of Applied Information Systems, vol. 4, no. 1, pp. 48–53, 2012.

[27] D. Davidov, O. Tsur, and A. Rappoport, "Enhanced sentiment learning using twitter hashtags and smileys," in Proceedings of the 23rd international conference on computational linguistics: posters, 2010, pp. 241–249.

[28] C. O. Alm, D. Roth, and R. Sproat, "Emotions from text: machine learning for text-based emotion prediction," in Proceedings of the conference on human language technology and empirical methods in natural language processing, 2005, pp. 579–586.

[29] C. Zhou, C. Sun, Z. Liu, and F. Lau, "A C-LSTM neural network for text classification," arXiv preprint arXiv:1511.08630, 2015.

[30] A. Krizhevsky, I. Sutskever, and G. E. Hinton, "ImageNet Classification with Deep Convolutional Neural Networks," in Advances In Neural Information Processing Systems, 2012, pp. 1–9, doi: http://dx.doi.org/10.1016/j.protcy.2014.09.007.

[31] M. Sivakumar and U. S. Reddy, "Aspect based sentiment analysis of students opinion using machine learning techniques," 2018, doi: 10.1109/ICICI.2017.8365231.

[32] X. Kang, F. Ren, and Y. Wu, "Exploring latent semantic information for textual emotion recognition in blog articles," IEEE/CAA Journal of Automatica Sinica, 2018, doi: 10.1109/JAS.2017.7510421.

[33] T. Rabeya, S. Ferdous, H. S. Ali, and N. R. Chakraborty, "A survey on emotion detection: A lexicon based backtracking approach for detecting emotion from Bengali text," in 20th International Conference of Computer and Information Technology, ICCIT 2017, Feb. 2018, vol. 2018-January, pp. 1–7, doi: 10.1109/ICCITECHN.2017.8281855.

[34] P. Agrawal and A. Suri, "NELEC at SemEval-2019 Task 3: Think Twice Before Going Deep," 2019.

[35] P. Kralj Novak, J. Smailović, B. Sluban, and I. Mozetič, "Sentiment of emojis," PLoS ONE, vol. 10, no. 12, p. e0144296, 2015, [Online]. Available: http://dx.doi.org/10.1371/journal.pone.0144296.

[36] S. M. Mohammad and P. D. Turney, "Emotions evoked by common words and phrases: Using Mechanical Turk to create an emotion lexicon," in Proceedings of the NAACL HLT 2010 workshop on computational approaches to analysis and generation of emotion in text, 2010, pp. 26–34.

[37] S. Poria, A. Gelbukh, A. Hussain, N. Howard, D. Das, and S. Bandyopadhyay, "Enhanced SenticNet with affective labels for concept-based opinion mining," IEEE Intelligent Systems, vol. 28, no. 2, pp. 31–38, 2013.

[38] R. Mahajan and M. Zaveri, "SVNIT $@$ SemEval 2017 Task-6: Learning a Sense of Humor Using Supervised Approach," in Proceedings of the 11th International Workshop on Semantic Evaluation (SemEval-2017), Aug. 2017, pp. 412–416, [Online]. Available: http://www.aclweb.org/anthology/S17-2069.

[39] A. P. Gopi, R. N. S. Jyothi, V. L. Narayana, and K. S. Sandeep, "Classification of tweets data based on polarity using improved RBF kernel of SVM," International Journal of Information Technology, 2020, doi: 10.1007/s41870-019-00409-4.

[40] M. Hall et al., "The WEKA Data Mining Software : An Update," ACM SIGKDD explorations newsletter, 2009.

[41] A. Chatterjee, U. Gupta, M. K. Chinnakotla, R. Srikanth, M. Galley, and P. Agrawal, "Understanding Emotions in Text Using Deep Learning and Big Data," Computers in Human Behavior, vol. 93, pp. 309–317, Apr. 2019, doi: 10.1016/j.chb.2018.12.029.

Monte Carlo Ray Tracing based Method for Investigation of Multiple Reflection among Trees

Kohei Arai
Faculty of Science and Engineering
Saga University, Saga City, Japan

***Abstract*—Monte Carlo Ray Tracing (MCRT) method for investigation of the multiple reflection among trees is proposed. For the forest research (Leaf Area Index: LAI, Normalized Difference Vegetation Index: NDVI, forest type, tree age, etc.) with spaceborne based optical sensor data, some errors due to influences of the multiple reflection among trees on the estimation of at sensor radiance have to be considered. The influence is difficult to formulate in a radiative transfer equation. The proposed method allows estimating the influence. Through experiment with miniature sized forest, it is found that the proposed method is validated. It is also found that a few to more than 10% of influence due to multiple reflections among trees are anticipated. Furthermore, the influence on the estimation of at sensor radiance is clarified. The potentialities of the code are then depicted over different types of forests including coniferous and broadleaf canopies.**

Keywords*—*Radiative transfer equation; Monte Carlo ray tracing: MCRT; multi reflection among trees; forest research; canopy reflectance; ellipse and cone shaped trees model

I. Introduction

Research on forest vegetation using earth observation satellite data is related to identification and identification of forest fires, logging areas surveys, forest maps, tree species discrimination, forest facies division map creation, etc. [1], carbon dioxide concentration, water vapor, latent heat in the ecosystem-atmosphere system There is a quantification of equal exchange and a tree structure analysis [2]. In addition, vegetation indexes, green ratio, amount of biomass, etc. are known as vegetation parameters that can be estimated from earth observation satellite data.

In addition to these, LAI (Leaf Area Index) for estimating growth and maintenance respiration of vegetation, leaf angle distribution characteristics, lignin (tree lignin, soil lignin cellulose index) for consumption and decomposition respiration calculation, growth, light utilization efficiency for photosynthetic activity (xanthophyll cycle, fluorescence), water stress (transpiration, leaf water content, etc.), temperature stress (leaf surface temperature), etc. for grasping maintenance process: LUE (Light Use Efficiency), photosynthesis effective Radiation: PAR (Photosynthetically Active Radiation), APAR (Absorbed PAR), fAPAR (Fraction of APAR), and basic production (NPP) have been estimated [3].

Lignin is synthesized by subjecting carbon compounds assimilated by photosynthesis (primary metabolism) to further metabolism (secondary metabolism). When a plant accumulated excessive reducing power in chloroplasts under conditions such as strong light, xanthophylls, which are auxiliary pigments of light-harvesting chlorophyll proteins, changed to substances with low light-harvesting efficiency, while becoming weak light. At that time, it changes to a substance with high light collection efficiency.

The purpose of this study is to clarify the optical characteristics of vegetation by using Monte Carlo method based on a three-dimensional tree structure model. From this characteristic, vegetation parameters such as tree shape and tree distance can be estimated. At this time, it is necessary to consider multiple reflection processes between trees and between trees and undergrowth, and absorption and multiple scattering processes by atmospheric air molecules and aerosols.

A model considering these has already been proposed by Goel & Thompson [9], but only individual factors such as the effect of multiple reflection between trees and the effect of multiple reflection including trees and undergrowth have not been grasped. The relationship between the parameters is not always clear. Originally, the Monte Carlo method stochastically inserts photons into the atmospheric cell and simulates its optical path, so that it is possible to understand the influence of each factor.

In particular, this paper separately evaluates the effects of multiple reflections between trees and between trees and undergrowth. This reveals the error in estimating the tree reflectance and the tree distance, ignoring these effects. That is, the reflectance of the tree obtained from the Earth observation satellite image reflects these influences, and the reflectance that is truly desired can be obtained by considering these influences.

The same applies to tree shapes and tree distances estimated based on these. In order to evaluate the validity of the Monte Carlo method used in this study, we compared and compared it with the experimental results using a scale model of a forest in which two trees of two relatively small sizes with different tree shapes were arranged two-dimensionally. As a result, the validity of the Monte Carlo method was shown, and the effects of inter-tree multiple reflection and tree shape on the radiance at the upper edge of the atmosphere were clarified. In addition, the proposed method was applied to ASTER / VNIR data, and we were able to understand these effects, so the author reports here.

In the following chapter, related research works and theoretical background including motivation of the research are described together with research background. Section 3 details the Monte Carlo method. In particular, the geometrical and optical models of trees and undergrowth hypothesized on the sun and sensors and the ground surface are detailed. In addition, the types of optical path patterns are enumerated, and the optical path patterns of multiple reflections including tree shapes, trees, and trees and undergrowth that are of interest in this study are described in detail. Section 4 introduces the scale model experiment conducted to evaluate the validity of the Monte Carlo method. Furthermore, an application example to ASTER / VNIR data is shown. In Section 5, the author considers the influence of tree reflection and multiple reflections including trees and undergrowth and tree shape on tree distance estimation.

Then, the experimental method together with experimental results is described. After that concluding remarks and some discussions are also described.

II. Related Research Works

In relation to the forest investigation from space, studies have been conducted on the estimation of tree species, tree shape, distance between trees, vegetation density, etc. [4]. In most of these studies, based on a single horizontally homogeneous tree model layer, vegetation parameters in the layer are estimated [5].

In recent years, a three-dimensional vegetation structure model consisting of several layers has been proposed and has come to be considered when estimating canopy clamps, albedo, LAI, etc. that consider bidirectional reflectance characteristics [6]. In addition, a model that considers inhomogeneity in the horizontal and vertical directions has been proposed, and the three-dimensional vegetation structure, which is indispensable for studies such as radiation balance on the surface of vegetation, carbon dioxide exchange with optical absorption and other physical processes, is considered. The author started to do it [7].

On the other hand, problem solving methods for radiative transfer equation, there are the following research works,

A radiative transfer model based on three-dimensional vegetation structure has been proposed [8]. A radiative transfer model based on the Monte Carlo method has also been proposed, which is useful for improving the accuracy of analysis of vegetation and biological / physical parameters considering the three-dimensional vegetation structure [9]. Furthermore, studies such as estimating the amount of chlorophyll from the hyperspectral data using the inverse problem solution based on the leaf scale model of conifers have been conducted [10]. Adjacency effect of layered clouds estimated with Monte-Carlo simulation is investigated [11]. Non-linear mixture model of mixed pixels in remote sensing satellite images based on Monte Carlo simulation is proposed [12].

Forest parameter estimation by means of Monte Carlo simulations with experimental considerations (Estimation of multiple reflections among trees depending on forest parameters) is conducted [13] together with forest parameter estimation, by means of Monte-Carlo simulations with experimental consideration of estimation of multiple reflections among trees depending on forest parameters [14].

Micro traffic simulation with unpredictable disturbance based on Monte Carlo simulation is conducted for validation of effectiveness of the agent cars of Sidoarjo hot mudflow disaster is reported [15] together with Monte Carlo ray tracing simulation for bi-directional reflectance distribution function and grow index of tealeaves estimation [16].

Monte Carlo simulation of polarized atmospheric irradiance for determination of refractive index of aerosols is conducted [17]. Also, Monte Carlo ray tracing simulation of polarization characteristics of sea water which contains spherical and non-spherical shapes of suspended solid and phytoplankton is conducted [18].

Monte Carlo based non-linear mixture model of earth observation satellite imagery pixel data is proposed [19]. On the other hand, Monte Carlo ray tracing based sensitivity analysis of the atmospheric and oceanic parameters on the top of the atmosphere radiance is conducted [20].

Monte Carlo ray tracing based nonlinear mixture model of mixed pixels in Earth observation satellite imagery data is also proposed [21]. Comparison between linear and nonlinear models of mixed pixels in remote sensing satellite images based on Cierniewski surface Bi-Directional Reflectance Distribution Function: BRDF model by means of Monte Carlo ray tracing simulation is conducted [22].

Monte Carlo Ray Tracing: MCRT based knowledge base system for texture mapping together with height estimation using objects' shadow with high spatial resolution remote sensing satellite imagery data is proposed [23]. Meanwhile, Monte Carlo ray tracing based adjacency effect and nonlinear mixture model for remote sensing satellite image data analysis is conducted [24].

Method for aureole estimation refinement through comparisons between observed aureole and estimated aureole based on Monte Carlo Ray Tracing is proposed and validated with experiments [25].

III. Theoretical Background and the Proposed Method

A. Monte Carlo Method

The Monte Carlo method is a method that treats sunlight as photons and probabilistically elucidates the behavior of photons in the atmosphere and on the ground surface [26]. Prerequisites are solar zenith angle, azimuth angle, sensor zenith angle, azimuth angle, observation wavelength, atmospheric cell size, atmospheric air molecule and aerosol optical thickness, surface reflectance: undergrowth and soil mixing (Lambertian surface) We give the tree size and the reflectance between trees (Lambertian surface).

Atmospheric composition molecules were only air molecules and aerosols. Since the observation wavelength range was set to visible near infrared, we decided to deal only with the composition that mainly contributes to absorption and scattering in this wavelength range. The ground surface is composed of trees and undergrowth. Trees have tree shapes such as spheres, ellipsoidal spheres, cylinders, and cones [27], [28].

In this study, from the viewpoint of the ease of constructing a scale model of a forest for the validation of the Monte Carlo method, the tree shapes that were relatively easily available were limited to elliptic spheres and cones. The photon is input to the atmospheric cell according to the following algorithm, the photon is counted when it is absorbed by the ground surface, trees, the atmosphere, and when it is captured in the sensor instantaneous visual field, and the optical path of the photon is terminated.

The photon is input to the atmospheric cell according to the following algorithm, the photon is counted when it is absorbed by the ground surface, trees, the atmosphere, and when it is captured in the sensor instantaneous visual field, and the optical path of the photon is terminated.

1) Assume the three-dimensional calculation cell shown in Fig. 1.

2) Photons are randomly generated and are incident from the top of the cell according to the solar zenith angle and azimuth angle.

3) Photons travel according to a free path determined by the optical thickness of the atmosphere.

4) If the end point of the free process of photons is in the atmosphere, either one of the photon molecules and the aerosol will be at a probability with the probability depending on the optical thickness of the aerosol.

5) Calculate the scattering angle of the photon and the remaining optical path length according to the scattering characteristics (phase function) of the air molecule and aerosol.

6) If the free process end point of the photon passes through the ground surface (trees / undergrowth), find the intersection with the tree / undergrowth, and reflect / absorb it. The reflection component reflects the remaining optical path length of the free process up to the intersection from the intersection.

7) If the end point of the free path of the photon is outside the cell, the photon is moved to the rest of the free path from the surface located exactly opposite the intersection of the free path vector and the cell wall surface.

8) The radiance at the top of the atmosphere is obtained based on the number of photons emitted from the upper surface of the cell into the instantaneous field of view of the sensor. The photon exiting the instantaneous visual field ends the optical path of the photon at that point.

9) A free process of photons and a log for each optical path are left so that the optical path locus of the photon can be traced.

For the random numbers, we use Mersenne Twister [29], which has a period of 2^{19937}-1 and is evenly distributed in a 623-dimensional hypercube. The number of photons and the number of random numbers generated are determined by numerical experiments. The radiance at the top of the atmosphere is stable when the number of photons exceeds 100,000, so the number of photons is set to 100,000.

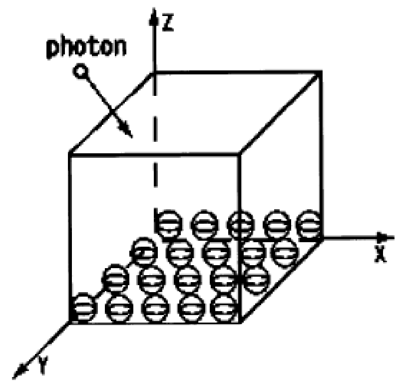

Fig. 1. Calculation Cell of Monte Carlo Simulation (Ellipsoidal Surface Objects are Trees).

Fig. 2 shows the possible optical paths of photons. The scattered light that is scattered only by the atmosphere and does not reach the ground surface is shown in Fig. 2(a), and the direct light that directly reaches the forest vegetation on the ground surface from the sun is shown in Fig. 2(b). Light path reaching the ground surface after scattering by the atmosphere Fig. 2(c) and Fig. 2(d) show the light path reaching the ground surface after multiple scattering by the atmosphere and undergoing multiple reflections between trees.

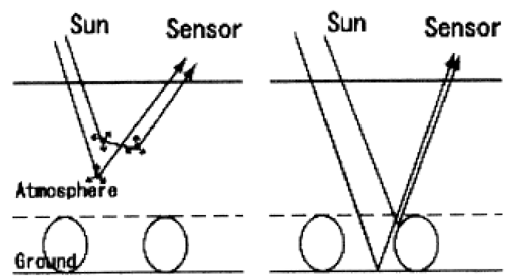

(a) Path Radiance. (b) Reflected Directly.

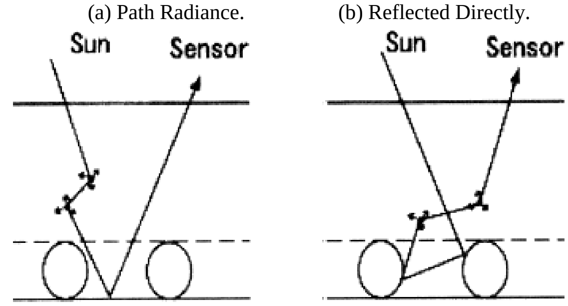

(c) Reflected by Sky Light and Ground. (d)Multiple Reflection among Trees.

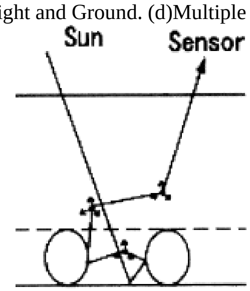

(e) Multiple Reflection among Trees, Sky Light and Ground.

Fig. 2. The Sun-atmosphere-ground Paths (Each Tree is Treated as each Individual Ellipse: Deciduous or cone: Coniferous Trees).

Fig. 2(e) shows the optical paths of trees and undergrowth, or multiple reflections between trees and multiple scattering due to the atmosphere after reaching the ground surface. These optical path types can be grasped for their contributions by performing atmospheric top radiance calculation for each optical path in Monte Carlo simulation.

B. Input Parameter

Photons are transmitted and scattered depending on the preset optical thickness of the air molecules and aerosol. In the case of scattering of air molecules, it is scattered according to the scattering phase function based on Rayleigh scattering, and in the case of aerosol, it is scattered according to the phase function based on Mie scattering.

The multiple refractive indices of the aerosol were 1.44 for the real part and 0.005 for the imaginary part. These are the values obtained by actually measuring in the winter (December 13, 2003) around Saga University using PROM-III (Japan) Sky Radiometer POM-III. The particle size distribution was the Junge distribution and the Junge parameter was 3. These are also the actual measured values around Saga University on the same day.

The aerosol scattering phase function was obtained using MODTRAN 4.0 Mie code (Software code to obtain scattering phase function by Mie scattering). Fig. 3 and 4 show the measured values of the real and imaginary parts of the complex refractive index and the Junge parameter, and the scattering phase function. The atmospheric optical thickness used in the Monte Carlo method is the measured value. The measured values are shown in Fig. 5. The surface of the tree is a Lambertian surface with uniform reflectance, and its shape is considered as an elliptical sphere or a cone as shown in Fig. 6.

Considering the distance between trees, we assumed a forest in which these trees were arranged in a grid. The state of the undergrowth was a Lambertian surface with a uniform reflectance. It is possible to consider bidirectional reflection distribution function (BRDF), Mineralt reflection law, trees based on fractal shape on the surface of trees and undergrowth [30], [31], where Lambert is used as the first approximation. The author assumed a face. In addition to these, measured values were used for the reflectance and shape of trees used in the Monte Carlo method.

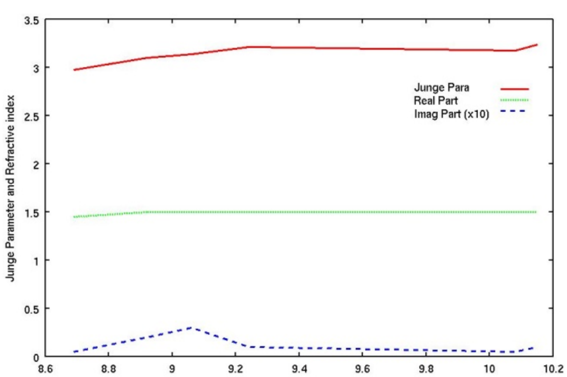

Fig. 3. Estimated Junge Parameter of Size Distribution and Real and Imaginary Part of Refractive Index of Aerosol with the Measured Data using POM-III of Sky-radiometer at the Saga University and its Surrounding on Dec. 13 2003.

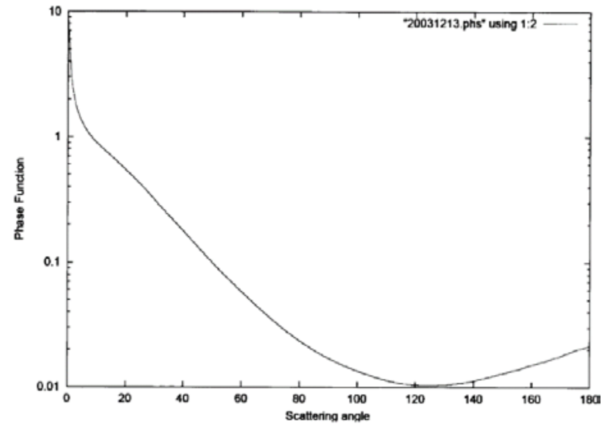

Fig. 4. Aerosol Phase Function used for Monte Carlo Simulation.

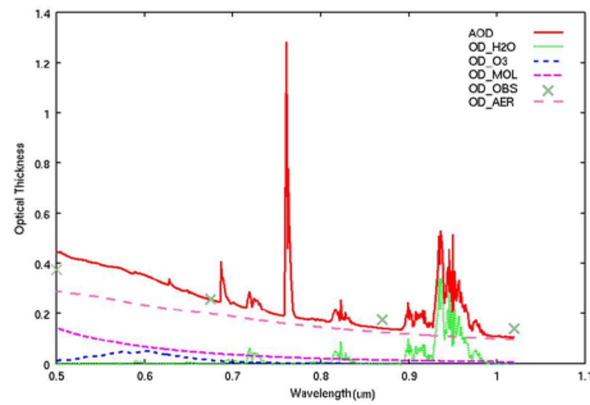

Fig. 5. Measured Optical Depths of Total Atmosphere (AOD), Water Vapor (OD_H20), Column Ozone (OD_03), Molecule (OD_MOL), and Aerosol (OD_AER) as well as Observed Optical Depth (OD_OBS) at Saga Test Site in Japan on Dec. 15 2004.

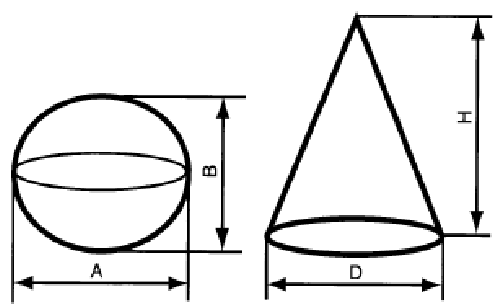

(a) Ellipse (b) Cone

Fig. 6. Two Kinds of Tree Models.

The author considers the parameter setting by using a comprehensive e-learning system with simulation capabilities for understanding of complex equations [32].

C. Output Parameters

The output parameters in the Monte Carlo method are the atmospheric top radiance and 10 types of photon statistical data:

1) The total number of photons incident on the cell from the cell top surface.

2) The number of photons emitted from the cell top surface, and trees.

3) The number of photons reflected by trees.
4) The number of photons reflected by undergrowth.
5) The number of photons absorbed by undergrowth.
6) The number of photons scattered by aerosols.
7) The number of photons absorbed by aerosol.
8) The number of photons scattered by air molecules.
9) The number of photons absorbed by air molecules.

IV. EXPERIMENT

A. Method for Experiment

Since it is difficult to measure multiple reflections between trees and between trees and undergrowth in natural forests, we decided to use the Monte Carlo method. For that purpose, the validity of the Monte Carlo method must be proved. Two types of relatively small size tree-shaped trees simulating a forest were arranged two-dimensionally, and a lawn was spread as undergrowth, and a black cloth was spread around it. The experimental configuration is shown in Fig. 7(a).

The experiment site is the center of the Saga University Athletic Ground, and the ground is surrounded by trees with a height of about 7 m, but the skyline is within about 2 degrees elevation when viewed from the center. The spectroradiometer used for measuring the ground surface reflectance was MS-720 manufactured by Eiko Instruments Co., Ltd. This is to measure the radiance by separating the wavelength range from 350 to 1050 nm into 256 channels at 3.3 nm wavelength intervals. As a standard white plate, Spectralon manufactured by Labsphere, USA was used. To monitor the direct light of the sun, GER2600 (measured radiance in the wavelength range of 400 to 2600 nm at 2 nm intervals) manufactured by GER, USA was used.

The height of the tree height of the MS720 radiometer with an opening angle of 45 degrees was set to 1.8 m. Therefore, the measurement range is within a circle with a radius of 74.56 cm centered directly under the radiometer. The lawn is a square with a side of 1.8 m, and the black cloth is a square with a side of 2.5 m. The above two types of trees were placed on this lawn. An overview of the tree is shown in Fig. 7(b).

Tree No. 1 is a conifer (Jerichoides, lateral diameter: 13 cm, vertical diameter: 12 cm), and No. 2 is a conifer (gold crest, bottom diameter: 11 cm, height: 26 cm). These were arranged two-dimensionally as shown in Fig. 8 to construct a forest scale model. In addition, Sky Radiometer POM-III is installed on the rooftop of the Faculty of Science and Engineering Building No. 7 (4 floors) about 100 m away from the ground, and direct observation of the sun, scattering, and ambient light is performed every day.

B. Experimental Results

Fig. 9 shows the spectral reflectance characteristics when the distance between trees is changed from 8 cm to 30 cm in 2.5 cm increments. The parameter in the legend in the figure is the distance between trees in cm. This is the characteristic of No. 1 tree, but it is almost the same for No. 2. This is a typical spectral reflectance characteristic of vegetation in which the reflectance is high in the green wavelength, low in the red wavelength, and highest in the near infrared wavelength range.

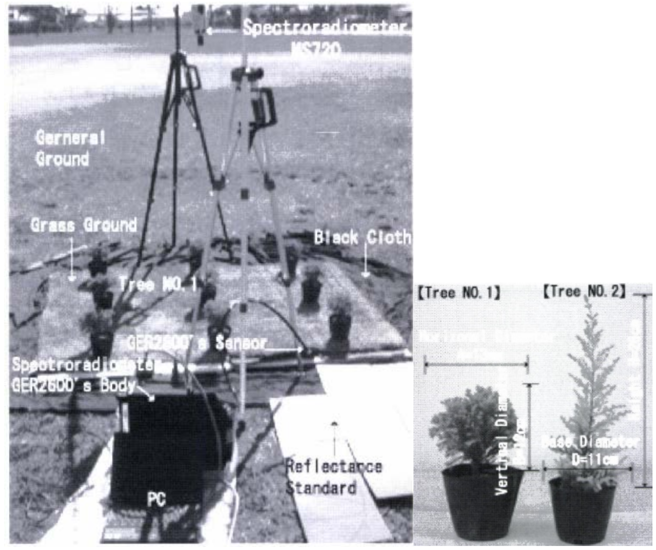

(a) Experiment configuration (b) Two types of trees

Fig. 7. Outlook of the Forested Trees and Grasses on the Land Surface together with the Measuring Instruments for Surface Reflectance (Spectralon : Standard Plaque, MS-720 and GER260O : Spectroradiometers).

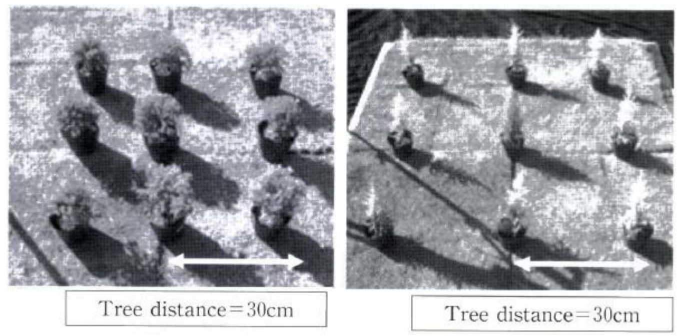

(a) Tree No.1 (b) Tree No.2

Fig. 8. Trees used in Experiment.

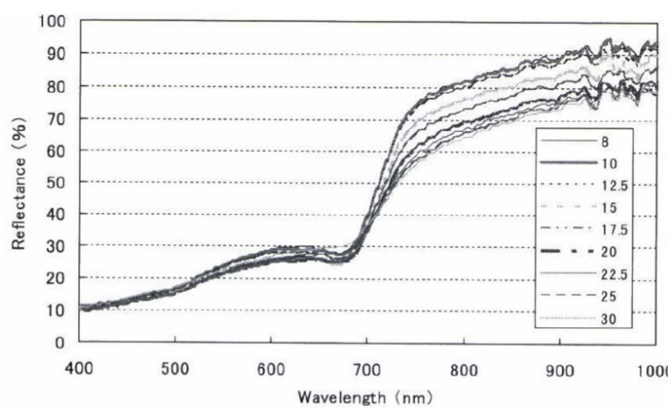

Fig. 9. Measured Reflectance of the Scale Model of the Two Dimensionally Aligned Trees (No.1) with the Tree Distance Ranges from 8 to 30cm (Legend shows the Tree Distance).

For the purpose of this study to clarify the effect of multiple reflections between trees and undergrowth on the upper radiance of the atmosphere, the reflectance changes significantly with the distance between trees 750,800,900,1000 nm (wavelengths that are less absorbed by atmospheric air molecules). Attention was paid to the reflectance at. Similarly, the spectral reflectance of grass, which is assumed to be undergrowth, was also measured.

Atmospheric optical thickness and geometric relationships with the sun, ground surface and sensors were investigated. Simultaneously with this experiment, we measured the optical thickness of the atmosphere at wavelengths of 368,500,675,778,862 nm, which avoids absorption of air molecules. The measuring instrument is MICROTOPS-II (Langley plot specification) manufactured by Solar Spectrum.

Fig. 5 shows the measurement results of the optical thickness. From this, the optical thickness of the aerosol was estimated by subtracting the total amount of ozone measured by scattering of air molecules (Rayleigh scattering) as a function of atmospheric pressure and wavelength and MICROTOPS-II (specification of ozone and water vapor) and absorption by total amount of water vapor.

The geometric parameters of the sun, ground surface and sensor were also obtained. These parameters are shown in Tables I and II. Here, the reflectance of a tree is measured from the top of the tree, and it is assumed that this reflectance is the same for all surfaces of a cone and an ellipsoid (Lambertian surface). Strictly speaking, there are differences in reflectance between the bottom and side surfaces of the cone, the upper and lower hemispheres of the ellipsoid, and the effects of multiple reflections, transmission, and scattering inside this shape, but the assumption was adopted as the first approximation.

Experiments using a forest scale model were compared with simulation results using the Monte Carlo method. Fig. 10(a) and 10(b) show a comparison of the distance between trees and sensor radiance characteristics by experiments using a forest scale model and simulations based on the Monte Carlo method. In the figure, the measured data (triangle, square, and diamond mark) and the data calculated by Monte Carlo simulation (solid line and broken line) are shown.

The top characteristic is the sensor radiance at 1000 nm, followed by 900, 800 and 750 nm. It can be seen that the sensor radiance decreases monotonically as the tree distance increases. This is probably because the effect of multiple reflections between trees and between trees and undergrowth on the sensor radiance decreases with the distance between trees. Moreover, the Monte Carlo method is valid because the two agree very well.

The parameters used for the Monte Carlo method were adapted to those of the forest scale model. That is, the cell size was a cube with the height of the light receiving part of the spectrometer as one side, the sensor aperture was 45 degrees full angle, and the other parameters shown in Tables I and II were used.

As a result, in Tree No. 1, the percentage of the total number of photons that reached the upper edge of the atmosphere after two or more reflections between trees at 750 nm was 8%, and reached 10% at a wavelength of 1000 nm. I found out that similarly, in the case of Tree No. 2, it was found to be 2.2% at 750 nm and 3.1% at 1000 nm. In other words, 10% of the reflectance in the near infrared of a forest on an ellipsoidal sphere based on satellite visible and near infrared radiometer data is due to the multiple reflections between trees, and the actual reflectance is about 10% lower. It can be said to be a value.

TABLE I. INPUT PARAMETERS FOR TREE NO. 1

Parameter	750nm	800nm	900nm	1000nm
Reflectance				
Grass reflectance	29%	33%	42%	53%
Tree reflectance	75%	82%	89%	93%
Optical depth				
Molecule	0.045	0.04	0.04	0.03
Aerosol	0.045	0.04	0.04	0.03
Sun-Sensor Geometry		Canopy properties		
Solar zenith angle	41°	Horizontal diameter (A)	13cm	
Solar azimuth angle	15°	Vertical diameter (B)	12cm	
View zenith angle	0°			

TABLE II. INPUT PARAMETERS FOR TREE NO. 2

Parameter	750nm	800nm	900nm	1000nm
Reflectance				
Grass reflectance	29%	33%	42%	53%
Tree reflectance	65%	75%	84%	92%
Optical depth				
Molecule	0.045	0.04	0.04	0.03
Aerosol	0.045	0.04	0.04	0.03
Sun-Sensor Geometry		Canopy properties		
Solar zenith angle	43°	Base diameter (C)	11cm	
Solar azimuth angle	29°	Height (D)	25cm	
View zenith angle	0°			

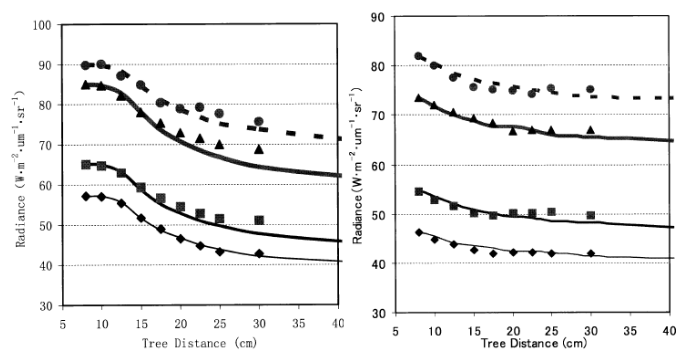

(a) (b)

Fig. 10. At-Sensor Radiance from the Scale Model of Trees and Grasses for Tree No.1 ((a): Left) and that for Tree No.2; ((b): Right). Upper Curve shows Radiance at 1000nm Followed by 900, 800, and 750nm. Solid and Dotted Lines show the Calculated Radiance based on Monte Carlo Simulation While Diamond, Square and Triangles show the Experimental Radiance with the Scale Model.

It was also found that this effect was less in the case of conical forests, which was a few percent. This effect depends on the distance between trees, and it can be seen that the multiple reflections between trees decrease rapidly as the distance between trees increases. From the effect of these multiple reflections between trees when evaluated by the ratio with the radiance at the upper edge of the total atmosphere, the effect of multiple reflections between trees can be inferred to be from several% to 10%. The effect of this multiple reflection between trees depends on the tree shape, distance between trees, tree species, etc. In this experiment, we examined only conifers, but in the case of broadleaf trees with a larger LAI, It can be inferred that the influence is even greater in the case of mixed forests when they are closer.

V. Conclusion

A radiation model of the atmosphere and forest vegetation was constructed by the Monde Carlo method. This makes it possible to evaluate the effects on the upper atmospheric radiance of only multiple reflections between trees and between trees and undergrowth that were not considered in the existing model. The validity of the Mon-Carlo method used in this study was confirmed by comparison with experimental values by a forest scale model in the field. Experiments using a forest scale model were performed by changing the distance between trees and the tree shape.

Comparing this experimental value and the simulation result by the Monte Carlo method, it was found that the radiance tends to gradually decrease as the distance between trees increases. This is a tendency that changes in reflectance due to changes in area coverage of undergrowth and trees overlap with the effects of multiple reflections between trees. And the effect of multiple reflections including trees and undergrowth can be understood.

The effect of the optical path that contributes to this multiple reflection on the radiance at the top of the atmosphere can be grasped from the Monte Carlo method, and it was confirmed that it ranges from several% to several tens of% (this effect also varies depending on the tree shape, It was found that it was about 10% in the case of an elliptical sphere and about 4% in the case of a cone).

This effect is in the near-infrared wavelength region and less in the visible wavelength region. In conclusion, the effect of multiple reflections between trees depends on tree shape, distance between trees, tree species (even single tree species change depending on age and season), LAI: Leaf Area Index, leaf angle distribution, etc. However, it is difficult to say how much it is, but it can be inferred that the impact is from several% to 10%.

Therefore, it can be seen that there is a risk that the reflectance of trees obtained from satellite images is estimated to be several to several tens of percent higher than the actual reflectance. Applying this method to understand the effects of multiple reflections between trees and undergrowth of trees to ASTER / VNIR band 3 data, the difference between the satellite data and the simulation results on bare land (no effect of multiple reflections) was 1.19%.

However, it is confirmed that it is as much as 7.47% in the coniferous forest (which is affected by multiple reflections). Therefore, most of the 7.47% difference is considered to be due to the multiple reflections between trees. It was also confirmed that the difference between the radiance obtained from the ASTER / VNIR band 3 data and that obtained from the Monte Carlo method was 11.28% when the tree shape was changed to an ellipsoidal shape. This fact suggests that tree shape discrimination is possible using these differences.

However, in the simulation by the Monte Carlo method, the tree shape, the distance between trees, etc. are provisionally set, and it is hard to say that the influence of the terrain inclination, undulation, etc. is strictly considered. Therefore, the effect of multiple reflections of several % to 10% is only an approximate number, but it is possible to argue that it is necessary to consider this effect when estimating reflectance of trees, distance between trees, and tree shape.

VI. Future Research Works

In the future, the author will conduct another experiment with actual remote sensing satellite data for the validation of the proposed method.

Acknowledgment

The author would like to thank Dr. Yaliu Ding of former student of Saga University for her contribution of this study. The author, also, would like to thank Professor Dr. Hiroshi Okumura and Professor Dr. Osamu Fukuda for their valuable discussions.

References

[1] Hall, F.G., Knapp, D.E. and Huemmrich, K.F., Physically based classification and satellite mapping of biophysical characteristics in the southern boreal forest, Journal of Geophysical Research, 102, D24, 29567-29580, 1997.

[2] Baldcchi, D., Kelliher, F.M., Black, T.A. and Javis, P.G., Climate and vegetation controls on boreal zone energy exchange, Global Change Biology, 6, Suppl. 1, 69-83, 2000.

[3] Nobel, P.S. and Long, S.P., Canopy structure and light interception, In : J. Coombs, D.O. Hall, S.P. Long and J.M.O. Scurlock (Edt.), Techniques in bioproductivity and photosynthe sis (2nd edt.) Oxford : Pergamon, 1985.

[4] Chen, J.M. and Cihlar, J., Plant canopy gap size analysis theory for improving optical mea surements of leaf area index, Applied Optics, 34, 6211-6222, 1995.

[5] Walthall, C.L., Loechel, S.E., Huemmrich, K. F., Brown de Colstoum, E., Chen, J., Markham, 65 B.L., Miller, J., and Walter-Shea, E.A., Spectral information content of the boreal forest, I : G. Guyot, and T. Phulpin (Edt.) Proc. of Physical Measures and Signatures in Remote Sensing, 607-611, 1997.

[6] Running, SW., and Coughlan J.C., A general model of forest ecosystem processes for regional applications : 1. Hydorologic balance, canopy gas exchange and primary production processes, Ecological Modeling, 42, 125-154, 1988.

[7] Chen, J.M., Liu, J., Leblanc, S.G., Lacaz, R. and Roujean, J.L., Multi-angular optical remote sensing for assessing vegetation structure and carbon absorption, Remote Sensing of Environ ment, 84, 4, 516-525, 2003.

[8] Gastellu-Etchegorry, J.P., Guillevie, P., Zagolski, F., Demarez, V., Trichon, V., Deering, D., and Leroy, M., Modeling BRF and radiation regime of boreal and tropical forests : I. BRF. Remote Sensing of Environment, 68, 3, 281-316, 1999.

[9] Goel, N.S. and Thompson, RI., A snapshot of canopy reflectance models and a universal model for the radiation regime, Remote Sensing Reviews, 18, 197-225, 2000.

[10] Zarco-Tejada, P.J. Miller, JR., Harron, J., Hu, B., Noland, TI, Goel, N.S., Mohammad, G. H. and Sampson, P., Needle chlorophyll content estimation through model inversion using byperspectral data from boreal conifer forest canopies, Remote Sensing of Environment, 89, 189-199, 2003.

[11] Kohei Arai, Adjacency effect of layered clouds estimated with Monte-Carlo simulation, Advances in Space Research, Vol.29, No.19, 1807-1812, 2002.

[12] Kohei Arai, Non-linear mixture model of mixed pixels in remote sensing satellite images based on Monte Carlo simulation, Advances in Space Research, 41, 11, 1715-1723, 2008.

[13] Yaliu Ding and Kohei Arai Forest parameter estimation by means of Monte Carlo simulations with experimental considerations -Estimation of multiple reflections among trees depending o n forest parameters-Online publication from Advances in Space Research, Elsevier 2008.

[14] Yaliu Ding, Kohei Arai, Forest parameter estimation, by means of Monte-Carlo simulations with experimental consideration of estimation of multiple reflections among trees depending on forest parameters, Advances in Space Research, 43, 3, 438-447, 2009.

[15] Kohei Arai, Tri Harsono, Achmad Basuki, Micro traffic simulation with unpredictable disturbance based on Monte Carlo simulation and effectiveness of the proposed agent cars of Sidoarjo hot mudflow disaster, Journal of EMITTER, 1, 1, 10-19, 2010.

[16] Kohei Arai, Monte Carlo ray tracing simulation for bi-directional reflectance distribution function and grow index of tealeaves estimation, International Journal of Research and Reviews on Computer Science, 2, 6, 1313-1318, 2011.

[17] Kohei Arai, Monte Carlo simulation of polarized atmospheric irradiance for determination of refractive index of aerosols, International Journal of Research and Review on Computer Science, 3, 4, 1744-1748, 2012.

[18] Kohei Arai, Y.Terayama, Monte Carlo ray tracing simulation of polarization characteristics of sea water which contains spherical and non-spherical shapes of suspended solid and phytoplankton, International Journal of Advanced Computer Science and Applications, 3, 6, 85-89, 2012.

[19] Kohei Arai, Monte Carlo based non-linear mixture model of earth observation satellite imagery pixel data, International Journal of Advanced Computer Science and Applications, 3, 8, 18-22, 2012.

[20] Kohei Arai, Monte Carlo ray tracing based sensitivity analysis of the atmospheric and oceanic parameters on the top of the atmosphere radiance, International Journal of Advanced Computer Science and Applications, 3, 12, 7-13, 2012.

[21] Kohei Arai, Monte Carlo ray tracing based nonlinear mixture model of mixed pixels in Earth observation satellite imagery data, International Journal of Advanced Computer Science and Applications, 4, 1, 148-152, 2013.

[22] Kohei Arai, Comparison between linear and nonlinear models of mixed pixels in remote sensing satellite images based on Cierniewski surface BRDF model by means of Monte Carlo ray tracing simulation, International Journal of Advanced Research in Artificial Intelligence, 2, 4, 1-7, 2013.

[23] Kohei Arai, Monte Carlo Ray Tracing: MCRT based knowledge base system for texture mapping together with height estimation using objects' shadow with high spatial resolution remote sensing satellite imagery data, International Journal of Advanced Research in Artificial Intelligence, 2, 6, 51-55, 2013.

[24] Kohei Arai, Monte Carlo ray tracing based adjacency effect and nonlinear mixture model for remote sensing satellite image data analysis, International Journal of Advanced Research in Artificial Intelligence, 2, 6, 56-64, 2013.

[25] Kohei Arai, Method for aureole estimation refinement through comparisons between observed aureole and estimated aureole based on Monte Carlo Ray Tracing, International Journal of Advanced Research in Artificial Intelligence, 2, 12, 1-8, 2013.

[26] Kohei Arai: Self-study remote sensing, Morikita Publishing, 2001.

[27] Sadamoto Watanabe: Sociology of trees, The University of Tokyo Press, pp.74-78, 1994.

[28] Toshio Tsutsumi: Forest Ecology, Asakura Shoten, pp.37-42, 1989.

[29] Mersenne Twister (MT), http://www.mathsci.hiroshima-u.ac.j p/~m-mat/MT/mt.html.

[30] Zarco-Tejada, P.J., Hyperspectral remote sensing of closed forest canopies : Estimation of chlorophyll fluorescence and pigment con tent. PhD Dissertation. Graduate Program in Earth and Space Science. York University, Toronto, 2000.

[31] Disney, M.I., P. Lewis, P.R. North, Monte Carlo ray tracing in optical canopy reflectance modeling, International Forum on BRDF Spe cial Issue, Remote Sensing Reviews, pp.1-50, 2000.

[32] Kohei Arai, Comprehensive e-learning system with simulation capabilities for understanding of complex equations, International Journal of Advanced Computer Science and Applications IJACSA, 10, 11, 330-335, 2019.

AUTHOR'S PROFILE

Kohei Arai, He received BS, MS and PhD degrees in 1972, 1974 and 1982, respectively. He was with The Institute for Industrial Science and Technology of the University of Tokyo from April 1974 to December 1978 also was with National Space Development Agency of Japan from January, 1979 to March, 1990. During from 1985 to 1987, he was with Canada Centre for Remote Sensing as a Post Doctoral Fellow of National Science and Engineering Research Council of Canada. He moved to Saga University as a Professor in Department of Information Science on April 1990. He was a councilor for the Aeronautics and Space related to the Technology Committee of the Ministry of Science and Technology during from 1998 to 2000. He was a councilor of Saga University for 2002 and 2003. He also was an executive councilor for the Remote Sensing Society of Japan for 2003 to 2005. He is a Science Council of Japan Special Member since 2012. He is an Adjunct Professor of University of Arizona, USA since 1998. He also is Vice Chairman of the Science Commission "A" of ICSU/COSPAR since 2008 then he is now award committee member of ICSU/COSPAR. He wrote 55 books and published 620 journal papers as well as 450 conference papers. He received 66 of awards including ICSU/COSPAR Vikram Sarabhai Medal in 2016, and Science award of Ministry of Mister of Education of Japan in 2015. He is now Editor-in-Chief of IJACSA and IJISA. http://teagis.ip.is.saga-u.ac.jp/index.html.

Recent Progress on Bio-mechanical Energy Harvesting System from the Human Body: Comprehensive Review

Mohankumar V[1]
Research Scholar, Department of Electronics and Communication Engineering
VTU, Belagavi, Karnataka, India

G.V. Jayaramaiah[2]
Professor and Head, Department of Electrical and Electronics Engineering, Dr. Ambedkar Institute of Technology, Bengaluru-560056, Karnataka, India

***Abstract*—Energy harvesting is a powerful technique to produce clean and renewable energy with better infrastructure improvement. The exhaustive review of recent progress and development in bio-mechanical energy harvesting (BMEH) techniques from human body is discussed in this manuscript. The BMEH from the human body is categorized into three parts, namely, piezoelectric energy harvesting (PEEH), triboelectric energy harvesting (TEEH), and Electro-magnetic Energy harvesting (EMEH). Each energy harvesting system is discussed with working principles with mathematical equations; each energy harvesting progress is discussed with a few work demonstrations. The applications of each energy harvesting from the recent research work are addressed in detail. The summary of each energy harvester from the human body or motion with advantages, limitations, performance metrics, current methods, and implemented human body parts are highlighted with Tabulation. The critical challenges/issues with possible solutions are also discussed.**

Keywords*—Bio-mechanical; energy harvesting; electromagnetic; human-body; piezoelectric; triboelectric

I. Introduction

Renewable energy resources are necessary to solve most of the significant challenges for sustainable development. The power is generated using the most commonly used energy resources like natural gas, petroleum, Hydraulic, nuclear energy, and coal. Energy harvesting is one of the essential processes to produce clean, renewable energy and improves infrastructure development. The energy harvesting (EH) process receives unused energy and is transformed into the most usable energy resource. The commonly used and available energy resources for the energy harvesting process are kinetic, solar, thermal, wind, hydro energies. The EH system is used to recharge batteries, increase the life span of electronic devices, and battery replacement in a low-power system. Firstly, the batteries are recharged easily by using energy harvesting. Next, the electronics devices' life cycle can be prolonged using an energy harvesting system. Lastly, the low-power circuits generally use 1mW total power, so integrate the energy harvesting method in small integrating circuits to consume less the 10 μW-100 μW total power [1-2].

The Human body needs energy and performs its day-to-day activities by consuming more and more energy. Nowadays most of the peoples use wearable devices and essence of home appliances while doing their activities. Metabolism produces enormous energy in the human body and is a prime resource for harvesting energy. Typical movements like walking, running, finger movement, and many other movements are performed daily to generate power in the human body. The heat, bio-chemical potentials, and limb movements produce the central part of the energy in the human body. Like lower limb movement, the body movement produces more energy because it has higher torque than other body parts [3-4]. The energy harvested from the human body is not affected much by day-to-day human life activities. Because of this, most of the current research is focused on human-body energy harvesting. The human body dissipates more energy every day. Even though the utilization ratio is minimal for the proportion of human energy, only micro to milliwatts of power are converted. Therefore, the Harvested power from the human body is insufficient to meet the electricity demand of people's daily Usage [5-6]. The human body energy resources are used in many ultra-lower applications with high efficiency. The various wearable, portable electronic devices, implantable medical devices are instantiated into people's daily Usage by using harvested human power. People use the human's energy resources for daily charging, battery replacement, replacement of implantable electronic devices, and other activities in an essential manner. The energy resources from the human body provide a reliable, flexible, safe environment and no side effects from environmental and space conditions. The human body energy is divided into three forms: Thermal, chemical, and mechanical energies. There is a need for an effective energy harvesting mechanism based on humans' biomechanical movement. The developments of a new form of electronic devices rely on energy harvesting technologies. Recent researches have improved the biomechanical energy harvesting system with suitable changes in the design and configurations of piezoelectric EH, triboelectric EH, and electromagnetic EH systems. The design and configuration are done by considering the particular energy harvesting technology challenges and achieving high energy harvesting. However still, various challenges exist in biomechanical energy harvesting techniques [7-9].

This review has made an exhaustive summary and analysis of the recent development of biomechanical energy harvesting from the human body. This work aims to provide insight into recent work on human-centric biomechanical energy harvesting systems using Piezoelectric, Triboelectric, and Electromagnetic modules. Section II discusses the energy distribution parameters in the human body. The working principles of the biomechanical energy harvesting systems are addressed in Section III. The recent progress of the biomechanical energy harvesting systems is analyzed in detail with a comparative study in Section IV. The challenges and possible solutions are highlighted in Section V. Lastly, the complete work is concluded with futuristic suggestions are incorporated in Section VI.

II. Energy Distribution in Human Body

The human body consumes and releases different forms of energy. For example, every movement and even breath produce energy all the time in the human body. The thermal, chemical and mechanical energies are the available potential energy resources in the human body. The potential energy resources and energy dissipation in the human body for different activities are represented in Fig. 1 [5, 7].

Every day human body consumes more amount of energy from metabolism to maintain the constant body -temperature. The thermal energy produced in the form of heat is exchanged between the body and its surroundings. The other forms of thermal energy are released with the help of respiration or breathing, evaporation heat produced from the sweat in the skin. Chemical energy is produced in the form of water (H2O), glucose, and lactic acid. The Human body digest and absorbs the food and is converted in the form of glucose. The glucose in blood glucose is distributed into other parts of the body to regenerate the energy in one other form. Additionally, the muscles produce the lactic acid by performing the exercise operations, and a few amounts of lactate decomposed in the muscle itself. The sweat is also produced while performing the exercise operations in the form of the substance of water. The mechanical energy is produced in the form of body movement, Heartbeat, Respiratory movement. The Limbs movements like steeping, arms turning, foot lifting, tapping, and other movements consume and release the mechanical energy. In addition to that, heartbeat, blood vessels relaxation and contraction, and respiratory movements are also consuming and releasing mechanical energy. The muscle's relaxation and contraction produce more mechanical energy to perform additional activities with continuous energy transmission.

The energy resources are evaluated further by analyzing the power utilization of different energy flows in the human body. The human body's energy is converted into electricity, which is less than the total amount of energy utilized in the typical energy flow of each human body's part. This is the primary concept and is discussed further with different energy harvesting methods for the human body. The human energy resources and their recent energy harvesting methods are represented in Fig. 1. The thermal energy is harvested using a pyroelectric and thermo-electric generator. Similarly, the chemical energy is harvested using a Hydro-voltaic effect generator and biofuel cell. Lastly, the mechanical energy is harvested using Piezoelectric, triboelectric and electromagnetic generators. In this article, the bio-mechanical energy harvesting techniques are discussed further with different applications.

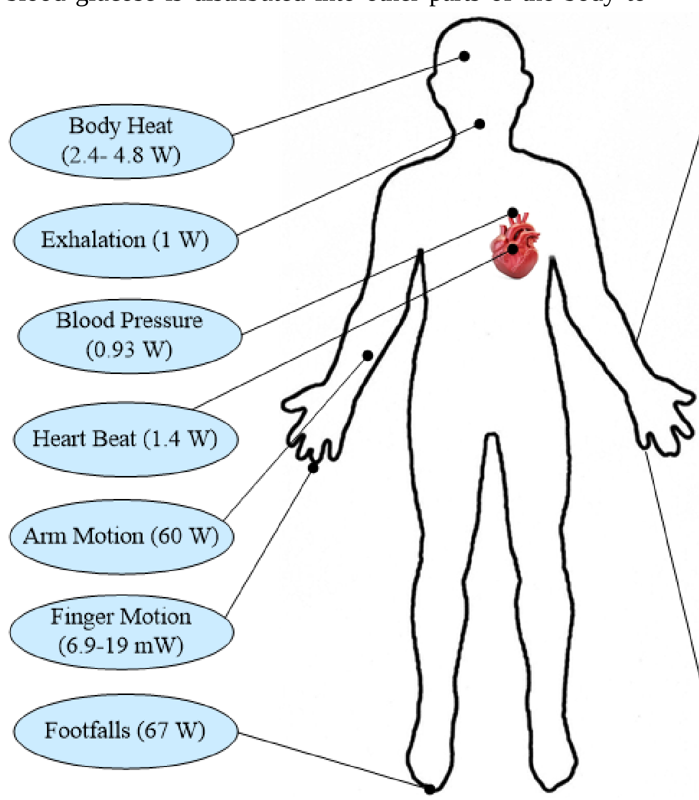

Source	Human Body Energy	EH Techniques
Thermal Energy	Body Temperature	Thermoelectric Generator
	Evaporation Heat	
	Respiration Heat	Pyroelectric Generator
Chemical Energy	H_2O	Bio-Fuel Cell,
	Lactic Acid	
	Glucose	Hydro-voltaic effect generator
Mechanical Energy	Body Movement	Piezo-electric generator
	Heart Beat	Tribo-electric generator
	Respiratory Movement	Electromagnetic generator

Fig. 1. Energy Distribution in Human Body and its Energy Harvesting Techniques [7]

III. Working Principles of Biomechanical Energy Harvesting

The biomechanical energy is harvested from the human body using the most common methods like Piezoelectric, Triboelectric, and Electromagnetic. The principles of the piezoelectric effect are used for the operation of piezoelectric materials. Many researchers can use the Piezoelectric Harvesting in humans to energize intelligent wearable devices like a smart watch, smart skin, smart shoes, portable and implantable devices. The most recent and advanced technologies are incorporated in Triboelectric energy harvesting. This approach uses the triboelectrification phenomenon for charging (electrical) the materials using frictional contact. The electricity is generated based on electrically charged materials with relative displacement. The recent human body-based energy harvesting is performed using triboelectric energy harvesting because of high power outputs, performance, and nanoscale designs. Electromagnetic Energy harvesting is working based on electromagnetic induction (Faraday's law). Faradays, law states that the electric current is induced based on the property of the materials used through a magnetic field. There are many kinds of research conducted based on electromagnetic energy harvesting for self-operated wearable electronic devices. However, these on electromagnetic energy harvesting system lacks with miniaturized designs and device size. The working principles, and recent work, and applications are discussed in the following sections.

A. *Piezoelectric Energy Harvesting (PEEH)*

Piezoelectric Energy harvesting (PEEH) is a widely used harvesting method due to its simple design and accessible materials usage. Piezoelectricity is observed macroscopically to produce electricity through molecular phenomena when some substances (i.e., piezoelectric devices) are deformed. The linear-piezoelectric effect (direct and indirect) [10-11] is represented in (1) and (2) as follows:

$$E_D = c\sigma + \in . EF_i \tag{1}$$

$$\varepsilon = s\sigma + cEF_i \tag{2}$$

Where σ and ε are stress and strain constants; The ED is electric displacement, and EF_i is electric field intensity; s is elastic compliance, ∈ is permittivity, and c is Piezoelectric (PE) co-efficient.

The direct effect of PE is defined in (1), which converts the mechanical energy into electric energy using PE materials. The electrical energy is produced by applying the mechanical force using crystalline materials (Quartz, salt, titanate) directly. In contrast, the indirect (converse) effect of PE is defined in (2), which converts the electric energy into mechanical energy using PE materials. When the electric field is applied to these materials, which produces mechanical energy in deformation. The Linear Piezoelectric energy harvester produces the narrow bandwidth for particular object frequencies, limiting the harvester compared to other non-harmonic systems. The nonlinear piezoelectric Energy harvesting system based on vibration overcomes the drawbacks of Linear PEEH [12].

The Piezo electrical materials [13-14] are categorized into two parts: Piezoceramics and Piezopolymers (PVDT). The Piezopolymers materials are easy to use and flexible but provide low-energy transformation rates and low electromechanical co-efficient. At the same time, Piezoceramics are complex and easily breakable. These materials provide high-energy transformation rates and significant electromechanical coefficients. The Piezoceramic materials like PZT8, PZT-5H, and Piezopolymers- (PVDT) have their material properties. The PEEH is classified further based on principles and materials used: Piezotronics mode, longitudinal mode (d31), and Transverse mode (d33). The PEEH limitation factor is that the energy harnessing will be significantly less; the energy produced only during mechanical stress and harnessing is very tough as the piezoelectric materials are very toxic. The predicted research of many researchers has suggested that Piezoelectricity's applicability can be effective in Nanotechnology.

B. *Triboelectric Energy Harvesting (TEEH)*

The TEEH works based on the principles of triboelectrification. The Energy transfer of the triboelectric effect works based on dissimilar polarities of two materials that can contact other two materials, which creates the opposite charges on each side of the electrical surface. The concept of triboelectricity was initiated long back, where electrostatic charges are generated when two materials are rubbed together. The materials of TEEH are placed in a single column, and one of the triboelectric series placed in the bottom gets a negative charge when they are rubbed with the above one. The primary Voltage (V_e) between two metal electrodes for the given charge accumulation (Q_c) on the surface is represented in (3) as follows [30]:

$$V_e = \frac{Q_c D_e}{\epsilon_0 S_e} \tag{3}$$

The External electrodes produce the Induced current (I_e) and are represented in the (4):

$$I_e = C_e \frac{\partial V_e}{\partial t} + V_e \frac{\partial C_e}{\partial t} \tag{4}$$

Where S_e, D_e, ϵ_0, C_e are metal electrode surface area, interlayer distance, Vacuum permittivity, and Capacitance of the Triboelectric system.

The triboelectric materials produce positive or negative charges based on the contact electricity in the human body. The Skin (Human body) gains the top similarity to lose a positive electron, and in contrast, the Fluoropolymer tends to gain negative electrons at a higher rate. The four different TEEH working operations are classified based on types of similar motion between two triboelectric materials and electrode position. The TEEH process operations include Single Electrode mode, sliding contact mode, Freestanding Mode, and Vertical contact separation mode. These TEEH are the most used technology in recent times for human motions. Most of these works are implemented on wearable and implantable electronic devices.

C. Electromagnetic Energy Harvesting (EMEH)

The Electromagnetic Energy Harvesters (EMEH) work is based on faraday's law with electromagnetic induction [47]. When both ends of the coils produce a nominal difference via a magnetic field. The Voltage (V) used across the coil is directly proportional to the rate of change of magnetic flux. The Voltage and magnetic flux (φ) are expressed in equation (5) as follows [67]:

$$V = N \frac{d\varphi}{dt} \text{ And } \varphi = \sum_{i=1}^{N} \int_A B.dA \quad (5)$$

Where 'N' represents the coil's number of turns, the overall area of the i^{th} coil is 'A', and the magnetic field is denoted by 'B'. The electricity is generated in EMEH using a magnet and conductor (relative motion of the coil). The EMEH is working with two modes of operation. (i) The coil area is changed while placing the coil perpendicular to the magnetic field. magnetic field's intensity is always uniform and constant across the conductor. (ii) The coil was moving parallel with the magnetic field's direction and followed by the magnetic field's intensity, constantly changing with the uniform coil's area. The three different types of EHEH working operations are classified based on mechanical motion. The EMEH working operations include oscillatory EH, rotational EH, and hybrid forms of EH.

IV. Recent Progress in Biomechanical Energy Harvesting System using Human Body

The recent progress in biomechanical energy harvesting techniques is discussed in this section.

A. Piezoelectric Energy Harvesting (PEEH)

The recent works on the PE-based energy harvesters are discussed for human motion in the section. Wang et al. [15] present the study of the Piezotronics and Piezophotochromic nanoarchitectures in addition to nanogenerators of Triboelectric, piezoelectric, and blue energy. The Usage and its application fields are analyzed for the same.

Granstrom et al. [16] present the energy harvesting of backpack instruction for piezoelectric shoulder straps. The design uses polyvinylidene fluoride (PVDF) materials for the backpack and consumes 45.6mW power while performing the simulation. The thickness of the shoulder straps is 52μm using PVDF material.

Calio et al. [17] discuss the study of Piezoelectricity and its material choice in detail with working operations. Pillatsch et al. [18] discuss the human motion energy harvester using wireless power transfer. The design uses the frequency up-conversion method for piezoelectric energy harvesting. Fan et al. [19] present a collection of energy from human lower limbs using the PEEH approach. The walking speed increases from 2km/h to 8 km /h when the PEEH's output voltage increases. The work also states that up-conversion is possible by using ultra-low frequencies of human motions. Wang et al. [20] discuss the nonlinear PEEH from human motion and analyze the frequency method's effectiveness to check the optimal resistance. The work is demonstrated on the Treadmill by placing the EH device on the Human leg. The motion speed is varying based on the resistance value changes. The EH utilizes 30.55 μW power at the 7 km/h speed.

Wang et al. [21] present the PEEH using a Bionic Single electrode electronic skin unit. The Single-electrode piezoelectric nanogenerators (SPENG) is designed using PVDF non-fibers to maintain steady-state sensing. The SPENG overcome the drawbacks of the Single-electrode triboelectric nanogenerators (STENG) for electronic skins. Kim et al. [22] present the multi-directional PEEH with flexibility for Human motion. The PEEH design incorporates the polydimethylsiloxane (PDMS) bump with PVDF material to maintain flexibility and access multidimensional inputs from human motion. Kakihara et al. [23] investigate the PEEH from walking using PVDF materials. The work produces less than 50 μW power with a kinetic energy of 500 μJ/s. Guido et al. [24] present the Aluminum Nitride (AlN) thin-film-based PEEH from human motion for the skin. The work is validated using the Finite Element Method (FEM) for electrical energy and mechanical deformation. Wu et al. [25] discuss the PE-based spring pendulum oscillator for low-frequency vibration harvesting systems with multi-directional features, represented in Fig. 2(a). The device consumes the 13.29mW power at 2.03Hz frequency, and it is applicable for low-power wearable applications. Qian et al. [26] present the PE footwear-based EH, which provides the average power of 9 mW/shoe with a walking speed of 4.8km/h. The footwear EH consumes 28mW with an open-circuit voltage of 20V. The polydopamine (PDA) based PE pressure sensor is designed by Yang et al. [72], and it is represented in Fig. 2(b). The PDA uses barium titanate (BTO) with PVDF composite film for human motion monitoring by using 9.3V output Voltage.

The applications of the PEEH using human motion are represented in Fig. 3. Smart Shoes, smart Textile, smart skin, Biomonitoring, and Implantable devices are the major applications of PEEH using human motions. Fig. 3(a) shows the PE-based shoulder straps [16] with backpack instrumentation for energy harvesting. The user (Human) and backpack are closely packed to improve the performance and harvest the energy. The PEEH module is fixed on the shoes [19] and analyzes the performance while running on Treadmill. The energy harvested results are displayed in the oscilloscope are represented in Fig. 3(b). The PENG-based electronic skin [21] is designed using a single electrode method shown in Fig. 3(c).

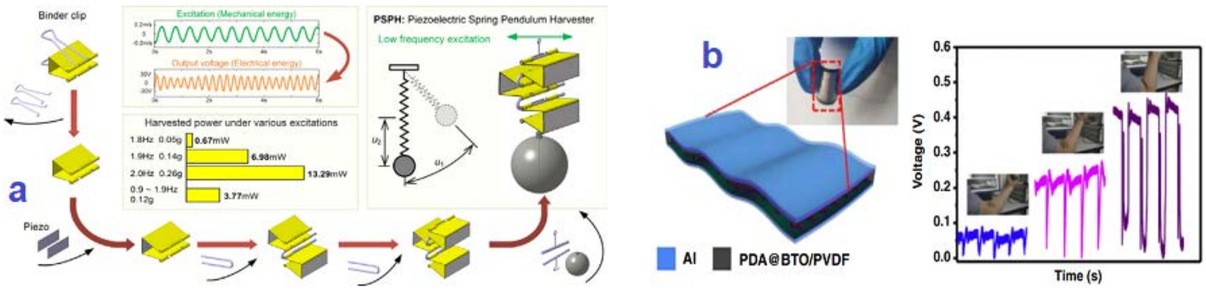

Fig. 2. PEEH Working Operations: (a) PE-based Spring Pendulum Harvester [25], (b) PDA based PE Pressure Sensor [72].

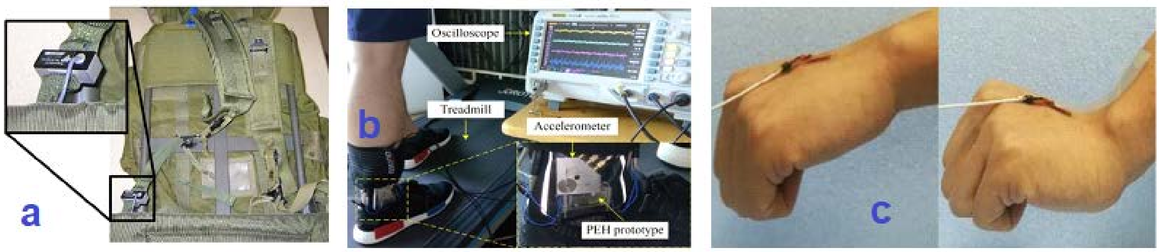

Fig. 3. Applications of PHEH: (a) Shoulder Straps [16], (b) Smart Shoes [19], (c) E-skin [21].

B. Triboelectric Energy Harvesting (TEEH)

The recent works on the TE-based energy harvesters are discussed for human motion in this section. Wang et al. [27] present the triboelectric-based EH to sustain the power in portable electronic devices. The arch-shape-based TE nanogenerator (TENG) is designed to direct electricity between the thin metal film and polymer thin film. The TENG is demonstrated on a Mobile phone to charge the Lithium battery is shown in Fig. 4(a). In addition, TENG [28] is used as a self-power sensor and provides better energy efficiency than the TENG [27]. The Sliding based TENG is designed based on In-plane charging separation (IPCS) method by Wang et al. [29]. The IPCS process is done using a relative sliding operation using two surface contacts. Fan et al. [30] present the Flexible nanogenerators for self-power electronics and also for EH. The hybrid nanogenerator mechanism is designed by using both PE nanogenerators (PENG) and TENG. Hybrid nanogenerators are used in many self-power devices and also for energy harvesting. In 8addition, that Hybrid generators using both PENG and TENG by Song et al. [31]. The work illustrated both wearable bio devices and bio-electronics. Wang et al. [32] present the TENG for EH from human motion or moving objects in non-contact and contact modes. The designed TENG supports freestanding features in the TE layer, which moves to and fro using external mechanical energy. Huang et al. [33] discuss the all-fiber TENG, which has PVDF PE nanofibers for human walking and wearable devices. The human walking results are analyzed, and it consumes 2.1mW power with 210V maximum output voltage. Tang et al. [34] present the High-performance TENG using the Liquid Metal electrode method, which provides instantaneous energy conversion with an efficiency of 70.6%, five times better than the Solid thin film-based electrode method. Ha et al. [35] present the TE-based generators and sensors for wearable electronic devices with self-powered features. The generators like Planar, Micro-patterned TEG, Multi-layered TEG, Rotary-type TEG are designed for Wearable devices like smart glass, watch=, smart band, smart ring, and smart lens. Lin et al. [36] present the TENG-based body sensor network (BAN) system is used in heart-rate monitoring system of human body with the self-power mechanism. Human walking is demonstrated, which consumes the power of 2.28mW with a conversion efficiency of 57.0%. Shen et al. [37] present the TENG for high - Performance-based Bio-mechanical EH system with a Humidity resisting feature. This work is demonstrated on human movements for wearable electronics. The device works at an output voltage of 345V, current of 28μA with 55% relative humidity.

Yu et al. [38] present the TEGN for textiles as power cloths using the Core-shell-Yarn method. The Textile based TENG work provides flexible, fashionable, comfortable features and is further used for large-scale textile manufacturing. Chen et al. [39] present the TENG using Ultra-thin Flexible Single - electrode method for Mechanical EH and instantaneous force sensing. Zhang et al. [40] discuss the stretchable electrode-based TENG using Air cushion features for human motions. The work outputs are validated with Lighting LEDs, power supplies for the calculator, and a digital thermometer. Ding et al. [41] explain the operation of TENG with a large scale for human sleep monitoring. The device supports a flexible sensor with self-powered features for monitoring human sleep with high-power output and high sensitivity. Ning et al. [42] discuss the Single-electrode based TENG with Textile structure (TS) for Wearable electronics with self-powered features. The design works with a current of 22 μA and consumes the output voltage of 1050V.

Song et al. [43] discuss the Smart bracelet-based TENG with high efficiency for portable electronics with a self-charging feature. The device obtains the peak voltage of 305V and consumes 300.4 μW power with 69.3% energy efficiency. Xia et al. [44] present the milk-based TENG for EH using Human body motions. The work consumes 4.67mW of power, 392V of peak voltage with a power density of 583.75μW /cm2 for food quality detection using the human arm. Wang et al. [45] present the skin-based TENG using transparent polyionic materials for human motion EH with highly flexible features. The design works consume the power of 1.12mW with an open-circuit voltage of 70V. Xiong et al. [46] discuss the Textile based TENG for Biomechanical EH with black phosphorous materials. The Textile-based TENG with Washable skin touched-actuated features is demonstrated, providing the 60V low Voltage from Cloth/skin and is used from human motion. Tian et al. [71] designed the TENG-based electrical stimulator, which supports osteoblasts differentiation and proliferation. The design is used for self-powered implantable devices and is shown in Fig. 4(b).

The applications of the TEEH using human motion are represented in Fig. 5. Biomedical monitoring, Smart footwear, smart clothes, smart watch, smart skin are the major applications of TEEH using human motions. The human walking controlled wearable TENG [33] is designed using electrospun PVDF non-fibers, shown in Fig. 5(a).

The Single electrode-based TENG is designed for wearable electronic devices, especially washable cloths [42] with self-power features in Fig. 5(b). The self-powered smart bracelet [43] is designed using freestanding TENG, and it's shown in Fig. 5(c). Finally, the transparent polyionic skin [45] based TENG is designed for human motion energy harvesting with flexible features represented in Fig. 5(d).

C. Electromagnetic Energy Harvesting (EMEH)

The recent works on the EM-based energy harvesters are discussed for human motion in this section. Dai et al. [48] discuss the electromagnetic generator (EMG) with hip-mounted features for EH using human motions. The amount of kinetic energy from walking and running is converted into electrical energy. The design consumes the open-circuit Voltage of 1V by consuming the 284 µW of power. Luciano et al. [49] present the EMEH for total knee prosthesis (TKP) of humans; the TKP works with internal loads to improve longer durations. The design consumes 1.7mw power for every 7.6s of walking by utilizing the 2V of Voltage. Zhang et al. [50] discuss the EMEH using coil arrays and magnets with magnetic springs for the energy generation from human motions. Dinuloyic et al. [51] present the EMEH system with rotational features. The design has multi-layer planar coils with magnets and a mechanical system for movement. The design consumes an 800mA short circuit current with an open-circuit voltage of 2V. Quan et al. [52] present the EM-TENG with hybrid features for a self-powered electronic wristwatch. The watch is operated continuously for 456 seconds by charging the capacitor of 100 µF in 39seconds. Bendame et al. [53] discuss the springless vibration EH system using EM impact, which supports wide bandwidth with low-level vibrations. Niroomand et al. [54] discuss the EM-microgenerator with rotary features for EH using human motions. The design uses the open-circuit Voltage of 0.3V and consumes the 284 µW of power by performing normal walking.

Geister et al. [55] present the nonlinear-based EMEH for wearable sensors with scaling effects. The design obtains the 150mV of Root means square (RMS) output voltage and consumes the 530 µW of load power. Brunner et al. [56] discuss the EMEH system for the upper extremity of the human body. The EM-linear Generator for Upper Limb is represented in Fig. 6(a). The module generates the gyrating mass, which consumes the average power of 50 µW with an output power of 2.2 mw. Halim et al. [57-58] present the EMEH using the rotational eccentric mass method, as shown in Fig. 6(b). The design uses the Swing arm motion for energy generation by consuming 55 µW of average power. In addition to that, the other EMEH using sprung eccentric rotor is designed from human motion with pseudo-walking. This works 61.3 µW power with 1 Hz frequency, which is greater than the upsprung rotor part. Zhang et al. [59] present EMEH using the circular Halbach array Method from bearing motion. The design utilizes the rotational speed is varied from 600-1000rpm by consumes the average power of 50.8-131.1 mW with a harvested output voltage of 2.79 V-4.59 V. Fan et al. [60] present the EMEH using nonlinear two-degree freedom features for human body motions. The works are applicable for Ultra-low-frequency vibrations and consume 2.58mW of power with an output voltage of 0 to 5V.

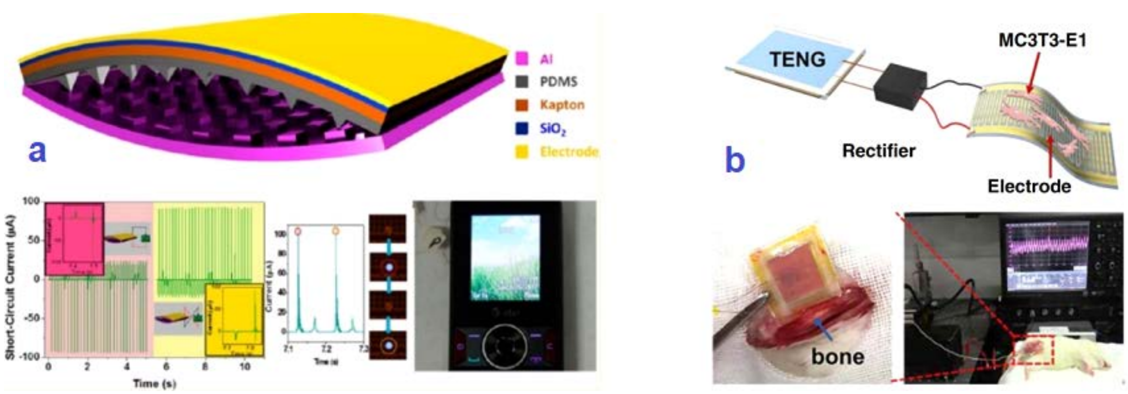

Fig. 4. TEEH Working Operations: (a) Arch Shaped TENG and its Results [27], (b) TENG based Implantable Stimulator [71].

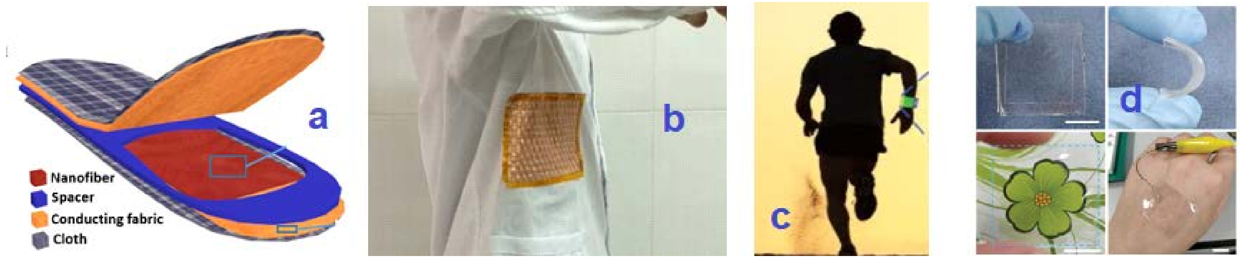

Fig. 5. Applications of TEEH: (a) Smart Shoes [33], (b) Smart Cloths [42], (c) Smart Watch [43], (d) Smart Skin [45].

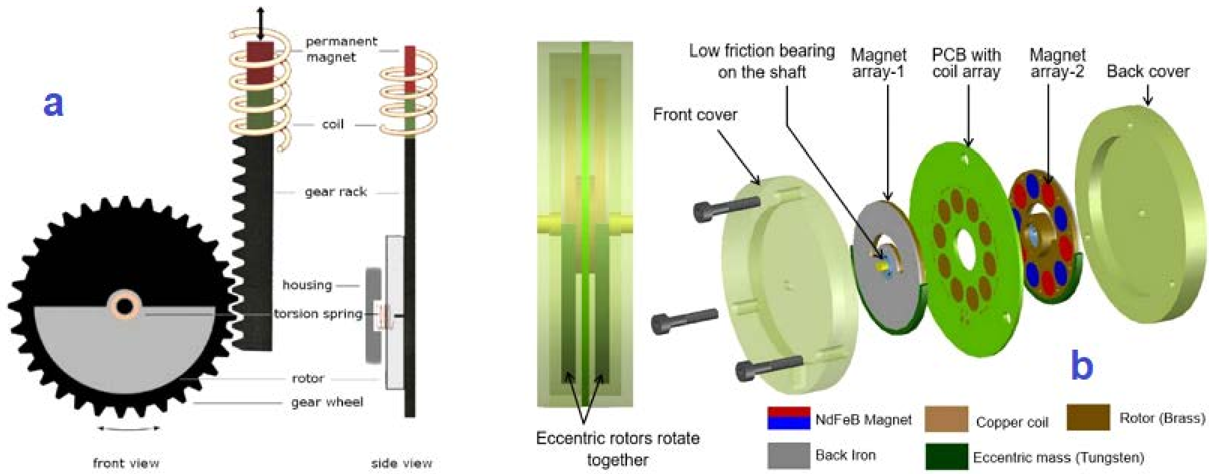

Fig. 6. EMEH Working Operations: (a) EM-Linear Generator for Upper Limb [56], (b) Rotational EMEH for Swing-Arm Motion [57].

Fig. 7. Applications of EMEH: (a) Hip Mounted Leg [48], (b) Smart Arms [60], (c) Smart Wrist Watch [68], (d) Smart Shoes [69].

The applications of the EMEH using human motion are represented in Fig. 7. Biomedical monitoring, Smart skin, smart clothes, smartwatch, smart shoes are the major applications of EMEH using human motions. The Hip mounted leg [48] using an EM generator is designed to harvest the energy, represented in Fig. 7(a). Fig. 7(b) shows the two-degree of freedom (2-DOF) based EMEH is designed for human arm with ultra-low frequency vibrations. The smart wristwatch [68] is designed using flux-guided magnet stacks in EMEH and is shown in Fig. 7(c). Fig. 7(d) shows the Three-degree of freedom (3-DOF) based human motion EMEH for smart shoes [69] using ferrofluid.

The human body produces the energy harvested using three different techniques like PEEH, TEEH, and EMEH. These EH's produces energy using specific human body parts and energy resource characteristics. The application (Smaller or big) requirements are categorized based on the amount of energy harvested. Many strategies are applied to produce the energy with the help of a human body for implantable and wearable devices [63-66]. The Summary of Wearable and implantable devices on the Human Body is tabulated in Table I.

D. Comparison between Different Energy Harvesters

The review of the recent works of bio-mechanical energy harvester systems on the Human body produces different applications, performance metrics, advantages, and limitations. The advantages and limitations of the different Energy harvesters on the Human body are summarized in Table II. The parameters like Power density usage, EH from human body parts, Usage of different methods, and recent development are summarized in Table III. Finally, the different energy harvesters produce the output power (W) and output voltages (V) using different human body parts and are summarized in Table IV.

TABLE I. SUMMARY OF WEARABLE AND IMPLANTABLE DEVICE ON HUMAN BODY

Human Body Part	**Wearable Device**	**Human Body Part**	**Implantable Devices**
Legs	Smart Power shoes	Brain	Deep Brain Stimulator
Legs	Socks: sweat analyzer	Muscle	Muscle stimulator
Body	Microneedle: Blood analyzer	Bladder	Bladder pressure sensor
Body	E-skin: Man-machine interface	Heart	Symbiotic Cardiac Pacemaker
Body	Clothing: Smart Fabrics	Aorta	Blood pressure sensor
Hand	Wristband: Pulse sensor	Stomach	Vagus Pressure Stimulator

TABLE II. ADVANTAGES AND LIMITATIONS OF DIFFERENT ENERGY HARVESTERS ON THE HUMAN BODY

Methods	**Advantages**	**Limitations**
Piezoelectric EH	Higher Power density; Produce Higher open circuit Voltages, Flexible and smaller in size, Highly sensitive to the applied strain Used for both Sensor technology and EH	Produces lower current and high impedance, Less-efficient for lower-frequency designs, Need of unique materials, High-performance PE materials are hard but easily breakable Requires higher cost to produces Higher energy output,
Triboelectric EH	Easy Fabrication, Low-cost, flexible, scalable, wide selection of materials, Produce very high-power density, Produce Higher output Voltages, Free from maintenance cost	The surface is rough and clean, Needs High voltage insulation, Initial understanding is limited, produces lower current density, Charge induction and polarity is depending on the material used Ambient Humidity causes the output performance
Electromagnetic EH	Produces higher output current Small size, Voltage requirement to run the operations is not required	Produces the Lower output voltage, Less flexible, challenging to make smaller-scale magnet and coils, Integration with microsystem is complex, Caused by Vibrations (Amplitude, frequency) and damping factors

TABLE III. DIFFERENT PARAMETERS SUMMARY OF DIFFERENT ENERGY HARVESTERS ON THE HUMAN BODY

Parameters	**Piezoelectric EH**	**Triboelectric EH**	**Electromagnetic EH**
Power Density	Wearables: 37 mW/cm^2 Implantables: 1.2 $\mu W/cm^2$	Wearables: -3 mW/cm^2	Wearables: 507 $\mu W/cm^2$ Implantables: -4 $\mu W/cm^2$
Human Body Parts	Shoulder straps [16] Lower Limbs [19] Human Leg [20] [23] Electronic Skin [21] [24] Walking [23] Footwear [26]	Shoe [33] Cloth [38] [42] Wrist Bracelet[43], Watch [61] Arm [44] Skin [45] Cloth/Skin [46]	Hip mounted [48] Knees [49] Watch [52] [68] Walking [54] [58][62] Arm [60], Shoes [69] Leg and Arm [70]
Methods	Circuit Usage [17] Frequency up-conversion [18] Non-linearity [20] Spring pendulum oscillator [25]	In-plane charging separation method [29] Liquid metal electrode [34] Core-shell structure method [38] Ultrathin flexible single-electrode [39] Air-cushion method [40]	Spring-less system [53] Spring clockwork Method [50] [56] Sprung eccentric rotor [58] Circular Halbach array Method [59] Non-linearity [55] [60] Frequency up-conversion [70]
Recent Developments	Flexible and stretchable PENG, Nanocrystals Usage in PENG	Nanocrystals Usage in TBNG, Flexible Generator, Cantilever-based TEG, Triboelectric Fabric [33]	Flexible Generator

TABLE IV. PERFORMANCE METRICS SUMMARY OF DIFFERENT ENERGY HARVESTERS ON THE HUMAN BODY

Methods	**Human body Part**	**Output Power (mW)**	**Output Voltage (V)**
Piezoelectric EH	Shoulder straps [16] Human Leg [20] Electronic Skin [24] Footwear [26]	45.6 30.55 0.0002 28	NA NA 0.7 20
Triboelectric EH	Shoe [33] Heart rate monitor [36] Cloth [42] Wrist Bracelet [43] Arm [44] Skin [45] Cloth/skin [46]	2.1 2.28 NA 0.3004 4.67 1.12 NA	210 NA 1050 305 392 70 60
Electromagnetic EH	Hip mounted [48] Knees [49] Walking [54] Upper limb [56] Arm [60] Shoes [69] Wrist Watch [68] Leg and Arm [70]	0.284 1.7 0.416 2.2 2.58 2.28 0.203 0.5	2.5 2 0.3 NA 0 to 5 0.5 1.12 0.24

V. CHALLENGES AND SOLUTIONS

The critical challenges for different bio-mechanical energy harvesters from human motion are addressed from the review observations.

- The PEEH produces very ultra-low frequencies around 1 Hz from human motion; however, The PEEH operated with very high bandwidth, compensating human motions. In addition, the Ceramic based piezoelectric materials are rigid and stiff but easily breakable. Therefore, the Linear PEEHs are challenging to extract the average power from human complex or multidimensional motions.
- The TEEH faces mechanical impact issues, which cause many problems (Output performance degradation, Reduction in life span, and safety hazards) and device failure. The moisture and dust particles cause the output
- Performance in the TEEH surface. So, there are chances to cause reliability, durability, and robustness issues. Humidity always affects the performance of the system. Washability issues, electrodes are not flexible in TENG operation,
- The EMEH system naturally uses low-frequency-based devices, which is challenging to produce the maximum output power. In contrast, ultra-lower frequencies are produced from human motion and unsuitable for producing the energy from human body or motion. Integration is a big challenge in EMEH and also tricky to miniaturizing the system. The size and height of the EMEH are enormous. The EMEH system is not flexible in Nature.

The possible solutions for the challenges and issues of the different biomechanical energy harvesters from human motion are addressed.

- The Usage of microfabrication methods like MEMS-based PEEH leads to produces in further progress the Nano PEEH to improve integration issues and output performance. In addition, the Cantilever beam designs are incorporated in PEEH to improve the flexibility in multidimensional motions.
- The Multi-layered encapsulation technique improves the reliability and durability problems irrespective of the environmental conditions. In addition, the TE material abrasion is reduced by using liquid-solid contact in TEEH, which also improves the humidity issues.
- The low-frequency-based springless oscillators are used in EMEH to improve the human motion energy harvesting from the ultra-low frequency range. Frequency-up conversion methods are adopted to improve the output power in the EMEH system (Spring-mass-damper system). Most of the researchers are using hybrid generators like EMEH with TEEH to reduce the size (miniaturization) and also improve the power output.

VI. CONCLUSION AND FUTURE SCOPE

In this manuscript, a detailed review of biomechanical energy harvesting from human motion is discussed. These biomechanical energy harvesters are mainly used in wearable and implantable electronic devices like smart shoes, smartwatches, smart skins, smart clothes, and many more. Harvesting the bi-mechanical energy from human motions is a challenging task. Human movements like walking, arm movement, muscle exercise produces very low frequencies (<10 Hz.). The Bio-mechanical energy harvesters are categorized into three parts PEEH, TEEH, and EMEH. The working principles of the three above energy harvesters are discussed with mathematical equations. The recent progress and development of the Biomechanical energy harvesters are discussing in detail with applications. The advantages and limitations of the PEEH, TEEH, and EMEH are summarized. The performance metrics, recent development, and methods are summarized in detail with Tabulation. Lastly, the Bio-mechanical energy harvesting system challenges and possible solutions are addressed. In the future, incorporate the bio-mechanical energy harvesters into the closed loop-bio electronic system with self-power features.

References

[1] I. Chopra, "Review of the state of the art of smart structures and integrated systems," *AIAA Journal*, vol. 40, no. 11, pp.2145-2187, 2002.

[2] A. Proto, L. Peter, M. Cerny, M. Penhaker, D. Bibbo, S. Conforto, and M. Schmid, "Human Body Energy Harvesting Solutions for Wearable Technologies," *In IEEE 20th International Conference on e-Health Networking, Applications and Services (Healthcom)*, pp. 1-5, 2018.

[3] S. Roundy, and S. T-McKinstry, "Materials and approaches for on-body energy harvesting," *MRS Bulletin*, vol. 43, no. 3, pp. 206-213, 2018.

[4] H. Shi, Z. Liu, and X. Mei, "Overview of human walking induced energy harvesting technologies and its possibility for walking robotics," *Energies*, vol. 13, no. 1, pp. 86, 2020.

[5] G. Rebel, F. Estevez, P. Gloesekoetter, and J. M. C-Secilla, "Energy harvesting on human bodies," *In Smart Health*, pp. 125-159, 2015.

[6] H. Wang, A. Jasim, and X. Chen, "Energy harvesting technologies in roadway and bridge for different applications–A comprehensive review," *Applied energy*, vol. 212, pp.1083-1094, 2018.

[7] Z. Yang, L. Bo, and Z. Li, "Recent progress in human body energy harvesting for smart bioelectronic system," *Fundamental Research*, vol.1, no. 3, pp. 364-385, 2021.

[8] C. Xu, Y. Song, M. Han, and H. Zhang, "Portable and wearable self-powered systems based on emerging energy harvesting technology," *Microsystems & Nanoengineering*, vol. 7, no. 1, pp. 1-14, 2021.

[9] J. Cui, H. Yoon, and B.D. Youn, "An omnidirectional biomechanical energy harvesting (OBEH) sidewalk block for a self-generative power grid in a smart city," *International Journal of Precision Engineering and Manufacturing-Green Technology*, vol. 5, no. 4, pp. 507-517, 2018.

[10] H.S. Kim, J-H. Kim, and J. Kim, "A review of piezoelectric energy harvesting based on vibration," *International journal of precision engineering and manufacturing*, vol. 12, no. 6, pp. 1129-1141, 2011.

[11] M-G. Kang, W-S. Jung, C-Y. Kang, and S-J.Yoon, "Recent progress on PZT based piezoelectric energy harvesting technologies," In Actuators, vol. 5, no. 1, p. 5. Multidisciplinary Digital Publishing Institute, 2016.

[12] Narita, Fumio, and Marina Fox. "A review on piezoelectric, magnetostrictive, and magnetoelectric materials and device technologies for energy harvesting applications." Advanced Engineering Materials 20, no. 5 (2018): 1700743.

[13] Elahi, Hassan, Marco Eugeni, and Paolo Gaudenzi. "A review on mechanisms for piezoelectric-based energy harvesters." Energies 11, no. 7 (2018): 1850.

[14] Priya, Shashank, Hyun-Cheol Song, Yuan Zhou, Ronnie Varghese, Anuj Chopra, Sang-Gook Kim, Isaku Kanno et al. "A review on piezoelectric energy harvesting: materials, methods, and circuits." Energy Harvesting and Systems 4, no. 1 (2019): 3-39.

[15] Wang, Zhong Lin. "Nanogenerators, self-powered systems, blue energy, piezotronics, and piezo-phototronics–A recall on the original thoughts for coining these fields." Nano Energy 54 (2018): 477-483.

[16] Granstrom, Jonathan, Joel Feenstra, Henry A. Sodano, and Kevin Farinholt. "Energy harvesting from a backpack instrumented with piezoelectric shoulder straps." Smart Materials and Structures 16, no. 5 (2007): 1810.

[17] Caliò, Renato, Udaya Bhaskar Rongala, Domenico Camboni, Mario Milazzo, Cesare Stefanini, Gianluca De Petris, and Calogero Maria Oddo. "Piezoelectric energy harvesting solutions." Sensors 14, no. 3 (2014): 4755-4790.

[18] Pillatsch, Pit, Eric M. Yeatman, Andrew S. Holmes, and Paul K. Wright. "Wireless power transfer system for a human motion energy harvester." Sensors and Actuators A: Physical 244 (2016): 77-85.

[19] Fan, Kangqi, Bo Yu, Yingmin Zhu, Zhaohui Liu, and Liansong Wang. "Scavenging energy from the motion of human lower limbs via a piezoelectric energy harvester." International Journal of Modern Physics B 31, no. 7 (2017): 1741011.

[20] Wang, Wei, Junyi Cao, Chris R. Bowen, Shengxi Zhou, and Jing Lin. "Optimum resistance analysis and experimental verification of nonlinear piezoelectric energy harvesting from human motions." Energy 118 (2017): 221-230.

[21] Wang, Xiaoxiong, Wei-Zhi Song, Ming-Hao You, Jun Zhang, Miao Yu, Zhiyong Fan, Seeram Ramakrishna, and Yun-Ze Long. "Bionic single-electrode electronic skin unit based on piezoelectric nanogenerator." Acs Nano 12, no. 8 (2018): 8588-8596.

[22] Kim, Min-Ook, Soonjae Pyo, Yongkeun Oh, Yunsung Kang, Kyung-Ho Cho, Jungwook Choi, and Jongbaeg Kim. "Flexible and multi-directional piezoelectric energy harvester for the self-powered human motion sensor." Smart Materials and Structures 27, no. 3 (2018): 035001.

[23] Kakihara, R., K. Kariya, Y. Matsushita, T. Yoshimura, and N. Fujimura. "Investigation of piezoelectric energy harvesting from human walking." In Journal of Physics: Conference Series, vol. 1052, no. 1, p. 012113. IOP Publishing, 2018.

[24] Guido, Francesco, Antonio Qualtieri, Luciana Algieri, Enrico Domenico Lemma, Massimo De Vittorio, and Maria Teresa Todaro. "AlN-based flexible piezoelectric skin for energy harvesting from human motion." Microelectronic Engineering 159 (2016): 174-178.

[25] Wu, Yipeng, Jinhao Qiu, Shengpeng Zhou, Hongli Ji, Yang Chen, and Sen Li. "A piezoelectric spring pendulum oscillator used for multi-directional and ultra-low frequency vibration energy harvesting." Applied energy 231 (2018): 600-614.

[26] Qian, Feng, Tian-Bing Xu, and Lei Zuo. "Design, optimization, modeling, and testing of a piezoelectric footwear energy harvester." Energy conversion and management 171 (2018): 1352-1364.

[27] Wang, Sihong, Long Lin, and Zhong Lin Wang. "Nanoscale triboelectric-effect-enabled energy conversion for sustainably powering portable electronics." Nano Letters 12, no. 12 (2012): 6339-6346.

[28] Wang, Zhong Lin. "Triboelectric nanogenerators as new energy technology and self-powered sensors–Principles, problems, and perspectives." Faraday discussions 176 (2015): 447-458.

[29] Wang, Sihong, Long Lin, Yannan Xie, Qingshen Jing, Simiao Niu, and Zhong Lin Wang. "Sliding-triboelectric nanogenerators based on in-plane charge-separation mechanism." Nano Letters 13, no. 5 (2013): 2226-2233.

[30] Fan, Feng Ru, Wei Tang, and Zhong Lin Wang. "Flexible nanogenerators for energy harvesting and self-powered electronics." Advanced Materials 28, no. 22 (2016): 4283-4305.

[31] Song, Peiyi, Guang Yang, Tingting Lang, and Ken-Tye Yong. "Nanogenerators for wearable bioelectronics and biodevices." Journal of Physics D: Applied Physics 52, no. 2 (2018): 023002.

[32] Wang, Sihong, Yannan Xie, Simiao Niu, Long Lin, and Zhong Lin Wang. "Freestanding triboelectric-layer-based nanogenerators for harvesting energy from a moving object or human motion in contact and non-contact modes." Advanced materials 26, no. 18 (2014): 2818-2824.

[33] Huang, Tao, Cheng Wang, Hao Yu, Hongzhi Wang, Qinghong Zhang, and Meifang Zhu. "Human walking-driven wearable all-fiber triboelectric nanogenerator containing electrospun polyvinylidene fluoride piezoelectric nanofibers." Nano Energy 14 (2015): 226-235.

[34] Tang, Wei, Tao Jiang, Feng Ru Fan, Ai Fang Yu, Chi Zhang, Xia Cao, and Zhong Lin Wang. "Liquid-metal electrode for high-performance triboelectric nanogenerator at an instantaneous energy conversion efficiency of 70.6%." Advanced Functional Materials 25, no. 24 (2015): 3718-3725.

[35] Ha, Minjeong, Jonghwa Park, Youngoh Lee, and Hyunhyub Ko. "Triboelectric generators and sensors for self-powered wearable electronics." Acs Nano 9, no. 4 (2015): 3421-3427.

[36] Lin, Zhiming, Jun Chen, Xiaoshi Li, Zhihao Zhou, Keyu Meng, Wei Wei, Jin Yang, and Zhong Lin Wang. "Triboelectric nanogenerator enabled body sensor network for self-powered human heart-rate monitoring." ACS Nano 11, no. 9 (2017): 8830-8837.

[37] Shen, Jiali, Zhaoling Li, Jianyong Yu, and Bin Ding. "Humidity-resisting triboelectric nanogenerator for high-performance biomechanical energy harvesting." Nano Energy 40 (2017): 282-288.

[38] Yu, Aifang, Xiong Pu, Rongmei Wen, Mengmeng Liu, Tao Zhou, Ke Zhang, Yang Zhang, Junyi Zhai, Weiguo Hu, and Zhong Lin Wang.

"Core–shell-yarn-based triboelectric nanogenerator textiles as power cloths." ACS Nano 11, no. 12 (2017): 12764-12771.

[39] Chen, Shu Wen, Xia Cao, Ning Wang, Long Ma, Hui Rui Zhu, Magnus Willander, Yang Jie, and Zhong Lin Wang. "An ultrathin flexible single-electrode triboelectric-nanogenerator for mechanical energy harvesting and instantaneous force sensing." Advanced Energy Materials 7, no. 1 (2017): 1601255.

[40] Zhang, Zengxing, Kang Du, Xi Chen, Chenyang Xue, and Kaiying Wang. "An air-cushion triboelectric nanogenerator integrated with stretchable electrode for human-motion energy harvesting and monitoring." Nano Energy 53 (2018): 108-115.

[41] Ding, Xiaoheng, Hailin Cao, Xinghong Zhang, Mingyu Li, and Yuntian Liu. "Large scale triboelectric nanogenerator and the self-powered flexible sensor for human sleep monitoring." Sensors 18, no. 6 (2018): 1713.

[42] Ning, Chuan, Lan Tian, Xinya Zhao, Shengxin Xiang, Yingjie Tang, Erjun Liang, and Yanchao Mao. "Washable textile-structured single-electrode triboelectric nanogenerator for self-powered wearable electronics." Journal of Materials Chemistry A 6, no. 39 (2018): 19143-19150.

[43] Song, Yu, Haobin Wang, Xiaoliang Cheng, Guoke Li, Xuexian Chen, Haotian Chen, Liming Miao, Xiaosheng Zhang, and Haixia Zhang. "High-efficiency self-charging smart bracelet for portable electronics." Nano Energy 55 (2019): 29-36.

[44] Xia, Kequan, Zhiyuan Zhu, Hongze Zhang, Chaolin Du, Jiangming Fu, and Zhiwei Xu. "Milk-based triboelectric nanogenerator on paper for harvesting energy from human body motion." Nano Energy 56 (2019): 400-410.

[45] Wang, Lingyun, and Walid A. Daoud. "Highly flexible and transparent polyionic-skin triboelectric nanogenerator for biomechanical motion harvesting." Advanced Energy Materials 9, no. 5 (2019): 1803183.

[46] Xiong, Jiaqing, Peng Cui, Xiaoliang Chen, Jiangxin Wang, Kaushik Parida, Meng-Fang Lin, and Pooi See Lee. "Skin-touch-actuated textile-based triboelectric nanogenerator with black phosphorus for durable biomechanical energy harvesting." Nature Communications 9, no. 1 (2018): 1-9.

[47] Saha, C. R., T. O'donnell, N. Wang, and P. McCloskey. "Electromagnetic generator for harvesting energy from human motion." Sensors and Actuators A: Physical 147, no. 1 (2008): 248-253.

[48] Dai, Dan, and Jing Liu. "Hip-mounted electromagnetic generator to harvest energy from human motion." Frontiers in Energy 8, no. 2 (2014): 173-181.

[49] Luciano, V., E. Sardini, M. Serpelloni, and G. Baronio. "An energy harvesting converter to power sensorized total human knee prosthesis." Measurement Science and Technology 25, no. 2 (2014): 025702.

[50] Zhang, Qian, Yufeng Wang, and Eun Sok Kim. "Power generation from human body motion through magnet and coil arrays with magnetic spring." Journal of Applied Physics 115, no. 6 (2014): 064908.

[51] Dinulovic, Dragan, Michael Brooks, Martin Haug, and Tomislav Petrovic. "Rotational electromagnetic energy harvesting system." Physics Procedia 75 (2015): 1244-1251.

[52] Quan, Ting, Xue Wang, Zhong Lin Wang, and Ya Yang. "Hybridized electromagnetic–triboelectric nanogenerator for a self-powered electronic watch." Acs Nano 9, no. 12 (2015): 12301-12310.

[53] Bendame, Mohamed, Eihab Abdel-Rahman, and Mostafa Soliman. "Electromagnetic impact vibration energy harvesters." In Structural nonlinear dynamics and diagnosis, pp. 29-58. Springer, Cham, 2015.

[54] Niroomand, Mehdi, and Hamid Reza Foroughi. "A rotary electromagnetic microgenerator for energy harvesting from human motions." Journal of applied research and technology 14, no. 4 (2016): 259-267.

[55] Geisler, M., S. Boisseau, M. Perez, I. Ait-Ali, and S. Perraud. "Scaling effects in a nonlinear electromagnetic energy harvester for wearable sensors." In Journal of Physics: Conference Series, vol. 773, no. 1, p. 012044. IOP Publishing, 2016.

[56] Brunner, Stephan, Maximilian Gerst, and Christian Pylatiuk. "Design of a body energy harvesting system for the upper extremity." Current Directions in Biomedical Engineering 3, no. 2 (2017): 331-334.

[57] Halim, M. A., R. Rantz, Q. Zhang, L. Gu, K. Yang, and S. Roundy. "Electromagnetic energy harvesting from swing-arm motion using rotational eccentric mass structure." In 2017 19th international conference on solid-state sensors, actuators, and microsystems (TRANSDUCERS), pp. 1863-1866. IEEE, 2017.

[58] Halim, M. A., R. Rantz, Q. Zhang, L. Gu, K. Yang, and S. J. A. E. Roundy. "An electromagnetic rotational energy harvester using sprung eccentric rotor, driven by pseudo-walking motion." Applied Energy 217 (2018): 66-74.

[59] Zhang, Ying, Junyi Cao, Hongyu Zhu, and Yaguo Lei. "Design, modeling and experimental verification of circular Halbach electromagnetic energy harvesting from bearing motion." Energy conversion and management 180 (2019): 811-821.

[60] Fan, Kangqi, Yiwei Zhang, Haiyan Liu, Meiling Cai, and Qinxue Tan. "A nonlinear two-degree-of-freedom electromagnetic energy harvester for ultra-low frequency vibrations and human body motions." Renewable Energy 138 (2019): 292-302.

[61] Leonov, Vladimir. "Energy harvesting for self-powered wearable devices." In Wearable monitoring systems, pp. 27-49. Springer, Boston, MA, 2011.

[62] Xie, Longhan, and Mingjing Cai. "Human motion: Sustainable power for wearable electronics." IEEE Pervasive Computing 13, no. 4 (2014): 42-49.

[63] Ghomian, Taher, and Shahab Mehraeen. "Survey of energy scavenging for wearable and implantable devices." Energy 178 (2019): 33-49.

[64] Khalifa, Sara, Guohao Lan, Mahbub Hassan, Aruna Seneviratne, and Sajal K. Das. "Harke: Human activity recognition from kinetic energy harvesting data in wearable devices." IEEE Transactions on Mobile Computing 17, no. 6 (2017): 1353-1368.

[65] Dagdeviren, Canan, Zhou Li, and Zhong Lin Wang. "Energy harvesting from the animal/human body for self-powered electronics." Annual review of biomedical engineering 19 (2017): 85-108.

[66] Pavelková, Radka, David Vala, and Kateřina Gecová. "Energy harvesting systems using human body motion." IFAC-PapersOnLine 51, no. 6 (2018): 36-41.

[67] Invernizzi, F., S. Dulio, M. Patrini, G. Guizzetti, and P. Mustarelli. "Energy harvesting from human motion: materials and techniques." Chemical Society Reviews 45, no. 20 (2016): 5455-5473.

[68] Halim, Miah A., Hyunok Cho, Md Salauddin, and Jae Y. Park. "A miniaturized electromagnetic vibration energy harvester using flux-guided magnet stacks for human-body-induced motion." Sensors and Actuators A: Physical 249 (2016): 23-31.

[69] Wu, Shuai, Patrick Chi-Kwong Luk, Chunfang Li, Xiangyu Zhao, Zongxia Jiao, and Yaoxing Shang. "An electromagnetic wearable 3-DoF resonance human body motion energy harvester using ferrofluid as a lubricant." Applied Energy 197 (2017): 364-374.

[70] Fan, Kangqi, Meiling Cai, Haiyan Liu, and Yiwei Zhang. "Capturing energy from ultra-low frequency vibrations and human motion through a monostable electromagnetic energy harvester." Energy 169 (2019): 356-368.

[71] Tian, Jingjing, Rui Shi, Zhuo Liu, Han Ouyang, Min Yu, Chaochao Zhao, Yang Zou, Dongjie Jiang, Jingshuang Zhang, and Zhou Li. "Self-powered implantable electrical stimulator for osteoblasts' proliferation and differentiation." Nano Energy 59 (2019): 705-714.

[72] Yang, Ye, Hong Pan, Guangzhong Xie, Yadong Jiang, Chunxu Chen, Yuanjie Su, Yang Wang, and Huiling Tai. "Flexible piezoelectric pressure sensor based on polydopamine-modified BaTiO3/PVDF composite film for human motion monitoring." Sensors and Actuators A: Physical 301 (2020): 111789.

CRS-iEclat: Implementation of Critical Relative Support in iEclat Model for Rare Pattern Mining

Wan Aezwani Wan Abu Bakar[1]
Faculty of Informatics and Computing
Universiti Sultan Zainal Abidin (UniSZA)
Besut Campus, 22200 Besut, Terengganu, Malaysia

Mustafa Man[2]
Faculty of Ocean Engineering Technology and Informatics
Universiti Malaysia Terengganu (UMT)
21030 Kuala Nerus, Terengganu, Malaysia

Zailani Abdullah[3]
Faculty of Entrepreneurship and Business (FEB)
Centre of Computing and Informatics (CCI), Universiti Malaysia Kelantan (UMK), City Campus, Malaysia

Mahadi B Man[4]
Faculty of Ocean Engineering Technology and Informatics
Universiti Malaysia Terengganu (UMT)
21030 Kuala Nerus, Terengganu, Malaysia

***Abstract*—The research purpose is to develop a performance enhancement in Incremental Eclat (iEclat) model by embedding Critical Relative Support (CRS) in mining of infrequent itemset. The CRS measure acts as an interestingness measure (filter) in iEclat model that comprises of i-Eclat-diffset algorithm, i-Eclat-sortdiffset algorithm and i-Eclat-postdiffset algorithm for infrequent (rare) itemset mining. The association rule is performed to reveal the relationships among itemsets in a transactional database. The task of association rule mining is to discover if there exist the frequent itemset or infrequent patterns in the database and if any, an interesting relationship between these frequent or infrequent itemsets can reveal a new pattern analysis for the future decision making. Regardless of frequent or infrequent itemsets, the persisting issues are deemed to execution time to display the rules and the highest memory consumption during mining process. CRS-iEclat engine is proposed to overcome the said issues. Prior to experimentation, results indicate that CRS-iEclat outperforms iEclat from 54% to 100% accuracy on execution time (ET) in selected database as to show the improvement of ET efficiency.**

***Keywords*—Critical relative support; equivalence class transformation (Eclat); iEclat model; interestingness measure**

I. Introduction

Association Rule is among the four (4) core domains in Data Mining. The rule or pattern generated determines the associations or similar structures among sets of items in the database transaction. Correlation or association allows the tendencies between one item and another item in one particular set of items in a typical dataset. The association rule implementation can be seen in market basket analysis to predict the potential item buying by customers, remedial medications for no vaccine disease, biological cells actions that constitutes to certain disease symptoms, offering banking or retail services [1-2]. There are two categories of item i.e. Frequent itemset (frequent occurring) and infrequent (rare occurring) itemset. Main contribution of frequent itemset is finding frequent correlation of items that constitutes to certain pattern in database transactions while infrequent itemset is finding the contradiction or peculiar or rare pattern. To determine either the itemset is frequent or infrequent, one threshold value must be set that is called minimum support (min_supp) or the maximum support (max_supp) where these values are pre-defined user settings. When the itemset is above min_supp, then it is considered as frequent itemset and vice versa. While frequent itemset discovers the normal operations i.e. buying types or disease occurrences, the rare itemset in contrast finds abnormal and peculiar association and correlation of abnormal itemsets. This abnormal consolidation may discover hidden or new findings that require for further attention by domain experts. Further investigation of the rare patterns generated would provide solutions for a significant difficulty through formulation in association rule mining algorithms. Setting of rare patterns depending upon certain predefined threshold value considering on lower than minimum occurrences of the itemsets from database transactions.

The rest of the sections are organized as follows. Section 2 describes the previous literatures, Section 3 illustrates the Eclat basic principles, Section 4 explains the design of iEclat model. Next Section 5 prescribes the experimentation settings while Section 6 discusses on the results achieved. Section 7 summarizes the conclusions as well as future recommendations.

II. Related Work

Regardless either mining data via frequent or infrequent association, the critical issues still remains on memory space consumption and data storage capacity [3-5]. To reduce memory and data consumption during mining process, the previous researches have made effort on the 2 searching strategy i.e. horizontal database record or breadth first searching [6] and vertical database record [7-8] or depth first searching. When the horizontal record drawback issues are subjected to storage and memory, thus contemporary works are then utilized on the vertical database for rules mining algorithms that are proposed in [8-10]. In ARM, the so-called state-of-the-art frequent/infrequent models are Apriori [1, 6] underlying on horizontal records. Meanwhile Eclat [9] and FP-Growth [14] are vertical database records practitioners.

To the best of our knowledge, Equivalent Class Transformation (Eclat) algorithm [8] outperforms because of its 'fast' intersection of its transaction-id-list to determine the minimum or maximum support threshold [9, 14]. The Eclat followers and the invariants are [9-13], [15-20], [22] and [26].

In response to its simple and quick method in finding the threshold value as the interestingness measure in mining, we have done an improvement in original Eclat where we have proposed Incremental Eclat (iEclat) model in our previous work [20], [22] and [26]. To continue, this research presents a deployment of Critical Relative Support (CRS) as the interestingness measure or filtering or pruning method in our Incremental Eclat (iEclat) model. Our proposed solution, CRS-iEclat algorithm is used in selected dense dataset to improve the performance of execution time.

III. Basic Principles of Eclat

Eclat works in two-steps i.e. first, generate candidate itemsets during intersecting and second is pruning. In step 1, each i-itemset candidate is generated by (i-1)-itemset and the number of frequency occurrences (support) are calculated. If the support<threshold, then pruning/removing it, if not, then is frequent itemsets later is set to generate (i+1)-itemset. Because of its depth first searching, start with the frequent items in the item base 1-itemset, then move to 2-itemset, next is 3-itemset and continues until all the depths of itemset trees are visited. The four algorithms underlying in i-Eclat model are tidset [9], diffset [9], sortdiffset [12] and postdiffset [20, 22, 26].

A. *Original Eclat (tidset)*

The i-itemset formulates when joining of (i-1)-itemset which have similar (i-2)-itemset, both (i-1)-itemsets are named as superclass itemsets of the i-itemset. Let {}, {ab} and {ac} are superclass of {abc}. To get rid of duplication, (i-1)-itemset are arranged in some order. For example, itemset {a, b, c, d, e} are arranged into alphabet order. Finding all 2-itemsets, items {a} is joined with {b,c,d,e} resulting into {ab, ac, ad, ae} then for the union of {b} with {c,d,e} resulting in {bc, bd, be}, similarly for {c} and {d}. Lastly, all candidate of 2-itemsets {ab, ac, ad, ae, bc, bd, be, cd, ce, de} are formulated that later used for formulation of 3-itemsets. The union process continues to the higher depths of itemset trees and finish when all items in the itemsets are visited. These operations are illustrated in Fig. 1.

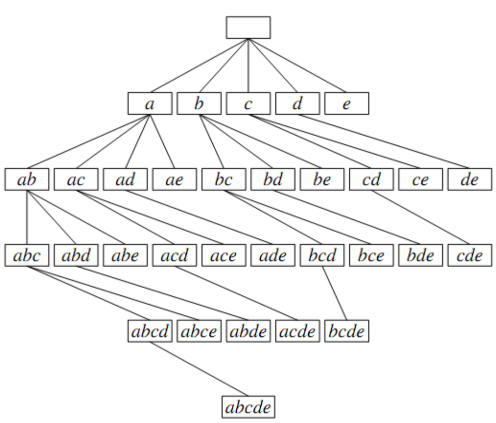

Fig. 1. Example of Candidate Generation with {a,b,c,d,e}.

B. *Eclat (diffset)*

The dEclat (where d stands for different set or diffset) as referred in [9] is the process of finding the different in prefix items among 2 tidsets (tid of itemsets and its prefix). When finding prefix items that differs, the matching correlation (cardinality) of itemsets is lesser and fasten the intersecting process and reduce memory consumption because candidate itemsets is vastly reduced. Let equivalence class with prefix F contains the itemsets X and Y [7]. Let t(X) to be the tidset of X while d(X) to be the diffset of X. In tidset, t(FX) and t(FY) are formed in the equivalence class and to obtain t(FXY). When we check the matching correlation of t(FX)∩t(FY) = t(FXY). Much simpler in diffset where we formulate d(FX) instead of t(FX) and d(FX) = t(F) – t(X), , the set of tids in t(F) but not in t(X). Then it results in d(FY) = t(F) – t(Y). Hence, the frequency occurrences (support) of FX does not constitute to diffset size. Refer to diffset process illustration in Fig. 2.

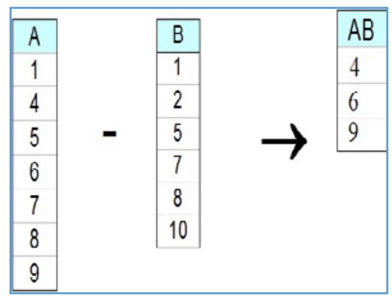

Fig. 2. Diffset between Itemset A and B.

C. *Sortdiffset Algorithm*

Diffset sorting [12] tries to improve dEclat [9] during intersecting process. Sorting takes place where switching is done to the itemsets. But during switching, it happens when certain tidsets are not eligible for the switching condition, thus instead of diffset, but these tidsets remains. For example, if the equivalence class with prefix E consisting of itemsets Xi, intersection of EXi with all EXj with j>i is processed to achieve a new prefix EXi class and itemsets XiXj. EXi and EXj potential to be found in either tidset format or diffset format. If EXi is in diffset format and EXj is in tidset format, the d(EXi)∩t(EXj) = d(EXjXi). Relatively for each itemset, tidset format must appear before diffset format in the order of their equivalence class according to Sortdiffset algorithm.

D. *Postdiffset Algorithm*

Postdiffset [22, 26-27] is proposed to answer the suggestion that is made in [12] to use tidset format in the first level of looping for sparse database and later switch to diffset format. The second level onwards of looping is done in diffset (difference intersection set) between i^{th} column and $i+1^{th}$ column before saving to database. For the first level looping, $Xi \cap Xj$ is performed while in second level looping, only candidates itemsets that differ in X_i is considered in differentiating process of X_i – X_i. From Fig. 3, the min_support value is given in percentage of min_support value over 100 and multiplies with total of transaction records of each dataset. If the min_supp is lower, then it is set to be rare itemsets and vice versa. Next, in the first loop, if the itemset support >= to min_support (that is set), then, tidset takes place in first looping and follows by diffset process in the second looping onwards between i^{th} column and $i+1^{th}$ column before saving it to database.

```
Input: E((i_1, t_1), ... (i_n, t_n))|P), s_min

Output: F(E, s_min)
Start
//get min_support
    min_supp=number_of_rows*percentage_min
    _support;
    run tidset for first loop;
    if(support<=min_support){
    add data to the next process;
    add data into db
    } end tidset
//for next loop
    start looping ;
    run diffset;
    if(support<=min_support){
    add data to the next process;
    add data into db
    } end looping.
    end diffset;
    flush value for current/last transaction data;
```

Fig. 3. Postdiffset Pseudocode.

Critical Relative Support (CRS) is designed by [20] is a measurement to mine the critical least association rules. The range of CRS is between 0 and 1. The value that is mostly reached 1 is considered to be the most significant and critical rule. CRS value plays around between 2 threshold value (i.e. lowest support, α and highest support, β). Detail explanation of CRS is given in Definition 13.

IV. Design of iEclat Model

A. Incremental Eclat (iEclat)

To improve performance and accuracy of itemset mining, recent researches are focus towards parallel and incremental mining approach [21-23]. Incremental mining in a dynamic database is established with regards to the itemsets or records of transaction [24-25]. Incremental in itemsets means an additional of new items being added or deleted to the existing itemsets in database whereas incremental in records of transaction means the additional transactions to the existing database transaction. The basic definitions of incremental mining concept are as follows:

Definition 1: (Incremental Database). Given a transaction itemset, T, and database, D and a sequence α. The support of D is denoted by supportD(α) is the frequency of items in D. When new data, δ is to be added to database D. Then D is said to be original database and δ is the incremental database. The updated database is denoted by (D + δ).

Definition 2: (Incremental Records and Itemsets Discovery Problem). Given an original database D and a new increment to the D which is δ, for all frequent itemsets in database (D + δ) with minimum possible recomputation and I/O overheads. The length of frequent itemsets in the updated database (D + δ) is called Incremental Records.

B. Critical Relative Support in i-Eclat

In this phase, a CRS-iEclat model is designed. First step is to design a base model in vertical approach of infrequent pattern models such as CRS in iEclat-diffset, CRS in iEclat-sortdiffset and CRS in iEclat-postdiffset. The enhancement of iEclat algorithm is required to suit for infrequent pattern mining. The completion of these steps produces an enhancement of iEclat model called as CRS-iEclat-diffset, CRS-iEclat-sortdiffset and CRS-iEclat-postdiffset format.

The outcomes are first, the embedded CRS definition in i-Eclat algorithm, second is the completion of incremental algorithm in CRS-iEclat-diffset, CRS-iEclat-sortdiffset and CRS-iEclat-postdiffset. Third, the completion of all artefact's compilation in the proposed hybrid algorithms.

Definition 3: (Least Items). An itemset X is called least item if $(a <= sup(X) <= b)$ where a and b is the lowest and highest support, respectively. The set of least item is denoted as.

$$Least\ Items\ =\ \{X \in I \mid a <=\ sup(X)\ <=\ b\}$$

Definition 4: (Infrequent Items). An itemset X is called infrequent item if $(sup(X)\ <=\ b)$ where b is the highest support. The set of infrequent item is denoted as.

$$Infrequent\ items\ =\ \{X \in I \mid sup\ (X)\ <=\ b\}$$

Definition 5: (Critical Relative Support). A CRS is a maximum of relative frequency among itemset and their Jaccard similarity coefficient. The value of Critical Relative Support denoted as CRS and.

$$CRS\ =\ max[(sup(A)/sup(B)), ((sup(A \longrightarrow B)/(sup(A) + sup(B) - sup(A \longrightarrow B)))]$$

The CRS value is ranging from 0 to 1, getting the results of multiplication of the highest value either antecedent support and divide by the consequence or otherwise with their Jaccard similarity coefficient. The measurement value refers to the level of CRS between combination of the both Least Items and Infrequent Items to be set as antecedent or consequence.

The architecture of CRS-iEclat is diagrammed in Fig. 4. From all infrequent items will be passed to the first pruning process, getaway G1. G1 is set with the CRS value. To set G1, total transaction records are scanned to be multiplied with the percentage of user-specified relative value of min_sup, max_sup and min_conf (minimum confidence) value. Once the value is obtained, only candidate of infrequent itemsets that passed the G1 value will be processed either through Eclat-tidset, Eclat-diffset, Eclat-sortdiffset or Eclat-postdiffset algorithms in Eclat engine. Second pruning process, getaway G2 takes place. Getaway G2 plays an important role in each itemset prior to generating frequent association rules where, filtered infrequent itemset is written to text file. Candidate itemsets are directed to hard disk storage, so that the resource of memory storage is automatically reduced to enable the processing and executing of full datasets.

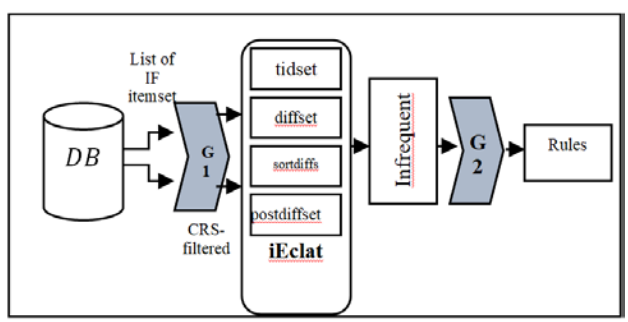

Fig. 4. CRS-iEclat Architecture.

V. Experimental Settings

A. Setup

In this phase, the proposed hybrid model will be implemented by converting all algorithms, data structures and measures into PHP-MySQL programming in a relational database management system (RDBMS) platform. The outcome is the completion of the workable prototype to mine infrequent AR.

B. Dataset

The retrieval of benchmark datasets is obtained from (Goethals, 2003) in a *.dat file format. The two (2) category of datasets are dense (i.e. a dimension with a high probability that one or more data points is occupied in every combination of dimensions) and sparse (i.e. a dimension with a low percentage of available data positions filled). The datasets descriptions are illustrated in Table I.

TABLE I. Database Source

Dataset	Description
Chess	lists the chess end game positions for king vs. King and rook
Mushroom	contains different attributes of 23 species of gilled mushrooms in the Agaricus and Lepiota family

The category of datasets is dense (i.e. a dimension with a high probability that one or more data points are occupied in every combination of dimensions). The overall characteristics of benchmark datasets is tabulated in Table II.

TABLE II. Database Characteristics

Database	#Size (KB)	#Length (attribute)	#Item	#Records (transaction)	Category
Chess	334	37	75	3196	Dense
Mushroom 557	23	119	8124	Dense	

VI. Result and Discussion

Performance of two dense datasets are measured based upon the formula in (1). The example of percentage of reduction ratio of execution time (ET) in B as compared to execution time (ET) in A is calculated based on (1) that determines the outperform percentage of B.

$$\frac{(ET\ in\ A)-(ET\ in\ B)}{2ET\ in\ A} x100 \quad (1)$$

We reveals the experimentation with only taking 50% min_supp threshold for iEclat engine whereas in CRS-iEclat, we take 30%, 40% and 50% of min_supp, min_conf and max_supp value respectively that we have tested for only 3 algorithms which are diffset, sortdiffset and postdiffset algorithms since tidset algorithms consistently to response in highest execution time both in iEclat as well as CRS-iEclat engine. Fig. 5 plots the graph of full chess dataset running in iEclat algorithm and the proposed CRS-iEclat algorithm. The CRS-iEclat outperforms iEclat engine in chess for diffset with 99% while in sortdiffset and postdiffset it shows 100% outperformance towards lesser execution time. Meanwhile, CRS-iEclat outperforms iEclat in diffset, sortdiffset and postdiffset with 54%, 66% and 79% respectively for mushroom dataset.

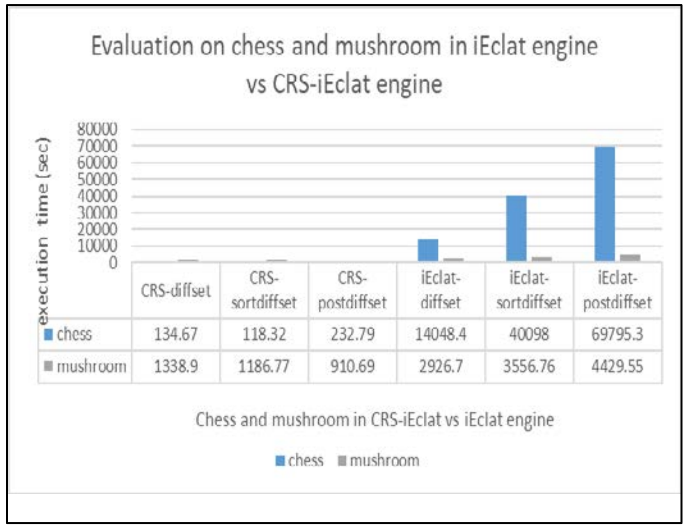

Fig. 5. Evaluation of ET between CRS-iEclat Vs iEclat Engine.

VII. Conclusion

The research proves that the more increment in itemset (column) resulting in the more usage of memory as compared to the increment of records of transaction. This is due to the increment of itemsets produces the higher cardinality of intersection between each item that needs to be conducted in vertical mining. That is why the much higher execution time can be seen in chess despite mushroom dataset. Our work also confirmed that when CRS measure is adopted in the filtering of support-confidence of our iEclat model, the execution time has drastically reduced. Either iEclat or CRS-iEclat engine, the performance of both engines is actually depending upon the nature of dataset itself when testing in diffset, sortdiffset and postdiffset algorithms. However, both engines conform that among these three algorithms, postdiffset outperforms other two algorithms by certain order of magnitude in all selected datasets. This research has proved that with CRS used as the value-added interestingness measure and filtering (pruning) in original iEclat engine, the performance is significantly improved in mining of infrequent itemsets. For our future work, the remaining test would undertake other FIMI dense datasets such as connect and pumbstar or sparse datasets such as retail or T10I4D100K to observe the performance of CRS-iEclat algorithm. The consistency of results obtained is important in determining the robustness of this model in mining process.

Acknowledgment

This project is funded by FRGS grant with reference code FRGS/1/2020/ICT06/UNISZA/03/1. A sincere gratitude goes to all faculty members of UniSZA and grant collaborators of UMT for supporting our work in reviewing for spelling errors and synchronization consistencies and also for the meaningful comments and suggestions.

References

[1] R. Agrawal and R. Srikant, “Fast algorithms for mining association rules,” in Proceedings of 20th International Conference on Very Large Data Bases (VLDB), 1215, pp. 487–499, 1994.

[2] S. Shrivastava and P.K. Johari, “Analysis on high utility infrequent ItemSets mining over transactional database,” InRecent Trends in

Electronics, Information & Communication Technology (RTEICT), IEEE International Conference on pp. 897-902, 2016.

[3] M.A. Thalor and S. Patil, "Incremental Learning on Non-stationary Data Stream using Ensemble Approach," International Journal of Electrical and Computer Engineering, Aug 1;6(4):1811, 2016.

[4] G. Bathla, et al., "A Novel Approach for clustering Big Data based on MapReduce," International Journal of Electrical and Computer Engineering (IJECE), Jun 1;8(3), 2018.

[5] M.B. Man, et al., "Mining Association Rules: A Case Study on Benchmark Dense Data," Indonesian Journal of Electrical Engineering and Computer Science on pp. 546-553, Sep 1;3(3), 2016.

[6] R. Agrawal, et al., "Mining association rules between sets of items in large databases," ACM SIGMOD Record, 22(2), pp. 207–216, 1993.

[7] J. Han, et al., "Mining frequent patterns without candidate generation," ACM SIGMOD Record, 29(2), pp. 1–12, 2000.

[8] M. J. Zaki, et al., "New algorithms for fast discovery of association rules," In Proceedings of the ACM SIGKDD international conference on Knowledge Discovery and Data Mining (KDD'97), pp. 283–286, 1997.

[9] M. J. Zaki and K. Gouda, "Fast vertical mining using diffsets," In Proceedings of the ninth ACM SIGKDD international conference on Knowledge Discovery and Data Mining, pp. 326–335, 2003.

[10] P. Singh, S. Singh, P. K. Mishra, and R. Garg. "RDD-Eclat: Approaches to Parallelize Eclat Algorithm on Spark RDD Framework." In *International Conference on Computer Networks and Inventive Communication Technologies*, pp. 755-768. Springer, Cham, 2019.

[11] P. Shenoy, et al., "Turbo-charging vertical mining of large databases," ACM SIGMOD Record, 29(2), pp. 22–33, 2000.

[12] T. A, Trieu and Y. Kunieda, "An improvement for declat algorithm," In Proceedings of the 6th International Conference on Ubiquitous Information Management and Communication (ICUIMC'12), 54, pp. 1–6, 2012.

[13] J. Hipp, et al., "Algorithms for association rule mininga general survey and comparison," ACM SIGKDD Explorations Newsletter, 2(1), pp. 58–64, 2000.

[14] J. Han, et al., "Frequent pattern mining: current status and future directions," Data Mining and Knowledge Discovery, 15(1), pp. 55–86, 2007.

[15] C. Borgelt, "Efficient implementations of apriori and eclat," In Proceedings of the IEEE ICDM Workshop on Frequent Itemset Mining Implementations (FIMI03), pp. 90, 2003.

[16] B. Goethals, and M. J. Zaki. "FIMI'03: Workshop on frequent itemset mining implementations." In *Third IEEE International Conference on Data Mining Workshop on Frequent Itemset Mining Implementations*, pp. 1-13. 2003.

[17] A. Savasere, et al., "An efficient algorithm for mining association rules in large databases," In Proceeding of the 21th International Conference on Very Large Data Bases (VLDB '95), pp. 432–444, 1995.

[18] T. Slimani and A. Lazzez, "Efficient analysis of pattern and association rule mining approaches," International Journal of Information Technology and Computer Science, 6(3), pp. 70–81, 2014.

[19] H. Toivonen, "Sampling large databases for association rules," In Proceeding of the 22nd International Conference on Very Large Data Bases (VLDB '96), pp. 134–145, 1996.

[20] M. Man, W. A. W. A. Bakar, M. A. Jalil, & J. A. Jusoh, "Postdiffset Algorithm in Rare Pattern: An Implementation via Benchmark Case Study." International Journal of Electrical & Computer Engineering (2088-8708) 8, 2018.

[21] Z. Abdullah, T. Herawan, N. Ahmad, and M. M. Deris. "Mining significant association rules from educational data using critical relative support approach." Procedia-Social and Behavioral Sciences 28, pp. 97-101, 2011.

[22] W. A. W. A. Bakar, Z. Abdullah, M. Y. M. Saman, M. A. Jalil, M. Man, and T. Herawan. "Vertical Association Rule Mining: Case study implementation with relational DBMS." In *2015 International Symposium on Technology Management and Emerging Technologies (ISTMET)*, IEEE, pp. 279-284, 2015.

[23] Q. Yong, "Integrating Frequent Itemsets Mining with Relational Database." In *2007 8th International Conference on Electronic Measurement and Instruments*, IEEE, pp. 2-543, 2007.

[24] G. Ramesh, M. William, and M. J. Zaki. "Indexing and Data Access Methods for Database Mining." In *DMKD*. 2002.

[25] J. Küng, J. Markus, and K. D. Tran, "IFIN+: a parallel incremental frequent itemsets mining in shared-memory environment." In *International Conference on Future Data and Security Engineering*, pp. 121-138, Springer, Cham, 2017.

[26] W. A. W. A. Bakar, M. A. Jalil, M. Man, Z. Abdullah, and F. Mohd., "Postdiffset: an Eclat-like algorithm for frequent itemset mining." *International Journal of Engineering & Technology* 7, no. 2.28, pp. 197-199, 2018.

[27] W. A. W. A. Bakar, M. Man, M. Man, and Z. Abdullah, "i-Eclat: performance enhancement of Eclat via incremental approach in frequent itemset mining." *Telkomnika* 18, no. 1, pp. 562-570, 2020.

Pre-trained CNNs Models for Content based Image Retrieval

Ali Ahmed
Faculty of Computing and Information Technology
King Abdulaziz University –Rabigh
Rabigh 21589, Saudi Arabia

***Abstract*—Content based image retrieval (CBIR) systems is a common recent method for image retrieval and is based mainly on two pillars extracted features and similarity measures. Low level image presentations, based on colour, texture and shape properties are the most common feature extraction methods used by traditional CBIR systems. Since these traditional handcrafted features require good prior domain knowledge, inaccurate features used for this type of CBIR systems may widen the semantic gap and could lead to very poor performance retrieval results. Hence, features extraction methods, which are independent of domain knowledge and have automatic learning capabilities from input image are highly useful. Recently, pre-trained deep convolution neural networks (CNN) with transfer learning facilities have ability to generate and extract accurate and expressive features from image data. Unlike other types of deep CNN models which require huge amount of data and massive processing time for training purposes, the pre-trained CNN models have already trained for thousands of classes of large-scale data, including huge images and their information could be easily used and transferred. ResNet18 and SqueezeNet are successful and effective examples of pre-trained CNN models used recently in many machine learning applications, such as classification, clustering and object recognition. In this study, we have developed CBIR systems based on features extracted using ResNet18 and SqueezeNet pre-trained CNN models. Here, we have utilized these pre-trained CNN models to extract two groups of features that are stored separately and then later are used for online image searching and retrieval. Experimental results on two popular image datasets Core-1K and GHIM-10K show that ResNet18 features based on the CBIR method have overall accuracy of 95.5% and 93.9% for the two datasets, respectively, which greatly outperformed the traditional handcraft features based on the CBIR method.**

Keywords—Pre-trained deep neural networks; transfer learning; content based image retrieval

I. Introduction

The great development of digital computers and various smart devices, in addition to the large and steady increase in the different storage media, led to a considerable increase in digital images and other types of multimedia components. The large amount of multimedia, especially digital images, are used in many fields of medical treatment, satellite data and remote sensing, digital forensics and digital evidence [1, 2]. The large and rapid increase of the size of the digital content of images relies basically on retrieving these images from their various sources so that they can be used in the specific field or application. The content-based image retrieval (CBIR) method is one of the modern and effective ways to retrieve images from various image repositories, as well as from the web. CBIR is defined as the process of image retrieval by extracting some useful information from their low-level features or contents, such as colour, texture and shape, or other level of characteristics. The efficiency and effectiveness of any content-based image retrieval (CBIR) system depends on the extracted features because it will be used as numerical values in calculating similarity between the query submitted by the end user and all the images stored in a repositories or data storage [3]. One of the main challenges facing any content-based image retrieval (CBIR) is the semantics gap, which is defined as missing or lost information as a result of representing or capturing an image using an imaging device and the human vision system (HVS) used to perceive that image. This semantics gap that exists between the visual information captured by the imaging device and HVS can be reduced either by including domain or field-specific knowledge or by using some machine learning techniques to be trained and act like HVS. There has been a great development in the last decades in machine learning techniques and methods; these techniques have proven successful in being used in many areas of application, such as classification, clustering as well as information retrieval. Many machine learning methods have achieved great success and good results in many studies related to image retrieval. The main reason for that success is the availability of large amounts of images and pre-classified data in addition to the high computing capabilities of modern computers. The convolutional neural network (CNN) is a group of nonlinear transforming processes that have the ability to learn from the input data. These networks learn different features, especially image features. It uses small squares of the input data, and then it applies a set of operations of filter scanning for the input pixel values, known as convolutional operations. Deep convolutional neural networks are used in many applications related to digital image processing, such as image clustering, image classification and pattern or object recognition. On the other hand, these convolutional neural networks require huge data, computational resources and processing time. Pre-trained deep learning neural networks are the latest developed methods of convolutional neural networks that have been applied recently and have demonstrated high accuracy and good results in many areas of research. The superior ability of pre-trained networks are the result of their training on large-scale images for a large number of classes. This facility enables users to benefit from the advantage of pre-training and the transfer learning concept in various processes of classification or feature extraction. These pre-trained CNN models, such as AlexNet, GoogleNet, SqueezeNet and ResNet-18, have been applied for solving many problems, such as pattern recognition, computer vision, natural language processing, and medical image classification. Due to the success and good performance of this type of neural network, in this study we propose the CBIR method that is based on the two popular types of these networks in extracting features, which will be used to retrieve images through their content. The remainder of this study is organized as follows: Section 2 refers to related studies and state-of-art methods and approaches used in the area of CBIR, while Section 3 presents and explains our proposed methodology in more detail. Results and findings are reported and discussed in Section 4, while in Section 5 we summarize and conclude our study.

II. Related Work

Image retrieval is an old research problem of which the idea is to retrieve images like the user's query from the image data repository. The traditional method used for this process, which is known as text based image retrieval (TBIR) has used keywords associated with each image. These keywords are designed and indexed manually and later used to search for similar images. There are many drawbacks in this method, including the human effort to design the keywords, cost and time, which is extremely labour intensive, in addition to the low accuracy and efficiency of the retrieval process because it relies on searching for index words and not the content of the images. Moreover, this traditional method does not enable the developers to describe the meanings and semantics of images content in databases, especially those that contain a large number of images. All of the previous limitations led to dispensing with this old method and replacing it with the new and modern method, which is known as content-based image retrieval (CBIR) [4, 5]. In this modern method of image retrieval, low level image representations are used in the comparison or similarity process. These representational properties or features are extracted directly from the images. In most content-based image retrieval (CBIR) systems, the lowest content representations of the query image are compared against the representations of all the images in the database, and then the most similar images are retrieved. The most common visual properties used in this method are the characteristics of colour, texture, and shape [6-8]. The colour feature is one of the most used characteristics in retrieving images in CBIR. The colour is one of the best distinguishing features at lower-level visual features of CBIR. The colour is also one of the effective, robust, and easy-to-implement properties and requires less storage capacity [9]. The histogram is one of the best methods of representing colours that can be used in CBIR [10]. The researchers in [11] have designed the CBIR systems using the global colour histogram method and they achieved acceptable results. The Hue Saturation Value (HSV) colour space representation is useful and has better retrieval results compared with the default Red Green Blue (RGB) colour space [12]. The texture descriptor is the second most widely used features representation space in CBIR. The gray-level co-occurrence matrix (GLCM) [13] is the popular method used to extract many useful texture features, such as uniformity, correlation, contrast and entropy [14]. Features learning algorithms based on convolutional neural networks (CNNs) have become popular and widely used in recent years, due to their capabilities and powerful in many disciplines in general and in image processes in particular due to their accuracy and good performance in retrieval tasks [15]. One major drawback that faces this type of new generation of neural networks is their need of huge training data, which is not available across various domains of knowledge [16]. Due to this training limitation, the latest generation of pre-training CNN is found to fit the needs for well-trained CNNs and has highly accurate results. These pre-training CNN models have the ability to transfer their knowledge because they were trained on big-scale annotated natural image data collections in ImageNet [17] and it was successfully applied in many image processing application area [18-22]. There are three different methods that could be used to obtain the benefits and utilized the power of these pre-trained CNN and transfer their learning capabilities. These methods are feature extraction, using their architectures with proper needed tuning and, lastly, we can train some layers of the model while freezing others. In this study we utilize the pre-trained CNN and propose the content-based image retrieval method based on the features extracted using their pre-trained architecture. The contributions of this study can be summarized as follows:

- To utilize the ResNet-18 and SqueezeNet pre-trained CNN model for feature extraction from images collections.
- To develop a retrieval method based on extracted features and Euclidean distance similarity measures for CBIR.
- To enhance the retrieval process and compare the performance of our proposed method with some other state-of-the-art methods.

III. Methodology

The proposed method of this study consists of two phases or processes − offline process and online process − as shown in Fig. 1. In the offline process, the pre-trained CNN model is used for feature extraction while the online phase is responsible for end user query manipulation and retrieval results. The pre-trained deep CNN models consist of many layers that apply their learning process in an incremental manner and execute many subsampling and convolutions process. Here, SqueezeNet and ResNet18 pre-trained deep CNN models are used for feature extraction, and the features vector is saved in the features database to be used later for a similarity calculation. The online phase is the most important phase in which the extracted features generated in the previous step is used instead of the image itself for matching and similarity computation, and then the top similar images are retrieved to the end user.

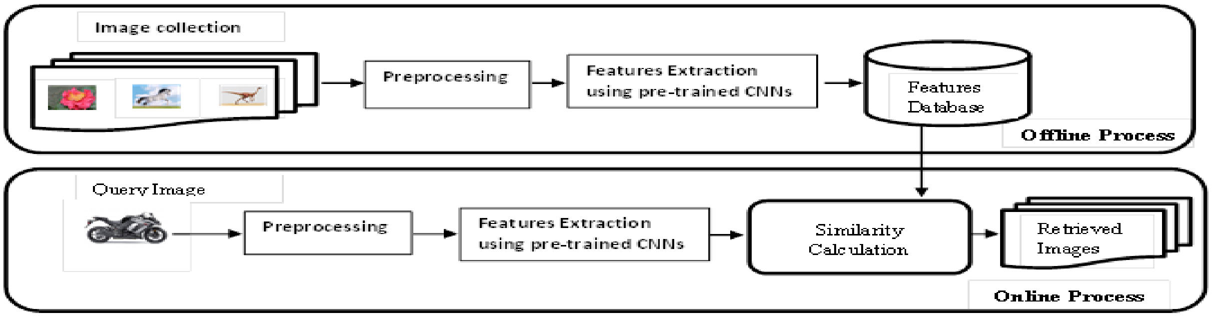

Fig. 1. Main Framework of CBIR.

A. SqueezeNet Pre-trained CNNs for Features Extraction

SqueezeNet is a simple and effective pre-trained CNN architecture with acceptable performance, and it has had successful usage recently. This model consists of 68 layers and it requires a 227x227x3 size input image [23]. After each image is set to the required size, the process in this model goes through 14 convolutions processing block elements with different rescaling and resampling operations, as shown in Fig. 2. Finally, a total of 1000 features are extracted and saved into a separated database for future use by the next online similarity and ranking process.

B. ResNet18 Pre-trained CNNs for Features Extraction

The second pre-trained CNN model used here is ResNet-18, a convolutional neural network that consists of 18 layers deep that was developed by [24]. Both this model and the previous model are trained on more than a million images from the ImageNet database [17]. This wide-range training process is very important for the transfer learning process as we mentioned earlier. A total of 512 features are extracted from the last fully connected layer, as shown in Fig. 3. The number of convolutional blocks and size of each block are also shown in Fig. 3. The group of features extracted here is saved again for a further similarity calculation process.

C. Visual Features based on Color and Texture Descriptors

In this method, a total of 18 colour features are extracted from each image using six colour moments. Each colour image is converted from the RGB colour space to HSV colour representation, and then six features are extracted from each channel. For the texture descriptor, four functions are used to extract texture features using the gray-level co-occurrence matrix (GLCM). Again, by using three channels of HSV, a total of 12 features are combined with the previous 18 colour features into a single vector of 30 features. The retrieval performance of these features is used as a based result to compare with our proposed method results and findings. The finding and performance of the features extracted by the previous two pre-trained CNN models and this group of traditional features are analyzed and compared at the next section.

D. Similarity Measure

The group features are extracted from both pre-trained deep CNN models, and traditional colour and texture features vectors are stored in separated databases to perform the similarity measures, which is considered an important online phase for the retrieval process. For this purpose, this study uses Euclidean distance that is considered the standard similarity coefficient used by many related studies [25]. For the two images vectors X and Y of numeric values, the similarity measure is calculated using the following equation.

$$[\sum_i^n (x_i - y_i)^2]^{\frac{1}{2}}.$$

where n is the number of dimensions of the X and Y vectors.

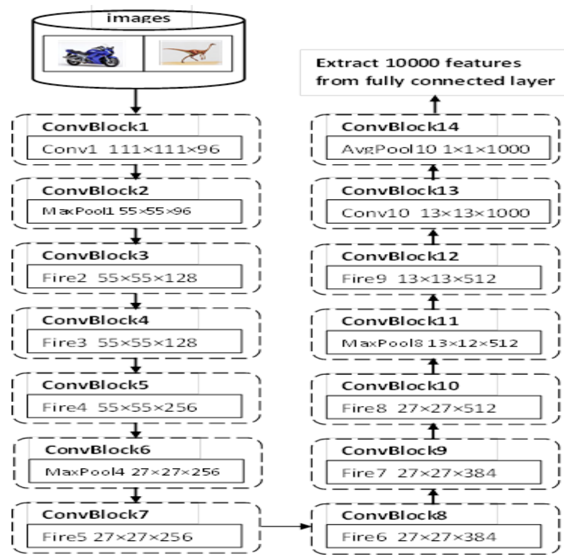

Fig. 2. SqueezeNet Model for Feature Extraction.

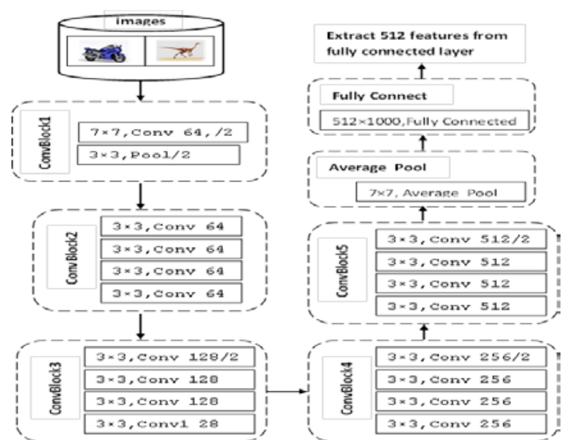

Fig. 3. ResNet18 Model for Feature Extraction.

IV. Experimental Results and Discussion

A. Images Datasets

For the experiments and evaluation of our proposed method, the study uses two of the most known image datasets. These two datasets were used widely in many studies related to CBIR and their recent usage found in [26]. First dataset is Corel-1K [27] and has a total of 1000 images divided into ten categories with 100 images for each class. The resolution of images is 256×384 or 384×256 pixels. GHIM-10K [28] is the second dataset used here; it consists of 10000 images divided equally into 20 classes with 500 images with a resolution of 300×400 pixels or 400×300 pixels. The second image dataset is 10 times larger, and it has more challenges than the previous one, since it contains more classes with a larger number of images. Samples from both datasets are shown in Fig. 4 and Fig. 5, where a single image from each class has been taken.

B. Performance Evaluation

Recall and precision are two performance measures used here. These two metrics could be used for evaluation of any retrieval model, especially the CBIR model. The performance based on these metrics could compute at any point of the top retrieved image, but for simplicity many researchers calculated their results at the top ten retrieved images. The general formula for these metrics is shown in the following equations.

$$\text{Recall} = \frac{\text{number of relevant images retrieved}}{\text{total number of retrieved images}}$$

$$\text{Precision} = \frac{\text{number of relevant images retrieved}}{\text{total number of relevant images}}$$

C. Results and Discussion

In this study, three different retrieval methods are developed and their results and findings are evaluated. The result of each experiment is reported; tables and figures of their findings are illustrated, as we will show in the coming paragraphs. The first retrieval method is based on traditional colour and texture features, which is considered the based model before the revolution of deep convolution models. These traditional image descriptors are wide image descriptors that have been used for CBIR for many years and have good performance results if followed and combined with some enhancement techniques such as relevance feedback or expansion processes. The second and third retrieval methods are based on SqueezeNet and ResNet18 features, respectively. For all our experiments, a random 10 images from each image class are selected for user queries and then average recall and precision at the top 10 retrieved images are calculated. The overall results of the Corel-1K images database for the three retrieval methods are shown in Table I. CL and GLCM refer to the first method since we use the colour moment functions for colour features and the GLCM method for texture features spaces. In this table, recall and precision for each of the 10 classes as well as the average values for the two metrics are shown. A fast inspection of these values illustrated that the two pre-trained CNN models outperformed the traditional colour and texture based retrieval method. Bolded cell values in both tables are used to represent the highest value of average precision of each class among the three retrieval methods, proving that ResNet18 has better retrieval results compared with SqueezeNet, as well as the traditional feature based retrieval method. For the GHIM-10K images database, which is considered more challenging; our two pre-trained CNN models also have better retrieval performance. For all 20 classes, ResNet18 has many highest retrieval values for xx classes out of 20 classes and moreover, the overall average recall and precision outperformed the SqueezeNet and the traditional method. The final result for this images database is shown in Table II. More analytical results are shown in Fig. 6 and Fig. 7 for both image databases. These two figures related images are retrieved in different top values (from 5 to 100) with precision values. The higher location of ResNet18 plotted lines proved that the good performance for these features outperformed the based model. Finally, visual retrieval performance in terms of top image retrieved for each query image for some selected classes for both images databases, show that ResNet18 has the best achievement. It was success to retrieve all correct images from the retrieved top 10 images as shown in Fig. 8. Part (a) of this figure represents the top retrieved images for the Bus class of the GHIM-10K dataset. Seven out of ten images are successfully retrieved using CL and GLCM features, compared with 10 out of 10 images retrieved using both ResNet18 and the SqueezeNet based model, as shown in part (b). Another example is shown in part (c), (d) and (e) for the Bikes class, 7 out of 10 and 9 out of 10 d are retrieved for GLCM and SqueezeNet, while all 10 images are retrieved using the ResNet18 model. Part (f) of Fig. 8 also represents the top retrieved images of Core-1K images. For the Dinosaurs class, our proposed pre-trained models and CL and GLCM traditional model have successfully retrieved all top 10 images. This is due to the simplicity of images of this class as its colour and texture properties are very clear and simple.

Fig. 4. Samples Images from Corel-1K Dataset.

Fig. 5. Samples Images from GHIM-10K Dataset.

TABLE I. AVERAGE RECALL AND PRECISION FOR COREL-1K DATASET

Class	CL and GLCM		SqueezeNet Features		ResNet18 Features	
	R	**P**	**R**	**P**	**R**	**P**
Africa	0.038	0.38	0.087	0.87	0.097	**0.97**
Beach	0.037	0.37	0.056	0.56	0.077	**0.77**
Building	0.051	0.51	0.077	0.77	0.089	**0.89**
Buses	0.072	0.72	0.1	**1**	0.1	**1**
Dinosaurs	0.1	**1**	0.1	**1**	0.1	**1**
Elephants	0.042	0.42	0.1	**1**	0.1	**1**
Flowers	0.086	0.86	0.1	**1**	0.1	**1**
Horses	0.071	0.71	0.096	0.96	0.099	**0.99**
Mountains	0.037	0.37	0.087	0.87	0.098	**0.98**
Food	0.029	0.29	0.091	0.91	0.095	**0.95**
Mean	0.0563	0.5630	0.0894	0.8940	**0.0955**	**0.9550**

TABLE II. AVERAGE RECALL AND PRECISION FOR GHIM-10K DATASET

Class	CL and GLCM		SqueezeNet Features		ResNet18 Features	
	R	**P**	**R**	**P**	**R**	**P**
Fireworks	0.0124	0.62	0.0188	0.94	0.02	**1**
Buildings	0.0064	0.32	0.0152	0.76	0.0196	**0.98**
Walls	0.0052	0.26	0.015	0.75	0.0182	**0.91**
Cars	0.0052	0.26	0.02	**1**	0.02	**1**
Flies	0.0074	0.37	0.016	0.8	0.0198	**0.99**
Mountains	0.0042	0.21	0.0134	0.67	0.0188	**0.94**
Flowers	0.0072	0.36	0.019	0.95	0.02	**1**
Trees	0.0098	0.49	0.018	0.9	0.0192	**0.96**
Green Grounds	0.0126	0.63	0.0178	0.89	0.0176	**0.88**
Beaches	0.0052	0.26	0.0142	0.71	0.0174	**0.87**
Aeroplanes	0.0074	0.37	0.0176	0.88	0.0198	**0.99**
Butterflies	0.007	0.35	0.0172	0.86	0.019	**0.95**
Forts	0.0058	0.29	0.0144	0.72	0.0156	**0.78**
Sunsets	0.0138	0.69	0.0186	0.93	0.02	**1**
Bikes	0.0064	0.32	0.0194	0.97	0.02	**1**
Boats	0.0058	0.29	0.02	**1**	0.02	**1**
Ships	0.0048	0.24	0.0162	0.81	0.0184	**0.92**
Chickens	0.0074	0.37	0.0188	0.94	0.02	**1**
Insects	0.0068	0.34	0.014	0.7	0.0138	**0.69**
Horses	0.0062	0.31	0.0176	0.88	0.0184	**0.92**
Mean	0.0074	0.3675	0.0171	0.8530	**0.0188**	**0.9390**

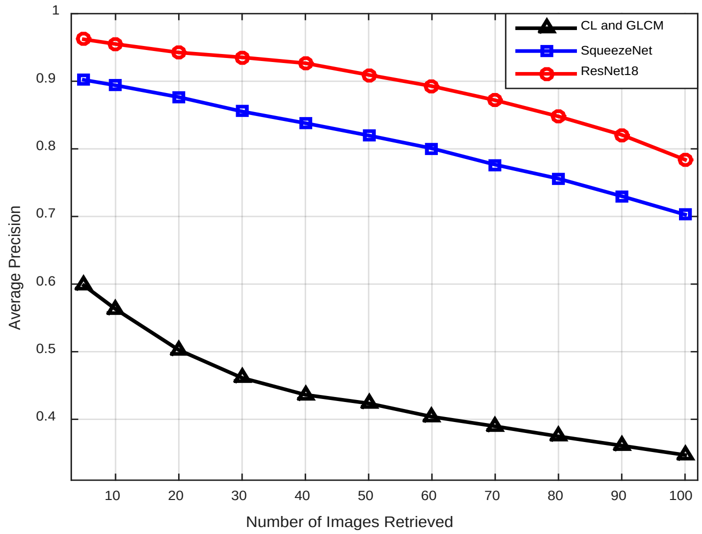

Fig. 6. Average Precision vs Number of Images Retrieved for Corel-1K

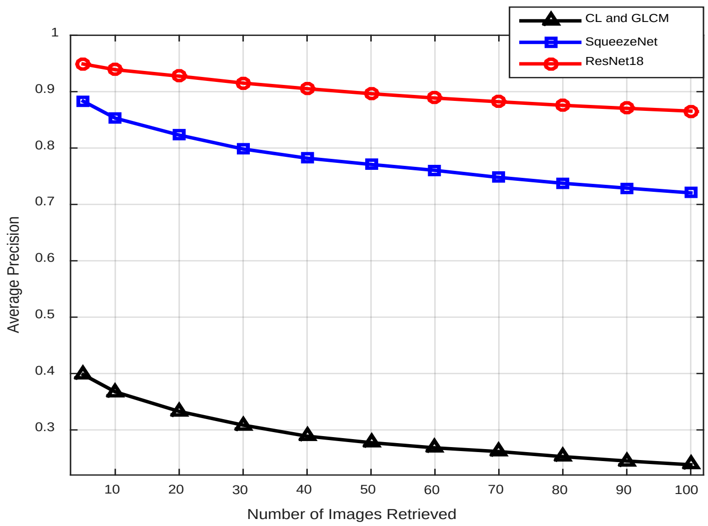

Fig. 7. Average Precision vs Number of Images Retrieved for GHIM-10K.

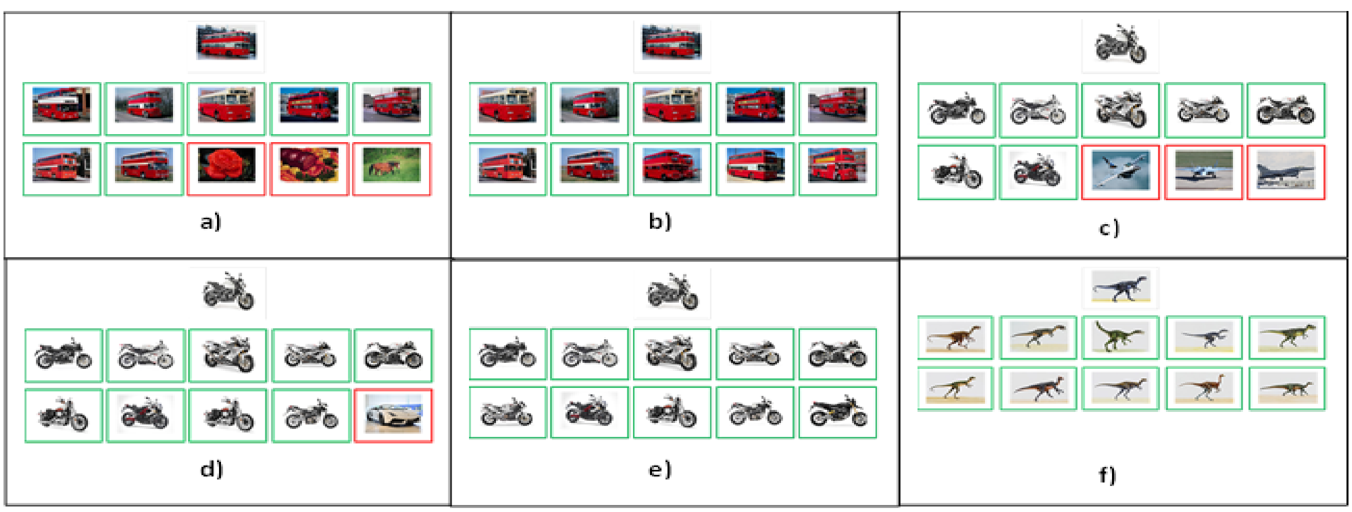

Fig. 8. Samples of Top Retrieved Images for some Classes from Corel-1k and GHIM-10K Datasets.

From visual inspection as shown in Fig. 8, the good retrieval performance of pre-trained CNN models for these most challenging GHIM-10K dataset images is clearly proved. There are similar best results in terms of top retrieved images found in other classes for both datasets such as Elephants and Flowers classes of Corel-1K and Sunsets and Boats of GHIM-10K dataset images.

V. Conclusion

In this study, we implemented and tested the CBIR method based on features extracted from two different pre-trained deep CNN models. CBIR models based on SqueezeNet and ResNet18 models are developed and tested on multi-class digital images datasets (Core-1K and GHIM-10K) and their results were compared with traditional CBIR, based on colour and texture features descriptors. The study achieved the average retrieval precisions of 89.40% and 95.50% for Corel-1K and 85.30% and 93.90% for GHIM-10K, using SqueezeNet and ResNet18 respectively, which clearly outperformed the CBIR model based on colour and texture-based features. Our average precisions of the ResNet18 based CBIR method are increased by 39.20% and 56.55%, compared with colour and texture based CBIR for Core-1K and GHIM-10K, respectively, which was clearly considered to be effective and has the best retrieval performance. Our retrieval performance results of ResNet18 have better performance compared with the SqueezeNet based CBIR method, and this could be due to accurate extracted features, compared with the large number of features extracted by the SqueezeNet pre-trained CNN model. For future efforts, other popular pre-trained CNN models could be used for feature extraction purposes, which could achieve better performance after proper and required tuning processes for their architectures.

References

[1] Lin, X., J.-H. Li, S.-L. Wang, F. Cheng and X.-S. Huang , Recent advances in passive digital image security forensics: A brief review. Engineering, 2018. 4(1): p. 29-39.

[2] Fonseca, L.M.G., L.M. Namikawa, and E.F. Castejon., Digital image processing in remote sensing. in 2009 Tutorials of the XXII Brazilian Symposium on Computer Graphics and Image Processing. 2009. IEEE.

[3] Liu, Y., D. Zhang, G. Lu and W.-Y. Ma ., A survey of content-based image retrieval with high-level semantics. Pattern recognition, 2007. 40(1): p. 262-282.

[4] Zare, M.R., R.N. Ainon, and W.C. Seng., Content-based image retrieval for blood cells. in 2009 Third Asia International Conference on Modelling & Simulation. 2009. IEEE.

[5] Sreedevi, S. and S. Sebastian., Content based image retrieval based on Database revision. in 2012 International Conference on Machine Vision and Image Processing (MVIP). 2012. IEEE.

[6] Latif, A., A. Rasheed, U. Sajid, J. Ahmed, N. Ali, N. I. Ratyal, B. Zafar, S. H. Dar, M. Sajid and T. Khalil ., Content-based image retrieval and feature extraction: a comprehensive review. Mathematical Problems in Engineering, 2019. 2019.

[7] Wang, S., K. Han, and J. Jin., Review of image low-level feature extraction methods for content-based image retrieval. Sensor Review, 2019.

[8] Thilagam, M. and K. Arunish., Content-Based Image Retrieval Techniques: A Review. in 2018 International Conference on Intelligent Computing and Communication for Smart World (I2C2SW). 2018. IEEE.

[9] Chen, Y., The image retrieval algorithm based on color feature. in 2016 7th IEEE International Conference on Software Engineering and Service Science (ICSESS). 2016. IEEE.

[10] Zhang, Z., W. Li, and B. Li., An improving technique of color histogram in segmentation-based image retrieval. in 2009 Fifth International Conference on Information Assurance and Security. 2009. IEEE.

[11] Chmelar, P. and A. Benkrid. Efficiency of HSV over RGB Gaussian Mixture Model for fire detection. in 2014 24th International Conference Radioelektronika. 2014. IEEE.

[12] Nazir, A., R. Ashraf, T. Hamdani and N. Ali., Content based image retrieval system by using HSV color histogram, discrete wavelet transform and edge histogram descriptor. in 2018 international conference on computing, mathematics and engineering technologies (iCoMET). 2018. IEEE.

[13] Weszka, J.S., C.R. Dyer, and A. Rosenfeld., A comparative study of texture measures for terrain classification. IEEE transactions on Systems, Man, and Cybernetics, 1976(4): p. 269-285.

[14] Ahmed, A. and S. Mohamed, Implementation of early and late fusion methods for content-based image retrieval. International Journal of Advanced and Applied Sciences, 8(7) 2021, Pages: 97-105.

[15] Rezazadeh, N., Initialization of weights in deep belief neural network based on standard deviation of feature values in training data vectors. Vol (6), 2017(6): p. 708-715.

[16] Han, D., Q. Liu, and W. Fan, A new image classification method using CNN transfer learning and web data augmentation. Expert Systems with Applications, 2018. 95: p. 43-56.

[17] ImageNet. http://www.image-net.org.

[18] Lou, Y., G. Fu, Z. Jiang, A. Men and Y. Zhou, PT-NET: Improve object and face detection via a pre-trained CNN model. in 2017 IEEE Global Conference on Signal and Information Processing (GlobalSIP). 2017. IEEE.

[19] Rajesh, K.B., Cybernetic microbial detection system using transfer learning. Multimedia Tools and Applications, 2018: p. 1-18.

[20] Marmanis, D., M. Datcu, T. Esch and U. Stilla ., Deep learning earth observation classification using ImageNet pretrained networks. IEEE Geoscience and Remote Sensing Letters, 2015. 13(1): p. 105-109.

[21] Hussain, M., J.J. Bird, and D.R. Faria. A study on cnn transfer learning for image classification. in UK Workshop on computational Intelligence. 2018. Springer.

[22] Akcay, S., M. E. Kundegorski, C. G. Willcocks and T. P. Breckon ., Using deep convolutional neural network architectures for object classification and detection within x-ray baggage security imagery. IEEE transactions on information forensics and security, 2018. 13(9): p. 2203-2215.

[23] Gopalakrishnan, K., S. K. Khaitan, A. Choudhary and A. Agrawal ., Deep convolutional neural networks with transfer learning for computer vision-based data-driven pavement distress detection. Construction and Building Materials, 2017. 157: p. 322-330.

[24] He, K., et al. Deep residual learning for image recognition. in Proceedings of the IEEE conference on computer vision and pattern recognition. 2016.

[25] Shirkhorshidi, A.S., S. Aghabozorgi, and T.Y. Wah, A comparison study on similarity and dissimilarity measures in clustering continuous data. PloS one, 2015. 10(12).

[26] Varish, N., A. K. Pal, R. Hassan, M. K. Hasan, A. Khan, N. Parveen, D. Banerjee, V. Pellakuri, A. U. Haqis and I. Memon ., Image retrieval scheme using quantized bins of color image components and adaptive tetrolet transform. IEEE Access, 2020. 8: p. 117639-117665.

[27] Li, J. and J.Z. Wang, Real-time computerized annotation of pictures. IEEE transactions on pattern analysis and machine intelligence, 2008. 30(6): p. 985-1002.

[28] Liu, G.-H., J.-Y. Yang, and Z. Li, Content-based image retrieval using computational visual attention model. pattern recognition, 2015. 48(8): p. 2554-2566.

Independent Task Scheduling in Cloud Computing using Meta-Heuristic HC-CSO Algorithm

Jai Bhagwan[1], Sanjeev Kumar[2]
Department of Computer Science and Engineering
Guru Jambheshwar University of Science and Technology
Hisar, India

***Abstract*—Cloud computing is a vital paradigm of emerging technologies. It provides hardware, software, and development platforms to end-users as per their demand. Task scheduling is an exciting job in the cloud computing environment. Tasks can be divided into two categories dependent and independent. Independent tasks are not connected to any type of parent-child concept. Various meta-heuristic algorithms have come into force to schedule the independent tasks. In this, paper a hybrid HC-CSO algorithm has been simulated using independent tasks. This hybrid algorithm has been designed by using the HEFT algorithm, Self-Motivated Inertia Weight factor, and standard Cat Swarm Optimization algorithm. The Crow Search algorithm has been applied to overcome the problem of premature convergence and to avoid the H-CSO algorithm getting stuck in the local fragment. The simulation was carried out using 500-1300 random lengths independent tasks and it was found that the H-CSO algorithm has beaten PSO, ACO, and CSO algorithms whereas the hybrid algorithm HC-CSO is working fine despite Cat Swarm Optimization, Particle Swarm Optimization, and H-CSO algorithm in the name of processing cost and makespan. For all scenarios, the HC-CSO algorithm is found overall 4.15% and 7.18% efficient than the H-CSO and standard CSO respectively in comparison to the makespan and in case of computation cost minimization, 9.60% and 14.59% than the H-CSO and the CSO, respectively.**

Keywords—Crow search algorithm (CSA); cat swarm optimization (CSO); H-CSO algorithm; HC-CSO algorithm; heft algorithm; SMIW (self-motivated inertia weight); independent tasks; particle swarm optimization (PSO); QoS (Quality of Service); virtual machines (VMs)

I. INTRODUCTION

At present, the IT industries having cloud infrastructure are providing on-demand services to their customers [1][2]. These services may include hardware storage, memory, software, applications development at remote locations [3]. To fulfill these services, cloud service providers provide virtual machines to the users in order to execute their tasks. It is necessary to map all the tasks on each virtual machine carefully to optimize the performance of the cloud [4][5]. A service level agreement needs to be signed by the user and the service provider. According to that agreement various QoS (Quality of Service) parameters need to be decided before starting a service. These QoS may be budget, deadline of all tasks, security, throughput, etc. Quick execution of all tasks is highly demanded [5]. Task scheduling always remains a burning topic of research in cloud computing due to its NP-Hard properties [6][7]. The most critical problem of a cloud is to schedule the tasks to the perfect resources [8][9]. The cloud service providers apply many techniques to reduce the makespan and cost of tasks scheduling. There may be two kinds of scheduling techniques: independent scheduling and dependent scheduling. In the case of dependent scheduling, the tasks are interconnected with each other in the form of a workflow. In independent scheduling the tasks are not dependent on each other; they are autonomous as per their nature [6]. Further, the scheduling policy can be classified into two categories static scheduling and dynamic scheduling. In static scheduling, the amount of the data is known before execution but in the event of dynamic scheduling, the amount of the data is not known [10]. Scheduling is an important issue to increase the performance of a cloud. Many scheduling meta-heuristic methods have entered the Information Technology market. For example, Ant Colony Optimization, Genetic Algorithm, Particle Swarm Optimization, Gravitation Search Algorithm, etc. [11]. In this research, various algorithms have been utilized and these are described as:

1) HEFT – The HEFT algorithm [10] is having two phases: setting a task priority and selecting a virtual machine. In the priority phase, the HEFT sets the ranks of all the tasks. In the virtual machine selection phase, the HEFT calculates the earliest finish time of all tasks on the VMs. After this in HEFT, the tasks are set in decreasing order of their ranks and assign to virtual machines.

2) Crow Search Algorithm – The CSA algorithm [8] is another meta-heuristic technique. This algorithm has been developed by considering the real behavior of the Crow bird. The Crow is one of the most intelligent birds in this universe. Its memory is very sharp and it can easily remember the thing for a long time. One of the characteristics of the Crow is to steal the food of other birds by chasing them cleverly. Based on the above characteristic, the algorithm has been designed by A. Askarzadeh in 2016. According to the author [12], there are two states of the CSA algorithm, and both states are combined in equation 1.

$$X^{i,itr+1} = \begin{cases} X^{i,itr+1} + r_i \times fl^{i,itr} \times (m^{j,itr} - X^{i,itr}) & r_j \geq AP^{j,itr} \\ a\ random\ position & else \end{cases} \quad (1)$$

Where r_i and r_j are random variables between [0 – 1], fl denotes the flight length of the $Crow_i$, and $AP^{j,itr}$ is the awareness probability of the $Crow_j$ at the itr iteration.

In the first state, the local searching is taking place whereas in the second state the global searching (random searching). If the awareness probability is less than or equal to the r_j variable then the global searching will be done otherwise local searching will be executed. The searching also depends on flight length (fl), a small value of fl will lead to local search. In above equation 1, it is also assumed that the $Crow_i$ will follow the victim $Crow_j$ and steal its food.

3) Cat Swarm Optimization – The CSO algorithm was designed by Chu and Tasi in the year 2006 based on two properties of a real cat, i.e. resting and hunting modes [13]. In the seeking mode, the cat moves freely in a random manner and remains alert. In the case of tracing mode, the cat has full of energy and moves towards the prey with high eagerness. Both the modes are described in detail in [14]. The pseudo-code [26] of the Cat Swarm Optimization is given in Fig. 1.

Cat Swarm Optimization Algorithm

```
Randomly initialize Cats of Size N
While Termination Condition Do
Distribute Cats into Tracing Mode and Seeking Mode as per MR Flag
  For K = 1 to N
    Evaluation Cat Fitness
    If Cat_K is in Seeking Mode Then
      Execute Seeking Mode
    Else
      Execute Tracing Mode
    End If
  End For
End While
```

Fig. 1. Pseudo-Code of Standard Cat Swarm Optimization.

4) H-CSO Algorithm – This algorithm was formulated by using the HEFT algorithm original Cat Swarm Optimization, and the SMIW method. The SMIW method is given in the methodology adopted section in detail.

The flaws of the H-CSO algorithm are observed and the work has been done to overcome those limitations by inserting a local searching part of the standard Crow Search Algorithm [25]. Basically, the H-CSO algorithm is a hybrid of standard CSO, HEFT algorithm, and SMIW method. Some drawbacks of the H-CSO are described as:

- The H-CSO algorithm has poor local searching capacity. Although, the outrange drawback of the velocity formula of the tracing mode of the standard CSO has been removed in the H-CSO using the SMIW method.
- Due to the resting of Cats for a maximum time in the seeking mode of the H-CSO, it gets frozen in the local fragment.

The objective of this research is to simulate the HC-CSO [25] algorithm for independent tasks and make comparisons with H-CSO and other existing standard algorithms. The remaining information is specified in the methodology adopted section.

The remaining of the paper is organized as: In Section II related work has been presented. Section III is describing the methodology adopted and the simulation setup is explained in Section IV. Simulation results are discussed in Section V. Final Section VI is representing the conclusion and future scope of this research.

II. Related Work

In this section, a study of various scientists is described. A hybrid CSO algorithm using the Simulated Annealing and Orthogonal Taguchi was designed by the scientists in [3]. The result analysis highlighted that the proposed method performs efficiently than MGA, MOACO, and MPSO for various QoS parameters. A task mapping approach using the PSO and Eagle Strategy was designed in [4]. The simulation results indicate that the proposed procedure is improved than the original PSO and other existing methods like RALBA, NMT-FOLS, etc. A joint task scheduling and resource placement policy was designed in the paper [5]. The makespan, degree of imbalance, resource utilization, and cost are improved using the newly designed policy as compared to existing GSO and GA methods. A new method named MHO was designed for task scheduling and load balancing in [6]. The proposed method having two phases MHOS-S and MHO-D were found better after results analysis as compared to other meta-heuristic methods. A new model for task allocation to virtual machines has been proposed in [8]. The experimental results summarized that the proposed ICSA algorithm reduced the makespan, waiting time, response time, and flow time as compared to FCFS and PSO methods. A Binary PSOGSA method was developed for the load balancing and task scheduling in the cloud in paper [11]. It is a bio-inspired load balancing algorithm used to manage the virtual machines for the load balancing issue. The outcome analysis demonstrated that the proposed method is efficient than originally developed Bin-LB-PSO and other techniques. An Average-Inertia Weight CSO algorithm (AICSO) was proposed in [14]. The simulation demonstrated that the AICSO is having a good convergence rate as compared to the standard CSO and ICSO algorithms. The authors proposed a cloud scheduling strategy named Genetic Algorithm-Chaos Ant Colony Optimization [15]. The proposed algorithm is optimal as compared to the ACO. A task scheduling strategy was designed using the PSO algorithm in the research paper [16]. The proposed method is a combination of Dynamic PSO and Cuckoo Search. It was identified by the results that the proposed algorithm worked fine than the original PSO. An adaptive cost-based method was developed in [17]. The proposed method was proved better by the simulation results in terms of various resources utilization like memory, bandwidth, CPU utilization, etc. A PSO-oriented load balancing method was proposed in [19]. The proposed method was designed by using a load balancing technique and was analyzed with traditional Round-Robin, the present PSO and load management method. The results were discussed by the authors and the new introduced technique was found efficient for balancing the cloud load. The paper [20] described that an improved PSO was developed using a discrete position updating strategy and the Gaussian Mutation operation. The proposed algorithm outperformed the existing algorithms. The researchers modified the PSO in [21] to overcome the problem of slow convergence. The proposed PSO having dynamic inertia weight worked fine for cost reduction as compared to the existing IPSO, PSO-ACO, and standard ACO algorithms. An IPSO algorithm was proposed for task mapping on virtual machines in [22]. The process was achieved by splitting the coming tasks into many batches. The author in experiments summarized that the Improve PSO was efficient than existing Round-Robin, Honey Bee, and Ant Colony algorithms. A multi-objective CSO technique was framed in paper [23]. It was observed by the analysis of the results that the proposed MOCSO is very effective than MOPSO for better makespan, cost, etc. A CSO algorithm based on heuristic scheduling was introduced in the paper [24]. The results of this paper depicted that the proposed Cat Swarm Optimization worked better than the existing PSO.

From the above study, the main key points are found as follows:

1) The ACO algorithm is having a poor global search characteristic, due to that the convergence of the ACO is poor. The standard CSO jumps out from the search space due to the unbalanced tracing mode's velocity formula.

2) The PSO algorithm is famous for global searching and superior to the ACO for scheduling purposes.

3) The CSO algorithm is superior to the PSO due to its better convergence than PSO, but it gets trapped in local optima due to the resting behaviour of numerous cats in seeking mode.

4) H-CSO algorithm improved than the CSO but it may get trapped in the local search or in tracing mode while increasing the number of iterations.

III. Methodology Adopted

To overcome the research gaps of the H-CSO described in the literature review section, a new algorithm has been designed named HC-CSO [25]. In the H-CSO, a local search portion of the CSA technique has been fused with the CSO. This technique balances the seeking and tracing modes which improve the searching capacity of the HC-CSO algorithm. The pseudo-code of the HC-CSO algorithm is given in Fig. 2.

As said earlier the HC-CSO method is a hybridization of the H-CSO and the Crow Search Algorithm's local searching portion. It has also been told earlier that the H-CSO is a combination of HEFT (described in the introduction section) and Self-Motivated Inertia Weight. The SMIW method is shown in equation 2.

$$\gamma = \gamma_{max} \times \exp\left(-c \times \left(\frac{itr}{itr_{max}}\right)^{c}\right) \quad (2)$$

Where, γ is a weight factor inserted in tracing mode of the CSO whereas γ_{max}, and c are constant factors greater than 1 i.e. 2.0.

As can be seen in Fig. 2 the local search portion of the CSA technique has been joined into the HC-CSO procedure. The functioning of the HC-CSO method is well-defined step by step as follows:

1) All the parameters are initialized at the beginning of the algorithm.

Some parameters used in the pseudo-code of the HC-CSO algorithm are: fl, r_K, V_K, c, γ_{max}, c1, MR flag, and number of iterations. The flight length of the crow is represented by the symbol fl. The Local and Global searching of the Crow Search Algorithm may be decided by the flight length. Flight length (fl) less than 1 is used for local searching, so, it has been set to 0.5. r_K and r1 are random numbers between [0, 1]. V_K is the initialized velocities of the cats. c and γ_{max} are constant values that are set to 2. MR flag (Mixing Ratio) is set randomly [0.2-0.3] which means 20-30% of the cats are distributed in the tracing mode and rests are distributed in the seeking mode.

After this, the HEFT will calculate the rank based on the average execution time of all independent tasks and will arrange them as per their ranks.

2) If the solution is optimized at the beginning then, the algorithm will be terminated immediately and returned the solution else the population produced by the HEFT algorithm will be given for local searching via the CSA algorithm (as shown in line number 17 of pseudo-code).

3) The population generated by the CSA local search method will be handed over to the H-CSO algorithm for local as well as global searching via seeking and tracing modes. The cats are distributed in the seeking and tracing modes as per the Mixing Ratio (MR) parameter as described above. If the present Cat_K is caught in the seeking mode then, the seeking mode will be executed otherwise the tracing mode will be processed.

4) In seeking mode, the S number of copies of the cats will be generated. Here, all cats are evaluated by the fitness function and the best cat is picked up randomly among various copies. After this, the current Cat_K will be replaced by the best cat.

5) In tracing mode, the velocity of the current Cat_K is updated by the modified velocity equation using the SMIW method (given in line number 28 in pseudo-code). Then, the position of the current Cat_K is updated. Now, the evaluation of the Cats is taken place and the best cat is found out.

6) The best cat is saved in the memory.

7) This practice is sustained until the criterion is not met. In the end, the optimum solution is returned from the memory in the shape of the optimum result (Best Cat).

HC-CSO Algorithm

Input (Tasks ($T_1, T_2, T_3 \dots T_n$), Virtual Machines ($VM_1, VM_2, VM_3 \dots VM_m$)
Output (Optimal Makespan and Cost of n Tasks on m VMs) // Mapping of tasks

BEGIN PROCEDURE

1. Initialize fl (flight length), r_K, (velocity factor) V_K, c, γ_{max}, Coefficient c1, r1, MR flag, and no. of iterations
/* Calculate Rank of independent tasks using HEFT Algorithm */
2. Feed the tasks in HEFT
3. **For** Each Task in List Do
4. Calculate average execution time of all VMs
5. **If** Task t_i is the last Task **Then**
6. Rank value of t_i = its average execution time
7. **Else**
8. $rank_u(t_i) = WAvg_i + \text{Max } t_j \in succ(t_i)\ (CAvg_{ij} + rank_u(t_j))$
Where $WAvg_i$ is average execution cost
Succ (t_i) is set of immediate successor of task t_i
$CAvg_{i,j}$ is average communication cost
9. **End If**
10. **End For**
11. Assign Tasks to VMs according to HEFT Rank
12. **If** Solution not Optimized **Then**
13. Generate a set of Crows by the Population generated by HEFT of Size N
14. **While** No. of Iterations not Exceeded **Do**
15. **For** K=1 to N
16. Update the positions by the following equation : // Do local search
17. $X_{K,D} = X_{K,D} + r_K \times fl_{K,D} \times (M_{L,D} - X_{K,D})$
Where, $X_{K,D}$ is current position of $Crow_K$, r_K is uniformly distributed random number [0, 1]
$fl_{K,D}$ is flight length (less than 1 i.e. 0.5) of the $Crow_K$ at current iteration
$M_{L,D}$ is present best location of $Crow_K$ in Dimension D
18. Feed the population generated by Local CSA in H-CSO // Do local and global search
19. Assign the velocity V_K to each Cat
20. According to Mixing Ratio (MR) flag Distribute Cats to Seeking and Tracing Modes
21. **If** current Cat_K is in Seeking Mode **Then**
22. Generate S (SMP) Copies of Cat_K and Spread them in D Dimensions where each Cat has a velocity ($V_{K,D}$)
23. Evaluate the Fitness value of all Copies and Discover Best Cats ($X_{BEST,D}$)
24. Replace Original Cat_K with the Copy of Best Cats ($X_{BEST,D}$)
25. **Else If** current Cat_K is in Tracing Mode **Then**
26. Compute and Update Cat_K velocity by following equations:
27. $\gamma = \gamma_{max} \times \exp\left(-c \times \left(\frac{itr}{itr_{max}}\right)^c\right)$
Where, γ is a weight factor calculated by Self-Motivated Inertia Weight method
γ_{max} and c are constant factors greater than 1, both are set as 2.0
28. $V_{K,D} = \gamma \times V_{K,D} + \left(c1 \times r1 \times (X_{BEST,D} - X_{K,D})\right)$
Where, D = 1, 2, 3, …, M.
c1 is acceleration coefficient, r1 is random number in the range of [0, 1]
29. Update the position of every dimension of Cat_K by using following equation:
30. $X_{K,D} = X_{K,D} + V_{K,D}$
31. Evaluate Fitness of all Cats and find out Best Cats ($X_{BEST,D}$) having Best Fitness
32. **End If**
33. Update Best Cats ($X_{BEST,D}$) in Memory
34. **End For**
35. **End While**
36. **End If**
37. return (Optimal Solution)
END PROCEDURE

Fig. 2. Pseudo-code of Meta-Heuristic HC-CSO Algorithm.

IV. Simulation Setup

For simulations of the independent tasks a computing machine was opted to have the configurations as Processor – Intel ® Core ™ i3-5005U 2.0 GHz speed, RAM – 4 GB, Hard Disk Drive – 1 TB, and Machine OS – Windows 10.

A. Parameters

For experimental tests, a PowerDatacenter was generated having the formation as number of Hosts - 1, RAM – 25 GB, Each VM MIPS – 1000, Storage – 1 TB, and Bandwidth – 5000 bps. The cloud nature is heterogeneous and all details are displayed in Table I.

B. Cost Plan

The cost plan for independent task scheduling is summarized in Table II. These charges will be applicable to the customer for using the datacenter services [27].

TABLE I. Simulation Parameters

PowerDatacenter	
Parameters	**Values**
Number of Hosts	1
System Architecture	x86
VMM	Xen
OS	Linux
Number of Cloudlets Cloudlets Length Type	500-1300 Independent Random Length (300-700)
Numbers of VMs	3, 5 and 8
CPU (PEs Number)	1
RAM per VM	512-1024 MB
Bandwidth	500-1000 bps
Processing Elements per VM	500 – 1000 MIPS
Image Size	10000 MB
Policy Type	Time Shared
PSO	
No. of Particles	100
Max. Iterations	300
Weights C1 and C2	1.5
Standard CSO and H-CSO	
No. of Cats	100
Max. Iterations	300
Weights (C1)	1.5
r1and r_k (Random Variables)	[0, 1]
Mixed Ratio Percentage	Random Range [0, 1]
HC-CSO	
No. of Cats	100
Max. Iterations	300
Weights (C1)	1.5
r1(Random Variable)	[0, 1]
Mixing Ratio (MR) Percentage	Random Range [0, 1] i.e. 0.2-0.3
fl (Flight Length)	0.5

TABLE II. Cost Plan (In Indian Rupees)

Resource	Processor	RAM	Storage	Bandwidth
Size	500-1000 MIPS	512 MB	Unlimited	1000 bps
Cost	Rs. 3.00 per processor	Rs. 0.05 per MB	Rs. 0.1	Rs. 0.10 per MB

C. Dataset Used

In the simulation studies, a group of 500, 800, and 1300 independent tasks having random lengths were opted and submitted to the VMs for execution.

D. Performance Metrics

The performance metrics taken for this research are described below:

1) Makespan: The makespan [18] is stated as the maximum finished time occupied for the accomplishment of the last task in a set. It is the utmost generally used and very important parameter to map the performance of any algorithm in task scheduling. The makespan is calculated by the formula specified in equation 3.

$$\text{Makespan} = \max\,(CT_i)_{\ t_i \in tasks} \tag{3}$$

Where, CT_i is the completion time of $task_i$

2) Computation cost: The computation cost should be as less as possible; this is not only the demand of customers but; the industries also want the same to stay in the competitive IT market. The computation cost can be computed by equation 4.

$$Total\ Cost = \frac{MF+CF}{2} \tag{4}$$

Where, MF is Movement Factor and CF is the Cost Factor

$$MF = \frac{1}{No.\ of\ Hosts/Datacenters}\left[\sum_{x=1}^{VMx}\left(\frac{Number\ of\ Migrations}{Used\ VM}\right)\right] \tag{5}$$

$$CF = \sum_{x=1}^{VMx}\left(\frac{Processing\ Cost \times Memory\ of\ Tasks}{VM \times Datacenter}\right) \tag{6}$$

Equations 5 and 6 are utilized for the scheming of the total computation cost which is represented in equation 4.

3) Fitness function: Equation 7 is displaying how to calculate a fitness function that has been used in this research paper. It is used to check the optimization at various levels as shown in Fig. 2.

$$F_X = \frac{1}{Datacenter \times VMj}\left[\sum_{i=1}^{DCi}\sum_{j=1}^{VMj}\frac{1}{VM}\,\frac{CPU\ Utilized}{CPUij} + \frac{Memory\ Utilized}{Memoryij} + \frac{Makespan\ Utilized}{Makespanij} + \frac{Bandwidth\ Utilized}{Bandwidthij}\right] \tag{7}$$

V. Simulation Results and Discussion

Previously, the HC-CSO algorithm was tested with scientific workflows [25]. Now, a set of three scenarios with 500-1300 independent tasks and a flock of 3, 5, and 8 VMs have been set in the CloudSim tool for the results analysis. The HC-CSO is compared with the PSO, CSO, and H-CSO algorithms. The simulation results in terms of makespan are shown in Table III. All algorithms were executed many times and the average results are displayed in the form of the makespan for each algorithm.

TABLE III. MAKESPAN ESTIMATION (IN SEC)

Scenarios	VMs	PSO	CSO	H-CSO	HC-CSO
Scenario - 1 500 Tasks	3	240.13	231.42	224.74	213.02
	5	225.29	213.27	203.89	195.24
	8	181.09	174.18	165.27	151.23
Scenario – 2 800 Tasks	3	425.35	417.21	401.93	387.54
	5	310.17	301.07	287.35	281.75
	8	279.85	263.17	255.03	243.29
Scenario – 3 1300 Tasks	3	722.13	712.28	697.13	681.08
	5	580.43	553.89	530.87	513.13
	8	452.24	437.23	433.11	400.39

Fig. 3, 4, and 5 are representing the virtual machines at the x-axis and makespan at the y-axis.

Fig. 3 is representing that for 500 independent tasks the HC-CSO algorithm is performing better than standard PSO, CSO, and H-CSO algorithms on all 3, 5, and 8 VMs. This is because the convergence of the HC-CSO method has been improved due to better local searching and a balanced velocity factor by inserting the SMIW method.

In Fig. 4, it can be seen that the makespan is improved in the case of the HC-CSO method. In the case of 800 independent tasks, the HC-CSO method performs better than the PSO, CSO, and H-CSO algorithms due to a better exploration and exploitation rate and it is possible due to the integration of the CSA algorithm in H-CSO.

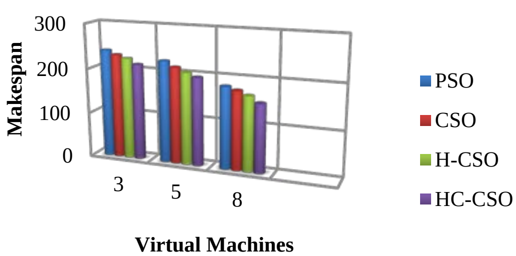

Fig. 3. Makespan Assessments for 500 Independent Tasks.

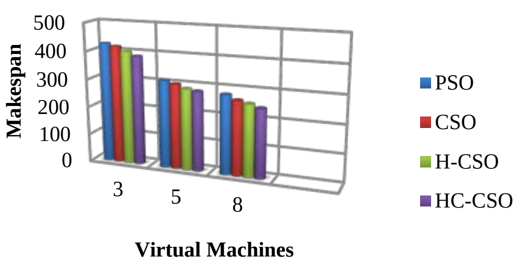

Fig. 4. Makespan Assessments for 800 Independent Tasks.

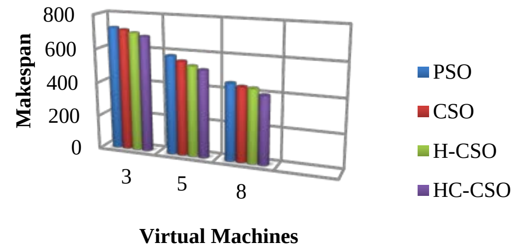

Fig. 5. Makespan Assessments for 1300 Independent Tasks.

Fig. 5 is justifying that the HC-CSO outperforms the PSO, H-CSO, and CSO with all flocks of VMs for 1300 independent tasks. The makespan is reduced due to better convergence of HC-CSO and a decent stability between seeking and tracing mode due to the collaboration of the CSA.

Table IV is briefing the cost consumptions for the execution of each algorithm with each scenario.

It can be seen that the virtual machines and cost are depicted at the x-axis and y-axis separately in Fig. 6, 7, and 8.

Fig. 6 is demonstrating that the cost is reduced by the HC-CSO algorithm with respect to all sets of VMs in the case of 500 tasks. Here, the HC-CSO is outperforming other algorithms depicted in Fig. 6 due to choosing of the best VM among all at a right time while mapping the independent tasks.

TABLE IV. COST CONSUMPTIONS (IN INDIAN RUPEES)

Scenarios	VMs	PSO	CSO	H-CSO	HC-CSO
Scenario - 1 500 Tasks	3	23.89	22.21	21.03	19.05
	5	30.23	28.20	27.52	28.29
	8	37.29	36.09	35.47	34.27
Scenario – 2 800 Tasks	3	41.13	38.33	37.08	33.51
	5	50.88	47.29	44.13	40.11
	8	65.58	62.13	59.15	54.01
Scenario – 3 1300 Tasks	3	70.03	67.51	64.53	59.24
	5	93.08	87.87	82.35	75.17
	8	117.13	113.25	103.89	85.87

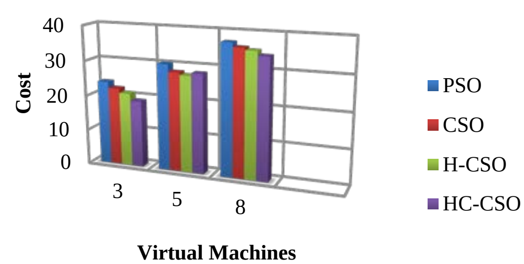

Fig. 6. Cost Assessments for 500 Independent Tasks.

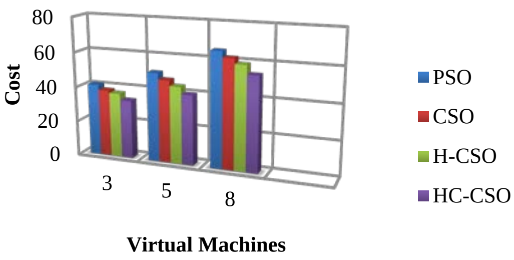

Fig. 7. Cost Assessments for 800 Independent Tasks.

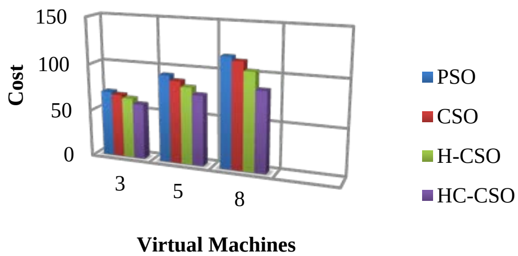

Fig. 8. Cost Assessments for 1300 Independent Tasks.

In Fig. 7, the performance comparison is done with 800 independent tasks on a flock of 3, 5, and 8 VMs. The HC-CSO algorithm won the race for reducing the cost as compared to the PSO, CSO, and H-CSO methods. It is due to the improvement of tracing mode by Self-Motivated Inertia Weight. The CSA gives the capacity of load adjustment to the HC-CSO algorithm in a better way by picking the best available virtual machine.

The HC-CSO algorithm is again working fine with 1300 tasks and a group of 3, 5, and 8 VMs. This can be observed in Fig. 8. The Cost is optimized here due to the good rate of task migration between under-loaded and over-loaded virtual machines. This happens because the HC-CSO algorithm is keeping a better global seeking property and local searching is improved by the CSA procedure. The outranged issue of the traditional Cat Swarm Optimization has been removed in the HC-CSO as well.

In the end, it is stated that the HC-CSO method has beaten all other techniques like PSO, H-CSO, and the traditional CSO concerning the makespan and computation cost due to better convergence, and the improved tracing mode. The Cats do not come out of the search space after inserting the SMIW method. The Self-Motivated Inertia Weight controls the velocity formula in tracing mode. So, it doesn’t matter whether the search space is small or large. The CSA algorithm improves the exploration and exploitation of the H-CSO algorithm.

VI. Conclusion and Future Scope

The cloud computing area is a burning topic of research nowadays. Many scientists have worked with GA, ACO, PSO, and CSO. It was seen that the CSO worked well in the name of makespan and processing cost. The scientists worked with dependent as well as independent tasks. The related work showed that the Cat Swarm Optimization worked better in many areas of cloud computing. In this research, a new algorithm named HC-CSO was utilized for experiments. This algorithm is a hybridization of three algorithms: HEFT, CSA, and H-CSO. The H-CSO was developed by the HEFT and SMIW formula.

After simulation, it was observed that the HC-CSO method outperformed the other techniques like the H-CSO, PSO, and CSO. The hybrid algorithm HC-CSO worked better with three scenarios having 500, 800, and 1300 independent tasks on 3, 5, and 8 virtual machines. After inclusion of all scenarios, it showed an overall 4.15% efficacy for makespan with minimization of 9.6% cost in comparison to the H-CSO and 9.60% efficacy with makespan for minimization of 14.59% cost than the CSO. The reason behind this good performance is the integration of the CSA algorithm in H-CSO. Also, the SMIW method controls the tracing mode velocity factor. This makes a check over the cats to escape out of the search space. It saves time as there is no need to initialize the velocity of the cats again and again.

This study proves that the HC-CSO technique is a generalized one as it has been tested on a different set of independent tasks. In the upcoming time, the HC-CSO algorithm can be tried for other objectives like energy consumption, resource utilization, load balancing, etc. Also, it can be applied in other areas of technology.

References

[1] R. A. Al-Arasi, and A. Saif, “Task Scheduling in Cloud Computing Based on Meta-Heuristic Techniques: A Review Paper,” EAI Endorsed Transactions on Cloud System, vol. 6, no. 17, pp. 1-19, 2020.

[2] A. M. Lonea, H. Tianfield, and D. E. Popescu, “Identity Management for Cloud Computing,” New Concepts and Applications in Soft Computing, vol. 417, Springer, Berlin, pp. 175-199, 2013.

[3] D. Gabi, A. S. Ismail, A. Zainal, Z. Zakaria, and A. AI-Khasawneh, “Hybrid Cat Swarm Optimization and Simulated Annealing for Dynamic Task Scheduling on Cloud Computing Environment,” Journal of ICT, vol. 17, no. 3, pp. 435-467, 2018.

[4] A. Kollu, and S. Vadlamudi, “Eagle Strategy with Cauchy Mutation Particle Swarm Optimization for Energy Management in Cloud Computing,” International Journal of Intelligent Engineering & Systems, vol. 13, no. 6, pp. 42-51, 2020.

[5] D. Alboaneen, H. Tianfield, Y. Zhang and B. Pranggono, “A Meta-Heuristic Method for Joint Task Scheduling and Virtual Machine Placement in Cloud Data Centers,” Future Generation Computer Systems, vol. 115, pp. 201-212, 2021.

[6] S. Peer Mohamed Ziyath, and S. Senthilkumar, “MHO: Meta Heuristic Optimization Applied Task Scheduling with Load Balancing Technique for Cloud Infrastructure Services,” Journal of Ambient Intelligence and Humanized Computing, 2020.

[7] H. Singh, S. Tyagi and P. Kumar, “Scheduling in Cloud Computing Environment using Metaheuristic Techniques: A Survey,” Emerging Technology in Modelling and Graphics, Advances in Intelligent Systems and Computing, vol. 937, pp. 753-763, 2020.

[8] A. Kousalya, P. Sinduja, V. H. Viswanathan, and Jeevitha, “Optimization of Task Scheduling using Improved Crow Search Algorithm in a Cloud Environment,” International Journal of Pure and Applied Mathematics, vol. 119, no. 16, pp. 219-230, 2018.

[9] J. Natarajan, “Parallel Queue Scheduling in Dynamic Cloud Environment Using Backfilling Algorithm,” International Journal of Intelligent Engineering & Systems, vol. 11, no. 2, pp. 39-48, 2018.

[10] A. Mazrekaj, A. Sheholli, D. Minarolli, and B. Freisleben, “The Experiential Heterogeneous Earliest Finish Time Algorithm for Task Scheduling in Clouds,” 9th International Conference on Cloud Computing and Services Science, pp. 371-379, 2019.

[11] T. S. Alnusairi, "Binary PSOGSA for Load Balancing Task Scheduling in Cloud Environment," International Journal of Advanced Computer Science and Applications, vol. 9, no. 5, pp. 255-264, 2018.

[12] A. Askarzadeh, "A Novel Metaheuristic Method for Solving Constrained Engineering Optimization Problems: Crow Search Algorithm," Computers and Structures, vol. 169, pp. 1-12, 2016.

[13] A. M. Ahmed, T. A. Rashid, and S. A. M. Saeed, "Cat Swarm Optimization Algorithm: A Survey and Performance Evaluation," Computational Intelligence and Neuroscience, vol. 2020, pp. 1-20, 2020.

[14] M. Orouskhani, M. Mansouri, and M. Teshnehlab, "Average-Inertia Weight Cat Swarm Optimization," Advances in Swarm Intelligence, Lecture Notes in Computer Science, vol. 6728, 2011.

[15] H. Cui, X. Liu, T. Yu, H. Zhang, Y. Fang and Z. Xia, "Cloud Service Scheduling Algorithm Research and Optimization," Security and Communication Networks, vol. 2017, pp. 1-7, 2017.

[16] A. Al-maamari, and F. A. Omara, "Task Scheduling Using PSO Algorithm in Cloud Computing Environments," International Journal of Grid Distribution Computing, vol. 8, no. 15, pp. 245-255, 2015.

[17] M. A. S. Mosleh, G. Radhamani, M. A. G. Hazber, and S. H. Hasan, "Adaptive Cost-Based Task Scheduling in Cloud Environment," Scientific Programming, vol. 2016, pp. 1-9, 2016.

[18] M. Kalra, and S. Singh, "A Review of Metaheuristic Scheduling Techniques in Cloud Computing," Egyptian Informatics Journal, vol. 16, pp. 275-295, 2016.

[19] F. Ebadifard, and S. M. Babamir, "A PSO-Based Task Scheduling Algorithm Improved Using a Load Balancing Technique for the Cloud Computing Environment," Concurrency and Computation Practice and Experience, Special Issue, pp. 1-16, 2017.

[20] G. Peng, and K. Wolter, "Efficient Task Scheduling in Cloud Computing using an Improved Particle Swarm Optimization Algorithm," 9th International Conference on Cloud Computing and Services Science, pp. 58-67, 2019.

[21] Z. Zhou, J. Chang, Z. Hu, J. Yu, and F. Li, "A Modified PSO Algorithms for Task Scheduling Optimization in Cloud Computing," Concurrency and Computation Practice and Experience, Special Issue, pp. 1-11, 2018.

[22] H. Saleh., H. Nashaat, W. Saber, and H. M. Harb, "IPSO Task Scheduling Algorithm for Large Scale Data in Cloud Computing Environment," IEEE Access, vol. 7, pp. 5412-5420, 2019.

[23] S. Bilgaiyan, S. Sagnika, and M. Das, "A Multi-Objective Cat Swarm Optimization Algorithm for Workflow Scheduling in Cloud Computing Environment," International Journal of Soft Computing, vol. 10, no. 1, pp. 37-45, 2015.

[24] S. Bilgaiyan, S. Sagnika, and M. Das, "Workflow Scheduling in Cloud Computing Using Cat Swarm Optimization," IEEE International Advance Computing Conference, pp. 680-685, 2014.

[25] J. Bhagwan, and S. Kumar, "An HC-CSO Algorithm for Workflow Scheduling in Heterogeneous Cloud System," International Journal of Advanced Computer Science and Applications, vol. 12, no. 6, pp. 484-492, 2021.

[26] S. Goyal, S. Bhushan, Y. Kumar, A. H. S. Rana, M. R. Bhutta, M. F. Ijaz, and Y. Son, "An Optimized Framework for Energy-Resource Allocation in a Cloud Environment Based on the Whale Optimization Algorithm," Sensors, pp. vol. 21, no. 5, 1-20, 2021.

[27] S. Elsherbiny, E. Eldaydamony, M. Alrahmawy, and A. E. Reyad, "An Extended Intelligent Water Drops Algorithm for Workflow Scheduling in Cloud Computing Environment," Egyptian Informatics Journal, vol. 9, pp. 33-55, 2018.

Detecting Website Defacement Attacks using Web-page Text and Image Features

Trong Hung Nguyen[1]
Faculty of Information Security
Academy of People's Security
Hanoi, Vietnam

Xuan Dau Hoang[2]
Faculty of Information Technology
Posts and Telecommunications
Institute of Technology
Hanoi, Vietnam

Duc Dung Nguyen[3]
Institute of Information Technology
Vietnam Academy of Science and
Technology
Hanoi, Vietnam

***Abstract*—Recently, web attacks in general and defacement attacks in particular to websites and web applications have been considered one of major security threats to many enterprises and organizations who provide web-based services. A defacement attack can result in a critical effect to the owner's website, such as instant discontinuity of website operations and damage of the owner's reputation, which in turn may lead to huge financial losses. A number of techniques, measures and tools for monitoring and detecting website defacements have been researched, developed and deployed in practice. However, some measures and techniques can only work with static web-pages while some others can work with dynamic web-pages, but they require extensive computing resources. The other issues of existing proposals are relatively low detection rate and high false alarm rate because many important elements of web-pages, such as embedded code and images are not processed. In order to address these issues, this paper proposes a combination model based on BiLSTM and EfficientNet for website defacement detection. The proposed model processes web-pages' two important components, including the text content and page screenshot images. The combination model can work effectively with dynamic web-pages and it can produce high detection accuracy as well as low false alarm rate. Experimental results on a dataset of over 96,000 web-pages confirm that the proposed model outperforms existing models on most of measurements. The model's overall accuracy, F1-score and false positive rate are 97.49%, 96.87% and 1.49%, respectively.**

Keywords—Website defacement attacks; website defacement detection; machine learning-based website defacement detection; deep learning-based website defacement detection

I. Introduction

Defacement attacks to websites and web applications are a type of web attacks that modify the content of web-pages and hence change their looks and feels [1][2]. According to the statistics on the Zone-h.org website, about 500,000 websites have been defaced worldwide in 2020 and this number is almost 200,000 websites in the first 5 months of 2021 [3]. Fig. 1 and Fig. 2 are defaced screenshots of the portal of AI Dhaid city, United Arab Emirates and the website of Nongkla district, Thailand in June, 2021 [3]. According to the messages left on the web-pages, AI Dhaid city's portal was defaced by the "B4X ~ M9z" hacking group and Nongkla district's website was attacked by the "s4dness ghost" hacking group.

There have been a number of known reasons that websites, web-portals and web applications were defaced. However, the major cause is critical security vulnerabilities exist in websites, web-portals and web applications, or their hosting servers, which allow hackers to carry out defacement attacks [1][2][4][5]. XSS (Cross-Site Scripting), SQLi (SQL injection), inclusion of local or remote files, improper account and password management and no-update software are the most common and critical security vulnerabilities existed in websites, web-portals and web applications.

A defacement attack to a website can cause serious consequences to the owner of the website. The defacement attack can immediately interrupt the normal operations of the website, damage the reputation of the owner and cause possible data losses. All of these problems may lead to big financial losses. Due to the wide spreading and severe consequences of defacement attacks to websites, web-portals and web applications, many measures and tools have been researched, developed and deployed in practice to defend against these attacks [6][7][8]. Existing countermeasures to website defacements can be divided into three groups:

- Group (A) consists of measures and tools to scan and fix security vulnerabilities in hosting servers and web applications, such as Acunetix Vulnerability Scanner [9], App Scanner [10] and Abbey Scan [11];
- Group (B) includes tools to monitor and detect web attacks, such as VNCS Web Monitoring [12], Nagios Web Application Monitoring Software [13], Site24x7 Website Defacement Monitoring [14] and WebOrion Defacement Monitor [15];
- Group (C) comprises of solutions to detect website defacement attacks. Typical solutions in this group will be discussed in detail in Section II.

Solutions to detect defacement attacks in Group (C) can be based on simple and complex techniques. Some solutions based on simple techniques can only work with web-pages that have static content or stable structures. Some other solutions based on complex techniques can work with dynamic web-pages, however they require intensive computing powers. Moreover, low detection rate and high false alarm rate are other issues with current proposals, which limit their applicability in practice. In order to address these issues, this paper proposes a website defacement detection model using the combination of text content and image features of web-pages, which belongs to Group (C). The main aim of the proposal is to increase the detection accuracy as well as to decrease the false alarm rates. The proposed detection model can work well with both static and dynamic web-pages. In the proposed model, first text features are extracted from HTML content of web-pages using a tokenizer and image features are extracted from web-pages' screenshots. Then, deep learning techniques, including BiLSTM [16] and EfficientNet [17] are used to construct two component detection models using text and image features, respectively. The Late fusion method is used to combine the detection results of component detection models to produce the final result.

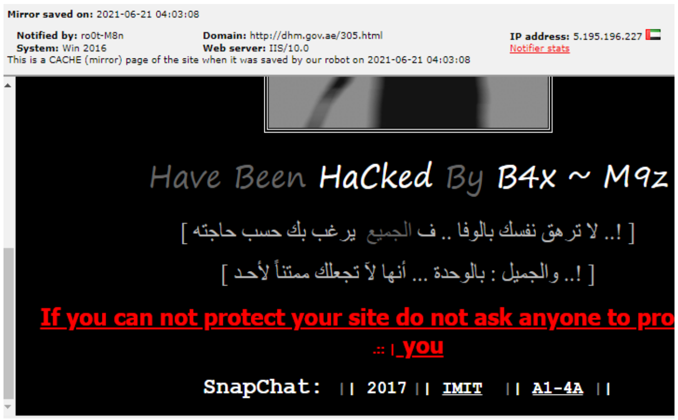

Fig. 1. The Portal of Al Dhaid city, UAE was Defaced in June, 2021.

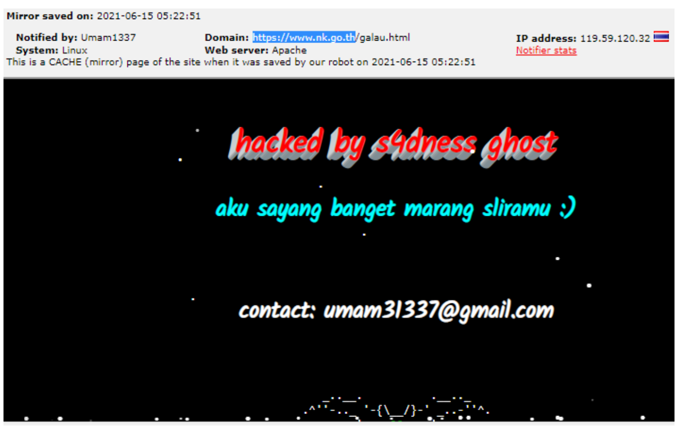

Fig. 2. The Website of Nongkla District, Thailand was Defaced in June, 2021.

The rest of this paper is organized as follows: Section II presents some closely related works; Section III describes the proposed combination detection model, and data preprocessing, model training and detection steps; Section IV shows experimental results and discussion; and Section V is the conclusion of the paper.

II. Related Work

As mentioned in Section I, a number of techniques, solutions and tools in Group (B) and Group (C) for monitoring and detecting website defacements have been proposed. However, we limit our survey on some closely related proposals of Group (C) in the scope of this paper. Group (C) consists of defacement detection solutions, which are based on simple and complex techniques [7]. Defacement detection solutions based on simple techniques include checksum comparison, DIFF comparison and DOM tree analysis of web-pages [7]. These techniques are relatively simple and fast. However, they are only work well with web-pages that have static content or stable structures. That means, solutions based on simple techniques cannot be used effectively for detecting defacement attacks on dynamic websites and web applications, such as online shops or discussion forums. On the other hand, defacement detection solutions based on complex techniques use complicated methods, such as statistics, generic programming and machine learning to construct detection models. These methods are generally more complicated, slower and computationally intensive. Nevertheless, solutions based on complex techniques can be used effectively to monitor and detect defacement attacks for both static and dynamic web-pages. Specifically, existing proposals selected to review include Kim et al. [18], Bartoli et al. [19], Davanzo et al. [20], Hoang [6] and Hoang et al. [7][8].

Kim et al. [18] proposed a statistical method for monitoring and detecting website defacement attacks. The proposed method uses 2-gram technique to build a "profile" from the training dataset of normal web-pages. Fig. 3 describes the defacement detection flow proposed by Kim et al. [18]. The proposed method is implemented in two phases: the training phase and the detection phase. To construct the "profile" in the training phase, the HTML content of each web-page in the training dataset is vectorized using 2-gram substrings and their corresponding appearance frequencies. Based on experiments, 300 2-grams with the highest appearance frequencies are selected to represent a web-page for the defacement detection. In the detection phase, the monitored web-page is first downloaded, and then its HTML content is vectorized using the processing technique done for training web-pages. Then, the vector of the monitored web-page is compared with the vector of the corresponding web-page in the "profile" to compute the similarity score using the cosine distance. If the calculated similarity score is less than a pre-defined detection threshold, an attack alarm is fired. The detection threshold is generated initially and then updated periodically using an algorithm for each web-page. The proposal's major advantage is it can create and adjust dynamic detection thresholds and thereby it can theoretically lower the false alarms. However, the method's major drawbacks are: (i) for web-pages with frequent changed content, the periodic adjusted thresholds may not be suitable and therefore the approach still generates more false alarms, and (ii) it requires extensive computing resources for the dynamic threshold adjustment for each monitored web-page.

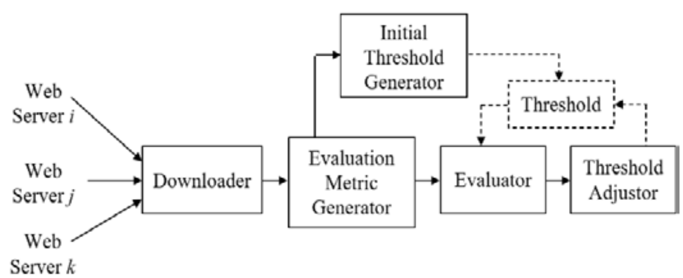

Fig. 3. Defacement Detection Flow Proposed by Kim et al. [18].

Bartoli et al. [19] and Davanzo et al. [20] proposed to use genetic programming techniques to construct the profile for detecting website defacement attacks. In order to collect web-pages' data, in the first step, they use 43 sensors in five groups for monitoring and extracting the information of monitored web-pages. In the next step, the collected information of each web-page is converted to a vector of 1,466 elements. The proposed approach is implemented in two phases: the training phase and detection phase. In the training phase, the information of normal working web-pages are collected and vectorized to build the detection profile using genetic programming techniques. In the detection phase, the information of the monitored web-page is collected, vectorized and then compared with the detection profile to find the difference. An attack alarm is fired if any significant difference is found. The method's major issue is that it requires highly extensive computing resources for building the detection profile due to large-size vectors of web-pages and expensive genetic programming techniques are used.

Hoang [6] proposed to use traditional supervised machine learning techniques for constructing website defacement detection models. Fig. 4 presents the proposed method's detection phase. In the proposed approach, HTML code of each web-page is vectorized using n-gram and term frequency techniques. The proposed method uses an experimental dataset of 100 normal web-pages and 300 defaced web-pages for training and testing. Experimental results on different scenarios using Naïve Bayes and J48 decision tree machine learning algorithms show that the proposed method produces high detection rate and low false alarm rate. However, the main disadvantages of Hoang [6] are (i) the experimental dataset is relatively small, which reduces the reliability of results and (ii) the method only processes the HTML code of web-pages while other important components of web-pages, such as JavaScript code, CSS code and images are not processed.

In order to address issues in Hoang [6], Hoang et al. [7] proposed a website defacement detection model using the combination of the signature-based and machine learning-based techniques. Fig. 5 shows the proposed approach's detection phase in three steps. In the first step, the signature-based detection component looks for pre-defined attack signatures in HTML code of the monitored web-page in order to improve the processing performance for known defacement attacks. In the next step, the machine learning-based detection component classifies the web-page using a classifier built in the training process. Finally, the integrity of embedded files in the web-page are validated using the hashing method. Experiments using a dataset of 1200 normal web-pages and 1200 defaced web-pages show that the proposed model achieves high detection performance. Although the combination model validates the integrity of embedded files in web-pages, the hashing-based technique can only work with static embedded files.

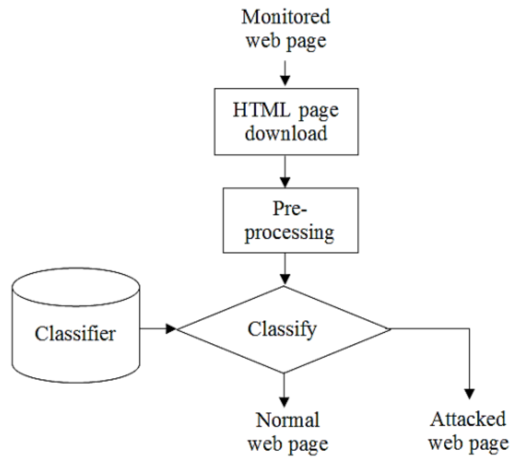

Fig. 4. Detection Phase Proposed by Hoang [6].

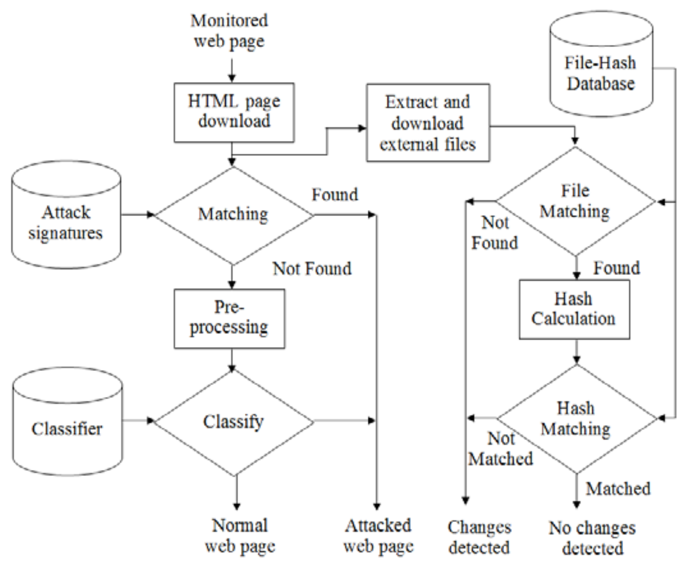

Fig. 5. Detection Phase Proposed by Hoang et al. [7].

In a further expansion of previous works [6][7], Hoang et al. [8] proposed a multi-layer model for website defacement detection. Fig. 6 describes the proposed model's detection phase in several consecutive steps. In this multi-layer model, the machine learning-based integrated model is used to detect defacement attacks for text components of web-pages, including HTML, JavaScript and CSS code. For embedded images in web-pages, the hashing technique is used for integrity checking. Experiments confirm that the multi-layer model can detect defacement attacks effectively on text components of web-pages. However, the proposed model's defacement detection on embedded images of web-pages is limited because only hashing-based integrity checking is used. For many web-pages, embedded images are crucial elements.

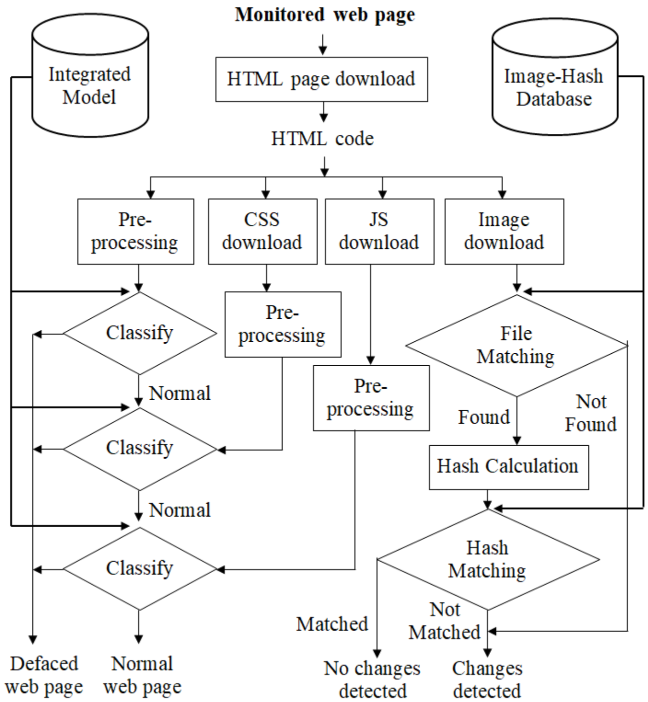

Fig. 6. Detection Phase Proposed by Hoang et al. [8].

In summary, the issues of existing solutions for website defacement detection are as follows:

- Solutions based on simple techniques, such as checksum, DIFF comparison and DOM tree analysis can only work with static web-pages;
- Some solutions require extensive computing resources because of using highly complicated detection models [19][20];
- Some solutions have a high level of false alarms and the detection performance depends heavily on the selection of detection thresholds [18];
- Some solutions can only process text content of the web-pages. Other important web-page elements, including embedded JavaScript, CSS and image files are not processed or processed using simple techniques, such as hashing-based integrity checking [6][7][8].

In order to address the above-mentioned issues, this paper proposes a combination model for website defacement detection. The proposed model aims at increasing detection accuracy and reducing the false alarm rate using the combination of text and image features of web-pages. The reason that text and image features are selected because they are the most important elements of many web-pages. In the proposed model, text features are extracted from pure text content of web-pages and image features are extracted from screenshot images of web-pages. Although a screenshot image of a web-page is not truly equivalent to the web-page's embedded images it provides the true layout and look & feel of the web-page. Therefore, web-pages' screenshot images are a suitable input for the defacement detection. Deep learning techniques, including BiLSTM [16] and EfficientNet [17] are used to build two component detection models using text and image features, respectively. The detection results generated by the component detection models are combined using the Late fusion method to produce the final detection result.

III. Proposed Combination Model

A. Introduction to the Combination Model

The proposed combination model for website defacement detection is implemented in two phases: (i) the training phase and (ii) the detection phase. The training phase as shown in Fig. 7 consists of the following steps:

- Preparing the training dataset: The training dataset includes a subset of normal web-pages and another subset of defaced web-pages. For each web-page in the training dataset, the page HTML code is first downloaded from its URL, then the pure text content is extracted and then the page's screenshot is captured using a set of tools;
- Preprocessing the data: The set of extracted text and page screenshots are processed to extract text and image features for the training of component detection models;
- Training: The preprocessed text subset is used to train the Classifier No. 1 using BiLSTM algorithm and preprocessed image subset is used to train the Classifier No. 2 using EfficientNet algorithm. BiLSTM and EfficientNet algorithms will be discussed in next section.

The detection phase as described in Fig. 8 includes the following steps:

- Retrieving data of the monitored web-page: From the monitored web-page's URL, the page HTML code is downloaded, then the text content is extracted and then the page's screenshot is captured;
- Preprocessing data: the web-page's text content and screenshot image are processed to extract features for next step;
- Classification: Preprocessed text content is classified using Classifier No.1 and preprocessed screenshot image is classified using Classifier No. 2;
- Aggregating the detection results: The output results of Classifier No.1 and Classifier No. 2 are combined using late fusion method to produce the final detection result that is the monitored web-page's status of either normal or defaced.

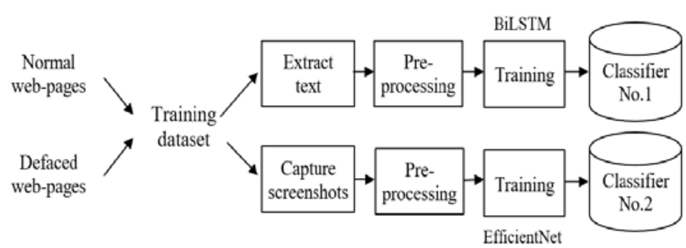

Fig. 7. The Proposed Combination Model: Training Phase.

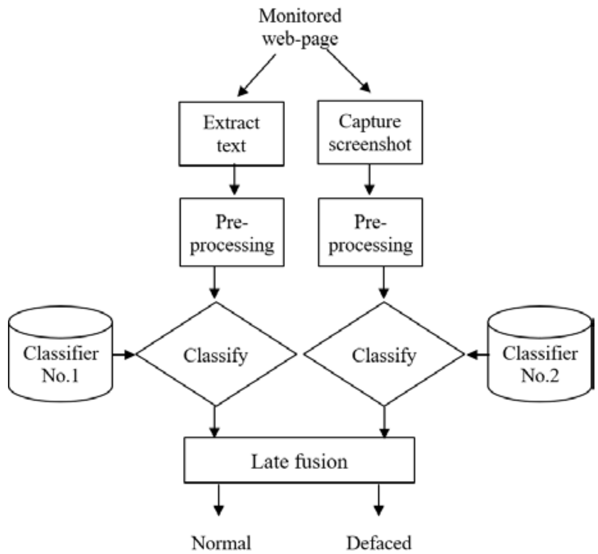

Fig. 8. The Proposed Combination Model: Detection Phase.

B. Data Preprocessing

The text content collected from web-pages is processed to extract text features for the model training. In which, each web-page's text content is converted a vector using the processing procedure as follows:

- The text content is tokenized into a set of words. Next, each word is mapped to a positive integer. In this paper, the Tokenizer technique supported by Google Tensorflow [21] library is used for word segmentation;
- In the set of words tokenized from the text content, the first consecutive 128 words are selected to be the input for the BiLSTM. 128 words are chosen because the amount of information obtained is just sufficient for the model computation, which makes the model training converge faster and reduces the requirements of computational resources. In addition, the selection of consecutive words ensures the BiLSTM algorithm not to omit information thanks to the relationship among adjacent words.

On the other hand, the screenshot images are processed using the following steps:

- The collected screenshot images are converted to the standard size of 224x224 pixels to be the input for the EfficientNet algorithm;
- The value of each pixel of screenshot images is converted to a value in the range of [0, 1]. This is an important step that makes the model training converge faster because neural networks usually process small weighted values [17][22].

C. Training, Detection and Measurements

1) Model training using BiLSTM and efficientnet: The preprocessed datasets of text content and screenshot images are used to train two component detection models, in which the text dataset is trained using BiLSTM algorithm and the image dataset is trained using *EfficientNet* algorithm. BiLSTM algorithm is an extension of LSTM (Long-Short Term Memory) algorithm. BiLSTM is considered more suitable with the processing of text data because it can predict the relationship among words at a longer distance. Therefore, it can limit the information omission [16][23]. Fig. 9 describes the structure of the BiLSTM used in this paper. BiLSTM structure consists of an Embedding layer, a SpatialDropout layer and a Bidirectinal(lstm) layer. The last Dense layer uses the Softmax function to compute the probability for predicting the web-page to be normal or defaced.

EfficientNet is currently considered one of the most powerful CNN (Convolutional Neural Networks) architectures in the field of image classification [17][22][24]. Based on the model zooming technique, EfficientNet is capable of achieving high image classification accuracy while it requires significant lower computing resources compared to previous architectures of neural networks [24]. For example, the smallest EfficientNet (B0) with only 5 million parameters has better classification performance than the famous ResNet50 model with 23 million parameters [24]. EfficientNet can significantly reduce the number of training parameters to gain the high efficiency by using MBConv blocks introduced in MobileNetV2 network. Furthermore, EfficientNet has the efficient zooming ability by balancing the model quantities: the depth, width, and resolution of the network [24].

With the above advantages of EfficientNet, the transition learning based on EfficientNet B0 network is selected for constructing the model for image classification to detect defacements using screenshot images in this paper. Fig. 10 shows the EfficientNet structure used. The EfficientNet network is stripped of the last fully-connected layer and replaced by fully-connected layers that classify the web-page's screenshot image as normal or defaced. The Batch Normalization technique is used to speed up the model convergence and partly prevent overfitting.

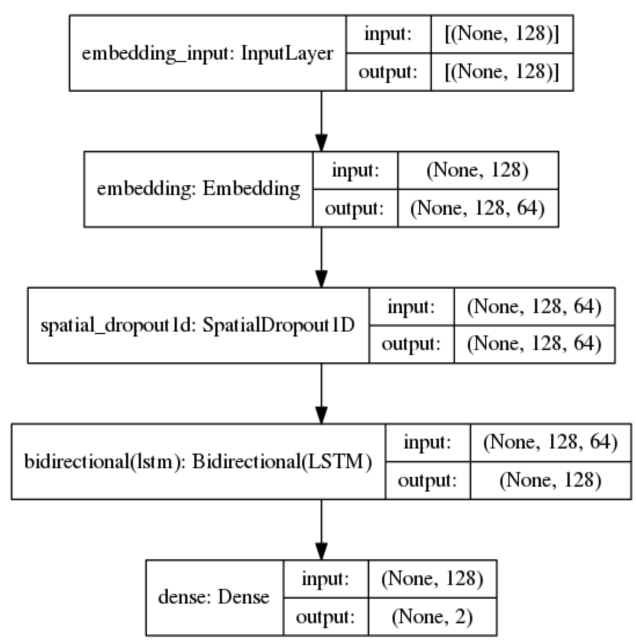

Fig. 9. BiLSTM Algorithm Structure.

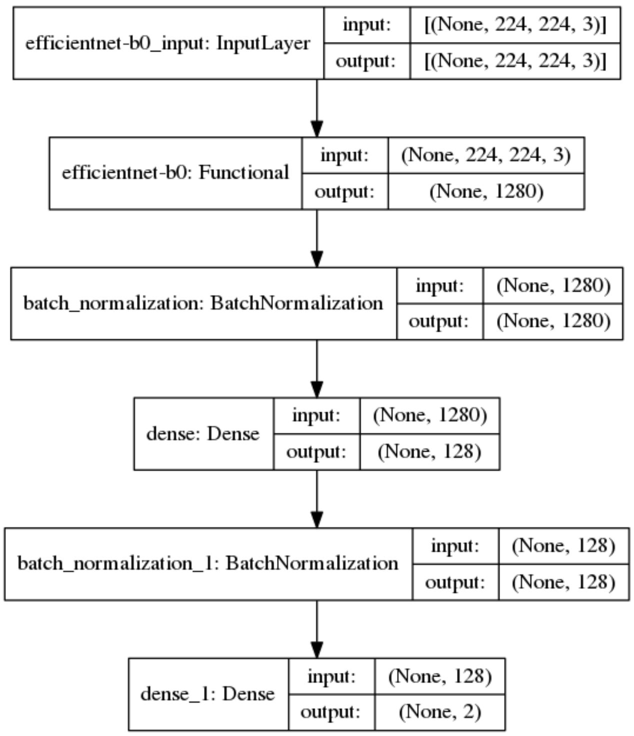

Fig. 10. EfficientNet Algorithm Structure.

2) Detection of defacement attacks: As discussed in section III.A, the detection phase consists of two detection layers based on two component detection models using text content and screenshot image of the web-page. The Late fusion method [25] is used to combine the detection results of the two component detection models. Late fusion allows to merge learned decision values with the following mechanisms: averaging, polling, or a learned model, etc. The advantage of this approach is that it allows different models to be used on different methods thus giving more flexibility. In addition, since each model gives its own prediction it is easier to deal with models that do not produce results [25]. This paper uses the soft voting method that is to calculate the average of the prediction probabilities produced by BiLSTM and EfficientNet component detection models.

3) Performance measurements: We use 6 measurements to measure the detection performance of the proposed detection model. The measurements include: PPV (Positive Predictive Value, or Precision), TPR (True Positive Rate, or Recall), FPR (False Positive Rate), FNR (False Negative Rate), F1 (F1 score) and ACC (Overall Accuracy). These measurements are calculated using the following formulas:

$$PPV = \frac{TP}{TP+FP} \tag{1}$$

$$TPR = \frac{TP}{TP+FN} \tag{2}$$

$$FPR = \frac{FP}{FP+TN} \tag{3}$$

$$FNR = \frac{FN}{FN+TP} \tag{4}$$

$$F1 = \frac{2TP}{2TP+FP+FN} \tag{5}$$

$$ACC = \frac{TP+TN}{TP+TN+FP+FN} \tag{6}$$

in which, TP, FP, FN, TN are model's output parameters of the confusion matrix given in Table I.

TABLE I. THE TP, FP, FN AND TN IN THE CONFUSION MATRIX

		Actual Class	
		Defaced	***Normal***
Predicted Class	***Defaced***	TP (True Positives)	FP (False Positives)
	Normal	FN (False Negatives)	TN (True Negatives)

IV. EXPERIMENTS AND DISCUSSION

A. Collection of the Experimental Dataset

The experimental dataset consists of a subset of normal working web-pages and a subset of defaced web-pages. Normal working web-pages are extracted from the list of top 1 million ranking websites listed by Alexa [26]. Defaced web-pages are downloaded from Zone-h.org [3]. The data collection procedure is carried out as follows:

- From each web-page's URL, its HTML code is downloaded and saved to a HTML file using a self-developed toolset written in JavaScript and run on NodeJS server;
- The screenshot image of the web-page is taken and saved to an image file using the Selenium WebDriver integrated in a web browser.

The collected main dataset includes:

- 57,134 HTML files and 57,134 screenshot image files retrieved from normal working web-pages. These files are labelled as 0 (normal);
- 39,100 HTML files and 39,100 screenshot image files retrieved from defaced web-pages. These files are labelled as 1 (defaced).

The main dataset is randomly divided into two parts:

- The train-set is 80% of the main dataset for training to construct the detection model. The train-set also consists of a text subset for the training of Classifier No. 1 and an image subset for the training of Classifier No. 2; and.
- The test-set is 20% of the main dataset for the model validation. The test-set also includes a text subset for the validation of Classifier No. 1 and an image subset for the validation of Classifier No. 2.

The ratio between the normal and defaced web-pages in the train-set and test-set is equivalent to that of the main dataset.

B. Experimental Results

We have carried out several experiments using train-set and test-set as described in Section IV.A on the following website defacement detection models:

- Models proposed by Hoang [6] using Naïve Bayes and decision tree algorithms;
- Hoang et al. [7] using the random forest algorithm;
- The proposed model with 3 options: (1) model based on EfficientNet using screenshot image features only, (2) model based on BiLSTM using text features only and (3) model based on the combination of BiLSTM and EfficientNet using text and screenshot image features.

Table II provides the experimental results on six measurements of ACC, F1, PPV, TPR, FPR and FNR for different defacement detection models, including:

- The first three lines of the table are the results of previous models based on Naïve Bayes [6], Decision Tree [6] and Random Forest [7];
- The last three lines of the table are the results of the proposed models: EfficientNet (Image) is the component model based on EfficientNet using screenshot image features only, BiLSTM (Text) is the component model based on BiLSTM using text features only, and BiLSTM+ EfficientNet (Text+Image) is the combination model with 2 independent detection sub-models using both text and image features. The late fusion method is used to combine the detection results of two independent detection sub-models to generate the final result.

C. Discussion

Based on the experimental results given in Table II, we have some comments as follows:

- It is clearly that component detection models based on BiLSTM or EfficientNet using text or image features produce much better detection results than previous models [6][7] using the same dataset on most performance measurements. For example, the overall accuracy (ACC) of BiLSTM (Text), EfficientNet (Image), Random Forest [7], Decision Tree [6] and Naïve Bayes [6] are 96.75%, 93.05%, 89.03%, 84.73% and 74.69%, respectively;
- The combination model based on deep learning techniques (BiLSTM and EfficientNet) outperforms previous models based on traditional machine learning techniques, including those based on Random Forest [7], Decision Tree [6] and Naïve Bayes [6].
- The combination model (BiLSTM+EfficientNet (Text+Image)) that processes both text and image information of web-pages achieves significant higher detection accuracy (ACC and F1) than that of the individual component detection models of BiLSTM (Text) and EfficientNet (Image). Specifically, the ACC and F1 of the combination model, and component models based on BiLSTM and EfficientNet are 97.49% and 96.87%, 96.75% and 95.91% and 93.05% and 91.41%, respectively;
- The combination model also reduces considerably the false alarm rates, including both the false positive rate and the false negative rate, compared to the individual component detection models. The FPR and FNR of the combination model, and component models based on BiLSTM and EfficientNet are 1.49% and 4.01%, 1.49% and 5.83% and 5.81% and 8.62%, respectively;
- The BiLSTM (Text) model gives better detection performance than that of the EfficientNet (Image) model. However, because embedded images are important elements of many web-pages, the component model based on EfficientNet plays an important role in the combination model in terms of improving the detection accuracy as well as lowering down the false alarm rates;
- The major shortcoming of the combination model and its component models is that they require high level of computational resources for the training phase to construct the detection models because expensive deep learning and image processing techniques are used. Nevertheless, the training process can be done offline and it does not cause any issues to the monitoring and detecting defacement attacks for web-pages using the constructed models.

TABLE II. EXPERIMENTAL RESULTS FOR DIFFERENT WEBSITE DEFACEMENT DETECTION MODELS

Measurements / Detection Models	ACC	F1	PPV	TPR	FPR	FNR
Naïve Bayes [6]	74.69	75.79	61.45	98.87	41.47	1.13
Decision Tree [6]	84.73	77.89	92.75	67.13	3.51	32.87
Random Forest [7]	86.03	79.92	94.28	69.35	2.81	30.65
EfficientNet (Image)	93.05	91.41	91.44	91.38	5.81	8.62
BiLSTM (Text)	96.75	95.91	97.72	94.17	1.49	5.83
BiLSTM+EfficientNet (Text+Image)	**97.49**	**96.87**	**97.76**	**95.99**	**1.49**	**4.01**

V. Conclusion

This paper proposes a website defacement detection model based on the combination of component models that process text content and screenshot images extracted from web-pages. The proposed combination model increases the detection accuracy as well as reduces the false alarm rates thanks to its ability to simultaneously process two main elements of web-pages, including text content and screenshot images. The deep learning techniques, including BiLSTM and EfficientNet algorithms are used to build the component detection models. The Late fusion method is used to merge the results of the component detection models to create the final detection result. Experiments on a dataset of 96,234 web-pages (57,134 normal web-pages and 39,100 defaced web-pages) confirm that the proposed combination model gives significant higher detection performance than previous models. In addition, the combination model also has higher detection accuracy and lower false alarm rates than the individual component models.

In the future, we continue our research to improve the combination model on two issues: (i) to further increase the detection accuracy and decrease false negative rate, and (ii) to reduce the requirements of computational resources for the model training and especially for the model detection in order to make it higher applicability in practice.

Acknowledgment

Authors sincerely thank the Cyber Security Lab, Posts and Telecommunications Institute of Technology, Hanoi, Vietnam for the facility support to complete the research project.

References

[1] Imperva, Website Defacement Attack, https://www.imperva.com/learn/application-security/website-defacement-attack/, last accessed in May 2021.

[2] Trend Micro, The Motivations and Methods of Web Defacement, https://www.trendmicro.com/en_us/research/18/a/hacktivism-web-defacement.html, last accessed in May 2021.

[3] Zone-H.org, http://zone-h.org/?hz=1, last accessed in May 2021.

[4] Banff Cyber Technologies, Best Practices to address the issue of Web Defacement, https://www.banffcyber.com/knowledge-base/articles/best-practices-address-issue-web-defacement/, last accessed in May 2021.

[5] OWASP, OWASP Top Ten, https://owasp.org/www-project-top-ten/, last accessed in May 2021.

[6] X.D. Hoang. A Website Defacement Detection Method Based on Machine Learning Techniques. In SoICT '18: Ninth International Symposium on Information and Communication Technology, December 6–7, 2018, Da Nang City, Viet Nam. ACM, New York, NY, USA, 6 pages. https://doi.org/10.1145/3287921.3287975.

[7] X.D. Hoang, N.T. Nguyen. Detecting Website Defacements Based on Machine Learning Techniques and Attack Signatures, Computers 2019, 8, 35; doi:10.3390/computers8020035.

[8] X.D. Hoang, N.T. Nguyen. A Multi-layer Model for Website Defacement Detection. In In SoICT'19: Tenth International Symposium on Information and Communication Technology, December 4 – 6, 2019 | Hanoi - Ha Long Bay, Vietnam. ACM, New York, NY, USA, 6 pages. https://doi.org/10.1145/3368926.3369730.

[9] Acunetix, Acunetix Vulnerability Scanner, https://www.acunetix.com/vulnerability-scanner/, last accessed in May 2021.

[10] Trustware, App Scaner, https://www.trustwave.com/Products/Application-Security/App-Scanner-Family/App-Scanner-Enterprise/, last accessed in May 2021.

[11] Misterscanner, Abbey Scan, https://misterscanner.com, last accessed in May 2021.

[12] Vietnam Cyberspace Security Technology, VNCS Web Monitoring, https://vncs.vn/en/portfolio/vncs-web-monitoring/, last accessed in May 2021.

[13] Nagios Enterprises, Web Application Monitoring Software with Nagios, https://www.nagios.com/solutions/web-application-monitoring/, last accessed in May 2021.

[14] Site24x7, Website Defacement Monitoring, https://www.site24x7.com/monitor-webpage-defacement.html, last accessed in May 2021.

[15] Banff Cyber Technologies, WebOrion Defacement Monitor, https://www.weborion.io/website-defacement-monitor/, last accessed in May 2021.

[16] How to Develop a Bidirectional LSTM For Sequence Classification in Python with Keras, https://machinelearningmastery.com/develop-bidirectional-lstm-sequence-classification-python-keras/, last accessed in May 2021.

[17] EfficientNet: Scaling of Convolutional Neural Networks done right, https://towardsdatascience.com/efficientnet-scaling-of-convolutional-neural-networks-done-right-3fde32aef8ff, last accessed in May 2021.

[18] W. Kim, J. Lee, E. Park, S. Kim. Advanced Mechanism for Reducing False Alarm Rate in Web Page Defacement Detection. National Security Research Institute, Korea, 2006.

[19] A. Bartoli, G. Davanzo and E. Medvet. A Framework for Large-Scale Detection of Web Site Defacements. ACM Transactions on Internet Technology, Vol.10, No.3, Art.10, 2010.

[20] G. Davanzo, E. Medvet and A. Bartoli. Anomaly detection techniques for a web defacement monitoring service. Journal of Expert Systems with Applications, 38 (2011) 12521–12530, doi:10.1016/j.eswa.2011.04.038, Elsevier, 2011.

[21] TensorFlow, https://www.tensorflow.org/api_docs/python/tf/keras/preprocessing/text/Tokenizer?fbclid=IwAR2cwjwyHGIB-KJfBHHMZg5ivbuI64qAJbTrDndkd8GhopvyyOf6ZFeS59I.

[22] N.K. Sangani, H. Zarger. Machine Learning in Application Security, Book chapter in "Advances in Security in Computing and Communications", IntechOpen, 2017.

[23] D-A. Clevert, T. Unterthiner and S. Hochreiter. Fast and accurate deep network learning by exponential linear units (elus), 2015. Available online: https://arxiv.org/abs/1511.07289.

[24] Mingxing Tan, Quoc V. Le. EfficientNet: Rethinking Model Scaling for Convolutional Neural Networks, International Conference on Machine Learning, 2019.

[25] Daniel Gibert , Carles Mateu, Jordi Planes. The rise of machine learning for detection and classification of malware: Research developments, trends and challenges, Journal of Network and Computer Applications, 2020.

[26] Alexa, Top 1 million domains, [Available online] http://s3.amazonaws.com/alexa-static/top-1m.csv.zip, last accessed in May 2021.

Preprocessing Handling to Enhance Detection of Type 2 Diabetes Mellitus based on Random Forest

Nur Ghaniaviyanto Ramadhan[1], Adiwijaya[2], Ade Romadhony[3]
School of Computing, Telkom University
Bandung, West Java
Indonesia

***Abstract*—Diabetes is a non-communicable disease that has a death rate of 70% in the world. Majority of diabetes cases, 90-95%, are of diabetes cases are type 2 diabetes which is caused by an unhealthy lifestyle. Type 2 diabetes can be detected earlier by using examination that contains diabetes-related parameters. However, the dataset does not always contain complete information, the distribution between positive and negative classes is mostly imbalanced, and some parameters have low importance to the decision class. To overcome the problems, this study needs to carry out preprocessing to improve detection precision and recall. In this paper, propose an approach on dataset preprocessing, which is applied to diabetes prediction. The preprocessing approach consists of the following process: missing value process, imbalanced data process, feature importance process, and data augmentation process. The data preprocessing process uses the median for missing value, random oversampling for imbalanced data, the Gini score in the random forest for feature importance, and posterior distribution for data augmentation. This research used random forest and logistic regression as classification algorithms. The experimental results show that the classification increased by 20% precision and 24% recall by applying proposed method and random forest method compared to without proposed method and random forest method.**

***Keywords*—Diabetes mellitus; data preprocessing; data augmentation; random forest; classification**

I. Introduction

Quoted from the 2016 WHO data, 70% of total deaths in the world are caused by diabetes, and 90-95% of diabetes cases are type 2 diabetes, which is mainly preventable because it is caused by an unhealthy lifestyle [1]. Diabetes mellitus is a chronic metabolic disorder caused by the pancreas not producing enough insulin or the body unable to use the insulin effectively [2]. In Indonesia, according to Basic Health Research (RisKesDas) in 2018 [2], people with diabetes from 2013 to 2018 increased gradually, where 6.9% of Indonesia population is diabetic. 69.6% of those with diabetes were undiagnosed, and 30.4% diagnosed. Meanwhile, in 2013, 5.7% were diabetic. As many as 73.7% of these people with diabetes, were undiagnosed and 26.3% were diagnosed. This data shows that diabetes mellitus is a dangerous disease since it can lead to various complications of other diseases, such as heart disease, kidney failure, stroke, and even paralysis and death [2].

The prevalence of diabetes mellitus (DM), based on a doctor's diagnosis in the population aged $\geqslant$ 15 years, is increased to 2% based on the report of Basic Health Research (RisKesDas) 2018 [2]. The largest DM sufferers are in the age range of 55-64 years and 65-74 years [2]. In 2018, the percentage of DM sufferers for female (1.8%) and male (1.2%) [2]. As for domicile areas, the percentage of DM sufferers in urban areas (1.9%) than in rural areas (1.0%) [2]. The highest estimate number of DM cases in Indonesia will occur in 2030, with a total population of 21.3 million [2]. Based on Basic Health Research (RisKesDas) diabetes data [2], undiagnosed patients can be detected beforehand. Diabetes detection could be performed by a doctor based on blood sugar and insulin levels or conducted automatically based on individual medical checkup data.

Prediction of diabetes diagnosis using data can determine whether the patients have diabetes or not. There are several studies that discussed diabetes diagnosis prediction based on data. Besides Pima Indian dataset [3-17], there is also data from Luzhou [4], Irvine [18], Kashmir [19,20], online questionnaire [21], and dr. Schorling [9,21]. There are various classification methods on diabetes diagnosis prediction like random forest, J48, naïve bayes (NB), support vector machine (SVM), logistic regression, neural network (NN), and K-Nearest Neighbors.

The explanation of paper contributions taken from some of the shortcomings of previous research is applied to diabetes prediction. In [8] discusses the process of missing value using the median in general and feature selection using this importance index and permutation importance index. Paper [10] discusses the problem of imbalanced data using general random oversampling. In [23] discusses data augmentation techniques for the problem of imbalanced data using a gaussian distribution.

In this paper, the contribution is firstly to replace the value of outliers using median for every six rows, secondly for imbalanced data using oversampling technique namely Random Oversampling by combining three imbalanced features, third for the selected feature process using feature importance technique in random forest model with Gini index value, fourth for data augmentation process using posterior distribution technique where latent data (Y) uses Karya Medika data. Comparison of the contribution of this study with several other studies can be seen in Table I. This paper aims to improve the precision and recall outcomes in diabetes prediction using data preprocessing.

TABLE I. COMPARISON OF CONTRIBUTIONS

Author	Missing Value	Imbalanced Data	Feature Selection	Data Augmentation
[8]	Yes	No	Yes	No
[10]	No	Yes	No	No
[23]	No	No	No	Yes
This Study	Yes	Yes	Yes	Yes

II. LITERATURE REVIEW

In previous studies, the classification and prediction of DM with Pima Indian data have been carried out using several machine learning methods. However, only a few studies discussed about preprocessing on Pima Indian dataset. The problem of missing value is discussed in a limited number of papers [8,13,14,15,17]. The problem of imbalanced data [10,11,17] and of feature selection [5,9,10,14] have been discussed too. Several models have been used in data preprocessing, such as missing value using median [8], Interquartile Range [13,14], mean [15], and Naive Bayes [17]. In imbalanced data, there is Synthetic Minority Over-sampling [10,11], Random Oversampling [10], and Adaptive Synthetic Sampling [17]. Meanwhile, in feature selection, there is Principal Component Analysis [5,9], Maximum Relevance and Minimum Redundancy [5], Fisher Discriminant Ratio [9], Analysis of Variance [9], Information Gain [10], and forward backward [14] models.

According to several prior studies on diabetes prediction, important factors that contribute to classification accuracy are imbalanced data, the presence or absence of missing values, and features that affect the results [4,7,11,13-17,19-22]. In addition, paper explains that data augmentation can improve the accuracy of diabetes prediction [23]. Data augmentation is an algorithm used to augment the observed X data with a quantity of Y, referred to as latent data [24]. In the Pima Indian dataset, imbalanced data occurs in the class label. Imbalanced data is a problem related to the performance of learning algorithms faced with underrepresented data, and the slope of the class distribution is severe [25]. The missing value is a problem that replaces the null value in a variable [9]. The maximum limit for missing value varies from 5-10% and 50% [26]. Feature selection is an important problem in machine learning since it gets the most informative features [9].

III. METHODS OF RESEARCH

To improve the precision and recall outcomes in DM prediction analysis, this research proposed data preprocessing on the binary classification of DM type 2. Fig. 1 shows the proposed system diagram performed in this study whilst Fig. 2 shows the proposed system in more detail.

A. Dataset

This study used two different diabetes datasets, namely Pima Indian and Karya Medika. Kumar et al. provides Pima Indian dataset description [14].

For data augmentation, other data with the same characteristics with the Pima Indian data were used. In this paper, this research used datasets of DM from Karya Medika in January to April 2020. This dataset was taken from an individual sample of Indonesians from the Slawi region, Central Java with a sample size of 630 and has nine features include class labels. In Karya Medika dataset also has problems with preprocessing. Table II shows the dataset of Karya Medika, where the body mass index (BMI) value can be obtained using the formula (1). The BMI formula was used during the data augmentation process, which will become a new feature called BMI.

$$\mathrm{BMI} = \frac{\text{Weight (kg)}}{\text{Height (meter)}*\text{Height (meter)}} \tag{1}$$

Table III presents a baseline of two different datasets, which used as a comparison. Same characteristics found in these two datasets are glucose level, diastolic blood pressure, BMI, age, and class types.

Table IV presents the features of missing values. Pima Indian has more outliers than Karya Medika dataset.

Table V compares features with an imbalanced value of two different datasets, where Karya Medika has more imbalanced features than Pima Indian.

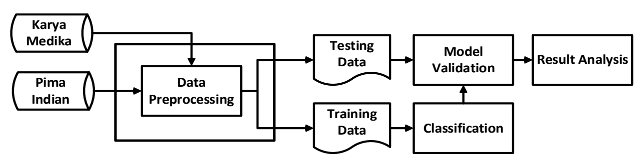

Fig. 1. Proposed System Diagram.

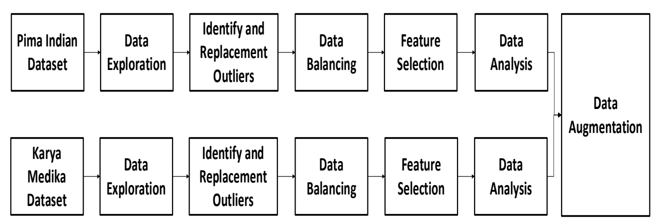

Fig. 2. Proposed System Diagram in Detail.

TABLE II. KARYA MEDIKA DATASET

No	Attribute Description	Unit	Attribute Type
1	Glucose	mg/dl	Numeric
2	Male (1) or Female (0)	-	Nominal
3	Systolic Blood Pressure	mmHg	Numeric
4	Diastolic Blood Pressure	mmHg	Numeric
5	Height	Kg	Numeric
6	Weight	cm	Numeric
7	Age	Year	Numeric
8	Fasting (1) or No-Fasting (0)	-	Nominal
9	Diabetes (1) or No-Diabetes (0)	-	Nominal

TABLE III. DATASETS STATISTIC COMPARISON

Dataset	Number of Observation	Number of Feature	Continuous Feature	Binary Feature	Categorical Feature	Class Type	Classes
Pima Indian	768	8	8	0	0	Binary	2
Karya Medika	630	8	6	2	0	Binary	2

TABLE IV. MISSING VALUES COMPARISON

Dataset	Feature of Missing Values					
Pima Indian	Pregnancies 14%	Glucose 0.65%	Diastolic Blood Pressure 4.5%	Skin Thickness 29.5%	Insulin 48.6%	BMI 1.4%
Karya Medika	Systolic Blood Pressure 10.63%	Diastolic Blood Pressure 10.63%	Height 8%	Weight 7.46%	Age 4.4%	

TABLE V. IMBALANCED DATA COMPARISON

Dataset	Feature of Imbalanced Data					
Pima Indian	Diabetes (268)			No Diabetes (500)		
Karya Medika	Male (264)	Female (366)	Fasting (452)	No Fasting (178)	Diabetes (290)	No Diabetes (340)

B. Outliers Identification and Replacement

In this process, identifying each dataset is whether each feature has a null value, as represented in NaN/{}/0. After determining the outliers, the value is calculated. The process of replacing the null value with a statistical method or machine learning model is carried out. This process can be referred to as missing imputation. In this study, the missing imputation process uses the median value. The median value is chosen since it only takes the middle value in the calculation process without considering other values. In this step, this research aim to find the median value with an even number of data because the imputation process will be carried out every six rows.

C. Data Balancing

In this step, this research uses the random oversampling (ROS) method, which will carry out the oversampling process for minor data to increase percentage. The ROS method was chosen because the data problem used occurred imbalanced in the minority class, which was suitable to use the oversampling method. Applying a re-sampling strategy to the pre-processing data process to obtain a more balanced data distribution is an effective solution to the imbalance problem [27]. ROS method also involves randomly duplicating samples from a minority class and adding them to the training dataset [27]. The process will also see the imbalanced ratio, which calculates the data set from two certain classes. The imbalanced ratio then can be calculated using formula (2) [12].

$$(\text{Instance Minority}/\text{Instance Majority}) \quad (2)$$

where, instance minority is the number of distributions of label class that is less, while instance majority is the number of distributions of label class that is more. So, to find the imbalanced ratio based on [12], namely, the distribution of minority divided by the distribution of the majority.

Table VI shows the imbalanced ratio in the two datasets of this study. The imbalanced ratio has a scale of 0-1, where if the result is close to the value of 1, then the class has only a few imbalanced data.

TABLE VI. IMBALANCED RATIO IN DATASET

Dataset	Feature	Imbalanced Ratio (%)
Karya Medika	Gender	0.72
	Fasting or No Fasting	0.39
	Class Label	0.85
Pima Indian	Class Label	0.53

D. Feature Selection

There are three feature selection techniques: univariate selection, feature importance, and correlation matrix with heat maps [28]. In this paper, this research performs the feature importance technique to solve predictive analysis problems [29]. This technique is carried out to provide a score for each feature against the label class, whether it has high or low attachment.

$$Gini = 1 - \sum_i^c P^2 i \quad (3)$$

where c is the number of values in the target attribute (number of classification classes) and P is the sample portion for the class i (diabetes and no diabetes).

In this paper, the feature importance technique uses the random forest model. Therefore, the calculation process uses the Gini function, as shown in equation (3) in the random forest model. The value of c is two classes, namely diabetes or no diabetes. Then Pi is the sample size for diabetes and no diabetes.

E. Data Augmentation

This study proposed other techniques in addition to using oversampling techniques on class balance problems. The proposed technique is data augmentation. This study uses data augmentation for the problem of lack of varied samples in the Pima Indian dataset, which will be done with additional data using dataset Karya Medika. The data augmentation process will provide a way to increase inference based on the posterior distribution [24]. The posterior distribution is shown in formula (4).

$$P(\vartheta|Y) = \int_X P(\vartheta|Y,Z)\, P(\vartheta|Z,Y) dZ \quad (4)$$

where $P(\vartheta|Y)$ denotes the posterior density of parameter ϑ given the dataset Pima Indian observation, $P(\vartheta|Z,Y)$ denotes the predictive density of the Karya Medika data Z given Pima Indian, and $P(\vartheta|Y,Z)$ denotes the conditional density of ϑ given the data augmented X=(Y,Z) namely augmented posterior [24].

This study will augment data from Pima Indian using Karya Medika data to produce data augmented (X) containing feature characteristics with similarities in both datasets. This study calculates the relative difference using equation (5) to calculate the increase in the original data changes with augmentation data.

$$RD = \left(\frac{\text{Result Augmentation} - \text{Result Original}}{\text{Result Original}}\right) \times 100\% \quad (5)$$

where Result Augmentation (RA) is the result after the Pima Indian dataset augmentation process with Karya Medika dataset. Result Original (RO) is the result before the dataset augmentation process is carried out.

Relative Difference (RD) is a measure that shows the percentage increase when an enlarged data set is used compared to the original data [23]. The instance value used from Karya Medika dataset for augmentation is 100%.

F. Classification

This process is data classification using supervised machine learning methods, namely random forest (RF) and logistic regression (LR), to see the precision and recall. This process also separates training data from data testing. This study split the dataset to train and to test dataset with the ratio of 75:25. Both models have been widely applied with success in various disciplines for classification and regression purposes [30]. The Random Forest used is entropy, as shown in equation (6), where *c* and Pi have been described above.

$$Entropy = \sum_i^c Pi \log 2\ Pi \quad (6)$$

IV. Result and Discussion

This section will discuss the results of the proposed method and analyze the results. Three experiments were conducted separately. First, using the Pima Indian dataset by applying the preprocessing algorithm and then conducting classification. Second, using the Karya Medika dataset by applying the preprocessing algorithm and then conducting classification. Third, using the augmented dataset by applying the preprocessing algorithm and then conducting classification.

As shown in Table VII, the Pima Indian dataset by applying the proposed preprocessing was compared to the original preprocessing increased by using RF and LR classification methods. In Karya Medika dataset by applying preprocessing proposal was compared to original preprocessing increased by using RF classification method compared to LR classification. The results indicated to be different in the Karya Medika dataset with the oversampling process of three features using LR experienced a decrease in precision of 7% and F1 score of 1% compared to the original data.

TABLE VII. Results

Dataset	Preprocessing	Classification	Result		
			Precision Diabetes (%)	***Recall Diabetes (%)***	***F1-Score Diabetes (%)***
Pima Indian	Original	Random Forest (RF)	70	53	61
	Median every six rows, Random Oversampling 1 Features Imbalanced (Class Label), Gini Index Rank 9 Features		83	88	86
	Original	Logistic Regression (LR)	77	55	64
	Median every six rows, Random Oversampling 1 Features Imbalanced (Class Label), Gini Index Rank 9 Features		78	74	76
Karya Medika	Original	Random Forest (RF)	88	83	85
	Median every six rows, Random Oversampling 3 Features Imbalanced (Gender, Fasting, and Class Label), Gini Index Rank 9 Features		98	99	98
	Median every six rows, Random Oversampling 1 Features Imbalanced (Class Label), Gini Index Rank 9 Features		92	98	95
	Original	Logistic Regression (LR)	88	81	84
	Median every six rows, Random Oversampling 3 Features Imbalanced (Gender, Fasting, and Class Label), Gini Index Rank 9 Features		81	84	83
	Median every six rows, Random Oversampling 1 Features Imbalanced (Class Label), Gini Index Rank 9 Features		91	84	87
Augmented Data	Median every six rows, Random Oversampling 1 Features Imbalanced (Class Label), Gini Index Rank 5 Features	Random Forest (RF)	94	96	95
	Median every six rows, Random Oversampling 1 Features Imbalanced (Class Label), Gini Index Rank 5 Features	Logistic Regression (LR)	82	67	74

In augmented datasets increased by using RF classification method when compared with the Pima Indian original dataset and original dataset of Medika Works. Different results in augmented datasets using LR classification method when compared to the original dataset of Karya Medika experienced a decrease in results. However, if augmented datasets using LR classification method compared to the Pima Indian original dataset experienced an increase in results.

So, for the overall RF classification experimentation is superior to LR by applying the proposed method of preprocessing. This happens because the LR classification performed better when the number of noise variables was less than or equal to the number of explanatory variables. Therefore, if the LR classification results were going to be improved, it was necessary to note the importance of each variable used.

Based on augmented dataset results, it showed that Karya Medika data was able to make the predicted results of DM in the Pima Indian dataset increase. However, the Pima Indian dataset was unable to make the DM prediction results in the Karya Medika dataset increase. The F1 score showed that after the imbalanced data method was applied, the results for the minority class increased. Precision and recall results show that the importance of preprocessing the dataset in advance to improve the predicted results of diabetes mellitus.

For the most important preprocessing process to improve diabetes detection results is missing value and balancing class. This is because the missing value process is a built-in problem in which the data used there is a value of 0/NaN/{} in which the value must be replaced with a guess of value, if the missing value is not executed then there will be an error during the classification process. Meanwhile, the process of balancing the class has a great influence on the results of diabetes detection because the ratio of the class of diabetes used as a sample tends to be less than the class that is not diabetic. This is evident after the process of balancing the class of classification results obtained has increased significantly.

V. Conclusion

Based on the results of the implementation and analysis, it can be concluded that this study on the preprocessing process can improve the precision and recall results of the random forest classification model. The results indicate that the classification method using a random forest is superior to logistic regression. The proposed preprocessing method can also be applied to the other augmentation result data from two different datasets by looking at the data characteristics. For the most important preprocessing process to improve diabetes detection results is missing value and balancing class. Data augmentation can also improve the precision and recall results of each original data. This study found that the data quality used is better for Karya Medika dataset than Pima Indian.

Further works need to be conducted by adding some other parameters to the data with samples such as insulin levels, history of diseases suffered, family history of people with diabetes or not, and other parameters related to diabetes. In addition, further studies can also be done using other medical data such as patient data on cancer, heart disease, stroke, and others, or using other combinations of machine learning models in any preprocessing or classification process.

Acknowledgment

The authors would like to thank the Pima Indian and the Karya Medika Lab for the datasets on diabetes. The authors declare no competing financial interest.

References

[1] Ministry of Health RI. "CEGAH, CEGAH, dan CEGAH: Suara Dunia Perangi Diabetes, Accessed December. 12, 2019, https://www.kemkes.go.id/article/view/18121200001/prevent-prevent-and-prevent-the-voice-of-the-world-fight-diabetes.html, 2018 (In Indonesian).

[2] Khairani, InfoDatin (Pusat Data dan Informasi Kementrian Kesehatan Republik Indonesia), Hari Diabetes Sedunia, Accessed December, 12, 2019. PDF article, https://pusdatin.kemkes.go.id/download.php?file=download/pusdatin/infodatin/infodatin-Diabetes-2018.pdf, 2018 (In Indonesian).

[3] Vigneswari, D., et al, Machine Learning Tree Classifiers in Predicting Diabetes Mellitus, 2019 5th International Conference on Advanced Computing & Communication Systems (ICACCS), IEEE, 2019.

[4] Zou, Quan, et al, Predicting diabetes mellitus with machine learning techniques, Frontiers in genetics 9, 515, 2018.

[5] Mercaldo, Francesco, Vittoria Nardone, and Antonella Santone, Diabetes mellitus affected patients classification and diagnosis through machine learning techniques, Procedia computer science, 112, 2519-2528, 2017.

[6] Tafa, Zhilbert, Nerxhivane Pervetica, and Bertran Karahoda, An intelligent system for diabetes prediction, 2015 4th Mediterranean Conference on Embedded Computing (MECO), IEEE, 2015.

[7] Saru, S., and S. Subashree, Analysis and Prediction of Diabetes Using Machine Learning, International Journal of Emerging Technology and Innovative Engineering, 5, 4, 2019.

[8] Maniruzzaman, Md, et al, Accurate diabetes risk stratification using machine learning: role of missing value and outliers, Journal of medical systems, 42, 5, 92, 2018.

[9] Ijaz, Muhammad, et al, Hybrid Prediction Model for Type 2 Diabetes and Hypertension Using DBSCAN-Based Outlier Detection, Synthetic Minority Over Sampling Technique (SMOTE), and Random Forest, Applied Sciences, 8, 8, 1325, 2018.

[10] Shi, Zhan, Improving k-Nearest Neighbors Algorithm for Imbalanced Data Classification, IOP Conference Series: Materials Science and Engineering, IOP Publishing, Vol. 719, No. 1, 2020.

[11] Tyagi, Shivani, and Sangeeta Mittal, Sampling Approaches for Imbalanced Data Classification Problem in Machine Learning, Proceedings of ICRIC 2019, Springer, Cham, 209-221, 2020.

[12] Devi, R. Delshi Howsalya, Anita Bai, and N. Nagarajan, A novel hybrid approach for diagnosing diabetes mellitus using farthest first and support vector machine algorithms, Obesity Medicine, 17, 100152, 2020.

[13] Nnamoko, Nonso, and Ioannis Korkontzelos, Efficient treatment of outliers and class imbalance for diabetes prediction, Artificial Intelligence in Medicine, 104, 101815, 2020.

[14] Raghavendra, S., and J. Santosh Kumar, Performance evaluation of random forest with feature selection methods in prediction of diabetes, International Journal of Electrical & Computer Engineering, 10, 2088-8708, 2020.

[15] Rajni, Amandeep, RB-bayes algorithm for the prediction of diabetic in PIMA Indian dataset, International Journal of Electrical and Computer Engineering (IJECE), 9, 6, 4866-4872, 2019.

[16] Azrar, Amina, et al, Data mining models comparison for diabetes prediction, Int J Adv Comput Sci Appl, 9, 2018.

[17] Wang, Qian, et al, DMP_MI: an effective diabetes mellitus classification algorithm on imbalanced data with missing values, IEEE, Access 7, 102232-102238, 2019.

[18] Kumar, N. Komal, et al, An Optimized Random Forest Classifier for Diabetes Mellitus, Emerging Technologies in Data Mining and Information Security, Springer, Singapore, 765-773, 2019.

[19] Mirza, Shuja, Sonu Mittal, and Majid Zaman, Decision Support Predictive model for prognosis of diabetes using SMOTE and Decision tree, International Journal of Applied Engineering Research, 13, 11, 9277-9282, 2018.

[20] Shuja, Mirza, Sonu Mittal, and Majid Zaman, Effective Prediction of Type II Diabetes Mellitus Using Data Mining Classifiers and SMOTE, Advances in Computing and Intelligent Systems. Springer, Singapore, 195-211, 2020.

[21] Wu, Han, et al, Type 2 diabetes mellitus prediction model based on data mining, Informatics in Medicine Unlocked, 10, 100-107, 2018.

[22] Abd Rahman, Muhammad Hafiz Fazren, Wan Wardatul Amani Wan Salim, and Mohd Firdaus Abd Wahab, Risk Prediction Analysis For Classifying Type 2 Diabetes Occurrence Using Local Dataset, Biological and Natural Resources Engineering Journal, 3, 1, 48-61, 2020.

[23] Moreno-Barea, Francisco J., José M. Jerez, and Leonardo Franco, Improving classification accuracy using data augmentation on small data sets, Expert Systems with Applications, 161, 113696, 2020.

[24] Tanner, Martin A, Tools for statistical inference: observed data and data augmentation methods, Springer Science & Business Media, Vol. 67, 53, 2012.

[25] He, Haibo, and Edwardo A. Garcia, Learning from imbalanced data, IEEE Transactions on knowledge and data engineering, 21.9, 1263-1284, 2009.

[26] Madley-Dowd, Paul, et al, The proportion of missing data should not be used to guide decisions on multiple imputation, Journal of clinical epidemiology, 110, 63-73, 2019.

[27] Branco, Paula, Luis Torgo, and Rita Ribeiro, A survey of predictive modelling under imbalanced distributions, arXiv preprint, arXiv:1505.01658, 2015.

[28] Verma, Anurag Kumar, and Saurabh Pal, Prediction of skin disease with three different feature selection techniques using stacking ensemble method, Applied Biochemistry and Biotechnology, 1-20, 2019.

[29] Kuo, Kuang-Ming, et al, A multi-class classification model for supporting the diagnosis of type II diabetes mellitus, PeerJ, 8, e9920, 2020.

[30] Couronné, Raphael, Philipp Probst, and Anne-Laure Boulesteix, Random forest versus logistic regression: a large-scale benchmark experiment, BMC bioinformatics, 19, 1, 270, 2018.

Grey Clustering Approach to Assess Sediment Quality in a Watershed in Peru

Alexi Delgado[1], Jossel Altaminarano[2], Luis Pariona[3]
Patricia Oscanoa[4], Stephany Esquivel[5], Wendy Mejía[6], Chiara Carbajal[7]
Mining Engineering Section, Pontificia Universidad Católica del Perú, Lima, Peru[1]
Environmental Engineering Faculty, Universidad Nacional de Ingeniería, Lima, Peru[2, 3, 4, 5, 6]
Administration Program, Universidad de Ciencias y Humanidades, Lima, Peru[7]

***Abstract*—The evaluation of sediment quality is a relevant topic that involves the analysis of various parameters that are altered by natural or anthropogenic causes. Therefore, the Grey Clustering method provides an alternative to evaluate sediment quality. In the present study, the sediment quality of the Chontayacu river watershed was evaluated considering the results of the monitoring of twenty-three points carried out in the early evaluations by the Environmental Impact Evaluation Agency (OEFA by its Spanish acronym). These twenty-three points were separated into three blocks considering the monitoring points upstream of the Uchiza town center and the Chontayacu Alto and Chontayacu Bajo hydroelectric plants. Seven parameters were analyzed: As, Cd, Cr, Cu, Pb, Hg and Zn, which were compared with Canadian sediment quality standards for the protection of aquatic life. The results of the assessment showed that all points in the Chontayacu River were classified as having unlikely adverse biological effects from heavy metals. However, a quality ranking was established between the points of each block where it was found that points P3, P4 and P17 correspond to the lowest values for the high CH, low CH and CP Uchiza blocks respectively. Finally, the results obtained will provide integrated information for decision making by the competent authorities in Peru, as well as indicate the level of sediment contamination that should be taken into account for the proposal of hydroelectric projects that influence sediment transport and entrainment.**

***Keywords*—Grey clustering; sediment quality; watershed**

I. Introduction

The Chontayacu River is a tributary of the left bank of the Huallaga River, belonging to one of the main basins of Peru due to its great water resource potential [1]. This river has potentially exploitable areas for hydroelectric purposes because there are no demands for water use, knowing that the few economic activities are limited to agriculture, livestock and forestry, therefore, the waters flow naturally without being exploited [2]. However, from an early evaluation of sediment quality, high concentrations of some heavy metals have been observed, which may be due to natural processes or anthropogenic factors [3].

The Chontayacu River originates in the eastern foothills of the Andes Mountains, above 4,000 m above sea level, flowing through the Aurecchico and Pumahuanunga Rivers, which converge at approximately 3,600 m above sea level, giving rise to the Chontayacu River up to the town of Uchiza, at 1,180 m above sea level. Along its course, the river receives contributions from numerous tributaries, the main ones being the Chonas, Lucmabamba and Frijol rivers on the right bank and Crisnejas on the left bank [4]. The sediment quality evaluation will be carried out from the upper part of the Santa Rosa de Oso hamlet to the jurisdiction of the Crisnejas hamlet (Blanco river), both belonging to the Chontayacu river basin.

During the development of the evaluation, the Grey Clustering method was used, which is mainly used to verify whether or not the study objects belong to predetermined classes so that they can be treated differently, i.e., classifying them according to their characteristics [5]. Therefore, the center-point triangular whitenization weight functions (CTWF) method was applied because it allows us to classify objects into definable classes, called Grey Classes [6].

Therefore, the specific objective of this study is to classify 23 points, divided into 3 major blocks of the Chontayacu River basin, based on Canadian Sediment quality levels for the protection of aquatic life [7], using the Grey Claustering method [15] based on triangular center-point whitening weighting functions (CTWF).

In the present study, Section II provides information on the literature reviewed. Section III details the CTWF method. Then, in Section IV, the case study is described, followed by the results and discussions in Section V. Finally, conclusions will be presented in Section VI.

II. Literature Review

Kejian and Min (2014) [9], applied the Grey Clustering method to evaluate the sediment quality of the coastal ocean of Jiangsu, central China. They established 3 grey clusters, between clean, low and high contamination for 39 coastal sediment samples. The evaluation results indicate that the surface sediment quality of the northern branch of the Yangtze River is comparatively better, while the quality of the abandoned yellow river mouth of Jiangsu province is the worst with the highest pollution. When analyzing the underlying reasons, pollutants discharged into the sea due to the increase of industrial and agricultural activities contributed to the pollution. Therefore, it is recommended to improve from the source to protect the marine ecosystem of the coastal area.

Delgado et al. (2017) [8], evaluated the water quality of the Santa river basin according to the parameters established by the Ministry of Environment in Peru, using the Grey Clustering method with triangular weight functions (CTWF). Monitoring data from the Peruvian National Water Authority of 2013 were used, where they analyzed twenty-one monitoring points in the Santa river basin. The results showed that 47.6% of the monitoring points presented good water quality for consumption by the population; 33.3% moderate water quality for consumption by the population; and 19.1% of the points presented low water quality for consumption by the population. The gray grouping method showed interesting results and could be applied to other studies on water quality or environmental quality in general.

According to Quanz et al. (2020) [10], they conducted an ecological risk assessment (ERA) to determine the potential effect of human activities and industries within an aquatic ecosystem on sediments using the Canada-Ontario Decision-Making Framework for Assessment of Great Lakes Contaminated Sediments (COA) method. Historical data (1996 to 2005) from South Baymouth were examined to determine contaminants of potential concern, especially bioaccumulative metals from a comparison with sediment quality standards (SQG). The results show that although the sediments presented negligible potential for ecological risk and did not require any remedial management action, this case study highlights the strengths of using COA for this IAS, but also highlights weaknesses that included unclear linkages between the cause and effects of aquatic contaminants.

III. Methodology

In this section we describe the Grey Clustering method [15] based on triangular center-point whitening weighting functions (CTWF), which has been used to evaluate sediment quality in the Chontayacu River, a tributary of the left bank of the Huallaga River [1], which is described as follows: first identify the monitoring points "m", then define the sediment quality parameters "p" and finally define the Grey Classes "g", according to the sediment quality monitoring values. $x_{ij} = (i = 1,2,\ldots,m; j = 1,2,\ldots,p)$. The steps of the Grey Clustering method in CTWF [15] are presented in Fig. 1.

Step 1: Determination of focal points

The criteria ranges are divided into three grey classes and the center points are calculated based on the Canadian Sediment quality levels for aquatic life protection [7].

Step 2: Sizing of standard data and monitoring data

For the calculation of the dimensioned standard values, the parameters of the sediment quality "p" and the Grey Classes "g" are established, which form the following matrix $A = [Aij;\ i = 1,2,\ldots,p;\ j = 1,2,\ldots,g]$; in that sense, it is normalized (Pij) for each criterion. The normalized value is calculated by (1).

$$Pij = \frac{\mathrm{A_{ij}}}{\sum_{\mathrm{j=1}}^{\mathrm{g}} \mathrm{A_{ij}}/g} \tag{1}$$

For the calculation of the dimensioned monitoring data, the parameters of the sediment quality "p" and the monitoring points "m" are established and form the following matrix $M = [Mij;\ i = 1,2,\ldots,p;\ j = 1,2,\ldots,M]$, which is normalized (Kij) for each criterion. The normalized value is calculated by (2).

$$Kij = \frac{M_{ij}}{\sum_{\mathrm{j=1}}^{\mathrm{g}} \mathrm{A_{ij}}/g} \tag{2}$$

Step 3: Determination of the triangular functions and their values

The grey classes use as reference the Canadian Sediment quality levels for aquatic life protection [7], which gave us the data to measure the sediment quality in this research, these quality levels gives us 3 quality levels for each parameter so there will be 3 functions for each parameter. The new sequence of center points is $\lambda 1$, $\lambda 2$ and $\lambda 3$. For class $g = 1,2\ and\ 3$; $j = 1,2,\ldots,p$ for an observed value xij. The calculation of the CTWF is shown using (3) – (5); and Fig. 2 shows the plot of the triangular functions.

$$f_j^1(x_{ij}) = \begin{cases} 1, & x \in \left[0, \lambda_j^1\right] \\ \frac{\lambda_j^2 - x}{\lambda_j^2 - \lambda_j^1}, & x \in \left]\lambda_j^1, \lambda_j^2\right[\\ 0, & x \in \left[\lambda_j^2, +\infty\right[\end{cases} \tag{3}$$

$$f_j^2(x_{ij}) = \begin{cases} \frac{x - \lambda_j^1}{\lambda_j^2 - \lambda_j^1}, & x \in \left]\lambda_j^1, \lambda_j^2\right] \\ \frac{\lambda_j^2 - x}{\lambda_j^2 - \lambda_j^1}, & x \in \left]\lambda_j^2, \lambda_j^3\right[\\ 0, & x \in \left[0, \lambda_j^1\right] \cup \left[\lambda_j^3, +\infty\right[\end{cases} \tag{4}$$

$$f_j^3(x_{ij}) = \begin{cases} \frac{x - \lambda_j^2}{\lambda_j^3 - \lambda_j^2}, & x \in \left]\lambda_j^2, \lambda_j^3\right[\\ 0, & x \in \left[0, \lambda_j^2\right] \\ 1, & x \in \left[\lambda_j^3, +\infty\right[\end{cases} \tag{5}$$

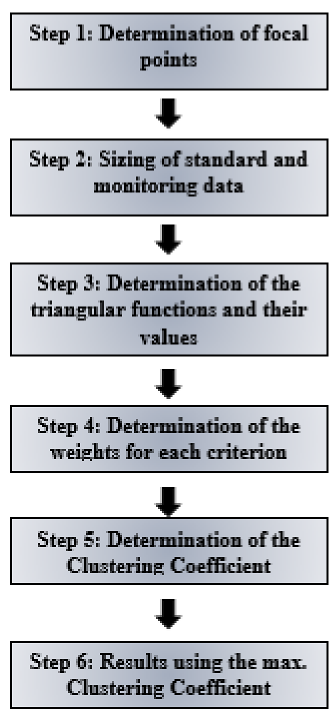

Fig. 1. Grey Clustering Method Diagram.

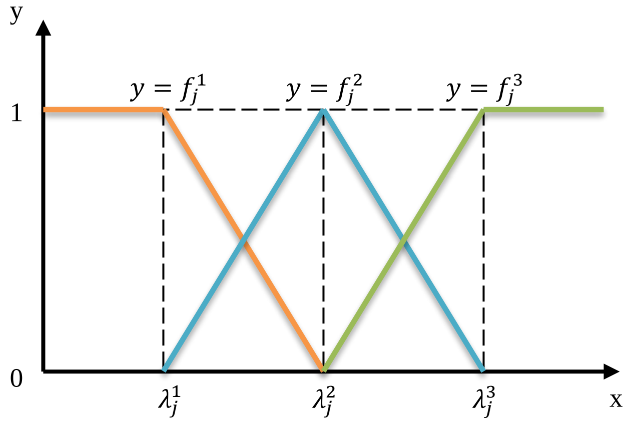

Fig. 2. Whitenization Functions.

Step 4: Determination of the weights for each criterion

The weights of each criterion known as Clustering weight (nij) is determined based on the dimensionless standard data, where Pij represents these, which were calculated in (1), to establish the values of nij will take into account the parameters of the sediment quality "p" and the Grey Classes "3" where (i=1,2, ..., p; j=1,2,3), the weights of each criterion are calculated by (6), as follows:

$$n_{ij} = \frac{\frac{1}{P_{ij}}}{\sum_{x=1}^{p} \frac{1}{P_{ij}}} \quad (6)$$

Step 5: Determination of the Clustering Coefficient

The values of the whitenization functions $(f_j^g(x_{ij}))$ are determined by (3) – (5) and the weights of each parameter (nij) are calculated by (6). Once these calculations are defined, the Clustering coefficient is calculated by (7).

$$\sigma_j^g = \sum_{j=1}^{p} f_j^g(x_{ij}) \times n_{ij} \quad (7)$$

Step 6: Results using the max. Clustering Coefficient

With the results obtained in the previous step, the maximum values of each sampling point classified by blocks are selected, with which it is identified which areas contain unlikely, occasional or frequent biological effects; it is calculated by (8):

$$max\{\sigma_i^g\} = \sigma_i^{g^*} \quad (8)$$

IV. Case Study

A. Description of the Context

The analysis of sediment quality was carried out in the Chontayacu River located in the micro-watershed of the Chontayacu River, belonging to the district of Cholon, province of Marañón, department of Huánuco. It is located in the upper basin of the Huallaga River, which has a total area of 89 416 km2 in the northeastern part of Peru, on the Atlantic slope [1], being the main tributary of the most important basin in northern Peru, which is represented in Fig. 3.

Fig. 3. Huallaga River Basin Location.

B. Definition of Objects of Study

For the evaluation of sediment quality in the upper Huallaga river basin, 23 points classified in three blocks (Upper Chontayacu Hydroelectric Plant, Lower Chontayacu Hydroelectric Plant and Uchiza Village Center), obtained from the early environmental assessment report on the future site of the upper and lower Chontayacu hydroelectric project and surrounding areas, in the district of Cholon, province of Marañón, department of Huánuco[3], were collected. These are detailed in Table I and represented in Fig. 4.

C. Definition of Evaluation Criteria

The evaluation criteria for the present study are determined by the Canadian Sediment Quality Standards for the Protection of Aquatic Life [7], which are presented in Table II.

D. Definition of Grey Classes

The Grey classes established for sediment quality assessment are three and are based on the Canadian Sediment quality levels for the protection of aquatic life [7], which are presented in Table III.

TABLE I. MONITORING POINTS OF THE EARLY EVALUATIONS CARRIED OUT BY OEFA

Block	Point	EAT Code	Description	This	North
Central Hydroelectric Chontayacu High (CH-ALTO)	P1	SED-RChon1	Point located on the left bank of the Chontayacu river, approximately 0.7 km upstream from the confluence with the Susto river and the Santa Rosa de Oso hamlet.	311828	9047095
	P2	SED-RSust1	Point located on the Susto river, approximately 20 m upstream from the Susto bridge and 100 m before the confluence with the Chontayacu river.	312476	9047252
	P3	SED-RChon2	Point located on the left bank of the Chontayacu River, approximately 0.5 km before the confluence with the Oso River, near the Santa Rosa de Oso hamlet.	313311	9047400
Central Hydroelectric Chontayacu Under (CH-BAJO)	P4	SED-RChon3	Point located on the left bank of the Chontayacu river, approximately 1 km before the confluence with the Esperanza river.	314222	9047247
	P5	SED-RChon4	Point located on the left bank of the Chontayacu river, approximately 950 m before the confluence with the Aragán river.	316141	9048347
	P6	SED-RArag1	Point located on the Aragán river, approximately 50 m upstream from the Aragán bridge and 120 m before the confluence with the Chontayacu river.	316987	9048655
	P7	SED-RChon5	Point located on the left bank of the Chontayacu river, approximately 320 m before the confluence with the Santillan river.	317794	9048774
	P8	SED-RSanti1	Point located on the Santillan river, approximately 50 m upstream from the Santillan bridge and 250 m before the confluence with the Chontayacu river.	318259	9048862
	P9	SED-RYana1	Point located on the Yanajanca river, approximately 250 m before the confluence with the Chontayacu river, near the Cocalito hamlet.	321126	9047235
	P10	SED-RChon6	Point located on the Chontayacu river, near the Cocalito hamlet, approximately 200 m before the confluence with the Yanajanca river.	321046	9047585
Center Village Uchiza (CP-Uchiza)	P11	SED-RChon7	Point located on the Chontayacu river, at the Nueva Galilea hamlet, before the confluence with the Ollas river.	323344	9047364
	P12	SED-ROlla1	Point located approximately 20 m upstream from the Ollas bridge, at the Nueva Galilea hamlet and before the confluence with the Chontayacu river.	323620	9047530
	P13	SED-RSAna1	Point located on the Santa Ana river, approximately 20 m from the Santa Ana bridge and 100 m before the confluence with the Chontayacu river, at the Nueva Unión de Santa Ana hamlet.	326359	9048903
	P14	SED-RChon9	Point located on the left bank of the Chontayacu river, before the confluence with the El Ají river, near the Nueva Unión de Ají hamlet.	327152	9049557
	P15	SED-RPAle1	Point located on the Puerto Alegre river (Pólvora river), approximately 350 m before the confluence with the Chontayacu river and downstream of the Puerto Alegre bridge.	329942	9051224
	P16	SED-RChon10	Point located on the left bank of the Chontayacu river, approximately 2 m from the Puerto Alegre bridge and 500 m before the confluence with the Pólvora river.	329085	9051345
	P17	SED-RChon12	Point located on the left bank of the Chontayacu River, approximately 200 m before the confluence with the San Antonio River, near the San Antonio de Padua population center.	330951	9051803
	P18	SED-RChon13	Point located on the left bank of the Chontayacu river, approximately 200 m before the confluence with the Camote river, downstream of the San Antonio de Padua population center.	332382	9053919
	P19	SED-RChon14	Point located on the left bank of the Chontayacu river, approximately 200 m after the confluence with the Blanco river, near the Blanco river hamlet.	332871	9054988
	P20	SED-RChon15	Point located on the left bank of the Chontayacu river, 100 m before the confluence with the Camote river, near the Crisnejas Base of the Peruvian Army.	333810	9055880
	P21	SED-RCamo1	Point located on the Camote River, approximately 500 m before the confluence with the Chontayacu River, at the Crisnejas Base of the Peruvian Army.	333544	9055269
	P22	SED-RCamo2	Located on the Camote river, approximately 300 m before the confluence with the Chontayacu river, near the Blanco river hamlet.	332617	9054011
	P23	SED-RChon16	Point located on the Chontayacu river, approximately 2 km downstream from the confluence with the Crisnejas river.	335740	9056944

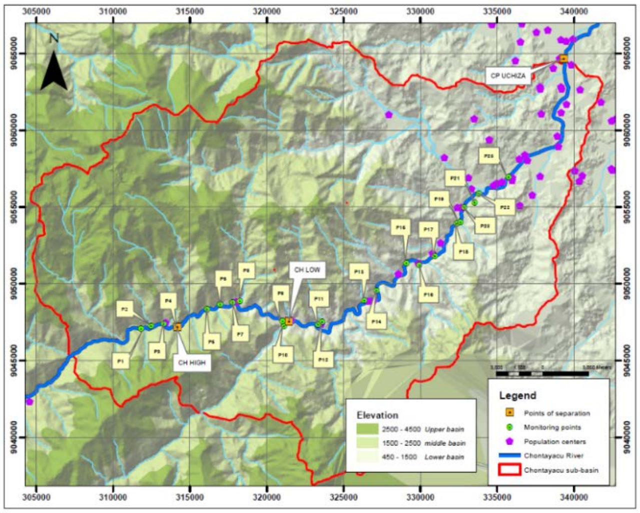

Fig. 4. Location of Sediment Quality Monitoring Points in the upper Huallaga River Basin.

TABLE II. EVALUATION CRITERIA FOR SEDIMENT QUALITY

Notation	Criteria	Units
C1	As	mg/kg
C2	Cd	mg/kg
C3	Cr	mg/kg
C4	Cu	mg/kg
C5	Pb	mg/kg
C6	Hg	mg/kg
C7	Zn	mg/kg

TABLE III. SEDIMENT QUALITY LEVELS FOR THE PROTECTION OF AQUATIC LIFE

Criteria	Biological effect		
	Unlikely	*Occasional*	*Frequent*
As (mg/kg)	5.9	<5.9-17>	
Cd (mg/kg)	0.6	<0.6-3.5>	3.5
Cr (mg/kg)	37.3	<37.3-90>	
Cu (mg/kg)	35.7	<35.7-197>	
Pb (mg/kg)		<35-91.3>	91.3
Hg (mg/kg)	0.17	<0.17-0.486>	0.486
Zn (mg/kg)		<123-315>	

E. Calculations using the CTWF Method

The calculations for the case study based on the gray clustering method (CTWF) are shown below:

Step 1: Determination of focal points

Based on the Canadian Sediment quality levels for the protection of aquatic life [7], the central values of the parameters to be analyzed are obtained, which are presented in Table IV.

Step 2: Sizing of standard data and monitoring data

The dimensionless values of the standard data calculated for each criterion according to the Canadian Sediment Quality Levels for the Protection of Aquatic Life [7] were determined through (1). These values are presented in Table V.

Similarly, based on data from the early environmental assessment report on the future site of the upper and lower Chontayacu hydroelectric project and surrounding areas, in the district of Cholon, province of Marañón, department of Huánuco (OEFA, 2017), the dimensioned values of the 23 monitoring points established for each criterion and separated by blocks were obtained using (2). These values are presented in Table VI.

Step 3: Determination of the triangular functions and their values

The triangular bleaching functions of the three grey classes for each parameter were obtained by replacing the values in Table IV in (3) – (5). As an example, the Clustering functions established for Arsenic are presented below.

$$f_j^{\,1}\begin{cases} 1\,, & x \in [0,0.515] \\ \frac{1-x}{1-0.515}, & x \in [0.515,1] \\ 0, & x \in [1,+\infty\rangle \end{cases} \tag{9}$$

$$f_j^{\,2}\begin{cases} \frac{x-0.515}{1-0.515}\,, & x \in [0.515,1\rangle \\ \frac{1.485-x}{1.485-1}, & x \in \langle 1,1.485\rangle \\ 0 & x \in [0,0.515] \cup [1.485,+\infty\rangle \end{cases} \tag{10}$$

$$f_j^{\,3}\begin{cases} \frac{x-1}{1.485-1}\,, & x \in \langle 1,1.485\rangle \\ 1, & x \in [1.485,+\infty\rangle \\ 0\,, & x \in [0,1] \end{cases} \tag{11}$$

TABLE IV. CENTRAL VALUES OF SEDIMENT QUALITY LEVELS FOR CANADA

Criteria	Biological effect		
	Unlikely	*Occasional*	*Frequent*
As (mg/kg)	5.9	11.45	
Cd (mg/kg)	0.6	2.05	3.5
Cr (mg/kg)	37.3	63.65	
Cu (mg/kg)	35.7	116.35	
Pb (mg/kg)		63.15	91.3
Hg (mg/kg)	0.17	0.33	0.486
Zn (mg/kg)		219	

TABLE V. STANDARD DIMENSIONLESS VALUES OF SEDIMENT QUALITY LEVELS FOR CANADA

Notation	Criteria	Unlikely	Occasional	Frequent
C1	As	0.515	1	1.485
C2	Cd	0.293	1	1.707
C3	Cr	0.586	1	1.414
C4	Cu	0.307	1	1.693
C5	Pb	0.554	1	1.446
C6	Hg	0.518	1	1.482
C7	Zn	0.562	1	1.438

TABLE VI. DIMENSIONED DATA OF THE MONITORING POINTS ESTABLISHED IN THE CASE STUDY

Block	Point	Criteria						
		C1	***C2***	***C3***	***C4***	***C5***	***C6***	***C7***
		As	***Cd***	***Cr***	***Cu***	***Pb***	***Hg***	***Zn***
Hydroelectric Power Plant Chontayacu Alto	P1	2.62	2.54	0.70	0.15	0.00	22.99	0.34
	P2	0.44	1.79	0.30	0.17	0.00	15.00	0.27
	P3	2.18	3.08	0.76	0.17	0.00	29.15	0.34
Hydroelectric Power Plant Lower Chontayacu	P4	2.18	2.87	0.77	0.17	0.00	34.45	0.37
	P5	1.83	2.70	0.72	0.18	0.00	31.71	0.35
	P6	0.03	2.45	0.31	0.36	0.00	22.96	0.37
	P7	1.83	2.75	0.76	0.15	0.00	26.04	0.36
	P8	0.03	1.15	0.06	0.05	0.00	13.63	0.20
	P9	2.18	0.13	0.54	0.19	0.00	29.30	0.40
	P10	2.45	0.09	0.69	0.20	0.00	30.40	0.37
Uchiza town center	P11	1.66	0.09	0.50	0.15	0.00	22.47	0.31
	P12	0.16	0.02	0.05	0.02	0.00	27.87	0.26
	P13	0.06	0.02	0.03	0.03	0.00	20.06	0.18
	P14	1.92	0.08	0.63	0.20	0.00	26.95	0.36
	P15	0.17	0.08	0.06	0.02	0.00	46.34	0.13
	P16	2.45	0.12	0.62	0.21	0.00	31.40	0.41
	P17	2.36	0.14	0.69	0.23	0.00	34.76	0.45
	P18	2.01	0.09	0.59	0.19	0.00	29.42	0.37
	P19	2.01	0.07	0.58	0.17	0.00	24.39	0.34
	P20	1.48	0.05	0.47	0.15	0.00	24.91	0.30
	P21	0.14	0.03	0.08	0.04	0.00	27.41	0.11
	P22	0.11	0.02	0.04	0.02	0.00	20.03	0.11
	P23	2.18	0.08	0.59	0.20	0.00	30.49	0.36

Step 4: Determination of the weights for each criterion

The values of the weights of each criterion evaluated were calculated using (6); the results are presented in Table VII.

Step 5: Determination of the Clustering Coefficient

The values of the clustering coefficients were calculated using (7) established in this study for the 23 monitoring points. The results of five monitoring points selected among the three blocks under study are presented in Table VIII.

Step 6: Results using the max. clustering coefficient

Finally, we selected the maximum values of the Clustering coefficients calculated using (8), with which we determined the biological effect presented by each monitoring point, which were separated by blocks, the results are presented in Tables IX, X and XI, where each maximum value was highlighted for its better appreciation.

TABLE VII. WEIGHTING OF EACH CRITERION EVALUATED IN THIS STUDY

Notation	**Criteria**	**Unlikely**	**Occasional**	**Frequent**
C1	As	0.123	0.143	0.146
C2	Cd	0.216	0.143	0.127
C3	Cr	0.108	0.143	0.153
C4	Cu	0.206	0.143	0.128
C5	Pb	0.114	0.143	0.150
C6	Hg	0.122	0.143	0.146
C7	Zn	0.112	0.143	0.151

TABLE VIII. CLUSTERING COEFFICIENTS FOR FIVE MONITORING POINTS

Block	Point	Criteria	C1	C2	C3	C4	C5	C6	C7	Results
Chontayacu Alto Hydroelectric Power Plant	P1	f_j^1(X)	0.00	0.00	0.72	1.00	1.00	0.00	1.00	0.510
		f_j^2(X)	0.00	0.00	0.28	0.00	0.00	0.00	0.00	0.040
		f_j^3(X)	1.00	1.00	0.00	0.00	0.00	1.00	0.00	0.419
Chontayacu Bajo Hydroelectric Power Plant	P4	f_j^1(X)	0.00	0.00	0.56	1.00	1.00	0.00	1.00	0.492
		f_j^2(X)	0.00	0.00	0.44	0.00	0.00	0.00	0.00	0.063
		f_j^3(X)	1.00	1.00	0.00	0.00	0.00	1.00	0.00	0.419
	P5	f_j^1(X)	0.00	0.00	0.67	1.00	1.00	0.00	1.00	0.505
		f_j^2(X)	0.00	0.00	0.33	0.00	0.00	0.00	0.00	0.047
		f_j^3(X)	1.00	1.00	0.00	0.00	0.00	1.00	0.00	0.419
Uchiza Village Center	P12	f_j^1(X)	1.00	1.00	1.00	1.00	1.00	0.00	1.00	0.878
		f_j^2(X)	0.00	0.00	0.00	0.00	0.00	0.00	0.00	0.000
		f_j^3(X)	0.00	0.00	0.00	0.00	0.00	1.00	0.00	0.146
	P13	f_j^1(X)	1.00	1.00	1.00	1.00	1.00	0.00	1.00	0.878
		f_j^2(X)	0.00	0.00	0.00	0.00	0.00	0.00	0.00	0.000
		f_j^3(X)	0.00	0.00	0.00	0.00	0.00	1.00	0.00	0.146

TABLE IX. RESULTS OF THE MAXIMUM SELECTED VALUE OF THE CLUSTERING COEFFICIENT CALCULATIONS IN THE CH - CHONTAYACU ALTO

Chontayacu Alto Hydroelectric Power Plant			
Points	**Unlikely**	**Occasional**	**Frequent**
P2	0.662	0.000	0.273
P1	0.510	0.040	0.419
P3	0.495	0.060	0.419

TABLE X. RESULTS OF THE MAXIMUM SELECTED VALUE OF THE CLUSTERING COEFFICIENT CALCULATIONS IN THE CH - CHONTAYACU BAJA

Chontayacu Bajo Hydroelectric Power Plant			
Points	**Unlikely**	**Occasional**	**Frequent**
P9	0.756	0.000	0.292
P10	0.728	0.036	0.292
P8	0.662	0.174	0.174
P6	0.646	0.011	0.273
P5	0.505	0.047	0.419
P7	0.494	0.061	0.419
P4	0.492	0.063	0.419

TABLE XI. RESULTS OF THE MAXIMUM SELECTED VALUE OF THE CLUSTERING COEFFICIENT CALCULATIONS IN THE CP-UCHIZA

Uchiza Village Center			
Points	**Unlikely**	**Occasional**	**Frequent**
P12	0.878	0.000	0.146
P13	0.878	0.000	0.146
P15	0.878	0.000	0.146
P21	0.878	0.000	0.146
P22	0.878	0.000	0.146
P11	0.756	0.000	0.292
P19	0.756	0.000	0.292
P20	0.756	0.000	0.292
P18	0.754	0.002	0.292
P23	0.754	0.002	0.292
P16	0.748	0.010	0.292
P14	0.743	0.017	0.292
P17	0.728	0.037	0.292

V. Results and Discussion

A. About the Case Study

Tables IX, X and XI show that the 23 points studied have a low probability of generating adverse biological effects to aquatic biota due to heavy metals for the three blocks established (CH-High, CH-Low and CP-Uchiza). In addition, we can point out that points P2, P9 and P12, which correspond to the highest values of clustering coefficients for the blocks CH High, CH Low and CP Uchiza respectively, represent very little bioavailability of heavy metals (As, Zn, Cu, Cd, Hg, Pb, among others) [11] in sediments. On the contrary, points P3, P4 and P17 present the lowest clustering values for each block, giving them greater importance due to their environmental implications, which will be explained in Fig. 5, 6 and 7.

In relation to the results, we must pay attention to the CP Uchiza block because the Clustering coefficient values are the highest in that block compared to CH-High and Low, and also because it is near the Uchiza locality with a high density of inhabitants.

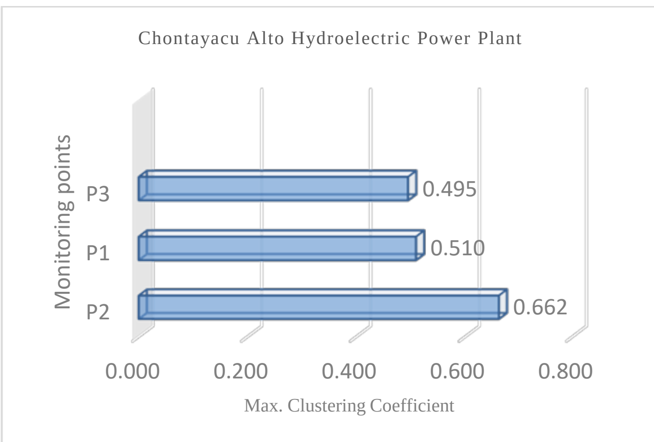

Fig. 5. Plot of Max. Monitoring Points for the Block (Chontayacu Alto Hydroelectric Power Plant).

According to Fig. 5, the following hierarchy is observed:

P2 > P1 > P3

Point P3 was sampled near the Santa Rosa de Oso hamlet, this population could have agricultural lands and pastures but upstream of their housing areas [12], which usually make use of fertilizers being a source of finding moderate and high concentrations of heavy metals such as Pb, Cr, Zn, As and Cd in soils and sediments, which could affect points P1 and P2. As a result of the scarce natural vegetation in the study area [2], soils can release heavy metals that flow through runoff flows, either in particulate or dissolved form, and can accumulate in sediments downstream of the river [13].

In addition, points P1 and P2, which are located exactly on the Chontayacu River, receive water from the upper part of the basin, where there are about 13 population centers approximately 11 km away, which carry out subsistence activities such as livestock, forestry and agriculture [2]. Likewise, this zone has little to moderate precipitation. However, in order for there to be a greater accumulation of toxic elements such as heavy metals in the sediment due to their transport or dragging, it is necessary to have heavy precipitation, thus generating rainfall runoff, as suggested by some studies [14].

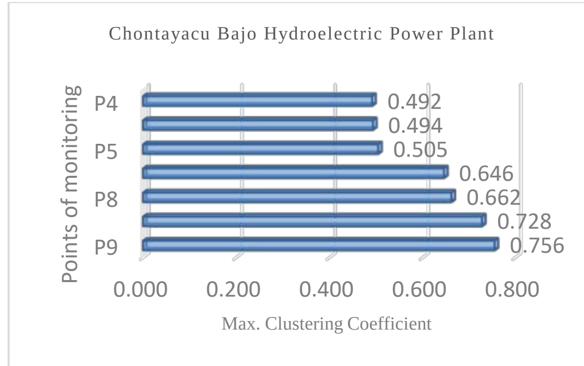

Fig. 6. Plot of Max. Monitoring Points for the Block (Chontayacu Bajo Hydroelectric Power Plant).

Fig. 6 shows the following hierarchy in relation to the clustering coefficient:

P9 > P10 > P8 > P6 > P5 > P7

Points P8, P9 and P10 show the highest values, mainly due to the increase in precipitation in the area [2], which removes deposited sediments and the presence of the Santillan and Cocalitos hamlets, respectively. These populations would be carrying out activities typical of the area, producing non-point sources of natural and anthropogenic origin that contribute to the increase in the concentration of heavy metals in sediments [3] at points P4 and P7. As part of the comprehensive ecological risk assessments in other rivers, the same problem of metal accumulation (Cu, Pb, Zn, Cr and Cd) [15]has been observed in nearby areas and the ecological impact [16]on aquatic biota, especially on the river's benthic communities [17].

On the other hand, point P5 also has a low value and is located in an intermediate zone of anthropogenic areas (grazing areas, livestock and farming activities and agriculture [2]), it may be affected by the geomorphology of the basin, which has varied slopes that could drag or accumulate sediments[18]. Regard, it is important to note that sediment entrainment can increase during periods of floods and high precipitation, which, together with agricultural activities [19] reduce the concentrations of As, Cd, Zn, among other metals. However, moderate concentrations of heavy metals may also be due to natural processes such as erosion, biological activity and volcanic emissions [3].

According to Fig. 7, we observe the following hierarchy of the Clustering coefficient values:

P12=P13=P15=P21=P22>P11=P19=P20>P18=P23>P16>P14 >P17

In relation to the present block, we observed that it is the most sensitive section due to the proximity to the Uchiza population center with a population of 21 285 censused for the year 2017 [20]. Therefore, the bioaccumulation of heavy metals in fish and aquatic biota [21] should be carefully monitored due to sediment transport as a result of the increase in precipitation recorded in the Uchiza station, in addition this section has little slope which facilitates the disposal of sediments [2]. On the other hand, as the results indicate, there is very little probability of generating an adverse biological effect, this is due to the fact that the metals under study have been analyzed in an integrated manner, being found in the ranges of low to moderate biological contamination in the short term [22]. But the accumulated risk could exceed the acceptable levels of toxic elements over a longer period [21].

On the other hand, hydroelectric power plant reservoirs have serious sediment accumulation problems [23], and their cleaning and treatment is complicated by the accumulation of heavy metals [24], and if the upstream sediment flow is not properly managed. Then water outflows could affect the health of the aquatic ecosystem located downstream, and several ecotoxicological studies [25] on organisms, mainly fish, even endanger the health of nearby populations, such as those in the Uchiza population center.

On the other hand, the retention of solids produced by reservoirs, which mainly belong to hydroelectric projects, modifies the transport of nutrients and organic matter [26]. The reduction in the granulometry of suspended sediment and the modification of the water regime leads to the transport of fine sediments [27], which may include heavy metals or others, resulting in the armoring of the riverbed and a modification of the river habitat that may endanger aquatic life as well as the riverbeds.

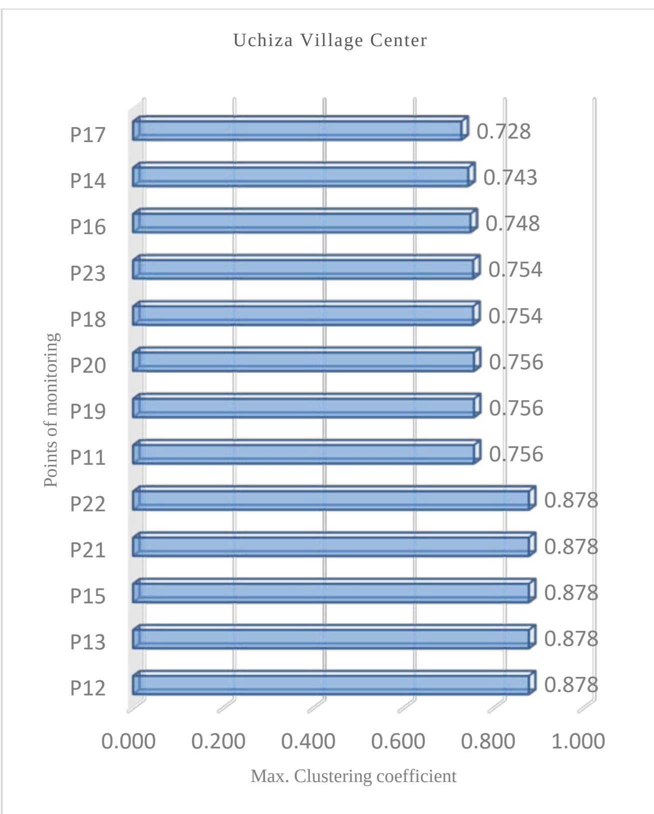

Fig. 7. Plot of Max. Monitoring Points for the Block (Centro Poblado Uchiza).

In relation to other studies [9], the Grey Clustering method was able to determine sediment quality in Jiangsu province, the results show serious contamination, pointing to the agricultural, energy and mining industries as the source of contamination.

B. About the Methodology

Unlike all the statistical methods that are traditionally used, Grey Clustering is a method that considers uncertainty in its analysis, which when performing the integration of the indicators in its evaluation; with respect to environmental pollution, it can be seen that there is a big problem regarding the high uncertainty presented in its different sources of pollution [28]. It can be evidenced that in the part of the contamination generated by the sediments produced by the different industrial activities [9], at the time of making their calculations they do not consider them synergistically, which indicates that their analysis is not the most appropriate. However, this method allows us to calculate in an appropriate way to classify and adequately evaluate the quality of sediments at an early stage of a project proposal.

VI. Conclusion

Sediment quality in the Chontayacu river basin was evaluated using the Grey Clustering method, which classified the 23 monitoring points according to each separation block. The results obtained will provide integrated information for decision making by the competent Peruvian authorities, as well as indicate the level of sediment contamination that should be taken into account for the proposal of hydroelectric projects that influence sediment transport and entrainment.

There are few studies on the application of the Grey Clustering method for the early evaluation of sediments from quality standards. It turns out to be very effective because it integrates several contamination parameters, as well as the consideration of uncertainty within the analysis.

Finally, for future research, it is necessary to establish standard values for measuring sediment quality according to the geomorphology of each river in Peru, in order to improve the results of the Grey Clustering method. Likewise, research should be proposed to use the Grey Clustering method for sediment evaluation in areas with mining activities, hydrocarbons, large-scale agricultural activities and mainly in hydroelectric power plants, in order to measure the effectiveness of the method with respect to this environmental component.

References

[1] Autoridad Nacional del Agua, “Informe de Monitoreo Participativo de la Calidad del Agua Superficial en la Cuenca del Río Huallaga - Febrero a Marzo del 2019”, Tarapoto, 2019. 2019.

[2] Hidroeléctricas Lima S.A., “‘Estudio Hidrológico para la Acreditación de la Disponibilidad Hídrica Superficial del Río Chontayacu para el Proyecto Central Hidroeléctrica Chontayacu Bajo,’” 2015.

[3] Organismo de Evaluación y Fiscalización Ambiental, “‘Informe de Evaluación Ambiental Temprana en el Futuro Emplazamiento del Proyecto Hidroeléctrico Chontayacu Alto y Bajo y Zonas Aledañas, en el distrito de Cholón, Provincia de Marañón, Departamento de Huánuco, durante el Año 2017,’” 2017.

[4] Servicio Nacional de Certificación Ambiental para las Inversiones Sostenibles, “Resolución Directoral N° 175-2019-SENACE-PE/DEAR", "APROBAR el Estudio de Impacto Ambiental Detallado del Proyecto ‘Centrales Hidroeléctricas Chontayacu Alto y Chontayacu Bajo,’” 2019.

[5] S. Liu, Y. Yang, and J. Forrest, Grey Clustering Evaluation Models. 2017.

[6] A. Delgado and I. Romero, "Applying the Grey Systems Theory to Assess Social Impact from an Energy Project," in Proceedings of the 2018 IEEE 25th International Conference on Electronics, Electrical Engineering and Computing, INTERCON 2018, 2018.

[7] Canadian Council of Ministers of the Environment, "Canadian Sediment Quality Guidelines for the Protection of Aquatic Life 'SUMMARY TABLES,'" Environ. Conserv., 2002.

[8] A. Delgado and H. Flor, "Selection of the best air purifier system to urban houses using AHP," in 2017 CHILEAN Conference on Electrical, Electronics Engineering, Information and Communication Technologies, CHILECON 2017 - Proceedings 2017-January, pp. 1-4.

[9] K. J. Chu and M. Tan, "Assessment of sediment quality in jiangsu coastal ocean based on grey clustering method," Appl. Mech. Mater., vol. 535, pp. 266–271, 2014.

[10] M. Quanz, R. Willis, D. Burr, R. Recoskie, and T. R. Walker, "Aquatic ecological risk assessment frameworks in Canada: a case study using a single framework in South Baymouth, Ontario, Canada," Environ. Monit. Assess., vol. 192, no. 8, 2020.

[11] A. Sormunen, Bioavailability assessment of sediment-associated organic compounds through desorption and pore-water concentration. 2008.

[12] S. Helfgott, S. Vargas, A. C. Gutiérrez, and M. Salvatore, "Aptitud de tierras y oportunidades para el desarrollo rural en perú," Bioenergia y Segur. Aliment. "BEFS," pp. 25–36, 2010.

[13] M. De Siervi, A. F. De Iorio, and C. I. Chagas, "Heavy metals in sediments and runoff waters in soils of the Matanza river basin, Argentina," Commun. Soil Sci. Plant Anal., vol. 36, no. 17–18, pp. 2303–2314, 2005.

[14] H. Jeong, J. Y. Choi, J. Lee, J. Lim, and K. Ra, "Heavy metal pollution by road-deposited sediments and its contribution to total suspended solids in rainfall runoff from intensive industrial areas," Environ. Pollut., vol. 265, p. 115028, 2020.

[15] H. G. Hoang et al., "Heavy metal contamination trends in surface water and sediments of a river in a highly-industrialized region," Environ. Technol. Innov., vol. 20, p. 101043, 2020.

[16] W. Ennaji, A. Barakat, M. El Baghdadi, and J. Rais, "Heavy metal contamination in agricultural soil and ecological risk assessment in the northeast area of Tadla plain, Morocco," J. Sediment. Environ., vol. 5, no. 3, pp. 307–320, 2020.

[17] R. B. Choueri et al., "Integrated sediment quality assessment in Paranaguá Estuarine System, Southern Brazil," Ecotoxicol. Environ. Saf., vol. 72, no. 7, pp. 1824–1831, 2009.

[18] I. Pérez and L. Rumbo, "Evaluación de la capacidad de transporte de sedimentos en el Rio Tinaco, municipio Tinaco del Estado Cojedes," vol. Vol. 14 (2, 2017.

[19] A. Kabata-Pendias, "Soil-plant transfer of trace elements - An environmental issue," Geoderma, vol. 122, no. 2-4 SPEC. IIS., pp. 143–149, 2004.

[20] Instituto Nacional de Estadística e Informática, "Perú: Crecimiento y distribucion de la poblacion total, 2017. Poblacion censada más población omitida," 2018.

[21] R. Fernandez-Maestre, B. Johnson-Restrepo, and J. Olivero-Verbel, "Heavy Metals in Sediments and Fish in the Caribbean Coast of Colombia: Assessing the Environmental Risk," Int. J. Environ. Res., vol. 12, no. 3, pp. 289–301, 2018.

[22] N. S. Buzzi and J. E. Marcovecchio, "Heavy metal concentrations in sediments and in mussels from Argentinean coastal environments, South America," Environ. Earth Sci., vol. 77, no. 8, pp. 1–13, 2018.

[23] Y. Huang, J. Wang, and M. Yang, "Unexpected sedimentation patterns upstream and downstream of the Three Gorges Reservoir: Future risks," Int. J. Sediment Res., vol. 34, no. 2, pp. 108–117, 2019.

[24] V. Angelaki and J. M. Harbor, "Impacts of flow diversion for small hydroelectric power plants on sediment transport, northwest washington," Phys. Geogr., vol. 16, no. 5, pp. 432–443, 1995.

[25] A. Serafim et al., "Evaluation of sediment toxicity in different Portuguese estuaries: Ecological impact of metals and polycyclic aromatic hydrocarbons," Estuar. Coast. Shelf Sci., vol. 130, no. May, pp. 30–41, 2013.

[26] J. Ruiz Bellet, J. Balasch, and A. Tena, "Suspended sediment transfer during a flood along the dam-regulated Segre river (NE Iberian Peninsula)," Cuaternario y Geomorfol., vol. 25, no. 3, pp. 87–101, 2011.

[27] C. Guo, Z. Jin, L. Guo, J. Lu, S. Ren, and Y. Zhou, "On the cumulative dam impact in the upper Changjiang River: Streamflow and sediment load changes," Catena, vol. 184, no. September 2019, p. 104250, 2020.

[28] A. Delgado and I. Romero, "Environmental conflict analysis on a hydrocarbon exploration project using the Shannon entropy," in Proceedings of the 2017 Electronic Congress, E-CON UNI 2017, 2018-January, pp. 1-4.

Dynamic Phrase Generation for Detection of Idioms of Gujarati Language using Diacritics and Suffix-based Rules

Jatin C. Modh[1]
Research Scholar
Gujarat Technological University
Ahmedabad, Gujarat, India

Jatinderkumar R. Saini[2]*
Professor and Director
Symbiosis Institute of Computer Studies and Research
Symbiosis International (Deemed University), Pune, India

***Abstract*—Gujarati is the language used for everyday communication in the state of Gujarat, India. The Gujarati language is also officially recognized by the constitution and the government of India. Gujarati script is based on the Devanagari script. An idiom is an expression, phrase, or word that has a different meaning from the literal meaning of the words in it. Idioms represent the cultural heritage of Gujarati language. Idioms are used in Gujarati language for effective communication and convey of an accurate message. No Machine Translation System does the accurate translation of Gujarati idioms to English or any other language. Different idiom phrases can be generated by adding diacritic(s) as well as suffix to the root or base form of the idiom. Many forms of single idiom make automatic idiom identification as well as machine translation more challenging. This paper focuses on the design and implementation of diacritics and suffix-based rules for dynamic phrase generation and detection of idioms of Gujarati language. This implementation helps in identifying Gujarati idiom present in any possible form in the Gujarati text. The obtained results with the execution of 7050 different Gujarati idiom phrases yield an accuracy of 99.73%. The results are encouraging enough to make the proposed implementation useful for Natural Language processing tasks related to Gujarati language idioms.**

Keywords*—Diacritic; Gujarati; idiom; machine translation system (MTS); natural language processing (NLP); suffix; unicode transformation format (UTF)

I. Introduction

Machine translation is the sub-field of Natural Language Processing (NLP) which is also a sub-field of Artificial intelligence (AI). Natural language processing is the study of any language by analyzing its structure and morphology. Natural language processing is challenging as different language has different grammatical structure. Vocabulary is important for the enrichment of the language. Idioms also contribute to the enrichment of the language. Idioms give impetus to the language. The idiom is an incomplete phrase as part of a sentence.

The people of Gujarat state are known as Gujarati. Idioms are the invaluable heritage of Gujarati language and for Gujarati people. Idiom in which a word or phrase becomes specific rather than its literal meaning. An idiom is in which a word or phrase becomes a specific meaning rather than its literal meaning. Gujarati idioms represent the customs, manners and beliefs of the people of Gujarat who speak Gujarati language. Gujarati idioms are the adornment of Gujarati language. Gujarati idioms are spoken in day-to-day communication and understood by every Gujarati.

When the speaker uses idioms, the listener is likely to mistakenly understand the literal meaning of the words if they do not already know the metaphor. Usually, idioms cannot be translated properly by any machine translation system. In most cases, the meaning changes when the idioms are translated into another language or it becomes misleading. In the Gujarati language, a particular idiom may have one or more forms or phrases. For the correct translation of Gujarati idioms into any other language, detection of all idiom forms or phrases is a very crucial task.

A. Gujarati Script

There are more than 46.1 million speakers of Gujarati language in the world. Gujarati is the 26th most spoken native language in the world [1]. Gujarati script is a script closely related to Devanagari script. It is a syllabic alphabet (abugida), in which every consonant carries the inherent vowel. Its principles are similar to Devanagari script principles [2]. It is distinguished from Devanagari script by not having a horizontal bar for its letter forms [3]. The Gujarati script is used to write the Gujarati language of Gujarat state in India. Gujarati language consist three different types of character: 34 independent consonants, 13 independent vowels and dependent vowel signs [3-5].

B. Gujarati Idioms

An idiom is a common phrase whose meaning is different from its literal meaning of the word. It is widely used and it has its popular meaning. For the correct translation of Gujarati idioms, identification of different forms of idioms from the input text is important. In Gujarati language, different and valid forms of idioms are possible by adding one or more specific diacritics marks to the base or root form of the Gujarati idiom. For example, હાથ આપ 'hath aap' is the base or root form of Gujarati idiom. It's one meaning is "to help" in English language. From root form હાથ આપ, other valid idiom forms like હાથ આપવો 'hath aapvo', હાથ આપી 'hath aapi', હાથ આપીને 'hath aapine', હાથ આપ્યો 'hath aapyo', હાથ આપેલો 'hath aapelo' etc. can be generated. Identification of all

*Corresponding Author

Gujarati idiom phrases is concentrated here. Surrounding words are important for the idioms having more than one literal meaning in Gujarati language [6-9]. But the dynamic generation, as well as identification of all Gujarati idiom forms from the base form of the idiom, are focused here only.

C. Diacritics

Diacritic or accent is a mark which is added to a word that changes its function, sense or pronunciation. A diacritical mark is attached to a letter or word to show appropriate stress or sound [10]. Diacritic marks are more common in Gujarati language. Diacritics can be inserted below, before, after or above to a letter or word. In Gujarati language, every consonant carries the natural vowel. Diacritic vowel signs are added after, before, above, or below a consonant. Table I shows the diacritics for Gujarati language [11].

D. Gujarati Idioms with Diacritics

Gujarati language is rich in its morphological structure. Even single idiom has many possible forms. For example મેથીપાક આપ 'methipak aap' is the base form of bigram idiom. Its English translation is "to beat", but the same idiom can be used by many ways in the Gujarati sentences. After applying all diacritics to base idiom મેથીપાક આપ 'methipak aap', other possible forms are generated like મેથીપાક આપા, મેથીપાક આપિ, મેથીપાક આપી, મેથીપાક આપુ, મેથીપાક આપૂ, મેથીપાક આપે, મેથીપાક આપૈ, મેથીપાક આપો, મેથીપાક આપૌ, મેથીપાક આપં, મેથીપાક આપૃ, મેથીપાક આપૅ, મેથીપાક આપૉ, મેથીપાક આપ્, મેથીપાક આપઁ, મેથીપાક આપઃ, મેથીપાક આપૄ, મેથીપાક આપ઼ .But these many forms of idioms are not used in sentences. Commonly idiom forms used in sentences are મેથીપાક આપી, મેથીપાક આપે, મેથીપાક આપો .Other forms are also possible like મેથીપાક આપીને, મેથીપાક આપ્યો, મેથીપાક આપવા, મેથીપાક આપેલો. So rules are needed to generate different idiom phrases or forms that can be used in sentences.

E. Unicode Transformation Format (UTF)

The Unicode standard is based on ISCII-1988 (Indian Script Code for Information Interchange). The Unicode Standard encodes the Devanagari characters, as well as the same layout, is followed for Gujarati language [3]. Unicode or Universal Transformation Format is a variable width character encoding. It is capable of all valid code points in Unicode. It is a superset of American Standard Code of Information Interchange (ASCII). UTF goes beyond 8-bits and supports all languages in the world.

TABLE I. DIACRITICS FOR GUJARATI LANGUAGE

◌ા ā	◌િ i	◌ી ī	◌ુ u	◌ૂ ū
◌ે E	◌ૈ ai	◌ો o	◌ૌ au	◌ં ṁ
◌ૃ r̥	◌ૅ Ē	◌ૉ Ō	◌્	◌ઁ
◌ઃ ḥ	◌ૄ rī	◌઼		

The rest of the paper is organized as follows: Section II presents the literature review related to the study of Gujarati morphology, diacritic identification methods, stemmer, and Gujarati idioms; Section III covers the methodology in which diacritics and suffix based rules are generated for dynamic idiom generation; it also describes proposed algorithm steps to identify the different Gujarati idiom phrases within the input text. In Sections IV and V, experiments with results, analysis, and observations are discussed; finally, the conclusion part is discussed in Section VI.

II. RELATED LITERATURE REVIEW

Various projects have been carried out for the study of different languages and their machine translation, but the scope of this paper is Gujarati language and related to idioms only.

Rakholia et al. [11] implemented diacritic identification and extraction Technique for Gujarati language using an 8-bit Unicode Transformation Format. They designed an independent tokenization algorithm for diacritic extraction from Gujarati documents. They claimed 99.58% accuracy in diacritic extraction.

Sheth et al. [12] proposed a stemmer called Dhiya for morphological level analysis for Gujarati language. They used inflections of Gujarati text and created rule sets and tested stemmer performance using EMILLE corpus. They claimed 92.41% accuracy of stemmer.

Patel et al. [13] proposed a hybrid morphological analyzer paradigm model for Gujarati language. They applied a supervised approach and used partial stemmer for the generation of word forms based on language-dependent rules. They built a manual dictionary of root words, classified words and covered 5000 nouns.

Baxi et al. [14] developed a morphological analyzer for Gujarati language using a hybrid combination of knowledge-based, statistical-based and paradigm-based approach. They claimed 92.34% accuracy with a knowledge-based hybrid model and 82.84% accuracy with a statistical hybrid model.

Fashwan et al. [15] proposed rule-based method for detecting the case ending diacritics but it was for modern standard Arabic texts. They applied morphological analysis, part of speech, syntactic analysis and word relation as well as position. They experimented with both morphological and syntactic processing levels for handling diacritization problem.

Dan et al. [16] described the languages that use diacritical characters and difficulty in recovery of missing diacritics. They evaluated and described a system for automatically recovering the missing diacritics in documents in the Romanian language. They suggested recovery suggestions for possible changes for Romanian diacritics.

Rakholia et al. [17] implemented a rules-based technique to identify stop words from the Gujarati text. They presented 11 rules to identify a complete list of Gujarati stop words. They applied an automatic and dynamic approach to identify stop words from Gujarati documents and claimed 94.08% average accuracy.

Research works involving Natural Language Processing (NLP) of Gujarati language have been presented for MTS for Sanskrit-Gujarati pair [18], comparison of morphologically analyzed words [19], bilingual dictionary implementation [20], constituency mapper [21], classification [22] and information retrieval [23] to name a few.

Based on this literature review and the analysis based on Gujarati diacritics, no researchers have identified various idiom forms from the input text using the rule-based diacritics insertion technique. No researchers have applied diacritics and suffix based rules on idiom base form to generate all possible idioms. Some researchers have experimented on diacritization but using different languages other than the Gujarati language. Some of the researchers have applied various techniques for creating rule-based stemmer and diacritics identification methods.

The proposed model deals with the Gujarati idioms and their possible forms of idioms. Due to many phrases or forms of Gujarati idioms, the detection of Gujarati idioms within input text is a challenging task. The proposed model detects all Gujarati idioms present in the text by generating and searching all possible forms of particular idiom within the text. The proposed model applies dynamic phase generation for the detection of Gujarati idioms using diacritics and suffix-based rules. All available machine translation systems encounter problems in translating Gujarati idioms. Idiom detection helps the researchers' community in translating the Gujarati idioms into any language.

III. Methodology

In Gujarati language, distinct 3240 n-gram Gujarati idioms were collected. But in Gujarati language, one idiom can be used in many ways i.e. one specific idiom may have many forms or phrases. Rules are generated and applied on idiom base form to generate all possible forms of idioms. So for the generation of idiom forms, the base idiom form is stored in the database and all possible forms of idioms are generated dynamically by inserting diacritics and suffix to the base idiom form by applying defined rules. This implementation is used to identify any forms of Gujarati idioms within input Gujarati text.

A. Rules Generation

Rules are generated and applied for n-gram idioms where n>=2. For bigram or 2-gram idioms, rules are applied on the 2nd word only and various idiom forms can be generated. For trigram or 3-gram idioms, rules are applied on 3rd word only and many idiom forms can be generated. For example, હાથ આપ 'hath aap' is the bigram idiom root form, so diacritic rules are applied on 2nd word આપ 'aap' only; whereas અક્કલ મારી જવ 'akkal mari jav' is the trigram idiom root form, so diacritic rules are applied on 3rd word જવ 'jav' only. In general, for n-gram idiom where n>=2, then many idiom forms can be generated by applying rules on last word of idiom root form. For 1-gram idioms as well as some n-gram idiom(s), different forms of idioms are not applicable.

Following Rules are identified to generate possible idiom forms from the given base form of n-gram idiom.

1) Rule 0: Root or base form only

For instance, idiom અધ્ધર રાખ 'adhdhar rakh', the same form is used in sentences as an idiom. So no diacritics need to be added on root verb રાખ.

2) Rule 1: Root form + Diacritics

For instance, idiom અધ્ધર રાખ 'adhdhar rakh', root verb is રાખ 'rakh'. Based on Table II, after adding single diacritics, possible other forms of idiom અધ્ધર રાખ 'adhdhar rakh' are 18: અધ્ધર રાખા, અધ્ધર રાખિ, અધ્ધર રાખી, અધ્ધર રાખુ, અધ્ધર રાખૂ, અધ્ધર રાખે, અધ્ધર રાખૈ, અધ્ધર રાખો, અધ્ધર રાખૌ, અધ્ધર રાખં, અધ્ધર રાખૃ, અધ્ધર રાખૅ, અધ્ધર રાખૉ, અધ્ધર રાખ્, અધ્ધર રાખઁ, અધ્ધર રાખઃ, અધ્ધર રાખૄ, અધ્ધર રાખ઼ .Out of these 18 generated forms, 05 common idiom forms used in Gujarati sentences are અધ્ધર રાખા, અધ્ધર રાખી, અધ્ધર રાખુ, અધ્ધર રાખે, અધ્ધર રાખો .Other 13 idioms forms are ignored as they are not used in general. By adding extra diacritics ં; other 02 commonly used forms are generated as અધ્ધર રાખાં and અધ્ધર રાખું.

TABLE II. Example of Diacritics Insertion to Letter ત 'T' and Word **આગ લાગ** 'AAG LAG'

Sr. No	Diacritics	Example **ત** + Diacritics	Example આગ લાગ + **Diacritics**
1	ા	**તા**	**આગ લાગા**
2	િ	**તિ**	**આગ લાગિ**
3	ી	**તી**	**આગ લાગી**
4	ુ	**તુ**	**આગ લાગુ**
5	ૂ	**તૂ**	**આગ લાગૂ**
6	ે	**તે**	**આગ લાગે**
7	ૈ	**તૈ**	**આગ લાગૈ**
8	ો	**તો**	**આગ લાગો**
9	ૌ	**તૌ**	**આગ લાગૌ**
10	ં	**તં**	**આગ લાગં**
11	ૃ	**તૃ**	**આગ લાગૃ**
12	ૅ	**તૅ**	**આગ લાગૅ**
13	ૉ	**તૉ**	**આગ લાગૉ**
14	્	**ત્**	**આગ લાગ્**
15	ઁ	**તઁ**	**આગ લાગઁ**
16	ઃ	**તઃ**	**આગ લાગઃ**
17	ૄ	**તૄ**	**આગ લાગૄ**
18	઼	**ત઼**	**આગ લાગ઼**

3) Rule 2: using suffix વ and diacritics

Root form + વ + Diacritic(s)

Example: for idiom અધ્ધર રાખ 'adhdhar rakh', રાખ 'rakh' is the root verb form. Based on Table II, possible other forms of idiom અધ્ધર રાખ 'adhdhar rakh' are 18: અધ્ધર રાખવા, અધ્ધર રાખવિ, અધ્ધર રાખવી, અધ્ધર રાખવુ, અધ્ધર રાખવૂ, અધ્ધર રાખવે, અધ્ધર રાખવૈ, અધ્ધર રાખવો, અધ્ધર રાખવૌ, અધ્ધર રાખવં, અધ્ધર રાખવૃ, અધ્ધર રાખવૅ, અધ્ધર રાખવૉ, અધ્ધર રાખવ્, અધ્ધર રાખવઁ, અધ્ધર રાખવઃ, અધ્ધર રાખવૄ, અધ્ધર રાખવ઼ .Out of these 18 generated forms, 04 common idiom forms used in Gujarati sentences are અધ્ધર રાખવા, અધ્ધર રાખવી, અધ્ધર રાખવુ, અધ્ધર રાખવો .Other idioms forms are ignored for considering rules generation.

By adding extra diacritics ં; other 02 commonly used forms are generated as અધ્ધર રાખવાં and અધ્ધર રાખવું.

Root form + વ + Diacritic ા + Diacritic ં

For idiom અધ્ધર રાખ,

અધ્ધર રાખ + વ + ા + ં = અધ્ધર રાખવાં

Root form + વ + Diacritic ુ + Diacritic ં

For idiom અધ્ધર રાખ,

અધ્ધર રાખ + વ + ુ + ં = અધ્ધર રાખવું

4) Rule 3: using suffix ય and diacritics

Root form + ્ + ય + Diacritic(s)

Example: for idiom અધ્ધર રાખ, રાખ is the root verb form. Common forms of idiom used in sentences are 5: અધ્ધર રાખ્યા, અધ્ધર રાખ્યાં, અધ્ધર રાખ્યુ, અધ્ધર રાખ્યું, અધ્ધર રાખ્યો

રાખ + ્ + ય + ા =રાખ્યા

રાખ + ્ + ય + ા + ં =રાખ્યાં

રાખ + ્ + ય + ુ =રાખ્યુ

રાખ + ્ + ય + ુ + ં =રાખ્યું

રાખ + ્ + ય + ો =રાખ્યો

5) Rule 4: using suffix ન and diacritics

Root form + Diacritic ી + ન + Diacritic ે

Example: for idiom સંસાર માંડ 'sansar mand', possible and common forms of idiom used in sentences are સંસાર માંડીને 'sansar mandine'

માંડ + ી + ન + ે = માંડીને

6) Rule 5: using suffix લ and diacritics

Root form + Diacritic ે + લ + Diacritic ા

Root form + Diacritic ે + લ + Diacritic ો

Example: for idiom અધ્ધર રાખ 'adhdhar rakh', Possible and common forms of idioms used in sentences are: અધ્ધર રાખેલા 'adhdhar rakhela', અધ્ધર રાખેલો 'adhdhar rakhelo'

રાખ + ે + લ + ા = રાખેલા

રાખ + ે + લ + ો = રાખેલો

7) Rule 6: using two suffixes and diacritics

Root form + વ + Diacritic ા + મ + Diacritic ા

Root form + વ + Diacritic ા + મ+ Diacritic ા + Diacritic ં

Example: for idiom અધ્ધર રાખ 'adhdhar rakh', Possible and common forms of idioms used in sentences are: અધ્ધર રાખવામા 'adhdhar rakhvama', અધ્ધર રાખવામાં 'adhdha rakhvaman'

રાખ + વ + ા + મ + ા = રાખવામા

રાખ + વ + ા + મ + ા + ં = રાખવામાં

8) Rule 7: using diacritic ે, suffix વ and diacritics

Root form + ે + વ + Diacritic(s)

Root form + ે + વ + ા

Root form + ે + વ + ી

Root form + ે + વ + ુ

Root form + ે + વ + ુ + ં

Root form + ે + વ + ો

If the last word of root form is રહ, then possible common forms of idioms used in sentences are રહેવા, રહેવી, રહેવુ, રહેવું, રહેવો

9) Rule 8: using diacritic ા, suffix and diacritics

Root form + ા + વ

Root form + ા + વ + ા

Root form + ા + વ + ા + ં

Root form + ા + વ + ી

Root form + ા + વ + ુ + ં

Root form + ા + વ + ો

Root form + ા + ય + ુ + ં

If the last word of root form is ભર 'bhar', then possible common forms of idioms used in sentences are ભરાવ, ભરાવા, ભરાવાં, ભરાવી, ભરાવું, ભરાવો, ભરાયું

10) Rule 9: using diacritic ો, suffix and diacritic(s)

For the last word of base idiom form is જ 'j'

Root form + ો + ઈ

Root form + ો + વ + ા

Root form + ો + વ + ા + ં

Root form + ો + વ + ી

Root form + ો + વ + ુ

Root form + ો + વ + ુ + ં

Root form + ો + વ + ો

If the last word of root form is જ, then possible common forms of idioms used in sentences are જોઈ, જોવા, જોવાં, જોવી, જોવુ, જોવું, જોવો

11)Rule 10: For the last word of base idiom form is જવ 'jav']Exception rule]

If the last word of root form is જવ, then possible common forms of idioms used in sentences are જવો, જવું, જવુ, જવી, જવાં, જવા, ગયો, ગયું, ગયુ, ગયાં, ગયા, ગઈ

12)Rule 11: For the last word of base idiom form is થવ 'thav' [Exception rule]

If the last word of root form is થવ, then possible common forms of idioms used in sentences are થવો, થવું, થવુ, થવી, થવાં, થવા, થયો, થયું, થયુ, થયાં, થયા, થઈ

13)Rule 12: For the last word of base idiom form is ખાવ 'khaav' [Exception rule]

If the last word of root form is ખાવ, then possible common forms of idioms used in sentences are ખાવો, ખાવું, ખાવુ, ખાવી, ખાવાં, ખાવા, ખાધી, ખાધાં, ખાધા

14)Rule 13: For the last word of base idiom form is લેવ 'lev' [Exception rule]

If the last word of root form is લેવ, then possible common forms of idioms used in sentences are લેવો, લેવું, લેવુ, લેવી, લેવાં, લેવા, લીધું, લીધુ, લીધાં, લીધા

15)Rule 14: For the last word of base idiom form is બેસ 'bes' [Exception rule]

If the last word of root form is બેસ, then possible common forms of idioms used in sentences are બેસી, બેસવો, બેસવું, બેસવુ, બેસવી, બેસવા, બેઠો, બેઠું, બેઠુ, બેઠી, બેઠાં, બેઠા

Table III shows all rules generated for inserting diacritics and suffix to root idiom form. Rule 0 is the original root form of idiom stored in the database. All rules from Rule 1 to Rule 9 are applied to all root forms of idioms. Rule 10 to Rule 14 are exception rules for idioms whose root form ends with જવ 'jav' થવ 'thav' ખાવ 'khaav' લેવ 'lev' બેસ 'bes'.

B. Proposed Model

To store the idiom database, MySQL was used for database software. PHP was used as a scripting language for the development platform. Visual Studio Code was used as an editor to write PHP coding. XAMP was used for the cross-platform local web server for the implementation of the model.

- Step 1: Data collection: A total of 3240 distinct Gujarati n-gram idioms were collected from different books and websites.
- Step 2: Pre-processing step: Except for 1-gram idioms, wherever applicable, the root form of each Gujarati idiom is generated; so diacritics and suffix can be added dynamically to the root form to generate various possible idiom forms.
- Step 3: Idiom database generated that contains idiom column in which root or base form of the idiom is stored once for each idiom. Idiom database contains root form idiom column with corresponding literal Gujarati meaning column for each idiom.
- Step 4: Accept input as text containing Gujarati idiom(s). Input text may contain any number of n-gram Gujarati idioms.
- Step 5: The algorithm searches all n-gram idioms from the input text by comparing input text with the idiom column of the idiom database.
- Step 6: Proposed algorithm generates all possible forms of idiom(s) for specific n-gram idiom. The algorithm uses the rules created and shown in Table III and generates all possible forms of idioms.
- Step 7: Generated various idiom form(s) are compared with the idiom form entered within the input text. If matching idiom form is found in the input text, the algorithm displays its possible literal meaning(s) in the Gujarati language; otherwise, it displays the text or idiom form as it is.

TABLE III. COMMON POSSIBLE IDIOM FORMS GENERATED USING RULE-0 TO RULE-14

Sr. No	Rule Description	Example for અધ્ધર રાખ 'adhdhar rakh'	Remarks
1.	Root Idiom	અધ્ધર રાખ	Rule 0
2.	Root Idiom + ા	અધ્ધર રાખા	Rule 1
3.	Root Idiom + ા + ં	અધ્ધર રાખાં	
4.	Root Idiom + ી	અધ્ધર રાખી	
5.	Root Idiom + ુ	અધ્ધર રાખુ	
6.	Root Idiom + ુ + ં	અધ્ધર રાખું	
7.	Root Idiom + ે	અધ્ધર રાખે	
8.	Root Idiom + ો	અધ્ધર રાખો	
9.	Root Idiom + **વ** + ા	અધ્ધર રાખવા	Rule 2
10.	Root Idiom + **વ** + ા + ં	અધ્ધર રાખવાં	
11.	Root Idiom + **વ** + ી	અધ્ધર રાખવી	
12.	Root Idiom + **વ** + ુ	અધ્ધર રાખવુ	
13.	Root Idiom + **વ** + ુ + ં	અધ્ધર રાખવું	
14.	Root Idiom + **વ** + ો	અધ્ધર રાખવો	
15.	Root Idiom + ્ + **ય** + ા	અધ્ધર રાખ્યા	Rule 3
16.	Root Idiom + ્ + **ય** + ા + ં	અધ્ધર રાખ્યાં	
17.	Root Idiom + ્ + **ય** + ુ	અધ્ધર રાખ્યુ	
18.	Root Idiom + ્ + **ય** + ુ + ં	અધ્ધર રાખ્યું	
19.	Root Idiom + ્ + **ય** + ો	અધ્ધર રાખ્યો	
20.	Root Idiom + ી + **ન** + ે	અધ્ધર રાખીને	Rule 4
21.	Root Idiom + ે + **લ** + ા	અધ્ધર રાખેલા	Rule 5
22.	Root Idiom + ે + **લ** + ો	અધ્ધર રાખેલો	
23.	Root Idiom+ **વ**+ ા +**મ** + ા	અધ્ધર રાખવામા	Rule 6
24.	Root Idiom+ **વ**+ ા +**મ** + ા + ં	અધ્ધર રાખવામાં	
	Rule Description	Example for માનમાં રહ	**Remarks**
25.	Root Idiom + ે + **વ** + ા	માનમાં રહેવા	Rule 7
26.	Root Idiom + ે + **વ** + ી	માનમાં રહેવી	
27.	Root Idiom + ે + **વ** + ુ	માનમાં રહેવુ	
28.	Root Idiom + ે + **વ** + ુ + ં	માનમાં રહેવું	
29.	Root Idiom + ે + **વ** + ો	માનમાં રહેવો	
	Rule Description	Example for ગળું ભર	**Remarks**
30.	Root Idiom + ા + **વ**	ગળું ભરાવ	Rule 8
31.	Root Idiom + ા + **વ** + ા	ગળું ભરાવા	
32.	Root Idiom + ા + **વ** + ા + ં	ગળું ભરાવાં	
33.	Root Idiom + ા + **વ** + ી	ગળું ભરાવી	
34.	Root Idiom + ા + **વ** + ુ + ં	ગળું ભરાવું	

35.	Root Idiom + ા + વ + ો	ગળું ભરાવો	
36.	Root Idiom + ા + ય + ુ + ં	ગળું ભરાયું	
	Rule Description	Example for પાણી જ	**Remarks**
37.	Root Idiom + ો + ઈ	પાણી જોઇ	Rule 9
38.	Root Idiom + ો + વ + ા	પાણી જોવા	
39.	Root Idiom + ો + વ + ા + ં	પાણી જોવાં	
40.	Root Idiom + ો + વ + ી	પાણી જોવી	
41.	Root Idiom + ો + વ + ુ	પાણી જોવુ	
42.	Root Idiom + ો + વ + ુ + ં	પાણી જોવું	
43.	Root Idiom + ો + વ + ો	પાણી જોવો	
EXCEPTION RULES			
Sr. No	**Rule Description**	**Possible forms of idioms used in sentences**	**Remarks**
44.	If last word of Root Idiom is **જવ** 'jav'	જવો જવું જવુ જવી જવાં જવા ગયો ગયું ગયુ ગયાં ગયા ગઇ	Rule 10
45.	If last word of Root Idiom is **થવ** 'thav'	થવો થવું થવુ થવી થવાં થવા થયો થયું થયુ થયાં થયા થઇ	Rule 11
46.	If last word of Root Idiom is **ખાવ** 'khaav'	ખાવો ખાવું ખાવુ ખાવી ખાવાં ખાવા ખાધી ખાધાં ખાધા	Rule 12
47.	If last word of Root Idiom is **લેવ** 'lev'	લેવો લેવું લેવુ લેવી લેવાં લેવા લીધું લીધુ લીધાં લીધા	Rule 13
48.	If last word of Root Idiom is **બેસ** 'bes'	બેસી બેસવો બેસવું બેસવુ બેસવી બેસવા બેઠો બેઠું બેઠુ બેઠી બેઠાં બેઠા	Rule 14

IV. Results

There is no automated tool available to measure accuracy in Gujarati language. The help of 2 or 3 linguists was taken, particularly for manual verification of results. Obtained results are recorded manually side-by-side to calculate accuracy. Individual idiom with their possible and valid forms is analyzed and tested each form for accuracy. For example, different forms of root form તરસ ખાવ 'taras khav' and હાથ આપ 'hath aap' are tested. The literal meaning of Gujarati idiom તરસ ખાવ is દયા બતાવવી 'daya batavavi' in Gujarati and 'showing kindness' in English.

INPUT TEXT=તરસ ખાવી તરસ ખાવા

FINAL OUTPUT=દયા બતાવવી દયા બતાવવી

INPUT TEXT=હાથ આપ હાથ આપવો હાથ આપી હાથ આપીને હાથ આપ્યો હાથ આપેલો

FINAL OUTPUT=મદદ કરવી મદદ કરવી મદદ કરવી મદદ કરવી મદદ કરવી મદદ કરવી

For experiments, overall 7050 different valid idiom phrases or forms were entered as input text and tested for results. Only 19 idiom forms were not correctly identified, whereas 7031 idioms forms were correctly identified by proposed system. The accuracy obtained for the correct identification of the Gujarati idiom(s) from the Gujarati text was 99.73%. Idiom phrases or forms which were not correctly identified due to similarity in their root forms; for example જામી જવું 'jami javu' and જામી જવી 'jami javi' both are distinct idioms with distinct literal Gujarati meaning but their root forms are same જામી જવ 'jami jav'. Other error issues were due to inclusion of comma, hyphen, space, non-breaking space between words for n-gram idioms where n>=2.

V. Analysis and Discussion

Some observations, results and language ambiguities came out during the experimentation.

1) Applied algorithm generates possible forms from the root idiom stored in the database. For example, અન્ન પાણી ઝેર થઈ જવ 'anna pani zer thai jav' is the root form stored in the database and it generates various forms and successfully identifies all forms like અન્ન પાણી ઝેર થઈ જવા, અન્ન પાણી ઝેર થઈ જવાં, અન્ન પાણી ઝેર થઈ જવું, અન્ન પાણી ઝેર થઈ ગયા, અન્ન પાણી ઝેર થઈ ગયું etc entered as input.

2) However, all collected idioms i.e. idiom root forms are inserted in the database, if the idiom does not exist in the database then algorithm won't able to identify its various forms. Therefore the algorithm returns particular idiom form as it is in the text without its literal Gujarati meaning.

3) For generating various idiom forms, algorithm inserts diacritic ં at the end of some idioms root forms and generates various idiom forms. For example, લેવુ and લેવું, લેવા and લેવાં, લીધુ and લીધું, લીધા and લીધાં etc are generated from the idiom root form *માથે લેવ* 'mathe lev'. This will help us in correcting any input spelling error of user and catches correctly all input idiom forms like *માથે* લેવુ and *માથે લેવું*, *માથે લેવા* and *માથે લેવાં*, *માથે લીધુ* and *માથે લીધું*, *માથે લીધા* and *માથે લીધાં.* and displays Gujarati literal meaning *જવાબદારી ઉઠાવવી* 'javabdari uthavavi'.

4) However, minimum and relevant rules are made; implemented algorithm may generate some general irrelevant idiom forms based on general examples. For example *અધ્ધર રાખ* 'adhdhar rakh' root form will generate *અધ્ધર રાખેવુ, અધ્ધર રાખેવું, અધ્ધર રાખેવો.* These extra forms are generated internally and it doesn't affect the output at all. Same rule will generate relevant forms for *માનમાં રહ* 'akkad rah' root form like *માનમાં રહેવુ, માનમાં રહેવું, માનમાં રહેવો.*

5) For 1-gram or unigram idioms, all idioms are stored as it is with its literal Gujarati meaning in the database. For example, *ઊંટવૈદ* 'untvaid', *ઝોડ* 'jhod', *ઢ* 'dh', *પ્રજ્ઞાચક્ષુ* 'pragnachakshu', *મખ્ખીચૂસ* 'makhkhichus', *લલ્લુ* 'lallu' etc are unigram idioms and are stored as it is in the database with its literal meaning in Gujarati language.

6) For n-gram idioms (n>=2), where root forms are irrelevant or only a single idiom form is possible, the same idiom phrase is entered in the idiom database. For example, *અટકળ પંચા દોઢસો* 'atkal pancha dodhso' is 3-gram idiom and its different forms are irrelevant in Gujarati language. So *અટકળ પંચા દોઢસો* 'atkal pancha dodhso' as it is stored in the idiom database instead of its root form. Another example, *અડિયલ ટટ્ટુ* 'adiyal tattu' is 2-gram idiom and its different forms are irrelevant in Gujarati language; so it is stored in the same form in the idiom database.

7) The algorithm additionally identifies nested idiom i.e. idiom within idiom from the input text. For example, *એક ઘાએ બે કટકા થવા* 'ek ghaae be katka thava' input produces intermediate output *તડ ને ફડ જવાબ થવો* 'tad ne fad javab thavo'; but *તડ ને ફડ* is also idiom and its literal meaning is *સ્પષ્ટ* 'spasht'; so for input text *એક ઘાએ બે કટકા થવા*, the final output is *સ્પષ્ટ જવાબ થવો* 'spasht javab thavo'.

An idiom database containing 3240 distinct idioms was created and tested 7050 different idiom phrases or forms. An implemented algorithm can find out all possible idiom phrases within Gujarati text by applying 15 rules of Table III on idiom root form whose root form or idiom is present in the idiom database. Spelling errors in Gujarati idioms can also be rectified by the proposed model.

VI. Conclusion

The proposed model that identifies all valid Gujarati idiom forms within Gujarati text and returns their literal Gujarati meaning was successfully implemented. Dynamic generation and identification of all Gujarati idiom phrases are focused here. By the exhaustive in-depth study of 3240 Gujarati idioms and their 7050 different idiom forms, 15 rules are generated. These rules are used to insert diacritic(s) and suffixes to the base or root form of Gujarati idiom. These dynamically generated different idiom forms are used to identify any idiom phrase inside the text. If the particular Gujarati idiom root form is not present in the database, then model returns the idiom as it is. So an entire assemblage of idioms is required for the success of the model. It is noteworthy that the proposed approach is not just diacritic based but also uses suffixes like વ, ય and ન.

Based on the results obtained from generating various possible idiom forms via rules implementation, it is advocated that the proposed rule-based system for generating various idiom forms is promising and worth implementation in the real world for the translation of Gujarati language idiom to any other language. Since Gujarati idioms are used in many forms in real life, all forms of idiom identification are challenging tasks for any machine translation system. The implemented rule-based system identifies most of the various forms of idioms. The proposed model opens the path for Gujarati idiom translation to any other language by finding all possible idioms forms within the input text. The task of context identification for multiple meanings idioms concerning the translation of Gujarati idioms is left for future scope.

References

[1] GujaratiLexicon, Gujaratilexicon.com, Available online: http://www.letslearngujarati.com/about-us (accessed May 23, 2021).

[2] Alejandro Gutman and Beatriz Avanzati, "Gujarati", The Language Gulper, Available online: http://www.languagesgulper.com/eng/Gujarati.html (accessed April 25, 2021).

[3] The Unicode® Standard Version 12.0 – Core Specification, Unicode, Inc., Available online: https://www.unicode.org/versions/Unicode12.0.0/ch12.pdf (accessed April 24, 2021).

[4] Wikipedia, "Gujarati language", https://en.m.wikipedia.org/wiki/Gujarati_language (accessed April 28, 2021).

[5] Xavier Nègre, "Multilingual Keyboard", Lexilogos 2002-2019, Available Online: https://www.lexilogos.com/keyboard/gujarati.htm (accessed April 28, 2021).

[6] Modh J. C. and Saini J. R., "Using IndoWordNet for Contextually Improved Machine Translation of Gujarati Idioms", International Journal of Advanced Computer Science and Applications(IJACSA), 12(1), 2021; Available online: http://dx.doi.org/10.14569/IJACSA.2021.0120128.

[7] Modh J. C. and Saini J. R., 2020, "Context Based MTS for Translating Gujarati Trigram and Bigram Idioms to English", 2020 International Conference for Emerging Technology (INCET), Belgaum, India, 2020, pp. 1-6, doi: 10.1109/INCET49848.2020.9154112; Available online: https://ieeexplore.ieee.org/document/9154112/.

[8] Modh J. C. and Saini J. R., 2018, "A Study of Machine Translation Approaches for Gujarati Language", International Journal of Advanced Research in Computer Science, Volume 9, No. 1, January-February 2018, pages 285-288; Available online: ijarcs.info/index.php/Ijarcs/article/download/5266/4497.

[9] Saini J. R. and Modh J. C., 2016, "GIdTra: A Dictionary-based MTS for Translating Gujarati Bigram Idioms to English", Fourth International Conference on Parallel, Distributed and Grid Computing (PDGC) 22-24 December 2016, pages 192-196, Available online: https://ieeexplore.ieee.org/document/7913143.

[10] Nordquist and Richard, "Examples of Diacritical Marks." ThoughtCo., Available online: https://www.thoughtco.com/what-is-a-diacritic-mark-1690444 (accessed April 24, 2021).

[11] Rakholia R.M. and Saini J.R., 2015, "The Design and Implementation of Diacritic Extraction Technique for Gujarati Written Script using Unicode Transformation Format", proc. of IEEE International Conference on Electrical, Computer and Communication Technologies (ICECCT-2015), Coimbatore, India, vol. 2, pages 654-659, Available online: https://ieeexplore.ieee.org/document/7226037.

[12] Sheth J. and Patel B., "Dhiya: A stemmer for morphological level analysis of Gujarati language," 2014 International Conference on Issues and Challenges in Intelligent Computing Techniques (ICICT), 2014, pp. 151-154, doi: 10.1109/ICICICT.2014.6781269.

[13] Patel C. and Patel M., 2016, "Paradigm Model based Hybrid Morph Analyzer for Gujarati using Partial Stemmer", IJSRD - International Journal for Scientific Research & Development Vol. 3, Issue 11, 2016, Available online: http://www.ijsrd.com/articles/IJSRDV3I110454.pdf.

[14] Baxi J, Patel P. and Bhatt B.,2015, "Morphological Analyzer for Gujarati using Paradigm based approach with Knowledge based and Statistical Methods", Twelfth International Conference on Natural

Language Processing (ICON-2015), Available online: https://cdn.iiit.ac.in/cdn/ltrc.iiit.ac.in/icon2015/icon2015_proceedings/PDF/49_rp.pdf.

[15] Amany Fashwan and Sameh Alansary, 2017, "SHAKKIL: An Automatic Diacritization System for Modern Standard Arabic Texts", Proceedings of The Third Arabic Natural Language Processing Workshop (WANLP), pages 84–93, Valencia, Spain, April 3, 2017, Available online: https://www.aclweb.org/anthology/W17-1311.pdf.

[16] Dan Tufiş and Alexandru Ceauşu, 2008, "DIAC+: A Professional Diacritics Recovering System", Institute for Artificial Intelligence, Romanian Academy, Available online: http://lrec-conf.org/proceedings/lrec2008/pdf/54_paper.pdf.

[17] Rakholia R.M. and Saini J.R., 2017, "A Rule-based Approach to Identify Stop Words for Gujarati Language", proc. of The 5th International Conference on Frontiers of Intelligent Computing: Theory and Applications (FICTA-2016), Bhubaneshwar, India, vol. 515, pages 797-806, Available online: https://link.springer.com/chapter/10.1007/978-981-10-3153-3_79.

[18] Raulji J.K. and Saini J.R., "A Rule Based Architecture for Sanskrit to Gujarati Machine Translation System", proc. of International Conference on Emerging Trends in Engineering, Science and Technology (ICRISET-2018), Anand, India, in press with IEEE.

[19] Raulji J.K. and Saini J.R., "Sanskrit Stopword Analysis through Morphological Analyzer and its Gujarati Equivalent for MT System", proc. of International Conference on ICT for Sustainable Development (ICT4SD-2019), Panaji, Goa, India, in press with Springer.

[20] Raulji J.K. and Saini J.R., "Bilingual Dictionary for Sanskrit – Gujarati MT Implementation", proc. of International Conference on ICT for Sustainable Development (ICT4SD-2019), Panaji, Goa, India, in press with Springer.

[21] Raulji J.K. and Saini J.R., "Sanskrit-Gujarati Constituency Mapper for Machine Translation System", proc. of IEEE Bombay Section Signature Conference (IBSSC- 2019), Mumbai, India, in press with IEEE.

[22] Rakholia R.M. and Saini J.R., 2017, "Classification of Gujarati Documents using Naïve Bayes Classifier", Indian Journal of Science and Technology, vol. 10(5), pages 1-9, Available online: http://indjst.org/index.php/indjst/article/view/103233/78147.

[23] Rakholia R.M. and Saini J.R., 2017, "Information Retrieval for Gujarati Language using Cosine Similarity based Vector Space Model", proc. of The 5th International Conference on Frontiers of Intelligent Computing: Theory and Applications (FICTA-2016), Bhubaneshwar, India, vol. 516, pages 1-9, Available online: https://link.springer.com/chapter/10.1007/978-981-10-3156-4_1.

Copy Move Forgery Detection Techniques: A Comprehensive Survey of Challenges and Future Directions

Ibrahim A. Zedan[1], Mona M. Soliman[2], Khaled M. Elsayed[3], Hoda M. Onsi[4]
Department of Information Technology
Faculty of Computers and Artificial Intelligence
Cairo University, Giza, Egypt

***Abstract*—Digital Image Forensics is a growing field of image processing that attempts to gain objective proof of the origin and veracity of a visual image. Copy-move forgery detection (CMFD) has currently become an active research topic in the passive/blind image forensics field. There has no doubt that conventional techniques and especially the keypoint based techniques have pushed the CMFD forward in the previous two decades. However, CMFD techniques in general and conventional techniques in particular suffer from several challenges. And thus, increasing approaches are exploiting deep learning for CMFD. In this survey, we cover the conventional and the deep learning based CMFD techniques from a new perspective. We classify the CMFD techniques into several classifications according to the detection methodology, the detection paradigm, and the detection capability. We discuss the challenges facing the CMFD techniques as well as the ways for solving them. In addition, this survey covers the evaluation metrics and datasets commonly utilized for CMFD. Also, we are debating and proposing certain plans for future research. This survey will be helpful for the researchers' as it master the recent trends of CMFD and outline some future research directions.**

Keywords—Image forensics; copy-move forgery detection (CMFD); conventional techniques; deep learning techniques

I. Introduction

Digital image forgery has already showed up in many disturbing forms and results in inestimable lose [1]. Digital image forgery is characterized as changing the original semantic meaning of an image by adding or erasing some significant features of the image for malicious aims [2], [3]. Digital image forgeries can be classified into three classes: Image Retouching, Image Splicing, and Copy-Move Forgery (CMF). Among the image forgery types, CMF is the most common and difficult forgery type. In CMF or image cloning, a part of an image (an authentic source region) is replicated and then pasted to another part of the same image (the forged region) [1], [4] in order to remove unwanted object or replicating desirable object [5]–[7]. Fig. 1 shows two examples of CMF where the cloned regions are marked with red color. The term cloned regions is commonly utilized to refer to the forged region as well as its source region.

To face the massive increase in image forgeries and its harmful effect, Digital image forensics (DIF) becomes an important area of recent research that verifies images reliability. DIF can be classified into passive and active techniques [7], [8]. Active forensic techniques require special hardware and software to embed authentication information such as digital watermark and digital signature into the image before distribution [7], [9]. To overcome such drawback, passive/blind forensic techniques are often used. Passive forensic techniques don't require any prior information about the image to be verified [10], [11]. This survey focuses on the passive forensic techniques proposed for copy-move forgery detection (CMFD) because CMF is a very challenging and popular forgery type. It is hard to differentiate between the actual and tampered images [12]. As the forged region is picked from the image itself, image properties are consistent all over the image and the forged region will be undetectable by methods that look for features inconsistencies [13], [14]. To make detecting CMF more difficult, several geometric and post-processing operations are performed [15].

As shown in Fig. 2, CMFD techniques can be classified according to its detection methodology into: visual similarity based, tampering artifacts based, and hybrid based techniques. Depending on visual similarity aims to specifically detect CMF and isn't able to detect any other forgery type. It can localize the forged region along with its source region based on assessing their similarity. Other forgery detection techniques are based on the fact that image forgery could present tampering artifacts that can be utilized to reveal the forgery. Depending on tampering artifacts is considered a general detection methodology for various forgery types. Applying such methodology for CMFD is only able to localize the forged region without its authentic source region. There are some works that combine the two detection methodologies together. Such works are able to detect and localize the cloned regions and can discriminate the forged region from its source region.

The CMFD techniques can be classified according to its detection paradigm into: conventional techniques, deep learning techniques, and the hybrid techniques. Also, CMFD techniques can be classified according to its detection capability or outcome. The outcome of a CMFD technique could be: (a) classifying an image as original or tampered, (b) localization of the cloned regions at the pixel level if the image is forged, and (c) classifying the cloned regions as source region or forged region [16][17].

Fig. 1. Examples of CMF. (a) CMF Image Processed by Noise Addition. (b) CMF Image with Ggeometric Ttransforms.

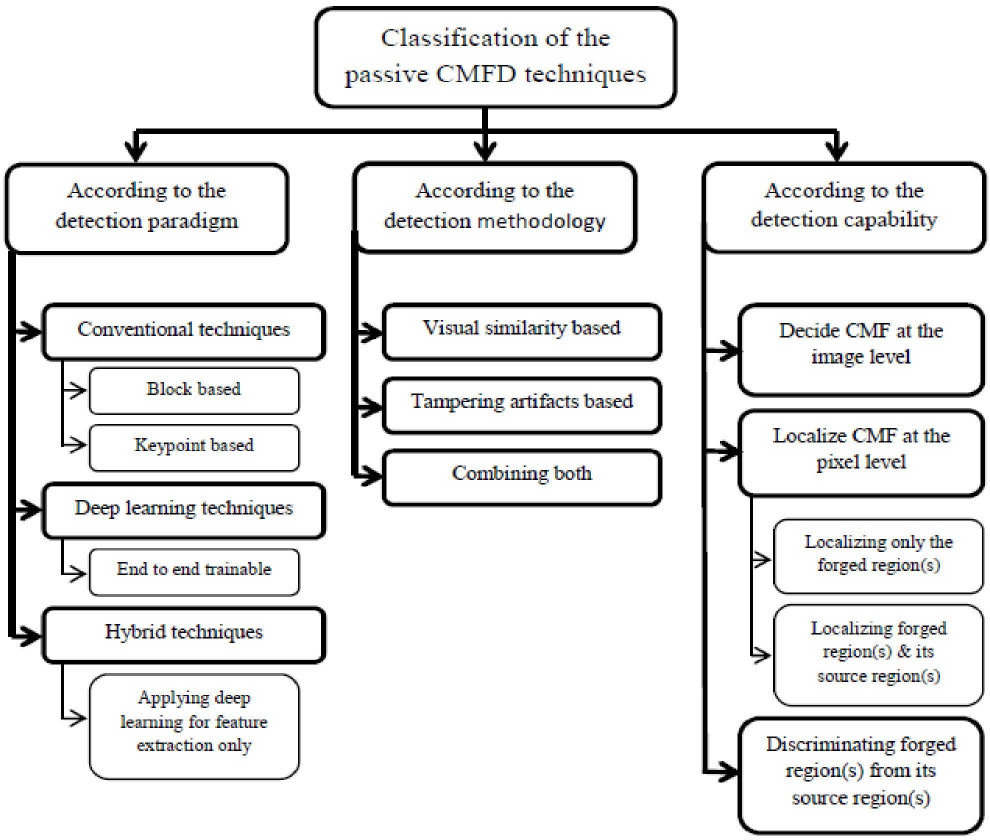

Fig. 2. Classification of the Passive CMFD Techniques.

Surveys such as [18]–[20] are recently proposed to summarize the CMFD techniques. Unlike previous surveys, we cover and organize the conventional techniques and the deep learning techniques for CMFD according to several aspects and with a new perspective. By analyzing the challenges facing CMFD along with the ways to solve them, a reader would be able to know the developing level of this field, and it also can inspire researchers to come up with new perspectives. In addition, we show how the performance of the CMFD techniques highly depends on the utilized dataset and the assessment mechanism. The rest of the survey is organized as follows. Section 2 presents the common procedure of the conventional CMFD techniques. Section 3 analyzes the challenges that face CMFD techniques and the solutions proposed to handle them. Section 4 presents the deep learning based CMFD techniques. Sections 5 and 6 present the standard evaluation metrics and the common datasets being utilized in literature, respectively. Section 7 highlights the important findings of the survey and outlines some future research directions. Finally, Section 8 concludes the survey.

II. Conventional CMFD Techniques

Conventional techniques are mostly adopt the visual similarity based detection methodology [13]. The majority of the conventional CMFD techniques are extract features that represent the image regions and assess the similarity between different regions to reveal the cloned regions [21]. Conventional CMFD techniques can be mainly classified into two categories: block based techniques, and keypoint based techniques [7], [17]. Conventional CMFD techniques have a common detection procedure that divided into three consecutive phases which are: feature extraction, feature matching, and forgery localization [17], [22]–[24].

A. Feature Extraction

It is common to convert RGB images into gray scale and extracting the image features from the intensity channel [22], [25]. Block based CMFD techniques divide the input image into fixed size overlapping square blocks [15], [26]. Numerous descriptors have been utilized in literature to extract the blocks features, e.g., Intensity-based features are utilized in [27], Discrete Cosine Transform (DCT) coefficients in [28]–[31], Principal component analysis (PCA) in [32], Singular Value Decomposition (SVD) [33], sector statistics [34], histogram of orientated gradients [35], Hu moments [36], [37], Local Binary Patterns (LBP) [38]–[41], zernike moments [42], [43], gaussian hermite moments [44], tetrolet features [45], tchebichef moments [46], blur moment invariants [47], polar complex exponential transform (PCET) moments [2], [48], etc.

For keypoint based CMFD techniques, the feature extraction phase consists of two steps: features detection and the description step [13], [17], [22]. Feature detection is to localize a set of keypoints/regions inside an image that are stable for geometric transformation [26]. In the description step, keypoints are described by encoding its surrounding region. SIFT, and SURF are the most popular algorithms utilized in CMFD which are able to perform the features detection and description. On the other hand, Harris corner detector, the maximally stable extremal regions (MSERs), and maximally stable color region are algorithms that only perform the features detection. Utilizing such features detectors requires using other algorithms for the features description.

B. Feature Matching

Image blocks or keypoints with similar descriptors should be matched [17], [23]. The regions of matched pairs are possibly cloned regions [22]. One way to match image features is to apply a global threshold on the distance between descriptors as in [29], [31], [33], [35], [43], [45]. Two blocks/keypoints are matched if the distance between their feature vectors is smaller than a threshold. This threshold can fluctuate from zero to one. A threshold closer to zero yields fewer but more accurate matches [13]. However, this matching method obtains a low accuracy [24], [26]. So, the two nearest neighbor (2NN) test is a widely utilized matching method in keypoint based CMFD techniques as in [10], [13], [17], [21]–[23], [49]. In the 2NN test, if the distance ratio between the nearest distance to the second nearest distance is less than a threshold, then the two keypoints are matched [26].

The 2NN test works well when a region is duplicated one time. As a result, the generalized nearest neighbor (g2NN) matching method is proposed to work when the region is cloned several times. The g2NN matching method iterates the 2NN test until the distance ratio become greater than the specified threshold [4], [5], [9], [14], [25], [26]. However, some matched keypoints still can't be recognized by the g2NN matching method. Accordingly, the transitive matching is utilized in [50] to enhance the matching relationship.

C. Forgery Localization

In the forgery localization phase, the geometric transform between the matched pairs is usually modeled. Such modeling is helpful to eliminate any mismatched pairs as cloned regions are commonly localized when detecting certain number of matched pairs with the same geometric transform [44]. Then, a forgery decision process is performed at the image level to decide if the given image is tampered with CMF or not. Finally, a localization process at the pixel level is performed to locate the cloned regions within tampered images.

In [30]–[32] the geometric transform between matched pairs is modeled by the shift vector between their coordinates. But, the shift vector concept is not suitable in case of rotation or scaling [44]. So, the geometric transform between the replicated regions is usually modeled by an affine homography [23]. Random Sample Consensus (RANSAC) is a widely used technique for accurate estimation of the affine homography that leads to the minimum error even when high number of mismatched pairs are exist [4]. So, RANSAC is utilized to estimate the affine transform and to filter some mismatched pairs in [51]–[53]. In [10] the Helmert transformation is utilized instead of the affine transformation because of its low degree of freedom and low computational complexity.

Several decision rules are utilized in literature to decide at the image level whether an image is tampered with CMF or not. In [27] The task of cloning detection is that of detecting two large similar regions bigger than an area threshold corresponds to certain percentage of the image size. The area threshold determines the smallest size of the cloned region to be detected. Large area threshold increase the misses while small values increase false alarms [28]. In [42] the forgery decision is specified if there are more than a particular number of matched pairs that meet the estimated affine transform and the similar regions are bigger than an area threshold.

Some works such as [34], [54]–[56] are just localize the cloned regions by depicting the matched pairs as lines. While other works reveal the cloned regions at the pixel level [24], [57]. Block based CMFD techniques are commonly localize CMF at the pixel level by relatively simple steps. First, a black image is created with the same size as the suspected image. Then, the blocks correspond to the matched pairs are simply assigned other color [30], [46], [47]. But, keypoint based CMFD techniques don’t have good localization power of cloned regions [10] as matched keypoints don’t cover completely the cloned regions [52]. To solve this issue, Cloned regions are commonly localized by the following steps [17]. First, the transformation matrices between the cloned regions are estimated. Then, all image pixels are transformed forward and backward. Next, the similarity between the original image and the transformed images is assessed with the correlation coefficients that are invariant to illumination changes. After that, correlation maps are smoothed to reduce the noise and transformed to binary images with a fixed correlation threshold [1], [26], [58], [59]. Finally, small isolated regions are eliminated and holes are filled [13], [16], [24], [36]–[38], [41], [60], [61]. Such final post processing can be accomplished by morphological operations, specially designed filter as in [39], or an area threshold as in [37], [62].

In [7], [8], [10], [49], [63] the cloned regions are localized by different methods rather than the common work flow described previously. In [63] to localize the cloned regions; image registration through bi-cubic interpolation is utilized. In [8] the cloned regions are localized by region growing technique through Hu's moments. In [49] cloned regions are localized based on multi-scale analysis and a voting process. Some works such as [7], [10] utilized the superpixels segmentation algorithms to localize the cloned regions.

III. Formulation of Challenges

This section analyzes the challenges that face the CMFD techniques in general and provides a comprehensive survey on different strategies adopted by the conventional CMFD techniques to handle these challenges. Table I shows the phases of the conventional CMFD techniques and the challenges that face each phase along with the solutions.

A. Geometric Transforms

Geometric transforms such as scaling, and rotation are usually applied to the forged regions to fit the scene and to mislead the human eye. Scaling or rotating an image region introduces some changes in the pixels values due to the interpolation error. Block based techniques fail when large rotation and scale are operated on the cloned regions [26] because of the de-synchronization in searching of matched blocks [60]. Dividing the image into overlapping square blocks with static size isn't able to detect CMF with large scaling and rotation regardless of whether the utilized features are scaling and rotation invariant. Utilizing circular blocks solves to some extent CMF with rotation. To handle CMF with scaling, adopting a pyramid model and performing the matching process across several scales are needed [42].

The majority of the keypoint based techniques are robust against geometric transformations, including large rotation and scale. But when utilizing a keypoints detector that wasn't robust by nature to certain geometric transforms, it is essential to make it invariant to geometric transforms such as [64], [65]. In [64], [65] to make Harris corners invariant to scaling, stable points across a scale space are only identified.

Conventional CMFD techniques such as [6], [13], [34], [62] tried to enhance its robustness against reflection because reflection needs special handling. In [34], [62] To detect CMF with flipping, a matching process between the feature vectors of the original image and the flipped image is performed. In [6], [13] a flip invariant SIFT descriptor is utilized in which each image keypoint is represented by two descriptors that reorganize the SIFT descriptor with both clockwise order and anticlockwise order. Among all the geometric transforms, deformation affect greatly the performance of the conventional CMFD techniques as it is a nonlinear transformation that can't be modeled well by an affine model [13]. Dealing with nonlinear geometric transformations still needs to be explored.

TABLE I. Conventional CMFD Techniques: Phases, Challenges and Proposed Solutions

Phases	**Challenges**	**Solutions**
Feature Extraction	Geometric Transforms	Utilizing invariant features
		Multi scale analysis & matching
		Utilizing circular blocks
	Post Processing Operations	Performing image enhancement before extracting features
	Dealing with Small or Smooth Cloned Regions	Increasing the image contrast and resolution
		Utilizing hybrid keypoints detectors
		Lowering the contrast threshold
		Adopting small block size
		Combining keypoint based and block based techniques
Feature Matching	Image Continuity	Avoid matching of neighboring features
	Handling Image Self-Similarity and Similar But Genuine Objects	Enhancing discrimination power of the descriptors
		Eliminating outlier matches
		Accurate estimation of the thresholds
		Accurate estimation and validation of the geometric transformations
	The Matching High Computational Complexity	Decreasing the image dimension and number of features
		Utilizing low dimensional and binary descriptors
		Sorting and organizing the image features before matching
		Matching search space reduction
		Searching for approximate matching
	Un Consistent Matching Order	Utilizing clustering or segmentation based algorithms
Forgery Localization	Dealing With Multiple Cloned Regions	Performing clustering of the matched pairs
		Performing iterative localization
	Discriminating Forged Region from its Source Region	Utilizing hybrid detection methodology

B. Post Processing Operations

Post processing operations are generally applied to make the detection of CMF harder to detect. The most utilized post processing operations are JPEG compression, image blurring, and noise addition [1]. CMFD techniques achieve better detection accuracy when the intensity of the post processing operation is minimal [16]. When handling low quality images or images with high noise, the performance of the CMFD algorithms is decreased because the pixel values are disturbed that result in less number of correct matched pairs, more false positives, and more false negatives [1], [34], [66].

Numerous conventional CMFD techniques tried to face image post-processing attacks. In [38], [39], [60] image is filtered by Gaussian low pass filter because the low frequencies are more steady to post processing operations. In [42] each image block is filtered by an adaptive wiener filter which can remove noise while preserving edges. In [67] the input image is enhanced before extracting the SIFT features. First, high pass filter (HPF) is applied. Then, Butterworth low pass filter (BLPF) is utilized for noise reduction. In [16], [29], [41] the stationary wavelet transform (SWT) is utilized to reduce the noise effect. Image blurring effect specially the performance of the keypoint based CMFD techniques [13] as a lot of keypoints are lost due to blurring. Dealing with blurring is similar to dealing with smooth or small cloned regions. Several solutions are reviewed in the next sub-section.

C. Dealing with Small or Smooth Cloned Regions

With small cloned regions, the performance of the CMFD techniques is low because of insufficient number of correct matched pairs [34]. Block-based CMFD techniques usually adopt small block size for revealing small cloned regions. But, small block size can't yield robust features [3] and results in large number of blocks that increases the computational cost. On the other hand, large block size decreases the computational cost but can't detect small cloned regions [3], [44]. So, block-based CMFD techniques face a difficulty in selecting the suitable block size [3]. It is worth noting that block based CMFD techniques work well in smooth regions.

Keypoint based CMFD techniques fail to detect the forgery if insufficient keypoints are identified that results in insufficient correct matched pairs, and that is the situation when dealing with smooth or small cloned regions or when the input image is of low resolution [4], [68]. One way to extract more keypoints is to utilize hybrid/multiple detectors such as in [5], [9], [26]. Other works such as [15], [25] applied the keypoints detectors on the opponent color space rather than the intensity channel to get an adequate number of keypoints.

Image keypoints are generally detected by applying certain contrast threshold [58]. Several works increase the keypoints in the whole image by simply lowering the contrast threshold of all images under investigation such as [9], [24]. As the suitable contrast threshold could varies from one image to another, other works tried to choose the suitable contrast threshold separately for each test image. In [17], [22], [23], [55], [69] particle swarm optimization (PSO) algorithm is utilized to generate customized parameter values for each image. Several works such as [1], [4], [56], [66], [70], [71] increase the entire image contrast or resolution instead of decreasing the contrast threshold. In [70] single image super resolution algorithm is utilized to increase the image resolution. Similarly in [4] the image is up-sampled. In [1], [56], [66] the contrast limited adaptive histogram equalization algorithm is utilized to increase the image contrast. Similarly in [71] the dynamic histogram equalization method is utilized.

Increasing the keypoints in the whole image by adopting a small contrast threshold has several drawbacks. Keypoints in the rough regions will increase quicker than in smooth regions [68] which is pointless. This phenomenon is called the non-uniform distribution of the image keypoints [58]. Also adopting a small contrast threshold will trigger numerous unstable keypoints, and expand false matching possibility. More redundant keypoints are located at nearby locations and its corresponding descriptors are similar [24].

Several works such as [12], [52], [54], [58], [68] aim to overcome the non-uniform distribution of the image keypoints. In [58] the non-maximum value suppression algorithm is utilized. First, all possible keypoints are initially selected. Then, redundant keypoints are filtered out. In [68] the image is segmented into smooth and rough layers. Swarm intelligence algorithm is applied for each layer separately to find its customized parameter values. In [12], [52], [54] image is segmented into non-overlapping superpixels. The way of localizing the keypoints varies from smooth regions to texture regions to make keypoints uniformly covering the entire image. Other works such as [5], [71] process specific regions within the image to extract more keypoints and more matched pairs. In [5] any suspicious region that contains insufficient number of matched keypoints is up-sampled and re-examined. In [71] matched keypoints are grouped into regions. The obtained regions are scaled up instead of scaling up the entire image.

As block based CMFD techniques work well in case of smooth regions, a combination of keypoint based and block based methods is proposed for effective CMFD as in [11], [61], [72]. In [11], [61] SIFT based method is utilized to detect forgery in rough regions. To detect forgery in smooth regions, Zernike moments are utilized in [61] while the Fourier Mellin transform (FMT) is utilized in [11]. In [72] to handle cloned regions with insufficient number of matched pairs, two regions centered on the keypoints location of each matched pair are obtained. These regions are examined by Zernike moments.

D. Image Continuity

Because of the continuity of images, the similarities of neighboring blocks/keypoints are high and hence are wrongly matched. Also in block based CMFD techniques, the image is usually divided into overlapping blocks. Blocks with an overlapping ratio are highly similar and wrongly matched. So, in [2], [28], [30], [32], [42], [47], [53], [60] matched pairs are removed if their spatial separation is below a threshold. The spatial separation threshold defines the smallest spatial distance between the cloned regions to be detected [47]. The choice of the spatial separation threshold should consider its relationship with the image content and size [61].

Other solution avoids the selection of the spatial separation threshold by segmenting the image into non-overlapping superpixels and requires that two image features are comparable if they are belonging to different superpixels [4], [58], [61], [73]. But, this solution isn't able to detect CMF in case of two cloned regions are in the same superpixel [73]. Similarly in [3] the image blobs are detected utilizing DoG and BRISK keypoints in different blobs are only matched.

E. Handling Image Self-Similarity and Similar But Genuine Objects

The intrinsic self-similarity of natural images is considered the other reason of wrong matching in addition to the image continuity [17]. In addition, images might have similar but genuine objects (SGO). CMFD techniques which are based on a simple hypothesis that similar regions in an image are often made by CMF are commonly produce false positives in images having SGO [64], [65], [74]. The ability to distinguish cloned regions from SGO is essential for a successful CMFD technique [64], [65]. In the next paragraphs, we discuss how the selected features, the matching method, and the choice of the thresholds can play a vital role to deal with image self-similarity and to distinguish cloned regions from SGO.

The majority of the conventional CMFD techniques extract its features from gray scale images. But, some CMFD techniques such as [58], [75] perform the feature extraction phase in a certain color space to enhance its discrimination power and hence its performance. In [75] each color channel is considered separately. Matched blocks that are common in all color channels are considered as forged. In [58] OpponentSIFT is utilized for feature extraction. OpponentSIFT describes all the channels of the opponent color space utilizing SIFT.

Texture descriptors are useful to differentiate between really cloned regions and SGO. Also, high dimensional descriptors are generally more distinctive. As a result, several works such as [52], [53], [57], [64], [65], [76] enhance its discrimination power and hence its matching performance by utilizing texture features or utilizing high dimensional descriptors. In [53] Image blocks are described by multiple LBP operators. In [76] two regions are verified as cloned if their GLCM contrast difference is below a threshold. In [57] SIFT descriptor is combined with the histogram of the reduced LBP. In [64], [65] LBP as well as DCT and SVD are utilized to describe the detected Harris keypoints. In [52] PCET is utilized to extract descriptors of the detected SURF keypoints.

Cloned regions are commonly chosen from meaningful objects [26]. As a result, false matched pairs of intrinsic self-similar regions are usually isolated and much more scattered. Based on such idea, several conventional CMFD techniques such as [47], [77]–[79] reduce the false matching rate basically by its matching process. In [47] two blocks are matched if its neighboring blocks are also matched to each other. The number of neighboring blocks to be checked for similarity defines the smallest size of the cloned region to be detected. In [77] a match is decided when the keypoints from an image and its k nearest neighbors are matched to that of the suspicious area. In [78] the matching process is done among objects rather than single point matching. In [79] clusters of keypoints are matched instead of single point matching.

Other way to reduce the false matching rate is to adopt an outlier removal process of wrong matches after performing the matching process as in [45], [66]. In [66] the outlier matches are eliminated by combining the guaranteed outlier removal algorithm with the RANSAC algorithm. In [45] Fast outliers filtering method is utilized instead of RANSAC. But, such few outlier matches might correspond to a CMF with small cloned regions and should be further verified.

Several conventional CMFD techniques utilize the segmentation or the clustering methods to eliminate false matches [24]. The regions/clusters that contain a few matched pairs are discarded [14], [26], [50], [59]. The segmentation and the clustering based algorithms suffer from high time and space complexity [66]. Also it is hard to decide a segmentation or clustering algorithm and its associated parameters that are suitable for all images [24]. The superpixel segmentation algorithms are commonly utilized. The initial superpixel size has significant impact on the forgery detection performance. An appropriate initial superpixel size should consider the image size and content. In case of textured images, an initial superpixel size of low value should be utilized. While, a high value should be adopted as an initial superpixel size when dealing with simple images [54]. Many works have taken into account the image size and content when selecting the initial superpixel size. But, no one has dealt with the fact that a single image could contain both a smooth part and a texture part and they should be segmented differently.

Clustering based algorithms such as [10], [13], [49] aim to filter out false matches by adopting the geometric inconsistency idea. In [13] the slope of all lines connecting matched pairs is grouped in different clusters. Within each cluster, outlier matched pairs are removed if its locations are far from the cluster centroid location. In [10], [49] matched pairs are grouped into clusters dependent on the spatial separation among them and the angle of the line that connects them relative to the x-axis. Furthermore, in [10] the Helmert transformation is utilized to merge clusters with similar transformation parameters. Despite the fact that the hierarchical agglomerative clustering (HAC) is the common clustering algorithm utilized in CMFD, it is sensitive to outliers and noise. So, in [21], [51], [66], [71] the DBSCAN (density-based spatial clustering of applications with noise) is utilized.

The thresholds related to the matching process acquire special significance in handling image self-similarity and SGO. To decide an appropriate value of the matching threshold, a training phase is needed. But, the matching threshold may change from one image to another [53]. So, in [2] an appropriate matching threshold is estimated for each image utilizing PSO and the histogram of block similarities. After localizing suspected regions within an image, it is common to compute the correlation coefficient between the suspected regions. Then, a correlation threshold is utilized to differentiate really cloned regions from SGO. High value of the correlation threshold increases the misses' rate while a low value increases the false alarm rate. Many works such as [17] have focused on selecting an appropriate value of the correlation threshold. In [17] customized correlation threshold is utilized to detect each image rather than utilizing a fixed threshold for all images.

It is essential to assess the accuracy of the estimated geometric transformation [5] as inaccurate estimation of the geometric transformation results in wrong localization of cloned regions. So, many CMFD techniques have focused on the accurate estimation and validation of the geometric transformation such as [5], [13], [24]. In [24] a homography validation and inlier selection technique is proposed. For each correctly matched keypoints, the difference of the dominant orientations should be consistent with the estimated homography. In [5] inaccurate affine transformations are filtered by utilizing the Bag of Word idea. In [13] the affine transformation parameters are refined iteratively.

F. The Matching High Computational Complexity

Feature matching is the main phase that consumes time [2], [60] because of the huge number of image features and their high dimensional descriptors [80], [81]. Keypoint based techniques have a lower computation cost compared to the block based techniques because the number of keypoints for an image is generally smaller than the number of blocks [26], [82]. However, several keypoint based CMFD techniques try to increase the number of keypoints inside an image to handle small or smooth cloned regions. In this case, the computational complexity also needs to be reduced.

One way to reduce the matching time is to decrease the number of image features to be extracted as in [15], [48]. In [48] the features are computed for only the fundamental objects rather than all the overlapping blocks of the image. In [15] Image is divided into MSERs. SIFT keypoints that aren't belong to any MSER are excluded to reduce the matching cost. Decreasing image dimension results in a reduction of the number of features. In [42] high resolution images are scaled down. In [27], [37] the image is decreased in dimension by Gaussian pyramid. In [21], [32], [36], [51], [53] the wavelet transform is utilized. However, decreasing the number of image features reduces the performance of the CMFD because the high details in the image have been lost [21].

Low dimensional descriptors and binary descriptors are more desired for fast matching. As a result, several works such as [2], [21], [28], [46], [47] tried to decrease the matching time by reducing the descriptor length through SVD or PCA. As SURF descriptor has low dimensional space compared to SIFT, so matching SURF descriptors is fast [81]. Also, binary descriptors are favored for fast matching as they are matched quickly by simple XOR operation through the hamming distance [83]. As a result, the BRISK binary descriptors are utilized in [83]. Similarly in [84] The SIFT descriptors are binarized and matched to reduce the matching time.

Several works tried to reduce the matching search space and decrease the number of comparisons needed by means of segmentation or clustering such as [3], [52], [80]. In [52] image regions are separated into texture regions and smooth regions. The image features are matched separately in smooth regions and in texture regions. In [3] the image background is eliminated prior to matching image features to speed up the matching process. In [80] image keypoints are grouped into clusters using the Fuzzy C means clustering technique. Each cluster center and its close keypoint are matched only to other clusters instead of matching all the image keypoints.

To reduce the matching time, it is common to sort or organize the image features before matching [43]. For block based CMFD techniques, Lexicographic sort is a widely utilized sorting method that makes comparable feature vectors closer to each other. A feature vector will be checked for similarity with just a specific number of neighboring vectors [40]. For computational efficiency, some conventional CMFD techniques such as [7], [60] utilized approximate matching instead of exact matching. In [1], [55], [62], [66], [81] the best bin first search algorithm is utilized which is based on a variant of the KD tree to search for approximate nearest neighbor. It is common to use the Euclidian distance to calculate the distance between image descriptors. But for computational efficiency, the cosine similarity is utilized in [25], [73], [79].

G. Inconsistent Matching Order

It is common to use RANSAC to estimate the geometric transform from the authentic source region to its forged region or vice versa. The estimation of the geometric transformation is order-dependent. If the geometric transform estimated from the source region to its forged region is T, then the geometric transform estimated from the forged region to its source region is T^{-1}. As a result, the matched pairs fed into RANSAC should have consistent matching order; otherwise they could result in erroneous estimation [24]. But in keypoint based CMFD techniques, keypoints are detected from the image without any spatial order. So, the matching process can't guarantee a consistent matching direction [24]. To solve this problem, the segmentation and the clustering based algorithms are utilized to facilitate a consistent matching direction from one region/cluster to the other region/cluster [24]. On the other hand, block based CMFD techniques aren't suffered from this problem at all.

H. Dealing with Multiple Cloned Regions

Some conventional CMFD techniques such as [22], [23] aren't able to handle images with multiple cloning. To handle images with multiple cloning, two issues should be considered. First, the adopted matching method should able to perform multiple matching if exist of the same block/keypoint. As mentioned before, matching methods such as G2NN and transitive matching are able to perform multiple matching. Second, the matched pairs may follow diverse geometric transformations in case of multiple cloned regions [24].

Multiple cloning is commonly handled through clustering the matched pairs and iterating the localization task [24], [26]. Clustering of matched pairs aims to group pairs that follow the same affine transformation [58], [70], [81]. In [24] the localization task runs in an iterative manner. In each iteration, RANSAC algorithm is utilized to estimate one affine homography using all the matched pairs from two contiguous local patches. In [26] the RANSAC algorithm is executed iteratively to estimate the transformation matrices. After each iteration, the inliers satisfying the previously estimated transformation are excluded from the next iteration.

Clustering based algorithms such as [1], [14], [61], [70], [81] clustered the matched pairs by their location utilizing HAC. Especially in keypoint based CMFD techniques, clustering of the matched pairs based on their location has two drawbacks: (i) the inability to separate the cloned region when cloned region is close to its source region and (ii) the difficulty to identify the cloned region as a single region, when it contains scattered keypoints [59]. To handle these drawbacks, in [58], [59] matched pairs are clustered using the J-Linkage algorithm based on a transformation domain rather than the spatial domain. In J-Linkage clustering, a number of affine transformation hypotheses are generated randomly. Each matched pair is assigned to an initial cluster. HAC process is operated on the clusters. To reduce the computational cost of J-Linkage clustering, image is segmented into superpixels in [58]. Then, the matched pairs are grouped based on the correspondence between the superpixels to produce a small number of initial clusters of the J-Linkage algorithm [58].

I. Discriminating Forged Region from its Source Region

The majority of the CMFD techniques lack the ability to classify the cloned regions into source and forged regions. Providing this capability enriches the CMFD technique. Depending on visual similarity to reveal the cloned region can't discriminate between the forged region and its source region. To provide such ability, detection of tampering artifacts should be integrated with the visual similarity based detection methodology as in [85]. In [85] a resampling based method is combined with SIFT based CMFD technique. The resampling based method takes as input the matched pairs that highlight any cloned regions. If the resampling factor of a certain region is different from its neighborhood, it is considered as forged region. Otherwise, it is considered as source region. The resampling based method fails to classify the cloned regions into source and forged regions if the forged region hasn't been modified geometrically.

IV. Deep Learning based CMFD Techniques

Conventional CMFD techniques with handcrafted features experience three limitations [86]. First, these techniques have an identical structure comprises of three phases. Each phase is trained separately and has numerous parameters that are manually tuned [86]–[88]. Second, these techniques are mostly tuned to accomplish great performance on specific dataset(s) yet fail in other datasets [86]. Third, handcrafted features are usually have restricted discrimination power [89], [90].

Deep learning exhibits a major achievement in various recognition tasks. As a result, numerous researchers attempt to adopt deep learning for CMFD [91]. Selection of the appropriate parameters/thresholds is the most important problem that conventional CMFD techniques faced, but deep learning models are able to automatically learn the suitable features for CMFD [87], [92]. To build a CMFD system using deep learning, a large number of training samples is required. But, existing CMF image datasets are limited in size [93]. One way to handle this problem is adopting transfer learning or utilizing deep learning methods to only extract the image features within a block or keypoint based CMFD techniques.

Transfer learning utilizes a pre-trained model for certain task and slightly re-train the model parameters with little training samples for other task [93]. These pre-trained models such as AlexNet, VGGNet, GoogLeNet, and ResNet are pre-trained from enormous training dataset and have a powerful generalization power [93]. Several works such as [92]–[94] utilized AlexNet for CMFD because of its simple construction. In [92][93] Alex Net is utilized for CMF classification at the image level. The proposed method in [93] fails to handle realistic CMF because its model is trained with simple CMF samples. In [92] the SVM classifier is trained with the features obtained from the fully connected layer of Alex Net. In [94] a modified AlexNet architecture is proposed for classifying various forgery types at the image level.

Several CMFD techniques such as [89], [95] utilized deep learning methods to only extract the image features within a block or keypoint based CMFD techniques. In [95] A block based CMFD technique in which Alex Net is utilized to describe the image blocks. In [89] GPU-based convolutional kernel network (CKN) is utilized to obtain local descriptors of the image keypoints. CKN is a deep convolutional network that combines neural networks with kernel methods. CKN aims to produce local descriptors that are invariant to various transformations. Also, in [89] the image is adaptively over-segmented into superpixels utilizing an efficient CNN based technique which is called the convolutional oriented boundaries (COB).

Adopting transfer learning or utilizing deep learning methods to only extract the image features have some drawbacks. CMFD techniques which utilize transfer learning are commonly deciding the forgery at the image level only. Also, CMFD techniques which utilize deep learning methods to only extract the image features aren't end to end trainable. So, several synthesized datasets that incorporates an enormous number of images with its localization binary masks are proposed to manage an end to end training process of the CMF localization task [90], [96]. In the next subsections, several deep learning based CMFD techniques are reviewed and organized according to its detection methodology. All the presented techniques are end to end deep learning based systems which are trained using huge synthesized datasets.

A. Visual Similarity Based

Deep learning based CMFD techniques which reveal the CMF on the basis of visual similarity are commonly mimic the same phases of the conventional CMFD techniques. However, each phase is accomplished by deep neural network (DNN) layers. A customized DNN layers are utilized to perform the feature matching phase. As a result of relying on visual similarity to locate CMF, similar but genuine regions may be treated as forged regions by mistake [87], [97].

Deep learning models such as [86]–[88], [97], [98] aim to localize CMF on the basis of visual similarity. In [87], [88], [97], [98] feature extraction is performed through the VGG16 architecture. BusterNet [87], [88] is considered the first end-to-end DNN model that aims to localize CMF at the pixel level. Other works such as [97], [98] aim to enhance BusterNet. For feature extraction, BusterNet utilized 4 blocks of the VGG16 network along with four pooling layers while in [98] the 4th pooling layer is removed to obtain features with higher resolution. Additionally, atrous convolution is utilized in [97], [98] to increase the filters field of views. As contextual information isn't captured well in BusterNet, the attention module is utilized in [97], [98] to capture contextual information, and enrich features. For feature matching, BusterNet performed single level feature matching while in [97], [98] hierarchical feature matching is enabled by considering features of multiple levels. To produce the CMF localization mask, BusterNet utilized a deconvolutional network which incorporates bilinear up-sampling layers and inception modules. Atrous spatial pyramid pooling (ASPP) is utilized in [97], [98] to localize CMF with scaling operation by exploiting image features in multiple scales. The CMF localization mask is refined in [97] using a residual refinement network. In [86] three dense inception blocks are combined to extract multi scale highly rich features. Three matching maps are obtained to yield a coarser to fine feature matching and then they are integrated by the loss layer to localize the CMF.

B. Tampering Artifacts Based

Several deep learning based CMFD techniques depend on the detection of tampering artifacts to reveal forgery in general. One example of such tampering traces is the unnatural characteristics that may appear at the forged regions boundary [91], [96]. To achieve visual consistency in a forged image, it is common to edit the forged region by various operations. The presence of multiple editing operations inside an image is also considered as a forgery indicator [99]. Additionally, geometric transformations and interpolation are commonly applied to the forged regions which results in periodic correlation artifacts. The resampling features can be utilized to catch such periodic correlation in the frequency domain [96].

Utilizing deep neural networks for detecting tampering artifacts is a difficult task. Deep neural networks (DNNs) are usually provides feature maps that describe image content rather than the forgery traces. So, utilizing DNNs for forgery detection needs some sort of adaptation to learn richer features correspond to the tampering artifacts [93], [99]. To be specific, the training of DNNs for the forgery detection purpose should be based on an information that describe the local relationship between adjacent pixels [99]. Such information could be captured through fixed spatial rich model (SRM) filters as in [100], [101], or a constrained convolutional layer that learns the filters weights as in [98], [99].

Realistic forged images show high similarity between its authentic and forged regions. So, depending only on CNN based architecture or single feature type for forgery localization isn’t enough. In [91], [96] a hybrid model consists of LSTM network and CNN is utilized to localize three image forgery types: copy-move, splicing, and removal. As LSTM network is able to handle sequential and contextual information, in [91], [96] LSTM is utilized to learn the transition between the authentic and forged regions. In [91] the proposed model comprises of an LSTM network and 5 convolutional layers. Image patches are gone through the first 2 convolutional layers to output a low-level feature map which is divided into blocks. Then, these blocks are gone through the LSTM network. The later 3 convolutional layers will get the LSTM feature map and produce the forgery localization mask. In [96] the proposed model comprises of an LSTM network and encoder-decoder network. Image is divided into blocks which are described by the resampling features. The resampling features go through the LSTM network. The encoder consists of residual units accepts the whole image as input and produce the spatial feature maps with global context. The encoder features and the LSTM features are fused and taken as input to the decoder to produce the forgery localization mask.

CNN networks are usually aim to classify an image into one of various classes by learning class-specific features. On the other hand, the Siamese network aims to discriminate various classes by learning more generic features along with a distance metric. The Siamese network comprises of twin sub-networks processing two images in parallel to decide whether the two images are similar or not [99]. In [99] a deep Siamese network is utilized to detect several types of image level post-processing operations that are usually aim to hide the forgery traces. Moreover, a forgery localization method is proposed in [99] by dividing an image into overlapping regions which are compared with each other through the Siamese network to decide whether the image regions are similarly processed or not. Image is considered as forged if its regions have different processing operations.

Several works such as [90], [100], [101] adapted object detection or segmentation networks to localize three image forgery types: copy-move, splicing, and removal. In [100] Faster R-CNN network with two parallel streams: RGB stream, and noise stream is proposed. The RGB stream models the global visual tampering artifacts. SRM filters are applied to the image to extract local noise features which go through the noise stream to figure out any noise inconsistency. A bilinear pooling layer is utilized to fuse the two streams features and enrich the network training. Object detection networks such as R-CNN, and Faster R-CNN are able to localize the forgery using bounding boxes. For this reason, object segmentation networks such as Mask R-CNN and U-net are preferred to precisely localize the forgery at the pixel level. In [90] an improved Mask R-CNN network is proposed. For precise forgery segmentation, a sobel based edge agreement head is joined to the mask prediction branch of the Mask R-CNN. In [101] a dense U-net based architecture is utilized. The image residual obtained by SRM filters is concatenated with the image pixels to enhance the learning process of the dense U-net. Through multi-scale up-sampling and concatenation, the features in the convolutional network are moved to the deconvolutional network to exploit the contextual features intersection for improving the forgery localization.

DNNs can easily localize splicing forgery utilizing the tampering traces [97]. But, this isn't the case in localizing CMF because almost all image properties are highly consistent [97]. So, in [100] the model's performance in detecting CMF is the worst compared to other forgery types. To handle CMF, a comparison mechanism between the image objects is needed. Also in [99] the experimental results provided for CMF localization isn’t enough.

C. Hybrid Detection Methodology

Discriminating forged region(s) from its source region(s) is favored task in forensic investigations. CMFD techniques with hybrid detection methodology such as [88], [98] are usually aim to discriminate forged regions from its source region besides localizing them at the pixel level. BusterNet [88] is considered the first end to end DNN that is able to discriminate forged region from its source region besides localizing them at the pixel level. BusterNet consists of two parallel branches that are fused together. One branch is responsible for localizing the forged region besides its source region based on visual similarity. The other branch is responsible for localizing at the pixel level only the forged region within the entire image based on visual artifacts. It comprises of a CNN based feature extractor and a deconvolutional network. But, BusterNet fails to discriminate the source region from its forged region if any of its branches wrongly locate the regions. So, the proposed model in [98] solves this problem and proposing more faster network with less parameters than BusterNet. The proposed model in [98] consists of two serial sub-networks. The first sub-network is responsible for localizing similar regions at the pixel level which will be cropped and transferred to the second sub-network as sub-images. The second sub-network follows the same structure of the constrained CNN and is responsible for deciding the class label of each sub-image if it is source region or forged region.

V. Evaluation Metrics

The outcome of a CMFD technique could be classifying an image as authentic/tampered, or localization of the cloned regions within the image at the pixel level. Such localization of the cloned regions requires classifying each image pixel as authentic/tampered. In this way, any CMFD technique can be viewed as a classifier and its performance could be measured at the image level or at the pixel level. However, the pixel-level evaluation is the most accurate and reliable way. The standard evaluation metrics for CMFD techniques are mostly depending on some measures which could operate at the image level or the pixel level. These measures are: $\mathrm{T_P}, \mathrm{F_P}, \mathrm{T_N}, and\ \mathrm{F_N}$ [106]. True Positive ($\mathrm{T_P}$) represents the No. of tampered images/pixels correctly recognized as tampered. False Positive ($\mathrm{F_P}$) represent the No. of authentic images/pixels erroneously recognized as tampered. True Negative ($\mathrm{T_N}$) represents the No. of authentic images/pixels correctly recognized as authentic. False Negative ($\mathrm{F_N}$) represents the No. of tampered images/pixels erroneously recognized as authentic.

From the above measures, different evaluation metrics can be computed at the image / pixel level as listed below [106]:

$$precision\ (p) = \frac{T_P}{T_P+F_P} \tag{1}$$

$$Recall\ (r)/TPR/sensitivity = \frac{T_P}{T_P+F_N} \tag{2}$$

$$F1 = \frac{2.p.r}{p+r} = \frac{2.T_P}{2.T_P+F_P+F_N} \tag{3}$$

$$Accuracy\ (Acc) = \frac{T_P+T_N}{T_P+F_P+T_N+F_N} \tag{4}$$

$$False\ positive\ rate\ (FPR) = \frac{F_P}{F_P+T_N} \tag{5}$$

The performance of CMFD techniques can also be evaluated through the receiver operating characteristics (ROC). The ROC curve examines the effect of various thresholds on the prediction result by plotting the TPR against the FPR. However, it is common to convert the ROC curve into single value by computing the area under the ROC curve (AUC). The AUC value of certain classification system represents its discrimination capability and hence facilitates the performance comparison of different classification systems [88].

As mentioned before, several attacks including the geometric operations and the post-processing operations are performed to make it difficult to detect the CMF. So, it is required to test the ability of the CMFD techniques to face these attacks. Such type of test is called the robustness test. In robustness test, the evaluation metrics mentioned above are usually measured for various attacks. Here comes the role of the evaluation datasets and how it covers various attacks.

VI. The CMFD Datasets

Many datasets are available for CMFD in which they vary according to some aspects such as the dataset volume, the way for expressing its ground truth, and the dataset complexity. Table II highlights the main CMFD datasets utilized in literature along with its main characteristics.

The dataset volume is determined by the number of authentic (A) & tampered (T) images it contains, the images size, and the images format. In general, evaluating the performance of CMFD techniques using datasets with massive number of images obtains reliable measures at the expense of the time complexity. Images with high resolution could provide more details that facilitate the forgery detection task. On the other hand, low image size is preferred for fast computation. CMFD datasets with compressed images add some difficulty for the forgery detection task because of missing some details.

The CMFD datasets commonly provide its ground truth at two levels: at the image level and/or at the pixel level. At the image level, each image should have a class label to indicate if it is authentic or tampered. Evaluating the pixel-level performance requires the presence of the ground truth localization masks. Not all the CMFD datasets provide binary masks that localize the cloned regions within the tampered images. But since most of the CMFD datasets provide the authentic images and its tampered images, it is possible to indirectly obtain the CMF localization mask through images subtraction followed by thresholding and morphological operations. This idea was adopted by the authors of [13] to get the localization masks for the CAISA dataset [107].

The dataset complexity is determined by the challenges it contains, attacks involved in creating the forged images, and the intensity of such attacks. The attacks include the geometric transforms and the post processing operations which are usually carried out in forged images. Also, the shape and size of the cloned regions greatly affect the detection performance of CMFD techniques. Small and irregularly shaped cloned regions poses a great challenge for CMFD techniques. Furthermore, images with multiple CMF pose other challenge. Several datasets are designed to intensively cover certain challenge(s). For example, the COVERAGE [105] dataset is intensively introduce SGO regions. Also, the GRIP [103] dataset introduced several small and smooth cloned regions.

TABLE II. SUMMARY OF THE CMFD DATASETS

Dataset	No. of images	Size of images	Format of images	Shape of cloned region(s)	Geometric transforms	Post processing operations	Existence of localization masks	Other notes
The CMFD datasets with single cloning								
MICC-F220 [14]	110 A + 110 T	722*480 to 800*600	JPEG	Square or rectangular	Scaling (S) & Rotation (R)	Not exist	Not exist	Size of forged region = 1.2% of the entire image
MICC-F2000 [14]	1300 A + 700 T	2048*1536	JPEG	Square or rectangular	S & R	Not exist	Not exist	Size of forged region = 1.12% of the entire image
SBU-CM16 [102]	240 T	800*580	PNG/JPEG	arbitrary shapes	Only R	Noise addition (NA), JPEG compression (JC), blurring (B)	Exist	Although the cloned regions vary from smooth to texture, they are not skillfully prepared
GRIP [103]	80 A + 3440 T	768*1024	PNG	arbitrary shapes	S & R	NA & JC	Exist	Provide small / smooth CMF. The complete dataset is obtained by executing perl scripts.
CMH [49]	216 T	845*634 to 1296*972	PNG/JPEG	arbitrary shapes	S & R	JC	Exist	
CVIP [104]	70 A + 970 T	1000*700 or 700*1000	BMP	arbitrary shapes	S & R	Not exist	Exist	The forged region varies in size from small to large.
COVERAGE [105]	100 A + 100 T	400*486 (on average)	TIF	arbitrary shapes	S, R, and free form	Illumination change	Exist	Have multiple SGO objects. Large size of forged region.
The CMFD datasets containing multiple cloning								
MICC-F8multi [14]	8 T	800*532 to 2048*1536	JPEG	arbitrary shapes	S & R	Not exist	Not exist	
MICC-F600 [14]	440 A + 160 T	800*533 to 3888*2592	JPEG/PNG	arbitrary shapes	S & R	Not exist	Exist	
FAU [106]	48 A	3000*2300	PNG/JPEG	arbitrary shapes	S & R	NA, JC, downscaling	Exist	Cloned regions with varied size and texture are exist. Forgeries could be generated on demand through scripts.
CAISA ITDE v1.0 [107]	800 A + 451 images with CMF	384*256	JPEG	Regular / Arbitrary	S, R, and distortion	Not exist	Not exist	Include images with CMF as well as splicing
CAISA ITDE v2.0 [107]	7200 A + 3274 images with CMF	320*240 to 800*600	JPEG / TIF / BMP	Mostly arbitrary shaped	S, R, and distortion	B	Not exist	Include images with CMF as well as splicing
CoMoFoD small [108]	5000 A + 5000 T	512*512	PNG/JPEG	arbitrary shapes	S, R, and distortion	NA, JC, B, Brightness change, Contrast adjustment, Color reduction	Exist	Post processing operations are applied to the authentic images as well as the forged images. The forged region varies in size from small to large.
CoMoFoD large [108]	1500 A + 1500 T	3000*2000	PNG/JPEG	arbitrary shapes	S, R, and distortion	Same as CoMoFoD small	Exist	Same as CoMoFoD small

VII. DISCUSSION AND FUTURE DIRECTION

Assessing the visual similarity for revealing the CMF is the most effective and common detection methodology. Such detection methodology can be implemented through the conventional techniques or the deep leaning techniques. Regardless of the implementation paradigm, the detection system usually consists of three stages as follows: feature extraction, feature matching, and forgery localization. Each stage suffers from certain challenges. In the feature extraction phase, it is required to deal with small, smooth cloned regions and low resolution images as well as the geometric transforms and post processing operations. In the matching phase, dealing with similar but genuine objects and reducing the false matching rate are of great importance. In the forgery localization phase, it is essential to deal with multiple cloning.

Among the conventional CMFD techniques, keypoint based techniques and hybrid techniques have been proved to provide better performance than the block based techniques. To handle CMF with small or smooth cloned regions, there are two options: either integrating block based techniques with keypoint based techniques or covering the entire image by enough keypoints. There are several alternatives to acquire an adequate number of keypoints covering the entire image such as utilizing multiple keypoints detectors, lowering the contrast threshold of the keypoint detector, and increasing the image resolution or contrast. Among all these alternatives, techniques that handle the non-uniform distribution of the image keypoints phenomenon are favored.

The matching complexity is a fundamental problem with conventional CMFD techniques. Also, increasing the extracted features from an image to handle CMF with small/smooth cloned regions makes the matching complexity problem more difficult. Adopting low dimensional descriptors can decrease the matching time but reduce the CMFD performance. On the other hand, matching search space reduction or utilizing approximate matching are favored techniques for reducing the matching time.

For accurate localization of cloned regions that avoid detecting SGO as cloned regions, it is important to utilize descriptors with high discrimination power, choose appropriate values of the thresholds, validate the estimated geometric transform and estimate it accurately. Conventional CMFD techniques are commonly utilizing clustering or segmentation techniques for different reasons: to eliminate false matching, facilitate consistent matching direction between the cloned regions, and localize multiple cloned regions.

Although the conventional CMFD techniques have created many solutions to deal with different challenges, there are two problems that remain without an efficient solution. First, CMFD techniques aim to localize the cloned regions with high accuracy whatever the applied geometric and post processing operations. Also, in the same time the CMFD technique should have reasonable time complexity. There is a tradeoff between these objectives and a way to balance between them is needed. Second, several parameters are utilized in conventional CMFD techniques. A way to automatically choose customized values for these parameters that are suitable for each image is also needed. On the other hand, deep learning can find a solution to these two problems, as it is the best way to learn features as well as the classification task.

Because of its massive learning power, deep learning techniques can overcome many of the challenges facing CMFD. Deep learning models are able to extract features with high description and discrimination ability. Such extracted features could be further enriched by adopting attention modules and utilizing the contextual information. Deep learning techniques have achieved an adequate level of invariance to geometric transformations, and post processing operation through the polling units and data augmentation. In addition, deep learning techniques achieve scaling invariance by adopting either the atrous spatial pyramid pooling or the inception modules. Atrous spatial pyramid pooling requires less number of parameters than the inception module. However, invariance to rotation and especially large rotation needs to be investigated. Deep learning techniques are commonly handle small cloned regions by performing multi-level matching. In other words, the matching process is performed between the low level features of early layers as well as the high level features of subsequent layers.

Although deep learning systems have several achievements in many areas, their use in the CMFD problem still needs more research to improve performance. In deep learning models, it is common to resize the training/testing images to specific size to fit the input layer. The effect of this resizing operation as well as the image resolution on the detection performance should be investigated. Some deep learning based models apply a preprocessing step to suppress the image content and highlights the relationship between image pixels to reveal the forgery. More preprocessing operations need to be investigated especially to resist against noise addition and blurring.

Depending on visual similarity to reveal CMF could result in false alarms. Conventional CMFD techniques are usually verifying the suspected regions by assessing the geometric transform between them. While in deep learning based CMFD techniques such verification step is missed. It is true that relying on tampering artifacts to reveal CMF isn't the best choice. But, combining it with the visual similarity based detection methodology helps to enhance the performance, reduce false alarms and discriminate forged regions from its source regions. Such hybrid training can be accomplished through deep learning from two streams: the image stream and the image residual stream.

The most recent CMFD techniques are summarized in Table III. All the reported performance results are at the pixel level. In case of measuring the performance of certain CMFD technique with respect to several attacks, the reported performance result is expressed as a range. From Table III, we can find that the performance of most CMFD techniques isn't mature enough, varies from dataset to another, and needs more enhancements. Some CMFD techniques are deceiving in terms of their efficiency as they were either evaluated with small subset of test images or evaluated under simple conditions. Detecting the forgeries in certain dataset may be more difficult than other dataset because some datasets include more challenges/attacks than other datasets. Also, it is common to have many datasets include certain challenge. But, the strength of applying such challenge could vary from one dataset to another.

TABLE III. SUMMARY OF THE RECENT CMFD TECHNIQUES

Paper	Details	Performance	Reviews
Block based CMFD techniques			
[44]	Overlapping square blocks division, Gaussian hermite moments, assess similarity through euclidian distance, RANSAC, Morphological opening.	CoMoFoD small: $F1_p$=[0.9555,0.8144] GRIP: $F1_p$= 0.9805 [Plain CMF] CVIP: $F1_p$= 0.9497 [Plain CMF]	**Pros**: less sensitive to noise, able to detect small/multiple CMF. **Cons**: high time complexity, detect scaling only in the range [80% -140%], test with simple rotations.
[45]	Overlapping square blocks division, tetrolet features, assess similarity through the absolute difference, Fast outliers filtering method, Morphological opening and closing.	CoMoFoD small: $F1_p$=[0.9564,0.8282]	**Pros**: enhanced time complexity, able to detect small /multiple CMF. **Cons**: detect CMF only where scaling in the range [80% -135%] and the quality factor is 80 or more.
[29]	SWT, overlapping square blocks division, DCT mean features, similarity through euclidian distance, Morphological opening.	CoMoFoD small: $F1_p$=[0.941,0.834]	**Pros**: adopting descriptors of reduced dimension. **Cons**: a tiny subset of the dataset has been utilized for evaluation, false alarms are exist.
[46]	Square blocks division, tchebichef moments, SVD, similarity through euclidian distance, Morphological opening.	CoMoFoD: $F1_i$= [0.9586-0.7786]	**Pros**: adopting descriptors of reduced dimension. **Cons**: robustness test against geometric transformations was missed.
[42]	Image size reduction, Pyramid model construction, overlapping circular blocks division, zernike moments, KD tree, RANSAC.	FAU: $F1_i$= 0.9717	**Pros**: able to handle large scaling & rotation. **Cons**: slow, bad performance against noise addition, and small cloned regions.
[2]	Circular blocks division, PCET+ SVD, similarity through euclidian distance, PSO optimization of the matching threshold.	374 test images from CoMoFoD & CASIA: $F1_i$= [0.9913-0.8572]	**Pros**: adopting descriptors of reduced dimension. **Cons**: fail to handle images with large smooth regions, small cloned regions, and large scaling.
Keypoint based CMFD techniques			
[8]	SIFT keypoints are described by Hu's moments, Global threshold, Region growing.	CoMoFoD small: $F1_p$=0.7672 [Plain CMF]	**Pros**: able to detect CMF with rotation/flipping. **Cons**: unable to detect small CMF.
[5]	Keypoints are detected by Harris-Laplace+Hessian-Laplace+SIFT and described by SIFT, G2NN, RANSAC, Bag of Word	FAU: $F1_p$=0.8022 [Plain CMF] MICC-F600: $F1_p$=0.7011	**Pros**: able to detect small /multiple CMF. **Cons**: false alarms are exist which reduced the precision.
[50]	SIFT+LIOP, G2NN+transitive matching, Require matching density through SLIC superpixels segmentation, RANSAC	FAU: $F1_p$=0.7442 [Plain CMF]	**Pros**: able to handle cloned regions with few keypoints, enhance the matching relationship. **Cons**: the precision needs enhancement.
[74]	Keypoints are detected by SURF and described by RLBP, G2NN through Euclidean distance, Hierarchal clustering, RANSAC	COVERAGE: Acc= [0.705 - 0.645] CoMoFoD small: Acc=0.701 FAU: Acc = 0.833	**Pros**: distinguish SGO regions from cloned regions. **Cons**: tested mostly without post processing operations. Only consider jpeg compression and blurring for the COVERAGE dataset.
[11]	Image is segmented into rough and smooth regions. In rough regions: SIFT + G2NN + HAC + RANSAC. In smooth regions: Fourier Mellin + Patchmatch. Morphological operations.	FAU: $F1_i$=[0.9697,0.7407] GRIP: $F1_i$=0.9581 [Plain CMF]	**Pros**: able to detect smooth /multiple CMF as well as CMF with large scaling/rotation. **Cons**: evaluation at the pixel level isn't provided.
[57]	SIFT, the histogram of the reduced LBP, 2NN, RANSAC, Correlation coefficient computation, standard thresholding.	MICC-F220: Acc_i=0.9682 CMH: Acc_p= [0.9772-0.9766] CVIP: Acc_p= [0.982- 0.9583] COVERAGE: Acc_i=0.675	**Pros**: combining the histogram of the reduced LBP with SIFT for enhancing the performance. **Cons**: not consider multi CMF, evaluated with datasets with minimal post-processing.
Deep learning based CMFD techniques			
[88]	BusterNet: DNN with two parallel branches. Mani-Det branch: VGG16, bilinear up-sampling layers, inception modules, binary classifier. Simi-Det branch: same as Mani-Det branch + Self-Correlation, Percentile Pooling.	CAISA ITDE v2.0: $F1_p$=0.456 COVERAGE: $F1_p$=0.618 CoMoFoD small: $F1_p$=0.493	**Pros**: discriminate forged regions from its source regions. **Cons**: contextual information is lost, difficulty in detecting small cloned regions.
[97]	DNN with single stream. VGG16, atrous convolution, attention module, hierarchical feature matching, ASPP, residual refinement network.	CAISA ITDE v2.0: $F1_p$=0.455 COVERAGE: AUC= 0.8488 CoMoFoD small: $F1_p$=0.501	**Pros**: Enrich the extracted features, the CMF localization mask is refined. **Cons**: Not distinguish well SGO regions from really cloned regions.
[98]	DNN with two serial sub-networks. CMSDNet: VGG16, atrous convolution, double level self-correlation, attention module, ASPP. STRDNet: constrained conv. layer, 4 conv. groups, fully connected classification network.	CAISA ITDE v2.0: $F1_p$=0.538 COVERAGE: $F1_p$= 0.677 CoMoFoD small: $F1_p$= 0.511	**Pros**: enhances the performance of BusterNet [88] as well as the computational time, able to discriminate forged regions from its source regions. **Cons**: The performance still needs enhancement.
[86]	End to end DNN. three dense inception blocks, hierarchical feature matching and post processing.	CAISA ITDE v2.0: $F1_p$=0.6429 CoMoFoD small: $F1_p$= 0.441 [averaged for several attacks]	**Pros**: detect unseen forged regions through learning the correlations of multi scale dense features. **Cons**: bad performance for the FAU dataset.
[89]	Adaptive over segmentation by COB, keypoints detection using DoG, keypoints description using CKN, matching through KD tree, RANSAC.	CoMoFoD small: $F1_p$= 0.6318 [with no post processing]	**Pros**: the processing time is reduced due to the GPU implementation of CKN and COB. **Cons**: scale invariance needs further enhancement.
[95]	Overlapping square blocks division, feature extraction using AlexNet, matching through global threshold, Morphological operations.	GRIP: $F1_p$=0.93 [Plain CMF]	**Pros**: able to handle CMF with SGO regions and smooth cloned regions. **Cons**: robustness test was missed.

VIII. Conclusion

In this survey, we have studied the CMFD problem in depth. We have categorized the CMFD techniques based on their detection methodology, their detection paradigm, and their detection capability. Different detection methodologies and paradigms have been analyzed and discussed regarding their advantages and disadvantages. Moreover, we have deeply examined the challenges that face the CMFD techniques in general and the conventional CMFD techniques in specific. Consequently, this survey gives an integrated and in-depth view of the CMFD techniques, challenges and recent trends.

The CMFD is a very challenging problem and still an open research area. The majority of the CMFD techniques aren't achieved yet good enough performance due to many conflicting challenges. In order ensure that a specific CMFD technique has achieved satisfactory results, it should be evaluated at the pixel level and evaluate its robustness against a wide range of challenges that might face the CMFD techniques. Consequently, additional work should be carried out to solve several conflicting challenges and there is a great need to further investigate and employ diverse deep learning capabilities in tackling the CMFD problem.

References

[1] Hegazi, A. Taha, and M. M. Selim, "Copy-Move Forgery Detection Based on Automatic Threshold Estimation," International Journal of Sociotechnology and Knowledge Development, vol. 12, no. 1, pp. 1–23, 2020.

[2] Y. Wang, X. Kang, and Y. Chen, "Robust and accurate detection of image copy-move forgery using PCET-SVD and histogram of block similarity measures," Journal of Information Security and Applications, vol. 54, pp. 1–11, 2020.

[3] P. Niyishaka and C. Bhagvati, "Copy-move forgery detection using image blobs and BRISK feature," Multimedia Tools and Applications, 2020.

[4] C. Lin, W. Lu, W. Sun, J. Zeng, T. X. J. Lai, and W. Lu, "Region duplication detection based on image segmentation and keypoint contexts," Multimedia Tools and Applications, vol. 77, pp. 14241–14258, 2018.

[5] C. Lin, W. Lu, X. Huang, K. Liu, W. Sun, and H. Lin, "Region duplication detection based on hybrid feature and evaluative clustering," Multimedia Tools and Applications, vol. 78, pp. 20739–20763, 2019.

[6] Y. Yu, G. Wang, and J. Zhao, "FI-SIFT Algorithm for Exposing Image Copy-Move Forgery with Reflection Attacks," International Journal of Network Security, pp. 1–8, 2019.

[7] A. Badr, A. Youssif, and M. Wafi, "A Robust Copy-Move Forgery Detection In Digital Image Forensics Using SURF," in 8th International Symposium on Digital Forensics and Security (ISDFS), 2020.

[8] C. Chen, W. Lu, and C. Chou, "Rotational copy-move forgery detection using SIFT and region growing strategies," Multimedia Tools and Applications, pp. 1–16, 2019.

[9] C. Wang, Z. Zhang, and X. Zhou, "An Image Copy-Move Forgery Detection Scheme Based on A-KAZE and SURF Features," Symmetry, vol. 10, no. 12, pp. 1–20, 2018.

[10] H. Huang and A. Ciou, "Copy-move forgery detection for image forensics using the superpixel segmentation and the Helmert transformation," EURASIP Journal on Image and Video Processing, vol. 68, 2019.

[11] K. B. Meena and V. Tyagi, "A hybrid copy-move image forgery detection technique based on Fourier-Mellin and scale invariant feature transforms," Multimedia Tools and Applications, 2020.

[12] Y. Liu, H. Wang, Y. Chen, H. Wu, and H. Wang, "A passive forensic scheme for copy-move forgery based on superpixel segmentation and K-means clustering," Multimedia Tools and Applications, vol. 79, no. 1, pp. 477–500, 2020.

[13] M. Jaberi, G. Bebis, M. Hussain, and G. Muhammad, "Accurate and robust localization of duplicated region in copy – move image forgery," Machine Vision and Applications, vol. 25, no. 2, pp. 451–475, 2014.

[14] I. Amerini, L. Ballan, R. Caldelli, A. Del Bimbo, and G. Serra, "A SIFT-Based Forensic Method for Copy – Move Attack Detection and Transformation Recovery," IEEE Transactions on Information Forensics and Security, vol. 6, no. 3, pp. 1099–1110, 2011.

[15] R. Dixit and R. Naskar, "Region duplication detection in digital images based on Centroid Linkage Clustering of key – points and graph similarity matching," Multimedia Tools and Applications, vol. 78, pp. 13819–13840, 2019.

[16] T. Mahmood, Z. Mehmood, M. Shah, and T. Saba, "A robust technique for copy-move forgery detection and localization in digital images via stationary wavelet and discrete cosine transform," Journal of Visual Communication and Image Representation, vol. 53, no. 1, pp. 202–214, 2018.

[17] F. Zhao, W. Shi, B. Qin, and B. Liang, "A Copy-Move Forgery Detection Scheme with Improved Clone Region Estimation," in Third International Conference on Trustworthy Systems and Their Applications, 2016, pp. 8–16.

[18] R. Agarwal, O. P. Verma, A. Saini, A. Shaw, and R. Patel, "The Advent of Deep Learning-Based Image Forgery Detection Techniques," Innovative Data Communication Technologies and Application. Lecture Notes on Data Engineering and Communications Technologies, vol. 59, pp. 679–693, 2021.

[19] M. Kharanghar and A. Doegar, "Copy-Move Forgery Detection Methods : A Critique," Advances in Information Communication Technology and Computing. Lecture Notes in Networks and Systems., vol. 135, pp. 501–523, 2021.

[20] R. Thakur and R. Rohilla, "Recent Advances in Digital Image Manipulation Detection Techniques: A brief Review," Forensic Science International, vol. 312, p. 110311, 2020.

[21] M. F. M. Mursi, M. M. Salama, and M. H. Habeb, "An Improved SIFT-PCA-Based Copy-Move Image Forgery Detection Method," International Journal of Advanced Research in Computer Science and Electronics Engineering (IJARCSEE), vol. 6, no. 3, pp. 23–28, 2017.

[22] S. H. I. Wenchang, Z. Fei, Q. I. N. Bo, and L. Bin, "Improving image copy-move forgery detection with particle swarm optimization techniques," China Communications, vol. 13, no. 1, pp. 139–149, 2016.

[23] F. Zhao, W. Shi, B. Qin, and B. Liang, "Analysis of SIFT Method Based on Swarm Intelligent Algorithms for Copy-Move Forgery Detection," Lecture Notes in Computer Science, vol. 10066, no. 1, pp. 478–490, 2016.

[24] Y. Li and J. Zhou, "Fast and Effective Image Copy-Move Forgery Detection via Hierarchical Feature Point Matching," IEEE Transactions on Information Forensics and Security, vol. 14, no. 5, pp. 1307 – 1322, 2019.

[25] G. Jiachang and G. Jichang, "Image Copy - Move Forgery Detection Using SURF in Opponent Color Space," Transactions of Tianjin University, vol. 22, no. 2, pp. 151–157, 2016.

[26] F. Yang, J. Li, W. Lu, and J. Weng, "Copy-move forgery detection based on hybrid features," Engineering Applications of Artificial Intelligence, vol. 59, no. 1, pp. 73–83, 2017.

[27] J. Wang, G. Liu, H. Li, Y. Dai, and Z. Wang, "Detection of Image Region Duplication Forgery Using Model with Circle Block," in International Conference on Multimedia Information Networking and Security, 2009, pp. 25–29.

[28] J. Zhao and J. Guo, "Passive forensics for copy-move image forgery using a method based on DCT and SVD," Forensic Science International, vol. 233, no. 1–3, pp. 158–166, 2013.

[29] F. H. Pugar, S. Muzahidin, and A. M. Arymurthy, “Copy-Move Forgery Detection Using SWT-DCT and Four Square Mean Features,” in International Conference on Electrical Engineering and Informatics (ICEEI), 2019, pp. 63–68.

[30] Y. Huang, W. Lu, W. Sun, and D. Long, “Improved DCT-based detection of copy-move forgery in images,” Forensic Science International, vol. 206, no. 1–3, pp. 178–184, 2011.

[31] M. Alkawaz, G. Sulong, T. Saba, and A. Rehman, “Detection of copy-move image forgery based on discrete cosine transform,” Neural Computing and Applications, vol. 30, no. 1, pp. 183–192, 2018.

[32] M. Zimba and S. Xingming, “DWT-PCA (EVD) Based Copy-move Image Forgery Detection,” International Journal of Digital Content Technology and its Applications, vol. 5, no. 1, pp. 251–258, 2011.

[33] X. Kang and S. Wei, “Identifying Tampered Regions Using Singular Value Decomposition in Digital Image Forensics,” in International Conference on Computer Science and Software Engineering, 2008, pp. 926–930.

[34] L. Chen, W. Lu, and J. Ni, “An Image Region Description Method Based on Step Sector Statistics and its Application in Image Copy-Rotate / Flip-Move Forgery Detection,” International Journal of Digital Crime and Forensics, vol. 4, no. 1, pp. 49–62, 2012.

[35] J. Lee, C. Chang, and W. Chen, “Detection of copy – move image forgery using histogram of orientated gradients,” INFORMATION SCIENCES, vol. 321, pp. 250–262, 2015.

[36] T. Mahmood, T. Nawaz, M. Shah, Z. Khan, R. Ashraf, and H. A. Habib, “Copy-move forgery detection technique based on DWT and Hu Moments,” International Journal of Computer Science and Information Security (IJCSIS), vol. 14, no. 5, pp. 156–161, 2016.

[37] G. Liu, J. Wang, S. Lian, and Z. Wang, “A passive image authentication scheme for detecting region-duplication forgery with rotation,” Journal of Network and Computer Applications, vol. 34, no. 5, pp. 1557–1565, 2011.

[38] P. Yang, G. Yang, and D. Zhang, “Rotation Invariant Local Binary Pattern for Blind Detection of Copy-Move Forgery with Affine Transform,” Cloud Computing and Security. ICCCS 2016. Lecture Notes in Computer Science, vol. 10040, pp. 404–416, 2016.

[39] L. Li, S. Li, and H. Zhu, “An Efficient Scheme for Detecting Copy-move Forged Images by Local Binary Patterns,” Journal of Information Hiding and Multimedia Signal Processing, vol. 4, no. 1, pp. 46–56, 2013.

[40] Y. Wang, L. Tian, and C. Li, “LBP-SVD Based Copy Move Forgery Detection Algorithm,” in IEEE International Symposium on Multimedia (ISM), 2017, pp. 553–556.

[41] T. Mahmood, A. Irtaza, Z. Mehmood, and M. T. Mahmood, “Copy - move forgery detection through stationary wavelets and local binary pattern variance for forensic analysis in digital images,” Forensic Science International, vol. 279, pp. 8–21, 2017.

[42] J. Ouyang, Y. Liu, and M. Liao, “Robust copy-move forgery detection method using pyramid model and Zernike moments,” Multimedia Tools and Applications, vol. 78, pp. 10207–10225, 2019.

[43] K. Mahmoud and A. Abu-alrukab, “Copy-Move Forgery Detection Using Zernike and Pseudo Zernike Moments,” The International Arab Journal of Information Technology, vol. 13, no. 6A, pp. 930–937, 2016.

[44] K. B. Meena and V. Tyagi, “A copy-move image forgery detection technique based on Gaussian-Hermite moments,” Multimedia Tools and Applications, vol. 78, pp. 33505–33526, 2019.

[45] K. B. Meena and V. Tyagi, “A copy-move image forgery detection technique based on tetrolet transform,” Journal of Information Security and Applications, vol. 52, pp. 1–9, 2020.

[46] T. Mahmood, M. Shah, J. Rashid, T. Saba, M. W. Nisar, and M. Asif, “A passive technique for detecting copy-move forgeries by image feature matching,” Multimedia Tools and Applications, 2020.

[47] B. Mahdian and S. Saic, “Detection of copy – move forgery using a method based on blur moment invariants,” Forensic Science International, vol. 171, no. 2–3, pp. 180–189, 2007.

[48] K. M. Hosny, H. M. Hamza, and N. A. Lashin, “Copy-move forgery detection of duplicated objects using accurate PCET moments and morphological operators,” The Imaging Science Journal, vol. 66, no. 6, pp. 330–345, 2018.

[49] E. Silva, T. Carvalho, A. Ferreira, and A. Rocha, “Going deeper into copy-move forgery detection : Exploring image telltales via multi-scale analysis and voting processes,” Journal of Visual Communication and Image Representation, vol. 29, no. 1, pp. 16–32, 2015.

[50] C. Lin, W. Lu, X. Huang, L. Wei, S. Hanhui, and L. Zhiyuan, “Copy-move forgery detection using combined features and transitive matching,” Multimedia Tools and Applications, vol. 78, pp. 30081–30096, 2019.

[51] M. Bilal, H. A. Habib, Z. Mehmood, T. Saba, and M. Rashid, “Single and Multiple Copy – Move Forgery Detection and Localization in Digital Images Based on the Sparsely Encoded Distinctive Features and DBSCAN Clustering,” Arabian Journal for Science and Engineering, 2019.

[52] C. Wang, Z. H. I. Zhang, Q. LI, and X. ZHOU, “An Image Copy-Move Forgery Detection Method Based on SURF and PCET,” IEEE Access, vol. 7, pp. 170032–170047, 2019.

[53] R. Davarzani, K. Yaghmaie, S. Mozaffari, and M. Tapak, “Copy-move forgery detection using multiresolution local binary patterns,” Forensic Science International, vol. 231, no. 1–3, pp. 61–72, 2013.

[54] Y. Liu, H. Wang, H. Wu, and Y. Chen, “An Efficient Copy-Move Detection Algorithm Based on Superpixel Segmentation and Harris Key-Points,” Cloud Computing and Security. ICCCS 2017. Lecture Notes in Computer Science, vol. 10602, pp. 61–73, 2017.

[55] L. Chen, W. Lu, J. Ni, W. Sun, and J. Huang, “Region duplication detection based on Harris corner points and step sector statistics,” JOURNAL OF VISUAL COMMUNICATION AND IMAGE REPRESENTATION, vol. 24, no. 3, pp. 244–254, 2013.

[56] W. Zhang, Z. Yang, S. Niu, and J. Wang, “Detection of Copy-Move Forgery in Flat Region Based on Feature Enhancement,” Digital Forensics and Watermarking. IWDW 2016. Lecture Notes in Computer Science, vol. 10082, pp. 159–171, 2017.

[57] J. Y. Park, T. A. Kang, Y. H. Moon, and I. K. Eom, “Copy-Move Forgery Detection Using Scale Invariant Feature and Reduced Local Binary Pattern Histogram,” Symmetry, vol. 12, no. 4, pp. 1–16, 2020.

[58] G. Jin and X. Wan, “An improved method for SIFT-based copy-move forgery detection using non-maximum value suppression and optimized J-Linkage,” Signal Processing: Image Communication, vol. 57, no. 1, pp. 113–125, 2017.

[59] I. Amerini, L. Ballan, R. Caldelli, A. Del, L. Del, and G. Serra, “Copy-move forgery detection and localization by means of robust clustering with J-Linkage,” Signal Processing : Image Communication, vol. 28, no. 6, pp. 659–669, 2013.

[60] M. Emam, Q. Han, and X. Niu, “PCET based copy-move forgery detection in images under geometric transforms,” Multimedia Tools and Applications, vol. 75, pp. 11513–11527, 2016.

[61] J. Zheng, Y. Liu, J. Ren, T. Zhu, Y. Yan, and H. Yang, “Fusion of block and keypoints based approaches for effective copy-move image forgery detection,” Multidimensional Systems and Signal Processing, vol. 27, no. 4, pp. 989–1005, 2016.

[62] X. Pan and S. Lyu, “Region Duplication Detection Using Image Feature Matching,” IEEE Transactions on Information Forensics and Security, vol. 5, no. 4, pp. 857–867, 2010.

[63] S. Samir, E. Emary, K. Elsayed, and H. Onsi, “Copy-Move Forgeries Detection and Localization Using Two Levels of Keypoints Extraction,” Journal of Computer and Communications, vol. 07, no. 09, pp. 1–18, 2019.

[64] Y. Zhu, T.-T. Ng, X. Shen, and B. Wen, “Revisiting copy-move forgery detection by considering realistic image with similar but genuine objects,” arXiv preprint arXiv:1601.07262, 2016.

[65] Y. Zhu, T. Ng, B. Wen, X. Shen, and B. Li, “Copy-move Forgery Detection in the Presence of Similar but Genuine Objects,” in IEEE 2nd International Conference on Signal and Image Processing (ICSIP), 2017, pp. 25–29.

[66] A. Hegazi, A. Taha, and M. M. Selim, “An improved copy-move forgery detection based on density-based clustering and guaranteed outlier removal,” Journal of King Saud University - Computer and Information Sciences, pp. 1–9, 2019.

[67] M. A. Elaskily, H. K. Aslan, M. M. Dessouky, and E. Fathi, “Enhanced Filter-based SIFT Apprroach for Copy-Move Forgery Detection,”

Menoufia Journal of Electronic Engineering Research (MJEER), vol. 28, no. 1, pp. 159–182, 2019.

[68] Z. Fei, S. H. I. Wenchang, Q. I. N. Bo, and L. Bin, “Image Forgery Detection Using Segmentation and Swarm Intelligent Algorithm,” Wuhan University Journal of Natural Sciences, vol. 22, no. 2, pp. 141–148, 2017.

[69] A. Gupta and I. Chawla, “An Efficient Copy-Move Forgery Detection Technique Using Nature-Inspired Optimization Algorithm,” in Recent Advances on Memetic Algorithms and its Applications in Image Processing. Studies in Computational Intelligence, vol 873. Springer, Singapore, Springer Singapore, 2020, pp. 153–166.

[70] M. M. Al-hammadi and S. Emmanuel, “Improving SURF Based Copy-Move Forgery Detection Using Super Resolution,” in International Symposium on Multimedia, 2016, pp. 341–344.

[71] M. Bilal, H. A. Habib, Z. Mehmood, R. M. Yousaf, T. Saba, and A. Rehman, “A robust technique for copy-move forgery detection from small and extremely smooth tampered regions based on the DHE-SURF features and mDBSCAN,” Australian Journal of Forensic Sciences, pp. 1–24, 2020.

[72] K. Liu, W. Lu, Y. Xue, C. Lin, X. Huang, X. Liu, and Y. Yeung, “Copy move forgery detection based on keypoint and patch match,” Multimedia Tools and Applications, vol. 78, pp. 31387–31413, 2019.

[73] K. Sachdev, M. Kaur, and S. Gupta, “A Robust and Fast Technique to Detect Copy Move Forgery in Digital Images Using SLIC Segmentation and SURF Keypoints,” in Proceeding of International Conference on Intelligent Communication, Control and Devices, 2017, pp. 787–793.

[74] A. Roy, R. Dixit, R. Naskar, and R. S. Chakraborty, “Copy-Move Forgery Detection with Similar But Genuine Objects,” Digital Image Forensics. Studies in Computational Intelligence, vol. 755, pp. 65–77, 2020.

[75] G. Muhammad, M. Hussain, and G. Bebis, “Passive copy move image forgery detection using undecimated dyadic wavelet transform,” Digital Investigation, vol. 9, no. 1, pp. 49–57, 2012.

[76] M. Chowdhury, H. Shah, T. Kotian, N. Subbalakshmi, and S. D. S, “Copy-Move Forgery Detection using SIFT and GLCM-based Texture Analysis,” in IEEE Region 10 Conference (TENCON), 2019, pp. 960–964.

[77] K. H. Paul, K. R. Akshatha, A. K. Karunakar, and S. Seshadri, “SURF Based Copy Move Forgery Detection Using kNN Mapping,” in Advances in Computer Vision. CVC 2019. Advances in Intelligent Systems and Computing, vol. 944, Springer International Publishing, 2020, pp. 234–245.

[78] M. A. Elaskily, H. A. Elnemr, M. M. Dessouky, and O. S. Faragallah, “Two stages object recognition based copy-move forgery detection algorithm,” Multimedia Tools and Applications, vol. 78, pp. 15353–15373, 2019.

[79] E. Ardizzone, A. Bruno, and G. Mazzola, “Detecting multiple copies in tampered images,” in IEEE International Conference on Image Processing, 2010, pp. 2117–2120.

[80] H. A. Alberry, A. A. Hegazy, and G. I. Salama, “A fast SIFT based method for copy move forgery detection,” Future Computing and Informatics Journal, vol. 3, no. 2, pp. 159–165, 2018.

[81] P. Mishra, N. Mishra, S. Sharma, and R. Patel, “Region Duplication Forgery Detection Technique Based on SURF and HAC,” The ScientificWorld Journal, 2013.

[82] C. S. Prakash, P. P. Panzade, H. Om, and S. Maheshkar, “Detection of copy-move forgery using AKAZE and SIFT keypoint extraction,” Multimedia Tools and Applications, vol. 78, pp. 23535–23558, 2019.

[83] T. Du, L. Tian, and C. Li, “Image Copy-Move Forgery Detection based on SIFT-BRISK,” in International Conference on Control, Automation and Information Sciences (ICCAIS), 2018, pp. 141–145.

[84] G. Muzaffer and G. Ulutas, “A Fast and Effective Digital Image Copy Move Forgery Detection with Binarized SIFT,” in 40th International Conference on Telecommunications and Signal Processing (TSP), 2017, pp. 595–598.

[85] D. V´azquez-Pad´ın and F. P´erez-Gonz´alez, “Exposing Original and Duplicated Regions Using SIFT Features and Resampling Traces,” Digital Forensics and Watermarking. IWDW 2011. Lecture Notes in Computer Science, vol. 7128, pp. 306–320, 2012.

[86] J. Zhong and C. Pun, “An End-to-End Dense-InceptionNet for Image Copy-Move Forgery Detection,” IEEE Transactions on Information Forensics and Security, vol. 15, no. 1, pp. 2134–2146, 2019.

[87] Y. Wu, W. Abd-almageed, and P. Natarajan, “Image Copy-Move Forgery Detection via an End-to-End Deep Neural Network,” in IEEE Winter Conference on Applications of Computer Vision (WACV), 2018, pp. 1907–1915.

[88] Y. Wu, W. Abd-almageed, and P. Natarajan, “BusterNet : Detecting Copy-Move Image Forgery with Source / Target Localization,” in Proceedings of the European Conference on Computer Vision (ECCV), 2018, pp. 168–184.

[89] Y. Liu, Q. Guan, and X. Zhao, “Copy-move forgery detection based on convolutional kernel network,” Multimedia Tools and Applications, vol. 77, no. 1, pp. 18269–18293, 2018.

[90] X. Wang, H. Wang, S. Niu, and J. Zhang, “Detection and localization of image forgeries using improved mask regional convolutional neural network,” Mathematical Biosciences and Engineering, vol. 16, no. 5, pp. 4581–4593, 2019.

[91] J. H. Bappy, A. K. Roy-chowdhury, J. Bunk, L. Nataraj, and B. S. Manjunath, “Exploiting Spatial Structure for Localizing Manipulated Image Regions,” in IEEE International Conference on Computer Vision (ICCV), 2017, pp. 4970–4979.

[92] A. Doegar, M. Dutta, and G. Kumar, “CNN based Image Forgery Detection using pre-trained AlexNet Model,” International Journal of Computational Intelligence & IoT, vol. 2, no. 1, pp. 402–407, 2019.

[93] J. Ouyang, Y. Liu, and M. Liao, “Copy-Move Forgery Detection Based on Deep Learning,” in 10th International Congress on Image and Signal Processing, BioMedical Engineering and Informatics (CISP-BMEI), 2017, pp. 1–5.

[94] S. Samir, E. Emary, K. El-sayed, and H. Onsi, “Optimization of a Pre-Trained AlexNet Model for Detecting and Localizing Image Forgeries,” Information, vol. 11, no. 5, p. 275, 2020.

[95] G. Muzaffer and G. Ulutas, “A new deep learning-based method to detection of copy-move forgery in digital images,” in Scientific Meeting on Electrical-Electronics & Biomedical Engineering and Computer Science (EBBT), 2019, pp. 1–4.

[96] J. H. Bappy, C. Simons, L. Nataraj, B. S. Manjunath, and A. K. Roy-chowdhury, “Hybrid LSTM and Encoder-Decoder Architecture for Detection of Image Forgeries,” IEEE Transactions on Image Processing, vol. 28, no. 7, pp. 3286 – 3300, 2019.

[97] Y. Zhu, C. Chen, G. Yan, Y. Guo, and Y. Dong, “AR - Net : Adaptive Attention and Residual Refinement Network for Copy - Move Forgery Detection,” IEEE Transactions on Industrial Informatics, vol. 16, no. 10, pp. 6714 – 6723, 2020.

[98] B. Chen, W. Tan, G. Coatrieux, Y. Zheng, and Y.-Q. Shi, “A serial image copy-move forgery localization scheme with source / target distinguishment,” IEEE Transactions on Multimedia, 2020.

[99] A. Mazumdar and P. K. Bora, “Siamese convolutional neural network-based approach towards universal image forensics,” IET Image Processing, vol. 14, no. 13, pp. 3105–3116, 2020.

[100] P. Zhou, X. Han, V. I. Morariu, and L. S. Davis, “Learning Rich Features for Image Manipulation Detection,” in IEEE Conference on Computer Vision and Pattern Recognition (CVPR), 2018, pp. 1053–1061.

[101] R. Zhang and J. Ni, “A dense u-net with cross-layer intersection for detection and localization of image forgery,” in IEEE International Conference on Acoustics, Speech and Signal Processing (ICASSP), 2020, pp. 2982–2986.

[102] M. Zandi, A. Mahmoudi-aznaveh, and A. Mansouri, “Adaptive Matching for Copy-Move Forgery Detection,” IEEE international workshop on information forensics and security (WIFS), pp. 119–124, 2014.

[103] D. Cozzolino, G. Poggi, and L. Verdoliva, “Efficient dense-field copy-move forgery detection,” IEEE Transactions on Information Forensics and Security, vol. 10, no. 11, pp. 2284 – 2297, 2015.

[104] E. Ardizzone, A. Bruno, and G. Mazzola, “Copy-Move Forgery Detection by Matching Triangles of Keypoints,” IEEE Transactions on Information Forensics and Security, vol. 10, no. 10, pp. 2084 – 2094, 2015.

[105] B. Wen, Y. Zhu, R. Subramanian, and T.-T. Ng, “Coverage – A Novel Database For Copy-Move Forgery Detection,” in IEEE International Conference on Image Processing (ICIP), 2016.

[106] V. Christlein, C. Riess, J. Jordan, C. Riess, and E. Angelopoulou, “An Evaluation of Popular Copy-Move Forgery Detection Approaches,” IEEE Transactions on Information Forensics and Security, vol. 7, no. 6, pp. 1841–1854, 2012.

[107] J. Dong, W. Wang, and T. Tan, “CASIA image tampering detection evaluation database,” in IEEE China Summit and International Conference on Signal and Information Processing, 2013, pp. 422–426.

[108] D. Tralic, I. Zupancic, S. Grgic, and M. Grgic, “CoMoFoD - New Database for Copy-Move Forgery Detection,” in Proceedings ELMAR, 2013.

LSTM, VADER and TF-IDF based Hybrid Sentiment Analysis Model

Mohamed Chiny[1], Marouane Chihab[2], Younes Chihab[4]
Laboratory of Computer Sciences
Ibn Tofail University
Kenitra, Morocco

Omar Bencharef[3]
Department of Computer Sciences
Cadi Ayyad University
Marrakesh, Morocco

***Abstract*—Most sentiment analysis models that use supervised learning algorithms consume a lot of labeled data in the training phase in order to give satisfactory results. This is usually expensive and leads to high labor costs in real-world applications. This work consists in proposing a hybrid sentiment analysis model based on a Long Short-Term Memory network, a rule-based sentiment analysis lexicon and the Term Frequency-Inverse Document Frequency weighting method. These three (input) models are combined in a binary classification model. In the latter, each of these algorithms has been implemented: Logistic Regression, k-Nearest Neighbors, Random Forest, Support Vector Machine and Naive Bayes. Then, the model has been trained on a limited amount of data from the IMDB dataset. The results of the evaluation on the IMDB data show a significant improvement in the Accuracy and F1 score compared to the best scores recorded by the three input models separately. On the other hand, the proposed model was able to transfer the knowledge gained on the IMDB dataset to better handle a new data from Twitter US Airlines Sentiments dataset.**

Keywords*—Sentiment analysis; hybrid model; long short-term memory (LSTM); Valence Aware Dictionary and sEntiment Reasoner (VADER); term frequency-inverse document frequency (TF-IDF); classification algorithm

I. Introduction

With the massive use of social networks such as Facebook, Twitter and Instagram, and dedicated platforms for sharing reviews and comments such as IMDB and Airbnb; it has become extremely difficult to track down published information, let alone extract relevant information such as reviews about a product or service, on the one hand, because of the abundance and variety of published data [1], and on the other hand because of the unstructured nature of the published texts, which makes it almost impossible to analyze them by classical computer methods [2].

The content produced by the social media community reflects one of the richest sources of data in terms of opinions and knowledge, and offers greater opportunities for businesses, governments, and society to extract valuable, expressive, and diverse knowledge, both in terms of the content itself and context-related knowledge [3]. Indeed, decision makers need to perceive how people feel about their services in order to improve the aspects that customers find unsatisfactory. Therefore, mining and analyzing the data left on these platforms with automated tools is crucial.

Sentiment analysis is a field of analysis that aims to determine the opinion and subjectivity of people's criticisms and attitudes towards entities and its attributes from unstructured written text [4]. A multitude of sentiment vocabulary analysis methods have been proposed over the past decades. As an example, based on the emotional attributes of words, Turny [5] used a simple unsupervised classification learning algorithm to compute pointwise mutual information to measure sentence sentiment polarity.

Wang et al. [6] proposed a topic-specific sentiment analysis method based on LSTM with attention mechanism, which focused on the features of different parts of the sentence through the attention mechanism, and achieved good performance on the task of classifying topic-specific sentiments. This work was conducted to address the problem that sentiment vocabulary generally changes with context information [7]. In [8] Pang et al. advocated for the first time the supervised learning model in sentiment classification, which performed significantly better than the traditional sentiment vocabulary-based parsing algorithms [9]. In addition, this study also pointed out that sentiment classification is more challenging than general classification tasks.

Although the models analyzed in the existing literature, which are characterized by the diversity of different features, improve performance that can be evaluated by metrics such as accuracy, Recall and F1-score, these supervised models have been trained on a large volume of data and, therefore, require a lot of labeled data, which is usually costly and leads to high labor cost in real-world applications [10,11].

On the other hand, the use of an intuitive lexicon-based classification does not work well, unlike a simple text classification. The reason is that among the overwhelming number of reviews, there are reviews that do not contain any intuitively subjective words and yet express a strong opinion. Other reviews contain very pejorative words and express a positive opinion (and vice versa) [12].

The idea of our work is to propose a sentiment analysis model that uses a low volume of labeled training data, while obtaining satisfactory results. Our approach is to combine three sentiment analysis models; the Long Short-Term Memory (LSTM) model, the Valence Aware Dictionary and sEntiment Reasoner (VADER) which is a rule-based sentiment analysis lexicon built on the wisdom of the crowd and the Term Frequency-Inverse Document Frequency (TF-IDF) weighting based sentiment analysis model. Each of these three input models returns a sentiment positivity score in the text to be analyzed. Then we included a classification model where each of the following five algorithms has been implemented: Logistic Regression, k-Nearest Neighbors, Random Forest, Support Vector Machine and Naive Bayes. This classification model returns a binary result that indicates the sentiment experienced in the input text.

Our model improved the Accuracy, Recall, F-Score obtained by the three input models used individually (LSTM, VADER and TF-IDF). In addition, its evaluation on data from a different field than the one that provided the training data indicates that it was able to transfer the knowledge gained on an IMDB dataset to better handle a new Twitter US Airlines Sentiments dataset.

II. Literature Review

A. Recurrent Neural Network and Long Short-Term Memory

Recurrent neural networks (RNNs) are artificial neural networks that model the behaviors of dynamic systems using hidden states [13,14]. They have been the answer to most sequential data and natural language processing (NLP) problems for many years. This is because traditional neural networks take in a fixed amount of input data at a time and produce a fixed amount of output each time. In contrast, RNN do not consume all the inputs at once. Instead, they take them one at a time and in a sequence. At each step, the RNN performs a series of calculations before producing an output. The output, called a hidden state, is then combined with the next input in the sequence to produce another output. This process continues until the model is scheduled to terminate or the input sequence ends.

However, a major shortcoming that affects the typical RNN is the problem of gradient disappearance/explosion. This problem arises during backpropagation through the RNN during formation, especially for networks with deeper layers. For this reason, the LSTM was proposed by Sepp Hochreiter and Jürgen Schmidhuber in 1997 [15].

Long Short-Term Memory (LSTM) is a type of RNN architecture implementation that is faster and more accurate than standard RNN. Indeed, LSTM leads to many more successful executions and learns much faster. It also solves complex tasks that have never been solved by previous recurrent network algorithms and shows better performance for long range sequences than conventional RNN architectures [16,15].

LSTM has found its application in many fields that require sequential models, in this case NLP and especially in sentiment analysis. For example, Thomas et al. [17] modeled the LSTM neural network to find the sentiment of transliterated text that has become the language of social media websites such as WhatsApp, Facebook and Twitter. A transliterated dataset is collected using scrapping of different websites. A sample of 10,000 datasets was prepared. Two of the layers were created for training and testing the data. Their model was trained with 65 units and a learning rate of 0.01. This work was able to achieve an average accuracy of 0.8151.

In order to solve sentiment analysis problems and improve the execution time, Zhixing et al. [9] proposed a fast sentiment analysis algorithm, called FAST-BiLSTM. The algorithm is realized by merging FastText and Bi-LSTM models. First, FastText has a fast speed for linear fitting and can generate pre-trained word vectors as a by-product. Second, Bi-LSTM uses the generated word vectors for training and then merges with FastText to perform full sentiment analysis. The results show that the temporal efficiency of the algorithm is improved by more than 30% and that FAST-BiLSTM can sufficiently extract contextual semantic information from texts.

In a similar context, a new architecture is proposed by Soubraylu et al. [18] by combining long-term memory (LSTM) with word embedding to extract the semantic relationship between neighboring words, and weighted self-attention is also applied to extract key terms from reviews. Based on the experimental analysis of the IMDB dataset, the authors showed that the proposed word-embedded self-attention LSTM architecture achieved an F1 score of 88.67%, while the LSTM and word-embedding based LSTM models resulted in an F1 score of 84.42% and 85.69%, respectively. In [6], Wang et al. propose an LSTM that provides an attention mechanism to focus on different parts of the opinion sentence, given several aspects. Embedding of the aspect expression is taken into account with word sequence folding to assign attention weights with respect to a given aspect to each word.

In order to propose software to extract Business Intelligence from SA using a modified LSTM algorithm by having a different activation function. Sreesurya et al. [20] analyzed the data using LSTM machine learning approach, evaluating the sentiments on a scale from -100 to 100. A new proposed activation function is used for LSTM giving the best results compared to the existing artificial neural network (ANN) techniques. In [21], Dhanalakshmi et al. propose an analytics system that collects employee comments from open forums and performs sentiment analysis using the RNN-LSTM algorithm. In the sentiment analysis, the employee comments are classified as positive or negative so that the organization can identify the social sentiments of its brand and can take corrective actions to retain the employees. This paper also captures the performance of various models in training and predicting the employee feedback dataset and the models evaluated are logistic regression, support vector machine, random forest classifier, AdaBoost classifier, gradient amplification classifier, decision tree classifier and Gaussian Naive Bayes. The classification ratio and accuracy of each model are captured. When training the RNN-LSTM algorithm with a dataset of size 30k, the accuracy was 88%.

LSTM networks have also shown good performances in various domains such as meteorology [22], finance [23,24], medicine [25,26], image description generation [27,28], motion prediction in video sequences [29,30] and machine translation [31,32].

B. Valence Aware Dictionary and Sentiment Reasoner Lexicon and Rule-based Sentiment Analysis

The specific nature of social media content poses serious challenges to applications of sentiment analysis due to its huge bias and big data nature [33, 34]. Indeed, traditional methods of textual sentiment analysis are mainly devoted to the study of extended texts, such as news stories and full documents. Microblogs are considered short texts that are often characterized by large noises, new words, and abbreviations. Previous emotion classification methods generally fail to extract meaningful features and produce a poor classification effect when applied to the processing of short texts or microtexts [35].

Valence Aware Dictionary and sEntiment Reasoner (VADER) is a rule-based lexicon and sentiment analysis tool that is specifically adapted to sentiments expressed in social media. VADER uses a sentiment lexicon which is a list of lexical features that are generally labeled based on their semantic orientation as positive or negative.

VADER is based on a wisdom of crowds (WotC) approach [36] to acquire a valid point estimate of the sentiment valence (intensity) of each lexical feature. The VADER evaluation was conducted by ten independent human raters (for a total of over 90,000 ratings), leading to the adoption of 7,500 lexical features with valence scores that indicate the polarity and intensity of sentiment on a scale of -4 (Extremely negative) to +4 (Extremely positive) [34]. This work has shown that VADER's performance exceeds even individual human raters.

VADER is sensitive to both the polarity and intensity (how positive or negative the sentiment is) of emotions, and it is adapted to the content of social networks that generally use informal writing (several punctuation marks, acronyms, emoticon, slang...). Indeed, some of the heuristics used by VADER to incorporate the impact of each subtext on the perceived intensity of the sentiment in the text are part of the writing style on social networks, in this case punctuation (such as the exclamation mark that increases the magnitude of the perceived intensity) and capitalization that emphasizes an important word for the sentiment in the presence of other non-capitalized words [34].

The fact that VADER is a pre-trained model gives it an advantage with respect to users. For example, Borg et al. [37] examine sentiment analysis among customers of a large Swedish telecommunications company. The dataset consists of 168010 emails with no sentiment information available. Therefore, the VADER model is used together with a Swedish sentiment lexicon to provide an initial labeling of the emails. It is after the labeling provided by VADER that the content is used to train two Support Vector Machine models in extracting and classifying the sentiment of the e-mails. In another work, Valdez et al. [38] analyzed the average daily sentiment of 86,581,237 U.S. time-series tweets with the VADER tool to understand what themes emerge from a corpus of U.S. tweets about COVID-19 and whether the sentiment changes in response to the pandemic. In [39], Al Mansoori et al. attempted to assess criminal behavior on Facebook and Twitter, and effectively classify the collected data as negative, positive, or neutral in order to identify a suspect by performing sentiment analysis using the VADER model. The VADER model was also used by Scholz et al [40] to perform an integrated semantic analysis to provide the sentiment of tweets retrieved between 2008 and August 2018 for the purpose of detecting tourism flows in the province of Styria in Austria.

C. *Term Frequency-Inverse Document Frequency*

Statistical approaches such as machine learning and deep learning work well with numerical data. However, natural language consists of words and sentences. Therefore, before a sentiment analysis model can be created, text must often be converted into numbers. For this purpose, several approaches have been developed, such as Bag of Words, N-grams, Word2Vec and TF-IDF.

The Term Frequency-Inverse Document Frequency (TF-IDF) algorithm [41, 42, 43] is used to evaluate the importance of words in a textual corpus. The importance is proportional to the number of times the words appear in the document and inversely proportional to the frequency of words appearing in the corpus. Indeed, in a simple Bag of Words, each word has the same importance. The idea behind TF-IDF is that words that appear more frequently in one document and less frequently in other documents should have more importance because they are more useful for classification.

TF represents the frequency of words, i.e. the number of times they appear in a corpus (Func 1). This consists in calculating the number of occurrences of the word out of the total number of words present in the corpus.

$$tf_i = \frac{n_i}{\sum_k n_k} \quad (1)$$

$$idf_i = \log \frac{|D|}{|\{d_j : t_i \in d_j\}|} \quad (2)$$

$$tfidf_i = tf_i \, idf_i \quad (3)$$

IDF is the measure of the importance of the term in the whole corpus. It consists in calculating the logarithm of the inverse of the proportion of documents in the corpus that contain the term (Func 2). This consists in calculating the total number of documents contained in the corpus over the number of documents where the word is present. It is the logarithm of this result that constitutes the value of the IDF.

The TF-IDF weight is calculated by multiplying the two measures (Func 3). Thus, the higher the weight, the more significant the word in question is within the corpus.

The TF-IDF algorithm is often applied to texts for sentiment analysis. For example, Soumya et al. [44] performed sentiment analysis of Malayalam tweets using machine learning techniques. They used TF-IDF and Unigram with Sentiwordnet for training feature vectors of the input dataset, before classifying them using different techniques such as Naive Bayes (NB), Support Vector Machine (SVM) and Random Forest (RF). In [45], Ullah et al. proposed an algorithm and method for sentiment analysis using both text and emoticons. The two modes of data were analyzed in combination and separately with machine learning and deep learning algorithms to find sentiments from Twitter-based airline data using several features such as TF-IDF, N-gram and emoticon lexicons. On the other hand, Ayo et al. [46] adopted an approach that proposes an improved hybrid integration with a topic inference method and an improved neural network for hate speech detection in Twitter data. The proposed method uses a hybrid nesting technique that includes TF-IDF for word-level feature extraction and LSTM long-term memory for sentence-level feature extraction.

III. Architecture of our Hybrid Sentiment Analysis Model

The objective of our study is to build a hybrid sentiment analysis model (Fig. 1) that is based on three input models:

- A model based on the use of LSTM layer and which was trained on a corpus of labeled IMDB reviews.
- The VADER lexicon which is a pre-trained model based mainly on the wisdom of the crowd.
- A TF-IDF model that takes into account the importance of words in the text to estimate the sentiment. This model was also trained on the same dataset as the LSTM model.

The scores calculated by these three models are then combined in a classification model that returns whether the sentiment of the input occurrence is positive or negative.

A. LSTM Model

LSTM is a class of powerful neural networks for modeling sequence data such as time series or natural language. An optimal use of LSTM layer requires the preparation of the text to be analyzed. This preparation consists of cleaning and filtering, followed by tokenization, then word embedding. The vector representation of the words in the sentence is the input to our LSTM model which uses Softmax as an activation function to produce a multi-class categorical probability distribution and the Cross Entropy loss function.

1) Cleaning and filtering: Once the sentence to be evaluated is available at the input of our model, it is first cleaned in order to eliminate all occurrences that may bias the subsequent processing, such as multiple spaces or spurious characters like excessive successions of punctuation marks.

The filtering operation was also carried out on the data used to train and test our model. This is an IMDB dataset containing 50,000 movie reviews for natural language processing, text analysis or binary sentiment classification [47].

2) Tokenization: Tokenization is a process used to divide text into single words (unigram) or combinations of successive words (n-gram). This operation also creates an index mapping dictionary using the vocabulary of all the words in the model training text.

The N-gram model is widely used in computational linguistics to predict the next element in such a contiguous sequence of n elements from a particular sample of text. However, in our case, and in order to use the GloVe model, the text has been divided into one-word tokens.

The resulting sequences have different lengths, and in order to handle both short and long criticisms, it is preferable that all entries have the same length. This length has been defined as the sequence length. This sequence length is identical to the number of time steps for the LSTM layer and is the maximum length calculated for a comment in the training corpus (1744 tokens).

3) Word Embedding with GloVe: Word embedding is a class of approaches for representing words using a dense vector representation. It is an improvement over traditional bag-of-words model coding schemes which consist in marking each word in a vector to represent an entire vocabulary. Since the latter is vast, then a given word will be represented by a large vector consisting mostly of null values.

Semantic vector space models of the language represent each word with a real-valued vector. Vectors can be used as features in various applications, such as document classification [48] or named entity recognition [49]. Indeed, Word embedding improves text classification by solving the sparse matrix and word semantics problem.

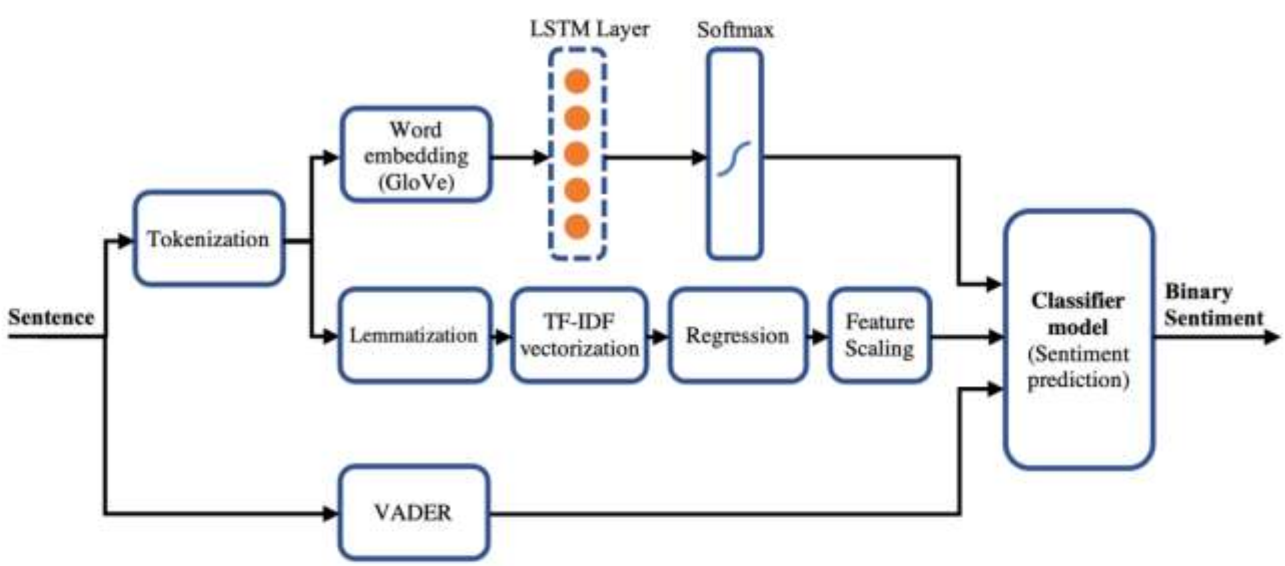

Fig. 1. Proposed LSTM, VADER and TF-IDF based Hybrid Sentiment Analysis Model.

The two most common word integrations are: Word2Vec and GloVe.However, GloVe (Global Vectors for Word Representation), as its name suggests, is better at preserving global contexts because it creates a global co-occurrence matrix by estimating the probability that a given word co-occurs with other words.

GloVe is an unsupervised learning algorithm for obtaining vector representations of words. Training is performed on global word-word co-occurrence statistics aggregated from a corpus, and the resulting representations have linear substructures of the word vector space [50]. 100-dimensional GloVe integrations of 400,000 calculated words were used.

4) LSTM layer: When defining the LSTM layer, 256 hidden units have been fixed. This layer is linked to a Softmax activation function. The Adam optimizer, which is one of the methods that compute the learning rate, known to work well in practice, and compares favorably with other adaptive learning algorithms has been used (Table I).

5) Softmax layer: The softmax function is a function that transforms a vector of K real values into a vector of K real values that sum to 1. Whatever the values of the input, the softmax transforms them into values between 0 and 1, so that they can be interpreted as probabilities.

Softmax is a generalization of logistic regression that can be used for multi-class classification. Many multi-layer neural networks end with a penultimate layer that produces real-valued scores that are not properly scaled and can be difficult to work with. Here, the softmax is very useful because it converts the scores to a normalized probability distribution.

In our case, the softmax layer outputs two probability scores that correspond to the positivity and negativity of the input sequence.

Training and evaluation of the LSTM model

From the 50,000 reviews available in the dataset, 5,000 reviews were selected from the train set and 2,000 from the test set of our LSTM model. We checked that the number of positive reviews and the number of negative reviews in the dataset were balanced. Most of these reviews consist of several hundred words, and some reviews exceed a thousand words. The average number of words used in the reviews in the dataset is 1309.

TABLE I. HYPER-PARAMETERS OF THE LSTM MODEL

Hyper-parameter	Value
Input vocab size	1744
Output embedding dimension	100
LSTM layer internal units	256
Optimizer	Adam
Loss	Categorical Crossentropy
Activation function	Softmax

B. VADER Lexicon

VADER (Valence Aware Dictionary and sEntiment Reasoner) is a rule-based lexicon and sentiment analysis tool that is specifically adapted to sentiments expressed in social media. VADER uses a combination of a sentiment lexicon and a list of lexical features (e.g., words) that are generally labeled according to their semantic orientation as positive or negative.

VADER produces four measures of sentiment from these word ratings. The first three, positive, neutral, and negative, represent the proportion of text that falls into these categories. The final metric, the composite score, is the sum of all lexicon scores that have been normalized between -1 and 1.

It should be recalled that the VADER model is sensitive to punctuation and capitalization [34]. Therefore, special characters have not been filtered out and text has not been converted to lowercase in order to capture the full sentiment.

Evaluation of the VADER model

The VADER model was evaluated on the same test dataset used for the evaluation of the LSTM model (2000 opinion). The composite score was retained after normalizing it between 0 and 1.

C. TF-IDF Model

The TF-IDF approach is used to create numerical feature vectors from text. It is a method very often used in text classification that gives information about the occurrence of words.

1) Data pre-processing: As for the LSTM model, the targeted sentence is first cleaned to eliminate all unnecessary occurrences such as multiple spaces, strings of numbers or URLs... Then all the text is converted to lowercase so as not to have 2 different dimensions for the same word at the time of vectorization

Stopwords have also been removed from the text. These are very common words in the studied language that do not bring any informative value for the understanding of the meaning of a document and corpus. In addition, they are very frequent and are part of the common vocabulary, which has the effect of significantly impacting the speed of the processing that follows.

2) Tokenization and lemmatization: The same tokenization module used for the LSTM model is used for the TF-IDF model, i.e. the input texts have been segmented into tokens of one word each (unigram) before being lemmatized.

Lemmatization refers to a lexical treatment of a text in order to analyze it. Stemming and lemmatization refer to text normalization in the field of natural language processing and are widely used in text mining.

The difference between stemming and lemmatization is that stemming simply removes the last characters, which often leads to incorrect meanings and sometimes even misspellings, whereas lemmatization considers the context and converts the word into its canonical form recorded in the dictionaries of the relevant base language.

For our model, WordNet lemmatizer which uses the WordNet repository database to search for word lemmas has been used. Indeed, Wordnet [51] is a large lexical database, freely and publicly available for the English language, aiming at establishing structured semantic relations between words. Nouns, verbs, adjectives and adverbs are grouped into cognitive synonym sets (synsets), each expressing a distinct concept. The majority of WordNet's relationships connect words from the same Part Of Speech (POS). Among the features it offers is one of the oldest and most commonly used lemmatizers.

3) TF-IDF vectorization: Unlike a Bag of Words (BoW) which converts text into a feature vector by counting the occurrence of words in a document without considering their importance, TF-IDF is based on the Bag of Words (BoW) model, which contains information about the most important and least important words in a document.

In order to convert a collection of raw documents into a TF-IDF feature matrix, a vocabulary which only considers the first 500 terms classified by term frequency in the corpus has been built, and then removed terms that appear too frequently (in more than 50% of documents) or infrequently (in less than 7 documents) (Table II). This allows us to ignore words that have very few occurrences to be considered significant, or conversely, too frequent in the corpus.

4) Linear regression: Regression is a method of modeling a variable (called target) as a function of independent predictors (called features), where the algorithm involved tries to find causal relationships between the variables [52].

Since the TF-IDF feature matrix contains 500 dimensions, and each of these dimensions represents a relevance score of each word ($tfidf_i$), our goal is to establish a regression model (Func 4) that will allow us to compute the relative weights (β_i) to the 500 most significant words in the corpus with respect to the sentiment score ($Score_i$).

$$Score_i = \sum_{i=1}^{500} \beta_i \, tfidf_i \tag{4}$$

In this kind of application (sentiment analysis), it is rather classification models that are used and not regression models. However, the objective is not to calculate a binary score, but a continuous value (like the scores calculated with the LSTM and VADER models). These three scores will constitute the inputs of the final classification model (Fig. 1).

In order to train the regression model, the same dataset as the one used for training the LSTM model (5000 reviews) was used.

TABLE II. HYPER-PARAMETERS OF THE TF-IDF MODEL

Hyper-paramter	Value
max_features	500
min_df	7 documents
max_df	50% of documents

5) Feature scaling: Many machine learning algorithms work better or converge faster when the features are relatively similar in scale and close to the normal distribution, including linear regression. However, the output of our regression model gives prediction values outside the interval [0,1] (unlike the LSTM and VADER models). In order to help the features arrive in a more suitable form to the Classifier model, normalization of the prediction values of this output was performed.

Evaluation of the TF-IDF model

The TF-IDF model was evaluated on the same test set used to evaluate the LSTM and VADER models (2000 reviews). The evaluation scores of the three models (LSTM, VADER and TF-IDF) are used as reference values to compare them to the scores of our proposed architecture in this study.

D. CLASSIFIER Model

We recall that our objective is to combine the 3 models of sentiment analysis of the input with a classification model in order to improve the performance of predictions on the sentiment conveyed through the input text. Indeed, the LSTM model, which is part of the RNN, is distinguished by its ability to adapt to sequential data. The VADER model has proven its efficiency in the microblogging domain. Finally, the TF-IDF model is characterized by its ability to handle the most significant words in a document. A higher Accuracy and F1 scores than those obtained by the three models used separately on the same data is expected. We also recall that the LSTM and TF-IDF models have been trained on IMDB review texts, while VADER is a pre-trained model.

Our classification model contains three inputs that are directly related to the outputs of the LSTM, VADER and TF-IDF models. The values of these inputs are continuous in a range of [0,1] and the output of the classification model returns a binary result (positive or negative) which is the prediction of the sentiment of the text of the full model input (Fig. 1).

5000 random reviews have been selected from the dataset that are different from the training set and test set data used for the LSTM and TF-IDF models. We ran them through the input of our global model to obtain the predictions computed by the LSTM, VADER and TF-IDF models. Then we divided these results into two batches (75% for the train set and 25% for the test set), in order to train and evaluate our binary classification model, implementing each of the following five classification algorithms: Logistic Regression (LR), k Nearest Neighbors (k-NN), Random Forest (RF), Support Vector Machine (SVM) and Naive Bayes (NB).

The hyper-parameters of each of the classification algorithms used were manipulated to have the best possible evaluations for our data set. Table III gives an overview of the most important hyperparameters that were applied to our classification models.

TABLE III. MOST IMPORTANT HYPER-PARAMETERS APPLIED TO THE ALGORITHMS IMPLEMENTED IN THE CLASSIFICATION MODEL

Algorithme	Hyper-parametre	Value
Logistic Regression	Inverse of regularization strength	1
k Nearest Neighbors	Number of neighbors	13
Random Forest	Number of trees in the forest Maximum depth of the tree	19 4
Support Vector Machine	Regularization parameter Kernel type	1 Linear
Naive Bayes	Var smoothing	1e-09

IV. RESULTS

A. Evaluation of the Binary Classification Model

The binary classification model is the block that returns the final result of the sentiment experienced in the input text of the full model. Its three inputs come from the three input models (LSTM, VADER and TF-IDF). Table IV lists the Accuracy of each classification model following its evaluation on the test data.

TABLE IV. ACCURACY EVALUATED FOR THE ALGORITHMS IMPLEMENTED IN THE CLASSIFICATION MODEL

Model	Accuracy
Logistic Regression	0.888
k Nearest Neighbors	0.868
Random Forest	0.876
Support Vector Machine	0.884
Naive Bayes	0.868

B. Evaluation of our Model with IMDB Dataset Data

In the following, the results obtained using the proposed architecture will be exposed. In order to better identify the performance improvement that it has allowed, the complete model was evaluated on the same test set that evaluated the LSTM, VADER and TF-IDF models separately.

Fig. 2 shows mean micro-averaged for the model by implementing the five different algorithms in the model Classifier. Table I shows that after training the LSTM model, its evaluation on the test set gave an accuracy of 0.829 and an F1 score of 0.835. As for the VADER model (which is a pre-trained model), its evaluation on the same testset gave an accuracy of 0.723 and an F1 Score of 0.766. With the TF-IDF model, an accuracy of 0.789 and an F1 score of 0.792 have been obtained. Between these three basic models, it turns out that the LSTM model shows higher scores in terms of accuracy, Recall and F1 score.

Table V displays the performance metrics (Accuracy, Recall and F1 score) of the 3 input models (LSTM, VADER and TF-IDF) on the IMDB test data.

TABLE V. PERFORMANCE METRICS EXPECTED BY THE THREE INPUT MODELS ON IMDB DATA

Model	Accuracy	Recall	F1 Score
LSTM	0.829	0.827	0.835
VADER	0.723	0.675	0.766
TF-IDF	0.789	0.803	0.792

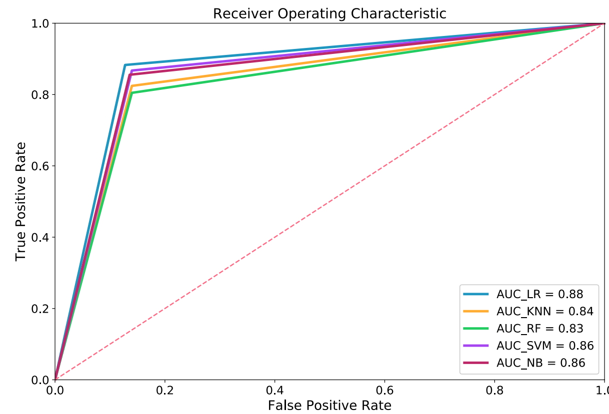

Fig. 2. AUC of the Proposed Model by implementing the different Classification Algorithms when Predicting Sentiment on IMDB Data.

After training and evaluating our model using the five proposed classification algorithms, the performance metrics shown in Table VI have been obtained.

TABLE VI. PERFORMANCE METRICS ACHIEVED BY OUR MODEL BY IMPLEMENTING THE 5 CLASSIFICATION ALGORITHMS ON IMDB DATA

Model	Accuracy	Recall	F1 Score
Logistic Regression	0.878	0.882	0.881
k Nearst Neighbors	0.841	0.824	0.842
Random Forest	0.831	0.804	0.830
Support Vector Machine	0.863	0.867	0.867
Naive Bayes	0.860	0.855	0.862

The evaluation scores obtained using our model is different depending on the classification algorithm used. However, whatever the algorithm, the scores are better than those obtained using the three models LSTM, VADER and TF-IDF separately, except for the F1 scores obtained using Random Forest (0.83) which is slightly lower than the F1 scores obtained using the LSTM model (0.835), but higher than the F1 scores obtained using VADER and TF-IDF (respectively 0.766 and 0.792).

The average Accuracy obtained using our model using the 5 classification algorithms separately (0.854) is 9.517% higher than the average Accuracy obtained using the three models LSTM, VADER and TF-IDF (0.780%), and the average F1 score obtained using the full model (0.856) is 7.363% higher than that obtained using the three models separately (0.797) (Table VI).

It should be noted that the Logistic Regression model offers a better Accuracy (0.878) compared to the accuracy obtained with the three models LSTM, VADER and TFIDF (respectively 0.829, 0.723 and 0.789), i.e. 5.91% higher than the accuracy obtained with LSTM which is the best score recorded among the 3 initial models. Logistic Regression also offers a better F1 score (0.881) which is 5.51% higher than the F1 score of LSTM (0.835) (Table VII).

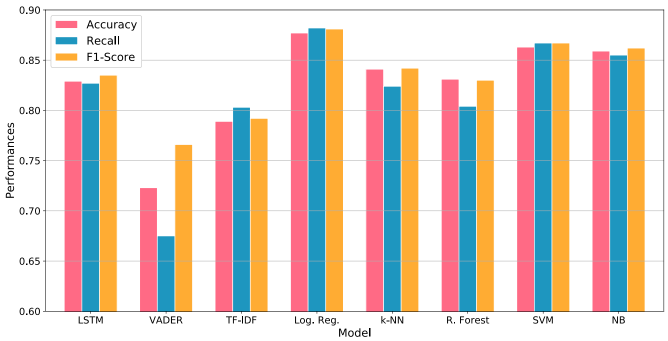

Fig. 3. Representation of the Evaluation Metrics on IMDB Data.

Overall, Fig. 3 shows that our model gave the best performance using the Logistic Regression, k-NN, SVM and Naive Bayes models. The Random Forest model on the other hand gave a slightly lower F1 score than the LSTM model, but still outperformed VADER and TF-IDF.

TABLE VII. RELATIVE IMPROVEMENT RECORDED BY EACH CLASSIFICATION ALGORITHM COMPARED TO THE BEST SCORES DISPLAYED BY THE INPUT MODELS ON THE IMDB DATA

Model	Accuracy improvement	F1 Score improvement
Logistic Regression	+5.91%	+5.51%
k Nearst Neighbors	+1.44%	+0.83%
Random Forest	+0.24%	-0.59%
Support Vector Machine	+4.10%	+3.83%
k-Means	+3.74%	+3.23%
Mean	+9.51%	+7.36%

C. Evaluation of our Model with Data from the Twitter Dataset

The proposed model has also been evaluated on a US Airlines Sentiments Twitter dataset available on Kaggle [53]. This is a set of labeled tweets that was posed as a binary classification problem. The dataset contains 14427 unique texts that were used as a test set for our models.

It should be noted that the structure of the data encompassed in this dataset is different from that of the IMDB movie review dataset. On the one hand, the tweets contain text that is too short (with an average of 104 words, compared to 1309 words for the IMDB reviews), and on the other hand, due to the nature of the topic being reviewed, the vocabulary used most likely contains words that our LSTM and TF-IDF models never saw during training.

Fig. 4 shows mean micro-averaged for the model by implementing the five different algorithms in the model Classifier. Obviously, the performance of the LSTM and TF-IDF models has dropped considerably. Indeed, the accuracy score and the F1 score of the LSTM model are respectively 0.66 and 0.67. For the TF-IDF model, these scores are respectively 0.667 and 0.637. On the other hand, the VADER model showed almost the same scores as for the IMDB data (Table VIII).

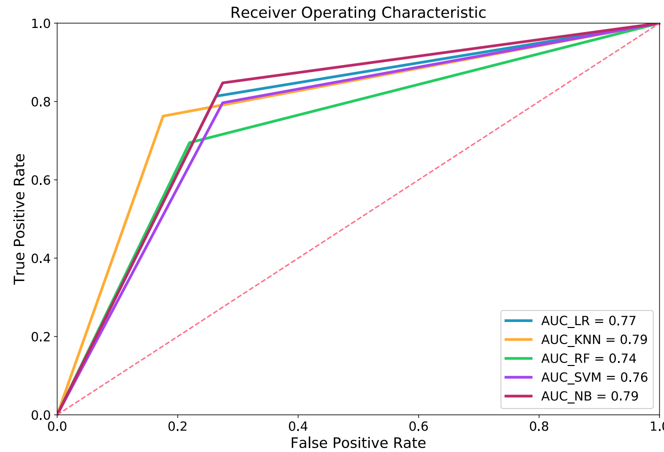

Fig. 4. AUC of the Proposed Model by Implementing the different Classification Algorithms when Predicting the Sentiment on the Twitter US Airlines Sentiments Data.

TABLE VIII. PERFORMANCE METRICS DISPLAYED BY THE 3 INPUT MODELS ON THE US AIRLINES SENTIMENTS TWITTER DATA

Model	Accuracy	Recall	F1 Score
LSTM	0.660	0.541	0.670
VADER	0.720	0.591	0.723
TF-IDF	0.667	0.556	0.637

However, the Accuracy score of our model remains higher than that of the LSTM, TF-IDF and VADER models (0.767, 0.8, 0.747, 0.754 and 0.773 for Logistic Regression, k Nearest Neighbors, Random Forest, SVM and Naive Bayes respectively). The same is true for the F1 score of the three models Logistic Regression, k-NN and Naive Bayes which are respectively 0.733, 0.75 and 0.746 (Table IX).

TABLE IX. PERFORMANCE METRICS ACHIEVED BY OUR MODEL BY IMPLEMENTING THE FIVE CLASSIFICIATION ALGORITHMS ON THE TWITTER US AIRLINES SENTIMENTS DATA

Model	Accuracy	Recall	F1 Score
Logistic Regression	0.767	0.813	0.733
k Nearst Neighbors	0.800	0.762	0.750
Random Forest	0.747	0.695	0.683
Support Vector Machine	0.754	0.797	0.717
Naive Bayes	0.773	0.847	0.746

The average Accuracy obtained using our model using the five classification algorithms separately is 12.58% higher than the average Accuracy obtained using the three models LSTM, VADER and TF-IDF, and the average F1 score obtained using the full model is 7.26% higher than that obtained using the three models separately (Table X).

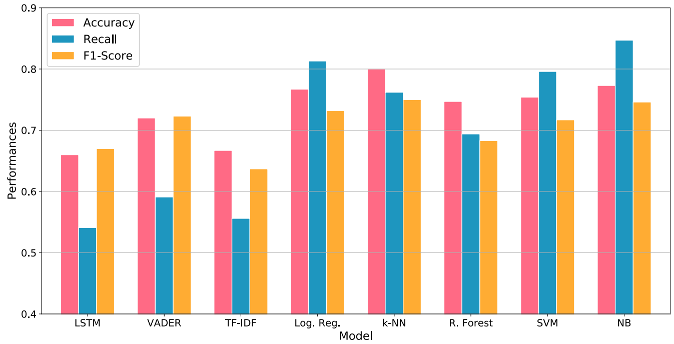

Fig. 5. Representation of Evaluation Metrics on US Airlines Sentiments Twitter Data.

If the VADER model which displayed the best scores (Accuracy=0.72 and F1 score=0.723) is taken as a reference, then we can notice that the proposed model recorded an improvement in accuracy and F1 score (respectively 11.11% and 3.73%) using the k-NN algorithm.

TABLE X. RELATIVE IMPROVEMENT RECORDED BY EACH CLASSIFICATION ALGORITHM COMPARED TO THE BEST SCORES DISPLAYED BY THE INPUT MODELS ON THE DATA AFTER THE EVALUATION OF OUR MODEL ON THE TWITTER US AIRLINES SENTIMENTS DATA

Model	**Accuracy improvement**	**F1 Score improvement**
Logistic Regression	+6.52	+1.38
k Nearest Neighbors	+11.11	+3.73
Random Forest	+3.75	-5.53
Support Vector Machine	+4.72	-0.83
Naive Bayes	+7.36	+3.18
Mean	+12.58	+7.26

Fig. 5 clearly illustrates that our model performed well (compared to the three input models), in this case if our classifier model implements the Logistic regression, k-NN and Naive Bayes algorithms.

V. DISCUSSION

According to the results obtained, the proposed model shows better performances in terms of accuracy and F1 score, and which can exceed the performances of the best among the three input models (LSTM, VADER and TF-IDF) by 5.91% for accuracy and 5.51% for F1 Score. This peak was obtained by implementing the Logistic Regression algorithm in our Classifier model and by evaluating our model on the IMBD dataset, knowing that the training data also comes from this same dataset.

On the other hand, when the proposed model has been evaluated using the Twitter US Airlines Sentiments dataset, the performance obviously decreased, but it remains globally more advantageous than those obtained using the three input models. Indeed, we were able to record a higher accuracy score of 11.11% and a higher F1 score of 3.73% using the k-NN algorithm. These comparisons were made with respect to the highest Accuracy and F1 scores that were displayed by the VADER model (0.72 and 0.723, respectively).

It would be useful to recall that the structure of the US Airlines Sentiments Twitter dataset is different from the IMDB movie review dataset in terms of text size and vocabulary used. However, our model managed to display better scores compared to the three input models (LSTM, VADER and TF-IDF).

This improvement could be explained by the combination of the different techniques used in the three input models. Indeed, LSTM is more adapted to sequential data such as time series, speech and text [16]. VADER is a pre-trained lexicon focused on the wisdom of the crowd and mainly adapted to microblog data [34]. TF-IDF, on the other hand, takes into account the presence of the most significant words in a textual corpus [41]. We can therefore conclude that the combination of these three basic models through a classification model has allowed this performance improvement by capturing each of the different features of the input text according to their operating mode.

On the other hand, considering that most machine learning algorithms are based on the assumption that the training dataset and the test dataset belong to the same descriptor space and follow the same probability distribution [19], our model was able to transfer the knowledge gained on an IMDB dataset to better process a new US Airlines Sentiments Twitter dataset. Although the scores obtained are not very high, they are still much better than those obtained by the LSTM, VADER and TF-IDF models separately.

VI. CONCLUSION

The content created by users of social media (such as Twitter, Facebook or Instagram) and dedicated platforms (such as IMDB or Airbnb) reflects one of the richest sources of data in terms of opinions and knowledge. The data they encompass offers great opportunities for companies to extract valuable and expressive knowledge. For this reason, a field like sentiment analysis, which seeks to determine the opinion and subjectivity of people's reviews from unstructured written text, is growing rapidly.

Although for more than a decade, many sentiment analysis models have been proposed, they are generally data-intensive and computationally expensive. Indeed, most of these models generally require a huge amount of training data to achieve satisfactory performance metrics, namely, accuracy and F1 score.

The objective of our study is to propose a hybrid sentiment analysis model based on three basic models, namely, LSTM, VADER and TF-IDF. Each of these models captures different specifications of the same text. These models are then combined in a classification model where each of the following five algorithms has been implemented: Logistic Regression, k-Nearest Neighbors, Random Forest, Support Vector Machine and Naive Bayes. The output of our model delivers a binary score that reflects the sentiment of the input text. The proposed model was trained on 5000 IMDB movie reviews and then evaluated on other reviews from the same dataset, then it was evaluated on Twitter US Airlines Sentiments which has a different structure in terms of text size and vocabulary used.

The results suggest that, depending on the classification algorithm implemented, our model displays higher Accuracy and F1 scores than those achieved by the three basic models. Indeed, with Logistic Regression, an improvement of 5.91% for the Accuracy and 5.51% for the F1 Score on the evaluation data of the IMBD dataset has been noted. These scores were calculated with respect to the best performances achieved by the three basic models.

After evaluating our model on the US Airlines Sentiment Twitter data, an overall decrease in performance has been noted. However, the performance of the model is still much higher than those recorded by the three basic models. Indeed, we were able to record a higher accuracy score of 11.11% and a higher F1 score of 3.73% using the k-NN algorithm, which indicates that our model was able to transfer the knowledge acquired on an IMDB dataset to better process a new US Airlines Sentiments Twitter dataset.

As a perspective, it would be interesting to improve the proposed model by implementing a BiLSTM model based on self-attention in order to capture the polarity of a whole sentence that may contain several term-aspects. Such an improvement would have a significant impact on the evaluation metrics, namely the accuracy and the F1 Score.

References

[1] Sepideh Bazzaz Abkenar, Mostafa Haghi Kashani, Ebrahim Mahdipour, Seyed Mahdi Jameii. Big data analytics meets social media: A systematic review of techniques, open issues, and future directions. Telematics and Informatics, 101517, 2020. doi:10.1016/j.tele.2020.101517.

[2] Soubraylu Sivakumar, Ratnavel Rajalakshmi. Analysis of Sentiment on Movie Reviews Using Word Embedding Self-Attentive LSTM, International Journal of Ambient Computing and Intelligence (IJACI)12(2), 2021.

[3] M. Baumgarten, Maurice Mulvenna, N. Rooney, J. Reid. Keyword-Based Sentiment Mining using Twitter, International Journal of Ambient Computing and Intelligence, 2015.

[4] Tetsuya Nasukawa and Jeonghee Yi. Sentiment analysis: Capturing favorability using natural language processing. In Proceedings of the 2nd international conference on Knowledge capture, pages 70–77. ACM, 2003.

[5] P. D. Turney. Thumbs up or thumbs down? Semantic orientation applied to unsupervised classification of reviews, 40th Annual Meeting on Association for Computational Linguistics, Stroudsburg, USA, 2002.

[6] WANG Y., HUANG M., ZHU X. & ZHAO L. Attention-based LSTM for aspect-level sentiment classification. In J. SU, X. CARRERAS & K. DUH, Eds., Proceedings of the 2016 Conference on Empirical Methods in Natural Language Processing, EMNLP 2016, Austin, Texas, USA, November 2016, p. 606–615 : The Association for Computational Linguistics.

[7] T. Mike, B. Kevan, P. Georgios, C. Di and K. Arvid. Sentiment in short strength detection informal text. Journal of the American Society for Information Science & Technology, vol. 61(12), 2010.

[8] B. Pang, L. Lee and S. Vaithyanathan. Thumbs up? Sentiment classification using machine learning techniques, Conf. on Empirical Methods in Natural Language Processing, Brussels, Belgium, 2018.

[9] Zhixing Lin, Like Wang, Xiaoli Cui, Yongxiang Gu. Fast Sentiment Analysis Algorithm Based on Double Model Fusion, Computer Systems Science & Engineering, 2020.

[10] F. Koto and M. Adriani. HBE: Hashtag-based emotion lexicons for twitter sentiment analysis, 7th Forum for Information Retrieval Evaluation, New York, USA, 2015.

[11] X. C. Huang, Y. H. Rao, H. R. Xie, T. L. Wong and F. L. Wang. Cross-domain sentiment classification via topic- related TrAdaBoost, Association for the Advancement of Artificial Intelligence Conf, San Francisco, USA, 2017.

[12] Anaïs Collomb, Crina Costea, Damien Joyeux, Omar Hasan, Lionel Brunie. A Study and Comparison of Sentiment Analysis Methods for Reputation Evaluation, Laboratoire d'InfoRmatique en Image et Systèmes d'information, 2013.

[13] K.-i. Funahashi and Y. Nakamura. Approximation of dynamical systems by continuous time recurrent neural networks, Neural networks, vol. 6, no. 6, pp. 801–806, 1993.

[14] A. Delgado, C. Kambhampati, K. Warwick. Dynamic recurrent neural-network for system-identification and control. IEE Proceedings – Contro, 1995.

[15] S. Hochreiter, J. Schmidhuber. Long Short-Term Memory. Neural Computation, 9(8), 1735–1780, 1997. doi:10.1162/neco.1997.9.8.1735.

[16] Y. J. Kim, S. Choi, S. Briceno, D. Mavris. A deep learning approach to flight delay prediction. 2016 IEEE/AIAA 35th Digital Avionics Systems Conference (DASC), 2016. doi:10.1109/dasc.2016.7778092.

[17] M. Thomas, C. A. Latha. Sentimental analysis of transliterated text in Malayalam using recurrent neural networks. Journal of Ambient Intelligence and Humanized Computing, 2020. doi:10.1007/s12652-020-02305-3.

[18] Soubraylu Sivakumar, Ratnavel Rajalakshmi, Analysis of Sentiment on Movie Reviews Using Word Embedding Self-Attentive LSTM, International Journal of Ambient Computing and Intelligence (IJACI)12(2), 2021.

[19] Matthew E. Taylor, Peter Stone. Transfer Learning for Reinforcement Learning Domains: A Survey, Journal of Machine Learning Research 10, 2009.

[20] I. Sreesurya, H. Rathi, P. Jain, T. K. Jain. Hypex: A Tool for Extracting Business Intelligence from Sentiment Analysis using Enhanced LSTM. Multimedia Tools and Applications, 2020. doi:10.1007/s11042-020-08930-6.

[21] R. Dhanalakshmi and T. Sri Devi. Adaptive cognitive intelligence in analyzing employee feedback using LSTM, Journal of Intelligent & Fuzzy Systems, 2020.

[22] S. X. Jian, C. Z. Rong, W. Hao, Y. D. Yan, W. W. Kin. Convolutional LSTM network: A machine learning approach for precipitation nowcasting, in Proc. Advances in Neural Information Processing Systems, Montreal, Canada, pp. 802–810, 2015.

[23] Xuan Zhang, Xun Liang, Aakas Zhiyuli, Shusen Zhang, Rui Xu and Bo Wu. AT-LSTM: An Attention-based LSTM Model for Financial Time Series Prediction, 2019 IOP Conf. Ser.: Mater. Sci. Eng. 569 052037.

[24] Jungsik Hwang. Modeling Financial Time Series using LSTM with Trainable Initial Hidden States, arXiv:2007.06848 [q-fin.ST].

[25] Trang Pham, Truyen Tran, Dinh Phung, Svetha Venkatesh. Predicting healthcare trajectories from medical records: A deep learning approach, Journal of Biomedical Informatics,Volume 69, May 2017.

[26] Jing Xia, Su Pan, Min Zhu, Guolong Cai, Molei Yan, Qun Su, Jing Yan, Gangmin Ning. A Long Short-Term Memory Ensemble Approach for Improving the Outcome Prediction in Intensive Care Unit, Computational and Mathematical Methods in Medicine, 2019.

[27] A. Karpathy and L. Fei-Fei. Deep visual-semantic alignments for generating image descriptions. In CVPR, 2015.

[28] K. Xu, J. Ba, R. Kiros, A. Courville, R. Salakhutdinov, R. Zemel, and Y. Bengio. Show, attend and tell: Neural image caption generation with visual attention. In ICML, 2015.

[29] M. Ranzato, A. Szlam, J. Bruna, M. Mathieu, R. Collobert, and S. Chopra. Video (language) modeling: a baseline for generative models of natural videos. arXiv preprint arXiv:1412.6604, 2014.

[30] N. Srivastava, E. Mansimov, and R. Salakhutdinov. Unsupervised learning of video representations using lstms. In ICML, 2015.

[31] Sutskever, I., Vinyals, O., and Le, Q. (2014). Sequence to sequence learning with neural networks. In Advances in Neural Information Processing Systems (NIPS 2014).

[32] Bahdanau, Dzmitry, Cho, Kyunghyun, and Bengio, Yoshua. Neural machine translation by jointly learning to align and translate. arXiv:1409.0473, September 2014.

[33] Parul Pandey, Simplifying Sentiment Analysis using VADER in Python (on Social Media Text), https://medium.com/analytics-vidhya/simplifying-social-media-sentiment-analysis-using-vader-in-python-f9e6ec6fc52f (2018).

[34] C.J. Hutto, Eric Gilbert. VADER: A Parsimonious Rule-based Model for Sentiment Analysis of Social Media Text, Conference: Proceedings of the Eighth International AAAI Conference on Weblogs and Social Media At: Ann Arbor, MI, 2015.

[35] D. Xu, Z. Tian, R. Lai, X. Kong, Z. Tan, W. Shi. Deep Learning Based Emotion Analysis of Microblog Texts. Information Fusion, 2020. doi:10.1016/j.inffus.2020.06.002.

[36] James Surowiecki. The Wisdom of Crowds: Why the Many Are Smarter Than the Few and How Collective Wisdom Shapes Business, Economies, Societies and Nations. Random House Large Print, 2004.

[37] A. Borg, M. Boldt. Using VADER Sentiment and SVM for Predicting Customer Response Sentiment. Expert Systems with Applications, 2020.

[38] Valdez Danny, Ten Thij Marijn, Bathina Krishna, Rutter Lauren A., Bollen Johan. Social Media Insights Into US Mental Health During the COVID-19 Pandemic: Longitudinal Analysis of Twitter Data, JOURNAL OF MEDICAL INTERNET RESEARCH, 2020.

[39] Al Mansoori Saeed, Almansoori Afrah, Alshamsi Mohammed, SalloumSaid A. Suspicious Activity Detection of Twitter and Facebook using Sentimental Analysis. TEM JOURNAL-TECHNOLOGY EDUCATION MANAGEMENT INFORMATICS, 2020.

[40] J. Scholz, J. Jeznik. Evaluating Geo-Tagged Twitter Data to Analyze Tourist Flows in Styria, Austria. ISPRS International Journal of Geo-Information, 9(11), 681, 2020. doi:10.3390/ijgi9110681.

[41] G. Kang, M. Tang, J. Liu, X. Liu, and B. Cao "Diversifying web service recommendation results via exploring service usage history", IEEE Transactions on Services Computing, vol. 9, 2016.

[42] A. Guo and T. Yang. Research and improvement of feature words weight based on TF-IDF algorithm. IEEE Information Technology, Networking, Electronic and Automation Control Conference, pp. 415–419, Chongqing, China, 2016.

[43] Shengqi Wu, Huaizhen Kou, Chao Lv, Wanli Huang, Lianyong Qi, Hao Wan. Service Recommendation with High Accuracy and Diversity, Wireless Communications and Mobile Computing Volume 2020.

[44] Soumya S, Pramod K. V. Sentiment analysis of malayalam tweets using machine learning techniques. ICT Express, 2020. doi:10.1016/j.icte.2020.04.003.

[45] M. A. Ullah, S. M. Marium, S. A. Begum,N. S. Dipa. An algorithm and method for sentiment analysis using the text and emoticon. ICT Express, 2020. doi:10.1016/j.icte.2020.07.003.

[46] F. E. Ayo, O. Folorunso, F. T. Ibharalu, I. A. Osinuga. Hate speech detection in Twitter using hybrid embeddings and improved cuckoo search-based neural networks. International Journal of Intelligent Computing and Cybernetics, 2020. doi:10.1108/ijicc-06-2020-0061.

[47] Kaggle. https://www.kaggle.com/lakshmi25npathi/imdb-dataset-of-50k-movie-reviews, 2019.

[48] Fabrizio Sebastiani. Machine learning in automated text categorization. ACM Computing Surveys, 34, 2002.

[49] Joseph Turian, Lev Ratinov, and Yoshua Bengio. Word representations: a simple and general method for semi-supervised learning. In Proceedings of ACL, 2010.

[50] Jeffrey Pennington, Richard Socher, Christopher D. Manning. GloVe: Global Vectors for Word Representation, Proceedings of the 2014 Conference on Empirical Methods in Natural Language Processing (EMNLP), 2014.

[51] Fellbaum, Christiane. WordNet and wordnets. In: Brown, Keith et al. (eds.), Encyclopedia of Language and Linguistics, Second Edition, Oxford: Elsevier, 665-670. 2005.

[52] Mohamed Chiny, Omar Bencharef, Moulay Youssef Hadi, Younes Chihab. A Client-Centric Evaluation System to Evaluate Guest's Satisfaction on Airbnb Using Machine Learning and NLP, Applied Computational Intelligence and Soft Computing, 2021.

[53] Twitter US Airline Sentiment. https://www.kaggle.com/crowdflower/twitter-airline-sentiment, February 2015.

Multiple Relay Nodes Selection Scheme using Exit Time Variation for Efficient Data Dissemination in VANET

Deepak Gupta[1], Rakesh Rathi[2], Shikha Gupta[3], Neetu Sharma[4]
Department of Computer Science and Engineering
Engineering College Ajmer
India

***Abstract*—Efficient Data dissemination in VANET is still the challenge because of variable speed of vehicles, road conditions, frequent fragmentation etc. In this article a selective forwarding data dissemination scheme using exit time differences in vehicles for highway lanes scenario is proposed that focuses on the solution of broadcast storm, less coverage, transmission delay and reliable data delivery. Our approach is selecting multiple forwarding nodes to increase coverage in less delay. In this article road lanes concept is used to identify the moving node direction. Redundant regions and zones technique in proposed approach is reducing the processing of parameters at significant extents. Simulation of proposed approach is done using NS2 and SUMO. Output of implementation is compared with unidirectional flooding, KB_Selective, and LT_Selective techniques. Result analysis shown that the proposed technique is much efficient and it increases the rate of coverage up to 23%. Also it reduces the delay up to 18% in data delivery ratio. This methodology also improves the performance of system by increasing the throughput and reducing the collision rate in comparison with other methods.**

***Keywords*—Broadcasting; disseminations; exit time; highway lanes; relay nodes; vehicle speed; vehicular ad hoc networks**

I. INTRODUCTION

The networks of moving vehicles are used to disseminate important information among vehicles which includes safety related information, driving support, entertainment, and other mobile commercial services using wireless communication. Communication through vehicular ad hoc network provides the facility of managing and monitoring the traffic services for improvement and maintaining the flow of vehicles on road [1]. VANETs have a fast changing topology where nodes (vehicles) are moving at high and variable speeds in various directions. Such networks are categorized in self-organising networks that can disseminate data with or without requiring any fixed infrastructure [2], [3]. Communication is possible when the vehicles involve in network are differ from normal vehicles. Vehicles in vehicular ad hoc networks are enabled with On Board Unit (OBU). OBU is special hardware in the form of embedded circuit board or ICs that has collection of sensors with processing capabilities to connect the other vehicle in the range. When vehicles are connected to other vehicles then it can transmit or receive the information or vehicles are able to exchange signal and related information in the form of packet transmission [4]. There is another important fixed unit along road side named as Road Side Unit or RSU. When RSU communicate with vehicles through their OBU then this is vehicle to infrastructure (V2I) communication. RSU temporarily stores the details of all vehicles in its range. This unit can connect to cloud, fog or other internet servers to send and receive information to and from other systems as per requirement. This is Infrastructure to Infrastructure (I2I) communication [5]. Periodic beacons are used to exchange the traffic-related information with OBU to aware the drivers of other connected vehicles for traffic and other related conditions [6]. RSUs also exchange information periodically for updating databases. As vehicles have radar at both front and rear side so it can communicate with vehicles moving in any directions [7]. Alert can be seen on display units or can be felt through vibrations, sounds or any other type of alarming options [8]. Fig. 1 is showing the typical VANET scenario consists of OBU enabled vehicles, RSUs, Cloud or other internet server. Remaining article is arranged as follows: Section 2 contains brief overview about data dissemination. In Section 3 the related work is explained followed by proposed methodology in Section 4. Section 5 includes experimental setup and comparison of results with existing schemes. Sections 6 and 7 presents conclusion and future scope of our approach.

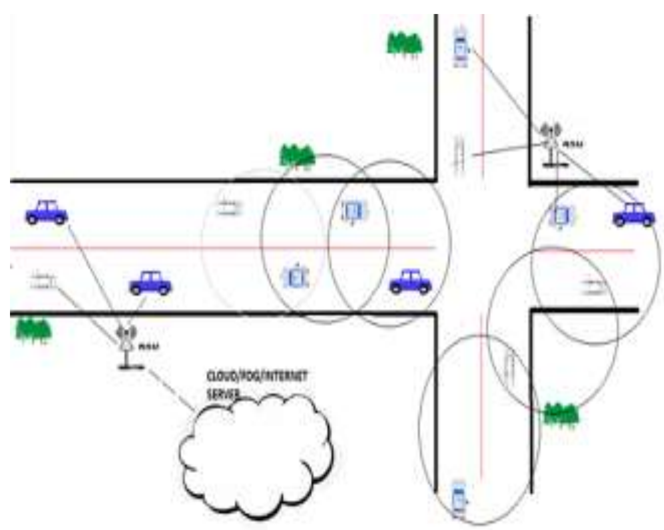

Fig. 1. Basic Vehicular ad HOC Network Scenario.

II. VANET DATA DISSEMINATION

As in Vehicle to Vehicle communication, vehicles are moving with variable speeds and directions, it is very difficult task to deliver data at proper time that is, the time when the data is valued for receiver for example there is no use of information received by a vehicle user regarding traffic support like jam due to road accident when vehicle already reached there and hang up in traffic [9]. This is the problem of discovering and distributing information quickly to nodes. Data dissemination is challenging because vehicular network changes rapidly, variables speed vehicles, different road conditions, frequent fragmentation or others parameters [10]. The process of delivering the data or information to other vehicles or nodes in distributed wireless network is called as data dissemination. Proper dissemination schemes are helpful in delivery of data to desired number of vehicles at in proper time [11]. This also helps in reducing the data congestion and traffic. Different characteristics of vehicular ad hoc networks like variable speeds, types of mobility models, communication flow etc. creates networking complications, which requires the solution for efficient and effective dissemination protocol [12]. Vehicles create a dynamic scenario due to variation in speed and therefore very short life span in several lanes. Many researchers proposed various schemes for improving the dissemination process between vehicles that can be categorized as infrastructure, broadcast and geocast [13]. RSU is basic requirement for infrastructure based schemes. In broadcast based the sender forward information to all nodes in network while in geocast, nodes are belongs to zone of relevance [14]. Some basic data dissemination schemes are shown in Fig. 2.

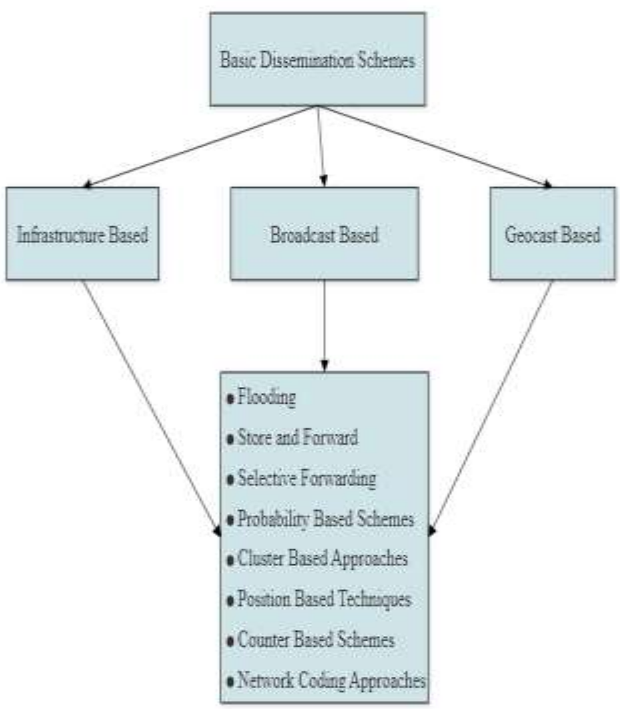

Fig. 2. FBasic Dissemination Schemes in VANET.

Broadcasting the information for dissemination in vehicles may create the problems like broadcast storms and network congestion. Another problem that arise during VANET data dissemination is the disconnected networks problem which mostly occurs in areas having sparse traffic that is, less number of connected vehicles are available for information transfer [15]. This problem of disconnected network may leads to loss of data or information before reaching to actual receiver or desired number of receivers. Many researchers worked on these problems and proposed solutions. We are discussing some in next section of the article.

III. RELATED WORK

Tian et al. [16] introduced Traffic Adaptive Data Dissemination (TrAD) Protocol that defines concept of a directional cluster which includes the vehicles around the sender whose direction of movement is same as of sender. There is a coordinator in the cluster which is the vehicle or node at the intersection whereas breaker is the vehicle which is about to leave the cluster. This scheme was supporting broadcast storm reduction and based on forwarding technique but there was more delay due to high processing at the intersections of roads in urban scenarios. Geocast based Information - Centric Opportunistic Data Dissemination scheme was proposed by Leal et al. [17] which classifying messages as periodic beacons and event driven messages named as Cooperative Awareness Messages (CAM) and Decentralized Environmental Notification Messages (DENM). In this the probability of retransmission of a message keeps on decreasing with distance of the vehicle from the event location. Density-based Gossiping protocol tries to address an issue of Geographic Gossiping Protocol which was not as much supportable as proposed in areas with non-uniform distribution of vehicles. Nikolovski et al. [18] proposed Delay Tolerant and Predictive protocol (DTP-DDP) of Dissemination, focused mainly to overcome from broadcast storm problem by reducing number of rebroadcasting. Message strength or power was computed for every received message and if it is less than 12 % then it immediately rebroadcast the message, assuming that it is very far from sender or it may be at transmission boundary of sender. For message having power more than the threshold, decision was based on distance and direction of receiver node with respect to event location which involved lots of processing and computing. This may produce delay in further broadcasting of information. Retransmission decision based on number of times of message received by node, in defined time duration is introduced by Bakhouya et al. [19] named as adaptive and decentralized approach (AID). Assumption behind this was that, in case of dense network of vehicle message can be forwarded from many other vehicles, so better to drop the message instead of further forwarding. This theory will help in reducing the congestion in network in dense network but not as much effective as proposed in sparse network due to overhead created for retransmission decision. Costa et al [20] introduced beacon based DDRX protocol for data dissemination in urban scenario that is depends on vehicle network density for TMS related applications claiming in overhead reduction and less delay by creating a graph of connected vehicles up to 2 –hop network. To have knowledge of 2-hop vehicles before transmission of information may produce delay which can be high in urban traffic. Ali et al. [21] introduced an infrastructure less scheme for data broadcasting was fully based on position of vehicles and clusters for emergency messages in high dense scenarios of vehicles. Vehicle's information like positions, speed and moving direction was exchanged using periodic beacons signals. Based on these parameters a node may be the cluster member or not. If a node was cluster member then only it would be the part of relay node selection process otherwise not. In distributed traffic management systems, Costa et al. [22] introduce a protocol for efficient data dissemination by selecting the best relay node for sending traffic management services messages to cover maximum nodes with less overhead and transmission delay. In selecting the relay node every vehicle must have knowledge of 1 and 2-hop neighbours, this may introduce delay in coverage. A probability based broadcasting approach for safety related messages was given by Sospeter et al. [23] named as Effective and Efficient Adaptive Probability Data (EEAPD) Dissemination. Information forwarder decision was based on the vehicle (source node) to vehicle distance, vehicle density and direction of message. Relationship between number of vehicles (vehicle density) and particular road segment is defined by a metric called redundancy ratio which was not highly effective in urban scenarios. Adaptive Data Dissemination Protocol (AddP) was introduced by Oliveira et al. [24], focusing on reliability of safety message dissemination. It was a multi-hop broadcast protocol where rebroadcasting was reduced through aggregation of data and network coding. A relay or forwarding node selection was based on local vehicle density and distance (from neighbour's nodes) involves huge processing at each node and may led to delay in dense networks. Baiocchi et al. [25] proposed Timer-Based Backbone Network (TBN) protocol. Forwarding or Rebroadcast decisions were taken using Monte Carlo algorithm for randomization method. As the approach was beacon-less and time based, therefore there were chances to not forward important information due to network delay or other after timer expired. Liu et al. [26] proposed an approach based on maximum flooding. This was an effective solution towards data dissemination but cannot handle the dense network due to broadcast storm as the focus was on mostly on maximum coverage. Chaqfeh et al. [27] proposed another approach to solve the congestion problem in heavy traffic during data transmission among vehicles, based on the concept of relay node selection but they have still not considered some other parameters which can solve the problem of broadcast storm more efficiently. Further the technique based on probability during flooding was proposed by Gutiérrez-Reina et al. [28] for data dissemination in VANET, but the problem of delay in coverage was still persists and overall throughput was not up to the mark as proposed in dense network due to less rate of coverage. Qureshi et al. [29] proposed cluster based approach for vehicular data dissemination. Making clusters of networks to process the information for dissemination was one of the efficient technique but to handle the cluster members and other overheads there is quite more processing was required on account of which an important and urgent information may have to suffer. With this survey we found that still the speed and lane of vehicles were rarely used by researchers which could be important parameters in dissemination process. These parameters may have important role in solving the problems or issues by broadcast storm like coverage, delay, collision etc. In section 4, we are proposing an effective solution in such relay networks where information from one network, is pass on to another using relay nodes. We have used speed as important parameter that covers some technical gaps and problems in relay node selection or selective forwarding approaches.

IV. Proposed Methodology

In the highway scenario of vehicular ad hoc communication, number of lanes is an important parameter that can be used in assignment of direction of moving vehicles and helps in the process of relay nodes selection effectively. Number of lanes, L on highway or highway lanes may vary as per the regions, states and countries, and always are even in number as in (1).

$$Lanes = \{ L : [(L \leq 16) \, and \, ((L \bmod 2) == 0)] \} \tag{1}$$

In our proposed technique we are assuming maximum 16 lanes. Periodically values of basic parameters like position, speed and lane number for every vehicles in 1-hop will exchange with each other. Nodes maintain the dynamic record of received coordinates of neighbor's and start the grouping of these records into the same or other direction vehicles with respect to itself. It has been assumed that vehicles on highway are either moving from left to right or right to left. Depending on direction of moving of source vehicles (N_{SOURCE}), other nodes in the transmission range of source will considered as same or opposite direction moving vehicles. Fig. 3 shows the vehicles scenario of proposed 1-hop neighbors of N_{SOURCE} (*black car moving right*) and respective mapping to regions according to moving directions in 8 lanes.

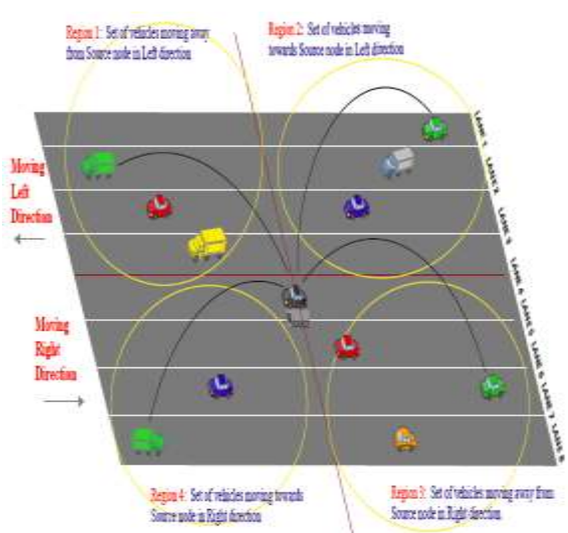

Fig. 3. Directions and Regions Mapping with respect to Source (Black Car).

If source is moving left then the defined procedures in later subsections of this article will change accordingly. We are separating all 1-hop neighbors into four regions that is, region 1, region 2, region 3 and region 4 with respect to source node.

A. Direction Assignment Process (DAP)

Direction assignment process of proposed technique is assigning directions with respect to source vehicle for each 1-hop vehicles in source transmission range; procedure *Direction_Assign* doing the work of direction assignment at N_{SOURCE} using the exchanged records of parameters.

Procedure: Direction_Assign (NLIST, L_ID, L)

```
Input:1-hop Node list (N_LIST) in source
      transmission range, Lane number of each
      neighbor (L_ID), Number of lanes on
      highway (L)

Output: Assignment of directions to 1-hop nodes

  for each {Ni ϵ N_LIST} do
   if L_ID <=|L/2|
   ML[ ] ← Ni // Moving Left Assignment
   otherwise,
    MR[ ] ← Ni // Moving Right Assignment
   return {ML[ ], MR[ ]}
```

After assignment of moving direction and using the position of vehicles, source node divides the ranged vehicles into the set of same and opposite directions from itself; having confidence in that the vehicles moving away from the source will provide faster coverage as compared to the vehicles moving towards source. Keeping this belief and to reduce processing, vehicles are divided into *Rejection and Selection zone*. Vehicles belongs to rejection zone will not include in the selection process for relay candidate. Flow of working approach is shown in Fig. 4.

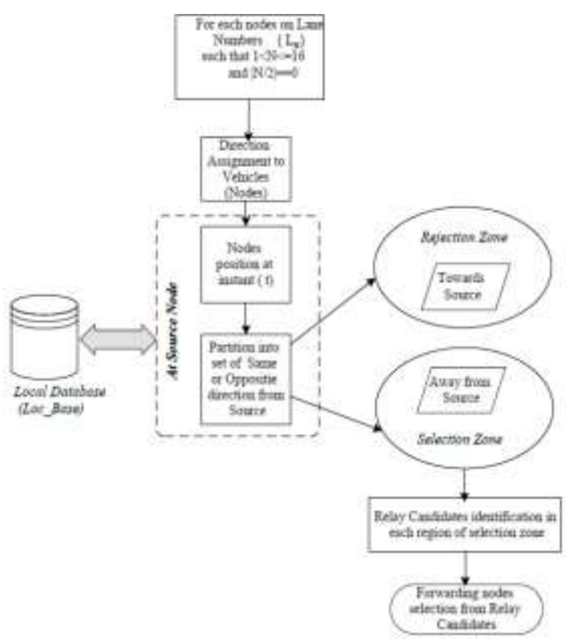

Fig. 4. Flow of Proposed Working Approach.

B. Region Assignment Process (RAP)

After assigning the direction of moving of nodes at N_{SOURCE}, region assignment of vehicles is performed. Various regions for proposed approach are defined as follows:

Region 1 ϵ Vehicles moving left and away from N_{SOURCE}.

Region 2 ϵ Vehicles moving left and towards from N_{SOURCE} .

Region 3 ϵ Vehicles moving right and away from N_{SOURCE} .

Region 4 ϵ Vehicles moving right and away from N_{SOURCE}.

Assignment of each 1-hop vehicle to respective region with respect to source is carried out by below procedure.

Procedure (at N_{SOURCE}): Region_Assign (N_{LIST})

```
for each N in N_LIST
   if Loc_Base(N_LOCATION) ϵ [(X < X_SOURCE ) AND
  (Y > Y_SOURCE )]
     Region1[ ]← N
     A1_N_SOURCE[ ]←N
    else if Loc_Base(N_LOCATION) ϵ [(X > X_SOURCE )
    AND (Y > Y_SOURCE )]
     Region2[ ]← N
     T1_N_SOURCE[ ]←N
    else if Loc_Base(N_LOCATION) ϵ [(X > X_SOURCE )
    AND (Y < Y_SOURCE )]
     Region3[ ]← N
     A2_N_SOURCE[ ]←N
     else Loc_Base(N_LOCATION) ϵ [(X < X_SOURCE )
    AND (Y < Y_SOURCE )]
     Region4[ ]← N
     T2_N_SOURCE[ ]←N
 return { Region[ ], T1_ N_SOURCE[ ], A1_
  N_SOURCE[ ], T2_ N_SOURCE[ ], A2_ N_SOURCE[ ]}
```

C. Zones Selecting and Rejecting Process (ZSRP)

Next to RAP for 1-hop moving vehicles with respect to source the system proceed to select the best relay node. In our work we are selecting two relay nodes instead of one to cover maximum area in less time. For this we are considering an important parameter that is speed of moving vehicles. This parameter is not focused in most of the earlier researches. In this approach with the help of speed of moving vehicle we are efficiently selecting the forwarder nodes from selection zone. In almost all previous approaches the farthest node from source was considered as the relay node but here we are also considering the node just behind the farthest node in both directions. It could possible that the node just behind farthest node may leave the transmission range of source first because of speed difference, it may overtake farthest node within the range itself.

This leave time computation can applied to all the nodes in selection zone but we are not calculating that, assuming that there is less probability of existence of node which have less leave time in comparison with farthest or behind farthest node.

Also if such vehicle exists then also the coverage by farthest or behind farthest node will be more as these nodes will be in early contact to 2- hop nodes.

Including computation of leave time for each node will increases overhead and processing which may introduce delay in coverage. Fig. 5, showing the representation of such nodes on x-y coordinate system. Here we are assuming that N_{SOURCE} is at (0, 0) in red colour. Green nodes are the relay candidates and their remaining distances from source are represent by *R1d1*, *R1d2* in region 1 while in region 3 they are represents by *R3d1* and *R3d2*. Vehicles in region 2 and region 4 belongs to rejection zone, so they are not considered for relay candidate and marked in black colour. Following possible cases occurs for rejection zone vehicles according to the source moving direction as in (2) and (3).

Case I: $$\left[\left(dir\left(N_{SOURCE}\right)=MR\right)\wedge\left(pos\left(N\right)\varepsilon\left(\left(x,y\right)\vee\left(-x,-y\right)\right)\right)\right] \quad (2)$$

Description: If any vehicle selected as forwarding node and belong to either (-*x*, -*y*) or (*x*, *y*) region when source moving towards positive *x*, then it would covers mostly those vehicles which are already in the range of source only. Node selected as relay, will forward the information as soon as it received and to cover the region outside the source transmission range will take some time by such nodes even having the minimum time of leave (*ttl*).

Case II: $$\left[\left(dir\left(N_{SOURCE}\right)=ML\right)\wedge\left(pos\left(N\right)\varepsilon\left(\left(x,-y\right)\vee\left(-x,y\right)\right)\right)\right] \quad (3)$$

Description: If any vehicle selected as forwarding node and belong to either (-*x*, *y*) or (*x*, -*y*) region when source moving towards negative *x*, then also it covers mostly the vehicles which are in the range of source and have already the information.

Remaining distance, let for green node in Fig. 6, is |AC=BD=$R_K d_K$ |in region *K*. Position of this node is represents as [(-*x*, *y*) ~ |*x*|, |*y*|)]. Transmission range of source (*T*) creating a circle of radius *T*. Also *OD*=|*x*| and *CD*=*AB*=|*y*|. Therefore value of $R_K d_K$ and remaining time to leave (*ttl*) from source range are computed using (4) and (5) respectively.

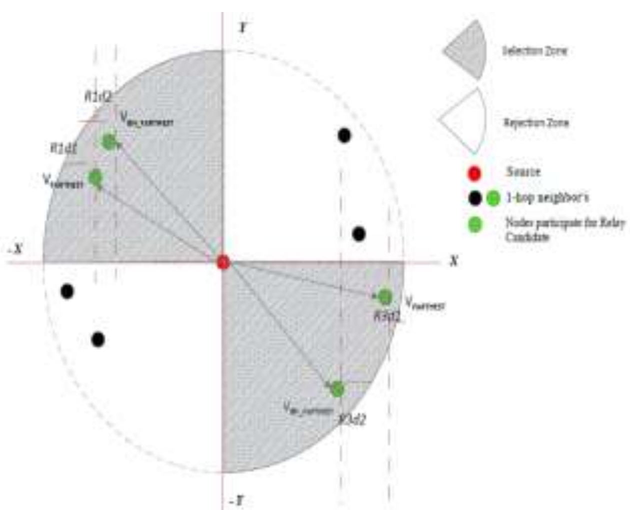

Fig. 5. Representation of 1-hop Nodes on x-y Coordinate System.

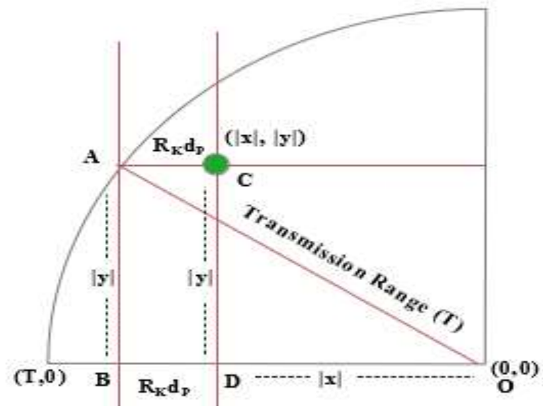

Fig. 6. Computation of Remaining Span from Source Transmission Range.

$$R_K d_P = \left\{\left(\sqrt{T^2-(|\,y\,|)^2}\right)-|\,x\,|\right\} \quad (4)$$

$$ttl[\ ] = \left\{\left(R_K d_P\right)*\left(\left[V_{FARTHEST}\right] or \left[V_{BH\_FARTHEST}\right]\right)K\right\} \quad (5)$$

K is region number and $P\ \varepsilon\ \{FARTHEST, BH\_FARTHEST\}$

D. Relay Nodes Selection Process (RNSP)

This subsection is explaining the process vehicle detection which will cover the next network earliest. RNSP is selecting two relay or forwarder nodes: *relay_node1 and relay_node2* in opposite directions from selection zones. The procedure is considering both farthest and behind the farthest vehicles in selection zones based on the assumption that the behind vehicle may leave the range first covering more vehicles outside the range of source in less time. So the aim of RNSP is vehicle detection which will leave the transmission range of source early between farthest node and behind the farthest node, in both regions having vehicles moving away from source. For this leave time calculation, speed and distance between these vehicles are obtained using global positioning system and other parameters exchanged periodically and stored in local database of nodes. Fig. 7 shows the steps of RNSP procedure.

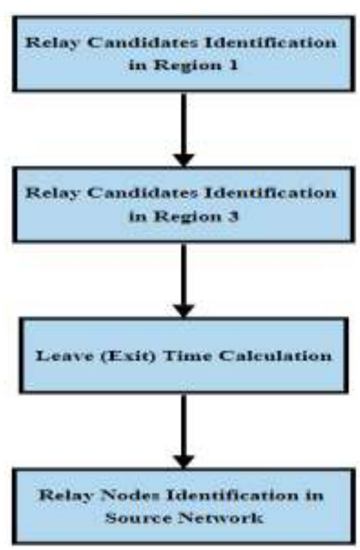

Fig. 7. Steps for RNSP.

Algorithm: RN_Election

Step 1: Relay Candidate Identification in Region 1
For each $N \in A1\_N_{SOURCE}$ **do**
$Distance\_R1[N] = |pos(N) - pos(N_{SOURCE})|$
$R1_{FARTHEST}$=Max($Distance\_R1$[])
$Distance\_R1[\,] \leftarrow |Distance\_R1[\,] \setminus R1_{FARTHEST}|$
$R1_{BH\_FARTHEST}$=Max($Distance\_R1$[])
Step 2: Relay Candidate Identification in Region 3
For each $N \in A2\_N_{SOURCE}$ **do**
$Distance\_R2[N] = |pos(N) - pos(N_{SOURCE})|$
$R2_{FARTHEST}$=Max($Distance\_R2[]$)
$Distance\_R2[\,] \leftarrow |Distance\_R2[\,] \setminus R2_{FARTHEST}|$
$R2_{BH\_FARTHEST}$=Max($Distance\_R2$[])
Step 3: Leave Time (Exit) Calculation
$ttl1=R1d1*V[R1_{FARTHEST}]$
$ttl2=R1d2*V[R1_{BH\_FARTHEST}]$
$ttl3=R2d1*V[R2_{FARTHEST}]$
$ttl4=R2d2*V[R2_{BH\_FARTHEST}]$
Step 4: Relay Nodes Identification in Source Network
if $tt1<=ttl2$
$relay\_node1 \leftarrow R1_{FARTHEST}$
else
$relay\_node1 \leftarrow R1_{BH\_FARTHEST}$
if $ttl3<=ttl4$
$relay\_node2 \leftarrow R2_{FARTHEST}$
else
$relay\_node2 \leftarrow R2_{BH\_FARTHEST}$
return (*relay_node1*, *relay_node2*)

E. Notation List

Table I is showing the list of notations and their interpretation used in our proposed methodology.

TABLE I. NOTATIONS LIST

Notations	Interpretation
L	Number of Lanes
V	Vehicle speed
t	Time instant
L_ID	Unique identification number of lane
N_{SOURCE}	Source node or vehicle
N_{LIST}	1-hop neighbors list of N_{SOURCE}
MR[ ]	Set of Nodes moving right with respect to N_{SOURCE}
ML[ ]	Set of Nodes moving left with respect to N_{SOURCE}
Loc_Base	Local database of each node
T1_ N_{SOURCE} [ ]	Set of vehicles from region 2, moving towards N_{SOURCE}
T2_ N_{SOURCE}[ ]	Set of vehicles from region 4, moving towards N_{SOURCE}
A1_ N_{SOURCE}[ ]	Set of vehicles from region 1, moving away from N_{SOURCE}
A2_ N_{SOURCE}[ ]	Set of vehicles from region 3, moving away from N_{SOURCE}
Distance_R1[ ]	Distance of all nodes $\in$ Region 1 from N_{SOURCE}
Distance_R2[ ]	Distance of all nodes $\in$ Region 3 from N_{SOURCE}
$R1_{FARTHEST}$	Farthest vehicle in region 1 from N_{SOURCE}
$R1_{BH\_FARTHEST}$	Vehicle behind $R1_{FARTHEST}$
$R2_{FARTHEST}$	Farthest vehicle in region 3 from N_{SOURCE}
$R2_{BH\_FARTHEST}$	Vehicle behind $R2_{FARTHEST}$
R1d1	Span remains to exit from source range by $R1_{FARTHEST}$
R1d2	Span remains to exit from source range by $R1_{BH\_FARTHEST}$
R2d1	Span remains to exit from source range by $R2_{FARTHEST}$
R2d2	Span remains to exit from source range by $R2_{BH\_FARTHEST}$
ttl	Remaining time to exit from source transmission range

V. PERFORMANCE EVALUATION

A. Simulation Environment

Proposed work is carried out in NS-2 environment with the supporting tools SUMO and MOVE. For comparing and analysis of results we have assigned the speed randomly to moving vehicles in the range of 20 mph to 80 mph. For better analysis we are taking the average of values obtained in 10 simulations. Various simulation parameters taken are shown in Table II. Work has been extended to real time highway fragment of radius 3 km using OpenStreetMap. Working approach has been examined in the terms of simulation duration and rate of flow of vehicles or vehicle density. Result of proposed work is compared with selective flooding, unidirectional flooding and selective forwarding proposed by Farooq et al. [30] and Pradhan R. [31]. Farooq et al. proposed unidirectional flooding and selective flooding based on knapsack problem (KB_Selective) of weight and profit assignment for optimal (maximum profit) solution. Pradhan R. proposed selective dissemination technique based on leave time (LT_Selective) calculation of nodes to select the forwarding node.

B. Metrics

- *Receiver Ratio (RR)*: Receiver ratio in (6) is the ratio of number of nodes received (N_R) the message transmitted by source to the total number of nodes (N) available in the region of interest for n simulations. More the value of this means more the coverage of nodes on highway.

$$RR = \left(\sum_{s=1}^{n} \frac{N_R}{N} \right) \Big/ n \tag{6}$$

- *Packet Delivery Ratio (PDR)*: This metric supports the trustworthiness of network and defined as the total number of packets successfully delivered from the total packets transmitted in source node range. High the *PDR* produces the reliability of network and belief on moving nodes.

$$Avg\_PDR = \left(\sum_{s=1}^{n} \frac{P_R}{P_R + P_L} \right) \Big/ n \tag{7}$$

- *Wait Time (WT)*: Wait time is defined as the amount of time taken by transmitted message (D) to reach at every node in the region. High waiting time is not acceptable in network for important and time bound information.

$$Avg\_WT = \left(\sum_{s=1}^{n} \left(\sum_{i=1}^{N_R} (D_i) \right) \Big/ N_R \right) \Big/ n \tag{8}$$

- *Collision Ratio (CR)*: Collision ratio is the total number of collided packets (P_C) to the total number of nodes in the network for given duration of time.

$$Avg\_CR = \left(\sum_{s=1}^{n} \left(\left(P_C / N \right) \right) \right) \Big/ n \tag{9}$$

- *Throughput*: This parameter is used to find the efficiency of network by computing the size of total message received (R) per unit time as shown in (10).

$$Throughput = \left(\sum_{i=1}^{t} R \Big/ t \right) \tag{10}$$

C. Simulation Parameters

The simulation parameters and their corresponding values considered for proposed scheme are listed below in Table II.

TABLE II. PARAMETERS USED FOR SIMULATIONS

Item	Values
Distance	3 km
Number of lanes	8
Simulation time	300 seconds
Number of simulations	10
Vehicle speed	[20 – 80] mph
Transmission range	400 m
Message size	1 KB
MAC Layer	802.11p
Traffic rate	[100-400] vehicles/hr
Simulation framework	NS 2.35
Mobility Simulator	SUMO 0.32
Map tool	OpenStreetMap

D. Simulation Results

This sub-section includes the results and analysis of simulation based on various parameters as we discussed earlier. Fig. 8 to 12 shows the effect on parameters behaviour with the simulation time by keeping maximum constant number of vehicles (300) in simulation for 300 seconds. As the proposed approach selecting two relay nodes in each direction of moving therefore we are considering half of total vehicles moving left and remaining half are moving right. That means 150 vehicles in each direction.

Table III represents the values of metrics with simulation time and comparison graphs for same are shown in Fig. 8-12. In the beginning of simulation less number of packets generated for transmission and hence most of them are successfully delivered to destination nodes but as the time increases more number of packets are transmitted which increases the collision and congestion. The variation in packets delivery is shown in Fig. 8. Results show that proposed technique is doing far better in comparison to others.

Variation in throughput at early phase of simulation is not changing rapidly. As the time increases it decreases speedily in each round of simulation. This is due to decrease in packet delivery and increases in retransmission. Fig. 9 shows the performance for throughput and it is found that proposed approach is giving better results in comparison to others.

Fig. 10 shows the result of coverage of information among nodes. Comparing to others proposed method is covering the network in approximately 4 min, while the others are covering up to 80 % to 90 % region in this duration. Though the vehicle density is constant and collisions are increasing the coverage is still reaching to 100 % because of packets delivery to some nodes and such nodes are further applying the approach to find the forwarding nodes. These selective forwarders increase the coverage and also transmit message to the nodes which haven't received the packets in previous transmission.

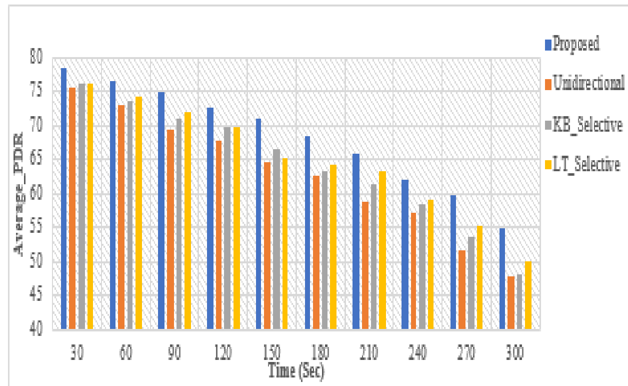

Fig. 8. Simulation Result for Packet Delivery Ratio versus Time.

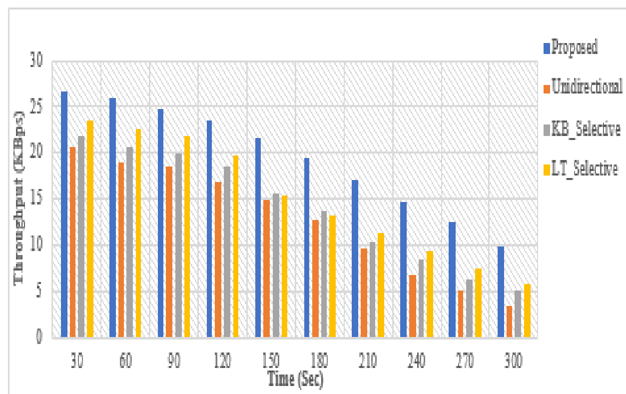

Fig. 9. Simulation Result for throughput versus Time.

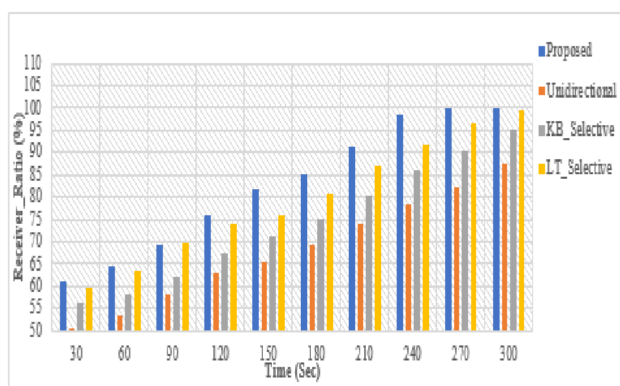

Fig. 10. Simulation Result for Receiver Ratio versus Time.

TABLE III. RESULT TABLE WITH SIMULATION TIME

Time (Sec)		30	60	90	120	150	180	210	240	270	300
PDR	Proposed	78.532	76.547	75.006	72.637	70.837	68.541	65.903	62.041	59.821	54.971
	Unidirectional	75.554	72.827	69.214	67.803	64.443	62.53	58.71	57.196	51.62	47.645
	KB_Selective	75.981	73.443	71.106	69.719	66.369	63.237	61.264	58.304	53.71	48.064
	LT_Selective	76.054	74.106	72.083	69.54	65.112	64.224	63.12	59.17	55.34	50.146
Throughput (KBps)	Proposed	26.78	25.96	24.85	23.57	21.73	19.42	17.05	14.56	12.41	9.75
	Unidirectional	20.75	19.06	18.51	16.87	14.92	12.78	9.72	6.67	4.96	3.37
	KB_Selective	21.96	20.77	20.06	18.41	15.71	13.64	10.32	8.51	6.33	4.97
	LT_Selective	23.48	22.69	21.87	19.68	15.38	13.23	11.22	9.28	7.41	5.79
Receiver_Ratio (%)	Proposed	61.219	64.296	69.451	76.145	81.781	85.116	91.407	98.391	100	100
	Unidirectional	50.612	53.437	58.295	62.805	65.457	69.421	74.103	78.306	82.116	87.362
	KB_Selective	56.221	58.234	62.143	67.224	71.361	75.104	80.224	85.849	90.244	95.361
	LT_Selective	59.753	63.68	69.758	73.842	75.886	80.731	87.221	91.784	96.576	99.748
Collision_Ratio (Avg)	Proposed	0	0.4	1.1	1.8	2.5	3.2	4.2	5.8	8.6	11.4
	Unidirectional	0	0.6	1.4	2.4	3.2	5.4	6.2	8.5	12.9	16.3
	KB_Selective	0	0.9	1.8	2.6	3.5	5.8	6.4	8.7	11.7	15.9
	LT_Selective	0	0.7	1.4	2	2.8	4.1	5.8	7.2	10.4	15.3
Wait_Time (Avg_Delay) (ms)	Proposed	92.812	96.173	101.44	112.67	121.86	134.58	152.38	175.18	210.12	248.6
	Unidirectional	95.059	101.29	109.73	119.54	138.58	164.28	187.28	221.15	266.51	321.41
	KB_Selective	98.561	104.13	110.54	121.71	136.15	155.07	178.41	206.04	244.64	304.18
	LT_Selective	96.43	100.04	107.08	116.84	133.09	150.69	170.3	195.46	229.83	278.42

Due to increases in transmission and retransmission of packets with the simulation time collision increases. As the nodes in network is almost constant therefore collision ratio is directly depends only on number of collided packets in defined duration. Fig. 11 shows the collision ratio for selective time duration in 10 simulations and it is less for our proposed work as compared to others.

Average wait time in milliseconds has been recorded for various simulations. This delay is increases in each simulation for every method because the network congestion increases. Packet retransmission is one of the major reasons for same. Also increase in nodes increases the delay. Deviation in delay or wait time with the increase in simulation time is shown in Fig. 12.

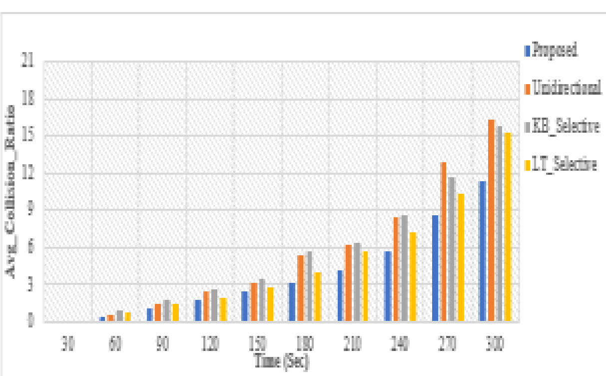

Fig. 11. Simulation Result for Collision Ratio Versus Time.

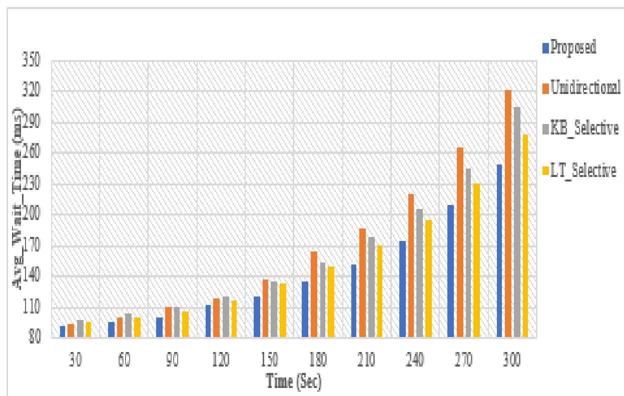

Fig. 12. Simulation Result for Wait Time Versus Time.

Further the analysis was done on the basis of node density in ad hoc network. Now we are varying the number of vehicles in the network from 40 to 400 vehicles per hour for simulation time. Recorded metrics are given in Table IV and performance comparisons for considered schemes are shown from Fig. 13 to 17.

With the increase in the node density in the network the average packet delivery ratio (PDR) is decreased. Reason for such type of changes in PDR is, data packets to be transmitted are increased with increase in number of vehicles. Tendency towards collision or loss of packets will increase which led to decrease in overall effective packet delivery ratio for simulation duration. Also in the proposed work PDR decreases but still it is performing much better as compared to others as shown in Fig. 13.

TABLE IV. RESULT TABLE WITH NODE DENSITY

Node Density		40	80	120	160	200	240	280	320	360	400
PDR	Proposed	91.09	90.24	89	87.56	85.91	83.99	81.81	79.41	76.7	73.66
	Unidirectional	84.06	82.96	81.53	79.82	77.89	75.68	73.02	70.18	67.18	63.21
	KB_Selective	85.23	84.03	82.67	80.99	79.19	77.03	74.5	71.8	68.8	65.01
	LT_Selective	86.45	85.5	84.21	82.71	80.96	78.91	76.45	73.77	70.8	67.12
Throughput (KBps)	Proposed	0.97	0.9388	0.9019	0.8623	0.8196	0.7729	0.7235	0.6714	0.6141	0.5549
	Unidirectional	0.88	0.8311	0.781	0.7232	0.6634	0.6012	0.5361	0.4687	0.3996	0.3282
	KB_Selective	0.9	0.8574	0.812	0.7623	0.7071	0.6482	0.5869	0.5225	0.4554	0.3861
	LT_Selective	0.94	0.9014	0.8603	0.8117	0.7594	0.7016	0.642	0.5818	0.5183	0.4525
Receiver_Ratio (%)	Proposed	81.63	83.304	85.006	86.77	88.568	90.413	92.319	100	100	100
	Unidirectional	75.28	76.564	77.875	79.222	80.59	81.974	83.395	84.837	86.304	87.774
	KB_Selective	78.63	79.958	81.347	82.813	84.306	85.813	87.36	88.921	90.504	92.096
	LT_Selective	80.09	81.517	82.956	84.424	85.916	87.447	89.031	90.653	92.334	94.096
Collision_Ratio (Avg)	Proposed	2.043	2.883	4.003	6.273	9.353	13.493	18.753	25.073	32.543	41.073
	Unidirectional	3.153	4.513	6.603	10.543	15.413	21.673	28.653	36.523	46.363	57.633
	KB_Selective	2.761	4.011	6.071	9.751	14.321	20.291	26.901	34.191	43.231	53.641
	LT_Selective	2.523	3.543	5.263	8.313	12.253	17.373	23.183	30.043	38.173	47.633
Wait_Time (Avg_Delay) (ms)	Proposed	97.44	101.56	108.02	116.77	127.85	142.6	160.43	182.49	210.38	244.93
	Unidirectional	116.84	125.51	136.7	152.34	173.46	202.15	243.82	298.78	364.02	435.66
	KB_Selective	111.71	119	128.08	141.87	159.79	180.97	207.85	244.02	286.83	342.5
	LT_Selective	107.27	113.68	122.67	135.12	150.99	169.41	193.15	224.37	262.8	312.08

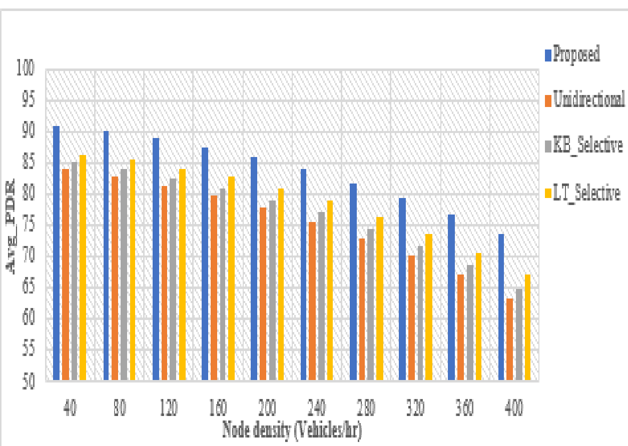

Fig. 13. Simulation Result for Packet Delivery Ratio versus Node Density.

With the increase in vehicle density, throughput of network is decreases because every node is not receiving the packets and also new nodes are continuously entering in network will cause the increase in network traffic for data packets. Therefore with the highest node density there will be least throughput. Our work is giving better result compared to other in simulation duration for network throughput with the variation in number of vehicles per hour as shown in Fig. 14.

Fig. 15 shows the fast coverage of information by proposed approach with the increase in node density compared to other approaches. Our methodology is delivering data packets by covering all the nodes in approximate 240 sec while others not.

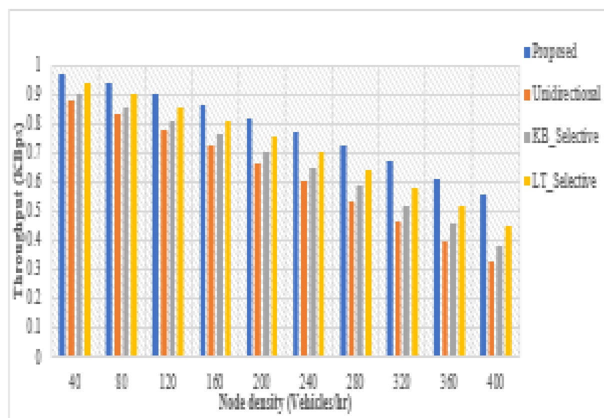

Fig. 14. Simulation Result for throughput versus Node Density.

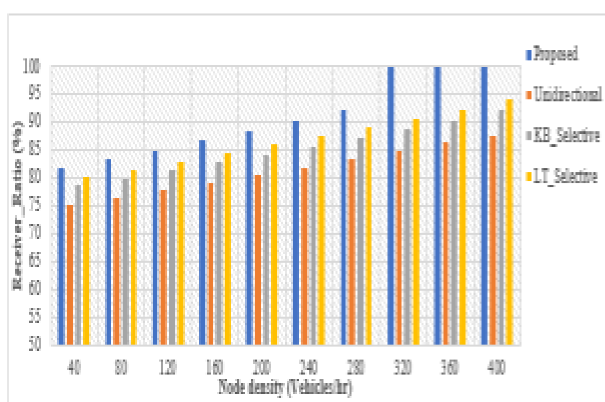

Fig. 15. Simulation Result for Receiver Ratio versus Node Density.

It is obvious that number of collisions will increase with the increase in vehicle density but how much efforts can be applied to reduce the collision ratio is more important. A better performance of our algorithms in comparison to others on collision ratio with the increase in node density has been shown in Fig. 16. Initially the collision ratio is not increasing rapidly. When node density increases to around 300 vehicles per hour there is growth in collision ratio for all approaches but minimum for our proposed approach.

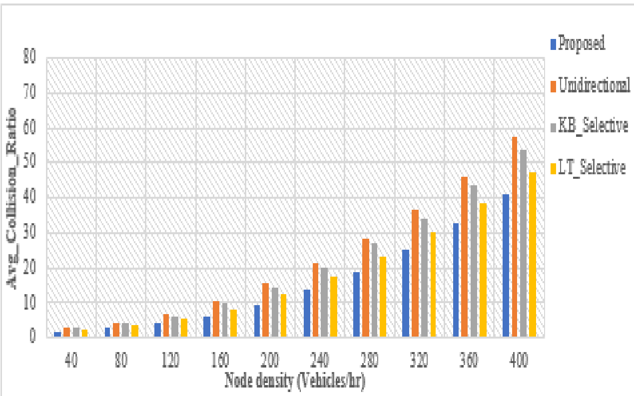

Fig. 16. Simulation Result for Collision Ratio versus Node Density.

Average delay for all simulations durations is increasing with the increase in node density of network. Average delay is approx. 90 milliseconds when we have taken minimum node density of 40 vehicles per hour. Up to density of 200 vehicles per hour, average delay is not increasing rapidly but after that it increases exponentially as shown in Fig. 17. Recorded values of simulations show the better performance for delay metrics in our proposed approach.

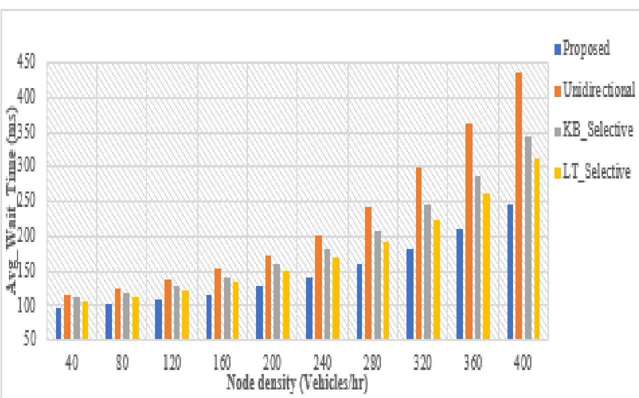

Fig. 17. Simulation Result for Wait Time versus Node Density.

VI. Conclusion and Future Work

In this article of proposed work for selective forwarders from 1-hop we can conclude that the performance for all metrics is better from other three approaches. Here the approach of choosing either farthest or behind the farthest node moving in similar direction based on their exit time calculation from source transmission range is providing effective reduction in overall delay and increase in throughput of network. Filtering of vehicles using region assignment also reducing the overall time taken by approach to select relay nodes. Overall transmission range of source is divided into regions and when vehicle entered in this range, it has been allotted to a particular region. During relay node selection if the vehicle belongs to rejection zones then it will not be the part of relay selection process. Therefore overhead for selection has been reduced effectively and this led to increase in system performance and approach is quite faster in relay node selection. Selective schemes for data dissemination give better results compared to unidirectional in the dense traffic. Various features of designed approach are, it covers the network rapidly, reducing the number of retransmissions and effectively reducing the average delay. Finally the proposed novel approach providing efficient and effective data dissemination in infrastructure less vehicle to vehicle communication.

Proposed technique of data dissemination can be further extended for comparison with some more type of similar approaches with different parameter values. Also the work can be extended to include the technique of cluster with head and members instead of regions creation and assignment. Proposed work may be examined for urban and infrastructure based scenarios with other parameters. Further scope in proposed approach to work on rank based message transmission where the priority can be assigned as per emergency, critical or important information.

References

[1] R. Kumar and M. Dave, “A review of various VANET data dissemination protocols,” *International Journal of u- and e- Service, Science and Technology*, vol. 5, No. 3, , pp. 27–44, September, 2012.

[2] R. Meneguette, G. Maia, E. R. M. Madeira, A. R. Pinto, A. A. F Loureiro and L. A. Villas, “A new Solution to perform Data Dissemination in Vehicular Networks,” Brazilian Symposium on Computer Networks and Distributed Systems, 2014, pp. 443–450. 10.1109/SBRC.2014.53.

[3] J.A Sanguesa, M. Fogue, P. Garrido, F. J. Martinez, J. C. Cano and C. T. Calafate, “A Survey and Comparative Study of Broadcast Warning Message Dissemination Schemes for VANETs”, Mobile Information Systems, vol. 2016 , pp. 1-18, 2016. https://doi.org/10.1155/2016/8714142.

[4] M. Sichitiu and M. Kihl, “Inter-vehicle communication systems: a survey,”.IEEE Communications Surveys & Tutorials, vol.10, No. 2, , pp. 88–105, 2nd Quarter, 2008. 10.1109/COMST.2008.4564481.

[5] Co-operative Networks for Intelligent Road Safety, [Online]. Available: https://trimis.ec.europa.eu/project/co-operative-networks-intelligent-road-safety.

[6] S. Allani, T. Yeferny, R. Chbeir, and S.B. Yahia, “A Novel VANET Data Dissemination Approach Based on Geospatial Data,” Procedia Computer Science, vol. 98, pp. 572–577, 2016. https://doi.org/10.1016/j.procs.2016.09.089.

[7] W. Viriyasitavat, O. Tonguz and F. Bai, “UV-CAST: an urban vehicular broadcast protocol,” IEEE Communications Magazine, vol. 49(11), pp. 116–124, Nov. 2011. 10.1109/VNC.2010.5698266.

[8] S. Allal and S. Boudjit, “Geocast Routing Protocols for VANETs: Survey and Guidelines,” Sixth International Conference on Innovative Mobile and Internet Services in Ubiquitous Computing (IMIS), Palermo, Italy 2012, pp. 323–328. 10.1109/IMIS.2012.133.

[9] B. Alsubaihi and A. Boukerche, “Semantic and Self-Decision Geocast Protocol for Data Dissemination over VANET (SAS-GP),” IEEE Wireless Communications and Networking Conference (WCNC), New Orleans, LA, USA, 2015, pp. 1948-1953. 10.1109/WCNC.2015.7127766.

[10] F. Cunha, G. Maia, A. Viana, R.A. Mini, L. Villas and A.A. Loureiro, “Socially Inspired Data Dissemination for Vehicular Ad Hoc Networks,” Proceedings of the 17th ACM International Conference on

Modeling, Analysis and Simulation of Wireless and Mobile Systems, MSWiM '14, ACM, New York, 2014, pp. 81–85. https://doi.org/10.1145/2641798.2641834.

[11] M. Bilal, P. M. L. Chan and P. Pillai, "Fastest-Vehicle Multi-hop Routing in Vehicular Ad hoc Networks," Proc. of 10th IEEE Int'l Conf. on Computer and Inf. Tech. (CIT), Bradford, UK , 2010, pp. 773-778. 10.1109/CIT.2010.148.

[12] I. Achour, T. Bejaoui, A. Busson and S. Tabbane, "SEAD: A Simple and Efficient Adaptive Data Dissemination Protocol in Vehicular Ad-hoc Networks," Wireless Network 22, pp. 1673–1683, 2016. https://doi.org/10.1007/s11276-015-1050-9.

[13] R. Kumar and M. Dave, "A comparative study of Various Routing Protocols in VANET," International Journal of Computer Science Issues (IJCSI), vol. 8, Issue 4, No.-4, pp. 643-648, July 2011.

[14] B. Bako, and M. Weber, "Efficient Information Dissemination in VANETs," Advances in Vehicular Networking Technologies, Dr Miguel Almeida (Ed.), ISBN: 978-953-307-241-8, April 2011, pp. 45-64. 10.5772/15533.

[15] F. J. Ros, P. M. Ruiz PM and I. Stojmenovic, "Acknowledgment-Based Broadcast Protocol for Reliable and Efficient Data Dissemination in Vehicular Ad Hoc Networks". IEEE Transactions on Mobile Computing, vol. 11(1).1, pp. 33–46, Jan. 2012. 10.1109/TMC.2010.253.

[16] B. Tian, K.M. Hou, and J. Li, "TrAD: Traffic Adaptive Data Dissemination Protocol for Both Urban and Highway VANETs," in IEEE, 30th International Conference on Advanced Information Networking and Applications (AINA), Crans-Montana, Switzerland, 2016, pp. 724-731. 10.1109/AINA.2016.20.

[17] M. A. Leal, M. Rockl, B. Kloiber, F. de. P. Muller and T. Strang, "Information-centric opportunistic data dissemination in Vehicular Ad Hoc Networks".13th International IEEE Annual Conference on Intelligent Transportation Systems, Funchal, Portugal, September 19-22, 2010, pp. 1072-1078. 10.1109/ITSC.2010.5625053.

[18] T. Nikolovski, and W.R. Pazzi, "Delay Tolerant and Predictive Data Dissemination Protocol (DTP-DDP) for urban and highway vehicular ad hoc networks (VANETs),". Proceedings of the 6th ACM Symposium on Development and Analysis of Intelligent Vehicular Networks and Applications - DIVANet '16, Malta, Malta, November 13-17, 2016, pp. 67-74. https://doi.org/10.1145/2989275.2989280.

[19] M. Bakhouya, J. Gaber, J., and P. Lorenz, "An adaptive approach for information dissemination in Vehicular Ad hoc Networks," Journal of Network and Computer Applications, vol. 34(6), pp. 1971–1978, Nov 2011. https://doi.org/10.1016/j.jnca.2011.06.010

[20] J. B. D. da Costa, A. M. de Souza, D. Rosário, E. Cerqueira and A. V. Leandro, "Efficient data dissemination protocol based on complex networks' metrics for urban vehicular networks," Journal of Internet Services and Applications, pp. 10-15, 2019. https://doi.org/10.1186/s13174-019-0114-y.

[21] M. Ali, A. W. Malik, A. U. Rahman, S. Iqbal, and M.M. Hamayun, "Position-based emergency message dissemination for Internet of vehicles," International Journal of Distributed Sensor Networks, vol. 15(7), pp. 1-12, June 2019. 10.1177/1550147719861585.

[22] J. Costa, D. Rosario, A. M. de Souza, L. A Villas and E. Cerqueira, "Data Dissemination Based on Complex Networks' Metrics for Distributed Traffic Management Systems," IEEE Symposium on Computers and Communications (ISCC), Natal, Brazil, 2018, pp. 01062-01067. 10.1109/ISCC.2018.8538601.

[23] J. Sospeter, D. Wu, S. Hussain and T. Tesfa, "An Effective and Efficient Adaptive Probability Data Dissemination Protocol in VANET," Data, MPDI, Vol. 4(1), 1, 2019. 10.3390/data4010001.

[24] R. Oliveira, C. Montez, A. Boukerche and M. S. Wangham, "Reliable Data Dissemination Protocol for VANET Traffic Safety Applications", Ad Hoc Networks, vol. 63, pp. 30-44, Aug 2017. 10.1016/j.adhoc.2017.05.002.

[25] A. Baiocchi, P. Salvo, F. Cuomo, I. Rubin, "Understanding Spurious Message Forwarding in VANET Beaconless Dissemination Protocols: An Analytical Approach," IEEE Transactions on Vehicular Technology, Vol. 65 (4), pp. 2243–2258, 2016. 10.1109/TVT.2015.2422753.

[26] L. Liu, C. Chen, T. Qiu, M. Zhang, S. Li and B. Zhou, "A data dissemination scheme based on clustering and probabilistic broadcasting in VANETs," Vehicular Communications, vol. 13, pp.78–88, July 2018. 10.1016/j.vehcom.2018.05.002.

[27] M. Chaqfeh, H. El-Sayed and A. Lakas, "Efficient data dissemination for urban vehicular environments," IEEE Transactions on Intelligent Transportation Systems, vol. 20, no. 4, pp.1226–1236, Aug 2018. 10.1109/TITS.2018.2850068.

[28] D. G. Reina, V. Sharma, I. You and S. Toral, "Dissimilarity metric based on local neighboring information and genetic programming for data dissemination in vehicular ad hoc networks (VANETs)," Sensors, Vol. 18, No. 7, pp.1-18, 2018. 10.3390/s18072320.

[29] K. N. Qureshi, H. Abdullah, F. B. Hussain, S. and K. Awan, "Cluster-based data dissemination, cluster head formation under sparse, and dense traffic conditions for vehicular ad hoc networks," International Journal of Communication Systems, vol. 31, no. 8, pp. 1-16, 2018. 10.1002/dac.3533.

[30] M. U. Farooq, K. U. R Khan and S. Mohammed, "Selective flooding techniques for dissemination in VANETs," IEEE International Conference on Contemporary Computing and Informatics (IC3I), Noida, India, 2016, pp.369–374. 10.1109/IC3I.2016.7917991

[31] R. Pradhan and T. De, "A selective forwarding technique for data dissemination in vehicular ad hoc networks based on traffic parameters," International Journal of Ad Hoc and Ubiquitous Computing, vol. 35, no. 4, pp.179–190 2020. 10.1504/IJAHUC.2020.111460.

IoT-based Closed Algal Cultivation System with Vision System for Cell Count through ImageJ via Raspberry Pi

Lean Karlo S. Tolentino[1,2], Sheila O. Belarmino[2], Justin Gio N. Chan[3], Oliver D. Cleofas Jr[4], Jethro Gringo M. Creencia[5], Meryll Eve L. Cruz[6], JC Glenn B. Geronimo[7], John Peter M. Ramos[8], Lejan Alfred C. Enriquez[9], Jay Fel C. Quijano[10], Edmon O. Fernandez[11],Maria Victoria C. Padilla[12]
Electronics Engineering Department, College of Engineering
Technological University of the Philippines, Manila, Philippines[1, 2, 3, 4, 5, 6, 7, 8, 9, 10, 11, 12]
University Extension Services, Technological University of the Philippines, Manila, Philippines[1]
Information Management and Computer Engineering Department, Integrated Research and Training Center
Technological University of the Philippines, Manila, Philippines[9]

***Abstract*—Spirulina platensis and other microalgae are now being considered in the different fields of research. It is due to the former's endless potential let alone, its high protein content. That is why, a stable demand of microalga production is now necessary. To achieve a high-protein spirulina, its cultivation using closed algal cultivation requires monitoring and maintenance of the bio-environmental factors and parameters affecting its growth to provide a stable and efficient production of microalgae. Meanwhile, laboratories that culture spirulina determine its cell count through manually counting the cells under a microscope – a tedious work. This establishes the need to construct a device that cultivates spirulina with maintaining and cell counting capabilities. Thus, the proponents developed a culturing device that has three main systems. The first system is tasked to maintain the bio-environmental parameters, such as the pH level, temperature, and light. The second system on the other hand speaks of the cell counting system through ImageJ's Image Processing. This system verifies the cell count and growth through counting the filaments of the spirulina. Lastly, a corresponding Android application, which was developed using Firebase and Android Studio, displays real-time values of the culture's parameter. Results show that the device was able to stabilize its parameters. Also, red LEDs exhibited 28.43% higher approximate cell count than red-blue LEDs. With this, the quality of the Spirulina that was produced throughout the study was improved. Lastly, the use of ImageJ's image processing feature showed no significant difference with manual counting. It also releases the results multiple times faster than the manual counting. Thus, being a better alternative to manual cell counting.**

Keywords*—*Spirulina platensis; ImageJ; image processing; closed algal cultivation; parameter monitoring; firebase

I. Introduction

Spirulina is a blue-green microalga that grows in alkaline lakes. Because of its high protein content, this microalga can be widely used in pharmaceutical, aquaculture as feed, and as a source of biofuel. That is why, it is currently in great interest [1]-[2]. Spirulina is now produced in large batches and is cultured in either open or closed systems. Open systems usually use ponds, while closed systems are in any container that has controlled parameters. Major disadvantages of open ponds are the contamination of the culture and the changing condition of the environment. Closed systems, on the other hand, has the defense for contamination. Essential parameters such as temperature, pH level, and oxygen level can also be monitored using closed systems [3]-[6]. Insufficient monitoring of the culture results to lower production of the aquaculture, technological solutions such as data monitoring using Internet of Things (IoT) devices and platform provides real-time tracking of the essential parameters [7]. Aeration is necessary for the maintenance of these parameters especially to the homogeneity of the light absorption of the culture. Also, aeration ensures that the nutrients are scattered all throughout the culture. As for the temperature, it is maintained by submerging the container to a pool of water, by using heat exchanger, or by spraying the outside of the container with water. Light is the most important parameter in culturing spirulina [8]. Since Spirulina platensis is under the phylum cyanobacteria, it is photoautotrophic. It utilizes the process photosynthesis in making own food [9].

Spirulina platensis cell counting is usually done in laboratories through a 'cell counting chamber' called Hemocytometer [10]. It is simple, direct, and cheap but it is also laborious and time consuming because of Spirulina platensis unusual cell shape and cell suspension making this method susceptible for human errors.

The amount of the spirulina obtained after the farming is important. It is desired to have great amount of spirulina produced in one cycle of culturing. It is also settled that the counting and the detection of Spirulina cells are extremely tedious to be done manually. From these, the implementation of image processing is considered since image processing as a means for cell counting proved its effectivity in numerous studies [11]. One of the main applications of digital image processing is estimating the total number of a specific object in each image.

The study investigates the contribution made by the microscopic vision system and the light of the closed cultivation system in the measurement of the cell density of

Spirulina platensis. It also identifies the extent of the proposed vision system in capturing the microscopic image of the spirulina and determining its cell count. Specifically, it aims to (1) build a device with maintenance and correcting system; (2) create a vision system that captures images of samples then counting the cells; and (3) create an Android application for the real-time monitoring of the parameters using IoT platform. Lastly, this device that counts the filaments is a great help for the spirulina farmers to save time and to have accurate cell counts is what the research is aimed at.

II. Related Work

A study by Aquino et al. [12]-[13] also measured, monitored, and corrected parameters essential in culturing Spirulina platensis. Their system also has a vision system that comprises of a camera and a sampling cube. Artificial neural network was trained and then used as an algorithm in analyzing the algal concentration. The detection and correction system in [13] were adapted in this past study [12], except for the dissolved oxygen parameter, vision system and the algorithm that were used in their image processing. Thus, said vision system was improved and the algorithm was also changed. Additional one difference between the past study [12] and this one [13] is the visualization of data. This study made use of an Android application that displays the data and their graphical representation for each parameter.

In [14], this study incorporates temperature, UV intensity, and water turbidity sensors, microcontroller, and cloud services for their spirulina culturing system. It also made use of the IoT platform and the Android app to acquire, visualize, and monitor data gathered within the smart micro farm. This study used ThingSpeak as database and MIT Appinventor to create their application. It also focused on the implementation of IoT and Android application. Parameters were only measured, not corrected.

A study in [15] uses an optical sensor unit that is responsible for measuring cell concentration and changes of the physiological status in the culturing system in real-time. This optical sensor was made up of three laser diodes different wavelengths. This study also developed a graphical user interface (GUI) in their control station. Environmental conditions, such as temperature, were controlled using this control station. The real-time data sent to the control station using Ethernet. The optical sensor unit in [14] utilizes flow cytometry, so air pump was used to acquire culture to pass through the unit. Culture passing through the pump might not get enough light and it might get stuck on the surface of the tube, affecting the flow rate. Their GUI and control system are not portable because they are attached to the system. Lastly, a study by Niangoran et al. [16] concludes that using red light in the culture produced more biomass than any other color of light.

To obtain a high protein alga, three key parameters such as pH level, temperature, as well as light should be considered. Previous works only took one or two parameters into account. Thus, in this paper, monitoring the said three key parameters were considered to prove that the said parameters were necessary in producing a greater growth of the microalgae. Moreover, a device that can ease the cell counting system was developed in this study. Through an algorithm which is purposely designed for scientific image processing. This image processing technique was made with ImageJ; furthermore, implementing the IoT concept with Firebase and Android Studio made monitoring and data acquisition easier. Because both is in real-time and can be done remotely.

III. Challenges and Limitations of Existing Approaches

The prior works of Spirulina culturing system [12]-[13] had a monitoring, measuring, and correcting features. However, they were not IoT-enabled. Thus, they cannot be monitored nor controlled via the Internet. Meanwhile, the two different culturing system's parameters [14], [17] can be measured and monitored through the Internet but not corrected. An IoT-based Spirulina [18] and microalgae [19]-[20] culturing system where its parameters can be monitored and corrected through the Internet were developed but the growth of the algae was measured using turbidity value [18] and microalgae biomass [19]-[20], respectively. The said limitations are summarized and listed as shown in Table I.

TABLE I. Existing Approaches and their Limitations

	[12]	[13]	[14]	[17]	[18]	[19]	[20]
IoT			✓	✓	✓	✓	✓
Parameter Monitoring	✓	✓	✓	✓	✓	✓	✓
Parameter Correction	✓	✓			✓	✓	✓
Growth Monitoring	✓	✓			✓	✓	✓

IV. Methodology

Fig. 1 shows the block diagram of the entire system. The culturing device has three main parts: the culturing system, the vision system, and the android application. The culturing system is responsible for the monitoring and maintenance of the parameters. Monitoring includes temperature and pH sensors. Data from the measured parameters will be sent to the Arduino and if the values of the parameters are out of the desired range, maintenance takes place by correcting the parameters. The Arduino opens or closes maintenance through a relay. The Arduino is also connected to the Raspberry pi which is responsible for sending data to the cloud. The Raspberry pi and cloud were also included in the android application as well as its interface. The application displays the data from the parameters and their graphs, including the cell counted from the vision system for the real-time monitoring. Finally, the vision system where the cell counting occurs is fitted in a small black box where the extracted 0.1 ml sample using a sterile syringe is transferred in a petri dish and is placed inside the platform of the vision system. After three images are taken per sample using a fixed hand-held microscope camera, the images are then processed, and cells are counted using ImageJ's morphological processes.

Fig. 2 on the other hand, shows the process of maintaining the parameters. Maintenance system starts off with the sensors simultaneously reading the pH level and temperature of the culture. The data gathered will be verified if it is in the ideal range. If the parameters, either pH or temperature were in the ideal range, the current data is sustained. However, if it is not in the ideal range, certain amount of chemical needed to maintain the system will automatically be added to the culture. If the pH level read is higher than the ideal range, Phosphoric acid will be added to the system. If it is lower, sodium hydroxide will be added. Likewise, if the temperature read is higher than the ideal range, the maintenance system will run the cooling fan. And if it is lower, the maintenance system will run the heater. This process will repeat unless the ideal range is maintained.

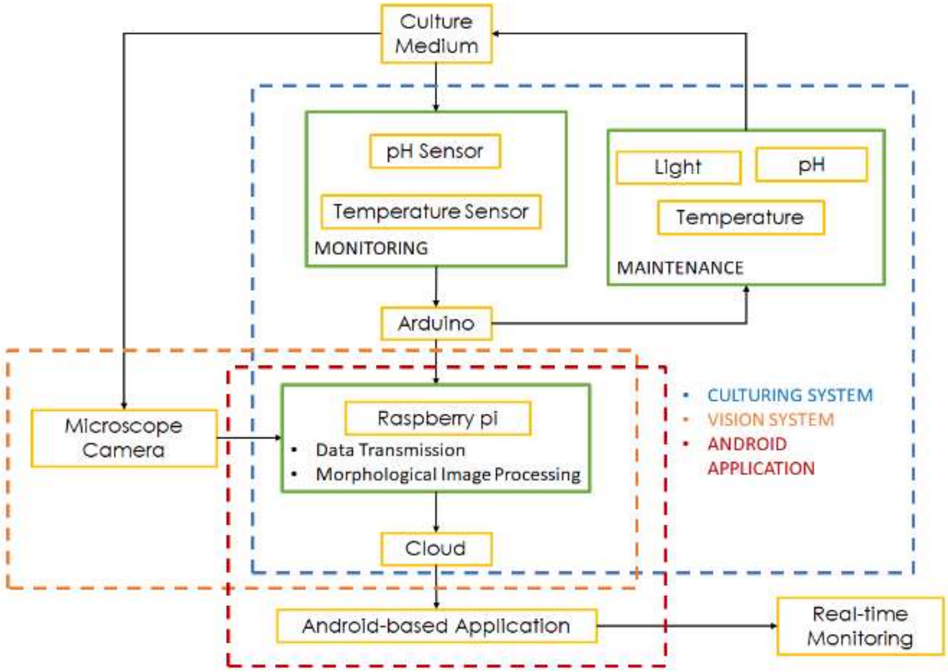

Fig. 1. The Block Diagram of the System.

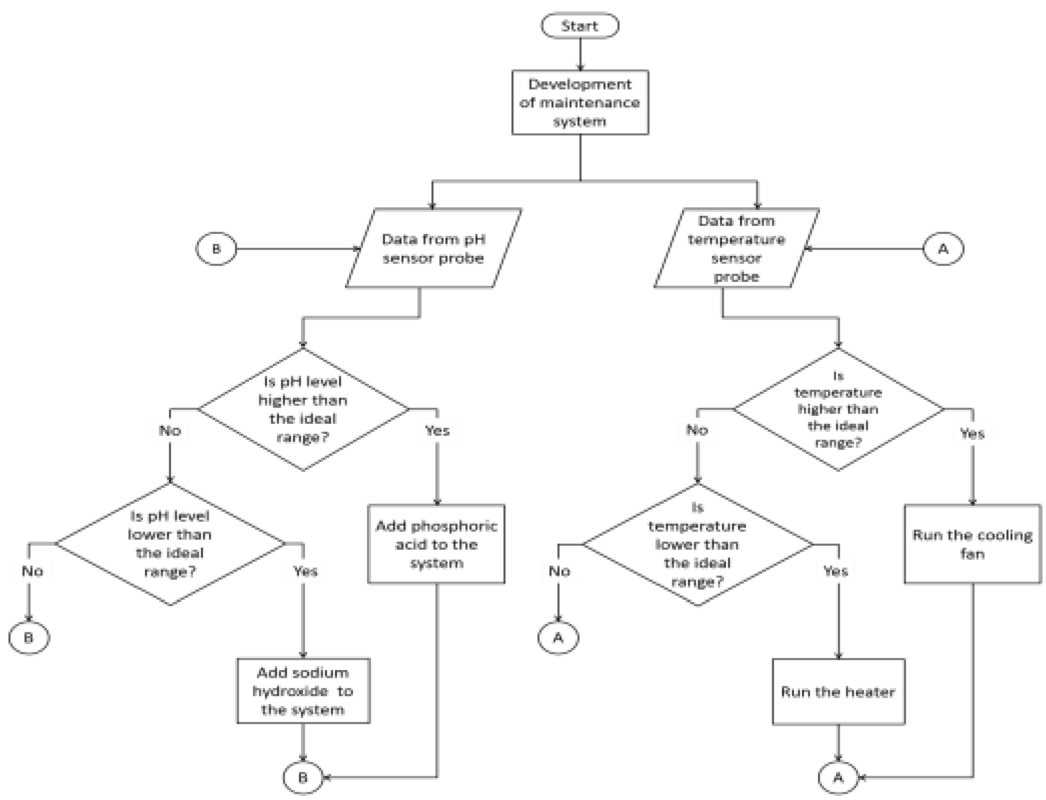

Fig. 2. Parameter Maintenance Flow Chart.

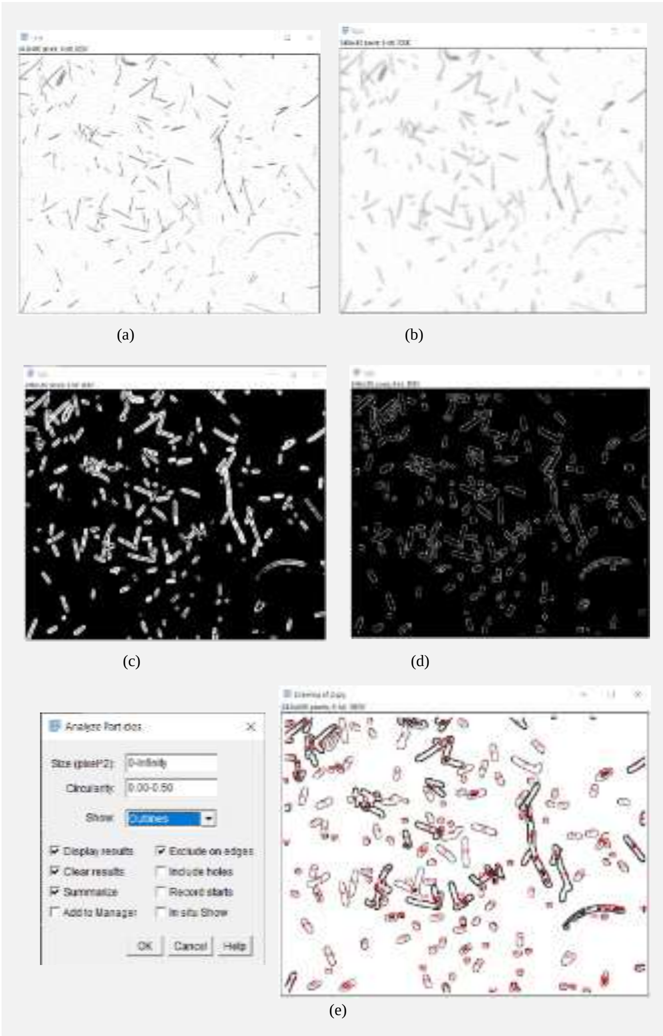

Fig. 3. ImageJ's Image Processing Steps: (a) Obtained Image in Binary, (b) Image after Gaussian Blur, (c) Thresholding, (d) Canny Edge Detection, (e) Counting of Detected Filaments.

Fig. 3 shows the functions done in the images and the counting of the filaments by the ImageJ's image processing. The images are initially evaluated by ImageJ's edge detection. This was done to effectively determine the location of the filaments present in the sample image with minimal error rate. Furthermore, the method used was Particle Analysis. This was utilized because it detects the edges with precision. The process began by converting the acquired image to binary. The thresholding is done twice to clearly detect the filament edges. The image should also pass through Gaussian blur. In this case, the sigma is set to 2. Then, run the Canny edge function. Lastly, through the output image of the Canny edge wherein it detected the cells in the image, is the analysis of the image by counting the identified particles.

Fig. 4 shows the isometric view of the device. It is made from a half-inch thick marine plywood and the edges were finished with aluminum angle bar. The wood box is C-shaped, and the aquarium is placed in the middle. At the top part of the box, above the aquarium, is where the electronic circuits, air pump, peristaltic pumps, and the power supply lie. They are fixed in a piece of acrylic so that they do not move easily. There is also a small hole that acts as a passage of wires. The back part houses the vision system and the two wash bottles. This part is for the tall components. The bottom part is a drawer. This drawer serves as a storage for the essential tools in culturing Spirulina, such as the syringe, the sampling dishes, and the plankton net. Moreover, Fig. 5 shows the actual device.

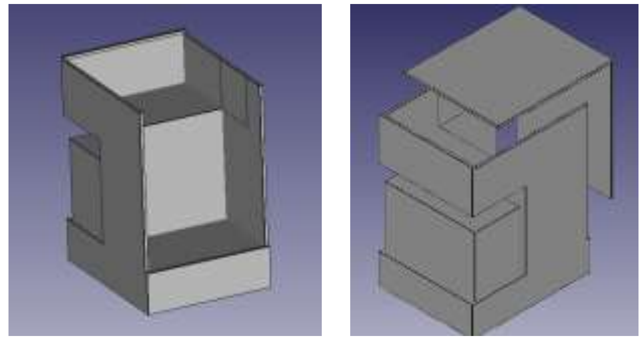

Fig. 4. The Design of the System.

Fig. 5. The Assembled Prototype.

Furthermore, the results obtained in this study were statistically evaluated. T-test was applied to determine if there is a significant difference in using a different color of LED as artificial light in culturing Spirulina platensis.

At the same time, regression analysis was utilized to determine the growth rate of Spirulina under different artificial lighting treatment over time.

The exponential analysis is given as:

$$y=\alpha e^{\beta x} \tag{1}$$

Where:

y = Cell count

α = equation coefficient

β = growth rate

x = number of days past

V. Result and Discussion

The culture prepared for this study was composed of 80% culture medium and 20% inoculum of pure Spirulina platensis. Three parameters were assessed for the constructed cultivation system. These are the temperature, the pH level, and the lighting. The constructed closed cultivation system underwent a 7-day test run to evaluate the parameter's functionality. The plotted graphs below would show the measured temperature and pH level obtained from the cultivating system for 7 days.

Fig. 6 shows the obtained temperature of the microalgae during the 7-day run. The system maintained the temperature within the specified target range of 29 to 32 degree Celsius. The starting temperature of the culture was 25.5°C and it progressively reached the specified range for the parameter's maintenance optimal range. The monitored temperature contains numerous changes but is still at the applicable set of temperature.

Fig. 7 proves that the device maintained the pH level of the culture during the test run. The culture began with a pH level of 7.28 because the water that was used for the culture was distilled. As it progresses, the culture's pH level immediately rose to the parameter's target optimal range which was between 8.5 and 9.5. Since then, the said parameter has been maintained. It also showed stability and it did not exceed the desired alkalinity for the microalgae.

Moreover, the vision system was programmed to automatically capture images of the sample using the Raspberry Pi, which will then be followed by detecting and counting the filaments on the captured image, as seen in Fig. 3. Furthermore, to determine its acceptability, 31 microscopic Spirulina images were assessed as the initial samples evaluated using ImageJ's particle analysis to effectively determine the location of the filaments present in the sample image. The samples were obtained using a sterile syringe and were placed in a sampling dish.

The obtained data from the vision system that uses ImageJ's Image Processing techniques were compared with manual counting of the filaments. T-test of two samples assuming equal variances was used for the statistical analysis of the system as shown in Table II. This was utilized to verify if the mean of the methods used would show a significant difference. And in turn, the result showed that the methods have no significant difference with each other. Since the obtained p-value is equal to 0.0729, which is greater than the significance level that is 0.025. Hence, the proponents have concluded that there is no significant difference between the methods. Thus, the constructed vision system which utilizes ImageJ plugins can be considered as an alternative in counting the filaments of the Spirulina platensis.

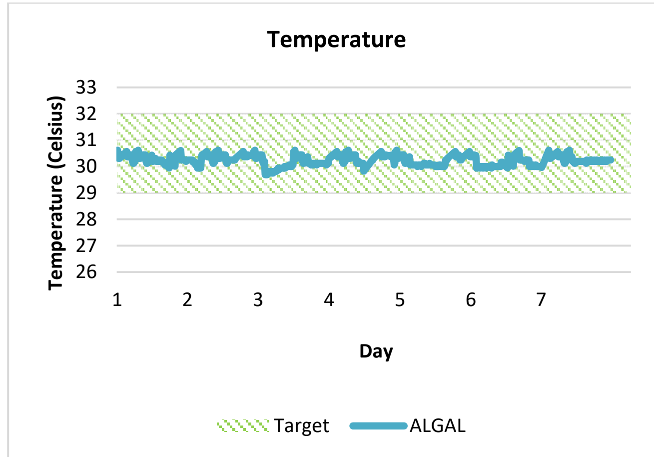

Fig. 6. Temperature of the System during the 7-day Test Run.

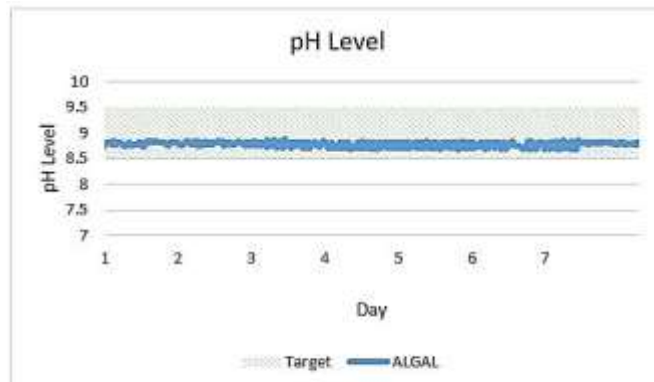

Fig. 7. pH Level of the System during the 7-day Test Run.

TABLE II. T-Test Validation for the Vision System

	Count (Manual)	Count (ImageJ)
Mean	37.16129032	33.77419355
Variance	54.13978495	52.58064516
Observations	31	31
df	60	
t Stat	1.825511902	
P(T<=t) one-tail	0.036450873	
t Critical one-tail	1.670648865	
P(T<=t) two-tail	0.072901747	
t Critical two-tail	2.000297822	
Decision	Accept H_{01}	
Interpretation	No Significant Difference	

The proposed system was compared with a previous study [12]-[13] to verify which set-up yields better growth of Spirulina platensis as shown in Table III. The former has been re-enacted with the same conditions except that this experiment uses 20% of inoculum. The medium used for each culture was SOT (Society of Toxicology) culture media. On the other hand, the bio-environmental factors such as pH level and temperature were monitored. Meanwhile, previous studies [12]-[13] proved that the culture's Dissolved Oxygen (DO) level remained on its ideal range which was 10-25 mg per liter. Thus, this study did not monitor the DO level of the culture anymore. The cultures were also aerated to obtain homogeneity in light absorption. This study uses Red LEDs as artificial lighting whereas the past study uses a Red-blue LEDs. For the vision system, to determine the cell count of the culture, the previous study used RGB analysis using Artificial Neural Network, while this study opted to made use of the microscopic image analysis using ImageJ. Furthermore, IoT implementation and Android application were implemented in this study, whereas the previous study did not.

The experimental setup also proved that Red-only LED helps increase the cell count of the Spirulina platensis culture compared to the previous research's Red-Blue LED setup. During its Lag phase, the Red-only displayed an early increase in growth as it progresses through the week resulting in a clear gap having a 28.43% more cell count per ml compared to Red-Blue on the seventh day. Fig. 8 shows the cell count for each light setup for 7 days.

Fig. 9 and 10, on the other hand shows the regression analyses for the two methods of artificial lighting. The growth rate of the Red LED is 0.388 while the Red-blue LED has 0.3021. The Red LED had 28.43% higher growth rate than the Red-blue LED.

Table IV shows the t-test for the comparison of Red-only and Red-blue LED. The p-value 0.02 is less than the 0.05 significance level. The decision is to reject the null hypothesis, which states that the color of LED used in culturing Spirulina does not affect its cell count. This means that there is a significant difference between the two means.

TABLE III. COMPARISON BETWEEN THE PREVIOUS WORK AND THE PROPOSED WORK

	Previous work [12], [13]	This work
Inoculum	10%	20%
Culture Medium	SOT	SOT
Bio-environmental factors (pH and Temperature)	Monitored	Monitored
Dissolved Oxygen	Yes	No
Aeration	Yes	Yes
Artificial light color	Red-blue	Red
Growth rate	30.2%	38.8%
Vision System	RGB analysis using ANN	Microscopic image analysis using ImageJ
IoT implementation	No	Yes
Android application	No	Yes

The Android application was able to obtain the data from the pH and temperature sensors. These sensors are connected to the Arduino using Raspberry Pi. Correspondingly, the Android application was programmed to fetch the upcoming data and to display the latest recorded entry the database has received per parameter. In turn, the accumulated data were presented into the developed application in graphical and numerical forms. These are shown in Fig. 11.

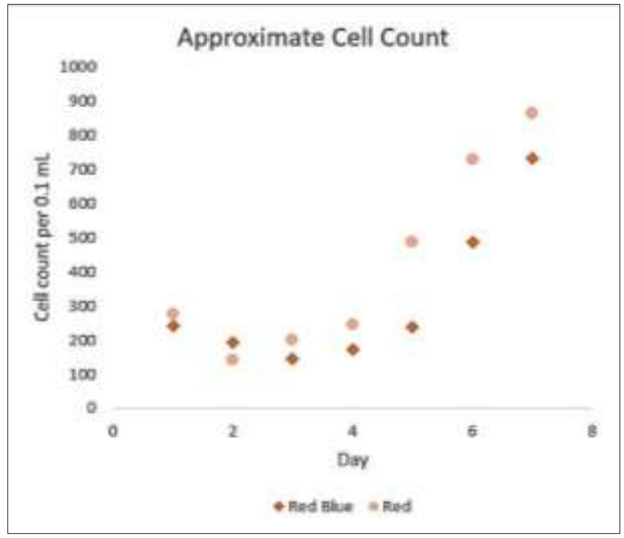

Fig. 8. Approximate Cell Count.

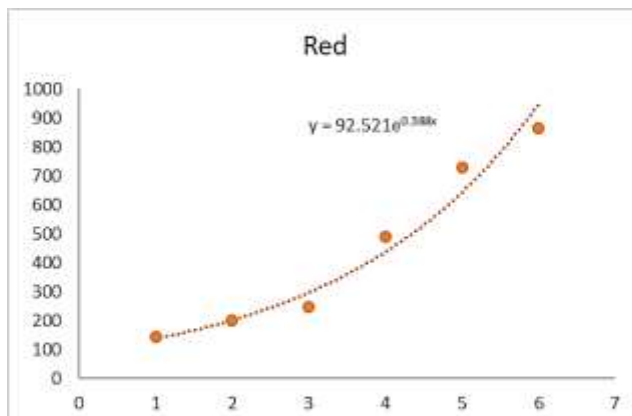

Fig. 9. Regression Analysis of Spirulina Platensis using Red LED.

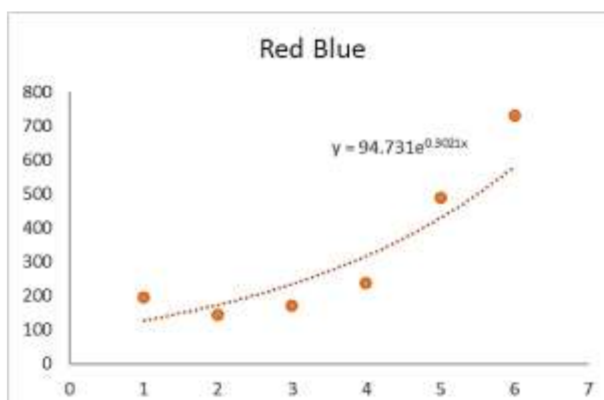

Fig. 10. Regression Analysis of Spirulina platensis using Red-Blue LED.

TABLE IV. T-TEST FOR THE LIGHTING TREATMENT TO BE USED IN CULTURING SPIRULINA

Test Statistic:	-2.511
Pearson's r:	0.934
P-value:	0.02
Decision	Reject H_{01}
Interpretation	Significant

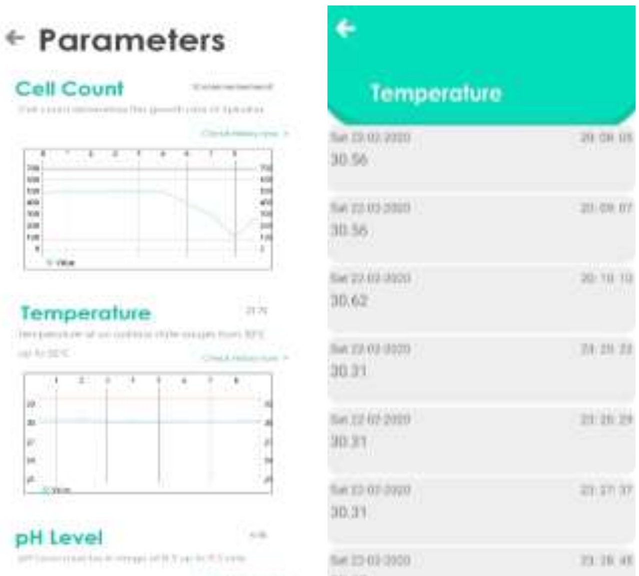

(a) (b)

Fig. 11. Parameter Data in (a) Graphical and (b) Numerical form in Spirulinapp.

VI. CONCLUSION

The proposed closed algal culturing system successfully and effectively maintained the parameters to its optimal level. Its maintenance system was consistent in keeping the parameters in their respective ideal range. The culture which was illuminated using red LED obtained more cell count than the ones with red and blue LED. This, in turn, improved the quality of the Spirulina that was produced throughout the study proper.

Since no significant statistical difference between the implemented ImageJ's image processing and the manual counting and the ImageJ-based vision system's counting took less than 10 seconds, the implemented ImageJ feature became a good substitute for counting cells manually. Lastly, the Android application was a great help for the cultivators since it showed convenience in monitoring the necessary parameters.

VII. FUTURE WORK

For future work, this study can be applied to other aquaculture systems especially other species of microalgae which requires an optimal range of bio-environmental factors to greatly improve its growth. Furthermore, the automation of collecting samples is advised as it can limit the frequency of opening the system, reducing the contamination of the culture. Improvement or alternative for the device's camera is also advised to further improve the sample's image resolution and quality. As for the IoT implementation, data encryption and improvement of the Android application's GUI is advised for security and quality of life. Lastly, it is advised to increase the images to be assessed by the system and the timeframe in conducting the study since microalgae are species that need proficiency and precision in cultivating.

ACKNOWLEDGMENT

The authors would like to thank the University Research and Development Services and University Extension Services of the Technological University of the Philippines for the support and grant. They would also like to acknowledge Dr. Frolan Aya and Mr. Reylan Gutierrez of SEAFDEC for sharing their knowledge answering all the questions and for providing and allowing to use the laboratory equipment and materials.

REFERENCES

[1] M. Ahsan, B. Habib, M. Parvin, T. C. Huntington, and M. R. Hasan, "A Review on Culture, Production and Use of Spirulina as Food for Humans and Feeds for Domestic Animals and Fish," FAO Fisheries and Aquaculture Circular (FAO), 2008.

[2] S. Kulkarni and D. Chavan, "Nutritional and Therapeutic Evaluation of Spirulina Platensis," *Asian Journal of Pharmaceutical and Clinical Research*, 2020.

[3] K. Srivastava and S. K. Sharma, "Temperature and Humidity Sensors With Arduino and Android," in *Handbook of Research on the Internet of Things Applications in Robotics and Automation*, pp. 367-398, 2020.

[4] S. Kumar, "Economic and Commercial Aspects of IoT in Agriculture Digitization," in *Handbook of Research on the Internet of Things Applications in Robotics and Automation*, pp. 160-168, 2020.

[5] R. Singh, A. Gehlot, V. Jain, and P. K. Malik, "Handbook of Research on the Internet of Things Applications in Robotics and Automation," IGI Global, pp. 1-433, 2020. doi:10.4018/978-1-5225-9574-8.

[6] P. K. Das, P. K. Malik, R. Singh, A. Gehlot, K. V. Gupta, and A. Singh, "Industrial hazard prevention using raspberry Pi," in *International Conference on Intelligent Computing and Smart Communication*, pp. 1487-1499, Dec. 2019.

[7] M. Cordova-Rozas, J. Aucapuri-Lecarnaque, and P. Shiguihara-Juarez, "A Cloud Monitoring System for Aquaculture using IoT," in *2019 IEEE Sciences and Humanities International Research Conference (SHIRCON)*, pp. 1-4, Nov. 2019.

[8] J. Masojıdek and G. Torzillo, "Mass Cultivation of Freshwater Microalgae," *Ecological Engineering*, pp. 2226-2235, 2008.

[9] A. Vonshak and A. Richmond, "Mass production of the blue-green alga Spirulina: an overview," *Biomass*, vol. 15, no. 4, pp. 233-247, Jan. 1988.

[10] P. Sharpe, "Methods of cell counting and assaying cell viability," in *Laboratory Techniques in Biochemistry and Molecular Biology*, vol. 18, Elsevier, pp. 7-17, 1988.

[11] J. G. A. Barberdo, "A review on methods for automatic counting of objects in digital images," *IEEE Latin America Transactions*, vol. 10, no. 5, pp. 2112-2124, Sept. 2012.

[12] A. U. Aquino, M. V. L. Bautista, C. H. Diaz, I. C. Valenzuela, and E. P. Dadios, "A Vision-Based Closed Spirulina (A. Platensis) Cultivation System with Growth Monitoring using Artificial Neural Network," in *2018 IEEE 10th International Conference on Humanoid, Nanotechnology, Information Technology, Communication and Control, Environment and Management (HNICEM)*, pp. 86-90, Dec. 2018.

[13] A. U. Aquino, M. E. M. Fernandez, A. P. Guzman, A. A. Matias, I. C. Valenzuela, and E. P. Dadios, "An Artificial Neural Network (ANN) Model for the Cell Density Measurement of Spirulina (A. platensis)," in *2018 IEEE 10th International Conference on Humanoid, Nanotechnology, Information Technology, Communication and Control, Environment and Management (HNICEM)*, pp. 81-85, Dec. 2018.

[14] E. Ariawan and S. Makalew, "Smart Micro Farm: Sustainable Algae Spirulina Growth Monitoring System," in *2018 10th International Conference on Information Technology and Electrical Engineering (ICITEE)*, pp. 587-591, Jul. 2018.

[15] F. Jia, “Multivariable And Sensor Feedback Based Real-Time Monitoring and Control of Microalgae Production System,” Ph.D. dissertation, Department of Agricultural and Biosystems Engineering, University of Arizona, 2015.

[16] U. Niangoran, F. Tian, L. Canale, C. T. Haba, D. Buso, and G. Zissis, “Study of the LEDs spectrums influence on the Spirulina platensis growth in batch culture,” in *2018 IEEE International Conference on Environment and Electrical Engineering and 2018 IEEE Industrial and Commercial Power Systems Europe (EEEIC/I&CPS Europe)*, pp. 1-4, Jun. 2018.

[17] M. Lafont, S. Dupont, P. Cousin, A. Vallauri, and C. Dupont, “Back to the future: IoT to improve aquaculture : Real-time monitoring and algorithmic prediction of water parameters for aquaculture needs,” in *2019 Global IoT Summit (GIoTS)*, pp. 1-6, Jun. 2019.

[18] I. Hermadi, I. R. Setiadianto, D. F. Al Zahran, M. N. Simbolon, G. Saefurahman, D. S. Wibawa, and Yandra Arkeman, “Development of smart algae pond system for microalgae biomass production,” in *IOP Conference Series: Earth and Environmental Science*, vol. 749, no. 1, pp. 1-8, 2021.

[19] S. Esposito, A. Cafiero, F. Giannino, S. Mazzoleni, and M. M. Diano, “A monitoring, modeling and decision support system (DSS) for a microalgae production plant based on internet of things structure,” *Procedia computer science*, vol. 113, pp. 519-524, Jan. 2017.

[20] F. Giannino, S. Esposito, M. Diano, S. Cuomo, and G. Toraldo, “A predictive Decision Support System (DSS) for a microalgae production plant based on Internet of Things paradigm,” *Concurrency and Computation: Practice and Experience*, vol. 30, no. 15, pp. 1-6, Aug. 2018.

(IJACSA) International Journal of Advanced Computer Science and Applications,
Vol. 12, No. 7, 2021

Feature Engineering Framework to detect Phishing Websites using URL Analysis

N.Swapna Goud[1]
Research scholar
Department of Computer Science and Engineering, Koneru Lakshmaiah Education Foundation
Vaddeswaram, AP, India

Dr. Anjali Mathur[2]
Assistant Professor
Department of Computer Science and Engineering, Koneru Lakshmaiah Education Foundation
Vaddeswaram, AP, India

***Abstract*—Phishing is a most popular and dangerous cyber-attack in the world of internet. One of the most common attacks in cyber security is to access the personal information of internet users through "Phishing Website". The major element through which hacker can do this job is through URL. Hacker creates an almost replica of original URL in which there is a very small difference, generally not revealed without keen observation. By pipelining various machine learning algorithms, the proposed model aims to recognize the important features to classify the URL using a recursive feature elimination process. In this work the data set of various URL records has been collected with 112 features including one target value. In this work a Machine Learning based model is proposed to identify the significant features, used to classify a URL, the wrapper method recursive feature elimination compares different bagging and boosting machine learning approaches .Ensemble algorithms, Bootstrap Aggregation Algorithms, Boosting and stacking algorithms are used for feature selection. The proposed work has five sections: work on the pre-processing phase, finding the relation between the features of the dataset, automatic selection of number of features using Extra Tree Classifier, comparison of the various ensemble algorithm and finally generates the best features for URL analysis. This paper, designs meta learner with XG BOOST classifier as base classifier and achieved an accuracy of 93% Out of 112 features, this model has performed an extensive comparative study on feature selection and identified 29 features as core features by performing URL analysis.**

***Keywords*—Recursive feature elimination; principal component analysis; standard scalar transformation; eXtreme gradient boosting classifier; correlation matrix**

I. Introduction

The world of digital suffers a lot from cyber security attacks. The phishing attack can be handled based on source code or URL or image. This research designed the model based on URL features. These URL features are further classified into 4 sub categories. The sub categorization is represented in the below Fig. 1.

With the increase of E-commerce applications, cyber-crimes are also increasing rapidly [1]. To solve this issue, researchers are focusing on the detection of phishing websites using Machine Learning and Deep Learning techniques. The dataset contains 112 attributes but all the attributes may not be important. This research tries to find the most important attributes that can determine whether it is a phishing website or not. Some of the websites access are marked as unauthorized by Google but it is difficult to identify all the unauthorized sites by Google search engine. In order to prevent those types of sites, the model compares the every component of the URL to mark it as "Phish Website" [7].

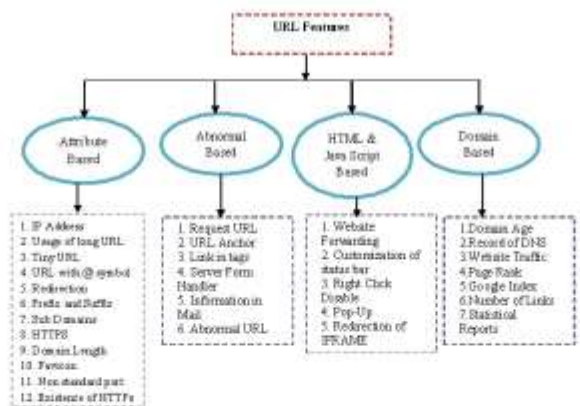

Fig. 1. Classification of URL based Features.

In the proposed research, the feature selection to detect the phishing website is solved using the ensemble algorithms. Ensemble algorithms are popular for their robust results and it designs the meta learners by combining the weak learners, which performed on the same dataset. There are three popular ensemble techniques. The algorithms are as follows.

1) Bootstrap aggregation algorithms: Bootstrap Aggregation is also known as "Bagging", in which execution of weak classifiers occurs concurrently (or) in parallel. In this method, a sample randomized subset is generated from the entire dataset. The traditional algorithms suffer from high variance. To solve this problem, a component known as "estimator" is added, which is used to create a random sub sample based on the classifier passed.

2) Boosting algorithms: In this type of algorithms, classifiers of same type are combined sequentially to generate a new model. In general, it solves the problem of label incorrectness, which is defined by the one or more models. Boosting also, address the problem of high variance by generating the output of various classifiers and then the average of their predictions are taken into account. It also plays an vital role in reduction of bias.

3) Stacking algorithms: It is more advanced than bagging and boosting algorithms because it combines heterogeneous classifiers rather than homogenous. It also designs a model in such way that it combines a meta learners with base learners. In these algorithms, after every iterations, it applies meta model based on the output generated by the previous iteration.

II. Related Work

In [8] Mehmet Korkmaz et al. analyzed URL features by comparing the performance of the model using three different datasets and eight machine learning algorithms. This model has analyzed every part of the URL for detection of fake website. The model has recognized 58 features as important features in URL analysis.

Among all the algorithms, Random forest has given best performance on all the three datasets.

In [2] M Somesha et al, proposed an efficient deep learning techniques in which URL's are passed as the input to the model and features are extracted from the selenium testing tool. The major components of extraction are:

a) Obfuscation Features: These are features are extracted from the URL itself. In general, there are 5 types of features as shown in Table I.

TABLE I. Obfuscation Features

S.NO	Feature Name
1	Number of dots in host name
2	@symbol in URL
3	URL Length
4	IP presence
5	HTTPS presence

b) Hyperlink-based Features: These features are extracted from the code snippet of the HTML page. Among 8 features, this model has identified six features as important to design the concept of information gain.

c) Third-Party-based Features: These features are extracted from the search engines and assisting devices. In this type of features, Alexa has obtained highest information gain. In information gain, it assumes that every feature is dependent on class label and all other features are independent of other features. Every feature is allocated with rank and the ranks less than the threshold value are ignored.

In the next step, the model splits the data into trained and cross validated data. The model had designed a multi feed forward network, with five DNN layers with hyper parameters. In this design, weight values are considered randomly. A Recurrent Neural Network as LSTM is designed to find the relation between the extracted. LSTM is good at handling the vanishing gradient problem. To avoid long term dependencies, LSTM has designed three gates with every gate has its own equation. A CNN with eight layers are designed with back propagation method to classify the URL as suspicious or not.

In [3] Paulius Vaitkevicius et al. conducted a comparative study on various machine learning algorithms and designed a unified ranking model for the detection of phishing website. During the training phase, the model has implemented a cross validation process with setting of hyper parameters and also it has the solved the problem of memorizing the data by decreasing the number of weak learning algorithms. Similarly, at the same time, overfitting and underfitting issues are handled by defining the high bias and high variance. Welch's T-test, compare the accuracies generated by the two classifiers and compute the statistical difference. Based on the accuracies produced, each classifier has assigned a unique value. Finally, the model has given unique ranking depending on the related work and libraries used.

In [9] Jitendra Kumar et al. proposed five classifiers for detecting phishing websites. Among these random forest and decision tree classifiers are given almost the same accuracy. Author used regular expressions to extract the components from the URL. The author has mainly focused on the three important features namely, URL based features, page based features and domain based features. The data are randomly distributed for forming training and testing dataset.

In [4] Ammar Odeh et al. designed a Multi-Layer Perceptron by considering the URL features. On the extracted features, performed selection, combination of ranking and single attribute evaluation is performed. Later, a subset from these features is generated and is passed as input to the neural network. In this, model is designed with fixed values of hyper parameters and has obtained an accuracy of 93.7%.

In [5] Yazan A et al, proposed AI meta learners combined with base algorithm known as "Extra Tree Classifier". The first meta learner is "ABET", this process is carried for 100 iterations and later normal distribution is performed. After training the classifier, it generated a hypothesis and computed the error rate. For every iteration, it updated the weight value and checked whether the threshold value 0.5 is satisfied or not. For the entire generated hypothesis, it computed the argmax function. The second meta learner is "RoFET", in which the dataset is randomly divided into five subsets, with each containing six features. It created a new dataset by using the bootstrap induction. The newly constructed dataset generated coefficients with the help of sparse rotation matrix. It generated class confidence to determine the class label of each record. The third meta learner is "BET", 150 iterations are performed over the training dataset and a new dataset is generated by inducer for base algorithm. Argmax concept is applied to find the most frequent predicted class label of the record. The fourth meta classifier is "LBET", all the weights are initialized to 1/n, where n is number of records in the dataset. The probability estimators are initialized as 0.5. For all the 100 iterations, calculated the weight based probability estimators, then fitted the least square regression function to the weights and updated the values of the weight. Summation of all the classifiers are used to predict the class label. Out of these 4 meta classifiers, LBET has performed better with 97.5% accuracy.

In [6] Waleed Ali et al. proposed PSO based feature weighting approach by encoding the features in a particle. The position and velocities are generated randomly to calculate the fitness of the function. The major goal of the fitness function is to update the local and global values by checking the threshold values regularly. After reaching the termination condition, it generates the optimal weights of all the features. Based on the weights, important features are considered for classification process. These features are passed as input to the five traditional machine learning algorithms and one neural network algorithm. The model has compared all the six algorithms in terms of all evaluation metrics and stated that back propagation neural network has achieved highest accuracy.

In [10] Suleiman Y. Yerima et al, designed 2-layer CNN and 3-layer CNN to detect the phishing websites. The 2-layered architecture contains one convolution and one max pooling layer. The flattened data is transferred to the eights units of neurons that are activated with the help of ReLu function. To prove the efficiency, author has constructed the network with different number of neurons and has achieved 96.6% accuracy for 64 neurons. In the 3-layered architecture additional max pooling layer is added and has achieved 97.1% accuracy for 64 neurons. This model clearly depicted that with the increase of layers and neurons, the accuracy of the model also increases.

III. Methodology

In this research, the major focus is to reduce the number of features for classifying a URL as phishing website or not. This research work is organized into five sections: Section 1 describes the pre-processing, Section 2 describes the process of finding the relation between the features of the dataset using correlation and principal component analysis (PCA), Section 3 describes the automatic selection of number of features using Extra Tree Classifier, Section 4 compares the bagging and boosting algorithms on the number of features generated using the pipeline mechanism and Section 5 generates the best features based on the best algorithm generated in Section 4.

The feature engineering helps the model to construct the explanatory attributes which plays a vital role in training the model. The major goal of feature selection is to reduce the computation time of the complex models. The process of feature engineering is illustrated in the Fig. 2.

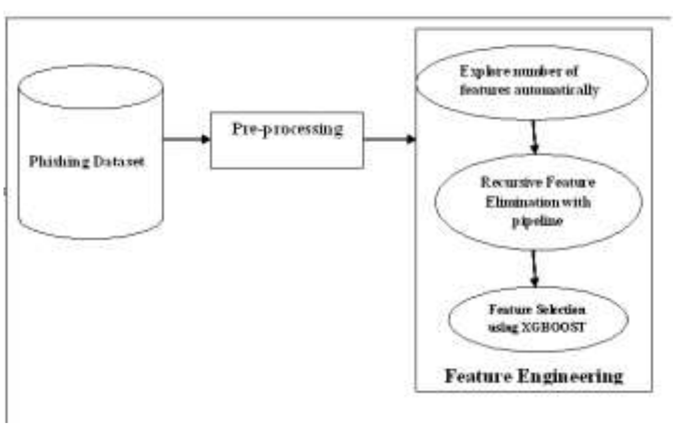

Fig. 2. Feature Engineering Framework for Detection of Phishing Websites.

A. Pre-Processing

The process of cleaning and transforming the data is known as “Pre-processing”. A dataset with missing and inconsistent values leads to the poor performance of the model. The dataset used in this research contains 112 features (Table VII in Appendix A) and all the features are numerical values. Used wrangling process to deal with missing and inconsistent values to reduce the computational time, the data should be normally distributed. Normal distribution is achieved by applying standard scalar mechanism.

The equation is

$$SC = \frac{A[i]-\mu}{\sigma} \quad (1)$$

Where,

A[i] , represents attribute(columns) of i^{th} index

μ, represents the mean

σ, represents the standard deviation

After applying standard scalar mechanism, for further processing of the model, the dataset is divided into 80% training data and 20% testing data.

B. Dependency between the Features

Implementing correlation function and PCA functions to find the relation among the features of the dataset. In correlation, the coefficient r, is denoted by 3 possible values [-1, 0, 1], which indicates negative, no relation and positive relation. In this research, Pearson method is implemented, which tries to draw a best fit line between the features. The calculation of Pearson coefficient is represented in the equation 2.

$$PC = \frac{np * \sum_{i=0}^{np} A_i A_j}{\sqrt{(np\sum_{i=0}^{np}(A_i)**2-(\sum_{i=0}^{np}(A_i))**2)*(np\sum_{i=0}^{np}(A_j)**2-(\sum_{i=0}^{np}(A_j))**2)}} \quad (2)$$

Where,

np, represents number of pairs.

Ai, A j, represents attribute values of corresponding indexes.

After applying PCA on our dataset, the result is observed as followed (the attributes whose coefficient value, PC is less than 0.95 and self-denoting correlation values are ignored) Table II.

Principal Component Analysis (PCA) creates a linear relationship among the attributes. The explained variance measures as rank in terms of PCA. It iterates from 1 to n components specified in the algorithm. It is a two-step process in which first one calculates the covariance matrix and second one computes the Eigen values, Eigen vectors for the covariance matrix. This proposed research made the threshold for covariance as 0.90 and obtained 20 features as important features. The results are tabulated in Table III.

TABLE II. PEARSON COEFFICIENT VALUES IN CORRELATION MATRIX

S.No	Attribute 1	Attribute 2	PC Value
1	qty_percent_url	qty_percent_params	0.950514
2	qty_equal_url	qty_and_params	0.960387
3	qty_and_params	qty_equal_params	0.966137
4	tld_present_params	qty_at_params	0.967140
5	qty_plus_params	qty_questionmark_params	0.969952
6	qty_plus_params	qty_exclamation_params	0.969952
7	qty_equal_url	qty_equal_params	0.970317
8	qty_equal_directory	qty_asterisk_directory	0.974202
9	qty_hashtag_params	qty_plus_params	0.976315
10	qty_slash_directory	qty_slash_url	0.977222
11	qty_equal_directory	qty_tilde_directory	0.978526
12	qty_equal_params	qty_params	0.979225
13	qty_equal_directory	qty_and_file	0.980746
14	qty_and_directory	qty_equal_directory	0.982878
15	qty_questionmark_directory	qty_equal_directory	0.983013
16	qty_asterisk_directory	qty_and_directory	0.986722
17	qty_exclamation_params	qty_questionmark_params	0.987444
18	qty_asterisk_directory	qty_and_file	0.988919
19	qty_dollar_directory	qty_asterisk_directory	0.988919
20	qty_tilde_directory	qty_and_directory	0.991102
21	qty_comma_file	qty_asterisk_directory	0.991163
22	qty_percent_file	qty_percent_directory	0.991288
23	qty_and_directory	qty_dollar_directory	0.993309
24	qty_and_file	qty_tilde_directory	0.993309
25	qty_dollar_params	qty_questionmark_params	0.993776
26	qty_exclamation_params	qty_space_params	0.993776
27	qty_dollar_directory	qty_and_file	0.995510
28	qty_hashtag_directory	qty_and_directory	0.995562
29	qty_dollar_file	qty_tilde_directory	0.995562
30	qty_plus_directory	qty_and_file	0.997758
31	qty_space_file	qty_dollar_directory	0.997758
32	qty_and_directory	qty_and_file	0.997778

TABLE III. EXPLAINED VARIANCE MEASURE OF PCA

S.No	Explained Variance Ratio
1	0.40925027
2	0.16526287
3	0.05252565
4	0.03512697
5	0.03213711
6	0.02153855
7	0.02043802
8	0.01887185
9	0.01696678
10	0.01528985
11	0.01430187
12	0.01369579
13	0.01319472
14	0.01253416
15	0.01178374
16	0.01158423
17	0.01125422
18	0.01058307
19	0.01013929
20	0.0098498

C. *Automatic Selection of Number of Features*

In this research, an ensemble technique known as “Extra Tree Classifier” is implemented. This model constructs unpruned decision trees and it considers majority voting to predict the class labels. It follows reverse approach to decision trees and random forest; it tries to fit the decision trees generated by the dataset. The algorithm has three hyper parameters, change of which may lead different evaluations. The hyper parameter k, determines the attribute selections, n-min determines the output noise average and m determines variance level. To evaluate the model, repeated stratified cross validation is performed. This research paper has opted repeated cross validation because in K-fold cross validation, because of the random distribution of the data, every time it is executed, and the output values may vary. To reduce this noisy data problem, in the proposed model the repeated cross validation, performs the same task for multiple times and the average of all the executions is taken into account. The number of models generated and executed is shown in the equation 3.

$$\text{Number of models generated} = k*r \tag{3}$$

Where,

k, represents K-folded cross validation

r, represents number of repetitions

Algorithm 1: Explore Number of Features
Input: Phishing Dataset, D **Output:** Accuracy for 2 to n-1 features
Start Step 1: Load the dataset, D Step 2: number_features=111 Step 3: create an empty dictionary, models Step 4: for i← 1 to number_features: a. call ExtraTreeClassifier(max_features=i) b. append to the models Step 5: cv←repeatedstratifiedcrossvalidation() Step 6: scores←cross_val_score() Step 7: for names, model in models.items(): Step 8: print scores Stop

D. Comparative Study

Bagging and boosting algorithms are identified as powerful ensemble algorithms. Pipelined four ensemble algorithms to study the performance of an algorithms on the number of features generated by the Extra Tree Classifier among them three are boosting algorithms and other is bagging algorithm with meta base estimator each algorithm is illustrated.

1) Bagging with meta base estimator: This model fits the randomly generated subsets to the base classifiers. The average predicted values of all the models generated by the subsets are taken in to consideration and the outcome is predicted based on the majority voting. The random subsets are generated based on the estimator specified in the model. In this research, the estimator considered is "Logistic Regression", which is better to draw the relationships between nominal, interval and ordinal data. The base classifier considered is "Decision Tree Classifier", in this at every node to split the data, it takes number of conditions into consideration. Using the concept of divide and conquer, the decision tree recursively partitions the data. The splitting of the data is taken care by the parameter, information gain. Here, the information gain is computed by subtracting the weighted sum node impurity of two child nodes from the node impurity of the parent node. The node impurity defines the homogeneity of the labels to which it belongs to.

2) Adaptive boost (AdaBoost) classifier: This algorithm trains the model sequentially by correcting the errors generated by the previous models. In this classifier, initially every record is assigned with a random weight (Generally, it is considered as 1/n, where n represents number of record in the dataset). A decision tree is constructed and is used to classify the records. The predictive labels generated by the decision tree are compared against the actual class labels of the training dataset. This comparison gives the results of correctly and incorrectly classified records. This misclassified data weights summation is assumed as error rate and theses errors are corrected by increasing the weights of incorrect decisions and decreasing the weights of correct decisions. This process is repeated continuously until correct predictions are made.

3) Gradient Boosting (GBM) Classifier: It is almost similar to AdaBoost classifier but it specifies the target values to the next model generator. The target value always depends on the rate of variation among the prediction models. If the error rate is high the target value is set to high otherwise it is set to low. The error value is determined by the gradient coefficient in the loss function. The loss function in this algorithm is considered as mean square error, the objective of this algorithm is to minimize it. It always tries to bring the error rate close to zero.

4) eXtreme Gradient BOOSTing (XGBOOST) Classifier: It is an extended version of gradient boosting algorithm. The major goal of this algorithm is to increase the computational power of the system and optimize the performance of the model as minimum as possible. All the trees construction occurs concurrently in this model. This parallelism improves the CPU utilization time.

Algorithm 2: Recursive Feature Elimination with pipeline Architecture
Input← Phishing Dataset, D **Output**← Accuracies of different machine learning algorithm
Start Step 1: Load the Dataset, D Step 2: create a two dimensional matrix, ID← store all the columns except the target column Step 3: create a one dimensional matrix, DD←store the target column Step 4: ID_train, DD_train, ID_test,DD_test←split the dataset Step 5: Update the ID_train and DD_train with the standard scalar values and fit the transformation Step 6: alg=get_alg() Step 7: create two empty lists, res and name Step 8: for n,m in alg: a. sco←eval_alg(m,ID_train,DD_train) b. append sco value to the res list c. append n to the name list d. print the mean of scores, mean(sco) and names n Stop

The feature selection has done using filtering methods, wrapper methods and embedded methods. In this research, the popular wrapper method known as “Recursive Feature Elimination” (RFE) is implemented. In this method, different classifiers are applied on the same model to find the number of important features. Initially, RFE considers all the features as important and it starts constructing subset by eliminating the unwanted features. RFE ranks the features based on their importance. The features with least absolute value are removed.

Procedure for get_alg():

1) create an empty list, algorithms

2) add logistic regression with decision tree classifier as meta estimator to pipeline

3) add adaboost algorithm to pipeline

4) add XGBoost classifier to pipeline

5) add Gradient Boosting classifier to pipeline

Procedure for eval_alg(m, ID_train,DD_train):

a) call the repeated cross validation function

b) call the cross evaluation score function

E. Generation of Best Features

The best features are obtained by passing XGBoost as estimator to the recursive feature elimination algorithm and number of significant features are 29. Support and rank are achieved for all the features.

Algorithm 3: Recursive Feature Elimination with XGBOOST Estimator

Input← Phishing Dataset, D

Output← Accuracies of different machine learning algorithm

Start

Step 1: Load the Dataset, D

Step 2: create a two dimensional matrix, ID← store all the columns except the target column

Step 3: create a one dimensional matrix, DD←store the target column

Step 4: ID_train, DD_train, ID_test,DD_test←split the dataset

Step 5: Update the ID_train and DD_train with the standard scalar values and fit the transformation

Step 6: Call RFE() method with XGBoostClassifier as estimator.

Step 7: fit the train data to the RFE() method

Step 8: for i←0 to len(D):

Print support[i], rank[i]

Stop

IV. Experimental Results

In this work the algorithms are good enough to find the significant features useful for classification process. The feature selection is based on their accuracy score and score for every feature is tabulated in Table IV.When the accuracy is calculated for all 111 features, it is observed that accuracy is more i.e., 94 % accuracy when the number of features are 29 and are tabulated in table new. The accuracy scores are plotted in Fig. 3. In the below graph, x-axis represents the number of features and y-axis represents the accuracy.

TABLE IV. Accuracy Values of each Feature

Feature Number	Accuracy Score	Feature Number	Accuracy Score	Feature Number	Accuracy Score	Feature Number	Accuracy Score	Feature Number	Accuracy Score
1	0.921	24	0.933	47	0.937	70	0.936	93	0.934
2	0.927	25	0.934	48	0.936	71	0.936	94	0.934
3	0.922	26	0.935	49	0.937	72	0.938	95	0.935
4	0.925	27	0.934	50	0.937	73	0.938	96	0.935
5	0.927	28	0.928	51	0.937	74	0.937	97	0.935
6	0.926	29	0.940	52	0.936	75	0.933	98	0.934
7	0.923	30	0.933	53	0.939	76	0.936	99	0.935
8	0.923	31	0.936	54	0.937	77	0.935	100	0.935
9	0.927	32	0.932	55	0.940	78	0.937	101	0.934
10	0.931	33	0.935	56	0.937	79	0.935	102	0.935
11	0.928	34	0.935	57	0.938	80	0.932	103	0.933
12	0.926	35	0.937	58	0.936	81	0.932	104	0.933
13	0.927	36	0.936	59	0.940	82	0.933	105	0.937
14	0.926	37	0.935	60	0.936	83	0.935	106	0.934
15	0.930	38	0.936	61	0.935	84	0.937	107	0.935
16	0.933	39	0.935	62	0.936	85	0.936	108	0.935
17	0.929	40	0.934	63	0.937	86	0.934	109	0.934
18	0.932	41	0.937	64	0.935	87	0.936	110	0.936
19	0.933	42	0.936	65	0.935	88	0.934	111	0.934
20	0.930	43	0.937	66	0.937	89	0.935		
21	0.932	44	0.938	67	0.937	90	0.937		
22	0.930	45	0.933	68	0.937	91	0.936		
23	0.930	46	0.939	69	0.935	92	0.937		

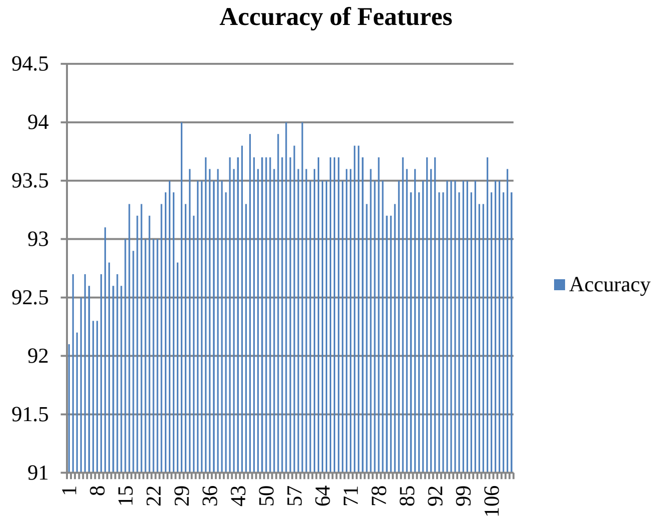

Fig. 3. Features Accuracies Plot.

On the selected number of features, four different algorithms are passed to the recursive feature elimination and the accuracies are tabulated in Table V, and the comparative study is plotted in Fig. 4.

TABLE V. MACHINE LEARNING ALGORITHM ACCURACIES

S.No	Algorithm Name	Accuracy
1	Logistic Regression (LR)	89.8
2	Ada Boost(Ada)	90.0
3	XGBoost	93.0
4	Gradient Boost (gbm)	92.8

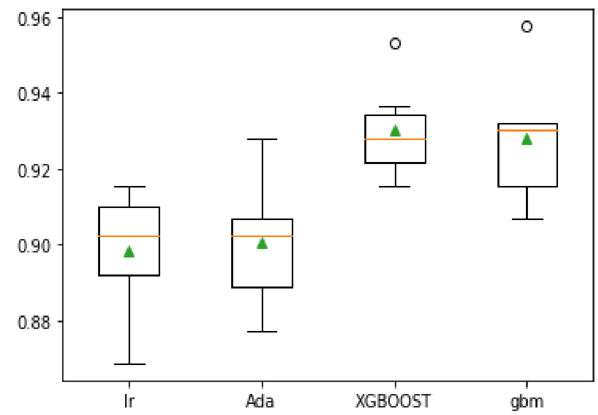

Fig. 4. Comparative Study on Selected Features.

The XGBoost classifier identifies the top 29 features and remaining is allocated with different ranking. The results are tabulated in Table VI.

TABLE VI. RANK AND SUPPORT VALUES FOR THE FEATURES

Feature Number	Feature Name	Support	Rank	Feature Number	Feature Name	Support	Rank
1	qty_dot_url	True	1.000	57	qty_percent_directory	True	1.000
2	qty_hyphen_url	True	1.000	58	directory_length	True	1.000
3	qty_underline_url	True	1.000	59	qty_dot_file	False	69.000
4	qty_slash_url	True	1.000	60	qty_hyphen_file	False	43.000
5	qty_questionmark_url	False	3.000	61	qty_underline_file	False	41.000
6	qty_equal_url	False	2.000	62	qty_slash_file	False	39.000
7	qty_at_url	True	1.000	63	qty_questionmark_file	False	37.000
8	qty_and_url	True	1.000	64	qty_equal_file	False	6.000
9	qty_exclamation_url	False	11.000	65	qty_at_file	False	10.000
10	qty_space_url	False	13.000	66	qty_and_file	False	12.000
11	qty_tilde_url	False,	15.000	67	qty_exclamation_file	False	14.000
12	qty_comma_url	False	17.000	68	qty_space_file	False	34.000
13	qty_plus_url	False	24.000	69	qty_tilde_file	False	35.000
14	qty_asterisk_url	False	19.000	70	qty_comma_file	False	16.000
15	qty_hashtag_url	False	21.000	71	qty_plus_file	False	33.000
16	qty_dollar_url	False	25.000	72	qty_asterisk_file	False	18.000
17	qty_percent_url	False	4.000	73	qty_hashtag_file	False	20.000
18	qty_tld_url	False	5.000	74	qty_dollar_file	False	22.000
19	length_url	True	1.000	75	qty_percent_file	True	1.000
20	qty_dot_domain	True	1.000	76	file_length	True	1.000
21	qty_hyphen_domain	False	38.000	77	qty_dot_params	False	48.000
22	qty_underline_domain	False	40.000	78	qty_hyphen_params	False	50.000
23	qty_slash_domain	False	42.000	79	qty_underline_params	False	52.000
24	qty_questionmark_domain	False	47.000	80	qty_slash_params	False	54.000
25	qty_equal_domain	False	49.000	81	qty_questionmark_params	False	56.000
26	qty_at_domain	False	51.000	82	qty_equal_params	False	58.000
27	qty_and_domain	False	53.000	83	qty_at_params	False	60.000
28	qty_exclamation_domain	False	55.000	84	qty_and_params	False	62.000
29	qty_space_domain	False	57.000	85	qty_exclamation_params	False	64.000
30	qty_tilde_domain	False	59.000	86	qty_space_params	False	66.000
31	qty_comma_domain	False	61.000	87	qty_tilde_params	False	68.000
32	qty_plus_domain	False	63.000	88	qty_comma_params	False	28.000
33	qty_asterisk_domain	False	65.000	89	qty_plus_params	False	7.000
34	qty_hashtag_domain	False	67.000	90	qty_asterisk_params	False	23.000

35	qty_dollar_domain	False	44.000	91	qty_hashtag_params	False	46.000
36	qty_percent_domain	True	1.000	92	qty_dollar_params	False	36.000
37	qty_vowels_domain	True	1.000	93	qty_percent_params	True	1.000
38	domain_length	False	27.000	94	params_length	False	26.000
39	domain_in_ip	False	29.000	95	tld_present_params	False	9.000
40	server_client_domain	True	1.000	96	qty_params	False	8.000
41	qty_dot_directory	True	1.000	97	email_in_url	True	1.000
42	qty_hyphen_directory	True	1.000	98	time_response	True	1.000
43	qty_underline_directory	True	1.000	99	domain_spf	True	1.000
44	qty_slash_directory	False	71.000	100	asn_ip	True	1.000
45	qty_questionmark_directory	False	73.000	101	time_domain_activation	True	1.000
46	qty_equal_directory	False	72.000	102	time_domain_expiration	False	31.000
47	qty_at_directory	False	70.000	103	qty_ip_resolved	True	1.000
48	qty_and_directory	False	30.000	104	qty_nameservers	True	1.000
49	qty_exclamation_directory	False	32.000	105	qty_mx_servers	True	1.000
50	qty_space_directory	False	74.000	106	ttl_hostname	True	1.000
51	qty_tilde_directory	False	76.000	107	tls_ssl_certificate	True	1.000
52	qty_comma_directory	False	78.000	108	qty_redirects	False	75.000
53	qty_plus_directory	False	80.000	109	url_google_index	False	77.000
54	qty_asterisk_directory	False	82.000	110	domain_google_index	False	79.000
55	qty_hashtag_directory	False	83.000	111	url_shortened	True	1.000
56	qty_dollar_directory	False	81.000				

V. Conclusion

This proposed model of feature engineering, trained the dataset in split ratio of 80% and 20%. This model evaluates the correlation matrix values and principal component analysis values. The values don't specify the relation between the features clearly. While comparing PCA values and filter values with wrapper methods we found more clarity between the features in terms of exploratory and performance by using wrapper methods. The proposed developed algorithm eXtreme Gradient finds the important features among all the existing 112 features. The major reason for selecting the XGB classification algorithm is when meta classifier i.e., the bagging algorithm, Ada Boost (Ada), XGBoost (XGB), and Gradient Boost (gbm) classifiers are applied, the XGB algorithm has achieved an accuracy of 93%. The Ensemble based recursive feature elimination mechanism constructs a subset, by eliminating the weak features. RFE identify significant feature with minimum number so good classifier is designed. Recursive feature elimination is developed by combining Meta classifier with base classifier and decision tree as a bagging algorithm. The most significant features are highlighted under the column support on the basis of the rank values. All the true values in support column are considered as significant values, these significant features has accuracy value as 1.000. The bagging algorithm, Logistic regression obtained 89.8% accuracy whereas boosting algorithms achieved more than 90% accuracy apart from all XGBoost gave 93.0% accuracy to retrieve the features to detect Phishing websites.

References

[1] Abdulhamit Subasi, Emir Kremic, Comparison of Adaboost with MultiBoosting for Phishing Website Detection, Procedia Computer Science, Volume 168, 2020, Pages 272-278, ISSN 1877-0509, https://doi.org/10.1016/j.procs.2020.02.251.

[2] Somesha, M., Pais, A.R., Rao, R.S. et al. Efficient deep learning techniques for the detection of phishing websites. Sādhanā 45, 165 (2020). https://doi.org/10.1007/s12046-020-01392-4

[3] Vaitkevicius, Paulius, and Virginijus Marcinkevicius. "Comparison of Classification Algorithms for Detection of Phishing Websites." Informatica, 2020, pp. 143–60. DOI.org (Crossref), doi:10.15388/20-INFOR404.

[4] Odeh, A., Keshta, I. & Abdelfattah, E. (2020). *Efficient Detection of Phishing Websites Using Multilayer Perceptron*. International Association of Online Engineering. Retrieved March 27, 2021 from https://www.learntechlib.org/p/217754/.

[5] Y. A. Alsariera, V. E. Adeyemo, A. O. Balogun and A. K. Alazzawi, "AI Meta-Learners and Extra-Trees Algorithm for the Detection of Phishing Websites," in *IEEE Access*, vol. 8, pp. 142532-142542, 2020, doi: 10.1109/ACCESS.2020.3013699.

[6] W. Ali and S. Malebary, "Particle Swarm Optimization-Based Feature Weighting for Improving Intelligent Phishing Website Detection," in *IEEE Access*, vol. 8, pp. 116766-116780, 2020, doi: 10.1109/ACCESS.2020.3003569.

[7] C. Singh and Meenu, "Phishing Website Detection Based on Machine Learning: A Survey," *2020 6th International Conference on Advanced Computing and Communication Systems (ICACCS)*, Coimbatore, India, 2020, pp. 398-404, doi: 10.1109/ICACCS48705.2020.9074400.

[8] M. Korkmaz, O. K. Sahingoz and B. Diri, "Detection of Phishing Websites by Using Machine Learning-Based URL Analysis," *2020 11th International Conference on Computing, Communication and Networking Technologies (ICCCNT)*, Kharagpur, India, 2020, pp. 1-7, doi: 10.1109/ICCCNT49239.2020.9225561.

[9] J. Kumar, A. Santhanavijayan, B. Janet, B. Rajendran and B. S. Bindhumadhava, "Phishing Website Classification and Detection Using Machine Learning," *2020 International Conference on Computer Communication and Informatics (ICCCI)*, Coimbatore, India, 2020, pp. 1-6, doi: 10.1109/ICCCI48352.2020.9104161.

[10] S. Y. Yerima and M. K. Alzaylaee, "High Accuracy Phishing Detection Based on Convolutional Neural Networks," *2020 3rd International Conference on Computer Applications & Information Security (ICCAIS)*, Riyadh, Saudi Arabia, 2020, pp. 1-6, doi: 10.1109/ICCAIS48893.2020.9096869.

Appendix A

TABLE VII. Dataset Used in Research with 112 Features

Feature Number	**Feature Name**
1	qty_dot_url
2	qty_hyphen_url
3	qty_underline_url
4	qty_slash_url
5	qty_questionmark_url
6	qty_equal_url
7	qty_at_url
8	qty_and_url
9	qty_exclamation_url
10	qty_space_url

11	qty_tilde_url
12	qty_comma_url
13	qty_plus_url
14	qty_asterisk_url
15	qty_hashtag_url
16	qty_dollar_url
17	qty_percent_url
18	qty_tld_url
19	length_url
20	qty_dot_domain
21	qty_hyphen_domain
22	qty_underline_domain
23	qty_slash_domain
24	qty_questionmark_domain
25	qty_equal_domain
26	qty_at_domain
27	qty_and_domain
28	qty_exclamation_domain
29	qty_space_domain
30	qty_tilde_domain
31	qty_comma_domain
32	qty_plus_domain
33	qty_asterisk_domain
34	qty_hashtag_domain
35	qty_dollar_domain
36	qty_percent_domain
37	qty_vowels_domain
38	domain_length
39	domain_in_ip
40	server_client_domain
41	qty_dot_directory
42	qty_hyphen_directory
43	qty_underline_directory
44	qty_slash_directory
45	qty_questionmark_directory
46	qty_equal_directory
47	qty_at_directory
48	qty_and_directory
49	qty_exclamation_directory
50	qty_space_directory
51	qty_tilde_directory
52	qty_comma_directory
53	qty_plus_directory
54	qty_asterisk_directory
55	qty_hashtag_directory
56	qty_dollar_directory
57	qty_percent_directory
58	directory_length
59	qty_dot_file
60	qty_hyphen_file
61	qty_underline_file
62	qty_slash_file
63	qty_questionmark_file

64	qty_equal_file
65	qty_at_file
66	qty_and_file
67	qty_exclamation_file
68	qty_space_file
69	qty_tilde_file
70	qty_comma_file
71	qty_plus_file
72	qty_asterisk_file
73	qty_hashtag_file
74	qty_dollar_file
75	qty_percent_file
76	file_length
77	qty_dot_params
78	qty_hyphen_params
79	qty_underline_params
80	qty_slash_params
81	qty_questionmark_params
82	qty_equal_params
83	qty_at_params
84	qty_and_params
85	qty_exclamation_params
86	qty_space_params
87	qty_tilde_params
88	qty_comma_params
89	qty_plus_params
90	qty_asterisk_params
91	qty_hashtag_params
92	qty_dollar_params
93	qty_percent_params
94	params_length
95	tld_present_params
96	qty_params
97	email_in_url
98	time_response
99	domain_spf
100	asn_ip
101	time_domain_activation
102	time_domain_expiration
103	qty_ip_resolved
104	qty_nameservers
105	qty_mx_servers
106	ttl_hostname
107	tls_ssl_certificate
108	qty_redirects
109	url_google_index
110	domain_google_index
111	url_shortened
112	Phishing(Target value)

The Impact of CALL Software on the Performance of EFL Students in the Saudi University Context

Ayman Khafaga[1]*
Department of English, College of Science and Humanities,
Prince Sattam Bin Abdulaziz University, Saudi Arabia, &
Department of English, Faculty of Arts and Humanities
Suez Canal University, Egypt

Abed Saif Ahmed Alghawli[2]
Department of Computer Science, College of Science and Humanities, Prince Sattam Bin Abdulaziz University, Aflaj
Kingdom of Saudi Arabia

***Abstract*—This paper investigates the extent to which Computer-Assisted Language Learning (CALL) contributes academically and pedagogically to the performance of students majoring English as a Foreign Language (EFL). The paper's main objective is to explore the extent to which CALL is effective in developing the linguistic and communicative competence of EFL students in the skill of reading. This paper uses both quantitative and qualitative approaches in the process of data collection. As an empirical study, the sample in this study was 47 students studying English at Prince Sattam bin Abdulaziz University. The participants were classified into two groups: experimental and control; each of which has been assigned specific reading activities. The experimental group has been allocated technological learning, by means of using the computer programs of Snagit[TM], Screencast; whereas the control group has been assigned traditional learning, i.e. without using computer. Results revealed that the use of CALL has more positive effects on the learning outcomes of the experimental group than those pertaining to the control group. This, in turn, accentuates the fact that the use and application of CALL into EFL contexts improves the students' learning outcomes concerning the skill of reading. The study recommends further integration of computer software into the designation of the different EFL courses.**

Keywords*—CALL; EFL students; Saudi university context; language skills; reading; Snagit[TM]; screencast; performance; effectiveness

I. Introduction

The overwhelming use and application of CALL (computer-assisted language learning) significantly influences the process of teaching and learning in all fields and disciplines in general, and in teaching and learning English as a foreign language (EFL) in particular. The employment of computer technologies in learning has caused unprecedented advancement beyond the limits of traditional and conventional sources of knowledge [1], [2]. The interest in digital technologies shapes all aspects of life; education is no exception. Educational technology dominates the process of learning and teaching EFL courses in the Saudi universities, specifically in recent years. This computer technology exceeds the boundaries of knowledge to the extent that contributes to the education of language skills and linguistic courses [3], [4].

As one innovative manifestation of technological advancement in learning, computer-assisted language learning (henceforth, CALL) is not intended to replace the traditional classroom instruction; however, its main concern is to enhance the performance of learners as well as to offer them further benefits on learning [5]. Students can easily use these computer software and applications in their learning regardless of time and place. They can use the different CALL programs to improve their linguistic competence and performance in the various language skills, including writing, reading, listening, speaking, vocabulary, etc. [6], as well as to practice their English language via specific interactive activities that can be followed by immediate feedback monitoring their linguistic progress [7].

CALL is a learning approach, whose theoretical, applied and pedagogical frameworks allow the use and application of computer programs and computer-based resources in teaching and learning English [8]. CALL is a technological system that can assist in not only the learning and teaching EFL courses, but also in improving the linguistic and communicative competence of EFL students [9]. According to [10], CALL is a computer program that is principally devised and developed to target educational purposes manifested in offering instructional help and support for both students and teachers in learning and teaching English. This program has been under a constant process of development since it has firstly been introduced to the field of learning and teaching EFL courses. Such a development has shifted the focus of this program from a simple digital program focusing on textbooks to very advanced digital programs that serve to grant students the opportunity of not only to learn English through the use of computer, but also to create and develop their own learning styles and outcomes. Crucially, the popularity CALL software has nowadays is due to the prominent impact of the information communication technology (ICT) that dominates both society and education [11], [12]. CALL provides both synchronously and asynchronously types of learning in a way that enables students to learn in a cooperative environment and to create communicative activities in pairs and in group [13].

In the Saudi educational system, CALL has relatively been a novel concept for many years because learning EFL is limited in practice and is confined to the classroom. Recently, CALL is introduced into EFL classes, particularly in Saudi universities. Nowadays, one can notice the application of CALL programs to almost all Saudi universities to the extent that some of these institutions have an independent course entitled CALL, as is the case for Prince Sattam bin Abdulaziz University, the setting where this study was conducted. This,

*Corresponding Author

in turn, reflects the interest of applying and using computers in the educational process, and also demarcates a shift towards a technological education that covers all educational fields. Crucially, this fast digital shift is accompanied with an incessant process of training for instructors and students to ensure that they are up-to-date with the latest developments of technology. This paper, therefore, tries to explore the impact of using CALL software on the performance of EFL students in terms of learning the skill of reading at Prince Sattam bin Abdulaziz University. In so doing, this article can be perceived as an empirical study that targets to test EFL students' attitudinal behaviors towards the use of CALL programs and the way it influences their linguistic performance as well as their learning outcomes.

A. Research Questions

Based on the abovementioned introduction as well as the main purpose of the study, this article tries to answer the following overarching research question:

1) To what extent is the application of CALL software effective in learning the skill of reading in the Saudi university context? This research question constitutes a number of subsidiary questions that are further sought to be answered throughout this paper. These are as follows:

a) How does the use of CALL in the skill of reading activate autonomous learning and contribute to students' learning independence?

b) To what extent can learning outcomes of EFL students in the skill of reading be influenced via using CALL programs?

c) Does the use of CALL software in EFL courses increase students' learning motivation and curiosity?

B. Research Objectives

The answer of the aforementioned research questions comprises the main objectives of the current study:

1) To explore the extent to which the use of CALL software is effective in EFL classes within Saudi university context.

2) To shed light on the way learning outcomes concerning reading skill can be improved by the use and application of CALL software into EFL courses. This is accompanied with demonstrating the discrepancy in learning outcomes arrived at by the application of CALL software and those achieved by traditional instruction.

The remainder of this article is structured as follows: Section II presents the general theoretical background of the study, in which a brief account of the nature of CALL is provided; in this section some previous studies pertinent to the application of CALL software to EFL classes are also reviewed. Section III offers the methodology of the study, wherein data collection and description, research design and setting, participants, research instruments, and analytical procedures are provided. In Section IV, the results of the study elicited from the collected data are demonstrated. Section V is dedicated to discussing the results in relation to the findings of previous studies relevant to the contribution pertaining to the current paper. Section VI concludes the article and recommends further studies in the field.

II. Literature Review

A. Computer-Assisted Language Learning (CALL)

CALL, the result of the Information Age as well as the information communication technology, is a method of teaching and learning a foreign language [10]. Beatty [14] offers a definition for CALL, in which he states that it is a digital tool of teaching and learning English, wherein a computer is utilized in the process of education by a learner in order to improve his/her language. For [14], CALL is a tool whose dynamic functionality serves to facilitate the process of teaching and learning in a way that enables teachers to create innovative techniques in teaching the different language skills, including reading, writing, listening, speaking, vocabulary, etc.

According to [15], CALL motivates the online discourse environment on the part of both teachers and students. It helps learners present, develop and defend their ideas concerning specific topics. In today's EFL settings, CALL has become the feature of almost all linguistic programs applied to EFL courses [8]. Despite the fact that the use and/or application of CALL varies from one user to another, it is obvious that it fosters autonomy in the process of learning on the part of students [3]. This anticipated independent environment of learning, according to [16], is manifested in some procedures pertaining to self-directed learning that enables learners to set their personal perspectives in learning in a way that guarantees autonomous learning of some language skills outside the classrooms. As such, by employing CALL programs, students' performance can be evaluated in terms of the different skills of language they are supposed to learn. Significantly, self-directed procedures in the process of learning serve to create pedagogical awareness on the part of learners and help them highlight their strengths as well as weaknesses during the process of learning [17].

Due to the rapid development in the computer technologies the whole world witnesses nowadays, using CALL software has occupied considerable significance in numerous studies, theoretically and empirically, that are concerned with learning and teaching EFL courses [18-22]. These studies shed light on the effective role of computers as digital tools assisting and facilitating a better educational environment, wherein learners feel motivated towards the realization of their educational goals, for example, [23] emphasizes that computers not only offer restrictive activities accompanied with simple graphics, but also provide further complicated activities that allow the integration of videos, sounds, animation and communication in today's world. This, in turn, functions to develop a better educational atmosphere that increases the motivational attitude of learners towards EFL learning.

In their attempts to assess the performance of students in terms of the application of CALL software to EFL classrooms, and the way this is activated by the learners' motivation, some researchers have clarified the reasons why computer technologies in general, and CALL software in particular play a significant and influential part in improving students' performance concerning the different skills of language [24-29]. These studies list a number of reasons that revolve around the following ideas: (i) the availability of independent and autonomous learning; (ii) the proper accessibility to work with new digital tool of learning, which can replace the traditional tools of learning; (iii) the opportunity to have immediate services, such as reviewing and editing, as well as immediate feedback; (iv) the varieties in language learning activities, practices, and materials that are often missed in the traditional learning; and (v) computers can effectively foster learning of language skills in times and places where human performance in such skills proves to be inadequate.

According to [30], the educational and pedagogical advantages gained as a result of applying and using CALL software have been observed in the different skills of language, including the productive skills (writing and speaking), the receptive skills (reading and listening), and the other skills of language (vocabulary and grammar). Now, the question is: if various computer technologies contribute to the different skills of language, to what extent does the application of CALL software in the skill of reading influence the performance of learners in the Saudi EFL contexts? This is the core concern of this article.

B. Previous Studies

Much research has been conducted on the use and application of CALL software in learning and teaching English as a foreign language [31-39]. For example, Moras [40] investigated the effectiveness of using CALL programs and the Internet in EFL teaching in Brazil. Moras's study showed the interest of the English language teachers in the use of computers in teaching their courses to students. The study revealed that CALL programs have an influential role in directing the teaching and learning process from a teacher-dependent towards student-independent process. This, in light of Moras's study, emphasizes the effective contribution CALL software provides for teaching and learning EFL courses.

The same results have been reported by [41], who also explored the extent to which CALL is effective in teaching and learning English in the American EFL context. This study supports the application of communication technology, including computers, the Internet and the educational software to the teaching and learning process, and concluded by confirming the contributive part CALL programs play in acquiring English as a foreign language. The same contributive effectiveness of the use of communication technology and CALL software in learning and teaching EFL courses in Georgia, USA was also reported by [42].

In another study, [43] addressed the Online Writing Labs (OWLs) as a featured function of CALL within EFL contexts. They proposed what they termed as 'product approach', which offers help for learners in the skill of writing. They maintained that this approach provides learners with certain resources to enhance their writing skill, by offering advices, including grammatical structures, vocabulary, text structures, reference style, cohesion, coherence, etc. For [3], the accessibility of the different CALL features and word-processing packages, such as hypertext, multimedia and hypermedia serve to help learners convey their ideas in the skill of writing.

Concerning the skill of reading, [44] argued that the use of CALL software allows non-linear reading via hypertexts, wherein learners can access other linked texts, highlight documents and construct their own interpretation and insights into the text under readership. They added that computer technologies in this case can provide learners with different reading aids that contribute to the general understanding of the reading texts and also increase the motivational attitude of students towards this skill. These technological tools constitute a variety of multimedia aids, including photographs, graphics, sound, animation, video, as well as other links to dictionaries and glossaries that serve to foster the process of learning the skill of reading and enhance students' performance [23].

In the Saudi EFL context, [45] investigated the possibility of integrating CALL in the education process by exploring the perceptions and attitudes towards using CALL in English among Saudi secondary EFL teachers. Alshumaimerie [45] used a sample from King Saud University constituting 183 participants to test their attitudes concerning the use of CALL into classroom instruction. The study revealed positive attitudes towards the integration of CALL as a digital tool in the teaching process, and clarified that the successful implementation of the information technology represented in CALL entirely depends on the attitudes of teachers and educators and contributes significantly to the whole process of teaching EFL courses.

In the same vein, Al-Mekhlafi [46] discussed the effectiveness of introducing CALL into EFL classes at preparatory schools. The study attempted to test the hypothesis of whether or not the use of computer increases the students' exposure to language, as well as the effect of this on the performance of students. The findings of Al-Mekhlafi's study showed that students who use computers in learning display better learning outcomes than those learn by traditional classes. The findings of this study accentuate the fact that the application and use of information technology, and more specifically CALL in EFL contexts is highly contributive to the process of learning and teaching.

III. Methodology

A. Research Design and Setting

This study is an empirical one conducted on students at the department of English, College of Science and Humanities, Prince Sattam bin Abdulaziz University, Saudi Arabia. The study constitutes two groups: experimental group and control group. Each group is assigned specific reading activities. The experimental group undergoes some reading activities technologically by the use of the two computer programs Snagit™ and Screencast; whereas the control group is assigned the same reading tasks by means of a traditional method of learning, that is, without the use of any computer programs. The study was conducted in the second semester of the academic year 2020-2021 and lasted for eight weeks. Interestingly, the department of English at Prince Sattam University teaches a course entitled 'Computer-Assisted Language Learning', also abbreviated as CALL. This, therefore, facilitates the task of researchers in supervising and monitoring the study in its different stages, given the fact that the two researchers are affiliated and work at the same institution. The existence of CALL as an independent course in the department of English also helps in the management of the whole study for two reasons. First, the reading activities required for the analytical purposes are naturally incorporated into the delivered elements of the course; and, second, it guarantees the avoidance of any artificiality bias, either in the procedures adopted in the study or the data collection procedures.

B. Participants

The participants in the current study were 47 level-seven Saudi students who are studying English as a foreign language at Prince Sattam University. All participants were aged 19-21, and were studying CALL as an obligatory course in the department of English. Among the participants were 36 female students (67%), while 11 participants were males (23%). The participants were divided into two groups: an experimental group constituting 24 students and a control group including 23 students.

C. Research Instruments

Two research instruments were used in this study. The first was an interview, in which participants were directly asked about their experiences concerning the use of computers and CALL programs in their study of the different courses, the time they spend using computer every week, the availability of the computer sets, and the accessibility of the internet services during their study. The second research instrument was a questionnaire designed to test the participants attitudinal behaviors concerning using computer and computer programs in reading, the different activities they are assigned in this skill, and the way they perceive computer programs in the learning the skill of reading. The questionnaire consisted of 15 items with a 5-point Likert scale, including the response categories of: strongly agree, agree, no idea, disagree, and strongly disagree. The two instruments were employed to investigate the impact of using CALL on the performance of EFL students at Prince Sattam University.

Importantly, the study used version 11.1 on Windows of the program Snagit™. This computer program is run by TechSmith Corporation and serves to help users capture the elements they see on their computer screens. This includes capturing a text, a video, an image, etc. One option of Snagit™ is called Snagit Editor, through which users can edit their captures and/or sharing them with any person and at any time. This option also helps users save their captures in various formats, including PDF, GIF, JPG, and EPS, insert them into different types of documents, including Word, PowerPoint or Excel, and share them through YouTube, Screencast, Facebook, Twitter and so forth. As for the Scrrencast, it is a computer program which enables users to record, save, and share any activities on their computer devices. This program also allows users to comment on each other's files and/or documents, which, in turn, serves to facilitate and support the process of interaction among users. The activities conducted via Screencast may include screen or webcam activities or both, and recorded activities may also be saved and shared as video file.

D. Research Procedures

The research procedures adopted in this study comprise two paralleled strands. The first is confined to the control group, whereas the second is dedicated to the experimental group. The procedural strands constitute three stages: pre-, in-, and post- process. The pre-process stage is a preparatory stage which offers general orientation to the two groups concerning the assigned reading tasks. The in-process is confined to the assigned reading tasks themselves pertaining to the two groups. This stage comprises three sub-stages: pre-reading, while-reading, and post-reading. The post-process is dedicated to the interpretation of results in terms of the assessment of participants' performance, either those who used CALL in conducting the required reading activities or those completed the activities traditionally, that is, without the use of computer programs. Importantly, when dealing with the experimental group, further specific procedures are applied. These include: (i) designing a questionnaire as well as an interview to provide the information concerning the experience of participants in dealing with computer programs in studying English as a foreign language; (ii) allowing the experimental group to conduct the activities by means of using the two computer programs of Snagit™ and Screencast, while the control group is only allowed to do the reading tasks assigned to the experimental group without using computers; and (iii) demonstrating the results elicited from the questionnaire and the interview after conducting the assigned tasks. After the completion of the three stages, a general interpretation of the results elicited from the research instruments used in the study is provided. In this stage, the obtained results are discussed in terms of the performance of the sampled participants. Results are also compared with previous studies approached the same topic. Significantly, the two groups were assigned the reading comprehension of one short story titled *Enter Dragoon*, written by Thomas Hardy in 1900. The assigned reading tasks are listed in Tables I and II.

TABLE I. ANALYTICAL PROCEDURES (CONTROL GROUP)

Control group			
Stage	**Manifestations**	**Procedures**	**Learning tools**
Pre-process	Reading orientation	-Preparing the group participants towards the assigned tasks	Traditional learning; no use of computer programs
In-process	Pre-reading activities	- Brainstorming	
	While-reading activities	- Identifying main themes in the text - Highlighting ideological words in the text - Classifying the characters in the text	
	Post-reading activities	- Answering some comprehension questions on the text	
Post-process	Results interpretation	- Assessing participants' performance	

TABLE II. ANALYTICAL PROCEDURES (EXPERIMENTAL GROUP)

Experimental group			
Stage	**Manifestations**	**Procedures**	**Learning tools**
Pre-process	Reading orientation	-Preparing the group participants towards the assigned tasks	Technological learning; using computer programs of Snagit™ and Screencast
In-process	Pre-reading activities	- Brainstorming	
	While-reading activities	- Identifying main themes in the text - Highlighting ideological words in the text - Classifying the characters in the text	
	Post-reading activities	- Answering some comprehension questions on the text	
Post-process	Results interpretation	- Assessing participants' performance	

IV. RESULTS

This part demonstrates the results obtained from the questionnaire and the interview pertaining to the experimental group. The results pertinent to the control group were only used to compare those of the experimental group in the discussion section. This is because the core concern of the study is to monitor and explore the impact of using CALL on the performance of EFL students, which necessitates the analytical focus to be on the experimental group rather than on the control one.

A. *The Interview*

TABLE III. PARTICIPANTS' EXPERIENCE ON USING COMPUTER

Question	Experience degree						
	Low		**Moderate**		**High**		**Total**
	N.	**%**	**N.**	**%**	**N.**	**%**	
To what extent do you generally use computer in learning English as a foreign language?	4	16.6	19	79.1	1	4.16	24
To what extent are you experienced in Snagit™ and Screencast?	22	97.5	1	4.16	1	4.16	24
Have you ever practiced reading comprehension by using any computer technologies?	15	62.5	7	29.1	2	8.32	24

TABLE IV. PARTICIPANTS' RESPONSES CONCERNING TIME SPENT ON COMPUTER

Question	Less than 5 hours		5-8 hours		More than 8		Total
How many hours have you spent in learning by means of computers per week?	**N.**	**%**	**N.**	**%**	**N.**	**%**	24
	13	54.1	7	29.1	4	16.6	

As indicated from Tables III and IV, the majority of the participants in the experimental group expressed positive attitude concerning the extent to which they use computers in learning English as a foreign language. 19 (79.17%) out of 24 participants have a moderate experience in terms of the use and/or applications of computer in the process of learning. This indicates that they are technologically familiarized to assign various reading activities by means of any technological tools. In question No. 2 which addresses the experience of the participants in the experimental group with regard to the use of the computer programs of Snagit™ and Screencast, a very high percentage of the participants display a negative attitude. Most of them (97.5%) emphasized that they have a poor experience concerning the two programs used in this study. This indication in question No. 2 is accentuated by the participants' responses to question No. 3, in which the majority of them (62.5%) stated that their experience in terms of using computer technologies in reading is low, whereas (29.16%) of them expressed a moderate degree in dealing with computer technologies when they read texts. The results obtained from Table III can be attributed, in one way or another, to the results displayed in Table IV, wherein experimental participants are asked about the number of hours they spend in learning by means of computer. In this regard, (54.18%) of the participants stated that they spent less than 5 hours per week in learning via computer; (29.16%) spent between 5 and 8 hours, whereas only (16.66%) learn via computer for more than 8 hours per week. Here, the general indication is that the majority of the participants have positive attitude concerning the use of computer in learning in general; however, they have a negative attitude towards the application of specific computer programs into the process of learning in general and the skill of reading in particular. This further explains the rationale for selecting the skill of reading rather than the rest of other language skills to be the core concern of this study.

B. *The Questionnaire*

Table V shows the participants' response concerning their attitudinal perception of the use and application of CALL software in the skill of reading, and the effect of this on their linguistic competence and performance.

TABLE V. PARTICIPANTS' RESPONSE TO THE QUESTIONNAIRE

No.	**Statement**	**SA**	**A**	**No idea**	**D**	**SD**	**Mean**
		Percent %					
1	I prefer to read texts via computer more than via textbooks.	20.83	66.67	4.17	4.17	4.17	3.96
2	Reading via computer increases my learning curiosity.	25.00	54.17	4.17	8.33	8.33	3.79
3	I think that using computer to practice reading is a waste of time.	4.17	8.33	4.17	70.83	12.50	2.21
4	Using computers increases reading chances.	16.67	62.50	12.50	4.17	4.17	3.83
5	Reading via computer saves time.	29.17	58.33	4.17	4.17	4.17	4.04
6	Computers enhance my reading skills in a positive way.	41.67	45.83	.00	8.33	4.17	4.13
7	Computers offer immediate feedback on my reading.	16.67	54.17	8.33	8.33	12.50	3.54
8	I understand texts well when I use computer in reading.	20.83	66.67	4.17	8.33	.00	4.00
9	Reading through computer develops my learning independence.	29.17	58.33	.00	8.33	4.17	4.00
10	I can check the meaning of difficult words via online dictionaries when I read via computer.	25.00	54.17	.00	8.33	12.50	3.71
11	Reading via computer hinders my comprehension of texts.	4.17	20.83	4.17	54.17	16.67	2.42
12	I prefer visual and audible information when I read via computer.	33.33	45.83	.00	12.50	8.33	3.83
13	Using computer programs in reading facilitates the various reading activities.	25.00	58.33	.00	8.33	8.33	3.83
14	Using computer in reading increases my motivation towards learning.	37.50	50.00	4.17	8.33	.00	4.17
15	I prefer to continue using computer to learn the different language skills.	33.33	54.17	4.17	4.17	4.17	4.08

Note: SA (Strongly Agree); A (Agree); SD (Strongly Disagree); D (Disagree)

As displayed in Table V, the questionnaire clarified one general fact: the attitudinal positivity in terms of the two response categories of strongly agree and agree. This, in turn, functions to emphasize the very positive attitude towards the use and application of computer and computer programs into learning the skill of reading. Responses in the above questionnaire indicate that a unanimous number of participants appeared to have high level of consent concerning using computer programs in reading. Through a simple observation of the questionnaire's items, one can identify five main points, all of which test the participants' attitudes in terms of the use of computer in reading. These are (i) preference of reading via computer and the intention to continue this in future (items 1,15); (ii) learning curiosity (items 2, 4); (iii) learning motivation (item 14); (iv) learning autonomy (item 9); and (v) improving reading skills (items 5, 6, 7, 8, 10, 12, 13). These besides two negative items (3, 11), which were intentionally included in order to verify whether or not the participants read the questionnaire's items while completing it.

Concerning the preference to use computer in reading as well the intention to continue using it to learn the different skills of language in the future, a very high percentage (20.83% for strong agreement and 66.67% for agreement) of the participants expressed their agreement that they prefer to practice reading by means of using computer. In terms of learning curiosity, the participants appeared to have a positive attitude (25% and 54.17% for strong agreement and agreement options, respectively) that their learning curiosity is improved when they use computer to read any texts. This attitudinal positivity is subsequently accentuated by the participants' response regarding item 4, wherein they stated that reading via computer serves to increase the chances of reading.

With respect to learning motivation, participants' responses also showed that they are highly motivated towards reading when they use computer (37.50% and 50% for the response categories of strongly agree and agree, respectively). This is statistically reflected by the high mean of (4.17) for the questionnaire item No. 14. The same positive attitude has also been reported regarding learning autonomy, where (29.17%) and (58.3%) of the participants expressed their agreement in response to item No. 9. They emphasized that the use of computer in reading helps them feel autonomous. The learning independence can be ascribed to the freedom they have when they practice reading; there is not control from teachers, no feeling of shyness to commit mistakes, and, therefore, they feel that what they do is entirely their own work. They further stated that using computer in reading offers them immediate feedback on their reading.

As for the questionnaire items addressing the improvement of the skill of reading, they were responded positively by the participants. This has statistically been reported by the high mean these items have shown (4.04, 4.13, 3.54, 4.00, 3.71, 3.83, and 3.83 for the items 5, 6, 7, 8, 10, 12, 13, respectively). Participants expressed their agreement that using computer in reading saves their time and helps them comprehend the reading texts in an easy way. They also agree that through the use of computer they can browse both visual and audible information pertinent to the text they are assigned to read.

V. Discussion

The results showed that the use and application of CALL software positively influences the performance of EFL students at Prince Sattam bin Abdulaziz University. This effectiveness is clearly clarified from the responses of the experimental group to the interview and the questionnaire, as well as the observable discrepancies in performance between the control group and the experimental group in terms of the fulfillment of the reading tasks assigned to the two groups. It is analytically observed that the participants of the experimental group showed higher level of performance in conducting the assigned tasks than that of the control group. This performance discrepancy can be ascribed to the different technological aids participants in the experimental group had by means of using computer in reading the assigned novel. More specifically, and unlike the control group, the experimental group managed to identify the main themes in the novel, highlight the ideological words in the text, and classify the characters in the novel in an easy, accurate and fast way. They also managed to answer all the comprehension questions on the reading text. This is successfully arrived at because they were assigned to use the two computer programs, namely Snagit™ and Screencast, which added more effectiveness to students' performance in reading. The participants in the control group, on the other hand, did not manage to meet all the assigned reading tasks, either in quality or in quantity. That is, they spent much time in order to achieve the targeted tasks and fail to fulfill some of the activities, such as answering some of the comprehension questions listed on the novel. They also reflect low degree of performance when they were asked to recognize the ideological weight of some words from the text, or to classify some of the characters and themes in the novel.

The analysis also demonstrated that the impact of CALL on the performance of the students in the experimental group may be attributed to some factors. First, the employment of computer programs in reading have positively contributed to students' performance in terms of accessibility regardless of time and place, variability of presentation, speed, accuracy, flexibility of use and control, and information reciprocity among users. These elements are often missed if the process of reading is conducted traditionally, i.e. without the help of computer. Second, reading via computer makes students feel free from any pressures that may cause them to be shy or reluctant in doing the tasks assigned to them. They become information-seekers rather than information-receivers, as is the case with their counterparts in the control group. Third, the use of computer in reading develops the feeling of independence on the part of students in a way that makes them create their own education environment, as well as to feel autonomous and in complete control over the whole process of their learning. Fourth, the use of Snagit™ and Screencast enables students in the experimental group to capture texts, images, videos related to the reading text, and to edit files, save them in particular format, and sharing them with their groupmates in a fast and accurate way. Fifth, computers allow experimental students to get immediate feedback on what they read, either in terms of answering specific questions on the assigned reading text or in relation to correcting and verifying mistakes. The majority of these factors were missed with the control group, which, in turn, emphasizes the reason why computer has a great influence on the performance of EFL students. Significantly, the above findings correlate with many previous studies, such as [31-35], [47- 49].These studies have acknowledged the positive impact of computer in learning English as a foreign language.

It is also evidenced from the results that the use of computer technologies in general and the two computer programs of Snagit™ and Screencast in particular serve to foster autonomous learning. These technological tools enable students to shape and reshape their educational contexts in a way that further serves to increase their curiosity and motivation towards learning. They also help them create an interactive type of communication, which influences their performance positively. This also goes in conformity with a number of previous studies, including [50-53] whose findings have emphasized the positively constructive impact of computers on the performance of EFL students.

A further interpretation pertinent to the impact of CALL software on the performance of EFL students concerning the skill of reading is the possibility of integrating visual and audible activities, such as those provided by Snagit™ and Screencast into the reading process. This is also anticipated to increase the learning motivation on the part of students and, thus, enhances their performance. This reconciles with [54] and [55], who highlighted the beneficial impact of the visual and audible sources on not only the skill of reading, but also on the other language skills, including writing, listening, speaking, and vocabulary. Crucially, the use, integration and application of CALL software in EFL classes have a very positive influence on the performance of Saudi EFL students, and greatly affect their learning outcomes.

VI. Conclusion

This paper investigated the impact of CALL software represented by the programs of Snagit™ and Screencast on the performance of Saudi EFL students at Prince Sattam bin Abdulaziz University concerning the skill of reading. The study attempted to test the hypothesis that the use of CALL software contributes positively to the performance of EFL students, and enhances their learning outcomes. The analysis clarified that there are many differences between the two groups in terms of the activities and tasks allocated for each one. Unlike the control group, participants in the experimental group managed to meet nearly all the required reading tasks in a fast, accurate and interactive way, which accentuates the constructively positive influence computer has on learning the skill of reading. The analysis further demonstrated that the use of CALL software in EFL classes increases students' motivation and curiosity towards learning, and develops a feeling of independence that serves to foster autonomous learning.

Finally, this paper recommends further studies that may meet its limitation, by extending the analytical scope as well as the sample to cover other universities within the Saudi EFL context. These studies can explore the impact of CALL programs on the performance of EFL students concerning courses other than those dealing with the skills of language. For example, to assess and evaluate the performance of EFL students, who study drama, poetry, phonology, syntax, etc. These studies are anticipated to reveal findings different and/or similar to those approached in this paper or in any other studies whose core concern is language skills. Crucially, extending the research focus of using CALL in EFL contexts to include all EFL courses (i.e., not only language skills) might contribute to the fields of applied and computational linguistics.

ACKNOWLEDGMENT

The researchers would like to thank Prince Sattam bin Abdulaziz University in Saudi Arabia alongside its Scientific Research Deanship for all technical support it has provided to complete this study.

REFERENCES

[1] L. Pedro, C. Barbosa, and C. Santos, “A critical review of mobile learning integration in formal educational contexts,” International Journal of Educational Technology in Higher Education, vol.15, no. 1, 2018.

[2] M. Eltahir, S. Al-Qatawneh, and S. Alsalhi, “E-Textbooks and their application levels, from the perspective of faculty members at Ajman University, U.A.E,” International Journal of Emerging Technologies in Learning, vol. 14, no. 13, pp. 88-104, 2019.

[3] K. Beatty, Teaching and researching computer-assisted language learning. Harlow: Longman Pearson, 2010.

[4] D. M. Ahmadi, “The use of technology in English language learning: A literature review,” International Journal of Research in English Education,vol. 3, no.2, pp. 115-125., 2018.

[5] C. A. Chapelle, Computer applications in second language acquisition: Foundations for teaching, testing and research. Cambridge, UK: Cambridge University Press, 2001.

[6] C. A. Chapelle, and J. Jamieson, Tips for teaching with CALL: Practical approaches to computer-assisted language learning. White Plains, NY: Pearson Education, 2008.

[7] R. S. Pinner, R. S., “Teachers’ attitudes to and motivations for using CALL in and around the language classroom,” Procedia - Social and Behavioral Sciences, vol. 34, pp. 188-192, 2012.

[8] G. Stockwell, Computer-assisted language learning: Diversity in research and practice. Cambridge: Cambridge University Press, 2018.

[9] E. Torlakovi and D. Deugo, “Application of CALL system in the acquisition of adverbs in English,” Computer-assisted Language Learning, vol. 17, no. 2, pp. 203-235, 2004.

[10] C. Vrasidas, A. S. Georgeou, and E. Papanastasiou, “Educational media and innovative practice: Challenges and visions,” Proceedings of September 2007conference on innovative learning environment. Nicosia, Cyprus: International Council for Educational Media, 2007.

[11] A. Zaytoon, Constructivism theory and its strategy in teaching science. Amman, Jordan: Al Shorroq Dar, 2007.

[12] A. Omar, A. F. Khafaga, and I. Shaalan, "The impact of translation software on improving the performance of translation majors," International Journal of Advanced Computer Science and Applications, vol. 11, no. 4, pp. 287-292 , 2020.

[13] A. F. Abu Seileek, Cooperative vs. individual learning of oral skills in a CALL environment. Riyadh, Saudi Arabia: King Saud University, 2009.

[14] K. Beatty, Teaching and researching computer-assisted language learning. Harlow: Longman Pearson, 2010.

[15] L. Harasim, “Shift happens: Online education as a new paradigm in learning,” The Internet and Higher Education, vol. 3, no. 1-2, pp. 41-61, 2000.

[16] J. Li, and A. Cumming, “Word processing and ESL writing: A longitudinal case study,” International Journal of English Studies, vol. 1, no. 2, pp. 127-152, 2001.

[17] K. Hyland, Second language writing. Cambridge: Cambridge University Press, 2003.

[18] Y. H. Chen, “Computer mediated communication: The use of CMC to develop EFL learners' communicative competence,” Asian EFL Journal, vol. 7, no. 1, pp. 167-182, 2005.

[19] H. Jarvis, and L. Pastuszka, “Electronic literacy reading skills and the challenges for English for academic purposes,” CALL-EJ Online, vol. 10, no. 1, 2008.

[20] I. G. Singh, “The computer mediated communication to develop ESL learners' communicative competence,” Journal of Literature, Culture & Media Studies, vol. 2, no. 3, pp. 72-85, 2010.

[21] S. S. Terrell, “Integrating online tools to motivate young English language learners to practice English outside the classroom,” International Journal of Computer-Assisted Language Learning and Teaching (IJCALLT), vol. 1, no. 2, pp. 16-24, 2011.

[22] A. Khafaga, “The perception of blackboard collaborate-based instruction by EFL majors/teachers amid COVID-19: A case study of Saudi universities,” Journal of Language and Linguistic Studies, vol. 17, no. 2, pp. 1160-1173; 2021.

[23] K. Beatty, Teaching and researching computer assisted language learning. New York: Longman, 2003.

[24] L. Lee, “Learners’ perspectives on networked collaborative interaction with native speakers of Spanish in the US,” Language Learning and Technology, vol. 8, no. 1, pp. 83-100, 2004.

[25] H.J. Shin, and J. B. Son, “EFL teachers' perceptions and perspectives on Internet-assisted language teaching,” CALL-EJ Online, vol. 8, no. 2, pp. 1-13, 2007.

[26] C. Y. Chiu, “The discourse of an English teacher in a cyber writing course: Roles and autonomy,” The Asian EFL Journal, vol. 10, no. 1, pp. 79-110, 2008.

[27] A. Barger, and K. Byrd, “Motivation and computer-based instructional design,” Journal of Cross-Disciplinary Perspectives in Education, vol. 4, no. 1, pp. 1-9, 2011.

[28] R. Dzekoe, “Computer-based multimodal composing activities, self-revision, and L2 acquisition through writing,” Language Learning & Technology, vol. 21, no. 2, pp.73-95, 2017.

[29] A. Khafaga, and I. Shaalan, “Mobile learning perception in the context of COVID-19: An empirical studyof Saudi EFL majors,” Asian EFL Journal, vol. 28, no. 1.3, pp.336-356, 2021.

[30] M. Sokolik, “Computers in language teaching,” in M. Celce-Murcia (Ed.), Teaching English as a second or foreign language (3rd ed.), Boston, MA: Heinle & Heinle, 2001, pp. 477-488.

[31] Q. Ma, “From monitoring users to controlling user actions: A new perspective on the user-centred approach to CALL,” Computer Assisted Language Learning, vol. 20, no. 4, pp. 297-321, 2007.

[32] T. Chiu, H. Liou, Y. Yeh, “A study of webbased oral activities enhanced by automatic speech recognition for EFL college learning,” Computer Assisted Language Learning, vol. 20, no. 3, pp. 209-233, 2007.

[33] A. AbuSeileek, “Cooperative vs. individual learning of oral skills in a CALL environment,” Computer Assisted Language Learning, vol. 20, no. 5, pp. 493-514, 2007.

[34] A. Al-Menei, “An investigation of the effect of computerassisted writing instruction on EFL Saudi learners’ ability,” Unpublished Master Thesis, King Saud University, Riyadh, KSA, 2008.

[35] K. Romeo, “A web-based listening methodology for studying relative clause acquisition,” Computer Assisted Language Learning, vol. 21, no. 1, pp. 51-66, 2008.

[36] I. A. Khan, “Diagnosis of learning difficulties in English: The Arabic bilingual context,” Elixir Psychology,vol. 36, pp. 3448-3454, 2011.

[37] C. Z. Javid., U. Farooq, and M. Umer, “An investigation of Saudi EFL learners’ writing problems: A case study along gender-lines,” Kashmir Journal of Language Research,vol. 16, no. 1, pp. 179-203, 2013.

[38] A. M. Mudawy, “An attempt at promoting undergraduate sudanese EFL students’ performance in academic writing skills,” Arab World English Journal, vol. 10, no. 1, pp. 218-230., 2019.

[39] A. Khafaga, and M. Aldawsari, “Ideological agency in Edward Bond’s Lear,” Applied Linguistics Research Journal, vol. 5, no. 2, pp. 11-23, 2021.

[40] S. Moras, “Computer-assisted language learning (CALL) and the internet,” Karen’s Linguistic Issues, 2001 Retrieved from http://www3.telus.net/linguisticsissues/CALL.html.

[41] A. Albarini, “Cultural perceptions: The missing element in the implementation of ICT in developing countries,” Computers and Education, vol. 52, pp. 588-598, 2009.

[42] K. J. Cobb, “Facilitating second language acquisition through computer-assisted language learning,” Artmanuscript, vol. 1, no. 1, 2002.

[43] A. Walker, and G. White, Technology enhanced language learning: Connecting theory and practice. Oxford: Oxford University Press, 2013.

[44] R-C. Li, and R. S. Hart, “What can the world wide web offer ESL teachers?” In J. C. Richards, and W. A. Renandya (Eds.), Methodology in language teaching: An anthology of current practice, Cambridge, UK: Cambridge University Press, 2002, pp. 368-373.

[45] Y. Alshumaimeri, “Perceptions and attitudes towards using CALL in English among Saudi secondary EFL Teachers,” The JALT CALL Journal, vol. 4, no. 2, pp. 29-46, 2008.

[46] A. G. Al-Mekhlafi, “The effect of computer-assisted language learning (CALL) on United Arab Emirates English as a foreign language school student’s achievement and attitude,” Journal of Active Learning Research, vol. 17, no. 2, pp. 121-142, 2006.

[47] C. A. Chapelle, and J. Jamieson, “Tips for teaching with CALL: Practical approaches to computer-assisted language learning. White Plains, NY: Pearson Education, 2008.

[48] A. AbuSeileek, “The effect of using a computer-based program on students’ writing ability in English. Unpublished Doctoral Dissertation, Arab University, Amman, Jordan, 2004.

[49] A. Khafaga, and I. Shaalan, “Using concordance to decode the ideological weight of lexis in learning narrative literature: A computational approach,” International Journal of Advanced Computer Science and Applications, vol. 11, no. 4, pp. 246-252 , 2020.

[50] D. R. Ferris, Treatment of error in second language student writing. Ann Arbor; MI: University of Michigan Press, 2020.

[51] C. Pim, “Emerging technologies, emerging minds: Digital innovations within the primary sector,” In G. Motteram (Ed.), Innovations in learning technologies for English language teaching, London: British Council, 2013, pp. 17-42.

[52] S-G. Wang, and C. Vásquez, “Web 2.0 and second language learning: What does the research tell us?” CALICO Journal, vol. 29, no. 3, pp. 412-430, 2012.

[53] A. Khafaga, and I. Shaalan, “Pronouns and modality as ideology carriers in George Orwell’s Animal Farm: A computer-aided critical discourse analysis,” TESOL International Journal, vol. 16, no. 4.2, pp. 78-102, 2021.

[54] A. Yeh, “Poetry from the heart,” English Today, vol. 21, no. 1, pp. 45-51, 2005.

[55] A. Oskoz, and I. Elola, “Digital stories: Overview,” CALICO Journal, vol. 32, no. 2, pp. 155-173, 2016.

A Novel Method for Handling Partial Occlusion on Person Re-identification using Partial Siamese Network

Muhammad Pajar Kharisma Putra[1], Wahyono[2]*
Department of Computer Science and Electronics, Universitas Gadjah Mada, Yogyakarta Indonesia[1, 2]
Faculty of Engineering and Computer Science, Universitas Teknokrat Indonesia, Lampung, Indonesia[1]

***Abstract*—Person-reidentification (Re-ID) is one of the tasks in CCTV-based surveillance system for verifying whether two detected objects are the same person or not. Re-ID visually matching one person or group in various situations obtained from different cameras or on the same camera but at different times. This method replaces the task of surveillance through surveillance cameras that was previously carried out conventionally by humans because it is prone to errors. The challenge of Re-ID is the pose of varied objects, occlusions, and the appearance of people who tend to be similar. Occlusion issues receive special attention since the performance of Re-ID can decrease due to partial occlusion. This can occur because the re-identification process relies on features of the person such as the color and pattern of clothing. The occlusion resulted in the feature not being caught by the camera resulting in a re-identification error. This paper proposed to overcome this problem by dividing the image into several parts (partial) and then processed in different neural network (NN) but with the same architecture. The research conducted is applying the CNN algorithm with the Siamese network architecture and applying the contrastive loss function to calculate the similarity distance between a pair of images. The test results show that the partial process obtained an accuracy of 86%, 77%, 68%, and 56% for occlusion data of 20%, 40%, 60%, and 80%. This accuracy is three to five percent higher than images without partial.**

Keywords—CCTV; CNN; video-surveillance; NN; contrastive-loss

I. Introduction

Today's surveillance cameras are common in public places such as shopping centers, airports, schools or offices. This technology has been used widely in applications related to vision such as video surveillance. With a surveillance camera, every event captured by the camera can be monitored or stored by the operator; therefore it can be analyzed if needed.

One application of video surveillance is for criminal problems. Often a criminal investigator needs to find out where certain people appear based on pictures taken by the camera [1]. However this is not without problems. Relying on human intervention performance for surveillance of more than one cam- era requires expensive and inaccurate costs. The operator assigned to monitor more than one camera and carry out a manual matching process, is prone to errors. In addition, human performance is determined subjectively based on the experience of each operator therefore it can lead to differences in performance between operators [2]. To handle this problem, monitoring activities are carried out by computers using the person re-identification (Re-ID) method.

Re-ID is the process of matching certain people through different cameras [3]. Unlike identification which aims to get the identity of the object identified, the purpose of Re-ID is to match the same person on different cameras or at different times but on the same camera [4]. The first stage of Re-ID is to detect people on the camera, which is then followed by identification. The identification stage is the most important stage of Re-ID, since at this stage it is concluded whether the person is the same person or not.

The challenge of Re-ID is the pose of varied objects, occlusions, and the appearance of people who tend to be similar [3]. Occlusion issues receive special attention since the performance of Re-ID can decrease due to partial occlusion. This problem is difficult to overcome since some parts of the body of people are covered by other people or objects in the environment [5]. On the other hand, performing a process of matching between detected images with a large number of images requires a long computational time [6].

Therefore, in this paper, the problem of partial occlusion at the re-identification stage can be dealt by dividing the image partially so that people can still be recognized even though some attributes are blocked from the camera. The image is divided into three parts, namely the head, body, and legs and then each part will be trained on a different neural network. This partial process can improve the accuracy of the data by occlusion [7]. Then the reidentification process uses the Siamese Network algorithm. The Siamese Network algorithm as a feature extraction is better in terms of accuracy compared to other methods, since this model has identical network layers and fewer datasets. The last layer of the Siamese Network as a layer to find the value of similarity between two objects with a distance function [8]. Siamese Network uses contrastive loss as a function of distance that is able to distinguish between objects in pairs [6].

Overall, this paper provides following major contributions: (1) Proposed a new strategy to apply partial regions division in Siamese Network based on human body proportion. (2) Utilize constructive loss for matching two difference objects. (3) Provide more detail investigation regarding to the effect of partial occlusion on person re-identification problem.

*Corresponding Author

II. Related Work

Some research on Re-ID has been done in recent years with various methods to overcome various problem. Ku *et al.* in 2018 doing research on Re-ID based on features extracted with CNN and manually selected [4]. In 2017, Gu *et al.* combined DPM and SVM for person reidentification [1]. J Liu *et al.* in 2017 proposed method a novel multi-part compact bilinear convolutional neural network (CNN) model, which consists of a bilinear CNN and two part-networks aiming to learn the global features and the finer local features simultaneously [9]. However, these method weak against occlusion since occlusion can block images from camera so that features from images can't be extracted. Another research about Re-ID for overcome occlusion problem was carried out by Song *et al* in 2017 by dividing the image into three equal parts [7] and Liu *et al* in 2017 by dividing the image into four parts with overlapping [10] then processed in a separate neural network.

Dividing the image into several parts of the same size allows an occlusion that blocks one part will have a significant impact on other parts because no part is prioritized. Based on previous research, our proposed method will modify images partial process by dividing images into three parts based on human body proportion consisting of head, body, and leg. This research also proposes the process of determining which parts are considered priority or have more features based on accuracy during the training process. Thus, occlusion that occurs in parts that are not a priority will not have a significant impact on the results of re-identification.

III. The Method

The system aims to re-identify human objects on the surveillance camera. This system implements the siamese network algorithm which is partially processed in each sub-region to overcome the occlusion problem in Re-ID. The research flow consists of data collection, pre-processing, feature extraction with CNN, similarity measurement with contrastive loss, and testing. While the design of the built algorithm is divided into two algorithms (i.e training and testing). The details of these stages will be explained in the following subsections.

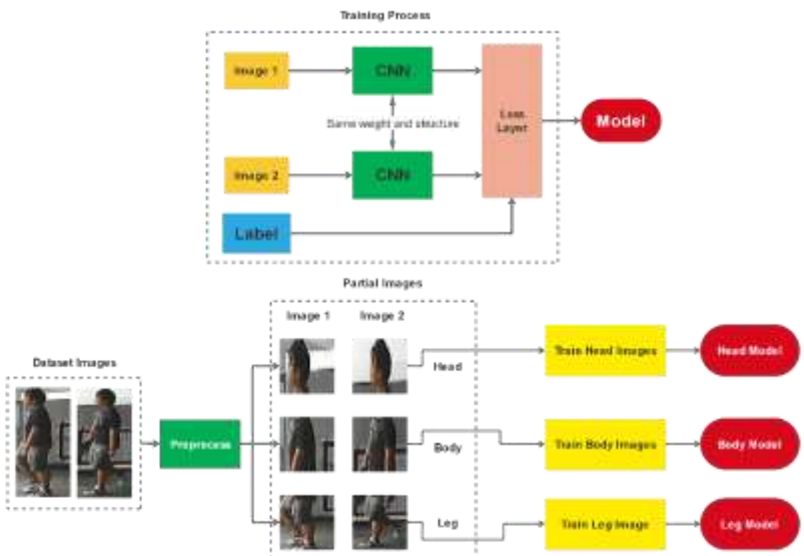

Fig. 1. Flowchart of the Proposed Method for Training Stage.

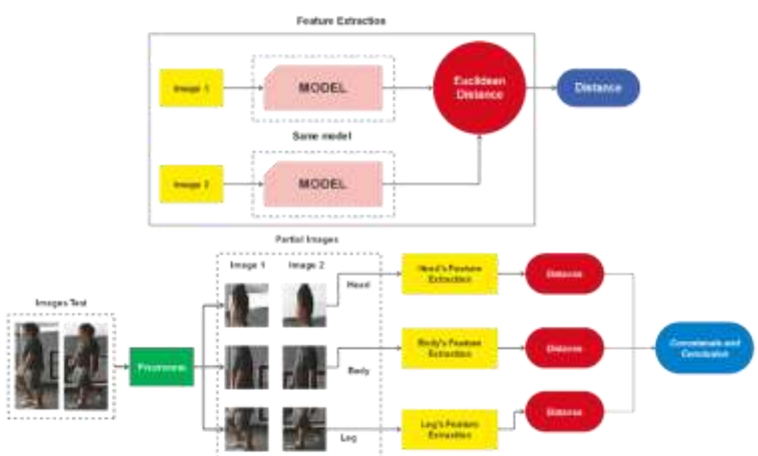

Fig. 2. Flowchart of the Proposed Method for Testing Stage.

Fig. 1 and 2 show the design of the training and testing algorithm. In the training algorithm, the two images are extracted using an identical CNN architecture [11]. The features obtained will be calculated using a loss function. This process will be carried out continuously until certain conditions or iterations. Each subregion is processed separately. The model produced at the training stage will be used at the testing stage. In the testing phase, the test image pair feature will be extracted using the trained model. Then the feature distance of this image pair will be calculated using the Euclidean Distance.

A. Data Collection

The dataset used in this research was obtained from CUHK03 dataset [12]. In the CUHK03 dataset there are 1360 identities and 13164 images, consisting of manual crop images and automatic detection. Fig. 3 shows the example of CUHK03 dataset.

B. Preprocessing

The input image will be divided into several sub-regions then resize so that both images have the same resolution as shown in Fig. 4. Later each of these sub-regions will be processed separately on different neural networks. The purpose of this stage is to avoid occlusion. The image will be divided into eight sub-regions vertically with the same size. The division of these eight sub-regions is based on the proportion of human body height that is equal to the height of the human head itself [13].

C. Feature Extraction using CNN

Feature extraction is the process of extracting features such as colors and textures from person images. CNN is the algorithm used in the process of extracting this feature. The CNN architecture design used is shown in Fig. 5.

Fig. 5 is an initial design that will be used in this study adopted from Liu dan Huang (2017) [10]. Overall the architecture consists of two inception modules, one convolution layer, and one fully connected layer. The first Inception module consists of 16 convolution kernels of 5×5 and 16 kernels of 3×3. The resulting map feature will be combined with input followed by 2×2 max pooling. The second inception module similar as the first inception module, except the convolutional kernel sizes are 3×3 dan 1×1. Different kernel sizes in the two inception modules aim to extract features from different resolutions. The last convolution layer consists of 16 kernels of 1×1 aims to reduce the depth of feature maps.

D. Similarity Measurement using Contrastive Loss

Similarity measurement is a function that provides the real value of the calculation results of the similarity between two objects. Similarity measurement is done to calculate the distance of similarity between a pair of person's images. The contrastive loss function used in this research will calculate the distance between images. The architecture of constrastive loss is shown in Fig. 6.

Contrastive loss can measure the distance between two images [6]. This function will encourage similar images to have a close distance and different images have at least an ecludian distance of a predetermined margin [14]. Contrastive loss is defined as follows:

$$l = \frac{1}{2} l D^2 + \frac{1}{2}(1 - \mathrm{l})\{max(0, m - D)\}^2 \quad (1)$$

where l is image label, m is margin, and D is Euclidean Distance of pair images. The output of this process is float value. The smaller number produced shows the closer similarity distance between two images and vice versa.

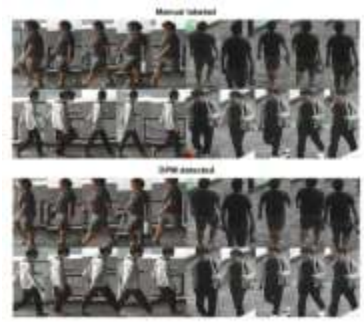

Fig. 3. Selected Samples of CUHK03 Dataset [12].

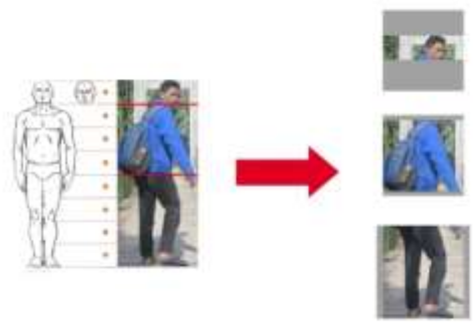

Fig. 4. Preprocessing Illustration.

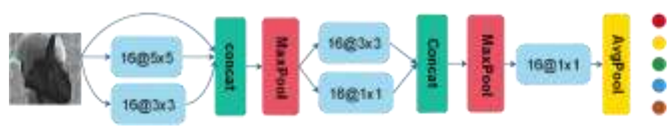

Fig. 5. The Proposed CNN Architecture.

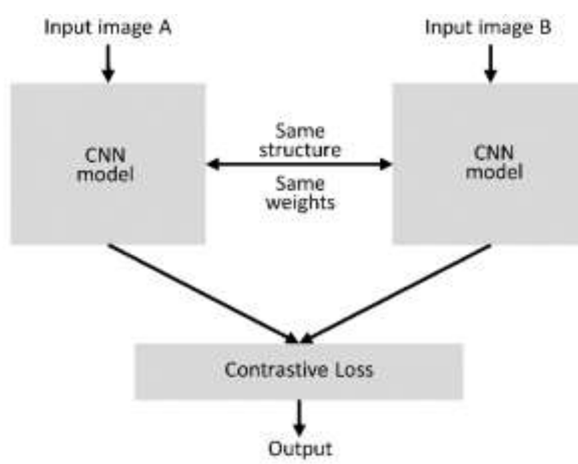

Fig. 6. Contrastive Loss Architecture.

In addition to contrastive loss, there is one other loss function that can be used, namely triplet loss. Training with triplet loss is done by comparing the baseline vector (anchor image) with a positive vector (truth image) and a negative vector (false image), so that three images are needed as input [15]. By applying a margin between pairs of faces with the same identity and faces with different identities, triplet loss keeps faces of the same identity closer than faces of different identities in the embedding space as in Fig. 7.

Triplet loss is defined as follows:

$$Loss = \max(d(A, P) - d(A, N) + margin, 0) \quad (2)$$

Where $d(A,P)$ is distance between anchor and positive images, $d(A,N)$ is distance between anchor and negative images.

E. Testing

The testing phase is the stage of evaluating the performance of the proposed algorithm. This stage will compare the performance of the proposed method with a model without a partial process. The measured performance is the ability of the model in reidentifying data with occlusion. This data is an augmentation image with occlusion of 20%, 40%, 60%, and 80%. Occlusions are randomly placed at the top or bottom of the image. An example of an occlusion image is shown in Fig. 8.

Test image using CUHK02 and RAiD dataset. CUHK02 was collected at the Chinese University of Hong Kong using two cameras. Overall, this dataset has 7,264 images consisting of 1816 identities [16]. RAiD dataset was collected at the Winstun Chung Hall of UC Riverside. It is a four camera dataset with two indoor and two outdoor cameras. The cameras are numbered as 1, 2, 3 and 4 where cameras 1 and 2 are indoor while cameras 3 and 4 are outdoor. 43 people walked in these camera views resulting in 6920 images. Among the 43 persons 41 people appeared in all the 4 cameras whereas person 8 is not present in camera 3 and person 34 is not present in camera 4 [17]. However only 250 images were used at the test stage.

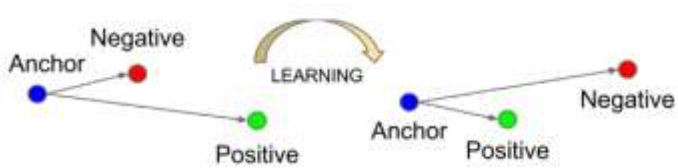

Fig. 7. Triplet Loss Illustration.

Fig. 8. Example Data with Occlusion.

F. Concatenate

Concatenate is a process that is done in the testing phase. Concatenate will combine each distance from each sub-region (i.e., head, body, and leg). Each sub-region has a different probability based on the accuracy value obtained after the model has been trained; the higher accuracy of the sub-region, the greater probability of the sub-region. Each distance and probability value from each sub-region will be multiplied then added to obtain the final score. The next step is to determine the threshold obtained during the training process. Two images that have a final score below the threshold will be summed up as the same person. The process of determining probabilities and final scores is shown in the following equation:

$$p_i = \frac{acc_i}{\sum_{i=1}^{n} acc_i} \quad (3)$$

where p_i is a probability of each sub-region dan acc_i is an accuracy of each sub-region. While the process of determining the final score is shown in the following equation:

$$D = \sum_{i=1}^{n}(d_i * p_i) \quad (4)$$

where D is final distance between pair images, d_i is distances of each sub-region, dan p_i is probability of each sub-region. Finally, the process of determining the image based on the threshold is shown in the following equation:

$$f(D) = \begin{cases} similar;\ D < threshold \\ disimilar;\ D \geq threshold \end{cases} \quad (5)$$

IV. Experiment and Results

At the training phase the model has been determined several hyperparameters that are considered optimal, namely batch size 32 and Adam optimizer. Large batch size (more than 512) decreases the quality of the model [18]. This is measured by the ability of the model to generalize data. While Adam's optimizer provides better performance in reducing error values compared to other optimizers such as SGD, AdaGrad, and RMS [19].

A. Loss Function Testing

As mentioned before, there are two common loss functions in Siamese network, namely, contrastive loss and triplet loss. This test aims to compare the performance of two loss functions and analyze the effect of margin parameters on training results. Margin defines the radius around the embedding space of the sample so that different sample pairs only contribute to the loss function if the distance between the sample pairs is within the margin [14]. The results are shown in Table I.

Table I shows that there is a significant difference between the two loss functions. Contrastive loss obtains a smaller loss value and higher accuracy in the train and validation data for every margin value except the margin value 3 for triplet loss, but requires a longer training time than triplet loss. This is because in contrastive, each data consists of two images and a label, while in triplet each data consists of three images, namely anchor, positive, and negative. Every two data on contrastive is equal to one data on triplet so contrastive loss requires a longer training time than triplet loss.

TABLE I. RESULTS LOSS FUNCTION TESTING

Loss Function	Margin	Loss Value		Acc	Time (minutes)
		Train	**Validation**		
Contrastive Loss	1.0	0.016	0.075	92.3	30:40
	2.0	0.036	0.222	94.5	29:12
	3.0	0.062	0.487	93.9	29:18
Triplet Loss	1.0	0.019	0.271	88.6	17:59
	2.0	0.045	0.821	89.2	17:59
	3.0	0.071	0.787	89.6	17:58

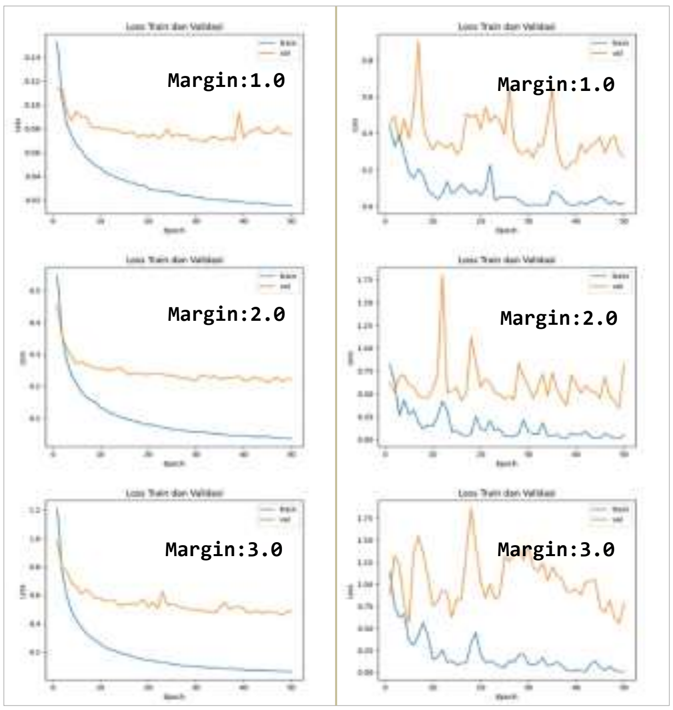

(a) Contrastive Loss (b) Triplet loss.

Fig. 9. Training Results Graph.

Fig. 9 shows that there is overfitting in both loss functions, but the contrastive loss has decreased consistently in each epoch for the data train. Meanwhile, in the validation data, the value of margin 2 shows a decreasing graph that is more consistent than margins 1 and 3. In the triplet loss test, in addition to obtaining a loss value that is greater than the contrastive loss, the loss value does not consistently decrease. As shown in equations (1) and (2), if the resulting loss value is negative, then the value will be normalized to zero. This results in the loss of some of the information in the data. For example, data with a loss value of -2 has a more significant similarity between anchor and positive images or a significant difference between anchor and negative images than data with a loss value of -1. However, with the normalization of the negative value to zero, it causes the two data to be considered the same. This has resulted in overfitting in the triplet loss test. Even though contrastive loss also applies the same normalization, as previously mentioned, if two data in a contrastive are equal to one data in a triplet, so that when normalization occurs, the contrastive only loses information on one data, namely the distance between two images is the same, while in a triplet it will lose information. Information on the distance between the two data, namely, the distance of the anchor image - positive and the image anchor - negative.

Furthermore, in the margin parameter, the margin value of 2 gives the best results. Reidentification process can work well if applied to objects with the same class. As previously explained, the purpose of the margin is to keep the image pair actually consisting of the same object (person and person object) so that the image pair that has a distance greater than the margin will not contribute to the loss function or will be ignored. A margin value that is too small to make a small difference between the two objects will be ignored and will not contribute to the loss function, while a margin value that is too large will cause a pair of objects that are far enough apart to have an impact on the loss function because they are still within the margin radius even though the object is a objects of different classes (person and non-person objects). The impact on this loss function will affect the backpropagation process and parameter weight updates so that an incorrect margin value will reduce accuracy even though the loss value obtained is smaller. It can be concluded that contrastive loss with a margin value of 2 gives the best results.

B. *Model Training*

Each sub-region that has been divided will be trained to obtain a model that will be used at the testing stage. The training process uses 50 epochs. This stage also compares the performance of the architecture used with the Adaptive Spatial Feature (ASF) architecture [7] and Multi-part Compact Bilinear CNN (MCBCNN) Architecture [9] using the same dataset and parameters. Loss value and training time obtained as shown in Table II.

The test results in Table II show that the ASF architecture requires the longest training time while the MCBCNN architecture requires the shortest training time. The length of time training is influenced by the number of parameters being trained. The ASF architecture has 289,470,848 parameters, while the proposed architecture has 89,160,288 parameters, and the MCBCNN architecture has 31,931,664 parameters. The number of parameters that must be trained makes the ASF architecture have the longest training time followed by the proposed architecture and the MCBCNN architecture. Meanwhile the training chart for each epoch is shown in Fig. 10.

TABLE II. CNN ARCHITECTURE TEST RESULTS

Architecture	Loss		Training Time
	Train	**Validation**	
Proposed	0.2076	0.2095	07:07:58
ASF	0.1167	0.2503	07:23:43
MCBCNN	0.3550	0.6209	04:27:07

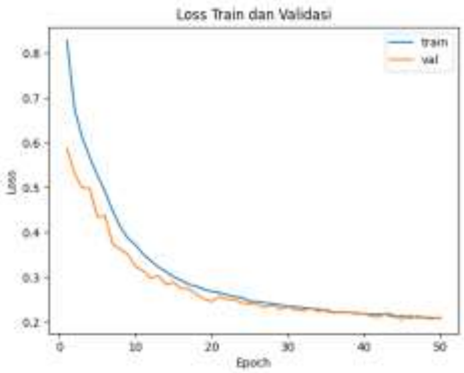

(a) Proposed Architecture.

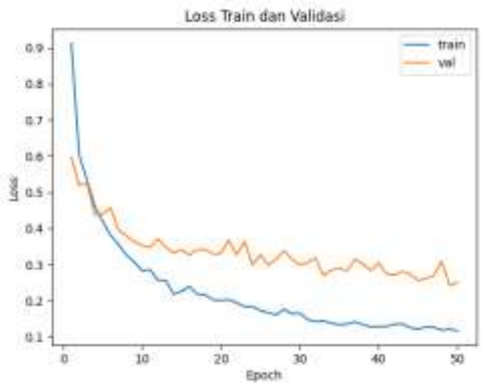

(b) ASF Architecture.

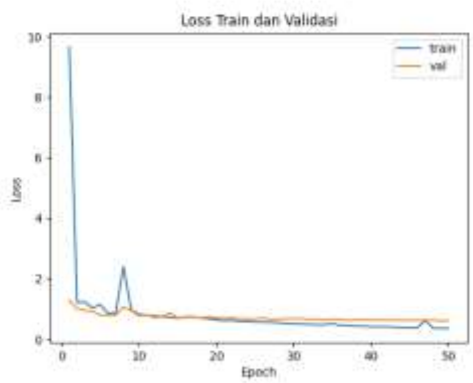

(c) MCBCNN Architecture.

Fig. 10. Loss Train and Validation.

Fig. 10 shows a gradual decrease in the loss value as the epoch increases both in the data train and validation for each architecture. However, in Fig. 10(a), it can be seen that there is no big difference between the train data and validation. Thus, the inception module applied to the convolution layer with the aim of extracting features from different resolutions proved to be able to overcome overfitting.

Fig. 10(a) shows the ASF architecture obtains the lowest loss value and the highest accuracy for the data train. In addition, there is also a decrease in the loss value as the epoch increases, but there is a large difference between the train and validation data so that it can be concluded that the ASF architecture is overfitting. One of the causes of overfitting is because each convolutional layer only uses one type of kernel with a small number of feature maps so that the features that can be extracted are limited. If you look at other CNN architectures that are sequential like VGG16 [20], there are 64 feature maps in the first and second convolution layers, as well as 512 feature maps in the last three covolution layers so you can still extract many features even though you only use one kernel type at each convolution layer.

C. Testing on Occlusion Data

Testing on occlusion data uses a model that has been previously trained and implemented on occlusion data as shown in Fig. 11. This test will also compare the proposed partial process with the partial process in Adaptive Spatial Feature (ASF) [7] and Body Structure Based Triplet CNN (BSTCNN) [10] using same dataset and parameter. ASF and BTCNN partial process show in Fig. 11.

Using a trained model, each sub-region obtains the accuracy, as shown in Table III.

The results of the accuracy of each sub-region in Table III show the body parts represented by sub-region two in the proposed partial process and ASF obtained higher accuracy than other parts since this section has more features such as motifs and clothing colors. The foot sub-region has the lowest accuracy of the three partial processes, since the colors and motifs that tend to be similar between one identity and another make not many features that can be extracted in this sub-region. Based on the accuracy in Table III, using equation (3) the probability of each sub-region is obtained as shown in Table IV.

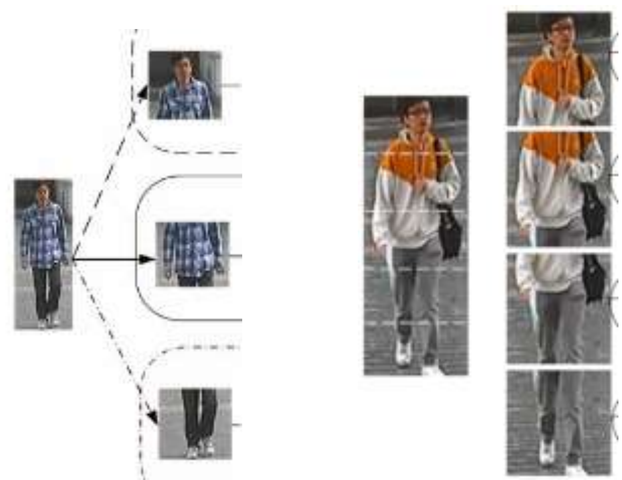

(a) (b)

Fig. 11. (a) ASF; (b) BSTCNN Partial Process.

TABLE III. ACCURACY OF EACH SUB-REGION

Sub-Region	**Accuracy (%)**		
	Proposed	**ASF**	**BSTCNN**
1	82	85	88
2	92	89	82
3	76	87	85
4	-	-	71

TABLE IV. PROBABILITY OF EACH SUB-REGION

Sub-Region	**Probability**		
	Proposed	**ASF**	**BSTCNN**
1	0.328	0.351	0.270
2	0.368	0.367	0.251
3	0.304	0.281	0.261
4	-	-	0.220

The probability value in Table IV is a reference in determining the distance between a pair of images. The final distance of a pair of images is calculated based on the distance and probability value of each sub-region using equation (4). The accuracy of each partial process on occlusion data is shown in Table V.

Table V shows that the proposed partial process has higher accuracy than other partial processes or images without partials on all occlusion data. Image without partials still obtained higher accuracy than partial ASF and BSTCNN processes at 20% occlusion, but the subsequent occlusion obtained the lowest accuracy compared to others. This is because the greater of occlusion in the image, the fewer features that can be extracted because some features are lost due to the occlusion. The occlusion of one part of the image will greatly affect the calculation of the distance in the image without partial because all images are extracted using the same model. Unlike the image without partials, in the partial process each image will be divided into several sub-regions and processed separately using each model, so that the occlusion of one sub-region with a small probability value will not have a big impact on the calculation of the distance of a pair of images.

TABLE V. ACCURACY OF OCCLUSION DATA

Occlusion (%)	**Partial Process**	**Accuracy (%)**
20	Without Partial	82
	Proposed	86
	ASF	81
	BSTCNN	81
40	Without Partial	73
	Proposed	77
	ASF	74
	BSTCNN	73
60	Without Partial	65
	Proposed	68
	ASF	68
	BSTCNN	66
80	Without Partial	51
	Proposed	56
	ASF	55
	BSTCNN	53

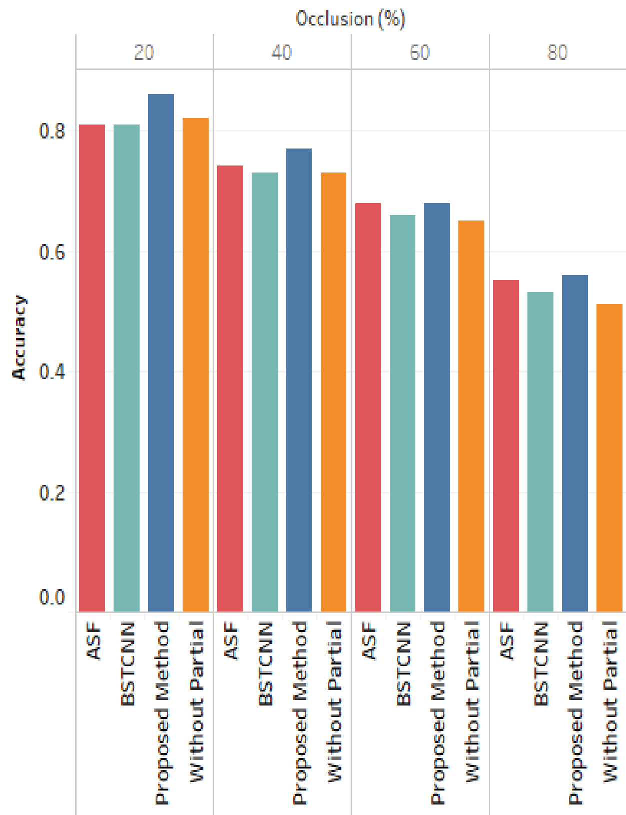

Fig. 12. Accuracy of Occlusion Data.

As shown in Fig. 12, the proposed partial process gets higher accuracy since dividing the image according to the proportions of the human body. The sub-region of the body that has the highest accuracy has a higher probability value as well because this section contains important features such as color and pattern of clothing. Two other partial processes divide the image by equal size. The small difference in probability values between sub-regions makes this partial process not much different from images without partial processing. Overall, partial processing has been shown to improve accuracy in occlusion data compared to images without partial processing.

D. Analysis and Discussion

The results in Table V show that the proposed method obtained better accuracy than other methods and succeeded in increasing the accuracy compared to the model without partial processing. However, there are still some weaknesses in proposed method.

Fig. 13 shows the error that occurs in the re-identification of the same pair. Part-2 and part-3 which are parts of the body and legs get a distance below the threshold value, while part-1 which is part of the head gets a distance above the threshold since there is occlusion in that part. In some cases, the proposed method cannot re-identify if there is occlusion in all parts of one of the sub-regions or sections. This occlusion makes the distance from the sub-region far above the threshold so that it affects the concatenate process.

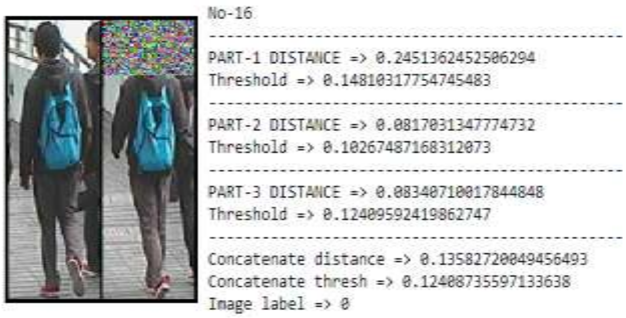

Fig. 13. Example Error Due to Occlusion.

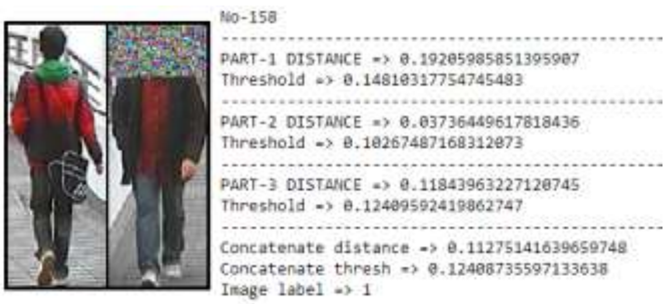

Fig. 14. Example Error due to Similar Feature.

Similar features between two images with different identities can also cause errors. Fig. 14 shows an error due to a similar feature, namely color. Part-2 and part-3 get a smaller distance than the threshold, which means that the two images are the same identity even though the image is a different identity. This error occurs since both objects are wearing red and black clothes. In addition, the legs-part of the two objects use pants which tend to be similar and the background in this part is gray.

Another factor that can cause re-identification errors is the difference in camera angles in recording images. Fig. 15 shows a pair of images of people with the same identity but taken by different cameras. Part-1, part-2, and part-3 get a distance greater than the threshold. The error in calculating this distance is caused by different feature conditions due to different camera angles. For example in part-2, there is a difference in the area of the blue bag object between the left and right images. Another example in part-1, a significant difference in the background of the object can affect the distance calculation because this part is also processed during feature extraction.

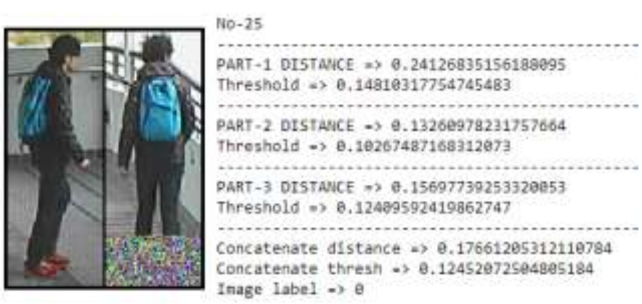

Fig. 15. Example Error due to taken by Different Cameras.

V. CONCLUSION

In this paper introduced the partial Siamese network method using CNN as a feature extraction and contrastive loss as a function of distance in overcoming occlusion in person re-identification. The CNN architecture used consists of two inception modules, one convolutional layer, and a fully connected layer. This architecture is proven to be able to get better performance than the other two architectures using the same dataset and parameters. In the testing phase, the distance of each sub-region will be multiplied by the probability value then added to obtain the final distance. An image pair that has a distance less than the threshold will be considered as a person with the same identity and vice versa. Overall, the proposed method is proven to be able to improve the accuracy of occlusion data compared to images without partiality, and two partial processes. In the future, several image enhancement methods [21] will be applied before the dataset is processed in a neural network so that it can overcome reidentification errors due to similar features.

ACKNOWLEDGMENTS

This research was partially supported by 2020 Research Grant on Graduate Program of Department of Computer Science and Electronics, Universitas Gadjah Mada, Indonesia.

REFERENCES

[1] X. Gu, X. Zou, J. Liu, and L. Zhang, “Person re-identification by using a method combining DPM and SVM,” in 2016 13th International Computer Conference on Wavelet Active Media Technology and Information Processing, ICCWAMTIP 2017, 2017, vol. 2018-Febru, pp. 124–127, doi: 10.1109/ICCWAMTIP.2017.8301463.

[2] R. Layne, T. Hospedales, and S. Gong, “Person re-identification by attributes,” in BMVC 2012 - Electronic Proceedings of the British Machine Vision Conference 2012, 2012, no. June 2014, doi: 10.5244/C.26.24.

[3] H. Huang, D. Li, Z. Zhang, X. Chen, and K. Huang, “Adversarially Occluded Samples for Person Re-identification,” Proc. IEEE Comput. Soc. Conf. Comput. Vis. Pattern Recognit., pp. 5098–5107, 2018, doi: 10.1109/CVPR.2018.00535.

[4] H. Ku, P. Zhou, X. Cai, H. Yang, and Y. Chen, “Person re-identification method based on CNN and manually-selected feature fusion,” ICNC-FSKD 2017 - 13th Int. Conf. Nat. Comput. Fuzzy Syst. Knowl. Discov., pp. 93–96, 2018, doi: 10.1109/FSKD.2017.8393401.

[5] R. Hou, B. Ma, H. Chang, X. Gu, S. Shan, and X. Chen, “VRSTC : Occlusion-Free Video Person Re-Identification,” in CVPR, 2019, pp. 7183–7192.

[6] I. Melekhov, J. Kannala, and E. Rahtu, “Siamese network features for image matching,” in Proceedings - International Conference on Pattern Recognition, 2016, vol. 0, pp. 378–383, doi: 10.1109/ICPR.2016.7899663.

[7] Z. Song, X. Cai, Y. Chen, Y. Zeng, L. Lv, and H. Shu, “Deep convolutional neural networks with adaptive spatial feature for person re-identification,” in 2017 IEEE 2nd Advanced Information Technology, Electronic and Automation Control Conference (IAEAC), Mar. 2017, pp. 2020–2023, doi: 10.1109/IAEAC.2017.8054370.

[8] G. Koch, R. Zemel, and R. Salakhutdinov, “Siamese Neural Networks for One-shot Image Recognition Gregory,” in International Conference on Machine Learning, 2015, vol. 37, no. 5108, p. 1355, doi: 10.1136/bmj.2.5108.1355-c.

[9] J. Liu, Z. Yang, T. Zhang, and H. Xiong, “Multi-part compact bilinear CNN for person re-identification,” in 2017 IEEE International Conference on Image Processing (ICIP), Sep. 2017, vol. 1, pp. 2309–2313, doi: 10.1109/ICIP.2017.8296694.

[10] H. Liu and W. Huang, “Body structure based triplet Convolutional Neural Network for person re-identification,” in 2017 IEEE International

Conference on Acoustics, Speech and Signal Processing (ICASSP), Mar. 2017, pp. 1772–1776, doi: 10.1109/ICASSP.2017.7952461.

[11] M.P.K. Putra, “Person Re-identifikasi Menggunakan Partial Siamese Network untuk Mengatasi Masalah Oklusi Parsial Pada Object (Person Re-Identification Using Partial Siamese Network for Handling Partial Occlusion on Object)”, Master Thesis, Universitas Gadjah Mada, Indonesia, 2020 (In Bahasa Indonesia).

[12] W. Li, R. Zhao, T. Xiao, and X. Wang, “DeepReID: Deep filter pairing neural network for person re-identification,” in Proceedings of the IEEE Computer Society Conference on Computer Vision and Pattern Recognition, 2014, pp. 152–159, doi: 10.1109/CVPR.2014.27.

[13] C. Hart, Figure It Out! Human Proportions. New York: Sixth & Spring Books, 2014.

[14] R. Hadsell, S. Chopra, and Y. LeCun, “Dimensionality reduction by learning an invariant mapping,” Proc. IEEE Comput. Soc. Conf. Comput. Vis. Pattern Recognit., vol. 2, pp. 1735–1742, 2006, doi: 10.1109/CVPR.2006.100.

[15] F. Schroff, D. Kalenichenko, and J. Philbin, “FaceNet: A unified embedding for face recognition and clustering,” in Proceedings of the IEEE Computer Society Conference on Computer Vision and Pattern Recognition, 2015, vol. 07-12-June, pp. 815–823, doi: 10.1109/CVPR.2015.7298682.

[16] W. Li and X. Wang, “Locally aligned feature transforms across views,” Proc. IEEE Comput. Soc. Conf. Comput. Vis. Pattern Recognit., pp. 3594–3601, 2013, doi: 10.1109/CVPR.2013.461.

[17] A. Das, A. Chakraborty, and A. K. Roy-Chowdhury, “Consistent re-identification in a camera network,” Lect. Notes Comput. Sci. (including Subser. Lect. Notes Artif. Intell. Lect. Notes Bioinformatics), vol. 8690 LNCS, no. PART 2, pp. 330–345, 2014, doi: 10.1007/978-3-319-10605-2_22.

[18] N. S. Keskar, J. Nocedal, P. T. P. Tang, D. Mudigere, and M. Smelyanskiy, “On large-batch training for deep learning: Generalization gap and sharp minima,” 5th Int. Conf. Learn. Represent. ICLR 2017 - Conf. Track Proc., pp. 1–16, 2019.

[19] D. P. Kingma and J. L. Ba, “Adam: A method for stochastic optimization,” 3rd Int. Conf. Learn. Represent. ICLR 2015 - Conf. Track Proc., pp. 1–15, 2015.

[20] K. Simonyan and A. Zisserman, “Very deep convolutional networks for large-scale image recognition,” 3rd Int. Conf. Learn. Represent. ICLR 2015 - Conf. Track Proc., pp. 1–14, 2015.

[21] S.S. Khan, M. Khan, and Y. Alharbi, “Multi Focus Image Fusion using Image Enhancement Techniques with Wavelet Transformation,” International Journal of Advanced Computer Science and Applications (IJACSA), Vol. 11, No 5, pp. 414-420, 2020. doi:10.14569/IJACSA.2020.0110555.

Validation of Requirements for Transformation of an Urban District to a Smart City

Rosziati Ibrahim[1], N.A.M. Asri[2]
Department of Software Engineering
Universiti Tun Hussein Onn
Malaysia (UTHM)
Parit Raja, Malaysia

Sapiee Jamel[3]
Dept. of Web Technology and
Information Security
Universiti Tun Hussein Onn
Malaysia (UTHM)
Parit Raja, Malaysia

Jahari Abdul Wahab[4]
Engineering R&D Department
SENA Traffic Systems Sdn. Bhd
Kuala Lumpur, Malaysia

***Abstract*—The concept of a smart city is still debatable and yet gives attention to every country around the globe to provide their community with a better quality of life. New ideas for the development of a smart city have always evolved to enhance the quality, performance, and interactivity of services. This paper presents a model of a smart city based on the comparison of the chosen smart cities in the world and used the model to validate the requirements for the transformation of an urban district to a smart city. The proposed model for a smart city in this paper focuses on two major components, which are by utilizing IoTs (Internet of Things) in forming a model for a smart city and incorporating culture diversity. The relationship of components and culture influence are the foundation of designing the model of a smart city. In this research, the model of a smart city has been validated based on the requirements analysis from the survey instrument and the results show that the average mean of each element used is more than 4 out of 5. The model of a smart city can be used as a guideline for transformation of an urban district to a smart city.**

Keywords*—*Smart city; Internet of Things (IoTs); requirements analysis; survey instrument

I. Introduction

The smart city development has been growing over years, with the concept highly debated in all countries. A smart city is the answer to the rise of globalization of cities by managing and implementing ICT (information and communication technology) in all dimensions of the city such as infrastructure, mobility, governance, buildings, health and education. A smart city has become a competition between countries to serve the best for its citizens. The development has become dilemmas for the governance as it is a long-term process, which requires a lot of hard work between public and private sector. A smart city [1] is defined as a city that has components for smart such as smart citizen, smart infrastructure, smart building, smart governance, smart transportation, smart technology, smart health care and smart energy. A smart city does not necessarily have all these components to label as smart but depends on the cost and availability of the technology.

The components of smart city have been discussed by many researchers such as in [1 - 5]. However, as far as the research on smart city, no smart urban district model has been formed yet. Therefore, the design of smart urban district model is important leading to a research question on how to design a smart urban district model. To answer this research question, the objectives of the research is to design a smart urban district model and to validate the model based on the survey instrument so the model can be used as a guideline for the transformation of an urban district to a smart city.

This paper discusses the validation of requirements for a model of a smart city. Survey instruments are used to validate the model. The survey consists of questionnaire, interview and observation at research area. The questionnaire is divided into five sections which are demographic data, awareness of a smart city, elements of a smart city, impact of forming a smart city and culture influence towards a smart city with the purpose to ease the researcher to analyze the data. Interviews and surveys are conducted to people who live within the research area. The data has been collected and analyzed using Statistical Package for the Social Sciences (SPSS) software.

II. Related Work

In Malaysia, Putrajaya has been proposed as a first smart city in Malaysia. Seven domains have been considered as important elements to make Putrajaya as a smart city [2]. These seven domains are highlighted in Fig. 1.

From Fig. 1, smart transportation and mobility are the first domain for making Putrajaya as a smart city by adopting an intelligent traffic management system [3]. Smart home and environment ensure the residents of Putrajaya safety, which include intelligent environments by utilizing Internet of Things (IoTs) such as Wi-Fi, CCTV, and RFID.

The architecture of smart city has been discussed in [4]. From the architecture that have been suggested in [4], there are four requirements which are infrastructure, IoTs, environment and culture as shown in Fig. 2. Based on the architecture proposed in [4], the model of smart city has four elements, which are infrastructure, IoTs, environment and culture elements. Infrastructure consists of hospital, school, recreation park and library while IoTs consists of WSN Wifi, CCTV, Smart Parking and RFID. Meanwhile, environment consists of waste management, renewable resource energy, waste management and recycling program and lastly, culture element consists of prayer place and town hall.

This work was supported by Minister of Higher Education (MOHE) under Fundamental Research Grant Scheme (FRGS) under grant Vote No FRGS/1/2018/ICT04/UTHM/01/1.

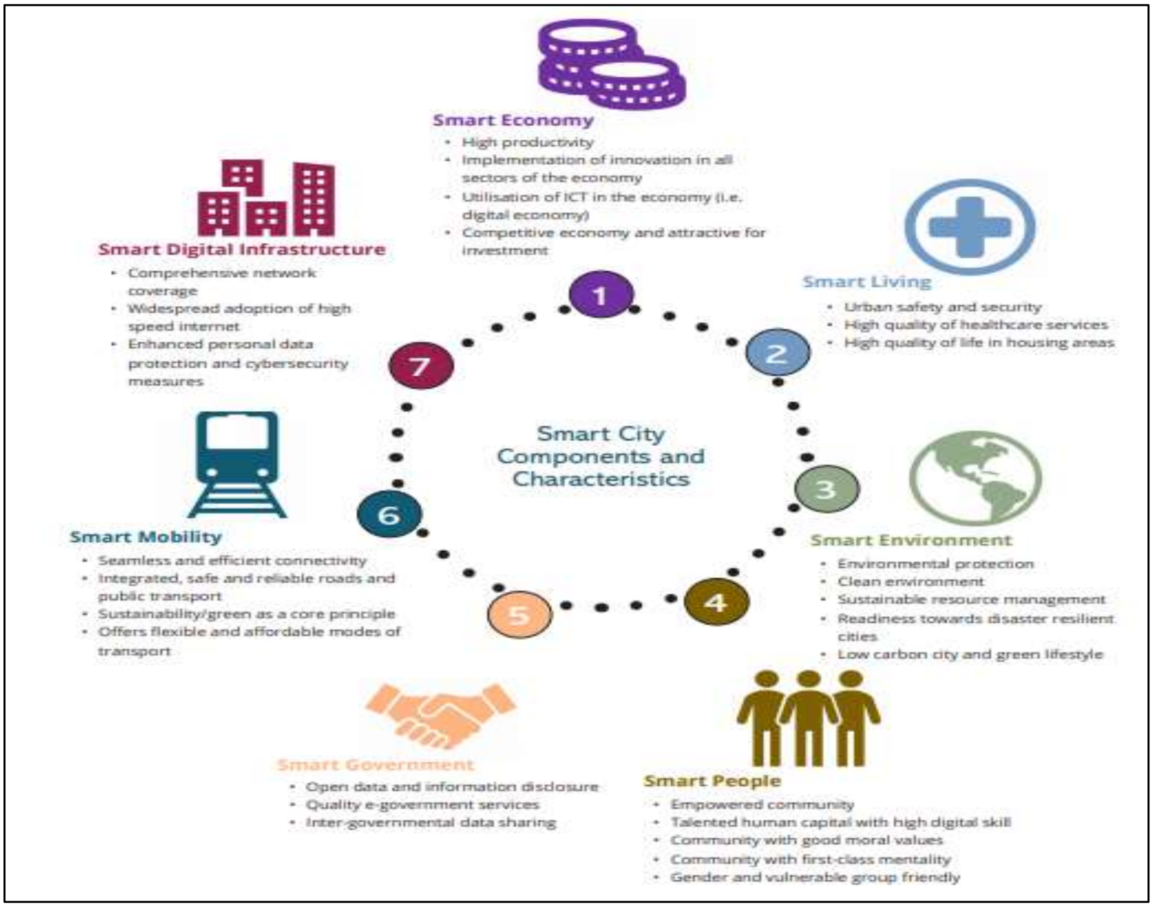

Fig. 1. Putrajaya Smart City Framework [2].

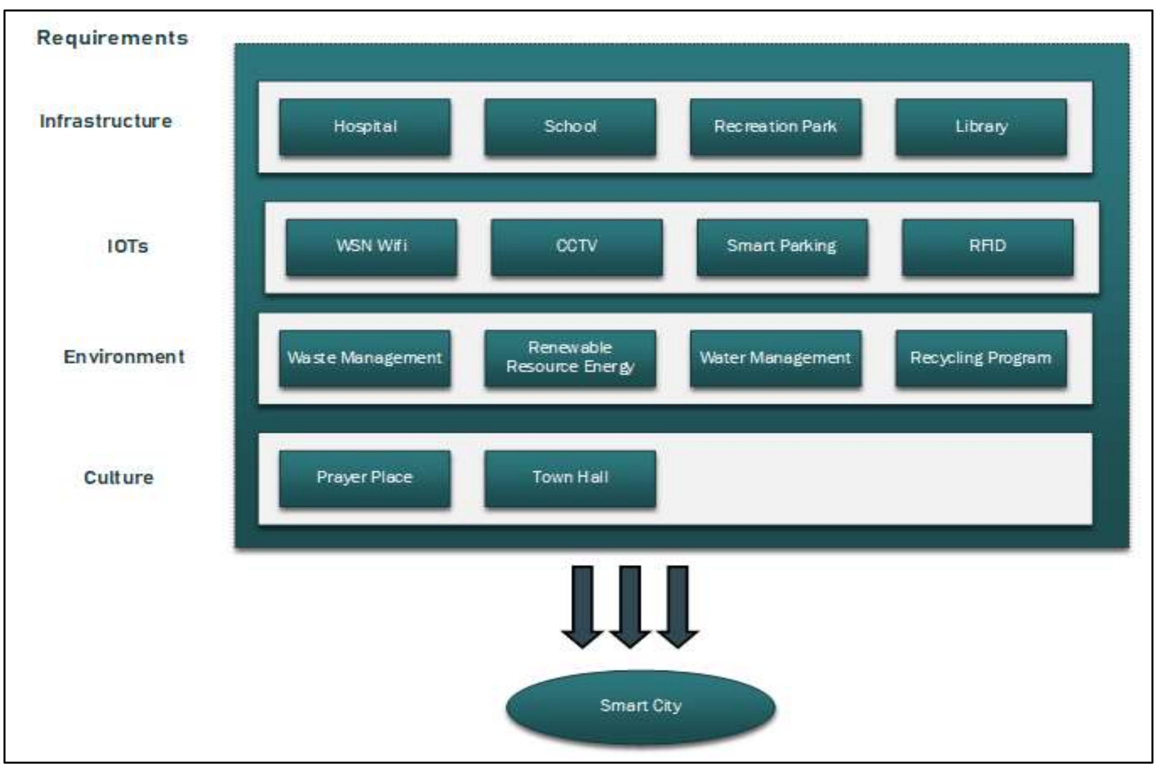

Fig. 2. The Architecture of a Smart City [4].

The proposed architecture in [4] was drawn from various studies such as [5] and [6]. Table I shows the summary of elements that have been cited by various researchers. The details clarifications are explained.

TABLE I. SUMMARY OF ELEMENTS

Elements	References
Infrastructure	[5], [6], [7], [8]
IoTs	[9], [10], [11], [12], [13]
Environment	[12], [13], [14]
Culture	[14], [15]

A. Infrastructure

Infrastructure has positively affected the smart city. The population growth has adapted to cities' services and infrastructures that tension to their limits and scalability. To build a smart city, the long-term scalability in term of housing, accessibility, transport system and sustainable growth should have taken into consideration in order to make a better life. Infrastructure in a smart city surround by the evolvement of all aspects of modern-day life such as transportation, healthcare, entertainment, work, business, social interactions, and governance [5 - 7].

Infrastructure defined broadly as the systems that provide water, energy, food, sheleter, transportation, communication, waste management and public spaces [6]. Khatoun et al. [7] stated that for sustainability and accessibility the development and growth from a city, the resource management such as safety and security, environment and transport, educational facilities, tourism and citizen's health are important to provide efficiency of urban life.

B. IoTs

The main engine for a smart city delivery is its technology. The technology drives the ICT and IoTs to make it more immersive and permissive. IoTs work amazingly in heterogeneous devices to communicate among those platforms to support smart city's vision in maximal exploits in communication.

IoTs links physical devices such as computer, sensors, electronics equipped with sensors connected to the internet and network connectivity enabling them to communicate [8]. Gartner [9] mentioned the IoTs units installed based will reach 20.8 billion by 2020 resulting in massive amount of data which will further highlight the security, customer privacy, storage management, and data centric network challenges.

Chang et al. [10] stated that the growing ubiquity and emerging applications of IoTs, especially in urban centres will enhance the usefulness of such systems to transform the manner in which social entities like individuals and organisations such as schools, healthcare, families, and community groups to interact with one another and their physical environment. IoTs connect everything together via the internet through specific protocols for information exchange and communications, achieving intelligent recognition, location, tracking, monitoring, and management. By interconnecting physical and virtual worlds with huge amounts of electric devices distributed in houses, vehicles, streets, buildings, and many other public environments, it can help in various kinds of services for both citizens and administrators [11].

C. Environment

Zygiaris [12] stated in his paper there is 7 layers for smart city conceptual model and of them is the green city layer that should practice in taking other alternative energy for city planning, water conservation, green transport practices, green building policies and CO2 reduction.

Tangauay et al. [13] included environment element in their dimensions of sustainable development of a smart city. To correspond to the concept of a quality of life, he studied indicators for sustainable development in an urban setting. They found that environmental challenges such as water pollution, soil contamination and air pollution can discontinuities the structural changes of the place.

Environment linked with natural resources and energy such as renewable energies, waste management and water management. Waste management focused on collecting, recycling, and disposing waste in correct ways; water management to analyze and manage the quantity and quality of water through hydrological cycle; renewable energy which exploits the natural resources that are regenerative such as heat, water and wind power [14].

D. Culture

A smart city rarely related with the culture of a city. Most researchers [5, 6, 8, 9] are mostly focus on other elements without taking culture element into consideration. Culture can build a city in term of raising the quality of life which encourage celebration in a way expressing creativity and show the individual identity and enhance or preserve the community's sense of place. Public involvement in exploiting the culture and attractiveness of a city's cultural heritage can facilitate in maintaining the attractive of a city [14].

Allam and Newman [15] highlighted that a smart city usually focused on ICT without taking cultural values into deliberation as it holds the legacies of the city. Their research proposed a framework that requires culture into consideration along with governance elements. Culture can contribute vitally to the economic growth as most visitors are attracted to one's cultural events. They also said the potential culture factor can revamp the urban areas.

III. RESEARCH METHODOLOGY

In this study, we have conducted an interview in the domain of the area. An interview is widely used in conducting research which requires a face-to-face interaction between an interviewee and an interviewer. An interview occurs when an interviewer asks one or more participants in general, open ended questions and record their answers [16]. Interviews are beneficial for getting the information behind a participant's experiences or knowledge. According to Giacoppo [17], interviews are also useful for pinpoint any potential areas for more detailed analysis.

A. Preliminary Study

A questionnaire is defined as a document containing questions and other types of items designed to solicit information appropriate to analysis [18]. During preliminary study, questionnaire design, questionnaire validation, pilot study, instrument reliability test, sample size population has been performed. After the collection of data, questionnaire response rate has been calculated. The questionnaire was designed based on closed-ended questions. Five-point Likert-Type scale [19] is used for this questionnaire to determine the degree of agreement of the respondents with the statements. They are Strongly Disagree, Disagree, Neutral, Agree and Strongly Agree.

Creswell [20] recommended that studies which involved in making questionnaires and interview must run a pilot study to modify the instruments based on feedback of small pool of respondents. A pilot study aims to reveal and eliminate the weakness of questionnaires [21]. A set of questionnaires were designed based on information from related prior studies which had investigated the elements of a smart city. The pilot study was carried out to examine each element and to test the feasibility of questionnaires. This study is necessary to verify the elements in the questionnaire whether they are reliable and free of errors. Therefore, for this study, the researchers had sent a set of questionnaires to 30 respondents for them to answer for the pilot study.

Reliability test is used for evaluating the reliability of the questionnaire based on Cronbach's alpha [22]. Table II shows the results for testing the reliability of the questionnaire.

TABLE II. INSTRUMENT RELIABILITY

Factor	Cronbach's alpha	No. of Items
Infrastructure	0.938	4
IoTS	0.877	4
Environment	0.891	4
Culture	0.940	2

Based on Table II, the Cronbach's alpha is greater than 0.7 for each element, hence the questionnaire is acceptable.

For the validation of the requirements for the model of a smart city, a total of 400 questionnaires were distributed in Sri Gading. From the total, only 391 questionnaires were received, and 374 questionnaires are able to be used. The remaining questionnaires cannot be used because of incomplete answers and missing information in several areas. Table III shows the questionnaire response rate for this study.

TABLE III. QUESTIONNAIRE RESPONSE RATE

Description	Frequency
Total Distributed Questionnaire	400
Total Received	391
Percentage of Response Rate	97.75%
Usable Questionnaires	374
Adjusted Response Rate	93.5%

B. Data Analysis

During the data analysis phase, data preparation that involves screening, checking missing data, suspicious response rate, outliers, and normality have been analysed. Data preparation performed to determine how to assign the numeric scores to the data. Before the process of analysing the data can be done, cleansing the data is important to ensure data is free from any error. Screening, checking missing data, suspicious response rate, outliers and normality are steps in preparing a valid data. The data is screened to detect and delete any kind of undesired data. The data were coded with characters and numbers and the responses were key in manually using SPSS. After that, the missing data is checked to overcome any error before proceeding with data analysis. SPSS is used to check the missing data. The result found that 0.431% is missing responses. Research analysis is acceptable if the neglecting responses with missing values are less than 10% [21].

The suspicious response rate has been identified for all dataset. The result found out that there is no suspicious response rate and can be considered error free. Suspicious response rate is the identification of the response pattern by the respondents which mark similar answer for all questions [22]. Outliers are to state the error rates and substantial distortions of parameter and statistic estimates when using either parametric or nonparametric tests [23]. This step was achieved by examining each individual construct using standard score. To analyze outliers, standardized Z-scores is created for the variables and the values are examined. If the Z-scores ranged between -3.29 and +3.29, it indicates no outliers [22]. Table IV shows the result of outliers analyzation. The Z-scores range is between -3.29 and +3.29, thus, no outliers are found in this dataset. Therefore, the data set is free from error.

TABLE IV. OUTLIERS

Construct	Max	Min	Outliers
Infrastructure	2.90	0.94	No
IoTs	3.16	0.97	No
Environment	3.21	1.14	No
Culture	2.66	1.11	No

Normality is used to regulate whether the data is well-modelled according to normal distribution. Holmes et al. [23] suggested that each construct item needs to be analyzed for their normalization. Value of skewness and kurtosis function estimate the symmetry and peak of data distribution. We tested our questionnaire for this and the standard error of skewness is 0.203 and the value of standard error of kurtosis is 0.403. The skewness for a normal distribution is zero, and any symmetric data should have a skewness near zero. Thus, this shows that standard error of skewness and kurtosis is not too far from normal distribution.

IV. STATISTICAL ANALYSIS AND RESULTS

The results based on the survey instrument are discussed in this section. Descriptive statistics are used to illustrate the data in two ways which are demographic frequencies and descriptive statistics and variables. The data has been analysed using statistical software, SPSS. Table V shows the demographic information obtained from the questionnaire.

Table V also shows the statistic of demographic frequencies of the respondents. A total number of 374 questionnaires were analyzed after eliminating the uncompleted data. Based on Table V, the respondents' characteristics include gender, race, occupation, income and residency. These characteristics were considered to provide in-depth understanding of the respondents.

Based on Table V, most of the respondents are dominated by females by 223 (59.6%) and 151 are males (40.4%). Most of them are Malay which 344 (92%), followed by Chinese is 19 (5.1%); Indian is 3 (9%) and others 4 people (2%). Most of them aged between 41 to 50 (31%); 24.3 % from age 31 to 40, 23.3 % from age over 50 years old followed by 12.8% for aged between 21 to 30 and 8.6% from under 20 years old. For occupation, respondents mostly are from private sector (37.2%) followed by self-employed (25.1%), not employed (17.9%) and 10.2% employed as government servant. Most respondents have income more than RM4000 and respondents with no stable income are 24.3%. Based on the survey, most respondents are from Sri Gading whom has stayed in for more than 10 years lead by 57% followed by 6 to 10 years (29.7%).

Descriptive statistics are represented to measures the tendency and frequencies of each item. Table VI shows the results obtained from the survey questionnaire. The results show the percentage for each layer of the proposed model of a smart city that has been shown in Fig. 2.

Based on Table VI, the descriptive statistics, and variables for four elements of a smart city are summarized for its mean value. Table VII shows the mean for each layers of the proposed model of a smart city. The average mean for infrastructure is 4.24; IOTs is 4.21; Environment is 4.30 and Culture is 4.15.

Based on Table VII, the mean of distribution is greater than 4 out of 5. Hence, this verified the requirements of the model of a smart city model based on Table VII. That is, firstly, a smart city should have infrastructure which consists of hospital, school, recreation park and library. Secondly, IoTs installation in the smart city such as Wi-Fi, CCTV, Smart Parking and RFID are needed as well. Thirdly, environment should also be recognized as one of a smart city element that includes waste management, renewable resource energy, water management, and recycling program. Lastly, the culture element is considered as well such as prayer places and a town hall. The urban district should have these four elements in order for the urban district to be transformed into smart city as shown in Fig. 2.

TABLE V. DEMOGRAPHIC INFORMATION

Item	Categories	Frequency	Percent	Valid Percent	Cumulative Percent
Gender	Male	151	40.4	40.4	40.4
	Female	223	59.6	59.6	100.0
Race	Malay	344	92.0	92.0	92.0
	Chinese	19	5.1	5.1	97.1
	Indian	9	2.4	2.4	99.5
	Others	2	0.5	0.5	100.0
Age (years)	Under 20	32	8.6	8.6	8.6
	21-30	48	12.8	12.8	21.4
	31-40	91	24.3	24.3	45.7
	41-50	116	31.0	31.0	76.7
	>50	87	23.3	23.3	100.0
Occupation	Government	38	10.2	10.2	10.2
	Private Sector	139	37.2	37.2	47.3
	Self-employed	94	25.1	25.1	72.5
	Student	36	9.6	9.6	82.1
	Not employed	67	17.9	17.9	100.0
Income (RM)	100-1000	70	18.7	18.7	18.7
	1001-2000	103	27.5	27.5	46.3
	2001-3000	59	15.8	15.8	62.0
	3001-4000	18	4.8	4.8	66.8
	>4000	33	8.8	8.8	75.7
	No income	91	24.3	24.3	100.0
Residency	< 1	18	4.8	4.8	4.8
	1-5	32	8.6	8.6	13.4
	6-10	111	29.7	29.7	43.0
	>10	213	57.0	57.0	100.0

TABLE VI. RESULTS BASED ON SURVEY QUESTIONNAIRE

Elements	Items	Strongly Agree (%)	Agree (%)	Neutral (%)	Disagree (%)	Strongly Disagree (%)
Infrastructure	Hospital	44.65	39.84	14.17	0.80	0.53
	School	43.65	43.85	11.23	0.80	0.53
	Recreation Park	33.69	54.01	8.82	3.21	0.27
	Library	38.50	48.65	10.43	1.87	0.53
IoTS	WSN WiFI	44.25	44.26	9.63	1.07	0.60
	CCTV	41.44	47.33	9.63	1.07	0.53
	Smart Parking	40.37	43.58	13.90	1.34	0.80
	RFID	32.62	47.33	15.78	3.48	0.80
Environment	Waste Management	39.57	47.33	11.50	0.80	0.80
	Renewable Resource Energy	33.96	48.13	16.04	1.34	0.53
	Water Management	41.44	47.33	9.63	1.07	0.53
	Recycling Program	40.47	48.66	9.09	0.80	1.07
Culture	Prayer Place	38.77	43.58	14.71	1.87	1.07
	Town Hall	34.76	45.99	16.31	2.41	0.53

TABLE VII. THE MEAN FOR EACH ELEMENT

Elements	Items	Mean	Average Mean
Infrastructure	Hospital	4.27	4.24
	School	4.29	
	Recreation Park	4.18	
	Library	4.23	
IOTS	WSN WiFI	4.28	4.21
	CCTV	4.28	
	Smart Parking	4.21	
	RFID	4.07	
Environment	Waste Management	4.24	4.30
	Renewable Resource Energy	4.14	
	Water Management	4.28	
	Recycling Program	4.26	
Culture	Prayer Place	4.17	4.15
	Town Hall	4.12	

V. COMPARISON AND DISCUSSION

The comparison of smart city model between Dubai, Brisbane, and Putrajaya had been made by reviewing some papers from various sources such as [2, 3, 4, 5, 24, 25].

Dubai as the fastest growing city has amazed the world by their vigorous movement towards an intelligent city. Dubai built its history in socio-economic, leading regional paradigm of digital transformation and sustaining the status of the city as a global hub. In six dimension of Dubai, Dubai municipalities has highlighted several elements such as health, infrastructure, transport, piped water, sanitation, electricity, road infrastructure, and building [24].

Brisbane is another example of a smart city. Brisbane is the second city in the world to implement a digital transformation strategy. With an eye towards a better city, Brisbane has introduced a smart, connected city concept for the purpose of delivering a more liveable, sustainable, and prosperous city. In the last few years, Brisbane municipality realised the opportunities of Brisbane in becoming an economic city that deliver the right environment for economic purpose in investment, collaboration, and growth. In order to do so, Brisbane [25] has presented six characteristics of its smart, connected city. Brisbane city council has highlighted transport, water, energy, telecommunications, waste management, social infrastructure, green space, and key district as main elements of Brisbane Smart City.

Meanwhile, Putrajaya is in progress of becoming the first smart city in Malaysia with the inclusion of Internet of Things (IoTs) and other information and communication technology (ICT) innovations as the main feature in building a global city. Putrajaya has a vision of transforming itself into a Green City by the year of 2025 [2]. In order to achieve the objective of becoming a smart city, Smart Putrajaya has highlighted the elements of Communication, Street & Compound Lighting, Facilities Management, and Waste Management System as the main features in developing a smart city.

The urban district should have four elements in order to be transformed into a smart city as shown in Fig. 2. Table VIII shows the results of transformation of urban district (in the case of Sri Gading) into a smart city.

Based on Table VIII, Sri Gading has few elements that can be considered to be a smart city. However, elements such as hospital, library, CCTV, smart parking, RFID, renewable resource energy and a town hall building are needed in order to transform Sri Gading into a smart city. This kind of elements can be used as recommendations to higher authorities in order to transform Sri Gading into the future of a smart city.

TABLE VIII. THE COMPARISON OF EACH ELEMENT

	Elements	Sri Grading	Smart City
Infrastructure	Hospital	No	Yes
	School	Yes	Yes
	Recreation Park	Yes	Yes
	Library	No	Yes
IoTs	Wi-Fi	Yes	Yes
	CCTV	No	Yes
	Smart Parking	No	Yes
	RFID	No	Yes
Environment	Waste Management	Yes	Yes
	Renewable Resource Energy	No	Yes
	Water management	Yes	Yes
	Recycling Program	Yes	Yes
Culture	Prayer Place	Yes	Yes
	Town Hall	No	Yes

VI. CONCLUSION AND FUTURE WORK

This paper discussed requirements analysis for validation of transforming the urban district to a smart city. The results for the validation of requirements based on survey instrument are very promising. Based on the results, most respondents agreed that infrastructure, IoTs, environments and culture are the four vital elements for a model of a smart city. For future work, the model of a smart city presented in this paper can be used as a guideline for transformation of an urban district to a smart city. Recommendation can be made based on the guideline whether the city can be transformed into a smart city or not.

ACKNOWLEDGMENT

The authors would like to thank Ministry of Higher Education (MOHE) for supporting this research study under Fundamental Research Grant (FRGS) entitled: Designing a Model for Smart City thru Digital Transformation, under grant Vote No FRGS/1/2018/ICT04/UTHM/01/1.

REFERENCES

[1] S.P. Mohanty, U. Choppali and E. Kougianos, "Everything you wanted to know about smart cities: The Internet of things is the backbone," *IEEE Consumer Electronics Magazine*, vol. 5, no. 3, pp. 60-70, July 2016.

[2] Putrajaya Smart City, *Putrajaya Smart City Blue Print, 2021*. [Online]. Available: https://smart.putrajaya.my

[3] Malaysian Communications and Multimedia Commission. *Framework on Smart Cities Standardisation in Relations to Information & Communication Aspects, 2021*. [Online]. Available: https://www.mcmc.gov.my/skmmgovmy/media/General/pdf/Framework-on-Smart-Cities-Standardisation.pdf

[4] R. Ibrahim, N.A.M. Asri and S. Jamel, "Utilization of IOTs in Developing the Architecture of Smart City in Malaysia," *2019 IEEE 9th International Conference on System Engineering and Technology, ICSET 2019 – Proceeding*, 2019, pp. 35-40, 8906398.

[5] R. Mehmood, B. Bhaiduri, I. Katib, "Smart Societies, Infrastructure, Technologies and Applications," *First International Conference, SCITA*, 2017, Jeddah, Saudi Arabia, November 27-29, Proceedings, 2017.

[6] European Commission Directorate, *General for Research and Innovation, Towards an EU Research and Innovation Policy Agenda for Nature-Based Solutions and Re-Naturing Cities*: Final Report of the Horizon 2020 Expert Group on 'Nature-Based Solutions and Re-Naturing Cities, 2015. DOI:10.2777/479582

[7] R. Khatoun and S. Zeadally, "Smart cities." *Communications of the ACM*, 59(8), 46–57, 2016.

[8] U. Ahmad, J. Chaudhary, M. Ahmad and A. A. Naz, "Survey of Internet of Things (IoT) for Different Industry Environment," *Annals of Emerging Technologies in Computing (AETiC)* Vol. 3, No., 2019.

[9] Gartner Inc., *Gartner says 4.9 billion connected things" will be in use in 2015*. [Online]. Available: http://www.gartner.com/newsroom/id/2905717, Nov 2014

[10] V. Chang, V. Kantere, M. Ramachandran, "Emerging services for internet of things," *Journal Network Computing* Appl. 89, 1–2, 2017.

[11] Y. Qian, D. Wu, W. Bao and P. Lorenz, "The Internet of Things for Smart Cities: Technologies and Applications," *IEEE Network*-March/April 2019.

[12] S. Zygiaris, "Smart City Reference Model: Assisting Planners to Conceptualize the Building of Smart City Innovation Ecosystems," *Journal of the Knowledge Economy*, 4(2), 217–231, 2012.

[13] G. A. Tangauay, J. Rajaonson, J. Lefebreve and P. Lanoie, "Measuring the Sustainability of Cities: A Survey-based analysis of the Use of Local Indicators". *SSRN Electronic Journal*. 2010. DOI:10.2139/ssrn.1336649

[14] P. Neirotti, A. De Marco, A. C. Cagliano, G. Mangano and F. Scorrano, "Current trends in Smart City initiatives: Some stylised facts." *Cities*, 38, 25–36, 2014.

[15] Z. Allam and P. Newman, "Redefining the Smart City: Culture, Metabolism and Governance". *Smart Cities*, 1(1), 4–25, 2018

[16] McNamara, Carter, *General Guidelines for Conducting Interviews. 1999.* [Online]. Available: https://managementhelp.org/businessresearch/interviews.htm

[17] S. Giacoppo, "Development Methods: User Needs Assessment & Task Analyses." Department of Psychology, Catholic University, 2001.

[18] B. Earl, "Survey Research Methods", Second Edition. California: Wadsworth Publishing Company, 1990.

[19] R. L. Armstrong, "The Midpoint on a Five-Point Likert-Type Scale." *Perceptual and Motor Skills*, 64(2), 359–362. doi:10.2466/pms.1987.64.2.359 , 1987.

[20] J. W. Creswell, "Planning, Conducting, and Evaluating Quantitative and Qualitative Research." University of Nebraska-Lincoln, 2012.

[21] L. J. Cronbach, "Response sets and test validity." *Educational and Physocological Measurement* 6(4): pp 475-494, 1946.

[22] L. Tabachnick and F. Fidell, "Using Multivariate Statistics."*Pearson Education Inc.* Vol. 28, 2017.

[23] S.P. Holmes, L. Coote and E. Cunningham, "Structural Equation and Modelling: From the fundamentals to advanced topics." Melbourne:Stream, 2006.

[24] Abdulla bin Hozaim and Vishwesh Laxmikant, "A Framework for transforming Dubai into a smart city." *The Fourth HCT Information Technology Trends (ITT 2017) Dubai, UAE, Oct 25-26, 2017.*

[25] Digital Brisbane. *Digital Brisbane 2.0- Empowering residents and businesses to thrive globally-connected, digitally-enabled world.* [Online]. Available: https://www.brisbane.qld.gov.au/about-council/governance-and-strategy/vision-and-strategy/smart-connected-brisbane

Cyberattacks and Vociferous Implications on SECS/GEM Communications in Industry 4.0 Ecosystem

Shams A. Laghari[1], Selvakumar Manickam[2]*, Shankar Karuppayah[3], Ayman Al-Ani[4], Shafiq Ul Rehman[5]
National Advanced IPv6 Centre (NAv6), Universiti Sains Malaysia (USM), Pulau Pinang, Malaysia[1,2,3,5]
Department of Biomedical Engineering, Faculty of Engineering, University of Malaya, Kuala Lumpur, Malaysia[4]

***Abstract*—Information and communications technology (ICT) is prevalent in almost every field of industrial production and manufacturing processes at present. A typical industry network consists of sensors, actuators, devices, and services to connect, track, and manage production processes to increase performance and boost productivity. The SEMI Equipment Communications Standard/Generic Equipment Model (SECS/GEM) is SEMI's Machine-to-Machine (M2M) protocol for equipment-to-host data communications. It is the most popular and profoundly used M2M communication protocol operating in the manufacturing industry. With Industry 4.0 as a guiding factor, connectivity to business networks is required for accessing real-time data whenever and wherever needed. This openness of connectivity raises security concerns as SECS/GEM protocol offers no security, which endangers exposing the manufacturing industries' business secrets and production processes. This paper discusses the key processes involved in SECS/GEM communications and how potential attackers can manipulate these processes to obtain illegal or unauthorized access. The experiments' results indicate that the SECS/GEM processes are entirely vulnerable to numerous attacks, including DoS attack, Replay attack, and False-Data-Injection-Attack. Thus, the future direction involves developing a prevention mechanism that aims at securing the SECS/GEM processes in the industrial network. This study's findings are useful as preliminary guidance for the infrastructure owners to plan for appropriate security measures to protect the industrial network.**

Keywords—SECS/GEM; cybersecurity; industry-4.0; machine-to-machine communication; industrial internet of things (IIoT)

I. Introduction

Over the past few decades, technological advancements have progressed so rapidly that we have reached the fourth industrial revolution called Industry 4.0, commonly termed as the Industrial Internet of Things (IIoT) or smart manufacturing [1]. Cyber-physical structures have been accoladed to map the physical world into a virtual one with the advent of the technological revolution. Cybersecurity, robotics, cloud computing, 5G networks, big-data analysis, machine learning, Internet of Things (IoT), and additive manufacturing are the prime developments of this modern-day technology, which bring forth groundbreaking changes in the life of individuals, society, industry as well as economy [2]. Industry 4.0 is vying for enhanced connectivity, machine learning, real-time data collection, the interaction between machine-to-machine on novice mechanisms, automation and advanced robotics, increasing industrial productivity, and modernizing the production process. Even though businesses, companies, and organizations are entirely different in scale and scope, they all face the same problem, i.e., the need for connectivity and real-time insights through manufacturing processes, products, material movement, and resource utilization for timely decision making [3].

Historically, manufacturers have been more concerned with protecting their Operational Technology (OT) environment, often almost entirely neglecting Information Technology (IT) security. The perpetrators are fully informed of this negligence and realize how easy it is to infiltrate and hack industrial networks. In accordance with the awareness that important, confidential information such as product types, product recipes, material details, system configurations, comprehensive equipment logs, equipment's communication patterns, etc., is held valuable by industries and thereby opens up an increasingly attractive prospect for threat-actors. Hackers and threat-actors have realized that the supply chain is a large and complex process with ample vulnerabilities, and therefore it is the perfect environment for attempting an attack to infect numerous suppliers and organizations at a massive scale.

Recent incidents of security breaches and cybercrimes have reached the epidemic stage in the manufacturing industry, rendering the manufacturing industry the most vulnerable and targeted sector by attackers [4]. According to EEF, a recent survey reveals that 48 percent of manufacturers have been subject to a cybersecurity incident at any point, and half of those firms have suffered financial losses or market disruption. Another study carried out by Cybersecurity Ventures has identified that cybercrime will cost corporations worldwide \$10.5 trillion a year by 2025, up from \$3 trillion in 2015 [5], while manufacturing has been catching up quickly in recent years, as can be seen in the Verizon Data Breach Investigation Report 2019, which detailed 352 incidents, 87 among manufacturers. The Taiwan Semiconductor Manufacturing Company (TSMC) computer virus attack was Taiwan's biggest information security infringement in its history. It fully exposed the information security weaknesses at production plants as the manufacturing industry embraces the fourth industrial revolution, or industry 4.0, with increasing automation and data exchange [6].

This work embodies an overview of SECS/GEM standard and uncovers lacunas in SECS/GEM, which eases launching of

*Corresponding Author

attacks on factory equipment with the help of attacks like False-Data-Injection attack (FDIA), Replay attack, Denial of Service (DoS) attack. This paper, therefore, includes a brief explanation of the relevant aspects of the SECS/GEM standard in order to fully comprehend the mechanics of these cyberattacks on industrial networks.

This paper is arranged into the following sections: A brief literature review of security features of popular industrial M2M communication protocols is covered in Section 2. SECS/GEM's overview and connection establishment processes are explained in Section 3. Attacks on SECS/GEM processes are discussed in Section 4. Scenarios, attacks, and experimental results are discussed in Section 5. The conclusion and future outlook are provided in Section 6.

II. Literature Review

Within the landscape of Industry 4.0, cybersecurity plays a leading role in preventing the loss of companies' competitiveness. However, when seen in the perspective of the industrial automation industry, cybersecurity has concentrated more on protecting corporate and operational perimeters, i.e., restricting unauthorized access to the industrial network. There are numerous messaging communication protocols for IIoT and industrial communications such as SECS/GEM, OPC UA, CoAP, DDS, MQTT, and many more. Industry 4.0 has brought these protocols under the spotlight once again. Most of these protocols have limited security features. A brief discussion on security features offered in the above-mentioned M2M protocols is provided in the following sub-sections.

A. *Message Queuing Telemetry Transport*

Message Queuing Telemetry Transport (MQTT) is an open-source messaging protocol developed by IBM for resource-constrained devices (i.e., devices having limited computational power, memory, storage, and battery backup). It adheres to the publish/subscribe interface paradigm and performs well in networks where communication requirements are less than optimal such as high latency with low bandwidth. It keeps bandwidth requirements to an absolute minimum, works ridiculously well with unstable networks, and is best suited for machine-to-machine (M2M) communications. MQTT is undoubtedly regarded as a de facto IoT normative protocol, and research on the offensive and defensive solutions to MQTT has attracted substantial interest from academia and industry for analysis on security issues [7].

The condition under which the MQTT protocol operates by default [18] can easily be linked to nearly all security concerns that occur. Since MQTT is meant to be lightweight, it does not encrypt the header or payload but rather exchanges data as plaintext, which is obviously a security problem. Thus, encryption must then be used as a separate function, such as by Transport Layer Security (TLS), which increases the computational overhead on the resource-constrained devices. Most MQTT brokers provide authentication support through the use of the Link control message. A few security solutions have been proposed to address MQTT's security concerns [8][9][10].

B. *Open Platform Communications – Unified Architecture*

Open Platform Communications – Unified Architecture (OPC-UA) is an M2M communication protocol developed by OPC Foundation for Industrial Automation [11]. OPC UA is built to ensure security and thus offers a wide variety of core security features, including authentication, integrity, confidentiality, and authorization. It provides different protection modes, such as no security, integrity only, integrity and confidentiality, as well as security policies predefining encryption and signature cryptographic algorithms for the establishment of secure communication. Depending on the message protection mode, the client chooses a security protocol to secure the messages exchanged during the handshake. Notably, one of the seven security policies available offers little security, and two have been discarded because of cryptographic primitives that are now vulnerable. Overall, OPC UA offers industrial automation with strong security features [12].

C. *Constrained Application Protocol*

Constrained Application Protocol (CoAP), as specified in RFC 7252[13], is an Internet Application Protocol specifically designed for resource-constrained devices and constrained networks [14]. It functions HTTP-like and follows REST-Architecture, and runs over User Datagram Protocol (UDP). To secure communication, CoAP does not use TLS since it runs over UDP, which is an insecure transport protocol, so DTLS is used by CoAP instead of using TLS as a security solution.

CoAPS is a security-enabled variant of the CoAP protocol, which is based on a TLS protocol with modifications needed to operate over unreliable UDP connections. Some of the TLS enhancements include features whereby CoAPS retains the connection in the event of missed or out-of-order packets and prevents link termination (i.e., teardown) as it is done in CoAP. There is a probability of retransmitting handshake messages as an example. With the exchanging of client and server 'hello' messages, the handshaking mechanism is quite similar to the one in TLS, but with the additional possibility for a server to send a verification query to ensure that the client sends its 'hello' message from the authentic source address. This added functionality helps in preventing DoS attacks.

D. *Data Distribution Service*

Data Distribution Service (DDS) [15] is an M2M protocol that follows the publish/subscribe pattern, and it is specifically designed to allow efficient, high-performance, interoperable data exchange for real-time systems. DDS can run on both TCP and UDP, so a security mechanism provides two distinct options for DDS. The security combination may be either TCP with TLS or UDP with Datagram Transport Layer Security (DTLS), depending on the underlined transport protocol. Both TLS and DTLS are not designed for constrained devices; thus, they incur too much computational overhead and are not suitable for a constrained environment. In order to solve the issue, OMG's proposed DDS security specifications describe a robust security architecture that is considered lightweight and acceptable for the IoT device.

Unlike all protocols mentioned above, SECS/GEM does not provide any security features. High-Speed SECS Message Services (HSMS) is a SECS/GEM's transport communication protocol and runs over TCP. It lacks security. Henceforth, data is not encrypted by any encryption algorithm. Moreover, credentials and certificates are not required for connection. Furthermore, validation of the connecting party is not carried out. However, obfuscation is applied to the data through the data packaging binary encoding process, which makes it incomprehensible for humans.

To our knowledge, no one has previously assessed SECS/GEM in terms of security features. In this paper, we have extensively analyzed the mechanism of SECS/GEM and have identified weak points that may be problematic if not patched in time would undoubtedly lead to catastrophic consequences, including financial and business losses.

III. SECS/GEM Processes and Connection States

SEMI (Semiconductor Equipment and Material International) is an association enjoying membership of more than two thousand companies worldwide. It deals with materials, services, and equipment required by the manufacturing industries. The SECS/GEM standard has been widely adopted in semiconductors, surface mount technology, electronics assembly devices, photovoltaic, and solar cell industries. SEMI has published several different specifications that coordinate communication between the host and the factory machinery, including E4, E5, E30, and E37. SEMI communication standards are collectively known as SECS/GEM. The SECS/GEM protocol is an industry-standard that is widely in operation across several industries worldwide [3][16][17]. It acts as a backbone of the semiconductor industry and is heavily used in the world's leading enterprises, including Intel, Samsung, TSMC, IBM, Qualcomm, Broadcom, UMC, SK Hynix, Micron, TXN, Toshiba, NXP, proving as a de facto communication protocol and control system since years[18].

High-Speed SECS-II Messaging Service (HSMS) serves as a transport protocol for SECS/GEM communications in industrial networks [19][20][21]. The HSMS protocol is derived from Transmission Control Protocol / Internet Protocol (TCP/IP). It utilizes virtually the same methods of forming a link as specified in RFC-793 but with minor essential modifications [22]. In accordance with the guidelines prescribed in RFC 793, either side of the communication link can initiate a request to create the connection. However, the HSMS protocol limits the standard practice of the formation of connections as defined in the RFC; and distinguishes two distinct types of connection modes, namely active and passive. The devices configured in passive mode act as a server, open a port, and listen for incoming connections, while the responsibility of initiating a connection request is destined to the devices configured in active mode. Upon a successful connection has been formed between the two communicating entities (i.e., host and equipment), HSMS protocol passes binary encoded SECS-II messages. The HSMS protocol keeps the connection alive, and data moves back and forth until either or both entities are purposely rendered offline (i.e., firmware or software updates, add/remove machines in the production line, maintenance, etc.). The HSMS message format is shown in Fig. 1, and a brief overview of the HSMS header fields is discussed in Table I. HSMS messages are packed in binary format and are transported as byte streams, where the first four bytes of the message are used to calculate the overall message length. The minimum and maximum size of a message carried out over an HSMS protocol is 10 bytes and 4.3 gigabytes, respectively.

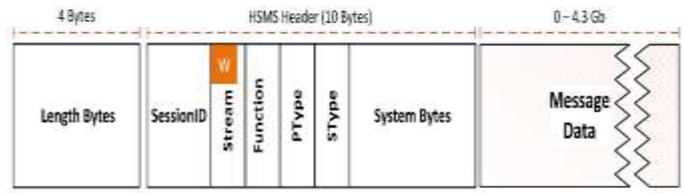

Fig. 1. HSMS Message Structure.

TABLE I. Brief Description of HSMS Header Fields Along with Possible Values

Bytes	Field	Description
0-1	Session ID	- Provides an association by reference between control messages and subsequent data messages
2	W-Bit & Stream	- Contains 0 or status code for control messages - When SType=0, it contains W-bit and Stream number for data messages
3	Function	- Contains 0 for control messages - When PType = 0, it contains SECS-II function
4	PType	- Contains 0 for SECS-II messages
5	SType	- 0 for data messages - 1-9 (8 is unused) for control messages
6-9	System Bytes	- Contains a unique value for each transaction - Same value for both Primary and its associated secondary (response) message

A. SECS/GEM Message Types

SECS/GEM messages are broadly divided into two categories, (1) control messages and (2) data messages. Control messages are used by the HSMS protocol for connection and link management. The SType header field of HSMS protocol may have values 1,3,5 and 9 to perform operations select.req, deselect.req, linktest.req, and separate.req, respectively. Each request message is acknowledged with a succeeding even number value for the paired control message except the separate.req, which does not require acknowledgment. In addition to the aforementioned control messages, there is an additional control message named reject.req with SType=7. This control message is used in response to any valid HSMS message received which is not supported by the receiver of the message or which is not valid at the time when that message was received [23] (for example, an HSMS message whose SystemBytes value is invalid or it does not match with any open transaction).

B. SECS/GEM Connections States

In order to establish a connection with equipment, it is important to understand the SECS/GEM connection state. There are two states at the fundamental level, NOT-CONNECTED and CONNECTED. As the name indicates, in the NOT-CONNECTED state, either an entity is listening on a

TCP port and waiting for incoming connection establishment requests, or all previously established connections have been terminated. Either way, an entity in a NOT-CONNECTED state does not engage in any communication. Upon a successful TCP connection establishment with the host, equipment enters the CONNECTED state. Two sub-states named NOT-SELECTED and SELECTED are in the CONNECTED state. The entities await the request for the HSMS link establishment upon entering the CONNECTED state.

Once the HSMS control message for the connection establishment is received, the entity enters the SELECTED state. Only when entities have reached the SELECTED state are the actual SECS-II messages and control messages exchanged between the two communicating entities. Fig. 2 depicts the HSMS State Model.

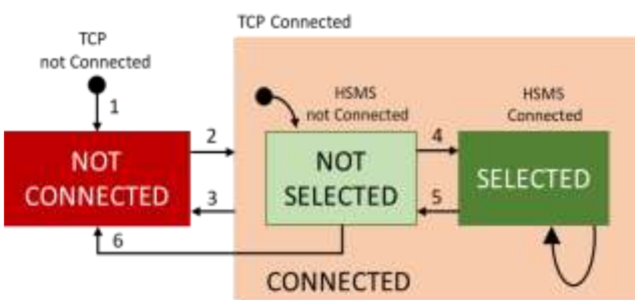

Fig. 2. HSMS Connection States.

C. HSMS Communication Processes

SECS/GEM messages exchanged between the host and equipment are highly important in order to control and monitor the equipment. In a normal communication mode, either side of the connection can request data. Upon receiving a request message, the target entity would reply with generated data for the specific request. SECS/GEM communication is carried out on HSMS protocol, which has a fixed header format and structure. If the SType field of the HSMS header in any message is 0, it means the message is a data message; otherwise, it will be considered a control message.

1) Connection establishment process: Fig. 3 represents the different SECS/GEM communications processes. The entity configured in active mode (i.e., usually host) must send a TCP request to the equipment entity that is typically configured in passive mode in order to initiate communication. Upon receiving a response from the equipment, the host will send an acknowledgment, and a TCP connection will be formed between the two communicating entities (i.e., Fig. 3(a)). The equipment will enter into the CONNECTED state at this point and wait for the establishment of an HSMS connection. At this stage, the host will request for the HSMS link establishment, and the equipment will respond to that message and change its state from NOT-SELECTED to SELECTED. Now, the link is complete and ready for the exchange of SECS-II messages (Fig. 3(e)). The process of creating TCP and HSMS connections is illustrated in Fig. 3(a) and Fig. 3(b).

2) Connection management process: The connections in industrial networks are kept alive for several days or even weeks. There are possibilities that there is no communication carried out for a certain period of time between the two entities; therefore, it is required to test the connectivity beforehand. Fig. 3(d) illustrates a scenario when such an inactive period is detected when there is no communication between the two entities. The control messages linktest.req and linktest.res are exchanged periodically based on timer T3 value in order to keep the connection alive.

3) Connection termination (tear-down) process: Two ways to teardown a link are specified by SECS/GEM specifications, i.e., by sending deselect.req or separate.req control messages. The difference between these two messages is that without waiting for an acknowledgment, separate.req abruptly disconnects the connection. Fig. 3(c) and Fig. 3(f) demonstrate the teardown phase of the connection.

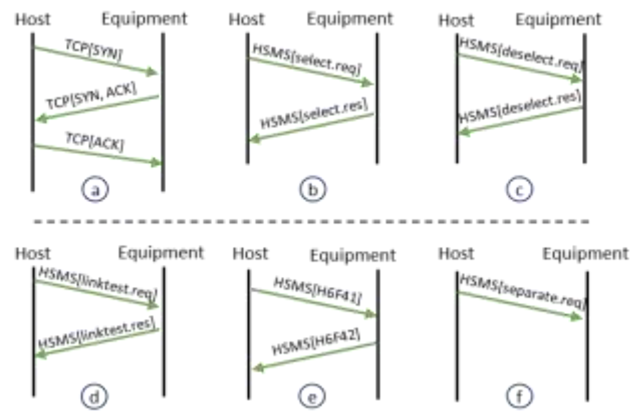

Fig. 3. SECS/GEM's Connection Establishment, Control and Data Message Processes.

IV. CYBERATTACKS ON SECS/GEM

Numerous cyber-attacks, such as DoS attack, Replay attack, spoofing attack, side-channel attack, covert-channel attack, False-Data-Injection-Attack, etc., can be launched on industrial networks[24] where SECS/GEM is used for M2M communications. However, this study focuses on DoS attack, replay attack, and FDIA. Fig. 4 depicts a typical industrial machines network layout and production line on the shop-floor.

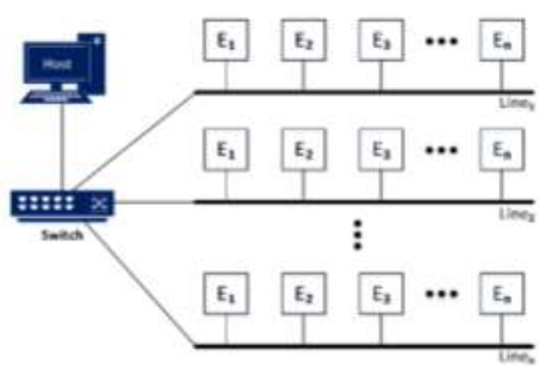

Fig. 4. A Simplified and Generalized OT Industrial Shop-Floor Network.

The first step that should be taken in order to carry out a successful attack on any network is to analyze network activity and communication patterns. A huge amount of data is usually generated by SECS/GEM-enabled machines, and this data is exchanged in plaintext and without any authentication. Fig. 5 shows the pattern of 20 hours of communication between a host and equipment that occurred in a production environment (for protection and privacy purposes, the organization's name and the machine's specifics are not discussed here). SECS/GEM messages are paired as primary and secondary messages, where request messages, and secondary messages are associated reply messages. Each primary message is usually responded with an associated secondary message (i.e., S6F11/S6F12 represents the pairing of Primary/Secondary messages), as shown in Fig. 5. It is important to note that a primary message can be sent at any time by both sides of the connection, and therefore it is essential to keep a record of the most recent SystemBytes value for a successful attack. The information presented in Fig. 5 also reveals that the preparators might not have yet carried out any successful attack on the industrial network; the intruders may still have the ability to effectively intercept data and steal sensitive product information by merely observing data shared between the host and the equipment.

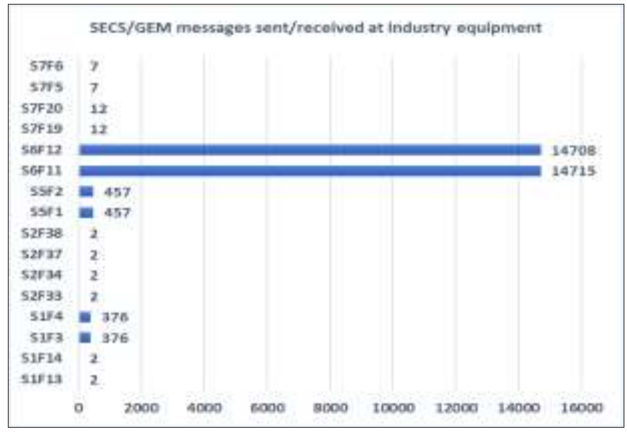

Fig. 5. Typical SECS/GEM Interaction Pattern as seen on a Factory Machine.

A. Denial-of-Service (DoS) Attack

In industrial communication networks, DoS is characterized as a particular cyberattack in which attackers try to ensure that access to the intended users is either temporarily or permanently inaccessible for the desired service or resource. There are numerous ways to achieve a DoS attack in SECS/GEM communications. For example, the perpetrators may capture and forge a bogus message of a legitimate host/equipment and send a deselect.req message to terminate the communication link. Upon using the port stealing mechanism, the attack-actors may perform a man-in-the-middle attack and then initiate the DoS attack, in which case the host will never know the connection is terminated [25].

We have exploited the HSMS's control messages to launch a DoS attack. We used the control message separate.req in this study to execute a successful DoS attack on HSMS communications. As discussed in the previous section, an HSMS message with SType=9 is used to terminate HSMS communications immediately. With the exception of the SType value, separate.req control message is identical to the Deselect.req message. Its purpose is to end HSMS communications immediately and without exception or notifying the host. No response or acknowledge message is required.

Fig. 6 illustrates in detail how a DoS attack on SECS/GEM communications is carried out. As it happens in most cases, the preparator scans the network and passively tries to determine the nodes that are listening on port 5000, which is usually used for HSMS communications. The attacker captures and monitors the network traffic and captures the most recent reply message sent from the target machine. It is important to note that the chances of a successful attack carried out on response messages are higher than request messages because it usually takes a while to request another set of data in quick succession.

The DoS attack in Fig. 6 follows the same analogy, and the attacker waits for a linktest.req and linktest.res pair of messages exchanged between the host and equipment. At this stage, the attacker would intercept any control message (ex. linktest.res), modify header field SType=9 (which represents separate.req message) and increment SystemBytes value by 1 to launch DoS attack. The attacker may send these messages to both host and the equipment, which will teardown connections between the host and the equipment abruptly. The received message is considered legitimate because there is no mechanism available in SECS/GEM to validate the authenticity of the received separate.req message. The attacker may periodically or at random time intervals launch a replay-attack to converge it as a full-fledge DoS attack. Both the host and the equipment will remain unaware of the attack. The attacker then can send a connection establishment request on port 5000 to equipment to hold the connection. During this time period, the legitimate host would remain disconnect and unable to reestablish the communication link as SECS/GEM is a point-to-point communication protocol and only allows one active connection at a time.

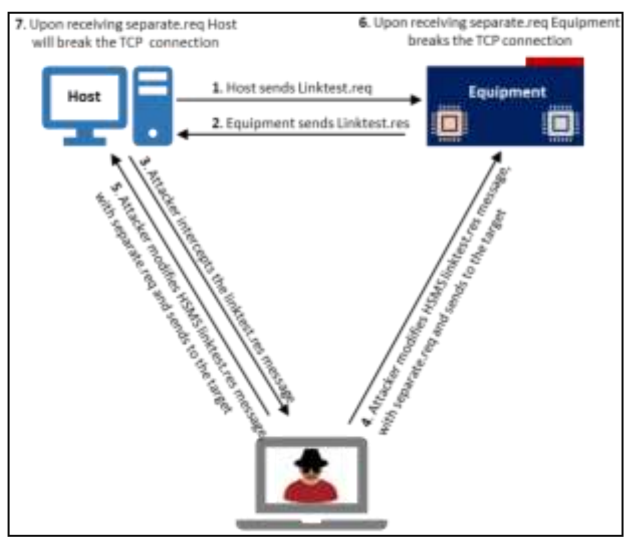

Fig. 6. Scenario of Capturing, Intercepting & Attacking SECS/GEM Communications.

Alternatively, by using TCP's RST flag to tear down the TCP connection established between the two communicating entities (i.e., host and the equipment), we were able to launch a DoS attack on SECS/GEM communications successfully. The equipment would change its status back to a NOT-CONNECTED state when it detects the broken TCP connection, and it would start listening for new incoming connection requests on the specified port address (i.e., usually 5000). At this stage, the attacker would establish a connection on the open port and hold a connection for an unspecified time. During this time frame, any attempt of connection establishment by the legitimate host will be ignored by the equipment. In our experiments, we witnessed that a simple application such as NC (a.k.a., Netcat) running on an attacker's machine suffices the requirement to establish a TCP connection with the equipment. This is because HSMS communication starts after successfully establishing a TCP connection (i.e., three-way handshake). We also found that the equipment continued to send requests for the HSMS link establishment to the attacker machine that simply did not respond to any of the equipment's messages. However, during this attack, the attacker held the TCP session, and the equipment will not accept any other connection until the current session expires. Hence, the attacker is able to hold the connection and disrupt the communication between a host and equipment as long as it is desired.

The DoS attack can also be launched on SECS/GEM communications using data messages. This is true because the HSMS standard limits HSMS connection to process messages as 1Hz, that is, one message per second. The attacker can send any data messages during this time to throttle that equipment's processing capabilities. Fig. 7 indicates the effective injection of the Separate.req message occurred in the HSMS connection establishment between the host and equipment, and subsequently, the equipment terminated the connection.

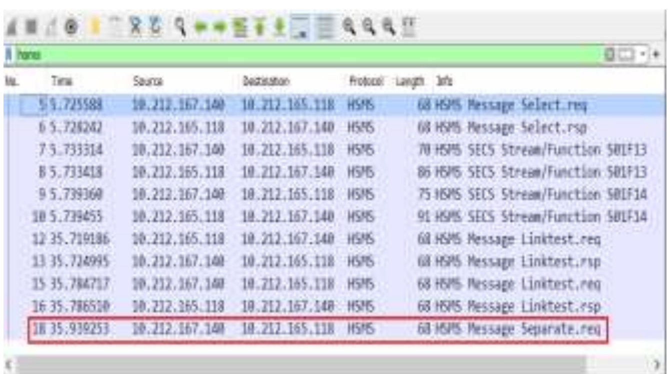

Fig. 7. The Successful Injection of Separate.Req Attack Message.

Detecting a DoS attack is difficult to traceback as it is never initiated by a rogue device; often, they are carried out by the footprints of a legitimate device from within the network.

B. Replay Attack

SECS/GEM messages exchanged between the host and equipment are highly important in order to control and monitor the equipment. In a normal communication mode, either side of the connection can request data. Upon receiving a request message, the target entity would reply with generated data for the specific request. SECS/GEM communication is carried out on HSMS protocol, which has a fixed header format and structure. If the SType field of the HSMS header in any message is 0, it means the message is a data message; otherwise, it will be considered a control message. Irrespective of the message type, an attacker may sniff the message and replay it with a changed payload to inflict damage or interrupt the overall production. HSMS has a sequence number field in its header called SystemBytes, which is monotonically increased for each transaction. A pair of request and response messages from host and equipment or vice-versa is called a transaction, and each transaction is identified with a unique sequence number (header field SystemBytes). However, each successive transaction will have a successive number of the previous transaction. This predictability enables attackers to launch a replay attack by just modifying SystemBytes contents. The replay attack would be devesting for the overall communication and may bring down overall communication, or it may adversely impact the equipment's behavior.

Upon receiving a connection establishment request, the attacker may intercept any control message (ex. select.res), modify header field SType=9 and increment SystemBytes header fields by 1 to launch a replay-attack, which will teardown connection between host and the equipment abruptly. The attacker may periodically or at random time intervals launch a replay-attack to converge it as a full-fledge DoS attack. Both the host and the equipment will remain unaware of the attack. At this stage, it will be very difficult to trace out such an attack on the equipment side; however, the careful investigation at the host will reveal that no such teardown command was initiated from the host, which will ultimately unfold the truth that the equipment was under DoS attack.

C. False Data Injection Attack

Originally in the smart grid domain, the definition of FDIA[4] was first introduced. Although the term sounds normal, it indicates that an intruder exploits sensor readings in such a way that undetected errors are inserted into state variables and calculated results. FDIA is not limited to the manufacturing industry only; cyber-criminals are involved in leveraging related attacks in other application areas such as healthcare, financial institutes, defense. Thus, FDIA has been one of the highest priority problems to contend with within today's highly perilous cyber world of dynamic adaptive systems.

Cyber-criminal can launch FDIA and inject falsified data into blind-trusted communication occurring between two SECS/GEM entities. The receiving entity cannot differentiate between a legitimate and a bogus message, and it will process it nevertheless. The impact and intensity of the falsified data injected depend on the purpose of the attack; however, it can be imagined that under such attack and ill-intention data injected into the production system might disrupt the overall processing or at least will undermine the quality of the product.

V. Experiments and Results

In this section, the various attacks are launched on different SECS/GEM communication processes carried out between a host and equipment. The details of hardware specifications are shown in Table II, and the Testbed attack scenario is illustrated in Fig. 8. The SECS/GEM communication has been started between a host and equipment E2 in production $Line_n$.

The experiments were conducted to observe the SECS/GEM behavior during various attacks. The Python implementation of SECS/GEM host and equipment was used to emulate SECS/GEM entities' behavior and functionality. The necessary code level changes have been adapted to mimic the attack behaviors in the host-side of the emulator. In order to successfully carry out cyber-attacks on SECS/GEM communications, it is important to eavesdrop and capture the packets while in transit and then modify them to launch attacks such as DoS attack, replay attack, and FDIA. For this purpose, the Python-based Scapy tool is used to capture, modify, and transmit forged packets to the target entity [26]. The attacks were repeated 30 times for each attack scenario, and results were measured for each process. The equation (1) below is implemented to measure the ability of the SECS/GEM processes in preventing the attacks carried on SECS/GEM communications [27]:

$$ATTACK_{SR} = 1 - F / N \quad (1)$$

where, $ATTACK_{SR}$ represents the specific attack's success rate, N represents the number of times forged messages are injected, and F signifies the specific attack type failed a number of times. According to the $ATTACK_{SR}$ definition, it was found that if $ATTACK_{SR}$ is 1, this means that the attack is successful. Nevertheless, if $ATTACK_{SR}$ is 0, this indicates that the specific attack on the SECS/GEM process can be susceptible to DoS. Table III illustrates the experimental results of each experiment conducted on SECS/GEM's processes, such as control messages and data messages.

Based on Table III, the results revealed that the SECS/GEM communication is completely vulnerable to cyber-attacks. Following are our findings:

- The key issue with SECS/GEM protocol is that it does not provide any security mechanism to guard against cyber-attacks; thus, all data and control messages can be intercepted and tampered with by attackers, and it is up to the mercy of attackers to determine whether to initiate an effective attack by any manner they want.
- SECS/GEM messages are packed in the binary-encoded format to achieve high data density with little overhead. However, these messages are still readable and can easily be intercepted and converted into plaintext. Binary encoding thus does not offer any safeguard against attacks or hinders attackers from extracting meaningful information.
- The communication can be initiated by any host/equipment or rouge machine anytime without any validity or verification of the legitimacy. There is no authentication mechanism to check the legitimacy of the originator of the message.
- SECS/GEM offers a method to assess the freshness of the message by using SystemBytes; however, the SystemBytes value is monotonically incremented, and therefore it is simpler to estimate the next potential value from the current value. As a result, the receiver of the message cannot discern whether a message has been altered just by analyzing the contents of SystemBytes.
- SECS/GEM messages are paired as primary and secondary messages. Primary messages are request messages, whereas secondary messages are reply messages. SECS/GEM messages are binary encoded and exchanged in plaintext; however, they are still readable, and there is no way to detect if the messages are modified while in transit.
- Messages are not encrypted; therefore, the entire communication is susceptible, and the attacker can easily profile communication details and steal valuable information and business secrets.

TABLE II. TESTBED DEVICES AND THEIR SPECIFICATIONS

Device Role	Specifications	OS
Host	**CPU:** Intel(R) Ci7-9750H @ 2.60GHz x 8 **RAM:** 24 GB	Win10
Equipment	**CPU:** Intel® Ci7-3770M @ 3.4GHz x 8 **RAM:** 8 GB	Win10
Attacker PC	**CPU:** Intel(R) Ci3-330M @ 2.13GHz x 2 **RAM: 8 GB**	Ubuntu 2020.3
Switch	Cisco Catalyst 2960 Fast Ethernet	-

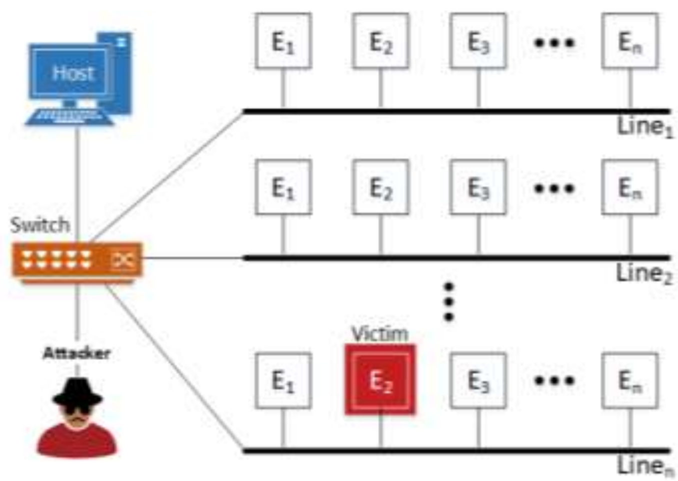

Fig. 8. Testbed Environment: An Attack Scenario.

TABLE III. EXPERIMENTAL RESULTS

Attack Type	Message Type	Experiment Count[N]	Attack Failure[F]	$ATTACK_{SR}$
DoS	Control TCP[RST]	20 20	0 0	1 1
Replay	Control Data	20 20	0 0	1 1
FDIA	Control Data	20 20	0 0	1 1

VI. Conclusion and Future Outlook

SECS/GEM has been seen as the cornerstone to semiconductor industries, and it has been in profound use since its inception. It aims to provide machine-to-machine communication, and it provides instantaneous (i.e., real-time) insights of factory equipment for effective decision making and performance boost up. SECS/GEM messages are binary encoded and exchanged plaintext without any authentication and encryption. As SECS/GEM does not offer any security mechanism, all these messages are subject to cyberattacks. The experimental results revealed that the SECS/GEM processes are vulnerable to cyberattacks. Therefore, there is a need for a comprehensive security framework that prevents these cyberattacks and offers authentication, confidentiality, and integrity for secure and reliable communication. The authentication mechanism will ensure that messages are exchanged between legitimate SECS/GEM entities. The integrity mechanism will ascertain that the contents within messages are not altered during transit, and the confidentiality mechanism will ensure that the messages are not readable while in transit. Our future direction is focused on all these issues and will provide a complete security framework that will protect SECS/GEM communications from cyberattacks discussed in this paper.

References

[1] E. Oztemel and S. Gursev, Literature review of Industry 4.0 and related technologies, *Journal of Intelligent Manufacturing*, Vol. 31, No. 1, pp. 127–182, January, 2020.

[2] G. *Culot*, F. Fattori, M. Podrecca, and M. Sartor, Addressing Industry 4.0 Cybersecurity Challenges, *IEEE Engineering Management Review*, Vol. 47, No. 3, pp. 79–86, September, 2019.

[3] S. A. Laghari, S. Manickam, and S. Karuppayah, A Review on SECS/GEM : A Machine-*to*-Machine (M2M) Communication Protocol for Industry 4 . 0, *International Journal of Electrical and Electronic Engineering & Telecommunications*, Vol. 10, No. 2, pp. 105–114, March, 2021.

[4] N. Tuptuk and S. Hailes, Security of smart manufacturing systems, *Journal of Manufacturing Systems*, Vol. 47, pp. 93–106, April, 2018.

[5] S. Morgan, 2021 Report: Cyberwarfare In the C-Suite, January, 2021.

[6] Sydney Peng, The Real Reason Behind the TSMC Cyber Attack, *CommonWealth Magazine*, November, 2018.

[7] F. Chen, Y. Huo, J. Zhu, and D. Fan, A Review on the Study on MQTT Security Challenge, *SmartCloud 2020: IEEE International Conference on Smart Cloud*, Washington DC, USA, 2020, pp. 128–133.

[8] S. Hernández Ramos, M. T. Villalba, and R. Lacuesta, MQTT Security: A Novel Fuzzing Approach, *Wireless Communications and Mobile Computing*, Vol. 2018, 2018.

[9] C. Patel and N. Doshi, A Novel MQTT Security framework In Generic IoT Model, Procedia *Computer Science*, Vol. 171, pp. 1399–1408, January, 2020.

[10] A. Rahman, S. Roy, M. S. Kaiser, and M. S. Islam, A Lightweight Multi-tier S-MQTT Framework to Secure Communication between low-end IoT Nodes, *5th International Conference on Networking, Systems and Security* (NSysS), Dhaka, Bangladesh, 2018, pp. 1–6.

[11] N. Mühlbauer, E. Kirdan, M. O. Pahl, and G. Carle, Open-Source OPC UA Security and Scalability, 25th *IEEE International Conference on Emerging Technologies and Factory Automation, ETFA*, Vienna, Austria, Vol. 1, 2020, pp. 262–269.

[12] Mühlbauer, Nikolas, Erkin Kirdan, Marc-Oliver Pahl, and Georg Carle, Open-Source OPC UA Security and Scalability, *25th IEEE International Conference on Emerging Technologies and Factory Automation*, Vienna, Austria, September, 2020, pp. 262-269.

[13] Z. Shelby, K. Hartke, and C. Bormann, The Constrained Application Protocol, RFC-7252, January, 2014.

[14] M. Iglesias-Urkia, A. Orive, and A. Urbieta, Analysis of CoAP Implementations for Industrial Internet of Things: A Survey, *Procedia Computer Science,* Vol. 109, No. 2016, pp. 188–195, January, 2017.

[15] M. Friesen, G. Karthikeyan, S. Heiss, L. Wisniewski, and H. Trsek, A comparative evaluation of security mechanisms in DDS, TLS and DTLS, *Kommunikation und Bildverarbeitung in der Automation*, Berlin, Heidelberg, 2020, pp. 201–216.

[16] F. T. Ewe, K. S. Yeo, S. C. Yeoh, and C. T. Khoh, Data Analysis on SMT Reflow Oven with SECS/GEM Communication Protocol, *ISCAIE 2020 - IEEE 10th Symposium on Computer Applications and Industrial Electronics*, Penang, Malaysia, 2020, pp. 118–124.

[17] F. Stoop, G. Ely, R. Menna, G. Charache, T. Gittler, and K. Wegener, Smart factory equipment integration through standardised OPC UA communication with companion specifications and equipment specific information models, *International Journal of Mechatronics and Manufacturing Systems*, Vol. 12, No. 3–4, pp. 344–364, 2019.

[18] A. Weber, B. Grey, B. Rubow, D. Francis, D. Lindsey, J. Lopez, J. Cravotta, M. Bennet, T. Hutchison, *Features & Benefits of GEM: A guide to some of the main features and benefits of GEM – SEMI Standard E30*, Cimetrix, 2019.

[19] G. Baweja and B. Ouyang, Data acquisition approach for real-time equipment monitoring and control, *13th Annual IEEE/SEMI Advanced Semiconductor Manufacturing Conference: Advancing the Science and Technology of Semiconductor Manufacturing*, Boston, MA, USA, 2002, pp. 223-227.

[20] A. B. Nelson, P. M. K. Chow, V. A. Snowball, S. Chung, and A. Majumdar, High-speed SECS message services (HSMS) pass-through including bypass. United States Patent US 8, January, 2012.

[21] L. Ma, N. Zhang, and Z. Zhang, Tool Efficiency Analysis model research in SEMI industry, *4th International Conference on Energy Materials and Environment Engineering (ICEMEE 2018)*, Selangor, Malaysia Vol. 38, 2018, pp. 1–5.

[22] J. Postel, Transmission control protocol, RFC- 793, September, 1981.

[23] T. Sauter and A. Treytl, Semiconductor equipment and materials international interface and communication standards: An overview with case studies, *Industrial Communication Technology Handbook,* Second Edition, CRC Press, 2015.

[24] J. E. Rubio, C. Alcaraz, R. Roman, and J. Lopez, Current cyber-defense trends in industrial control systems, *Computers & Security*, Vol. 87, p. 101561, November, 2019.

[25] S. Pfrang and D. Meier, On the detection of replay attacks in industrial automation networks operated with profinet IO, *3rd International Conference on Information Systems Security and Privacy*, Porto, Portugal, 2017, pp. 683–693.

[26] A. Al-Ani, M. Anbar, S. A. Laghari, and A. K. Al-Ani, “Mechanism to prevent the abuse of IPv6 fragmentation in OpenFlow networks,” PLoS One, vol. 15, no. 5, 2020.

[27] A. K. Al-Ani, M. Anbar, A. Al-Ani, and D. R. Ibrahim, Match-Prevention Technique Against Denial-of-Service Attack on Address Resolution and Duplicate Address Detection Processes in IPv6 Link-local Network, IEEE Access, Vol. 8, pp. 27122-27138, January, 2020.

A Similarity Score Model for Aspect Category Detection

Zohreh Madhoushi[1], Abdul Razak Hamdan[2], Suhaila Zainudin[3]
Faculty of Information Science and Technology
Universiti Kebangsaan Malaysia 43600 Bangi, Selangor, Malaysia

***Abstract*—Aspect-based Sentiment Analysis (ABSA) aims to extract significant aspects of an item or product from reviews and predict the sentiment of each aspect. Previous similarity methods tend to extract aspect categories at the word level by combining Language Models (LM) in their models. A drawback for the LM model is its dependence on a large amount of labelled data for a specific domain to function well. This work proposes a mechanism to address labelled data dependency by a one-step approach experimenting to decide the best combinatory architectures of recurrent-based LM and the best semantic similarity measures for fostering a new aspect category detection model. The proposed model addresses drawbacks of previous aspect category detection models in an implicit manner. The datasets of this study, S1 and S2, are from standard SemEval online competition. The proposed model outperforms the previous baseline models in terms of the F1-score of aspect category detection. This study finds more relevant aspect categories by creating a more stable and robust model. The F1 score of our best model for aspect category detection is 79.03% in the restaurant domain for the S1 dataset. In dataset S2, the F1-score is 72.65% in the laptop domain and 75.11% in the restaurant domain.**

Keywords—Aspect category detection; language model; semantic similarity

I. Introduction

The first task in Aspect-based Sentiment Analysis (ABSA) is to detect aspects of an item or product from reviews and categories each aspect into a specific group. There are different methods to detect aspects; namely, language rule methods or LM, sequential methods, topic model methods, deep learning methods, and hybrid methods, which are the combination of the above methods [1]. We have seen exciting outcomes in various NLP tasks in recent years using these emerging models [2]–[5]. Regardless of the existing techniques, the most crucial point in any Natural Language Processing (NLP) task is to find a way to make machines understand language or text.

Deep learning techniques automate the process of representation learning in multi computational layers. These techniques have enabled researchers to improve state of the art for many NLP tasks such as Sentiment Analysis (SA) [6], [7] significantly and in other domains (image, speech, etc.). A drastic advancement happened in the text representation, and many LMs were developed, such as Word2Vec [8], deep LM [9], [10]. However, these emerging LMs have not yet fully addressed aspect category detection, mainly because there is no study to design experiments assessing the effect of different recent advanced LMs on the specific task of aspect category detection. This work hypothesis is that a general deep LM can be used for any specific task in NLP. As [11] states, using a pre-trained LM is better than starting a model with random weights therefore Deep LM is used as a form of transfer learning in this work. The task of a simple LSTM-based LM is to predict the next word in a large corpus. Instead of learning from scratch using random weights, the representation created with the proposed LM can be a better starting point for another LM. Then, it can be used for a specific task in a more related domain.

On the other hand, previous ABSA methods tend to extract aspect terms and categories them in two separate steps. Also, they set model threshold values and seed words for aspects categories manually. Domain-specific models are often not practical for this task. Various semantic similarity measures were proposed in the literature such as WordNet, NGD, Cosine and Soft Cosine. A few works utilize these semantic similarity measures to extract aspect categories in one phase; however, all works performed word-level similarity measurement. Recent works find the semantic similarity of a pair of text [12], [13] at the sentence level. But there is a lack of investigation addressing the effect of semantic similarity measures for the aspect category detection task at sentence level in the literature.

The main contributions of this paper are summarized as follows. First, this study presented a mechanism based on two semantic similarity measures and two standard LMs. The proposed mechanism is based on sentence-level similarity measurement, which extracts aspect categories in one step. The best combination of recurrent language and semantic similarity measures is investigated. This helps the researchers to find the best recent options for semantic similarity measure and neural LM for this task. Second contribution is that the model developed based on the above mechanism works in one step instead of two steps by utilizing semantic similarity measures at both word and sentence level and identifies aspect categories related to implicit aspects, mainly because of using the neural LM and still working in two different areas without any labeled data. The model works without setting seed words for each aspect category. The last contribution is solving the problem of setting several thresholds manually. The model proposed by current study set the thresholds automatically without any human intervention. Therefore, the model has reduced the amount of manual human intervention by removing the need for seed words and automatically setting thresholds. The proposed similarity score model is able to fine-tune to any new domain by only adding pre-known aspect categories for the new domain and more related domain reviews without any labeled data.

This paper is organized as follow. In Section 2, the literature for aspect category detection is reviewed. Section 3 proposed a new model based on existing deep LM and semantic similarity measure. The experiment and result discussion on the dataset of this study is presented in Section 4. Finally, the study is concluded in Section 5.

II. Background of Study

There are many current works that focus on Language Rules Models [14]–[17]. These effective syntactic LM still have room for improvement. However, it is challenging to design a set of rules to perform well due to natural languages' flexibility. It also appears from the review that researchers mostly focused on extracting the aspect term instead of aspect category. Aspect category detection is similar to explicit and implicit aspect extraction and then grouping under one category. Explicit aspects are those that one can find the aspects clearly stated as nouns or noun phrases in a review, for example,' picture quality' in "The picture quality of this phone is great." Implicit aspects are not clearly stated in a review but are implied indirectly, for example, 'price' in "This laptop is so expensive". There are language rule models in the literature that extract implicit aspects. These models' problem is that they always need to extract an explicit or implicit aspect term to group them under one category. The above causes several category names creation for one unique category in new datasets. In other words, there are no predefined standard categories that one can assign aspect terms to those categories. They cannot identify aspect categories directly from a review text. However, most of these model does not group the extracted terms into predefined categories in the literature [16], [18]. For the aspect category detection model to be practical, one crucial step is to propose a model that works in fewer steps.

Until recently, a few studies [15], [19] attempted to extract aspect categories directly from review text in a single step using language rule methods. The intermediate task of aspect term extraction is required for most models [16], [20], [21] However, it is hard to use these models on new datasets since manual tuning of various thresholds is required [15], [22]. Another problem of recent models is that they need to find some synonyms for each aspect, in which the result depends on the selection of these synonyms words. They need these lists for every aspect and for every domain, which is a time-consuming activity. Various manual thresholds setting required for new datasets in the models that use similarity to predefined categories [15], [19].

The number of models focused on implicit aspect extraction increased in recent years. While aspect category detection can handle the implicit aspects and explicit aspects, it is much harder to extract implicit aspects with aspect term extraction. Sequential supervised models [23], [24] are better than language rule models to extract implicit aspects. These models' problem is that they need lots of labeled data, which is not easy to get for each area and domain separately. Again, for the aspect category detection models to be practical, the models must work in multiple domains or at least easy to apply or transfer to any new domain. Sequential and Modern deep learning models cannot work in different domain or need lots of training data in each domain [25]–[29]. Topic models on the other hand are too statistical centric which this study can hardly find improvement for it.

This study continues [19] for the model not to use any labeled data. The difference is that, instead of clustering and getting the similarity of a cluster with aspect categories, this study utilizes a representation from sentence-level deep LM. The proposed model does not require any seed words to be set for each aspect category anymore. There is a recent similar work in the literature solving the same issue. [30] rely on the similarity of sentence words and some seed aspects utilizing Word2Vec, Glove and Fastext. They state that their model performs the same as recent neural models for aspect extraction with a less computational cost. Their model is very similar to our similarity score model. However, the approach of finding more than one aspect category for a sentence is not explained clearly.

We have performed a comparison to prove the novelty of the proposed model. The state of the art is summarized via Table I.

The limitations of the previous models are summarized in the last column. The main limitations are first they perform the task of aspect category extraction in two separate phases; second, they need labeled data in every domain; third, only the word level similarity is performed, lastly, they need to set the parameters manually.

TABLE I. ASPECT CATEGORY DETECTION MODELS

Method of aspect category detection	**Steps of aspect category detection**	**Author**	**Dataset**	**Domain**	**Result (average)**	**Limitation**
Language rule (Dependency relation + similarity)	2	Garcia et al. (2014)	SemEval 2015	Laptop Restaurant Hotel	F-score aspects category: Laptop: 24.94 Restaurant: 41.85 Acc. Sentiment: Laptop 68.38 Restaurant 69.46 Hotel 71.09	- Cannot find implicit aspects and sentiment. -It cannot detect context orientation of opinion word.
Language rule (Graph based)	1	Schouten et al. (2017)	SemEval 2014	Restaurant	F1-score:67.0	-Needs to set synonym words for every aspect. -Lots of parameter setting is required.
Language rule (Similarity)	1	Ghadery et al. (2018)	SemEval 2014	Restaurant	F1-score:76.98	-Needs to set synonym words for every aspect. -Word level similarity is performed
Language rule (Similarity)	2	Gaillat et al. (2019)	SE-2015	Financial Microblogs	Accuracy: 42.5	The Word2Vec model is trained on the Google news corpus -Word level similarity is performed
Language rule (Lexicon based)	2	Alqaryouti et al. (2019)	Dataset of (Alqaryouti et al. 2019)	government smart apps	Aspect category detection: Precision Recall F-score 92.63. 84.03 88.12 Sentiment Accuracy: 93.01%	Intermediate task of aspect term extraction is required.
Deep Learning (Auto-encoder with attention)	1	He et al. (2017)*	Citysearch corpus BeerAdvocate	Restaurant review beer review	F1-score: Restaurant: 79.25 Beer: 73.56	-It is domain dependent. Needs large labeled data.
Deep Learning (LSTM)	1	Ma et al. (2018)	SemEval-2015	Restaurant	Aspect extraction: F1-score: 0.75 Sentiment detection Acc. 74.11	It is domain dependent. Needs large, labeled data.

III. PROBLEM STATEMENT

A group of similarity techniques emerged with the advance of text representations in language rule methods to extract aspect categories were summarized in Table I. Nevertheless, only one of these models perform the task in one single step. It is also hard to use these models on new datasets since manual tuning of various thresholds is required. Another problem of these models is that they need to find some synonyms for each aspect which the result depends on the selection of these synonym words. They need these lists for every aspect and for every domain, which is a time-consuming task. All these methods utilize the word level similarity measure.

Distributed representation of sentences and neural LMs are a good source of semantic similarity measurement in the literature. To the best of our knowledge, combining the sentence similarity measurement techniques and deep LMs have not been addressed for the aspect category detection task. Considering that deep learning model that used in the literature for this task are supervised and domain-dependent, this study aims to propose a mechanism for aspect category detection using sentence similarity measurement and recurrent-based LM without using labeled data.

The author in [31] defines recurrent language model where an input vector sequence x = (x1, . . . , xT) is passed through weighted connections to a stack of N recurrently connected hidden layers to compute first the hidden vector sequences hn = (hn1 , . . . , hn T) and then the output vector sequence y = (y1, . . . , yT). Each output vector yt is used to parameterize a predictive distribution Pr(xt+1|yt) over the possible next inputs xt+1. The first element x1 of every input sequence is always a null vector whose entries are all zero; the network, therefore, emits a prediction for x2, the first real input, with no prior information.

The hidden layer activations are computed by iterating the following equations from t = 1 to T and from n = 2 to N. W terms denote weight matrices in equation below. Wihn is the weight matrix connecting the inputs to the nth hidden layer, Wh1h1 is the recurrent connection at the first hidden layer, and so on. The b terms denote bias vectors, and H is the hidden layer function. Given the hidden sequences, the output sequence is computed as follows:

$$h_t^1 = H(W_{ih^1}x_t + W_{h^1h^1}h_{t-1}^1 + b_h^1)$$

$$h_t^n = H(W_{ih^n}x_t + W_{h^{n-1}h^n}h_t^{n-1} + W_{h^nh^n}h_{t-1}^n + b_h^n)$$

$$\hat{y}_t = b_y + \sum_{n=1}^{N} W_{h^ny}h_t^n$$

$$y_t = \mathcal{Y}(\hat{y}_t)$$

where y̑ is the output layer function. The objective function is cross entropy error as the sum over the entire vocabulary at time-step t. |V| is the vocabulary size.

$$J^{(t)}(\theta) = -\sum_{j=1}^{|V|} y_{t,j} \times log(\widehat{y_{t,j}})$$

The entire network therefore defines a function, which is parameterized by the weight matrices, from input histories x1:t to output vectors yt. The output vectors yt are used to parameterize the predictive distribution Pr(xt+1|yt) for the next input. Network direction, layers and variation can be experimented to find the best combination for the LM.

Based on the above discussion and limitations discussed in previous section, there are two general problems in this study.

1) Lack of utilizing existing recurrent-based LMs and experiment on finding the best combinatory architectures of LMs and the best semantic similarity measures for aspect category detection task.

2) Lack of aspect category detection model for fetching aspect categories without the intermediate task of aspect (explicit and implicit) term extraction using no labeled data.

IV. Materials and Methods

The idea to extract the most related aspect category is that with a suitable vector representation of a sentence and pre-known aspects both, a comparison can be performed to find the similarity. The data sets of this study include a list of aspect categories for each area. Even if the list is not available, people usually talk about these aspects found in online review websites. These pre-known aspects are a good source of detecting other aspects with similar meanings. Therefore, a pre-trained Word2Vec LM is used for training. Then, another LM is trained on top of the initial LM with Amazon product review dataset in fourteen areas at the sentence level, and then the model is fine-tuned for the in-domain dataset which is on laptop, restaurant and hotel. Fine-tuning means training an existing model with a new dataset or continuing the current LM training with more data. Fine-tuning in deep learning model means only the model architecture or weights of the model is used in a new model. In this study the initial layers are frozen, not to change the weights of the pretrained LM and top layer are trained. This approach has been used in recent LMs [10], [32]. In this study, the existing Skip-gram LM is fine-tuned with a new dataset and LSTM-based LM is fine-tuned by freezing the initial layer and continuing the training with the more related dataset.

Once the specific LM is trained, the sentence representation that is created can be used for any NLP task. Therefore, for any piece of text a meaning that this LM creates can be represented. This information is a good source for comparing texts. Texts or sentences with similar meaning are close in space. The sentence representation of the final LM is used to extract aspect category detection by comparing the representation of a list of aspects with each review in our in-domain dataset. Therefore, for this LM, the unlabeled S1 and S2 datasets, the list of our aspect categories, a piece of text with meaning and dataset M, is appended. The second and final LM representation will be used to get the semantic similarity of review text and aspect categories. Fig. 1 shows the proposed idea in action. The first LM from left is famous Skip-gram LM which has been pre-trained on Google News. The second LM is the same Skip-gram LM that was fine-tuned on Amazon review dataset (A) with 14 areas and S1 and S2, which are laptop, restaurant, and hotel area. The third and fourth LMs are LSTM-based LMs which simply predicts the next word. The unlabeled datasets S1 and S2 and dataset A are appended.

The bidirectional form of LSTM is used for the LM. This study does not use the LM for text generation; therefore, predicting the next word in both directions is useful for getting better representation of words and sentences. The network is fed with representation of each word in the string that is gained from the training. The model is used for aspect string set (A) and sentence string set (S). Aspect string and sentence string is defined as follow:

$$a = x_{a_1}, x_{a_2}, \dots, x_{a_j}$$

$$s = x_1, x_2, \dots, x_j$$

Where x_j, x_{aj} are vector representation of each word in sentence and aspect string respectively which is gained from the LSTM LM. After freezing the model, maximum, minimum, average and last cell representation are concatenated to define each sentence vector (h_j) and each aspect vector (h_{aj}). If the Soft Cosine similarity of h_j with any of aspects vector (h_{aj}) is more than a specific threshold then the candidate aspect is remained, otherwise it will be ignored. Cosine similarity is a measure of similarity between two vectors of an inner product space that measures the cosine of the angle between them. The Soft Cosine of two vectors is introduced by Sidorov et al. (2014). They propose to modify the calculation of cosine similarity taking into account similarity of features. They named the traditional cosine as “hard cosine”, which ignores similarity of features. Given two vectors of attributes, a and b, the Soft Cosine can be derived by using the following formula:

$$soft - cosine(a, b) = \frac{\sum\sum_{i,j=1}^{N} a_{ij} b_{ij}}{\sqrt{\sum\sum_{i,j=1}^{N} a_{ij}^2}\sqrt{\sum\sum_{i,j=1}^{N} b_{ij}^2}}$$

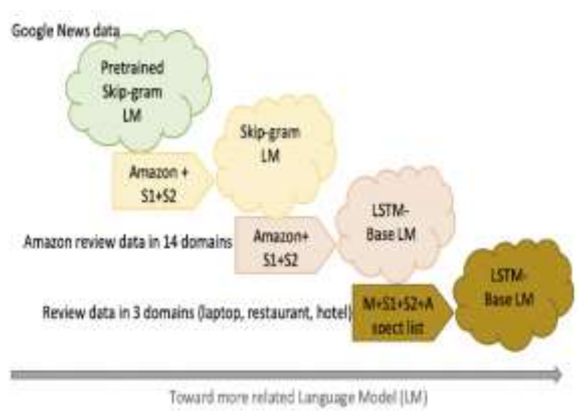

Fig. 1. Fine-tuning LM for the Specific Domain.

To speed up, get rid of for loops and reduce the complexity, vectorization is used for the implementation of similarity measurement. Instead of using each sentence and aspect vector at a time to measure the Soft Cosine similarity, vectorization gets a whole set of sentence and aspect vectors as matrix and compute the similarity of two matrices. Sentence matrix H and aspect matrix H_a is defined as follow, where *n* and *m* are the number of samples in sentence set (S) and aspect set (A) respectively:

$$H = [h_{j1}, h_{j2}, \ldots \ldots, h_{jn}]$$

$$H_a = \left[h_{aj1}, h_{aj2}, \ldots \ldots, h_{ajm}\right]$$

If the similarity surpasses a specific threshold, the model adds it to aspect set one. The similarity score model has two modules of deep and non-deep learning. The deep learning module is explained above. Fig. 2 shows the process of this model. This model finds the best result with a simple linear search. A score function is used to calculate a similarity score for each category in our dataset.

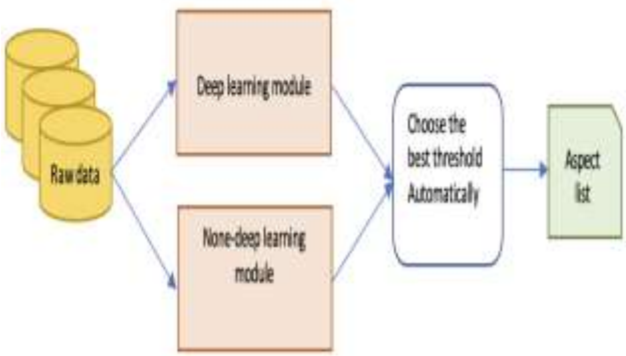

Fig. 2. Similarity Score Model Process.

The similarity score is a combination of the deep and non-deep learning score. Let |pos| be a set of all nouns, verbs, adjectives, and adverbs of a given sentence x and |aspect| be a set of our pre-known aspects. The similarity of the non-deep learning part for one aspect category of the given sentence is calculated from the maximum Soft Cosine similarity of that category to all words of that review after pos-tagging, which this work named it |pos|, is shown in Equation 1. Let h and h_a be the sentence and aspect representation that is taken from our LSTM based LM for the same given sentence and aspect respectively. The similarity of the deep learning part for this aspect category is calculated from the Soft Cosine similarity of h and h_a. Equation 3 shows the calculation of this score. Also, both similarity scores are calculated using sigmoid function on deep and non-deep learning similarity result same as our first model as in equation 2 and 4. Our final score is calculated with the interpolation of second score within the first score as shown in equation 5.

V. Experiment

Previous sections presented our models for aspect category detection. This section explains about the dataset that is used in this study and discusses the evaluation method for this task. We are interested in producing a sentence representation that keeps the sentiment of several aspects from different areas. Therefore, this study chooses the Amazon product review dataset (A) introduced in [33] as a training corpus to learn the distributed representation of the sentences. This dataset contains over 82 million product reviews from May 1996 to July 2014, amounting to over 38 billion training bytes. The second dataset is the dataset of SemEval 2014 competition task 4 (S1).

A. Baselines

The model is compared to the state-of-the-art models for aspect category detection. To have a fair comparison, the comparison partners should be aspect category detection models with no labeled data. Also, they should work on a multi-domain dataset. But due to lack of enough similar work for this task, this study shall compare the model with nearest work available. The models are compared with seven baselines. These baselines are for aspect category detection and not for aspect term extraction. Two baselines are on S1, three baselines are on S2 and one baseline is on both datasets. The following subsections describe about these baselines separately. Language rule baselines are presented in subsections a, b and c. Deep learning baselines including the winner of SemEval 2015-task 12 is remined in sub section d. The result of aspect category detection is presented in these works either as a direct task or as a subtask of aspect term extraction.

The first baseline is V3 [20] is a language rule model on both S1 and S2 that does not need labeled data. They use a similar implementation of [34] on SemEval 2014 task 4 dataset to extract aspect terms first and then compare with the category words using the similarity measure. The category with the highest similarity measure is then selected if it surpasses a manually set threshold. And d is SemEval 2014 task 4 baselines.

|pos| = p1, ..., ps
|aspect| = a_1, ..., a_k

$$SentSim1_{ai}(x) = Max_{j=1}^{|p|}\left(Softcosim\left(p_j, a_i\right)\right) \quad (1)$$

$$SentScore1_{ai}(x) = \frac{e^{SentSim1\_ai\,(x)}}{1+e^{SentSim1_{ai}(x)}} \quad (2)$$

$$SentSim2_{ai}(x) = Softcosim(h, h_{ai}) \quad (3)$$

$$SentScore2_{ai}(x) = \frac{e^{SentSim2\_ai\,(x)}}{1+e^{SentSim2_{ai}(x)}} \quad (4)$$

$$Aspect\_Score = \alpha * SentScor1 + (1-\alpha) * SentScore2$$
(5)

Spreading activation is the second baseline. [15] developed a model called spreading activation that does not need labeled data. They used some seed words and co-occurrence matrix of words to create a digraph for aspect category detection using association rule mining. The similarity baselines are the closest baselines to our model since they try to find the similarity of a given sentence to some pre-known categories. The baseline is [19] model. They use similarity of average word vectors to pre-known aspect categories. They cluster sentences and use the closest cluster's similarity to a given sentence as different similarity measurement. Our model is very similar to [19]. The difference is instead of averaging the word embedding of all the words in a sentence; the sentence embedding is gained from the LSTM based LM. Also, instead of clustering sentences to get the second similarity measurement to the pre-known aspect categories, sentences are POS-tagged. The similarity of each selected word to the pre-known aspect categories is calculated.

One of the deep learning baselines is SemEval 2015-task 12, NLANGP [35], on S2. They used feedforward network with sigmoid to train binary classifiers for each category in the training set. Another recent deep learning baseline is [36]. They proposed an LSTM base model which combines implicit and explicit knowledge. The model adopted a sequence-encoder and a self-attention mechanism to calculate and incorporate common-sense knowledge into LSTM-based model to jointly extract aspect categories and predict sentiment for them.

B. Result and Discussion

The developed models can solve the problems that we discussed in the previous models. Both models use no labeled data. They performed the aspect category detection in one single step. The models can identify aspect categories for implicit aspect as well.

Cosine is the most common similarity measurement method, and Soft Cosine is an improvement over it. There are also modern LMs in the literature which Word2Vec and LSTM-based LMs are most common among them. We compare the F1-score of aspect category detection using two similarity measurement method, namely Cosine and Soft Cosine and two LMs, namely Word2Vec and recurrent base LM, with a few architecture differences on S1 and S2 respectively. Soft Cosine with two layers Bi-LSTM initialized with Word2Vec trained on Amazon dataset shows better performance than other combinations by scoring F1 score of 76.25 for Laptop and 75.11 for Restaurant. Therefore, this combination is used for the rest of the comparisons with baselines of this study for aspect category detection.

The comparison is done comparing the baselines F1 score for aspect category detection in two domains. Consider that the similar work in the baselines, [15], [19], need to set a large number of seed words for each aspect category. The result is undoubtedly related to choosing the right list of seed words. The model of this study does not need to choose a set of synonyms for each aspect category. Also, this model sets the similarity threshold automatically which makes it more robust and applicable to different datasets and areas. The F1-score results of dataset S1 and S2 are presented in Tables II and III on S1 and S2, respectively. Since there is no work in the baselines reported on the S1 laptop dataset; therefore, the presented results for S1 are only on the restaurant domain. Also, no work is reported to the author's knowledge on the aspect term or aspect category detection performance on the hotel domain on the S2 dataset. The presented results are from baseline's reported results, which have been explained in this study's scope. The result on S1 shows that the similarity score model performs better than the unsupervised language rule baseline V3 and only outperform by two supervised baselines. V3 is suitable to extract explicit aspects, but it performs so poorly when it comes to implicit aspects. Because the dataset is full of implicit aspects, its performance is lower than the similarity score model. This fact is more precise about the results on S2, and the reason is that most of the reviews contain implicit aspects. The similarity score model performs better than Ghaderi [19]. The model uses the average word vectors from pre-trained Word2Vec on Google news to represent each sentence, while for the similarity score model, the LSTM based LM is trained on a large related review dataset (A) to get the representation for sentences.

As presented in Section 4.3, 77% of the aspect categories are related to implicit aspect in this dataset. This number is 83% in S2. Therefore, the model can find explicit aspects and many of the implicit aspects in two different domains. The result also shows that the similarity score model is more stable than the baselines in various domains. As stated above a drawback of [19] and Spreading activation models is that the models need a set of manually pre-known aspect seeds for each category. They reported the result on S1 only. The number of aspect categories for laptop domain is 70. In this study, the work is replicated on the restaurant area for S2 dataset but not on laptop area because the seed data is not available for this area. To develop their model, one needs to generate an extensive list of seed words for 70 aspect categories which is not available in this study.

To find the best threshold alpha for the similarity score model a linear search is performed. Fig. 3 shows the sensitivity of the similarity score model to different thresholds. It shows that the optimum value for alpha is around 0.75 for laptop domain, about 0.70 for restaurant domain and around 0.65 for hotel domain.

Because of the high number of aspect categories in each domain, the results of classifiers NLANGP Toh & Su (2015) and Ma et al. (2018) are lower than similarity score model. Another drawback of these models is that they need a large number of labeled data to improve their performance on any dataset and domain.

TABLE II. ASPECT CATEGORY DETECTION F1-SCORE RESULTS ON S1.

Model/dataset	Restaurant
V3	60.20
Spreading activation	67.0
(Ghadery et al., 2018) [18]	76.98
Similarity score model	79.03

TABLE III. ASPECT CATEGORY DETECTION F1-SCORE RESULTS ON S2.

Model	Laptop	Restaurant
V3	24.94	41.85
NLANGP	50.86	62.68
(Ma et al. 2018) [34]	69.85	75.00
(Ghadery et al., 2018) [18]	-	73.96
Similarity score model	72.65	75.11

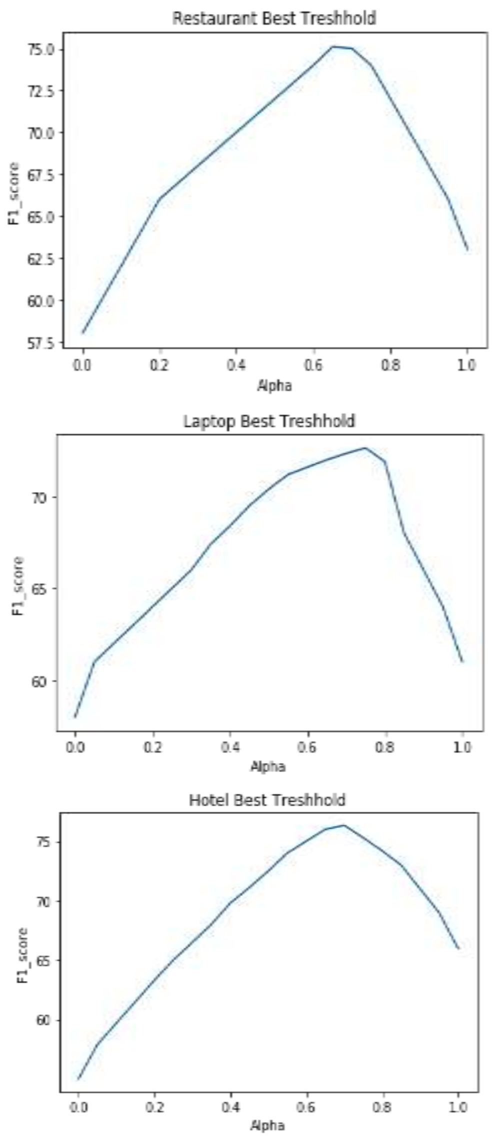

Fig. 3. Best Alpha Thresholds for our three Areas.

VI. Conclusion and Future Work

This study presented a new mechanism based on recurrent-based LM and semantic similarity measure for aspect category detection. A new model for aspect category detection was proposed, combining the above mechanism with existing language rules to extract aspect category in one step. The proposed similarity score model sets the similarity threshold automatically with a linear search. The f1-score results are presented for aspect category detection and compared with the baselines of this study on two datasets of S1 and S2. The work shows the priority of the proposed model compares to baselines on both datasets.

Unsupervised deep LMs may be effective in other NLP tasks since the context of previous and next sentences in a review affects the aspect category detection of the whole review. A direction for future is to work on review level instead of sentence level and extract all aspect categories of a given review. Also, one can investigate the best approach to replace ambiguous words in the review. For example, in a review with two sentences “the sushi is one of the best. You will find it delicious if you try it”. One can do dependency parsing to find out that ‘it’ relates to Sushi in the sentence and replace ‘it’ with sushi.

Acknowledgment

Acknowledgement for grants GUP-2020-089 dan TT-2020-015 from Universiti Kebangsaan Malaysia for the support.

References

[1] Z. Madhoushi, A. R. Hamdan, and S. Zainudin, “Aspect-Based Sentiment Analysis Methods in Recent Years,” Asia-Pacific J. Inf. Technol. Multimed., vol. 08, no. 01, pp. 79–96, 2019, doi: 10.17576/apjitm-2019-0801-07.

[2] Z. Madhoushi, A. R. Hamdan, and S. Zainudin, “Sentiment analysis techniques in recent works,” 2015, doi: 10.1109/SAI.2015.7237157.

[3] I. S. Ahmad, A. Abu Bakar, M. R. Yaakub, and M. Darwich, “Beyond sentiment classification: A novel approach for utilizing social media data for business intelligence,” Int. J. Adv. Comput. Sci. Appl., vol. 11, no. 3, pp. 437–441, 2020, doi: 10.14569/ijacsa.2020.0110355.

[4] S. M. Al-Ghuribi, S. A. Mohd Noah, and S. Tiun, “Unsupervised Semantic Approach of Aspect-Based Sentiment Analysis for Large-Scale User Reviews,” IEEE Access, vol. 8, no. December, pp. 218592–218613, 2020, doi: 10.1109/ACCESS.2020.3042312.

[5] J. Awwalu, A. A. Bakar, and M. R. Yaakub, “Hybrid N-gram model using Naïve Bayes for classification of political sentiments on Twitter,” Neural Comput. Appl., vol. 31, no. 12, pp. 9207–9220, 2019, doi: 10.1007/s00521-019-04248-z.

[6] D. S. Sachan, M. Zaheer, and R. Salakhutdinov, “Revisiting LSTM networks for semi-supervised text classification via mixed objective function,” 33rd AAAI Conf. Artif. Intell. AAAI 2019, 31st Innov. Appl. Artif. Intell. Conf. IAAI 2019 9th AAAI Symp. Educ. Adv. Artif. Intell. EAAI 2019, pp. 6940–6948, 2019, doi: 10.1609/aaai.v33i01.33016940.

[7] C. Raffel et al., “Exploring the limits of transfer learning with a unified text-to-text transformer,” arXiv, vol. 21, pp. 1–67, 2019.

[8] Y. Li, P. Xu, and M. Pang, “Adversarial Attacks on Word2vec and Neural Network,” in ACAI 2018: Proceedings of the 2018 International Conference on Algorithms, Computing and Artificial Intelligence, 2018, pp. 1–5, doi: 10.1145/3302425.3302472.

[9] Y. Gu et al., “An enhanced short text categorization model with deep abundant representation,” World Wide Web, vol. 21, no. 6, pp. 1705–1719, Nov. 2018, doi: 10.1007/s11280-018-0542-9.

[10] A. Radford, R. Jozefowicz, and I. Sutskever, “Learning to Generate Reviews and Discovering Sentiment,” arXiv Prepr., 2017, Accessed: Aug. 13, 2017. [Online]. Available: https://arxiv.org/pdf/1704.01444.pdf.

[11] L. Li et al., “On Robustness and Bias Analysis of BERT-based Relation Extraction,” pp. 1–17, 2020, [Online]. Available: http://arxiv.org/abs/2009.06206.

[12] H. T. Nguyen, Q. H. Vo, and M. Le Nguyen, “A Deep Learning Study of Aspect Similarity Recognition,” Proc. 2018 10th Int. Conf. Knowl. Syst. Eng. KSE 2018, pp. 181–186, 2018, doi: 10.1109/KSE.2018.8573326.

[13] H. Gong, T. Sakakini, S. Bhat, and J. Xiong, “Document similarity for texts of varying lengths via hidden topics,” ACL 2018 - 56th Annu. Meet. Assoc. Comput. Linguist. Proc. Conf. (Long Pap., vol. 1, pp. 2341–2351, 2018, doi: 10.18653/v1/p18-1218.

[14] S. Poria, E. Cambria, L.-W. Ku, C. Gui, and A. Gelbukh, “A rule-based approach to aspect extraction from product reviews,” Soc. 2014, p. 28, 2014.

[15] K. Schouten, O. Van Der Weijde, F. Frasincar, and R. Dekker, “Supervised and Unsupervised Aspect Category Detection for Sentiment Analysis With,” IEEE Trans. Cybern., pp. 1–13, 2017.

[16] T. Gaillat, B. Stearns, G. Sridhar, R. McDermott, M. Zarrouk, and B. Davis, “Implicit and Explicit Aspect Extraction in Financial

Microblogs," pp. 55–61, 2019, doi: 10.18653/v1/w18-3108.

[17] C. Henríquez, F. Briceño, and D. Salcedo, "Unsupervised model for aspect-based sentiment analysis in Spanish," IAENG Int. J. Comput. Sci., vol. 46, no. 3, 2019.

[18] R. Panchendrarajan, N. Ahamed, B. Murugaiah, P. Sivakumar, S. Ranathunga, and A. Pemasiri, "Implicit Aspect Detection in Restaurant Reviews using Cooccurence of Words," pp. 128–136, 2016, doi: 10.18653/v1/w16-0421.

[19] E. Ghadery, S. Movahedi, H. Faili, and A. Shakery, "An Unsupervised Approach for Aspect Category Detection Using Soft Cosine Similarity Measure," 2018, [Online]. Available: http://arxiv.org/abs/1812.03361.

[20] A. Garcıa-Pablos, M. Cuadros, and G. Rigau, "V3: Unsupervised Aspect Based Sentiment Analysis for SemEval-2015 Task 12," SemEval-2015, pp. 714–718, 2015, [Online]. Available: https://www.aclweb.org/anthology/S15-2121.

[21] F. Nurifan, R. Sarno, and K. R. Sungkono, "Aspect based sentiment analysis for restaurant reviews using hybrid ELMo-wikipedia and hybrid expanded opinion lexicon-senticircle," Int. J. Intell. Eng. Syst., vol. 12, no. 6, pp. 47–58, 2019, doi: 10.22266/ijies2019.1231.05.

[22] T. A. Rana and Y. N. Cheah, "A two-fold rule-based model for aspect extraction," Expert Syst. Appl., vol. 89, pp. 273–285, 2017, doi:10.1016/j.eswa.2017.07.047.

[23] S. Chatterji, N. Varshney, and R. K. Rahul, "AspectFrameNet: a frameNet extension for analysis of sentiments around product aspects," J. Supercomput., vol. 73, no. 3, pp. 961–972, 2017, doi: 10.1007/s11227-016-1808-6.

[24] W. Wang, S. J. Pan, D. Dahlmeier, and X. Xiao, "Recursive Neural Conditional Random Fields for Aspect-based Sentiment Analysis," 2016, Accessed: Nov. 11, 2017. [Online]. Available: https://arxiv.org/pdf/1603.06679.pdf.

[25] S. Kiritchenko, X. Zhu, C. Cherry, and S. Mohammad, "NRC-Canada-2014: Detecting aspects and sentiment in customer reviews," in Proceedings of the 8th International Workshop on Semantic Evaluation (SemEval 2014), 2014, pp. 437–442.

[26] D. Marcheggiani, O. Täckström, A. Esuli, and F. Sebastiani, "Hierarchical multi-label conditional random fields for aspect-oriented opinion mining," Lect. Notes Comput. Sci. (including Subser. Lect. Notes Artif. Intell. Lect. Notes Bioinformatics), vol. 8416 LNCS, pp. 273–285, 2014, doi: 10.1007/978-3-319-06028-6_23.

[27] M. Yang, W. Tu, J. Wang, F. Xu, and X. Chen, "Attention-Based LSTM for Target-Dependent Sentiment Classification," pp. 5013–5014, 2017, doi: 10.1146/annurev.neuro.26.041002.131047.

[28] E. Cambria, B. B. Schuller, Y. Xia, and C. Havasi, "Building a Sentiment Summarizer for Local Service Reviews," IEEE Intell. Syst., vol. 28, no. 2, pp. 15–21, 2013, doi: 10.1109/MIS.2013.30.

[29] Y. Ma, H. Peng, T. Khan, E. Cambria, and A. Hussain, "Sentic LSTM: a Hybrid Network for Targeted Aspect-Based Sentiment Analysis," Cognit. Comput., vol. 10, no. 4, pp. 639–650, 2018, doi: 10.1007/s12559-018-9549-x.

[30] D. S. Vargas, L. R. C. Pessutto, and V. P. Moreira, "Simple Unsupervised Similarity-Based Aspect Extraction," 20th Int. Conf. Comput. Linguist. Intell. Text Process. (CICLing 2019), 2020, [Online]. Available: http://arxiv.org/abs/2008.10820.

[31] A. Graves, "Generating Sequences With Recurrent Neural Networks," Arxiv, pp. 1–43, 2013, [Online]. Available: http://arxiv.org/abs/1308.0850.

[32] R. Kiros et al., "Skip-Thought Vectors," Adv. neural in- Form. Process. Syst., pp. 3294–3302, 2015, doi: 10.1017/CBO9781107415324.004.

[33] J. McAuley, C. Targett, Q. Shi, and A. Van Den Hengel, "Image-based recommendations on styles and substitutes," SIGIR 2015 - Proc. 38th Int. ACM SIGIR Conf. Res. Dev. Inf. Retr., pp. 43–52, 2015, doi: 10.1145/2766462.2767755.

[34] G. Qiu, B. Liu, J. Bu, and C. Chen, "Opinion word expansion and target extraction through double propagation," Comput. Linguist., vol. 37, no. 1, pp. 9–27, 2011.

[35] Z. Toh and J. Su, "NLANGP: Supervised Machine Learning System for Aspect Category Classification and Opinion Target Extraction," Proc. 9th Int. Work. Semant. Eval., vol. 14, no. SemEval, pp. 496–501, 2015.

[36] Y. Ma, H. Peng, and E. Cambria, "Targeted Aspect-Based Sentiment Analysis via Embedding Commonsense Knowledge into an Attentive LSTM," 2018.

SRAVIP: Smart Robot Assistant for Visually Impaired Persons

Fahad Albogamy[1]
Turabah University College, Computer Sciences Program
Taif University, Saudi Arabia

Turk Alotaibi[2], Ghalib Alhawdan[3]
Mohammed Faisal*[4]
College of Applied Computer Sciences, King Saud University, Saudi Arabia

***Abstract*—Vision is one of the most important human senses, as visually impaired people encounter various difficulties due to their inability to move safely in different environments. This research aimed to facilitate integrating such persons into society by proposing a robotic solution (Robot Assistance) to assist them in navigating within indoor environments, such as schools, universities, hospitals, airports, etc. according to a prescheduled task. The proposed system is called the smart robot assistant for visually impaired persons (SRAVIP). It includes two subsystems: 1) an initialization system aimed to initialize the robot, create an environment map, and register a visual impaired person as a target object; 2) a real-time operation system implemented to navigate the mobile robot and communicate with the target object using a speech-processing engine and an optical character recognition (OCR) module. An important contribution of the proposed SRAVIP is the user-independent, i.e. it does not depend on the user, and one robot can serve unlimited users. SRAVIP utilized Turtlebot3 robot to realize SRAVIP and then tested it in the College of Computer and Information Sciences, King Saud University, AlMuzahmiyah Campus. The experimental results confirmed that the proposed system could function successfully.**

Keywords—Mobile robot; robotics; robot assistance; and visually impaired persons

I. Introduction

At present, a large number of persons have various physical impairments. The World Health Organization (WHO) has evaluated that according to examination in 2019 approximately 2.2 billion people worldwide live with a form of vision impairment, among which 36 million people are blind [1]. Visual impairment is a noteworthy issue that prevents from moving freely. Such people usually require the assistance of unimpaired individuals to identify and follow a target direction or to provide guidance while passing stairs and turns. Most visually impaired individuals cannot determine their path freely in an unfamiliar zone.

In general, there are many tools and ways to help the blind people: 1) Traditional ways, e.g. Help by other people, White Stick, and Guide dogs; 2) Technical-based such as Wearable device and Navigation Robot.

The recently introduced technologies, such as Blind Stick, have facilitated them to move freely; however, the implemented procedures are deemed insufficiently reasonable and practical. At present, the rapid technical development has enabled introducing many types of robots, such as ones intended for the commercial use and delivery. In addition, there are several applications in hospitals and hotels, for example, a DoorDash robot employed to deliver food to customers via an application [2]. The other type of robots includes those that are similar to humans, such as Sofia designed by the company Hanson Robotics[1]. These robots have been developed to learn and adapt to human behavior. Other types of existing robots inhibit various features: they can behave independently, identify their way to specific locations in the buildings, and so on.

This study aimed to assist the blind people to reach their target (classroom in schools/universities, and gates in airports) using a robot-based solution. Therefore, a solution that utilizes robotics to assist visually impaired individuals is developed. Robot-based solutions can be applied to assist visually impaired and blind people to walk and move in various environments, such as schools, universities, hospitals, airports, shopping malls, etc. For example, when a visually impaired person enters an airport, a mobile robot can be utilized to enable navigation to a required gate according to the boarding ticket information. As the other example, we can consider the situation in which a robot can assist a student in navigating to a target classroom according to the timetable. The concept of robotic assistance should be grounded on understanding the needs of visually impaired individuals. In the present study, we focus on a task of navigating a visually impaired person to a predefined location within a particular indoor environment.

In the future, we are planning to enhance the proposed SRAVIP system by adding more features such as fingerprint or face recognition, supporting Arabic languages, and enabling remote maintenance.

The remainder of this paper is organized as follows. In Section 2, the related literature review is presented. The proposed system structure is outlined in Section 3. In Section 4, we describe the experimental setup and discuss the obtained results. The discussion is provided in Section 5. And the conclusion provided in section6.

II. Literature Review

Several systems and techniques have been proposed to assist visually impaired persons by means of a wearable device, a smart cane, or a robotic assistant.

*Corresponding Author

[1] https://www.hansonrobotics.com/sophia/

A. Wearable Devices

Wearable devices have been incorporated in various modern techniques to assist visually impaired people. In [6], a smart assistant called Tyflos has been proposed to assist while walking, navigating, and working in an indoor environment. Tyflos consists of seven main elements: a pair of glasses, vision cameras, laser range scanner, microphone, portable computer, ear speaker, and a communication system. Two optical cameras are implemented to capture 3D images of a target environment. The system can operate in a continuous mode that registers the information about the environment in video format, converts it into verbal descriptions for each shot, and provides a user with obtained description. Alternatively, as an assistant describing the environment upon a user request, the system provides an ability to investigate surroundings through verbal communication.

Lee Y. and Medioni [3] have proposed a vest-type gadget with an embedded RGB-D camera for real-time navigation with obstacle avoidance (Fig. 1). Here, the RGB-D camera is used to capture the depth imagery data, and traversability is implemented to identify free and occupied spaces (obstacles). Directions, such as "Go straight" and "Stop" are provided to a user by means of four micro vibration motors on a vest.

One more system that employs a similar vest differently has been proposed in [4] that is implemented as a stereo vision system for visually impaired systems (Fig. 2). Using a visual odometer and feature-based metric-topological and simultaneous localization and mapping (SLAM), the system generates a 3D map representation corresponding to the vicinity of a user that can be utilized for obstacle detection and traversability map development.

Fig. 1. RGB-D Camera [3].

Fig. 2. Robot Vision [4].

In [16], the researchers have constructed a model aimed to control movements, perceive protests, and maintain a distance from obstacles in an indoor environment for visually impaired individuals. The framework comprises a module with a headset, a camera, a marker, an inertial estimation unit, and laser sensors mounted on a user's chest (Fig. 3).

Communication between the system and users is established through speech recognition and synthesis modules. The laser sensors registered the data required to maintain a safe distance. The camera is utilized to capture scenes and send it to the system for navigation or recognition.

Bai and Wang [5] have developed a low-cost wearable device aimed to assist visually impaired persons in navigating and avoiding obstacles based on the dynamic subgoal strategy. The device is composed of an ultrasonic rangefinder, a depth camera, a fisheye, an earphone, a pair of see-through glasses, and an embedded CPU board. The visual SLAM is utilized to define a virtual trajectory based on the depth and RBG images. The device identifies a short path by applying the A* algorithm to a point-of-interest. However, the problem associated with this device is that ultrasonic sensor data may vary depending on weather, which may lead to misdirection (Fig. 4).

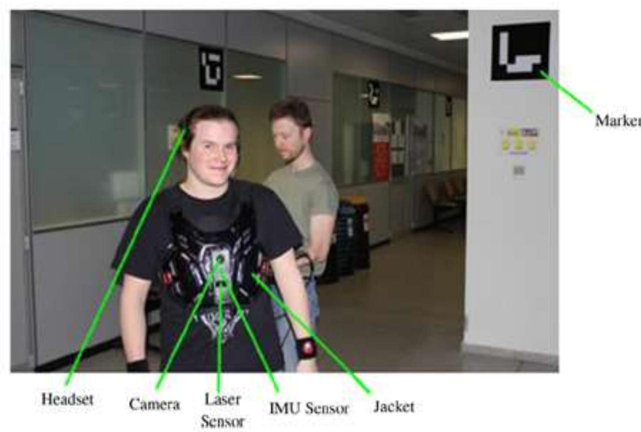

Fig. 3. Photo of the Prototype [16].

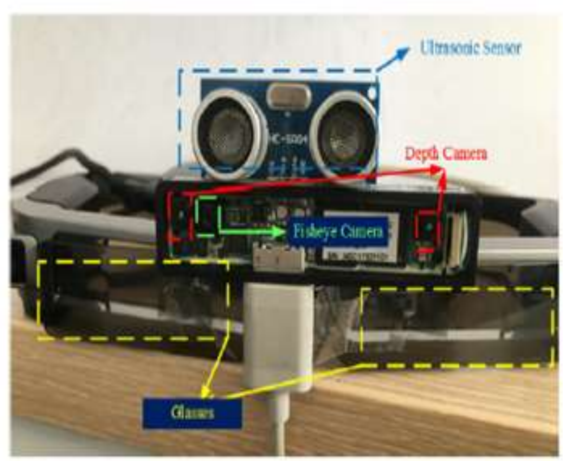

Fig. 4. Navigation Device [5].

B. Smart Cane

Visually impaired individuals may encounter numerous dangers that may threaten their security, as there are multiple regular things in their surroundings that may act as obstructions. Therefore, an inside framework presented in [7] is considered as a powerful arrangement between a several segments used at the stage of capturing and handling the data that are then utilized to define the path and transmit route messages to a user while moving in an inner zone. This framework contains key apparatuses including a white stick equipped with different lights, two infrared cameras, a portable computer with a product application to manage the whole framework, and a cell phone to convey the route data to a user through voice messages (Fig. 5).

Navigating indoor environments for visually impaired persons is usually difficult; therefore, in [8], the authors have proposed a system that can assist blind people in identifying the best path to arrive to a target destination. This system implies embedding RFID tags within paths and capturing them by a RFID reader using a cane antenna (Fig. 6).

In [9], a system called AKSHI has been proposed to assist visually impaired people in walking. The system has been implemented using Raspberry Pi, a GSM module, ultrasonic sensor, RFID tags, and a reader. The RFID reader is attached to the bottom of the cane. In the middle of the cane, an ultrasonic sensor has been mounted; the box containing Raspberry Pi 2, GPS, and GSM modules has been mounted above the sensor. Moreover, a mobile application to track the user location has been developed. However, the problem associated with this system is that the utilized sensor cannot function accurately in dirty or muddy environments.

Muñoz and other authors [10] have proposed a system using Tango devices within a mobile computing platform and have implemented a method for obstacle detection based on TSM-KF using RGB-D camera. The automated map generation process has been established by developing an indoor map editor to parse a CAD model of an architectural floor map, as well as implementing a smart cane as a human-machine interface and communication tool.

C. Robotics

The authors in [11] have proposed a suitcase-shaped navigation robot called Cabot to assist visually impaired persons in navigating to a target destination and avoiding obstacles. It comprises a stereo camera, a LIDAR sensor, a tactile handle, a portable computer, batteries, a motorized wheel, and a clutch. It can be used to receive feedback from a handle and to provide the information about the required direction. However, it does not consider dynamic elements. To enable a robot to move and recognize a target environment, many techniques and algorithms have been used [17-23]. A specific framework has been proposed in [12]. Here, the RGB and depth images are employed to achieve the purpose. The scheme represented in Fig. 7 can be used to understand the general structure of this proposed framework, which can be divided into two sequential stages: the offline work stage including the establishment of the structure and the electronic stage in which the model is applied to identify a target item according to the predefined map.

Fig. 5. Components of the Navigation System [7].

Fig. 6. Navigation Device Attached to a user with a Headphone and a Cane with a Buil-in RFID Antenna [8].

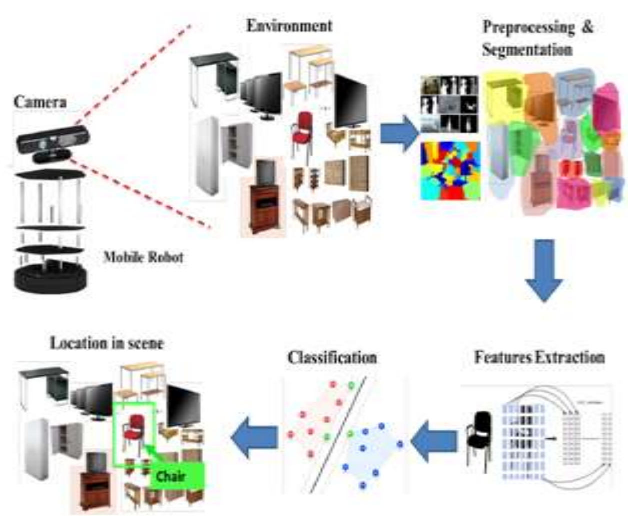

Fig. 7. Structure of the Proposed System [11].

Jalobeanu [13] has developed a framework based on a Kinect sensor to map indoor environments. This framework combines a grid map based on the truncated signed distance function with a particle filter used in a real-time mode. This framework exploits the noisy depth data and can be used to increase the field of view by establishing virtual views from local maps. In [14], the researchers have combined the LIDAR and sonar sensors. Such multi-sensor combination techniques have been applied to identify objects while performing SLAM. In the case when various sensors are used to analyze a similar obstacle, they can confirm the obtained information and improve the estimation precision of each other. Kumar [15] has proposed a robotic navigation system including two controllers. The first one is intended to compute the path from the current position to a target point without considering potential obstacles. The other controller is based on fuzzy logic and is utilized to deal with obstacles by processing the input from a laser sensor and then sending the output to the robot aiming to avoid the identified obstacle.

III. Proposed System

In this study, we developed a system called SRAVIP aimed at integrating visually impaired persons into society. To do this, we attempted to construct a mobile robotic solution intended to assist such persons in walking and navigating in an indoor environment. SRAVIP is aimed at assisting the blind people to reach the target location (such as classrooms in schools/universities or gates in airports) using a robotic solution, as presented in Fig. 8. The proposed SRAVIP has the following structure:

1) Initialization system (Offline)

a) Map Construction: establishing a map of a target environment;

b) User Registration: registering a user in the system.

2) Real-time operation system (Online)

a) Robot Navigation and Path Planning: navigating the robot;

b) User Interface: communicating with a user (through a speech-processing engine or an OCR system).

An important contribution of the proposed SRAVIP is the user-independent, i.e. it does not depend on the user, one robot can serve unlimited users. In this section, we provide an overview of the proposed system and discuss the interaction between its components, explaining each component in detail.

A. System Initialization

This phase is implemented to initialize the system. It includes two steps: constructing the map of a target environment and registering users in the system.

- Map Construction

First, we execute system/robot initialization by determining where a mobile robot is located with respect to the surrounding environment (using simultaneous localization and mapping). Enabling the robot to move from the current location to the destination one according to the predefined map, we utilize an encoder, an IMU sensor, and a distance sensor to avoid obstacles. We will employ a 2D occupancy grid map (OGM) to construct the map based on the distance information obtained using the sensors and the pose information of the robot itself (Fig. 9). Finally, the system saves the map.

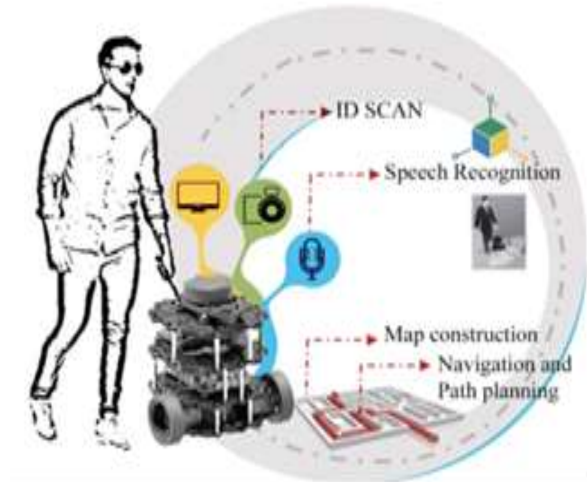

Fig. 8. The Core Components of the Proposed System.

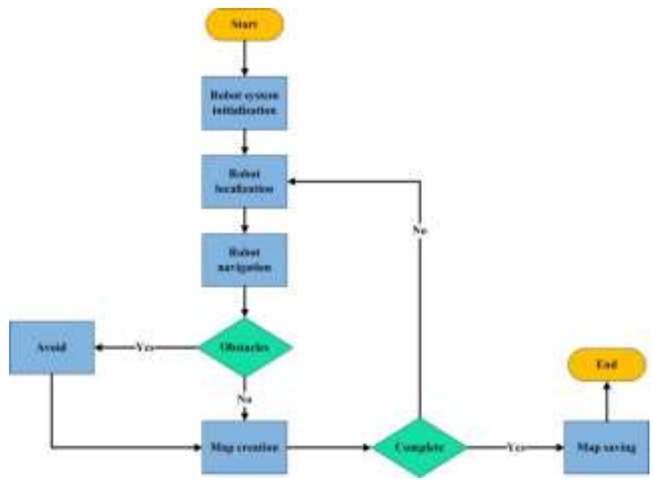

Fig. 9. System Initialization Diagram.

- User Registration

In this step, the robot operator registers the information about a user manually in the database of the target organization (school, university, airport, etc.). When the registration is completed, the robot can identify a user when he or she requires assistance in reaching the target destination by using ID scan or speech commands.

B. Real Time Operation

This phase is online and is intended to perform robot navigation, path planning, and user interaction (Fig. 10).

After a user interacts with the robot through telling the ID number or presenting the ID card, the robot can identify the user and retrieve the information about this user from the database (a student timetable or a flight information). Then, it identifies the target location and specifies the current one according to the predefined map of the building. The target and current locations and the map serve as the inputs into the path-planning algorithm. The robot defines a path aiming to avoid obstacles and to identify the shortest route. Then, the robot initiates moving along the defined path. At this time, even if an unexpected obstacle is suddenly detected, the robot will be able to avoid it and to proceed moving to the target destination. During the movement, the current location of the robot is identified with respect to its environment using simultaneous localization and mapping. If the robot reaches the destination, it will go back to its initial location; otherwise, it continues executing the localization steps to proceed with the operation. When the robot reaches the initial location, it stops; otherwise, it continues executing the robot localization step.

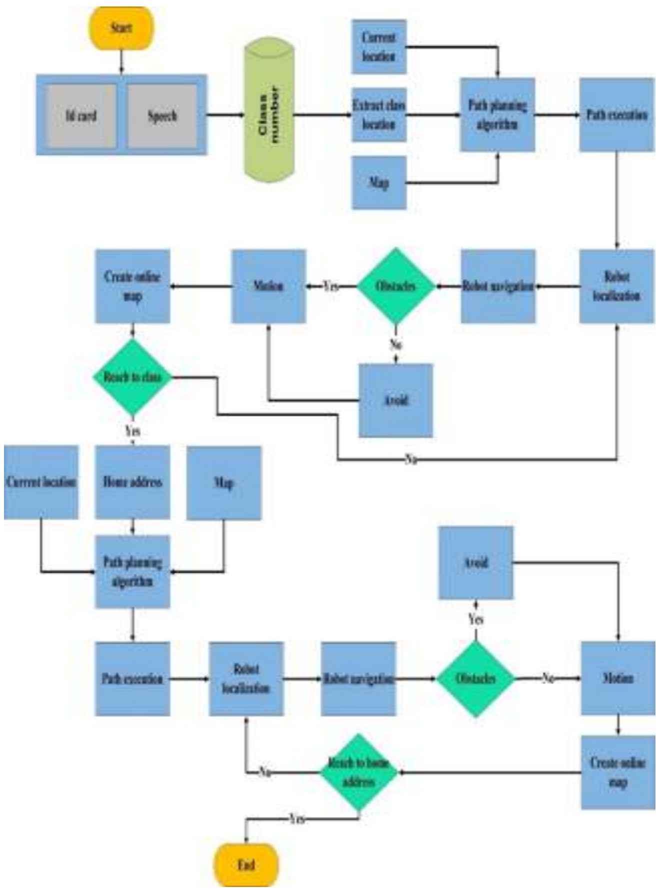

Fig. 10. Flowchart of the Real Time Operation Phase.

IV. SRAVIP IMPLEMENTATION

In this section, we describe the implementation of the proposed SRAVIP, which consists of two parts: the first part is the initialization of the system (offline), and the second part is real-time operation (online). In SRAVIP, we have utilized Turtlebot3 and then, we have tested the proposed system within the College of Computer and Information Sciences, King Saud University, AlMuzahmiyah Campus.

Turtlebot3 has the following features: Raspberry Pi 3 Model B and B+; a laser distance sensor (LDS) is a 360 LDS-01. We have modified it mounting a camera to facilitate recognizing a university card and a microphone for speech recognition. We have utilized a robot operation system (ROS) as a robotic platform. ROS is an open-source robotics software platform. In addition, we have employed Gazebo and RViz simulations.

A. Offile Implementation System Initialization Phase

1) Map construction: We construct the map using the gmapping package, implementing the laser-based simultaneous localization and mapping (SLAM) technique to create a 2D occupancy grid map (Fig. 11).

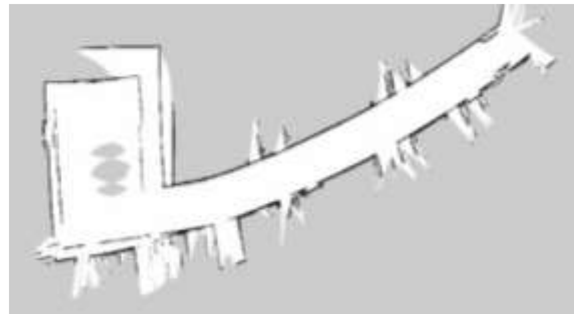

Fig. 11. Building Map of a Corridor of the College.

2) User registration: In the user registration step, we employ MYSQL as relation database management system to register users in the system. The entity relationship (ER) diagram is illustrated in Fig. 12.

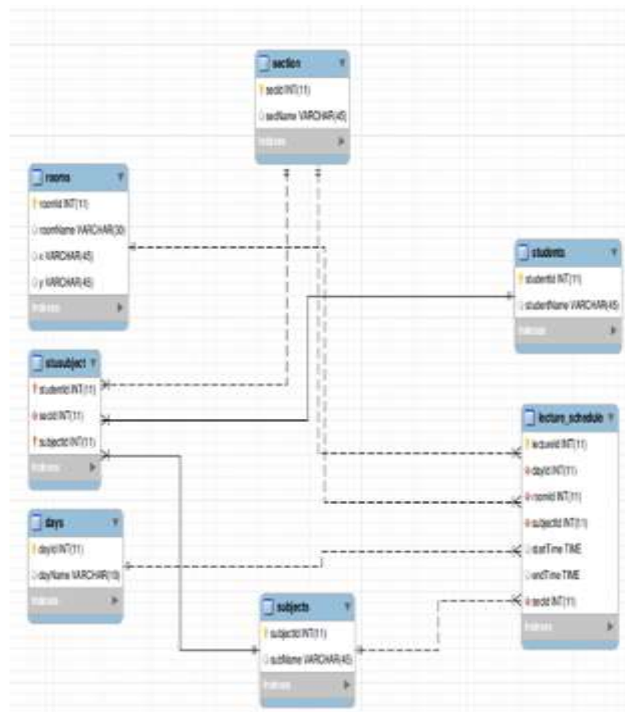

Fig. 12. ER Diagram of Blind Registration.

B. Real Time Operation (Online)

In this part, we implement the interaction between a user and the robot either by scanning a university card through the OCR system or using the speech recognition system to identify the university ID number. The real time operation modules include two main steps: user interaction and robot navigation/path planning.

1) User interface implementation: In this section, we explain the details of how a user interacts with the robot through the developed user interface (UI). To enable this option, we have implemented the code in Python. In UI (Fig. 13), a user has two options: to provide a user ID card so as to identify the ID number by means of the optical character recognition (OCR) system from the database, or to say the ID number so that the robot could detect it through the speech recognition module. If the user is registered in the system correctly, the id number appears on the screen.

We implement UI using the tkinter package, the standard Python UI available in the tk graphical user interface toolkit.

Fig. 13. Robot GUI.

2) OCR implementation: Optical character recognition (OCR) is a technology that can be used to extract the ID number based on a student card. To do this, we have implemented several stages, as illustrated in Fig. 14, using various libraries. The first library is NUMBY that allows generating arrays and data-followed processes. Then, we have employed TensorFlow library using a neural network trained on 500 images. Lastly, we utilized the OpenCV library intended for executing clustering operations.

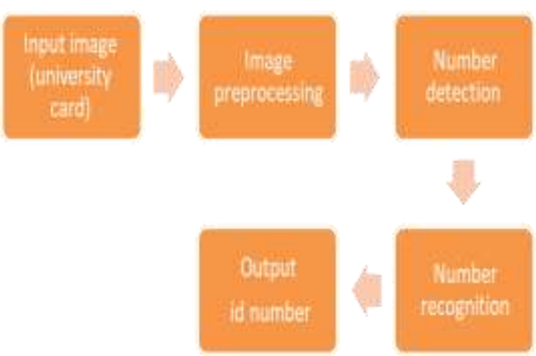

Fig. 14. Flowchart of the OCR System.

3) Speech recognition implementation: Speech recognition includes several stages described in Fig. 15, the most important step is to represent the relationship between the language units of speech and voice signals. The other module is used to match linguistic modeling sounds with number sequences to allow distinguishing between numbers that look similar. Using the speech recognition module, the system allows recognizing the ID number pronounced by a user. If the user is registered in the system, the ID number is processed using the database and is represented on the system screen. According to the ID number, the user data and schedule are extracted from the database, and the robot navigates the user to the target location.

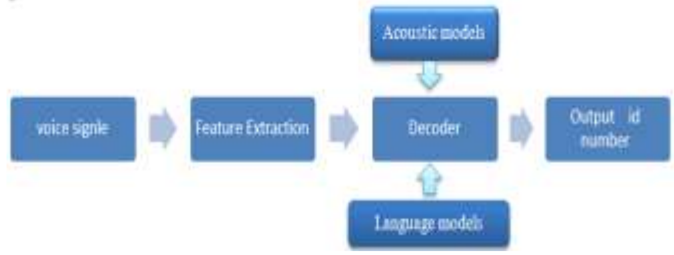

Fig. 15. Flowchart of the Speech Recognition System.

4) Robot navigation and path planning: Using the constructed map and after the student loaded from the database, SRAVIP can define the class coordinates and automatically save them in a text file. Thereafter, the system can process them to set up a coordinate target for navigation, and the robot automatically executes path planning to move from the initial location to the requested one. After the robot reaches the target location, it returns to the initial point.

V. SRAVIP EXPERIMENT AND TESTING

We tested the SRAVIP system within the simulation environment established in College of Computer and Information Sciences, King Saud University, AlMuzahmiyah Campus. In the experiment, we considered the two possible scenarios of the interaction between the proposed system and users. In the first scenario, experiment participants utilized the OCR system, and in the second scenario, the speech recognition system was employed. The experiment procedure was specified as follows. When the participant entered the college building from the main gate, the robot could be found on the right side of the door, and this location was fixed for a robot as "Home Adder." The first scenario implied utilizing the OCR system (Fig. 16). In the beginning, participant A had to demonstrate the university card (Fig. 17) to the robot so as to extract the student ID number.

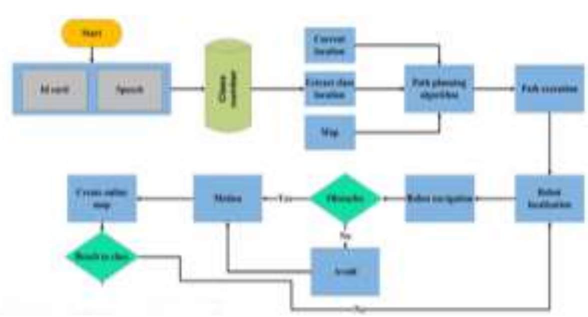

Fig. 16. Flowchart of the Experimental Scenarios using OCR and Speech Recognition.

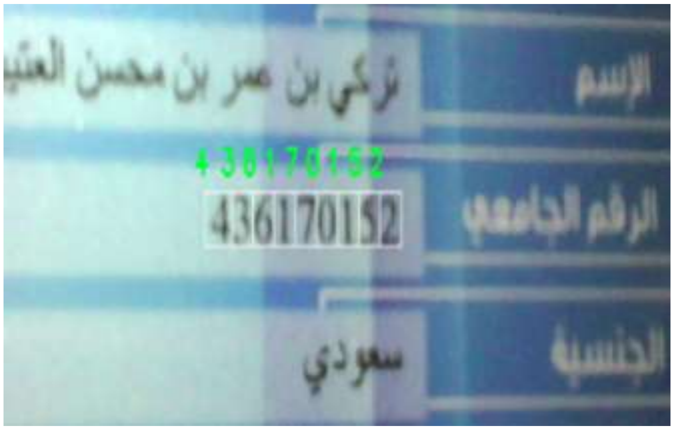

Fig. 17. Extraction of a University ID Number using the OCR System.

Thereafter, the system was able to gain the information about the student schedule and define the coordinates of a target class for this user. Then, the coordinates were processed by the robot navigation system (Fig. 18).

Fig. 18(a) shows that the robot at the Home Adders location and waiting for the path to the target class (Fig. 18(b)) to be generated by the robot navigation system. Then, the student goes to his class with assist from the robot (Fig. 18(c)), finally, the robot automatically returns to home address to be able to serve other students.

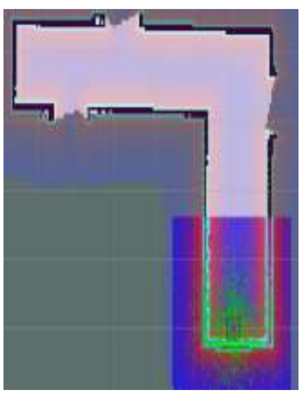

a) Robot at the "Home Adders" Location.

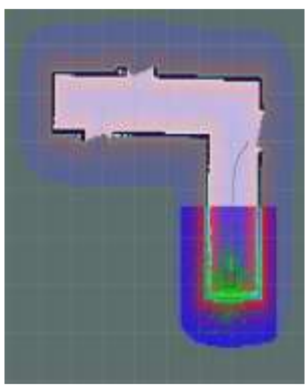

b) Generated Path to the Class 98.

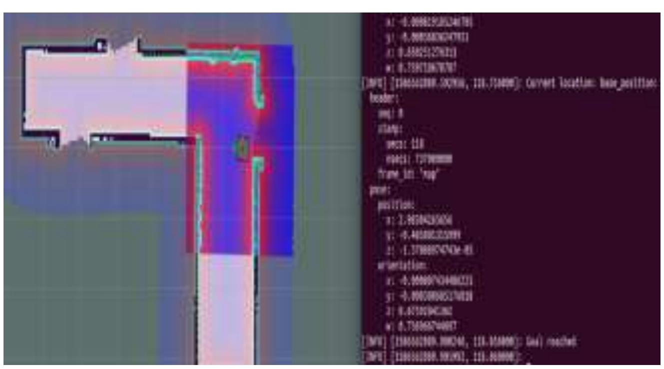

c) Navigation and Path Planning to the Class 98.

Fig. 18. Robot Navigation System used in the First Scenario.

The second scenario considered employing the speech recognition system (Fig. 16). In this case, participant B told the university number to the robot for extraction and identification of the user information from the database using the speech recognition technology. After that, the system was able to load the information about the student schedule and coordinates of a target class for this user. Then, the coordinates were employed by the robot navigation system to construct a trajectory (Fig. 19).

Fig. 19(a) shows that the robot at the Home Adders location and waiting for the path to the target class (Fig. 19(b)) to be generated by the robot navigation system. Then, the student goes to his class with assist from the robot (Fig. 19(c)), finally, the robot automatically returns to home address to be able to serve other students.

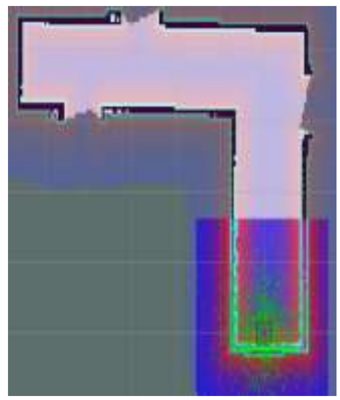

a) Robot at the "Home Adders" Location.

b) Generated Path to the Class 98.

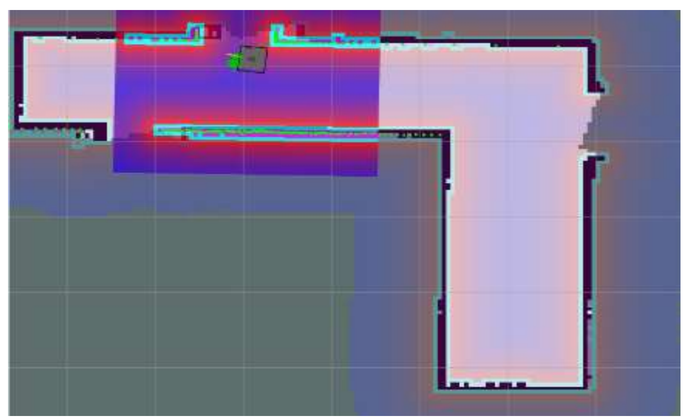

c) Navigation and Path Planning to the Class 97.

Fig. 19. Robot Navigation System used in the Second Scenario.

VI. Discussion

As we have seen in the literature review, several systems and techniques have been proposed to assist visually impaired persons by means of a wearable device, a smart cane, or a robotic assistant. All those solutions are user-dependent solution, and work as one to one solution. It means that one device only can be used by one blind person. An important contribution of the proposed SRAVIP is the user-independent property, i.e. it does not depend on the user. It is one to many solutions, i.e. one robot can serve unlimited number of users.

VII. Conclusion

In the present paper, we proposed a robotic solution to assist visually impaired people to walk and navigate within various indoor environments, such as schools, universities, hospitals, airports, etc. according to a prescheduling task. An important contribution of the proposed system is the user-independent property, i.e. it does not depend on the user, it is one to many solutions, i.e. one robot can serve unlimited number of users. While the previous solutions work as one to one solutions. It means that one device only used by one blind person.

The proposed system called a smart robot assistant for visually impaired persons (SRAVIP) was composed of two subsystems: the initialization module and the real-time operation one. We employed Turtlebot3 to implement the proposed system. Then, we tested it in many scenarios within the College of Computer and Information Sciences, King Saud University, AlMuzahmiyah Campus. The experimental result indicated that the proposed system could be utilized successfully. In the future, we are planning to enhance the proposed SRAVIP system by enabling remote maintenance, adding more features such as fingerprint or face recognition, speech recognition, and supporting different languages such as Arabic.

Acknowledgment

The authors extend their appreciation to the Deanship of Scientific Research at King Saud University for funding this work through research group no RG-1441-503.

References

[1] W. H. Organization, "World report on vision," 2019.

[2] M. S. S. Schaudt, "Delivery robots, a transport innovation for the last mile Market survey and modelling the logistic system," LITERATURE SERIES, p. 87, 2018.

[3] Y. H. Lee and G. Medioni, "RGB-D camera based navigation for the visually impaired," in Proceedings of the RSS, 2011.

[4] V. Pradeep, G. Medioni, and J. Weiland, "Robot vision for the visually impaired," in 2010 IEEE Computer Society Conference on Computer Vision and Pattern Recognition-Workshops, 2010, pp. 15-22.

[5] J. Bai, S. Lian, Z. Liu, K. Wang, and D. Liu, "Virtual-blind-road following-based wearable navigation device for blind people," IEEE Transactions on Consumer Electronics, vol. 64, pp. 136-143, 2018.

[6] N. G. Bourbakis and D. Kavraki, "An intelligent assistant for navigation of visually impaired people," in Proceedings 2nd Annual IEEE International Symposium on Bioinformatics and Bioengineering (BIBE 2001), 2001, pp. 230-235.

[7] L. A. Guerrero, F. Vasquez, and S. F. Ochoa, "An indoor navigation system for the visually impaired," Sensors, vol. 12, pp. 8236-8258, 2012.

[8] S. Chumkamon, P. Tuvaphanthaphiphat, and P. Keeratiwintakorn, "A blind navigation system using RFID for indoor environments," in 2008 5th International Conference on Electrical Engineering/Electronics, Computer, Telecommunications and Information Technology, 2008, pp. 765-768.

[9] V. Kaushalya, K. Premarathne, H. Shadir, P. Krithika, and S. Fernando, "'AKSHI': Automated help aid for visually impaired people using obstacle detection and GPS technology," International Journal of Scientific and Research Publications (IJSRP), vol. 6, 2016.

[10] B. Li, J. P. Munoz, X. Rong, Q. Chen, J. Xiao, Y. Tian, A. Arditi, and M. Yousuf, "Vision-based mobile indoor assistive navigation aid for blind people," IEEE transactions on mobile computing, vol. 18, pp. 702-714, 2018.

[11] A. C. Hernández Silva, C. Gómez Blázquez, J. Crespo Herrero, and R. I. Barber Castaño, "Object detection applied to indoor environments for mobile robot navigation," 2016.

[12] M. Jalobeanu, G. Shirakyan, G. Parent, H. Kikkeri, B. Peasley, and A. Feniello, "Reliable kinect-based navigation in large indoor environments," in 2015 IEEE International Conference on Robotics and Automation (ICRA), 2015, pp. 495-502.

[13] T. Zhang, Z. Chong, B. Qin, J. Fu, S. Pendleton, and M. Ang, "Sensor fusion for localization, mapping and navigation in an indoor environment," in 2014 International Conference on Humanoid, Nanotechnology, Information Technology, Communication and Control, Environment and Management (HNICEM), 2014, pp. 1-6.

[14] N. Kumar, M. Takács, and Z. Vámossy, "Robot navigation in unknown environment using fuzzy logic," in 2017 IEEE 15th International Symposium on Applied Machine Intelligence and Informatics (SAMI), 2017, pp. 000279-000284.

[15] J. Guerreiro, D. Sato, S. Asakawa, H. Dong, K. M. Kitani, and C. Asakawa, "CaBot: Designing and Evaluating an Autonomous Navigation Robot for Blind People," in The 21st International ACM SIGACCESS Conference on Computers and Accessibility, 2019, pp. 68-82.

[16] M. L. Mekhalfi, F. Melgani, A. Zeggada, F. G. De Natale, M. A.-M. Salem, and A. Khamis, "Recovering the sight to blind people in indoor environments with smart technologies," Expert systems with applications, vol. 46, pp. 129-138, 2016.

[17] M. Faisal, R. Hedjar, M. Al Sulaiman, and K. Al-Mutib, "Fuzzy logic navigation and obstacle avoidance by a mobile robot in an unknown dynamic environment," International Journal of Advanced Robotic Systems, vol. 10, p. 37, 2013.

[18] M. Faisal, M. Algabri, B. M. Abdelkader, H. Dhahri, and M. M. Al Rahhal, "Human expertise in mobile robot navigation," IEEE Access, vol. 6, pp. 1694-1705, 2017.

[19] F. Abdessemed, M. Faisal, M. Emmadeddine, R. Hedjar, K. Al-Mutib, M. Alsulaiman, and H. Mathkour, "A hierarchical fuzzy control design for indoor mobile robot," International Journal of Advanced Robotic Systems, vol. 11, p. 33, 2014.

[20] M. Faisal, K. Al-Mutib, R. Hedjar, H. Mathkour, M. Alsulaiman, and E. Mattar, "Multi modules fuzzy logic for mobile robots navigation and obstacle avoidance in unknown indoor dynamic environment," in Proceedings of the 2013 International Conference on Systems, Control and Informatics, 2013, pp. 371-379.

[21] M. Faisal, R. Hedjar, M. Alsulaiman, K. Al-Mutabe, and H. Mathkour, "Robot localization using extended kalman filter with infrared sensor," in 2014 IEEE/ACS 11th International Conference on Computer Systems and Applications (AICCSA), 2014, pp. 356-360.

[22] O. Çatal, T. Verbelen, T. Van de Maele, B. Dhoedt, and A. Safron, "Robot navigation as hierarchical active inference," Neural Networks, vol. 142, pp. 192-204, 2021.

[23] C. K. Verginis and D. V. Dimarogonas, "Adaptive robot navigation with collision avoidance subject to 2nd-order uncertain dynamics," Automatica, vol. 123, p. 109303, 2021.

Modelling the Player and Avatar Attachment based on Student's Engagement and Attention in Educational Games

Nooralisa Mohd Tuah[1], Dinna @ Nina Mohd Nizam[2], Zaidatol Haslinda A. Sani[3]
Faculty of Computing & Informatics
Universiti Malaysia Sabah, Labuan International Campus, 87008 Labuan F.T, Malaysia

***Abstract*—The Player and Avatar attachment help to motivate a student to strengthen their engagement in gameplay. The different types of avatar designs deployed in a game have an impact on students' engagements. The avatars are designed with different roles, wherein each role offers varying motivational effects on students' engagement. Several research in human and computer interaction have assessed user engagement and user attention in a computer or system application as well as in gameplay. Among the usual approaches to assess user engagement are using questionnaire and eye-tracking. Investigating the possible use of these approaches in determining the player and avatar attachment, particularly the attachment that associated with the various avatar designs and their effect on students' engagement are inconclusive and remains untapped. Essentially, studying students' engagement and attention perception while learning enriches one's comprehension about engagement in the education segment. As such, this study proposes a new model of player and avatar attachment based on the students' engagement and focus attention on the gameplay of digital educational games (DEGs). The model is developed follows a stepwise approach consisting component identification, relationship of the components, model development, and model validation. Several components were scrutinized, summarized, and developed into the model proposed in this study. A significant attachment can determine the avatar design that may influence a student's engagement in gameplay. Hence, this study offers several constructive recommendations for future avatars in game design for education purpose, which may validate the user's engagement based on his or her focus attention.**

Keywords—Avatar; engagement; attention; digital educational games

I. Introduction

The player-avatar attachment (PLAVA) in gameplay refers to the relationship developed between a player (student) and his or her in-game virtual representation, which is the representation also known as an avatar [1, 2]. A player develops a relationship with the avatar via in-game engagement, particularly when one is having fun while learning [1] as he or she indulges in the game activities [2]. Research conducted by Kim et al. [3] shows that the degree of attachment is one of the predictors that identifies a positive relationship that brings identification between a player and the in-game character (avatar). Such positive relationship motivates players in sustaining their engagement in gameplay.

Previously, several studies had researched the effects of player and avatar attachment, relationship, and user engagement in gameplay and in learning in an educational game (i.e. [4 - 8]). However, among the studies, the approach to synchronize the different types of avatar designs and their effect on student's engagement in learning was not explored extensively. Thus, it remains under research. Moreover, to extend the study of the player attachment and in-game engagement, engaging this research with an eye-tracker can contribute to visual attention perception while learning Digital Educational Games (DEGs).

As in previous research by Mohd Tuah et al. [6], Banks & Bowman [7], and Hwang & Mamykina [9], they had summarized a spectrum of avatar design in a game. This spectrum varies from actual human design to abstract human design. Each of the design spectrum is exploring different roles of an avatar in gameplay, such in [5, 6, 8]. As such, the following question is posed: Can students' engagement and their attention toward their avatar design and roles be modelled in defining PLAVA in the context of DEG gameplay?

Therefore, in this study, we developed a Player-Avatar attachment model by implementing avatar design types and their roles adapted to learning on DEGs. We developed the model to demonstrate how the player, which is a student, and avatar attachment can affect the way they engage based on visual attention in a game. The visual attention is modelled based on the eye-tracking metrics, which can precisely quantify the user's attention and gaze. Hence, enrich understanding of engagement in learning. We aim to investigate the Player and Avatar attachment effects on each avatar design to the avatar roles in gameplay. The significant attachment will determine which type of designs could influence the student's engagement in a game and how visual attention can validate the result. This research provides a constructive recommendation for future Avatar's game design in education and validates user's engagement based on the user's focused attention.

The remaining of this paper is structured as follows. The next section presents the background study of the avatar design, roles, the player and avatar relationship, and the user engagement evaluation. Following the literature is the method used to develop the model, in which the processes involved in model development and validation are discussed in detail. After that, this paper presents the proposed model in the result section, as well as the outcome of the model validation study.

This work is funded by a research grand under Universiti Malaysia Sabah (grant no: SLB0198-2019)

Moving on, the evaluation study plan is described to future endeavor. Finally, a summary of this study and the concluding remarks are presented.

II. Background Study

An avatar denotes the representation of a player in a gameplay. Notably, an avatar is the resemblance of a player in a virtual setting [1] with its human quality and features [1, 5 - 6]. Avatar designs exist in varying forms of humanism, such as in iconic form, cartoonish, or a combination of designs between them. For instance, Kao and Harrel [5] found that three avatar designs; scientist avatar (i.e., Einstein), athlete avatar (i.e., Michael Jordan), and shape avatar (i.e., square, hexagon, etc.), had influenced both game performance and game experiences in educational games. The scientist avatar emerged as the most significant avatar in science, technology and mathematic educational game. This finding is consistent with the criteria of an effective role model in boosting academic performance, particularly for competent, in-group member, and success domains. Banks & Bowman [7] outlined four categories of avatar designs (object, 'me' (oneself), symbiote, and the social other) to determine the social relationship between a player and his or her avatar in the gameplay. Upon validating the merged metric for player avatar interaction, the study identified four essential factors (emotional investment, anthropomorphic autonomy, suspension of disbelief, and sense of player control) that dictated the player–avatar interaction. Another study classified the avatar designs into several characters, including lifelike, human cartoon, medium human-like, hybrid, and abstract characters [6]. These classifications of anthropomorphic characters enable designers to develop more significant interactions for individuals in promoting a long-term relationship. Hence, this study investigated the various types of avatar designs that affected the players' engagement in gameplay.

Several studies have examined the effects among PLAVA, relationship, and user engagement in gameplay [7 – 8, 10]. The player-avatar relationship signifies how a player perceives and responds to social interaction as if the player has a real social relationship with the avatar [7]. This social relationship is built while being engaged in a particular environment. Studies based on Human-Computer Interaction such as in [8, 11 – 13] perceived being engaged as the amount of time users spend doing their work (add, use or manipulate the content) or interacting with other users on the application/software/system. The social relationship between players and their avatar denotes the way players perceive themselves toward their online version (avatar) [10]. In the context of this present study, the amount of time indicates a series of temporal interaction a player spends in gameplay.

Temporal interactions exist when players spend time toward completing the assigned tasks or achieving the goal of the game. In this sense, when players are attached to their avatar, they tend to develop a social relationship and a sense of immersion in the gameplay [3]. The PLAVA is materialized when players recognize and respond to their avatar as though they are connected, similar to the social attachment established in the gameplay [7]. When playing, the player and its avatar are considered as a 'unified person'. A positive 'unified person' yields a high level of engagement. This notion emphasizes the sense of being attached to an avatar that can significantly affect the user's experience and enjoyment in the game [3 - 5].

In light of students' engagement and their avatar attachment in digital educational games (DEGs), several studies have assessed the player-avatar correlation in learning [14 - 16]. Game-based learning on DEGs makes a formal learning environment into a fun and enjoyable situation within the digital setting. According to Qian and Clark [17], use of games in classroom is integral to enhance students' motivation in learning. Similarly, Huizenga et al. [16], who studied the perception of teachers on DEGs in a classroom, revealed that DEGs increased both engagement and motivation amongst students in learning. Therefore, DEGs sustain engagement amongst students throughout the learning process, while simultaneously increasing their cognitive skills after several attempts playing the game [17]. Following All et. al. [18], this not only improves the learning effect, but also achieves the learning outcomes stipulated in each DEG. These studies disregarded the effect of each avatar design on students' engagement in learning. Therefore, more studies are called to determine avatar designs that may establish better attachment with the players, so as to make learning activities fun.

Despite the various types of avatar designs in educational games, avatars typically represent a student's self-representation [14] or as a tutor or a virtual teacher [19]. The use of avatar should not be restricted to the representation of a user, but should cover specific roles to encourage social interaction, including as a customization tool [20], as an in-game strategy [9], or as a personal identification [6, 8, 15]. As a customization tool, users may freely customize their avatars based on the purpose and the rules of the game [1]. For instance, players can change the appearance of their avatar (e.g., shirt, shoes, hair, eyes, nose, etc.), or add accessories to the avatar (e.g., bag, umbrella, skateboard, etc.). Meanwhile, for an avatar as an in-game strategy, the avatar appearance can be part of the game strategy to gain a winning point or to achieve the goal of the game [9]. The best avatar may be selected by the player to deal with the challenges in the game. Avatar with a stronger character (bold, fierce, and muscular) is usually chosen in strategizing the gameplay. Framing the player’s real-life situations can also be part of gaming strategies for personal improvement and motivation [21]. In personal identification, the players may integrate their personalities with the avatar [16, 22], but limited to the options available in the game.

Further exploration into the type of avatar design yields its significant impact on a player's engagement, which reflects a reliable 'unified person' deployed in DEGs. A 'unified person' indicates the attachment between a player and its avatar, which is significantly connected to the DEG gameplay. Past studies had assessed engagement among players through their avatar in gameplay using questionnaires [7 - 8]. The questionnaire has been applied to collect individual perceptions on the use of games for particular purposes. This method captures important information concerning engagement and can further support one's perception toward his or her engagement in a gameplay. Another viable measurement tool is eye-tracking. In this method, the players' engagement with their avatar and environment is measured through visual attention perception, thus making this tool particularly useful for DEGs. In this case, it is for the purpose of learning using DEGs.

The eye-tracking method gathers a user's behaviour by tracking the eye movement in a natural interaction setting [23]. Several studies had applied the eye-tracking technology to examine the effects of graphics [24], reading [22], and recently, DEGs in young children [25]. Several indicators, including fixation duration, total number of fixations, and time-to-first-fixation, are grounded measures of attention paid to objects of interest [26]. Visual attention or focused attention refers to the attention span during interaction and how one loses track of time when interacting in a given environment [11]. One gets absorbed when one has full concentration on mental activities while ignoring the rest [11]. By deploying this eye-tracking method, visual attention is measured using fixation-based metrics, as detailed in [27]. The metrics refer to the attention that spans in a certain duration associated with intensive facial expression and eye movements [22]. Analyzing the fixation duration on a defined Area of Interest (AOI) in DEG environment determines if an avatar design has an impact on the relationship with and on the behavior of a student's gameplay engagement. The longer a player focuses on the defined AOI from the fixation duration, the more information can be captured if the fixation duration is linked with the player's engagement behavior. In studying the effect of PLAVA on a user's engagement, it is essential to investigate the correlation between the type of avatar design and its related roles in the game.

This paper proposes a player-avatar attachment (PLAVA) model. The model is developed to assess the impact of PLAVA on the player's interaction with varying avatar designs and their designated roles in gameplay. Following the player's interaction, a significant attachment can determine the type of avatar designs that may influence his or her engagement in a game. The model is composed of two aspects, as mentioned earlier, namely avatar design types and avatar roles in learning using DEGs. In the model, the relationship between player and avatar is perceived through the components of engagement and attention. The component of engagement is modelled to understand the player's perception toward his or her connection with the avatar. The model incorporates the engagement component derived from questionnaires developed by [7] and [11]. Meanwhile, the attention component is retrieved from visual attention attributes and eye-tracking metrics, in order to precisely quantify the attention and gaze of the users. Hence, the student's perceptions toward engagement are supported by their visual attention data captured using the eye-tracking method. The data input can enrich the understanding of engagement in learning. Lastly, this study provides several constructive recommendations for future avatars in game design for education purpose, besides validating the users' engagement based their focused attention. This study significantly contributes to the body knowledge pertaining to creative content in DEGs and eye-tracking technology.

III. Methodology

In the model development, a step-by-step approach was followed to ensure the applicability of the model whether in research or in practice. However, when developing the model, it is deemed necessary to confirm the significance of each components identified in the model. The model development processes will be explained in detail followed by the explanation of expert review studies in validating the proposed model.

A. The Model Development Process

A stepwise approach was adopted to develop the proposed model. In the initial step, the development process began with component identification. In this process, variables related to the PLAVA, as well as students' engagement and attention, were identified, analyzed, and refined by reviewing articles published since a decade ago (2010-2020). Articles published in the area of human-computer interaction and educational games were incorporated. There on, details of the sought components were scrutinized after considering the importance and the relevance of each article. After identifying all the components, each component and sub-component had been defined. Defining both the scope and the purpose of each component can be plausibly helpful in model creation.

In the second step, input and output variables for each component were listed. By doing so, potential relationships or connections among the variables were further explored to develop the model. In particular, this step determined the flow and link between input and output of the components. As for the third step, the selected components and the inter-connection among the components were embedded to build the conceptual model for this study. In the final step, a validation study was conducted to validate the idea and concept of the model. Fig. 1 illustrates the model development process.

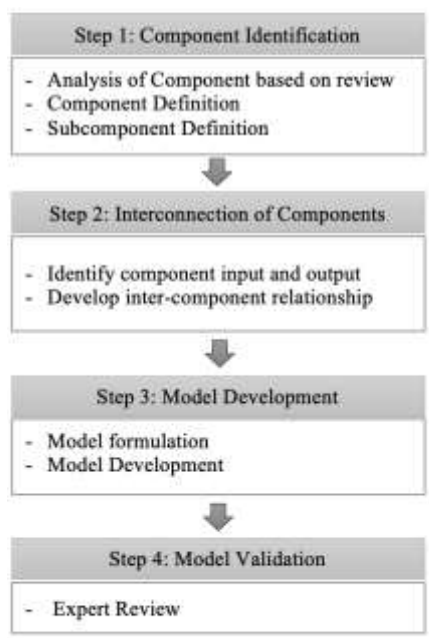

Fig. 1. The PLAVA Model Development Process.

B. Component Identification

Prior studies have excluded the engagement component in PLAVA in light of avatar roles. Most of the past studies had looked into agency as a tool to measure engagement [3, 5]. In view of this, the agency has been linked with the user's sense of agency with autonomy toward body ownership. Several considerations must be weighed in to measure the level of engagement based on PLAVA, including the method and the motivation of measurement. For instance, Hookham [13] had identified many strategies deployed to measure engagement in a series of game field and categorized them into interviews, focus groups, questionnaires, as well as direct and indirect observations. Meanwhile, Doherty et al. [12] classified the methods in a more structured and explicit manner. They categorized the methods of measuring engagement into two; subjectivity- oriented and objectivity-oriented. Subjectivity-oriented refers to perception and usually adopts the questionnaire as a tool, such as the User Engagement Scale (UES) [11] and the Game Engagement Questionnaire (GEQ) [28]. The UES is a tool that evaluates engagement in a setting of information search, system application or video games environment. Meanwhile, GEQ is used to specifically measure the impact of engagement on playing video games. As for objectivity-oriented, it is a measurement of engagement without directly questioning the users. For example, the electroencephalography (EEG) is applied to trace the behavior displayed by users in exerting action/transaction, as well as the eye-tracking method [25]. The methods were adopted based on the study purpose; either to comprehend the fundamentals of engagement, to design engagement and practice it, or to implement the components of engagement in system development [12].

Focused attention is one of the attributes used to measure the level of user engagement in gameplay. It refers to the feel of being absorbed in the game during interaction and how they lose track of time when interacting [11]. The feeling of being absorbed happens when users completely concentrate on mental activities while ignoring the rest [11]. In most engagement measurement tools, such as GEQ [28] and UES [11], focused attention is measured in accordance with the users' perceptions of their concentration and loss of time in their gaming experiences. The tools weigh in users' subjectivity measures. These perceptions, nonetheless, may be further comprehended when they are quantified using other methods, such as the eye-tracking method.

On the other hand, attachment had been assessed in past studies based on the effect of players' game experiences, interaction, and enjoyment. A study using the PLAVA model by [7] contended that there are other significant elements in the model, namely sociality and character attachment. Sociality includes emotional investment, anthropomorphic autonomy, suspension of disbelief, and sense of control. Banks & Bowman assessed all these components to measure the extent of players' sense of themselves in gameplay in terms of agency, presence, and engagement. These components are applicable to DEGs as well. The attachment that a player has to an avatar can significantly affect physical presence, emotional presence, and narrative presence, particularly when the environment involves avatar customization [3]. As reported in [3], the attachment established between a player and an avatar can significantly affect enjoyment as well.

A study by Mohd Tuah [29] modelled the motivational design of avatar based on its role in gameplay. The roles are inclusive of a player's profile identification or in-game character. For profile identification, players may set their profile by selecting the available avatar as their affiliation and also as their in-game character. The players are allowed to choose their preferred avatars to represent themselves in the gameplay. The relationship established between the player and the avatar is based on the avatar roles in the game. Nevertheless, the model excluded other method(s) to validate the relationship. Apparently, the application of avatar, at some point, will effectively motivate the users, thus engage the players. However, this engagement varies depending on the condition and the environment where the avatar is applied – if the avatar is designed in 3D/2D model or if it is merely a flat image or if it is animated with the variation of avatar design types. Table I lists the variation of avatar design types reported in past studies. The interpretation of avatar types are as follows: 1) human character (lifelike or cartoonish), 2) hybrid (unrealistic human mix between human and animal design), and 3) abstract human form design.

On another note, DEG is also a part of serious games; whereby in a healthcare environment, DEG is used mainly to assist patients in learning and comprehending their condition, as well as for health self-management. For example, Hwang and Mamykina [9] applied DEGs to encourage a healthier lifestyle. They used an avatar as the player's representation that changed based on the choices of high- or low-calorie snacks intake. The players (patients) eventually learnt about nutrition intake and its impact on their body. Their study revealed that DEGs could significantly affect the healthcare environment on a larger scale.

TABLE I. SUMMARY OF AVATAR DESIGN TYPES

Article	**Human lifelike character**				**Abstract Human Form Design**
[31]	Real Human Image (1)	High (anthropomorphism) (2)	Medium (anthropomorphism) (3)		Low (anthropomorphism) (4)
[5]	the scientist avatar (1)		athlete avatar (2)		shape avatar (3)
[7]	Me (oneself) (1)	Symbiote (2)	Object (3)		social other (4)
[6]	Human lifelike character (1)	human cartoon character (2)	medium human-like character (3)	hybrid character (4)	abstract character (5)
[4]	Human (high anthropomorphism) (1)		Robot (high anthropomorphism) (2)		Block-like (low anthropomorphism (3)
[30]	Realistic humans (1)	Humanoid machine (2)	Unrealistic human (3)		Abstract human form (4)
[19]	Kinect-Video (Human) (1)	Human-Model (2)	Robot-Model (human-robot) (3)		Hybrid (Real Human + Robot) (4)

Hence, investigating the aspect of engagement based on avatar types and roles using the platform of DEGs can shed light on the personal avatar effects, as well as the best way to deliver them. In DEGs, it is integral to identify the learning outcome of the game, which serves as a measurable indicator in determining the player's achievement.

Following the above discussion, several components were identified as the factors in modelling the PLAVA in light of students' engagement and attention in DEGs. The components include avatar designs and roles in DEGs; player's demographic, learning outcome, and engagement – attention; aesthetics appeal; perceived usability; reward; character attachment; and sociality.

C. Definition of Components

Based on the processes exemplified above, the definition of each component is as follows:

- The avatar design – It denotes the avatar and its roles. Notably, the avatar and its roles can affect the way a player engages in the DEG environment. This component specifies the selection of avatar type and its implementation in the games, as described previously for avatar design roles.
- The learning outcome – each educational game has its learning outcome to be achieved at the end of the game. Learning outcomes provide further insight into the relationships among the engagement components (attention, character, aesthetic usability, and rewards), particularly on the significance of the attributes in achieving the learning outcome of the games.
- The engagement – This component is about measuring the engagement of the players in DEGs. Several measurements can be considered, including 1) character attachment and sociality adopted from Banks & Bowman [7], 2) game engagement scale by O'Brien et al. [11], and 3) focus attention using the eye-tracking method to extract fixation-based data.

D. Interconnection among the Components

The PLAVA is interrelated between the setting fixed for the DEG environment and the components that determine the players' engagement in the DEG. The DEG environment takes into account three sub-components, namely player's demographic profile, learning outcome, and avatar design. These three components are interrelated to strongly justify the DGE environment. The determined learning outcome can influence the selection of avatar type and design. One with vital gaming skill and knowledge in the context of games environment can positively affect the PLAVA or vice versa.

In determining the engagement among students, several measurement factors are inter-related to each other. As defined earlier, the engagement components include measuring avatar attachment with sociality, game engagement, and focus attention. For avatar and game, the measurement tool is survey-based tools to measure PLAVA and the player's engagement with DEGs. To further support the survey data, fixation-based data were incorporated to assess engagement. By using the fixation-based data, which were gathered from the eye-tracking method, the players' focus attention was calculated and compared with the survey data.

E. Model Development and Validation

Following the component identification and their intercomponent relationships, the conceptual model was developed, as presented in the result section. In the development stage, the focus was on refining the flow of the components, particularly on how the components interacted with each other. Several attempts to formulate the model were made via idea brainstorming and discussions. The final developed model was then agreed upon after considering all issues discussed in this paper. As we discussed earlier, the developed model requires validation. Next, this paper explains the validation studies conducted in this study.

1) Validation study with expert review: Insights from research experts will be beneficial in validating the model. Conducting an expert review will helps to uncover the model limitations, uncertainties and problems that might not detected from the literature [32]. Thus, an expert review is planned and conducted to validate the model. For that, this study employed a focus group discussion. The focus group discussion is mainly to get further feedback on the developed model and the developed games as well as to put in place the future work related to the model. We asked these experts to identify any components that ambiguous and related comments for adjustments to improve the model. From this expert review studies, it helped the authors to answer some questions and rectified the misconceptions during the model development stage.

2) Participant and design: We conducted a focus group discussion to the experts in the field. The review studies were participated with five experts. A minimum of five experts are plausible to find average proportion of problems in heuristics evaluation [33]. The five experts are identified based on their expertise in the field of human-computer interaction, especially in user experiences, educational games, and aesthetics. All identified experts agreed to participated.

The review session is designed to be conducted via online meeting. The experts are invited to participate in the study via email. Once they agreed, details and materials of the meeting are sent to them for further action. Their consent to the studies is collected via email prior to the meeting. During the session, procedures of the discussion especially related to question-and-answer session were briefed beforehand. After the briefing, introduction to the model is presented followed by the discussion. The online meeting lasts two hours.

IV. Result and Discussion

A. The Player and Avatar Attachment Model

After analyzing the related components and synthetizing the relationships among the components for PLAVA in DEGs, the conceptual model for this study was built. Fig. 2 illustrates the proposed conceptual model for this study.

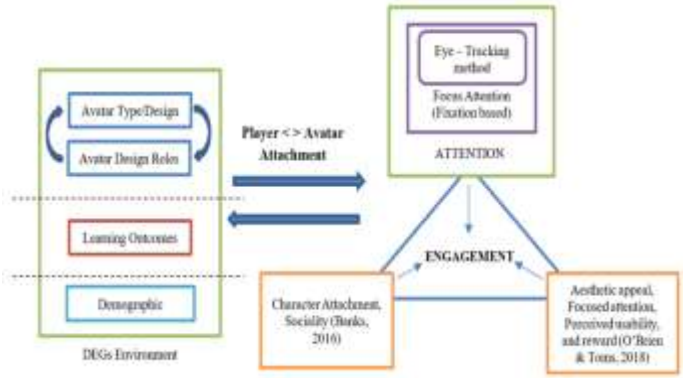

Fig. 2. The Player-Avatar Attachment Model.

In the PLAVA model, the DEGs environment involved with avatar type, avatar design roles, DEGs learning outcomes, and student's demographic. For engagement, it involved with attention, character attachment and sociality, and game engagement. From the PLAVA model, the main hypothesis is the avatar type (humanoid (x)) applied as (avatar design roles (y)) has positively affected the way a player engages in DEGs. Whereby x is a human character, hybrid design, and abstract design. Variable y is the identification and in-game character.

Meanwhile, as of the engagement, the PLAVA model has incorporated the elements to measure the player's engagement effect of the avatar in DEGs. Following the proposed model, it is assumed that the selected indicators have an integral role in defining the PLAVA within the context of DEG gameplay. Hence, the validation study in this area could address each component embedded in the PLAVA Model, so as to determine the effect of all the model components on the players in DEGs gameplay.

B. *Result of the Expert Reviews*

Five experts participated in the review studies. The demographic of the experts is summarized in Table II. The distribution of experts is appropriate considering their years of experiences, field of expertise, and the employment status. Three main questions were asked during the session.

1) What do you think about the model?
2) Do you find any ambiguous components in the model?
3) Do you have any comments to improve the model?

We analyzed the findings for the first question and summarized them in Table III. For the first question, findings in Table III show that all experts had agreed that the element of engagement and attention were the main factors in defining player attachments towards their avatar and the games. These factors were consistent with the reviews of engagement and attention in the component identification section in this paper. Two experts find that demographic component does not totally matters in the model. However, the other three experts contended the demographic is needed to analyze the player's perspective based on their background. Thus, the demographic component remains in the model. Therefore, based on the analysis of first question, the experts mutually have accepted the proposed model.

TABLE II. EXPERT DEMOGRAPHIC

Demographic	**No**
Gender	
Female	3
Male	2
Age	
35 - 40	3
40 - 45	2
Employment Status	
Senior Lecturer	3
Researcher	1
Post-Doctorate	1
Field of Expertise	
User experiences	2
Educational games	2
Aesthetics	1
Years of experiences in the field	
3 - 5	1
6 - 9	3
10 and Above	1

For the second question, there were a consistent remark from the experts on two issues that need further clarification. The issues are: 1) if the model should adopt all the items or adapt only some items accordingly, and 2) which type of avatar designs should be used to assess PLAVA and which avatar should be planned comprehensively. For the first issue, the PLAVA model incorporated all measurement items derived from Banks & Bowman [7] and O'Brien et al. [11]. In total, 30 (five items for each factor) items were used in the PLAVA model. As for the avatar type of design, five avatar designs were implemented (real human character, human cartoonish, a mix design between human and animal design, hybrid design (between animal and abstract design), and abstract design). These avatar designs were retrieved from [6].

TABLE III. EXPERT PERSPECTIVE ABOUT THE PROPOSED MODEL

Component	**Experts Agreement**				
	E1	***E2***	***E3***	***E4***	***E5***
DEGs Environment					
Avatar Type / Design	√	√	√	√	√
Avatar Design Roles	√	√	√	√	√
Learning Outcomes	√	√	√	√	√
Demographic	x	x	√	√	√
Engagement					
Character Attachment Sociality	√	√	√	√	√
Attention (focus attention)	√	√	√	√	√
Aesthetic appeal, focus attention, perceived usability, rewards	√	√	√	√	√

As of the third question, the comments were mainly discussing about the evaluation study. Two important points were highlighted in planning and conducting the evaluation study. One is associated with the completeness of the games, while the second is about the eye-tracking experimental setup. Game completeness is important to avoid bias. Bias may result from a player's confused state, mainly because instead of responding about the engagement, the player's responses could be influenced by the game usability. The second point is linked with the eye-tracking method. A step-by-step procedure should be outlined prior to the experiment.

As a result, the plan for the evaluation study is as follows: Two different games were installed to imply each one of the two different avatar roles (customization and personal identification). Each game deployed all the avatar types in the gameplay. Thus, with the two conditions (roles) and five variables (avatar types), ten sets of games were prepared to perform the evaluation study. The students were required to play each game for 20-30 minutes. In the end, they would have to reach a specific goal as the point of achieving the learning outcome(s) of the game.

V. Conclusion

Using Player-Avatar attachment as a method to define which avatar design and what roles that can be used to develop a sustainable engagement and attention in the DEG's gameplay require a careful attention. In general, having a well-presented avatar can help to boost a player's motivation to engage in the gameplay. However, the type of avatar design that can offer optimum attachment in DEG gameplay remains untapped. In order to understand the student's engagement in learning, methods other than the self-reflecting/preferences questionnaire tool should be employed. Essentially, the mixed method is bound to enrich the findings. One may further explore the player's visual attention by using the eye-tracking method. Upon combining these varying methods, there is high potential to develop an all-comprehensive PLAVA for future DEG design. Hence, this paper proposes a model for players (student) and their in-game avatar attachment in the context of DEG gameplay. The attachment could improve students' engagement in many different ways. By determining the avatar design type that can influence the PLAVA in DEG gameplay, suitable avatar designs may be applied for educational games in the future. For future work, an evaluation experiment will be performed to assess the PLAVA using the game that was created for this purpose. The design of the evaluation experiment will be derived from the validation study performed in this paper. Overall, ample opportunities are present for an avatar to serve as a significant social model for effective learning via game.

Acknowledgment

Authors would like to thank the university for the support and opportunities given in conducting the research as well as the participants who participate in completing this study.

References

[1] Turkay, S., & Kinzer, C. K., "The Effects of Avatar-Based Customisation on Player Identification", International Journal of Gaming and Computer-Mediated Simulations, vol. (6), no. (1), pp. 1–25, 2014.

[2] Wang, W., Zhao, Y., "Attributions of human-avatar relationship closeness in a virtual community", Lecture Notes in Computer Science (including subseries Lecture Notes in Artificial Intelligence and Lecture Notes in Bioinformatics), vol. (5288 LNAI), pp. 61-69, 2008.

[3] Kim, K., Schmierbach, M. G., Bellur, S., Chung, M. Y., Fraustino, J. D., Dardis, F., & Ahern, L., "Is it a sense of autonomy, control, or attachment? Exploring the effects of in-game customisation on game enjoyment", Computers in Human Behavior, vol. (48), pp. 695–705, 2015.

[4] Kao, D., & Harrell, D. F. "Toward avatar models to enhance performance and engagement in educational games", In Proceeding of the IEEE Conference on Computational Intelligence and Games, pp. 246–253, 2015.

[5] Kao, D., & Harrell, D. F., "Exploring the impact of role model avatars on game experience in educational games", In Proceedings of the 2015 Annual Symposium on Computer-Human Interaction in Play, pp. 571–576, 2015.

[6] Mohd Tuah, N., Wills, G., & Ranchhod, A., "The Characteristics and Application of Anthropomorphic Interface: A Design Spectrum", In Proceeding of The Ninth International Conference on Advances in Computer-Human Interactions, Venice, 24-28 Apr 2016, ThinkMinds, pp. 398–402, 2016.

[7] Banks, J., & Bowman, N. D., "Emotion, anthropomorphism, realism, control: Validation of a merged metric for a player–avatar interaction (PAX)", Computers in Human Behavior, vol. (54), pp. 215–223, 2016.

[8] Wiebe, E. N., Lamb, A., Hardy, M., & Sharek, D., "Measuring engagement in video game-based environments: Investigation of the User Engagement Scale", Computers in Human Behavior, vol. (32), pp. 123–132, 2014.

[9] Hwang, M., & Mamykina, L., "Monster Appetite: Effects of Subversive Framing on Nutritional Choices in a Digital Game Environment", In Proceedings of the 2017 CHI Conference on Human Factors in Computing Systems, ACM, Denver, CO, USA, pp. 4082–4096, 2017.

[10] Sibilla, F., & Mancini, T, "I am (not) my avatar: A review of the user-avatar relationships in Massively Multiplayer Online Worlds", Cyberpsychology: Journal of Psychosocial Research on Cyberspace, vol. (12), no. (3), article 4, 2018.

[11] O'Brien, H. L., Cairns, P., & Hall, M., "A practical approach to measuring user engagement with the refined user engagement scale (UES) and new UES short form", International Journal of Human-Computer Studies, vol. (112), pp. 28–39, 2018.

[12] Doherty, K., & Doherty, G., "Engagement in HCI: Conception, theory and measurement", ACM Computing Surveys, vol. (51), no. (5). 2019.

[13] Hookham, G., & Nesbitt, K., "A Systematic Review of the Definition and Measurement of Engagement in Serious Games", In Proceedings of the Australasian Computer Science Week Multiconference (ACSW 2019), ACM, New York, USA, Article 42, pp. 1-10, 2019.

[14] Barata, G., Gama, S., Fonseca, M. J., Gonçalves, D., & Jorge, J., "Improving student creativity with gamification and virtual worlds", In Proceedings of the First International Conference on Gameful Design, Research, and Applications - Gamification '13, New York, NY, USA: ACM, pp. 95–98, 2013.

[15] Birk, M. V., Atkins, C., Bowey, J. T., & Mandryk, R. L., "Fostering Intrinsic Motivation through Avatar Identification in Digital Games", Proceedings of the 2016 CHI Conference on Human Factors in Computing Systems - CHI '16, pp. 2982–2995, 2016.

[16] Huizenga, J. C., ten Dam, G. T. M., Voogt, J. M., & Admiraal, W. F., "Teacher perceptions of the value of game-based learning in secondary education", Computers and Education, vol. (110), pp. 105–115, 2017.

[17] Qian, M., & Clark, K. R., "Game-based Learning and 21st century skills: A review of recent research", Computers in Human Behavior, vol. (63), pp. 50–58, 2016.

[18] All, A., Nuñez Castellar, E. P., & Van Looy, J., "Assessing the effectiveness of digital game-based learning: Best practices", Computers and Education, vol. (92), no. (93), pp. 90–103, 2016.

[19] Woodworth, J. W., Lipari, N. G., & Borst, C. W., "Evaluating teacher avatar appearances in educational VR", In Proceeding of 26th IEEE Conference on Virtual Reality and 3D User Interfaces, pp. 1235–1236. 2019.

[20] Lin, L., Parmar, D., Babu, Sƒ. V., Leonard, A. E., Daily, S. B., & Jörg, S., "How character customisation affects learning in computational thinking", In Proceedings of the ACM Symposium on Applied Perception - SAP '17, pp. 1–8, 2017.

[21] Tuah, N.M., Yoag, A., Ahmedy, F., & Baharum, A., "A Gamification and Avatar Self-representation application for Diabetes Self-Management", International Journal of Advanced Trends Computer Science Engineering, vol. (8), no. (1.6), pp. 401-407, 2019.

[22] Hector R Ponce and Richard E Mayer., "An eye movement analysis of highlighting and graphic organiser study aids for learning from expository text", Computers in Human Behavior, Vol. (41), pp. 21–32, 2014.

[23] Moayad Mokatren, Tsvi Kuflik, Ilan Shimshoni, "Exploring the potential of a mobile eye tracker as an intuitive indoor pointing device: A case study in cultural heritage", Future Generation Computer Systems, vol. (81), pp. 528-541, 2018.

[24] Marta Koć-Januchta, Tim Höffler, Gun-Brit Thoma, Helmut Prechtl, Detlev Leutner, "Visualizers versus verbalizers: Effects of cognitive style on learning with texts and pictures – An eye-tracking study", Computers in Human Behavior, vol. (68), pp. 170-179, 2017.

[25] Mohd Nizam, Dinna & Law, Lai-Chong., "In the Eyes of Young Children: A Study on Focused Attention to Digital Educational Games", In Proceedings of the 32nd International BCS Human-Computer Interaction Conference (HCI), Belfast, 4 - 6 July 2018.

[26] Steichen, B., Wu, M. M. A., Toker, D., Conati, C., & Carenini, G., "Te,Te,Hi,Hi: Eye Gaze Sequence Analysis for Informing User-Adaptive Information Visualisations", In V. Dimitrova, T. Kuflik, D. Chin, F. Ricci, P. Dolog, & G.-J. Houben (Eds.), User Modeling, Adaptation, and Personalisation. UMAP 2014, Lecture Notes in Computer Science, vol. (8538), pp. 183-194, 2014.

[27] Borys, M., & Plechawska-Wójcik, M., "Eye-tracking metrics in perception and visual attention research", European Journal of Medical Technologies, vol. (3), pp. 11-23. 2017.

[28] Brockmyer, J. H., Fox, C. M., Curtiss, K. A., McBroom, E., Burkhart, K. M., & Pidruzny, J. N., "The development of the Game Engagement Questionnaire: A measure of engagement in video game-playing", Journal of Experimental Social Psychology, vol. (45), no. (4), pp. 624–634, 2009.

[29] MohdTuah, N., Wanick, V., Ranchhod, A., & B Wills, G., "Exploring avatar roles for motivational effects in gameful environments", EAI Endorsed Transactions on Creative Technologies, vol. (4), no. (10). 2017.

[30] Lugrin, J.-L., Latt, J., & Latoschik, M. E., "Anthropomorphism and Illusion of Virtual Body Ownership", In Proceedings of the 25th International Conference on Artificial Reality and Telexistence and 20th Eurographics Symposium on Virtual Environments, pp. 1–8, 2015.

[31] Gong, L., "How social is social responses to computers? The function of the degree of anthropomorphism in computer representations", Computers in Human Behavior, vol. (24), no. (4), pp. 1494–1509. 2008.

[32] Sweetser, P., Johnson, D., Wyeth, P., Anwar, A., Meng, Y., & Ozdowska, A., "Game Flow in Different Game Genres and Platforms", Computer Entertainment, vol. (15), no. (3), article 1, pp. 1-24, 2017.

[33] Nielsen, J., "Estimating the number of subjects needed for a thinking aloud test", International Journal of Human-Computer Studies, vol. (41), no. (3), pp. 385–397. 1994. http://doi.org/10.1006/ijhc.1994.1065.

Assessment of Emotion in Online News based on Kansei Approach for National Security

Noor Afiza Mat Razali[1], Nur Atiqah Malizan[2], Nor Asiakin Hasbullah[3]
Norul Zahrah Mohd Zainuddin[4], Normaizeerah Mohd Noor[5]
Faculty of Defence Science and Technology
National Defence University of Malaysia
Sungai Besi, Kuala Lumpur, Malaysia

Khairul Khalil Ishak[6]
Center for Cybersecurity and Big Data
Management and Science University
Shah Alam, Selangor, Malaysia

Sazali Sukardi[7]
CyberSecurity Malaysia
Selangor
Malaysia

***Abstract*—Securing a nation is more complicated in modern days than how it was decades ago. In the era of big data, massive information is constantly being shared in cyberspace. Online rumours and fake news could evoke negative emotions and disruptive behaviours that possibly can jeopardize national security. Real-time detection and monitoring of unsettling emotions and potential national security threats should be further developed to help authorities manage the situation early. Text in the online news could be weighted with emotions that possibly lead to a misunderstanding that can affect national security and trigger chaos. Thus, understanding the emotion included in the online news and the relationship with national security is crucial. Kansei approach was determined as a methodology capable of interpreting human emotions towards an artefact. This research explores the emotion assessment using Kansei for text in online news and summarized the emotion variable factors that are likely to have a relationship with an individual state of mind towards one of the national security elements which are political security. The result determines that the identified variables of factors were "Frustrated," Consent," Resentful" and "Attentive". This gives an understanding of the significant effect of people's emotions represented in the text for political security elements.**

***Keywords*—Online news; kansei; national security; political security**

I. Introduction

The increased use of the Internet by the community due to the development and advancement of information technology enables the utilisation of social networks on the digital media platform. According to the statistic of internet user's data by "statista" which is one of the well-known data statistic websites, in the early year of 2021, there are more than 4 billion active internet users across the world. People are connected in cyberspace via various types of existing social networks such as blogs and online news that create massive online data. Online news reports various types of issues that occurred in the country and world near to real-time and may have a potential risk of national security if not being monitored. National security is essential to maintain the survival of the nation and also a critical factor in ensuring national sovereignty through the use of economic power, diplomacy, power projection and political power. Threats related to national security need to be constantly monitored to retain the stability of a country. Moreover, with today's advancement in technology, mass information sharing has become one of the threats to political security.

Political security is one of the most significant elements of national security as it plays a major role in securing the nation's political institution from any threats that can weaken national security. Political institution stability plays a crucial role in sustaining community unity and upholding the rule of law in a country. The necessity for economic development, social harmony and the supremacy of the law is political stability. The rise of political issues can make the political environment unstable and indirectly poses a threat to the state of national security.

Personal convictions based on feelings and sensations are capable of influencing public sentiment than objective evidence [1]. Negative information in the news decreases positive effects due to the influence of negative effects on an emotion such as increased sadness, worries and anxiety [2]. To further understand the relationship between emotion in the text broadcasted in online news, this study proposed the application of the Kansei philosophy approach to evaluate human emotions toward artefacts in form of text gathered from online news. Kansei approach is mainly being utilised in the business and product services domain to obtain users feedback and emotional reaction [3]. However, there is a limited study being done in the national security domain using this approach. This support our research objective which is to assess emotions in national security elements from the online news text, focusing on political security. This study surveys the emotions laid in the online news text by evaluating the sample's reaction towards the text found in the online news. This research will contribute to understanding emotion that exists in online news text and its relationship with political security.

As for the following sections, it is organized as follows. In the second section, we give a detailed explanation of the background studies. For the next sections, we stated the overview of emotion assessment for online news using the Kansei approach for national security and also discussed the details of the methodology for the assessment of emotion in National Security elements. In Section IV, we present the result and findings of the experiment that had been executed. In the final section, as the conclusion, we summarize the main points of this research paper and discuss the future work plan for this research.

II. Background Studies

A. Security Elements and Political Security

National security is a very important feature as a protection control for any country [4]. There are several national security dimensions including economic growth and development, the structure of the economic process, welfare of citizens, variability of climatic conditions, preservation of natural resources and political stability [5]. Balzach discussed eight elements of national security which are military security, political security, cybersecurity, human security, homeland security, economic security, environmental security, energy and natural resources security [4]. Meanwhile, other researchers discussed that there are two basic elements in national security, namely, military and non-military. Military security is the competency of a nation to defend itself or intercept military aggression from the outside. The non-military element encompasses political security, cybersecurity, food security, economic security, human security, energy and natural resources security, environmental security, border security and health security [6], [7].

The concept of national security has been explained by emphasising that politics is one of four major national security dimensions [8]. Political security focuses on the stability of institutions and governments. Robert Mandel stated that political security is a concern with the organisational stability of the state's systems of government and the ideologies that give them legitimacy [9]. The role of political security in national security is important since political security acts as a defender in defence of the nation from any form of political oppression that can affect national security. Political oppression can lead to an unvisitable event such as a riot and civil war, which can disturb the unity of people [10]. To avoid these events, there is a need to ensure that the political state is in a stable environment and able to increase the quality of political security.

Political stability becomes a vital interest for national security because there are several threats that come from the political aspect which can harm the nation and weaken the state political security such as violations of the rule of law caused by tensions between communities. Thus, the good stability of the political security can strengthen the national security. A study in India underlined that national security needs to be viewed in political security terms to protect and promote national security goals and objectives [11].

Threats that can shake the country's political security stability are political violence, technology, and political upheaval, which possibly threaten the country's peace. Nowadays, the political issue can be easily expanded in cyberspace because of the sophisticated use of the Internet that can pose a threat to the political atmosphere of the country [12].

B. Online News and Emotions related to National Security Elements (Political Security)

Digital media such as Twitter and Facebook provide cognitive, affective and behavioural communication platforms that allow individuals to communicate collaboratively [13] and offer news and data mobilisation to individuals and allow them to share their views with many others, enabling them to participate in public engagement [14].

In the field of national security, the study of fear and anger in the political dimension found that these emotions can affect political behaviour and public opinions [15]. The relationship between emotion and the elements of national security can also be seen through human reactions towards environmental security issues. For example, ‘hope’ is an emotion that is shown by individuals with pro-environmental behaviours in relation to their feelings towards climate change policies [16]. The attachment of emotion can also be found in cybersecurity. Nowadays, cyberspace has become one of the potential threats to the country’s national security through the spread of fake news and hate speeches [17], especially when people believe and spread them. This is a concern for national security because it could harm the entire nation [18]. The relationship between emotion and hate speech in cyberspace is undeniable because cyberspace has an emotionally rich nuance and space where people can share their feelings, emotion, and thoughts [19].

A study also shows that national security can be strengthened by monitoring text that is being shared online because in the current online system, information is mostly displayed in text form [20] and words can reveal information like individual preferences, thoughts, emotions, and behaviours. A large amount of textual data has been generated because it is typical for an individual or persona to express emotion in words or text in cyberspace [21].

C. Kansei Approach

Kansei is a Japanese term for the sensibility and emotions that individuals have about a product or the environment [22]. Kansei can relate sensitivity, feeling and emotion. A study by Khairul discussed the application of Kansei Engineering in developing the Kansei Information Security Assessment (KISA) for developing a framework for user’s emotional assessment in the security domain, which employed the Kansei Engineering methodology in assessing human emotion factors in the designs and implementations of information security policies [23]. Other studies had used the Kansei approach in assessing the concept of trust in the information security domain by analysing the emotion of positive and negative that can influence the concept of trust [24].

Also, another research has been done focusing on user’s rage assessment for information security by using Kansei Engineering methodology. The artefacts were utilised as the specimen to evaluate the rage emotion on chatbot [25]. The research had shown that the Kansei approach could also be utilised on other applications or research related to the assessment of emotion including the information security domain. This supports the present study in implementing Kansei for political security related emotion assessment.

III. Emotion Assessment for Online News using Kansei Approach for National Security

In this work, we proposed that Kansei can be utilised as an approach to measure users' emotion in a text from the online news where the result can show the relationship between emotion and the national security elements. We utilised the KJ Method to determine the KW for the national security domain.

A. Conceptual Model for Relationship between the National Security, Physical Segment and Psychological Segment

Kansei's most common approach involves an evaluation activity using a pre-defined artefact accompanied by a statistical analysis of data. Kansei approach can evaluate the relation of emotion towards the artefact according to the research objectives. Many traditional methods seek to generalise such sensitivity through an average assessment of subjects. Relationships are formed between the average Kansei judgments and the specimen attributes [26].

The measurement approaches in Kansei are divided into physical and psychological segments. Eight elements of national security discussed by Balzacq are military security, political security, cybersecurity, human security, homeland security, economic security, environmental security, energy and natural resources security [4]. The additional elements discussed by [6], [7] are food security, border security and health security. The elements of national security are defined as the physical segment. The physical segment consists of stimulus in form of artefact. In this research, the artefacts are the sample of text from the online news.

Kansei evaluation is important to obtain users' evaluation in national security. The attribute set is defined as an emotional descriptor or Kansei Word (KW) that is taken from a noun or an adjective. This method has been used in many studies related to the characterisation of human emotions for various purposes of science such as analysis of emotional video material, emotional effects on viral video, digital learning content and retrieval of images [27]. KW is a word that can be used to represent a user's emotions. Generally, the selection of KW is made based on the literature review, experts' advice and magazine. The use of Kansei Word was follow up in the domain of research [28]. The use of the Kansei approach is to convey the psychological feelings of a product or an environment assembled with it. Fig. 1 shows the conceptual model for the relationship between the national security elements defined by Balzacq, Bahadur and Thakuri and Kshetri with actions stimulated by senses generated by psychological elements. The emotional elements are cited from research by [24] which are emotion, motivation, appraisal and perception.

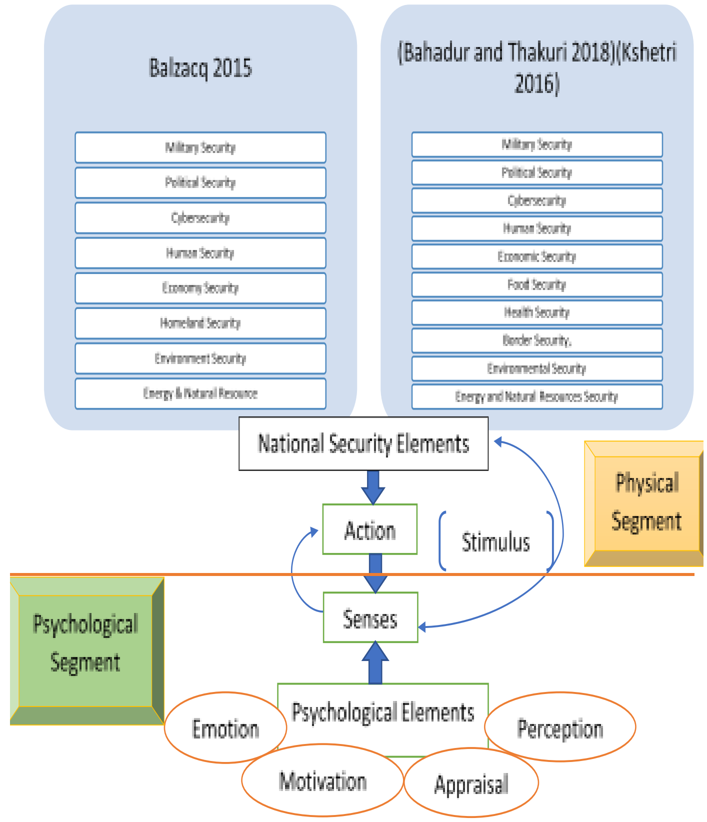

Fig. 1. Conceptual Model for Relationship between National Security Elements, Physical Segment and Psychological Segment.

Human mental states such as behaviour, act, expression and impression, is addressed by the psychological segment that can be measured using self-reporting systems such as the Different Emotional Scale (DES), the Semantic Differential (SD) scale or the free labelling method [25], [29]–[32]. Also, several methods using sensory measures including the SD have been used to determine the accuracy of Kansei objects represented by KW.

B. Emotion Assessment using Kansei

This section focuses on the related processes in Kansei evaluation measurement that was executed to measure the relationship between the emotion and the text in the online political news. Our focus for this study is political security which is one of the elements of national security. The Kansei evaluation measurements are based on responses gathered using the Kansei Checklist, a form of a questionnaire that includes emotional keywords or known as Kansei Words (KW) [33]. The evaluation was done in four phases. Phase 1 is Instrument Preparation, Phase 2 is the Establishment of Kansei Words (KW), Phase 3 is Kansei Evaluation Procedure and Activity, and Phase 4 is Kansei Result Assessment. The methodology for the assessment of emotion in national security elements focusing on political security used in this research is shown in Fig. 2.

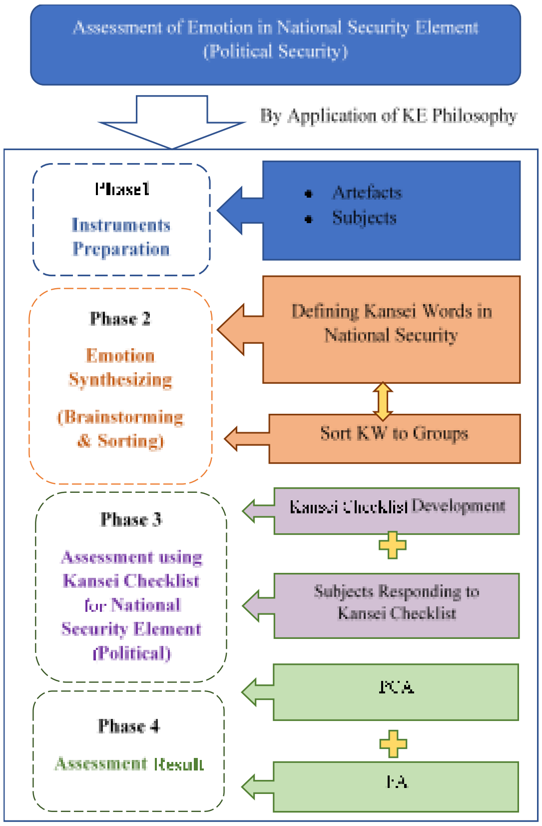

Fig. 2. Methodology for Assessment of Emotion in National Security Elements.

1) Phase 1: Instrument preparation: This step determines the instruments which are the Kansei artefacts and the subjects that will be used in research. Artefacts include the text in the online news that have a relationship with national security elements etc., whereas subjects are people that have an understanding of national security. In this study, the Cadet officers at the National Defence University are our subjects.

2) Phase 2: Establishment of kansei words: Kansei Word (KW) is used for the concept of perception in the chosen product or research domain. The selected Kansei Word should be related and capable of defining the domain for this study. For this study, the focus domain is national security. Significant words in online news that were presumed to give an impact on the state's national security was taken into consideration while establishing the KW[34]. To develop the list of KW related to national security, the KJ method, also known as part of the affinity diagram was used. KJ method was founded by Jiro Kawakita as a tool for grouping and summarising emotional keywords into their group preferences [28]. The purpose of the affinity diagram is to assess the group members as they are related to the choice of research domain [35]. The key idea behind the KJ method is to organise ideas. Various methods are used for creative thinking, such as brainwriting, mind maps, and spatial hypertext. KJ method is a part of the creative thinking methods, which involve brainstorming and structuring the idea [36]–[38]. The KJ method could also be utilised for any mechanism because it is a universal method [39].

Based on the Kansei affinity cluster methodology used by [40] we implemented this phase in three steps which are: i) the initial study step; ii) the exploratory study step, and iii) the KJ application step. The first step was required to emphasise the national security domain as a reference to generate the KW. This phase acquired a common type of results. This is because the key point for the idea is related only to the general idea of the national security domain. It was viable as the first action in this research method. The initial KW would be generated according to the national security domain. The process of synthesising the initial KW was done by referring to the literature on national security and experts.

The second step required human participants. It utilised the results of the initial set of words from the first step. Experts in national security and psychology were recruited to brainstorm KW for the national security domain. Next, multiple processes, cross-searches, and review of synonyms and antonyms from dictionaries and glossaries were performed to make sure that all possible KW for the national security domain has been gathered during this phase. A literation process was also conducted for this phase until all possible KW have been searched and identified. The second step was conducted with all possible lists of KW.

In the third step, participants were recruited to perform an activity based on the KJ Method. The participants are the Cadet officers at the National Defence University, who have the knowledge and exposure to national security. To start the experiment in a controlled environment, each KW was written down on a piece of card or paper. Each word was displayed on a large surface and arranged in random ways for the participants to sort according to their understanding of the national security concept.

This clustering session required a facilitator that acted as a guide for the participants. The participants were required to search for two words that have a relation with each other and to put the linked words together. Other words that were not related were placed aside. The main priority was for words that have a similar relation. If a word has other aspects of relation, a new group was created and the word was set in that group. This repetitive process was considered done when the participants have finished arranging and putting all words together according to their relationships. Words that did not belong to any group were excluded from these groups and the participants put the word into a new group. Each of these words has its headers.

Once the participants have completed the word grouping, a header was assigned to each group. The participants had to develop a question between participants to create the header for the words that represented the group. This phase was concluded with precise keywords that could help the discussion run smoothly. This session could also begin by creating the header first and then word listing and grouping each word that has a relationship with the existing header. Participants need to discuss and decide on the need to create a super header, where the super header will act as a parent to one header or more.

Lastly, the participants had manually evaluated the words that have been grouped under each header. Then, they were required to check the final diagram to confirm that the headers and groups were represented according to their right cluster.

3) Phase 3: Kansei evaluation procedure and activity: After determining the KW for national security, Kansei evaluation was conducted using the KW for national security. For this phase, we choose political security, the elements of national security as the focus of our Kansei Evaluation. To accomplish the objective, the Kansei assessment for this study was carried out with 20 participants selected to took part in the tests. The activity was conducted in two separate sessions. There were 10 people involved in the first session and another 10 people for the second session. For phase 3, a set of stimuli focusing on the political security element was prepared.

a) Stimuli: Stimuli was produced from 30 sample texts from political news from various news platforms in Malaysia. The selection process took the most time and effort to complete before finalising the number of sample texts. There were several steps taken in examining the sample texts. The first step was looking for the digital platform news that is popular among societies in Malaysia, such as “The Star,” “New Straits Times,” and “Malaysiakini.” The second step was searching for news that focuses on the aspects of politics in the chosen news platform. The next steps were to select and examine certain texts in the chosen political news. The text samples were defined in regard to certain control parameters and the prerequisite for matching the domain research. The procedure was repeated for each chosen news platform. The precision of the text sample specimen has to be considered when finalising the text sample. All 30 sample texts were collected since the assessment focused on text features that only require textual material to be displayed and evaluated by the participant. Examples of sample text are shown in Fig. 3.

b) Participants: 20 people were recruited for the evaluation and the experiments were performed in Malaysia. These participants were from the state security field. Participants preferred not to have a visual disability problem and agreed to see textual visualisation that may contain harsh words. Participants comprised 11 men and 9 women aged between 19 and 30 years. Subjects were asked to respond to questioners on the basis of their feelings for each of the text samples displayed in front of them.

Sample No:	Text
1	Malaysia refutes racism claim by news network ,the government has slammed a report carried in Al Jazeera's 101 East, in which it accused Malaysia of racism in handling illegal immigrants during the Covid-19 pandemic
2	The common good of the nation requires less of power politics and substantive consensus to move the nation forward to confront an existential threat. The service for the common good should be core principles that inspire political behaviour among politicians.
3.	With its leadership tossed into uncertainty again, Malaysia risks delays and loss of new investments, analysts and business groups say, as anxiety bubbles among foreign investors worried about policy disruption and reforms stalling
4	The persistent uncertainty associated with an unstable political environment has undermined investor confidence, weakened consumer sentiment and reduced pace of economic development
5.	A change of government at this juncture could upset a wide range of activities planned to contain the pandemic and the socio-economic problems.

Fig. 3. Examples of Sample Text.

c) Procedure: The people who took part in all sessions participated in their own will and were allowed to self-report their emotional reactions on the assessment sheet. The evaluation began with a briefing on consent statements and guidance for the participants. For each of the 30 sample texts, a checklist containing KW adapted from an affinity cluster for national security in political security aspects was added.

Kansei Checklist was created to measure emotions after the KW was defined. Kansei Checklist was represented as a sort of a questionnaire that consists of KW. Fig. 4 shows the sample of Kansei Checklist Evaluation forms containing a checklist of 25 KW for each sample text that was distributed to all participants to prevent response bias. The order of the Kansei words for each sample text was in a random arrangement.

The participants were asked to complete Kansei word ratings in conjunction with their emotional reactions to the sample text. Participants gave ratings on their feelings after viewing each sample text in the shape of a 5-degree bipolar of semantic differential (SD). The semantic differential method developed by Osgood is a common scaling device for quantifying subjective consumer emotions [41]. The purpose of the semantic differential approach is to provide quantitative support to encourage users to provide an objective assessment of the specimen's psychological value. This involves descriptive scales with adjectives to assess the similarity or difference between subjects. A semantic differential of 5 points was used in this present analysis because these scales appear to be more easily interpreted by respondents than more point score methods. Fig. 4 shows that the Kansei checklist established was arranged in a 5-point semantic differential scale and consisted of 25 KW. The rating scale was (1=" not at all; "5=" very much”). Each session lasted for 1 hour; before moving to the next sample text, the participant was given 5 minutes to complete the rating, and similar instructions were given for all 30 sample texts.

4) Phase 4: Kansei result assessment: The final phase is the Kansei assessment result discussed in the next chapter.

Subject ID: __________ Sample No: __________

			Contempt			
Very much	5	4	3	2	1	Not at all
			Questioning			
Very much	5	4	3	2	1	Not at all
			Resentment			
Very much	5	4	3	2	1	Not at all
			Embarrassment			
Very much	5	4	3	2	1	Not at all
			Rejection			
Very much	5	4	3	2	1	Not at all
			Hatred			
Very much	5	4	3	2	1	Not at all
			Downhearted			
Very much	5	4	3	2	1	Not at all
			Tolerance			
Very much	5	4	3	2	1	Not at all

Fig. 4. The Sample of Kansei Checklist.

IV. Result and Findings

A. Result on Kansei Affinity Diagram

Kansei most common approach involves an evaluation activity using a pre-defined artefact accompanied by a statistical analysis of data. Kansei approach can evaluate the relation of emotion towards the artefact according to the research objectives. Many traditional methods seek to generalise such sensitivity through an average assessment of subjects. Relationships are formed between the average Kansei judgments and the specimen attributes [34]. The measurement approaches in Kansei are divided into physical and psychological segments.

Eight elements of national security discussed by Balzacq are military security, political security, cybersecurity, human security, homeland security, economic security, environmental security, energy and natural resources security [4]. The additional elements discussed by [6], [7] are food security, border security and health security. The elements of national security are defined as the physical segment. The physical segment consists of stimulus in form of artefact. In this research, the artefacts are the sample of text from the online news.

The results from the initial study were then used in the exploratory study as a reference for experts to derive more Kansei Words and to perform cross-checks from the glossaries. The number of Kansei Words from the initial study has increased from 41 to 236, which included "embarrassment", "loathing", "apprehension", "appalling", "despair", "woefulness", "horrified", "shock", "relief", and "bitter". Identified Kansei Words is shown in Table I.

After utilizing the KJ method to organise these KWs into "affinity groups", eleven clusters were created by Cadet's students who participate in this study. The compiled KW in each cluster was developed into a dictionary of emotion based on national security, as shown in Table II. The clusters are political security, economic security, border security, cybersecurity, human security, energy and natural resources security, environmental security, military security, food security, health security and personal security.

TABLE I. Identified Kansei Words

References	Kansei Words (KW)
[42]	Trust, Empathy, Hope
[43],[44]	Fear
[44]	Anger, Hatred, Contempt, Shame, Guilt, Envy, Love, Care, Pity, Anxiety
[45]	Helplessness, Interest, Sadness, Depression, Disgust, Worry
[46]	Doubt
[47]	Grief
[48]	Alarm, Cautious, Disengaged, Doubtful, Dismissive
[49]	Calmness, Optimism, Tolerance, Prosperity, Ease, Conformity, Concern, Stiffness, Disquietude, Upset, Confidence Nervousness, Sympathy, Aggression

TABLE II. Kansei Affinity Clusters based on National Security

Cluster	Kansei Word
Political security	Contempt, Questioning, Resentful, Embarrassment, Resentment, Rejection, Hatred, Downhearted, Disgruntled, Cynical, Anger, Disbelief, Rejecting, Pissed, Enraged, Fear, Dejection, Agony, Wrath, Tolerance, Irritated, Aversion, Eagerness, triumph, contentment, Satisfaction, Adoration, Affection, Attraction, Compassion,
Economic security	Bargaining, Peeved, Distracted, Interest, Perplexed, Loathing, Neglect, Impatient, Dislike, Irritation, Grief, Shaky, Envy, Care, Disappointment, Scary, Aggravation, Misery, Insult, Stress, Guilt, Trust, Anxiety
Border security	Afraid, Scared, Anguish, Worry, Distrust, Apprehension, Off Guard, Frightened, Beastly, Exasperation, Ferocity, Bitterness, Hate, Apprehensive, Enthusiasm
Cybersecurity	Trouble, Insecurity, Anxious, Disturbed, Astonished, Suspicious, Unsure, Confuse, Sceptical, Denial, Doubt, Concern, Frustrated, Appalling, Rage, Spite, Gloom, Disapproving, Furious, Nervousness
Human security	Joyful, Irritable, Dismay, Offended, Love, Calmness, Upset, Sad, Happy, Optimism, Humiliation, Ease, Proud, Angry at self, Disgusted with self, Scornful, Disquietude, Confident, Bold, Daring, Annoyed, Vengefulness, Jealousy, Despair, Regret, Nervous, Horrify, Insulted, Irate, Contentment
Energy and natural resources security	Depression, Distress, Empathy, Blue, Disgust, Torment, Devastating, Jittery, Blameworthy, Conformity, Mortification, Annoyance, Revulsion, Isolation, Mad, Woefulness
Environmental security	Alarm, Concerned, Cautious, Disengaged, Doubtful, Dismissive, Helplessness, Uncomfortable, Hope, Hurt, Sadness, Horrified
Military Security	Hostility, Terror, Chaotic, Goosebumps, Suffering, Pride, Terrify, Strong, Hostile, Stiffness, Petrified, Shock, Fury, Defeat, Serenity, On Edge, Alienation, Mistrust, Aggravated, Vengeful, Gloomy, Panic, Grieve, Amazed, Astonished, Thrill, Exhilaration
Food Security	Relief, Unhappy, Vindictive, Depressed, Unhappiness, Outrage, Dread, Desperate, Melancholy, Grouchiness, Grumpiness, Desolation, Satisfaction, Pleasure
Health Security	Pity, Displeasure, Lost, Prosperity, Confidence, Delighted, Hopeless, Excitement, Disappointed, Compassion, Amusement, Reluctant, Grouchy, Disdain, Hesitant, Agitated, Edgy, Nauseated, Tenderness,
Personal security	Fearless, Infuriated, Safety, Surprise, Moody, Lonely, Contrary, Bitter, Shame, Cold Feet, Loneliness, Hysteria, Horror, Satisfaction, Inhibited, Sorrow, Remorse, Relaxed, Cheerful, Guilty, Ashamed, Hopelessness, Miserable, Dissatisfied with self, Alone, Timid, Sentimentality

From the result in Table II, we found out that 25 KW were clustered and listed in the affinity cluster of keywords under the political security aspects. The KW for political security included "fear, compassion, contempt, disbelief," which describe the political perception and emotions of people based on political security aspects of national security. The results from this procedure are shown in Fig. 5.

Contempt	Resentment	Questioning	Embarrassment	Rejection
Hatred	Downhearted	Disgruntled	Cynical	Anger
Disbelief	Enraged	Fear	Wrath	Agony
Tolerance	Irritated	Aversion	Eagerness	Triumph
Contentment	Satisfaction	Adoration	Attraction	Compassion

Fig. 5. Kansei Words for Political Security Element.

B. Result from the Kansei Assessment

This sub-section discusses the analysis performed over the result obtained from the experiment. First, the validity of the test was validated by the Cronbach Alpha reliability test. Next, the correlation of the Kansei words towards the sample text was analysed. The result was analysed using PCA and FA. PCA and FA is a statistical method that is able to construct a well-organised Kansei space with the selected Kansei words for specific purposes. The statistical analysis that comes from PCA and FA can give clear explanations and visual output. It also contains a descriptive graph that is easy to be analysed and understood. It also directly translates numerical data into useful information. For example, radar plots and profiles for Kansei words can be used to check similarities among words.

PCA is an abbreviation from the word Principal Component Analysis (PCA). It is a commonly used multivariate technique that helps to understand the underlying data structure. This method in the preference matrix was resolved into a set orthogonal preference dimension represented both Kansei words and artefact. The KWs were represented in the first two principal components, giving a visual representation of the semantic space. The located Kansei words (the responses) was shown on a scatterplot with the first principal components displaying similarly perceived responses.

Factor Analysis or abbreviated as FA, is helpful to direct the process of concept mapping by clustering the Kansei Words into smaller groups. FA is a technique of statistical data reduction used to observe the variability of correlations in random variables or minor differences in random variables that are then compared. This reduction is important as the level of any attribute is influenced by the effects of other attributes. Usually, FA may reduce the data level of different attributes to some important degrees. Inductive analysis can be done through factor analysis. The outcome is evaluated by measuring a coefficient of correlation between each variable and another variable. The FA is often used to analyse Kansei's study concept and psychological structure due to the data structure generated from the data collection.

In this research, reliability analysis was performed to expose the reliability and efficacy of the Kansei Checklist survey questionnaire. A high-reliability coefficient value means that the Kansei Checklist survey questionnaire is reliable. The accuracy of the results from the survey carried out over various lengths was evaluated. To test internal accuracy, the Cronbach alpha of the Kansei Checklist was determined. Cronbach's alpha is the statistic commonly used today to estimate internal consistency. It explains that alpha is maximised when each item on a scale shares a common variance with at least some other items on the scale [50]. Several reports suggested that the benchmark value for Cronbach's alpha of 0.70 above is acceptable; nevertheless, 0.80 or higher is preferred.

Based on Fig. 6, this study yielded a Cronbach's total alpha value of 0.969, which is greater than the 0.7 typical benchmark value. The reliability of the Kansei checklist was verified by this.

Reliability Statistics

Cronbach's Alpha	Cronbach's Alpha Based on Standardized Items	N of Items
.969	.973	750

Fig. 6. Reliability Analysis.

This research focused on the impact of the emotion in the text on political news. Thus, for this research, the evaluation was done by PC loading because it can help in representing the evaluation between the Kansei words and specimen; first, the visibility of distributed emotions across the semantic space is studied to deliver an indication that the assessment of emotions is effective. Effective evaluation is needed to explain the importance of the data on emotion to further evaluate operations. It can be shown from Fig. 7 that there was a decent distribution of KW on both axes, suggesting an efficient evaluation of emotion. After that, the emotional structure axes were observed.

The plot reveals the emotions that generated large negative loads of the first PC (x-axis), which were led by 'Satisfaction.' The field on the left side of the chart corresponded to those emotions. On the other side, emotions generated by large positive PC loads were "Rejection," "Embarrassment" and "Downhearted." Also, the dense section at the most right of the semantic space was presented by them. Then, this axis was named as the 'Emotional' axis. From there, it can predict those variables with high score values on this component, which have a higher sense of emotion.

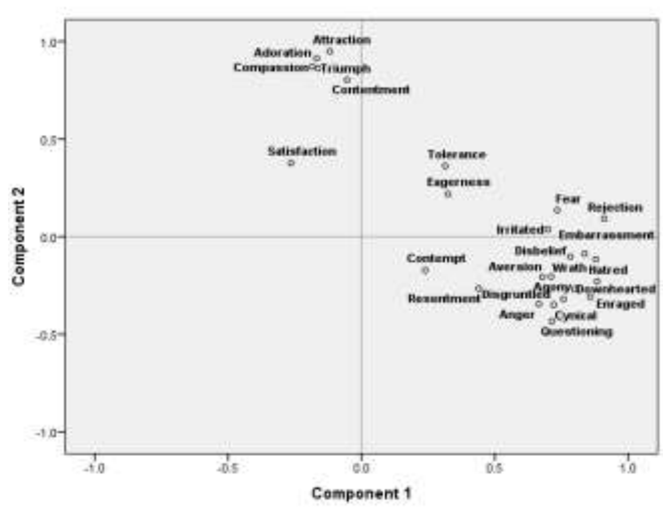

Fig. 7. Result of PC Loading.

For the second component loading (y-axis), emotions that have larger positive loading were “Attraction” and “Adoration”. The emotions on the side larger negative loadings were “Questioning,” “Anger,” and “Cynical.” The research identified this PC as the 'Acceptance' axis. Low-score factors in this component were more toward having high acceptance characteristics and vice versa.

FA was used to recognise important Kansei factors for the emotion of sample texts in political news that could affect the unity of people and state national security. FA is widely used to extract the psychological structure of the emotional component that constitutes the fundamental principle of the study domain [51]. Based on statistical data, FA demonstrates a reduction technique to explain variability among observed random variables in terms of unobserved random variables called factors. To reduce the number of complex variables and enhancement the interpretation of variables, FA was performed by the Varimax rotation. This was accomplished by analysing the contribution of variables after the rotation of varimax. Kaiser introduced the Varimax rotation in 1958, which then became the most common rotation approach for simplifying the understanding of variables [52]. This research used the average assessment value between specimens to find the factors. Table III summarises the contributory variable outcomes.

TABLE III. FACTOR ANALYSIS RESULT

Factor	**Contribution and Accumulated Contribution**	
	Contribution (%)	***Accumulated contribution (%)***
1	38.920	38.920
2	20.760	59.680
3	19.029	78.709
4	7.299	86.008

Table III shows that the first factor explains 38.920% of the result, which represents the majority of the key factor contribution and has a significant impact on Kansei words. 20.760% of the data were explained by the second factor, while the third factors have a small factor contribution of the 19.029% and the fourth factor has a small percentage contribution of 15.09%. The first factor alone constituted 38.920% of variability, while the second variable described 60.759% of the variability.

The inclusion of the second factor was assumed considerable; thus, much of the data may be clarified by the first two factors. Whereas Factor 3 and Factor 4 contributed 78.709% and 86.008%, correspondingly. Slight segments of the third factor and the fourth factor were considered to be significant since they can be summed as the contribution rate that represents all the data results. The results of factor loading in ascending order are shown in the following Table IV. The result classified a big value of variables into groups. This data needs to be analysed to help to clarify the emotional connection towards the sample texts. Variables with a higher score are considered important factors.

TABLE IV. THE FACTOR LOADING OF THE 25 VARIABLES USING FOUR FACTORS

Variables/ Adjectives	**Factors**			
	Factor 1	***Factor 2***	***Factor 3***	***Factor 4***
Rejection	0.910			
Hatred	0.883			
Embarrassment	0.878			
Enraged	0.858			
Disbelief	0.837			.
Downhearted	0.798			
Wrath	0.783			.
Agony	0.757			
Fear	0.734			
Cynical	0.721			
Questioning	0.713			
Disgruntled	0.710			
Irritated	0.699			
Aversion	0.678			
Anger	0.665			
Attraction		0.948		
Adoration		0.913		
Compassion		0.870		
Triumph		0.862		
Contentment		0.802		
Contempt			0.880	
Resentment			0.810	
Satisfaction			-0.649	
Tolerance				0.796
Eagerness				-0.680

The structure of KW can be seen and observed in the analysed findings of this research. This research defined the value of 0.7 as average. However, a slightly lower score can also be known as a substantial concept [53]. From Table IV above, it is clear that the significant factors for a sample text in political news specimens were defined by 4 factors. The list of content in the first factor included “Rejection,” “Hatred,” “Embarrassment,” “Enraged,” “Disbelief,” “Downhearted,” “Wrath,” “Agony,” “Fear,” “Cynical,” “Questioning,” “Disgruntled,” “Irritate,” “Aversion,” and “Anger.” This research labelled this Kansei space as “Frustrated.”' The second factor consists of “Attraction,” “Adoration,” “Compassion,” “Triumph,” and “Contentment.” This research labelled this Kansei space as “Consent.” The third factor included “Contempt,” “Resentment,” and “Satisfaction.” This Kansei space was labelled as “Resentful.”

After that, the fourth factor involved “Tolerance” and “Eagerness.” This research labelled this Kansei space as “Attentive.” When labelling all the factors or deciding the term for Kansei space, this research followed the standard practice in Kansei of choosing representative terms that one would believe and effectively characterise the group of factors or Kansei space. There was no conditional decision for this since there was no correct or incorrect judgment of the chosen keywords. As long the chosen keywords can be parameters that match the variable of the group factors.

These four variables together accounted for 86.008% of the total results. The outcome result from the FA proof that the Kansei concept for sample texts from political news was structured by four factors. The four factors were “Frustrated,” Consent,” Resentful,” and “Attentive.”

The first two factors with more than 59.680% of data variance are important concepts for texts in political news emotional concepts. The result indicates that Factor 1 was the most important Kansei concept for text in political news since it consists more than the percentage value of data variance that influences the result. Meanwhile, Factor 2 contained fewer correlations than Factor 1 but could be defined as potential variables against the factor.

The insertion of the third and fourth factors tended to be significant, even if the contribution was lower for these two factors, which was 19.029% and 7.299%. This research agreed to preserve the third and fourth factors because of the importance of the KWs toward the sample text specimens. These two factors could be adding as an important concept of text in political news, which could be used as supporting factors for the main factors above described by the first and second factors. Although the first and second variables may have been concluded as major significant Kansei concepts, other factors should be used to support the comprehension of the emotion towards the political news that could impact the people and state national security.

It can be observed from the above results that the text in political news influences people's emotions. The sample texts in political online news used as an artefact for this research produced emotional feedback and most likely toward negative views. From the data analysis, it can be understood that the type of word in the text has a significant influence on a particular emotion. This research managed to conclude four labels of emotions that have a significant relationship with political security elements in the national security domain.

V. Conclusions

This research explored the utilization of Kansei approach as a methodology to assess texts in online news that touch on national security issues and try to understand the relationship between the text and emotion that may affect the political stability in national security. This study has therefore adopted the KJ method in finding the KWs emotion words for national security to test the emotional response toward the subjects.

This research has shown four important factors that established Kansei's basic concepts for text in political security elements that could impact the state national security. “Frustrated,” Consent,” Resentful” and “Attentive” were the identified variables of factors. Consequently, these four variables were likely to give a high level of political understanding, awareness and effect on the individual’s state of mind in regard to the political issues. This analysis selected text on various news platforms including “the Star” and “News Strait Times” online newspaper. This research selected texts on political issues with the text viewing and reading experience; the subjects reacted to it with mixed opinions that consisted of negative and positive reactions.

VI. Discussion and Future Work

This research is an ongoing study that shows the pilot result regarding people's emotions extracted from text in political online news. Emotions of human beings are influenced by what they see and depends on how the eyes and brain are functioning together to generate the reaction. The results of this study can be utilised as a foundation to understand the relationship between emotion and political knowledge from textual representations in digital media. Our next step is to perform activities with a larger group of participants to obtain more comprehensive data for the analysis. The process of evaluating the respondents’ results needs to be carefully managed especially during the process of entering the data into the data analysis software. It is to prevent the unmatching and wrong results. Other than that, the limitation of this study is the result was only referred to the emotion words in the text without specific emotion weight value being determined. Given the importance of the weight score for each word in opinion mining, the mechanism to determine the weight score is also essential, thus, an extended study can be done to identify and analyse the method that can be implemented to measure the weight of the emotion word that is related to national security. Furthermore, a detailed analysis including a thorough assessment and evaluation of emotion is required for expanding the research outcomes. The results also can be utilised to establish national security dictionary that can be utilised for opinion mining.

For future work, we are planning to investigate and observe people emotions in the text that are being published on other digital platforms such as social media by using the Kansei approach. The research will help to understand more areas on national security elements in cyberspace with any type of digital platform. Also, potential future research will be the adoption of automation of Kansei approach using machine learning technique for the development of dictionary for national security domain to be used in opinion mining.

Acknowledgments

The authors would like to thank all experts and participants for their precious contribution in provided their insight and expertise that greatly assisted towards the whole research activities. This research is fully supported by the National Defence University of Malaysia (UPNM) under Short Grant UPNM/2020/GPJP/ICT/5. The authors fully acknowledged UPNM and the Ministry of Higher Education Malaysia (MOHE) for the approved fund, which makes this research viable and effective.

REFERENCES

[1] L. Bode and E. K. Vraga, "In Related News , That Was Wrong : The Correction of Misinformation Through Related Stories Functionality in Social Media," vol. 65, pp. 619–638, 2015, doi: 10.1111/jcom.12166.

[2] N. De Hoog, "Is the news making us unhappy ? The influence of daily news exposure on emotional states," pp. 157–173, 2020, doi: 10.1111/bjop.12389.

[3] Z. Li, Z. G. Tian, J. W. Wang, and W. M. Wang, "Extraction of affective responses from customer reviews: an opinion mining and machine learning approach," Int. J. Comput. Integr. Manuf., vol. 33, no. 7, pp. 670–685, 2020, doi: 10.1080/0951192X.2019.1571240.

[4] T. Balzacq, "What is national security?," What is Natl. Secur., vol. 52, no. 4, pp. 33–50, 2015, doi: 10.3917/ris.052.0033.

[5] J. and A. B. Scheffran, "Climate and conflicts: The security risks of global warming," Reg. Environ. Chang., vol. 11, pp. 27–239, 2011, doi: 10.1007/s10113-010-0175-8.

[6] B. Bahadur and S. Thakuri, "Human Security : Concept , Dimensions & Challenges Running Head : Human Security Human Security : Concept , Dimension And Challenges An Article Submitted to Lt . Gen . (Retd .) Balananda Sharma For the Partial Fulfillment of the Internal Evaluation of th," no. April, 2018.

[7] N. Kshetri, "The quest to cyber superiority: Cybersecurity regulations, frameworks, and strategies of major economies," Quest to Cyber Super. Cybersecurity Regul. Fram. Strateg. Major Econ., pp. 1–240, 2016, doi: 10.1007/978-3-319-40554-4.

[8] R. Vxyrnen, "Conceptual Analysis by Robert Mandel BOOK REVIEWS Concepts of Security Revisited," no. May, 2014.

[9] B. Buzan, "New Patterns of Global Security in the Twenty-First Century," Int. Aff. (Royal Inst. Int. Aff. 1944-), vol. 67, no. 3, pp. 431–451, 1991.

[10] L. Ronken, H. Eilers, and G. Re, "Strike , Riot and Civil Commotion – An Increasingly Significant Form of Cover," no. September, 2020.

[11] D. Enclave, R. Tula, and R. Marg, Institute for Defence Studies and Analyses (IDSA), no. 1. 2019.

[12] R. Sandoval-almazan and J. R. Gil-garcia, "Towards cyberactivism 2 . 0 ? Understanding the use of social media and other information technologies for political activism and social movements," vol. 31, pp. 365–378, 2014.

[13] B. D. Loader and D. Mercea, "Information , Communication & Society NETWORKING DEMOCRACY ?," 2011, doi: 10.1080/1369118X.2011.592648.

[14] S. Klar, "How Partisan Online Environments Shape Communication with Political Outgroups," vol. 13, pp. 2287–2313, 2019.

[15] T. G. Coan, J. L. Merolla, and E. J. Zechmeister, "Emotional Responses to Human Security Threats : Evidence from a National Experiment," pp. 1–26, 2012.

[16] I. Lorenzoni, S. Nicholson-Cole, and L. Whitmarsh, "Barriers perceived to engaging with climate change among the UK public and their policy implications," Glob. Environ. Chang., vol. 17, no. 3–4, pp. 445–459, 2007, doi: 10.1016/j.gloenvcha.2007.01.004.

[17] G. Belova and G. Georgieva, "Fake News as a Threat to National Security," Int. Conf. KNOWLEDGE-BASED Organ., vol. 24, no. 1, pp. 19–22, 2018, doi: 10.1515/kbo-2018-0002.

[18] E. Relations, "Cybersecurity : A National Security Issue ?," pp. 1–7, 2018.

[19] M. Yassine and H. Hajj, "A framework for emotion mining from text in online social networks," Proc. - IEEE Int. Conf. Data Mining, ICDM, pp. 1136–1142, 2010, doi: 10.1109/ICDMW.2010.75.

[20] C. Smeureanu, I., & Bucur, "Applying Supervised Opinion Mining Techniques on Online User Reviews," Inform. Econ. J., vol. 16, no. 2, pp. 81–91, 2012.

[21] A. F. Ab Nasir et al., "Text-based emotion prediction system using machine learning approach," IOP Conf. Ser. Mater. Sci. Eng., vol. 769, no. 1, 2020, doi: 10.1088/1757-899X/769/1/012022.

[22] P. Lévy and T. Yamanaka, "Towards a definition of Kansei TOWARDS A DEFINITION OF KANSEI," no. May, pp. 1–4, 2014.

[23] K. K. Ishak, N. A. M. Razali, A. M. Lokman, and K. Toshiyuki, "Kansei Information Security Assessment (KISA): Characterizing Trust as Stimuli for User Emotional Assessment in Information Security," Indian J. Sci. Technol., vol. 9, no. S1, pp. 1–6, 2016, doi: 10.17485/ijst/2016/v9is1/106846.

[24] A. Noor and K. K. Ishak, "The Assessment of Trust in Information Security Using Kansei," vol. 1, pp. 194–202, 2020, doi: 10.1007/978-981-15-7801-4.

[25] N. A. M. Razali, K. K. Ishak, N. J. A. MdSaad, N. M. Zainudin, N. A. Hasbullah, and M. F. M. Amran, "Conceptualization of Use as Rage Assessment Using Chatbot Interface by Implementing Kansei Engineering Methodology for Information Security," in Proceedings of the 8th International Conference on Kansei Engineering and Emotion Research, 2020, pp. 184–193.

[26] A. M. Lokman and M. Nagamachi, Kansei Engineering: A Beginners Perspective. University Pub. Centre (UPENA), 2010.

[27] R. E. Guadagno, D. M. Rempala, S. Murphy, and B. M. Okdie, "What makes a video go viral ? An analysis of emotional contagion and Internet memes," Comput. Hum. Behav., vol. 29, no. 6, p. 2312 2319, 2013.

[28] S. T. W. Schütte, J. Eklund, J. R. C. Axelsson, and M. Nagamachi, "Concepts, methods and tools in kansei engineering," Theor. Issues Ergon. Sci., vol. 5, no. 3, pp. 214–231, 2004, doi: 10.1080/1463922021000049980.

[29] J. Schütte, S., Schütte, R., Eklund, "Affective Values of Lift Trucks - an Application of Kansei Engineering," 2005.

[30] M. Ishihara, K., Nakagawa, R., Ishihara, S., Nagamachi, "An E-Commerce Site to Propose Gift Flower Arrangements That Fit Kansei and Social Manners.," 2007.

[31] M. Lokman, A.M., Noor, N. M., Nagamachi, "ExpertKanseiWeb – A Tool To Design Kansei Website," 2009.

[32] Y. Hashizume, A., Masaaki, K., Toshimasa, "Relative Importance of Design and Usability of Cell Phone in Terms of Age and Gender.," 2010.

[33] A. Hadiana, "Analysis Learners ' Preference in E-Learning System Using Kansei Kansei Approach Using Approach," Trends in E-learning, 2018, doi: 10.5772/intechopen.75620.

[34] A. M. Lokman and K. A. Kamaruddin, "Kansei affinity cluster for affective product design," Proc. - 2010 Int. Conf. User Sci. Eng. i-USEr 2010, no. January 2015, pp. 38–43, 2010, doi: 10.1109/IUSER.2010.5716719.

[35] J. Pitaktiratham, T. Sinlan, P. Anuntavoranich, and S. Sinthupinyo, "Application of Kansei Engineering and Association Rules Mining in Product Design," World Acad. Sci., Eng., Tech., vol. 69, no. 9, pp. 198–203, 2012.

[36] U. Neupane, K. Nishimoto, M. Miura, and S. Kunifuji, "Random display of hints and its effect on generating ideas in brain-writing groupware," Lect. Notes Comput. Sci. (including Subser. Lect. Notes Artif. Intell. Lect. Notes Bioinformatics), vol. 5178 LNAI, no. PART 2, pp. 863–870, 2008, doi: 10.1007/978-3-540-85565-1-107.

[37] T. Buzan, The ultimate book of mind maps: unlock your creativity, boost your memory, change your life. London: HarperThorsons, 2006.

[38] C. C. Marshall and F. M. Shipman, "Spatial Hypertext: Designing for Change," Commun. ACM, vol. 38, no. 8, pp. 88–97, 1995, doi: 10.1145/208344.208350.

[39] R. Scupin, "The KJ method: A technique for analyzing data derived from Japanese ethnology," Hum. Organ., vol. 56, no. 2, pp. 233–237, 1997, doi: 10.17730/humo.56.2.x335923511444655.

[40] N. J. A. M. Saad et al., "Kansei Engineering Approach for Measuring Political Propaganda: A Case of Malaysia," Int. J. Eng. & Technol. Vol 7, No 4.29 Spec. Issue 29DO - 10.14419/ijet.v7i4.29.21838 , vol. 7, no. November, pp. 31–35, 2018, [Online]. Available: https://www.sciencepubco.com/index.php/ijet/article/view/21838.

[41] P. H. Osgood, Charles E.; Suci, George J.; and Tannenbaum, The Measurement of Meaning. Urbana. Illinois: University of Illinois Press, 1957.

[42] T. A. Myers, M. C. Nisbet, E. W. Maibach, and A. A. Leiserowitz, "A public health frame arouses hopeful emotions about climate change: A

Letter," Clim. Change, vol. 113, no. 3–4, pp. 1105–1112, 2012, doi: 10.1007/s10584-012-0513-6.

[43] J. S. Lerner, "Improving national security through research on emotion and decision making," pp. 1–3, 2016.

[44] A. Crawford and S. Hutchinson, "Mapping the contours of 'everyday security': Time, space and emotion," Br. J. Criminol., vol. 56, no. 6, pp. 1184–1202, 2016, doi: 10.1093/bjc/azv121.

[45] N. Smith and A. Leiserowitz, "The role of emotion in global warming policy support and opposition," Risk Anal., vol. 34, no. 5, pp. 937–948, 2014, doi: 10.1111/risa.12140.

[46] J. Hesterman, "The Emotional Traps of Soft Target Security," ASIS International. .

[47] L. Retter, E. Frinking, S. Hoorens, A. Lynch, F. Nederveen, and W. Phillips, "Relationship between the economy and national security security policy in the Netherlands," 2020.

[48] E. Asekun-Olarinmoye et al., "Public perception of climate change and its impact on health and environment in rural southwestern Nigeria," Res. Rep. Trop. Med., no. August 2015, p. 1, 2014, doi: 10.2147/rrtm.s53984.

[49] O. Zotova, "Emotional Security of People," J. Sib. Fed. Univ. Humanit. Soc. Sci., vol. 8, no. 9, pp. 1816–1833, 2015, doi: 10.17516/1997-1370-2015-8-9-1816-1833.

[50] K. S. Taber, "The Use of Cronbach ' s Alpha When Developing and Reporting Research Instruments in Science Education," 2016, doi: 10.1007/s11165-016-9602-2.

[51] A. M. Lokman, "KE as affective design methodology," pp. 7–13, 2013.

[52] H. F. Kaiser, "The Varimax Criterion for Analytic Rotation in Factor Analysis," no. 3, 1958.

[53] D. Passig, "The Interaction between Gender , Age , and Multimedia Interface Design," pp. 241–250, 2001.

Arbitrary Verification of Ontology Increments using Natural Language

First Order Logic (FOL) based Algorithmic Approach

Kaneeka Vidanage[1], Noor Maizura Mohamad Noor[2], Rosmayati Mohemad[3], Zuriana Abu Bakar[4]
Faculty of Computing, Department of Data Science, NSBM Green University, Sri Lanka[1]
Faculty of Ocean Engineering Technology & Informatics, University Malaysia Terengganu (UMT), Malaysia[1, 2, 3, 4]

***Abstract*—Parallel to the advancement of practical use cases in computers, the trend toward collaborative ontology engineering is accelerating. Both domain experts and ontologists must collaborate in collaborative ontology engineering processes. However, the bulk of domain experts are not computer experts (i.e. lawyers, medical doctors, bankers, etc.). Question and Answer on Linked Data (QALD) is a suggested method for non-computer domain experts to engage with the ontology increments as they evolve. Existing QALD methods and systems, on the other hand, have a number of drawbacks, including significant setup requirements, domain dependence, and user discomfort. As a result, a new QALD algorithm and QALD system designed with the usage of First Order Logic (FOL) are presented in order to address the shortcomings of current QALD mechanisms. The suggested FOL based, QALD mechanism was tested quantitatively and qualitatively over three distinct ontology increments. This experiment had an overall acceptance rate of 79 percent from all stakeholders.**

***Keywords*—First order logic; linked data; ontologist; iterative framework**

I. Introduction

Ontology increment verification using QALD is critical for evaluating the correctness and relevance of a given ontology increment. Existing QALD methods, on the other hand, have a number of flaws that will be discussed in this article.

Both domain experts and ontologists must work in unison and with mutual understanding during collaborative ontology engineering [1]. Specialists in certain domains will help ontologists by sharing their specific domain expertise (i.e. COVID-19, Criminal Law, Aquaculture, etc.) [23]. On the other side, ontologists will conceive and build ontologies using the information collected from domain experts [24]. Thus, the information contained in the resultant ontology will become both human and machine readable [2], thereby allowing for an unbounded wide variety of application options.

However, the process of developing an ontology is iterative and incremental [3]. At the conclusion of each cycle, the ontologists will generate an ontology increment. Domain experts must then evaluate the ontology increment generated by the ontologists. When information is transferred from domain experts to ontologists, there is a possibility of misinterpretations and ambiguities that result in cognitive glitches. As a result, it is possible that the ontologists do not always replicate the precise cognitive interpretations conveyed by domain experts. Because neither ontologists nor domain experts are ontologists. Consequetly, there are many ways for knowledge errors to result in an incorrect schematic conceptualization at the ontology level. This might be hazardous if such ontologies were to be published directly into the production environment and produced illogical outcomes [4, 25]. QALD is a favored method for bridging this knowledge gap between domain experts and ontologists. Effectively built QALD systems may significantly aid domain experts in their ontology augmentation evaluation process. As a result, domain experts and ontologists may collaborate to debate and implement necessary improvements to the ontology increment under review [5-7].

However, current QALD systems have a slew of problems and restrictions that limit their potential. The bulk of them have a complicated technical curve that excludes non-computer domain experts such as bankers, attorneys, medical practitioners, and marketers from eligibility. it is not possible [8-10]. Therefore, this study introduces a new domain specialist-friendly, domain- and schema-independent, configuration-free algorithm to aid the QALD process in a more effective manner.

II. Literature Review

SPARQL or SQWRL querying capabilities are a high-level capabilities that cannot be acquired overnight. Even if that barrier is resolved, an individual cannot construct a valid SPARQL or SQWRL query without first understanding the schematic structure of the corresponding ontology increment. To understand the schematic structure of an ontology increment, one must be familiar with the semantic web's fundamental notions, such as triple concepts, data and object properties, and individuals. All of them are extra and unnecessary costs for domain experts, which may demotivate their participation [8-10]. However, in collaborative ontology engineering, the domain experts' participation in evaluating ontology increments is critical [2]. The following Table I summarizes an evaluation of various recently implemented QALD systems and their shortcomings.

TABLE I. EXISTING QALD SYSTEM ANALYSIS

QALD Tool	**Deficiency**
Neural Machine Translation [6]	-Training for the deep learning technique takes about 20 days. -Assemble and organize the domain-specified dataset. This is a vast overhead. -The accuracy of the SPARQL queries produced by the deep learning model is insufficient. Results that are ambiguous. -Because the dataset is required, the tool's whole operation is domain-dependent, since domain-independent datasets are not feasible.
Schema-Agnostic QALD [5]	-Using similarity assessment logic, SPARQL queries are generated based on the contents of the natural language query. -Accuracy is very low. Results that produces tempt to be very ambiguous.
Question and Answering on Linked Data (QALD) [11]	- The QALD tool is statically associated with a single ontology. It is incompatible to work with all other ontologies. -Extremely domain-specific. But the requirement is for domain independency
Regular Language to SPARQL questions [12]	-Based on the tool's domain-specific rule sets. -Generates numerous SPARQL queries, even for a single purpose. -Extensive operational overhead and extremely low precision.
ORAKEL [13]	-Protracted period of domain-specific setup utilizing the FrameMapper program. -Intense human interaction throughout the setup process.

In addition to that, an assessment of some of the latest existing QALD algorithms was conducted as depicted in Table II.

TABLE II. EXISTING QALD ALGORITHM ANALYSIS ACCORDING

QALD Algorithm	Deficiency
SPE Algorithm [14]	-An extensive domain-specific configuration effort needs the intense involvement of domain experts. -It is necessary to create predefined question and response pairings.
Conversational Question and Answering (CQA) with BERT [15]	This is accomplished via the use of a sophisticated machine learning model that has been trained on 104 languages. The BERT architecture is not suitable for querying linked data using SPARQL or SQWRL.
Visual Genome and Visual Question Answering [16]	-This is based on the visual genome dataset and a deep neural network trained on it. As a result, it is statically bound to a domain.
QA Optimization pipeline Algorithm [17]	-Frankenstein Framework is the basis for this algorithm. It is intended for the purpose of determining the optimum QA pipeline from 360 configurations and is not tailored to QALD needs.
Template-Based Question and Answering [18]	-Defining templates is a time-consuming manual process that needs significant human participation. -Additionally, each specified template is domain-specific.

As shown in Tables I and II, the current QALD methods have a number of drawbacks. The primary weakness of current QALD methods is as follows:

1) Domain-dependence.
2) Schema dependence.
3) Extensive effort required for manual configuration.
4) Inconvenience to the user.

The purpose of this study is to develop a more user-friendly, domain- and schema-independent QALD method that does not need knowledge of SPARQL or SQWRL to verify ontology increments. Additionally, this is free of lengthy manual setup procedures.

III. METHODOLOGY

The research methodology used in this study is shown in Fig. 1.

After numerous brainstorming sessions with ontologists and domain experts, the nature of the issue and the importance of resolving it were justified. Following that, a systematic evaluation of the most recent available tools and algorithms was performed to identify unsolved gaps. Thus, the objective of "need for a more user-friendly QALD method for verifying ontology increments" was created. Finally, the brainstorming findings resulted in the introduction of the following algorithm. As shown in Fig. 2, the suggested method is divided into four distinct stages.

The algorithm's first phase is responsible for extracting information from the associated ontology increment file. The corresponding ontology increment files may be in OWL (Web Ontology Language) or RDF (Resource Description Framework)format. To begin, this method requires a file containing the ontology increments. Phase I will extract and store the knowledge in a relational database. Below is a representation of the pseudocode for phase-I execution.

Fig. 1. Research Process.

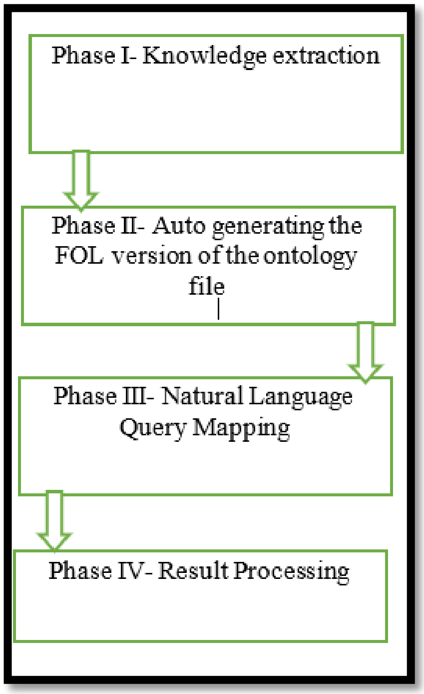

Fig. 2. Phases of the Algorithm.

Phase-I - [Knowledge Extraction]

Start
Upload relevant RDF / OWL file of the ontology increment to be verified.
Conduct format verification as either RDF or OWL.
According to the verified format, trigger the relevant RDF / OWL extraction logics.
While [Until EOF]
Extracts class info from the ontology increment file.
[i.e. Inheritance class info / Disjoint class info…]
Extract property associated info from the ontology increment file
[i.e. Data / Object properties]
IF [INDIVIDUALS Exists]
Extract INDIVIDUAL specific object and data properties
End IF

Store extracted info in the relevant relations of the database Schema without violating mapping sequences.

End While
End

The portion of the code snippet associated with the practical implementation of the pseudocode phase -I is depicted in Fig. 3.

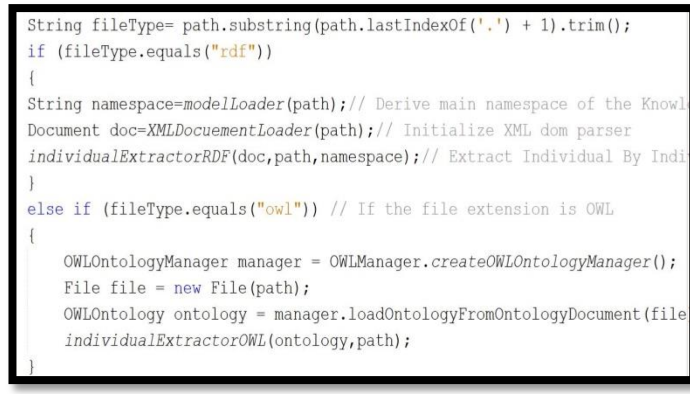

```
String fileType= path.substring(path.lastIndexOf('.') + 1).trim();
if (fileType.equals("rdf"))
{
String namespace=modelLoader(path);// Derive main namespace of the Knowl
Document doc=XMLDocuementLoader(path);// Initialize XML dom parser
individualExtractorRDF(doc,path,namespace);// Extract Individual By Indi
}
else if (fileType.equals("owl")) // If the file extension is OWL
{
    OWLOntologyManager manager = OWLManager.createOWLOntologyManager();
    File file = new File(path);
    OWLOntology ontology = manager.loadOntologyFromOntologyDocument(file
    individualExtractorOWL(ontology,path);
}
```

Fig. 3. Implementation of the Phase-I of the Pseudocode.

Phase II is in charge of creating the FOL (First Order Logic) version of the ontology increment by accessing the database's relevant knowledge embeddings. This will be completely automated, with no human intervention required. The pseudocode below illustrates the execution of Phase II.

Phase-II - [Auto-generation of the First Order Logic Knowledge base]

Start
ArrayList<String> folStoreArr=new ArrayList<> () // To store FOL elements
Connection con=DriverManager.getConnection(ConnectionString) // DB connection
Statement stmt=con.createStatement()
ResultSet rs=stmt.executeQuery("select count(*) from table") // Deriving the count of tuples from the relation

While(rs.next())
Extract semantic element from the DB table.
Determine the type of the semantic element
[Either data/object property, class relationship etc..]

* / Organization of semantic elements to be presented in the First Order Logic (FOL) format /*

Initialize identification flags accordingly for conditional formatting of the values retrieved from the table.
Check the semantic type of the extracted element and re-write it in the appropriate standardized FOL format.
folStoreArr. Add //Append all semantic elements re-formatted into its FOL version, one by one

End While
FileWriter fw=new FileWriter("prologue.pl")
BufferedWriter bufferedWriter = new BufferedWriter(fw);
bufferedWriter.write(Iterate through the contents stored in folStoreArr);
End

The portion of the code snippet associated with the practical implementation of the pseudocode phase II is depicted in Fig. 4. Similarly, the autogenerated first-order logic (FOL) version of the inspecting ontology increment is depicted in Fig. 5. This FOL version of the inspecting ontology increment is completely autogenerated as an outcome of phase II of the algorithm.

Phase II transforms the RDF/OWL file's semantic components to a standardized FOL format series. For instance, among the specified standard format series are the following:

1) Classes are converted as:= "Class(Class Name)".

2) Inheritance relationships are converted as:=" Inheritance(Child Class, Parent Class)".

3) Disjoint relationships as :=" Disjoint(Class-1, Class-2)"

4) Individuals as:= "Individual(Class Name, Object Name)"

5) Data Properties as:="dProp(Individual, d_prop_1_name, d_prop_1_value, Domain).

6) Object Properties as:="oProp(Individual-1,obj_prop_name, Individual-2, Domain, Range).

```
public static void writePrologFile(String alst, String flag) throws IOException
 {
     if(j==0)
  {
      File file = new File("C:/phd/prolog.pl");
      if(file.exists())
          file.delete();
  }
     BufferedWriter writer = new BufferedWriter(new FileWriter("C:/phd/prolog.pl", true));
     String str = "";
     if(flag.equals("class"))
     {
      str=flag+'('+alst+')'+"."+"\n";
      writer.append(str);
     }
     if(flag.equals("inheritance"))
     {
      String[]v=alst.split(":");
      str="class"+'('+v[1]+')'+"."+"\n";
      writer.append(str);
      str=flag+'('+v[0]+','+v[1]+')'+"."+"\n";
      writer.append(str);
     }
```

Fig. 4. Implementation of Phase II of the Pseudocode.

```
class('offences_of_weights_and_meassures').
class('crime_classifications').
inheritance('offences_of_weights_and_meassures','crime_classifications').
class('offence_of_forces').
class('crime_classifications').
inheritance('offence_of_forces','crime_classifications').
class('fine').
class('punishments').
inheritance('fine','punishments').
class('sexual_harrasment').
class('offence_to_human_body').
inheritance('sexual_harrasment','offence_to_human_body').
class('offences_to_public_health').
class('crime_classifications').
inheritance('offences_to_public_health','crime_classifications').
class('mens_rea').
class('crime_elements').
inheritance('mens_rea','crime_elements').
class('hurt').
class('offence_to_human_body').
inheritance('hurt','offence_to_human_body').
class('unsound_mind').
class('general').
inheritance('unsound_mind','general').
class('general').
class('excemptions').
inheritance('general','excemptions').
class('special').
class('excemptions').
inheritance('special','excemptions').
class('simple').
class('imprisonment').
inheritance('simple','imprisonment').
```

Fig. 5. Auto-Generated FOL Version of the Ontology Increment.

The relevant values retrieved and stored in the RDBMS, which was accomplished in phase I, will be replaced with the associated parameter values accessible in the generated standardized FOL rules displayed earlier. These standardized FOL rules along with the replaced parameter values will be utilized for the autogeneration of the FOL file as shown in Fig. 5. Therefore, the phase II of the algorithm converts the entire contents of the ontology increment into it`s respective FOL format. The algorithm's third phase is responsible for locating the FOL components that correspond to the plain language queries. Here, domain experts may immediately ask the necessary queries in English, obviating the requirement for SPARQL or SQWRL literacy entirely. The following pseudocode illustrates the execution of Phase III.

Phase-III - [Natural Language Query Mapping]

Start
Accept natural language (i.e. English) user query.
Activate Part of Speech Tagging (POS) for the user query classification.
Derive POS sequences for the user query.
Locate positioning of various lexicons and special terms and update flag variables accordingly to classify the user query.
Remove all prepositions, modal verbs, pronouns. Nouns and Verbs will only be remaining.

Locate the nouns and verbs of concern by executing a verification prologue query on the generated prologue knowledge base (i.e. Fig. 5)

Eliminate all unnecessary nouns and verbs after the prologue verification.

IF [Verified nouns / verbs . Has Both Domain && Range]
    Segment those as object properties.
End If
Else If [Verified nouns/verbs. Has Only a Domain && No Range]
    Segment those as data properties
End If

Derive the structure of the user query by analyzing the POS pattern sequences of the flag variables updated.
Map the POS pattern sequence of the flag updation with respective prologue query generation rules.

Generate appropriate chained prologue query
Locate the missing elements.

Execute it on the FOL knowledge base.
End.

The code snippet below (i.e. Fig. 6) illustrates the categorization and updating of flag variables depending on the Part Of Speech (POS) of the user inquiry. This technique can be used to extract particular requests for data or object attributes from a natural language-based user inquiry. The following figure (i.e. Fig. 7) illustrates the updating of POS sequence-specific flag variables and the creation of chained prologue queries. The chained prologue query structures are parameterized in this section. An appropriate parameterized chained prologue query will be initiated based on the POS sequences in the natural language user inquiry. At the moment, specified parameterized prologue query structures mapped to the user query's POS sequences are capable of extracting nearly all object and data property queries.

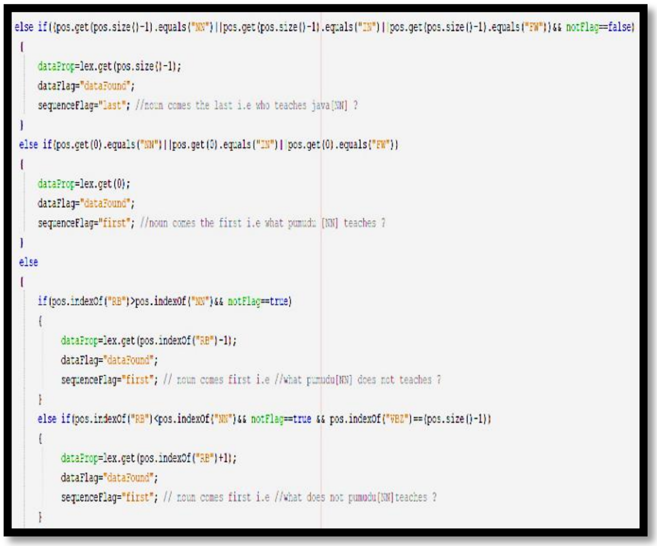

```
else if((pos.get(pos.size()-1).equals("NN")||pos.get(pos.size()-1).equals("IN")||pos.get(pos.size()-1).equals("FW"))&& notFlag==false)
{
    dataProp=lex.get(pos.size()-1);
    dataFlag="dataFound";
    sequenceFlag="last"; //noun comes the last i.e who teaches java[NN] ?
}
else if(pos.get(0).equals("NN")||pos.get(0).equals("IN")||pos.get(0).equals("FW"))
{
    dataProp=lex.get(0);
    dataFlag="dataFound";
    sequenceFlag="first"; //noun comes the first i.e what pumudu [NN] teaches ?
}
else
{
    if(pos.indexOf("RB")>pos.indexOf("NN")&& notFlag==true)
    {
        dataProp=lex.get(pos.indexOf("RB")-1);
        dataFlag="dataFound";
        sequenceFlag="first"; // noun comes first i.e //what pumudu[NN] does not teaches ?
    }
    else if(pos.indexOf("RB")<pos.indexOf("NN")&& notFlag==true && pos.indexOf("VBZ")==(pos.size()-1))
    {
        dataProp=lex.get(pos.indexOf("RB")+1);
        dataFlag="dataFound";
        sequenceFlag="first"; // noun comes first i.e //what does not pumudu[NN]teaches ?
    }
```

Fig. 6. User Query Classification and Property Extraction.

```
if(notFlag==false)
 {

    // who teaches java [NN] ??

     if(arr.contains("dataFound")&&arr.contains("objectFound")&& arr.contains("last"))
    {
        // String qry="dProp(X,_,"+dataProp+",_),oProp(Y,"+objectProp+",X,_,_),dProp(Y,B,Z,_).";
         String qry="dProp(X,_,"+dataProp+",_),oProp(X,"+objectProp+",Y,_,_),dProp(Y,B,Z,_).";
         Query q=new Query(qry);
         if (q.hasNext()==false)
         {
             qry="dProp(X,_,"+dataProp+",_),oProp(Y,"+objectProp+",X,_,_),dProp(Y,B,Z,_).";
         }
          q=new Query(qry);
         StringBuilder stringBuilder = new StringBuilder();
         int i=0;
           while(q.hasMoreSolutions())
           {
              Map<String,Term> rslt=q.nextSolution();
             // if(i==0)
             // {
               stringBuilder.append("Data Property :-"+rslt.get("B").toString()+"\n");
               stringBuilder.append("Data Property Values:-"+rslt.get("Z").toString()+"\n");
             // }
              stringBuilder.append(",");
              stringBuilder.append(" ");
            i++;
           }
           val.add(stringBuilder.toString());
```

Fig. 7. Part of Speech Tag Pattern Specific Parameterized Chained Prologue Queries.

Phase IV is in charge of processing the output in natural language (i.e. English) and ensuring that it is readily understandable by domain experts. The pseudocode below illustrates the execution of Phase IV.

Phase-IV - [Results Processing]

Start
  Use StringBuilder to append all returned results with "\n" as the delimiter.
  Split the appended output by the delimiter "\n"
  Return the result in Natural Language (i.e. English)
End

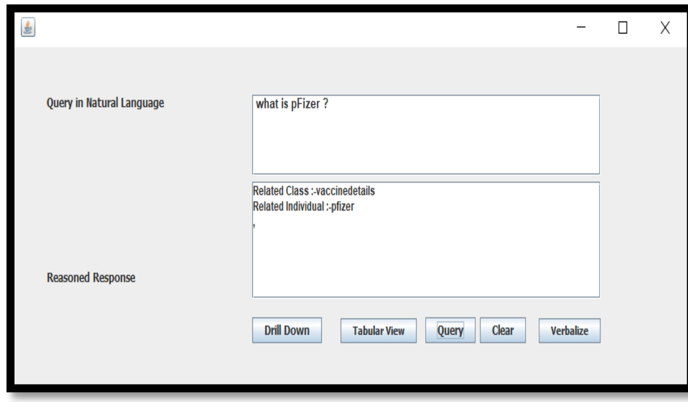

Fig. 8. Natural Language Interrogation on Ontology Increment.

The QALD interface designed is shown in Fig. 8 above. The user just has to enter the desired question in English and click the query button. Then, as visible, the relevant findings will be presented in natural language.

Let us attempt to understand the execution of this algorithm using a simple real-world scenario. Assume you have been given a university ontology increment that includes information of professors who teach various courses. Thus, the domain expert may simply ask the query in plain language (i.e. English) to verify that correct mappings are included to the ontology increment.

For instance, who teaches Financial Accounting?

After completing the first levels of processing, the aforementioned English question will be converted into its new structure as teach [VERB] "Financial Accounting" [NOUN]. Thus, a simple Prologue verification query on the phase II-generated 'Prologue. pl' file will validate "teach" as an object property and "Financial Accounting" as a data property. Because "teach" is a property of an object, it will have both a domain and a range. However, "Financial Accounting" will have a domain-exclusive scope. Due to the axiomatic difference between object and data, properties can readily be distinguished with a simple IF condition. Thus, extracted knowldge elements may be represented as follows using the specified standard FOL representation rules:

dProp(Individual, d_prop_1_name, "Financial Accounting", Domain).

Likewise, teach can be represented as:-

oProp(Individual-1," teach", Individual-2, Domain, Range)

As per the question asked our concern is to find a person. Therefore, we can negate the unnecessary fields of the prologue query as mentioned below.

dProp(Individual,_, "Financial Accounting", _).
oProp(Individual-1," teach", Individual-2, _, _)

Henceforth, a chained prologue query can be formulated as:

dProp(X,_," Financial Accounting ",_),oProp(Y,"teach",X,_,_),dProp(Y,B,Z,_).

Once the above-chained prologue query is executed in the fact base following conclusions can be derived.

dProp(X,_," Financial Accounting ",_) → X (Individual) => "Subject-1"

After, assign the result to the second prologue query.

oProp(Y,"teach",Subject-1,_,_) → Y(Individual)=>"Lect-1"

Henceforth, assign the result to the third prologue query.

dProp("Lect-1",B,Z,_).

Hence, B represents the data property names and the Z represents the data property values.

The algorithm's fourth step allows for the formatting and representation of returning results as cleaned string outputs, resulting in the names of individuals who teach Financial Accounting.

According to Lampa's comprehensive experiment report [19], prologue searches are straightforward and close to 10 times quicker than SPARQL or SQWRL queries. The primary reason for this is because the Prologue reasoning engine uses a backtracking search technique to explore the fact base in search of necessary axioms. SPARQL requires the generation of a parse tree after finding the ontology's schema, which is a highly complicated and resource-intensive operation [20]. As a result, our SPARQL-free natural language interrogation technique represents a major addition.

IV. Result and Discussion

The algorithm described above was exposed in three distinct ontology increments, one for COVID-19, one for aquaculture, and one for criminal law. This experiment included a total of fifteen stakeholders. Nine were domain experts, while the remaining six were professional ontologists. The appendix of this article contains snapshots of the three ontology increments used in this experiment. We did not go into detail on such ontology increments since they are outside the scope of this article.

The evaluation workflow for the suggested new algorithm is depicted in Fig. 9. This suggested evaluation workflow took into account both quantitative and qualitative perspectives.

Prior to it, the operationalization phase was accomplished. We prepared a list of open-ended questions regarding the study's goals. Operationalization entails matching questionnaire items to the research objective [21]. This guarantees that the questionnaire's questions elicit highly relevant and consistent answers. The following is a collection of open-ended questions that correspond to the assessment's study aim:

1) Have you been informed of the NLI processes that are currently in place?

2) In comparison to them, what are the favorable characteristics of this mechanism that you identified?

3) Do you believe it will ease the ontology increment verification function?

4) Could you expand on how this would ease the inspectors' work?

5) What flaws did you discover in the suggested verbalization mechanism?

Both ontologists and domain specialists were shown a specially created synoptic video clip about the research as part of the pre-warm-up setup. This phase acts as a retrospective, summarizing the major findings of the research performed by the evaluation's stakeholders. This was done prior to the formal commencement of the assessment process in order to clear up any remaining questions about the procedure.

A face-to-face interview series with nine domain experts in criminal law, COVID-19, and aquaculture was done during the controlled interview session. The five questions outlined above served as the basic foundation for the nine domain experts' interviews. All controlled interview sessions were videotaped to aid in subsequent analysis. All participants gave their previous permission and consent to the recording, which was utilized only for research purposes and not for personal benefit.

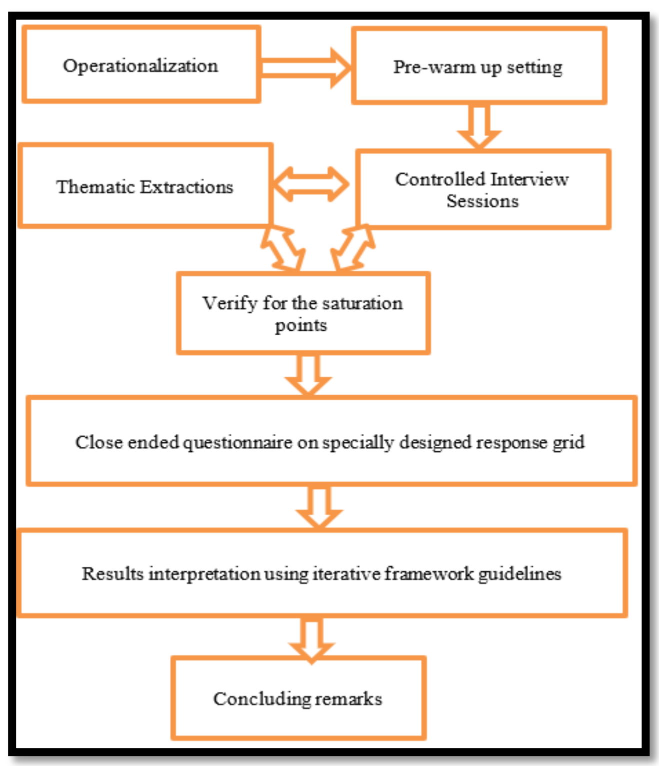

Fig. 9. Evaluation Workflow.

During the thematic extraction process, all recorded interviews were transcribed into textual format. Following that, the research team iteratively analyzed the transcribed texts for numerous turns. The data gathered over the course of the repetitive study were categorized into a few broad themes. At the outset of the research, new themes developed rapidly; however, as the study progressed to the ninth transcription, the development of new topics slowed significantly, while the same motifs reappeared repeatedly. This characteristic was identified as approaching saturation.

The extraction of themes facilitated the identification of the most intriguing aspects of the research. It was difficult to elicit all important views simply via quantitative procedures. As a consequence of the qualitative phase, which was conducted through controlled interview sessions, important user insights were identified.

Following that, we created a series of closed-ended questions to extract more information on the highlighted themes. This enables us to focus our attention on particular subjects while simultaneously emphasizing their numerical importance. Fig. 10 illustrates the process of extracting quantitative stakeholder views using a customized rating grid.

10	20	30	40	50	60	70	80	90	100
Very Poor	Fairly OK – Major Revisions				Good & Acceptable – Minor Revisions			Exceptional	

Fig. 10. Close-Ended Response Grid.

The four questions below were given in a closed-ended manner, with respondents invited to evaluate their level of agreement with the quantitative inspection criteria.

1) SPARQL / SQWRL is not required, and interrogations may be initiated using plain language (i.e. English).

2) Addresses needs for on-demand, ad-hoc knowledge verifications.

3) Operations are domain and schema-independent and configuration-free.

4) The retured findings were accurate.

5) How would you evaluate the tool support's NLI assistance?

The mean answer scores received from nine domain experts from three distinct domains and the ontologists participating in this research are summarized in Table III.

The following Table IV summarizes the qualitative interpretations elicited during the controlled interview session.

TABLE III. AVERAGED RESPONSE SCORES FROM DOMAIN SPECIALISTS

Natural Language Interrogation [NLI]	Law	80%
	COVID-19	76%
	Aquaculture	83%
	Averaged	**79%**

TABLE IV. QUALITATIVE RESPONSE SYNTHESIS

Natural Language Interrogation [NLI]	-Completely automated, configuration-free operation that is domain and schema agnostic. -Assists with ad-hoc, on-demand consolidation analysis during ongoing discussions -Eradicates technological obstacles associated with SPARQL or SQWRL -Comprehensible user inquiries expressed in natural language by domain specialists (i.e., English) -Perfect for arbitrary knowledge verification in real-time. - Returned findings are readily understandable and precise

The iterative framework was utilized as the last stage of the assessment process to keep the emphasis on the research objective. Iterative framework [22] is well-established method for evaluating the effectiveness of rationally accomplishing research objectives. Three different but connected questions control the iterative framework's functioning. Each part must provide reflective proof. Table V summarizes the discussion of iterative framework measurements.

TABLE V. ITERATIVE FRAMEWORK ASSESSMENT

Steps in Iterative Framework	Reflective Evidence
01 → What are the data telling me?	Quantitative Metrics: As shown in Table III above, various domain-specific qualitative opinion ratings were utilized to verify the efficacy and operational effectiveness of the developed QALD algorithm. It had yielded favorable outcomes. Qualitative Evaluation: The QALD algorithm was experimentally assessed with the involvement of stakeholders who participated to the development of the ontology increments. Precision, usability, and "technical help offered" were all cited as critical characteristics of the returned findings. Additionally, as indicated in Table IV above, the themes of stakeholders' reflective views were documented. The entire research yielded acceptable findings in both the quantitative and qualitative experimental stages.
02 → What do I want to know?	Need for a domain specialist friendlier QALD mechanism for the ontology increment`s arbitrary verification
03 → Is there a dialectical relationship between step 01 & 02?	The QALD method was exposed to multiple ontology increments in three different domains throughout the quantitative assessment phase. Quantitative matrices were utilized to evaluate the overall efficacy of the QALD algorithm in each of these tests, and it was apparent that the overall operation was a success. Throughout the qualitative assessment process, the views of stakeholders were analyzed thematically, and the distilled findings are summarized in Table IV. The quantitative and qualitative assessment stages were both completed successfully. As a consequence of the iterative framework's reasoning, it is feasible to infer that the connection between stages 01 and 02 is positive and acceptable, indicating the effectiveness of the newly suggested QALD algorithm.

V. CONCLUSION

QALD mechanisms will be very helpful throughout the collaborative ontology engineering process for doing ad-hoc verifications of the knowledge embeddings contained in the ontology increments. As previously mentioned, mutual understanding between domain experts and ontologists is critical for the successful development of applied ontologies. Domain experts, on the other hand, such as medical physicians, attorneys, bankers, and marketers, are not computer specialists fluent in SPARQL, SQWRL, or Semantic principles. Thus, establishing English-language-based QALD mechanisms will be critical for domain experts to communicate successfully with ontologists and accomplish their assigned tasks.

As previously stated, current QALD methods have a number of flaws, as shown in Tables I and II above. As a result, this study proposes a new algorithm that addresses those problems by enabling domain- and schema-independent, configuration-free QALD intervention. The proposed method was evaluated in three distinct domains and produced successful results with an overall of 79% acceptance from the involved stakeholders, as shown in Tables III, IV, and V. Therefore, it may be characterized as a new and important addition to the field of semantic technologies. In the future, it is planned to test the algorithm's effectiveness across a variety of other areas and to incorporate the chatbot capability to further enhance human-computer interaction views.

REFERENCES

[1] De Nicola, A., & Missikoff, M. (2016). A lightweight methodology for rapid ontology engineering. Communications of the ACM, 59(3), 79-86. doi:10.1145/2818359doi:10.1093/bib/6.3.239.

[2] Abeysiriwardana, P. C., & Kodituwakku, S. R. (2012). Ontology-Based Information Extraction for Disease Intelligence. International Journal of Research in Computer Science, 2(6), 7-19. doi:10.7815/ijorcs.26.2012.051 ACIS 2011 Proceedings. 80.

[3] Spasic, I., Ananiadou, S., McNaught, J., & Kumar, A. (2005). Text mining and ontologies in biomedicine: Making sense of raw text.Briefings in Bioinformatics, 6(3), 239-251.

[4] Ingram, J., & Gaskell, P. (2019). Searching for meaning: Co-constructing ontologies with stakeholders for smarter search engines in agriculture. NJAS - Wageningen Journal of Life Sciences, 100300. doi:10.1016/j.njas.2019.04.006\.

[5] Strohmaier, M., Walk, S., P Pschko, J., Lamprecht, D., Tudorache, T., Nyulas, C. Noy, N. F. (2013). How Ontologies are Made: Studying the Hidden Social Dynamics Behind Collaborative Ontology Engineering Projects. SSRN Electronic Journal. doi:10.2139/ssrn.3199036.

[6] Steinmetz, N., Arning, A., & Sattler, K. (2019). From Natural Language Questions to SPARQL Queries: A Pattern-based Approach. BTW.

[7] Soru, T., Marx, E., Valdestilhas, A., Esteves, D., Moussallem, D., & Publio, G. (2018). Neural Machine Translation for Query Construction and Composition. ArXiv, abs/1806.10478.

[8] Hamon, T., Grabar, N., & Mougin, F. (2017). Querying biomedical Linked Data with natural language questions. Semantic Web, 8, 581-599.

[9] Trokanas, N., & Cecelja, F. (2016). Ontology evaluation for reuse in the domain of Process Systems Engineering. Computers & Chemical Engineering, 85, 177-187.doi:10.1016/j.compchemeng.2015.12.003.

[10] Munir, K., & Anjum, M. S. (2018). The use of ontologies for effective knowledge modelling and information retrieval. Appl Comput Inform., 14(2): 116–126, ISSN 2210-8327.

[11] Elve, A. T., & Preisig, H. A. (2019). From ontology to executable program code. Computers & Chemical Engineering, 122, 383-394.

[12] Fathalla, S., Lange, C., & Auer, S. (2019). A HumanFriendly Query Generation Frontend for a Scientific Events Knowledge Graph. TPDL.

[13] Pradel, C., Haemmerlé, O., & Hernandez, N. (2013). Natural language query interpretation into SPARQL using patterns.

[14] Cimiano, P., Haase, P., Heizmann, J. (2007). Porting natural language interfaces between domains: an experimental user study with the orakel system. In: IUI '07: Proceedings of the 12th international conference on Intelligent user interfaces, 180–189. ACM, New York, NY, USA.

[15] Lai, Y., Lin, Y., Chen, J., Feng, Y., & Zhao, D. (2016). Open Domain Question Answering System Based on Knowledge Base. NLPCC/ICCPOL.

[16] Otegi, A., Gonzalez-Agirre, A., Campos, J.A., Soroa, A., & Agirre, E. (2020). Conversational Question Answering in Low Resource Scenarios: A Dataset and Case Study for Basque. LREC.

[17] Noh, H., Kim, T., Mun, J., & Han, B. (2019). Transfer Learning via Unsupervised Task Discovery for Visual Question Answering. 2019 IEEE/CVF Conference on Computer Vision and Pattern Recognition (CVPR), 8377-8386.

[18] Singh, K., Radhakrishna, A.S., Both, A., Shekarpour, S., Lytra, I., Usbeck, R., Vyas, A., Khikmatullaev, A., Punjani, D., Lange, C., Vidal, M., Lehmann, J., & Auer, S. (2018). Why Reinvent the Wheel: Let's Build Question Answering Systems Together. Proceedings of the 2018 World Wide Web Conference.

[19] Punjani, D., Singh, K., Both, A., Koubarakis, M., Angelidis, I., Bereta, K., Beris, T., Bilidas, D., Ioannidis, T., Karalis, N., Lange, C., Pantazi, D., Papaloukas, C., & Stamoulis, G. (2018). Template-Based Question Answering over Lilnked Geospatial Data. Proceedings of the 12th Workshop on Geographic Information Retrieval.

[20] Lampa, S. (2010). SWI-Prolog as a Semantic Web Tool for semantic querying in Bioclipse: Integration and performance benchmarking.

[21] Jespersen, L.N., Michelsen, S.I., Holstein, B., Tjørnhøj-Thomsen, T., & Due, P. (2018). Conceptualization, operationalization, and content validity of the EQOL-questionnaire measuring quality of life and participation for persons with disabilities. Health and Quality of Life Outcomes, 16.

[22] Srivastava, P., & Hopwood, N. (2009). A Practical Iterative Framework for Qualitative Data Analysis. International Journal of Qualitative Methods, 8, 76 - 84.

[23] Narock, T., & Fox, P. (2015). The Semantic Web in Earth and Space Science. Current Status and Future Directions. Amsterdam, Netherlands: IOS Press.

[24] McDaniel, M., &Storey, V. C. (2019). Evaluating Domain Ontologies. ACM Computing Surveys, 52(4), 1-44. doi:10.1145/3329124.

[25] Façanha, R. L., Cavalcanti, M. C., & Campos, M. L. (2019). A Systematic Approach to Review Legacy Schemas Based on Ontological Analysis. Metadata and Semantic Research, 63-75. doi:10.1007/978-3-030-14401-2_6.

APPENDIX

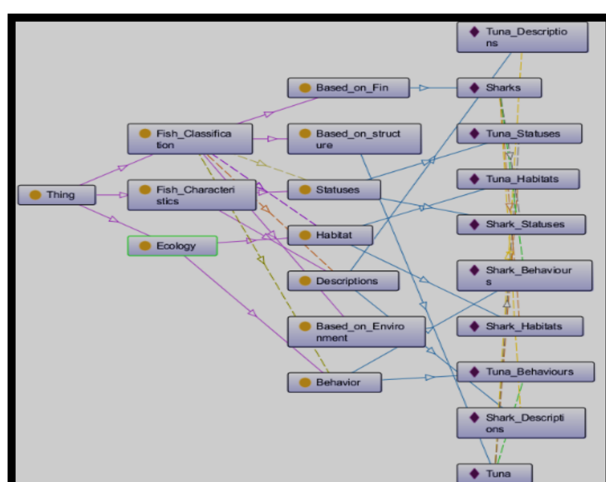

Fig. 11. Ontology Increment for Aquaculture Domain.

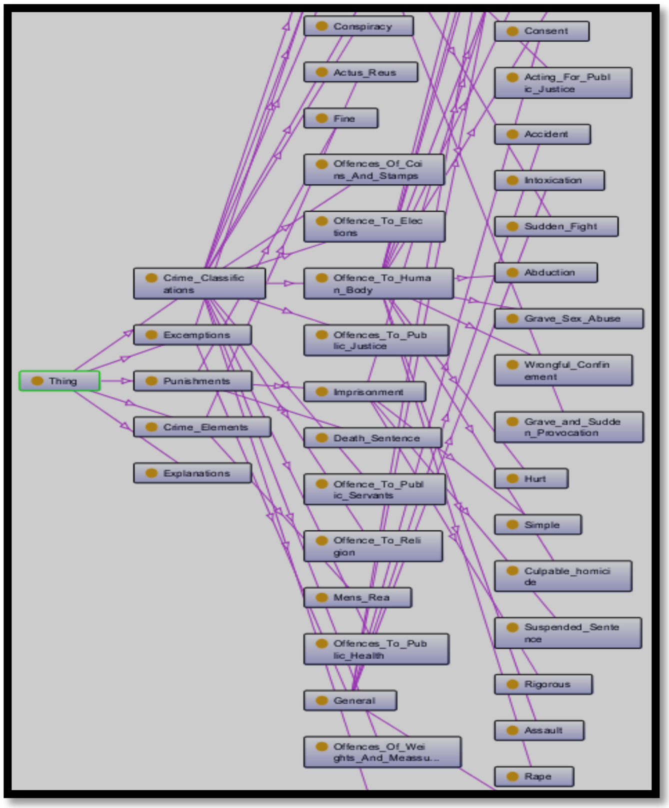

Fig. 12. Ontology Increment for Criminal Law.

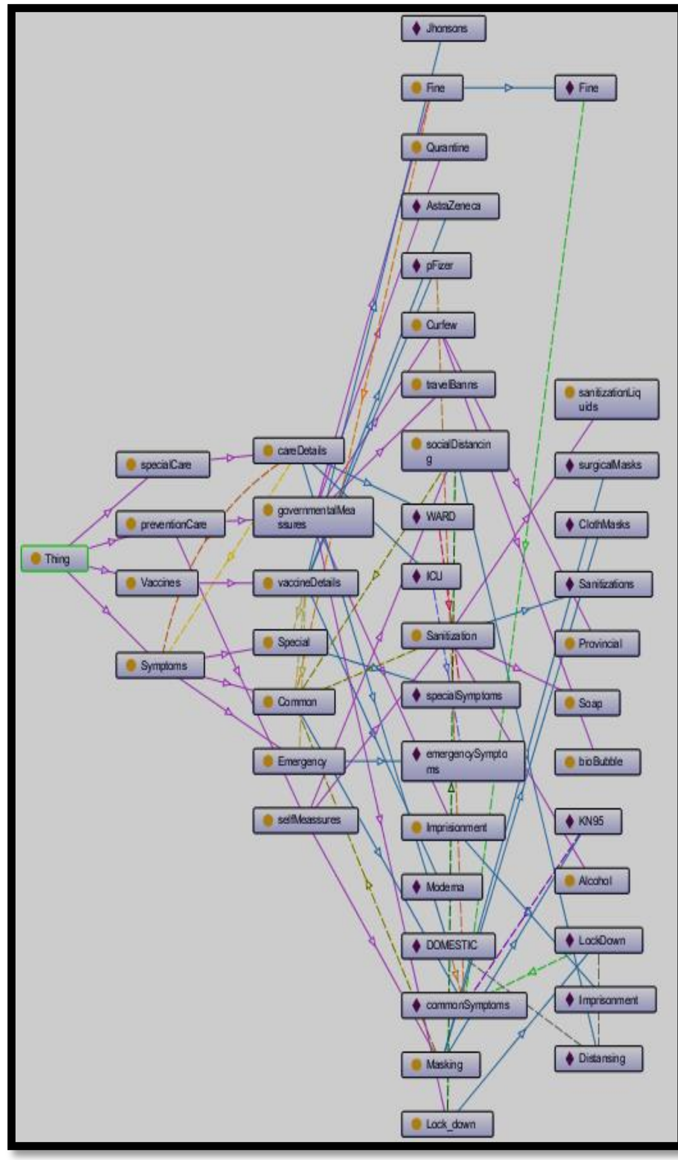

Fig. 13. Ontology Increment for COVID-19.

An Improvised Facial Emotion Recognition System using the Optimized Convolutional Neural Network Model with Dropout

P V V S Srinivas[1], Pragnyaban Mishra[2]
Department of Computer Science and Engineering
Koneru Lakshmaiah Education Foundation (KLEF), Guntur, India

Abstract*—Facial expression detection has long been regarded as both verbal and nonverbal communication. The muscular expression on a person's face reflects their physical and mental state. Using computer programming to integrate all face curves into a categorization class is significantly more important than doing so manually. Convolutional Neural Networks, an Artificial Intelligence approach, was recently developed to improve the task with more acceptance. Due to overfit during the learning step, the model performance may be lowered and regarded underperforming. There is a method dropout uses to reduce testing error. The influence of dropout is applied at convolutional layers and dense layers to classify face emotions into a distinct category of Happy, Angry, Sad, Surprise, Neutral, Disgust, and Fear and is represented as an improved convolutional neural network model. The experimental setup used the datasets namely JAFEE, CK48, FER2013, RVDSR, CREMAD and a self-prepared dataset of 36,153 facial images for observing train and test accuracy in presence and absence of dropout. Test accuracies of 92.33, 96.50, 97.78, 99.44, and 98.68 are obtained on Fer2013, RVDSR, CREMA-D, CK48, and JAFFE datasets are obtained in presence of dropout. The used features are countably large in the computation as a result the higher computation support of NVDIA with the capacity of GPU 16GB, CPU 13GB and memory 73.1 GB are used for the experimental purposes.

Keywords*—*Convolutional neural network (CNN); facial emotion recognition (FER); dropout; FER 2013; CREMAD; RVDSR; CK48; JAFFE

I. Introduction

The face expressions connect to emotions; they are essential identifiers for human sentiments. Most of the time, a person's facial expression is a nonverbal means of expressing emotion, and it may be used as tangible proof of human state. Human–computer interaction, psychiatric observations, intoxicated driver recognition, and lie detection are all viable uses facial emotion recognition.

The convolutional layers which act as a backbone for classification with artificial intelligence in several applications few of them are cancer detection [1], Brain Tumor Segmentation, Object detection [2], and crowd counting [3]. The CNN takes input facial image data, modify it using kernels, and then transmit the outputs to the next convolution layer. The final CNN layer's output is flattened and sent into the Feed Forward Neural Network for categorization into an emotion class. The learning stage entails training the model, while the evaluation stage entails putting it to the test and determining the acceptance percentage. Due to the impact of overfitting, it is more likely that the training phase is more fitted implies reduction of the test accuracy. By avoiding overfitting [4], the under described model expresses a research direction of reaching higher accuracy of facial emotion recognition.

The remaining of the paper is organized as follows: Section 2, Related Studies and Motivations; Section 3, Research Method; Section 4, Result and discussion; and Section 4, Conclusion.

II. Related Studies and Motivations

Image is a set of pixels represented by the function $f(x, y)$ such that the scalar quantity of an image's $x \in domain(x-axis)$ and $y \in range(y-axis)$ is equivalent to the amount of energy emitted from the location where the image was captured. Assume that $f(a, b)$ denotes a continuous variable picture that is transformed to a digital image in the form of $f(x, y)$ with $x \in \{0,1,2,..,\mathrm{M}-1\}$ and $y \in \{0,1,2,..,\mathrm{N}-1\}$ Here M, N are the length and breadth of the digital image [5].

$$f(x, y) = \begin{pmatrix} f(0,0) & \cdots & f(0, M-1) \\ \vdots & \ddots & \vdots \\ f(N-1,0) & \cdots & f(N-1, M-1) \end{pmatrix}$$

CNN is a Deep Learning method that can take an image as input, assign importance of learnable weights and biases to distinct aspects in the image, and distinguish one from the other. When compared to other classification methods, the amount of pre-processing required by a CNN is significantly less. While basic techniques need hand crafted of filters, CNN can learn these filters or characteristics with enough training [6] and successfully capture the Spatial and Temporal dependencies in a picture. Due to the reduced number of parameters involved and the reusability of weights, the architecture performs superior trained to better recognition of the image. The goal of the CNN is to compress the images into a structure that is easier to process while preserving important elements for a successful prediction. By retaining picture features, the CNN's flow from layer to layer minimises the dimension. Different kernels and pooling layers of CNN can accomplish this task. The residue left over after a few repetitions of the previous stages is fed into the dense layer for categorization according to the need and model specification.

Current techniques largely focus on face study while keeping the surrounding intact, resulting in a variety of redundant and erroneous features that hamper CNN training. Happy, Angry, Sad, Surprise, Neutral, Disgust, and Fear are the seven basic face emotion classes that the model learns during learning stage. Recently [7] [8], researchers have achieved remarkable progress in facial expression identification with higher number of classes [9], leading to advancements in neurology and applied mathematics, etc that are boosting research in the field of facial expression further. Moreover, advances in computer vision and machine learning have made emotion recognition more accurate tools of classification.

Dropout changed the idea of learning all the weights in the network in each training cycle to learning a proportion of the weights in the network. This problem is solved by addressing overfitting [10] in networks with many neurons, which are then associated with weights. Regularization was an important study topic prior to Dropout. Regularization approaches in neural networks, such as L1 and L2 weight penalties, are introduced. These regularizations, however, did not entirely alleviate the overfitting problem [11].

Co-adaptation is a key challenge when learning networks with high neurons. If all the weights are learnt at the same time in such a network, it is likely that certain connections will be more predictive than others, As the network is trained repeatedly in this case, the stronger connections are learned more, while the weaker ones are ignored. The traditional regularization, such as the L1 and L2, could not avoid this. The reason for this is that they also regularize depending on the connections' prediction abilities. As a result, they approach determinism in selecting and rejecting weights. As a result, the strong become stronger and the weak become weaker.

The researchers Nitish Srivastava et al. [10] extensively studied the impact of dropout and concluded that increasing the size of the neural network would not help. As a result, neural networks' size and accuracy have been limited. Dropout is a co-adaption strategy that can help to avoid these problems.

As seen below, there are numerous examples of major contributions in this field in the literature.

With the CK48 [12] and FER2013 [13] datasets, Mollahossei [14] proposed CNN for FER [13] obtained 93.2% and 61.1% accuracy, respectively. Using the CK48 dataset, [15] investigated the impact of data pre-processing prior to training the network on emotion categorization and found that it improved accuracy by 96.76%. Using the CK48 [12] dataset, [16] used the notion of action units and achieved 97.01% accuracy. [17] suggested a unique architecture based on Sparse Batch normalization, estimating the model's accuracy at 95.24% for JAFEE [18] and 96.87% for the CK48[12] dataset. Using the FER2013[13] database, Agrawal et Mittal [19] investigated the influence of adjusting CNN parameters on classification results and found a 65.23% average accuracy without dropout and 65.77% with dropout. The author in [20] used the datasets JAFEE [18] and CK48 [12] to train the model, achieving 95.23 % and 93.24 % accuracy, respectively.

Similar tests with datasets CREMAD [21] & RVDSR [22] were done by researchers [23] with accuracy notes of 65%, 58.33%, [24] 52.52%, 47.11 %, [25] 74.0 %, 67.5 % and [26] 62.84% only for CREMAD [21] dataset.

III. Research Method

A. Proposed CNN Model

The convolutional neural network proposed in this section is an optimal framework that contains layers namely an input, an interleaved Z grouped convolutional, a batch normalization, a polling, a fully connected, a dropout, a flatten and a dense that forward to an output layer at the end. The fully connected layer is resulted after slicing the convolutional, batch normalization and max pooling layers that are connected through a cross-layer connection as shown in the Fig. 1.

The input image to the proposed framework is a three-dimensional array with dimensions $h \times w \times n$ where h, w are spatial dimensions and n is the channel whose value is 1 as gray scale images are considered as input, $*$ It is used to perform the convolution operation and Act plays the role of activation function. The output of the convolutional layer is represented as follows.

$$hl_{2n,j}^{l} = conv_{n+1,j}^{l} = Act\left(u_{2n,j}^{l}\right)$$

$$= Act\left(\sum_i hl_{2n-1,i}^{l} * W_{i,j}^{2n}\right), \quad 1 \le n \le Z \tag{1}$$

Where as $W_{i,j}^{2n}$ represents the weight matrix between the feature space of $(2n-1)th$ hidden layer that belongs to i and feature space of $(2n)th$ hidden layer which belongs to j. $conv_{n+1,j}^{l}$ is j^{th} feature plane of $(n+1)th$, $hl_{2n,j}^{l}$ represents i^{th} feature space of the hidden layer $(2n-1)$ and $hl_{2n-1,i}^{l}$ represents the j^{th} feature space of hidden layer $(2n)$.

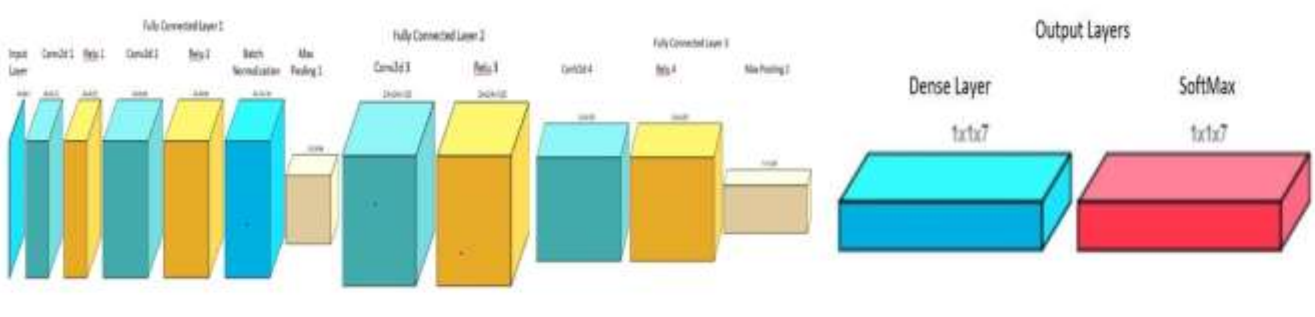

Fig. 1. Proposed CNN Architecture.

The output of the convolution layer obtained from Equation 1 is given to the Batch normalization layer where the batch of inputs is represented as $BT = \{hl^l_{1,2,3,\dots,2n}\}$ and the mean of the batch is given as.

$$E[hl^l_{BT}] = \frac{1}{m}\sum_{j=1}^{2n} hl^l_{2n} \tag{2}$$

And the variance of the batch is

$$Var[hl^l_{BT}] = \frac{1}{m}\sum_{j=i}^{n}(hl^l_{2n} - E[hl^l_{BT}])^2 \tag{3}$$

$$hl^{\wedge}_{BT} = \frac{hl^l_{2n} - E\left[hl^l_{BT}\right]}{\sqrt{var[hl^l_{BT}] + \varepsilon}} \tag{4}$$

Where $hl^{\wedge}_{BT}$ represents the normalized values

After calculating mean, variance, and normalized values. The output of the batch normalization layer is given as

$$hl^l_{2n+1,j} = Bat^l_{n+1,j} = \alpha * hl^{\wedge}_{BT}\ , 1 \leq BT \leq Z \tag{5}$$

$hl^l_{2n+1,j}$ represents j^{th} feature space of $(2n)th$ hidden layer, $Bat^l_{n+1,j}$ represents the batch normalization of layers j^{th}feature space of sample l

The output of the Batch normalization layer is fed as an input to the max polling layer in which fixed step sized feature space is used. The output of the polling layer is calculated by the following equation.

$$hl^l_{2n+2} = Max\ polling\{hl^l_{2n+1,j}\} \quad 1 \leq n \leq Z \tag{6}$$

In the proposed model a convolutional layer, a Batch normalization layer, and a Max Polling layer forms one fully connected layer. And the output of the fully connected layer is given to dropout layer where some of the neurons will be removed before going to the next fully connected layer. hl^l_{2n+2} is the output of a fully connected layer and will be given as input to the dropout layer. The output of the dropout layer is calculated as given below.

$$hl^l_{2n+3} = Act\left(\left(W^{[2n+2]} .* Drop^{[2n+2]}\right) hl^l_{2n+2}\right),$$
$$1 \leq n \leq Z \tag{7}$$

$W^{[2n+2]}$ is the weights associated to layer $2n+2$, $Drop^{[2n+2]}$ amount of dropout applied on layer $2n+2$, hl^l_{2n+2} is the output of fully connected layer and .* It is called Hadamard product.

The above process is repeated for all the fully connected layers of the proposed convolutional neural network model and the fully connected form of the proposed model which is also called flattening is given as mentioned below.

$$hl^l_{2Z+1} = (a_1 hl^l_1, a_2 hl^l_2, a_3 hl^l_3, \dots, a_{2Z} hl^l_{2Z}) \tag{8}$$

The binary string $AI = a_1, a_2, a_3, \ldots, a_{2Z-1}$ represents a crossover indicator which indicates the cross-layer connection. For example $AI = 111,\dots,1$ says that all $(2Z-1)$ convolution, batch normalization, polling, dropout which forms a fully connected layer are connected to the final fully connected layer which is also called as flatten layer, the representation $AI = 100,\dots,0$ says that only the first one is the fully connected layer and the remaining are normal convolutional layers and the representation $AI = 000,\dots,0$ says that there are no fully connected layers and all the layers in the network are just convolution layers. For the proposed model in this paper $AI = 1{,}0{,}1$ that says that we have a fully connected layer followed by a convolutional layer which was followed by a fully connected layer again. After performing flattening operation resulted from Equation 8 is fed as an input the dense layer in which Relu activation function is used followed by dropout layer which was again followed by a dense layer where the output is obtained. SoftMax function is used in the final dense layer to classify the output.

$$out^l_{Dense1} = Dense\left(Den_N, Act_{Relu}(hl^l_{2Z+1})\right) \tag{9}$$

out^l_{Dense1} denotes the output of the first hidden layer, Den_N represents the number of hidden neurons used in the dense layer, Act_{Relu} says the Relu Activation function is used here for activating the neurons and hl^l_{2Z+1} is nothing but the output of the flatten layer or final fully connected convolutional layer.

$$out^l_{Drop} = Act\left(\left(W^{[2Z+2]} .* Drop^{[2Z+2]}\right) hl^l_{2Z+2}\right) \tag{10}$$

out^l_{Drop} is the output of the dropout layer after the dense layer, Act is the activation function, $W^{[2Z+2]}$ and $Drop^{[2Z+2]}$ are respective weights assigned and the amount of dropout applied. And, finally the output of the last dense layer where the classified output is obtained as given below.

$$out^l_F = Dense\left(Den_C, Act_{Softmax}\left(out^l_{Drop}\right)\right) \tag{11}$$

out^l_F is the final output of the proposed convolutional neural network, Den_C represents the total classes to classify, $Act_{softmax}$ is the SoftMax activation function.

For the sample l, the optimization model that was propose uses the formulas given below to calculate the activation of all Convolutional, Batch Normalization, Max Polling, Fully connected, Dropout, Dense layers.

$$hl^l_{2n,j} = conv^l_{n+1,j} = Act\left(u^l_{2n,j}\right)$$
$$= Act\left(\textstyle\sum_i hl^l_{2n-1,i} * W^{2n}_{i,j}\right),\ 1 \leq n \leq Z$$
$$hl^{\wedge}_{BT} = \frac{hl^l_{2n} - E[hl^l_{BT}]}{\sqrt{var[hl^l_{BT}] + \varepsilon}}$$
$$hl^l_{2n+1,j} = Bat^l_{n+1,j} = \alpha * hl^{\wedge}_{BT}, \qquad 1 \leq BT \leq Z$$
$$hl^l_{2n+2} = Max\ polling\{hl^l_{2n+1,j}\}, 1 \leq n \leq Z$$
$$hl^l_{2n+3} = Act\left(\left(W^{[2n+2]} .* Drop^{[2n+2]}\right) hl^l_{2n+2}\right)$$
$$hl^l_{2Z+1} = (a_1 hl^l_1, a_2 hl^l_2, a_3 hl^l_3, \dots, a_{2Z} hl^l_{2Z})$$
$$out^l_{Dense1} = Dense\left(Den_N, Act_{Relu}(hl^l_{2Z+1})\right)$$
$$out^l_{Drop} = Act\left(\left(W^{[2Z+2]} .* Drop^{[2Z+2]}\right) hl^l_{2Z+2}\right)$$
$$out^l_F = Dense\left(Den_C, Act_{Softmax}\left(out^l_{Drop}\right)\right)$$

B. The effect of Drop Out on FER Classification

Dropout is a process of dropping a %age of connection with probability (1-p). The Expectation with dropout $Ep(d)$ is represented as:

$$Ep(d) = \frac{1}{2}(t - \sum_{i=1}^{m} \delta_i w_i I)^2 \quad (12)$$

where δ is a dropout rate: δ ~ Bernoulli(p).

The Bernoulli(p) satisfy the properties listed below.

If $X$is a random variable with Bernoulli distribution, then:

$$P_r(X = 1) = p = 1 - P_r(X = 0) = 1 - q \quad (13)$$

The probability mass function f on this distribution, over possible outcomes k, is.

$$f(k;p) = \begin{cases} p & if\ k = 1 \\ q = 1 - p & if\ k = 0 \end{cases}$$

$$f(k;p) = p^k(1-p)^{1-k} \ \ \forall\, k \in \{0,1\}$$

$$f(k;p) = pk + (1-p)(1-k) \ \ \forall\, k \in \{0,1\} \quad (14)$$

Lemma 1: Dropping network connections increases generalization over non-dropout.

Let a weight $w_{pq}$is associated in between two consecutive hidden layers of p and q with absolute Mean Square Error E for a neural network. The projection for respective connections is represented as

$$\omega(p,q) = \frac{\partial^2 E}{\partial w_{pq}^2} \gamma^2(p,q) \quad (15)$$

$\gamma(p,q)$ is the parameter that control the Connection [27] with high projection improves the generalization of the Neural network. The generalization potential of the network with normalization is represented as

$$G_a = \prod_{\forall (a,b)} \omega'(p,q) \quad (16)$$

Where $\omega'$is the normalized view of the $\omega(p,q)$.

After few of the connection dropped the generalization of the neural network measured as

$$G_b = \prod_{\forall (a,b:\exists\omega\prime(\cdot)\to 0)} \omega'(p,q) \quad (17)$$

$$\forall Dout_{ab}: \exists\gamma(\cdot) \to 0 \ \Rightarrow \omega(\cdot) \to 0. \quad (18)$$

$$\therefore G_b > G_a \quad (19)$$

As can be seen from the equation above, dropping connections can result in a high degree of generalization.

Theorem 1: With every rise in hidden layer, the frequency of activation neuron falls.

To simplicity, the number of hidden layers is an even and it is n. An adaptive probability density function [28] for any hidden layer $l \ \ where\ 1 \le l \le n$ is defined as:

$$f(l) = 1 - (\sigma\sqrt{2\pi})^{-1} \int_{-\infty}^{l} exp\left(\frac{\left(l - \frac{n}{2}\right)^2}{2\sigma^2}\right) dl \quad (20)$$

The derivative of the function $f'(l) = (\sigma\sqrt{2\pi})^{-1} e^{(ln/2)^2 / 2\sigma^2}$

$\because f'(l) < 0 \ \Rightarrow f(l)\ is\ monotonically\ decreasing$

$\therefore f(n) < f(l) < f(1)$

$$\{f(l)\}_{mx} = 1 - (\sigma\sqrt{2\pi})^{-1} \int_{-\infty}^{1} exp\left(\frac{(l - \frac{n}{2})^2}{2\sigma^2}\right) dl < 1$$

$$\{f(l)\}_{mn} = 1 - (\sigma\sqrt{2\pi})^{-1} \int_{-\infty}^{n} exp\left(\frac{\left(l - \frac{n}{2}\right)^2}{2\sigma^2}\right) dl > 0 \quad (21)$$

it is cleared from above two equations that min and max ranges in between 0 and 1 is $0 < f(l) < 1$, Hence Proved.

IV. Experimentation and Results

A. About Datasets

For experimentation six different datasets are considered namely FER2013 [13], RVDSR [22], CREMAD [21], CK48 [12], JAFFE [18] and own dataset each of which consists of gray scale images of dimensions 48 x 48. For own dataset images and videos are collected from different web resources, all the images are converted to gray scale and resized to 48x48, the videos are converted to frames and preprocessed manually by considering only those frames which are of good. FER 2013[13] and own dataset consists of images belonging to seven different classes namely Angry, Disgust, Fear, Happy, Neutral, Sad and Surprise, whereas CREMAD [21] and RVDSR [23] datasets consist of images belonging to six different classes namely Angry, Disgust, Fear, Happy, Neutral, and Sad. FER 2013[13] consists of 35557, RVDSR [22] consists of 61,673, CREMAD [21] Consists of 61,309 CK48[12] and JAFFE [18] consists of 3540 and 3406, own dataset consists of 36,153 images, respectively. RVDSR [22] and CREMAD [21] datasets consist of videos of different expressions, all the videos are converted to frames. While converting the videos to frames, only the frame for every second is considered, after which the images are resized to 48x48 and taken for experimentation. The details of the images in the dataset are given in Table I.

TABLE I. DESCRIPTION OF THE DATASETS USED FOR EXPERIMENTATION

No of Images Per Category	Name of the Dataset				
	Fer2013	CREMA-D	RVDSR	JAFFE	CK48
Happy	8989	9861	10887	448	621
Sad	6077	8835	9814	496	336
Angry	4953	10672	9612	486	540
Disgust	547	9298	11223	464	531
Fear	5121	11576	10112	512	336
Surprise	4022	NA	NA	472	996
Neutral	6198	11067	8914	528	216
Total Images	35887	61309	61673	3406	3540

B. About Experimentation Setup and Resources

As the datasets consists of a huge number of images, implementation on the systems with general configuration will take more time. So, the support of Kaggle cloud platform was taken for performing the implementation that has the NVDIA GPU support of 16GB, CPU support of 13GB and memory support of 73.1GB, respectively.

B. Experimentation

The implementation is done on the four datasets mentioned above in which three cases were considered. In Case 1, a Convolutional Neural Network model where the dropout layer was included in between the fully connected layers and after the flattening layer was considered. After the flatten layer, the dropout layer was added in between two dense layers. The amount of dropout percentage applied in between the fully connected layers is 0.25, whereas in between the dense layers is 0.5. Along with dropout l2. Kernel regularizer and l2. Bias regularizer of 0.01 and 0.01 were added to the convolutional and dense layers. Each fully connected layer consists of a convolutional layer, batch normalization layer and a max polling layer. Three fully connected layers, three dropout layers, one flatten layer and two dense layers are used to construct the model.

In Case 2, the same Convolutional Neural Network with slight modifications is used. In this case will have a dropout layer only between the denser layers and no dropout layers were used in between the fully connected layers. 0.5 is the dropout percentage applied in between the dense layers, l2. Kernel regularizer and l2. Bias regularizer are used in the same way as Case1. Whereas in Case 3 no Dropout layers were used, and the remaining considerations are the same as in Case 1 and Case 2. The total parameters used by the proposed convolutional network are 32,115,718 out of which 32,115,078 are trainable parameters and 640 are non-trainable parameters. The detailed description of the results obtained for all the three cases on the respective datasets is given in the tables and figures given below. An observation from the results after experimentation is overall performance of the model has been increased after using dropouts in between fully connected layers as well as dense layers and the over fitting and under fitting problems normally a CNN Model has been outshined by using dropouts, l2 kernel and bias regularization techniques.

Fig. 2(a) to 2(f), 3(a to 3(f), 4(a) to 4(f) and 5(a) to 5(f) shows the Model Accuracy on FER 2013, RVDSR, CREMAD and own datasets in all the three cases which were explained above. Fig. 2(a) and 2(b), Fig. 3(a) and 3(b), Fig. 4(a) and 4(b), and Fig. 5(a) and 5(b) gives the Model Accuracy and loss in the case where dropout is used in between convolutional layers and in between dense layers, Fig. 2(c) and 2(d), Fig. 3(c) and 3(d), Fig. 4(c) and 4(d) and Fig. 5(c) and 5(d) gives model accuracy and loss in the case where dropout is used only after flattening the layer, i.e., between dense layers whereas Fig. 2(e) and 2(f), Fig. 3(e) and 3(f), Fig. 4(e) and 4(f) and Fig. 5(e) and 5(f) gives the model accuracy and loss of the case where dropout is not considered. It is observed that the case where dropouts are considered produced high accuracy and low loss when compared to other cases. The detailed description of Train and Test Accuracies, Train and Test Loss, Macro-average of Precision, Recall and f1-score, Weighted-average of Precision, Recall and f1-score are given in Table II to Table V. All the Experiments are done with 50 Epochs.

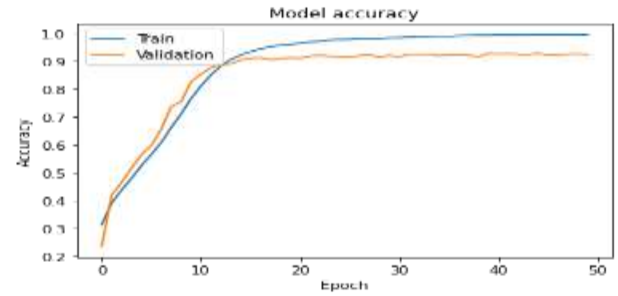

(a). Model Accuracy of the Proposed Model with Dropout on FER 2013 Dataset.

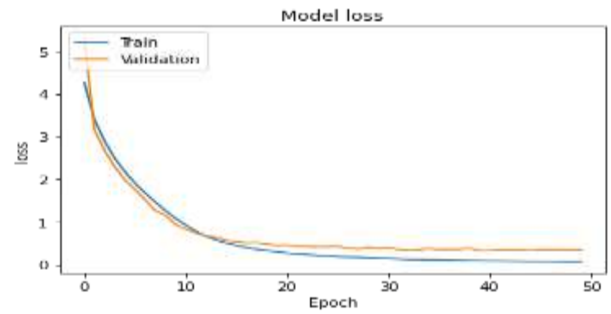

(b). Model Loss of the Proposed Model with Dropout on FER 2013 Dataset.

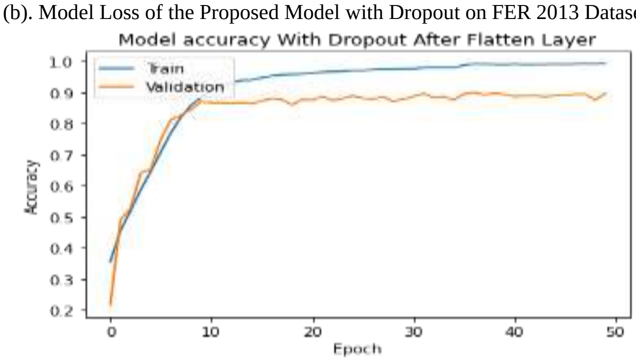

(c). Model Accuracy of the Proposed Model with Dropout only after Flatten Layer on FER 2013 Dataset.

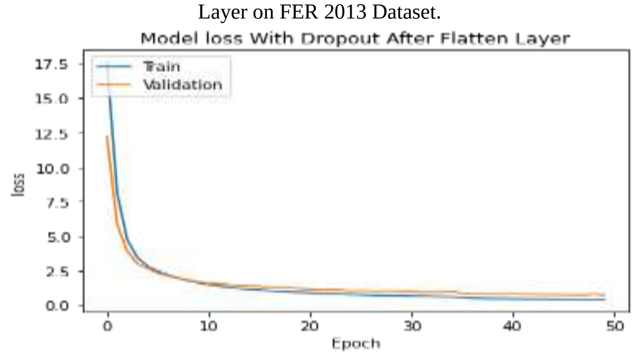

(d). Model Loss of the Proposed Model with Dropout only after Flatten Layer on FER 2013 Dataset.

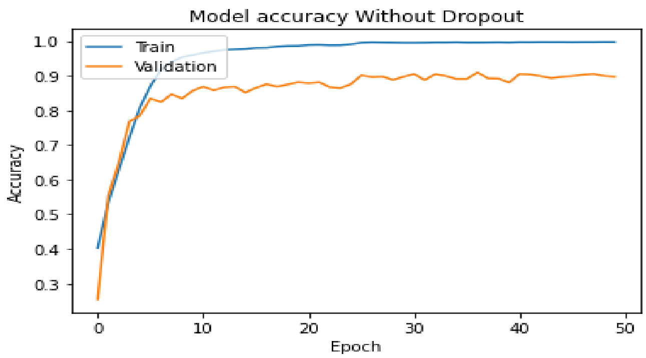

(e). Model Accuracy of the Proposed Model without Dropout on FER 2013 Dataset.

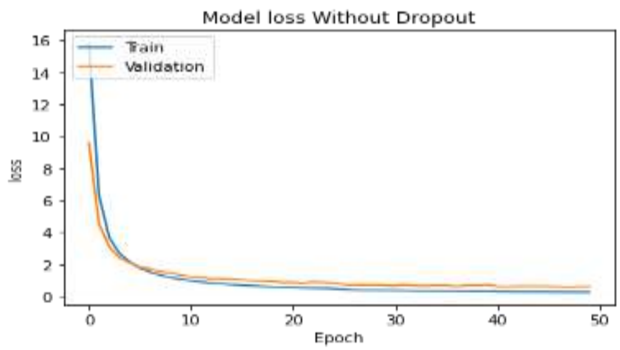

Fig. 2. (f). Model Loss of the Proposed Model without Dropout on FER 2013 Dataset.

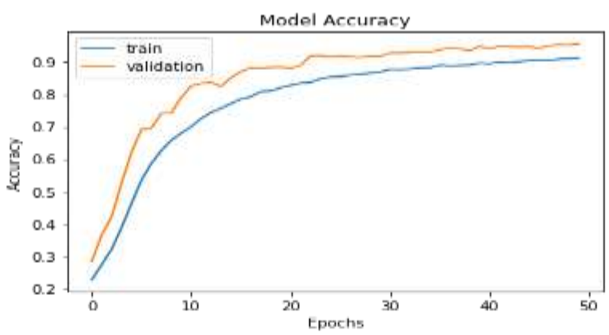

(a) Model Accuracy of the Proposed Model with Dropout on RVDSR Dataset.

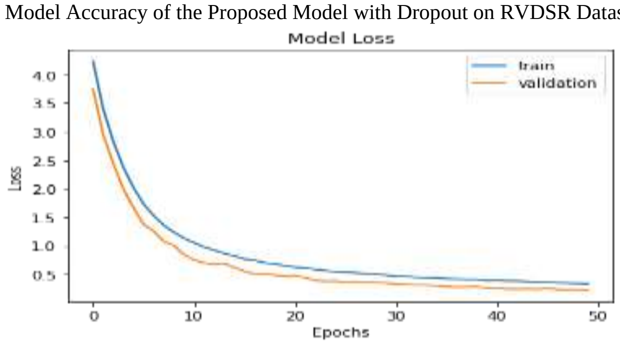

(b). Model Loss of the Proposed Model with Dropout on RVDSR Dataset.

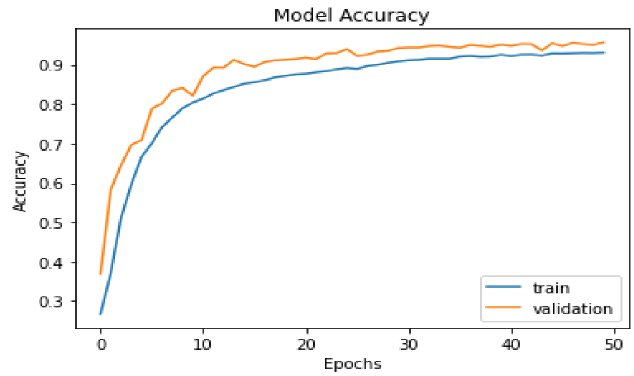

Fig 3(c). Model Accuracy of the Proposed Model with Dropout only after Flatten Layer on RVDSR Dataset.

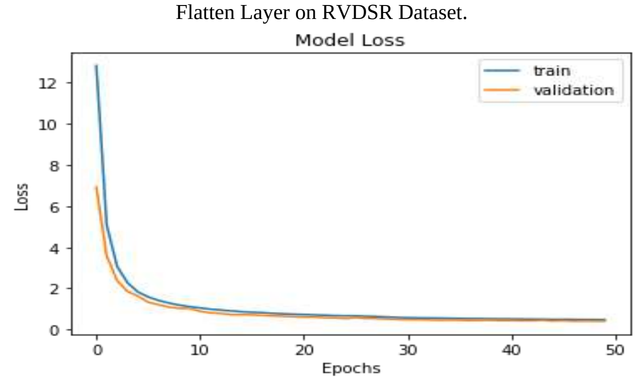

(d). Model Loss of the Proposed Model with Dropout only after Flatten Layer on RVDSR Dataset.

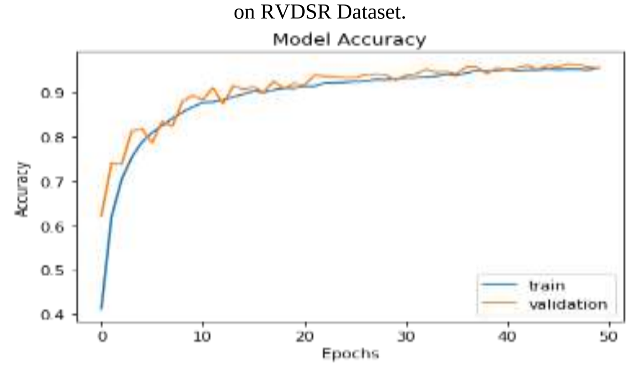

(e). Model Accuracy of the Proposed Model without Dropout on RVDSR Dataset.

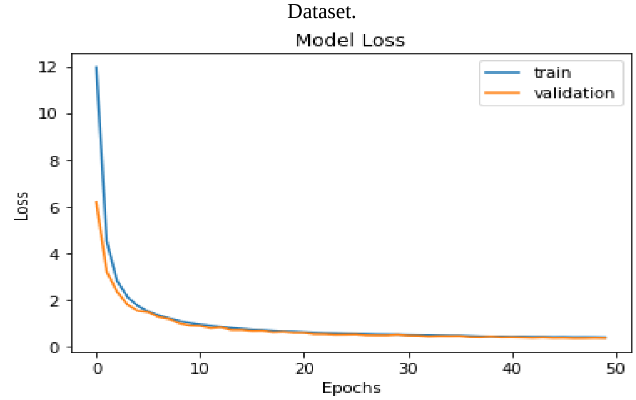

Fig. 3. (f). Model Loss of the Proposed Model Without Dropout on RVDSR Dataset.

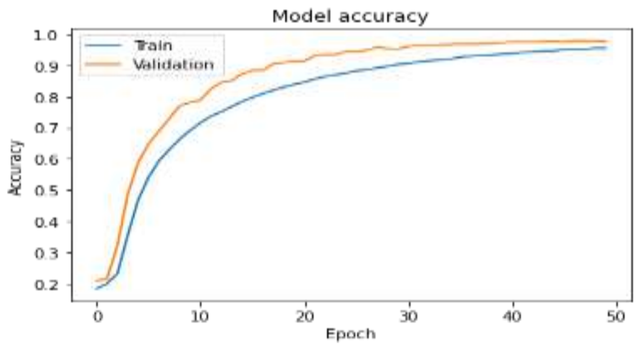

(a). Model Accuracy of the Proposed Model with Dropout on CREMA-D Dataset.

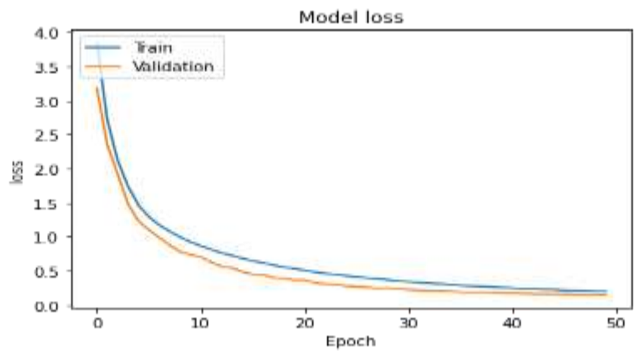

(b) Model Loss of the Proposed Model with Dropout on CREMA-D Dataset.

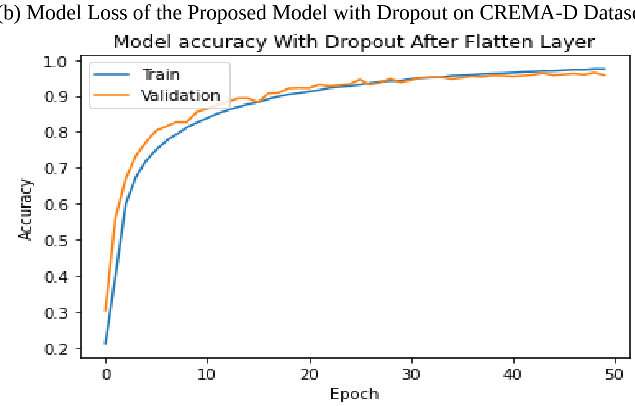

(c). Model Accuracy of the Proposed Model with Dropout only after Flatten Layer on CREMA-D Dataset.

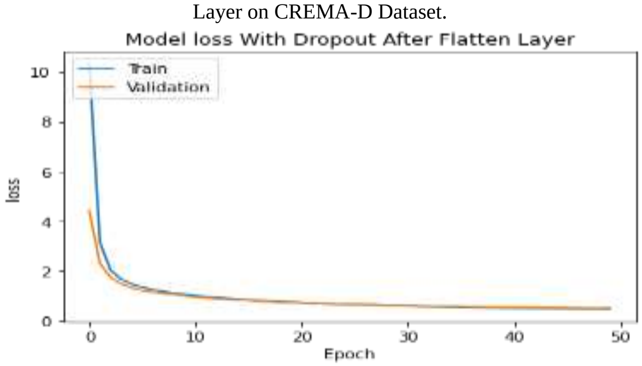

(d). Model Loss of the Proposed Model with Dropout only after Flatten Layer on CREMA-D Dataset.

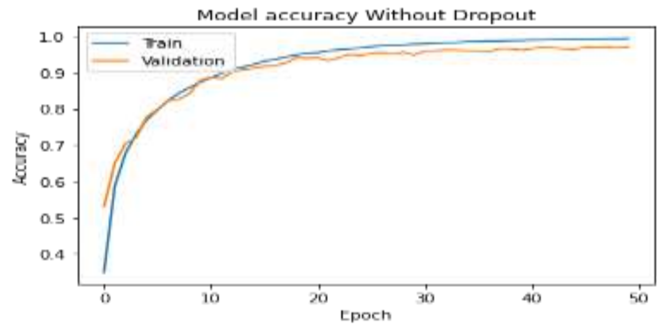

(e). Model Accuracy of the Proposed Model without Dropout on CREMA-D Dataset.

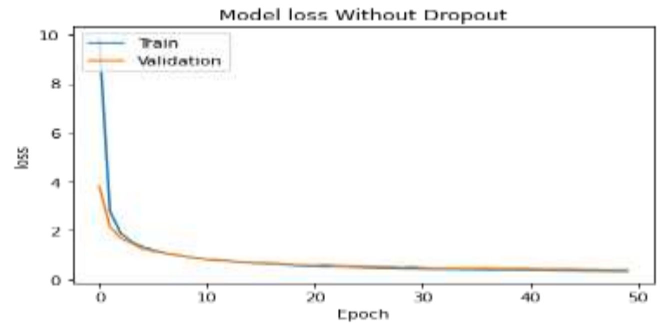

Fig. 4. (f). Model Loss of the Proposed Model without Dropout on CREMA-D Dataset.

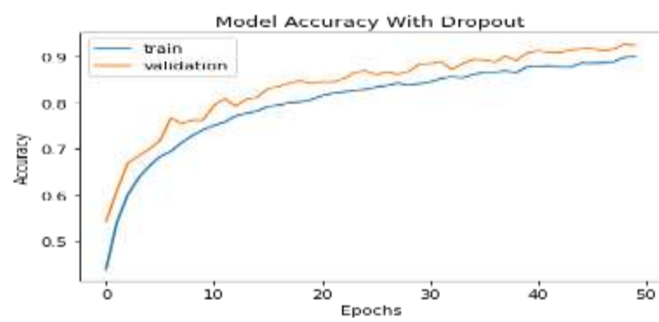

(a). Model Accuracy of the Proposed Model with Dropout on Own Dataset.

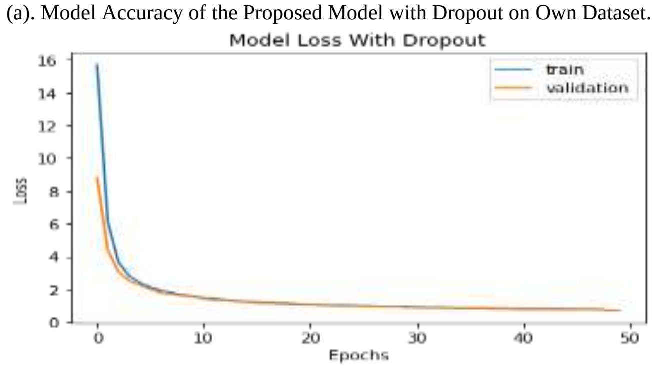

(b). Model Loss of the Proposed Model with Dropout on Own Dataset.

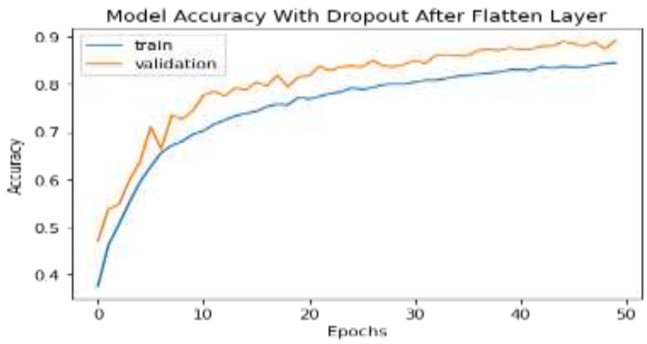

(c). Model Accuracy of the Proposed Model with Dropout only after Flatten Layer on Own Dataset.

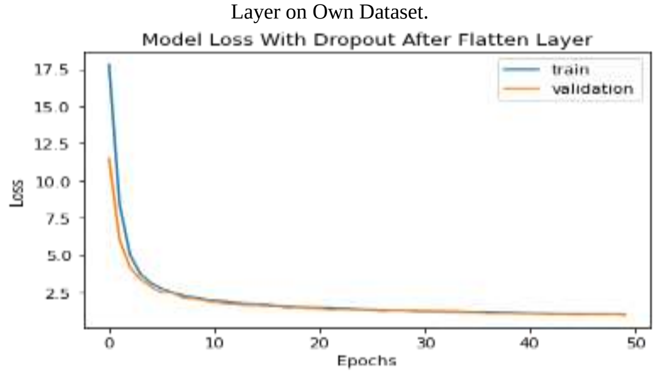

(d). Model Loss of the Proposed Model with Dropout only after Flatten Layer on Own Dataset.

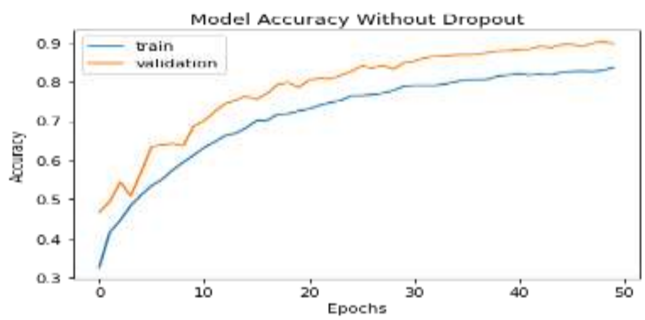

(e). Model Accuracy of the Proposed Model without Dropout on Own Dataset.

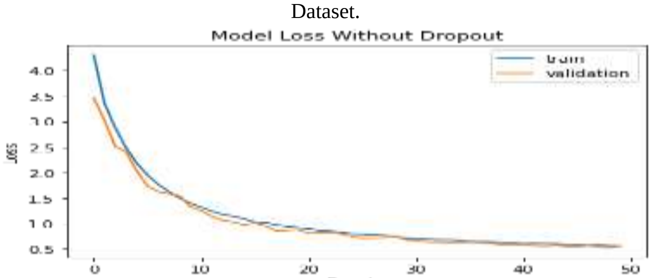

Fig. 5. (f). Model Loss of the Proposed Model without Dropout on Own Dataset.

Table VI gives the performance comparison of proposed CNN model over the existing work done and found that the proposed model obtained a better performance when the datasets Ck48, JAFFE, FER 2013, RVDSR, CREMAD and Own dataset are considered for evaluation.

TABLE II. PERFORMANCE COMPARISON OF THE MENTIONED THREE CASES ON FER2013 DATASET

Performance Measure	Case 1	Case 2	Case 3
Train Accuracy	99.32	99.38	99.74
Test Accuracy	92.33	89.61	89.24
Train Loss	0.0728	0.3908	0.2572
Test Loss	0.3248	0.7305	0.6737
Macro Avg of Precision	0.94	0.91	0.91
Macro Avg of Recall	0.93	0.90	0.91
Macro Avg of f1-Score	0.93	0.90	0.90
Weighted Avg of Precision	0.93	0.90	0.90
Weighted Avg of Recall	0.92	0.90	0.90
Weighted Avg of f1-Score	0.92	0.89	0.89
Time Taken Per Epoch	9 Sec	10 Sec	10 Sec

TABLE III. PERFORMANCE COMPARISON OF THE MENTIONED THREE CASES ON RVDSR DATASET

Performance Measure	Case 1	Case 2	Case 3
Train Accuracy	95.58	95.08	95.39
Test Accuracy	96.50	95.29	95.16
Train Loss	0.23	0.39	0.43
Test Loss	0.24	0.37	0.41
Macro Avg of Precision	0.96	0.95	0.94
Macro Avg of Recall	0.95	0.94	0.94
Macro Avg of f1-Score	0.95	0.94	0.93
Weighted Avg of Precision	0.95	0.94	0.93
Weighted Avg of Recall	0.94	0.93	0.93
Weighted Avg of f1-Score	0.94	0.93	0.92
Time Taken Per Epoch	55 Sec	56 Sec	57 Sec

TABLE IV. PERFORMANCE COMPARISON OF THE MENTIONED THREE CASES ON CREMAD DATASET

Performance Measure	Case 1	Case 2	Case 3
Train Accuracy	95.53	97.73	99.03
Test Accuracy	97.78	95.81	96.09
Train Loss	0.1978	0.4428	0.3676
Test Loss	0.1508	0.4995	0.4418
Macro Avg of Precision	0.97	0.96	0.96
Macro Avg of Recall	0.97	0.96	0.96
Macro Avg of f1-Score	0.97	0.96	0.96
Weighted Avg of Precision	0.97	0.96	0.96
Weighted Avg of Recall	0.97	0.96	0.96
Weighted Avg of f1-Score	0.97	0.96	0.96
Time Taken Per Epoch	123 Sec	125 Sec	126 Sec

TABLE V. PERFORMANCE COMPARISON OF THE MENTIONED THREE CASES ON OWN DATASET

Performance Measure	Case 1	Case 2	Case 3
Train Accuracy	90.52	86.86	89.91
Test Accuracy	92.45	89.68	89.19
Train Loss	0.6938	0.9604	0.4292
Test Loss	0.7083	0.9764	0.5534
Macro Avg of Precision	92	89	89
Macro Avg of Recall	92	89	89
Macro Avg of f1-Score	91	89	88
Weighted Avg of Precision	92	89	88
Weighted Avg of Recall	92	89	88
Weighted Avg of f1-Score	91	88	87
Time Taken Per Epoch	43 Sec	45 Sec	47 Sec

TABLE VI. PERFORMANCE COMPARISON OF PROPOSED CNN MODEL WITH EXISTING WORK DONE

<table>
<tr><th>Name of The Author</th><th>Datasets Used</th><th>Percentage of Test Accuracy</th><th>Proposed Model Test Accuracy</th></tr>
<tr><td>Mollahosseini et al. [14]</td><td>CK48</td><td>93.2</td><td rowspan="11">FER2013: 92.33
CK48: 99.44
JAFFE: 98.68
CREMAD: 97.78
RVDSR: 96.50</td></tr>
<tr><td>Mollahosseini et al. [14]</td><td>FER 2013</td><td>61.1</td></tr>
<tr><td>Lopes et al. [15]</td><td>CK48</td><td>96.76</td></tr>
<tr><td>Mohammadpour et al. 16]</td><td>CK48</td><td>97.01</td></tr>
<tr><td>Cai et al. [17]</td><td>JAFFE</td><td>95.04</td></tr>
<tr><td>Cai et al. [17]</td><td>CK48</td><td>96.87</td></tr>
<tr><td>Agarwal et al. [19]</td><td>FER 2013</td><td>65%</td></tr>
<tr><td>Deepak jain et al. [20]</td><td>JAFFE</td><td>95.23</td></tr>
<tr><td>Deepak jain et al. [20]</td><td>CK48</td><td>93.24</td></tr>
<tr><td>Rory Beard et al. [23]</td><td>CREMAD</td><td>65</td></tr>
<tr><td>Rory Beard et al. [23]</td><td>RVDSR</td><td>58.33</td></tr>
</table>

V. CONCLUSION AND FUTURE WORK

It is demonstrated in the proposed method that the use of dropout handled overfitting, resulting in a 3.09 percent gain in test accuracy in the category of CNN Model that uses dropout in fully connected convolutional layers and a 0.37 percent gain in test accuracy in the other category of CNN Model that uses dropout in dense layers using FER2013 dataset. Also, it has been noticed that there is a significant improvement of test accuracy for other datasets namely JAFEE, CK48, RVDSR, CREMAD and a self-prepared. Some FER recent developments in the literature were compared to the proposed model and found to be greater due to the implementation of dropout, as shown in Table VI.

The future scope of this paper will be to investigate the trade-off between overfitting and underfitting for FER by CNN models and developing mathematical models for managing a percentage of overfitting and or underfitting to achieve higher accuracy.

REFERENCES

[1] Bodavarapu, Pavan Nageswar Reddy, et al. "Optimized Deep Neural Model for Cancer Detection and Classification Over ResNet." *Smart Technologies in Data Science and Communication*. Springer, Singapore, 2021. 267-280.

[2] Mandhala, Venkata Naresh, et al. "Object detection using machine learning for visually impaired people." *International Journal of Current Research and Review* 12.20 (2020): 157-167.

[3] Mishra, et al. "Crowd Counting Using CSR-Net Architecture," *International Journal of Advanced Trends in Computer Science and Engineering*, Vol 8, no. 6, p. 2762-2767, 2019, 10.30534/ijatcse/2019/13862019.

[4] NarasingaRao, M. R., et al. "A survey on prevention of overfitting in convolution neural networks using machine learning techniques." *Int. J. Eng. Technol* 7.2.32 (2018): 177-180.

[5] RC Gonzalez, et al., "Digital Image Processing, Global Edition.", 2017, ch. 4, p. 203–303.

[6] Pan, Xin, and Jian Zhao. "A central-point-enhanced convolutional neural network for high-resolution remote-sensing image classification." International Journal of Remote Sensing 38.23 (2017): 6554-6581.

[7] Ashok Kumar, P. M., Jeevan Babu Maddala, and K. Martin Sagayam. "Enhanced Facial Emotion Recognition by Optimal Descriptor Selection with Neural Network." *IETE Journal of Research* (2021): 1-20.

[8] Videla, Lakshmi Sarvani, and PM Ashok Kumar. "Facial Expression Classification Using Vanilla Convolution Neural Network." 2020 7th International Conference on Smart Structures and Systems (ICSSS). IEEE, 2020.

[9] Srinivas, P. V. V. S., and Pragnyaban Mishra. "Facial Expression Detection Model of Seven Expression Types Using Hybrid Feature Selection and Deep CNN." *International Conference on Intelligent and Smart Computing in Data Analytics: ISCDA 2020*. Springer Singapore, 2021.

[10] Srivastava, Nitish, et al. "Dropout: a simple way to prevent neural networks from overfitting." *The journal of machine learning research* 15.1 (2014): 1929-1958.

[11] Hinton, Geoffrey E., et al. "Improving neural networks by preventing co-adaptation of feature detectors." *arXiv preprint arXiv:1207.0580* (2012).

[12] Lucey, Patrick, Jeffrey F. Cohn, Takeo Kanade, Jason Saragih, Zara Ambadar, and Iain Matthews. "The extended cohn-kanade dataset (ck+): A complete dataset for action unit and emotion-specified expression." In *2010 ieee computer society conference on computer vision and pattern recognition-workshops*, pp. 94-101. IEEE, 2010.

[13] Wolfram Research, "FER-2013" from the Wolfram Data Repository, 2018.

[14] Mollahosseini, Ali, David Chan, and Mohammad H. Mahoor. "Going deeper in facial expression recognition using deep neural networks." *2016 IEEE Winter conference on applications of computer vision (WACV)*. IEEE, 2016.

[15] Lopes, André Teixeira, et al. "Facial expression recognition with convolutional neural networks: coping with few data and the training sample order." *Pattern Recognition* 61 (2017): 610-628.

[16] Mohammadpour, Mostafa, et al. "Facial emotion recognition using deep convolutional networks." *2017 IEEE 4th international conference on knowledge-based engineering and innovation (KBEI)*. IEEE, 2017.

[17] Cai, Jun, et al. "Facial expression recognition method based on sparse batch normalization CNN." *2018 37th Chinese Control Conference (CCC)*. IEEE, 2018.

[18] Lyons, Michael, Miyuki Kamachi, and Jiro Gyoba. "Japanese female facial expression (JAFFE) database.", 2017.

[19] Agrawal, Abhinav, and Namita Mittal. "Using CNN for facial expression recognition: a study of the effects of kernel size and number of filters on accuracy." *The Visual Computer* 36.2 (2020): 405-412.

[20] Jain, Deepak Kumar, Pourya Shamsolmoali, and Paramjit Sehdev. "Extended deep neural network for facial emotion recognition." *Pattern Recognition Letters* 120 (2019): 69-74.

[21] Cao, Houwei, David G. Cooper, Michael K. Keutmann, Ruben C. Gur, Ani Nenkova, and Ragini Verma. "Crema-d: Crowd-sourced emotional multimodal actors dataset." *IEEE transactions on affective computing* 5, no. 4 (2014): 377-390.

[22] Livingstone, Steven R., and Frank A. Russo. "The Ryerson Audio-Visual Database of Emotional Speech and Song (RAVDESS): A dynamic, multimodal set of facial and vocal expressions in North American English." *PloS one* 13, no. 5 (2018): e0196391.

[23] Beard, Rory, et al. "Multi-modal sequence fusion via recursive attention for emotion recognition." *Proceedings of the 22nd Conference on Computational Natural Language Learning*. 2018.

[24] Athanasiadis, Christos, Enrique Hortal, and Stylianos Asteriadis. "Audio–visual domain adaptation using conditional semi-supervised Generative Adversarial Networks." *Neurocomputing* 397 (2020): 331-344.

[25] Ghaleb, Esam, Mirela Popa, and Stylianos Asteriadis. "Multimodal and temporal perception of audio-visual cues for emotion recognition." *2019 8th International Conference on Affective Computing and Intelligent Interaction (ACII)*. IEEE, 2019.

[26] Ristea, Nicolae-Cătălin, Liviu Cristian Duţu, and Anamaria Radoi. "Emotion recognition system from speech and visual information based on convolutional neural networks." *2019 International Conference on Speech Technology and Human-Computer Dialogue (SpeD)*. IEEE, 2019.

[27] LeCun, Yann, John S. Denker, and Sara A. Solla. "Optimal brain damage." *Advances in neural information processing systems*. 1990.

[28] An, Feng-Ping, and Jun-E. Liu. "Medical Image Segmentation Algorithm Based on Optimized Convolutional Neural Network-Adaptive Dropout Depth Calculation." *Complexity* 2020 (2020).

An Exploration on Online Learning Challenges in Malaysian Higher Education: The Post COVID-19 Pandemic Outbreak

Ramlan Mustapha[1]
Akademi Pengajian Islam Kontemporari
Universiti Teknologi MARA Pahang
Raub Campus, Malaysia

Maziah Mahmud[2], Norhapizah Mohd Burhan[3]
Akademi Pengajian Islam Kontemporari
Universiti Teknologi MARA Pahang
Jengka Campus,
Malaysia

Hapini Awang[4]
School of Computing, College of Art and Science,
Universiti Utara Malaysia, Malaysia

Ponmalar Buddatti Sannagy[5]
Othman Yeop Abdullah Graduate School of Business
(OYAGSB) Universiti Utara Malaysia, Malaysia

Mohd Fairuz Jafar[6]
School of Education, College of Art and Science, Universiti
Utara Malaysia, Malaysia

***Abstract*—Flexible online programmes and learning are gaining popularity as a means of educating students. It can also facilitate the delivery of knowledge to pupils, as well as facilitating the learning process. The purpose of this study was to investigate Online Learning Challenges following the Covid-19 pandemic outbreak in Malaysia. This study employs the qualitative and Fuzzy Delphi Method in collecting the data. In the qualitative research phase, open-ended questions were distributed to 118 participants, while in the Fuzzy Delphi phase, expert questionnaires were distributed to 7 experts in the field of study. Qualitative data were analysed using Atlas-ti software, whereas Fuzzy Delphi data was analysed using Fudelo 1.0 software. The qualitative study discovered that students confront seven significant challenges: internet coverage, mental fatigue, learning devices, environmental disturbance, pedagogical challenges, lack of motivation, and social interaction.Meanwhile, the fuzzy Delphi analysis of the expert consensus of the theme is at a reasonable level. The overall expert consensus agreement findings exceed 75%, the overall value of the threshold (d) is 0.2, and the -cut exceeds 0.5. The study provides important insights into online learning issues and the fields for further improvement. This study also discusses the avenue for future research by future researchers for more significant benefits and contributions to knowledge in general.**

Keywords*—Online learning; COVID-19; outbreak; fuzzy delphi method; expert consensus

I. Introduction

The transition from the non-digital period to the digital era occurs at a frenetic pace in this century. Digital changes are not a new phenomenon; they have been a constant presence in universities for several years [1]. With current changes, the demand for technical components is increasing and pervading numerous sectors, most notably in the higher education sector. Whether we like it or not, adapting to online technology, the Internet, and new media is regarded as a critical prerequisite of this current era. The digital transformation of higher education institutions is an issue that must be dealt with by various stakeholders in education. It is incumbent to universities to equip potential professionals to address difficulties and propose solutions to apply ICT in every field of life [2]. Digital transformation can be perceived as a summary of all the digital processes needed for the transformation, equipping universities with the opportunity to implement digital technology optimally [1-3]. This process includes adequate strategic preparation, trust creation, process reflection, merging and strengthening all participating parties, mutual collaborative and organisational knowledge [3]. In light of this, researchers believe that technological mastery, readiness, preparedness, and expertise are all essential when dealing with technology-centered learning. However, as service providers, certain parties, such as educational institutions, must consider a number of factors in its implementation. The purpose of learning is to equalise knowledge, but if technology is the cause of knowledge delivery dropouts, then technology's function in higher education is underutilised.

II. Related Work

A. Online Learning

Today's new generation, lives in a sophisticated and rapidly expanding technological community that is in sync with current technology. The current generation expects a new set of learning standards based on technology, new learning styles, and new modern ways [4-5]. After the Covid-19 outbreak, educational institutions throughout the world have felt startled. This leads most schools to turn to alternate teaching instead of halting learning sessions. Based on the current situation, online learning is the best option to continue learning.

Online learning refers to online learning where teachers and learners teach and learn, using suitable learning platforms [6]. Online learning includes online training, e-learning, web learning, cyber learning, computer education or network-based instruction [7]-[4]. In 2010, about 30% of higher education registration was expected to be done online. [8]-[4]. By providing opportunities for working parents, adult learners, and students who are unable to attend classrooms, online education produces a diverse student population. This means that online learning is essential for student achievement today, and higher education institutions should provide programmes that meet their students' needs [9].

B. Online Learning Challenge in Post Covid Outbreak in Malaysia

The global outbreak of covid-19 had a tremendous influence on all sectors of the world. The economy and education are two significant sectors that have been severely impacted by the pandemic. Following the spread of this pandemic, many educational institutions were closed, and teaching and learning activities were halted immediately. Many universities around the world have digitalized their activities in order to completely comprehend the critical requirements for this current condition [10]. Even if the educational institution is closed to physical learning activities, this approach should be implemented for continuous educational institutions. When compared to the previous concentration on face-to-face and physical learning, the integration of virtual learning activities began to be fostered consistently. To some extent, social distance instruction is detrimental to the learning process. From this point on, all educational institutions began to explore for alternatives in continuing teaching and learning activities. Online learning is one of the options that can be adopted [10].

Malaysia is also among those hit by the pandemic. Following the outbreak of the pandemic, the entire school system was shut down. Many institutes of higher learning continue to engage in online teaching and learning activities today. However, in today's world, many educators prefer face-to-face learning activities [11]. In Malaysia, which has a diverse demographic, there are various challenges in the implementation of this OLL. The hilly terrain, remote areas, villages, and no internet coverage is a daunting challenge in the implementation of OLL [11]. Similarly, [12] it's been discovered that face-to-face classroom instructions were perceived as an obstructive pupil environment, and that its structure could be stressful and daunting.

Many studies have been conducted in Malaysia related to the challenges in implementing online learning in Malaysia. Meanwhile, [13], it's noted that in Malaysia, there is a significant disparity in internet coverage between urban and rural areas. At the same time, the data shows that users in the city account for 70% of all users. This disparity reflects a disparity in learning styles between urban and rural residents, since students in urban regions are more likely to use the Internet for learning than students in rural areas. This creates conflict because rural people miss out on information as a result of limited internet connectivity [14]-[15. [16] stated that most Malaysian universities embrace blended learning in tandem with face-to-face learning. This provides students with reassurance because it is vital to combine face-to-face teaching approaches with online learning. However, the shift to more online-focused teaching techniques causes students to feel apprehensive and overwhelmed by abrupt shifts, a lack of preparation, and hasty implementation.

Furthermore, for people who are poor and who reside in rural areas, the learning environment at home to conduct OLL is an issue [17]. Fast access, electronic learning tools, internet data, and a conducive environment are all essential for OLL sessions [18]. This, however, makes it difficult for those living in rural and isolated places to gain access to educational information. Students and professors face considerable challenges as a result of OLL. According to the head of the University of Malaya Association of New Youth, most students struggle and are frustrated with online learning because professors tend to provide more assignments than lectures [19]. If there are any concerns or questions, students are unable to interact actively and directly with the professor [20].

III. Methodology

The research used a qualitative descriptive approach to understand the challenges in online learning among higher education students in Malaysia. Qualitative research employs a subjective, systematic approach to exploring and describing student barriers, which might highlight new themes [21]. Researchers employed this approach to explore and describe in depth the phenomena, obstacles, and challenges encountered by students when conducting online learning activities during the Covid pandemic 19. Furthermore, using the Fuzzy Delphi method, the researchers triangulated the data with expert agreement analysis to confirm the factors and challenges of students adopting online learning. The Fuzzy Delphi technique is ideal for reaching agreement on an issue or study [22].

A. Data Collection

The data collection process in this study used an open-ended questionnaire distributed to 118 students of higher learning institutions in Malaysia. All these questions are distributed using google Forms. The distribution of questions to participants were conducted via online. Before the researcher distributed the questionnaire, the researcher contacted the study participants to obtain their consent. Once the study participants agreed, the researcher provided a link to the study questions for them to answer. Most of the study participants answered the questions well, and the researcher analysed the answers based on the feedback sheet obtained.

B. Participants

The study participants involved in this study were undergraduate students from several public universities in Malaysia. A total of 118 undergraduate students in public universities were distributed links containing open-ended questions. The selection of study participants was made by purposive sampling. All participants provided excellent cooperation, and answers were received from participants in the shortest possible time using electronic media to facilitate participants to answer the research questions. Meanwhile, for the phase of obtaining expert agreement, the researcher distributed expert questionnaires to nine experts skilled in this field of study (refer to Table I).

TABLE I. LIST OF EXPERTS

Expert list	Field of expertise	Institution
2 Professors	• Higher education	• Public University
2 Assct. Professor	• Educational multimedia	
3 Senior lecturers	• Information Technology	
2 Lecturer	• ICT	• Private university

C. Data Analysis

The data analysis of this study is divided into three parts. The first part was descriptive data analysis to collect participants profiling data. Data were analysed using SPSS version 20. Analysis of participants profiling such as gender, university and field of specialisation were collected. The second part contains data analysis of open-ended questions to obtain feedback and comments from study participants. Content analysis was then carried out on open-ended questionnaires to assess student comments and identify common patterns among written answers [23]. Content analysis involves the process of coding written answers (open-ended) into the form of patent categorisation obtained from participants' responses [24]. The last section covers the data triangulation phase through expert agreement on elements or themes extracted from open-ended questions. Fuzzy Delphi data were analysed using Fudelo 1.0 software in obtaining expert agreement.

Meanwhile, for Fuzzy Delphi analysis, the researcher used the Fuzzy Delphi method analysis by using the following formula, which contains some specific steps: The first step is in determining the linguistic scale by transforming all linguistic variables into fuzzy triangles (fuzzy triangular numbers). This stage also entails translating the language variables by adding fuzzy numbers [25]. The Fuzzy triangular number reflects m1, m2 and m3 (m1, m2, m3). The m1 value is the lowest value, the m2 value is the acceptable value, and the m3 value is the maximum value. The second step involved the Determination of Linguistic Variables and Average Responses. This method is known as the identification of each fuzzy number's constant answer [26]. The third step involved the determination of the threshold value "d". Distance is measured using the formula for each fuzzy number m = (m1, m2, m3) and n = (m1, m2, m3):

$$d\left(\bar{m},\bar{n}\right)=\sqrt{\frac{1}{3}\left[\left(m1-n1\right)^{2}+\left(m2-n2\right)^{2}+\left(m3-n3\right)^{2}\right]} \quad .$$

The fourth step involved identifying the alpha-cut aggregate level of fuzzy assessment. It is involved by adding a fuzzy number for each item. The calculation and determination of fuzzy values are using the formula: Amax = (1)⁄4 (m1 + 2m2 + m3). The fifth process known as defuzzification process, by uses the formula Amax = (1) ⁄4 (a1 + 2am + a3). If the researcher uses Average Fuzzy Numbers or average responses, the resulting score number is a number that is in the range of 0 to 1 [27]. In this process, there are three formulas, namely: i. A = 1/3 * (m1 + m2 + m3), or; ii. A = 1/4 * (m1 + 2m2 + m3), or; iii. A = 1/6 * (m1 + 4m2 + m3). A-cut value = median value for ‘0’ and ‘1’, where α-cut = (0 + 1) / 2 = 0.5. If the resulting A value is less than the α-cut value = 0.5. According to [28], the alpha cut value should exceed 0.5. It is supported by [29], who stated that the α-cut value should be more than 0.5. The last step is the ranking process by selecting defuzzification values based on an expert consensus, where the most significant position is the one with the highest value [30].

IV. STUDY’S FINDINGS

In this section, the researcher will describe the study's findings based on three phases of data analysis. Phase one is the descriptive analysis of participants who participated in this study. The second phase is the qualitative data analysis (Open-ended question) and the third phase is the data triangulation phase using Fuzzy Delphi Method.

A. First Phase Finding (Descriptive Analysis)

Table II shows the distribution of participants' gender data. 57% (50) of respondents were male, while 57% (68) were female.

B. Second Phase Finding (Qualitative)

In this section, the researcher will describe the qualitative findings (open-ended). In the results of the analysis, several themes can be inferred by the researcher based on the responses received from the participants. The themes are summarised in the Table III.

TABLE II. PARTICIPANTS

Gender	Total participants	Percentage
Male	50	43%
Female	68	57%

TABLE III. THEME AND PARTICIPANTS RESPONSE SUMMARY

Theme	• Participants responce
Internet coverage	• *"I don't really care about the class, my only problem is the internet coverage is very bad in my place"* ***(P1, 19,29,90)*** • *"It's a bit difficult for me to join this ODL class, because in my house the internet coverage is not very good"* ***(P18)*** • *"This covid ge class is quite challenging, because it is made online. My problem is that the internet is not very good in my area"* ***(P28,29)*** • *"I hope that covid 19 ends soon, I can't stand this OLL class anymore, because the internet problem in my place is very critical, know that I am in the village, not on campus"* ***(P60, 17,35,67)*** • *"I prefer face -to -face classes, because it's easier. If I don't like online classes, because internet coverage often bothers me. Sometimes it's ok and sometimes it's bad, it's hard"* ***(P87, 78,89,79)***
Mental fatigue	• *“Sometimes I feel tired with this online class, because I sit in front of the screen without doing anything for a long time, boring” (**P46, 67, 89, 93**)* • *“My brain is tired, because I prefer face to face. When sitting online in front of the screen, it feels like it's useless and tiring. as if we were talking alone”* ***(P98, 17.6,90)*** • *“If the class is ok, it's ok. sometimes the class is not ok, I will feel tired, boring”.* ***(P20,P68, 75,99)*** • *I feel uncomfortable and sometimes feel tired, exhausted. more comfortable face to face* ***(P112, P92)***
Learning Device	• *"I share the device with other siblings. It's a bit difficult to manage my class"* ***(P8,9,17.26)*** • *"This device is also a problem, because I need an ok device. But I have a laptop, but when I'm at home I*

	have to share it with my siblings sometimes." ***(P74.98,101,102)*** • *"During class, I had to use a mobile phone because I could access it outside the house because at home I had access to it was a bit poor.* ***(P22,16,81,90)***
Environmental disturbances	• *"During Covid, I studied at home, so there were a lot of disturbances, noisy, sometimes my younger siblings bothered me, I had to do my homework and so on"* ***(P15,17, 28, 29, 65)*** • *"My biggest challenge is the environment because I sit at home around the campus. When I am at home, there are many challenges, siblings, noise and so on.* ***(P1, 16, 90, 87, 102)*** • *"I can study anywhere, only if there is a disturbance that is a bit difficult for me. Noise disturbance, environmental disturbance bothers me* ***(P18,19, 35, 78, 98)*** • *"It's really challenging to use this OLL, because when we don't study on campus, the atmosphere will be different. If there is a lot of disturbance at home, it's noisy, not conducive and so on"* ***(P15,19,76,87,90,94)***
Pedagogical Challenge	• *"Learning online is ok for me, only if the lecturer doesn't teach using fun lessons, I'm so boring"* ***(P16, 78, 87,65, 90)*** • *"The challenge for me is if the class is not interesting, I'm lazy to join the class, sometimes I'm silent and I don't pay much attention to lectures"* ***(P1, 16, 45, 54,67)*** • *"I will join the class and give help if the class is interesting"* ***(P90,101, 67, 57)*** • *"If the lecturer does not provide interesting materials and presentations during the lecture session, it is difficult for me to give full concentration. I really want to concentrate if the class is not interesting".* ***(P13, 25, 17, 47,39)*** • *"I hope the lecturers prepare well for teaching, add activities online. Most lecturers only use one method, so it's hard for me to pay attention"* ***(P78,89,95)***
Lack of Motivation	• *"It's really challenging when it's OLL. Since covid happened suddenly, I initially lost weight and motivation because it happened suddenly"* ***(P16,18,90,104)*** • *"I will lose motivation and interest if the class is not interesting even more when it is this covid season"* ***(P15,18,78,67,90)*** • *"I'm very tense right now, because studying online. Actually online is ok because it's flexible, but when there are distractions and troubles I lose motivation and interest in learning"* ***(P15,18,26,58,89,90)***
Social interaction	• *"The challenge I feel is to interact with my friends because we live in different places, so it's hard to talk"* ***(P67,78, 90, 100, 107)*** • *"When there are group assignments, it's a bit difficult to discuss, everything is online. Sometimes there are those who can't cooperate for various reasons. It's difficult for me"* ***(P17, 26,57,89)*** • *"I really lose motivation when there are distractions and obstacles. I am frustrated because when online class, it requires a device, good Internet. I live in the village, coverage problems, gadgets and others make my mood disappear. Sometimes I feel depressed"* ***(P13, 47, 78, 89)*** • *"I'm ok with this online class. It's just that sometimes I lose my mood and motivation when there are unavoidable interruptions such as internet coverage, insufficient data, etc. All this makes me stress"* ***(P4, 9, 17, 78, 91)***

The bolded threshold value is over 0.2 (> 0.2) as a result of the data analysis (refer to Table IV). This indicates that there are opinions of experts which are either inconsistent or inconsistent on some issues only. However, all themes average values. suggest a threshold value (d) < 0.2, which is 0.06456. If the average threshold value of (d) is less than 0.2, the item is agreed upon by the experts [31]-[32]. Meanwhile, the total percentage of the expert agreement is 93% greater than (> 75%) for the fulfilment of the expert agreement terms of this item. Furthermore, all defuzzification value of Alpha-cut value exceeds α-cut = > 0.5 (average fuzzy responses). The alpha cut value should be higher than 0.5 [33]-[34] and discarded if less than 0.5. The analysis results demonstrate that all of the OLL challenges have been agreed upon by the qualified experts. The elements approved by the agreement of the experts are prioritised, as indicated in Table V.

TABLE IV. FUZZY DELPHI ANALYSIS RESULT

Results	Item1	Item2	Item3	Item4	Item5	Item6	Item7
Expert 1	0.05132	0.07698	0.12189	0.00642	0.01283	0.01283	0.10906
Expert 2	0.12189	0.01925	0.00642	0.06415	0.07057	0.07057	0.06415
Expert 3	0.05132	**0.2117**	0.05132	0.06415	0.07057	0.01283	0.10906
Expert 4	0.05132	0.01925	0.00642	0.10906	0.01283	0.01283	0.06415
Expert 5	0.12189	0.07698	0.00642	0.06415	0.01283	0.10264	0.06415
Expert 6	0.06415	0.01925	0.00642	0.00642	**0.21811**	0.07057	0.00642
Expert 7	0.05132	0.07698	0.00642	0.06415	0.01283	**0.21811**	0.06415
Expert 8	0.06415	0.01925	0.05132	**0.22453**	0.01283	0.07057	0.10906
Expert 9	0.16679	0.09623	0.05132	0.06415	0.01283	0.07057	0.06415

TABLE V. FUZZY SUMMARY

Statistics	Item 1	Item2	Item3	Item4	Item5	Item6	Item 7
Value of the item	0.08268	0.06843	0.03422	0.07413	0.04847	0.07128	0.0727
Value of the "D" construct	0.06456						
Item < 0.2	9	8	9	8	8	8	9
% of item < 0.2	100 %	88%	100%	88%	88%	88%	100 %
Average of % consensus	93%						
Defuzzification	0.928889	0.86667	0.92111	0.87889	0.87778	0.87778	0.88889
Rank	1	6	2	4	5	5	3
Status	Accept	Accept	Accept	Accept	Accept	Accept	Accept

V. Detailed Finding

In this section, the researcher will describe in detail the findings of the study of both phases of the study, namely the qualitative phase and data triangulation phase using expert consensus (Fuzzy Delphi). After analyzing the qualitative data (open-ended), the researcher summarized the findings to seven main themes based on the responses from the participants of this study, as stated in Table III. Then the researcher triangulated the data by obtaining expert consensus using the Fuzzy Delphi method. The results show that the main factor of the OLL challenge theme based on expert rankings (see Table V) as follow:

A. Internet Coverage Factor

As we know, the implementation of OLL requires good and robust internet coverage. If coverage cannot be adequately provided, the OLL teaching implementation process cannot be carried out well and effectively because the primary medium of OLL is the Internet. In Malaysia, not all students during Covid 19 have good (internet access). Most students are in rural areas where internet coverage is not as good as in urban areas. This shows the imbalance of the digital divide between urban and rural areas [35]-[11]. [13] Reported that in Malaysia, there is a huge gap between urban and rural areas pertaining to the issue of internet coverage. Concurrently, the data shows that users in the city account for 70% of all users. This gap reflects a disparity in learning styles between urban and rural residents, since students in urban areas are more likely to use the Internet for learning than students in rural areas. This creates conflict as rural communities miss out on information due to poor internet access problems [35] As [36] stated in his study in South Africa, it shows an unbalanced gap between urban and rural (undemocratic citizenry). In addition, [37]-[38], the response as socio-demographic inequalities raised by rural students lags compared to urban students who are more comfortable with better internet access. In addition, the absence of inadequate facilities for high-performance internet technology has also contributed to a significant problem [39]. This is a difficult challenge because the internet facilities in some places are unstable, problems with internet quota, and a lack of smartphones [39]. There are also difficulties pertaining to streaming or downloading huge size video lecture files with Internet connections and insufficient bandwidth. Rural students commonly complain about difficulties with live streaming of conferences and attending virtual conferences [40]. Students with little or no socio-economic potential to buy broadband connections are more prone to fall behind or face extra obstacles to meet others during Online Learning [41]. Based on the descriptions and findings, some respondents stated that internet coverage was the biggest challenge for them in following OLL classes. Apart from that, the experts also acknowledged that internet coverage is an issue in the Malaysian context, especially in rural areas.

B. Learning Device

One of the requirements in the implementation of online learning is a learning device. Most lecturers or teachers will use laptops, mobile phones, tablets, and other gadgets as the main medium, so electronic gadgets become mandatory in OLL. Based on the researcher's findings, the learning device is a constraint among students (see Table III). They face problems such as lack of devices, sharing devices with siblings and devices that do not support certain applications. "I share the device with other siblings. It's a bit difficult to manage my class" (P8, 9, 17.26), "This device is also a problem, because I need an ok device. But I have a laptop, but when I'm at home I have to share it with my siblings sometimes." (P74.98, 101,102). In the context of Malaysia, not all individuals in society can own electronic gadgets in large numbers. Some families with many children need to share electronic gadgets with their children to join OLL—as such, owning gadgets for learning is indeed a big challenge in some societies. This is supported by the opinion [42] that online learning entirely depends on technological equipment and the Internet. Lecturers, teachers and students with bad Internet connectivity are subject to access denial of internet learning. The reliance on online learning and the supply of technology equipment was a major problem for institutions, lecturers and students.

C. Social Interaction

In implementing this OLL, many challenges will be faced by both lecturers and students. In the context of students, it must be more challenging because the lecturer only teaches and gives input, assignments and others. Hence, in the context of students, OLL has a significant impact on social interaction between students and other friends in the class. Students usually need to interact with others at the tertiary level, especially when creating assignments and presentations. To complete assignments and presentations, they need to interact and discuss with each other. However, the constraints in terms of the Internet and the difficulty of face-to-face discussions present a significant barrier to students. As a result of the analysis, the researcher found that students expressed such problems "The challenge I feel is to interact with my friends because we live in different places, so it's hard to talk" (P67,78, 90, 100, 107), "When there are group assignments, it's a bit difficult to discuss, everything is online. Sometimes there are those who can't cooperate for various reasons. It's difficult for me" (P17, 26, 57, 89), "I really lose motivation when there are distractions and obstacles. I am frustrated because when online class, it requires a device, good Internet. I live in the village, coverage problems, gadgets and others make my mood disappear. Sometimes I feel depressed" (P13, 47, 78, 89), "I'm ok with this online class. It's just that sometimes I lose my mood and motivation when there are unavoidable interruptions such as internet coverage, insufficient data, etc. All this makes me stress" (P4, 9, 17, 78, 91). This data shows that aspects of social interaction have an impact on students. As [43]-[44] agreed that in the online course, it was emphasized that students are physically far from college, as these often influence student success and experience so that students cannot utilize or consider the resources and interactions available to them. A lack of social interaction with peers makes students feel isolated and online learning seem impersonal [44]. The researcher also has concluded that online interaction could reduce the extent of communication asynchronously; however, those who take traditional classes can be assessed successfully, with substantial delays in receiving answers. Likewise, the absence of face-to-face and social interaction found the online teaching as a disadvantage in the classroom environment.

D. Environmental Disturbance

Environmental challenges will exist if the surrounding environment presents disturbances and threats to individuals. In implementing OLL, students and lecturers will be at home or certain designated places while implementing teaching and learning sessions. Most of the students during their MCO will be in their respective homes along with other siblings. They will face a tight schedule of implementation of their respective cells. Environmental disturbances such as noise disturbances, siblings, homework and the learning environment become a threat and constraint. As a result of the analysis, the researchers found that the environmental aspect is also a major challenge in students undergoing the OLL process. They admit, “During Covid-19, I studied at home, so there were many disturbances, noisy, sometimes my younger siblings bothered me, I had to do my homework and so on” (P15, 17, 28, 29, 65), “My biggest challenge is the environment because I sit at home around the campus. When I am at home, there are many challenges, siblings, and noise and so on.” (P1, 16, 90, 87, 102), “I can study anywhere, only if there is a disturbance that is a bit difficult for me. Noise disturbance, environmental disturbance bothers me” (P18, 19, 35, 78, 98), “It is challenging to use this OLL because when we do not study on campus, the atmosphere will be different. If there is much disturbance at home, it is noisy, not conducive and so on” (P15, 19, 76, 87, 90, 94). However, [45] acknowledges that students will feel disturbed by noisy noise, and locations with a bad environment disturb students’ emotions. Disruptions and disturbances, however, are not only problematic to understand. Although orientation away from study activities may have implications for student learning, it can also be helpful to prevent cognitive overload of working memory [46].

E. Pedagogical Challenge

To get a quality teaching session, good pedagogy and andragogy aspects need to be given attention. If this aspect is not given special and robust attention and preparation, the teaching sessions are conducted without focus or attention and attraction from the students. Lecturers who teach also need to be prepared to present a good style and pedagogy to attract students' attention. Not only technology issues are related to innovation, but new educational pedagogy also arises. Online learning means the methods utilized for one-to-one classes are revised [47]. As a result of the shortcomings shown in the teaching methods, it makes students to become bored and not interested in following the teaching classes. The results of the analysis made by the researcher, the study participants admitted as follows, "Learning online is ok for me, only if the lecturer does not teach using fun lessons, I am so boring" (P16, 78, 87,65, 90) "The challenge for me is if the class is not interesting, I am lazy to join the class, sometimes I am silent and I do not pay much attention to lectures" (P1, 16, 45, 54,67), "I will join the class and give help if the class is interesting" (P90,101, 67, 57), “If the lecturer does not provide interesting materials and presentations during the lecture session, it is difficult for me to give full concentration”, "I want to concentrate if the class is not interesting". (P13, 25, 17, 47, 39) & "I hope the lecturers prepare well for teaching, add activities online. Most lecturers only use one method, so it is hard for me to pay attention". Many students admit that one thing that makes it a challenge for them to join the classes is that the learning taught is not interesting. In addition, the class is conducted online, so this aspect becomes a turning point for those who are not interested in participating in the class. The provision of unattractive teaching materials, poor pedagogy causes this problem to occur in online classrooms. Indeed, [48] stated that online learning requires lecturers to change their mindset from face to face learning to learning technology. [49] Said that "as online learning continues to grow, a lot of us recommend that we think differently about our pedagogy and move beyond face-to-face imitation". Based on this data, a good and solid pedagogical aspect is essential to attract students. Students acknowledge that if the teaching methods are not good and interesting, it causes them to be less interested and become a big challenge for them to stay and join the class consistently.

F. Lack of Motivation

Motivation is a natural thing that human beings need to do. If there is no motivation and less in oneself, it leads to human reluctance to do something. Things involving this motivation are also a big challenge among students to participate in online learning classes (OLL). In the context of students in Malaysia, lack of motivation is a matter of cause and challenge; this is related to their confession such as "It's really challenging when it's OLL. Since Covid-19 happened, I initially lost weight and motivation because it happened suddenly" (P16, 18, 90, 104), "I will lose motivation and interest if the class is not interesting even more when it is this Covid-19 season" (P15, 18, 78, 67, 90), "I'm very tense right now, because studying online. Actually online is ok because it's flexible, but when there are distractions and troubles I lose motivation and interest in learning" (P15, 18, 26, 58, 89, 90). Participants admitted that one of the reasons for the lack of motivation was that online classes had to be conducted in a hurry due to the outbreak of Covid-19. In addition to the rush and lack of careful planning towards OLL, it was causing students to feel less motivated and less enthusiastic. In addition, external disturbances and problems involving OLL are also a cause of loss of motivation among students. [50] Stated that one of the things that can motivate students towards OLL is to design exciting learning. However, [51] declared that online learning requires interaction between students and lecturers online without face-to-face interaction. So, student content must be rigorous, exciting and able to motivate students. If this does not happen, then the class will not be able to be implemented properly and will not motivate the students. Meanwhile, [52] [53] highlighted motivation and engagement for an online learning environment as the contextual interest and activities and information that maintain students' attention depend on the situational interest. However [54] further recommended that students must get help suited to their requirements in order to reduce their worry and uncertainty. The literature and the support of previous researchers' opinions show that the lack of motivation acknowledged by higher education students in Malaysia is supported by previous literature. Based on this description and theme, the researcher concluded that the lack of motivation is one of the main challenges in implementing OLL among higher education students in Malaysia.

G. Mental Fatigue

Mental health needs to be taken into account in creating an excellent emotional atmosphere during the teaching and learning process. Mental health needs to be taken into account in forming an excellent emotional atmosphere during the teaching and learning process. Mental fatigue will lead to difficulties in shaping situations, emotions and catalysts to the learning mood. This study's data revealed a great challenge among students in dealing with OLL, i.e. mental fatigue for some reason. Their confession is recorded as follows: "Sometimes I feel tired with this online class, because I sit in front of the screen without doing anything for a long time, boring" (P46, 67, 89, 93) "My brain is tired, because I prefer face to face. When sitting online in front of the screen, it feels like its useless and tiring. As if we were talking alone" (P98, 17.6, 90), "If the class is ok, it's ok. Sometimes the class is not ok, I will feel tired, boring". (P20, P68, 75, 99) & I feel uncomfortable, and sometimes feel tired, exhausted. More comfortable face to face (P112, P92). This acknowledgement indicates that they acknowledge being tired, useless and exhausted of interacting online. In the view of researchers, online learning should be fun and easy. However, these external things and disturbances cannot be controlled and sometimes burden students who cause mental fatigue. The average student admits being tired and exhausted with online classes is not due to that online, but due to things that bother them, such as internet data, environmental disruption, other assignments, etc. In addition, in Malaysia, not all students have good internet access, especially in rural areas, so it is a factor of mental fatigue and a big challenge.

VI. Conclusion

To conclude, this study aimed to explore the online learning challenge in the Malaysian Higher education setting. The open-ended question was given to students who were undergoing online learning during the Covid-'19 MCO. As a result of the responses received from them, the researchers analysed and formed specific themes in identifying the challenges faced by students in undergoing online learning in Malaysia. The responses received by the researcher were internet coverage factor, mental fatigue, learning device, environmental disturbance, pedagogical challenge, lack of motivation and social interaction. These challenges become an essential contribution of the study that will consider certain parties in formulating online learning policy, then try to overcome them to maximize learning better. In addition, with this disclosure, those who provide teaching input, such as lecturers in institutions of higher educations, need to pay attention to the existing weaknesses and improve them so that the learning system and knowledge transfer can be done better.

VII. Guideline for Further Research

This study has certain limitations. This study focuses on students in public universities in Malaysia. Future studies could focus on private universities in Malaysia as well as elsewhere. In addition, this study uses qualitative methods and data triangulated with the Fuzzy Delphi Method, and future studies can be conducted using quantitative methods by testing the variables produced in this study. In addition, this study used open-ended questions and distributed online because there were certain constraints to meet face to face with participants. Future studies can be explored in more detail, using interviews in-depth, and data can be obtained in more depth and interesting. Other aspects of teaching methodologies, institutional capabilities and lecturer efficacy can be studied in more depth in future studies.

Acknowledgment

The author would like to thank Universiti Teknologi MARA Pahang (UiTM) for providing research facilities when conducting this study.

References

[1] Kopp, M., Gröblinger, O., & Adams, S. (2019). Five common assumptions that prevent digital transformation at Higher Education Institutions. INTED2019 Proceedings, 1448-1457.

[2] Bond, M., Marín, V. I., Dolch, C., Bedenlier, S., & Zawacki-Richter, O. (2018). Digital transformation in German higher education: student and teacher perceptions and usage of digital media. International Journal of Educational Technology in Higher Education, 15(1), 1-20.

[3] Adedoyin, O. B., & Soykan, E. (2020). Covid-19 pandemic and online learning: the challenges and opportunities. Interactive Learning Environments, 1-13.

[4] Mustapha, R. (2021). Development of e-xtvt guidelines in promoting active online learning in higher education: the fuzzy delphi approach. Psychology and Education Journal, 58(1), 5681-5696.

[5] Arghode, V., Brieger, E. W., & McLean, G. N. (2017). Adult learning theories: implications for online instruction. European Journal of Training and Development.

[6] Kanuka, H., & Anderson, T. (2007). Ethical issues in qualitative e-learning research. International Journal of Qualitative Methods, 6(2), 20-39.

[7] Urdan, T. A., & Weggen, C. C. (2000). Corporate elearning: Exploring a new frontier.

[8] Moloney, J. F., & Oakley, B. (2010). Scaling online education: Increasing access to higher education. Journal of Asynchronous Learning Networks, 14(1), 55-70.

[9] Dhawan, S. (2020). Online learning: A panacea in the time of COVID-19 crisis. Journal of Educational Technology Systems, 49(1), 5-22.

[10] Rieley, J. B. (2020). Corona Virus and its impact on higher education. Research Gate.

[11] Tukiman, N., Khalid, A. K., Onn, M., Foong, N. S., & Amran, M. A. M. (2020). Online Learning Challenges and Students' Preference on Mode of Learning during COVID-19 Pandemic. International Journal of Advanced Research in Education and Society, 2(3), 72-79.

[12] Arumugam, T. (2020). Covid19: Education sector grapple with technology virtual online classrooms. In New StraitsTimes. New Straits Times Press (M) Bhd.

[13] Pui Yee, "COVID-19: (2020) Impact on the tertiary education sector in Malaysia," 'Crisis Assessment,' Penang Institute, Pulau Pinang, Malaysia, Tech. Rep., 2020. [Online]. Available: https://penanginstitute.org/wpcontent/uploads/2020/05/IMPACT-ON-THE-TERTIARY-EDUCATIONSECTOR-IN-MALAYSIA.pdf.

[14] Nassr, R. M., Aborujilah, A., Aldossary, D. A., & Aldossary, A. A. A. (2020). Understanding Education Difficulty During COVID-19 Lockdown: Reports on Malaysian University Students' Experience. IEEE Access, 8, 186939-186950.

[15] Aliyyah, R. R., Rachmadtullah, R., Samsudin, A., Syaodih, E., Nurtanto, M., & Tambunan, A. R. S. (2020). The perceptions of primary school teachers of online learning during the COVID-19 pandemic period: A case study in Indonesia. Journal of Ethnic and Cultural Studies, 7(2), 90-109.

[16] Lim, I. (2020). Reality for Malaysia's university students: Online learning challenges, stress, workload; possible solutions for fully digital future until Dec. Malay Mail, 16.

[17] Lau, J. (2020). Will Online Education Widen Asia's Digital Divide. In The World University Rankings. Times Higher Education.

[18] Arumugam, T. (2020). Covid19: Education sector grapple with technology virtual online classrooms. In New StraitsTimes. New Straits Times Press (M) Bhd.

[19] Sia, J. K. M., & Adamu, A. A. (2020). Facing the unknown: pandemic and higher education in Malaysia. Asian Education and Development Studies.

[20] Rafidi, R. (2020). Address e-learning challenges, students urge. New Straits Times.

[21] Burn, N., & Grove, S. K. (2010). Understanding nursing research: Building an evidence based practice. Elsevier Health Science, Maryland Height.

[22] Mustapha, R., & Darusalam,G. (2018), Aplikasi kaedah Fuzzy Delphi dalam penyelidikan sains sosial. Penerbit Universiti Malaya. Kuala Lumpur

[23] Chambers, T., & Chiang, C. H. (2012). Understanding undergraduate students' experience: a content analysis using NSSE open-ended comments as an example. Quality & Quantity, 46(4), 1113-1123.

[24] Moretti, F., van Vliet, L., Bensing, J., Deledda, G., Mazzi, M., Rimondini, M., ... & Fletcher, I. (2011). A standardised approach to qualitative content analysis of focus group discussions from different countries. Patient education and counseling, 82(3), 420-428.

[25] Hsieh, T. Y., Lu, S. T., & Tzeng, G. H. (2004). Fuzzy MCDM approach for planning and design tenders selection in public office buildings. International journal of project management, 22(7), 573-584.

[26] Benitez, J. M., Martín, J. C., & Román, C. (2007). Using fuzzy number for measuring quality of service in the hotel industry. Tourism management, 28(2), 544-555.

[27] Said, S., Cheng, L. S., Ridhuan, M., Jamil, M., Yusop, Y. M., Azeez, M. I. K., & Ni, N. P. (2014). Analisis masalah dan keperluan guru Pendidikan Khas integrasi (masalah pembelajaran) peringkat sekolah rendah tentang pendidikan seksualiti. Jurnal Pendidikan Bitara Universiti Pendidikan Sultan Idris, 7, 1-9.

[28] Bodjanova, S. (2006). Median alpha-levels of a fuzzy number. Fuzzy Sets and Systems,157(7), 879–891. doi: 10.1016/j.fss.2005.10.015.

[29] Tang, C.W. and , Wu, C.T. (2010). Obtaining a picture of undergraduate education quality: a voice from inside the university, Springer. Higher Education, 60, 269-286.

[30] Fortemps, P., & Roubens, M. (1996). Ranking and defuzzification methods based on area compensation. Fuzzy sets and systems, 82(3), 319-330.

[31] Lin, W. S., & Chen, C. S. (2002). Robust adaptive sliding mode control using fuzzy modelling for a class of uncertain MIMO nonlinear systems. IEE Proceedings-Control Theory and Applications, 149(3), 193-202.

[32] Jani, N. M., Zakaria, M. H., Maksom, Z., Haniff, M. S., & Mustapha, R. (2018). Validating antecedents of customer engagement in Social Networking Sites using fuzzy delphi analysis. International Journal of Advanced Computer Science and Applications, 9(9), 294-304.

[33] Tang, C.W. and , Wu, C.T. (2010). Obtaining a picture of undergraduate education quality: a voice from inside the university, Springer. Higher Education, 60, 269-286.

[34] Bodjanova, S. (2006). Median alpha-levels of a fuzzy number. Fuzzy Sets and Systems,157(7), 879–891. doi: 10.1016/j.fss.2005.10.015.

[35] Nassr, R. M., Aborujilah, A., Aldossary, D. A., & Aldossary, A. A. A. (2020). Understanding Education Difficulty During COVID-19 Lockdown: Reports on Malaysian University Students' Experience. IEEE Access, 8, 186939-186950.

[36] Du Preez, P., & Le Grange, L. (2020). The COVID-19 pandemic, online teaching/learning, the digital divide and epistemological access. Unpublished paper.

[37] Mbodila, M. (2020). Online learning–the pandemic cannot change reality. University World News: Africa Edition.

[38] Friemel, T. N. (2016). The digital divide has grown old: Determinants of a digital divide among seniors. New media & society, 18(2), 313-331.

[39] Atmojo, A. E. P., & Nugroho, A. (2020). EFL classes must go online! Teaching activities and challenges during COVID-19 pandemic in Indonesia. Register Journal, 13(1), 49-76.

[40] Farooq, F., Rathore, F. A., & Mansoor, S. N. (2020). Challenges of online medical education in Pakistan during COVID-19 pandemic. J Coll Physicians Surg Pak, 30(6), 67-9.

[41] Fishbane, L., & Tomer, A. (2020). As classes move online during COVID-19, what are disconnected students to do? Brookings.

[42] Adedoyin, O. B., & Soykan, E. (2020). Covid-19 pandemic and online learning: the challenges and opportunities. Interactive Learning Environments, 1-13.

[43] Tareen, H., & Haand, M. T. (2020). A case study of UiTM post-graduate students' perceptions on online learning: Benefits & challenges. International Journal of Advanced Research and Publications, 4(6), 86-94.

[44] Appana, S. (2008). A review of benefits and limitations of online learning in the context of the student, the instructor and the tenured faculty. International Journal on E-learning, 7(1), 5-22.

[45] Braat-Eggen, P. E., van Heijst, A., Hornikx, M., & Kohlrausch, A. (2017). Noise disturbance in open-plan study environments: A field study on noise sources, student tasks and room acoustic parameters. Ergonomics, 60(9), 1297-1314.

[46] Dau, S., & Ryberg, T. (2014, October). Disruptions and Disturbance as Challenges in a Blended Learning (BL) Environment and the Role of Embodied Habit Orientation. In European Conference on E-Learning (p. 156). Academic Conferences International Limited.

[47] Ferri, F., Grifoni, P., & Guzzo, T. (2020). Online learning and emergency remote teaching: Opportunities and challenges in emergency situations. Societies, 10(4), 86.

[48] Devlin, M., & McKay, J. (2016). Teaching students using technology: Facilitating success for students from low socio-economic status backgrounds in Australian universities. Australasian Journal of Educational Technology, 32(1).

[49] Shearer, R., Aldemirb L., Hitchcock T., Resig, J.J., Driver, J. and Kohler, M. (2019), "What students want: a vision of a future online learning experience grounded in distance education theory", American Journal of Distance Education, Vol. 34 No. 1, pp. 36-52.

[50] Kim, K. J., & Frick, T. W. (2011). Changes in student motivation during online learning. Journal of Educational Computing Research, 44(1), 1-23.

[51] Knowles, E., & Kerkman, D. (2007). An Investigation of Students Attitude and Motivation toward Online Learning. InSight: A Collection of Faculty Scholarship, 2, 70-80.

[52] De Barba, P. G., Kennedy, G. E., & Ainley, M. D. (2016). The role of students' motivation and participation in predicting performance in a MOOC. Journal of Computer Assisted Learning, 32(3), 218-231.

[53] Meşe, E. & Sevilen, Ç. (2021). Factors influencing EFL students' motivation in online learning: A qualitative case study. Journal of Educational Technology & Online Learning, 4(1), 11-22.

[54] Chambers, T., & Chiang, C. H. (2012). Understanding undergraduate students' experience: a content analysis using NSSE open-ended comments as an example. Quality & Quantity, 46(4), 1113-1123.

An Advanced Stress Detection Approach based on Processing Data from Wearable Wrist Devices

Mazin Alshamrani
The Custodian of the Two Holy Mosques Institute for Hajj and Umrah Research (HURI)
Umm Al-Qura University, Makkah, Saudi Arabia

***Abstract*—Today's busy lifestyle often leads to frequent stress, the accumulation of which may lead to severe consequences for humans. Smartwatches are widely distributed and accessible, and as such deserve intelligent solutions that deal with the processing of such collected data and ensuring the improvement of the quality of life of end-users. The goal of this research is to create a stress detection technology that can correctly, constantly, and unobtrusively monitor psychological stress in real time. Due to the importance of stress detection and prevention, many traditional and advanced techniques have been proposed likewise we provide a unique stress-detection technique that is context-based. Due to the importance of stress detection and prevention, many traditional and advanced techniques have been proposed. In this research, a novel approach to designing and using a deep neural network for stress detection is presented. To provide a desirable training environment for network development, an open-source data set based on motion and physiological information collected from wrist and chest-worn devices was acquired and exploited. Raw data were analyzed, filtered, and preprocessed to create the best possible training data. For the proposed solution to have wide use value, further focus was placed on the data recorded using only smartwatches. Smartwatches are widely distributed and accessible, and as such deserve intelligent solutions that deals with the processing of such collected data and ensuring the improvement of the quality of life of end-users. Finally, two network types with proven capabilities of processing time series data are examined in detail: a fully convolutional network (FCN) and a ResNet deep learning model. The FCN model showed better empirical performances, and further efforts were made to select an optimal network structure. In the end, the proposed solution demonstrated performance similar to state-of-the-art solutions and significantly better than some traditional machine learning techniques, providing a good foundation for reliable stress detection and further development efforts.**

Keywords*—*Fully convolutional neural network; stress detection; smartwatch; data pre-processing; semi-supervised learning

I. Introduction

The definition of stress emphasizes that it is a natural phenomenon that occurs when an organism tries to adapt to a life problem, life challenge, event, or situation. In that sense, stress is any negative reaction of the organism that occurs due to an attempt to adapt the organism to some sudden or unpleasant influence. It is commonly manifested by mental or physical suffering. As one type of emotion, stress is, unfortunately, an almost everyday phenomenon in people's lives, and as such, it has always been a complex challenge for its prevention, analysis, and monitoring. There are three main features that make measuring stress a difficult and worthwhile topic to investigate. The stress is quite subjective as it has a stimulus that initiates the stress response in one individual may not initiate it in another. In addition, the ground truth for stress detection is difficult to define because of the high subjectivity and ongoing nature of the stress process, defining the onset, length, and severity of a stress event is challenging. Furthermore, stress cannot be directly measured as its reaction is made up of physiological, behavioral, and emotional components [1, 2]. Therefore, wearable devices can directly measure a portion of the physiological reaction (e.g., increased heart rate, increased sweating rate, etc.). However, there are no direct ways to measure the other two components of the stress response (behavioral and emotional reaction). With the advancement of technology and many approaches to the treatment of stress data, artificial, and intelligent approaches for solving this issue have emerged. Some interesting research on different methodologies for treating emotions and even stress data can be seen in [1-5]. Using various previously listed papers and conducted research, hidden knowledge and unknown data patterns can be found. Even predictions of stressful events can be generated in an accurate manner.

The motivation for this new research is based on the wearable stress and affects detection (WESAD) data set from the University of California Irvine (UCI) machine learning repository, which was publicly introduced and presented for the first time in [6]. WESAD data, a collection of curated databases, are maintained by the UCI and freely available to the worldwide machine learning community. In [6] is included research that examines motion and physiological information acquired from the chest and wrist-worn devices while worn by 15 participants (12 male and three female participants), with an average age 27.5 years. Examined WESAD data includes three different affective states: neutral, stress, and amusement. Furthermore, in [6] is presented the classification linear discriminant analysis (LDA) model for processing data that achieved an F1-score accuracy of 91%. Another complete approach by the same author from [6] of identifying and labeling affective states is presented in [7]. Applicability of the WESAD data set is shown in a few other research papers, where the authors tried to achieve improved accuracy performances by exploiting different intelligent algorithms. For example, in [8], only wrist sensor measurements from the WESAD data set are exploited, highlighting that wrist data measuring techniques are non-intrusive and widely available for acquiring. The research [8] uses three different machine learning models (i.e., logistic regression, decision tree, and random forest) without any previous feature engineering processes. The best performances were achieved with the random forest model, achieving an accuracy between 88% and 99%, depending on the exploited feature. The article [9] examines if stress can be reliably detected only by using sensor data from a smartwatch. For experimental purposes, the authors used only wrist WESAD data and demonstrated satisfactory stress detection accuracy by using three different models: LDA, quadratic discriminant analysis (QDA), and random forest. Once again, as in [6], LDA showed the best performances. The research of [9] is also valuable from the perspective that it provides insights into what combination of different sensors can provide the most useful data for stress detections, highlighting the next three measuring devices: heart rate (HR) sensors, blood volume pulse (BVP), and skin temperature (ST) sensors. The most recent state-of-the-art research for automated stress detection in real life [8], [9] suggest an approach that employs a chest sensor. In their method, they first fine-tune their machine-learning model in the lab before applying it in real-world situations with certain simplifications, such as excluding times of moderate to high activity. They propose smartwatches as a source of physiological data in the future, as well as improved handling of physical activity and adding context information in the process of stress detection. All of these concerns are addressed in this research effort by using a source of physiological data is a wrist gadget. This used to recognize the user's activity by utilizing a machine-learning technique to analyze the acceleration data from the wrist device. This model is using a real-world contextual information in the machine-learning process to increase the method's effectiveness. Furthermore, we study the problem of stress detection under laboratory settings first, using an off-the-shelf wrist gadget outfitted with bio-sensors, and then apply the derived laboratory knowledge to real life, using data obtained entirely in the wild. In addition to laboratory expertise, real-world context information is collected to ensure that the approach may be effectively applied to real-world data. The context information is necessary to distinguish between real-life psychological stress and the various circumstances that cause comparable physiological arousal (e.g., exercise, eating, hot weather, etc.).

Unlike in [6, 8, 9], in [10] are applied deep learning (DL) techniques are applied in [10] to provide desired results in processing the WESAD data set. The DL model is designed to possess the ability to receive data from network inputs with different sampling rates. For that purpose, four different classification sub-models are proposed, each processing a single input with a specified sample rate and making individual predictions on its output. Final classification values are calculated by applying the fusion mechanism and applying the random forest model to generate all sub-models' predictions. Fundamental information about the fusion mechanisms can be acquired in [11]. Another recent study based on DL techniques in processing the WESAD data is presented in [12], where self-supervised learning (SSL) methodology was used to augment the initial data. This paper is different from the others listed here because it used an additional three data sets in pair with the WESAD data set and exploited only the electrocardiogram (ECG) feature. The methodology in [12] includes two main learning steps: unsupervised and supervised. In the unsupervised part of the model, its goal was to detect and recognize previously applied data transformations without introducing any pre-defined labels and creating the features. In the second part, a transfer learning approach from [13] was used for the supervised classification of affective states by using previously created features. Another study that is based on applying SSL techniques to the WESAD data set is presented in [14]. The paper uses a "pretext task" to train the model without using labeled data, where it must be determined whether the raw data and the wavelet transformations are temporally aligned. The proposed model in [14] is evaluated in two ways: using a linear classifier on top of the SSL component and assessing the number of used samples for the supervised learning process. The first evaluation approach includes a direct comparison of the features created by SSL with the features designed with expert knowledge, as in [6]. The second one is based on every participant's feedback, where they were individually asked to interactively provide input information when they field stress. The algorithm utilized this feedback information to classify stress for every subject of examination. This approach is possible only if an intelligent model does not require an extensive database with labeled data and can learn from very few provided labels. Another paper that proposes an efficient semi-supervised network architecture for classification purposes is presented in [15]. The highlighted advantages of the model are its good applicability to big data in medical diagnosis. One interesting fact of the model from [15] is that it can be applied in processing structured, semi-structured, and unstructured data at the same time.

The goal of the novel research in this paper is to propose an intelligent framework for stress detection by using only wrist dana acquired from a smartwatch. By reviewing previously introduced papers [6, 8, 9, 10, 12], it can be concluded that the current stress detection methodologies suffer from two significant deficiencies: 1) common usage of highly intrusive ECG and electroencephalogram (EEG) sensors that are not available to a broad public and 2) difficulties in getting high quality and reliable data due to the complexity of reading affective state values from appropriate sensors. As in [9], this research will also seek to avoid intrusive sensors for collecting data and will focus only on wrist sensors available on commercial smartwatches. Additionally, good practices in work with SSL models in treating the WESAD data from [12, 14] will be used as a starting point for developing a novel SSL methodology. A review of exploited methods for collecting, processing, and evaluating data collected by wearables (smartwatches and bands) is presented in [16]. It provides useful insights into techniques for intelligent algorithms' practical applicability while operating with wearable sensing equipment. It is also shown that HR sensors, galvanic skin responses, and body temperature sensors should be of leading interest in collecting data when devices are restricted to smartwatches.

In [17], another modeling effort of the WESAD data set is presented that includes both feature engineering and DL techniques for processing the data. It was proven that the combination of multiple deep neural networks could provide high performances with an average of 97.2% recall and 97.7% precision within all examined classes. The proposed solution's downside is the high complexity and significant computation costs caused by utilizing one separate network for processing data of one single sensor. Information from all the networks is finally concatenated, and final classifications are produced. One other DL application for stress and affect detection is presented in [18]. The approach utilizes recurrent neural networks and provides high-accuracy results, with 97.5% of accurately detected values.

Another approach to human stress level examination is presented in [19]. The influence of the urban environment causes stress, and the article is of interest for new research, bearing in mind that the data are collected only by using the wrist devices. Thirty people participated in the study, and the raw unlabeled data was recorded during the 30 h of the experiment. The data format is suitable for our future self-supervised training procedure, and this experiment will further be explained in following sections.

II. Research Methodology

The previous section presented the summation of different intelligent approaches in treating the multimodal WESAD data set. The main goal in all these approaches was data classification and predictions of the stress conditions of involved participants. Introduced state-of-the-art research was used as an initial foundation for designing a novel intelligent solution in the domain of stress detection and was presented in the following parts of this research paper.

To start with an in-depth analysis of the proposed solution, the examined data was presented first. Included WESAD features represented physiological and motion data recorded from both chest and wrist-worn devices. The following biological parameters were examined: BVP, electrocardiogram, electrodermal activity, electromyogram, respiration, body temperature, and three-axis acceleration. The data included expert features crafted by using widely established physiological knowledge and medical procedures that are mostly utilized to interpret respiration results and the heartbeat rate. Furthermore, the dataset contained information about three different affective states of participants (neutral, stress, and amusement), which represented the most critical parameters for this research. However, it should be highlighted that the stress conditions were restricted to public speaking exercises, and no other types of stress causes were analyzed. This is the primary deficiency of utilized data, considering that a model trained on this data might not perform at a desirable level on the general population. Besides the WESAD features, the previously introduced article [19] represents an essential base for additional data. It includes three different and associated open-source data sets that provide more than 50 h of raw Empatica E4 wrist measurements were used in this research for the semi-supervised learning phase. Furthermore, the specific Empatica E4 wrist device from [19] is of central importance for new research because it was used in our laboratory environment and in the original WESAD experiment. This implies that it was possible to combine or compare the measurement results from the described research with the measurement results in this study, ultimately leading to an accurate and reliable evaluation of the novel model. Besides building intelligent applications on the WESAD data set, many independent attempts were made to analyze emotions and extract meaningful insights from collected data of emotional parameters [20–22]. In [20, 21], different techniques were used to recognize various emotions, understand these emotions, and understand the overall reasons for their occurrence. Additionally, in [22], the Deep Multi-Net CNN Model was used for violence recognition in video surveillance. In this paper, another emotional state that caused violent behavior was examined, but not by using internal human conditions and measurement of biological parameters, but by using recorded participants' video shots.

Finally, based on the previously introduced articles, it was concluded that there were few studies based on utilizing DL techniques on wrist data wearables. This research tried to fill the observed scientific gap and propose a new approach based on the combination of a DL algorithm with a semi-supervised learning mechanism. The methodology focused on the following four phases: data exploration and preparation, design and tuning of suitable DL models, application of prepared models on the optimized data set, and evaluation of performances and analysis of obtained results. In the next section, the first phase and applied exploratory data analysis are presented on the research data.

III. Exploratory Data Analysis

Seventeen subjects (persons) participated in the original WESAD research, where they were labeled S1 to S17. This analysis is based on the WESAD data collection, which is freely available to the public. It comprises data collected from 17 individuals using the Empatica wrist-worn gadget. This gadget has accelerometers (ACC) as well as sensors for measuring skin temperature (ST), electrodermal activity (EDA), blood volume pulse (BVP), heart rate (HR), and heart rate variability (HRV). WESAD incorporates data from the chest-worn RespiBAN device, as well as questionnaires linked to participants' moods during the data collection session, in addition to E4 data. However, due to unreliable sensor results acquired in two cases, S1 and S12, these two specific subjects were removed from the research data in this paper. The rest of the data were used for building the required experimental data sets. Exploratory data analysis in this research was performed by using subjects S2 to S10 from the WESAD database as the features of the training set. The remaining subjects were assigned to the test and validation sets. With the purpose of preparing the data optimally for future DL processing, the initial data were treated in the following way. At first, the responses of all wrist sensors were aligned at the same timeline f = 700Hz. Moreover, all recorded sensor data from all included subjects were merged, and the overall data set was created accordingly. The data exploration phase was performed exclusively on the training data consisting of 40 million data rows. Keeping in mind that this research's main focus was stress detection, training data was initially analyzed from the perspective of the types of information within the set and the influence they could individually have on the stress feature. For the beginning, Fig. 1 graphically represents all subject activities that are registered during the measurement phase and saved to the training data set.

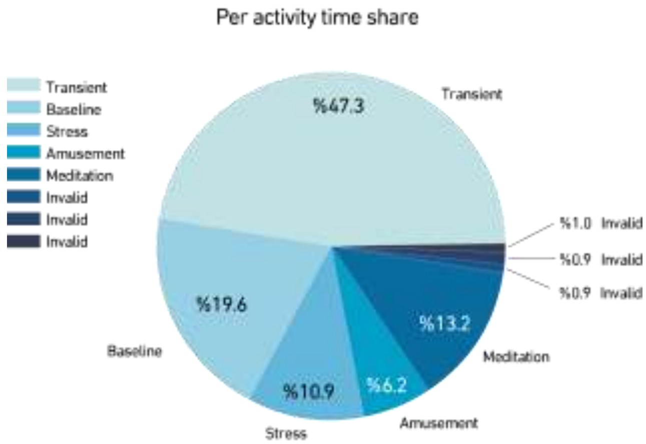

Fig. 1. The Share of Individual Activities within the Training Set.

It is easy to conclude by examining Fig. 1 that the utilized data set is imbalanced from the stress feature's perspective: Only 11% of training data is associated with stress occurrence. However, the quantity of the stress data expressed through time is 4 h, which should be sufficient material for a future model's training. Moreover, 3% of data are explicitly labeled by the data set authors as invalid and are to be removed from further work. Another question that should be answered concerning the research goal is which sensor and which recorded features have the most correlation to the stress status. For that purpose, correlation analysis was performed, and graphical results are presented in Fig. 2. It can be concluded from the figure that the acceleration and electrodermal activities (EDA) have the most correlation with the stress feature, recorded both on wrist and chest devices. This agrees with the intuitive and judgmental conclusions that stress generally causes an increase in breathing rate, chest acceleration, and sweating.

In the next phase of the data analysis and pre-processing, the outlier removal technique was performed. Each sensor was pre-defined with acceptable ranges of values, and measured values outside of these ranges were deleted and replaced by the closest valid values. Table I presents all needed information about exploited features and defined ranges.

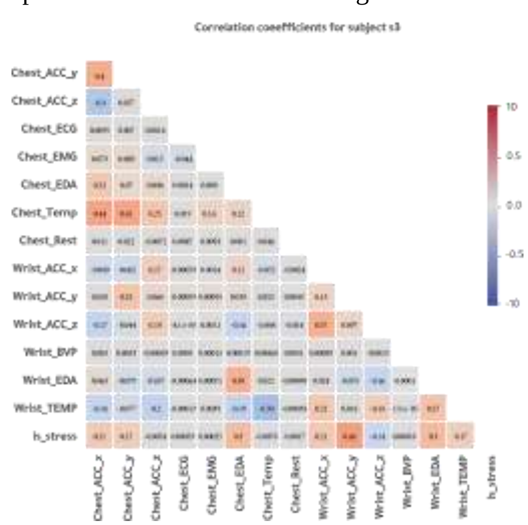

Fig. 2. Correlation Analysis of Training Data Set Concerning the Stress Feature.

TABLE I. EXAMINED SENSORS AND RELATED FREQUENCIES

Sensor	Sampling frequency (HZ)	Cutoff frequency	Defined range
Chest acceleration	700	70	X: [0;2] Y: [-0.5;0.5]. Z: [-2:2]
Chest ECG	700	70	[-1;1]
Chest EMG	700	70	[-0.5;0.5]
Chest EDA	700	2	[0;18]
Chest temperature	700	0.5	[30;36]
Chest respiration	700	2	[-10:10]
Wrist acceleration	32	16	X: [-100;150] Y: [-75;75] Z: [-75:100]
Wrist BVP	64	32	[-200;200]
Wrist EDA	4	2	[0;5]
Wrist temperature	4	2	[28;36]

Further, when working with environmental and real sensor measurements, the occurrence of noise is a common situation. Generally, any sensor signal is divided into two parts: a signal component that includes valuable information and a random noise component. In order to remove the noise component, a low-pass filter was utilized to remove the noise frequencies and undesirable data. The filtering procedure was performed as follows: a specific cutoff frequency was selected for each sensor, which represented the sensor's highest meaningful frequency values. The cutoff frequencies were selected by visual inspection of the signals, and their numerical values were provided in Table I. Next, a second-order Butterworth low-pass filter with the four corresponding cutoff information were utilized to process the signal. The example of successful filtering of one of the examined features is presented in Fig. 3.

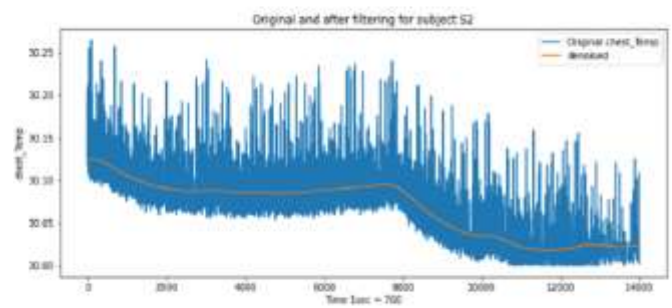

Fig. 3. An Example of Original and De-noised Signals of the Chest Temperature Feature.

IV. Application of the Fully Convolutional Network to Stress Detection Tasks

To design a model useful to a broad audience and applicable to almost any interested party, the training processes of neural network models focused only on using smartwatch WESAD data (wrist data). Following [9], all other sensor data from the initial data set that are not widely available in commercial smartwatches (like EDA sensors) were removed from the training data. For programming purposes, popular Python environments TensorFlow and Keras were used. Finally, a Google cloud machine with Nvidia K80 GPU was exploited to provide optimal computational power.

For research purposes, an FCN and a ResNet DL model from [23] were used for binary classification of baseline and stress states of the subjects. These models proved reliable and capable of a quality prediction of time series, especially the FCN model, a simple but effective model for time series classifications as shown in Fig. 4. Both networks were based on convolution layers, where the main difference between the two was in the number of layers: FCN was designed with 3, while ResNet possessed nine convolution layers. In general, a convolutional layer is a linear layer, like any other dense layer. However, the convolution layer structure was adapted for work with temporal information, which provided faster processing and improved accuracy of time series in comparison to a dense layer. In addition to these two types of networks, good results in DL analysis for emotion detection were presented [24].

After three convolutional layers of FCN, a global average pooling and the final SoftMax layer continued. At the end of each convolution, a batch normalization layer influencing training and convergence performances was applied. The main batch parameters, feature maps and striding, were tuned with special attention. Feature maps affected the total number of neurons within a network, while striding influenced how the network processed and sampled the time series data. The best empirical performances were achieved to combine four, two, and two strides for each of the three convolution layers of FCN. This combination was applied to the structure of the network. Feature maps layers 1 to 3 were selected by following the procedure from [23], and the following configuration was utilized: 64, 128, 256. The approach from [23] was also applied for selecting an Adam optimizer learning rate equal to 0.001, which was the default configuration for FCN. Two hundred and fifty learning epochs were specified, and the model that showed the best performances on the validation set was selected. Finally, ReLU activation functions [25] were chosen for building artificial neurons and DL models. Another approach to optimizing network parameters for a neural network-based emotion recognition framework was presented in [26].

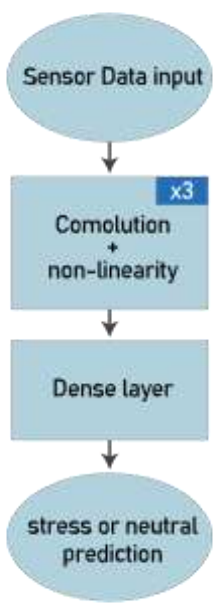

Fig. 4. Simplified Diagram of FCN Model.

For evaluation purposes, Leave-one-out cross-validation (LOO) from [27] was performed. The LOO experiment was performed on 15 folds, where for each tested subject, the data was trained on 12 other subjects, and two additional subjects were used for building the validation set. For example, if the test data was defined as S2, validation data variables were randomly selected to be S3 and S5, and all other variables were used for the training data set. By utilizing this kind of approach of treating acquired data, 15 different data sets were created through the experimental phase, and they allowed 15 different testing environments for the proposed intelligent algorithm, providing robust and reliable results in the end.

Different configurations of FCN and ResNet models were tested on the prepared training data, and it was observed that FCN was significantly faster (8 min) than ResNet (1h 30 min), and additionally, it performed better on processing the data (accuracy on examined sample: 81%–77%). The specific model configuration was selected by comparing achieved performances after a fixed number of epochs versus choosing the best model on the validation set. It was experimentally shown that the second approach provided more reliable performances, so the main testing parameter of the selection process was achieved on the validation set.

V. Results Analysis

In Fig. 5, the model performances for each examined subject are presented. An in-depth review of the achieved performances of the proposed model is presented in Table II. Metrics within the table can be explained as follows: accuracy—the number of correct classifications over total samples; balanced accuracy—the average of the proportion corrects for each class individually; F1—a harmonic average of precision and recall for the “stress” class; WEIGHTED-F1—similar to F1, this is an averaging of the “stress” and the “non-stress” class; area under curve (AUC)—a classification metric not impacted by class imbalance; precision—true “stress” detection overall stress detections; recall—true “stress” detections of overall stress samples.

Summarized results from Table II and the overall classification results of this research are presented in Table III. The average accuracy of the proposed model is approximately 0.85, while for the same training conditions, a conventional naive classifier achieved an accuracy of 0.78. Achieved results compares with the results from [8], where smartwatch data was also used. It is shown that the model from [8] provided slightly better accuracy from the model in this research (0.874 in comparison to 0.85). On the other hand, they performed 255 different runs during the training process of their model compared to only 15 performed runs in this research. It can be concluded that the proposed model in this research demonstrated satisfactory prediction performances with a small number of training cases. Furthermore, it should be reliably assumed that the model will likely further improve performance by providing additional training data and test cases and making additional tuning attempts.

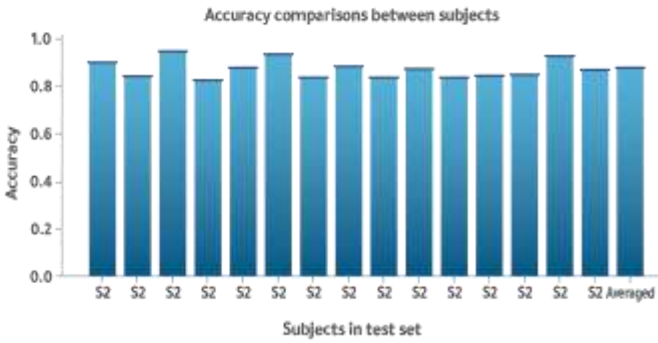

Fig. 5. Model Performances per each Examined Subject.

TABLE II. ACCURACY PER SUBJECT

Subject	Accuracy	Balanced Accuracy	F1	Weighted F1	AUC	Precision	Recall
S2	0.87	0.85	0.73	0.88	0.92	0.67	0.8
S3	0.81	0.67	0.5	0.8	0.86	0.61	0.43
S4	0.92	0.82	0.78	0.91	0.99	0.96	0.65
S5	0.8	0.87	0.68	0.82	0.98	0.52	0.99
S6	0.85	0.75	0.63	0.85	0.89	0.69	0.57
S7	0.91	0.91	0.81	0.91	0.96	0.72	0.91
S8	0.81	0.66	0.47	0.79	0.8	0.64	0.37
S9	0.86	0.7	0.56	0.84	0.82	0.82	0.43
S10	0.81	0.66	0.49	0.79	0.85	0.69	0.38
S11	0.85	0.78	0.67	0.85	0.9	0.67	0.67
S13	0.81	0.69	0.53	0.8	0.87	0.58	0.48
S14	0.82	0.63	0.4	0.79	0.87	0.82	0.27
S15	0.82	0.71	0.57	0.82	0.8	0.64	0.51
S16	0.9	0.92	0.81	0.9	0.97	0.7	0.96
S17	0.84	0.73	0.62	0.83	0.87	0.76	0.52
Averaged	0.85	0.76	0.62	0.84	0.89	0.7	0.6

TABLE III. IN-DEPTH ANALYSIS OF ACHIEVED RESULTS

Metric	FCN
Accuracy	0.85
Recall “baseline”	0.92
Precision “baseline”	0.89
F1 score “baseline”	0.90
Recall “stress”	0.59
Precision “stress”	0.68
F1 score “stress”	0.63

VI. CONCLUSION

In this research, a deep convolutional neural network model for stress detection was proposed. The model was implemented by exploiting only commercial smartwatch data because of the desire to provide a broad audience with a universal intelligent solution. Stress is a major issue in today's society, with both social and economic consequences. The results show that these works have a high accuracy for identifying stress. However, because stress levels in everyday life can differ considerably from stress levels generated in laboratory conditions, daily life studies have gained popularity in the scientific community. Another important reason why everyday life stress detection studies are more appealing to researchers is because consumers do not desire intrusive measuring techniques employed in laboratory settings. Inconspicuous wearable gadgets can be used to assess stress levels in everyday life without disturbing the users. We covered open research issues for everyday life stress detection in this part, and there is still space for development in this area. Furthermore, the accuracies of stress detection methods in everyday life are significantly lower than those in laboratory conditions. The ultimate goal of stress detection is to create a high-accuracy scheme in everyday life by conquering unsolved difficulties and employing emotion management strategies to reduce the users' stress.

REFERENCES

[1] Lisetti, C. L., and Nasoz, F. (2004) Using non-invasive wearable computers to recognize human emotions from physiological signals. EURASIP journal on applied signal processing, 2004, 1672–1687.

[2] Pollreisz, D., and Taheri, N. (2017) A simple algorithm for emotion recognition, using physiological signals of a smart watch. 39th Annual International Conference of the IEEE Engineering in Medicine and Biology Society (EMBC), Jeju Island, Korea, 11-15 July, 2353– 2356, IEEE, New York, USA.

[3] Albraikan, A., Hafidh, B., and Saddik, A. El. (2018) iaware: A real-time emotional biofeedback system based on physiological signals. IEEE Access, 6, 78 780–78 789.

[4] Ragot, M., Martin, N., Em, S., Pallamin, N., and Diverrez, J. M. (2017) Emotion recognition using physiological signals: laboratory vs. wearable sensors. In International Conference on Applied Human Factors and Ergonomics, Los Angeles, California, 17- 21 July, 15-22, Springer, Berlin, Germany.

[5] Zhao, Z., Wang, Z. Y., and Guo, B. (2018) Emotionsense: Emotion recognition based on wearable wristband. In 2018 IEEE Smart World, Ubiquitous Intelligence & Computing, Advanced & Trusted Computing, Scalable Computing & Communications, Cloud & Big Data Computing, Internet of People and Smart City Innovation (Smart-World/SCALCOM/UIC/ATC/CBDCom/IOP/SCI), China, 8-12 October, 346-355, IEEE, New York, USA.

[6] Schmidt, P., Reiss A., Duerichen R., Marberger, C., and Laerhoven, K. V. (2018) Introducing WESAD, a Multimodal Dataset for Wearable Stress and Affect Detection. ICMI '18: Proceedings of the 20th ACM International Conference on Multimodal Interaction, Boulder CO USA, 16-20 October, 400-408, ACM, New York, USA.

[7] Schmidt, P., Reiss, A., Dürichen, R., and Laerhoven, K. V. (2018) Labelling affective states in the wild: Practical guidelines and lessons learned. In Proceedings of the 2018 ACM International Joint Conference and 2018 International Symposium on Pervasive and Ubiquitous Computing and Wearable Computers, Singapure, 9-11 October, 654–659, Association for Computing Machinery, New York, United States.

[8] Indikawati, F. I., and Winiarti, S. (2019). Stress Detection from Multimodal Wearable Sensor Data. IOP Conference Series: Materials Science and Engineering, Yogyakarta, Indonesia, 16 November, 1-6, IOP Publishing Ltd, Bristol, United Kingdom.

[9] Siirtola, P. (2019) Continuous stress detection using the sensors of commercial smartwatch. UbiComp/ISWC '19 Adjunct: Adjunct Proceedings of the 2019 ACM International Joint Conference on Pervasive and Ubiquitous Computing and Proceedings of the 2019 ACM International Symposium on Wearable Computers, London, United Kingdom, 11-13 September, 1198–1201, Association for Computing Machinery, New York, NY, United States

[10] Lin, J., Pan, S., Lee, C., and Oviatt, S. L. (2019) An Explainable Deep Fusion Network for Affect Recognition Using Physiological Signals. CIKM '19: Proceedings of the 28th ACM International Conference on Information and Knowledge Management, Beijing, China, 3-7 November, 2069-2072, Association for Computing Machinery, New York, United States.

[11] Popescu, A., Mocanu, I., and Cramariuc, B. (2020) Fusion Mechanisms for Human Activity Recognition Using Automated Machine Learning. IEEE Access, 8, 143996-144014.

[12] Sarkar, P., and Etemad, A. (2020) Self-supervised ECG Representation Learning for Emotion Recognition. IEEE Transactions of Affective Computing, early access, accepted for publication.

[13] Weiss, K., and Khoshgoftaar, T. (2017) Evaluation of Transfer Learning Algorithms Using Different Base Learners. IEEE 29th International Conference on Tools with Artificial Intelligence (ICTAI), Boston, USA, 6-8 November, 187-196, IEEE, New York, USA.

[14] Saeed, A., Salim, F. D., Ozcelebi, T., and Lukkien, J. (2020) Federated Self-Supervised Learning of Multi-Sensor Representations for Embedded Intelligence. IEEE Internet of Things Journal, early access, accepted for publication.

[15] Wang, L., Qian, Q., Zhang, Q., Wang, J., Cheng, W., Yan, W. (2020) Classification Model on Big Data in Medical Diagnosis Based on Semi-Supervised Learning, The Computer Journal, bxaa006.

[16] Saganowski, S., Dutkowiak, A., Dziadek, A., Dzieżyc, M., Komoszyńska, J., Michalska, W., Polak, A., Ujma, M., and Kazienko, P. (2020) Emotion Recognition Using Wearables: A Systematic Literature Review. IEEE International Conference on Pervasive Computing and Communications Workshops (PerCom Workshops), Austin, TX, USA, 23-27 March, 1-6, IEEE, New York, USA.

[17] Chakraborty, S., Aich, S., Joo, M., Sain, M., and Kim, H. C. (2019) A Multichannel Convolutional Neural Network Architecture for the Detection of the State of Mind Using Physiological Signals from Wearable Devices. Journal of Healthcare Engineering, 2019, 1-17.

[18] Ragav, A., Krishna, N. H., Narayanan, N., Thelly, K., and Vijayaraghavan, V. (2019). Scalable Deep Learning for Stress and Affect Detection on Resource-Constrained Devices. 18th IEEE International Conference on Machine Learning And Applications (ICMLA), Boca Raton, Florida, USA, 16-19 December, 1585-1592, IEEE, New York, USA.

[19] Ojha, V. K. et al. (2019) Machine Learning Approaches to Understand the Influence of Urban Environments on Human's Physiological Response. Information Sciences, 474, 154-169.

[20] Ratre, A. (2020) Stochastic Gradient Descent–Whale Optimization Algorithm-Based Deep Convolutional Neural Network To Crowd Emotion Understanding, The Computer Journal, 63(2), 267–282.

[21] Afdhal, R., Ejbali, R., and Zaied, M. (2020) Emotion Recognition by a Hybrid System Based on the Features of Distances and the Shapes of the Wrinkles, The Computer Journal, 63(3), 351–363.

[22] Mumtaz, A., Sargano, A. B., and Habib, Z. (2020) Fast Learning Through Deep Multi-Net CNN Model For Violence Recognition In Video Surveillance, The Computer Journal, bxaa061.

[23] Wang, Z., Yan, W., and Oates, T. (2017) Time series classification from scratch with deep neural networks: A strong baseline. International Joint Conference on Neural Networks (IJCNN), Anchorage, Alaska, USA, 14-19 May, 1578-1585, IEEE, Piscataway, New Jersey, USA.

[24] Kanjo, E., Younis, E. M., and Ang, C. S. (2019) Deep learning analysis of mobile physiological, environmental and location sensor data for emotion detection. Information Fusion, 49(-), 46–56.

[25] Glorot, X., Bordes, A. and Bengio, Y. (2010) Deep Sparse Rectifier Neural Networks. Journal of Machine Learning Research, 15, 315-323.

[26] Nakisa, B., Rastgoo, M. N., Rakotonirainy, A., Maire, F. and Chandran, V. (2018) Long short-term memory hyperparameter optimization for a neural network-based emotion recognition framework. IEEE Access, 6, 49 325–49 338.

[27] Vehtari, A., Gelman, A. and Gabry, J (2017). Practical Bayesian model evaluation using leave-one-out cross-validation and WAIC. Statistics and Computing, 27, 1413–1432.

An Evaluation of the Accuracy of the Machine Translation Systems of Social Media Language:

Google's Arabic-English Translation as an Example

Yasser Muhammad Naguib Sabtan[1]*
College of Arts and Applied Sciences
Dhofar University, Salalah, Oman
Faculty of Languages and Translation
Al-Azhar University, Cairo, Egypt

Hamza Ethelb[3]
Translation Department
Faculty of Languages
University of Tripoli
Tripoli, Libya

Mohamed Saad Mahmoud Hussein[2]
Department of Curriculum & Instruction
Faculty of Education
Assiut University
Assiut, Egypt

Abdulfattah Omar[4]
Department of English
College of Science & Humanities
Prince Sattam Bin Abdulaziz University
Faculty of Arts, Port Said University, Egypt

Abstract*—In this age of information technology, it has become possible for people all over the world to communicate in different languages through social media platforms with the help of machine translation (MT) systems. As far as the Arabic-English language pair is concerned, most studies have been conducted on evaluating the MT output for the standard varieties of Arabic, with fewer studies focusing on the vernacular or colloquial varieties. This study attempts to address this gap through presenting an evaluation of the performance of MT output for vernacular or colloquial Arabic in the social media domain. As it is currently the most widely used MT system, Google Translate (GT) has been chosen for evaluating the reliability of its output in the context of translating the Arabic colloquial language (i.e., Egyptian/Cairene Arabic variety) used in social media into English. With this goal in mind, a corpus consisting of Egyptian dialectal Arabic sentences were collected from social media networks, i.e., Facebook and Twitter, and then fed into GT system. The GT output was then evaluated by three human translators to assess their accuracy of translation in terms of adequacy and fluency. The results of the study show that several translation problems have been spotted for GT output. These problems are mainly concerned with wrong equivalents, inappropriate additions and deletions, and transliteration for out-of-vocabulary (OOV) words, which are mostly due to the literal translation of the Arabic vernacular sentences into English. This can be due to the fact that Arabic vernacular varieties are different from the standard language for which MT systems have been basically developed. This, consequently, necessitates the need to upgrade such MT systems to deal with the vernacular varieties.

Keywords*—*Colloquial Arabic; Google translate; machine translation evaluation; reliability; social media

I. Introduction

Arabic is a diglossic language. For many years, however, writing used to be confined to Modern Standard Arabic (MSA) which was and still considered by some to be more prestigious [1]. With the development of social media networks and platforms, however, millions of users in the Arab world have been using their vernacular and colloquial dialects in expressing themselves. In other words, social media networks have given legacy to the colloquial forms of Arabic [2]. Millions of Arab users are using these forms in reflecting on different issues and there is an increasing demand from institutions and individuals for translating a lot of this stuff. Political agencies, manufacturers, branders, and researchers are often concerned with understanding what people say and think about. It is impossible for human translators to meet these translation needs of institutions and individuals.

In response to these needs, various machine translation (MT) systems including Google Translate, Microsoft Translator, Amazon Translate, Bing Translator have been developed. Despite the effectiveness of these systems in providing reliable translation services, many questions are still raised concerning the accuracy and quality and thus reliability of MT systems of Arabic social media [3]. This can be attributed in part to the lack of evaluation studies of the performance of MT systems with Arabic social media [4]. Therefore, this study seeks to address this gap in the literature through the evaluation of Google Translate Arabic into English translation of Arabic social media language. The rationale behind choosing Google Translate for the current study is that Google Translate is the most widely used MT system for Arabic-English translations.

Data from Facebook and Twitter will be collected for the purposes of the study. Length and representativeness issues will be considered. Manual evaluation methods will be used for evaluating the performance of Google Translate. The rest of the paper is organized as follows. Section 2 is a brief survey of the evaluation studies of Google Translate. Section 3 describes the methods and procedures of the study. Section 4 reports on the results of the translation of Google Translate of the selected

*Corresponding Author

data. Section 5 is a discussion and interpretation of the results. Section 6 concludes the paper with suggestions for further research.

II. Literature Review

Omar, et al. [5] argue that social media platforms accommodate colossal varieties of dialectal communications of Arabic. Such inclusion of different varieties has necessitated a wide use of automatic translation on social media networks. Irrespective of the purpose that pushed towards this type of translation, which can be economic or political, etc., this study is concerned with the reality that machine translation is heavily counted on in social media, amongst these is Google Translate. Zantout and Guessoum [6] illustrate that Arabs who are unable to interact or use English have lesser chance to be familiar with 50% of the content of the Web. This explains the reason that people in the Arab world resort to using machine translation. They further pinpoint the fact that it is momentous to use machine translation as it allows access to the technological advances happening in the world.

Zughoul and Abu-Alshaar [7] deduce that machine translation, also known as automatic translation, is a process that involves statistical approaches of using "rules and assumptions to transfer the grammatical structure" from one source language into another target language. Machine Translation can be defined as "the application of computers to the task of translating texts from one natural language to another" [8]. Machine translation has been developed in the field of computer science and it has been deemed of great value to a number of areas where technological endeavours are aspired for [9]. The future of machine translation, especially in the light of unprecedented development of social media tools, is booming. This has been stressed by Technology Review cited in [7] that "Universal translation is one of 10 emerging technologies that will affect our lives and work in revolutionary ways within a decade". Indeed, the Arab world is now open to all tools of social media and Arabic language is one of the languages that is available on Google Translate and other machine translation systems. Zantout and Guessoum [6] state that the Arab world is in shortage of human translators that make it follow the technological advances the world witnesses. This situation has increased the pressure of heavily relying on machine translation in order for the Arab people to keep up to date with the renovation of knowledge in all disciplines.

The process of translating knowledge or information is challenging and tedious. It could be deemed time-consuming when done by human translators. Penrose [10] cited in [11] explains that the idea of machine translation is that it imitates human minds. Given the fact that a human mind can perform complicated and sometimes enigmatic tasks, then it is possible to construct a machine that can perform this duty in an accelerated manner. This requires uploading all linguistic knowledge into software with constant input of information. In fact, technology has made it possible for people to communicate in different languages through social media platforms with the help of machine translation systems. The need to real-time translators in immediate exchange of interactions in business or socio-political situations has lessened; even though, the faults of the machine could be insurmountable. This is what this study is dealing with, as it attempts to present an evaluation of machine translation output in relation to Arabic through social media texts with special focus on Google Translate. This study assumes that the Arab people are able to interact and exchange information among cultures and across the globe without being knowledgeable of the target language; nonetheless, they are able to manage their messages through. In this respect, and in relevance to our argument, Hadla, et al. [12] argue that "most of the people with Arabic as their mother tongue use dialects in their communications at home". However, such use is even greater on social media, we argue. In fact, many studies have been conducted to evaluate the effectiveness, accuracy and reliability of machine translation, but before we visit those studies, it is relevant and crucial to explore Google Translate system, being the one that is mostly used on such platforms.

Google Translate was introduced in 2006 and is considered one of the most popular machine translation systems. It is highly used by most people all over the world [13]. Sherman [14] states that Google Translate is a statistical, phrase-based machine translation (PBMT) model. Later in 2016, it was updated with a Neural Machine Translation (NMT) model. NMT is a sophisticated method that outrates statistical methods [15]. Cheng [16] mentions that NMT employs a neural network that deals with input through various layers before it goes out. It uses deep learning techniques that results in quicker translation outcomes [17]. This enhancement of Google Translate is marked with both high-quality processing of translation and speed. It is stated that NMT uses algorithms that are capable of comprehending the linguistic rules in a way that outperforms the old statistical approach [16]. Mahmood and Al-Bagoa [13] illustrate that Google Translate translates more than 100 billion words per day to support 107 languages and more than 500 million people use it. Mahmood and Al-Bagoa [13] further explain that Google Translate can translate full web pages, spoken languages, text images, render handwritten pattern and can also provide pronunciation and read out translations.

However, with such high-tech in-built introduction to Google Translate, it has been under constant evaluation by translation studies scholars. In this research, we try to describe the reliability of the system by using social media texts. It is worth mentioning that there have been a number of studies, including Arabic, evaluating the quality of Google Translate translations. Hadla, et al. [12] show that there are three main categories used in the process of evaluating machine translation systems: human evaluation, automatic evaluation, and embedded application evaluation. In this section, we explore a number of studies related to human evaluation and automatic evaluation. Alkhawaja, et al. [17] say that the product of machine translation can be evaluated by human translators who have access to both the source and target languages. They evaluate a text in terms of adequacy, fluency, accuracy and cognition. They can also compare two outputs of machine translation to scrutinize the differences and similarity between them. The literature exhibits that there are a quite number of evaluation studies carried out on Google Translate; however, research in Arabic remains decent in this area.

Al-khresheh and Almaaytah [18] use Google Translate to evaluate the translation of English proverbs into Arabic in a small-scale study. They compared the output of the machine to a translation done by students. This study concluded that the translation of Google Translate was inaccurate in terms of rendering syntactic and lexical patterns. It can be argued that the structure of proverbs is a challenge to the machine at the moment. In a similar vein, Hadla, et al. [12] used non-proverbial Arabic sentences in their study to evaluate and compare the outcomes of Google Translate and Babylon. They used a corpus of 1033 sentences in these two machine systems and compared them to model translations. The results of their study indicated that Google translate outperformed Babylon on grounds of precision and accuracy. Further, their findings concur Al-khresheh's in that the system was incapable of handling Arabic sayings and proverbs. The ungrammatical structure that Google Translate unintelligibly produces is usually related to wrong word order, mispositions of verbs in the sentences, lexicosemantic slips and probably incorrect tense concordance [17]. Inaccuracy of Google Translation output was also evident in a study conducted by Hijazi [19] who evaluated the translation of English into Arabic legal texts. It could be argued that the newly introduced NMT update of Google Translate would produce more accurate results when it comes to legal texts. Hijazi's research was in 2013, three years before the update which was in 2016. It is recommended that a new research comparing legal texts by using machine translation and Neural Machine Translation is conducted to offer better highlights on the accuracy and adequacy of meaning.

Al-Dabbagh [20] conducted a study to evaluate the quality of Google Translate in relation to Arabic texts. The study uses a variety of text types: journalistic, economic and technical. It showed that the translation outputs of Google Translate have been marked with grammatical and textual blunders and sometimes lexical inaccuracies. The outcome of Google Translate, as pointed out by Al-Dabbagh [20], sometimes appears to be incomprehensible to readers. Moreover, the effect of Arabic from/into English translation as per Google Translate has been measured to indicate that there is no consistent frequency of flaws [12]. Discrepancies of Google Translate between Arabic appeared, as well, on verb constructions. In a detailed study on the translation of Arabic verb via Google Translate, Carpuat, et al. [21] detect that the position and the order of the Arabic verb seem to be altered by Google Translate. This, in fact, is in line with Alqudsi, et al. [22] who find that the production of Google Translate seemed literal and fallacious. Further, Jabak [23] concludes that in the light of Arabic/English automatic translation, the output of Google Translate is marked with "inadequacy, ineffectiveness and defectiveness".

Evaluation studies of Google Translate in other languages is abundant; nonetheless, the machine is relatively new and on constant development and improvement. Aiken [24] indicates that recent results of Google Translate assessment are highly encouraging. He mentions that the quality of the machine has been enhanced scoring "3.694 (out of 6) to 4.263, nearing human-level quality at 4.636" (p. 253). Aiken [24] offers further improvement statistics in these language combinations of Google Translate: "English to Spanish (87%), English to French (64%), English to Chinese (58%), Spanish to English (63%), French to English (83%), and Chinese to English (60%), for an average improvement of 69% for all pairs". The figures in Aiken's study are based on a study conducted by Wu, et al. [25] titled Google's Neural Machine Translation System: Bridging the Gap between Human and Machine Translation, which investigates the neural machine translation system.

As indicated, the literature reveals that the enhancement of Google Translate yielded more accurate results. Thus, this study explores Arabic social media texts to evaluate translation adequacy and fluency in order to reach a verdict on the system's reliability. It goes without saying that translation could be perfect in different stylistic constructions. However, we attempt to evaluate the closeness of the output of Google Translate to a logical human translation that reads fluent with adequate and accurate meaning. Social media language holds the impression of the heavy use of dialects that Arabic is renowned with. It will be interesting to see how the system is flexible in handling dialects with less counterpart phrases stored in it. The study seeks to explore whether Google Translate algorithms can construct a meaningful written utterance with probably less processing data. Puchała-Ladzińska [11] reports that the accuracy of Google Translate could differ among languages as he states that "English and Spanish works very well, but translating between English and Japanese is not nearly as effective". This study will look at this harmony by seeing if the dialectal nature of social media works well with English on Google Translate.

III. Methods and Procedures

Thirty passages with variation in document length were randomly selected. These included short, middle, and long passages. Short passages (1-10) were about 1000-1200 characters. Middle passages (11-20) were about 2000-2400 characters. Long passages (21-30) were about 3600-3900 characters. This corpus-based study aims to evaluate the dialectal Arabic-English translation of the social media content. Dialectal Arabic is a spoken phenomenon that makes it hard to find written material in the slang language except in the social media platforms. Hence the corpus consisted of dialectal Arabic sentences, mainly Egyptian (Cairene) Arabic collected from monolingual Arabic Facebook and Twitter comments on posts covering wide spectrum of genres including sports, religion, and politics. Data were filtered and comments which are completely or mostly made up of MSA words were eliminated. Only comments mostly composed of dialectal words were retained. The sentences were fed into Google Translate and the translation outputs were evaluated by the three evaluators specialized in translation for the potential errors of translation. Errors were, then, analyzed and classified according to their type. A graded rubric was designed by the researchers to guide the evaluation work of the three annotators, as seen in Table I.

Evaluators were asked to highlight the error they come across in the process of their evaluation. Table II details the evaluators' estimation of each of the passages included in the corpus.

TABLE I. A GRADED RUBRIC FOR TRANSLATION EVALUATION

Point	Criterion description
1.0	The passage exhibits major sematic, syntactic and pragmatic errors that render incomprehensible meaning(as compared to the ST)
2.0	The passage exhibits major sematic, syntactic and pragmatic errors that render partially comprehensible meaning. (as compared to the ST)
3.0	The passage exhibits slight sematic, syntactic and pragmatic errors that render mostly comprehensible meaning. (as compared to the ST)
4.0	The passage exhibits no sematic, syntactic and pragmatic errors that render completely comprehensible meaning. (as compared to the ST)

TABLE II. GOOGLE TRANSLATE SCORES BY THE ANNOTATORS

Passage No.	Annotator 1	Annotator 2	Annotator 3	Average
1.	2	2	3	2.3
2.	2	2	3	2.3
3.	3	3	2	2.6
4.	3	2	3	2.6
5.	3	3	3	3
6.	2	2	3	2.3
7.	3	2	2	2.3
8.	2	2	2	2
9.	2	3	3	2.6
10.	3	3	3	3
11.	2	3	2	2.3
12.	1	1	2	1.3
13.	2	1	2	1.6
14.	2	2	2	2
15.	2	2	3	2.3
16.	2	1	1	1.3
17.	2	3	2	2.3
18.	2	1	2	1.6
19.	1	1	2	1.3
20.	1	1	1	1
21.	1	2	2	1.6
22.	2	1	1	1.3
23.	2	1	2	1.6
24.	2	3	2	2.3
25.	1	1	2	1.3
26.	2	1	1	1.3
27.	2	3	2	2.3
28.	2	1	2	1.6
29.	2	1	2	1.6
30.	2	2	2	2

A summary of the results can be seen in Table III.

TABLE III. A SUMMARY OF THE EVALUATION RESULTS

Passages	Score average
Short passages	TABLE IV. 2.5
Middle passages	TABLE V. 1.7
Long passages	TABLE VI. 1.69
Overall average	TABLE VII. 2.0

The evaluation of the MT quality is inspired by some more general criteria. Adequacy and fluency are the general parameters against which machine translation is assessed; the former is about conveying ideas contained in the source text or how accurate the translated text as compared with the source text. The latter is concerned with the grammaticality of the target text [26, 27]. Likewise, Popović [28] argues that the quality of the MT outputs is always assessed against three quality norms: adequacy, comprehensibility and fluency. The bilingual standard of adequacy is concerned with the accuracy of conveying the meaning of the source text to the target text. The monolingual criterion of comprehensibility deals with the extent to which a reader is able to understand the resultant translation without having to go back to the source text. Fluency reflects how much the translated text adheres to the structural system of the target language. Fluency and adequacy are described by Koehn and Monz [29] as the most widely employed as manual evaluation metrics. As thus, evaluation of the MT translation in terms of semantic, syntactic and pragmatic features seems to be a kind of breaking down of these more holistic terms of adequacy, comprehensibility and fluency. Accordingly, evaluators were asked to assess each sentence along two phases. The first is monolingually-directed in which the target text was assessed for comprehensibility. The second phase compared the two texts to examine the accuracy of rendering the source text into the target text.

IV. ANALYSIS

Three annotators were given the selected passages to judge in terms of their adequacy and fluency quality. A rubric of five points was prepared by the researchers to guide annotators. The annotators were asked to comment on the salient problematic elements they come across in the outputs that render the translation defective. Annotators pinpointed different types of errors that affected the quality of the Google Translate performance. They spotted many errors covering the lexico-semantic, syntactic and pragmatic levels. Table IV details the number and of each error category as identified by the evaluators.

TABLE VIII. ERROR TYPES AS IDENTIFIED BY THE ANNOTATORS

Passages	Error types				Total
	Lexico-semantic	Syntactic	Pragmatic	Other	
Short passages (1-10)	18	16	23	7	64
Middle passages (11-20)	22	19	26	11	78
Long passages (21-30)	25	21	27	13	86

The lexcio-semantic errors are proliferent in the Google Translate (GT) outputs. For example, in the following example:

ST	إن شاء الله الرد هيكون يوم الوقفه مع نهاءي الدوره الرمضانيه 'in sha' allh alradu hayikun yawm alwaqfih mae naha'i aldawrih alramdanih
GT Output	God willing, the response will be on the day of the endowment with the end of the Ramadan session

Translating “الوقفة’ *alwaqfah* with “endowment” which denotes “to furnish with an income” is a reprehensive example of a semantic error as the proper translation that conveys the propositional content of the phrase is “the eve of the feast”. Similarly, the choice of “session” to translate “الدوره” *aldawrah* is a manifestation of lexical and semantic error as the word used in the output means “a meeting” whereas the intended meaning is “tournament”. One more instance of semantic errors, which annotators highlighted, is in the following output:

ST	والله العظيم انت كلام على الفاضي ولا هتعملوا حاجه بتضحكو على جمهوركم بأى كلام wallah aleazim 'ant kalam ealaa alfadi wala taemaluu hajah bitadhuk ealaa jumhurikum ba'aa kalam
GT Output	By God Almighty, you are talking about the empty space, and you will not do anything by laughing at your audience with any words.

In this example, Google Translate transferred the formulaic expression of “انت كلام على الفاضي” *'ant kalam ealaa alfadi* into “talking about the empty space” which constitutes a major semantic problem severely affecting the meaning and distorting the connotations of the source text. The literal translation of بتتعبو نفسكم *bitataeibu nafsikum* into “how tired you are” is another example of the lexico-semantic problems faced in Google Translate translations.

The syntactic problems or the errors related to structure and the word order of the sentence appeared now and then in the machine translation outputs. Sometimes they follow from the semantic errors; however they can also occur independently from the semantic errors. In the following output, syntactic errors appeared coupled with the semantic problem.

ST	محدش مودينا ف داهيه غيرك انت ي جرجيري muhadash mwdina f dahyh ghyrk 'ant y jrjyri
GT Output	No one, Modena, Dahia, other than you, you are watercressers

In this example, the system failed to recognize/identify the meaning of “مودينا ف داهيه” *Mwdina f Dahyh* as it mistakenly identified it as referring to named entities that should be written capitalized. This creates semantic and syntactic problems. The semantic content of the source utterance is not conveyed to the translated text bringing about a meaningless sentence. This semantic error is intertwined with a syntactic one as the sentence is missing a necessary verb and a predicate. The sentence has another instance of synchronous semantic-syntactic error occurring in the second half of the sentence when the system uses the plural form of watercressers to refer to the second person singular pronoun “you”. The use of the word “watercressers” as the English equivalent of the Arabic word”جرجيري ” *jrjyri* is semantically wrong since it is used here to refer to the name of the post author(with some phonological modification) with the purpose of mocking him. Another example to show the association of semantic errors with the syntactic one is found in the following output:

ST	😂والله الواحد م غيرر الزمالك مش عارف كان هيلاقي الضحك فين wallah alwahid m ghyrr alzamalik msha earif kan hilaqi aldahk fyn
GT Output	By God, the One M changed Zamalek, I don’t know where I would have laughter

Using the indefinite pronoun” the one” as the subject of the sentence and at the same time using the first person singular pronoun “I” to refer to it is an example of syntactic malfunction not to mention the structurally incorrect use of the definite article “the “before it. The subject “الواحد’ *alwahid* meaning “one “ refers to the author of the comment who is the speaker and as thus should be referred to using the first person pronoun “I” . The sentence should be restructured to be “By God, I don’t know without Zamalek,….” This syntactic issue seems to be based on a semantic problem as the system failed to convey the propositional content of “م غيرر الزمالك” m *ghyrr alzamalik* which is a prepositional phrase meaning “without Zamalek”.

The pragmatic errors, which reflect insensitivity to the contextual and cultural aspects of the text, popped out persistently in the translation outputs. Take for example, the following outputs:

ST	اذا بليتم فاستتروا يا اخي اختشي علي دمك ya 'akhi akhtashi ealiun damak 'iidha balaytum fastatiruu
GT Output	My brother, fear for your blood If you bleach, then take cover.

In this output, the system rendered the Arabic formulaic expression اختشي علي دمك *akhtashi ala damak* to “fear for your blood “which is a word for word translation that misses important cultural dimensions. It is an idiomatic expression used to implicate the illocutionary force of blame or rebuke. It is better to be translated into the functional equivalent of “shame on you” or “you should be ashamed of yourself”. Another bad word choice is that caused by lack of diacritics. The word بليتمis identified by the system as meaning “wear away” when the intended meaning is taken from the Arabic word بُلِيَ *bulia* to mean “be afflicted” which means “if you are afflicted by or find it indispensable to commit shameful things you should do this privately or secretly not in public”. The best equivalent is another proverb in English which says “Don't wash your dirty linen in public”. Here is another manifestation of the occurrence of pragmatic ambiguity in the GT translation’s output:

ST	بتجيبو مراره منين تتفرجو ع الحجات دي bitajibu mararih mnyn tatafaraju e alhajat di
GT Output	Btjebo bitterness from where you look at these pilgrimages

In this example, the system was not able to translate”بتجيبو ” *bitajibu* and identified it as a named entity causing a syntactic error that produced a distorted meaning. The literal translation of بتجيبو مراره منين *bitajibu mararih mnyn* is a sign of a pragmatic issue which should be transferred so that it reflects the illocution of surprise or disbelief. As the expression is an idiomatic one in Arabic, it is better to be translated by another English equivalent idiom, if possible, to give similar connotation and convey the intended speech act. The best functional equivalent in English is "how on earth you have the patience to ". The last part of the ST الحجات دي is translated by GT system as "these pilgrimages" and not "these things". This is due to the fact that sometimes the spelling form "الحجات" is used in colloquial Arabic to mean "things" but it is used in Modern Standard Arabic to refer to the plural form of the word "pilgrimage". The standard Arabic form for "things" is الحاجات *alhaajat.*

The addition to or deletion of words from the translation output is also an issue that can affect the translation quality especially with regard to the deletion. Deletion might jeopardize the appropriate convey of the full connotation of the utterances of the source text. Izwaini [30] came across similar cases of word deletion and suggested that such deletion might result in awkward translation. Numerous cases of deletion occurred in the translation of the comments with negative influence on meaning. Take the following example:

ST	والله العظيم انت كلام على الفاضي ولا هتعملوا حاجه بتضحكو على جمهوركم بأى كلام wallah aleazim 'ant kalam ealaa alfadi wala taemaluu hajah bitadhuk ealaa jumhurikum ba'aa kalam
GT Output	By God Almighty, you are talking about the empty space, and you will not do anything by laughing at your audience with any words.

In this example there are two instances of addition which has no equivalent in the source text; the first is the addition of the word "space" which is semantically wrong as it does not convey any propositional content and at the same time caused severe semantic ambiguity. The second instance is the addition of the preposition "by" that refers to the means through which something is done, a meaning not meant in this context and not included in the source text as a lexeme. For deletion, here is an example:

ST	يا عم بتتعبو نفسكم ليه مش بتقولو أن الدوري أفضل من افريقيا ya em bttebw nafsikum lih msh btqwlw 'ana aldawria 'afdal min 'afriqia
GT Output	Oh, how tired you are, why don't you say that the league is better than Africa?

In this example, the word"عم" *em* to mean buddy is deleted which causes the meaning to lose an important pragmatic connotation that show the informality of the communication and that the addresser and the addressee are mostly strangers. The addition of the question word "how" is not supported in the source text bringing about semantic ambiguity and conveying meaning which is neither said nor meant by the writer.

V. Discussion

This small-scale exploration of the MT's translation quality of the social media content revealed a wide range of errors that covered the Lexical, syntactic and pragmatic levels affecting the overall translation performance and rendering unintelligible outputs in most cases. This is in line with Jabak [23] who, albeit focused on MSA, challenged the validity of the GT system and advocated human intervention. Al-khresheh and Almaaytah [18] noted that the polysemous vocabulary and the difference in grammar caused the GT to face multitude of difficulties that affected the translation quality. Likewise, Al-Dabbagh [31] disclosed that English-Arabic translation of varied text types via Google Translate produced the full range of errors from the lexical level up to the contextual level. Omar and Gomaa [32] questioned the reliability of GT due to the many errors surveyed that relate to different lexical, structural, and pragmatic types of errors. Hadla, et al. [12] highlighted the tendency of MT systems including Google Translate to translate literally overlooking the pragmatic aspects. Hijazi [19] concluded that GT was unable to produce accurate translation to legal texts and that this kind of genre presented high difficulties lexically and syntactically. The system could not provide the readers with a general idea about the translated texts.

In the same vein, Jabak [23] revealed that GT is not a valid tool to translate from Arabic to English as its outputs lack accuracy due to the many sematic and syntactic errors committed which necessarily needs human intervention. Abdelaal and Alazzawie [33] used Google Translate to render informative news from Arabic to English to pinpoint the most common errors committed by the system. Results referred to two types: omission and bad word choice. Ali [34] revealed that three MT systems, namely, Google Translate, Microsoft Bing, and Ginger, performed insufficiently. Google translate came last in terms of accuracy. The study again highlighted the need for human post editing. However, given this stress on the necessity of a human role in translation, the question that poses itself in this regard is the feasibility of human intervention in this almost real time communication which means that the luxury of post editing and human interference is not possible.

The reason of this inherent poor quality of Google Translate is mostly due to the distant relation between Arabic and English in terms of their linguistic systems and underlying cultures, which makes MT highly challenging for GT [22, 23]. The challenges faced by the MT system due to this linguistic distance touch a wide scope of linguistic performance including the orthographic, semantic, syntactic and pragmatic levels [35-38]. The difference in lexical schemes between the two languages including phenomena like homophony [33] polysemy, and multiword expressions ([39] mainly lend themselves well to the lexico-semantic problems. The difference between the two languages with regard to the grammatical rules governing the structuring of sentences causes syntactic issues that constitute major challenges for Google Translate bringing about defective translation [18].

Orthography is another challenge that affects the GT performance. One manifestation of this challenge is the one-letter words in Arabic. Such words are so scarce in Arabic and they are mostly prepositions. They are always joined to the next words and as thus never appear as distinct words in the Arabic sentence structure. Examples are (ك) 'like', (ب)' with'.in addition, there are some imperative verbs that are reduced to one letter like (ق)'protect' and (ع) 'beware". For dialectal Arabic, the lack of standardized orthographic system leads to variation in orthographic representations/ resulting in an absence of uniformity concerning the writing system [40]. These one-word letters constituted barriers to the GT system as it failed to correctly process many instances of these one-letter words (peculiar to dialectal Arabic) occurring in the comments.

The lack of unified writing systems for vernacular Arabic means that within the one dialect the same words can be written in a variety of ways and spelled as it comes [41]. In other words, people's writing of the dialectal Arabic follows dialectal pronunciation, and ,as thus, lacks standard spelling conventions [42]. The system failure to address the challenge of improvised encoding of the dialectal language was clear in many examples of the comments translated by the study.

Orthography also affects the MT system's processing of lexemes. For example, when diacritical marks are added many of the semantic and lexical problems are solved. This is clear in translating "بليتم" and "حاجات" in the example shown earlier. Similarly, poor named entities recognition seems more evident in Arabic posing high challenge on the MT systems. Examples of the system's inability to address such challenge are the incorrect translation of "بتجيبو' and "داهية" detailed in the examples. This is actually due to the fact that Arabic writing system doesn't have the uppercase and lower case letter conventions found in English [39].

Degree of Dialectness of the source text is an important challenge that determines the effectiveness of the MT systems. Habash, et al. [43] break down dialectness into four levels which each has a degree of impact on the performance of GT system. They categorize dialecteness along a continuum with the extremes of pure MSA and Pure dialectal. The other two levels cover the mixed cases between the two extremes. The pure dialectness and the code switching between MSA and the Arabic dialect cause the system to work relatively improperly and render defective translations. In this regard, Omar and Gomaa [32] argue that the degree of colloquialism determines how accurate and reliable machine translation is due to the elastic nature of the dialectic coding system lexically or syntactically.

The contextual and cultural dimensions play a vital role in determining the MT quality. Drawing on information previously mentioned in the text is a context sensitive skill that relates to pragmatics. Pragmatics is concerned with how a language user can mean more than what s/he says. Pragmatics presupposes that the referential meaning of the utterance should be seen in light of the contextual aspects so as to be able to capture the speaker /writer's intention which often goes beyond what is said. Linguistic elements by themselves are not enough to carry the full-fledged meaning intended. Pragmatics is about the implied meaning which is not carried through words or the indirect meaning that can be derived from the text and context. "When it comes to translation, the key issue is how to capture indirectness in human communication and how to invest the resources available in both languages when rendering it" [44]. What is explicitly expressed in the ST can be faithfully transferred into the TT. However, this might create a pragmatic ambiguity resulting from not clarifying elements in the context. The pragmatic ambiguity constitutes the most common error type in the current study compared to the other lexico-semantic and syntactic error types. Notably, in most cases of semantic and syntactic errors, a pragmatic ambiguity ensues as a result.

It is worthy to note that reviewing the studies that explored the MT performance concerning literary texts [32, 44, 45] and proverbs genre [18, 45, 46] have common denominator with social media texts. Though different in their type of texts, they all agree in that high degree of cultural aspects exists in them that determine the translation quality. This makes human intervention through post editing necessary. Malika [45] reaffirms this argument that:

The cultural context of proverbs and poetry is of major importance, and since this context is out of reach for the machine, the outcome is stylistically ambiguous and culturally inappropriate translations. When the source language and the target language belong to two different families, like Arabic and English, the outcome is what Gellerstram called "Translationese " i.e., awkwardness and ungrammicality [45].

It is worthy to note that the Machine translation systems have their tools to deal with aforementioned challenges to produce as accurate translation as possible. However, the point is not as concerned with the availability of such tools as it is with the quality and compatibility of such tools. Following are a brief exploration of the specific processing techniques needed to improve the translation quality of the MT systems.

The lexico-semantic problems persist in the translated outputs despite the existence of word sense disambiguation (WSD) techniques .This might be logical due to the special case of the Arabic morphological system as characterized with being highly inflectional [47] and the unique orthographic system of Arabic with its loose and nonconventionalized scheme of writing [48]. The morphological and orthographic systems of the Arabic vernacular languages seem to be even more complicated and pose more challenge. Existing word sense disambiguation' (WSD techniques need to be honed and even more Arabic-compatible techniques that address the unique features of Arabic should be developed.

The Out of vocabulary (OOV) words stood out clearly in the translated outputs in two instances to disclose the system failure to engender accurate translation. These out of vocabulary words always appear in the translated output as transliterated words. Meereboer [49] confirms that an inherent weakness in any machine translation system is Out-Of-Vocabulary (OOV) words which is supposedly not to be included in the training data. Translating from morphologically rich languages to another less rich ones often leads to the OOV words [50]. Aqlan, et al. [51] argue that these missing or unknown words are caused by the highly inflected words peculiar to the Arabic language .As a matter of fact, with low resource languages that have limited parallel data, out of vocabulary (OOV) words are more likely to happen [52]. Dealing with this challenge should be based on the type of the missing words. According to Gujral, et al. [52], unknown words fall under three categories; "named entities, borrowed words, compound words, spelling or morphological variants of seen words or content words unrelated to any seen word" [52]. This challenge was addressed via different techniques [43, 50].

In addition, for optimal translation out of the system, morphological segmentation schemes need to be developed to cover the wide complex variation in the morphological behaviour of the dialectal Arabic. Some of the errors committed by the system, especially concerning the out-of-vocabulary, are likely to be due to the failure of the system to discover the different possible morphological variants that can associate specific roots. Some words, which the system failed to recognize and produced as out of vocabulary, were fed again to the system with different morphemes and the system was able to recognize and interpret these words. in their study of the Semitic language of *Tigrinya,* Tedla and Yamamoto [53] call for developing new morphological segmentation models that fit the highly inflected nature of their language, a thing which is applicable to Arabic as belonging to the same language family.

It is clear from the examples shown that some of the resultant problems are brought about by the poor boundary recognition of the system. The sentence boundary detection is the foundational first step for natural language processing. What follows is that more work is needed to hone the sentence boundary detection tools to address the complicated sentence structure of the typical social media communication. The social media content is primarily composed of non-punctuated stream of words which essentially presents a seemingly insurmountable challenge that so often hinders the system from executing properly. Systems need more training to be able to address the inherent flurry sentence boundaries of the social media communications. In their investigation of the sentence boundary detection for social media texts, Rudrapal, et al. [54] concluded that the current systems are limited in terms of sentence boundary detection and highlighted the needs for more advancements in this regard to capture the peculiarities of the coarse nature of social medial contents. They explained that the language of the social media texts "tend to be full of misspelled words, show extensive use of home-made acronyms and abbreviations, and contain plenty of punctuation applied in creative and non-standard ways.

VI. Conclusion

Several studies have been conducted on evaluating the performance of a number of MT systems, including Google Translate (GT), for the Arabic-English language pair. However, while most studies were focused mainly on the modern standard form of Arabic, very few studies handled the translation of Arabic dialects or the so-called colloquial Arabic or vernaculars. The current study has attempted to address this gap through evaluating the performance of automatic translation of the colloquial forms of Arabic in the social media networks and platforms, including Facebook and Twitter. In the current age of information technology social media is extensively used by people across the globe to communicate in different languages with the help of MT systems. GT, which is the most widely used MT system for the Arabic-English translation, has been chosen for evaluating the reliability of its output in the context of translating Arabic social media language into English. The evaluation has been carried out manually by human translators who assessed the accuracy of translation in terms of adequacy and fluency. The evaluators spotted a number of errors on the lexico-semantic, syntactic and pragmatic levels, which rendered the translation unintelligible in most cases. Most of the texts investigated were translated literally by GT, which resulted in inappropriate translation in the TL output. This literal rendition resulted in wrong equivalents, inappropriate additions and deletions, and transliteration for out-of-vocabulary (OOV) words.

This poor quality of GT output can be attributed to a number of reasons, most important of which is the distant relation between Arabic and English in terms of their linguistic systems. The difference in the linguistic system between both languages gives rise to a number of linguistic challenges including polysemy, homophony and multi-word expressions. Another similarly important reason is the peculiar nature of Arabic which is generally described as morphologically rich and syntactically free. This complex nature of Arabic, commonly known as a highly inflected language, poses great challenges for the computational processing of the language for NLP applications, including machine translation. A third reason which is particularly related to the vernacular varieties used in social media is the lack of a standardized orthographic system which consequently leads to variation in orthographic representations. This means that in colloquial Arabic the same words can be written in a variety of ways as they follow dialectal pronunciation and do not adhere to standard spelling conventions.

In order to overcome the problems encountered in the GT output of Arabic social media texts, NLP techniques, such as morphological analyzers, part-of-speech (POS) taggers, syntactic parsers and word sense disambiguation (WSD), systems need to be enhanced and even more Arabic-compatible techniques that address the unique features of Arabic should be developed, particularly for processing the Arabic vernacular varieties.

The current study is an attempt to shed light on the problems facing MT in the context of Arabic vernacular varieties used in social media. The study was focused on evaluating one MT system, i.e., GT, in this regard. Further studies are still needed in the area of machine translation of dialectal Arabic. One such study can address the translation of vernacular Arabic by a number of MT systems and compare and contrast between the outputs of the systems under investigation to uncover more problems and suggest possible solutions.

References

[1] Omar and M. Alotaibi, "Geographic Location and Linguistic Diversity: The Use of Intensifiers in Egyptian and Saudi Arabic," International Journal of English Linguistics, vol. 7, no. 4, pp. 220- 229, 2017.

[2] A. Omar, H. Ethelb, and Y. Gomaa, "The Impact of Online Social Media on Translation Pedagogy and Industry," 2020 Sixth International Conference on e-Learning, pp. 369-373.

[3] F. Mallek, B. Belainine, and F. Sadat, "Arabic Social Media Analysis and Translation," Procedia Computer Science, vol. 117, pp. 298-303, 2017/01/01/ 2017.

[4] A. Shazal, A. Usman, and N. Habash, "A Unified Model for Arabizi Detection and Transliteration using Sequence-to-Sequence Models," in Proceedings of the Fifth Arabic Natural Language Processing Workshop, Barcelona, Spain, 2020, pp. 167–177.

[5] A. Omar, H. Ethelb, and M. E. Hashem, "Mapping Linguistic Variations in Colloquial Arabic through Twitter A Centroid-based Lexical Clustering Approach," International Journal of Advanced Computer Science and Applications, vol. 11, no. 11, pp. 73-81, 2020.

[6] R. Zantout and A. Guessoum, "Arabic Machine Translation: A Strategic Choice for the Arab World," Journal of King Saud University - Computer and Information Sciences, vol. 12, pp. 117-144, 2000.

[7] M. R. Zughoul and A. M. Abu-Alshaar, "English/Arabic/English MachineTranslation: A Historical Perspective," Meta, vol. 50, no. 3, pp. 1022–1041, 2005.

[8] T. Poibeau, Machine Translation. Cambridge, Massachusetts: MIT Press, 2017.

[9] A. Trujillo, Translation Engines: Techniques for Machine Translation. Springer London, 2012.

[10] R. Penrose, Nowy umysł cesarza. O komputerach, umyśle i prawach fizyki (The Emperor's New Mind. About computers, mind and the laws of physics). Używana: Wydawnictwo Naukowe PWN, 1996.

[11] K. Puchała-Ladzińska, "Machine translation: A threat or an opportunity for human translators? ," Studia Anglica Resoviensia, vol. 13, no. 9, pp. 89- 98, 2016.

[12] L. S. Hadla, T. M. Hailat, and M. Al-Kabi, "Evaluating Arabic to English Machine Translation," International Journal of Advanced Computer Science and Applications, vol. 5, no. 11, pp. 68-73, 2014.

[13] M. I. Mahmood and M. A. Al-Bagoa, "The Translation of Adverbial Beta Clause Functions by Using Google Translate," International Journal of English Linguistics, vol. 11, no. 2, pp. 118-125, 2021.

[14] C. Sherman, Google Power. McGraw-Hill Education, 2005.

[15] S. W. Chan, Routledge Encyclopedia of Translation Technology. London; New York: Routledge, 2014.

[16] Y. Cheng, Joint Training for Neural Machine Translation. Singapore: Springer Nature Singapore Ltd, 2019.

[17] L. Alkhawaja, H. Ibrahim, F. Ghnaim, and S. Awwad, "Neural Machine Translation: Fine-Grained Evaluation of Google Translate Output for English-to-Arabic Translation " International Journal of English Linguistics, vol. 10, no. 4, pp. 43-60, 2020.

[18] M. H. Al-khresheh and S. A. Almaaytah, "English Proverbs into Arabic through Machine Translation," International Journal of Applied Linguistics & English Literature, vol. 7, no. 5, pp. 158-166, 2018.

[19] B. A. Hijazi, "Assessment of Google's Translation of Legal Texts," PhD Degree PhD Thesis, English Department, University of Petra Petra, Jordan, 2013.

[20] U. Al-Dabbagh, "Free Online Machine Translation Services as Providers of Gist Translation: A Fiction or a Reality," presented at the Paper presented at the 2nd Jordan International Conference on Translation, Amman, Jordan, November 30, 2010, 2010.

[21] M. Carpuat, Y. Marton, and N. Habash, "Improving Arabic-to-English Statistical Machine Translation by Reordering Post-verbal Subjects for Alignment," in Proceedings of the ACL 2010 Conference, Uppsala, Sweden, 2010, pp. 178–183.

[22] A. Alqudsi, N. Omar, and K. Shaker, "Arabic machine translation: a survey," Artificial Intelligence Review, vol. 42, no. 4, pp. 549-572, 2014/12/01 2014.

[23] O. O. Jabak, "Assessment of Arabic-English translation produced by Google Translate. ," International Journal of Linguistics, Literature and Translation (IJLLT), vol. 2, no. 4, pp. 238-247, 2019.

[24] M. Aiken, "An Updated Evaluation of Google Translate Accuracy," Studies in Linguistics and Literature, vol. 3, no. 3, pp. 253-260, 2019.

[25] Y. Wu et al., "Google's Neural Machine Translation System: Bridging the Gap between Human and Machine Translation," ArXiv, vol. abs, pp. 1-23, 2016.

[26] H. P. Krings, S. Litzer, G. S. Koby, G. M. Shreve, and K. Mischerikow, Repairing Texts: Empirical Investigations of Machine Translation Post-editing Processes. Kent State University Press, 2001.

[27] P. Koehn, Statistical Machine Translation. Cambridge: Cambridge University Press, 2010.

[28] M. Popović, "Informative manual evaluation of machine translation output," in Proceedings of the 28th International Conference on Computational Linguistics, Barcelona, Spain (Online), 2020, pp. 5059-5069: International Committee on Computational Linguistics.

[29] P. Koehn and C. Monz, "Manual and automatic evaluation of machine translation between European languages," in Proceedings on the Workshop on Statistical Machine Translation, New York City, The United States, 2006, pp. 102-121: Association for Computational Linguistics.

[30] S. Izwaini, "Problems of Arabic Machine Translation: Evaluation of Three Systems," in Proceedings of the International Conference "The Challenge of Arabic for NLP/MT", London, United Kingdom, 2006, pp. 118-148.

[31] U. Al-Dabbagh, "Assessing the Quality of Free Online Machine Translation Services," International Journal of Translation-IJT, vol. 25, no. 2, 2013.

[32] A. Omar and Y. Gomaa, "The Machine Translation of Literature: Implications for Translation Pedagogy " International Journal of Emerging Technologies in Learning (iJET), vol. 15, no. 11, pp. 228-235, 2020.

[33] N. M. Abdelaal and A. Alazzawie, "Machine Translation: The Case of Arabic-English Translation of News Texts. ," Theory & Practice in Language Studies, vol. 10, no. 4, pp. 408-418, 2020.

[34] M. A. Ali, "Quality and Machine Translation: An Evaluation of Online Machine Translation of English into Arabic Texts," Open Journal of Modern Linguistics, vol. 10, pp. 524-548, 2020.

[35] F. Alliheibi, A. Omar, and N. Alhorais, "An Evaluation of Automatic Text Summarization of News Articles: The Case of Three Online Arabic Text Summary Generators," International Journal of Advanced Computer Science and Applications, vol. 12, no. 5, 2021.

[36] A. Omar, "An Evaluation of the Localization Quality of the Arabic Versions of Learning Management Systems," International Journal of Advanced Computer Science and Applications, vol. 12, no. 2, pp. 443-449, 2021.

[37] A. Omar and W. Hamouda, "The Effectiveness of Stemming in the Stylometric Authorship Attribution in Arabic," International Journal of Advanced Computer Science and Applications, vol. 11 no. 1, pp. 116-122, 2020.

[38] A. Omar and W. Hamouda, "Document Length Variation in the Vector Space Clustering of News in Arabic: A Comparison of Methods," International Journal of Advanced Computer Science and Applications, vol. 11 no. 2, pp. 75-80 2020.

[39] M. Ameur, F. Meziane, and A. Guessoum, "Arabic machine translation A survey of the latest trends and challenges," Computer Science Review, vol. 38, pp. 1-22, 2020.

[40] R. Zbib et al., "Machine Translation of Arabic Dialects," presented at the Paper presented at the 2012 Conference of the North American Chapter of the Association for Computational Linguistics: Human Language Technologies, Montr ́eal, Canada, June 3-8, 2012, 2012.

[41] N. Habash, M. Diab, and O. Rambow, "Conventional Orthography for Dialectal Arabic," Proceedings of the Eighth International Conference on Language Resources and Evaluation (LREC'12), pp. 711-718, 2012.

[42] H. Sajjad, K. Darwish, and Y. Belinkov, "Translating dialectal Arabic to English," in Proceedings of the 51st Annual Meeting of the Association for Computational Linguistics, Sofia, Bulgaria,, 2013, pp. 1-6: Association for Computational Linguistics.

[43] N. Habash, O. Rambow, M. Diab, and R. Kanjawi-Faraj, "Guidelines for annotation of Arabic dialectness," Proceedings of the LREC Workshop on HLT & NLP within the Arabic world: Arabic Language and local languages processing Status Updates and Prospects, pp. 49-53, 2008.

[44] M. Farghal and A. Almanna, "Some pragmatic aspects of Arabic/English translation of literary texts," Jordan Journal of Modern Languages and Literature, vol. 6, no. 2, pp. 93-114, 2014.

[45] B. Malika, "The Deficiencies of Machine Translation of Proverbs and Poetry: Google and Systran Translations as a case study," Revue Maghrébine des Langues, vol. 10, no. 1, pp. 222-240, 2016.

[46] S. Hamdi, K. Nakae, and M. A. Okasha, "Online Translation of Proverbs between Availability and Accuracy," presented at the Conference: 2013 International Symposium on Language, Linguistics, Literature and Education, Osaka, Japan, 2013.

[47] Y. M. N. Sabtan, "Bilingual Lexicon Extraction from Arabic-English Parallel Corpora with a View to Machine Translation," Arab World English Journal (AWEJ), vol. 5, no. Special Issue on Translation, pp. 317–336, 2016.

[48] A. Omar and M. Aldawsari, "Lexical Ambiguity in Arabic Information Retrieval: The Case of Six Web-Based Search Engines," International Journal of English Linguistics, vol. 10, no. 3, pp. 219- 228, 2020.

[49] S. Meereboer, "Comparing solutions for the OOV word problem in Neural Machine Translation," Master Master thesis, School of Humanities, Tilburg University, Tilburg, 2016.

[50] N. Habash and H. Metsky, "Automatic learning of morphological variations for handling out-of-vocabulary terms in Urdu-English machine translation," presented at the Proceedings of the Association for Machine Translation in the Americas (AMTA-08), Waikiki, HI., Waikiki, Hawaii, USA, October 21-25, 2008, 2008.

[51] F. Aqlan, X. Fan, A. Alqwbani, and A. Al-Mansoub, "Improved Arabic–Chinese Machine Translation with Linguistic Input Features," Future Internet, vol. 11, no. 22, pp. 1-17, 2019.

[52] B. Gujral, H. Khayrallah, and P. Koehn, "Translation of Unknown Words in Low Resource Languages," presented at the Twelfth Conference of The Association for Machine Translation in the Americas, Austin, United States, 28 Oct 2016 - 1 Nov 2016, 2016.

[53] Y. Tedla and K. Yamamoto, "Morphological Segmentation for English-to-Tigrinya Statistical MachineTranslation," International Journal of Asian Language Processing, vol. 27, no. 2, pp. 95-110, 2017.

[54] D. Rudrapal, A. Jamatia, K. Chakma, A. Das, and B. Gambäck, "Sentence boundary detection for social media text," presented at the Proceedings of the 12th International Conference on Natural Language, Trivandrum, India, December 2015, 2015.

AUTHORS’ PROFILE

Yasser Muhammad Naguib Sabtan is an Assistant Professor of Linguistics and Translation in the Department of English Language and Literature, College of Arts and Applied Sciences, Dhofar University, Oman. He is also affiliated to the Department of English, Faculty of Languages and Translation, Al-Azhar University, Egypt. Dr. Sabtan has a PhD in Computational Linguistics from the University of Manchester, UK. His research interests include computational linguistics, translation studies, machine translation, corpus linguistics and EFL. ORCID: https://orcid.org/0000-0002-4389-285X.

Hamza Ethelb is an Assistant Professor in Translation Studies, Department of Translation, Faculty of Languages, University of Tripoli, Libya. He obtained his PhD degree in Translation Studies at the School of Modern Languages and Cultures, University of Glasgow, UK, in 2019. His research interests include translation studies, discourse analysis, ideology, political discourse, news translation, and language learning and teaching. ORCID: https://orcid.org/0000-0002-6075-255X.

Mohamed Saad Mahmoud Hussein is a language instructor, translator, and interpreter. His research interests include Applied Linguistics, English Language Teaching (ELT), and Translation Studies. ORCID: https://orcid.org/0000-0003-2259-7533.

Abdulfattah Omar is an Associate Professor of English Language and Linguistics in the Department of English, College of Science & Humanities, Prince Sattam Bin Abdulaziz University (KSA). Also, he is a standing lecturer of English Language and Linguistics in the Department of English, Faculty of Arts, Port Said University, Egypt. Dr. Omar received his PhD degree in computational linguistics in 2010 from Newcastle University, UK. His research interests include computational linguistics, digital humanities, discourse analysis, and translation studies. ORCID: https://orcid.org/0000-0002-3618-1750.

Impact of Data Compression on the Performance of Column-oriented Data Stores

Tsvetelina Mladenova[1], Yordan Kalmukov[2], Milko Marinov[3], Irena Valova[4]
Department of Computer Systems and Technologies
University of Ruse, Ruse, 7017, Bulgaria

***Abstract*—Compression of data in traditional relational database management systems significantly improves the system performance by decreasing the size of the data that results in less data transfer time within the communication environment and higher efficiency in I/O operations. The column-oriented database management systems should perform even better since each attribute is stored in a separate column, so that its sequential values are stored and accessed sequentially on the disk. That further increases the compression efficiency as the entire column is compressed/decompressed at once. The aim of this research is to determine if data compression could improve the performance of HBase, running on a small-sized Hadoop cluster, consisted of one name node and nine data nodes. Test scenario includes performing Insert and Select queries on multiple records with and without data compression. Four data compression algorithms are tested since they are natively supported by HBase - SNAPPY, LZO, LZ4 and GZ. Results show that data compression in HBase highly improves system performance in terms of storage saving. It shrinks data 5 to 10 times (depending on the algorithm) without any noticeable additional CPU load. That allows smaller but significantly faster SSD disks to be used as cluster's primary data storage. Furthermore, the substantial decrease in the network traffic is an additional benefit with major impact on big data processing.**

***Keywords*—Column-oriented data stores; data compression; distributed non-relational databases; benchmarking column-oriented databases**

I. Introduction

The main factors that put pressure on the centralized relational model and play a key role in the development of NoSQL DBMS are: Volume, Velocity, Variety and Agility [1]. Volume and Velocity are referred to the possibility of management of big sets of data that is generated with high speed and should be processed fast. Variety is the existence of various structures and formats of data (structured, semi-structured and unstructured). Agility is the likelihood of an organization reacting to changes in the business [2].

Usually, the relational database management systems are seen as the best possibility of data storage, data retrieval and data processing. Regardless, the constant growing needs of scalability and the emerging needs for specific applications posed various challenges to the conventional relational databases [3,4]. For example, the continuous growth of user-generated data led to an increase in the types (structured, semi-structured and unstructured) and the volume of the data that has to be stored and processed. In practice, the fast growth in the volume of the data created a big problem for the conventional databases that require a pre-known defined schema of the data, based on relations. In fact, the pre-known schema became inadequate in many different scenarios.

The desire to meet this challenge led to the creation of NoSQL DBMS [2,5]. For the purposes of the distributed databases, NoSQL is defined in [6] as follows: NoSQL is a set of ideas and concepts that allow for fast and efficient processing of datasets with an emphasis on performance, reliability and speed. One of the challenges for the users of NoSQL is that there are a large number of different architectural data models to choose from (key-value, column-oriented, document-based, graph stores).

Compression of data elements in traditional database management systems significantly improves system performance by [7,8]: (1) decreasing the size of the data, (2) increase the productivity of input/output operations by reducing search time, (3) reduction of data transfer time in the communication environment (less data is transferred to the computer network) and (4) increasing the relative speed of the input-output buffer. For requests that are limited in terms of data input or retrieval speed, the CPU load resulting from the decompression is offset by I/O system improvements at the operating system level. All this has a significant effect when working with large amounts of data.

In the column store, each attribute is stored in a separate column, so that the sequential values of this attribute are stored sequentially on disk [4,9]. This data model provides more opportunities for improved performance as a result of applying algorithms to compress data elements compared to row-oriented architectures. In the column-oriented model, the use of different compression schemes that encode multiple values at once is natural. In tuple-oriented systems, such schemes do not work well because the individual attribute is stored as part of the whole tuple, so combining the same attribute from different tuples together into one value will require some way to "mix" tuples.

The main objective of the current research is to test the capabilities of a small-sized cluster when performing the operations Insert and Select to Hbase. The operations are performed with and without the supported Hbase compression algorithms. This article aims to observe the behavior of the cluster when performing the experiments.

The article is structured as follows: Section 2 reviews some related research. Section 3 presents column-oriented data model properties. Section 4 outlines the nature of Hbase.

Section 5 presents the conducted experiment. Finally, in Section 6 the authors make conclusions and offer ideas for further research.

II. Related Work

Many authors are doing extensive research on the topic of data compression in Hbase and are proposing some additional algorithms and strategies for optimization of the compression process.

To avoid the hot-spot issue in the Regional Servers, the authors in [10] are proposing sorting of the data before the compression. Another part of the proposed solution is the usage of different compression algorithms for different data types.

In [11] the authors are overviewing some common compression algorithms and through experiments are comparing the methods. The results from these experiments are used for the decision of how to compress a particular data column. As a result, they propose an architecture for query executor. The authorsalso pay attention to the order of the columns.

A short survey of data compression techniques for column-oriented databases is presented in [12]. The results show that the LZO and Snappy compressions have comparable compression rates and speeds.

An analysis on compression of data, presented in relational format is done in [13] resulting in the authors proposing a strategy for compressing similar data together. The authors are noting that the traversal strategy has a significant impact on the compression ratio.

The compression algorithms of Hbase are considered in [14]. A series of experiments are conducted and several aspects are analyzed - used memory, CPU utilization, network utilization and disk space usage. The results show that the usage of some form of compression is beneficial when dealing with large clusters and large jobs. In terms of query time execution, Snappy is the best performing algorithm.

III. Column-oriented Data Model Properties

The systems based on column families are important architecture models of NoSQL data because they can easily expand (scale horizontally) while processing big volumes of data. Column-oriented data models can be viewed as one multi-dimensional table (Table I), to which queries can be made using the primary key. In this type of data storage, the key can be the identifier of the row (Row ID) and the name of the column. The first dimension of the table is the RowKey, which denotes the row of the physical storage of the data in the table. The second dimension is the column family, which is similar of the attributes in the relational data model. The third dimension is the qualificator of the column. In theory, every column can have an unlimited number of qualificators. The fourth dimension is the timestamp which is automatically assigned and represents the moment of the cell creation in nanoseconds. The structure of the key can be seen in the following manner:

The advantages of column-oriented systems are as follows [1,2,5,9]:

- A high degree of scalability – in essence, column-oriented systems have the property of scalability, which means that when there is a high intensity of data addition, more general-purpose nodes have to be added to the cluster. With a good design of the cluster can be achieved a linear relation between the way the data is expanding and the number of the needed nodes. The main reason for this relation is the manner in which the Row identifier and the column names are being used when identifying a cell. With the maintenance of a simple interface, the system which works in a background mode, can distribute the queries between a large number of nodes without the need of performing any merge and join operations.
- A high degree of availability – by building a system that is easily scalable, the need for data duplication arises. Because column-oriented systems use effective communication, the replication cost is low. The lack of join operations allows the storage of individual portions of the column matrix on remote servers. This means that if one of the nodes that contain some of the matrix data, falls, and the other nodes will provide the services to these cells.
- Easy data addition – the column-oriented model does not require a pre-detailed design before the data insertion begins. The column names should be known prior to the insertion, but the identifier of the rows and the column qualifiers can be created at any given moment.

Improved data compression – storing data from the same domain increases the locality of the processing and thus improves the degree of data compression (especially if the attribute is sorted). The requirements for the transfer speed in the computer network are further reduced when transferring compressed data. The coefficient of the compression is higher in the column-oriented data storages as the sequential values that are being stored in the column are from the same data type, while the neighboring attributes in the tuple can be different types. When every value in the column has the same size, the speed of decompression can be high, especially when taking into account the super-scalar properties of today's processors. The columns can be further sorted which in turn will increase the potential of compression. The compression methods used in the column-oriented systems improve the CPU performance by allowing data manipulators to work directly on the compressed data without having to decompress.

TABLE I. KEY STRUCTURE IN COLUMN-ORIENTED SYSTEMS

Key				
Row-ID	Column family	Column qualifier	Time stamp	**Value**

IV. HBASE OVERVIEW

Apache HBase (http://hbase.apache.org) is a distributed, fault-tolerant, column-oriented database modeled after Google's Bigtable [15]. Similarly, as Bigtable is built on top of the Google's distributed file system, HBase relies on the data storage provided by the Hadoop's distributed file system (HDFS). It is an open-source software, written in Java. Its primary goal is to provide random, fast (real-time) read/write access to very large tables (containing billions of rows and millions of columns) running on clusters of cheap commodity servers.

As a non-relational database, it does not rely on SQL to access the data; however the Apache Phoenix project [16] offers an additional SQL layer on top of HBase, and a JDBC driver that allows external JAVA applications to communicate with the database. Furthermore, data are accessible through Java API, REST API and Avro or Thrift gateway APIs.

HBase features linear horizontal scalability, strictly consistent reads and writes, automatic failover support between RegionServers, data compression, in-memory operation, and Bloom filters on a "per-column" basis as implemented in Bigtable [10].

HBase is a widely deployed database, used by large number of companies, ranging from IT giants (Facebook, Twitter, Yahoo!, Adobe, Meetup, OCLC – WorldCat's data storage, and others) to smaller companies and research projects. Before 2018 Facebook fully relied on HBase to store private messages (multimedia content) exchanged through "Messenger". Then they switch to MyRocks - Facebook's open source database project that integrates RocksDB as a MySQL storage engine [17]. Twitter uses HBase as a distributed backup of their production database (implemented in MySQL). Benipal Technologies utilizes a 35-node HBase cluster that holds over 10 billion rows with hundreds of datapoints per row. They compute over 1018 calculations daily using MapReduce directly on HBase.

Data compression is a method that is used to improve the performance and reduce the storage space. Hbase supports four different compression algorithms, which can be directly applied on the ColumnFamily. That includes SNAPPY [18], LZO [19], LZ4 [20] and GZ [21] compressions. When creating a table every ColumnFamily is defined separately meaning that some families can have a compression algorithm applied to them and some may not. Using a compression algorithm can lead to a significantly reduced storage space as it is seen from the conducted experiments.

V. EXPERIMENTAL ANALYSIS

A. Experimental Environment and Dataset

A cluster of 10 servers is being used to conduct this experiment. A Name Node having two CPUs: Intel Xeon Silver 4110, 8 cores and a total of 32 threads, and 64GB RAM; 9 data nodes – each data node have one CPU Intel Xeon E-2124, 4 cores and 4 threads, and 16GB RAM; and 1 additional server, having the same technical specifications as the data nodes, that is not being featured in the cluster but is located in the same network as the cluster.

Every experiment consists of a Python code that initiates an Insert or Select queries to the Name Node. The python code is developed with the help of some additional Python libraries and packages. Most important of which is the HappyBase library. HappyBase is a library, developed on the ThriftPy2 Package. Essentially, the ThriftPy2 is used to establish the connection between the cluster (more precisely - the Name Node) and the client. All of the test scenarios are being performed from the additional server, the one that is located in the same network but is not featured in the cluster.

The data that is being sent and retrieved to the server consist of over 4 900 000 different sensor measurements. The description of the dataset can be seen in Table II.

TABLE II. DATASET DESCRIPTION

Attribute	Column Family
house_id	house:mac
date_time	house:datetime
ch1_watts to ch3_watts	ch:1 to ch:3
temp	readings:temp
gas_reading	readings:gas
appliance_1 to appliance_10	app:1 to app:10

While performing the experiment the sequential data transmission from the sensors is stimulated, as can be expected in real-life scenarios. Therefore, all of the Insert tests are done in the manner of several thousand queries being sent to the server instead of performing a single Load Dump. We strive to test the capabilities of the cluster as close to real-life situations as possible. Nevertheless, the experiments are performed in an almost sterile environment, as the cluster does not handle any additional tasks while inserting and selecting the data.

B. Comparative Experiment on Query Execution Time

1) Insert queries: The Insert Test Cases are done under the following conditions:

- The table that will store the row is created at the beginning of the test.
- The number of the versions of the cells is left at the default value – three.
- A total of fifteen Insert tests cases are performed – three tests without any compression and twelve tests with compression (four compressions multiplied by three times).
- Every test is performed with 200 000, 400 000, 600 000, 800 000 and 1 000 000 different queries send to the server.

The inconsistent manner of the insert query execution is notably visible in these tests. The number of requests per second is around 400 to 430. That difference is small enough to be considered insignificant. Fig. 1 shows the number of requests per second, per compression in detail. When inserting 200 000 rows, the LZO Compression, the SNAPPY compression and the control test without compression behave in similar manner. The GZ and LZ4 compressions are a fraction slower. The insertion of 400 000 rows is similar regardless of the chosen compression and starting from the 600 000 and upward clearer differences in the execution time and the number of requests per second can be observed. What makes an impression are the spikes in the LZO compression and the test without any compression. In the tests with 800 000 and 1 000 000 rows, the cases without compression and the LZO compression behave best, respectively.

2) Select queries: The select test cases are performed on the same tables that have been created when conducting the Insert experiments. Meaning that the select queries are performing full table scans on the compressed data. For every combination of dataset and compression, a total of three test scenarios are done – querying 25%, 50% and 75% of the data. Fig. 2 shows the execution time of the conducted tests. Almost every compression is behaving as expected – with the increase of the queried rows, the execution time increases linearly. LZO is the only compression that does not follow this behavior – it has some notable spikes when selecting 150 000, 300 000 and 450 000 rows. A possible explanation of that can be the locality of the data and it is worth a further examination.

C. Comparative Experiment on Physical Storage

The physical storage of the data (the Persistent Memory) is also an area that is worth looking into. The column-oriented systems are characterized by improved data compression. Moreover, that can be seen in Fig. 3 in which it is obvious that the tests run with no compression are taking up a lot of physical memory on the cluster. Tables with more than 1 000 000 rows can be as large as 1GB. Fig. 4 shows the physical memory of the data without the outlier – the tests with no compression. In this figure, the difference between the four compressions is more distinguishable.

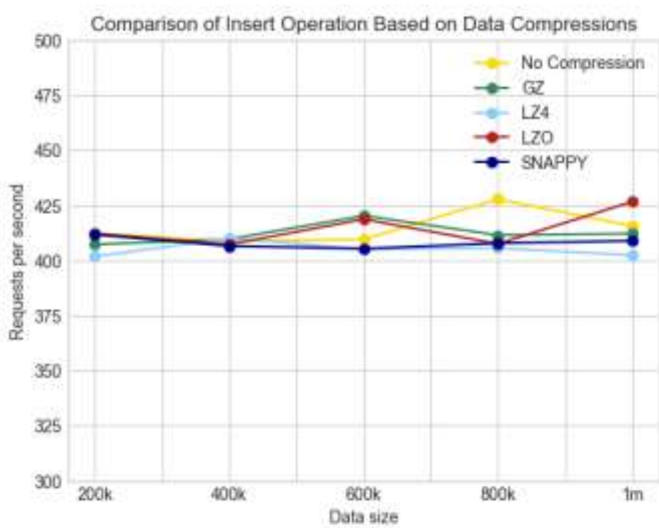

Fig. 1. Comparison of Insert Operation.

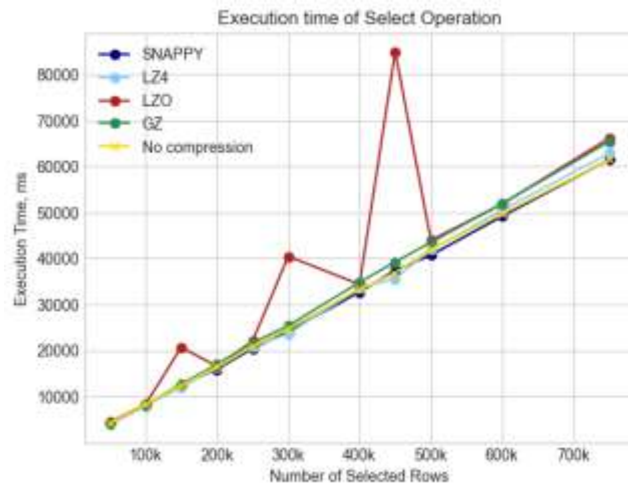

Fig. 2. Comparison of Select Queries.

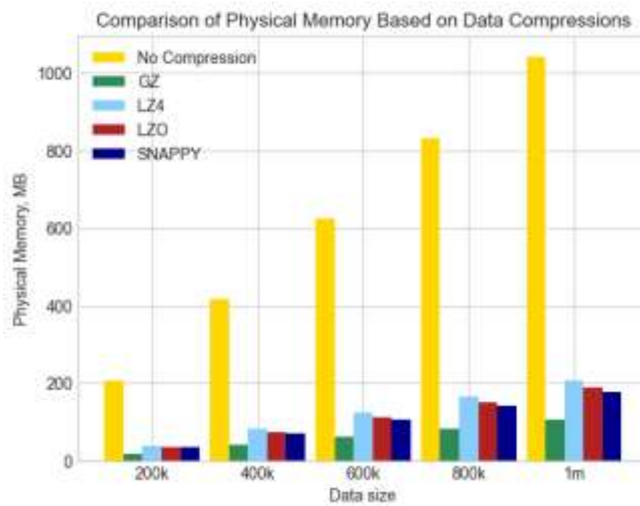

Fig. 3. Comparison of Physical Memory for all Test Cases.

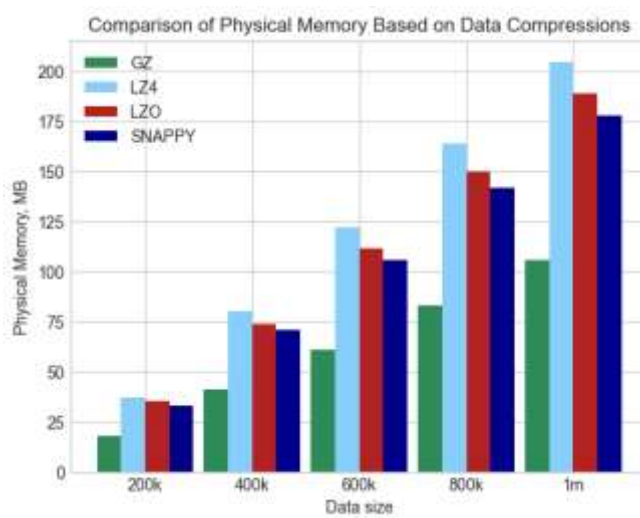

Fig. 4. Comparison of Physical Memory for the Compression Tests.

The GZ compression is clearly the most sparing of the four, storing 1 000 000 rows in little more than 100MB; in other words, 10 times less than the insertion without compression. The GZ compression is followed by SNAPPY compression and the LZ4 compression is the one that takes up most storage space.

D. Comparative Experiment on Number of RegionServers

The number of the RegionServers is another indicator that is taken into consideration. It confirms the benefit of using data compression algorithms. Although the difference in the number of RegionServers when using compression and not, is small, it does affect the whole performance of the cluster when inserting and selecting multiple records. The number of the occupied RegionServers while inserting rows without compressions is up to two for more than 600 000 inserted rows, while using any compression results in one reserved server every time.

E. Cluster CPU Load

Fig. 5 shows the load of the Cluster CPU while performing 400 000 insert queries. The left part of the figure shows the CPU load of the cluster when insert data without any compression and the right part shows the CPU with the LZO compression. Clear from the figure is that regardless of the used compression, or the lack of, the CPU is loaded the same.

Fig. 6 denotes the data transferred through the HDFS with and without any compression. The left side of the figure is the insertion of 400 000 rows of uncompressed data and the right side – the same number of rows with LZO compression. As expected, the compressed data is less and therefore the I/O operations on the HDFS are less. What makes an impression is that regardless of the data that is being transferred and the additional processed linked to the compression, the time of the whole insert operation is almost even.

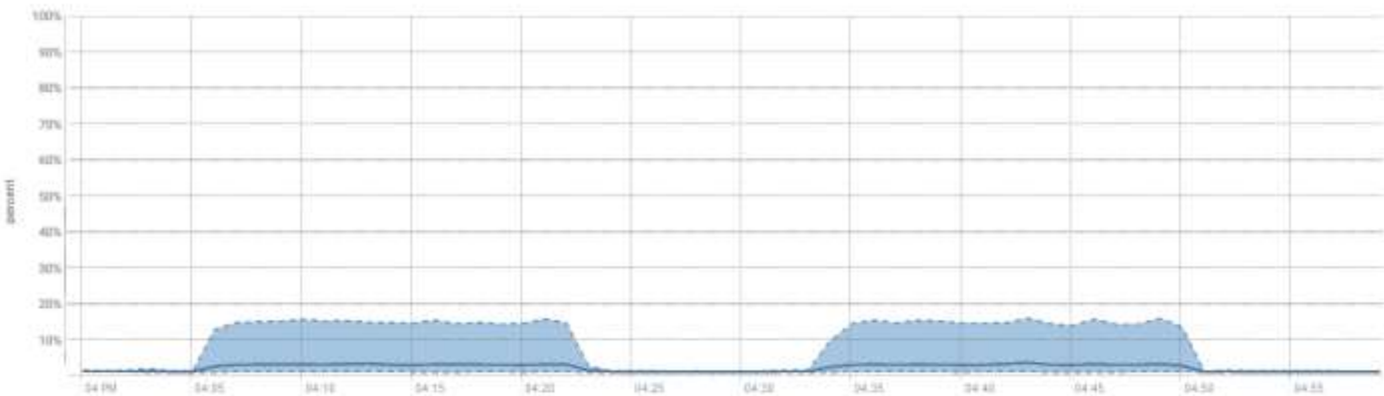

Fig. 5. Cluster CPU Load.

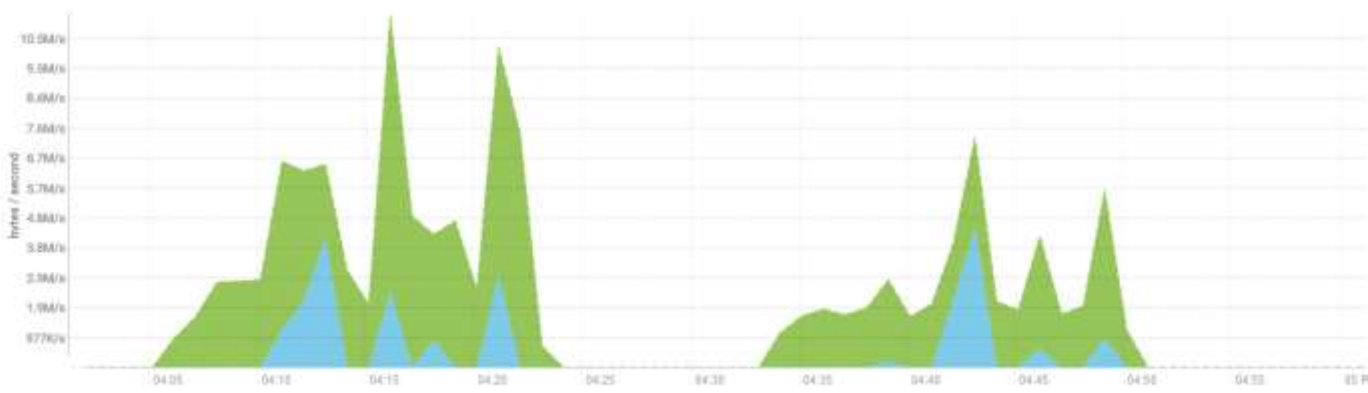

Fig. 6. HDFS I/O.

VI. Conclusions and Future Work

The aim of this research is to determine if data compression could improve the performance of HBase, running on a Hadoop cluster, consisted of one name node and nine data nodes. After performing a series of experiments, we can conclude that:

- Data compression highly improves system performance in terms of storage saving. It could shrink data 5 to 10 times (depending on the algorithm) without any noticeable additional CPU load.
- The substantial decrease in the network traffic could have a significant positive impact on large clusters with many data nodes or in clusters with higher data replication factors.
- The GZ algorithm achieves the highest compression ratio from all four applied algorithms.
- The cluster does not need any additional computational resources or CPU time to compress or decompress data, as it was expected.
- Regardless of the used compression, or the lack of it, the time for inserting and selecting thousands of rows does not change in noticeable manner. Neither the requests per second. When running the experiments, the active nodes' CPU load was less than 20%. All these measurements may suggest that there is some kind of limitation setting in the Thrift server or in the ThriftPy2 package. Further research and analysis are needed.

In future, we plan to extend our work and:

- Find a way to increase the number of processed requests per second. Obviously not the hardware is the limitation factor in the present experiments.
- Add more sources of data and simulate a parallel cluster usage from multiple clients.
- Increase the replication factor and analyze how data compression impacts the cluster performance in that case.

References

[1] F. Bajaber, S. Sakr, O. Batarfi, A. Altalhi, A. Barnawi, "Benchmarking big data systems: A survey," Computer Communications, 149, 241–251, 2020.

[2] A.H. Abed, "Big Data with Column Oriented NOSQL Database to Overcome the Drawbacks of Relational Databases," Int. J. Advanced Networking and Applications, 11(05), 4423–4428, 2020.

[3] W. Ali, M.U. Shafique, M.A. Majeed, A. Raza, "Comparison between SQL and NoSQL databases and their relationship with big data analytics," Asian Journal of Research in Computer Science, 1–10, 2019.

[4] J. Agnelo, N. Laranjeiro, J. Bernardino, "Using Orthogonal Defect Classification to characterize NoSQL database defects," Journal of Systems and Software, 159, 110451, 2020.

[5] R. Yangui, A. Nabli, F. Gargouri, "Automatic transformation of data warehouse schema to NoSQL data base: comparative study," Procedia Computer Science, 96, 255–264, 2016.

[6] D. McCreary, A. Kelly, "Making sense of NoSQL," Shelter Island: Manning, 19–20, 2014.

[7] S. Wandelt, X. Sun, U. Leser, "Column-wise compression of open relational data," Information Sciences, 457, 48–61, 2018.

[8] P. Raichand, "A short survey of data compression techniques for column oriented databases," Journal of Global Research in Computer Science, 4(7), 43–46, 2013.

[9] R. Čereš\vnák, M. Kvet, "Comparison of query performance in relational a non-relation databases," Transportation Research Procedia, 40, 170–177, 2019.

[10] J. Sun, T. Lu, "Optimization of column-oriented storage compression strategy based on HBase," in 2018 International Conference on Big Data and Artificial Intelligence (BDAI), 24–28, 2018.

[11] D. Abadi, S. Madden, M. Ferreira, "Integrating compression and execution in column-oriented database systems," in Proceedings of the 2006 ACM SIGMOD international conference on Management of data, 671–682, 2006.

[12] Raichand, P., & Aggarwal, R. R. (2013). A short survey of data compression techniques for column oriented databases. Current Trends in Information Technology, 3(2), 1-6.

[13] Wandelt, S., Sun, X., & Leser, U. (2018). Column-wise compression of open relational data. Information Sciences, 457, 48-61.

[14] Raichand, P., & Aggarwal, R. R. G. (2013). Query execution and effect of compression on nosql column oriented data-store using hadoop and hbase (Doctoral dissertation).

[15] F. Chang, J. Dean, S. Ghemawat, W.C. Hsieh, D.A. Wallach, M. Burrows, T. Chandra, A. Fikes, R.E. Gruber, "Bigtable: A distributed storage system for structured data," ACM Transactions on Computer Systems (TOCS), 26(2), 1–26, 2008.

[16] Apache Phoenix project: http://phoenix.apache.org/.

[17] X. Li, T. Georgiou, Migrating Messenger storage to optimize performance. Facebook Engineering, 2018: https://engineering.fb.com/2018/06/26/core-data/migrating-messenger-storage-to-optimize-performance/

[18] Fang, J., Chen, J., Al-Ars, Z., Hofstee, P., & Hidders, J. (2018, September). A high-bandwidth Snappy decompressor in reconfigurable logic: work-in-progress. In Proceedings of the International Conference on Hardware/Software Codesign and System Synthesis (pp. 1-2).

[19] Prasanth, T., Aarthi, K., & Gunasekaran, M. (2019, April). Big Data Retrieval using HDFS with LZO Compression. In 2019 International Conference on Advances in Computing and Communication Engineering (ICACCE) (pp. 1-6). IEEE.

[20] Jiang, H., & Lin, S. J. (2020). A rolling hash algorithm and the implementation to LZ4 data compression. IEEE Access, 8, 35529-35534.

[21] Packer, C., & Holder, L. B. (2017, August). GraphZip: Mining graph streams using dictionary-based compression. In SIGKDD Workshop on Mining and Learning in Graphs (MLG).

IoT-based Cyber-security of Drones using the Naïve Bayes Algorithm

Rizwan Majeed[1], Nurul Azma Abdullah[2], Muhammad Faheem Mushtaq[3]
Faculty of Computer Science and Information Technology[1, 2]
Universiti Tun Hussein Onn Malaysia (UTHM), Parit Raja 86400, Johor, Malaysia[1, 2]
Department of Artificial Intelligence, The Islamia University of Bahawalpur, 63100 Bahawalpur, Pakistan[3]

***Abstract*—Recent advancements in drone technology are opening new opportunities and applications: in various fields of life especially in the form of small drones. However, these advancements are also causing new challenges in terms of security, adaptability, and consistency. Small drones are proving to be a new opportunity for the civil and military industries. The small drones are suffering from architectural issues and the definition of security and safety issues. The rapid growth of the Internet of things opens new dimensions for drone technology but posing new threats as well. The tiny flying intelligent devices are challenging for the security and privacy of data. The design of these small drones is yet not matured to fulfill the domain requirements. The basic design issues also need security mechanisms, privacy mechanisms, and data transformations. The aspects like intrusion and interception in the domain of the Internet of Drones (IoD) need to be investigated to make these timely drones more secure and more adaptable. In this paper, we have used intelligent machine learning approach to design an IoT aided drone. This approach will provide intelligent cyber security system which will help in detecting network security threats using Blockchain.**

Keywords*—Drone technology; security; internet of things; internet of drones; machine learning; blockchain

I. Introduction

Internet usage is increasing as a powerful tool nowadays because of its unlimited benefits and applications. It is a global trend in which computers and devices are interconnected through some predefined rules and standards. Day-to-day information is carried by these communication networks over the internet. Nowadays, Internet of Things (IoT) is the most widely used network among all networks [1]. IoT is an interconnection of devices that are using the internet to share their information. These devices can be small household objects or can be large industrial machines that are communicating to perform their operations. IoT devices can be used to monitor objects, the performance of machines, bank transactions as well as industrial tasks [2, 3]. There are 90 million IoT objects by the end of 2020 which can be 25 billion in 2021[4]. These IoT objects can communicate intelligently with other devices by consuming low energy. Fig. 1 shows the impact of IoT devices on different areas of life. The manufacturing and health sector has the major share of IoT devices. IoT is most widely used in smart cities, surroundings observing, health, commerce, inventory, and business administration [5].

The main issue with IoT objects is security and privacy. Security means provide authorized access to information and protecting it from unauthorized users. Security includes confidentiality and integrity. IoT-specific security issues include cyber-attacks. With the advancement of technology, security challenges are growing day by day. Cloud technology has increased the risk of unauthorized access to information [6]. This Research [7] Identified cyber security challenges of IoT networks and other sources such as software, hardware, data, and applications. Attacks associated with IoT networks include transmission protocol disaster, denial of service, jamming, spoofing, and messaging attacks.

The advancement of technology and expansion of the economy allows the use of drone technology in many areas of life [8]. Drone technology provides several advantages and benefits for human beings. It helps in day-to-day activities as well as the military and monitoring of weather. However, several privacy and safety concerns are associated with their advantages [9]. At the same time, it also provides openings for cyber-criminals to eavesdrop on drone communication for harmful purposes. Unmanned Aerial Vehicles (UAV) were used in the past with major security threats and extortions. These devices were also used for harmful attacks on communication which increases the chances of distorted warfare. The Internet of Drone Things (IoDT) [10] or Internet of Drones (IoD's) [11] are emerging concepts towards smart commercial drones that can be used for precision agriculture, product delivery, security purposes, etc.

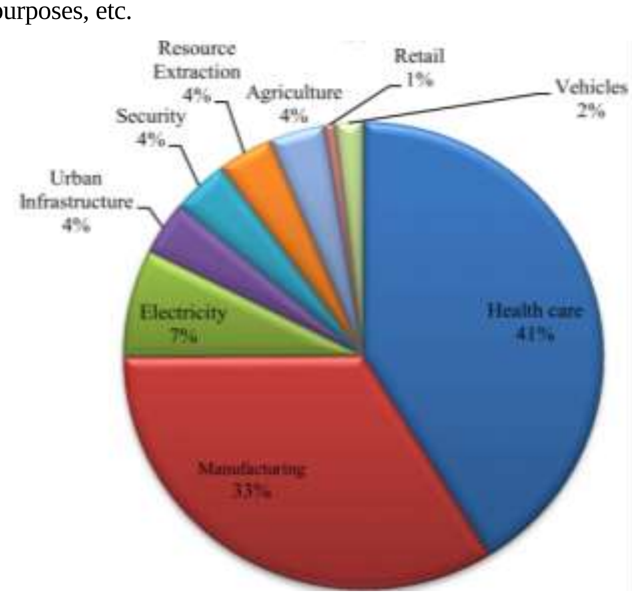

Fig. 1. Financial Influence of IoT Devices.

A major challenge in drone security is the generation of heavy computation and communication load for drones and other IoT devices [12]. The execution of computation-intensive and latency-sensitive security procedures becomes tough to ask for heavy drone data streams due to limited resources of drones such as limited memory, restricted computation, limited radio bandwidth, and limited battery resources. A secure authentication procedure for Drones and other IoT devices to identify the secure nodes and mitigate the identity-based attacks such as spoofing, etc. [13]. A robust access control method is required to prevent the unauthorized need to access the IoT resources [14-17]. A secure offloading technique is required that enables drones to perform computational-intensive tasks while interacting with the storage resources of the server and other edge devices [11].

Currently, there is no efficient platform exists for secure and smart industrial drones. Previously, industrial drones are being flown with a camera and a GIS sensor without having any platform support for drone security and data privacy, which could result in hacking of drones, and interception or loss of drone data [18]. Secure drone flight and privacy of drone data are needed to provide safe and secure surveillance of smart buildings. Additionally, machine intelligence (such as machine learning) support is also needed for drone data analytics along with the support of mobile and Web apps to visualize and disseminate the results [11]. There is a need to investigate and design a secure and intelligent mechanism for the authentication procedure for IoT devices, access control method, and secure offloading [19].

In the modern architectures of drones, the industrial drones are transmitting raw sensor data directly to a cloud platform whereas, the telecommunication channels are not secure. Here, absence of platform support for secure drone data transmission, the possibility exists that a drone with a security hole may be left unattended. A mechanism to manage and upgrade drone-side security and data privacy is necessary. Previously, machine learning has been used to provide secure mechanisms for wireless networks. However, there is a need for blockchain and machine-learning-based intelligent security systems to provide a secure channel for data transmission to the edge side for drones. Previously, blockchain is being used in IoT systems for secure authentication of devices [20], but the security mechanism for secure access control and secure offloading is still an open challenge.

This study will play a significant role in making these tiny flying devices intelligent, smart, and secure. However, the absence of a platform to ensure security and intelligence for these small drones is a bottleneck that makes it difficult to use these tiny drones for commercial, business, or industrial purposes. The proposed research will improve the basic design of small drones to ensure safety from cyber security threats, data privacy threats, and data interception threats. The proposed research is presenting an improved layered architecture that adds new layers from the implementation of security mechanisms and data analysis mechanisms in the traditional architecture of drones. Such, layered architecture will help to handle security and data analytics separate from the other conventional operations of drone handling mechanisms. Additionally, the proposed improvement in layered architecture will not only help in simple implementation but also will support easy regeneration for future enhancements. Furthermore, the secure drone flight and privacy of drone data will help in providing safe and secure surveillance of smart buildings and the raw-sensors data will safely reach IoT Hub for detailed data analytics. Finally, the support for machine intelligence (such as machine learning) will help in improved drone data analytics along with the support of mobile and Web apps to visualize and disseminate the results.

The rest of the paper can be organized as follows: Section 2 explains the research methodology of this research. Section 3 discusses the result and discussion based on the proposed methodology. Section 5 mentioned the conclusion and future work of this research.

II. Research Methodology

This research mainly focused to improve the basic design drones in order to ensure the security threats of drones such as data interception, data privacy and common cybersecurity threats. In the proposed approach, new layers are added in the layer architecture to help the implementation of security and data analysis mechanisms in the traditional drone's architecture. The improvement of layer architecture will support the easy regeneration for future enhancements. Fig. 2 shows the addition of security and privacy layer with the updating in the data processing layer through the components of machine intelligence.

A. *Drone Layer*

The first layer of industrial drones is the drone layer where camera needs to attach with the mini drone or quadcopter. In this layer, smart sensors are used such as altitude sensor, radar, GPS sensor and camera. The purpose of this layer to sense, record and transmit the recorded information y drones to the next layer. DJI phantom 3 drone are deployed that consist of communication link and custom remote controller.

B. *Edge Processing Layer*

This layer forwards the IoT raw data and drone data to the security and privacy layer where it verify the data come from authenticated devices. The IoT gateways are used in this layer for wireless communication that provides a fast transmission of the information. This layer is responsible for data flooding, protecting and cashing. For the purpose of cloud communication, it uses the Azure IoT gateway.

C. *Security and Privacy Layer*

This layer is responsible to provide the authentication to the devices and secure the access control through the machine learning algorithms. In this layer, some privacy threats are occurred such as physical, behavior and location privacy threat. Third party is secretly monitored and capture the drone information that effects the personal information of someone compromised. In behavior privacy, the unauthorized person can monitor someone's activities and behavior. Threats using location privacy involves to capture the location by authorized persons. These threats can be managed through the protocols and authentication schemes. Furthermore, machine learning algorithms are used by device authentication to alert and detect the security attacks.

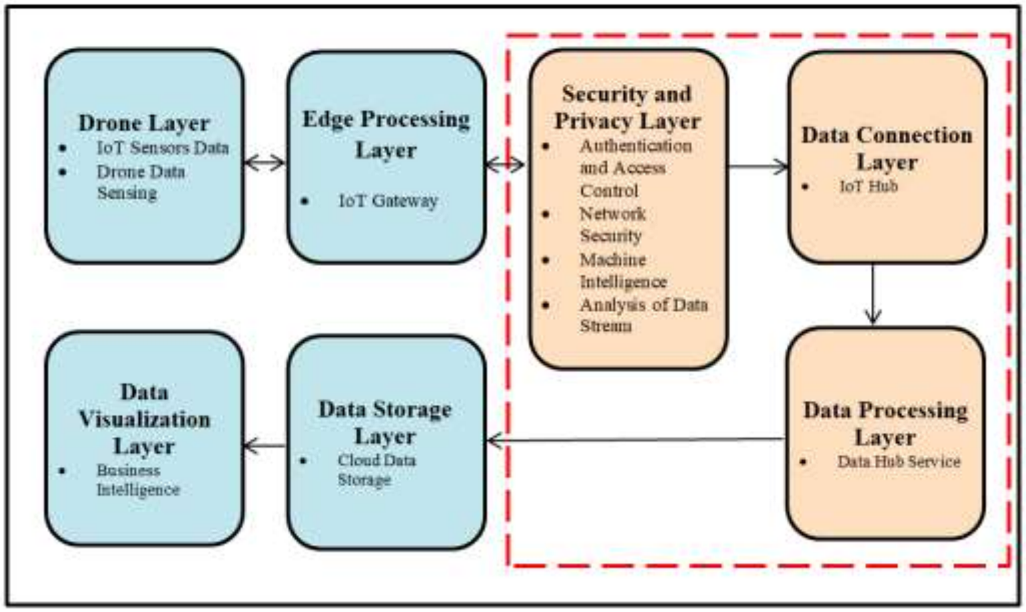

Fig. 2. Proposed Architecture.

D. Device Connection Layer

The security and privacy layer play an vital role to provide the communication link to a cloud based IoT Hub at the base station and new module is added in this layer for security automation and orchestration which ensures the connection between the authenticated devices. In the IoT network, message passing between cloud system and IoT devices is allowed by the IoT hub. IoT security and devices is provided by Blockchain mechanism in real-time.

E. Data Processing Layer

In order to analyze the drone data in stream, IoT hub data is passed to the data processing layer. In this layer, two new modules are developed such as machine intelligence that carried out the intelligent data analysis and data hub service that helps in simple and smooth cloud data storage. Naïve Bayes model are used in this layer that is intelligent machine learning algorithm. Flight data of drone is used for training and testing.

F. Data Storage Layer

Drones generate the data storage results for the cloud-based NoSQL database. It contains the IoT sensors data with the drone and network information. The purpose to use NoSQL database provides less storage schema of information that makes easily retrieve and access data in a short time.

G. Data Visualization Layer

This layer allows the monitoring of data with multiple services and tools. In our proposed work, Microsoft Azure services are used for storage and hub services. The data visualization layer shows the predictions made by proposed intelligent model about the security level of a drone and identified with the intelligent Naïve Bayes model.

III. Results and Discussion

In this section, results produced by the model as well as the experiment are explained. The performance is evaluated using precision, recall, and cost which are arithmetical methods to estimate performance. This experiment is performed on real-time data of drones, KDD'99 dataset. The proposed machine learning model such as Naïve Bayes is applied for good performance.

A. Naïve Bayes Model Results

The proposed Naïve Bayes model provides an overall accuracy of 96.3%. The confusion matrix of the trained Naïve Bayes model depicts true and predicted classes of data provided to the model as shown in table 6.2. Class precision for the DOS, Jamming, and Spoofing category is 96%, 99%, and 93% respectively. Similarly, class recall is also shown in the confusion matrix for three categories. Fig. 3 shows the drone routing id and route length information.

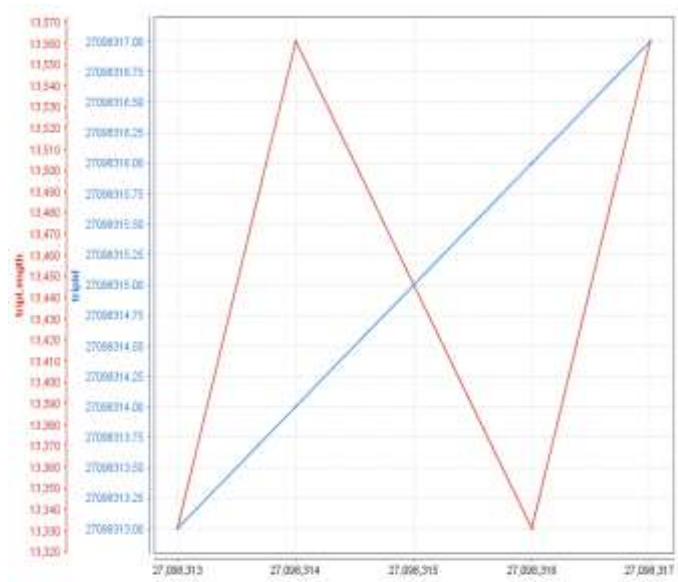

Fig. 3. Trip Id and Trip Length of Drone.

In the graph, trip id is plotted on x-axis and route length of drone is plotted on y axis. Blue and red lines represent this information in a line graph.

Fig. 4 shows the trip id, pattern id and stop length of DJ phantom 3 drone which is used in the experiment. Fig. 5 shows the true positive and false positive rate in training dataset. Fig. 5(a) shows the histogram and 5(b) shows the ROC curve of this training data. -15 is used as a threshold value to separate the normal communication from the malicious traffic.

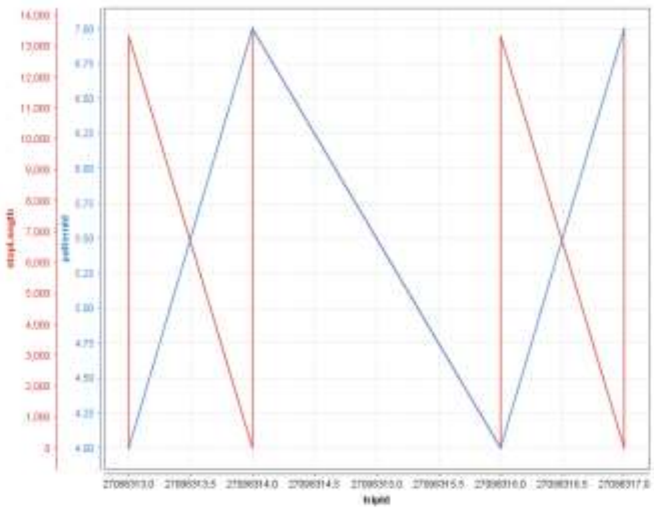

Fig. 4. Drone Flight Information.

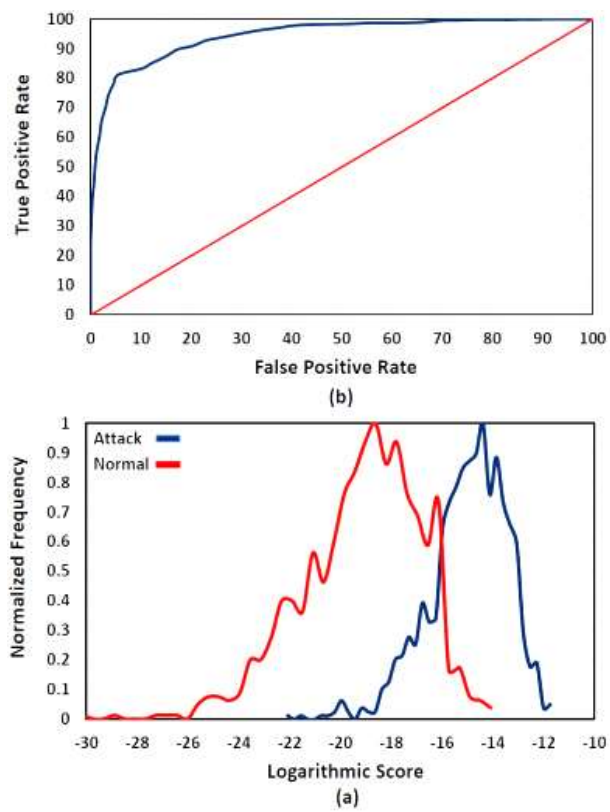

Fig. 5. Threshold Categorization of Training Data i.e. (a) Histogram, (b) ROC.

Fig. 6 shows the training data categorization with -64 threshold value. This training data is generated by the experimentation. Fig. 6(a) shows the histogram and 6(b) shows ROC cure. The ROC curve for the spoofing attach identification is shown in Fig. 7.

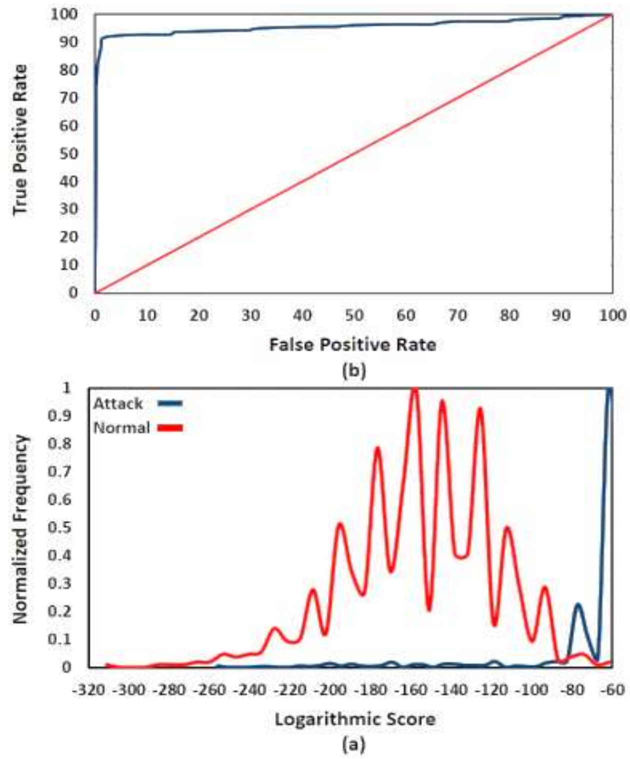

Fig. 6. Threshold Categorization of Training Data with -64 Threshold Value.

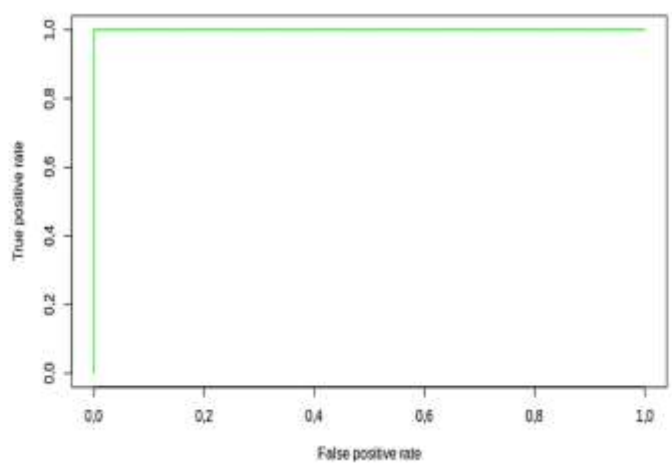

Fig. 7. Spoofing Attack Identification ROC Curve.

The confusion matrix for the Naïve Bayes classifier indicates the accuracy of the proposed machine learning algorithm shown in Fig. 8. True classes are shown as columns and predicted classes are shown as rows. Classification of data is performed by using three classes DOS attack, Jamming, and Spoofing. In this classification process, 96.3% accuracy is achieved which is the best for the cyber security decision-making process.

True Class / Predicted Classes	DOS	JAM	SPF	Class Precision
DOS	4	1	27	96%
JAM	6	9	6	99%
SPF	0	1	5	93%
Class Recall	99.3%	97.5%	83.16%	

Fig. 8. Confusion Matrix for Naive Bayes Classifier.

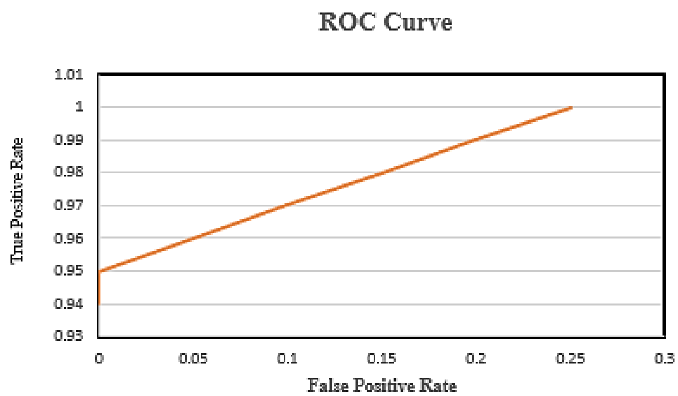

Fig. 9. ROC Curve for Intrusion-Detection Model.

In Fig. 9, the ROC curve of our proposed Naïve Bayes model is shown the number of true positive instances and the number of false-positive instances predicted by the Naïve Bayes model. True positive cases are shown on y and false-positive are shown on the x-axis. The area under ROC is 0.996. Fig. 10 shows the Roc curve for multiple cyber-attacks.

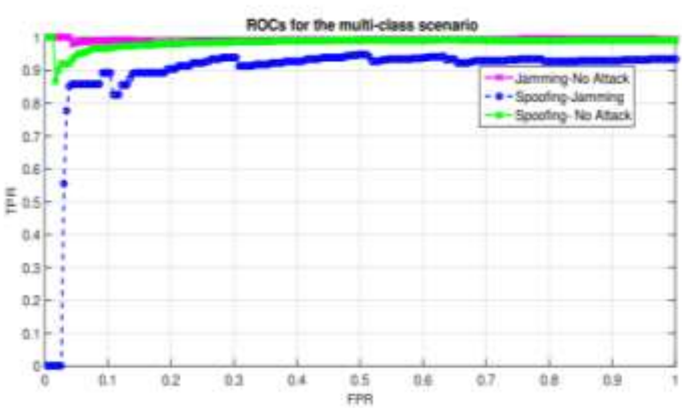

Fig. 10. ROC Curve for Multiple Cyber Attacks.

IV. Conclusion and Future Work

This paper proposes IoT-based cyber-security of drones using the Naïve Bayes algorithm. This model uses IoT sensors data, drones, and network information to generate patterns of security levels and identified the security attacks using these patterns. With this pattern, the model was able to identify attacks in the dataset. This model is tested with two datasets and achieves higher accuracy in real-time security attack detection. The accuracy achieved by the model is 96.3% which is higher and acceptable as compared to previous machine learning approaches. Precision recall and cost are calculated to estimate the performance. The Naïve Bayes model works by predicting items using two layers of processing in which independence between information items is assumed which shows a drawback in this suggested model. In the future, this problem will be addressed using a more efficient algorithm.

Acknowledgment

The authors would like to thank the Faculty of Computer Science and Information Technology, Universiti Tun Hussein Onn Malaysia (UTHM), Johor, Malaysia for supporting this research.

References

[1] Nayyar, A., Nguyen, B. L., and Nguyen, N. G., "The Internet of Drone Things (IoDT): Future Envision of Smart Drones", International Conference on Sustainable Technologies for Computational Intelligence. Springer, Singapore. pp. 563-580, 2020.

[2] R. Koslowski and M. Schulzke, "Drones along borders: border security UAVs in the United States and the European Union", International Studies Perspectives, vol. 19, pp. 305-324, 2018.

[3] Trevor Hastie, R. T., Jerome Friedman. *The Elements of Statistical Learning*. 2009.

[4] C. Lin, D. He, N. Kumar, K.-K. R. Choo, A. Vinel, and X. Huang, "Security and privacy for the internet of drones: Challenges and solutions", IEEE Communications Magazine, vol. 56, no.1, pp. 64-69, 2018.

[5] R. Lombreglia, "The Internet of things," Boston Globe, pp. 76–83, 2005.

[6] M. F. Mushtaq, U. Akram, I. Khan, S. N. Khan, A. Shahzad and A. Ullah, "Cloud Computing Environment and Security Challenges: A Review" International Journal of Advanced Computer Science and Applications, vol. 8, no. 10, 2017.

[7] W. Zhou, Y. Jia, A. Peng, Y. Zhang and P. Liu, "The Effect of IoT New Features on Security and Privacy: New Threats, Existing Solutions, and Challenges Yet to Be Solved," in IEEE Internet of Things Journal, vol. 6, no. 2, pp. 1606-1616, April 2019, doi: 10.1109/JIOT.2018.2847733.

[8] B. Bera, S. Saha, A. K.. Das, N. Kumar, P. Lorenz, and M. Alazab, "Blockchain-Envisioned Secure Data Delivery and Collection Scheme for 5G-Based IoT-Enabled Internet of Drones Environment", IEEE Transactions on Vehicular Technology, 2020.

[9] Kerns, A.J., Shepard, D.P., Bhatti, J.A. and Humphreys, T.E. (2014), Unmanned Aircraft Capture and Control Via GPS Spoofing. J. Field Robotics, 31: 617-636.

[10] M. Gharibi, R. Boutaba, S. L. Waslander "Internet of Drones", IEEE Access, 2016.

[11] Z. Feng, N. Guan, M. Lv, W. Liu, Q. Deng, X. Liu, and W. Yi, "Efficient drone hijacking detection using onboard motion sensors," in Design,Automation&TestinEuropeConference&Exhibition(DATE), 2017. IEEE, 2017, pp. 1414–1419.

[12] Z. Lv, "The security of Internet of drones", Computer Communications, vol. 148, pp. 208-214, 2019.

[13] M. Shahroz, M. F. Mushtaq, M. Ahmad, S. Ullah, A. Mehmood, G. S. Choi, “IoT-based smart shopping cart using radio frequency identification”, IEEE Access, vol. 8, pp. 68426-68438, 2020.

[14] R. Altawy and A. M. Youssef, “Security, Privacy, and Safety Aspects of Civilian Drones: A Survey”, ACM Trans. Cyber-Phys. Syst. Vol. 1, No. 2, 2017.

[15] M. F. Mushtaq, S. Jamel, S. R. B. Megat, U. Akram, M. M. Deris, “Key Schedule Algorithm using 3-Dimensional Hybrid Cubes for Block Cipher”, International Journal of Advanced Computer Science and Applications, Vol. 10, no. 8, pp. 427-442, 2019.

[16] R. Majeed, N. A. Abdullah, I. Ashraf, Y. B. Zikria, M. F. Mushtaq and M. Umer, “An Intelligent, Secure, and Smart Home Automation System”, Scientific Programming, 2020.

[17] M. F. Mushtaq, S. Jamel, K. M. Mohamad, S. K. A. Khalid, and M. M. Deris, “Key Generation Technique based on Triangular Coordinate Extraction for Hybrid Cubes,” J. Telecommun. Electron. Comput. Eng., vol. 9, no. 3–4, pp. 195–200, 2017.

[18] F. A. Narudin, A. Feizollah, N. B. Anuar, and A. Gani, “Evaluation of machine learning classifiers for mobile malware detection,” Soft Computing, vol. 20, no. 1, pp. 343–357, 2016.

[19] D. Hussain, M. A. Khan, S. Abbas, R. A. Naqvi, M. F. Mushtaq, A. Rehman and A. Nadeem, “Enabling Smart Cities with Cognition Based Intelligent Route Decision in Vehicles Empowered with Deep Extreme Learning Machine”, Computers, Materials & Continua, 2020.

[20] V. Chang, P. Chundury, and M. Chetty, “Spiders in the sky: User perceptions of drones, privacy, and security”, Proceedings of the 2017 CHI conference on human factors in computing systems, 2017.

Data Mining to Determine Behavioral Patterns in Respiratory Disease in Pediatric Patients

Michael Cabanillas-Carbonell[1]
Facultad de Ingeniería
Universidad Privada del Norte
Lima, Perú

Randy Verdecia-Peña[2]
ETSI de Telecomunicación
Universidad Politécnica de Madrid
Madrid, Spain

José Luis Herrera Salazar[3]
Facultad de Ingeniería y Negocios
Universidad Norbert Wiener
Lima, Perú

Esteban Medina-Rafaile[4]
Escuela Profesional de Ingeniería de Sistemas e Informática
Universidad Nacional Santiago Antúnez de Mayolo
Áncash, Perú

Oswaldo Casazola-Cruz[5]
Facultad de Ingeniería Industrial y de Sistemas
Universidad Nacional del Callao
Callao, Perú

***Abstract*—There are several varieties of respiratory diseases which mainly affect children between 0 and 5 years of age, not having a complete report of the behavior of each of these. This research seeks to conduct a study of the behavior of patterns in respiratory diseases of children in Peru through data mining, using data generated by the health sector, organizations and research between the years 2015 to 2019. This process was given by means of the K-Means clustering algorithm which allowed performing an analysis of this data identifying the patterns in a total of 10,000 Peruvian clinical records between the years mentioned, generating different behaviors. Through the grouping obtained in the clusters, it was obtained as a result that most of the cases in all the ages studied, they presented diseases with codes between the range of 000 and 060 approximately. This research was carried out in order to help health centers in Peru for further study, documentation and due decision-making, waiting for optimal prevention strategies regarding respiratory diseases.**

***Keywords*—Respiratory diseases; data mining; cluster algorithms; K-Means algorithm**

I. Introduction

The use of technologies has played an important role in the health sector, providing benefits that contribute to the fight against diseases. This context the use of data mining makes the processing and distribution of data more feasible, optimizing time, labor and costs [1]. Gathering large amounts of data to enable decision-making and strategic guidance is crucial for the analysis of the health situation in Peru [2]. According to [3], the health care industry in Peru is moving towards a personalized care model supported by new technologies to improve management and quality of service. Some of the processes where ICT has been implemented are telemedicine, remote diagnosis, informative applications, databases, cloud computing, etc.; however, more work still needs to be invested to close the existing gaps [3], [4], as the need to analyze big data and the analysis of population health is not yet fully covered.

Respiratory diseases have been mutating considerably over the years, causing the lack of a complete report of the behavior of these diseases for their proper prevention. According to MINSA and CDC [2], higher incidence rates were shown in children under 5 years of age with respect to acute respiratory infections and pneumonia between 2015, 2016, 2017 and 2018.

The situation of the health sector in Peru with respect to the use of data mining as a predictive tool is not many, although there are technological initiatives, such as regulating electronic medical records, or creating information systems that help the processes of health entities, there are still things to be done.

In the research [5], a prediction of academic performance was performed by data mining, through the use of three techniques, obtaining that using data mining it was possible in 82.87%, to make predictions of the academic performance of entrants in a timely manner.

Identifying that respiratory diseases are one of the main causes of mortality in infants in Peru, especially in children under five years of age [2], [6]-[8], the project aims to analyze population data to identify patterns of respiratory diseases in infant patients. The aim of this research is to generate results that will reveal the behaviors associated with respiratory diseases in children from 0 to 5 years of age, and may help health centers in Peru to create prevention strategies regarding respiratory diseases that are more frequent in infants and thus achieve a decrease in the number of deaths.

II. Theoretical Basis and Related Work

A. Respiratory Diseases

The upper respiratory tract includes the nose, mouth, nasal passages, pharynx and larynx, and the lower respiratory tract includes the trachea, main bronchus and lung (Fig. 1).

This whole system directs the inhalation of the outside air into the lungs for breathing to take place. An acute respiratory tract infection that we will call for research as "respiratory disease", [9], [10] is an infectious process it is an infectious process that occurs within the airways, either upper or lower.

One of the most common causes why most people tend to get sick and attend the environment are upper respiratory tract infections, which produce variable symptoms ranging from runny nose, sore throat, cough, shortness of breath and lethargy [9], being one of the main ills afflicting preschool children [11].

B. Classification of Respiratory Diseases

These are classified as upper respiratory tract infections (SSRIs) and lower respiratory tract infections (ITRI), the most common being SSRIs, which compromises the airways, starting from the nostrils, larynx, sinuses and middle ear [9], [11], [12].

C. Pattern Recognition in Respiratory Diseases

Respiratory diseases generally present a pattern (standard or model) of behavior by which a physician can diagnose whether a patient is suffering from this condition as either a lower respiratory tract infection or an upper respiratory tract infection.

D. Data Mining

According to [13], [14], data mining is a process of extracting useful information by analyzing big data. Data mining is the process of knowledge discovery by analyzing interesting patterns that large amounts of data to be analyzed have in common (Fig. 2).

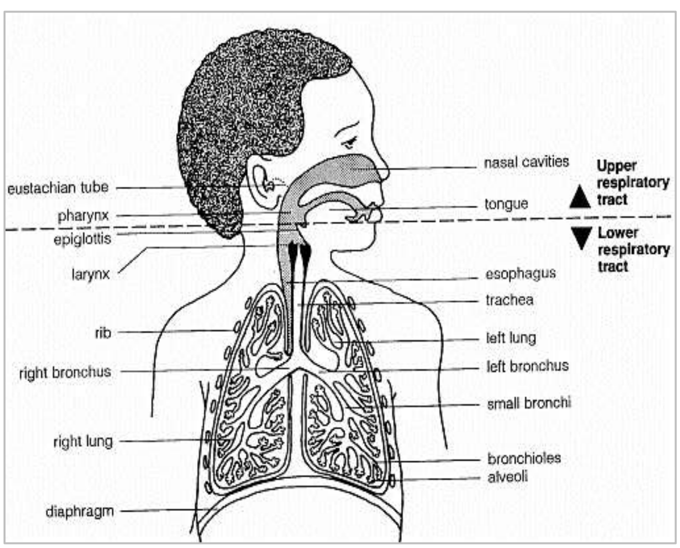

Fig. 1. Airway Components [9].

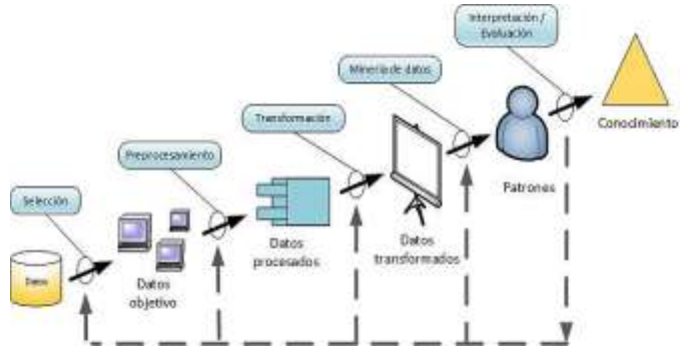

Fig. 2. Knowledge Discovery Process [13].

E. Clustering Algorithms

These algorithms aim at clustering data according to their classification (see Fig. 3), with the objective of finding the set of patterns for an efficient representation that characterizes the presented population [14]-[16].

The most widely used clustering algorithm is K-Means due to its good scalability with the use of data fulfilling initialization, assignment and update steps [15], [17].

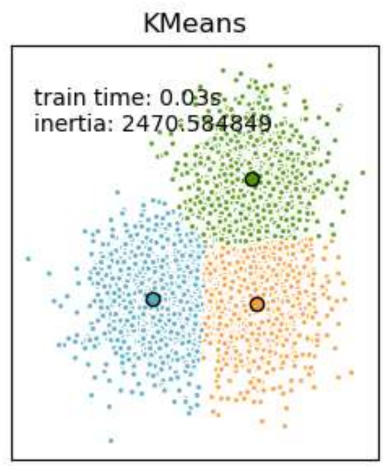

Fig. 3. K-Means Algorithm [18].

III. Methodology

The research is of the applied correlational type since it attempts to establish a degree of association between the variables under study.

The method of analysis and synthesis will be used in the development of the research. The methodology that was implemented allows having an order and an adequate procedure to carry out the respective analysis and to be able to obtain the adequate results that are desired for this research work.

A. Population

The health sector is one of the sectors that generate large volumes of information and data capture of their patients. The population to be taken into account for this research was 10,000 Peruvian clinical records between the years 2015 to 2019, for cluster analysis, from which the variables extracted were type of disease, year, age, case number and gender.

B. Data Processing and Analysis Technique

After evaluating and critiquing the data to ensure accuracy and reliability, we proceeded to debug unnecessary data, using appropriate statistical tools, using software such as Ms Excel and Clementine v 11.1.

1) Methodology processes

a) Obtaining databases: The extraction sources searched were from the Sergio E. Bernales Hospital, Daniel Alcides Carrion Hospital, WHO, research articles, MINSA, SISPRO, UNICEF and Red Cross, the sources were qualified according to some selection criteria that are associated with data quality, to finally define the variables taking into account the altitude, city of origin, amount of CO (carbon monoxide, EPS, stratum, date, date of measurement of air quality, inhabitants, mortality rate, amount of NO2 (nitrogen dioxide), maximum temperature, minimum temperature and average temperature obtained.

b) Obtain the data analysis tool to be used: The data analysis tool to be used is searched, in this case the RapidMiner tool was chosen.

c) Apply the databases in the analysis tool: The data obtained from the extraction sources are applied within the data analysis tool.

d) Apply the search algorithms: In order to identify behavioral patterns within the databases applied in the analysis tool, for this reason, a Clustering algorithm is selected to run it in RapidMiner.

e) Perform the search for data to identify patterns of behavior in these diseases: The algorithm is run on the data to be analyzed in the data analysis tool.

f) Obtain the search results: The results obtained from the search in the data analysis tool for the identified patterns are extracted.

g) Documentation of the results obtained: Documentation is made according to the results obtained from the data analysis tool.

C. Design

This section will show the design of how the data is handled through the information point of view with its corresponding diagrams, according to the data model proposed by TOGAF.

1) Data architecture design: To identify the aspects for the appropriate use of data, it is proposed to use the TOGAF framework which provides methods and tools that facilitate decision making in conjunction with data mining [19].

2) Selection of clustering algorithms: After performing an evaluation for an optimal selection of the clustering algorithm, based on two types of clustering, partition-centered and hierarchical, the K-Means algorithm was chosen. This algorithm was in charge of the development of the partitions at the same level to then group the data according to their category. For this research, four clusters were taken into account according to the distribution made by the K-Means algorithm, which allowed the analysis and distribution of the data according to the established parameters.

3) K-Means clustering algorithm: The process of this algorithm was applied in RapidMiner. Normalization, clustering, performance, de-normalization and new model application components were used to develop the process (see Fig. 4). To begin with, a Ripley-Set is taken that contains the data to be analyzed and then sent to the normalization, which is responsible for matching the data values for uniformity between them and thus achieve a correct execution of the algorithm. The normalized table is then sent to the clustering process for the execution of the k-means algorithm, and at the same time the un-normalization process is executed to return the table to its normal values to be sent to the application of a model.

After the execution of the clustering algorithm, it is sent to the performance process which measures distances with respect to its centroids. This process is necessary for a better grouping of each cluster with respect to its variables. Finally the normalized table and the cluster model go through the model aggregation process so that the results are performed on the original data values in a normalized way.

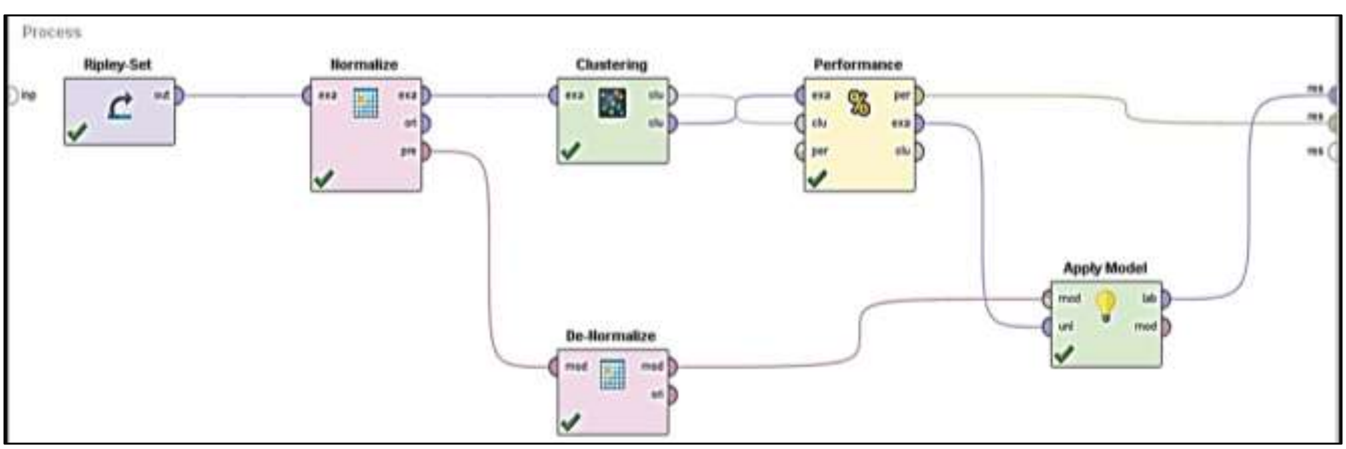

Fig. 4. Process for the K-Means Clustering Algorithm.

IV. Results

A. Cluster Graph

The graphs that show the grouping of each of the variables in the clusters generated by the analysis tool are presented.

1) Cluster vs disease graph: The graph is distributed according to the number of clusters according to the disease code (see Annexure 1).

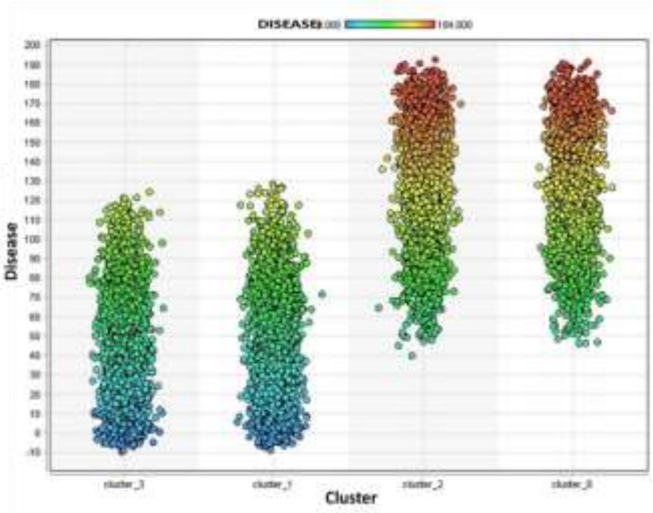

Fig. 5. Graphical Representation of Cluster vs Disease.

2) Cluster vs year graph: The graph is distributed according to the number of clusters according to the range of years analyzed 2015-2019.

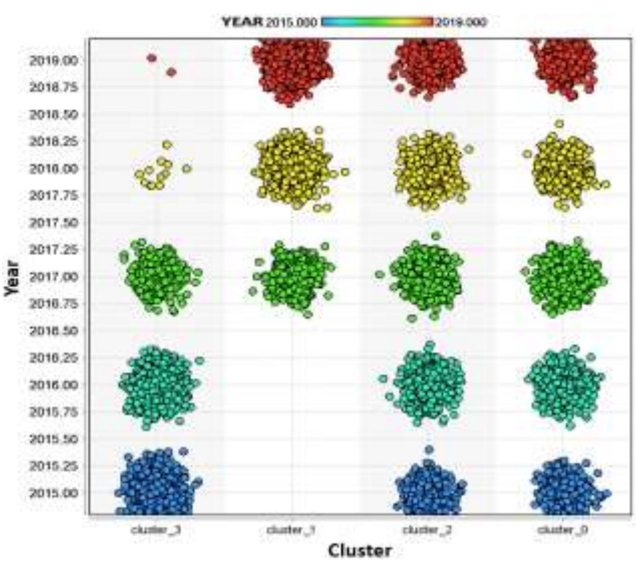

Fig. 6. Graphical Representation of Cluster vs Year.

3) Cluster vs age graph: The graph is distributed according to the number of the cluster according to the age range analyzed from 0 to 5 years old.

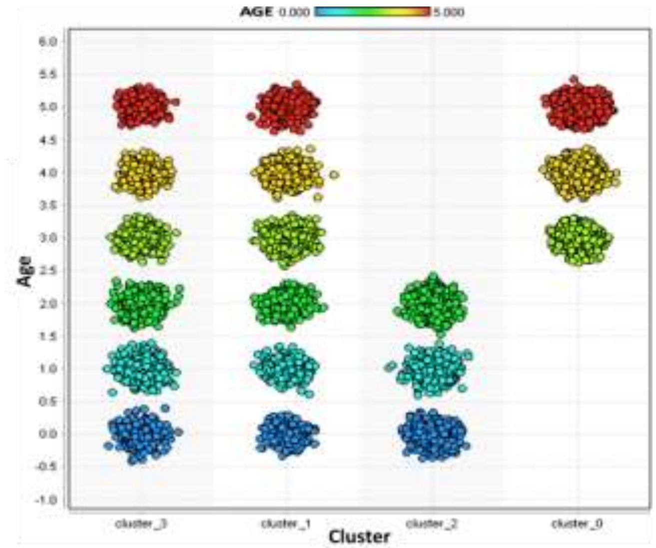

Fig. 7. Graphical Representation of Cluster vs Age.

4) Cluster vs. gender graph: The graph is distributed according to the number of clusters according to gender: male (0) and female (1).

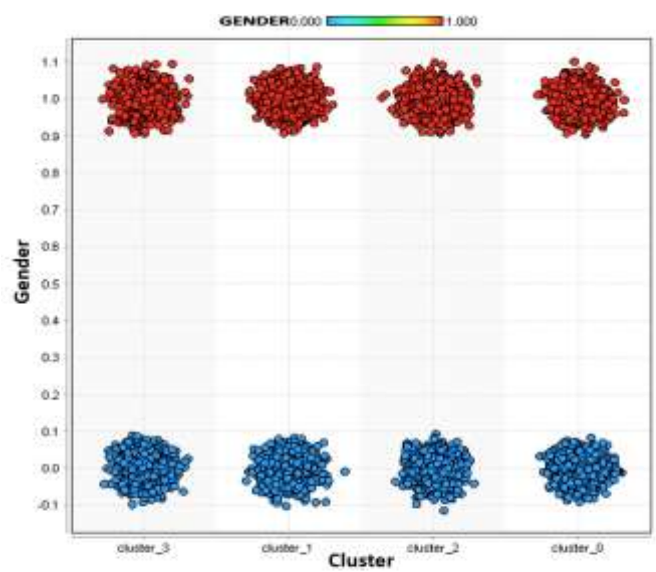

Fig. 8. Graphical Representation of Cluster vs Gender.

5) Cluster vs. number of cases graph: The graph is distributed according to the number of the cluster according to the cases analyzed.

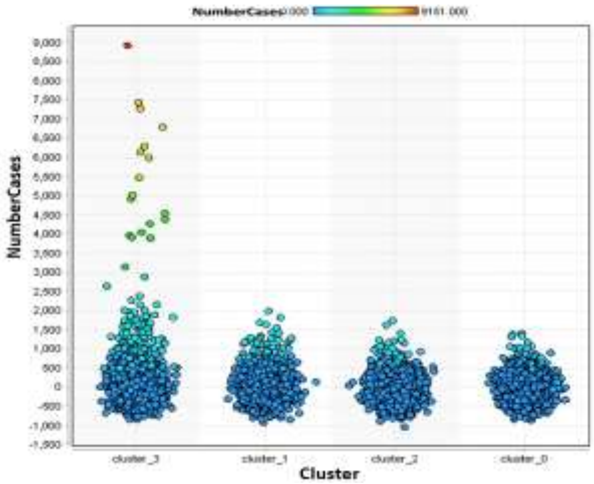

Fig. 9. Graphical Representation of Cluster vs. Number of Cases.

Graph of the distribution of the number of cases in each cluster.

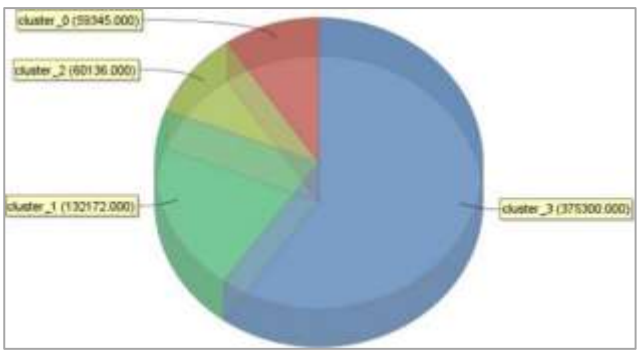

Fig. 10. Graphical Representation of the Number of Cases in each Cluster.

B. Cluster Analysis

1) Cluster 0: The following cluster has a total of 2,426 records, associated with 115 types of diseases analyzed for this cluster, with a total of 59,345 cases distributed in each of the types of diseases (see Fig. 9 and 10 section cluster_0), between the ages of 3 and 5 years (see Fig. 7 section cluster_0), with the majority being 5 year old children and with 51% male and 49% female (see Fig. 8 section cluster_0).

This cluster presented a lower incidence in the type of disease "CHRONIC RHINOPHARYNGITIS" resulting in 0.09% with a total of 88 cases for the ages of 5 years between female and male gender. It is observed that in the year 2017 in children aged 4 and 5 years there is a greater number of the disease type "ASTHMA, NOT SPECIFIED", occupying 19% compared to the other years analyzed, being mostly of male gender. For the years 2018-2019 it is observed that there was a significant decrease decreasing the number of cases by 39% for female gender and 41% for male gender.

Regarding "TRACHEAL AND BRONCHIAL DISEASES, NOT CLASSIFIED ELSEWHERE" represents 25.3% being present in the entire range of years studied 2015-2019 being present in the years from 3 to 5 years in both genders, observing an exponential growth increasing by 69.68%.

2) Cluster 1: The following cluster has a total of 2,520 records, associated with 112 types of diseases analyzed for this cluster, counting a total of 59,345 cases distributed in each of the types of diseases (see Fig. 9 and Fig. 10 section cluster_1), between the ages of 0 to 5 years (see Fig. 7 section cluster_1) corresponding to the years 2017-2019 (see Fig. 6 section cluster_1).

In the present cluster, it was identified that the least present type of disease is 126 with 0 cases reported in 2019. Likewise, it is observed that the type of disease with more presence is "OTHER ALLERGIC RHINITISES", with a total of 8112 cases being 46.72% of female gender and 53.98% of male gender being present in all the evaluated ages, being the year 2018 its peak.

There is a similarity with cluster 0 with respect to the gender variable, where the male gender represents 49.5% of the cases analyzed and 50.5% the female gender.

3) Cluster 2: The cluster has a total of 2509 records, associated with 116 types of disease analyzed for this cluster, counting a total of 59,345 cases distributed in each of the types of diseases (see Fig. 9 and Fig. 10 section cluster_2), between the ages of 0 to 2 years (see Fig. 7 section cluster_2) between the years 2015-2019 (see Fig. 6 section cluster_2), where the types of disease grouped together correspond to codes 047 to 176 and 184 according to Annex 1, within this cluster it was identified that the least present disease are 057 and 058 (see Fig. 5 and Fig. 9 section cluster_2).

There is a similarity with cluster 0 with respect to the gender variable, where the male gender represents 50.29% of the cases analyzed and 49.71% the female gender (see Fig. 8 section cluster_2).

4) Cluster 3: The present cluster has a total grouping of 2,541 records associated with 115 types of diseases for this cluster, counting a total of 59,345 cases distributed in each of the types of diseases (see Fig. 9 and 10 section cluster_3), between the ages of 0 to 5 years (see Fig. 7 section cluster_3) corresponding to the years 2015-2017 (see Fig. 6 section cluster_3), where disease codes 000 to 119 correspond according to Annex 1, within this cluster it was identified that the least present diseases are those of code 112, 114, 116, 117, 118 and 119 finding a lower amount of data in the year 2018 with 0.47% and in the year 2019 0.07% of data was found.

There is a similarity with cluster 0 with respect to the gender variable, where the male gender represents 50.13% of the cases analyzed and 49.86% the female gender (see Fig. 10 section cluster_3).

V. Discussion

The results obtained from the clusters after the application of data mining in child patients aged 0 to 5 years, through the discovery of patterns in respiratory diseases in the period 2015 - 2019 (see Fig. 5, 6, 7 8, 9 and 10), were relevant for decision making.

After performing the analysis to the results of cluster 0 it could be identified that there was an exponential growth of "Diseases of the trachea and bronchus, not elsewhere classified", starting with 2572 cases in 2017, reaching with 3819 cases by 2019. If promotion and prevention strategies will be implemented for the coming years then many future cases in children 0-5 years old would be avoided.

After analyzing the results of cluster 1, it was possible to identify that if prevention plans had been applied during the period 2017-2018, the 334% increase in cases of "Other allergic rhinitis" for children between 0 and 5 years of age, where the female population was the most affected, would have been avoided.

According to the results of cluster 2, if measures are taken for prevention in ages 0 to 2 years for diseases with codes 047 to 176 and 184 (Annex 1), then the number of cases and affected would begin to decrease, this is because these diseases mainly affect this segment of the population.

After analyzing the results of cluster 3, it was possible to identify that diseases such as 112, 114, 116, 117, 118 and 119, and the other diseases from codes 000 to 119 had little presence in recent years for this number of cases. This is understood to mean that preventive measures are being taken with respect to these diseases; however, they are not sufficient since these diseases are still frequent despite their decrease.

Different behaviors were obtained through the grouping obtained in the clusters generated, with the result that most of the cases in all ages presented diseases with codes between the range of approximately 000 to 060.

VI. Conclusion

Data mining models based on algorithms are suitable for the prediction and description of the relationships that exist between indicators or variables, for the identification of patterns within the analysis of the results, optimizing the processing of large amounts of data. The management of these data allowed structuring them and subsequently converting them into information by means of RapidMiner.

The implementation of the K-Means algorithm allowed taking different metrics for the evaluation of the functionalities with respect to the classification of clustering algorithms, which by means of graphical representations identifies the behavior of the data to subsequently make decisions about the generation of future prevention programs in Peruvian health centers.

The aim of this research is to demonstrate the great help that can be provided by models that show a pattern of patient behavior and serve as a basis for redirecting resources in the Peruvian health sector. This data extraction allows future research to be carried out.

References

[1] D. Perna and A. Tagarelli, “Deep auscultation: Predicting respiratory anomalies and diseases via recurrent neural networks,” Proc. - IEEE Symp. Comput. Med. Syst., vol. 2019-June, pp. 50–55, 2019, doi: 10.1109/CBMS.2019.00020.

[2] M. Hinostroza, G. Rosell, O. Broggi, M. Loayza, A. Gutierrez, and C. Munayco, “Analisis de Situación de Salud del Peru 2018,” Lima, 2019. Available: http://www.minsa.gob.pe/portada/est_san/tbc.htm.

[3] E. Sánchez, “Tecnología, cada vez más inmersa en la salud,” 2017. Available:http://www.madrid.org/cs/Satellite?blobtable=MungoBlobs&blobcol=urldata&blobkey=id&blobwhere=1158619206279&ssbinary=true&blobheader=application/pdf.

[4] M. C. Brian, A. D. Witman, A. Luis, G. M. Julio, and R. G. Avid, “Advances and Uses of ICT in Public Health of Peru,” Proc. 2018 IEEE Sci. Humanit. Int. Res. Conf. SHIRCON 2018, 2018, doi: 10.1109/SHIRCON.2018.8593132.

[5] E. Yamao, L. Celi Saavedra, R. Campos Pérez, and V. de J. Huancas Hurtado, “Predicción del rendimiento académico mediante minería de datos en estudiantes del primer ciclo en una universidad peruana,” Campus, vol. 23, no. 26, pp. 151–160, 2018, doi: 10.24265/campus.2018.v23n26.05.

[6] Organización Panamericana de la Salud (OPS), “Infecciones respiratorias agudas en el Perú: Experiencia frente a la temporada de bajas temperaturas,” Organ. Mund. la Salud, pp. 2–22, 2014. Available: https://iris.paho.org/bitstream/handle/10665.2/28549/iras2014-spa.pdf.

[7] Ministerio de Salud, “Situación de salud de IRAS, Neumonías Perú,” 2018. Available: http://www.dge.gob.pe/portal/docs/tools/02.pdf.

[8] MINSA, “Boletín Epidemiológico del Perú SE 02-2020,” Boletín Epidemiológico del Perú, vol. 29, pp. 32–59, 2020. Available: http://www.dge.gob.pe/portal/docs/vigilancia/boletines/2020/02.pdf.

[9] World Health Organization (WHO), Acute respiratory infections in children: Case management in small hospitals in developing countries. Washington, D.C., 1994.

[10] S. B. Lambert, K. M. Allen, R. C. Carter, and T. M. Nolan, “The cost of community-managed viral respiratory illnesses in a cohort of healthy preschool-aged children,” Respir. Res., vol. 9, no. May 2014, 2008, doi: 10.1186/1465-9921-9-11.

[11] L. M. Trandafir, L. V. Boiculese, G. Dimitriu, and M. Moscalu, “Recurrent respiratory tract infections in children,” 2017 E-Health Bioeng. Conf. EHB 2017, pp. 741–744, 2017, doi: 10.1109/EHB.2017.7995530.

[12] Foro de las Sociedades Internacionales de Enfermedades Respiratorias, El impacto mundial de la Enfermedad Respiratoria, 2nd Editio. Unidos por la Salud Pulmonar, 2017.

[13] J. Jiawei Han and M. Kamber, Data Mining: Concepts and Techniques, 3rd Editio. United States of America: Elsevier Science, 2012.

[14] J. Minguillón, J. Casas, and J. Minguillón, Minería de datos: modelos y algoritmos. Barcelona: Editorial UOC, 2017.

[15] C. N. Bouza-Herrera, “Una Mirada a Los Métodos Y Algoritmos,” Una Mirada a Los Métodos Y Algoritm. Del Análisis Clústeres, no. May, 2017, Available: https://www.researchgate.net/publication/317237054%0AUNA.

[16] J. Oyelade et al., “Data Clustering: Algorithms and Its Applications,” Proc. - 2019 19th Int. Conf. Comput. Sci. Its Appl. ICCSA 2019, no. July, pp. 71–81, 2019, doi: 10.1109/ICCSA.2019.000-1.

[17] E. Rendon Lara and I. M. Abundez Barrera, “RENTOL: Un algoritmo de agrupamiento basado en K-means,” Res. Comput. Sci., vol. 128, no. 1, pp. 149–157, 2016, doi: 10.13053/rcs-128-1-14.

[18] F. Pedregosa et al., “Scikit-learn: Machine Learning in Python - Clustering,” J. Mach. Learn. Res., vol. 12, pp. 2825–2830, 2011, Accessed: May 24, 2021. Available: https://scikit-learn.org/stable/modules/clustering.html.

[19] R. Yuliana and B. Rahardjo, “Designing an agile enterprise architecture for mining company by using TOGAF framework,” Proc. 2016 4th Int. Conf. Cyber IT Serv. Manag. CITSM 2016, 2016, doi: 10.1109/CITSM.2016.7577466.

ANNEXURE 1

Nomenclature of disease variable codes is shown in Table I.

TABLE I. TABLE OF DISEASES

Respiratory Diseases	
Diseases	***Code***
INFLUENZA WITH PNEUMONIA, DUE TO INFLUENZA VIRUS IDENTIFIED.	000
INFLUENZA WITH OTHER RESPIRATORY MANIFESTATIONS, DUE TO INFLUENZA VIRUS IDENTIFIED	001
INFLUENZA, WITH OTHER MANIFESTATIONS, DUE TO VIRUSES OF THE IDENTIFIED INFLUENZA.	002
INFLUENZA WITH PNEUMONIA, UNIDENTIFIED VIRUS.	003
INFLUENZA WITH OTHER RESPIRATORY MANIFESTATIONS, UNIDENTIFIED VIRUSES.	004
INFLUENZA WITH OTHER MANIFESTATIONS, UNIDENTIFIED VIRUSES.	005
PNEUMONIA DUE TO ADENOVIRUS.	006
PNEUMONIA DUE TO RESPIRATORY SYNCYTIAL VIRUS.	007
PNEUMONIA DUE TO PARAINFLUENZA VIRUS.	008
PNEUMONIA DUE TO OTHER VIRUSES.	009
VIRAL PNEUMONIA, NOT SPECIFIED.	010
PNEUMONIA DUE TO STREPTOCOCCUS PNEUMONIAE.	011
PNEUMONIA DUE TO HAEMOPHILUS INFLUENZAE.	012
PNEUMONIA DUE TO KLEBSIELLA PNEUMONIAE.	013
PNEUMONIA DUE TO PSEUDOMONAS.	014
PNEUMONIA DUE TO STAPH.	015
PNEUMONIA DUE TO GROUP B STREPTOCOCCALS.	016
PNEUMONIA DUE TO OTHER STREP.	017
PNEUMONIA DUE TO OTHER GRAM-NEGATIVE AEROBIC BACTERIA.	018
PNEUMONIA DUE TO MYCOPLASMA PNEUMONIAE.	019
OTHER BACTERIAL PNEUMONIA.	020
BACTERIAL PNEUMONIA, NOT SPECIFIED.	021
PNEUMONIA DUE TO CHLAMYDIA.	022
PNEUMONIA DUE TO OTHER SPECIFIED INFECTIOUS MICROORGANISMS.	023
BACTERIAL PNEUMONIA, NOT SPECIFIED. J160 - PNEUMONIA DUE TO CHLAMYDIA.	024
PNEUMONIA DUE TO CHLAMYDIA.	025
PNEUMONIA DUE TO OTHER SPECIFIED INFECTIOUS MICROORGANISMS.	026
BRONCONEUMONIA, NOT SPECIFIED.	027
LOBAR PNEUMONIA, NOT SPECIFIED.	028
HYPOSTATIC PNEUMONIA, NOT SPECIFIED.	029
OTHER PNEUMONIA, UNS SPECIFIED MICROORGANISM.	030
NEUMONIA, NOT SPECIFIED.	031
ACUTE BRONCHITIS DUE TO MYCOPLASMA PNEUMONIAE.	032
ACUTE BRONCHITIS DUE TO HAEMOPHILUS INFLUENZAE.	033
ACUTE BRONCHITIS DUE TO STREP.	034
ACUTE BRONCHITIS DUE TO COXSACKIE VIRUS.	035
ACUTE BRONCHITIS DUE TO HAEMOPHILUS INFLUENZAE.	036

Respiratory Diseases	
Diseases	***Code***
ACUTE BRONCHITIS DUE TO STREP.	037
ACUTE BRONCHITIS DUE TO COXSACKIE VIRUS.	038
ACUTE BRONCHITIS DUE TO ECHO VIRUS.	039
ACUTE BRONCHITIS DUE TO OTHER SPECIFIED MICROORGANISMS.	040
ACUTE BRONCHITIS, NOT SPECIFIED.	041
ACUTE BRONCHITIS DUE TO ECHO VIRUS.	042
ACUTE BRONCHITIS DUE TO OTHER SPECIFIED MICROORGANISMS.	043
ACUTE BRONCHITIS, NOT SPECIFIED.	044
UNSOFIED ACUTE LOWER RESPIRATORY TRACT INFECTION	045
VASOMOTOR RHINITIS	046
ALLERGIC RHINITIS DUE TO POLLEN.	047
OTHER SEASONAL ALLERGIC RHINITIS.	048
OTHER ALLERGIC RHINITIS.	049
ALLERGIC RHINITIS, UNS SPECIFIED.	050
CRONICA RHINITIS.	051
CRONICA RHINOPHARYNGITIS.	052
CRONICA PHARYNGITIS.	053
CRONICA MAXILLA SINUSITIS.	054
CRONICA FRONT SINUSITIS.	055
CHRONOIC ETHMOIDAL SINUSITIS.	056
CHRONIC SPHENOIDAL SINUSITIS.	057
PANSINUSITIS CRONICA.	058
OTHER CHRONIC SINUSITIS.	059
CHRONIC SINUSITIS, NOT SPECIFIED.	060
NASAL CAVITY POLYPO.	061
PARANASAL SINUS POLYPOID DEGENERATION.	062
OTHER BREAST POLYPS PARANASALS.	063
NASAL POLYPO, NOT SPECIFIED.	064
ABSCESS, FURUNCULO AND ANTRAX OF THE NOSE.	065
CYST AND MUCOCELE OF THE NOSE AND SINUS PARANASAL.	066
DEVIATION OF NASAL SEPTUM.	067
HYPERTROPHY OF NASAL CORNETS.	068
OTHER SPECIFIED DISORDERS OF THE NOSE AND PARANASAL BREASTS.	069
CRONICA TONSILLITIS.	070
TONSIL HYPERTROPHY.	071
ADENOID HYPERTROPHY.	072
HYPERTROPHY OF TONSILS WITH ADENOID HYPERTROPHY.	073
OTHER CHRONIC DISEASES OF TONSILS AND ADENOIDS.	074
CHRONIC TONSIL AND ADENOID DISEASE, NOT SPECIFIED.	075
PERIAMIGDALINO ABSCESS.	076
CHRONIC LARYNGITIS.	077
CHRONIC LARYNGOTRACHEITIS.	078

Respiratory Diseases	
Diseases	***Code***
VOCAL CORD AND LARYNX PARALYSIS.	079
VOCAL CORD AND LARYNX POLYPO.	080
VOCAL CORD NODULES.	081
OTHER VOCAL CORD DISEASES.	082
LARYNX EDEMA.	083
LARYNX SPASM.	084
LARYNX STENOSIS.	085
OTHER LARYNX DISEASES.	086
RETROPHARYNX AND PARAPHARYNX ABSCESS.	087
OTHER ABSCESSES OF THE FARINGE.	088
OTHER PHARYNGE DISEASES.	089
HYPERSENSITIVITY REACTION OF THE UPPER RESPIRATORY TRACT, SITE NOT SPECIFIED.	090
OTHER SPECIFIED UPPER RESPIRATORY TRACT DISEASES.	091
UPPER RESPIRATORY TRACT DISEASE, NOT SPECIFIED.	092
BRONCHITIS, NOT SPECIFIED AS ACUTE OR CHRONIC.	093
BRONCHITIS CRONICA SIMPLE.	094
BRONCHITIS CRONICA MUCOPURULENTA.	095
SIMPLE AND MUCOPURULENT MIXED CRONICA BRONCHITIS.	096
CHRONIC BRONCHITIS NOT SPECIFIED.	097
MACLEOD SYNC.	098
PANLOBULAR EMPHYSEMA.	099
CENTROLOBULAR EMPHYSEMA.	100
OTHER TYPES OF EMPHYSEMA.	101
EMPHYSEMA, UNSPECIFIED.	102
CHRONIC OBSTRUCTIVE PULMONARY DISEASE WITH ACUTE LOWER RESPIRATORY TRACT INFECTION, UNSPECIFIED LOWER RESPIRATORY TRACT INFECTION.	103
CHRONIC OBSTRUCTIVE PULMONARY DISEASE WITH ACUTE EXACERBATION, UNSPECIFIED.	104
OTHER SPECIFIED CHRONIC OBSTRUCTIVE PULMONARY DISEASES.	105
CHRONIC OBSTRUCTIVE PULMONARY DISEASE, UNSPECIFIED.	106
ASTHMA PREDOMINANTLY ALLERGIC.	107
NON-ALLERGIC ASTHMA.	108
MIXED ASTHMA.	109
ASTHMA, UNSPECIFIED.	110
STATUS ASTHMATICUS.	111
BRONCHIECTASIS.	112
COAL WORKERS' PNEUMOCONIOSIS.	113
PNEUMOCONIOSIS DUE TO OTHER SILICA-CONTAINING DUSTS.	114
SIDEROSIS.	115
PNEUMOCONIOSIS, UNSPECIFIED.	116
BYSSINOSIS.	117
AIRWAY DISEASE DUE TO OTHER SPECIFIED ORGANIC	118

Respiratory Diseases	
Diseases	***Code***
DUSTS.	
FARMER'S LUNG.	119
VENTILATOR PNEUMONITIS DUE TO AIR CONDITIONER AND HUMIDIFIER.	120
PNEUMONITIS DUE TO HYPERSENSITIVITY TO OTHER ORGANIC DUSTS.	121
PNEUMONITIS DUE TO HYPERSENSITIVITY TO UNSPECIFIED ORGANIC DUSTS.	122
BRONCHITIS AND PNEUMONITIS DUE TO INHALATION OF GASES, FUMES, VAPORS AND CHEMICALS.	123
UPPER RESPIRATORY INFLAMMATION DUE TO INHALATION OF GASES, FUMES, VAPORS AND CHEMICALS, NOT ELSEWHERE CLASSIFIED.	124
OTHER ACUTE AND SUBACUTE RESPIRATORY CONDITIONS DUE TO INHALATION OF GASES, FUMES, VAPORS AND CHEMICALS, NOT ELSEWHERE CLASSIFIED, FUMES, VAPORS AND CHEMICALS.	125
CHRONIC RESPIRATORY DISORDERS DUE TO INHALATION OF GASES, FUMES, VAPORS AND CHEMICALS.	126
OTHER RESPIRATORY DISORDERS DUE TO INHALATION OF GASES, FUMES, VAPORS AND CHEMICALS. CHEMICAL SUBSTANCES.	127
UNSPECIFIED RESPIRATORY CONDITIONS DUE TO INHALATION OF GASES, FUMES, VAPORS AND CHEMICALS.	128
PNEUMONITIS DUE TO ASPIRATION OF FOOD OR VOMIT.	129
PNEUMONITIS DUE TO ASPIRATION OF OILS AND ESSENCES.	130
PNEUMONITIS DUE TO ASPIRATION OF OTHER SOLIDS AND LIQUIDS.	131
ACUTE PULMONARY MANIFESTATIONS DUE TO RADIATION.	132
CHRONIC PULMONARY AND OTHER MANIFESTATIONS DUE TO RADIATION.	133
DRUG-INDUCED ACUTE INTERSTITIAL LUNG DISORDERS.	134
CHRONIC DRUG-INDUCED INTERSTITIAL LUNG DISORDERS.	135
RESPIRATORY CONDITIONS DUE TO OTHER SPECIFIED EXTERNAL AGENTS.	136
RESPIRATORY CONDITIONS DUE TO UNSPECIFIED EXTERNAL AGENTS.	137
ADULT RESPIRATORY DISTRESS SYNDROME.	138
PULMONARY EDEMA.	139
PULMONARY EOSINOPHILIA, NOT ELSEWHERE CLASSIFIED.	140
ALVEOLAR AND ALVEOLOPARIETAL CONDITIONS.	141
OTHER INTERSTITIAL LUNG DISEASES WITH FIBROSIS.	142
OTHER SPECIFIED INTERSTITIAL LUNG DISEASES.	143
INTERSTITIAL LUNG DISEASE, UNSPECIFIED.	144
GANGRENE AND NECROSIS OF THE LUNG.	145
LUNG ABSCESS WITH PNEUMONIA.	146
LUNG ABSCESS WITHOUT PNEUMONIA.	147
MEDIASTINAL ABSCESS.	148
PYOTHORAX WITH FISTULA.	149
PYOTORAX WITHOUT FISTULA.	150
PLEURAL EFFUSION NOT ELSEWHERE CLASSIFIED.	151
PLEURAL EFFUSION IN CONDITIONS CLASSIFIED ELSEWHERE.	152

Respiratory Diseases	
Diseases	***Code***
PACHYPLEURITIS WITHOUT ASBESTOSIS.	153
SPONTANEOUS PRESSURE PNEUMOTHORAX.	154
OTHER SPONTANEOUS PNEUMOTHORAX.	155
OTHER PNEUMOTHORAX.	156
PNEUMOTHORAX, UNSPECIFIED.	157
CHYLOTHORAX.	158
HEMOTHORAX.	159
OTHER SPECIFIED CONDITIONS OF THE PLEURA.	160
PLEURAL INVOLVEMENT, UNSPECIFIED.	161
TRACHEOSTOMY MALFUNCTION.	162
ACUTE PULMONARY INSUFFICIENCY FOLLOWING THORACIC SURGERY.	163
ACUTE PULMONARY INSUFFICIENCY FOLLOWING EXTRATHORACIC SURGERY.	164
CHRONIC PULMONARY INSUFFICIENCY FOLLOWING SURGERY.	165
MENDELSON'S SYNDROME.	166
SUBGLOTTIC STENOSIS FOLLOWING PROCEDURES.	167
OTHER RESPIRATORY DISORDERS FOLLOWING PROCEDURES.	168

Respiratory Diseases	
Diseases	***Code***
UNSPECIFIED DISORDER OF THE RESPIRATORY SYSTEM, CONSEQUENTIAL TO PROCEDURES	169
ACUTE RESPIRATORY FAILURE.	170
CHRONIC RESPIRATORY INSUFFICIENCY.	171
RESPIRATORY INSUFFICIENCY, UNSPECIFIED.	172
DISEASES OF THE TRACHEA AND BRONCHI, NOT ELSEWHERE CLASSIFIED.	173
COLLAPSED LUNG.	174
INTERSTITIAL EMPHYSEMA.	175
OTHER DISORDERS OF THE LUNG.	176
DISEASES OF THE MEDIASTINUM, NOT ELSEWHERE CLASSIFIED.	177
DISORDERS OF THE DIAPHRAGM.	178
OTHER SPECIFIED RESPIRATORY DISORDERS.	179
RESPIRATORY DISORDER, UNSPECIFIED.	180
RHEUMATOID LUNG DISEASE (M05.1†).	181
RESPIRATORY DISORDERS IN OTHER DIFFUSE CONNECTIVE TISSUE DISORDERS.	182
RESPIRATORY DISORDERS IN OTHER DISEASES ELSEWHERE CLASSIFIED.	183
PACHYPLEURITIS WITH ASBESTOSIS.	184

Image Encryption Enabling Chaotic Ergodicity with Logistic and Sine Map

Mohammad Ahmar Khan[1]
College of Commerce and Business Administration
Dhofar University, Oman

Jalaluddin Khan[2]*
School of Computer Science and Engineering
University of Electronic Science and Technology of China
Chengdu, 611731, China

Abdulrahman Abdullah Alghamdi[3]
College of Computing and Information Technology
Shaqra University, Shaqra 11961, Saudi Arabia

Sarah Mohammed Awadh Bait Saidan[4]
College of Commerce and Business Administration
Dhofar University, Oman

***Abstract*—Chaotic systems with complicated characteristics of ergodicity, impredictability as well as sensitivity to beginning stages are commonly utilized in the world of cryptography. A 2D logistic-adjusted-sine (LS) map is implemented in this article. Performance assessments reveal superior ergodicity as well as unpredictable and even a broader spectrum of chaotics than numerous previous chaotic maps. This research also develops a 2D-LS-based image encryption system and proposed LS-IES. The notion of diffusion as well as confusion is properly complied with enabled encryption functions. Research outcomes as well as security analyses demonstrate that LS-IES can swiftly encrypting different parameters in various images with a great resistance towards security threats.**

Keywords—Image encryption; ergodicity; logistic sine map; security; privacy

I. Introduction

Nowadays the advancement within digital technology as well as communications infrastructure, yet more digitized information is produced constantly communicated across networks, containing all sources of material in world [1]. Digital pictures include a common two-dimensional (2D) piece of content, typically contains a lot of information. The following are two illustrations: A image of a battleship can communicate not just about their dimensions as well as arms but rather about its geographical position as well as combat operation: a personalized photograph may sometimes indicate how it appears corresponding, and therefore its estimated physical state. As the digital image can hold significant indistinguishable content, image cybersecurity is becoming increasingly attractive. Picture encrypted among many types of image security methods is a visible means of changing a valuable actual image into something like an encrypted image that is not known as well as noise-less[2]–[4].

A digitized image is treated as dichotomous sequence as well as encrypted to most established systems including cryptographic benchmark as well as enhanced cryptography specification, as that of best technique among the encryption algorithm. Therefore, pixel consists usually 8 or even additional bits but there can be considerable association amongst consecutive frames. The significant correlation can persist while encoding a digital file in terms of binary sequence despite incorporating pixel characteristic as well as encryption effectiveness can still be relatively low. Consequently, various image-encoding systems were offered by numerous sorts of approaches, including magical cube [5], wavelet transform [6], [7], wave disturbance [8]and chaotic maps [9]–[12], in view of specific features of digitized images. As several scholars have indicated highlighted, although since mid-nineties numerous characteristics of chaos theory comparable to those encryption [13]–[16], analytical solutions were frequently utilized in image-based encryption but were extremely appropriate towards cryptography [17]–[19]. Whenever chaotic schemes are utilized in visual cryptography, the trustworthiness of privacy preservation depends heavily heavily onto performance of chaotic classifications implemented. For certain chaotic 1D processes, its chaotic cycles are very basic as well as completely predictable. After some data is collected, certain strategies can be used to approximate individual starting states [20]–[23].

The chaotic classification that has a straightforward nonlinear characteristic makes it easy to exploit appropriate image encryption technique [24]–[28]. A high-dynamic chaotic scheme feature complex chaotic conduct then are hard to anticipate future unpredictable orbits. Furthermore, technologies even have certain drawbacks, including difficult identification of problems as well as significant installation costs [5]. This study presents a novel, chaotic characteristics two dimensional map, with incorporation of logistics as well as sine map in terms of 2D LS-IES. Logistic map is used to regulate entrance of Sine map then afterwards expands their amplitude level between one dimensional to two dimensional. The assessments of efficiency demonstrate 2D-LS to be more chaotic, more ergodic as well as unpredictable than other current chaotic maps. This work also uses 2D-LS to create a 2D-LS image encryption technique (LS-IES). The confusion as well as diffusion are performed around pixel level. Simulation findings as well as security analyses demonstrate the LS-IES can randomly encrypted numerous photographic files (image) thus it is strongly able to prevent malicious activities.

*Corresponding Author

The remaining article proceeded at the section-based descriptions such as: Section II provides preliminaries about complex chaotic functions. Section III described the proposed concept about 2D LS-IES. Section IV is discussed with incorporated simulation and experimental setup of 2D LS-IES. Section V is illustrated with security analysis and comparative study of 2D LS-IES and at last concludes with Section VI.

II. Preliminaries about Chaotic Functions

The preliminaries about the chaotic functions in terms of one dimensional and two-dimensional functions including logistic as well as sine map represented as following:

A. Logistic Maps

The logistic function is a discreet analogue of something like logistic equation involving increasing population [29]. A logistic map is expressed quantitatively as following Eq. (1),

$$X_{i+1} = 4Kx_i\left(1 - x_i\right) \tag{1}$$

where K is well inside [0, 1] domain and logistic function is K [0.89,1], the logistic function declared within this rage is chaotic in nature.

B. Sine Maps

If function of sine has intakes that lie inside [0, π] region, their outcomes occur inside [0, 1] target area. Sine map is constructed through translating their parameters at [0, 1] as generating sine function. It has been characterized as following Eq. (2),

$$X_{i+1} = \mathrm{D}\,Sin\left(\pi x_i\right) \tag{2}$$

Here variable D is set to factor D [0, 1]. The complex chaotic sequence of Sine map is formally noticeable in nature such as D [0.87, 1].

C. Logistic Adjusted Sine Map

Here incorporating the 2D-LS algebraic formulation including each two well-known chaotic function such as logistic as well as sine as following Eq. (3):

$$\begin{cases} X_{i+1} = \{ \ Sin\left(\pi\zeta\left(y_i+2\right)x_i\left(1-x_i\right)\right) \\ Y_{i+1} = \{ \ Sin\left(\pi\zeta\left(x_i+2\right)y_i\left(1-y_i\right)\right) \end{cases} \tag{3}$$

When variable ζ [0, 1] is assigned to [0, 1]. 2D-LS is constructed using logistic as well as sinus mapping. The logistic polynomial x_i (1 − x_i) is initially normalized by something like a coefficient of ζ as well as supplied through Sine map insight. The frequency field is again stretched between 1-diamention and 2-diamention. 2D-LS simultaneously affects two parameters as well as outcome couples (x_i+1, y_i+1) spread over the 2D phase plane. That has an additional significant action thus its results are harder to gauge comparing other Sine as well as Logistic Mapping.

III. 2D LS-IES Image Encryption

Employing 2D-LS, this part establishes a different LS-IES image encryption system, wherein cryptographic keys are being utilized to establish a minimum 2D-LS configuration to produce chaotic S matrix. Confusion as well as diffusion algorithms are useful to periodically adjust pixel placements as well as to alter number of pixels. The confusion as well as dispersion activities a single image can be encoded in a bunch of high randomized encrypted images. Fig. 1 shows the entire design of LS-IES.

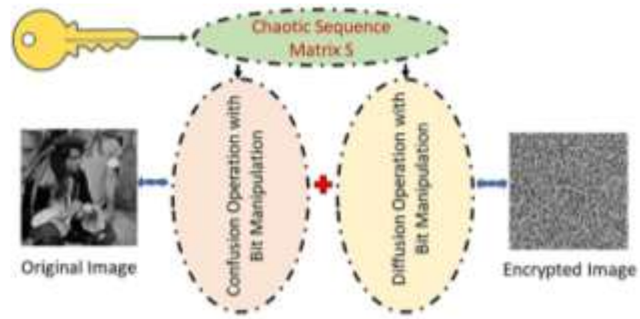

Fig. 1. The Concrete of 2D LS-IES Image Encryption.

A. Generation of Key

The generalization ability among the chaos-oriented encryption technique must ≥ 2^{100} to withstand the assault by brute force [30]. We have a cryptographic key of 232 bits, K = {X_0, Y_0, α, m, β, £} to meet this criterion as well as adjust it to the construction of the LS-IES. It comprises of four pieces, whereas β, £ are two interfering intensities (X_0, Y_0, α) as well as m are the interfering parameters. The activities of confusion as well as diffusion are adjusted onto pixel level. These protected findings seem to have the same formatting as both the actual pictures. LS-IES can therefore be used to digitized photos about any source.

B. Confusion through Bit Manipulation

The characteristics of confusion which demonstrates the number of outcomes would vary sensibly mostly on confidential key [31], [32]. The confusion of bit arbitrarily shifts pixel coordinates inside the image based on current chaotic binary sequence.

TABLE I. Bit Manipulation Algorithm

Confusion through Bit manipulation algorithm	
Input	Image I with chaotic sequence S and size of element K×L
Output	G operated result
	H initiated matrix of size K×L
	f=$\mathbf{log_2}(\boldsymbol{KL})$
	for i =1: K
	for j=1: L
	a= (i-1) L+ j
	ab=Bin (a, f)
	Hi,j =Joint(Si,j, ab,Ii,j)
	end
	end
	H=SortH(H)
	H=SortC(H)
	G=FetEnd ($H_{1:K\ 1:L}$, p)

Table I is explained about the processing algorithm in the certain steps, initially it takes input parameter in terms of original image with complex chaotic sequences S with the size of K×L. The whole algorithm is incorporated and generated with the confusion outcomes from the optimized bit manipulation process from the algorithm.

C. Diffusion through Bit Manipulation

The diffusion possessions showed that perhaps encrypted message must be highly responsive to unencrypted changes, meaning where each bit inside encrypted data can be altered with about fifty percent likelihood of occurrence [31], [32]. LAS-IES employs earlier pixel as well as a chaotic complex matrices S component to modify within contemporary pixel. The alteration through one pixel can be extended throughout the image sequence during computations within the proposed setup. Assume complex chaotic matrices S as well as confusion outcome G for bit manipulation algorithm are K × L, so that diffusion for bit manipulating is defined as following Eq. (4):

$$U_{i,j} = \begin{cases} G_{i,j} \oplus G_{K,L} \oplus S_{i,j}; \text{ for i=1; j=1;} \\ G_{i,j} \oplus U_{i-1,L} \oplus S_{i,j}; \text{ for j=1; } i \neq 1; \\ G_{i,j} \oplus U_{i,j-1} \oplus S_{i,j}; \text{ for } j \neq 1; \end{cases} \tag{4}$$

Whereas U recognizes as a consequence of bit diffusion manipulating, sign of ⊕ is bitwise XOR function. The methodology of decryption of whole portion is to perform reverse procedure stated as following Eq (5):

$$G_{i,j} = \begin{cases} U_{i,j} \oplus U_{i,j-1} \oplus S_{i,j}, \text{ for } j \neq 1; \\ U_{i,j} \oplus U_{i-1,L} \oplus S_{i,j}, \text{ for } i \neq 1, j=1; \\ U_{i,j} \oplus G_{K,L} \oplus S_{i,j}, \text{ for i=1 , j=1;} \end{cases} \tag{5}$$

After the confusion as well as diffusion of bit manipulating with separate complex chaotic vectors, a single original image can indeed be scrambled into an unidentifiable cipher-image matrix. The proposed concept at the entire setup recognizes that excellent diffusion as well as confusion effects can be achieved because premise of diffusion as well as confusion has been achieved. A high encrypted communications performance may be achieved as LS-IES requires only bit-level confusion in addition broadcast techniques. This has strong noise resistance or information leakage assault dependability. LAS-IES can indeed capture entire image having good graphical fidelity whenever an encrypted image contains turbulence or certain loss of data.

IV. Simulation and Discussion

We estimate the benefits of image encryption and it is supposed to encrypt various aspects of digital photos (Image data) using unpredictable cipher images. Mostly with the encryption credentials (key) can such a cipher picture to be deciphered successfully. This report outlines the LS-IES measured data as well as evaluates their dependability. We utilize R2018a MATLAB to construct LS-IES as well as deploy it to several digital image formats hereunder. Fig. 2 and Fig. 3 demonstrated the grayscale image simulated results. Using Fig. 2, we can also see that LS-IES may encrypted images (as mentioned A to C and A' to C') with a uniformly distributed to randomized cryptographic images. With the right equipment (Keys), the actual pictures can also be totally reconstructed. As illustrated in Fig. 2(A' to C') and Fig. 3(E' to G') the histograms of the underlying gray image as well as it is distributed randomly. In such scenarios, the intruders have difficulties accessing statistical data. The simulation work organized in the ecosystem which is Intel (R) Core (TM) i3-4030U CPU @ 1.90 GHz personal computer, Microsoft Windows 10 pro with 8GB RAM. Since individually encryption procedure is equally composite towards diverse undisclosed keys, LS-IES is technically more robust in contradiction of adversarial attack.

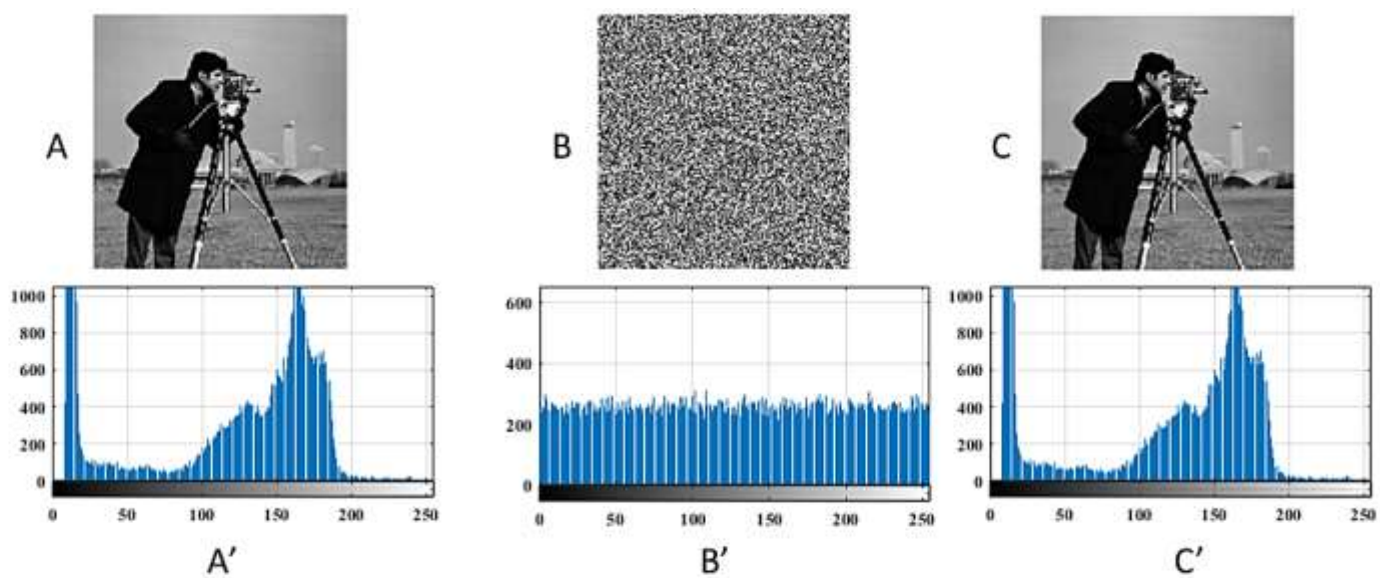

Fig. 2. Image Encryption Outcomes for the Cameramen Image.

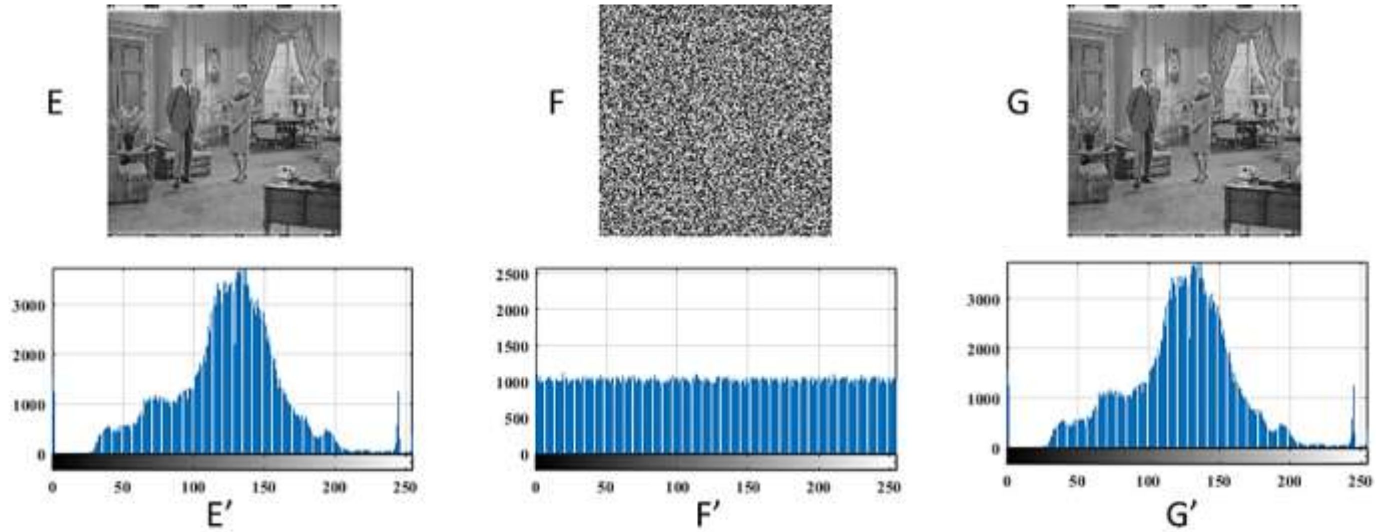

Fig. 3. Image Encryption Outcomes for the Meeting Image.

V. Security Analysis

This subsection shows effectiveness of its encryption algorithm to examine secure communication of LS-IES as well as its capacity to withstand conventional safety threats. The entire experimental setup is used gray scale test image from 'Miscellaneous' image dataset of USC-SIPI [33]. We compared this with other published state-of-the-art mechanism in the similar field of image encryption to highlight its benefits of LS-IES. Several simulation findings were used for the comparison of published data and cited that article with the references as mentioned at the reference section for the more clarity.

A. Histogram Analysis

Histogram is a homogenous as well as significantly separate histogram diagram only for idealized encrypted images, therefore prevents the adversary from getting significant evidence in the epidemiology including its encrypted images. This experiment showed histograms of the actual picture as well as encrypted image in Fig. 2(A', B' and C') and Fig. 3(E', F' and G'). Fig. 2 (B') and Fig. 3(F') demonstrates how cipher image histograms are consistent; those are unique histograms of actual pictures. These contains uniformly characteristics as a flat representation of cipher images. This encryption algorithm suggested about the enhanced and successfully avoidable any kind of statistical attacks.

B. Correlation Analysis

Throughout this investigation the actual as well as encrypted images have been picked by random means for the correlation testing of 1000 combinations of consecutive frames and afterwards coefficient of correlation have been computed in terms of directional such as horizontal (H), vertical (V) and diagonal (D). The coefficient of determination computation procedure incorporated from Eq. 6-11, whereas x and y indicate the gray values of consecutive frames.

$$CC_{xy} = \frac{\text{Covariance}(x,y)}{\sqrt{K(x)L(y)}} \tag{6}$$

$$\text{Covariance}(x,y) = \frac{1}{N}\sum_{i=1}^{N}\left(x_i - A(x)\right)\left(y_i - B(y)\right) \tag{7}$$

$$K(x) = \frac{1}{N}\sum_{i=1}^{N}\left(x_i - A(x)\right)^2 \tag{8}$$

$$L(y) = \frac{1}{N}\sum_{i=1}^{N}\left(y_i - E(y)\right)^2 \tag{9}$$

$$A(x) = \frac{1}{N}\sum_{i=1}^{N} x_i \tag{10}$$

$$B(y) = \frac{1}{N}\sum_{i=1}^{N} y_i \tag{11}$$

Table II reveals that perhaps the correlations of unencrypted images are near 1; the encrypted images are near 0 that further confirms that the methodology implemented removes the interaction amongst neighboring pixels of unencrypted images.

TABLE II. Correlation Coefficient on Experimented Images

Image	**Plain Images**			**Encrypted Images**		
	H	**V**	**D**	**H**	**V**	**D**
5.1.14	0.8890	0.9186	0.8730	0.0040	0.0031	-0.0048
5.1.12	0.9649	0.9423	0.9289	0.0060	-0.0020	-0.0040
5.1.09	0.9280	0.9081	0.9121	-0.0049	-0.0030	0.0018

C. Differential Attacks

The demonstration of the differential attack is based on two premium criteria such as number of pixels change rate (NPCR) as well as unified average changing intensity (UACI). These two are key factor to distinguishing about the differential attacks exist at any image during the image encryption methods. These two are mythically demonstrated on Eq. 12 to 14 as following:

$$NPCR = \frac{\sum_{i,j} H(i,j)}{M \times N} \times 100\% \tag{12}$$

$$H(i,j) = \begin{cases} 0 & if\ C_1(i,j) = C_2(i,j) \\ 1 & if\ C_1(i,j) \neq C_2(i,j) \end{cases} \tag{13}$$

$$UACI = \frac{1}{M \times N}\left[\sum_{i,j} \frac{|C_1(i,j) - C_2(i,j)|}{255}\right] \times 100\% \tag{14}$$

in which $C_1(i, j)$ signifies cipher picture value of each pixel. C_2 (i j) indicates encrypted image value of the pixel where actual picture modifies its pixel values.

The received outcomes of Table III, the NPCR and UACI from the image dataset demonstrated about the efficacy of the used encryption methodology. It is acknowledging that the output of the NPCR is approaching towards hundred and UACI is reaching one-third of the hundred. This is also justifying about the withstand of any type of differential attacks with the utilization of 2D LS-IES mechanism.

D. Entropy Analysis

The entropy of any image is fundamentally recognized towards reflecting picture information uncertainty. Basically, the entropy quality of information is determined via formula 15. The highest entropy value is 8 if probability among gray levels is precisely same. Entropy can be computationally obtained through Eq. (15) which is as followed:

$$Z(r) = -\sum_{i=1}^{255} P(r_i)\log_2 P(r_i) \tag{15}$$

Whereas Z(r) is the calculated information entropy of experimented images and its probability as shown by P(r). Table IV is illustrated optimize setup with the produced information entropy which are experimentally comes through dataset images.

E. Key Analysis

The generalization ability among the chaos-oriented encryption technique must $\geq 2^{100}$ to withstand the assault by brute force [30]. We have a cryptographic key of 232 bits, K = $\{X_0, Y_0, \alpha, m, \beta, £\}$ to meet this criterion as well as adjust it to the construction of the LS-IES.

F. Comparative Study

This section is illustrated efficiently of proposed outcomes and compared with earlier well-known published state-of-art methods on Table V. After comparison, we found that our proposed 2D LS-IES method is comparatively satisfactory in terms of result generated by 2D LS-IES methodology.

TABLE III. NPCR AND UACI VALUES OF ENCRYPTED IMAGES

Images	**NPCR**	**UACI**
5.1.14	99.59	33.30
5.1.12	99.49	33.31
5.1.09	99.60	33.32

TABLE IV. ENTROPY OF THE EXPERIMENTED IMAGES

Images	**5.1.14**	**5.1.12**	**5.1.09**
Plain image	7.3321	6.6050	6.6027
Encrypted	7.9985	7.9945	7.9956

TABLE V. COMPARATIVE STUDY OF 2D LS-IES

Methods	Image	Key	Entropy	NPCR	Correlation Coefficient	UACI
Proposed	5.1.14	2^{232}	7.9985	99.59	0.0031	33.30
[34]	5.1.09	2^{232}	7.9971	99.66	-0.0017	33.30
[35]	512×512 [3]	2^{256}	7.9991	99.6212	0.0015	33.4406
[36]	Lena	2^{279}	7.9969	99.62	NA	33.50
[37]	512×512 [3]	2^{256}	7.9996	99.6383	0.0010	33.3516
[38]	Lena	2^{312}	7.9993	99.60	0.0020	33.4754
[39]	Lena	2^{262}	7.9993	99.62	0.0023	33.46
[40]	5.1.09	2^{512}	NA	99.6185	0.0593	33.45
[41]	5.1.09	2^{224}	7.997	99.60	-0.00033	33.45
[42]	5.1.09	2^{256}	7.9026	99.6094	NA	33.5253

VI. CONCLUSION

This research initiated a unique 2D-LS chaotic. The logistical map's outcome is used to alter associated sine map insight, and after that transition period is extended to one dimension to two dimensions. A variety of empirical techniques and its examination have been offered to indicate why 2D-LS has greater ergodicity as well as chaotic spectrum compare to all those current one dimension as well as two-dimensional cryptosystems. This research is also suggested an innovative image encryption system named LS-IES utilizing 2D-LS. It has two fundamental characteristics, including misunderstanding over bit manipulation as well as diffusion through bit manipulation. Uncertainty as well as dispersion are accomplished at bit scale to reach the confusion as well as diffusion premise. Research outcomes as well as security concern have shown that LS-IES can easily encrypts many picture formats with producing high security randomized cryptographic images. For the future work, this work can carry with different types of images and some improved encryption methods in terms of critical security with medical healthcare systems.

ACKNOWLEDGMENT

We are thanking to the Dhofar University, Sultanate of Oman for constantly help and support.

REFERENCES

[1] W. D. Ferreira, C. B. R. Ferreira, G. da Cruz Júnior, and F. Soares, “A review of digital image forensics,” Comput. Electr. Eng., vol. 85, p. 106685, Jul. 2020.

[2] M. Yu, “Film and television culture dissemination based on ZYNQ embedded digital image processing,” Microprocess. Microsyst., vol. 82, p. 103921, Apr. 2021.

[3] Y. Zhang and L. Y. Zhang, “Exploiting random convolution and random subsampling for image encryption and compression,” Electron. Lett., vol. 51, no. 20, pp. 1572–1574, 2015.

[4] Y. Zhang, D. Xiao, W. Wen, and K.-W. Wong, “On the security of symmetric ciphers based on DNA coding,” Inf. Sci. (Ny)., vol. 289, pp. 254–261, Dec. 2014.

[5] G. Ye, “Image scrambling encryption algorithm of pixel bit based on chaos map,” Pattern Recognit. Lett., vol. 31, no. 5, pp. 347–354, Apr. 2010.

[6] J. Ramya, H. C. Vijaylakshmi, and H. Mirza Saifuddin, “Segmentation of skin lesion images using discrete wavelet transform,” Biomed. Signal Process. Control, vol. 69, p. 102839, Aug. 2021.

[7] C. Ye, J. Peng, and S. Kong, “Implementation of wavelet transform on optical computer,” Opt. Commun., vol. 486, p. 126761, May 2021.

[8] Y. Wu, Y. Zhou, S. Agaian, and J. P. Noonan, “A symmetric image cipher using wave perturbations,” Signal Processing, vol. 102, pp. 122–131, Sep. 2014.

[9] A. Elghandour, A. Salah, and A. Karawia, “A new cryptographic algorithm via a two-dimensional chaotic map,” Ain Shams Eng. J., May 2021.

[10] J. S. Muthu and P. Murali, “A new chaotic map with large chaotic band for a secured image cryptosystem,” Optik (Stuttg)., vol. 242, p. 167300, Sep. 2021.

[11] M. Z. Talhaoui and X. Wang, “A new fractional one dimensional chaotic map and its application in high-speed image encryption,” Inf. Sci. (Ny)., vol. 550, pp. 13–26, Mar. 2021.

[12] Y. Peng, S. He, and K. Sun, “A higher dimensional chaotic map with discrete memristor,” AEU - Int. J. Electron. Commun., vol. 129, p. 153539, Feb. 2021.

[13] X. Wang, W. Zhang, W. Guo, and J. Zhang, “Secure chaotic system with application to chaotic ciphers,” Inf. Sci. (Ny)., vol. 221, pp. 555–570, Feb. 2013.

[14] Yicong Zhou, Zhongyun Hua, Chi-Man Pun, and C. L. P. Chen, “Cascade Chaotic System With Applications,” IEEE Trans. Cybern., vol. 45, no. 9, pp. 2001–2012, Sep. 2015.

[15] J. Khan, H. Abbas, and J. Al-Muhtadi, “Survey on Mobile User’s Data Privacy Threats and Defense Mechanisms,” Procedia Comput. Sci., vol. 56, pp. 376–383, 2015.

[16] J. Khan et al., “Medical Image Encryption Into Smart Healthcare IOT System,” in 2019 16th International Computer Conference on Wavelet Active Media Technology and Information Processing, 2019, pp. 378–382.

[17] X. Wang, N. Guan, and J. Yang, “Image encryption algorithm with random scrambling based on one-dimensional logistic self-embedding chaotic map,” Chaos, Solitons & Fractals, vol. 150, p. 111117, Sep. 2021.

[18] C. Luo, B. Q. Liu, and H. S. Hou, “Fractional chaotic maps with q–deformation,” Appl. Math. Comput., vol. 393, p. 125759, Mar. 2021.

[19] B. Khokhar, S. Dahiya, and K. P. S. Parmar, “Load frequency control of a microgrid employing a 2D Sine Logistic map based chaotic sine cosine algorithm,” Appl. Soft Comput., vol. 109, p. 107564, Sep. 2021.

[20] Z. Feixiang, L. Mingzhe, W. Kun, and Z. Hong, “Color image encryption via Hénon-zigzag map and chaotic restricted Boltzmann machine over Blockchain,” Opt. Laser Technol., vol. 135, p. 106610, Mar. 2021.

[21] K. A. K. Patro, A. Soni, P. K. Netam, and B. Acharya, “Multiple grayscale image encryption using cross-coupled chaotic maps,” J. Inf. Secur. Appl., vol. 52, p. 102470, Jun. 2020.

[22] M. Alawida, A. Samsudin, and J. Sen Teh, “Enhanced digital chaotic maps based on bit reversal with applications in random bit generators,” Inf. Sci. (Ny)., vol. 512, pp. 1155–1169, Feb. 2020.

[23] A. A. Śliwiak, N. Chandramoorthy, and Q. Wang, “Ergodic sensitivity analysis of one-dimensional chaotic maps,” Theor. Appl. Mech. Lett., vol. 10, no. 6, pp. 438–447, Nov. 2020.

[24] T. Zhao, L. Yuan, and Y. Chi, “Image encryption using linear weighted fractional-order transform,” J. Vis. Commun. Image Represent., vol. 77, p. 103098, May 2021.

[25] Y. Zhang, L. Zhang, Z. Zhong, L. Yu, M. Shan, and Y. Zhao, “Hyperchaotic image encryption using phase-truncated fractional Fourier transform and DNA-level operation,” Opt. Lasers Eng., vol. 143, p. 106626, Aug. 2021.

[26] D. Arroyo, R. Rhouma, G. Alvarez, S. Li, and V. Fernandez, “On the security of a new image encryption scheme based on chaotic map lattices,” Chaos An Interdiscip. J. Nonlinear Sci., vol. 18, no. 3, p. 033112, Sep. 2008.

[27] C. Li, Y. Liu, L. Y. Zhang, And M. Z. Q. Chen, “Breaking A Chaotic Image Encryption Algorithm Based On Modulo Addition And Xor Operation,” Int. J. Bifurc. Chaos, vol. 23, no. 04, p. 1350075, Apr. 2013.

[28] C. Li, D. Arroyo, And K.-T. Lo, “Breaking A Chaotic Cryptographic Scheme Based On Composition Maps,” Int. J. Bifurc. Chaos, vol. 20, no. 08, pp. 2561–2568, Aug. 2010.

[29] R. M. May, “Simple mathematical models with very complicated dynamics,” Nature, vol. 261, no. 5560, pp. 459–467, Jun. 1976.

[30] G. Alvarez And S. Li, “Some Basic Cryptographic Requirements For Chaos-Based Cryptosystems,” Int. J. Bifurc. Chaos, vol. 16, no. 08, pp. 2129–2151, Aug. 2006.

[31] D. Xiao, X. Liao, and S. Deng, “One-way Hash function construction based on the chaotic map with changeable-parameter,” Chaos, Solitons & Fractals, vol. 24, no. 1, pp. 65–71, Apr. 2005.

[32] Z. Hua and Y. Zhou, “Image encryption using 2D Logistic-adjusted-Sine map,” Inf. Sci. (Ny)., vol. 339, pp. 237–253, Apr. 2016.

[33] Digital Test Image, “Usc-sipi image database for research in image processing, image analysis, and machine vision.” [Online]. Available: http://sipi.usc.edu/database/. [Accessed: 29-Jun-2021].

[34] X. Gao, “Image encryption algorithm based on 2D hyperchaotic map,” Opt. Laser Technol., vol. 142, p. 107252, Oct. 2021.

[35] J. Khan et al., “SMSH: Secure Surveillance Mechanism on Smart Healthcare IoT System With Probabilistic Image Encryption,” IEEE Access, vol. 8, pp. 15747–15767, 2020.

[36] S. Zhang and L. Liu, “A novel image encryption algorithm based on SPWLCM and DNA coding,” Math. Comput. Simul., vol. 190, pp. 723–744, Dec. 2021.

[37] J. Khan et al., “Efficient secure surveillance on smart healthcare IoT system through cosine-transform encryption,” J. Intell. Fuzzy Syst., vol. 40, no. 1, pp. 1417–1442, Jan. 2021.

[38] Q. Cun, X. Tong, Z. Wang, and M. Zhang, “Selective image encryption method based on dynamic DNA coding and new chaotic map,” Optik (Stuttg)., vol. 243, p. 167286, Oct. 2021.

[39] N. Khalil, A. Sarhan, and M. A. M. Alshewimy, “An efficient color/grayscale image encryption scheme based on hybrid chaotic maps,” Opt. Laser Technol., vol. 143, p. 107326, Nov. 2021.

[40] X. Wang and M. Zhao, “An image encryption algorithm based on hyperchaotic system and DNA coding,” Opt. Laser Technol., vol. 143, p. 107316, Nov. 2021.

[41] R. Wang, G.-Q. Deng, and X.-F. Duan, “An image encryption scheme based on double chaotic cyclic shift and Josephus problem,” J. Inf. Secur. Appl., vol. 58, p. 102699, May 2021.

[42] H. Zhu, Y. Zhao, and Y. Song, “2D Logistic-Modulated-Sine-Coupling-Logistic Chaotic Map for Image Encryption,” IEEE Access, vol. 7, pp. 14081–14098, 2019.

An Optimized Neural Network Model for Facial Expression Recognition over Traditional Deep Neural Networks

Pavan Nageswar Reddy Bodavarapu[1], P.V.V.S Srinivas[2]
Department of Computer Science and Engineering
Koneru Lakshmaiah Education Foundation, Vijayawada, India

Abstract*—Emotions have a key role in Feedback analysis to provide a good customer service, the main seven emotions are Anger, Disgust, Fear, Happy, Neutral, Sad and Surprise. There are several advantages, an efficient Facial Emotion Recognition model can help us in self-discipline and control over the drivers, while they are driving the vehicle. Low resolution and Low-reliable images are main problems in this field. We proposed a new model which can efficiently perform on Low resolution and Low-reliable images. We created a low resolution facial expression dataset (LRFE) by collecting various images from different resources, which contains low resolution images. We also proposed a new hybrid filtering method, which is a combination of Gaussian, Bilateral, Non local means filtering techniques. Densenet-121 achieves 0.60 0.68 accuracy on fer2013 and LRFE respectively. When hybrid filtering method is combined with Densenet-121, it achieved 0.95 accuracy. Similarly Resnet-50, MobileNet, Xception models performed effectively when combined with the hybrid filtering method. The proposed convolutional neural network(CNN) model achieved 0.65 accuracy on fer2013 dataset, while the existing models like Resnet-50, MobileNet, Densenet-121 and Xception obtained 0.60 0.57 0.60 0.52 accuracies on fer2013 respectively. The proposed model when combined with hybrid filtering method achieved 0.85 accuracy. Clearly the proposed model outperforms the traditional methods. When the hybrid filtering method is combined with the CNN models, there is significant increase in the accuracy.

Keywords*—*Facial expression recognition; deep learning; filtering techniques; convolutional neural network; emotion

I. Introduction

The raw data consists of noise like random variation of brightness or color information, removing noise from the images drastically improves the performance of the facial emotion recognition models. To eliminate noise from images there are many denoising techniques such as gaussian blur, bilateral filter, non-local means filtering. Gaussian Blur helps in blurring the edges and reducing the contrast, but it reduces the details [1]. Bilateral Filter decreases the noise by preserving the edges by replacing the intensity of pixels with weighted average of intensity from surrounding pixels [2]. Gaussian Filter, Bilateral Filter and other traditional filtering techniques can remove image noise, but the image structure information is not retained enough. Non Local Means Filtering averages neighbours with similar neighbourhoods, with much greater clarity and smaller extent loss of detail post-filtering. The limitation of this technique is, efficiency is slightly lower when compared to traditional techniques. The computation complexity is quadratic in number of pixels in the image, so it is expensive to apply. To speed up the execution many techniques were designed, one such technique is fast Fourier transform, it determines the similarity between two pixels by speeding up the algorithm by factor of 50 and also maintains the quality of result [3][4].

When compared grayscale images with RGB images, grayscale images achieves more accuracy in object recognition field. The other benifit of using grayscale images is, cost of computation will decrease [5][6]. Due to continuous gradient updating, overfitting is one of the basic issues in neural networks. This results in poor performance of the neural network model [7]. For a deep learning model to perform well, it needs a large amount of samples. Gathering more number of samples or large dataset might be expensive, so an possible way is, to automatically generate new samples, this process is called data augmentation. Data Augmentation is used to improve neural network model performance by decreasing data bias and improving the model generalization [8]. Batch normalization is used to increase the stability of a neural network and allows us to use higher learning rates. For as much as dropout can decrease overfitting in a model, a batch normalized neural network can remove or reduce the overfitting [9]. The traditional way for training a CNN is via stochastic gradient descent [10]. Instead of decreasing the learning rate, increase the batch size during the training. This method shows identical performance with lesser parameter updates [11][12][13].

Haar feature-based cascade classifier is a machine learning approach, where the cascade function is trained on positive and negative images. This approach is useful in object detection in images [14][15]. The best way to distinguish a neutral facial emotion from other emotions is to check whether the person’s mouth is open or closed. If the mouth seems to open, then that it does not belongs to neutral Facial emotion. A lot of research is being done in mobile applications for Emotion recognition tasks. Even though the present mobile devices have enough memory and processing power, when compared to previous generation smart phones, we cannot directly use solutions from computer to smart phones in respect of facial emotion recognition [16][17]. Social robots are very much needed for the society, they can behave as consort for old people, help doctors during operations. In facial emotion recognition mouth, eyes, eyebrows play a key role for emotion recognition, Gabor filter helps to obtain these features from an image [18][19].

Our major contributions in this research paper can be outlined as: (1) designed a novel convolutional neural network, Fig. 4 represents the proposed model architecture; (2) presented hybrid denoising method; (3) low resolution facial expression (LRFE) dataset is created for facial expression recognition; (4) compared with traditional methods. We applied various filtering techniques such as Average filtering, Median filtering, Gaussian filtering, Non local means filtering, Bilateral filtering and Hybrid denoising method to both FER2013 and LRFE dataset and compared the results. The Hybrid denoising method is presented by combining Gaussian, Bilateral and Non local means filtering techniques. The proposed model is compared with traditional methods, the batch size used in this research is 32 and trained for 100 epochs. Various techniques like dropout, L2 regularization are used to avoid overfitting. We build a novel convolutional neural network because the existing methods are not working well on the test sets and are very large in size(more number of layers when) and taking more time to train them. So our proposed convolutional neural network overcomes all these problems. In section III proposed work we explained about the dataset used in this paper and the algorithm of the proposed model. Next, in experiment and result section, we pointed out all the experimental results along with graphs of all the techniques used. Table I outlines the description of FER2013 and LRFE datasets, respectively.

TABLE I. OUTLINE OF FER2013 AND LRFE DATASET

Category	FER2013	LRFE
Downloadable	YES	NO
No.of emotions	7	7
Gender	FEMALE/MALE	FEMALE/MALE
No.of images	35887	6100

II. RELATED WORK

Zhiding Yu et al [20] proposed a method based on ensemble of three face detectors, followed by a classification module with ensemble of various convolutional neural networks. Each convolutional neural network model is pre-trained and fine-tuned on Facial Expression Recognition challenge 2013 and SFEW 2.0, respectively. This method achieved 61.29% on test set of SFEW 2.0. Zhihao Zhang at al [21] designed a convolutional neural network to extract features from video clips and a feature matrix processing method is used for identifying the apex frame from such a long video. By combining feature extraction and feature matrix processing methods, the model achieved smaller Mean Absolute Error (MAE). Samira Ebrahimi Kahou et al [22] proposed a hybrid convolutional neural network (CNN) – recurrent neural network (RNN) method for facial expression recognition. Recurrent Neural Networks produced state-of-art performance on diverse set of sequence analysis tasks. The results show that higher recognition accuracy can be achieved by combining feature-level and decision-level fusion networks.

Bing Feiwu et al [23] proposed a model, which can solve the problem of customizing the general model without the label information of the testing samples. The model resulted an improve in accuracy by 3.01% 0.49% 5.33% when tested on extended Cohn-Kanade (ck+), Radboud Faces Database (RaFD) and Amsterdam Dynamic Facial Expression set (ADFES) respectively. Shamim Hossain et al [24] designed a model for mobile application, which can detect the facial emotions with less computation, since a mobile device has limited processing power we need a model which can recognize facial emotions with computationally less expensive. The proposed model takes only 1.4 seconds to recognize one instance of emotion and obtained an 99.8% 99.7% accuracies on JAFFE database and CK database respectively. Jia Deng et al [25] proposed conditional generative adversarial network approach to reduce the intra-class variations. The proposed approach consists of a generator G and discriminators (Di, Da and Dexp). For learning the generative and discriminative representations, three loss functions were designed. But there is one limitation in this approach is that the model is trained individually for each different datasets, a model which is trained on a particular dataset may result in poor accuracy on another dataset.

Hongli Zhang et al [26] designed a method based on convolutional neural network and edge detection for facial emotion recognition. For testing this they created a simulation experiment by combining the fer-2013 database with LFW dataset. The average recognition obtained by this method is 88.56% and the train speed on the training dataset is 1.5 times faster than the traditional method. Yingying Wang at al [27] proposed a hybrid transfer learning model, which is based on Convolution Restricted Boltzmann Machine (CRBM) model and a Convolutional Neural Network (CNN) model, since there are some content differences between the datasets during traditional transfer learning, which affects the classification performance of the model. In this model CRBM replaces the full connection layer in the CNN model. The added CRBM layer learns about the unique statistical characteristics of the target set. This helps in eliminating the content differences between the datasets.

Ronak Kosti et al [28] presented “Emotions in context Database” (EMOTIC), this dataset contains images of people in context in non-controlled environments with 26 emotional categories. They trained a convolutional neural network model on EMOTIC dataset that can analyze the person and the whole scene to classify the emotion states. There model is able to make notable guesses on the emotion states, when the face of the person is not visible. Jianzhu Guo et al [29] created ICV-MEFED dataset. It includes 50 classes of compound emotions (e.g., happy-disgusted and sadly-fearful) and labels that are evaluated by psychologists, since the labels that are obtained automatically by machine learning based algorithms could lead to inaccuracies. They have organized a challenge on the ICV-MEFED dataset at FG workshop 2017. After analyzing the top three methods, the experimental results indicate that pairs of compound emotions (e.g., happily-surprised vs surprisingly-happy) are more difficult to recognize.

III. Proposed Work

A. Filter Description

The main aim of our research is to compare the Facial Emotion recognition accuracy of Gaussian, Bilateral, Non local means, Average, Median, Hybrid denoising techniques. A hybrid denoising method is proposed by combining the Gaussian, Bilateral, Non-local Means denoising techniques. Guassian filter is a 2D convolution filter, which blur the image, helping in remove the noise. The only limitation with this technique is, the loss of image details is high when compared to other techniques. Bilateral is a non-linear filtering technique used to remove noise from the image by preserving the edges. The limitation of this technique is that it introduces false edges in the image. Non local means filter, unlike taking the mean value of a group of pixels, non local means takes a mean of all pixels and unlike other techniques which blur the image, non local means can restore the texture of image.Median filter is one of the non-linear digital filtering technique, used to remove the noise from the images. It removes the noise from the images by preserving the edges. For removing salt and pepper noise, median filter is most effective.Average filtering helps in removing the noise from the images by replacing each value with average of neighbouring pixels; decreases the intensity variation among neighbouring pixels.

B. Dataset Description

1) FER2013 dataset: This dataset contains nearly 35887 images of various people facial expressions. It is a publicly available dataset, which enables to do research in the field of facial expression recognition. It contains both male and female gender images. The no. of emotions in fer2013 are seven (Happy, Sad, Neutral, Fear, Disgust, Anger, Surprise). This dataset is then divided in the ratio of 80:20 for training and testing purpose. Thus, the training and testing set contains 28709 and 7178 images respectively. Fig. 1 shows the sample images of FER2013 dataset.

2) LRFE (Low resolution facial expression) dataset: We collected images and videos from different resources belonging to seven different Facial Emotions (Anger, Disgust, Sad, Neutral, Fear, Happy, Surprise). All the videos are split into images and these images are organized into their respective directories based on the Facial Emotion. The dataset contains 35000 images belonging to seven different Facial Emotions. The raw images collected are of different formats (file extensions with .png, .gif, .tiff, .jpg). So we converted all the images with file extension other than .JPG into .JPG format. Next, we converted all the images into grayscale format from RGB format. After converting the images into grayscale, we resized all the images to 48X48 pexels. Fig. 2 shows the sample images of LRFE dataset.

3) Mixed dataset: Randomly various images from each emotion category are mixed together from FER2013 and LRFE dataset to form the mixed dataset. This dataset contains nearly 35000 images belonging to seven different facial expressions (Happy, Sad, Neutral, Fear, Disgust, Anger, Surprise). Later different types of denoising techniques like Bilateral, Non local means, Gaussian, Average, Median filtering are applied to all images. Fig. 3 shows the sample images of Mixed dataset.

Fig. 1. Sample Images in FER2013 Dataset.

Fig. 2. Sample Images in LRFE Dataset.

Fig. 3. Sample Images in Mixed Dataset.

C. Algorithm

Step 1: Input of image dataset containing seven different facial emotions.

Step 2: Firstly, convert all the images into JPG format.

Step 3: Secondly, convert all the RGB images into gray scale format.

Step 4: Thirdly, re-size all the corresponding gray scale images to 48X48 pixels.

Step 5: Now, Assign labels to all the images after re-sizing.

Step 6: Split the dataset into 80:20 ratio for training and testing the model for classification of image.

Step 7: Train the model on the training set and evaluate the model on the testing set.

Step 8: Finally, output the classification of image based on the emotion expressed in the image.

D. Model Architecture

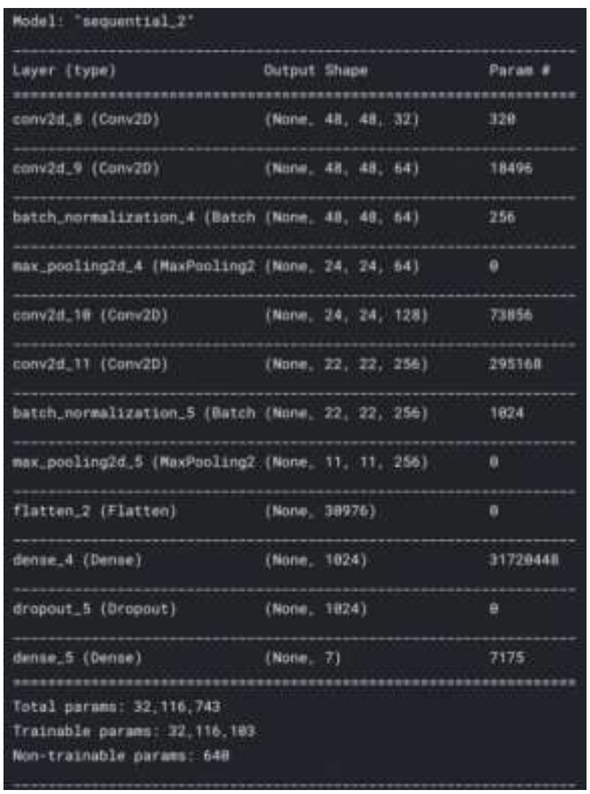

```
Model: "sequential_2"
_________________________________________________________________
Layer (type)                 Output Shape              Param #
=================================================================
conv2d_8 (Conv2D)            (None, 48, 48, 32)        320
_________________________________________________________________
conv2d_9 (Conv2D)            (None, 48, 48, 64)        18496
_________________________________________________________________
batch_normalization_4 (Batch (None, 48, 48, 64)        256
_________________________________________________________________
max_pooling2d_4 (MaxPooling2 (None, 24, 24, 64)        0
_________________________________________________________________
conv2d_10 (Conv2D)           (None, 24, 24, 128)       73856
_________________________________________________________________
conv2d_11 (Conv2D)           (None, 22, 22, 256)       295168
_________________________________________________________________
batch_normalization_5 (Batch (None, 22, 22, 256)       1024
_________________________________________________________________
max_pooling2d_5 (MaxPooling2 (None, 11, 11, 256)       0
_________________________________________________________________
flatten_2 (Flatten)          (None, 30976)             0
_________________________________________________________________
dense_4 (Dense)              (None, 1024)              31720448
_________________________________________________________________
dropout_5 (Dropout)          (None, 1024)              0
_________________________________________________________________
dense_5 (Dense)              (None, 7)                 7175
=================================================================
Total params: 32,116,743
Trainable params: 32,116,103
Non-trainable params: 640
_________________________________________________________________
```

Fig. 4. Model Architecture.

IV. Experiment and Results

A. Performance on FER2013 Dataset

The Table II (fer2013 dataset) is divided in the ratio of 80:20 for training and testing purpose, the batch size is 32 and all the models are trained for 100 epochs. During model implementation, 80 percent of fer2013 dataset is used for training the model and remaining 20 percent is divided into validation and testing the model.

Table III shows the accuracy and loss comparison of different deep learning models and proposed FerExpNet model on Fer2013 dataset. The proposed FerExpNet achieves an accuracy of 0.79 0.65 on training and testing sets of Fer2013 respectively. The results clearly indicate that the proposed FerExpNet is performing better than the state-of-models on Fer2013 dataset. The state-of-art VGG variants VGG16, VGG19 obtained 0.60 0.53 accuracy on Fer2013 dataset. The Xception model achieved only 0.52 accuracy on Fer2013 dataset, which makes it less efficient in Facial expression recognition, when compared with ResNet-50 and Densenet-121 on Fer2013 dataset. A mobile application efficient model MobileNet achieved 0.57 accuracy on Fer2013 dataset. Among all the models implemented, Xception model is not performing better on Fer2013 for facial expression recognition. The results show that Xception model train accuracy is 0.53 and train loss is 1.29, indicating that it under-performance on fer2013 for facial expression recognition. The latest EfficientNet-B7 obtained an 0.60 accuracy on Fer2013 dataset. In Fig. 5(a), 5(b) and 5(d) we can see that train loss and test loss converges quickly, as the number of epochs increases the train loss and test loss decreases quickly. In Fig. 5(c), we can see that the Xception model is taking much more number of epochs to decrease the train loss and test loss, when compared to proposed FerExpNet model. In Fig. 5(e), we can see that the DenseNet121 model is taking much more number of epochs to decrease the train loss and test loss, when compared to proposed FerExpNet model The Fig. 5(f) shows the accuracy vs loss comparison graph of proposed FerExpNet model. After analyzing all the results, the proposed FerExpNet model is performing better than the existing state-of-art models on Fer2013 dataset for facial expression recognition in terms of accuracy and loss.

Table IV shows the results of FerExpNet on Fer2013, when different filtering techniques are applied. We designed a novel Hybrid filtering method (HDM), which is a combination of Gaussian, bilateral and non-local means filtering techniques. When the proposed FerExpNet is combined with average filtering technique, the model achieved 0.70 accuracy on Fer2013 dataset. The proposed model without any filtering technique achieved 0.65 accuracy on Fer2013 dataset, there is a significant increase in accuracy after applying the average filter. When the proposed FerExpNet is combined with Gaussian filtering technique, the model achieved 0.65 0.55 on train set and test set of Fer2013, respectively. The accuracy of this approach is only 0.55 which is less, when compared to FerExpNet without filtering techniques, because when Gaussian filter is applied a lot of details in the images will be lost. When the designed hybrid filtering method (HDM) is combined with FerExpNet, the model achieved 0.87 0.85 accuracy on train and test sets of Fer2013 respectively. There is a significant increase in both accuracy and loss, when compared to FerExpNet without filtering techniques. The results in Table IV show that the FerExpNet with hybrid filtering method is performing better than other filtering techniques on Fer2013 dataset. The Fig. 6(a), 6(b) and 6(c) represents the comparison of accuracy and loss of various denoising techniques on proposed model when applied on FER2013 dataset, respectively.

TABLE II. OUTLINE OF FER2013 DATASET

Dataset	Name & No. of images in each emotion						
	Happy	Sad	Angry	Disgust	Sad	Surprise	Neutral
Fer2013	8989	6077	4953	547	6077	4002	6198

TABLE III. OUTLINE OF ACCURACY AND LOSS OF VARIOUS MODELS ON FER2013 DATASET

S.no	Model Name	Dataset	Train Accuracy	Test Accuracy	Train Loss	Test Loss
1	VGG16	Fer2013	0.63	0.60	1.01	1.10
2	VGG19	Fer2013	0.54	0.53	1.22	1.20
3	Resnet-50	Fer2013	0.63	0.60	0.97	1.09
4	MobileNet	Fer2013	0.59	0.57	1.10	1.15
5	Xception	Fer2013	0.53	0.52	1.29	1.39
6	EfficientNetB7	Fer2013	0.63	0.60	1.10	1.09
7	DenseNet121	Fer2013	0.61	0.60	1.06	1.08
8	FerExpNet	Fer2013	0.79	0.65	0.69	1.07

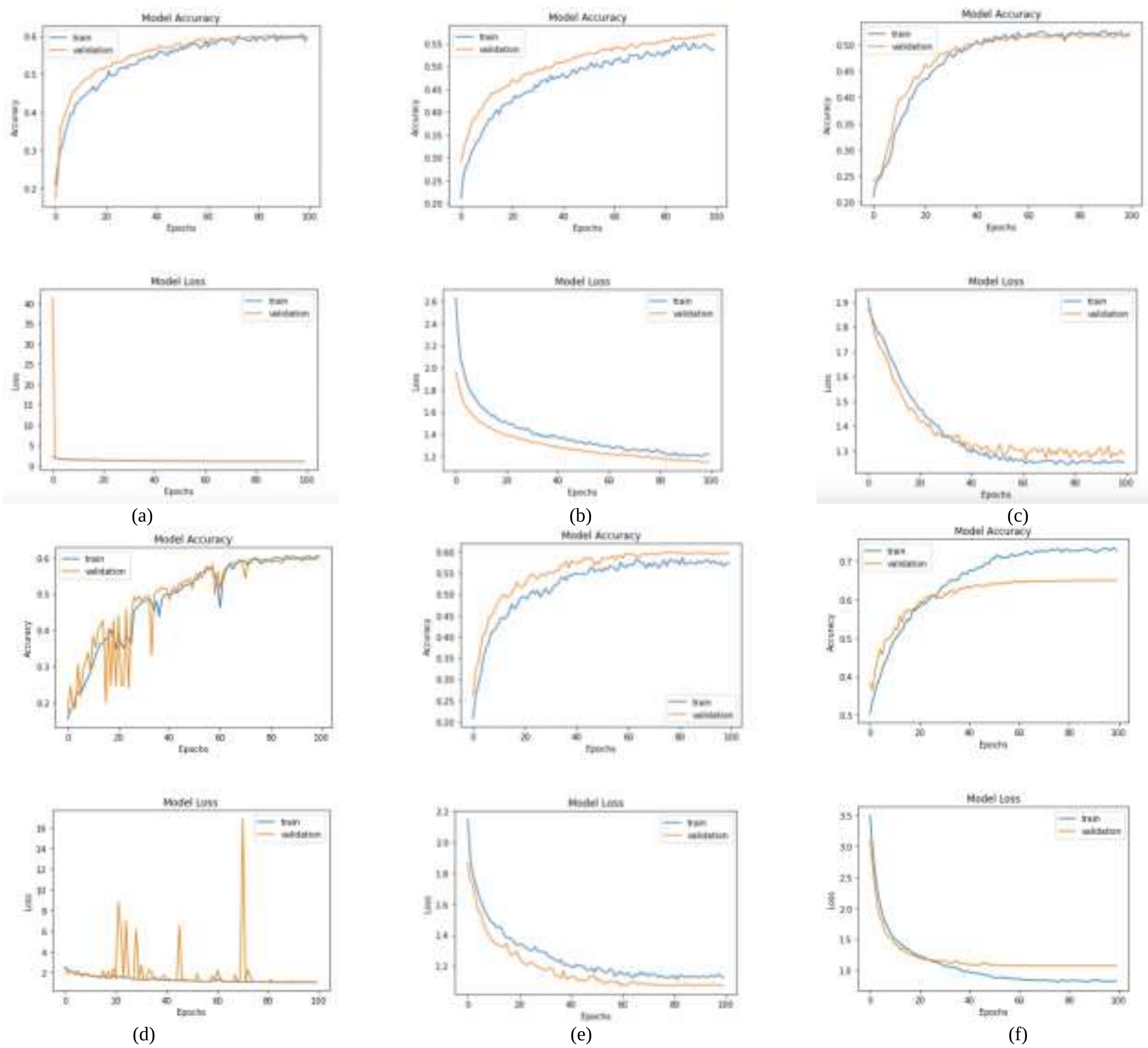

Fig. 5. (a) Accuracy and Loss of Resnet-50 on Fer2013 (b) Accuracy and Loss of MobileNet on Fer2013 (c) Accuracy and Loss of Xception on Fer2013. (d) Accuracy and Loss of EfficientNetB7 on Fer2013 (e) Accuracy and Loss of DenseNet121 on Fer2013 (f) Accuracy and Loss of FerExpNet on Fer2013.

TABLE IV. OUTLINE OF ACCURACY AND LOSS OF PROPOSED FEREXPNET ON FER2013 DATASET AFTER APPLYING VARIOUS FILTERING TECHNIQUES

S.no	Model Name	Dataset	Train Accuracy	Test Accuracy	Train Loss	Test Loss
1	FerExpNet_Average	Fer2013	0.91	0.70	1.45	2.39
2	FerExpNet_Median	Fer2013	0.76	0.60	0.79	1.19
3	FerExpNet_Bilateral	Fer2013	0.80	0.65	0.69	1.09
4	FerExpNet_Gaussian	Fer2013	0.65	0.55	1.05	1.33
5	FerExpNet_NonLocal Means	Fer2013	0.79	0.65	0.71	1.09
6	FerExpNet_HDM	Fer2013	0.87	0.85	0.47	0.56

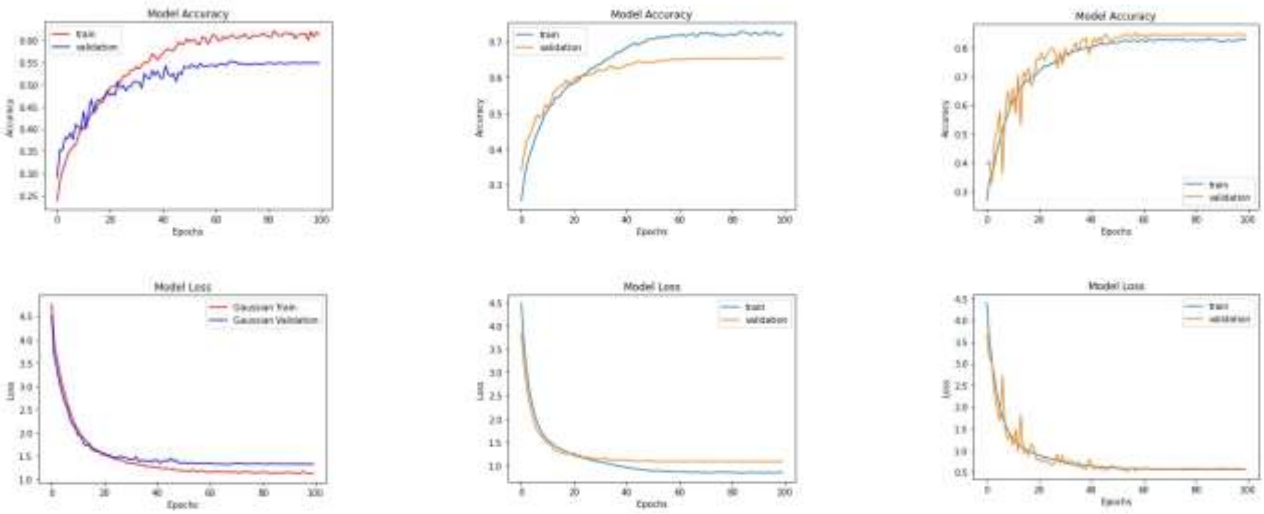

(a) (b) (c)

Fig. 6. (a) Accuracy and Loss of FerExpNet_Gaussian on Fer2013 (b) Accuracy and Loss of FerExpNet_NonLocal Means on Fer2013 (c) Accuracy and Loss of FerExpNet_HDM Means.

B. Performance on LRFE Dataset

The LRFE dataset is divided in the ratio of 80:20 for training and testing purpose, the batch size is 32 and all the models are trained for 100 epochs. During model implementation, 80 percent of LRFE dataset is used for training the model and remaining 20 percent is divided into validation and testing the model.

Table V shows the accuracy and loss comparison of different deep learning models and proposed FerExpNet model on Low resolution Facial Expression (LRFE) dataset. The proposed FerExpNet achieves an accuracy of 0.95 0.71 on training and testing sets of LREF dataset, respectively. The results clearly indicate that the proposed FerExpNet is performing better than the state-of-models on LRFE dataset. The state-of-art VGG variants VGG16, VGG19 obtained 0.69 0.66 accuracy on LRFE dataset. The MobileNet model achieved only 0.65 accuracy on LRFE dataset, which makes it less efficient in Facial expression recognition, when compared with Xception and FerExpNet on LRFE dataset. The Xception model achieved 0.69 accuracy on LRFE dataset, which is second best after the FerExpNet on LRFE dataset. The latest EfficientNet-B7 obtained an 0.65 accuracy on LRFE dataset. In Fig. 7(a), 7(b) and 7(d) we can see that train loss and test loss converges quickly, as the number of epochs increases the train loss and test loss decreases quickly. In Fig. 7(c) and 7(e) we can see that the Xception and DenseNet121 models are taking much more number of epochs to decrease the train loss and test loss, when compared to proposed FerExpNet model. The Fig. 7(f) shows the accuracy vs loss comparison graph of proposed FerExpNet model. After analyzing all the results, the proposed FerExpNet model is performing better than the existing state-of-art models on LRFE dataset for facial expression recognition in terms of accuracy and loss.

TABLE V. OUTLINE OF ACCURACY AND LOSS OF VARIOUS MODELS ON LRFE DATASET

S.no	Model Name	Dataset	Train Accuracy	Test Accuracy	Train Loss	Test Loss
1	VGG16	LRFE	0.87	0.69	0.40	1.16
2	VGG19	LRFE	0.84	0.66	0.47	0.96
3	Resnet-50	LRFE	0.89	0.69	0.28	0.95
4	MobileNet	LRFE	0.85	0.65	0.40	0.98
5	Xception	LRFE	0.95	0.69	0.27	1.99
6	EfficientNetB7	LRFE	0.79	0.65	0.71	1.09
7	DenseNet121	LRFE	0.89	0.68	0.30	0.98
8	FerExpNet	LRFE	0.98	0.74	0.16	1.19

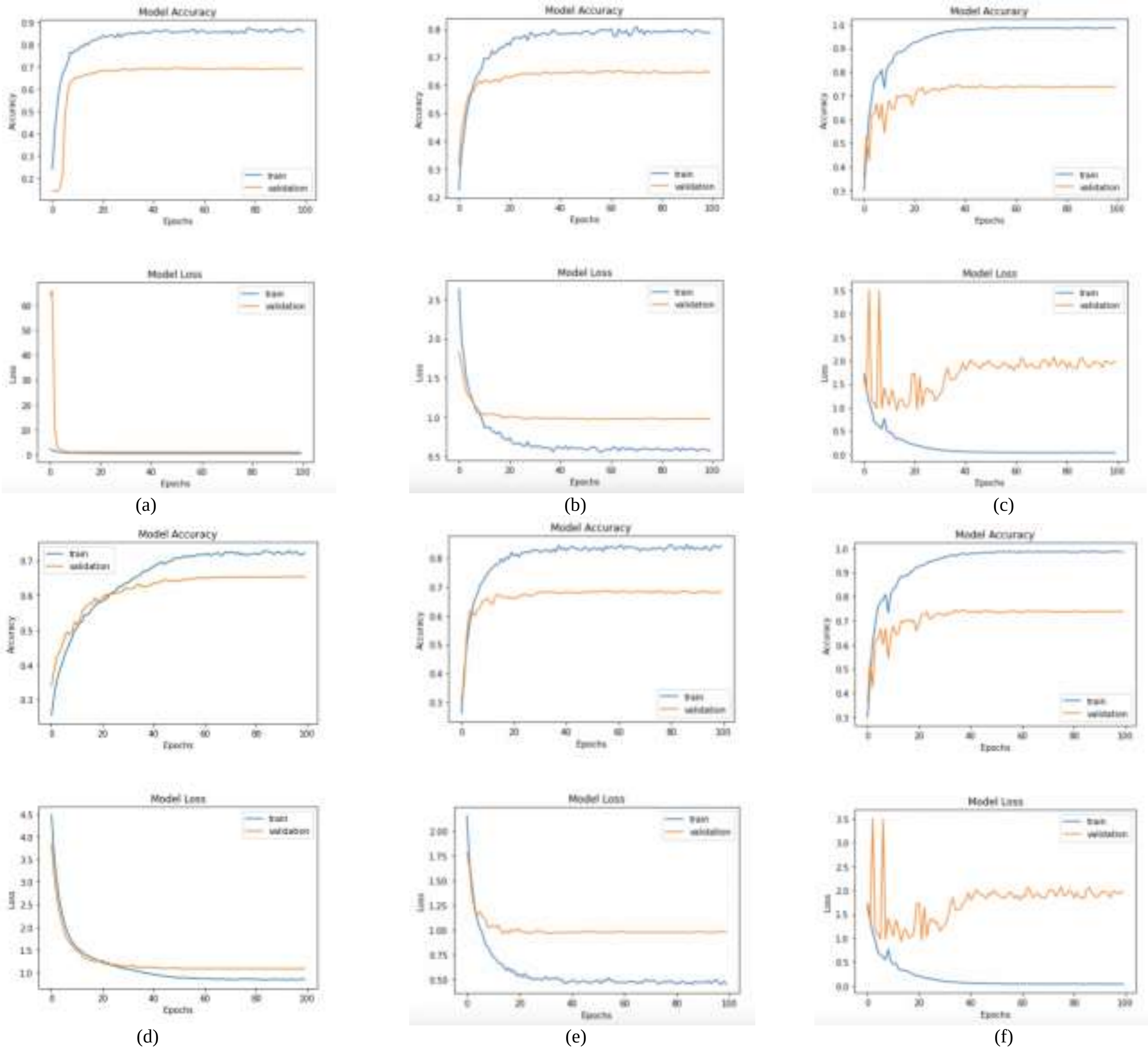

Fig. 7. (a) Accuracy and Loss of Resnet-50 on LRFE dataset (b) Accuracy and Loss of MobileNet on LRFE dataset (c) Accuracy and Loss of Xception on LRFE dataset. (d) Accuracy and Loss of EfficientNetB7 on LRFE dataset (e) Accuracy and Loss of DenseNet121 on LRFE dataset (f) Accuracy and Loss of FerExpNet on LRFE dataset.

Table VI shows the results of FerExpNet on LRFE dataset, when different filtering techniques are applied. We designed a novel Hybrid filtering method (HDM), which is a combination of gaussian, bilateral and non-local means filtering techniques. When the proposed FerExpNet is combined with average filtering technique, the model achieved 0.70 accuracy on LRFE dataset. The proposed model without any filtering technique achieved 0.65 accuracy on LRFE dataset, there is a significant increase in accuracy after applying the average filter. When the proposed FerExpNet is combined with Gaussian filtering technique, the model achieved 0.98 0.58 on train set and test set of LRFE dataset respectively. The accuracy of this approach is only 0.58 which is less, when compared to FerExpNet without filtering techniques, because when gaussian filter is applied a lot of details in the images will be lost. When the designed hybrid filtering method (HDM) is combined with FerExpNet, the model achieved 0.98 0.95 accuracy on train and test sets of Fer2013, respectively. There is a significant increase in both accuracy and loss, when compared to FerExpNet without filtering techniques. The results in Table VI show that the FerExpNet with hybrid filtering method is performing better than other filtering techniques on LRFE dataset. The Fig. 8(a), 8(b) and 8(c) represents the accuracy and loss comparison of various denoising techniques on proposed model on LRFE dataset, respectively.

C. Performance on Mixed Dataset

Randomly various images from each emotion category are mixed together from FER2013 and LRFE dataset to form the mixed dataset. Later, the dataset is divided in the ratio of 80:20 for training and testing purpose, the batch size is 32 and all the models are trained for 100 epochs. During implementation, 80 percent of dataset is used for training and 20 percent of dataset is used for validation and testing purpose.

Table VII shows the comparison of various deep learning models and FerExpNet on Mixed dataset. This mixed dataset is created by mixing different emotions from Fer2013 and LRFE dataset into one directory. The dataset is then divided into training and testing sets in the ratio 80:20. The proposed FerExpNet achieved 0.96 accuracy on Mixed dataset. The state-of-art models like MobileNet, DenseNet and Xception achieved 0.91 0.95 0.92 accuracy on mixed dataset respectively. The results clearly show that the proposed FerExpNet is performing slightly better than the traditional methods on mixed dataset for Facial expression recognition.

TABLE VI. OUTLINE OF ACCURACY AND LOSS OF PROPOSED FEREXPNET ON LRFE DATASET AFTER APPLYING VARIOUS FILTERING TECHNIQUES

S.no	Model Name	Dataset	Train Accuracy	Test Accuracy	Train Loss	Test Loss
1	FerExpNet_Average	LRFE	0.91	0.70	1.45	2.39
2	FerExpNet_Median	LRFE	0.99	0.73	0.23	1.59
3	FerExpNet_Bilateral	LRFE	0.98	0.63	0.43	2.52
4	FerExpNet_Gaussian	LRFE	0.98	0.58	0.30	3.00
5	FerExpNet_NonLocal Means	LRFE	0.93	0.61	0.79	2.32
6	FerExpNet_HDM	LRFE	0.98	0.95	0.07	0.33

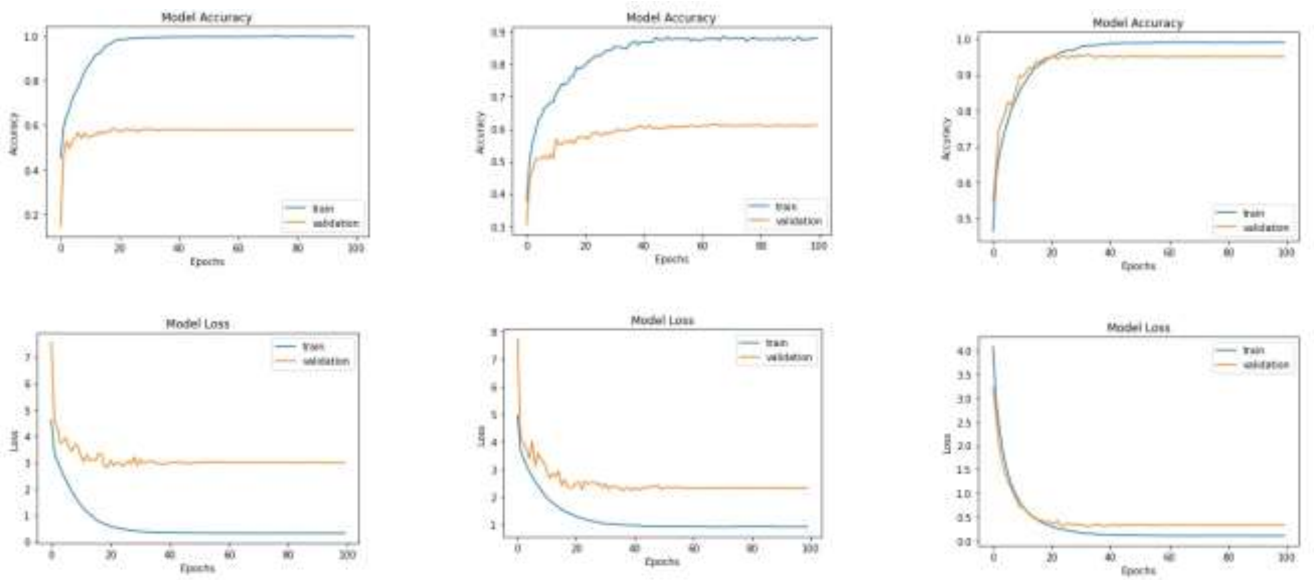

(a) (b) (c)

Fig. 8. (a) Accuracy and Loss of FerExpNet_Gaussian on LRFE (b) Accuracy and Loss of FerExpNet_NonLocal Means on LRFE (c) Accuracy and Loss of FerExpNet_HDM on LRFE.

TABLE VII. OUTLINE OF ACCURACY AND LOSS OF VARIOUS MODELS ON MIXED DATASET

S.no	Model Name	Dataset	Train Accuracy	Test Accuracy	Train Loss	Test Loss
1	FerExpNet	Mixed	0.99	0.96	0.05	0.38
2	MobileNet	Mixed	0.95	0.91	0.16	0.28
3	DenseNet	Mixed	0.99	0.95	0.05	0.19
4	Xception	Mixed	0.95	0.92	0.23	0.38

V. CONCLUSION

A Novel optimized neural network on basis of convolutional neural network is proposed in this paper. We also designed a new hybrid filtering method, which is a combination of Gaussian, bilateral and non-local means filtering techniques. This hybrid filtering method is used for removing any noise present in the images. All the datasets are divided in the ratio of 80:20 for training and testing purpose. The proposed FerExpNet achieved 0.65 accuracy on Fer2013 dataset and this model is performing better than the state-of-art models on Fer2013. When the hybrid filtering method is combined with the proposed FerExpNet, the model achieves 0.85 accuracy on Fer2013 dataset. There is a significant increase in the accuracy when hybrid filtering method is applied. The proposed FerExpNet obtained 0.74 accuracy on LRFE dataset, outperforming the existing models, similarly when the hybrid filtering method is combined with FerExpNet the accuracy increased to 0.95 on LRFE dataset. The results show that the proposed FerExpNet is performing better than the existing models. The average time taken for each epoch on LRFE dataset is 1sec, similarly the average time taken for each epoch on Fer2013 is 5sec for FerExpNet respectively. The future work of this paper is to build a more sophisticated convolutional neural network model which can be integrated into a mobile device for wide use in real-world applications.

ACKNOWLEDGMENT

I sincerely thank P.V.V.S Srinivas for guiding me in this research work and helping through difficult times.

REFERENCES

[1] Kopparapu, Sunil Kumar, and M. Satish. "Identifying Optimal Gaussian Filter for Gaussian Noise Removal." 2011 Third National Conference on Computer Vision, Pattern Recognition, Image Processing and Graphics (December 2011). doi:10.1109/ncvpripg.2011.34.

[2] Tomasi, C., & Manduchi, R. (n.d.). Bilateral filtering for gray and color images. Sixth International Conference on Computer Vision (IEEE Cat. No.98CH36271). doi:10.1109/iccv.1998.710815.

[3] Deledalle, C.-A., Duval, V., & Salmon, J. (2011). Non-local Methods with Shape-Adaptive Patches (NLM-SAP). Journal of Mathematical Imaging and Vision, 43(2), 103–120. doi:10.1007/s10851-011-0294-y.

[4] Ashok Kumar, P. M., Jeevan Babu Maddala, and K. Martin Sagayam. "Enhanced Facial Emotion Recognition by Optimal Descriptor Selection with Neural Network." *IETE Journal of Research* (2021): 1-20.

[5] Bui, H. M., Lech, M., Cheng, E., Neville, K., & Burnett, I. S. (2016). Using grayscale images for object recognition with convolutional-recursive neural network. 2016 IEEE Sixth International Conference on Communications and Electronics (ICCE). doi:10.1109/cce.2016.7562656.

[6] Videla, Lakshmi Sarvani, and PM Ashok Kumar. "Facial Expression Classification Using Vanilla Convolution Neural Network." In *2020 7th International Conference on Smart Structures and Systems (ICSSS)*, pp. 1-5. IEEE, 2020.

[7] Salman, Shaeke, and Xiuwen Liu. "Overfitting mechanism and avoidance in deep neural networks." *arXiv preprint arXiv:1901.06566* (2019).

[8] Tran, Toan, Trung Pham, Gustavo Carneiro, Lyle Palmer, and Ian Reid. "A bayesian data augmentation approach for learning deep models." In *Advances in neural information processing systems*, pp. 2797-2806. 2017.

[9] Ioffe, Sergey, and Christian Szegedy. "Batch normalization: Accelerating deep network training by reducing internal covariate shift." *arXiv preprint arXiv:1502.03167* (2015).

[10] Sainath, Tara N., Brian Kingsbury, Hagen Soltau, and Bhuvana Ramabhadran. "Optimization techniques to improve training speed of deep neural networks for large speech tasks." *IEEE Transactions on Audio, Speech, and Language Processing* 21, no. 11 (2013): 2267-2276.

[11] Smith, Samuel L., Pieter-Jan Kindermans, Chris Ying, and Quoc V. Le. "Don't decay the learning rate, increase the batch size." arXiv preprint arXiv:1711.00489 (2017).

[12] Inthiyaz, Syed, M. Muzammil Parvez, M. Siva Kumar, J. Sri sai Srija, M. Tarun Sai, and V. Amruth Vardhan. "Facial Expression Recognition Using KERAS." In *Journal of Physics: Conference Series*, vol. 1804, no. 1, p. 012202. IOP Publishing, 2021.

[13] Mahesh, D. Sri Sai, T. Maneesh Reddy, A. Sai Yaswanth, C. Joshitha, and S. Sudarshan Reddy. "Facial detection and recognition system on Raspberry Pi with enhanced security." In *2020 International Conference on Emerging Trends in Information Technology and Engineering (ic-ETITE)*, pp. 1-5. IEEE, 2020.

[14] Viola, Paul, and Michael Jones. "Rapid object detection using a boosted cascade of simple features." In *Proceedings of the 2001 IEEE computer society conference on computer vision and pattern recognition. CVPR 2001*, vol. 1, pp. I-I. IEEE, 2001.

[15] Srinivas, P. V. V. S., and Pragnyaban Mishra. "Facial Expression Detection Model of Seven Expression Types Using Hybrid Feature Selection and Deep CNN." In *International Conference on Intelligent and Smart Computing in Data Analytics: ISCDA 2020*, pp. 89-101. Springer Singapore, 2021.

[16] Suk, Myunghoon, and Balakrishnan Prabhakaran. "Real-time mobile facial expression recognition system-a case study." In *Proceedings of the IEEE conference on computer vision and pattern recognition workshops*, pp. 132-137. 2014.

[17] Abinaya, R., Lakshmana Phaneendra Maguluri, S. Narayana, and Maganti Syamala. "A Novel Biometric Approach for Facial Image Recognition Using Deep Learning Techniques." *International Journal of Advanced Research in Engineering and Technology* 11, no. 9 (2020).

[18] Ruiz-Garcia, Ariel, Mark Elshaw, Abdulrahman Altahhan, and Vasile Palade. "Emotion recognition using facial expression images for a robotic companion." In *International Conference on Engineering Applications of Neural Networks*, pp. 79-93. Springer, Cham, 2016.

[19] Jahnavi, P., Enireddy Vamsidhar, and C. Karthikeyan. "Facial expression detection of all emotions and face recognition system." *International Journal of Emerging Trends in Engineering Research* 7, no. 12 (2019): 778-783.

[20] Lopes, Nuno, André Silva, Salik Ram Khanal, Arsênio Reis, João Barroso, Vitor Filipe, and Jaime Sampaio. "Facial emotion recognition in the elderly using a SVM classifier." In *2018 2nd International Conference on Technology and Innovation in Sports, Health and Wellbeing (TISHW)*, pp. 1-5. IEEE, 2018.

[21] Yu, Zhiding, and Cha Zhang. "Image Based Static Facial Expression Recognition with Multiple Deep Network Learning." Proceedings of the 2015 ACM on International Conference on Multimodal Interaction - ICMI '15 (2015). doi:10.1145/2818346.2830595.

[22] Zhang, Zhihao, Tong Chen, Hongying Meng, Guangyuan Liu, and Xiaolan Fu. "SMEConvNet: A Convolutional Neural Network for Spotting Spontaneous Facial Micro-Expression From Long Videos." IEEE Access 6 (2018): 71143–71151. doi:10.1109/access.2018.2879485

[23] Ebrahimi Kahou, S., Michalski, V., Konda, K., Memisevic, R., & Pal, C. (2015). Recurrent Neural Networks for Emotion Recognition in Video. Proceedings of the 2015 ACM on International Conference on Multimodal Interaction - ICMI '15. doi:10.1145/2818346.2830596

[24] Wu, Bing-Fei, and Chun-Hsien Lin. "Adaptive Feature Mapping for Customizing Deep Learning Based Facial Expression Recognition Model." IEEE Access 6 (2018): 12451–12461. doi:10.1109/access.2018.2805861.

[25] Hossain, M. Shamim, and Ghulam Muhammad. "An Emotion Recognition System for Mobile Applications." IEEE Access 5 (2017): 2281–2287. doi:10.1109/access.2017.2672829.

[26] Deng, Jia, Gaoyang Pang, Zhiyu Zhang, Zhibo Pang, Huayong Yang, and Geng Yang. "cGAN Based Facial Expression Recognition for Human-Robot Interaction." IEEE Access 7 (2019): 9848–9859. doi:10.1109/access.2019.2891668.

[27] Zhang, Hongli, Alireza Jolfaei, and Mamoun Alazab. "A Face Emotion Recognition Method Using Convolutional Neural Network and Image Edge Computing." IEEE Access 7 (2019): 159081–159089. doi:10.1109/access.2019.2949741.

[28] Wang, Yingying, Yibin Li, Yong Song, and Xuewen Rong. "The Application of a Hybrid Transfer Algorithm Based on a Convolutional Neural Network Model and an Improved Convolution Restricted Boltzmann Machine Model in Facial Expression Recognition." IEEE Access 7 (2019): 184599–184610. doi:10.1109/access.2019.2961161.

[29] Kosti, Ronak, Jose M. Alvarez, Adria Recasens, and Agata Lapedriza. "Emotion Recognition in Context." 2017 IEEE Conference on Computer Vision and Pattern Recognition (CVPR) (July 2017). doi:10.1109/cvpr.2017.212.

Development of a Low-Cost Bio-Inspired Swimming Robot (SRob) with IoT

Mohd Aliff[1], Ahmad Raziq Mirza[2], Mohd Ismail[3]
Instrumentation and Control Engineering
Malaysian Institute of Industrial Technology
Universiti Kuala Lumpur
Johor, Malaysia

Nor Samsiah[4]
Center for Artificial Intelligence Technology (CAIT)
Faculty of Information Science and Technology
Universiti Kebangsaan Malaysia
Selangor, Malaysia

***Abstract*—Now-a-days, exploring underwater is a difficult activity to do and requires specialized equipment to explore it. Many studies so far have proven that bio-inspired robotic fish such as stingray robots have many advantages for use as underwater exploration. One of them is the manta ray which can show excellent swimming ability by flapping the pectoral fins with large amplitude. By studying the movement behavior of *genus Mobula*, the development of biomimetic robots has grown exponentially in recent years. But this technology requires expensive development costs, and the prototypes produced are heavy. Therefore, the development of low-cost bio-inspired Swimming Robot (SRob) using embedded controller with internet of things (IOT) is proposed and presented in this paper. SRob is designed with a small size and lightweight compared to other conventional swimming robots and is well equipped with 6 servo motors, ADXL335 accelerometer 3-axis, 2 Lipo batteries 7.4V, ESP01 Wi-Fi module and Arduino Mega. The RemoteXY app that works like a remote control will be connected to the Arduino Mega using the ESP01 Wi-Fi module to control servo motors and obtain readings of the sensors. Based on the experimental results, the servo motor used to produce flapping motion can be controlled precisely while producing a large amplitude of motion. In addition, the position control for the compact SRob can be realized and determined correctly while swimming in the water.**

Keywords—Stingray robot; angle of flapping motion; remote control; position control; compact SRob

I. Introduction

Numerous studies have demonstrated that robots are particularly effective in medical [1], rehabilitation [2-7], rescue operations [8-10], automobiles, and manufacturing [11-12]. Robotics has been used in a variety of industries for many years and has provided humans with numerous benefits. Furthermore, as the internet has grown in popularity, more intelligent devices and systems have emerged. The concept of internet or web-based controls for robots and the home environment is still in its early stages. The Internet offers low-cost communication routes and can be used for telephony. Many issues still need to be addressed before a viable real-world application can be realized. Researchers across the world are interested in using the internet to control robots as part of the Fourth Industrial Revolution (4IR).

Manta rays are the world's largest and most intelligent rays. The swimming capabilities of the manta ray has recently attracted the interest of researchers around the world and focusing on its movement performance, maneuverability, and stability [13]. Relevant research has been conducted based on this movement pattern and prototypes such as fish robots have been developed. However, the previous research on this swimming robot only focuses on the design and propulsion performance in addition to its expensive production cost and its large and heavy size.

Currently, many research studies have developed underwater vehicles fitted with propellers for use in challenging water environments. While it is easy to operate, there are some drawbacks on its movement mode such as loud noise, large scale, poor performance and even low speed maneuvers. There are also some underwater vehicles such as Autonomous Underwater Vehicles (AUV) and Unmanned Underwater Vehicle (UUV) that rely heavily on the design of manta rays and are able to glide in water without human control. Both robotic vehicles are heavily equipped with various types of sensors and cameras to be able to collect various types of data while used in rescue operations or exploration in the water to find out the environmental conditions.

Bio-inspired robotics provides biologists the equipment to study animal behavior and test beds for research and evaluation of biological algorithms for potential engineering applications [14]. Various studies involving animals including invertebrates and vertebrates have been conducted for different purposes. One of the research projects involving bio-inspired robots is used to answer simple biological questions or build classical mechatronic structures [15]. The development of swimming robot is particularly promising, not only as a testbed for learning how fish swim, but also for different underwater applications such as underwater discovery, patrol, and aquatic surveillance. Despite their appearance, current robotic fish are still substantially slower and less durable than their biological counterparts, necessitating further research into swimming mechanisms and control methods. Rajiforms are a type of underwater animal that have long wavy fins and they have a variety of swimming methods. The ray species that demonstrate this two-fin swimming method are manta rays with swinging flaps and stingrays with wavy movements. Rays can make large deformations on the fins because their bodies have no bone structure. In particular, manta rays can produce large amplitudes of deformation with fast duration and large thrust [16].

The main objectives of this project are to develop the manta ray swimming robot (SRob) using Arduino and WiFi module, to control and monitor manta ray swimming robot using RemoteXY application and ADXL335 accelerometer and to evaluate the movement of manta ray swimming robot based on angle of servo motor. The scope of this project focuses on control system using embedded controller along with IoT for manta ray robot prototype while solving the problem of conventional swimming robots by developing lightweight prototype at low cost.

II. Literature Review

Although bionic manta ray research has progressed significantly in recent years, robot mobility still differs significantly from that of genuine manta rays. To begin with, most existing bionic manta rays use an oscillating propulsion mode, and the mechanical construction is typically simplified. A prototype's skeleton is usually built of stiff material. As a result, the majority of prototypes are rigid. Second, the bionic prototype's control algorithm cannot quite match the genuine movement of manta rays, especially during the transition between motor patterns. As a result, to improve control performance, a more robust and reasonable control algorithm is necessary. The bionic manta ray robot with flexible pectoral fin was proposed in response to the mechanical structure and motion control algorithm shortcomings of previous bionic manta rays [17]. The longitudinal structure of the pectoral fins was created using 3D printing technology and joined by flexible beams and metal wires. As a result, these pectoral fins' geometrical form was more akin to that of actual manta rays. CPG was used to recreate the mobility pattern of manta rays based on observations of their periodic movement. However, the prototype that was invented was still quite huge and heavy. The bionic manta ray robot is 48.5 cm long, 70.0 cm wide, and 6.0 cm tall. It weighs 6 kg and has a maximum speed of 0.4 m/s with a flapping frequency of 2.5 Hz.

Alvarado et al. using a new method that can provide an advantage in its robotic stingrays, which are made of a soft material and only require one actuator per fin [18-21]. Chew et al. demonstrated a Robot Manta Ray prototype in which each fin's oscillatory motion is controlled by a single servo motor [22]. The fin is constructed with a leading-edge structure/spare that supports a flexible fin film material consisting of PVC film of uniform thickness, with a flapping fin frequency of 1.1Hz and a maximum speed of 1.783 BL/s. The replaced servomechanism was clamped above the water while the fin was flapping near the water surface to measure thrust created by a single fin. However, the effect of the water surface and the movement of the separated actuator may not be consistent with the robot manta ray, and the thrust performance of a Robo manta ray has not been evaluated using this measurement setup.

Batoids achieve extraordinary mobility and propulsive performance thanks to their huge pectoral fins. The robot is made to move in an undulatory rajiform pattern. Because of its full autonomy, extended battery life, and wireless recharging capabilities, the design is under-actuated, simple, and sturdy, making it ideal for propulsive performance investigations. The robot has an overall length of 180 mm with a top speed of 0.93 body length per second [23]. Based on the experimental results, both thrust and side forces are found to rise as flapping frequency and amplitude increase, but frequency effects are more obvious. The proposed robot designs greatest swimming speed is close to 1 BL/s. For the identical input parameters, side forces were greater than thrust forces for the geometry and swimming mode matched by the design [23].

III. Methodology

Fig. 1 shows the schematic wiring diagram for controlling SRob. SRob has been equipped with various components, including 6 servo motors, an ADXL335 3-axis accelerometer, 2 Lipo batteries, an ESP01 WiFi module, and an Arduino Mega, to achieve the desired movement and speed. On the hardware development side, AutoCAD 2017 was used to create the 3D design, while Fritzing was used to create the wire diagrams for the control system. The servo motor consists of three colors of wire that the black wire connects to the GND, the white or yellow wire connects to the pin and the red wire connects to the power supply. The servo motor requires a voltage of around 4.8V-6.0V. The speed of the servo motor stays 0.14sec / 60 degrees for 4.8V and 0.12sec / 60 degrees for 6.0V. ADXL335 is an accelerometer sensor that works based on the principle of Piezoelectric effect. Each time the sensor is tilted, the ball will move in that direction due to the force of gravity. The wall is made of Piezoelectric elements and if every time the ball touches the wall, an electric current will be generated which will be interpreted in the form of a value in any 3D space. In addition, the ADXL335 will provide acceleration values on three axes and will provide three output values. The bandwidth of this sensor is adjustable as it has a single capacitor per axis. Analog interfaces are made to communicate with other devices such as Arduino. This accelerometer sensor requires a voltage of around 1.8 V to 3.6 V.

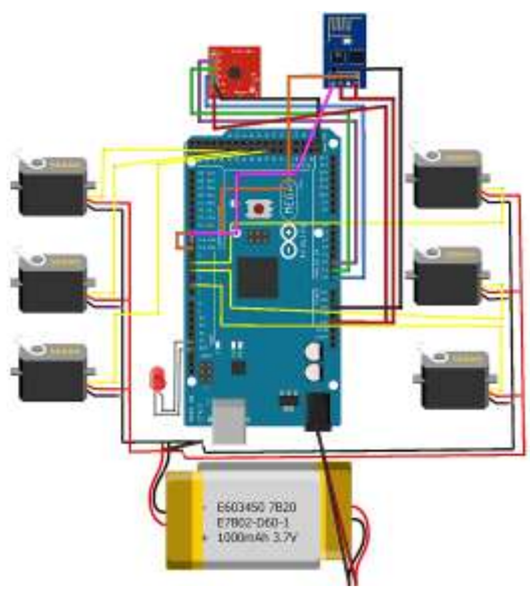

Fig. 1. Schematic Wiring Diagram.

Serving as the brain for the SRob, the Arduino Mega 2560 is one of the microcontroller boards used to control the movement of the swimming robot. This microcontroller has 54 digital input and output pins where 15 pins can be used as PWM output. The ESP01 Wi-Fi module is a complete and standalone solution for Wi-Fi networks that can carry application services and connect SRob to the internet. This Wi-Fi module is very important making the SRob can be controlled remotely and wirelessly. This feature makes it easier for the operator to control the movement of the SRob effectively without having to be in a hazardous environment. The ESP8266 high frequency clock is used to drive two Tx and Rx mixers provided by the internal oscillator and the external oscillator. The frequency of the floating crystal is 26MHz to 52MHz. The ESP01 Wi-Fi module requires a 3.3V power supply and an ambient temperature of 25 degrees Celsius. Then, from the internet cloud, SRob will be connected directly to the RemoteXY application which serves as a remote control to navigate SRob from a smartphone. The control process starts from the power source which is the Lipo battery which will activate the microcontroller, sensor, and actuator. Then, the accelerometer will calculate the exact body force and angular rate so that the exact position of the SRob can be determined. Finally, the servo motor will be activated and will operate according to the instructions from the remote control whether moving forward, turning right, left, or turning 360 degrees.

IV. Control System

Fig. 2 shows the 3D design of the SRob. Each side of the main body is fitted with three servo motors that are used to generate thrust. These three servo motors have been set up to have different delays from each rotation and can produce large wave motion. Thus, this will allow the SRob to move forward or change direction turning to the right or left in a short time. The main body of the SRob is made of durable acrylic and has a specific weight that is suitable to make the SRob sink and float in water. This main body houses all the components including the Arduino Mega, ADXL335 accelerometer-3axis, Lipo battery, and ESP01 WiFi module. The pectoral fin material must be flexible and waterproof so that swimming movements can be produced smoothly. The height of the robot manta ray is 6 cm, width and length are 80 cm and 30 cm, respectively.

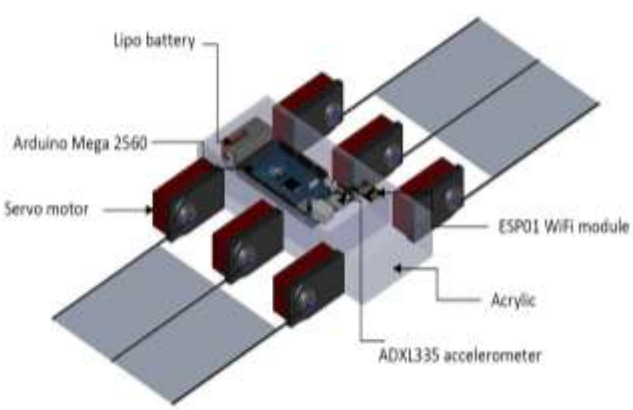

Fig. 2. 3D Design of the SRob.

Fig. 3 shows the flowchart of the SRob control system. After connecting all the parts together, the RemoteXY app must be connected to the Arduino Mega using WiFi to control all the servo motors. After that, the SRob can be activated on the smartphone, and at the same time, the accelerometer sensor will measure and calculate the axial position of the SRob. This will help the operator to know the initial position of the SRob before any operation is carried out. To control the movement of the SRob, there are five different types of modes have been set. The first mode is a command for the robot to stop. When the *A* button is pressed on the remote control using the RemoteXY application on the smartphone, all servo motors will turn off. The second mode is to move forward. When button *B* is pressed, all servo motors will be turned on and thrust will be generated making the SRob move forward. The third mode is to move forward to the right. When the *C* button is pressed, all servo motors on the right will be turned off causing only the left side to produce movement. The fourth mode is to move forward to the left. The same command as to the right is used but only the servo motor on the left will be turned off while the servo motor on the right will be turned on. Lastly is the fifth mode which is a 360˚ rotation round. When the *E* button is pressed, each side of the servo motor will produce the opposite direction so that the SRob can rotate up to 360˚.

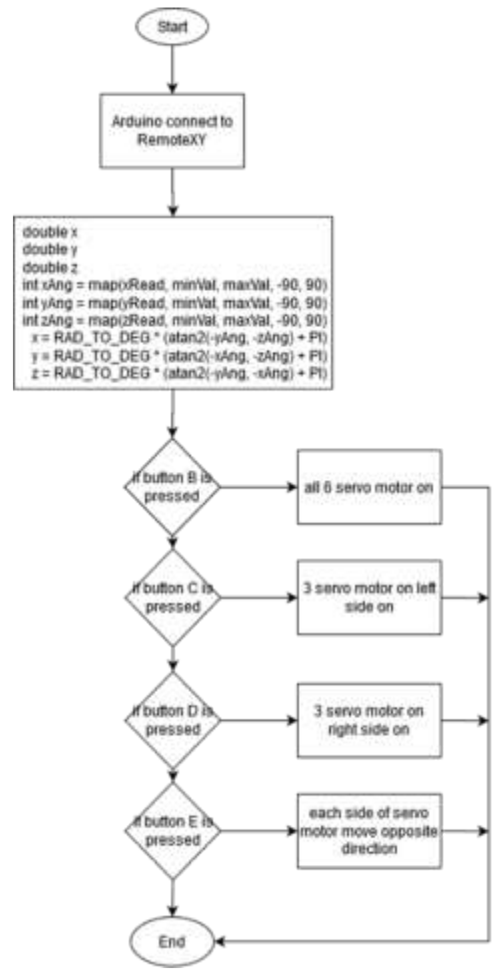

Fig. 3. Flowchart of the Swimming Robot (SRob) Control System.

V. RESULT AND DISCUSSION

Fig. 4 shows the speed of the SRob against time. From this graph, SRob takes 10 seconds to move forward 2 m in the pool. The maximum speed that can be reached by the prototype is 20 m/s and takes 1 second to reach the maximum speed. Based on the graph, the data shows that the time increases when the speed reaches 1 second and remains the same up to 10 seconds. Fig. 5 shows the flapping motion angle relative to the time for moving forward produced by 6 servo motors. The angle for the servo motor to operate is between 70˚ to 110˚, while the difference value between the initial angle and the final angle is 40˚. According to the findings of the research, improper angles result in imbalanced speed and movement. As a result, a 40-degree angle was set on the microcontroller to achieve maximum speed and smooth movement. Based on this graph it is also found that the servo motor takes 0.75 seconds to complete one cycle.

Fig. 6 shows the flapping motion angle relative to the time to move to the right. The three straight lines in this graph indicate the 3 servo motors on the right that are not energized while the three sinusoidal lines are the three servo motors that are energized on the left side of the SRob. When the *C* button is pressed, servo motor 1, 2 and 3 on the left will be actuated while the other servo motors are not activated. The graph also shows that a servo motor takes 0.45 seconds to complete one cycle compared to 0.75 seconds found in Fig. 5. This function is important to ensure that the SRob can turn right or left faster. Fig. 7 shows the flapping motion angle relative to the time to move to the left. This graph, like the method of turning to the right, includes three straight lines indicating that the three servo motors on the left are not powered and three sinusoidal lines indicating that the three servo motors on the right are energized. When the *D* button is pressed, the servo motor 4, 5 and 6 on the right will be actuated while the other servo motors are not energized.

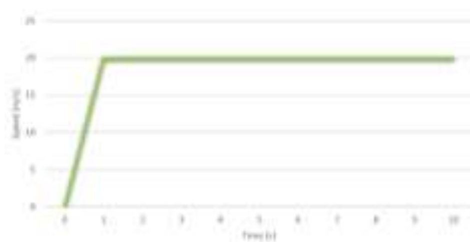

Fig. 4. Speed of the SRob vs Time.

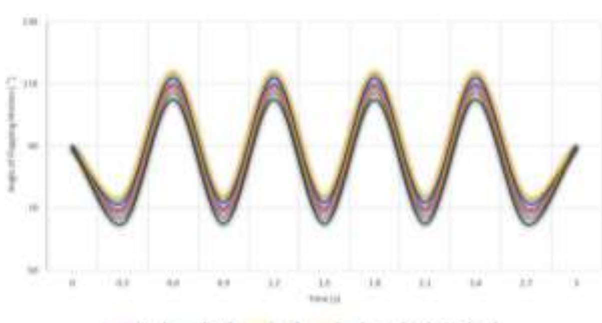

Fig. 5. Angle of Flapping Motion vs Time for Moving Forward.

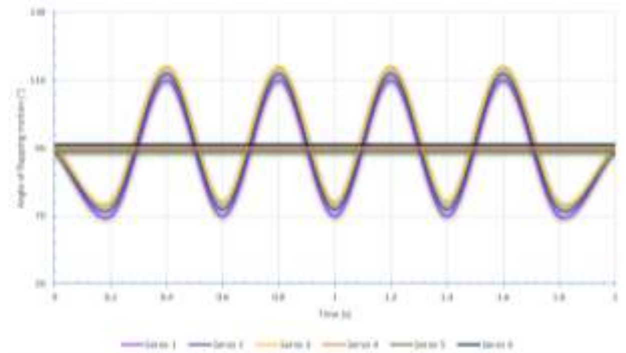

Fig. 6. Flapping Motion Angle Relative to the Time to Move to the Right.

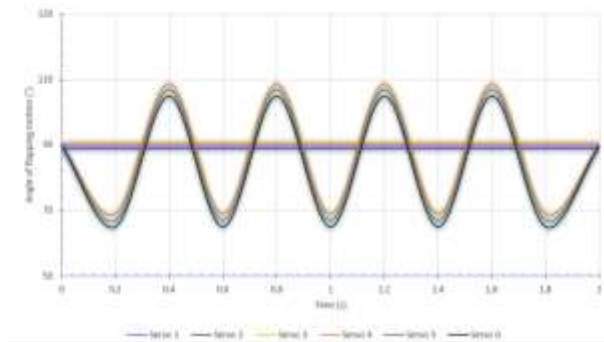

Fig. 7. Flapping Motion Angle Relative to the Time to Move to the Left.

Fig. 8 shows the flapping motion angle relative to the time to rotate 360˚. There are two sinusoidal graphs representing each servo motor for the SRob. To ensure that the SRob can rotate 360˚, the initial angle of the three servo motors on the right is set to 110˚, while the initial angle of the three servo motors on the left is set to 70˚. When the *E* button is pressed, the three servo motors on the right will undulate from 70˚ to 110˚ while the three servo motors on the left will undulate from 110˚ to 70˚. As a result, by setting the angle accurately, it will produce two sinusoidal graphs, and the SRob will be able to rotate at a fast and effective rate. Data for the position of the SRob were taken using an ADXL335 accelerometer sensor placed on the main body on the flat surface. Data is collected when the SRob is connected to WiFi using the ESP01 WiFi module. Due to the water vibration caused by the servo motor, the data for the x-axis and y-axis showed tiny difference values during the testing, whereas the z-axis had large values.

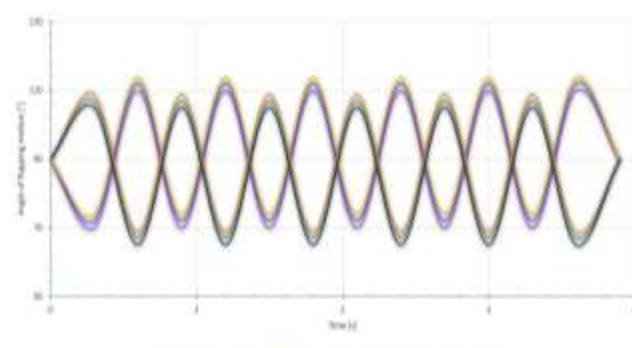

Fig. 8. Flapping Motion Angle Relative to the Time to Rotate 360˚.

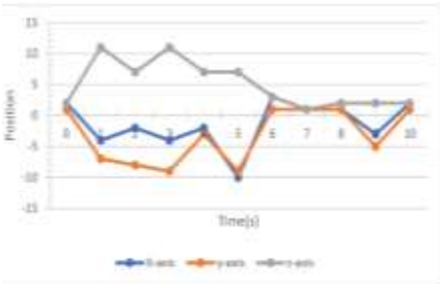

(a) Moving Forward.

(b) Turning to Right.

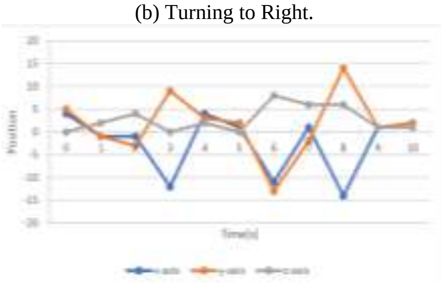

(c) Turning to Left.

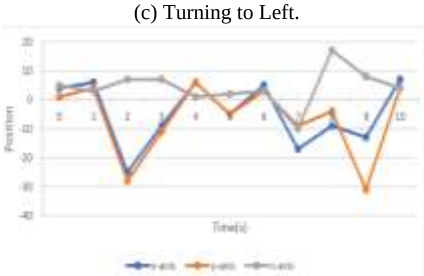

(d) Rotate 360˚.

Fig. 9. SRob Position Graphs for x-axis, y-axis, and z-axis vs Time.

Fig. 9 shows the SRob position graphs for x-axis, y-axis, and z-axis vs time for (a) moving forward, (b) turning to right, (c) turning to left, and (d) rotate 360˚. For the forward motion test, from 0 seconds to 6 seconds, there was a very large degree difference between the 3 axes. At 10 seconds, the positions of the SRob on the x-axis, y-axis and z-axis were 2˚, 1˚ and 2˚, respectively. As the SRob moves to the right, from the 8th to the 10th second, there is a very large difference of degree between the three axes. At 10 seconds, the positions of SRob on the x-axis, y-axis and z-axis were at 17˚, 21˚ and 4˚, respectively.

Then, when the SRob moves to the left, starting at the 2nd to 9th second, there is a large degree of difference between the three axes. At 10 seconds, the positions of SRob on the x-axis, y-axis and z-axis were at 1˚, 2˚ and 1˚, respectively. Finally, for a 360˚ rotation, from the 1st second to the 4th second and from the 7th second to the 10th second, there is a very large degree of difference between the three axes. At 10 seconds, the positions of SRob on the x-axis, y-axis and z-axis were at 7˚, 4˚ and 4˚, respectively. From the observations during the experiments performed, due to the water vibration caused by the servo motors, the data for the x-axis and y-axis show small difference values during the testing, whereas the z-axis has large difference values.

VI. Conclusion

The development of a low-cost bio-inspired swimming robot (SRob) with IoT can be summarized as follows. The first objective of this study is to develop the SRob swimming robot using Arduino and WiFi modules. The inexpensive and compact prototype has been successfully developed using a durable acrylic material and equipped with several essential components such as an Arduino Mega, six servo motors, a WiFi module, and an accelerometer sensor. Then, to control and monitor the SRob, the RemoteXY app was used on the smartphone as a remote control for the SRob. With this IoT feature, operator can control the SRob easily without having to be in a dangerous area. From the experimental results, it can be concluded that the z-axis has a small difference value of only 4˚ compared to the x-axis and y-axis, which have a big degree difference of 17˚ and 21˚, respectively. By using an accelerometer sensor, the position and condition of the SRob can be determined effectively. Finally, the rotational angle range of the servo motor for fluctuate is between 70˚ and 110˚ and the maximum speed of the SRob that can be achieved is 20 m/s. The soft fins' material characterization and design will be the subject of future research. Maneuverability will also be examined further. Furthermore, multiple navigation algorithms will be used to further investigate autonomy.

Acknowledgment

The authors gratefully acknowledge to the Ministry of Higher Education (MoHE) Malaysia for financial supports given under the Fundamental Research Grant Scheme (FRGS/1/2019/TK04/UNIKL/02/11).

References

[1] S. Jeelani, A. Dany, B. Anand, S. Vandana, T. Maheswaran, and E. Rajkumar, "Robotics and medicine: A scientific rainbow in hospital," Journal of pharmacy & bioallied sciences, 2015, 7(Suppl 2), S381–S383.

[2] M. Aliff, F. Danieal, M. F. Mohamed, A. 'Athif, T. Akagi, and N. Samsiah, "Development of Flexible Pneumatic Rehabilitation Actuator for Knee Injury," TEST Engineering & Management, 83, 2020, pp. 12849 – 12855.

[3] H. Obayashi, T. Akagi, S. Dohta, W. Kobayashi, Y. Matsui, S. Shimooka, T. Shinohara, and M. Aliff, "Development of Portable Rehabilitation Device Driven by Low-Cost Servo Valve Using Tap Water," International Journal of Mechanical Engineering and Robotics Research, 9(3), 2020, pp. 353 – 359.

[4] M. Aliff, M. A. Dinie, I. Yusof, and N. Samsiah, "Development of Smart Glove Rehabilitation Device (SGRD) for Parkinson's Disease," International Journal of Innovative Technology and Exploring Engineering (IJITEE), 9(2), 2019, pp. 4512 – 4518.

[5] M. Aliff and N. Samsiah Sani, "Robot Arm Analysis based on Master Device Pneumatic Actuators," International Journal of Advanced Computer Science and Applications (IJACSA), 10(8), 2019, pp. 199 – 204.

[6] M. Aliff, S. Dohta, and T. Akagi, "Control and analysis of simple-structured robot arm using flexible pneumatic cylinders," International Journal of Advanced and Applied Sciences, 4(12), 2017, pp. 151-157.

[7] M. Aliff, S. Dohta, and T. Akagi, "Simple Trajectory Control Method of Robot Arm Using Flexible Pneumatic Cylinders," Journal of Robotics and Mechatronics, 27 (6), 2015, pp. 698-705.

[8] M. Aliff, I. S. Amry, M. I. Yusof, A. Zainal, A. Rohanim, and N. S. Sani, "Development of Smart Rescue Robot with Image Processing (iROB-IP)," International Journal of Electrical Engineering and Technology, 11(9), 2020, pp. 08-19.

[9] M. Aliff, N. Firdaus, N. Rosli, M. I. Yusof, N. Samsiah, and S. Effendy, "Remotely Operated Unmanned Underwater Vehicle for Inspection," International Journal of Innovative Technology and Exploring Engineering (IJITEE), 9(2), 2019, pp. 4644 – 4649.

[10] M. Aliff, N. S. Sani, M. I. Yusof, and A. Zainal, "Development of Fire Fighting Robot (QRob)," International Journal of Advanced Computer Science and Applications (IJACSA), 10(1), 2019, pp. 142 – 147.

[11] C. P. Day, "Robotics in Industry—Their Role in Intelligent Manufacturing," Engineering, 4(4), pp. 440-445.

[12] M. Aliff, A. H. Hamdi, I. Yusof, and N. Samsiah, "Development of Control System for Dual NC Machine with Single 6-Axis Robot," International Journal of Innovative Technology and Exploring Engineering (IJITEE), 9(2), 2019, pp. 4505 – 4511.

[13] G. Li, Y. Deng, O. L. Osen, S. Bi, and H. Zhang, "A bio-inspired swimming robot for marine aquaculture applications: From concept-design to simulation," OCEANS 2016 - Shanghai, 2016, pp. 1-7.

[14] Q. Shi, H. Ishii, Y. Sugahara, A. Takanishi, Q. Huang, and T. Fukuda, "Design and Control of a Biomimetic Robotic Rat for Interaction With Laboratory Rats," IEEE/ASME Transactions on Mechatronics, vol. 20, no. 4, 2015, pp. 1832-1842.

[15] J. Yu, C. Zhang, and L. Liu, "Design and Control of a Single-Motor-Actuated Robotic Fish Capable of Fast Swimming and Maneuverability," IEEE/ASME Transactions on Mechatronics, vol. 21, no. 3, 2016, pp. 1711-1719.

[16] M. Hassanalian, H. Abdelmoula, S. Mohammadi, S. Bakhtiyarov, J. Goerlich, and U. Javed, "Aquatic animal colors and skin temperature: Biology's selection for reducing oceanic dolphin's skin friction drag," Journal of Thermal Biology, vol. 84, 2019, pp. 292-310.

[17] Y. Zhang, S. Wang, X. Wang, and Y. Geng, "Design and Control of Bionic Manta Ray Robot With Flexible Pectoral Fin," IEEE 14th International Conference on Control and Automation, pp. 1034- 1039.

[18] P. V. y Alvarado, S. Chin, W. Larson, A. Mazumdar, and K. Youcef Toumi, "A soft body under-actuated approach to multi degree of freedom biomimetic robots: A stingray example," in Biomedical Robotics and Biomechatronics (BioRob), 2010 3rd IEEE RAS and EMBS International Conference on, pp. 473–478.

[19] P. V. y Alvarado, "Hydrodynamic performance of a soft body underactuated batoid robot," in Robotics and Biomimetics (ROBIO), 2011 IEEE International Conference on, pp. 1712–1717.

[20] A. Cloitre, V. Subramaniam, N. Patrikalakis, and P. V. y Alvarado, "Design and control of a field deployable batoid robot," in Biomedical Robotics and Biomechatronics (BioRob), 2012 4th IEEE RAS & EMBS International Conference on, pp. 707–712.

[21] K. S. Sekar, M. Triantafyllou, and P. y Valdivia y Alvarado, "Flapping actuator inspired by lepidotrichia of ray-finned fishes," in Intelligent Robots and Systems (IROS 2014), 2014 IEEE/RSJ International Conference on, pp. 1120–1126.

[22] C. M. Chew, Q. Y. Lim, and K. S. Yeo, "Development of propulsion mechanism for Robot Manta Ray," in Robotics and Biomimetics (ROBIO), 2015 IEEE International Conference on, pp. 1918–1923.

[23] T. V. Truong, V. K. Viswanathan, V. S. Joseph and P. V. y. Alvarado, "Design and Characterization of a Fully Autonomous Under-actuated Soft Batoid-like Robot," 2019 IEEE/RSJ International Conference on Intelligent Robots and Systems (IROS), 2019, pp. 5826-5831.

Multicriteria Handover Management by the SDN Controller-based Fussy AHP and VIKOR Methods

Najib Mouhassine[1], Mohamed Moughit[3]
LaSTI Laboratory, National School of Applied Sciences
Sultan Moulay Slimane University
Khouribga, Morocco

Mostapha Badri[2]
MASI Laboratory,Polydisciplinary Faculty of Nador
Mohammed first university
Oujda,Morocco

***Abstract*—A wireless environment is characterized by its dynamic nature, inherent uncertainty, and imprecise parameters and constraints. Network settings such as speed, RSS, network delays, etc. are inherently imprecise. Due to this vagueness, accurately measuring these network parameters in a wireless environment is a difficult task. As a result, a fuzzy logic approach appears to work best when used to design systems in such environments. Although conventional techniques based on precise values can be used to reduce transmission delay, they cannot produce intelligent and efficient transfer decisions that take into account all the constraints of the network. Thus, using one criterion only can lead to service disruption, unbalanced network load, and inefficient handoff. Therefore, to guide the Horizontal handover process in wireless networks towards making a better choice for VoIP in congested environments, we propose the integration of the Fuzzy-AHP and VIKOR method in SDN (Software Defined Networking) controller on several criteria (the signal-to-noise ratio plus interference (SNIR), packet loss, jitter, delay, throughput). However, the results of this work show that our contribution maintains a good quality of service for real-time applications.**

Keywords—SDN; QoS; WLAN; Handover; F-AHP; VIKOR

I. Introduction

In an uncertain environment, multi-criteria decision-making methods (MADM) consist of constructing a Global Preference Relation (optimal choice) for a set of alternatives (set of choices) evaluated by several criteria.

Each decision-making problem has several alternatives that a decision-maker tries to filter or classify in a decision-making process, also the attributes are essentially the criteria used to evaluate the alternatives. These attributes are grouped into attributes of cost and other benefits or risk. For example, mobile communication with a less noisy channel is advantageous, while the number of subscribers has a cost.

Each attribute can have its unit. The normalization is necessary to eliminate the effect of the different units; it consists of transforming the values of the alternatives into a scale included in the interval [0 1]. To reflect the importance of the attributes, they are assigned a weighting factor either by the decision-maker or calculated with a mathematical method.

MADM Problems can be formalized in matrix or vector form, where the columns and rows present the attributes (criteria) and the alternatives (choices). The elements of the matrix present the evaluation of the performance of the alternative against the attribute. For example, in the advantage attribute group (less noisy channel) alternatives with a higher score are preferred. In contrast, the cost attribute group (number of subscribers) alternatives with a low score are optimal.

In this work the F-AHP method presents the importance of each criterion over the other with the elements of the pairwise comparison matrix. After fuzzification and defuzzification come to assign a weight to each criterion.

Subsequently builds the selection matrix with the VIKORE method where the columns denote the weights of the criteria and the rows the choices (access point). Then calculate a coefficient which is used to classify the access points in order of importance. The values of the matrix are collected from OpenFlow access points in direct connection with the SDN controller.

Based on this classification made by the SDN controller, a message containing the order of priority is sent to the mobile which requests the change of the access point. The latter proceeds to trigger the Handover towards the right choice. Hence, this work is an improvement to our contribution [1].

II. Background

The mathematical methods of multicriteria analysis can be grouped into two approaches:

A. *The Scalar Methods*

- Simple Additive Weighting method (SAW) [2].

Consists of weighting the different criteria of the multi-criteria decision problem with real numbers called weights which represent the importance of each criterion in the decision process. Once the importance of the different criteria is quantified, the method chooses the action that minimizes or maximizes the weighted sum of the criteria.

Mathematical formulation:

Starting data

m actions $A_1, A_2, A_3 ... A_m$.

n criteria $C_1, C_2, C_3 ... C_n$.

Weight vector $(W_1, W_2, ..., W_n)$ et $W_j > 0$.

$a_{ij} = U_{ij}(A_i)$, Quotient cardinal utility function. Represents the performance of each action on each of the criteria.

Data transformation:

1) Normalization of aij.
2) Normalization of the weights.
3) Implementation of the weighted sum method (1).

$$R(a_i) = \sum_{j=1}^{n} w_j a_{ij} \;\; \forall i \in [1, m] \tag{1}$$

Single criterion for any action i.

- Weighted Product Mode (WPM) [2].

Similar to SAW, also called exponent weighting, the main difference is that we will have a multiplication instead of the addition. It allows comparing alternatives against several criteria. This comparison is made by dividing the values of all criteria by one of them and then multiplying those ratios. Each ratio is raised to the exponent equivalent to the weight of the corresponding criterion.

Mathematical formulation (2):

$$P\left(\frac{A_k}{A_L}\right) = \prod_{j=1}^{N} \left(\frac{a_{kj}}{a_{Lj}}\right)^{w_j} \quad k, L = 12,3, \dots \tag{2}$$

Where N represents the number of criteria.

m the number of actions (or alternatives).

wj the weight of criterion j.

$\mathbf{A_k}$ and $\mathbf{A_L}$ two alternatives to compare.

$\mathbf{a_{Kj}}$ and $\mathbf{a_{Lj}}$ the weights of the alternative A_k and A_L

Compared to criterion j.

We can also calculate the overall weight of an alternative by the following formula (3):

$$P(A_k) = \prod_{j=1}^{N} (a_{kj})^{w_j} \; k = 1,2, \dots m \tag{3}$$

- Method of Weighted Metrics (MWM).

Selects a vector of criteria that minimizes the distance to a reference solution R = (R_1, ..., R_k). The vector R is either the ideal point or the reference solution fixed by the decision-maker according to its preferences.

- Analytic Hierarchy Process (AHP) [3].

Allows calculating an aggregate synthetic score based on a ranking and weighting of all the criteria considered in the decision. It consists of four stages:

1) Establish the hierarchy of criteria and alternatives.
2) Perform pairwise comparisons of the criteria, and estimate the weights of the criteria and the relative performance values of the alternatives concerning each criterion.
3) Aggregate the weights and performance values for the alternative priority.
4) Check the consistency of judgments to verify the result

The limitation of this method is the instability of the classification of the different alternatives if the problem to be treated contains a large number of alternatives.

- Analytical Network Process (ANP) [4].

It is an extension of the AHP and allows the consideration of the interdependence among and between the levels of criteria and alternatives.

- Multi Attribute Utility Theory (M.A.U.T) [5].

Method developed in the late 1960s by Ralph Keeney and Howard Raiffa attempting to modelize the preferences of the decision-maker by a so-called utility function using different mathematical tools. These methods are often of the aggregation type, in the sense that the resulting utility function is often an aggregation of several "sub-functions," which can be the objective functions of each criterion or a combination of two or more of them.

- The Technique for the Order of Preference by Similarity of Ideal Solution (TOPSIS) [6].

This technique proposed by [Yoon and Hwang, 1981] allows choosing the best solution which maximizes the profit criteria and minimizes the cost criteria. Firstly, it aims to reduce the number of disambiguation scenarios by discarding the dominated scenarios and, secondly, to rank the effective scenarios according to their calculated overall scores.

TOPSIS can sometimes be used to replace AHP in the process of ranking alternatives. In other words, it often happens that the AHP is used to assign the weight of the selection criteria while the TOPSIS is applied to prioritize the selection alternatives.

B. Ranking Methods

- Elimination And Choice Translating Reality (ELECTRE I) [7].

This method of Bernard Roy, allows a partial aggregation through the construction of comparison relations of the performances for each pair of solutions.

- Preference Ranking Organization METHod for Enrichment Evaluations (PROMETHEE) [8].

Consists of establishing a process of numerical comparison of each action in relation to all the other actions. Thus it is possible to calculate the plus or minus optimal of each action compared to all the others. The result of this comparison allows the orderly classification of the actions.

- VIKOR (VIsekriterijumska optimizacija i KOmpromisno Resenje) [9].

Multicriteria optimization and compromise solution: It is a ranking method for a finite set of alternatives and allows solving a discrete multicriteria problem with non-commensurable (different units) and contradictory criteria.

III. Related Work

In the context of our research, we can separate the work due to improving the Handover in three parts:

A. Multi-Criteria or Multi-Attribute Decision-Making Algorithms (MCDM)

R.Bikmukhamedov et al [10] evaluated the performances of SAW, GRA (Gray relational analysis) [11], TOPSIS and VIKOR algorithms, and they showed by simulations for the same criteria (RSSI, Available Bitrate and Cost) that VIKOR and GRA are optimal.

The VIKOR method was developed under the name Dynamic VIKOR (D-VIKOR) by Xiaohong Li et al [12], it reduces time complexity by frequently evaluating dynamic attributes. This helps to minimize the Handover delay, otherwise the execution time.

K. savita et al [2], carried out a comparative study between the two methods WPM and SAW for the attributes: delay, jitter and cost, to choose the best wireless network that offers minimal transmission delay. Without results, the judgment postulated on the performance of the WPM method remains useless.

M.Alhabo et al [13], propose two modified TOPSIS methods to reduce the number of unnecessary handovers and radio link failure, plus improving the average throughput for each user. One integrates the entropy weighting of metrics (PE-TOPSIS), and the other integrates the weighting of the standard deviation (PSD-TOPSIS) to note the importance of each criterion (here the angle of movement, time of stay, the signal-to-noise ratio plus interference). The simulation is done with a constant mobility speed and random deviation angles. The results are evaluated in terms of the number of handovers, radio link failures, and average user throughput compared to the two network-controlled methods Handover and TOPSIS.

Another implementation of TOPSIS was carried out by R.Abdullah and Z.Zukarnain [14], to select the most relevant wireless access technology (LTE, WiMAX, WLAN). Three types of priority are defined, namely equal priority, Mobile priority and Network priority. The simulation results prove that the network priority is better than the two other.

B. The Fuzzy Logic Theory

Network parameters such as delay, jitter, noise, effective throughput, etc. are generally imprecise and unpredictable, measurements are approximate and probabilistic. Therefore, fuzzy logic allows us to model this imprecision for each parameter by linguistic variables, that each variable corresponds to a membership function having a value in the interval [0,1].

Implementation of fuzzy logic made by A.Sadik et al. [15], aims to choose the best AP (access point) and reduce the handover delay. They chose the RSSI and the direction from the mobile node to the AP as selection criteria.

The classification of the network for the desired application according to user preferences and also network parameters has been the research objectives of M. Krichna et al. [16]. The chosen method uses the concept of fuzzy logic in three steps, the first is the initiation phase of the Handover based on two parameters, QoS and the power of the signal (RSS), which are the inputs of FIS (Fuzzy Inference System) mamdani, the second is the preselecting phase which takes into account the speed of mobility and user preferences, finally the classification of WLAN, WIMAX and cellular networks based on the type of application chosen.

M.sharma [17], had also introduced fuzzy logic (criterion: RSS, Bandwidth, Users Preference) to trigger the Handover towards choosing the optimal network between WLAN and WWAN.

C. Fuzzy Logic Combined with MCDM Algorithms

In heterogeneous wireless networks, mobile equipment is equipped with various wireless access technologies, to allow it to intelligently choose the one that offers the best quality of communication. F.kaleem et al. [18], has just proposed a combined technique in two steps. The first consists of estimating the need to trigger the Handover towards another technology based on the fuzzy multicriteria decision. The second is the selection of a target PoA (Point-of-Attachment) based on ranking algorithms, namely TOPSIS with AHP weighting, TOPSIS with F-AHP (Fuzzy AHP) weighting and FTOPSIS (fuzzy TOPSIS). The fuzzy system input parameters are, predicted RSS, mobility speed, the distance between mobile stations and PoA, and degree of QoS. the output of the system is the Vertical Handover Factor. The degree of QoS is calculated according to the class traffic type requirements currently used. According to the network parameters, the weights assigned to each class are calculated with the AHP or Fuzzy AHP method (throughput, jitter, delay, and packet loss rate).

M.Alkhawlani et al. [19], implemented a decision-making system based on the combination of fuzzy logic and TOPSIS, for the choice between three types of networks.

To remove the ambiguity, the criteria present the input of the fuzzy logic system. At the same time, the outputs of the latter, are the inputs of the MCDM TOPSIS system, which allows after construction of the decision matrix, weighting and determination of the best and worst value for each attribute by the max-min-distance method, to select the network that offers an optimal solution. The results are compared to each criterion with the proposed system.

S. Zhang et al. [20], had suggested the Fuzzy GRA method for solving multicriteria problems. Fuzzy numbers are defined in triangular value intervals, criteria weighting and selection are calculated by the GRA method.

In most research, the criteria weighting step is done with the AHP method or its Fuzzy-AHP Enhanced Version to determine the importance of each attribute. Drissi et al [21], evaluated the performance of the F-AHP method compared to AHP for different decision algorithms (MEW, SAW, VIKOR, TOPSIS) and different types of traffic. The results show better QoS by combining F-AHP with the VIKOR method.

IV. Problem Statement and Proposed Model

According to the comparison of previous research focused on maintaining a good quality of service in wireless networks, the rest of this article proposes the management of multicriteria handover by the SDN controller based on the F-AHP and VIKOR. The problem can be formalized as described in "Fig. 1", where each access point calculates its parameters and sends them to the controller, which ranks them in order of QoS priority.

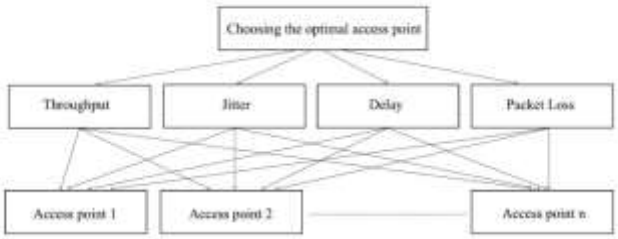

Fig. 1. The Graphical Formalism of the Problem.

The solution of the problem is divided into two stages:

A. *Weighting of Criteria by the F-AHP Method*

1) Creation of the pairwise comparison matrix "Table I": The weighting vectors give more importance to the delays then the jitter and finally the loss of the packets, the throughput in the case of VoIP is not so important because the packets are small and can be transmitted at a low rate.

2) Fuzzification "Table II": creation of the fuzzy AHP pairwise comparison matrix.

The fuzzy geometric mean value "Table III" is calculated by this formula (4) (Buckley 1985) [22].

$$r_i = \left(\prod_{j=1}^{n} a_{ij}\right)^{1/n} \tag{4}$$

Product of two fuzzy numbers.

$$\widetilde{A}_1 \otimes \widetilde{A}_2 = (l_1, m_1, U_1) \otimes (L_2, m_2, U_2)$$

$$= (l_1 * l_2, m_1 * m_2, U_1 * U_2)$$

Criteria matrix $\bar{A} = [a_{ij}]$

TABLE I. PAIRWISE COMPARISON MATRIX

Conversation	Packet Loss	Delay	Jitter	Throughput
Packet Loss	1	1/7	1/5	3
Delay	7	1	1/3	7
Jitter	5	3	1	7
Throughput	1/3	1/7	1/7	1

TABLE II. FUZZY AHP PAIRWISE COMPARISON MATRIX

Conversation	Packet Loss	Delay	Jitter	Throughput
Packet Loss	(1,1,1)	(1/8,1/7,1/6)	(1/6,1/5,1/4)	(2,3,4)
Delay	(6,7,8)	(1,1,1)	(1/4,1/3,1/2)	(6,7,8)
Jitter	(4,5,6)	(2,3,4)	(1,1,1)	(6,7,8)
Throughput	(1/4,1/3,1/2)	(1/8,1/7,1/6)	(1/8,1/7,1/6)	(1,1,1)

TABLE III. FUZZY GEOMETRIC MEAN VALUE RI

Conversation	r_i value
Packet Loss	(0.45, 0.54, 0.64)
Delay	(1.73, 2.01, 2.38)
Jitter	(2.63, 3.20, 3.72)
Throughput	(0.70, 0.29, 0.34)

This formula (5) calculates the fuzzy weights for each criterion "Table IV".

$$W_i = r_i \otimes (r_1 \oplus r_2 \oplus \dots \oplus r_n)^{-1} \tag{5}$$

Sum of two fuzzy numbers.

$$\widetilde{A}_1 \oplus \widetilde{A}_2 = (l_1, m_1, U_1) \oplus (L_2, m_2, U_2)$$

$$= (l_1 + l_2, m_1 + m_2, U_1 + U_2)$$

So

$(r_1 \oplus r_2 \oplus \dots \oplus r_n)$ = (0.45 +1.73 + 2.63 + 0.70, 0.54 + 2.01+ 3.20 + 0.29, 0.64 + 2.38+ 3.72+0.34)

= (5.51, 6.04, 7.08)

$$(r_1 \oplus r_2 \oplus \dots \oplus r_n)^{-1} = \left(\frac{1}{7.08}, \frac{1}{6.04}, \frac{1}{5.51}\right)$$

TABLE IV. FUZZY WEIGHTS FOR EACH CRITERIA

	Fuzzy geometric mean value r_i	Fuzzy weights W_i
Packet Loss	(0.45, 0.54, 0.64)	(0.064, 0.089, 0.12)
Delay	(1.73, 2.01, 2.38)	(0.244, 0.332, 0.431)
Jitter	(2.63, 3.20, 3.72)	(0.371,0.530, 0.675)
Throughput	(0.70, 0.29, 0.34)	(0.099, 0.048, 0.062)

3) Defuzzification to get crisp numerical values "Table V": The defuzzification method used here is center of area (CoA) (6).

$$w_i = \left(\frac{l+m+u}{3}\right) \tag{6}$$

TABLE V. CRISP NUMERICAL VALUES

	Weight w_i	Normalised weight
Packet Loss	0.137	$\frac{0.137}{1.068} = 0{,}128$
Delay	0.336	$\frac{0.336}{1.068} = 0{,}315$
Jitter	0.525	$\frac{0.525}{1.068} = 0{,}492$
Throughput	0.070	$\frac{0.070}{1.068} = 0{,}065$
Sum	1.068 >1	1

B. *Access Points Classification by VIKOR Method*

1st step: find the best "x_i^+" (7) and the worst "x_i^-" (8) value for each criteria j = 1, 2, …, n "Table VI".

$$x_i^+ = \{(\max(n_{ij})|j \subset M_p)\ ;\ \{(\min(n_{ij})|j \subset M_c)\} \quad i = 1,2, \cdots m \tag{7}$$

$$x_i^- = \{(\min(n_{ij})|j \subset M_p)\ ;\ \{(\max(n_{ij})|j \subset M_c)\} \quad i = 1,2, \cdots m \tag{8}$$

With i = 1,2, ⋯ m presents the alternatives (Access point).

Where Mp and Mc are the sets of performance and cost parameters, respectively.

2nd step: compute S_i (9) and R_i (10) value for each access point "Table VII".

$$S_i = \sum_{j=1}^{n} w_j \cdot \left(\frac{x_i^+ - x_{ij}}{x_i^+ - x_i^-}\right) \tag{9}$$

$$R_i = \max_j [\, w_j . \left(\frac{x_i^+ - x_{ij}}{x_i^+ - x_i^-}\right)] \tag{10}$$

"Table VIII" shows the values (S^*, R^*) and (S^-, R^-) which respectively present the minimum and maximum value of Si and Ri for each access point.

$S^* = \min_i S_i;\ R^* = \min_i R_i;$

$S^- = \max_i S_i;\ R^- = \max_i R_i.$

3rd step: compute Q_i value (11) "Table IX".

$$Q_i = \nu . \frac{S_i - S^*}{S^- - S^*} + (1-\nu) . \frac{R_i - R^*}{R^- - R^*} \tag{11}$$

where $\nu = 0,5$.

TABLE VI. BEST AND THE WORST VALUE FOR EACH CRITERION

Weight	0,128	0,315	0,492	0,065
Criteria	**Packet Loss**	**Delay**	**Jitter**	**Throughput**
AP1	0.01	150 ms	30 ms	20 Mb/s
AP2	0.03	100 ms	15 ms	15 Mb/s
AP3	0.02	250 ms	20 ms	10 Mb/s
Best (x_i^+)	0.01	100	15	20
Worst (x_i^-)	0.03	250	30	10

TABLE VII. S_i AND R_i VALUE FOR EACH ACCESS POINT

Weight	0,128	0,315	0,492	0,065	S_i	R_i
AP_1	0	0,105	0,492	0	0,597	0,492
AP_2	0,128	0	0	0,0325	0,1605	0,128
AP_3	0,064	0,315	0,164	0,065	0,608	0,315

TABLE VIII. (S* , R*) AND (S^-, R^-) VALUE FOR EACH ACCESS POINT

	S_i	R_i
AP_1	0,597	0,492
AP_2	0,1605	0,128
AP_3	0,608	0,315
S^* , R^*	0,1605	0,128
S^- , R^-	0,608	0,492

TABLE IX. COMPUTE QI VALUE

	S_i	R_i	Q_i	Rank base on Q_i
AP_1	0,597	0,492	0,988	3
AP_2	0,1605	0,128	0	1
AP_3	0,608	0,315	0,756	2
S^* , R^*	0,1605	0,128		
S^- , R^-	0,608	0,492		

Based on the calculated Qi values, the access points are ranked in order of QoS priority.

V. IMPLEMENTATION, SIMULATION AND RESULTS

Fig. 2 shows the algorithm implemented to manage Handover. The SDN controller periodically collects every 5 seconds the information from the access points namely jitter, delay, packet loss and Throughput, on which it calculates the order of QoS priority for each access point. A mobile that sees a SNIR value below the threshold sends a request to the controller, which responds with the list of access points already classified. The mobile connects to the access point which offers a good quality of service.

To evaluate our contribution, we tried to make a comparative study of two codecs G711 and G729, for a network architecture with SDN and other SDN based on F-AHP and VIKOR methods. The following "Table X" shows some characteristics of the two codecs.

TABLE X. CODECS CHARACTERISTICS

Codec	Bit Rate (Kbit/s)	Link Utilization (Kbit/s)	Delay (ms)	Loss(%)
G.711	**64**	**87.2**	**0.125**	**7-10**
G.729	**8.0**	**31.2**	**15**	**<2**

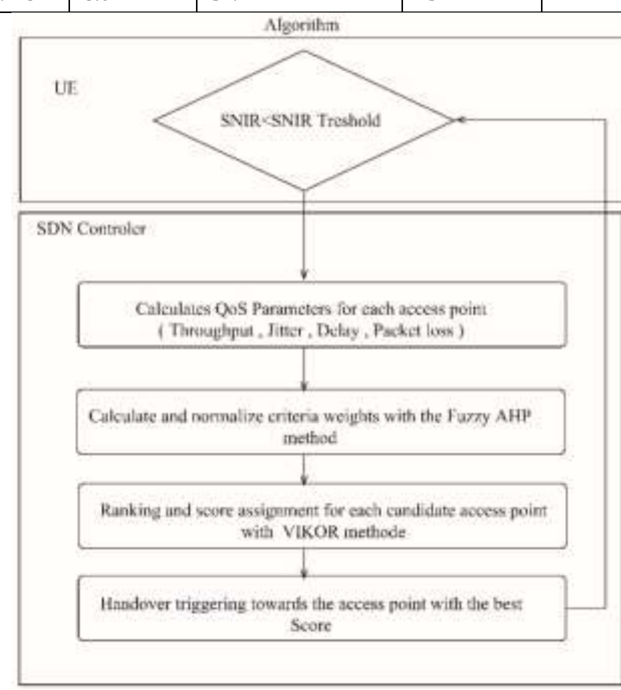

Fig. 2. The Proposed Model Flowchart.

Also, the simulation architecture "Fig. 3" is composed of three APs (access point) that support the OpenFlow v1.3 protocol; thus, an SDN controller and a VoIPStreaming server. More than 20 nodes follow linear mobility with variable speed, and communicate progressively over time with the server. The simulator chosen for this experiment is OMNeT ++ 5.5.1.

Our controller is configured to perform both functions, classification of access points according to QoS priority and switching. The simulations are repeated ten times per experiment, and the results illustrated below present their averages.

A. End-to-end Delay

The end-to-end delay represents the propagation delay plus the delay introduced by the equipment, also the coding, decoding and packing time.

The mobile no longer makes a blind choice without prior knowledge of the quality of service offered by the access points, the decision calculated and taken by the controller based on information collected periodically from them, then sent on request to the mobile. So, the time that will commit the motive for the calculation of the decision before the execution of the Handover is reduced. Also, the delay in processing packets by the access points is minimized. The controller is responsible for instructing the access points on how to route the packets to the recipient. This explains the results obtained "Fig. 4", where the end-to-end delay was significantly reduced for both codecs by implementing our solution. In the case of the G729, the delay no longer exceeds 100 ms. While for G711 is limited to 200 ms.

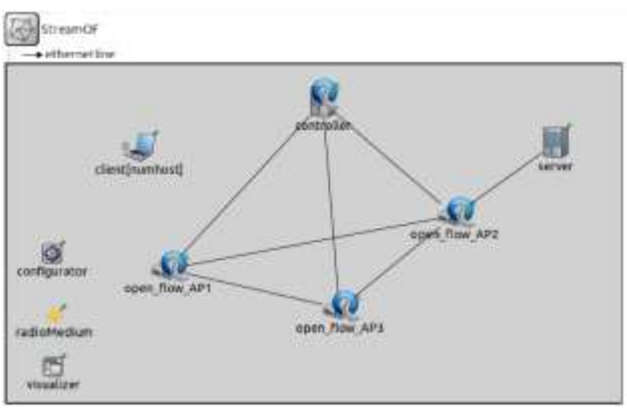

Fig. 3. Simulation Architecture.

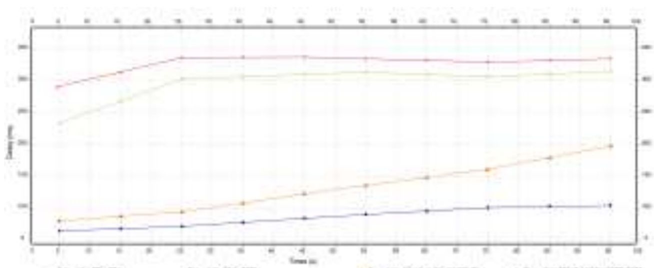

Fig. 4. Delay Comparison between SDN and SDN based F-AHP & VIKOR.

B. Jitter

It refers to the difference in end-to-end transmission delay between different packets of the same stream when transmitting from one system to another; hence, the reason for the results presented in the following figure "Fig. 5". The SDN controller, which incorporates the multicriteria choice technique based on F-AHP and VIKORE produced good jitter values no longer exceeding 18 ms for the G711 codec, also note that the G729 codec is still more powerful than G711 and has values no longer exceeding 13 ms.

C. Packet Loss

Packet loss occurs when one or more data packets passing through a computer network cannot reach their destination. Usually in wireless networks, it is caused by data transmission errors, interference, very low radio power, or network congestion. The following formula (12) gives the percentage value of lost packets:

$$PL\ \% = \frac{\text{packets sent} - \text{packets received}}{\text{packets sent}} \quad (12)$$

According to the results shown in "Fig. 6", the G711 codec maintains its packet loss resistance with SDN technology based on multicriteria choice, it does not cross the 1% limits. Even for G729 in the worst cases, reached an acceptable value below 2%.

D. Mean Opinion Score (MOS)

Model E (ITU G.107) [23] provides a powerful means of evaluating and predicting the quality of calls in data networks. The calculated result of model E is a single scalar, called "R-value", which is derived based on the delay and degradation factors of the equipment. Once the R value is obtained, it can be mapped to the estimated MOS, it ranges from 100 to 0, where 100 is excellent and 0 is poor. When the signal is not altered, the quality is perfect, we write (13):

$$R = R0 \quad (13)$$

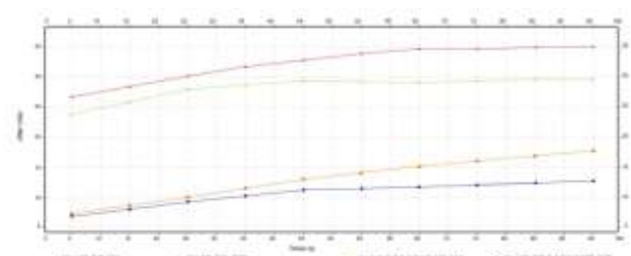

Fig. 5. Jitter Comparison between SDN and SDN based F-AHP & VIKOR.

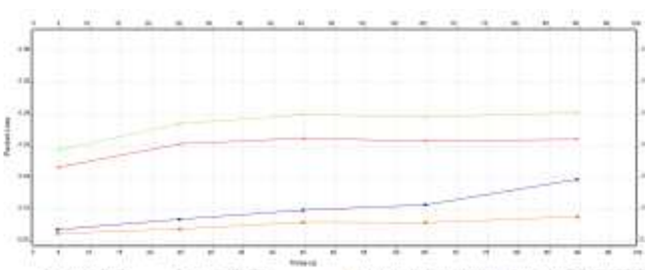

Fig. 6. Packet Loss Comparison between SDN and SDN based F-AHP & VIKOR.

In reality, the signal is influenced by the equipment and the constraints of the network, which degrades its quality from end to end (14).

$$R = R0 - Id - Ie + A \tag{14}$$

With:

- **Id** is the end-to-end delay.
- **Ie** impairment introduced by the equipment.
- **R0** Basic signal-to-noise ratio.
- **A** Advantage factor.

These values are related to data loss, jitter and delay, also the chosen codec. The choice of codec is a compromise between the desired quality of service and the ability of the IP infrastructure to deliver bandwidth and QoS parameters that will impact this quality. For example, the G711 codec offers a better quality of the channel since it does not perform any compression, therefore less delay and less sensitive to datagram losses. While other codecs like G729 and G723 consume less bandwidth, allowing simultaneous calls to be made on the same segment, but introduce more delay due to compression. These are sensitive to datagram loss. SDN technology provides fair quality for the G729 codec and good for the G711 codec. Fig. 7 shows that the integration of our SDN solution based on F-AHP and VIKORE helps the mobile node to make a good decision and brought an improvement in audio quality.

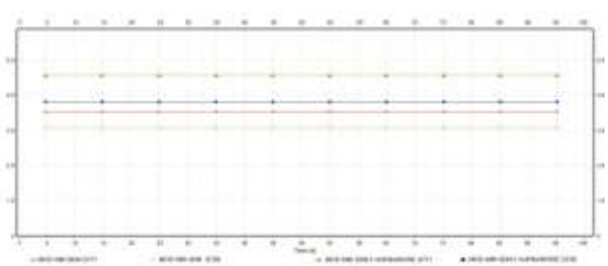

Fig. 7. MOS Comparison between SDN and SDN based F-AHP & VIKOR.

VI. Conclusion

SDN technology presents good quality in wired networks, contrary to a wireless architecture influenced by constraints of an unpredictable nature. To solve this problem, we tried to integrate the multi-criterion management of Handover by SDN controller based on F-AHP and VIKOR.

The results showed a good quality of service for real-time applications, since the multi-criterion choice is based on a weighting technique which takes into account the fuzzy nature of the network parameters and also the importance of each criterion in relation to each other depending on the type of traffic chosen.

The VIKOR classification method consumes less resources which generates flexibility in the decision, and decreases the time required to trigger the handover. The mobile node is in front of a safe choice, without leaning into computations that decrease battery power and also increase the handover trigger delay or packet loss.

For large networks, it is possible to envisage processing distributed by several SDN controllers based on F-AHP and VIKOR.

References

[1] N. Mouhassine, M. Moughit, and F. Laassiri, “Improving the Quality of Service of Voice over IP in Wireless Sensor Networks by Centralizing Handover Management and Authentication Using the SDN Controller,” *2019 3rd International Conference on Intelligent Computing in Data Sciences, ICDS 2019*, 2019, doi: 10.1109/ICDS47004.2019.8942345.

[2] K. Savitha and Dr. C. Chandrasekar, “Vertical Handover decision schemes using SAW and WPM for Network selection in Heterogeneous Wireless Networks,” Global Journal of Computer Science and Technology, vol. 11, no. 9, p. 7, 2011, doi: 10.5120/3125-4300.

[3] T. L. Saaty, “Transport planning with multiple criteria: The analytic hierarchy process applications and progress review,” Journal of Advanced Transportation, vol. 29, no. 1, pp. 81–126, 1995, doi: 10.1002/atr.5670290109.

[4] The analytic network process, vol. 195. 2013.

[5] R. L. Keeney, H. Raiffa, and R. F. Meyer, Decisions with multiple objectives: preferences and value trade-offs. Cambridge university press, 1993.

[6] C.-L. Hwang and K. Yoon, “Methods for multiple attribute decision making,” in Multiple attribute decision making, Springer, 1981, pp. 58–191.

[7] BENADLA Abdelhalim, “Etude du Multihoming dans les Terminaux Mobiles (Sélection d’Interface),” pp. 2012–2013, 2013.

[8] J. P. Brans and B. Mareschal, “The PROMETHEE methods for MCDM; the PROMCALC, GAIA and BANKADVISER software,” in Readings in multiple criteria decision aid, Springer, 1990, pp. 216–252.

[9] S. Opricovic and G. H. Tzeng, “Extended VIKOR method in comparison with outranking methods,” European Journal of Operational Research, vol. 178, no. 2, pp. 514–529, 2007, doi: 10.1016/j.ejor.2006.01.020.

[10] R. Bikmukhamedov, A. Nadeev, Y. Yeryomin, and J. Seitz, “Simulating multi-criteria handover algorithms in OMNeT++,” 2017 International Siberian Conference on Control and Communications, SIBCON 2017 - Proceedings, 2017, doi: 10.1109/SIBCON.2017.7998466.

[11] Y. Kuo, T. Yang, and G.-W. Huang, “The use of grey relational analysis in solving multiple attribute decision-making problems,” Computers & industrial engineering, vol. 55, no. 1, pp. 80–93, 2008.

[12] X. Li, F. Liu, Z. Feng, G. Xu, and Z. Fu, “A novel optimized vertical handover framework for seamless networking integration in cyber-enabled systems,” Future Generation Computer Systems, vol. 79, pp. 417–430, 2018, doi: 10.1016/j.future.2017.03.031.

[13] M. Alhabo and L. Zhang, “Multi-criteria handover using modified weighted TOPSIS methods for heterogeneous networks,” IEEE Access, vol. 6, no. April 2020, pp. 40547–40558, 2018, doi: 10.1109/ACCESS.2018.2846045.

[14] R. M. Abdullah and Z. A. Zukarnain, “Enhanced handover decision algorithm in heterogeneous wireless network,” Sensors (Switzerland), vol. 17, no. 7, 2017, doi: 10.3390/s17071626.

[15] A. S. Sadiq, K. Abu Bakar, and K. Z. Ghafoor, “a Fuzzy Logic Approach for Reducing Handover Latency in Wireless Networks,” Network Protocols and Algorithms, vol. 2, no. 4, pp. 61–87, 2011, doi: 10.5296/npa.v2i4.527.

[16] M. V. S. Krishna and L. Rajesh, “Implementation of fuzzy logic for network selection in next generation networks,” International Conference on Recent Trends in Information Technology, ICRTIT 2011, pp. 595–600, 2011, doi: 10.1109/ICRTIT.2011.5972475.

[17] M. Sharma, “Fuzzy Logic Based Handover Decision System,” International Journal of Ad hoc, Sensor & Ubiquitous Computing, vol. 3, no. 4, pp. 21–29, 2012, doi: 10.5121/ijasuc.2012.3403.

[18] F. Kaleem, A. Mehbodniya, K. K. Yen, and F. Adachi, “A fuzzy preprocessing module for optimizing the access network selection in wireless networks,” Advances in Fuzzy Systems, vol. 2013, 2013, doi: 10.1155/2013/232198.

[19] M. M. Alkhawlani, K. A. Alsalem, and A. A. Hussein, "Multi-criteria vertical handover by TOPSIS and fuzzy logic," 2011 International Conference on Communications and Information Technology, ICCIT 2011, pp. 96–102, 2011, doi: 10.1109/ICCITECHNOL.2011.5762703.

[20] S. F. Zhang, S. Y. Liu, and R. H. Zhai, "An extended GRA method for MCDM with interval-valued triangular fuzzy assessments and unknown weights," Computers and Industrial Engineering, vol. 61, no. 4, pp. 1336–1341, 2011, doi: 10.1016/j.cie.2011.08.008.

[21] M. Drissi, M. Oumsis, and D. Aboutajdine, "A Multi-Criteria Decision Framework for network selection over LTE and WLAN," Engineering Applications of Artificial Intelligence, vol. 66, no. February, pp. 113–127, 2017, doi: 10.1016/j.engappai.2017.08.019.

[22] J. J. Buckley, "Fuzzy hierarchical analysis," Fuzzy Sets and Systems, vol. 17, no. 3, pp. 233–247, 1985, doi: 10.1016/0165-0114(85)90090-9.

[23] D. Systems, "ITU-T," 2015.

ROI Image Encryption using YOLO and Chaotic Systems

Sung Won Kang[1]
Dept. Information Security
Pukyong National University
Busan, South Korea

Un Sook Choi[2]*
School of Artificial Intelligence
Tongmyong University
Busan, South Korea

***Abstract*—In this paper, we design a cellular automata (CA)-based ROI (region of interest) image encryption system that can effectively reduce computational cost and maintain an appropriate level of security. The proposed image encryption system obtains a cryptographic image through three steps. First, a region of interest with high importance is extracted from the entire image using deep learning. We use the YOLO (You Only Look Once) algorithm to extract the ROI from a given original image. Next, the detected ROI is encrypted using the Chen system, a chaotic-based function with high security. Finally, the execution time is effectively reduced by encrypting the entire image using a hardware-friendly CA. The safety of the proposed encryption system is verified through various statistical experiment results and analyses.**

***Keywords*—Image encryption; cellular automata; YOLO algorithm; deep learning; Chen system; region of interest**

I. Introduction

The development of information and communication technology has brought many changes in our society. Recently, with the emergence of new communication technologies such as the IoT (Internet of Things) and big data, various types of information are efficiently and conveniently transmitted and applied in various ways. The factory automation system improves productivity. It is possible to quickly and conveniently collect and utilize information using computers and mobile devices, and expand opportunities for social participation through SNS (social networking services). In addition, the demand for real-time data transmission has increased in applications such as medical service, the military, finance and education. And problems related to personal information protection such as personal information leakage and cyber terrorism are also frequently occurring. In particular, image security is an essential part of today's communication technology, and very important for safe transmission.

Due to the recent epidemic such as COVID-19, many changes have occurred in the daily life of our society [1]. Changes in daily life such as real-time non-face-to-face online meetings, education, telemedicine, and online collaboration have increased traffic to the network and increased demand for real-time security of multimedia. Multimedia traffic, including video, audio and image content, is very large and has a very high correlation between pixels. Unfortunately, traditional cryptographic algorithms such as DES (Data Encryption Standard), AES (Advanced Encryption Standard), IDEA (International Data Encryption Algorithm) are suitable for text data, but not for images or video in real-time applications. Many techniques have been developed to protect images [2].

Among these technologies, image encryption is the most intuitive and effective method of converting an image into an unrecognizable image. Through this method, it is possible to prevent theft and illegal reading of personal images, and to prevent leakage of personal information when sending images.

Chaos theory is a dynamic system that is very sensitive to time changes and initial conditions. Chaos theory can effectively generate a random sequence because a logical law exists even in a chaotic state that seems disorderly. The chaos-based encryption system is the most used technology for image encryption due to its many advantages such as high randomness, complexity, sensitivity to initial conditions, and system parameters. The chaos-based image encryption algorithm was introduced by Fridrich [3], and many research results have been proposed over the past 20 years [2-16]. The chaos-based cryptographic algorithm is processed through two steps. The first step is a diffusion process that randomly changes pixel values using a random sequence generated based on a chaotic function. At this time, in order to obtain high security and reliable encryption image, an encryption system that is very sensitive to the key must be used. Another process is the confusion process, which effectively change the position of the pixels. This step is a necessary process to protect the image against unexpected noise generation or deletion attacks in the process of transmitting the encrypted image.

X. Zhang et al. [7] designed an encryption system by introducing a bi-direction diffusion technique to compensate for the weaknesses of the image encryption method. In order to effectively perform permutations in the encryption stage, they proposed a method of wholly constructing permutations by combining small permutations. W. Zhang et al. [8] proposed a chaotic-based image cryptographic algorithm using both a chaotic cat map and a logistic map. They changed pixel planes to each other at the stage of changing the pixel position of the image. Tang et al. [9] proposed a method of an image encryption by dividing it into small blocks and encrypting the image using a chaos function. Zahmoul et al. [10] proposed an effective cryptosystem by designing a new chaos map based on the beta function frequently used in statistics and probability theory. They showed that the proposed beta chaotic function has higher sensitivity and security than other chaotic functions. Wang et al. [16] proposed the logistic-dynamic Arnold coupled logistic map lattice model. They used the proposed model as

*Corresponding Author

the key sequence generator of the image encryption system. Their proposed encryption system uses a dynamic coupling method based on a logistic map, and then applies the Arnold coupled logistic map lattice based on the Arnold map proposed in [6].

Although the cryptographic algorithm based on the chaos function has a high level of security, it is based on mathematical calculations, which increases the calculation cost.

In this paper, we design a CA-based ROI image encryption system that can effectively reduce computational cost and maintain an appropriate level of security. The proposed cryptographic system obtains a cryptographic image through three steps. First, an ROI with high importance is extracted from the entire image using deep learning. Next, the detected ROI is encrypted using a chaotic-based function with high security. Finally, the execution time is effectively reduced by encrypting the entire image using a hardware-friendly cellular automata. The safety of the proposed encryption system is verified through various statistical experiment results and analyses.

II. Background

A. YOLO

YOLO (You Only Look Once) proposed by Redmon et al. [17] is a 1-stage detector suitable for real-time detection. YOLO is composed of one neural network, so it predicts the bounding box surrounding the object and the class probability of which class the object belongs to with one calculation for the entire image. YOLO has superior performance compared to the existing object detection model based on R-CNN. The advantages of YOLO are as follows: 1) Because it is a single neural network structure, the configuration is simple and fast. 2) Because it learns surrounding information and processes the entire image, the background error is small. 3) Detection accuracy is high even for new images not seen in the training stage. Although it is less accurate than the state-of-the-art object detection model. But speed and accuracy are in a trade-off relationship. In this paper we use YOLO to extract the ROI of the original image in this paper.

B. Cellular Automata

CA is a system for analyzing dynamic systems in discrete time and finite discrete space. Cells, the basic unit for storing states of 0 and 1, are connected in a certain shape, and the states of each cell are updated simultaneously by local interaction of cells by a given state transition function [18]. CAs are classified according to the shape in which each cell is arranged. If they are arranged linearly, they are called one-dimensional CAs, if they are arranged in a plane, they are called two-dimensional CAs, and CAs arranged in a cubic shape are classified as three-dimensional CAs. Cells participating in the state transition of each cell are called neighbors. The most basic form is a 1-dimensional 3-neighbor CA with a radius of 1 relative to itself, and a CA with a radius of 2 including itself is called a 1-dimensional 5-neighbor CA. CA can effectively generate a random pattern with good randomness because it is connected to its neighbors by associative logic and its shape is composed of a regular arrangement.

For this reason, CA is applied to cryptographic systems [19-22]. In CA, where the state transition rule applied to each cell of the CA is expressed by XOR logic, the state transition function can be expressed as a matrix. If the characteristic polynomial of the state transition matrix of a given CA is a primitive polynomial, the sequence generated by the CA becomes the maximum periodic sequence [23]. This CA is referred to as a one-dimensional 5-neighbor maximum length CA (FNMLCA). Eq. (1) is a state transition function of a one-dimensional 5-neighbor CA.

$$u_i^{t+1} = a_i u_{i-2}^t \oplus b_i\, u_{i-1}^t \oplus c_i u_i^t \oplus d_i u_{i+1}^t \oplus e_i\, u_{i+2}^t \qquad (1)$$

where u_i^t is the state of the *i*th cell at time t, and $u_i^t = \{0,\ 1\}$, $a_i, b_i, c_i, d_i, e_i \in \{0, 1\}$. In this paper. we use a one-dimensional symmetric FNMLCA in which a_i, b_i, d_i, e_i in Eq. (1) are all 1. One-dimensional symmetric FNMLCA can generate high-quality random sequences than 1-D 3-neighbor 90/150 MLCA [23], and the diffusion rate is twice as fast. Fig. 1 shows the structure of an 8-cell one-dimensional symmetric FNMLCA with the state transition rule <00111010>. Each element of the state transition rule is each $c_i (i = 1,2, \cdots ,8)$in (1). The characteristic polynomial for the state transition matrix in Fig. 1 is $c(x) = x^8 + x^6 + x^5 + x^3 + 1$, and $c(x)$ is primitive.

C. Chen System

Chen system is a structure applied in chaotic dynamic control, synchronization, turbulence modeling and controlled weather model [24]. One of the chaotic dynamic system models, the Chen system, has similar properties to the Lorenz system. The Chen system can generate chaotic sequences sensitive to initial values.

Since the sequence generated by the Chen system has very high randomness, the system is used in key generation of the OTP (one time password) cryptosystem and key image generation in the image encryption process. The Chen system is expressed as a system of third-order nonlinear differential equations as shown in (2).

$$\begin{cases} \dot{x} = a(y - x) \\ \dot{y} = (c - a)x - xz + cy \\ \dot{z} = xy - bz \end{cases} \qquad (2)$$

where a=35, b=3, c=28. Fig. 2 shows the attractor of the Chen system.

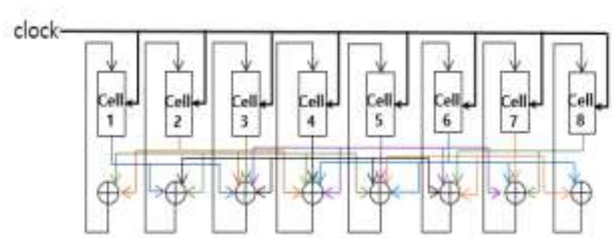

Fig. 1. The Structure of 1-Demensional Sysmetric FNMLCA with Transition Rule <00111010> and Characteristic Ploynomial $x^8 + x^6 + x^5 + x^3 + 1$.

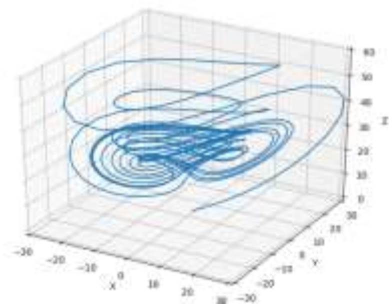

Fig. 2. The Attractor of the Chen System.

III. Proposed Algorithm

In this section, we propose a 1-D FNMLCA-based ROI image encryption algorithm. The proposed algorithm consists of three steps. The first step is ROI detection for the original image, and the second step is the encryption of the ROI.

The encryption of the ROI consists of shuffling the pixels of the ROI image and changing the pixel values using a sequence generated by the Chen system. Finally, the third step consists of encrypting the entire image.

A. Detecting of the ROI

YOLO divides the original image into $n \times n$ grids, and if there is an object in a grid cell, the grid cell detects the object. Assume that L bounding boxes are detected in the image [17]. The coordinates of the four vertices of the ith bounding box can be expressed as $(x_{i,1}, y_{i,1})$, $(x_{i,2}, y_{i,1})$, $(x_{i,1}, y_{i,2})$ and $(x_{i,2}, y_{i,2})$, where $x_{i,2} > x_{i,1}$ and $y_{i,2} > y_{i,1}$. The smallest rectangular area including all L boxes becomes the ROI. The four vertices $(rx_{i,1}, ry_{i,1})$, $(rx_{i,2}, ry_{i,1})$, $(rx_{i,1}, ry_{i,2})$ and $(rx_{i,2}, ry_{i,2})$ of the ROI are calculated as follows.

$$rx_{i,1} = \min(\{x_{i,1} \mid i = 1, 2, \cdots, L\}) \tag{3}$$

$$ry_{i,1} = \min(\{y_{i,1} \mid i = 1, 2, \cdots, L\}) \tag{4}$$

$$rx_{i,2} = \max(\{x_{i,2} \mid i = 1, 2, \cdots, L\}) \tag{5}$$

$$ry_{i,2} = \max(\{y_{i,2} \mid i = 1, 2, \cdots, L\}) \tag{6}$$

Fig. 3 shows the process of detecting the ROI by detecting the bounding box using YOLO for the original image.

B. Encryption of the ROI

ROI encryption consists of shuffling pixel positions and randomly changing pixel values. First, pixel positions are shuffled using one-dimensional symmetric FNMLCA for ROI, which is the minimum area including all bounding boxes detected using YOLO. Unlike mathematical operation-based chaotic functions, one-dimensional symmetric FNMLCA is very efficient because it is easy to implement in hardware and can be implemented in hardware-friendly even when implemented in software. The one-dimensional symmetric FNMLCA F_n having $p_n(x)$ as the characteristic polynomial is synthesized by selecting the primitive polynomial $p_n(x)$ of degree n corresponding to the selected n. For effective synthesis, F_n is synthesized using the state transition function T_n of the one-dimensional 3-neighbor MLCA corresponding to $p_n(x)$.

Fig. 3. The Process of Detecting the ROI for the Original Image.

A sequence generated using F_n and the initial state is arranged according to the size of the ROI, and row positions of the ROI are rearranged using the arranged sequence. Reorder the column positions in the same way for the shuffled ROI image in the row positions. In the same way, the row-column pixel shuffling process is repeated k times. To increase the security level, different $F_n s$ and initial values are selected for each round of color component and row-column shuffling of the ROI.

The next step is to change the value of each pixel of the shuffled ROI image to an arbitrary value. Let the size of the ROI detected from the original image be $\mathrm{W} \times \mathrm{H}$, where W and H are $W = (rx_{i,2} - rx_{i,1})$ and $H = (ry_{i,2} - ry_{i,1})$ from (3)-(6). Using the selected initial value and Chen chaotic system, a sequence of size $\mathrm{W} \times \mathrm{H} \times 3 (= \mathrm{M})$ is generated. In order to generate an efficient chaotic sequence in which the correlation with the initial value is removed, the values generated from the first to the 2000th are discarded and the values generated from the 2001th are used. The ith value $s_i (i = 0, 1, \cdots, M-1)$ of the generated sequence is calculated using (7) to obtain an integer value $k_i (i = 0, 1, \cdots, L-1)$ between 0 and 255.

$$k_i = (s_i \times 10^{14}) \; mod \; 256 \;\; (\mathrm{i} = 0, 1, \; \cdots, \mathrm{M} - 1) \tag{7}$$

By rearranging the generated integer sequence k_i, a $\mathrm{W} \times \mathrm{H}$ color key image with the same size as the ROI is created and XORed with the shuffled ROI image.

C. Encryption of the Entire Image

After performing ROI encryption, the entire image is encrypted. Like the ROI image encryption process, the final encrypted image is obtained through a shuffling step that changes the pixel position and a diffusion step that randomly changes pixel values.

In the entire image, areas excluding the ROI are generally less important than the ROI. Therefore, in the ROI image encryption process, since encryption was first performed using a function with high security strength, the entire image is encrypted with priority over performance speed rather than security strength. In the proposed system, the hardware-friendly one-dimensional symmetric FNMLCA is used to speed up the shuffling process of pixel positions. And it is used to change pixel values for the entire image in the diffusion process.

In the pixel shuffling step, the pixel shuffling process in row-column units is appropriately repeated in the same way as the shuffling process in the ROI encryption process.

To generate a key image for changing pixel values, generate a sequence using FNMLCA and initial values that are appropriately large as much as the entire image size, and adjust the values to fit the range of image pixel values. For example, if the color value of one pixel has values ranging from 0 to 255 for each R, G, and B, the value generated through the state transition of one-dimensional symmetric FNMLCA is processed as mod 256 and XORed with the pixel value. Repeat for the R, G, and B color planes.

D. Proposed FNMLCA-based ROI encryption Algorithm

The FNMLCA-based ROI encryption algorithm proposed in this paper is performed through the following five steps. Among the main algorithms below, FNMLCA is used for the pixel shuffling step and the pixel value change step of the entire image. Algorithm 1 is a sequence generation function using FNMLCA, and Algorithm 2 is a pixel shuffling function using a sequence generated from FNMLCA. Algorithm 3 is the proposed main encryption algorithm. Algorithm 4 is a decoding algorithm. After performing ROI encryption, the entire image is encrypted. Like the ROI image encryption Fig. 4 shows the block diagram of the proposed ROI image encryption system in this paper. Table I shows the proposed ROI image encryption algorithm.

In order to perform the ROI decryption algorithm, the sender needs to transmit the coordinates of the ROI together with the key to the receiver. And the ROI decoding algorithm performs the following processes:

TABLE I. THE PROPOSED ROI IMAGE ENCRYPTION ALGORITHM

Algorithm 1 FNMLCA sequence generator

n is a number of cells
R_n is a rule of FNMLCA
v^t is a state vector of the CA at the time t
seq is a list $[v^0]$
def FNMLCA(R_n, v^t, k):
  for i in range(0, k):
    $v^{i+1} \leftarrow (v^i//4)+(v^i//2)+(v^i \wedge R_n)+(v^i*2)+(v^i*4) \bmod 2^n$
      seq.append(v^{i+1})
  return seq

Algorithm 2 FNMLCA shuffling

P is the input image
W is the width of the P
H is the height of the P
seq1, seq2 are sequences generated by *Algorithm 1*
def shuffling(P, seq1, seq2):
  S is the empty image with the size W×H
  for i in range(0, W}:
    S[i, :] ← P[seq1[i], :]
  for j in range(0, H):
    S[:, j] ← P[:, seq2[j]]
  return S

Algorithm 3 ROI Encryption Algorithm

Input : Original image
Output : Encryption image
1: Detect the ROI from the original image using the pre-trained YOLO algorithm.
2: Shuffle the ROI using FNMLCA (Algorithm 2).
3: XOR the key image generated from Chen attractor with the shuffled
ROI image.
4: Shuffle the entire ROI-encrypted image using FNMLCA (Algorithm 2).
5: Create a key image (KImg) with the same size as the original image
using FNMLCA (Algorithm 1).
6: XOR the image obtained in step 4 with KImg to generate a encrypted image.

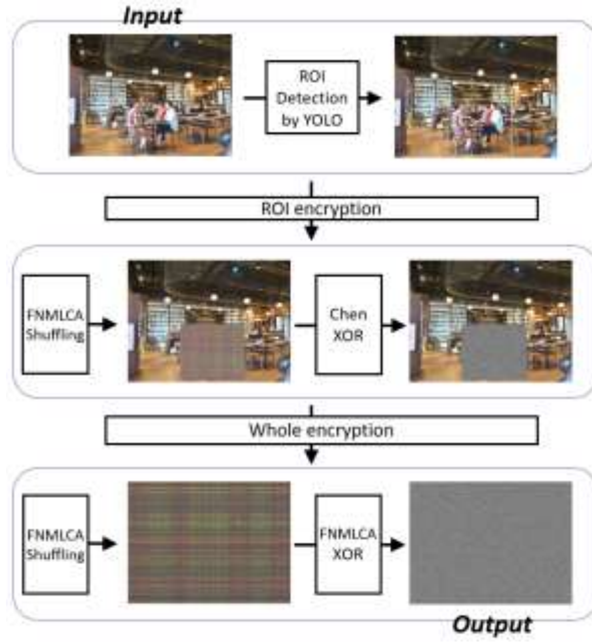

Fig. 4. The Block Diagram of the Proposed ROI Image Encryption System.

- Step 1. After using FNMLCA to create a key image of the same size as the entire area (Algorithm 1), XOR it with the image to be decrypted.
- •Step 2. Shuffle the image of Step 1 using FNMLCA (Algorithm 2).
- Step 3. XOR the key image generated from Chen attractor on the received ROI coordinate area.
- Step 4. Shuffle the ROI image using FNMLCA (Algorithm 2). The image obtained at this time is a decoded image.

IV. EXPERIMENT RESULTS AND SECURITY ANALYSIS

In this section, the results of statistical analysis are presented. Photographs of people in various forms were used as original images for simulation. Fig. 5 shows some of the original image samples of various sizes used in the experiment. For each original image, the serial number is subsequently referenced in the data representing the experimental results. The number in (•) next to each image number is the width × height of the image.

A. Histogram Analysis

In order to defend against statistical attacks, the encryption technique must uniformly spread the pixel values of a given image. Fig. 6 is an image encrypted by the proposed algorithm for each original image in Fig. 5. According to Fig. 6, the encrypted image cannot recognize the original image with the naked eye. Fig. 7 shows the histograms for the original image in Fig. 5 and the encrypted image in Fig. 6. Comparing the histograms for each original image and the encrypted image in Fig. 7, it can be seen that the histogram of the original image has a non-uniform color distribution that reflects the feature of the image. On the other hand, the histogram of the encrypted image shows all pixel values uniformly.

Fig. 5. Original Images and their Image Sizes.

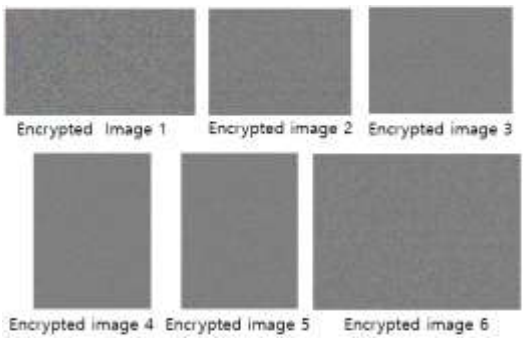

Fig. 6. Images Encrypted by the Porposed Algorithm for each Original Images.

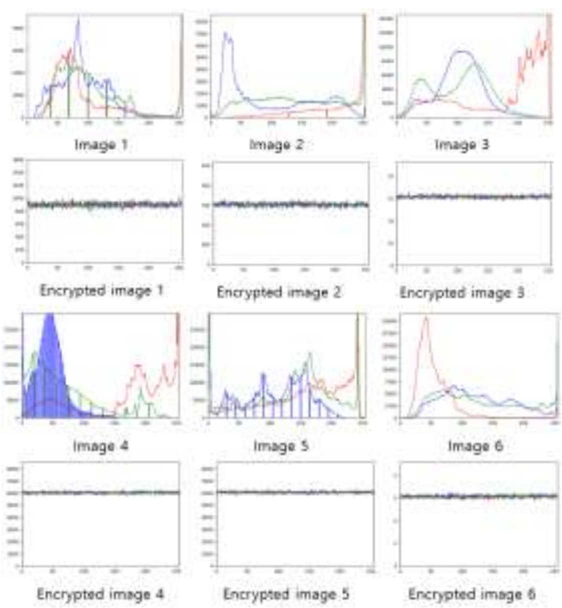

Fig. 7. The Histograms for Original/Encrypted Images.

Therefore, it can be seen that the statistical characteristics of the original image are removed in the encrypted image through the histogram result.

B. Correlation Analysis

The image has a characteristic that the values of adjacent pixels are almost the same. Since a statistical attack can also use this characteristic, the encryption technique must ensure that the values of adjacent pixels vary. The correlation coefficient is used as a measure of the degree of relation between adjacent pixels in image encryption. The degree of correlation is between -1 and +1, and the closer to ±1, the higher the correlation, and the closer to 0, the lower the correlation.

The correlation coefficient is calculated using (8) to show that the correlation between adjacent pixels has disappeared with respect to the image encrypted by the proposed method.

$$\rho_{xy} = \frac{\sum_{i=1}^{N}(X_i-\bar{X})(Y_i-\bar{Y})}{\sqrt{\sum_{i=1}^{N}(X_i-\bar{X})^2}\sqrt{\sum_{i=1}^{N}(Y_i-\bar{Y})^2}} \quad (8)$$

$\bar{X} = \sum_{i=1}^{N} X_i/N$, X and Y are the values of two adjacent pixels in (8). Table II shows the correlation coefficients of pixels adjacent to each other in the horizontal, vertical, and diagonal directions of the original image and the encrypted image.

TABLE II. THE CORRELATION COEFFICIENTS OF PIXELS ADJACENT TO EACH OTHER IN THE HORIZONTAL, VERTICAL AND DIAGONAL DIRECTIONS

Image	color	Horizontal	Vertical	Diagonal
Original image 1	R	0.97972	0.98736	0.97314
	G	0.98040	0.98729	0.97318
	B	0.97956	0.98759	0.97295
Encrypted image 1	R	-0.00422	-0.00824	0.00192
	G	0.00615	0.00269	-0.00280
	B	0.00085	0.00088	-0.00025
Original image 2	R	0.86795	0.85358	0.76400
	G	0.84946	0.83211	0.78305
	B	0.85573	0.84011	0.74209
Encrypted image 2	R	0.00704	-0.00400	0.00102
	G	-0.00069	0.00819	0.00527
	B	0.01022	0.00596	0.01056
Original image 3	R	0.94519	0.95867	0.91887
	G	0.92337	0.94256	0.88494
	B	0.93120	0.94944	0.90104
Encrypted image 3	R	-0.00118	-0.00328	-0.00008
	G	-0.00642	0.00764	-0.00086
	B	-0.00171	-0.00723	0.00518
Original image 4	R	0.98992	0.99155	0.98368
	G	0.99161	0.99385	0.98785
	B	0.99084	0.99327	0.98603
Encrypted image 4	R	0.00146	0.00259	-0.00012
	G	-0.00111	-0.00268	0.00368
	B	0.00242	0.00373	-0.00660
Original image 5	R	0.96853	0.99446	0.95757
	G	0.98370	0.99730	0.97965
	B	0.97507	0.99589	0.96875
Encrypted image 5	R	0.00100	0.00062	-0.00220
	G	-0.00712	-0.00571	-0.01348
	B	0.00328	-0.00475	0.00885
Original image 6	R	0.93681	0.95447	0.92919
	G	0.95735	0.96808	0.94631
	B	0.94541	0.95920	0.93359
Encrypted image 6	R	-0.00012	0.00271	0.00157
	G	0.00115	0.00419	0.00538
	B	-0.00051	0.00255	0.00153

The correlation coefficient was calculated from 2500 samples randomly extracted from the image, and a more accurate correlation coefficient was calculated by calculating the average of the results of 300 repetitions. Also, correlation analysis can be expressed using a scatter plot. In Fig. 8, the scatter plots of pixels adjacent to each other in the horizontal, vertical and diagonal directions for the original image (image 1) in Fig. 5 and the encrypted image for the original image are shown. It can be confirmed that the scatter of the original image has a high positive correlation, and it can be confirmed that the scatter of the encrypted image has a very low correlation. From the results of Table II and Fig. 8, it can be seen that the strong correlation between pixels of the original image has disappeared in the encrypted image by the proposed algorithm. Table III is a comparison of the correlation coefficients of images encrypted by the proposed method and other methods.

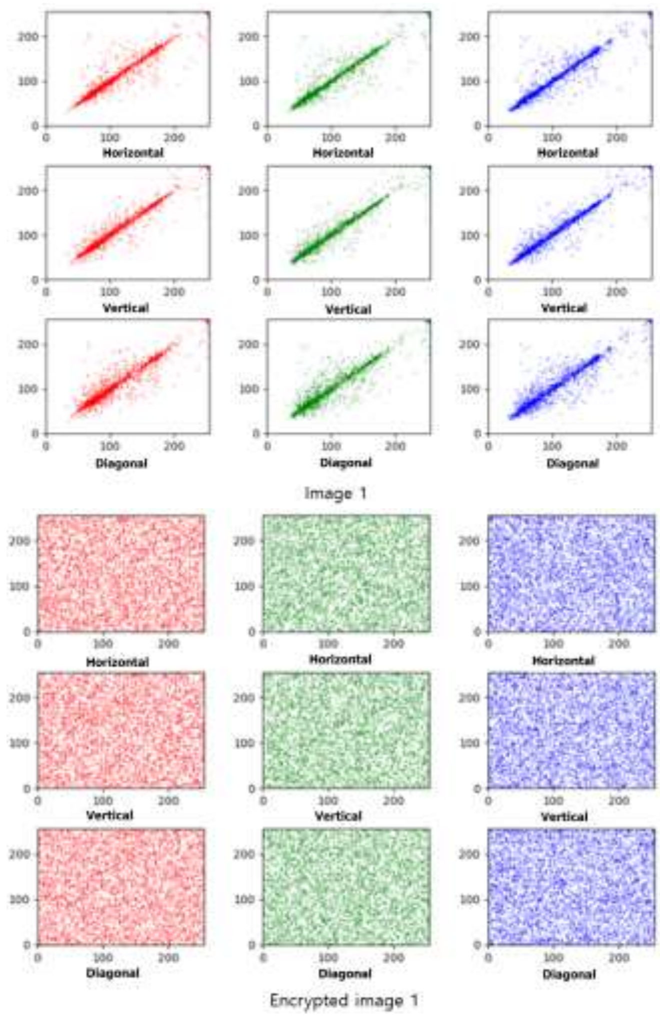

Fig. 8. The Correlation Scatter Plots of Pixels Adjacent to each other in the Horizontal, Vertical and Diagonal Directions for the Original/Encrypted Image (Image 1).

TABLE III. THE COMPARISON OF CORRELARION COEFFICENTS OF IMAGES ENCRYPTED BY THE PROPOSED METHOD AND OTHER METHODS

Method		Correlation coefficient	
Proposed		0.0006	
Kamal et al. [25]		-0.0024	
Wade et at. [26]		0.0401	
Yang et al. [27]		-0.0034	
Hua et al. [28]		0.0030	
B	7.56390	B	7.99975

C. Entropy Analysis

The uncertainty of the information should be increased by the encryption technology. In information theory, entropy is used as a measure of information uncertainty. Information entropy means the minimum average bit required to represent a given data. Entropy can be obtained from the distribution of pixel values of a given image. Calculate entropy using (9).

$$\mathrm{H(X)} = -\sum_{i=0}^{2^n-1} p(x_i) log_2 p(x_i) \quad (9)$$

, where $\mathrm{p}(x_i)$ is a probability distribution of a pixel value x_i. In a general 8(=*n*) bit format image, the maximum value of entropy is 8, and the maximum entropy means that the given information is uncertain.

Table IV shows the entropies of the given original and encrypted images in Fig. 5 and Fig. 6. The encrypted images by the proposed encryption method have the entropies very close to 8. And Table V shows the comparison of entropy of images encrypted by the proposed algorithm and other methods.

TABLE IV. THE ENTROPIES OF THE GIVEN ORIGINAL AND ENCRYPTED IMAGES

Original color		Entropy	Encrypt. color		Entropy
image 1	R	6.99289	image 1	R	7.99917
	G	7.18091		G	7.99932
	B	7.09116		B	7.99917
image 2	R	6.96075	image 2	R	7.99945
	G	6.93752		G	7.99953
	B	6.94867		B	7.99933
image 3	R	7.59813	image 3	R	7.99977
	G	7.71103		G	7.99978
	B	7.62290		B	7.99976
image 4	R	7.28923	image 4	R	7.99989
	G	7.61027		G	7.99986
	B	7.51687		B	7.99987
image 5	R	7.69426	image 5	R	7.99988
	G	6.85420		G	7.99989
	B	7.72390		B	7.99987
image 6	R	7.43362	image 6	R	7.99977
	G	7.70272		G	7.99973

TABLE V. THE COMPARISON OF ENTROPY OF IMAGES ENCRYPTED BY THE PROPOSED METHOD AND OTHER METHODS

Method	Entropy
Proposed	7.9997
Kamal et al. [25]	7.9973
Wade et at. [26]	7.9422
Zhong et al. [29]	7.9972
Hua et al. [30]	7.9977

D. Difference Analysis

A differential attack is achieved through a selective plaintext attack. This is a way for malicious users to find vulnerabilities in cryptographic systems by using encryption and decryption using different keys.

To be safe from this differential attack, the cryptographic system must be sensitive to even small changes in keys. PSNR, NPCR, and UACI are representative measures to analyze the sensitivity of cryptographic systems. The peak signal-to-noise ratio (PSNR) is the ratio between the original image and the encrypted image. The higher the PSNR, the smaller the difference between the two images. PSNR is calculated by (10).

$$PSNR = 10 \log_{10}(255^2/MSE) \tag{10}$$

where the mean square error (MSE) is the mean squared difference between the original input image and the encrypted image. It is calculated in pixels by squaring the difference of all pixels and dividing by the total number of pixels. MSE is calculated by (11).

$$\mathrm{MSE} = \sum_{i,j} \left(a_{i,j} - b_{i,j}\right)^2 / (W \times H) \tag{11}$$

where W and H are the width and height of the given image, and $a_{i,j}$ and $b_{i,j}$ are the pixel values of the cryptographic image encrypted with another key.

Other metrics used to evaluate the cryptographic strength of image encryption algorithms with respect to differential attacks are NPCR and UACI. NPCR is a measure of the absolute pixel change rate between two images, and UACI is the average color intensity difference between the two images. For two cryptographic images C_1 and C_2 generated by different keys with only a 1-bit change, NPCR and UACI are calculated by (12) and (13).

$$\mathrm{NPCR} = \frac{\sum_{i,j} D(i,j)}{W \times H} \times 100(\%) \tag{12}$$

$$\mathrm{UACI} = \frac{\sum_{i,j} |C_1(i,j) - C_2(i,j)|}{W \times H \times 255} \times 100(\%) \tag{13}$$

where $D(i,j)$ is 0 for $C_1(i,j) = C_2(i,j)$ and 1 for $C_1(i,j) \neq C_2(i,j)$. Also, $C_1(i,j)$ and $C_2(i,j)$ are the pixel values for each position of C_1, C_2, and W and H are the width and the height of C_1 and C_2.

Table VI shows the difference analysis results for the two images encrypted by the proposed method using different keys for the original images in Fig. 5. Here, the two keys used to encrypt each original image differ only by one bit. The results in Table VI are within the reference value range [32]. Therefore, the proposed image encryption system can sufficiently withstand differential attacks. Table VII shows the comparison of NPCR and UACI of images encrypted by the proposed method and several methods.

E. Robustness Analysis against Data Corruption and Deletion Attacks

Malicious attackers attempt several illegal activities when images are transmitted. In this process, abnormal noise data may be inserted and the image may be damaged. Therefore, cryptographic systems must be robust against variety of data corruption and deletion attacks. Fig. 9 is the result of decrypting the encrypted image with data corruption due to various reasons by the proposed algorithm. It can be seen that the original image is decoded without serious damage when the image in which one part is intensively lost is decoded in the proposed system.

TABLE VI. DIFFERENTIAL ANALYSIS BETWEEN TWO ENCRYPTED IMAGES GENERATED USING DIFFERENT KEYS FOR EACH ORIGINAL IMAGES

Image color		NPCR (%)	UACI (%)	PSNR
image 1	R	99.58724	33.49941	7.73394
	G	99.62847	33.50500	7.74525
	B	99.61632	33.43314	7.75461
image 2	R	99.62603	33.46946	7.74767
	G	99.61883	33.44007	7.77723
	B	99.59722	33.32345	7.75534
image 3	R	99.61255	33.48647	7.74219
	G	99.59920	33.48335	7.74559
	B	99.61688	33.47931	7.75331
image 4	R	99.60663	33.46790	7.74482
	G	99.61496	33.48184	7.74805
	B	99.60042	33.45623	7.74559
image 5	R	99.61692	33.46269	7.74720
	G	99.60322	33.46984	7.74805
	B	99.59699	33.49762	7.73960
image 6	R	99.60988	33.50102	7.73592
	G	99.61230	33.44299	7.75711
	B	99.60874	33.42345	7.75698

TABLE VII. THE COMPARISON OF NPCR AND UACI OF IMAGES ENCRYPTED BY THE PROPOSED METHOD AND OTHER METHODS

Method	NPCR (%)	UACI (%)
Proposed	99.6096	33.4624
Kamal et al. [25]	99.6223	33.4406
Wade et at. [26]	99.6136	31.3253
Yang et al. [27]	99.6122	33.4155
Hua et al. [28]	99.6459	33.3797
Zhong et al. [29]	99.606	33.456
Hua et al. [30]	99.9974	33.2716
Thanikaiselvan et al. [31]	99.5945	33.0644

Fig. 9. Decryption Result of the Encrypted Image with Data Loss.

Therefore, the proposed encryption system can be said to be robust against data corruption and deletion attacks.

F. Analysis of Keyspace

In cryptosystems, the keyspace must be large enough to resist brute force attacks. The number of available keys in a cryptographic system determines the size of the keyspace. In the proposed encryption system, the initial value of the Chen system used to generate the key image in ROI image encryption is used as the key. And the cell size, transition rule, and initial vector of FNMLCAs used in the shuffling process of the ROI image and the whole image and the pixel value change process of the whole image are used as keys.

The size n of the cell of FNMLCA is sufficiently large than 8 which is the number of pixel bits of the image. At this time, the number of transition rules is 2^5 for each cell, so the total number of transition rules is 2^{5n} and the number of initial vectors is 2^n. In this FNMLCA shuffling step, different FNMLCA and different initial vectors are selected in each color plane and in the row and column shuffling step, so the number of keys in one shuffling encryption process is $(2^{6n})^6$. Therefore, the number of keys used in the ROI image shuffling, whole image shuffling, and entire image pixel value change steps is $(2^{18\times6})^6)^3 = 2^{108\times18}$ when n=18. The initial number of Chen system used to generate a key image for changing the pixel value of the ROI image is $10^{16} \approx 2^{53}$. Therefore, the size of the keyspace is large enough to be about $2^{53+108\times18} = 2^{1997} (\gg 2^{128})$ when the size of FNMLCA is 18. Therefore, the proposed cryptosystem can sufficiently resist brute force attacks.

G. Performance Speed Analysis

The proposed encryption system can detect ROI faster than other deep learning models by adopting the YOLO model in the ROI detection process. Most of the chaotic map-based image encryption algorithms encrypt the entire original image using the chaotic map. However, the proposed method minimizes the algebraic operation by using the chaotic map only in the process of changing the pixel value of the ROI with high importance among the original image. This effectively reduced execution time while maintaining security over key areas of the image. And by adopting the FNMLCA system for both the shuffling of the encryption system and the diffusion process for the entire image, the proposed system can be implemented in a hardware-friendly manner. The FNMLCA-based encryption system uses only logical and shift operations. In particular, in the process of changing the position of the pixel during the shuffling process, it is very effective in terms of execution speed because it relocates the pixel position by row and column units rather than by pixel unit. For this experiment, we used Python 3.8 and Intel(R) Core(Tm) i7-4770 CPU 3.40GHz on Windows 10 OS. The proposed algorithm is very fast enough to perform real-time image encryption. Table VII shows the execution time for each partial process in the process of encrypting the original images in Fig. 5 by the proposed algorithm. ROI detection time, ROI shuffling time, ROI diffusion process time, entire image shuffling time, and entire image diffusion process time are shown separately and the encryption execution time of the entire process is shown. In Table VIII, it can be seen that the ROI detection time for image 1 takes more than average time, the ROI detection time is very effective in most images, and it is very effective to perform the diffusion process using only the ROI using the Chen system.

TABLE VIII. THE EXECUTION TIME FOR EACH PARTIAL PROCESS IN THE PROCESS OF ENCRYPTING ORIGINAL IMAGES OF VARIOUS SIZES

	Image 1	Image 2	Image 3
Image size (W × H)	640×360	720×540	1024×768
ROI size (W × H)	123×122	519×274	173×592
ROI detection (sec.)	1.0342	0.4336	0.4335
ROI shuffling (sec.)	0.0156	0.0156	0.0156
ROI diffusion (sec.)	0.0781	0.6929	0.4699
Entire image shuffling (sec.)	0.0156	0.0156	0.0156
Entire image diffusion (sec.)	0.4062	0.6774	1.3075
Total encryption time (sec.)	1.6037	1.8351	2.2421
	Image 4	Image 5	Image 6
Image size (W × H)	1080×1433	1080×1441	1024×768
ROI size (W × H)	348×798	468×1162	407×353
ROI detection (sec.)	0.4233	0.5445	0.4692
ROI shuffling (sec.)	0.0156	0.0156	0.0156
ROI diffusion (sec.)	1.3980	2.6088	0.6561
Entire image shuffling (sec.)	0.0469	0.0781	0.0156
Entire image diffusion (sec.)	2.8169	2.6400	1.2966
Total encryption time (sec.)	4.7034	5.8870	2.4531

V. CONCLUSION

In this paper, we designed a new ROI image encryption system based on FNMLCA. The proposed algorithm can encrypt quickly in terms of speed, and at the same time, it can also increase security for high-value areas. The proposed algorithm detects ROI quickly by using YOLO among deep learning models, and because only the ROI image uses a chaotic map, it is effective in speed compared to other chaotic-based encryption algorithms. In particular, the key sequence was effectively generated through the hardware-friendly FNMLCA. In the pixel shuffling process, the overall encryption speed is improved by performing shuffling in row/column units rather than pixels. In addition, to enhance security, the ROI image is shuffled twice at pixel positions and pixel values by the proposed encryption system. The security strength is strengthened because the replacement process is performed. We plan to apply it to video encryption in the future.

ACKNOWLEDGMENT

This research was supported by the Tongmyong University Research Grants 2018(2018A046).

REFERENCES

[1] T. Favale, F. Soro, M. Trevisan, I. Drago, and M. Mellia, “Campus traffic and e-Learning during COVID-19 pandemic,” Comput. Networks, vol. 176, no. 20, Jul. 2020. doi: 10.1016/j.comnet.2020.107290.

[2] P. Zhen, G. Zhao, L. Min, and X. Jin, "Chaos-based image encryption scheme combining DNA coding and entropy," Multimed. Tools Appl., vol. 75, no. 11, pp. 6303–6319, Jun. 2016. doi: 10.1007/s11042-015-2573-x.

[3] J. Fridrich, "Symmetric ciphers based on two-dimensional chaotic maps," Int J Bifurcation and Chaos, vol. 8, no. 6, pp.1259–1284, Jun. 1998. doi: 10.1142/S021812749800098X.

[4] X. Wang, J. Zhao, and Z. Zhang, "A chaotic cryptosystem based on multi-one-dimensional maps," Mod. Phys. Lett. B, vol. 23, no. 2, pp. 183–189, Jan. 2009. doi: 10.1142/S0217984909017947.

[5] M.S. Azzaz, C. Tanougast, S. Sadoudi, and A. Dandache, "Robust chaotic key stream generator for real-time images encryption," J. Real-time Image Process., vol. 8, pp. 297–306, Sept. 2013. doi: 10.1007/s11554-011-0219-4.

[6] Y.Q. Zhang, and X.Y. Wang, "Spatiotemporal chaos in Arnold coupled logistic map lattice," Nonlinear Anal. Model. Control, vol. 18, no. 4, pp. 526–541, Oct. 2013. doi: 10.15388/NA.18.4.13977.

[7] X. Zhang, and Z. Zhao, “Chaos-based image encryption with total shuffling and bidirectional diffusion,” Nonlinear Dyn, vol. 75, no. 1-2, pp. 319–330, Jan. 2014. doi: 10.1007/s11071-013-1068-4.

[8] W. Zhang, H. Yu, and Z. Zhu, “Color image encryption based on paired interpermuting planes,” OPT COMMU, vol. 338, no. 1, pp. 199–208, Mar. 2015. doi: 10.1016/j.optcom.2014.10.044.

[9] Z. Tang, X. Zhang, and W. Lan, "Efficient image encryption with block shuffling and chaotic map," Multimed. Tools Appl., vol. 74, no. 15, pp. 5429-5448, Aug. 2015. doi: 10.1007/s11042-014-1861-1.

[10] R. Zahmoul, R. Ejbali, and M. Zaied, “Image encryption based on new Beta chaotic maps,”Opt. Lasers Eng., vol. 96, pp. 39-49, Sept. 2017. doi: 10.1016/j.optlaseng.2017.04.009.

[11] J.S. Khan, and J. Ahmad, "Chaos based efficient selective image encryption," Multidim Syst Sign Process, vol. 30, no. 2, pp.943-961, May 2019. doi: 10.1007/s11045-018-0589-x.

[12] A.Y. Niyat, M.H. Moattor, and M.N. Torshiz, "Color image encryption based on hybrid hyper-chaotic system and cellular automata," Opt. Lasers Eng. vol. 90, pp.225–237, Mar. 2017. doi: 10.1016/j.optlaseng. 2016.10.019.

[13] Y. Zhang, "The unifed image encryption algorithm based on chaos and cubic S-Box," Inf. Sci., vol.450, pp. 361–377, Jun. 2018. doi: 10.1016/j.ins.2018.03.055.

[14] R. Parvaz, and M. Zarebnia, "A combination chaotic system and application in color image encryption," Opt. Laser Technol. vol. 101, pp. 30–41, May 2018. doi: 10.1016/j.optlastec.2017.10.024.

[15] H.M. Ghadirli, A. Nodehi and R. Enayatifar, "An overview of encryption algorithms in color images," Signal Processing, vol. 164, pp. 163–185, Nov. 2019. doi: 10.1016/j.sigpro.2019.06.010.

[16] X. Wang, L. Feng, R. Li, and F. Zhang, "A fast image encryption algorithm based on non-adjacent dynamically coupled map lattice model," Nonlinear Dyn. vol.95, no.1, pp. 2797-2824, Mar. 2019. doi: 10.1007/s11071-018-4723-y.

[17] J. Redmon, S. Divvala, R. Girshick, and A. Farhadi, "You only look once: unified, real-time object detection," Proc. of 2016 IEEE Conference on Computer Vision and Pattern Recognition (CVPR), pp.779-788, 2016. doi: 10.1109/CVPR.2016.91.

[18] S. Wolfram, "Random sequence generation by cellular automata," Adv. Appl. Math., vol. 7, no. 2, pp. 123-169, Jun. 1986. doi: 10.1016/0196-8858(86)90028-X.

[19] P. Ping, J. Wu, Y. Mao, F. Xu, and J. Fan, "Design of image cipher using life-like cellular automata and chaotic map," Signal Processing, vol. 150, pp. 233-247, Sep. 2018. doi: 10.1016/j.sigpro.2018.04.018.

[20] G. Kumaresan and N.P. Gopalan, "Reversible data hiding in encrypted images using public cloud and cellular automata, J. Appl. Secur. Res., vol. 14, no. 4, pp. 427-444, Sept. 2019. doi: 10.1080/19361610.2019.1656472.

[21] W. Zhang, Z. Zhu, and H.Yu, "A symmetric image encryption algorithm based on a coupled logistic–Bernoulli map and cellular automata diffusion strategy," entropy, vo. 21, no. 5, 504(23pages), May 2019. doi: 10.3390/e21050504.

[22] U.S. Choi, S.J. Cho, J.G. Kim, S.W. Kang and H.D. Kim, "Color image encryption based on programmable complemented maximum length cellular automata and generalized 3-D chaotic cat map," Multimed. Tools App., vol. 79, no. 10, pp. 1-18, Aug. 2020. doi: 10.1007/s11042-020-09033-y.

[23] S.J. Cho, U.S. Choi, H.D. Kim, Y.H. Hwang, J.G. Kim and S.H. Heo, “New synthesis of one-dimensional 90/150 linear hybrid group cellular automata,” IEEE T COMPUT AID D, vol. 26, no. 9, pp. 1720-1724, Sept. 2007. doi: 10.1109/TCAD.2007.895784.

[24] P. Sooraksa, and G. Chen, “Chen systems as a controlled weather model – physical principle, engineering design and real applications,” Int. J. Bifurcation and Chaos, vol. 28, no. 4, 1830009, 2018. doi: 10.1142/S0218127418300094.

[25] S.T. Kamal, K.M. Hosny, T.M. Elgindy, M.M. Darwish, and M.M. Fouda, "A New Image Encryption Algorithm for Grey and Color Medical Images," IEEE Access, vol. 9, pp. 37855-37865, Mar. 2021. doi: 10.1109/ACCESS.2021.3063237.

[26] M.I. Wade, M. Chouikha, T. Gill, W. Patterson, T.M. Washington, and J. Zeng, "Distributed Image Encryption Based On a Homomorphic Cryptographic Approach," Proc. of 2019 IEEE 10th Annual Ubiquitous Computing, Electronics & Mobile(UEMCON), Feb. 2020. doi: 10.1109/UEMCON47517.2019.8993025.

[27] F. Yang, J. Mou, Y. Cao, and R. Chu, "An Image Encryption Algorithm Based on BP Neural Network and Hyperchaotic System," China Communications, vol. 17, no.5, pp 21-28, May 2020. doi: 10.23919/JCC.2020.05.003.

[28] Z. Hua, B. Xu, F. Jin, and H. Huang, "Image Encryption Using Josephus Problem and Filtering Diffusion," IEEE Access, vol. 7, pp. 8660-8674, Jan. 2019. doi: 10.1109/ACCESS.2018.2890116.

[29] Y. Zhong, H. Liu, X. Sun, R. Lan, and X. Luo, "Image Encryption Using 2D Sine-Piecewise Linear Chaotic Map," Proc. of 2018 International Conference on Wavelet Analysis and Pattern Recognition (ICWAPR), Chengdu, China, July, 2018. doi: 10.1109/ICWAPR.2018.8521240.

[30] Z. Hua, S. Yi, and Y. Zhou, "Medical image encryption using highspeed scrambling and pixel adaptive diffusion," signal processing, vol. 144, pp 134-144, Mar. 2018. doi: 10.1016/j.sigpro.2017.10.004.

[31] V. Thanikaiselvan, S. kumar, and R. Gera, "New Image Encryption using Chaotic Map in Wavelet Domain," Proc. of 2019 International Conference on Vision Towards Emerging Trends in Communication and Networking (ViTECoN), Vellore, India, Mar. 2019. doi: 10.1109/ViTECoN.2019.8899365.

[32] Y. Wu, J.P. Noonan and, S. Agaian, “NPCR and UACI randomness Tests for image encryption,” Cyber Journals: Multidisciplinary Journals in Science and Technology, Journal of Selected Areas in Telecommunications (JSAT), pp 31–38, Apr. 2011.

Multi-point Fundraising and Distribution via Blockchain

Abdullah Omar Abdul Kareem Alassaf[1], Fakhrul Hazman Yusoff[2]
Faculty of Computer Science and Mathematical Sciences
Universiti Teknologi MARA
Shah Alam, Malaysia

***Abstract*—Trust and transparency are significant facets that are much esteemed by charitable organizations in achieving their mission and encouraging donations from the public. However, after many high-profile scandals, the faith in charities is questionable, heralding the need for an increased level of transparency among such organizations. Fortunately, leveraging Blockchain technology in charities' systems could help to rebuild the integrity of these organizations. This study aims to raise the level of integrity showcased by charities by creating a multi-point fundraising approach using smart contracts. The proposed system offers a transparent fundraising platform through its integration of charity organization evaluators. Various steps were deployed to satisfy the intended target. Firstly, the study investigated the potentials of Blockchain in improving the level of transparency. Secondly, a probing process was undertaken to choose a suitable platform as a server-side in the system. This process involved garnering salient features in Blockchain platforms based on the proposed system requirements. After the probing process, a Decision Support System (DSS) was utilized to investigate the most suitable Blockchain platform. Results garnered proved that the Ethereum platform is best for the proposed system.**

Keywords—Blockchain; smart contract; transparency; charity

I. Introduction

The desire to help and to be of service to others is the nature of human behaviour. Donations to charities are one of the ways people help each other and this is positively reflected on the community. Charities play an essential role in fields like education, healthcare, and other social services [1]. In addition, all religions preach and encourage philanthropy, for instance, Islam makes it obligatory and calls it Zakat [2].

Trust and confidence are fundamental for charitable bodies to achieve their mission in getting donors and donations [3]. Higher trust levels could increase the amount of donations received by these charities [1]. However, after many high-profile scandals, charities have been criticized for misusing donated money [4], and donors have begun to lose trust in charities; hence calls for more transparency have increased [5].

For instance, recent events and evidences show that public trust and confidence in charities in the UK has been damaged. As a result, the activities of individual charities could be limited, and the sustainability of the whole sector reduced [6].

The following figure is a survey has been done in North Ireland to explore the views on the charity sector; Fig. 1 shows a question related to transparency in charities.

Fig. 1 shows that 92% of the people, who answered the survey, agreed on that charities should be transparent about how public donations are spent, and how important it is that charities must demonstrate how they benefit the public, while 40% know how to find information about how charities are run. Also, only 32% know where they can find information about how charities are spending their money [7].

According to the facts and findings mentioned above, transparency is a crucial element in charity sector. Yet, it is one of the biggest vulnerabilities in the existing charity systems, as addressed in many studies [1], [3], [5], and [7]. Therefore, it should be enhanced.

With the advent of blockchain, many studies suggested that blockchain has a great potential to benefit various sectors and industries such as education [8] and travel [9].

Similarly, Blockchain is reputedly able to solve the transparency issues in charity systems [10]. Thus, leveraging blockchain technology in charity systems could help in rebuilding the image of charity. Hence, studies and researches are investigating different approaches to take the advantages of this technology.

This study aims to tackle the transparency issue. Therefore, a donation system will be implemented to promote transparency in charitable organizations' campaigns by using smart contracts to hold donors' donations till it gets verified based on multi-point model to ensure that donations reach those who need help. The deployed smart contracts store on a suitable blockchain platform which will be selected after identifying the important features in blockchain platforms to get the ideal platform for charity systems. The system offers a transparent environment for all parties including charitable organizations, donors, recipients, and charity evaluator organizations. As well as, all transactions will be made through this system will be accessible and traceable for the public.

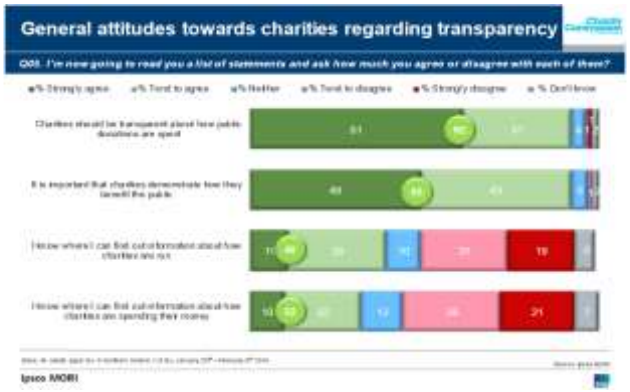

Fig. 1. General Attitudes towards Charities Regarding Transparency in North Ireland [7].

II. Related Work

Blockchain technology can play a significant role in philanthropy to overcome many challenges. So, some studies have tried to utilize blockchain in a charity system. Firstly, Nor et al. [11] proposed Sadaqa system for disaster aid crowd funding. The system focuses on transferring funds to the people in need during the disaster using Ethereum smart contract to avoid problems of the modern day transactions related to transaction fees, potential fraud, absence of accountability, and transaction time.

Secondly, Hu et al. [12] proposed a charity system using Ethereum smart contracts, they leverage Blockchain to improve the transparency in charities and increase the public trust, the system allows donors to vote on the request of a beneficiary to involve donors in fundraising and enhance transparency.

Lastly, D. Jayasinghe et al. [13] built a Bitcoin payment system that can be used in both an offline environment via the existing GSM network, as well as, online environment to provide aid for people living in a challenging geographical environments with limited internet availability.

Based on the abovementioned studies, this article will investigate the crucial features in blockchain platforms to find the most suitable platform for charity system, and then it will propose a blockchain charity system that relies on a new model concentrates on enhancing transparency; the model contains elements that have not been addressed in the previous studies.

III. Blockchain

Blockchain technology has gained widespread attention in recent years, as it promotes trust and transparency. In 2015 a report by the UK Charities Aid Foundation [14] points out that for charities, Blockchain helps to increase transparency, openness and confidence while reducing transaction costs and providing new opportunities for fundraising.

Blockchain can be identify as a public ledger, in which all transactions are stored in a chain of blocks; the ledger constantly grows when new blocks get approved and added by the network members [15].

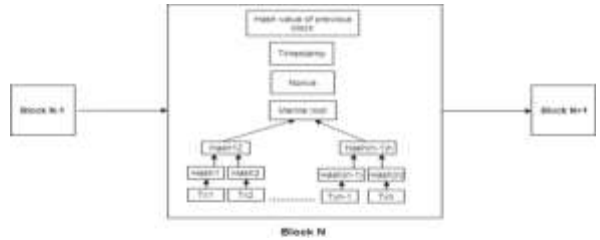

Fig. 2. Blockchain Structure.

Blockchain sorts and encrypts the information inside the block before adding the block to the chain. What makes the chain traceable is the blocks are linked with each other in the chain, giving each block encryption code called a hash [16]. Blockchain contains blocks where each block records transactions sent between users, hash code which is a unique code created when a new block is discovered, and a reference code of the previous block [17]. Fig. 2 illustrates how blocks are connected to form the Blockchain. Each block consists of transactions (Tx) that is represented in a hash number using Merkle tree, as well as other values such as hash value of previous block (N-1), timestamp, and nonce which is a random number that can be used just once, these values will be used to represent the hash value of the current block (N), and this hash will be stored in the next block (N+1).

IV. Key Benefits of Blockchain for Business

Nguten and Hoang [18] pointed out the key benefits of blockchain technology that makes it attractive for many types of businesses, the benefits are:

1) Decentralized: blockchain networks are not controlled by a central party, which helps to avoid a single point of failure and take over the network by a small group of users. Users in Blockchain participate in a distributed network managed by consensus mechanism to reach the agreement on the network state.

2) Transparency: All network participants can see the stored data; in other words, the data stored in a blockchain is visible to the public.

3) Immutability: Once the data are stored in the Blockchain, it cannot be changed.

4) Security and privacy: One of the important features in the Blockchain is the cryptographically secure mechanism because it helps in promoting privacy and security. Furthermore, users in the network use a public and private key for identification and verification. When a transaction occurs, a user can be easily verified by his digital signature.

V. Choosing a Suitable Blockchain Platform

First of all, two crucial features have to be determined in the blockchain platform. The first step is to decide on the type of network, and then to decide whether Crypto-currencies is needed or not [19].

A. Network Type

Data cannot be exchange without networks; therefore, networking plays an important role in any field related to information technology. That is why there are vicarious network attacks such as mentioned by [20], [21], [22] , and [23].

With regard to the first step, there are three types of networks in blockchain: public network, private network, and consortium network.

1) *Public network:* It's a permission-less or open network, not controlled by any organization, anyone can join the network, and all users are equal; they can read and write without any restrictions. These blockchain networks are considered as fully decentralized. Transparency is the most significant advantage of the public network. However, there are some disadvantages of Public Network and that includes slow transaction speed as compared to other networks, and scalability issue though some steps are already taken to solve this problem such as off-chain, examples of public network Bitcoin and Ethereum [24].

2) *Private network:* The second type of the blockchain network is the private or permissioned network; it is centralized or partially-centralized as compared to the public network; it is controlled by a single organization that has the permission to write in the ledger, read can be public or restricted by participants. The advantages of this network are the transaction speed, and it is considered more scalable than a public network; however, it is not transparent since a single organization controls it. An example of a private network is Heyperledger, one of the popular private network platforms [25].

3) *Consortium network:* It is a semi-private network owned and controlled by a preselected group of members. This group of members has permission to write in the ledger, and read can be public or restricted by participants, it is more secure and has better scalability; however, it is less transparent. Marco Polo platform is an example of a consortium network [26].

Each blockchain network has unique features to offer; therefore, choosing a suitable platform would rely on the system requirements, for a charity system transparency has the highest priority. Thus, the public network is ideal for organizations that thrive on trust and transparency.

B. Crypto-Currency

The second feature is to decide on the need for crypto-currencies. It is a currency that only exists digitally, that usually has no central issuing or regulating authority but instead uses a decentralized system to record transactions and handle the issuance of new units, and that relies on cryptography to avoid counterfeiting and fraudulent transactions.

The most important feature about crypto-currency is that it is not controlled by any central authority or a third party. It can be sent directly between two parties with minimum transaction fees and allow users to avoid the high fees that traditional institutions impose [13].

The crypto-currency was the first application of Blockchain presented by Nakamoto [27] in 2008 and it is known as Bitcoin. Since then, a lot of crypto-currencies have arisen, such as Ethereum, Tether, and many others.

There are many benefits that can be gained from Blockchain that would positively affect the existing charity systems. As pointed in previous studies [13] and [14], the benefits that can be obtained from using crypto-currency are:

1) *Reducing transaction cost:* One of the notable features of Blockchain is its low international transaction fees.

2) *Transaction speed:* In Ethereum, once a user clicks on send, the transaction will broadcast immediately, it takes some time to get confirmed, the time can be determined based on the gas amount that users are willing to pay.

3) *Donation provisioning:* Sending the donations to the recipient can be challenging in some cases. For instance, humanitarian financial aid distribution in war zones can be blocked if the country's bank system is subject to sanctions, Ethereum transactions can reach the recipient without needing to use any bank system.

C. Smart Contract

The third important feature is the smart contract. It is a computer program that allows the charity system to control the transferring of crypto-currencies and assets between users and these contracts are stored in a decentralized ledger. Many studies have suggested Smart Contract as a primary factor for charity system based blockchain [7], [10], and [13]. The first use of the smart contract was made by Ethereum [28].

It can also be defined as a set of instructions represented in computer code published on a distributed network that receives inputs, executes instructions, and provides outputs. It can enable a charity to over other features such as routine provisioning of donations, record keeping, donation requests to donors, and automatic audit reports of a charity activity [13].

D. Consensus Algorithm

The fourth important feature that should be taken into account is consensus algorithm or mechanism which is the backbone of the Blockchain and the core element of any blockchain platform. It plays a vital role to ensure the network's security, integrity, and performance [18], and [29].

The most popular consensus mechanism is Proof of Work (PoW) that was first introduced by Nakamoto [27]. It relies on the computing power to distribute a new block among network peers. PoW is used by many platforms such as Bitcoin and Ethereum. The second popular consensus is Proof of Stake (PoS) that was created as an alternative to PoW mechanism because of the high energy consumption of PoW consensus; PoS relies on the participant's stake rather than computing power. Different protocols have been introduced PoS approach with slight differences; such as Ouroboros [30] and Casper by Ehereum [31], another study suggested combining POW and POS such as Proof of Activity (POA) [24].

Furthermore, some platforms implement PoS, such as Peercoin, However, studies are still needed for more analysis and investigation for the Proof of Stake mechanism [29]. Thus, a specific algorithm will not be chosen, since it is currently under study, and it can be changed in the future. For example, Ethererum is planning to switch from PoW to PoS [31].

VI. Decision Support System

Choosing a suitable platform for any type of business is an essential step before implementing blockchain [19]. However, there are many varieties of available blockchain platforms with multiple features. This problem called Multi-Criteria Decision-Making (MCDM), which is defined by "making preference decisions (such as evaluation, prioritization, and selection) over the available alternatives that are characterized by multiple, usually conflicting attributes" [32]. To cope with this problem, Farshidi et al.'s system [19] will be used.

Farshidi et al.'s system is called Decision Support System (DSS). The system formulates the Blockchain selected platform as an MCDM problem to find a suitable platform that supports the required features. They have extracted a set of blockchain features from online documentation of blockchain platforms. A list of the important features has been identified by researchers and experts.

Based on the DSS they are other features that need to be taken into account along with the abovementioned features to get the most suitable Blockchain platform, however, they are not crucial as the mentioned features, but they can help to differentiate between platforms. The features are:

1) Market positioning: It is measured by the Numerical feature like transaction speed, popularity in market and platform's maturity, and by Boolean feature, which is the number of innovations that platforms support, such as; Internet of Things and Artificial Intelligence, etc.

2) Capacity: It is measured by scalability technologies used, such as side-chains, Sharding, Plasma-chains, Off-chian-state-channels and On-Chain Transactions.

3) Development: It is measured by programming languages support, such as; Soildity, Python, JavaScripit, C++,.Net and Golang.

4) Flexibility: It is measured by resilience technologies such as Sybil attack resistant, Spam-attack resistant, Quantum-computing resistant, Instant transaction Finality, and Hard-fork resistant.

5) Integration: Which means a platform that can integrate with the other systems, and it is measured by Interoperability technologies that supported by the platform such as Atomic Swap, Cross-chain technology, Enterprise system Integration.

The score will be indicated on a scale from *0 to 100*, where *0* represents the least suitable platform and *100* represents the most suitable platform. The following figure shows the result of the top 10 feasible platforms for the proposed system based on these features:

- Network type: public network.
- Smart contracts: yes.
- Crypto-currencies: yes.
- Consensus algorithms: Proof of Work or Proof of Stake.
- Market Positioning: High Transaction Speed, High Maturity, High Popularity, High Innovation.
- Programming languages support: Solidity, JavaScript and python.
- Interoperability technologies: any (Not specified).
- Scalability technologies: any (Not specified).
- Resilience technologies: any (Not specified).

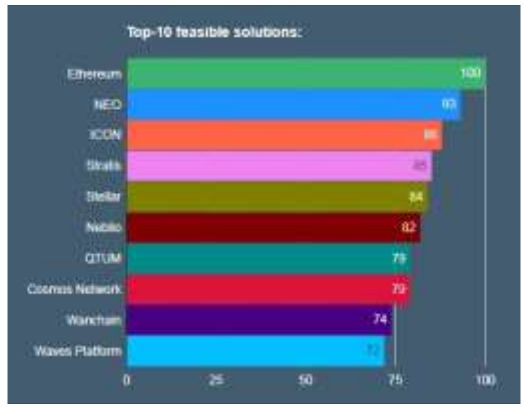

Fig. 3. The Result for the Suitable Platform based on Decision Support System [19].

Fig. 3 shows that Ethereum scored 100, which is the highest score among other platforms; because it supports all the selected features. NEO is the second platform scored 93; it has a lower score than Ethereum, because it does not support all features.

VII. Additional Elements to Improve Transparency

As addressed above transparency issue in the current charitable organizations; and presented Blockchain as a solution that will help in tackling this issue. In addition to Blockchain other elements can be used, the following section discusses two important elements that can help in improving the transparency in charities.

A. Monitoring Charitable Organization

Evaluation and assessment of charitable organizations by another type of non-profit organization specialized in charity evaluation is one of the solutions to improve the transparency and give donors more confidence to contribute. This kind of organization called charity evaluator, and their job is ensuring that fundraising in charitable organizations is being organized and performed in a satisfactory manner and that the administration of the collected funds is adequate, one example on this organization is International Committee on Fundraising Organizations (ICFO) [33].

Therefore, having a Charity Evaluator organization in a charity will help in improving transparency and encouraging donors to donate confidently. It will also provide an additional layer of assurance in the prevention and detection of misuse of donors' funds.

B. Offering a Refund Option

Donazzan, Erkal, and Koh experiment showed that offering a refund option has a positive impact on giving behaviour and increasing confidence [34]. Another experimental study also showed that offering a refund option could increase the contributions [35]. Therefore, offering a refund option in a charity system has a potential to increase the confidence and the amount of contributions.

VIII. System Model

Fig. 3 displays system processes flow; the system's main processes accrue through two main pages login page that lead to the user profile and view campaigns page to view campaign details.

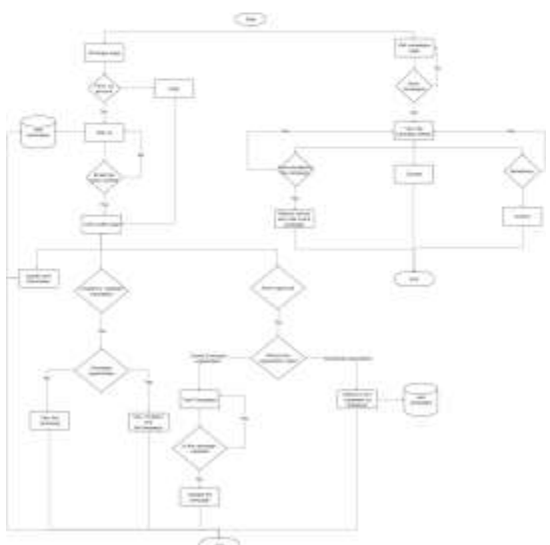

Fig. 4. System Flow Diagram.

According the Fig. 4, the system starts with two main processes, first login process for two types of user charitable organizations and evaluator organizations, they should login to interact with their campaign, to do so, they need the admin approval, if they received the approval, charitable organizations can create and deploy new campaigns on Ethereum network, and evaluator organizations can validate them.

On the other hand, campaigns will be accessible to the public without the need for logging in, so that donors, beneficiaries, and visitors can view campaigns' details that have been created by charitable organizations.

IX. The Design of the System

Fig. 5 illustrates the proposed system design; the system is a decentralized web application (Dapp), where the web application is (client side) that is connected to the Ethereum Network (server side) through web3 that allows the system to interact with the Ethereum network. Users are required to use Metamask Ethereum wallet in order to interact with the system smart contracts, donors however, can donate by using Metamask or any other Ethereum wallet.

The Dapp will deploy the Campaign Factory smart contract once, so that the system users in particular the charitable organization can interact with this contract to deploy their campaigns. Additionally, the system will be able to track all campaigns that have been deployed through it.

Dapp users and visitors can view details of all campaigns contracts that have been deployed by charitable organizations. Donors can send money to the contract directly without the need to sign up, whereas, Charitable Organization and Charity Evaluator Organization should submit their information and wait till their application gets approved by Administrator. Once the Charitable organization's application is approved, they can interact and create any number of campaigns they want through a predefined Metamask wallet address. On the other hand, Charity Evaluator organizations are responsible for monitoring and evaluating charitable organizations' performance and campaigns.

Smart contract details with all transactions will be stored in the Ethereum blockchain network. Mysql database is used to store charitable organization and Charity Evaluator credentials and information.

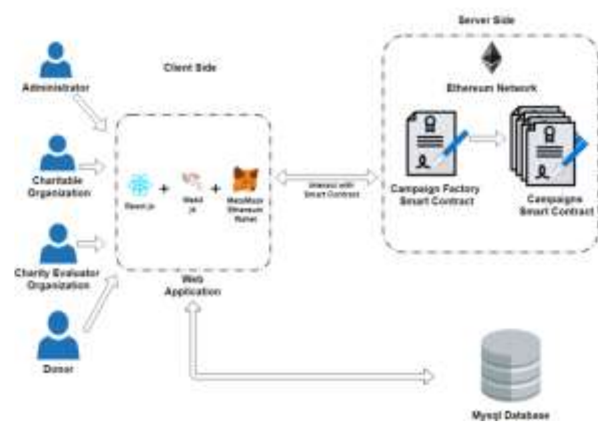

Fig. 5. Client Server System Architecture.

Fig. 6. Use Case Diagram.

As shown in Fig. 6 they are four types of users in the proposed system:

1) Administrator: the Administrator is responsible for accepting or rejecting users' applications, as well as deleting users. He can also terminate any campaign's contract if he feels that the campaign does not meet the requirements.

2) Charitable organizations: this type of users has a profile; so, charitable organizations are required to provide information about the charitable organization's name, address, email, contact number, registration number, number of employees, mission and goals of the organization, in order to sign up to the Dapp. Then they need to verify their email address, upon which they will then be able to create new campaigns if their applications get approved by the Administrator. Charitable organizations' profile will be available and accessible to the public.

3) Charity evaluator organizations: they are similar to charitable organizations in terms of the signup process; however, their job is overseeing and monitoring the charitable organizations' campaigns and evaluating their performance.

4) Donors: they are not required to login in. Donors can send money through Metamask wallet or any Ethereum wallet to all campaigns' smart contract, and they also can get their money refunded any time during the lifetime of the campaign.

X. System's Smart Contracts

The proposed system has two smart contacts.

A. Campaign Factory Smart Contract

Campaign Factory is a smart contract that has been deployed before the launch of the Decentralized Application (Dapp). This is to enable the charitable organization to deploy their smart contract (Campaigns) through Campaign Factory. Therefore, Dapp will be able to track all campaigns that have been deployed by the charitable organizations. This contract has two functions:

- To create a campaign: this function invokes by a charitable organization to create a new contract, the function's parameters are minimum target amount of Ether needed to finalized the campaign, originator Metamask wallet address, description about the campaign, campaigns parties' information, beneficiary wallet address, and the end date of the campaign.
- To list deployed campaigns: the Dapp calls this function to display a list of all campaigns that have been deployed by charitable organizations.

B. Campaign Smart Contract

A charitable organization deploys this contract through the Campaign Factory smart contract; parties involved in this contract are Charitable Organization, Charity Evaluator, Donors and Beneficiary. Campaign smart contract shows information about the campaign and receives Ether from donors, as well as, holds donors Ether until all conditions stated in the contract are fulfilled. Later, it will allow a charitable organization to finalize its campaign; once the campaign gets finalized, the funds will be sent to the beneficiary. Once the campaign is completed, no one can interact with the finalized contract, and it will remain as a reference that stored all transaction and information. The Campaign contract performs the following functions:

- Donate(): this function allows donors to donate for the campaign through the website application by using Meta mask Ethereum Wallet extension in the browser. When a user clicks on a donate button, the website will invoke the donate function from the Campaign smart contract, and Ether will be sent to the contract.
- Receive(): this function gets called when the donors send money from any Ethereum wallet other than Metamask wallet. It allows the Campaign smart contract to receive Ether from anywhere.
- Refund(): this function gives donors the right to get their money refunded at any time they want as long as the contract has not been finalized.
- CharityEvaluatorApproval(): Any charity evaluator organization can execute this function, it will change the value of ApprovedByEvaluator from false to true, and this will indicate that a charity evaluator organization has approved the campaign.
- BeneficiaryApproval(): Similar to the Charity Evaluator Approval function, beneficiary confirmation is also required; beneficiary only can call this function.
- Finalize(): This function can be called only by contract originator (the charitable organization) in order to transfer the money to the beneficiary.
- TerminatetheCampaign(): The contract originator or the Administrator can call this function. It sends the Ether back to donors and blocks any future interactions with this campaign.
- VotetoTerminate(): The function can be called by a donor who has donated to the campaign to vote for termination of the campaign.
- GetSummary(): This function gets called by the Dapp to display campaign details to the public.

Note that Metamask Ethereum wallet is required for all parties if they want to interact with the deployed contract, except, contribution or sending money to the campaign can be either by Metamask or other Ethereum wallets. Campaign smart contract rules are:

- Once the contract gets deployed, funds will be held in the smart contract in the Ethereum blockchain network till the campaign ends.
- When the campaign ends, only a charitable organization can finalize the contract to transfer the funds to the beneficiary address.
- A charitable organization cannot finalize the campaign without other parties' confirmation (Charity Evaluator and Beneficiary), should have passed campaign end

date, and the funds should reach the minimum amount of Ether.

- During the lifetime of the campaign contract, donors can get their Ether refunded at anytime they want.
- During the lifetime of the campaign donors can vote to terminate the campaign if they are not satisfied. If end date has already passed and 50% of the donors are not satisfied with the campaign the charitable organization (campaign originator) will not be able to finalize the contract, and they will be required to terminate the campaign.
- If the campaign end date has already passed, and the contract's conditions are not fulfilled, a charitable organization or Administrator can refund Donors money by calling the termination function.
- Once funds are sent successfully to the beneficiary, the campaign will not accept any new transaction, and no one can interact with it. However, all transactions and information will remain available and accessible to the public.
- Charitable organization (campaign originator) and Administrator can terminate the campaign at any time, when they do so, consequently, funds will be sent back to donors and the campaign will not accept any other transactions.

XI. Multi-Point Model

Fig. 7 illustrates how the Multi-point approach has been applied in the campaign smart contract; the campaign should go through seven processes, each of which is designed for a certain player.

For example when a charitable organization wants to finalize its campaign, the request through MetaMask wallet will be sent to the campaign smart contract in a transaction form to invoke the 'finalize function'. The campaign contract will first check if the sender ID is same as the contract originator ID to ensure that only the campaign originator (charitable organization) can finalize the campaign. It will then check if the campaign is validated by a charity evaluator organization, and verify that the beneficiary has confirmed the campaign and that 50% or more of donors are satisfied with the campaign. The campaign contract will then check if the campaign target is achieved and the campaign has reached its end date. Only when these conditions are met, will the transaction be confirmed and the campaign is finalized.

As shown in Fig. 6 the first step is to check the campaign status. If the campaign is finalized by its originator, users will no longer be able to interact with the finalized campaign. They can however continue to read the campaign details. The important point of this approach is to ensure that before the campaign is finalized or completed, it has to go through Multi-point campaign finalization process. This process would involve various parties in the fundraising process.

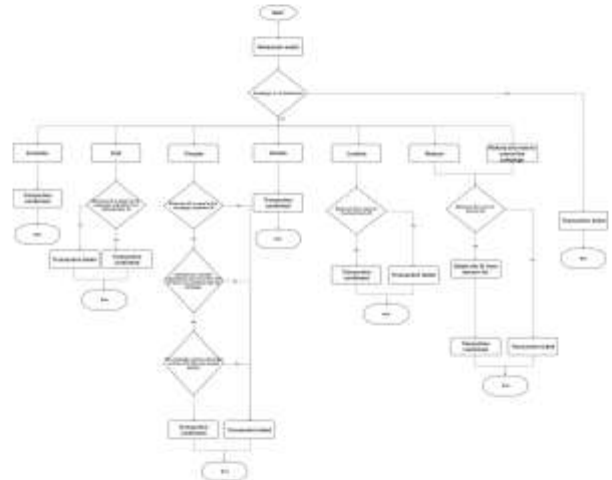

Fig. 7. Multi-point Model.

XII. System Interface

The system pages will be shown in this section, the system is a Dapp. The following points and figures illustrate the system pages, the Dapp interface consists of:

- Home page layout: Fig. 8 shows the home page of the Dapp. It is the first page that will be displayed for users - the first page that users will view in the website.

This page provides a short description about Blockchain and Smart Contract, as well as the latest two campaigns run by charitable organizations are displayed. From the navigation menu, user can go to the campaigns, about us, login and sign up pages.

- Campaigns page layout: as shown in Fig. 9 on this page users can check all campaigns that have been created by charitable organizations through the Campaign Factory smart contract. A list of campaigns will be displayed, consisting its campaign title, charitable name, short description about the campaign, and campaign status (to show if the campaign is completed).

Fig. 8. Home Page Layout.

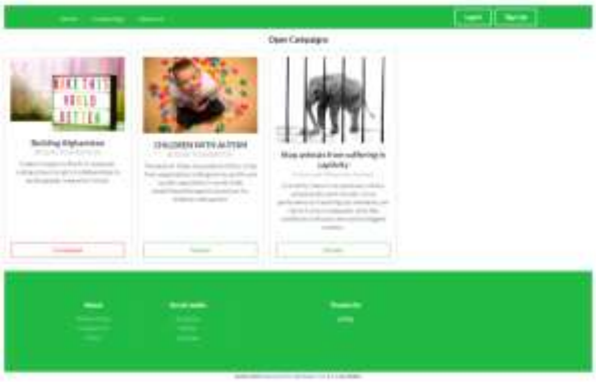

Fig. 9. Campaigns Page Layout.

- About us page: This page includes system directors' personal information such as name and email address. This page is also accessible to the website visitors to enable them to get in touch with the board members should the needs arise. Fig. 10 shows this page layout.

Fig. 10. About us Page Layout.

- Signup page layout: Fig. 11 illustrates this page layout. On this page the two types of users allowed to sign up are the charitable organization and charity evaluator organization. Users are required to fill fields that are divided into four main sections; first section is login information which includes user email and password. The second section includes organization name, mission and goals (for charitable organization) and standards (for charity evaluator organization), number of employees, address, and the registration number of the organization. The third section is the contact information such as phone number, email, and website. In the last section users are required to enter theirs Ethereum wallet address.

- Login page: as shown in Fig. 12 from this page users can access their accounts once their credentials are keyed in. The two fields that users are required to fill in are their email and password. If a user doesn't have an account yet, he/she should go to the sign up page through a hyperlink provided underneath the fields form, or through the menu bar to create a new account.

Fig. 11. Signup Page Layout.

Fig. 12. Login Page Layout.

- Campaign details page: as Fig. 13 shows, this page displays all the details of a campaign; it is the main page of the Dapp since most of the interactions with the Campaign smart contract will take place on this page. Here, donors can donate to a campaign. The second section is used to show information about the originator of the campaign (charitable organization), which includes name and Ethereum address of the organization as well as a button to visit the organization's profile and a hyperlink to send users to the Etherscan to check its account. Details on the charity evaluator information are also displayed here. 'Waiting for validation from evaluator' message will be prompted if the campaign has yet to be validated by a charity evaluator. The beneficiary information is shown at the bottom of the page: as who is/are the beneficiary/ies, their physical address along with their Ethereum address and a hyperlink to visit their account in the Ethereum network. Underneath the beneficiary information section, unhappy donors could claim for a refund and vote to cancel the campaign. In addition, campaign information is shown under the campaign image - campaign title, short description about the campaign, and campaign status (it will be funded if the campaign is still running and completed if the campaign is completed and does not accept a new transaction). The minimum amount of funding needed for this the campaign is displayed with a progress bar to show the percentage of the campaign balance, and donors rating (if a donor had requested for a refund of his Ether and voted to cancel the campaign hence affecting the rating). The same page also displays the campaign details such as start and end date, campaign target (the minimum amount), campaign balance, number of donors, number of unsatisfied donors, campaign manager name and email, campaign Ethereum address, and campaign goals.

Unlike the general users, the two types of logged in users (charitable organization and evaluator organization) can also see/access to the following buttons:

1) Evaluator organization's button: This button is for evaluator organizations to validate a campaign.

2) Charitable organization's button: Only charitable organizations can see this button to either finalize or terminate the campaign.

- Charitable organization's profile: After a user has verified his account and logged in, he needs to wait until his account gets approved by the admin. If approved, new campaign button will be appeared on the user's page as it is shown in Fig. 14 and he will then be able to update certain information such as address, number of employees, phone number, contact email, missions and goals, and email. The user will also be able to see his campaigns and access it to finalize, terminate, or just check on the campaign status.

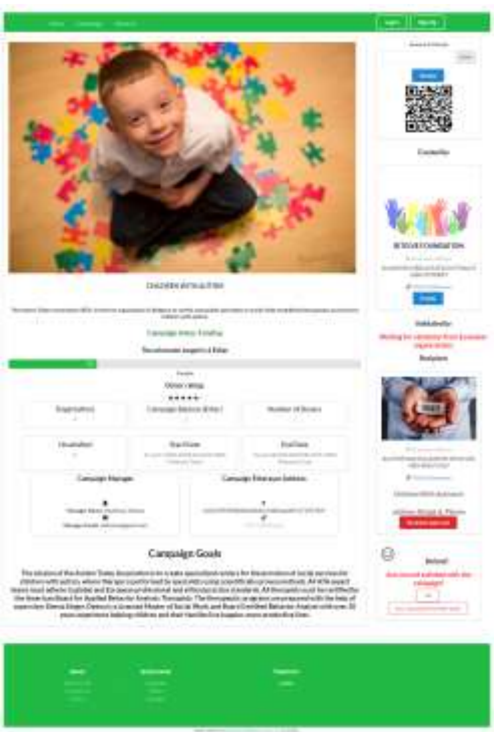

Fig. 13. Campaign Details Page Layout.

Fig. 14. Charitable Organization's Profile Layout.

As shown in Fig. 15, if the user wants to create a new campaign, a new page will be opened. This page is only accessible to the charitable organizations. To create a new campaign, the user will furnish some relevant information on the campaign, i.e. title, short description about the campaign, minimum target needed to fulfil campaign goals, beneficiary Etherum address so that the funds will be automatically transferred to this account after the campaign is completed and finalized, campaign goals, beneficiary information, campaign manager information, and end date.

Fig. 15. Create New Campaign Page Layout.

The user must use his predefined Metamask address so that after clicking on the create button, his MetaMask wallet will pop up and display the transaction fee. Once the user clicks on the confirm button, only then will his new campaign be deployed in the Ethereum network.

- Charity Evaluator Organization: as Fig. 16 shows the charity evaluator organizations' profile is very similar to the charitable organization. After a user verifies his account and logged in, he needs to wait until he gets the admin's approval.

Fig. 16. Charity Evaluator's Profile Layout.

Similarly, when the user account gets approved, a campaign button will be appeared in his account and the user will be able to update certain information such as address, number of employees, phone number, contact email, standards, and email address.

Fig. 17. Charity Evaluator Campaigns Page Layout.

The user can also see those campaigns that have been validated by him as shown in Fig. 17. When the evaluator clicks on the campaigns buttons on the page, a list of campaigns will be displayed and the user can then access to information such as the campaign details and whether or not the campaigns are validated.

XIII. Test System's Smart Contract

The Dapp contracts have been tested locally; Rinkeby Ethereum test network is used during the test to obtain virtual Ethereum tokens for donation and expenses required for the test.

Infura provides a suitable entry point for the Rinkeby network. MetaMask wallet was used to store the Ethereum tokens and complete the corresponding transactions. At the same time, a Web3 instance completes the interaction between the website and the Ethereum network. Table I shows accounts and their balances that have been utilized for testing before the campaign is being deployed.

The campaign includes a description of the campaign, goals, information about the Originator and the Beneficiary, end date of the campaign to notify the public that the Originator will be able to finalize the campaign after that date, it also displays the campaign balance along with all transactions that have been made and the minimum target amount needed to achieve campaign's goals (the minimum target for this campaign is 1 Ether).

Table II illustrates all interactions with System contracts; the first transaction made by Originator to create a new campaign. 0.00141 ETH of the gas limit was used to execute the create function in the campaign factory smart contract. The second transaction was made by the Donor A to send 0.25 Ether from his wallet to the testing campaign smart contract, the gas fee used to execute this transaction was 0.00012 Ether. Donor B also donated with Ether to the campaign at a different amount of 0.10 Ether. After that, the Originator tried to finalize the campaign, but the transaction failed because some requirements have not yet been fulfilled.

TABLE I. ETHEREUM ACCOUNTS THAT HAVE BEEN USED FOR TESTING THE SMART CONTRACT

Account	***Address***	***Balance (ETH)***
Originator	0x38e7be22eaFc465042f1b92c13D685342Bb034AC	1
Monitor	0xbB1E68cE914f95b4aB86d81581Bb25aB5C2B3402	1
Beneficiary	0x4a6F69e31BE1a5A3E4d7A794ba76a2Ba71f9DB93	0.0007
Donor A	0x21A1292D940090AB830eF88D0fb1891F0A220596	1
Donor B	0x0C69Ff3624c607Bc3Aca6BF8f2D5f93bb3B4bDD3	1
Donor C	0x2700556Ab9a1eb2D39c1D53C22b40E5982671457	1

TABLE II. ALL INTERACTIONS WITH THE CAMPAIGN SMART CONTRACT

Originator	***Action***	***Message***	***Notes***
Manager	Create a new campaign	Confirmed Transaction	-
Donor A	Donate (0.25 Ether)	Confirmed Transaction	Contract balance 0.25 Ether
Donor B	Donate (0.10 Ether)	Confirmed Transaction	Contract balance 35.0 Ether
Originator	Finalize the campaign	Failed Transaction	Failed transaction: because the contract has not been confirmed and verified by the beneficiary and the monitor.
Beneficiary	Approval	Confirmed Transaction	-
Originator	Approval	Confirmed Transaction	-
Manager	Finalize	Failed Transaction	Failed transaction: the end date has not passed yet, and the target balance has not reached.
Donor C	Donate (0.65 Ether)	Confirmed Transaction	Contract balance is 1 Ether
Originator	Finalize	Failed Transaction	Failed Transaction: because the end date has not passed yet.
Originator	Finalize	Confirmed Transaction	The contract finalized and the Ether sent to the beneficiary, no more interaction can be done.

The campaign includes a description of the campaign, goals, information about the Originator and the Beneficiary, end date of the campaign to notify the public that the Originator will be able to finalize the campaign after that date, it also displays the campaign balance along with all transactions that have been made and the minimum target amount needed to achieve campaign's goals (the minimum target for this campaign is 1 Ether).

Finally, the originator was able to finalize the contract and transfer the money to the Beneficiary when all the requirements and conditions have been fulfilled.

Table III presents the accounts' balance after the Testing Campaign has been finalized. All of the Testing Campaign's transactions with time and fees are recorded on Ethereum blockchain as shown in Fig. 18. The figure is taken from Etherscan website, a search engine that lets users look up, confirm and validate transactions on the Ethereum network.

TABLE III. ETHEREUM ACCOUNT AFTER THE CAMPAIGN SMART CONTRACT IS FINALIZED

Account	***Address***	***Balance (ETH)***
Originator	0x38e7be22eaFc465042f1b92c13D6853 42Bb034AC	0.998501
Monitor	0xbB1E68cE914f95b4aB86d81581Bb2 5aB5C2B3402	0.99997
Beneficiary	0x4a6F69e31BE1a5A3E4d7A794ba76a 2Ba71f9DB93	1.000616
Donor A	0x21A1292D940090AB830eF88D0fb1 891F0A220596	0.749872
Donor B	0x0C69Ff3624c607Bc3Aca6BF8f2D5f9 3bb3B4bDD3	0.89988
Donor C	0x2700556Ab9a1eb2D39c1D53C22b40 E5982671457	0.349902

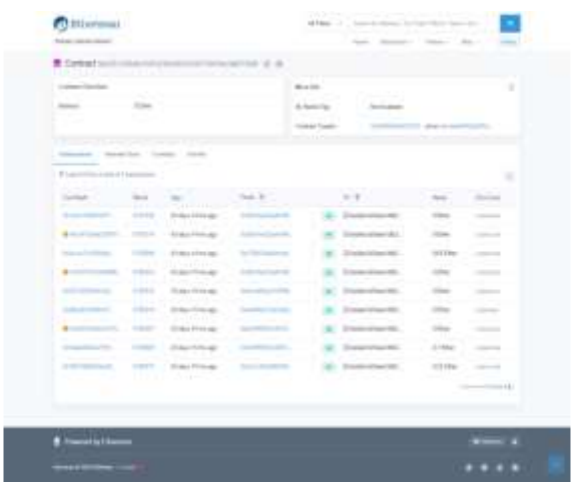

Fig. 18. Etherscan All Transaction Details.

XIV. DISCUSSION AND RESULTS

The study proposes the Multi-point approach to tackle transparency issue, in which the fundraising process should go through multi acceptance and specific conditions before it gets finalized. In other words, rather than having a campaign managed and controlled by one party, this approach involves other parties between the charitable organization and the beneficiary and empower them to improve the transparency in fundraising. Thus, that could help in strengthening the relationship between the charitable organization and donors. Furthermore, it will create a transparent environment that could affect positively on the charitable organizations and increase the quantity and amount of donations to charities, as well as boost donors trust.

The biggest issue in the existing Dapps' campaigns is that they are fully controlled by one party which is the campaign's originator, so they can spend funds anytime and anywhere without any constraints. The proposed Dapp allows donors to play a significant role in the campaign. When the contract gets finalized by the originator the funds will be sent automatically to one direction (beneficiary address) that has already been defined in the campaign.

In addition, existing Dapps do not offer refund option nor do they ensure that the donated funds are sent to the beneficiary. On the other hand, the proposed Dapp ensures that donors can get their money back at any time during the lifetime of the campaign.

The Multipoint approach in fundraising is concerned about empowering donors and involving charity evaluator organizations in the fundraising, between a charitable organization and a beneficiary, in which, charity evaluator organizations are responsible for evaluating and monitoring charitable organizations' campaigns. With the presence of the charity organization evaluators who act as a party ensuring transparency and authenticity of a charity body, donors involved in the fundraising process are protected from fraudulent charities. Moreover, donors can evaluate campaigns and play a major role in the fundraising process. The Dapp interacts with two smart contracts: the Campaign Factory smart contract that uses for creating and tracking charities' campaigns, and the Campaign smart contract that creates by a charitable organization to receive and hold donors funds. Based on certain conditions such as the campaign status, charity evaluator's evaluation, and donor satisfaction, the smart contract determines whether or not the funds can be sent. Besides, all interactions (transactions) with the Campaign smart contract are accessible and traceable and they will be recorded in the Ethereum blockchain.

Finally, based on the above discussion the Dapps's smart contract has been tested and has proven that it can deal with the lack of transparency issue in charity, in consequence, rebuild trust and confidence in charity.

XV. CONCLUSION

Many people have a passion for contributing to society, and they want to donate generously to charitable organizations. However, the lack of transparency in charity caused a trust issue. Transparency is essential in fundraising to maintain public trust, and should be the top priority for charity organizations. Therefore, the research proposed a Multi-point approach based on the usage of Blockchain technology to overcome the transparency issue in charity. First, it investigated the potentials of Blockchain can improve transparency, and then it analyzed the important features related to Blockchain that should exist in the charity's Blockchain platform. The significant features are public network, crypto-currency, smart contract, and consensus algorithm. Finally, the system was tested and proved that it can enhance transparency.

ACKNOWLEDGMENT

Special thanks to Faculty of Computer and Mathematical Science (FSKM) at Unversiti Technolgi MARA, Shah Alam for all the reference resources and support.

REFERENCES

[1] O. Dijk and M. Holmén, "Journal of Behavioral and Experimental Economics Charity , incentives , and performance R," vol. 66, pp. 119–128, 2017.

[2] E. Ahmad, "Pakistan Institute of Development Economics Food Insecurity in Pakistan :," no. September, 2018.

[3] N. Hyndman and D. Mcconville, "Trust and accountability in UK charities : Exploring the virtuous circle," Br. Account. Rev., vol. 50, no. 2, pp. 227–237, 2018.

[4] J. T. A. Prakash, "Will You Trust Me ?: How Individual American Donors Respond to Informational Signals Regarding Local," Volunt. Int. J. Volunt. Nonprofit Organ., vol. 28, no. 2, pp. 621–647, 2017.

[5] D. Mcdonnell and A. C. Rutherford, "Promoting charity accountability : Understanding disclosure of serious incidents ☆," Account. Forum, no. September 2017, pp. 1–11, 2018.

[6] A. Hind, "New development: Fundraising in UK charities—stepping back from the abyss," Public Money Manag., vol. 37, no. 3, pp. 205–210, 2017.

[7] I. Mori, C. Commission, and N. Ireland, "Public trust and confidence in charities," 2016.

[8] A. MacHado, M. Sousa, and Á. Rocha, "Blockchain Technology in Education," ACM Int. Conf. Proceeding Ser., vol. 12, no. 5, pp. 130–134, 2020.

[9] H. B. M. Hadzir and F. H. Bin Yusoff, "Blockchain Based Data Structure for Travel Entourage Tracking System," 2019 4th Int. Conf. Inf. Syst. Comput. Networks, ISCON 2019, pp. 538–541, Nov. 2019.

[10] H. F. Atlam and G. B. Wills, Technical aspects of blockchain and IoT, 1st ed. Elsevier Inc., 2018.

[11] R. M. Nor, M. M. H. Rahman, and T. Rahman, "Blockchain Sadaqa Mechanism for Disaster Aid Crowd Funding," no. 211, pp. 400–405, 2017.

[12] B. Hu and H. Li, "Research on Charity System Based on Blockchain," IOP Conf. Ser. Mater. Sci. Eng., vol. 768, no. 7, 2020.

[13] D. Jayasinghe, S. Cobourne, and K. Markantonakis, "Philanthropy On The Blockchain," 2012.

[14] Charities Aid Foundation, "Giving Unchained: Philanthropy and the Blockchain," Charities Aid Foundation, 2015. [Online]. Available: https://www.cafonline.org/about-us/publications/2015-publications/ giving-unchained-philanthropy-and-the-blockchain.

[15] X. Chen, "Blockchain challenges and opportunities : a survey Zibin Zheng and Shaoan Xie Hong-Ning Dai Huaimin Wang," vol. 14, no. 4, pp. 352–375, 2018.

[16] M. A. Jamison and P. Tariq, "Five things regulators should know about blockchain (and three myths to forget)," Electr. J., vol. 31, no. 9, pp. 20–23, 2018.

[17] J. Herbert and A. Litchfield, "A Novel Method for Decentralised Peer - to - Peer Software License Validation Using Cryptocurrency Blockchain T echnology," no. January, pp. 27–30, 2015.

[18] C. T. Nguyen and D. T. Hoang, "Proof-of-Stake Consensus Mechanisms for Future Blockchain Networks : Fundamentals, Applications and Opportunities," vol. 7, pp. 85727–85745, 2019.

[19] S. Farshidi, S. Jansen, S. Espana, and J. Verkleij, "Decision Support for Blockchain Platform Selection: Three Industry Case Studies," IEEE Trans. Eng. Manag., vol. PP, pp. 1–20, 2020.

[20] N. S. Selamat, F. H. M. Ali, and N. A. A. Othman, "Polymorphic malware detection," 2016 6th Int. Conf. IT Converg. Secur. ICITCS 2016, Nov. 2016.

[21] M. A. M. Yusof, F. H. M. Ali, and M. Y. Darus, "Detection and Defense Algorithms of Different Types of DDoS Attacks Using Machine Learning," Lect. Notes Electr. Eng., vol. 488, pp. 370–379, 2018.

[22] S. M. Jawi and F. H. M. Ali, "Rules and results for SSL/TLS nonintrusive proxy based on JSON data," 2016 6th Int. Conf. IT Converg. Secur. ICITCS 2016, Nov. 2016.

[23] M. Azizi and M. Ariffin, "Data Leakage Detection in Cloud Computing Platform Investigation and Review of Cloud Computing Security View project," Artic. Int. J. Adv. Trends Comput. Sci. Eng., vol. 8, no. 1, pp. 400–408, 2019.

[24] I. Bentov, C. Lee, and A. Mizrahi, "Proof of Activity : Extending Bitcoin ' s Proof of Work via Proof of Stake," no. 240258, pp. 1–19, 2013.

[25] W. Viriyasitavat and D. Hoonsopon, "Journal of Industrial Information Integration Blockchain characteristics and consensus in modern business processes," J. Ind. Inf. Integr., vol. 13, no. June 2018, pp. 32–39, 2019.

[26] A. Banerjee, Blockchain with IOT: Applications and use cases for a new paradigm of supply chain driving efficiency and cost, 1st ed., vol. 115. Elsevier Inc., 2019.

[27] S. Nakamoto, "Bitcoin : A Peer-to-Peer Electronic Cash System," 2008.

[28] Ethereum, "Ethereum Whitepaper | Ethereum.org," 2013. [Online]. Available: https://ethereum.org/whitepaper/. [Accessed: 11-Jun-2020].

[29] E. Deirmentzoglou and G. Papakyriakopoulos, "A Survey on Long-Range Attacks for Proof of Stake Protocols," IEEE Access, vol. 7, pp. 28712–28725, 2019.

[30] A. Kiayias, A. Russell, B. David, and R. Oliynykov, "Ouroboros : A Provably Secure Proof-of-Stake Blockchain Protocol," 2019.

[31] V. Buterin and V. Griffith, "Casper the Friendly Finality Gadget," pp. 1–10, 2019.

[32] C. L. Hwang and K. Yoon, "Multi-objective decision making–methods and application. A state-of-the-art study," New York Springer-Verlag, 1981.

[33] W. Burkhard, "Monitoring Charitable Organizations: Criteria and Assessment Methods," Comp. Gen. Pharmacol., no. March, pp. 25–26, 2003.

[34] M. Donazzan, N. Erkal, and B. H. Koh, "Impact of rebates and refunds on contributions to threshold public goods: Evidence from a field experiment," South. Econ. J., vol. 83, no. 1, pp. 69–86, 2016.

[35] J. A. List and D. Lucking-Reiley, "The effects of seed money and refunds on charitable giving: Experimental evidence from a university capital campaign," J. Polit. Econ., vol. 110, no. 1, pp. 215–233, 2002.

Power System Controlled Islanding using Modified Discrete Optimization Techniques

N.Z. Saharuddin[1]
Faculty of Electrical Engineering
Universiti Teknikal Malaysia Melaka
Melaka, Malaysia

I. Z. Abidin[2]
Department of Electrical and Electronics Engineering
Universiti Tenaga Nasional
Selangor, Malaysia

H. Mokhlis[3]
Department of Electrical Engineering
Universiti Malaya
Kuala Lumpur, Malaysia

M.Y. Hassan[4]
Department of Electrical Engineering
Universiti Teknologi Malaysia
Johor, Malaysia

***Abstract*—Controlled islanding is implemented to save the power system from experiencing blackouts during severe sequence line tripping. The power system is partitioned into several stand-alone islands by removing the optimal transmission line during controlled islanding execution. Since selecting the optimal transmission lines to be removed (cutsets) is important in this action, a good technique is required in order to determine the optimal islanding solution (lines to be removed). Thus, this paper developed two techniques, namely Modified Discrete Evolutionary Programming (MDEP) and Modified Discrete Particle Swarm Optimization (MDPSO) to determine the optimal islanding solution for controlled islanding implementation. The best technique among these two which is based on their capability of producing the optimal islanding solution with minimal objective function (minimal power flow disruption) will be selected to implement the controlled islanding. The performance of these techniques is evaluated through case studies using the IEEE 118-bus test system. The results show that the MDEP technique produces the best optimal islanding solution compared to the MDPSO and other previously published techniques.**

Keywords*—Controlled islanding; modified discrete evolutionary programming (MDEP) technique; modified discrete particle swarm optimization (MDPSO) technique; minimal power flow disruption; power imbalance

I. Introduction

Cascading failures that occur due to severe transmission line outages is the main contribution to power system blackout. This cascading event causes the system to form few unstable islands (unintentional islanding) that finally lead the system to lose its stability and experience a blackout. According to the blackout cases happened around the world, cascading failures is the main reason for the blackout occurrence [1]-[2]. Therefore, prevention on cascading failures which causes the unintentional islanding is important in order to save the system from total collapse. Therefore, controlled islanding is implemented for this purpose. Generally, controlled islanding is executed by disconnecting the selected islanding cutsets in order to forms few stable stand-alone islands. These stand-alone islands are capable to operate independently and generate electrical power to consumers until the system back to its normal operating condition. The selected islanding cutsets must be optimal and do not cause the system to face any other instability issue after islanding implementation. However, the selection of optimal islanding cutsets is complicated as the search space of possible islanding cutsets is huge and increase proportionally when the system size increased.

Numerous methods on controlled islanding have been proposed by previous researches in recent years [3]. Ordered Binary Decision Diagrams (OBDD) is one of the methods proposed to determine the proper islanding strategy for a power system network [4]-[5]. This method simplifies the huge possible islanding solution using node simplification technique. Another method namely slow coherency approach was proposed to find the suitable islanding cutsets by determining the weakest connection in the network [6]. This method further used in [7] which considers minimal number of line removed with minimal power flow and graph partitioning technique in [8]. Author in [9] further proposed the slow coherency with blackstart unit in each island formed during controlled islanding. Through this, the load and generation balance in each island can be achieved and restoration action can be planned if required. A linear programming technique namely mixed integer linear programming (MILP) which uses DC power flow equation is proposed in islanding cutsets determination in [10]. This method further improved using AC power flow in [11] for better feasible islanding solution determination. Another MILP technique for controlled islanding considering coherent groups of generators is then proposed in [12]. A Heuristic technique which utilizes the possible search technique to determine the best islanding solution is proposed in [13]. Other techniques, which are the meta-heuristic techniques for intentional islanding are proposed by authors in [14]-[15]. These techniques use BPSO [14] and AMPSO [15] to determine the optimal islanding solution using minimal power imbalance as their objective function. Another meta-heuristic technique is proposed in [16] which uses Tabu Search algorithm to determine the islanding solution using similar objective function as in [14],[15].

Since determining the optimal islanding cutsets is imperative in controlled islanding, two discrete optimization techniques which are Modified Discrete Evolutionary Programming (MDEP) and Modified Discrete Particle Swarm Optimization (MDPSO) are developed and analysed in this paper. Minimal power flow disruption is used as the objective function in these techniques. The usage of this objective function helps to enhance the transient stability in each island by reducing the power flow change during islanding implementation [17]. The utilization of discrete optimization technique in this work is in line with islanding problem which is discrete in nature. This is because the selection of optimal islanding cutsets (line to be removed) involved with discrete value such as line 2-8, line 9-11 and line 12-13. The main objective of this paper is to select the best technique among the two developed techniques for controlled islanding determination.

II. Developed Techniques

In this paper, two different techniques, namely Modified Discrete Evolutionary Programming (MDEP) and Modified Discrete Particle Swarm Optimization (MDPSO) were developed and analysed for controlled islanding determination. The aim of this paper is to select the best technique that capable to find the optimal islanding solution with minimal power flow disruptions.

There are four main stages involved in this work. In stage 1, the power system network is modelled using the graph theory approach. This approach is vital to identify the transmission line connection during controlled islanding execution. Since the search space for possible islanding solution is huge, an appropriate initial solution is required in order to helps the discrete optimization techniques to find the optimal islanding solution. As such, suitable initial solution for controlled islanding is obtained using initialization based graph theory approach in stage 2. This initial solution is determined based on the specified constraints which are: i) number of the islands formed, and ii) coherent groups of generator. In this approach, the same coherent generators are grouped together and the numbers of total islands are represented by the total number of generators group. Next, the nearest adjacent nodes (next node) are grouped to the nearest coherent group and the process is continued until all line are assigned to their appropriate coherent groups. The initial cutsets are the line that located between the different coherent generator groups. Further explanation on the implementation of this approach can be found in [18].

In stage 3, the initial solution is then used to assist the discrete optimization techniques in determining the optimal islanding solution. The best technique which capable of determining better optimal islanding solution is identified and controlled islanding is further executed. Then, the load-generation balance checking procedure will be performed on each island after intentional islanding execution. This checking is important in order to ensure that each island formed is balanced and capable to operate as a stand-alone island. In the case of any imbalance is detected, the load shedding scheme will be activated in stage 4. The voltage magnitude at each bus and the power flow at each line in all islands are checked and verified to ensure the voltage limit and line capacity is not violated. Fig. 1 shows the stages involved in the proposed technique.

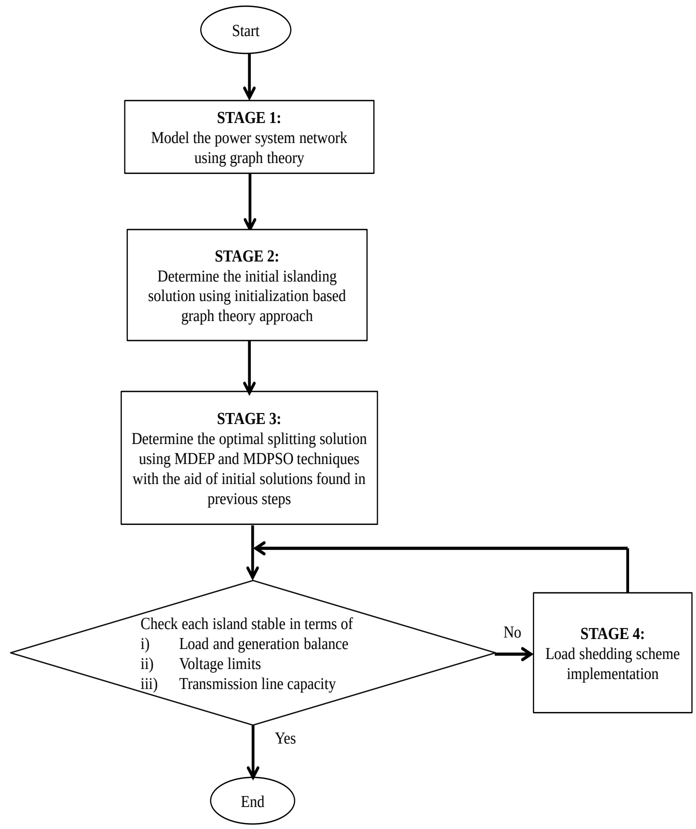

Fig. 1. Flowchart of the Proposed Techqniue.

III. Methodology

Controlled islanding is a discrete problem and the islanding solution is represented by the integer numbers such as line 3-6, 8-9, 10-13 and 11-15. Therefore, the modified discrete optimization technique is utilized in this work. Two different modified discrete optimization techniques (MDEP and MDPSO) are developed in this work in order to determine the optimal islanding solution. This section describes the methodology adopted to develop the two controlled islanding techniques to obtain the optimal islanding solution.

A. Modified Discrete Evolutionary Programming (MDEP)

The Modified Discrete Evolutionary Programming (MDEP) is developed as one of the controlled islanding technique. The process involved in determining the optimal islanding solution using the MDEP technique is illustrated by the flowchart shown in Fig. 2.

Based on Fig. 2, the initial solution obtained from graph theory approach is used as the initial populations (parents), x_i in the MDEP technique. The objective function (minimal power flow disruption) is then calculated using the equation below:

$$min\{g(x) = \left(\sum_{a=1}^{a_{line}} |P_a|\right)\} \quad (1)$$

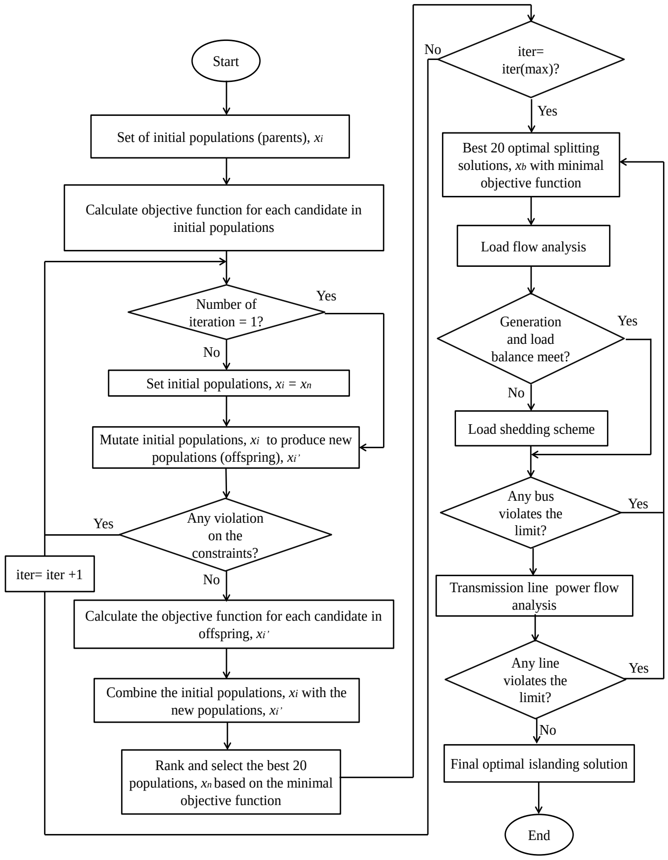

Fig. 2. MDEP Optimization Technique.

where P_a is the active power flow in the transmission line (cutsets candidate), and a_{line} is the total number of cutsets that disconnected to forms the islands.

Then, the mutation process starts by mutating the initial populations, x_i to produce the new populations (offsprings), x_i' using three different techniques. In the first technique, the mutation is carried out by mutating each cutset in a diagonal form, randomly from the possible transmission lines, S_T as shown in Table I. The possible transmission lines, S_T is the total number of transmission line, $TL=\{TL_p\}$ in the system where $p=1,2,3….total\ number\ of\ lines$.

TABLE I. MUTATION PROCESS OF MDEP TECHNIQUE IN TECHNIQUE 1

	Initial cutsets from graph theory approach	Z_1	Z_2	Z_3	Z_4	Z_5	Z_6	Z_n
1	1st cutset is randomly changed	a_{i1}	Z_2	X_3	Z_4	Z_5	Z_6	Z_n
2	2nd cutset is randomly changed	Z_1	a_{i2}	X_3	Z_4	Z_5	Z_6	Z_n
3	3rd cutset is randomly changed	Z_1	Z_2	a_{i3}	Z_4	Z_5	Z_6	Z_n
4	4th cutset is randomly changed	Z_1	Z_2	X_3	a_{i4}	Z_5	Z_6	Z_n
5	5th cutset is randomly changed	Z_1	Z_2	X_3	Z_4	a_{i5}	Z_6	Z_n
6	6th cutset is randomly changed	Z_1	Z_2	X_3	Z_4	Z_5	a_{i6}	Z_n
7	nth cutset is randomly changed	Z_1	Z_2	X_3	Z_4	Z_5	Z_6	a_{in}

According to Table I, each cutset from the initial solution ($Z_1, Z_2 … Z_n$) which is obtained from the graph theory approach is mutated and replaced by a random value, a_{in}. For example, if the initial solution contains seven cutsets, the mutation process in technique 1 will produce another new seven mutated islanding solution.

Taking into consideration that the initial solution might produce better optimal islanding solution with less or more number of cutsets, technique 2 and technique 3 are performed as shown in Table II and Table III.

Once the mutation process involving the three techniques completed, the total new populations (mutated islanding solution) obtained from the mutation process above will undergo the constraints checking (desired number of islands and coherent groups of generators). Next, the objective function for each candidate in the new populations is calculated and stored. Then, the combination of the new populations with the initial populations is carried out and the best 20 populations, x_n with minimal objective function are ranked and selected for the next iteration. The process continues until it reached the maximum number of iteration specified. Finally, the 20 final best solutions, x_b with minimal power flow disruptions are selected as the best possible islanding solution.

TABLE II. MUTATION PROCESS OF MDEP TECHNIQUE IN TECHNIQUE 2

	Initial cutsets from graph theory approach	Z_1	Z_2	Z_3	Z_4	Z_5	Z_6	Z_n
1	1st cutset is randomly changed	a_{i1}	Z_2	Z_3	Z_4	Z_5	Z_6	0
2	2nd cutset is randomly changed	Z_1	a_{i2}	Z_3	Z_4	Z_5	Z_6	0
3	3rd cutset is randomly changed	Z_1	Z_2	a_{i3}	Z_4	Z_5	Z_6	0
4	4th cutset is randomly changed	Z_1	Z_2	Z_3	a_{i4}	Z_5	Z_6	0
5	5th cutset is randomly changed	Z_1	Z_2	Z_3	Z_4	a_{i5}	Z_6	0
6	6th cutset is randomly changed	Z_1	Z_2	Z_3	Z_4	Z_5	a_{i6}	0

TABLE III. MUTATION PROCESS OF MDEP TECHNIQUE IN TECHNIQUE 3

	Initial cutsets from graph theory approach	Z_1	Z_2	…	…	Z_n	Z_{n+1}
1	1st cutset is randomly changed	a_{i1}	Z_2	…	…	Z_n	a_{n+1}
2	2nd cutset is randomly changed	Z_1	a_{i2}	…	…	Z_n	a_{n+1}
3	3rd cutset is randomly changed	Z_1	Z_2	…	…	Z_n	a_{n+1}
4	4th cutset is randomly changed	Z_1	Z_2	…	…	Z_n	a_{n+1}
5	5th cutset is randomly changed	Z_1	Z_2	…	…	Z_n	a_{n+1}
6	6th cutset is randomly changed	Z_1	Z_2	…	…	Z_n	a_{n+1}
7	nth cutset is randomly changed	Z_1	Z_2	…	…	a_{in}	a_{in+1}
8	n+1th cutset is randomly changed	Z_1	Z_2	…	…	Z_n	a_{in+1}

The first islanding solution from the final best solutions, x_b is selected as the optimal islanding solution. Load flow analysis is then performed and the power imbalance criterion is checked on each island. In the case of any imbalance is found on any island, the load shedding scheme is executed in order to produce the balanced island. Once the power imbalance criterion is fulfilled, the voltage magnitude at each bus and transmission line power flow at each line is checked and analysed. If the voltage limit or line capacity in any islands is violated, the islanding solution is considered not feasible and the next optimal islanding candidate will be selected for evaluation. The islanding solution is considered an optimal solution if the power imbalance, voltage limit and line capacity are fulfilled.

B. Modified Discrete Particle Swarm Optimization (MDPSO)

Another modified discrete optimization, namely Modified Discrete Particle Swarm Optimization (MDPSO) is developed to validate the performance of MDEP in determining the optimal islanding solution. The flowchart in Fig. 3 shows the process involved to obtain the optimal islanding solution using the MDPSO technique.

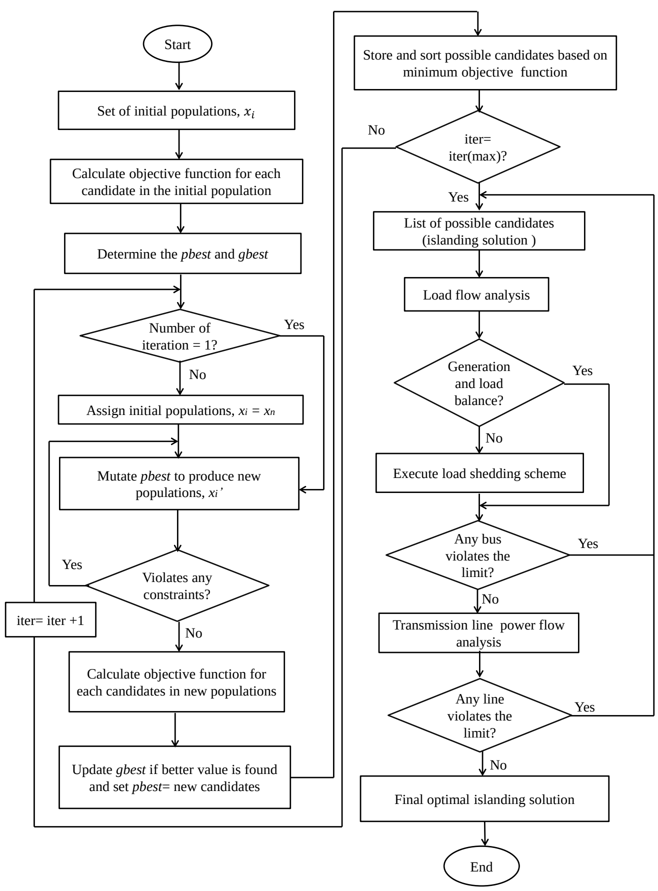

Fig. 3. MDPSO Optimization Technique.

Referring to Fig. 3, the initial solution obtained from the graph theory approach is used as the initial population, x_i in the MDPSO technique. Then, the objective function (minimal power flow disruption) is then calculated for each candidate using the equation in (1). The initial *pbest* and *gbest* are determined and the mutation process is begun. The similar mutation techniques used in the MDEP technique is utilized in the MDPSO technique to produce new populations, x_i'. Then, the constraints checking process for all the new populations are performed, similar to the MDEP technique. The objective function for each candidate in the new populations is then calculated and stored. The *gbest* is updated if a better objective function is found and the process continues until it reaches the maximum number of iteration. The new population, x_i' is used as the *pbest* for each iteration in this technique.

The best possible islanding solution is selected as the optimal islanding solution and load flow analysis is further carried out. Then, the power imbalance (load-generation balance), voltage limits and transmission line capacity are checked and analyzed as performed in the MDEP technique. Finally, the optimal islanding solution which fulfilled these checking criteria is selected as the final optimal islanding solution in this technique.

IV. Result and Analysis

The IEEE 118-bus system is used to demonstrate and validates the developed MDEP and MDPSO techniques. This system consists of 19 generators and 186 transmission lines. This work uses the MATLAB R2015a on an Intel® Core™ i7-5500U CPU at 2.40GHz with 8GB of RAM is used to code the developed techniques.

A. Case I: IEEE 118-bus System

In Case I, the controlled islanding is performed by splitting the system into two stand-alone island based on their coherent group of generators, G_1 = {10,12,25,26,31} and G_2 = {46,49,54,59,61,65,66,69,80,87,89,100,103,111} [9],[16]. The initial solution obtained using the graph theory approach is shown in Table IV. The initial solution of six cutsets with minimal power flow disruption of 100.164 MW is obtained in this case. Through the utilization of this approach, the huge possible combination of islanding solution ($2^{\text{no.of trans. line}} = 2^{186} \approx 9.808 \times 10^{55}$) is reduced to five cutsets as an initial solution.

The initial solution is then used in the MDEP and MDPSO technique to obtain the optimal islanding solution. The results are then compared with other published techniques as illustrated in Table V. It is observed that the MDEP technique provides a better optimal solution with minimal power flow disruption (81.4477 MW) as compared to MDPSO and other published techniques.

TABLE IV. Initial Solution for Case I

Initial Solution	**$\sum P_{disrup}$ (MW)**
19–34, 33–37, 30–38, 24–70, 71–72	100.164

TABLE V. Comparison of Optimal Islanding Solution – Case I

Technique	**Optimal Islanding Strategy**	**$\sum P_{disrup}$ (MW)**
Tabu Search [16]	22-23, 23-25, 23-32, 33-37, 34-36, 34-37, 34-43, 37-38, 38-65	890.7296
Controlled Islanding [9]	24 – 70, 34 – 43, 38 – 65, 40 – 41, 40 – 42, 71 - 72	232.7722
MDPSO	15 – 33, 19 – 34, 30 – 38, 23 – 24	83.7969
MDEP	15 – 33, 19 – 34, 30 – 38, 24 – 70, 24 - 72	81.4477

The optimal solution using MDEP technique is used to implement the controlled islanding solution which forms two stand-alone islands and the information of this execution is shown in Table VI.

Referring to Table VI, the total generation, Pgen in both Island 1 and Island 2 are more than the total load demand, Pload. Therefore, the load shedding scheme is not required in both islands. Then, the voltage limit at each bus and power flow at each line are checked for both islands in order to ensure that the voltage limit and power flow capacity is not exceeded after controlled islanding execution.

B. *Case II: IEEE 118-bus System*

In Case II, the controlled islanding is performed by splitting the system into three stand- alone island based on their coherent group of generators, G_1 = {10,12,25,26,31}, G_2 = {46,49,54,59,61,65,66,69}, and G_3 = {80,87,89,100,103,111}. The initial solution obtained using the graph theory approach is shown in Table VII.

This initial solution is then used to assist the developed MDEP and MDPSO techniques to determine the optimal islanding solution. The results are then compared with other published techniques as illustrated in Table VIII. It is proved that the MDEP technique provides a better optimal solution with minimal power flow disruption (296.0604 MW) as compared to the MDPSO and other published techniques.

TABLE VI. OPTIMAL INTENTIONAL ISLANDING SOLUTION FOR CASE I

Islands	**Buses Info**	**Active Power (MW)**		**Load Shed (MW)**
		Total Pgen	**Total Pload**	
Island 1	1~32, 113~115, 117	1011.153	976.0	-
Island 2	33~112, 116, 118	3363.901	43.0	-

TABLE VII. INITIAL SOLUTION FOR CASE II

Initial Solution	**$\sum P_{disrup}$ (MW)**
19 – 34, 33 – 37, 30 – 38, 24 – 70, 71 – 72, 78-79, 77-80, 77-80, 80-81, 77-82	314.9342

TABLE VIII. COMPARISON OF OPTIMAL ISLANDING SOLUTION – CASE II

Technique	Optimal Islanding Strategy	$\sum P_{disrup}$ (MW)
Controlled Islanding [9]	40 – 41, 40 -42, 34-43, 38-65, 71-72, 24-70, 75 -77, 76-118, 69-77, 68-81	385.8167
MDPSO	15 – 33, 19 -34, 30-38, 24-70, 71-72, 78-79, 77-80, 77-80, 68-81, 77-82	304.6849
MDEP	15 – 33, 19 -34, 30-38, 24-70, 24-72, 78-79, 77-80, 77-80, 68-81, 77-82	296.0604

TABLE IX. OPTIMAL INTENTIONAL ISLANDING SOLUTION FOR CASE II

Islands	**Buses Info**	**Active Power (MW)**		**Load Shed (MW)**
		Total Pgen	**Total Pload**	
Island 1	1~32, 113~115, 117	1011.153	976.0	-
Island 2	33~78 116, 118	2173.212	2102.0	-
Island 3	79~112	1192.906	1164.0	-

The optimal solution using MDEP technique is used to implement the controlled islanding solution which forms three stand-alone islands and the information of this implementation is shown in Table IX.

Referring to Table IX, the three islands formed in this case are balance in terms of power balance criterion. This is due to the fact that the total generation, Pgen in all three islands; Island 1, Island 2 and Island 3 are more than the total load demand, Pload. Therefore, load shedding scheme is not required in any of these islands. Once the power balance criterion is fulfilled, the voltage limit at each bus and power flow at each line are checked for all islands in order to ensure that the voltage limit and power flow capacity is not exceeded after controlled islanding execution.

V. CONCLUSION

This paper investigates two different techniques that developed to determine the optimal islanding solution. The effectiveness of the developed techniques, MDEP and MDPSO are evaluated through case studies using the IEEE 118-bus system. The results proved that the MDEP technique capable on determining the optimal islanding solution with minimum power flow disruption as compared to MDPSO and other published works in Case I and Case II, respectively. As such, MDEP technique is selected as the best technique to implement the controlled islanding action. This research emphasizes on obtaining the optimal islanding solution with lower power flow disruptions, as it helps to improve the transient stability in each island after the implementation of controlled islanding.

In the future study, the implementation of controlled islanding taking into account the severe outages will be investigated and analyzed using the selected MDEP technique.

ACKNOWLEDGMENT

The author would like to express her appreciation to Ministry of Higher Education Malaysia (MOHE) via FRGS Grant (FRGS/1/2018/TK07/UNITEN/01/1) to fund this research. In addition, the author would like to thank Universiti Teknikal Malaysia Melaka (UTeM) and Universiti Tenaga Nasional (UNITEN) for their support in this research.

REFERENCES

[1] N. Z. Saharuddin, I. Z. Abidin, H. Mokhlis, and K. Naidu, “Intentional islanding methods as post fault remedial action: A review,” Indones. J. Electr. Eng. Comput. Sci., vol. 12, pp. 182–192, 2018.

[2] G. Andersson et al., “Causes of the 2003 Major Grid Blackouts in North America and Europe , and Recommended Means to Improve System Dynamic Performance,” IEEE Trans. Power Syst., vol. 20, no. 4, pp. 1922–1928, 2005.

[3] S. Larsson and A. Danell, “The black-out in southern Sweden and eastern Denmark, September 23, 2003,” in 2006 IEEE PES Power Systems Conference and Exposition, 2006.

[4] Q. Zhao, K. Sun, D. Zheng, J. Ma, and Q. Lu, “A study of system splitting strategies for island operation of power system: a two-phase method based on OBDDs,” IEEE Trans. Power Syst., vol. 18, no. 4, pp. 1556–1565, 2003.

[5] K. Sun, D. Z. Zheng, and Q. Lu, “Splitting strategies for islanding operation of large-scale power systems using OBDD-based methods,” IEEE Trans. Power Syst., vol. 18, no. 2, pp. 912–923, 2003.

[6] H. You, V. Vittal, and X. Wang, “Slow Coherency-Based Islanding,” IEEE Trans. Power Syst., vol. 19, no. 1, pp. 483–491, 2004.

[7] X. Wang, S. Member, and V. Vittal, "System Islanding Using Minimal Cutsets with Minimum Net Flow," in Power System Conference and Exposition, 2004, pp. 1–6.

[8] G. Xu, S. Member, and V. Vittal, "Slow Coherency Based Cutset Determination Algorithm for Large Power Systems," IEEE Trans. POWER Syst., vol. 25, no. 2, pp. 877–884, 2010.

[9] J. Q. Tortos and V. Terzija, "Controlled islanding strategy considering power system restoration constraints," IEEE Power Energy Soc. Gen. Meet., pp. 1–8, 2012.

[10] P. A. Trodden, W. A. Bukhsh, A. Grothey, and K. I. M. Mckinnon, "MILP Formulation for Islanding of Power Networks," IEEE Trans. POWER Syst., vol. 29, pp. 1–8, 2014.

[11] P. A. Trodden, W. A. Bukhsh, S. Member, A. Grothey, and K. I. M. Mckinnon, "Optimization-based Islanding of Power Networks using Piecewise Linear AC Power Flow," IEEE Trans. POWER Syst., vol. 29, 2014.

[12] P. Demetriou, A. Kyriacou, E. Kyriakides, and C. Panayiotou, "Applying Exact MILP Formulation for Controlled Islanding of Power Systems," in 51st International Universities Power Engineering Conference (UPEC), 2016.

[13] M. R. Aghamohammadi and A. Shahmohammadi, "Electrical Power and Energy Systems Intentional islanding using a new algorithm based on ant search mechanism," Int. J. Electr. Power Energy Syst., vol. 35, no. 1, pp. 138–147, 2012.

[14] W. Liu, L. Liu, and D. A.Carter, "Binary Particle Swarm Optimization Based Defensive Islanding Of Large Scale Power Systems," Int. J. Comput. Sci. Appl., vol. 4, no. 3, pp. 69–83, 2007.

[15] L. Liu, W. Liu, D. A. Cartes, and I. Chung, "Slow coherency and Angle Modulated Particle Swarm Optimization based islanding of large-scale power systems," Adv. Eng. Informatics, vol. 23, no. 1, pp. 45–56, 2009.

[16] F. Tang, H. Zhou, Q. Wu, H. Qin, J. Jia, and K. Guo, "A Tabu Search Algorithm for the Power SystemIslanding Problem," Energies, vol. 8, no. 10, pp. 11315–11341, 2015.

[17] L. Ding, F. M. Gonzalez-longatt, S. Member, P. Wall, V. Terzija, and S. Member, "Two-Step Spectral Clustering Controlled Islanding Algorithm," IEEE Trans. POWER Syst., vol. 28, no. 1, pp. 75–84, 2013.

[18] N. Saharuddin, I. Zainal Abidin, H. Mokhlis, A. Abdullah, and K. Naidu, "A Power System Network Splitting Strategy Based on Contingency Analysis," Energies, vol. 11, no. 2, p. 434, 2018.

Development of Technology to Support Large Information Storage and Organization of Reduced User Access to this Information

Serikbayeva Sandugash Kurmanbekovna[1]
Sadirmekova Zhana Bakirbaevna[4]
Department of Information Systems
L.N. Gumilyov Eurasian National University
Nur-Sultan, Kazakhstan

Batyrkhanov Ardak Gabitovich[2]
Department of Information Systems
L.N. Gumilyov Eurasian National University
Atyrau State University Named after H. Dosmukhamedov
Nur-Sultan, Atyrau, Kazakhstan

Sambetbayeva Madina Aralbaevna[3]
L.N. Gumilyov Eurasian National University
Institute of Information and Computational Technologies
CSMES RK
Nur-Sultan, Almaty, Kazakhstan

Yerimbetova Aigerim Sembekovna[5]
Institute of Information and Computational Technologies
CSMES RK
Almaty, Kazakhstan

***Abstract*—This article solves the problem of developing a technology for supporting large information storages and organizing delimited user access to this information, which provides a service both for managing these objects and organizing access to these objects. Solving the problem will allow you to create a conceptual model with the allocation of basic entities among information objects and the establishment of relationships between them. It will also allow the development of technical documentation reflecting the results of the first stage of creating an information system: solving problems of syntactic and technical interoperability, developing a single interface, interacting with users, etc. In existing DL developments, as a rule, search and access to information are provided only through visual graphical interfaces. The task of the subsystem for integrating various digital resources is to provide other subsystems with a single interface for access to information stored in the data sources of the system. That is, any resource must be cataloged in a standard way, provided with metadata, access rules, and a unique identifier. To implement search functions outside of graphical interfaces, support for special network services and query languages is required. Ideally, all IS should support a single search profile and a single query language.**

Keywords*—Information systems; digital library; metadata; collection; privilege; rights; administrator

I. Introduction

Information systems (IS) to support scientific and educational activities operate with various kinds of information, such as publications, digital documents, electronic collections, ontological descriptions, data arrays, logical descriptions, etc. As a rule, these resources, which are in demand by different groups of researchers, are inaccessible due to the impossibility of their search and identification. Semantic links between information resources increase their value and provide additional opportunities for information retrieval and identification. Data integrated into open semantic space is a body of knowledge about a certain subject area in the form of a semantic structure, based on which qualitatively new scientometric measurements and studies of the structural properties of the body of scientific knowledge become possible.

The main purpose of the study is to develop a conceptual vision technology of using the digital library management system as a typical system for storing and accessing information resources and a description of the basic requirements for its implementation and operation.

Information storage technology is a kind of integrated technology designed to implement procedures, methods, and means of storing and using a database complex in solving user problems. Large amounts of data can be stored on one or more servers. These arrays are usually called information storage [1].

Data presentation; As a subject area, the materials of the scientific heritage in the field of IT technologies were considered. In the information space, events, facts, and any other entities of the real world exist only in the form of documents. The document is the main object involved in any information system (IS). The main function of the document is informational, i.e. the ability to satisfy the information needs of a person. Many documents containing factual information, having the same physical structure and logical, informative purpose, form collections. Collections, according to [2], are characterized by their descriptions and descriptions of the structure of documents from which it consists, and represent a systematized collection of documents, united by some criterion of belonging, for example, by content, purpose, access method, etc. provided with meta description (metadata) under standards and data schemas. Collections can be nested within each other, but one collection can only have one parent collection. Any document can be placed in several collections.

Metadata is created in the process of explicit or implicit cataloging and corresponds to one or another generally accepted area. To extract metadata, algorithms are used for parsing the title page, extracting keywords in their absence, an algorithm for constructing an abstract, based on a graph connected to the text. The main catalog of information resources of the IS metadata server is built under the metadata schema. The developed schema takes into account the basic requirements of the Dublin Core metadata schema. In what follows, our metadata schema will be called internal.

Data storage: For long-term storage of documents, the institutional repository Dspace [3] was used, due to its ability to expand the list of supported metadata, which allows it to be customized for different subject areas. To support the process of populating full-text databases, workflows and user interfaces were configured: the created metadata profiles were registered in the DSpace system.

Data exchange: To implement the exchange of metadata between DSpace, under the extended profile, a service in XSLT was created that converts metadata schemas from the internal DSpace schema to the metadata server schema and the Dublin Core schema using qualifiers. The OAI service is also implemented, which periodically, in batch mode, under the schedule, synchronizes the metadata of the repository and the metadata server. To fill the main catalog of metadata under the created metadata schemas, controlled vocabularies from the reference block of the system are used [4, 27].

Environment functioning: Based on the use of Z39.50 and LDAP protocols. At the same time, mechanisms are provided for converting data from subject schemas to the abstract schema of the Z39.50 protocol. The virtual environment consists of a registry of objects and resources, the main Z39.50 servers, several functional modules, and a web interface with public and administrative sections for accessing various functions of the environment. For each source, a separate Z39.50 servers is installed, which transforms data from the source schema into an abstract data schema [5, 28].

Collecting data from external sources: The chosen technology of integration of the developed information system to support research on scientific heritage with a DD (digital depository) allows using any other DD implementations that support the OAI protocol. To work with external data centers that support the OAI protocol, service has been implemented that converts the Dublin Core metadata schema into the system's internal metadata schema.

Metadata extracted from external data centers is also placed in the database of the digital library (metadata server). If this is possible for a specific DD, then the metadata is extracted in an XML schema with further transformation into a GOST schema. If the data schema of the external data center is unknown, then the metadata is converted from the Dublin Core-based schema to the GOST metadata schema.

To integrate the digital library with external systems and applications using the OAI protocol, transformation services of the internal metadata schema are used, for example, in MARC XML 20 schema or RUSMARC, etc. If necessary, the same approach can be used to transform metadata into other schemas of the MARC family.

Search for data: The functionality of searching for documents (information resources) is available to end-users in three ways: through the user interface of the information system (metadata server), through a specialized search service (for external applications), and the user interface of the DSpace DD [3]. However, in any case, the documents themselves are always stored in the DD, therefore, through whatever interface the user finds the document he needs, the document will be directly retrieved via the HTTP protocol from the DD.

User access control: At all levels of user interfaces (metadata server, services, and DD), user access control to the resources of the information system is carried out based on identification information under the LDAP protocol. DSpace has built-in support for LDAP, and in programmed services and the metadata server, support is provided by the services of the information system.

The proposed technology for supporting large information storages is based on the client-server architecture of the IS and meets the requirements described in [4]: {{1}}.

- a unification of the process of exchange of scientific research results;
- operating with data and documents integrated into an open semantic space;
- provision of services for transforming heterogeneous resources that implement means of description, presentation, automatic linking of resources, as well as interaction with search and classification mechanisms by the needs of users.

II. Management System for Digital Libraries

A. *Administrative Collections*

The information system consists of objects - elementary units of documents, from documents - information units. Many documents containing factual information, having the same physical structure and logical, informative purpose, form collections. Collections are characterized by their descriptions and descriptions of the structure of documents from which it consists.

A collection is a set of documents united by semantic attributes and having the same structure.

A collection is a set of documents with a dedicated fixed structure, the content of which has the same thematic focus. From the point of view of unification of work with documents, we will represent the information system as a set of collections [6].

A collection is a common form of organization of information resources, which is determined by its parameters (style, attributes) and the structure of the documents included in it and is a systematized set of documents, united by some criterion of belonging, for example, by content, purpose, access method, etc., provided with meta description (metadata) following data standards and schemas. The document is characterized by its parameters (style, attributes) and the structure of the objects of which it consists. An object is determined by the type of data (following the selected data schema) that it contains, the description of the properties and methods of the object.

Metadata Server digital library management system (DLMS) contains an administrative (service) collection of the Main Catalog contains descriptions of the QDC metadata schema, extended with metadata and for MECOF compliance and descriptions of service metadata describing the structure of objects, user interfaces, associative links between documents, access lists to documents to differentiate access rights to the object by the rights of the actors (if desired, it can be extended with new metadata) [7].

Fig. 1 is represented by administrative collections: users (actors), sets of metadata schemas and access lists to documents (collections).

A metadata schema is a set of metadata elements used, for example, to describe specific types of information resources. A set of metadata elements are defined by the DL super administrator that defines various schemes, from relatively simple text materials to more complex multimedia objects and DL collections, at the earliest stages of library creation, taking into account the needs of all potential users. However, over time, it can be expanded and the metadata schema will be adjusted to meet new requirements.

The system operates with the following types of information objects - collections, documents, objects.

From a functional point of view, information resources of a collection are divided into data (document) and metadata. Metadata is specially prepared, machine-readable, structured information about a resource, representing the properties that the resource has, the services that the resource provides.

Collection metadata is a set of values of some of its properties and properties of information resources belonging to it. The specific functions of metadata and their composition can vary significantly, depending on the specifics of DL and a particular collection. In our case, the set of metadata is divided into the following classes, such as: unique (identifier (UID)), automatic (owner, record modification date), public (informational content of the record), and service (administrative metadata, access rights, user data, etc.) metadata. Accordingly, each of which is also subdivided according to the level of access: automatic, administrative, and public [8].

Fig. 1. Administrative Collection.

The metadata system is the central logical component of any collection of documents. Collection metadata describes the properties of documents, sections, and the collection as a whole. Metadata describes the structure of the collection, determines the composition of the collection, and ensures correct interpretation and processing of the documents presented in it. Collection metadata also describes the structural properties of documents (types, relationships), their presentation formats, access control, resource content, information about authors, the collection's classification system, etc.

Thus, the main element of the considered scheme is structural metadata (that is, formalized descriptions of the structure of stored information). It makes it easy to build a library with a distributed data warehouse: the connection between the warehouse and the system will provide meta-descriptions of the warehouse data.

The digital library management system is an information system that provides the development and administration of digital library systems, as well as the integration of software that offers advanced and specialized additional features.

Fig. 2 shows a scheme for managing collections and documents in the electronic library management system.

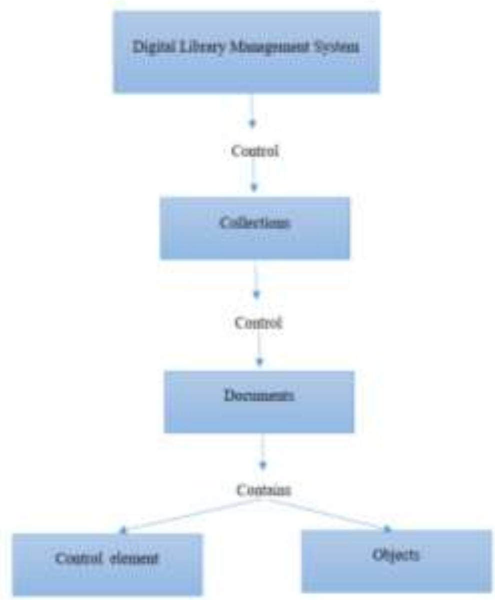

Fig. 2. Digital Library Management Systems.

Main functions of the Digital Library Management System:

- Access to resources-navigation through DL collections, query processing, location detection, extraction, resource transformation.
- Resource management – creating new information objects and collections, adding, deleting, etc.
- Metadata and dictionary management-creation, up-to-date maintenance and development, the composition of metadata and dictionaries is determined by agreements, taking into account international standards.

- User management – their registration, registration of rights, personal information.
- System administration – installation, configuration, recovery, maintenance, data security.

B. Basic Concepts in Access Control

Identification-assigning identifiers to users (unique names or labels) under which the system "knows" the user. In addition to user identification, user groups, system resources, and so on can be identified. Identification is also needed for other system tasks, such as event logging. In most cases, identification is accompanied by authentication [9, 10].

Authentication - authentication-verification of the identity of the user presented to them. For example, at the beginning of a session in the system, the user enters a name and password. Based on this data, the system performs identification (by user name) and authentication (by matching the user name and the entered password).

Access control is a method of protecting information by regulating the use of all system resources.

The identification and authentication system is one of the key elements of the infrastructure of protection against unauthorized access of any information system.

The access model operates with the terms "entity", "subject", "object".

Entity – any named component of the system being developed.

A subject is an active entity that can initiate resource requests and use them to perform any operations. The subject can be a program running in the system or a "user" (not a real person, but the essence of the system).

An object is a passive entity used to store or retrieve information. An object can be considered, for example, a collection, a document, etc.

Access – interaction between a subject and an object, as a result of which information is transferred between them.

Two fundamental types of access: a read-an operation that results in the transfer of information from the object to the subject; a write-an operation that results in the transfer of information from the subject to the object.

The basis of the mandatory security policy of the system is the mandatory access control, which implies that:

- all subjects and objects must be identified;
- a hierarchy of information security levels is set;
- each object of the system is assigned a level of protection that determines the value of the information contained in it – its level of availability;
- each subject of the system is assigned a restriction level, which determines the level of trust in it – its access level; and
- the decision to allow the subject to access the object is made based on the type of access and the comparison of the hierarchy of the subject and the object.

The main purpose of the mandate model is to prevent access to resources of objects with a high level of access to objects with low-level access.

In the model, objects and subjects are categorized according to the hierarchical mandatory access principle.

The basis of this approach (the condition for its application) is the introduction of a hierarchy (implemented on any principles) of access objects and subjects and access rights within the compiled hierarchy [11,12.13].

The most typical solution is to introduce a hierarchy of access objects based on the level of confidentiality (public, for official use, no access, etc.) of the documents stored in them, and a hierarchy of access subjects based on their status.

The introduced hierarchy of subjects and access objects allows you to enter permissions (formalize rights) to access resources, for example, after registration, the subject has access with minimal limited rights and privileges (search and view only open collections), the administrator (super administrator) of the upper zero levels has all rights and permissions, the first-level administrator inherits rights and permissions except for some (such as system collections, user data, etc.) and registers other low-level administrators, etc. this principle allows you not to violate the integrity of the system and save information in the system.

The above can be illustrated as follows. Let the sets $S = \{S_1..., S_k\}$ and $O = \{O_1..., O_k\}$ be linearly ordered sets of access subjects (subject) and access objects (object), respectively. As an access subject Si, i = 1..., k is considered as a separate subject, and a group of subjects with the same access rights and privileges, respectively, as an access object O_i, i = 1..., k can also be considered as a separate object and a group of objects characterized by the same access rights to them. Let's introduce the following hierarchy of subjects and access objects: the larger the object's sequence number *i*, the fewer rights and privileges to system resources (documents), respectively, the smaller the subject's sequence number *i*, the more access rights to information it has. Let $R = \{R_1..., Rn\}$ (Rj, where j = 1..., n, (for example, view, edit, link, delete, etc.) be the set of access rights. Where each subject Si uniquely corresponds to Rj a set of rights (privileges) of a set of objects from Oi. For example, subject S1 owns the entire set of rights (privileges) from Rj and has access to all objects of Oi. That is, each subject or group of subject's Si corresponds to a certain set of privileges (privileges) from Rj to certain objects Oi. Where the greater the ordinal number of the subject from *i*, the smaller the set of rights (privileges) from Rj, respectively, has fewer objects from Oi [14,15,16].

Thus, a mandatory access control mechanism is one of the possible ways to implement the principles of rights (powers) to control access to resources. The purpose of the mandate mechanism is to simplify the administration of the system, increase the level of protection of the document during its processing, and allows you to maintain the integrity of the system as a whole.

The basis of the principle of mandatory access control to resources, as noted, is the assignment of access rights of subjects to objects based on their authority. However, in general, several users (subjects) can have the same permissions at the same time, which are taken into account when assigning access rights, for example, several users have the same form of access to work with documents (when setting access control rules (privileges), a set of Rj must be assigned, as a result, these users (subjects) must have the same access rights, i.e. they can work with the same documents). However, the access rights of users (subjects) to documents may differ. Thus, the mandatory access control model implements a fully decentralized principle of organizing and managing the access control process. This approach provides the flexibility to configure the access control system in the database for a specific set of users and resources [17].

III. Technology of Storage Creation and Organization of Access to Information Resources

The developed resource access control model uses a Mandatory Hierarchical Access Control Model. In which each subject has a set of rights (rules) in the system. Each right (rule), in turn, contains a set of privileges that grant access to certain resources. Using elements of the hierarchical access control model. This ensures the decentralization of the management of actors, i.e. the presence in the system of a set of administrators (actors who expose a set of rights (rules) to users) of different levels. A system administrator can delegate some of their authority to lower-level administrators. The system under development supports three main types of actors: actors, a group of actors, and others [18, 19, 20].

The actor – those subjects that are related to the system. Most of the actors in one form or another are users of information resources of the digital library.

A group of actors is a set of actors that have some similar functions when interacting with information resources. And the rest are all registered users who only have access to public collections (search and view information).

In the management of subjects, the following principles are used:

1) Each subject (actor) is assigned classification levels (hierarchy levels), reflecting their place in the corresponding access to objects (collections, documents).

2) Each subject has a set of rules in the system, which is determined by its status in the system being developed. Each of the rights, in turn, contains a set of privileges that grant access to certain resources (objects).

3) Subjects belonging to a certain group inherit a set of rights of this group, i.e. the rights assigned to a group of subjects.

4) Using elements of the hierarchical access control model. The use of this principle means the decentralization of user management, i.e. the presence in the system of many administrators (acting, granting rights to users) of different levels. A system administrator can delegate some of their authority to lower-level administrators. This approach allows, for example, to transfer the responsibility for managing the rights of lower-level entities to a higher level, thereby removing the burden from the system support service.

5) A significant part of the rights of subjects is assigned by their status, or by the subject's belonging to a particular group.

6) The access rights setting is separate from the settings for each of the resources. In other words, the system component that provides the administrator with an interface for editing access rights does not depend on the logic of the resources, including the set of resources itself. Similarly, the resources themselves do not directly depend on the logic of the access control system, which is accessed only by periodic requests to confirm that the current user has a particular privilege.

To describe the operation of the digital library management system, you need to write out the main entities: service (system) collections, collections open for viewing, editing, and closed, metadata contains elements that are divided into the following classes: P-public (for example, DC metadata), A-automatic (owner and date of entry, modifications, etc.), S-service (access rights, class of the metadata element, access to the element, etc.), M-meta (link to pages (dictionary)), U-unique (resource identifier) and each class, in turn, has access to the element (P – all, S-super admin (0 - level), A - admins (1, 2-level).; and documents.

Table I considered the set of privileges and rights of administrative collections divided into five stages.

In addition to the above, the system has system and service collections such as the genre type of the resource (document_type), the data schema (privileges: view and add), user data - privileges (view), on which only the super administrator of the system has rights and privileges [21, 22].

Administrator-level privileges for editing the structure and contents of a collection depend on the attributes of the collection.

If collection access is allowed, then everyone can search and browse the collection, otherwise only the administrator of this collection, the super administrator, and the 1st level administrator.

The administrator can have access to different collections with different privileges to view and edit the collection and edit the records of the collection (documents) as shown in the table.

In addition to the above, the system has system and service collections such as the genre type of the resource (document_type), the data schema (privileges: view and add), user data - privileges (view), on which only the super administrator of the system has rights and privileges [23].

TABLE I. PRIVILEGES AND RIGHTS COLLECTIONS

	Rights to collections							
Privileges	**open**					**closed**		
	1	**2**	**3**	**4**	**5**	**1**	**2**	**3**
1. Collections								
1.1. Create a collection	+	+				+		
1.1.1. Collection data schema (from metadata)	+	+				+		
1.1.2. Document output in the collection	+	+				+		
1.1.3. Displaying (template) a document in a collection	+	+				+		
1.1.4. Sorting a document in a collection	+	+				+		
1.1.5. Structure of documents in the collection	+	+				+		
1.1.6. Description of the collection	+	+				+		
1.1.7. Collection Attributes								
1.1.7.1. Name of the collection	+	+				+		
1.1.7.2. Collection access (open for viewing, open for editing)	+	+				+		
1.2. Delete a collection	+	+				+		
1.3. Access to the collection (allowed)	+	+				+	+	
1.4. Establish a link between collections								
1.4.1. Family relations (according to the content of the collection)	+	+				+	+	
1.4.2. Establishing hard links (links)	+	+				+	+	
1.4.3. Establishing a connection with the rubricator	+	+				+	+	
1.5. Change								
1.5.1. Issuing a document in the collection	+	+	+			+	+	+
1.5.2. Displaying (template) a document in a collection	+	+	+			+	+	+
1.5.3. Sorting a document in a collection	+	+	+			+	+	+
1.5.4. The structure of documents in the collection	+	+	+			+	+	+
1.5.5. Description of the collection	+	+	+			+	+	
1.5.6. Change (attributes)	+	+				+	+	
2. Metadata								
2.1. Create (add) an element	+	+				+		
2.2. Edit an item	+					+		
2.3 Delete an item								
3. Document								
3.1. Create a document	+	+	+	+	+	+	+	
3.2. Edit the document	+	+	+	+	+	+	+	
3.3. Search and view the document	+	+	+	+	+	+	+	
3.4. Delete the document	+	+	+	+	+	+	+	
3.5. Importing a document	+	+	+	+	+	+	+	
3.6. Exporting a document	+	+	+	+	+	+	+	
3.7. Access to the document	+	+				+		
3.8. Change document properties								
3.8.1. Change the document owner	+	+				+		
3.8.2. Change the versioning of the document	+	+	+			+		
3.8.3. Change the document template	+	+				+		
3.8.4. Restrictions on viewing the document (who can see the document)	+	+	+			+		
4. Registration of administrators	+	+	+	+		+		
5. User Privileges								
5.1. Local network access	+	+	+					
5.2. Access to registered users	+	+	+					

Administrator-level privileges for editing the structure and contents of a collection depend on the attributes of the collection.

If collection access is allowed, then everyone can search and browse the collection, otherwise only the administrator of this collection, the super administrator, and the 1st level administrator.

The administrator can have access to different collections with different privileges to view and edit the collection and edit the records of the collection (documents) as shown in the table.

For each administrator or group of administrators in the system, according to the hierarchy level, a certain set of rights and privileges by default is granted to edit the collection and documents (as shown in the table). If necessary, the top-level administrator can add/remove privileges for editing collections and documents. For example, for an administrator who works only with documents, you can give meta description privileges for a collection for an individual collection, or for an administrator who works only with his records in a collection, grant editing privileges to all records of a particular collection [24, 25, 26].

Each administrator-level determines what rights are given to view and edit the collection and what privileges it has, that is:

- permission to view the collection (documents);
- permission to edit the collection, add, edit or delete objects;
- permission to edit collection documents (create, modify and delete a document);
- permission to change the order of collection objects;
- permission to change the format of issuing collection objects;
- permission to add a new object (metadata item);
- Allowing registration of lower-level administrators.

Table II shows the system of hierarchical levels of administration in the system. Administrator-level privileges for editing the structure and contents of a collection depend on the attributes of the collection.

An administrator can have access to different collections with different privileges to view and edit collections and edit collection records (documents). Each collection (depending on the type) has a minimum required set of metadata. Depending on the level of administration, the collection administrator can define a collection metadata schema based on the available metadata from the main catalog [27, 28]. Description of the structure of privileges and rights of administrative collections is shown in Table III.

TABLE II. THE SYSTEM IMPLEMENTS A HIERARCHICAL SIX-LEVEL SYSTEM (MANAGEMENT) OF ADMINISTRATION

Admin Levels	**Has Access**	**Works (Edits)**
0	All collections, documents, schemas, dictionaries, etc.	All collections systems and documents
1	All collections and documents except official ones	All collections and documents except (service and system collections)
2	Only your own and open collections	Structure (meta description of the collection), documents (templates, properties) of the collection record.
3	Open collections	Open collections (meta description of a collection), document structure, and records
4	Open collections	Only records of open collections (also, in some cases, it can work with the structures of individual collections and documents)
5	Open collections	Documents in open collections (only with their records)

TABLE III. RIGHTS AND PRIVILEGES FOR VIEWING EDITING THE STRUCTURE AND DESCRIPTION OF THE COLLECTION

		Rights	Privileges
Collections		Open for viewing,	Search and view a collection
Data schema	Collection metadata	Open for editing	Add an item Edit an item
Meta Description of the collection	Collection Parameters,	open for editing	Change the collection structure, Change the order, Change the format of the document output, Add a new element.
		Open for viewing	Viewing the collection structure
Metadata	Metadata Schema	Open for viewing,	Search and view an item
		Open for editing	Add, Delete, Edit Search and view an item
Document	Documents in the collection	Open for editing	To create, Edit, Remove, Import Export Search and view
		Open for viewing	Search and view a document
	Document Properties	Open for editing	Change the document owner, Change the document versioning, Change the document template
Administrator Registration		Allowed	Add an administrator Remove Administrator

The access rights (privileges) model also allows you to perform the following functions:

- create system administrator accounts;
- creating groups of system administrators with the same default privileges;
- assigning access rights to collections and documents, both for groups of administrators and individual system administrators;
- creating templates for access rights to documents of various types, both for groups and individual users;
- assign access rights to the collection and document structures for the system administrator.

Administrators can be grouped into groups of administrators, which are the following structures:

- name of the group;
- list of administrators;
- a set of rights (privileges) for specific collections and documents;
- a set of rights for document types [29, 30].

In Fig. 3, we discussed the scheme of access to administrative collections and its tasks. Administrator access depends on the level (hierarchy of administrators) of the administration and the attributes of the collection. As noted above, in the system, collections can be divided into Administrative and Content Collections. Each Content collection consists of documents. The document, in turn, contains Information Content, an Annotation, and a Link (that is, a pointer to the data warehouse (repository) where the full text is stored, to an archive file, a separate fragment (figure, table, etc.). The document also has a Meta Description, Genre Document Type, Versioning, and Record Owner. The meta description of the collection documents, in turn, has a Template, Structure, Rules for ordering and displaying the document.

Document versioning is a document that corresponds to a certain stage (stage) of document development. Each version represents the state of the document at some point in time. Users can only view the full versions of the document. Document management is the process of tracking such information, ensuring, for example, that there is only one original copy of a document and that archived copies of all previous versions are stored in the order in which they appear [31, 32].

Abstract - A brief description of the document, explaining its content, purpose, form, and other features. Annotation, information about an object for which the main purpose is to annotate the "target" Resource (or its scope). Examples of such Annotation Objects include notes, structured comments, and links. Annotations help in interpreting the target resource, or about support or objections, i.e. more detailed explanations. A relationship is a relationship between an entity and what is associated with it.

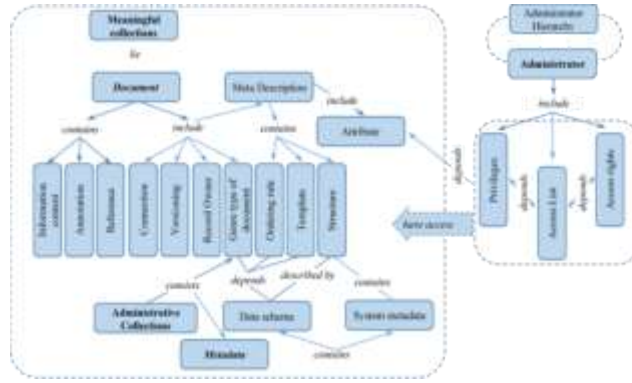

Fig. 3. System for Managing Administrator Access to Collections.

Connections — This is what the Digital Library consists of. The relationships between the data are identified by the type of relationship and the direction. The nature of the type and direction of the relationship can be reflected by its name (named relationship, relationship characteristics). Relationships allow objects in one collection to link to other objects not only in a given system but also to other remote distributed systems. There are two types of communication (relationships):

- Internal relationships – An order relationship between documents that builds a hierarchy of subordination in a collection, for example, a relationship of subordination between documents;
- External relations – The relationship between documents regardless of the structure of subordination.

A reference is an entry in a document that points to another part of that document or another document. A link can point to a data warehouse (repository) where the full text is stored, to an archive file, or a separate fragment (figure, table).

Ordering rule – The system also arranges the list of documents according to certain weights that are assigned to the documents during the search. Cataloging implements the basic paradigm of organizing information and ensures its search by pre-defined criteria (for example, by list size, alphabetically) [33, 34].

The owner of the record is the actor who creates, modifies documents in collections, and establishes relationships between them. The owner of the document record is responsible for the storage, correctness, and presentation of the document by the users of the system. Also, the document may not belong to the system, i.e. its “owner” may be another information system, and our system contains only its description or a link to this document.

Attribute - A feature that characterizes an object or entity, its properties, a data descriptor that contains one of its characteristics (for example, name, type, access elements, presentation form, etc.).

Structure - A fixed ordered set of objects and relationships between them (information about its logical division).

A template is a model for creating a collection document. The template stores a variety of elements that make up the basis of the document: the structure of the document together with the attributes assigned to them; document page parameters; a list of available styles; macros (a sequence of actions that automate working with the document); custom toolbars. Document template describes the basic structure of the document, which is processed and filled with real data by the filling function. To create a new collection, you must primarily use document templates to ensure that the documents are designed under the Organization's accepted style [35, 36].

Fig. 4 shows a picture of changing the characteristics of administrative colleges.

Each available collection of the administrator contains a meta description as shown in Fig. 4 above (edit) and delete where it has the right to search for documents, view documents, enter a new document, and a meta description of the collection. In the meta description of a collection, you can change the order of objects (the document display rule), change the collection parameters (i.e., the attributes are closed or open for viewing and editing), change the format of object output (the collection structure), add a new object (add a metadata element), and edit the information in the collection (edit the document).

Each available collections of the administrator contains a meta description, as shown in Fig. 5 above (edit) and delete where it has the right to search for documents, view documents, enter a new document and a meta description of the collection.

Editing a document has a minimum set of privileges such as shown in Fig. 6: add (entering a new document, importing a new document), view (show), edit/edit (edit), establish a link (link) and delete a document (delete). Depending on the access of the collection and the structure of the collection itself, these privileges may be minimal.

Collections: Persons in the collection of computer science training courses (persona_cat), Mixed learning: Key terms (term_cat), List of sections of the course "Modern problems of Computer Science" (temas_class) minimum set of privileges.

Fig. 4. For Example, Admin Page.

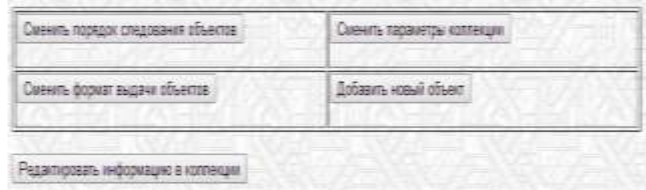

Fig. 5. Meta Description of the Collection.

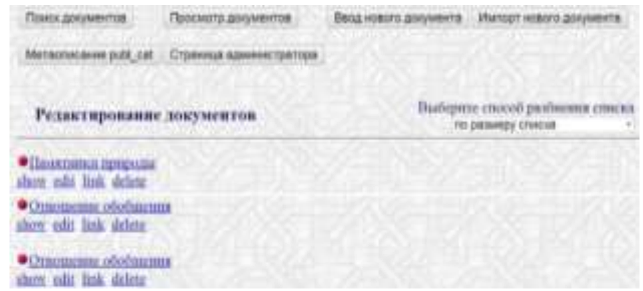

Fig. 6. For Example, Resources in the Computer Science Course Collection (publ_cat) contains the above Privileges.

The system implements a hierarchical six-level system (management) of administration, as shown in Fig. 7.

Each of the administrators also has the right to view open collections, register other lower-level administrators, and have all the rights and privileges of low-level administrators.

This access control method allows you to control user access to information based on the status in the system. The use of this method involves determining the rights (rules) in the system. The concept of law (rules) can be defined as a set of actions and powers related to a certain type of activity. So, instead of specifying all the access types for each user to each object, it is enough to specify a set of object access rules. And users, in turn, specify their privileges [37].

Rights are a set of rules (rights) that determine what privileges and over what objects the user who is assigned this set will have. Rules that make up a set of rights can be permissive (allow acting on a certain group of objects) or forbidding (prohibit performing the corresponding actions).

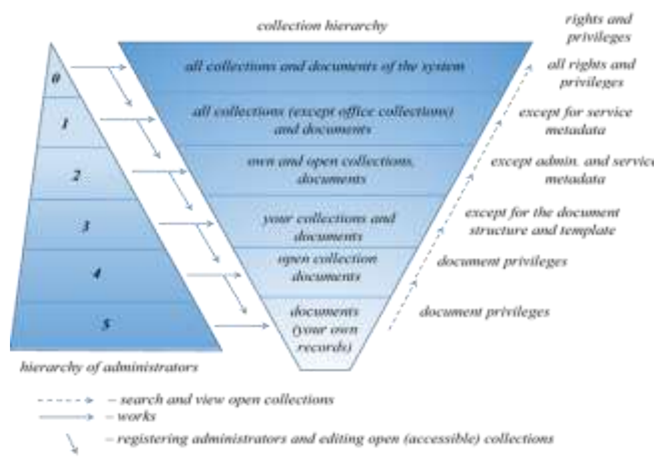

Fig. 7. Collection Hierarchy.

A privilege is all possible actions of a user (administrator) to perform any actions about objects (collections and documents) of the system, which requires a certain differentiation of access to this action. In principle, it is possible to combine several such actions into one privilege, but only if this combination of the simplest actions is required in all possible situations.

In other words, the user can perform different actions in different situations. The same set of rights (rules) can be used by several different users. In the system, a user can also have multiple rights (rules) at the same time.

The main advantages of this access control model are:

Easy administration – separation of rights (rules), privileges, and users allows you to split the task into parts: defining user rights and defining access rights to the object to perform certain functions. This approach simplifies the administration process since when changing the user's area of responsibility for objects, it is enough to change his previous rights (rules) and assign other appropriate ones for this situation [38].

Hierarchy of rights - the system of rights (rules) can be configured so that it reflects the real processes much more closely by building a hierarchy of rights. Each right (rule), along with its privileges, can inherit the privileges of other rules. This approach also significantly simplifies the administration of the system.

The principle of least privilege allows the user to register in the system with the least rights, allowing him to perform limited tasks. Users who have multiple rights do not always need all of their privileges to perform a specific task.

The principle of least privilege is very important to ensure the integrity of the data in the collection. It requires users to be given only those of the privileges allowed to it that it needs to perform a specific task.

To do this, you need to find out the goals of the task, the set of privileges required for its execution and restrict the user's privileges to this set. Prohibiting user privileges that are not required to perform a certain task allows you to maintain the integrity of the data in the system [39].

Separation of responsibilities is one important principle in the access control system. The system of mandatory access control helps to solve this problem with maximum simplicity. The system of mandatory access allocation allows you to distribute the problems of sharing responsibility between administrators and privileged users of the system and provides a multi-stage security level of the entire system.

The model consists of the following entities: users, sets of rights (rules), and privileges. A user is either a person or a program running on behalf of the user. This includes not only people but also external (relative to the digital library) software and hardware.

Thus, the advantage of this model is the ease of administration: assigning users a set of access rights (rules). At the same time, it does not allow you to manage different parts of the system separately and even more so - to delegate such powers to any user - ensures the integrity of the system. This model combines the protection and restriction of rights applied to data, collections, and system collections designed to prevent their unwanted use.

Classification of the hierarchy of entities and objects (resources) have rights and permissions (such as creating, editing, deleting, registering, controlling access, etc.)

After identification and authentication, each Sk user (subject) is assigned a minimum set of rights (privileges) Rj to objects from the Oi (for example, search and view documents that are open for viewing). Further, depending on the work in the system or the status of the administrator (subject), the top-level administrator grants the rights (privileges) to the corresponding level of administration to the corresponding objects, etc. or vice versa. This control method, as noted above, allows you to control the operation of the system and preserves the integrity of the system as a whole. Also, top-level administrators give part of their authority to lower-level administrators and thus freeing themselves from a large load of work in the system [40].

IV. Conclusion

The article is devoted to the history of the creation and description of the technological solutions used in the creation of the system. The article describes the architecture of the information system and the principles of integration with external sources, the rules for the representation and transformation of metadata, as well as the work with dictionaries that are used to systematize and classify information resources, and modeling the relationships between them.

An important component of the EC is a digital repository or repository of digital objects, the main purpose of which is to store these objects with all their possible variants and versions. In a broader sense, a digital repository is not only a repository of digital objects but also a system that provides a service for both managing these objects and organizing access to these objects. The International Organization for Standardization (ISO) has proposed the ISO-14721 (Open Archive Information System – OAIS) standard for organizing a system of long-term storage of information resources (a repository of digital objects) [8]. The reference model for the OAIS standard is a conceptual model based on the extended DublinCore data schema (Dublin Core, Dublin Core, DC), and is a set of metadata elements for representing the domain ontology.

Acknowledgment

This research has been funded by the Science Committee of the Ministry of Education and Science of the Republic of Kazakhstan (Grant No. AP08857179).

References

[1] Shokin Yu. I., Fedotov A.M., Guskov A. E., Zhizhimov O. L., Stolyarov S. V. Digital libraries - the way of integration of information resources of the Siberian Branch of the Russian Academy of Sciences. Series: Mathematics, Mechanics, Computer science. - 2005. - Almaty: KazNU. - No. 2. - S. 115-127. - ISSN 1563-0285.

[2] Law of the Russian Federation (No. 149-FZ) "On information, information technologies and information protection" dated July 27,

2006 // - the Federal law dated 27 07 2006 N 149-FZ (as amended on 07 06 2013). - 2006.

[3] GOST ISO / IEC 2382-1-99. Information technology. Dictionary. Part 1. Basic terms and definitions / / - Minsk: Mezhgos. council for Standardization, Metrology and Certification. - 1999. - 40 c.

[4] GOST 34.320-96. Information technologies. Database standards system. Concepts and terminology for the conceptual scheme and information base / / - Gosstandart of Russia, M.: IPK Publishing House of Standards. - 2001. - 14 p.

[5] GOST 7.0-99. The system of standards for information, library and publishing. Information and library activities. Bibliography. Terms and definitions.

[6] Golitsyna O. L., Maksimov N. V. Information systems / Moscow International Institute of Econometrics, Informatics, Finance and Law. - Moscow: 2004. - 329 p.

[7] Izbachkov Yu. S., Petrov V. N. Information systems: Textbook for universities. 2nd ed. - St. Petersburg: Piter, 2006. - 656s.

[8] Karminsky A.M., Chernikov B. V. K24 Information systems in the economy: In 2 ch. Ch. 1. Methodology of creation: Textbook. - M.: Finance and Statistics, 2006. - 336 p.: ill.

[9] Soviets, B. Ya. Information technologies: textbook for universities / B. Ya. Soviets, V. V. Tsekhanovsky. - M.: Higher School, 2005.

[10] Kogalovsky M. R. Perspective technologies of information systems. - M.: DMK Press; IT Company, 2003. - 288 p.

[11] Berg A. I. "Questions of cybernetics", VK-72 / Ed. by R. M. Suslov and A. P. Reutov. - M.: Scientific Council of the USSR Academy of Sciences "Cybernetics".

[12] Big systems and management (ed. by V. I. Chernetsky). Izd. LVVIK im. A. F. Mozhaisky, Leningrad, 1969. 206 p.

[13] Telemtaev M. M. Information systems. Moscow: MTS, 2010, 98 p.

[14] Kutsenogiy K. P., Kutsenogiy P. K., Molorodov Yu. I., Fedotov A.M. Development of the metadata structure for atmospheric aerosols based on an information model. 2004. Vol. 9. Special Issue: Proceedings of the International Conference "Computing and Information Technologies for Environmental Sciences" (CITES 2003). Tomsk, September 1-11, 2003 Part 2. pp. 25-33.

[15] Shokin Yu. I., Fedotov A.M., Zhizhimov O. L., Fedotova O. A. Management system of digital libraries [Digital resource] / / Distributed information and computing resources (DICR-2014): materials of the XV Russian Conference with international participation (digital edition). - 2014. - Novosibirsk: Institute of Computing Technologies of the Siberian Branch of the Russian Academy of Sciences. - State Register. No.: 0321500379.

[16] Larkov N. S. Documentovedenie: Uchebnoe posobie / N. S. Larkov. - M.: AST: Vostok-Zapad, 2006.

[17] Pavlenko N. A. Istoriya pisma. Minsk, 1987.

[18] Larkov N. S. Documentovedenie: Digital textbook. Tomsk: TSU 2002.

[19] Otle P. Biblioteka, bibliografiya, dokumentatsiya: Izbrannye trudy pionera informatiki [Library, bibliography, documentation: Selected works of the pioneer of Informatics]. - Moscow: FAIR-PRESS: Pashkov House, 2004. - 348, [1] p.- (Special publishing project for libraries). - Bibliogr.: pp. 312-327. - Names. decree: pp. 340-342. - ISBN 5-8183-0624-0.

[20] GOST R ISO / IEC TO 10000-2-99. Information technology. Fundamentals and taxonomy of functional standards. Part 2. Principles and taxonomy of VOS profiles.

[21] Shvetsova-Vodka G. N. General theory of the document and the book: textbook. manual / G. N. Shvetsova-Vodka. - M.: Rybari ; K.: Knowledge, 2009. - 487 p.

[22] Stolyarov Yu. N. "There is no alternative to the document" / Yu. N. Stolyarov / / Nauch. and tech. b-ki. – 2000. – № 3.

[23] Stolyarov Yu. N. The theory of relativity of the document / Yu. N. Stolyarov / / Ibid. – 2006. – № 7.

[24] Sokolov A.V. Social communications: textbook. - method. manual: in 2 ch. Ch. I. / A.V. Sokolov-Moscow: Profizdat, 2001. - 222 p. - ("Modern library". Issue 16).

[25] Dvoinosova G. A. / Functions of the document / / Scientific and technical information. Ser. 1: Organization and methodology of information work. - 2013. - № 2.

[26] Kushnarenko N. N. Documentovedenie: ucheb. / N. N. Kushnarenko. - 2nd ed., pererab. and additional – Kiev: Knowledge, 2000. - 459 p.

[27] V. V. Pogulyaev Commentary to the Federal law "On the mandatory copy of documents".

[28] Tkachev A.V. The legal status of computer documents: main characteristics. M., 2000.

[29] Ozhegov S. I., Shvedova N. Yu. Explanatory dictionary of the Russian language. M., 1993. P. 241.

[30] Oblavets A. A. Legal regulation of digital document management//Vestnik MSU. Ser. 11. Pravo. 1997. No. 4, p 51.

[31] Walk, V. V., E. A. Morgunova Comments to the Federal law "On information, Informatization and protection of information". M., 2004, P. 14.

[32] Federal law of December 29, 1994 N 78-FZ "On librarianship" (with amendments and additions).

[33] Federal law No. 217354-4 "On information, information technologies information security".

[34] Federal law of October 22, 2004 No. 125-FZ "On archival business in the Russian Federation" (with amendments and additions).

[35] GOST R 52292-2004 Information technology. Digital exchange of information. Terms and definitions.

[36] GOST R 52292-2004 Information technology. Digital information exchange Terms and definitions.

[37] Fedotov A.M. Methodologies for constructing distributed systems / / Selected reports of the X Russian Conference "Distributed Information and Computing Resources" (DICR-2005), Novosibirsk, October 6-8, 2005 / Computational Technologies. 2006. - Vol. 11. - p. 3-Novosibirsk: IVT SB RAS. - ISSN 1560-7534.

[38] Kogalovsky M. R. Metadata in computer systems/M. R. Kogalovsky / / Programming, 2013, N No. 4. – p.

[39] 28-46 39. Kogalovsky M. R. Scientific collections of information resources in digital libraries. Proceedings of the First All-Russian Scientific Conference "Digital Libraries: Promising Methods and Technologies, Digital Collections", St. Petersburg, October 1999. St. Petersburg University Press, 1999.

[40] Kogalovsky M. R. Metadata, their properties, functions, classification and means of representation // Proceedings of the 14th All-Russian Scientific Conference "Digital Libraries: Promising Methods and Technologies, Digital Collections" - RCDL-2012, Pereslavl-Zalessky, Russia, October 15-18, 201.

Open Text Ontology Mining to Improve Retrievals of Information

Mohd Pouzi Hamzah[1], Syarifah Fatem Na'imah Syed Kamaruddin[2]
Faculty of Ocean Engineering Technology and Informatics
University of Malaysia Terengganu
Terengganu, Malaysia

Abstract—**Information retrieval is the main task to extract relevant information from documents. Mostly, the information retrieval system is based on the keyword approach to extract the knowledge of relevant documents. The experiment shows the ontology can improve the result to overcome the weakness of keyword approach. Ontology implementation method is based on phrase formation and semantic relationships between words. This study tested 10 Malay documents using ontology to retrieve information. The results obtained were compared with the result obtained from manual information retrieval done by experts for precision and recall measure. In this study, there are three semantic relationships between words that are capable of expressing knowledge in documents. They are taxonomy relationship, attribute relationship and non-taxonomy relationship. The relationship of ontology can be formed by using taxonomy relationships algorithm, attribute relationships algorithm and non-taxonomy relationships algorithm based on the linguistic rules of the Malay language. The result of precision and recall for this experiment shows that the ontology approach can enhance the performance of information retrieval from the relevant documents.**

Keywords*—*Information retrieval; ontology; Malay text; taxonomy relationship; non-taxonomy relationship

I. Introduction

An increase in volume of documents will make the task to extract relevant information or knowledge complicated for users. Obstacles and challenges faced by users to obtain relevant and useful information increases with increased data. Information retrieval system helps users to retrieve a relevant document and rank them. Information retrieval is a process that extracts relevant document from an unstructured document that is meaningful to the user. There are four levels of processing in information retrieval. They are string processing, morphological processing, syntactic processing and semantic processing [1].

We need a data in order to process information and to stimulate knowledge. Data is referring to a fact that can be used in calculating, analysing or processing. The data then becomes information once it has been processed into a form that is useful and meaningful to the user. From the information, we can extract and synthesis more knowledge.

There are some basic elements required in information retrieval systems which are document, query and related comparisons between document and query. Van Rijsbergen [2] has presented the process of information retrieval system as illustrated in Fig. 1. The information retrieval system will start from the input section, which is a query and a document. This query is an interaction between a user and a computer.

The previous researcher also use knowledge representation approach to extract knowledge such as semantic nets, systems architecture, frames, rules, and ontology [3]-[6]. Understanding the limitations of keyword-based information retrieval, this study seeks solutions through knowledge based on documents using ontologies approach. It has been proposed that Malay documents develop ontologies so that knowledge representation of the document can be made. There are implicit relationships between words in the form of phrases, as well as semantic relations between words. These include taxonomic relationships, attribute relationships, and non-taxonomic relationships, among others. Natural language processing is used to establish these semantic relations. They are based on the Malay linguistic rules.

In this paper, we will discuss on the effectiveness of ontology approach in information retrieval. Ontology is a model that explains the world or a particular subject field that consists of a set of properties and a set of relationships between them. In 2001, Hendler defined ontology as "a set of knowledge terms, including the vocabulary, semantic interconnections, and simple rules of inference and logic for some particular topic" [7]. Ontology approach in the search process between query and documents provide an interaction between machine and human. Ontology is also able to achieve a relationship between different types of semantic knowledge.

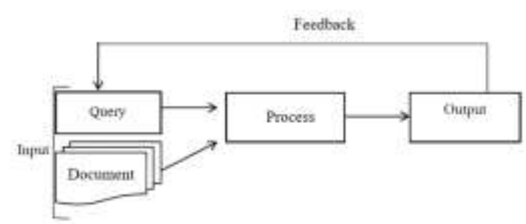

Fig. 1. Information Retrieval Process.

Recently, domain ontologies are also applied in data modelling and information retrieval using semantic-based approaches [8]. The ontology-based approach can improve a semantic gap between the documents and query. The main objective for ontology-based information retrieval is to get more accurate result of the query request by improving the interface between data and search requests. An ontology-based approach is more efficient in retrieval compared to the tf-idf weighting scheme and latent semantic indexing model [9]. Ontology-based semantic search is one of the search techniques based on the semantic or the meaning of query rather than the syntax of query, and helps to find more relevant information. In general, ontology can be described as in Fig. 2. Fig. 3 shows some of the ontologies in the construction domain. Ontology is very useful because it makes the knowledge in certain subject areas structured and literal. The knowledge can be reused and shared. Due to the richness of semantic information, ontology is widely used in knowledge management systems, artificial intelligence, data mining, knowledge engineering, natural language processing, question and answer systems, information extraction and information retrieval. Chi and Chen [10] used ontology and semantic law to infer knowledge from the characteristics of the news in the document.

The rest of this paper is organized as follows. Section II describes the related work of ontology and Section III represent the Malay test collection. Then, Section VI will cover the methodology of the MyGenOntology. Section V presents and discuss the finding in this study. Section VI is the conclusion to the study.

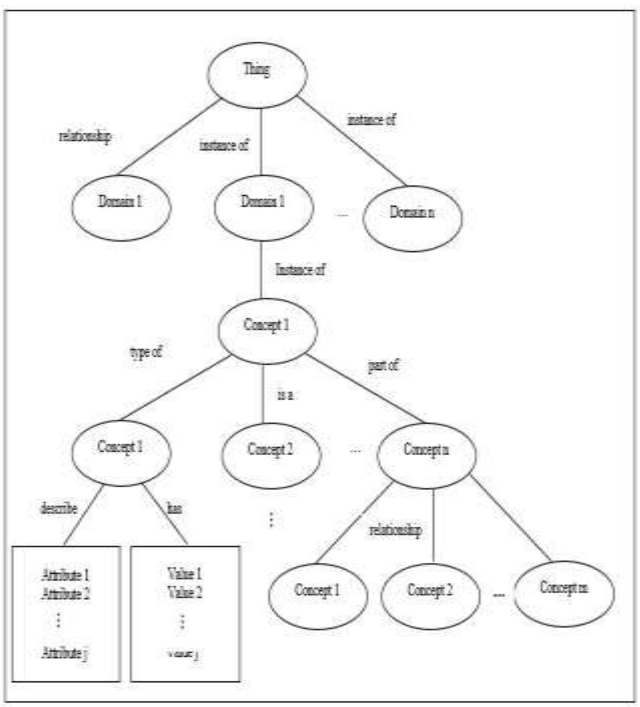

Fig. 2. Ontology.

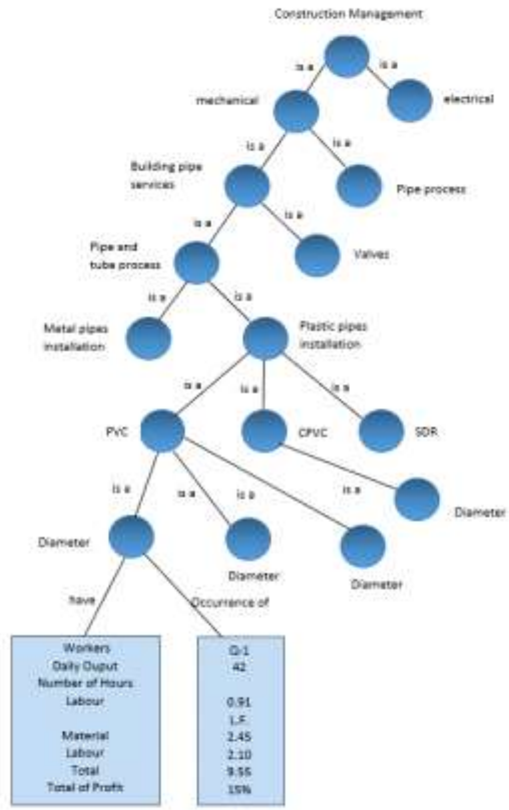

Fig. 3. Ontology of Construction Domain (Source: [11]).

II. Related Work

Most traditional information retrieval systems based on conventional models use only a keyword for document representation. Studies in information retrieval to only keyword based on Boolean models and conventional vector spaces have reached a saturated level with small achievements. Users have difficulty finding the right keywords to get the information they want using Internet search engines such as Google and Yahoo. This difficulty is due to the indexing system used by the search engine. It is based on the keywords found in the document and not based on a concept published from the analysis of the content of the indexed document. However, some search engines have taken the initiative to improve the retrieval process by indexing phrases in documents based on the classification or category of phrase. These methods, however, have their limitations and do not provide encouraging results that fulfil the needs or wants of users, the study has change to semantic aspects that are expected to be able to improve document representation and further enhance relevant document retrieval.

The studies from semantic aspects using thesaurus, phrases, and taxonomies have been extensively reviewed. Although these techniques show improvements, it is still not enough to give high results in information retrieval. Later on, semantic studies are done based on ontology, whereby the representation of documents is based on knowledge organization. The results of this study show that the representation of documents based on ontology can improve the effectiveness and efficiency of information retrieval. However, most of these ontology-based documents representations are made limited to documents in specific domains and not in the general domain.

Representation of a keyword-based cannot express the knowledge of the document. Words with the same meaning (synonyms) are not shown in the representation, while homonyms (words with different meanings) are not distinguished (polysemy). Sánchez [12] states that keyword-based information retrieval models are unable to explain the relationship between phrase and weaknesses in linguistic phenomena such as polysemy and synonyms. Therefore keyword-based information retrieval systems are not able to find relevant documents effectively. Woods [13] stated that two main problems in traditional information retrieval techniques are morphological problems using stemming and semantic problems using query expansion techniques through synonyms. He further explained with the use of "subsumption" technology in which the phrase is arranged in a conceptual taxonomic structure and was tested with specific paragraph retrieval algorithm, it got better results when compared to the results of commercial search engine searches. Using this technology, experiments conducted by Woods [14] on 10 documents obtained a recall value of 38.6% and a precision value of 7.3% compared to the method tf.idf whereby the recall value is 14.8% and the precision value is 2.9%. Yoon [15] who has conducted knowledge-based information retrieval research on specific domains, UMLS ("Unified Medical Language Systems") and SNOMED ("Systematized Nomenclature of Medicine") found that retrieval performance increased by 37% when compared to retrieval performance using traditional vector space.

Research conducted by Yi [16] using ontology-based information retrieval among university students in the United States, got a recall average of 76% when compared to a thesaurus-based information retrieval system of only 43%. Research in the field of information retrieval and knowledge representation based on ontology is accelerating with the advent of semantic web technology. The purpose of semantic web is to make information in the unstructured web meaningful, understandable and can be processed by a computer. The backbone to the semantic web to realize this purpose is ontology. Kumar [17] used an ontology-based semantic indexing approach to show the gap and narrow between text-based websites and semantic websites by using ontology. In 2009, Muhammad [18] proved that stemming algorithm based on stemming order can improve precision and recall. A method based on semantic information can improve the effectiveness of retrieval compared to a method based on keyword.

The methodology of ontology development consists of a set of principles, practices, processes, methods and activities developed to design, construct, evaluate and use ontology [7]. Several ontology development methodologies are reported in the literature. Generally, the development of ontology is made either fully automatic or semi-automatic. Most of the methodologies discussed in the literature use semi-automated methods with a focus on ontological development in specific domains. Uschold and King [19] have developed enterprise ontology for enterprise process modelling. The framework-based methodology of Noy and McGuinness [20] consists of the elements which are identify the domain and scope of ontology, consider the reuse of existing ontology, name the important terms in ontology, define the classes and class hierarchy, define class properties and create class events. The methodology developed by Uschold and Gruninger [21] provides in-depth needs analysis methods and involves four steps which are identify the purpose and scope of ontology, build Ontology, assessment, and documentation. Darlington and Curley [22] used the methodology provided by Noy and McGuinness [20] and Uschold and Gruninger [21] to develop ontologies to support the process of obtaining engineering design requirements. From the Table I below, the precision and recall of ontology is increase from the previous ontology system [23].

TABLE I. PREVIOUS ONTOLOGY SYSTEM

Ontology	Precision	Recall	Accuracy
Google	42.5	100	42.5
Kngine	25	100	25
UsWolfram-Alpha	30	100	30

III. TEST COLLECTION (CORPUS)

Language is an important element in research of information retrieval. There are various test collections that have been developed in different languages; Chinese language used by Di [24] in research of named entity recognition, a collection of Persian language tests developed by Ahmadi [25], and the collection of Malay language tests used by Sazali, Chekima and Sidi [26]-[28]. The example of Malay language used by Sazali is a classical Malay text as a collection document.

This research will focus on the extraction from a Malay text. The texts are collection of Malay texts taken from Berita corpus. The corpus is collected from daily reports and common texts. The corpus is tagged, according to knowledge base. The system will automatically tag proper words according to its class. 10 documents are tagged from a sample of the report at the early stage. They are tagged with a coarse tagset consisting of four main different tags which are noun, verb, adverb and adjective. A linguistic study of Malay words and grammatical structures is required before extracting the most appropriate structures for common forms of Malay sentence.

There are three main systems in language, namely phonological, grammar and semantic systems [29]. Phonological systems are in terms of sound and intonation of language, grammar system is of formation of words and sentences, and semantic system focuses on the meaning contained in language. Grammar system is divided into two main components, which are morphology and syntax. The morphology of the Malay language is a study of two aspects of the language, namely, the process of formation and categorization of words, while the syntax Malay language also is a field of study that examines aspects related to Malay sentences [30]. Since language is a system that has a certain structure, careful analysis of its components needs to be carried out to get meaning from it. To extract meaning, this study focuses on the analysis in the field of morphology and syntax of each sentence in the document.

In Malay language, the sentences have two main parts which are subject and predicate. Subject is the focused matter that is told or described while predicate is the description or story of the focused matter in the subject [31]. The subject section consists of Noun Phrases or other phrases that serve as Noun Phrases. The predicate section may consist of Noun Phrase (FN), Verb Phrase (FK), Adjective Phrase (FA) or Adverb Phrase (FSN). Ramli Md. Salleh [32] stated that in the Malay language, there are four sentence structure bases. They are the first phrase name (subject) + Noun Phrase (predicate), second phrase name (subject) + Verb Phrase (predicate), third phrase name (subject) + phrases Adjectives (predicate) and fourth Noun Phrase (subject) + Adverb Phrase (predicate). In short, construction verses in Malay language consist of four patterns as shown in Table II.

TABLE II. BASIC SENTENCE PATTERN

Pattern	Subject	Predicate
1. FN + FN	Othman	guru sekolah (is a teacher).
2. FN + FK	Syahirah	sedang makan (is eating).
3. FN + FA	Pemuda itu (that young man)	rajin.(is diligent)
4. FN + FSN	Datuk (grandfather)	di kebun.(is in a garden)

IV. METHODOLOGY

Document representation using ontology makes an information retrieval system more effective. This is because ontology can store meaning to words and is able to make inferences through the semantic relationship between words [33]. By enabling inference through hierarchy, ontology is one of the most popular and powerful tools in the representation of knowledge [34]. Ontology can also convert knowledge in unstructured texts into structured forms. This structured knowledge can be understood and processed by computers to be applied in various fields [35]. Therefore, there is a lot of research in the field of ontology development to enable knowledge to be shared and reused [36]. This is no exception in the field of information retrieval to find a more accurate document representation method to produce a more effective information retrieval system.

This section will describe the methods for the development of automatic ontologies for Malay language documents in the general domain. The process will be conducted based on the Malay language system and its development process are combined in a prototype system. This system is called MyGenOntologi. The development of ontology involves the process of extracting ontological components from the text of a general domain without being guided by a pre-defined structure. The extraction system is based on the Malay language system and does not refer to any lexical dictionary. As illustrated in Fig. 4, the ontological components are as follows:

- Concept - An entity or object whether it exists in reality or abstract.
- Attributes - Characteristics or attributes that describe a concept or attributes that describe the identifier of the relationship between concepts.
- Taxonomic Relationships - The hierarchical relationship between concepts.
- Non-taxonomic relationships - Non-hierarchical relationships between concepts.

Fig. 5 show a process of ontology development from texts document. The steps in the ontology development process are as follows:

- Process and analyse documents.
- Extract the phrase from the document.
- Obtain concepts from documents and build taxonomic relationships between concepts.
- Find the concept attributes and attributes to the relationship identifier between the concepts.
- Find non-taxonomic relationships between concepts.

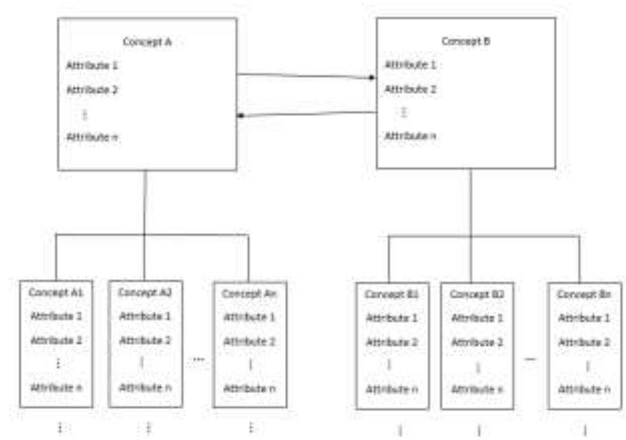

Fig. 4. Ontology Components.

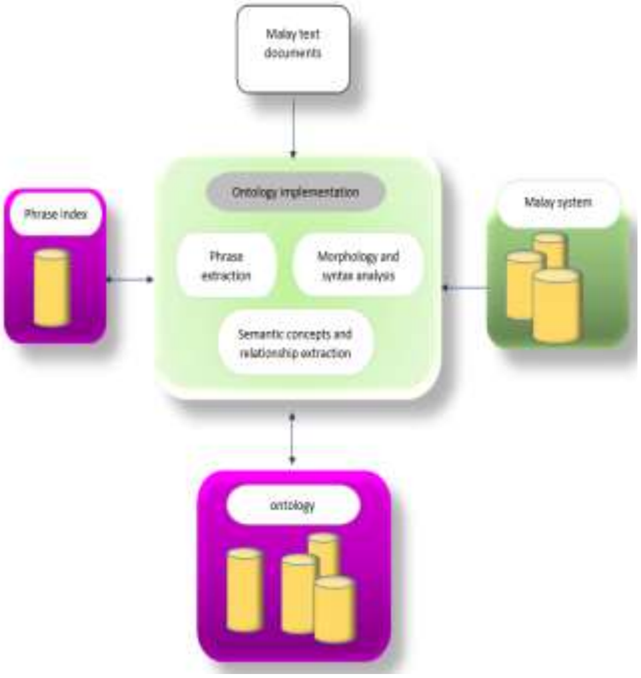

Fig. 5. Process of Ontology Development.

V. Result and Discussion

This section discusses about the issue and the result of the ontology process. There are several errors during the analysis process especially in labelling, segmentation and word disambiguation [24]. These issues are related to the language of corpus. Mostly, the analysis of tagging or labelling will not achieve 100% result because there maybe are spelling errors or the dictionary used does not include certain words. Besides that, the errors may happen because the system cannot detect ambiguous words, or polysemy, and the context of its meaning. Another issue in information retrieval is pertaining to an element of semantic, such as the relationship between words or sentences. These issues can be resolved while improving an ontology or ruled based technique [35].

To identify the effectiveness of ontology quality that has been developed by the MyGenOntology system, the extraction of ontological components from a set of experimental tests consisting of 10 documents from three different online newspapers was carried out. In addition, the manual extraction of ontological components from the same set of experimental tests was also performed by five experts. These manually extracted ontology components are then compared to ontologies developed by the system. Taxonomic relationships show the hypernyms or hyponyms between concepts. The average of recall value is 88% and the precision value achieved is 79%, deeming the experiments conducted as successful. Overall, the recall interval value in percentage is [76,95] and the precision interval value is [62,93]. Comparison of recall value and precision value between documents can be seen more clearly using bar charts as illustrated in Fig. 6.

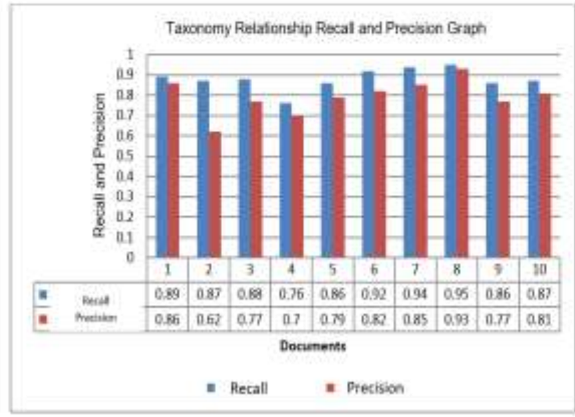

Fig. 6. Taxonomic Relationship Recall and Precision Graph.

The level of precision of the taxonomic relationship is lower than recall. This is because the system forms a taxonomic relationship from the content of the document and the relationship is not included in the list of manually created taxonomic relationships. This problem is due to the weakness during the phrase labelling process and the implementation of taxonomic law. The formation of incorrect compound phrase will affect the form of taxonomic relationships. For example, due to the absence of a comma after the word "beliau" (he) in the sentence “Kata beliau rakyat di Bukit Gantang, Bukit Selambau dan Batang Ai juga...” (He said the people in Bukit Gantang, Bukit Selambau and Batang Ai also ...) from the test collection, the system has produced a phrase of “beliau rakyat” (he people), thus forming a taxonomic relationship between concepts "beliau" (“people”) with the sub-concept "beliau rakyat". In addition, the weakness of the labelling process is due to words that are polysemic. For example, the phrase, “Kesemua pelajar cemerlang terbabit menerima wang tunai RM300, dua buah buku motivasi dan sijil penghargaan” (All the students received RM300 in cash, two motivational books and a certificate of appreciation) resulted in the wrong definition. In the sentence, the word "buah" (a) in the context of the sentence is a collective noun but has been labelled by the system as a noun word causing the system to form a phrase of "buah buku" (a book), thus forming a taxonomic relationship between the concept of "buah" (a) and the sub-concept "buah buku" (a book). Although the recall result is high, there are also taxonomic relationships provided manually that cannot be detected by the system. This is due to several problems. The first problem is the labelling of phrase that are not in the dictionary, such as the taxonomic relationship between the concept of "litar"(circuit) and "litar tertutup"(closed circuit). The word "litar" (circuit) was not found in the Malay dictionary causing the system inability to form the phrase "litar tertutup"(closed circuit). The second problem is the effect of the formation of a compound phrase of two words of the noun in “Chor berkata, ia adalah antara langkah penambahbaikan dari segi pematuhan peraturan dan...”. (Chor said, it was among the improvement measures in terms of regulatory compliance and”.) The system has labelled “segi pematuhan peraturan” (in terms of compliance and regulations) as a compound phrase, causing the taxonomic relationship between the concept of "pematuhan" ("compliance") and the sub-concept of "pematuhan peraturan" (compliance rules) to be undetected manually. Next problem is the grammatical weaknesses. This affects the retrieval of taxonomic relationships. The proper noun "orang kurang upaya" (disabled person) in the sentence "Katanya, 10 peratus lagi adalah untuk pelajar dari Sabah dan Sarawak manakala 10 peratus lagi dikhaskan bagi kes tertentu seperti pelajar orang kurang upaya (OKU)" ("he said another 10 per cent was for students from Sabah and Sarawak while another 10 per cent was reserved for certain cases such as students with disabilities) was written in lower case at the beginning of the sentence. This causes the system failure to identify the concept of "orang kurang upaya oku"(disabled person) and cannot form a taxonomic relationship between "pelajar" ("student") and "pelajar orang kurang upaya oku" ("disabled student). The formation of these incorrect taxonomic relations affects the degree of precision of taxonomic relations.

Another process in the ontology development is the attribute relationship formation. Fig. 9 demonstrates the effectiveness of the formation of the relationship of concepts and attributes. It shows that the effectiveness is moderate with an average recall of 80% and the precision achieved is 54%. Overall, the recall interval value in percentage is [74,90] and the precision interval value is [29,69]. Comparison of values of recall and precision between documents can be seen more clearly using bar charts as in Fig. 7.

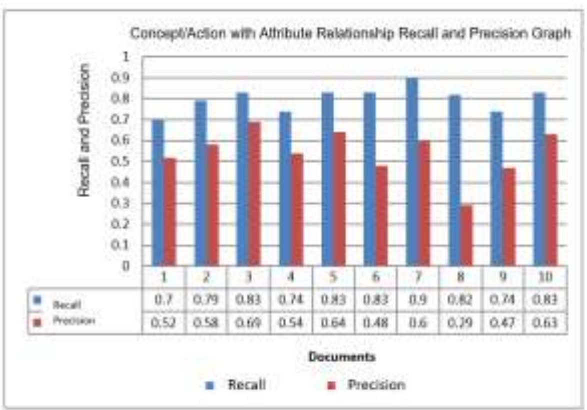

Fig. 7. Attribute Relationship Recall and Precision Graph.

The precision value of the attribute relationship obtained from the tests conducted is low compared to the recall value. This is because the system tries to detect as many phrases as possible that will be attributes to the concept or action in order to increase recall. In general, the weaknesses and problems that affect the precision and recall of taxonomic relationships also affect the precision and recall of the relationship between concepts and actions with attributes. The weaknesses and problems that form incorrect compound phrase will form incorrect attribute relationships, in turn affecting the precision. For example, from the formation of compound phrase "negara tahun"(country year), it will produce an attribute relationship between the concept of "negara"(country). and the concept of "tahun" (year). The problem of labelling a compound phrase from a sequence of more than two nouns as in the sentence "...insiden kematian atau kecederaan orang tahanan berulang" (... incidents of death or injury of detainees are repeated") affects the precision of attribute relationships. This is because the system produces two nouns phrase namely "kecederaan orang" (injuries people) and "tahanan" (prisoner). This makes the attribute relationship between "insiden kematian" ("incident death") and "orang tahanan" (prisoner) and the attribute relationship between "kecederaan" (injuries) and "orang tahanan" (prisoner) undetectable by the system. In the sentence "chor berkata melalui semakan dan kajian yang teliti...", (Chor said through careful review and study ...) the formation of the compound phrase "melalui semakan" (through review") causes the system to not be able to form and detect the attribute relationship between "semakan"(review) and "teliti"(thorough). The normalization problem of the phrase also affects the precision of the test. In the sentence "Bagaimanapun, jelasnya, biasiswa yang ditawarkan kepada pelajar Sabah dan Sarawak adalah khusus untuk bumiputera sahaja" (However, he explained, the scholarships offered to Sabah and Sarawak students are specifically for bumiputera only), the phrase Sarawak is not normalized to "kepada pelajar sarawak" (to Sarawak students) causing the system unable to form and trace the attribute relationship between "ditawarkan" (offered) and "kepada pelajar sarawak" (to Sarawak students).

The next process in the ontology development is the formation of non-taxonomic relationship. Fig. 8 illustrates the effectiveness of detecting non-taxonomic relationships between concepts with an average of recall value of 60% and the precision value achieved is 63%. Overall, the recall interval value in percentage is [38,88] and the precision interval value is [33,100]. Comparison of recall and precision between documents can be seen more clearly using bar charts as in Fig. 8.

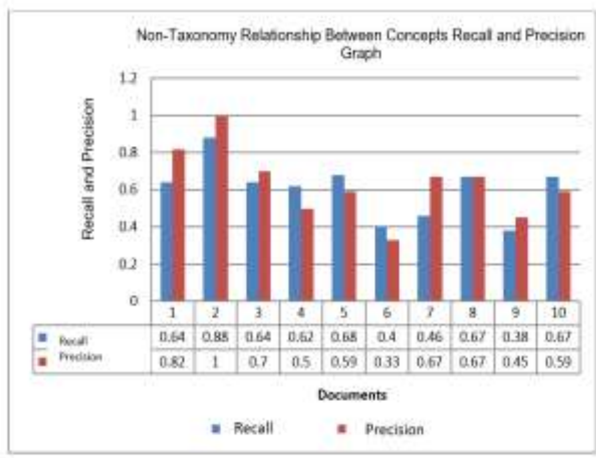

Fig. 8. Non-Taxonomic Relationship Recall and Precision Graph.

Non-taxonomic relationships involve the relationship of three phrases, which are two phrases of nouns and one phrase of verbs, as compared to taxonomic and attribute relationships involving only two phrases. The weaknesses and problems that affect the precision and recall of retrieval to taxonomic and attribute relationships from the process of formation of phrase will affect the precision and recall of non-taxonomic relationship. This is because the taxonomic relationship involves the relationship between the three phrases. The average recall of non-taxonomic relationships is (60%), lower than the average recall of taxonomic relationships (88%) and attribute relationships (80%). However, the average precision of taxonomic relationship (63%) was higher than the average precision of attribute relationship (54%) but lower than the average prevision of taxonomic relationship (79%). This is because the rules of non-taxonomic relationship search are more limited than the rules of attribute relationship search.

Based on the experiments conducted, it has been found that the cause of inaccuracy of non-taxonomic relationship retrieval is inherited from the factors of weakness and problems that affect the inaccuracy of taxonomic and attribute relationships. The problem of labelling phrase of nouns as in the sentence “Adakah mereka mendapat keperluan nutrisi yang diperlukan?”, (“Do they get the nutritional needs they need?) has caused the system to label "adakah mereka" (are they) as a noun phrase, causing the system inability to form a taxonomic relationship "mereka-mendapat-keperluan nutrisi" (they-get-nutritional needs). Instead, the system formed a taxonomic relationship "adakah mereka-mendapat-keperluan nutrisi" (they-get-the-nutritional needs). In addition to the aforementioned weaknesses and problems, this study also found certain sentence patterns that caused the system to form incorrect non-taxonomic relationships. The words from nouns and verbs are connected with the conjunction word "and". This can be seen in the sentence "Selain itu, pengalaman dan kreativiti guru-guru dalam..." (In addition, the experience and creativity of teachers in ..."). It causes the system to form a non-taxonomic relationship "pengalaman-kreativiti-guru-guru" (experience-creativity-of-teachers).

The results of the experiments found that the effectiveness of the taxonomic relationship between concepts is high with an average recall of 88% and average precision of 79%, the effectiveness of the concept relationship and action between attributes is moderate with an average retrieval of 80% and accuracy of 54%, and the effectiveness of non-taxonomic relationships between concepts is low with an average retrieval of 60% and an accuracy of 63%. Although the effectiveness of the detection of the components of ontologies derived from this experiment is not very high, it is still considered as a success and can be used as a basis for the development of ontology for Malay documents.

VI. Conclusion

In conclusion, there are some important findings have been found from this study. The findings provide a major contribution in the field of information retrieval to Malay documents which are development of detection and generation of taxonomic relations algorithm, attribute relationships algorithm and non-taxonomic relationships algorithm.

Based on the result, it can be concluded that the representation of Malay documents using an ontology-based knowledge repository can help and support information retrieval.

References

[1] T. M. T. Sembok, "Knowledge Representation in Information Retrieval", 2015.

[2] C. J. V. Rijsbergen, Information Retrieval, Butterworth- Heinemann, 1979.

[3] T. Xu, D. W. Oard, T. Elsayed and A. Sayeed, “Knowledge representation from information extraction”, Proceedings of the 8th ACM/IEEE-CS joint conference on Digital libraries. Pittsburgh PA, PA, USA, ACM: pp. 475-475, 2008.

[4] S. Roychoudhury, V. Kulkarni and N. Bellarykar, “Mining enterprise models for knowledgeable decision making”, Proceedings of the Fourth International Workshop on Realizing Artificial Intelligence Synergies in Software Engineering, Italy, IEEE Press: pp. 1-6, 2015.

[5] C. M. d. O. Rodrigues, F. L. G. d. Freitas and R. R. d. Azevedo, “An Ontology for Property Crime Based on Events from UFO-B Foundational Ontology”, Brazilian Conference on Intelligent Systems (BRACIS), 2016.

[6] Y. Chouni, "Information retrieval system based semantique and big data." Procedia Computer Science, vol. 151: pp. 1108-1113, 2019.

[7] D. Gasevic, D. Djuric, and V. Devedzic, “Model Driven Architecture and Ontology Development” Springer, 2006.

[8] K. Munir and M. Sheraz Anjum, "The use of ontologies for effective knowledge modelling and information retrieval." Applied Computing and Informatics, vol. 14(2), pp. 116-126, 2018.

[9] J. Paralic and I. Kostial, "Ontology-based Information retrieval." Information and Intelligent Systems, Croatia, pp. 23-28, 2003.

[10] Y. Chi and H. Chen, “Ontology and semantic rules in document dispatching”, The Eletronic Library, vol. 27(4), 694-707, 2008.

[11] C.J. Anumba, R.R.A. Issa, J. Pan, and I. Mutis, “Ontology-based information and knowledge management in construction”, Construction Innovation, vol. 8(3), pp. 218-239, 2008.

[12] M.F. Sánchez, “Semantically enhanced information retrieval: An ontology-based approach”, Tesis Ph.D. Autonoma University De Madrid, 2009.

[13] W. A. Woods, “Searching vs finding: Why systems need knowledge to find what you really want”, ACM Queue, hlm. pp. 2-35, 2004.

[14] W. A. Woods, L. A. Bookman, A. Houston, R. J. Kuhns, P. Martin, and S. Green, “Linguistic knowledge can improve information retrieval”, Proceedings of ANLP-2000, Seattle, WA, hlm. pp. 1-6, 2000.

[15] C. Yoon, “Domain-Specific Knowledge-based information retrieval model using knowledge reduction”, Tesis Ph.D. University of Florida, 2005.

[16] M. Yi, “User performance using an ontology-driven information retrieval (ONTOIR) system”, Tesis Ph.D. Florida State University,2006.

[17] S. Kumar, R. Rana and P. Singh, “Ontology based semantic indexing approach for information retrieval system”, International Journal of Computer Applications, vol. (12), pp. 0975 – 8887, 2012.

[18] M. T. Abdullah, F. Ahmad, R. Mahmod and T. M. T. Sembok, “Rules frequency order stemmer for Malay language”, IJCSNS International Journal of Computer Science and Network Security, vol. 9(2), pp. 433-438, 2009.

[19] M. Uschold and M. King, “Towards a methodology for building ontologies”, IJCAI95 Workshop on Basic Ontological Issues in Knowledge Sharing. Montreal, 1996.

[20] N. Noy and L. McGuinness, “Ontology development 101: A guide to creating your first ontology”, Stanford Knowledge Systems Laboratory Technical Report KSL-01-05 and Stanford Medical Informatics Technical Report SMI-2001-0880, 2001.

[21] M. Uschold and M. Gruninger, “Ontologies: Principles, Methods and Applications”, Knowledge Engineering Review, vol. 11 (2), 1996.

[22] M. J. Darlington and S. J. Culley, “Investigating ontology development for engineering design support”, Advanced Engineering Informatics, vol. 22(1), pp. 112-134, 2008.

[23] A. Sayed, and A. Al Muqrishi, “IBRI-CASONTO: Ontology-based semantic search engine”, Egyptian Informatics Journal, vol. 18(3), pp. 181-192, 2017.

[24] Y. Di, W. Song, H. Wang and L. Liu, “Research on open domain Named entity recognition based on Chinese query logs”, Proceedings of 2016 IEEE Advanced Information Management, Communicates, Electronic and Automation Control Conference, IMCEC, 2017.

[25] F. Ahmadi and H. Moradi, "A hybrid method for Persian Named Entity Recognition", Conference on Information and Knowledge Technology, IKT, 2015.

[26] S. S. Sazali, N. A. Rahman and Z. A. Bakar, "Information extraction: Evaluating named entity recognition from classical Malay documents", International Conference on Information Retrieval and Knowledge Management, CAMP 2016", 2017.

[27] K. R Chekima, Alfred and K. O. Chin, "Rule-Based Model for Malay Text Sentiment Analysis", Lecture Notes in Electrical Engineering, vol. 488, pp. 172-185, 2018.

[28] F. Sidi, "MalayIK: An Ontological Approach to Knowledge Transformation in Malay Unstructured Documents." International Journal of Electrical and Computer Engineering (IJECE), vol. 8(1), 2018.

[29] Ahmad Khair Mohd Nor., Pengantar sintaksis bahasa Melayu, Kuala Lumpur: Utusan Publications & Distributions Sdn. Bhd, 2003.

[30] Zulkifley Hamid, Konsep Bahasa, dlm. Zulkifley Hamid, Ramli Md. Salleh, Rahim Aman. (pnyt.). Linguistik Melayu. Bangi: Penerbitan Universiti Kebangsaan Malaysia, 2006.

[31] Abdul Ghalib Yunus, Dr. Ghazali Lateh, Panduan revisi esensi bahasa Malaysia PMR. Longman: Pearson Sdn. Bhd.,2009.

[32] Ramli Md. Salleh, Zulkifley Hamid, Ramli Md. Salleh, Rahim Aman. (pnyt.). Linguistik Melayu. Bangi: Penerbitan Universiti Kebangsaan Malaysia, 2006.

[33] B. Selvalakshmi and M. Subramaniam, "Intelligent ontology based semantic information retrieval using feature selection and classification", Cluster Computing, vol. 22(5), pp. 12871-12881, 2019.

[34] G.P. Zarri and E. Jennex. Murray, "Knowledge Management: Concepts, Methodologies, Tools, and Applications", Premier Reference Source, IGI Global, 2008.

[35] K. Munir, and M. S. Anjum, "The use of ontologies for effective knowledge modelling and information retrieval." Applied Computing and Informatics, vol. 14(2), pp.116-126, 2018.

[36] S. B., Rodzman, "Domain specific concept ontologies and text summarization as hierarchical fuzzy logic ranking indicator on malay text corpus."Indonesian Journal of Electrical Engineering and Computer Science, vol. 15(3), 2019.

Adaptive Control Technique Effects on Single Link Bilateral Articulated Robot Arm

Nuratiqa Natrah Mansor[1], Muhammad Herman Jamaluddin[2], Ahmad Zaki Shukor[3]
Faculty of Electrical Engineering, Universiti Teknikal Malaysia Melaka (UTeM)
Durian Tunggal, Melaka, Malaysia

***Abstract*—This paper describes a technique for addressing the issue of instability within force controller by developing a model of a bilateral master-slave haptic system that incorporates a Disturbance Observer (DOB) in a robotic simulation. The suggested modeling is used in conjunction with conventional controllers to be correcting undesired noise that occurs inside the working system of a particular joint of the youBot arm. To acquire the target position, the controller will additionally compensate for interference by changing its position response. Two tests were carried out to examine and compare the system's feedback that employed the proposed approach and another system with the conventional and standard-setting. The experimental findings demonstrate the resilience of the suggested system, as the system integrated with observers is more precise and faster. All of the system feedbacks from conducted experiments are measured in the simulation platform.**

Keywords*—Force and position controller; disturbance observer; simulated bilateral system; adaptive control; manipulator arm

I. Introduction

In technology pieces of machinery, a bilateral control system and autonomous robot is cutting-edge technology that allows humans to engage with situations that are inaccessible to them, owing to that the location is situated distant or dangerous. Because the robot is small-scale in size and adaptable, it is simple to control and moved freely and easily. At the same time, it also transfers the haptic sense of an isolated place. Studies in [1] reviewed that this automation has been utilized in a variety of sectors, including telesurgery, autonomous teleoperation for sea and space operations as well as dealing with explosive or high radiation operations. Since the year of 1980, haptic technology has expanded and numerous researchers have explored studies on many parts including its working control system, machine learning, architectures, communication, and applications in many landscapes [2].

Regardless of how the bilateral control system's functionality is proved to behave superiorly with directly corresponds to its pair of manipulators or devices, it is vital to maintain its high feedback gains in both position and force control for acquiring transparency. Typically, to measure the amount of torque acting upon the motor of the manipulator link, force sensors are responsible for doing the calculations.

However, the use of traditional approaches such as force sensors as part of the component as mentioned in [3] was appeared to be some limitations and disadvantages for the running system. Aside from the limited shelf life and costly price, it brings certain uncertainties, instability, and delays to the operating control system, including in robots [4]. Plus, to optimum the budget for purchasing the sensors, most works and studies focusing on upgrading the operationality of a premade assistive device like electronic joysticks, keyboards, data gloves, and custom-built manipulators [5]. These input devices communicate its direction and tasks of various aspects to the device it is controlling but never experiencing two sides tactile perceptions aside from its unilateral common vibration feedback based on onscreen actions.

On the other hand, a simpler approach for a better framework of bilateral control system can be attained by using Disturbance Observer (DOB). From past studies, the control action and feedback inside a bilateral control system may be improved up to 90% inaccuracy, compared to the standard system without DOB. As records, [6] observed that the prior system suffered around 25% to reach the ideal efficiency value. Following the implementation of DOB, contributes to the infallibility of the control process simultaneously and improving the response process within the system. This out-turn should be prioritized in designing a function-based controller design deal for a bilateral control system. Plus, this control technique is practical and offers better capability as shown in [7] to the telerobotic and robot manipulator control system which has been validated and proved in past research.

Considering the notion of programmable task handling and knowledge in controller design, this study presented an adaptive approach for bilateral control system design for industrial arm robots. KUKA youBot is chosen as the manipulator and also interfaces for creating a model of bilateral master and slave robotic control system as it has open interfaces that can use for various experiments and also a mobile industrial manipulator. Furthermore, the integration of adaptive design of force and position controller into the robotic arm bilateral system is expected to demonstrate the disparity and uniqueness when operating in an industrial robotic arm, in contrast to smaller and common assistive devices like being studied in [4] and [8].

In summary, the purpose of this work is to demonstrate the proposed idea of implementing the DOB technique into a bilateral master-slave control system and its relations with an industrial robotic arm. Section 2 goes into further detail on the approach and procedure used to carry out the experiments. Section 3 will show the data and information gathered from the experiment, which has been tabulated and plotted into multiple graphs. Following that, the feedback of the stated

Zamalah Scheme, Universiti Teknikal Malaysia Melaka (UTeM)

system from the simulation of the bilateral master-slave arm manipulator is reviewed in Section 4. While in Section 5, conclusions and recommendations for forthcoming works are commented here. The study presented in this paper is limited to provide a way to design an adjustable system that is capable to improve the complexity and effectiveness of the bilateral control system on a robotic arm manipulator with a type of robust control tool (DOB).

II. METHODOLOGY

The whole workflow for this study can be visualized in diagram Fig. 1 below for a clear understanding of the work process and to illustrate the step-by-step activities.

A. *Modeling for Disturbance Observer (DOB)*

The primary objective of this project is to use a software simulation to create a simpler framework of a bidirectional master-slave haptic system on the industrial robotic arm. As discussed priorly in the introduction, a close loop system response carries noise and experiences delay in its operation. The robustness and sensitivity of the system are typically subpar and difficult to maintain. To address such an issue, an idea for incorporating a robust control tool into the close loop control systems is required. By eliminating uncertainty and undesirable information within the system, DOB implementation might increase system infallibility. Additionally, this technique facilitates robot navigation and task manipulation between the operator and target objects. Also, force measurement through a force sensor can be substituted with this observer due to the sensors' notable drawbacks [7]. On the other hand, using conventional controllers for the control system is insufficient due to certain limitations.

In comparison to these common controllers, proportional derivative (PD) is very suitable to combine with DOB when designing a new framework control system for the bilateral robotic arm. In many engineering applications, DOB is widely approached in absence of a force sensor. Commercial force sensors are practically less robust, not cost-effective, and have limited bandwidth for sensing [8]. Hence, this intuitive robust control technique can estimate the disturbance force, F_{dis}, and calculate the compensatory current, I_{cmp}, required to achieve robust motion control. Information estimated from the observer is used in conjunction with the input signal as feedback to reject any instabilities and achieve robust stability of providing high-accuracy readings for accurate tracking. To that end, the analogous system for (1) is depicted as a system block diagram in Fig. 2 and Fig. 3 below. F_{dis} is composed of the following components:

$$F_{dis} = F_{ext} + F_{int} + F_{fric} + (M - M_n)\, s^2 X_{res} + (K_{tn} - K_t)\, I_a^{ref} \tag{1}$$

The disturbance force, F_{dis} equation is the result of a modeling error in the nominal mass, M_n, and thrust coefficient, K_{tn}. Under interactive force, F_{int}, the components examined are Coriolis term, centrifugal term, and gravity term. As a consequence, F_{dis} is calculated in the following manner using the low pass filter (LPF):

$$F_{dis} = \frac{g_{dis}}{s+g_{dis}} F_{dis} \tag{2}$$

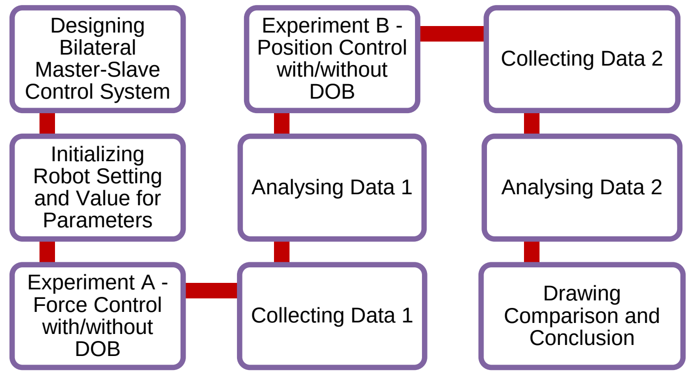

Fig. 1. The Work Process for the Study.

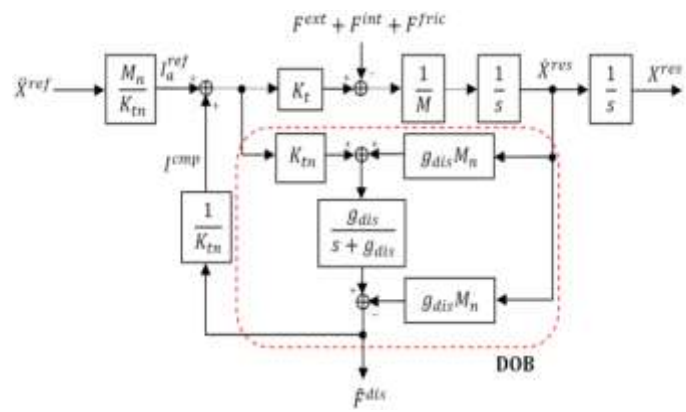

Fig. 2. Disturbance Compensation by DOB.

To put it another way, DOB assists the system in achieving solid acceleration control. Fig. 3 illustrates the block diagram of an acceleration-based position control system.

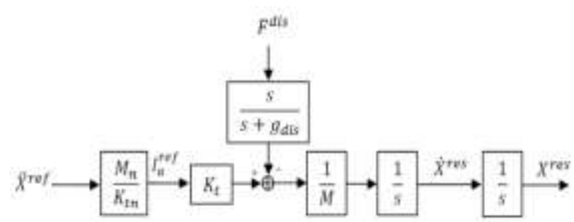

Fig. 3. Robust Acceleration Control.

Position controller, C_p is:

$$C_p = K_p + sK_v \tag{3}$$

While the related position response is described as:

$$x_{res} = \frac{C_p}{s^2}(x_{cmd} - x_{res}) \tag{4}$$

Equation (4) has been rearranged and converted into (5) as follows:

$$\frac{x_{res}}{x_{cmd}} = \frac{C_p}{s^2 + C_p}$$

$$\frac{x_{res}}{x_{cmd}} = \frac{sK_v + K_p}{s^2 + sK_v + K_p}$$

$$\frac{x_{res}}{x_{cmd}} = \frac{2\xi\omega_n s+\omega_n{}^2}{s^2+2\xi\omega_n s+\omega_n{}^2} \quad (5)$$

The natural angular frequency, ω_n is equal to $\sqrt{K_p}$ or ½ K_v whereas the damping ratio, ξ can be adjusted to 1.0 to get a critical damping effect.

B. Framework Design of Bilateral Master-Slave Control with DOB Based

Following the integration of DOB into the system, the bilateral control system as a whole is illustrated in Fig. 4. The combination of the information from the said observer and the input signal produced feedback that compensates for any modeling error or interference that occurs. The total acceleration, $\ddot{x}_{dif}$ for position controller C_p in Differential Mode, and total force, $\ddot{x}_{com}$ for the force controller C_f in Common Mode, are equated as in (6) and (7) for this master and slave bilateral paradigm.

$$\ddot{x}_{dif}^{ref} = C_p(s)(x_s^{res} - x_m^{res}) \quad (6)$$

$$\ddot{x}_{com}^{ref} = C_f(s)(f_s^{ext} - f_m^{ext}) \quad (7)$$

C. Simulation and Experiment Setup

The work platform for this project is robotic simulation software. To determine if the proposed system is ideal and follows the rule of action and reaction in bilateral control systems, the simulation is performed in the Virtual Experimentation Platform (VREP), a 3D Robot Simulation Software with beginning parameters pre-configured similarly to in the actual environment. VREP software includes a pre-configured KUKA youBot.

The scene, models, and object attributes included therein are simple to manage and have a plethora of choices to be controlled and numerous functionalities. To implement the system's bilateral communication with a DOB-based robust control technique, KUKA youBot incorporates a model of the bilateral master-slave control system, as seen in Fig. 5.

Both the Python command script and the remote Application Programming Interface (API) function are used to link the two robots to the system. Although youBot is a mobile robot with five ° of freedom and has multiple links, this study focused only on 'Joint0' (the first joint located on the lower robot component). This is because to decrease the complexity of operating the haptic test and speed up the time required operating further joints and trajectory movement. Essentially, the setup and workstation for a bilateral master-slave robotic arm have been modeled in VREP. Fig. 6 illustrates the perspective view of the robot setup and environment utilized in each experiment.

In general, both systems and robot settings are equivalent. Constant variables such as the starting position of Joint0 of both robots are fixed at 0°. The obstacle's mass placed alongside the slave is set to 500N. Throughout the simulation's execution for all experiments, the procedure is specified in flowchart Fig. 7 and presented in Fig. 8 and 9.

In summary, this section discussed the modeling designations for the specified controller and introduced observer to the close loop system, new block diagrams for bilateral control master-slave system, and robot setup in VREP simulation staged for further experiments. Procedures and workflow for experiments have been described to provide insight into how the tests are conducted.

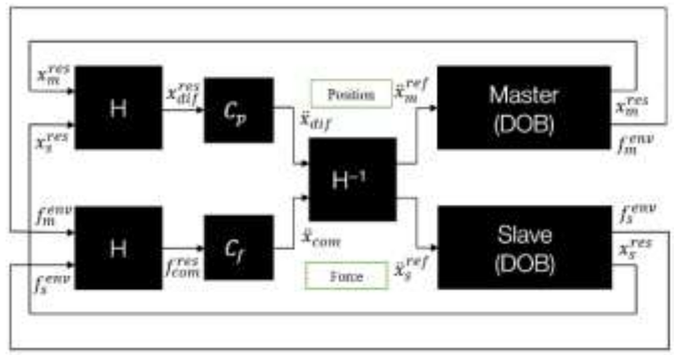

Fig. 4. Block Diagram of the Bilateral System with the Construction of DOB.

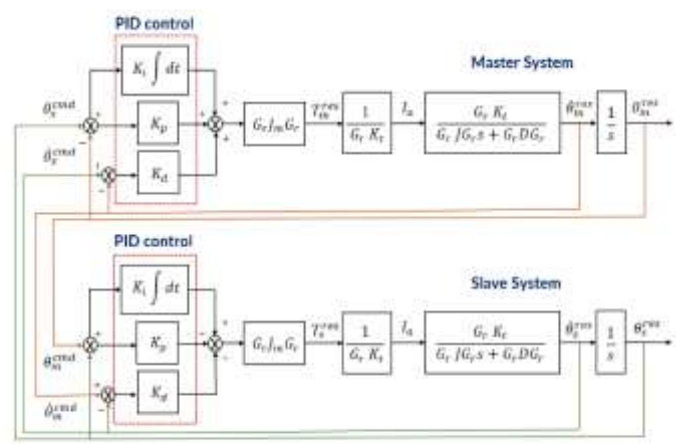

Fig. 5. Block Diagram of Master-Slave Control System with PID Controller.

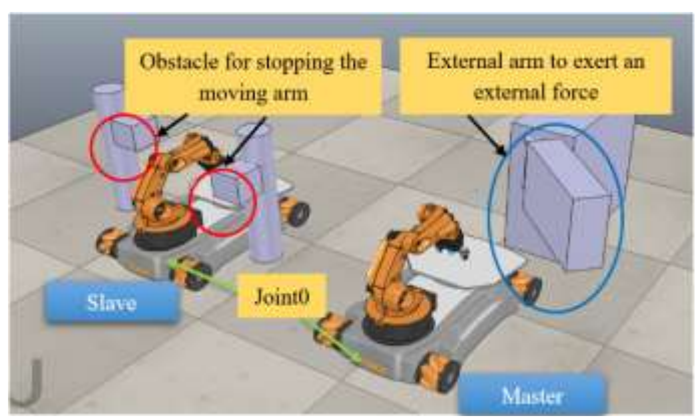

Fig. 6. Bilateral Robot Setup from Perspective view for Experiments.

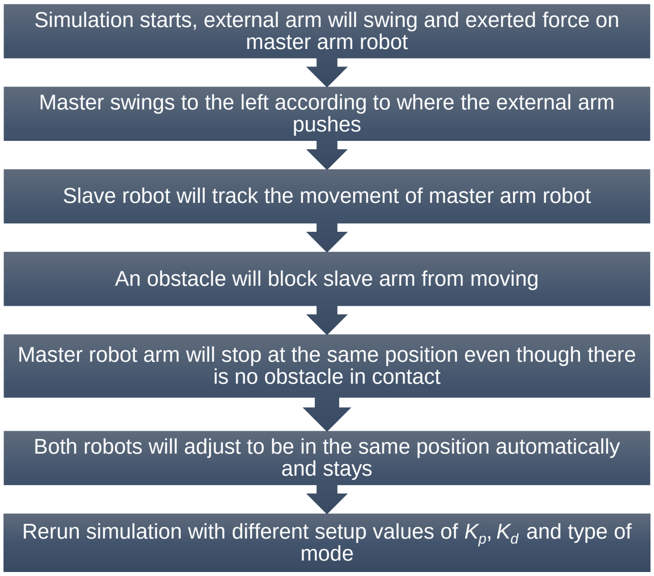

Fig. 7. Steps in the Operation of Bilateral Control System Experiment.

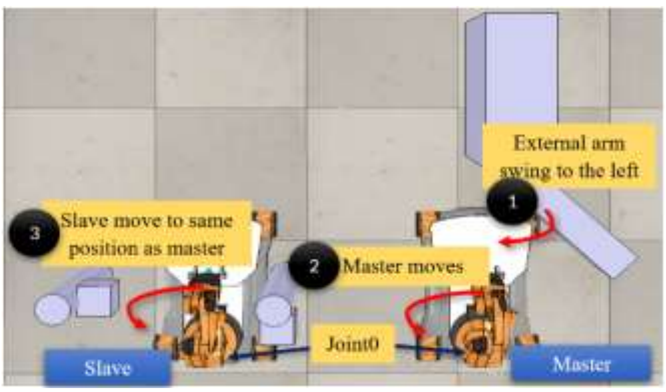

Fig. 8. Illustration A for Bilateral System Operation.

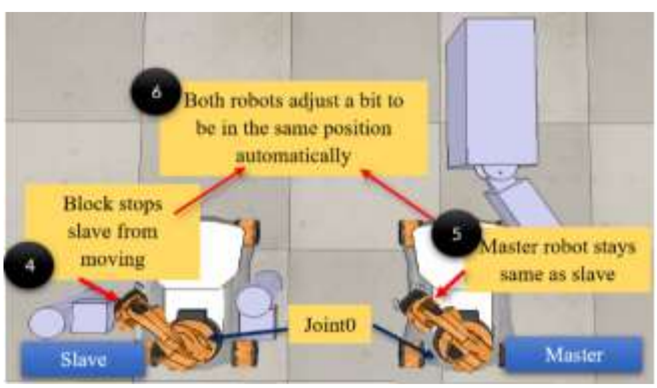

Fig. 9. Illustration B for Bilateral System Operation.

III. Result and Analysis

To demonstrate the second law of bilateral control system which is a total difference of position reading in master and slave must be equal to zero, the experiment was solely focused to prove on the differential mode law. Next, the purpose of this experiment is to observe whether the input feed carried by DOB can be used to improve the system's performance or reducing noise that occurs internally. PD controller is also paired with DOB for the proposed system.

The findings from the simulation are portrayed in this section. Response from the DOB-based control system for the articulated bilateral arm manipulator is shown in this subsection in the form of tables and graphs. Each experiment is repeated three times with a different value set of variables. K_p and K_d are independent variables while the initial value of the robot joint is the controlled variable. Values for independent variables are shown in Table I below. These parameters are chosen using an experimental validation technique that involves selecting a range of the best acceptable values from a large number of trials ranging from low to high. Every value of variables was necessary to repeat thrice to get the mean value before plotting into graphs accordingly.

TABLE I. Ω_N, K_P AND K_D VALUES FOR DOB EXPERIMENT

ω_n	$K_p\,(\omega_n)^2$	$K_d\,(2\omega_n)$
1	1	2
2	4	4
5	25	10
10	100	20
20	400	40
50	2500	100
100	10000	200
200	40000	400
500	250000	1000

A. DOB based for Force Control (Part A)

The graphs in Fig. 10 to Fig. 18 illustrate the force readings at Joint0 recorded for both master and slave youBot arms.

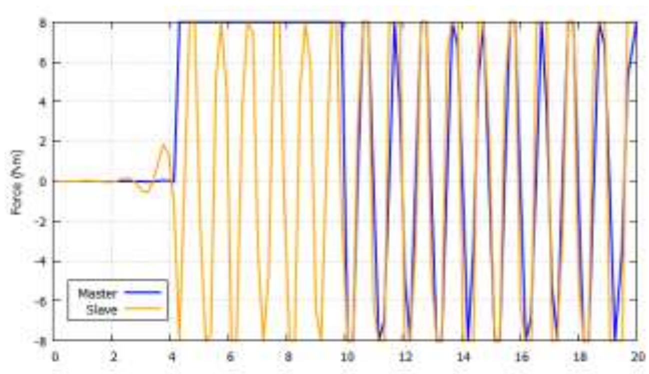

Fig. 10. Force of Master and Slave Arm vs. Time for ω_n = 1.

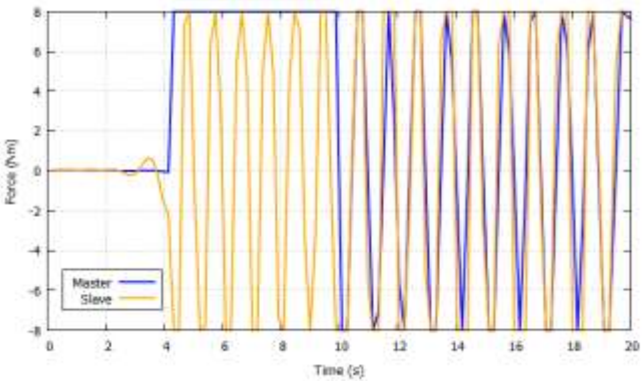

Fig. 11. Force of Master and Slave Arm vs. Time for ωn = 2.

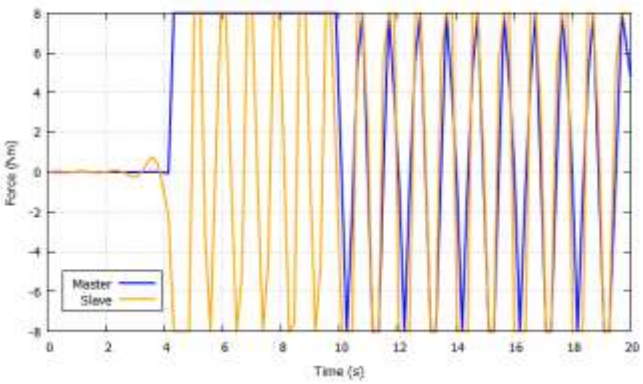

Fig. 12. Force of Master and Slave Arm vs. Time for ωn = 5.

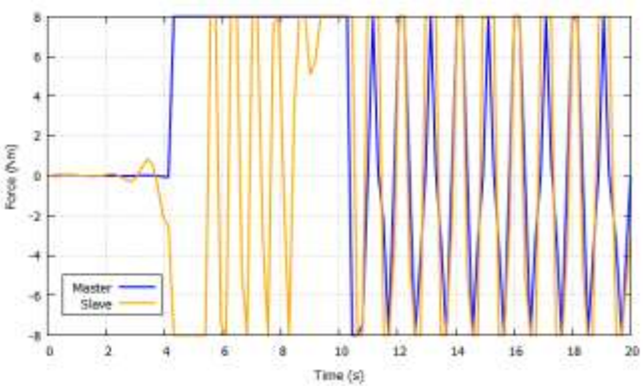

Fig. 13. Force of Master and Slave Arm vs. Time for ωn = 10.

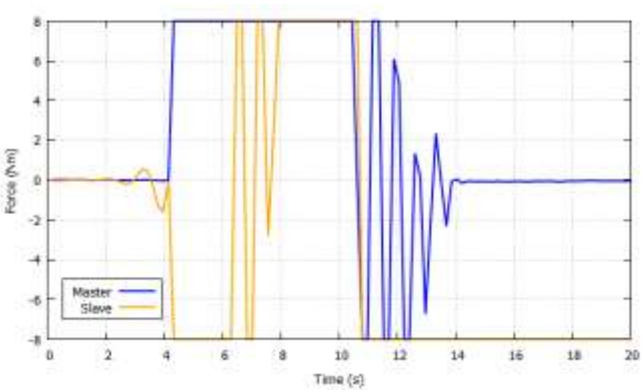

Fig. 14. Force of Master and Slave Arm vs. Time for ωn = 20.

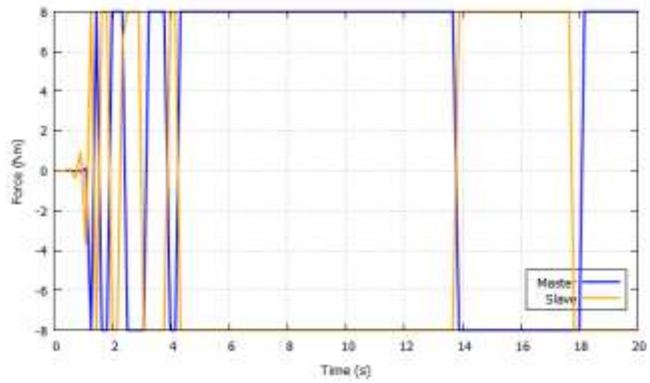

Fig. 15. Forces of Master and Slave Arm vs. Time for ωn = 50.

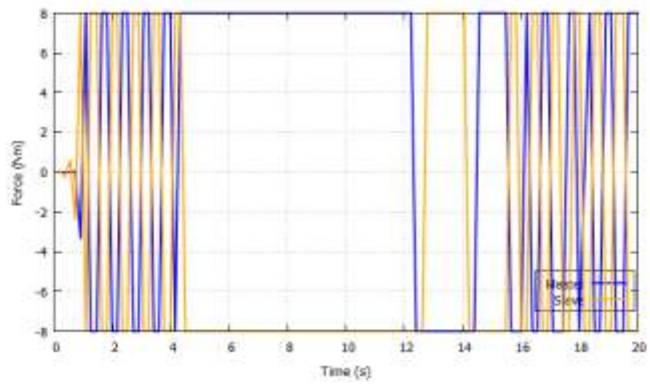

Fig. 16. Force of Master and Slave Arm vs. Time for ωn = 100.

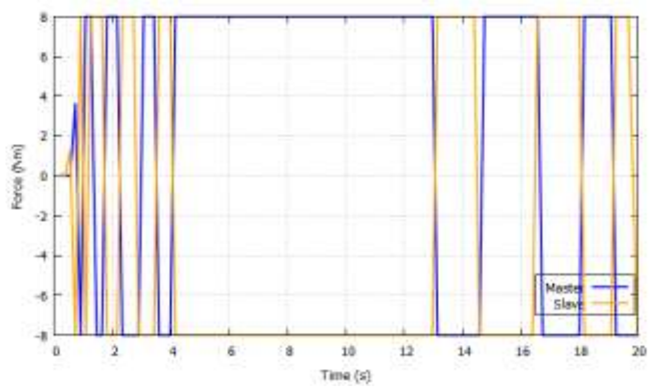

Fig. 17. Force of Master and Slave Arm vs. Time for ωn = 200.

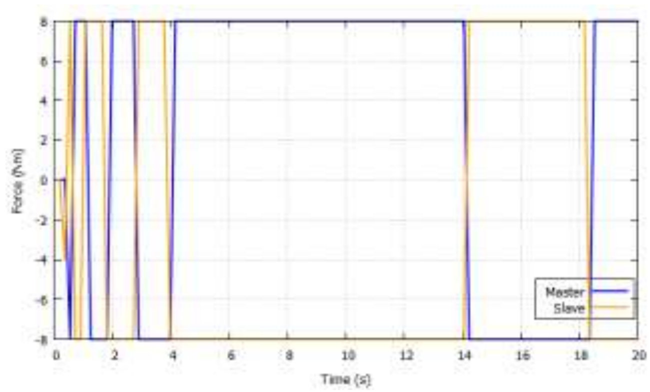

Fig. 18. Force of Master and Slave Arm vs. Time for ω_n = 500.

All graphs from Fig. 10 to Fig. 18 illustrate the feedback in torque reading on the single joint of both master and slave system in various parameter values, ranging specify at value ω_n=1 to ω_n=500. The graph line formed in blue color represents the torque reading for the master robot, while the orange line shows the torque reading recorded on the slave robot. The preset maximum torque value for Joint0 in both articulated robots is 8 Nm. In Fig. 10 to Fig. 14, when force reading in master increased to 8 Nm after being forced by the external manipulator, the reading value on the slave robot started to create series of progressive variations in the force reading. At this moment, the slave remains stationary from its initial position. This is because the value of gain K_p and K_d are relatively small and unfit to generate a working bilateral scheme. Although force exerted on master robot getting an increase for a brief period after the push, system on slave side considered the information feed from the other pair to be disregarded. The slave robot is unable to read the data that passes through, as reading is unstable and constantly changing. This situation also occurred after the external manipulator returned to its initial position and ceased pushing the master youBot arm ahead. Hence, torque readings for both master and slave are continually fluctuating and show no evidence of colliding or contacting with other external forces.

Whereas the force reading in the slave improved and matched the force reading recorded in the master's as shown in Fig. 15 to 18. This is because, at t = 4s, the external arm began pushing the master youBot. After receiving information from its pair, the slave sensing the same applied force and move ahead as well for a certain period until obstructed by another block. Slave youBot instantly exerting a reaction force against the barrier and attempting to go forward. From the graph, the lines formed indicate that the master youBot arm applied its maximum torque of +8Nm to go further, while the slave youBot arm attempted to withstand the greater force applied by an external obstacle, resulting in a value of -8Nm in torque. The bigger gain values for the controllers demonstrate the connection between the magnitudes of the input and output signals at a steady state. For example, when the external manipulator returned to its position after 12s and ceased its 8Nm push on the master robot, joint reading for both subsystems (master-slave robot) wavered and unstable. To improve the system stability, increasing the value of gain controller for both subsystems will cause the bilateral system to operate ideally and obey the bilateral law of the control system, as illustrated in Fig. 15 to Fig. 18 when the value of gain is respectively set at K_p = 2500 and K_d = 100, K_p = 10000 and K_d = 200, K_p = 40000 and K_d = 400 and K_p = 250000 and K_d = 1000. Thus, whenever the force reads on Joint0 of the master is +8Nm, Joint0 on the slave will be giving a counter at -8Nm.

B. DOB based for Position Control (Part B)

For this experiment, position control is backed up by trials that demonstrate the DOB's capability to the bilateral system after being paired with the PD controller. Thus, graphs in Fig. 19 to Fig. 27 showed the position readings of both master-slave robots at specified Joint0.

All graphs from Fig. 19 to Fig. 27 illustrates the feedback in position reading on the single joint of both master and slave system in various parameter values, ranging specify at value ω_n=1 to ω_n=500. Graph line formed in blue color denotes the reference angle or step input, while the green line signifies the position reading logged on master robot and red line denotes the joint position recorded on slave robot. The preset maximum torque value for Joint0 in both articulated robots is 8 Nm and the position angle was initially set at 0° for both pairs of manipulators. Reading for the position of the master reaches a maximum around t >8.5s and is maintained until 20s, looking from graphs in Fig. 18 to Fig. 23.

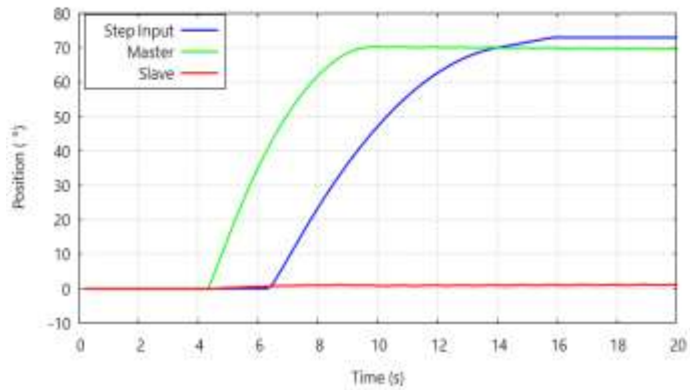

Fig. 19. Position of Master and Slave Arm vs. Time for ωn = 1.

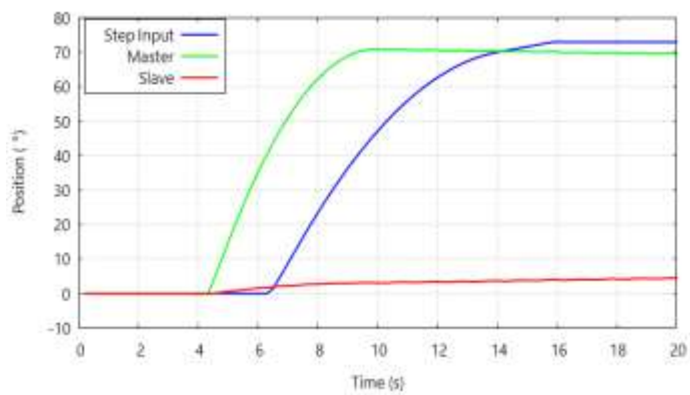

Fig. 20. Position of Master and Slave Arm vs. Time for ωn = 2.

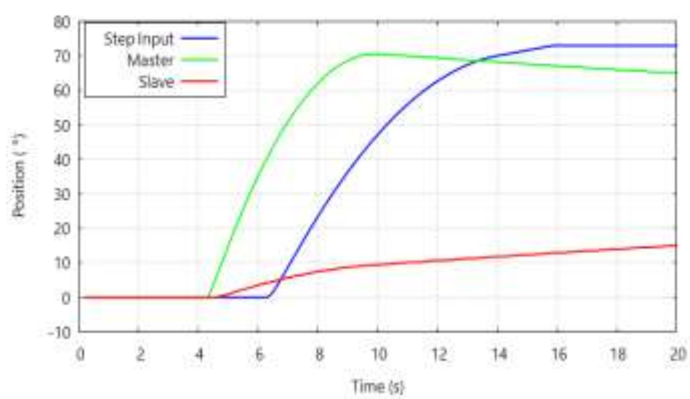

Fig. 21. Position of Master and Slave Arm vs. Time for ωn = 5.

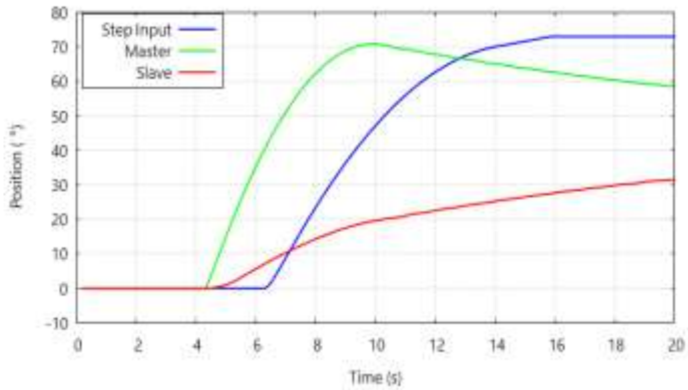

Fig. 22. Position of Master and Slave Arm vs. Time for ωn = 10.

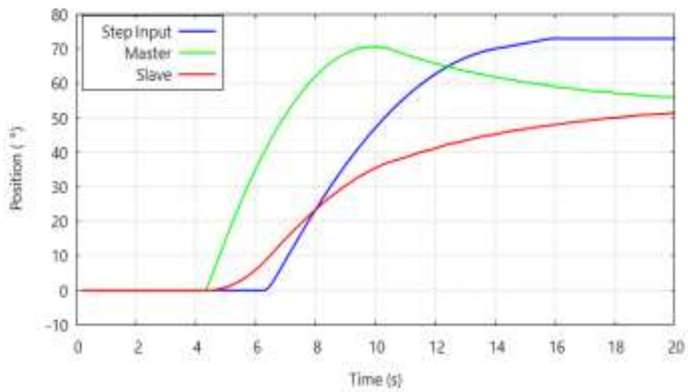

Fig. 23. Position of Master and Slave Arm vs. Time for ωn = 20.

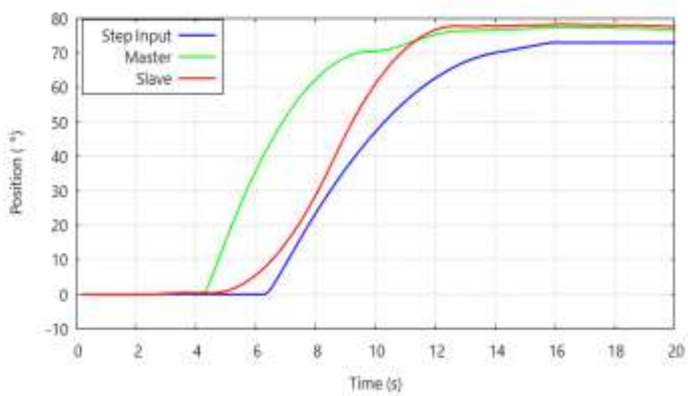

Fig. 24. Position of Master and Slave Arm vs. Time for ωn = 50.

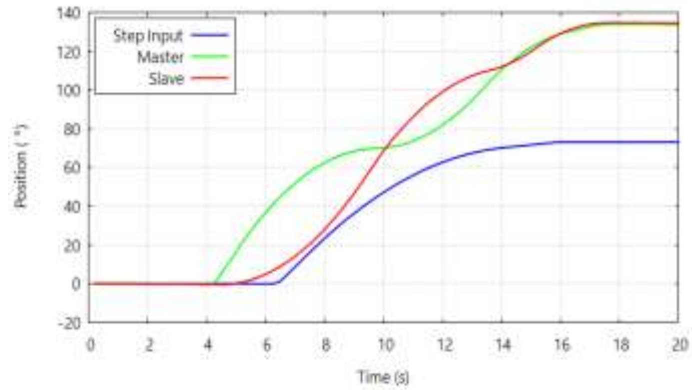

Fig. 25. Position of Master and Slave Arm vs. Time for ωn = 100.

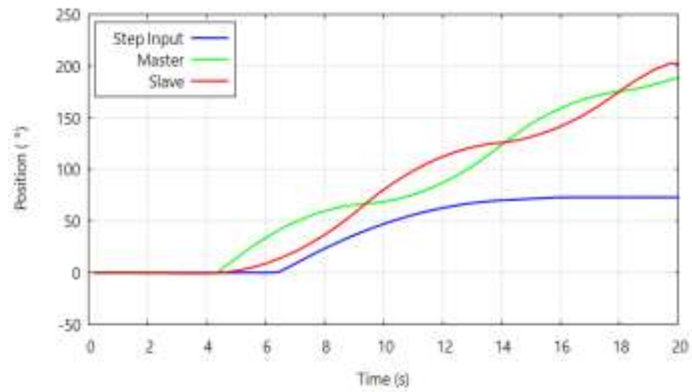

Fig. 26. Position of Master and Slave Arm vs. Time for ωn = 200.

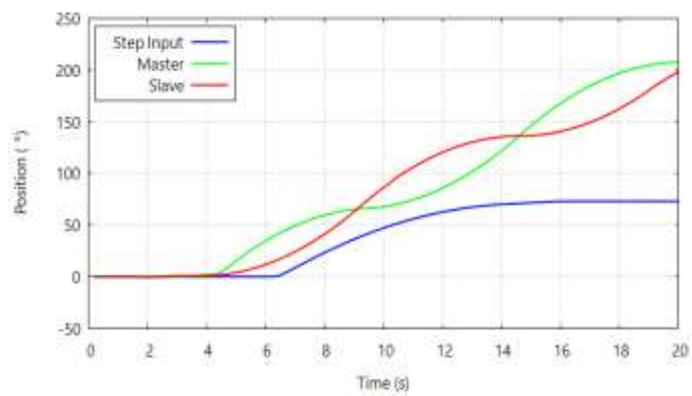

Fig. 27. Position of Master and Slave Arm vs. Time for ω_n = 500.

Individually, the position of the slave achieved maximum position angle at 51° in Fig. 23, 20° in Fig. 22, 15° in Fig. 21, and 5° in Fig. 20. After t > 5s, the slave's position grew slightly but no distinct disparity with the first three graphs. On the other hand, at t = 9s, the graph in Fig. 19 to Fig. 23 showed that the position of the master topped across 70° and roughly reached 80° for Fig. 24. Different situations were observed from graphs 25, 26, and 27, respectively. Both robots swinging forth and back while steadily increase in their positions. It appears that the position readings at the master side continue to rise after an external force is exerted on the master robot.

Meanwhile, the pattern of the graph in Fig. 19 to Fig. 21 shows that the angle position expands slightly as being compared to the master because the value of the PD controller is insufficient to reach an overshoot or settling time. Following the increased value of gain, the position angle of the slave robot extended and advanced, peaked at 78° in maximum position with a stable condition as portrayed in Fig. 24 and 200° in unstable condition, formed in each graph in Fig. 26 and 27. Simultaneously, the position angle for the master robot began to converge with the slave's position, as seen in Fig. 24 and Fig. 25.

Reading of angle at Joint0 on slave robot according to Fig. 25 to Fig. 27 showed that it went further to catch up with the master's position, while the master robot is attempting to catch up with the slave's position as well. Delays between the two subsystems occurred during exchanging the data, which caused the angle to vary continuously. When ω_n = 100, both robots were able to achieve the same position at 137° after fluctuating for about 13s. The position values of the master and slave exceeded the reference angle after the value of ω_n is set at 50 to 500. Error value in position angle between master and slave and the reference angle is smallest, approximately -5° as shown in Fig. 24 and largest (-125°) in Fig. 27. Table II summarizes the accuracy for values of ω_n in the stated controller.

TABLE II. ACCURACY FOR CONTROL SYSTEM WITH DOB

ω_n	$K_p\,(\omega_n)^2$	$K_d\,(2\omega_n)$	Accuracy *(%)*
1	1	2	1.78
2	4	4	6.49
5	25	10	23.09
10	100	20	53.79
20	400	40	91.82
50	2500	100	98.94
100	10000	200	99.54
200	40000	400	92.66
500	250000	1000	95.31

Three systems have an accuracy of greater than 95%. The system with ω_n=100 has the best accuracy at 99.54%, followed by the system with ω_n=50 at 98.94% and the system with ω_n=500 at 95.31%. Although the last system acquired the highest accuracy, both robots swayed further before settling into the same position relative to one another. Meanwhile, there are two systems with an accuracy rate of less than 10%. The system has an accuracy of 1.78% when ω_n=1 while another system with precision of 6.49% when ω_n=2. Conferring to graph shape in Fig. 24, the optimal design for a control system with DOB based for position control is K_p=2500 and K_d=100 since both bilateral master and slave robot reached the same position fixedly after 11s, has a smaller error in steady-state, and attained a critical damped. For force control, the optimal design for a control system is the value of K_p=250000 and K_d=1000. Due to force readings recorded at Joint0 inside master and slave systems is indicated at zero for summation of torque and has the least feedback noise, as seen in Fig. 18.

IV. Discussion and Conclusion

Tables III and IV summarized the best values for controllers and observations made from the analysis in simulation and graph patterns from all experiments.

Overall, this study successfully met all the objectives and was supported by two different experiments with a variety of different parameter sets to validate the system response. All results have been recorded and transformed into graphs to show the feedback pattern. The control system response with the proposed adaptive technique is also evaluated and discussed in form of accuracy, time delay, and settling time. It is shown that the adopted control technique as discussed by Jing *et al.*, in [8] improves the stability and performance of the bilateral control system and is practical to apply in various systems including industrial robot simulations. The application of the observers by replacing the old-style force sensors on the robot control system has improved the dynamics inside the whole system, estimates the disturbance inside to improve the errors, and adjusting the input signal to achieve robust control motion, like the outcome of control system observed in [6].

TABLE III. SUMMARY FOR DOB IN COMMON MODE LAW

Common Mode Law	
Best values	K_p = 250000 and K_d = 1000
Worst values	K_p = 1 and K_d = 2
Force reading	Total in force between master and slave are equal to zero
Force pattern	More vibrations, not stable

TABLE IV. SUMMARY FOR DOB IN DIFFERENTIAL MODE LAW

Differential Mode Law	
Best values	K_p = 2500 and K_d = 100
Worst values	K_p = 250000 and K_d = 1000
Time delay	+0.5*s*
Overshoot	9.0*s* to 9.5*s*
Accuracy	98.94%
Position reading	Difference in total position between master and slave are almost zero

For future work, another control tool called Reaction Force Observer (RFOB) could be introduced to the framework design of the bilateral control system to improve enhances the system's feedback and resilience. RFOB is known to have the ability to subtract the system uncertainties from the DOB input. It cancels out disturbance signals such as gravity forces, viscous damping friction, or Coriolis forces within both the internal system and internal motor located at the robot joint.

Acknowledgment

The authors would like to express their gratitude for the funds and support provided by Universiti Teknikal Malaysia Melaka (UTeM) under the Zamalah Scheme to conduct this study. Additionally, the authors would like to express appreciation to the Faculty of Electrical Engineering's Robotics and Industrial Automation Research Group.

References

[1] B., Abeer, A. K., Hend, and A. S., Abdulmalik, “Haptics-Based Systems Characteristics, Classification, and Applications”, USA: Advanced Methodologies and Technologies in Artificial Intelligence, Computer Simulation, and Human-Computer Interaction, 2019, pp.778-794.

[2] G., G. Shankar, M., Yaser, and Z., Kourosh, “An Application-Based Review of Haptics Technology”, Robotics 2021, vol. 10, no. 29, 2021, pp. 1-18.

[3] N., Hiroshi, O., Kiyoshi, Y., Yuki, K. Naoki, M., Toshimasa, T., Akifumi, “Force Sensorless Fine Force Control Based on Notch-Type

Friction-Free Disturbance Observers", IEEJ J. Ind. Appl., vol. 7, 2018, pp. 117-126.

[4] L., Xiangxing, Z., Guokun, Z., Jiaji, and W., Jiajin, "Sensorless Force Estimation of End-Effect Upper Limb Rehabilitation Robot System with Friction Compensation", Int. J. Adv. Robot. Syst., vol., 16, 2019, pp. 1-11.

[5] A. R. Maouche and H. Meddahi, "A Fast Adaptive Artificial Neural Network Controller for Flexible Link Manipulators", Int. J. Adv. Comp. Sci. and App. (IJACSA), vol. 7, no. 1, 2016, pp. 298-308.

[6] E. Sariyildiz, and K. Ohnishi, "A Comparison Study for Force Sensor and Reaction Force Observer-based Robust Force Control Systems", Proc. IEEE 23rd Int. Con. Ind. Electron, 2014, pp. 1156-1161.

[7] L., Sichao, W., Lihui, and W., Vincent, "Sensorless Force Estimation for Industrial Robots Using Disturbance Observer and Neural Learning of Friction Approximation", Robot Comput. Integr. Manuf., vol. 71, 2021, pp. 1-11.

[8] B. Jing, H. Duan, J. Na, and S. Wang, "Unknown System Dynamics Estimator based Control for Bilateral Teleoperation Systems", 2021 IEEE 10th Data-Driven Control and Learning Systems Conf. (DDCLS), 2021, pp. 1552-1557.

A Novel Method for Rainfall Prediction and Classification using Neural Networks

K. Varada Rajkumar[1]
Research Scholar, Department of CSE
Koneru Lakshmaiah Education Foundation
Vaddeswaram, AP, India

Dr. K. Subrahmanyam[2]
Professor, Department of CSE
Koneru Lakshmaiah Education Foundation
Vaddeswaram, AP, India

***Abstract*—In the field of food production, it is an important and difficult job to maintain water sources for major population centres and reduce the risk of flooding, to forecast rainfall reliably and accurately. Accurate and genuine forecasts of rainfall on monthly and seasonal time scales help to provide beneficiaries with knowledge on the control of water supplies, farm forecasting and integrated crop insurance applications. Present rainfall prediction is the challenging task for the researchers and most of the rainfall prediction techniques are fail in accuracy. For this we propose a new effective hybrid approach for forecasting and classifying rainfall using the neural network and ACO method. The collected rainfall data were preprocessed by filling missing data and normalized by min-max normalization, the processed data is given to various classifiers for evaluating its performance. The performance of the existing and proposed models is compared. Performance comparison of existing feed-forward, cascade-forward and pattern recognition NN classifier and the proposed ACO+feed-forward backpropagation, ACO+ cascade-forward backpropagation and ACO+ pattern recognition NN classifier are done. The entire HNN forecasting protocol consists of pre-processing and choosing the input vector and maximising the number of hidden nodes using ACO and ANN modelling.**

Keywords—Pattern recognition; ant colony optimization; artificial neural network; rainfall prediction; feed-forward; cascade-forward; data processing

I. Introduction

Precipitation, which is heavily dependent on space and time, is one of the most dynamic atmospheric systems. Knowledge of the rainfall phenomenon remains a challenging problem and it is also a vital job to efficiently and correctly predict rainfall, since it is important to preserve water supplies for major population centers in the food production sector and to minimize the risk of floods [1]. Reliable and true rainfall predictions help to provide beneficiaries with information on water supply control, farm planning and their integrated crop insurance applications on monthly and seasonal time scales [2,3]. In recent days, different methods have been suggested for rainfall prediction. These approaches, such as dynamic and empirical, are split into two different groups. General circulation models (GCMs) are usually based on the laws of physics and are a form of dynamic model used for climate forecasting [4].

GCM models, however, are highly complicated, so empirical models are often used to forecast monthly and seasonal precipitation during their usage in agricultural forecasting [5]. Predictive simulations are usually based on the theoretical relationships of predicate variables with various other predictors. The idea is to work out the spatial and temporal characteristics of past reports of rainfall and forecast variables in this system and to model expected rainfall. Traditional numerical model rainfall prediction approaches are carried out in order to test uncertain parameters by considering some kind of appropriate attribute through the application of regression or some other methods of data optimization [6]. The analytical techniques include statistical simulations and artificial neural networks [7,8]. Although ANN is the recipient of the simulation phase of the physical system, this model is not increased in terms of its precision as the time series is gradually non-stationary and when the hydrological function works on a broad time scale [9]. The pre-processing of input and output is achieved by normalization and function selection in order to deliver better performance in ANN models.

In this paper we propose a new effective hybrid approach for forecasting and classifying rainfall using the neural network and ACO method. The collected rainfall data were preprocessed by filling missing data and normalized by min-max normalization, the processed data is given to various classifiers for evaluating its performance. The performance of existing and proposed model is compared. Performance comparison of existing feed-forward, cascade-forward and pattern recognition NN classifier and the proposed ACO+feed-forward backpropagation, ACO+ cascade-forward backpropagation and ACO+ pattern recognition NN classifier are done. The entire HNN forecasting protocol consists of pre-processing and choosing the input vector and maximizing the number of hidden nodes using ACO and ANN modelling.

II. Literature Survey

With the support of the k-means algorithm, a two-step prediction model, mixed Neural Network, and neural network was proposed by Chatterjee et.al [10]. This contrasts the proposed model with the MLP-FFN classifier. The data source is the Dumdum meteorological station. The proposed model outperforms by achieving 84.26 percent accuracy without feature selection and 89.54 percent accuracy with feature selection. Graf et. al. [11] suggests a dual mix of discrete wavelet transforms and an artificial neural network for water temperature forecasting. It is applied in Poland on the Warta River. The findings of the implementation showed that WT-ANN models were used in measuring river water temperature. The combination of one-dimensional Convolutional Neural Network (Conv1D) and Multi-Layer Perceptron (MLP) is suggested for regular rainfall prediction by M., a hybrid deep learning approach. Both I. Khanand R.aMaity [12] are then contrasted with Multi-Layered Perceptron (deep MLP) and another machine learning solution, Support Vector Regression (SVR), and the findings indicate that the hybrid Conv1D-MLP model is more efficient. The bootstrap aggregated classification tree-artificial neural network (BACT-ANN) model for predictive rainfall prediction is a hybrid model focused on artificial intelligence [13]. It is being introduced in the Langat River Basin of Malaysia. The stochastic secret form of Markov, which is non-homogeneous, is compared to (NHMM). The comparative findings suggest that the paradigm of BACT-ANN outperforms. With the assistance of the hybrid approach of two pre-processing techniques (Seasonal Decomposition and Discrete Wavelet Transformation) and two feed-forward neural networks (Artificial Neural Network and Seasonal Artificial Neural Network), Anh et.al., [14] proposes a monthly rainfall forecast-processing is performed, and the pre-processing performance is provided to the two-feed forward NN. The results of the success suggest that the wavelet transformation offers accurate forecasting of monthly rainfall along with SANN. For the prediction of typhoon precipitation and groundwater level change, a hybrid combination of artificial neural network (ANN) and multiple regression analysis (MRA) is proposed by Hsieh et. al. [15]. In the Zhuoshui River Delta, it is being introduced. An overall accuracy of 80% is obtained, and this technique is effective in predicting typhoons before they occur. Dhar et. al. [16] utilises the advantages of the deep neural network for weather forecasting. This is enforced by supplying the senses of DNN of such attributes such as temperature, relative humidity, vapour and friction. The output prediction result is accurate with respect to the input data given. Roshni et. al. has developed a Feedforward Artificial Neural Network (FFANN) and the hybrid WANN model to model spatio-temporal fluctuations in groundwater levels [17]. The efficiency of these hybrid models is calculated using goodness-of-fit. The experiment showed that the performance of the GT-WANN hybrid model Chen et al. [18]. The findings obtained from this experiment are evaluated and correlated with parameters of Root mean square error (RMSE), Nash Sutcliffe performance (NSE) coefficient and Pearson correlation coefficient (R). A Hybrid Particle Swarm Optimization (HPSO) and Genetic Algorithm (GA) to resolve limited optimization effects and local convergence [19]. It used three techniques, Elitist strategy, PSO strategy and GA strategy, and these strategies are added to the RBF-NN design. Compared to pure GA, the experiment is measured, and the outcome obtained has a greater ability to explore internationally and avoids premature convergence. He et al. invoked the X.A Hybrid Wavelet Neural Network (HWNN) model [20]. The artificial neural network (ANN) models for this HWNN have been combined with Multi Resolution Research (MRA), Mutual Information (MI) and Particle Swarm Optimization (PSO). With 255 rain gauge stations, the HWNN experiment was conducted where positive results were obtained at inland stations in south-east and west Australia. C.C Young et al used a physically based and machine learning hybrid approach [21]. This physically dependent and machine learning hybrid method was used during severe typhoon incidents. This process was evaluated with a total data set of 1200 in terms of model calibration and validation for seven storms. The effects of the experiment were correlated mechanically with the hydrological model, the artificial neural network, and the vector support framework to predict hourly runoff discharges in the Chishan Creek basin of southern Taiwan. S has stimulated a hybrid artificial neural network. Asadi et al [22]. This experiment utilised data pre-processing mixture methods, genetic algorithms and the Levenberg Marquardt (LM) algorithm and findings obtained from the hybrid artificial neural network relative to Artificial Neural Network (ANN) and Adaptive Neuro Fuzzy Inference System (ANFIS) models. A. Altunkaynak et al used the Combined Season Multilayer Perceptron (SAS-MP) and hybrid Wavelet Season Multilayer Perceptron (W-SAS-MP) [23]. SARIMAX (Seasonal Auto Regressive Combination Moving Average with exogenous input)-ANN model and wavelet-ANFIS model used by V. Nourani et al. [24]. The effects of the Combined Season Multilayer Perceptron and hybrid Wavelet Season Multilayer Perceptron experiments were compared to CE values 0.911 and 0.909 as one-day prediction lead time and other CE values of 0.588 and 0.570 as five-day prediction lead time. The SARIMAX model is an ANN model that finds that the non-linear relationship between the fitted linear SARIMAX residuals is related to T. Creative Feed forward back propagation (FFBP) of T. The ANFIS theory and the key time series for the calculation of rainfall runoff discharges in Azerbaijan Partal et al. [25], Role of radial base and transition of wavelets. This Wavelet Neural Network has been used to assess daily precipitation predictions and offers expertise to model the function of the physical phase.

A. *Background Methodology*

1) Data transformation: Data transformation is the stage at which the data is converted into an appropriate form for its usage in data mining. As the first step, the data is converted from hard copy to soft copy. In the next step the tables that are separated for 24 stations are combined into one dataset. Here we have expressed rainfall in terms of 0 and 1. Zero is used if the amount of rainfall is lesser than or equal to 0.1mms and one is used if the amount of rainfall is greater than 0.1mms. Finally, the data is saved in CVS (Commas Separated Value) file format.

2) Data pre-processing: The obtained data consists of some noise and there exists some lost data values and some unwanted data. So, our task here is to clean the data by removing the unnecessary information and by filling the lost data values. At this stage, a stable format for data model was constructed by adding the lost data, recognizing the duplicate data, and removing the bad data. This process makes use of PCA algorithm that takes care in replacing all the lost data values in the dataset.

3) Feature selection: The collection of features is typically an important step in data processing prior to implementing the learning algorithm. The decreased dimensionality of the attribute would lead to a better interpretation of the model and make it easy to use the various visualization tools, and it is a task in which all obsolete data and unnecessary information are found and extracted if possible. It helps to reduce the dimensionality of data and makes it easier and more effective for learning algorithms to operate. In the future classification, the precision of the findings will be improved. It determines the minimum set of attributes in such a way that the resulting probability distribution is identical to the initial distribution of the data groups.ACO dependent role collection is used here.

4) Data normalization: One of the steps of data pre-processing is data normalization. Normalization is introduced here. It is used because normalization is commonly assumed to enhance the precision and efficacy of mining algorithms with the intervention of distance measurements. Harmony and equilibrium between data must be created because the information must be standardized between 0 and 1. For normalizing our dataset Eq. (1) was used. Here, x represents the actual data, and Xmin represents the minimum value of the values of the original attribute, and Xmax represents the maximum value of the values of the original attribute.

III. Existing Methodology

A. *Artificial Neural Network*

The versions of the Artificial Neural Network (ANN) are used to solve immense real-world problems. The key benefit of ANN over conventional approaches is that the comprehensive processing steps in the mathematical form of the process formed in it do not need to be complicated in nature [8].

1) Feed forward backpropagation model: The most popular ANN model in hydrologic modelling is also known as multilayer feed forward neural networks (FFNN) with back-propagation (BP) training algorithm (ASCE Task Committee, 2000b; [22]). There are a set of layers in the FFNN Multilayer, like a sheet of data, one or two secret layers, and a layer of performance. These layers consist of artificial neurons that have contacts with all the neurons found in the next layer. The association between these artificial neurons is measured in terms of the weight meaning represented by the weight interaction. The Input signals spread layer by layer in the forward direction. The weight value relation is calculated by the weight of the input output and its input values and sums the output and transfers the sum product via a nonlinear transfer function to the result. To test relation weights and connection trends, this analysis uses the LM learning algorithm. The LM learning algorithm teaches multilayer FFNN by using the gradient descent technique to reduce errors between the actual output values and the goal values that modify the randomly selected weights of the nodes. To internally evaluate the weight weights, input and output are measured. The teaching loop fails if the errors are reduced or obey a different stopping condition. As a solution to the question of schooling, the entire combination of weights was added. The LM algorithm can be represented in the following equations (1). The feedback from each hidden layer neuron is produced by the input layer until the input vector (x1, x2, , xNI) is supplied to the input layer.

$$h_j = g\left(\sum_{i-1}^{NJ} W_{ji} X_i + b_j\right) \quad (1)$$

Where $\left(\sum_{i-1}^{NJ} W_{ji} X_i + b_j\right)$ represents the activation function of hidden layer, hj denotes the neuron j output, wji denotes the weight given to input i by neuron j, and bj is the j-neuronbias. The performance of the network is given by

$$\hat{y}_k = f\left(\sum_{i-1}^{NJ} W_{kj} h_j + b_k\right) \quad (2)$$

Where $\left(\sum_{i-1}^{NJ} W_{ji} X_i + b_j\right)$ shows the output layer activation function and NJ denotes the number of neurons in the hidden layer. For all entries, the computation procedure is repeated and produces an output vector y_k. The training method entails weight changes using an iterative technique to lower the error between the expected and real performance of the network. Output is compared using the error function with the target output yk. The error is then propagated backwards from the output layer to the input layer to update the weight of each connection as follows:

$$W_{Kj}^{m+1} = W_{Kj}^{m} + \eta \in_k + \delta\left(W_{kj}^{m} - W_{kj}^{m-1}\right) \quad (3)$$

Where m denotes the degree of iteration, εk denotes the output layer's error word, η denotes the learning rate, and δ is a momentum vector that defines the effect on the current directionof travel of past weight shifts.

2) Cascade forward model of back propagation: Cascade forward (CF) models mimic feed forward networks, but from the input to each layer to the successive layers, they have a weight relationship. In its ideal relationship, the ANN easily discovers the additional links needed to reinforce its alliance [26-31]. The CFBPNN model also looks like FFBPNN, which uses a weight-updating back-propagation algorithm, but the key symptom of this network is that all previous neuron layers are connected to another layer of neurons. The customized status can be accomplished by Tan-transformation sigmoid’ s function. In predicting transformer oil parameters, the neural network cascade has improved efficiency. In this study, the CFBPNN model is used to estimate monthly rainfall.

3) Pattern-recognition Neural network (PatternNet): The Pattern-recognition Neural Network (PatternNet), a special kind of FFBPNN, is used for pattern recognition and classification issues. Pattern Recognition NN (PatternNet) is a type of ANN that can be used for pattern recognition problems to evaluate the different classes of input data sets. It is essentially a supervised FFBPNN learning method, where binary values representing 1 representing the hereditary class and 0 representing the hereditary class are the goal data. A specific type of FFBPNN which evaluates pattern recognition and classification problems is known as Pattern-recognition Neural network (PatternNet) belongs to ANN. It has objective to abstract the input data sets of various classes. The Pattern-recognition Neural network (PatternNet) has been trained by FFBPNN based on advanced learning for compressing target data as binary such 1's as defined inherited class and 0's as otherwise.

4) Modified ACO-CS based optimized KNN classifier: There are many numbers of classification algorithm considered and observed for the implementation of rainfall prediction. It is the fact from the observation that neural networks give absolute results when compared with SVM, KNN and tree classifier. The major problem with KNN algorithm is the calculation and assumption of hyperparameter k. In case if k is kept smaller, then the algorithm will be sensitive to outliers, and if the k is chosen to be larger than the neighborhood may include too many points from other classes. Thus, selecting the value of k is the demanding task in using KNN algorithm. Optimum k is selected by ACO. In addition to this, cuckoo search algorithm is used to abandon the worst K in the process. This enhancement reduces the allocation time. By using logarithmic scale of evenly spaced the number of neighbors can be calculated approximately. The error in the classification is estimated to correctly estimate the value of k. Then the design of classifier with the estimated optimal nearest neighbor can be done. This increases the performance of the classifier. The training data comprises of Nv-*N*-dimensional pattern.

ALGORITHM

Step 1: Select Number of neighbors by approximately evenly spaced on a logarithmic scale.

Step 2: select k randomly by cuckoo search algorithm

Step 3: for selected ant (k)Find classification error

Step 4: update pheromone

Step 5: update global best

Step 4: design KNN classifier with global best (k)

Step 5: Train the model

Step 6: Test the model

Step 7: Validate the existing model

The number of nearest neighbors is approximated with the help of evenly spaced log scale. Next the classification error is calculated by ACO with CS algorithm. In this way the optimal nearest neighbor is selected, that gives minimum error. Then the design of KNN is done with optimum number of nearest neighbors. Then the testing and evaluation phase isdone.

IV. Proposed Methodology

The Proposed design methodology ensures the optimization of convergence behavior of neural network by implementing a method known as swarm-based intelligence method. The Main objective is to optimize neural network parameters to narrow down convergence by implementing ACO method. The Performance of this system can be improved by combining machine learning approaches with neural network.

A. *ACO Algorithm*

It emboldens the social actions of ants. There is no vision for world ants, but it has the potential to determine the shortest route between a food supply and their nest by using such chemical materials known as pheromones, which are expelled while passing on identical pathways for a phase of lesser ejection. Initially, step pheromone is initialized to 0. With this skill, actual ants determine the shortest paths where the shortest route leads to a higher rate of ant traversal over time and it will proceed before another shortest path is identified. For time optimization, the Pheromone update is used. Ant treats the number of classes in the training set as Ant.

1) Ant colony optimization metaheuristic approach: The meta heuristic has the optimization problem with the combination of ant colony algorithm that has been formalized by Dorigo et. al. It has entire link graph such as G (V, E) to build an artificial ACO by traveling across, where V denotes a set of vertices and E denotes set of edges. This solution has been conducted from a set of components in graph built either by denoting components vertices or by edges. The Ant constructs a solution incrementally by moving from one vertex to another along the edge. The ACO meta heuristics is presented in Algorithm 1.

Algorithm 1: The Ant Colony Optimization Meta heuristics

Step1: Set parameters, initialize pheromone trails

Step2: while Termination condition does not meet do

Step3: Construct Ant solutions.

Step4: apply Local search

Step5: Update Pheromones

Step6: end while

The above algorithm will be combined with machine learning approach.

B. *Hybrid Neural Networks*

Choosing hidden node is the challenging task in NN. Here Ant colony optimization is used to select the optimized hidden node. Here each ant is initialized with different hidden node. Pheromones are initialized as zero. For each ant fitness is calculated (RMSE) and pheromone is updated, and the heuristic information received. In every iteration globel best also updated. By this optimal hidden node is chosen for proposed model. Feature extraction stage is like existing method which results as an optimized parameter that decides the rainfall.

PROPOSED ALGORITHM

Step 1: Data collection

Step 2: processing of data

Step 3: Select optimum node using ACO Initialize pheromone, no. of. Ants; For 1: number of ant

Train NN model with initialized parameter and validate it; Evaluate fitness function (RMSE);

Update pheromone;

If Ant fitness < global best fitness Update global best;

Else

Update global best;

End if End for loop

The Optimal number of hidden nodes

Step 4: Develop a proposed model using optimal node

Step 5: Train the model

Step 6: Test the model

Step 7: Validate and compare the proposed model with existing model

The algorithm for the proposed methodology is given above. First step in this process is collection of rainfall data. Monthly rainfall of Andhra Pradesh is collected from Indian metrological department. Then the data is processed and missing data in the dataset is detected and imputed using PCA. Several pre-processing is done. To select the optimized node Ant Colony Optimization is used in proposed algorithm. Here each node is considered as ants. For every ant, NN model has been trained with initial parameters. Then the model has been validated. Then fitness function (RMSE) has been evaluated. Pheromone for each ant has been updated. Finally, global best has been updated by comparing ant fitness function. Now the optimal number of hidden nodes has been chosen. Next step is to develop the NN model with optimal number of hidden nodes. Here three type of NN model has been implemented, Feed forward backpropagation model, cascade forward backpropagation model and Pattern-recognition Neural network (Pattern Net). After success of developing the proposed model, it has been trained using training dataset and tested using testing dataset. Finally, the proposed model has been validated and compared with the existing model. Fig. 1 shows the flow chart of the ACO algorithm to determine the number of hidden nodes in ANN.

In this section, new hybrid neural network (HNN) models are introduced by combining ACO with various models of neural networks. The entire HNN forecasting protocol consists of pre-processing and choosing the input vector and maximizing the number of hidden nodes using ACO and ANN modelling. The whole HNN mechanism is seen in the flow map (Fig. 2). Here three proposed algorithms are presented.

In conventional methods the networks work on fully connected network topology, whereas in the proposed method the network nodes are optimized using the ACO algorithm. ACO optimizes the neural network based on the dataset. The ACO with Cascade Feed forward backpropagation increases the optimization process in addition to the nonlinear relation between input and output improvements. Here the incremental search of hidden layers is optimized using the ACO method computationally.

In Pattern-recognition Neural network (PatternNet) the abstraction of the input data sets of various classes is correlated for pattern identification in the rainfall data. The Pattern-recognition Neural network (PatternNet) -FFBPNN based on advanced learning for compressing target data to required class through the ACO algorithm.

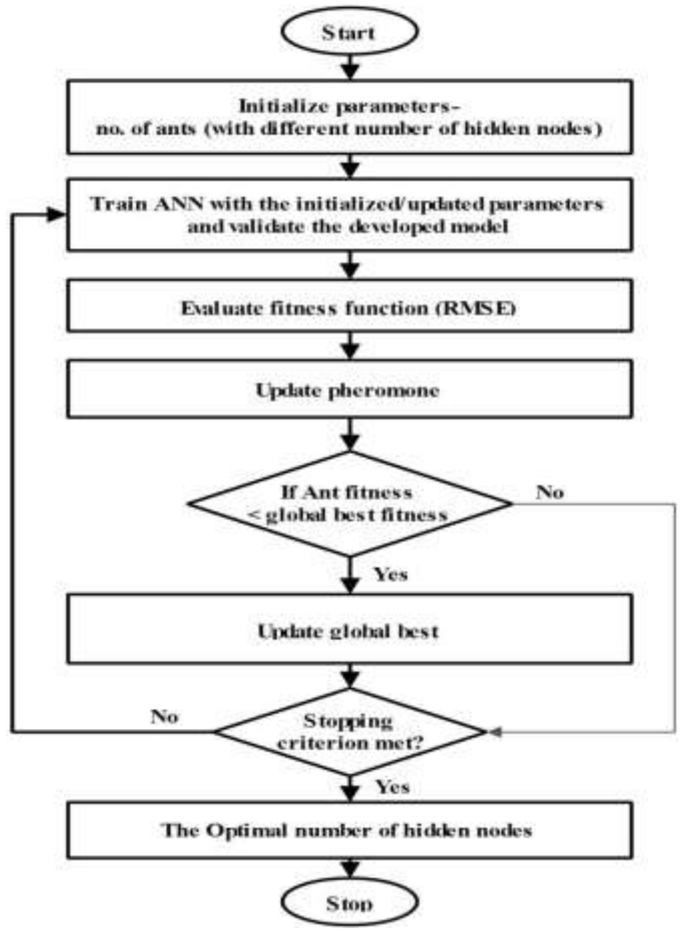

Fig. 1. Flow Chart of the ACO Algorithm to Determine the Number of Hidden Nodes in ANN.

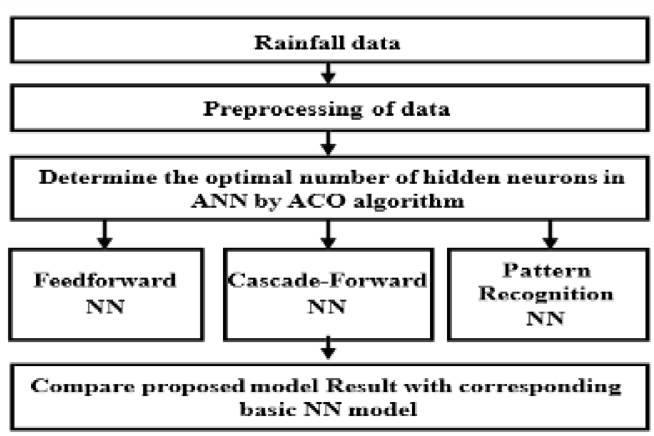

Fig. 2. Flow Chart of the HNN Model for Forecasting Monthly Rainfall.

V. Result Analysis

A. Data Set Taken

The meteorological data that used in this research has been brought from Indian meteorological Department, based on previous 120 years data set calculation of Monthly Rainfall prediction made in Andhra Pradesh, India.

B. Result and Discussion

The experiments were performed using monthly rainfall data sets that are downloaded from Indian meteorological Department (IMD). Monthly rainfall for years 1901 to 2019 are taken for analysis. Data were preprocessed by filling missing data and normalized by min-max normalization. Then the processed data is given to various classifiers for evaluating its performance. The performance of existing and proposed model is compared. Table I gives the Performance Comparison of existing Feed-Forward, cascade-Forward and Pattern Recognition NN Classifier. Table II gives the Performance of proposed ACO+Feed-Forward, ACO+ cascade-Forward and ACO+ Pattern Recognition NN Classifier. Table III gives the comparison of existing and proposed model run time. In addition to the improved accuracy our proposed model also increases the speed of the network. Table IV gives the comparison of number hidden nodes used in existing and proposed model. Here optimized hidden node selected for network design is less than existing model. Hence memory required for proposed method is less than the existing method. Fig. 3 shows the chart for existing FFNN and proposed hybrid ACO+FFNN model. Here our proposed model gives good accuracy than existing one. Similarly, Fig. 4 shows the chart for existing CFNN and proposed hybrid ACO+CFNN and Fig. 5 shows the chart for existing patternnet and proposed hybrid ACO+patternnet model.

TABLE I. Performance Comparison of Feed-Forward, Cascade-Forward and Pattern Recognition NN Classifier

Parameters	Feed - Forward NN	Cascade-Forward NN	Pattern Recognition NN	Modified KNN
Total (T)	40	40	40	40
True Positive (TP)	22	22	22	22
False Negative (FN)	0	0	0	0
False Positive (FP)	2	3	1	2
True Negative (TN)	16	15	17	16
Precision (%)	91.67	88	95.65	91.67
Sensitivity (%)	100	100	100	100
Specificity (%)	88.89	83.33	94.44	88.89
Accuracy (%)	95	92.50	97.50	95

TABLE II. Performance Comparison of Proposed Optimized Feed-Forward, Cascade- Forward and Pattern Recognition NN Classifier

Parameters	ACO+Feed -Forward NN	ACO+Cascade-Forward NN	ACO+Pattern Recognition NN
Total (T)	40	40	40
True Positive (TP)	22	22	22
False Negative (FN)	0	0	0
False Positive (FP)	0	2	0
True Negative (TN)	18	16	18
Precision (%)	100	91.67	100
Sensitivity (%)	100	100	100
Specificity (%)	100	88.89	100
Accuracy (%)	100	95	100

TABLE III. Time Comparison of Existing and Proposed Optimized Feed-Forward, Cascade-Forward and Pattern Recognition NN Classifier

Network	Existing	Proposed Method
FFNN	3.116459	0.632611
CFNN	0.977369	0.786527
PATTERNNET	1.000454	0.812689

TABLE IV. Comparison of Number of Hidden Nodes used in Existing and Proposed Optimized Feed-Forward, Cascade-Forward and Pattern Recognition NN Classifier

Network	Existing Model	Proposed Method
FFNN	10	6
CFNN	10	2
PATTERNNET	10	4

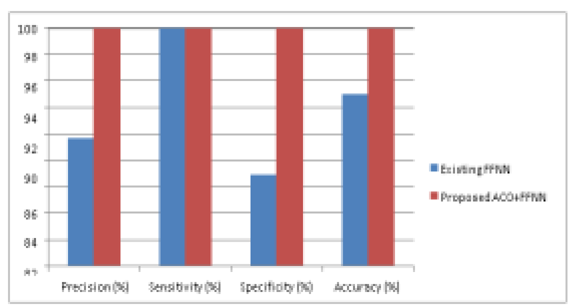

Fig. 3. Comparison Chart of Existing and Proposed Model 1.

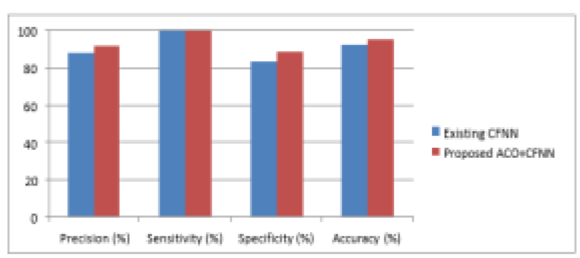

Fig. 4. Comparison Chart of Existing and Proposed Model 2.

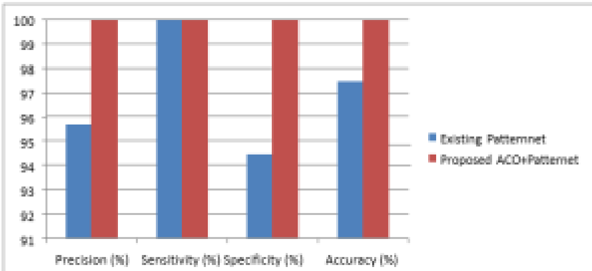

Fig. 5. Comparison Chart of Existing and Proposed Model 3.

VI. Conclusion

The paper presents the hybrid methods proposed using ACO and three neural network structures. The Hybrid Methods proposed were ACO+Feed-Forward backpropagation, ACO+ cascade-Forward backpropagation and ACO+ Pattern Recognition NN Classifier. The methods are designed by combining Neural Network and ACO Method. The performance of the existing and proposed models was compared, and the results were presented. It's been found that the proposed methods are better in performance when compared to the existing Feed-Forward, cascade-Forward and Pattern Recognition NN Classifiers. Real time data from meteorological department were used for testing and verification. Future work needs to focus on more accurate efficient rainfall prediction mechanism.

References

[1] J. Abbot and J. Marohasy, "Application of artificial neural networks to rainfall forecasting in Queensland, Australia," Adv. Atmos. Sci, vol. 29, pp. 717–730, 2012, doi: 10.1007/s00376-012-1259-9.

[2] Y. Everingham, C. Baillie, G. Inman-Bamber and J. Baillie, "Forecasting water allocations for Bundaberg sugarcane farmers," Clim. Res, vol. 36, pp. 231–239, 2008, doi: 10.3354/cr00743.

[3] J.D. Garbrecht, X.C. Zhang, J.M. Schneider and J.L. Steiner, "Utility of seasonal climate forecasts in management of winter-wheat grazing," Appl. Eng. Agric, vol. 26, pp. 855–866, 2010, doi: 10.13031/2013.34949.

[4] E.P. Lim, H.H. Hendon, D. Hudson, G.M. Wang and O. Alves, "Dynamical forecast of inter-El Niño variations of tropical SST and Australian spring rainfall," Monthly Weather Rev, vol. 137, pp. 3796–3810, 2009, doi: 10.1175/ 2009MWR2904.1.

[5] H. Meinke, , M.V.K. Sivakumar, , R.P. Motha and R. Nelson, "Preface: climate predictions for better agricultural risk management," Aust. J. Agric. Res, vol. 58, pp. 935–938, 2007, doi: 10.1071/ARv58n10_PR.

[6] A.K. Sahai, M.K. Soman, V. Satyan, "All India summer monsoon rainfall prediction using an artificial neural network," Climate Dyn, vol. 16, pp. 291–302, 2000, doi: 10.1007/s003820050328.

[7] M. Karamouz, S. Razavi and S. Araghinejad, "Long-lead seasonal rainfall forecasting using timedelay recurrent neural networks: a case study," Hydrol. Processes, vol. 22, pp. 229–241, 2008, doi: 10.1002/hyp.6571.

[8] R.V. Ramana, B. Krishna, S.R. Kumar and N.G. Pandey, "Monthly rainfall prediction using wavelet neural network analysis," Water Resour. Manage, vol. 27, pp. 3697– 3711, 2013, doi: 10.1007/s11269-013-0374-4.

[9] V. Nourani, M. Komasi and M.T. Alami, "Hybrid wavelet-genetic programming approach to optimize ANN modelling of rainfall–runoff process," J. Hydrol. Eng, vol. 17, pp. 724–741, 2012, doi: 10.1061/(ASCE)HE.1943-5584.0000506.

[10] S. Chatterjee, B. Datta, S. Sen, N. Dey and N. C. Debnath, "Rainfall prediction using hybrid neural network approach," 2018 2nd International Conference on Recent Advances in Signal Processing, Telecommunications & Computing (SigTelCom), Ho Chi Minh City, pp. 67-72, 2018, doi: 10.1109/SIGTELCOM.2018.8325807.

[11] R. Graf, S. Zhu and B. Sivakumar, "Forecasting river water temperature time series using a wavelet–neural network hybrid modelling approach," Journal of Hydrology, 124115, 2019, doi: 10.1016/j.jhydrol.2019. 124115.

[12] M. I. Khan and R. Maity, "Hybrid Deep Learning Approach for Multi-Step-Ahead Daily Rainfall Prediction Using GCM Simulations," in IEEE Access, vol. 8, pp. 52774-52784, 2020, doi: 10.1109/ACCESS.2020.2980977.

[13] C. Y. Lian, Y. F. Huang, J. L. Ng, M. Mirzaei, C. H. Koo and K. W. Tan, "A proposed hybrid rainfall simulation model: bootstrap aggregated classification tree– artificial neural network (BACT-ANN) for the Langat River Basin, Malaysia," Journal of Water and Climate Change, 2019, doi:10.2166/wcc.2019.294.

[14] D. Tran Anh, T. Duc Dang and S. Pham Van, "Improved Rainfall Prediction Using Combined Pre-Processing Methods and Feed-Forward Neural Networks," J 2019, vol. 2, pp. 65-83, 2019, doi: 10.3390/j2010006.

[15] P.-C. Hsieh, W.-A. Tong and Y.-C. Wang, "A hybrid approach of artificial neural network and multiple regression to forecast typhoon rainfall and groundwater-level change," Hydrological Sciences Journal, pp. 1-44, 2019, doi:10.1080/02626667.2019.1677905.

[16] D. Dhar, S. Bagchi, C.K. Kayal, S. Mukherjee, S. Chatterjee, "Quantitative Rainfall Prediction: Deep Neural Network-Based Approach," In: Chakraborty M., Chakrabarti S., Balas V., Mandal J. (eds) Proceedings of International Ethical Hacking Conference 2018, Advances in Intelligent Systems and Computing, Springer, Singapore, vol. 811, pp. 455-463, 2019, doi: 10.1007/978-981-13-1544-2_37.

[17] T. Roshni, , M.K. Jha, , R.C. Deo, et al, "Development and Evaluation of Hybrid Artificial Neural Network Architectures for Modeling Spatio-Temporal Groundwater Fluctuations in a Complex Aquifer System," Water Resour Manage, vol. 33, pp. 2381–2397, 2019, doi: 10.1007/s11269-019-02253-4.

[18] N. Chen, C. Xiong, W. Du, C. Wang, X. Lin and Z. Chen, ''An Improved Genetic Algorithm Coupling a Back-Propagation Neural Network Model (IGA-BPNN) for Water-Level Predictions,'' water, 2019, vol.11, pp. 1-18.

[19] J. Wu, J. Long, M. Liu, ''Evolving RBF neural networks for rainfall prediction using hybrid particle swarm optimization and genetic algorithm,'' Neurocomputing, vol.148, pp. 136–142, 2015, doi: 10.1016. /j.neucom.2012.10.043.

[20] X. He, H. Guan and J.Qin, ''A hybrid wavelet neural network model with mutual information and particle swarm optimization for forecasting monthly rainfall,'' Journal of Hydrology, vol.527, pp. 88–100, 2015, doi: 10.1016/j.jhydrol.2015.04.047. C.C Young, W.C Liu and M..C Wu, ''a physically based and machine learning hybrid approach for accurate rainfall runoff modelling during extreme typhoon events,'' Applied Soft Computing, vol.53, pp.205-216, 2017, doi:10.1016/j.asoc.2016.12.052.

[21] Asadi, J. Shahrab, P. Abbaszadeh, S. Tabanmehr, ''A New hybrid artificial neural networks for rainfall–runoff process modelling,'' Neurocomputing, vol.121, pp.470- 480, 201, doi:10.1016/j.neucom. 2013.05.023.

[22] A. Altunkaynak and T.A Nigussie, ''Prediction of daily rainfall by hybrid wavelet season neuro technique,'' Journal of Hydrology, vol.529, pp.287-301, 2015, doi:10.1016/j.jhydrol.2015.07.046.

[23] V.Nourani, O.Kisi and M. Komasi, ''Two Hybrid Artificial Intelligence approach for modelling rainfall runoff process,'' Journal of Hydrology, vol.402 (1-2), pp.59, 2011, doi:10.1016/j.jhydrol.2011.03.002.

[24] T. Partal, H.K Cigizoglu and E. Kahya, ''Daily precipitation predictions using three different wavelet neural network algorithms by meteorological data,'' Stochastic Environmental Research and Risk Assessment vol.29, pp. 1317–1329, 2015,

[25] Shi, X., Chen, Z., & Wang, H. (2015). Convolutional LSTM Network. Nips, 2–3. https://doi.org/[].

[26] Wahyuni, E. G.Fauzan, L. M.F.Abriyani, F.Muchlis, N. F., & Ulfa, M. (2018). Rainfall prediction with backpropagation method. Journal of Physics: Conference Series, 983(1). https://doi.org/10.1088/1742-6596/983/1/012059.

[27] Zeyi Chao, Fangling Pu, Yuke YinLing, B. and X. (2018). Research on real-time local rainfall prediction based on MEMS sensors. Journal of Sensors, 2018. https://doi.org/10.1155/2018/6184713.

[28] Etuk, E. H., & Mohamed, T. M. (2014). Time Series Analysis of Monthly Rainfall data for the Gadaref rainfall station, Sudan, by Sarima Methods. International Journal of Scientific Research in Knowledge, July, 320–327. https://doi.org/10.12983/ijsrk- 2014- p0320-0327.

[29] Kar, K., Thakur, N., & Sanghvi, P. (2019). Prediction of Rainfall Using Fuzzy Dataset. International Journal of Computer Science and Mobile Computing, 8(4), 182–186. https://ijcsmc.com/docs/papers/April2019/V8I4201937.pdf.

[30] KavithaRani, B., & Govardhan, A. (2014). Effective Features and Hybrid Classifier for Rainfall Prediction. International Journal of Computational Intelligence Systems, 7(5), 937–951. https://doi.org/10.1080/18756891.2014.960234.

[31] Prabakaran, S., Naveen Kumar, P., & Sai Mani Tarun, P. (2017). Rainfall prediction using modified linear regression. ARPN Journal of Engineering and Applied Sciences, 12(12), 3715–3718.

A Hybrid Model to Profile and Evaluate Soft Skills of Computing Graduates for Employment

Hemalatha Ramalingam*[1], Raja Sher Afgun Usmani*[2], Thulasyammal Ramiah Pillai[4]
School of Computer Science and Engineering
Taylor's University, Subang Jaya, Malaysia

Ibrahim Abakar Targio Hashem[3]
College of Computing and Informatics
Department of Computer Science
University of Sharjah, 27272 Sharjah, UAE

***Abstract*—Emerging tools such as Game Based Assessments have been valuable in talent screening and matching soft skills for job selection. However, these techniques/models are rather stand alone and are unable to provide an objective measure of the effectiveness of their approach leading to mismatch of skills. In this research study, we are proposing a Theoretical Hybrid Model, combining aspects of Artificial Intelligence and Game Based Assessment in profiling, assessing and ranking graduates based on their soft skills. Firstly, an Intelligent Controller is used to extract and classify the graduate skill profile based on data findings extracted using traditional assessment methods of self-evaluation and interview. With motivation and engagement as a competitive difference, an existing Game Based Assessment (OWIWI) is then used to assess the soft skills of these graduates hence generating a Graduate Profile based on results of the game. Moving forward, a ranking technique is then applied to match the profile to selected job requirements based on soft skills required for the job and the graduate strength. Finally, a comparison analysis is concluded based on the soft skills profile obtained before employment (pre-employment) and objective measure feedback of soft skills obtained after employment (post-employment) to provide a validity check to study the effectiveness of the overall Hybrid Model. Specifically, data obtained from this study can be useful in solving issues of unemployment due to mismatch of soft skills at the Higher Learning Institution level.**

Keywords*—Soft skills; artificial intelligence; intelligent controller; game based assessment; graduate profile; hybrid model

I. Introduction

The graduate employment landscape has drastically transformed in recent years. Attributing factors include the emergence of technologically driven process, changing nature of work environments as well as the diversified need of clientele and globalization. Evident to this is the apparent change in Talent Requirement of soft skills which is becoming a crucial priority for long term job success and performance comparatively to hard/technical skills. Soft skills or Human skills as they are sometimes termed, are skills that facilitate the work process of an organization. They are a "set of achievement skills"', understanding and personal attributes that makes individuals more likely to gain employment and to be successful in their chosen occupations. They were once considered as value added but have become an integral component to graduate employability, cutting horizontally across all industries and vertically across all jobs [1]. Soft skills are becoming hard requirements and no longer a 'nice to have' but a 'must have' for graduates. Supporting this is the study conducted by Stanford Research Institute and Carnegie Melon Foundation involving Fortune 500 CEOs. It revealed that individual soft skills accredit to 75% of getting and maintaining a job successfully, while only 25% relies on hard skills or technical knowledge [2].

On the contrary, amongst computing graduates, there is still an obsession on technical skills which creates a false divide that privileges these skills over soft skills. Soft skills are being discounted, dismissed, disappearing and what more, difficult to be assessed and identified. Assessment are used to fit a maximum fit between employee's qualities, the role and the hiring organization. Traditionally, most established assessment methods to evaluate soft skills remain align and well and have been used over a century. Supporting this is conclusive evidence from over 100 years of Industrial Organization (I/O) Psychology together with meta-analyses, support the validity of face to face interviews, personality inventories, assessment centers, 360-feedback ratings, biodata check, situational judgment test, and resume data in extracting and assessing soft skills [3].

Nonetheless, today, with technological advancement and the development of Internet, the prediction of data volume growth to 40 zettabytes in 2020 [4], and the avalanche of size and variety of applications, machines with intelligence algorithms and design methods are required. These new methods are used for filtering, extracting, classifying and assessing data, thus assisting humans in effective decision making in selection of potential talents. Adding to that, with data available via various online platforms, vast amount of human behavior data is generated from digital record consisting of individual preference, values and reputation. Hence, these techniques have become less intuitive, but more data driven, and evidence based.

With motivation, engagement and innovation as a driving factor, the use of Games in assessment has taken a forefront in hiring decisions of many organizations today. Various form of gaming techniques namely Gamification, Game Based Assessment and Serious Games have attracted the attention of Human Resource practitioners. Relying on neuro- science based Artificial Intelligence techniques, these games re-create real world situation disclosing true candidate reactions. A form of stealth assessment, these games are on the rise of adoption as they solve traditional assessment challenges, namely faking and social desirability attainment.

Today, many organizations are engaging third party game assessment tools used in assessing their potential hires for

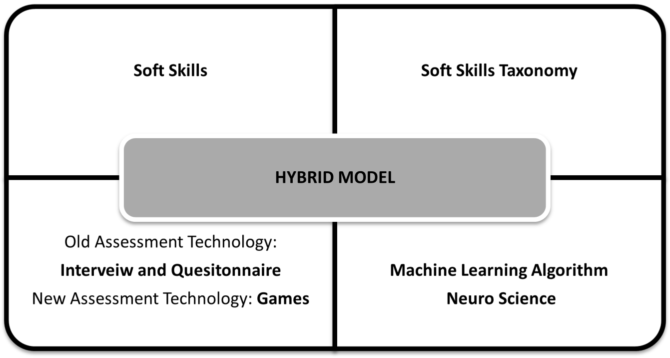

Fig. 1. Hybrid Model - Domain of Coverage.

long term job success. Many of these services and are stand alone and provide high quality data which reveals individual traits, they achieve the intended objective of pre-assessing the relevant soft skills required based on requirements of job roles. However, these new tools and innovations, although having revolutionized the way organizations identify, engage and assess talents, many are stand alone and incomplete in supporting the Human Resource functions of effective talent selection. Furthermore, these assessments fail to justify the validity, effectiveness and value of assessing the candidate's soft skills pre and post-employment. These individual tools and innovations are unable to profile, validate and rank the behavioral traits of candidates, matching the intended skills required for the specified job leading to potential employment.

Present studies incorporating these tools/innovations have not considered the assessment of the validity of traits obtained, verified against the job performance, given a duration of employment. Hence, the purpose of our research is to propose a Theoretical Hybrid Model in filtering, assessing and ranking Computer Graduates soft skills for employment selection. The domains of coverage is as illustrated in Figure 1 above. The objective of this Theoretical Hybrid Model is to propose an improvement in soft skills assessment of graduate selection enabling a effective job match.

II. Literature Review

The rise of Artificial Intelligence and automation is changing the job market in the 21st century. The importance of soft skills amongst employers which identified 10 out of 16 21st century crucial proficiencies are related to employee soft competencies [5]. There have been many research studies that have provided the definitions and classifications of soft skills. Patacsil and Tablatin terms them as behavioral elements referring to the capability of how individuals perform a job well as well as his/her level of performance [6]. Hurrell, in his research study relates these skills to a vast range of interpersonal and social qualities and competencies which are deemed transferable across economic sections and industries [7]. With reference to employability amongst young graduates as noted by O'Reilly, these skills include Entrepreneurial Skills, which includes the capacity to creatively deal with a given problem, ability to work in teams, learning to learn, effectively communicate with peers and superiors, adaptation to different cultural settings, problem solving, management of conflicts and endurance to deal with complicated or stressful situations enabling them to successfully move from an academic setting to the labor market [8].

Soft skills sets are guided by taxonomies. Various soft skills taxonomies are crucial in employment as well as talent acquisition depending on specific domain of job requirements and industries. In studies of job advertised on four online portals in North America, Europe, Asia and Australia, findings summarized on job title found Communication, Interpersonal, Analytical and Problem Solving and Team Skills to be most critical taxonomies. In a more related research study, a survey concluded by [9] for entry level IS position (graduates), conducted amongst Information Technology global employers, listed Intrapersonal/Interpersonal, Willingness to Learn, Critical Thinking and Attitude as crucial soft skills. A study conducted by [10] noted that the 10 commonly noted soft skills related to jobs in the fields of Business and Computer Technology were Communication, Critical and Decision making, Interpersonal, Negotiation, Problem solving, Self-confidence, Self-management, Team work and Work ethics. On the local front in Malaysia, [11] stated that soft skills that would need to be assessed amongst graduates in Higher Education Institutions for work readiness include Responsibility, Positivity, Time Management, Teamwork, Communication, Leadership, Creative and Innovation . More specific toward this research study of using games in assessing graduate employability [12] elaborated on eight(8) soft skills that seemed to become more and more relevant and prevalent in today's demanding working environment which include Resilience, Adaptability, Flexibility/Willingness to Change and Decision making, Teamwork, Learning Agility, Accountability and Integrity. This skill taxonomy had been adopted to an online Game Based Assessment (OWIWI) deployed by his team which has been tested and deployed.

With reference to soft skills assessments, technological advancements such as Big data, big spatial data [13], Artificial Intelligence and Data Mining techniques have emerged revolutionizing the way organizations identify, develop and engage talents. [14] reported talent assessment in the human resource world is shifting from the traditional methods of assessments to a range of new, novel, efficient tools and techniques for evaluating employee behavior making them less intuitive, more evidence based and data driven. [15] study revealed that with the development in machine learning algorithms, computer based personality judgments are more accurate than those made by humans. Table I lists some of the old and new assessments techniques.

One such novel technique that motivates and engages talents in the area of Human Resource assessment is the use of Games. It is the process of enhancing services with motivational affordance in order to invoke game-full experiences and behavioral outcomes as noted in a research by [16]. [17] further elaborates that, although interactive simulations have been used in assessments and selection methods for decades, efforts have been made to make them more game like hence fun and attractive, thus encouraging/increasing engagement, novelty, competitiveness and visually appeal making it difficult to fake. This can be further supported in a recent study by [18] that reported higher level of process satisfaction, fairness and organizational attractiveness as compared to traditional

TABLE I. OLD AND NEW TALENT ASSESSMENT METHODS AND TOOLS

Old Methods	New Tools	Dimension Assessed
Interviews	Digital Interviews Voice Profiling	Expertise, Social Skills, Motivation and Intelligence
Biodata Supervisory Ratings IQ	Big Data	Past Performance, Current Performance, Intelligence, Job Related Knowledge and Big Five Personality Traits or Minor Traits
Situational Judgment Test Self-Reports	Gamification	
Self-Reports	Social Media Analytics	Big Five Personality Traits and Values (Identity claims)
Resume	Professional Social Networks	Experience, Past Performance and Technical Skills and Qualifications
360	Crowdsourced Reputation/Peer Ratings	Any personality Trait, Competencies and reputation

methods. [19] and [20] too reported on the same points as previously and in conclusion positively affects applicant's job pursuit behaviors towards an organization. [21] further reported on game platforms being more realistic upon conducting a research study that measured the effectiveness of using Epistemic Games as a stimulus medium in presenting SJTs. Here is was stated that SJTs connected with other evidence based assessment increases the measurable validity in predicting job performance. In a more related study/findings by [12] reported that converting a SJT (Situational Judgment Test) to an adventure story with game elements confirms the construct validity of the measure of Resilience, Adaptability, Flexibility and Decision Making hence revealing positive results. In his research a fully working game called OWIWI is used which is also currently a readily available Game service provided by the authors. This game is available at www.owiwi.co.uk.

A. Machine Learning Algorithm – Classification Techniques for Skills

Machine Learning enables machines with algorithms in place to learn and make data driven predictions. The self-learning algorithms such as ANN and its modified forms [22], [23] uses forms of statistics to draw models from large data sets. In the domain of recruitment and selection, Machine Learning Algorithms are used to create patterns from job posts, applicants resume, social media activities and interview response.

In the study done by [24] in employing Machine Learning Technique to classify research's self evaluated questionnaires based on a set of pre-defined soft skills taxonomy for job hire, it was noted that the feature selection task was challenging and the Support Vector Machine (SVM) classifier was the best choice of classifying the skills taxonomy. Support Vector Machine (SVM) type classification technique has been much favorable and has visibly been applied in domains of pattern recognition, face detection and spam filtering as reported in study done by Allahyari [25]. Further findings from survey compiled by [26] on different weighting methods and classification techniques, reported that different techniques perform differently depending on dataset (long and short). A noted finding was a combination of KNN and TF- IDF term weighting scheme performed well in several classification algorithms. Adding to this, more specific to skills sets pertaining to job hire, [27] looked into using Web Scrapping and Machine Learning Technique for classifying skills required for Big Data professions. Job posted online was analyzed and a methodology was proposed. A semi-automated analytical process using AI tools was used to review jobs posted.

B. Adaptive Neuro Fuzzy Inference Systems (ANFIS) used for HR Recruitment and Selection

Neural Networks is a group of algorithms for machine learning that deals with logic structure of how conclusions will be drawn by humans and is a subset of machine learning. Neuro Fuzzy Inference Systems was introduced by Jang [28] which combines human like reasoning style of Fuzzy Systems with the learning and connectionist structure of Artificial Neural Networks in 1993. Survey findings have noted that, Neuro Fuzzy Inference Systems provide flexible and powerful universal approximations with the ability to explore interpretable IF-THEN rules. The application of Neuro Fuzzy Inference Systems has proliferated and have been evidently applied and developed between the years 2000-2012 covering both social and technological sectors. Applications and domains include medical systems, economic systems, electrical and electronics system, traffic control, student modelling system, image processing and feature extraction, forecasting and predictions, manufacturing and system modelling, enhancements and social sciences.

Adaptive Neural Fuzzy Inference Systems (ANFIS) on the other hand, is a superimposed Fuzzy Inference System over a Neural Layer architecture, in which the Fuzzy Inference Systems learns the training procedure in Neural Network and upon that, behaves exactly as the Neural Network. Notably in various research studies, the most common Adaptive Neural Fuzzy Inference Systems (ANFIS) algorithms is the Tagaki-Sugeno Fuzzy Model. Based on the Literature study surveyed by [29] of Adaptive Neural Fuzzy Inference Systems (ANFIS) applications, it is widely used in the field of diagnostic control, medical research and civil engineering. In another domain, the study concluded by [30] presented a Neuro Fuzzy based methodology to forecast short term stock trends during turbulent stock market periods. The methodology was able to make accurate forecast and results demonstrated solid and superior performance in terms of percentage of forecasting accuracy of stock market trend during crisis.

More specific in the domain of Human Resources, the research concluded by [31], assist HR managers in the assessment of employability of candidates during recruitment process. Here, the employability level of candidates was able to be computed based on three input values of Education, Personal Development and Understanding Power using the Sugeno type inference.

Trailing on, the development of an adaptive information filtering system using Adaptive Neural Fuzzy Inference Systems (ANFIS) was done in the research study concluded by [32]. The procedure of personnel assortment of candidates was automated based on specific Human Resource criterion of skills, vacancies and experience. A model theory was proposed to determine job characteristics defined by experts and record the ranking decisions made. The information obtained was used to provide personalized information filtering system done by analyzing user behavior on web history. Moving more specific to a related research study, [33] focused on creating a framework for soft skill profile of jobseekers. Using the Sugeno Fuzzy Inference System, it was aimed at supporting the evaluation of PhD's profiles by calculating the inference rule and selecting the most performing soft skills to be recommended to the HR Manager.

C. Ranking Technique used for HR Recruitment and Selection

Analytical Hierarchy Process (AHP) is a Multi Attribute Decision Making (MCDM) model, developed by Saaty [34]. It is a powerful and flexible weighted scoring decision making process to help people set priorities, allowing the selection of the best amongst the alternative based on several conflicting criteria [35]. It has been widely used in industrial practice and academic research to solve multi-criteria decision making [36]. Extending on this, Fuzzy AHP, an analytical extension of AHP, allows for a more accurate description of the decision making process where linguistic variables and Triangular Fuzzy Numbers (TFNs) are used for better consistency and accuracy in decision making as reported in the study done by [35]. Areas of application of this method of problem solving have been concluded in Human Resource Management of personnel recruitment and selection , network pre-negotiation service evaluation, company inventory control and classification, water quality management, selection of measuring instruments for undergraduate engineering institution, hydrogeology groundwater management and measurement of object oriented software usability [35].

More specific, in the domain of Human Resource recruitment, [35] research study applied a combination of Fuzzy AHP, triangular Fuzzy Numbers (TFN) and linguistic variable to improve human expert decision making for recruiting academic staff of University. This study noted that Fuzzy AHP proved to be more useful tool for solving multi-criteria decision problems with inherent uncertainty and deviations in Decision Maker's opinions. In a study conducted by [36], in the automotive industry in Pakistan, the use of AHP for supplier selection based on ranking was proposed as a methodology. There were noted reduction in incoming rejection of suppliers, however aspects of service quality using this technique were difficult to quantify. This led to the consider improved version of AHP, which included Fuzzy AHP and Fuzzy TOPSIS. In another study of ranking potential candidates for selection of human resource conducted by [37], explored the use of Linear Regression and Support Vector Regression. Here, in the job application module, the candidates register and provides a twitter handle and fills an online CV. The emotional aptitude evaluation module estimates the emotional findings by extracting tweets based on the Big Five Personality model. In the grading module, it combines the eligibility criteria from CV and personality assessment from social handle and assigns a relevance score.

In summary, the digital revolution has transformed Human Resource assessments. No doubt traditional methods in profiling and assessing soft skills remain reliable and valid given many research findings, they have become outdated, mundane, resource and time consuming. Hiring decisions today, are moving towards being more data driven and evidence based. Behaviors are recorded and unprecedented qualities of data are available to quantify human potential given new technologies in Human Resource assessment.

However, these new tools and innovations, although having revolutionized the way organizations identify, engage and assess talents, many are stand alone and incomplete in supporting the Human Resource functions of effective talent selection. Adding to this, these assessments fail to justify the validity, effectiveness and value of assessing the candidate's soft skills pre- and post employment. These individual tools and innovations are unable to profile, validate and rank the behavioral traits of candidates, matching the intended skills required for the specified job leading to potential employment. Present studies incorporating these tools/innovations have not considered the assessment of the validity of traits obtained, verified against the job performance, given a duration of employment. How similar or dissimilar were the traits as compared to before (pre) and after (post) employment? Still in a hypothetical stage due to many empirical unknowns.

III. Research Framework

A. Instrument and Dataset

In relation to this study, purposive sampling technique using a total population sampling will be employed to identify the respondents/informants of the study. The findings from these data will be used to form a judgment analysis based on this sampling techniques. With that, there will be three groups of informants. The first group of informants will be Graduates taking on their Internships from three private Universities in Malaysia, respectively. The Internship timeline varies between 3 and 6 months respective of the individual Universities. The second group of informants will be Academic Supervisors assigned to each internship graduate placement. Individual interviews are conducted with each graduate in evaluating and assessing their soft skills prior to the start date of internship. The final group of information would be the Industry Supervisors of hiring companies assigned to each intern pertaining to their internship roles and responsibilities in the respective companies.

This study is a descriptive research in nature as it seeks to provide accurate descriptions of the characteristics of a graduate in terms of their soft skill traits. With that, a descriptive survey is designed for the Graduates to extract relevant soft skills they possess through experience and their self-evaluated strengths. These questions consist of open ended questions that leads the graduates to reason on the eight(8) given skills addressed in this research study. Feature engineering [38], [39], [40], an important step in data science studies, will be performed on the questionnaire attempted by the Graduates to perform text pre-processing, extraction and classification.

The soft skills used for assessments are based on the eight (8) skills adopted in the Game Based Assessment (OWIWI) and adopted in the study done by [41] and [12]. These soft skills include Resilience, Adaptability, Accountability, Willingness to Change, Decision Making, Integrity, Resilience and Teamwork. Supporting this would be the measure of validity as highlighted in Table II for each skill. Internship graduates have been selected for this study as that there is careful assessment of their performance observed by both the Academic and Industry Supervisor during the three/six month internship period hence feedback can be obtained. With that, the validity and effectiveness of the framework/model can be

TABLE II. SOFT SKILLS MEASURES

Skills Assessed	Definitions	Construct Validity Measures
Resilience.	The developable capacity to rebound or bounce back from adversity, conflict and failure or even positive events, progress and increased responsibility [42].	Scale by [43]
Adaptability.	Related to change and how people deal with it. People's adjustment to changing environment [44]	Scale by [45]
Willingness to Change	A positive behavioral intention towards the implementation of modifications in an organization's structure, or work and administrative processes, resulting in efforts from the organization member's side to support or enhance the change process [46]	Scale - HEXACO Personality Inventory [47]
Decision Making.	The intellectual process leading to a response to circumstances through selection among alternatives [48].	[49]
Teamwork	Extent to which a team member is able to meet the team's output goals, ,the expectations of other members, or its cost and time objectives [50].	Scale - Teamwork Quality (TWQ) [51]
Learning Agility.	The willingness and ability to learn new competencies in order to perform under first-time tough, or different conditions [52].	Scale - HEXACO Personality Inventory [53]
Accountability.	Perceived expectation that one's decisions or actions will be evaluated by a salient audience and that rewards or sanctions are believed to be congruent on this expected evaluation [54].	Scale - [55]
Integrity.	It describes a set of beliefs and attitudes and actions reflecting one's personal values and morals [56].	Subscale "morality/ethics" [57]

ascertained given the completion of the internship duration i.e. post-employment.

B. Graduate Profile – (Pre-Employment – Self Evaluation and Interview)

As depicted in the Proposed Hybrid Model (Fig. 2), to generate a Graduate Soft Skills Profile, input is obtained from both Graduates and Academic Supervisors. Using the advantage of traditional assessment strategies, graduates will attempt a self-evaluation survey of their soft-skills whereby a Machine Learning Algorithm will be used to classify relevant soft skills according to the measures adopted thus generating a Machine Learning (ML) vector of their soft skills. Parallel to this, the Academic Supervisors would interview the graduates assessing all eight soft skills again adopting the same measures of validity consistently. Following this, an Intelligent Based Controller with an Adaptive Neuro Fuzzy Inference System (ANFIS) mechanism will then be used to generate a final Graduate Soft Skills Profile combining both the details of soft skills obtained from the Graduate as well as the Soft Skills Interview results obtained from the Academic Supervisor.

C. Graduate Profile (Pre- Employment - Game Based Assessment)

As depicted in the Proposed Hybrid Model (Fig. 2), an existing Game Based Assessment called OWIWI will be used to generate the Graduate Soft Skills Profile. Adopting a gamified Situational judgment Test (SJT) using various game mechanics, the players (Graduates) are immersed into a gaming environment assessing the pre-defined eight soft skills. Many trials will await the players assessing these eight skills and the players Situational judgment will be thoroughly tested. Each player will receive eight separate scoring report of each of the eight soft skills. The updated version of OWIWI 2.0 has much improvements which include, a total of eight soft skills, a redesigned User Interface with Progress Bar and Scenario Titles. The soft skills assessed here are skills adopted as the Taxonomy of study for this research study. Following this, the Analytical Hierarchical Process (AHP) methodological approach will be adopted in ranking and decision making of Graduates for selected jobs for recruitment. Upon this, graduates are then classified to hired or not hired for the job. Candidates who are hired are then fit for their Internship tenure. Once the internship is completed, the HR/Industry Supervisor then assess the graduates based on the same eight soft skills providing a Graduate Profile (Post-Employment).

D. Comparison Analysis (Graduate Profile – Pre-Employment VS Post-Employment)

A Comparison Analysis is performed to validate the effectiveness of the proposed Hybrid Model. In achieving this, both Pre-Employment Soft Skills Graduate Profile obtained using the traditional method in Section III-B and the Graduate Profile obtained in Section III-C via Game Based Assessment, is compared with the Post-Employment Graduate Profile obtained from the HR/Industry Supervisor upon completion of Internship. The comparison of these profiles would justify the effectiveness of the hybrid model.

IV. DISCUSSION AND CONCLUSION

The Youth unemployment rate in Malaysia has seen a gradual increase between 2014-2018. Fresh graduate unemployment is an issue in Malaysia with 11.3% reported amongst Computing graduates. Two main attributing factor on unemployment rates in Malaysia is mismatch of skills, job search and recruitment, and shortage of relevant skills as reported by the Ministry of Education and Department of Statistics Malaysia. Today's workplace, employers want their employees to remain highly skilled and employable. However, based on the Economic Report 2018, employers faced difficulty in finding talent, primarily because of lack of required soft and interpersonal skills as observed in literature study conducted by [58]. The skills gap among graduates is however not limited to Malaysia but is a global phenomenon.

Based on the QS Global Skills Gap in the 21st century report, there is sizable and consistent disparity between employer expectations and student skills based on insights provided by 11,000 employers and 16,000 students across the world. It is noted that subject knowledge skills and technical skills are no longer the determinant factor of employability; however, soft skills are the crucial mechanism for long term job success. With that, Higher Education Institutions (HEI) worldwide are under pressure to produce the right fit among the employable graduates [59].

Nonetheless, although soft skills are extremely valuable and vital, the one thing machines can't replace, assessing them accurately is still an uphill task. Only 41% of companies have

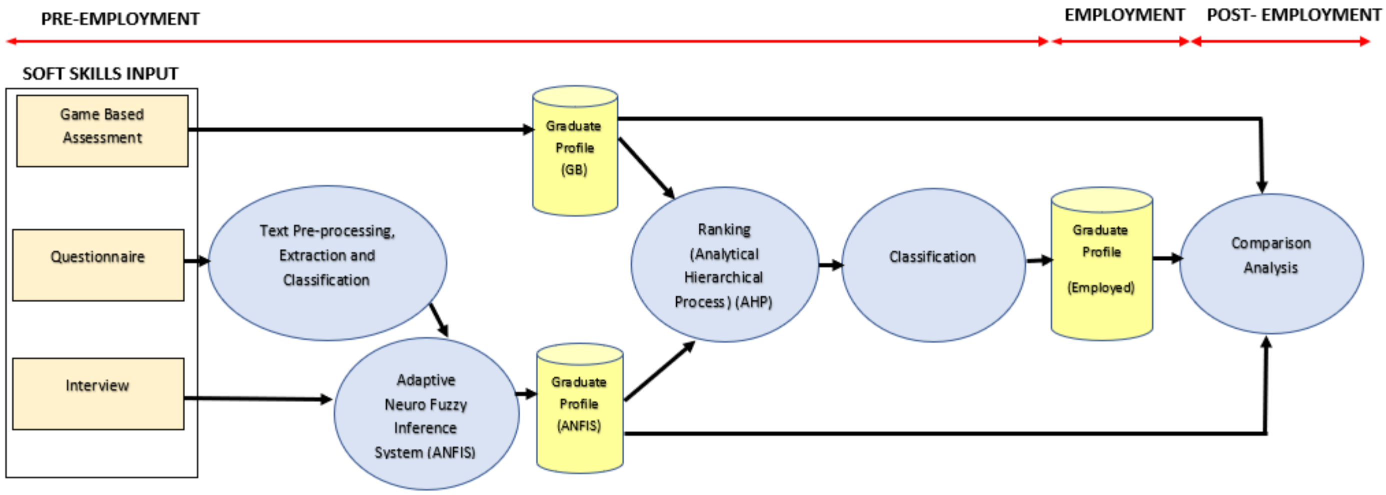

Fig. 2. Hybrid Model.

formal process in place to measure these skills. As noted in the Global Work Trend 2019 report produced by LinkedIn, there is a growing gap between the demands for soft skills and the inability to identify them. No doubt many companies have turned to Artificial Intelligence (AI) powered technological solutions such as games, which are evidence based and data drive to solve this issue, however, much has not been done to assess the validity of these techniques with regards to post-employment performance. This is further supported with many research findings that have deployed games in assessment of soft skills and with an gap of missing objective measures in place to support the validity of such technique.

In solving this gap, this research work aims to explore the proposal of a theoretical hybrid model to profile and evaluate soft skills of computing graduates for employment. The proposed theoretical hybrid model seeks to contribute to an effective mechanism in filtering, assessing, and selecting crucial soft skills amongst graduates thus able to validate the effectiveness of both the traditional assessment techniques as well as the game-based technique. Therefore, in achieving this, this theoretical model proposes a combined assessment of both the traditional assessment strategies of interview and questionnaire as well as an existing game in providing a graduate soft skills profile, respectively. In future work, when implemented, a comparison analysis will be generated between the profile obtained before employment (pre-employment) as well as after employment (post-employment) to justify the validity of the techniques adopted as an objective measure of outcome. Hence, this study is limited to a theoretical proposal and future work will look into implementing the model thus evaluating the effectiveness of this study.

In summary, this model is intended to solve the problems of unemployment amongst graduates, which reportedly among many reasons is caused by mismatch of skills, recruitment, and industry requirement/expectations. This is achieved with the creation of a Graduate Profile, clearer verification of the profile via assessment using Gaming technologies inculcating motivation and engagement as well as ranking them based on these skills with regards to job requirements put forth by the hiring company. Further to this, data obtained from this study can be input provided to respective Higher Learning institution as a support mechanism to look into improving their curricular framework emphasizing the industry need of essential soft skills amongst their graduates for successful employment in the 21st century.

REFERENCES

[1] N. H. Omar, A. A. Manaf, R. H. Mohd, A. C. Kassim, and K. A. Aziz, "Graduates' employability skills based on current job demand through electronic advertisement," *Asian Social Science*, vol. 8, no. 9, p. 103, 2012.

[2] R. S. Malhi, "The hard truth about graduate employability and soft skills," *ADEPT: Higher Education Leadership Research Bulletin*, vol. 3, pp. 45–56, 2009.

[3] T. Chamorro-Premuzic and A. Furnham, *The psychology of personnel selection*. Cambridge University Press, 2010.

[4] J. Gantz and D. Reinsel, "The digital universe in 2020: Big data, bigger digital shadows, and biggest growth in the far east," *IDC iView: IDC Analyze the future*, vol. 2007, no. 2012, pp. 1–16, 2012.

[5] C. Succi and M. Canovi, "Studies in Higher Education Soft skills to enhance graduate employability : comparing students and employers ' perceptions," vol. 5079, 2019.

[6] F. F. Patacsil and C. L. S. Tablatin, "Exploring the importance of soft and hard skills as perceived by it internship students and industry: A gap analysis," *Journal of Technology and Science Education*, vol. 7, no. 3, pp. 347–368, 2017.

[7] S. A. Hurrell, "Rethinking the soft skills deficit blame game: Employers, skills withdrawal and the reporting of soft skills gaps," *Human Relations*, vol. 69, no. 3, pp. 605–628, 2016.

[8] J. O'Reilly, W. Eichhorst, A. Gábos, K. Hadjivassiliou, D. Lain, J. Leschke, S. McGuinness, L. M. Kureková, T. Nazio, R. Ortlieb *et al.*, "Five characteristics of youth unemployment in europe: Flexibility, education, migration, family legacies, and eu policy," *Sage Open*, vol. 5, no. 1, p. 2158244015574962, 2015.

[9] K. Jones, L. N. K. Leonard, G. Lang, K. Jones, L. N. K. Leonard, and G. Lang, "Desired Skills for Entry Level IS Positions : Identification and Assessment Desired Skills for Entry Level IS Positions : Identification and Assessment," vol. 4417, 2018.

[10] A.-M. C. Williams, "Soft skills perceived by students and employers as relevant employability skills," 2015.

[11] I. Abdul, G. Azmi, and R. C. Hashim, "THE EMPLOYABILITY SKILLS OF MALAYSIAN UNIVERSITY STUDENTS," pp. 1–14, 2018.

[12] I. Nikolaou, K. Georgiou, and V. Kotsasarlidou, "Exploring the relationship of a gamified assessment with performance," *The Spanish journal of psychology*, vol. 22, 2019.

[13] R. S. A. Usmani, I. A. T. Hashem, T. R. Pillai, A. Saeed, and A. M. Abdullahi, "Geographic information system and big spatial data: A review and challenges," *International Journal of Enterprise Information Systems (IJEIS)*, vol. 16, no. 4, pp. 101–145, 2020.

[14] T. Chamorro-Premuzic, R. Akhtar, D. Winsborough, and R. A. Sherman, "The datafication of talent: how technology is advancing the science of human potential at work," *Current Opinion in Behavioral Sciences*, vol. 18, pp. 13–16, 2017.

[15] W. Youyou, M. Kosinski, and D. Stillwell, "Computer-based personality judgments are more accurate than those made by humans," *Proceedings of the National Academy of Sciences*, vol. 112, no. 4, pp. 1036–1040, 2015.

[16] K. Huotari and J. Hamari, "A definition for gamification: anchoring gamification in the service marketing literature," *Electronic Markets*, vol. 27, no. 1, pp. 21–31, 2017.

[17] M. B. Armstrong, R. N. Landers, and A. B. Collmus, "Gamifying recruitment, selection, training, and performance management: Game-thinking in human resource management," in *Emerging research and trends in gamification*. IGI Global, 2016, pp. 140–165.

[18] K. Georgiou and I. Nikolaou, "Are applicants in favor of traditional or gamified assessment methods? exploring applicant reactions towards a gamified selection method," *Computers in Human Behavior*, p. 106356, 2020.

[19] D. S. Chapman and D. Mayers, "Recruitment processes and organizational attraction," in *Employee Recruitment, Selection, and Assessment*. Psychology Press, 2015, pp. 39–54.

[20] J.-L. McCord, J. L. Harman, and J. Purl, "Game-like personality testing: An emerging mode of personality assessment," *Personality and Individual Differences*, vol. 143, pp. 95–102, 2019.

[21] S. Rambhatla and D. Gupta, "Effectiveness of epistemic games as a medium to incorporate situational judgement tests," in *2018 IEEE Tenth International Conference on Technology for Education (T4E)*. IEEE, 2018, pp. 158–161.

[22] A. M. Abdullah, R. S. A. Usmani, T. R. Pillai, I. A. T. Hashem, and M. Marjani, "Prediction of traffic emissions using an optimized artificial neural network (oann) model," *International Journal of Advanced Computer Science and Applications*, vol. 12, no. 6, 2021.

[23] R. S. A. Usmani, T. R. Pillai, I. A. T. Hashem, M. Marjani, R. Shaharudin, and M. T. Latif, "Air pollution and cardiorespiratory hospitalization, predictive modeling, and analysis using artificial intelligence techniques," *Environmental Science and Pollution Research*, pp. 1–13, 2021.

[24] A. Azzini, A. Galimberti, S. Marrara, and E. Ratti, "A classifier to identify soft skills in a researcher textual description," in *International Conference on the Applications of Evolutionary Computation*. Springer, 2018, pp. 538–546.

[25] M. Allahyari, S. Pouriyeh, M. Assefi, S. Safaei, E. D. Trippe, J. B. Gutierrez, and K. Kochut, "A brief survey of text mining: Classification, clustering and extraction techniques," *arXiv preprint arXiv:1707.02919*, 2017.

[26] A. I. Kadhim, "Survey on supervised machine learning techniques for automatic text classification," *Artificial Intelligence Review*, vol. 52, no. 1, pp. 273–292, 2019.

[27] A. De Mauro, M. Greco, M. Grimaldi, and P. Ritala, "Human resources for big data professions: A systematic classification of job roles and required skill sets," *Information Processing & Management*, vol. 54, no. 5, pp. 807–817, 2018.

[28] C.-T. Sun and J.-S. Jang, "A neuro-fuzzy classifier and its applications," in *[Proceedings 1993] Second IEEE International Conference on Fuzzy Systems*. IEEE, 1993, pp. 94–98.

[29] Z. J. Viharos and K. B. Kis, "Survey on neuro-fuzzy systems and their applications in technical diagnostics and measurement," *Measurement*, vol. 67, pp. 126–136, 2015.

[30] G. S. Atsalakis, E. E. Protopapadakis, and K. P. Valavanis, "Stock trend forecasting in turbulent market periods using neuro-fuzzy systems," *Operational Research*, vol. 16, no. 2, pp. 245–269, 2016.

[31] R. Kumari, V. K. Sharma, and S. Kumar, "Adaptive neural fuzzy inference system for employability assessment," *assessment*, vol. 3, no. 3, pp. 159–164, 2014.

[32] S. Khan, P. Khodke, and A. Bhagat, "Neuro fuzzy based user queries categorization," in *2015 International Conference on Innovations in Information, Embedded and Communication Systems (ICIIECS)*. IEEE, 2015, pp. 1–7.

[33] A. Azzini, S. Marrara, and A. Topalovic, "A neuro-fuzzy approach to assess the soft skills profile of a phd," in *International Workshop on Fuzzy Logic and Applications*. Springer, 2018, pp. 134–147.

[34] T. L. Saaty, "Decision making with the analytic hierarchy process," *International journal of services sciences*, vol. 1, no. 1, pp. 83–98, 2008.

[35] D. E. Asuquo and F. E. Onuodu, "A fuzzy ahp model for selection of university academic staff," *International Journal of Computer Applications*, vol. 141, no. 1, pp. 975–8887, 2016.

[36] F. Dweiri, S. Kumar, S. A. Khan, and V. Jain, "Designing an integrated ahp based decision support system for supplier selection in automotive industry," *Expert Systems with Applications*, vol. 62, pp. 273–283, 2016.

[37] V. M. Menon and H. Rahulnath, "A novel approach to evaluate and rank candidates in a recruitment process by estimating emotional intelligence through social media data," in *2016 International Conference on Next Generation Intelligent Systems (ICNGIS)*. IEEE, 2016, pp. 1–6.

[38] A. M. Abdullah, R. S. A. Usmani, T. R. Pillai, I. A. T. Hashem, and M. Marjani, "Feature engineering algorithms for traffic dataset," *International Journal of Advanced Computer Science and Applications*, vol. 12, no. 4, 2021. [Online]. Available: http://dx.doi.org/10.14569/IJACSA.2021.0120435

[39] R. S. A. Usmani, T. R. Pillai, I. A. T. Hashem, N. Z. Jhanjhi, A. Saeed, and A. M. Abdullahi, "A spatial feature engineering algorithm for creating air pollution health datasets," *International Journal of Cognitive Computing in Engineering*, vol. 1, pp. 98–107, 2020.

[40] R. S. A. Usmani, W. N. F. B. W. Azmi, A. M. Abdullahi, I. A. T. Hashem, and T. R. Pillai, "A novel feature engineering algorithm for air quality datasets," *Indonesian Journal of Electrical Engineering and Computer Science*, vol. 19, no. 3, pp. 1444–1451, 2020.

[41] K. Georgiou, A. Gouras, and I. Nikolaou, "Gamification in employee selection: The development of a gamified assessment," *International Journal of Selection and Assessment*, vol. 27, no. 2, pp. 91–103, 2019.

[42] F. Luthans, "The need for and meaning of positive organizational behavior," *Journal of Organizational Behavior: The International Journal of Industrial, Occupational and Organizational Psychology and Behavior*, vol. 23, no. 6, pp. 695–706, 2002.

[43] G. Wagnild and H. Young, "Development and psychometric evaluation of the resilience scale," *Journal of Nursing Management*, vol. 1, no. 2, pp. 165–178, 1993.

[44] A. Hamtiaux, C. Houssemand, and P. Vrignaud, "Individual and career adaptability: Comparing models and measures," *Journal of Vocational Behavior*, vol. 83, no. 2, pp. 130–141, 2013.

[45] A. J. Martin, H. Nejad, S. Colmar, G. A. D. Liem *et al.*, "Adaptability: Conceptual and empirical perspectives on responses to change, novelty and uncertainty," *Australian Journal of Guidance and Counselling*, vol. 22, no. 1, p. 58, 2012.

[46] E. E. Metselaar, "Assessing the willingness to change," *Huispers Vrije Universiteit, Amsterdam*, 1997.

[47] M. C. Ashton and K. Lee, "The hexaco–60: A short measure of the major dimensions of personality," *Journal of personality assessment*, vol. 91, no. 4, pp. 340–345, 2009.

[48] G. D. Nelson, "Assessment of health decision making skills of adolescents." 1984.

[49] C. Mincemoyer and D. Perkins, "Assessing youth decision-making skills and influences on decisions," in *Forum for family and consumer sciences*, vol. 8, no. 1, 2003.

[50] D. G. Ancona and D. F. Caldwell, "Bridging the boundary: External activity and performance in organizational teams," *Administrative science quarterly*, pp. 634–665, 1992.

[51] N. Meslec and P. L. Curşeu, "Are balanced groups better? belbin roles in collaborative learning groups," *Learning and Individual Differences*, vol. 39, pp. 81–88, 2015.

[52] M. M. Lombardo and R. W. Eichinger, "High potentials as high learners," *Human Resource Management*, vol. 39, no. 4, pp. 321–329, 2000.

[53] K. Lee and M. C. Ashton, "Psychometric properties of the hexaco personality inventory," *Multivariate behavioral research*, vol. 39, no. 2, pp. 329–358, 2004.

[54] A. T. Hall and G. R. Ferris, "Accountability and extra-role behavior," *Employee Responsibilities and Rights Journal*, vol. 23, no. 2, pp. 131–144, 2011.

[55] N. P. Mero, R. M. Guidice, and S. Werner, "A field study of the antecedents and performance consequences of perceived accountability," *Journal of Management*, vol. 40, no. 6, pp. 1627–1652, 2014.

[56] J. P. Meriac, D. J. Woehr, and C. Banister, "Generational differences in work ethic: An examination of measurement equivalence across three cohorts," *Journal of Business and Psychology*, vol. 25, no. 2, pp. 315–324, 2010.

[57] J. P. Meriac, D. J. Woehr, C. A. Gorman, and A. L. Thomas, "Development and validation of a short form for the multidimensional work ethic profile," *Journal of Vocational Behavior*, vol. 82, no. 3, pp. 155–164, 2013.

[58] N. M. Salleh, J. Mapjabil, and R. Legino, "Graduate work-readiness in malaysia: Challenges, skills and opportunities," in *The Transition from Graduation to Work*. Springer, 2019, pp. 125–142.

[59] G. Grotkowska, L. Wincenciak, and T. Gajderowicz, "Ivory-tower or market-oriented enterprise: the role of higher education institutions in shaping graduate employability in the domain of science," *Higher Education Research & Development*, vol. 34, no. 5, pp. 869–882, 2015.

System Dynamics Modeling for Solid Waste Management in Lima Peru

Margarita Giraldo Retuerto[1], Dayana Ysla Espinoza[2], Laberiano Andrade-Arenas[3]
Faculty of Engineering Sciences
University of Science and Humanities
Lima, Peru

***Abstract*—This research work focuses on environmental care based on the treatment of solid, organic and inorganic waste. These inappropriate wastes cause deterioration of the environment and the ozone layer. This is why we are currently seeing an abrupt change in climate and diseases caused by environmental pollution. The objective of the research work is to perform a system dynamics modeling for effective and efficient solid waste management in Lima Peru, and thus contribute to the scientific community to achieve a future vision for solid waste management. The methodology used was system dynamics, which made it possible to analyze and understand the behavior of a complex solid waste system in a given time. In addition, vensim software was used for system dynamics modeling, creating the causal diagram and forrester diagram for solid waste management. The results obtained are the system dynamics modeling proposed for solid waste management, which were modeled from 2020 to 2030, where by 2030 it will be reduced in favorable equilibrium to 23,066 tons. Thanks to this system dynamics modeling, society will be made aware of the need to sort and use solid waste, in order to reduce environmental pollution. Likewise, having a healthy environment that will benefit health, agriculture and education will benefit society as a whole.**

***Keywords*—Causal diagram; environmental pollution; forrester diagram; systems dynamics; vensim**

I. Introduction

Solid waste management is a major problem worldwide and 90 percent of cities are affected by population growth. The inefficient process of industries, businesses and changing patterns in living standards have increased the generation of solid waste in cities and towns. Solid wastes are those organic and inorganic wastes that are created by the process of transformation, construction or implementation of goods and services. If such solid waste is not handled correctly, it generates environmental pollution and health hazards for individuals [1].

Solid waste includes all waste from humans and animals. From the following, it can be said that solid waste is the consequence of life itself, in a direct way the production of waste. There are several causes, such as improper placement of garbage bins in the city. City Corporation's inadequate waste collection system. More specifically, people are not aware enough to use garbage bins properly [2].

Coastal residents generate the largest proportion of Peru's garbage. In Lima alone, where the largest city is located, home to well over 8 million people, an average of 2,123,016 tons of waste is created each year. Each individual produces approximately 0.61 kilograms per day, which implies a significant increase in solid waste [3]. In Lima Peru in recent years, solid waste has increased aggressively in all corners of the city [4].

Solid waste management is a chain that includes many elements, including proper waste collection, organized transportation, and trained personnel. Proper waste disposal lines and fully automated monitoring systems, and awareness of what the public should and should not do [5]. This is as important as any other survival system in a city like Lima. This paper describes how to use system dynamic modeling as a decision support tool for waste management and planning of the total amount of waste generated in Lima. With more than 9,000 tons, landfills are the most accepted solution for waste disposal. However, improperly selected sites can have many environmental, economic and ecosystemic impacts [6].

To know what a system dynamics is, first of all, This term is often used, even if there are different exceptions. Just as we speak of a system as a way of doing, then we mention that we have a system to solve a problem and achieve a goal [7]. In this way, system dynamics allows the behavior of a solid waste system, how it behaves in a given time. of a solid waste system, how it behaves in a given time. Likewise, system dynamics makes a simulation in years and times and is based on 2 types of diagrams, the casual diagrams and the forrester diagrams, which have their origin in the general theory of systems.

The importance of the research is to contribute to the scientific community to reach a future vision for solid waste management. Under the modeling of a dynamic system. Since there is a lot of pollution from the citizens in Lima Peru.

The objective of this work is to carry out a System Dynamics modeling for the effective and efficient management of solid waste in Lima, Peru.

This paper is structured as follows: In Section II the literature review was performed, in Section III the methodology, in Section IV the results and discussions are shown, finally in Section V the conclusions and future work are presented.

II. Literature Review

This section cites solid waste treatment requirements papers and system dynamics modeling papers that continue to engage in research and provides the resources needed to address this work.

According to the author [8], exposes the problem related to sanitary waste and the current management of solid waste treatment. on the other hand, those that can be returned to the production cycle are wasted, this is also known as the recovery industry. They represent a direct risk to health and the environment and have hazardous properties such as toxicity, flammability, chemical reactivity, corrosiveness, explosiveness, reactivity, radioactivity.

On the other hand, the author [9], emphasizes that the benefit of good solid waste management can be obtained from many compus, since organic waste decomposes and turns into methane, which is a greenhouse gas. It can also reduce waste in the toilet and increase the service life. It also reduces soil and water pollution.

Likewise, the author [10], synthesizes that informational awareness is useful, since it makes waste segregation possible. In the principles there are significant incidences in the proportion of solid waste. As in sanitary landfills and in the prices associated with the production, disposal and collection of solid waste from households in urban regions.

In this category the author [11], indicates that it can be seen that participants categorize firm waste into plastic, paper and cardboard. In the preparation of products, they use plastic with greater demand and less frequently cardboard and paper, because in this virtual teaching environment the consumption of this material by students has decreased, showing that from home they are strengthening the ecological behavior and good practices of environmental conservation.

Finally, the author [12], states that they have used the systems dynamic model to analyze solid waste. It proposes a long-term solution for new generations with an environmental cultural program that promotes environmental care focused on the recovery of natural resources. Providing education to society based on system dynamics modeling, with casual diagrams and forrester diagrams.

III. Methodology

The methodology used is system dynamics, which is a tool for creating simulation models in vensim. This model is used to help visualize temporal behavior in complex environments. It is based on the identification of repetitive sequences in instructions based on causal diagrams and forrester diagrams. In order to develop correctly and thus achieve the objectives, it is applied with formulas and equations shown, in order to be able to run a good model of system behavior based on certain periods. Fig. 1 shows the relationship of system dynamics, consisting of the levels of decision, action and information. They are related to decision functions, flow channels and sources of information.

A. Causal Diagram

A causal diagram is one that is connected by an arrow that shows the causal relationships and collaborations that variables have with each other [13]. A negative (-) or positive (+) symbol is added to the arrows to indicate the change generated in the dependent variables when the variables change to independent [14].

It is also known as a causal loop diagram, because, within each type of loop, it turns in the same direction as the loop it belongs to, and this could be clockwise or counterclockwise [15]. It is worth mentioning that a correctly applied causal diagram is beneficial for the construction and analysis of a real system, since it can help in the planning and processes of a system [16].

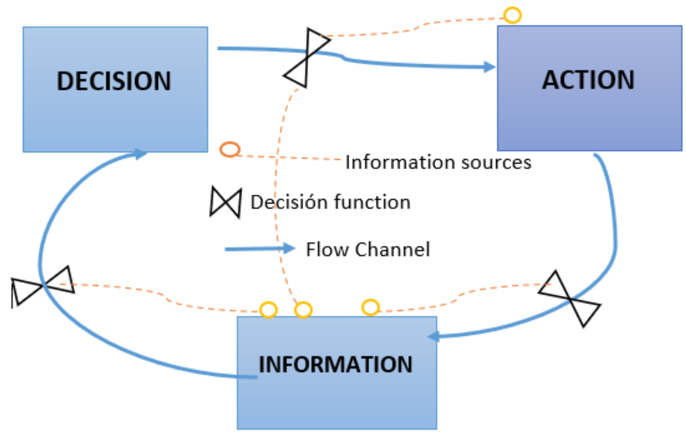

Fig. 1. Dynamic of Systems.

After the above mentioned causal diagram, we put into practice with the following Fig. 2, which shows that, with an increase in the population, there is a growth in the proportion of waste produced.Similarly, as a result of systematic collection, the proportion of garbage collection has increased. The proportion of solid waste in landfills increases due to the impact on the environment. It will increase pollution and generate deterioration of the quality of life and population growth.

The stress created by the growth, the proportion of waste caused by the people, means that they must collect a larger proportion of waste. This will make it possible to minimize the proportion of waste, if there is a lower proportion of the population for collection. This leaves us with little collection capacity to cope with population growth and the waste that everyone leaves behind simply because they live.

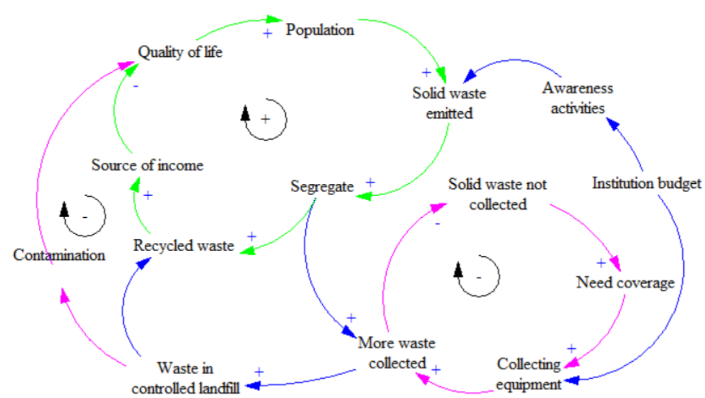

Fig. 2. Solid Waste Management System Causal Diagrama [1].

B. Forrester Diagram

In this section, the causal diagram seen in Fig. 1, already once classified the resources that appear in changing state, flows and auxiliaries. From the causal diagram was used to make the Forrester Diagram, with the required data.

In addition, the behavior of the solid waste system is being analyzed through the causal diagram and the forrester diagram using the data, equations and mathematical formulas of the system that is being developed. Among the attributes that make up the modeling of the system, there are also the well-known feedback loops [17].

We use system dynamics to represent or transform the interaction of these effects into dynamical systems that help create the behavior. It assigns values and limits based on data collected from existing systems, using formulas that describe the type and strength of all interrelationships between sets of changes.

Therefore, the vensim program was used to plot the interactions of influence and by means of the forrester diagram of the solid waste, the specifications of the mathematical equations were provided [18]. Looking at the flow diagram and inventory of Forester's solid waste diagram in Fig. 3, the whole system under study can be seen and some conclusions can be drawn.

First there is the fact that the three huge primitive feedback loops are being suppressed. This provides clear guidance on how to proceed if one part of the relevant change set has changed. Not only does it affect other parts of the system, but changes after some time will affect the same variable that caused the change [19].

C. Equations

Table I shows in summary form the sets of equations of the variables and parameters of the three level variables for the system dynamics modeling results.

1) variable level: : They are those that assume an accumulation in time and vary with other variables of system states, called flows. They characterize the pattern of the general population, the amount of solid waste on the streets.

2) Variable flow:: Variable flow: they explicitly manifest the alteration of the time units of the levels. The flow variable feeds or decreases the grade, determining the variations in levels. As well as birth variables, deaths, incoming waste, recycled waste, uncollected waste and collection [20].

3) Auxiliary variables and constants:: They suggest changing help in the model and are based on collaborating with the flow variables within the model and representing them in graphs, with the following level variations of solid waste modeling. Determined by variations in environmental quality, leachate emission, gas emission, contamination, amount of waste generated, source of income, recycling.

D. Data

Table II shows the data used in the forrester diagram for the graphs of waste generated, total recycling. Also for the controlled landfill waste graph that was made in the vensim tool.

TABLE I. FORMULAS [1]

Variables	Formulas
Variable Level	-Population = Births - Deaths -Amount of waste in the streets = IF THEN ELSE (Waste not collected - Collection.. -Waste in controlled landfill = Incoming waste - Recycled waste.
Variable flow	-Births = Population * Growth rate. -Deaths = (life expectancy + Quality of life) * Population. -Incoming waste = (Collection + Amount of waste collected) * (1 - Utilization Rate). -Recycled Waste = Waste in Controlled Landfill * Recycled Waste Rate. -Waste not collected = Segregation - Recycling - Waste collected. -Collection = Quantity of collection equipment 2 * Truck capacity 2 * Collection frequency 2.
Auxiliary and constant variables	-Collection = Amount of collection equipment 2 * Truck capacity 2 * Collection frequency 2. -Emission of leachate = RANDOM UNIFORM (0.01, 0.1, 0.001). -Contamination = (Leachate Emission + Gas Emission) * Waste in Landfill. -Quantity of waste generated = Population * Solid waste generation rate-Sensitized population. -Quantity of collected waste = (Number of collecting equipment * Truck capacity * Collection frequency. -Source of income = Average Price * Total recycled. -Recycled = Segregation * Recycling rate.

TABLE II. DATA

Num	Data
1	-Truck capacity = 2600
2	-Truck capacity 2 = 2600
3	-Average Price = 0.5
4	-Budget = 395000
5	-Realization rate = 0.2
6	-Growth rate = 0.013
7	-Solid waste generation rate = 1.17
8	-Recycling rate = 0.2Units: Kg / (day * person)
9	-Rate of Recycled Waste from the Dump = 0.09

IV. RESULT AND DISCUSSION

A. About Modeling

The system dynamics model allows the behavior of a complex system.To assist in decision making, whether tactical, strategic and policy design; how to act in a general system to drive it towards the desired behavior. The structure of the system dynamics modeling was built on causal diagrams and forrester diagrams. From the variables and data required by the system.

In addition, vensim software was used to create causal and forrester diagrams for system dynamics modeling for solid waste. Since Vensim is a software that allows simulation to improve the system performance and model quality [21].

Fig. 4, 5 and 6 show the notation of the values of the three scenarios, with their respective line graphs as: Equilibrium scenario, which are the red lines and are numbered 2, favorable scenario, which are the green lines and are numbered 3, and unfavorable scenario, which are the blue lines and are numbered 1.

In Fig. 4, the activity of the sub-variables is shown. Residuals are unavoidable in all situations.The results of the equilibrium scenario are used as a reference for the behavior of the solid waste produced. As expected, the movement tends to be greater than the balance in the opposite scenario. By 2022, the volume of industrial waste will reach 12,270, tons. On the other hand, the growth rate of waste generated tends to be low in favorable scenarios. On the other hand, the growth rate of waste generated tends to be low in favorable scenarios. 27.03

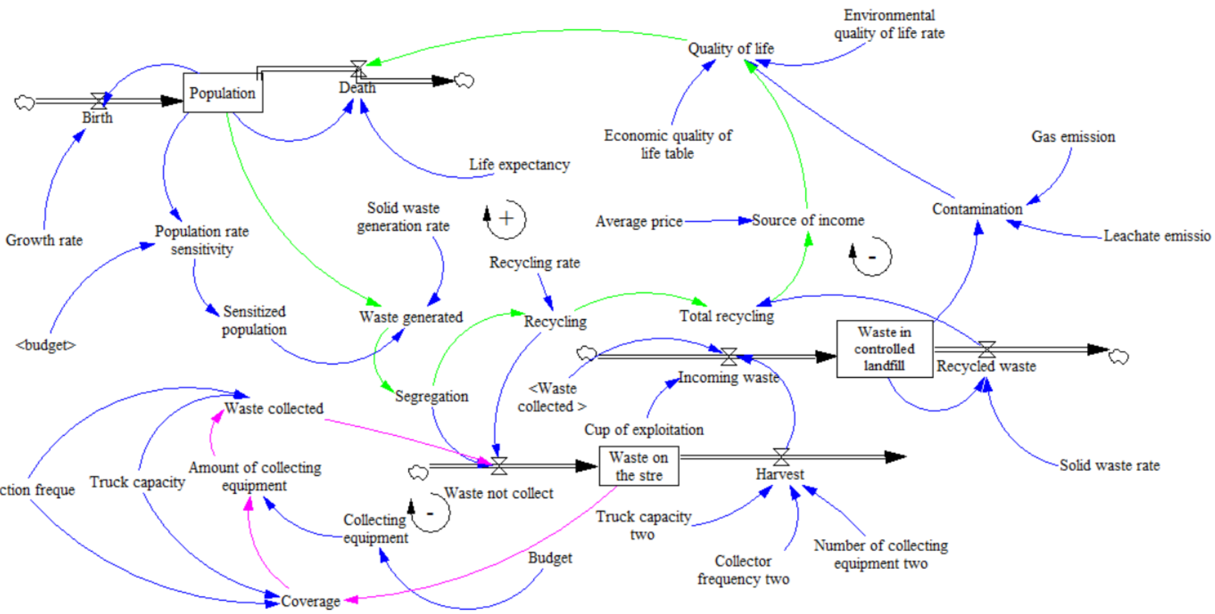

Fig. 3. Solid Waste Management System Forrester Diagram[1].

tons in 2023.

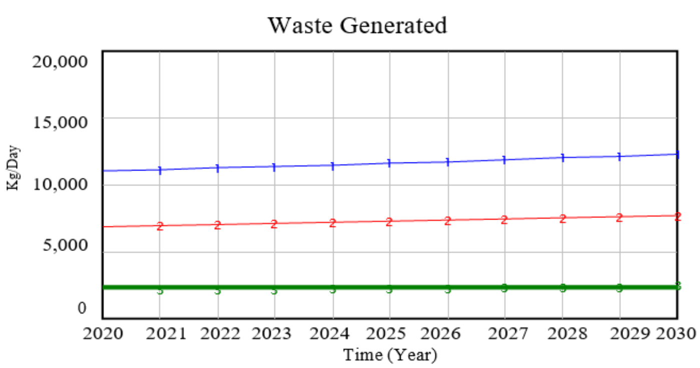

Fig. 4. Waste Generated.

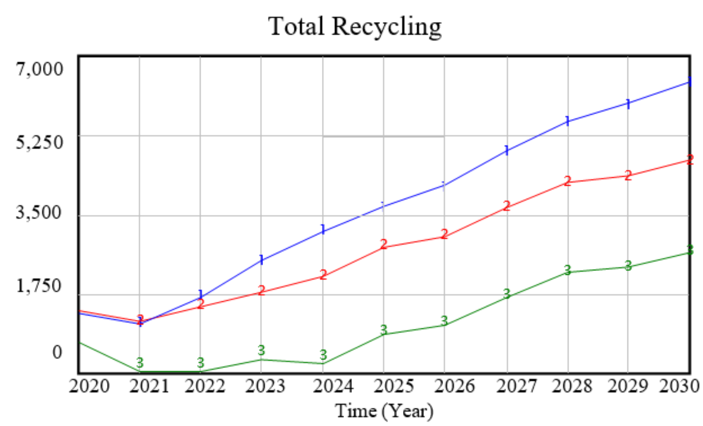

Fig. 5. Total Recycling.

Fig. 5 below shows the behavior of the secondary variables and waste recycling in each scenario. Here it can be seen that solid waste generation has a direct impact on recycled waste. The result of the balanced scenario serves as a benchmark for the rest of the performance [22]. In the unfavorable scenario, the behavior has a high growth trend, due to the growth of waste, reaching 6,429.56 tons of recycled waste in 2024. In the favorable scenario, the behavior has a trend that preserves in a stable degree with respect to the Equilibrium scenario, the rate of recycled hard waste will reach 2668 tons in 2024.

The following Fig. 6 shows the behavior of the variables at the level of solid waste at the landfill in metropolitan Lima. Here we will observe the behavior of the direct influence of the waste generated and the waste recycled from the population. In the unfavorable scenario, as expected, there is a growing trend, where rigid waste in the landfill increases significantly. Reaching 55,078 tons of waste by 2025. While in the favorable scenario it has a less increasing behavior. Landfilled solid waste is managed to be significantly reduced compared to the equilibrium scenario. By 2026, the amount of solid waste in landfills will be 21,033 tons.

Similarly, by 2030, the proportion of solid waste will be reduced in a favorable balance to 23,066 tons.

B. About the Methodology

For the discussion section, the tool comparison tables are shown. Used for the development of a system. Depending on the methodology applied in the work of the system. Table III shows the comparison between two important methodologies. System dynamics is a methodology for analyzing and modeling the temporal behaviors of complex environments [23]. It is based on the identification of feedback loops between resources, such as information and document delays in the system. On the other hand, Design Thinking is a methodology that considers exploration and thinking as fundamental as intuition in solving problems.

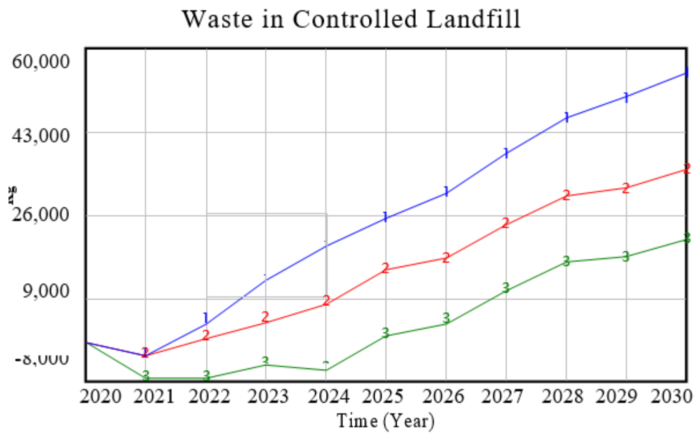

Fig. 6. Waste in Controlled Landfill.

TABLE III. DYNAMIC OF SYSTEMS-DESIGN THINKING

Dynamic of systems	Design thinking
Allows entry and exit to a jurisdiction.	You have creativity, elaboration, and learning through trial and error.
Line of ordered products. & He constantly works in multidisciplinary teams.	
Maximum power and very good volume of use. & Apply to achieve tangible and consistent results.	
Inventory management is very good because there is only one for each line See. & It greatly enhances the competitive strategy of companies.	

Table IV shows the comparison of the Vensim and Powesim studio software tools. Vensim is a simulation software developed by Ventana Systems. Primarily supports continuous simulation, with various agent-based and discrete-event modeling capabilities [24]. On the other hand, we have the powersim studio software, which is a fully equipped simulation model development environment, which makes it easy for you to create and perform analysis and simulation runs.

TABLE IV. VENSIM-POWERSIM STUDIO

Vensim & PowerSim studio
It is a simulation tool in which it simulates a dynamic model of systems. & It is a software library, which is used in applications that include simulation in Windows applications.
Provides a simple way to create simulation models (diagrams, flowcharts). & Create models and perform fully equipped analysis.
It is useful to simulate a projection of growth, population of certain markets. & Provides multi-user simulation game creation.

The comparison between the vensim software and the powerSim studio is that both do system modeling. The comparison between the vensim software and powerSim studio is that both do systems modeling. That is why the comparison is made that the vensim software allows to simulate and plot causal diagrams and forrester diagrams, a case that powerSim studio does not. In addition, the vensim software performs studies and forecasts of different scenarios with sensitivity analysis, using mathematical functions, such as data, equations and is very dynamic, user-friendly and acceptable to the public, it has many advantages. On the other hand, the powerSim studio studio, while it is true that it is very old, also does modeling, but it is a little more limited. That is why the comparison is made to see why the vensim software was used more and why not the other software that are similar to it, such as PowerSim studio, stella among others.

V. CONCLUSIONS AND FUTURE WORK

In conclusion, the system dynamics modeling allowed us to have a holistic view of the problem and thus provide a proposal for good management of solid waste from the authorities in Lima, Peru, which were modeled from 2020 to 2030. Thanks to these system dynamics modeling showed that environmental pollution will slowly reduce and will benefit society to raise awareness and sort solid waste, so as to have a healthy environment.

With respect to the methodology, system dynamics was used to analyze and understand the behavior of solid waste. Also, with the help of the vensim tool, it was possible to create a simulation of the models based on the causal diagram and forrester diagram for solid waste management.

One limitation of the research work is that it was not possible to contact the authorities in order to interview them about the solid waste problem and also to make a qualitative analysis of it. As a future work, it is suggested that it be complemented with a comparative study of the different countries of South America with respect to solid waste. Also explore the use of other modeling software such as Stella, powersim and Dinamo.

REFERENCES

[1] F. A. Condor Paucar and E. L. Lima Ataucusi, "Modelo prospectivo para el manejo de los residuos sólidos del distrito de pampas de la provincia de tayacaja," 2017.

[2] T. S. Vasagade, S. S. Tamboli, and A. D. Shinde, "Dynamic solid waste collection and management system based on sensors, elevator and gsm," in *2017 International Conference on Inventive Communication and Computational Technologies (ICICCT)*, 2017, pp. 263–267.

[3] F. A. Condor Paucar and E. L. Lima Ataucusi, "Prospective model for the management of solid waste from the district of pampas of the province of tayacaja," 2017.

[4] S. Zeeshan, Z. Shahid, S. Khan, and F. A. Shaikh, "Solid waste management in korangi district of karachi using gps and gis: A case study," in *2018 7th International Conference on Computer and Communication Engineering (ICCCE)*, 2018, pp. 1–4.

[5] A. Popov and A. Kuzmina, "Justification of the common information space components for the solid waste management," in *2018 IEEE International Conference"Management of Municipal Waste as an Important Factor of Sustainable Urban Development" (WASTE)*, 2018, pp. 25–27.

[6] S. Zeeshan, Z. Shahid, S. Khan, and F. A. Shaikh, "Solid waste management in korangi district of karachi using gps and gis: A case study," in *2018 7th International*

Conference on Computer and Communication Engineering (ICCCE), 2018, pp. 1–4.

[7] J. C. Hadiwibowo, S. Halim, B. N. Yahya, K. Agustin, and I. H. Sahputra, "A policy strategy evaluation for covid-19 pandemic in the city of surabaya using vensim ventana dynamic system simulation," in *2021 3rd East Indonesia Conference on Computer and Information Technology (EIConCIT)*, 2021, pp. 215–221.

[8] D. J. Gamarra Parra and J. e. L. Sanabria Gamboa, "Strategies for the use of organic solid waste a in the production on of renewable energy in colombia," 2020.

[9] M. B. G. Wegener, I. Buxeda, A. y Malmquist, and I. Anders y Herrera, "Polygeneration systems ’o n in the á urban area: advantages and disadvantages today," in *XIII CTV 2019 Proceedings: XIII International Congress of Virtual City and Territory: "Challenges and paradigms of the contemporary city": UPC, Barcelona,October 2-4, 2019*. Center de Politica de Sol i Valoracions, CPSV / Universitat Polytechnic, 2019.

[10] F. A. Condor Paucar and E. L. Lima Ataucusi, "Prospective model for the management of solid waste from the district of pampas of the province of tayacaja," 2017.

[11] J. S. Y. Vicente, M. R. V. Tomás, D. M. H. Acha, and M. D. B. De La Cruz, "Ecological behavior and environmental culture, fostered through virtual education in students from lima-peru," *Revista de ciencias sociales*, vol. 27, no. 1, pp. 385–398, 2021.

[12] "Solid waste management models: literature review," in *2018 2nd International Conference on Smart Grid and Smart Cities (ICSGSC)*.

[13] N. M. Sagar del Campo and L. Zamora-Matamoros, "Graphical methods in biomedical causality research," *Electronic magazine Dr. Zoilo E. Marinello Vidaurreta*, vol. 44, no. 4, 2019.

[14] V. Tower, "Analysis of variations in inventories through the causal diagram, case study construrama-tubyco de martínez," in *INTERDISCIPLINARY ENGINEERING CONGRESS ’I AS*, 2017, p. 26.

[15] C. F. Naranjo Viteri, "Reconstrucción del concepto de alienación en marx desde la dinámica de sistemas," B.S. thesis, PUCE, 2017.

[16] V. D. G. Vera and J. C. G. Vera, "Seguridad informática organizacional: un modelo de simulación basado en dinámica de sistemas," *Scientia et technica*, vol. 22, no. 2, pp. 193–197, 2017.

[17] C. Estay-Ossandon and A. Mena-Nieto, "Modelling the driving forces of the municipal solid waste generation in touristic islands. a case study of the balearic islands (2000–2030)," *Waste management*, vol. 75, pp. 70–81, 2018.

[18] F. A. Condor Paucar and E. L. Lima Ataucusi, "Prospective model for the management of solid waste from the district of pampas of the province of tayacaja," 2017.

[19] N. Phonphoton and C. Pharino, "A system dynamics modeling to evaluate flooding impacts on municipal solid waste management services," *Waste Management*, vol. 87, pp. 525–536, 2019.

[20] X. Meng, Z. Wen, and Y. Qian, "Multi-agent based simulation for household solid waste recycling behavior," *Resources, conservation and recycling*, vol. 128, pp. 535–545, 2018.

[21] E. Korchagina and O. Shvetsova, "Analysis of environmental consequences of tourism activity in baikal lake area: Regional practice of solid waste management," in *2018 IEEE International Conference"Management of Municipal Waste as an Important Factor of Sustainable Urban Development" (WASTE)*, 2018, pp. 19–21.

[22] N. P. Adriyanti, A. Gamal, and O. C. Dewi, "Solid waste management models: Literature review," in *2018 2nd International Conference on Smart Grid and Smart Cities (ICSGSC)*, 2018, pp. 37–40.

[23] S. A. H. Morales and L. Andrade-Arenas, "Inventory management analysis under the system dynamics model," *International Journal of Advanced Computer Science and Applications*, vol. 12, no. 1, 2021. [Online]. Available: http://dx.doi.org/10.14569/IJACSA.2021.0120174

[24] R. R. A. Marreros, K. V. N. Dionisio, L. A. R. Tuanama, J. A. Q. Gutarra, and L. Andrade-Arenas, "Study of post-covid-19 employability in peru through a dynamic model, between 2020 and 2025," *International Journal of Advanced Computer Science and Applications*, vol. 12, no. 1, 2021. [Online]. Available: http://dx.doi.org/10.14569/IJACSA.2021.0120171

Analysis of Distance Learning in the Professional School of Systems Engineering and Informatics

Eleazar Flores Medina[1]
Departamento de Estudios Generales
Universidad de Ciencias y Humanidades
Lima, Perú

Yrma Principe Somoza[2]
Departamento de Estudios Generales
Universidad de Ciencias y Humanidades
Lima, Perú

Laberiano Andrade-Arenas[3]
Facultad de Ciencias e Ingeniería
Universidad de Ciencias y Humanidades
Lima, Perú

Janet Corzo Zavaleta[4]
Departamento de Estudios Generales
Universidad de Ciencias y Humanidades
Lima, Perú

Roberto Yon Alva[5]
Departamento de Estudios Generales
Universidad de Ciencias y Humanidades
Lima, Perú

Samuel Vargas Vargas[6]
Departamento de Estudios Generales
Universidad de Ciencias y Humanidades
Lima, Perú

***Abstract*—The distance modality exponentially accelerated the use of technological tools in times of pandemic. In this context, educational institutions at all levels implemented actions to strengthen teaching work through training. The present study was carried out in the University of Sciences and Humanities considering the distance teaching process that is based on three dimensions: teaching strategy, resources and pedagogical materials, and evaluation. The study objective to analyze the distance learning process in its 3 dimensions to propose solutions in virtual teaching. The applied methodology was of a mixed approach; that is, qualitative through focus group and quantitative through student survey. The student population of 159 and a sample of 113 with a confidence level of 95% and margin of error 5%.The result obtained in the focus group shows that teachers have difficulties in the application of teaching strategies in the virtual modality evidenced in the management of digital tools, elaboration of rubrics to evaluate learning, and in the use of resources and pedagogical materials. This is complemented with surveys that show partial acceptance of teaching work in the distance modality; that is, the teaching strategy has an average of 3,76 and standard deviation (S.D) ,63 and 58,41% agrees with the teacher's teaching strategy; likewise, the pedagogical resources and materials dimension was obtained an average of 3,72 and S.D ,74 and agrees 51,33%.Also in the evaluation, an average of 3,76 and S.D ,72 were obtained with a 55,75% according to the way the teacher evaluates.The research work serves as input for future curricular designs in the distance modality.**

Keywords*—Distance modality; evaluation; focus group; resources and pedagogical materials; teaching strategy

I. Introduction

Distance education requires, in addition to resources, the preparation of teaching and administrative staff, accessibility and motivation of students for integrated learning based on ICT [1]. In Peru the access to internet has been steadily increasing these last years [2]. In March 2020, the first case of COVID-19 was detected in Peru, which led the central government to take economic and political measures that impacted on the Peruvian education, one of these being the suspension of classes at all levels [3]. Likewise, the Ministry of Education (MINEDU) established measures for distance education; so universities, professors and students had to adapt to the new context [4].

Later, the University of Sciences and Humanities (UCH) implemented the distance modality as an emergency measure. In this context, it was evidenced that although the teaching staff had experience and acceptance in the face-to-face modality, they lacked the management of methodologies and strategies at a virtual level [5]. Teachers had difficulty applying teaching strategies, using resources and pedagogical materials, as well as evaluating their students' learning. For this reason, trainings were carried out with teachers before classes began and during the semester [6].

The trainings focused on the use of digital tools, such as digital whiteboards, technological resources, among others; thus also in the proper use of the MOODLE platform where teachers upload their pedagogical resources and materials; furthermore, at the university, teachers and students use Zoom videoconferencing to interact in the teaching and learning process [7]. Faced with the COVID-19 pandemic, institutions have opted for virtual learning through the MOOC model that focuses on the student (LCM) and the MOODLE learning system. To increase the effectiveness of this process, a feedback and evaluation system has been incorporated. Also, a series of structures such as dialogues, videos, activities, learning experience interactions and questionnaires.

From the problem presented, the following question is formulated. What is the perception of the students, about the teaching process, in the distance modality of the Professional School of Systems Engineering and Informatics?

The objective of this research is to analyze the perception of students about the teaching process in the distance modality, taking into consideration the teaching strategy, the pedagogical resources and materials and the evaluation, of the Professional School of Systems Engineering and Informatics, through the focus group and surveys with the students. This in order to contribute to the continuous improvement and educational quality of the university.In this sense, this research work is relevant because it allows approaching teaching work in the distance modality and contributing to the university community, since it is specifically directed to the academic aspect. It also seeks to propose new actions that enhance the teaching process and the application of strategies in the distance modality

The article presents the following structure: Section I, the introduction, Section II presents the review of the Literature, where the background is explained; In Section III, the methodology is exposed, detailing the steps to follow in each stage of the process; then Section IV indicates the results obtained, in Section V discussions, and finally, we have Section VI with conclusions and future work.

II. Literature Review

In his research work, analyzes the consequences of moving from classroom teaching to distance learning during the COVID-19 pandemic; where it emphasizes that the teaching strategy and the evaluation system are different in these modalities [8]. It also presents the contingency plans that were put in place so that teaching is not affected. At the same time, he emphasized the strategies to reduce student desertion, among which stands out, having teachers who adapt to the distance modality; For this reason, trainings were developed for teachers in technological resources, virtual teaching strategy, among others.

In his article, he conducted a survey of students who point out that distance education has positive and negative aspects; likewise, teachers must be trained in the teaching process and in the use of educational platforms to face this new modality [9].

In his study on education in times of pandemic points out that teachers must enhance their technological and pedagogical knowledge [10]. To do this, surveys were conducted with students and teachers, reaching the conclusion that teachers have to be able to innovate, reflect and transform their didactic proposals in order to provide quality education.

The importance of the use of technological resources by teachers, so that they can interact with their students in the teaching process [11]. In the conclusions obtained, they highlighted that teachers must be trained in the use of educational platforms and digital tools to reduce dissatisfaction on the part of students in distance learning.

In addition, a study carried out on the perception of students, in relation to learning in the distance and face-to-face modality, was carried out by [12], with students from the University of Indonesia. The results show that students have a greater perception of face-to-face learning compared to virtual learning. Among the aspects that stand out we have: presence and social interaction and satisfaction. Despite the results, the difference between both learning modalities is not significant, since some students indicated that they felt comfortable learning in the distance modality, because it allowed them to innovate through technology.

The study carried out by [13], examines the attitudes of Portuguese university students in the remote mode during the COVID-19 pandemic. The surveyed students agree with the teaching and evaluation methodologies in this new modality; however, they feel the need for face-to-face classes for practical and laboratory classes.

On the other hand, the study carried out by [14], aimed to capture the teaching experiences in the process of transition to virtual education in its early stages. To this end, a questionnaire was distributed to six groups of Swedish teachers through Facebook groups on preparing teachers and schools for distance education. The results indicate that there are four fundamental pedagogical activities for this teaching modality: teacher and school preparation, strategies for distance education, pedagogical activities, and positive experiences and challenges. It is concluded that distance education leads to a rapid change that can become more complex; For this reason, it is necessary to use technological tools, that is, to focus on the available devices and applications, but the teachers lacked previous experience; Likewise, activities such as communication, collaboration, exchange of learning materials, workload, evaluation and exams were emphasized.

III. Methodology

The research was carried out at the University of Sciences and Humanities in Lima, Peru and this presents a qualitative-quantitative approach, of an exploratory-descriptive scope, not experimental.Teaching at the university under study was synchronous. The study variable is teaching with the 3 dimensions (D) shown in Fig. 1. The dimensions come to disaggregate the teaching variable.

A. Focus Group to Students

The focus group was carried out virtually (evidence in Fig. 2) and had the participation of nine students from the fifth to the tenth semester of the Professional School of Systems and Informatics, where the recording of the focus group and the evidence of the photo It was with the consent of the students and respecting the code of ethics of the university. The purpose of the focus group was to collect information on the perception of students in relation to teaching, from the dimensions of Fig. 1. The interview was structured, for which an eight question guide was prepared, validated by experts in the field. In Fig. 3, the processes that were carried out in the focus group are shown:

- Start: Those involved were identified: students, researchers and the moderator of the interview. The selected students were nine.
- Planning: The requirements for the focus group were compiled and the activities and tasks to be carried out on scheduled dates were defined.
- Execution: The implementation of the focus group was directed to guarantee and ensure the event.
- Closing: The recording and writing of the report of the Focus group was carried out.

B. Student Surveys

TABLE I. Expert Judgment

Question	Expert1	Expert2	Expert3	Percent
1	80%	85%	90%	85%
2	75%	80%	85%	80%
3	70%	90%	80%	80%
4	90%	90%	90%	90%
5	80%	80%	80%	80%
6	90%	90%	90%	90%
7	70%	90%	80%	80%
8	90%	90%	90%	90%

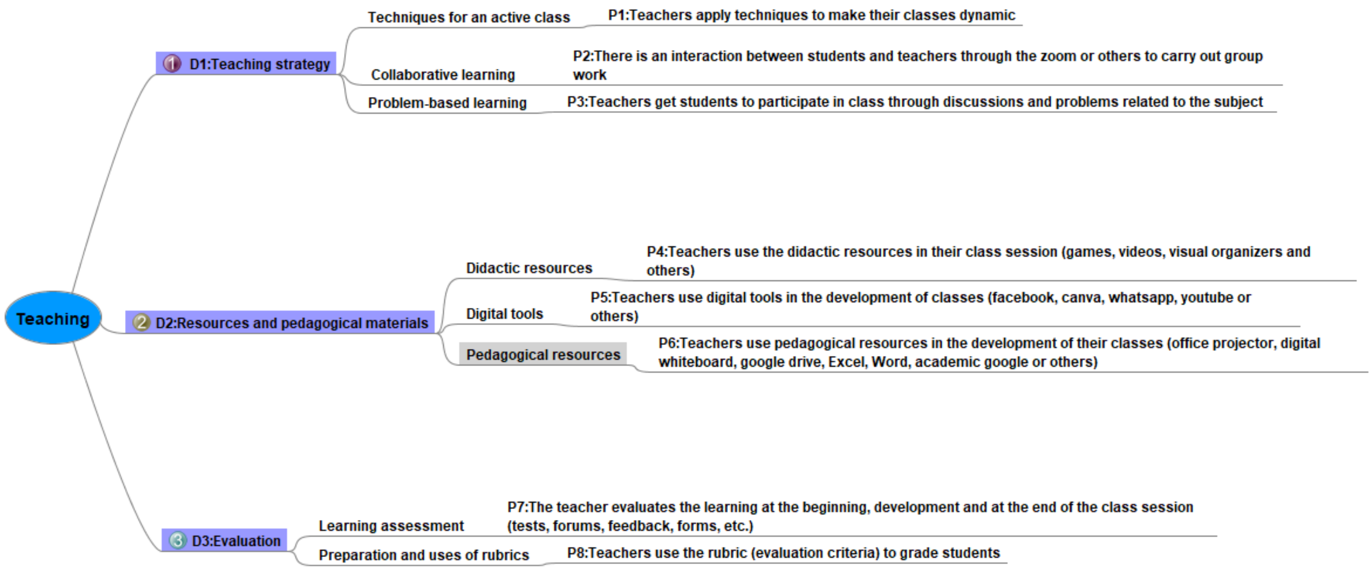

Fig. 1. Teaching Dimensions.

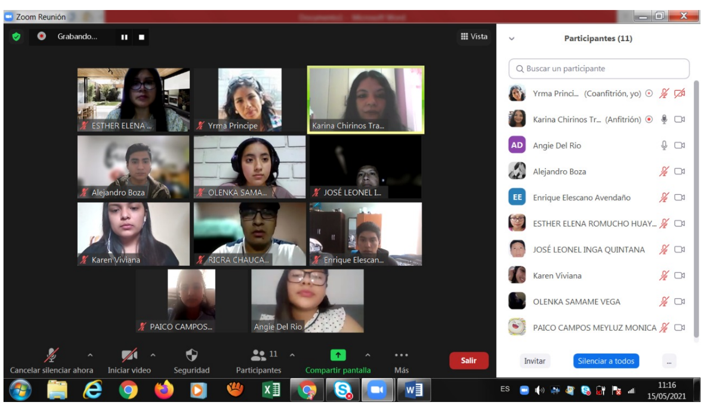

Fig. 2. Focus Group to Students.

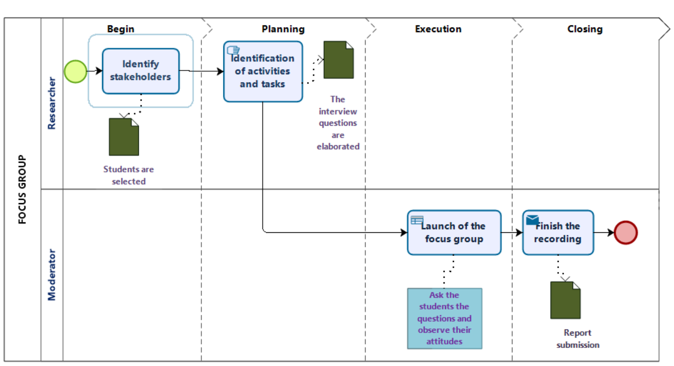

Fig. 3. Focus Group Process.

The student population of the Professional School of Systems and Informatics consists of a total of 159 students. Simple random sampling was applied, obtaining as a sample (N) 113 students, with a confidence level of 95% and margin of error of 5%. The survey link is: https://n9.cl/7at2k

The first three questions focus on the first dimension: teaching strategy; From the fourth question to the sixth, the second dimension was applied, which is pedagogical resources and materials, and the seventh and eighth questions cover the evaluation dimension. Likewise, the Likert scale from 1 to 5 was applied, with 1 strongly disagreeing, 2 disagreeing, 3 moderately agreeing, 4 agreeing, 5 strongly agreeing.

The content of the instrument was validated by expert judgment, as shown in Table I, based on the following criteria:

- Drafting: The questions are clear and precise.
- Relevance: The questions asked are appropriate and timely.
- Coherence: There is a logical coherence between the dimensions and the questions asked.
- Understanding: There is a comprehensive understanding of all questions.

To carry out the assessment, each criterion was sought to have an interval of 25 points (one point equals 1 %) For example: expert 1 placed 20 points on the first question to write(20%), relevance 25% consistency 25% y understanding 10%; where the sum of them is 80 %. Then in Table I it is placed 80% and so on until the entire table is filled with the scores that the other experts placed. After filling in the table, the average of the last column is taken, obtaining as a result 84,375%. The general average must be greater than 75% To give the content as Validated, therefore, it can be noted that the instrument has been validated by expert judgment.

A pilot test was carried out with 16 students representing 10% o of the sample where no observations were found. Likewise, the reliability and internal consistency test and validation of the instrument shown in Table II were carried out, obtaining Cronbach's Alpha 0,921, which shows high reliability, since its value is close to 1; on the other hand, the validation was obtained using Factorial Analysis with the Kaiser Meyer and Olkin (KMO) index, obtaining 0,753, thus demonstrating that the scale is valid because it is greater than 0.5; likewise, in Bartlett, 0.000 was obtained, being less than 0,05. Therefore, the instrument is reliable and validated; all this was done using the SPSS statistics 23 software.

TABLE II. RELIABILITY AND VALIDATION OF THE INSTRUMENTS

Cronbach's Alpha	KMO	Bartlett
Reliability	Validation	Validation
It must be greater than or equal to 0,7	It must be greater than or equal to 0,5	It must be p less than 0,05
0,921	0,753	0,000

IV. RESULTS

A. Analysis of the Data on the Focus Group

After the Focus Group recording, the video was observed on several occasions. Likewise, the audio was transcribed and then the most significant responses of the students were underlined. Subsequently, the questions in rows and the refined answers in columns were placed in a matrix.

In Fig. 4, the procedure for the analysis of the Focus Group data is shown, through a flow chart, from the beginning, which is the collection of data obtained from the recording, until the closing, which is the writing after having passed for validation.

-Analysis by dimensions

1) Teaching strategy: In this dimension, three questions were asked.

Question 1. Do you think that your teachers apply techniques so that their classes are active?
The students stated that the teachers partially use the techniques to make their classes active. The sections and techniques that are carried out in distance classes must be supported by tools to fulfill the objective of being more dynamic teaching. However, they observe that teachers do not use these tools adequately to motivate students and thus be dynamic in their classes. According to the author [15], in his research, classes become dynamic when they use digital tools appropriately; so it is necessary to train in its use; that is, university teachers should have more training so that their classes are more active and motivating using digital tools as a complement.

Question 2. Is interaction between students observed in group work carried out by the teacher to improve their learning?

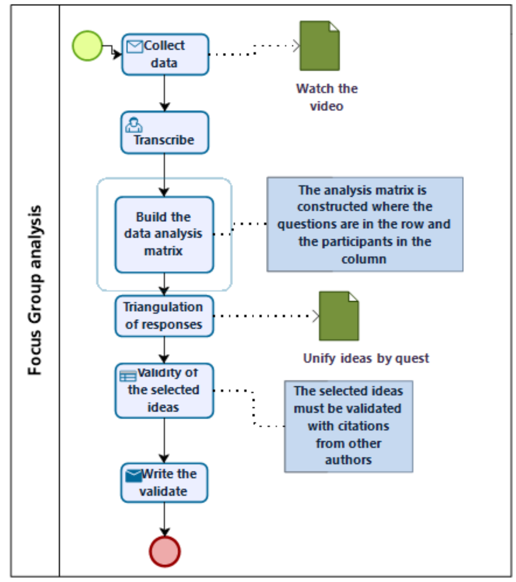

Fig. 4. Focus Group Procedure.

Students point out that interaction in group or collaborative work is not what is expected. But if there are teachers who use collaborative tools through Zoom, they have the option to form groups with students and also chat; since, through these means, teachers and students interact. According to the author [16], is important that teachers know how to handle the Zoom videoconference, such as the group room, so that their students can carry out their work in class where the teacher plays the role of mediator.

Question 3. Do you think that teachers make students be participative and not passive in the development of the class?

According to the students, most of the teachers, at the beginning, dictated as they did in the face-to-face modality, but as they were trained they improved in the teaching process and this made their students more participatory in the forums of debates, in class sessions. Likewise, the majority of students use mobile phones more than computers, which means that teachers must develop strategies to promote the participation of students from their cell phones. The author [17], in his study indicates that the teacher must apply strategies so that the students are more participative in the distance mode, based on the use of virtual tools, since the students use various devices, mainly mobile phones.

2) Resources and pedagogical materials: In this dimension, three questions were asked.

Question 4. How do teachers use the teaching resources in their class session?

Students responded that teachers use visual and audiovisual teaching resources such as videos, some virtual tools and the Internet. The difficulty they present is that most of the students use mobile phones and that is a limitation due to the little data and time that they can use it for a class of several hours; as well as, they have internet connectivity and stability problems. According to the author of the article, distance learning allows interaction from any space between the teacher and students, as well as between students; however, it is a complication for the teacher of not having all the hardware and software accesses to carry out a session of appropriate class using teaching resources.

Question 5. What is your opinion about the use of digital tools in the development of the class?

WhatsApp is the digital communication tool most frequently used by teachers and students. They create groups for classrooms and communicate to carry out tasks, tests to be carried out and notices. Therefore, what must be done is to bear in mind the rules of coexistence from the beginning on the use of this tool. Online applications and tools in teaching [18] they are fundamental, since the students partially use the computer, and rather use mobile phones as their main means, and communications are generally carried out through WhatsApp.

Question 6. How do teachers use pedagogical resources in the development of their classes?

Teachers use pedagogical resources with limitations, but the materials are shared in the Moodle platform or virtual classroom and these are used in synchronous classes. Likewise, teachers use a digital blackboard, teach their students the use of Google drive so that they can organize their information; students also use information search engines. As for the tools that the teacher has on the Moodle platform, these are used during class, but they are not fully explored. The author [19], points out that the students' perception of the use of technological resources is that it served as support in their learning process and facilitated progress in the organization of their knowledge.

3) Evaluation: In this dimension, two questions were asked.

Question 7. Do you think that the teacher evaluates at the beginning, development and at the end of his class session?

In classes, few teachers evaluate at the beginning of the process and at the end of the class. Generally, they carry out their classes according to the syllable; and some teachers evaluate through the Moodle platform; while others use technological tools such as Mentimeter and Quizizz. The author analyzes the use of LMS (learning management system),for example Moodle,which is the platform used by the university under study, pointing out that on this platform evaluations can be carried out through questionnaires and other tools that the platform offers, carried out by their teachers after having been trained in the use of it.

Question 8. Do you think that teachers use the rubric criteria appropriately in their evaluation?

For students, some teachers apply rubrics, but the vast majority do not. Likewise, the teachers who use the rubrics in their evaluation system in the exams, graded practices or others do so in an inappropriate way, since they do not present them to the students, nor do they explain them; Therefore, the students do not know the criteria by which they will be evaluated. The author [20], in his research, analyzes the use of rubrics and their scores according to each criterion established in the evaluation and disseminates this with his students as they will be evaluated. In summary, the students point out the need to train teachers in the management and elaboration of rubrics.

B. About Student Survey

1) Analysis of the dimensions: In the dimension of teaching strategy, 58,41% points out that teachers apply strategies with a mean of 3,76 and S.D ,63 (see Fig. 5), however, a 17,70% moderately agrees on the use of the teaching strategy.

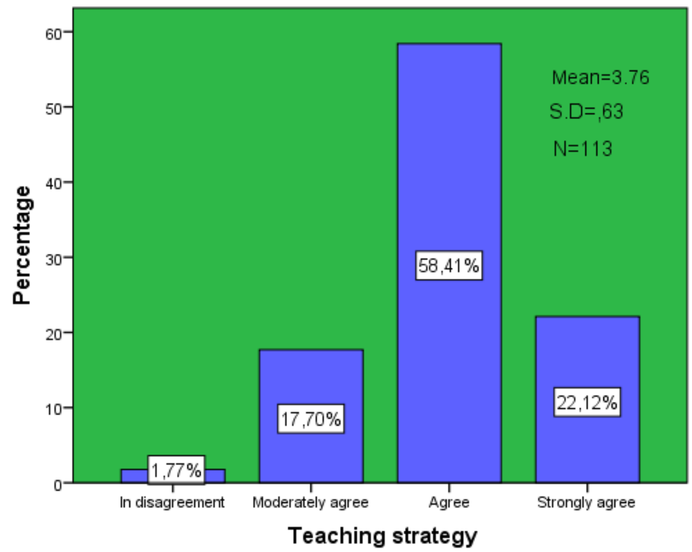

Fig. 5. Dimension 1: Teaching Strategy.

Also, in Fig. 6, the 51,33% agrees on the use of pedagogical resources and materials, that is, teachers upload their materials to the virtual classroom and 18,58%, moderately agree. This dimension has a mean of 3,72 with a standard deviation of, 74 which indicates that it is slightly above normal. El 55,75%

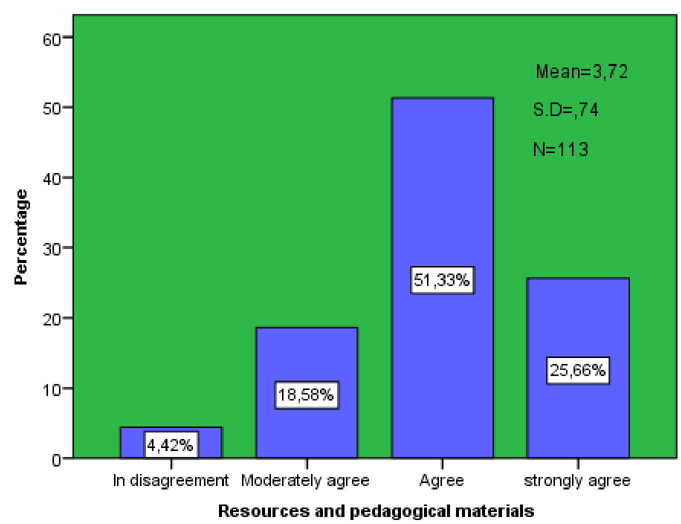

Fig. 6. Dimension 2: Resources and Pedagogical Materials.

agree that teachers partially use evaluation at the entrance, process and exit of a class session. There is also 19.47 % that moderately agrees, see (Fig. 7).

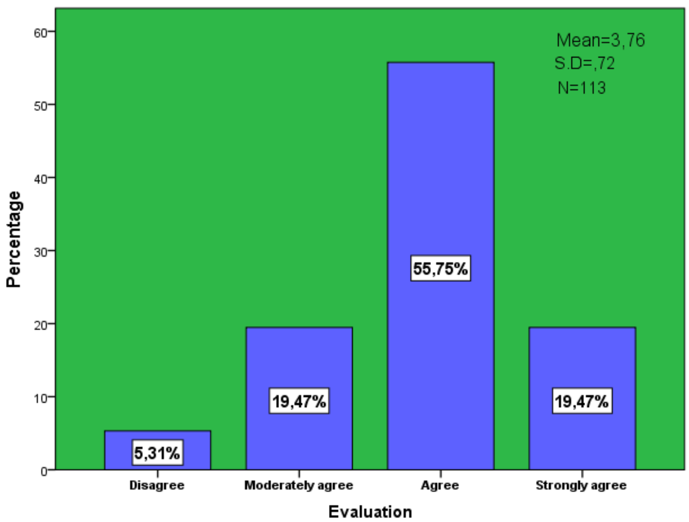

Fig. 7. Dimension 3: Evaluation.

2) Analysis by questions: Each question that was placed as affirmations is analyzed (See Fig.1).

P1: Teachers apply techniques to make their classes dynamic

In the question about the techniques for active and dynamic classes, an average of 3,72 was obtained and S.D of, 761. That is, the teachers have partial acceptance; in addition, 28,32% moderately agree, (see Fig. 8).

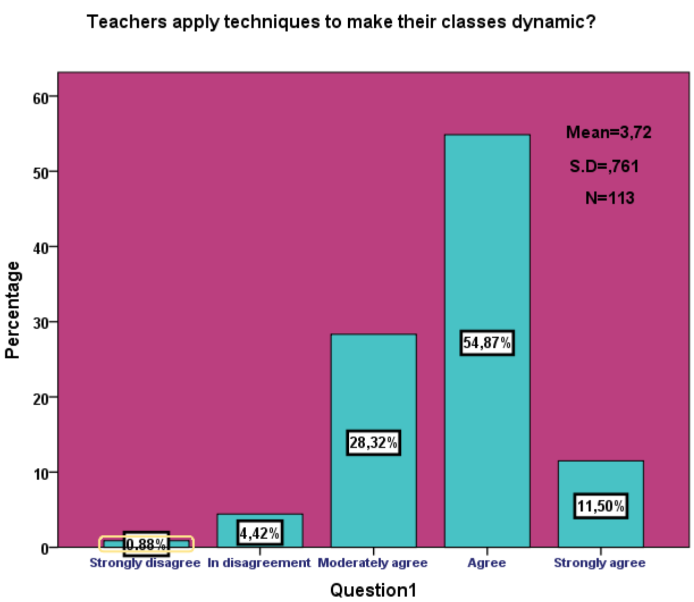

Fig. 8. Analysis of Question 1.

P2: There is an interaction between students and teachers through the zoom or others to carry out group work The interaction between teachers and students through group work such as the Zoom videoconference with its group work option has an average of 3,88 and S.D of ,746 (see Fig. 9). It is also observed that 56,64% agree

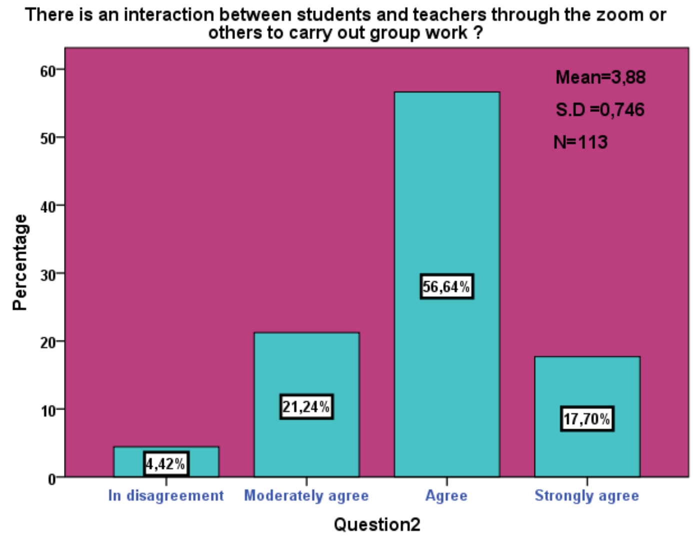

Fig. 9. Analysis of Question 2.

P3: Teachers get students to participate in class through discussions and problems related to the subject

It is observed in Fig. 10, that a 54,87% it agrees. Although it is true, there is some acceptance from the students, but not in its entirety, since there is 26,55 % who moderately agree; In other words, there are teachers who still carry out their classes in a traditional way. This question has a mean of 3,70 and S.D ,789.

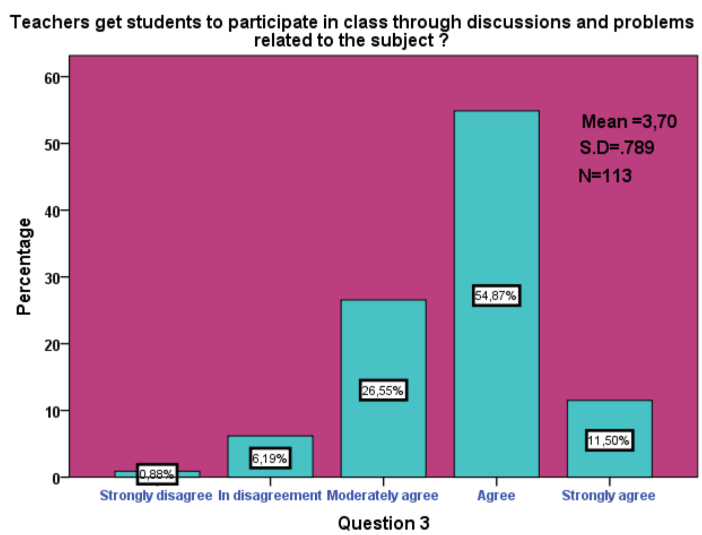

Fig. 10. Analysis of Question 3.

P4: Teachers use the didactic resources in their class session (games, videos, visual organizers and others)

There is a 44,25 % who agree that teachers use didactic resources in the class session. Of the 8 questions, it is the lowest in percentages that agree. It has a mean of 3,58 and a standard deviation of ,989 (see Fig. 11).

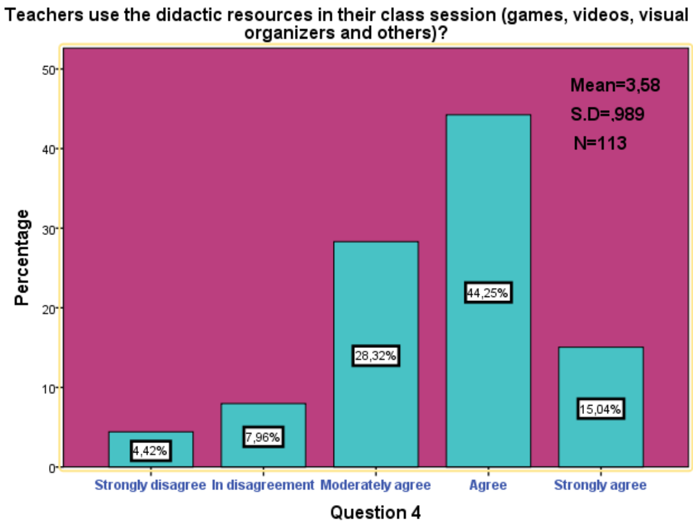

Fig. 11. Analysis of Question 4.

P5: Teachers use digital tools in the development of classes (facebook, canva, whatsapp, youtube or others)

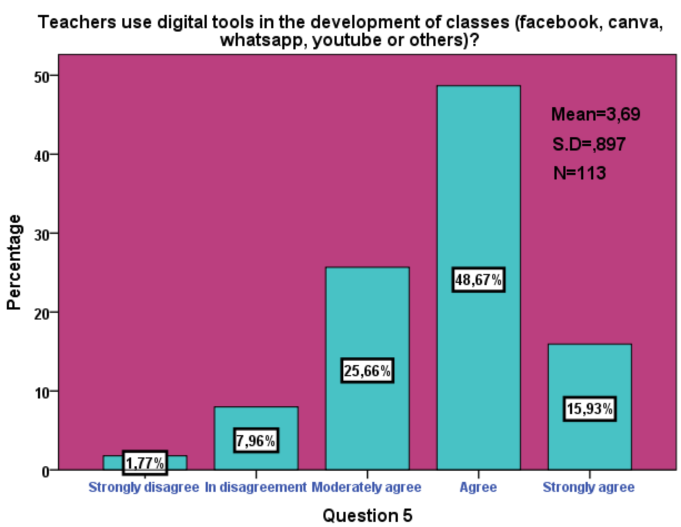

Fig. 12. Analysis of Question 5.

It is seen in Fig. 12. that less than 50 % agree that teachers use digital tools in their class session, with a mean of 3,69 and a standard deviation of, 897. There is a 7,96 % that disagrees.

P6: Teachers use pedagogical resources in the development of their classes (office projector, digital whiteboard, Google drive, Excel, Word, academic Google or others)

The use of pedagogical resources by the teacher in their class session is 48,67 % with a mean of 3,89 and a standard deviation of ,870. There is a percentage of teachers, partially, who use pedagogical tools as a complement in their teaching (see Fig. 13).

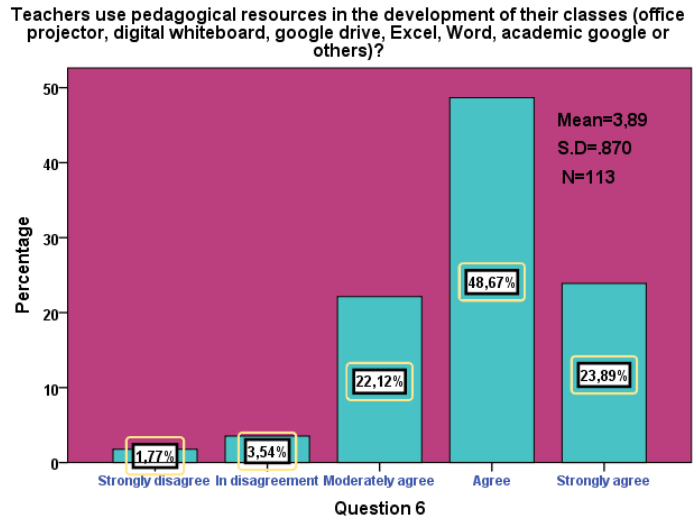

Fig. 13. Analysis of Question 6.

P7: The teacher evaluates the learning at the beginning, development and at the end of the class session (tests, forums, feedback, forms, etc.)

The students state that the teachers agree with 52,21 % in the learning evaluation. However, there is 7,08 % who disagree, since it has a mean of 3,59 and a standard deviation of, 862, (see Fig. 14).

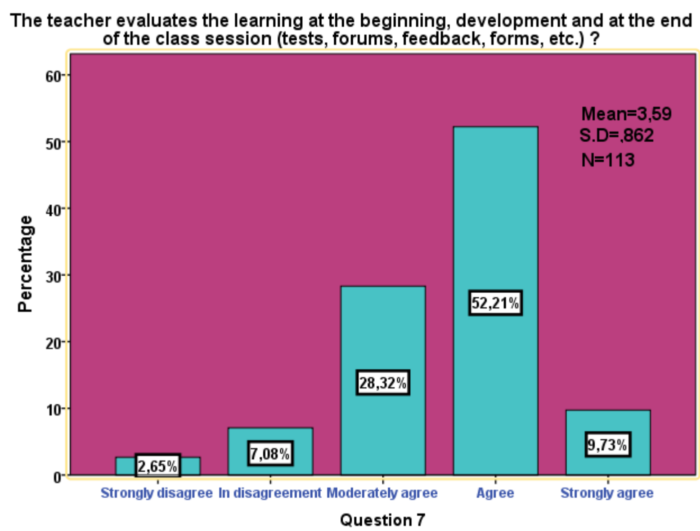

Fig. 14. Analysis of Question 7.

P8: Teachers use the rubric (evaluation criteria) to grade students

In Fig. 15 it is observed that 54,87 % indicate that teachers correctly apply their evaluation system with the use of rubrics and 2,65% disagree with a mean of 3,93 and S.D, 776.

3) Box and whisker analysis: The 3 dimensions were analyzed using box and whiskers from Fig. 16 and Table III. The first dimension, which is the teaching strategy, the score of the mean that is represented on the vertical axis and its

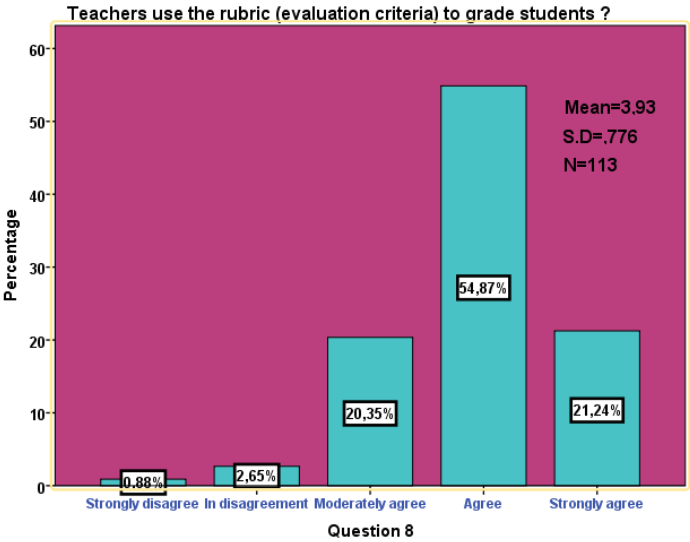

Fig. 15. Analysis of Question 8.

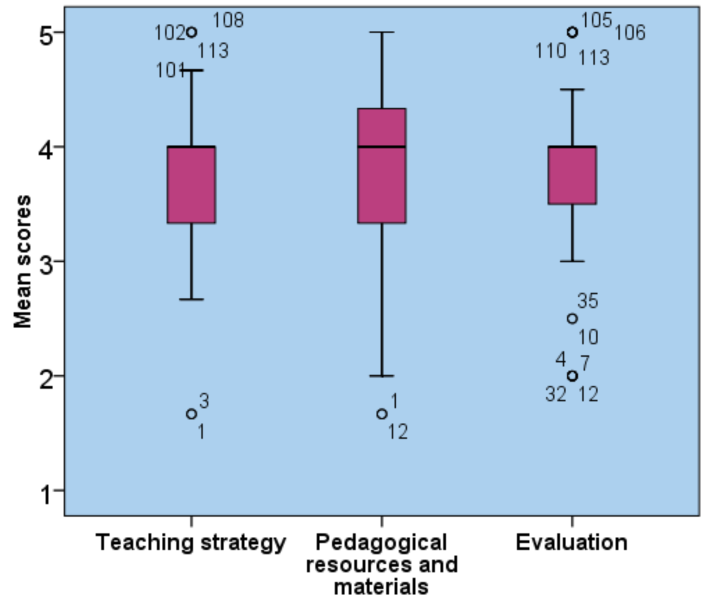

Fig. 16. Boxes and Whiskers.

TABLE III. Percentile Analysis

Dimension	Percentile 25	Percentile 50	Percentile 75	Percentile 95
D1:Teaching strategy	3,33	4	4	4,66
D2:Educational resources and materials	3,33	4	4,33	5
D3:Evaluation	3,25	4	4	5

median is 4, which represents quartile 2 of the 50th percentile of 4, which coincides with quartile 3 of 75 with a value of 4; but it is observed in the whiskers that there is a symmetry; Furthermore, extreme values are observed in the upper part, where a mean score of 5 was obtained for 4 cases, and in the lower part, a mean score of less than 2 was obtained, which was only one case. In dimension 2, pedagogical resources and materials, the median is also 4; but it is asymmetrical, since one mustache is shorter than the other; Furthermore, it is observed in the box that the highest concentration of the mean score is found between quartile 2 of the 50th percentile with a value of 4 and quartile 3 of the 75th percentile, taking the value of 4.33, since it is denser; In addition, 2 cases are observed in the lower part that are extreme points to evaluate with a mean score lower than 2. The evaluation dimension represents a symmetry in the distribution of the mean score, this is validated by the size of the mustache, its median is 4 coinciding with quartile 2 of percentile 50 of value 4 and quartile 3 of percentile 75 taking the value of 4. It also has extreme values both in the upper and lower part that requires further evaluation. In the upper part it has 4 cases with a mean score 5 and in the lower part it has 4 cases with a mean score of 2 and 2 cases with a mean score slightly higher than 2.

4) Confidence interval analysis (CI): It is shown in Fig. 17 and Table IV, the comparison of the mean D (mean dimension) with the average of the scores with the 95% Confidence Interval (95% CI) that is located in the vertical. A dispersion is observed in all dimensions; having a lower lower limit in the mean D2 dimension (resources and pedagogical materials) with 36,85 and an upper limit in the mean dimension 3 (evaluation) with 3,89. Likewise, it is observed that the mean total dimension has a lower interval 3,62 and an upper limit 3,86 %, where dimension 1 is close to it, which is the teaching strategy.

TABLE IV. Confidence Interval for the Mean at 95 % (95 % CI)

Dimension	Lower limit (95 % CI)	Upper limit (95 % CI)	Median	Mean	S.D
D1 mean:Teaching strategy	3,64	3,88	4	3,76	,63
D2 mean:Resources and pedagogical materials	3,58	3,85	4	3,72	,74
D3 mean:Evaluation	3,62	3,89	4	3,76	,72
D total mean:Mean total dimension	3,62	3,86	4	3,74	,63

V. Discussion

The analysis of the focus group and the student surveys have allowed us to triangulate, cross and compare the student's perception qualitatively with the quantitative part about teaching at the university.

The distance learning strategy has not allowed direct human interaction between teachers and students, since face-to-face teaching is different from distance learning [8]. Distance learning, carried out at the university under study, is under development, as it is focusing on training its teachers in the proper use of digital tools. However, training alone does not guarantee an education according to the pedagogical model of the university. In other words, pedagogical guidelines are required in distance learning. Likewise, the trainings oriented to the methodology of the distance modality would help to strengthen teaching. The author [9], states that training in

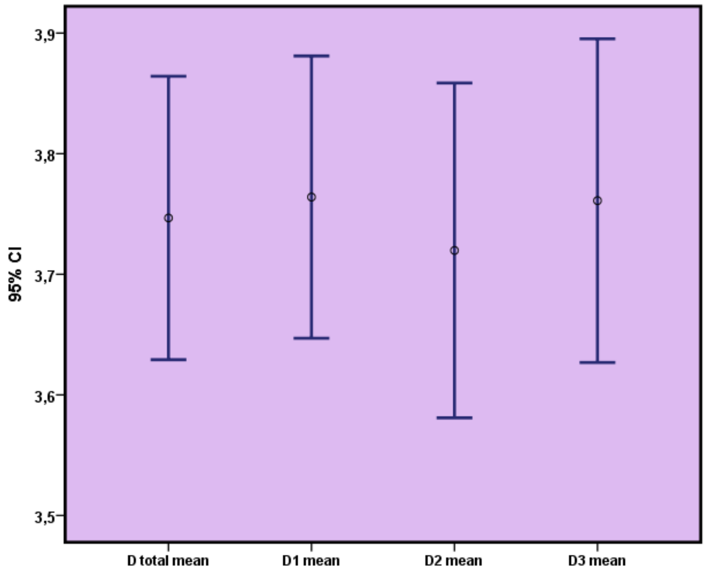

Fig. 17. Confidence Interval Analysis.

digital tools and educational platforms should be developed. However, in our study, information was obtained that teachers should be trained not only in the use of digital tools but also in distance learning strategies. Regarding the uses of resources and pedagogical materials, students partially agree that teachers use them appropriately; However, there are other aspects that prevent the development of distance classes, such as connectivity problems and limited access to the Internet, and to this is added the fact that the majority of students use mobiles that have limited connectivity. El autor [11], agree in their results regarding that teachers should be trained in digital tools to promote student learning. On the other hand, in the dimension of the evaluation of the learning of the students, the teachers presented limitations to evaluate in the distance modality; but this was partially overcome with training and the use of virtual classroom tools. In summary, the students stated that distance education is partially accepted, since the interaction between those involved is minimal, coinciding with the author [12] in their conclusions, regarding the fact that face-to-face teaching has a greater impact on the interaction between student and teacher.

VI. Conclusion and Future Work

After carrying out the qualitative and quantitative analysis, we conclude that teachers must further strengthen the strategies for teaching their classes, as well as the way to carry out evaluations in the distance mode and make the appropriate use of resources and educational materials. The pedagogical aspect is different between face-to-face teaching and distance learning, so the latter aspect should be strengthened. It is recommended to develop constant training not only in the use of digital tools but also in the didactics of teaching strategies. The connectivity problem and the internet have been limitations in the teaching process and in the evaluation system, since the majority of students used mobile computers and some did not have cameras for evaluation. There was a difficulty in the teamwork among the students to be able to carry out their assignments, forums and group works of exposition. We suggest as future work to carry out a comparative analysis of distance, face-to-face and blended classes involving university teachers and authorities. In addition, we also suggest to carry out a study about the digital gap that exists among the students, since internet connectivity problems emerged.

Acknowledgment

This work was sponsored by the University of Sciences and Humanities and the research direction. To acknowledge Dr. Carlos Sotomayor Beltrán for the suggestions in the article.

References

[1] W. Ali, “Online and remote learning in higher education institutes: A necessity in light of covid-19 pandemic.” *Higher education studies*, vol. 10, no. 3, pp. 16–25, 2020.

[2] C. Sotomayor-Beltran and L. Andrade-Arenas, “A spatial assessment on internet access in peru between 2007 and 2016 and its implications in education and innovation,” in *2019 IEEE 1st Sustainable Cities Latin America Conference (SCLA)*, 2019, pp. 1–4.

[3] B. Williamson, R. Eynon, and J. Potter, “Pandemic politics, pedagogies and practices: digital technologies and distance education during the coronavirus emergency,” *Learning, Media and Technology*, vol. 45, no. 2, pp. 107–114, 2020.

[4] L. Li, Y. Chen, Z. Li, D. Li, F. Li, and H. Huang, “Online virtual experiment teaching platform for database technology and application,” in *2018 13th International Conference on Computer Science Education (ICCSE)*, 2018, pp. 1–5.

[5] N. Asadi, F. Khodabandeh, and R. R. Yekta, “Comparing and contrasting the interactional performance of teachers and students in traditional and virtual classrooms of advanced writing course in distance education university,” *Turkish Online Journal of Distance Education*, vol. 20, no. 4, pp. 135–148, 2019.

[6] J. G. Coello, J. T. Salazar, and M. L. N. Taborda, “Peruvian students in pandemic: Digital gap and what is done from engineering programs?” in *2020 IEEE International Symposium on Accreditation of Engineering and Computing Education (ICACIT)*, 2020, pp. 1–4.

[7] K. Kedraka and C. Kaltsidis, “Effects of the Covid-19 pandemic on university pedagogy: students’ experiences and considerations,” *European Journal of Education Studies*, vol. 7, no. 8, 2020.

[8] S. Elmendili and S. Saaidi, “The Distance learning practices in Moroccan universities in the coronavirus era,” *The Journal of Quality in Education*, vol. 10, no. 16, 2020.

[9] O. Yarmak, T. Shkaiderova, E. Strashko, M. Bolshakova, and L. Garas, “Institution of higher education transformation and society’s response to distance learning during the covid 19 pandemic,” vol. 244, 2021.

[10] S. T. Calvo, L. Cervi, F. Tusa, and A. Parola, “Educación en tiempos de pandemia: reflexiones de alumnos y profesores sobre la enseñanza virtual universitaria en españa, italia y ecuador,” *Revista Latina de Comunicación Social*, no. 78, pp. 1–21, 2020.

[11] S. Deb Roy, “Application of ICTs in Teaching-Learning Process,” *International Research Journal of Interdisciplinary & Multidisciplinary Studies (IRJIMS) A Peer-*

Reviewed Monthly Research Journal, vol. 1, no. VII, 2015.

[12] S. Bali and M. Liu, "Students' perceptions toward online learning and face-to-face learning courses," in *Journal of Physics: Conference Series*, vol. 1108, no. 1. IOP Publishing, 2018, p. 012094.

[13] S. P. Gonçalves, M. J. Sousa, and F. S. Pereira, "Distance learning perceptions from higher education students—the case of portugal," *Education Sciences*, vol. 10, no. 12, p. 374, 2020.

[14] N. Bergdahl and J. Nouri, "Covid-19 and Crisis-Promted Distance Education in Sweden," *Technology, Knowledge and Learning*, 2020.

[15] L. Andrade-Arenas, D. L. Nunez, and C. Sotomayor-Beltran, "Leveraging digital tools for a better virtual teaching-learning process in a private university of lima," in *EDUNINE 2021 - 5th IEEE World Engineering Education Conference: The Future of Engineering Education: Current Challenges and Opportunities, Proceedings*, 2021. [Online]. Available: www.scopus.com

[16] A. D. Rio-Chillcce, L. Jara-Monge, and L. Andrade-Arenas, "Analysis of the use of videoconferencing in the learning process during the pandemic at a university in lima," *International Journal of Advanced Computer Science and Applications*, vol. 12, no. 5, 2021. [Online]. Available: http://dx.doi.org/10.14569/IJACSA.2021.01205102

[17] Q. Kharma, K. Nairoukh, A. Hussein, M. Abualhaj, and Q. Shambour, "Online learning acceptance model during covid-19: An integrated conceptual model," *International Journal of Advanced Computer Science and Applications*, vol. 12, no. 5, 2021. [Online]. Available: http://dx.doi.org/10.14569/IJACSA.2021.0120561

[18] G. Georgieva-Tsaneva and I. Serbezova, "Online training and serious games in clinical training in nursing and midwife education," *International Journal of Advanced Computer Science and Applications*, vol. 12, no. 5, 2021. [Online]. Available: http://dx.doi.org/10.14569/IJACSA.2021.0120539

[19] H. H. Razami and R. Ibrahim, "Distance education during covid-19 pandemic: The perceptions and preference of university students in malaysia towards online learning," *International Journal of Advanced Computer Science and Applications*, vol. 12, no. 4, 2021. [Online]. Available: http://dx.doi.org/10.14569/IJACSA.2021.0120416

[20] C. Rodriguez-Sabiote, J. Alvarez-Rodríguez, and R. D. P. Gámez-Durán, "Methodological limitations and feasible solutions in the assessment and grade calculation obtained through the rubrics as skills assessment strategies of higher education students and other levels," *Meta: Avaliacao*, vol. 10, no. 30, pp. 621–637, 2018. [Online]. Available: www.scopus.com

An ICU Admission Predictive Model for COVID-19 Patients in Saudi Arabia

Hamza Ghandorh[1], Muhammad Zubair Khan[2]
College of Computer Science and Engineering,
Taibah University
Medina 42353, Saudi Arabia

Raed Alsufyani[3]
Research and Knowledge Director
Aathar Alkhair Holding Company
Jeddah Governorate, Saudi Arabia

Mehshan Khan[4]
Department of EE
HITEC University
Museum Road, Taxila, Pakistan

Yousef M. Alsofayan[5], Anas A. Khan[6], Ahmed A. Alahmari[7]
Global Center for Mass Gatherings Medicine Ministry of Health,
P.O. Box 1146 Riyadh, 11176, Saudi Arabia

***Abstract*—Globally, COVID-19 already emerged in around 170 million confirmed cases of infected people and, as of May 31, 2021, affected more than 3.54 million deaths. This pandemic has given rise to numerous public health and socioeconomic issues, emphasizing the significance of unraveling the epidemic's history and forecasting the disease's potential dynamics. A variety of mathematical models have been proposed to obtain a deeper understanding of disease transmission mechanisms. Machine Learning (ML) models have been used in the last decade to identify patterns and enhance prediction efficiency in healthcare applications. This paper proposes a model to predict COVID-19 patients admission to the intensive care unit (ICU). The model is built upon robust known classification algorithms, including classic Machine Learning Classifiers (MLCs), an Artificial Neural Network (ANN) and ensemble learning. This model's strength in predicting COVID-19 infected patients is shown by performance analysis of various MLCs and error metrics. Among other used ML models, the ANN model resulted in the highest accuracy, 97.9% over other models. Mean Squared Error showed that the ANN method had the lowest error (0.0809). In conclusion, this paper could be beneficial to ICU staff to predict ICU admission based on COVID-19 patients' clinical characteristics.**

Keywords*—*Covid-19; ANN; ensemble learning method; prediction; ICU admission; Saudi Arabia

I. Introduction

The 2019 coronavirus disease (COVID-19) emerged as a global public health emergency on December 12, 2020, affecting 220 countries worldwide. This disease is caused by an extreme acute respiratory syndrome called coronavirus 2 (SARS-CoV-2) [1, 2], first identified in Wuhan, China. This new virus began to transmit rapidly globally, and the WHO declared the epidemic to be International Public Health Emergency of International Concern (PHEIC), and soon after it was declared a pandemic [3, 4]. Around 170 million confirmed cases and more than 3.54 million deaths were registered worldwide, with a Case Fatality Rate (CFR) of 2 as of May 31, 2020, [5]. In the same time interval, the Kingdom of Saudi Arabia has registered a lower CFR 1.7 similar to the international clinical manifestation and risk factors of COVID-19 [6, 7, 8].

Various prevention measures have been promoted, namely encouraging the use of face masks, isolation, quarantine, lockdowns, and travel bans promoted locally and by the World Health Organization (WHO) [9, 10]. As soon as COVID-19 infections appeared in a few developed countries, COVID-19 cases have been exponentially dispersed in developing countries. All over the world, scientists have made incredible efforts to cope with COVID-19; there are still many missing puzzle pieces they do not understand about the disease [11]. For instance, asymptomatic cases [12] could be between 5 % and 80 %of individuals who test positive for COVID-19, including children and young adults. The Centers for Disease Control and Prevention (CDC) stated that there are 11 common symptoms for COVID-19 [13], yet many COVID-19 infected patients did not develop vital sign abnormalities.

One of the most pressing questions about COVID-19 that was not answered is how deadly COVID-19 is. It is challenging to be confident about the death rate within a designated geographical area. Currently, between 0.02 % - 0.82 % of people infected with the virus are estimated to die [14], although the mortality rate could be lower if there are large numbers of asymptomatic patients. While in Saudi Arabia, it is estimated that there have been more than 7,362 death. Moreover, 1,438 critical cases have been recorded until March 2021, which is depicted in Fig. 1.

The massive volume and the increasing velocity of COVID-19 data pose an enormous challenge. Because they play a crucial role in disease transmission, asymptomatic carriers and healthcare workers should be given special consideration. The recent rapid and exponential rise in the number of infected patients has impelled accurate prediction models, for instance, Artificial Intelligence (AI), for potential outcomes.

Machine Learning (ML) and self-learning concepts have become tightly coupled terminology over the last decade. ML models have been used to detect patterns and improve prediction performance using statistical modeling. ML models operate upon input data and empirical information without direct programming. Probabilistic reasoning, trial and error, and other computational-intensive methods are key players in ML models [16].

ML has proved to be a major research area in the resolution of many highly complex and advanced real-world problems Rustam et al. [17]. These days, one of the main areas of ML application is healthcare. For example, Petropoulos and Makridakis [18] provided live projections with reported cases

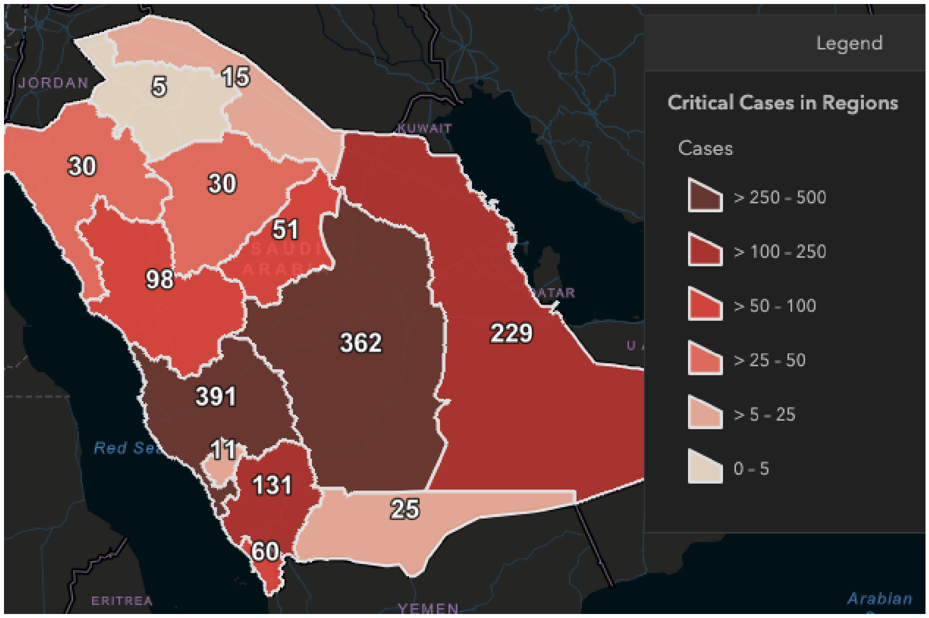

Fig. 1. Overview of Critical Cases Recorded in Saudi Arabia Until May 2021 [15].

of COVID-19. Grasselli et al. [19] also focused on predicting the epidemic and the early response to COVID-19. In the same way, these predictive systems can help manage current scenarios to direct early interventions to manage these diseases very efficiently.

There is a need for a novel model based on ML methods to investigate and predict the severity of the asymptomatic carriers and the possible death rate from the conditions mentioned earlier. This paper aims to propose a model to predict COVID-19 patients admission to the intensive care unit (ICU). The model is built upon robust known classification algorithms, including classic Machine Learning Classifiers (MLCs), Artificial Neural Network (ANN) and ensemble learning. The model may use clinical characteristics of COVID-19 on a national scale.

The contribution of this work is two-folded:

- This work presents a comparative analysis of multiple MLCs that intended to process COVID-19 patients' dataset in Saudi Arabia where an ANN and ensemble learning method were identified as good models for ICU admission prediction.
- This work serves as a starting point for the research community to explore different ML classifiers for better prediction of ICU admission.

The rest of the article is organized as follows: Section II demonstrates a few related works in which MLCs have been used for COVID-19 prediction. Section III describes the model details along with the dataset description and the data analysis. Section IV depicts the performance of the proposed model. Section V sheds a light upon a further discussion, and Section VI provides a conclusion and the future direction.

II. Related Work

This section demonstrates the most popular MLCs and the architecture of the proposed model.

This pandemic has led to various public health and socioeconomic concerns, highlighting the importance of unraveling the disease's evolution and predicting future dynamics. Various mathematical paradigms have often played a significant part in providing a deeper understanding of disease transmission mechanisms, adding significant insights to controlling the disease's spread. Calafiore et al. [20] and Nesteruk [21] have argued in favor of Mckendrick's suggested Susceptible Infectious Removed (SIR) disease model, and subsequently, one of the family models for human-to-human transmission is reasonably predictive. The Susceptible Exposed Infectious Removed (SEIR) model was created with many variants to forecast the possible dynamics of an outbreak. In a model that is based on population, integrating such real-world dynamics is still very difficult. Indeed, due to the lack of suitable actual historical data, research and prediction could go wrong. Instead, various models that focused on stochastic agents have been used as effective methods for monitoring the fine-grained effects of heterogeneous disease intervention policies on multiple disease outbreaks [22, 23, 24, 25]. However, due to the network structures' time-varying existence, this method's consistency can be a critical problem.

For reported and unreported infections, Li et al. [1] suggested an SEIR model after the virus's outbreak, integrating a meta-population framework, considering journeys between major cities in China. Their research discovered that before traveling was banned on January 23, 2020, about 86% of cases went unreported in Wuhan. As per their estimate, about 55% of asymptomatic spreaders were infectious on an individual basis, resulting in 79% of newly infected cases. In Verity et al. [26] later projected that about 63% of Italy cases were under-reported by reviewing an updated SIR model. Applying the Susceptible-Infectious-Recovered-Deceased (SIRD) model to a Chinese official's statistics, Anastassopoulou et al. [27] estimated the COVID-19 pandemic's propagation dynamics in Hubei, using linear regression to assess the parameters of the model.

A more comprehensive SEIDIUQHRD[1] model has been proposed considering the above limitations of different proven mathematical models, taking into account all potential interactions, which can provide a more precise and stronger short-term and long-term estimation of the future COVID-19 dynamic model. As of May 11, the early stage's mathematical model parameters have changed dramatically. However, due to the strict containment measures and large-scale testing strategy, the outbreak has improved in many countries [28]. Considering the features of coronavirus infection reported by health organizations or quantitatively assessed in the literature, the model parameters' nominal values were considered [1, 26, 29, 30].

A few efforts aimed to provide a deeper understanding of the disease's spread and healthcare management aspects. ML models' capacity to predict the number of potential patients affected by COVID-19 is shown by Rustam et al. [17]. In this study, four typical forecasting models have been used to predict the threatening factors of COVID-19, such as linear regression (LR), minimum absolute shrinkage and selection operator (LASSO), support vector machine (SVM), and exponential smoothing (ES). The findings show that followed by LR and LASSO; the ES performed best out of all the models used, which performs well in predicting newly recorded incidents, death rate, and recovery rate, while SVM performs poorly in all projection scenarios given the available dataset.

The author in Iwendi et al. [31] provided a fine-tuned method for the Random Forests (RF) algorithm boosted by AdaBoost. This model uses the geographical, travel, health, and demographic data of COVID-19 patients and calculates the potential outcome of recovery or death. This study has a 94% accuracy and an F1 score of 0.86 for the used dataset.

Kutia et al. [32] attempted to break down consumer perceptions on China's eHealth applications and Ukraine's eHealth platform, which subsequently generated bits of knowledge and recommendations for refining an eHealth application (eZdorovya) specifically for health information benefits.

The proposal by Ardabili et al. [33] presented a relative analysis of ML and soft computing methods to forecast the COVID-19 pandemic. These two models present essential outcomes (i.e. multi-layered perceptron, adaptive network-based fuzzy inference system) based on the complexity of work that showed ML models were effective compared to their peers.

The study was given by Yan et al. [34], examining 404 infected patients' blood samples in the Wuhan region of China to classify critical predictive biomarkers of the seriousness of the disease. Three biomarkers that predict individual patients' survival with more than 90 % accuracy have been selected through ML tools for this function: lactic dehydrogenase (LDH), lymphocyte, and high-sensitivity C-reactive protein (hs-CRP). In particular, relatively high levels of LDH alone seem to play a crucial role in distinguishing the overwhelming number of incidents that required immediate medication. This finding was consistent with a current medical understanding that various diseases, including pulmonary disorders (e.g. pneumonia) are correlated with elevated levels of LDH, causing tissue breakdown. Overall, the authors proposed an exact and operable formula for quickly predicting patients at the highest risk, enabling them to prioritize and potentially lower the mortality rate.

[1]SEIDIUQHRD stands for Susceptible-Exposed-Symptomatic Infectious-Asymptomatic Infectious-Quarantined-Hospitalized-Recovered-Dead model.

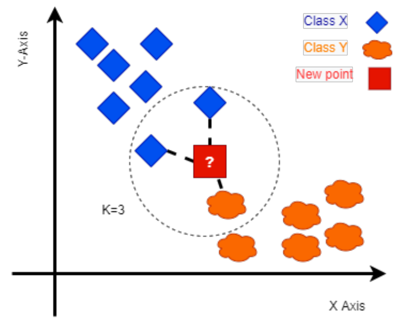

Fig. 2. Calculating Distance between a New Data point and Finding Closest Neighbors Through k-NN Classifier.

The research proposed by Pinter et al. [35] aimed to construct a hybrid approach to ML to predict COVID-19 and uses Hungary-based data to exemplify its potential. To forecast the time series mortality rate for infected individuals, the adaptive network-based fuzzy inference system (ANFIS) and multi-layered perceptron-imperialist competitive algorithm (MLP-ICA) hybrid ML methods are recommended. The online COVID-19 tracker suggested by Hamzah et al. [36] was used to interpret world sentiment trends on the dissemination of relevant health information and determine the political and economic effect of the virus's spread.

III. Material and Methods

This section demonstrates the most popular MLCs and the architecture of the proposed model.

A. Background

1) k-Nearest Neighbors (k-NN): k-Nearest Neighbors (k-NN) is a simple supervised [16] ML model. It stores all input data and computes the distance between each new data point and all existing data points (i.e. neighbors). k-NN expects to label a new data point in a class based on the closest data points. Whenever many of the neighboring points become the majority, they will be designated as a class [37]. Fig. 2 depicts an overview of the k-NN model. The distance between a current data point and its neighbors is calculated as Eq. 1.

$$D\left(x,y\right)=\sqrt{\left(x_1-y_1\right)^2+\left(x_2-y_2\right)^2}, \qquad (1)$$

where D is the distance between x and y points.

Although k-NN is known for its accuracy and user-friendliness, it cannot tolerate multi-dimensional data with multiple features [16].

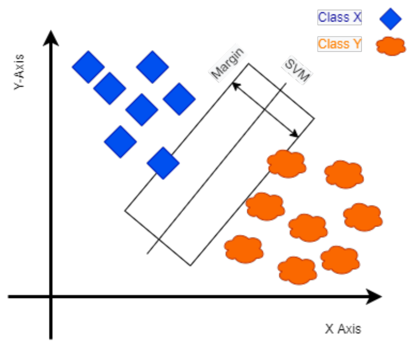

Fig. 3. Predicting the Class of a New Data Point using SVM Classifier.

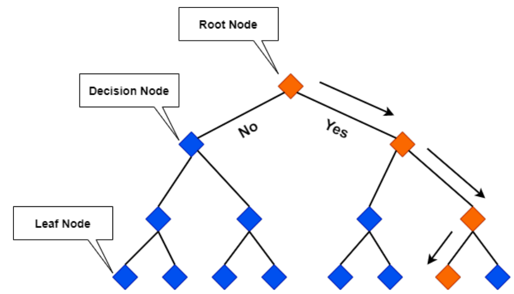

Fig. 4. Navigating Toward Optimum Split a the Tree Features through of DT Classifer.

2) Support Vector Machine (SVM): Support Vector Machine (SVM) is an MLC used to predict categorical-based dataset decisions. SVM uniquely classifies data points by filtering them into binary or multiclass variables. It maintains a plane (i.e. hyperplane) to cover several dataset features. The maximum margin will be calculated in each plane, and the sides of the plane will be assigned to different classes. The plane is also a reinforcement used for future data points to be classified on either side of the plane's sides. Fig. 3 shows an overview of the SVM model. The maximum margin and the data point classification are calculated as Eq. 2, where the hypothesis function is h, vector x, and vector w.

$$h(x_i) = \begin{cases} +1 & \text{if } w.x + b >= 0 \\ -1 & \text{if } w.x + b < 0 \end{cases} \tag{2}$$

Since SVM is useful in detecting complex relationships between classes, it is less sensitive to outliers and anomalies [16].

3) Decision Tree (DT): Decision tree (DT) classifier intends to maintain a decision based upon learning a hierarchy of if\else tests of each decision point within a hierarchy of connecting nodes, starting from the root node to leaf node. It navigates all possible tests within the hierarchy and finds the most informative test of a target variable. Fig. 4 depicts an overview of a DT model. Gini index and entropy criteria are important measures to determine the optimum split of the tree features and are calculated through Eq. 3 and Eq. 4, respectively.

$$Gini_{index} = 1 - \sum_j p_j^2, \tag{3}$$

where $0 \leq Gini_{index} \leq 1$ and p_j is the probability of class j.

$$Entropy \ = - \sum_j p_j \cdot log_2 \cdot p_j, \tag{4}$$

where p_j is the probability of class j.

Although DT is known to be used for classification and regression tasks and tends to work well with completely different scale features, it is over-fitting and may provide poor generalization performance for models [37].

4) Random Forests (RF): Random Forests (RF) is a well-known regression and classification model. RF encompasses the collection of decision trees in which each tree could override part of the dataset. RF averages each tree's final results at the end of the prediction process and finalizes it. Fig. 5 provides an overview of the RF model.

Although RF surpasses the individual DT and its deficiencies, handles vast datasets, and its training stage can be rapidly executed in parallel, RF does not operate well on very high-dimensional or sparse data. Moreover, it requires massive computing resources for prediction tasks [37].

5) Artificial Neural Network (ANN): An ANN is an advanced ML model used to construct prediction models. It mimics the slender projection's structural function through human brain nerve cells [16]. ANN has been seen as a generalization of linear models, executing different processing segments to reach a decision [37]. ANN consists of interconnected functions, known as nodes, that interact with each other through axon-like edges to maintain a network of nodes. Each input node then passes information through the network's edges to the next layer of nodes. The model's predicted output is compared with the actual output, which is understood to be right, using supervised learning. The expense's magnitude defines the difference between these two outcomes. Conventional neural networks can be subdivided into input, hidden, and output layers. Input (i.e. datasets' points) is initially received through the input layer, where the features are detected. The hidden layer(s) will then analyze and process the input features, and the final result will be shown as the output layer. The training goal is to reduce the value of the cost until the estimation of the model accurately reflects the correct output. One of the main advantages of neural networks is that they can detect the information contained in massive amounts of data given adequate time for computing, data and careful tuning. Fig. 6 depicts an overview of the ANN model. The cost of an ANN is calculated through the activation function as demonstrated in Eq. 5.

$$\hat{y} = w[0] * x[0] + w[1] * x[1] + ... + w[p] * x[p] + b, \tag{5}$$

where $\hat{y}$ is the weighted sum of the input features $x[0]$ to $x[p]$, and weighted by the learned coefficients $w[0]$ to w[p].

It often takes a long time to train neural networks, especially large/strong ones. Besides, they require proper pre-processing of the information. Also, they work best with

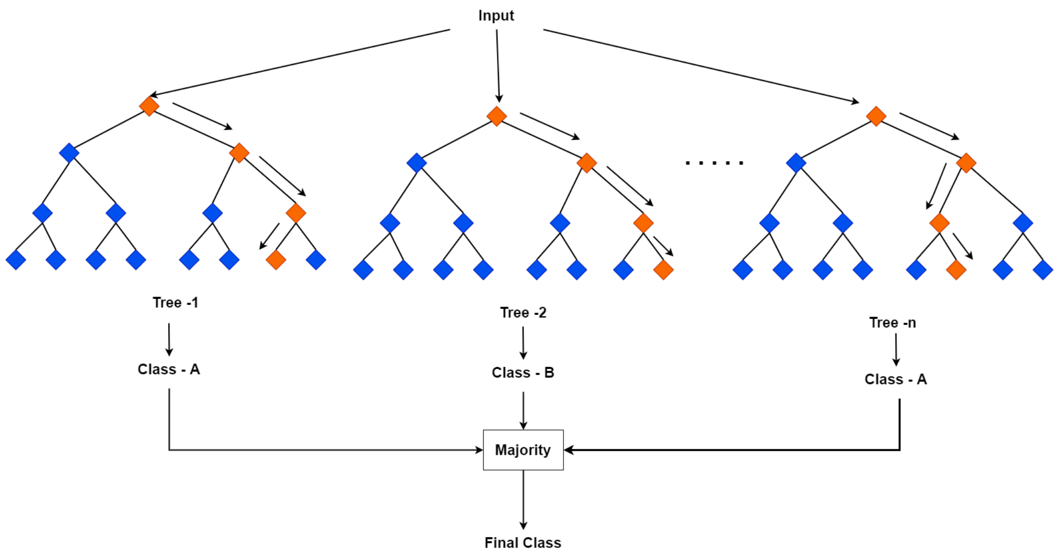

Fig. 5. Averaging each DT's Results to Arrive at the Final Class Through RF Classifier.

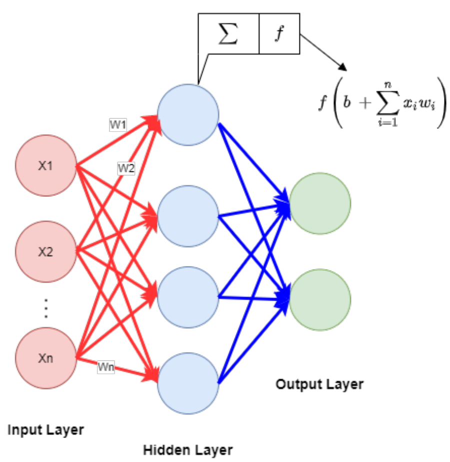

Fig. 6. Overview of ANN Classifier with Three General Layers, where x_i Represents an Input, w_i is Corresponding Weight, b is bias, and f is the Activation Function to be Applied to the Weighted Sum of the Inputs.

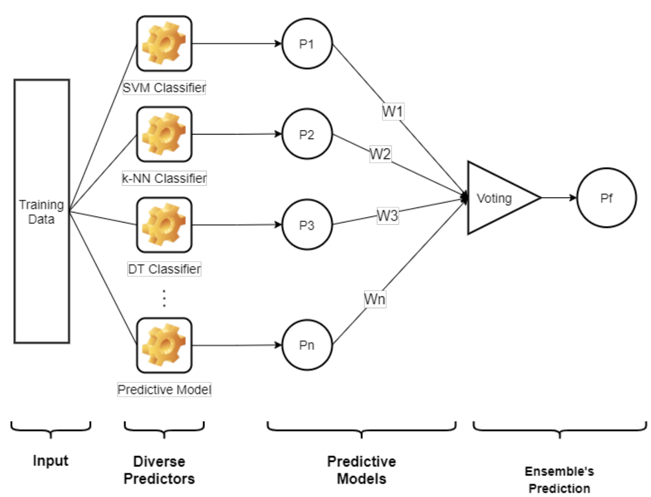

Fig. 7. Overview of an Aggregate of the Predictions of MLCs and the Prediction of Predict the Class that Gets the Most Votes, where P_n Represents Model Feature, W_n Represents Model Weight, and P_f Represents the Majority Vote.

"homogenous data", where all features have similar meanings [16].

6) Ensemble Learning Method: Ensemble learning method - advanced ML classification model - considers and tests more than one ML model and finds the best model for input data to combine ML models. The ensemble learning method integrates various ML models into a single prediction using a complete analysis data voting system. These two methods, together, provide additional benefit over any homogeneous model. Fig. 7 depicts an overview of an ensemble learning method.

While the ensemble learning method performance exceeds a single algorithm in many other homogeneous models, the degree of complexity and sophistication of the method can be a potential drawback. The ensemble learning method produces the same advantages as the single ML model, where transparency and ease of interpretation are surrendered to the accuracy of a more complex algorithm, such as RF, bagging or boosting [16].

B. Proposed Model

The current rapid and exponential increase in the number of infected patients has necessitated an accurate estimation of suitable ML models' potential outcomes. We propose a novel model based on MLCs to investigate and predict the severity of the asymptomatic carriers and the possible death rate. The model entails various MLCs, including k-NN (refer to Section III-A1), DT (refer to Section III-A3), RF (refer to Section III-A4), SVM (refer to Section III-A2) and the ensemble learning method (refer to Section III-A6). The model uses a private dataset's clinical characteristics in Saudi Arabia (refer to Section III-B1). In addition, model performance has been evaluated in terms of accuracy based on the confusion matrix [38]. The proposed model can be built from scratch or by using the existing pre-trained models. Data acquired from the hospital(s) will be separated into training and testing clusters.

The proposed model architecture consists of five main phases, namely data acquisition, pre-processing, feature extraction, feature selection, and classification. An overview of the proposed model is presented as Fig. 8, and the primary taken stages are presented in Pseudocode 1.

Algorithm 1: Proposed algorithm to investigate and forecast the incidence and the potential death risk of the asymptomatic carriers.

```
Input: COVID-19 Positive Patients (CPP) Dataset
Output: Recovery from ICU, Recovery Without ICU,
        Death
Extract features from CPP Dataset
Pre-process features
Normalize input dataset
Select feature from the dataset
Initialize dataset_train & dataset_test
Train and validate (dataset_train, dataset_test)
[X_train, X_test, Y_train, Y_test]
Initialize ML models
Input the readings to the model
Train the ML model
Test unseen input dataset
for each Fold in range (10) do
    Evaluate Loss, Validation Loss
    Evaluate Accuracy and Validation Accuracy
    Evaluate Precision, F-Score, Roc Curve and
      Confusion matrix
end
```

First, we acquired the private dataset in Saudi Arabia. Second, pre-processing was performed on the acquired dataset, and the entire health dataset was cleaned for prediction purposes. Third, the model used Principle Components Analysis (PCA) for feature selection and vital known classification methods from the dataset. Then, the selected features were utilized to train and test the MLCs. Finally, various classification methods were used to classify testing data.

1) COVID-19 Positive Patients (CPP) Dataset: Across all Saudi Arabian regions, a private COVID-19 Positive Patients (necessitated) dataset [6] was collected between March 1, 2020, and March 31, 2020, with no exclusion criteria. The diagnosis of COVID-19 was conducted based on the performance of real-time reverse transcription-polymerase chain reaction (RRT-PCR) tests in a quantitative study undertaken at the Saudi National Health Laboratory. The patients' data were stored at the Saudi Health Electronic Surveillance Network Database (HESN)[2] under the authority of the Global Center for Mass Gatherings Medicine. The HESN contains demographic characteristics, COVID-19-positive clinical, lab, and raw outcome data in all Saudi Arabian regions. All efforts have been made to preserve the data's confidentiality and autonomy. A study identification number was allocated to all subjects. In the dataset, 12.5 % of all patients served in healthcare facilities, and 17.3 % were asymptomatic.

[2]Site: https://hesn.moh.gov.sa/webportal/

Table I depicts an overview of the dataset, and Table II presents an overview of the dataset features' profile. The dataset contains 18 numerical variables, 15 Boolean variables, and 11 categorical variables. The dataset has 639 records with 44 features, and it contains demographic and clinical data for live patients.

2) Data Pre-processing: Since the dataset was unbalanced, there were many missing values, each variable was unique, and data were imputed to handle the missing entries as necessary. This dataset has three variable types: 1) Boolean, 2) numerical, and 3) categorical. The "Outcome" feature was designated as an independent variable, and the other features were designated as dependent variables during the models' training."Outcome" feature has three classes, namely "Active ICU or Recovery with history of ICU", "Death", and "Recovery No ICU". In the dataset, we have a record of 639 patients. Out of 639 patients, 563 patients belong to the "Recovery No ICU" class, 65 patients belong to the "Active ICU or Recovery with history of ICU" class, and only 11 patients belong to the "Death" class. Due to shallow death cases in training data, sometimes the classifiers cannot correctly predict the "Death" classes. The Synthetic Minority Over-sampling Technique (SMOTE) [39] was applied to the whole dataset to deal with its unbalanced nature. SMOTE aims to balance the dataset by oversampling the minority class and duplicating the same entities without any new information. After applying SMOTE to the dataset, we have 563 patients in each class.

Boolean features ("Fever_PRESENT", "SoreThroat", "RunnyNose_PRESENT") entail "Yes" and "No" values where "Yes" means the symptom was present and "No" means the symptom was not present. In order to unify the code system within the entries, we replaced the "Yes" with "1" and "No" with "0" notations. In the "age_65" feature, there were two entries, "1" and "2" where "1" means a person was younger than 65, and "2" means a person was older than 65. In this variable, "1" was replaced with "0" and "2" was replaced with "1". Empty entries in these variables are replaced with "0" assuming that the symptom is not present. Other Boolean variables ("any_comorbidity", "DM1", "HTN1", "CRF1", "cardiac1", "asthma1", "cancer_immunodefecincy1", "C_lungdisease") used the binary code system "0" and "1". Therefore, they are left untreated in the pre-processing part.

Numerical features ("comorbidities", "LOSdays", "Smoking", "dayofExposureifknown", "Incubation", "Temperature", "HEART_RATE", "RESPIRATOR", "SBP", "DBP", "SATURATION", "WHITE_CELLS", "CREATININE", "LYMPHOCYTES", "PLATELET", "NEUTROPHILS", "BLOOD") entailed missing values that were replaced with a median of their corresponding variable. Besides, categorical features ("ClassificationGroup", "Gender", "Nationality", "Outcome") had some missing values that were replaced with others. Other numerical features ("Myalgiaonset", "GIsymptomsonset", "Headacheonset" entailed different scales that did not contribute equally to the models fitting. The "MinMax" scaler was applied to all these variables to scale the values on the same scale and prevent the problems caused by these values.

Categorical features ("Myalgiaonset", "GIsymptomsonset", "Headacheonset") entailed intervals, for instance, "1_2" that implied an individual read of a symptom occurred every two

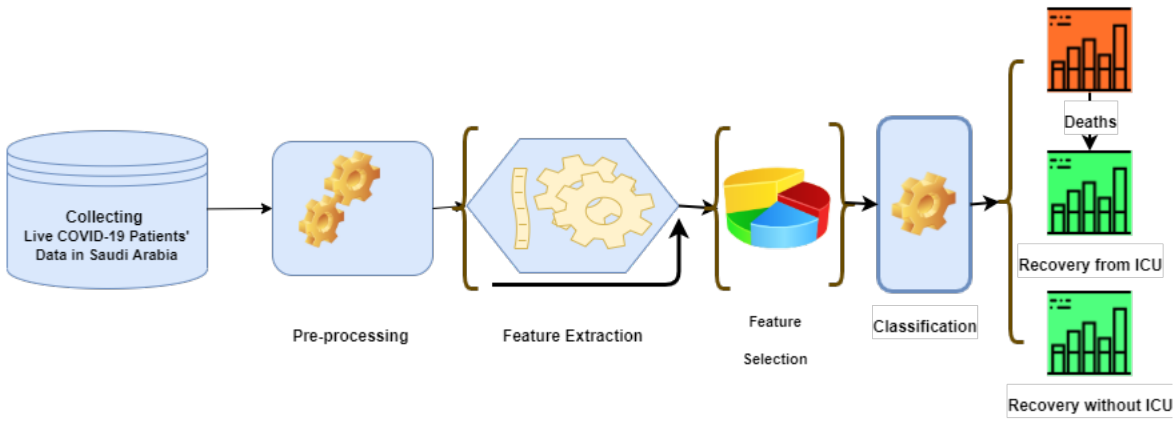

Fig. 8. Architecture of the Proposed Model to Investigate and Forecast the Incidence and the Potential Death Risk of the Asymptomatic Carriers.

TABLE I. DESCRIPTION OF THE 2019 CORONAVIRUS DISEASE (COVID-19) POSITIVE PATIENTS (CPP) DATASET.

Feature	Description	Initial Value	Null values(%)	Datatype
InvID	-	-	0	Categorical
ClassificationGroup	Epidemiological criteria	Case, Contact	0	Categorical
ClientName	-	-	0	Categorical
Outcome or Outcome_Modified	Admission status outcome	Recovery No ICU, Recovery with history of ICU, Death	0	Categorical
LOSdays	length of stay in days	-	1.3	Numerical
HCW_totalpop	Patient's occupation (Medical staff, Military, others)	"0", "1", "2"	0	Categorical
comorbidities	-	-	0.2	numerical
any_comorbidity	Any comorbidity?	(Yes, No)	0	Categorical
morethan2comorbidities	Two or more comorbidities?	(Yes, No)	0	Categorical
DM1	Diabetes?	(Yes, No)	0	Categorical
HTN1	Hypertension?	(Yes, No)	0	Categorical
CRF1	Chronic kidney disease?	(Yes, No)	0	Categorical
cardiac1	Heart diseases?	(Yes, No)	0	Categorical
asthma1	Asthma and chronic lung disease?	(Yes, No)	0	Categorical
cancer_immunodeficiency1	immunodeficiency?	(Yes, No)	0	Categorical
C_lungdisease	Lung disease?	(Yes, No)	0	Categorical
Smoking	Smoker?	(Yes, No)	0.2	Categorical
age_65	Age Above 65?	(Yes, No)	0	Categorical
Gender	Patient gender	Male, Female	0	Categorical
Nationality	nationality	Saudi Arabia, Egypt, Philippines, Sudan, India, and many others.	5.6	Categorical
SYMPTOMATIC	Symptomatic?	(Yes, No)	57.7	Categorical
Fever_PRESENT	Fever?	(Yes, No)	38	Categorical
Cough_PRESENT	Cough?	(Yes, No)	65.1	Categorical
SoreThroat_PRESENT	Sore Throat?	(Yes, No)	77.6	Categorical
RunnyNose_PRESENT	Runny nose?	(Yes, No)	85	Categorical
Headacheonset	Headache frequency	"0", "1_1", "1_2", "1_3"	21.6	Categorical
Myalgiaonset	Myalgia frequency	"0", "1_1", "1_2", "1_5"	21.6	Categorical
GIsymptomsonset	GI symptoms frequency including abdominal pain, vomiting, or diarrhea	"0", "1_1", "1_2", "1_3", "1_4"	21.6	Categorical
dayofExposureifknown	-	-	64.9	Numerical
Incubation	-	-	65.1	Numerical
Temperature	oral temperature of 38° or higher	-	58.5	Numerical
HEART_RATE	Heart beats per minute	-	82.2	Numerical
RESPIRATORY	number of breaths for an entire minute	-	83.6	Numerical
SBP	Systolic Blood Pressure	-	82.3	Numerical
DBP	Diastolic Blood Pressure	-	82.2	Numerical
SATURATION	Oxygen level	-	59.9	Numerical
WHITE_CELLS	White cell count	-	94.7	Numerical
CREATININE	Creatine phosphate from muscle and protein metabolism count	-	96.9	Numerical
LYMPHOCYTES	lymphocyte count of less than 1,500 per 1 Mio. m^3		96.4	Numerical
PLATELET	Platelet counts in the blood	-	94.8	Numerical
NEUTROPHILS	White blood cell type level	-	95.6	Numerical
SEVERITY	Patients' conditions	"0","3"	0	Categorical

TABLE II. PROFILE INFORMATION OF THE CPP DATASET

Feature	Min.	Max.	Mean	Std. deviation
LOSdays	0	60	7.71	9.59
comorbidities	0	5	0.47	0.87
age_computed	0	84	36.59	15.57
dayofExposureifknown	1	30	8.5	6.30
Incubation	1	30	7.21	6.12
Temperature	0	39.1	37.05	2.37
HEART_RATE	63	125	89.82	14.19
RESPIRATORY	14	30	19.87	2.48
SBP	60	188	125.12	17.22
DBP	57	116	75.03	10.46
SATURATION	69	100	96.68	3.63
WHITE_CELLS	0	17	6.53	3.96
CREATININE	0	145	64.55	43.63
LYMPHOCYTES	6.3	58.1	24.43	13.00
PLATELET	107	572	246.52	92.53
NEUTROPHILS	1.37	93.4	48.68	32.52

TABLE III. SAMPLE OF CONFUSION MATRIX

		Actual class	
		P	N
Predicted class	P	T_P	F_P
	N	F_N	T_N

days. There were some empty entries in these variables, and they were replaced with the median of each variable.

"Client name" and "InvID" are removed because these variables have no role in classification.

C. Experimental Setup

In this work, the ML methods were executed using Python programming language (version 3.7) in Google Colaboratory (Colab)[3]. Colab is a web-based platform intended to run python code and customized for AI and data analysis tasks. Colob provides on-demand computing services for ML-related tasks. The following specifications were used: CPU (Intel Xeon 2.20 GHz, family 6, Model 79), RAM (1 GB), and Storage (Google Drive with 69 GB), including all the necessary libraries: Pandas, sklearn, NumPy, Seaborn, SciPy, Keras, ELI5, and TensorFlow.

D. Performance Evaluation Metrics

To accurately predict ICU admission depending on multiple COVID-19 symptoms and patients' clinical characteristics, accuracy is vital. A comparative analysis has been conducted between MLCs and the ensemble learning method for COVID-19 infected patient classification in this study. Based on the confusion matrix parameters, "accuracy", "precision", and "f-score" will be calculated to investigate the accuracy of the proposed approach. The confusion matrix is represented in Table III.

A few notations are used within the evaluation metrics. True Positive (T_P) is the number of true positives classified by the prediction model. True Negative (T_N) is the number of true negatives classified by the prediction model. False Positive (F_P) is the number of false positives classified by the prediction model. False Negative (F_N) is the number of false negatives classified by the prediction model.

1) Accuracy: The accuracy predictor is the ratio between the total accurate predictions ($TP + TN + FP + FN$) and the total data points of the classifier. Accuracy defines the full variety of correct predictions laid out in percentage. Eq. 6 calculates Accuracy as follows:

$$Accuracy = \frac{T_P + T_N}{T_P + T_N + F_P + F_N}, \tag{6}$$

$where\ 0.0 < Accuracy < 1.0$

2) Precision: The ratio of the True Positive (TP) samples to the sum of the True Positive (TP) and False Positive (FP) samples is equal to the precision predictor. Precision is outlined because of the entire range of correct positive predictions portrayed in percentage. Eq. 7 calculates Precision as follows:

$$Precision = \frac{T_P}{T_P + F_P} \tag{7}$$

3) F Score: The F score is defined as the harmonic mean of precision and recall of the model. Eq. 8 calculates F Score as follows:

$$F\ score = 2 \times \frac{Precision \times Recall}{Precision + Recall} \tag{8}$$

E. Error Metrics

We calculated four error metrics: Root Mean Squared Error (RMSE), Relative Squared Error (RSE), Mean Absolute Error (MAE), and Relative Absolute Error (RAE).

1) Root Mean Squared Error (RMSE): RMSE determines the mean of the magnitude of the error. Eq. 9 calculates RMSE as follows:

$$RMSE = \sqrt{\frac{\sum_{i=1}^{n}(p_i - a_i)^2}{n}}, \tag{9}$$

where a is the actual target, and p is the predicted target.

2) Relative Squared Error (RSE): RSE compares the sum of errors of the model compared to a simple predictor (using the average). Eq. 10 calculates RSE as follows:

$$RSE = \frac{\sum_{i=1}^{n}(p_i - a_i)^2}{\sum_{i=1}^{n}(\bar{a} - a_i)^2} \tag{10}$$

3) Mean Absolute Error (MAE): MAE measures the average of all the absolute errors. Eq. 11 calculates MAE as follows:

$$MAE = \frac{\sum_{i=1}^{n}|p_i - a_i|}{n} \tag{11}$$

4) Relative Absolute Error (RAE): RAE calculates the square root of the relative squared error. Eq. 12 calculates RAE as follows:

$$RAE = \frac{\sum_{i=1}^{n}|p_i - a_i|}{\sum_{i=1}^{n}|\bar{a} - a_i|} \tag{12}$$

[3]Site: https://colab.research.google.com/

TABLE IV. COMPARISON OF THE PROPOSED MODEL WITH THE RELATED MODELS

ML Architecture	Accuracy (%)
Pal et al. [40]	77.6
Tang et al. [41]	87.5
Yan et al. [34]	90
Iwendi et al. [31]	94
Proposed	97.93

TABLE V. OVERVIEW OF PERFORMANCE EVALUATION METRICS OF VARIOUS MLCS AND THE ENSEMBLE LEARNING METHOD

Classifiers	Accuracy	Precision	AUC	F-Score
k-NN	0.87968	0.889014	0.7997	0.86935
SVM	0.94872	0.949557	0.9115	0.94746
DT	0.88166	0.882669	0.8138	0.87966
RF	0.96647	0.96691	0.9358	0.96585
ANN	0.9783	0.97937	0.9508	0.97778
Ensemble learning method	0.94675	0.949887	0.9048	0.9445

IV. RESULTS

This section demonstrates our results from the constructed ML models and the associated evaluation metrics.

A. Comparative Analysis of Various Classifiers

We presented an evaluation of the proposed model for COVID-19 predictive models with the related methods presented in [40], [41], [34], and [31] in Table IV. The proposed model provided 97.93% accuracy, while the comparative models attained an average accuracy of 87.28%, so that the proposed model showed a 10.7% performance gain.

We measured various performance metrics of the used classifiers: Accuracy, Precision, Area Under the ROC Curve (AUC), and F-score. We calculated ANN's results by comparing them with the outcomes obtained from MLCs and the ensemble learning method. We divided the COVID-19 dataset using the beforementioned classifiers into 30% of the dataset for the testing mode and 70% of the dataset for the training mode. All the classifiers' execution time took 0.03 seconds, except ANN, which took 45 seconds.

The performance of the ML methods was calculated and is shown in Fig. 9 and portrayed in tabular form in Table V. Accuracy, Precision, AUC, and F1-score scores of all the classifiers are represented in Fig. 10, Fig. 11, Fig. 12, Fig. 13, respectively.

Using MAE, RMSE, RAE, and RRSE, the error rate of each predictor was calculated and shown in Fig. 14 or Table VI. In Fig. 15, Fig. 16, Fig. 17, and Fig. 18, the different error rates obtained for different classifiers are shown, respectively.

MAE is used to calculate the average absolute difference between the expected and the observed set of values, given that the weight of each difference is the same. The following figure shows that ANN gives the lowest error at 8%, whereas the decision tree is 42%, SVM is 17%, and RF is 13%. Therefore, the ANN model provides a 92% match to actual values with 8% error, while RF provides an 87% match to actual values with only 13% error. The MAE graph is shown in Fig. 15.

TABLE VI. DIFFERENT ERROR METRICS GIVEN BY VARIOUS MLCS AND THE ENSEMBLE LEARNING METHOD

Classifiers	MAE	RMSE	RAE	RRSE
k-NN	0.3452	0.5875	0.2912	0.7247
SVM	0.1755	0.419	0.1382	0.5168
DT	0.426	0.6527	0.3294	0.8051
RF	0.1341	0.3662	0.1	0.4518
ANN	0.0809	0.2844	0.0618	0.3508
Ensemble learning method	0.1598	0.3997	0.1323	0.493

RMSE also calculates the median magnitude of the variations as MAE (i.e. errors). The square root of the mean of the square deviations is RMSE. As RMSE is more suitable than MAE, the ANN model has 28% RMSE, indicating a 78% accurate classification of COVID-19 ICU recoveries, death, and recoveries with 28% error, while RMSE falls between 39% and 60% of the remaining ML models. The RMSE graph is shown in Fig. 16.

RAE is the same as RRSP, which is determined by dividing MAE by the simple classifier error received. The smaller the value of RAE, therefore, the better the prediction. Fig. 17 shows that the proposed ANN method attained 6% of RAE, a superior RAE value.

RRSP provides the forecasts' squared error relative to every data value's mean. It gives more accurate results than simple classifiers by normalizing the values obtained from the simple classifiers (e.g. k-NN or ANN). RRSP divides the total squared error by splitting it with ASE (absolute squared error) obtained from the simple classifiers. Furthermore, the error is minimized by producing a normalized value square root. As shown in Fig. 18, the ANN model exceeds 35%, while other classifiers are greater than RRSE.

The different proposed methods (k-NN, SVM, DT, ANN, RF, and the ensemble learning method) for classification on the CPP dataset yields 87.96%, 94.87%, 88.16%, 97.83%, 96.64%, and 94.67%, respectively. The accuracy of various ML and the ensemble learning methods was ensured compared to the evaluation of classifier error rates by Table VI, as it considers the relative significance of each factor found in the study. Thus, the ANN model provides greater precision than other variants on the CPP dataset by alleviating data inconsistencies.

Table VII shows the p-values obtained using the student test while examining possible significant differences by various pairs of classifiers. We calculated p-values between MLCs against each other, and then calculated p-values between MLCs and the ensemble learning method. By comparing the ANN and k-NN classifiers, the p-values are smaller than 0.05, by which there was no significant difference (i.e. rejecting the null hypothesis). Comparing ANN, RF and the ensemble learning method, the p-values are smaller than 0.05, by which there was no significant difference (i.e. rejecting the null hypothesis).

However, when we compare ANN and SVM against RF, the p-values are larger than 0.05, by which there was a significant difference (i.e. accepting the null hypothesis). When we compare k-NN and SVM against RF, the p-value is smaller than 0.05, by which there was no significant difference (i.e. rejecting the null hypothesis). When we compare k-NN and

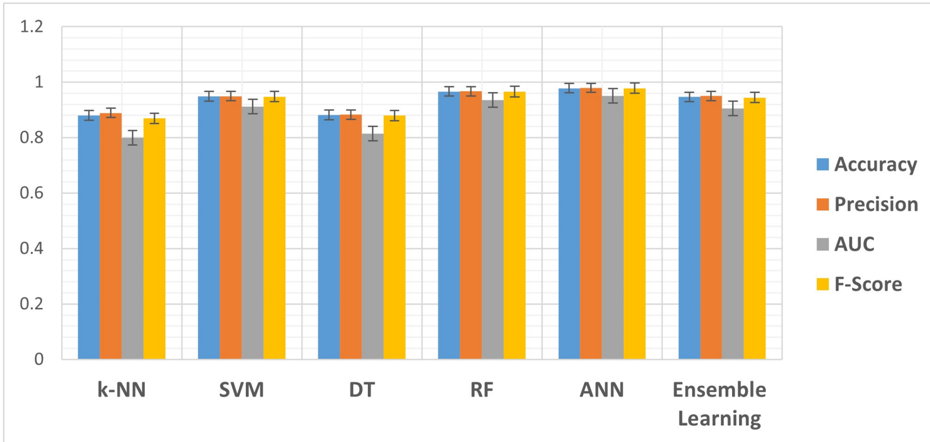

Fig. 9. Comparison of Performance Analysis of Various MLCs and the Ensemble Learning Method.

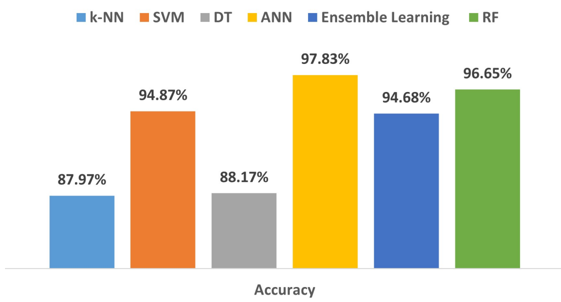

Fig. 10. Accuracy Scores of Various MLCs and the Ensemble Learning Method.

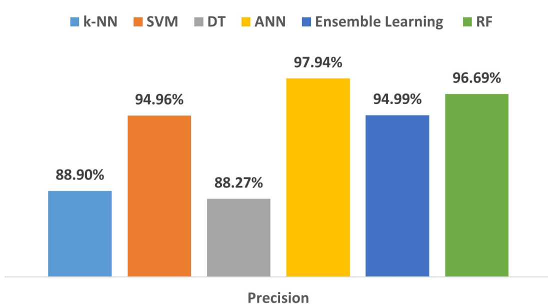

Fig. 11. Precision Score of Various MLCs and the Ensemble Learning Method.

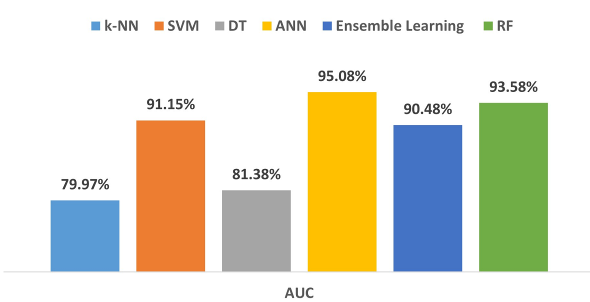

Fig. 12. AUC Scores of Various MLCs and the Ensemble Learning Method.

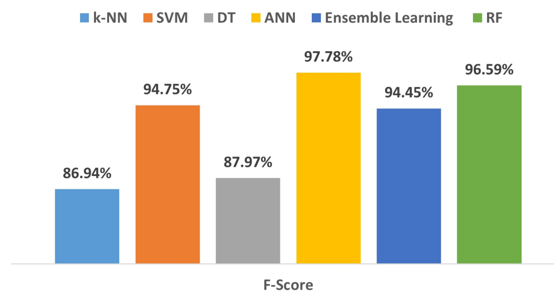

Fig. 13. F-Score Scores of Various MLCs and the Ensemble Learning Method.

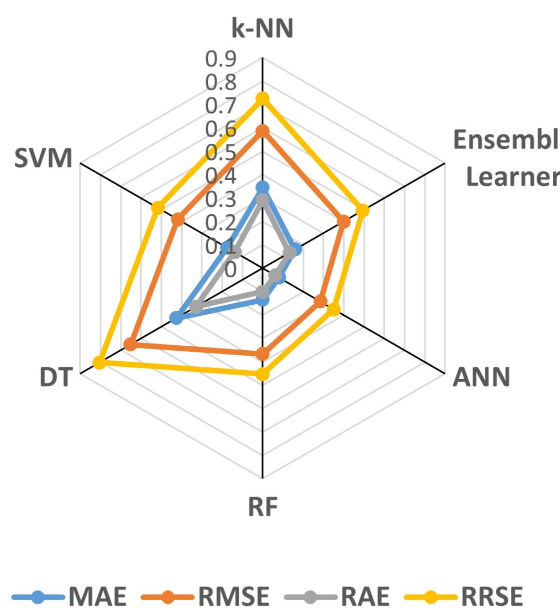

Fig. 14. Different Error Metrics Given by Various MLCs and the Ensemble Learning Method.

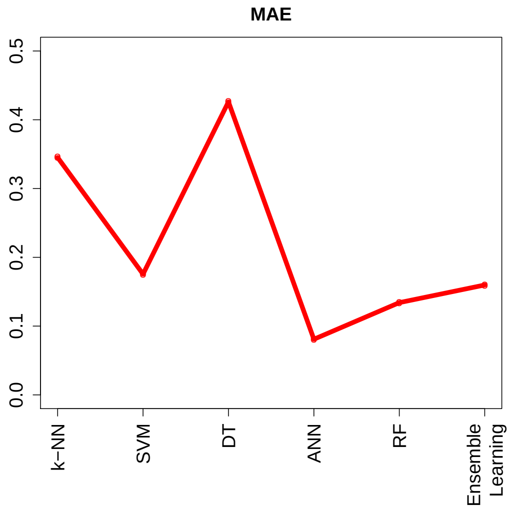

Fig. 15. Mean Absolute Error (MAE) Analysis of Individual MLCs and the Ensemble Learning Method.

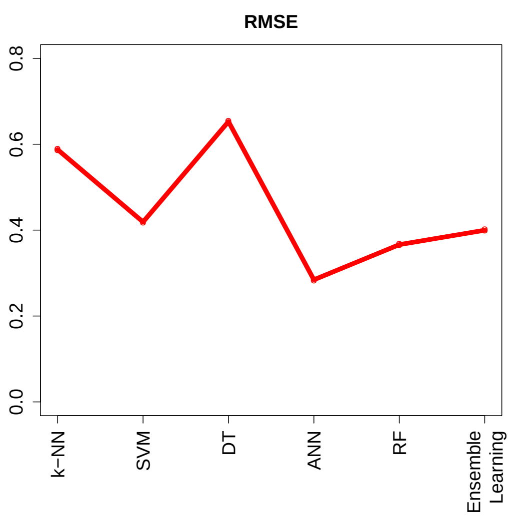

Fig. 16. Root Mean Square Error (RMSE) Analysis of Individual MLCs and the Ensemble Learning Method.

TABLE VII. P-VALUES OF VARIOUS CLASSIFIER SCORES

Algorithms	t-test	p value
ANN - k-NN	3.191458	0.012775
ANN - SVM	0.910476	0.38918
ANN - DT	2.106662	0.06822
ANN - RF	-0.81257	0.439975
ANN - Ensemble learning method	3.191458	0.012775
k-NN - SVM	-2.80261	0.023105
k-NN - DT	-1.06956	0.316024
k-NN - RF	-4.12081	0.00334
k-NN - Ensemble learning method	0	1
SVM - DT	1.596006	0.149154
SVM - RF	-2.15321	0.063458
SVM - Ensemble learning method	2.802612	0.023105
DT - RF	-2.99951	0.017085
DT - Ensemble learning method	1.069559	0.316024
RF - Ensemble learning method	4.120807	0.00334

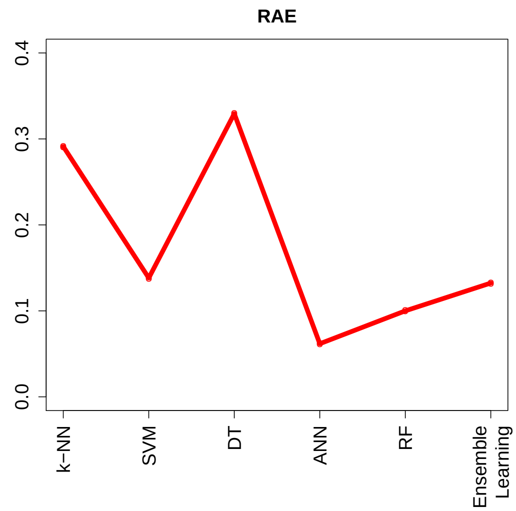

Fig. 17. Relative Absolute Error (RAE) from Various MLCs and the Ensemble Learning Method.

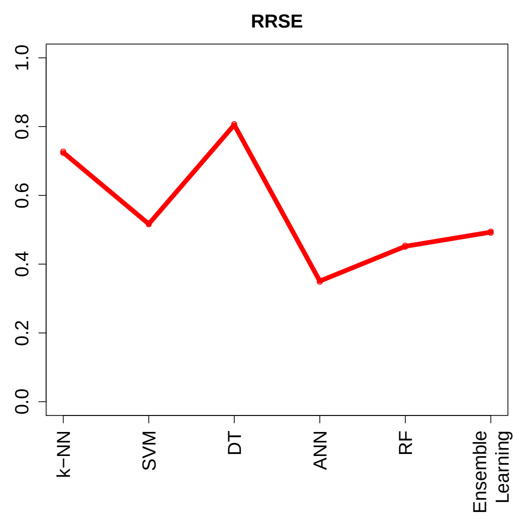

Fig. 18. Root Relative Squared Error (RRSE) from Various MLCs and the Ensemble Learning Method.

DT against the ensemble learning method, the p-value is larger than 0.05, by which there was a significant difference (i.e. accepting the null hypothesis). Similarly, the null hypothesis was accepted, and there was a significant difference when comparing SVM against RF. When comparing SVM with the ensemble learning method, the p-value was less than 0.05, by which there was no significant difference (i.e. rejecting the null hypothesis). Finally, when we compare DT's p-value with RF and RF with the ensemble learning method, the null hypothesis is rejected, so there is no significant difference among them. However, when comparing DT with the ensemble learning method, the null hypothesis was accepted.

V. DISCUSSION

Early COVID-19 prediction could help reduce healthcare systems' enormous burden by diagnosing patients with it. In

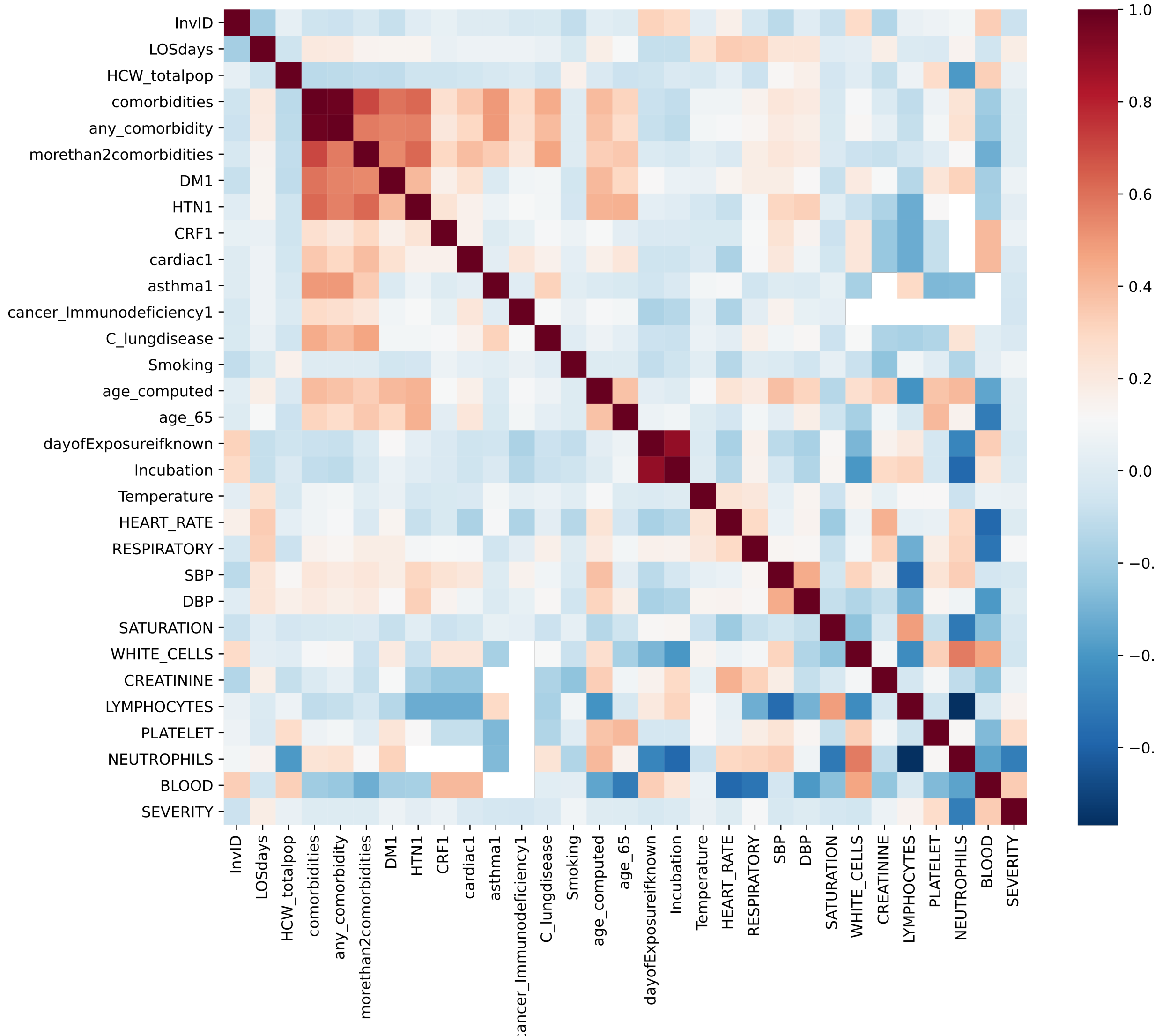

Fig. 19. Heatmap of Correlation Coefficient of CPP Dataset Features.

this study, k-NN, SVM, DT, RF, ANN, and the ensemble learning methods were constructed to predict patients' ICU admission with a CPP dataset for Saudi Arabian residents. Accuracy, Precision, AUC, and F-score were used to measure all models' performance.

Fig. 19 demonstrates various characteristics, including clinical conditions (fever, cough, sore throat, runny nose, headache, myalgia), GI symptoms, and blood work indicators (oxygen saturation, immune cells, creatinine, lymphocytes, platelet, neutrophils) and others, against the ”Outcome“ feature, which is an independent variable. Besides, commodities increase “LoSdays” and “Severity”. Also, “age_65” correlates with “commodities”. It was not expected that there would be no correlation between smoking and “LoSdays” or “Severity”.

The feature importance for the dataset is shown for ANN and the ensemble learning method in Fig. 20 and Fig. 21, respectively.

From Fig. 20, the ANN model indicated that “LOSdays” is the most important feature among all the dependent features, while some clinical characteristics, such as “Myalgiaonset” or “Headacheonset”, are the least important features of the dataset. From Fig. 21, the ensemble learning method indicated that a patient's occupation and “LOSDays” are the most important features among all the dependent features of the dataset, while some clinical characteristics, such as cough or hypertension, are the least important features.

VI. Conclusion and Future Work

Non-clinical methods, for instance, ML models, have been utilized as an alternative means for diagnosis and prognosis. In this study, a model was proposed to predict COVID-19 patients admission to the ICU was established with the CPP dataset using MLCs and the ensemble learning method in Saudi Arabia. The models were trained with 70% of the training data and tested with 30% of the data remaining. In terms of precision, the model developed with ANN was the best model among all models with 97.83%. This study

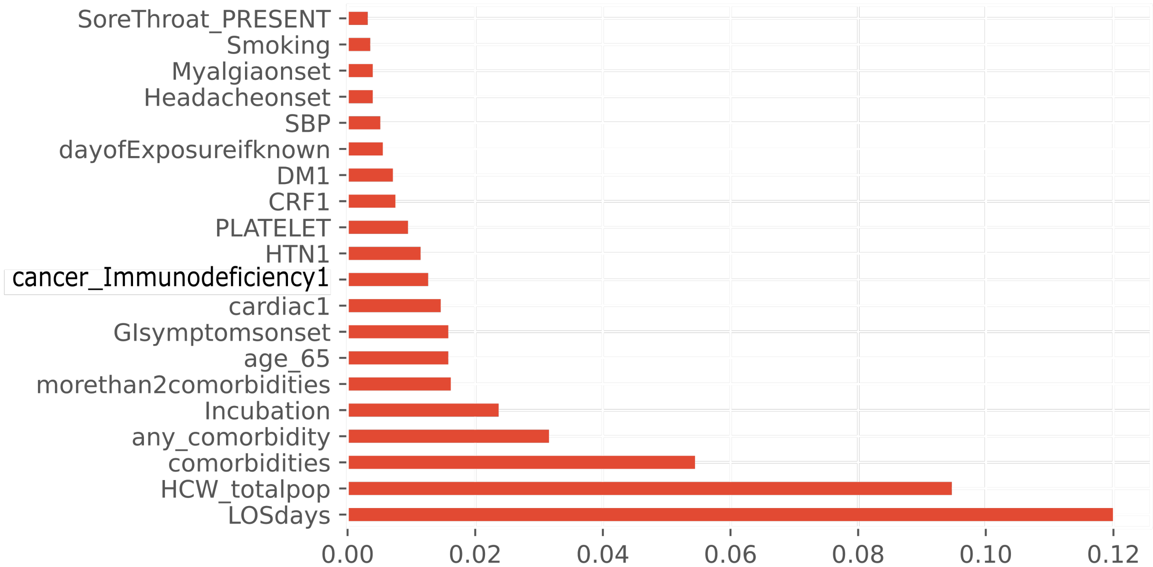

Fig. 20. Feature Importance Computed from ANN that was Fitted to CPP Dataset.

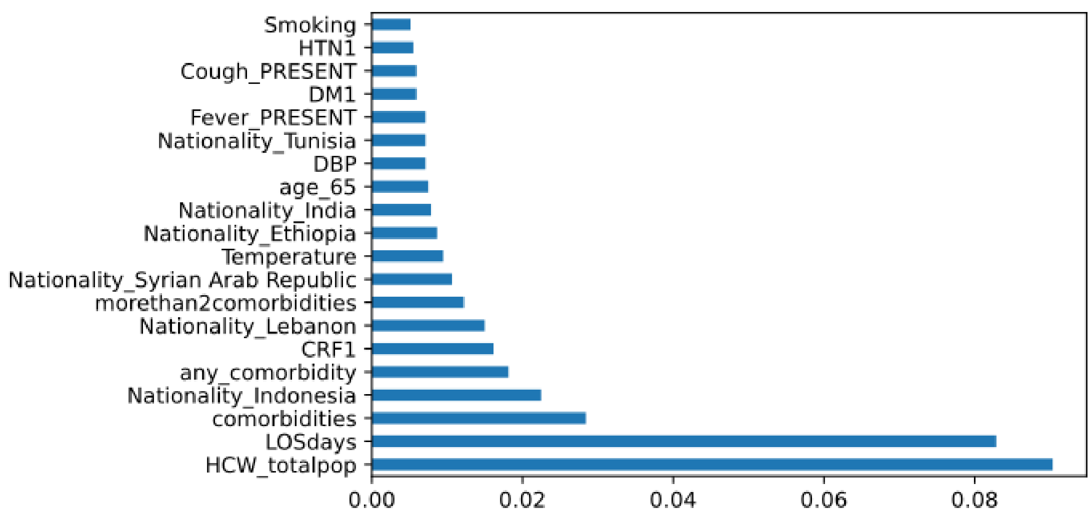

Fig. 21. Feature Importance Computed from the Ensemble Learning Method that was Fitted to CPP Dataset.

shows how it is possible to develop, validate, and use ML Predictive COVID-19 infection models as tools for ICU admission prediction. The models developed would potentially be vital in the battle against COVID-19 in healthcare. Future work will compare the current ML models against another prediction model, for instance, Ada boost. The developed models could be incorporated into decision–support systems for semi-autonomous diagnostic devices with rapid screening and diagnosis of possible outbreaks.

A. *Data Availability Statement*

The dataset presented in this study is private property for the Global Center for Mass Gatherings Medicine.

B. *Authors Contributions*

MZK, YA, RA, AA, AAK: idea conceptualization and project administration. HG, MZK, RA: methodology, investigation, data curation, and writing—original draft preparation. HG, MK: software. HG, MZK: validation and visualization. HG, MZK: formal analysis. YA, RA, AA: resources. HG, MZK, YA, RA, AA: writing—review and editing, supervision. The authors declared that they have read and agreed to the manuscript's published version.

C. *Funding*

There is no funding for the project.

D. *Conflict of Interests*

All authors declared that there are no conflicts of interest.

Acknowledgment

This project has resulted from the collaboration between the Global Center for Mass Gatherings Medicine and the College of Computer Science and Engineering in Taibah University, starting from October 1, 2020 until February 20, 2021.

References

[1] R. Li, S. Pei, B. Chen, Y. Song, T. Zhang, W. Yang, and J. Shaman, "Substantial undocumented infection facilitates the rapid dissemination of novel coronavirus (SARS-CoV-2)," *Science*, vol. 368, no. 6490, pp. 489–493, May 2020. [Online]. Available: https://www.sciencemag.org/lookup/doi/10.1126/science.abb3221

[2] F. Zhou, T. Yu, R. Du, G. Fan, Y. Liu, Z. Liu, J. Xiang, Y. Wang, B. Song, X. Gu, L. Guan, Y. Wei, H. Li, X. Wu, J. Xu, S. Tu, Y. Zhang, H. Chen, and B. Cao, "Clinical course and risk factors for mortality of adult inpatients with COVID-19 in Wuhan, China: a retrospective cohort study," *The Lancet*, vol. 395, no. 10229, pp. 1054–1062, Mar. 2020. [Online]. Available: https://linkinghub.elsevier.com/retrieve/pii/S0140673620305663

[3] World Health Organization, "Statement on the second meeting of the International Health Regulations (2005) Emergency Committee regarding the outbreak of novel coronavirus (2019-nCoV)," Jan. 2020, publisher: World Health Organization. [Online]. Available: https://cutt.ly/tkrihlz

[4] ——, "WHO Director-General's opening remarks at the media briefing on COVID-19 - 11 March 2020," Mar. 2020, publisher: World Health Organization. [Online]. Available: https://cutt.ly/KkrikaE

[5] "WHO COVID-19 Dashboard," 2020. [Online]. Available: https://covid19.who.int/

[6] Y. M. Alsofayan, S. M. Althunayyan, A. A. Khan, A. M. Hakawi, and A. M. Assiri, "Clinical characteristics of covid-19 in saudi arabia: A national retrospective study," *Journal of Infection and Public Health*, vol. 13, no. 7, pp. 920–925, 2020. [Online]. Available: http://www.sciencedirect.com/science/article/pii/S1876034120304925

[7] World Health Organization, "Saudi Arabia: WHO Coronavirus Disease (COVID-19) Dashboard," publisher: World Health Organization. [Online]. Available: https://covid19.who.int

[8] A. Khan, S. Althunayyan, Y. Alsofayan, R. Alotaibi, A. Mubarak, M. Arafat, A. Assiri, and H. Jokhdar, "Risk factors associated with worse outcomes in COVID-19: a retrospective study in Saudi Arabia," *Eastern Mediterranean Health Journal*, vol. 26, no. 11, pp. 1371–1380, Nov. 2020. [Online]. Available: https://applications.emro.who.int/emhj/v26/11/1020-3397-2020-2611-1371-1380-eng.pdf

[9] Ministry of Health, KSA, "MOH Publications - Saudi Arabia's Experience in Health Preparedness and Response to COVID-19 Pandemic," The Saudi Ministry of Health, Riyadh, Saudi Arabia, Tech. Rep., Aug. 2020. [Online]. Available: https://www.moh.gov.sa/en/Ministry/MediaCenter/Publications/Pages/Publications-2020-10-27-001.aspx

[10] World Health Organization, "Operational planning guidance to support country preparedness and response," World Health Organization, Geneva, Switzerland, Tech. Rep., May 2020. [Online]. Available: https://cutt.ly/pkriWU0

[11] J. Gallagher, "Coronavirus: What we still don't know about Covid-19," *BBC News*, Mar. 2020. [Online]. Available: https://www.bbc.com/news/health-52006988

[12] C. Heneghan, J. Brassey, and T. Jefferson, "COVID-19: What proportion are asymptomatic?" Apr. 2020. [Online]. Available: https://www.cebm.net/covid-19/covid-19-what-proportion-are-asymptomatic/

[13] Centers for Disease Control and Prevention, "Coronavirus Disease 2019 (COVID-19) – Symptoms," Dec. 2020. [Online]. Available: https://www.cdc.gov/coronavirus/2019-ncov/symptoms-testing/symptoms.html

[14] G. Meyerowitz-Katz and L. Merone, "A systematic review and meta-analysis of published research data on COVID-19 infection-fatality rates," Epidemiology, preprint, May 2020. [Online]. Available: http://medrxiv.org/lookup/doi/10.1101/2020.05.03.20089854

[15] Ministry of Health, KSA, "COVID-19 Dashboard: Saudi Arabia," 2021. [Online]. Available: https://covid19.moh.gov.sa/

[16] O. Theobald, *Machine learning for absolute beginnners: a plain English introduction*. Scatterplot Press, 2018.

[17] F. Rustam, A. A. Reshi, A. Mehmood, S. Ullah, B.-W. On, W. Aslam, and G. S. Choi, "COVID-19 Future Forecasting Using Supervised Machine Learning Models," *IEEE Access*, vol. 8, pp. 101 489–101 499, 2020. [Online]. Available: https://ieeexplore.ieee.org/document/9099302/

[18] F. Petropoulos and S. Makridakis, "Forecasting the novel coronavirus COVID-19," *PLOS ONE*, vol. 15, no. 3, p. e0231236, Mar. 2020. [Online]. Available: https://dx.plos.org/10.1371/journal.pone.0231236

[19] G. Grasselli, A. Pesenti, and M. Cecconi, "Critical Care Utilization for the COVID-19 Outbreak in Lombardy, Italy: Early Experience and Forecast During an Emergency Response," *JAMA*, vol. 323, no. 16, p. 1545, Apr. 2020. [Online]. Available: https://jamanetwork.com/journals/jama/fullarticle/2763188

[20] G. C. Calafiore, C. Novara, and C. Possieri, "A Modified SIR Model for the COVID-19 Contagion in Italy," *arXiv:2003.14391 [physics]*, Mar. 2020, arXiv: 2003.14391. [Online]. Available: http://arxiv.org/abs/2003.14391

[21] I. Nesteruk, "Statistics-based predictions of coronavirus 2019-nCoV spreading in mainland China," Epidemiology, preprint, Feb. 2020. [Online]. Available: http://medrxiv.org/lookup/doi/10.1101/2020.02.12.20021931

[22] N. Ferguson, D. Laydon, G. Nedjati Gilani, N. Imai, K. Ainslie, M. Baguelin, S. Bhatia, A. Boonyasiri, Z. Cucunuba Perez, G. Cuomo-Dannenburg, A. Dighe, I. Dorigatti, H. Fu, K. Gaythorpe, W. Green, A. Hamlet, W. Hinsley, L. Okell, S. Van Elsland, H. Thompson, R. Verity, E. Volz, H. Wang, Y. Wang, P. Walker, P. Winskill, C. Whittaker, C. Donnelly, S. Riley, and A. Ghani, "Report 9: Impact of non-pharmaceutical interventions (NPIs) to reduce COVID19 mortality and healthcare demand," Mar. 2020. [Online]. Available: http://spiral.imperial.ac.uk/handle/10044/1/77482

[23] S. L. Chang, N. Harding, C. Zachreson, O. M. Cliff, and M. Prokopenko, "Modelling transmission and control of the COVID-19 pandemic in Australia," *Nature Communications*, vol. 11, no. 1, p. 5710, Nov. 2020. [Online]. Available: https://www.nature.com/articles/s41467-020-19393-6

[24] B. Wilder, M. Charpignon, J. Killian, H.-C. Ou, A. Mate, S. Jabbari, A. Perrault, A. Desai, M. Tambe, and M. S. Majumder, "the role of age distribution and family structure on Covid-19 dynamics: A preliminary modeling assessment for Hubei and Lombardy," 2020.

[25] M. A. Ruiz Estrada and E. Koutronas, "The Networks Infection Contagious Diseases Positioning System (NICDP-System): The Case of Wuhan-COVID-19," *SSRN Electronic Journal*, 2020. [Online]. Available: https://www.ssrn.com/abstract=3548413

[26] R. Verity, L. C. Okell, I. Dorigatti, P. Winskill, C. Whittaker, N. Imai, G. Cuomo-Dannenburg, H. Thompson, P. G. T. Walker, H. Fu, A. Dighe, J. T. Griffin, M. Baguelin, S. Bhatia, A. Boonyasiri, A. Cori, Z. Cucunubá, R. FitzJohn, K. Gaythorpe, W. Green, A. Hamlet, W. Hinsley, D. Laydon, G. Nedjati-Gilani, S. Riley, S. van Elsland, E. Volz, H. Wang, Y. Wang, X. Xi, C. A. Donnelly, A. C. Ghani, and N. M. Ferguson, "Estimates of the severity of coronavirus disease 2019: a model-based analysis," *The Lancet Infectious Diseases*, vol. 20, no. 6, pp. 669–677, Jun. 2020. [Online]. Available: https://linkinghub.elsevier.com/retrieve/pii/S1473309920302437

[27] C. Anastassopoulou, L. Russo, A. Tsakris, and C. Siettos, "Data-based analysis, modelling and forecasting of the COVID-19 outbreak," *PLOS ONE*, vol. 15, no. 3, p. e0230405, Mar. 2020. [Online]. Available: https://dx.plos.org/10.1371/journal.pone.0230405

[28] Q. Lin, S. Zhao, D. Gao, Y. Lou, S. Yang, S. S. Musa, M. H. Wang, Y. Cai, W. Wang, L. Yang, and D. He, "A conceptual model for the coronavirus disease 2019 (COVID-19) outbreak in Wuhan, China with individual reaction and governmental action," *International Journal of Infectious Diseases*, vol. 93, pp. 211–216, Apr. 2020. [Online]. Available: https://linkinghub.elsevier.com/retrieve/pii/S120197122030117X

[29] J. M. Read, J. R. Bridgen, D. A. Cummings, A. Ho, and C. P. Jewell, "Novel coronavirus 2019-nCoV: early estimation of epidemiological parameters and epidemic predictions," Infectious Diseases (except HIV/AIDS), preprint, Jan. 2020. [Online]. Available: http://medrxiv.org/lookup/doi/10.1101/2020.01.23.20018549

[30] J. T. Wu, K. Leung, and G. M. Leung, "Nowcasting and forecasting the potential domestic and international spread of the 2019-nCoV outbreak originating in Wuhan, China: a modelling study," *The Lancet*, vol. 395, no. 10225, pp. 689–697, Feb. 2020. [Online]. Available: https://linkinghub.elsevier.com/retrieve/pii/S0140673620302609

[31] C. Iwendi, A. K. Bashir, A. Peshkar, R. Sujatha, J. M. Chatterjee, S. Pasupuleti, R. Mishra, S. Pillai, and O. Jo, "COVID-19 Patient Health Prediction Using Boosted Random Forest Algorithm," *Frontiers in Public Health*, vol. 8, p. 357, Jul. 2020. [Online]. Available: https://www.frontiersin.org/article/10.3389/fpubh.2020.00357/full

[32] S. Kutia, S. H. Chauhdary, C. Iwendi, L. Liu, W. Yong, and A. K. Bashir, "Socio-technological factors affecting user's adoption of ehealth functionalities: A case study of China and Ukraine ehealth systems," *IEEE Access*, vol. 7, pp. 90 777–90 788, 2019. [Online]. Available: https://ieeexplore.ieee.org/document/8744204/

[33] S. F. Ardabili, A. Mosavi, P. Ghamisi, F. Ferdinand, A. R. Varkonyi-Koczy, U. Reuter, T. Rabczuk, and P. M. Atkinson, "COVID-19 Outbreak Prediction with Machine Learning," Health Informatics, preprint, Apr. 2020. [Online]. Available: http://medrxiv.org/lookup/doi/10.1101/2020.04.17.20070094

[34] L. Yan, H.-T. Zhang, J. Goncalves, Y. Xiao, and M. Wang, "A machine learning-based model for survival prediction in patients with severe COVID-19 infection," Epidemiology, preprint, Mar. 2020. [Online]. Available: http://medrxiv.org/lookup/doi/10.1101/2020.02.27.20028027

[35] G. Pinter, I. Felde, A. Mosavi, P. Ghamisi, and R. Gloaguen, "COVID-19 Pandemic Prediction for Hungary; A Hybrid Machine Learning Approach," *Mathematics*, vol. 8, no. 6, p. 890, Jun. 2020. [Online]. Available: https://www.mdpi.com/2227-7390/8/6/890

[36] F. A. B. Hamzah, C. H. Lau, H. Nazri, D. V. Ligot, G. Lee, C. L. Tan, M. K. B. M. Shaib, U. H. B. Zaidon, A. B. Abdullah, M. H. Chung, C. H. Ong, and P. Y. Chew, "CoronaTracker: World-wide COVID-19 Outbreak Data Analysis and Prediction," nCoV, preprint, Mar. 2020. [Online]. Available: http://www.who.int/bulletin/online_first/20-255695.pdf

[37] A. C. Müller and S. Guido, *Introduction to machine learning with Python: a guide for data scientists*, 1st ed. Sebastopol, CA: O'Reilly Media, Inc, 2016.

[38] S. V. Stehman, "Selecting and interpreting measures of thematic classification accuracy," *Remote Sensing of Environment*, vol. 62, no. 1, pp. 77 – 89, 1997. [Online]. Available: http://www.sciencedirect.com/science/article/pii/S0034425797000837

[39] K. W. Bowyer, N. V. Chawla, L. O. Hall, and W. P. Kegelmeyer, "SMOTE: synthetic minority over-sampling technique," *CoRR*, vol. abs/1106.1813, 2011. [Online]. Available: http://arxiv.org/abs/1106.1813

[40] R. Pal, A. A. Sekh, S. Kar, and D. K. Prasad, "Neural network-based country wise risk prediction of COVID-19," *Applied Sciences*, vol. 10, no. 18, p. 6448, Sep. 2020, arXiv: 2004.00959. [Online]. Available: http://arxiv.org/abs/2004.00959

[41] Z. Tang, W. Zhao, X. Xie, Z. Zhong, F. Shi, J. Liu, and D. Shen, "Severity Assessment of Coronavirus Disease 2019 (COVID-19) Using Quantitative Features from Chest CT Images," *arXiv:2003.11988 [cs, eess]*, Mar. 2020, arXiv: 2003.11988. [Online]. Available: http://arxiv.org/abs/2003.11988

Applying Custom Algorithms in Windows Active Directory Certificate Services

Alaev Ruhillo
Faculty of Applied Mathematics and Intelligent Technologies
National University of Uzbekistan named after Mirzo Ulugbek, NUUz
Tashkent, Uzbekistan

***Abstract*—The article presents a solution to the problem of not recognizing the O'zDst 1092:2009 algorithm by the operating system and the problem of using digital certificates generated using the O'zDst 1092:2009 algorithm and O'zDst 1106:2009 algorithm. These algorithms were adopted in 2009. But these algorithms are still not recognized by the operating system. For other cryptographic algorithms used in Windows, cryptographic service providers have been developed that provide cryptographic operation functions to other software. These cryptographic service providers do not support the above algorithms. From here it becomes necessary to develop the cryptographic provider supporting the O'zDSt 1106:2009 hashing algorithm and the O'zDSt 1092:2009 signature algorithm. But to work with digital certificates, one cryptographic provider is not enough. Special extensions are also required to encode and decode digital certificate data. Therefore, the development of an extension for cryptographic providers is given. Also, for managing digital certificates and key lifecycle, a method of integrating cryptographic providers with Windows Active Directory Certificate Services is presented. Developed cryptographic providers are composed of 3 types of providers such as hash provider, signature provider, and key storage provider. The architecture of the key storage provider, a method for secure storage of cryptographic keys, as well as key access control are proposed. The description of the O'zDst 1092:2009 algorithm and the implementation of the functions of the Key storage provider interface are shown.**

Keywords*—O'zDSt 1106:2009 hashing algorithm; the O'zDSt 1092:2009 signature algorithm; active directory certificate services; digital certificate; key access control; key storage provider

I. Introduction

Electronic digital signature technology is widely used to ensure the integrity and identification of the owner of an electronic document. Presently in Uzbekistan, tools and methods that allow using O'zDst 1092:2009 signature algorithm do not provide document signing, signature validation and key management, through standard interfaces such as CryptoAPI, Cryptography Next Generation API [1] and PKCS [2], [3], [4], [5], [6]. This raises the problem of using the O'zDst 1092:2009 algorithm in information systems, such as not recognizing the O'zDst 1092:2009 algorithm by the operating system, working with digital certificates generated using the O'zDst 1092:2009 algorithm and O'zDst 1106:2009 algorithm. In Windows, cryptographic service providers are used to work with digital certificates, signing an electronic document, checking the digital signature. Starting with Windows Vista, Microsoft is offering a new Cryptography Next Generation API (CNG API) [1] to perform cryptography operations for applications. Microsoft provides several CNG providers that work with CNG API.

The list of CNG providers developed by Microsoft is shown in Table I.

TABLE I. The List of CNG Providers Developed by Microsoft

CNG Provider	Description
Microsoft Primitive Provider	It supports the following functions: hashing with SHA1, SHA256, SHA384, SHA512, MD2, MD4, MD5 algorithms; signing and signature verification with RSA, DSA and ECDSA algorithms; symmetric encryption and decryption with AES, DES, 3DES, DESX, RC2 and RC4 algorithms; asymmetric encryption and decryption with RSA algorithm; key exchange with DH and ECDH algorithms; random number generation.
Microsoft Software Key Storage Provider	It performs operations on key pairs, especially persistent keys. It creates, exports, imports, deletes and stores key pairs. Key pairs generated by the Microsoft Primitive Provider are not persisted, so the Software Key Storage Provider is used for persistent keys.
Microsoft SSL Protocol Provider	It performs key management operations in SSL and TLS. It is used to establish a secure connection using SSL and TLS on Windows.
Microsoft Smart Card Key Storage Provider	It is used to store keys and digital certificates on smart cards. It creates, exports, imports, deletes, and stores key pairs as Software Key Storage Provider, but unlike it stores keys on smart cards.
Microsoft Key Protection Provider	It provides secure storage of keys. Also it allows you to protect content to a group in an Active Directory forest.

Vendors such as "CryptoPro", "Infoteks", "Validata", "Signal-COM" and "Lissi-Soft" develop CNG providers that support both algorithms of international standards and Russian cryptographic algorithms.

CNG providers such as CryptoPro CSP, ViPNet CSP, Signal-COM CSP, Validata CSP, Lissi CSP, Tumar CSP and AVEST CSP support GOST R 34.11-94, GOST 34.11-2012, GOST R 34.10-2001, GOST 34.10-2012 and GOST 28147-89 algorithms. In addition AVEST CSP supports STB RB 1176.1-99, STB RB 1176.2-99, STB 34.101.18-2009, STB 34.101.31-2011, STB 34.101.45-2013, STB 34.101.47-2017 and STB 34.101.50-2019 algorithms.

CNG also offers a mechanism for implementing a new cryptographic algorithm in the operating system. For each algorithm, a separate cryptographic provider is developed, which is registered in the system for a certain class of algorithms. To manage cryptographic keys of digital signature algorithm, the tools, that supports this algorithm, are required. Only some digital signature algorithms support such tools. These tools can be hardware or software.Some implementations of hardware key management provide hardware-level key management capabilities; signing and signature verification is performed in software.

Key management tools allow you to automate the process of using keys in information systems, such as generating, storing, exporting, importing, destroying keys, encryption and decryption with a key, and key access control. Public Key Infrastructure (PKI) provides cryptographic key management [7]. PKI is a collection of services for managing keys and digital certificates of users, systems and networks.

PKI uses public key cryptography to identification of electronic exchange participants, control the integrity of information.

A Certificate Authority (CA) is main part of the PKI that issues a certificate to validate the rights of users or systems requesting. It creates the certificate and signs it using the CA private key. Another important part of PKI is the Certificate repository. Certificate repository is a store of valid certificates and certificate revocation lists (CRLs). Applications check the validity of the certificate using the CRL in the repository.

PKI performs the following main functions:

1) *Registration* is the process of collecting information about a user and verifying its authenticity.
2) *Certificate Issuance*. Once the CA has signed the certificate, it is issued to the applicant and/or sent to the certificate store. CA affixes a validity period to the certificates, thus requiring periodic renewal of the certificate.
3) *Certificate Revocation*. A certificate can become invalid before expiration for various reasons: the user has left the company, changed his name, or if his private key has been compromised. Under these circumstances, the CA will revoke the certificate by entering its serial number on the CRL.
4) *Key Recovery*. A PKI function that allows to recover data or key.
5) *Key and certificate Lifecycle Management* - maintenance of certificates in PKI, including renewal, recovery and archiving of keys.

All international PKI standards are based on the ITU-T X.509 standard [8], which defines the format of the digital certificate and CRL.

In CNG to manage keys, the key storage providers are used. Windows provides Active Directory Certificate Services (ADCS) for working with key store providers. ADCS is PKI system for Windows clients. ADCS by default works with signature algorithms such as RSA[9], Diffie Hellman (DH)[10], [11], Elliptic Curve Diffie Hellman (ECDH)[12] and Elliptic Curve Digital Signature Algorithm (ECDSA) [13].

Only a key storage provider is not sufficient to perform cryptographic operations. The CNG provides the following types of providers for this purpose: hash provider, cipher provider, asymmetric encryption provider, random number generator provider, secret agreement provider, signature provider, key derivation provider. Applications interact with CNG providers through CNG routers that provide CNG APIs [14]. The CNG API is divided into two groups:

1) *BCrypt API* – CNG Cryptographic Primitive Functions for cryptographic operations such as hashing, signing and signature verification, random number generation, encryption, asymmetric encryption, key derivation;
2) *NCrypt API* – CNG Key Storage Functions for working with cryptographic keys and CNG SSL Provider Functions.

Each type of algorithms has its own type of CNG router. Several CNG providers can be implemented for the algorithm.

The organizational structure of this article is as follows. Section 2 refers to related work. Section 3 provides a description of the O'zDSt 1092: 2009 signature algorithm, such as key pair generation, signing, and verification process. Section 4 provides the system architecture of the created ARH Primitive provider and ARH Key Storage provider. Section 5 presents the OIDs of the algorithms and the main parameters of the algorithms. Section 6 describes the implementations of the Key Storage provider interface functions. Section 7 describes the implementations of the Provider extension interface functions. The results will be presented and discussed in Section 8. Finally, Section 9 contains the conclusion.

II. Related Work

A review of Microsoft's next-generation providers and the analysis of their supporting algorithms, types of providers were discussed in [15]. Windows default CNG providers do not support signature algorithm O'zDSt 1092:2009 [15]. The design and implementation of the key storage provider, which provides management keys' life cycle, were discussed in [16]. But the detailed description and integration with the Active Directory certification service has not been discussed. K. Lee and others [17] analyzed the possible vulnerabilities of the CNG library. The structures, functionality, and security issues of CNG have been discussed in [18], [19]. Cryptographic modules are not only developed as a cryptographic provider. The design and implementation of such elliptic curve cryptographic electronic signature systems were discussed in [20], [21], [22], [23]. But such cryptographic modules are not compatible with CNG, and therefore such solutions are not suitable for new custom algorithms. The development of a cryptographic provider for the hashing algorithm and the encryption algorithm was considered in the work [24]. It proposes a method of applying the symmetric algorithm O'zDSt 1105:2009, and the hashing algorithm O'zDSt 1106:2009 to ensure the confidentiality of electronic documents in MS Office. The authors of [25] discussed the development of a cryptographic provider that supports the CryptoAPI interface. They gave a detailed review of the cryptographic transformations of the encryption algorithm O'zDst 1005:2009, presented the architecture and modules of the CryptoAPI provider that they developed. But the CryptoAPI is already being replaced by a more advanced CNG API.

The above works analyze CNG libraries, the security of their key storage, provide a review of CNG API, discuss the development of the Key storage provider and the CryptoAPI provider. But the application of the new algorithm presented in this article in ADCS was not provided, and the problem of not recognizing digital certificates based on the O'zDSt 1092:2009 signature algorithm has not been resolved.

Therefore, we created CNG providers that support the above algorithms and provider extensions to address the issue of Windows digital certificates not being recognized. This article presents the architecture of these providers, describes the functions and modules, and proposes a solution to the problem of unrecognizing digital certificates.

III. The First Signature Algorithm of the O'zDSt 1092:2009 Standard

O'zDSt 1092:2009 is the State Standard of Uzbekistan. The standard includes two algorithms for creating and verifying an electronic digital signature. In this article, the first algorithm of the standard is discussed.

A. Definition

The following definitions are defined in the algorithm:

M– message to be signed, represented in binary code, arbitrary finite length; p – module, prime number, for software cryptographic module $p < 2^{1023}$;
q – a prime number that is a factor (prime factor) of $p - 1$, where $2^{254} < q < 2^{256}$;
R – a natural number, parameter;
(x, u) – a pair of integers – the private key of the signature algorithm;
(y, z) – a pair of integers – the public key of the signature algorithm;
(r, s) – a pair of integers – the signature value of M;
$H(M)$ – hash function that computes the hash value of M;
md – mode of signing; for the mode with a session key $md = 1$, and for the mode without a session key $md = 0$.
R_1 – an integer number – the control key
y_1 – an integer number – the session key

B. Special Operations

$X^{\backslash e}(mod\ p)$ - the operation of raising the base x to the power e modulo p with the parameter R. For example, for $e = 41$.

$x^{\backslash 41}(mod\ p) => x^{\backslash 32+8+1}(mod\ p) =$
$(((((x^{\backslash 2})^{\backslash 2})^{\backslash 2})^{\backslash 2})^{\backslash 2} **(x^{\backslash 2})^{\backslash 2})^{\backslash 2} ** x(mod\ p)$.

where $x^{\backslash 2}(mod\ p) \equiv x(2 + xR)(mod\ p)$.

$X ** Y(mod\ p)$ – the operation of multiplication of two integer numbers modulo p with parameter R. It is defined as follows:

$$X ** Y mod\ p \equiv X + (1 + XR)Y mod\ p \tag{1}$$

'

$X^{\backslash -1}$ – the operation of the modular inverse of an integer X modulo p with parameter R. It is defined as follows:

$$X^{\backslash -1} \equiv -X\,(1 + XR)^{-1}\,(mod\ p) \tag{2}$$

C. Key Generation

Algorithm 1 uses a one-way function in a group with a parameter, which is used in multiplication, exponentiation, and group inversion. Each user of Algorithm 1 has a private key and a public key:

1) (x, u) - private key numbers, randomly or pseudo-randomly generated integers satisfying the condition $1 < x, u < q$;
2) (y, z) - public key numbers calculated by the formula:

$$y \equiv g^{\backslash x}(mod\ p) \tag{3}$$

$$z \equiv g^{\backslash u}(mod\ p) \tag{4}$$

where g is a private or public parameter, which is an integer, calculated according to the formula:

$$g \equiv h^{(p-1)/q}(mod\ p) \tag{5}$$

where: $h < p$ – is a natural number satisfying the condition $g^{\omega}\,(modp) \equiv 0$, ω in the range of values $1, \ldots, q$ if and only if $\omega = q$

D. Sign Process

Input parameters: M, md, x, u, R_1

Output: if $(md = 0)$ $\{r, s\}$, else $\{r, s, y_1\}$

Step 1: $m = H(M),\ c = x$

Step 2: $k = H(m + (1 + mR)c)$

Step 3: if $(k = 0)$ then $c = c + 2$ and go to Step 2.

Step 4: $T \equiv g^{\backslash -k}(mod\ p)$ with parameter R

Step 5: $r \equiv m + (1 + mR)T(mod\ p)$

Step 6: if $(r = 0)$ then $k = k + 1(mod\ p)$ and go to Step 4.

Step 7: $s_1 \equiv k - rx(mod\ q)$

Step 8: if $(s_1 = 0)$ then $k = k + 1(mod\ p)$ and go to Step 4.

Step 9: $s \equiv s_1 u^{-1}(mod\ q)$

Step 10: if $(md = 0)$ then return $\{r, s\}$ as signature values, else go to Step 11.

Step 11: $r_1 \equiv R_1 + (1 + RR_1)r(mod\ q)$

Step 12: if $(r_1 = 0)$ then $k = k + 1(mod\ p)$ and go to Step 4.

Step 13: $x_1 \equiv (k - suR_1)r_1^{-1}(mod\ q)$

Step 14: if $(x_1 = 0)$ then $k = k + 1(mod\ p)$ and go to Step 4.

Step 15: $y_1 \equiv gR_1^{\backslash x_1}(mod\ p)$ with parameter RR_1.

Step 16: return $\{r, s, y_1\}$ as signature values.

E. Signature Verification Process

Input parameters: $M, md, \{y, z\}, r, s$; and $y1$ if $md = 1$

Step 1: $m = H(M)$

Step 2: if $L(s) \leq L(q)$ and $L(r) \leq L(p)$ then go to Step 3 else signature is not valid

Step 3: $z_0 \equiv z^{\backslash s}(mod\ p)$ with parameter R

Step 4: $r' \equiv r(mod\ q)$

Step 5: $y_2 \equiv y^{\backslash r'}(mod\ p)$ with parameter R

Step 6: $z_1 \equiv z_0 + (1 + z_0 R)y_2(mod\ p)$

Step 7: $y_3 \equiv z_1 + (1 + z_1 R)r(mod\ p)$

Step 8: if $(md = 0)$ and $(m = y_3)$ then signature is valid else if $(md = 0)$ and $(m = y_3)$ then go to Step 9, else if $(m \neq y_3)$ then signature is not valid;

Step 9: $g_3 \equiv z_1 R_1^{-1}(mod\ p)$

Step 10: $s_1 \equiv sR_1(mod\ q)$

Step 11: $r_1 \equiv R_1 + (1 + RR_1)r'(mod\ q)$

Step 12: $z_2 \equiv z + R_1^{-1}(mod\ p)$

Step 13: $y_4 \equiv y_1(mod\ p)$

Step 14: $z_3 \equiv z_2^{\backslash s_1}(mod\ p)$ with parameter RR_1

Step 15: $y_5 \equiv y_4^{\backslash r_1}(mod\ p)$ with parameter RR_1

Step 16: $g_4 \equiv z_3(1 + z_3 RR_1)y_5(mod\ p)$

Step 17: if $(g_3 = g_4)$ then signature is valid else signature is not valid

IV. System Architecture

Applications for working with cryptographic keys use the key storage provider, for symmetric encryption they use the cipher provider, for hashing data they use the hash provider, for signing and verifying the signature they use the signature provider, etc. In turn, the key storage provider uses the signature provider to generate, export and import keys, sign data and verify the signature. To encrypt data with simmetric algorithms it uses the cipher provider, to compute a hash value of data, it uses the hash provider. Therefore, a key storage provider and a custom algorithm provider were developed to integrate with ADCS. The custom algorithm provider implements three interfaces: hash interface for algorithm O'zDst 1006:2009, signature interface for algorithm O'zDst 1092:2009 and cipher interface for algorithm O'zDst 1005:2009. The architecture of the developed system consists of four main parts (Fig. **??**): ARH Primitive Provider – the custom algorithm provider, ARH Key Storage Provider – the key storage provider, Provider extension – the extension module of provider, PKCS #11 - a module that implements the functions of the PKCS #11 interface and cryptographic algorithms.

V. Main Parameters

The following constants are defined for the algorithms:

"ARH Primitive Provider" – the name of the custom algorithm provider

"ARH Key Storage Provider" – the name of the key storage provider

"O'zDSt 1092:2009 Alg1" – the name of the 1st algorithm of the O'zDst 1092:2009 standard

"O'zDSt 1092:2009 Alg2" – the name of the 2nd algorithm of the O'zDst 1092:2009 standard

"O'zDSt 1006:2009 Alg1" – the name of the 1st algorithm of the O'zDst 1006:2009 standard

"O'zDSt 1006:2009 Alg2" – the name of the 2nd algorithm of the O'zDst 1006:2009 standard

"O'zDSt 1005:2009 Alg1" – the name of the algorithm of the O'zDst 1005:2009 standard

"O'zDSt 1106:2009 Alg1/1092:2009 Alg1" – the name of the double algorithms "O'zDSt 1092:2009 Alg1" and "O'zDSt 1106:2009 Alg1"

"O'zDSt 1106:2009 Alg2/1092:2009 Alg2" – the name of the double algorithms "O'zDSt 1092:2009 Alg2" and "O'zDSt 1106:2009 Alg2"

1.2.860.3.15.1.1.1.1 – the OID of the 1st algorithm of the O'zDst 1092:2009 standard for sign

1.2.860.3.15.1.1.1.1.1 – the OID of test parameters of the first algorithm of the O'zDst 1092:2009 standard for sign

1.2.860.3.15.1.1.2.1 – the OID of the 2nd algorithm of the O'zDst 1092:2009 standard for sign

1.2.860.3.15.1.1.2.1.1 – the OID of test parameters of the second algorithm of the O'zDst 1092:2009 standard for sign

1.2.860.3.15.1.3.1 – the OID of the 1st algorithm of the O'zDst 1006:2009 standard

1.2.860.3.15.1.3.1.1 – the OID of test parameters of the first algorithm of the O'zDst 1006:2009

1.2.860.3.15.1.3.2 – the OID of the 2nd algorithm of the O'zDst 1006:2009 standard

1.2.860.3.15.1.3.2.1 – the OID of test parameters of the second algorithm of the O'zDst 1006:2009

1.2.860.3.15.1.1.1.2.2.1 the OID of the double algorithm "O'zDSt 1106:2009 Alg1/1092:2009 Alg1"

1.2.860.3.15.1.1.2.2.2.2 the OID of the double algorithm "O'zDSt 1106:2009 Alg2/1092:2009 Alg2"

The OIDs of algorithms and parameters are registered with the operating system.

VI. Implementing Key Storage Provider Interface Functions

The following functions are implemented according to the requirement for the key storage provider interface:

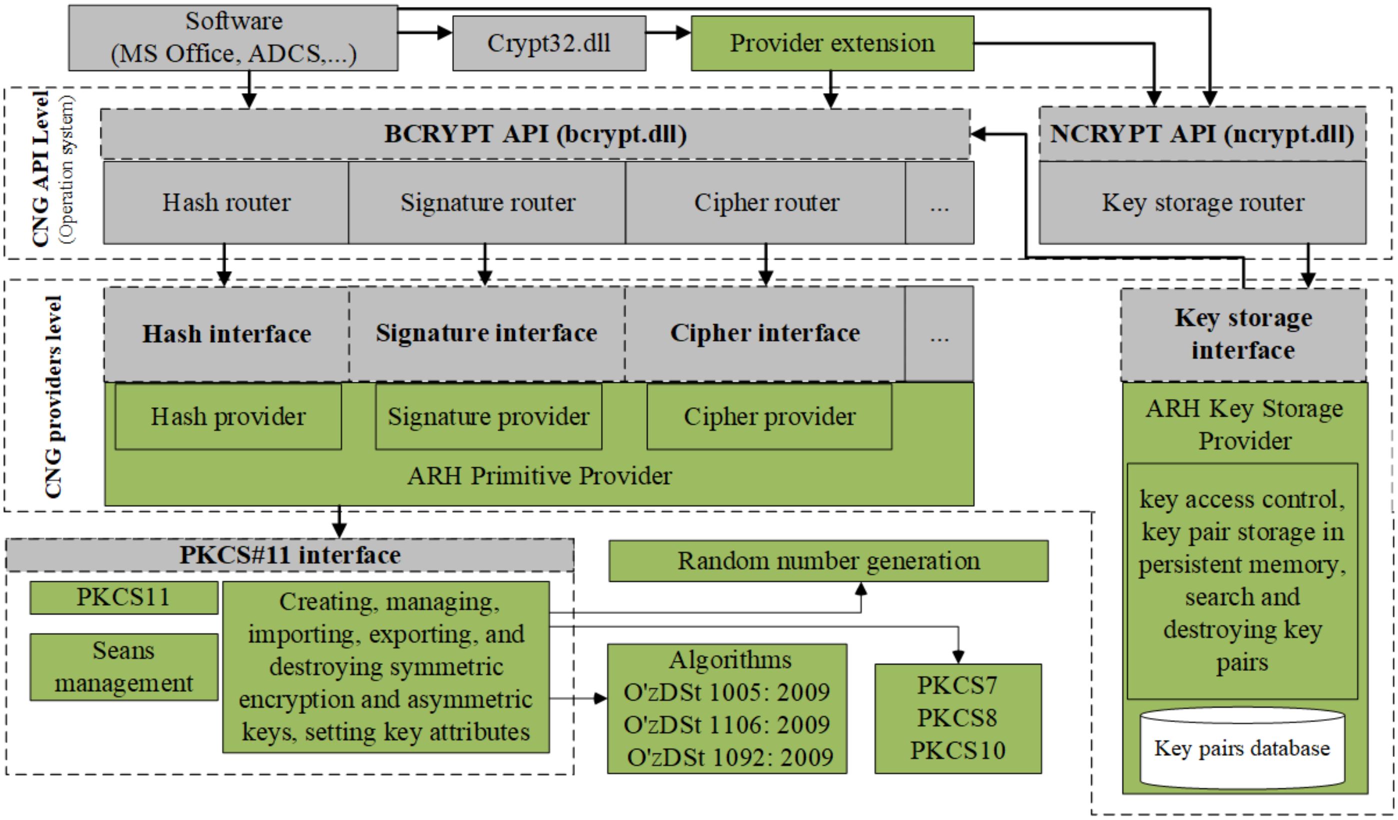

Fig. 1. The System Architecture.

- *GetKeyStorageInterface* function
- Key storage provider interface functions:
  - *OpenProvider*
  - *OpenKey*
  - *CreatePersistedKey*
  - *GetProviderProperty*
  - *GetKeyProperty*
  - *SetProviderProperty*
  - *SetKeyProperty*
  - *FinalizeKey*
  - *DeleteKey*
  - *FreeProvider*
  - *FreeKey*
  - *FreeBuffer*
  - *Encrypt*
  - *Decrypt*
  - *IsAlgSupported*
  - *EnumAlgorithms*
  - *EnumKeys*
  - *ImportKey*
  - *ExportKey*
  - *SignHash*
  - *VerifySignature*
  - *PromptUser*
  - *NotifyChangeKey*
  - *SecretAgreement*
  - *DeriveKey*
  - *FreeSecret*
  - *KeyDerivation*

The *GetKeyStorageInterface* function is used by the CNG router to get the address of the Key storage provider interface functions. The function takes the name of the key storage provider as an input parameter. An object of the *NCRYPT_KEY_STORAGE_FUNCTION_TABLE* structure is returned as an output parameter, which stores the addresses of the key storage provider interface functions. Later, the GNG router uses it to call interface functions of the Key storage provider.

The *OpenProvider* function is called by the CNG router when an application establishes a connection to the key storage provider. The function takes the name of the key storage provider as an input parameter and returns the handle of the provider. This handle serves as an identifier for the current connection. Also, this handle is used as an input parameter in many interface functions. The function initializes a provider object of type *ALPKSP_PROVIDER* and returns provider object addresses as handle of the provider.

ALPKSP_PROVIDER struct:

```
typedef struct _ ALPKSP_PROVIDER
{
        ALP_OBJECT_HEADER Header;
        //the size of the object
        // and magic number
        DWORD dwFlags;
        LPWSTR pszName;
        // the name of the provider
        BCRYPT_ALG_HANDLE hAlgorithm;
```

```
        //the handle of the
        //ARH Key Storage Provider
        LPWSTR pszContext;
        //context
} ALPKSP_PROVIDER
typedef struct _ALP_OBJECT_HEADER
{
        DWORD cbLength;
        // the size of the object
        DWORD dwMagic;
        // magic number
}
ALP_OBJECT_HEADER
```

The *CreatePersistedKey* function is called by the CNG router when generation of a key pair is required. It takes as input parameters the handle of the provider, the name of the algorithm, the name of the key, the type of key { *AT_KEYEXCHANGE* the key is a key exchange key, *AT_SIGNATURE* the key is a signature key, 0}, as well as a flag indicating the key of the current user or the local computer. If the key was created for the current user, then the user who created the key can use this key. In the case of a local computer, the key can be used by all users of the local computer. This method is often used in service applications. The function initializes a key object of type *ALPKSP_KEY*. The function will not generate key pair, it starts the key generation process of the key pair. Typically, after calling the *CreatePersistedKey* function, the *SetKeyProperty* function is used to specify the length of the key, and the value of other parameters. The key generation process ends with a call to the *FinalizeKey* function. To generate the key pair, the *CreatePersistedKey* function uses the ARH Primitive Provider through the signature interface and calls the *GenerateKeyPair* function.

Syntax of the *ALPKSP_KEY* struct:

```
typedef struct _ALPKSP_KEY
{
        ALP_OBJECT_HEADER Header;
        PALPKSP_PROVIDER hAlgoritm;
        DWORD dwKeyBitLen;
        BOOL isFinished;
        // whether the key is finalized
        BCRYPT_KEY_HANDLE hPublicKey;
        // the handle of public key
        BCRYPT_KEY_HANDLE hPrivateKey;
        // the handle of private key
        DWORD dwExportPolicy;
        // the export policy flag
        DWORD dwFlags;
        //{NCRYPT_MACHINE_KEY_FLAG,
        //NCRYPT_OVERWRITE_KEY_FLAG}
        LPWSTR pszKeyName;
        //the name of the key (key file)
        DWORD dwKeyUsagePolicy;
        //the key usage policy
        DWORD dwLegacyKeySpec;
        //the type of the key
        //{AT_KEYEXCHANGE,AT_SIGNATURE,0}
        //encrypted private key blob
        PBYTE pbPrivateKey;
        DWORD cbPrivateKey;
        //hash value of pin
        PBYTE pbPinHash;
        DWORD cbPinHash;
        //handle to cryptography
        //providers needed to perform
        //operations with the key.
        BCRYPT_ALG_HANDLE hBCryptProvider;
        //security descriptor to be
        //set on the private key file.
        DWORD dwSecurityFlags;
        PBYTE pbSecurityDescr;
        DWORD cbSecurityDescr;
        NCRYPT_UI_POLICY_BLOB *pkeyUIPolicy;
        LIST_ENTRY PropertyList;
        //list of properties.
} ALPKSP_KEY;
```

The *FinalizeKey* function is called by the CNG router when an application needs to complete the key pair generation process. The function takes as input parameters the handle of the provider, the handle of the key. This function sequentially calls ARH Primitive Provider signature interface functions such as *FinalizeKeyPair* and *ExportKey*. The function encrypts the key blob and stores it on disk. If a pin code is specified, then the key is encrypted using the formula (6):

$$Ke = E(Kp, Kb) \tag{6}$$

Kp – the encryption key, Kb – the generated private key, E – the O'zDst 1105:2009 encryption algorithm.

The encryption key Kp calculated using the formula (7):

$$Kp = H(H(H(pin))) \tag{7}$$

pin – the pin code value, H – the O'zDst 1106:2009 hash function.

If the pin code is not specified, then the private key is encrypted using the *CryptProtectData* function.

The *"system"* and *"hidden"* attributes are set for the key file. If the key is applied to the local computer, full permission on the key file is assigned to the *System account* and the *Administrators group*, otherwise, to the current user account.

The *GetProviderProperty* function is used by the CNG router when an application needs to determine the value of the Key storage provider properties.

The *GetKeyProperty* function is used by the CNG router when an application needs to determine the value of the key properties. The function takes the handle of the key, property name as input parameters and returns the attribute value as an output parameter.

The *SetProviderProperty* function is used by the CNG router when an application needs to set the value of the Key storage provider properties.

The *SetKeyProperty* function is used by the CNG router when the value of the key attributes needs to be set. The function accepts the handle of the key, the attribute name, the new value of the attribute as input parameters.

The *OpenKey* function is called by the CNG router when an application opens an existing key. The function accepts as input parameters the handle of the provider, the key name, the key type, a flag indicating whether the key is for the current user or the local computer. The function initializes the key object of the *ALPKSP_KEY* type from the key file.

The *DeleteKey* function takes the handle of the key as an input parameter, deletes the key file from persistent storage, and also destroys the key object.

The *FreeProvider* function is called by the CNG router when an application closes the current connection to the key storage provider. The function takes the handle of the provider as an input parameter, frees the memory occupied by the provider object, which was created when calling the *OpenProvider* function. It closes the session with the pkcs11 module.

The *FreeKey* function takes the handle of the key as an input parameter and destroys the key object.

The *FreeBuffer* function takes a buffer address as an input parameter and frees memory.

The *Encrypt* function encrypts a block of data. The function uses the ARH Primitive Provider.

The *Decrypt* function decrypts the data block. The function uses the ARH Primitive Provider.

The *ImportKey* function imports the key that is exported by the *ExportKey* function. The function takes a key blob, a key blob type {*BCRYPT_PUBLIC_KEY_BLOB* – public key blob, *BCRYPT_PRIVATE_KEY_BLOB* – private key blob} as input parameters, and returns the handle of the key. If the key blob type is *BCRYPT_PRIVATE_KEY_BLOB*, then it saves the key to a file. The function initializes a key object of type *ALPKSP_KEY*.

The *ExportKey* function exports the key. The function takes as input parameters, the handle of the key, the key blob type, and returns the key blob through the *pbOutput* output parameter. The public key blob consists of the key identifier, key version, OID of the key, algorithm parameter values, and public key parameters. The private key blob consists of the key identifier, key version, OID of the key, algorithm parameter values, public/private key.

The *SignHash* function is used by the CNG router when an application needs to sign data. The function takes the handle of the key, a hash value as input parameters, and returns the generated signature. The function uses the ARH Primitive Provider.

The *VerifySignature* function is called by the CNG router when the signature needs to be verified. The function takes as input parameters the handle of the key, a hash value, the signature to be verified, and returns the verification result. The function uses the ARH Primitive Provider.

To integrate CNG providers with Windows Active Directory Certificate Services, they must be registered with the CNG router.

Therefore, the ARH Primitive Provider is registered to the hash, signature and cipher interface.

The ARH Key Storage Provider is registered to the key storage provider interface.

VII. Implementation of Integration Functions

The Provider extension is developed to work with digital certificates. It implements the following callback functions:

The function *PFN_CRYPT_EXPORT_PUBLIC_KEY_INFO_EX2_FUNC* encodes and exports the public key blob. The function takes the handle of the key, an encoding type {*X509_ASN_ENCODING*, *PKCS_7_ASN_ENCODING*}, the public key as input parameters, and returns an object of type *CERT_PUBLIC_KEY_INFO*, which contains information about the public key. The function uses the ARH Key Storage Provider.

The function *PFN_IMPORT_PUBLIC_KEY_INFO_EX2_FUNC* decodes the public key algorithm identifier and imports the key. The function uses the ARH Primitive Provider.

The function *PFN_CRYPT_SIGN_AND_ENCODE_HASH_FUNC* signs and encodes the hash value. The function takes the handle of the key, encoding type, signature algorithm identifier, signature parameters, OID of the double algorithm, hash algorithm identifier, hash value as input parameters and returns the created signature. The function uses the ARH Primitive Provider.

The function *PFN_CRYPT_VERIFY_ENCODED_SIGNATURE_FUNC* decodes the signature and verifies the signature. The function takes as input parameters the type of encoding, the address of an object of type *CERT_PUBLIC_KEY_INFO*, which contains the public key, the OID of the signature algorithm, the identifier of the signature algorithm, signature parameters, the identifier of the hash algorithm, hash value, the signature to be verified, and returns the verification result. The function uses the ARH Primitive Provider.

These callback functions are called by the operating system to decode the algorithm OID fields in the certificate and to validate the certificate.

The provider extension is registered in the system using the *CryptRegisterOIDInfo* function to encode and decode the data of the digital certificate generated using the O'zDst 1092:2009 algorithm and O'zDst 1106:2009 hash algorithm.

VIII. Result and Discussion

After registering CNG providers and provider extension, the Windows ADCS is installed and configured to work with the O'zDst 1092:2009 signature algorithm and O'zDst 1106:2009 hash algorithm.

Registered algorithm OIDs are located in the registry under the path HKEY_LOCAL_MACHINE\SOFTWARE\Microsoft\Cryptography\OID\EncodingType 0\CryptDllFindOIDInfo.

A Windows registry key is created for each algorithm OID. For example: [HKEY_LOCAL_MACHINE\SOFTWARE\Microsoft\Cryptography\OID\EncodingType 0\

CryptDllFindOIDInfo\1.2.860.3.15.1.1.1.2.2.1!4]
"Name" = "O'zDSt 1106:2009 Alg1/1092:2009 Alg1"
"Algid" = dword:ffffffff
"ExtraInfo" = hex:fe,ff,ff,ff
"Flags" = dword:00000001
"CNGAlgid" = "O'zDSt 1106:2009 Alg1"
"CNGExtraAlgid" = "O'zDSt 1092:2009 Alg1"

This registry key is created for the double algorithm(hash and signature algorithm) used in certificates. The key name includes the OID of the algorithm.

The registered provider extension functions are located in the registry under the following paths, respectively:

1) HKEY_LOCAL_MACHINE\SOFTWARE\Microsoft\Cryptography\OID\EncodingType 1\CryptDllExportPublicKeyInfoEx2;
2) HKEY_LOCAL_MACHINE\SOFTWARE\Microsoft\Cryptography\OID\EncodingType 1\CryptDllImportPublicKeyInfoEx2
3) HKEY_LOCAL_MACHINE\SOFTWARE\Microsoft\Cryptography\OID\EncodingType 1\CryptDllSignAndEncodeHash
4) HKEY_LOCAL_MACHINE\SOFTWARE\Microsoft\Cryptography\OID\EncodingType 1\CryptDllVerifyEncodedSignature

For each OID of the signature algorithm and dual algorithm, a key is created in the registry under the paths listed above. For example: [HKEY_LOCAL_MACHINE\SOFTWARE\Microsoft\Cryptography\OID\EncodingType 1\CryptDllVerifyEncodedSignature\1.2.860.3.15.1.1.1.2.2.1]
"Dll" = "C:\Program Files\ARHCrypto\ARHCNG\provext64.dll"
"FuncName" = "ARHVerifyEncodedSignature".

"ARHVerifyEncodedSignature" is the name of the *PFN_CRYPT_VERIFY_ENCODED_SIGNATURE_FUNC* function implemented in the provider extension.

Registered providers are in the path HKEY_LOCAL_MACHINE\SYSTEM\ControlSet001\Control\Cryptography\Providers.

The comparison results by supported algorithms of Microsoft CNG providers with the created CNG providers are shown in Table II and Table III.

TABLE II. THE COMPARISON RESULTS OF MICROSOFT SOFTWARE KEY STORAGE PROVIDER AND ARH KEY STORAGE PROVIDER

Functions	Microsoft Software Key Storage Provider	ARH Key Storage Provider
Generate, export/import, use and delete of key pairs of RSA, DSA and ECDSA algorithms	+	-
Generate, export/import, use and delete of key pairs of O'zDSt 1092:2009 algorithm	-	+
PIN based Authentication	-	+
Machine key type support	+	+
User key type support	+	+
Kernel mode(using from drivers)	+	-
User mode	+	+

TABLE III. THE COMPARISON RESULTS OF MICROSOFT PRIMITIVE PROVIDER AND ARH PRIMITIVE PROVIDER

Functions	Microsoft Primitive Provider	ARH Primitive Provider
Hashing with SHA1, SHA256, SHA384, SHA512, MD2, MD4, MD5 algorithms	+	-
signing and signature verification with RSA, DSA and ECDSA algorithms	+	-
symmetric encryption and decryption with AES, DES, 3DES, DESX, RC2 and RC4 algorithms	+	-
asymmetric encryption and decryption with RSA algorithm	+	-
key exchange with DH and ECDH algorithms	+	-
random number generation	+	+
signing and signature verification with O'zDSt 1092:2009 algorithm	-	+
hashing with O'zDSt 1106:2009 algorithm	-	+
symmetric encryption and decryption with O'zDSt 1105:2009 algorithm	-	+
Kernel mode(using from drivers)	+	-
User mode	+	+

CNG providers, developed by Russian companies, work with their national algorithms, they also do not support O'zDSt 1092:2009, O'zDSt 1105:2009 and O'zDSt 1106:2009 algorithms.

A new certificate request has been created to test the system. Then a certificate is issued on request through ADCS.

The certificate content:

——BEGIN CERTIFICATE——
MIIDjDCCAtOgAwIBAgITLwAAAAc1JEX561oNaAAAAA
AABzAPBgsqhlwDDwEBAQICAQUAMBAxDjAMBgNVBA
MTBWFscENBMB4XDTIwMDgyMjExMTc1NloXDTIxMDg
yMjExMjc1NlowQTELMAkGA1UEBhMCVVoxDTALBgNV
BAoTBE5VVXoxIzAhBgkqhkiG9w0BCQEWFG1yLnJ1aGls
bG9AZ21haWwuY29tMIIBMDAlBgkqhlwDDwEBAQEwGA
YKKoZcAw8BAQEBAQYKKoZcAw8BAwEBAQOCAQUAB
IIBABQyfDPMWddMPpIIuRPC22IxhjlUw3ciPb2ugMQUsF8
ooshYXQyzkkL00BI8LQwmTEWcQJdGihZC0CCM+0KUYS
4A3aJbpjhnSWmkmE+v9gTfVUgUzdkA2uDcN4njUFJrSN7jz
/Fyo+IZutDze732QaIxC3ENwOkDtxNOsN/b//v/C6b7K/T0qsO
3LlJ1eH5VNF+rUdA9Ya9bRaLWzWE5UJGHz1NYJpSqld0R
8u6ft5Oo/lFPWWJH/S1qc1ku/tMw693Z8pVC4EzPzfJAyIsEO
V9O1KOkSKNJSI3wrE26pwZ8KDGkkWkC6WBwOxWMsu
IlbyHziNDuGdN6tyAUcBzbzbOjgfwwgfkwDgYDVR0PAQH/
BAQDAgSQMB0GA1UdDgQWBBREVPgsiLr5lss6Y5+uOR
w/An/jPzAfBgNVHSMEGDAWgBRBN7Hcr4RnJBtxH/f0i9d/
riFMTzA+BgNVHR8ENzA1MDOgMaAvhi1maWxlOi8vLy9
XSU4tN09FUkhLTFJDOUEvQ2VydEVucm9sbC9hbHBDQS
5jcmwwWQYIKwYBBQUHAQEETTBLMEkGCCsGAQUF
BzAChj1maWxlOi8vLy9XSU4tN09FUkhLTFJDOUEvQ2Vy
dEVucm9sbC9XSU4tN09FUkhLTFJDOUFfYWxwQ0EuY3J
0MAwGA1UdEwEB/wQCMAAwDwYLKoZcAw8BAQECAg
EFAAOBoQAhs9NcO8eECJIE8wmHlsNwL0HPB1aXpUolgk
NmN0mF8wpqFFRi90YREVsC3Kg/lTDy79yYNMZ8yRQ3Te
tE0Aj+w9n8T7THf9okYPDYE6xl4N+K4DQi+YulGyuPpzpLQ

Remr35snqXQj92KTJ8cgkkLjde5avD9V0eGVKKPNVPd4u5/
9wQPAoxn9sIiS1NuOwliwuyunVaVd6JgcyFC7Syq
——END CERTIFICATE——

By default Windows cannot verify the integrity of the certificate and cannot recognize the OID algorithms (Fig. **??**, Fig. **??**).

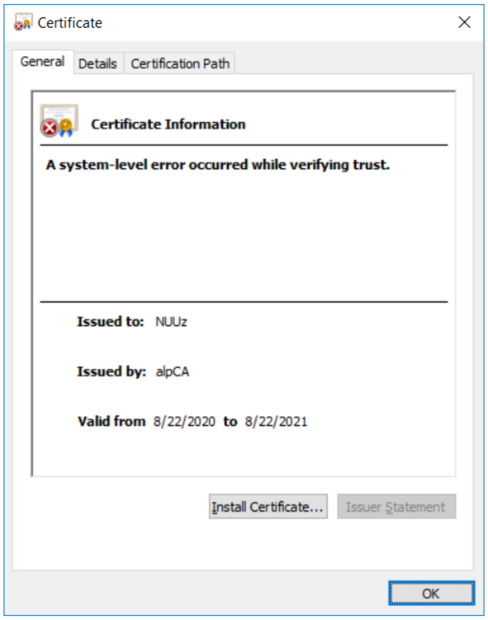

Fig. 2. Unrecognized Certificate.

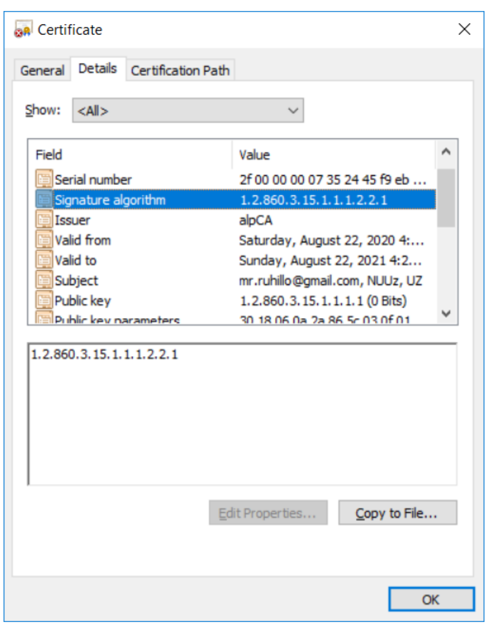

Fig. 3. Unrecognized Certificate Details.

This certificate is recognized by Windows that has both the ARH Primitive Provider and the ARH Key Storage Provider installed (Fig. **??**, Fig. **??**).

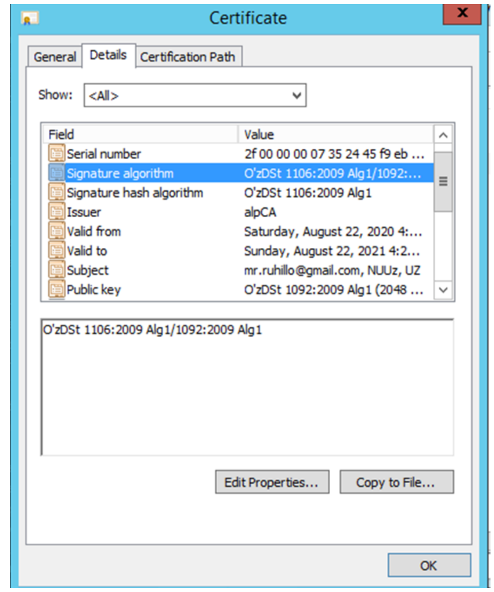

Fig. 4. Certificate Details.

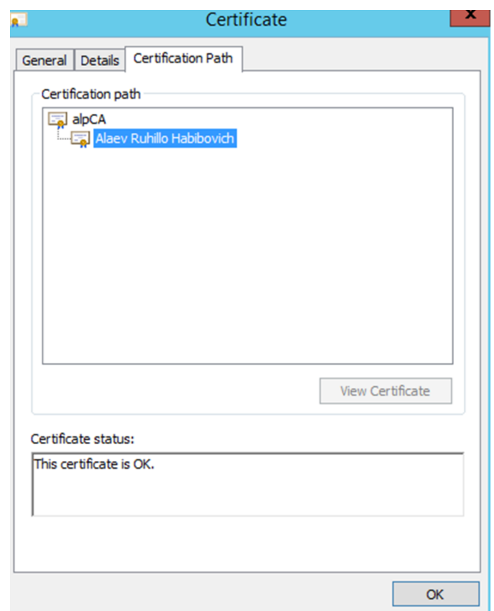

Fig. 5. Certification Path.

IX. Conclusion

The architecture of the custom algorithm provider and key storage provider was provided. The description of the key storage provider interface functions was discussed. The implementation of the key storage provider interface functions was presented. The ARH Primitive Provider has been developed which implements the signature interface, the hash interface and the cipher interface, and also supports the O'zDst 1105:2009, O'zDst 1106:2009 and O'zDst 1092:2009 algorithms. The ARH Key Storage Provider has been developed, which implements the key storage provider interface. The ARH Key Storage Provider provides secure storage, use, export and import of national signature algorithm keys. The

ARH Key Storage Provider supports storage, export/import of signature keys in PKCS#7 and PKCS#8 formats, as well as generation of PKCS#10 requests for a digital certificate via the CertEnroll API. The description and implementation of the ADCS integration functions were provided.

The developed system solves the problem of not recognizing digital certificates generated based on the O'zDst 1106:2009 and O'zDst 1092:2009 algorithms. The CNG providers included in Windows by default do not address this issue.

The solution to the problem allows users to verify the integrity of the certificate generated based on the O'zDst 1106:2009 and O'zDst 1092:2009 algorithms. This, in turn, allows users to verify the integrity of data and documents signed with the private key of the certificate.

The methods proposed here can be used to apply other signature algorithms that are not supported by the Windows by default.

In addition, these CNG providers provide the ability to use these algorithms in existing information systems that work with other CNG providers. Because they already work with the CNG API to perform cryptographic operations. Sometimes this is achieved with just a few system settings, as a result, it is very easy to apply different algorithms in the system without additional costs and resources.

Acknowledgment

I would like to acknowledge the reviewers for their valuable feedback.

References

[1] Singh, Abhishek. Identifying Malicious Code Through Reverse Engineering. 2009, 10.1007/978-0-387-89468-3.

[2] B. Kaliski. RFC2315: PKCS #7: Cryptographic Message Syntax Version 1.5. RFC Editor, 1998, USA.

[3] Kaliski, B. Public-Key Cryptography Standards (PKCS) #8: Private-Key Information Syntax Specification Version 1.2. RFC, 5208, 2008.

[4] M. Nystrom and B. Kaliski. RFC2986: PKCS #10: Certification Request Syntax Specification Version 1.7. RFC Editor, 2000, USA.

[5] PKCS #11 Cryptographic Token Interface Base Specification Version 2.40, Committee Specification 01. OASIS Open (September 2014), http://docs.oasis-open.org/pkcs11/pkcs11-base/v2.40/cs01/pkcs11-base-v2.40-cs01.html

[6] K. Moriarty, M. Nystrom, S. Parkinson, A. Rusch, and M. Scott, "PKCS #12: Personal Information Exchange Syntax v1.1" RFC 7292, 2014.

[7] Johannes A. Buchmann, Evangelos Karatsiolis, and Alexander Wiesmaier. Introduction to Public Key Infrastructures. Springer Publishing Company, Incorporated. 2013.

[8] ITU-T Recommendation X.509 "Information technology - Open Systems Interconnection - The Directory: Public-key and attribute certificate frameworks ". 2000.

[9] Qi, N., Wei, W., Zhang, J., Wang, W., Zhao, J., Li, J., Hu, J. Analysis and research of the RSA algorithm. Information Technology Journal, vol.12(9), pp. 1818–1824, 2013, 10.3923/itj.2013.1818.1824.

[10] Diffie, W., Diffie, W., & Hellman, M. E. New Directions in Cryptography. IEEE Transactions on Information Theory, vol.22(6), pp. 644–654, 1976, 10.1109/TIT.1976.1055638.

[11] Maurer, U.M., Wolf, S. The Diffie–Hellman Protocol. Designs, Codes and Cryptography 19, pp. 147–171, 2000, 10.1023/A:1008302122286.

[12] Wei, W., Chen, J., Li, D., & Zhang, B. Research on the Bit Security of Elliptic Curve Diffie-Hellman. Journal of Electronics and Information Technology, vol.42(8), pp. 1820–1827, 2020, 10.11999/JEIT2_190845.

[13] M. Al-Zubaidie, Z. Zhang, J. Zhang, Efficient and secure ECDSA algorithm and its applications: A survey. International Journal of Communication Networks and Information Security. vol.11(1), pp. 7–35, 2019.

[14] Sean Turner and Russ Housley. Implementing Email and Security Tokens: Current Standards, Tools, and Practices. Wiley Publishing. 2008.

[15] Y. Ahmad. "A study on algorithms supported by CNG of Windows operating system" International Journal of Modern Engineering Research. vol.2(1) pp. 276–280, 2012.

[16] Z. Lina. "Design and implementation of KSP on the next generation cryptography API" Physics Procedia, International Conference on Medical Physics and Biomedical Engineering (ICMPBE2012). pp. 1640–1646, 2012.

[17] K. Lee, Y. Lee, J. Park, K. Yim, and I. You, "Security issues on the CNG cryptography library (Cryptography API: Next generation)" in 2013 Seventh International Conference on Innovative Mobile and Internet Services in Ubiquitous Computing. pp. 709–713, 2013.

[18] K. Lee, H. Lee, Y. Lee, and K. Yim, "Analysis on the key storage mechanism of the CNG library" in 2016 10th International Conference on Innovative Mobile and Internet Services in Ubiquitous Computing (IMIS), pp. 499–502, 2016.

[19] K. Lee, I. You, and K. Yim, "Vulnerability analysis on the CNG crypto library" in 2015 9th International Conference on Innovative Mobile and Internet Services in Ubiquitous Computing, pp. 221–224, 2015.

[20] Khalique, A., Singh, K., & Sood, S. "Implementation of elliptic curve digital signature algorithm" International Journal of Computer Applications. vol.2(2) 2010.

[21] A. Abidi, B. Bouallegue, and F. Kahri, "Implementation of elliptic curve digital signature algorithm (ECDSA)" in 2014 Global Summit on Computer Information Technology (GSCIT), pp. 1–6, 2014.

[22] S. F. Temitope O.S. Olorunfemi, B.K. Alese and O. Fajuyigbe. "Implementation of elliptic curve digital signature algorithms" Journal of Software Engineering, vol.1(1), pp. 1–12, 2007. 10.3923/jse.2007.1.12.

[23] B. Chen, W. Wu, and Y. Zhang, "The design and implementation of digital signature system based on elliptic curve" in Proceedings of the 2012 International Conference on Cybernetics and Informatics, edited by S. Zhong (Springer New York, New York, NY, 2014) pp. 2041–2047.

[24] M.M. Aripov, R. H. Alaev. "Research of the application of the new cryptographic algorithms: Applying the cipher algorithm O'zDSt 1105:2009 for MS Office document encryption" in Proceedings of the 5th International Conference on Engineering and MIS, ICEMIS'19 (Association for Computing Machinery, New York, NY, USA, 2019). 10.1145/3330431.3330434

[25] M. Nurullaev and R. D. Aloev, "Software, algorithms and methods of data encryption based on national standards," IIUM Engineering Journal, vol.21(1), pp. 142–166, 2020. 10.31436/iiumej.v21i1.1179

Robust Real-time Head Pose Estimation for 10 Watt SBC

Emad Wassef[1], Hossam E. Abd El Munim[2]
Department of Computer and Systems Engineering, Ain Shams University, Cairo, Egypt

Sherif Hammad[3], Maged Ghoneima[4]
Department of Mechatronics Engineering, Ain Shams University, Cairo, Egypt

***Abstract*—Head Pose Estimation has always been an essential part for many applications such as autonomous driving and driving assist systems and hence performance optimization provides better performance as well as lower computing and power needs that allows us to run such applications over embedded devices inside these systems. In this article we present an implementation over a Single board computer for a new system of 3D Head pose estimation that estimates the Head pose of a person in real-time for applications such as Driver monitoring systems, Drones, Gesture recognition and tracking devices. The system is developed over a single board computer (SBC) that is suitable for very low powered applications, it only utilizes the data provided through the IR camera sensor to estimate both the Head and camera pose without any need for external sensors. This system will combine methods that include traditional image processing techniques for image projection, feature detection, key point description and 3D pose estimation along with Machine Learning techniques for face detection and facial landmarks detection.**

Keywords*—*Head Pose Estimation; real-time; face detection; face landmarks localization; single board computing; SBC; GPU optimization

I. Introduction

Realtime head pose estimation is a critical problem for many applications in the current industry. Applications such as autonomous driving where it provides assistance for the driver to monitor his attentiveness and drowsiness. This technique can also be used to provide real-time face recognition for tracking and monitoring systems on low cost boards, it can support future work in gesture and facial impressions recognition. In this approach we target the detection of head pose to support many applications like Driver monitoring systems, tracking drones, Gesture controls and augmented reality. This information is needed to detect the focus point and the concentration of the monitored person as well as to compensate for his motion to take the proper action accordingly. Our approach is to provide a system that is supposed to utilize low power profile consuming less than 10 watts while maintaining real-time operation.

As an example in a driver monitoring system, the driver assist camera need to check if the driver is concentrating on the road ahead or if he noticed the road signs and provide assistance and alerts, It can also support if he is trying to take a turn it can detect if he checked the side mirrors and that he is aware of the vehicles behind and his surroundings. Another example is in drone systems where it can be controlled by gestures and detect real gestures targeting the drone and not to be confused with fake gestures as part of his normal behavior by detecting the pose is front facing the drone. It can be used for video surveillance systems where it's always tracking and centered over certain person and needs to provide a good follow up for his face.

Our proposed system is supposed to address these kind of applications taking into consideration the challenges imposed when using limited low cost hardware capabilities and provide low power consumption.

While several Head pose estimation techniques exists with very high accuracy like the state of the art Face Alignment technique of V. Kazemi[1], X. Zhu and D. Ramanan's method [2] and others, these methods among others all focus on the accuracy and discard other aspects like performance and efficiency, these two aspects depending on the application that the model is needed for can be considered as a limitation like in our situation for the use case of the use inside a very small single board computer board to be installed inside a low powered application. This is where our model comes in hand as we will discuss we can achieve higher computational efficiency from these models without sacrificing the accuracy.

There are several approaches and techniques to address the same problem, either by using full AI methods, Geometric methods, Tracking methods and lastly the Hybrid methods which combines multiple methods together.

In our system, we will follow the Hybrid method approach which is based on Geometric method with additional tracking algorithm. This shall provide robust pose estimation specially in case of tracking a moving person or using a movable camera. The tracking method will provide information that comes to hand to support in recovery from failure and in occlusion. Our proposed system will be based on a normal geometric method with a layer of Kalman filter to provide a tracking method on top of our geometric analysis.

In this paper we will present our proposed head pose estimation technique illustrated in Fig. 1 which consists of Face detection, Facial landmarks detection, Head Pose Estimation and Kalman filter. We will be discussing the problem definition of 3D head pose estimation in Section II followed by a survey analysis for the proposed techniques on the building blocks such as Face detection, Facial landmarks detection and Point to point mapping techniques as well as the different proposals and their challenges in the real-time manner showing the reliability of such system in Section III. Later on in Section IV we will discuss our new system and the hardware environment used in a production grade system specifying our selected

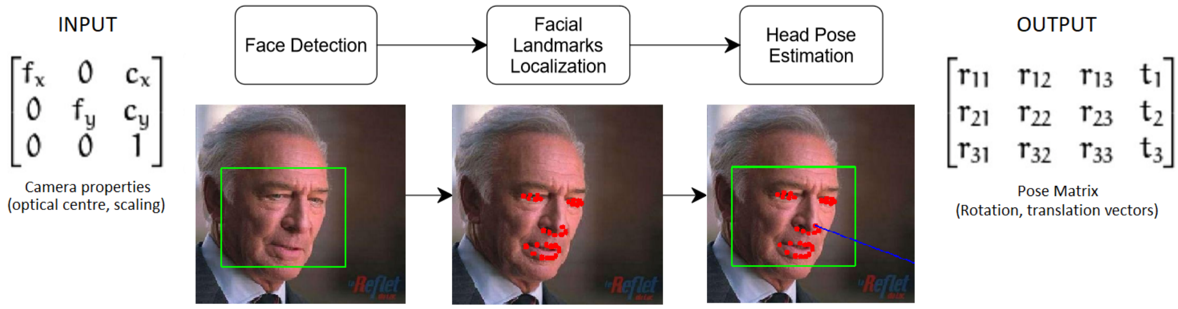

Fig. 1. A Block Diagram to Describe the Building Blocks of our Proposed System.

techniques and showing the relation between each phase with an illustrative algorithm and images for each phase. In Section V we will discuss our results and compare to the most famous state of the art techniques to provide a good insight of the performance and finally will concluded our research in Section VI.

II. 3D Head Pose Estimation

Pose estimation is a very popular topic in computer vision. It's problem definition is to find the extrinsic parameters of the camera matrix which are as following:

$$\begin{bmatrix} R_{3*3} & T_{3*1} \\ 0_{1x3} & 1 \end{bmatrix}_{4*4}$$

R & T represents the extrinsic parameters which transforms the coordinate system from 3D world coordinates to 3D camera coordinates. This means the Yaw, Pitch and Roll angles of the object in the 3D world coordinates system can be transformed to the camera coordinates system using linear equations give by:

$$\begin{bmatrix} X \\ Y \\ Z \end{bmatrix} = R \begin{bmatrix} U \\ V \\ W \end{bmatrix} + t$$

It also incorporates the usage of a 3D model to map the 2D detected points on the image plan over a 3D plan so that we can get the U, V & W 3D world coordinates. Using this method to find the extrinsic parameters in real-time for human's head R and T matrices to estimate the pose. Our system needs to utilize the geometric method where it needs to find the 2D coordinates of specific points in any human's head, This means we need to find the face from within the image frame and then find the pre define points in this image frame. These preselected points are needed to be mapped to the 3D model using point to point perspective for a generic Human head. In order to do so, the system needs first to do Face Detection, followed by Landmarks localization for these pre selected points, given these points we shall use PnP and solve for Pose Estimation, this workflow can be illustrated from Algorithm 1. Other methods are also applicable to combine steps together to find the 2D coordinate of these points.

Algorithm 1 Head Pose Estimation Geometric Method

Require: Camera Intrinsic parameters Cam_Mat
Require: Face Detector Model FD_model
Require: Facial Landmark detection Model FL_model
Require: Head Model Reprojection Matrix RP_Mat
  while New image frame **do**
    $img \leftarrow imageframe$
    $Faces \leftarrow FD\_model(img)$
    if $Length(Faces) > 0$ **then**
      for $Face$ in $Faces$ **do**
        $Landmarks \leftarrow FL\_model(Face)$
        $SolvePnP(RP\_Mat, Landmarks, Cam\_Mat)$
        $R\_vec, T\_vec \leftarrow SolvePnP$
        $R\_Mat = Rodrigues(R\_vec)$
        $Pose\_Mat[Face] \leftarrow R\_Mat, T\_vec$
      end for
    end if
  end while

III. Realtime Head Pose Estimation Candidate Techniques

While our primary goal is to find a robust yet real-time solution to the Head pose estimation problem based on the Geometric approach we selected, several techniques were suggested to achieve the best computational performance without sacrificing accuracy. The geometric approach consist of three main parts that may be combined in technique consists of a single model or the general technique of a standalone model for each stage, these stages are as follows:

1) Face Detection Technique.
2) Facial Landmarks Localization Technique.
3) Point to Point perspective for Head pose estimation.

A. Face Detection Technique

Here we discuss different techniques for face detection from within the image, the purpose of this step is to identify the face and return a bounding box identifying the location of the face within the image as illustrated in Fig. 2. If a face is detected, it's location will further on be supplied to the Facial landmarks detector for further processing, most of face detection approaches are based on machine learning models that are trained on object detection.

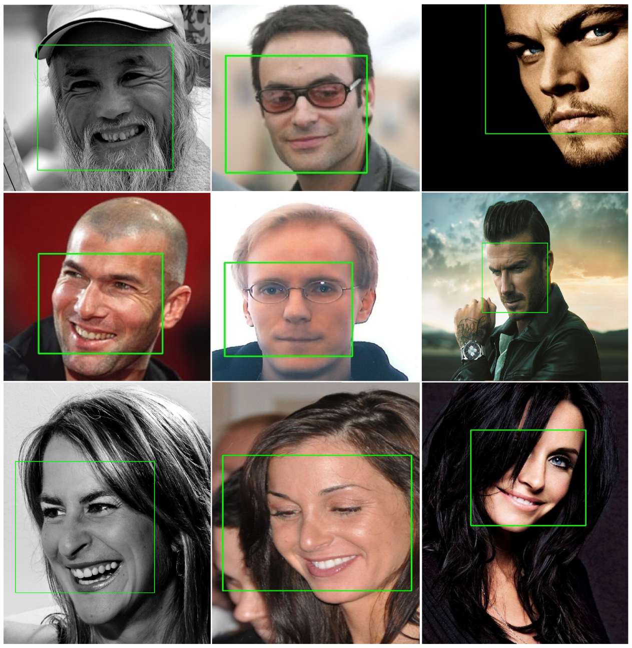

Fig. 2. A Face Detection Sample of the Hybrid Algorithm using MMOD Technique[6].

The first proposed technique was the well known Haar feature-based cascade classifiers which was proposed by Viola and Jones [3][4], this technique consists of three main stages Haar features acting as the convolution kernel and plenty of these features are calculated, then selection process over these feature to provide with relevant and informative features and discard the week features using adaptive boosting technique. The classifier is the combination of the strong features. This technique provides good accuracy and has good computing efficiency but suffers greatly under occlusion and non-frontal faces.

Another proposed technique is using the Histogram of Oriented Gradients, the HOG method for face detection is based on the same concept of object detection as depicted by the well known pedestrian detection technique 'Histograms of oriented gradients for human detection' [5], the HOG descriptions using sliding windows are extracted for positive and negative samples then used for training a linear SVM, of course the sliding windows and multiscale windows are used to detect objects within the image frame regardless of their location and scale then we suppress the non-maxima bounding boxes as we will end up having multiple detection for the same object. While HOG method provides better performance than the Haar cascade classifiers method in terms of occlusions, non-frontal facing and illumination invariance, it's still computationally expensive as sliding windows techniques are usually expensive specially when we are doing operations like gradient calculations in HOG yet still faster in and offers superior performance than that of the previous Haar cascade classifiers.

Another technique like Max-Margin object detection [6] for HOG CNN based features was taken into consideration, This technique is known to be slower than the HOG method but provides superior performance in facial detection in cases of occlusion and hard detection cases.

While there are many more techniques that contributes to the same issue like TinyFaces, DSFD [7] and ASFD and many others that perform great in terms of multiple faces detection with various benchmarking datasets like WIDER [8] and FDDB [9] yet this increased accuracy for detection of multiple faces is irrelevant to our application as we only need to detect single face, also they are much more computational intensive than that of our system can't provide. These previous methods are concerned for face detection only, there are also techniques that can do extra task, in particular some techniques can do both the face detection as well as landmarks localization, these techniques shall be taken into consideration against the previously suggested alternatives for face detection integrated with the face landmark detection techniques altogether for fair judgment, for this we will discussing them in the next section with face landmark detection.

B. *Facial Landmarks Localization Technique*

Face landmarks detection is the last step before Head pose estimation to detect the preselected points in Human's face, it starts by providing the algorithm with location of the face within the image frame bounded by a box as in Fig. 2, the model then processes this bounding box to provide the location of some points in the face as in Fig. 3 where we can identify the eye, eyebrows, nose, mouth and jawline if needed. There are many datasets that differentiates between the facial landmarks. Our selected dataset was based on iBUG dataset "a semi-automatic methodology for facial landmark annotation" [10], [11], [12], this base dataset contains 68 landmark points and it's created from several other datasets including the LFPW [13], HELEN [14] and other datasets which results in 7674 images in total, these images were annotated using a semi-automated annotation process, this provides a vast number of training and testing data that are very rich in variations in conditions and imposes more challenging situations for the proposed techniques.

Another notable mention is the HELEN dataset [14] that originally provides 194 localization points as facial landmarks instead. It consists of 2000 images for training and 330 for testing. Usually more localization landmark points translates to better accuracy, but also this comes at the cost of computational needs during technique's inference operation in runtime. Among the vast proposals of face landmarks localization techniques we have the ensemble of regression trees V. Kazemi and J. Sullivan's technique [1], this technique was claimed to have one millisecond performance per image, this technique provides good benchmarks compared to many state of the art techniques, we put this among our proposed solution for this reason however, they didn't mention the Hardware used to benchmark their claimed computational needs. Another technique was proposed by S. Ren LBF technique [15] which claims to reach 3000 fps while providing better results by utilizing the concept of local binary features search instead of using a global one over the whole image frame which provides better error rate when validated over the two datasets of our choice. Other techniques that can do multiple operations like the one introduced by Multi-task Cascaded Convolutional Neural Networks MTCNN technique[16], this technique can directly identify the face and also do five point facial landmarks

Fig. 3. Facial Landmarks Localization Output using our Proposed Method.

detection, this technique stands out in real life results for both face detection and Landmarks localization but it's five landmark points only which will not provide enough information for applications such as drowsiness behavior or emotion state, it's also performing much worse in terms of computational needs as it provides less than one fps thus can't be utilized for real-time operations for low power applications, another suggested technique is proposed by Zhu and Ramanan [2], this technique does all, the face detection, landmark localization and the pose estimation which is quite very useful as it sums up all the stages for pose estimation, yet still it has huge cost in terms of computational need as they claim it takes 40 seconds per image to provide high accuracy compared to the commercial existing solutions.

C. Point to Point perspective for Head Pose Estimation

Lastly, Point to Point perspective needed to calculate head pose estimation. At first we need to compensate for scale variation by using the size of the face box according to the face detection algorithm, afterwards we need to have an estimated 3D model for the face in order to map each facial 2D point to it's corresponding 3D face model, this mapping is needed to find the Head Pose from this 2D-3D correspondence. Many proposed methods exist for such called perspective point problem (PNP), one of the methods is based on Levenberg-Marquardt optimization another which provides higher efficiency is the Effective PNP method [17] and lastly is a method using the direct least square solutions for PNP [18] which provides better accuracy and error rates without sacrificing real-time operation than the previous two methods. Other approaches exist that rely on noise free points Like P3P and P4P approaches but they proven not suitable for our application as they provide inaccurate results when there are higher noise in these selected points. After estimating the Pose, we apply Kalman filter for further filtering the output in order to have a smooth transitions and better correlation between each frame and the preceding which reflects real life behaviors.

IV. Single Board Implementation for 3D Head Pose Estimation

A. Our Proposed System

Aiming to target real-time performance on a production ready solution we selected a well known and stable platform that supports low power applications with industry grade performance and capabilities that also supports easy expandability. Our Selected control board is Jetson Nano board provided by Nvidia depicted in Fig. 4. This system specifications are illustrated in Table I. It's constructed of a Quad-core ARM Cortex-A57 MPCore processor along with NVIDIA Maxwell GPU with 128 NVIDIA CUDA cores to support image manipulation and model inference functions included in our algorithm. This single board computer (SBC) module consumes less than ten Watts with all peripherals connected. This board is 69.6 mm x 45 mm in size which is smaller than a credit card in size which makes it very suitable in small low powered applications, to have imagination about how low is it's power consumption, When installed in any product, Our system's power needs is less than the tenth of the power needed by the smallest motor installed in a small drone, it's almost the same power consumed by a toy DC motor. This proves how efficient it can be used in low-powered embedded applications.

TABLE I. NVIDIA Jetson Nano Main System Specifications.

CPU	Quad Core ARM Cortex A-57 1.43GHz
GPU	128 Maxwell Cores
Memory	4 GB 64 bit LPDDR4 25.6 GB/s
Storage	16GB eMMC
Camera	12 MIPI CSI-2 DPHY 1.1 lanes 1.5Gbps
Peripherals	PCIE USB3.0 SDIO SPI SysIO GPIOs I2C
Power Consumption	5 Watt or 10 Watt modes

This board runs Linux operating system environment, this allows us to use many libraries such as OPENCV and DLIB[19], also models that are built using Caffe, Pytorch or TensorFlow. This is amazing feature to run a lot of variations as well as building our custom models.

The rest of our system is constructed of a single IR camera sensor accompanied by IR LED lights to provide good illumination for the image and to prevent distraction and confusion with no additional sensors are used in our system. This camera sensor supports frames of resolution up to 1,920x1,080 for 30 frames per second with scalable viewing angle and focus. This system is supposed to provide the rotation matrix parameters Yaw, Pitch and Roll for both the head pose in case of movement. The camera is assumed to have a constrained range of motion around all three-axes assuming that no sudden far jumps can happen so that there will always be a correlation between a frame and it's preceding one.

As illustrated earlier, Our system shall consist of several stages as shown in Fig. 1, Each stage contribute to our problem definition as shown in Algorithm 1. We expect that the human

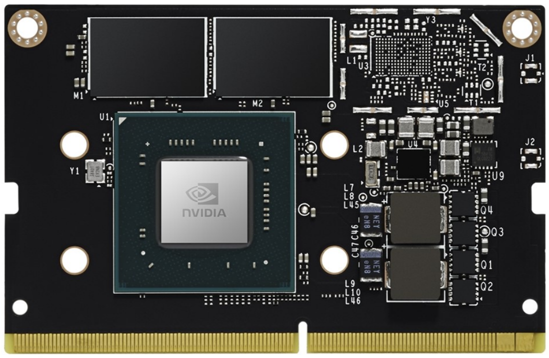

Fig. 4. NVIDIA Jetson Nano Production Module.

will have a front facing camera with a constrained movement that majorly will be facial facing but encounter change in yaw, pitch and roll angles. Our system will perform all the stages on video stream in real-time manner to provide robust tracking of the Head's pose using the Hardware we presented. We split the system into these three main stages where we can address each at a time:

1) Initialization.
2) Our Head Pose Estimation System.
3) Tracking Kalman Filter.

B. Initialization

As mentioned earlier our system consists of a single camera sensor, this sensor is like any camera needs to be calibrated, this calibration process is needed to find the intrinsic parameters of the camera sensor whish is done using checkerboard method [20], the checkerboard method measures the intrinsic parameters in terms of focal length and the principal point, also it measures the extrinsic parameters, these data is used to build the calibration matrix needed later on in both the Camera and Head pose estimation, the extrinsic parameters defines the 3-D location of the camera with respect to the world coordinate which are used to translate from the 3-D camera coordinate system to world coordinate system, the intrinsic parameters is used in the transformation from 2-D coordinate system in the image to the 3-D camera coordinate system, lastly camera distortion matrix can also be calculated which can be used in correcting image distortions like radial and tangential distortions but they are not mandatory.
This step is done for a single camera sensor at the first setup and these values later on to be used as standard configuration for the system, they need to be done for autofocus sensors and provide some kind of look up table or through equation as these parameters are dependent on the focal point.

C. Our Head Pose Estimation System

Geometric method of head pose estimation as we discussed earlier constitutes of 3 main parts, Here we will state our selected techniques from the ones we suggested earlier and in Section V we shall see comparison of it's performance and how our selected techniques compares to others.

Using a real-time video stream, we shall feed our face detection algorithm on a frame by frame basis based on Max-Margin object detection [6] method, This method provides more robust results than the other two methods in field tests,

This method is supposed to be slower than HOG method however, using GPU accelerated implementation of this method it performed great in our test that somehow surpassed the other approaches due to it's higher accuracy. MMOD method provides two points representing the bounding box for the head location which is suitable to be provided to our own custom model of head landmarks detection needed for face alignment problem.

Max-Margin Object detector technique is a generic technique that's trained over face detection dataset FDDB [9], the MMOD uses similar approach to HOG in building HOG descriptors using sliding window classification method and utilizing random projection based locality sensitive hash for determining which bin the calculated HOG descriptor belongs to, this projection process is less in computational cost than the original HOG method, yet the whole process is more expensive due to the sliding window operation. This method was selected to elevate the accuracy of face detection as it's the corner stone of the Head pose estimation to correctly identify the head from within each image frame.

In the other hand, for the facial landmarks localization technique, we build our own custom model to be used which is based on the ensemble of regression trees similar to V. Kazemi's [1] but with a modification in the set of facial landmark points, this approach was done over three phases to get the best computational efficiency without sacrificing the accuracy. The first phase is to select feature points that gives us relevant information regarding our needed aspects as shown in Fig. 5 where it illustrates the most important landmarks that provides comparable results according to 68 Landmarks Dataset, Fig. 5b shows our selected points are those that describes eye lid opening, head orientation and mouth contour, which are the points that contributes mostly to the drowsiness behavior, emotional state, and has higher impact on determining face orientation. Secondly analyzing the impact of each model parameter on the overall performance of the model and selecting the optimum range for these parameters. The last phase is to do parameter optimization over 150 combinations of the selected ranges for each model parameter and calculate metrics for overall accuracy over both train and test data, training and inference speed and lastly size, these metrics are used for comparative analysis with the original models as well as other alternative solutions.

Lastly, Point to point perspective, we used the direct least square PNP [18] which provides both accuracy and real-time operation. This function is already implemented in OPENCV library and can be used directly by providing it the Model points and the corresponding points from the previous step of Facial landmarks localization. Solving this PnP problem we get our R_vec and T_vec which constitutes the pose matrix

D. Tracking Kalman Filter

Kalman filter named after Rudolf E. Kálmán is a modeling technique used for predicting the next state from the history of previous data. This technique is widely used in cases of trajectory and motion planning as well as signal processing algorithms as it provides robustness to statistical noises and

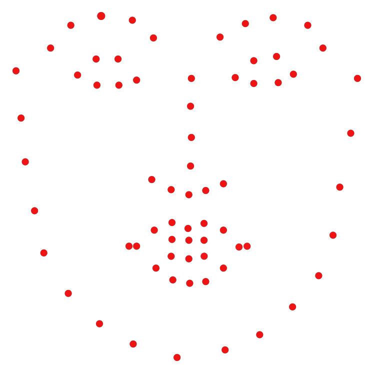

(a) Original 68 Facial Landmark Points based on the 300-W Dataset[10], [11], [12].

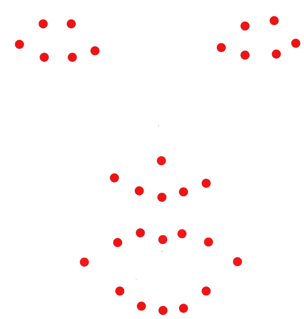

(b) Our Model's Selected set of Facial Landmarks.

Fig. 5. Our Proposed Selected Set of Facial Landmark Points Compared to the Original 68 Landmark Points[10], [11], [12].

sudden abrupt changes that are not following the trajectory pass according to the previous state. In it's simplest form, it follows linear equations however, this filter contains many complex variations and can predict the state of 2D, 3D and more complex non linear equations states with many variations like Extended Kalman filter, unscented, Hybrid and many other variations. Here in our applications we used the simple form of Kalman filter to predict the pose estimation to provide it as the simplest for of tracking algorithm to the head pose. We firstly start by constructing the Kalman filter and then by starting the application we feed the filter with data after each phase until the filter converges and then it shall provide filtration from occlusion and drop or incorrect data during operation for sudden short periods of time.

V. Experimental Results

In our experimental test we will show how each of the Face Detection and Facial Landmarks localization techniques perform in respect of Realtime operation and accuracy of detection. Also we will be showing the Benchmark results of them compared to each other in terms of error rate to show how accurate each technique shall perform.

For the Face detection operation we will be comparing between Viola and Jones technique [3] [4], HOG technique[5] and Max-Margin object detection [6] technique in terms of the speed of inference and error rate as depicted in Fig. 6. Our diagram shows how each technique compares to each other in terms of speed and accuracy of detection. Our accuracy of detection method is according to FDDB metrics of the ROC curves based on continuous score method for the True positive rate at 1000 False positive samples threshold. Our results indicate that the FaceDetection process is the bottle neck of the whole algorithm as the frame rate are much lower than the other parts of the algorithm.

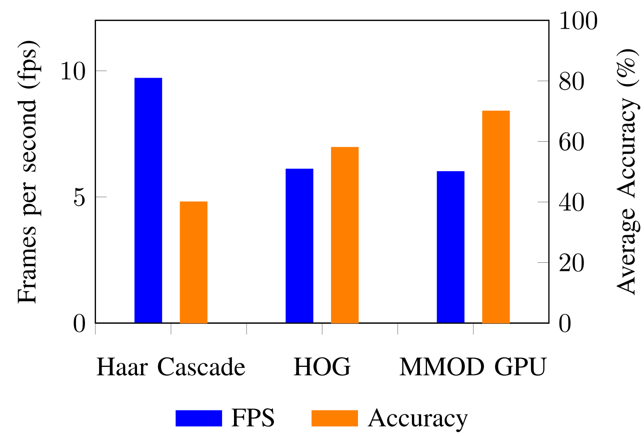

Fig. 6. Comparison between the three Proposed State of the Art Face Detection Techniques in terms of Accuracy and Performance as Frames Per Second.

In terms of Face landmarks localization, in Fig. 7 we show how our reduced feature points technique performance is compared to the original S. Ren LBF technique and V. Kazemi ERT technique using our hardware configuration. We will apply same approach of V. Kazemi's technique where only 31 points are selected instead of the full 68 landmark points of the 300-W dataset in order to maximize speed without sacrificing accuracy.

This illustrated accuracy is calculated using 1000 images from testing dataset in addition to 6674 from the training dataset of combined datasets including iBUG dataset [10], [11], [12], LFPW [13] and HELEN [14] for testing purpose using the same criteria as described by V. Kazemi. Calculation of the accuracy was done using their provided function of DLib library, this function calculates the distance of each landmark to the ground truth position, this value is divided by the interocular distance to get the normalized distance of the landmark. Using the average of this normalized distance we can get the error and hence the accuracy as depicted in our diagram. Our technique shows very good results compared to other techniques while on a larger dataset with much more sparse training and testing data. As illustrated in Fig. 8, We showed a sample of images from the three datasets we used AFW, HELEN, IBUG and LFPW where multiple faces are detected correctly with different poses and lighting conditions as well as immunity to different occlusion types and glasses wearing yet there are certain scenarios that the system fails in either identifying the face or to locate the landmarks correctly, this normally happens in very minor situations when it's in a very acute pose, or when the occlusion is severe that eliminates crucial parts of the face and makes it hard to detect the distinctive facial features.

Also using AFLW2000-3D dataset [21] which is 2000

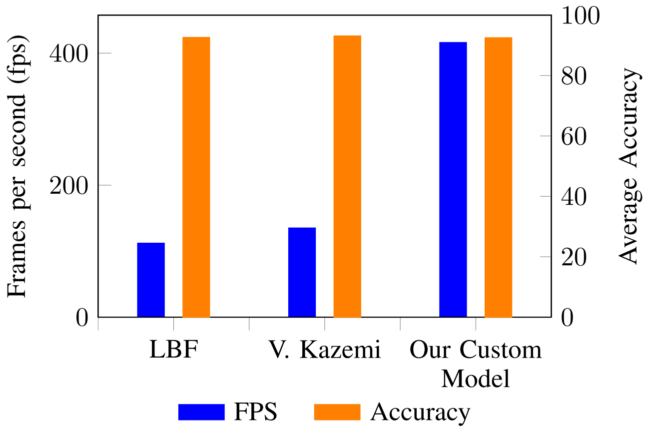

Fig. 7. Comparison of Face Landmarks Localization Techniques between our Custom Model Versus the well known Models of LBF [15] and V. Kazemi [1] in Terms of Performance and Accuracy of Detection.

image can be used for 3D face alignment evaluation, our system which is based on DLib approach with reduced number of points showed Mean average error of 16 degrees versus 9 of the Ground Truth landmarks.

Our benchmarking tests of the full system performs with total frame rate around five frames per second for sampling a 640x480 monochrome image which is very good performance. This is done utilizing only the GPU of our evaluation board, leaving the Quad-core ARM Cortex-A57 almost free for other application threads that will utilize the output of this algorithm. This leaves more room for further parallelization, optimization and off loading to the Quad-Core CPU if needed.

VI. Conclusion

We presented a real-time full system for head pose estimation for embedded infrared camera sensor, that's capable of compensating for the motion of the camera and provide the 3D Head pose estimation accordingly. We presented our new system including the techniques of Face detection, Facial landmarks localization and Point to point mapping that are optimized for operation over embedded low powered devices that has limited computational abilities. We also presented the challenges in each step as well as the possible techniques that are suitable for our applications presenting our own modification for the Face landmark localization technique showing both speed and accuracy of operation. Lastly we presented the pose estimation calculations and Kalman filter for smoothing out fluctuations and better tracking. As for the future direction, Our model can be enhanced to use the detected facial landmarks of the human and analyzes his drowsiness and detect this facial emotions and provide further more information beyond the pose estimation.

References

[1] V. Kazemi and J. Sullivan, "One millisecond face alignment with an ensemble of regression trees," in *2014 IEEE Conference on Computer Vision and Pattern Recognition*, 2014, pp. 1867–1874.

[2] X. Zhu and D. Ramanan, "Face detection, pose estimation, and landmark localization in the wild," in *2012 IEEE Conference on Computer Vision and Pattern Recognition*, 2012, pp. 2879–2886.

[3] P. Viola and M. Jones, "Rapid object detection using a boosted cascade of simple features," in *Proceedings of the 2001 IEEE Computer Society Conference on Computer Vision and Pattern Recognition. CVPR 2001*, vol. 1, Dec 2001, pp. I–I.

[4] ——, "Robust real-time face detection," in *Proceedings Eighth IEEE International Conference on Computer Vision. ICCV 2001*, vol. 2, 2001, pp. 747–747.

[5] N. Dalal and B. Triggs, "Histograms of oriented gradients for human detection," in *2005 IEEE Computer Society Conference on Computer Vision and Pattern Recognition (CVPR'05)*, vol. 1, 2005, pp. 886–893 vol. 1.

[6] D. King, "Max-margin object detection," *ArXiv*, vol. abs/1502.00046, 2015.

[7] J. Li, Y. Wang, C. Wang, Y. Tai, J. Qian, J. Yang, C. Wang, J. Li, and F. Huang, "Dsfd: Dual shot face detector," in *2019 IEEE/CVF Conference on Computer Vision and Pattern Recognition (CVPR)*, 2019, pp. 5055–5064.

[8] S. Yang, P. Luo, C. C. Loy, and X. Tang, "Wider face: A face detection benchmark," in *2016 IEEE Conference on Computer Vision and Pattern Recognition (CVPR)*, 2016, pp. 5525–5533.

[9] V. Jain and E. Learned-Miller, "Fddb: A benchmark for face detection in unconstrained settings," University of Massachusetts, Amherst, Tech. Rep. UM-CS-2010-009, 2010.

[10] C. Sagonas, E. Antonakos, G. Tzimiropoulos, S. Zafeiriou, and M. Pantic, "300 faces in-the-wild challenge: database and results," *Image and Vision Computing*, vol. 47, pp. 3–18, 2016, 300-W, the First Automatic Facial Landmark Detection in-the-Wild Challenge. [Online]. Available: https://www.sciencedirect.com/science/article/pii/S0262885616000147

[11] C. Sagonas, G. Tzimiropoulos, S. Zafeiriou, and M. Pantic, "A semi-automatic methodology for facial landmark annotation," in *2013 IEEE Conference on Computer Vision and Pattern Recognition Workshops*, 2013, pp. 896–903.

[12] ——, "300 faces in-the-wild challenge: The first facial landmark localization challenge," in *2013 IEEE International Conference on Computer Vision Workshops*, 2013, pp. 397–403.

[13] P. N. Belhumeur, D. W. Jacobs, D. J. Kriegman, and N. Kumar, "Localizing parts of faces using a consensus of exemplars," *IEEE Transactions on Pattern Analysis and Machine Intelligence*, vol. 35, no. 12, pp. 2930–2940, 2013.

[14] V. Le, J. Brandt, Z. Lin, L. Bourdev, and T. S. Huang, "Interactive facial feature localization," in *Computer Vision – ECCV 2012*, A. Fitzgibbon, S. Lazebnik, P. Perona, Y. Sato, and C. Schmid, Eds. Berlin, Heidelberg: Springer Berlin Heidelberg, 2012, pp. 679–692.

[15] S. Ren, X. Cao, Y. Wei, and J. Sun, "Face alignment at 3000 fps via regressing local binary features," in *2014 IEEE Conference on Computer Vision and Pattern Recognition*, 2014, pp. 1685–1692.

[16] K. Zhang, Z. Zhang, Z. Li, and Y. Qiao, "Joint face detection and alignment using multitask cascaded convolutional networks," *IEEE Signal Processing Letters*, vol. 23, pp. 1499–1503, 2016.

[17] V. Lepetit, F. Moreno-Noguer, and P. Fua, "Epnp: An accurate o(n) solution to the pnp problem," *International Journal of Computer Vision*, vol. 81, 02 2009.

[18] J. A. Hesch and S. I. Roumeliotis, "A direct least-squares (dls) method for pnp," in *2011 International Conference on Computer Vision*, 2011, pp. 383–390.

[19] D. E. King, "Dlib-ml: A machine learning toolkit," *Journal of Machine Learning Research*, vol. 10, pp. 1755–1758, 2009.

[20] Zhengyou Zhang, "Flexible camera calibration by viewing a plane from unknown orientations," in *Proceedings of the Seventh IEEE International Conference on Computer Vision*, vol. 1, 1999, pp. 666–673 vol.1.

[21] X. Zhu, Z. Lei, X. Liu, H. Shi, and S. Z. Li, "Face alignment across large poses: A 3d solution," in *2016 IEEE Conference on Computer Vision and Pattern Recognition (CVPR)*. Los Alamitos, CA, USA: IEEE Computer Society, jun 2016, pp. 146–155. [Online]. Available: https://doi.ieeecomputersociety.org/10.1109/CVPR.2016.23

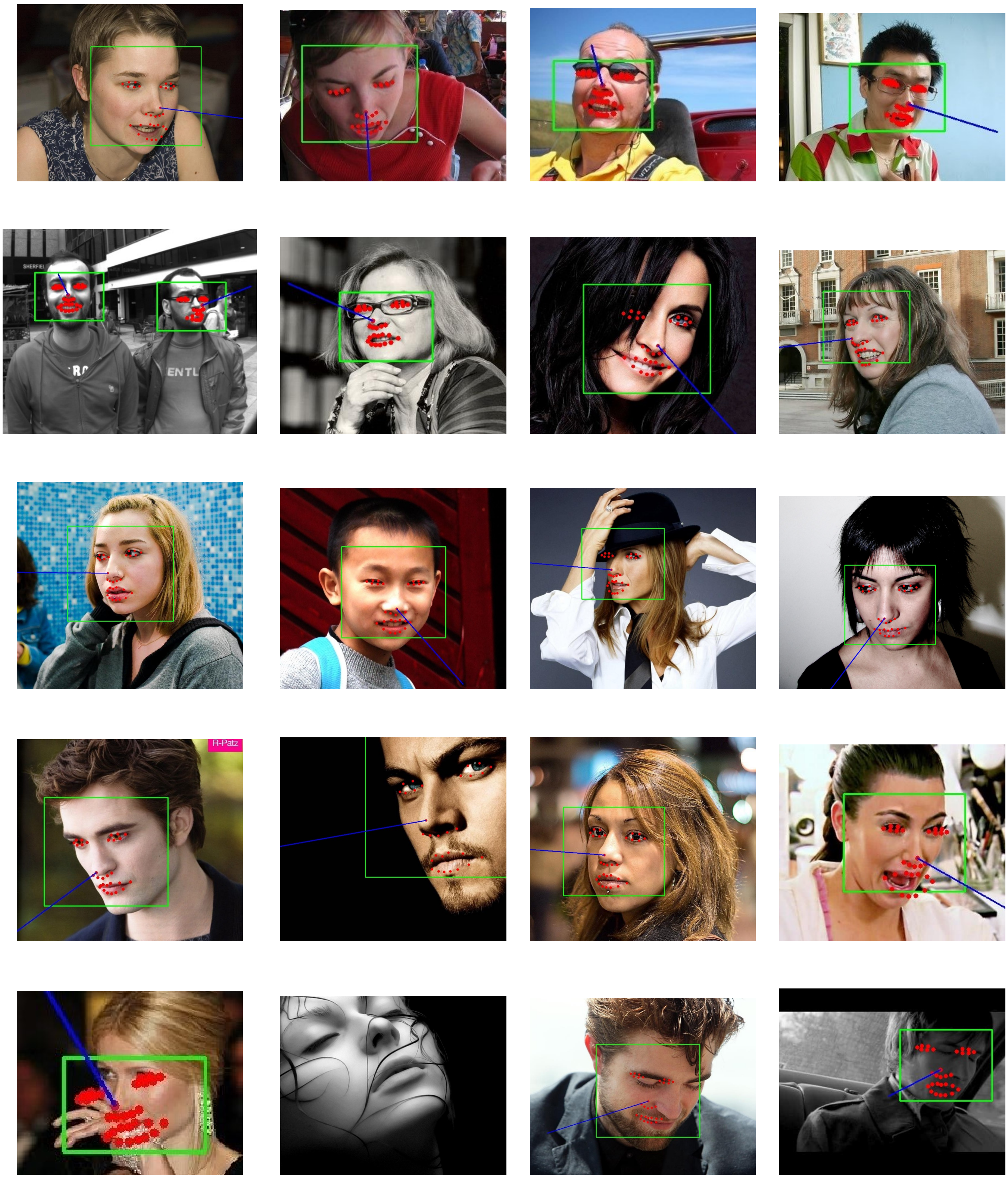

Fig. 8. Sample of the Output from our used Datasets to show Immunity to Partial Occlusion, Lighting Conditions, Wearing of Glasses and Different Poses with the Last set Showing Scenarios of a Negative Result.

SIP-MBA: A Secure IoT Platform with Brokerless and Micro-service Architecture

Lam Nguyen Tran Thanh[1], Nguyen Ngoc Phien*[2], The Anh Nguyen[3], Hong Khanh Vo[4], Hoang Huong Luong[5], Tuan Dao Anh[6], Khoi Nguyen Huynh Tuan[7], Ha Xuan Son[8]
VNPT Information Technology Company, Ho Chi Minh city, Vietnam[1]
Center for Applied Information Technology, Ton Duc Thang University, Ho Chi Minh City, Viet Nam[2]
Faculty of Information Technology, Ton Duc Thang University, Ho Chi Minh City, Vietnam[2]
Department of Computer Science, Faculty of Electrical Engineering and Computer Science,
VSB-Technical University of Ostrava, Ostrava, Czech Republic[2]
FPT University, Can Tho City, Viet Nam[3,4,5,6,7]
University of Insubria, Varese, Italy[8]

Abstract— **The Internet of Things is one of the most interesting technology trends today. Devices in the IoT network are often geared towards mobility and compact in size, thus having a rather weak hardware configuration. There are many light weight protocols, tailor-made suitable for limited processing power and low energy consumption, of which MQTT is the typical one. The current MQTT protocol supports three types of quality-of-service (QoS) and the user has to trade-off the security of the packet transmission by transmission rate, bandwidth and energy consumption. The MQTT protocol, however, does not support packet storage mechanisms which means that when the receiver is interrupted, the packet cannot be retrieved. In this paper, we present a broker-less SIP-MBA Platform, designed for micro-service and using gRPC protocol to transmit and receive messages. This design optimizes the transmission rate, power consumption and transmission bandwidth, while still meeting reliability when communicating. Besides, we implement users and things management mechanisms with the aim of improving security issues. Finally, we present the test results by implementing a collect data service via gRPC protocol and comparing it with streaming data by using the MQTT protocol.**

Keywords—Internet of Things (IoT); gRPC; Single Sign-On; brokerless; micro-service; MQTT; message queue; security

I. Introduction

In recent years, Internet of Thing (IoT) applications have grown and applied in most fields such as smart city, health-care, supply chains, industry, agriculture, etc. According to estimates, by 2025, the whole world will have approximately 75.44 billion IoT connected devices [1]. Timothy et al. [2] claimed that the IoT system architecture consists of 5 layers in order from low to high: Things, Connect, Collect, Learn and Do.

Specifically, the Things layer is the class of actuators to control physical devices or sensors to collect environmental parameters. The Connect layer connects devices with applications and users. The Collect layer is responsible for aggregating the data returned by the Things layer devices. Finally, Learn layer is used to analyze data to give suggestions to Do layer in response to received data. Eventually, the Things and Connect layers are the two most important ones because these provide the input data for the upper layers.

The Things layer consists of devices in the IoT which have limitations in network connectivity, power, and processing capabilities [3]. Therefore, the question is how can we optimize the processing capacity and power consumption of the devices, while still have to meet some requirements of communication speed as well as the confidentiality of information on transmission lines. This problem is determined by the protocol itself within the Collect class.

For interfaces in constrained networks, MQTT and CoAP are proposed to use [4]. We found that MQTT protocol had faster Packet transmission and creation time twice as fast as CoAP protocol. Besides, for developers of low bandwidth and hardware configuration devices, MQTT is the most preferred protocol [5]. Comparison of energy consumption, Mart et al. [6] found that the MQTT protocol consumes less energy than CoAP. For the above reasons, in this paper, we evaluate the aspects of power consumption, hardware capacity capacity as well as security risks (security risks) present of The platforms use the MQTT protocol.

The MQTT protocol uses a publish / subscriber [7] architecture, with the MQTT broker at the center. The MQTT subcriber (client), connects to the broker and sends messages to topics. Brokers rely on topic for packet routing, meaning that subscribers who subscribe to a topic receive all messages sent to that topic. This means that when the MQTT broker crashes, the whole system will be affected.

The MQTT protocol has four levels of QoS, ranging from 0 to 2[1] and these QoS levels are related to the level of confidence in the transmission of the packet (QoS has the lowest confidence level and QoS-2 has the confidence level. highest reliability). According to the article [8], the ratio of packet loss and packet transmission rate of QoS-0 level is highest. However, according to the article [9], the energy consumption of the QoS-0 level is only about 50% of the QoS-2 level and the communication bandwidth of QoS-0 is also lower than that of QoS-2. The MQTT protocol runs on TCP [10] and each TCP connection can only make one request and one response. This means that in order to send a message at the QoS-2 level, each client in the system using

[1]https://mqtt.org/

MQTT must make four TCP connections [11]. This results in systems using MQTT consuming a lot of bandwidth and the device's hardware processing capabilities. In addition, by using a publish / subscribe architecture, in order for subscribers to be ready to receive incoming messages on topics, the subscriber must maintain a persistent connection to the MQTT broker. The time to keep connection is determined by the parameter keep alive. Article [12] has shown that the shorter the keep alive cycle, the higher the energy consumption. On the other hand, according to the article [13], MQTT was created for transmission purpose. Therefore, it does not provide message storage capability and does not guarantee the order of the message when it reaches the receiver. These are also two important issues that need to be considered as the weaknesses of the system using MQTT.

In terms of security, the current MQTT protocol only provides identity, authentication and authorization for the security mechanism [14] but is very simple. Therefore, there are a lot of security risks. Lundgren et al. [15] indicates that we can obtain data by subscribing to any topic of the MQTT broker that is public on the internet - a serious security risk. If the attacker subscribes to MQTT topics with the client ID, the victim will experience a denial of service status and all information sent to the victim is passed on to the attacker - a serious risk factor [16]. Regarding the Authentication mechanism, MQTT supports authentication by username and password pairs, but the authentication mechanism is optional and not encrypted. The MQTT client authenticates itself by sending the username and password plaintext in the CONNECT package. Attacker attacks are made easily by blocking packets [14]. Zaidi et al. [17] survey of Shodan, the world's first IoT search engine for Internet-connected devices, found that there were 67,000 MQTT servers on the public Internet with most of them not authentic. MQTT has support for Authorization mechanism to access specific topic based on access list (ACL). This access list must be predefined in the configuration file of the MQTT broker and we must restart the MQTT broker service if we want to apply the new access list configuration. This is inconvenient and difficult to scale especially for systems with billions of devices and these devices may only have the authority to take action for a specified period of time on specific topics. Access control and authorization are a major challenge [18].

In this paper, we summarize the weaknesses of platforms using MQTT protocol, such as bandwidth issue, hardware processing power, power consumption, no message storage mechanism, and security risks. Since then, the paper proposes the SIP-MBA Platform model to use brokerless architecture to limit the weaknesses of brokered architecture. Our SIP-MBA Platform is designed in micro-service, devices and services communicate directly with each other by peer-to-peer communication model for fast communication speed. In the system architecture, we also added message queues to store messages when communicating between services, helping to ensure that when a service fails, it is still possible to receive messages during recovery. The communication process of the components in our SIP-MBA Platform will take place proactively, without requiring a constant connection to reduce energy and bandwidth consumption. To do this, we use gRPC as the communication protocol between devices and services. This work presents a method of combining gRPC and Oauth to complement the Authentication and Authorization mechanism for SIP-MBA Platform. Besides, we introduces a management model of users and things and channels information to prevent denial-of-service attacks and impersonation of participating systems.

The rest of paper is organized as follows. In Section 2 we provide knowledge about the technology used in this work. Section 3 discusses related work. In Section 4, we introduce our proposed system Architecture and in Section 5 is software architecture. Section 6, we implement Collect data service - this is the most important service in our architecture. Section 7, we discuss our test results. In Section 8, we conclude the paper and discuss the potential future work.

II. Background

A. gRPC and http/2

gRPC[2] (general-purpose Remote Procedure Calls) is an open-source high performance framework of Remote Procedure Call Protocol (RPC) developed by Google. gRPC is built on http/2 protocol. Improvements in http/2 over previous versions allow for better and more efficient http performance connections. One of the most important features of http/2 is multiplexing, which sends and receives multiple packets in a single connection. The activity comparison between http/1.1 and http/2 is shown in Fig. 1:

gRPC has four types of communication as follows [19]:

- Unary: Similar to traditional client-server communication. The client sends a request to the server, waits for the server to process it, and then returns the results to the client.
- Server streaming: In this mode, the client sends a request to the server and then waits for the server to return a stream of data. The client read messages from that stream until no more messages are returned. The order of messages for each stream is guaranteed to be the same between client and server.
- Client streaming: Similar to Server streaming RPCs, in this type, the client is the side that sends the data stream to the server, the server read the stream and perform the necessary processing, and then return the data to the client.
- Bi-direction streaming: This is the type of method where the data is sent in a stream from both client and server directions, the data stream in both directions is independent of each other, and the client and server can process that streamed data independently. That means when the client sends a message to the server, the server can process it to perform a certain task (while still receiving other messages) and send the result back to the client (while the client is still sending another message).

B. Oauth Protocol and Single Sign-On

Oauth basically is an authentication mechanism that enables third-party applications to be authorized by the user

[2]https://grpc.io/

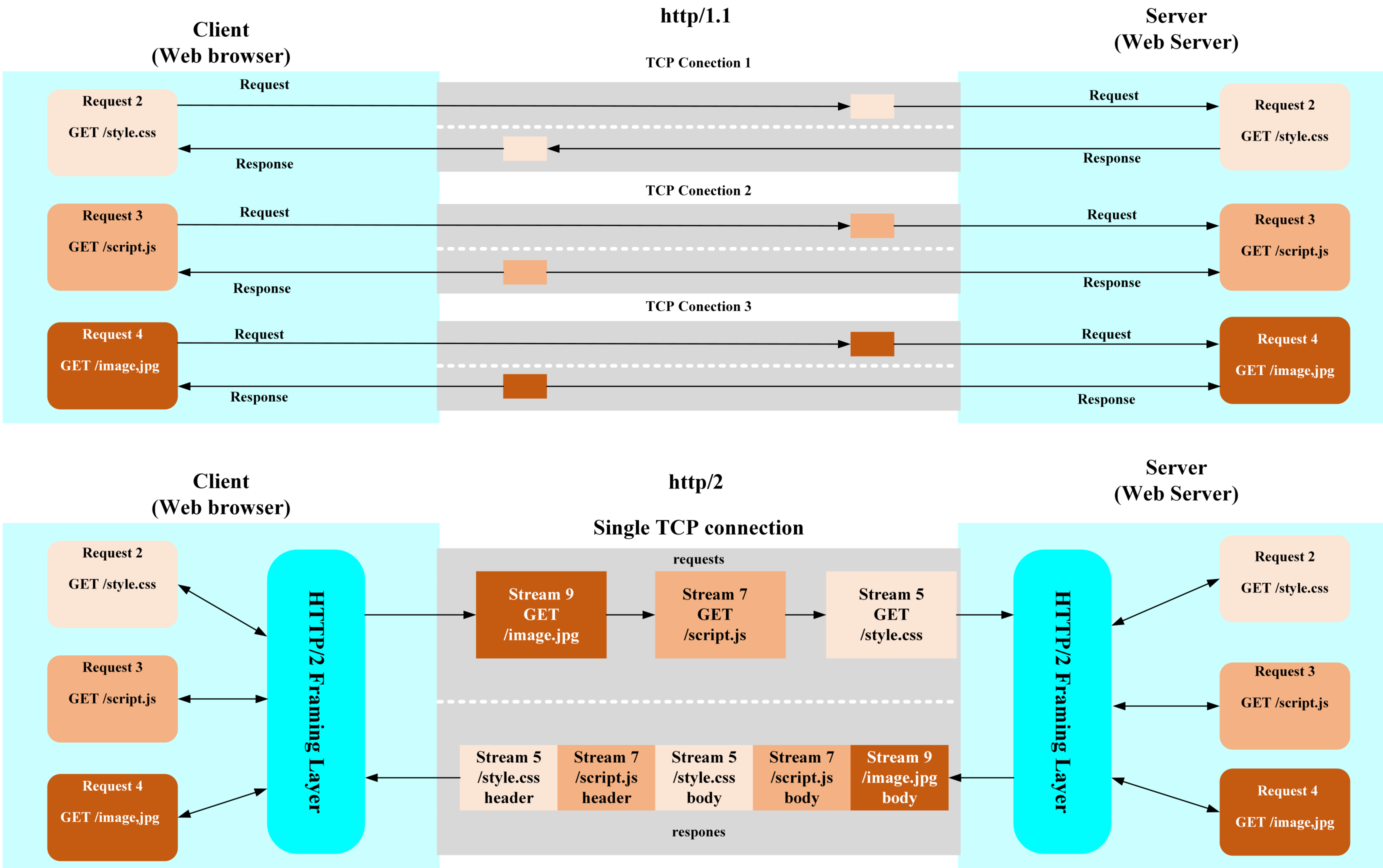

Fig. 1. The Activity Comparison between http/1.1 and http/2 [19].

to access the user's resources located on another application. Oauth version 2.0 is an upgrade of Oauth version 1.0, an authentication protocol that allows applications to share a portion of resources with each other without the need to authenticate via username and password as the traditional way. That helps limit the hassle of having to enter a username, password in too many places or register too many accounts for many applications that the user cannot remember all.

In Oauth, there are four basic concepts [3]:

- Resource owners: are the users who have the ability to grant access, the owner of the resource that the application wants to get.
- Resource servers: are the places which store resources, capable of handling access requests to protected resources
- Clients: are third-party applications that want to access the shared resource of the owner (i.e. prior to access, the application needs to receive the user's Authorization).
- Authorization servers: are the authentications that check the information the user sent from there, grants access to the application by generating access tokens. Sometimes the same Authorization server is the resource server.

[3]https://oauth.net/2/

Token is a random code generated by the Authorization server when a request comes from the client. There are two types of tokens, namely the access token and the refresh token. The former is a piece of code used to authenticate access, allowing third-party applications to access user data. This token is sent by the client as a parameter in the request when it is necessary to access the resource in the Resource server. The access token has a valid time (e.g., 30 minutes, 1 hour), when it expired, the client had to send a request to the Authorization server to get the new access token. Whereas, the latter is also generated by Authorization server at the same time with accessed token but with different function. Refresh token is used to get the new access token when it expires, so the validity period is longer than the access token.

Single Sign-On (SSO) is a mechanism that allows users to access multiple applications with just one authentication. SSO simplifies administration by managing user information on a single system instead of multiple separate authentication systems. It makes it easier to manage users when they join or leave an organization [20]. SSO supports many authentication methods such as Oauth, OpenID, SAML, and so on.

III. Related Work

A. *Brokerless Architecture*

Alif Akbar Pranata et al. [21] build a water quality monitoring system according to brokerless pub/sub architecture.

The paper uses two nodes including: relay node (publisher) to collect data from sensor and gateway node (subscriber) to receive data from relay node and send information to server. The paper uses Zigbee to send and receive messages in communication at close distances. However, the paper does not give methods to expand the system as well as security mechanisms.

Lam et al. [22] presented an architecture that combines MQTT broker and kafka message queue to connect different IoT service providers. This architecture allows individual service providers to communicate with each other easily without changing the existing architecture too much. In addition, Lam et al. [23] also evaluates power consumption, transfer speed, communication reliability, and security when using a combination of MQTT broker and kafka message queue. With Kafka's capabilities, we don't need to trade off transmission speed and reliability for power consumption (this is related to QoS-0 and QoS-2 levels). Moreover, these authors demonstrated an architecture that combines MQTT broker, Single Sign On, and kafka message queue [24]. This combination allows no need to trade-off speed and reliability when communicating with power consumption (this is related to QoS-0 and QoS-2 levels) while still ensuring security. of the system.

B. Oauth and Internet of Things

Paul Fremantle et al. [18] demonstrated using Oauth to enable to enable access control via the MQTT protocol. The results of the paper show that IoT client can fully use Oauth token to authenticate with MQTT broker. This indicates that Oauth is not only suitable for web application but also applicable for low hardware devices. The paper demonstrates implementing the Web Authorization Tool to create the access token, then embedded it (embedded) MQTT client. In addition, the paper presents the combined implementation of Oauth and MQTT for internal communication between MQTT broker and MQTT client. However, the paper uses RESTful over HTTP/1.1 to transfer the packet. This can be a waste of bandwidth and energy of IoT devices as discussed in Introduction. In our paper, we will use Oauth in conjunction with Single Sign-On to build into a service responsible for device authentication. Devices will communicate with this service through gRPC to take its advantages.

IV. System Architecture

The SIP-MBA Platform is designed in a micro-service architecture to ensure the system is horizontal scale that is shown in Figure 2. The architecture consists of three layers namely the Things layer, the Server layer and the User layer. Each class has components that play a different role.

The Things layer includes physical devices capable of collecting data from the environment (pH, temperature, humidity, etc.). After the collection process, the data are transferred to the Server layer according to the gRPC protocol. Things layer also receives a control command from the User layer or from the data processing service of the the Server layer to control the behavior of Things based on the information it collects.

The Server layer consists of micro-services that handle the following tasks:

- Collect data service: collect data from the (authenticated) things in Thing Layer. In addition, the collect data service also passes control commands from users or data processing service to things.
- SSO service: is responsible for authenticating things and users according to the Oauth protocol.
- Objects management service: allows to manage users and things participating in the system.
- Control service: allows the user to command control of things.
- Data processing service: analyze collected data to respond to users, store system logs and issue commands to control things according to pre-set triggers.
- Message Queue: is responsible for transporting messages interacting between services within the Server layer.

Finally, the User layer uses the Internet of Things service. Only users authenticated by the SSO service can interact with the Server layer.

V. Software architecture

To meet the goals set out by the SIP-MBA Platform, we provide several definitions of the components participating in the system and their interactions.

A. Users

Users are people who use IoT services. By constructing a user hierarchy model tree with the child's user_parent_id value equal to the parent user's username, our SIP-MBA Platform allows the creation and management of multiple levels of users without being bounded. The term depends on the characteristics of the organization. This tree-modeled user hierarchy makes the SIP-MBA Platform suitable for companies, especially when authorizing a specific user or changing the operation state for a series of child users at the same time w.r.t crashes (only ACTIVE users can request access token). User information is generated when a user registers to use an IoT service or is created by the parent user and provided to his or her child user.

Each user has a unique user_id value that conforms to the standard UUID[4] and is managed by the Objects-management service. When issuing commands to manipulate things, the user must pass in the access token obtained from the Single Sign On service. This token is authenticated by the Single-Sign-On service. In this way, we have enhanced the authentication mechanism, the authorization mechanism for the user as well as minimized the risk of a denial-of-service attack when a hacker impersonates a user repeatedly sending control commands.

B. Things

Things represent information about physical devices or applications owned by the user. To create things, the user that owns the things will have to pass in his valid Oauth token.

[4]https://tools.ietf.org/html/rfc4122

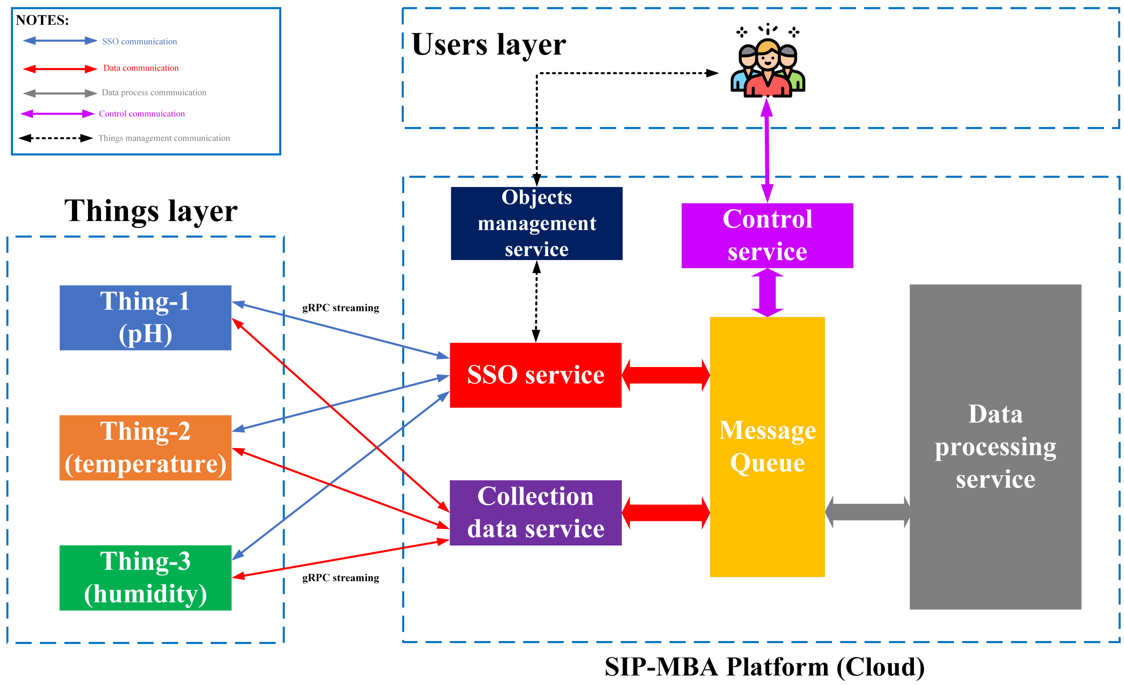

Fig. 2. SIP-MBA Platform as Micro-service Architecture.

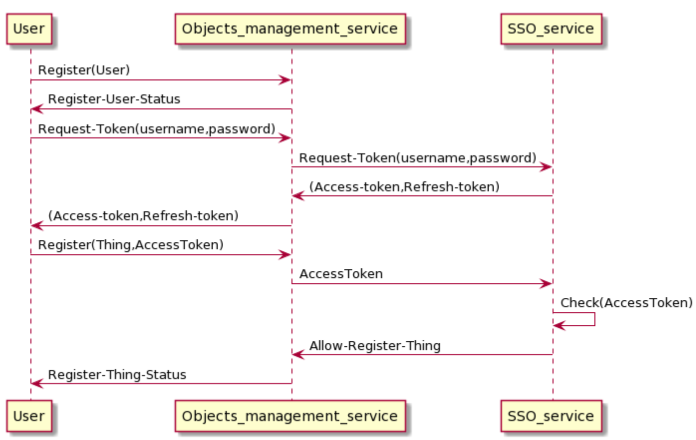

Fig. 3. The User and Thing Initialization Processes.

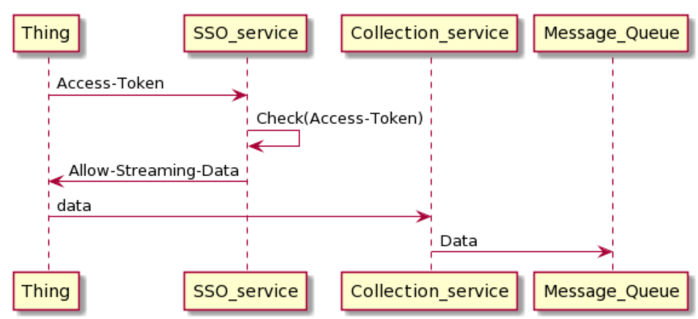

Fig. 4. Data Collection Process.

After creating things, users must embed their access token into things. Embedding the access token is out of the scope of this paper. Only things that own a valid access token communicate with the Collect-data service. Similar to the user, this way to create device management information, helps increase security and reduce the risk of denial-of-service attacks.

C. Communication Workflow

1) Initialization workflow: As mentioned in Sections V-A and V-B, a user must be registered to use the Internet of thing service. After registration, the user makes a request for access token with username and password information. The system will return the user access token and refresh the token according to the Oauth standard. The user then performs registration of the thing by passing in his access token. The access token is authenticated by the SSO service. Finally, the Objects-management service will enable the creation of things information. The thread process initializes the user and thing as shown in Fig. 3

2) Data collection process: Things first send their access token to the SSO service. If the access token is authenticated by the SSO service then the thing is allowed to stream data to the Collection service. The collection service collects the data and passes it to the message queue. Other services like Data processing service access the data stream through the message queue. Thing after completing streaming data will disconnect from the Server layer and go to sleep to save energy. The protocol used in the Collect data process is gRPC. Process collect data is presented in Fig. 4

3) Control workflow: The user can issue commands to control the thing remotely by sending the access token and command to the Control service. The access token is authenticated through the SSO service. If the access token is valid, the

Control service forward the command to the Message Queue. Ultimately the collection service sends this command to things. The protocol used in the Control process is gRPC. The entire procedure is shown in Fig. 5

VI. Implementation

A. Database

In this paper we deploy the most important service is the collection data service, the remaining components will be present in our upcoming paper. The deployment model is shown in Fig. 6

The deployment model consists of two components. Firstly, the Raspberry Pi module plays the role of Thing in the System Architecture presented in Section 2. Raspberry Pi is a small computer packed with powerful hardware capable of running the operating system and installing many applications on it. With a price of only a few tens of dollars, Raspberry is currently the most prominent mini computer today. Initially, the Raspberry Pi Foundation developed the Raspberry project with the main goal of teaching computers to children and creating a cheap tool (only a few tens of dollars) for students to study and study. Currently, Raspberry Pi is commonly used in IoT systems because of its powerful processing capabilities, multitasking and exceptionally low cost. The second is Collect data service deployed on an Amazon EC2 server. The roles of the components are as follows:

- Raspberry Pi Module is responsible for collecting data from sensors and sending to the server via gRPC protocol.
- Collect data service is a service deployed on the server, in charge of receiving data sent from the client through the gRPC protocol.

The configuration of the two components is shown in Table I

VII. Evaluation

A. Environment Setting

After implementing the Collection data service, we set up a script to test the performance of the SIP-MBA Platform. This scenario tests the message delivery speed of a broker-less architecture, uses the gRPC protocol with a brokered architecture, and uses the MQTT protocol. The two of scenarios' source code is shown in our Github repository for collection data service[5] and MQTT streaming [6]. The testing scenarios are shown in Fig. 7.

We set up two test environments consisting of two Raspberry Pi modules and two Amazon EC2 Servers with similar configurations. The Raspberry Pi-1 and Server-1 pair implements the Collect data service and uses the gRPC protocol to transmit the packet. The Raspberry Pi-2 and Server-2 pair respectively deploy the MQTT client, the MQTT broker and use the MQTT protocol to transmit packets.

[5]https://github.com/thanhlam2110/iot-platform-collect-data-service
[6]https://github.com/thanhlam2110/mqtt-streaming

B. Message Delivery Speed Test Case

We perform a rate test of one million packets that are an integer between 1 and 1,000,000 on both test environments and record when the message was sent and when it was received. In our test, each sender message follows this structure **"hello + i"** with i comes from 1 to 1.000.000 For the environment using MQTT protocol, we perform the test with two levels of QoS-0 and QoS-2. The tests were performed 3 times and averaged. The results of the process obtained are shown in Table II

From the results noted in the Table II, we found that SIP-MBA Platform uses a broker-less architecture and gRPC protocol that has a much faster message delivery speed than systems using brokered architecture and MQTT protocol. Particularly in the case of MQTT QoS-2, Raspberry module can only send 65423, 65534 and 65672 messages, the MQTT broker hangs and does not continue to receive messages. This makes sense because gRPC runs on an http/2 protocol that allows sending and receiving messages with multiple packets in a single connection. Finally, gRPC is also a peer-to-peer communication instead of a broker like MQTT protocol.

C. Broken Connection Test Cases

In addition, we also have taken test scenario with broken connection between publisher and subscriber. We compare number of receive messages in case with and without using SIP-MBA platform when occurred broken connection. The test model is shown in the Fig. 8.

The test result show that, in case without using SIP-MBA platform, subscriber only receive one message - the newest message that publisher send when occurred broken connection. This is the retain function of MQTT protocol. When we enable retain flag, MQTT broker is ability to keep only newest message that publish by publisher. This message is received by subscriber after it reconnects to MQTT broker[9]. However, when using SIP-MBA platform, subcriber can receive all message that published by publisher. This is ability of kafka message queue therefore the system is guaranteed lost data.

D. Future Work

To develop a larger scenario and increase the number of devices/users authorized quickly, other security issues such as security, privacy, availability for objects are still the challenges. For the security aspect, further works will be deployed in different scenarios like healthcare environment [25], [26], [27], cash on delivery [28], [29]. For the privacy aspect, we will exploit attribute-based access control (ABAC) [30], [31] to manage the authorization process of the SIP-MBA Platform via the dynamic policy approach [32], [33], [34]. Finally, we will apply the blockchain benefit to improve the availability issues [35], [36], [37].

VIII. Conclusion

In this paper, we present the model of the SIP-MBA Platform in a broker-less and micro-service architecture. We use gRPC as the medium of communication to take advantage of its advantages. Besides, we also offer a solution to supplement

[9]http://docs.oasis-open.org/mqtt/mqtt/v3.1.1/os/mqtt-v3.1.1-os.html

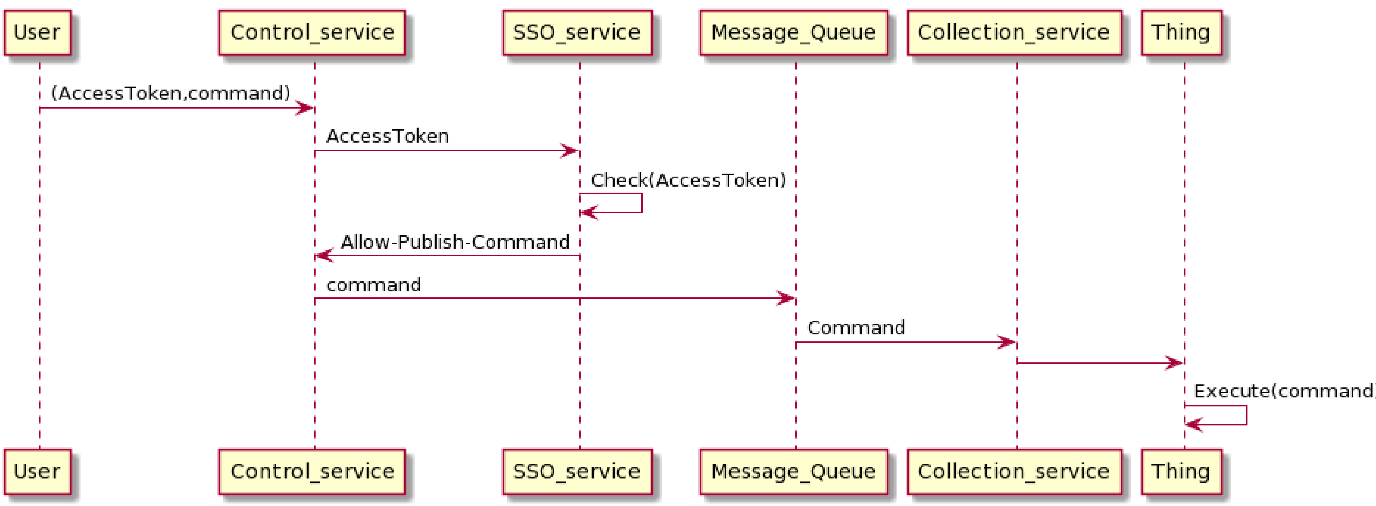

Fig. 5. Control Workflow.

TABLE I. Configuration of the Raspberry Pi Module and Collect data Service

	CPU	RAM
Raspberry Pi (module 3B)	Broadcom BCM2837, ARMv8 (64bit) quad-core, 1.2 Ghz	RAM 1GB
Collection Data Service (Server)	1vCPU	RAM 1GB

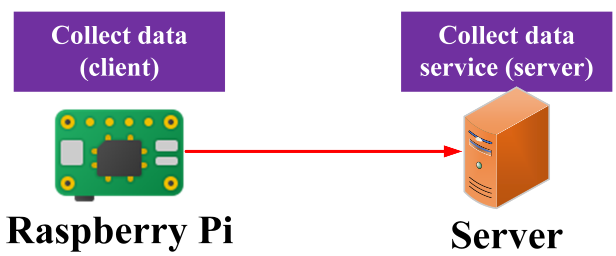

Fig. 6. The Collect Data Service Operators.

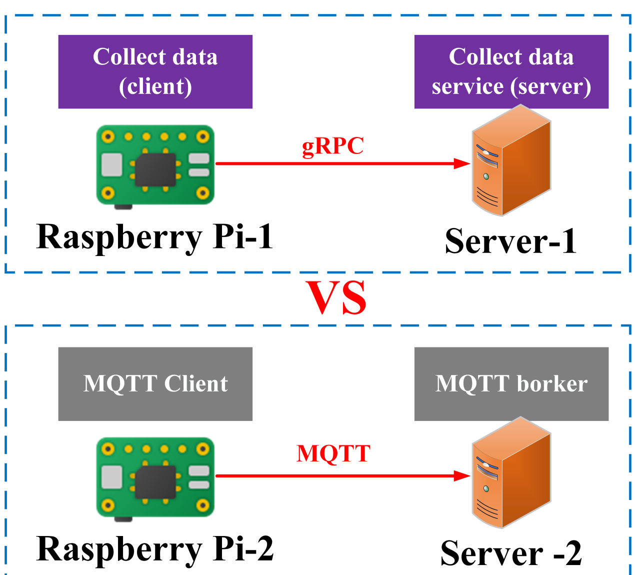

Fig. 7. The Scenarios of Communication Speed between gRPC and MQTT.

TABLE II. Results of Performance (seconds) Comparison between Two Scenarios (i.e., gRPC vs MQTT(QoS-0; QoS-2)).

Sending time	gRPC	MQTT (QoS-0)	MQTT (QoS-2)
1st	55s	266s	can't complete test
2nd	53s	268s	can't complete test
3rd	57s	272s	can't complete test
Average	55s	267s	can't complete test

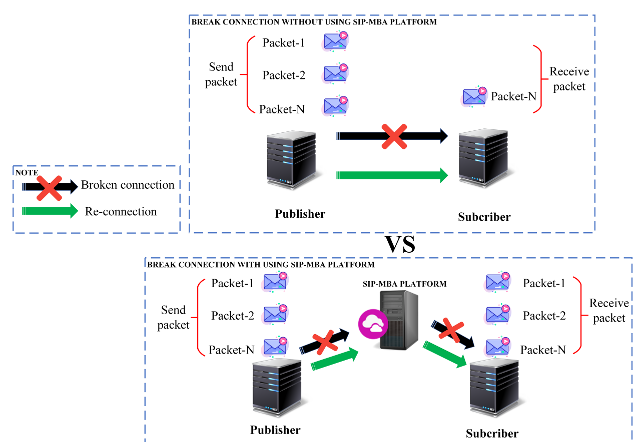

Fig. 8. Number of Receive Messages when System Recover after Broken Connection Issue.

the security mechanism for the system using Single Sign-On and Oauth. We also add a message queue system that stores and transports packets between services within the system. This ensures that when a service is not available, the message is still not lost. In the future, we will develop the remaining services and build a complete SIP-MBA Platform.

REFERENCES

[1] T. Alam, "A reliable communication framework and its use in internet of things (iot)," *CSEIT1835111— Received*, vol. 10, pp. 450–456, 2018.

[2] T. Chou, *Precision-Principles, Practices and Solutions for the Internet of Things*. McGraw-Hill Education, 2017.

[3] V. Karagiannis, P. Chatzimisios, F. Vazquez-Gallego, and J. Alonso-Zarate, "A survey on application layer protocols for the internet of things," *Transaction on IoT and Cloud computing*, vol. 3, no. 1, pp. 11–17, 2015.

[4] S. P. Jaikar and K. R. Iyer, "A survey of messaging protocols for iot systems," *International Journal of Advanced in Management, Technology and Engineering Sciences*, vol. 8, no. II, pp. 510–514, 2018.

[5] B. H. Çorak, F. Y. Okay, M. Güzel, Ş. Murt, and S. Ozdemir, "Comparative analysis of iot communication protocols," in *2018 International symposium on networks, computers and communications (ISNCC)*. IEEE, 2018, pp. 1–6.

[6] M. Martí, C. Garcia-Rubio, and C. Campo, "Performance evaluation of coap and mqtt_sn in an iot environment," in *Multidisciplinary Digital Publishing Institute Proceedings*, vol. 31, no. 1, 2019, p. 49.

[7] D. Soni and A. Makwana, "A survey on mqtt: a protocol of internet of things (iot)," in *International Conference On Telecommunication, Power Analysis And Computing Techniques (ICTPACT-2017)*, vol. 20, 2017.

[8] S. Lee, H. Kim, D.-k. Hong, and H. Ju, "Correlation analysis of mqtt loss and delay according to qos level," in *The International Conference on Information Networking 2013 (ICOIN)*. IEEE, 2013, pp. 714–717.

[9] J. Toldinas, B. Lozinskis, E. Baranauskas, and A. Dobrovolskis, "Mqtt quality of service versus energy consumption," in *2019 23rd International Conference Electronics*. IEEE, 2019, pp. 1–4.

[10] B. Mishra, "Performance evaluation of mqtt broker servers," in *International Conference on Computational Science and Its Applications*. Springer, 2018, pp. 599–609.

[11] N. Q. Uy and V. H. Nam, "A comparison of amqp and mqtt protocols for internet of things," in *2019 6th NAFOSTED Conference on Information and Computer Science (NICS)*. IEEE, 2019, pp. 292–297.

[12] Y. Kwon and J. Lee, "Energy optimization model with variable keep-alive cycle algorithm in wireless sensor network," *International Journal of Control, Automation and Systems*, vol. 17, no. 10, pp. 2531–2540, 2019.

[13] H. C. Hwang, J. Park, and J. G. Shon, "Design and implementation of a reliable message transmission system based on mqtt protocol in iot," *Wireless Personal Communications*, vol. 91, no. 4, pp. 1765–1777, 2016.

[14] D. Mendez Mena, I. Papapanagiotou, and B. Yang, "Internet of things: Survey on security," *Information Security Journal: A Global Perspective*, vol. 27, no. 3, pp. 162–182, 2018.

[15] L. Lundgren, "Light-weight protocol! serious equipment! critical implications!" *Defcon 24*, 2016.

[16] J. J. Anthraper and J. Kotak, "Security, privacy and forensic concern of mqtt protocol," in *Proceedings of International Conference on Sustainable Computing in Science, Technology and Management (SUSCOM), Amity University Rajasthan, Jaipur-India*, 2019.

[17] N. Zaidi, H. Kaushik, D. Bablani, R. Bansal, and P. Kumar, "A study of exposure of iot devices in india: Using shodan search engine," in *Information Systems Design and Intelligent Applications*. Springer, 2018, pp. 1044–1053.

[18] P. Fremantle, B. Aziz, J. Kopeckỳ, and P. Scott, "Federated identity and access management for the internet of things," in *2014 International Workshop on Secure Internet of Things*. IEEE, 2014, pp. 10–17.

[19] B. Pollard, *HTTP/2 in Action*. Manning, 2019.

[20] V. Radha and D. H. Reddy, "A survey on single sign-on techniques," *Procedia Technology*, vol. 4, pp. 134–139, 2012.

[21] A. A. Pranata, J. M. Lee, and D. S. Kim, "Towards an iot-based water quality monitoring system with brokerless pub/sub architecture," in *2017 IEEE International Symposium on Local and Metropolitan Area Networks (LANMAN)*. IEEE, 2017, pp. 1–6.

[22] L. N. T. Thanh *et al.*, "Toward a unique iot network via single sign-on protocol and message queue," in *International Conference on Computer Information Systems and Industrial Management*. Springer, 2021.

[23] ——, "Toward a security iot platform with high rate transmission and low energy consumption," in *International Conference on Computational Science and its Applications*. Springer, 2021.

[24] ——, "Uip2sop: A unique iot network applying single sign-on and message queue protocol," *IJACSA*, vol. 12, no. 6, 2021.

[25] H. X. Son and E. Chen, "Towards a fine-grained access control mechanism for privacy protection and policy conflict resolution," *International Journal of Advanced Computer Science and Applications*, vol. 10, no. 2, 2019.

[26] N. Duong-Trung, H. X. Son, H. T. Le, and T. T. Phan, "Smart care: Integrating blockchain technology into the design of patient-centered healthcare systems," in *Proceedings of the 2020 4th International Conference on Cryptography, Security and Privacy*, ser. ICCSP 2020. New York, NY, USA: Association for Computing Machinery, 2020, p. 105–109.

[27] ——, "On components of a patient-centered healthcare system using smart contract," in *Proceedings of the 2020 4th International Conference on Cryptography, Security and Privacy*. New York, NY, USA: Association for Computing Machinery, 2020, p. 31–35.

[28] H. T. Le, N. T. T. Le, N. N. Phien, and N. Duong-Trung, "Introducing multi shippers mechanism for decentralized cash on delivery system," *money*, vol. 10, no. 6, 2019.

[29] N. T. T. Le, Q. N. Nguyen, N. N. Phien, N. Duong-Trung, T. T. Huynh, T. P. Nguyen, and H. X. Son, "Assuring non-fraudulent transactions in cash on delivery by introducing double smart contracts," *International Journal of Advanced Computer Science and Applications*, vol. 10, no. 5, pp. 677–684, 2019.

[30] N. M. Hoang and H. X. Son, "A dynamic solution for fine-grained policy conflict resolution," in *Proceedings of the 3rd International Conference on Cryptography, Security and Privacy*, 2019, pp. 116–120.

[31] H. X. Son and N. M. Hoang, "A novel attribute-based access control system for fine-grained privacy protection," in *Proceedings of the 3rd International Conference on Cryptography, Security and Privacy*, 2019, pp. 76–80.

[32] S. H. Xuan, L. K. Tran, T. K. Dang, and Y. N. Pham, "Rew-xac: an approach to rewriting request for elastic abac enforcement with dynamic policies," in *2016 International Conference on Advanced Computing and Applications (ACOMP)*. IEEE, 2016, pp. 25–31.

[33] Q. N. T. Thi, T. K. Dang, H. L. Van, and H. X. Son, "Using json to specify privacy preserving-enabled attribute-based access control policies," in *International Conference on Security, Privacy and Anonymity in Computation, Communication and Storage*. Springer, 2017, pp. 561–570.

[34] H. X. Son, T. K. Dang, and F. Massacci, "Rew-smt: a new approach for rewriting xacml request with dynamic big data security policies," in *International Conference on Security, Privacy and Anonymity in Computation, Communication and Storage*. Springer, 2017, pp. 501–515.

[35] X. S. Ha, H. T. Le, N. Metoui, and N. Duong-Trung, "Dem-cod: Novel access-control-based cash on delivery mechanism for decentralized marketplace," in *2020 IEEE 19th International Conference on Trust, Security and Privacy in Computing and Communications (TrustCom)*. IEEE, 2020, pp. 71–78.

[36] X. S. Ha, T. H. Le, T. T. Phan, H. H. D. Nguyen, H. K. Vo, and N. Duong-Trung, "Scrutinizing trust and transparency in cash on delivery systems," in *International Conference on Security, Privacy and Anonymity in Computation, Communication and Storage*. Springer, 2020, pp. 214–227.

[37] H. X. Son, T. H. Le, N. T. T. Quynh, H. N. D. Huy, N. Duong-Trung, and H. H. Luong, "Toward a blockchain-based technology in dealing with emergencies in patient-centered healthcare systems," in *International Conference on Mobile, Secure, and Programmable Networking*. Springer, 2020, pp. 44–56.

IoHT-MBA: An Internet of Healthcare Things (IoHT) Platform based on Microservice and Brokerless Architecture

Lam Nguyen Tran Thanh[1], Nguyen Ngoc Phien*[2], The Anh Nguyen[3], Hong Khanh Vo[4],
Hoang Huong Luong[5], Tuan Dao Anh[6], Khoi Nguyen Huynh Tuan[7], Ha Xuan Son[8]
VNPT Information Technology Company, Ho Chi Minh city, Vietnam[1]
Center for Applied Information Technology, Ton Duc Thang University, Ho Chi Minh City, Viet Nam[2]
Faculty of Information Technology, Ton Duc Thang University, Ho Chi Minh City, Vietnam[2]
Department of Computer Science, Faculty of Electrical Engineering and Computer Science,
VSB-Technical University of Ostrava, Ostrava, Czech Republic[2]
FPT University, Can Tho City, Viet Nam[3,4,5,6,7]
University of Insubria, Varese, Italy[8]

***Abstract*— Internet of Thing (IoT), currently, is one of the technology trends that are most interested. IoT can be divided into five main areas including: Health-care, Environmental, Smart city, Commercial and Industrial. The IoHT-MBA Platform is considered the backbone of every IoT architecture, so the optimal design of the IoHT-MBA Platform is essential issue, which should be carefully considered in the different aspects. Although, IoT is applied in multiple domains, however, there are still three main features that are challenge to improve: i) data collection, ii) users, devices management, and iii) remote device control. Today's medical IoT systems, often too focused on the big data or access control aspects of participants, but not focused on collecting data accurately, quickly, and efficiently; power redundancy and system expansion. This is very important for the medical sector - which always prioritizes the availability of data for therapeutic purposes over other aspects. In this paper, we introduce the IoHT Platform for Healthcare environment which is designed by microservice and brokerless architecture, focusing strongly on the three aforementioned characteristics. In addition, our IoHT Platform considers the five other issues including (1) the limited processing capacity of the devices, (2) energy saving for the device, (3) speed and accurate of the data collection, (4) security mechanisms and (5) scalability of the system. Also, in order for the IoHT Platform to be suitable for the field of health monitoring, we also add realtime alerts for the medical team. In the evaluation section, moreover, we describe the evaluation to prove the effectiveness of the proposed IoHT Platform (i.e. the proof-of-concept) in the performance, non-error, and non affected by geographical distance. Finally, a complete code solution is publicized on the authors' GitHub repository to engage further reproducibility and improvement.**

Keywords—Internet of Health Things (IoHT); microservice; brokerless; gRPC; kafka; single sign-on; RBAC

I. Introduction

The Internet of Thing (IoT) applications, currently, are increasingly diverse including smart city, healthcare, supply chains, industry, agriculture, etc. It is estimated that the number of IoT-connected devices worldwide will increase to 43 billion by 2023, three times that of 2018 [1]. Investments in IoT technology are expected to grow at 13.6% per year until 2022 [1], of which, the rate of IoT adoption in the healthcare sector accounts for 20%, second only to smart city with the density of 29% [2]. However, the IoT apps still have three main evaluation issues, namely: response time (27%), energy consumption (18%) and realiability (14%) [2]. Iot Platform is an intermediary system that acts as a glue to attach devices to users. Therefore, the IoT platform development optimizes the three aforementioned issues is very vital since it is a platform with all the more advanced features. There are many architectures for the IoT Platform, the most popularity is build in the five-layer architecture from low to high, namely Things, Connect, Collect, Learn and Do [3]. We found that the the main evaluation factors of IoT correspond to the design requirements of the three classes of Things, Connect and Collect.

Things (the physical devices) collect data directly or perform an action based on a control command from the user. The device is designed to fulfill the mobility requirements, hence it has limited power, processing capacity and bandwidth [4].

Connect includes tailored protocols that are suitable for the hardware and networking capabilities of the Things layer. Pratim et al. [5] evaluated the pros and cons of 9 protocols being applied for IoHT including: MQTT, CoAP, HTTP, XMPP, AMQP, RESTful, Websocket, SMQTT and DDS. In which, DDS (Data Distribution Service) protocol satisfies two criteria of response time and reliability. DDS uses M2M communication and brokerless architecture suitable for medical devices. However, the paper also points out the weakness of DDS is its low security and lack of support for many types of programming languages, especially python. Beside, the paper has not evaluate an assessment of the energy consumption of DDS compared to the rest of the protocols.

Collect layer is the collection software to collect data generated by Things through the Connect class. Therefore, the Collect layer architecture is determined by the protocol used in the Connect. This paper considers the brokering architecture at Collection layer with the MQTT protocol used in Connect layer, as this protocol is commonly used in IoT frameworks (including IBM, Amazon and Microsoft) [6]. The MQTT protocol uses a publish / subscriber architecture [7], with the MQTT broker at the center. The MQTT subscriber (client), connects to the broker and sends messages to topics. Brokers rely on topic to route the packet, meaning that subscribers who subscribe to a topic will receive all messages sent to that topic. This can easily lead to a single point failure [8] at the central broker location. Besides, MQTT is created for transmission purposes. Thus, MQTT broker does not provide message storage capabilities and does not guarantee the order of messages when it reaches the receiver [9]. Finally, it also considers the weaknesses of brokering architectures using MQTT.

From the analysis of evaluation criteria and the three most basic functional layers of all IoT platforms, this paper focus on giving a new platform built on brokerless and microservice architecture for the healthcare environment (a.k.a IoHT-MBA Platform). We build the brokerless architecture on the Collection class using the gRPC protocol on the Connection class. Similar to DDS, the gRPC protocol also uses M2M communication and a brokerless architecture. However, gRPC supports more programming languages, which is convenient for developers. Also, gRPC consumes lower CPU and RAM compared to other IoHT protocols such as MQTT, CoAP, XMPP. The brokerless architecture does not have a central broker to coordinate topic-based messages, but instead is a service that communicates directly with the device to collect data. Collected data will be transferred to storage and distributed to advanced processing services (the function equivalent of Learn and Do classes). Besides, our IoHT-MBA Platform is designed based on the microservice architecture, ensuring fault tolerance, scaling horizontally, and ensuring the availability and capacity of the system as introduced in [10]. In addition, to ensure the security of the system, we also build a management model of the components participating in the IoHT-MBA Platform such as users and things. The management model is built according to Role-base Access Control (RBAC) architecture combined with hierarchical management of users according to the model tree.

The rest of the paper is organized as follows. In Sections 2 and 3, we provide the knowledge of the technology used and the work involved, respectively. Section 4 introduces the IoHT-MBA Platform and we build a prototype system to verify the effectiveness in Section 5. Section 6, we discuss the evaluation outcomes. Finally, Section 7 concludes the summarize and discusses further work.

II. Background

A. gRPC and http/2

gRPC[1] (general-purpose Remote Procedure Calls) is an open-source high performance framework of Remote Procedure Call Protocol (RPC) developed by Google. gRPC is built on http/2 protocol. Improvements in http/2 over previous versions allow for better and more efficient http performance connections. One of the most important features of http/2 is multiplexing, which allows us to send and receive multiple packets in a single connection. gRPC supports a variety of programming languages and is fully compatible with embedded devices [11]. This protocol provides four communication types as follows:

- Unary: Similar to traditional client-server communication. The client sends a request to the server, waits for the server to process it, and then returns the results to the client.
- Server streaming: In this mode, the client sends a request to the server and then waits for the server to return a stream of data. The client read messages from that stream until no more messages are returned. The order of messages for each stream is guaranteed to be the same between client and server.
- Client streaming: Similar to Server streaming RPCs, in this type, the client is the side that sends the data stream to the server, the server read the stream and perform the necessary processing, and then return the data to the client.
- Bi-direction streaming: This is the type of method where the data is sent in a stream from both client and server directions, the data stream in both directions is independent of each other, and the client and server can process that streamed data independently. That means when the client sends a message to the server, the server can process it to perform a certain task (while still receiving other messages) and send the result back to the client (while the client is still sending another message).

B. Kafka Message Queue

Kafka[2] is a distributed messaging system. It is capable of transmitting a huge number of messages in realtime. In the case that the receiver has not received the message, this message is still stored on the message queue and the disk to achieve the safety transaction.

The Kafka architecture includes the four main components, namely producer, consumer, topic, and partition. Kafka producer is a client to publish messages to topics. Data is sent to the partition of the topic stored on the broker. Kafka consumers are clients that subscribe and receive messages from topic, consumers are identified by group names. Many consumers can subscribe to the same topic. Data is transmitted in Kafka via the corresponding topic, when it is necessary to transmit data for different applications, it is possible to create many different topics. Partition is where to store data on the specific topic where each might have one or more partitions. On each partition, the data is stored permanently and assigned an ID called offset. Besides, a set of Kafka server (a.k.a broker and the zookeeper) is a service to manage the brokers.

C. OAuth and Single Sign-On Protocol

Oauth is an authentication mechanism that helps third party applications be authorized by the user to access the user resource located on the other application. OAuth version 2.0, an authentication protocol, is an upgrade version of OAuth version 1.0 and allows the applications to share a portion of resources with each other without provides the username and password as the traditional approach. That limits the hassle of having to enter the username, password in too many places or

[1] https://grpc.io/

[2] https://kafka.apache.org/

register too many accounts or applications. In OAuth includes four concepts[3].

- **Resource owners**: are users who have the ability to grant access, the owner of the resource that the application wants to collect.
- **Resource server**: a place to store the resource (resource), capable of handling access requests to protected resources.
- **Clients**: are third-party applications that want to access the shared resource as of the resource owner.
- **Authorization server**: authenticates, checks the information the user sent from there, grants access to the application by generating access tokens. Sometimes the authorization server is the resource server as well.

The token is a random code generated by the Proxy server when a request comes from the client. There are second type tokens which are i) access tokens and ii) refresh tokens. An access token is a code used to confirm access, allowing third-party applications to access user data. This token is sent by the client as a parameter in the request when needing access to the resource server's resource. The access token has a certain valid time (e.g., 30 minutes, 1 hour). When this expires, the client must request the proxy server to get the new access token. Although the refresh token is also generated by the proxy server simultaneously as the access token but differs in functionality. The refresh token is used to get a new access token when it expires, hence the longer duration than the access token.

D. Zabbix

Zabbix[4] is an open source that support to solve system monitoring issues. Zabbix could monitor network parameters, server status and data in real time. Zabbix offers the ability to set alarm thresholds and send alerts to subscribers via email, SMS or telegram, etc.

III. Related Work

A. IoT Architecture for Healthcare

Maktoubian et al. [12] has built an architecture that allows data collection from medical devices. This architecture collects data based on a combination of the MQTT protocol and the Kafka Message Queue. In addition, the architecture also performs big data analysis using Apache Spark. We appreciate the use of Kafka as it allows for secure data transmission. However, the use of MQTT protocol and brokering architecture brings many weaknesses as we discussed in Introduction. In addition, MQTT has 3 levels of Quality-of-Service (QoS) from 0 to 2. Selecting these QoS levels is a trade-off between reliability of packet transmission (rate of loss on the transmission line), transmission rate and energy consumption. The QoS-0 level has the fastest transmission rate but has the lowest reliability [13], the opposite is the QoS-2 level. According to the article [14] the energy consumption of the QoS-0 level is only about 50% of the QoS-2 level. The report also did not specify the level of MQTT QoS that the system uses. In terms of security, the article mentioned security risks, but did not specify how to fix it.

Taher et al. [15] building an IoT-cloud system to collect and process medical data. The system by the authors has full features, however, operating based on the MQTT protocol, there are many weaknesses in the security mechanisms [16] and the brokering architecture [8] that may cause single point failure.

Partha Pratim Ray [17], builds medical data collection system based on websocket and HTTP. However, according to Bansal et al. [5], websocket requires more RAM and HTTP header is a big challenge for low hardware devices. Besides, security aspect has not been considered.

Ha Xuan Son et al. [18] has built an emergency system for the patient. The system launched by the authors applies Blockchain technology on Hyperledger fabric platform with a strong focus on access control. However, the authors have not describe the collecting data method from patients. Moreover, the authors did not mention a specific architecture, so they cannot prove the scalability of the system. Also, the paper did not provide any evaluation on the processing speed of the system.

B. Microservice and Brokerless Architecture for IoHT

Jita et al. [19] developed an in-home medical care system (IHMCS), a system designed in a highly available and scalable micro service architecture. The system also uses blockchain to enhance security. However, in the implementation part, the system uses Zetta IoT Platform - a platform that uses HTTP and RESTful protocols to perform the communication process with the device. These two protocols are not suitable for devices with low hardware [5].

Martino et al. [20] provided a review of the most common architectural solutions available (i.e. pros and cons) to shape an IoT system, ranging from already standardized architecture to commercial ones. In healthcare fields, some studies [21], [22], [23] claimed the field of public healthcare using a service oriented architecture modeled as a multi-agent and multi-type policy system. Besides, these papers emphasized the importance of microservice in healthcare but it has not been clarified as a major contribution.

Di Zeng el at. [24] has launched research on medical systems according to micro service and brokerless architecture. This is a fairly complete functional system that a health care system must have and ensure scalability. However, the authors only give a research model but have not deployed the system.

Lam et al. [25] presented an architecture that combines MQTT broker and kafka message queue to connect different IoT service providers. This architecture allows individual service providers to communicate with each other easily without changing the existing architecture too much. In addition, Lam et al. [26] also evaluates power consumption, transfer speed, communication reliability, and security when using a combination of MQTT broker and kafka message queue. With Kafka's capabilities, we don't need to trade off transmission speed and reliability for power consumption (this is related to QoS-0 and QoS-2 levels). Moreover, these authors demonstrated

[3]https://oauth.net/2/
[4]https://www.zabbix.com/

an architecture that combines MQTT broker, Single Sign On, and kafka message queue [27]. This combination allows no need to trade-off speed and reliability when communicating with power consumption (this is related to QoS-0 and QoS-2 levels) while still ensuring security. of the system.

IV. System architecture

The proposed platform is designed according to microservice and brokerless architecture including three layers, namely, Things layer, User layer and Platform layer as shown in Fig. 1. The Things layer (physical device) the devices implement two independent services: collection data service (client) and control service (client). The former is responsible for streaming data collected from the environment according to a predetermined cycle to the collection data server (server) at the IoHT-MBA Platform. This data stream is only performed when the client is authenticated and checked the things' role by the Single Sign On service. The latter receives control commands from the control service (server) through the message queue system.

The user class (user group) registered to use the IoHT service. The user has the right to control and monitor the device state through the Control service (server), which will be performed after going through the authentication phase and verifying phase (i.e. the user's role) by the Single Sign-On service. Besides, the users can manage device information (for instance create / delete / disable / active) as well as manage their child users (for instance register / disable / active) through the Object Management Service. The information for managing the thing and the user is stored in the database and the Single Sign-On service also relies on this information to authenticate and verify the permissions of the Things and Users.

IoHT platform (system load balancer) includes Message Queue Service (MQS), Data Processing Service (DPS). MQS is in charge of routing the control packet from the Users to the Things and the data collected from the Things layer. Also, it stores messages going through the IoHT-MBA Platform, ensuring that when a service fails, it can still receive messages after recovery. Whereas, DPS does data analysis in depth. DPS is in charge of analyzing data according to medical parameters predetermined by IoHT service provider and as the input of Zabbix server. The Zabbix server system allows the user to configure the warning thresholds (a.k.a. the trigger) that sends notification to the user via the telegram-bot when the data output of the data processing service hits the threshold. For example, the user can configure to send the notification when the patient's heart rate reaches over 140bmp in 5 minutes. This post focuses on the three layers of things, connect and collect so we are temporarily using Telegram as the third party to send the notification to users.

V. Implementation

The article implementing the services outlined in the proposal section includes: collection data service[5], single sign on service[6], control service[7], message queue service[8] and object management service[9]. The deployment model and interaction between the symbolic services in Fig. 1 is as follows: (1a-7a) collect the data handler and send the notification, (1b-5b) control the device flow, (1c) manage the object.

The collect data stream details are shown in Fig. 2. Things collects data from sensors and periodically sends them back to the IoHT-MBA Platform (sending data periodically to help save energy). The collection data service (client) on things creates a single gRPC connection that both sends token credentials, role checks, and streaming data. This is the advantage that gRPC brings, discussed in Section 2.1 (process 1a). The collection data service (server) passes the token and role information to the single sign on service (process 2a), the test result is returned (process 3a). If things is authenticated and has a valid role, it will start streaming bulk of collected data, whereas Collection data service (server) will close gRCP connection. Data received by the Collection data service (server) will be sent to the Kafka Message Queue (process 4a) and forwarded to an in-depth analysis at the Data Processing service (process 5a). Data after being analyzed later will be monitored by Zabbix server (process 6a). The user has also set the notification threshold on the Zabbix server. When data read by the Zabbix server hits the threshold, it sends an notification to the user via Telegram-bot (process 7a).

Details of flow control are shown in Fig. 3. User sends information about the `access token`, `thingID` and `control command` to the Control service server (process 1b). The control service server will pass the above information to the Single Sign-On server to authenticate the user through the token, check the users'role based on the control command submitted by the user and check if the user owns it. On the other hand it is assigned the thing based on thingid (process 2b). The test result is returned to the Control service server (process 3b), if it is valid this service sends the control command to the Message Queue (process 4b). The Control service (client) deployed on Things opens a gRPC connection to read all the control commands in a pre-set cycle (process 5b).

Object flow is simply we provide APIs for users to interact with the database. The Single Sign-On service will also use the data stored here to authenticate and verify the roles of users and things.

We apply RBAC model in conjunction with Single Sign-On to provide role-based authentication and authorization for Things and Users. However, the concepts of user roles and things are different. We define the users' role including permissions that affect the thing and child user such as: create or delete thing/assign or unassign thing (for another user) / control thing / active or disable child user. Whereas things' roles are related to their services; for instance things are capable of collecting 3 information such as: heart rate, blood pressure and coordinates. If the thing don't have role **"heart rate"**, it could not allowed to send this data to the IoHT-MBA Platform, although still collected and stored locally. While if it have role **"blood pressure"** and **"coordinates"**, it could send blood pressure and coordinates data to the IoHT-MBA Platform. These role of things only set by the owner user.

[5]https://github.com/thanhlam2110/collection-service-new
[6]https://github.com/thanhlam2110/service-sso
[7]https://github.com/thanhlam2110/user-control-service
[8]https://github.com/thanhlam2110/tcp-kafka-producer
[9]https://github.com/thanhlam2110/object-management-service

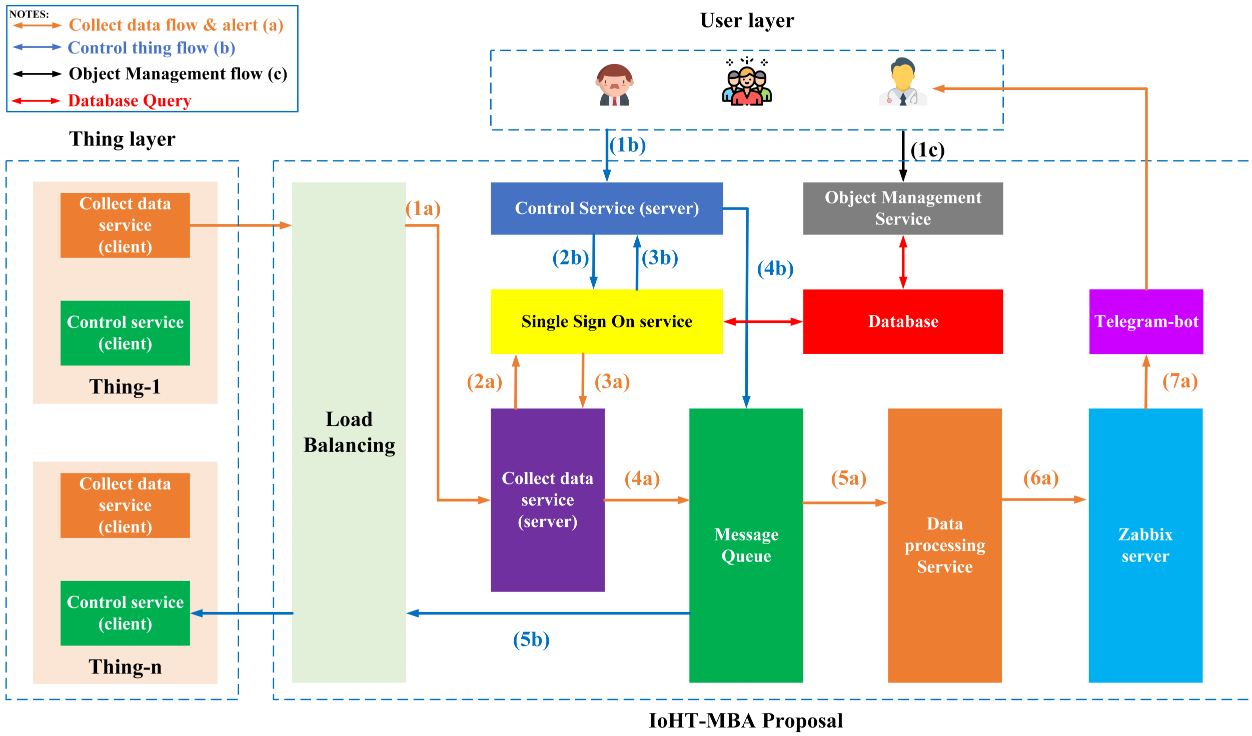

Fig. 1. IoHT-MBA Platform Proposal.

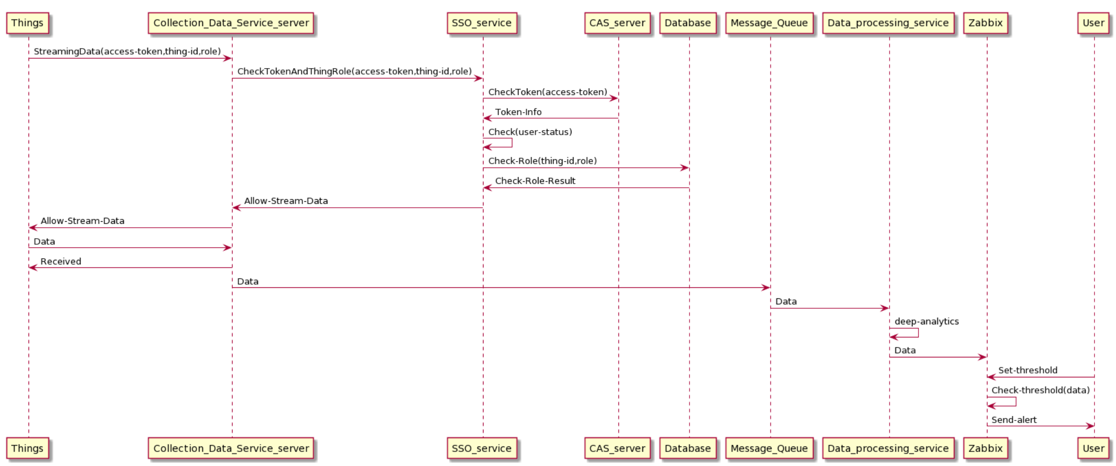

Fig. 2. Collection Data and Send Alert Flow.

This allows you to be flexible and proactive in sharing their information.

We implement the user management by model tree with the child user's `user_parent_id` field equal to the parent user's username. This allows our IoHT-MBA Platform to be flexibly applied to the business of performing hierarchical HR management. A parent user can `DISABLE` all of their child users (via user-status values) on the fly.

VI. Evaluation

A. Environment Setting

Our IoHT-MBA Platform is designed by microservice architecture. To perform the evaluation, we deploy these services to the Amazon EC2[11] platform with each service equivalent to a virtual machine with 1GB RAM and 1 vCPU configuration. For the device, we deploy collection data service (client) and control service (client) on the Raspberry Pi 3 model B+[12] module with Broadcom BCM2837, ARMv8 (64bit) quad-core, 1.2 GHz and 1GB RAM.

[11] https://aws.amazon.com/
[12] https://www.raspberrypi.org/products/raspberry-pi-3-model-b/

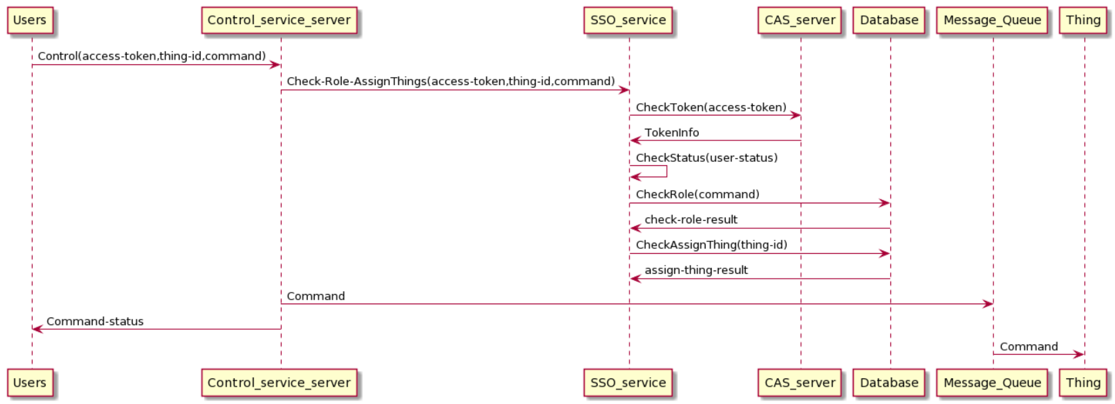

Fig. 3. The Control Flow.

B. Round Trip Time Test Cases

We measure Round Trip Time (RTT) from the moment things are streaming data to receiving it at Message Queue. We also look at the error rate (number of messages lost out of total messages). In addition, we also create EC2 VMs with a configuration equivalent to the Raspberry Pi model B + module in different geographical areas (except in Vietnam deployed on the real module) to simultaneously assess the impact of the site location. the delay time and error rate when streaming data Measured results are shown in Table I. The measurement results show that when we only deploy evaluation on low-profile servers, the processing time is completely unaffected by geographical distance. We realize that the data transfer rate is very fast and the error rate is 0, which is very suitable when applying the IoHT-MBA Platform for medical applications. All messages are received in full and in order. By using gRPC which allows sending multiple messages on one connection, we achieve very fast transfer speed while still satisfy the whole process of checking and validating before streaming data as described in Section 5.

C. Broken Connection Test Cases

Also, we have taken test scenario with broken connection between publisher and subscriber. We compare number of receive messages in case with and without using IoHT-MBA platform when occured broken connection. The test model is shown in the Fig. 4.

The test result show that, in case without using IoHT-MBA platform, subscriber only receive one message - the newest message that publisher send when occurred broken connection. This is the retain function of MQTT protocol. When we enable retain flag, MQTT broker is ability to keep only newest message that publish by publisher. This message is received by subscriber after it reconnects to MQTT broker[13]. However, when using IoHT-MBA platform, subcriber can receive all message that published by publisher. This is ability of Kafka message queue therefore the system is guaranteed lost data.

D. Future Work

To develop a larger scenario and increase the number of devices/users authorized quickly, other security issues such as security, privacy, availability for objects are still the challenges. For the security aspect, further works will be deployed in different scenarios like healthcare environment focusing on the smart care approaches [28], cash on delivery (CoD) [29], [30]. For the privacy aspect, we will exploit attribute-based access control (ABAC) [31], [32] to manage the authorization process of the IoT Platform via the dynamic policy approach [33], [34], [35]. Besides, we will apply the blockchain benefit to improve the availability issues [18], [36], [37]. Finally, we have a plant to develop data processing service to analyze the collected data.

[13] http://docs.oasis-open.org/mqtt/mqtt/v3.1.1/os/mqtt-v3.1.1-os.html

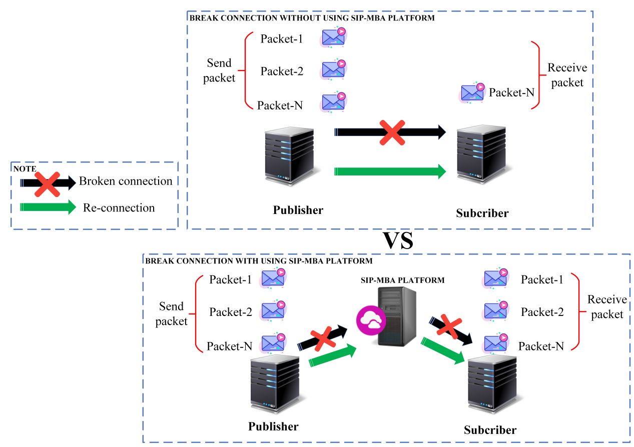

Fig. 4. Number of Receive Messages when System Recover after Broken Connection Issue.

VII. Conclusion

In this paper, we present the model IoHT-MBA Platform according to brokerless and microservice architecture. The scope of articles is oriented towards architecture that meets the most basic requirements and satisfies the top three evaluation criteria of IoHT Application, namely response time, energy consumption, and realibility. The microservice and brokerless architecture allows us to scale the system horizontally, while also ensuring availability, which is crucial in real systems. We take advantage of gRPC's advantages to define the data collection protocol. We also added the message queue system to store and transport packets between services within the

TABLE I. THE TEST RESULT

Location	Factor	1000	5000	10000	50000	100000
N.California	RTT(s)	3.30	14.02	26.17	132	261.38
	Error(%)	0	0	0	0	0
Stockholm	RTT(s)	3.27	14	26.05	131.55	261.5
	Error(%)	0	0	0	0	0
Ho Chi Minh city	RTT(s)	3.15	13.65	25.66	130.51	260.66
	Error(%)	0	0	0	0	0
Sydney	RTT(s)	3.19	13.72	25.8	131.05	261.15
	Error(%)	0	0	0	0	0

system. This ensures that when a service is not available, the message is still not lost and does not cause errors for the whole system. In addition, we also offer a solution that complements the security and decentralization of users and things through the RBAC model using Single Sign-On and OAuth. IoHT-MBA Platform is an open system, when we ensure a fast, accurate and energy-efficient data collection platform, developing advanced application layers using these data will be advantageous. more for developers. In the future, we will upgrade the platform's authentication and authorization mechanism by using Attribute-based Access Control to accommodate the increasingly complex nature of controlling things and users participating in the IoHT-MBA Platform.

REFERENCES

[1] F. Dahlqvist, M. Patel, A. Rajko, and J. Shulman, "Growing opportunities in the internet of things," *McKinsey, July*, 2019.

[2] P. Asghari, A. M. Rahmani, and H. H. S. Javadi, "Internet of things applications: A systematic review," *Computer Networks*, vol. 148, pp. 241–261, 2019.

[3] T. Chou, *Precision-Principles, Practices and Solutions for the Internet of Things*. McGraw-Hill Education, 2017.

[4] A. Pratap, R. Gupta, V. S. S. Nadendla, and S. K. Das, "On maximizing task throughput in iot-enabled 5g networks under latency and bandwidth constraints," in *2019 IEEE International Conference on Smart Computing (SMARTCOMP)*. IEEE, 2019, pp. 217–224.

[5] M. Bansal *et al.*, "Application layer protocols for internet of healthcare things (iot)," in *2020 Fourth International Conference on Inventive Systems and Control (ICISC)*. IEEE, 2020, pp. 369–376.

[6] J. C. Fuentes Carranza and P. W. Fong, "Brokering policies and execution monitors for iot middleware," in *Proceedings of the 24th ACM Symposium on Access Control Models and Technologies*, 2019, pp. 49–60.

[7] D. Soni and A. Makwana, "A survey on mqtt: a protocol of internet of things (iot)," in *International Conference On Telecommunication, Power Analysis And Computing Techniques (ICTPACT-2017)*, vol. 20, 2017.

[8] P. Lv, L. Wang, H. Zhu, W. Deng, and L. Gu, "An iot-oriented privacy-preserving publish/subscribe model over blockchains," *IEEE Access*, vol. 7, pp. 41 309–41 314, 2019.

[9] H. C. Hwang, J. Park, and J. G. Shon, "Design and implementation of a reliable message transmission system based on mqtt protocol in iot," *Wireless Personal Communications*, vol. 91, no. 4, pp. 1765–1777, 2016.

[10] M. Ali, S. Ali, and A. Jilani, "Architecture for microservice based system. a report," 2020.

[11] N. Karcher, R. Gebauer, R. Bauknecht, R. Illichmann, and O. Sander, "Versatile configuration and control framework for real time data acquisition systems," *arXiv preprint arXiv:2011.00112*, 2020.

[12] J. Maktoubian and K. Ansari, "An iot architecture for preventive maintenance of medical devices in healthcare organizations," *Health and Technology*, vol. 9, no. 3, pp. 233–243, 2019.

[13] M. B. Yassein, M. Q. Shatnawi, S. Aljwarneh, and R. Al-Hatmi, "Internet of things: Survey and open issues of mqtt protocol," in *2017 international conference on engineering & MIS (ICEMIS)*. IEEE, 2017, pp. 1–6.

[14] J. Toldinas, B. Lozinskis, E. Baranauskas, and A. Dobrovolskis, "Mqtt quality of service versus energy consumption," in *2019 23rd International Conference Electronics*. IEEE, 2019, pp. 1–4.

[15] N. C. Taher, I. Mallat, N. Agoulmine, and N. El-Mawass, "An iot-cloud based solution for real-time and batch processing of big data: Application in healthcare," in *2019 3rd International Conference on Bio-engineering for Smart Technologies (BioSMART)*. IEEE, 2019, pp. 1–8.

[16] J. J. Anthraper and J. Kotak, "Security, privacy and forensic concern of mqtt protocol," in *Proceedings of International Conference on Sustainable Computing in Science, Technology and Management (SUSCOM), Amity University Rajasthan, Jaipur-India*, 2019.

[17] P. Pratim Ray, D. Dash, and N. Moustafa, "Streaming service provisioning in iot-based healthcare: An integrated edge-cloud perspective," *Transactions on Emerging Telecommunications Technologies*, vol. 31, no. 11, p. e4109, 2020.

[18] H. X. Son, T. H. Le, N. T. T. Quynh, H. N. D. Huy, N. Duong-Trung, and H. H. Luong, "Toward a blockchain-based technology in dealing with emergencies in patient-centered healthcare systems," in *International Conference on Mobile, Secure, and Programmable Networking*. Springer, 2020, pp. 44–56.

[19] H. Jita and V. Pieterse, "A framework to apply the internet of things for medical care in a home environment," in *Proceedings of the 2018 International Conference on Cloud Computing and Internet of Things*, 2018, pp. 45–54.

[20] B. Di Martino, M. Rak, M. Ficco, A. Esposito, S. Maisto, and S. Nacchia, "A survey: Internet of things reference architectures, security and interoperability."

[21] R. Hill, D. Shadija, and M. Rezai, "Enabling community health care with microservices," in *2017 IEEE International Symposium on Parallel and Distributed Processing with Applications and 2017 IEEE International Conference on Ubiquitous Computing and Communications (ISPA/IUCC)*. IEEE, 2017, pp. 1444–1450.

[22] N. Duong-Trung, H. X. Son, H. T. Le, and T. T. Phan, "On components of a patient-centered healthcare system using smart contract," in *Proceedings of the 2020 4th International Conference on Cryptography, Security and Privacy*. New York, NY, USA: Association for Computing Machinery, 2020, p. 31–35.

[23] H. X. Son and E. Chen, "Towards a fine-grained access control mechanism for privacy protection and policy conflict resolution," *International Journal of Advanced Computer Science and Applications*, vol. 10, no. 2, 2019.

[24] D. Zheng, X. Zhang, and L. Chen, "Research of new integrated medical and health clouding system based on configurable microservice architecture," in *2020 IEEE 23rd International Conference on Computational Science and Engineering (CSE)*. IEEE, 2020, pp. 78–85.

[25] L. N. T. Thanh *et al.*, "Toward a unique iot network via single sign-on protocol and message queue," in *International Conference on Computer Information Systems and Industrial Management*. Springer, 2021.

[26] ——, "Toward a security iot platform with high rate transmission and low energy consumption," in *International Conference on Computational Science and its Applications*. Springer, 2021.

[27] ——, "Uip2sop: A unique iot network applying single sign-on and message queue protocol," *IJACSA*, vol. 12, no. 6, 2021.

[28] N. Duong-Trung, H. X. Son, H. T. Le, and T. T. Phan, "Smart care: Integrating blockchain technology into the design of patient-centered healthcare systems," in *Proceedings of the 2020 4th International Conference on Cryptography, Security and Privacy*, ser. ICCSP 2020. New York, NY, USA: Association for Computing Machinery, 2020, p. 105–109.

[29] H. T. Le, N. T. T. Le, N. N. Phien, and N. Duong-Trung, "Introducing multi shippers mechanism for decentralized cash on delivery system," *money*, vol. 10, no. 6, 2019.

[30] N. T. T. Le, Q. N. Nguyen, N. N. Phien, N. Duong-Trung, T. T. Huynh, T. P. Nguyen, and H. X. Son, "Assuring non-fraudulent transactions in cash on delivery by introducing double smart contracts," *International Journal of Advanced Computer Science and Applications*, vol. 10, no. 5, pp. 677–684, 2019.

[31] N. M. Hoang and H. X. Son, "A dynamic solution for fine-grained policy conflict resolution," in *Proceedings of the 3rd International Conference on Cryptography, Security and Privacy*, 2019, pp. 116–120.

[32] H. X. Son and N. M. Hoang, "A novel attribute-based access control system for fine-grained privacy protection," in *Proceedings of the 3rd International Conference on Cryptography, Security and Privacy*, 2019, pp. 76–80.

[33] S. H. Xuan, L. K. Tran, T. K. Dang, and Y. N. Pham, "Rew-xac: an approach to rewriting request for elastic abac enforcement with dynamic policies," in *2016 International Conference on Advanced Computing and Applications (ACOMP)*. IEEE, 2016, pp. 25–31.

[34] Q. N. T. Thi, T. K. Dang, H. L. Van, and H. X. Son, "Using json to specify privacy preserving-enabled attribute-based access control policies," in *International Conference on Security, Privacy and Anonymity in Computation, Communication and Storage*. Springer, 2017, pp. 561–570.

[35] H. X. Son, T. K. Dang, and F. Massacci, "Rew-smt: a new approach for rewriting xacml request with dynamic big data security policies," in *International Conference on Security, Privacy and Anonymity in Computation, Communication and Storage*. Springer, 2017, pp. 501–515.

[36] X. S. Ha, H. T. Le, N. Metoui, and N. Duong-Trung, "Dem-cod: Novel access-control-based cash on delivery mechanism for decentralized marketplace," in *2020 IEEE 19th International Conference on Trust, Security and Privacy in Computing and Communications (TrustCom)*. IEEE, 2020, pp. 71–78.

[37] X. S. Ha, T. H. Le, T. T. Phan, H. H. D. Nguyen, H. K. Vo, and N. Duong-Trung, "Scrutinizing trust and transparency in cash on delivery systems," in *International Conference on Security, Privacy and Anonymity in Computation, Communication and Storage*. Springer, 2020, pp. 214–227.

A Survey on the Effectiveness of Virtual Reality-based Therapy and Pain Management

Fatma E. Ibrahim[1], Neven A. M. Elsayed[2], Hala H. Zayed[3]
Department of Computer Science,
Faculty of Computers & AI,
Benha University, Egypt

***Abstract*—Virtual reality refers to the technology used to create multi-sensory three-dimensional environments that can be navigated, manipulated, and interacted by a user. This paper's objective is to categorize the most common areas that use virtual reality (VR) for managing pain (psychological and physical). To our knowledge, this is the first survey that summarizes all of these areas in one place. This paper reviews the conducted studies that used VR for psychological treatment, especially with phobias. Also, this paper summarizes the current literature on using virtual reality interventions for managing acute, chronic, and cancer pain. Based on the review, virtual reality shows great potential for controlling acute pain - such as pain associated with burn wound care. However, limited studies only investigated the impact of using virtual reality on patients with chronic pain. The findings indicated that VR distraction has a great impact on pain and distress related to cancer and its treatments. This paper also discusses the challenges and limitations of the current research. Notably, the identified studies recommend VR distraction as a promising adjunct for pain reduction and psychological treatment. However, further research needs to be conducted to determine under what conditions VR distraction will provide more analgesic effects.**

***Keywords*—Virtual reality; mental health; cancer pain; distraction; pain management**

I. Introduction

Pain is a sensory and emotional experience, which affects negatively physical, mental, and social function [1]. The definition of pain - according to the International Association for Study of Pain (IASP) [2], is "an unpleasant sensory and emotional experience associated with actual or potential tissue damage or described in terms of such damage". Most hospitalized patients experience pain, which can be acute or chronic [3]. Acute pain is associated with an injury to the body and developed slowly or quickly. It can last for a few minutes to six months and goes away when the injury heals. On the other hand, chronic pain persists for more than six months beyond the expected time for recovering [4]. Another type of pain that occupies a separate category is cancer pain, patients with cancer frequently suffer from pain related to the disease itself and/or pain caused by treatment such as chemotherapy, radiation, and other painful procedures [5]. Cancer pain has components of both acute and chronic, this makes experts of pain categorize it in a separate class [6]. Managing the pain associated with painful medical procedures is still one of the greatest challenges in health care. Accordingly, it is valuable for all health care institutions to understand the benefits of managing pain during these medical procedures.

The most commonly used approach to manage pain is the pharmacological methods relying largely on opioids [7]. However, the analgesic effects of these methods diminish with repeated use and may cause many unwanted physical side effects and different types of mental disorders [8], [9]. Therefore, researchers pay great attention to non-pharmacological methods as alternatives for managing pain related to painful medical procedures [8]. Non-pharmacological approaches include physical methods (e.g. positioning, pressure, hot and cold treatments) and cognitive-behavioral methods (e.g. guided imaginary, relaxation techniques, and distraction activities such as music, reading, and video games) [10], [11], [12].

Recently, distraction is the most common method of non-pharmacological techniques for pain management. Distraction is an effective technique that diverts the attention of patients away from painful stimuli to decrease the experienced pain [10]. Melzack and Wall [13] explained the logic of why distraction reduces pain by presenting the gate control theory. Their theory states that the perception of pain will be reduced if the patient is well distracted. Due to the efficacy of distraction interventions, there is a growing interest to propose more immersive and interactive distraction interventions, such as using VR for pain control.

VR refers to technology that involves immersive and interactive three-dimensional (3D) computer-generated environments. VR systems have two main characteristics: immersion and presence [14]. Immersion strongly depends on the VR system's interface and display [15]. VR presence depends on the user's perceived value of seeing, hearing, touching the virtual world. Presence makes users feel while being in the virtual world as if they were in a real-world [16]. VR systems use multi-sensory to enhance the immersive experience. The multi-sensory embeds sensors in HMD to control users' virtual visual and audio content based on users' head position [17]. During the last years, VR distraction gains massive popularity as an alternative for pain management. Accordingly, many successful trials have been conducted for managing pain during painful medical procedures [18] as well as the treatment of many psychological disorders such as phobias [19].

Previous reviews of research have presented many controlled investigations of the effectiveness of VR distraction for managing pain. However, none provided the most common areas in health care that use VR distraction. To this aim, we categorize for the first time the major areas that use VR interventions for pain management and treatment. This will help to determine the main characteristics of the conducted studies to be considered in future research. This survey indicated two main categories based on the type of pain: psychological and physical. Through the article, a literature review of the conducted studies that used VR for the treatment of many types of phobia was provided. Also, presents the effect of using VR distraction for managing acute, chronic, and cancer pain. Moreover, we present the key findings of these studies and limitations that need more research work.

Through the following sections, our paper summarizes the clinical use of VR interventions for managing pain and psychological treatment. Section 3 includes the literature review on using VR for many mental health treatments especially phobias. Research studies that were conducted to measure the effect of using VR for acute pain management are presented in Section 4. Then Section 5 presents the research papers that studied the impact of VR on patients with chronic pain. Section 6 summarizes the research studies which were performed for managing cancer pain. Finally, the challenges and limitations of using VR distraction in health care along with conclusions are included in Section 7 and 8, respectively.

II. Method of Survey

This survey aims to summarize and highlight the most common areas that use VR interventions for pain management. To this aim, literature searches of web-based scientific databases were conducted to include studies that used VR for managing physical pain as well as including studies that used VR for treating many psychological disorders (phobias). In this survey, we restrict the searches to include studies that use different ways of investigating the efficacy of VR distraction. We were interested to include the studies that used VR distraction under different model designs (within or between-subjects). Also, we included studies that used different conditions where VR distraction was used alone or was compared with at least one alternative intervention or no-treatment control condition in reducing pain. We selected these studies of different settings to show that VR distraction is a promising tool for managing pain. A broad literature search of the IEEE Xplore, Science Direct, Google Scholar, Scopus, and MedLine databases as well as an examination of other reviews in this area. We performed the search using as main terms "virtual reality distraction", "pain management", "VR for cancer", and "chronic".

In addition, there were no date restrictions to be able to search all citations in each database. We include all the retrieved studies that investigated the impact of immersive VR distraction during painful medical procedures. Also, the reference lists of all retrieved papers were reviewed to identify other relevant articles. We excluded the studies in which it was not possible to identify how VR was used and failed to be used in comparative data. The studies in this survey are organized into the following four groups, according to the type of pain: (a) psychological pain; (b) acute pain; (c) chronic pain; and finally (d) cancer pain. A total of 39 studies were analyzed and included in this survey (see Fig. 1).

III. Virtual Reality for Mental Health

The standard methods used for mental health treatment are Cognitive behavioral therapy (CBT) and Vivo exposure therapy. CBT is a type of talking therapy that aims to help patients learn some strategies for dealing with their phobia. On the other hand, patients in Vivo will face a feared object, situation,

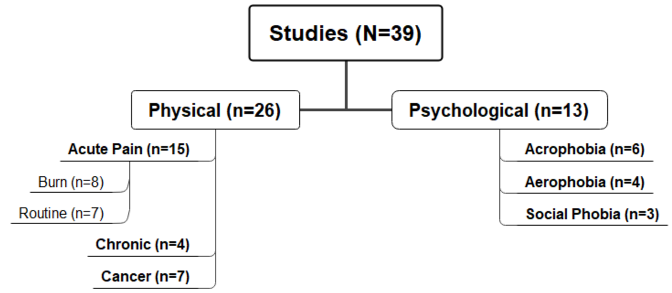

Fig. 1. Summary of the Included Studies.

or activity in real life. Vivo type of treatment is impractical, difficult, and sometimes dangerous. Recently, VR technology provides an alternative solution for Vivo exposure, with better safety and cost-effective characteristics. In this section, we will focus on the most common types of phobias; fear of heights (*acrophobia*), flying phobia (*aerophobia*), and *social phobia*, and review the conducted VR studies for treating them. Table I summarizes the characteristics of the included studies.

A. VR for Acrophobia Treatment

Since the mid of 1990's many studies were conducted to explore the effect of using VR interventions to treat acrophobia [33]. Rothbaum et al. [20] conducted one of the studies in this area, involving twenty participants, who suffered from acrophobia. Through the study, participants were assigned to treatment using VR exposure therapy against the waiting list. Participants in VR therapy experienced three different conditions for eight weekly sessions. Three different self-reported questionnaires were used to measure the VR treatment impact. Only ten participants completed the treatment sessions. The results from all assessment measures indicated that there was a significant reduction in means of all questionnaire scores for the VR group.

Valuable results from the conducted studies in the 90s opened the door for further research in this era. After a few years, another acrophobia study was conducted by Emmelkamp et al. [21] to compare VR exposure against Vivo exposure therapy. Thirty-three patients participated in the extended study and were divided randomly into two equivalent groups: the VR group and the Vivo group. All participants attended three sessions of treatment per week, each session lasted for one hour. Both groups showed improvements in anxiety and avoidance even after 6 months of follow-up. Results from this study revealed that the two types of therapy showed a significant improvement in anxiety and avoidance. The VR therapy was found to be more effective concerning the attitudes towards heights questionnaire. The main finding from this study is that VR treatment had the same effect as Vivo exposure.

Research studies started to focus on investigating whether the type of VR may affect its analgesic effect. Krijn et al. [22] conducted a study to compare the effect of using different types of VR exposure on thirty-seven patients with acrophobia. Participants were partitioned randomly into three groups: (1) VR group (using HMD), (2) VR group (using CAVE), or (3) control list group. The treatment included

TABLE 1. KEY FEATURES OF STUDIES USED VR FOR MENTAL HEALTH TREATMENT

Study	Sample	No.Sessions	Conditions	Findings	Disorder Treated
Rothbaum et al. [20]	20 students mean 20 years	8 sessions	VRE* / WL*	Acrophobia decreased for VR compared to WL	Acrophobia
Emmelkamp et al. [21]	33 patients mean 43 years	3 sessions 6 months follow up	VRE / Vivo	No differences in anxiety and avoidance for VR and Vivo	Acrophobia
Krijn et al. [22]	37 patients mean 50.6 years	3 sessions 6 months follow up	VRE(HMD)/ VRE(CAVE)/ WL	Acrophobia reduced for both VR groups with no differences in effect between them	Acrophobia
Suyanto et al. [23]	10 patients 21-25 years	4 tests	VRE	Reduced acrophobia when use VR exposure therapy	Acrophobia
Freeman et al. [24]	100 patients mean 30 years	6 sessions 4 Weeks follow up	Automated VR / C*	Automated VR reduced acrophobia compared to C	Acrophobia
Donker et al. [25]	74 patients 18-65 years	9 sessions 3 months follow up	VRE / WL	Acrophobia decreased consistently with the challenge presented in self-guided VR exposure	Acrophobia
Rothbaum et al. [26]	49 patients mean 40 years	8 sessions 6-12 months follow up	VRE / SE* / C	VRE and SE were equally effective greater than C	Aerophobia
Muhlberger et al. [27]	45 patients 25-65 years	1 sessions 6 months follow up	VR-mot*/VR-no-mot*/CBT*	VR treatment reduced aerophobia compared to CBT	Aerophobia
Rothbaum et al. [28]	83 patients mean 40 years	8 sessions 6-12 months follow up	VRE/ SE/ WL	VRE and SE were equally effective compared more than WL	Aerophobia
Tortella-Feliu et al. [29]	60 patients mean 36 years	6 sessions one year follow up	VRE/ CAE-T*/ CAE-SA*	Three treatment conditions were equally effective	Aerophobia
Klinger et al. [30]	36 patients 18-65 years	12 sessions	VRE / CBT	VRE was more effective than CBT	Social phobia
North et al. [31]	16 students	5 sessions	VRE / C	VRE reduced social phobia compared to C	Social phobia
Kampmann et al. [32]	60 patients mean 37 years	10 sessions 3 months follow up	VRE/ Vivo/ WL	VR was effective in treating social phobia	Social phobia

*VRE-virtual reality exposure; WL-waiting list; C-control; SE-standard exposure; VR-mot–VR motion simulator; VR-no-mot–VR without motion simulator; CBT-cognitive behavioral therapy; CAE-T–computer aided exposure with a therapist; CAE-SA–self-administrated computer aided exposure;

three 1.5 hour sessions. Gradually, participants who used VR were exposed to four different virtual environments. Using a (0-10) scale, patients rated their anxiety during exposure therapy. Results from self-reported questionnaires such as the acrophobia questionnaire showed that both groups (1 and 2) significantly improved compared to the third group. Also, there was no notable difference in results between groups (1) and (2). These results proved that VR therapy using an HMD had the same impact as using the CAVE.

According to the encouraging benefits of VR, there is an ongoing body of research to explore its treatment capabilities. Recently, ten patients aged (21-25) years participated in a study that integrated VR with Kinect to evaluate the efficacy of VR for reducing acrophobia [23]. The virtual system used in the study was a simulation game called “Acrophobia Simulator”. The game included three different stages where difficulty was increased gradually. Participants experienced the VR application using Google cardboard. After the VR experience, the application was assessed using the state-trait anxiety inventory measurement. According to the results, patients reported a decrease in anxiety levels and an increase in improvements towards heights.

A year later, Freeman et al. [24] conducted another study to investigate whether VR technology can be used to automate acrophobia. One hundred patients participated and were divided randomly into two groups the automated VR group and the control group. The VR intervention used was “Now I Can Do Heights” which was developed for use without the help of any therapist. The treatment using VR included six sessions over two weeks with a VR experience last for 30 minutes. Many different measurements were used to assess the VR experience and data were collected. The results indicated a significant decrease in anxiety and acrophobia scores for those who used VR compared to the control group.

Recently, another clinical study was conducted to investigate the efficacy of using fully self-guided VR therapy delivered via low-cost VR hardware [25]. Totally seventy-four patients aged (18-65) years who suffered from acrophobia symptoms participated. Participants were randomized into two groups either the VR group or the wait-list group. Participants experienced a VR system called “Zerophobia”, which consisted of six animated modules that differed in the engaging level. The VR therapy started from module three and the time range among modules was between 5 and 40 minutes. The game included a series of tasks with increasing levels of challenge (5 levels). The study included around nine sessions over three weeks. In case of decreasing anxiety levels, participants can experience VR in a standing-up fashion. A different set of questionnaires were used to assess the experiment. The results showed that a linear pattern existed between the anxiety score and the difficulty experienced at each level of the game (most reduction of anxiety occurred during level five). Moreover, it was shown that this fully self-guided application can be effectively used in the home setting.

B. VR for Aerophobia Treatment

Other several experimental studies also found encouraging results when used VR for treating aerophobia. In one study, conducted by Rothbaum et al. [26] forty-nine patients with aerophobia participated and randomly were assigned to one of three groups. The groups were: (1) a VR group that used a virtual airplane, (2) a standard exposure group who used an actual airplane, or (3) a waiting list group with no treatment. In

VR exposure patients experienced flying in a virtual airplane with different weather conditions, where the standard group experience actual flying using a stationary plane. Both groups (1) and (2) showed a significant improvement compared to the waiting list control with no notable differences between the same two groups. According to the 12 monthly follow up, results showed that the short-term VR treatment had a lasting effect with no need for relapse sessions.

Later on, one study was conducted to investigate the efficiency of one session VR treatment by Muhlberger, Wiedemann, and Pauli [27]. Forty-five patients with aerophobia participated and were randomly partitioned into three cognitive treatment groups: VR exposure with motion simulation (VR-mot), VR exposure without motion simulation (VR-no-mot), or cognitive treatment alone. All participants received cognitive therapy for 50 minutes. Both VR groups (VR-mot and VR-no-mot) used an HMD and experienced four VR flights with a 5-10 minute break between flights. Post-treatment and 6 months follow-up, results showed that there was a reduction in fear of flying for both VR exposure groups in contrast to the cognitive treatment group. The results of the two VR exposure groups were also compared and recorded that motion simulation didn't improve the treatment effects.

After the success of their previous research, authors Rothbaum et al. [26] conducted another study on eighty-three patients [28]. Randomly, participants were divided into three groups (1) therapy using VR (VRE), (2) therapy using standard Vivo (SE), and (3) waiting group (WL). The treatment duration lasted for six weeks including eight individual sessions. Over the first four sessions, both VRE and SE groups received the same treatment techniques and methodology. For the remaining sessions, the VRE group experienced VR exposure therapy and on the other hand, the SE group received the Vivo exposure therapy. Many self-reported questionnaires such as fear of flying inventory (FFI) were used to assess this clinical trial. Results indicated that there wasn't a significant difference between both VRE and SE groups. However, both groups significantly differed from the WL group. Also, after the follow-up period, the conducted analysis revealed that participants in both VRE and SE groups were more likely to fly (12.7) times over the WL group.

Another study was conducted to compare the efficacy of using VR exposure therapy against computer-aided therapy [29]. Sixty patients with aerophobia were eligible to participate in the study. The participants were randomly assigned to either (1) VR exposure therapy, or (2) computer-aided exposure with therapist (CAE-T), or (3) self-dependent computer-aided exposure (CAE-SA). Treatment using VR exposure included different scenarios with different situations gradually increased in difficulty through sessions. Therapists attended all CAE-T exposure sessions, where patients received six sequences of different tasks and were asked to rate fear at the end of each sequence. The final group received the same treatment as the CAE-T group except it was self-administrative. Results showed that there was no significant difference between the three treatment methods, they were equally effective in reducing the fear of flying disorder. Also, this study suggested that the therapist rule can be excluded during computer-based treatments.

C. VR for Social Phobia Treatment

Through last years, VR also helps people who suffered from social anxiety disorders. VR Therapy is promising for these patients as it provides different situations that are difficult to be handled in real life. Klinger et al. [30] conducted a study to compare VR therapy to cognitive therapy with thirty-six patients participated. Participants in the VR therapy attended 45 min sessions for 12 weeks where the VR intervention included four different scenes. After each session, all participants from both groups performed some tasks in vivo for practicing. Results indicated that patients treated using the VR therapy significantly improved as well as those in the cognitive group.

According to the considerable efficacy of VR therapy, another study was conducted with sixteen students who participated and were assigned to either the VR therapy group or the comparison group [31]. The VR therapy included a virtual environment for public speaking with a virtual wooden stage and a speaker's stand. A microphone attached to the HMD was used for speaking and generating the simulated echo in the hall. On the other hand, a simple VR scene was used to treat participants in the comparison group. Also, participants were motivated to control their fear using either visualization methods or self-exposure conditions. Both groups attended 10-15 min sessions for five weeks. Results indicated that anxiety symptom significantly reduced for those who used the VR intervention in contrast to the comparison group.

Kampmann et al. [32] conducted a study to investigate the effect of using VR exposure therapy for social phobia treatment. Sixty participants were divided randomly into three groups: (1) VR exposure therapy (VRET), (2) Vivo exposure therapy (iVET), and (3) waiting group. Participants during the VRET treatment sessions received different one-to-one and group situations to reduce their social anxiety symptoms. On the other hand, participants in Vivo exposure experienced real-life situations. Information from the statistical analysis revealed that both VRET and iVET improved compared to the waiting list group. However, results indicated that iVET is more efficient than VRET. This was because participants in iVET experienced a variety of social situations compared to VRET. So, this study suggested using the same situations with all active groups to be able to generalize results. Other several VR interventions were developed and effectively used to treat other types of phobia such as fear of driving [34], [35], [36] and fear of spiders [37], [38], [39].

Notably, VR-based treatments for different mental health problems have observed positive findings. The results of the presented studies showed that VR therapy is as effective as Vivo therapy. However, VR therapy has many key features over Vivo; it is a stable application, cheap and controlled, can be used repeatedly, can experience difficult situations safely, and provide more confidentiality. Also, findings indicated that using HMD or CAVE to deliver VR therapy resulted in an equal treatment impact, but HMD VR is cheap, easy, and more appropriate compared to the CAVE VR. Another key issue revealed from the controlled studies is that VR therapy is more effective than cognitive-behavioral therapy. Finally, as the cost of VR software and hardware has decreased, VR therapy may become increasingly available.

IV. VR for Acute Pain Management

VR provides a unique distraction with multisensory, immersive, and interactive environments. Therefore, VR is effectively used in various types of health care applications especially for managing pain associated with different medical procedures. A lot of research studies have been conducted to explore the relationship between immersion and VR distraction effects. The findings of these studies reported that VR is a promising alternative for managing acute pain related to burn wound care and other routine medical procedures. Through this section, we will present the literature on using VR distraction interventions for managing acute pain. We will focus on presenting the conducted studies for reducing pain in patients with severe burn pain and other types of routine medical procedures (see Table 2).

A. VR for Burn Pain Management

Wound care after burn injury is one of the most painful medical procedures. In favor of wound healing, it is required to repeat the procedure of wound care dressing changes regularly. Treatment of severe burns usually includes tanking sessions, which required the removal of old bandages and dead skin in a hydro tank, then taking a dose of antibiotics and putting a new bandage. Patients with severe burns can also experience extreme pain due to physical therapy exercises, which play an important role during treatment and afterward. This may discourage patients especially children from complying with their physical therapy [55]. VR technology gains a growing interest as an alternative for managing pain in adolescents with burn injuries, as indicated by many successful controlled studies with children and adults [56].

Hoffman et al. [40] investigated the effect of using VR for severe burn pain management. The study included eleven patients aged (9-40) years who suffered from severe burns and required burn wound dressing changes in a hydrotherapy tank. To ensure safety, the study was conducted using a custom fiber optic VR system suitable for water use. The virtual environment used in the study was "SnowWorld" [57], which is the first environment designed for distracting burn patients. The 6-minutes wound care session for each patient is divided into two equivalent portions. During one portion, the patient used VR distraction for pain relief. The patient spent the other portion of the session without any distractor. Randomly, patients were assigned to one of two conditions: VR-first or VR-last. All patients reported that while being in VR they spent less time thinking about pain. Besides, patients with severe pain intensity showed a reduction of pain by (41%) while being in VR compared to the control condition. The study results indicated that VR distraction has a great impact on reducing pain associated with the wound care procedure.

Kipping et al. [41] through another study demonstrated the effectiveness of using VR system "off-the-shelf" with adolescents undergoing burn wound care. The main research questions included whether "off-the-shelf" VR is more effective than the standard distraction, besides investigating the impact of using VR on wound care procedures length. The randomized controlled trial included forty-one adolescent participants aged (11-17) years. Patients were assigned to one of two groups: the VR group (VRG) or the standard distraction group (SDG). The trial ensured applying the same medical procedures with all participants and to be conscious during their wound care dressing change. According to the results from the nursing staff, patients in the VR group experienced less pain during wound care dressing compared to the other group. Concerning the length of treatment, participants who used VR required a lower time for the dressing process (10 minutes) against (12 minutes) for the standard group.

In a related study, thirty adolescents aged (10-17) years participated and were divided into three groups: VR active distraction (SnowWorld VE), passive distraction (watching a movie) and standard care [42]. To include patients with facial burns, the VR group used a helmet device with a tripod instead of using the HMD. To assess pain Adolescent Pediatric Pain Tool word-graphic rating scale (APPT-WGRS) measurement was used [58], which is a 100-millimeter line word graphic scale to rate pain scores. The results showed that the VR distraction group reported a significant reduction in pain in contrast to the other two groups. Besides, the only group that reported a decrease in pain perception during burn wound care compared to pre-procedure pain was the VR distraction group.

Brown et al. [43] used a multi-model VR inspired intervention titled "Ditto" with manual control. The Ditto medical device is suitable for children aged (3-12) years and is used to distract the child during medical procedures by using interactive games or stories. The child in the preparatory phase of the device should know details of the medical procedures to reduce his fear and distress. Participants in this study were assigned to either the Ditto distraction group or the standard practice group. Before and immediately post to the burn wound care process, data from physiological measures and other scales were recorded. Results showed that patients receiving Ditto distraction recovered faster than those in the standard group by an average of two days. Moreover, self-reported pain and anxiety in pediatric patients who used Ditto decreased compared to the other group.

Overall results from the conducted studies showed that VR is an effective tool for reducing pain in burn patients. These results along with the availability of VR technology have motivated authors to investigate whether low-cost VR distraction will be effective as well. One study with inexpensive Oculus Rift goggles was on a boy aged eleven years during his occupational treatment [44]. He suffered from severe electric and flash burns on different parts of his body. For three consecutive days, he received three treatment sessions included one 20-minute session with no VR, then one with VR, and finally a session with no VR. The patient reported less pain perception and reduced discomfort, besides feeling more fun during physical therapy when used VR. Another related study was conducted to evaluate the effect of using inexpensive VR technology on patients with burn injuries [45]. Ten adult patients from an outpatient clinic participated in this study during their burn wound care procedure. Both patients and providers completed a satisfaction survey that summarized their experience with VR. Results proved that distraction using inexpensive VR technology is effective during burn wound care and/or dressing changes.

Through the last two decades, enormous studies showed that VR has great potential for managing pain associated with burn care procedures in both adolescents or adults. However,

TABLE 2. KEY FEATURES OF STUDIES USED VR FOR ACUTE PAIN MANAGEMENT

Study	Sample	No.Sessions	Conditions	Findings	Pain Type
Burn Injury					
Hoffman et al. [40]	11 patients 9-40 years	1 session	VR* / C*	VR reduced extreme burn pain compared to C	Burn injury
Kipping et al. [41]	41 patients 11-17 years	Not provided	VR / SD*	Mean pain scores for SD was higher than VR	Burn injury
Jeffs et al. [42]	30 patients 10-17 years	1 session	VR/ PD*/ SC*	The mean pain scores for PD was the highest	Burn injury
Brown et al. [43]	75 patients 4-13 years	Not provided	Ditto / SD	Pain and anxiety levels for Ditto were lower than SD	Burn injury
Hoffman et al. [44]	A boy aged 11 years	3 sessions	VR+SC / SC	VR reduced pain intensity and pain unpleasant compared to SC	Burn injury
Ford et al. [45]	10 patients mean 40 years	1 session	VR	Inexpensive VR is also effective during burn wound care	Burn injury
Khadra et al. [46]	15 patients 2 months-10 years	1 session	ProVR*	ProVR was an effective in reducing pain in children $\leq$ 4 years	Burn injury
Hoffman et al. [47]	48 patients 6-17 years	4 sessions	VR / C	Children's worst pain decreased when used VR	Burn injury
Routine Procedures					
Gold et al. [48]	57 patients 8-12 years	1 session	VR(HMD)/ VR(Desktop)/ SD/ C	VR via HMD is more effective than the other three groups	Blood draw
Gold et al. [49]	20 patients 8-12 years	1 session	VR / SC	SC felt pain of IV* placement four-times greater than VR	IV placement
Piskorz and Czub [50]	38 patients 7-17 years	1 session	VR / C	Pain and stress during blood draw reduced with VR	Blood draw
Hoffman et al. [51]	Two patients 51-56 years	1 session	VR / SD / C	VR reduced dental pain compared to other groups	Dental
Furman et al. [52]	38 patients mean 45 years	1 session	VR / SD / C	VR provided an analgesic effect greater than SD and C	Dental
Aminabadi et al. [53]	120 patients 4-6 years	3 sessions	VR / C	VR decreased pain and anxiety compared to C	Dental
Tanja-Dijkstra et al. [54]	69 patients mean 33 years	1 session	AVR* / PVR* / C	AVR increased presence more than PVR, AVR achieved the least aware of the surroundings	Dental

*VR-VR distraction; C-control; SD-standard distraction; PD-passive distraction; SC-standard care; ProVR-projector-based VR
AVR–active VR; PVR–passive VR; IV–intravenous

using VR to control pain in children aged less than 4 years has not been studied as much. One pioneering study was conducted by Khadra et al. [46], which used a projector-based VR system to distract children suffered from burn injuries. Fifteen children with ages ranged from two months to ten years were participated. The research group developed a 3D video game called "Bubbles" to be used in the study. The difficulty level of the game was consistent with the child's age. The game was started once the wound care session was started. This projector-based VR distraction was combined with the standard care medications. The VR experience involved only one session and the pain was assessed through five time periods. Results proved the feasibility and acceptability of the proposed VR system for managing procedural pain in children less than 4 years.

Many burn patients who have burns on their heads can't receive the VR intervention using an HMD. To solve this issue, a recent study was conducted and used for the first time a new portable water-friendly VR system especially for patients with severe burns [47]. The study included forty-eight patients aged (6 - 17) years. The study used a within-subject design where each patient experienced either VR or control conditions for five minutes during the same wound care session. The order of receiving the conditions was randomized. Patients played "SnowWorld" during the VR proportion, while received the standard wound care in the other proportion. The study used the graphic rating scales (GRS) to keep track of the worst pain, pain unpleasantness, and time spent thinking about pain. Post to the wound care session, each patient rated the pain intensity experienced in both conditions. The patient's worst pain score significantly decreased from (8.52) during standard care to (5.10) while using VR. For pain unpleasant score, it was decreased from (6.40) during the standard care against (3.47) while using VR. Also, patients spent less time thinking about pain when using VR.

B. VR in Routine Medical Procedures

Stress and anxiety in pediatrics are common symptoms associated with most hospital procedures especially needle-related procedures. VR offers a great opportunity for distracting patients during routine painful medical procedures [59]. Gold et al. [48] conducted a trial including fifty-seven participants aged (8-12) years to explore the effect of using VR distraction during the procedure of blood draw. Children were divided into four groups: (1) perceiving VR using an HMD, (2) perceiving VR using a desktop, (3) standard distraction, or (4) control group. For achieving visual occlusion, all participants received blood draw by passing their arm through a wall. Many self-reported and observational scales were used to assess pain before and post to the procedure. Results showed that participants in the HMD based VR group reported a reduction in pain compared to the other three groups. Also, children reported less pain during the procedure when used the HMD VR compared to the other two distraction groups. The same author performed another randomized control trial on twenty children requiring intravenous (IV) placement [49]. Randomly, children were assigned to one of two groups: (1) VR group, or (2) standard care group. For participants who received VR, the experience started 5 minutes before the IV placement and lasted for 5 minutes after. On the other hand, a local anesthetic spray was used with participants in the standard control group without receiving any VR intervention. The results showed that the children who used VR didn't report any increase in pain after the IV placement compared to a four-time increase for the other group.

Lately, many authors have designed a VR game with difficulty levels adjusted with the child's age. Also, they used the concept of multiple object tracking (MOT) in their game hence attracting most of the child's attention. The study involved thirty-eight patients aged (7-17) years during their blood draw in a clinic for pediatric [50]. Participants were partitioned into two groups: (1) VR group, or (2) control group. Children in the VR group started using the VR intervention just before the blood draw and continued until after the procedure was finished. On contrarily, children in the control group didn't receive any distraction during the blood-draw procedure. Both groups were asked to describe their blood draw experience and provide a report that included stress level and pain score. Results indicated that there was a significant reduction in pain for participants who used VR compared to the standard control group. Those who used VR reported a (59%) reduction in pain intensity score against the other group.

VR's unique characteristics also attracted authors to investigate its efficacy in controlling the pain related to different dental procedures. Many controlled studies demonstrated the impact of using VR on dental pain. Hoffman et al. [51] conducted a study involving two dental patients to explore the analgesic effect of VR. Each patient received his dental treatment under three different situations: (1) VR distraction, (2) standard distraction, or (3) control condition. Both patients spent an equal interval of time in each condition, besides the order of conditions was random. Both patients rated their pain intensity and provided the time spent thinking about the medical procedure. Patient 1 reported a mild pain score (1.2) during VR compared to severe pain (7.2) during the other conditions. On the other hand, patient 2 reported no pain score (0.6) during VR against mild pain (3.3) in the standard condition and moderate pain (4.4) during the control condition.

In a close study, thirty-eight dental patients participated and each one experienced three different treatment conditions: (1) VR distraction, (2) watching a movie, or (3) control condition [52]. The sequence of treatment conditions for each patient was chosen randomly. During the study, participants were asked to report their pain intensity and unpleasantness level using the visual analog scale (VAS). The mean VAS scores for VR, standard, and control groups were (1.76 vs 2.57 vs 3.95) respectively. Results also revealed that both distraction conditions (VR and watching a movie) led to a significant pain reduction in comparison with the control condition.

To date, a few research studies were conducted to investigate the impact of VR on children with dental pain. Aminabadi et al. [53] presented one study to explore the effect of using VR technology for distracting pediatric patients during dental treatment. The study included one hundred and twenty children aged (4-6) years partitioned randomly into two groups. The treatment procedure included three sequential sessions where all children in both groups received fluoride therapy in their first session. During the second session, groups 1 and 2 received restorative treatment procedures with and without VR respectively. Finally, the third session included the same treatment procedures as the second session with exchanging groups 1 and 2 conditions. To assess pain intensity a "Wong Baker FACES" scale was used and measured after each session for both groups. Results demonstrated that VR interventions can be used successfully to decrease pain severity and anxiety during dental procedures. For both groups, the pain intensity scores were lower when using VR (group1: 1.89, group2: 2.05) compared to sessions without VR (group1: 3.00, group2: 3.05).

The valuable benefits of using VR for dental pain reduction motivated other authors for further research. Another study was conducted including sixty-nine adult patients, randomly they were assigned to one of three conditions: active VR, passive VR, or control [54]. Besides, at the beginning of the study participants were divided into two groups according to their dental anxiety (high and low). A simulated dental area was established with heart rate measured during the treatment and blood pressure measured immediately after finishing. Participants in the active VR group reported a higher presence (mean 6.21) against (mean 5.16) for the passive VR group. Also, results showed that distraction from VR could influence the patient's memory after the treatment sessions ended.

As a whole, the presented studies in this section showed that VR distraction is an effective adjunct for controlling pain during burn wound care and routine medical procedures. Due to the nature of burns, a lot of studies used specially designed hardware to deliver VR. However, the findings of these studies supported the analgesic effect of VR on pain reduction. Besides, low-cost VR proved to be effective and hence may become more affordable. Also, VR distraction was used safely and effectively with children less than four years. Furthermore, studies indicated that the impact of interactive VR was greater than the passive one. Finally, immersive VR distraction showed a reduction in pain than non-immersive VR.

V. VR for Chronic Pain Management

Unlike acute pain, the duration of chronic pain starts from six months and continues after the expected period of recovery [4]. Chronic pain may include chronic headache, back or limb pain, and also complex regional pain syndrome. Despite the large number of studies that support the efficacy of VR for reducing acute pain, limited was conducted for the use of VR with chronic pain [60], [61]. In one pilot study, Sato et al. [62] investigated the effect of using VR for reducing complex regional pain syndrome in adults. Five adult patients aged (46-74) years with complex regional pain syndrome participated and experienced a non-immersive VR system along with mirror visual feedback. The study included four to eight outpatient sessions. Results indicated that four out of the five patients reported (50%) less pain. The authors recommended conducting further research studies with larger samples to be able to generalize these results.

Another study was conducted to explore the use of VR as an alternative therapy for reducing chronic pain [63].

Participants were forty patients aged (22-68) years exposed to a 15-minute VR session using an HMD. The pain scores of patients were measured before and during the VR experience, but not after the experience was completed. To assess pain, data from self-reported measures, heart rate, skin temperature, and pain intensity rates were collected. Patients reported that their pain ratings significantly decreased while exploring the VE (mean pain score approximately 0.8) compared to the control condition (mean pain score approximately 2.3). Results from the study suggested that VR can be effectively used for reducing chronic pain.

Jones, Moore, and Choo [64] conducted a study on thirty patients aged at least 18 years to investigate the impact of using VR applications for controlling chronic pain syndromes. The patients who participated in the study were exposed to a VR experience for five minutes. The VR application used in the study was called "COOL!", and there were two ways to deliver VR one using HMD and the other using DeepStream 3D Viewer. Participants were asked to assess their pain intensity prior to, during, and after the VR session using the 0-10 numerical rating scale. Participants reported a decrease in pain intensity by (60%) from pre-session during VR session, and a decrease in pain intensity by (33%) from pre-session to immediately after the VR session was completed.

The same author continued his research by conducting another study to answer the question previously posed in [64]. The research question was about whether longer VR sessions will result in a larger analgesic effect when used repeatedly with chronic pain. This pilot study included ten patients aged at least 18 years old primarily diagnosed with one of the chronic neuropathic pain types [65]. Participants delivered three 20-minute VR sessions (COOL! intervention) in three consecutive weeks. The 0-10 numerical rating scale was used to measure the pain severity experienced by patients before, during, and immediately after the VR session. Patients reported significant analgesia during and immediately after the VR session with decreased pain intensity (65% reduction during VR session and (45%) after the session). Overall, based on the results from the presented studies, VR interventions can be effectively used for controlling chronic pain [66].

VI. VR for Cancer Pain Management

Cancer patients usually experience pain as a common consequence of both the disease and its treatment. Today, chemotherapy is the leading cancer treatment. However, physical symptoms such as fatigue, pain, sleep disturbances, and other symptoms frequently start during the administration of chemotherapy sessions. As a result, cancer patients frequently suffering from distress, depression, and helplessness leading to incomplete treatment with decreasing chances of recovery. VR distraction interventions showed great potential in decreasing pain related to common painful cancer procedures whether diagnostic or treatments (see Table 3).

Many studies have been conducted to investigate the usability and analgesic capabilities of VR for reducing cancer pain. Schneider and Workman [67] performed a study on eleven children aged (10-17) years during receiving their chemotherapy session. This study included three different VR scenarios: Magic Carpet, Seventh Guest, and Sharlek Holmes. Children used the VR application for 5 minutes before the chemotherapy session to get familiar with it. The VR experience continued until the end of the session and then the VR headset was removed. Most of the children preferred the seventh guest scenario because its graphics were clear, easy to use, and included little instructions used. Results indicated that (82%) of the children preferred treatment with VR compared to previous chemotherapy treatments and they are interested in using VR in future treatments.

There is a scientific concern about the influence of VR on time perceived by patients during receiving their chemotherapy treatment. Many studies proved that experiencing VR interventions during receiving the chemotherapy treatment decreased the amount of perceived treatment time compared to the actual elapsed time. In one study, twenty adult women aged (18-55) years participated during their chemotherapy session for breast cancer [68]. This study used a within-subject design where each participant experience VR therapy and control conditions. Randomly, participants were divided into two groups (A and B). The difference between the two groups was whether exposed to the VR intervention in the first treatment session or the second. During the session without VR, participants were provided with different standard care methods. This study included three different VR scenarios: sea diving, walking in a museum, and solving a mystery. The symptom distress (SDS) and revised piper fatigue (PFS) scales were used to assess pain in this study. The lowest scores of the two scales (SDS: 16.6 and PFS: 1.85) occurred immediately after the chemotherapy session while using VR. Besides, the patients reported a lower estimated time duration while using VR (42 minutes) compared to the actual treatment time (67 minutes). No significant changes in both measures were reported after two days of follow-up. These results showed that using VR technology resulted in a significant reduction in symptom distress and fatigue during chemotherapy treatment.

Cancer patients essentially use ports and venous puncture of a vein for delivering chemotherapy. Gershon et al. [69] performed a study on fifty-nine children aged (7-19) years during their port access procedure. Children who participated were divided into three treatment groups including (1) distraction using VR group, (2) standard distraction group, or (3) control group. Both groups (1 and 2) experienced the same intervention called "Virtual Gorilla" [75] where the VR group used an HMD and the standard group used a computer monitor. For 5-minutes before the port access process, participants in groups (1 and 2) started using their distractors, while the control group did nothing. According to the information provided by the pulse rate measurement, there was a notable difference between all groups during the port access procedure (VR: 96.3, standard: 103.8, and control: 110.3). Depending on that study's finding, distraction using the illusion of VR has potential benefits in reducing pain during painful medical procedures.

Schneider and Hood [70] conducted another study that conformed the findings from [68]. This study included one hundred and twenty-three adult patients who suffered from different types of cancer. The authors used the same methodology and assessment measures as in their previous study. Participants reported that while using VR, they perceived a lower estimated time (47 minutes) against the actual chemotherapy

TABLE 3. KEY FEATURES OF STUDIES USED VR FOR CHRONIC AND CANCER PAIN MANAGEMENT

Study	Sample	No.Sessions	Conditions	Findings	Pain Type
Chronic					
Sato et al. [62]	5 patients 46-74 years	6 session	VRMVF*	VRMVF reduced chronic pain by more than 50%	Chronic pain
Wiederhold et al. [63]	40 patients 22-68 years)	1 session	VR*	VR reduced level of pain and anxiety	Chronic pain
Jones et al. [64]	30 patients 35-79 years	1 session	VR	VR decreased the sensation of chronic pain	Chronic pain
Jones et al.[65]	10 patients at least 18 years	3 sessions	VR	Reduction in pain ratings occurred using VR	Chronic pain
Cancer					
Schneider and Workman [67]	11 patients 10-17 years	1 session	VR	VR improved the chemotherapy treatment session	Cancer pain
Schneider et al. [68]	20 patients 18-55 years	2 sessions	VR / C*	VR reduced the distress and fatigue of chemotherapy	Cancer pain
Gershon et al. [69]	59 patients 7-19 years	1 session	VR / SD* / C	Lower ratings of pain when using VR	Cancer pain
Schneider and Hood [70]	123 patients mean age 54 years	2 sessions	VR / C	VR reduced the perceived time of chemotherapy	Cancer pain
Nilsson et al. [71]	42 patients 8-15 years	1 session	VR / C	Non-immersive VR provided a decrease in observational pain	Cancer pain
Schneider, Kisby, and Flint [72]	137 patients at least 18 years	2 sessions	VR / SC*	VR led to an underestimation of chemotherapy duration	Cancer pain
Birnie et al. [73]	17 patients 8-18 years	1 session	VR	VR increased sense of presence and hence reduced pain	Cancer pain
Sharifpour et. al [74]	30 patients mean age 14.8	8 session	VR / C	A significant reduction in pain scores for the experimental groups against the control group	Cancer pain

*VRMVF–VR mirror visual feedback; VR–VR distraction; C–control; SD–standard distraction; SC–standard care

treatment time (58 minutes).

Nilsson et al. [71] conducted a study to evaluate the effectiveness of using a non-immersive VR application for reducing pain during different needle-related procedures. Forty-two children and adolescent patients aged (5-18) years who were diagnosed with one of the childhood cancers participated during receiving their therapy. The participated subjects were divided into two groups, the first used a VR distraction intervention and the second didn't receive any distraction. The VR application used was a 3D game called "The hunt of the diamonds", which presented on a desktop monitor rather than using an HMD. To assess the observational pain experienced by the participants, the FLACC scale was used [76]. The FLACC pain scores for the VR group did not increase during the medical procedure compared to the control group. With respect to the heart rate scale, there was no significant difference between the two groups. The results of the interviews conducted with patients who used VR recommended that the VR application should be consistent with the patient and the medical procedure.

Another related study was conducted to explore the influence of many variables such as age, gender, and other variables on time perceived by cancer patients during receiving their chemotherapy while using VR applications [72]. Patients participated aged at least 18 years old and diagnosed with breast, colon, or lung cancer. Randomly, participants received the VR distraction intervention during either the first treatment session or the next. During the treatment session without VR, patients received any type of standard care techniques. The anxiety and fatigue ratings were assessed before and post to the two conditions (VR and standard care). Also, the researcher of the study recorded the estimated time perceived by each patient while using VR and compare it with the actual treatment time. According to the results, there was a significant reduction in time perceived by patients with an average of 23 min with breast, 12 min with colon, and less than 4 min with the lung.

Again another study proved that using VR technology during needle-related procedures offered promise for pain and distress reduction [73]. The study included seventeen participants aged (8-18) years who suffered from cancer and their treatment required the insertion of an implantable venous access device (IVAD). The study included three cycles for testing the usability of VR distraction capabilities and the participants were assigned to one of these cycles. Participants in the first cycle, experienced the VR application before their IVAD insertion to guarantee the application safety and if it may result in any side effects. While through cycles 2 and 3, participants were exposed to the VR application while inserting their IVAD device. After procedure completion, which lasted for 5 to 10 minutes, all participants were required to have a 5-min interview to evaluate the functionality of the VR distraction intervention. Concerning the baseline pain and symptoms scale which is a 0-10 numeric scale (0-no pain, 10-high pain), (70%) of patients reported no pain and (29%) reported mild to moderate pain intensity. Both nursing staff and patients reported that the distraction from VR has great potential in decreasing pain and distress related to the IVAD access procedure.

Recently, another study was conducted to assess the efficacy of using VR therapy for reducing chemotherapy-related pain symptoms [74]. The study included thirty adolescents with different types of cancer. Using a between-subject design, participants were randomly assigned to (1) the experimental VR group or (2) the control group. The experimental group received VR for 30 minutes once a week for two months. On the other hand, the control group didn't experience any distraction interventions. Participants in VR watched a VR movie that included a journey to the depths of the ocean and deliver it using a Samsung gear headset. Different pain measurements were used to assess the perceived pain. Also, these data were maintained after two intervals of follow-up (7 days and 1 month). Results indicated a significant reduction in pain intensity and anxiety scores for the VR group compared to the control group. This is another study to prove that VR technology had a significant positive effect on patients with cancer pain.

The findings of the controlled studies we discussed in this section indicated the efficacy of VR distraction in reducing chronic as well as cancer pain. Chronic pain is a common health problem that needs effective distraction techniques for managing. However, limited research studies have been conducted for exploring the effect of using VR in chronic pain. The presented studies provided the efficacy of using VR for a short time duration. As chronic pain is persistent, there is a need to investigate the effect of usage for repeated and long time durations. So, VR distraction can be used successfully with patients in their homes. Also, more research on exploring the duration of the analgesic effect of VR is important. Chronic and cancer pain share a common limitation, their studies neither compare VR with other distraction techniques nor control conditions. Comparing VR with other distractions is valuable to adjust the VR applications accordingly to obtain higher analgesic effects. Moreover, most of the cancer studies used a within-group design. Using the between-group design will help to ensure the efficacy of VR distraction. Finally, patients with cancer increase every day, and cancer pain is combined with many emotional and behavioral problems that need to be managed effectively. VR distraction may become an essential tool for managing and reducing cancer pain. According to all studies mentioned in this survey and others which can be found in [77], [78], VR technology proved to be a promising distraction tool with unique characteristics for controlling pain associated with different medical and clinical procedures.

VII. Discussion

We categorized the most common areas that use VR technology for managing pain as shown in (Fig. 2). Based on the referred studies in this survey and other identified reviews, we found that VR can be used in one of two directions. The first one is using VR in many psychological treatments, while the other is using VR for reducing physical pain. The most well-known area in psychology that makes benefits from the illusion of VR is treating phobias, and there is continuing research to generalize using it. On the other hand, VR is effectively being used for controlling many types of physical pain: 1-acute, 2-chronic, and 3-cancer pain. Also, growing research studies is being conducted to investigate deeply the analgesic effect of VR for managing physical pain. One day, VR will be used widely in many applications that assist the healthcare sector.

According to the presented studies, we found that all studies in psychological treatment used specially designed VR environments and an HMD to deliver VR. For studies that used VR during burn wound care, many of them utilized a “SnowWorld” environment [40], [42], [44], [47], and others used specially designed VR environments [41], [43], [45], [46]. All of the studies for burn wound care used specially designed HMD to experience VR, except for one study that used normal HMD [45] and excluded patients with face and/or neck burn injury. The HMDs of type i-glasses were commonly used to deliver VR during dental procedures [51], [52], [53], [54], and other routine medical procedures used normal HMD [48], [49], [50]. All routine medical procedure studies used specially designed environments, except [51] used “SnowWorld” system. The other category of studies that used VR for chronic pain management used specially designed VR environments and an HMD to deliver VR [62], [63], [64], [65]. Only one study used a non-immersive computer-based VR system [62]. Variations of VR hardware were used with cancer patients during receiving their chemotherapy treatment. Some used the i-glasses HMDs [67], [68], [70], [72], while [69], [73], [74]used normal HMD, and [71] used a standard personal computer. All of these studies used specially designed VR environments. Tables 4 and 5 summarize the VR hardware and software used in the presented studies.

The main challenge found is that the observations can’t be generalized. For each pain type, each study used a different procedure with different settings along with different sample sizes. This is why we can’t generalize the results from the conducted studies. The results of controlled studies showed that VR technology has the potential in treating different types of phobias. Most of these studies indicated that VR therapy has the same analgesic effect as Vivo therapy [21]. However, VR therapy is considered a stable application, cheap, and controlled. Also, it can be used repeatedly, can experience difficult situations safely, and provide more confidentiality. These features can encourage conducting more research to support using VR therapy. Also, studies that compared VR(HMD) against VR(CAVE) revealed that they are equally effective [22]. With the decreasing cost of VR technology, VR(HMD) will be cheap, easy, and more appropriate compared to VR(CAVE). Another key issue reported from the controlled studies is that VR therapy is more effective than cognitive-behavioral therapy [30].

Besides, many considerable issues were found in the presented studies. First of all, most of the research studies involved a small number of participants [23], [40], [45], [46], [62], [65], [67]. So, further research studies with a larger number of participants have to be conducted to confirm the efficacy of VR distraction in managing pain. Another issue, most of the studies depended on self-reported scales or observational scales to assess pain related to the medical procedure [24], [32], [49], [70]. To ensure a reliable assessment of pain, future studies should use other physiological or behavioral measures along with subjective ones. When designing a future VR study, it is valuable to consider comparing the effect of using VR against other standard distraction techniques [20], [31], [40], [64], [68]. Comparing VR therapy with other distraction techniques will help to determine the appropriate mechanisms of using VR interventions that will result in the most distraction effect. Moreover, future studies should develop new VR applications consistent with the patient’s pain threshold and the pain type [65], [47]. Consequently, these applications will ensure the best analgesic effect of VR distraction.

A scientific research question about using VR for managing pain is that the VR analgesic effect could decrease due

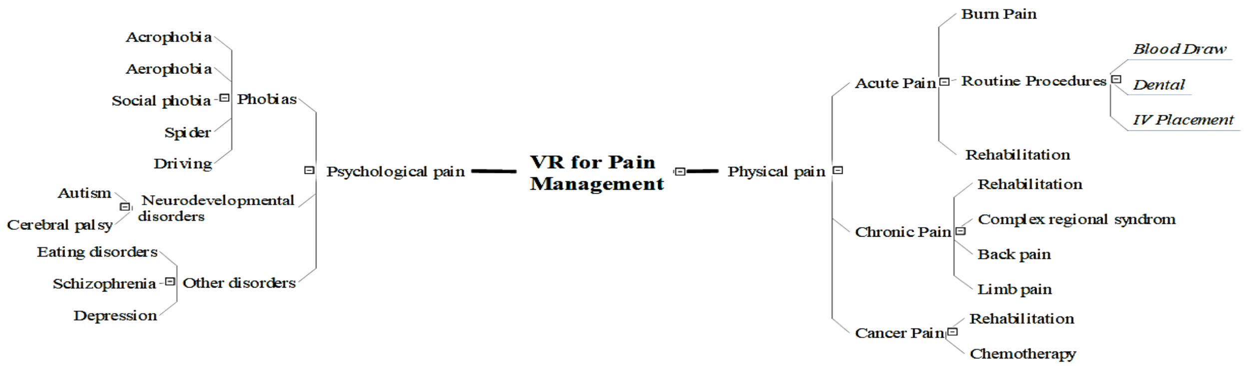

Fig. 2. VR for Pain Management in Healthcare.

to repeated use. To investigate this issue, few studies were conducted and showed that the effect of using VR interventions was not lost across repeated exposures [79], [80], [81]. However, more research is needed to ensure these findings. Thus, further research studies with a larger sample size along with applying VR intervention repeatedly are required to investigate the benefits of using VR for long-term treatment [45], [68], [72], [71]. Other scientific questions that need more investigation in future studies include whether VR therapy will effectively distract patients especially children during longer medical procedures [50] and if longer VR sessions will be more effective than the shorter ones [64].

Several studies have reported that VR technology has a promising ability to reduce acute pain. VR distraction provides an effective alternative for reducing pain during burn wound care and routine medical procedures. Despite using different types of VR hardware with burn patients [44], [46], the findings indicated the effectiveness of VR in reducing pain. Besides, using low-cost VR technology proved to be effective for managing pain. Hence VR distraction may become more available [45]. Also, VR distraction was used safely and effectively with children less than four years [46]. In contrast, few studies assessed the effect of using VR with chronic pain. The presented studies proved the efficacy of using VR for a short time duration [63], [64]. Further research is needed to investigate the effect of using VR distraction repeatedly and for long time durations [64], [65].

Pain from cancer is different; it is complex and has multidimensional sensory, affective, cognitive, and behavioral components [82]. Cancer-related pain can result from the disease itself, medical treatments such as chemotherapy and radiation therapy, and needle procedures such as blood draws, port access, and lumbar punctures [83], [84]. Also, as a result of chemotherapy patients experience some physical symptoms such as nausea, anxiety as well as depression, helplessness, and difficulty in concentrating [85]. To date, most cancer-related pain can be effectively managed using pharmacological and non-pharmacological strategies [86]. However, emotional and behavioral problems such as sleep disorders, procedural distress, restriction of social activities, and depression still need to be controlled especially for children with cancer [84]. VR provides a multisensory three-dimensional experience that diverts the attention of the patient away from painful stimuli. Recent advances in software and hardware besides cost reductions made VR promising for managing pain and other emotional problems related to cancer [87]. Another direction of research for VR distraction that may produce more analgesic effects is integrating VR distraction with Cognitive behavioral therapy. To our knowledge, few studies investigated the effect of integration [27], [88]. So, future research studies may consider this direction that that may increase the impact of VR distraction.

Our findings are consistent with previous reviews, which have shown that VR is effective in managing different types of pain. In sum, VR has emerged as a powerful non-pharmacological treatment intervention. According to the presented studies, effective VR distraction can be achieved using several resources and different settings. So, today VR is being used in numerous medical applications to help treat many psychological disorders and control pain. Despite the promising results indicated from the literature, we found that there is no study focused on investigating the impact of different visual parameters on human perception in VR. It is highly demanded to conduct further research to determine the visual effects that perceive most of the patient's attention and in turn provide more distraction and more pain tolerance. Finally, to ensure the effectiveness of the used VR application, more research is needed to determine how VR works to reduce the experienced pain and what is the best form of VR that provides a much analgesic effect.

VIII. Conclusion

Nowadays non-pharmacological analgesics including VR have great potential in managing pain related to different health care problems. This survey showed that VR technology is quickly gaining attention as a promising alternative for distracting patients during painful medical procedures. All studies presented in this survey have investigated the impact of using VR in controlling pain (acute, chronic, or cancer) experienced by adults or children. Findings from the presented studies showed that using any type of distraction is better than no distraction. In addition, interactive distraction is more effective than passive distraction. With VR distraction interventions, results indicated that high technology equipment provides much more immersion and presence than low technology, so pain intensity significantly decreased. So, the more quality of the VR system, the more analgesic effect occurs.

TABLE 4. VR HARDWARE AND SOFTWARE EQUIPMENT FOR PSYCHOLOGICAL TREATMENT

References	VR Software Equipment	VR Hardware Equipment
Acrophobia		
Rothbaum et al. [20]	Special designed environments (footbridges, balconies, and elevator)	HMD
Emmelkamp et al. [21]	Special designed environments (a mall, a fire escape, and a roof garden)	HMD
Krijn et al. [22]	Special designed environments (a mall, a fire escape, a roof garden,and a building site)	HMD & CAVE
Suyanto et al. [23]	A special designed game (Acrophobia simulator)	HMD
Freeman et al. [24]	A special designed application (Now I can do heights)	HMD
Donker et al. [25]	A special designed application (ZeroPhobia)	HMD
Aerophobia		
Rothbaum et al. [26]	A special designed virtual airplane	HMD
Muhlberger et al. [27]	A special designed simulated flights	HMD
Rothbaum et al. [28]	A special designed virtual airplane	HMD
Tortella-Feliu et al. [29]	A special designed virtual flight software	5D Technologies HMD
Social phobia		
Klinger et al. [30]	Four special designed environments	HMD
North et al. [31]	A special designed software to generate a fearful public speaking situations	HMD
Kampmann et al. [32]	A special designed virtual social environments (one-to-one and group situations)	HMD

TABLE 5. VR HARDWARE AND SOFTWARE EQUIPMENT FOR PHYSICAL PAIN REDUCTION

References	VR Software Equipment	VR Hardware Equipment
Burn Pain		
Hoffman et al. [40],Jeffs et al. [42] Hoffman et al. [44],Hoffman et al. [47]	SnowWorld VR system	A special designed VR system (VR helmet mounted to articulated arm)
Kipping et al. [41]	Chicken Little™ and Need for Speed™ games	A special designed VR system (off-the-shelf VR system)
Brown et al. [43]	Ditto™ intervention	An immersive hand-held device (Ditto)
Ford et al. [45]	Eight special designed environments	Sunny peak VR headset
Khadra et al. [46]	A special designed Bubbles video game	A special designed VR system (a projector-based VR system)
Routine Procedures		
Hoffman et al. [51]	SnowWorld VR system	i-glasses HMD
Furman et al. [52],Aminabadi et al. [53] Tanja-Dijkstra et al.[54]	A special designed VR environment	i-glasses HMD
Gold et al. [48],Gold et al. [49] Piskorz and Czub [50]	A special designed VR environment	HMD
Chronic Pain		
Sato et al. [62]	A special designed virtual environment	Non-immersive computer-based VR system
Wiederhold et al. [63]	A special designed virtual environment	HMD
Jones et al. [64],Jones et al.[65]	VR application called COOL	Oculus Rift DK2
Cancer Pain		
Schneider et al. [67], [68], [70], [72]	A special designed VR environments	i-glasses HMD
Gershon et al. [69],Birnie et al. [73]		HMD
Nilsson et al. [71]		Non-immersive computer-based VR system
Sharifpour et. al [74]	VR movie	Samsung Gear VR

Moreover, few studies have identified that the VR analgesic effect did not diminish during repeated use. Besides, patients reported a shorter time perception during the treatment when using VR distraction. One study has suggested that longer VR sessions have a much more analgesic effect than shorter sessions. In conclusion, VR emerges as a valuable distraction tool with unique characteristics suitable for reducing pain associated with different painful medical procedures. Also, this survey demonstrated that VR interventions were effectively used for treating different psychological problems such as phobias. Finally, with advances in using VR in many health care applications, patients may need fewer opioids during painful procedures and also may need a fewer number of treatment sessions.

REFERENCES

[1] M. Rajagopal *et al.*, "Pain–basic considerations," *Indian J Anaesth*, vol. 50, no. 5, pp. 331–334, 2006.

[2] H. Merskey, "Pain terms: a list with definitions and notes on usage. recommended by the iasp subcommittee on taxonomy," *Pain*, vol. 6, pp. 249–252, 1979.

[3] L. Li, F. Yu, D. Shi, J. Shi, Z. Tian, J. Yang, X. Wang, and Q. Jiang, "Application of virtual reality technology in clinical medicine," *American journal of translational research*, vol. 9, no. 9, pp. 3867–3880, 2017.

[4] P. Swieboda, R. Filip, A. Prystupa, and M. Drozd, "Assessment of pain: types, mechanism and treatment," *Annals of agricultural and environmental medicine : AAEM*, vol. Spec no. 1, pp. 2–7, 2013.

[5] R.-D. Treede, W. Rief, A. Barke, Q. Aziz, M. I. Bennett, R. Benoliel, M. Cohen, S. Evers, N. B. Finnerup, M. B. First *et al.*, "A classification of chronic pain for icd-11," *Pain*, vol. 156, no. 6, pp. 1003–1007, 2015.

[6] P. H. Berry, C. Chapman, E. Covington, J. Dahl, J. Katz, C. Miaskowski, and M. McLean, "Pain: current understanding of assessment, management, and treatments," *National Pharmaceutical Council and the Joint Commission for the Accreditation of Healthcare Organizations, VA, USA*, p. b44, 2001.

[7] G.-J. Hejdi, V. Pernille, Nygaard, O. L.-L. Viktoria, and E. Ingrid, "Acute pain management in burn patients: Appraisal and thematic analysis of four clinical guidelines," *Burns*, vol. 40, no. 8, pp. 1463 – 1469, 2014.

[8] H. Retrouvey and S. Shahrokhi, "Pain and the thermally injured patient - a review of current therapies," *Journal of Burn Care & Research*, vol. 36, no. 2, pp. 315–323, 2015.

[9] J. R. Holtman, Jr. and W. S. Jellish, "Opioid-induced hyperalgesia and burn pain," *Journal of Burn Care & Research*, vol. 33, no. 6, pp. 692–701, 2012.

[10] D. Koller and R. D. Goldman, "Distraction techniques for children undergoing procedures: A critical review of pediatric research," *Journal of Pediatric Nursing*, vol. 27, no. 6, pp. 652 – 681, 2012.

[11] K. Olsen and E. Weinberg, "Pain-less practice: Techniques to reduce procedural pain and anxiety in pediatric acute care," *Clinical Pediatric Emergency Medicine*, vol. 18, no. 1, pp. 32 – 41, 2017.

[12] K. Neziha, G. Dilek, and A. Yesim, Yaman, "Non-pharmacological interventions for pain management used by nursing students in turkey," *Kontakt*, vol. 18, no. 1, pp. 22 – 29, 2016.

[13] R. Melzack and D. Wall, Patrick, "Pain mechanisms: a new theory," *Science*, vol. 150, no. 3699, pp. 971–979, 1965.

[14] M. Gutierrez, F. Vexo, and D. Thalmann, *Stepping into virtual reality*. Springer Science & Business Media, 2008.

[15] A. A. Laghari, A. K. Jumani, K. Kumar, and M. A. Chhajro, "Systematic analysis of virtual reality & augmented reality." *International Journal of Information Engineering & Electronic Business*, vol. 13, no. 1, 2021.

[16] M. Slater and S. Wilbur, "A framework for immersive virtual environments (five): Speculations on the role of presence in virtual environments," *Presence: Teleoperators & Virtual Environments*, vol. 6, no. 6, pp. 603–616, 1997.

[17] A. Pourmand, S. Davis, D. Lee, S. Barber, and N. Sikka, "Emerging utility of virtual reality as a multidisciplinary tool in clinical medicine," *Games for health journal*, vol. 6, no. 5, pp. 263–270, 2017.

[18] B. Ridout, J. Kelson, A. Campbell, K. Steinbeck *et al.*, "Effectiveness of virtual reality interventions for adolescent patients in hospital settings: Systematic review," *Journal of Medical Internet Research*, vol. 23, no. 6, p. e24967, 2021.

[19] P. M. Emmelkamp and K. Meyerbröker, "Virtual reality therapy in mental health," *Annual Review of Clinical Psychology*, vol. 17, pp. 495–519, 2021.

[20] B. O. Rothbaum, L. F. Hodges, R. Kooper, D. Opdyke, J. S. Williford, and M. North, "Effectiveness of computer-generated (virtual reality) graded exposure in the treatment of acrophobia." *The American journal of psychiatry*, vol. 152 4, pp. 626–628, 1995.

[21] P. Emmelkamp, M. Krijn, A. Hulsbosch, S. de Vries, M. Schuemie, and C. van der Mast, "Virtual reality treatment versus exposure in vivo: a comparative evaluation in acrophobia," *Behaviour Research and Therapy*, vol. 40, no. 5, pp. 509 – 516, 2002.

[22] M. Krijn, P. M. Emmelkamp, R. Biemond, C. de Wilde de Ligny, M. J. Schuemie, and C. A. van der Mast, "Treatment of acrophobia in virtual reality: The role of immersion and presence," *Behaviour Research and Therapy*, vol. 42, no. 2, pp. 229 – 239, 2004.

[23] E. M. Suyanto, D. Angkasa, H. Turaga, and R. Sutoyo, "Overcome acrophobia with the help of virtual reality and kinect technology," *Procedia computer science*, vol. 116, pp. 476–483, 2017.

[24] D. Freeman, P. Haselton, J. Freeman, B. Spanlang, S. Kishore, E. Albery, M. Denne, P. Brown, M. Slater, and A. Nickless, "Automated psychological therapy using immersive virtual reality for treatment of fear of heights: a single-blind, parallel-group, randomised controlled trial," *The Lancet Psychiatry*, vol. 5, no. 8, pp. 625–632, 2018.

[25] T. Donker, C. v. Klaveren, I. Cornelisz, R. N. Kok, and J.-L. Van Gelder, "Analysis of usage data from a self-guided app-based virtual reality cognitive behavior therapy for acrophobia: a randomized controlled trial," *Journal of clinical medicine*, vol. 9, no. 6, p. 1614, 2020.

[26] B. O. Rothbaum, L. Hodges, S. Smith, J. H. Lee, and L. Price, "A controlled study of virtual reality exposure therapy for the fear of flying." *Journal of consulting and Clinical Psychology*, vol. 68, no. 6, p. 1020, 2000.

[27] A. Muhlberger, G. Wiedemann, and P. Pauli, "Efficacy of a one-session virtual reality exposure treatment for fear of flying," *Psychotherapy Research*, vol. 13, no. 3, pp. 323–336, 2003.

[28] B. O. Rothbaum, P. Anderson, E. Zimand, L. Hodges, D. Lang, and J. Wilson, "Virtual reality exposure therapy and standard (in vivo) exposure therapy in the treatment of fear of flying," *Behavior therapy*, vol. 37, no. 1, pp. 80–90, 2006.

[29] M. Tortella-Feliu, C. Botella, J. Llabrés, J. M. Bretón-López, A. R. del Amo, R. M. Baños, and J. M. Gelabert, "Virtual reality versus computer-aided exposure treatments for fear of flying," *Behavior Modification*, vol. 35, no. 1, pp. 3–30, 2011.

[30] E. Klinger, P. Légeron, S. Roy, I. Chemin, F. Lauer, and P. Nugues, "Virtual reality exposure in the treatment of social phobia." *Studies in health technology and informatics*, vol. 99, pp. 91–119, 2004.

[31] M. M. North, S. M. North, and J. R. Coble, "Virtual reality therapy: an effective treatment for the fear of public speaking," *International Journal of Virtual Reality (IJVR)*, vol. 3, no. 3, pp. 1–6, 2015.

[32] I. L. Kampmann, P. M. Emmelkamp, D. Hartanto, W.-P. Brinkman, B. J. Zijlstra, and N. Morina, "Exposure to virtual social interactions in the treatment of social anxiety disorder: A randomized controlled trial," *Behaviour Research and Therapy*, vol. 77, pp. 147–156, 2016.

[33] Y. H. Choi, D. P. Jang, J. H. Ku, M. B. Shin, and S. I. Kim, "Short-term treatment of acrophobia with virtual reality therapy (vrt): A case report," *CyberPsychology & Behavior*, vol. 4, no. 3, pp. 349–354, 2001.

[34] D. Walshe, E. Lewis, K. O'Sullivan, and S. I. Kim, "Virtually driving: are the driving environments" real enough" for exposure therapy with accident victims? an explorative study," *CyberPsychology & Behavior*, vol. 8, no. 6, pp. 532–537, 2005.

[35] H. M. Zinzow, J. O. Brooks, P. J. Rosopa, S. Jeffirs, C. Jenkins, J. Seeanner, A. McKeeman, and L. F. Hodges, "Virtual reality and cognitive-behavioral therapy for driving anxiety and aggression in veterans: a pilot study," *Cognitive and behavioral practice*, vol. 25, no. 2, pp. 296–309, 2018.

[36] S. Schoch, Y. Kaussner, A. Kuraszkiewicz, S. Hoffmann, P. Markel, R. Baur-Streubel, and P. Pauli, "Driving simulation as virtual reality exposure therapy to rehabilitate patients with driving fear after traffic accidents," 2019.

[37] H. G. Hoffman, A. Garcia-Palacios, A. Carlin, T. A. Furness Iii, and C. Botella-Arbona, "Interfaces that heal: Coupling real and virtual objects to treat spider phobia," *international Journal of Human-Computer interaction*, vol. 16, no. 2, pp. 283–300, 2003.

[38] Y. Shiban, I. Schelhorn, P. Pauli, and A. Mühlberger, "Effect of combined multiple contexts and multiple stimuli exposure in spider phobia: a randomized clinical trial in virtual reality," *Behaviour research and therapy*, vol. 71, pp. 45–53, 2015.

[39] A. Miloff, P. Lindner, P. Dafgård, S. Deak, M. Garke, W. Hamilton, J. Heinsoo, G. Kristoffersson, J. Rafi, K. Sindemark *et al.*, "Automated virtual reality exposure therapy for spider phobia vs. in-vivo one-session treatment: A randomized non-inferiority trial," *Behaviour research and therapy*, vol. 118, pp. 130–140, 2019.

[40] G. Hoffman, Hunter, R. Patterson, David, E. Seibel, M. Soltani, L. Jewett-Leahy, and R. Sharar, Sam, "Virtual reality pain control during burn wound debridement in the hydrotank," *The Clinical journal of pain*, vol. 24, no. 4, pp. 299–304, 2008.

[41] B. Kipping, S. Rodger, K. Miller, and M. Kimble, Roy, "Virtual reality for acute pain reduction in adolescents undergoing burn wound care: a prospective randomized controlled trial," *Burns*, vol. 38, no. 5, pp. 650–657, 2012.

[42] D. Jeffs, D. Dorman, S. Brown, A. Files, T. Graves, E. Kirk, S. Meredith-Neve, J. Sanders, B. White, and C. J. Swearingen, "Effect

of virtual reality on adolescent pain during burn wound care," *Journal of Burn Care & Research*, vol. 35, no. 5, pp. 395–408, 2014.

[43] J. Brown, Nadia, M. Kimble, Roy, S. Rodger, S. Ware, Robert, and L. Cuttle, "Play and heal: randomized controlled trial of ditto intervention efficacy on improving re-epithelialization in pediatric burns," *Burns*, vol. 40, no. 2, pp. 204–213, 2014.

[44] G. Hoffman, Hunter, J. Meyer III, Walter, M. Ramirez, L. Roberts, J. Seibel, Eric, B. Atzori, R. Sharar, Sam, and R. Patterson, David, "Feasibility of articulated arm mounted oculus rift virtual reality goggles for adjunctive pain control during occupational therapy in pediatric burn patients," *Cyberpsychology, Behavior, and Social Networking*, vol. 17, no. 6, pp. 397–401, 2014.

[45] G. Ford, Cameron, M. Manegold, Ellen, C. L. Randall, M. Aballay, Ariel, and L. Duncan, Christina, "Assessing the feasibility of implementing low-cost virtual reality therapy during routine burn care," *Burns*, vol. 44, no. 4, pp. 886–895, 2018.

[46] C. Khadra, A. Ballard, J. Déry, D. Paquin, J.-S. Fortin, I. Perreault, D. R. Labbe, H. G. Hoffman, S. Bouchard, and S. LeMay, "Projector-based virtual reality dome environment for procedural pain and anxiety in young children with burn injuries: a pilot study," *Journal of pain research*, vol. 11, p. 343, 2018.

[47] H. G. Hoffman, R. A. Rodriquez, M. Gonzalez, M. Bernardy, R. Peña, W. Beck, D. R. Patterson, and W. J. Meyer III, "Immersive virtual reality as an adjunctive non-opioid analgesic for predominantly latin american children with large severe burn wounds during burn wound cleaning in the intensive care unit: A pilot study." *Frontiers in human neuroscience*, vol. 13, p. 262, 2019.

[48] J. Gold, G. Reger, A. Rizzo, G. Buckwalter, S. Kim, and M. Joseph, "Virtual reality in outpatient phlebotomy: evaluating pediatric pain distraction during blood draw," *The Journal of Pain*, vol. 6, no. 3, p. S57, 2005.

[49] J. I. Gold, S. H. Kim, A. J. Kant, M. H. Joseph, and A. S. Rizzo, "Effectiveness of virtual reality for pediatric pain distraction during iv placement," *CyberPsychology & Behavior*, vol. 9, no. 2, pp. 207–212, 2006.

[50] J. Piskorz and M. Czub, "Effectiveness of a virtual reality intervention to minimize pediatric stress and pain intensity during venipuncture," *Journal for Specialists in Pediatric Nursing*, vol. 23, no. 1, p. e12201, 2018.

[51] H. G. Hoffman, A. Garcia-Palacios, D. R. Patterson, M. Jensen, T. Furness III, and W. F. Ammons Jr, "The effectiveness of virtual reality for dental pain control: a case study," *CyberPsychology & Behavior*, vol. 4, no. 4, pp. 527–535, 2001.

[52] E. Furman, T. R. Jasinevicius, N. F. Bissada, K. Z. Victoroff, R. Skillicorn, and M. Buchner, "Virtual reality distraction for pain control during periodontal scaling and root planing procedures," *The Journal of the American Dental Association*, vol. 140, no. 12, pp. 1508–1516, 2009.

[53] N. A. Aminabadi, L. Erfanparast, A. Sohrabi, S. G. Oskouei, and A. Naghili, "The impact of virtual reality distraction on pain and anxiety during dental treatment in 4-6 year-old children: a randomized controlled clinical trial," *Journal of dental research, dental clinics, dental prospects*, vol. 6, no. 4, p. 117, 2012.

[54] K. Tanja-Dijkstra, S. Pahl, M. P. White, J. Andrade, C. Qian, M. Bruce, J. May, and D. R. Moles, "Improving dental experiences by using virtual reality distraction: a simulation study," *PLoS One*, vol. 9, no. 3, p. e91276, 2014.

[55] D. M. Ehde, R. Patterson, David, and E. Fordyce, Wilbert, "The quota system in burn rehabilitation," *The Journal of burn care & rehabilitation*, vol. 19, no. 5, pp. 436–440, 1998.

[56] S. Y. Joo, Y. S. Cho, S. Y. Lee, H. Seok, and C. H. Seo, "Effects of virtual reality-based rehabilitation on burned hands: a prospective, randomized, single-blind study," *Journal of clinical medicine*, vol. 9, no. 3, p. 731, 2020.

[57] "Vr pain," http://www.vrpain.com, [Online; accessed 6-March-2021].

[58] M. C. Savedra, W. L. Holzemer, M. D. Tesler, and D. J. Wilkie, "Assessment of postoperation pain in children and adolescents using the adolescent pediatric pain tool." *Nursing research*, 1993.

[59] C. L. Wong, M. M. W. Lui, and K. C. Choi, "Effects of immersive virtual reality intervention on pain and anxiety among pediatric patients undergoing venipuncture: a study protocol for a randomized controlled trial," *Trials*, vol. 20, no. 1, p. 369, 2019.

[60] F. J. Keefe, D. A. Huling, M. J. Coggins, D. F. Keefe, M. Z. Rosenthal, N. R. Herr, and H. G. Hoffman, "Virtual reality for persistent pain: a new direction for behavioral pain management," *Pain*, vol. 153, no. 11, p. 2163, 2012.

[61] D. Gromala, X. Tong, C. Shaw, and W. Jin, "Immersive virtual reality as a non-pharmacological analgesic for pain management: Pain distraction and pain self-modulation," in *Virtual and Augmented Reality: Concepts, Methodologies, Tools, and Applications*. IGI Global, 2018, pp. 1176–1199.

[62] K. Sato, S. Fukumori, T. Matsusaki, T. Maruo, S. Ishikawa, H. Nishie, K. Takata, H. Mizuhara, S. Mizobuchi, H. Nakatsuka *et al.*, "Nonimmersive virtual reality mirror visual feedback therapy and its application for the treatment of complex regional pain syndrome: an open-label pilot study," *Pain medicine*, vol. 11, no. 4, pp. 622–629, 2010.

[63] B. K. Wiederhold, K. Gao, C. Sulea, and M. D. Wiederhold, "Virtual reality as a distraction technique in chronic pain patients," *Cyberpsychology, Behavior, and Social Networking*, vol. 17, no. 6, pp. 346–352, 2014.

[64] T. Jones, T. Moore, and J. Choo, "The impact of virtual reality on chronic pain," *PloS one*, vol. 11, no. 12, p. e0167523, 2016.

[65] T. Jones, R. Skadberg, and T. Moore, "A pilot study of the impact of repeated sessions of virtual reality on chronic neuropathic pain." *International Journal of Virtual Reality*, vol. 18, no. 1, 2018.

[66] K. B. Chen, M. E. Sesto, K. Ponto, J. Leonard, A. Mason, G. Vanderheiden, J. Williams, and R. G. Radwin, "Use of virtual reality feedback for patients with chronic neck pain and kinesiophobia," *IEEE Transactions on Neural Systems and Rehabilitation Engineering*, vol. 25, no. 8, pp. 1240–1248, 2017.

[67] S. M. Schneider and M. Workman, "Virtual reality as a distraction intervention for older children receiving chemotherapy," *Pediatric Nursing*, vol. 26, no. 6, pp. 593–593, 2000.

[68] S. M. Schneider, M. Prince-Paul, M. J. Allen, P. Silverman, and D. Talaba, "Virtual reality as a distraction intervention for women receiving chemotherapy." in *Oncology nursing forum*, vol. 31, no. 1, 2004.

[69] J. Gershon, E. Zimand, M. Pickering, B. O. Rothbaum, and L. Hodges, "A pilot and feasibility study of virtual reality as a distraction for children with cancer," *Journal of the American Academy of Child & Adolescent Psychiatry*, vol. 43, no. 10, pp. 1243–1249, 2004.

[70] S. M. Schneider and L. E. Hood, "Virtual reality: a distraction intervention for chemotherapy," in *Oncology nursing forum*, vol. 34, no. 1. NIH Public Access, 2007, p. 39.

[71] S. Nilsson, B. Finnström, E. Kokinsky, and K. Enskär, "The use of virtual reality for needle-related procedural pain and distress in children and adolescents in a paediatric oncology unit," *European Journal of Oncology Nursing*, vol. 13, no. 2, pp. 102–109, 2009.

[72] S. M. Schneider, C. K. Kisby, and E. P. Flint, "Effect of virtual reality on time perception in patients receiving chemotherapy," *Supportive Care in Cancer*, vol. 19, no. 4, pp. 555–564, 2011.

[73] K. A. Birnie, Y. Kulandaivelu, L. Jibb, P. Hroch, K. Positano, S. Robertson, F. Campbell, O. Abla, and J. Stinson, "Usability testing of an interactive virtual reality distraction intervention to reduce procedural pain in children and adolescents with cancer," *Journal of Pediatric Oncology Nursing*, vol. 35, no. 6, pp. 406–416, 2018.

[74] S. Sharifpour, G. R. Manshaee, and I. Sajjadian, "Effects of virtual reality therapy on perceived pain intensity, anxiety, catastrophising and self-efficacy among adolescents with cancer," *Counselling and Psychotherapy Research*, vol. 21, no. 1, pp. 218–226, 2021.

[75] D. Allison, B. Wills, D. Bowman, J. Wineman, and L. F. Hodges, "The virtual reality gorilla exhibit," *IEEE Computer Graphics and Applications*, vol. 17, no. 6, pp. 30–38, 1997.

[76] S. K. Jaskowski, "The flacc: A behavioral scale for scoring postoperative pain in young children," *AACN Nursing Scan In Critical Care*, vol. 8, no. 1, p. 16, 1998.

[77] B. M. Spiegel, "Virtual medicine: how virtual reality is easing pain, calming nerves and improving health," *Medical Journal of Australia*, vol. 209, no. 6, pp. 245–247, 2018.

[78] B. Spiegel, G. Fuller, M. Lopez, T. Dupuy, B. Noah, A. Howard, M. Albert, V. Tashjian, R. Lam, J. Ahn *et al.*, "Virtual reality for management of pain in hospitalized patients: A randomized comparative effectiveness trial," *PloS one*, vol. 14, no. 8, 2019.

[79] G. Hoffman, Hunter, R. Patterson, David, J. Carrougher, Gretchen, D. Nakamura, M. Moore, A. Garcia-Palacios, and A. Furness III, Thomas, "The effectiveness of virtual reality pain control with multiple treatments of longer durations: A case study," *International Journal of Human-Computer Interaction*, vol. 13, no. 1, pp. 1–12, 2001.

[80] S. Schmitt, Yuko, G. Hoffman, Hunter, K. Blough, David, R. Patterson, David, P. Jensen, Mark, M. Soltani, J. Carrougher, Gretchen, D. Nakamura, and R. Sharar, Sam, "A randomized, controlled trial of immersive virtual reality analgesia, during physical therapy for pediatric burns," *Burns*, vol. 37, no. 1, pp. 61–68, 2011.

[81] W. Faber, Albertus, R. Patterson, David, and M. Bremer, "Repeated use of immersive virtual reality therapy to control pain during wound dressing changes in pediatric and adult burn patients," *Journal of Burn Care & Research*, vol. 34, no. 5, pp. 563–568, 2013.

[82] N. Ovayolu, Ö. Ovayolu, S. Serçe, D. Tuna, L. Pirbudak Çöçelli, and A. Sevinç, "Pain and quality of life in turkish cancer patients," *Nursing & health sciences*, vol. 15, no. 4, pp. 437–443, 2013.

[83] L. Van Cleve, E. Bossert, P. Beecroft, K. Adlard, O. Alvarez, and M. C. Savedra, "The pain experience of children with leukemia during the first year after diagnosis," *Nursing Research*, vol. 53, no. 1, pp. 1–10, 2004.

[84] P. Tutelman, C. Chambers, Ph.D., J. Stinson, J. Parker, C. Fernandez, H. O. Witteman, P. Nathan, M. Barwick, F. Campbell, L. Jibb, and K. Irwin, "Pain in children with cancer: Prevalence, characteristics, and parent management," *The Clinical Journal of Pain*, vol. 34, no. 3, pp. 198–206, 07 2017.

[85] C. Miaskowski and K. A. Lee, "Pain, fatigue, and sleep disturbances in oncology outpatients receiving radiation therapy for bone metastasis: A pilot study," *Journal of Pain and Symptom Management*, vol. 17, no. 5, pp. 320 – 332, 1999.

[86] L. A. Jibb, P. C. Nathan, B. J. Stevens, L. Yohannes, and J. N. Stinson, "Psychological and physical interventions for the management of cancer-related pain in pediatric and young adult patients: an integrative review," in *Oncology nursing forum*, vol. 42, no. 6. Oncology Nursing Society, 2015, p. E339.

[87] V. C. Tashjian, S. Mosadeghi, A. R. Howard, M. Lopez, T. Dupuy, M. Reid, B. Martinez, S. Ahmed, F. Dailey, K. Robbins *et al.*, "Virtual reality for management of pain in hospitalized patients: results of a controlled trial," *JMIR mental health*, vol. 4, no. 1, 2017.

[88] D. R. Patterson, M. P. Jensen, S. A. Wiechman, and S. R. Sharar, "Virtual reality hypnosis for pain associated with recovery from physical trauma," *Intl. Journal of Clinical and Experimental Hypnosis*, vol. 58, no. 3, pp. 288–300, 2010.

Improved Medical Image Classification Accuracy on Heterogeneous and Imbalanced Data using Multiple Streams Network

Mumtaz Ali[1]
School of Computer Science,
Huazhong University of Science and Technology,
Wuhan & Department of Computer Systems Engineering,
Sukkur IBA University, Pakistan

Riaz Ali[2]
Department of Computer Science
Sukkur IBA University
Pakistan

Nazim Hussain[3]
Department of Mathematics
Sukkur IBA University
Pakistan

***Abstract*—Small and massively imbalanced datasets are long-standing problems on medical image classification. Traditionally, researchers use pre-trained models to solve these problems, however, pre-trained models typically have a huge number of trainable parameters. Small datasets are challenging for them to train a model adequately and imbalanced datasets easily lead to overfitting on the classes with more samples. Multiple-stream networks that learn a variety of features have recently gained popularity. Therefore, in this work, a quad-stream hybrid model called QuadSNet using conventional as well as separable convolutional neural networks is proposed to achieve better performance on small and imbalanced datasets without using any pre-trained model. The designed model extracts hybrid features and the fusion of such features makes the model more robust on heterogeneous data. Besides, a weighted margin loss is used to handle the problem of class imbalance. The QuadSNet is trained and tested on seven different classification datasets. To evaluate the advantages of QuadSNet on small and massively imbalanced data, it is compared with six state-of-the-art pre-trained models on three benchmark datasets based on Pneumonia, COVID-19, and Cancer classification. To assess the performance of QuadSNet on general classification datasets, it is compareed with the best model on each of the remaining four datasets, which contain larger, balanced, grayscale, color or non-medical image data. The results show that QuadSNet handles the class imbalance and overfitting better than existing pre-trained models with much fewer parameters on small datasets. Meanwhile, QuadSNet has competitive performance in general datasets.**

Keywords*—Medical image classification; convolutional neural networks; class imbalance; small dataset; margin loss

I. Introduction

Typically, a huge amount of data is needed to train the neural networks for natural and medical image classification. However, along with the scarcity of sufficient samples, generally, the medical image datasets are massively imbalanced and they possess very limited positive cases. Thus, to obtain high-performance results by incorporating small and imbalanced datasets is a very perplexing task. In recent years, researchers have tried various algorithm-level and data-level methodologies to handle such challenges.

The algorithm level approaches have evolved since the reemergence of deep learning. Transfer learning [5], few-shot learning [18], zero-shot learning [6], Siamese networks [8], network ensembles [4] and most recent algorithms based on generative adversarial networks [2] have been applied to small and imbalanced datasets. The algorithm level approaches commonly rely on pre-trained models. Despite decent signs of progress, the pre-trained models orthodoxly use millions of parameters and complex architecture to achieve competitive results, which appear to be enormous for a small dataset to train a good model.

Along with the issue of a small dataset, the class imbalance is another challenge. Overmuch parameters of pre-trained models typically lead to overfitting if the classes are imbalanced. Weighting class labels is a very prevalent technique in handling class imbalance. The weighted class label approach produces better results when the model is trained with a suitable loss function and optimization method.

The data level approaches are mainly based on data augmentation, oversampling and undersampling. In medical image processing, conventional data augmentation techniques are sometimes problematic. For instance, a chest X-ray image traditionally depicts the heart at the lower left side, but when the image is augmented with a mirror effect, it will depict the heart at the right side of the chest. Similarly, effects of filliping, zooming, or rotation may change the meaning of a medical image completely. Hence, efficiently designed deep learning models and algorithms may be a superior option for medical image processing.

However, despite good performance, data and algorithm level approaches tend to use very complex models with a large number of parameters. According to [3], recent hybrid models using multiple streams and feature fusion have produced competitive results for small and highly imbalanced datasets. In this work, the algorithm level approaches are followed and a quad-stream hybrid model, called QuadSNet, with separable as well as conventional convolutional neural networks is proposed to classify medical images on small and imbalanced datasets.

The performance of QuadSNet is evaluated together with the state-of-the-art pre-trained models, including DenseNet121 (DN) [12], InceptionV3 (IN) [25], MobileNet (MN) [11], ResNet50 (RN) [9], VGG16 (VG) [24] and Xception (XC) [7]. The proposed model QuadSnet is trained and tested on six medical image datasets and one famous MNIST handwritten digits dataset. QuadSNet is intended to handle the problem of class imbalance with weighted margin loss on small datasets. Consequently, out of these seven datasets, the three smallest and most imbalanced medical datasets are used as benchmarks to compare the performance of QuadSNet with pre-trained models. For comprehensiveness, two of the three benchmark datasets are grayscale and one is colored. Other than the three benchmark datasets, the remaining four datasets are used to analyze the performance of QuadSNet on the larger, balanced, grayscale, color or non-medical image data.

The proposed technique could well handle the challenges of small datasets and class imbalance using a less complex model. Competitive results are obtained by using a fewer number of trainable parameters than most state-of-the-art pre-trained models. The feature fusion technique makes QuadSNet robust on a range of data. The training data size, type of images, number of classes and number of samples in each class are controlled with QuadSNet at an agreeable level.

The rest of the paper is organized as follows. In Section II, the proposed QuadSNet model and its architecture in detail is discussed. Section III presents a clear demonstration of the datasets, training procedure and experimental results. The best results in all the tables are in **bold**. Discussion and conclusion are in the end.

II. The Proposed QuadSNet

The proposed QuadSNet model uses a quad-stream approach, as illustrated in Fig. 1. Out of the four streams, two streams use conventional convolutional neural networks [16], denoted as $CS1$ and $CS2$, and two streams use separable convolutional neural networks [7], denoted as $SS1$ and $SS2$, respectively. Each stream is based on blocks, whose detailed design is depicted in Fig. 1.

Each of the streams, $CS1$, $CS2$, $SS1$ and $SS2$, consists of four blocks. The design of the streams helps them to extract different features because of dissimilar kernel sizes and different forms of convolutional mode. Due to such a technique, the model becomes wider rather than deeper, and a wider approach helps to reduce the number of trainable parameters without losing accuracy. Features extracted from each stream are concatenated to make a fusion of the learned features. The model learns various features simultaneously. Therefore the training time is drastically reduced.

Separable convolutional neural networks are faster than conventional convolutional neural networks because of their depth-wise and point-wise feature extraction mechanism [7]. They perform fewer multiplications during operation than conventional convolutional neural networks. Therefore, both types of convolutional neural networks in are used in the model to make it faster and more robust. Model functions in a conventional manner as any convolutional neural network may operate. Thus, the quad-stream approach helps the model to learn features simultaneously on a single input image.

A. Feature Representation and Fusion

Formally, $\mathbf{F}_{CS1}$, $\mathbf{F}_{CS2}$, $\mathbf{F}_{SS1}$ and $\mathbf{F}_{SS2}$ are represented as the extracted features of the streams $CS1$, $CS2$, $SS1$ and $SS2$ respectively. The features $\mathbf{F}_{CS1}$ and $\mathbf{F}_{CS2}$ are generated through conventional convolutional neural networks, whereas $\mathbf{F}_{SS1}$ and $\mathbf{F}_{SS2}$ are the features generated through the streams of separable convolutional neural networks. The $CS1$ and $SS1$ streams use the kernel size of 3×3 for conventional convolutional layers and separable convolutional layers respectively, and use 2×2 for maxpooling layers. Similarly the $CS2$ and $SS2$ streams use the kernel size of 5×5 for conventional convolutional layers and separable convolutional layers, respectively, and 2×2 for maxpooling layers.

The features generated by $CS1$ and $CS2$ are concatenated into $\mathbf{F}_{cs}$. Likewise the features obtained through the streams $SS1$ and $SS2$ are concatenated into $\mathbf{F}_{ss}$. Finally the features $\mathbf{F}_{cs}$ and $\mathbf{F}_{ss}$ are concatenated into $\mathbf{F}_{total}$, as shown in Equation 1.

$$\mathbf{F}_{cs} = \begin{pmatrix} \mathbf{F}_{CS1} \\ \mathbf{F}_{CS2} \end{pmatrix}, \mathbf{F}_{ss} = \begin{pmatrix} \mathbf{F}_{SS1} \\ \mathbf{F}_{SS2} \end{pmatrix}, \mathbf{F}_{total} = \begin{pmatrix} \mathbf{F}_{cs} \\ \mathbf{F}_{ss} \end{pmatrix} \quad (1)$$

The feature fusion in $\mathbf{F}_{total}$ is eventually average-pooled to retain effective features and shrink the size of feature vectors.

B. Micromanagement of Over-fitting

The model handles over-fitting at the micro-level on each block of the model. Each block includes a dropout layer and a batch normalization layer. The dropout layer uses a fixed value of 0.3. The batch normalization layer depends upon two important parameters, momentum and epsilon. The momentum parameter is set to 0.99 and the ϵ is set to 0.0001.

Other than the block-level dropout layers, there is a dropout layer after the average-pooling layer as well. Customarily the dropout layers using a value more than 0.5 in medical image classification are not considered in best practices. Therefore, it is purposefully kept at 0.3.

C. Margin Loss

The margin loss [28] with dynamic weights is adopted to handle the class imbalance and unnecessarily instant over-fitting of the model due to a smaller training set. Preliminary experiments showed that the margin loss performs better than the cross-entropy loss. Therefore, the margin loss is opted to be used, as represented in Equation (2).

$$\begin{aligned} \Gamma_\kappa = T_\kappa max(0, m^+ - \|\nu_\kappa\|^2) \quad + \\ \lambda(1 - T_\kappa) max(0, \|\nu_\kappa\|^2 - m^-) \end{aligned} \quad (2)$$

In Equation (2) $\kappa = 1$ if κ class is present, $m^+ = 0.9$, $m^- = 0.1$ and $\lambda = 0.5$ is down-weighting. Here ν_κ represents the feature vector with κ number of classes. The proposed model can be used not only for binary classification but also for multi-class classification. Therefore κ can be any finite discrete number. The values of m^+, m^- and λ dynamically handle the value of total loss Γ_κ. Ultimately the loss is minimized gradually by controlling the imbalance among the κ classes.

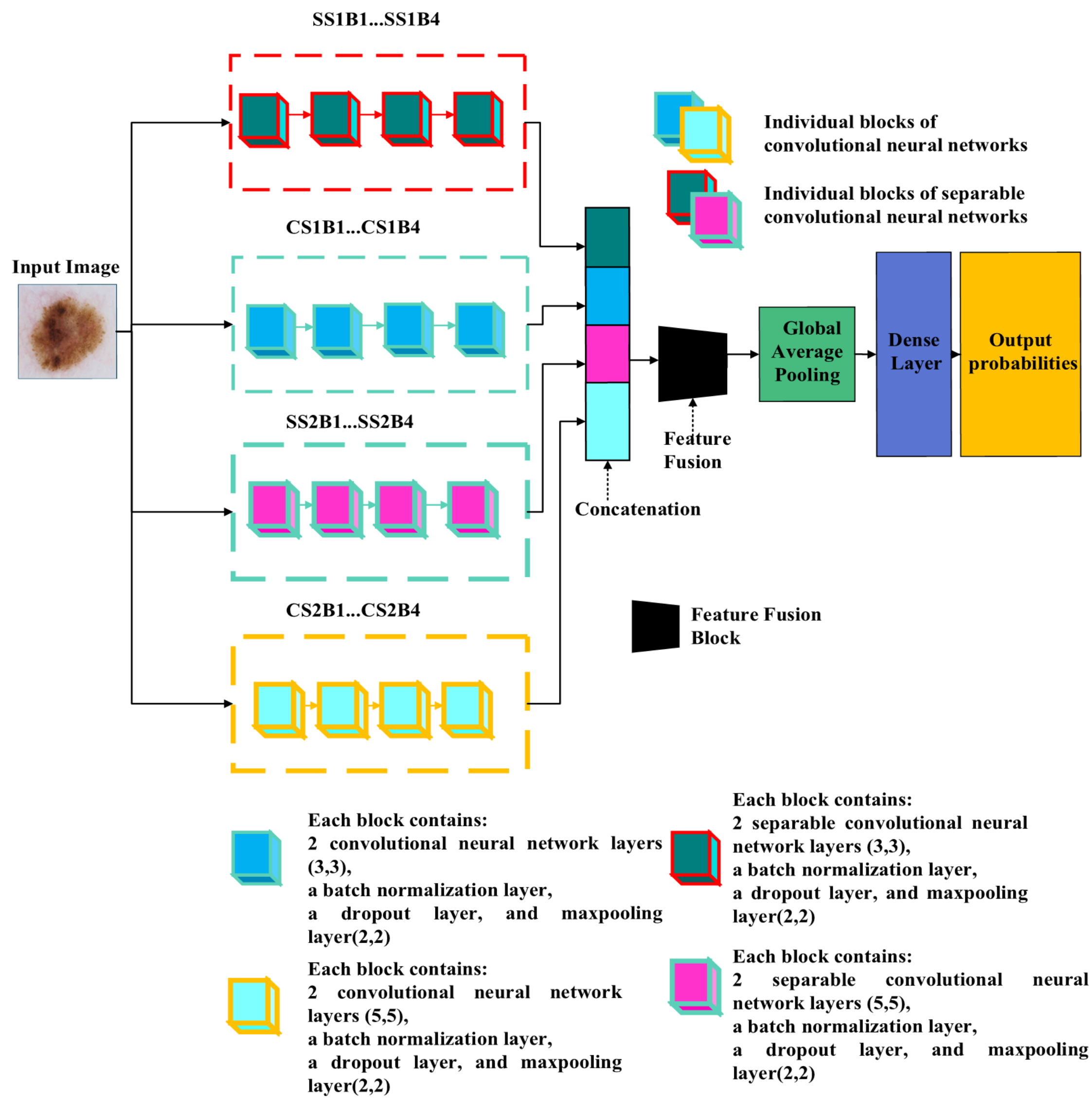

Fig. 1. Block Diagram of the QuadSNet Architecture. There are Four Streams and Each Stream Contains four Individual Blocks.

III. Experiments

A. Datasets

The proposed QuadSNet model and six state-of-the-art pre-trained models are trained and tested on six different types of medical datasets and one non-medical image dataset. For convenience, the seven datasets are symbolically, named, as Θ_1, Θ_2, ..., up to Θ_7 and the six pre-trained models as DN, IN, MN, RN, VG and XC, respectively.

1) Brief description of datasets: Each of the datasets in the list serves a unique purpose because of images' types and classes' degree of balance. Most datasets are imbalanced other than Θ_7, the MNIST dataset. Table I illustrates details of the datasets. The Θ_1, Θ_2, and Θ_3 are used as the benchmark datasets. Dataset Θ_1 consists of chest X-ray images in grayscale. Similarly, Θ_2 consists of CT-scan images in grayscale. Dataset Θ_3 is a colored dataset because of the dermoscopic images. As two of the benchmark datasets are grayscale and one is colored, the models have a fair chance of depicting efficacy. The QuadSNet and each of the six pre-trained models are trained on these datasets. The obtained results are then compared and analyzed comprehensively. Three benchmark datasets are described as follows:

TABLE I. Brief Description of Datasets. DR: Diabetic Retinopathy

Symbol	Dataset	#Samples
Θ_1	Pneumonia Classification	10855
Θ_2	COVID-19 Classification	746
Θ_3	Skin Lesion Classification	3297
Θ_4	DR Classification on Fundus Photographs	18632
Θ_5	DR Classification on OCT Data	84484
Θ_6	Malaria Cell Classification	27500
Θ_7	MNIST Handwritten Digit Classification	60000

1) Pneumonia (Θ_1): Θ_1 is a chest X-ray dataset for pneumonia classification [14]. This dataset is officially available at

https://www.kaggle.com/paultimothymooney/chest-xray-pneumonia/.

2) COVID-19 (Θ_2): Θ_2 is about COVID-19 (the data is from CT-scans) [29] and it is officially presented at https://covid-ct.grand-challenge.org.
3) Cancer (Θ_3): Dataset Θ_3 is RGB dataset based on dermoscopic images for skin lesion classification [26]. The dataset is a random subset of the dataset present at https://challenge2019.isic-archive.com/data.html.

Other than benchmark datasets, QuadSNet is also trained on Θ_4, Θ_5, Θ_6, Θ_7 to test its capabilities on a variety of image data. A brief description of the remaining datasets is presented as follows:

1) DR Classification on fundus photographs (Θ_4): Θ_4 is a relatively larger dataset than Θ_1, Θ_2 and Θ_3; it is based on color fundus photographs. The data is officially presented at https://www.kaggle.com/c/diabetic-retinopathy-detection/data.
2) DR Classification on OCT images (Θ_5): Θ_5 is the largest dataset among all the datasets and it is massively imbalanced due to the very high number of normal samples and the smaller number of diseased samples [14]. It is a multi-class classification data based on OCT (Optical Coherence Tomography) images of the retina of diabetic patients. This dataset contains four classes, called Choroidal Neovascularization (CNV), Diabetic Macular Edema (DME), DRUSEN, and Normal. This dataset is officially hosted at https://www.kaggle.com/paultimothymooney/kermany2018.
3) Malarial Cell Classification (Θ_6): Θ_6 is for Malarial cell classification. It is a balanced dataset [23]. This dataset is officially available at https://lhncbc.nlm.nih.gov/publication/pub9932. This dataset contains two classes based on Malarial and Non-Malarial cell images.
4) Hand Written Digit Classification MNIST (Θ_7): This dataset is based handwritten digits [17] from 0 to 9. The dataset Θ_7 is used to investigate the capabilities of QuadSNet on non-medical image datasets. Officially this dataset is present at http://yann.lecun.com/exdb/mnist/.

The main objective of using the seven different datasets is to analyze the diversity of the QuadSNet on a variety of image data. A few of the datasets are smaller and imbalanced except MNIST. The selected datasets are based on colored or grayscale images. Hence QuadSNet is tested accordingly.

B. Training and Testing

The QuadSNet and pre-trained models are trained and tested on a Windows 10 PC equipped with NVidia Gforce GTX 1060, having 16 GB of RAM, Intel Ci7 64 bit processor. All the simulations are performed on Keras with Tensorflow at the backend. The pre-trained models are individually trained on each of the three benchmark datasets.

Essential supplements and parameters, for instance, the learning rate $\gamma = 0.0001$, the optimizer, batch size $\beta = 32$, momentum $\mu = 0.009$, and input image size has been kept the same for all the models, including QuadSNet. Adam [15] optimizer has been used throughout the training. The models have been trained up to their maximum potential to nullify any unfairness.

TABLE II. COMPARISON OF QUADSNET WITH STATE-OF-THE-ART PRE-TRAINED MODELS IN TERMS OF THE TRAINABLE PARAMETERS

Abbr.	Model	#Trainable parameters
DN	DenseNet121	8,062,504
IN	InceptionV3	23,851,784
MN	MobileNet	**4,253,864**
RN	ResNet50	25,636,712
VG	VGG16	138,357,544
XC	Xception	22,910,480
QN	QuadSNet	**5,235,944**

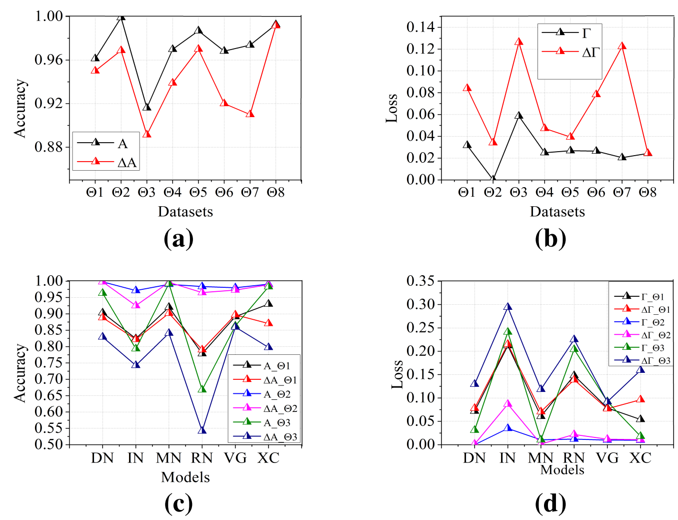

Fig. 2. (a) The Final Training Accuracy (A) and Validation Accuracy (ΔA) of QuadSNet on all Datasets, (b) The Final Training Loss (Γ) and Validation Loss ($\Delta\Gamma$) of QuadSNet on all Datasets, (c) The Final Training Accuracy (A) and Validation Accuracy (ΔA) Curves for Θ_1, Θ_2 and Θ_3 of Different Models and (d) The Final Training Loss (Γ) and Validation Loss ($\Delta\Gamma$) Curves for Θ_1, Θ_2, and Θ_3 of Different Models.

Fig. 2 shows the training accuracy (A), the validation accuracy (ΔA), the final training loss (Γ), and the validation loss ($\Delta\Gamma$) of the QuadSNet model on all the datasets. The distribution of individual datasets into train, validation, and test sets has been kept identical for all the models. The QuadSNet model has been trained on all the datasets, whereas the pre-trained models have been trained only on the three benchmark datasets.

IV. DISCUSSION

The training accuracy A and the validation accuracy ΔA of the pre-trained models and QuadSNet, as presented in Figure 2, exhibit the upshot of training with margin loss. As in this paper the weighted margin loss is used, it noticeably helps to control the effect of imbalance and scarceness of data with the help of QuadSNet. QuadSNet is trained from scratch. Therefore the micromanagement of over-fitting at the block level assists the model to handle it instantaneously.

The pre-trained models traditionally are trained on ImageNet [10], which is mostly based on natural images. In the transfer learning approach, the intended dataset and type of images play a vital role in a model's performance. If the results produced by pre-trained models are studied, datasets Θ_1 and Θ_2 were much easier because of precise edges and object-like structures. Whereas dataset Θ_3 looks harder for the models to extract features due to the lack of natural objects like features.

The same conditions of pre-trained models apply to QuadSNet as well. Therefore it yields higher accuracy on datasets Θ_1 and Θ_2 than on dataset Θ_3. The massive advantage of QuadSNet over pre-trained models in feature extraction is the fusion of multiple features obtained from various streams. Such features are rich due to different convolution techniques and different sizes of the kernels. The streams in QuadSNet are based on both separable and conventional convolutional neural networks; therefore, the features can be complementary with each other and contribute to the model's accuracy on diverse data. Therefore, QuadSnet achieves a reasonable accuracy on heterogeneous image data.

A. Experimental Results

The systematic analysis of the experimental results of QuadSNet and the pre-trained models after the training reveals a massive difference between the number of trainable parameters. Table II shows the details about the number of trainable parameters for each of the models. QuadSNet and MobileNet have the fewest trainable parameters, which are about one-fifth of the average parameters.

Traditionally accuracy is not considered as a better performance metric for medical image classification on imbalanced data, therefore, sensitivity, specificity and F_1 score are used.

All the datasets are distributed in three portions (Training, Validation and Test). The main objective is to analyze the performance of QuadSNet in comparison with pre-trained models on imbalanced and smaller datasets. Therefore, the chosen three benchmark datasets, Θ_1, Θ_2 and Θ_3, are the smallest and most imbalanced among the seven datasets.

The performances of pre-trained models and QuadSNet on Θ_1, Θ_2 and Θ_3 are depicted in Table III. It can be concluded that QuadSNet achieves the best performance in all the benchmark datasets at almost all the metrics.

Except for the six state-of-the-art pre-trained models, QuadSNet is compred with some of the latest publications on each of the datasets which have better performance on the particular dataset. The results can be observed from Table IV. Each of the compared methods is designed for a particular disease. QuadSNet exhibits competitive accuracy, specificity and sensitivity in comparison with existing works. Most existing works listed in Table IV utilize pre-trained models having a huge number of parameters and use data augmentation techniques, whereas QuadSNet produces comparable results with a few trainable parameters and without any data augmentation. The dataset Θ_7 is a non-medical image dataset. Therefore the results based on accuracy are compred only.

B. Limitations of the Study and Future Work

The proposed model has been thoroughly tested on the datasets described in Section III-A1. However, the proposed model has not been tested on 3-D medical image data, which may impact the performance. Similarly, the proposed model has not been tested in multi-input or multi-output settings where multiple tasks are performed simultaneously. In the future, the QuadSNet's efficacy may be tested on multimodal or 3-D medical image data.

TABLE III. THE PERFORMANCE OF PRE-TRAINED MODELS AND QUADSNET ON Θ_1, Θ_2 AND Θ_3 DATASETS

Dataset	Model	Sensitivity	Specificity	Accuracy	F_1 Score
Θ_1	DN	0.978	0.875	0.920	0.915
	IN	0.987	0.792	0.865	0.846
	MN	1.000	0.926	0.960	0.958
	RN	0.924	0.771	0.830	0.809
	VG	0.990	0.952	0.970	0.969
	XC	0.929	0.912	0.920	0.919
	QN	**0.990**	**0.971**	**0.980**	**0.980**
Θ_2	DN	0.877	1.000	0.891	0.934
	IN	0.956	1.000	0.964	0.977
	MN	0.926	1.000	0.938	0.961
	RN	0.867	1.000	0.881	0.928
	VG	0.961	0.949	0.959	0.974
	XC	**0.987**	0.892	0.964	0.976
	QN	0.962	**1.000**	**0.969**	**0.980**
Θ_3	DN	0.932	0.734	0.817	0.810
	IN	0.711	0.796	0.738	0.785
	MN	0.867	0.807	0.838	0.848
	RN	**0.985**	0.504	0.552	0.305
	VG	0.887	0.804	0.846	0.853
	XC	0.809	0.793	0.802	0.821
	QN	0.937	**0.917**	**0.928**	**0.945**

TABLE IV. COMPARISON OF QUADSNET WITH SOME OF THE LATEST STATE-OF-THE-ART METHODS ON Θ_1, Θ_2 AND Θ_3, Θ_4 , Θ_5, Θ_6 AND Θ_7 DATASETS. SEN: SENSITIVITY, ACC: ACCURACY

Datasets	Author	Sen	Spe	Acc
Θ_1	Rahman et al. [22]	0.990	0.970	0.980
	QN	**0.999**	0.970	**0.981**
Θ_2	Li et al. [20]	0.826	**1.000**	0.976
	QN	**0.960**	**1.000**	**0.977**
Θ_3	Kassem et al. [13]	0.798	**0.970**	0.943
	QN	**0.937**	0.910	**0.945**
Θ_4	Wan et al. [27]	0.880	**0.950**	0.900
	QN	**0.995**	0.858	**0.915**
Θ_5	Li et al. [19]	0.960	0.980	0.970
	QN	**0.960**	**1.000**	**0.990**
Θ_6	Masud et al. [21]	**0.970**	0.940	**0.970**
	QN	0.959	0.923	0.940
Θ_7	Ali et al. [1]	—	—	0.990
	QN	—	—	**0.999**

V. CONCLUSION

Compared with popular image datasets such as ImageNet for classification, medical datasets are usually small and class imbalance. This work introduces a new model called QuadSNet that can effectively handle over-fitting and class imbalance on small datasets without using transfer learning and data augmentation to handle such issues for image data. In general, QuadSNet outperforms the pre-trained models in terms of sensitivity, specificity, accuracy, and F_1 score on three medical benchmark datasets. Additionally, QuadSNet has competitive results compared to several state-of-the-art works focusing on a certain disease, demonstrating the effectiveness of the model. QuadSNet exhibits efficacy on a variety of datasets, including grayscale and color images. Due to the ability to handle diverse data, QuadSNet has the potential of becoming a universal model for medical image classification on small datasets. This paper uses margin loss only, but QuadSNet can be trained and tested using other loss functions to analyze its effectiveness.

Acknowledgment

Thanks to Chao Li for organizing the paper and thanks to professor Kun He for guidance and support.

References

[1] Ali S, Li J, Pei Y, Aslam MS, Shaukat Z, Azeem M (2020) An effective and improved cnn-elm classifier for handwritten digits recognition and classification. Symmetry 12(10):1742

[2] Ali-Gombe A, Elyan E (2019) Mfc-gan: class-imbalanced dataset classification using multiple fake class generative adversarial network. Neurocomputing 361:212–221

[3] Amin SU, Alsulaiman M, Muhammad G, Mekhtiche MA, Hossain MS (2019) Deep learning for eeg motor imagery classification based on multi-layer cnns feature fusion. Future Generation computer systems 101:542–554

[4] An N, Ding H, Yang J, Au R, Ang TF (2020) Deep ensemble learning for alzheimer's disease classification. Journal of Biomedical Informatics p 103411

[5] Apostolopoulos ID, Mpesiana TA (2020) Covid-19: automatic detection from x-ray images utilizing transfer learning with convolutional neural networks. Physical and Engineering Sciences in Medicine p 1

[6] Chen YJ, Chang YJ, Wen SC, Shi Y, Xu X, Ho TY, Jia Q, Huang M, Zhuang J (2020) Zero-shot medical image artifact reduction. In: 2020 IEEE 17th International Symposium on Biomedical Imaging (ISBI), IEEE, pp 862–866

[7] Chollet F (2017) Xception: Deep learning with depthwise separable convolutions. In: Proceedings of the IEEE conference on computer vision and pattern recognition, pp 1251–1258

[8] Dunnhofer M, Antico M, Sasazawa F, Takeda Y, Camps S, Martinel N, Micheloni C, Carneiro G, Fontanarosa D (2020) Siam-u-net: encoder-decoder siamese network for knee cartilage tracking in ultrasound images. Medical Image Analysis 60:101631

[9] He K, Zhang X, Ren S, Sun J (2016) Deep residual learning for image recognition. In: Proceedings of the IEEE conference on computer vision and pattern recognition, pp 770–778

[10] Hinton GE, Krizhevsky A, Sutskever I (2012) Imagenet classification with deep convolutional neural networks. Advances in neural information processing systems 25:1106–1114

[11] Howard AG, Zhu M, Chen B, Kalenichenko D, Wang W, Weyand T, Andreetto M, Adam H (2017) Mobilenets: Efficient convolutional neural networks for mobile vision applications. arXiv preprint arXiv:170404861

[12] Iandola F, Moskewicz M, Karayev S, Girshick R, Darrell T, Keutzer K (2014) Densenet: Implementing efficient convnet descriptor pyramids. arXiv preprint arXiv:14041869

[13] Kassem MA, Hosny KM, Fouad MM (2020) Skin lesions classification into eight classes for isic 2019 using deep convolutional neural network and transfer learning. IEEE Access 8:114822–114832

[14] Kermany DS, Goldbaum M, Cai W, Valentim CC, Liang H, Baxter SL, McKeown A, Yang G, Wu X, Yan F, et al. (2018) Identifying medical diagnoses and treatable diseases by image-based deep learning. Cell 172(5):1122–1131

[15] Kingma J (2014) Adam: A method for stochastic optimization. arXiv preprint arXiv:14126980

[16] LeCun Y, Bengio Y, et al. (1995) Convolutional networks for images, speech, and time series. The handbook of brain theory and neural networks 3361(10):1995

[17] Lecun Y, Cortes C, Burges C (1999) The mnist dataset of handwritten digits(images)

[18] Li C, Zhang D, Tian Z, Du S, Qu Y (2020) Few-shot learning with deformable convolution for multiscale lesion detection in mammography. Medical Physics

[19] Li F, Chen H, Liu Z, Zhang Xd, Jiang Ms, Wu Zz, Zhou Kq (2019) Deep learning-based automated detection of retinal diseases using optical coherence tomography images. Biomedical Optics Express 10(12):6204–6226

[20] Li K, Fang Y, Li W, Pan C, Qin P, Zhong Y, Liu X, Huang M, Liao Y, Li S (2020) Ct image visual quantitative evaluation and clinical classification of coronavirus disease (covid-19). European radiology pp 1–10

[21] Masud M, Alhumyani H, Alshamrani SS, Cheikhrouhou O, Ibrahim S, Muhammad G, Hossain MS, Shorfuzzaman M (2020) Leveraging deep learning techniques for malaria parasite detection using mobile application. Wireless Communications and Mobile Computing 2020

[22] Rahman T, Chowdhury ME, Khandakar A, Islam KR, Islam KF, Mahbub ZB, Kadir MA, Kashem S (2020) Transfer learning with deep convolutional neural network (cnn) for pneumonia detection using chest x-ray. Applied Sciences 10(9):3233

[23] Rajaraman S, Antani SK, Poostchi M, Silamut K, Hossain MA, Maude RJ, Jaeger S, Thoma GR (2018) Pre-trained convolutional neural networks as feature extractors toward improved malaria parasite detection in thin blood smear images. PeerJ 6:e4568

[24] Simonyan A Karen (2014) Very deep convolutional networks for large scale image recognition. arXiv preprint arXiv:14091556

[25] Szegedy C, Liu W, Jia Y, Sermanet P, Reed S, Anguelov D, Erhan D, Vanhoucke V, Rabinovich A (2015) Going deeper with convolutions. In: Proceedings of the IEEE conference on computer vision and pattern recognition, pp 1–9

[26] Tschandl P, Rosendahl C, Kittler H (2018) The ham10000 dataset, a large collection of multi-source dermatoscopic images of common pigmented skin lesions. Scientific data 5:180161

[27] Wan S, Liang Y, Zhang Y (2018) Deep convolutional neural networks for diabetic retinopathy detection by image classification. Computers & Electrical Engineering 72:274–282

[28] Xiao Q, Luo H, Zhang C (2017) Margin sample mining loss: A deep learning based method for person re-identification. arXiv preprint arXiv:171000478

[29] Zhao J, Zhang Y, He X, Xie P (2020) Covid-ct-dataset: a ct scan dataset about covid-19. arXiv preprint arXiv:200313865

A Randomized Hyperparameter Tuning of Adaptive Moment Estimation Optimizer of Binary Tree-Structured LSTM

Ruo Ando[1]
National Institute of Informatics
2-1-2 Hitotsubashi, Chiyoda-ku, Tokyo
101-8430 Japan

Yoshiyasu Takefuji[2]
Musashino University
Musashino University Faculty of Data Science
3-3-3 Ariake, Koto-Ku, Tokyo 1358181, JAPAN

***Abstract*—Adam (Adaptive Moment Estimation) is one of the promising techniques for parameter optimization of deep learning. Because Adam is an adaptive learning rate method and easier to use than Gradient Descent. In this paper, we propose a novel randomized search method for Adam with randomizing parameters of beta1 and beta2. Random noise generated by normal distribution is added to the parameters of beta1 and beta2 every step of updating function is called. In the experiment, we have implemented binary tree-structured LSTM and adam optimizer function. It turned out that in the best case, randomized hyperparameter tuning with beta1 ranging from 0.88 to 0.92 and beta2 ranging from 0.9980 to 0.9999 is 3.81 times faster than the fixed parameter with beta1 = 0.999 and beta2 = 0.9. Our method is optimization algorithm independent and therefore performs well in using other algorithms such as NAG, AdaGrad, and RMSProp.**

***Keywords*—Adaptive moment estimation; gradient descent; tree-structured LSTM; hyperparameter tuning**

I. Introduction

Optimization is involved in many deep learning algorithms. Analytical optimization is the basis of design algorithms. Neural network training is the most challenging problem of all the many optimization fields.

Among the hyperparameters to tune, learning rate is one of the most difficult because it drastically affects model performance. In general, the momentum algorithm can handle and mitigate the problem of being highly sensitive to some directions in parameter space. Adopting a separate learning rate for each parameter and these learning rates make sense about the directions of sensitivity.

Adaptive optimization is the algorithm to adapt the learning rate of model parameters based on many incremental or mini-batch based methods. Naturally, the choice of which algorithm to use is an unavoidable question. However, the algorithm selection much depend on the user's familiarity. In this paper, we will follow the assumptions below.

Hypothesis 1. There is no theorem or algorithm to determine which adaptive optimization is the best.

Then, as long as the optimal algorithm cannot be determined, we need to invent a method that can be commonly used to refine any algorithm. Parameter randomization is the promising approach to develop a speeding up procedure which is the adaptive optimization independent.

Hypothesis 2. According to Hypothesis 1, no optimization algorithms will be able to prove their own superiority over another algorithm.

Concerning the solution for Hypothesis 2, we propose the novel method concerning randomized hyperparameter tuning of adaptive moment estimation optimizer. The thrust of this paper is that the proposed method is adaptive optimization independent.

This paper is organized as follows. In Section II, three basic and popular algorithms are introduced: AdaGrad, RMSProp, and Adam. In Section III of related work, we introduce the related works of recurrent neural networks, recursive neural networks, LSTM, and adaptive optimization algorithms. In Section IV, we discuss the proposed method based on the binary tree of LSTM, linear activation unit, and constrained breadth-first search. In Section V, we discuss the research methodology for improving backpropagation, recurrent neural networks, and adaptive optimization algorithm. Experimental results are shown in Section VI. Our randomized hyperparameter tuning method is applied for Adam. In Section VII, we provide insights into the current situation of the research efforts of hyperparameter optimization. Then we conclude our paper in Section VIII.

II. Theoretical Background

A. AdaGrad

AdaGrad [18] algorithm adopting the learning rates with gradually changing them in proportion to the square root of the sum of all the historical squared values of the gradient.

$$s \leftarrow s + \bigtriangledown_\theta J(\theta) \tag{1}$$

$$\theta \leftarrow \theta - \eta \bigtriangledown_\theta J(\theta) \oslash \sqrt{s+\epsilon} \tag{2}$$

In equation (1), the square of gradients is accumulated into the vector s. Each S_i calculates the squares of the partial derivative of the cost function corresponding to the point to the parameter θ_i. In the case that the cost function is steep along the i^th dimension, s_1 will get larger and larger at each iteration.

Parameter s_1 will get larger and larger at each iteration as long as the cost function is steep along the i^th dimension,

Equation (2) is almost identical to one of Gradient Descent. However, there is one big difference. That is, the gradient vector is scaled down by a factor of $\sqrt{s+\epsilon}$.

AdaGrad is called an adaptive learning rate because AdaGrad decays the learning rate so that the learning rate for steep dimensions is faster than gentler slopes. The parameters of AdaGrad decrease rapidly in their learning rate corresponding to the largest partial derivative of the loss. On the other hand, the parameters decrease in their learning rate with the small partial derivatives. As a result, if the learning process has the more moderately directions of parameter space, the effect whole becomes greater.

B. RMSProp

RMSProp [19] algorithm improves AdaGrad to perform better in the nonconvex setting. AdaGrad is designed to converge with changing the gradient accumulation into an exponentially weighted moving average. Generally, a nonconvex function is used to train a neural network. The learning trajectory eventually reaches a region that is a locally convex bowl after the trajectory goes through many different structures. RMSProp has advantages compared with AdaGrad in the point that AdaGrad slows down rapidly and consequently finished never converging the global optimum.

For doing this, the RMSProp accumulates only the gradients from the most recent iterations.

$$s \leftarrow \beta s + (1-\beta)\,\nabla_\theta\, J(\theta) \otimes \nabla_\theta J(\theta) \quad (3)$$

$$\theta \leftarrow \theta - \eta\,\nabla_\theta\, J(\theta) \oslash \sqrt{s+\epsilon} \quad (4)$$

In equation (3), exponential decay is used. The decay rate β is typically set to 0.9. Except for very simple problems, this optimizer almost always performs much better than AdaGrad. In fact, it was the preferred optimization algorithm of many researchers until Adam algorithm came around.

C. Adam

Adam [20] is an adaptive learning rate optimization algorithm. The name Adam derives from the phase Adaptive moments. Adam can be described as a variant on the hybrid of momentum and RMSProp with some important distinctions. Adam incorporates momentum directly as an estimation value of the first-order moment. The first-order moment is called as exponential weighting. Adam adopts momentum and bias corrections. Momentum is used in combination with rescaling, which have a clear theoretical motivation. Bias corrections are used to estimate both first-order moments and second-order moments to account for their initialization at the origin.

III. Related Work

Recurrent neural networks [1], or RNNs are feedforward neural networks for processing sequential data by extending with incorporating edges that span adjacent time steps. In general, RNNs suffer the difficulty of training by gradient-based optimization procedures. Local numerical optimization includes stochastic gradient descent or second-order methods, which causes the exploding and the vanishing gradient problems [13][14][15]. Werbos et al. [11] propose the backpropagation through time (BPTT), which is a training algorithm for RNN. BPTT is derived from the popular backpropagation training algorithm used in MLPN training [12]. Derivatives of errors are computed with backpropagation over structures [6].

Recursive neural networks are yet another representation of the generalization of recurrent networks by using a different form of computation graph. The computation graph adopted in recursive neural networks is a deep tree instead of the chain-like structure of RNNs. Pollack [2] proposes recursive neural networks. Bottou [3] discuss the potential use of the recursive neural network in learning to reason. In [4] and [5], recursive neural networks are more effective in performing on different problems such as semantic analysis in natural language processing and image segmentation.

There is a long line of research efforts on extending the standard LSTM [7] in order to adopt more sophisticated structures. Tai et al. [8] and Zhu et al. [9] tree-structured LSTMs extended from chain-like structured LSTMs by adopting branching factors. They demonstrated that such extensions outperform competitive LSTM baselines on several tasks such as semantic relatedness prediction and sentiment classification. Furthermore, Li et al. [10] show the effectiveness of tree-structured LSTM on various tasks and situations in which tree-like structure is effective.

Boris Polyak proposes Momentum optimization with terminal velocity [21]. In 1983, Yurii Nesterov proposes Nesterov Momentum Optimization (NAG) [22]. NAG adopts the gradient of the cost function which is not measured in the local position but slightly ahead in the direction of the momentum. RMSProp [19] is an improved version of AdaGrad. RMSProp extends AdaGrad by accumulating the gradients from the most recent iterations. Adam [20] is based on the idea of both Momentum optimization and RMSProp. Adam keeps track of an exponentially decaying average of past gradients and an exponentially decaying average of past squared gradients.

Santa (Stochastic Annealing Thermostats with Adaptive Momentum) [23] is an adaptation method of Adam and RMSprop by leveraging MCMC (Markov Chain Monte Carlo) methods. In GD by GD (Gradient Descent by Gradient Descent) [24] is based on the idea that the optimization algorithm is a learning problem, and the optimization structure is determined by learning. They also propose LSTM optimizer.

In Adam, RMSProp, exponential decay by exponential moving average was adopted. However, it has been reported that when the gradient in that mini-batch disappears immediately due to exponential decay, consequently, Adam and RMSProp does not converge to the optimal solution. Therefore, AMSGrad [25] is an improved version of Adam that prevents important gradient information from disappearing immediately.

In Adam, the adaptive learning rate is efficient for fast learning, but even after learning has progressed, the validation error is not well converged due to high volatility in the learning rate. On the other hand, in SGD, which uses a fixed learning rate, the final validation error can be reduced, but it takes too much time to get to that point. Concerning these drawbacks, AdaBound and AMSBound were proposed as optimization

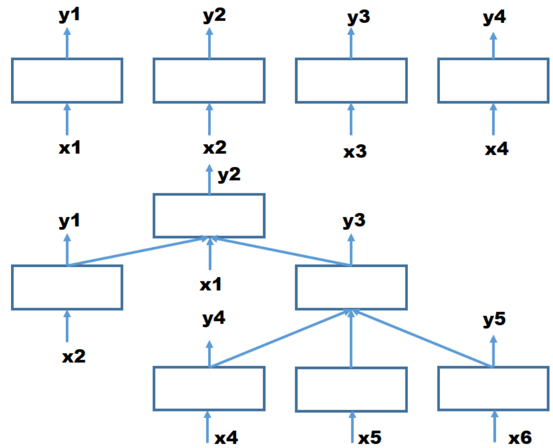

Fig. 1. True-structured LSTM with Arbitrary Branching Factor.

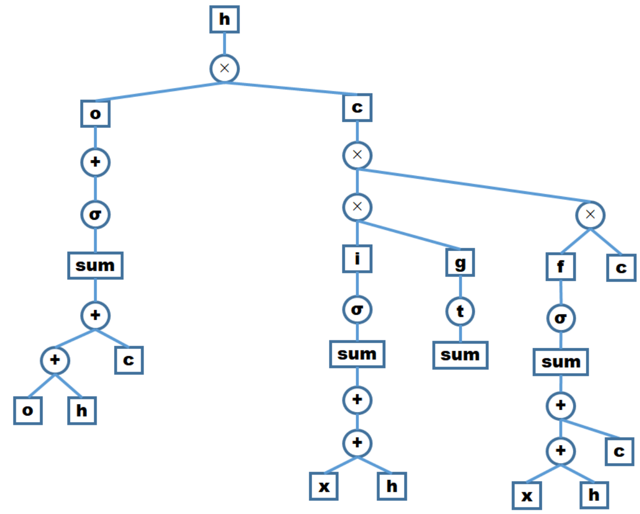

Fig. 2. Binary-tree-LSTM with Unary Operator.

methods as the combination Adam in the beginning and like SGD, in the end, [26].

As we have introduced in this section, adaptive optimization algorithms are constantly evolving, but there is still no theorem or algorithm to judge which algorithm is the best. Even one of the latest algorithm of [26] has not proven to be superior to everything else.

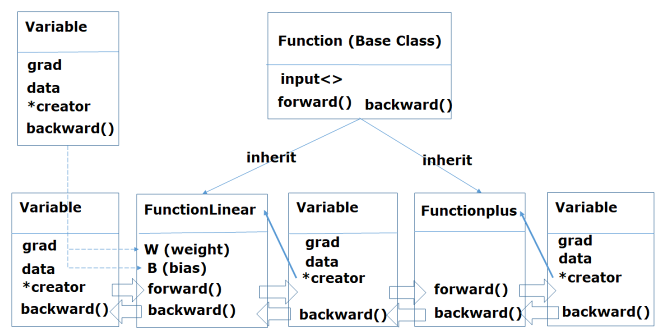

Fig. 3. Implementation of Linear Activation unit by Object-oriented Programming Language. The base Class of Function has the Inheritance of FunctionLinear.

IV. Proposal Model and Method

A. Binary Tree of LSTM

The Tree-LSTM is a generalization of long short-term memory (LSTM) networks to tree-structured network topologies, introduced in [9]. Here, the core design concept introduces syntactic information for language tasks by extending the chain-structured LSTM to a tree-structured LSTM.

Fig. 1 shows the comparison of two kinds of LSTM network structures. The upper side of Fig. 1 shows a chain-structured LSTM network. The lower side of Fig. 1 depicts a tree-structured LSTM network with an arbitrary branching factor. It is shown that Tree-structured LSTM has a good performance in the case that the networks cope with the combination of words and phrases in natural language processing [8].

Recursion is a fundamental process in any different modalities. It is associated with many phases. A recursive procedure and hierarchical structure is formed commonly indifferent modalities. Also, recursion is a core technique for traversing the binary tree. Fig. 2 depicts the representation of binary-tree-LSTM with the unary operator. A binary tree is a tree whose elements have at most two children.

If each element in a binary tree includes only two children, these two children are typically called as the left and right child. In the case of the forward computation of a S-LSTM memory block, it is represented in the following equations.

$$i_t = \sigma(W^L_{hi} h^L_{t-1} + W^R_{hi} h^R_{t-1} + W^L_{ci} c^L_{t-1} + W^R_{ci} c_{t-1} R + b_i) \tag{5}$$

$$f^L_t = \sigma(W^L_{fl} h^L_{t-1} + W^R_{hfl} h^R_{t-1} + W^L_{cfl} c^L_{t-1} + W^R_{cfl} c_{t-1} R + b_{fl}) \tag{6}$$

$$f^R_t = \sigma(W^L_{ft} h^L_{t-1} + W^R_{hfr} h^R_{t-1} + W^L_{cfr} c^L_{t-1} + W^R_{cfr} c_{t-1} R + b_{fr}) \tag{7}$$

$$x_t = W^L_{hx} h^L_{t-1} + W^R_{hx} h^R_{t-1} + b_x) \tag{8}$$

$$c_t = f^L_t * c^L_{t-1} + f^R_t * i_t * tanh(x_t) \tag{9}$$

$$o_t = \sigma(W^L_{ho} h^L_{t-1} + W^R_{ho} h^R_{t-1} + W_{co} c_t + b_o) \tag{10}$$

$$h_t = o_t * tanh(c_t) \tag{11}$$

Here, σ is the element-wise logistic function. σ is adopted to restricts the gating signals to be in the range of [0, 1]. f_L and f_R denotes the left (L) and right (R) forget gate. b is biased, and W is the weighting matrices of the network. Finally, the sign * is a Hadamard product which is also called element-wise product.

More importantly, equation (14)-(20) consists of a binary operator. Therefore, this equation can be represented as a binary tree. A binary tree is a fundamental data structure in different modalities. In binary tree, the elements have at most two children. We typically name them the left and right children because each element in a binary tree can have only two children, In computation, a binary tree consists of nodes, where each node contains a L("left") reference, a R("right") reference, and a data element. The topmost (or bottommost) node in the tree is called the root node.

Algorithm 1 recursive function

$variable \rightarrow generator \rightarrow backward(grad)$
while $i \leq variable \rightarrow generator.inputs\_size()$ **do**
  $nv = variable \rightarrow generator.inputs()$
  if $nv = isGetGrad$ **then**
    $this \rightarrow backward(nv.get())$
  end if
end while

B. Linear Activation Unit

Fig. 3 depicts our implementation of a linear activation unit for the reverse-mode auto diff of linear activation. In artificial neural networks, a node's activation function defines the output of that node given an input or set of inputs. The input-output model is defined as follows:

$$f(x) = \psi * (\sum_{i=0}^{n} w_i * x_i + b)$$

Here, ψ is an activation function such as Tanh and RELU. Class FunctionLinear implements the function of $\sum_{i=0}^{n} w_i * x_i + b$. The notation of *creator is the pointer to the function which generates its variable. For example, FunctionLinear outputs r which is equal to $\sum_{i=0}^{n} w_i * x_i + b$ and is passed to FunctionTanh. The creator of variable r is FunctionLinear. Fig. 3 also illustrates the detailed implementation of the inheritance of functions and variables of tree-structured LSTM. Inheritance in the middle of Fig. 3 enables us to define classes for modeling relationships among types by sharing what is common and specializing only on that which is inherently different. Its derived classes inherit members defined by the base class. We can use derived class without change. Deriving class do not depend on the specifics of the derived type. Those operations redefine those member functions depending on its type, specializing the function to take into account the peculiarities of the derived type. Consequently, a derived class may define additional members beyond those it inherits from its base class.

C. Constrained Breadth-first Search

As we discussed in Section I-B, a tree-structured LSTM graph is generated for each mini-batch. Fig. 4 depicts the model of a few tree-structured LSTM graphs for mini-batches. As usual, a breadth-first search (BFS) is applied for the recursive search of the tree structure. However, other procedures on our model, such as loss, MSE (Mean-Square Error), and Tanh should be skipped before the program reaches the LSTM tree, as shown in the lower-left side of Fig. 4.

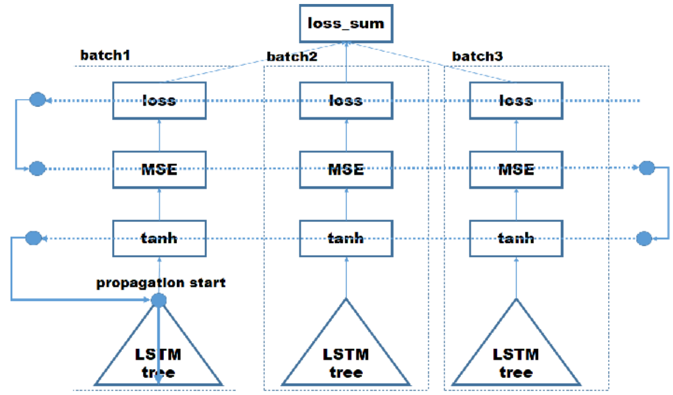

Fig. 4. Constrained Breadth First Search.

We modify the recursion algorithm as shown in Algorithm 1. Broadly, the breadth-first search is an algorithm for the traversal of tree (or graph) data structures. BFS begins at the tree root. It then searches all of the neighbor nodes at the present depth before it proceed to the nodes at the next depth.

Algorithm 2 Constrained model traversal

if $v \rightarrow last_{opt} \neq NULL \wedge \rightarrow opt = *v \rightarrow last_{opt}$ **then**
  $*v \rightarrow is\_last\_backward = true$
end if
if $if(v \rightarrow is\_last\_backward \neq NULL \wedge *v \rightarrow is\_last\_backward = false$ **then**
  $return$
end if
$back\_propagation()$

V. Research Methodology

A. Truncated Backpropagation through Time

Backpropagation through Time, or BPTT, is a specific application of backpropagation in neural networks for coping with sequence to sequence data like a time series. A recurrent neural network has one input each time step and predicts one output. Conceptually, BPTT performs by unrolling all input time steps, as shown in Fig. 5. In each time step, BPTT has one input time step and one copy of the network s_t , and one output o_t. Errors are then calculated and accumulated for each time slot with w.

Fig. 5 has outputs at each time step. The network is rolled back up, and the weights are updated. BPTT would be impractical in an online manner because its memory footprint grows linearly with time.

Truncated Backpropagation Through Time (TBPTT), which is an online version of BPTT, is proposed in [16]. TBPTT works analogously to BPTT. But, the sequence is calculated one-time step at a time periodically. The BPTT update is performed back for a fixed number of time steps. In [16], the accumulation stops after a fixed number of time steps. Truncated BPTT performs well if the truncated chains are effective in learning the recursive target functions.

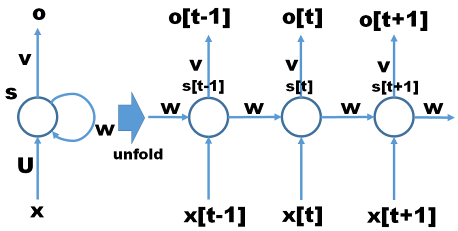

Fig. 5. Back Propagation through Time. It Works by Unrolling All Input Time Steps.

B. LSTM

Long short-term memory (LSTM) [7] is a family of recurrent neural networks. Like other recurrent neural networks, LSTM has feedback connections. Concerning the memory cell itself, it is controlled with a forget gate, which can reset the memory. unit with a sigmoid function. In detail, given a sequence data $x_1, ..., x_T$we have the gate definition as follows:

$$f_t = \sigma(W_{fh}h_{t-1} + W_{fx}x_t + P_f * c_{t-1} * b_f) \tag{12}$$
$$i_t = \sigma(W_i x_t + U_i h_{t-1} + P_i * c_{t-1} * b_i) \tag{13}$$
$$g_t = tanh(W_g x_t + U_g h_{t-1} + b_g) \tag{14}$$
$$c_t = i_t \Theta g_t + f_t \Theta c_{t-1} \tag{15}$$
$$o_t = \sigma(W_o x_t + U_o h_{t-1} + P_o * c_t + b_o) \tag{16}$$
$$h_t = o_t \Theta tanh(c_t) \tag{17}$$

where f_t is forget gate, i_t input gate, ot output gate and $g_t$input modulation gate. Particularly $P_f, P_i P_o$ indicates the peephole weights for the forget gate. The peephole connections introduced in [17] enable the LSTM cell to inspect its current internal states. Then, the backpropagation of the LSTM at the current time step t is as follows:

$$\delta o_t = tanh(c_t)\delta h_t \tag{18}$$
$$\delta c_t = (1 - tanh(c_t)^2) o_t \delta h_t \tag{19}$$
$$\delta f_t = c_{t-1}\delta c_t \tag{20}$$
$$\delta c_{t-1} = f_t \theta \delta c_t \tag{21}$$
$$\delta i_t = g_t \delta c_t \tag{22}$$
$$\delta g_t = i_t \delta c_t \tag{23}$$

C. Adam

Adam [20] stands for adaptive moment estimation. Adam optimization is the hybrid based on the ideas of momentum optimization and RMSProp. In Adam, momentum optimization keeps track of an exponentially decaying average of past gradients. On the other hand, RMSProp keeps track of an exponentially decaying average of past squared gradients.

$$m \leftarrow \beta_1 m - (1 - \beta_1) \bigtriangledown_\theta J(\theta) \tag{24}$$
$$s \leftarrow \beta_2 * s + (1 - \beta_2) \bigtriangledown_\theta J(\theta) \otimes J(\theta) \tag{25}$$
$$m \leftarrow \frac{m}{1 - \beta_1^t} \tag{26}$$
$$s \leftarrow \frac{m}{1 - \beta_2^t} \tag{27}$$
$$\theta \leftarrow \theta + \eta m \oslash \sqrt{s + \epsilon} \tag{28}$$

As far as steps 1, 2 and 5, Adam is closely similar to both momentum optimization and RMSProp.

The only difference is that instead of an exponentially decaying sum in momentum optimization and RMSProp, step 1 of Adam computes an exponentially decaying average rather than an exponentially decaying sum. Actually, these decaying sums are equivalent except for a content factor.

Steps 3 and 4 are technically specific detail. In steps 3 and 4, m and s are initialized at 0 at default. Then, m and s will be biased towards 0 at the starting phase of training. Consequently, steps 3 and 4 will help boost m and s in the early phase of training.

VI. Experiment

In this section, we describe the experimental results of the training and generating a sine wave. In the experiment, we use a workstation with Intel(R) Xeon(R) CPU E5-2620 v4 (2.10GHz) and 252G RAM.

Adam uses the moving average of gradient m_t as well as v_t, which is the squared moving average adopted by RMSProp and AdaDelta.

$$m_t = \beta_1 * m_t - 1 + (1 - \beta_1) g_t \tag{29}$$
$$v_t = \beta_2 * v_t - 1 + (1 - \beta_2) g_t^2 \tag{30}$$

Optimization problem requires the search for good hyperparameters. The hyperparameters are variable to decide. The cost to be optimized is the validation set error. For evaluating our method, we generate a sin wave with random noise by the normal distribution. Then, we apply curve fitting to the generated sin wave.

For hyperparameter tuning, we use three test scenarios. In first case, we set the parameter $\beta 1$ and $\beta 2$ fixed to 0.9 and 0.999. In second case, we set the parameter $\beta 1$ ranging from 0.89 to 0.91 and $\beta 2$ ranging from 0.9985 to 0.9995. Finally, we set the parameter $\beta 1$ ranging from 0.88 to 0.92 and $\beta 2$ ranging from 0.9980 to 0.9999.

Fig. 6, 7, and 8 are the results of the curve fitting of three test cases. Fig. 9 shows the comparison of validation loss of three test cases. It turned out that test case 3 with the parameter $\beta 1$ ranging from 0.88 to 0.92 and $\beta 2$ ranging from 0.9980 to 0.9999 has the best performance. The plot of test case 3 decreases rapidly comaware to the other two cases.

The results in Fig. 9 suggest that early stopping may be applicable. Early stopping is another approach to regularize iterative learning algorithms, including Adam and Gradient

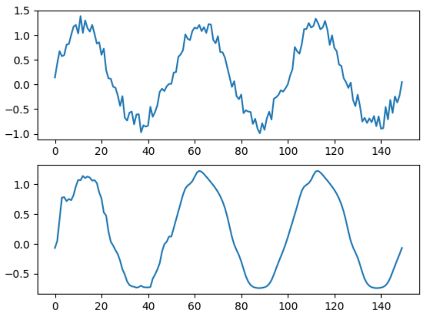

Fig. 6. $\beta1 = 0.9/\beta2 = 0.999$.

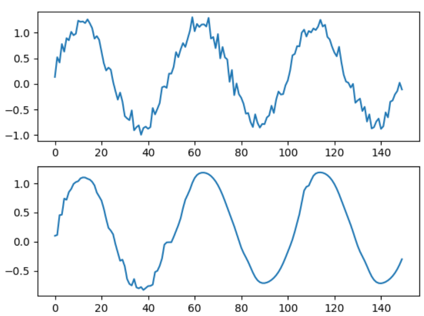

Fig. 7. $\beta1 = 0.89 - 0.91/\beta2 = 0.9985 - 0.9995$.

Descent, to stop training immediately after the validation loss reaches out a minimum value. In other words, leveraging early stopping, we control and terminate training as soon as the validation loss falls to a minimum. Early stopping is a simple and powerful regularization technique.

Table I shows the validation loss of three test cases. At step 5 with epoch size 750, elapsed time of the third case with $\beta1$ ranging from 0.88 to 0.92 and $\beta2$ ranging from 0.9980 to 0.9999 is 0.0493266. The elapsed time of 0.0493266 is 1.81 times faster than the second case and 3.81 times faster than the first case.

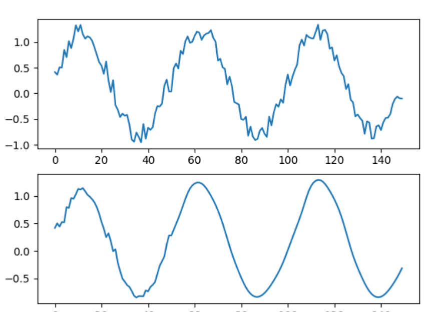

Fig. 8. $\beta1 = 0.88 - 0.92/\beta2 = 0.9980 - 0.9999$.

TABLE I. COMPARISON OF THREE TEST CASES

	Elaplse time in epoch=750 (sec)		
	0.9/0.999	0.89-0.91/0.9985-0.9995	0.88-0.92/0.9980-0.9999
1	0.392805	0.155601	0.140308
2	0.310886	0.130887	0.0976786
3	0.259277	0.113318	0.0733389
4	0.219546	0.100228	0.059955
5	0.187943	0.0893164	0.0493266

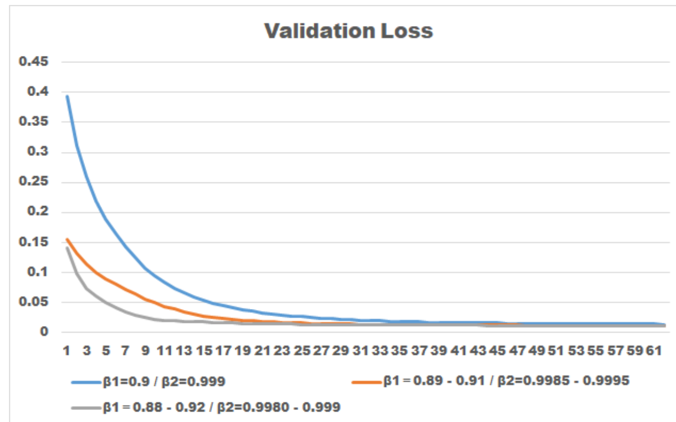

Fig. 9. Validation Loss with Parameter $\beta1$ and $\beta2$ Changed.

VII. DISCUSSION

In the process of discussing a series of optimization algorithms, a question now arises - which algorithm should one choose?

Schaul et al. [27] presents a comparative study of a large number of optimization algorithms across a wide range of learning tasks. According to this, although the series of optimization algorithms with adaptive learning rates such as RMSProp and AdaDelta works fairly robustly, no single best algorithm has emerged.

On the other hand, the drawback common to most hyperparameter optimization algorithms is the need for a training experiment to run before they can retrieve any information from the experiment. A more sophisticated (automated) random search is usually much less efficient than a manual search by a human practitioner. Partly because the set of hyperparameters is often completely pathological. Broadly, in this context, the choice of which algorithm to use largely depends on the user's familiarity with the algorithm.

Generally, adaptive optimization algorithms are recommended. However, Ashia C. Wilson et al. [28] pointed out that AdaGrad, RMSProp, and Adam generalize poorly on some datasets. According to this, it follows that we may stick to other alternatives such as Momentum optimization or Nesterov Accelerated Gradient as long as researchers have a better understanding of this issue. In this situation, we can conclude that our method is helpful and practical because our method is optimization algorithm independent.

VIII. CONCLUSION

Adam (Adaptive Moment Estimation) is one of the promising techniques for parameter optimization of deep learning.

In this paper, we propose a novel random search method for Adam with randomizing parameters of $\beta1$ and $\beta2$. Random noise generated by normal distribution is added to the parameters of $\beta1$ and $\beta2$ every step of updating function is called. In the experiment, we have implemented binary tree-structured LSTM and adam optimizer function.

There have been lots of research efforts on algorithms which each seek to address the challenge of optimizing deep models by adapting the learning rate for each model parameter. However, there is currently no consensus on which algorithm is best to choose. Our method of randomized hyperparameter tuning is an optimization method independent. Therefore, our method can be applied for various kinds of algorithms such as NAG, AdaGrad and RMSProp, and so on. Updating function is called. In the experiment, we have implemented binary tree-structured LSTM and adam optimizer function. It turned out that in best case, randomized hyperparameter tuning with $\beta1$ ranging from 0.88 to 0.92 and $\beta2$ ranging from 0.9980 to 0.9999 is 3.81 times faster than the fixed parameter with $\beta1$ = 0.999 and $\beta2$ = 0.9. We can conclude that adding random noise to the fixed-parameter of $\beta1$ and $\beta2$ is effective and reasonable compared with a naive manual search.

REFERENCES

[1] Rumelhart, David E.; Hinton, Geoffrey E., Williams, Ronald J., Learning representations by back-propagating errors. Nature 323 (6088): 533-536, 1986/10

[2] Jordan B. Pollack: Recursive Distributed Representations. Artif. Intell. 46(1-2): 77-105 (1990)

[3] Leon Bottou: From Machine Learning to Machine Reasoning. CoRR abs/1102.1808 (2011)

[4] Socher, Richard, Lin, Cliff C., Ng, Andrew Y., and Manning, Christopher D. Parsing Natural Scenes and Natural Language with Recursive Neural Networks. In Proceedings of the 26th International Conference on Machine Learning (ICML), 2011.

[5] Socher, Richard, Perelygin, Alex, Wu, Jean Y., Chuang, Jason, Manning, Christopher D., Ng, Andrew Y., and Potts, Christopher. Recursive deep models for semantic compositionality over a sentiment treebank. In Proceedings of the Conference on Empirical Methods in Natural Language Processing, EMNLP ?f13, Seattle, USA, 2013. Association for Computational Linguistics.

[6] Goller, Christoph, and Kohler, Andreas. Learning task-dependent distributed representations by backpropagation through structure. In In Proc. of the ICNN-96, pp. 347-352, Bochum, Germany, 1996. IEEE.

[7] Sepp Hochreiter and J.Nurgen Schmidhuber. 1997. Long short-term memory. Neural Computation 9(8):1735-1780.

[8] Kai Sheng Tai, Richard Socher, and Christopher D. Manning. 2015. Improved semantic representations from tree-structured long short-term memory networks. In Proceedings of the 53rd Annual Meeting of the Association for Computational Linguistics and the 7th International Joint Conference on Natural Language Processing. ACL, pages 1556-1566.

[9] Xiaodan Zhu, Parinaz Sobhani, and Hongyu Guo. 2015. Long short-term memory over recursive structures. In Proceedings of the 32nd International Conference on Machine Learning. ICML, pages 1604-1612.

[10] Jiwei Li, Minh-Thang Luong, Dan Jurafsky, and Eduard Holy. 2015. When are tree structures necessary for deep learning of representations. In Proceedings of the 2015 Conference on Empirical Methods in Natural Language Processing. EMNLP, pages 2304-2314.

[11] P. J. Werbos, Backpropagation through time: What does it does and how to do it. In Proc. IEEE, vol. 78, no. 10, pp. 1550-1560, Oct. 1990.

[12] P. J.Werbos, The Roots of Backpropagation: From Ordered Derivatives to Neural Networks and Political Forecasting, 1st ed. Hoboken, NJ:Wiley, 1994.

[13] Yoshua Bengio, Patrice Simard, and Paolo Frasconi. Learning long-term dependencies with gradient descent is difficult. IEEE transactions on neural networks, 5(2):157-166, 1994.

[14] John F. Kolen and Stefan C. Kremer. Gradient Flow in Recurrent Nets: The Difficulty of Learning LongTerm Dependencies, pages 464-479. Wiley-IEEE Press, 2001.

[15] Razvan Pascanu, Tomas Mikolov, and Yoshua Bengio. On the difficulty of training recurrent neural networks. In Proceedings of the 30th International Conference on International Conference on Machine Learning - Volume 28, ICML?f13, pages III310-III318. JMLR.org, 2013.

[16] Ronald J. Williams and Jing Peng. An efficient gradient-based algorithm for online training of recurrent network trajectories. In Neural Computation, 1990.

[17] Gers, F. A., and Schmidhuber, J. (2001). LSTM recurrent networks learn simple context-free and context-sensitive languages. IEEE Trans. Neural. Netw., 12(6), 1333-1340.

[18] J. Duchi, E. Hazan, and Y. Singer., Adaptive subgradient methods for online learning and stochastic optimization, Journal of Machine Learning Research 12 (Jul): 2121–2159 (2011)

[19] Tijmen Tieleman, Geoffrey Hinton, Rmsprop: Divide the gradient by a running average of its recent magnitude. Coursera: Neural networks for machine learning, COURSERA Neural Networks Mach. Learn, 2012

[20] Diederik P. Kingma, Jimmy Ba, Adam: A Method for Stochastic Optimization, ICLR (Poster) 2015

[21] BT Polyak, Some methods of speeding up the convergence of iteration methods, USSR Computational Mathematics and Mathematical Physics 4 (5), 1-17,1964

[22] NESTEROV Y., A method for unconstrained convex minimization problem with the rate of convergence o(1/k$\hat{2}$), Doklady AN USSR 269, 543-547, 1983

[23] Changyou Chen, David E. Carlson, Zhe Gan, Chunyuan Li, Lawrence Carin: Bridging the Gap between Stochastic Gradient MCMC and Stochastic Optimization. ASSISTANTS 2016: 1051-1060

[24] Marcin Andrychowicz, Misha Denil, Sergio Gomez Colmenarejo, Matthew W. Hoffman, David Pfau, Tom Schaul, Nando de Freitas: Learning to learn by gradient descent by gradient descent. NIPS 2016: 3981-3989

[25] Alexandre Défossez, Léon Bottou, Francis R. Bach, Nicolas Usunier: On the Convergence of Adam and Adagrad. CoRR abs/2003.02395 (2020)

[26] Liangchen Luo, Yuanhao Xiong, Yan Liu, Xu Sun: Adaptive Gradient Methods with Dynamic Bound of Learning Rate. CoRR abs/1902.09843 (2019)

[27] Tom Schaul, Ioannis Antonoglou, David Silver: Unit Tests for Stochastic Optimization. ICLR 2014

[28] Ashia C. Wilson, Rebecca Roelofs, Mitchell Stern, Nati Srebro, Benjamin Recht: The Marginal Value of Adaptive Gradient Methods in Machine Learning. NIPS 2017: 4148-4158

Encryption on Multimodal Biometric using Hyper Chaotic Method and Inherent Binding Technique

Nalini M K[1]
IEEE member,
BMS College of Engineering,VTU,
Bangalore, India - 560 019

Dr. Radhika K R[2]
Senior IEEE Member,
Professor, BMS College of Engineering,VTU,
Bangalore, India - 560 019

***Abstract*—Chaotic maps are non-convergent and highly sensitive to initial values. The applications include secure digital identity in distributed systems. Face and fingerprint biometric templates are subjected to hyper-chaotic map leading to encrypted image. Encrypted image is fed as an input to deoxyribonucleic acid (DNA) sequence. Dimensionality of generated DNA sequence is reduced by hashing. The intra-variation for a subject is measured with inter-quartile range. Image set with minimal variation value is identified for selecting the consistent image of a subject. 256 bit Key is generated from the consistent image. Generated key is reduced to 128 bits by eliminating subject specific outliers and redundant values. User specific features are extracted for both the traits using ResNet 50 convolutional neural network and are fused by addition. Final key is bound to feature vector by permutation function and time taken towards key binding is estimated with benchmark database SDUMLA-HMT. Outcome reveals that time taken for key binding varies between 45ms and 58ms for an image of size 80 MB.**

***Keywords*—Chaotic systems; DNA sequences; cryptographic techniques; Convolutional Neural Networks (CNN); key binding**

I. Introduction

Securing biometric template by binding it with cryptographic key is known as key binding. Fuzzy vault and fuzzy commitment are two well-known approaches in key binding. Helper data is generated during enrollment phase and decrypted to retrieve key in authentication phase. Sutcu et.al (2007) proposed a new framework to bind cryptography keys with signature biometric using correlation filters. Results shows that smaller size images reduces the security and EER for recognition is 0.08%. Christian Rathgeb et al. (2011) developed a key binding system using fuzzy commitment scheme with iris biometric. Implementation states that for128 bits key FAR is less than 0.01%. Daniel et al. (2016) designed a method using function minimization for key binding with iris biometric and proved False acceptance rate is 0.0% for 256 bits key.

Biometric encryption is the technique of binding cyptographic key to a biometric template. The encryption procedure generates cryptographic key from biometric trait and finally template or key is retrieved for authentication [1], [2].The rapid growth of online transactions, multimedia communications, realtime applications, cloud technologies, etc. entails additional security meant for data protection. Safeguarding digital image against malicious threats is an enormous challenge in distributed networks [3]. Several approaches such as cryptographic algorithms, passcodes, etc. are currently available to secure digital image in real time applications [4]. However, the above mentioned techniques fail to differentiate between legitimate user and an attacker who has fraudulently acquired the passcode [5]. Several studies confirm that biometric encryption is resistant to multiple attacks and as such is highly recommended for verification and authentication [6].

Biometric authentication offers an innovative approach to key security which bestow direct connection between passcode and key [7]. The secured template must satisfy properties such as diversity, revocability, security and accuracy. Individual traits are incredibly imperative and eminent; therefore the templates should be protected using a highly secure technique [8]. In the past, several methods have been advanced using cryptographic techniques and cancelable biometrics to develop template security [9]. Revocable and non-invertible transformations are executed to obtain cancelable biometrics [10].

Biometric image have high resolution, high redundancy and strong correlations among adjacent pixels and occupies large storage space, as a result of which bio- metric image cannot compete with traditional encryption methods. We are looking to develop a system where the image is sensitive to even slight changes made to initial conditions, pseudo randomness, etc. Chaotic systems meet these obligations of the encryption system [11]. Strong parallel computing technique is realized by DNA sequences [12] and multimodal biometrics is brought to bear to increase the security level. The different forms of multimodal biometrics available are multi-sensor, multi-instance and multi-algorithmic, etc. Multimodal biometrics is used in several applications [8]. Accuracy is enhanced as various fusion techniques are used to pool multiple traits, is highly reliable and provide heightened security such that even if one trait fails, another trait can be used for authentication [13]. Multimodal biometrics is impenetrable to attacks and is used in several applications where high level of security is desired [14].

The key generated using chaotic maps and DNA sequences are extremely secure and effective [15]. Strength of the key is assessed using several security tests, such as histogram, key space, key sensitivity, correlation and information entropy analysis [16]. Implementation results results illustrate that the algorithm enhances security and is resistant to multiple attacks.

mds

July 1, 2021

II. Chaotic Map

Chaotic maps have a virtuous property of randomness and acute sensitivity to initial conditions. Chaos help to intersperse the original data prohibitively which is highly invertible and therefore is best suited for image encryption. Chaotic sequence is generated by scrambling pixels either by substitution or diffusion etc. Numerical methods such as phase diagrams method, Lyapunov index method, power spectral method, etc. are harnessed to magnify complexity in chaotic system [15]. Some of the widely used chaotic maps for encryption are Logistic chaotic map [17], sine map [18], cosine map, baker map, tent map, Lorenz map [19], Chens map [20]. Several chaotic maps are pooled together to form multidimensional chaotic maps [21]. 1D Logistic chaotic system is defined in equation (1) and 2D Logistic chaotic system is designated in equation (2).

$$\begin{aligned} &X_(n+1) = f(x) = \mu X_n(1-X_n)) \\ &where \mu\epsilon(0,4), X_n\epsilon(0,1), n = 0,1,2,\ldots \end{aligned} \tag{1}$$

The results of the proposed system prove that when $3.56994 < \mu <= 4$ the system is chaotic.

$$\begin{aligned} &X_(i+1) = \mu_1 x_i(1-x_i) + \gamma_1 y_i^2 \\ &y_(i+1) = \mu_2 y_i(1-y_i) + \gamma_2(x_i^2 + y_i x_i) \end{aligned} \tag{2}$$

when "$2.75 < \mu_1 <= 3.4, 2.75 < \mu_2 <= 3.45, 0.15 < \gamma_1 <= 0.21, 0.13 < \gamma_2 <= 0.1$",two sequences in the region [0, 1] are generated which is chaotic. The multidimensional chaotic system such as 3D or 4D chaotic system is designed by combining three or four 1D chaotic system. Equation (3) describes sine map chaotic system [22]:

$$X_(n+1) = f(x) = \mu 5_i sin(\pi X_n) \tag{3}$$

where $\mu 5_i\epsilon(0.87,1)$ are parameters. Equation (4) describes cosine map chaotic system and Equation (5) describes baker's map chaotic system [23].

$$X_(n+1) = f(x) = \mu_6 cos(\pi|X_n - 0.5|) \tag{4}$$

where $\mu_6 = 0.98$.
$(x(n+1,)y(n+1)) =$

$$\{ \begin{array}{ll} (x_n/p, py_n) & 0 < x \leq p \\ ((x_n-p)/(1-p), (1-p)y_n + p) & p < x \leq 1 \end{array} \tag{5}$$

where $p = 0.5$ for standard bakers map.Equation (6) describes tent map,

$$x(i+1) = F_p(x_i) = \begin{cases} x_i/p & if x_i \leq p \\ (1-x_i)/(1-p) & if p < x_i \end{cases} \tag{6}$$

where $p\epsilon(0,1)$ is a control parameter.Equation (7) describes Lorenz chaotic map [19],

$$\begin{cases} x_i = \sigma(y_i - x_i) \\ y_i = \sigma x_i - y_i - x_i z_i \\ z_i = x_i y_i - \beta z_i \end{cases} \tag{7}$$

where x_i, y_i, z_i are first time derivatives,$\sigma = 10, \sigma = 28, \beta = 8/3$. Equation (8) describes Chen's chaotic map,

$$\begin{cases} \dot{p} = a(q-p) \\ \dot{q} = -pr + dp + cq - s \\ \dot{r} = pq - br \\ \dot{s} = p + k \end{cases} \tag{8}$$

where a, b, c, d, k are system parameters. when $a = 36, b = 3, c = 28, d = 16$ and$-0.7 \leq$k≤ 0.7 the system behaves hyper chaotic by generating four chaotic sequences. Equation (9) describes 4D nonlinear hyper chaotic system [24],

$$\begin{cases} (x_1) = a_1x_1 + a_2x_4 - x_2x_3 \\ (x_2) = -a_3x_1 + a_4x_2 + b_1x_1x_3 \\ (x_3) = a_5x_3 + b_2x_1x_2 + b_3x_1x_4 \\ (x_4) = a_6x_2 + a_7x_4 - b_4x_1x_3 \end{cases} \tag{9}$$

where $a_i < 0, i = 1,2,3\ldots7, b_i > 0, x_j\epsilon R, j = 1,2,3,4$. Equation (10) describes 5D hyper-chaotic maps [25],

$$\begin{cases} x_1 = a(x_2 - x_1) + x_2x_3x_4 \\ x_2 = b(x_1 + x_2) + x_5 - x_1x_3x_4 \\ x_3 = -cx_2 - dx_3 - ex_4 + x_1x_2x_4 \\ x_4 = -fx_4 + x_1x_2x_3 \\ x_5 = -g(x_1 + x_2)) \end{cases} \tag{10}$$

where "a, b, c, d, e, f, g" are system control parameters.when "$a = 30, b = 10, c = 15.7, d = 5, e = 2.5, f = 4.45, g = 38.5$",the system generates five choatic sequences and behaves hyperchaotic [26].

Chaotic maps are classified based on properties and complexity of the system. Logistic chaotic map is less complex and highly efficient system with linear and non-linear dynamic function. Spatiotemporal is highly dynamic in nature, which improves complexity during cryptography process. Efficiency is also enhanced during encryption and decryption. Hyper chaotic is highly random which generates more Lyapunov components. Based on the number of Lyapunov components the complexity of the system is decided. The system which is non-linear and hyper chaotic, generates an highly chaotic image.

III. DNA Coding Sequences

DNA sequence has four nucleic acid bases such as "Adenine (A), Cytosine (C), Guanine (G) and Thymine (T)" in which A and T, G and C are complement to each other. Based on the similarity and uniqueness of complementary properties, DNA and binary values are related together [27]. In binary 0 and 1 are complementary, similarly 00 and 11, 01 and 10 are complementary pairs in DNA encoding. Pairing mode of DNA base and binary is given in Table I. About $c_4^4 c_2^1 = 8$types of pairing rules are available. Maximum length of DNA sequence is 4 for each pixel in an image. When C, A, T, G are denoted as 11, 00, 01, 10 and

TABLE I. DNA Encoding

	A	T	C	G
Rule 1	00	11	10	01
Rule 2	00	11	01	10
Rule 3	11	00	10	01
Rule 4	11	00	01	10
Rule 5	10	01	00	11
Rule 6	01	10	00	11
Rule 7	10	01	11	00
Rule 8	01	10	11	00

TABLE II. DNA ADDITION AND SUBTRACTION

+	A	C	T	G	-	A	C	T	G
A	C	A	G	T	A	C	G	A	T
C	A	C	T	G	C	A	C	T	G
T	G	T	C	A	T	G	T	C	A
G	T	G	A	C	G	T	A	G	C

TABLE III. DNA COMPLEMENTARY RULE

Original base	A	C	T	G
Complementary base	T	G	A	C

for 8 bit grey images, the DNA sequence length is 4 (e.g. 10101101 is encoded in to DNA sequence GGCT). DNA addition and DNA subtraction [Table II], DNA complementary [Table III], DNA XOR rule [28] and DNA XNOR rule [29] [Table IV] are shown below.

TABLE IV. DNA XOR AND DNA XNOR

XOR	A	G	C	T	XNOR	A	C	T	G
A	A	G	C	T	A	C	A	G	T
G	G	A	T	C	T	T	G	C	A
C	C	T	A	G	C	A	C	T	G
T	T	C	G	A	G	T	G	A	C

IV. ENCRYPTION TECHNIQUES

Biometric template protection is performed by feature transformation or biometric cryptosystem. There are few feature transformation techniques which are salting and non-invertible transform whereas biometric cryptosystem includes key binding and key generation [17], [30].

The properties of template protection are, there should be no cross matching across databases, able to reproduce new template based on same biometric data, computationally hard to obtain original template. The cryptosystem techniques used for template protection are Fuzzy vault, Fuzzy commitment, shielding function etc. Chaotic maps and DNA sequences are also used for image encryption which generates highly secured image. Few methods are discussed below.

Zhang et al, proposed a method with three round scrambling-diffusion structure. Hill matrix permutation is computed based on hyper-chaotic chen's chaotic values and scrambles the pixel position [27]. DNA coding rules are used as key for 'F' function of fiestal network and finally image encryption is obtained by XOR operation of previous pixel. This method effectively resists plaintext attack, differential attack and statistical attack. Chakraborty et al, proposed a system with josephus traversing and mixed chaotic map [31] . Traversing scrambles the plain image followed by diffusion which includes four 1D chaotic maps. Finally XOR operation is performed to obtain the encrypted image. This method is resistant to several security attacks. Fu et al, proposed a method using CML chaotic system for scrambling and DNA complementary rule for generating encrypted image. Analysis proves that this system is safe and effective [32].

Li et al., proposed a method where initially Bit level scrambling and pixel level scrambling is performed. Using 5D hyperchaotic system and DNA XOR coding rule is applied to generate image encryption [25]. The above method is proved to be highly secured and reliable. Ye Tian et al., proposed a method using CT cascade map, NC map and DNA encoding rule. Chaotic maps are used for scrambling S-box followed by DNA addition and XOR operation to generate encrypted image. Results of the proposed system handles several security analysis and are resistant to attacks.

The image encryption algorithm with DNA masking, SHA-2 and Lorenz system developed by Zhang et al. [27] have high key sensitivity, large key space, which enhances the security against statistical attacks and exhaustive attacks. The results show that the algorithm improves encoding efficiency. Secured image encryption algorithm was developed by combining logistic and spatiotemporal chaotic systems along with DNA encoding technique and the system was proposed by Wang et al. [22]. The experimental results show that the proposed system enhances security to various attacks such as brute-force attack, statistical attack and differential attacks. The algorithm based on Lorenz and Chen's chaotic systems with Dynamic S-boxes was proposed by Ahmad et al. [24]. The results show that the proposed scheme is resistant to several attacks and have very good efficiency. A new 1D chaotic system for image encryption was designed by Chai et al. [33]. To enhance the security level, several 1D chaotic maps are combined and the proposed system results show that the scheme is resistant to various attacks. The DNA encoding along with chaotic systems generates 192 bit key, which was implemented by Wu et al. [34]. The proposed system results show that the image is highly chaotic and resistant to several security analyses. The 4D hyper chaotic system with DNA sequence was proposed by Maddodi et al. [35]. The system provides hyper chaotic sequence, which is pseudo random in nature. The chaotic sequence is converted in to DNA sequence and the image blocks are diffused. The proposed system implementation states that the system is capable of handling known-plaintext and chosen-plaintext attacks.

V. EXISTING KEY GENERATION TECHNIQUES

There are several key generation techniques using chaotic systems and DNA sequences where few are discussed in this section. Fu et al [36] developed key stream sequence as shown in equation (11). The logistic chaotic map is used to generate permutation and substitution key stream sequences. Al et al [37] introduces the scheme that takes a master key of 320 bit and produces a group of sub keys with length 32 bit, 128 bit using tent chaotic map as shown in equation (12). Chai et al [38] and Al et al [39] proposed SHA256 key generation sequences for initial values of 2D logistic-adjusted-Sine-map and Lorenz chaotic system. The initial values are expressed as 8-bit blocks and four 52 bit sequences as shown in equation (13) and equation (14). Li et al [29] proposed four pairs 48 bit key sequences generation using chaotic logistic map and DNA substitution method as shown in equation (15). Abanda et al [21] generated the secret key made of two triplets of initial values and a coefficient. The secret key uses mixed chaotic maps of Colpitts and Duffing Oscillators.

$$\begin{aligned} pk_m = pos(pk_m) + (1 + mod(sig \\ (abs(ps_m, \alpha), ((len(imgdata) - 1) - pos(pk_m)))) \end{aligned} \tag{11}$$

where pk_m is the permutation key stream sequence.

$$\text{key(i)} = concat(\text{SK, Chao, compkey , Chao(i+1)}) \quad (12)$$

where SK is the SubKey,$compKey$ is the complement of SK, $Chao, Chao_(i+1)$ is the chaotic keys from the Tent map.

$$K = K_1, K_2...K_{32} subjectto" K(i,0), K(i,1), K(i,7)" \quad (13)$$

where $K(i,j), i$ denotes the "character number" and j is the "bit number" in K_i.

$$x_h = digits(x_0 - floor(x_0), 52) \quad (14)$$

where x_0 is the initial secret key and x_h is the key value generated.

$$\begin{array}{l} b1b2b3b4 \ldots b12 \\ (b1b2b3b4) XOR (b5b6b7b8) XOR (b9b10b11b12) \\ r1r2r3r4 \end{array} \quad (15)$$

where $r1 \ldots r4$ are four pairs of 48 bit key sequences.

VI. Pre-trained Deep Networks

The convolutional neural network has several architectures which are pre-trained to solve complex problems [40]. The pre-trained models uses a benchmark dataset to achieve the solution [41],[42].

A. LeNet5

The LeNet5 architecture model [43] was developed for identification of handwritten character recognition. This mainly concentrates on automatic learning than hand-designed heuristics. The architecture comprises of 7 Layers with three convolutional layers (C1, C3, C5), two sub-sampling layer (S2, S4) and one output function (F6). The number of trainable parameters and connections are given in the Table V.

TABLE V. Entropy Analysis

Layers	Trainable Parameters	Connections
C1	156	304
S2	12	5880
C3	1516	151600
S4	32	2000
C5	10612	48120

F6 represents the Euclidean Radial Basis Function units (RBF) in the output layer. Each RBF output is calculated as given in equation (16),

$$y_i = \sum_j (x_j - w_{ij})^2 \quad (16)$$

where x_j is the state of unit j, w_ij is the weight of the respective input function. The pretrained model used MNIST database with 60000 parameters which gives error rate 0.95% without deformation and dropped to 0.8% with distortion.

B. ImageNet

ImageNet architecture model [44] was developed for classification of images. This architecture comprises of eight layers with five convolutional layers (C1 –C5) and three fully connected layers (F1-F3). The input image size is $224 \times 224 \times 3$, F1- F3 have 4096 neurons each. The model uses stochastic gradient descent with batch size of 128 examples, momentum of 0.9 and weight of 0.0005 for training and weight is updated as in equation (17).

$$v_{i+1} = 0.9 \cdot v_i - 0.0005.\epsilon \cdot w_i - \epsilon \cdot \langle dL|dw|w_i \rangle D_i \quad (17)$$

Where "i is the iteration index, v is the momentum variable,ϵ is the learning rate, $\langle dL|dw|w_i \rangle D_i$ is the average over ith batch D_i of the derivative with respect to w, evaluated at w_i". The network is trained for 60 million parameters in the entire architecture. GPU trains the model for ILSVRC-2010 dataset with error rate 17.0%

C. GoogleNet

GoogleNet architecture model [45] was developed with deep convolutions for classification and detection with increased accuracy rate. The network comprises of 22 layers deep with accuracy 0.6%. GoogleNet used 5 million (V1) and 23 million (V3) parameters used in the network. ILSVRC 2014 database is used with error rate of 6.67%.

D. ResNet

Residual network was mainly developed for deeper networks [46]. Research concludes that adding more layers may degrade the final performance of the system. Residual blocks are implemented with residual function and are placed in the intermediate layers of a block. Residual function helps to adjust the input feature map for high quality features. When the distinct feature extraction is not required, the weight of the residual function is reduced to zero.

Residual network was enhanced by increasing the network's width (channel depth) and is considered as the most effective way of expanding the capacity of the entire network as shown in Fig. 1. This was implemented in ResNet34 architecture and ResNet50 architecture [47].

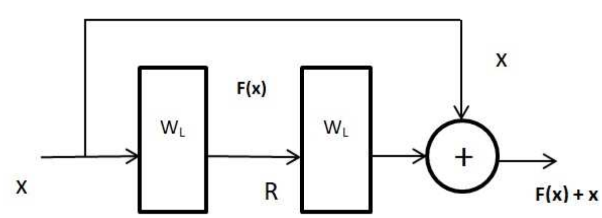

Fig. 1. Residual Model.

where W_L is the weight layer, R is the relu function, x is the input and F (x) is the residual function.

ResNet50 model replaces each two layer residual block with a three layer bottleneck block as shown in Fig. 1. The residual layer uses 1x1 convolutions in the implementation, which reduces and subsequently restores the channel depth as shown in Fig. 2. when calculating the 3x3 convolution the computational load is significantly reduced. It uses "25 million parameters" with 80% accuracy rate.

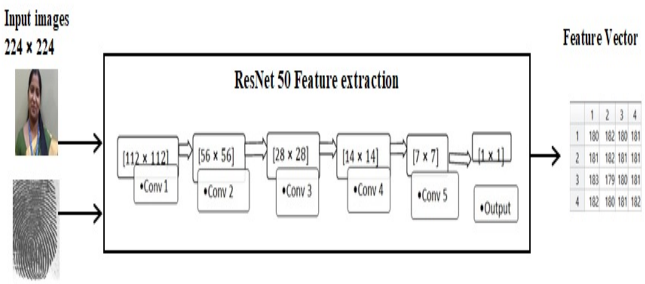

Fig. 2. ResNet50 Feature Extraction.

E. ResNeXt

The architecture of ResNeXt [48] is an extension of the deep residual network. In this network the standard residual block is replaced by one of the Inception models. The block's input is represented into a series of lower (channel) dimensional representations where convolution filters are applied before merging the results. The implementation is done using 8 GPUs with a mini batch size of 128. There are about 25 million parameters used for implementation.

F. DenseNet

Within the dense block, both the feature map and input are concatenated.

$$\text{Dense block} \ => \ \text{Feature map} \sim \\ \text{input of each successive layer}$$

Features are reused within the network by concatenating feature-maps learned by different layers. When the features of different layers are concatenated the efficiency is improved. Variation in the input of subsequent layers increases. DenseNet [41] is capable to work with very small output channel depths by reducing the number of parameters. The parameters used for implementation is 40 million with 3.46% error rate.

VII. Proposed Key Generation Technique

Key generation procedure combines chaotic theory and DNA sequence as shown in Fig. 3. The procedure for key generation is stated below

Step 1: Input two Images and convert in to equal binary blocks. Consider $I1 and I2$ are input images and divide the images in to two blocks $B1, B2$.

Step 2: Beta chaotic map sequence is generated with initial values $[x1, x2, c1, c2, b1, b2, k] are chosen.$

Step 3: The blocks are converted in to scrambled images using chaotic sequence values $|p, q, z, r|$

Step 4: The scrambled images are encoded using DNA addition.

Step 5: The complement value is generated using DNA complement.

Step 6: The blocks are combined and SHA 256 is applied to generate the fixed size key for encryption.

Step 7: Outliers are eliminated in the key sequences and finally only one key is accepted.

Key generated is highly sensitive to initial parameters, more efficient and resistant to several attacks.

A. Pre-processing Techniques

Zhang et al used global bit scrambling to generate binary sequence [49]. Ahmad et al applied the size of the resultant matrix obtained after chaotic map sequences to resize the image [24]. Girdhar et al converted the image to fixed size blocks for pre-processing and scrambling is performed using chaotic sequences [19]. The proposed system uses arnold chaotic map for scrambling input images.

B. Beta Chaotic Map

Ahmad et al used Beta chaotic map which is determined from beta function which has high chaotic behavior [24] . The mapping is polynomial and is given in equation (18). chaotic map generates four chaotic map sequences. The variables generated in the chaotic sequence have high randomness with two positive Lyapunov exponents.

$$x_(n+1) = k * \beta(x_n; x_2, p, q) \tag{18}$$

where $p = b_1 + c_1 * a$ and $q = b_2 + c_2 * a$ with b_1, c_1, b_2 and c_2 are constants. The parameter is used to control amplitude of the beta map and denote the bifurcation parameter. The beta function is given in equation (19).

$$Beta(x_n; x_2, p, q) =$$

$$\{ \begin{array}{ll} ((x - x_1)/(x_c - x_1))^p, & \\ ((x_2 - x)/(x_2 - x_c))^q if x\epsilon |x_1, x_2| & \\ 0 & otherwise \end{array} \tag{19}$$

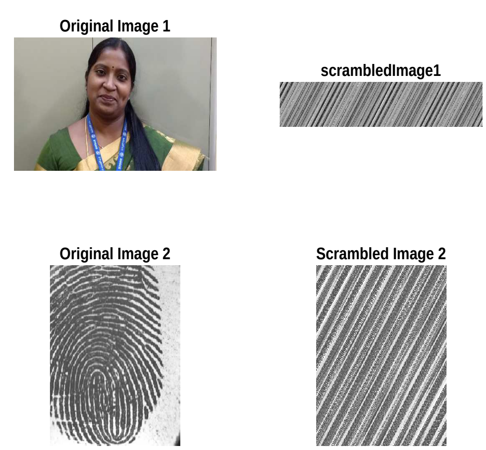

Fig. 3. Encrypted Images.

Algorithm 1: Key generation

1: The input from database folder of face and fingerprint is read.
2: im1 is the image from face database folder and im2 is the image from fingerprint database folder.
3: The input image is resized and stored it in B1 and B2.
4: The binarized values of the input images are stored in to bim1 and bim2.
5: The chaotic variables are initialized to $a = 0.8, x1 = -1, x2 = 1, k = 0.85, b1 = 5, c1 = 1, b2 = 3, c2 = -1.$
6: Beta chaotic map values are calculated **for** $i \leftarrow 0$ ***to*** n **do**
  $p \leftarrow b1 + c1 * a;$
  $q \leftarrow b2 + c2 * a;$
  $z \leftarrow ((p * x2) + (q * x1))/(p + q);$
  $r \leftarrow ((B1(i)-x1)/(z-x1))^p*((x2-B1(i))/(x2-z))^q;$
  $B1(1 + i) \leftarrow k * r;$
7: Images are scrambled using chaotic variable values **for** $inc \leftarrow 1$ ***to*** $num1$ **do**
  for $row \leftarrow 1$ ***to*** $rown$ **do**
    for $col1 \leftarrow 1$ ***to*** $coln$ **do**
      $nrowp \leftarrow row;$
      $ncolp \leftarrow col;$
      for $ite \leftarrow 1$ ***to*** inc **do**
        $newcord \leftarrow [11; 12] * [nrowpncolp];$
        $nrowp \leftarrow newcord(1);$
        $ncolp \leftarrow newcord(2);$
      $newim1(row, col) \leftarrow im1((mod(nrowp, rown) + 1), (mod(ncolp, coln) + 1));$
8: Repeat step 7 to get newim2 by scrambling
9: Image1 is encoded using DNA addition $bases \leftarrow' ATGC';$
  $scbin1 \leftarrow im2bw(newim1);$
  for $k \leftarrow 1$ ***to*** $length(scbin1)$ **do**
    $index \leftarrow 2 * scbin1(k) + scbin1(k + 1) + 1;$
    $result1((k + 1)/2) \leftarrow bases(index);$
10: Repeat step 9 to encode image2 using DNA condition
11: Compute DNA complement for encoded image1 **for** $o \leftarrow 1$ ***to*** $length(result1)$ **do**
  if $result1(o) =' A'$ **then**
    $l1(o) =' T';$
  if $result1(o) =' G'$ **then**
    $l1(o) =' C';$
  if $result1(o) =' T'$ **then**
    $l1(o) =' A';$
  else
    $l1(o) =' G';$
12: Repeat step 11 for encoded image2
13: Call SHA256 for image1 and image2
  $im1sha256 \leftarrow uint8(l1)$
  $im2sha256 \leftarrow uint8(l2)$
  $Key \leftarrow im1sha256 + im2sha256$
14: Intraclass variation of keys function is called
15: Outlier elimination function is called
16: Final key is accepted after eliminating outliers

C. Key Generation

Beta chaotic map is highly sensitive to its parameters, has strong chaotic behavior, more efficient and resistant to several attacks. The proposedkey generation procedure is shown in Fig. 4.

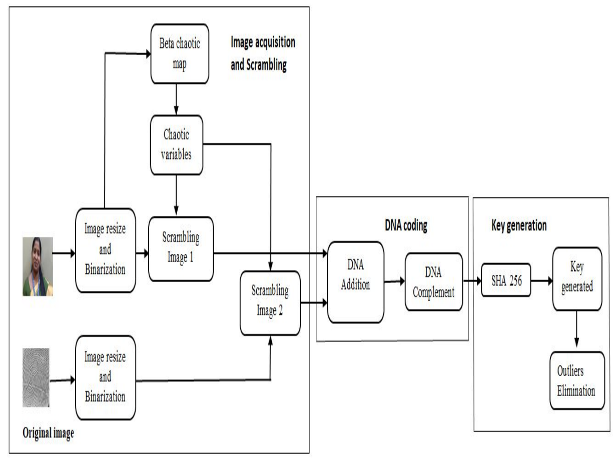

Fig. 4. Key Generation.

D. Scrambling Techniques

Liu et al. used permutation and substitution to obtain scrambled sequence. Input bits are transformed to output bits using S-boxes and P-boxes. The key introduced in each round is derived from beta chaotic map [15].

Zhan et al applied global bit scrambling technique to generate binary sequence [49]. Here 1D binary sequence b^0 contains binary digits where each digit represents intensity value of each pixel. k^x is the hyper-chaotic sequence in ascending order. b^0 is scrambled with k^x sequence as shown in equation (20). The author in [30] experimented with shuffling algorithm and substitution algorithm to rearrange the pixels. Assume m*n is the length of the input binary sequence, a_i is the shuffling sequence, $d_i$is the sequence after shuffling. Equation (21) explains shuffling sequence. Li et al experimented with pixel level scrambling [25] as shown in equation (22) and bit level scrambling as shown in equation (23).

$$b_i^1 = b_(k_i^x)^0 i\epsilon[1, 8_m * n] \quad (20)$$

$$d_(a_i) = c_i 1 \leq i \leq m * n \quad (21)$$

If F is the m×n substitution matrix, B is the resultant matrix after shuffling and then substitution is performed as shown in equation (24).

$$FoB = G_ij|G_ij = F_ij + B_ij(mod256) \quad (22)$$

$$q^{'}(i,j) = q(i^{'},j^{'}), q(i^{'},j^{'}) = q(i,j) \tag{23}$$

where "$q^{'}(i,j)$ is the scrambling image positioned at (i,j), $q(i^{'},j^{'})$and $q(i,j)$are the original image positioned at $(i^{'},j^{'})$ and $(i,j), i = 1,2,\dots m, j = 1,2,\dots n.$". Equation 24 shows the circular shift operation.

$$CS(r) = circshift[Q^{'}(r), LSB(k_3^{'}(r)), k_3^{'}(r)] \tag{24}$$

where "$circshift[u,q,v]$ means $v-$bit cycle shift on the binary sequences u. LSB(z) means the least bit of z. A right cycle shift or a left cycle shift will be decided by q =1 or q =0."

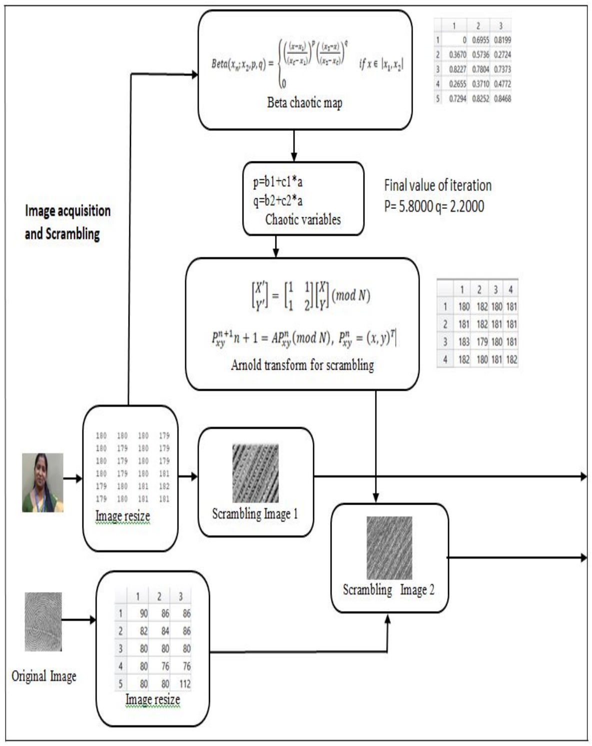

Fig. 5. Scrambling.

Arnold transform [28] is used in our proposed method for scrambling as shown in Fig. 5, because it is a reversible map without any attractor. Therefore, this transform is best used for scrambling and generalized 2D transform is shown in equation (25).

$$(x_(n+1)y_(n+1)) = ((ab)(cd))(x_n y_n)modN \tag{25}$$

Where "a,b,c,d are positive integers and gcd(ad-bc,N)=1".

E. DNA Coding

In the proposed system, DNA addition and DNA complement is used for encoding as shown in Fig. 6. For example, if the pixel of an image is 82 and 174, the equivalent binary sequence is 10100100 and 10101110. According to DNA encoding rule-1, we obtain CCGA and CCTC. Additionally, after applying DNA addition we get CCAA and applying complement rule the final encoded value is GGTT. DNA addition operation is implemented by Li et al [26] and Kumar et al. [50] proposed a system to obtain the encrypted sequence. Zhan et al used DNA addition, DNA complement rule and DNA XOR between the hyperchaotic sequence and DNA sequence [49]. The sequence generated in the proposed system gives a robust encryption performance. Li et al. used DNA operations rules to diffuse gray images [29]. The DNA operations (XOR, XNOR, +, -) are executed randomly as shown in equation (26) to obtain transitional images.

$$\begin{aligned} op &= [x3] + 1 \\ pr^{'} &= propKI_e \\ pg^{'} &= pgopKI_e \\ pb^{'} &= pbopKI_e \end{aligned} \tag{26}$$

where op is the selected DNA operation, pr, pg, pb are plain image, $pr^{'}$, $pg^{'}$, $pb^{'}$ are transitional images. Zheng et al. implemented DNA addition and XOR rule to obtain encrypted image [51].

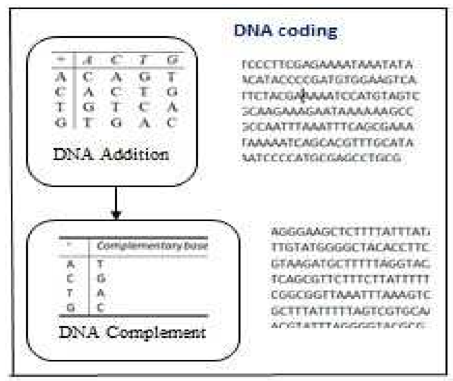

Fig. 6. DNA Coding.

F. SHA 256

Hashing is one of the widely used common cryptographic techniques due to its high security, uniqueness and integrity. It generates unique 256 bit (32 byte) signature for text which can be used as a key. In our proposed system, DNA encoded blocks of two images is combined and SHA-256 algorithm is implemented to obtain a key for encryption.

G. Intra-class Variation of Keys

After the generation of keys for all the traits, intra-class variation between the samples is calculated which is depicted in Fig. 7. The steps followed for intra-class variation of keys are as follows:

Step 1: Each column values are subtracted with the adjacent column to check the similarities between the samples of same class.

Step 2: All the column values are sorted and outliers are calculated based on zeros in the column values.

Step 3: The sample which has more zeros are considered as a class with more similarity therefore the sample is given low priority for selecting the final key.

Step 4: The above step is repeated for all the samples and the sample with minimum zero count is given high priority and the sample is used for selecting final key.

Step 5: Outliers are removed for the selected sample and final key is generated.

Algorithm 2: Intraclass variation

1: Each trait values are arranged column wise
2: **for** $i = 1$ *to* 12 **do**
    for $j = 1$ *to* 7 **do**
        $A_j = A_j - A_{j+1}$
    if i==7 **then**
        $A_j = A_j - A_1$
3: **for** $i = 1$ *to* 84 **do**
    $Sort(A)$

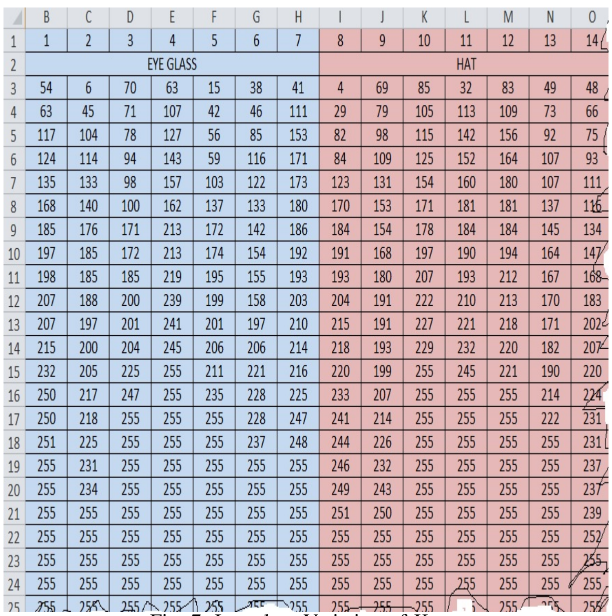

	B	C	D	E	F	G	H	I	J	K	L	M	N	O
1	1	2	3	4	5	6	7	8	9	10	11	12	13	14
2	EYE GLASS							HAT						
3	54	6	70	63	15	38	41	4	69	85	32	83	49	48
4	63	45	71	107	42	46	111	29	79	105	113	109	73	66
5	117	104	78	127	56	85	153	82	98	115	142	156	92	75
6	124	114	94	143	59	116	171	84	109	125	152	164	107	93
7	135	133	98	157	103	122	173	123	131	154	160	180	107	111
8	168	140	100	162	137	133	180	170	153	171	181	181	137	116
9	185	176	171	213	172	142	186	184	154	178	184	184	145	134
10	197	185	172	213	174	154	192	191	168	197	190	194	164	147
11	198	185	185	219	195	155	193	193	180	207	193	212	167	168
12	207	188	200	239	199	158	203	204	191	222	210	213	170	183
13	207	197	201	241	201	197	210	215	191	227	221	218	171	202
14	215	200	204	245	206	206	214	218	193	229	232	220	182	207
15	232	205	225	255	211	221	216	220	199	255	245	221	190	220
16	250	217	247	255	235	228	225	233	207	255	255	255	214	224
17	250	218	255	255	255	228	247	241	214	255	255	255	222	231
18	251	225	255	255	255	237	248	244	226	255	255	255	255	231
19	255	231	255	255	255	255	255	246	232	255	255	255	255	237
20	255	234	255	255	255	255	255	249	243	255	255	255	255	237
21	255	255	255	255	255	255	255	251	250	255	255	255	255	239
22	255	255	255	255	255	255	255	255	255	255	255	255	255	252
23	255	255	255	255	255	255	255	255	255	255	255	255	255	255
24	255	255	255	255	255	255	255	255	255	255	255	255	255	255
25	255	255	255	255	255	[illegible]	255	255	255	255	[illegible]	255	[illegible]	255

Fig. 7. Intraclass Variation of Keys.

H. Outlier Elimination

Outliers are patterns in the data which is not defined with the actual range of data values. Outliers are classified as point Outliers and contextual outliers based on the distribution of data points. The individual data, which is identified as distinct compared to rest of data, the instance is known as point outlier. If the data is distinct to a specific context then the data is a conditional outlier (or contextual outlier). The specific context is referred as either contextual attributes or behavioural attributes.

Outlier Detection using Indegree Number (ODIN) is the one of the outlier detection scheme proposed by Hautamaki et al. [52] that works based on local density. ODIN method is generally used for cluster thinning by removing vectors that are overlapping with other regions. Overlapping between clusters happen with the assumption that the regions are of low density. All the higher density regions grouped near the cluster centroid. The outlyingess of x_i is given in equation (27).

$$OL_i = \frac{1}{ind\,(x_i) + 1} \tag{27}$$

where "$ind(x_i)$ is the indegree of the vertexx_i, i.e. the number of edges pointing to x_i".

The outlyingness factor for each vector by finding the minimum distance to centroid dmax as shown in the equation (28).

$$d_{\max} = \max_i \{\|\boldsymbol{x}_i - \boldsymbol{c}_{p_i}\|\}, \quad i = 1, \ldots, N \tag{28}$$

The outlyingess of x_i is given in equation (29),

$$o_i = \frac{\|\boldsymbol{x}_i - \boldsymbol{c}_{p_i}\|}{d_{\max}} \tag{29}$$

where x_i is the vector, c_p is the centroid and d_max is the distance. The factors that are responsible for an outlier, in the dataset are normalized to the scale [0, 1]. The vector with greater value is considered as an outlier. The proposed system uses Interquartile Range technique as shown in Fig. 8. The outliers in the key generated are calculated by considering, that the outliers lie either on the first quarter or on the last quarter of the given data after sorting the key values. The final key generated is shown in Fig. 9. The steps followed are

Step 1: The point furthest from the mean of data is calculated.

Step 2: IQR is calculated by finding the difference between the mean of the upper quartile(q2) and mean of the lower quartile(q1).

Step 3: The fence is calculated using the formula, F=1.5 * IQR

Step 4: Lower bound and upper bound are calculated.

LB=q1 – F, UB=q2+F

Step 5: The values between the lower bound and upper bound are accepted for the final key.

Step 6: The accepted key size should not exceed 128 bits. If the size of the key is greater than 128 bits, steps 3 to step 5 are repeated.

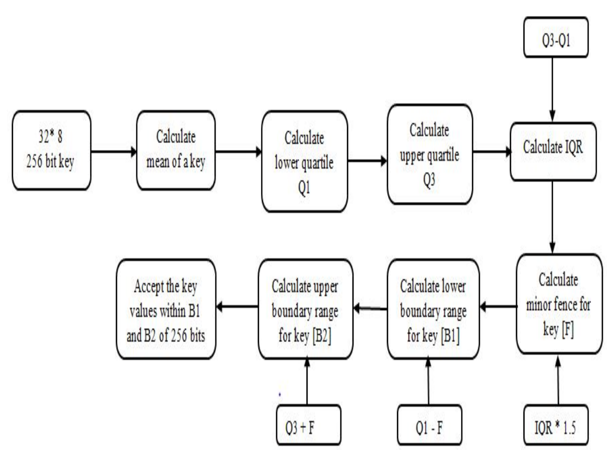

Fig. 8. Outlier Elimination.

Algorithm 3: Outlier elimination

1: Upper quartile(Q2) and lower quartile(Q1) are calculated using the given formula,

$$Q1 = \frac{1}{16}\Sigma_{1=1}^{16} k_i$$

$$Q2 = \frac{1}{16}\Sigma_{i=17}^{32} k_i$$

2: Inter Quartile Range is calculated using Q1 and Q2 $IQR = Q2 - Q1$

3: Upperbound(UB) and lower bound(LB) are calculated,

$$\mathrm{LB} = \mathrm{Q1} - \mathrm{F}, \mathrm{UB} = \mathrm{Q2} + \mathrm{F}$$

4: The values between the upperbound and lowerbound are considered for Final key is LB <= Key <= UB

5: **if** *Final key* > 128 *bits* **then**

    Repeat Step 2 to 4 till the key is 128 bits

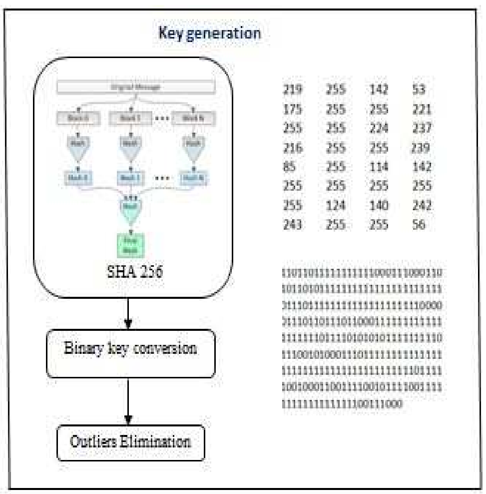

Fig. 9. Final Key.

I. Feature Extraction using CNN

ResNet increases the seed of training the deep networks, reduces the number of parameters by increasing the depth of the networks instead of widening the network, helps to vanish Gradient problem and gives high accuracy in network performance.

During the training period some neuron can die and cause information loss which is known as Gradient problem. The above problem is rectified by using residual network, by mapping non-linear function H(x) to F(x) which is defined as H(x) – x. The output of the second layer adds F(x) to x and carries important information to the next layer (Relu). Therefore, information loss is reduced and no gradient problem in ResNet. Increasing the depth of the network may result in bias problem but ResNet avoids negative outcomes, increases accuracy, fast training of the network while the network depth increases. ResNet is classified in to three models, 50, 101, 152 based on the depth of networks. The feature extraction analysis using CNN for Resnet50 network is shown in Fig. 12.

Algorithm 4: CNN Feature Extraction

1: Multimodal sample images are read
2: The sample images are divided for testing and training
3: The pre-trained ResNet-50 network is loaded
4: Features are extracted from the deeper layer of a pre-trained network
5: The training features are used to train the classifier
6: The accuracy level is calculated

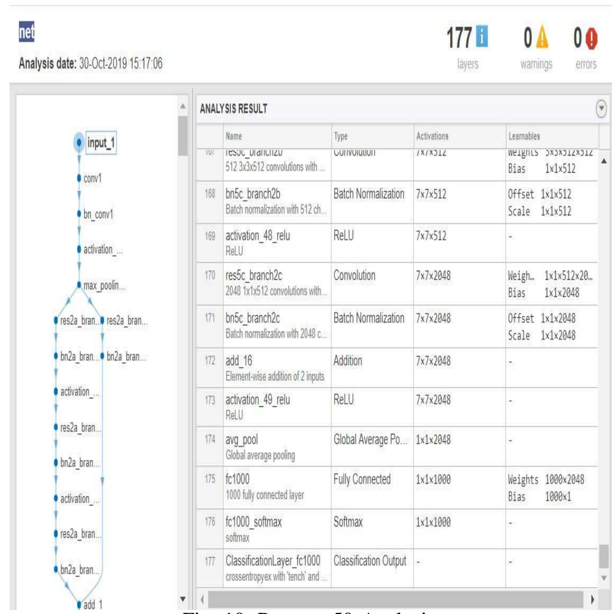

Fig. 10. Resenet 50 Analysis.

J. Key Binding Technique

The feature extraction is performed using Resnet 50 CNN as shown in Fig. 10. The training features are extracted for both the traits and fused using additive operation to get the original vector. The generated key of the respective trait is embedded with the original vector using random permutation function. The permutation function used is randi which returns the array of integers from discrete uniform distribution on the given interval. $X = \mathrm{randi}\left(\left[\mathrm{imin}_{\alpha}\, 1\, \mathrm{max}\right], \mathrm{sz}\, 1, \mathrm{szn}\right)$ Random positions are generated with respect to the key size in the original template vector. Now the random position values are replaced with the key value. Final image is the key embedded within the template as shown in Fig. 11. The steps followed for key binding are,

Step 1: Original fused vector of face and fingerprint is loaded.

Step 2: Random positions are generated using permutation function.

Step 3: The key values are replaced to the random positions of the original vector.

Step 4: The key is now embedded with the biometric template.

Algorithm 5: Key binding

1: V - Original vector, imin, imax - min and max position of V, SZ1,SZN - min and max position of Key, K - Key
2: index = randi([imin,imax], SZ1,SZN)
3: V(index) = K
4: New vector (NV) = embedded image

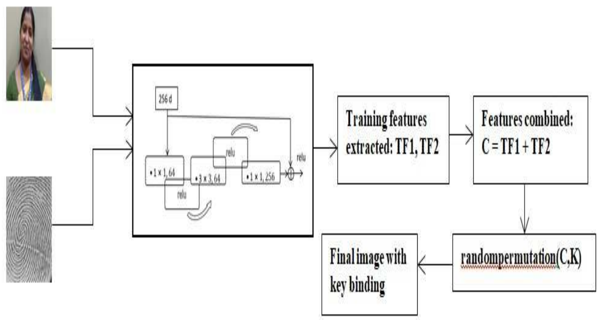

Fig. 11. Key Binding.

VIII. Security Analysis for Key

A. Key-Space Analysis

The iterative procedure of checking all possible keys to find the decryption key is known as Key space analysis. The proposed system ensures that the key generated is 256-bit hash value and reduce to 192 bits, which handles Brute force attack effectively.

B. Key Sensitivity Analysis

The perfect image encryption key should be sensitive so that the key will be highly secured and inaccessible by hackers easily. The minor change in initial parameter of the chaotic system will alter the entire key because of which the generated key in our proposed system is highly sensitive. A small change in the parameter results in a large variation in the encryption process. The variation measures the sensitivity of the generated key.

C. Statistical Analysis

Statistical analysis measures the performance of image encryption system. The encrypted image histogram is different from the original image histogram so that the hacker will not be able to get the original image through encrypted image histogram.

D. Pixel Correlation Analysis

The adjacent pixels correlation in both original and the encrypted image either horizontally or vertically or diagonally is known as correlation co-efficient analysis as shown in equation (30). When the similarity between the original and encrypted image is less, then the value of correlation coefficient is low. The values obtained by calculating Correlation coefficient shows that the system is capable of handling statistical attacks. Table VI gives the correlation values of the proposed system with the existing techniques.

$$r = \frac{\sum_m \sum_n \left(A_{mn} - \overline{A}\right)\left(B_{mn} - \overline{B}\right)}{\sqrt{\left(\sum_m \sum_n \left(A_{mn} - \overline{A}\right)^2\right)\left(\sum_m \sum_n \left(B_{mn} - \overline{B}\right)^2\right)}} \tag{30}$$

where $\overline{A} = \text{mean}\,2(A),$ and $\overline{B} = \text{mean}\,2(B)$

TABLE VI. Correlation Analysis

Image	Reference	Correlation
Pepper	Ref.1	0.2650
Lena	Ref.2	0.0214
Lena	Ref.3	0.0015
Lena	Ref.5	-0.0012
Lena	Proposed system	-0.0044

1) Differential Analysis: The sensitivity of the encrypted image is determined by Differential analysis. Minor variation in the original image gives more impact on the encrypted image. “Number of pixels changed between the original and the encrypted image is calculated using NPCR [number of pixels change rate]”. It gives the ratio of the two encrypted images when there is a slight variation in the input image. NPCR is calculated as given in equation (31). Table VII gives the NPCR analysis of the proposed system with the existing techniques.

$$NPCR = \frac{\sum_{i,j} D(i,j)}{M * N} * 100 \tag{31}$$

Where, “D is the auxiliary matrix which is created when $C1(i,j) = C2(i,j), then D(i,j) = 0$, otherwise D(i,j) = 1”.

TABLE VII. NPCR Analysis

Image	Reference	NPCR
Pepper	Ref.1	99.62
Lena	Ref.2	99.60
Lena	Ref.7	99.48
Lena	Ref.5	99.50
Lena	Proposed system	99.51

The calculation of the average intensity between the same cipher images is known as “unified average change intensity [UACI]”. When the values are high, the parameters shows that the minor variation in original image gives more impact in encrypted image. UACI is calculated as given in equation (32). Table VIII gives the UACI analysis of the proposed system with the existing techniques.

$$UACI = 1/(MxN)[(i=0)^(M-1)(i=0)^(N-1)|C_1(i,j) \\ -C_2(i,j)|/255]100 \tag{32}$$

TABLE VIII. UACI Analysis

Image	Reference	UACI
Pepper	Ref.1	34.26
Lena	Ref.2	33.44
Lena	Ref.7	28.45
Lena	Ref.5	35.65
Lena	Proposed system	33.16

2) MSE: The mean square error value between the decrypted image(I_2) and plain image (I_1). If there is more data loss the value is high or the value is low. The formula is given in equation (33).

$$MSE = 1/(MxN)(i=1)^M(J=1)^N I_1(i,j) - I_2(i,j)^2 \tag{33}$$

3) PSNR: "PSNR [Peak Signal to Noise Ratio] is used to test the quality of the attacked encrypted image". The formula is calculated as given in equation (34).

$$PSNR = 10xlog_10((255x255)/MSE)(dB) \tag{34}$$

E. Information Entropy Analysis

The robustness of encrypted image is verified by information entropy analysis. For an image, 8 bit length random system is generated and entropy of both images are calculated as given in equation (35). When the "Entropy value of cipher image is approximately 8 then the system is proved to be resistant to entropy analysis".

$$H(x) = -(i=1)^n(x_(i)logp(x_(i)) \tag{35}$$

Where, "x is a set of symbols, n is the total number of symbols, $x_(i)\epsilon x, p(x_(i))$is the probability of $x(i)$in x". Table IX gives the entropy value of the proposed system with the existing techniques.

TABLE IX. ENTROPY ANALYSIS

Image	Reference	Entropy
Pepper	Ref.1	7.9993
Lena	Ref.2	7.9993
Lena	Ref.3	7.9994
Lena	Ref.5	7.9982
Lena	Proposed system	7.7795

F. Time Analysis of Key Binding Technique

Biometric template of 80MB size is considered for the experiment. Result shows that the time taken for key binding of several template varies from 40ms to 58ms as shown in Fig. 12.

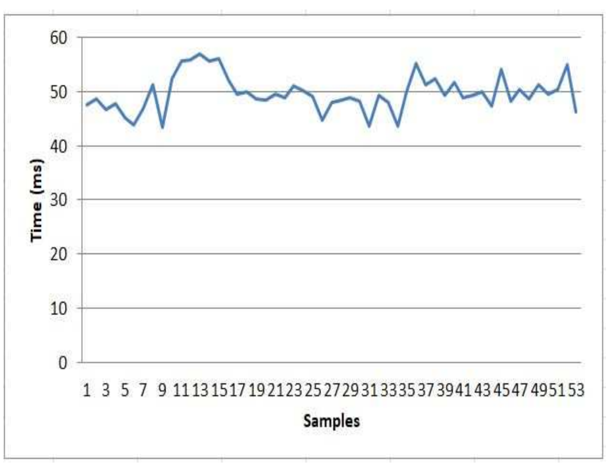

Fig. 12. Time Taken for Key Binding.

IX. CONCLUSION AND FUTURE WORK

An innovative algorithm has been proposed for key generation and key binding. Results prove that the key generated is highly secured as intraclass variations are applied to remove outliers and takes less time for key binding. The proposed system uses chaotic, DNA and CNN concepts and implemented using Matlab R2019b. The database used is SDUMLA-HMT which is a multimodal biometric of face and fingerprint with 106 traits of 96 samples each. The above work can be enhanced for touchless real-time biometric samples and measure the performance of the system.

ACKNOWLEDGMENT

I like to thank School of computer science and technology, Shandong university for providing multimodal biometric database SDUMLA-HMT for my experiment.

REFERENCES

[1] C.-C. Lee, C.-T. Chen, P.-H. Wu, and T.-Y. Chen, "Three-factor control protocol based on elliptic curve cryptosystem for universal serial bus mass storage devices," *IET Computers & Digital Techniques*, vol. 7, no. 1, pp. 48–55, 2013.

[2] D. G. Martínez, F. J. G. Castano, E. A. Rúa, J. L. A. Castro, and D. A. R. Silva, "Secure crypto-biometric system for cloud computing," in *2011 1st International Workshop on Securing Services on the Cloud (IWSSC)*. IEEE, 2011, pp. 38–45.

[3] M. Upmanyu, A. M. Namboodiri, K. Srinathan, and C. Jawahar, "Blind authentication: a secure crypto-biometric verification protocol," *IEEE transactions on information forensics and security*, vol. 5, no. 2, pp. 255–268, 2010.

[4] V. Matyáš and Z. Říha, "Security of biometric authentication systems," in *2010 International Conference on Computer Information Systems and Industrial Management Applications (CISIM)*. IEEE, 2010, pp. 19–28.

[5] M. Rahman and P. Bhattacharya, "Remote access and networked appliance control using biometrics features," *IEEE Transactions on Consumer Electronics*, vol. 49, no. 2, pp. 348–353, 2003.

[6] A. K. Jain and K. Nandakumar, "Biometric authentication: System security and user privacy." *IEEE Computer*, vol. 45, no. 11, pp. 87–92, 2012.

[7] Y. J. Lee, K. R. Park, S. J. Lee, K. Bae, and J. Kim, "A new method for generating an invariant iris private key based on the fuzzy vault system," *IEEE Transactions on Systems, Man, and Cybernetics, Part B (Cybernetics)*, vol. 38, no. 5, pp. 1302–1313, 2008.

[8] A. K. Jain, L. Hong, and Y. Kulkarni, "A multimodal biometric system using fingerprint, face and speech," in *2nd Int'l Conf. AVBPA*, vol. 10, 1999.

[9] R. Ang, R. Safavi-Naini, and L. McAven, "Cancelable key-based fingerprint templates," in *Australasian conference on information security and privacy*. Springer, 2005, pp. 242–252.

[10] C. Rathgeb and A. Uhl, "A survey on biometric cryptosystems and cancelable biometrics," *EURASIP*

Journal on Information Security, vol. 2011, no. 1, p. 3, 2011.

[11] R. Guesmi, M. A. B. Farah, A. Kachouri, and M. Samet, "A novel chaos-based image encryption using dna sequence operation and secure hash algorithm sha-2," *Nonlinear Dynamics*, vol. 83, no. 3, pp. 1123–1136, 2016.

[12] P. Zhen, G. Zhao, L. Min, and X. Jin, "Chaos-based image encryption scheme combining dna coding and entropy," *Multimedia Tools and Applications*, vol. 75, no. 11, pp. 6303–6319, 2016.

[13] K.-A. Toh, W.-Y. Yau, and X. Jiang, "A reduced multivariate polynomial model for multimodal biometrics and classifiers fusion," *IEEE Transactions on Circuits and Systems for Video Technology*, vol. 14, no. 2, pp. 224–233, 2004.

[14] T. B. Long, T. Hanh *et al.*, "Multimodal biometric person authentication using fingerprint, face features," in *Pacific Rim International Conference on Artificial Intelligence*. Springer, 2012, pp. 613–624.

[15] L. Liu, S. Miao, H. Hu, and M. Cheng, "N-phase logistic chaotic sequence and its application for image encryption," *IET Signal Processing*, vol. 10, no. 9, pp. 1096–1104, 2016.

[16] K. Radhika and M. Nalini, "Biometric image encryption using dna sequences and chaotic systems," in *2017 International Conference on Recent Advances in Electronics and Communication Technology (ICRAECT)*. IEEE, 2017, pp. 164–168.

[17] H. Ren, J. Wang, and Q.-H. Wang, "An image encryption scheme of logistic modulation using computer-generated hologram and chaotic map," *Journal of Electrical and Computer Engineering*, vol. 2018, 2018.

[18] B. Awdun and G. Li, "The color image encryption technology based on dna encoding & sine chaos," in *2016 International Conference on Smart City and Systems Engineering (ICSCSE)*. IEEE, 2016, pp. 539–544.

[19] A. Girdhar and V. Kumar, "A rgb image encryption technique using lorenz and rossler chaotic system on dna sequences," *Multimedia Tools and Applications*, vol. 77, no. 20, pp. 27 017–27 039, 2018.

[20] J. Zhang, D. Hou, and H. Ren, "Image encryption algorithm based on dynamic dna coding and chens hyperchaotic system," *Mathematical Problems in Engineering*, vol. 2016, 2016.

[21] Y. Abanda and A. Tiedeu, "Image encryption by chaos mixing," *IET Image Processing*, vol. 10, no. 10, pp. 742–750, 2016.

[22] X. Wang, X. Zhu, and Y. Zhang, "An image encryption algorithm based on josephus traversing and mixed chaotic map," *IEEE Access*, vol. 6, pp. 23 733–23 746, 2018.

[23] L. Liu, S. Hao, J. Lin, Z. Wang, X. Hu, and S. Miao, "Image block encryption algorithm based on chaotic maps," *IET Signal Processing*, vol. 12, no. 1, pp. 22–30, 2017.

[24] M. Ahmad, M. Doja, and M. S. Beg, "Security analysis and enhancements of an image cryptosystem based on hyperchaotic system," *Journal of King Saud University-Computer and Information Sciences*, 2018.

[25] Y. Li, C. Wang, and H. Chen, "A hyper-chaos-based image encryption algorithm using pixel-level permutation and bit-level permutation," *Optics and Lasers in Engineering*, vol. 90, pp. 238–246, 2017.

[26] T. Li, M. Yang, J. Wu, and X. Jing, "A novel image encryption algorithm based on a fractional-order hyperchaotic system and dna computing," *Complexity*, vol. 2017, 2017.

[27] X. Zhang, Z. Zhou, and Y. Niu, "An image encryption method based on the feistel network and dynamic dna encoding," *IEEE Photonics Journal*, vol. 10, no. 4, pp. 1–14, 2018.

[28] Y. Tian and Z. Lu, "Novel permutation-diffusion image encryption algorithm with chaotic dynamic s-box and dna sequence operation," *AIP Advances*, vol. 7, no. 8, p. 085008, 2017.

[29] X. Li, C. Zhou, and N. Xu, "A secure and efficient image encryption algorithm based on dna coding and spatiotemporal chaos." *IJ Network Security*, vol. 20, no. 1, pp. 110–120, 2018.

[30] Y. Zhang, "Test and verification of aes used for image encryption," *3D Research*, vol. 9, no. 1, p. 3, 2018.

[31] S. Chakraborty, A. Seal, M. Roy, and K. Mali, "A novel lossless image encryption method using dna substitution and chaotic logistic map," *International Journal of Security and Its Applications*, vol. 10, no. 2, pp. 205–216, 2016.

[32] X.-Q. Fu, B.-C. Liu, Y.-Y. Xie, W. Li, and Y. Liu, "Image encryption-then-transmission using dna encryption algorithm and the double chaos," *IEEE Photonics Journal*, vol. 10, no. 3, pp. 1–15, 2018.

[33] X. Chai, X. Zheng, Z. Gan, D. Han, and Y. Chen, "An image encryption algorithm based on chaotic system and compressive sensing," *Signal Processing*, vol. 148, pp. 124–144, 2018.

[34] X. Wu, K. Wang, X. Wang, H. Kan, and J. Kurths, "Color image dna encryption using nca map-based cml and one-time keys," *Signal Processing*, vol. 148, pp. 272–287, 2018.

[35] G. Maddodi, A. Awad, D. Awad, M. Awad, and B. Lee, "A new image encryption algorithm based on heterogeneous chaotic neural network generator and dna encoding," *Multimedia Tools and Applications*, vol. 77, no. 19, pp. 24 701–24 725, 2018.

[36] C. Fu, G.-y. Zhang, M. Zhu, Z. Chen, and W.-m. Lei, "A new chaos-based color image encryption scheme with an efficient substitution keystream generation strategy," *Security and Communication Networks*, vol. 2018, 2018.

[37] H. M. Al-Mashhadi and I. Q. Abduljaleel, "Color image encryption using chaotic maps, triangular scrambling, with dna sequences," in *2017 International Conference on Current Research in Computer Science and Information Technology (ICCIT)*. IEEE, 2017, pp. 93–98.

[38] X. Chai, Z. Gan, K. Yuan, Y. Chen, and X. Liu, "A novel image encryption scheme based on dna sequence operations and chaotic systems," *Neural Computing and Applications*, vol. 31, no. 1, pp. 219–237, 2019.

[39] O. M. Al-Hazaimeh, M. F. Al-Jamal, N. Alhindawi, and A. Omari, "Image encryption algorithm based on lorenz chaotic map with dynamic secret keys," *Neural Computing and Applications*, pp. 1–11, 2017.

[40] C. Szegedy, V. Vanhoucke, S. Ioffe, J. Shlens, and Z. Wojna, "Rethinking the inception architecture for computer vision," in *Proceedings of the IEEE conference on computer vision and pattern recognition*, 2016, pp.

2818–2826.

[41] G. Huang, Z. Liu, L. Van Der Maaten, and K. Q. Weinberger, “Densely connected convolutional networks,” in *Proceedings of the IEEE conference on computer vision and pattern recognition*, 2017, pp. 4700–4708.

[42] K. Simonyan and A. Zisserman, “Very deep convolutional networks for large-scale image recognition,” *arXiv preprint arXiv:1409.1556*, 2014.

[43] Y. LeCun, L. Bottou, Y. Bengio, P. Haffner *et al.*, “Gradient-based learning applied to document recognition,” *Proceedings of the IEEE*, vol. 86, no. 11, pp. 2278–2324, 1998.

[44] A. Krizhevsky, I. Sutskever, and G. E. Hinton, “Imagenet classification with deep convolutional neural networks,” in *Advances in neural information processing systems*, 2012, pp. 1097–1105.

[45] C. Szegedy, W. Liu, Y. Jia, P. Sermanet, S. Reed, D. Anguelov, D. Erhan, V. Vanhoucke, and A. Rabinovich, “Going deeper with convolutions,” in *Proceedings of the IEEE conference on computer vision and pattern recognition*, 2015, pp. 1–9.

[46] S. Zagoruyko and N. Komodakis, “Wide residual networks,” *arXiv preprint arXiv:1605.07146*, 2016.

[47] K. He, X. Zhang, S. Ren, and J. Sun, “Identity mappings in deep residual networks,” in *European conference on computer vision*. Springer, 2016, pp. 630–645.

[48] S. Xie, R. Girshick, P. Dollár, Z. Tu, and K. He, “Aggregated residual transformations for deep neural networks,” in *Proceedings of the IEEE conference on computer vision and pattern recognition*, 2017, pp. 1492–1500.

[49] K. Zhan, D. Wei, J. Shi, and J. Yu, “Cross-utilizing hyperchaotic and dna sequences for image encryption,” *Journal of Electronic Imaging*, vol. 26, no. 1, p. 013021, 2017.

[50] M. Kumar, A. Iqbal, and P. Kumar, “A new rgb image encryption algorithm based on dna encoding and elliptic curve diffie–hellman cryptography,” *Signal Processing*, vol. 125, pp. 187–202, 2016.

[51] W. Zheng, F.-Y. Wang, and K. Wang, “An acp-based approach to color image encryption using dna sequence operation and hyper-chaotic system,” in *2017 IEEE International Conference on Systems, Man, and Cybernetics (SMC)*. IEEE, 2017, pp. 461–466.

[52] V. Hautamäki, S. Cherednichenko, I. Kärkkäinen, T. Kinnunen, and P. Fränti, “Improving k-means by outlier removal,” in *Scandinavian Conference on Image Analysis*. Springer, 2005, pp. 978–987.

Evaluation of Routing Protocols and Mobility in Flying Ad-hoc Network

Emad Felemban
College of Computer & Information Systems,
Umm Al-Qura University, Makkah, Saudi Arabia

Abstract*—The ability of dynamic reconfigurability, quick response and ease of deployment has made Unmanned Aerial Vehicles (UAVs), a paramount solution in several areas such as military applications. Flying ad-hoc network (FANET) is a network of UAVs connected wirelessly and configured continuously without infrastructures. Routing on its own is not significant, but the mobility sequence of a UAV in FANETs is a more significant factor and an interesting research topic. The routing protocols gives us a certain and better perception of routing structure for FANETs. In this paper, routing protocols such as Ad-hoc On-Demand Vector (AODV), Dynamic Source Routing (DSR), Temporally Ordered Routing Algorithm (TORA), Geographic Routing Protocol (GRP) and Optimized Link State Routing (OLSR) are compared using performance parameters such as number-of-hops, packet loss ratio, throughput, end-to-end delay and throughput. The mobility models like Pursue Mobility Model (PRS), Semi-Circular Random Movement (SCRM), Manhattan Grid Mobility Model (MGM) and Random Waypoint Mobility (RWPM). The evaluation is carried out with three scenarios including one sender node and one receiver node, all senders one receiver and all senders all receivers are considered for above protocols and mobility models. For all evaluation scenarios, the performance of OLSR is the most efficient among the five routing protocols under four different performance parameters due to its proactive nature which makes the routing information up to date with the help of MPR (Multi Point Relay) in the network, resulting in the reduction of routing overhead in the network.

Keywords*—Flying ad-hoc network (FANET); mobility models; adhoc routing protocols; OPNET; Unmanned Aerial Vehicles (UAVs)

I. Introduction

Current development in UAVs is offering different opportunities at reasonable price. As a result, the ability of dynamic reconfigurability, quick response and ease of deployment has enabled UAVs to be a paramount solution in several applications [1][2]. Although UAVs are advantageous, high mobility is essential for the networks which need adequate control over UAVs. FANETs belong to an important class of UAVs, where many UAVs are connected in ad-hoc manner. UAV networking was given a new terminology due to modernization of Internet of Things (IoT), but it has the same functioning as Internet of Drones (IoD) shown in Fig. 1. IoD is a layered network control architecture for coordinating unmanned aerial vehicles to control airspace for navigation services.

As opposed to the traditional (MANET), the main feature of FANET is the highly dynamic scenario, which signifies that nodes move in higher mobility and in the meantime the network topology changes more quickly, so protocols under such circumstances are more challenging.The main advantage of the FANET networks is not to depend on a physical infrastructure; each node will be able to access the nodes through its closer resources, trusting the cooperation and collaboration of the other nodes and this get through them to their destination. Typical examples are applications that range from networks in the armed forces, to the applications of business, to reach the applications in case of natural disaster or terrorist acts. FANET network will offer services like absence of centralization, ability to configure networks automatically, 3D mobility, ability to exploit the resources of a working group and comfort. The important research concerns are whether MANET routing protocols are suitable for FANET, which performs better in high dynamic scenarios and the effect of nodes mobility on network performance.

The stability of Ad-Hoc networks [4] is compromised due to inadequate protocols. We can achieve improved efficiency in the passage of information in time and quality but achieving transparency is challenging. The end user does not have to make a different connection type according to the type of network (fixed or mobile) to extend them to a greater number of users [5]. In addition, due to wireless and dynamic nature of Ad-hoc networks, there is packet loss due to transmission error.

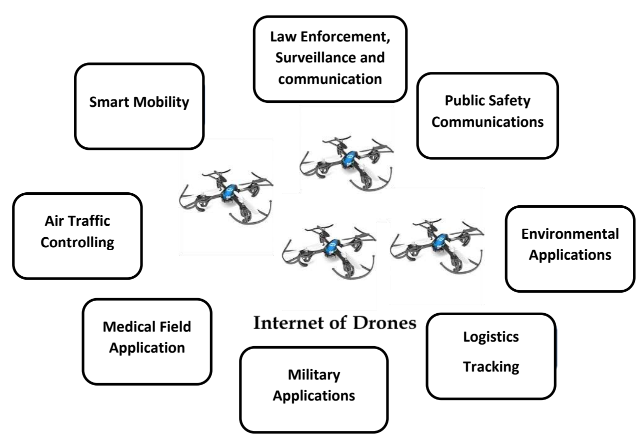

Fig. 1. A Summary of Internet of Drones (IoD) Application Services [3].

FANETs are a group of UAVs that can perform the different functions without human service. It is a network without infrastructure that has an autonomous set of mobile nodes that collaborate together to share information [6]. These mobile nodes can be constituted in any network topology as router through wireless communication. It has the ability to connect to the Internet or the cellular wireless network [7]. Each device in a FANET has the freedom to fly freely in all directions and it can alter its connections to other nodes constantly. Each node must forward traffic not related to itself. Consequently, and because of this it can function as a router [8]. FANET topology continues to change due to the mobility of the UAVs, it make them less secure networks. To overcome the threats it is crucial to use some security technologies in the network. For an ad-hoc network, not every node could be within the transmission reach between them, therefore nodes are compelled to forward network traffic on behalf of other nodes. For instance, we can contemplate a simple scenario, two nodes, a sender node (S) sends data to the destination node (D), which is three jumps away, and the data traffic will arrive at its destination. The procedure of forwarding network traffic from sender to destination is called routing. FANETs can assist networks which are operated to enable wireless connectivity in the places where deployment of physical infrastructure is hard or costly.

During the research in modeling FANET networks, it was possible to verify the importance of protocol evaluation. There is a need to model FANETs and analyze the performance of proactive and reactive routing protocols. Due to several applications, FANETs have captivated several research institutions and automotive industries. The main problem is the implementation of a proper routing mechanism as the result of various issues. Routing on its own is not significant, but the mobility sequence of a UAV in FANETs is also a more significant factor. Ad-Hoc routing protocols are categorized into many different classifications, one of which is topology based. It is analyzed that these routing protocols gives us a better perception for routing structure of FANETs. The evaluation of routing protocols is required using different mobility models for FANETs.

The main objective of this paper is to introduce FANETs and compare existing routing protocols (OLSR, AODV, DSR, TORA and GRP) and mobility models (RWPM, MGM, SCRM and PRS) for FANETs. The performance parameters include end to end delay, packets loss ratio, number of hops and throughput. The affect of speed over network performance is also evaluated. The rest of the paper is organized as follows. A detailed literature review is provided for routing protocols and mobility models in Section II. The Section III comprises of performance evaluation. Section IV draws conclusion with future work.

II. Literature Review

Wireless networks are formed by connecting radio transmitters to electronic devices (computers, smartphones, balloons, drones, etc.), with the support of a central access point to manage the network. Wireless standards include detailed requirements for the data link layer, physical layer and medium access control (MAC) regarding terminology introduced by IEEE 802.11 standards. There are many essential characteristics of wireless networks including high mobility, flexible communication system, simplicity and scalability.

Generally, The wireless network is divided in two classes based on their infrastructure as can be seen in Fig. 2. A network that has fixed base stations is called infrastructure-based network. These networks accommodate coordination among the mobile UAVs [9]. Infrastructure-less networks does not have any well defined infrastructure. They are a group of dynamically situated UAVs that keep the interconnections among UAVs by changing topology.

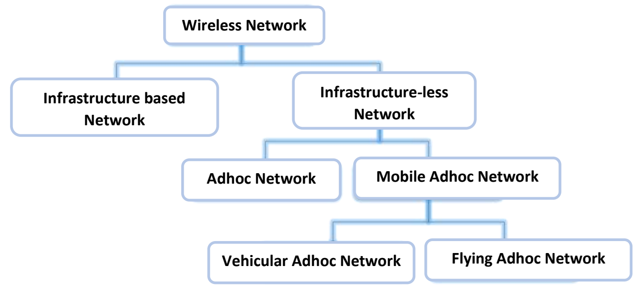

Fig. 2. Wireless Network Classifications.

The background of Ad-Hoc networks is related to the creation of the PRNET (Packet Radio Network) by the DoD (US Department of Defense) in 1972. The aim was to connect a network of computers to provide packet exchanges to mobile elements used in the battlefield e.g soldiers, aircraft, etc. The current proliferation of portable devices and the diffusion of wireless technology have permitted ad-hoc wireless networks to thrive. Moreover, interest in communication among ad-hoc wireless networks has raised consistently [9]. Ad-hoc network can be formed when you want to exchange data in the absence of a centralized access point (access point): the network is formed “spontaneously”. The advantage of being free from any infrastructure constraints helps these networks in obtaining an intrinsic ease and speed for installation [10]. Each node of ad-hoc network can act as a router. A node, instead of directly sending the packets to the recipient node, can route the packets to another node within its radio visibility.

In air-to-air wireless communications, UAVs are connected to each other in ad-hoc manner. These UAVs are independent of any restriction on transmission ranges between them [14]. In air-to-ground-wireless communications, UAVs can extend their connectivity by communicating with infrastructures and improve quality of service [15]. In this paper, we have focused on air-to-air communication i.e infrastructure-less protocols. MANETs are a self-configuring infrastructure-less network [9]. Each device can relocate without restriction within network. Vehicular Ad-Hoc network is a derived class from MANETs (As shown in Table I). In VANET, vehicles are connected via wireless communication. VANET is a distributed and self-formation network [11]. VANET can create new systems to provide safety and comfort in toll-tax payment to save time. FANETs can be described as a group of Unmanned Aerial Vehicles, which communicate with each other without the need of any access point, while at least one among the group acts as the server or satellite. These are automated systems, which don’t involve any human input for their basic operations [12]. All activity of the network including the discovery of its topology or the sending of messages is carried out by the nodes that integrate it. This type of network has arbitrary topology. The main consequence of this mobility is that links can be formed and broken frequently, which implies that the network

TABLE I. THE MAIN DIFFERENCES BETWEEN MANETS, VANETS, AND FANETS [13]

Types Parameters	MANET	VANET	FANET
Node Mobility	Low Compactness	Medium Compactness	High Compactness
Mobility Model	Random	Regular	Regular for pre determined paths
Node Density	Low	Medium	Very Low
Topology Change	Slow	Average Speed	Fast
Radio Propagation Model	Near to earth (2D)	Near to earth (2D)	Over to earth (3D)
Power Consumption	Energy efficient protocols	Not required	Energy efficacy for mini UAV & small UAVs
Computat ional Power	Limited	Above average	Above average

must be self-organized. The path between an origin and a certain destination that crosses several intermediate nodes can be modified and When this happens, the network must be able to re-organize itself to establish new path in least possible time. This functionality requires that each member of the network will be able to forward data on behalf of other members act as a router. The nodes of a FANET network have components or associated factors that must be considered when carrying out an efficient routing. These factors include auto configuration, bandwidth, distance, energy, routing path, partitions/unions, speed and variation in the routing path. The FANET networks are based on the concept of Peer-to-Peer (P2P) where peers are mostly UAVs.

The routing protocols can be classified into five major categories including static routing, position-based routing and Hierarchical routing, position-based routing, swarm-based routing, hierarchical routing and topology-based routing. Static routing protocols follow a static routing table loaded in the UAV's during the mission which cannot be changed further. The protocols cannot update the table dynamically in case of failure so they are not suitable for dynamic networks. Static protocols are further categorized in swarm intelligence and topology based routing protocols. Swarm based routing protocols are inspired from behavior of natural organisms. The algorithm in swarm intelligence is motivated by the behavior of different insects such as ants, bees, fireflies and fish etc. Swarm intelligence based algorithms offer efficient solutions for UAVs. The authors in [17] [18] presents Bee Ad-Hoc and APAR. Position based routing protocols establish route between UAVs using their geographical locations. Each UAV can use either hierarchical position, grid position or reactive position service. The examples include Delay Tolerant (DTN), Non-DTN and Heterogeneous Protocols [19]. The hierarchical protocols are other set for routing solution for FANET, which are founded in accordance with addressing the network scalability problem where the network contains of numerous clusters of different mission zones. The hierarchical protocols for FANET include clustering algorithm and mobility prediction clustering. In the clustering algorithm the network includes over many clusters. Every cluster has a cluster head (CH). All nodes in the cluster can directly communicate with cluster head. This type of model may generate improved performance of outcomes when the number of UAVs is higher and the mission range is large [20]. The mobility prediction algorithm can solve this issue by making cluster updates frequently. It uses a tree structured prediction algorithm [21].

The topology-based routing protocols are classified into reactive, proactive and hybrid routing. Reactive Routing is suitable for FANETS in the discovery of a path between nodes which is unavailable for UAVs. This kind of routing also leads to high latency. Multicast Ad hoc On-Demand Distance Vector (M-AODV) is an example of reactive routing [16]. Proactive routing tables are constantly shared periodically among nodes to assure availability of routing paths among UAVs. For example OLSR, Directional Optimized Link State Routing Protocol (D-OLSR), Cartography Enhanced OLSR (CE-OLSR) and DSDV [16] belong to this category. Hybrid routing solves the high latency problem of reactive protocols. The examples of this type are Hybrid Wireless Mesh Protocol (HWMP), GRP and TORA.

This paper is committed to the most critical topology-based routing protocols recommended for FANETs namely AODV, DSR, TORA, GRP and OLSR. AODV was introduced as an evolution of DSDV. It deals with sequence numbers and routing tables. It also provides on-demand routing as it saves information of nodes that intervene in data transmission. This protocol keeps all routes in cache memory when they are required and discard them when they are not needed [22] [23].

The DSR protocol follows routing at source. The nodes having a destination maintains cache to save list of nodes in this path. The methods such as detection and route maintenance are responsible to provide updates as new routes are learnt. It has on demand features but it is not table-driven. The UAV sends a packet to specify the route. The entire path information is put in the packet by the source [23]. It differs from table-driven and link-state routing. It collects the addresses of all the middle nodes between itself and the desired destination when finding routes.

The TORA protocol follows link reversal routing. It maintains a directed graph from source to destination without presence of any cycle. The network load is minimized in TORA and it keeps the shortest route. It is considered an efficient protocol because it does not saturate network traffic unnecessarily [25] [26]. If a node wants to know the path to destination, it will broadcast a query packet that propagates until it reaches a node having path to destination or the recipient node. The responding node is served by a User Datagram Protocol (UDP) that will add its weight and broadcasts it to allow all intermediate nodes to know about this modification.

GRP detects the location of nodes using global positioning system to obtain information about network. The route is discovered by source node and transfers data from source to destination using route. This concept is referred as hybrid routing protocol. There are several methods to find out the location of network nodes such as GPRS and GPS, etc. [24]. The transmission in this protocol is dependent on the neighbors located at one hop distance and destination node. The data is forwarded using greedy forwarding and face-2

TABLE II. FANET APPLICATIONS USING DIFFERENT MOBILITY MODELS [13].

Application Class	Mobility Model	Scenario Description
Search and rescue	MGM SRCM RWPM	Random exploration on a definite target zone. Scanning in a circular area Each UAV chooses the scan pattern in random location
Traffic and urban monitoring	MGM SRCM	Surveillance of city roads Patrolling of a crash event before the rescue team reaches
Survey and Patrolling	SRCM	Surveillance of a target
Target tracking	Pursue (PRS)	Crime tracking Pursuing of a critical moving target
SRCM: Semi-Random Circular Movement, PR: Pursue mode; MGM; Manhattan Grid Mobility, RWPM: Random waypoint model		

routing perimeter [21][23].

The OLSR protocol keeps the information about network in a table format in every node. Whenever a change take place in network, it triggers an update broadcast to inform all nodes about it. Consequently, it may cause packet overhead that affect throughput, energy and bandwidth of network. The main advantage is that each node is aware about routes to destination all the time without any route discovery mechanism but it faces performance issues in case of high mobility or large network size [26]. It utilizes hello, interface declaration (MID) and topology information control messages for its working.

The mobility models for FANETs are divided into four classes including MGM, RWPM, PRS and SCRM. MGM utilizes grid path topology (Fig. 3) and introduces a probable approach that whether a vehicle will keep on moving in same direction or change it [15]. In this model, the UAVs can move around in vertical and horizontal angles only. Although this model offers flexibility to change direction but puts geographic restrictions on node mobility. It is suitable in only a few UAVs scenarios.

In RWPM model, UAV begins movement by waiting in a place for a few times. Once it finishes, it selects a new random speed and location within a specified region [27]. This process is repeated with a short break everytime. Fig. 4 elaborates this model.

In PRS mobility model, the UAVs tracks a target which can be elaborated using this relation: $Newlocation = oldplace + randomvector + acceleration[target - oldplace]$. The acceleration specifies the movement of UAVs in direction of specified target [28]. The random vector is an offset to measure movement of individual UAV. Fig. 5 shows detail of his model, we can see the randomness of all UAVs is controlled to maintain tracking.

SCRM is different from RWPM model due to its predetermined flight plan [29]. The route is hexagon in this model. The aircraft is placed in different locations within a square area and desired object is chosen as shown in Fig. 6. In this way, information is collected for simulating UAV's in curved movement scenarios (Table II).

III. FANET SIMULATION MODEL

In this section, a detailed discussion is provided on available network simulators and our choice of simulator for experimentation. The design of FANET simulation model is elaborated. The evaluation and performance techniques are also presented. Three different scenarios are considered for performance evaluation.

A. Network Simulators

Before starting with the design of the network model, a search for network simulators was carried out to design and simulate network models in several viewpoints. The available softwares include MATLAB, OMNeT ++, NS-3, GNS3 and OPNET Modeler, which are well-known simulators in the area of telecommunications networks. NS-2 and NS-3 are open source programs. GNS-3 is open source but with graphic development. Few platforms are licensed but there are student versions that allow their use free of cost. For the OPNET simulation tool, it is commercial, and the source code is not open to everyone. However, OPNET has a broad integrated development environment to design and simulate network models. To carry out experimental evaluation, OPNET Modeler has been adopted based on the Microsoft Windows platform. The protocols available in the library are reactive, proactive and hybrid as compared to other commercial simulators. The OPNET Modeler simulation platform has several parameters in communication system environments especially wireless communications. For this work, FANET is evaluated for different routing protocols. OPNET provides graphical user interfaces known as editors to catch the specifications of installed networks, equipment, and protocols. The three essential editors are project, node and process editors. The network parameters to be measured are delay and performance. These are substantially affected by the algorithms of the routing protocols. Therefore, the parameters play a vital role in finding a suitable routing protocol for FANETs [30]. OPNET Modeler users can make customized models and simulate several scenarios. It is object-oriented and ensures a hierarchical approach to model communication networks. The performance parameters for FANETs include delay, throughput, packet hop count and packet loss using proactive and reactive routing protocols.

B. Design of FANET Model

The simulation scenarios are designed on the OPNET Modeler platform with help of different FANET network configuration parameters. The parameters such as profile, mobility and application configuration, wireless server and work stations are used in network design. Only 2D scenarios are discussed here. The selected protocols are AODV, DSR, TORA, OLSR and GRP. For the tests, OPNET simulator was used. Test scenarios were generated in area of 1500x2000 meters, in which 15 nodes were randomly arranged and the speed of nodes was set to 5 and 40 m/s. Furthermore, mobility models chosen were PRS, MGM, RWPM and SCRM. The nodes generated CBR traffic (Constant Bit Rate). The evaluated metrics are delay, transmission failures, packet hop count and throughput. There are other previous works where comparison tests were carried out between ad-hoc routing protocols. The traffic corresponding to the routing protocols will have a high priority so that routes can be formed more quickly. For this

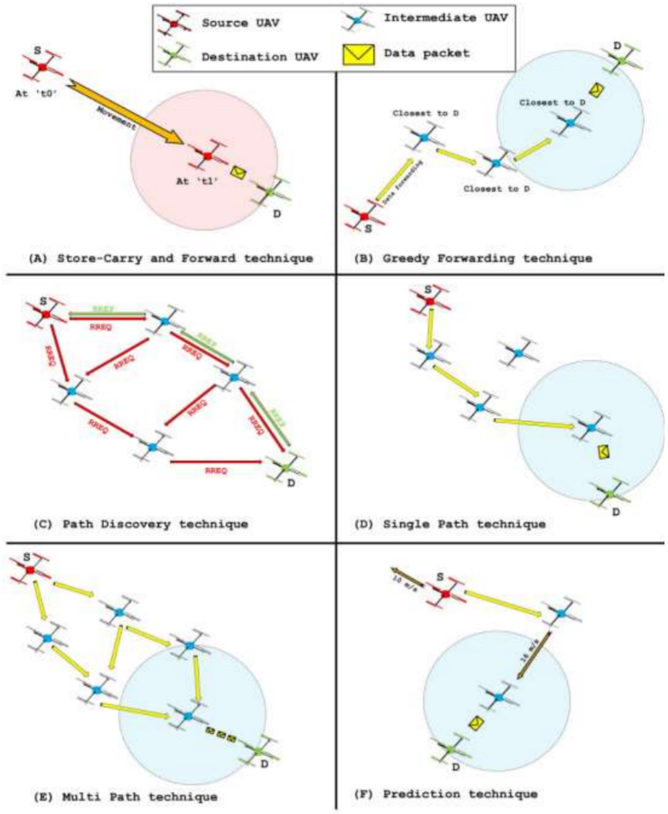

Fig. 3. A Manhattan Grid Topology with Two-Way Roads.

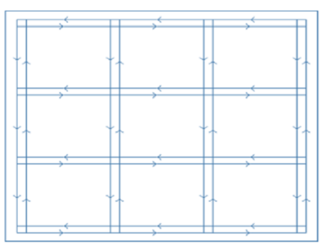

Fig. 4. A Random Waypoint Model.

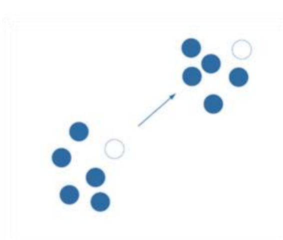

Fig. 5. An Example of a Pursue Mobility Model.

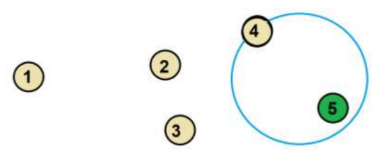

Fig. 6. An Example of a SCRM Model.

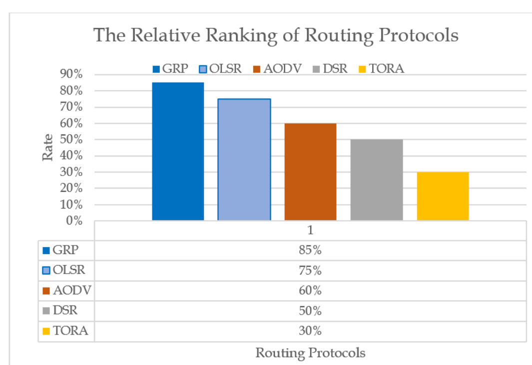

Fig. 7. The Relative Ranking of Routing Protocols in Scenario 1.

modification, we will use the IEEE 802.11n standard, which allows the use of quality of service in wireless networks.

C. Performance Evaluation

The present study has focused on the performance evaluation on the basis of mobility, congestion and the reliability of

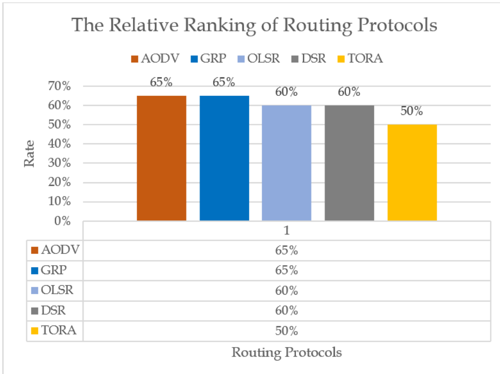

Fig. 8. The Relative Ranking of Routing Protocols in Scenario 2.

the route of the routing algorithm used to establish communications. The mobility model defines the speed, start time and stop time of nodes in network. The trajectory of movement was selected as 2000 meters at maximum. It is essential to perceive the mobility configuration to estimate mobility model of nodes. The movement of UAVs is controlled with parameters such as start and stop time, pause time and speed. The experiments are designed in such a way that performance of routing protocols is assessed using different mobility models in one sender one receiver, one sender all receivers and all senders and all receivers scenarios. A comparison is also performed among all routing protocols.

1) Scenario #1: One sender to one receiver situation: In our simulation parameter (One to one) in scenario 1, the numbers of UAVs are 15 and have fixed sender/receiver. The time taken of the simulation is 600 seconds, CBR traffic and data payload of 1024 bytes/packet. All routing protocols are evaluated and compared using performance parameters.

The simulated results show that shown in Fig. 7 indicate comparative ranking of routing protocols in our simulation results. It show that routing protocols can differ related to mobility model. The comparative ranking relies on the UAV speed because of the existence of the mobility that indicates frequent link failures. Each routing protocol plays an important role when link fails. Unlike OLSR, AODV and DSR, the Hybrid protocol GRP shows stable performance for all mobility models. TORA shows high delay and packet loss ratio in most scenarios. The algorithm of TORA keeps the “direction of the next destination” for packet forwarding. As a result, the source node follows downstream paths to the destination between several nodes. This will not be utilized if source node does not require path information before any topological changes.

2) Scenario # 2: All sender to one receive : In scenario 2 simulation, 15 nodes can be sent traffic to the base station. The speed of UAVs fluctuates between 5 and 40 m/sec. The simulation time is 600s, data payload of 1024 bytes/packet and CBR traffic.

Fig. 8 provide detailed results for scenario 2. The Reactive (AODV) and the Hybrid (GRP) have the same record with all existing mobility models. TORA shows higher delay in most scenarios.

3) Scenario #3: All senders to All receiver situation: In simulation scenario 3, the numbers of UAVs are 15 and every node can be treated as a source, destination, or routing node. The duration of simulation is 600 seconds, and traffic type considered is CBR. Regarding performance of different mobility moadels as shown in Fig. 9, we find that DSR and TORA have comparatively the lowest throughput. Finally, it is found that OLSR performs best in terms of throughput. It can be noticed that GRP and AODV are similar to each other in values fortunately.

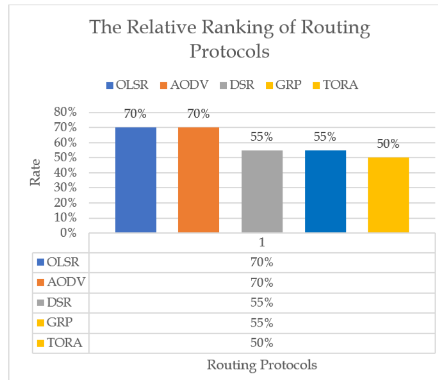

Fig. 9. The Relative Ranking of Routing Protocols in Scenario 3.

Now, we evaluate all mobility models based on performance parameters including delay, throughput, drop ratio and number of hops. Fig. 10 (a) shows performance of all protocol for PRS mobility model. It shows average result of all three scenarios mentioned above. Using PRS mobility model, TORA shows high delay and number of hops. MGM mobility model is evaluated in Fig. 10 (b). DSR routing protocols takes more time for end-to-end transmission and number of hops as compared to other protocols but provides maximum throughput and least packet drop ratio. AODV routing protocol takes minimum time for transmission and number of hops are slightly less than DSR, drop ratio is higher than DSR but less than other protocols which results in lesser throughput than DSR but higher throughput as compared to other protocols.

Using RWPM mobility model, DSR routing protocol outperforms other protocols as shown in Fig. 10 (c). Whereas after DSR, AODV performs really well. DSR has maximum throughput and least packet drop ratio although delay and number of hops a bit higher than other protocols.

Fig. 10 (d) shows performance of all protocol for SCRM mobility model. It shows average result of all three scenarios mentioned above. Using SCRM mobility model, DSR and AODV show high throughput. AODV shows minimum end-to-end delay and DSR shows minimum packet drop ratio.

IV. Conclusion and Future Work

Depending on the simulation results, the effect of node movement on performance is higher than the effect of node speed on performance. OLSR (proactive protocol) and GRP (hybrid protocol) are stable, TORA (hybrid protocol) is vulnerable and AODV/DSR (reactive protocols) are moderate in nature. It is noticed that node mobility results in rapid topology changes which affects network performance more than speed.

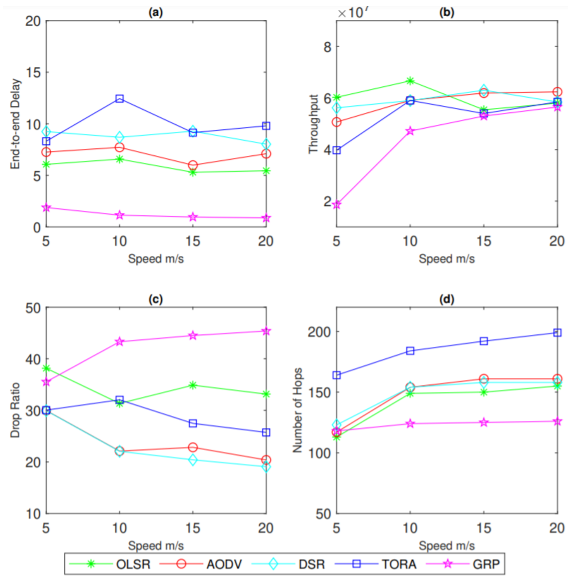

(a) Performance Evaluation of all scenarios with PRS Mobility Model

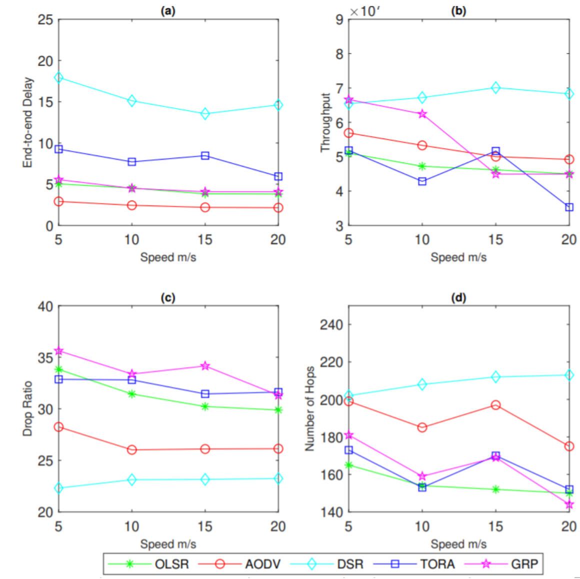

(b) Performance Evaluation of all scenarios with MGM Mobility Model

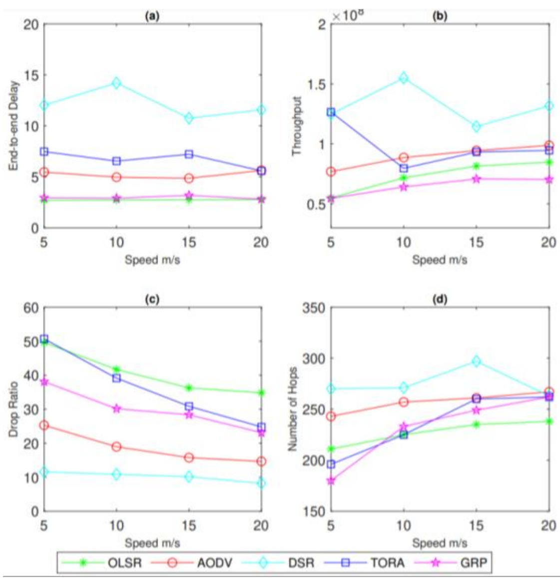

(c) Performance Evaluation of all scenarios with RWPM Mobility Model

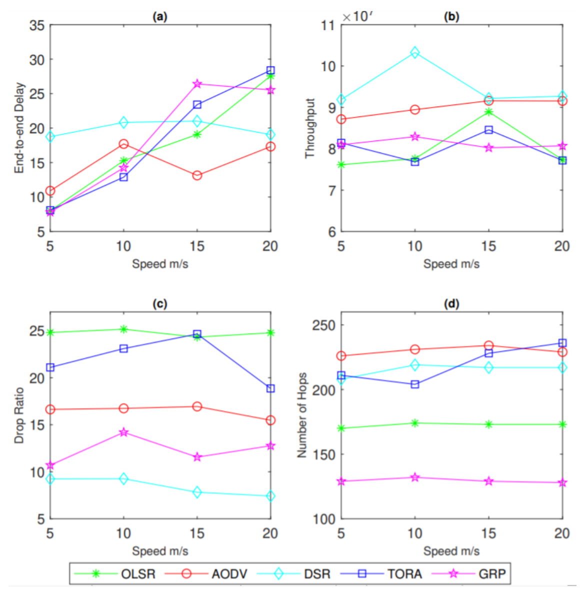

(d) Performance Evaluation of all scenarios with SCRM Mobility Model

Fig. 10. Performance Evaluation of Different Mobility Models and Routing Protocols.

Each mobility model undergoes topology changes differently. Among four mobility models, SCRM is the most competitive in high-speed environments. OLSR outperforms using MGM and PRS mobility models than other mobility models. While designing routing protocols, it is wise to make appropriate improvements on existing ones according to specific needs.

In addition, we discussed routing protocols along with their working and limitations. We also have provided a brief qualitative review of the aforementioned routing protocols on the basis of significant parameters. All these factors affect the performance of FANETs. We also have provided a simulation-based study of the topology-based routing protocols.

There are specific restrictions of FANETs because of its characteristics such as dynamic topology, security, limited bandwidth and UAVs management. One other problem is routing in swarm behaviour within FANETs. Because they work with each other to create a network, how they interact together also has importance in communication. The future work involve routing protocol depending on the swarm intelligence which will be helpful in setting efficient routing protocols for FANET environment in $3D - space$ mobility of UAVs.

ACKNOWLEDGMENT

This work is supported by grant number 43208008, Deanship of Scientific Research (DSR) of Umm al Qura University, Kingdom of Saudi Arabia. The authors would like to express their gratitude for the support and generous contribution towards pursuing research in this area

REFERENCES

[1] G. Pajares, "Overview and current status of remote sensing applications based on unmanned aerial vehicles (uavs)," Photogrammetric Engineering & Remote Sensing, vol. 81(4), p. 281–329, 2015.

[2] George, Joel, P. B. Sujit, and João B. Sousa, "Search strategies for multiple UAV search and destroy missions," J. Intell. Robot. Syst., vol. 61, p. 355–367, 2011.

[3] Choudhary, Gaurav, et al, "Internet of Drones (IoD): Threats, Vulnerability, and Security Perspectives," in The 3rd International Symposium on Mobile Internet Security, At Cebu, Philippines, 2018.

[4] M. A. Khan, A. Safi, I. M. Qureshi, and I. U. Khan, "Flying ad-hoc networks (FANETs):A review of communication architectures, and routing protocols," in IEEE First International Conference on Latest trends in Electrical Engineering and Computing Technologies (INTELLECT), Karachi, Pakistan, 2017.

[5] Bujari, Armir and et al, "Flying ad-hoc network application scenarios and mobility models," International Journal of Distributed Sensor Networks, vol. 1550147717738192, 2017.

[6] Pandit, Krushna J., and Shah Niyati, "Topology control in MANET for efficient energy conservation," International Journal of Advanced Computer Research, vol. 3.2, p. 108, 2013.

[7] Kaur, Kulwinder, and Barinderpal Singh, "Survey analysis of routing protocols and mobility models in manets," International Journal of Advanced Science and Technology , vol. 85 , pp. 55-64, 2015.

[8] Patel, S., Patel, H., Patel, S., and Patel, V, "A Study of Topology control in MANET," Presentado en SIEICON, International Journal of Advance Engineering and Research Development, p. 1–4, 2017.

[9] Robinpreet Kaur and Mritunjay Kumar Rai, "A Novel Review on Routing Protocols in MANETs," Undergraduate Academic Research Journal, vol. 1, no. 1, p. 2278 – 1129, 2012.

[10] Sarkar, Subir Kumar, Tiptur Gangaraju Basavaraju, and C. Puttamadappa, "Ad-hoc mobile wireless networks: principles, protocols, and applications," in CRC Press, 2016.

[11] J. e. a. Liu, "A survey on position-based routing for vehicular ad hoc networks," in Telecommunication Systems, 2016, pp. 15-30.

[12] O. K. Sahingoz, "Networking models in flying ad-hoc networks (FANETs): Concepts and challenges," Journal of Intelligent & Robotic Systems, Vols. 74(1-2), pp. 513-527, 2014.

[13] Maistrenko, Vasily A., Leonov V. Alexey, and Volkov A. Danil., "Experimental estimate of using the ant colony optimization algorithm to solve the routing problem in," in International Siberian Conference on Control and Communications (SIBCON)., IEEE, 2016.

[14] Leonov, Alexey V., and George A. Litvinov, "Applying aodv and olsr routing protocols to air-to-air scenario in flying ad hoc networks formed by mini-uavs,"in 2018 Systems of Signals Generating and Processing in the Field of on-Board Communications, IEEE, 2018.

[15] Nayyar and Anand, "Flying Adhoc Network (FANETs): Simulation Based Performance Comparison of Routing Protocols: AODV, DSDV, DSR, OLSR, AOMDV and HWMP," in 2018 International Conference on Advances in Big Data, Computing and Data Communication Systems (icABCD), IEEE, 2018.

[16] Yadav, Krishan, Amit Nain, and Sunil Maakar, "Routing protocols in FANET: Survey," in Proceedings of National Conference on Innovative Trends in Computer Science Engineering , (ITCSE-2015), ISSN, 2015.

[17] Nayyar, Anand, and Rajeshwar Singh, "Ant colony optimization—computational swarm intelligence technique," in 2016 3rd International conference on computing for sustainable global development , (INDIACom). IEEE, 2016.

[18] Nayyar, Anand, and Rajeshwar Singh, "A comprehensive review of ant colony optimization (ACO) based energy-efficient routing protocols for wireless sensor networks," International Journal of Wireless Networks and Broadband Technologies (IJWNBT) , vol. 3.3, pp. 33-55, 2014.

[19] Jailton, J., Carvalho, T., Araújo, J., and Francês, R, "Relay Positioning Strategy for Traffic Data Collection of Multiple Unmanned Aerial Vehicles Using Hybrid Optimization Systems," A FANET-Based Case Study, p. 11, 2017.

[20] Liu, Kesheng, Jun Zhang, and Tao Zhang, "The clustering algorithm of UAV networking in near-space," in 2008 8th International Symposium on Antennas, Propagation and EM Theory, IEEE, 2008.

[21] Maistrenko, Vasily A., Leonov V. Alexey, and Volkov A. Danil, "Experimental estimate of using the ant colony optimization algorithm to solve the routing problem in FANET," in In Control and Communications (SIBCON), 2016 International Siberian Conference on, 2016.

[22] Bendale, Lubdha M., Roshani L. Jain, and Gayatri D. Patil, "Study of various routing protocols in mobile ad-hoc networks," International Journal of Scientific Research in Network Security and Communication, vol. 6.01, pp. 1-5, 2018.

[23] D. e. a. Zhang, "Novel dynamic source routing protocol (DSR) based on genetic algorithm-bacterial foraging optimization," International Journal of Communication Systems, vol. e3824, 2018.

[24] Prasanth K. and Sivakumar P, "Location Based Routing Protocol – A Survey," in International Conference on Computer Communication and Informatics (ICCCI 2014), 2014 .

[25] Bruzgiene, Rasa, Lina Narbutaite, and Tomas Adomkus, "MANET network in internet of things system," in Ad Hoc Networks, 2017, p. 89.

[26] Jubair, Mohammed Ahmed, et al, "Performance Evaluation of Ad-Hoc On-Demand Distance Vector and Optimized Link State Routing Protocols in Mobile Ad-Hoc Networks," International Journal on Advanced Science, Engineering and Information Technology, pp. 1277-1283, 2018.

[27] F. Bai and A. Helmy, "A Survey of Mobility Models in Wireless Adhoc Network," in University of Southern California , USA, 2004.

[28] Vijayavani, G. R., and G. Prema. , "Performance comparison of MANET routing protocols with mobility model derived based on realistic mobility pattern of mobile nodes," in 2012 IEEE International Conference on Advanced Communication Control and Computing Technologies (ICACCCT), IEEE, 2012.

[29] K Kumari, S Maakar, B sah, "A Survey: Different Mobility Model for FANET," International Journal of Advanced Research in Computer Science and Software Engineering, 2015.

[30] R. Technology, "OPNET," 2019 . [Online]. Available: https://www.riverbed.com/gb/products/steelcentral/opnet.html.

Combining Word Embeddings and Deep Neural Networks for Job Offers and Resumes Classification in IT Recruitment Domain

Amine Habous*[1], El Habib Nfaoui[2]
LISAC Laboratory, Faculty of Sciences Dhar EL Mehraz,
Sidi Mohamed Ben Abdellah University,
Fez, Morocco

***Abstract*—Now-a-days, the use of web portals known as job boards for publishing job offers by recruiters has grown considerably. The candidates in their turn, apply to the job positions via the job boards. Since the opportunities are available on a wide range and the job application process is fast and straightforward, the data flow is transformed to large-volume data sets which are hard to handle. Most companies tend to automate the candidate selection process that aims to match the job offers with suitable resumes. In this paper, we propose a supervised learning approach to classify the job offers and CVs shared in the recruitment sites in order to enhance automatic recruitment process. We used natural language processing techniques for job offers and CV preprocessing. Next, we used word embeddings and deep neural networks to train two models, the first one categorizes recruitment documents based on job skills, and the second one predicts the expertise degree class. The experiment results show that our proposal is very efficient.**

Keywords*—*IT recruitment; word embeddings; deep neural networks; text classification; natural language processing

I. Introduction

Recruitment is the process of searching and selecting personnel for job positions in the staff of a company [1]. The use of the internet for recruitment purposes has known a prominent increase [2]. The appearance of job boards has made the advertising process easier and more cost-less compared with the old method that uses journal papers and magazines. Furthermore, these job boards provide more advanced services along with publishing job offers for recruiters and candidates curriculum vitae. With the swift development of Information and communication technologies, these portals now support the automatic matching between candidates resumes and their corresponding job offers [3]. The advantages that offer the e-recruitment encourage the companies recruiters and job seekers to upload more data that could be hard to process. Consequently, the data classification task is highly required in order to minimize the effort of handling vast data flows.

The job offer and candidate resume are unstructured textual documents that could have multiple formats. Thus these documents need a delicate process before applying the machine learning algorithms for achieving the classification task [4],[5]. The first phase in this process is the preprocessing task that aims to reduce the multiple forms of words in order to extract relevant features to feed the classification algorithms. Therefore, it reduces the dimensionality of the resulted features, which is an essential part of building an efficient model [6]. The features extraction is a vital part of the whole process, that has a direct impact on the classification model accuracy and performance. The classical model of document representation is the bag of words(BOW), which has many drawbacks regarding the features vector dimensionality and the model accuracy since it ignores the semantics and the contextual relations between the words [7].

Word embeddings presentations carry the semantic meanings beyond the words in textual documents. In 2013, Mikolov et al. proposed the word2vec model [8] that has been widely used in the text processing fields such as sentiment analysis, translation and document summarization, etc. Word2Vec consists on two learning models continuous bag of words (CBOW) and Skip-gram[9]. The CBOW model predicts the current word according to the context words, while Skip gram model predicts the surrounding context words according to the given word.

The IT sector is dynamic and booming in terms of employment, and an essential economic factor, source of national and international development. This sector is growing and evolving rapidly, that's why we have chosen to provide an effective solution to facilitate the processing of 'CV' applications and recruiters job offers. We have decided to address two essential points in the recruitment process, the first being the candidates talent related to the technical skills that they use. The second concerns the degree of expertise related to their experience and other knowledge and academic orientations that distinguish them from others.

In this paper, we propose a solution for text classification using deep neural networks and word embeddings for textual documents in the IT recruitment domain. We aim to classify these documents according to two levels, the first one concerns professional skills and the second is about the degree of expertise. These levels are combined to divide the huge IT jobs databases into smaller subsets to make their processing more easier. For instance, if we have a corpus of 1000000 CVs and 9 classes in the first level and 4 for the second. Thus using our method will allow us to process only 27000 ($\approx$ 1000000/(9$\times$4) considering that the sets are equivalent) to retrieve CVs from the corpus.

The rest of this paper is organized as follows. Section 2 presents the background. Section 3 contains the preliminaries to understand the rest of the paper. Section 4 presents the methodology. Section 5 details and discusses the experiments.

Finally, Section 6 concludes this paper.

II. Background and Related Work

A. Text Classification using Machine Learning

The objective of text classification is to assign a textual document into a set of predefined classes basing on its content. Classification is a supervised learning task where the machine uses labeled data to recognize hidden patterns to classify new documents. Several works have used the traditional techniques of machine learning in text classification combining the SVM (Support Vector Machine) algorithm with the TF-IDF weighting method for documents representation [10],[11] and [12]. Many other works have proposed machine learning based solutions; in [13],[14], the authors used the KNN algorithm and the Naive Bayes probabilistic representation for classifying the text documents. While [15] proposed a technique to enhance the document representation basing on the Naive Bayes method, which estimates the conditional probabilities of Naive Bayes using a deep feature weighting method for text classification.

B. Text Classification using Word Embeddings

Many works have integrated word embeddings based on contextual information for reliable representation instead of using the classical bag of words to classify text documents [16]. The authors in [17] used the deep neural networks methods with pre-trained word embeddings for enhancing Turkish text documents classification. Both of [18] and [19] proposed a solution based on an optimized TF-IDF along with word2Vec for text representation and convolutional neural networks to train the classification model. While [20] use convolutional neural networks on top of pre-trained word vectors for several sentence-level classification tasks. The authors of [21] present an approach that uses topic models based on LDA and word embeddings to represent documents in text categorization problems.

C. Text Classification in the Recruitment Field

Text classification is a vital task in the recruitment process; many techniques have been proposed to precisely classify job seekers resumes, and job offers into the right categories. In [22] paper, the authors presented a machine learning-based solution for binary classification to identify IT job offers on the world wide web. In [23], the authors proposed a deep neural network model for classifying personal basing on competency analysis in the human resources field. The authors in [24] and [25] proposed a text classification method basing on the personality traits in the recruitment domain. [26] proposed a solution for classifying job applicants documents into 27 categories using convolutional neural networks; Since it is hard to obtain resumes, they used free job description snippets for training the model then apply it to the candidates resumes. [27] presented an ontology-based solution for job offers classification, along with [28] that used the same technique for text classification to assist job hazard analysis. In [29], the authors proposed a solution aiming to identify the job skills in a textual document using recurrent neural networks. This method predicts if a word is a skill or not based on its context in the text.
The research works discussed above provide some solutions for textual documents classification in the recruitment process. While they give priority to the relevance of the technological choices and the implementation methods, they lack a business oriented model compared to our solution. Indeed, our proposal is efficient in terms of the chosen technologies and meets the recruitment process requirements.

III. Preliminaries

A. Problem Definition

In this paper, we propose a solution for job offers and candidate CV classification under a set of predefined categories. Let $D = \{x_1, ..., x_n\}$ the set of job offers/CV and $C = \{c_1, ..., c_k\}$ the list of the categories. The classifier estimates probability distribution over categories, and the probability of the correct category should be the highest. The input of the classifier is the training data which is a finite sequence of $\{(x_1, c_1), ..., (x_n, c_k)\}$ pairs from $D \times C$. While the output of the classifier is a function $f : D \to C$ that predicts $c \in C$ for new samples from D.

B. Word Embeddings

The word embeddings presented by [30] is a way to represent the words in textual documents that consist of extracting the contextual relationships between them. This model maps the words or phrases into a low-dimensional continuous space where each dimension represents a specific context. Thus the similar words will have similar vectors. Figure 1 shows an example of the spatial representation of five words according to three contexts.

One of the significant advantages of this model is to deal with dimensionality. As we said before, each word in the text is mapped to a point in a real continuous m-dimensional space that we choose beforehand. Contrary to one-hot encoded feature vector methods such as N-Grams, bag of words, and TF-IDF, the resulted feature vector is enormous. For example, if the corpus size is 100000, and we want to represent a sentence of 5 words, our feature vector will be a 100000-dimensional one-hot encoded vector where only five indexes will have 1.
The words embeddings models can be divided into two categories:

- Count-based methods
- Predictive methods

In count-based models, the semantic similarity between words is obtained by counting the co-occurrence frequency. Technically, we deduce the related words using the co-occurrence matrix. In the predictive models, the word vectors are generated using the predictive ability, i.e., by minimizing the loss between the target word and the context word. Thus the related word vectors are close to each other in space.

C. Deep Neural Networks (DNN)

Generally, the neural network is a technology built to simulate the activity of the human brain in pattern recognition through various layers of simulated neural connections. 'Deep learning' is used to describe those networks which represent a specific form of machine learning where technologies use aspects of AI that seek to classify and order information in ways

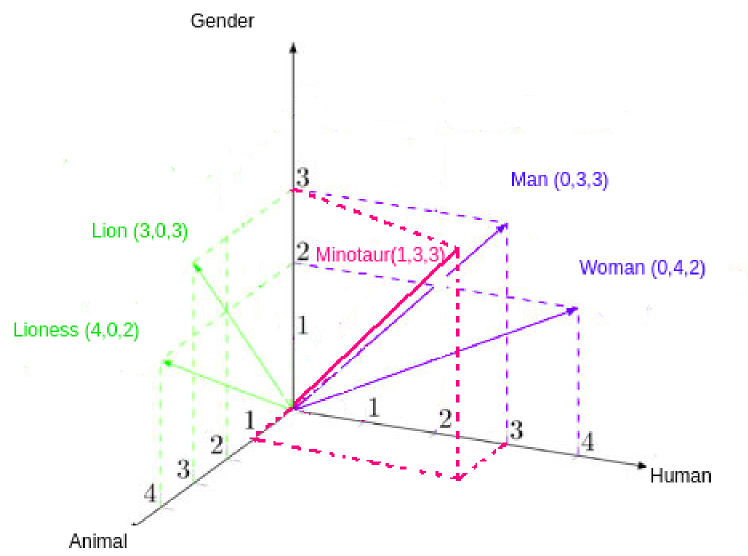

Fig. 1. Special Representation of Words According to Textual Contexts.

that go beyond simple input/output protocols. Mathematically, Deep neural networks are defined as a tuple (L, T, Φ) [31]:

$$L = \{L_k | k \in \{1...K\}\} \quad (1)$$

where L_1 is the input layer, L_K the output one and the other layers are called hidden layers.

$$T \subseteq L \times L \quad (2)$$

is the set of connections between layers

$$\Phi = \{\phi_k | k \in \{2...K\}\} \quad (3)$$

is the set of functions for each layer (non-input layer)

Each layer L_k consists of s_l neurons, each one is associated with two variables: $u_{k,l}$ and $v_{k,l}$ for recording its values before and after an activation function, respectively. There are many activation functions in the literature like the Binary Step function, Linear function, Sigmoid function, Than function and Relu function which is the most popular one for deep neural networks. Except for inputs, every neuron is connected to neurons in the preceding layer by pre-trained parameters such that for all k and l:

$$u_{k,l} = b_{k,l} + \sum_{h=1}^{s_{k-1}} w_{k-1,h,l} \cdot v_{k-1,h} \quad (4)$$

Where :

- $w_{k-1,h,l}$ is the weight of the connection between the h-th neuron of layer k-1 and the l-th neuron of layer k.
- $b_{k,l}$ the bias for neuron $s_{k,l}$
- $v_{k-1,h}$ the result of the activation function for $u_{k-1,l}$

For each input, The DNN assigns a label, that is, the index of the node of the output layer with the largest value $u_{k,l}$. Figure 2 shows the structure of a deep neural network with 4 layers.

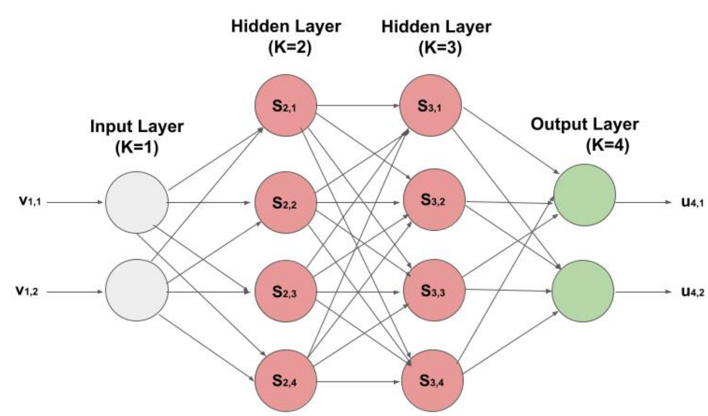

Fig. 2. Example of DNN Composed by 4 Layers.

IV. Methodology

Figure 3 shows the overall proposed architecture. The sub-sections below give all details about each module. In the first sub-section, we describe the labeling process that we use for each model training phase. In further sub-sections, we explain in detail the two models used in the last two sections.

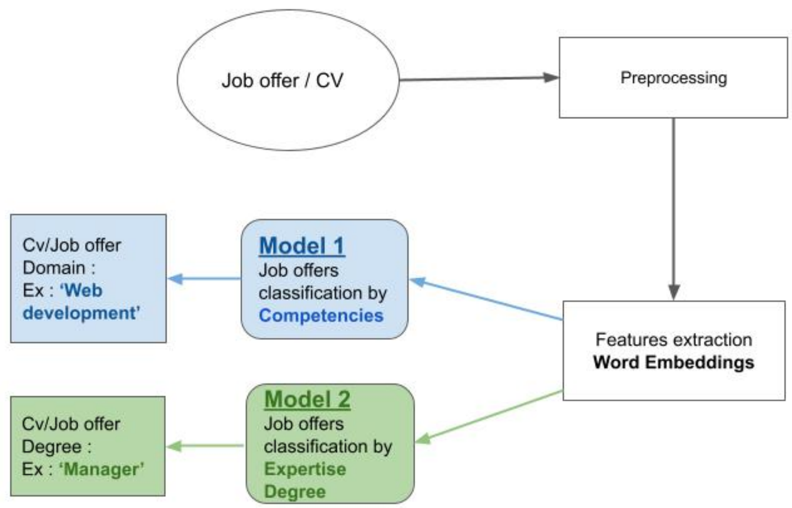

Fig. 3. The Overall Proposed Architecture.

A. The Process of Labeling Job Offers using Job Profiles

In IT recruitment, the job offer is a half structured textual document. It is composed of two parts; the first part is the job header, a set of information about the position, such as the type of contract, the salary, etc. The second part is the job description containing the free text that describes the employer needs, such as job qualifications, technical skills, etc. Most job boards share the same structure as the published job offers. Figure 4 shows an example of a job offer captured from Monster.com

Our work consists of a supervised multi-labeled text classification that takes the training data set with its labels as inputs. Therefore, we utilized the tagging concept using the job profiles to assign the correct labels to text data captured from the job boards. The tagging concept is the process of labeling short textual descriptions or key-words(tags) to information objects [32]. Table I shows some examples of tags that we use for each classification level.

TABLE I. EXAMPLE OF USED TAGS FOR LABELS ASSIGNMENT

	Model 1		Model 2	
Labels	Big data	Web development	engineer	Manager
Tags	Big data - Hadoop Hdfs - Spark	Front end - Back end Full stack Web developper	engineer engineering	Manager Director

We used only the tags that are very representative to avoid any ambiguity in the labeling process. For instance, we used key technologies or IT domains as tags to refer to a category.

B. Preprocessing Step

To preprocess the textual data, we used the traditional method in Natural Language Processing (NLP) [33], [34]:

- **Tokenization**: This step aims to transform our textual data into a set of distinct words (tokens)
- **Stop word removal**: After dividing the text into words, we remove the stop words which do not carry any sense using a predefined list of those words.
- **Stemming**: We transform the terms to their stems to unify the document units and reduce the corpus vocabulary size that we will construct in the next step.

These various text preprocessing steps are widely used for dimensionality reduction in the first level. It also helps to enhance the quality of data to promote the extraction of meaningful insights from it.

C. Features Extraction

Generally, the features extraction step in text classification aims to transform a list of words that we extract from the corpus into numerical vectors usable by a classifier. To minimize the vector dimension, we used a predefined list of IT technology fields and their synonyms that we obtained from a domain ontology. Thus we can unify the representation of all the technology fields in the textual corpus. For example, we represent the terms 'BI', 'Business Intelligence' and 'Decision Support System' as the same concept 'BI'; Consequently, it reduces the vector dimension due to the large number of those concepts in the IT recruitment. We can certainly find several open source ontologies such as O*net, ROME, and ESCO. Technically, we used O*net to create a sub-graph of the IT domain fields concepts with their synonyms.

The next step is building the corpus vocabulary, in which every word (token) is indexed based on its frequency in this corpus. Thus we transform each job offer from the corpus to a sequence of integers that correspond to the vocabulary

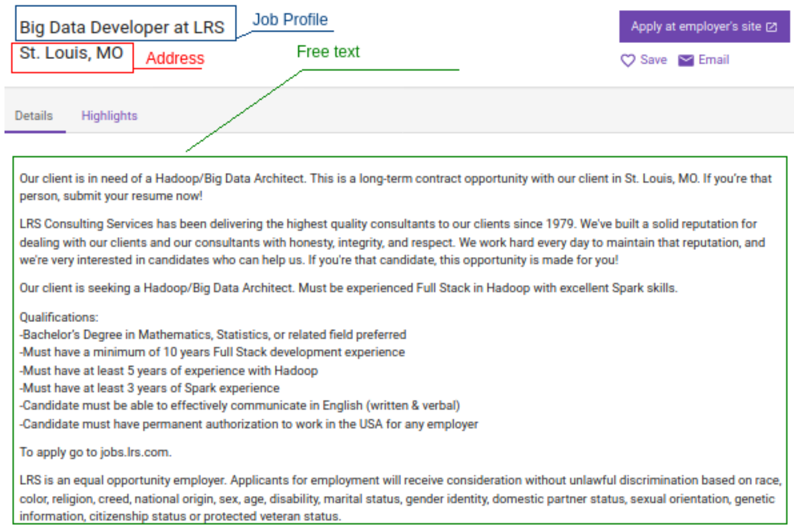

Fig. 4. Example of a Job Offer.

indexes. Since we will use the sequential deep neural networks for training the models, we use sequence padding to ensure that all sequences have the same length. Fig. 5 illustrates the feature extraction process.

D. Model 1: Job Offer Classifications According to Job Competencies

Job competencies are a set of abilities, knowledge, and skills needed to fill a job position or a role within a work environment. In addition to the work experiences that candidates achieve, Those competencies are learned and developed through academic studies. According to IBM corporation, job competencies are categorized as follows:

- Core competencies
- leadership management/business interpersonal
- Job functional competencies
- Job technical competencies
- Technical - task specific

In our context, we will focus on the last two types of competencies. Job technical competencies are the set of knowledge and skills related to the technologies of the IT domain. In contrast, task-specific competencies are the set of missions to perform in a specific role in the IT domain.

As we said before, the published job offers contain a free text part in where the recruiters specify the job requirements needed to fill a given post in his company. We use this data from our corpus to train the first model to classify the new job offers and CVs according to their skills and competencies in the IT domain.

E. Model 2: Job Offer Classifications According to Expertise Degree

In IT recruitment, the degree of expertise of a profile is related to the experience acquired and the employee tasks nature. Thus it is considered as a critical parameter to rank the IT recruitment job offers and candidates. In our paper, we divided these degrees into four separated degrees :

- **Technician**:The technician role is considered as the primary level in IT recruitment. Generally, its academic course does not exceed the Bachelor's degree.
- **Engineer**: The engineering level may require an additional academic degree compared to the technician; in the IT field, an engineer is oriented to be more autonomous in performing tasks. This degree also requires the mastery of many technical and personal skills.
- **Project chief**: This level is more privileged than the others; the project chief manages the cycles of IT projects, so he has many responsibilities requiring more advanced personal skills.
- **Manager/Consultant**: This degree gathers advanced technical, personal, and leadership skills. Managers and Consultants are also experimented with compared to the other levels.

In the IT recruitment field, there are so many ways to classify these roles according to expertise. Thus we focus on finding decisive differences between the chosen ones to train an efficient model for this level.

V. Result and Discussion

In this section, we present the data set that we used to train the proposed models and discuss the experimental results.

A. Data Set

We went through a data capture phase to construct a corpus of job offers and CVs documents from the IT recruitment domain. We have gathered job offers published on the job boards and the recruitment portals using web scraping tools and techniques. We targeted job offers for two reasons :

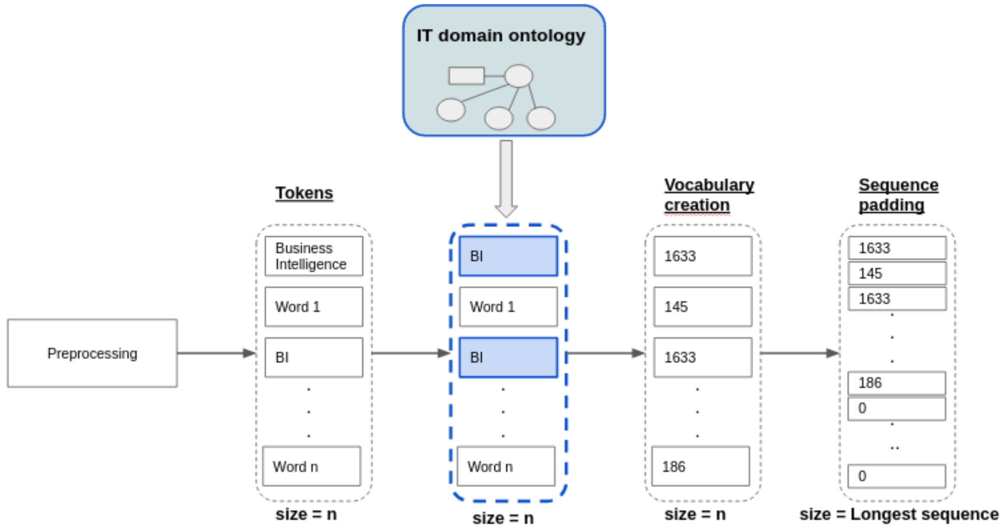

Fig. 5. Features Extraction Steps.

- The job offers are widely available and free compared to candidate CVs which are rarely published and shared on job boards; Consequently, it is challenging to create a CV corpus.
- The job offers are published according to a job profile that we use to define the class for supervised learning; whereas, the CVs contain a set of job profiles that the candidate achieved in his career.

We gathered about 10 000 documents from E-recruitment sites that share french job offers. Therefore, our tests concern French language. We preprocessed those documents following the steps explained in section IV.B above.

In the next step, we focused on filtering the job offers by removing the redundant ones. Then we filter the job offers having job profiles that don't contain the tags which makes the process of labeling more difficult. Table II and Table III describe the data that we used to train the two models.

TABLE II. THE DESCRIPTION OF THE DATA SET USED TO TRAIN MODEL 1

Class	Number of job offers
Web/software development	1115
Network engineering	1061
Embedded software engineering	796
Testing engineering	758
Business intelligence	740
Big data development	635
Data science	396
Information systems management	307
Database administration	245
Total	6053

To evaluate the two models performance, we split the data set for each of them as follows:

- Train set : 60 %
- Validation set : 20 %
- Test set : 20 %

TABLE III. THE DESCRIPTION OF THE DATA SET USED TO TRAIN MODEL 2

Class	Number of job offers
Technician	437
Engineer	4486
Project chief	1635
Consultant/Manager	1554
Total	8112

B. *Experimental Results*

To implement the solution, we used the Python language for implementing and evaluating our algorithms on an HP 4540s computer with an Intel i5 CPU running at 3.20 GHz with Ubuntu 18.04 (64-bit) and 8GB of RAM.
We used the NLTK library for the NLP tasks and the OWL-Ready2 to browse the IT ontology in the features extraction step. We trained the deep learning models using the KERAS toolkit. Our DNN models are composed of an embedding layer in the input. Then, two hidden layers with dropout ones to avoid overfitting.

The Table IV shows the two models performance using the accuracy, recall and f-score measures.

TABLE IV. MODEL 1 AND 2 PERFORMANCE RESULTS

	Model 1	Model 2
Accuracy	90.41 %	82.93 %
Recall	85.85 %	75.10 %
F-Score	88.07 %	78.82 %

The confusion matrices for job offers classification are shown in Fig. 6 and Fig. 7 for model 1 and 2 (resp.)

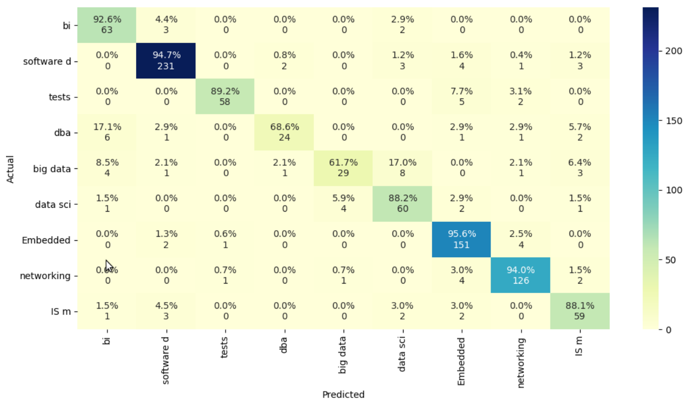

Fig. 6. Resulted Confusion Matrix for Model 1.

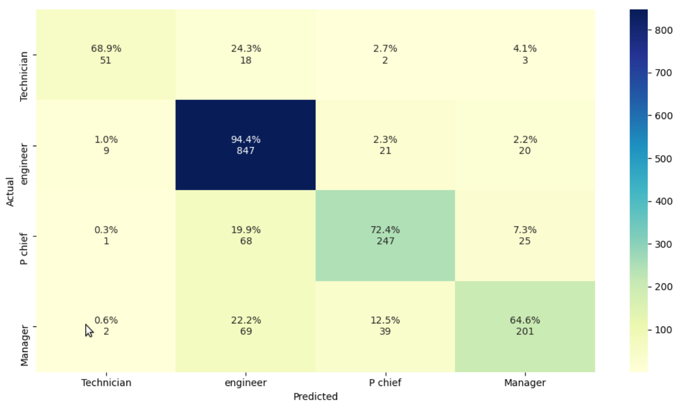

Fig. 7. Resulted Confusion Matrix for Model 2.

The results of the job offers classification show a good performance regarding the two models. They prove the relevance of the optimal choices that we made. The confusion matrix from figure 6 tells us that the minimum precision value for model 1 is 61 % for the "big data" class, which is justified by the complexity of the IT recruitment field. For example, in some cases, we can confuse a "data scientist" and a "big data developer" given a large number of technical skills in common. Concerning model 2, the confusion matrix from Fig. 7 shows us a low precision for the "manager" degree, which is predictable given few the job offers used for training the models.

In the implementation phase, we have tried multiple methods for textual classification in the recruitment process. First, we have trained a word2Vec model to catch similarities for the job offers corpus. We have also used the pre-trained model Glove for word embeddings. In both cases, the first results obtained with the Keras embedding layer outperform the other methods. The specific context of IT recruitment helps in semantic relationships capture with the deep neural network embedding layer. However, to train an embedding model, a large volume of data is necessary, which is not available in our case. In general, the pre-trained Glove model works well for text classification, but our solution concerns a specific context of words.

VI. Conclusion

In this paper, we proposed a technique for CV and job offers classification to facilitate their processing in massive data flows. We used the deep learning networks combined with word embeddings to build two efficient models. The first one aims to categorize CV and job offers according to the technical competencies in the IT domain, while the second one classifies these documents basing on the required or the recommended expertise degree.

The tests have shown that the constructed models give efficient results in terms of classification measures. We have well described the data set used in the results section, to show the efficiency of the models in such a complex context.

For future work, we plan to increase the classification classes number to have more subsets of the massive data; therefore, we gain additional performance in their processing. In addition, we aim to apply this solution to several other business sectors other than the IT field.

References

[1] V. Lytvyn, V. Vysotska, P. Petro, g. Bobyk, and B. Pakholok, "A method for constructing recruitment rules based on the analysis of a specialist's competences," *Eastern-European Journal of Enterprise Technologies*, vol. 6, pp. 4–14, 12 2016.

[2] J. Chen, Z. Niu, and H. Fu, "A novel knowledge extraction framework for resumes based on text classifier," in *Web-Age Information Management* (X. L. Dong, X. Yu, J. Li, and Y. Sun, eds.), (Cham), pp. 540–543, Springer International Publishing, 2015.

[3] A. Kmail, M. Maree, M. Belkhatir, and S. Alhashmi, "An automatic online recruitment system based on exploiting multiple semantic resources and concept-relatedness measures," 11 2015.

[4] S. Lai, L. Xu, K. Liu, and J. Zhao, "Recurrent convolutional neural networks for text classification," in *Twenty-ninth AAAI conference on artificial intelligence*, 2015.

[5] M. P. Akhter, Z. Jiangbin, I. R. Naqvi, M. Abdelmajeed, A. Mehmood, and M. T. Sadiq, "Document-level text classification using single-layer multisize filters convolutional neural network," *IEEE Access*, vol. 8, pp. 42689–42707, 2020.

[6] A. I. Kadhim, "An evaluation of preprocessing techniques for text classification," *International Journal of Computer Science and Information Security (IJCSIS)*, vol. 16, no. 6, 2018.

[7] B. Heap, M. Bain, W. Wobcke, A. Krzywicki, and S. Schmeidl, "Word vector enrichment of low frequency words in the bag-of-words model for short text multi-class classification problems," *arXiv preprint arXiv:1709.05778*, 2017.

[8] X. Rong, "word2vec parameter learning explained," *CoRR*, vol. abs/1411.2738, 2014.

[9] L. Ma and Y. Zhang, "Using word2vec to process big text data," in *2015 IEEE International Conference on Big Data (Big Data)*, pp. 2895–2897, 2015.

[10] G. Forman, "Bns feature scaling: An improved representation over tf-idf for svm text classification," pp. 263–270, 01 2008.

[11] K. Chen, Z. Zhang, J. Long, and H. Zhang, "Turning from tf-idf to tf-igm for term weighting in text classification," *Expert Systems with Applications*, vol. 66, pp. 245 – 260, 2016.

[12] F. Luo, C. Li, and Z. Cao, "Affective-feature-based sentiment analysis using svm classifier," in *2016 IEEE 20th International Conference on Computer Supported Cooperative Work in Design (CSCWD)*, pp. 276–281, 2016.

[13] V. Bijalwan, V. Kumar, P. Kumari, and J. Pascual, "Knn based machine learning approach for text and document mining," *International Journal of Database Theory and Application*, vol. 7, no. 1, pp. 61–70, 2014.

[14] P. Bolaj and S. Govilkar, "Text classification for marathi documents using supervised learning methods," *International Journal of Computer Applications*, vol. 155, no. 8, pp. 6–10, 2016.

[15] L. Jiang, C. Li, S. Wang, and L. Zhang, “Deep feature weighting for naive bayes and its application to text classification,” *Engineering Applications of Artificial Intelligence*, vol. 52, pp. 26–39, 2016.

[16] A. El Mahdaouy, E. Gaussier, and S. O. El Alaoui, “Arabic text classification based on word and document embeddings,” in *Proceedings of the International Conference on Advanced Intelligent Systems and Informatics 2016* (A. E. Hassanien, K. Shaalan, T. Gaber, A. T. Azar, and M. F. Tolba, eds.), (Cham), pp. 32–41, Springer International Publishing, 2017.

[17] M. Aydoğan and A. Karci, “Improving the accuracy using pre-trained word embeddings on deep neural networks for turkish text classification,” *Physica A: Statistical Mechanics and its Applications*, vol. 541, p. 123288, 2020.

[18] L. Li, L. Xiao, W. Jin, H. Zhu, and G. Yang, “Text classification based on word2vec and convolutional neural network,” in *Neural Information Processing* (L. Cheng, A. C. S. Leung, and S. Ozawa, eds.), (Cham), pp. 450–460, Springer International Publishing, 2018.

[19] T. Zhang and L. Wang, “Research on text classification method based on word2vec and improved tf-idf,” in *Advances in Intelligent Systems and Interactive Applications* (F. Xhafa, S. Patnaik, and M. Tavana, eds.), (Cham), pp. 199–205, Springer International Publishing, 2020.

[20] A. Mandelbaum and A. Shalev, “Word embeddings and their use in sentence classification tasks,” 10 2016.

[21] J. M. Lima and J. Maia, “A topical word embeddings for text classification,” pp. 25–35, 10 2018.

[22] E. ul haq Dar and J. Dorn, “Classification of job offers of the world wide web,” in *2018 International Conference on Computing, Mathematics and Engineering Technologies (iCoMET)*, pp. 1–8, 2018.

[23] Q. Guohao, W. Bin, W. Bai, and Z. Baoli, “Competency analysis in human resources using text classification based on deep neural network,” in *2019 IEEE Fourth International Conference on Data Science in Cyberspace (DSC)*, pp. 322–329, IEEE, 2019.

[24] E. Faliagka, A. Tsakalidis, and G. Tzimas, “An integrated e-recruitment system for automated personality mining and applicant ranking,” *Internet research*, 2012.

[25] S. Bharadwaj, S. Sridhar, R. Choudhary, and R. Srinath, “Persona traits identification based on myers-briggs type indicator(mbti) - a text classification approach,” in *2018 International Conference on Advances in Computing, Communications and Informatics (ICACCI)*, pp. 1076–1082, 2018.

[26] L. Sayfullina, E. Malmi, Y. Liao, and A. Jung, “Domain adaptation for resume classification using convolutional neural networks,” in *Analysis of Images, Social Networks and Texts* (W. M. van der Aalst, D. I. Ignatov, M. Khachay, S. O. Kuznetsov, V. Lempitsky, I. A. Lomazova, N. Loukachevitch, A. Napoli, A. Panchenko, P. M. Pardalos, A. V. Savchenko, and S. Wasserman, eds.), (Cham), pp. 82–93, Springer International Publishing, 2018.

[27] E. ul haq Dar and J. Dorn, “Ontology based classification system for online job offers,” in *2018 International Conference on Computing, Mathematics and Engineering Technologies (iCoMET)*, pp. 1–8, 2018.

[28] N.-W. Chi, K.-Y. Lin, and S.-H. Hsieh, “Using ontology-based text classification to assist job hazard analysis,” *Advanced Engineering Informatics*, vol. 28, no. 4, pp. 381 – 394, 2014.

[29] D. Baad *et al.*, “Automatic job skill taxonomy generation for recruitment systems,” 2019.

[30] G. E. Hinton *et al.*, “Learning distributed representations of concepts,” in *Proceedings of the eighth annual conference of the cognitive science society*, vol. 1, p. 12, Amherst, MA, 1986.

[31] Y. Sun, X. Huang, and D. Kroening, “Testing deep neural networks,” *CoRR*, vol. abs/1803.04792, 2018.

[32] I. Katakis, G. Tsoumakas, and I. Vlahavas, “Multilabel text classification for automated tag suggestion,” in *Proceedings of the ECML/PKDD*, vol. 18, p. 5, 2008.

[33] V. Gurusamy and S. Kannan, “Preprocessing techniques for text mining,” 10 2014.

[34] S. Vijayarani, M. J. Ilamathi, and M. Nithya, “Preprocessing techniques for text mining-an overview,” *International Journal of Computer Science & Communication Networks*, vol. 5, no. 1, pp. 7–16, 2015.

Mean Value Estimation of Shape Operator on Triangular Meshes

Ahmed Fouad El Ouafdi[1]
Research laboratory Labsiv, Faculty of Sciences
Ibn Zohr university, Agadir, Morocco

Hassan El Houari[2]
LaGuardia Community College,
CUNY, New York, USA

***Abstract*—The principal curvatures, eigenvalues of the shape operator, are an important differential geometric features that characterize the object's shape, as a matter of fact, it plays a central role in geometry processing and physical simulation. The shape operator is a local operator resulting from the matrix quotient of normal derivative with the metric tensor, and hence, its matrix representation is not symmetric in general. In this paper, the local differential property of the shape operator is exploited to propose a local mean value estimation of the shape operator on triangular meshes. In contrast to the stat-of-art approximation methods that produce a symmetric operator, the resulting estimation matrix is accurate and generally not symmetric. Various comparative examples are presented to demonstrate the accuracy of proposed estimation. The results show that the principle curvature arising from the estimated shape operator are accurate in comparison with the standard estimation in the literature.**

***Keywords*—Curvature estimation; shape operator; triangular meshes; discrete differential operator**

I. Introduction

Surface curvatures are a significant intrinsic geometry component that describe the geometrical structure of a regular object surface. As the three-dimensional shape of objects is progressing substantially, measuring such curvatures is becoming more common in a variety of areas such as physics-based modeling, variational modeling, geometric data processing and computer graphics.

Although differential geometry has a longstanding heritage of computing curvatures on smooth surfaces, such curvatures, as well as other features, lose their continuity when a smooth surface is approximated by a triangle mesh due to the mesh's discrete nature. There is therefore the necessity to create approaches for the estimate of surface curvatures of triangular meshes, as precision and effectiveness remain the essential ingredients for the development of discrete evaluation methods. Over the last years, curvatures estimations problem has been extensively studied, since it is a crucial phase in mesh data processing due to its several applications in computer and robot vision, computer graphics, geometric modeling, and industrial and biomedical engineering [4], [13], [16], [17], [3]. Although there are various proposed methods for estimating curvature in the literature, the algorithm that aims for maximum estimation precision still always needed to be developed.

The shape operator, whose eigenvalues are the principal curvatures, has captivate a lot of attention since it is an essential ingredient to construct an accurate curvature estimate. In the smooth setting, computing a surface's shape operator is crucial, since the shape operator is equal to the gradient of the surface normal field. The first discretization of shape operator dates back to Taubin [18], who described the operator as a weighted average of normal curvatures. Since then, several other approaches to discretize shape operator on triangular meshes has been developed in the literature [2], [20], [7], [10], [22], [6], and most of these methods treated the shape operator as a local operator extracted from the matrices quotient of normal derivative with the metric tensor, which generally result a symmetrical matrix representation, even for object with unsymmetrical shape operator. In this paper, we use the local differential property of the shape operator to propose a convolutional based approach to estimate the shape operator on triangular meshes. The resulting estimation matrix is accurate and not necessarily symmetrical, unlike the stat-of-the-art approximation methods producing a symmetric operator.

II. Relative Work

Curvatures estimation has been the subject of considerable research due to its several practical applications, leading to the development of a variety of curvature estimators. Most of the existing estimation approaches can be classified into two categories depending on whether the approach based on directional normal derivative approximation or local surface interpolation. In what follows, we briefly review some curvature estimation approaches from each category.

The first category estimate to shape operator on triangular face to develop an estimation of the curvature directly or through the curvature tensor. In [2], a discretization of the curvature surface tensor is based on the theory of normal cycles that estimates the curvature at the sampled smooth surfaces. Another approach based on degrees of freedom associated with normal vector is represented in [8], the curvature is estimated by formulating the shape operator from variational problems on general meshes. In [22], the finite difference approach is applied to discretize the directional derivative normal surface on each face. This method was later adopted by [1] using a collection of nearby sampling points combining the quadratic difference forms and the finite-difference normal directional derivative approximation. Another approach to estimating the surface's principal curvatures based on inversion-invariant local surface-based differential forms is proposed [23].

In [11], a per-face discrete curvature estimation approach is proposed in terms of discrete shape operator, the method is based on adapting the optimal estimation technique into a non-linear diffusion process for normal and curvature consistencies. Another face-based method for estimating the curvature of triangle meshes focused on the concept of osculating circles in regular planes is discussed in [24]. More recently, a component analysis-based method is presented to estimate the curvatures in [25]. The approach identifies principal components that are dominant in the shape fields, resulting the first and second fundamental forms used in the curvature estimation.

The second category deals with determining the most accurate approximation of the surface patch for each data point neighborhood. In this direction, Theisel in [19] proposed a face-based approach for computing shape operators using linear interpolation of normal. In [21], an approach is introduced for estimating mean and Gaussian curvature and the shape operator matrix as well, it relies on the periodic structure of the normal curvatures to ensure that the quadrature are exact. In [14] a new method is proposed to estimate the curvature at different scales by adapting suitable fitting technique and applying it to different-sized neighborhood depending on scale. In [12] the interpolation of three end points and the corresponding normal vectors of each triangular vertex to construct a curved patch was introduced as a curvature estimate approach for meshes. In [15] a screen space method is proposed for estimating the mean and Gaussian curvature at interactive rates from the second fundamental form matrix by using positions and normal.

A. Contribution

The most proposed approximations of the shape operator are formulated in term of a symmetrical matrix that produces an inaccurate curvatures estimation, especially for object with unsymmetrical shape operator. As the shape operator is locally defined by a directional differential normal vector, we propose to estimate the shape operator by a mean value expression of normal difference at each vertex of triangular mesh. In contrast to the standard shape operator approximation methods, the resulting estimation matrix is generally not symmetric. We compare the principal curvatures, eigenvalues of the estimated shape operator, to the one arising from analytic expression. Various comparative examples are presented to demonstrate the accuracy of proposed curvatures estimation method.

The rest of the paper is organized as follows: In Section III we present a brief theoretical background that describes the construction of shape operator. In Section IV, we formulate the expression of the shape operator by neighborhood mean value formulation, and then we propose the new shape operator discretization algorithm whose evaluation through numerous substantiating examples is provided in Section V. We finally give some concluding remarks in Section VI.

III. Preliminary Background

In this section, we briefly review some definition related to the shape operator background, for more rigorous details, we refer interested reader to the standard differential geometry textbooks [5], [26].

Let us consider a smooth regular surface $\mathbb{M} \subseteq \mathbb{R}^3$ locally parameterized by (x, y), where $T_p\mathbb{M}$ denoted the tangent plane of $\mathbb{M}$ at $p = p(x, y) \in \mathbb{M}$. The space $T_p\mathbb{M}$ is spanned by the partial derivatives $\mathrm{U} = \frac{\delta p}{\delta x}$ and $\mathrm{V} = \frac{\delta p}{\delta y}$ and it is equipped with

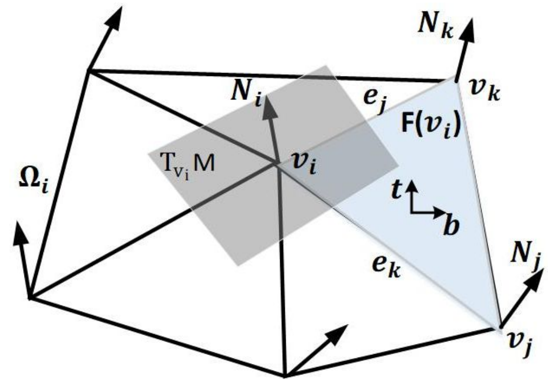

Fig. 1. Discrete Vertex Neighbourhood.

the standard inner product $(\cdot)$ in $\mathbb{R}^3$. The Riemannian metric tensor, called also first fundamental form, is defined as

$$I = \begin{pmatrix} E & F \\ F & G \end{pmatrix} = \begin{pmatrix} \mathrm{U} \cdot \mathrm{U} & \mathrm{U} \cdot \mathrm{V} \\ \mathrm{V} \cdot \mathrm{U} & \mathrm{V} \cdot \mathrm{V} \end{pmatrix} \tag{1}$$

The matrix I is symmetric and positive definite. At every point $p(x, y) \in \mathbb{M}$, the unit normal vector field is defined by

$$N(x, y) = \frac{\mathrm{U} \times \mathrm{V}}{|\mathrm{U} \times \mathrm{V}|} \tag{2}$$

which allows to define the second fundamental form $II = II(u, v)$ by

$$II = \begin{pmatrix} L & M \\ M & N \end{pmatrix} = \begin{pmatrix} \frac{\delta p}{\delta x \delta x} \cdot \mathrm{N} & \frac{\delta p}{\delta x \delta y} \cdot \mathrm{N} \\ \frac{\delta p}{\delta y \delta x} \cdot \mathrm{N} & \frac{\delta p}{\delta y \delta y} \cdot \mathrm{N} \end{pmatrix} \tag{3}$$

or in term of normal directional derivative

$$II = -\begin{pmatrix} \frac{\delta p}{\delta x} \cdot \frac{\delta N}{\delta x} & \frac{\delta p}{\delta x} \cdot \frac{\delta N}{\delta y} \\ \frac{\delta p}{\delta y} \cdot \frac{\delta N}{\delta x} & \frac{\delta p}{\delta y} \cdots \frac{\delta N}{\delta y} \end{pmatrix} \tag{4}$$

More generally, given a tangential vector $\mathrm{E} \in T_p\mathbb{M}$ at a point $p \in \mathbb{M}$, then the directional derivative $D_{\mathrm{E}}N$ of the the normal vector in the direction of vector E is defined by

$$\mathcal{S}_p(\mathrm{E}) = -D_{\mathrm{E}}N(p) \tag{5}$$

where $\mathcal{S} : T_p\mathbb{M} \leftrightarrow T_p\mathbb{M}$ is a *linear map* called Shape operator that can be expressed in term of the first and second fundamental forms as

$$S = I^{-1}II = \begin{pmatrix} \frac{FM-GL}{EG-F^2} & \frac{FL-EM}{EG-F^2} \\ \frac{FN-GM}{EG-F^2} & \frac{FM-EN}{EG-F^2} \end{pmatrix} \tag{6}$$

It should be noted that the above shape operator matrix need not to be symmetric in general, its eigenvalues, denoted with k_1 and k_2, are called the principal curvatures. The product and the mean of the principal curvatures are respectively called the Gaussian curvature $K = k_1 k_2$ and the mean curvatures

$$H = \frac{k_1 + k_2}{2} \tag{7}$$

In what follow, we propose a mean value based approach toward shape operator matrix estimation on triangular surfaces.

IV. Shape Operator Estimation on Meshes

For an arbitrary surface, the exact expression of the shape operator can rarely be expressed explicitly, hence, only an estimation on discrete surfaces can be performed. In the discrete setting, the surface $\mathbb{M}$ is sampled at n_p points $P = \{v_1, ..., v_{n_p}\}$. The points are then connected by n_e edges $E = \{e_1, ..., e_{n_e}\}$ and n_f faces $F = \{F_1, ..., F_{n_f}\}$ forming a triangular mesh (V, E, F) noted $\mathcal{M}$. An orthogonal and normalized tangential reference frame $(\mathbf{t}, \mathbf{b})$ is attached to each triangle $f \in F$ as well as a normal vector N_f. As the shape operator is defined on a local surface, we consider a local discrete surface $\Omega_i = \cup F(v_i)$ around the point $v_i \in P$ as shown in Fig. 1. To estimate locally the shape operator at v_i on the Ω_i, we propose to use the following mean local value expression

$$S_{v_i} = \frac{1}{|\Omega_i|} \int_{\Omega_i} \mathcal{S}_v \; dv \tag{8}$$

where $|\Omega_i|$ denoted the area of the local surfaceΩ_i. As $\Omega_i = \cup F(v_i)$, where $F(v_i)$ is a face sharing the vertex v_i depicted in Fig. 1, the local formulation of the shape operator (8) boils down to

$$S_{v_i} = \frac{1}{|\Omega_i|} \sum_{F \in \Omega_i} \int_F S_v \; dv \tag{9}$$

Hence, to estimate the shape operator over Ω_i, it is sufficient to evaluate its expression on each incident face F. To this end, assume that the face $F(v_i, v_j, v_k)$ is determined by the three vertex v_i, v_j and v_k. As the two vectors $e_j = v_i - v_k$ and $e_k = v_j - v_i$ are edges of the face F, hence, the two edges vectors can be fully expressed in the orthogonal frame $(\mathbf{t}, \mathbf{b})$ of F as

$$e_j = \underbrace{(e_j \cdot \mathbf{t})}_{e_{j\mathbf{t}}} \mathbf{t} + \underbrace{(e_j \cdot \mathbf{b})}_{e_{j\mathbf{b}}} \mathbf{b} \quad \text{and} \quad e_k = \underbrace{(e_k \cdot \mathbf{t})}_{e_{k\mathbf{t}}} \mathbf{t} + \underbrace{(e_k \cdot \mathbf{b})}_{e_{k\mathbf{b}}} \mathbf{b} \tag{10}$$

Using the expression of the shape operator in term of the normal directional derivative (5) along the two edges vector e_j and e_k give arise

$$S_v \cdot e_j = -D_{e_j} N(v) \quad \text{and} \quad S_v \cdot e_k = -D_{e_k} N(v) \tag{11}$$

Following Rusinkiewicz [22], we approximate the derivative of the normal vector N in the direction of the two vector $e_j = v_i - v_j$ and $e_k = v_k - v_i$ on the face F as

$$S_v \cdot e_j = -D_{e_j} N \;\; \approx \;\; \begin{pmatrix} (N_i - N_k) \cdot \mathbf{t} \\ (N_i - N_k) \cdot \mathbf{b} \end{pmatrix} \;\; \text{and} \tag{12}$$

$$S_v \cdot e_k = -D_{e_j} N \;\; \approx \;\; \begin{pmatrix} (N_j - N_i) \cdot \mathbf{t} \\ (N_j - N_i) \cdot \mathbf{b} \end{pmatrix} \tag{13}$$

which leads to an approximation of the shape operator matrix S_v of the normal vector N inside the face F as

$$S(F) \approx \begin{pmatrix} e_{j\mathbf{t}} & e_{j\mathbf{b}} \\ e_{k\mathbf{t}} & e_{j\mathbf{b}} \end{pmatrix}^{-1} \begin{pmatrix} (N_i - N_k) \cdot \mathbf{t} & (N_i - N_k) \cdot \mathbf{b} \\ (N_j - N_i) \cdot \mathbf{t} & (N_j - N_i) \cdot \mathbf{b} \end{pmatrix} \tag{14}$$

As the above estimation of the shape operator is locally constant over the face F, the integral formulation (9) can be expressed as

$$S_{v_i} = \frac{1}{|\Omega_i|} \sum_{F \in \Omega_i} |F| \cdot S(F) \tag{15}$$

Algorithm 1: Mean Value Hodge Operator Estimation.

1 **forall** *point* $v_i \in V$ **do**
2 Initialze S_{v_i} with a zero matrix
3 **foreach** *face F sharing the vertex v_i* **do**
4 Compute the estimation of the shape operator $S(F)$ on the face F by (14)
5 Compute the face area $|F|$.
6 $\tilde{S}_F \leftarrow projec\_to\_tangent\_plan(S(F))$
7 $S_{v_i} \leftarrow S_{v_i} + |F| \cdot \tilde{S}_F$
8 **end**
9 $S_{v_i} \leftarrow S_{v_i} / \sum_{F \in \Omega_i} |F|)$
10 **end**

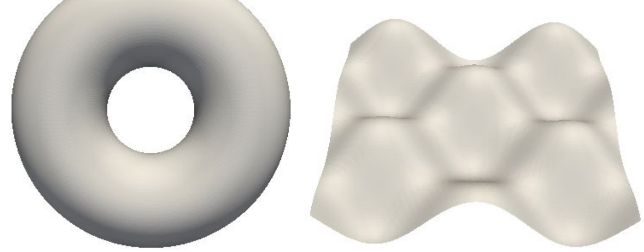

(a) Torus mesh (b) Sinusoidal mesh

Fig. 2. Explicit Meshes Arising from Analytic Parametric Torus and Sinusoidal Surfaces.

The following algorithm summarize the shape operator estimation procedure on a triangular mesh: A per-processing step of the algorithm 1 is to estimate the normal vector of each point v_i, then, we compute in the step 4 the shape operator (14) for each face F incident to the vertex v_i, the obtained face based shape operator is projected back onto tangent plan of the vertex v_i in the step 6, and then summed up and normalized in the step 9.

V. Experimental Results

In the following, we report evaluation and comparison of the proposed Convolution Based Estimation algorithm (CBE) with three stat-of-art methods: the finite Difference curvature Estimation Method (DEM) proposed by Rusinkiewicz [22], the Multi-Scale Curvature (MSC) Estimation methods (CCM) [14] and the Normal Cycle Curvature (NCC) estimation method [2]. For each comparative method, the shape operator is estimated on a set of standard triangular meshes. In the following, a set of quantitative and qualitative comparison experiments of the four methods are performed.

A. Quantitative Evaluation

In the first set of quantitative experiments, two explicit synthetic triangular meshes in Fig. 4 are selected, such that an analytic expression of the shape operator is available. The first mesh reported in Fig. 2(a) is the torus object with major radius 2 and minor radius 1, the analytic expression of the shape operator of torus is represented by a *symmetric* matrix [26].

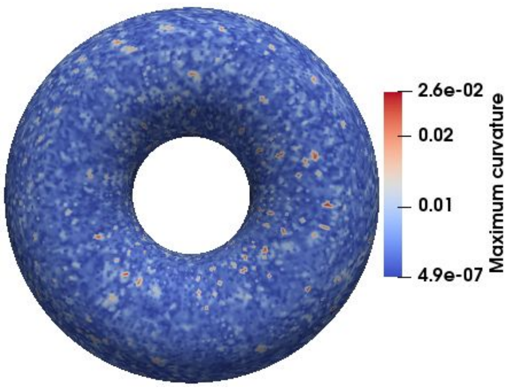

(a) CBE result

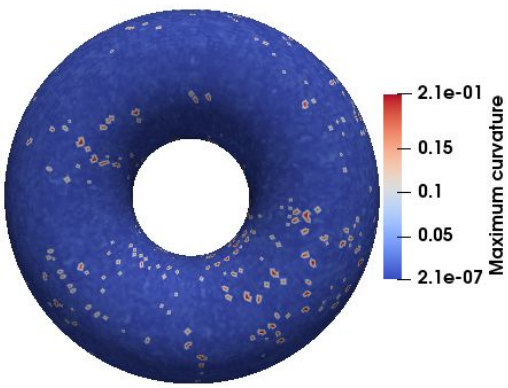

(b) DEM result

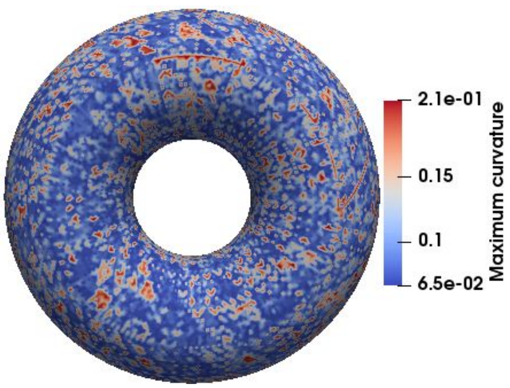

(c) MSC result

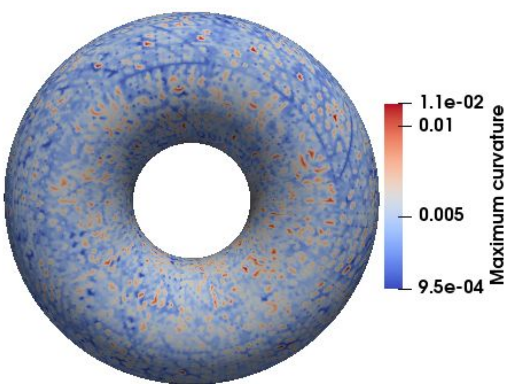

(d) NCC result

Fig. 3. Explicite Meshes Arising from Analytic Parametric Torus Surfaces.

The second triangular mesh reported in Fig. 2(b) is generated form the analytic sinusoidal parametric surface $(x, y, \sin(x)\cos(y))$ [9]. The analytic expression of the shape operator for the sinusoidal surface is represented by a *not symmetric* matrix. For the four comparative method, we first estimate the shape operator and then we compute the principal curvature represented by the two eigenvalues of each estimated operator.

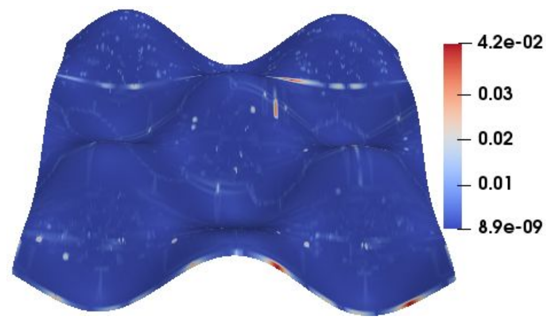

(a) CBE result

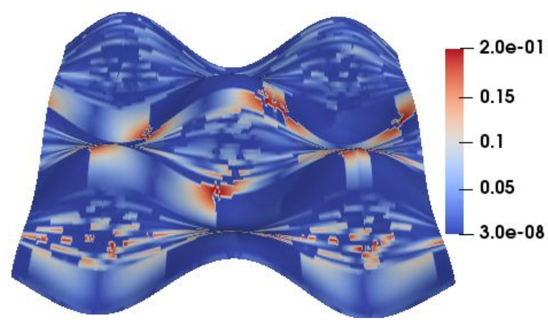

(b) DEM result

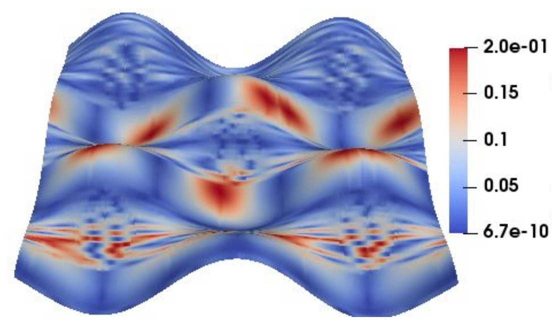

(c) MSC result

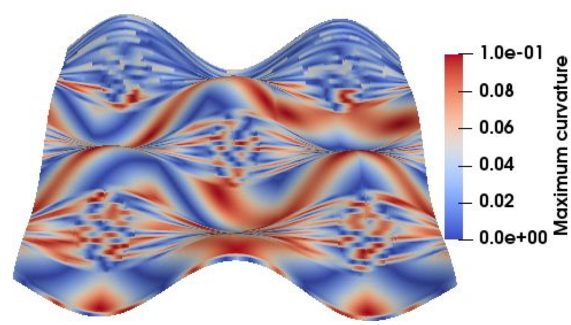

(d) NCC result

Fig. 4. Explicite Meshes Arising from Analytic Parametric Sinusoidal Surfaces.

The eigenvalue corresponding to the maximum curvature is then compared to the maximum curvature arising from the analytic expression of the shape matrix. For the torus mesh with symmetric shape operator, the absolute difference between the estimated and analytic maximum curvatures is reported in Fig. 3. As can clearly seen in Fig. 3(a), the lowest values of error difference between the exact and estimated maximum curvature is achieved by the proposed shape operator estimation method. For the sinusoidal mesh with unsymmetrical shape operator matrix, it can be clearly noticed that the proposed shape operator estimation method outperform the stat-of-art methods in term of accuracy. In Fig. 4(a), we notice the domination of blue color characterizing lowest error between estimated and exact curvature values. Also, due to the averaging shape operator estimation expression (8), the blue color is also uniformly distributed along the mesh. The

TABLE I. ABSOLUTE MEAN ERROR BETWEEN ESTIMATED AND EXACT MAXIMUM CURVATURE ON TORUS AND SINUSOIDAL MESHES.

	Torus mesh Symetric operator	Sinusoidal mesh Unsymetric operator
CBE	$1.02\ 10^{-4}$	$2.02\ 10^{-4}$
DEM	$4.50\ 10^{-4}$	$6.75\ 10^{-3}$
MSC	$2.32\ 10^{-2}$	$3.43\ 10^{-2}$
CCM	$1.50\ 10^{-3}$	$5.50\ 10^{-3}$

absolute mean errors between estimated and exact maximum curvature on torus and sinusoidal meshes are reported in Table I. On the torus mesh with symmetric shape operator, a little difference between the proposed method and the DEM is noticed; however, for unsymmetrical shape operator arising from the sinusoidal surface, the proposed approach largely outperform all comparative methods. To evaluate convergence rate of the four shape operator estimation methods, we report in Fig. 5 the evolution of the mean error difference values in term of mesh resolution for the torus and sinusoidal meshes. In the case of torus mesh with symmetrical shape operator, we observe that the four methods have almost the same rat of convergence, with a small advantage of the proposed method. In contrast to the sinusoidal mesh with unsymmetrical shape operator, we can clearly distinguish the net performance the proposed CBM in comparison with the stat-of-art methods.

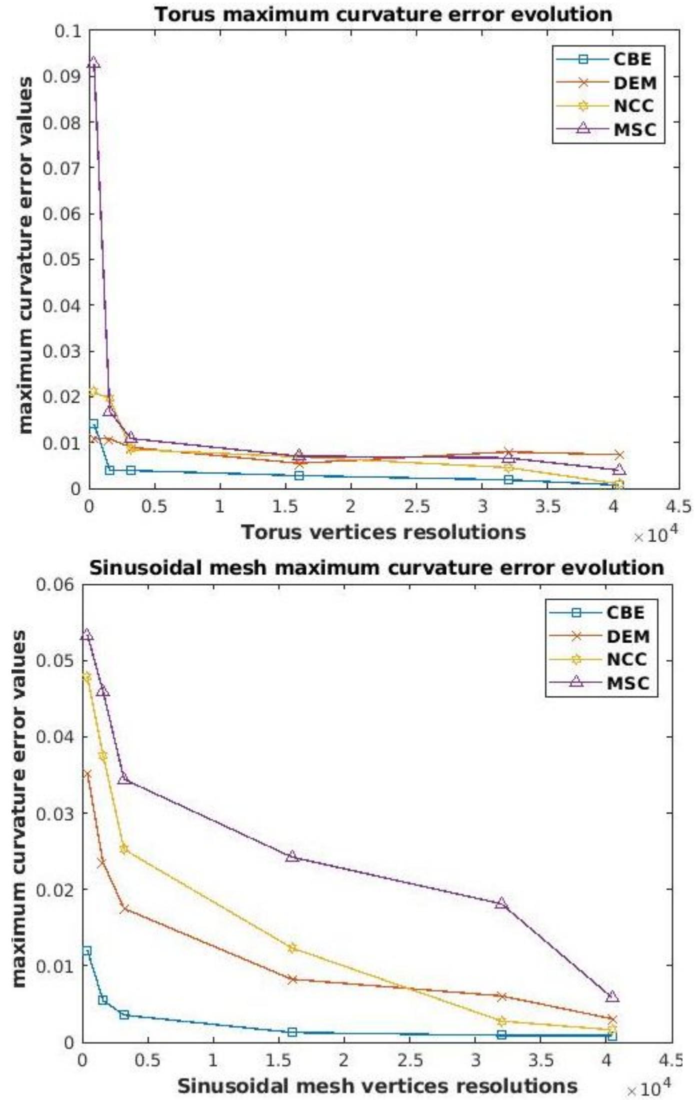

Fig. 5. Maximum Error Metric Evolution of Maximum Principal Curvatures Computed by the Comparative Estimation Methods on Torus and Sinusoidal Meshes.

B. Qualitative Evaluation

The second set of evaluation tests concern two triangular meshes: the catenoid mesh generated by the javaiew software and the standard Fandisk meshes with sharp features reported in Fig. 6(b). The catenoid mesh reported in Fig. 6(a) is a revolution surface generated by rotating catenary curve about an axis [9], it is a minimal surface, which means that it occupies the least area when bounded by a closed space. A minimal surface is essentially characterized by a vanishing mean curvatures elsewhere, that is, $H(v) = 0$ for each vertex v of the mesh. Recall that the mean curvature is the average of the principles curvatures (7). In the Fig. 7, we report the absolute average mean curvature values achieved by the four estimation methods for the minimal catenoid surface mesh. We notice that the proposed Shape operator estimation methods presents the smallest absolute error value flowed together with the Multi-Scale Curvature (MSC) Estimation methods (CCM) and the Normal Cycle Curvature (NCC), the worst values ares achieved by the finite Difference curvature Estimation Method (DEM).

In computer aided 3D design and mesh reprocessing applications, the maximum curvature is largely used to determine sharp features like edges and corners. Such geometric characteristics are characterized by a higher maximum curvature values. In Fig. 8 we consider a gain the catenoid and the fandisk meshes and we compute the maximum curvature values by the proposed shape operator estimation method. From the color map of maximum curvature values for the the catenoid and fandisk meshes depicted in Fig. 8(b), we observe that the sharp features like edges and corners are well identified by the proposed curvature estimation methods. The maximum curvature can also be used to detect defects that my arise during the fabrication process. The Fig. 8(a) shows the color map of the maximum curvature values for the catenoid mesh, we can clearly observe the crack along mesh that cannot be visually detected in the original object in Fig. 6(a). The experimental results show the effectiveness of the proposed mean value shape operator estimation method.

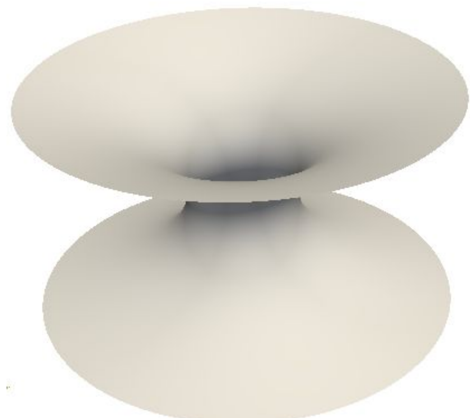

(a) Catenoid mesh

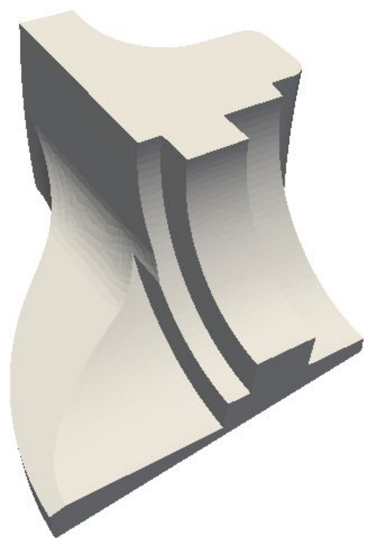

(b) Fandisk mesh

Fig. 6. Explicite Meshes Arising from Analytic Parametric Torus and Sinusoidal Surfaces.

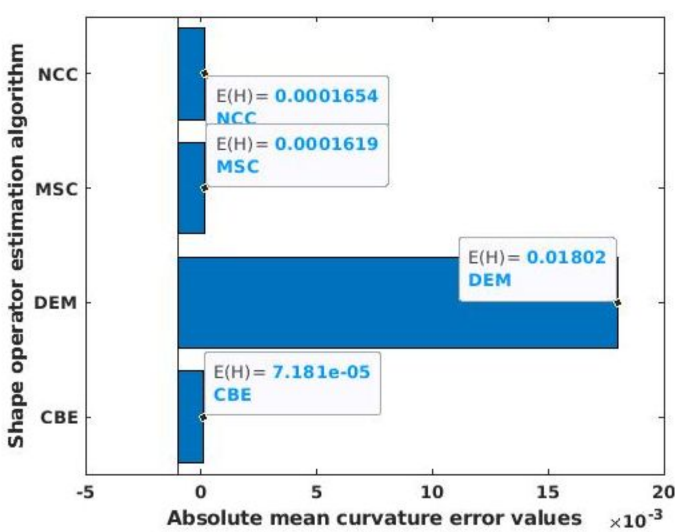

Fig. 7. Mean Curvature Errors Values for the Catenoid Minimal Surface Mesh.

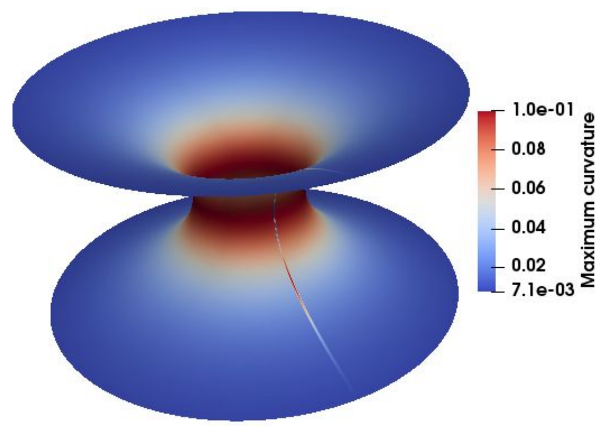

(a) Catenoid color map

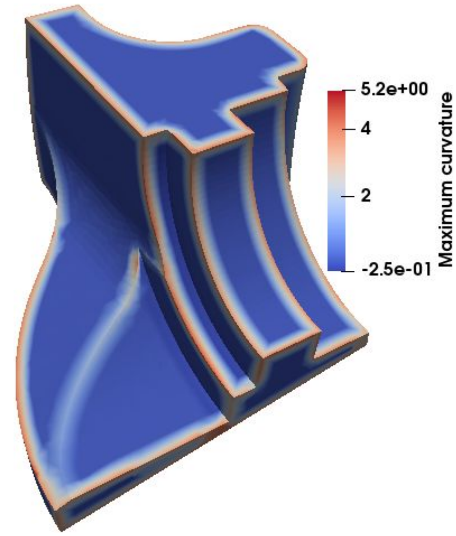

(b) Fandisk color map

Fig. 8. Maximum Curvature Color Map.

C. Discussion

The results show that the proposed operator performs better compared with outperformed some the stat-of-art shape operator estimation methods. It is clear from the above experiments that the shape operator estimation approaches based on the faces finite difference largely outperform the local surface fitting approaches. In future work we plan to adapt the proposed approach to estimate the shape operator method on noisy surface. Due to the complexity and irregularity of mesh data, the challenge is to build a mesh neural network to learn shape operator values directly from mesh data.

VI. Conclusion

In this paper we proposed a mean value based approach to estimate the shape operator on the triangular meshes. In contrast to the state-of-art estimation methods that produce a symmetric shape operator matrix, the proposed algorithm proposed in this work is derived directly from the theoretical definition of the shape operator, and hence produced an estimation that mimetic the continues unsymmetrical nature of the shape operator. To demonstrate the performance of our approach, different tests on a variety of standard meshes are conducted by a quantitative and qualitative comparative study are presented.

REFERENCES

[1] Batagelo, H., Wu, ST. *Estimating curvatures and their derivatives on meshes of arbitrary topology from sampling directions* Visual Comput. 23, pp. 803–812 (2007). https://doi.org/10.1007/s00371-007-0133-8

[2] COHEN-STEINER, D., AND MORVAN, *Restricted Delaunay Triangulations and Normal Cycle* In Proc. Symposium on Computational Geometry (2003). https://doi.org/10.1145/777792.777839

[3] Demir, J. Kehrer and R. Westermann, *Screen-space silhouettes for visualizing ensembles of 3D isosurfaces* 2016 IEEE (PacificVis), (2016), pp. 204-208. doi: 10.1109/PACIFICVIS.2016.7465271.

[4] Deng H, Zhang W, Mortensen E, Dietterich T and Shapiro L *Principal curvature-based region detector for object recognition*, Computer IEEE. (2007),pp. 1–8. doi: 10.1109/CVPR.2007.382972

[5] do Carmo, M. P. *Differential geometry of curves and surfaces*, Prentice Hall,(1976).

[6] El Ouafdi A. F., El Houari H., Ziou D. *Anisotropic adaptive method for tri.angular meshes smoothing* IET Image Process. 9 (6), (2015), 516-526. doi: 10.1049/iet-ipr.2014.0447

[7] Evangelos Kalogerakis, Patricio Simari, Derek Nowrouzezahrai, and Karan Singh. *Robust Statistical Estimation of Curvature on Discretized Surfaces*. In Symposium on Geometry Processing. (2007), 13–22. doi: 10.2312/SGP/SGP07/013-022

[8] Grinspun, E., Gingold, Y., Reisman, J., Zorin, D *Computing discrete shape operators on general meshes.* Comput Graph. Forum, 25(3),(2006), 547-556. https://doi.org/10.1111/j.1467-8659.2006.00974.

[9] K. Khadem S., E.Preus and, Reitebuch U., *Publication of Interactive Visualizations with JavaView*, http://www.javaview.de/, retrieved in Mai 2021.

[10] Klaus Hildebrandt and Konrad Polthier. *Generalized shape operators on polyhedral surfaces*. Comput. Aided Geom. Des. 28(5), (2011), 321–343. doi: https://doi.org/10.1016/j.cagd.2011.05.001

[11] M. Liu, Y. Liu and K. Ramani, *Anisotropic filtering on normal field and curvature tensor field using optimal estimation theory* (SMI '07), (2007), 169-178. doi: 10.1109/SMI.2007.5.

[12] Mao Zhihong, Cao Guo, Ma Yanzhao , Kunwoo Lee *Curvature estimation for meshes based on vertex normal triangles* Comput. Aided Geom. Des., 43(12), (2011), 1561-1566 https://doi.org/10.1016/j.cad.2011.06.006

[13] Merigot Q, Ovsjanikov M, Guibas L. *Robust Voronoi-based curvature and feature estimation*, Geometric and physical modeling, (2009), 1–12. doi/10.1145/1629255.1629257

[14] Panozzo, D., Puppo, E., Rocca, L. *Efficient multi-scale curvature and crease estimation* 2nd International Workshop on Computer Graphics, Computer Vision and Mathematics, GraVisMa 2010 - Workshop Proceedings, (2010), 9-16.

[15] M. Prantl, L. Vása, I. Kolingerová *Fast Screen Space Curvature Estimation on GPU* Published in VISIGRAPP, (2016), 10.5220/0005676801490158

[16] Tang, Y., Sun, X., Huang, D., Morvan, J.M., Wang, Y., Chen, L. *3D face recognition with asymptotic cones based principal curvatures* IEEE (ICB), (2015) 466–472. doi: 10.1109/ICB.2015.7139111

[17] Tang, Y., Li, H., Sun, X. et al *Principal Curvature Measures Estimation and Application to 3D Face Recognition* J Math Imaging Vis 59, 211–233 (2017). https://doi.org/10.1007/s10851-017-0728-2

[18] TAUBIN, G. *Estimating the Tensor of Curvature of a Surface from a Polyhedral Approximation*, IEEE (ICCV), (1995), 902-907. doi: 10.1109/ICCV.1995.466840.

[19] H. Theisel, C. Rossi, R. Zayer and H. P. Seidel, *Normal based estimation of the curvature tensor for triangular meshes* 12th Pacific Conference on Computer Graphics and Applications, (2004), 288-297, doi: 10.1109/PCCGA.2004.1348359

[20] W.-S. Tong and C.-K. Tang, *Robust estimation of adaptive tensors of curvature by tensor voting* IEEE Trans. Pattern Anal. Mach. Intell., 27(3), (2005), pp. 434–449. doi:10.1109/TPAMI.2005.62

[21] Torsten Langer Alexander Belyaev Hans-Peter Seidel *Exact and Interpolatory Quadratures for Curvature Tensor Estimation* Comput. Aided Geom. Des. 24, (2007) 443-463, https://doi.org/10.1016/j.cagd.2006.09.006

[22] S. Rusinkiewicz, *Estimating curvatures and their derivatives on triangle meshes* Proceedings. 2nd International Symposium on 3D Data Processing, Visualization and Transmission, (2004), 486-493. doi: 10.1109/TDPVT.2004.1335277.

[23] S. Yoshizawa, A. Belyaev, H. Yokota and H. Seidel, *Fast and Faithful Geometric Algorithm for Detecting Crest Lines on Meshes* (PG'07), (2007), 231-237. doi: 10.1109/PG.2007.24.

[24] Szilvási-Nagy, M. *Face-based Estimations of Curvatures on Triangle Meshes* J. Geom. Graph. 12 (2008), 63–73.

[25] S. Sharma, S. Vinuchakravarthy and S. J. Subramanian *Estimation of surface curvature from full-field shape data using principal component analysis* 2016 IOP Publishing Ltd Measurement Science and Technology, Volume 28, Number 1 Citation Sameer Sharma et al 2017 Meas. Sci. Technol. 28 015003

[26] Shifrin. T. *DIFFERENTIAL GEOMETRY: A First Course in Curves and Surfaces*, 2015,Lecture notes, University of Georgia, http://alpha.math.uga.edu/ shifrin/ShifrinDiffGeo.pdf.

Content-based Image Retrieval using Tesseract OCR Engine and Levenshtein Algorithm

Charles Adjetey[1]
Department Computer Science
Lancaster University Ghana
Accra, Ghana

Kofi Sarpong Adu-Manu[2]
Department Computer Science
University of Ghana
Legon-Accra, Ghana

***Abstract*—Image Retrieval Systems (IRSs) are applications that allow one to retrieve images saved at any location on a network. Most IRSs make use of reverse lookup to find images stored on the network based on image properties such as size, filename, title, color, texture, shape, and description. This paper provides a technique for obtaining full image document given that the user has some portions of the document under search. To demonstrate the reliability of the proposed technique, we designed a system to implement the algorithm. A combination of Optical Character Recognition (OCR) engine and an improved text-matching algorithm was used in the system implementation. The Tesseract OCR engine and Levenshtein Algorithm was integrated to perform the image search. The extracted text is compared to the text stored in the database. For example, a query result is returned when a significant ratio of 0.15 and above is obtained. The results showed a 100% successful retrieval of the appropriate file base on the match even when partial query images were submitted.**

Keywords*—*Image Retrieval Systems; image processing; Optical Character Recognition (OCR), text matching algorithm, Tesseract OCR engine, Levenshtein Algorithm

I. Introduction

Advances in internet technology, creativity, innovation and the tremendous increase in digital image creation in documents have given rise to the use of techniques to detect and query images on the web. **Content-based image retrieval systems are well studied and a number of researchers have proposed a number of techniques [1], [2], [3], [4]. Some of the authors proposed a new computational backend model that includes a dataset and OCR services for Arabic document information retrieval (ADIR)[1], multimodal features for similarity search we apply re-ranking according to averaged or maximum scores [2] and diagram image retrieval and analysis, with an emphasis on methods using content-based image retrieval (CBIR), textures, shapes, topology and geometry [5].**

The use of sophisticated computer software and multimedia tools on the market has led to the production of digital information and digital images stored in different repositories and cloud servers around the globe. The web content may be searched using keywords or images to retrieve relevant documents or images using search engines. There are general-purpose search engines used for text-based information collections and specialized search engines that allow for special image collections on the web [6].

Search Engines (SEs) give users indexed lists that provide essential information on high-quality websites [7]. Search Engine (SE) may be explained as a program that scans for and recognises items in a database that relates to keywords or characters determined by the users [8]. SEs are utilized mainly to find specific sites on the World Wide Web (WWW) that contain relevant information of interest after querying databases that contain or potentially matching the user keywords. The WWW contains an immense amount of material that require search engines to act as filters to retrieve information on the web. SEs make it easier and serves as a quicker means for users to discover information significant to them without wading through the copious number of insignificant web pages [9].

Different kinds of SEs require the user to input text which serves as the keyword for the search to take place. Searching for specific information via text on the web is a daunting task because users keywords are expected to match the indexing data structure to gain relevant feedback or information. Apart from searching the WWW for information using text, searching via images have also gained more prominence over the past two decades using image search engines (ISEs). ISEs require an image as the input item for the search to take place.

There is a lot of documents and files with multimedia content (that is text and images) of which users seek to retrieve using portions of the file, similar files or other documents [10], [11]. Recently, researchers have aimed at designing algorithms that support image querying that is capable of retrieving images, documents containing images and extracting images within vast scale databases. Content-based image retrieval systems (CBIRS) are required to retrieve specific image descriptors from digital libraries efficiently. CBIRS may operate based on low-level or high-level semantics [9]. The approaches used in CBIRS include deep learning methods, Scale Invariant Feature Transform (SIFT) algorithm, Clustered-scale Invariant (CSI) algorithm, deep learning and compressed domain, convolutional neural networks (CNN), Dot-Diffused Block Truncation Coding (DDBTC), and the Relevance Feedback (RF) Model [12]. All these methods take user input, processes and return the retrieval results to the user. It is expected that the retrieval systems provide the exact results that are semantically similar to the user query.

Most CBIRS use visual content to identify relevant images. In these systems, three key issues arise: how the image is represented, organized, and the image similarity measurements. The general framework of CBIRS may be classified into two stages, the offline and the online stage [6].

Deep learning techniques such as deep belief network are recent approaches used for feature extraction in CBIR applications. In this paper, we based on the strength of the Tesseract OCR to recognize text (that is, makes documents editable and searchable) in an image and we then use our novel algorithm to extract the text from the image. After extracting the text from the image document, we apply the Levenshtein text-matching algorithm to find the similarity between the texts extracted from the images saved in the database. The Levenshtein serves as an edit-distance algorithm to provide information about the least number of edits needed to modify one string to obtain another. For example, a distance of zero (0) indicates that the two strings are identical anything else means they are not the same. The more prominent the distance, the more extraordinary the strings.

Many factors influence search results; among these factors, the quality of keywords depends on the users. Most users enter short queries and avoid using anything other than the primary search engine index; when the search results are returned, users typically would focus on the first few results that appear in the search results. They are primarily unlikely to modify the query. With the CBIR, the search query is not dependent on the user instead the features in the image hence eliminating biases that will lead to poor search.

In this paper, we focus on reverse image search engines (that is, query by example). There are two main techniques used when searching for images in a reverse image search engines: 1) searching with keywords, and 2) searching with pictures/images. In this paper, we search by images. A resulting document-image is retrieved from the database when there is a similarity with the search image. The uniqueness of our approach is that any portion of the image is capable of retrieving the full image-document from the database.

II. Related Work

Content-based image retrieval is gaining more attention in the research community and has been one of the growing areas of research in the past decade. In this section, we provide previous works and approaches related to content-based image retrieval systems. These approaches have used different metrics to retrieve contents of documents from repositories across the world. Over the years, several low-level feature descriptors proposed for image representation have depended on extracting underlying features such as colour, position, edge, shape, texture, GIST, CENTRIST, and bag-of-words (BoW) models using local feature descriptors such as SIFT and SURF. In what follows, we provide brief descriptions of previous works done in the CBIR systems.

In [12], the authors proposed a multi-feature image retrieval technique that was capable of combining features such as colour, edge, and texture to retrieve an image. They made use of a deep belief network (DBN) of Deep Learning to extract these features from an image. The retrieval performance of their approach depended on the feature representation and similarity measurement. In their approach, the DBNs applied in CBIR proposed by authors aided in understanding learning and mapped the various features extracted from the images provided by users. A thorough investigation of feature extraction, mapping, zero paddings, residual learning and loss function were discussed. Their results showed that for a data set of 1000 images, an accuracy rate of about 98.6% was obtained during real-time data extraction. The authors in [13], [12], [11] designed a web content-based image retrieval system referred to as Anaktisi. The search for images is based on various descriptors which include colour and texture. Input from the user can be any image or keyword. Based on the input, the search is conducted in the various databases. The user is presented with images similar to the search input. The presentation of the images is base on the following descriptors: colour and edge directivity descriptor, the fuzzy colour and texture histogram, join composite descriptor, and their compact variants. The authors recommended that future work should include the capacity to seek document images by word spotting.

In [14], the authors developed an interactive content retrieval system. The system had a Graphical User Interface (GUI) that use colour, texture, and shape of a given image and performs a similarity search of the image. The application is made up of three sections. The image laboratory section presents the low-level features of the image used by the application for the retrieval procedure. The image retrieval section makes use of three different search options to retrieve the image, and the extras section of the system incorporates other application to check for the existence of an image. The searches of the images did not consider text that may be embedded in the query images in this system.

In [15], [16], the authors designed an automated system for search and retrieval of trademarks. In their work, they introduce a software that will enable the searching, comparing and retrieving of trademarks. The software comprised of: (i) annotation and storing trademarks in a database; (ii) text-based search and retrieval of trademarks based on annotations; and (iii) content-based search and retrieval based on trademark images. The system was not capable of recognising different trademark features due to the inefficiency of the algorithm used. The system's matching accuracy of trademark images was low and was not capable of assessing real-time data store containing trademarks. In their system, they did not specifically address how their system would deal with the text that is embedded in the word-in-mark trademarks.

The authors in [16] designed a mobile visual search using images and text features. In their work, they propose a mobile visual search system that uses both text and low-bit image features. They described how a phone enabled with a camera can be used to take a photo of a document image and search for the document in online databases. In the detection of text, the authors make use of OCR to detect the text. After the detection of the text, the system identifies the title text. The title text is the one identified because the most informative keywords to search for a document is in the title; hence it is extracted. Based on the features that are characterised by text titles such as size and stroke width, they are identified. Before the extracted features are passed to the OCR, they are rectified, to improve the accuracy of the features. Even though the query image is used as the source of the query and the focus is on the embedded text, it only considers the title text of documents for obvious reasons, and this may not be good enough in situations where the document title may not be available.

In [17], the authors proposed techniques to extract image descriptors using scale-invariant feature transform (SIFT) after which *k-means* clustering is performed on the features extracted with SIFT. These techniques were adopted due to their efficiency in retrieving realistic images in large databases. Experimental results, as reported by authors, showed that the proposed approach was efficient. The proposed approach when compared with the traditional Bag of Words (BoW) approach and the Spatial pyramid matching (SPM) yielded 92.69% mean Average Precision (mAP) whereas BoW and SPM achieved 82.00%and 88.80% mAP, respectively. In [18], the authors used 1400 binary and gray-scale images grouped into 70 categories with 20 images in each of the 70 categories were obtained from MPEG-7, COIL-20 and ZuBuD image databases. The authors observed that for both binary and gray-scale images, similar objects were retrieved. SIFT was used to perform the feature extraction to detect key-points within the datasets. The key-point descriptors were initially computed using the gradient magnitude and the orientation of the image at each image sample point within the chosen region. For example, the authors computed a 2X2 descriptor from a 4X4 set and 8X8 descriptor from a 16X16 image set samples. In the experiment results, the precision and recall graph of images such as octopus, hammer, apple and spoon revealed that images of octopus outperformed the remaining images due to the number of corners observed in an octopus. Hence, the SIFT algorithm was seen to perform better with images with more corners.

In the work of [9], the author designed an experiment and used datasets from the SUN database. The author classified the images into eight classes (that is, water, car, mountain, ground, tree, building, snow, sky and unknown - containing all other classes). Three thousand (3000) images placed into 41 categories were collected from the database. The images were further categorized into training images (1900), testing images (600) and validation images (500). Convolutional neural network (CNN) was employed for extracting required features. The CNN was repeatedly applied as a function across the sub-regions of the entire image. The focus was the input image with a linear filter, with an added bias term and further applying a non-linear function. The CNN was trained by passing the compressed train, test, and validation datasets. The system design comprised of the query image, trained neural network, and annotation index to obtain the results. From the authors evaluation results, it turned out that CNN outperformed Bag-of-Words (BoWs) in retrieving the different images (that is, water, car, mountain, ground, tree, building, snow, sky) but BoWs recorded fewer error rates in identifying a tree, building and sky. In Table I, a comparison of some existing content-based retrieval systems are provided. The comparison highlighted the techniques used for feature extraction, the query technique used, the testing environment, and the features used for the extraction.

From the literature review analysis, we observed that most of the research works in CBIR have focused on extracting images from database repositories using different feature extraction techniques. Besides the query by example scheme adopted in most projects, other query schemes such as querying by keyword and in some instances querying by colour layout have been used in recent implementations. Existing CBIR systems use the query by example scheme to retrieve similar images from databases. Most of these CBIR systems focused on retrieving images that contain objects from databases. In our work, we focused on the text feature of the query by example to retrieve text-based documents converted to image using part of the image as the query to retrieve the full documentation that contains the said text. This novel approach is relevant in searching large database repositories that contain an enormous amount of scanned text documents.

III. METHODOLOGY

A. Methods and Techniques

The system analysis and design tools used to model the system included Data Flow Diagram (DFD) and Unified Modelling Language (UML). Also, the incremental development and the reuse-oriented software engineering models were adopted for the development of the system. The main philosophy of this process is to develop an initial implementation, get feedback from the user and evolve the software until there is satisfaction with the functionalities of the software. Reuse-oriented software engineering approach was adopted because of its significant number of reusable components. The choice of the OCR engine influenced the usage of the model. The OCR engine adopted is the Tesseract-OCR. The use of the OCR engine decreases the amount of software to be developed. Also, it decreases the cost and risk that comes with using this approach [23].

Algorithm 1 Administrator Algorithm

Input: UPLOAD Image files
Output: Image
1: NAME Uploaded files
2: CALLS OCR module to extract text
3: SAVE extracted text to Database
4: SAVE Uploaded files (under the given Name) to a file location
5: **return** Image

B. Conceptual Model

Fig. 1 describes the conceptual framework for system implementation. The framework is in three compartments: the Query, Processing and Output, and Load. This framework guided the implementation of the proposed image retrieval system. The administrator activities are shown in Algorithm 1, and the user activities are also shown using Algorithm 2. In what follows, we provide a detail description of the activities involved in image retrieval. The system operates based on the following algorithms. The entire process flow is shown in Fig. 2 and Fig. 3.

C. Tools

The Tesseract OCR engine was used as the OCR engine for the system. The version used in our development supports multiple languages. It supports multiple image formats supported by Leptonica and supports layout analysis [24], [21]. ASP.NET MVC framework with C# framework was used for the development. Thus, the application does not need any installation on client computer beyond the usage of a web browser; making the application hardware independent

TABLE I. COMPARATIVE STUDY OF EXISTING CBRIS

Reference	CBIR Technique used for extraction	Brief Description	Query Techniques used and features extracted	Testing Environment
[12]	Deep belief network (DBN) method of deep learning	Proposed an efficient algorithm to search large databases and retrieve digital images using the feature representation and similarity measurements.	Query by example/colour, radiance, luminance, structures, frequency	Simulation [the type of simulator was not stated though by the authors]
[17]	Scale-invariant feature transform (SIFT)	The CBIR techniques introduced by the authors overcame the memory usage and matching time problem in SIFT. k-means clustering was employed to cluster the entire matrix into 16-clusters (that is a matrix of size 8X16). After this, a second approach is used to further reduced size 1 X 18	Query by example/Image scale, noise and illumination	Experimental testbed [Caltech 101 (with 9144 images) and Li database (with 2360) images]
[18]	Scale Invariant Feature Transform (SIFT) algorithm for binary and gray scale images	SIFT was employed to detect images and extract features of the image.	Query by example/Corners, edges, scale, rotation and translation	Experimental (MATLAB)
[9]	Convolutional Neural Networks (CNN)	The worked employed CNN to retrieve images from a database containing 3000 images that were placed into 41 categories and 8 classes	Query by example/colour and texture	Experimental
[19]	Convolutional Neural Networks (CNN) model and Dot-Diffused Block Truncation Coding (DDBTC)	In this work, two metrics (i.e., average precision rate and recall rate) to examine datasets to measure the retrieval rate. They employed deep learning with compression for image retrieval.	Query by colour and Exam-ple/Texture and colour	Experimental
[20]	Not provided	The work mainly focused on identifying problems existing in CBIR systems, biometric systems, and problems related to image feature extraction	Query by example/Shape, colour and texture	Investigation
[21]	Optical Character Recognition (OCR).	The work sought to improve OCR quality of digitizing historical collections in a national library in Finland. To show the improvement of their approach to other approaches, they employed morphological analyzer and character accuracy rate	ABBYY FineReader v.11 and Tesseract re-OCR	Evaluation
[22]	Relevance Feedback (RF) Model/ Deep Learning	The authors used the Rocchio algorithm to obtain the image vector trained in CNN model in a sorted database based on a similarity metric. The results obtained from an experimented design showed that the Precision-Recall results outperforms them on the Caltech256 datasets with the distance learning metric.	Empirical Studies/ Experimental	Experimental

Algorithm 2 Searcher Algorithm

Input: Query Image File
Output: Image
Initialisation:
1: CALL OCR module to extract text
LOOP Process
2: SAVE extracted text to temporary location
3: CALL Matching module
4: **if** (Match found) **then**
5: DISPLAY Results of Matches
6: RETRIEVE Document associated with Match from File location
7: **end if**
8: **return** $Image$

and ubiquitous. ASP.NET MVC allows the creation of web application by dividing the application into the model (M), views (V), and controllers (C) and this reduces the complexity of managing the broader application. The MVC framework provides the need for the separation of the business logic layer of the web application from its presentation layer. Unlike the Web Form framework, the MVC allows one to have absolute control on HTML and HTTP. MVC is extensible, providing developers with the ability to customize the framework [25].

1) Searcher Query: This is the part that interfaces with the user. The Searcher submits the query image file via the GUI, as shown in Fig. 4. The image file is sent to the processing and output section. The Query part serves as the front end of the system. The Searcher then searches for a particular document and uploads the image into the system. After the necessary processing has been performed on the image, a notification is

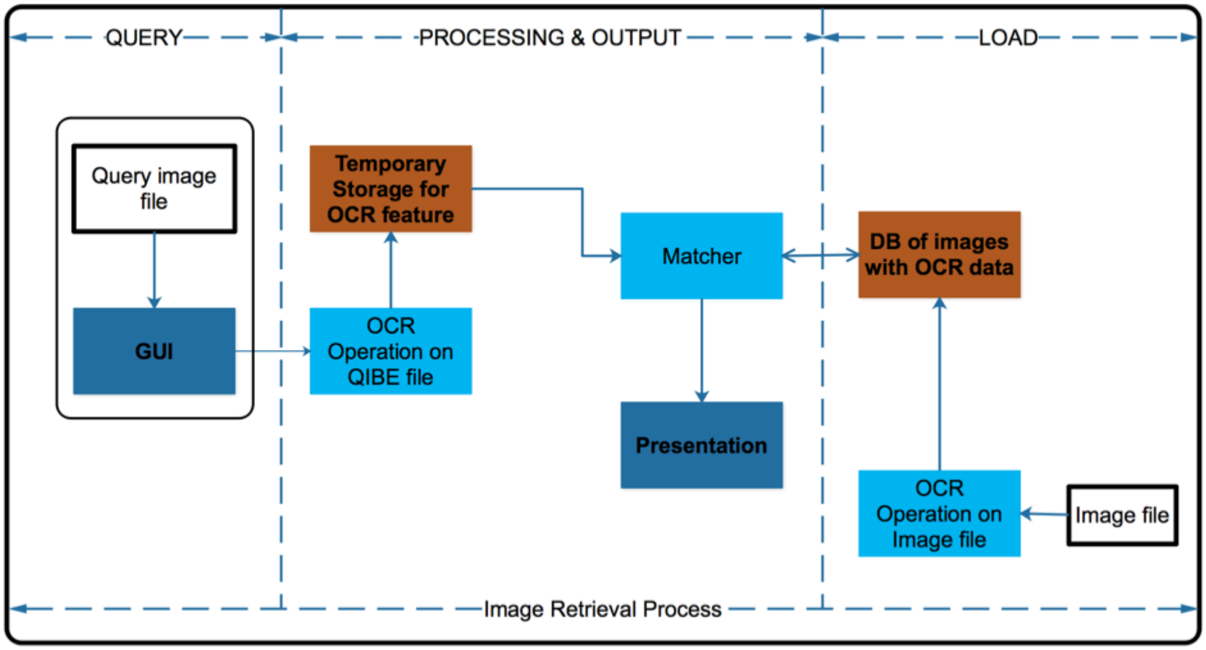

Fig. 1. Conceptual Framework for the CBIR System.

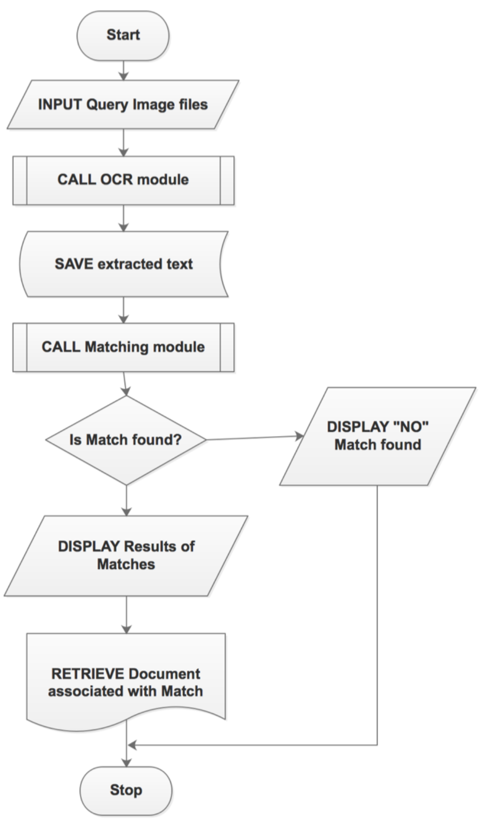

Fig. 2. Flowchart - Admin Side.

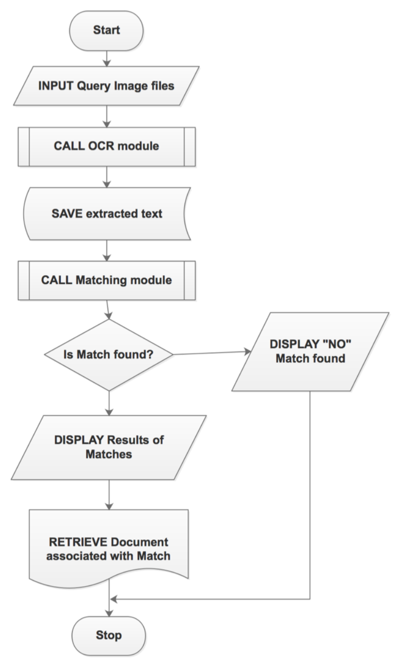

Fig. 3. Flowchart - user Side.

given to the Searcher [25].

2) Processing and Output: The query image file submitted is processed, and desired output is presented to the Searcher/User, as shown in Fig. 4. OCR operation is performed on the query image file to obtain the text feature of the file. This information is stored in a temporary storage location. The text features are sent to the matcher comparison. The Processing and Output section is between the front-end and the back-end (see Fig. 4). The processing and output part

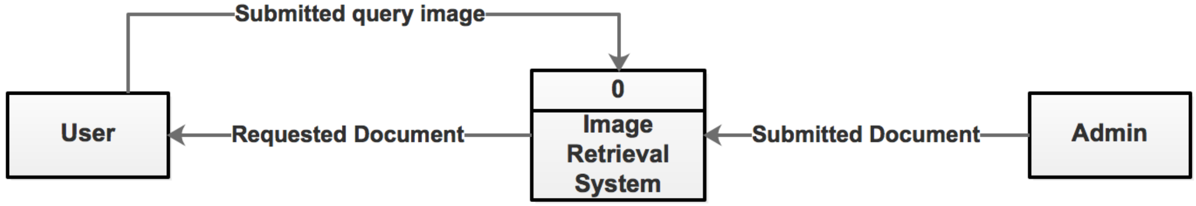

Fig. 4. Context Level Diagram of the CBIR System.

that acts as the *workhorse* for the system. The image upload by the user is processed in this section. Text matching to find the entire document and the display output is performed here. The Tesseract OCR engine evaluates the query image upload by the user, and the extracted text is saved in a temporary location. The content is saved in a string variable and compared to all extracted images uploaded by the Admin. The improved Levenshtein algorithm makes a comparison. The operation of the Levenshtein Algorithm on the implementation are discussed in Section IV. After the comparison is made the output is shown to the user. The outputs are ranked from the top to the bottom according to the similarity index found in the database, with the highest index at top. The user selects the appropriate link to download the document [26].

3) Load: The Load part stores information for Searcher/User retrieval. It serves as the database repository during the search process, which is similar to searching over the web. The image files are loaded into the system, then OCR operation is performed on the image to make the text recognisable. The recognised texts are stored with the image in the database. The Load part serves as the back-end to the system. It is in this section that the Administrator uploads the image files of a document to the system. Once the files have been uploaded the Tesseract OCR engine acts on it, and the extracted text is saved in the database. The file remains on the server but not saved in the database. However, the file path leading to where the file is saved is instead saved in the database. This makes the database lighter, hence, improving the system's performance.

IV. Analysis of the Tesseract OCR and Levenshtein Algorithm

A. Tesseract OCR

The primary purpose of the Tesseract OCR is to recognise characters in a given image. After the characters have been recognised, it is then extracted and saved. The characters extracted are group into words. A word is series of character without white space. Words recognised do have a confidence level. The confidence level of a word shows the accuracy level of the recognised word. Fig. 5 shows a sample image document that was uploaded to test the working of the OCR. Fig. 5 contains 595 words. At different resolutions, the number of words that the OCR recognised is as follows:

- Results of words at 2167 x 3064 pixel - 609 words
- Results of words at 724 x 1024 pixel - 91 words
- Results of words at 566 x 800 pixel - 20 words

The 609 words recognised in the 2167 x 3064 is because the OCR recognise some punctuations as words. It is clear that the lower the resolution, the fewer words were recognised, and this is in line with the work done by [25]. Each word recognised by the OCR has a confidence level. The confidence of a word is the certainty of the accuracy of that word. Lower values indicate high certainty whereas, higher values indicate low certainty. Also, lower resolutions provided low confidence values even with the same words recognised in the different resolution. With the data obtained from the OCR, it shows that high resolution also provides better *meaningful words*. Meaningful words are all words that when checked in the document exists as it has been recognised. The observation made from the data can express as follows:

- $R \propto W_n$
- $W_n \propto W_m$
- Hence, $R \propto W_m$
- $W_n \propto C$
- Hence, $R \propto C$
  where R is the Resolution, W_n is the number of words recognised, W_m is the number of meaningful words, and C is the confidence of a word.

B. Levenshtein Algorithm

The Levenshtein algorithm, also known as the Edit-Distance algorithm was developed by Vladimir Levenshtein [27]. The algorithm provides information about the least number of edits needed to modify one string to obtain another string. Levenshtein algorithm measures similarity and matches approximate strings with fuzzy logic. Thus, the difference between the two strings is not presented as either absolutely true or false [28]. The distance between two character strings is the difference in the strings due to the number of deletions, insertions, or substitution. A distance of zero (0) indicates that the two strings are identical anything else means they are not the same. The more prominent the distance, the more unique the strings are [25]. In order to test how the system is working concerning the algorithm, four (4) different files (image documents) which sum up to 13 pages was uploaded from the administrator's side of the system.

The first file constituted the first four pages in the database; the second file constituted the next three pages, the third file the next two pages and the fourth file the last four pages. From the user's side, a query image was submitted to the system. The query image that was used in the first instance is shown in Fig. 5. The second and third instance made use of portions of Fig. 5, these portions are shown in Fig. 6 and Fig. 7, respectively.

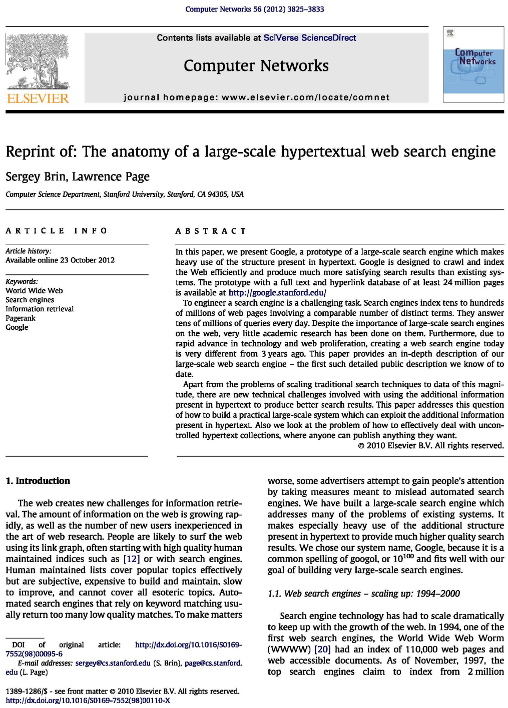

Computer Networks 56 (2012) 3825–3833

Contents lists available at SciVerse ScienceDirect

Computer Networks

journal homepage: www.elsevier.com/locate/comnet

ELSEVIER

Reprint of: The anatomy of a large-scale hypertextual web search engine

Sergey Brin, Lawrence Page

Computer Science Department, Stanford University, Stanford, CA 94305, USA

ARTICLE INFO

Article history:
Available online 23 October 2012

Keywords:
World Wide Web
Search engines
Information retrieval
Pagerank
Google

ABSTRACT

In this paper, we present Google, a prototype of a large-scale search engine which makes heavy use of the structure present in hypertext. Google is designed to crawl and index the Web efficiently and produce much more satisfying search results than existing systems. The prototype with a full text and hyperlink database of at least 24 million pages is available at http://google.stanford.edu/

To engineer a search engine is a challenging task. Search engines index tens to hundreds of millions of web pages involving a comparable number of distinct terms. They answer tens of millions of queries every day. Despite the importance of large-scale search engines on the web, very little academic research has been done on them. Furthermore, due to rapid advance in technology and web proliferation, creating a web search engine today is very different from 3 years ago. This paper provides an in-depth description of our large-scale web search engine – the first such detailed public description we know of to date.

Apart from the problems of scaling traditional search techniques to data of this magnitude, there are new technical challenges involved with using the additional information present in hypertext to produce better search results. This paper addresses this question of how to build a practical large-scale system which can exploit the additional information present in hypertext. Also we look at the problem of how to effectively deal with uncontrolled hypertext collections, where anyone can publish anything they want.

© 2010 Elsevier B.V. All rights reserved.

1. Introduction

The web creates new challenges for information retrieval. The amount of information on the web is growing rapidly, as well as the number of new users inexperienced in the art of web research. People are likely to surf the web using its link graph, often starting with high quality human maintained indices such as [12] or with search engines. Human maintained lists cover popular topics effectively but are subjective, expensive to build and maintain, slow to improve, and cannot cover all esoteric topics. Automated search engines that rely on keyword matching usually return too many low quality matches. To make matters worse, some advertisers attempt to gain people's attention by taking measures meant to mislead automated search engines. We have built a large-scale search engine which addresses many of the problems of existing systems. It makes especially heavy use of the additional structure present in hypertext to provide much higher quality search results. We chose our system name, Google, because it is a common spelling of googol, or 10^{100} and fits well with our goal of building very large-scale search engines.

1.1. Web search engines – scaling up: 1994–2000

Search engine technology has had to scale dramatically to keep up with the growth of the web. In 1994, one of the first web search engines, the World Wide Web Worm (WWWW) [20] had an index of 110,000 web pages and web accessible documents. As of November, 1997, the top search engines claim to index from 2 million

DOI of original article: http://dx.doi.org/10.1016/S0169-7552(98)00095-6
E-mail addresses: sergey@cs.stanford.edu (S. Brin), page@cs.stanford.edu (L. Page)

1389-1286/$ - see front matter © 2010 Elsevier B.V. All rights reserved.
http://dx.doi.org/10.1016/S0169-7552(98)00110-X

Fig. 5. Sample Image Document.

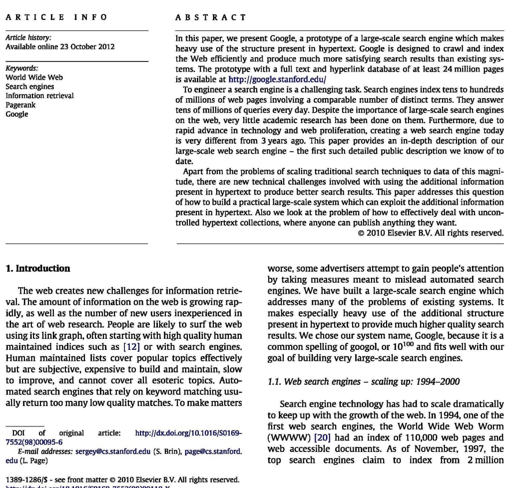

ARTICLE INFO

Article history:
Available online 23 October 2012

Keywords:
World Wide Web
Search engines
Information retrieval
Pagerank
Google

ABSTRACT

In this paper, we present Google, a prototype of a large-scale search engine which makes heavy use of the structure present in hypertext. Google is designed to crawl and index the Web efficiently and produce much more satisfying search results than existing systems. The prototype with a full text and hyperlink database of at least 24 million pages is available at http://google.stanford.edu/

To engineer a search engine is a challenging task. Search engines index tens to hundreds of millions of web pages involving a comparable number of distinct terms. They answer tens of millions of queries every day. Despite the importance of large-scale search engines on the web, very little academic research has been done on them. Furthermore, due to rapid advance in technology and web proliferation, creating a web search engine today is very different from 3 years ago. This paper provides an in-depth description of our large-scale web search engine – the first such detailed public description we know of to date.

Apart from the problems of scaling traditional search techniques to data of this magnitude, there are new technical challenges involved with using the additional information present in hypertext to produce better search results. This paper addresses this question of how to build a practical large-scale system which can exploit the additional information present in hypertext. Also we look at the problem of how to effectively deal with uncontrolled hypertext collections, where anyone can publish anything they want.

© 2010 Elsevier B.V. All rights reserved.

1. Introduction

The web creates new challenges for information retrieval. The amount of information on the web is growing rapidly, as well as the number of new users inexperienced in the art of web research. People are likely to surf the web using its link graph, often starting with high quality human maintained indices such as [12] or with search engines. Human maintained lists cover popular topics effectively but are subjective, expensive to build and maintain, slow to improve, and cannot cover all esoteric topics. Automated search engines that rely on keyword matching usually return too many low quality matches. To make matters worse, some advertisers attempt to gain people's attention by taking measures meant to mislead automated search engines. We have built a large-scale search engine which addresses many of the problems of existing systems. It makes especially heavy use of the additional structure present in hypertext to provide much higher quality search results. We chose our system name, Google, because it is a common spelling of googol, or 10^{100} and fits well with our goal of building very large-scale search engines.

1.1. Web search engines – scaling up: 1994–2000

Search engine technology has had to scale dramatically to keep up with the growth of the web. In 1994, one of the first web search engines, the World Wide Web Worm (WWWW) [20] had an index of 110,000 web pages and web accessible documents. As of November, 1997, the top search engines claim to index from 2 million

DOI of original article: http://dx.doi.org/10.1016/S0169-7552(98)00095-6
E-mail addresses: sergey@cs.stanford.edu (S. Brin), page@cs.stanford.edu (L. Page)

1389-1286/$ - see front matter © 2010 Elsevier B.V. All rights reserved.
http://dx.doi.org/10.1016/S0169-7552(98)00110-X

Fig. 6. Partial Image of Fig. 5 for Query.

In Fig. 8, we show the comparison ratio that was attained based on the three different query images that were used. The query image Fig. 6 that was used in the first query is the entire page 1 of the first file in the database. This return, the highest comparison ratio of 1, in other words, 100% match, as depicted in Fig. 9. The second and the third query as already indicated, was based on partial images of Fig. 6, and the highest comparison ratio return were 0.88 and 0.22, respectively. From these results, it is clear that the more words found in a query image, the higher the comparison ratio. Further tests indicate that when a file of a particular image document is used as the search query, the results that are the comparison ratio were close to 1. In Fig. 9, the individual pages of *document1* were uploaded as the search query, the results

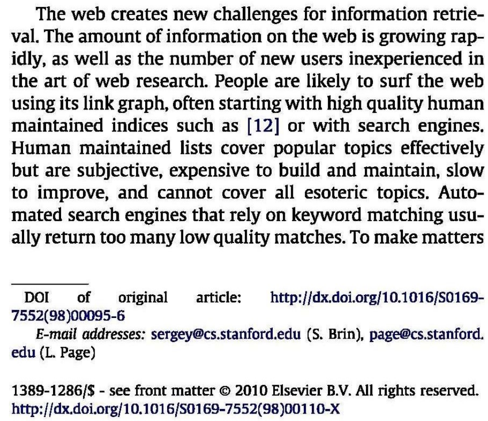

The web creates new challenges for information retrieval. The amount of information on the web is growing rapidly, as well as the number of new users inexperienced in the art of web research. People are likely to surf the web using its link graph, often starting with high quality human maintained indices such as [12] or with search engines. Human maintained lists cover popular topics effectively but are subjective, expensive to build and maintain, slow to improve, and cannot cover all esoteric topics. Automated search engines that rely on keyword matching usually return too many low quality matches. To make matters

DOI of original article: http://dx.doi.org/10.1016/S0169-7552(98)00095-6
E-mail addresses: sergey@cs.stanford.edu (S. Brin), page@cs.stanford.edu (L. Page)

1389-1286/$ - see front matter © 2010 Elsevier B.V. All rights reserved.
http://dx.doi.org/10.1016/S0169-7552(98)00110-X

Fig. 7. Partial Image of Fig. 6 for Query.

indicate that page 1 returned a comparison ratio of 0.99, page 2 returned 0.92, page 3 returned 0.98 and page 4 returned 0.99. Similar results were obtained from the experiment conducted, and these are shown in Fig. 10, 11, and 12.

Files that cannot get a comparison ratio of 0.15 and above in any of its pages is excluded from the search results. So in the third query were only the first file had a page with a comparison more significant than the 0.15 criteria, only the first file was return as the search results. However, the first and second query returned all the files as the search result since they were the page (s) in each files having a comparison ratio 0.15. Other tests were done with different query image, and these test yielded similar trends as discussed above. Also, future work can be that of having a crawler attached to the system that will crawl the web if its implementation is to be used universally on the internet. This crawler's purpose is to get images with their URL. The system can then extract the text content of these images and then link them to the URL where they were gotten from so that when a user submits a query image, the search results will be the URL links.

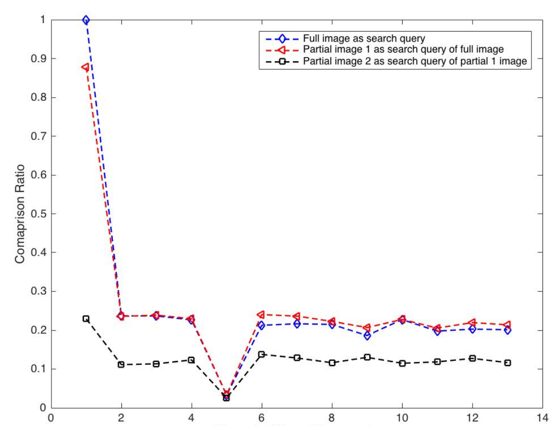

Fig. 8. Comparison Ratio of Fig. 5, 6, and 7.

In Fig. 13, the full page of an image *sample image - file 4* were uploaded as the search query, the results indicated in

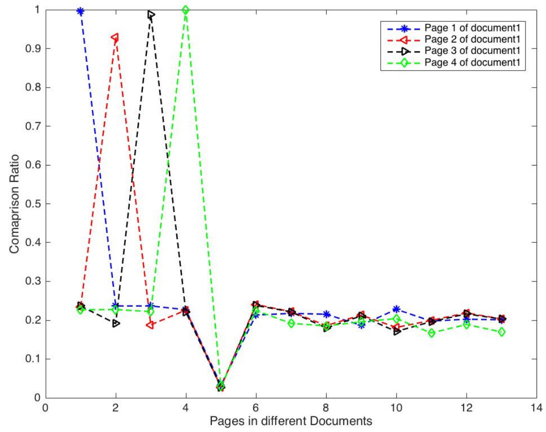

Fig. 9. Comparison Ratio of Pages 1 to 3 of Different Document.

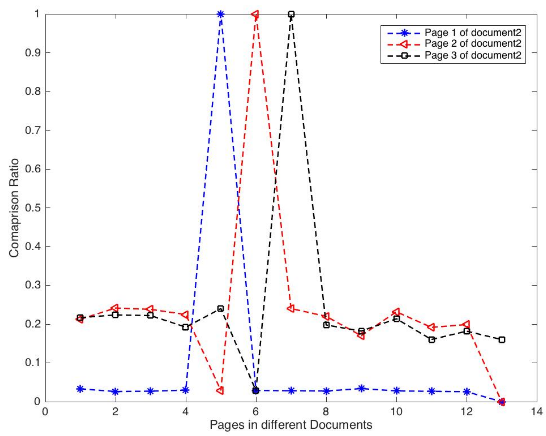

Fig. 10. Comparison Ratio of Pages 1 to 3 in the Database.

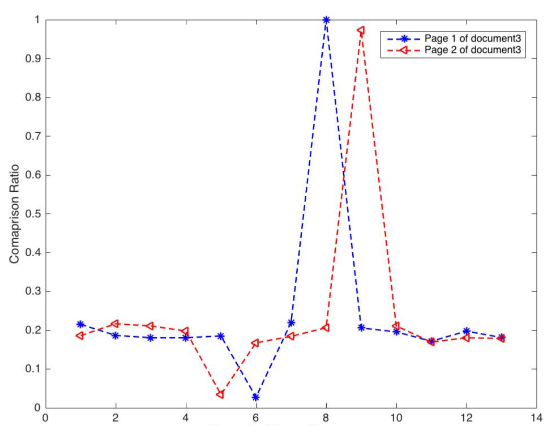

Fig. 11. Comparison Ratio of Page 1 and 2 of Different Document.

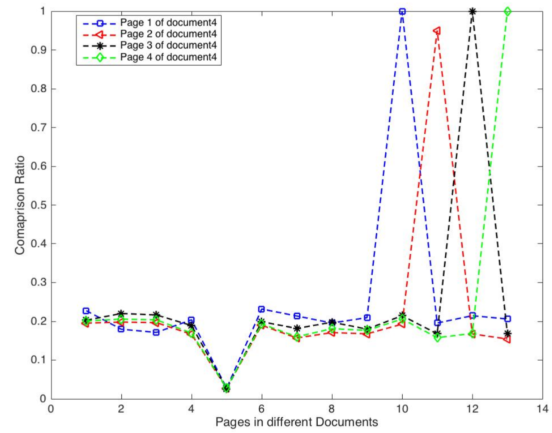

Fig. 12. Comparison Ratio of Pages 1 to 4 of Different Document.

2011 International Joint Conference of IEEE TrustCom-11/IEEE ICESS-11/FCST-11

Security Issues in NoSQL Databases

Lior Okman
Deutsche Telekom Laboratories
at Ben-Gurion University,
Beer-Sheva, Israel

Nurit Gal-Oz, Yaron Gonen, Ehud Gudes
Deutsche Telekom Laboratories
at Ben-Gurion University,
and Dept of Computer Science,
Ben-Gurion University,
Beer-Sheva, Israel

Jenny Abramov
Deutsche Telekom Laboratories
at Ben-Gurion University and
Dept of Information Systems Eng.
Ben-Gurion University,
Beer-Sheva, Israel

Abstract—**The recent advance in cloud computing and distributed web applications has created the need to store large amount of data in distributed databases that provide high availability and scalability. In recent years, a growing number of companies have adopted various types of non-relational databases, commonly referred to as NoSQL databases, and as the applications they serve emerge, they gain extensive market interest. These new database systems are not relational by definition and therefore they do not support full SQL functionality. Moreover, as opposed to relational databases they trade consistency and security for performance and scalability. As increasingly sensitive data is being stored in NoSQL databases, security issues become growing concerns.**

This paper reviews two of the most popular NoSQL databases (Cassandra and MongoDB) and outlines their main security features and problems.

Index Terms—**NoSQL; Security; Cassandra; MongoDB;**

I. INTRODUCTION

The recent advance in cloud computing and distributed web applications has created the need to store large amount of data in distributed databases that provide high availability and scalability. In recent years, a growing number of companies have adopted various types of non-relational databases, commonly referred to as NoSQL databases and as the applications they serve emerge, they gained extensive market interest. Different NoSQL databases take different approaches. Their primary advantage is that, unlike relational databases, they handle unstructured data such as documents, e-mail, multimedia and social media efficiently. The common features of NoSQL databases can be summarized as: high scalability and reliability, very simple data model, very simple (primitive) query language, lack of mechanism for handling and managing data consistency and integrity constraints maintenance(e.g., foreign keys), and almost no support for security at the database level.

The CAP theorem introduced by Eric Brewer [1], refers to the three properties of shared-data systems namely data consistency, system availability and tolerance to network partitions. The theorem [2] states that only two of these three properties can be simultaneously provided by the system. Traditional DBMS designers have prioritized the consistency and availability properties. The rise of large web applications and distributed data systems, makes the partition-tolerance property inevitable, thus imposing compromise on either consistency or availability.

The main promoters of NOSQL databases are Web 2.0 companies with huge, growing data and infrastructure needs such as Amazon and Google. The Dynamo technology developed at Amazon [3] and the Bigtable distributed storage system developed at Google [4], have inspired many of today's NoSQL applications.

In this paper we analyze the security problems of two of the most popular NoSQL databases, namely: Cassandra and MongoDB. Cassandra [5] is a distributed storage system for managing very large amounts of structured data spread out across many commodity servers, while providing highly available service with no single point of failure. Cassandra aims to run on top of an infrastructure of hundreds of nodes. At this scale, components fail often and Cassandra is designed to survive these failures. While in many ways Cassandra resembles a database and shares many design and implementation strategies therewith, Cassandra does not support a full relational data model; instead, it provides clients with a simple data model that supports dynamic control over data layout and format. Cassandra was designed to support the Inbox search feature of Facebook [6]. As such it can support over 100 million users which use the system continuously.

MongoDB [7] is a document database developed by 10gen. It manages collections of JSON-like documents. Many applications can thus model data in a more natural way, as data can be nested in complex hierarchies and still be query-able and indexable. Documents are stored in collections, and collections are in turn stored in a database. A collection is similar to a table in relational DBMS, but a collection lacks any schema. MongoDB also provides high availability and scalability by using Shardings and Replica sets (see below).

The increasing popularity of NoSQL databases such as Cassandra and MongoDB and the large amounts of user-related sensitive information stored in these databases raise the concern for the confidentiality and privacy of the data and the security provided by these systems. In this paper we review the main security features and problems of these two database systems. We start with a brief overview of Cassandra and MongoDB functionality in section II. We then discuss security features of Cassandra and MongoDB in sections III and IV respectively. We conclude in section V. Since much of the discussion is based on open-source Internet documents, it naturally reflects the situation at the time this paper is written

978-0-7695-4600-1/11 $26.00 © 2011 IEEE
DOI 10.1109/TrustCom.2011.70

541

IEEE computer society

Fig. 13. Sample Image - File 4.

Table II shows the various comparison ratios.

V. CONCLUSION

The paper employed the use of the Tesseract OCR engine and an improved Levenshtein Algorithm in content-based image retrieval system to extract text from an image and use the text-image to search for the full document containing the text. The text content of the image was used as the base. The system as it stands now can be used for the storing and retrieving of image documents. Just by providing a query image, the right document will be provided to the User once it exists in the database. This system can be employed in areas where

TABLE II. SEARCH RESULTS USING FULL IMAGE FILE (PAGE 1 OF FILE 4 OF FIG. 13).

Image File Pages	Comparison Ratio
File 1 Pg 1	0.227470472
File 1 Pg 2	0.179640725
File 1 Pg 3	0.171515763
File 1 Pg 4	0.2040605
File 2 Pg 1	0.027760513
File 2 Pg 2	0.231821
File 2 Pg 3	0.21379739
File 3 Pg 1	0.195773765
File 3 Pg 2	0.2104827
File 4 Pg 1	1
File 4 Pg 2	0.196395278
File 4 Pg 3	0.214626059
File 4 Pg 4	0.204474822

there is a need to digitised documents into images for onward retrieval base on the query image. From the experimental results, our approach a showed 100% match when the query image matches its page in the database; otherwise, lower values would be obtained when the extracted text does relate to other text.

VI. FUTURE WORK

In this section, we discuss some important research directions that require additional attention to improve content-based image retrieval systems.

A. Machine Learning Algorithms and Artificial Neural Networks

In most CBIR systems, the query techniques employed by authors are query by example to obtain the relevant features. These features are not adequate in themselves. Hence, advanced knowledge-based techniques and approaches capable of extracting multiple features from documents may efficiently improve the search criteria. These machine learning algorithms and artificial neural networks methods may also validate the extracted features, perform classification on the images and select relevant aspects for the search query. By this means, query features that are not capable of providing accurate results will be eliminated.

B. Multi-level Text Matching

Current approaches in CBIR systems based on text features rely mainly on single-level text matching. It is recommended that future CBIR systems implement a multi-level text matching capable of improving retrieval efficiency to improve the efficiency of the document retrieved.

C. Searching by Cluster of Words (or paragraph)

One of the significant limitations for searching with the current approach is lower image resolution. Hence, instead of word by word matching, we recommend that future work focuses on a cluster of words (or paragraph) matching, which will significantly increase the accuracy.

D. Gathering Data using Crawlers

A crawler can be attached to the system that will crawl the web if the system is implemented and used universally on the web. This crawler's purpose is to get images with their respective URL. The system can then extract the text content of these images and then link them to the URL where they were gotten from so that when a user submits a query image, the search results will be the URL links.

ACKNOWLEDGMENT

The authors would like to thank colleagues who supported us in diverse ways to get this manuscript ready for publication.

REFERENCES

[1] H. M. Al-Barhamtoshy, K. M. Jambi, S. M. Abdou, and M. A. Rashwan, "Arabic documents information retrieval for printed, handwritten, and calligraphy image," *IEEE Access*, vol. 9, pp. 51 242–51 257, 2021.

[2] K. Pustu-Iren, G. Bruns, and R. Ewerth, "A multimodal approach for semantic patent image retrieval," 2021.

[3] P. Ghadekar, S. Kaneri, A. Undre, and A. Jagtap, "Digital image retrieval based on selective conceptual based features for important documents," in *Evolutionary Computing and Mobile Sustainable Networks*. Springer, 2021, pp. 569–579.

[4] K. M. Lakshmi *et al.*, "An efficient telugu word image retrieval system using deep cluster," *Turkish Journal of Computer and Mathematics Education (TURCOMAT)*, vol. 12, no. 11, pp. 3247–3255, 2021.

[5] L. Yang, M. Gong, and V. K. Asari, "Diagram image retrieval and analysis: Challenges and opportunities," in *Proceedings of the IEEE/CVF Conference on Computer Vision and Pattern Recognition Workshops*, 2020, pp. 180–181.

[6] W. Zhou, H. Li, and Q. Tian, "Recent advance in content-based image retrieval: A literature survey," *arXiv preprint arXiv:1706.06064*, 2017.

[7] A. Jain, "The role and importance of search engine and search engine optimization," *International Journal of emerging trends & technology in computer science*, vol. 2, no. 3, pp. 99–102, 2013.

[8] N. Höchstötter and D. Lewandowski, "What users see–structures in search engine results pages," *Information Sciences*, vol. 179, no. 12, pp. 1796–1812, 2009.

[9] A. V. Singh, "Content-based image retrieval using deep learning," 2015.

[10] B. Wang, X. Zhang, and N. Li, "Relevance feedback technique for content-based image retrieval using neural network learning," in *2006 International Conference on Machine Learning and Cybernetics*. IEEE, 2006, pp. 3692–3696.

[11] A. Rashno and E. Rashno, "Content-based image retrieval system with most relevant features among wavelet and color features," *arXiv preprint arXiv:1902.02059*, 2019.

[12] R. R. Saritha, V. Paul, and P. G. Kumar, "Content based image retrieval using deep learning process," *Cluster Computing*, vol. 22, no. 2, pp. 4187–4200, 2019.

[13] K. Zagoris, S. A. Chatzichristofis, N. Papamarkos, and Y. S. Boutalis, "img (anaktisi): A web content based image retrieval system," in *2009 Second International Workshop on Similarity Search and Applications*. IEEE, 2009, pp. 154–155.

[14] K.-M. Wong, K.-W. Cheung, and L.-M. Po, "Mirror: an interactive content based image retrieval system," in *2005 IEEE International Symposium on Circuits and Systems*. IEEE, 2005, pp. 1541–1544.

[15] F. Karamzadeh and M. A. Azgomi, "An automated system for search and retrieval of trademarks," in *Proceedings of the 11th International Conference on Electronic Commerce*, 2009, pp. 374–377.

[16] B. Girod, V. Chandrasekhar, R. Grzeszczuk, and Y. A. Reznik, "Mobile visual search: Architectures, technologies, and the emerging mpeg standard," *IEEE MultiMedia*, vol. 18, no. 3, pp. 86–94, 2011.

[17] G. A. Montazer and D. Giveki, "Content based image retrieval system using clustered scale invariant feature transforms," *Optik*, vol. 126, no. 18, pp. 1695–1699, 2015.

[18] S. A. Bakar, M. S. Hitam, and W. N. J. H. W. Yussof, "Content-based image retrieval using sift for binary and greyscale images," in *2013 IEEE International Conference on Signal and Image Processing Applications*. IEEE, 2013, pp. 83–88.

[19] P. Liu, J.-M. Guo, C.-Y. Wu, and D. Cai, "Fusion of deep learning and compressed domain features for content-based image retrieval," *IEEE Transactions on Image Processing*, vol. 26, no. 12, pp. 5706–5717, 2017.

[20] R. S. Choras, "Image feature extraction techniques and their applications for cbir and biometrics systems," *International journal of biology and biomedical engineering*, vol. 1, no. 1, pp. 6–16, 2007.

[21] M. Koistinen, K. Kettunen, and J. Kervinen, "How to improve optical character recognition of historical finnish newspapers using open source tesseract ocr engine," *Proc. of LTC*, pp. 279–283, 2017.

[22] H. Xu, J.-y. Wang, and L. Mao, "Relevance feedback for content-based image retrieval using deep learning," in *2017 2nd International Conference on Image, Vision and Computing (ICIVC)*. IEEE, 2017, pp. 629–633.

[23] I. Sommerville, "Software engineering 9th edition," *ISBN-10*, vol. 137035152, p. 18, 2011.

[24] M. Smitha, P. Antony, and D. Sachin, "Document image analysis using imagemagick and tesseract-ocr," *International Advanced Research Journal in Science, Engineering and Technology (IARJSET)*, vol. 3, pp. 108–112, 2016.

[25] S. Smith, "Overview of asp .net core mvc," *Microsoft. Last modified January*, vol. 7, 2018.

[26] J. S. Valacich, J. F. George, and J. S. Valacich, *Modern systems analysis and design*. Pearson Education Limited London, 2017.

[27] G. Naganjaneyulu, A. Narasimhadhan, and K. Venkatesh, "Performance evaluation of ocr on poor resolution text document images using different pre processing steps," in *TENCON 2014-2014 IEEE Region 10 Conference*. IEEE, 2014, pp. 1–4.

[28] M. Gilleland *et al.*, "Levenshtein distance, in three flavors," *Merriam Park Software: http://www. merriampark. com/ld. htm*, 2009.

New Data Placement Strategy in the HADOOP Framework

Akram ELomari[1], Larbi Hassouni[2], Abderrahim MAIZATE[3]
RITM-ESTC / CED-ENSEM, University Hassan II
Casablanca, Morocco

***Abstract*—Today, the data quantities generated and exchanged between information systems continues to increase. Storing and exploiting such quantities require can't be done without bigdata systems with mechanisms capable of meeting technological challenges commonly grouped under the four Vs (Volume, Velocity, Variety and Veracity). These technologies include mainly the Distributed File System (DFS). Like Hadoop, which is based on HDFS, the main Big Data systems use a data distributed storage where a subsystem is responsible for subdividing data (data striping) and replicating it on a network of nodes called Grid. In the typical case of Hadoop, a Grid generally consists of many nodes, grouped in multiple Racks. The logic of distributing the stored data through the Grid respects a simple strategy that guarantees the durability of the data and a certain speed of writing. This strategy does not take into consideration neither the technical characteristics of nodes, nor the number of requests on the data, which means a considerable loss in processing capacity of the grid. In this work we proposed a new placement strategy based on exploitation analysis of new information integrated into the HDFS metadata model. A significant 20% improvement in overall processing time was reached through the simulations we conducted on Hadoop.**

Keywords—Big data; data storage; Hadoop; DFS; HDFS; data striping; chunks; placement strategy; performance optimization

I. Introduction

The amount of data generated and processed by current information systems continues to increase, and the generation of digital information has never been more abundant. While the volume of data created was estimated at 2 ZB in 2010, it is estimated that it has reached 47 ZB in 2020 and will increase to 175 ZB in 2025 and 2142 ZB in 2035 [1].

Also, taking advantage of data mines has become a complex and demanding operation. As a result, Big Data systems are positioned as effective [2], scalable, and efficient solutions to exploit this quantity of Data.

The purpose of big Data systems is therefore to store and analyze very large masses of data, while ensuring an adequate level of data security and accessibility.

In this context, most Big Data systems, such as the Apache Hadoop [3], delegate data storage management to distributed file systems (DFS).

The Hadoop Big Data system is based on HDFS (the standard DFS of HADOOP). In combination with other layers of data processing, Hadoop can achieve complex calculations on extended clusters. The main objective of HADOOP is to distribute complex operations on multiple machines while bringing those operations closer to the concerned data and thus improve the global performances.

The capacity and performance of similar platforms, such as Facebook and Google also depend on this distributed architecture based on DFS [4].

HDFS thus manage several storage nodes dedicated only to storage or to storage and computing at the same time, grouped generally in racks and interconnected by local or wide networks.

HDFS machines do not have specific characteristics; they are usually low-cost machines, easily replaceable. The protection against breakdowns is provided by a data placement strategy based on striping and replication of data blocks called chunks. This strategy is based on simple principles [5]:

Create multiple copies(replicas) of the same data.

Place replicas on several machines distributed on several racks (as much as possible).

The placement of replicas, however, does not take in consideration the nature of the demand on each data or its evolution over time [6]. The performance of machines is not considered too, even if HDFS allows integrating machines of different characteristics on the same cluster.

These shortcomings in HDFS' data placement strategy have prompted us to propose an improvement in this strategy as a novel algorithm, which takes into consideration the history of reading operations and proposes a redistribution of data over the cluster.

Our research starts with a deep understanding of the working mechanisms of HADOOP as a whole and of HDFS, to design an algorithm that is applicable and implementable.

Our test simulations were conducted on small cluster to control data transfers and thus demonstrate the efficiency of the algorithm even on a small scale.

The rest of the paper is as follows. Section 2 provides an overview of HADOOP Architecture. Section 3 presents the new proposed placements strategy of chunks. Section 4 presents testing and simulation approach. Section 5 the results and discussion and section 6 provide a conclusion of the work.

II. Hadoop Architecture Overview

Our research method was based on an in-depth analysis of how Hadoop's HDFS works, in order to better understand the problematic raised by the chunk placement strategy. The aim of this analysis is to bring a considerable improvement to this strategy, by using new algorithms which exploit new metadata integrated into the architectural model of HDFS.

Our analysis begins with an understanding of HDFS and its logic of data stripping and replication, followed by a critical analysis of the strategy currently used by HDFS to distribute replicas across the cluster. We then proposed new metrics to be calculated and integrated with chunk metadata managed by HDFS, as well as an algorithm that is based on these metrics and offers a new and more efficient way to place chunks.

Hadoop is Apache's known big data system, based on an open-source implementation of Google's famous MapReduce. It is a complex ecosystem that aims to optimize storage and calculations made on data in large quantities.

The main purpose of Hadoop is to distribute very large data processing on clusters composed mainly of entry-level machines. The goal is to bring processing closer to data instead of moving data to processing, to minimize network bandwidth occupation. Hadoop's strength comes from the fact that it can manage platforms ranging from a few servers to clusters of thousands of machines, while accepting a high tolerance for hardware failures given the wide variety of machines supported.

By offering a software-managed service continuity model regardless of hardware quality, Hadoop can detect hardware failures at the application level and take the necessary steps to return to normal in case of failure in a transparent manner for system users. Hadoop is a flexible, scalable, and highly tolerant solution to hardware failures which guarantees a very good cost/effective rate.

A. *Hadoop Architecture*

There are three major implementations of Hadoop, the 1.x launched for the first time in 2012, the 2.x first appeared in 2013 and the 3.x first launched in December 2017.

Hadoop's overall architecture has not changed much since its first release; it's based on a Model of Master/Slaves/Users.

Two layers are still present:

- The storage layer of data represented by HDFS (Hadoop Distributed File System) which manages the distribution of data through the cluster and always ensures the integrity and persistence of this Data. This layer also manages storage servers (DataNode).
- The data processing layer that manages the parallelization of calculations across the cluster, based on the MapReduce model.

Therefore, two types of Master exist on Hadoop: the NameNode in charge of the HDFS component and the JobTracker (replaced in version 2.x by YARN (Yet Another Resource Negotiator)) which takes care of the implementation of MapReduce.

The NameNode is duplicated for high availability purpose (even tripled on version 3.0).

The rest of the cluster consists of nodes running the DataNode process for storage distribution (communicates exclusively with HDFS NameNode) and TaskTraker for data processing (communicates exclusively with YARN JobTracker or resource manager)

YARN uses the ResourceManager which manages several NodeManager responsible for distributing tasks and reporting the status of nodes to the ResourceManager.

The client communicates with both masters and Slaves to write or read data or give instructions on how this data should be processed.

Fig. 1 gives a basic representation of Hadoop's organization.

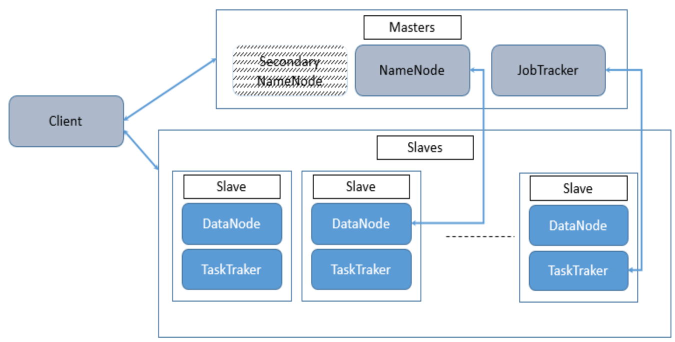

Fig. 1. Hadoop Architecture.

While reading process, the client wishing to read data contacts the NameNode to get the locations of the data blocks, and then reads the contents of the block from the nearest DataNode. When writing, the client asks NameNode to name a suite of three (by default three but can be configured) DataNodes to host replicas of the blocks. The user then writes the data in the DataNodes as a pipeline, user to node1, then node 1 to node 2 and node 2 to node 3.

The current design has only one active NameNode for each cluster. The cluster can have thousands of DataNodes and tens of thousands of HDFS clients per cluster, because each DataNode can perform multiple application tasks simultaneously.

The data processing goes through the JobTracker, the client constitutes his MapReduce job and submits it to the JobTracker which subdivides it into multiple Map/Reduce tasks and assigns each one to a TaskTracker of a DataNode containing concerned data. The user can retrieve the results through direct readings on HDFS.

B. *Hadoop Distributed File System*

HDFS is the distributed file storage system used by default by Hadoop. It has the particularity of being able to run on machines of low cost and consequently to be very tolerant to hardware failures.

For its implementation, several hypotheses have been made:

- The predisposition of equipment used to failures requires a high capacity to detect these failures and restore service.
- HDFS is better prepared for batch treatments and not for user-by-user interactions. POSIX semantics have been particularly relaxed in order to facilitate streaming and increase data flow.
- HDFS is geared to handle very large data. Files stored on HDSF can reach terabytes and therefore the size of the cluster and its architecture must support these sizes.
- Files on HDFS are usually written only once by a single owner but they are read several times. Actions that may change the files are Append or Truncate.
- HDFS allows applications to move data near processing. The other sense (bring data into processing) can be very bandwidth consuming especially when the data is very large.
- HDFS has been developed with JAVA which allows it to turn on many different platforms.

These assumptions frame the architecture of HDFS and allow the optimization of several aspects [7], especially data security and processing speed.

HDFS expose a Filesystem, called Namespace, similar to most traditional Filesystems; it can contain folder hierarchies, user can create, rename, move or delete files from the system. It can also include access rights or quotas per user.

1) Architecture of HDFS: The architecture of HDFS is based on a single active Master (called NameNode) and several Slaves (called DataNode).

The NameNode manages the state of DataNodes in the cluster and handle distribution of storage throughout the cluster.

The NameNode also regulates user's access to data, every write or read operation starts by requesting information from the NameNode [8].

However, the NameNode is not involved in the transfer of data between the user and dataNodes, since data blocks information (Metadata) are separated from the data itself and stored on the NameNode, it simply transfers a list of DataNodes concerned by the user's query as well as the metadata of chunks.

The user then communicates with the DataNode without overloading the NameNode. This greatly simplifies the architecture of HDFS and prevents the NameNode from becoming a bottleneck.

The persistence of the NameNode is guaranteed by two main files:

- A transaction log called EditLog that records all changes made to HDFS metadata (e.g., replica number change).
- A data file called FsImage, which contains all the information about the system as the locations of the blocks and the properties of the system.

FsImage reflects the exact state of HDFS; however it is not updated directly after data modification operations. Operations are recorded in real time on EditLog and flashed in bulk on the FsImage at the starting of HDFS or at specific times called checkpoints.

These two files constitute the heart of HDFS, and their corruption can cause the total shutdown of the service. So, the NameNode constitute a real SPOF (Single point of Failure) of the system.

To reduce the risk associated with this SPOF, the NameNode can maintain several copies of these two files and keep them meticulously synchronized, or else set up several NameNodes (possibility to put 2 on version 2 of Hadoop or more on version 3), where one is active, and the others are passive but ready to provide a fast "Failover" if needed. In this case the DataNodes are all conFig.d to recognize all NameNodes and transmit them the same data transmitted to the Active NameNode.

This can be combined with the use of a distributed EditLog called Journal which consists of the definition of several machines on the cluster (JournalNodes or JNs) that will house copies of the EditLog. The Active NameNode is responsible for transmitting the Editlog changes to the majority of the JNs. Other passive NameNodes see these changes and applicate them onto their own Namespace. In a disaster recovery situation, a passive NameNode makes sure to execute any changes made to the EditLog before turning into the active NameNode.

2) Replication in HDFS: Because HDFS often runs on convenience equipment, hardware failures can occur at any time, which can result in partial or total data loss [9]. To mitigate this risk, HDFS uses a replication technique that aims to ensure the sustainability of the data in case of hardware or network technical problems.

Fig. 2 explains the overall pattern of the HDFS replication model.

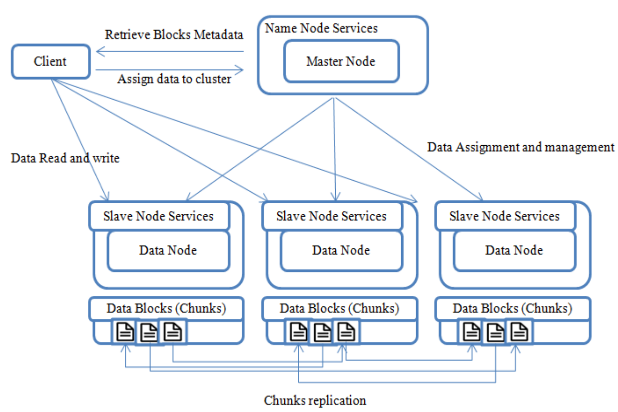

Fig. 2. Replication Process in HDFS.

In HDFS, the files are split into several Blocks of equal sizes (except the last one) called chunks. This manipulation, called Data Stripping, allows HDFS to parallelize data access by storing these blocks on different DataNodes and thus improve response times. HDFS then replicates each Block in several copies (usually three copies but it is configurable) and places each copy on a DataNode determined according to a predefined strategy.

The number of replicas, also called replication factor, is managed by the NameNode and can be changed at any time and for each file separately.

To keep the NameNode up to date, it receives regularly information from each DataNode. Two types of information are received:

- The HeartBeat that allows the NameNode to ensure that the DataNode is still up and running.
- The BlockReport through which DataNode provides NameNode with a list of all valid data blocks it contains.

When creating a file, the NameNode provides the user with a list of DataNodes that can host that data (the list contains N DataNode where N is the replication factor). The user starts transmitting the data in pieces to the first DataNode which writes it locally and begins to transmit it to the second DataNode in the list and so on until the Nth DataNode.

3) The placement of replicas on HDFS: To designate the DataNode that will house the Blocks during a write operation, HDFS applies a policy that considers both the risk of failure and the speed of access.

HDFS is often set up as a cluster consisting of several racks where several DataNodes are housed. Communication between machines of different racks necessarily passes through switches which make the exchange between machines of the same rack generally faster than the exchange between machines of different racks [10].

It will therefore make sense to select DataNode from the same rack to place all the replicas of a block, given the saving of time and bandwidth that this can provide. However, in this way it will increase the fragility of the system in case of a failure affecting an entire rack.

That is why HDFS has a strategy that takes these two aspects in consideration:

As illustrated in Fig. 3, in the common case where the replication factor is 3, two of the replicas are placed on two DataNodes of the same rack while the third is placed on a DataNode of a different rack, depending on the availability of storage space.

If the replication factor is greater than three then these conditions are supplemented by the condition of not putting more than two replicas on the same Rack or the same Data Node as far as possible.

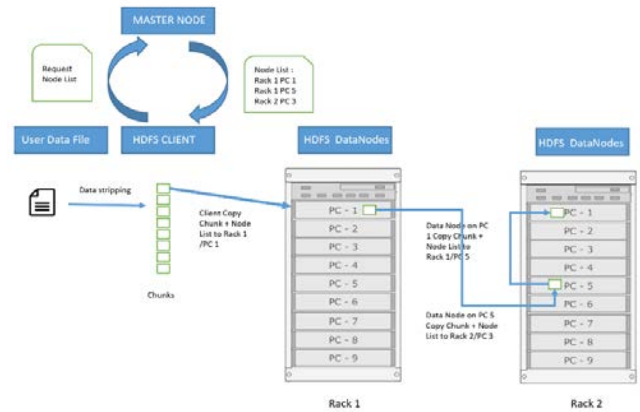

Fig. 3. Chunk's Placement Strategy in HDFS.

The problem statements:

This strategy allows better data availability in case of a network, rack or switch failure, and also optimizes writing times since one-third of the data is exchanged in a single rack.

However, this strategy may reduce the overall parallel playback bandwidth since the data is available only on two racks and not three (where 3 is the replication factor).

This strategy also shows another more important disadvantage [11]; it determines the DataNode where replicas are placed at creation of the chunk and never takes in consideration the evolution of traffic or demand on the replicas, nor the capacity of the nodes chosen for the hosting of the data.

Indeed, at the time of the creation of the chunks, the first replica is created on a DataNode close to the "writer", but our simulations have shown that the demand on the replicas can evolve to another location. In addition, since Hadoop cluster is built using convenience hardware that can fail or simply become obsolete [12], the structure and composition of the cluster may evolve rapidly and radically.

This suggests moving most requested Data (according to a cluster operations analysis) to machines most willing to process them as quickly as possible [13].

These points make the placement strategy used by default by HDFS, a possible source of loss of processing performance due to the poor distribution of data on the cluster.

Our work consists of proposing a method for analyzing the demand on replicas and develops an algorithm for replacing replicas based on the recurrence of demand and machines performances [14], [15].

4) Related work: Many works have tried to improve the strategy of placing chunks in DFS. Some works have proposed to change the storage method by reducing the number of small files by grouping them into larger files [5], or to optimize the replication factor and the size of chunks to improve internal exchanges inside the cluster [6], [7]. Another approach is to try to assign the data to the best node according to the known physical capacities of each node. The limitation of these methods is that it is based on data inputs that never updates, even in evolving environments like HADOOP where the hardware is constantly changing because of its possibly low-cost nature.

Our approach allows building a dynamic database based on collected response times and not the hardware characteristics of the Grid, then use this data to move the chunks to better locations and improve the overall response time of the grid.

III. Improved Placement of Chunks

A. *Evaluation of Demand on Chunks*

To assess the need to change the location of a chunk in the grid we propose to add two metadata to the chunks metadata managed by HDFS. Those metadata will be calculated by the DataNode and transmitted in the block report to the MasterNode. They will be updated every time a chunk is consulted.

These two metadata are:

- C: The chunk consultation rate, which is the number of times the chunks has been downloaded during a configurable period (such as one month)
- Tc: The mean read time of the chunk during the same period as defined in (1).

$$\mathrm{Tc} = \frac{\sum_{i=1}^{C} t_i}{C} \quad (1)$$

C : The number of consultations.

t_i : Read time at Nth consultation.

Mean read time is calculated by the HDFS daemon running on the DataNode after each read operation.

The NameNode will have a consolidated and sorted table of all the chunks as the example Table 1:

TABLE I. Sample of Chunks Consultation Statistics

Id chunks	C	Tc (ms)
A	200	10
B	100	6
C	50	12
D	40	7

A perfectly ordered table should contain the chunks at the beginning with a maximum C corresponding to a minimum Tc.

However, analysis of the data recovered from a simulation cluster shows cases where highly requested chunks have relatively high response times.

Our goal is to be able to move the most requested chunks to the Nodes that give the best reading times (Pn).

Through metadata we can calculate the mean performance of each node through the formula (2):

$$\mathrm{Pn} = \frac{\sum_{i=1}^{k} T_{ci} C_i}{\sum_{i=1}^{k} C_i} \quad (2)$$

Pn: Mean performance of the node n

k : Number of chunks in the node n

Ci: Number of consultations of Chunk i placed in the node n.

Tci : Mean read time of the Chunk i placed in the node n.

Moving a chunk to a location with better reading times does not necessarily mean that response times on this chunk will improve, as the mean response times also depend on the nature of the request (location of reading requests, processing on the data...), but Tc's evaluation algorithm will continue to collect response times for the moved chunks on its new location and will allow to reassess the need or not to move it to a better location.

After one to several iterations of chunks moves, the improvement on the mean consultation time will eventually be observable or at least stagnate in its minimum value, meaning that the chunks are on the best location in terms of response time.

The number of chunks moves must be limited so as not to saturate the network more than necessary.

Movements of Data should be made at a time when data access is low or absent, so that the bandwidth will not be over occupied by this operation.

B. *Algorithms*

<u>Optimizer</u>

The Optimizer function (Fig. 4) scans the table of statistics of chunks consultation starting from the greatest number of consultations, which corresponds to the most requested chunks. This chunk should be placed in the best Node in terms of response time. In the best case the chunks with highest C will have to be moved to the Node whose have lowest Pn. The algorithm will try to retrieve an available Node with the best Pn.

```
Function Optimizer(Table chunks_Table)
{
--Table ordered by decreasing number of consultations –

Chunks_OrdredDescByC = OrderDescByC(chunks_Table);
        Foreach (chunk in Chunks_OrdredDescByC)
        {
                DestinationNode=
                GetBestNodeForchunks(Chunk chunk);

                MoveChunkToNode(chunk,
                DestinationNode)


        }
}
```

<u>GetBestNodeForchunks</u>

The GetBestNodeForchunks (Fig. 5) function allows retrieving the Node which offers the best average consultation time (Pn) which suggests it is a better location for a given chunk.

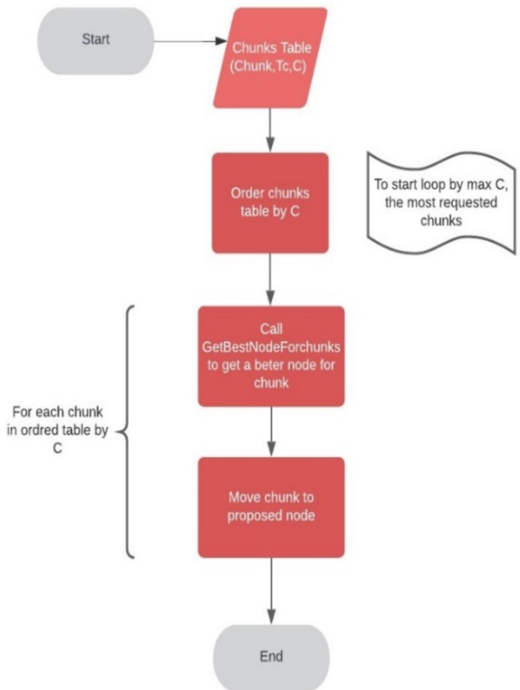

Fig. 4. Replacement Algorithm.

To do this, we calculate Pn for each node in the table and we go through the table of means of consultation time of the chunks, ordered up wards according to Pn, we check for each node its eligibility to receive the chunk passed in parameter.

Eligibility is based on four criteria:

1) The node is different from the one where the chunk is already placed.

2) The availability of space on the node.

3) The Node does not already contain a chunk replica.

4) The Node is not in the same rack as two other replicas.

Those criteria comply with Hadoop's basic policy, i.e., no more than two replicas in the same rack.

```
Function Node GetBestNodeForchunks(Chunk chunk)
{

--Table ordered by decreasing number of consultations –

Chunks_OrdredAscByPn = OrderDescByC(chunks_Table);
Foreach (betterPnChunk in Chunks_OrdredAscByPn)
          {
            If (betterPnChunk.Pn< chunk.Tc
                    {
                 Node node = getChunkNode(betterPnChunk);
                If (Eligible(node,chunk)
                                {Return node;}
                    }
            }
          Return Null;
}
```

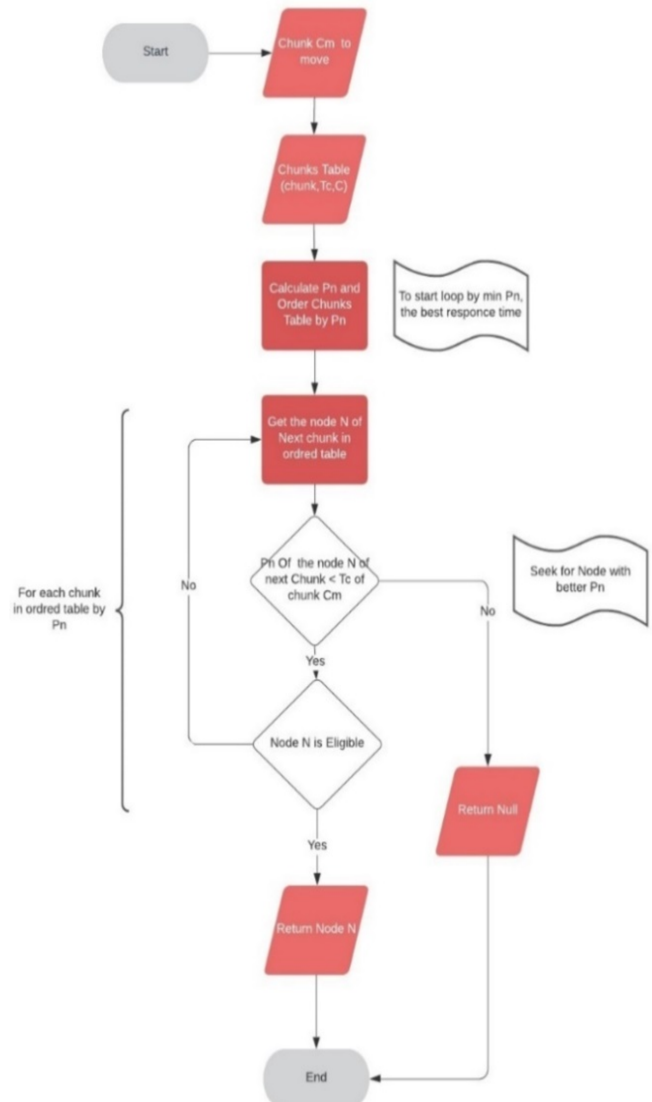

Fig. 5. Best Node Algorithm Selection.

IV. Testing Protocol

To make the performance measurements, we conducted simulations on a test grid consisting of 12 nodes.

The testing environment of the response time improvement algorithm consists of three racks (Fig. 6), each composed of four nodes of identical storage capacity and equal to three times the size of one chunk size (3x64MO).

Choosing this size allows us to limit the storage capacity of a node to a maximum of three chunks, in this way we will quickly saturate the nodes and the algorithm's ability to take this into consideration will be tested.

The performance characteristics of the nodes are heterogeneous; each of the three racks consists of the nodes of Table II.

TABLE II. GRID'S NODES CONFIGURATION

Node ID	RAM (GO)	Processor (Cores * speed)	Storage capacity
1	2	1 * 2GHz	192 MO
2	4	1 * 2GHz	192 MO
3	6	2 * 2GHz	192 MO
4	8	4 * 2GHz	192 MO

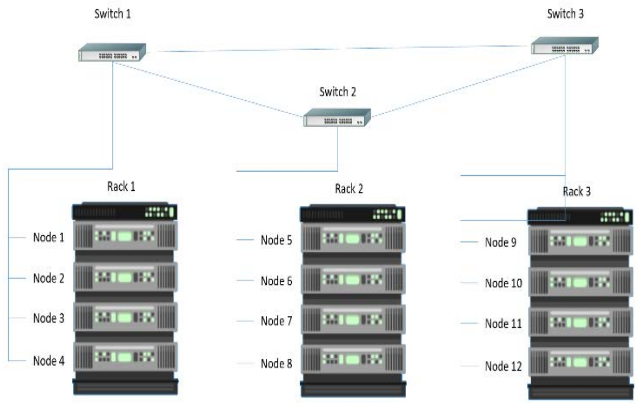

Fig. 6. Test Grid Architecture.

The bandwidth inside the same rack is 1 GB/s.

The direct bandwidth between the racks is set up according to the matrix in Table III (in MO/s).

TABLE III. GRID'S BANDWIDTH CONFIGURATION

	Rack 1	Rack 2	Rack 3
Rack 1	1000	100	10
Rack 2	100	1000	10
Rack 3	10	10	1000

The version of Hadoop used in the simulation is 2.5.0.

The simulations were conducted using 12 files with a unit size of 64MB.

The Size block configured on Hadoop is 64MO and the replication factor is 3.

Our TestJob consists of performing a variable number of jobs (map tasks) from the 12 nodes of the Grid on each of the 12 files distributed evenly on the Grid.

Each job is calling only one file, son the consultation rate C is equal to the number of executed jobs.

Testing protocol:

We followed a test protocol as shown in Fig.7:

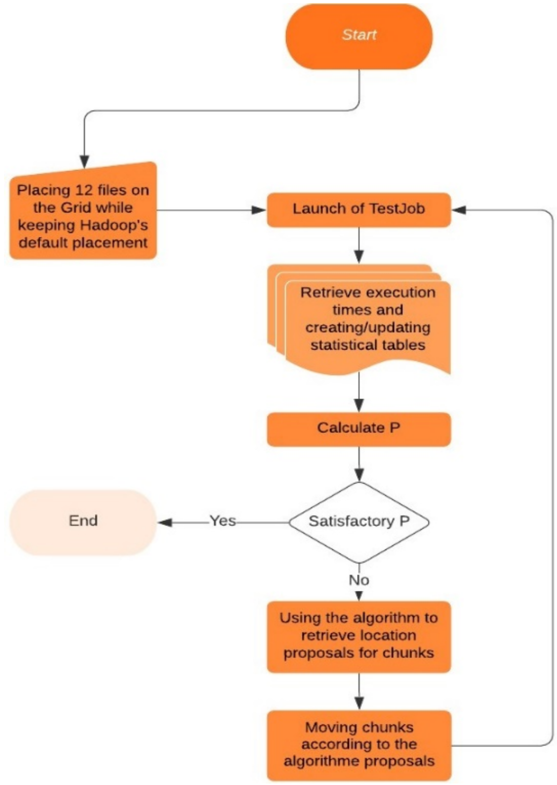

Fig. 7. Testing Protocol.

The phases were repeated over several iterations and after each iteration, we calculated the overall performance P of the cluster.

V. RESULTS AND EVALUATION

The main objective of running the test simulation is to calculate P before and after using the proposed algorithm. Thus, we can observe the evolution of P and assess the relevance of our approach.

The results collected on the first iteration of jobs are represented in the Table IV:

TABLE IV. INITIAL CHUNKS STATISTICS TABLE

Chunk Id	Id Node	C	Tc (ms)
0	0	12	20000,33
1	1	11	21626,64
2	2	10	23117,40
3	3	9	20143,00
4	4	8	16487,00
5	5	7	9967,00
6	6	8	26891,00
7	7	9	19819,44
8	8	10	31952,60
9	9	11	38492,09
10	10	12	35360,33
11	11	9	35135,00

C is the number of executed Jobs witch is equal to the consultation rate because each job is calling only one file.

The file is corresponding to only one chunk because of the chosen size of file and chunk configuration.

Tc is the mean job time of each file (MJT)

The overall performance of the Simulation Grid is then:

P1 = 25594.86 ms

The Tc calculated at this step is reflecting the default situation using the initial Hadoop placement strategy.

Running the relocation algorithm gives the locations suggestions in Table V:

TABLE V. CHUNK'S RELOCATION SUGGESTIONS TABLE

Id chunks	Id Node	Suggested Destination Node Id
0	0	5
10	10	5
1	1	4
9	9	4
2	2	7
8	8	7
3	3	None
7	7	None
11	11	0
4	4	None
6	6	3
5	5	None

The Algorithm proposes to relocate eight files to a new location.

Four files were not relocated because no improvement in the executions times is supposed to happen with any of available locations.

TABLE VI. CHUNKS STATISTICS TABLE AFTER FIRST RELOCATION

Id Chunks	Id Node	C	Tc (ms)
0	5	12	20000,33
1	4	11	21207,73
2	7	10	23117,40
3	3	9	20143,00
4	4	8	16487,00
5	5	7	9967,00
6	3	8	29259,00
7	7	9	19819,44
8	7	10	22736,60
9	4	11	17127,73
10	5	12	20000,33
11	0	9	19876,33

After moving the chunks to the suggested nodes and running the same set of jobs, the collection of response times gives the Table VI where Tc was recalculated:

The overall new performance of the grid is:

P2 =20125.21 ms

This value represents an improvement of 21.3% compared to P1.

Fig. 8 shows the evolution of the mean response time up to the third iteration.

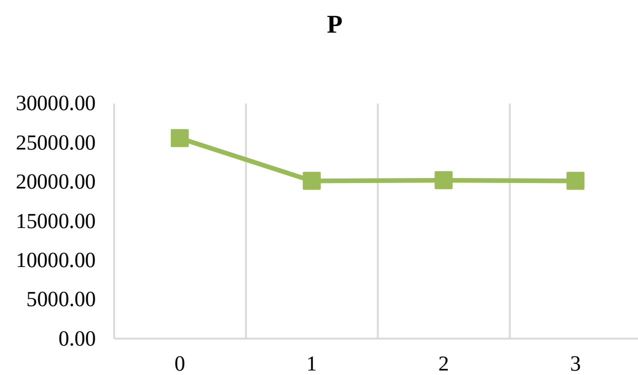

Fig. 8. Overall Performance Evolution.

After the first iteration P stabilizes. Changing the locations of the chunks according to the algorithm's proposals hardly affects the overall performance of the Grid.

We can conclude that the chunks are in an optimal node from the first iteration of replacement of chunks.

The overall performance improvement of the Cluster is nearly 20%. This improvement has been achieved after a single chunk replacement operation.

VI. CONCLUSION

The HADOOP system is a powerful and flexible big data system. Through its architecture it makes it possible to carry out complex operations on mass data distributed on grids which can range to thousands of machines whose characteristics can be very different.

Data striping and replication are among its strong features, thanks to them it manages to maintain the integrity of the system. But its basic chunk location strategy does not take advantage of all the capacity that the characteristics of the grid can offer.

In this research we conducted a deep analysis of how HDFS works to propose an improvement in the replica location strategy, and we demonstrated through our simulation that a substantial gain of more than 20% on the overall performance of the cluster is possible, while respecting the basic rules of HDFS initial chunk placement strategy.

In our future works we plan to integrate a module determining the best locations for data from the first writing, based on an artificial intelligence model capable of predicting the response time of a node for a given chunks. This will reduce data movements in the clusters and avoid unwanted bandwidth usage.

References

[1] Statista. “Volume of data/information created, captured, copied, and consumed worldwide from 2010 to 2025” Statista Digital Economy Compass https://www.statista.com/ (accessed Feb. 2019)

[2] M. D. Assunção, R. N. Calheiros, S. Bianchi, M. A. Netto, and R. Buyya, “Big data computing and clouds: Trends and future directions,” J. Parallel Distrib. Comput., vols. 79-80, pp. 315, May 2015.

[3] Y.Wu, F.Ye, K. Chen, and W. Zheng, “Modeling of distributed file systems for practical performance analysis," IEEE Trans. Parallel Distrib. Syst.,vol. 25, no. 1, pp. 156-166, Jan. 2014.

[4] C. Verma and R. Pandey, "Comparative Analysis of GFS and HDFS: Technology and Architectural landscape," 2018 10th International Conference on Computational Intelligence and Communication Networks (CICN), 2018, pp. 54-58, doi: 10.1109/CICN.2018.8864934.

[5] W. Dai, I. Ibrahim and M. Bassiouni, "A New Replica Placement Policy for Hadoop Distributed File System," 2016 IEEE 2nd International Conference on Big Data Security on Cloud (BigDataSecurity), IEEE International Conference on High Performance and Smart Computing (HPSC), and IEEE International Conference on Intelligent Data and Security (IDS), 2016, pp. 262-267, doi: 10.1109/BigDataSecurity-HPSC-IDS.2016.30.

[6] V. Venkataramanachary, E. Reveron and W. Shi, "Storage and Rack Sensitive Replica Placement Algorithm for Distributed Platform with Data as Files," 2020 International Conference on COMmunication Systems & NETworkS (COMSNETS), 2020, pp. 535-538, doi: 10.1109/COMSNETS48256.2020.9027494.

[7] T. Ma, F. Tian and B. Dong, "Ordinal Optimization-Based Performance Model Estimation Method for HDFS," in IEEE Access, vol. 8, pp. 889-899, 2020, doi: 10.1109/ACCESS.2019.2962724.

[8] The Apache Software Foudation. ”Apache Hadoop 3.3.1” Apache Hadoop. https://hadoop.apache.org/docs/current/ (accessed Mars 2021).

[9] J. Liu et al., "A Low-Cost Multi-Failure Resilient Replication Scheme for High-Data Availability in Cloud Storage," in IEEE/ACM Transactions on Networking, doi: 10.1109/TNET.2020.3027814.

[10] V. Venkataramanachary, E. Reveron and W. Shi, "Storage and Rack Sensitive Replica Placement Algorithm for Distributed Platform with Data as Files," 2020 International Conference on COMmunication Systems & NETworkS (COMSNETS), 2020, pp. 535-538, doi: 10.1109/COMSNETS48256.2020.9027494.

[11] J. Xie, S. Yin, X. Ruan, Z. Ding, Y. Tian, J. Majors, A. Manzanares, and X. Qin, “Improving MapReduce performance through data placement in heterogeneous Hadoop clusters,” in Proceedings of the 2010 IEEE International Symposium on Parallel & Distributed Processing, pp. 1-9, Atlanta, USA, 2010.

[12] Alshammari, Hamoud & Lee, Jeongkyu & Bajwa, Hassan. (2016). H2Hadoop: Improving Hadoop Performance using the Metadata of Related Jobs. IEEE Transactions on Cloud Computing. PP. 1-1. 10.1109/TCC.2016.2535261.

[13] Alanazi, Rayan & Alhazmi, Fawaz & Chung, Haejin & Nah, Yunmook. (2020). A Multi-Optimization Technique for Improvement of Hadoop Performance with a Dynamic Job Execution Method Based on Artificial Neural Network. SN Computer Science. 1. 10.1007/s42979-020-00182-3.

[14] Z. Li, H. Shen, W. Ligon and J. Denton, "An Exploration of Designing a Hybrid Scale-Up/Out Hadoop Architecture Based on Performance Measurements," in IEEE Transactions on Parallel and Distributed Systems, vol. 28, no. 2, pp. 386-400, 1 Feb. 2017, doi: 10.1109/TPDS.2016.2573820.

[15] M. Hajeer and D. Dasgupta, "Handling Big Data Using a Data-Aware HDFS and Evolutionary Clustering Technique," in IEEE Transactions on Big Data, vol. 5, no. 2, pp. 134-147, 1 June 2019, doi: 10.1109/TBDATA.2017.2782785.

A Proposed Framework for Big Data Analytics in Higher Education

Beenu Mago[1], Nasreen Khan[2]
Assistant Professor, School of Information Technology, Skyline University College, Sharjah, U.A.E[1]
Assistant professor, SZABIST University, Dubai, UAE[2]

***Abstract*—Students, faculties, and other members of the higher education (HEd) system are increasingly reliant on various information technologies. Such a reliance results in a plethora of data that can be explored to obtain relevant statistics or insights. Another reason to explore the data is to acquire valuable insight regarding the novel unstructured forms of data that are discovered and often found to have a connection with elements of social media such as pictures, videos, Web pages, audio files, etc. Moreover, the data can bring additional valuable benefits when processed in the context of HEd. When used strategically, Big Data (BD) provides educational institutions with the chance to improve the quality of education from all the perspectives and steer students of HEd toward higher rates of completion. Further, this will improve student persistence and results, all of which are facilitated by technology. With this aim, the current research proposes a framework that analyzes the data collected from heterogeneous sources and analyzes using BD analytics tools to do various types of analysis that will be beneficial for different learners, faculties and other members of HEd system. Moreover, current research also focuses on the challenges of acquiring BD from various sources.**

Keywords—Big data analysis; higher education; learning analytics; academic analytics

I. Introduction

Many people in the twenty-first century are interested in pursuing careers as data scientists [1]. Large amounts of data are being collected and analyzed, which is the source of the inspiration for this newly growing demand. BD analytics is the act of analyzing large amounts of data to uncover hidden patterns using computational algorithms, programming, and statistical modeling tools in order to discover significant and timely correlations [2, 3]. This enables the extraction of actionable information that may be used to impact internal company decision-making. As well as this, it assists in the discovery of patterns and the detection of anomalies across a wide range of data sources. Education is not an exception to the growing demand for BD in a variety of industries [4], which is increasing all the time. Certain parties, on the other hand, are still unwilling to engage with BD as a result of the application's specific constraints. Example: BD sets are frequently too enormous to be collected, stored, and analyzed correctly using typical database approaches [5, 2], and there is frequently no consistent structure for the data that has been gathered. According to Reference [6], consumers have evolved into a "continuous initiator of both structured, transactional data as well as contemporary unstructured behavioral data." It is possible to quickly overcome the difficulties to using BD by integrating novel technologies with freshly created approaches for data analysis [7]. Therefore, organizations that employ dynamic platforms for BD may profit through the enhanced corporate skills of critical thinking and taking appropriate decisions, which contributes to the broad usage of BD analytics across industries [8]. However, only a small number of papers and industrial accounts explicitly focus on the use of BD in tandem with HEd [2,10,11], despite the fact that several researchers have looked into the applicability, data availability, affordability, competence, privacy, relevance, and ownership of BD in many domains [9,10].

BD functions as a previously undiscovered opportunity for HEd institutions. The basic structural organization of the campus, the networks in use, servers, relevant apps, learning management systems (LMS), and other end-user systems generate data in huge volumes which, upon proper evaluation, may reveal substantial information and a new understanding concerning the various challenges that govern HEd [13, 14, 15]. As such, implementing BD in a HEd environment may result in enhanced skills involving the process of making decisions. It is the goal of this study to further add to the existing research on BD by analyzing the application of BD analytics in HEd institutions.

This paper is structured into different sections. First, the authors review the role of BD in HEd followed by importance of data analytics in HEd. Authors provide deep insight about the educational analytics. Post the review of literature, authors propose the conceptual framework followed by conclusion, future research and limitations of the current study.

II. BD and Education

Graduating students' learning processes are frequently chastised for failing to adequately prepare different stakeholders by not providing them the knowledge, relevant tools and mindsets, and values which are essential in future, yet, the huge data produced by the infrastructure various systems of today's digital campus that includes data produced or collected from the network applications of campus, various other internal applications used for serving various needs of HEd. It is observed that HEd rarely use Learning Management System (LMS), mobile or other devices, which are used by different stakeholders of HEd, to gain important details about the issues that are affecting or can affect current educational institutions [16]. This proves that the use of promising techniques such as BD is still in its infancy in HEd. Owing to various educational concerns, there has been a rise in the number of useful suggestions and propositions offered to ensure that HEd institutions can flourish in every way possible which can be summed up under the category of increased transparency and accountability involving all stakeholders including students, parents, taxpayers, and others [5] It is important to understand that using BD or LA in HEd is the best method of not only accumulating but also evaluating data regarding the advancement of the students and the educational environment. It not only offers educational content information to instructors, but identifies activities that improve teaching and evaluation procedures [2]. Much of the motivation for employing analytics in HEd stems from more stressed university finances and increased cost awareness. Students are also becoming more demanding as stakeholders, asking proof that their tuition is being spent wisely.

The advanced new integrative platforms have the ability to reduce the cost of education, improve operations, and frame more refined learning techniques [21]. This is possible because these platforms can access and interpret data that is collected from diversified sources that embraces log files, firewall data, remote sensors, legacy applications, structured databases, LMS, web servers, networks, student registration systems, and mobile and online learning apps, in addition to detecting problems, risks, and opportunities using untapped machine data [2]. A more convincing and engaging educational experience can be achieved by combining the digital and physical worlds. AA can help decision-makers make better decisions by focusing on trends that signal student performance and academic brilliance.

The following part will review the three primary research cores areas of data analytics in HEd. These First core area is Learning Analytics (LA). The second area is Academic Analytics (AA). Next, researcher has discussed Educational Data Mining used as EDM in short in this research. Next, it will present an overview of each research stream after which an integrated picture of the entire process will be presented.

III. Data Analytics in HEd

Educational analytics is the deep and detailed analysis of large amounts of educational data to gain valuable insights. Teaching Analytics, LA, AA, and EDM are some of the academic areas through which the power of analytics is utilized for this process [16].

A. Learning Analytics (LA)

Although a variety of terminology and concepts have been used to define the developing study subject of LA, it is best understood as the application of data diagnostic in the context of learning and teaching. Unlike AA and EDM, this technique is heavily focused on the learners and their learning process, gathering, integrating, and evaluating static and dynamic data on the learners' profiles, educational resources, and learning context. It hopes to achieve this by providing descriptive modeling and prediction of learning elements in real-time.

“The measurement, collection, analysis, and reporting of data about learners and their contexts for the purposes of understanding and optimizing learning and the environments in which it occurs,” is what LA is according to the Society for LA Research. This interpretation has recently gained widespread acceptance in the scholarly community [11,18].

B. Content Analysis

Many people are interested in analyzing hypertexts discovered on websites because of the ongoing advancements in the techniques related to web analytics such as machine learning, algorithms, web crawling, etc. [10].

The contextualized interpretations of textual documents are dealt by a branch of LA which is known as Content Analysis [19]. This method analyzes texts to understand their underlying meanings, either manually or with the assistance of technology. Despite the availability of various textual educational sources, this technique divides the texts into five groups for analysis purposes: written, oral, iconic, audiovisual, and hypertexts.

C. Discourse Analytics

To extract the relevant information related to the features of the used languages from the learning outline. It includes the study of user engagement. From the empirical data, the Content Analysis reveals the meaningful data while Discourse Analytics mainly concentrates on the learners’ language. Through the platforms where the employees communicate like, online learning pages, it addresses to the learners. The interaction will contribute the procedure of the knowledge production [20, 22]. Along with the platforms that connect the learners to the content items, the learning can be considered as socio-constructivist procedure [23]. The analytics of the discourse data and metadata is now possible because of log follow up and data mining. On the other hand, the Discourse Analytics focuses on the data and language that has been employed in learning process while the Social LA concentrate more on the involvement of the learners.

D. Social LA

Social LA is a unique branch of LA related to the cooperation and coordination between the learners [24]. In education, the Social LA studies a learning procedure from the social point of view and states that attaining newer information and skills are not only a person’s achievement while the Discourse Analytics examine the learners’ language. The way social interactions and platforms influence learning routine has been explained by many prior researches [25]. Like social network analysis (SNA) was carried out by [24] in order to determine the link between educational performance and contacts through social platforms. The outcomes of this research will help us to know whether we can depend on social network factors to act as indicators of student progress but on the other hand, for the calculations, this study discourages to entirely depend on social groups aspects. Also, for the social learning analytics, the data visualization is effective according to this study.

E. Disposition Analysis

The theoretical information about the learners’ back ground and their involvement in learning is discussed by Disposition Analytics which will help to determine the character of students along with their connection with the education procedure [26]. That means, the aspects, brought by the learners in the learning process to recognize the learning behaviors and anticipate the better learning attitudes for the better performance of both educating and learning, are studied by the LA technique. This is evident in [26], where the disposition analytics were used to study the influence of different features on the learner's progress and the teacher will be able to take informed decisions, regarding specific option and optimal instructing methods and approaches, by understanding this dynamic.

F. Academic Analytics (AA)

AA is precisely defined corporate intelligence in education and particularly, it refers to the procedure of determining the insightful patterns in educational data in order to maintain calculated management and to predict scholastic issues like drop out ratio [11]. The method mainly talks in the favor of organizational executive bodies and educationists but it has been assumed by the students that data analytics are used anticipate and laud their educational progress. In order to supervise and improve the academic the Key Performance Indicators (KPIs), like student retention, the organization's management will use the AA. It has been referred to, as a development for the provision of advanced educational institutes with the info that is required to support the functional an economic management [17].

Through the disclosing the important factors contributing to the learners' achievement, helping to understand the useful methods and increasing the scholarship of learning and educating, the AA support the staff. In the higher schooling, the student's accomplishment is considered to be among the primary key performance indicators (KPIs) so; majority of staff is interested in supervising and anticipating student success. Also, relevant and important information is collected from the academic data by AA in order to allow the teaching staff to make educational alterations to fulfill students' necessities and to examine the most useful methods.

To back their management, the executive bodies may extract required information from the AA. A unique set of KPIs is offered by AA which traditional educational systems do not possess them. For instance, the vice chancellor may force for the supervision of the learning and teaching methods upon knowing the ratio of at-risk students. The AA are also used maximize the employment of resources by the administrative team. The AA may play a part in development of the organization's answerability and improve the institute's image [30]. Regardless of many advantages, managements often highlight the expenses incurred in the AA plan [28,29], when the system is functioning, they might be worried about the security threat and privacy.

IV. Education Data Mining (EDM)

The EDM comes with the target of solving academic crisis and exploring the hidden info, talks about the usage of the data mining methods on scholastic data [29]. This information can extract learners' demographic information and their attitude towards the educational activities like, quizzes, interactive class exercises/tasks in a learning space and use data from team of learners who work together in a project, discussion platform, teacher data, managerial information, demographic and cognitive information. To attain the data regarding education of student, the EDM can be used which will help to improve the educational processes and monitor the leaning for the feedback. The information can be employed to give suggestions to adjust with the leaning attitude of the students depending on their learning patterns along with the unexpected leaning attitudes [31]. Like, the way of how the learning tasks of students were anticipated with the usage of k-means clustering algorithm according to Reference [30]. A machine-algorithm was used by [33] to know about the undergrads at engineering colleges who dropped out in their freshmen year. To conduct, student identification and to classify them according to their academic assessments that will comprise of quiz scores, assessment grades, exam scores and practical test scores, [34] used various data mining algorithms.

There are various kinds of EDM. All the types of academic data mining could be classified into five categories: prediction, clustering, relationship mining, discovery with models, and distillation of data for human judgment according to [35]. The initial three groups are generally considered by the EDM research team while, the last two groups are just dominant in the area of academic data mining [31]. The term prediction, in the EDM targets to show case the educational finding from the other information factors. Input factors are referred as predictor variable whereas the forecast factor is mentioned as predicted variable. The clustering is the second form of academic data mining that targets on grouping the unprocessed information into sets of clusters and identifying the borders in the groups. As said by [35], this category of academic info mining techniques can take predefined theories or no following studies into account.

The relationship mining is the third category of the academic data mining that aims to examine the existent connections in the datasets with different variables. It is divided in to four sub groups that are: association rule mining, causal data mining, correlation mining, and sequential pattern mining [35, 36]. The association rule mining will reveal the if-then rulings in the variables. To be specific, data mining techniques determine the links where any set of variables is described and other variable will have certain value. For example, [33] used shared the association rule mining as it was recommended to propose the guidelines like, the assignment score might be increased if the responded messages number in the discussion is high.

Approaches of Causal Data Mining are utilized to discover "casual relationships" in which one occurrence causes another. Both unidirectional and bidirectional causal relationships are possible [27]. Relationship Mining and Correlation Mining are remaining two types. They are looking for positive or negative linear correlations between variables whereas Sequential Pattern Mining is looking for temporal relationships. Reference [37], employed Sequential Pattern mining to integrate metacognitive judgments and eye movements to explore processes underpinning multimedia learning. Discovery with Models is deemed as the fourth sort of EDM; it builds a model of a phenomenon using existing EDM approaches or knowledge engineering and then using it as a component in another research. Discovery with Models, according to [35], finding with frameworks usually implies the substantiated adaptation of a forecasting model throughout several environments. The principal application of this EDM class is the finding of relationships among student conduct and subjective variables in the teaching environment [32].

V. BD Analytics in HEd

As a result of the massive amount of data being generated on a daily basis, contemporary system of integrated innovative technology demands has reached an all-time high. As a result, BD has emerged. There have been numerous studies conducted on the use of BD in a variety of sectors, with particular emphasis on the availability of data, cost of acquiring data, application, and importance of BD [8]. Despite this, only a few papers [9] [10] have documented the integrative application of BD in HEd. HEd institutions have access to an enormous amount of data that is stored in a variety of different sources and is managed by a variety of different processes. In this way, BD has the ability to harness institutional data that can improve the future of the education sector, particularly in terms of decision-making, and so improve the future of society. The evaluation of a diverse variety of organizational and functional information collected via the methods conducted to assess organizational efficiency and improvement in predicting long term growth and manage possible problems in academic programming, research, teaching, and learning is referred to as BD in HEd [13,20]. Many stated that HEd should employ insights as a mechanism to meet the demands of higher efficiency. A proportion of researchers have claimed that the BD paradigm is well suited to dealing with some of the core challenges that HEd faces as a new discipline within academia.

At this moment, much of the analytics work in HEd is integrative, involving the fields of Educational Technology, Statistics, Mathematics, Computer Science, and Information Science. The present work on analytics in education is centered on data mining.

In HEd, database systems that store vast volumes of longitudinal data about students, down to extremely specific transactions and activities relevant to learning and teaching, are referred to as BD [12]. Students leave data trails when they interact with learning tools, which can expose their attitudes, social connections, intentions, and aspirations. This data can be used by researchers to examine trends in student performance over time, such as from one semester to the next or from one year to the next.

On a higher level, the ability to find meaningful data and turn it into useable information by identifying patterns and deviations from patterns might be said to constitute BD's added value. According to [4], BD is now in a good position to begin tackling some of the major difficulties that HEd is currently experiencing. It could serve as the foundation for HEd to rethink both its financial model and the evidence used to make judgments about educational outcomes [2].

From the viewpoint of organizational learning, the analysis of appropriate data is well recognized, and today's technologies enable institutions to obtain insights from data at previously unimaginable levels of sophistication, speed, and accuracy [3, 7]. The production of essential information by students, computer programs, and systems is increasing as technology continues to permeate all sectors of HE [1].

BD Analytics may also be used to evaluate student replies to a course exam, discussion board postings, blog entries, and wiki activity, all of which can result in hundreds of transactions per student each course. These data would be collected in real-time or near-real-time as transactions occur, then evaluated to suggest actions. “[Learning] analytics are a foundational tool for informed change in education,” according to [38], and they provide evidence on which to create knowledge and make informed (rather than impulsive) decisions.

With the widespread use of information and communication technology, the amount of data that may be transmitted on the smart education platform grows exponentially [39]. When data is scattered over numerous unconnected diverse data systems in institutions, iLMS works closely with the learners serving many learners at a time and tailored according to the individual needs [40]. With innovation in technology, the data becomes so vast and takes the form of BD. The data is definitely unstructured and semi-structured, petabytes are produced on a daily basis, and traditional relational databases cannot effectively scale to support real-time analytics based on the data [41]. Further, it is also observed that analysis of this BD can help with the issues of obtaining information at the correct time. BD can help increase decision-making capability by exploring ways to aggregate data across platforms.

Despite growing interest in investigating and unlocking the possibilities of growing data in the HEd environment, there is a lack of research on BD in HEd.

- This work adds to HEd's theoretical and conceptual understanding of BD and Analytics.
- It defines BD and discusses how it relates to HEd.
- It presents a conceptual framework based on this expanding field of study.

VI. Proposed Framework, Future Research and Limitations

With the falling cost of BD storage, open source software such as Apache Hadoop and NoSQL databases, network bandwidth, and on-demand access to resources provided by cloud computing, complicated technologies are becoming more accessible to a broader range of people. To emphasize this, it should be noted that, as the cost of BD and Analytic tools continues to decline, they are becoming significantly easier to use [30]. This, in turn, opens the door to the use of these tools by businesses and educational institutions to achieve better outcomes while also making more efficient use of available resources. BD in HEd is being driven by a number of causes, including stakeholder expectations of good practices and accountability, as well as an increased desire for evidence-based guidelines to assist in decision-making. This means that the first stage in establishing a method to achieve this goal is to identify acceptable technology platforms that will enable BD analytics in addition to relevant technological talents, such as data scientists. Due to the fact that data is no longer viewed as just a back-office accounts-settling tool, but rather as a real-time decision-making tool that can be used by data scientists to extract useful information from terabytes of data that would otherwise remain hidden [16], data is becoming increasingly valuable. By utilizing virtual and online learning systems, information technology is transforming education and broadening the scope of the educational environment beyond traditional lecture halls and classrooms to accommodate learners who require flexibility in terms of both time and distance [6] [4]. The educational system is progressively being pressed to respond to economic, political, and social developments, such as the need to expand the number of students enrolled in specific subjects and the need to teach graduates with the skills and traits demanded by industry, among other things. These schools must use information technologies such as BD, which have significant potential in HEd, if they are to be responsive to these shifts in the marketplace. The majority of educational data has traditionally been collected through traditional assessments, but it is now increasingly being collected through online educational systems, educational games, and simulations, resulting in a large amount of data, which in turn opens the door to BD analytics opportunities. In the context of today's technology-enabled learning, the student is at the heart of a network of information-rich relationships in the educational system, which is offering opportunities for BD analytics, according to [17]. The author in [14] argues that HEd institutions are functioning in increasingly complicated situations, and that, as a result, it is essential that they employ BD to provide the finest learning environments for the benefit of the entire society. There are opportunities to use BD to link research and education, by making effective use of the most recent research techniques and outcomes to guide teaching and to enable the conduct of research activities as part of educational activities, for example. Students generate massive volumes of potentially valuable information during the course of their learning processes in areas such as course selection and registration, financial information, class participation, online resource usage, and textbook purchases, all of which can be used as raw material for BD analysis and redeployment to assist administrators and students in making better decisions. As a result of the digital revolution, HEd institutions are gathering more data than they have ever collected before.

Many colleges and universities have proved that analytics may help an institution considerably advance in such important areas as resource allocation, student achievement, and financial planning and administration. When leaders of institutions of HEd read about innovations occurring at other institutions as a result of BD analytics, they begin looking for methods to implement analytic programs in their own institutions [31]. Several studies, including the McKinsey Global Institute Report on BD [33], have found that the most developed regions, such as Europe, have the most potential to create value through the use of BD. BD adoption and widespread use in other regions, particularly in poor countries, has been bolstered as a result of this development. In accordance with [32], the diffusion of BD gives an account of how BD goes from discovery to widespread use, and how this is aided by steps taken by service providers of important technologies necessary to enhance the resources and capacities of academic institutions. [34] Stated that countries may take advantage of the numerous BD opportunities that are accessible to them in order to gain value from the huge volumes of data that are generated and, in the long term, aid in their development. BD and analytics in HEd have the potential to be transformative, affecting existing processes of administration, teaching, and learning, as well as contributing to policy outcomes by assisting in the resolution of existing difficulties facing educational institutions [4, 35]. The following are some examples of how successful institutions have made use of BD. First and foremost, we must cultivate a culture of completion and outplacement. 2) Decrease in the number of nonproductive credits. 3) Rethinking the way in which teaching is delivered. 4) Redesigning essential support services such as human resources, academic services, and finance in order to generate data that is valuable for strategic decision-making. 5) Improving the efficiency of non-core services and operations [17].

BD may have an impact on HEd practice in a multitude of ways, including improving student experience, academic programming, scientific proof judgement, and tactical responses to changing economic trends. BD has the ability to turn complex, often unstructured data into actionable information. Reference [14] claims that BD is a cost-effective approach to improve judgement. In order to organize the available literature and build a study technique to aid in the establishment of a set of choices for investigation, reference [2] presented a conceptual framework to describe BD in HEd along four components (Learning Analytics, Institutional Analytics, and AA and information Technology analytics). Following Fig. 1 shows the diagrammatic representation of it.

There is a wide range of administrative and operational data gathering processes that are used to assess institutional performance and progress in order to predict future performance. Reference [42] describe a wide range of administrative and operational data gathering processes that are used to identify potential issues related to academic programming, research, teaching, and learning. Data is rising in HEd institutions, but the majority of it is distributed among computers and departments, and it comes in a variety of formats, making it impossible to retrieve or consolidate the information. Having the ability to analyze diverse information sets, regardless of where they come from, is required for effective use of these data. Consolidating data stored in silos within institutions, managing and governing the data while protecting sensitive information across databases is a key requirement for implementation of BD in HEd [42]. A better basis for making better decisions about essential business and technological demands is provided by consolidated data from many sources across an institution, minimizing redundancy and the loss of valuable time gathering data from multiple sources. Though it can be incredibly challenging to combine data sets from across a number of disconnected systems, doing so results in more complete insights that inevitably lead to enhanced predictive modeling skills. Based on these existing deficiencies, the researcher of the current study develops a framework for utilizing large amounts of data from a variety of sources. Following Fig. 2 shows the proposed framework for the current study.

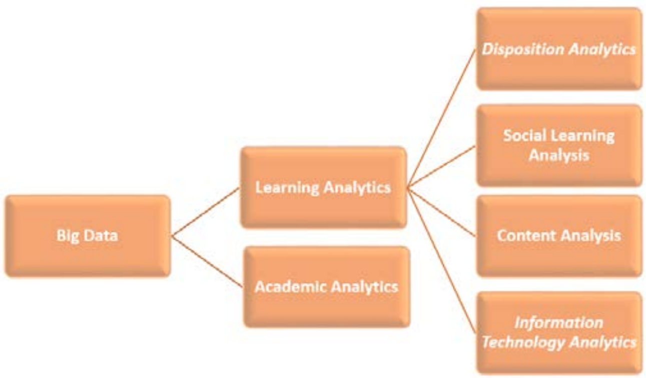

Fig. 1. Components of BD.

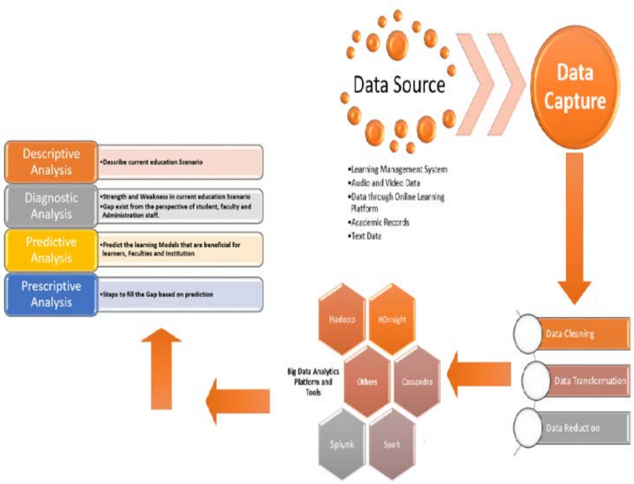

Fig. 2. Proposed Framework for Analyzing BD in HEd.

Based on the above framework, the BD which can be collected from various heterogeneous sources and can provide benefits which can be summarized as shown in Fig. 3.

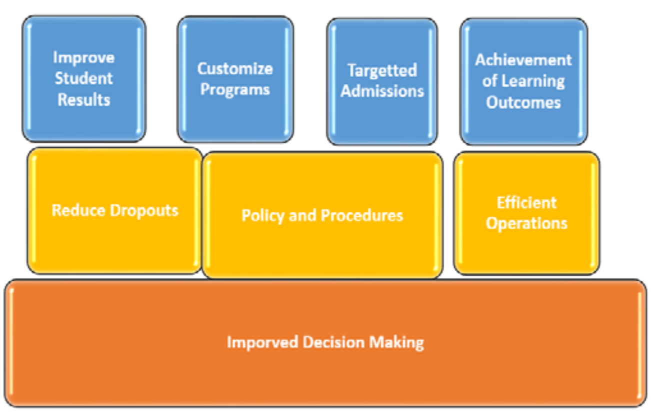

Fig. 3. Benefits of Analysis of BD in HEd.

VII. Conclusion, Future Research and Limitaions

As a result of the explosion of data, BD has evolved as a means of processing huge amounts of data from a number of sources. Universities with strong research and development capabilities can reap significant benefits from this technology. HEd institutions must consider the long-term implications of implementing BD analytics, which has the potential to broaden the scope of their teaching-learning orientation. Among the recommendations made by executives are that administrators and educators assist the system and gain value from practical applications, such as creating a culture of data use for educational decision-making, being keen on data users by asking critical questions about market deals and suggesting the most beneficial uses and features, involving IT departments in data collection, application planning, and starting with a pilot program, among others. As a result, institutions can save money while also making attempts to incorporate pedagogical abilities and make more informed decisions, which is beneficial. As a thoughtful contribution to curriculum design for instructors and learners in education in particular, and as a sustained competitive advantage for the education sector in general, this framework is intended to facilitate the development of innovative teaching-learning orientations for the performance of educational institutions, as well as for the performance of educational institutions as a whole.

Furthermore, the integration of BD analytics is not an easy process. The lack of skills and expertise in the HEd sector of will pose a challenge in data storage, collection and management of data [4]. Data privacy will be another concern along with the potential ethical concerns such as purpose of data collection and analysis. Hence, it is suggested that the key stakeholders of HEd sector should be involved to gain acceptance.

References

[1] J. Gagliardi, A. Parnell, and J. Carpenter-Hubin, “The Analytics Revolution in Higher Education,” Change: The Magazine of Higher Learning, vol. 50, no. 2, pp. 22–29, 2018.

[2] B. Daniel, "Big Data and analytics in higher education: Opportunities and challenges", vol. 46, no. 5, pp. 904–20. 2014.

[3] R. Kitchin, The Data Revolution: Big Data, Open Data, Data Infrastructures and Their Consequences. London: Sage.2014.

[4] M. I. Baig, “Big Data in Education: A State of the Art, Limitations, and Future Research Directions.” International Journal of Educational Technology in Higher Education, vol. 17, no. 1, 2020. Crossref, doi:10.1186/s41239-020-00223-0.

[5] M. Attaran, J. Stark, and D. Stotler, „Opportunities and challenges for big data analytics in US higher education. Industry and Higher Education”, vol. 32, no.3, pp 169–182,2018. https://doi.org/10.1177/0950422218770937.

[6] S. Erevelles. “Big Data Consumer Analytics and the Transformation of Marketing.” Journal of Business Research, vol. 69, no. 2, pp. 897–904,2016. Crossref, doi: 10.1016/j.jbusres.2015.07.001.

[7] H. Davenport, Thomas. “How Strategists Use ‘Big Data’ to Support Internal Business Decisions, Discovery and Production.” Strategy & Leadership, vol. 42, no. 4, pp. 45–50,2014. Crossref, doi:10.1108/sl-05-2014-0034.

[8] D. Trabucchi, and B. Tommaso, “Data-Driven Innovation: Switching the Perspective on Big Data.” European Journal of Innovation Management, vol. 22, no. 1, pp. 23–40,2019. Crossref, doi:10.1108/ejim-01-2018-0017.

[9] S. Zillner et al. “Big Data-Driven Innovation in Industrial Sectors”. In: Cavanillas J., Curry E., Wahlster W. (eds) New Horizons for a Data-Driven Economy. 2016, Springer, Cham. https://doi.org/10.1007/978-3-319-21569-3_9.

[10] N. Nistor, and A. Hernández-Garcíac, “What Types of Data are used in Learning Analytics? An Overview of Six Cases”. Computers in Human Behavior, vol.89, pp 335–338,2018.

[11] S. S. Chaurasia, D. Kodwani, H. Lachhwani, and M.A. Ketkar, “Big Data Academic and Learning Analytics”. International Journal of Educational Management, vol.32, no.6, pp 1099–1117,2018.

[12] S. Parack, Z. Zahid, F. Merchant, Application of data mining in educational databases for predicting academic trends and patterns. In Proceedings of the 2012 IEEE International Conference on Technology Enhanced Education (ICTEE), Kerala, India, 3–5 January 2012; pp. 1–4.

[13] A. Nguyen, L. Gardner, and D. Sheridan, A Multilayered Taxonomy of Learning Analytics Applications. In Proceedings of the Pacific Asia Conference on Information Systems, Article 54.2017.

[14] M. Hilbert, “Big Data for Development: A Review of Promises and Challenges.” Development Policy Review, vol. 34, no. 1, pp. 135–74,2015. Crossref, doi:10.1111/dpr.12142.

[15] U. Sivarajah, et al. “Critical Analysis of Big Data Challenges and Analytical Methods.” Journal of Business Research, vol. 70, pp. 263–86, 2017. Crossref, doi: 10.1016/j.jbusres.2016.08.001.

[16] N. Bousbia, I. Belamri, “Which contribution does EDM provide to computer-based learning environments?” In Educational Data Mining; Springer: Berlin/Heidelberg, Germany, pp. 3–28,2014.

[17] Black, Paul, and Dylan William. “Classroom Assessment and Pedagogy.” Assessment in Education: Principles, Policy & Practice, vol. 25, no. 6, 2018, pp. 551–75. Crossref, doi:10.1080/0969594x.2018. 1441807.

[18] A. Nguyen, L.A. Gardner, and D. Sheridan, “A Framework for Applying Learning Analytics in Serious Games for People with Intellectual Disabilities”. British Journal of Educational Technology, vol.49, no.4, pp 673–689,2018a.

[19] D. Clow, “An overview of learning analytics”. Teaching in Higher Education, vol.18, no.6, pp. 683–695,2013.

[20] J.A. Howell, L.D, Roberts and V.O. Mancini,” Learning Analytics Messages: Impact of Grade, Sender, Comparative Information and Message Style on Student Affect and Academic Resilience.” Computers in Human Behavior, vol.89, pp 8–15,2018.

[21] S. Ayesha, T. Mustafa, A.R. Sattar, M.I. Khan, “Data mining model for higher education system.” Eur. J. Sci. Res. vol.43, 24–29,2010.

[22] C. Kent, E. Laslo, and S. Rafaeli, “Interactivity in Online Discussions and Learning Outcomes. “Computers & Education, vol.97, pp 116–128,2016.

[23] D.T. Hickey, “Motivation and Contemporary Socio Constructivist Instructional Perspectives”. Educational Psychologist, vol.32, no.3, pp. 175–193,1997.

[24] P. Vlachopoulos, S. K. Jan, and L. Lockyer. “A Comparative Study on the Traditional and Intensive Delivery of an Online Course: Design and Facilitation Recommendations”. Research in Learning Technology, vol. 27, Mar. 2019, doi:10.25304/rlt. v27.2196.

[25] E. Vrieling, “Facilitating Social Learning in Teacher Education: A Case Study.” Studies in Continuing Education, vol. 41, no. 1, pp. 76–93,2018. Crossref, doi:10.1080/0158037x.2018.1466779.

[26] S. Bharara, S. Sabitha, and A. Bansal, “Application of learning analytics using clustering data Mining for Students' disposition analysis”. Education and Information Technologies, vol.23, no.2, pp. 957—984, 2018.

[27] P. Baepler, and C. Murdoch. “Academic Analytics and Data Mining in Higher Education.” International Journal for the Scholarship of Teaching and Learning, vol. 4, no. 2, 2010. Crossref, doi:10.20429/ijsotl.2010.040217.

[28] D. Raju and S. Randall, “Comparing Data Mining Models in Academic Analytics.” International Journal of Knowledge-Based Organizations, vol. 6, no. 2, pp. 38–54,2016. Crossref, doi:10.4018/ijkbo.2016040103.

[29] P. Mishra, et al. “Educational Data Mining and Learning Analytics in Higher Education.” MERI-Journal of Management & IT, vol. 12, no. 1, p. 85,2018. Crossref, doi:10.25089/meri/2018/v12/i1/180120.

[30] S. Pal, “Mining educational data to reduce dropout rates of engineering students” Int. J. Inf. Eng. Electron. Bus. vol.4, no.1. 2012,

[31] F. Alshareef, et al. “Educational Data Mining Applications and Techniques.” International Journal of Advanced Computer Science and Applications, vol. 11, no. 4, 2020. Crossref, doi:10.14569/ijacsa.2020.0110494.

[32] G. Ramaswami, et al. “Using Educational Data Mining Techniques to Increase the Prediction Accuracy of Student Academic Performance.” Information and Learning Sciences, vol. 120, no. 7/8, pp. 451–67,2019 Crossref, doi:10.1108/ils-03-2019-0017.

[33] Y. Salal, S. Abdullaev, and M. Kumar, “Educational data mining: Student performance prediction in academic,” IJ of Engineering and Advanced Tech, vol. 8, no. 4C, pp. 54–59, 2019.

[34] K. Agarwal, E. Maheshwari, C. Roy, M. Pandey, and S. S. Rautray, “Analyzing student performance in engineering placement using data mining,” in Proceedings of International Conference on Computational Intelligence and Data Engineering, pp. 171–181, Springer, 2019.

[35] Baker, R. S. J. D., & Yacef, K. (2009). The state of educational data mining in 2009: A review and future visions. Journal of Educational Data Mining, 1(1), 3-17.

[36] A. Peña-Ayala, Alejandro. “Educational Data Mining: A Survey and a Data Mining-Based Analysis of Recent Works.” Expert Systems with Applications, vol. 41, no. 4, pp. 1432–62, 2014.Crossref, doi: 10.1016/j.eswa.2013.08.042.

[37] R. Azevedo, N.V. Mudrick, M. Taub, and A.E. Bradbury, Self-regulation in computer-assisted learning systems. In J. Dunlosky & K. A. Rawson (Eds.), The Cambridge handbook of cognition and education (pp. 587–618). Cambridge University, 2019.

[38] G. Siemens, “The Journal of Learning Analytics: Supporting and Promoting Learning Analytics Research.” Journal of Learning Analytics, vol. 1, no. 1, 2014, pp. 3–5. Crossref, doi:10.18608/jla.2014.11.2.

[39] Ateeq, K., Mago, B. & Pradhan, M.R. “A novel flexible data analytics model for leveraging the efficiency of smart education.” Soft Computing (2021). https://doi.org/10.1007/s00500-021-05925-9.

[40] Alkhatib, O., & Mago, B. (2017) “ilearning Management System: An Innovative Approach to E-Learning.”, International Journal of Information Technology & Management Information System, 8(2).

[41] Mago B., “Analyzing Unstructured Data Using Mining Techniques”, Proceedings of the The 7th International Research Symposium of the SGBED: Managing Business in a Digital Age: Opportunities and Challenges, 17 December–19 December, 2018, Skyline University College, UAE, pp. 241–251.2018.

[42] B. K. Daniel, and R. Butson, Technology enhanced analytics (TEA) in higher education, Proceedings of the International Conference on Educational Technologies, 29 November–1 December, 2013, Kuala Lumpur, Malaysia, pp. 89–96.2013.

Fine-tuned Predictive Model for Verifying POI Data

Way to Trusted Crowd Sourced GeoTagged Data

Monika Sharma[1]
Research Scholar, Dept. of Computer Engineering
Poornima University, Jaipur, Rajasthan, India

Dr. Mahesh Bundele[2]
Principal and Director
Poornima College of Engineering
Jaipur, Rajasthan, India

Vinod Bothale[3]
Associate Director, NRSC
ISRO, Balanagar, Hyderabad, India

Dr. Meenakshi Nawal[4]
Associate Professor
Dept. of Computer Engineering
Poornima University, Jaipur, India

***Abstract*—Mapping websites and geo portals are playing a vital role in daily life due to the availability of geo-tagged data. From booking a cab to search a place, getting traffic information, review of the place, searching for a doctor or best school available in the locality, we are heavily dependent on the map services and geo portals available for finding such information. There is voluminous data available on these sources and it is getting increasing every moment. These data are majorly collected through crowdsourcing methods where people are contributing. As a basic principle of Garbage in garbage out, the quality of this data impacts the quality of the services based on this data. Therefore, it is highly desired to have a model which can predict the quality/accuracy of the geotagged Point of interest data. We propose a novel Fine-Tuned Predictive Model to check the accuracy of this data using the best suitable supervised machine learning approach. This work focuses on the complete life cycle of the model building, starting from the data collection to the fine-tuning of the hyperparameters. We covered the challenges particularly to the geotagged POI data and remedies to resolve the issues to make it suitable for predictive modeling for classifying the data based on their accuracy. This is a unique work that considers multiple sources including ground truth data to verify the geotagged data using a machine learning approach. After exhaustive experiments, we obtained the best values for hyperparameters for the selected predictive model built on the real data set prepared specifically to target the proposed solution. This work provides a way to develop a robust pipeline for predicting the accuracy of crowdsourced geotagged data.**

Keywords—Crowdsourced; fine-tuning; geotagged data; hyperparameters; predictive model

I. Introduction

We have been witnessing the data generation era where each day voluminous data is getting generated by people on different platforms like social media websites, microblogging websites, geo portals, web mapping websites, etc. Among these platforms, mapping websites and geo portals provide a wide variety of map data which has several important applications like traffic conditions, finding the route, business listing, etc. These maps contain a wide variety of Point of interest data such as public services like healthcare, schools, hotels, monuments, religious places, courts, open areas, business points, etc. The collection of such huge data is not possible without crowdsourcing. POI data are also known as geotagged data which includes the geographical information of a place along with the metadata. Many times, these data are contributed by general people hence there is no control over the quality of POI data. On the other hand, these data are used in various services like location route-finding which may lead to the wrong place if the metadata or geospatial data are not correct. There may be critical consequences of the wrongly tagged data. Hence, it is important to measure the quality of geotagged data. These data are voluminous hence there should be an automatic method or model to check the accuracy. As per our best knowledge, based on the published researches, there is no previous work available that can grade the POI data based on its accuracy so that users can decide the risk involved in using incomplete or less accurate data [1]. Therefore, the proposed research work has great significance in terms of quality assessment of POI data available on map websites or geo portals. The proposed approach includes multi-sourced verification methods to overcome the limitation of each source where we included ground truth data, web data, and some inferential data to check the accuracy of the tagged data. The proposed system categorizes the POI data into four different classes based on their accuracy level. The risk involved in using data from each category can be assessed based on the use case. Further we propose the fine-tuned predictive model to predict the appropriate class of the data based on its accuracy using state-of-the-art methods and techniques. The main contribution of this paper is given below:

- Defining classification criteria for different target labels for the desired dataset (Section III).
- Data preparation and conversion for desired dataset (Section IV).
- Improve the dataset after removing class imbalance and non-standardization issues (Section V).
- Implementing multiple learning algorithms to get the best model suitable for this dataset (Section VI).
- Fine-tuning of the hyperparameters for the suitable learning model (Section VII).

The rest of the paper is organized into eight sections: Section II describes the related work; Section III gives the problem description in detail along with the terminologies used in the paper. In Section IV, detailed data preparation processes are discussed. Model building is discussed in Section V. Section VI is about the experiments and results discussion. Fine-tuning of hyperparameters is explained in Section VII and at last, we conclude the work.

II. Related Work

Crowdsourced data available on geo portals are huge data with great potential where it can be used for better citizen-centric services. Therefore, it becomes important to analyze this data deeply to harness its power for robust applications. During this research work, we have explored various research papers related to POI data verification and Predictive machine learning models. This in-depth study is presented in three main categories as “POI data verification”, “Imbalance class dataset” and “Predictive modeling”. Research work related to each category is given below:

A. POI Data Verification

Researchers assessed the quality of POI data available on Different platform like Facebook, flicker, etc. and concluded that different level of accuracy is required for different use cases [1]. However, they considered very few parameters which are not sufficient to assess the accuracy of the POI. Authors searched the missing POI on Google Maps by using unsupervised learning methods where they extracted addresses from the web and enhanced the missing POI [2]. Outdated POI was searched using a semi-supervised method which includes decision tree classifier and Adaboost [3]. Finding the obsolete POI is an important work as the outdated POI may mislead the user. The authors formulated the Integer Linear Programming approach to identify the visited POI which is useful in handling the POI recommendation [4]. Researchers proposed detection of the POI boundaries using Boundary-dependent Explicit Semantic analysis [5]. POI data density is used to identify the urban functional area which can be used for future planning in that region [6]. Boundaries of the commercial centers were also identified using POI data [7]. These works are useful in planning regional events and business growth. Many times, multiple tags are available for the same data hence it is important to remove the duplicate information. The author suggested a non-negative matrix factorization method based on the maximum likelihood estimation to find the similarity between different labels assigned to the same POI [8]. Researchers work on the POI data organization using multidimensional ranking organization to arrange the POI data which can be retrieved easily during the recommendation process [9]. Mapping the POI data on correct location and category was suggested which can be used in POI recommendation [10]. Authors provide the statistics for POI accuracy on available sources that is useful in future development in this domain [11]. Lots of work is being done in the POI recommendation area [12-13]. POI data classification was done using various techniques including bounding box methods, land use identification and gazetteer information [14-17]. During the quality assessment for POI data, the researcher faced the limitation in obtaining the reference data [18]. We didn’t find many works done in POI verification or accuracy measurement of the crowdsourced geotagged POI data.

B. Imbalance Class Dataset

There is no readily dataset available which can claim for corresponding reference data. Hence, to conduct any experiment in this direction, desired dataset must be prepared. Data set preparation is done using real data available on different map services and geo portals as explained in Section IV. This dataset is imbalanced where each classification category has different number of instances that induce significant differences in accuracy of the predictions. Therefore, the available method for balancing such imbalanced dataset is explored. Authors experimented on various datasets and indicated the difficulties in using imbalanced data and summarized various available methods to make the classes balanced [19-21]. They proposed the method to identify the boundary case example from the given data set and discussed the sampling methods like SMOTE, SPIDER etc. Some researchers assessed the multi label classification problem in imbalanced dataset and suggested the metrics SCUMBLE and SCUMBLELbl to assess the hard label problems [22]. They proposed the new method of resampling to overcome minority class issues. Metrics to assess the performance of the model built using imbalance dataset are suggested [23]. CatBoost and LogitBoost are superior for such datasets and MMMC is the best metrics to judge the performance [24]. Author suggested skew normalized scores to assess the performance of skewed data [25].

C. Predictive Modelling

Predictive modelling approaches were explored for different domains as we hardly found the research work done for accuracy prediction of POI data. Authors proposed for popularity prediction of the POI data for recommendation system [26]. POI classification using machine learning approaches were studied [27-28]. Some researchers compared POI data extracted from different sources and observed the variations [29]. Machine learning methods were used to compare POI datasets extracted from different sources. Most of the work done in this domain is related to POI recommendation [30-31]. As there are very few research articles available with respect to POI data and predictive modelling, we explored other domains where predictive modelling was applied [32-35].

D. Review Summary

Geotagging is the important activity to generate POI data and many researchers worked in this domain [36-39]. Some authors suggested the techniques to inference the geographical location based on text, image and categories [40-47]. Authors explained that even incomplete data can also be useful hence we divided the dataset into four classes and proposed a method to categorize the POI in a suitable class [48]. As per our best knowledge, such categorization and labeling of POI data available on geoportal are not tried before using predictive modeling where multiple parameters including ground truth data are used. Our proposed solution is considering many sources to extract the relevant features from the trusted sources such as Layout urban planning and development map of that region and the repositories of public service POI data. The proposed model is based on state-of-the-art methods and techniques for a better solution.

III. Problem Setting

First, we give a brief introduction of the terms and abbreviations, and then formulate the problem for measuring the accuracy of geotagged data. Categorical Classes are defined in this section according to the net value calculated based on the penalty and gain as described in detail in Section IV.

A. Definitions

- Crowd sourcing is a data collection technique where a large number of people share the data on a common platform and collected data are called crowdsourced data.
- Geotagged POI data determines the Point of interest data that includes geographical information of a place along with other relevant metadata such as name, address, category, latitude, and longitude. It is used as tagged data interchangeably at some places.
- Ground truth data are the location data that are verified and provided by trusted contributors. This is considered as the reference data in this study.
- Category is a place type e.g. education, healthcare, bank, religious place, etc.
- In this work, the user is a contributor who has geotagged the data on some geoportal or mapping website. It could be anyone like an owner, local guide, and general user.
- Web Sources are the websites that give some information about the searched geotagged place. It must include the name and address of the searched tagged data.
- The geotagged data are said to be verified if some process is applied to check its accuracy which categories these in one of the classes specified as “Correct”, “Incorrect”, “Partially Correct” and “Almost Correct”.

List of notations are given in Table I.

TABLE I. NOTATIONS

Notation	Description
GT	Ground Truth
POI	Point of Interest
Lat	Latitude
Long	Longitude
GIS	Geographical-Information System
Pincode	Postal Code
CS	Crowdsourced
Sr No	Serial Number

B. Tagging the Label

As we explained earlier, there is no required dataset available to work on this problem hence, we have prepared the dataset and defined the criteria to label the target parameter based on its class. Proposed work is our extended work where we conceptualized the verification Model for POI data [49]. In this model, ground truth data are involved in verification where the layout plan and the trusted repositories are considered as GT data. Corresponding geotagged data are extracted from geo portals or map websites that are considered as CS data. A layout plan was georeferenced and the detail of each asset is converted in to attribute table. The main features of the asset like name, address, pin code, latitude, longitude, and category are incorporated in model building. The formulation for accuracy label tagging is explained in the below subsection.

C. Problem Definition

Let’s take G as the set of GT data and P as the set of POI data available on the geoportals or Map websites. Assuming A as the set of features or metadata, associated with POI data. L is the set of labels given to the target, based on the net values. “n” is the total number of records available in the data set. T is a set of target values as shown in “(1)” and “(2)”. These sets and their relationship are described in below equations:

$$G=\{g_i\},\ \text{where } i=1 \text{ to } n;\ P=\{p_i\},\ \text{where } i=1 \text{ to } n;\ A=\{a_j\},\ \text{where } j=1 \text{ to } x; \tag{1}$$

$$L=\{\text{“correct”}, \text{“incorrect”}, \text{“partial correct”}, \text{“almost correct”}\},\ T=\{t_i\},\ \text{where } i=1 \text{ to } n; \tag{2}$$

$$f\,(g_i, p_i) =\{gain/penalty\},\ \forall a_j \text{ where } j=1 \text{ to } x \tag{3}$$

$$\sum_{j=1}^{k}(gain) - \sum_{j=1}^{k}(penalty) = netvalue,\ \forall a_j \text{ where } j=1 \text{ to } x \tag{4}$$

$\forall t_i,\ f(t_i,(netvalue)) \in L$. where,

$$l_i=\begin{cases} incorrect, if\ netvalue \le 5 \\ partial\ correct\ , if\ 5 > netvalue \le 10 \\ almost\ correct, if 10 > netvalue \le 15 \\ correct, if\ netvalue > 15 \end{cases} \tag{5}$$

Comparison functions are applied on GT and corresponding CS data to get the gain and penalty as shown in “(3)”. The parameters that provide positive support towards accuracy, referred to as “gain” and the negatively contributing parameters are referred to as “penalty”. Details of the functions are covered in the next section. Once the net value is calculated based on the “(4)”, entire dataset is labeled with four different classes as described in “(5)”.

IV. Data Preparation

The success of any prediction model is entirely dependent on the training dataset. Hence, it is essential to get a correct, valid, consistent, and real dataset to get the actual image of the real data. For the proposed model, we need the GT data and the corresponding CS data. Therefore, we prepared the desired dataset by following the Process shown in Fig. 1. There are four main modules involved in dataset preparation. GT data are collected via two ways such as layout plans constructed for urban development and trusted repositories. For each GT data entity, CS data are extracted from geo portals and map websites using API provided by these service providers. Important features of both the dataset are name, address, pin code, category, Latitude, Longitude, Geo boundary, Asset area, user profile, Time stamp, and reviews.

Intersecting features of these two datasets were selected for comparison and few strong evidential features were also added like contributor's profile data, distinct web sources and the freshness of the data. Contributor's profile exposes the locality where it belongs to. So, the chances are higher to provide correct POI information from that place by the contributor. A number of distinct web sources are directly proportional to the accuracy due to the availability of the same information at various sources. The latest timestamp found in the web source data provides the measurement of the freshness of the POI data. Logic for web scrapping to extract the additional features is explained in the flowchart shown in Fig. 2. Search engine URL and the search string having the name and address of the POI are provided to the web scraping process. HTML is parsed using Beautiful Soup Library of Python, and all the distinct URLs are fetched. Once the entire URL list is processed, the count will be returned. Specifically, we obtained the latest date information found in the web sources to measure the freshness.

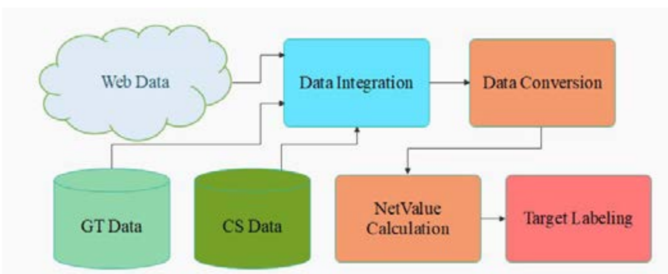

Fig. 1. Flow Diagram of Data Preparation.

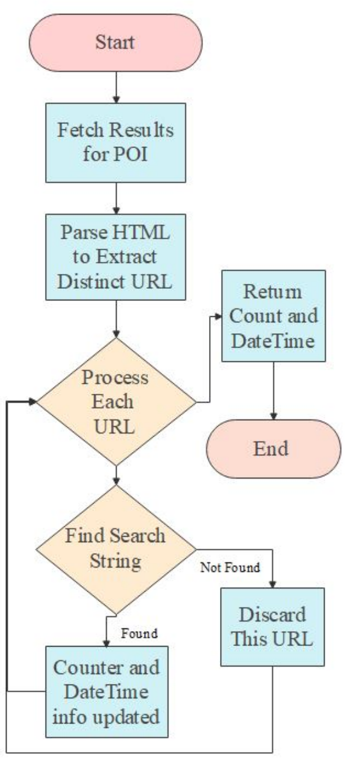

Fig. 2. Web Scrapping Process to Get Additional Information.

The integrated data are processed further to remove the incomplete, erroneous, and duplicate data in the data preparation module. Sample record of this integrated data is shown in Table II. Various comparison methods are applied to compare different features such as wordnet corpus of NLTK is used to compare the category data to consider semantic similarities [50]. Cosine similarity method is used for exact matching. For measuring the deviation in a location with respect to Geo Spatial Points, Haversine formula is used where we obtained the variation in Km. Sample data of comparison outcome values for two records R1 and R2 are shown in Table III. Gain and Penalty are required to calculate the Net value as given in "(4)". These are explained below.

1) Gain: Similarity Score is considered as gain because it supports the correctness of the data. A higher similarity score means more accurate data. Therefore, Name similarity, Address similarity, Pin code similarity, and a category similarity score are treated as gain values. Similarly, the higher web sources count is a positive sign of correctness. Hence it should be added to the gain. Higher user type is inclined towards more trusted users so it is also taken as gain. These user types are general user, local guide, surveyor, owner, or admin. General user has less credential and admin has the highest credential. These values are from 1 to 5. The higher the number, the better the chances to get the correct information.

2) Penalty: Higher variation in data pushes it towards an incorrect state. Therefore, variation is considered as a penalty. Location variation is the important factor to decide the correctness of the data. Using the haversine formula, variation distance is calculated and this deviation is subtracted from the threshold value which is considered as 1 km for this POC just for simplicity. Similarly, Staleness score is also taken as a penalty because a larger value signifies the staleness of the data that is inversely proportional to the accuracy. Hence it is added to the penalty.

After plug-in all the values of penalty and gain in "(4)", the net value is calculated which will be further considered to categorize the target data. Target values are categorized using "(5)" and the entire dataset is classified into four categories as explained in Section III.

TABLE II. SAMPLE DATA AFTER COMPARISON

Feature	Data value
Sr No	4973
Name Similarity	0.1176470
Add Similarity	0.300552458
PIN Similarity	1
Location Variation	533.690
Category Similarity	1
User Type Coding	3
Web Src Count	7
Staleness value	0

TABLE III. SAMPLE DATA AFTER TARGET LABELLING

Feature	Data value(R1)	Data Value(R2)
Sr_No	4973	6237
Name Similarity	0.1176470	1
Add Similarity	0.300552458	0.527072476
PIN Similarity	1	1
Location Variation	533.690	-0.77525
Category Similarity	1	1
User Type Coding	3	3
Web Src Count	7	8
Staleness value	0	0
Net Value	-520.27180484	15.30
TargetLabel	Incorrect	Correct

V. MODEL BUILDING

The Statistical analysis is required to understand the characteristics of the dataset to choose the appropriate approach for model building. Details of the statistical analysis and the treatment applied to the dataset are given in the following subsections.

A. Data Analysis

Once the data set is prepared as explained in the above section, JASP 0.14.1 software is used for statistical analysis to understand the characteristics of the data as displayed in Table IV.

Data shown in this table provides the basic statistical values including valid record, missing values, the mean value in each case, standard deviations, skewness, error in skewness, minimum values, and maximum value. There are lots of differences in the number of records in each class and the class "Correct" is a minority class. The range of the values is also wide which can impact the perfect model building. For some algorithms, higher values may dominate and results could be biased. The distribution graph is plotted for each feature with respect to each class specified in the target value. One of the graphs is shown in Fig. 3 and the detail of the other attributes is given in Appendix I.

TABLE IV. DESCRIPTIVE STATISTICS FOR NET VALUE AND THE TARGET CLASSES

Statistics	Almost Correct	Correct	Partial Correct	Incorrect
Valid	221	13	168	111
Missing	0	0	0	0
Mean	11.544	16.176	7.840	-456.775
Std. deviation	1.150	0.795	1.369	1441.913
Skewness	0.952	0.896	-0.346	-4.587
Std. Error of skewness	0.164	0.616	0.187	0.229
Minimum	10	15	5	-9413.181
Maximum	14.874	18	9.937	4.999

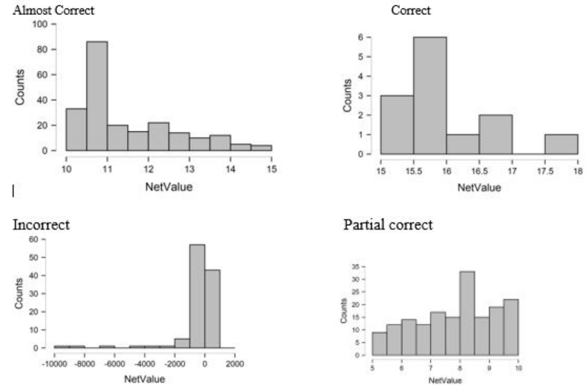

Fig. 3. Distribution Graph for All Four Classes v/s Netvalue.

It is observed that only partial correct data are closer to normal distribution. Distribution for the other classes is skewed as shown in the Fig. 3. High skewness may inject biased results and a false impression of the accuracy of the model could be achieved. Hence, before moving ahead, the dataset must be treated to overcome these issues related to the imbalanced classes and the wider range in the listed features. These processes are explained in the below sections.

B. Standardization and Class Balancing

In skewed data, learning may not be correct as the features having a large magnitude will dominate the objective function. Therefore, learning from other features will not happen impartially. We used MinMaxScaler class of sci-kit learn preprocessing package and set the range between -1 and 1 for required features. The impact of this normalization is shown in the results section.

To make the dataset balance for all the classes, SMOTE oversampling method is used [51]. In this method, interpolation is used to generate the synthetic instance based on the KNn approach. Selecting the number of neighbors is configurable and the default value is taken as 5. After interpolation, a fit-resample is applied to make sure the sufficient number of instances in test and training datasets before dividing it for model building. SMOTE method is available in oversampling package of the "imblearn" library of Python.

C. Model Selection Process

There must be a benchmark to measure the performance of the implemented model and there is a ZeroR classification method that provides the baseline performance for the selected model. It is a basic classification method that predicts the majority class without considering the available predictors in the dataset. After getting the benchmark value, other models need to be applied and compared. As per the statistics and the characteristics of the dataset, it is a multiclass classification problem. Suitable models for this problem are explained below in brief.

1) Logistic regression: Logistic regression is suitable for multi-class classification because it gives the probability of the classes available in the target variable based on the independent variable. By default, it can classify binary classes however using One vs one and One vs rest make it suitable for multiclass classification as well. This modified version is based on the SoftMax formula for a better approximation of the expected target class.

2) Decision tree: It is a supervised learning algorithm that can be used for classification and regression. It splits the data at the decision node according to certain rules based on the data. The entire dataset is considered at root note and the split logic is applied recursively on this dataset. Leaf node represents the class to which data belongs to. Splitting logic plays a vital role in a tree's classification accuracy.

3) Random forest: Random Forest is an ensemble of multiple decision trees and can be used in both regression and classification. It works on the principle of many weak learners rather than the one strong learner. It starts creating a decision tree corresponding to each instance and based on the majority voting, prediction results are generated. It overcomes the overfitting issue of the decision tree by dropping some features in each tree randomly. Based on the mode where the most frequently occurring outcome for the given data is chosen.

4) K-nearest neighbors: It is a supervised learning classifier based on lazy learning where the entire dataset is used as training data. Euclidian distance is calculated for available data points and the nearest similar items are picked. The accuracy of the model depends upon the data and it may not be able to classify the boundary cases.

5) Multi-Layer perceptron: It is a simple Artificial neural network which works based on the feed-forward principle. There are multiple layers divided into three parts. An input layer, an output layer, and the hidden layers. The input layer receives the input and passes it to the hidden layer where the SoftMax function is used as the activation function. The final prediction task is done at the output layer. There could be more than one hidden layer. The number of neurons on the output layers depends on the number of classes considered for the classification task.

VI. Experimental Set Up

To choose an appropriate algorithm, we have executed multiple tests using Weka 3.9 and all the selected algorithms were applied to the dataset. To apply the above-described algorithm, two well-known approaches, Cross-validation, and split train test was adopted. Both the approaches are given below in brief.

- Cross-validation: It is also known as k-fold cross-validation. In this approach, the dataset is split in to k subsets and the model is trained using k-1 subsets and the kth set is used for testing the performance of the model. The algorithm is executed in k iteration and the final prediction error is the average error observed in each iteration. This approach provides the insight to check the overfitting or selection bias issues.
- Split-Train-Test: The idea is to divide the dataset randomly into two parts where a bigger chunk is used to train the model which is called the training set. The leftover is used as the testing dataset which is unseen for the model and used to evaluate the performance of the model being used.

For cross-validation, K is set as ten which means the dataset is divided into ten parts and a total of ten iterations were executed. In the case of the split-train-test, the dataset is divided into two parts in 70-30 percentage, which means 70% of the data are used for training the model, and the rest 30 % are used as a test data set. The number of iterations is set as ten for this schema. Systematic analysis done for each model is presented in the following subsection.

A. *Experimental Results*

We analyzed the result obtained in each cycle for the different algorithms being used. Results are discussed below in the ordered way as they are executed.

1) Obtaining base performance: Zero R is used for base performance checks. Performance metrics obtained using ZeroR is set as a benchmark for other models. As shown in the Table V, accuracy and the kappa statistics are decreased after using a balanced class dataset. Hence 20.7009% is set as the benchmark accuracy level for other models. A negative value of Kappa statistics says that this model is very far from the optimum solution.

2) Multiple models application: Selected models were applied on the normalized dataset using both approaches as discussed in the previous section. Results using “Cross vaalidation” are given in Table VI. Logistic, Multilayer Perceptron, IBK, Multiclass Classification, decision tree, and the random forest are applied on the balanced and imbalanced dataset. Results shown in bold are the best performer. Here we can observe that Logistic regression is the best one.

Results obtained using the Split-Train-Test approach is shown in Table VII. As shown in the table, the best performance is shown by Logistic regression. Random forest and the Decision Tree are showing the second and third better performance. We have selected these top performer models for further analysis and once again executed them in python where we got almost same results. Therefore, we have plotted the learning curve for these three models as shown in Fig. 4. For decision tree and random forest models, learning on the small set of data are happening quickly whereas, for rest of the data it is taking time. It could be a case of local maxima so results may be biased. In the case of logistic regression model, the learning curve is much better as it is utilizing the maximum possible records from the dataset before converging. Hence the results obtained through logistic regression are more reliable. Therefore, logistic regression is selected for the final model building. There are certain hyperparameters that can be tuned to improve the performance. These hyperparameters and their impact are explained in the next section.

TABLE V. RESULTS OF ZEROR CLASSIFIER ON TWO DATASETS

Metrics	**Imbalanced Class Data set**	**Balanced Class dataset**
Accuracy	43.0799 %	**20.7009** %
Kappa Statistics	0	**-0. 0573**
MAE	0. 3303	0. 3753
RMSE	0. 4061	0. 4334

TABLE VI. PERFORMANCE RESULTS FOR CROSS VALIDATION SETUP

Model	**With Class balancer (Cross validation)**					**Without Class balancer (Cross validation)**				
	Accuracy	***Kappa***	***RMSE***	***F1***	***Time***	***Accuracy***	***Kappa***	***RMSE***	***F1***	***Time***
Logistic	97.81	0.9709	0.1063	0.978	0.09	99.61	0.9941	0.0491	0.994	1
Multilayer Perceptron	79.61	0.7282	0.2973	0.793	0.36	78.55	0.6641	0.2958	0.776	0.38
IBK	70.16	0.6022	0.3843	0.702	0	69.98	0.5442	0.383	0.700	0
Decision Tree	85.14	0.802	0.2597	0.853	0	86.93	0.8019	0.2419	0.870	0
Random Forest	**87.72**	**0.8363**	**0.2209**	**0.879**	**1**	**90.05**	**0.8484**	**0.1903**	**0.901**	**0.09**

TABLE VII. PERFORMANCE RESULTS FOR SPLIT-TRAIN-TEST SETUP

Model	**With Class balancer (Split-Train-Test)**					**Without Class balancer (Split-Train-Test)**				
	Accuracy	***Kappa***	***RMSE***	***F1***	***Time***	***Accuracy***	***Kappa***	***RMSE***	***F1***	***Time***
Logistic	**97.41**	**0.9654**	**0.1085**	**0.968**	**0.1**	**96.75**	**0.951**	**0.1192**	**0.952**	**0.1**
Multilayer Perceptron	80.09	0.7324	0.2874	0.808	0	77.92	0.659	0.3136	0.767	0
IBK	76.65	0.6864	0.3391	0.752	0.0	73.37	0.588	0.3629	0.722	0.01
Decision Tree	87.27	0.8293	0.2382	0.873	0	86.36	0.791	0.2591	0.863	0.01
Random Forest	**89.75**	**0.8625**	**0.1824**	**0.897**	**0**	**88.961**	**0.8304**	**0.2083**	**0.888**	**0**

Fig. 4. Learning Curve for Decision Tree, Random Forest and Logistic Regression.

VII. Fine Tuning

Each algorithm has some hyperparameters which needs to be tuned to make the model efficient on the desired data set as there is no pre-stated rule to choose the value of these hyperparameters. For decision tree and random forest models, learning on the small set of data happen quickly whereas, for rest of the data it is taking time. It could be a case of local maxima so results may be biased. In the case of logistic regression model, the learning curve is much better as it is utilizing the maximum possible records from the dataset before converging. Therefore, Logistic regression model is selected for final fine tuning to obtain the best performance.

In the case of logistic regression, we considered below explained three parameters for fine tuning of the model.

A. Solver

It's a mathematical model which helps to calculate the optimum prediction by reducing the loss factor. There are different methods available in logistic regression such as "saga", "lbfgs", "newton-cg", "sag", "liblnear", etc. to achieve the best optimization based on the characteristics of the dataset available to work on. Newton-cg uses the quadratic function for loss minimization which makes it expensive. It can handle the loss in case of multiclass problems easily. Limited-memory Broyden–Fletcher–Goldfarb–Shanno (lbfgs), stores only a few vectors that support the approximations for the next terms. It can also handle the multinomial loss easily and it is used as the default solver in sci-kit learn library of python. Liblinear uses the coordinate descent algorithm for optimization purposes. It applies automatic parameters selection and suitable for large predictors dataset. Stochastic Average Gradient (SAG) uses smooth convex functions and suitable for large data set as it easily gets converge. SAGA is a variant of SAG which supports sparse multinomial logistic regression and suitable for a very large dataset.

B. Regularization

It is also known as the penalty method. It is a way to avoid the overfitting of a model. Regularization overcomes the overfitting issue by adding some bias using tuning parameters. There are multiple methods available that are L1, L2, and Elastic Net. These methods are to regularize the higher coefficient values. L1 uses the absolute magnitude values of the coefficient and ignores the Zero values. L2 takes the square of the magnitude to avoid the sparse coefficient matrix. Elastic net is a combination of L1 and L2 and mostly used where the number of predictors is larger than the number of observations [52]. It groups the strongly correlated predictors so the contribution or removal of these variables is done together.

C. C-Value

This is the inverse of the solver strength. As per the documentation of the sci-kit learn, a smaller value indicates the stronger regularization.

All the solvers don't support each penalizing method. Table VIII shows the solver and the penalty supported by them. From the below table, we observe that penalty L2 is applicable with each solver so we are considering L2 for further analysis with different combinations of c value and the solver choice. The logic for getting the accuracy with standard deviation in each case is given in Algorithm 1.

TABLE VIII. Solver and Compatible Regularization Method

Solver	**Compatible Regularization Method**
Newton – cg	L2
Sag	L2
Saga	L2, Elastic net
Lbfgs	L2

The solver list, penalty method list, and solver strength list are passed as the input parameters. RepeatedStratifiedKFold class from sci-kit learn of python is used as a cross validator for taking different random records for repeating n times.

ALGORITHM 1: Analysis of Hyperparameters

```
Input:
solverList= {'newton-cg', 'lbfgs', 'liblinear'},
penaltyList={'l2','none'}, cValues = [100, 10, 1.0, 0.1, 0.01],
executionScheme= {simple logistic, k fold logistic, stratified k
fold}, dataset
Output:
outcomeList
        for each cValues do
         for each executionScheme
         cv = createInstanceOf_ExecutionScheme ()
         gs = GridSearchCV (estimator, param_grid, cv, scoring,
error_score)
         fitGridSearchOnDataset ()
         SetOutcome (accuracy, stdDeviation)
         endFor
 endFor
output outcomeList
```

After that, GridSearchCV of model selection package from sci-kit learn is used for executing the process for various parameters. It takes a model function as the estimator, param_grid as the list or dictionary of the parameters which need to be applied. It also takes the cross-validator estimator, a scoring list that may have multiple scoring parameters and an error score. We have tested for penalty "L2" and 'none' as the other options are not applicable. Best accuracy is observed with Newton-cg and the C value as 100. Accuracy decreases for other values of the C parameter. Solver Sag and Saga show minor change and low accuracy. If the penalty is set as "None" then Liblinear is out from the choice as it doesn't support any regularization method apart from L2. For the rest of the solver, again the Newton-CG performed the best with 100 as the C value. L2 regularization method gives the best result for Newton-cg solver and 100 as the strength value however it must be verified the same with a large dataset.

VIII Conclusion

In this research, the proposed predictive model was built and fine-tuned via exhaustive experiments done on the prepared dataset. Results show that the performance varies for an imbalanced dataset which is just half when applied to a balanced dataset. It removes the overfitting chances that lead for more accurate, nonbiased results. We also applied different models on the data set for two different approaches known as Cross-validation and Split-train-test to obtain the best model. Logistic regression is found as the best performer among six different models however random forest and decision tree were also good but they were suffered from the local maxima issue. Hence the logistic regression is chosen for the final model and it was fine-tuned for various parameters using exhaustive experiments. The final model is obtained with Newton-CG solver, L2 penalty and 100 as the solver strength parameter for this dataset. The proposed model gives 96.40% accuracy on unseen data. This is a novel predictive model, based on multiple sources of information to judge the accuracy of the geotagged data. This work provides the way to move forward for various use cases depends on the geotagged data for better development work for citizens. There are many preprocessing steps involved to make the data useful for prediction. As of now, these processes are discrete and costly in terms of execution time. Going forward, we are planning to increase the dataset with the small threshold value for location variation and build a robust pipeline to cover the data preprocess work using the state-of-the-art framework available for the machine learning pipeline. Proposed work opens the way to ensure the quality of geotagged data available on mapping websites and geoportals.

VIII. Supplementary Material

Detailed descriptive statistical analysis of dataset is provided in Appendix I.

References

[1] Jonietz, David, and Alexander Zipf. “Defining Fitness-for-Use for Crowdsourced Points of Interest (POI).” ISPRS International Journal of Geo-Information 5, no. 9 (August 24, 2016): 149. doi:10.3390/ijgi5090149.

[2] Chang, Chia-Hui, Hsiu-Min Chuang, Chia-Yi Huang, Yueng-Sheng Su, and Shu-Ying Li. “Enhancing POI Search on Maps via Online Address Extraction and Associated Information Segmentation.” Applied Intelligence 44, no. 3 (October 15, 2015): 539–556. doi:10.1007/s10489-015-0707-5.

[3] Chuang, Hsiu-Min, and Chia-Hui Chang. “Verification of POI and Location Pairs via Weakly Labeled Web Data.” Proceedings of the 24th International Conference on World Wide Web (May 18, 2015). doi:10.1145/2740908.2741715.

[4] Suzuki, Jun, Yoshihiko Suhara, Hiroyuki Toda, and Kyosuke Nishida. “Personalized Visited-POI Assignment to Individual Raw GPS Trajectories.” ACM Transactions on Spatial Algorithms and Systems 5, no. 3 (September 25, 2019): 1–28. doi:10.1145/3317667.

[5] Bui, Thanh-Hieu, Yong-Jin Han, Seong-Bae Park, and Se-Young Park. “Detection of POI Boundaries through Geographical Topics.” 2015 International Conference on Big Data and Smart Computing (BIGCOMP) (February 2015). doi:10.1109/35021bigcomp.2015.7072827.

[6] Hu, Sheng, Zhanjun He, Liang Wu, Li Yin, Yongyang Xu, and Haifu Cui. “A Framework for Extracting Urban Functional Regions Based on Multiprototype Word Embeddings Using Points-of-Interest Data.” Computers, Environment and Urban Systems 80 (March 2020): 101442. doi: 10.1016/j.compenvurbsys.2019.101442.

[7] Lifang, Zhu, Chen Yixin, Liu Yang, Zhang Yue, and Wang Jing. “POI Data Applied in Extracting the Boundary of Commercial Centers.” 2017 IEEE 2nd International Conference on Big Data Analysis (ICBDA)((March 2017). doi:10.1109/icbda.2017.8078693.

[8] Zhou, Jingbo, Shan Gou, Renjun Hu, Dongxiang Zhang, Jin Xu, Airong Jiang, Ying Li, and Hui Xiong. “A Collaborative Learning Framework to Tag Refinement for Points of Interest.” Proceedings of the 25th ACM SIGKDD International Conference on Knowledge Discovery & Data Mining (July 25, 2019). doi:10.1145/3292500.3330698.

[9] Liu, Lei, Jingwen Li, and Suxian Ye. “Research on the Method of Constructing POI Data Model Based on AP-MRO.” 2018 IEEE 4th Information Technology and Mechatronics Engineering Conference (ITOEC) (December 2018). doi:10.1109/itoec.2018.8740599.

[10] Li, Yurui, Hongmei Chen, Lizhen Wang, and Qing Xiao. “POI Representation Learning by a Hybrid Model.” 2019 20th IEEE International Conference on Mobile Data Management (MDM) (June 2019). doi:10.1109/mdm.2019.00010.

[11] Hochmair, Hartwig H., Levente Juhász, and Sreten Cvetojevic. “Data Quality of Points of Interest in Selected Mapping and Social Media Platforms.” Progress in Location Based Services 2018 (December 9, 2017): 293–313. doi:10.1007/978-3-319-71470-7_15.

[12] Liu, Shudong. “User Modeling for Point-of-Interest Recommendations in Location-Based Social Networks: The State of the Art.” Mobile Information Systems 2018 (2018): 1–13. doi:10.1155/2018/7807461.

[13] Massimo, David, and Francesco Ricci. “Harnessing a Generalised User Behaviour Model for Next-POI Recommendation.” Proceedings of the 12th ACM Conference on Recommender Systems (September 27, 2018). doi:10.1145/3240323.3240392.

[14] Janowicz, K., and C. Keßler. “The Role of Ontology in Improving Gazetteer Interaction.” International Journal of Geographical Information Science 22, no. 10 (October 2008): 1129–1157. doi:10.1080/13658810701851461.

[15] Jiang, Suhui, Yu Kong, and Yun Fu. “Deep Geo-Constrained Auto-Encoder for Non-Landmark GPS Estimation.” IEEE Transactions on Big Data 5, no. 2 (June 1, 2019): 120–133. doi:10.1109/tbdata.2017.2773096.

[16] Xing, Hanfa, Yuan Meng, Dongyang Hou, Fangjie Cao, and Haibin Xu. “Exploring Point-of-Interest Data from Social Media for Artificial Surface Validation with Decision Trees.” International Journal of Remote Sensing 38, no. 23 (August 23, 2017): 6945–6969. doi:10.1080/01431161.2017.1368101.

[17] Yuanrong He, Yuanmao Zheng, Jian Deng, and Huoping Pan. “Design and Implementation of a POI Collection and Management System Based on Public Map Service.” 2016 Fourth International Conference on Ubiquitous Positioning, Indoor Navigation and Location Based Services (UPINLBS) (November 2016). doi:10.1109/upinlbs.2016.7809971.

[18] De Tré, Guy, Daan Van Britsom, Tom Matthé, and Antoon Bronselaer. “Automated Cleansing of POI Databases.” Quality Issues in the Management of Web Information (2013): 55–91. doi:10.1007/978-3-642-37688-7_4.

[19] Krawczyk, Bartosz. “Learning from Imbalanced Data: Open Challenges and Future Directions.” Progress in Artificial Intelligence 5, no. 4 (April 22, 2016): 221–232. doi:10.1007/s13748-016-0094-0.

[20] Napierala, Krystyna, and Jerzy Stefanowski. “Types of Minority Class Examples and Their Influence on Learning Classifiers from Imbalanced Data.” Journal of Intelligent Information Systems 46, no. 3 (July 9, 2015): 563–597. doi:10.1007/s10844-015-0368-1.

[21] Vluymans, Sarah. “Learning from Imbalanced Data.” Studies in Computational Intelligence (November 24, 2018): 81–110. doi:10.1007/978-3-030-04663-7_4.

[22] Charte, Francisco, Antonio J. Rivera, María J. del Jesus, and Francisco Herrera. “Dealing with Difficult Minority Labels in Imbalanced Mutilabel Data Sets.” Neurocomputing 326–327 (January 2019): 39–53. doi: 10.1016/j.neucom.2016.08.158.

[23] Chawla, Nitesh V. “Data Mining for Imbalanced Datasets: An Overview.” Data Mining and Knowledge Discovery Handbook (n.d.): 853–867. doi:10.1007/0-387-25465-x_40.

[24] Tanha, Jafar, Yousef Abdi, Negin Samadi, Nazila Razzaghi, and Mohammad Asadpour. “Boosting Methods for Multi-Class Imbalanced Data Classification: An Experimental Review.” Journal of Big Data 7, no. 1 (September 1, 2020). doi:10.1186/s40537-020-00349-y.

[25] Jeni, Laszlo A., Jeffrey F. Cohn, and Fernando De La Torre. “Facing Imbalanced Data--Recommendations for the Use of Performance

Metrics.” 2013 Humaine Association Conference on Affective Computing and Intelligent Interaction (September 2013). doi:10.1109/acii.2013.47.

[26] Yang, Yang, Yaqian Duan, Xinze Wang, Zi Huang, Ning Xie, and Heng Tao Shen. “Hierarchical Multi-Clue Modelling for POI Popularity Prediction with Heterogeneous Tourist Information.” IEEE Transactions on Knowledge and Data Engineering 31, no. 4 (April 1, 2019): 757–768. doi:10.1109/tkde.2018.2842190.

[27] Jiang, Shan, Ana Alves, Filipe Rodrigues, Joseph Ferreira, and Francisco C. Pereira. “Mining Point-of-Interest Data from Social Networks for Urban Land Use Classification and Disaggregation.” Computers, Environment and Urban Systems 53 (September 2015): 36–46. doi: 10.1016/j.compenvurbsys.2014.12.001.

[28] Raj, Pethuru, and Chellammal Surianarayanan. “Digital Twin: The Industry Use Cases.” The Digital Twin Paradigm for Smarter Systems and Environments: The Industry Use Cases (2020): 285–320. doi: 10.1016/bs.adcom.2019.09.006.

[29] Zhou, Yang, Mingjun Wang, Chen Zhang, Fu Ren, Xiangyuan Ma, and Qingyun Du. “A Points of Interest Matching Method Using a Multivariate Weighting Function with Gradient Descent Optimization.” Transactions in GIS 25, no. 1 (October 5, 2020): 359–381. doi:10.1111/tgis.12690.

[30] Yu, Ruiyun, Dezhi Ye, and Jie Li. “RePiDeM: A Refined POI Demand Modeling Based on Multi-Source Data*.” IEEE INFOCOM 2020 - IEEE Conference on Computer Communications (July 2020). doi:10.1109/infocom41043.2020.9155294.

[31] Zhang, Zhiqian, Chenliang Li, Zhiyong Wu, Aixin Sun, Dengpan Ye, and Xiangyang Luo. “NEXT: a Neural Network Framework for Next POI Recommendation.” Frontiers of Computer Science 14, no. 2 (August 30, 2019): 314–333. doi:10.1007/s11704-018-8011-2.

[32] Asniar, and Kridanto Surendro. “Predictive Analytics for Predicting Customer Behavior.” 2019 International Conference of Artificial Intelligence and Information Technology (ICAIIT) (March 2019). doi:10.1109/icaiit.2019.8834571.

[33] Bindra, Simranjeet Kour, Akshay Girdhar, and Inderjeet Singh Bamrah. “Outcome Based Predictive Analysis of Automatic Question Paper Using Data Mining.” 2017 2nd International Conference on Communication and Electronics Systems (ICCES) (October 2017). doi:10.1109/cesys.2017.8321154.

[34] Lu, Yafeng, Robert Kruger, Dennis Thom, Feng Wang, Steffen Koch, Thomas Ertl, and Ross Maciejewski. “Integrating Predictive Analytics and Social Media.” 2014 IEEE Conference on Visual Analytics Science and Technology (VAST) (October 2014). doi:10.1109/vast.2014.7042495.

[35] Wazurkar, Parth, Robin Singh Bhadoria, and Dhananjai Bajpai. “Predictive Analytics in Data Science for Business Intelligence Solutions.” 2017 7th International Conference on Communication Systems and Network Technologies (CSNT) (November 2017). doi:10.1109/csnt.2017.8418568.

[36] Arenga, Delan Zoe H., Jennifer C. Dela Cruz, Franch Maverick A. Lorilla, and Paul A. Tangian. “Cloud-Based Flora Repository System with Geo-Location Mapping for Mt. Hamiguitan Sanctuary Exploration.” 2018 IEEE Region Ten Symposium (Tensymp) (July 2018). doi:10.1109/tenconspring.2018.8692056.

[37] Singh, Sanket Kumar, and Davood Rafiei. “Strategies for Geographical Scoping and Improving a Gazetteer.” Proceedings of the 2018 World Wide Web Conference on World Wide Web - WWW ’18 (2018). doi:10.1145/3178876.3186078.

[38] Yoshikatsu, Nagata. “Geographic Names on Old Maps of Early 20th Century Toward a Spatio-Temporal Gazetteer: A Study on Their Accuracy in Northeast Thailand.” 2017 Pacific Neighborhood Consortium Annual Conference and Joint Meetings (PNC) (November 2017). doi:10.23919/pnc.2017.8203528.

[39] Yu Liu, Runqiang Li, Kaichen Chen, Yihong Yuan, Lingli Huang, and Hao Yu. “KIDGS: A Geographical Knowledge-Informed Digital Gazetteer Service.” 2009 17th International Conference on Geoinformatics (August 2009). doi:10.1109/geoinformatics.2009.5293495.

[40] Abbas, S. Syed Ameer, S. K. Ajin, and P. Deepak Sundar. “Realization of Multimodal Geo-Tag Using ARM-A53 with Python.” 2017 International Conference on Intelligent Computing and Control (I2C2) (June 2017). doi:10.1109/i2c2.2017.8321905.

[41] Jurgens, T. Finethy, J. Mccorriston, Y. T. Xu, and D. Ruths, “Geolocation Prediction in Twitter Using Social Networks: A Critical Analysis and Review of Current Practice,” pp. 188–197. doi=10.1.1.700.5386.

[42] Niu, Wei, James Caverlee, Haokai Lu, and Krishna Kamath. “Community-Based Geospatial Tag Estimation.” 2016 IEEE/ACM International Conference on Advances in Social Networks Analysis and Mining (ASONAM) (August 2016). doi:10.1109/asonam.2016.77522.

[43] Qian, Xueming, Yisi Zhao, and Junwei Han. “Image Location Estimation by Salient Region Matching.” IEEE Transactions on Image Processing 24, no. 11 (November 2015): 4348–4358. doi:10.1109/tip.2015.2462131.

[44] Radke, Mansi A., Nitin Gautam, Akhil Tambi, Umesh A. Deshpande, and Zareen Syed. “Geotagging Text Data on the Web—A Geometrical Approach.” IEEE Access 6 (2018): 30086–30099. doi:10.1109/access.2018.2843814.

[45] Ssin, Seung Youb, Joanne E. Zucco, James A. Walsh, Ross T. Smith, and Bruce H. Thomas. “SONA: Improving Situational Awareness of Geotagged Information Using Tangible Interfaces.” 2017 International Symposium on Big Data Visual Analytics (BDVA) (November 2017). doi:10.1109/bdva.2017.8114625.

[46] Utomo, Muhammad Nur Yasir, Teguh Bharata Adji, and Igi Ardiyanto. “Geolocation Prediction in Social Media Data Using Text Analysis: A Review.” 2018 International Conference on Information and Communications Technology (ICOIACT) (March 2018). doi:10.1109/icoiact.2018.8350674.

[47] Zhang, Hang, Lin Li, Wei Hu, Wenjing Yao, and Haihong Zhu. “Visualization of Location-Referenced Web Textual Information Based on Map Mashups.” IEEE Access 7 (2019): 40475–40487. doi:10.1109/access.2019.2907570.

[48] Zhang, Liming, and Dieter Pfoser. “Using OpenStreetMap Point-of-Interest Data to Model Urban change—A Feasibility Study.” Edited by Michael Szell. PLOS ONE 14, no. 2 (February 25, 2019): e0212606. doi: 10.1371/journal.pone.0212606.

[49] Sharma, M., Bothale, V., Bundele, M. and Nawal, M. “Geotagging: Systematic Anatomization and Conceptual Model for POI Verification.” International Journal of Innovative Technology and Exploring Engineering 9, no. 11 (September 10, 2020): 339–348. doi:10.35940/ijitee.k7820.0991120.

[50] Princeton University "About WordNet." WordNet. Princeton University. 2010.

[51] Chawla, N. V., K. W. Bowyer, L. O. Hall, and W. P. Kegelmeyer. “SMOTE: Synthetic Minority Over-Sampling Technique.” Journal of Artificial Intelligence Research 16 (June 1, 2002): 321–357. doi:10.1613/jair.953.

[52] Scikit-learn: Machine Learning in Python, Pedregosa et al., JMLR 12, pp. 2825-2830, 2011.

APPENDIX I

Attribute wise Descriptive Statistical Analysis of the original dataset is presented here. The number of records is not the same for each class as shown in the respective tables. The range for minimum and maximum values is also varying for some attributes. Hence the class balancing and standardization methods were applied before model building.

A. *Name Similarity*

Name of the POI is matched in GT data and corresponding CS data, and compared using wordnet English language corpus. Very few records have exact same name in the Ground Truth data set and the Crowdsourced data available on Geoportals or mapping websites. Comparison score varies from 0 to 1 where 1 shows the perfect matching as shown in Table IX.

TABLE I. DESCRIPTIVE STATISTICS FOR NAME SIMILARITY BASED ON THE TARGET CLASSES

Descriptive Statistics	**Almost Correct**	**Correct**	**Incorrect**	**Partial Correct**
Valid	221	13	168	111
Missing	0	0	0	0
Mean	0.955	0.919	0.785	0.812
Std. deviation	0.151	0.031	0.326	0.311
Minimum	0	0.889	0.118	0
Maximum	1	1	1	1

B. *Address Similarity*

Address of the POI is matched in GT data and corresponding CS data and compared using wordnet English language corpus of NLTK library of Python. Here we considered the semantic meaning of the words like clinic, hospital, and medical institute all were considered as matching. Therefore, the mean value in case of almost correct is 0.715 which is acceptable as shown in Table X.

TABLE II. DESCRIPTIVE STATISTICS FOR ADDRESS SIMILARITY BASED ON THE TARGET CLASSES

Descriptive Statistics	**Almost Correct**	**Correct**	**Incorrect**	**Partial Correct**
Valid	221	13	168	111
Missing	0	0	0	0
Mean	0.715	0.919	0.335	0.453
Std. deviation	0.277	0.160	0.216	0.216
Minimum	0.087	0.527	0	0
Maximum	1	1	1	1

C. *PIN Similarity*

Pin code of the POI is matched in GT data and corresponding CS data and compared using the cosine similarity method. Here we considered exact matching based on the number of digits. As pin code in India has six digits where initial two digits give the information about the state code so if these two digits are not matching then it must go in incorrect however if only last digit is varying that means the variation is within the same locality so it can be considered as Almost Correct as shown in Table XI.

TABLE III. DESCRIPTIVE STATISTICS FOR PIN SIMILARITY BASED ON THE TARGET CLASSES

Descriptive Statistics	**Almost Correct**	**Correct**	**Incorrect**	**Partial Correct**
Valid	221	13	168	111
Missing	0	0	0	0
Mean	0.920	1	0.635	0.805
Std. deviation	0.254	0	0.470	0.357
Minimum	0	1	0	0
Maximum	1	1	1	1

E. *Distance Variation*

Distance variation is the GPS location variation in GT data and corresponding CS data and comparison is done using the Haversine distance calculation method. For implementing the idea, we have kept the threshold as one kilometer just for simplicity. If the variation is within the threshold value, it is considered as matching otherwise not. There is a large difference between minimum and maximum values which needs to be standardized before using in model building as shown in Table XII.

TABLE IV. DESCRIPTIVE STATISTICS FOR DISTANCE VARIATION BASED ON THE TARGET CLASSES

Descriptive Statistics	**Almost Correct**	**Correct**	**Incorrect**	**Partial Correct**
Valid	221	13	168	111
Missing	0	0	0	0
Mean	-0.778	-0.958	464.041	-0.109
Std. deviation	0.334	0.085	1442.937	1.173
Minimum	-1	-1	-1	-1
Maximum	1.292	-0.775	9156.581	4.639

F. *Category Similarity*

Category of the POI is matched in GT data and corresponding CS data and compared using wordnet English language corpus of NLTK library of Python. Here we considered the semantic meaning of the words as taken in case of Name and address contents. As the mean value suggests, even for the incorrect data, most of the records shows the similarity value more than 0.7 as shown in Table XIII.

TABLE V. DESCRIPTIVE STATISTICS FOR CATEGORY SIMILARITY BASED ON THE TARGET CLASSES

Descriptive Statistics	**Almost Correct**	**Correct**	**Incorrect**	**Partial Correct**
Valid	221	13	168	111
Missing	0	0	0	0
Mean	0.809	1	0.736	0.762
Std. deviation	0.314	0	0.347	0.352
Minimum	0.111	1	0	0
Maximum	1	1	1	1

G. *UserType Coding*

There are five types of contributors/users such as general user, local guide, surveyor, owner, or admin who tag the data. Admin is the system admin who is inserting verified geotagged data. Hence there are few less chances to get the wrong data. Surveyor is the authorized person who is manually verifying the locations and tagging. They also considered trusted users. The local guide has more knowledge about the vicinity to which they belong. The rest of the users are considered a general user. Therefore, encoding is done based on their trust factor, and the admin is assigned the highest value whereas the general user is given the lowest value within the range of 1 to 5. Statistics are shown in Table XIV.

TABLE VI. DESCRIPTIVE STATISTICS FOR USERTYPECODING BASED ON THE TARGET CLASSES

Descriptive Statistics	**Almost Correct**	**Correct**	**Incorrect**	**Partial Correct**
Valid	221	13	168	111
Missing	0	0	0	0
Mean	3.059	3.692	1.685	1.738
Std. deviation	1.682	1.316	0.991	0.930
Minimum	1	1	1	1
Maximum	5	5	5	5

I. *WebSrc Count*

Using Web scrapping, POI data are searched on the web and distinct web sources are identified which give the same address and name information about that POI. A number of distinct web sources are directly proportional to the accuracy of the data. However, few exceptional cases may arise due to the new business setup. In these scenarios, other parameters like user type and latency period are considered to categorize the data in one of the four classes. Table XV gives the statistical idea about related data.

TABLE VII. DESCRIPTIVE STATISTICS FOR WEBSRCCOUNT BASED ON THE TARGET CLASSES

Descriptive Statistics	**Almost Correct**	**Correct**	**Incorrect**	**Partial Correct**
Valid	221	13	168	111
Missing	0	0	0	0
Mean	4.905	9.154	4.090	4.280
Std. deviation	3.266	0.899	2.310	1.876
Minimum	1	8	1	1
Maximum	10	10	10	9

J. *Latency Period*

This attribute gives the idea about the freshness of the data. The latest timestamp is found through the process of web scraping and the data availability on the geoportals. The most recent is considered as better which is calculated by taking the difference in the current data and the latest timestamp. The smaller the difference leads to better accuracy. Statistics of this data are given in Table XVI.

TABLE VIII. DESCRIPTIVE STATISTICS FOR LATENCY PERIOD BASED ON THE TARGET CLASSES

Descriptive Statistics	**Almost Correct**	**Correct**	**Incorrect**	**Partial Correct**
Valid	221	13	168	111
Missing	0	0	0	0
Mean	0.597	0	1.000	1.119
Std. deviation	0.922	0	1.514	1.218
Minimum	0	0	0	0

A New Secure Algorithm for Upcoming Sensitive Connection between Heterogeneous Mobile Networks

Omar Khattab
Department of Computer Science and Engineering
Kuwait College of Science and Technology (KCST), Doha, Kuwait

***Abstract*—One of the most important concepts in the heterogeneous mobile networks is Vertical Handover (VHO). The VHO is a vital process taken place by Mobile Users (MUs) in order to satisfy their preferences of security and cost, in addition to the rest of parameters of network and terminal such as latency and velocity, respectively. However, a proactive security for upcoming sensitive connection and performing VHO between heterogeneous mobile networks have not been considered. This paper therefore comes up with a new secure algorithm to address this issue: Proactive Security for Upcoming Sensitive Connection (PSUSC). Analysis of the PSUSC algorithm proves reducing potential attacks extremely compared with previous works which rely on using less secure RAT.**

Keywords—Vertical handover security; mobile networks; wireless networks; heterogeneous wireless

I. INTRODUCTION

The Mobile Users (MUs) are always keen for using all available communication services anywhere, anytime regardless of any potential technical issue and/or technological constraint might associated with the different Radio Access Technologies (RATs): Wi-Fi, 2G (GSM), 3G (UMTS), 4G (WiMAX and LTE) and 5G.

In fact, a RAT itself is not able to satisfy MUs' preferences all the time as each RAT has its own restricted capabilities in terms of security, data rate, coverage, etc. For example, the 5G itself is not sufficient for providing ubiquitous wireless access without cooperating with the rest of RATs [1].

The VHO performance is measured by different factors such as latency, packet loss, cost signaling, connection failure and security. However, this paper focuses on the security as one of the most crucial factors for the MU to secure upcoming sensitive connection.

Although there are hundreds VHO approaches have been proposed in the literature, it is noticed that a proactive security for upcoming sensitive connection and performing VHO between heterogeneous mobile networks have not been considered. Therefore, this paper presents a new secure algorithm to address this issue: Proactive Security for Upcoming Sensitive Connection (PSUSC).

The rest of the paper is organized as follows: Section II presents related works in securing roaming issues. In Section III, a design of the proposed algorithm is presented. Section IV presents an analysis of the proposed algorithm. Finally, a conclusion and future work are given in Section V.

II. RELATED WORK

In [2], 132 VHO approaches have been reviewed and classified into two categories: VHO security based category and VHO non-security based category for which their characteristics have been discussed. It has been concluded in [2] that the VHO non-security based category takes a large portion of previous works (93%) compared with the VHO security based category (7%). Where, the majority works of this modest percentage of VHO security based category have mainly focused on the role of security parameter in selecting the best available RAT [3].

In [4-11] multi-criteria input parameters considered are (delays, user satisfactions), (Received Signal Strength (RSS), bandwidth, network, coverage, Quality of Service (QoS)), (RSS, Signal to Noise Ratio (SNR), bandwidth), (RSS, bandwidth, cost, velocity of the user), (user speed, RSS, network), (RSS, QoS, bandwidth, network coverage and current and predicted optical link status, traffic rate, active Access Points (APs), and traffic load of adjacent APs), respectively.

However, a proactive security for upcoming sensitive connection and performing VHO between heterogeneous mobile networks has not been considered.

III. DESIGN OF PSUSC ALGORITHM

The VHO consists of three phases: Initiation (Collecting Information), Decision and Execution [12-19]. The proposed secure algorithm takes into account the critical phases of decision and execution in order to secure upcoming sensitive connection between heterogeneous mobile networks. This is shown in Fig. 1.

A. Decision Phase

Unlike previous works which only focus on the role of security parameter in selecting the best available RAT for an imminent VHO, this proactive phase is responsible for selecting the best available secure RAT for the upcoming sensitive connection. Hence, it extremely reduces any potential attack might be launched due to using a current less secure RAT.

Based on Table I, the PSUSC algorithm descendingly orders all available RATs in terms of security into two levels [2]: L1: higher security for 5G (M=5), L2: high security for LTE (M=4), less high security for UMTS (M=3), medium security for WiMAX & GSM (M=2) and low security for Wi-Fi (M=1).

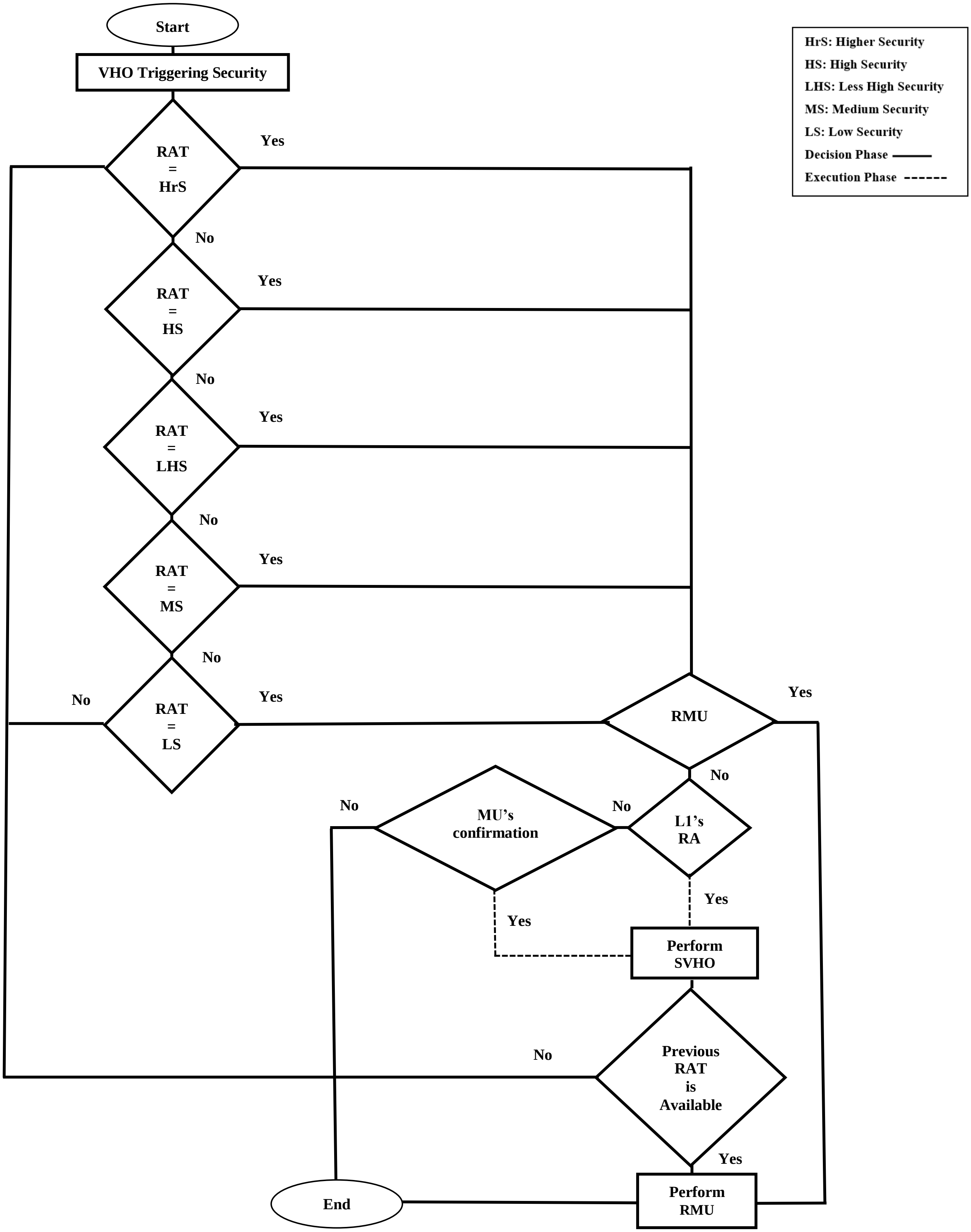

Fig. 1. The PSUSC Algorithm.

TABLE I. SECURITY COMPARISON OF RATS

RAT	Generation	Security	Metric (M)	Level (L)
5G	Fifth	Higher	5	One
LTE	Fourth	High	4	Two
UMTS	Third	Less High	3	
WiMAX	Fourth	Medium	2	
GSM	Second			
Wi-Fi	-	Low	1	

Once the VHO is triggered for a security session, the algorithm's precedence is to secure the upcoming sensitive session and it therefore selects the best available secure RAT, taking into account that the sole VHO to 5G (L1) is automatically taken place without MUs' confirmation. Otherwise, the MU could confirm whether proceeding VHO from available L2's RATs or not. Finally, when the VHO ongoing sensitive session is successfully performed, the MU is returned back to a previous RAT as long as it is still available. Otherwise, the MU is connected to the best available secure RAT.

B. *Execution Phase*

This phase is responsible for securing roaming between heterogeneous mobile networks. The critical moment during the phase is that the VHO between any two RATs (from a source RAT to a destination RAT) might face attackers who exploit such a process for achieving their malicious goals.

MIPv4 and MIPv6 are the best mobility management protocols used to maintain VHO ongoing sessions [20]. However, the MIPv6 is more secure than MIPv4 as it provides Internet Protocol Security (IPSec) for all security requirements [21].

IV. ANALYSIS OF PSUSC ALGORITHM

In this analysis, there are five available RATs: 5G, LTE, UMTS, GSM and Wi-Fi, as shown in Fig. 2. The MU is currently connected with Wi-Fi at office and intending to make online bank transactions. Once the MU proceeds to fill sensitive information, the VHO is triggered in order to secure the upcoming sensitive session by selecting the best available secure RAT. It is obvious in this scenario that the transactions' session is handovered to the most available secure RAT and therefore the security is effectively improved compared with using Wi-Fi as a less secure RAT.

Where the PSUSC algorithm guarantees ordering all available RATs descendingly in terms of security: higher security for 5G, high security for LTE, less high security for UMTS, medium security for GSM and low security for Wi-Fi. This is shown in Fig. 3 to Fig. 6.

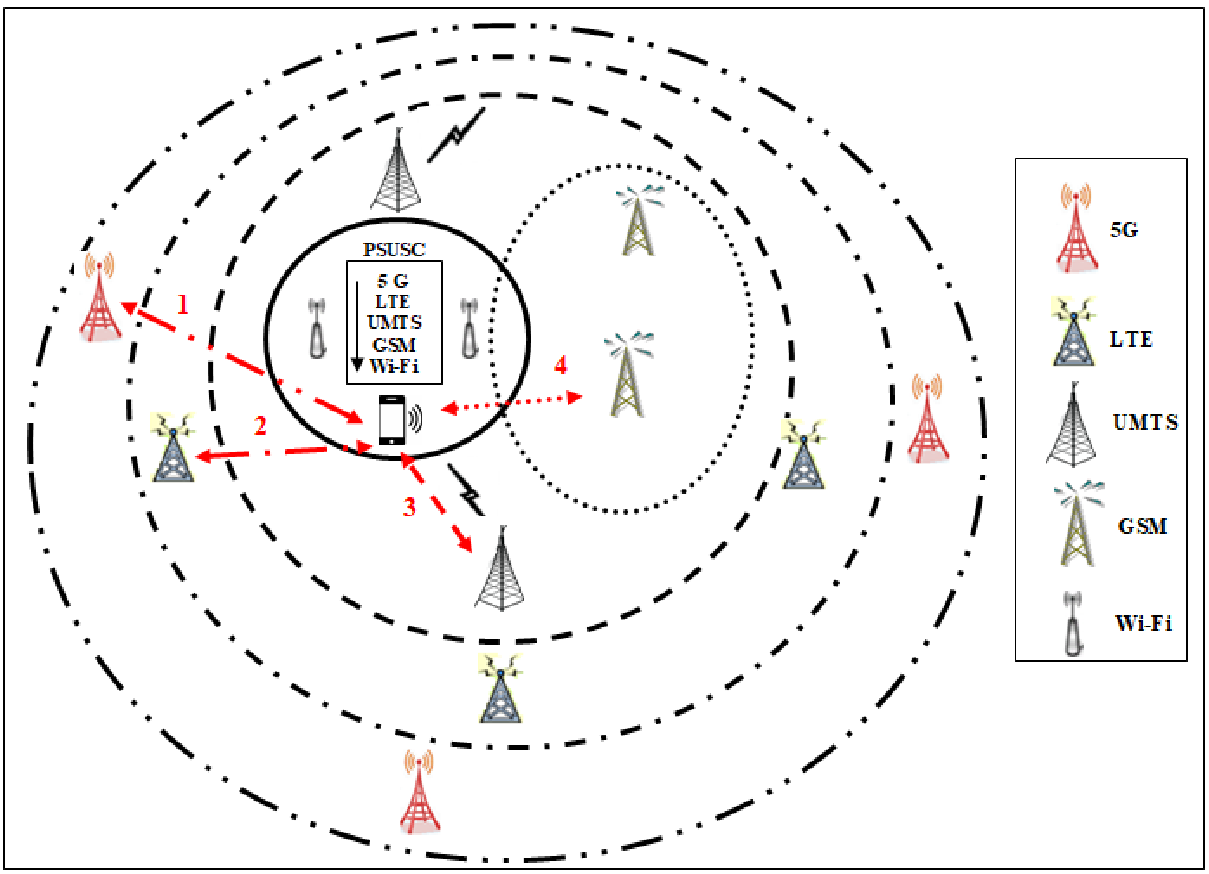

Fig. 2. Scenario of PSUSC Algorithm.

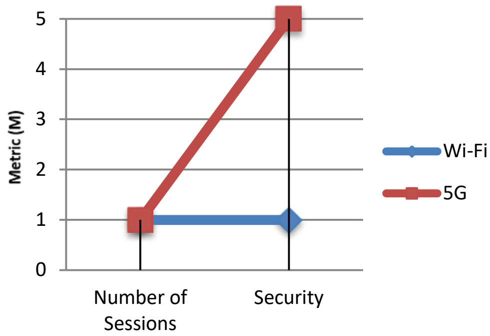

Fig. 3. 5G vs. Wi-Fi.

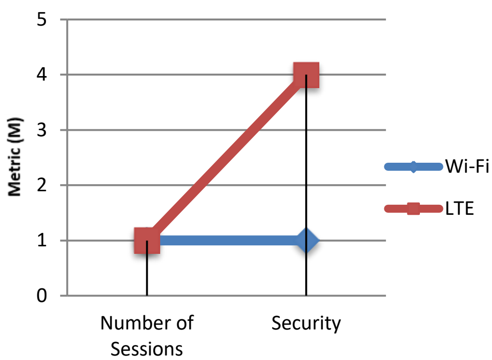

Fig. 4. LTE vs. Wi-Fi.

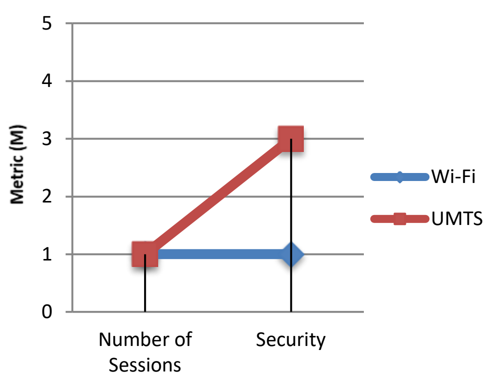

Fig. 5. .UMTS vs. Wi-Fi.

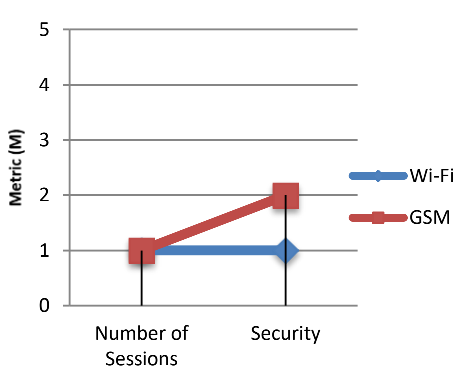

Fig. 6. GSM vs. Wi-Fi.

V. Conclusion

This paper has presented design and analysis of new proactive security algorithm for upcoming sensitive connection and performing VHO between heterogeneous mobile networks. The analysis has noticeably showed reducing potential attacks compared with previous works which rely on using less secure RAT. However, we intend to perform more analysis as well as simulation on the proposed algorithm to address security issues, which might face the execution phase as a result of using mobility management protocols during VHO.

References

[1] O. Khattab, "Vertical handover study on 4G category vs. 5G category for 3GPP generation mobile systems and non-3GPP wireless network", Transactions on Networks and Communications, vol. 6, no. 2, pp. 1-9, 2018.

[2] O. Khattab, "An overview of VHO security vs. VHO non-security in mobile networks: approaches", IOSR Journal of Electronics and Communication Engineering, vol. 13, no. 2, Ver. I, pp. 72-75, 2018.

[3] O. Khattab, "A Comprehensive survey on vertical handover security attacks during execution phase", International Journal of Advanced Trends in Computer Science and Engineering (IJATCSE), vol. 8, no. 5, pp. 1965-1968, 2019.

[4] D. Wang, Q. Sun, Y. Wang, X. Han and Y. Chen, "Network-assisted vertical handover scheme in heterogeneous aeronautical network", Asia-Pacific Conference on Image Processing, Electronics and Computers (IPEC), pp. 148-152, 2020.

[5] S. Goutam and S. Unnikrishnan, "QoS based Vertical Handover Decision Algorithm using Fuzzy Logic", International Conference on Nascent Technologies in Engineering (ICNTE), pp. 1-7, 2019.

[6] A. Debnath and N. Kumar, "Simple Additive Weighted Algorithm for Vertical Handover in Heterogeneous Network," 2nd PhD Colloquium on Ethically Driven Innovation and Technology for Society (PhD EDITS), pp. 1-2, 2020.

[7] S. Goutam, S. Unnikrishnan and A. Karandikar, "Algorithm for Vertical Handover using Multi Attribute Decision Making Techniques," IEEE International Conference on Communication, Networks and Satellite (Comnetsat), pp. 306-313, 2020.

[8] N. A. Ezz-Eldien, M. F. Abdelkader, M. I. Abdalla and H. M. Abdel-Atty, "Handover Performance Improvement in Heterogeneous Wireless Network," 11th IEEE Annual Information Technology, Electronics and Mobile Communication Conference (IEMCON), pp. 821-830, 2020.

[9] S. Goutam, S. Unnikrishnan and N. Kudu, "Decision for Vertical Handover using k-Means Clustering Algorithm," IEEE Bombay Section Signature Conference (IBSSC), pp. 31-35, 2020.

[10] Z. -Y. Wu, M. Ismail, E. Serpedin and J. Wang, "Artificial Intelligence for Smart Resource Management in Multi-User Mobile Heterogeneous RF-Light Networks," IEEE Wireless Communications, pp. 1-7, 2021.

[11] H. T. Yew, A. Chekima, A. Kiring, A. I. Mbulwa, J. A. Dargham and S. K. Chung, "RSS Based Vertical Handover Schemes in Heterogeneous Wireless Networks: Past, Present & Future," IEEE 2nd International Conference on Artificial Intelligence in Engineering and Technology (IICAIET), pp. 1-5, 2020.

[12] M. Zekri, B. Jouaber and D. Zeghlache, "Context aware vertical handover decision making in heterogeneous wireless networks", IEEE 35th Conference on Local Computer Networks (LCN), pp. 764-768, 2010.

[13] M. Kassar, B. Kervella and G. Pujolle, "An overview of vertical handover decision strategies in heterogeneous wireless networks", Computer Communications, vol. 31, no. 10, pp. 2607-2620, 2008.

[14] E. Stevens-Navarro and V.W.S. Wong, "Comparison between vertical handoff decision algorithms for heterogeneous wireless networks", IEEE 63rd VehicularTechnology Conference (VTC), vol. 2, pp. 947-951, 2006.

[15] P.M.L. Chan, R.E. Sheriff, Y.F. Hu, P. Conforto and C. Tocci, "Mobility management incorporating fuzzy logic for heterogeneous a IP environment", IEEE Communications Magazine, vol. 39, no. 12, pp. 42-51, 2001.

[16] W.T. Chen, J.C. Liu, and H.K. Huang, "An adaptive scheme for vertical handoff in wireless overlay networks", Tenth International Conference on Parallel and Distributed Systems (ICPADS), pp. 541- 548, 2004.

[17] J. McNair and F. Zhu, "Vertical handoffs in fourth-generation multinetwork environments", IEEE Wireless Communications, vol. 11, no. 3, pp. 8- 15, 2004.

[18] Y. Gyekye-Nkansah and J. Agbinya, "Vertical handoffs decision algorithms using fuzzy logic", International Conference on Wireless Broadband and Ultra Wideband Communications, pp. 1-5, 2006.

[19] D. Sourav, R. Amitava and B. Rabindranath, "Design and simulation of vertical handover algorithim for vehicular communication", International Journal of Engineering Science and Technology, vol. 2. no. 10, pp. 5509-5525, 2010.

[20] J. Rodriguez, M. Tsagaropoulos, I. Politis, S. Kotsopoulos and T. Dagiuklas, "A middleware architecture supporting seamless and secure multimedia services across an intertechnology radio access network", IEEE Wireless Communications, vol. 16, no. 5, pp. 24-31, 2009.

[21] Nokia Networks (2001). White paper on introducing mobile IPv6 in 2G and 3G mobile networks, (pp. 1-16): Finland.

A Planar 2×2 MIMO Antenna Array for 5G Smartphones

A. K. M. Zakir Hossain[1*], Nurulhalim Bin Hassim[2], W. H. W. Hassan[3], Win Adiyansyah Indra[4]
Centre for Telecommunication Research & Innovation (CeTRI), Fakulti Teknologi Kejuruteraan Elektrik & Elektronik (FTKEE), Universiti Teknikal Malaysia Melaka (UTeM), Melaka

Safarudin Gazali Herawan[5]
Industrial Engineering Department, Faculty of Engineering
Bina Nusantara University, Jakarta
Indonesia 11480

Mohamad Zoinol Abidin Bin Abd. Aziz[6]
Centre for Telecommunication Research & Innovation (CeTRI), Fakulti Kejuruteraan Elektronik & Kej. Komputer (FKEKK), Universiti Teknikal Malaysia Melaka (UTeM)
Melaka

***Abstract*—Here, a planar 2×2 MIMO configuration for the 5G smartphone has been presented. A single element modified planar tree profile shape (MPTPS) antenna is implemented to investigate the suitability in future 5G communication for different sub-6 GHz spectrum band. The size of the single MPTPS antenna is 40 × 25 mm^2. The electronic band gap (EBG) and partial ground plane (PGP) techniques have been utilized to tune this antenna. The antenna works from 2.81 – 7.23 GHz, with a (VSWR < 2) bandwidth of 4.42 GHz that covers all the mid-range sub-6 GHz 5G frequencies. It also has a comparatively good gain of 3.14 dBi, high efficiency of 96% and a bi-directional radiation pattern. The antenna has been implemented in a 145 × 75 mm^2 smartphone mainboard with MIMO configuration using polarization diversity. More than -21.1 dB isolation has been found between different ports. A good gain of as high as 6.59 dBi is observed for the MIMO in the band. Also, as MIMO performance, excellent envelope correlation coefficient of less than 0.0029 and minimum diversity gain of 9.9853 has been observed. The investigation has been further stretched by adding a liquid crystal display (LCD) for radiation performance and a hand phantom to assess the performance in terms of specific absorption rate (SAR). It is observed that the SAR value is as low as 0.887641 at 3.5 GHz. This design will motivate the researcher to develop high performance MIMO arrays for 5G smartphones.**

Keywords*—MIMO; smartphone antenna; isolation; envelope correlation coefficient; diversity gain; specific absorption rate (SAR)

I. Introduction

Nowadays, in wireless communication, the latest addition is 5G technology. The emergence of the 5G technology will enable improve connectivity, excellent speed and data rate and these all features will come with a very low latency [1]. In terms of the frequency of operation there are two different band of 5G: Sub-6 GHz (below 6 GHz bands) and the millimeter wave band. The millimeter wave band lays between 24 to 30 GHz in different regions. In the sub 6-GHz 5G band, there few sub bands such as lower band (700 MHz), mid band (3.4 to 3.6 GHz) and high band (4.8–6 GHz) [2]. Different countries from different regions have decided to choose different sub-6 GHz band for their future 5G rollout operation. Due to this shuttle change in the working frequencies, all the necessary hardware related to the base transceiver stations (BTS), handphone/smartphones and other user equipment (UE) need to be redesigned or tuned to fit those chosen frequencies. Among various components of those equipment, the antenna is one of the most significant part of the system. The antenna works as the main gateway for any wireless interface by converting the electrical signal to electromagnetic radiation [3]. So, a good design of antenna would impose less stress on other components such as power amplifiers (PAs), low noise amplifiers (LNAs) and etc. Recently, multiple input multiple output (MIMO) array techniques and configurations for smartphones provide a nice edge to the transmission and reception of the wireless signal, enabling low crosstalk, high signal selectivity and channel capacity [4]. In addition, it inherently comes with a better directivity, enhanced beamforming and beam-steering ability. However, it's still challenging for the designers to design a MIMO antenna array that fits inside a smartphone along with the other circuitry element without harming the performance of the entire system to cover the entire mid-range sub-6 GHz frequency range by still keeping the MIMO performance intact in terms of port isolation, envelope correlation coefficient (ECC), diversity gain (DG), and SAR.

II. Literature Review

Recently, research on 5G MIMO array design has got a lot of attention among the researcher and the design engineers. In [5] the authors have proposed a two element MIMO antenna array that works for the sub-6 GHz bands (3.5 and 4.3 GHz) and also in millimeter wave (mmWave) band from 24 – 38 GHz. The authors here have proposed the planar inverted-F (PIFA) structure for the single antenna element. The results show that the minimum isolation between the ports is -21 dB and the ECC is less than 0.05 throughout all the working frequencies. However, the authors have not performed any SAR analysis. As this antenna is intended to be working in the smartphones, it is a necessary to analyze the exposer around any human tissue.

*Corresponding Author

A four port 2 × 2 MIMO antenna array has been proposed using slotted rectangular shaped antenna element works for 5G new radio (NR) band 77, 78 and 79 which covers 3.3 to 4.2 GHz, 3.3 to 3.8 GHz and 4.4 to 5 GHz respectively (sub-6 GHz middle bands) [6]. The authors used E and L shaped slots in the rectangular planar patch to crate the desired resonant frequency bands and also used novel un-protruded multi-slot (UPMS) to isolate the ports. The results show that the ECC is less than 0.01 and, the isolations between the port 1 & 2 and port 3 & 4 are good below -25 dB. However, based on the results presented its can be seen that the isolation between port 2 & 4 and 1 & 3 it is as high as -15 dB which is not desired also. Another point of this proposal is the authors have not done any SAR analysis which is very important for the implementation of this design in the smartphone. A quad port 2 × 2 MIMO antenna for smartphones has been proposed in [7]. The single antenna element for the MIMO is based on the combination of L-shaped, rectangular shaped and Z-shaped strips. The antenna is designed for 3.5GHz (3.4-3.6 GHz) and 5GHz (4.8-5 GHz) bands for 5G application. The isolation between the ports is found to be larger than -16.5 dB and the ECC is less than 0.01 for this proposal. However, the SAR analysis is still missing in the analysis. One more proposal has been made for four element MIMO base on planar dipole single element antenna for smartphone which works 3.5 and 4.7 GHz sub-6 GHz 5G bands [8]. A thorough SAR analysis in this proposal with head and hand phantom defined in the simulator. The SAR value can been seen for the results are 1.8 W/Kg and 1.7 W/Kg for 3.5GHz and 4.7 GHz respectively for 10g tissue mass. Also, a good ECC of below 0.005 has been observing. However, in terms of the isolation between the ports it can be seen that the isolation, even though within the acceptable range, goes as low as -15 dB.

In [9], the authors have proposed a shared dipole antenna structure for the working frequency NR band 77/78/79. The authors have proposed this eight element array design especially for the laptop application. From the presented results it seen that the mutual coupling between ports as less as -19dB. However, the authors have not disclosed the single element antenna gain. Also, some important MIMO parameters such as ECC, (DG) and etc. are missing which are essential to assess the performance of the proposed design. Another 8 element antenna MIMO array has been proposed [10] for 5G smartphones that works between 3.4 to 3.6 GHz. The authors have proposed the MIMO array which can fit on the side edge of the smartphone and comprises with single monopole structures and the total size of the board is chosen to be 145 × 75 mm^2 structure. The configuration exhibits a good ECC of 0.1 and single element gain around 3.5. However, the minimum isolation between the ports comparatively low, dropping around -12 dB which is undesirable. Similarly, a different 8 element 8×8 MIMO antenna configuration has been proposed in [11] which works for sub-6 GHz frequency region. The single element antenna utilized here is a folded monopole with a dimension of 17.85 × 5 mm^2. The work reveals a good ECC of less than 0.06, the mean effective gain varies between 4.18 to 5.67 dBi and the maximum SAR value reaches 0.941 W/Kg. However, one important parameter, the isolation between the ports is not so high, as it drops to -17 dB between the ports which would degrade the whole system performance. Table I summarize the recent works and also make a comparison with this proposed work.

In this article, a modified tree profile shaped (MPTPS) antenna has been proposed and implemented in a 2 × 2 MIMO configuration for smartphones that has a working bandwidth (BW) 2.81 to 7.23 GHz to cover the entire mid-range sub-6 GHz 5G frequencies. The MIMO antenna has comparatively better isolation between the ports. It has better isolation between ports, superior ECC, DG and SAR values compared with the other existing proposals which would improve the overall performance of the smartphone for 5G communication.

TABLE I. SUMMARY OF THE RECENT WORKS WITH THE PROPOSED WORK

References	**Isolation (dB)**	**ECC**	**SAR (W/Kg)**
[5]	- 21	0.05	na
[6]	- 15	0.01	na
[7]	- 16.5	0.01	na
[8]	- 15	0.005	1.7
[9]	- 19	na	na
[10]	- 12	0.1	na
[11]	- 17	0.06	0.941
Proposed work	**- 21.1**	**0.0022**	**0.887641**

*na = not available

This article is organized as: Section II, Literature Review (where the recent related research has been discussed). Section III, MPTPS antenna and MIMO design (this section includes the thorough elaboration and illustration of the design procedure of a single element MTPS antenna and the MIMO design as well). Section IV, Results and Analysis (in this section a deep discussion and analysis has been done by presenting the relevant responses related to the proposed design) and Section V, Conclusion (the article is concluded here and further aspect of this research has been revealed).

III. MPTPS ANTENNA AND MIMO DESIGN

Fig. 1 comprises the front and back view geometry of the proposed MPTPS antenna structure. The antenna comprises one square shape and three circular shape patches to make it an MPTPS structure. One of the circular shapes' center is on the middle point of the upper side of the square patch. The other two circular patches' centers are on the middle point of the left and right side of the square patch. The Bottom side of the square patch is connected with the 50 Ω feed transmission line (TL). The back view of the antenna shows the partial ground plane (PGP) with its electronic band gap (EBG). Fig. 2 reveals the dimensions of the antenna which has been estimated and later optimized by (1)-(9) [12-16].

It is seen that the MPTPS antenna has an overall dimension of 25×40 mm^2 with a GP dimension of 17×18.9 mm^2 at the back of the antenna. The diameter of the each circle in the tree profile patch is 11 mm (radius, r = 5.5 mm) and the length of the sides of the square is same as the diameter of the circular shapes. The width of the 50 Ω feed TL is 1.24 mm and the length has been chosen as 20 mm as it is the one third of the free space wavelength (λ/3), where λ = 60 mm at center frequency 5 GHz, is the best optimized feed length for this design.

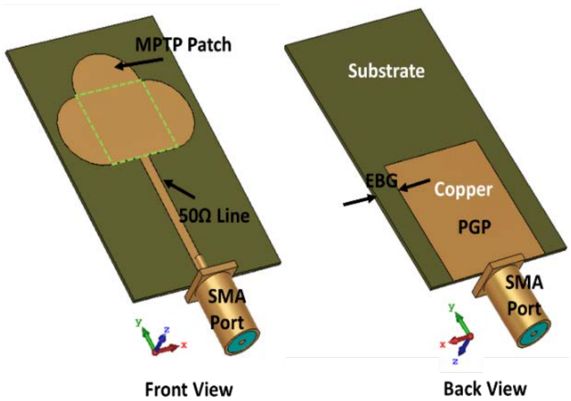

Fig. 1. The Front and the Back Geometry of the Proposed Single Element MPTPS Antenna.

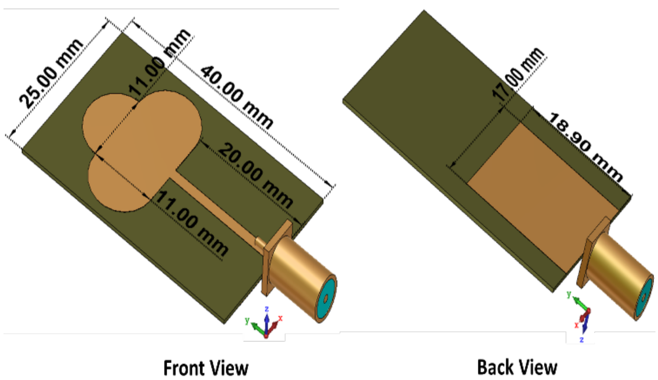

Fig. 2. The Detailed Dimension of the Proposed Antenna.

$$W = \frac{c_0}{2f_c\sqrt{\frac{(\varepsilon_r+1)}{2}}} \quad (1)$$

$$\varepsilon_e = \frac{\varepsilon_r+1}{2} + \frac{\varepsilon_r-1}{2}\left[1 + 12\frac{h}{W_p}\right]^{-\frac{1}{2}} \quad (2)$$

$$L_e = \frac{c_0}{2f_c\sqrt{\varepsilon_e}} \quad (3)$$

$$\Delta L = 0.412h\frac{(\varepsilon_e+0.3)(\frac{W_k}{h}+0.264)}{(\varepsilon_e-0.258)(\frac{W_k}{h}+0.8)} \quad (4)$$

$$L = L_e - 2\Delta L \quad (5)$$

$$L_g = 6h + L_k \quad (6)$$

$$W_g = W_g = 6h + W_k \quad (7)$$

$$r = \frac{F}{\left\{1+\frac{2h}{\pi\varepsilon_r F}\left[ln\left(\frac{\pi F}{2h}\right)+1.7726\right]\right\}^{\frac{1}{2}}} \quad (8)$$

$$F = \frac{8.791\times10^9}{f_c\sqrt{\varepsilon_r}} \quad (9)$$

Where, r is the radius of the circular patches. L and W are the length and the width of the any rectangular patch on the antenna. However, in this design, L = W since it's a square patch. The Lg and Wg are the length and width of the ground plane (GP) respectively. The substrate material for this proposed design is Rogers 3003 which has a dielectric constant (ε_r) of 3.00, the loss tangent ($tan\delta$) of 0.0019 and the substrate height (h) of 0.51 mm. After finalizing the single element design, the antenna has been used to be implemented for a 2 × 2 MIMO design configuration.

Fig. 3 shows the MIMO structure of the proposed array for smartphone. It can be seen from Fig. 3 that there are two pairs of antennas on the both side of the main board of the smartphone. Each pair has a combination of a 90^0 polarization diversity between them which actually give theoretically zero cross talk between them. The antenna 1 (A1) and antenna 2 (A2) is a pair and the other pair consists of antenna 3 (A3) and antenna 4 (A4). The total size of the main smartphone board is 145 × 75 mm^2 which represents the dimension of 5.5 inch display phone.

After this, in the MIMO configuration, a liquid crystal display (LCD) glass has been added to see the effect on the parameters (see Fig. 4). The material for the LCD is a lead glass which has a dielectric constant of 6, material density of 4200 kg/m^3, electrical conductivity of 1e-12 S/m and the thermal expansion coefficient of 8.18e-6 /K. The thickness of the LCD is chosen to be twice of the height of the substrate (1.1 mm) and the gap between the main board and the LCD is kept as 0.51 mm.

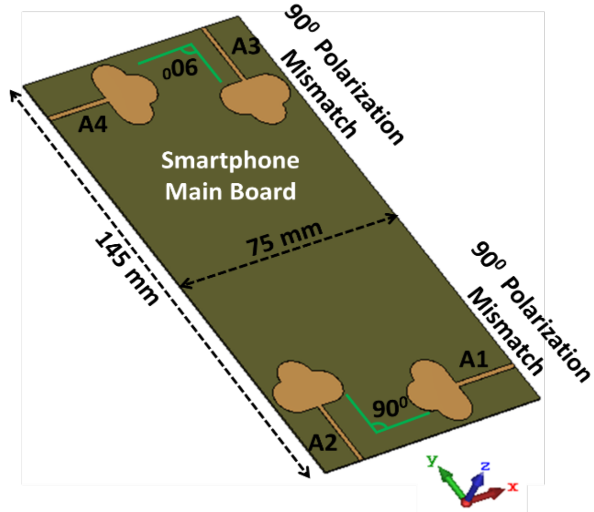

Fig. 3. The Proposed 2 × 2 MIMO Configuration for Smartphone.

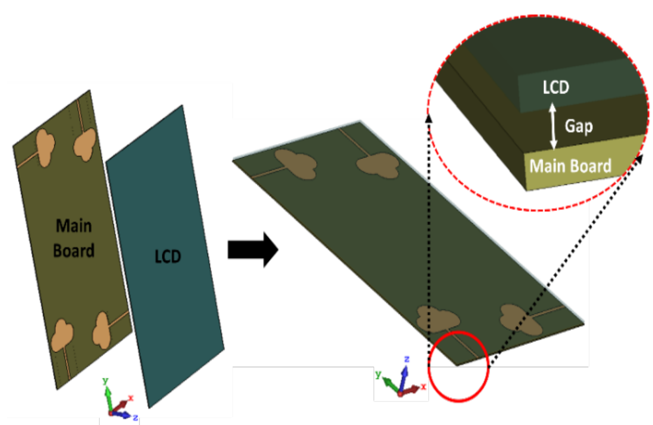

Fig. 4. MIMO Array with LCD.

Finally, to analyze the SAR performance of the antenna, a phantom model of hand tissue has been added to the structure. Fig. 5 represents the arrangement of the antenna with LCD and the added hand phantom. The simulation has been performed with the full 3-D electromagnetic simulator CST MWS 2021. In the next section all necessary result parameters and responses have been presented and analyzed.

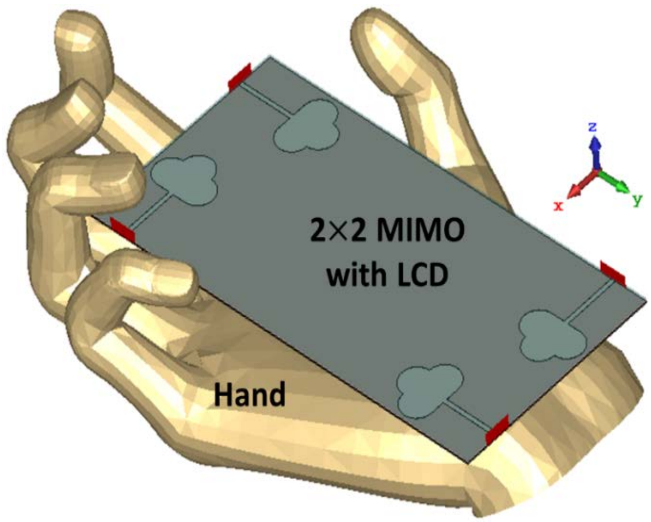

Fig. 5. MIMO Array with LCD and Hand Phantom.

IV. Result and Discussion

At first, the single element MPTPS antenna has been represented for analysis and discussion. Fig. 6 comprises the reference impedance (Fig. 6a), the S-parameter (S_{11}) (Fig. 6b) and the voltage standing ratio (VSWR) (Fig. 6c) of the antenna. In the beginning, it is important to see the impedance of the antenna. Since it is designed for a 50 Ω system, the reference impedance needs to be as close as 50 Ω value and from Fig. 6(a) it can be seen exactly the same as the impedance is 50 Ω throughout the BW. Now, to determine the working frequency BW it is necessary to check the S_{11} and the VSWR response of the antenna. From Fig. 6(b) it can be seen that the value $S_{11} \leq$ -10 dB starts from 2.83 GHz and stays below -10 dB until 7.16 GHz. So, it can be understood that the -10 dB BW is 4.33 GHz. To investigate further on the BW confirmation, the VSWR response has been analyzed. The condition VSWR $\leq$ 2 is commonly used to determine the working frequency of the antenna and it is seen from the Fig. 6(c) that the condition is satisfied from 2.81-7.23 GHz which increases the BW to 4.42 GHz.

Next, the efficiency, realized gain (RG) and the radiation pattern has been observed to assess the performance of the single MPTPS antenna. Fig. 7(a) and (b) comprise the radiation efficiency (RE) & total antenna efficiency (TAE), and the RG of the single MPTPS antenna respectively. Also, Fig. 8 comprises the 3-D and 2-D (polar) far-field radiation pattern at 3.5 GHz, 4.8GHz and 5.8 GHz. It can be seen from Fig. 7(a) that the RE and TAE both never go below 80% whereas goes as high as 96% at around 3 GHz. The realized gain (Fig. 7b) reveals that it reaches as high as 3.14 dBi which is very good considering the small size of the MPTPS antenna. Fig. 8(a), (c) and (e) comprise the 3-D far-field radiation pattern of the proposed MPTPS antenna at 3.5 GHz, 4.8 GHz and 5.8 GHz respectively. Furthermore, Fig. 8(b), (d) and (f) comprise the 2-D polar (the E- and H-plane) pattern of the antenna at those frequencies respectively. It can be seen that at all frequencies (from both 3-D and 2-D pattern) the far-field radiation pattern is bi-directional.

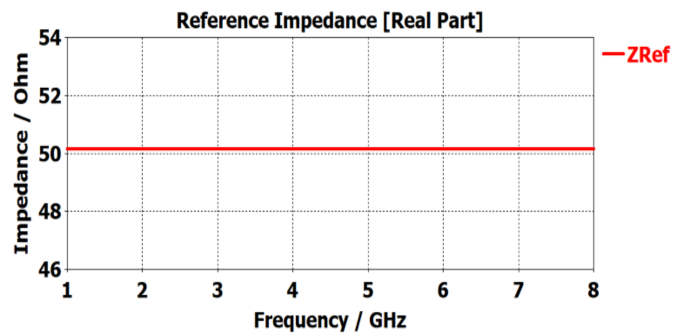

(a) Reference Impedance.

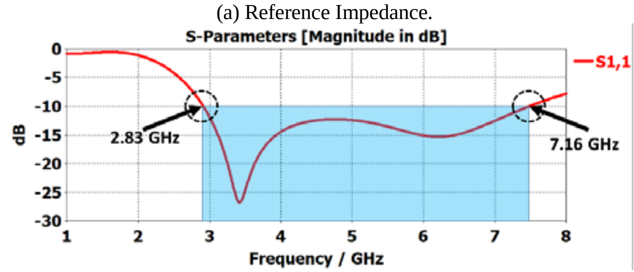

(b) S-Parameter (S_{11}).

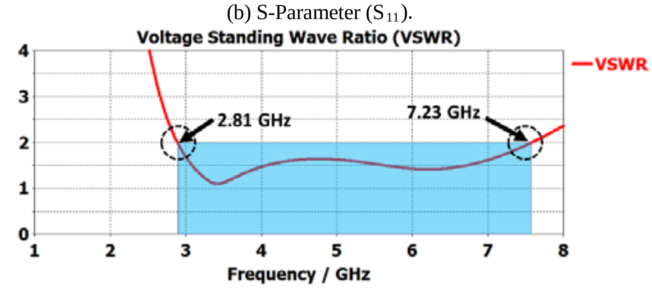

(c) VSWR.

Fig. 6. The (a) Reference Impedance, the (b) S-Parameter (S11) and the (c) VSWR of the Single Element MPTPS Antenna.

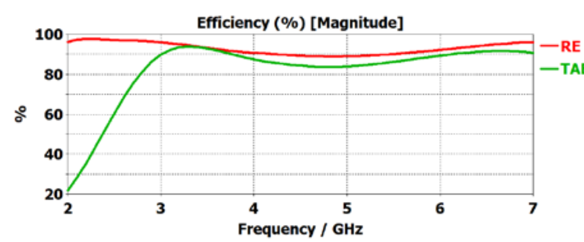

(a) RE and TAE of the MPTPS Antenna.

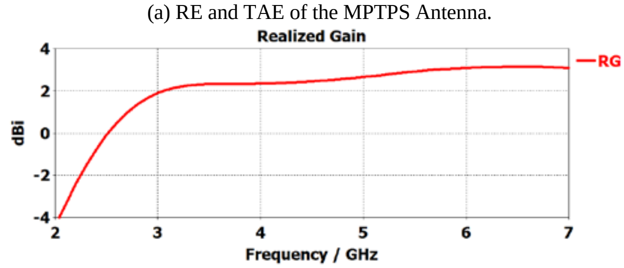

(b) Realized Gain of the MPTPS Antenna.

Fig. 7. Efficiencies and Realized Gain of the Single Element MPTPS Antenna.

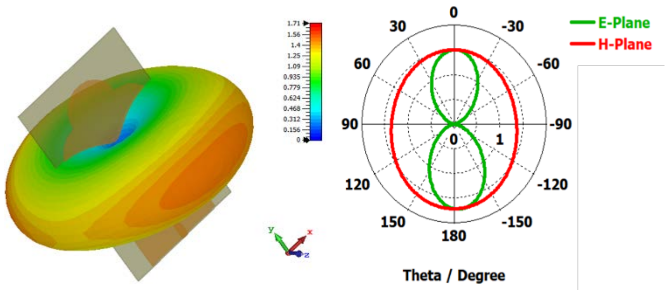

(a) 3.5 GHz. (b) 3.5 GHz.

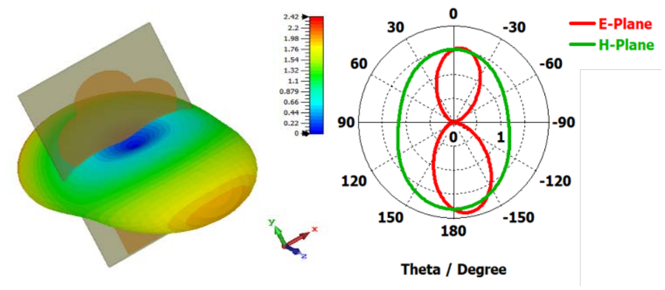

(c) 4.8 GHz. (d) 4.8 GHz.

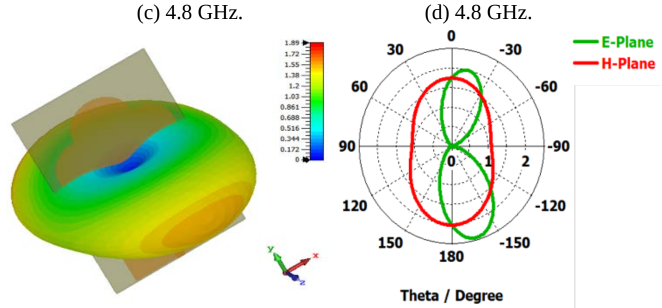

(e) 5.8 GHz. (f) 5.8 GHz.

Fig. 8. Far-Field Radiation Pattern at different Frequencies of the MPTPS Antenna.

After the confirmation of the performance assessment of the single element antenna, now, the next step is to investigate the performance of the proposed antenna in 2 × 2 MIMO configuration. Fig. 9(a) comprises the S-parameter's reflection parameter responses (S_{11}, S_{22}, S_{33} and S_{44}) of the four ports of the MIMO configuration. Similarly, Fig. 9(b) consists of the VSWR responses of the four different ports of the MIMO antenna. From both figures it can be seen that they are mostly same as the single element MPTPS antenna with a very little deviation. So, it is conclusive that in terms of the BW, the MIMO configuration keeps the working BW intact.

Fig. 10 illustrates the isolation between the ports which is one of the most important parameters to assess the performance of any MIMO array antenna. Since the array has two pairs of orthogonal configuration it is enough to investigate the port 1 and port 2 only. Fig. 10(a) comprises the S_{11}, S_{21}, S_{31} and S_{41} and Fig. 10(b) comprises the S_{12}, S_{22}, S_{32}, S_{42} and S_{34} to observe the isolations between different ports where S_{12}/S_{21} defines the isolation between port 1 and 2, S_{31} defines the isolation between and port 1 & 3, S_{41} defines the isolation between port 1 & 4 and S_{34} defines the isolation between port 3 & 4. Similarly, S_{32} and S_{42} defines the isolation between port 2 & 3 and port 2 & 4 respectively. It can be seen form both of the figure that except S_{42} (-21.1 dB), the rest of the isolation between different ports are below -30 dB. As the standard is less than -15 dB [6], this proposed MIMO exhibits an excellent isolation performance that is suitable for smartphones. Next, Fig. 11 comprises the surface current accumulation of the MIMO configuration at port 1 and port 2. It can be seen that due to the excitation at port 1 or port 2 other port does not accumulate much surface current and this is another justification on the good isolation between the ports in this MIMO configuration.

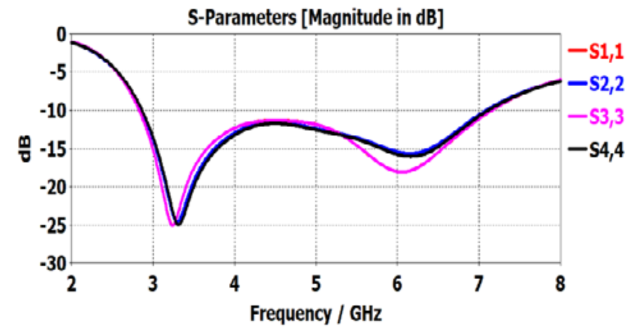

(a) S-Parameter of different Ports.

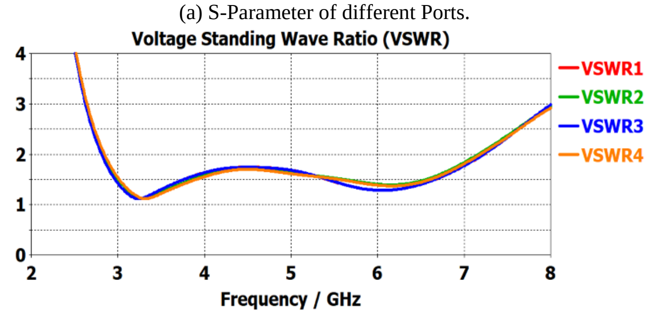

(b) VSWR of different Ports.

Fig. 9. (a) S-Parameters and (b) VSWRs of different Ports of the 2 × 2 MIMO Configuration.

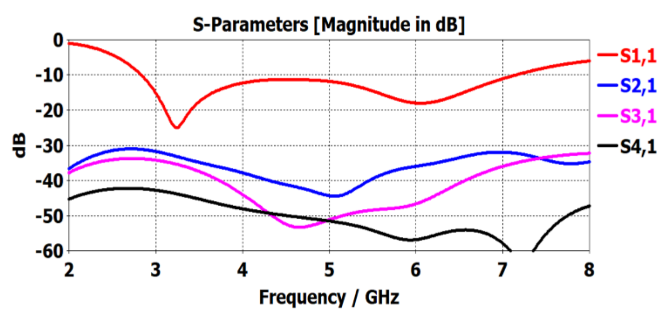

(a) Isolation with Respect to Port 1.

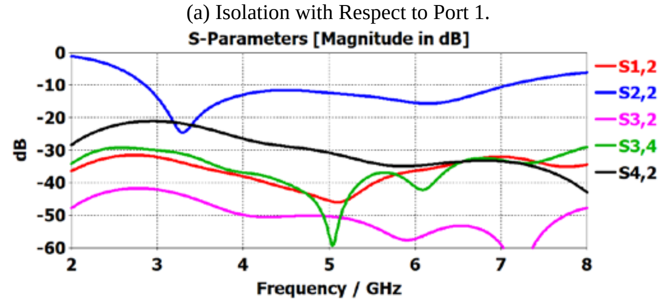

(b) Isolation with Respect to Port 2.

Fig. 10. Isolation between different Ports of the MIMO.

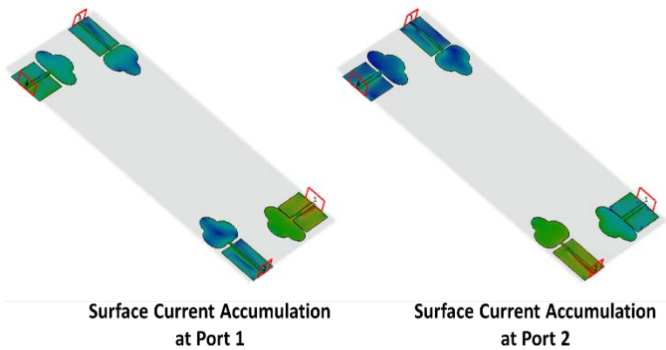

Fig. 11. Surface Current Accumulation at different Ports.

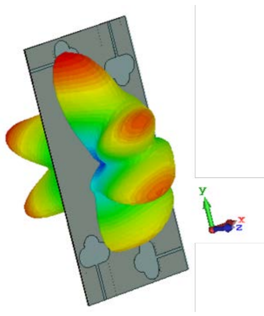

(a) Port 1.

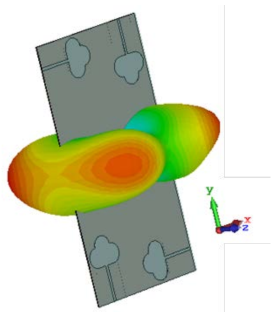

(b) Port 2.

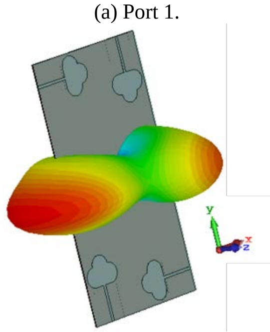

(c) Port 3.

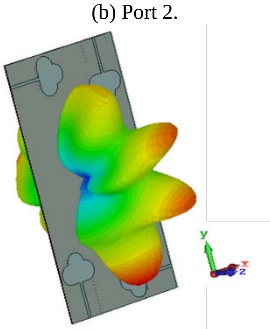

(d) Port 4

Fig. 12. 3-D Radiation Pattern for different Ports at 3.5 GHz.

The 3-D radiation patterns at 3.5 GHz in different ports can be seen in Fig. 12. The pattern at port 1 and 4 exhibit the front and back side radiating nature. On the other hand, port 2 and port 3 exhibit the radiation pattern at the right and left sides of the main board of the smartphone. So, it apparent that the combination of the four ports together covers all four directions of the radiation which makes this proposed configuration suitable for this specific application. As the assessment of the isolation and radiation performance is done, it is crucial to observe and analyze the other parameters such as the combined RG, the ECC and the DG of the array. Fig. 13(a), (b) and (c) discloses those parameters respectively. Since it's a four port MIMO, there will be three ECCs (ECC_{12}, ECC_{13} & ECC_{14}) and three DGs (DG_{e12}, DG_{e13} & DG_{e14}). The ECC for different forts can be calculated by (10)-(12) and similarly the DG can be estimated by (13)-(15) [17].

$$ECC_{12} = \frac{|S_{11}^*S_{12}+S_{12}^*S_{22}+S_{13}^*S_{32}+S_{14}^*S_{42}|^2}{(1-(|S_{11}|^2+|S_{12}|^2)+(|S_{13}|^2+|S_{14}|^2))^2} \quad (10)$$

$$ECC_{13} = \frac{|S_{11}^*S_{13}+S_{12}^*S_{23}+S_{13}^*S_{33}+S_{14}^*S_{43}|^2}{(1-(|S_{11}|^2+|S_{12}|^2)+(|S_{13}|^2+|S_{14}|^2))^2} \quad (11)$$

$$ECC_{14} = \frac{|S_{11}^*S_{14}+S_{12}^*S_{24}+S_{13}^*S_{34}+S_{14}^*S_{44}|^2}{(1-(|S_{11}|^2+|S_{12}|^2)+(|S_{13}|^2+|S_{14}|^2))^2} \quad (12)$$

$$DG_{e12} = 10\sqrt{1-|ECC_{12}|^2} \quad (13)$$

$$DG_{e13} = 10\sqrt{1-|ECC_{13}|^2} \quad (14)$$

$$DG_{e14} = 10\sqrt{1-|ECC_{14}|^2} \quad (15)$$

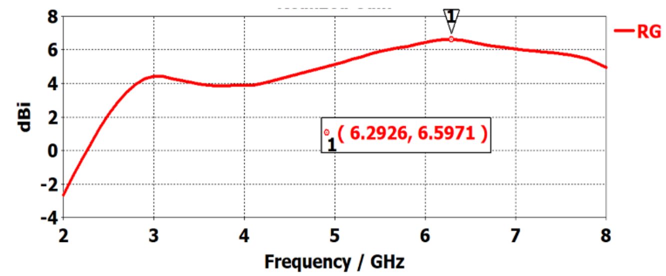

(a) Combined Realized Gain of the MIMO Array.

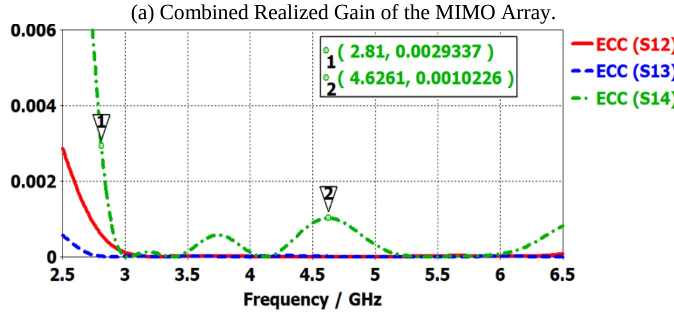

(b) ECC of the MIMO Array.

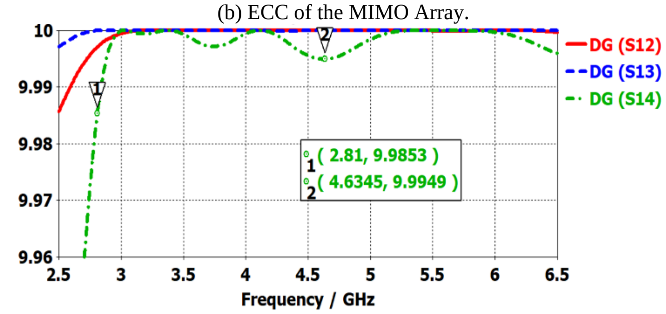

(c) Diversity Gain of the MIMO Array.

Fig. 13. The (a) Realized Gain, (b) ECC and (c) Diversity Gain of the MIMO Array.

The combined RG of the MIMO array (seen in Fig. 13a) never goes below 4 dBi throughout the entire BW of operation, whereas, it goes as high as 6.6 dBi around 6.3 GHz. From 3 to 6 GHz the RG stays between 4-6 dBi. From Fig. 13(b), the ECCs of the array can be observed. A lower value of ECC indicates the good isolation among the radiating elements of any MIMO array structure. It can be seen that throughout the whole BW the value starts with 0.0029 at 2.81 GHz and in most of the BW, it never goes higher than 0.001. As the standard for ECC should be less than 0.3 [17], it can be concluded that the value of the ECC for this proposed MIMO array is excellent. Similarly, the DG responses seen from Fig. 13(c), are also in agreement with the ECC responses, staying higher than the value of 9.9978 throughout the BW. Whereby most of the working BW is more than 9.9949. Lastly, the SAR values are illustrated in Fig. 14(a), (b) and (c) for 3.5 GHz, 4.8 GHz and 5.8 GHz, respectively. The SAR measures the amount of radiation energy would dissipated into a human body. So, the value is desired to be keep as low as possible as the higher radiated power may harm human tissue. As long as the SAR value is below standard specification, any design can be acceptable for human body proximity centric applications such as smartphones. The standard of the SAR value is SAR < 2 W/Kg for 10g mass [11]. At 3.5 GHz, it is seen that the SAR value is very low dropping at 0.887641 W/Kg which is remarkable. Similarly, at 4.8 GH it increases a little up to 0.90636 W/Kg and at 5.8 GHz the value goes to 0.950047 W/Kg. With these SAR results it is conclusive that the proposed design is not harmful for human body and well below within the acceptable standard value of SAR.

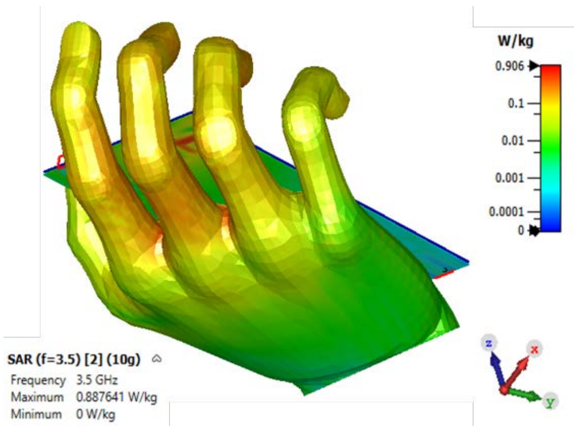

(a) SAR at 3.5 GHz.

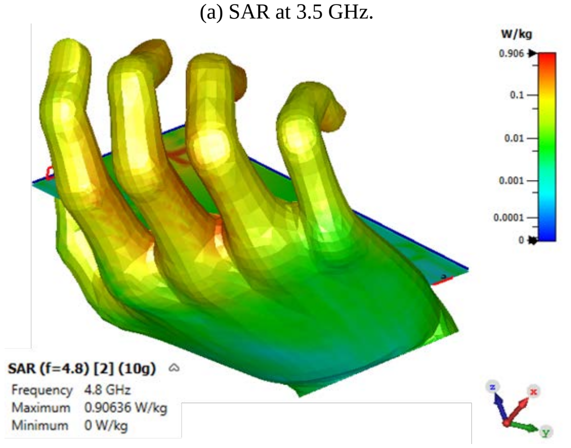

(b) SAR at 4.8 GHz.

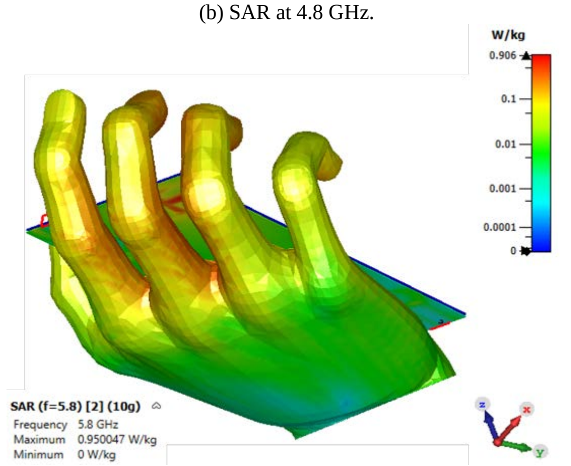

(c) SAR at 5.8 GHz.

Fig. 14. The SAR Values for (a) 3.5 GHz, (b) 4.8 GHz and 5.8 GHz.

V. Conclusion

The MPTPS single antenna has been presented here. The antenna working frequency is between 2.81 – 7.26 GHz covering all the 5G NR 77/78 and 79 bands for mobile communication. The antenna has a bi-directional radiation pattern and single antenna gain is up 3.14 dBi. Also, the antenna efficiency is good around 96% and it never goes below 80% throughout the BW of the antenna. Later, the proposed antenna has implemented in a 2×2 MIMO configuration of 2 pairs with the polarization diversity of 90^0 between the elements of the each pair. A good isolation of more than -30 dB is observed between the port except between port 2 and 4 where it drops as low as -21.1 dB which is still better that the existing antennas for smartphones. The MIMO configuration has a good far-field radiation pattern with covering all four directions together with four ports. The combined RG is up to 6.6 dBi. The ECC is as low as 0.0029 and mostly stays below 0.001 throughout the BW. Similarly, the DG responses of the MIMO configuration are also mostly below 9.9949 throughout the entire BW. One more aspect of this array is the SAR (10g) value. It is remarkably very low at 3.5 GHz with a value of 0.887641 W/Kg which is far below than the acceptable standard value of 2.0 W/Kg indicating the safeness for its application around human body proximity centric applications. The future aspect of this research is realized and validates this proposed design in the real world environment through experimentation. This design will motivate the antenna engineers to design a highly isolated and efficient MIMO array antenna for smartphone applications.

Acknowledgment

This work has been funded by the grant PJP/2020/FTKEE/PP/S01753 from the center for research and innovation management (CRIM), University Teknikal Malaysia Melaka (UTeM).

References

[1] Pant, A., Singh, M., & Parihar, M. S. (2021). A frequency reconfigurable/switchable MIMO antenna for LTE and early 5G applications. AEU - International Journal of Electronics and Communications, 131 doi:10.1016/j.aeue.2021.153638.

[2] https://fccid.io/frequency-explorer.php. Last accessed on 30th May 30, 2021.

[3] Guo, J., Cui, L., Li, C., & Sun, B. (2018). Side-edge frame printed eight-port dual-band antenna array for 5G smartphone applications. IEEE Transactions on Antennas and Propagation, 66(12), 7412-7417. doi:10.1109/TAP.2018.2872130.

[4] Li, G., Zhai, H., Ma, Z., Liang, C., Yu, R., & Liu, S. (2014). Isolation-improved dual-band MIMO antenna array for LTE/WiMAX mobile terminals. IEEE Antennas and Wireless Propagation Letters, 13, 1128-1131. doi:10.1109/LAWP.2014.2330065.

[5] Kumar, N., & Khanna, R. (2021). A two element MIMO antenna for sub-6 GHz and mmWave 5G systems using characteristics mode analysis. Microwave and Optical Technology Letters, 63(2), 587-595. doi:10.1002/mop.32626.

[6] Kulkarni, J., Desai, A., & Sim, C. -. D. (2021). Wideband four-port MIMO antenna array with high isolation for future wireless systems. AEU - International Journal of Electronics and Communications, 128 doi:10.1016/j.aeue.2020.153507.

[7] Huang, J., Dong, G., Cai, J., Li, H., & Liu, G. (2021). A quad-port dual-band mimo antenna array for 5g smartphone applications. Electronics (Switzerland), 10(5), 1-9. doi:10.3390/electronics10050542.

[8] Jamshed, M. A., Ur-Rehman, M., Frnda, J., Althuwayb, A. A., Nauman, A., & Cengiz, K. (2021). Dual band and dual diversity four-element mimo dipole for 5G handsets. Sensors (Switzerland), 21(3), 1-13. doi:10.3390/s21030767.

[9] Lee, C. & Su, S. (2021). Decoupled multi-input multi-output antennas with a common dipole for wideband 5G laptop computers. Microwave and Optical Technology Letters, 63(4), 1286-1293. doi:10.1002/mop.32736.

[10] Kiani, S. H., Altaf, A., Abdullah, M., Muhammad, F., Shoaib, N., Anjum, M. R., Damasevicius, R., Blažauskas, T. (2020). Eight element side edged framed MIMO antenna array for future 5G smart phones. Micromachines, 11(11). doi:10.3390/mi11110956.

[11] Serghiou, D., Khalily, M., Singh, V., Araghi, A., & Tafazolli, R. (2020). Sub-6 GHz dual-band 8 × 8 MIMO antenna for 5G smartphones. IEEE Antennas and Wireless Propagation Letters, 19(9), 1546-1550. doi:10.1109/LAWP.2020.3008962.

[12] Islam, M. S., Ibrahimy, M. I., Motakabber, S. M. A., & Hossain, A. Z. (2018, September). A Rectangular Inset-Fed Patch Antenna with Defected Ground Structure for ISM Band. In 2018 7th International Conference on Computer and Communication Engineering (ICCCE) (pp. 104-108). IEEE. doi:10.1109/ICCCE.2018.8539260.

[13] Zakir Hossain, A. K. M., Hassim, N. B., Alsayaydeh, J. A. J., Hasan, M. K., & Islam, M. R. (2021). A tree-profile shape ultra wide band antenna for chipless RFID tags. International Journal of Advanced Computer Science and Applications, 12(4), 546-550. doi:10.14569/IJACSA.2021.0120469.

[14] Azam, S. M. K., Islam, M. S., Hossain, A. K. M. Z., & Othman, M. (2020). Monopole antenna on transparent substrate and rectifier for energy harvesting applications in 5G. International Journal of Advanced Computer Science and Applications, 11(8), 84-89. doi:10.14569/IJACSA.2020.0110812.

[15] Zakir Hossain, A. K. M., Hassim, N. B., Kayser Azam, S. M., Islam, M. S., & Hasan, M. K. (2020). A planar antenna on flexible substrate for future 5g energy harvesting in malaysia. International Journal of Advanced Computer Science and Applications, 11(10), 151-155. doi:10.14569/IJACSA.2020.0111020.

[16] Zakir Hossain, A. K. M., Indra, W. A., Jamil Alsayaydeh, J. A., & Herawan, S. G. (2021). A planar monopole UWB antenna with partial ground plane for retransmission-based chipless RFID. International Journal of Intelligent Engineering and Systems, 14(4), 539-547. doi:10.22266/ijies2021.0831.47.

[17] Elfergani, I.; Iqbal, A.; Zebiri, C.; Basir, A.; Rodriguez, J.; Sajedin, M.; Pereira, A.d.O.; Mshwat, W.; Abd-Alhameed, R.; Ullah, S. (2020). Low-profile and closely spaced four-element mimo antenna for wireless body area networks. Electronics (Switzerland), 9(2) doi:10.3390/electronics9020258.

Machine Learning Approach of Hybrid KSVN Algorithm to Detect DDoS Attack in VANET

Ms.Nivedita Kadam[1]
PhD Research Scholar
Department of Computer Science and Engineering
Koneru Lakhmaiah Education Foundation
Vaddeswaram, A.P., India

Dr. Krovi Raja Sekhar[2]
Professor
Department of Computer Science and Engineering
Koneru Lakhmaiah Education Foundation
Vaddeswaram, A.P., India

***Abstract*—Most of the self-driving vehicles are suspect of the of the different types attacks due to its communication pattern and changing network topology characteristics, these types of vehicles are dependent on external communication sources of VANET, which is a vehicular network, It has attracted great interest of industry and academia, but it is having a number of issues like security, traffic congestion, road safety which are not addressed properly in recent years. To address these issues it's required to build secure framework for the communication system in VANET and to detect different types of attack are the most important needs of the network security, which has been studied adequately by many researchers. However to improve the performance and to adapt the scenario of VANET, here in this paper we proposed a novel Hybrid KSVM scheme which is based on KNN and SVM algorithm to build a secure framework to detect Distributed Daniel of Service attack *which* is the part of Machine Learning approach. The experimental results shows that this approach gives the better results as compared to different Machine Learning based Algorithms to detect Distributed Daniel of Service attack.**

Keywords—K-Nearest neighbor (KNN); support vector machine (SVM); DDoS (distributed denial of service attack)

I. Introduction

Vehicular Ad Hoc Networks (VANETs) are a sub type of mobile ad hoc network used for communication from vehicles to vehicle and vehicle to roadside units. VANETs is a new technology for the wide range of applications, including traffic congestion monitoring and controlling traffic, and is associated with the passenger and the driver safety program For example, a vehicle on the road where the accident occurred, is able to warn each other in order to find an alternate route to avoid the traffic congestion that occurs after an accident. The special characteristics of VANET, such as high mobility, dynamic network topology, etc., that compromises the quality of service of the application. [1] As vehicles are moving from normal to fully autonomous generation and its era is changed in to the driverless cars, they are providing the lots of information to their surroundings like Vehicle to vehicle, Vehicle to infrastructure and RSU's, as they are interconnected with each other. WAVE protocol is used for communication in VANET. The rising transport network has been thought to be a vital element of the event of the intelligent transportation system (ITS) and smart cities. It's expected to modify an entire new set of applications, starting from road safety improvement to traffic potency optimization. This new generation of networks can ultimately have a profound impact on society and also the daily lives of a lot of folks around the world. A Machine -learning approach is roughly divided into 3 major categories: supervised, un-supervised and reinforcement learning. Classification algorithms assign a categorical label to every sample which is in the system. In wireless networks, the classification detect whether or not the networks are misbehaving node or elements of the system are not functioning properly. The algorithms such as Bayesian classifiers, k-nearest neighbors, decision trees, support vector machines, and neural networks are considered.[2] In machine learning knowledge driven higher cognitive process approach is employed to overcome the new issues coming in transport networks, it is necessary to rethink ancient approaches to wireless network style, particularly given the made sources of knowledge from numerous on board sensors, margin observation facilities, historical transmissions, and then forth. Indeed, it's extremely fascinating to plot economical ways to interpret and mine the huge amounts of knowledge and facilitate a lot of data-driven higher cognitive process to enhance transport network performance. Machine learning represents smart tool to serve such functions with evidenced good performance in an exceedingly wide range of applications.[2].

DDoS attack uses the client/server technology with multiple computers as an attack platform to perform attacks on one or more targets to increase the power of the attack is becoming most of the intense major now a days however, because of the diversity of DDoS attack modes and the variable size of attack traffic, there is not any full proof model which gives the accurate detection method of attack presently.[3-4]. Confidentiality, integrity and availability are the main properties of the any communication in VANET [5] for security, network nodes are vulnerable to capture, hack, and communicate with attackers, and node messages may be eavesdropped and fake messages introduced or replayed into the network. Malicious nodes interfere purposefully with the regular actions of the network, aiming to disrupt the ordinary functionalities of the network. These issues would have a wide-scale effect on Vehicular network implementation, due to this the defence at vehicular network has more complex task, and such issues are the absence of data connectivity due to the low performance of wireless networks between different nodes and the lack of a source-destination connection. Therefore, it is extremely necessary for vehicular network to be highly flexible to respond to any situation. So to overcome these issues a framework is required which detects the intrusion and store the information in communication by preserving the data integrity. By applying ML algorithms the privacy and data integrity issues can be overcome. There are many unaddressed issues of the security in previous work. This paper is divided in to the following sections: Section 2, Related work; Section 3, Methodology and workflow; Section 4, Experimental results and Discussion; Section 5, Conclusion.

II. Related Work

Literature study has done by considering various papers which are based on intrusion detection systems in vanet through machine learning approach and various algorithms which are used for security in vanet. Elvin Eziama proposed the trust based model with classification approach using Bayesian NN(BNN). This model is generic in nature with classification approach. Author says that when trust mechanism is applied to this framework it gives better results with respect to performance prediction, classification accuracy and low detection latency. And when it is compared with Neural Network, with the uncertainty in the information it leads to result in over-fitting of the data which are collected from the nodes during the training phase. Timing attack, sybil attack and false positioning attack are considered in this work.[6] Carlos H. O. O. Quevedo, Ana M. B. C. Quevedo and Ahmed Serhrouchni Proposed a SyDVELM system for detection of Sybil attack which fast fast, scalable with low complexity Vehicle mobility pattern is considered as vector matrix, for displacement movements of the sybil attack. For some features of Vehicular nodes it applies the Extreme Learning machine. SyDVELM's proposed approach elaborates that from the urban scenarios the mobility pattern of the vehicle nodes are compared with real vehicle reliability in terms of inaccuracies in the relocation of Sybil nodes. The advantage of this mechanism is that it confirms a versatile detection process for sybil attacks with high detection rate, very low error rates and improves the scalability. But it this mechanism is not suitable for the low density scenarios, for more than 300 epochs its detect attacks quickly but when epochs are small, it limits the result. Other ML approaches can be applied with ELM for better results for detection. The authors in [7] Fabio Goncalves and Bruno Ribeiro explains in their work about different types of attacks are identified including the intrusion detection systems with anomaly detection by Machine learning algorithms. Like for malicious packet attack hierarchical IDS used to detect anomaly by applying learning automata algorithm. Based on their survey it is observed that no specific information is provided regarding datasets and its operations which are performed on it like training, validating of data and detection of attacks and beacon messages in communication. The authors in [8] Mohammad Asif Hossain and Wahidah Md Shah proposed they have considers the award and penalty scheme which is based on the case of student and teacher learning process. With this scheme it can reduce the network overhead and delay. The authors in [9] Stefan Mihai, Nedzhmi Dokuz and Meer Saqib Ali in this work explains on technical advances of leading to a wired, mobile, cooperative transport system. And the most important safety consequences of VANETs which provide a complete analysis of existing possible methods for keeping vehicle network communications private, stable and confidential. Different types of security issues and attacks they have elaborated in their work. The issues they have raised about the Mass acceptance depend on closing the gap in terms of both secure automobile accessibility and road networks. Flexibility and reliability while upholding appropriate levels of security and privacy is also the main concern [10]. Steven So, Prinkle Sharma and Jonathan Petit, proposed the misbehaviour detection scheme for VANET, by applying the plausibility checks feature of vector for machine learning models under the SVM algorithm for classification with this KNN- 1-NN algorithm is applied. Data set is KDD for flooding attack detection is possible in WSN VeReMi dataset is used for Detecting and classifying location spoofing misbehavior, this dataset is balanced by normal to attack ratio(70:30) is trained and Check is done by precision-recall curve. Drawback is that it considered only next neighbor for this work. The authors in [10] Francisco Sales de Lima Filho and 1 Frederico A. F. Silveira proposed the method for identify the DoS/DDoS attack by applying the Random Forest Tree algorithm, which segregates the samples collected from the flow protocol directly from network devices. It gives the better results with respect to better data rate, false alarm rate and precision. With this it is possible to to separate the attacks such as TCP, UDP and HTTP flood, HTTP slow. The authors in [11] Uzma Khana, Shikha Agrawala and Sanjay Silakaria proposed that Node centric detection scheme, this algorithm provides the better throughput, high packet delivery ratio and less end to end delay considers.

When considered the load, distance and distrust value, based on these parametersThey suggested that PSO can be selected to enhance the optimization. The author in [12] Abdulaziz Alshammari, Mohamed A. Zohdy, Debatosh Debnath and George Corser proposed the classification approach for the IDS in Vehicular networks, Machine learning techniques to cluster and classify the intrusions in VANET by applying KNN and SVM algorithms. It uses the CAN protocol by considering its request and response time for evaluating the time interval and offset ratio. Focus of this is to compare and detect the Dos attack and Fuzzy. Here KNN gave better results as compared to SVM on predefined data sets. CAN is more prone to attacks as it is a bus communication protocol. The author in [13] Khaoula Jeffane and Khalil Ibrahimi proposed the method DoS attacks detection with packet delivery ratio metric on the physical and MAC layers. Here black list is encrypted which is to be sent to the Road side unit by distributing to the users of the network to thwart packets sent by attackers. Also, they have suggested that DOS problem can be studied based on the stochastic learning game. The author in [14] Wenjia Li proposed the An SVM based Security Framework for VANET, SVM is used as a classifier to classify and train the patterns of the misbehaving nodes It gives better results with higher precision and recall values with less communication overhead. The author in [15] Kajal Rai et.al worked on the IDS based on the Decision Tree algorithm, which gives near about 80% uniform weightage to all attribute values. Drawback of this system is unknown attacks detection fails and no data Pre-processing is done. The author in [16] Mabayoje also proposed the Gain ratio and decision tree classifier for intrusion detection, in which 97 % accuracy for

DoS attack and drawback is prone to unknown attacks and no pre-processing is done on the data. K. M. A. Alheeti, A. Gruebler, and K. D. McDonald proposed a method to identify the Black Hole attack by observing the anomalies and misuse of the network, and Neural Network ML approach is used. It is observed in this paper accuracy and efficiency is less for detection of Black Hole attack because they used less data for training [17].

III. Methodology and Workflow

In ML approach, a huge variety of methods are developed for the classification approach such as K-NN, SVM, ANN, Deep Learning/CNN, out of that SVM is a most demanding and robust classifier. SVM uses the kernel functions to map the data of non –linearly to high dimensional space.[18] In proposed work, as indicated in Fig. 1 firstly we collect the data from different sources here in this paper we have collected data from kaggle for DDoS attack, this is the input to the system. Then we are training this data by considering the 70-30 percent ratio. 70 % data is trained properly. After that we are applying the SVM algorithm for classification purpose to detect the normal and malicious activity in database we have used the DDoD attack field. Then we are applying the KNN algorithm for finding the nearest neighbours which are trained and tested properly then simulation is done on dataset and it gives the results like if malicious node or attack is detected it predicts and provide security otherwise it send the normal report [19]. For this work input is taken as a text file of collected different IP addresses.

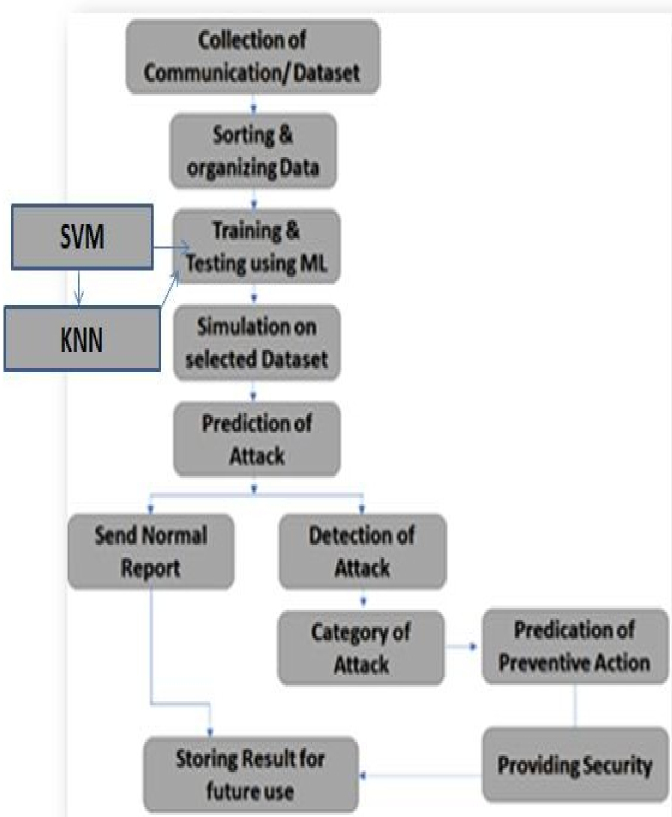

Fig. 1. Proposed System Workflow.

Proposed hybrid algorithm of KSVM for training and validating the data:

- Training set Ta={x1,x2,x3..xn}
- Testing set Tb={x1,x2,…xn}
- T=Ta U Tb

1. begin
   int i,j,k; // test samples i=1,2,3..n , j=1,2,3,..m.
2. SVM:T- > SV_{ij};
3. input X_k;Calculate nearest neighbour dist. of X_k and SV_{ij};
4. Put in to the nearest neighbour
5. k=k+1;// add all samples

Repeat step 3 to 5 until all samples values are calculated end.

Proposed Algorithm for data prediction and Accuracy is given below:

Algorithm (Predict, Accur) = Hybrid KSVM (W+O) (Train, Div, Test, Test-Final, θ)

Require: Train, Div, Test, Test-Final, Datasets;

θ - Termination condition

Ensure: Predict→ Predicted sentiment output;

Accur→ Accuracy

1: Net → Create_Network()
2: Network_initialize(Net)
3: for error >= θ do
4: error Netwrok_Train(Net, Train, Div)
5: end for
6: /* Training completed */
7: Featureopt → CSVM (Train, Div)
8: HTrain → GetTop_HiddenLayer (Net, Train)
9: Train_combined ← HTrain + Featureopt
10: ModelSVM ← SVMLinear (Traincombined)
11:HTest←GetTop_HiddenLayer(Net, Test)
12: Testcombined← HTest + Featureopt
13: Predict ←SVMLineart(ModelSVM , Testcombined)
14: Accur← Evaluation (Test-Final, Predict)
15: return (Predict, Accur)

By using above algorithm, we are trying to find the misbehaving activity in network with secure communication between the Autonomous Vehicles.

IV. Experimental Results and Discussion

The aim of this proposed work is to detect DDoS attack in a vehicular network where the network is choked. This would prevent those cars from having enough access to systems. This leads to the field of prediction using the machine learning method, to incorporate more accurate and stable security results. Client-server model is created for the experiment in python.

The DDoS attack is a method to spread an internet service or web-site by overburdening it with massive traffic floods caused by several outlets. In contrast to a service-default attack, that involves one device and an Internet link, a DDoS attack uses several machines and several Internet access. Data is collected from Kaggle dataset. Name of dataset is DDos data. The attributes of dataset are like protocol which is used for communication, source and destination IP address, source and destination port no. etc., predefined IP address is considered for this work to detect the malicious activity, if any message encountered in the system with different IP address which not from the predefined set then this is detected as malicious node. The evaluation criteria are based on the prediction and accuracy algorithm which performs the training and testing of data from the data set. Implementation is done using the python language. Different ML algorithms are considered which are shown below in the simulation results as indicated that our KSVM hybrid algorithm is giving the better results with different parameters like in the Fig. 2, the accuracy of data is more when we compare other ML algorithms. In Fig. 3, sensitivity results are better by comparing other ML algorithms. In Fig. 4, precision and in Fig. 5, recall parameters are giving the better results. And in Fig. 6, error percentage is less as compared to other algorithms of machine learning algorithms.

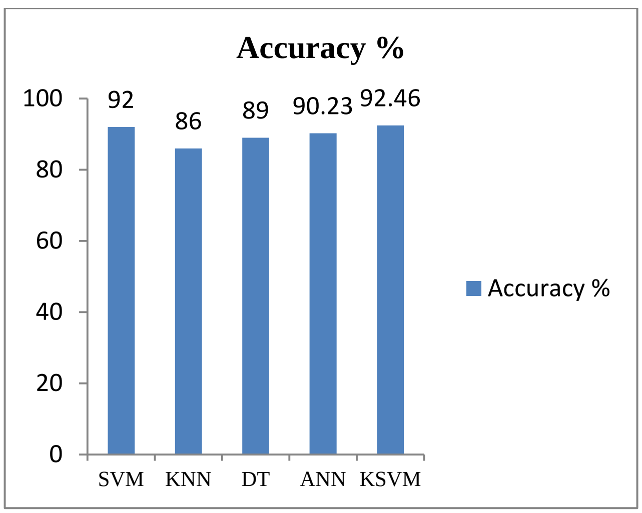

Fig. 2. Accuracy % as Compared to other ML Algorithms.

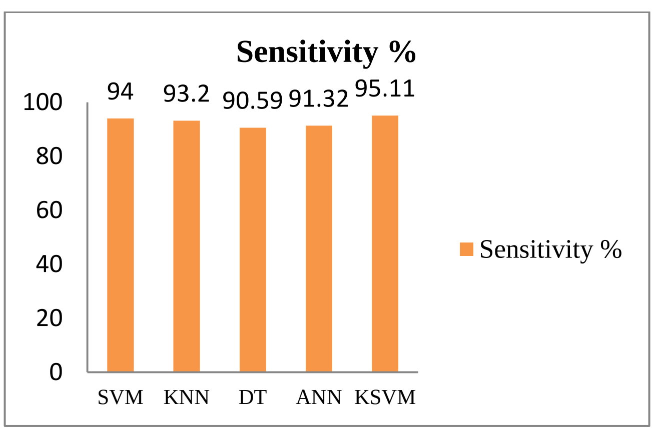

Fig. 3. Sensitivity % as Compared to other ML Algorithms.

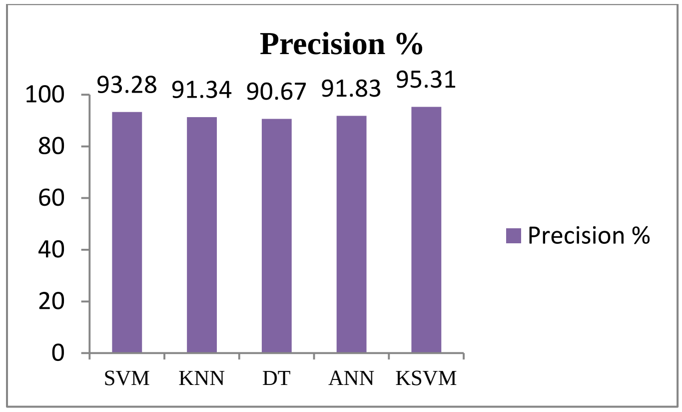

Fig. 4. Precision % as Compared to other ML Algorithms.

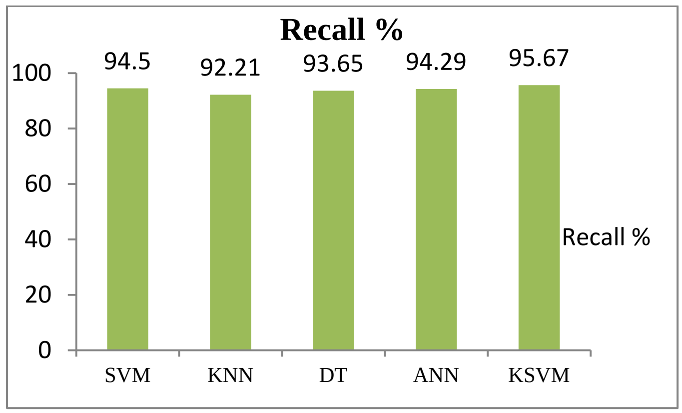

Fig. 5. Recall % as Compared to other ML Algorithms.

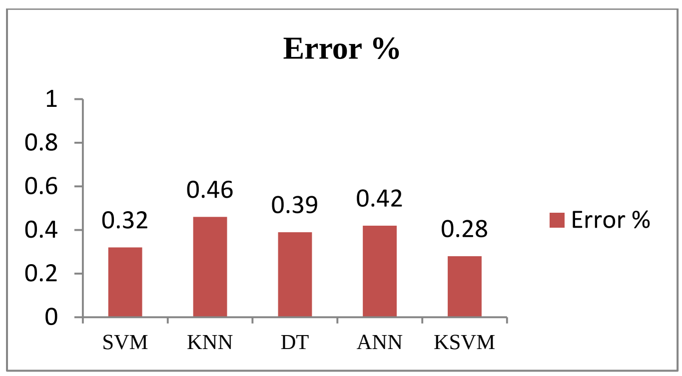

Fig. 6. Error % as compared to other ML algorithms

V. Conclusion and Future Scope

Here in this work, different ML approaches and proposed algorithm Hybrid KSVM for DDoS attack to detect malicious activity is considered with respect to a. accuracy b. sensitivity c. precision d. recall and e. error are shown in above figures and as compare to other ML algorithms our Hybrid KSVM is giving better results. Future scope of this work is further we can apply the same method to detect different attacks like Dos, Sybil. The more secure framework can be built for communication which preserves the privacy and integrity of the message in transit by considering different network security algorithms.

References

[1] Kadam N.N., Sekhar K.R. (2019), "Secure and congestion free routing techniques in vehicular Ad-Hoc Network (VANET)", International Journal of Recent Technology and Engineering, 8(0), PP.915-922.

[2] Hao ye, le liang, geoffrey ye li, joonBeom Kim, lu lu, and may Wu," Machine Learning For Vehicular Networks",2018 IEEE

[3] Zargar S T，Joshi J，Tipper D.,"A survey of defense mechanisms against distributed denial ofservice(DDoS)flooding attacks"．IEEE Corn— munications Surveys＆Tutorials.2013，15(4)：2046—2069.

[4] Jiangtao Pei1, Yunli Chen1*, Wei Ji1*,"A DDoS Attack Detection Method Based on Machine Learning",ICSP 2019 conference.

[5] Stefan Mihai, Nedzhmi Dokuz, Meer Saqib Ali, Purav Shah, and Ramona Trestian" Security Aspects of Communications in VANETs",. @2020IEEE.

[6] Elvin Eziama, Kemal Tepe, Ali Balador, Kenneth Sorle Nwizege and Luz M. S. Jaimes ," Malicious Node Detection in Vehicular Ad-Hoc Network Using Machine Learning and Deep Learning,2018 IEEE.

[7] Carlos H. O. O. Quevedo, Ana M. B. C. Quevedo, Ahmed Serhrouchni , "An Intelligent Mechanism for Sybil Attacks Detection in VANETs", 978-1-7281-5089-5/20/$31.00 ©2020 IEEE.

[8] Fabio Gonc¸alves, Bruno Ribeiro, Oscar Gama,"A Systematic Review on Intelligent Intrusion Detection Systems for VANETs", 978-1-7281-5764-1/19/$31.00 ©2019 IEEE.

[9] Mohammad Asif Hossain,Wahidah Md Shah, "Faster Convergence of Q-Learning in Cognitive Radio-VANET Scenario" , Springer 2019.

[10] Steven So , Prinkle Sharma, Jonathan Petit ," Integrating Plausibility Checks and Machine Learning for Misbehavior Detection in VANET",2018IEEE.

[11] Francisco Sales de Lima Filho ,1 Frederico A. F. Silveira," Smart Detection: An Online Approach for DoS/DDoS Attack Detection Using MachineLearning", HindawiSecurity and Communication Networks Volume 2019, Article ID 1574749.

[12] Uzma Khana, Shikha Agrawala, Sanjay Silakaria, "Detection of Malicious Nodes (DMN) in Vehicular Ad-Hoc Networks", ELSEVIER, 2015.

[13] Abdulaziz Alshammari1, Mohamed A. Zohdy1, Debatosh Debnath1, George Corser2, "Classification Approach for Intrusion Detection in Vehicle Systems" , Wireless Engineering and Technology SciRP 2018.

[14] Khaoula Jeffane, Khalil Ibrahimi, "Detection and identification of attacks in Vehicular Ad-Hoc Network" , IEEE 2016.

[15] WANG TONG, AZHAR HUSSAIN , WANG XI BO , AND SABITA MAHARJAN ,"Artificial Intelligence for Vehicle-to-Everything: a Survey", 2169-3536 (c) 2019 IEEE.

[16] Kajal Rai et.al," Decision tree based algorithm for intrusion detection", International Journal Advanced Networking and Applications,2015.

[17] Mabayoje, "Gain ratio and decision tree classifier for intrusion detection", Int. Journal of Computer applications.2015.

[18] K. M. A. Alheeti, A. Gruebler, and K. D. McDonald- Maier, "An Intrusion Detection System against Black Hole Attacks on the Communication Network of Self-Driving Cars," 2015 Sixth International Conference on Emerging Security Technologies (EST), pp. 86–91, 2015.

[19] Gulnaz Alimjan, Tieli Sun, Yi Liang, Hurxida Jumahun and Yu Guan,."A New Technique for Remote Sensing ImageClassi¯cation Based on Combinatorial Algorithm of SVM and KNN", International Journal of Pattern Recognitionand Artificial Intelligence, Vol. 32, No. 7 2018.

An Intelligent Approach for Data Analysis and Decision Making in Big Data: A Case Study on E-commerce Industry

EL FALAH Zineb[1], RAFALIA Najat[2], ABOUCHABAKA Jaafar[3]
Department of Computer Science
Computer Research Laboratory LaRI, Faculty of Sciences
Ibn Tofail University, Kenitra, Morocco

***Abstract*—A recent informational phenomenon has emerged as one of the considerable innovations in information systems, commonly referred to as "Big Data". The latter is currently trendy, both in academia and industry, and is used to describe a wide range of concepts, from data extraction, storage, and management, to data processing and analysis using well-known schemas, to extract patterns in hidden relationships in order to make better decisions and to derive new knowledge using analytical techniques and solutions. The technology that enables the potential of big data to be exploited is called "Big Data Analytics". Big data analytics is a major challenge that enables researchers, analysts and business users to make better decisions faster. Big Data became an important part of marketing research and marketing strategies. The e-commerce industry is one of the industries that currently benefits most from the potential of big data collection and analysis. This paper therefore aims to demonstrate the use of big data to understand customers and to improve and facilitate the decision making process. In this research, we apply multiple machine learning (ML) models on large dataset present in the e-commerce area by studying several practical cases on online markets.**

Keywords—Big data; data analytics; decision making; big data analytics; big data analysis; machine learning; marketing; e-commerce

I. Introduction

The world has become an information society that is highly dependent on data. Due to this technological revolution, millions of people generate huge amounts of data every day, every second due to the increased use of devices (smartphone, iot.). An interesting engine related to this topic mentions that data growth is unlimited. What is the company going to do about data overload? How to manage and furthermore process and analyze all data to extract value? It seems that we have the "Big Data" problem [1]. The term "big data" was coined when the era of big data began. The latter is an era described by rapidly expanding volumes of data, far beyond what most people imagined. The large volume of data does not only allow us to classify this period as one of big data[2], because there have always been larger volumes of data than our ability to work effectively with data has ever existed. What distinguishes the current era of the big data era is that businesses, governments and non-profit organizations have experienced a change in behavior. Before the big data era began, companies placed relatively low value on the data they collected that had no immediate value. When the big data era began [3], this investment in collecting and storing data for its potential future value has changed, and organizations have made a conscious effort to retain each potential data element.

Our challenge is not to get data [4][5], but to get the right data and use computers to increase our knowledge of the field and identify patterns that we didn't see or couldn't find before. In any fast-moving field such as Big Data, there is always room for innovation. It is widely recognized, and widely supported by research and case studies, that organizations that use data to make decisions over time actually make better decisions, leading to a stronger, more reliable business. With the speed at which data is created increasing at such a rapid rate, the companies responded by retaining all the data they could capture and assessing the future potential of this data higher than in the past.

A key aspect of this topic is that the ability to analyze and extract information from data for big data decision making is currently seen as an important competitive weapon. Traditional mode analytics, in terms of "Big Data", consists of acquiring data that may or may not be necessary for analysis. All of this requires a different approach, architecture or infrastructure, if necessary. The adoption of new technologies requires processing, discovery and analysis of these massive data sets that cannot be processed using traditional databases and architectures due to lack of resources in terms of computing and storage capacity. Today, data generation is increasing dramatically. This brings new challenges [6] for data analysis, storage, processing and how to get useful information from large datasets. The challenge of analyzing large datasets is to find patterns within them. Therefore, Big data Analytics [7][8] is an appropriate solution to current industrial problems.

Its objective is to "turn data into information" for better decision making and its capability can be turned into a competitive advantage [9][10]. Although Big Data has been one of the most popular topics for many years, how to conduct Big Data Analytics effectively is a great challenge for every field. To analyze big data, institutions are increasingly using analytical solutions. These solutions include predictive and prescriptive analytical techniques [11][12], often using AI and ML and Deep learning in particular, to understand and recommend actions based on the analysis of large volumes of data from multiple sources, internal or external.

By applying big data, it is possible to simplify data analysis and understand some of the characteristics of large data sets. In terms of decision-making, big data analysis [13] will be the next challenge for innovation, competition and productivity. Many solutions will emerge to meet all the challenges in this context. Now, the big challenge for companies is not just to store data, but to analyze it, and that analysis has implications for smarter, more effective decisions [14][15]. Advanced analytics provides solutions to "complex problems" in areas such as production, marketing, human resources or distribution, among others.

Although it may appear that Big Data is mostly employed in scientific fields, in the business world it must also be very present when important decisions are made. In the marketing area, it has become a fundamental piece to carry out large-scale campaigns. Big data is now influencing important marketing decisions. This refers to the application and study of complex, large data sets that cannot be processed by traditional data processing applications. The application of the right technology improves the quality of decision making and detail processes [16]. The term Big Data Marketing [24] emerged as a solution to the needs that marketing has posed since its inception on aspects such as market and consumer analysis. This concept refers to the processes, tools, techniques, and technology used to process large amounts of data in real time, allowing us to analyze consumer behavior, for example, in order to develop better strategies and reach a larger number of people who are interested in our product in a more effective and personalized way.

Indeed, the activity in social media, mobile and e-commerce makes us live in a world of Big Data. Big data technology helps us with advanced segmentation, being able to detect completely new areas of interest of customers. And with this, gain insights to create personalized offers, at the right touchpoint, targeted to the right audience and in real time. Artificial intelligence and machine learning [21] help to understand these metrics and create meaningful trends that indicate future changes in marketing and sales strategy.

Customer relationship management (CRM) [32] becomes a fundamental issue for business operation as a result of big data, which makes the marketing focus of enterprises change from products to customers. Currently, the majority of the E-commerce applications revolve around customer segmentation models, retail analytics, and the use of sentiment analysis to improve business decision making. By conducting this research, we apply an intelligent approach based on Machine learning (ML) to these applications making well-informed decision based on comprehensive data analysis in big data area.

This paper aims to answer the following questions: how to reduce large-scale problems to a scale that humans can understand and act upon? What role can big data play in digital marketing success? And how big data can help e-commerce industry to better understand customers? Based on concrete studies about online markets.

This paper is organized as follows: Section 1 gives an introduction of the research. In Section 2 discuss the theoretical background of this research by providing a general summary and overview of big data and its application on data analysis and decision making. In Section 3 presents literature review on big data applications about customer in marketing. In Section 4 briefs related work about big data techniques applied to marketing. In Section 5, we show the experimentation and results by giving three different case studies in e-commerce industry to see how customers will act in the future based on their present behavior patterns using machine learning approach. Finally, Section 6 gives the conclusion.

II. Background

A. Big Data

1) Definition: Big Data, the synonym for the intelligent handling of such large and at the same time heterogeneous data volumes, is one of the major challenges of our time. Big Data [1] holds great potential for science and industry. It can bring about a lasting change in the way companies make decisions and in the way they conduct research in a wide range of scientific disciplines. Big Data will create scientific progress and innovations and thus increase the competitiveness of our science and our companies.

At the same time, however, it requires a particularly responsible approach to data and the new intelligent Big Data technologies. Big Data refers to the enormous data growth that many companies are currently experiencing. A relatively established definition of Big Data is based on the 3-V model [2][3]. The 3-V model distinguishes three challenges of data growth: volume, velocity and variety. Volume refers to the growing amount of data. Volumes that are considered "big" are in the range of terabytes and more. Velocity describes the speed at which new data are created, but also the speed at which data can be accessed during analysis Variety describes the scope of diverse types and data sources, which can be more or less structured. Some definitions add other V the characteristics of Big Data. Big data can be defined as: "high-volume information assets or varieties that require cost-efficient and innovative ways of processing information and enable better understanding, manufacturing and automation of decision-making processes".

2) Big data challenges: In this section, we mention some important challenges related to big data and discuss in more detail some of the technological issues still open to research.

In the Big Data environment, organizations face the challenge [4][5][6] of integrating raw, unprocessed, real-time updated and extremely complex information. But the key issue is not the ability to collect and store voluminous data. It is not enough to simply enter and store a large amount of data, you need to know how to organize, refine and convert it into relevant information that enables you to take market positions. Raw information has only potential value; it is its analysis and systematization that enables organizations to increase their capacity for innovation. Thus, the processing of large volumes of data requires the following steps:

- Acquisition: The data will come from traditional data sources (EDW, relational databases and transactional data files), and from a large number of unstructured data sources that can be stored in NoSQL and "in-memory" databases.

- Organization of information: Preparing and processing information in order to obtain the best possible results, and on which advanced analytical techniques can be applied as effectively as possible.
- Analysis: Analyze all information with access to all data using advanced statistical tools such as social and opinion mining, or apply techniques developed with the R programming language, specifically to the design of advanced statistics. From an overall perspective, it would be practical for the analytics provider to offer tools for querying and reporting, data mining, data visualization, predictive modeling, and decision optimization.
- Decision making: Make decisions in real time or as quickly as possible so that they can have a positive effect on the company's activities. This step is inseparably linked to the analysis step, indeed many suppliers offer these tools integrated with the decision tools. The decision must be made in real time based on the results obtained in the analysis, so that the raw data is converted into usable knowledge to be integrated into dashboards, prospective dashboards and visualization tools; and thus, predict the behavior of a product or service to consumers.

These many challenges [7] require long-term research to work with big data. Data analysis is more difficult than just locating, identifying and understanding the data. It is not always possible to extract the collected data, through an extraction process, and then transform it into a structured structure suitable for analysis. In addition, another major data challenge is the incompleteness, scale, timeliness and complexity of the process. For large-scale analyses, the extraction process must be automated, which requires that differences in the structure and semantics of the data be expressed in a computer-readable way so that the data can be analyzed.

Another challenge is the management of Big Data, effectively managing big data is essential to facilitate the extraction of reliable information and to optimize spending. Indeed, good data management is the basis of Big data analytics. Big data management means cleaning data to ensure reliability, aggregating data from different sources and coding data to ensure security and confidentiality. It also means ensuring efficient storage of Big Data and role-based access to multiple distributed endpoints.

However, these challenges must be overcome in order to maximize large data sets, as the amount of information exceeds our operating capabilities. Based on an in-depth reading of several articles [4][5][8] which discuss the authors' opinions and perspectives on data analysis regarding the new opportunities and challenges created by the big data movement.

B. Big Data Analytics

The primary objective of analytics is to enable informed decision-making and the resolution of business problems. Thus, analytics is a knowledge repository composed of statistical and mathematical tools, machine learning algorithms, data management processes such as data extraction, transformation and loading (ETL), and computer technologies such as Hadoop that create value by developing actionable elements from data. Analytics refers to BI & A technologies that are mainly based on data mining and statistical analysis. Most of these techniques are based on the mature commercial technologies of relational DBMS, data warehousing, ETL, OLAP. Data analytics refers to the procedures and activities that are meant to collect and analyze data in order to extract usable information. The results of data analytics can be used to: identify key areas of risk, fraud, error or misuse; improve business processes; verify the effectiveness of processes and influence the decisions of the business.

Advanced analytics [8] are implementations of specific forms of analytics that consist of a set of techniques and related types of tools, typically including predictive analysis, data mining, statistical analysis and complex SQL, although the list covers data visualization, artificial intelligence, natural processing languages and the capabilities of analytical databases such as MapReduce, in-memory database analysis and columnar data stores. Big data analytics does not require data to be clean and standardized. In fact, they make no assumptions about data standardization. Data analytics [9] can analyze many varieties of data to provide insights into models and ideas that are not humanly possible. They use advanced statistics, artificial intelligence techniques, machine learning, deep learning, feedback, and natural language processing (NLP) to exploit data. Data analytics today is influenced by all kinds of devices and social media, such as data from GPS, NFC and RFID chips, barcodes and QR codes, and others within the Internet of Things, or data from social networks (Facebook, Twitter). All of them linked to data transit in all types of businesses such as banking, department stores, media, industries, etc.

Big data analytics [10] is the science and technology of organizing big data, analyzing and discovering knowledge, patterns and information from big data, visualizing and reporting the discovered knowledge to aid decision making. Big data analytics is the application of advanced analytical techniques to operate on large sets of large data.

In reality, what is being done is to unite two fields with their own entity: Big Data as a massive amount of detailed information, and advanced analysis which is actually a set of different types of tools, including those based on predictive analytics, data mining, statistics, artificial intelligence, natural processing languages, etc. Also known as process to create sustainable competitive advantages, by exploiting, on the one hand, the pools of knowledge resulting from the fine analysis of new data sources and, on the other hand, the capacity for anticipation, or even prediction, built up from this analysis. Big Data analytics is the use of analytical techniques applied to large data sets.

Therefore, Big Data analytics is really two things: analytics and Big Data. The first one helps to discover those data that have changed in the business to know how to react; big data must help to turn the challenges produced by the spectacular growth of the Big Data. Analytics is the best way to discover new customer segments, identify the best suppliers, associate products by affinity, understand sales by seasonality, etc.

C. Big Data Analysis

Data analysis and business analysis [13] are long-standing disciplines that have experienced remarkable growth in all areas of knowledge and, in particular, in organizations and businesses, due to the need for tools that analyze data and make effective and efficient decisions. Data analysis has evolved as data volumes have increased. Business intelligence tools have brought together OLAP (online analytical processing), reporting and querying, visualization and, most importantly, data mining technologies with their already established categories of web mining and text mining, and innovative social media data analysis, which has relied on techniques for analyzing feelings and opinions, or opinion mining and sentiment, as it is also known. There are a variety of software tools used in data analysis and methods used. The most used techniques are: queries and reports (querying and reporting), visualization, data mining, predictive data analysis, fuzzy logic, optimization, streaming audio, video or photography, etc.

Data analysis is also considered the science of examining raw data for the purpose of drawing conclusions about the information contained therein. It is used in many industries to enable organizations and businesses to make improvements in the of decisions. This term is widely used in the field of business intelligence, and depending on the software tool manufacturer, it can cover a wide variety of terms: OLAP, CRM, dashboard etc [18]. In the era of large volumes, we can consider five major categories in data analysis:

- Data analytics (analytics) in organizations and companies that analyze traditional data: transactional and operational.
- Web analytics or data traffic analysis on a website.
- Social analytics or social media data analysis (blogs, wikis, social networks, RSS.)
- Mobile analytics on mobile devices in order to analyze the data that send, receive or transit these devices.
- Big Data Analysis or analysis of large volumes of data.

Big Data analysis [14] is done with software tools normally used as part of the discipline of advanced analytics. So the usual tools are:

- Advanced SQL queries.
- Queries and reports (querying and reporting).
- Advanced statistical analysis.
- Data visualization.
- Data mining, text mining, web mining and social mining.
- Analysis and predictive modeling.
- Optimization.
- Awareness raising.
- Dashboards and scorecards.

The technologies associated with Big Data mainly include data warehouses, data marts, NoSQL and "in memory" databases, Hadoop and MapReduce frameworks. Big Data, as recognized by all serious studies on the subject by the consulting firms and tool manufacturers, it is an opportunity more than a problem.

Big data analysis [19] is a very active area of research that has a significant impact on industrial and scientific fields, where it is important to analyze very large and complex data repositories. It has found applications in many sectors through its ability to transform huge amounts of data into information for informed business and operational decisions.

D. Decision Making

Decision-making [15][16] has become a key tool in any organization, moving from a process based on experience and intuition to one that is increasingly established in data analysis. Since the early 1990s, data warehousing systems have provided the ability to capture, debug and explore data for support purposes. This triggered the development of decision support systems. From there efficient and intelligent techniques and algorithms to discover hidden information were developed in large databases, known as data mining and later generalized under the concept of Business Intelligence. The fundamental characteristic of these systems was that they ran on large volumes of internal data.

In the age of information and technology, data analysis is essential to forecast business scenarios. Thus, big data has become the main decision-making tool. The digital age has made a large amount of data available to businesses, making it a major asset for improved decision-making in all areas and sectors. Processing this large volume of data, through advanced analytics of Big Data architectures, helps to improve and automate decision making in a company's day-to-day business processes. Big data represent a fundamental change in the way business decisions are made. Sentiment analysis is probably the most widely used tool for decision making based on social network data. For good decision making [17] it is essential that in addition to being the right one, it must be done in a timely manner and with the minimum cost. With big data tools, the crossing of information from multiple sources is possible, which helps to obtain accurate and varied information for decision making. Data management tools suitable for volumes handled by big data are essential.

Data-centric approaches such as big data and related Business Intelligence and Analytics (BI&A) [18] approaches have recently attracted a lot of attention because of their promise of huge improvements in organizational performance based on new business insights and better decision making. Integrating data-centric approaches into organizational decision-making processes is a challenge, especially with big data, and it is not clear that the expected benefits will be realized. Previous studies [16][17] have identified the lack of research focus on the context of decision-making processes in data-centric approaches. Using “big data” to improve decision-making has recently become a highly practice area and active. Business Intelligence, the strategic decision-making tool [20].

E. Applications of Big Data in Machine Learning

Machine learning [22] consists of a set of techniques that enable computer systems to predict, classify, sort, order, make decisions , in general, extract knowledge from data without the need to explicitly define the rules for performing these tasks. It is a subfield of artificial intelligence that aims to teach computers the ability to perform example-based tasks without explicit programming. Big data extracts and processes data to make it available to machine learning algorithms. It can be said that big data is the source of data ingestion for ML and DL [22].

Machine learning takes the data processed by big data and analyzes it to generate business insights or learn to perform certain tasks automatically. Deep learning ingests the most important data from big data to learn about it at much deeper levels and to perform more complex tasks. Our target is to study how big data analytics can assist in segmenting online sales data and how to manage a marketing decision making with sentiment analysis on online customer reviews.

F. Big Data in Marketing Area

Marketing and sales are perhaps the areas of greatest application of big data today [23]. Data is used to gain a better understanding of consumers, their habits, and their preferences. Companies are willing to augment traditional data centers with social media, browsing logs, text analytics and sensor data to get a complete picture of their customer. Although Big Data applications to marketing bring innumerable advantages, it is still complicated for many companies to access them [24]. The main challenges stem from the difficulty of choosing the right information from the vast amount available. In addition, there is the challenge of implementing data analytics that knows how to extract valuable and actionable information. Finally, the biggest challenge has to do with people and lies in ensuring that all levels of the company, including top management, assume a culture based on data analysis.

Big Data is the biggest and best tool that marketers can use for their campaigns and strategies. With Big Data, we can analyze in real time large amounts of data and generate personalized profiles of our customers. This helps us to better understand their interactions with our company and purchase intentions. Big data can make more accurate real-time decisions in marketing. Big data allows companies to better focus on the primary needs of customers by developing quality and informative content. It enables us to study how to do a good job of customer segmentation and clustering, analyze customer demands and needs, optimize marketing strategy distribution models by the use of sentiment analysis to understand how customers feel, improve the real estate marketing system [25][26].

III. Literature Review

In this Digital Era we have at our disposal a large amount of data that defines the behavior of our customers [23]. Understanding the customer is a key element of the marketing strategy. With the fast changes in the market, marketing strategies based on the change in customer behavior relative to the problems caused over time has been a challenge.

In this section a review of literature on customer segmentation, retail analytics, sentiment analysis.

A. Review on Customer Segmentation

Customer Relationship Management (CRM) [31][32] is a competitive strategy for understanding a company's customers. But the question is: On which customers should efforts be focused to build successful and competitive relationships, considering that not all of them have the same importance for the company? To determine this level of importance, the use of customer segmentation techniques is useful and decisive in identifying those customers who are really profitable, and allows focusing more resources on them, maximizing their value, and also, optimally using resources in terms of attracting, retaining or recovering them.

In 1956, Wendell R. Smith revolutionized marketing by introducing his segmentation theory. Segmentation is the practice of classifying customers into different groups, based on their multidimensional information (socio-demographic characteristics, purchasing and usage patterns, preferences, needs and attitudes). Customer segmentation [27] is crucial to creating a marketing strategy, as it allows you to better understand the composition of the audience and then propose a marketing mix that precisely meets the needs of each user belonging to a targeted segment.

B. Review on Retail Analytics

The most of publications on big data analytics are focused on technical algorithms or systems development. The advantages of using big data analytics are not limited to a particular industry. The retail business has entered the Big Data age. Using Big Data, retailers can identify certain issues through customer activity, feedback, comments, and reviews on social media and reduce the problem by stocking products with higher demand thus increasing sales potential. Today’s retailers are up against a perfect storm of challenges. Consumer expectations and behaviors are changing, and a rapidly evolving consumer decision-making journey. Big data is to blame for a massive transformation in the retail sector [28] .

C. Review on Sentiment Analysis

Sentiment analysis (also known as opinion mining) is the process of determining or measuring the tone, attitude, opinion and emotional state of responses, to decide whether a conversation or opinion is positive, negative or neutral. Its use occurs in environments ranging from airlines, insurance, clothing sales and financial institutions, to political decisions. Sentiment analysis [29] is a common research Topic in the Natural Language Processing field (NLP). Natural Language Processing (NLP) is a field within the area of artificial intelligence, computing and linguistics. Its main objective is to facilitate and make effective communication between people and computers through the use of protocols such as natural languages. It transforms text into a language that the machine can understand, Big Data collects large amounts of data to obtain a more accurate analysis by improving the performance of the algorithms, and Artificial Intelligence (AI) uses the information provided by NLP to determine the categories of feelings and their corresponding polarities.

One of the techniques applied to large amounts of data is sentiment analysis. Its objective is focused on analyzing the vocabulary of a text in order to determine the opinion that a person has about a certain topic based on the ideas expressed in a text. NLP enables researchers to gather and analyze such data in order to determine the basic meaning of such writings. The field of sentiment analysis, which is used in a variety of fields, is highly reliant on NLP techniques. Opinion mining is a sub-domain of text mining, which consists in analyzing texts in order to extract information related to opinions and feelings (Sentiment Analysis).

IV. Related Work

E-commerce has evolved over the last few decades, and today there are millions of electronic transactions, i.e., purchases that are made over the Internet (online). Our target is to study how big data can aid in segmenting online sales data for better marketing strategies, and how big data analysis can help retailers to make strategic, effective and timely decisions [30].

In this section, we introduce the application of big data in Marketing and its uses for customer segmentation, retail analytics, and sentiment analysis. In this section, we are going to discuss related works and techniques proposed by various researchers that relate to big data analysis in marketing field.

An approach for business customer segmentation that integrates clustering and multi-criteria decision making is developed by [30]. This study extends the traditional RFM model by including five novel segmentation variables for business markets. The results of the application show that the proposed approach for business customer segmentation can effectively be used in practice. By increasing the effectiveness of CRM strategies, the proposed segmentation can help firms gain a sustainable competitive advantage in the market.

Another study [31] aims to determine the best approach to customer segmentation and to deduce associated rules for this based on recency, frequency and monetary (RFM) considerations as well as demographic variables. In this research, the impacts of RFM and demographic attributes have been challenged in order to enrich variables that aid comprehension to customer segmentation. The results show that the weights of RFM attributes have a positive effect on rule association performance. A study [32] examines particular e-commerce enterprises by using cluster analysis and logistic regression analysis to predict and analyze customer segmentation and customer and churn retention.

The aim of this research [33] is to demonstrate how big data analytics can be used in customer segmentation. The authors analyze various data analytics algorithms, especially K-Means and SOM. Although K-Means produced promising clustering results, SOM outperformed in terms of speed, quality of clustering, and visualization. This study discusses how these segmentation analysis approaches can be helpful in studying consumer interests.

A survey research on parallel processing systems [34], gives overview of the existing parallel data processing systems categorized by the data input as stream processing, graph processing, batch processing, and machine learning processing and discusses how the MapReduce architecture works and how efficient it is for data processing. It implements Spark as an easy-to-use cluster computing platform. It includes parallel operation features such as reduce, for each, and collect, which allow users to perform filter, map and reduce operations using functions.

The main focus of this study [35] is to use the Hadoop framework to analyze clickstream data collected from an online retail e-commerce website. In order to handle big data efficiently, the author use a variety of technologies such as Pig, Hive, and Sqoop, which are based on the Map-reduce.

A research [36] uses a big data platform to do sentiment analysis on a huge collection of tweets by examining user social data on a certain topic.

The author in [37] proposed implementation of the Spark framework for analyzing Twitter data. Spark offers and provides efficient solutions to analyze large amounts of data. Spark was able to process the tasks within short time which shows the high efficiency of the framework.

In this research [38], Apache Hive and Apache Pig are used to analyze the performance of various ECG Big Data datasets. Different ECG Big Data factors were examined, and the findings revealed that Apache Pig was more efficient and systematic than Apache Hive in terms of delivering rapid results in less time.

Since 2002, a large number of articles citing Sentiment Analysis have been published, focusing on the classification of comments and their polarity (positive or negative). Many researches have focused on opinion texts about products or political discussions. A research [39] propose a preference based sentiment analysis. It uses Hadoop technology to analyze various products. This paper shows the importance of analysis in a huge amount of data. This study proposed sentiment analysis of tweets, but accuracy and data size are very low.

A research [40] propose sentiment analysis of Twitter data using basic machine learning algorithms. To classify the text data. The author used basic machine learning algorithms such as KNN and SVM.

The aim of this research [41] is to improve marketing intelligence by developing a better understanding of consumers online generated contents in terms of positive and negative feedback. It focuses on the collection of tweets referring to three fast fashion retailers of various sizes operating in the UK market, and then analyzed and evaluated through a sentiment analysis based on machine learning. It provides an efficient and systematic approach to accessing the rich data set on customer experiences based on the vast amount of information that customers produce and share online, as well as investigating this massive amount of data to achieve perspectives that can affect retailers marketing intelligence.

The importance of log files in the E-commerce word is discussed in this study [42]. It proposes a predictive prefetching system based web log preprocessing using Hadoop MapReduce, which deliver accurate results in the shortest time possible for e-commerce business operations.

V. Experimentation

In this section, we have treated several case studies based on e-commerce industry to demonstrate the role of big data as a major marketing tool in understanding customers and improving the decision making process. Big data is a powerful tool to analyze and obtain very valuable information in any field. Applied to marketing, it allows us to study large volumes of data to extract information about customers, their interests or their consumption habits and thus be able to design more effective strategies. In this way, we are moving to marketing intelligence [43], which uses big data to understand customers, their environment, and make more strategic decisions. Big Data Analysis offers the analysis of large volumes of data to detect relationships between them that can provide useful information to companies, facilitating decision making in all processes and areas of the organization. The potential of big data can be fully exploited by corporate marketing departments to make decisions based on customer data. Machine learning presents a huge growth opportunity for online retailers. With machine learning, smart e-commerce companies can boost sales, reduce waste, and increase overall efficiency while actively engaging with consumers. It is a great tool for making better decisions.

In this paper, the experimentation will be separated in three subsections as follows.

A. Case study 1 : Approach K-Means and RFM to Study the Evolution of Customer Segmentation in Big Data Area

Rooted in recent literature [43][44][45], we focused on the landscape of big data analysis through the lens of a marketing mix framework [43]. The digital transformation enables enterprises to mine big data for marketing intelligence on customers, markets, products. The customer segmentation pillar of the marketing strategy. Segmentation is a way of dividing a problem into simpler parts, which help to prioritize efforts and locate business opportunities. Not all is a way of dividing a problem into simpler parts, which help to prioritize efforts and locate business opportunities. Not all customers are the same or have the same needs. Companies must therefore understand this and adapt their value proposition to each target group. Segmentation [45] is the process of dividing a population into homogeneous groups based on needs, behaviors, characteristics or attitudes and characterizing the resulting groups to discover what distinguishes them from one another.

Clustering [50] [51] is a machine learning method widely used in marketing for customer segmentation. A very useful way to segment and understand what kind of population we are studying is to see how their individuals naturally organize themselves. Today, clustering algorithms are commonly used in the commercial field, such as customer analysis, and this application has achieved a positive impact and good effect.

1) Proposed methodology: This research proposes a case study of building a customer segmentation model using data mining methods, K-means clustering, and RFM analysis, we used the k-means [52] and RFM [53] approach to study the evolution of customer segmentation in the era of big data [45][52]. The proposed methodology is shown in Fig. 1.

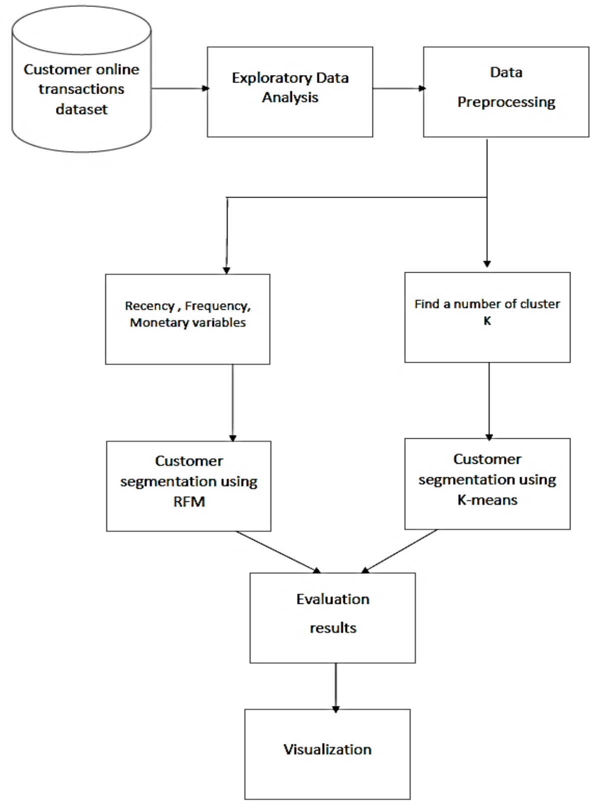

Fig. 1. Proposed Methodology for Customer Segmentation.

2) Dataset: The dataset used in this case study was collected from UCI Machine Learning Repository. This dataset is very hierarchical, with 541909 transactions and 8 attributes that describe these transactions, it contains all transactions recorded over an eight-month period (01/12/2010-09/12/2011) for a UK-based online retail company.

3) Data Pre-processing: In this stage, cleansing of the dataset was performed using Python programming language in Jupyter. Pre-processing of this data collection includes eliminating NAs, validating numerical values, removing invalid data points, and normalizing data.

4) Method: To achieve an efficient customer segmentation we, this study starts with K-means clustering [50] by the following steps to find customer groups with similar behaviors:

- Choose the number of clusters k.
- Set the k cluster centroids to their initial values.
- Assign the n data points to the clusters that are closest to them.
- Using the data points in each cluster, update the centroid.

- Repeat steps 3 and 4 until the variations in centroids' positions are zero.

a) K-Means Algorithm: K-means [52] algorithm requires knowledge of the number of groups in advance and therefore two internal evaluation methods were applied to determine this parameter: elbow method and silhouette method. In Fig. 2, the result of the elbow method is shown, the X-axis represents the cluster number and the Y-axis represents the sum of squares for the clusters (within-cluster sum of squares (WCSS)) according to. The appropriate cluster solution is defined at the moment when a dramatic reduction of the sum of squares in the cluster occurs. Based on Fig. 2, the extreme decrease of the sum of squares is pointed in the k=4 This produces a "bend" in the frame and in this case this bend can be seen in the number of four clusters. To validate the interpretation of this graph, the number of groups was also obtained using the silhouette index, with the highest index also being obtained in four groups.

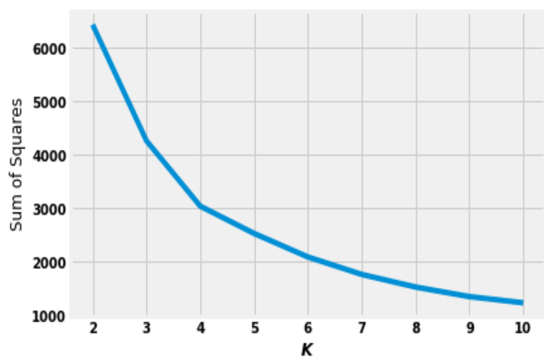

Fig. 2. Elbow Method for k-Means Algorithm.

b) RFM: To build a successful customer relationship management, companies must start with the identification of the true value of their customers as this provides the foundation for implementing more targeted and personalized marketing strategies. RFM (Recency- Frequency – Monetary) analysis is a data driven customer behavior segmentation technique.

RFM [53] based on three metrics that determine their purchase habits: Recency (the date since the last purchase), Frequency (how much the customer makes purchases), and Monetary value (the total value of all a customer's purchases). Customers purchase dates are typically sorted by RFM terms, which are determined by the number of appropriate time intervals. The quantile values are given a top score 4 and other 3, 2, 1. The quantile method is used to sort customer data in descending order (high to low), and the RFM scoring method is referred to as the customer quantile method.

RFM analysis enables businesses to properly forecast which consumers are more likely to make future purchases, how much income comes from new (vs repeat) clients, and how to convert infrequent consumers into habitual ones.

5) Results and disscusions: Based on the results of cluster analysis, 4 is the optimal number of clusters for this analysis. For the interpretation of the customer segments provided by these clusters. As shown in Fig. 4 customer segment in Red has low total sales and a low number of orders, which means that they are low value-added customers. On the other hand, Yellow customers have a high total sales and a high number of orders, indicating that they are the customers with the highest value. For Fig. 3, we could look at customers in the red group and try to find ways to increase their orders with e-mail reminders or targeted SMS notifications based on certain other identifying factors. The Fig. 5 confirms the previous two charts by identifying the Yellow cluster as the customers with the highest value, the red as the customers with the lowest value, and the blue and green as the customers with the highest opportunity. Customer segmentation can be carried out by taking into a multitude of different variables, such as demographic, geographical, psychological (preferences, etc.) or purchasing behavior data, which are increasingly important. Based on RFM analysis, Fig. 6 helps us decide which customer groups to target and how we can communicate with them.

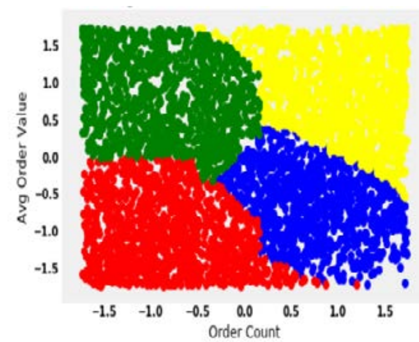

Fig. 3. Avg Order Value vs Order Count Clusters.

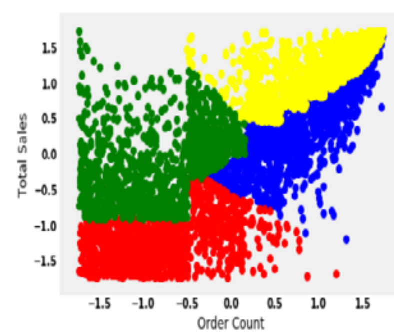

Fig. 4. Total Sales vs Order Count Clusters.

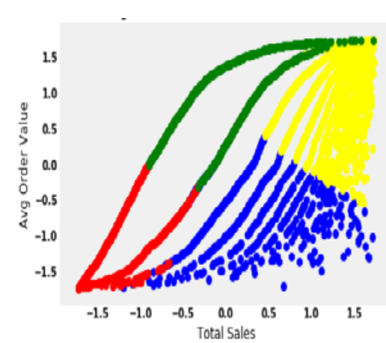

Fig. 5. Avg. Order Value vs Total Sales.

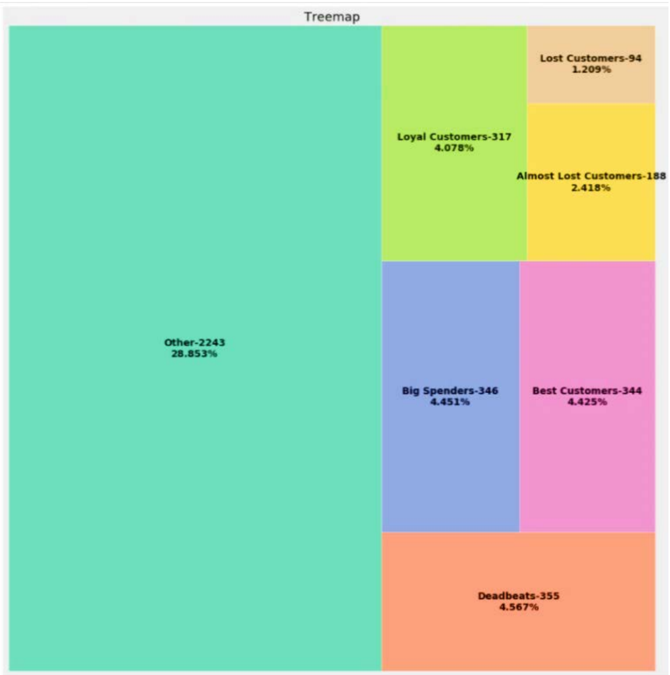

Fig. 6. Summary Report on Customer Segmentation using RFM.

6) Challenges and limitations: There are many challenges identified in this study, this analysis is usually performed in the form of a snapshot analysis where segments are identified at a specific point in time. However, it doesn't take into account the fact that customer segments are highly volatile and that segments change over time. Once the segments change, the entire analysis must be repeated and the strategies adapted. This is the origin of the grouping of flows as a tool to mitigate this problem. One of the biggest challenges is that customer segmentation is often based on a customer's transaction history.

As this data changes over time [49], it is necessary to update clients that have already been included in the bundle. We suggest the use of Stream clustering[46][47][48] is an extension of traditional clustering that manages a continuous flow of new observations. It updates the underlying classification over time without the need to recalculate the entire model. While it seems promising to apply flow aggregation for customer segmentation, it comes with several challenges. This customer segmentation is based on customer transactions. If we had data on customer demographics (i.e., gender, age, location, annual salary), we might discover more interesting information.

B. Case Study 2 : A Distributed Computing Approach to Analyze and Improve Retailing Business using Big Data Framework

Due to the complexity of big data, there are many obstacles to analyzing the dataset. The time span of the analysis is significant and important because it influences how quickly decisions can be taken in response to a change in the business environment. Analyzing the massive amounts of data produced by such transactions is critical for business growth and development [54]. Most research on big data in retail has focused on how to gain greater consumer insights to implement marketing activities and how to aid retail business owners in better understanding their customers' buying demands.

In this study, we used a distributed computing approach to analyze and improve retailing business using big data framework. It focused on online retail analytics using the same dataset used in the previous study.

1) Proposed architecture: The following proposed architecture Fig. 7 illustrates the analysis of Online retail transactions using Apache pig, Hive, Spark, Apache Zeppelin. For analyzing these large amounts of data a power tool is required using Hadoop and we also need efficient analytical tools which work on the top of Hadoop, Apache hive and Apache pig [54][55]. The first step was to install the necessary tools and the configuration between the set of big data analytics tools in order to build this architecture.

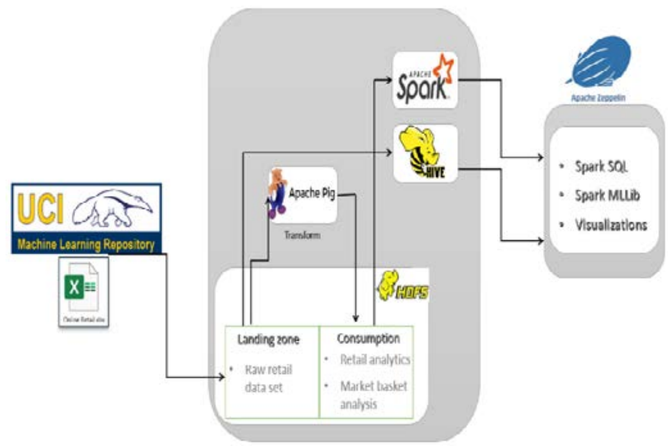

Fig. 7. Proposed Architecture based Big Data Tools.

2) Environement: For the analysis, many preliminary settings needed to be completed before moving to code development. The first step was to install Hadoop and install Apache pig, Apache Hive on top of it. Each tool has its own set of requirements, so how these tools are used is determined by the importance of the data and the needs of the organization or business. Due to the large amount of data that we need to be constantly analyzed, we attempted to exploit a physical server. Since Virtual machines are vulnerable to performance problems as a result of an overflow of virtual servers in a physical servers. However, in a large industrial environment, VMs may not be efficient because scalability of the processing equipment can be a problem. The performance should be considered in our case. In fact, Physical servers are much more powerful and efficient than VMs.

- Hive: It would be impossible to analyze massive databases without taking into account the technology's performance. Hive is a robust data warehouse platform built on Apache Hadoop. For big data analysis, the two together have stable storing and processing capability.

- Pig: Pig allows us to analyze and process the large datasets quickly and easily. It is also known as dataflow language. Ensures the originality of data by decreasing coding lines and replication.
- Spark: Apache Spark is another tool that has a large following. One of the great advantages of Spark is that it is able to store a lot of the processing data in memory and on disk, which can be much faster. However, one of the most interesting qualities is its ability to run on a single local machine, making it far more easier to use.

3) Proposed methodology

There are many steps Fig. 8 for the analysis of Online retail: :

- Step 1: Collect consumer transactions datasets from web resources.
- Step 2: Load dataset using Hadoop command line.
- Step 3: Store the data on HDFS which is very reliable for storing complex or large data size.
- Step 4: The data Ingestion, Cleanup and aggregation using Apache Pig, and SQL on Hadoop using Hive.
- Step 5: Analyze data and manipulate SQL in Hadoop using Hive. Also the analysis and visualization using SparkSQL on Apache Zeppelin.

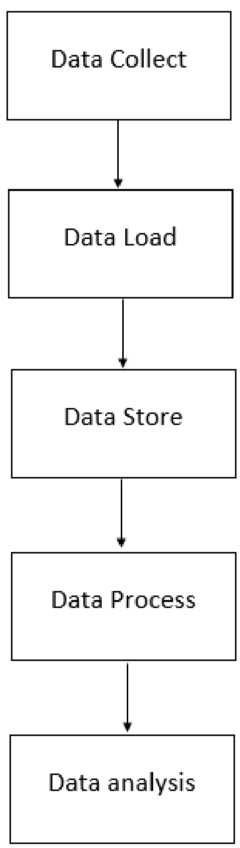

Fig. 8. Proposed Methodology to Analyze Retailing Business.

4) Result and disscusion: The below are some of the problem statements that have been analyzed in this study:

- The sales report by analyzing daily and hourly sales activities is done; this can help in decision making and aid in finding potential new market opportunities.
- To increase sales, an analysis of Basket size distribution is done. It aids in the identification of target audiences, the acquisition, retention, and growth of customers.
- In order to enable online marketers and online retails to build their business strategy around the most valuable customers, an analysis of customer lifetime value is done.

This study experimentally validates the effectiveness of the proposed architecture for retailing business. Big data analytics using pig and Hive [55] highlight major problems faced by consumers and help institutions or companies to solve these problems, provide appropriate consumer satisfaction, improve services, monitor problems and strengthen goodwill in the market place.

Query languages like as Hive and Pig became popular in the analysis of customer data to ensure that customers continue to have a convenient experience and businesses continue to provide excellent services. Two major factors make big data analysis the most meaningful leap in the history of data analysis. The low cost of computer hardware and availability make the analysis of big data the current trend of this era [54]. Large datasets amount to terabytes and require very complex operations and algorithms to be executed, but results are achieved in minutes, sometimes even seconds [56].

C. Case Study 3: A Machine Learning Approach for Statistical Analysis on Customer's Reviews with Sentiment Classification

1) Motivation and background: Consumers online posts, interactions, rating and ranking, reviews of products/ restaurants/attractions provide a large amount of data that marketers might access to enhance and improve the decision-making process, by influencing the competitive and marketing intelligence. Sentiment analysis is a contextual study that tries to determine people's feelings, views, outlooks, emotions, and moods regarding entities and their features. Companies are starting listen to social media as a tool to understand their customers in order to further improve their products and/or services. As part of this trend, text analysis has become an active research field in computational linguistics and natural language processing. One of the most popular problems in this area is the classification of texts . Today, understanding how customers feel is important key in marketing strategies. Sentiment analysis focuses on the understanding of emotions and the analysis in text patterns. Sentiment analysis in machine learning is a natural language processing (NLP) problem. NLP [57] is a field of artificial intelligence related to the understanding and processing of language. Both methods are very important for companies as they determine the public reaction to certain topics, products and/or services on digital platforms.

The aim of this study is to use sentiment analysis to find an accurate classification method for customer reviews based on online women clothing reviews by building a classification model to predict whether the customer will recommend the product or not. We used the power of text mining [58][58] to do an in-depth analysis of customer reviews.

2) Dataset: For this study, we used a real commercial data Women's e-commerce clothing reviews dataset revolving around the reviews written by customers. To maintain the data privacy, company name is replaced with word "retail" and customer names are excluded. It includes 23,486 rows and 10 feature variables in one CSV file. Each row corresponds to one customer review. The choice of the clothing e-commerce company as a population because this market is very interesting and attractive.

This application attempts to understand the correlation of different variables in the reviews and opinions of customers on a women's clothing e-commerce, and to classify each review according to whether or not it recommends the product under review and whether it is a positive, negative or neutral feeling.

3) Proposed methodology

This study was accomplished through a series of steps by following the entire process Fig. 9.

- Step 1: Collect real-time customers' data from Kaggle.
- Step 2: Analyze and plot each of the features in the dataset, this step covers four statistical analysis and visualization to gain insights on the features into the dataset and generate our hypotheses.
- Step 3: This step involves a lot of steps. Cleaning of data by removing outliers, Data Encoding, handling missing values and removing redundant features.
- Step 4: This step comes under data preprocessing. It includes cleaning and preparing text data to reduce the text with useful words that we need for our NLP goals. This covers a many approaches using NLTK libraries to extract stop words, formatting and removing unnecessary characters by eliminating delimiters, tokenization, Normalization.
- Step 5: Sentiment analysis is the process of analyzing customer sentiment with the use of NLP, text analysis, and statistics. It is accomplished by the use of algorithms to identify words as positive, negative, or neutral. This analysis tells us the polarity score of online reviews. Polarity is a float ranging from -1 to 1. Using the polarity score, we classify each of reviews into these three categories (positive, negative, neutral). Word cloud is used to extract the most used words and classify their polarity.
- Step 6: This step contains our classification models that are built using a detailed analysis of customer review text data as well as other numerical, categorical data. For our study, we used four models Decision Tree, Logistic Regression, Support Vector Machine and Naive Bayes to build a sentiment classifier.

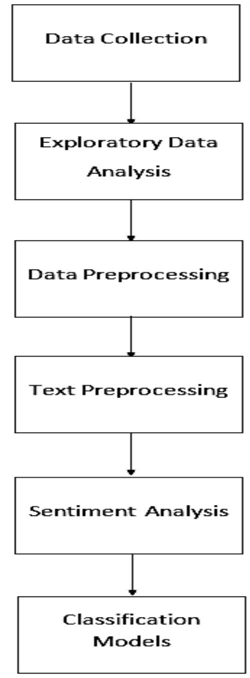

Fig. 9. Proposed Methodology for Sentiment Analysis.

4) Result and disscusion: In this experiment, we used supervised and unsupervised techniques [59] to predict the customer sentiment from reviews. We build our classification models based on a detailed analysis of customer review text data as well as other numerical, binary, and categorical data. As previously stated, the target variable here is whether or not the customer will recommend the product. We utilized four models: SVM, Logistic Regression, Decision Tree and Naive Bayes. To evaluate the performance of our model accuracy, precision, F1-score, recall scores calculated.

$$Accuracy = \frac{TN+TP}{TN+TP+FN+FP} \quad (1)$$

$$Precision = \frac{TP}{TP+FP} \quad (2)$$

$$Recall = \frac{TP}{TP+FN} \quad (3)$$

$$F1\ score = \frac{2*Precision*Recall}{Precision+Recall} \quad (4)$$

TABLE I. ALGORITHMS AND METRICS

Algorithm	**Metrics**			
	Accuracy	***Precision***	***Recall***	***F1-score***
SVM	0.95	0.98	0.92	0.95
Logistic Regression	0.95	0.98	0.93	0.95
Decision Tree	0.95	0.98	0.92	0.95
Naive Bayes	0.65	0.86	0.36	0.51

The Table I above showed the experimental results, it was obvious that expect Naive Bayes all other Classifier models perform well in Accuracy and F1-score as well as other metrics. The accuracy, precision and F1-score was the same as SVM, Logistic regression, Decision tree, which was 95%, 98% and 95%, respectively. However, Logistic regression had the highest Recall of four algorithms, which was 93%. In classification, naive Bayes converges faster but has greater error rates than other models. On small datasets, Naive Bayes is preferred, but as the training set size rises, other models are likely to outperform Naive Bayes. Based on the accuracy and F1 score in the chart Fig. 10, we can conclude that, with the exception of Naive Bayes, all classifiers can be utilized to analyze customer reviews.

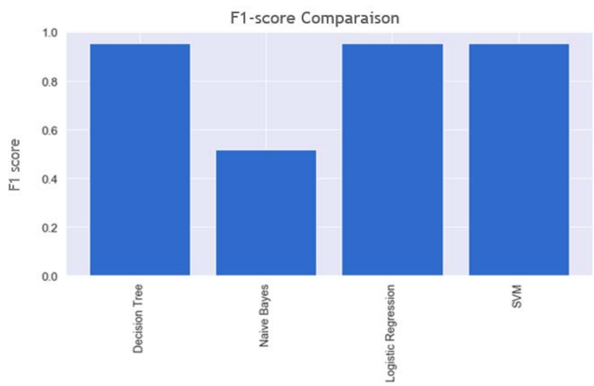

Fig. 10. Performance Comparaison of Models.

VI. Conclusion and Future Work

Big Data, as an emerging and continuing trend, is widely considered, studied and implemented in various sectors. While the level of implementation varies from sector to sector, it is important to understand what it takes to implement, reap the benefits of using Big Data. Big Data in e-commerce acts as the intelligent system that helps in the understanding of data and its transformation into valuable information, allowing us to better control all the processes of the online business. With the help of Big Data, online retailers may get more accurate information about the market, their users, and their customers, making it much easier to make decisions that will help them increase their return on investment. Otherwise, the ability to analyze and extract information from big data is currently seen as an important competitive weapon. Big data analytics is the field in which advanced analytical techniques operate on big data. These techniques are based on algorithms that help us obtain insights, patterns, correlations and associations that could not be understood with traditional small data. It also represents a real advance in the quality and customer service that any e-commerce company can and should offer. In the future, e-commerce will profit from efficient Big Data analysis and processing.

In conducting this research, it became clear that Big Data can improve decision making especially in e-commerce, it is critical for personalizing the strategies implemented, creating dynamic pricing, improving customer support before, during, and after transactions, better managing purchases, and making predictions. Big data has been responsible for some of the most significant innovations that have revolutionized the e-commerce industry.

An intelligent approach for data analysis and decision making in big data is demonstrated using a marketing cases study based on e-commerce industry by applying several machine learning models. The objective of this paper, as mentioned in the introduction, was to obtain and review knowledge about data science, particularly the field of big data, as well as to explore the existing literature on the fundamental concepts of big data and big data analytics and also demonstrate the role of big data as a major marketing tool in understanding customers and improving the decision making process based on practical case studies on online markets.

This research was done by a various case studies on e-commerce to study the evolution of customer segmentation in big data area using Online retail dataset with k-means and RFM, to analyze and improve retailing business using Big data framework, and to find an accurate classification method for customer reviews based on online women clothing reviews. Research on big data and their potential value in e-commerce industry is still very limited. When it comes to leveraging data, the volume of data, and the speed at which it accumulates the variety of data are the biggest challenges for e-commerce enterprises to overcome. To effectively utilize the benefits of Big Data in E-commerce, advanced research should be conducted in order to overcome application and existing technological challenges. The set of applications carried out has helped us to discover and better understand this topic, in particular the contribution of big data analysis and decision making in big data by looking for challenges and perspectives in e-commerce industry.

In addition to this research, the future work should be focus on including new data integration tools, new reporting tools, and new querying tools which can work efficiently with the challenges of big data.

References

[1] Kumar D., Mohanty M.N. (2019) A Survey: Classification of Big Data. In: Mallick P., Balas V., Bhoi A., Zobaa A. (eds) Cognitive Informatics and Soft Computing. Advances in Intelligent Systems and Computing, vol 768. Springer, Singapore. https://doi.org/10.1007/978-981-13-0617-4_29J. Clerk Maxwell, A Treatise on Electricity and Magnetism, 3rd ed., vol. 2. Oxford: Clarendon, 1892, pp.68–73.

[2] M. D. A. Praveena and B. Bharathi, "A survey paper on big data analytics," 2017 International Conference on Information Communication and Embedded Systems (ICICES), 2017, pp. 1-9, doi: 10.1109/ICICES.2017.8070723.

[3] R. Patgiri and A. Ahmed, "Big Data: The V's of the Game Changer Paradigm," 2016 IEEE 18th International Conference on High Performance Computing and Communications; IEEE 14th International Conference on Smart City; IEEE 2nd International Conference on Data Science and Systems (HPCC/SmartCity/DSS), 2016, pp. 17-24, doi: 10.1109/HPCC-SmartCity-DSS.2016.0014.

[4] S. R. Sukumar, "Open research challenges with Big Data — A data-scientist's perspective," 2015 IEEE International Conference on Big Data (Big Data), 2015, pp. 1272-1278, doi: 10.1109/BigData.2015.7363882.

[5] P. V. Desai, "A survey on big data applications and challenges," 2018 Second International Conference on Inventive Communication and Computational Technologies (ICICCT), 2018, pp. 737-740, doi: 10.1109/ICICCT.2018.8472999.

[6] Oussous, et Benjelloun. 2018. «Big Data technologies: A survey.» Journal of King Saud University-Computer and Information Sciences, pp. 431-448.

[7] Tsai Chun-Wei et al., "Big Data Analytics" in Big Data Technologies and Applications, Springer International Publishing, pp. 13-52, 2016.

[8] C. Komalavalli and C. Laroiya, "Challenges in Big Data Analytics Techniques: A Survey," 2019 9th International Conference on Cloud Computing, Data Science & Engineering (Confluence), 2019, pp. 223-228, doi: 10.1109/CONFLUENCE.2019.8776932.

[9] S. K. Bhatt and Srinivasan, "Survey on Big Data Analytics:Domain Areas and Features," 2020 2nd International Conference on Advances in Computing, Communication Control and Networking (ICACCCN), 2020, pp. 254-258, doi: 10.1109/ICACCCN51052.2020.9362939.

[10] S. Ahmad, P. Singh and A. K. Sagar, "A Survey on Big Data Analytics," 2018 International Conference on Advances in Computing, Communication Control and Networking (ICACCCN), 2018, pp. 256-260, doi: 10.1109/ICACCCN.2018.8748774.

[11] S. Kumar and M. Singh, "A novel clustering technique for efficient clustering of big data in Hadoop Ecosystem," in Big Data Mining and Analytics, vol. 2, no. 4, pp. 240-247, Dec. 2019, doi: 10.26599/BDMA.2018.9020037.

[12] S. Mittal and O. P. Sangwan, "Big Data Analytics using Machine Learning Techniques," 2019 9th International Conference on Cloud Computing, Data Science & Engineering (Confluence), 2019, pp. 203-207, doi: 10.1109/CONFLUENCE.2019.8776614.

[13] Akhil, M., Shravya, M., & Uma, K. (2017). Survey on the challenges and issues on big data analytics. International Journal of Mechanical Engineering and Technology, 8(12), 138-149.

[14] Sivarajah, U., Kamal, M. M., Irani, Z., & Weerakkody, V. (2017). Critical analysis of Big Data challenges and analytical methods. Journal of Business Research, 70, 263–286. doi:10.1016/j.jbusres.2016.08.001.

[15] S. Agarwal, K. Narayanan, M. Sinha, R. Gupta, S. Eswaran and T. Mukherjee, "Decision Support Framework for Big Data Analytics," 2018 IEEE World Congress on Services (SERVICES), 2018, pp. 53-54, doi: 10.1109/SERVICES.2018.00040.

[16] Elgendy, N., & Elragal, A. (2016). Big Data Analytics in Support of the Decision Making Process. Procedia Computer Science, 100, 1071–1084. doi:10.1016/j.procs.2016.09.251.

[17] J. Lu, Z. Yan, J. Han and G. Zhang, "Data-Driven Decision-Making (D3M): Framework, Methodology, and Directions," in IEEE Transactions on Emerging Topics in Computational Intelligence, vol. 3, no. 4, pp. 286-296, Aug. 2019, doi: 10.1109/TETCI.2019.2915813.

[18] Lim, et Chen. 2013. «Business intelligence and analytics: research directions.» ACM Trans. Manage. Inf. Syst., vol. 3, no. 4 1–10.

[19] M. S. Mahmud, J. Z. Huang, S. Salloum, T. Z. Emara and K. Sadatdiynov, "A survey of data partitioning and sampling methods to support big data analysis," in Big Data Mining and Analytics, vol. 3, no. 2, pp. 85-101, June 2020, doi: 10.26599/BDMA.2019.9020015.

[20] Wang, H., Xu, Z., Fujita, H., & Liu, S. (2016). Towards felicitous decision making: An overview on challenges and trends of Big Data. Information Sciences, 367-368, 747–765. doi:10.1016/j.ins.2016.07.007.

[21] Athmaja, S., Hanumanthappa, M., & Kavitha, V. (2017). A survey of machine learning algorithms for big data analytics. 2017 International Conference on Innovations in Information, Embedded and Communication Systems (ICIIECS). doi:10.1109/iciiecs.2017.8276028.

[22] G. Pal, G. Li and K. Atkinson, "Big Data Real Time Ingestion and Machine Learning," 2018 IEEE Second International Conference on Data Stream Mining & Processing (DSMP), 2018, pp. 25-31, doi: 10.1109/DSMP.2018.8478598.

[23] Hofacker, C.F., Malthouse, E.C. and Sultan, F. (2016), "Big Data and consumer behavior: imminent opportunities", Journal of Consumer Marketing, Vol. 33 No. 2, pp. 89-97. https://doi.org/10.1108/JCM-04-2015-1399.

[24] ORTIZ MORALES, Marsy Dayanna; AGUILAR, Luis Joyanes and GIRALDO MARIN, Lillyana María. The Marketing Challenges in the Big Data Age. E-Ciencias de la Información [online]. 2016, vol.6, n.1, pp.16-45. ISSN 1659-4142. http://dx.doi.org/10.15517/eci.v6i1.19005.

[25] S. Yu and C. Song, "Research on Real Estate Marketing Innovation System in the Era of Big Data," 2020 2nd International Conference on Machine Learning, Big Data and Business Intelligence (MLBDBI), 2020, pp. 309-312, doi: 10.1109/MLBDBI51377.2020.00066.

[26] W. Gan, "Design of Network Precision Marketing Based on Big Data Analysis Technology," 2020 International Conference on E-Commerce and Internet Technology (ECIT), 2020, pp. 77-81, doi: 10.1109/ECIT50008.2020.00026.

[27] Christy, A. J., Umamakeswari, A., Priyatharsini, L., & Neyaa, A. (2018). RFM Ranking – An Effective Approach to Customer Segmentation. Journal of King Saud University - Computer and Information Sciences. doi:10.1016/j.jksuci.2018.09.004.

[28] Kaur, Ramandeep and G. Jagdev. “Big Data in Retail Sector - An Evolution that Turned to a Revolution.” (2017).

[29] H. Kaur, V. Mangat and Nidhi, "A survey of sentiment analysis techniques," 2017 International Conference on I-SMAC (IoT in Social, Mobile, Analytics and Cloud) (I-SMAC), 2017, pp. 921-925, doi: 10.1109/I-SMAC.2017.8058315.

[30] Güçdemir, H. and Selim, H. (2015), "Integrating multi-criteria decision making and clustering for business customer segmentation", Industrial Management & Data Systems, Vol. 115 No. 6, pp. 1022-1040. https://doi.org/10.1108/IMDS-01-2015-0027.

[31] Sarvari, P.A., Ustundag, A. and Takci, H. (2016), "Performance evaluation of different customer segmentation approaches based on RFM and demographics analysis", Kybernetes, Vol. 45 No. 7, pp. 1129-1157. https://doi.org/10.1108/K-07-2015-0180.

[32] Wang, L., & Liu, S. (2020). Research on E-commerce customer relationship management based on data analysis. Paper presented at the ACM International Conference Proceeding Series, 20-26. doi:10.1145/3414752.3414776.

[33] Qadadeh, W., & Abdallah, S. (2018). Customers Segmentation in the Insurance Company (TIC) Dataset. Procedia Computer Science, 144, 277–290. doi:10.1016/j.procs.2018.10.529.

[34] Y. Zhang et al., "Parallel Processing Systems for Big Data: A Survey," in Proceedings of the IEEE, vol. 104, no. 11, pp. 2114-2136, Nov. 2016, doi: 10.1109/JPROC.2016.2591592.

[35] P. M. Anand, G. S. Vamsi and P. R. Kumar, "A Novel Approach for Insight Finding Mechanism on ClickStream Data Using Hadoop," 2018 Second International Conference on Inventive Communication and Computational Technologies (ICICCT), 2018, pp. 446-449, doi: 10.1109/ICICCT.2018.8473232.

[36] Jatwani, P., Tomar, P., & Dhingra, V. (2018). Framework for analyzing user behavior using big data technology. Paper presented at the Proceedings of the 8th International Conference Confluence 2018 on Cloud Computing, Data Science and Engineering, Confluence 2018, 598-603. doi:10.1109/CONFLUENCE.2018.8442467.

[37] K. Aziz, D. Zaidouni, and M. Bellafkih, “Real-time data analysis using spark and hadoop,” in 2018 4th International Conference on Optimization and Applications (ICOA). IEEE, 2018, pp. 1–6.

[38] M. Ahmad, S. Kanwal, M. Cheema and M. A. Habib, "Performance Analysis of ECG Big Data using Apache Hive and Apache Pig," 2019 8th International Conference on Information and Communication Technologies (ICICT), 2019, pp. 2-7, doi: 10.1109/ICICT47744.2019.9001287.

[39] Kumar, M., Bala, A.: Analyzing Twitter sentiments through big data. In: 2016 3rd International Conference on Computing for Sustainable Global Development (INDIACom), New Delhi, pp. 2628–2631 (2016).

[40] Huq, M.R., Ali, A., Rahman, A.: Sentiment analysis on Twitter data using KNN and SVM. Int. J. Adv. Comput. Sci. Appl. (IJACSA) 8(6), 19–25 (2017).

[41] Pantano, E., Giglio, S. and Dennis, C. (2019), "Making sense of consumers’ tweets: Sentiment outcomes for fast fashion retailers through Big Data analytics", International Journal of Retail & Distribution Management, Vol. 47 No. 9, pp. 915-927. https://doi.org/10.1108/IJRDM-07-2018-0127.

[42] S. Suguna, M. Vithya and J. I. C. Eunaicy, "Big data analysis in e-commerce system using HadoopMapReduce," 2016 International Conference on Inventive Computation Technologies (ICICT), 2016, pp. 1-6, doi: 10.1109/INVENTIVE.2016.7824798.

[43] Fan, S., Lau, R. Y. K., & Zhao, J. L. (2015). Demystifying Big Data Analytics for Business Intelligence Through the Lens of Marketing Mix. Big Data Research, 2(1), 28–32. doi:10.1016/j.bdr.2015.02.006.

[44] Nguyen Anh Khoa Dam, Thang Le Dinh, and William Menvielle, " Marketing Intelligence from Data Mining Perspective — A Literature Review," International Journal of Innovation, Management and Technology vol. 10, no. 5, pp. 184-190, 2019.

[45] Arunachalam, et Kumar. 2018. «Benefit-based consumer segmentation and performance evaluation of clustering approaches: an evidence of data-driven decision-making.» Expert Syst. Appl., 111 (2018) 11-34.

[46] Matthias , Carnein, et Trautmann Heike . 2019. «Customer Segmentation Based on Transactional Data Using Stream Clustering.» Advances in Knowledge Discovery and Data Mining 280-292.

[47] Ding, S., Wu, F., Qian, J. et al. Research on data stream clustering algorithms. Artif Intell Rev 43, 593–600 (2015). https://doi.org/10.1007/s10462-013-9398-7.

[48] Kokate, U., Deshpande, A., Mahalle, P., & Patil, P. (2018). Data Stream Clustering Techniques, Applications, and Models: Comparative Analysis and Discussion. Big Data and Cognitive Computing, 2(4), 32. doi:10.3390/bdcc2040032.

[49] Zubaroğlu, A., & Atalay, V. (2020). Data stream clustering: a review. Artificial Intelligence Review. doi:10.1007/s10462-020-09874-x.

[50] P. S. Badase, G. P. Deshbhratar and A. P. Bhagat, "Classification and analysis of clustering algorithms for large datasets," 2015 International Conference on Innovations in Information, Embedded and Communication Systems (ICIIECS), 2015, pp. 1-5, doi: 10.1109/ICIIECS.2015.7193191.

[51] T. Sajana, C. Sheela Rani and K. Narayana, "A Survey on Clustering Techniques for Big Data Mining", Indian Journal of Science and Technology, vol. 9, no. 3, 2016.

[52] Mugdha Jain, et Chakradhar Verma. September 2014. «Adapting k-means for Clustering in Big Data.» International Journal of Computer Applications (0975 – 8887) 1.

[53] Christy, et Joy. 2018. «RFM ranking–an effective approach to customer segmentation.» J. King Saud Univ.-Comput. Inf. Sci. (2018).

[54] S. Cha and M. Wachowicz, "Developing a real-time data analytics framework using Hadoop", 2015 IEEE International Congress on Big Data, pp. 657-660, June 2015.

[55] Urmila R. Pol. June 2016. «Big Data Analysis: Comparision of Hadoop MapReduce, Pig and Hive.» International Journal of Innovative Research in Science, Engineering and Technology Vol. 5, Issue 6.

[56] B. Yadranjiaghdam, N. Pool and N. Tabrizi, "A Survey on Real-Time Big Data Analytics: Applications and Tools," 2016 International Conference on Computational Science and Computational Intelligence (CSCI), 2016, pp. 404-409, doi: 10.1109/CSCI.2016.0083.

[57] Khader, M., Awajan, A., & Al-Naymat, G. (2018). The Effects of Natural Language Processing on Big Data Analysis: Sentiment Analysis Case Study. 2018 International Arab Conference on Information Technology (ACIT).

[58] Hossein Hassani, Christina Beneki, et Stephan Unger. January 2020. «Text Mining in Big Data Analytics.» Big Data and Cognitive Computing.

[59] M. Somvanshi, P. Chavan, S. Tambade and S. V. Shinde, "A review of machine learning techniques using decision tree and support vector machine," 2016 International Conference on Computing Communication Control and automation (ICCUBEA), 2016, pp. 1-7, doi: 10.1109/ICCUBEA.2016.7860040.

Improved Incentive Pricing Wireless Multi-service Single Link with Bandwidth Attribute

Nael Hussein[1], Kamaruzzaman Seman[2], Fitri Maya Puspita[3], Khairi Abdulrahim[4], Mus'ab Sahrim[5]
Faculty of Engineering and Built Environment, Universiti Sains Islam Malaysia, Nilai, 71800 Negeri Sembilan, Malaysia[1, 2, 4, 5]
Sriwijaya University, Indralaya, South Sumatra, 30662, Indonesia[3]

***Abstract*—Several objectives that service providers have to achieve are to determine the increase or decrease in the price change due to the change in service quality and the amount of service quality value. Multi-service wireless Internet pricing schemes that apply the quality of the bandwidth advantage are designed to take into account the need of ISPs to provide high-quality services to users and increase their revenue, considering the limited bandwidth of the resources. The modified model is an improvement of the original model by adding variables and parameters to the multiple service network model by specifying the base price for QoS (alpha) and premium quality (β) as variables, parameters, and service class load factor, Pregnancy basis factor and differentiation factor. The models are solved by the program Lingo 18.0 to get the best solution. The results prove that the modified model is the best and yields the best profit for the service provider when the cost of all changes in quality of service is increased and the variable α and β is set as constant or variable.**

Keywords—Optimal solution; multi service network; wireless pricing scheme; bandwidth QoS attribute

I. Introduction

The Internet plays a big role in developing the economy and is seen as an important catalyst for restructuring business activities [1]. The volume of demand on the Internet has increased, especially with the emergence of the IOT and its multiple uses that require an Internet connection to display the results of the sensors [2]. Quality of service in networks is defined as the mechanisms that allow distinguishing network services based on their unique service requirements [3].

The DiffServ and IntServ architectures allow the implementation and differentiation of QoS to different specifications on a given network [4]. The pricing works to regulate the use of the Internet by providing appropriate pricing that is equivalent to the quality of service, which is reflected in improving network performance and avoiding congestion [5]. Internet service providers should provide an appropriate internet pricing mechanism and a better and different quality of service [6]. The best way to prevent network congestion and distinguish its services is through usage-based pricing schemes [7]. The author in [8] Improved the reverse charging scheme of a multi-service connection in a wireless network with an bit error rate feature, in addition take in to account basic cost ,quality of service, and reached optimal profit when adjusting the basic costs as fix and quality as variable. Designed the reverse charging model within a multi-link network in the wireless network, based on the end to end feature [9]. The Internet service provider must take into account the provision of prices, the price is affected by quality and variable depending on the quality of the service [10].

Avoiding congestion requires studying consumer behavior, knowing peak times, and working on balancing loads in multi-service networks to avoid congestion [11]. Internet service providers suffer during peak usage times from congestion, and therefore there is a need for an appropriate pricing scheme that seeks to control usage at peak times to prevent network collapse and encourage consumers to rationalize their consumption during peak times [12].

Designed a model to price the Internet in multiple links depending on the incentive mechanism so that the service provider chooses to either recover the cost or promote a particular service [13]. The author in [14] proposed a mathematical model of the Paris metro pricing Scheme for charging the packet networks, which is based on dividing the networks into sub-networks or classes, and fees are imposed on their customers at different prices.

The optimal solution is determined by the basic price, either it is a fixed price for the purpose of recovering the cost or the price is variable for the purpose of competition, determining the quality premium and the level of service quality to enable the user to choose the categories [15]. The author in [16] improved the Bundle Pricing model in the wireless internet model on the multiple QoS network by integrating the quasi-linear utility function with the bundle problem and the consumer problem. And they concluded that the best solution is in the feature of Bit Error Rate on the flat fee and two-part tariff internet pricing scheme.

The author in [17] discussed a wireless pricing scheme on a multi-category single link models with the bandwidth attribute and taking into account the addition of the base value of the price and the variable of quality premium. The author in [18] explained a wireless pricing scheme on a multi-category model with the Bit Error Rate (BER) QoS attribute and taking into account the addition of the base value of the price and the variable of quality premium. In [19], the author discussed improving the wireless internet pricing scheme using different features of the multiple QoS network.

The authors in [20], [21] explained that the Internet pricing scheme is based on three strategies, namely, the flat fee , two-part tariff, and usage based. We note that the topic of Internet pricing in wireless networks has been covered recently in several papers. Optimization needs prior study about understanding user behavior and when demand will rise, as well as knowing what kind of service is badly needed. Thus, by determining the basic demand factor in the network and the demand factor for users, as well as knowing the magnitude of differentiation between service classes and the demand for them by users, this will provide a more accurate and more profitable pricing scheme for the service provider. In this paper [22], we present multi-service wireless single network incentive pricing scheme based on the bandwidth attribute.

This paper is organized as follows: the research methodology and case study used are described in the second section. The third section explains the analysis and comparison of the results of the different models. Finally, the main conclusions are summarized in the conclusion section. Pricing models will be solved to reach the optimal solution using the Lingo program.18, the data used to test the model consists of three types of traffic classes, which are mail and files and an IP camera, obtained from a local server. The results will be compared between our pricing scheme in wireless network with bandwidth attribute , the original model [22] and a model that has been developed in wireless network with the attribute of bandwidth [17], all results will be shown in the tables presented in the results section.

II. Research Method

In [22], we work to improve the model presented by [11] in the pricing of wireless multi-service Internet with bandwidth QOS attribute by looking at the model as an optimization problem that can be solved in the optimization tool using Lingo 18, which simulates formulas and search results.

In this paper, we contribute to the QOS multiservice wireless internet pricing model, and provide better results than model [22], [17].

The idea originated mainly from [3], [11], [22] the goal is to improve wireless Internet networks for a single link. The model consists of the objective function that will be maximized and the constraints of the model that form the framework that cannot be crossed during the solution and that consists of limits and controls.

We seek to get the best solution that represents the best profit for the provider by transforming the problem of pricing the Internet in the networks of one link and multiple services into an improvement model and trying to solve it to get the best solution that will help explain the problems that include pricing of services, the load in the network with its multiple services and the volume of Bandwidth required by the user. The goal of this optimization is to maximize the gain based on the load; parameter in the multicast, the base load factor and the diversity factor, bandwidth.

A. *Original Models using Bandwidth Qos Attribute*

In this section, we explain the meaning of the variables contained in the original model.

PR_{ik}: The cost to connect to the QoS provided.

$\mathrm{P}Q_{ik}$: Changes in the cost of all the changes QoS.

X : Amount of increase or decrease in the value of QoS.

Q_{Pik}: Nominal value attribute QoS in the network operator.

PB_{ik} : The basic cost for a connection with the service I and links k.

Lx : Linearity factor

T_l : Traffic load

a_{ik}: linear price factor for each service (i) and links(j).

a : Linear parameter set.

B : Linear parameter set.

F, g, h: A predetermined minimum value for a service provider.

a_{ik} : The maximum value that has been set for the service provider.

T_l: The minimum amount of load traffic that is allowed.

T_{ik} : The maximum amount of traffic goods that is

allowed.

The Wireless bandwidth schema is divided by the original form into four sections depending on the value of X. the objective function as follows:

$$MAX\ R = \sum_{k=1}^{r} \sum_{i=1}^{s} (\mathrm{PR}_{ik} \pm PQ_{ik}) \tag{1}$$

Subject to:

$$\mathrm{P}Q_{11} = (1\pm \mathrm{x}/2000)\ \mathrm{PB}_{11}\ L_x \tag{2}$$

$$\mathrm{P}Q_{12} = (1\pm \mathrm{x}/2000)\ \mathrm{PB}_{12}\ L_x \tag{3}$$

$$\mathrm{P}Q_{21} = (1\pm \mathrm{x}/2000)\ \mathrm{PB}_{21}\ L_x \tag{4}$$

$$\mathrm{P}Q_{22} = (1\pm \mathrm{x}/2000)\ \mathrm{PB}_{22}\ L_x \tag{5}$$

$$\mathrm{P}B_{11} = a_{11}(\mathrm{e}\text{-}e^{-xB})\ T_l/100 \tag{6}$$

$$\mathrm{P}B_{12} = a_{11}(\mathrm{e}\text{-}e^{-xB})\ T_l/100 \tag{7}$$

$$\mathrm{P}B_{21} = a_{21}\ (\mathrm{e}\text{-}e^{-xB})\ T_l/100 \tag{8}$$

$$\mathrm{P}B_{22} = a_{22}(\mathrm{e}\text{-}e^{-xB})\ T_l/100 \tag{9}$$

$$L_X = (\mathrm{e}\text{-}e^{-xB}) \tag{10}$$

$$0.05 \le a_{11} \le 0.15 \tag{11}$$

$$0.06 \le a_{12} \le 0.14 \tag{12}$$

$$0.07 \le a_{21} \le 0.13 \tag{13}$$

$$0.08 \le a_{22} \le 0.12 \tag{14}$$

$$50 \le T_l \le 1000 \tag{15}$$

$$0 \le x \le 1 \tag{16}$$

$$0.8 \le \mathrm{B} \le 1.07 \tag{17}$$

$$a = 1 \tag{18}$$

B. *Modified Models*

The model was developed to improve its results by combining a multi-service wireless network model and adding parameters and variables, where the basic price (α) and premium quality (β) for each service category will be determined in addition to the load factor and the variance factor. The model, variables, and decision parameters are formulated within the constraints and determinants of the network.

We improve models by four cases:

1) α and β constants.
2) α constants and β variable.
3) α and β variables.
4) α variables and β constants.

Parameters used in the modified models are as follows:

i: priority of the service.

C: bandwidth capacity of link K.

L_{base}: base load factor for the network.

Z_{ik}: requested bandwidth in class I in link k.

R_{ik} : price service class I at link k.

p_{ik}: load factor for service class I at link k.

L_{ik}: load of service class I at link k.

I_{i}: Quality of service index *i.*

a_{ik}: *price service I in link k.*

m_{I} : Minimum QoS for service *i.*

Ii: The minimum premium for the service *i.*

b_{i}: The maximum premium for the service i.

y: The minimum base price for service i.

z: The maximum base price for service i.

5) Modified model case α and β constants: Wireless pricing schemes in the first case, the objective function is as follows:

$$MAX\ R = \sum_{k=1}^{r} \sum_{i=1}^{s} (\mathrm{PR}_{ik} \pm PQ_{ik}) + (\alpha + \beta . I_i) + \mathrm{R}_{ik} * \mathrm{Z}_{ik} * \mathrm{P}_{ik}) \quad (19)$$

Subject to:

$$\mathrm{P}Q_{11} = \left(1 \pm \frac{\mathrm{X}}{2000}\right) \mathrm{PB}_{11}\ L_x \quad (20)$$

$$\mathrm{P}Q_{21} = \left(1 \pm \frac{\mathrm{X}}{2000}\right) \mathrm{PB}_{21}\ L_x \quad (21)$$

$$\mathrm{P}Q_{31} = \left(1 \pm \frac{\mathrm{X}}{2000}\right) \mathrm{PB}_{31}\ L_x \quad (22)$$

$$PB_{11} = a_{11}(\mathrm{e}\text{-}e^{-xB})\ T_l/100 \quad (23)$$

$$PB_{21} = a_{21}(\mathrm{e}\text{-}e^{-xB})\ T_l/100 \quad (24)$$

$$\mathrm{P}B_{31} = a_{31}\ (\mathrm{e}\text{-}e^{-xB})\ T_l/100 \quad (25)$$

$$\mathrm{P}L_X = (\mathrm{e}\text{-}e^{-xB}) \quad (26)$$

$$0.05 \le a_{11} \le 0.15 \quad (27)$$

$$0.06 \le a_{24} \le 0.14 \quad (28)$$

$$0.07 \le\ a_{31} \le 0.13 \quad (29)$$

$$50 \le T_l \le 1000 \quad (30)$$

$$0 \le \mathrm{x} \le 1 \quad (31)$$

$$0.8 \le \mathrm{B} \le 1.07 \quad (32)$$

$$a = 1 \quad (33)$$

$$P11 = \left(\frac{1 - L_{base}}{1 - L_{11}}\right)^n \quad (34)$$

$$P21 = \left(\frac{1 - L_{base}}{1 - L_{11}}\right)^n \quad (35)$$

$$P31 = \left(\frac{1 - L_{base}}{1 - L_{11}}\right)^n \quad (36)$$

$$\mathrm{L11} < 1 \quad (37)$$

$$\mathrm{L21} < 1 \quad (38)$$

$$\mathrm{L31} < 1 \quad (39)$$

$$0 \le \mathrm{Lbase} \le 1 \quad (40)$$

$$\mathrm{n} > 1 \quad (41)$$

$$\mathrm{L11} + \mathrm{L21} + \mathrm{L31} = 1 \quad (42)$$

$$\mathrm{Z}_{11} <= \mathrm{C} \quad (43)$$

$$\mathrm{Z}_{21} <= \mathrm{C} \quad (44)$$

$$\mathrm{Z}_{31} <= \mathrm{C} \quad (45)$$

$$I_1 P_{11} \le a_{11} \quad (46)$$

$$I_2 P_{21} \le a_{21} \quad (47)$$

$$I_3 P_{31} \le a_{31} \quad (48)$$

$$I_1 P_{11} + I_2 P_{21} + I_3 P_{31} \le \mathrm{C} \quad (49)$$

$$a_{11} + a_{21} + a_{31} = 1 \quad (50)$$

$$0 \le a_{11} \le 1 \quad (51)$$

$$0 \le a_{21} \le 1 \quad (52)$$

$$0 \le a_{31} \le 1 \quad (53)$$

$$0.01 \le I_1 \le 1 \quad (54)$$

$$0.01 \le I_2 \le 1 \quad (55)$$

$$0.01 \le I_3 \le 1 \quad (56)$$

By modifying the index of quality of services (I_i) we obtain

$$I_i = I_{i-1} \quad (57)$$

$$I_2 - I_1 = 0 \quad (58)$$

$$I_3 - I_2 = 0 \quad (59)$$

6) Modified model case α constants and β variable: Wireless pricing schemes in the second case, the objective function is as follows:

$$MAX\ R = \sum_{k=1}^{r} \sum_{i=1}^{s} (\mathrm{PR}_{ik} \pm PQ_{ik}) + (a + \beta_i . I_i) + \mathrm{R}_{ik} * \mathrm{Z}_{ik} * \mathrm{P}_{ik}) \quad (60)$$

With subject to equation: (2)-(33), as well as the added constraints.

$\beta_2 I_2 \geq \beta_1 I_1$ (61)

$\beta_3 I_3 \geq \beta_2 I_2$ (62)

$0.01 \leq \beta_1 \leq 0.5$ (63)

$0.01 \leq \beta_2 \leq 0.5$ (64)

$0.01 \leq \beta_3 \leq 0.5$ (65)

$\beta_1 = \beta_{1-1}$ by modifying the service quality index, I (Ii) and the premium quality of service then added constraints

$\beta_2 - \beta_1 = 0$ (66)

$\beta_3 - \beta_2 = 0$ (67)

7) Modified model case α and β variables: Wireless pricing schemes in third case, the objective function is as follow:

$$MAX\ R = \sum_{k=1}^{r} \sum_{i=1}^{s} (\mathrm{PR}_{ik} \pm PQ_{ik}) + (a_i + \beta_i . I_i) + \mathrm{R}_{ik} * \mathrm{Z}_{ik} * \mathrm{P}_{ik}) \quad (68)$$

With subject to equation: (2)-(33) and equation. (46) – (50), as well as the added constraints

$a_2 + \beta_2 I_2 \geq a_1 + \beta_1 I_1$ (69)

$a_3 + \beta_3 I_3 \geq a_2 + \beta_2 I_2$ (70)

$0 \leq a_1 \leq 1$ (71)

$0 \leq a_2 \leq 1$ (72)

$0 \leq a_3 \leq 1$ (73)

$a_{\mathrm{I}} - = a_{1-1}$ by modifying the service quality index i(l_1) and set a base price and premium service and added constraints :

$a_2 - a_1 = 0$ (74)

$a_3 - a_2 = 0$ (75)

8) Modified model case α variables and β constants: Wireless pricing schemes in fourth case, the objective function is as follow:

$$MAX\ R = \sum_{k=1}^{r} \sum_{i=1}^{s} (\mathrm{PR}_{ik} \pm \mathrm{P}Q_{ik}) + (a_i + \beta . I_i) + \mathrm{R}_{ik} * \mathrm{Z}_{ik} * \mathrm{P}_{ik}) \quad (76)$$

with subject to equation. (2)- (32), (34)-(42). (54)-(56), with added constraints as follows

$a_2 + I_2 \geq a_1 + I_1$ (77)

$a_3 + I_3 \geq a_2 + I_2$ (78)

III. Result and Discussion

In this section, the results for the four cases are presented separately. The solution consists of three tables. Table I shows the optimal solution for the paper [17] and Table II shows the optimal solution for the modified model [23], which is the value of the objective function. The Table III represents the value of the variables in the modified model, Results Original Model:

- α and β constants in bandwidth QoS

TABLE I. Optimal Solution for [17] Model for a and β Constants in bandwidth QoS

Var	pqij increase x increase	pqij increase x decrease	Pqij decrease x increase	Pqij decrease x decrease
Model Class	INLP	INLP	INLP	INLP
State	Local Opt	Local Opt	Local Opt	Local Opt
Objective	125.681	125.625	67.7576	67.7576
Infeasibility	0	0	0	0
Iter	13	13	45	45
GMU	32K	32K	32K	32K
ER	0	0	0	0

TABLE II. Optimal Solution for Models for a and β Constants in Bandwidth QoS

Var	pqij increase x increase	pqij increase x decrease	Pqij decrease x increase	Pqij decrease x decrease
Model Class	NLP	NLP	NLP	NLP
State	Local Opt	Local Opt	Local Opt	Local Opt
Objective	791.567	791.560	733.511	733.511
Infeasibility	0	0	0	0
Iter	14	14	14	14
GMU	41	41	41	41
ER	0	0	0	0

Based on the objective function (19) with equation, (20) to (59), the optimal solution in each case on bandwidth QoS attributes solved using LINGO 18.0 are presented in Table II and Table III.

Based on Tables III and IV, the value achieved the most optimal results in the first case is equal to 791.567. These results obtained by 13 iterations of the infeasibility of 0. Generated Memory Used (GMU) that is 32K and Elapsed Runtime I is 0 seconds.

We note the difference between the model [17] and the modified model, where the difference is clear in the value of the objective function between the four cases in each model Thus, by comparing the best value of the objective function in the model [17] in the case of fixed alpha and beta, it is equal to 125.681, while in the modified model it is equal to 791.567.

- α constant and β variable in Bandwidth Qos

Based on the objective function (60) and the equations from (2) to (32) and (61) to (65): The optimal solution is summarized in Tables V and VI for each case of the bandwidth features that were solved using Lingo18.

From Tables IV and V, we notice that the first case achieved the best results compared to the rest of the cases, where the objective is 791.434, where the results are reached after 14 repetitions. Zero invisibility, 43 memory usage, and zero runtime. The results of the values of the first and second cases are similar, while the results of the third and fourth cases are identical. By comparing the objective value between the two models, we see that our model outperforms the previous model by about 665.753.

TABLE III. OPTIMAL SOLUTION FOR MODEL FOR α AND β CONSTANTS IN BANDWIDTH QOS

Var	pqij increase x increase	pqij increase x decrease	Pqij decrease x increase	Pqij decrease x decrease
PQ11	8.487065	8.458654	0.2214369	0.2214369
PQ21	7.921260	7.894743	0.2066745	0.2066745
PQ31	40.17211	40.03763	1.048135	1.048135
X	1	1	0	0
PB11	3.562910	3.562910	0.042957	0.042957
PB21	3.325383	3.325383	0.060139	0.060139
PB31	16.86444	16.86444	0.068731	0.068731
PR11	0.5	0.5	0.5	0.5
PR21	0.6	0.6	0.6	0.6
PR31	0.7	0.7	0.7	0.7
a11	0.15	0.15	0.05	0.05
a21	0.14	0.14	0.06	0.06
a31	0.71	0.71	0.07	0.07
Lx	2.375273	2.375273	1.718282	1.71828
Tl	1000	1000	50	50
a	1	1	1	1
B	1.07	1.07	0.8	0.8
I1	0.2983710	0.2983710	0.2983710	0.2983710
I2	0.2983710	0.2983710	0.2983710	0.2983710
I3	0.2983710	0.2983710	0.2983710	0.2983710
P11	0.5072075	0.5072075	0.5072075	0.5072075
P21	0.4717468	0.4717468	0.4717468	0.4717468
P31	0.4258186	0.4258186	0.4258186	0.4258186
L11	0,3	0.3	0.3	0.3
L21	0.33	0.33	0.33	0.33
L31	0.37	0.37	0.37	0.37
R11	0.00007	0.00007	0.00007	0.00007
R21	0.0006	0.0006	0.0006	0.0006
R31	0.005	0.005	0.005	0.005

TABLE IV. OPTIMAL SOLUTION FOR ORIGINAL MODELS FOR α CONSTANT AND β VARIABLE IN BANDWIDTH QOS

Var	pqij increase x increase	pqij increase x decrease	Pqij decrease x increase	Pqij decrease x decrease
Model Class	INLP	INLP	INLP	INLP
State	Local Opt	Local Opt	Local Opt	Local Opt
Objective	125.681	125.625	67.7576	67.7576
Infeasibility	0.015	0.011	0	0
Iter	24	24	13	13
GMU	34K	34K	34K	34K
ER	0s	0s	0s	0s

TABLE V. OPTIMAL SOLUTION FOR MODELS FOR α CONSTANT AND β VARIABLE IN BANDWIDTH QOS

Var	pqij increase x increase	pqij increase x decrease	Pqij decrease x increase	Pqij decrease x decrease
Model Class	NLP	NLP	NLP	NLP
State	Local Opt	Local Opt	Local Opt	Local Opt
Objective	791.434	791.378	734.563	733.511
Infeasibility	0	0	0	0
Iter	14	14	14	14
GMU	43	43	43	43
ER	0	0	0	0

TABLE VI. VARIABLE VALUES FOR MODELS FOR α CONSTANT AND β VARIABLE IN BANDWIDTH QOS

Var	pqij increase x increase	pqij increase x decrease	Pqij decrease x increase	Pqij decrease x decrease
PQ11	8.467116	8.458654	0.2214369	0.2214369
PQ21	7.902640	7.894741	0.2066745	0.2066745
PQ31	40.07769	40.03763	1.048135	1.048135
X	1	1	0	0
PB11	3.562910	3.562910	0.1288711	0.1288711
PB21	3.325382	3.325382	0.1202797	0.1202797
PB31	16.86444	16.86444	0.6099900	0.6099900
PR11	0.5	0.5	0.5	0.5
PR21	0.6	0.6	0.6	0.6
PR31	0.7	0.7	0.7	0.7
a11	0.15	0.15	0.15	0.15
a21	0.14	0.14	0.14	0.14
a31	0.71	0.71	0.71	0.71
Lx	2.375273	2.375273	1.718282	1.71828
Tl	1000	1000	50	50
a	1	1	1	1
B	1.07	1.07	0.8	0.8
β 1	0.5	0.5	0.5	0.5
β 2	0.5	0.5	0.5	0.5
β 3	0.5	0.5	0.5	0.5
I1	0.2983710	0.2983710	0.2983710	0.2983710
I2	0.2983710	0.2983710	0.2983710	0.2983710
I3	0.2983710	0.2983710	0.2983710	0.2983710
Λ11	0,3	0.3	0.3	0.3
Λ21	0.33	0.33	0.33	0.33
Λ31	0.37	0.37	0.37	0.37
P11	0.00007	0.00007	0.00007	0.00007
P21	0.0006	0.0006	0.0006	0.0006
P31	0.005	0.005	0.005	0.005

- α and β variable in bandwidth QoS:

Based on the objective function (68) and the equations from (2) to (32) and (46) to (50) and additional constraints (60) to (66): The optimal solution is summarized in Tables VII and VIII for each case of the bandwidth features that were solved using Lingo18.

We note from Table VIII that the first case achieved the best result, I need to get the results 14 iterations and the value of the memory used is 45. From Table IX, we notice that the values of the variables in the first and second cases are close, while in the 3 and 4 the results are identical. The first case gives the best results for the values of the variables. By comparing the objective value between the two models, we see that our model outperforms the previous model is 164.449

TABLE VII. OPTIMAL SOLUTION FOR ORIGINAL MODELS FOR α AND β VARIABLE IN BANDWIDTH QOS

Var	pqij increase x increase	pqij increase x decrease	Pqij decrease x increase	Pqij decrease x decrease
Model Class	INLP	INLP	INLP	INLP
State	Local Opt	Local Opt	Local Opt	Local Opt
Objective	629.681	692.625	634.758	634.758
Infeasibility	0	0	1.1x10-16	1.1x10-16
Iter	12	12	13	13
GMU	35K	35K	35K	35K
ER	0s	0s	0s	0s

TABLE VIII. OPTIMAL SOLUTIONS FOR MODELS FOR α AND β VARIABLE IN BANDWIDTH QOS

Var	pqij increase x increase	pqij increase x decrease	Pqij decrease x increase	Pqij decrease x decrease
Model Class	NLP	NLP	NLP	NLP
State	Local Opt	Local Opt	Local Opt	Local Opt
Objective	794.130	794.076	736.211	736.211
Infeasibility	0	0	0	0
Iter	14	14	14	14
GMU	45	45	43	43
ER	0	0	0	0

TABLE IX. VARIABLE VALUES FOR MODELS FOR α AND β VARIABLE IN BANDWIDTH QOS

Var	pqij increase x increase	pqij increase x decrease	Pqij decrease x increase	Pqij decrease x decrease
PQ11	8.467110	8.458654	0.2214369	0.2214369
PQ21	7.902642	7.894743	0.2066745	0.2066745
PQ31	40.07768	40.03763	1.048135	1.048135
X	1	1	0	0
PB11	3.562910	3.562910	0.1288711	0.1288711
PB21	3.325383	3.325383	0.1202797	0.1202797
PB31	16.86444	16.86444	0.6099900	0.6099900
PR11	0.5	0.5	0.5	0.5
PR21	0.6	0.6	0.6	0.6
PR31	0.7	0.7	0.7	0.7
a11	0.15	0.15	0.15	0.15
a21	0.14	0.14	0.14	0.14
a31	0.71	0.71	0.71	0.71
Lx	2.375273	2.375273	1.718282	1.71828
***T*i**	1000	1000	50	50
α	1	1	1	1
B	1.07	1.07	0.8	0.8
β 1	0.5	0.5	0.5	0.5
β 2	0.5	0.5	0.5	0.5
β 3	0.5	0.5	0.5	0.5
I1	0.2983710	0.2983710	0.2983710	0.2983710
I2	0.2983710	0.2983710	0.2983710	0.2983710
I3	0.2983710	0.2983710	0.2983710	0.2983710
α 1	1	1	1	1
α 2	1	1	1	1
α 3	1	1	1	1
L11	0,3	0.3	0.3	0.3
L21	0.33	0.33	0.33	0.33
L31	0.37	0.37	0.37	0.37
R11	0.00007	0.00007	0.00007	0.00007
R21	0.0006	0.0006	0.0006	0.0006
R31	0.005	0.005	0.005	0.005

- α variable and β constants in bandwidth Qos

Based on the objective function (67) and the equations from (2)-(32), (34)-(42), (54)– (56), and additional constraints (68) and (69). The optimal solution is summarized in Tables XI and XII for each case of the bandwidth features. We note from Table XI that the first case achieved the best result; it needs to get the results 14 iterations and the value of the memory used is 45.

From Table XII we notice that the values of the variables in the first and second cases are close, while in the 3 and 4 the results are identical. The first case gives the best results for the values of the variables. By comparing the optimal solution between the original model in Table X and the modified models in Table XI, we see that our model outperforms the previous model by 101.453.

- Comparison of optimal solutions between modified model [23] , [17] , and [22].

In this section, we compare the three models that used the bandwidth attribute in a single-link wireless network.

By comparing the results, we notice that our model [13] is better as it reaches the best profit (794.134) the results showed in Table XV. While in the model [17] , the best solution was (692,681) as showed in Table XIV. In the model [22], the best profit was 32.68 as shed in Table XIII.

TABLE X. OPTIMAL SOLUTION FOR ORIGINAL MODELS FOR α VARIABLE AND β CONSTANT IN BANDWIDTH QOS

Var	pqij increase x increase	pqij increase x decrease	Pqij decrease x increase	Pqij decrease x decrease
Model Class	INLP	INLP	INLP	INLP
State	Local Opt	Local Opt	Local Opt	Local Opt
Objective	692.681	692.625	634.758	634.758
Infeasibility	0	0	0	0
Iter	13	13	14	14
GMU	35K	35K	35K	35K
ER	0s	0s	0s	0s

TABLE XI. OPTIMAL SOLUTIONS FOR MODELS FOR α VARIABLE AND β CONSTANTS IN BANDWIDTH QOS

Var	pqij increase x increase	pqij increase x decrease	Pqij decrease x increase	Pqij decrease x decrease
Model Class	NLP	NLP	NLP	NLP
State	Local Opt	Local Opt	Local Opt	Local Opt
Objective	794.130	794.076	736.211	736.211
Infeasibility	0	0	0	0
Iter	14	14	14	14
GMU	45	45	43	43
ER	0	0	0	0

TABLE XII. VARIABLE VALUES FOR MODELS FOR α VARIABLE AND β CONSTANTS IN BANDWIDTH QOS

Var	pqij increase x increase	pqij increase x decrease	Pqij decrease x increase	Pqij decrease x decrease
PQ11	8.467110	8.458654	0.2214369	0.2214369
PQ21	7.902642	7.894743	0.2066745	0.2066745
PQ31	40.07768	40.03763	1.048135	1.048135
X	1	1	0	0
PB11	3.562910	3.562910	0.1288711	0.1288711
PB21	3.325383	3.325383	0.1202797	0.1202797
PB31	16.86444	16.86444	0.6099900	0.6099900
PR11	0.5	0.5	0.5	0.5
PR21	0.6	0.6	0.6	0.6
PR31	0.7	0.7	0.7	0.7
a11	0.15	0.15	0.15	0.15
a21	0.14	0.14	0.14	0.14
a31	0.71	0.71	0.71	0.71
Lx	2.375273	2.375273	1.718282	1.71828
Tl	1000	1000	50	50
a	1	1	1	1
B	1.07	1.07	0.8	0.8
β 1	0.5	0.5	0.5	0.5
β 2	0.5	0.5	0.5	0.5
β 3	0.5	0.5	0.5	0.5
I1	0.2983710	0.2983710	0.2983710	0.2983710
I2	0.2983710	0.2983710	0.2983710	0.2983710
I3	0.2983710	0.2983710	0.2983710	0.2983710
α 1	1	1	1	1
α 2	1	1	1	1
α 3	1	1	1	1
Λ11	0,3	0.3	0.3	0.3
Λ21	0.33	0.33	0.33	0.33
Λ31	0.37	0.37	0.37	0.37
P11	0.00007	0.00007	0.00007	0.00007
R21	0.0006	0.0006	0.0006	0.0006
R31	0.005	0.005	0.005	0.005

TABLE XIII. OPTIMAL SOLUTION OF ORIFGINAL MODELS OF WIRELESS INTERNET PRICING SCHEME ON BANDWIDTH QOS ATTRIBUTE [22]

Var	pqij increase x increase	pqij increase x decrease	Pqij decrease x increase	Pqij decrease x decrease
Model Class	NLP	NLP	NLP	NLP
State	Local Opt	Local Opt	Local Opt	Local Opt
Objective	32.68	32.68	1.816	1.816
Infeasibility	0	0	1.3×10^{-17}	$1.3\text{x}10^{-17}$
Iter	11	11	11	11
GMU	24k	25k	25k	25 k
ER	0	0	0	0

TABLE XIV. OPTIMAL SOLUTION MODELS OF WIRELESS INTERNET PRICING SCHEME ON BANDWIDTH QOS ATTRIBUTE [17]

Var	α and β constant	α constant and β variable	α and β variable	α variable and β constant
Model Class	INLP	INLP	INLP	INLP
State	Local Opt	Local Opt	Local Opt	Local Opt
Objective	125.681	125.681	692.625	692.681
Infeasibility	0	0	0	0
Iter	13	13	13	13
GMU	32K	32K	35K	35K
ER	0	0	0	0

TABLE XV. OPTIMAL SOLUTION OF MODIFIED MODEL OF WIRELESS INTERNET PRICING SCHEME ON BANDWIDTH QOS ATTRIBUTE [13]

Var	α and β constant	α constant and β variable	α and β variable	α variable and β constant
Model Class	NLP	NLP	NLP	NLP
State	Local Opt	Local Opt	Local Opt	Local Opt
Objet	791.567	791.434	794.120	794.134
Infeasibility	0	0	0	0
Iterations	14	14	14	14
GMU	44k	44k	44k	44k
ER	0s	0s	0s	0s

IV. CONCLUSION AND FUTURE WORK

The basic price of the service has a major role in increasing the profit when it is variable, even though the quality of the service is constant, and this is proven by the results we have reached through the comparisons shown in the previous tables. In addition, an increase in the cost of service quality, and a variance in service quality categories, which will be reflected in an increase in service cost. In our improved model, we see that the best result is 794.134, which is in the case that the basic price (α) is variable and the premium quality (β) is constant. For more future studies, it is possible to apply other features of the model and compare the various features to get the best scheme in addition to addressing the topic in terms of multi-links.

ACKNOWLEDGMENT

The research leading to this paper was financially supported by the Ministry of Higher Education Malaysia for support through Fundamental Research Grant Scheme 2020, Research Code: USIM-FRGS-FKAB-055002/53619.

REFERENCES

[1] E.-I. Apăvăloaie, “The impact of the internet on the business environment,” Procedia Econ. Financ., vol. 15, pp. 951–958, 2014.

[2] N.Husein, A.Rahman, and D.Dahnil, “Evaluation of LoRa-based Air Pollution Monitoring System,” Evaluation, vol. 10, no. 7, 2019.

[3] J. Byun and S. Chatterjee, “A strategic pricing for quality of service (QoS) network business,” AMCIS 2004 Proc., p. 306, 2004.

[4] C. A. Martínez, D. A. L. Sarmiento, J. J. R. Ochoa, and R. D. G. Tovar, “Performance assessment of diffserv and intserv services in qos on an academic network using ns2,” Tecciencia, vol. 7, no. 14, pp. 65–75, 2013.

[5] Indrawati, Irmeilyana, Puspita, F. M., & Sanjaya, O. (2015). Internet pricing on bandwidth function diminished with increasing bandwidth utility function. TELKOMNIKA, 13(1), 299-304

[6] Puspita, F. M., Seman, K., Taib, B. M., & Abdullah, I. (2017). The Comparison Of Internet Pricing Scheme In Multi Link Bottleneck Multi Service Network. Paper presented at the 6th International Conference on Computing and Informatics 2017 (ICOCI2017). Universiti Utara Malaysia, Sepang, Malaysia.

[7] G. Kesidis, A. Das, and G. de Veciana, “On flat-rate and usage-based pricing for tiered commodity internet services,” in 2008 42nd Annual Conference on Information Sciences and Systems, 2008, pp. 304–308.

[8] F. M. Puspita, E. Yuliza, W. Herlina, Y. Yunita, and R. Rohania, “Improved Multi Service-Reverse Charging Models for the Multi Link Internet wireless Using QOS Bit Error Rate QoS Attribute,” Sci. Technol. Indones., vol. 5, no. 1, pp. 6–13, 2020.

[9] F. M. Puspita, W. Herlina, S. Anggraini, B. Arisha, and Y. Yunita, “Improved internet wireless reverse charging models under multi link service network by end-to-end delay QoS attribute,” in 2019 International Seminar on Research of Information Technology and Intelligent Systems (ISRITI), 2019, pp. 182–187.

[10] R. Sitepu, F. M. Puspita, A. N. Pratiwi, and I. P. Novyasti, “Utility Function-based Pricing Strategies in Maximizing the Information Service Provider’s Revenue with Marginal and Monitoring Costs.,” Int. J. Electr. Comput. Eng., vol. 7, no. 2, 2017.

[11] C. Gu, S. Zhuang, and Y. Sun, “Pricing Incentive Mechanism based on Multi-stages Traffic Classification Methodology for QoS-enabled Networks,” J. Networks, vol. 6, no. 1, p. 163, 2011.

[12] P. Loiseau, G. Schwartz, J. Musacchio, and S. Amin, “Incentive schemes for internet congestion management: Raffles versus time-of-day pricing,” in 2011 49th Annual Allerton Conference on Communication, Control, and Computing (Allerton), 2011, pp. 103–110.

[13] M. S. N.Hussein, K.Seman, F.Puspita, K.Abdulrahim, “Improved Model of Internet Pricing Incentive Mechanism based on Multi bottleneck Links in Multi QoS Networks,” 2021.

[14] D. Ros and B. Tuffin, “A mathematical model of the Paris metro pricing scheme for charging packet networks,” Comput. Networks, vol. 46, no. 1, pp. 73–85, 2004.

[15] S. Wu, P. Y. Chen, and G. Anandalingam, “Optimal pricing scheme for Information Services,” Univ. Pennsylvania Philadelphia, 2002.

[16] F. M. Puspita and M. Oktaryna, “Improved bundle pricing model on wireless internet pricing scheme in serving multiple qos network based on quasi-linear utility function,” in 2017 International Conference on Electrical Engineering and Computer Science (ICECOS), 2017, pp. 38–43.

[17] Irmeilyana, Puspita, F. M., Indrawati, Agustin, R. T., & Ulfa, M. (2017). Wireless single link pricing scheme under multi service network with bandwidth QoS attribute. ARPN Journal of Engineering and Applied Sciences. , 12(12).

[18] I. Irmeilyana, F. M. Puspita, I. Indrawati, and T. A. Rahayu, “Bit Error Rate (BER) QoS Attribute in Solving Wireless Pricing Scheme on Single Link Multi Service Network,” Int. J. Electr. Comput. Eng., vol. 8, no. 1, p. 236, 2018.

[19] Irmeilyana, Puspita, F. M., & Husniah, I. (2016). Optimization of Wireless Internet Pricing Scheme in Serving Multi QoS Network Using Various QoS Attributes. TELKOMNIKA, Telecommunication, Computing, Electronics and Control, 14(1).

[20] S. Sain and S. Herpers, “Profit maximization in multi service networks-an optimization model.,” in ECIS, 2003, pp. 1653–1669.

[21] I. Indrawati, I. Irmeilyana, F. M. Puspita, and M. P. Lestari, “Cobb-Douglass Utility Function in Optimizing the Internet Pricing Scheme Model,” TELKOMNIKA (Telecommunication Comput. Electron. Control., vol. 12, no. 1, pp. 227–240, 2014.

[22] E. Wallenius, T. Hpmhihinen, I. P. M. Networks, and M. I. Technology, “PRICMG MODEL FOR 3G/4G NETWORKS,” no. 1, pp. 187–191, 2002.

[23] N.Hussein, K.Seman, F.Puspita, K.Abdulrahim,M.Saharim “Improved Incentive Pricing Wireless Multi-Service Single Link With Bandwidth Attribute,” Int. J. Adv. Comput. Sci. Appl., vol. 12 No 7 Ju, 2021.

Drip Irrigation Detection for Power Outage-Prone Areas with Internet-of-Things Smart Fertigation Managemant System

Dahlila Putri Dahnil[1], Zaihosnita Hood[2], Afzan Adam[3]
Center for Software Technology and Management[1, 2]
Center for Artificial Intelligence and Technology[3]
Faculty of Information Sciences and Technology
Universiti Kebangsaan Malaysia, Bangi, Selangor, Malaysia

Mohd Zulhakimi Ab Razak[4]*, Ahmad Ghadafi Ismail[5]
Institute of Microenginnering and Nanoelectronics
Universiti Kebangsaan Malaysia
Bangi, Selangor, Malaysia

***Abstract*—In drip irrigation agriculture or fertigation technique, sufficient amount of water and nutrients are crucial for a plant's growth and development. An electronic timer is usually used to control the plant watering automatically and the scheduling is set according to different levels of plant growth. The timer has to be adjusted frequently since the required amount of water is different according to the growth stages. In power outage-prone regions, the problem with scheduled irrigation using timer becomes worsen since the watering schedule is disrupted by occasional black-outs, leading to an insufficient supply of water and nutrients, which leads to poor crop yields. Typical solution for such problems is by hiring field works to monitor the functionality of the automated system, plant health, and to re-adjust the timer once a power outage occurs. However, this solution is ineffective, time-consuming, and acquires high overhead costs. This paper proposes a systematic irrigation method using the internet-of-things (IoT) framework in order to improve the monitoring of plant growth and consequently improves the efficiency of the workflow. This systematic fertigation monitoring system consists of power outage alerts, and on-line notifications of plant irrigation, pesticide delivery, and polybag cleaning schedule. As a result, by using the proposed system, higher efficiency in farming management is achieved, with a 40% reduction in manpower, as compared to a typical fertigation-based farming system. This system demonstrates greater control over irrigation scheduling, plant growth, recording of pesticide scheduling automatically, and polybag cleaning, all of which will improve crop yields significantly.**

Keywords*—Irrigation technique; water and nutrient; automatic drip irrigation; crop; power-outage

I. Introduction

The advancement in technology has influenced modern farming methods significantly and agricultural environment particularly. The agricultural landscape has shifted from conventional farming to digitized farming with the merging of interrelated computing devices, sensors, and cloud edge [1-5]. In addition, the combination of engineering and computing technology, equipped with sensors for agricultural activities, has enabled smart farming [6]. As the demand for food sources increases around the world, irrigation has grown even more necessary to prevent famine and nutritional deaths [7].

Advanced irrigation techniques are essential in order to achieve efficient irrigation management, and an optimal agriculture management system will ensure productivity, and environmental and economic viability [7-10]. Most techniques, such as regulated deficit irrigation [11], automated drip fertigation [10,12-13] and precision irrigation systems offer the opportunity to conserve irrigation water, improve fruit quality, increasing crop yield and decreasing costs while contributing to environmental sustainability [14-15].

The motivation of this study is to improve the management system of the irrigation scheduling by providing farmers with real-time feedback during irrigation so that they are notified of any abrupt loss of electricity, and can act based on the information provided by the system. This enables farmers to decide which nutrients should be received by the plant by controlling the timing of the irrigation. The system is easy to deploy in existing drip fertigation systems, with a plug-and-play module insertion. The application also aims to provide farmers and farm workers with a user-friendly tool that facilitates the management of pesticides and drip maintenance. Instead of manually entering records, farmers can track pesticide schedules through the system, which makes the process more manageable. It is expected that the proposed system could improve the crops yield as well as equipped the farmers with an improved and smart farming management system. The results demonstrated that the developed system could effectively facilitate fertigation management for outage-prone areas and substantially decrease the need for on-site monitoring.

The rest of the manuscript is organized as follows. Section 2 describes related work in the area of advanced irrigation. Section 3 describes the user-friendly platform of the proposed system. This section also describes the real-time irrigation feedback, which records current and past irrigation durations, as well as the alert system, which notifies farmers of any absence of electricity. Section 4 describes the implementation of the system and discusses the results, and Section 5 presents the concluding remarks and future research.

*Corresponding Author

II. Overview of Drip Fertigation Methods

Drip fertigation system is gradually gaining acceptance, and is becoming more attractive to many farmers since it supplies nutrients and water to the plant root zone more effectively than conventional planting [16]. To date, [17] have attempted to design an automatic irrigation system, but its implementation on actual farming sites has not been fully investigated. Another study to improve the drip irrigation technique was recently designed by [18]. Using this technique, farmers do not have to manually mix the fertilizer, which requires them to read the EC and pH of the mixture. Slow adoption of drip fertigation technology might be caused by low exposure, lack of expert techno-logical support, and the high cost of implementation, which includes hardware with computing, storage, and communication capabilities.

The automated drip fertigation system is more appealing to farmers worldwide, and has been gradually replacing conventional methods of farming. This is mainly due to the improvement in the quality of crops and agricultural products, as adequate nutrition is delivered directly to the plant root zone [19]. Such system saves significant amount of time when scheduled irrigation is performed remotely by turning pumps and valves on and off [20]. In a study done by [21], productivity for crops such as ginger shows increment in net income due to an increase in the yields of ginger. The crop productivity is almost doubled per hectare with an automatic drip fertigation system, compared to more conventional methods. Although the drip fertigation system requires a large amount of initial capital, the cost will be compensated by high crop productivity. In [22], the authors introduce a real-time irrigation system, named REUTIVAR, which calculates irrigation timing and fertilizer amount required in real-time using reclaimed water to watering olive tree. This technique will determine the timing of irrigation and fertigation events and can optimize fertilizer injection, the stabilization time and cleaning phase.

The development of useful new models based on the decision support system (DSS) has improved the automatic irrigation system [23-24]. An optimized DDS with a modified fertigation systems (DSS-FS) is designed primarily for drip and sprinkler irrigation, based on an environmental sustainability approach [25]. Meanwhile, [20] developed a DSS system to provide insight into the irrigation time required for a given crop and how irrigation schedules would change with soil types. All of these DSSs and models are very helpful in optimizing the use of water and fertilizer, and managing the centralized fertigation system in a water distribution network. However, the effects of occasional power outages on a scheduled drip fertigation system have not been investigated. Occasional power failures disrupt the time required for irrigation, unfortunately lead to an insufficient supply of water, and will affect crop growth.

In order to improve network performance to achieve more reliable smart farming system, an adaptive technique was introduced to maintain reliable network connection to transmit sensor data to base station by adaptively change the communication protocol between IEEE 802.11ac and LoRaWAN [26]. This technique is particularly useful to manage large farming sites at different location. On the other hand, Agri-Info, a cloud based autonomic resource management technique for agriculture service was introduced in order to maintain required level of QoS. This method makes use of Fuzzy logic for making decisions based on defined rules to diagnose status as well as schedule the resources automatically [27].

In Malaysia, farmers have started to use the automatic drip fertigation system. However, due to poor technical knowledge and the initial development cost of the system, the farmers prefer not to use the DSS, and decide to manage their planting based on their experience instead. This is also the reason farmers opt to hire workers to man-age scheduled irrigation through on-site monitoring during power failure, which is very tedious and time-consuming, and in doing so, results in high man-power utilization.

The lack of technological advancement in drip fertigation has left farmers with no option but to use the commercial irrigation controllers available at the market, which are pre-programmed to supply water at predefined intervals. Typical drip fertigation system uses a timer and a valve to turn on the water pump for irrigation. Fig. 1 shows a typical fertigation system that consists of a water tank, a timer, a water filter, a water pump, garden accessories, and a piping system to channel water to individual pots [28-29]. These pots are arranged horizontally on the ground or vertically with supporting poles. The water supply is pre-program and follows a preset schedule. The amount of water and nutrients required by each plant is different each week, and normally depends on the stage of growth. Table I shows the required amount of water and nutrients required during the first three weeks of growth [30]. This table indicates that 600 ml is the total amount of water required per day for vegetables such as spinach and eggplants [31].

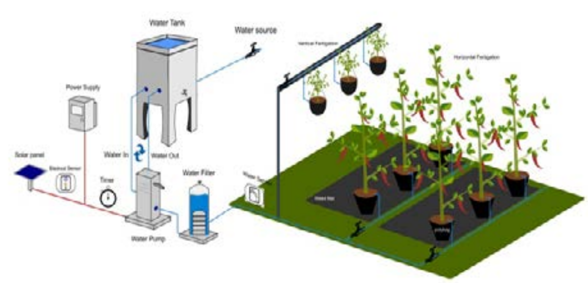

Fig. 1. The Fertigation System.

TABLE I. Volume of Water Required in Three Weeks Growth

No	Time (hrs)	Description
1	0730	150ml water and nutrient
2	0830	150ml water and nutrient
3	1100	150ml water
4	1700	150ml water

Medium- and small-scale drip fertigation farms still use the old and conventional method of observing the plantation site to check the growth of the plants. Field workers are required to monitor faults in the irrigation system and to perform regular checks on the plants' leaves and roots for possible plant disease infection. The only way to deter-mine poor plant growth is to examine the condition of the leaves and roots. Yellowish or wilting leaves are signs of poor growth. This farming workflow results in inefficient monitoring, especially when the plantation site holds thou-sands of pots. Fig. 2 shows the process in a fertigation system implemented for a local chili variety called Centil.

Centil (Capsicum Frustecens) is a type of red chili currently grown in Johor, Malaysia on a farming area with 1,000 pots [32]. Workers observe the irrigation process for 20 minutes in the morning and 20 minutes in the afternoon, and spend an additional 40 minutes every evening inspecting plants for general health and wilting leaves. They spend another 20 minutes in the evening inspecting for pests and diseases and administering pesticides. They perform maintenance and polybag cleaning once a week for 30 minutes. These processes are repeated until harvesting day. The detailed activities of the farming process are presented in Table II.

In areas where occasional power outages occur, the irrigation schedule, which is based on the needs of each plant, is often disturbed. Instead of turning to technological solutions, farmers prefer to hire more workers to look for faults in the irrigation system. With the current practice of having workers observe on-site, adding more workers to monitor faults results in inefficient irrigation management and high costs in labor, which in turn fails to offset the initial investment. Such a fertigation strategy defeats the purpose of an automatic irrigation and water management system, and could worsen depending on the solution taken by the farmers.

Previous work in the irrigation field focused on calculating irrigation requirements, where crop details fetched from the user were taken as input to estimate water requirements with the help of sensors. However, with scheduled irrigation, water and nutrient requirements cannot be fulfilled when the process is disturbed by an electrical power outage. Detailed information on the nutrients supplied is lost and irretrievable. The system shuts down, and the sensors do not capture information during the absence of electricity. This condition will go unnoticed without any notification to the farmers, and will last until power returns, which may take hours or even days. The problem becomes more serious during dry seasons and in remote farming areas, where farmers are not aware of such situations.

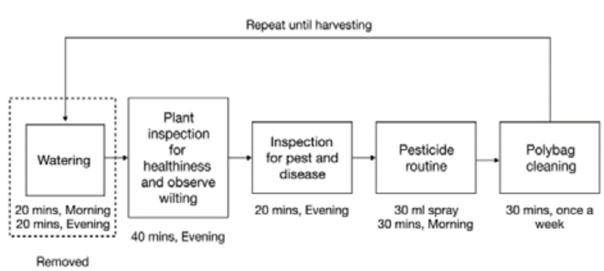

Fig. 2. Manual Process of Monitoring Plant Growth.

TABLE II. DETAILED ACTIVITIES FOR FERTIGATION FARMING

Activity	Detailed activity	Note	Duration	Frequency	No of People
Preparation of plant bag	1. Turn on the water pump to see if there is a pipe leak or a clog.	2-5 days before planting	15 mins	once a day	5
	2. Turn on the water pump to moisten the soil before planting the seedlings.		15 mins	once a day	5
Supervision after planting	1. Turn on the water pump to water the seedlings.	1-2 days after planting	20 mins	morning	5
	2. Ensure the seedlings are not infected with pests and diseases.		20 mins	afternoon	
			20 mins	once a day	5
	3. Turn on the water pump to fertilise the seedlings for the first time and pour out the stagnant water.	3 days after planting	20 mins	morning	5
			20 mins	afternoon	
	4. Turn on the water pump once every morning to fertilise the plants.	4-7 days after planting	30 mins	morning	5
			40 mins	Afternoon	
	5. Plant inspection to check whether the plants are healthy.		30 mins	once a day	5
	6. Note if the plant starts to wither. If yes, check the piping system.		30 mins	once a day	5
	7. Fertilise the plants twice a day using the fertigation system.	7 days after planting	20 mins	morning	5
			20 mins	afternoon	

All of these works provide interesting information on advanced technologies for irrigation systems, mostly focusing on optimizing water usage and crop productivity. However, any sensor data or video images of a given farm can-not be transmitted to a processing center or server in the absence of electricity. Under these circumstances, a system cannot perform real-time monitoring, which is crucial for agricultural applications. Real-time monitoring is essential because it provides timely information on the actual status of farming sites, such as the volume of water and fertilizer received, which is an important factor in improving crop production. Thus, having a system to access real-time data through a mobile application during power failure would allow farmers to respond and act to the situation in timely manner.

III. Methodology of the Proposed Solution

In this section, we describe the complete system of the proposed automated monitoring system for watering and power outage alerts, with pesticide and polybag cleaning notifications. The proposed monitoring system comprises of three main components: (i) the overall system architecture; (ii) the sensor systems; and (iii) the mobile and web applications monitoring interfaces, as shown in Fig. 3.

In Fig. 3, a system administrator is in charge of the farming system. This figure also shows that the farmers will use the mobile application to monitor the system, receiving alerts and notifications, and interact with the system for pesticide scheduling and polybags maintenance. The watering and power outage sensors are designed to detect whether the plants have been watered, and to alert farmers through mobile notifications when a power failure occurs. The notifications and alerts are sent through Global System for Mobile Communications (GSM) to the internet service provider [33], then to a cloud server for data storage and processing.

A. System Architecture

Our proposed monitoring system, as shown in Fig. 4, consists of integration of sensors with the existing fertigation system. The water sensor will be installed in the main distribution pipe, and on the other hand, the power outage sensor will be installed on the power supply line. The proposed system was developed by taking into account the important layers of the IoT architecture [34]. We introduced another layer for troubleshooting and debugging the sensors. This includes fixing the devices' programming errors. In the second layer, we have our proposed watering and power outage detection sensors, which are connected to an Arduino-based processor for data processing. For data transmission to the cloud server, the devices connect wirelessly via a GSM module, which is on the third layer. The cloud server is on the fourth layer, where all data is sent using the "post" application programming interface (API) via a GSM module to the backend cloud processor. The cloud services will cover all "post" and "get" APIs from the GSM module and mobile applications. Lastly, we have a mobile application for monitoring and interaction, and a web server for managing the system, as shown in Fig. 5.

The interaction between the hardware, backend processor, and mobile applications is shown in Fig. 6. Arduino will send the "post" API to the backend processor on the cloud via a GSM module. When the backend processor receives the API, it will log it and update the record in the database. If a notification is required, backend processor will trigger the Firebase server, which will then push the notification to our mobile application so that farmers will receive the notification on their smartphones. For information updates, the mobile application will send the "post" and "get" APIs to request that the data be updated on the app. The cloud server acts as an intermediary between the sensors and the mobile application.

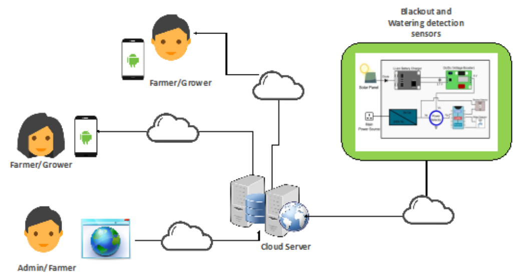

Fig. 3. Components of the Fertigation System.

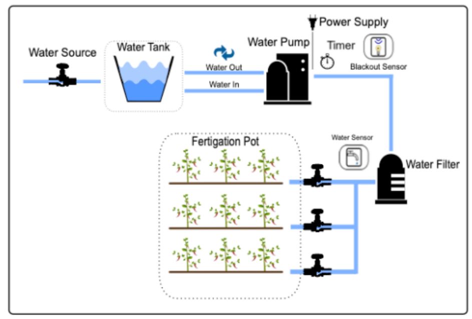

Fig. 4. The Proposed Fertigation System.

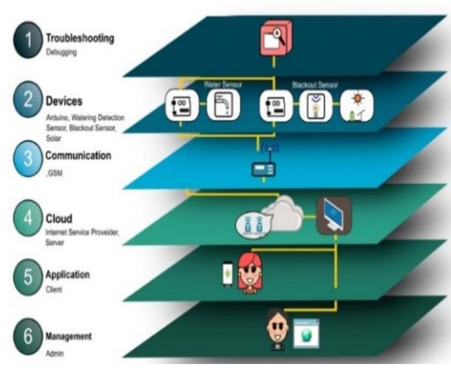

Fig. 5. Proposed System Architecture.

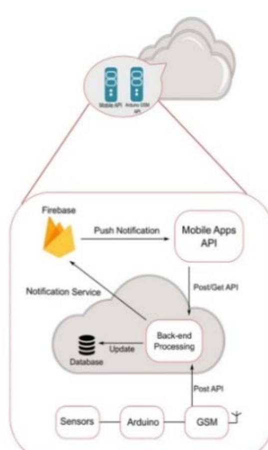

Fig. 6. The Interaction between Hardware, Mobile Apps and the Backend Server.

B. Sensor System

The power outage sensor is powered by a 240 VAC main power source that in turn is converted to a direct current (DC), which provides nine VDC to the system by using an adaptor, as shown in Fig. 7. This is the main power source for the fertigation system. The auxiliary power comes from the solar panel, which charges a 3.7V 18650 Li-ion battery. The voltage from the battery is then boosted to 9V and fed to a power selector circuit prior to Arduino. The power selector takes the power in such a way that the power always comes from the main power source, except during a power outage, when it takes the power from the charged battery.

This power switch is instantaneous, similar to an uninterrupted power supply (UPS), so that Arduino does not re-boot. In the event of a power outage, the system will automatically switch to the solar-powered battery. While the system is using the battery, the transition causes the system to send a "power down" API token through a GSM module to the backend processing cloud server. When the server receives the "power outage" API token, a power outage notification is sent to a Firebase server, which will then push it to the mobile application. The dashboard will display the power outage status, which will read "blackout has occurred" in red. This function notifies growers immediately when the system is no longer using the main power source. Thus, action can be taken to troubleshoot and to fix the problem. When the power outage sensor detects that the main source is functioning again, it will send the "power up" API to the server. Fig. 8 shows the flow of the power outage sensor. The flowchart shows that the "power down" API and the "power up" API are sent to the server only when there is a change in state.

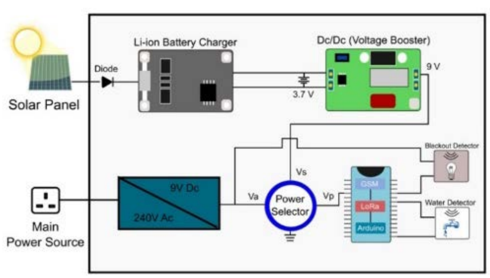

Fig. 7. The Watering and Power Outage Sensors for Fertigation System (Type A Module).

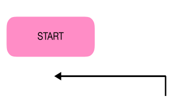

Fig. 8. Flow Chart for Power Outage Detection.

In the fertigation system, the watering schedule uses a timer to activate a water pump. The water pump releases water to the main pipe for a period of time determined by the volume of water needed for each plant. Therefore, it is crucial to know that the plant has been watered according to the schedule set by the farmers. In our proposed system, the water detection sensor is installed in the main pipe, where it will detect the presence of water. Water detection only happens if there is a change in the sensor as follows:

1) State 0 to 1 (No water is detected to Water is detected), API "watering start" is called.

2) State 1 to 0 (Water detected to No water) API "watering stop" is called.

Water detection is taken as an analogue input to Arduino. Upper and lower boundaries are required for water detection. The upper boundary is required to determine the presence of water, and the lower boundary lets the water subside in the pipe after the water pump has been turned off. The flowchart for watering detection is shown in Fig. 9.

Two states of mobile display are described as follows to let the farmers know the watering status.

1) Watering has started: Indicates that watering has been executed as scheduled and the water pump has been activated for a duration specified by user. This is activated when the sensor detects water, and the API "watering start" is called.

2) Watering has stopped: Indicates that watering has stopped, and the API "watering stop" is called when the sensor detects that the water has subsided below the lower boundaries.

We designed two modules, type A and type B, for watering and power outage sensors. For type A, the watering and power outage sensors are combined in one module. This design is suitable for fertigation sites where watering sensors can be installed in close proximity to the power outage sensor.

The type B module shown in Fig. 10 is designed for large fertigation sites. The type B module allows the watering and power outage sensors to be installed in different locations, thus increasing the flexibility for extended range. We used Long Range (LoRa) connectivity [35-37] for greater connection between the watering and power outage detection sensors before data is sent to the cloud server via the GSM module. The GSM module requires a lot of power to transmit data to the server. The LoRa wireless transmission cannot run on the Arduino Uno processor due to its large memory requirement.

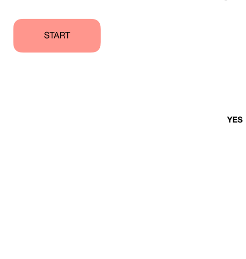

Fig. 9. Flow Chart for Watering Detection.

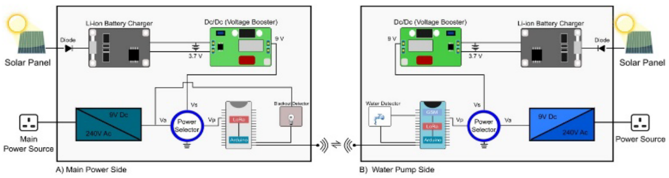

Fig. 10. The Watering and Power-outage Detection Sensors for Fertigation System (Type B Module).

C. Software System and Mobile Monitoring Interfaces

To ensure our watering and power outage detection sensors are functional 24 hours a day, Arduino will send the "I am alive" API to the server every hour. The backend processor will receive this "post" API and update the database. This information will be sent to the mobile apps when they send the "get" API, and the "sensor is online" status will appear on the mobile app dashboard. The "I am alive" flowchart is shown in Fig. 11. However, if the server does not receive this API, it will state that the system is not working and post this status on the mobile app's dashboard.

Table III shows all the "get" APIs, from the hardware to the backend processor. The backend processor will act according to the API, whether it receives data to record changes in the database or to send a notification to a Firebase server.

The proposed system consists of a web application for a system administrator or head farmer to efficiently manage the planting cycle. Fig. 12 shows the administrator page, where the administrator is responsible for adding the following information to the system.

1) *Planting schedule:* The planting schedule will have the total time of growth, from first transplanting to harvesting. The schedule contains information on when to spray pesticides and when the polybag should be maintained by which group of farmers.

2) *Authorizing the users (farmers)* in the system and assigning them to specific groups.

3) *Watering schedule:* How many times the farmers need to water the plants.

4) *Adding the pesticide routine* and assigning different groups to perform the activity.

5) *Assigning polybags cleaning* to different groups.

Fig. 11. "I am Alive" Flowchart to System Checking.

TABLE III. APIS USED FROM HARDWARE TO BACKEND SERVER

API	Descriptions
Watering Start	Water is detected. Change of state from water=0 to water=1
Watering Stop	Water is not detected. Change of state from water=1 to water=0
Power up	Main supply is detected. Change of state from power=solar to power=main
Power down	Main supply is not detected. Change of state from power=main to power=solar
I am alive	Indicates the hardware is functioning properly. If alive, status=1. If not, status=0

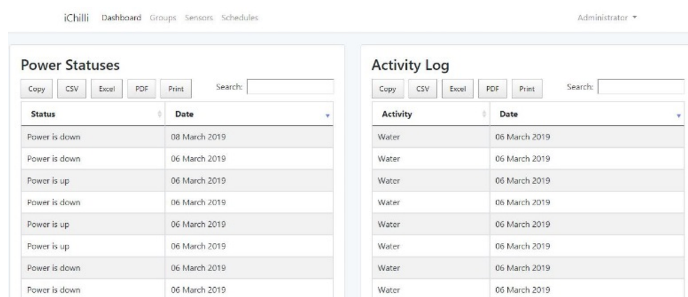

Fig. 12. The Webpage for System Administrator.

A smartphone application, called iChilli, was developed to manage planting activities more efficiently. Table IV shows the functionality of the iChilli user interface (UI). The iChilli apps displays the front page, registration page, blackout status, polybag cleaning, history, pesticide control status, and schedules. The Android-based application was developed for the following purposes:

1) To alert farmers when a power failure occurs so they can respond to it.

2) To notify farmers of the watering status so they can follow the schedule.

3) To show the history of watering so farmers can estimate the volume of water their plants received.

4) To manage pesticide activity and record the type and volume of pesticide used.

5) To assign farmers to maintain the fertigation site with activities such as cleaning and weeding.

6) To manage the planting cycle by showing the schedule for planting activities.

TABLE IV. FEATURES OF THE SMART PHONE

Dashboard	Blackout status
	Watering status
	Pesticide
	Polybag cleaning
Blackout history	By selected date
Watering history	By selected date
Pesticide control	Status: Done/Not Done
	Type: Organic/Non organic
	Quantity in Litre
Polybag cleaning	Status: Done/Not Done
	Which group performed the task
Full schedule	Day-date-time activities

D. Implementation and Evaluation

To validate our system, type A watering and power outage sensors were installed at the fertigation site. A water tank with a capacity of 70 litres and a water piping system capable of watering 1000 pots of plants are shown in Fig. 13. The farming activities under the fertigation system for the red chili Centil were used for benchmarking.

E. Wireless Connection to Cloud Server via Internet Service Provider

A GSM module is used to send data to a server in the cloud. The module is connected to the internet service provider, enabling APIs to be sent to the server. The GSM module has an LED indicator that blinks rapidly every second the GSM is not connected to the network. When the module is sending a request signal to connect to the network, the LED blinks every three seconds, and, when the blinking reaches an even slower speed, it indicates that the net-work connection has been established. Since connecting to the network requires a high current consumption, an adaptor with power ration of 9V 2A is used to power up the GSM module as shown in Fig. 14.

Fig. 13. The Fertigation Site where the System is Installed.

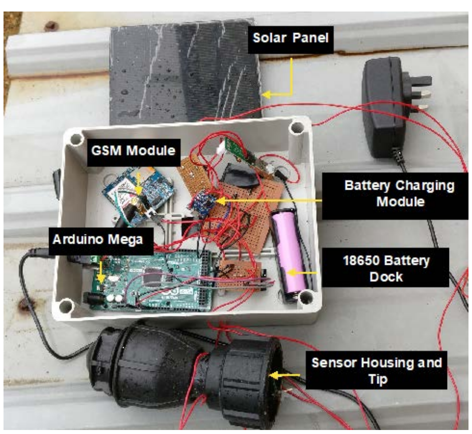

Fig. 14. The Electronic Hardware of the System.

IV. Result and Discussion

We discuss two elements for improvement. The first element involves the farming work-flow, and the second involves design-related module performance.

A. Improving Farming Work-Flow by the System

The proposed system automates the first block in Fig. 2 (namely "watering"), which has been identified as inefficient in growth monitoring. Workers are required to be on-site to observe the watering for 20 minutes in the morning and 20 minutes in the afternoon. The proposed system improved the farming work-flow by reducing manpower while maintaining the same yield production. Manpower was calculated based on three variables: project duration, number of hours per worker, and number of workers. The project duration for the chili Centil, from transplant to harvest, was six months. A worker worked for five days a week to perform daily tasks, as shown in Fig. 2 that include:

1) Observe watering: 40 minutes.
2) Plant inspection to check for health: 40 minutes.
3) Inspection for disease: 20 minutes.

Thus, the three tasks required 100 minutes (1.67 hours) for each worker per day. The calculation considered 20 working days per month for six months (120 days). The manpower calculation is shown in Table V.

A typical fertigation-based system requires 200.4 hours, whereas the proposed system requires 120 hours. Thus, with this system, we reduce man-power by 40%. The man-hour reduction would be more significant for a big farming site that requires extensive monitoring. Five workers are required for 1,000 plants, which means a larger farm's manpower can be further reduced. In the cost relationship shown in Fig. 15, the reduction in man-hours not only improved the operational cost, but increased the yield production as well.

TABLE V. MAN-POWER CALCULATION

Parameter	Current system	Proposed system
Project running days (day) 120 120	120	120
Working hours (hour)	1.67	1
Numbers of workers (person)	1	1
Man-power(hours) = day x hour x person	***200.4***	***120***

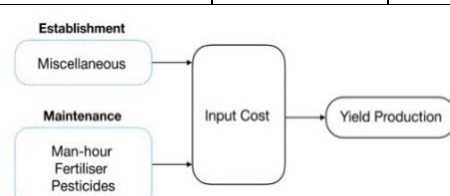

Fig. 15. Relationship between Man-hour to Yield Production.

B. Water Detection Sensor

The experiments were performed using two types of watering detection sensors. The first type was custom designed with two protruding gold pins. The pins are not connected electrically, and act as a switch. Without water presence, the sensor has an extremely low voltage (around 0.0-0.4 volts). However, when water is flowing, depending on how submerged the pins are or how strong the flow is, when more of the pins' surface area is covered with water, the voltage will increase. At the highest water flow, it is possible to achieve over 2.8 volts across the pins. In a perfect water flow system, the value will drop or rise instantly between the “water detection” and “water not detected” stages. However, due to the nature of the pipes used, some excess water may still be present in the pipes when the water stops flowing. Thus, the voltage drop is not instantaneous.

For example, from high water flow we will get 2.8 volts, and the voltage drops to 2.5 volts when the pump is stopped. As time progresses, the voltage will decrease as the water flows towards the end of the piping system and water levels drop slowly. However, this value is constantly fluctuating due to the formless nature of water, which causes some motion within the pipe. As such, it can be deduced that an optimal “water detection” voltage value would be any voltage higher than 2.7 volts (upper boundary) and “water not detected” can be any value below that (lower boundary). When the water pump is activated, there will be an instant rise in voltage, exceeding the upper boundaries, and a sudden drop in voltage to below the lower boundaries over a short period of time. Therefore, a few seconds are given for the sensor to stabilize before the API “watering start” is sent to the server.

Other experiments were conducted with a typical inline water flow sensor made for an Arduino-based environment with three pole connections for 5V voltage input, one digital data pin, and a ground pin. However, the digital pin does not connect to the standard digital input pins on Arduino, but must be connected to Arduino where Pulse Width Modulation (PWM) is allowed. This connection enables Arduino to make the necessary calculations to transcribe data from the sensor into a readable format for the user. The sensor functions through the rotational motion created by an electric rotor. The rotational speed of this rotor depends on the rate of water travelling through the sensor. The sensor, which is based on the Hall effects phenomenon, will then send a corresponding pulse signal to Arduino. The rate at which the pulse signal is received will directly correlate to the rate of water flow: that is, slower pulses mean a lower flow rate, while faster pulses mean a higher rate.

An “API Start” API token is sent when the upper boundary is reached. We calculated the upper boundary by measuring the reading of the irrigation system. The lower boundary for sending the “watering stop” API token was set to zero. This is because when the water flow stops, even though there may still be water in the pipes, the value of the water flow will be set to 0 as long as the water is not moving. The measured value of the water flow was calculated in liter per minute (l/m). Some precautionary steps were taken when using the water flow sensor. Firstly, the water flow sensor had a small diameter to allow a pipe to fit on it. Appropriate adaptors were used when the pipe was larger than the hole of the water flow sensor. Secondly, most commercial Arduino-based water flow sensors have a maximum flow rate of 30 (l/m). In addition, it is unclear if higher water flow directly influences the accuracy and efficiency of the water flow sensor. It is currently unclear if this damages or adversely affects the sensor in any way.

C. Battery-Powered Solar Cell Charging and Discharging Rate

Since the system is operated by a back-up battery in the case of power failure, we analyzed the total operating time of the back-up supply by studying the battery’s charge and discharge time. To control the charging process as well as to protect the battery from overcharging, the level at which the battery will supply sufficient power was noted.

An experiment was conducted to study the rate of power loss for the 18650 battery over time without direct power from the mains. The experiment was conducted with the system running, and voltage measurements were taken across the battery. The experiments were conducted a few times, and the average readings were calculated. The result of the discharge time is illustrated in Fig. 16.

Experiment 1 in Fig. 16 shows the voltage loss over time for a battery initially charged up to 4V. There is a slow semi-linear loss of voltage over time until around 3.3V, where the voltage will reduce exponentially until a value of 2.2V is reached. Experiment 2 was conducted to determine whether this pattern could be replicated. Experiment 2 shows the voltage loss over time for a battery that has been fully charged to 4.17V. Similar to the first experiment, the voltage indicates a slow, semi-linear decrease until around 3.3V, where the rate of voltage discharge increases tremendously in an exponential fashion. It can also be seen that the final voltage of 2.2 V will remain for a period of time and will not decrease further. During these experiments, the system was able to run as long as the voltage was above 2.2V; however, after this point, although the voltage did not decrease further, Arduino and the GSM module would be off. This indicated that the system did not have the required power to run. Experiment 1 showed that the sys-tem can run up to 6.7 hours, whereas experiment 2 showed that the system can last for 8.3 hours de-pending on the initial charged voltage of the battery.

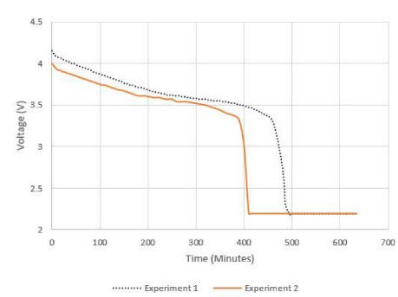

Fig. 16. Discharge Voltage over Time for Battery Powered Solar Cell.

D. Study of Switching during Power Outage

In the event of power failure, supply is cut off from the main. The designed circuit instantaneously switches to the battery charged by the solar cell. The switching processes from main supply to battery and vice versa were observed in terms of response time. In this case, the transient response of the transition time for both cases was observed. There is a small period in which the module switches to a new power source when another has stopped. Fig. 17(a) shows the voltage against the transition time between main supply and battery-powered operation. On the contrary, Fig. 17(b) shows the transient result of the voltage of the switching state between battery-operated to the adaptor-operated supplies.

Fig. 17 shows that it took 400 microseconds for both situations to switch from one state to another, as de-noted by the bandwidth of both pulses. Essentially, when the states are switched from one power source to another, this creates a transient that can be measured as denoted by the peaks in the graph. Thus, the time it takes for the switching to occur is measured by the time it takes for the transient peak to rise and fall. A short switch time is ideal, as it ensures that the system will have constant power and can efficiently switch between power sources with minimal transition. Arduino will go to reset state if the transition takes too long, and the whole system will be reset.

E. Comparison Study

Table VI highlights the comparison between the proposed system and the previously developed intelligent systems in term of key features that record real-time irrigation of plants, the duration of scheduled irrigation for each cycle, the history of nutrients supplied to the plants, and, more importantly, an alert sent to farmers so that quick action can be taken during a power outage to prevent severe damage to the plants. Our monitoring system is an attempt to present a solution that records the length of the irrigation process, notifies farmers in the event of power failure, and tracks the irrigation history through an easy-to-use mobile application that guides farmers and farm workers. The solution is a user-friendly platform that does not require any knowledge of programming.

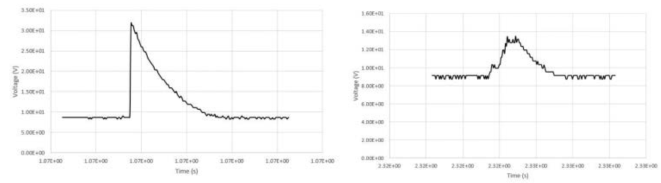

(a) (b)

Fig. 17. Switching Time Tansitions: (a) Transition between Adaptor-operated to Battery-operated Power Supplies, (b) Transition Time between Battery-operated to Adaptor-operated Power Supplies.

TABLE VI. COMPARISON TABLE OF PREVIOUS WORK

	Features					
Work	**Feature 1**	**Feature 2**	**Web or Mobile Apps**	**Agriculture Domain**	**Connectivity**	**Cloud Resources**
[1]	Monitoring and automatic irrigation system on crop water needs and real time and history of farm data	Neural based irrigation decision for ecient irrigation	Yes	Greenhouse irrigation	WiFI	Yes
[4]	a flexible platform able to cope with soilless culture needs in full recirculation greenhouses using moderately saline water	three-tier open source software platform that distributes computing at Cyber Physical Systerm, edge and cloud planes	No	Precision agriculture, greenhouse	Microwave radio link, fiber optic, DSL	Yes
[5]	a scalable network architecture for monitoring and controlling agriculture and farms in rural areas	a cross-layer-based channel access and routing solution for sensing and actuating	No	Smart farming	LoWPAN, IEEE 802.15.4, WiFi	Yes
[22]	REUTIVAR-calculates in real-time irrigation time and fertilizer amount required to olive tree using reclaimed water	Adaptive fertigation scheduling according to the actual weather conditions and adjusted the water allocation along the irrigation season	Yes	Irrigation	Mobile Server, SqLite	No, local server
[23]	a user-friendly decision support system tool for the optimization of the design and management of on-farm fertigation	determine the timing of irrigation and fertigation events and optimize fertilizer injection, the stabilization time and cleaning phase	No	Drip fertigation	No	No
[26]	Improve network performance to achieve more reliable smart farming system	Adaptive technique to maintain reliable network connection to transmit sensor data to base station by adaptively change the communication protocol between IEEE 802.11ac and LoRaWAN	No	Smart farming	LoRaWan and IEEE802.11ac	No
[27]	Agri-Info, a cloud based autonomic resource management technique for agriculture service and maintain required level of QoS	Fuzzy logic for making decisions based on defined rules to diagnose status as well as schedule the resources automatically	Yes	Agriculture-as-a-Service	Agriculture-as-a-Service	Yes
Our proposed system	Real-time irrigation tracking and record with alert to notify farmer during power outage	Tracking and recording for pesticide and maintenance	Yes	Drip fertigation	GSM module	Yes

F. Limitation and Future Work

The developed system was developed for chili fertigation farming of 1000 pots of plant. So far, it also only been tested in a location that is prone to electrical blackout. Although, the results show significant improvement over the conventional method applied on the same scope, the results and performance will be more accurate if the system is tested over various kinds of plants with larger pots (~2000 pots and more) and the data are observed over longer period of time i.e. three to six months. Furthermore, the proposed system should also be tested in various locations that are prone to blackouts to further evaluate is effectiveness and efficiency.

V. Conclusion

In this paper, we have demonstrated a systematic and automated method for monitoring large-scale chili fertigation area in order to improve the farm management efficiency and consequently to improve plant growth in a power-outage-prone area. The system, which consists of sensors for detecting irrigation activities and power outages, a mobile application to manage scheduling for pesticide delivery and polybag cleaning, and a web application to al-low farmers to manage planting schedules has shown improvement in efficiency in farming management, with a 40% reduction in manpower in this power outage-prone area, compared to a typical fertigation-based farming sys-tem in such area. The proposed system also exhibited greater control over plant growth and automatically records pesticide schedules and polybag cleaning, all of which could improve crop yields. We believe the findings and the method of using IoT platform as a systematic monitoring mechanism, presented in this paper, will pave the way and encourage further use in broader plant types, which could prove useful in a large farming area in rural sites.

Acknowledgment

The research was supported by research grants: DCP-2018-001/2, FRGS/1/2020/STG07/UKM/02/3, and GUP-2017-068.

References

[1] N. K. Nawandar, V. R. Satpute, “IoT Based Low Cost and Intelligent Module for Smart Irrigation System”. Computers and Electronics in Agriculture, Vol. 162, 2019, pp. 979-990.

[2] W. Wang, Y. Cui, Y. Luo, Z. Li, J. Tan, “Web-Based Decision Support System for Canal Irrigation Man-agement”. Computers and Electronics in Agriculture, Vol. 161, 2019, pp.312-321.

[3] A. Goap, D. Sharma, A. Shukla, C. R. Krishna, “An IoT Based Smart Irrigation Management System using Machine Learning and Open source Technologies”. Computers and Electronics in Agriculture, Vol. 155, 2018, pp.41-49.

[4] M. A. Zamora-Izquierdo, J. Santa, J. A. Martinez, V. Martinez, A. F. Skarmeta, “Smart Farming IoT Plat-form Based on Edge and Cloud Computing”. Biosystems Engineering, Vol. 177, 2019, pp.4-17.

[5] N. Ahmed, D. De, I. Hussain, “Internet of Things (IoT) for Smart Precision Agriculture and Farming in Ru-ral Areas”. IEEE Internet of Things Journal, Vol. 5, No. 6, 2018, pp.4890-4899.

[6] D. Pivoto, P. D. Waquil, E. Talamini, C. P. S. Finocchio, V. F. Dalla Corte, G. de Vargas Mores, “Scientific Development of Smart Farming Technologies and Their Application in Brazil”. Information Processing in Agriculture, Vol. 5, No. 1, 2018, pp.21-32.

[7] E. A. Abioye, M. S. Z. Abidin, M. S. A. Mahmud, S. Buyamin, M. H. I. Ishak, M. K. I. Abd Rahman, A. O. Otuoze, P. Onotu, M. S. A. Ramli, “A Review on Monitoring and Advanced Control Strategies for Precision Irrigation”. Computers and Electronics in Agriculture, Vol. 173, 2020, pp.105441.

[8] R. G. Perea, E. C. Poyato, P. Montesinos, J. R. Diaz, “Prediction of Irrigation Event Occurrence at Farm Level using Optimal Decision Trees”. Computers and Electronics in Agriculture, Vol. 157, 2019, pp.173-180.

[9] Y. Osroosh, R. T. Peters, C. S. Campbell, Q. Zhang, “Comparison of Irrigation Automation Algorithms for Drip-Irrigated Apple Trees”. Computers and Electronics in Agriculture, Vol. 128, 2016, pp.87-99.

[10] S. A. Nikolidakis, D. Kandris, D. D. Vergados, C. Douligeris, “Energy Efficient Automated Control of Irriga-tion in Agriculture by Using Wireless Sensor Networks”. Computers and Electronics in Agriculture, Vol. 113, 2015, pp.154-163.

[11] N. Zapata Ruiz, I. Chalghaf, E. Nerilli, B. Latorre Garces, C. Lopez Marin, A Martinez-Cob, J. Girona, E. Playan Jubillar, “Software for On-Farm Irrigation Scheduling of Stone Fruit Orchards Under Water Limita-tions”. Computers and Electronics in Agriculture, Vol. 88, 2012, pp.52-62.

[12] K. X. Soulis, S. Elmaloglou, “Optimum Soil Water Content Sensors Placement for Surface Drip Irrigation Scheduling in Layered Soils”. Computers and Electronics in Agriculture, Vol. 152, 2018, pp.1-8.

[13] E. A. Dar, A. Brar, K. Singh, “Water Use and Productivity of Drip Irrigated Wheat Under Variable Climatic and Soil Moisture Regimes in Northwest India”. Agriculture, Ecosystems & Environment, Vol. 248, 2017, pp.9-19.

[14] D. Yang, S. Li, S. Kang, T. Du, P. Guo, X. Mao, L. Tong, X. Hao, R. Ding, J. Niu, “Effect of Drip Irrigation on Wheat Evapotranspiration, Soil Evaporation and Transpiration in Northwest China”. Agricultural Wa-ter Management, Vol. 232, 2020, pp.106001.

[15] R. Liu, Y. Yang, Y. S. Wang, X. C. Wang, Z. Rengel,W. J. Zhang, L. Z. Shu, “Alternate Partial Root-Zone Drip Irrigation with Nitrogen Fertigation Promoted Tomato Growth, Water and Fertilizer-Nitrogen Use Effi-ciency”. Agricultural Water Management, Vol. 233, 2020. pp.106049.

[16] E. Suarez-Rey, M. Gallardo, M. Romero-Gamez, C. Gimenez, F. Rueda, “Sensitivity and Uncertainty Analysis in Agro-Hydrological Modelling of Drip Fertigated Lettuce Crops under Mediterranean Condi-tions”. Computers and Electronics in Agriculture, Vol. 162, 2019, pp.630-650.

[17] A. Rasyid, N. Shahidan, M. Omar, N. Hazwani, J. Choo, “Design and Development of Irrigation System for Planting Part 1”, in 2nd Integrated Design Project Conference (IDPC), pp. 1-22. 2015.

[18] B. Aisham, A. Rahim, “Design of Reservoir Tanks Modelling to Mix Several Types of Fertilizer for Fertiga-tion Planting System: Part B”, in Journal of Physics: Conference Series, IOP Publishing. Vol. 1150, No. 1, p. 012022. 2019.

[19] R. Prabha, E. Sinitambirivoutin, F. Passelaigue, M. V. Ramesh, “Design and Development of an IoT Based Smart Irrigation and Fertilization System for Chilli Farming”, in 2018 IEEE International Conference on Wireless Communications, Signal Processing and Networking (WiSPNET), pp. 1-7. 2018.

[20] E. Wang, S. Attard, A. Linton, M. McGlinchey, W. Xiang, B. Philippa, Y. Everingham, “Development of a Closed-Loop Irrigation System for Sugarcane Farms using the Internet of Things”. Computers and Elec-tronics in Agriculture, Vol. 172, 2020, pp.105376.

[21] M. Y. Suhaimi, A. M. Mohamad, M. N. F. Hani, “Potential and Viability Analysis for Ginger Cultivation using Fertigation Technology in Malaysia”. International Journal of Innovation and Applied Studies, Vol. 9, No. 1, 2014, pp.421.

[22] C. A. Zaragoza, R. G. Perea, I. F. Garcia, E. C. Poyato, J. A. R. Diaz, “Open Source Application for Opti-mum Irrigation and Fertilization using Reclaimed Water in Olive Orchards”. Computers and Electronics in Agriculture, Vol. 173, 2020, pp.105407.

[23] R. G. Perea, M. Moreno, J. Ortega, A. del Castillo, R. Ballesteros, “Dynamic Simulation Tool of Fertigation in Drip Irrigation Subunits”. Computers and Electronics in Agriculture, Vol. 173, 2020, pp.105434.

[24] N. J. Car, “Using Decision Models to Enable Better Irrigation Decision Support Systems”. Computers and Electronics in Agriculture, Vol. 152, 2018, pp.290-301.

[25] J. M. Barradas, S. Matula, F. Dolezal, “A Decision Support System-Fertigation Simulator (DSS-FS) for De-sign and Optimization of Sprinkler and Drip Irrigation Systems”. Computers and Electronics in Agricul-ture, Vol. 86, 2012, pp.111-119.

[26] R. M. Rusyadi, P. T. Daely, D. S. Kim, J. M. Lee, “IoT-Based Adaptive Network Mechanism for Reliable Smart Farm System”. Computers and Electronics in Agriculture, Vol. 170, 2019, pp.105287.

[27] S. Singh, I. Chana, R. Buyya, “Agri-Info: Cloud Based Autonomic System for Delivering Agriculture as a Service”. Internet of Things, Vol. 9, 2020, pp.100131.

[28] R. Thompson, I. Delcour, E. Berckmoes, E. Stavridou, The Fertigation Bible: Technologies to Optimise Fertigation in Intensive Horticulture, 2018.

[29] J. M. Salih, A. Adom, A. M. Shaakaf, “Solar Powered Automated Fertigation Control System for Cucumis Melo L. Cultivation in Green House”. APCBEE Procedia, Vol. 4, 2012, pp.79-87.

[30] Z. Sayuti, H. Ahmad, A. K. Sandrang, Inovasi Pertanian Bandar. Penerbit MARDI. 2018.

[31] N. A. S. Hanifah, M. A. Rashid, A. Jupri bin Ahmat, “Fruit Yield, Fruit Quality and Seed Yield of Four Chilli Varieties Grown in Open-Field as Affected by Conventional System in Peat Soil Area and Fertigation Sys-tem”, in 15th International Peat Congress, Sarawak, Malaysia, August 2016.

[32] A. Adam, K. P. Ee, N. Sahari, A. Tida, C. Y. Shang, K. M. Tawie, S. Kamarudin, H. Mohamad, et al., “Dr. Lada: Diagnosing Black Pepper Pest and Diseases with Decision Tree”. International Journal on Ad-vanced Science, Engineering and Information Technology, Vol. 8, 2018, pp.1584-1590.

[33] M. Zaman, R. Azim, N. Misran, M. Asillam, T. Islam, “Development of a Semielliptical Partial Ground Plane Antenna for RFID and GSM-900”. International Journal of Antennas and Propagation, Vol. 2014, 2014.

[34] S. Axryd, T. Chari, “A Digital Solution Towards Data-Driven Agriculture in Malaysia”. https://www.digitalnewsasia.com/insights/digital-solution-towards-data-driven-agriculture-malaysia, Febu-ary 2019.

[35] N. A. A. Husein, A. H. A. Rahman, D. P. Dahnil, “Evaluation of Lora-Based Air Pollution Monitoring Sys-tem”. International Journal of Advanced Computer Science and Applications, Vol. 10, No. 7, 2019, pp.391-396.

[36] M. Shahidul Islam, M. T. Islam, A. F. Almutairi, G. K. Beng, N. Misran, N. Amin, “Monitoring of the Hu-man Body Signal Through the Internet of Things (IoT) Based Lora Wireless Network System”. Applied Sciences, Vol. 9, No. 9, 2019, pp.1884.

[37] M. Hossinuzzaman, D. P. Dahnil, “Enhancement of Packet Delivery Ratio During Rain Attenuation for Long Range Technology”. International Journal of Advanced Computer Science and Applications, Vol. 10, No. 10, 2019, pp.219-225.

View-independent Vehicle Category Classification System

Sara Baghdadi[1], Noureddine Aboutabit[2]
IPIM Laboratory. National School of Applied Sciences, Khouribga
Sultan Moulay Slimane University, USMS
Beni-mellal, Morocco

***Abstract*—Vehicle category classification is important, but it is a challenging task, especially, when the vehicles are captured from a surveillance camera with different view angles. This paper aims to develop a view-independent vehicle category classification system. It proposes a two-phase system: one phase recognizes the view angles helping the second phase to recognize the vehicle category including bus, car, motorcycle, and truck. In each phase, several descriptors and Machine Learning techniques including traditional algorithms and Deep neural networks are employed. In particular, we used three descriptors: HOG (Histogram of Oriented Gradient), LBP (Local Binary Patterns) and Gabor filter with two classifiers SVM (Support Vector Machine) and k-NN (k-Nearest Neighbor). And also, we used the Convolutional Neural Network (CNN, or ConvNet). Three experiments have been elaborated based on many datasets. The first experiment is dedicated to choosing the best approach for the recognition of views: rear or front. The second experiment aims to classify the vehicle categories based on each view. In the third experiment, we developed the overall system, the categories were classified independently of the view. Experimental results reveal that CNN gives the highest recognition accuracy of 94.29% in the first experiment, and HOG with SVM or k-NN gives the best results (99.58%, 99.17%) in the second experiment. The system can robustly recognize vehicle categories with an accuracy of 95.77%.**

Keywords—Vehicle category classification; view recognition; machine learning; deep learning; convolutional neural network

I. Introduction

Actually, with the increasing number of vehicles and surveillance cameras, it is necessary to automate vehicle recognition to collect traffic data [1]. Automatic vehicle recognition is an integral part of Intelligent Transportation Systems and has become an important subject of study for monitoring and surveillance issues [2]. It presents a particularly challenging problem in contemporary road safety. Various computer systems have been proposed to detect and classify vehicles according to several criteria (category, color, brand, size, views…) where the type (category) of a vehicle is the most important and essential characteristic [3].

Category classification plays an essential role in intelligent traffic systems and can be used extensively for various purposes such as highway surveillance, toll collection, traffic flow statistics [1], automatic parking, preventing heavy trucks from entering city bridges [4]. It can also be used to specify speed limits for each category to monitor traffic rules and regulation systems (sending warnings). For example, trucks have different speed limits than other vehicles. Vehicle category classification can also be used in self-guided vehicles to alert, for example, the driver that a truck is approaching. This work is a part of our project that aims to detect automatically prohibited overtaking of vehicles from a static camera. Thus, the future system must take into account special situations to allow, for example for motorcycles to overtake traffic without sending a warning for violation laws. In fact, the classification of vehicle categories is influenced by changes in viewing angles. This makes this task more challenging. This paper aims to create a system that classifies vehicle categories (Bus, Car, Motorcycle, and Truck) independently of the view angle (Front/ rear angles). The system has two phases: view recognition phase and vehicle category classification phase.

The motivation to take this challenge is that first, many previous studies have worked on classifying vehicles from the side. Unfortunately, there has been relatively little research on classifying vehicles from front and rear views [5]. Classifying vehicles, from their front or/and rear views, is more challenging. Most vehicle categories have the same characteristics in their view structures such as windshield, forward lighting, mirrors, bumper, etc. (Example: Fig. 1/ Front view). Second, most researchers have used just one, two or three methods in their comparative studies. Third, there is not a lot of work being done on vehicle view recognition [2]. Forth, no one has previously developed a view-independent classification system for vehicle categories.

Fig. 1. Example of Front View Structure of Trucks, Buses and Cars.

In this work, Machine Learning and Deep Learning techniques were used to classify the views and categories of vehicles. Object classification is a broad field of computer vision and machine learning research that aims to classify objects in images into meaningful categories [6]. This involves predicting the class of a new object in an image according to the information obtained from the training set of data whose category class is known [7]. This work is constituted of three experiments. The first experiment is devoted to vehicle view classification. The second one is dedicated to vehicle category classification. The third one presents the overall system using the best models we obtained. To accomplish this, we used three descriptors (LBP, HOG and Gabor filter), two classifiers, and Convolutional Neural Networks.

The rest of the paper is organized as follows. Section 2 presents the works that are closely related to vehicle classification. In Section 3, we present an overview of the system. Section 4 describes in detail all techniques used for vehicle view and category classification. The experimental results and comparisons are presented in Section 5. The last section presents the conclusions and future works.

The next section presents the previous research on vehicle classification.

II. Related Work

This section presents some information on some previous works related to vehicle classification. [8] used size and shape measurements as features with SVM and random forest classifiers to classify vehicles into four categories: car, van, bus and bicycle/motorcycle. The results showed that the SVM outperformed RF with an accuracy of 96.26%. [9] proposed a real-time classification of vehicle types from surveillance videos. Vehicles are classified as small cars, large cars or motorbikes using the HOG descriptor with SVM classifier. [3] proposed a vehicle-types recognition based on improved HOG_SVM. The authors used HOG to extract features from images and PCA to reduce the dimension and complexity of feature vectors. SVM is used as a classifier to classify vehicle types. The improved HOG_SVM model has an accuracy of 92.6%. In [4], the authors proposed for the vehicle type classification a cascade ensemble classifier using Multiple Layer Perceptron (MLP) and K-Nearest Neighbor (K-NN) as base classifiers. HOG, LBP and the combined feature HOG-LBP are used as inputs. [10] used two feature extractors the Pyramid Histogram of Oriented Gradients (PHOG) and Curvelet Transform and the classifiers MLP, SVM, kNN and Random Forest to classify the type and make of vehicles. The authors combined the PHOG with Curvelet Transform and applied for classification the RF/MLPs ensemble on a database of 600 images from 21 makes of cars/vans. The method achieved an accuracy of 96,5%. [11] proposed a method based on a linear SVM to solve vehicle make and model classification problems. For the feature extraction step, the authors used SIFT (Scale Invariant Transform Feature). They reported an accuracy of 89%. [12] classified three classes: vehicle taxi, a mini-bus, and a double-decker by estimating the width, length, and height. The model achieved an accuracy of 92.5%. In [13] used Logistic Regression, neural networks, and SVM as classifiers. LR was the best one compared to the other method with an accuracy of 93.4%. [14] proposed a new method of detecting and classifying vehicles into six types, such as SUV type, sedan type, RV type, based on images of visible light and thermal cameras. The authors extracted features by measuring the texture, the contrast, the homogeneity, the entropy and the energy of the images of the front view. The visible image classifier has an accuracy of 92.7% and the thermal image classifier has 65.8%. [15] proposed a multimodal method to address this task of vehicle type classification from traffic scenario videos. The method extracts image and audio features and fuses them to feed an SVM classifier. To extract features from images, the authors used the pre-trained networks AlexNet [16] and GoogleNet [17]. The model classified the vehicles as an armored vehicle, construction vehicle, crane vehicle, rescue vehicle, military vehicle, motorcycle, and rescue vehicle. It achieved an accuracy of 72.1%.

In recent years, Deep learning and especially Convolutional Neural Networks have been used to tackle the task of vehicle type classification but with different approaches and datasets [6]. CNNs have demonstrated better performance in image classification. [18,1,6,5] used Convolutional Neural Networks to classify vehicle types. [18] proposed a method based also on a semi-supervised convolutional neural network with Laplacian Filters for kernels. The authors constructed the BIT-Vehicle dataset of front view images. The method achieved an accuracy of 96.1% in daytime conditions and 89.4% in nighttime conditions. [1] combined two steps. The first is data augmentation and the second is the CNN model training. In [6], the authors used also the CNNs with low-resolution images from a frontal view. The model achieved an accuracy of 93.90%. Also, [5] developed a model using CNN, but, on rear view images. The model achieved an accuracy of 97.88 %.

Unfortunately, there is no previous work on vehicle view classification topic except our last work [2]. We developed a classification system of the vehicle's front and back using two descriptors HOG and LBP with two classifiers SVM and kNN. The system achieved an accuracy of 97,47%.

III. System Overview

This section provides an overview of the overall system, which is summarized in Fig. 2. The system has two phases. The first phase is to recognize the view of the vehicle helping the second phase to recognize the vehicle category, including bus, car, motorcycle, and truck.

We provide above an overview of each phase. So, as we said, we used Machine Learning techniques to recognize vehicle views and categories. Machine Learning is a branch of Artificial Intelligence. It analyzes data to build a model by itself. There are three types of Machine Learning: Supervised Learning, Unsupervised Learning and Reinforcement Learning [19]. The problem in each phase is classified under Supervised Learning, in particular, in the classification category.

The next section presents in detail the vehicle view classification phase.

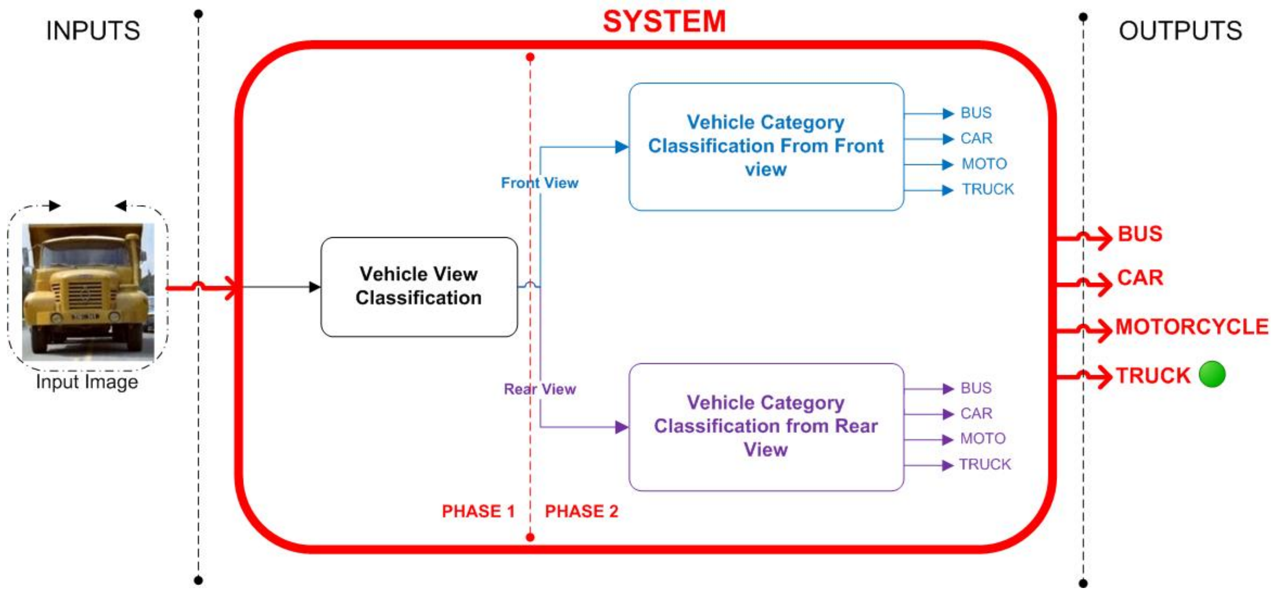

Fig. 2. Overall System.

Fig. 3. Flow Chart for Building a Vehicle View Classification Model.

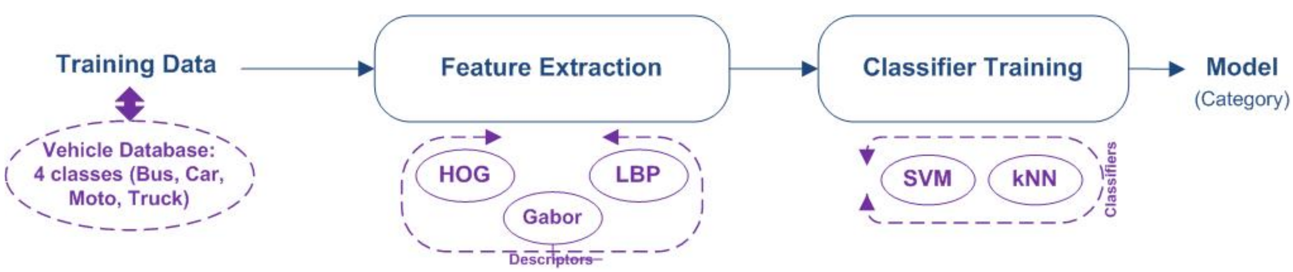

Fig. 4. Flow Chart for Building a Vehicle Category Classification Model.

A. Vehicle View Classification

Several factors make the recognition of rear and front views very difficult, including the similarity of shape, size, and color [2]. In this step, we used Machine Learning techniques including traditional algorithms and Convolutional Neural Networks. Fig. 3 shows all the steps involved in building the model from the data. Here, we used a dataset containing two classes (Front/Rear views). Several features are computed to characterize the shape of the vehicle view using descriptors like HOG, LBP or Gabor. For traditional ML techniques, features are extracted manually however CNNs extract features automatically. The feature vector associated with each image enters the classifier such as SVM or k-NN. We described in detail all descriptors and classifiers we used, in Section 4.

B. Vehicle Category Classification

This step aims to fit a model classifying the vehicle categories from the front view and another for rear view. So here, we used two databases. Each database contains the images of one view with four classes in which each class contains the images of a category. As explained before, building a model requires two steps (Fig. 4): feature extraction and classification. We extract features from the training data using three different kinds of descriptors: LBP, HOG and Gabor filter. Then, we train a classifier using these features to understand how the given input variables relate to the class, here we used, SVM and k-NN classifiers. We can call the process of constructing a model the training, learning or modeling step.

The following section presents all the methods we used.

IV. Methodology

In this section, we present all the methods used to resolve the vehicle category classification and view recognition problems. This section is divided into three parts. The first part presents the descriptors (HOG, LBP, and Gabor). The second part describes the classifiers (SVM, k-NN). The third part defines Convolutional Neural Networks in detail.

A. Descriptors

The key to efficient vehicle classification is to select a good feature descriptor that can characterize the vehicle view shape. As we said, we used three types of descriptors. These descriptors are summarized as it's written below.

1) Histogram of Oriented Gradients (HOG): HOG is proposed by Dalal et al. [20]. The HOG feature extraction process is based on the pixel gradient. The gradient corresponds to the first derivative of the image along the vertical and horizontal axes [21]. Features are calculated as follows: the gradient value and gradient direction value ("(1)" & "(2)") of each pixel I(x,y) of a cell are calculated and then grouped into a 9-bins [3] as shown in Fig. 5. Cells are grouped in blocks and then all vectors of all blocks are combined in series to obtain the final feature vector for classification [22].

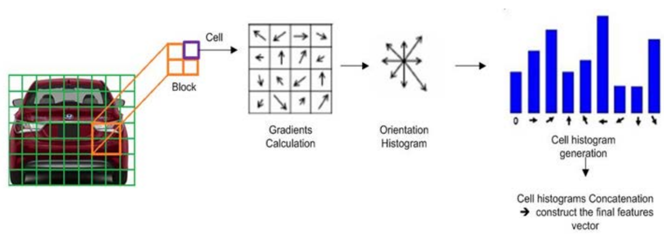

Fig. 5. HOG Features [4].

$$G(x,y) = \sqrt{G_x(x,y)^2 + G_y(x,y)^2} \quad (1)$$

$$\theta(x,y) = \arctan(\frac{G_y(x,y)}{G_x(x,y)}) \quad (2)$$

$G_x(x,y)$ is the horizontal gradient "(3)" and $G_y(x,y)$ is the vertical gradient "(4)".

$$G_x(x,y) = I(x,y) - I(x-1,y) \quad (3)$$

$$G_y(x,y) = I(x,y) - I(x,y-1) \quad (4)$$

As we can see, the orientation histogram varies from 0 to 180° (20° per bin) [3].

A cell is composed of n × n pixels, with the increase of n, the number of features in the image decreases [22].

2) Local Binary Pattern (LBP): The LBP is a texture descriptor. Its general purpose is to create a feature based on order for each pixel by comparing its intensity value with that of its neighboring pixels [23].

The LBP feature vector is created using the following process:

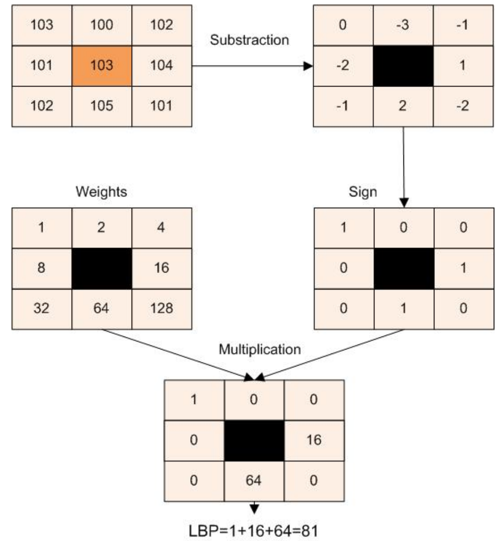

Fig. 6. LBP Operator [25].

The image is divided into cells of size 3x3. LBP labels the center pixel of each cell with a binary number called LBP code. This code is calculated as described in Fig. 6. The central pixel p_c is subtracted from the 8 neighboring pixels p_i (3 × 3 neighborhood, i = 0, 1, ..., 7). If the result is negative, the neighboring pixel is coded with "0". If it is positive, it is coded with "1", as in the following formula:

$$s(p_i - p_c) = \begin{cases} 1, if\ p_i \geq p_c \\ 0, if\ p_i < p_c \end{cases} \quad (5)$$

Where p_i and p_c are the grayscale values of the neighbor and center pixels, respectively.

The result code is an 8-bit number, so it is converted into a decimal value (Label), as the following equation shows [24]:

$$LBP(p_c) = \sum_{i=0}^{7} s(p_i - p_c).2^i \quad (6)$$

In addition, the LBP descriptor is calculated in its general form as follows [24]:

$$\text{LBP}(p_c) = \sum_{i=0}^{M-1} s(p_i - p_c).2^i,\ s(d) = \begin{cases} 1, if\ d \geq 0 \\ 0, \quad else \end{cases} \quad (7)$$

where p_c is the gray level value of the central pixel and p_i is the values of the M neighboring pixels.

Then, the obtained decimal values are used to construct the histogram for each cell by calculating the frequencies of the obtained values of all pixels. This histogram is considered as a feature vector with $256 = 2^8$ dimensions. The histograms of all the cells are concatenated to give a feature vector for the whole image.

3) Gabor features: The Gabor Filter (named after the English physicist Dennis Gabor) is a linear filter used for texture analysis, edge detection, feature extraction, etc. It is defined by the product of a complex sinusoid (known as the carrier) and a Gaussian function (known as the envelope) [26]. Then, in a spatial domain of dimension 2 (if it is an image), the Gabor function is presented as follows:

$$G(x,y) = s(x,y).g(x,y) \tag{8}$$

with *s(x,y)* is the complex sinusoid. It is defined as follows:

$$\mathrm{s(x,y)} = \exp(2\mathrm{j}\pi.(u_0.x + v_0.y) + \varphi) \tag{9}$$

(u_0, v_0) and φ define the spatial frequencies and phase of the sinusoid, respectively. The real and imaginary parts of this sinusoid are [26] :

$$Re\big(s(x,y)\big) = \cos(2\pi(u_0.x + v_0.y) + \varphi) \tag{10}$$

$$Im\big(s(x,y)\big) = \sin(2\pi(u_0.x + v_0.y) + \varphi) \tag{11}$$

g(x,y) is the Gaussian function. Its formulation is given by :

$$g(x,y) = \exp(-\left(\frac{(x-x_0)^2}{\sigma_x^2} + \frac{(y-y_0)^2}{\sigma_y^2}\right)) \tag{12}$$

where *(x0,y0)* is the peak Gaussian envelope g, σ_x (respectively σ_y) is the standard deviation of g from the *x*-axis (resp. *y*-axis) [26].

The Gabor function can be represented by a real component "(13)" and an imaginary component "(14)" whose directions are perpendicular (phase shift of 90 degrees).

$$\mathrm{Gr(x,y)} = \cos(2\pi(u_0.x + v_0.y) + \varphi)\,.\exp(-\left(\frac{(x-x_0)^2}{\sigma_x^2} + \frac{(y-y_0)^2}{\sigma_y^2}\right)) \tag{13}$$

$$\mathrm{Gi(x,y)} = \sin(2\pi(u_0.x + v_0.y) + \varphi)\,.\exp(-\left(\frac{(x-x_0)^2}{\sigma_x^2} + \frac{(y-y_0)^2}{\sigma_y^2}\right)) \tag{14}$$

This Gabor function is applied to a convolution mask, to define a convolution filter called Gabor filter. The application of this filter *G* to an image *I* is therefore the convolution of the image with the Gabor mask or kernel *N*, as shown in the following formula:

$$G(I) = I * N \tag{15}$$

where "*" is the convolution operator.

B. Classifiers

In the classification stage, we used two types of classifiers SVM and k-NN. We describe each classifier below:

1) Support Vector Machine (SVM): SVM is a classifier proposed by Cortes and Vapnik in 1995 [27], their main idea was separating the training data by a hyperplane without error. SVM classification is essentially a binary classification technique with category labels having only two values, 1 and -1 respectively. It is modified to handle multiclass tasks in real-situations. Two methods are proposed for this adaptation include techniques "One Against One" 1A1 and "One Against All" 1AA [28]. The 1AA approach represents the oldest and most common SVM multiclass approach [29] and involves the division of an N class dataset into two classes. In contrast, the 1A1 approach involves constructing a machine for each pair of classes, giving N(N-1)/2 machines. When applied to a test point, each classification gives a vote to the winning class and the point is tagged with the class with the most votes. This approach can be further modified to weight the voting process. According to the theory of machine learning, it is accepted that the 1AA approach has more disadvantages than 1A1; its performance can be compromised due to unbalanced learning data sets. However, the 1A1 approach requires more computation because the results of the SVM pairs have to be calculated [28].

2) k-Nearest Neighbor (kNN): K-Nearest Neighbor (kNN) is the extension of the minimum distance and the nearest neighbor classifiers. It calculates the distance between the test sample *x* and all the training samples and defines the distances in decreasing order. Then, it selects the *k* training samples closest to the test sample *x* and counts the category of *k* selected training samples. The test sample belongs to the category with the highest number of votes in the same category [30] [31].

3) Convolutional neural networks: As known, Deep Learning has recently attracted a great deal of interest especially in the field of computer vision and in particular image classification. Briefly, Deep Learning is a machine learning technique that uses deep neural networks [19]. It refers to Artificial Neural Networks (ANN) with multiple layers [14]. This section briefly describes the Convolutional Neural Network (CNN), one of the most popular deep neural networks. It is specialized in image recognition. Its name means that the network uses a linear mathematical operation called convolution.

In fact, CNN is an old technique that was developed in the 1980s and 1990s. However, it has been forgotten for some time because it was not practical for real-world applications [19]. There was no GPU to help training, and even CPUs were slow. Increasingly, data was becoming more and more available and accessible to people by making the databases public like ImageNet, CIFAR and MNIST. And CPUs were getting faster, and GPUs became a multipurpose computing tool. Both data and computing power made the CNN revived in 2012.

Using directly the original images for recognition gives poor results. Thus, feature maps are provided instead of the original images. As illustrated in Fig. 7, CNN consists of a feature extractor and a classification neural network. The feature extractor consists of pairs of convolution and pooling layers. The output from the convolution layer passes through an activation function like ReLU, Sigmoid or Tanh. The classifier is a fully connected neural network consisting of at least one layer. The final results of this part are transformed into a one-dimensional vector and then enter into the classifier network that generates the output [19].

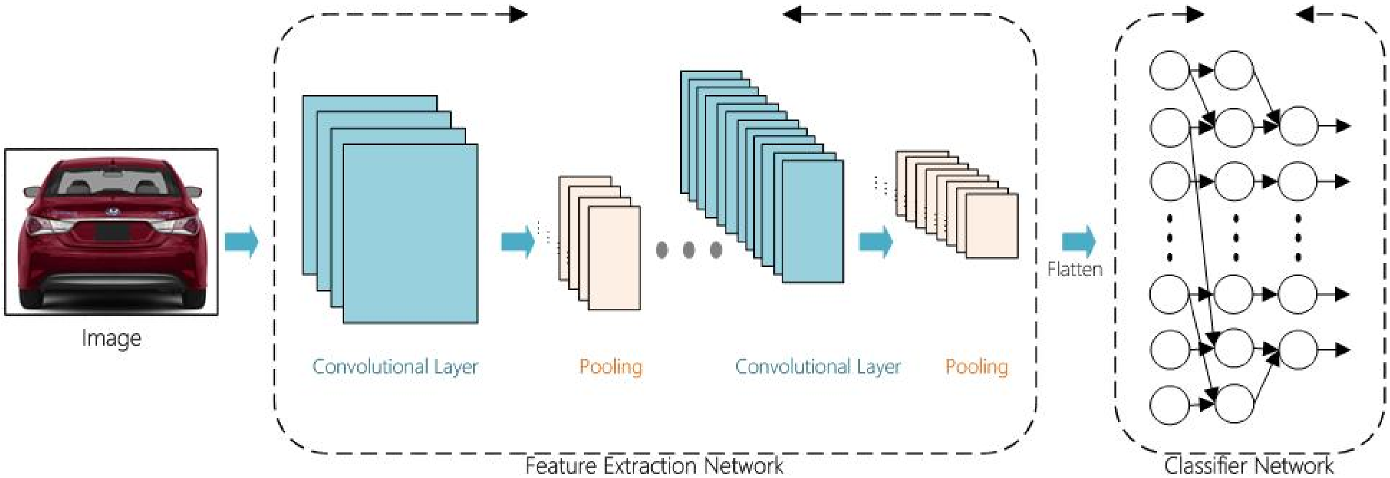

Fig. 7. Typical CNN Architecture.

The convolutional layer converts the images via the convolution operation, and the pooling layer reduces the dimensions of the image. It combines the neighboring pixels into a single pixel [19]. We will define these two layers in detail in the following sections.

- Convolution Layer

The convolution layer generates new images called feature maps using convolution filters. The feature map is a 2D grid of features; it highlights the features of the original image. The number of feature maps is identical to the number of convolution filters. The filters are two-dimensional matrices whose elements are the hidden weights. As shown in Fig. 8, the filter starts with the upper-left region. Each region is a submatrix which has the same size as the convolutional filter.

Thus, for each submatrix, the convolution result is the sum of the products of values having the same position with the filter kernel values [19]. In the same way, the filter slides across the image from left to right and top to bottom until the feature map is produced. The feature map dimension is presented as follows:

$$f = \frac{(D-K)}{S} + 1 \quad (16)$$

D and K are the dimensions of the image and filter respectively. S is the stride which is the number of pixels by which the filter is allowed to slide on the image.

- Activation function

It is necessary to use Activation functions in CNNs and artificial neural networks. Without them, the CNNs would be just a series of linear operations. An activation function is a non-linear transformation of the output of a neuron in a layer, like ReLU, Tanh, and Sigmoid [32].

a) Rectified Linear Unit (ReLU): ReLU is the most used activation function nowadays. It is presented by the equation "(17)". As shown in Fig. 9, when the input is equal to or greater than zero, the output is identical to the input. When it is less than zero, the output is zero [32].

$$f(x) = \max(0, x) \quad (17)$$

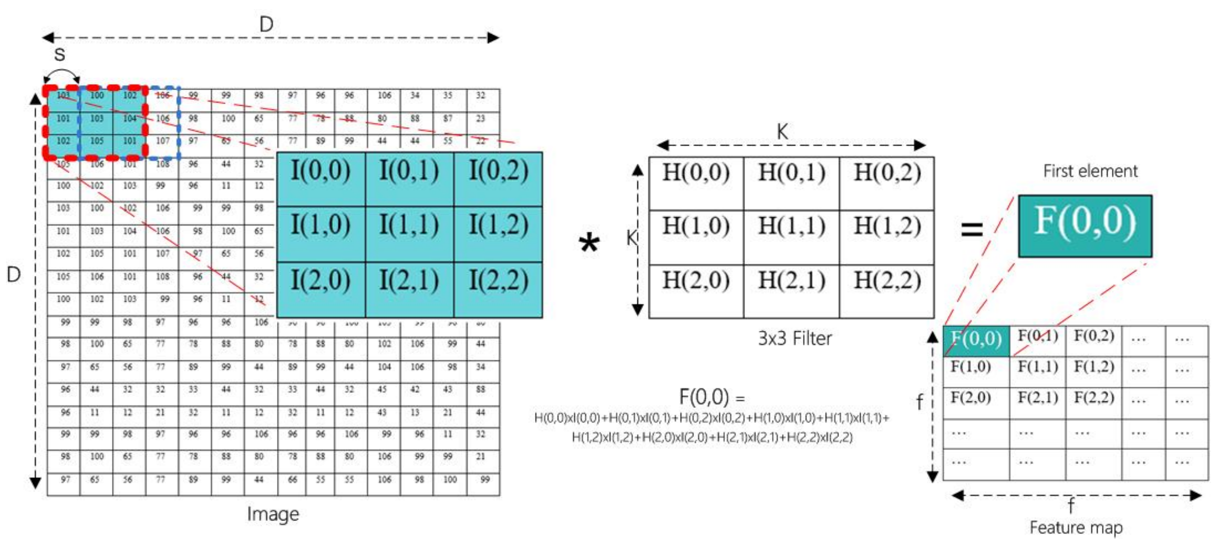

Fig. 8. Convolution Operation.

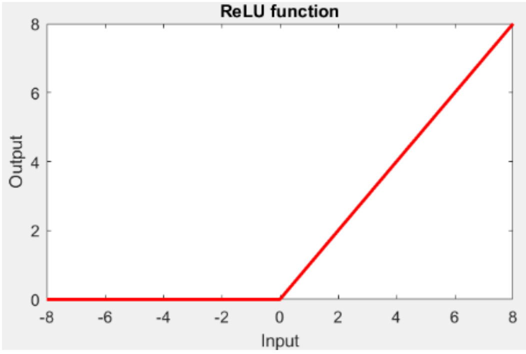

Fig. 9. Rectified Linear Unit.

b) Sigmoid: The Sigmoid or logistic function is presented by the equation "(18)" [32]. As shown in Fig. 10, Sigmoid has the output between the values of 0 and 1.

$$f(x) = \frac{1}{1+e^{-x}} \tag{18}$$

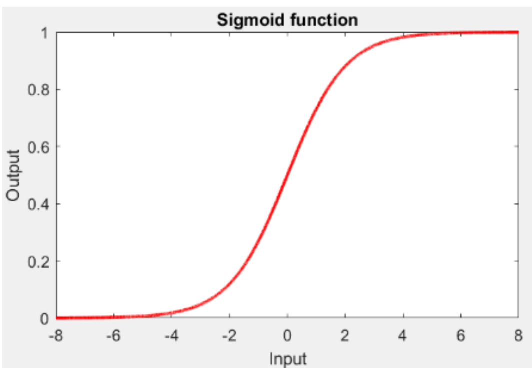

Fig. 10. Sigmoid Function.

Recently, it has lost favor because of several disadvantages, such as the problem of vanishing gradient.

c) Tanh: The hyperbolic tangent function (Tanh) is presented by the "(19)" [32]. As we see in Fig. 11, Tanh is very similar to the sigmoid function, it centered around 0. Tanh has the output between the -1 and 1.

$$f(x) = \frac{1-e^{-2x}}{1+e^{-2x}} \tag{19}$$

In practice, Tanh is usually preferred to the sigmoid, but it still suffers from the problem of the vanishing gradient.

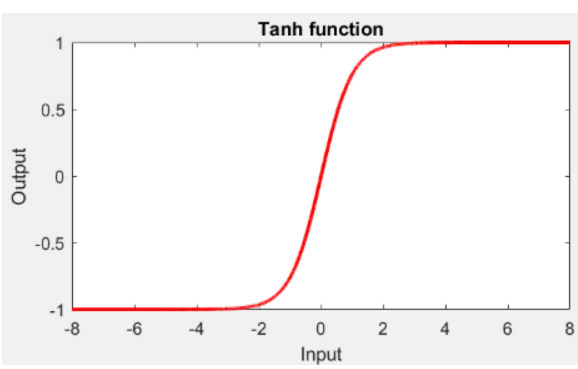

Fig. 11. Hyperbolic Tangent.

- Pooling Layer

The pooling layer reduces the size of feature maps. It replaces neighboring pixels by their maximum or average value. Fig. 12 illustrates the two operations.

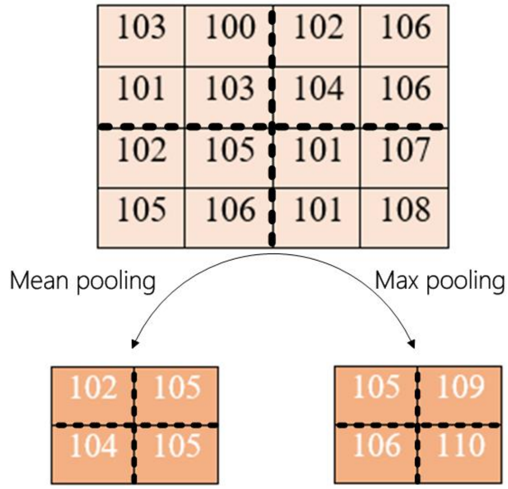

Fig. 12. Pooling Operations.

a) Mean Pooling: Mean pooling operation compresses a feature map by taking the average value of each block "(20)" [33]. Pooling is performed on non-overlapping blocks.

$$P_{i,x,y} = \frac{1}{d^2} \sum_{v,h} F_{i,(x+v),(y+h)} \tag{20}$$

$F_{i,x,y}$ is the value at the position *x,y* of the i^{th} feature map. *v* is a vertical index in the local neighborhood. *h* is a horizontal index in the local neighborhood. *d* is the dimension of the block.

b) Max pooling: Max-pooling operation is similar to the mean pooling, except that instead of taking the average, we take the max presented by the following equation "(21)" [33]:

$$P_{i,x,y} = \max_{v,h}(F_{i,(x+v),(y+h)}) \tag{21}$$

$F_{i,x,y}$ is the value at the position *x,y* of the i^{th} feature map. *v* is a vertical index in the local neighborhood. *h* is a horizontal index in the local neighborhood.

V. Result and Discussion

Various experiments are conducted to evaluate the performance of the methods we described below. In this section, we present the experimental results.

A. Dataset Construction & Implementation Details

In practice, several factors make the classification of vehicle categories very challenging. Among them: the unavailability of databases; none of the existing datasets are suitable for our work. We find only a few databases/top view or only databases for cars/side and rear views. Thus, we have collected, from many websites, thousands of images containing buses (Appendix/ Fig. 23 & Fig. 27), cars (Appendix/ Fig. 24 & Fig. 28), motorcycles (Appendix/ Fig. 25 & Fig. 29), and trucks (Appendix/ Fig. 26 & Fig. 30) from front and rear views. We built three datasets. The first is for the view classification. It contains 4000 images with two classes: one for front view images and the other for rear view images. The two other datasets are used for the classification of vehicle categories: a dataset for front vehicle images (2182 images), the other for rear vehicle images (2000 images). Each of these two datasets contains four classes: each class for one category (500 images under each class).

All the images were resized to a fixed size of 150*150 pixels. From each dataset, two sets are created with a random split: a training set and a test set. Eighty percent of the images were included in the training set. The remaining 20% were included in the test set. These images are selected under different weather conditions.

We executed the algorithms on a Lenovo ThinkPad with a processor Intel® Core™ i5 7th Generation CPU @ 2.50GHz 2.71GHz, RAM 8Go. We implemented the algorithms in Matlab.

B. Performance Metrics

To evaluate the performance of the constructed models, we calculated many metrics using the confusion matrices extracted for each model. The rows and columns show the true and predicted classes, respectively. The values in the diagonal represent the correct classification rates while those outside the diagonal represent classification errors.

In this work, we have two problems: binary classification (Rear/ Front) and multi-class classification (Displayed in Fig.13) with four classes in the order of Bus, Car, Moto, and Truck. Thus, for a confusion matrix with more than two-classes, we calculated the metrics (True Positives TP, False Positives FP, False Negatives FN) of each class as follows:

- The TP for each class is the corresponding value in the main diagonal. For example, the TP of the Motorcycle class is: TPM.

- The FN for each class is the sum of the values of the corresponding row excluding the main diagonal element TP. For example, the FN of the Truck class is:

FNT = ERTB+ ERTC + ERTM (22)

- TP+FN=100%

- The FP for each class is the sum of the values of the corresponding column excluding the TP. For example, the FP of the Bus class is:

FPB = ERCB+ ERMB+ ERTB (23)

C. Experiments

This section aims to compare the constructed models to find which of these models provides significant results. The best models in each classification have been selected to create a robust system. To accomplish this, three experiments are conducted. The first experiment is devoted to the recognition of the vehicle view: back or front. The second experiment aims to classify the vehicle categories according to each view. In the third experiment, we created the global system; the categories were classified independently of the view.

In the learning stage, each model is trained on three subsets of training data using the resampling method 4-fold cross-validation. In total, we generated 12 models for each method making different prediction errors on test data. And then we calculated the average performance. This process leads to a more stable prediction than those of any individual member model.

Among the traditional ML algorithms, we have used k-NN. As explained before, to classify a sample the k-NN starts by finding all the closest k training samples, and then predict the class by majority vote [10]. So here in experiments, we simply chose k=1 and the distance metric=Euclidean. On the other hand, in front and rear vehicle classification, we used SVM with the linear kernel. For the category classification, we used the SVM multiclass approach “1A1”.

The features of HOG have been extracted from the front and rear vehicle images as shown in Fig. 14 [2]. The inputs are 150 × 150 color images. Firstly, we converted the color images into gray images. Every input RGB three-channel image is converted into a single-channel image, the transformation formula is as follows:

$$Gry = 0{,}3.R + 0{,}59.G + 0{,}11.B \quad (24)$$

The feature vector is obtained by using the histograms of each block. Here, each block is represented by 8x8 cells, and each cell is represented by 9 bins. Thus, each block is represented by the vector 8x8x9=576 features. By combining all the vectors of all the blocks in series, we obtain the final HOG feature vector for the whole image for use in the classification step.

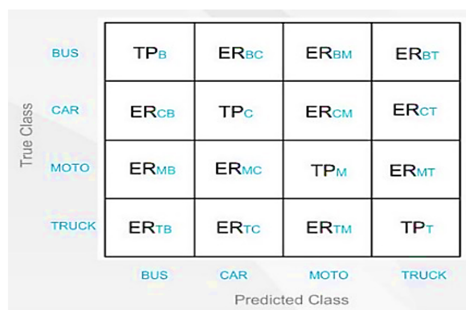

Fig. 13. Multi-Class Confusion Matrix (4 Classes).

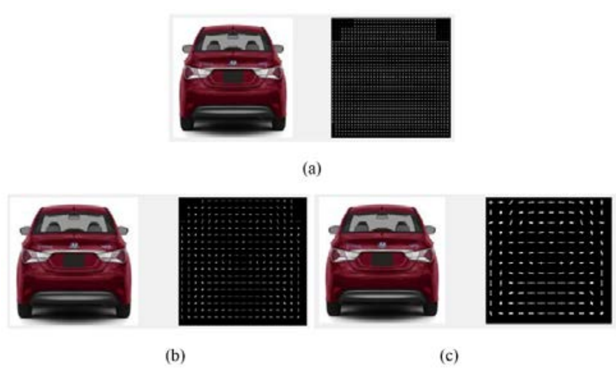

Fig. 14. (a). HOG Features of Rear-View Vehicle (Cell Size 4*4), (b). HOG Features (Cell Size 8*8).

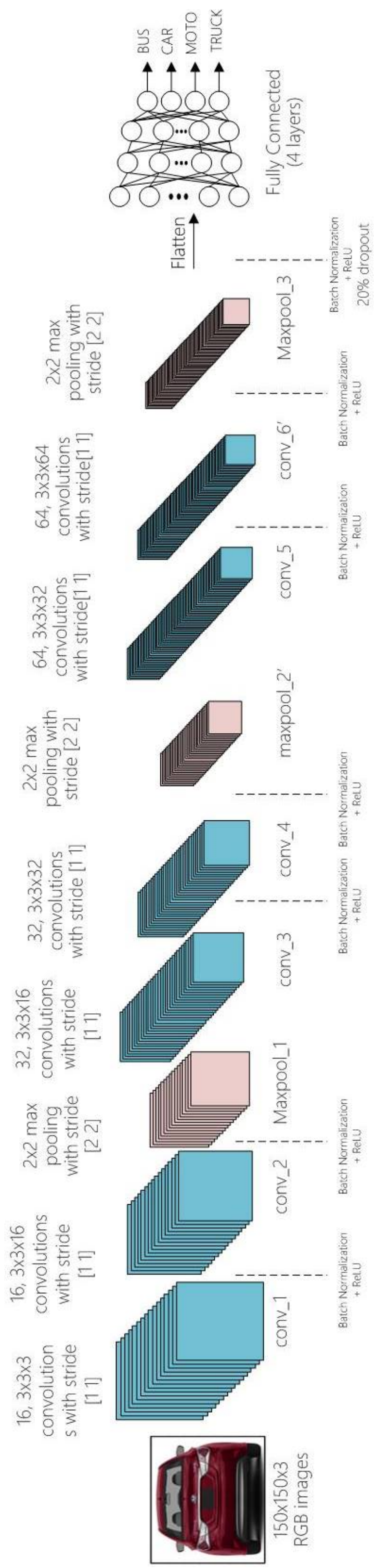

Fig. 15. CNN Architecture for Category Classification.

For CNNs, the input image of a convolution layer has a dimension D × D × c, where D is the height and width, and c is the number of channels. For RGB images, c = 3 [34]. In the experiments, we have D=150 and c=3. As shown in Fig. 15, the image passes through the convolution layer, the pooling layer, and then the fully connected layer. The network consists of six convolution layers using the ReLU activation function. The second and fourth convolution layers are followed by max-pooling layers. We add the Dropout layer at the end to regularize the network. In the classification network, we used a fully connected layer followed by a Softmax classifier. The size of the output layer is identical to the number of classes we expect.

CNNs automatically learn filter values (weights) by training the network on large amounts of data using a concept called backpropagation, continuing to have a minimal classification error. In the first layers, the network tries to recognize certain aspects of images, such as edges, shapes (squares, triangles, circles), and colors. More and more layers learn complex patterns until all of these patterns can help the network to learn the classification of the input [32].

1) Experiment 1 (Vehicle view classification): Fig. 16 presents a summary of the comparison of the obtained accuracy and error results. From the graph, we can easily see that CNN outperformed the other methods. It reached an accuracy of 94.29%, higher than LBP+SVM by a difference of 30.65%. We can also notice that HOG with SVM and k-NN obtained the same accuracy.

From Table I, we can notice that CNN produced 92.91% rear view images. But for the class/Front, the TP rate of HOG+kNN was higher than CNN (accuracy difference 1.01%).

When we trained the Convolutional Neural Networks, we monitored the training progress by plotting various metrics. Thus, we can determine if and how quickly the accuracy and error of the network are improving. Fig. 17 and Fig. 18 show these metrics at every iteration. Each iteration estimates the gradient and updates the network parameters.

Fig. 17 presents the training progress of one CNN model. It illustrates the evolution of training accuracy and its smoothed version according to the number of epochs. Each epoch is marked using a shaded background. An epoch is a full pass through the entire dataset.

We can observe that the accuracy increases progressively according to the number of epochs (total 24 epochs) to reach its best level. The model has become more generalized, especially from epoch 7. The graph shows also the classification accuracy across the entire validation set.

In the following Fig. 18, we show the curve evolution of the training loss and its smoothed version according to the number of epochs. As shown, the loss function decreases as the number of epochs increases.

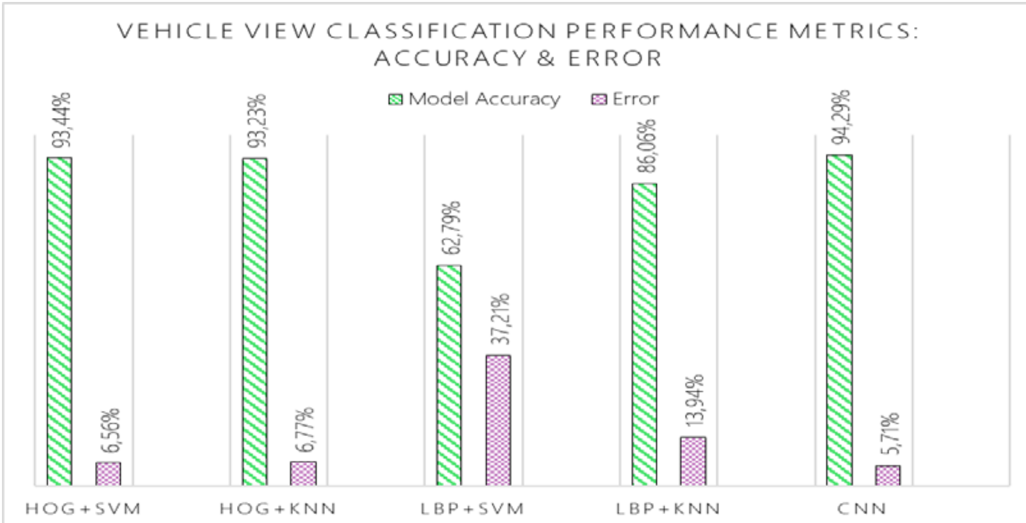

Fig. 16. Vehicle View Classification Accuracy.

TABLE I. VIEW CLASSIFICATION RESULTS

Models	Class : Rear		Class : Front	
	TP	FN	TP	FN
HOG+SVM	90.94%	9.06%	95.64%	4.06%
HOG+KNN	89.76%	10.24%	96.70%	3.30%
LBP SVM	32.68%	67.32%	92.89%	7.11%
LBP+KNN	85.83%	14.17%	86.29%	13.71%
CNN	92.91%	7.09%	95.69%	4.31%

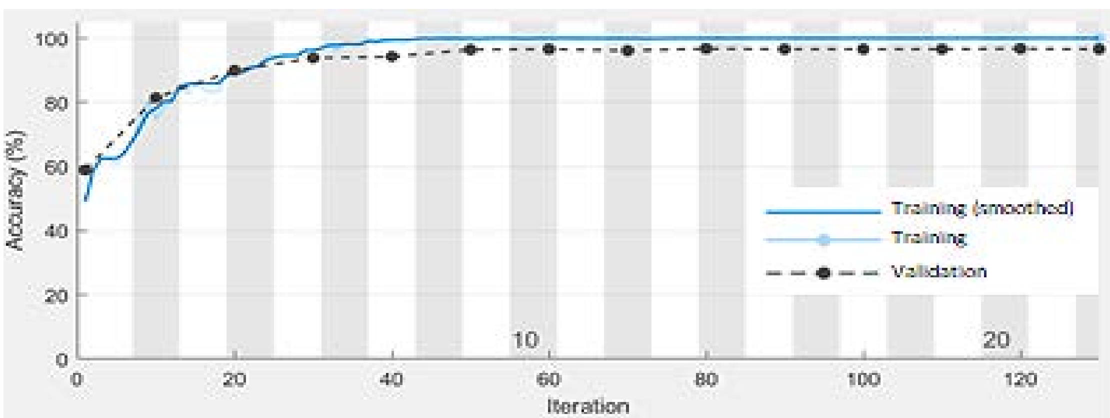

Fig. 17. The Evolution of Training Accuracy.

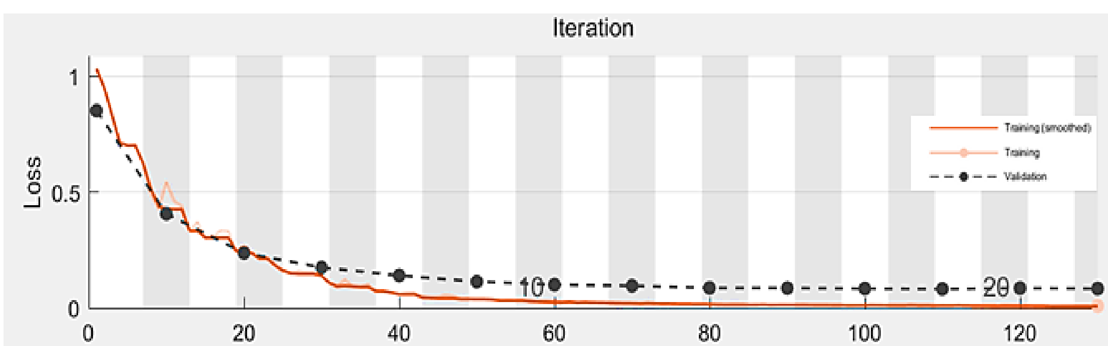

Fig. 18. Error Function.

During the execution of the algorithms, we observed that the CNNs take a very long time to be trained compared to the other models. If the number of layers increases, the training and testing time increase. On the other hand, the performance of the network becomes better [14]. In CNN, the most important layer is the convolution layer. Thus, this latter takes the most training time. Moreover, we have already worked on the classification of front and rear views but only for cars [2] (97.47% obtained by HOG+kNN). However, in this experiment, we classified the views of the four vehicle categories. This classification is more difficult, especially for motorcycles. Both views (front and rear) have the same shape.

2) Experiment 2 (Vehicle category classification)

a) Front view: In this experiment, we tested the algorithms with the front view dataset. The evaluation was based on the metrics we presented. The results were demonstrated in Fig. 19 and Table II.

Fig. 19 presents the overall accuracy and error of each model. Table II summarizes the comparative performance between all models; it shows the percentage of the accuracies and errors FP and FN of each category. We present the results of vehicle type classification basing on test data. Several observations can be made from this table. First, the combination of HOG and k-NN performs much better than the other combinations. It outperforms LBP and CNN. [3] also found that the accuracy of HOG features is higher than the convolutional neural network's accuracy (by 2,3%). Because HOG is a dense grid; it is used as low-level features, so it can extract richer information from the images [10]. Second, the Gabor filter is least efficient among all descriptors we tested. Gabor and LBP perform less efficiently with SVM, but when they are combined with k-NN, they provide better results. All descriptors work very well in combination with the k-NN classifier.

As shown in Fig. 19, the order of the best models, in this experiment, according to the accuracy is as follows: HOG+kNN, HOG+SVM, CNN, and LBP+kNN.

For each category, we calculated TP, FN, and FP as shown in Table II. We can see that all models (except Gabor+SVM and LBP+SVM) classified very well the three classes MOTO, CAR, and TRUCK. The MOTO class was obviously the easiest to be correctly classified.

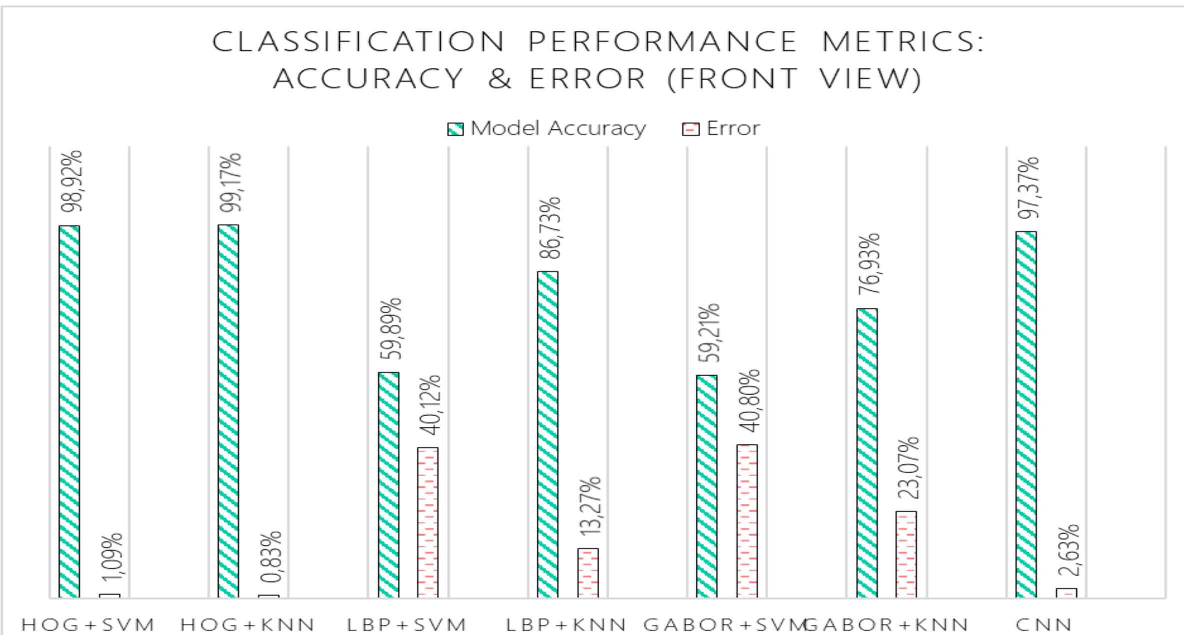

Fig. 19. The Accuracy and Error Obtained for Each Model (Front View).

TABLE II. CLASSIFICATION METRICS FOR EACH CATEGORY (FRONT VIEW)

Models	Class BUS			Class CAR			Class MOTORCYCLE			Class TRUCK		
	TP (%)	FN (%)	FP (%)	TP (%)	FN (%)	FP (%)	TP (%)	FN (%)	FP (%)	TP (%)	FN (%)	FP (%)
HOG+SVM	95.835	4.17	0	**99.8225**	0.1775	0	**100**	0	0	**100**	0	4.3475
HOG+kNN	**97.40**	2.60	0.26	**99.8225**	0.1775	0.257	**100**	0	0	**99.485**	0.515	2.7825
LBP+SVM	39.8475	60.16	7.99	95.1775	4.8175	127.04	78.75	21.2525	3.02	25.775	74.4	22.405
LBP+kNN	71.355	28.65	7.6705	92.8575	7.1425	16.89.5	94.585	5.42	4.115	88.145	11.8575	22.85
Gabor+SVM	70.05	29.9575	50.695	75	25	53.36	41.2525	58.7525	7.83	50.515	49.48	51.305
Gabor+kNN	63.5425	36.4625	16.6825	82.32	17.6775	33.9885	75	25	9.005	86.8575	13.1475	32.615
CNN	91.494	8.5049	0.402466	**99.2275**	0.772466	0.7741	**99.72166**	0.27833	0.0866	**99.0558**	0.9441	9.23663

The experimental results show that HOG+SVM produced errors $FN_{BUS} = 4.17\%$, $FN_{CAR} = 0.1775\%$ and $FP_{TRUCK} = 4.3475\%$. We observe that $FN_{BUS} + FN_{CAR} = FP_{TRUCK}$, this means that 4.17% of buses and 0.1775% of cars are classified as trucks. The same observation for the model HOG+kNN, 2.6% of buses and 0.1775% of cars are classified as trucks, but also 0.515% of trucks are classified as buses (0.26%) and cars (0.257%). This misclassification is due to the similarity of the appearance of these categories from the front view.

The next experiment aims at testing the same algorithms on the rear-view dataset.

b) Rear view: The second experiment was elaborated to verify the performance of the algorithms for vehicle category classification from the rear-view. Fig. 20 shows the classification performance of every constructed model. As observed from the figure, the models HOG+SVM, HOG+kNN and CNN, in the testing sets, achieved higher classification accuracies 99.58%, 99.47%, and 97.43%, respectively. The metrics of each class are listed in Table III. As concluded in the first experiment, HOG achieved the best results and k-NN outperforms SVM. For example, for the class BUS, when LBP is combined with SVM, it provided an accuracy of 9.09% whereas when it is combined with k-NN it provided an accuracy of 93.1825%. However, when k-NN and SVM are combined with HOG, they work slightly similar.

Table III shows the TP, FN, and FP per class.

In this experiment/both views, it is easy to see that the difficult category to classify was the BUS, especially from the front view. This is because most buses contain the same details and information as trucks from the front view compared to the rear-view. In both experiments, the HOG descriptor was the key to this classification. It delivered better performance in characterizing the shape and appearance of vehicles. HOG is considered as one of the most accurate feature descriptors for visual classification problems [35].

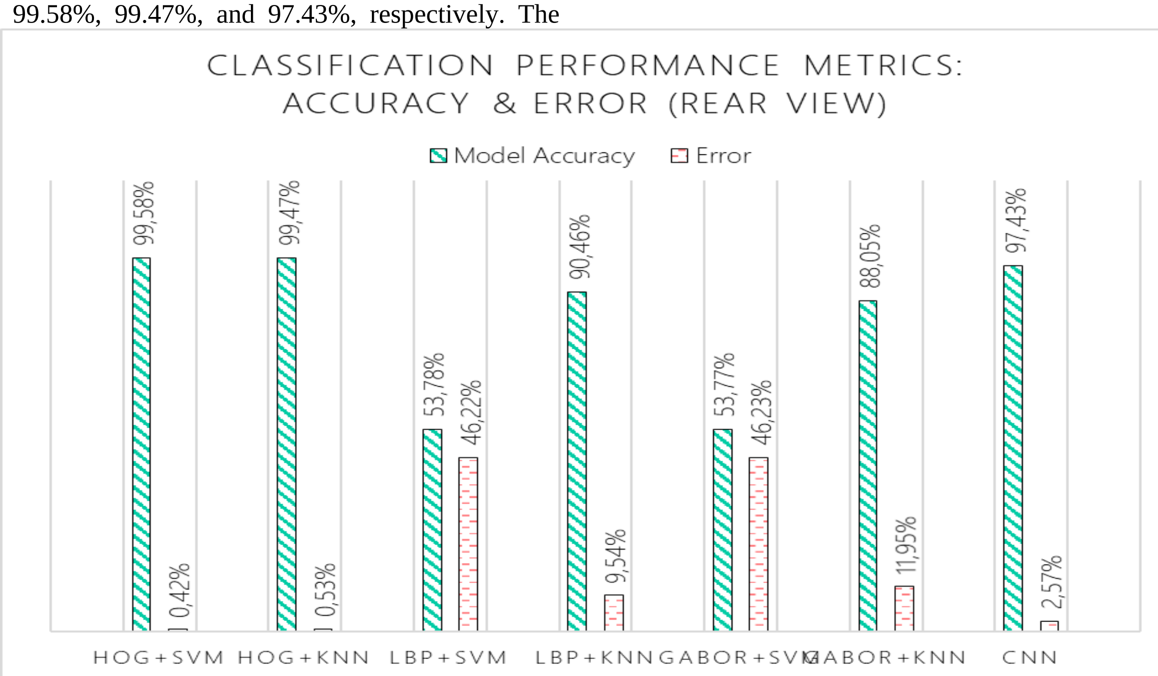

Fig. 20. The Accuracy and Error Obtained for Each Model (Rear View).

TABLE III. CLASSIFICATION METRICS FOR EACH CATEGORY (REAR VIEW)

Models	Class BUS			Class CAR			Class MOTORCYCLE			Class TRUCK		
	TP(%)	FN(%)	FP(%)	TP(%)	FN(%)	FP(%)	TP(%)	FN(%)	FP(%)	TP(%)	FN(%)	FP(%)
HOG+SVM	**99.4325**	0.5675	0.2875	**99.7125**	0.2875	0	**99.5825**	0.4175	0.425	**99.5975**	0.425	0.985
HOG+kNN	**98.295**	1.705	0.425	**100**	0	0	**100**	0	0	**99.5975**	0.425	1.705
LBP+SVM	9.09	90.9075	4.3175	95.1125	4.8875	135.01	63.335	36.6625	15.1725	47.5825	52.4225	30.38
LBP+kNN	93.1825	6.8175	11.195	93.675	6.325	10.495	96.25	3.75	3.58	90.7275	9.2925	4.6725
Gabor+SVM	17.0425%	82.955	8.975	85.9225	14.08%	97.22	50.4175	49.585	61.2725	61.6925	38.3075	17.46
Gabor+kNN	82.9525%	17.045	6.2675%	86.21%	13.8	21.445	86.665	13.3325	13.545	96.3725	3.6275	6.5475
CNN	96.0216%	3.9775%	4.04716%	96.8375%	3.16232	1.923326	**99.5825**	0.41746	0.47916	**97.3125**	2.687166	3.7948

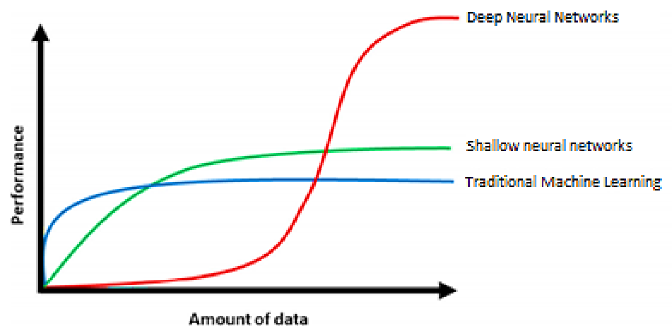

Fig. 21. Impact of Data Availability on the Algorithms [36].

CNN outperformed other methods in the vehicle view classification experiment. However, it was surpassed by HOG with k-NN and SVM in the vehicle category classification experiment. This is due to the impact of data availability. In the first experiment, we used a larger database than in the second one. Fig. 21 illustrates, in general, this impact on the performance of traditional machine learning methods and neural networks. Traditional methods reach better results with small amounts of data. However, deep learning can outperform all other methods with a large amount of data [36].

It was difficult to compare our results with those of other works on vehicle category recognition since no reference image set contains the categories from their front and rear views. And also, most of the works did not use the same methods we used. However, the results of previous works are as follows (Table IV). [8] achieved an accuracy of 96.26%. The author in [1] achieved accuracy of 93.90% using CNNs on vehicle frontal-view images. In [5], the CNN model achieved an accuracy of 97.88% on rear view images. In [3] achieved an accuracy of 92,6% on the BIT vehicle dataset. In [18], the author used the same dataset and reached 96.1% in daytime conditions and 89.4% in nighttime conditions. Unfortunately, this dataset has been removed from the website [37].

TABLE IV. COMPARISON OF VEHICLE CATEGORY CLASSIFICATION RESULTS WITH THE EXISTING WORKS

Study	View	Approach	Performance
[8]	Side	SVM and Random Forest	96.26%
[1]	Front	CNN	93.90%
[5]	Rear	CNN	97.88%
[3]	Front	Improved HOG_SVM	92,6%
[18]	Front	Semi-supervised CNN	96.1% / daytime 89.4% / nighttime
Proposed	Front and Rear	HOG, LBP, Gabor, SVM, k-NN, CNN	99.58% / Rear 99.17% / Front

3) Experiment 3 (Overall system): After building the models, we chose the best ones to create the global system (Fig. 22) in order to know which category an input image belongs to.

Experimental results demonstrated that CNN model achieved the best performance to recognize vehicle views, the HOG+kNN model has the highest accuracy in classifying vehicle categories from the front view, and the HOG+SVM model for the rear-view.

To evaluate the performance of the system, we tested it with a list of 209 images (different from those used in the datasets). This evaluation was based on many metrics: overall accuracy, accuracy for each view, runtime for each image. The evaluation results are presented in Table V. As shown, the system achieved an accuracy of 95.7746% and a runtime of 12.46 seconds per image.

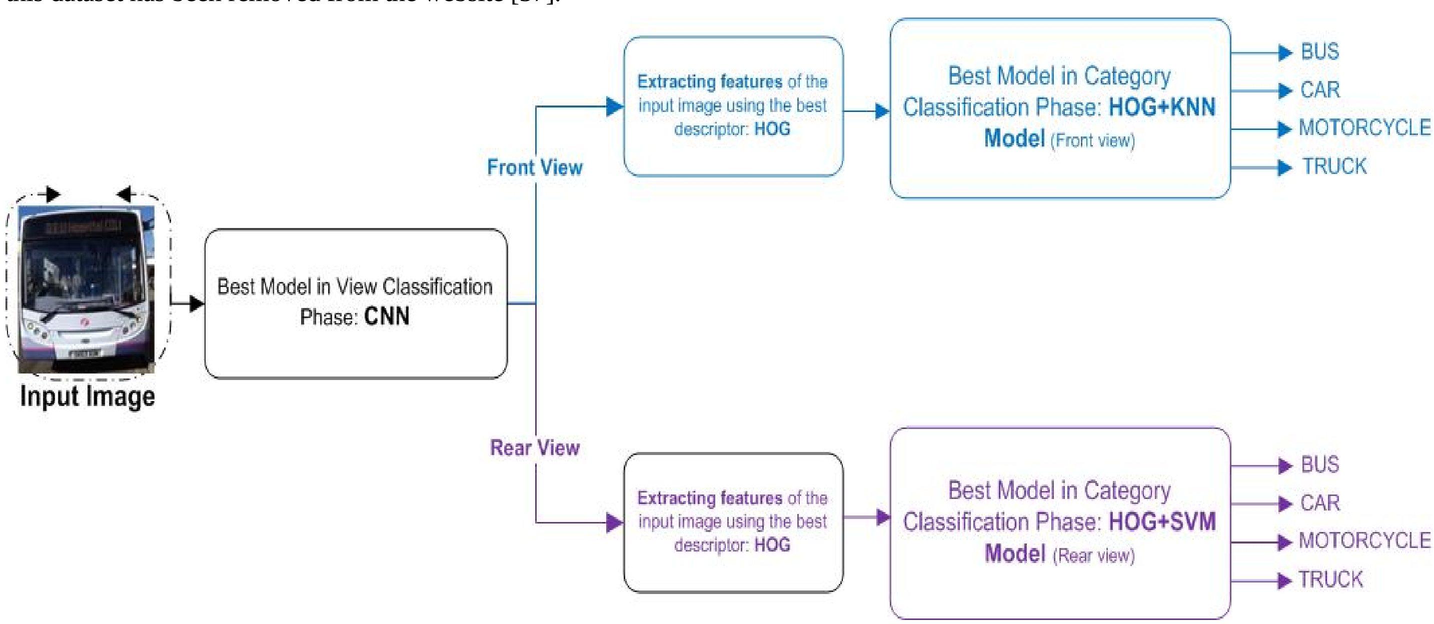

Fig. 22. System Flowchart.

TABLE V. SYSTEM PERFORMANCE METRICS

	Overall Accuracy		**Error**		**Time /Image (Second)**
System	**95.7746%**	Front : 98.29%	4.22%	Front : 1.709%	12.46
		Rear : 92.5%		Rear : 7.5%	

VI. CONCLUSION

In this paper, we have proposed a view-independent classification system for vehicle categories (Bus, Car, Motorcycle, and Truck) using traditional machine learning algorithms and CNNs. The system uses a two-phase approach. The first phase is used to recognize the vehicle view. The second recognizes the categories. To evaluate the built models, we used the three databases we built ourselves. The first dataset includes 4000 images, the second contains 2182 front vehicle images and the third contains 2000 rear vehicle images. The results showed that CNN provides the highest accuracy with the lowest error rate in the view classification step. But at the vehicle category classification step, the HOG features were efficient compared to Gabor and LBP features. they characterized well the vehicle's view orientations, making it more resistant to geometric and lighting variations. In fact, in this classification, it was easy to see that Motorcycle class was the easiest to be correctly classified with an accuracy of 100% / for both views. However, buses and trucks were misclassified due to their similar shapes. HOG achieved an accuracy of 99,58% with SVM, for the rear-view and 99,17% with k-NN for the front view. Finally, the overall system achieved an accuracy of 95,7746%. We can notice that, in classification, two main factors affect the performance of the system: the characteristics selected and the availability of data. The results we have obtained show that the system can be successfully exploited for many applications.

In future work, we will train CNNs with larger datasets, and detect and classify vehicles in traffic videos.

REFERENCES

[1] B., Hicham, A. Ahmed, M. Mohammed (2018). Vehicle Type Classification Using Convolutional Neural Network. *2018 IEEE 5th International Congress on Information Science and Technology (CiSt)*, 313-316. Doi: 10.1109/CIST.2018.8596500.

[2] S. Baghdadi, N. Aboutabit, Front and Rear Vehicle Classification, *Advanced Intelligent Systems for Sustainable Development (AI2SD'2019)*, vol.4, no.142. doi:10.1007/978-3-030-36674-2_28.

[3] Ge., Penghua and Hu., Yanping, Vehicle Type Classification based on Improved HOG_SVM. *Proceeding . 3rd International Conference on Mechatronics Engineering and Information Technology (ICMEIT 2019)*. Doi: 10.2991/icmeit-19.2019.102.

[4] J., Lian, J., Zhang, T., Gan and S., Jiang. Vehicle Type Classification using Hierarchical Classifiers. *Journal of Physics: Conference Series*. 2018. Vo.1069.doi: 10.1088/1742-6596/1069/1/012099.

[5] Y. Chen, W. Zhu, D. Yao and L. Zhang, "Vehicle type classification based on convolutional neural network," *2017 Chinese Automation Congress (CAC)*, Jinan, 2017, pp. 1898-1901. doi: 10.1109/CAC.2017.8243078.

[6] N., Roecker, Max, M. G., Yandre Costa, L. R., João Almeida and H. G., Gustavo Matsushita. "Automatic Vehicle type Classification with Convolutional Neural Networks." *2018 25th International Conference on Systems, Signals and Image Processing (IWSSIP)* (2018): 1-5.

[7] S. Kul, S. Eken and A. Sayar, "A concise review on vehicle detection and classification," *2017 International Conference on Engineering and Technology (ICET)*, Antalya, 2017, pp. 1-4. doi: 10.1109/ICEngTechnol.2017.8308199.

[8] Z. Chen, T. Ellis and S. A. Velastin "Vehicle type categorization: A comparison of classification schemes", *14th IEEE Annual Conference on Intelligent Transportation Systems*, the George Washington University, Washington, DC, USA. pp. 74-79, Oct. 5-7, 2011.

[9] Y. C. Wang, C. C. Han, C. T. Hsieh, and K. C. Fan, Vehicle type classification from surveillance videos on urban roads, in Ubi-Media Computing and Workshops (UMEDIA), 2014 7th International Conference on, 2014, pp. 266–270.

[10] Z., bailing and Z., Yifan. Vehicle type and make recognition by combined features and rotation forest ensemble. *International Journal of Pattern Recognition and Artificial Intelligence*. Vol. 26, No. 03, 1250004 (2012). Doi : 10.1142/S0218001412500048.

[11] M. A. Manzoor, Y. Morgan ,"Vehicle Make and Model Classification System using Bag of SIFT Features", 7th IEEE Annual Conference on Computing and Communication Workshop and Conference (CCWC), Las Vegas, NV, USA. pp. 572 577, 02 March 2017.

[12] A.H.S. Lai , G.S.K. Fung , N.H.C. Yung, "Vehicle Type Classification from Visual-Based Dimension Estimation", Intelligent Transportation Systems, 2001. Proceedings. 2001 IEEE, Oakland, CA, USA, pp. 201-206, 25-29 Aug. 2001.

[13] D. Kleyko, R. Hostettler, W. Birk, E. Osipov, "Comparison of Machine Learning Techniques for Vehicle Classification Using Road Side Sensors", 2015 IEEE 18th Int. Conf. Intell. Transp. Syst., pp. 572-577, 2015.

[14] S. Albawi, T. A. Mohammed and S. Al-Zawi, "Understanding of a convolutional neural network," *2017 International Conference on Engineering and Technology (ICET)*, Antalya, 2017, pp. 1-6. doi: 10.1109/ICEngTechnol.2017.8308186.

[15] B. Selbes and M. Sert, Multimodal vehicle type classification using convolutional neural network and statistical representations of MFCC. *2017 14th IEEE International Conference on Advanced Video and Signal Based Surveillance (AVSS)*, (2017) 1-6. Doi: 10.1109/AVSS.2017.8078514.

[16] A. Krizhevsky, I. Sutskever, and G. E. Hinton, "Imagenet classification with deep convolutional neural networks," in *Advances in Neural Information Processing Systems 25*, F. Pereira, C. J. C. Burges, L. Bottou, and K. Q. Weinberger, Eds. Curran Associates, Inc., 2012, pp. 1097–1105.

[17] C. Szegedy, W. Liu, Y. Jia, P. Sermanet, S. Reed, D. Anguelov, D. Erhan, V. Vanhoucke, and A. Rabinovich, "Going deeper with convolutions," in *Computer Vision and Pattern Recognition (CVPR)*, Boston, MA, USA, June 2015.

[18] Z. Dong, Y. Wu, M. Pei, and Y. Jia, "Vehicle type classification using a semisupervised convolutional neural network," *IEEE Transactions on Intelligent Transportation Systems*, vol. 16, no. 4, pp. 2247–2256, August 2015. doi:10.1109/TITS.2015.2402438..

[19] K., Phi, book, Matlab Deep Learning: with Machine learning, neural network and artificial intelligence. 2017. ISBN-13 (pbk): 978-1-4842-2844-9. ISBN-13 (electronic): 978-1-4842-2845-6. DOI 10.1007/978-1-4842-2845-6.

[20] N., Dalal, B., Triggs. Histograms of oriented gradients for human detection, in: *IEEE Computer Society Conference on Computer Vision and Pattern Recognition*, pp. 886–893. 2005.

[21] R., Scherer. Computer Vision Methods for Fast Image Classification and Retrieval. 2020. ISSN 1860-949X. ISSN 1860-9503 (electronic). https://doi.org/10.1007/978-3-030-12195-2.

[22] Y., Sinha, P., Jain, N. Kasliwal: Comparative Study of Preprocessing and Classification Methods in Character Recognition of Natural Scene Images. In: Machine Intelligence and Signal Processing. Advances in Intelligent Systems and Computing, vol. 390. Springer, New Delhi (2016). doi: 10.1007/978-81-322-2625-3_11.

[23] A. I. Awad and M. Hassaballah, Image Feature Detectors and Descriptors, Foundations and Applications, Switzerland: Springer, 2016.

[24] M., Bereta, W., Pedrycz, M., Reformat. Local descriptors and similarity measures for frontal face recognition: A comparative analysis. *J. Visual Communication and Image Representation*, vol. 24, pp. 1213-1231. 2013. doi: 10.1016/j.jvcir.2013.08.004.

[25] S., Baghdadi, N., Aboutabit: Illumination Correction in a Comparative Analysis of Feature selection for Rear-View Vehicle Detection. *International Journal of Machine Learning and Computing (IJMLC)*, vol 9 n.6 .2019. doi: 10.18178/ijmlc.2019.9.6.863.

[26] J. R. Movellan, "Tutorial on Gabor Filters".

[27] T.-J., Alhindi, S., Kalra, K.-H., Ng, A., Afrin, H.-R., Tizhoosh: Comparing LBP, HOG and deep features for classification of histopathology images. In: International Joint Conference on Neural Networks (IJCNN) (2018). doi: 10.1109/IJCNN.2018.8489329.

[28] C.-W., Hsu and C.-J., Lin. A Comparison of Methods for Multi-class Support Vector Machines. *IEEE Transactions on Neural Networks* 13(2):415-25. 2002. doi: 10.1109/72.991427.

[29] F., Melgani, and L., Bruzzone. Classification of hyperspectral remote sensing images with Support Vector Machines. IEEE Transactions on Geoscience and Remote Sensing, 42, 1778 – 1790. 2004.

[30] S., Baghdadi, N., Aboutabit: A Comparative Study of Vehicle Detection Methods, Advanced Intelligent Systems for Sustainable Development (AI2SD2018), Springer, vol. 5, pp. 111 (2019). doi: 10.1007/978-3-030-11928-7_83.

[31] Sh., Lin, Ch., Zhao, and X., Qi: Comparative Analysis of Several Feature Extraction Methods in Vehicle Brand Recognition. In: 10th International Conference on Sensing Technology (ICST) (2016). doi: 10.1109/ICSensT.2016.7796337.

[32] M., Salvaris, D., Dean, W., Hyong Tok. *Deep Learning with Azure*. ISBN-13 (pbk): 978-1-4842-3678-9. ISBN-13 (electronic): 978-1-4842-3679-6. https://doi.org/10.1007/978-1-4842-3679-6.

[33] K., Jarrett, K., Kavukcuoglu, M.A., Ranzato, and Y., LeCun. What is the best multi-stage architecture for object recognition? 2009 IEEE 12th International Conference on Computer Vision. doi:10.1109/iccv.2009.5459469.

[34] F., Özyurt, T., Tuncer, E., Avci, *et al.* A Novel Liver Image Classification Method Using Perceptual Hash-Based Convolutional Neural Network. *Arab J Sci Eng* 44, 3173–3182 (2019). https://doi.org/10.1007/s13369-018-3454-1.

[35] L., Xuesong, J., Jo, S., Youngbo and D., Stantic. "Detection and Classification of Vehicle Types from Moving Backgrounds." *RiTA* (2017).

[36] P. Savadjiev, J. Chong, A. Dohan, M. Vakalopoulou, C. Reinhold, N. Paragios, B. Gallix. Demystification of AI-driven medical image interpretation: past, present and future.

[37] http://iitlab.bit.edu.cn/mcislab/vehicledb/.

AUTHORS' PROFILE

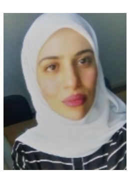

Sara Baghdadi is a Ph.D. Student at the National School of Applied Sciences in Khouribga (Sultan Moulay Slimane University, Morocco). She received her engineering diploma in Networking and Telecommunications in 2015 from the same school.

Her main research interest includes Machine Learning and Image Processing.

Noureddine Aboutabit is actually an Associate Professor in Telecommunications and multimedia processing at the National School of Applied Sciences, Kh-ouribga (Sultan Moulay Slimane University, Morocco) since October 2011. He teaches in the Department of Networking and Telecommunication primarily in the areas of computer vision, signal processing and image processing. In 2007, he received his Ph. D. degree in Signal Image Speech Telecom from Grenoble INP (France). He received his M.S. degree in 2004 from the same institute. In 2003, he obtained his engineering diploma from Ecole Normale Suprieure d'Ingnieurs Electriciens de Grenoble (ENSIEG).

His current research interests include computer vision, machine learning, artificial intelligence, and multimedia processing.

APPENDIX

Some samples of the datasets containing four types: Bus, Car, Motorcycle, and Truck.

Fig. 23. Samples from Bus Class (Front View).

Fig. 24. Samples from Car Class (Front View).

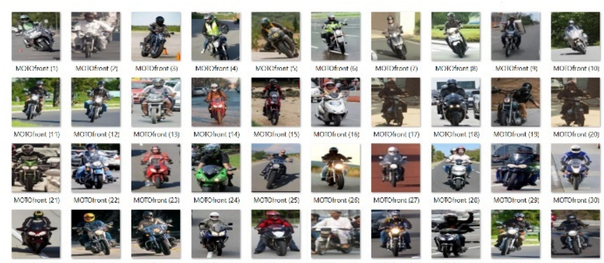

Fig. 25. Samples from Motorcycle Class (Front View).

Fig. 26. Samples from Truck Class (Front View).

Fig. 27. Samples from Bus Class (Rear View).

Fig. 28. Samples from Car Class (Rear View).

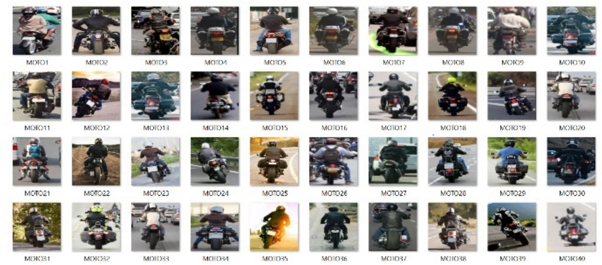

Fig. 29. Samples from Motorcycle Class (Rear View).

Fig. 30. Samples from Truck Class (Rear View).

Machine Learning Predictors for Sustainable Urban Planning

Sarojini Devi Nagappan[1], Salwani Mohd Daud[2]
Advanced Informatics School
Razak Faculty of Technology and Informatics
Universiti Teknologi Malaysia
Kuala Lumpur, Malaysia

***Abstract*—While essential for economic reasons, rapid urbanization has had many negative impacts on the environment and the social wellbeing of humanity. Heavy traffic, unexpected geohazards are some of the effects of uncontrollable development. This situation points its fingerto urban planning and design; there are numerous automation tools to help urban planners assess and forecast, yet unplanned development still occurs, impeding sustainability. Automation tools use machine learning classification models to analyze spatial data and various trend views before planning a new urban development. Although there are many sophisticated tools and massive datasets, big cities with colossal migration still witness traffic jams, pollution, and environmental degradation affecting urban dwellers' quality. This study will analyze the current predictors in urban planning machine learning models and identify the suitable predictors to support sustainable urban planning. A correct set of predictors could improve the efficiency of the urban development classification models and help urban planners to enhance the quality of life in big cities.**

Keywords—Urban planning; sustainable development; urban development classification model; machine learning; urban development predictors

I. Introduction

Growing cities, due to socioeconomic activities, witness the challenges of rapid urbanization much faster. Rapid urbanization, once seen as a positive change, has brought many challenges to sustainable development. Some of the research cited challenges include environmental degradation, social equality, climate issues [1]. The United Nations has projected an increase of 60 per cent increase in urbanization in developing countries, and the situation could lead to unmanaged urban development if not handled wisely [2]. The author in [2] has pointed out urbanization is shaped by spatial and urban planning. However, the rapid growth in the city has brought in much unmannered urban development. The continuous development of facilities to feed the needs of the city population and fuel economic growth has led to challenges from various dimensions, including pollution, health issues, infrastructure congestion and massive traffic.

While much care is taken to ensure the ecosystem during city planning, the increase in geohazards such as flash floods and unbearable climate change is alarming [3-5]. Unmanageable city development has also led to overcrowding cities with uncontrollable traffic conditions and disoriented land development.

The increase of people and vehicles on the road increases the traffic index daily in cities, contributing to accidents and health issues such as anxiety and pollution. An improved sustainable urban planning methodology can control uncontrollable development and minimize its negative impact.

Although numerous urban planning support systems and various large amounts of data, unplanned development still happens in many major cities. The author in [6] have pointed out that urban planners can better support city planning by analyzing a city's density and compactness. The algorithmic analysis will help urban planners better study the city development patterns to help the decision-making process for the further development of a busy town. Some quantifiable metrics mentioned by [6] are used by urban planners for decision making include density, compactness, clustering and connectivity. However, the evidence of these metrics on their efficiency and relationship is still inconclusive.

Discussion on land development often leads to the topic of land use land cover (LULC). Modelling the land use change (LUC) process is essential in urban planning as it enables the urban planners and policymakers to make an informed decision in planning a city's infrastructure [7]. Many urban planning automation tools use machine learning models to classify the current development in a given area in urban planning simulation [8]. Models developed with these machine learning algorithms talks about the correlation between spatial indicators and land use classes but does not expand to the study of estimating LUC for forecasting or prediction [7].

The author in [7] stressed that a good machine learning framework with a suitable prediction model is necessary for urban planning. Many scholars study the classification of the attributes on the land cover using ML techniques to classify the characteristics on lands such as forest, water, buildings, and the intensity of land use change based on human activities for a given area. Recent research by [9] has indicated remote sensing data can provide information on natural attributes of ground components, but it does not show information of socio-economic features caused by human activities, which is contributing to challenges in urban land use classification.

The classification machine learning algorithms require the right set of features to classify urban development accurately. An excellent urban planning model allows the urban planners and policymakers to decide to plan a city's infrastructure [7].

The main objective of this paper is to explore machine learning urban planning classification models and propose new urban predicator categories to improve sustainable urban development. Section 2 of this paper will discuss the concepts in three domains, namely sustainability, urban planning and machine learning. Section 3 outlines the methodology used for this review. Section 4 presents the finding of the review coupled with the discussion of the findings.

II. Problem Background

Environment degradation, poor health and spread of disease, increasing urban crime are some of the challenges faced with rapid urbanization. Urbanization does equally provide a good transformation for the economic growth and citizens wellbeing; however, with the large scale migrating to the busy cities, the positive impact is now slowly fading. The author in [3] has highlighted adverse effects to environments are due to urban activities. An increase in urban population also speeds up the expansion for physical built up which exacerbate the warming climate of city dwellers [4]. The author in [10] also pointed out the fact that rapid urbanization causes problems to climate change, social inequalities and land scarcity. Sustainable development goals spearheaded by the United Nation s[2] outlines the required services or necessary resources to support the wellbeing of a certain percentage of the population. Sustainable development aims to achieve these goals via various activities, and one of them is sustainable urban planning.

Sustainable urban planning is related to the physical and spatial planning to optimize the distribution of land allocation to support human activities [11]. In an urban context, this implies creating both resource-efficient systems and good, engaging urban design for attractive cities with good quality of life [12].

The recent paradigm shift on urbanization has also awakened the realization of the need for sustainable urban planning to support sustainability goals. Land development along with land transactions in the cities is a forced change by urbanization. Nevertheless, when global migration to significant cities happens rapidly, this change is viewed as a positive relationship between land development and land-based revenue growth [13]. Due to this, policymakers and urban planners are often bounded by the economic growth indicator to decide on further development. The development of residential, commercial and other amenities is continuously increased as the need of city dwellers increase. As a result, the infrastructure eco system becomes unstable, causing traffic congestion, climate change, urban crimes and many other negative effects.

These recent advancements have exposed the need for urban planners to support sustainable development is now increasingly evident. They hold the key responsibility to decide on the need and impact of further development in a city with rapid urbanization. Fortunately, with the rise of smart cities and big data, there is an explosion of different types of data from various sources for the urban planner to analyze and predict the need and impact of further development in a compact city. With the advancement in the planning support systems, big data and artificial intelligence (AI), urban planners are now able to use data and urban models not only to evaluate the need but to predict the consequences of rapid development. Although there are many areas of focus in urban planning supporting sustainable planning, there is an increasing research interest in the study of land use land cover (LULC). Research by [14] mentions LULC is a major driver to globalization as well as a great support to sustainable development. This research has pointed out how the LULC change analysis employed in prediction models are helpful to monitor LULC to understand the historical events of change on landcover and forecast the impact of future development to mankind. LULC analysis largely depends on remote sensing data, and the accuracy depends on the machine learning model employed to process the data. While there were claims on the unavailability of spatial data previously [15], Google Earth has brought in many data sets on the cloud to make the LULC not only easier but also faster coupled with visualization, making it easier for urban planners to ingest the data [16]. Despite the availability of large datasets, there is little evidence on the classification, simulation or prediction of land use domain that involves human interaction in urban development [17]. This study aims to review existing classification models and predictors used in LULC classification to understand the missing predictors to support sustainable urban planning. Urban development models with the right set of predictors supporting sustainable urban development can help urban planners better decide on future developments and impacts in highly urbanized cities.

III. Related Work

Related works in this study are derived from three different domains, including sustainability, urban planning and machine learning. Table I lists the concepts gathered in the literature review used directly or indirectly in this study.

A. Sustainable Development

Sustainability is initially defined as the mechanism of how natural systems produce and provide to the ecosystem in a balanced way. Sustainability originally defines as the mechanism of how natural systems produce and provide to the ecosystem in a balanced way. This concept has been evolving since its conceptualization in 1946 by Sir John Hicks [18]. According to [18] there is a high correlation between human activities and the stability of the natural ecosystem. Human activities influence on the natural ecosystem or environment can be from economic, social and political grounds. Hence to create a sustainable solution, it is crucial to have the three pillars: economic, social and environmental systems to work in harmonization [18].

Brundtland commission popularized the concept of sustainable development (SD) and defined it as the “development that meets the current needs without compromising the ability of future generation needs” [19]. Sustainable development indicators can be divided into economic, social and environmental indicators. There are three pillars of sustainability which is the foundation to drive sustainable development. Sustainable development indicators should be understandable, adaptable and measurable for future development. Indicators provide the means of performance measurement for urban sustainability. It is therefore important to select the best indicators to achieve the optimum performance of urban sustainability.

This study concentrates on the indicators to achieve sustainable development goal 11(SDG 11), which has the target to develop safe, resilient, and sustainable cities. There are ten targets with 15 indicators to be addressed by SDG 11, and they are strongly related to the urban transformations to sustainability. This includes four focus areas of the SDG 11 indicators, namely, inclusivity, urban safety, resiliency and sustainability, with the following target indicators:

- Safe and Affordable Housing.
- Affordable and sustainable transport systems.
- Inclusive and sustainable urbanization.
- Protect the world's cultural and natural heritage.
- Reduce the adverse effects of natural disasters.
- Reduce the environmental impacts of cities.
- Provide access to safe and inclusive green and public spaces.
- Strong national and regional development planning.
- Implement policies for inclusion, resource efficiency and disaster risk reduction.

This study refers to indicators from the need for improved urban planning and management techniques to develop sustainable cities in SDG 11 and map it to the current features used in urban development model classifications use for LULC monitoring. Once the mapping is done, the missing indicator will be used in the classification to enhance the urban development classification to support sustainable urban planning.

B. *Urban Planning Concepts*

Urban planning is a cyclic process encompassing many phases and stakeholders' involvement at many intervals and entirely bounded by the legal framework. It is a domain associated with the process of open land development as well as redesigning the unutilized space effectively to promote sustainable urban development [20]. Urban planning is deemed an important tool to promote sustainable urban development and keep the authorities informed on infrastructure development, land investments and demand, or urban population growth [21].

Urban planning tools employ land use land cover (LULC) models to study the change analysis in the landscape. This change analysis provides an insight into historical land use patterns as a base to forecast future developments [22]. Land cover defines the area covered by forest, wetlands, impervious surfaces, agriculture and other land and water types on earth surfaces and land use describe how the land has been used by socioeconomic activities to change the natural landscape into urban built land, cultivated or recreational areas [23]. LULC change analysis uses remote sensing geographical information system (GIS) data to simulate and forecast changes in many areas like deforestation, climate change and population movement [23]. LULC monitoring plays an important role in urban planning [24]. The change analysis allows the urban planner to take an informed decision for future development for a designated area. LULC change analysis is also used in understanding the effects of urbanization, ecosystem degradation, the impact of pollution on the quality of life [23, 25, 26]. Urban development models use machine learning techniques like SVM, Random Forrest (RF) are widely used to study the change analysis LULC. These models use spatial data to classify LULC and are used by urban planners to evaluate the impact on domains like climate, pollution, traffic via GIS tools. To minimize the impact of rapid urban development, it is important to have the right set of features included in the machine learning models. The right set of features will classify LULC at a higher accuracy to give urban planners a better understanding of the study area before moving forward with a development decision.

Land use land cover monitoring plays a vital role in sustainable development planning [27] because it shows the changes to land cover historically. Revisiting the urban planning decision and management policies is crucial to achieving sustainable urban development. With an improved LULC classification, it would be easier to make informed decisions to drive sustainable development for a better future generation.

Many modelling techniques have been employed to measure the land use land cover change (LULCC). It provides the continuous assessment of the current situation as well as provides the capability to predict future land use change [28]. The author in [29] argue that the performance of the individual indicators or predictors plays a significant role in modelling the land use change (LUC) dynamics. Hence the ability to model LULCC and simulate LUC is firmly based on the predictors used in the urban simulation model.

C. *Urban Planning Predictors*

Urban development or urban expansion are terms used in urban planning to denote the development of a given land area. At present, the evaluation of land use change patterns has gained research popularity again. It was evident that environmental degradation was due to uncontrollable human activities on the land surface. Hence urban simulation using geospatial data is now popular again. Machine learning is currently being employed to achieve better classification and improve and improve the accuracy of existing machine learning models. The machine learning models' performance depends on the features used to measure the land use change simulation. In this study, predictors are referred to as the features used in the urban simulation model to simulate and predict a land use change. Simulating urban development patterns using these predictors provides an early assessment of urban planning before its implementation [30]. The role and selection of predictors are solely dependent on using the model in the defined area.

D. *Machine Learning in Urban Planning*

Many researchers have utilized machine learning in urban planning and design to develop and monitor city planning in recent years. Urban analytics and urban simulations employ machine learning is used for predictive analysis for a given domain. Several techniques and algorithms have been employed in simulation to enable urban planners to improve decision-making for strategic planning. Recent research by [28] stressed the importance of high prediction accuracy to monitor land use change. The same study has also pointed out the need for a suitable model for different applications to ensure accuracy and fitness.

Urban planner uses GIS tools to collect, manage, analyze and visualize geospatial data [30]. Commonly GIS tools use a simulation model to evaluate, predict and analyze complex urban interactions and processors [31]. These urban development models can also identify the urban development trends and their impact with various views to help urban planners understand better the area they are working on. The efficiency of urban planning would depend on the predictors used in the urban classification model. A good predictor enables the urban development classification model to analyze the current geospatial data pattern and simulate future sustainability growth.

TABLE I. KEY CONCEPTS

Concept	Definition
Sustainable Development	Sustainable development (SD) is the development that meets the current needs without compromising the ability of future generation needs."
Urban Planning	Urban planning is a cyclic process encompassing many phases and stakeholders' involvement at many intervals and entirely bounded by the legal framework.
Urban Planning Predictors	Urban planning predictors are referred to as the features used in the urban simulation model to simulate and predict a land use change.
Urban development classification model	An urban development classification model would analyze the current pattern of geospatial data and simulate future growth with a good set of predictors

IV. LITERATURE REVIEW METHODOLOGY

A literature review study was carried out to have a concise understanding of concepts and capture the relevant literature on sustainable development and machine learning predictors in urban planning. The purpose of the review is to understand what and how sustainable development goals play a role in urban planning and how the indicators can be used to define additional features or predictors for a better urban development classification model.

This study uses the Preferred Reporting Items for Systematic reviews and Meta–Analyses (PRISMA) to validate the relevancy of the literature's collated before reporting the conclusion. PRISMA advocates four phases for literature review, starting from identification of the record source, screening of the records, setting the eligibility criteria and finally compiling the records to be included for the identified research [32]. Fig. 1 illustrates the PRISMA flowchart adopted for this study.

In the identification phase, the source of the records is determined to avoid the irrelevant search. For this study, literature will be extracted from five databases, including IEEE, Scopus, Springer, Science Direct and Web of Science.

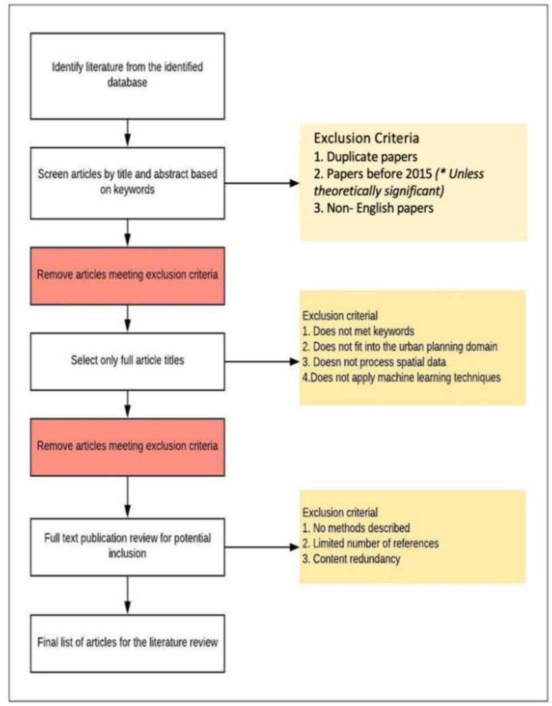

Fig. 1. PRISMA Flow Chart used for Literature Review.

The next process is screening the records. Records are screen based on the keywords found from the first level of record retrieval. The first screening exclusion criteria to be applied is as follows:

- Duplicate papers. As there are many sources of the database the records will be retrieved from, there are high chances of duplicate records.
- Papers which are before the year of 2015 will not be considered unless it defines a standard terminology or significantly prominent for the research. Also, for the purpose of this study.
- Non-English papers are to be removed.

In the first phase of screening, the articles will be screened by title and abstract based on the list of keywords. The list of keywords is listed in Table II.

The second round of screening only takes into account full text records. Records with only abstracts are not included in the screening. The third level of screening is based on the actual content. The content of the articles must be complete with the methods without content redundancy. Records with below ten references are omitted. The screening process includes setting the inclusion and exclusion criteria that have been listed earlier. The last stage of the flow is to compile the final list of records to be included in the final literature review.

The review was done to

- Gather the sustainable development goal indicators for urban planning.
- Analyze the concepts in urban planning and evaluate the human activities on land.

- Review the features used by different urban classification models.

TABLE II. KEYWORD USED IN THE LITERATURE SEARCH STRINGS

Domain	**Keywords**
Sustainable Development	• sustainability • sustainable development • sustainable development goals • sustainable urban planning • sustainable urban planning indicators
Urban Planning	• Urban planning • Urban planning classification model • Urban planning indicators • Urban planning simulation • Urban planning assessment • Urban planning measurement metrics • Urban planning density
Machine Learning	• Machine learning models in urban planning • Machine learning features in urban planning • Machine learning algorithm performance • Machine learning accuracy • LULC classification

V. FINDINGS AND DISCUSSION

The following six urban models have been analyzed from scholarly reviews to understand the predictors or indicators used to simulate urban expansion and tabled out in Table III. These models were actively used to simulate land use changes since 2011 cited in a review done by [30].

- Cellular Automata.
- Regression Models.
- Artificial Neural Networks.
- Agent Based Models (ABM).
- Tree Based Models.
- Support Vector Machines (SVM).

Some of the reviews have detailed out the criteria, like the indicators used in the SVM model. This gives an indication to know the popularity of the model employed in this field. Another interesting finding is the gaining interest in the Agent-Based Model (ABM) model to which is widely used in land-use change and transport line models. This model is gaining interest as it considers three main stakeholders in the urban planning process. However, this model has its limitation because its dependency on agents' predictors is highly variable.

TABLE III. URBAN DEVELOPMENT MODELS AND ITS PREDICTORS

Urban Development Model	Predictor	Reference
Cellular Automata model (CA)	proximation roads, expressways, railways and town centers, land use types and topography and population density	[33, 34]
Artificial neural networks (ANN)	elevation, slope, annual population growth rate, land use types and distance	[35, 36]
Linear Regression (LR) Predictors	easting and northing coordinates, land use types, slope, restricted areas, population density, distances to main active economic centres, a central business district, roads and urbanized area	[37, 38]
Agent Based Model (ABM) Predictors	**Dwellers** -accessibility to education centers, favourite elevation, favourite slope, accessibility to health services, accessibility to metro stations, distance from disposal area, accessibility to fruit garden accessibility to sports centers, accessibility to the road network, accessibility to recreation areas, accessibility to business districts distance to railway **Developers**- residential density,employment density,commercial intensity/density,investment profit minimum unseen profit maximum profit Government river streams risk zone, roads network buffer, highways buffer, airports risk buffer, military facility risk zone, power facility risk zone, parks buffer on a suitable slope	[39] [40] [36] [41] [42]
Decision Tree Model(DT)	development history, elevation details, land type, proximities to neighbourhood amenities and densities of residential, commercial	[43]
Support Vector Machines (SVM)	land-use types land use densities proximities to: roads, expressways, railways and town centres, as well as land-use types and topography neighbouring land characteristics built area unbuilt area	[30] [44] [45] [46] [40]

The land-use change patterns, which are the main urban development metrics, cannot be just determined by only one factor. The relationship between various factors provides a better evaluation of urban development. The author in [36] explain the urban growth and development indicators differs based on the model and data used to evaluate or predict the urban pattern change.

A. Urban Development Models Predictor Evaluation

According to [30], predictors in urban development modelling can be further categorized as site specific proximity and neighbourhood characteristics. Site specific characteristics describe built and unbuilt areas as well as commercial and residential buildings. Proximity predictors refer to the distance of access to a specific facility, like the distance to roads, highways, urban built areas, green space and water bodies. The neighborhood characteristics refer to predictors which will affect LULC in future including the number of cells corresponding to wetlands, forest, barren lands, developed areas. Table IV below shows a summary mapping between the existing urban land indicator categories by [47] and predictor categories by [30]. If the predictors match the indicators, it is indicated as “complies”.

Table V shows that the urban development models are commonly used by tools or applications to model urban growth. All the models have used site-specific and proximity predictors. Remote sensing data gives a good source for site-specific and proximity indicators, which is one reason why it's a commonly used predictor category in all models. The neighborhood category defines its attribute in the number of cells usually found on maps. This measurement is very suitable for fractal development models as it works best with maps. In a fractal model, structures are produced by iterations of the same principle in a given pattern of points, lines or surfaces. The model's accuracy depends on the model. The last two categories are population, and crowd mobility is the least used predictor category in the urban development models analyzed in this study. Mobility of the city dwellers and the population indicators are not used in the urban expansion models. This information is not easily made available in a single source data source like remote sensing data. Research by [9] has pointed out that although including socioeconomic data would improve the accuracy of classification accuracy, there is very little evidence to show its usage. However, due to rapid urbanization, the increase of traffic and environmental hazards warrants the inclusion of these predictors in the urban development model. research has used these data to improve accuracy. Agent based models are now considering factoring these predictors as it may improve the transit-oriented model.

TABLE IV. URBAN DEVELOPMENT MODEL PREDICTOR CATEGORIES COMPLIANCE TO LAND USE

Land Use Predictor Categories	Urban Development Model Predictor Categories		
	Site Specific	Proximities	Neighbourhood
Neighbourhood	-	-	-
Employment	-	-	-
Infrastructure	Complies	Complies	Complies
Access to Basic Facilities	-	Complies	Complies
Legislation	-	-	-
Environment	Complies	-	-

TABLE V. PREDICTORS CATEGORIES USED IN SELECTED URBAN DEVELOPMENT MODELS

Urban Development Models	Urban Development Model Predictor Derived from Research Article (1986 – 2018)					
	Application	Site Specific	Proximities	Neighbourhood	Population Density	Crowd Mobility
Cellular Automata	Large Scale Urban Simulation	√	√			
Artificial Neural Network	Modelling of Urban Growth	√	√		√	
Fractals	Urban Growth Experience	√	√	√		
Linear/ Logistic Regression	Prediction of urban growth pattern	√	√		√	
Agent Based Model	Modelling and simulation of land use and land cover dynamics	√	√		√	
Decision Tree	Prediction of Urban Growth	√	√			
Support Vector Machine	Prediction of Urban Expansion	√	√	√		

Fig. 2. Urban Development Model Predictors: Existing and Proposed.

The above finding concludes that urban development models have used various predictors to simulate urban expansion. However, the current extensive list of predictors for these research resources does not include population and crowd mobility as key predictor categories in the urban development models. Fig. 2 shows the existing and new categories along with their predictors for the urban development model.

Rapidly urbanizing countries often show rapid land usage; however, population factors are not explicitly included in the urban models [48]. Urbanization warrants more urban built up in dense cities and converts prime land to support the needs of the growing population [17]. This scenario takes place because the spatial analysis of the built-up area is limited to building-like structures. Urban development models do not capture the external factors such as traffic, population maturity in LULC classification. Traffic congestion is a cycle effect, a higher population growth rate in an area warrants more development, and more development increases traffic. However, urban development models do not capture this effect, limiting the LULC analysis for the urban planners. Sustainable urban design framework includes indicators for mobility and transport indicators are for a better environment and economy. The author in [49] highlighted how mobility and transport indicators are key for health and the environment in a sustainable city, supporting the need to have these predictors to assess urban planning. The traffic layer or properties and urban growth included in the urban development model can improve urban-built in LULC monitoring. Instead of classifying the urban built-up based on infrastructure properties, the inclusion of vehicular information for a period of time gives the urban planners insight into how dense the area is both in traffic and built-up area.

A sustainable city development should not forget the social aspects to improve quality of life. Hence, this study proposes that population and crowd mobility predictors should be included to improve the urban development classification model.

VI. Proposed Future Work

Developing geospatial classification models using Google Earth Engine has been the recent research trends [16, 50-52] as it allows to process large sets earth imagery data without the need to have high end software or hardware requirements. The availability historical data sets and the ability to preprocess the data in Google Earth Engine allows fast simulation of LULC change analysis therefore developing enhanced application with improved feature is faster using the web interface.

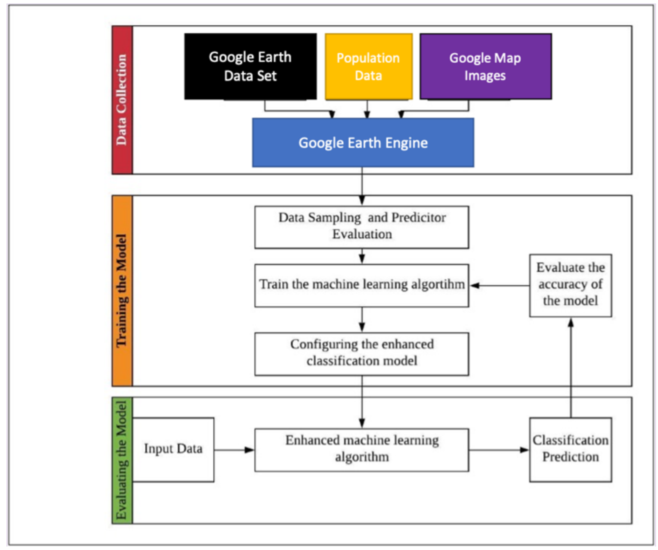

Fig. 3. Poposed Enhanced Urban Development Classification Model Development Framework.

An enhanced urban development classification model will be developed using the development methodology in Fig. 3. The proposed development framework will derive its dataset for Google Earth and use the Google Earth Engine as a platform to develop and train the classified model. The enhanced urban development classification model will evaluate the impact of the newly identified indicator in this study on the LULC classification. Specifically, the classification model will use the existing features from the land use land cover properties, traffic or mobility data, and urban demographic data to increase the accuracy of LULC classification, particularly the urban built classification. Similar research employing the traffic layer classified as spatial static temporal dynamic data for intelligent transportation [53] will be closely adopted in the urban classification model development framework.

VII. Conclusion

Effects of rapid urbanization are simply inevitable, and however, with appropriate measures, it can be controlled. The recent paradigm shift on urbanization has also awakened the need for sustainable urban planning to support sustainability goals. This study has pointed out the shortfall in urban development models, which could be the factor for uncontrolled urban planning with the exponential population growth. The shortfall of the urban development models include:

- Urban development models do capture traffic intensity and population attributes in land use land cover monitoring.
- Urban development models use predictors available only directly from remote sensing data and do not combine data from different sources, limiting the analysis.
- The urban development model classifies LULC, but its accuracy highly depends on the data available in the area of interest. Thus, the urban planning forecast relies

very much on what type of classification algorithm is used in the model.

- Urban development classifies the urban built-up land as residential, commercial and services, industrial, communication and utilities, mixed urban or built-up land but does not include vehicular properties as part of the classification predictor.

This study proposes two new predictor categories: population and crowd mobility, also known as socioecological indicators, to enhance the urban development classification model further. Traffic analysis will provide the crowd mobility predictors for urban development models to simulate the optimum crowd movement, land change, and population growth. Many urban development models concentrate on classifying the attributes on the surface land to affect future urban expansion; however, based on the discussions earlier on sustainable development, it is pointless only to analyze the land cover changes. LUC is beneficial from economics as it promotes industrial development; however, to achieve urban sustainability, the models should consider the social, economic indicator as it affects the human wellbeing and the stability of the environment. Moving forward, data for this predictor will be gathered to assess the accuracy of the urban development classification model.

Acknowledgment

The authors would like to express greatest appreciation to Universiti Teknologi Malaysia (UTM) and Ministry of Higher Education (MOHE), Malaysia for the financial support (grant number: Q.K130000.2456.08G28). Last but not least, we also appreciate Advanced Informatics at Razak Faculty of Technology and Informatics (FTIR), UTM for their support in conducting this research.

References

[1] K. Anarfi, R. A. Hill, and C. Shiel, "Highlighting the sustainability implications of urbanisation: A comparative analysis of two urban areas in ghana," Land, vol. 9, no. 9, 2020.

[2] D. o. E. a. S. A. United Nations, Population Division "World urbanization prospects: The 2018 revision ", New York, 2019 2019. [Online]. Available: https://population.un.org/wup/Publications/Files/WUP2018-Report.pdf.

[3] A. Mersal, "Sustainable urban futures: Environmental planning for sustainable urban development," Procedia Environmental Sciences, vol. 34, pp. 49-61, 2016.

[4] Q. Cao, D. Yu, M. Georgescu, J. Wu, and W. Wang, "Impacts of future urban expansion on summer climate and heat-related human health in eastern china," Environ Int, vol. 112, pp. 134-146, Mar 2018.

[5] S. H. Mahmoud and T. Y. Gan, "Long-term impact of rapid urbanization on urban climate and human thermal comfort in hot-arid environment," Building and Environment, vol. 142, pp. 83-100, 2018.

[6] J. Ogle, D. Delparte, and H. Sanger, "Quantifying the sustainability of urban growth and form through time: An algorithmic analysis of a city's development," Applied Geography, vol. 88, pp. 1-14, 2017.

[7] M. Samardžić-Petrović, M. Kovačević, B. Bajat, and S. Dragićević, "Machine learning techniques for modelling short term land-use change," ISPRS International Journal of Geo-Information, vol. 6, no. 12, 2017.

[8] M. Batty, "Big data and the city," Built Environment, vol. 42, no. 3, pp. 321-337, 2016.

[9] W. Mao, D. Lu, L. Hou, X. Liu, and W. Yue, "Comparison of machine-learning methods for urban land-use mapping in hangzhou city, china," Remote Sensing, vol. 12, no. 17, 2020.

[10] Y. Tan, H. Xu, and X. Zhang, "Sustainable urbanization in china: A comprehensive literature review," Cities, vol. 55, pp. 82-93, 2016.

[11] D. Geneletti, D. La Rosa, M. Spyra, and C. Cortinovis, "A review of approaches and challenges for sustainable planning in urban peripheries," Landscape and Urban Planning, vol. 165, pp. 231-243, 2017.

[12] C. Haaland and C. K. van den Bosch, "Challenges and strategies for urban green-space planning in cities undergoing densification: A review," Urban Forestry & Urban Greening, vol. 14, no. 4, pp. 760-771, 2015.

[13] J. Chen, F. Guo, H. Wang, Z. Wang, and Y. Wu, "Urban land revenue and sustainable urbanization in china: Issues and challenges," Sustainability, vol. 10, no. 7, 2018.

[14] C. Liping, S. Yujun, and S. Saeed, "Monitoring and predicting land use and land cover changes using remote sensing and gis techniques-a case study of a hilly area, jiangle, china," PLoS One, vol. 13, no. 7, p. e0200493, 2018.

[15] D. Li, S. Wang, and D. Li, Spatialdatamining theory and application. SpringerNature, 2015.

[16] R. Goldblatt, K. Deininger, and G. Hanson, "Utilizing publicly available satellite data for urban research: Mapping built-up land cover and land use in ho chi minh city, vietnam," Development Engineering, vol. 3, pp. 83-99, 2018/01/01/ 2018.

[17] J. Gao and B. C. O'Neill, "Data-driven spatial modeling of global long-term urban land development: The select model," Environmental Modelling & Software, vol. 119, pp. 458-471, 2019.

[18] N. R. Khalili, Theory and concept of sustainability and sustainable development. Palgrave Macmillan, New York, 2011.

[19] B. Purvis, Y. Mao, and D. Robinson, "Three pillars of sustainability: In search of conceptual origins," Sustainability Science, vol. 14, no. 3, pp. 681-695, 2018.

[20] R. Wennersten, "Development of new sustainable urban areas: Horizontal or vertical planning systems for resource efficient cities," in An overview of urban and regional planning, 2018, ch. Chapter 6.

[21] O. M. Dede, "The analysis of turkish urban planning process regarding sustainable urban development," in Sustainable urbanization, 2016, ch. Chapter 12.

[22] N. Hashem and P. Balakrishnan, "Change analysis of land use/land cover and modelling urban growth in greater doha, qatar," Annals of GIS, vol. 21, no. 3, pp. 233-247, 2014.

[23] M. Mohamed, J. Anders, and C. Schneider, "Monitoring of changes in land use/land cover in syria from 2010 to 2018 using multitemporal landsat imagery and gis," Land, vol. 9, no. 7, 2020.

[24] C. B. Karakuş, "The impact of land use/land cover (lulc) changes on land surface temperature in sivas city center and its surroundings and assessment of urban heat island," Asia-Pacific Journal of Atmospheric Sciences, vol. 55, no. 4, pp. 669-684, 2019/11/01 2019.

[25] H. Bagan and Y. Yamagata, "Land-cover change analysis in 50 global cities by using a combination of landsat data and analysis of grid cells," Environmental Research Letters, Article vol. 9, no. 6, 2014, Art no. 064015.

[26] A. Navara and R. Vedamuthu, "Ecosystem services-based approach to sustainable development in a peri-urban area of chennai, india," Environment, Development and Sustainability, 2021/06/09 2021.

[27] F. Ahmad, L. Goparaju, and A. Qayum, "Lulc analysis of urban spaces using markov chain predictive model at ranchi in india," Spatial Information Research, vol. 25, no. 3, pp. 351-359, 2017.

[28] M. Ahmadlou, M. R. Delavar, A. Basiri, and M. Karimi, "A comparative study of machine learning techniques to simulate land use changes," Journal of the Indian Society of Remote Sensing, vol. 47, no. 1, pp. 53-62, 2018.

[29] M. C. Cheruto, M. K. Kauti, P. D. Kisangau, and P. Kariuki, "Assessment of land use and land cover change using gis and remote sensing techniques: A case study of makueni county, kenya " Assessment of Land Use and Land Cover Change Using GIS and Remote Sensing Techniques: A Case Study of Makueni County, Kenya, 2016.

[30] F. Karimi, S. Sultana, A. Shirzadi Babakan, and S. Suthaharan, "An enhanced support vector machine model for urban expansion prediction," Computers, Environment and Urban Systems, vol. 75, pp. 61-75, 2019.

[31] D. Fecht, L. Beale, and D. Briggs, "A gis-based urban simulation model for environmental health analysis," Environmental Modelling & Software, vol. 58, pp. 1-11, 2014.

[32] C. Pizzi et al., "Prevalence of cardiovascular medication on secondary prevention after myocardial infarction in china between 1995-2015: A systematic review and meta-analysis," PLoS One, vol. 12, no. 4, 2017.

[33] S. Deep and A. Saklani, "Urban sprawl modeling using cellular automata," The Egyptian Journal of Remote Sensing and Space Science, vol. 17, no. 2, pp. 179-187, 2014/12/01/ 2014.

[34] E. d. N. Vaz, P. Nijkamp, M. Painho, and M. Caetano, "A multi-scenario forecast of urban change: A study on urban growth in the algarve," Landscape and Urban Planning, vol. 104, no. 2, pp. 201-211, 2012.

[35] S. Mohammady, M. R. Delavar, and P. Pahlavani, "Urban growth modeling using an artificial neural network a case study of sanandaj city, iran," ISPRS - International Archives of the Photogrammetry, Remote Sensing and Spatial Information Sciences, vol. XL-2/W3, pp. 203-208, 2014.

[36] S. I. Musa, M. Hashim, and M. N. M. Reba, "A review of geospatial-based urban growth models and modelling initiatives," Geocarto International, vol. 32, no. 8, pp. 813-833, 2016.

[37] A. A. A. Alsharif and B. Pradhan, "Urban sprawl analysis of tripoli metropolitan city (libya) using remote sensing data and multivariate logistic regression model," Journal of the Indian Society of Remote Sensing, vol. 42, no. 1, pp. 149-163, 2013.

[38] P. Tripathy, A. Bandopadhyay, R. Raman, and S. K. Singh, "Urban growth modeling using logistic regression and geo-informatics: A case of jaipur, india," Environment & We An International Journal of Science & Technology, vol. 13, 2018.

[39] H. Motieyan and M. S. Mesgari, "An agent-based modeling approach for sustainable urban planning from land use and public transit perspectives," Cities, vol. 81, pp. 91-100, 2018.

[40] A. Shirzadi Babakan and M. Taleai, "Impacts of transport development on residence choice of renter households: An agent-based evaluation," Habitat International, vol. 49, pp. 275-285, 2015.

[41] Q. Zhang, R. R. Vatsavai, A. Shashidharan, and D. Van Berkel, "Agent based urban growth modeling framework on apache spark," in Proceedings of the 5th ACM SIGSPATIAL International Workshop on Analytics for Big Geospatial Data, BigSpatial 2016, 2016, pp. 50-59.

[42] C. Wray and K. Cheruiyot, "Key challenges and potential urban modelling opportunities in south africa, with specific reference to the gauteng city-region," South African Journal of Geomatics, vol. 4, no. 1, 2015.

[43] H. Jin and G. Mountrakis, "Integration of urban growth modelling products with image-based urban change analysis," International Journal of Remote Sensing, vol. 34, no. 15, 2013.

[44] H. Kim, S. Sultana, and J. Weber, "A geographic assessment of the economic development impact of korean high-speed rail stations," Transport Policy, vol. 66, pp. 127-137, 2018.

[45] M. Samardžić-Petrović, S. Dragićević, M. Kovačević, and B. Bajat, "Modeling urban land use changes using support vector machines," Transactions in GIS, Article vol. 20, no. 5, pp. 718-734, 2016.

[46] Y. Deng and S. Srinivasan, "Urban land use change and regional access: A case study in beijing, china," Habitat International, vol. 51, pp. 103-113, 2016.

[47] F. Samara, S. Tampekis, S. Sakellariou, and O. Christopoulou, "Sustainable indicators for land use planning evaluation: The case of a small greek island," presented at the International Conference on Environmental Management, Engineering, Planning and Economics (CEMEPE), Mykonos, Greec, 2013.

[48] J. Gao and B. C. O'Neill, "Mapping global urban land for the 21st century with data-driven simulations and shared socioeconomic pathways," Nat Commun, vol. 11, no. 1, p. 2302, May 8 2020.

[49] A. López Chao, A. Casares Gallego, V. Lopez-Chao, and A. Alvarellos, "Indicators framework for sustainable urban design," Atmosphere, vol. 11, no. 11, 2020.

[50] T. N. Phan, V. Kuch, and L. W. Lehnert, "Land cover classification using google earth engine and random forest classifier—the role of image composition," Remote Sensing, vol. 12, no. 15, 2020.

[51] P. Arévalo, E. L. Bullock, C. E. Woodcock, and P. Olofsson, "A suite of tools for continuous land change monitoring in google earth engine," Frontiers in Climate, vol. 2, 2020.

[52] N. A. Wahap and H. Z. M. Shafri, "Utilization of google earth engine (gee) for land cover monitoring over klang valley, malaysia," IOP Conference Series: Earth and Environmental Science, vol. 540, p. 012003, 2020/08/05 2020.

[53] H. Yuan and G. Li, "A survey of traffic prediction: From spatio-temporal data to intelligent transportation," Data Science and Engineering, vol. 6, no. 1, pp. 63-85, 2021

Designing Strategies for Autonomous Stock Trading Agents using a Random Forest Approach

Monira Aloud
Department of Management Information System
College of Business Administration, King Saud University, Saudi Arabia

Abstract—**Machine learning-based autonomous agents are valuable for back-testing stock trading strategies, including algorithmic trading. Several studies in the financial literature have proposed artificial intelligence-based algorithms that support decision making for financial investment, but few studies have provided systematic processes for designing intelligent trading agents. This paper overviews the steps involved in designing agents that forecast stock prices in a trading strategy. These steps include data preprocessing, time-series segmentation, dimensionality reduction, clustering, and others. Our main contributions are: (i) a systematic process that guides the design and development of trading agents, and (ii) a random forest forecasting model.**

***Keywords*—Decision trees; financial forecasting; machine learning; random forest; trading agents; trading strategy**

I. Introduction

The success of a stock trading strategy depends on the quality of the information underlying its decision-making process. Most importantly, a successful trading strategy must quickly respond to data inputs for making informed decisions. Forecasting the level of a financial market index or individual stock is a classic problem. The efficient market hypothesis claims that forecasting stock prices is infeasible and that financial time series follow a random walk [1]. However, technical analysts consider that information regarding stocks and stock market indexes are reflected in historical prices and that prices can be forecasted. Financial market time-series forecasting has been widely studied in various disciplines, including finance, economics, engineering, computer science, and mathematics [2].

Financial market time series are commonly analyzed and forecasted by fundamental analysis [3, 4] and technical analysis [5–7]. The fundamental approach, typically used for long-term decision making on financial investments, focuses on the macroeconomic and company-specific factors that can influence the movements of stock index prices. Fundamental analysis is less common in the financial forecasting literature, because forecasting models that identify the reason(s) for stock price changes are difficult to construct. In contrast, technical analysis recognizes the patterns in a historical financial time series and implicitly assumes that some patterns are exploitable. Analytical and forecasting models based on technical analysis indicators are widely used in the financial literature (Murphy 1986, 1999).

Several machine learning techniques have been applied to financial time series [5, 8-13]. Machine learning techniques identify the patterns in financial time series using a data driven approach. Common machine learning techniques for forecasting financial time series are decision trees [14], random forest (RF) [15-17], artificial neural networks (ANNs) [18-22] and evolutionary algorithms, such as genetic algorithms [23-27] and genetic programming (GP) [28-33]. Machine learning applications of financial time-series forecasting are reviewed in [34-35].

Automated trading in financial markets, including the foreign exchange (FX) and stock markets, is among the most logical applications of autonomous agents. The systematic design and evaluation of active trading strategies requires a detailed understanding of market mechanisms and operations and an awareness of the issues common to trading strategies. The present study provides a systematic process that guides the design and development of a stock market trading strategy for autonomous trading agents. The study also identifies the essential attributes representing the inputs of a machine learning algorithm for financial forecasting and discusses the potential and impact of these attributes. Designing and evaluating trading agents for financial markets is a non-trivial task giving the complexity and dynamic nature of financial data.

To accomplish our goals, we build a classification model that forecasts stock market prices using attribute selection and an RF algorithm. The characteristics and importance of the attributes are described in detail, and the most relevant attributes for forecasting and hence generating the trading rules are identified. The RF model is trained on the seasonality data's attribute space, directional changing price events, fundamental and technical indicators, and other financial data. Based on the attribute subset obtained from the attribute search space, the classifier computes the forecasting results, which are then used in designing the trading strategy. The impact of number of trees in the RF model and length of the training period are carefully evaluated. The agent strategy (and hence the performance of the generated trading rules) is evaluated in a stock market simulation of three datasets: the daily trade data of Standard and Poor (S&P100), Financial Times Stock Exchange (FTSE 100), and the Deutscher Aktienindex (DAX) indices of German stock. To identify the profitable trading opportunities over various time scales within the trading run, we connect the machine learning algorithm to the appropriate attribute space. Our RF learning algorithm can help traders to generate profitable trading strategies and bridge the gap between attribute selection and trading-strategy design.

The remainder of this paper is structured as follows. Section 2 briefly reviews the related literature. Section 3

*Corresponding Author

systematically describes the agent design process, including attribute selection and the RF algorithm. Section 4 demonstrates and examines the experimental results. Section 5 offers concluding remarks.

II. Related Work

Agent-based modeling is an efficient and cost-effective method for analyzing complex dynamic phenomena, such as trading in financial markets and portfolio management [36-39]. By finding the optimal attribute sets and associations between the inputs and outputs of agent-based models, we can better understand the dynamics of financial markets and the modeled trading strategy. The financial literature includes several methods that explain and simplify the identification of attribute relationships through sampling and modeling [40-44].

Machine learning techniques provide a broad set of tools for the systematic design of trading and trading-agent algorithms [35, 45]. Among these techniques, supervised learning algorithms efficiently capture the nonlinear relationships between the inputs and outputs, inferring functional relationships from the data. Machine learning algorithms for stock forecasting include the support vector machine approach [46-48], ANNs [18-22], genetic algorithms [23-27], GP [28-33, 43, 44], support vector regression models [49], RF [15-17], extreme gradient boosting (XGB) [11, 17], and reinforcement learning [50]. Two reviews [34, 35] cover the recent significant studies on machine learning algorithms for stock market forecasting. The most relevant studies are [14, 16, 17]; and [51] who initially applied machine learning (particularly RF) to financial forecasting.

The work by [51] proposed a hybrid system that forecasts the future levels of a stock market index. They introduced a two-stage fusion approach using support vector regression (SVR) in the first stage and an ANN, RF, and SVR in the second stage, yielding three fusion prediction models: SVR–ANN, SVR–RF, and SVR–SVR. The second stage reduces the overall forecasting error. Patel et al. in [51] input ten technical analysis indicators to each forecasting model and emphasized the importance of providing adequate information to the model. To evaluate the effectiveness of their results, they compared the forecasting performance with single-stage models based on ANN, RF, and SVR.

The work by [17] applied deep ANNs, gradient-boosted decision trees (GBDTs), RF, and a combination of these methods (referred to as an ensemble) to the S&P 500 index. They forecasted the daily price returns by binary classification after training the four models on the momentum feature space. The average profits predicted by the ensemble (0.45% per day) were higher than those predicted by deep learning (0.33% per day), GBDT (0.37% per day), and RF (0.43% per day). Their results suggest that machine learning algorithms can provide sustainable profit opportunities in the short term.

The authors in [16] proposed an algorithmic trading strategy for the intraweek FX market trading based on an RF model and Probit regression. The RF model forecasted the medium-term evolution, whereas the Probit model was applied to the technical analysis indicators for predicting the price value of the next day. The profitability of the proposed model was evaluated on USD/EUR, UDS/JPY, and USD/GBP from January 2014 to 2019. Their strategy improved the prediction accuracy and helped to identify the best times of entering and exiting the market.

The work in [14] built an experimental prediction framework based on a tree classifier, which analyzes the prices up to n days earlier, and forecasts whether prices will rise or fall. They trained two algorithms, RF and GBDT (using XGBoost), on technical analysis indicators, and varied the time interval of the analysis. The authors highlighted the importance of flexibility enabled by different features, each giving a specific interpretation.

The present study makes three contributions to the literature. First, it provides a simplified, systematic process for designing trading agents. We provide guidelines for determining the minimal set of attributes needed for an effective design, offering essential insights into agent design. Second, we evaluate the performance of the trading strategy using the existing standards in the financial forecasting literature. Third, we generate a diverse set of trading rules with a focus on attribute selection, allowing an extended training phase and trading rules that best exploit the RF algorithm.

III. Methods

As mentioned above, trading agents developed by machine learning techniques can forecast financial time-series data. This section sets a framework to describe the main components in designing and developing intelligent trading agents to guide developers and practitioners in building such agents. The works by [52, 53] present the operational steps of an intelligent trading system that focuses on forecasting price movements in financial time series.

Simplicity is an essential characteristic of trading agents, because intricate design and complex trading rules will confuse the trading decisions and the dynamics of the trading rules. Forecasting of a price time-series significantly depends on the set of attributes used in the model. Therefore, selecting the right set of attributes for the trading agent is essential. Understanding the role of the attributes and settings can benefit investment profitability.

Our design of an intelligent trading agent proceeds through the following steps: (1) data preprocessing, (2) time-series segmentation, (3) dimensionality reduction, (4) algorithm definition, (5) training, and (6) evaluation. Fig. 1 depicts the framework of designing an intelligent trading agent for predicting the stock market.

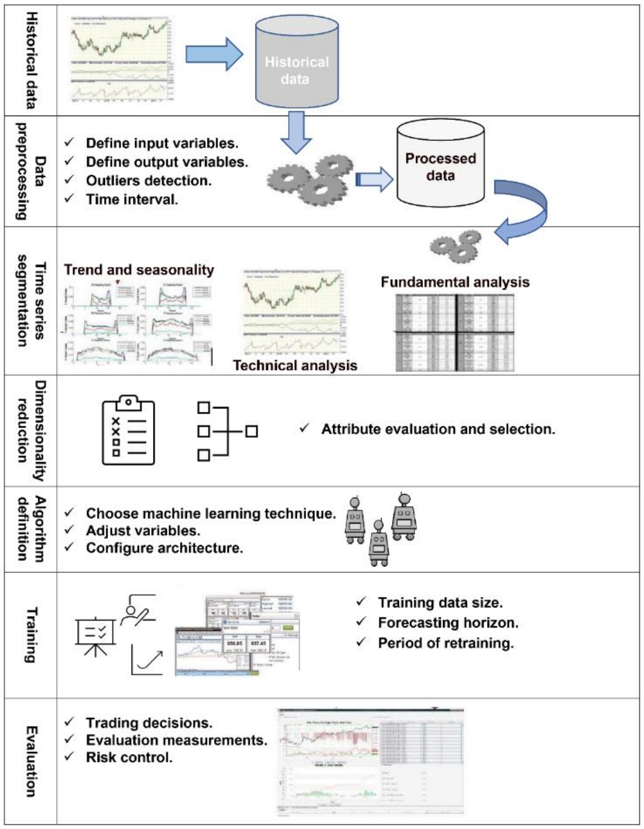

Fig. 1. Framework for Designing an Intelligent Agent for Stock Market Trading.

A. Data Preprocessing

The first step pre-processes the data utilized in the learning process. The main tasks in this step are defining the input and output variables, detecting the outliers, and structuring the data within a specified time interval. Data preprocessing ensures a reliable and accurate forecasting performance.

1) Defining the input and output variables: When designing a trading agent, we must first define the input variables used by the machine learning technique and the output signals to be forecasted. The sets of input and output variables define the trading rules and control risk, respectively. Technical analysis indicators are considered as the primary modeling inputs. Trading agents for short forecasting horizons are thought to require the technical analysis indicators, whereas those for long-term forecasting mainly use the fundamental input variables. Intraday seasonality statistics are the essential inputs of a forecasting model. The output variables are binary classifications of three class values signifying the buy, sell, and hold signals, which predict the direction and size of price movements throughout the trading period.

2) Outlier detection: After defining the input and output variables, the data are processed to remove noise and outliers, and the data elements are normalized and structured within a specified time interval. This process includes filtering the outliers and eliminating dimensionality from the data, data reduction, normalization, and detrending [54, 55]. Some studies [54, 55, 56-58] suggest removing conditional transactions, late transactions, transactions reported out of sequence, and transactions with special settlement conditions. If these outlier transactions remain, they create noise and possibly erroneous data signals.

3) Time interval: As prices in a financial time series arrive at unequal time intervals, designing the trading rules is a challenging task. In particular, the time interval affects the technical analysis of the time series. Most of the reported intelligent forecasting models compute the technical parameters using the prices (open, high, low, and close) during a trading day, without measuring the magnitude of the price change. Therefore, the input data are considered as continuous data values (an interval-based dataset). This approach has proven effective in several studies [59-62] that assess whether today's closing asset price will extend yesterday's price trend.

Alternatively, trend-deterministic data can be analyzed within a directional change (DC) event framework [59, 61], which treats the input data as discrete entities to be sampled at irregular time intervals. The sampling interval is decided by the magnitude of a price change defined by the trader. The DC approach, which converts the discrete nature of a pricing series into a continuous DC event, has been critical in the FX market [43, 59-61, 63] and stock markets [28, 29, 64].

B. Time-Series Segmentation

The time-series data of financial prices are naturally dynamic and unevenly spaced in time. These attributes complicate the analysis phase and forecasting investment opportunities, as discussed in subsection 3.1.3. To reduce the number of dimensions for later analysis, the time series is commonly segmented in a preprocessing step. The resulting time series contains less data, allowing better detection of its significant patterns. Well-known financial time-series segmentation methods are intraday seasonality statistics [15, 60], scaling laws [61], and technical analysis indicators [6, 7]. By identifying trends and patterns in the segmented data, a trading agent can lower the computational costs and improve the forecasting accuracy.

1) Trend and seasonality: Seasonality analysis identifies periodic patterns in the historical data and formulates predictions based on the behavior patterns of earlier periods. Periodic past behaviors are assumed as the most likely future scenarios [14, 28, 65]. Therefore, seasonality statistics can reveal the most active trading hours of a stock index, the volume of transactions throughout a given day, and the probable development of trading flows. The intraday seasonality in a time series is defined as the hourly activity changes over a specified period of the time series. For example, the intraday seasonality can be represented by the aggregate number of pricing data points observed in each hour of a single day (hour 0–23), divided by the total number of pricing data points in the same period.

2) Technical analysis indicator: Technical analysis forecasts the prices and returns of actively traded financial instruments, such as individual stocks, market indices, and FX.

This approach assumes that patterns appear in historical prices. In statistical terms, technical indicators measure the various features in the time series of a given stock or market index, such as price trends, volatility, and momentum. Various technical indicators have been used for forecasting future price movements and developing rules of trading decisions [6, 66].

In this study, the trading agent was modeled using eight popular technical indicators calculated from historical price data. The calculation formulas of these indicators are given in Table I.

TABLE I. TECHNICAL ANALYSIS INDICATORS USED BY THE TRADING AGENTS IN THE PRESENT STUDY

Indicator	Formula
Moving Average	$MA(L,t) = \frac{p(t) - (\frac{1}{L}\sum_{i=1}^{L} p(t-i))}{\frac{1}{L}\sum_{i=1}^{L} p(t-i)}$
Trade Break Out	$TRB(L,t) = \frac{p(t) - \max\{p(t-1), \dots, p(t-L)\}}{\max\{p(t-1), \dots, p(t-L)\}}$
Filter	$FLR(L,t) = \frac{p(t) - \min\{p(t-1), \dots, p(t-L)\}}{\min\{p(t-1), \dots, p(t-L)\}}$
Volatility	$VOL(L,t) = \frac{\sigma(p(t), \dots, p(t-L+1))}{\frac{1}{L}\sum_{i=1}^{L} p(t-i)}$
Momentum	$Mom(L,t) = p(t) - p(t-L)$
Momentum Moving Average	$MomMA(L,t) = \frac{1}{L}\sum_{i=1}^{L} Mom(L, t-i)$

The first technical indicator is the moving average (MA). The MA indicator continuously updates the average price within a specified window of time. In this study, the forecasting model inputs a 10-day MA and provides a short-term prediction. If the current price is above or below the MA, the price trend is upward or downward, respectively.

To understand the trade break out (TBR) indicator, we must define two concepts: support and resistance. At the support and resistance points, the price trend is expected to stop declining and rising, respectively. The TBR assumes that price trends will reverse at the support and resistance points; however, when these points represent a break out, possibly because new information emerges on the market or (for an individual stock) the company, the price trend is expected to continue in the same direction. Traders watching these break-outs will buy when a price trend exceeds the point of resistance and sell when the price trend falls below its support level.

The filter (FLR) technical indicator signifies a buy or sell signal depending on whether the price trend has been reversed by a predefined threshold. For example, if the price rises by a defined percentage of its earlier low value (reversing a downward price trend), the FLR issues a “buy” order.

Price volatility (VOL) is the standard deviation calculated from the historical prices over a specified period. The VOL indicator suggests a buying opportunity when the volatility is declining, as the price may be trending upward. In contrast, a cycle of increasing volatility may signify a downward price trend, presenting a “sell” opportunity.

Momentum (Mom) is a simple trend-following indicator defining the rate or strength of the price movement. The Mom indicator relates the very recent closing price to the previous closing price over a time interval specified by the analyst. The Mom indicator also determines the momentum MA (MomMA).

Return on investment (ROI) in the trading context (distinct from the ROI of the data in a company’s financial statements) relates the trading profits to the strategy’s capital. Here, the ROI is the ratio of the price return to invested capital over a specified period. In our decision support system framework, the average price return is determined throughout the previous *n* days. The ROI is real-valued and can be positive (indicating a profit) or negative (indicating a loss).

The relative strength index (RSI) is a momentum indicator that contrasts the sizes of the recent upward and downward price trends over a defined period. This measure evaluates the rate and change of an asset’s price movements. To define an upward price-trend change, we set $Uptrend_t = p_t - p_{t-1}$ *if* $pt > p_{t-1}$ and 0 otherwise; conversely, we define a downward price trend as $Downtrend_t = p_{t-1}$- p_t if $p_t < p_{t-1}$ and 0 otherwise. The relative strength RSI(n) is then defined as the average of the last n upward price-trend changes divided by the average of the last n downward price-trend changes. The RSI fluctuates between zero (average upward price change = 0) and 100 (downward price change = 0). In typical scenarios, an asset or overall market is overbought when the RSI exceeds 70 and is oversold when the RSI falls below 30.

3) Fundamental analysis: A fundamental analysis of a time series of securities prices investigates the likely factors affecting the time-series dynamics. These factors are derived from various sources, including financial statements, liquidity measures, market capitalization, and earnings announcements. Several studies have confirmed the relationships between these financial data and future price returns [3, 67].

The core mechanism of fundamental analysis is estimating an asset's fundamental value using the financial data from all available sources. A trader can compare a fundamental value with the asset's current price and make a trade decision based on that comparison. If an asset's price exceeds its fundamental value, it is regarded as overvalued, and a sell order is recommended. Conversely, if the price is below its fundamental value, the asset is considered undervalued and a buy is recommended.

The trading strategy can consider the fundamental price value [67] or more than one value [3]. In the present analysis, an agent considers one fundamental price value as in [67]. Throughout the model run, the asset's fundamental value is described by an exogenic random procedure:

$$f_t = f_{t-1} + \eta_t, \tag{1}$$

where f_t denotes the fundamental value of the asset price at time t and η_t is a normal noise process with mean μ and standard deviation σ.

C. Dimensionality Reduction

Restricting the number of attributes in the trading-agent model is essential, as not all attributes are valuable for forecasting a trade signal, and some are irrelevant. Reducing the attribute number and feature dimensionality improves the learning time, shortening the computational time, and improving the scalability. This step is particularly important for adaptive learning algorithms, which depend on the learning speed to route the streaming data over a suitable timeframe. Reducing the dimensionality reduces the memory and data-storage requirements, and simplifies the behavior of the trading agents. It also captures the dependencies and correlations among the attribute features.

D. Algorithm Definition

During learning by a machine learning technique, the agents continuously interact with the environment and thus learn the optimal trading rules to achieve a specific goal. The setting involves current price movements and historical data of stock market trading provided by an extensive array of raw data and technical analysis indicators. When selecting a machine learning technique, these historical data and technical indicators are prerequisites for designing agents that observe the price time-series environment and learn the stock trading rules. Most of the total design time is expended in providing the agents with informative data and tools, which is performed in the first three phases (data preprocessing, time-series segmentation, and dimensionality reduction). Although each phase generates inputs for the subsequent phase, the progression is unsteady and moves back and forth between the phases to optimize the result. After processing and reducing the data, the trading rules are generated from the selected input data by a machine learning technique, and the output signals are forecasted.

1) RF methodology: Forecasting by a machine learning technique is subjected to many factors: processing speed, pattern learning capability, natural interpretation of the trading strategy, knowledge simplification after learning, flexibility and adaptability to changes, and strategic optimizers for the retraining and forecasting horizons. Decision trees and RF are popular algorithms for forecasting price changes and developing automated trading agents. The RF algorithm has been successfully used in feature pruning (attributes in our case) owing to its broad capability and strength. In this study, the RF algorithm generates the trading rules for the trading agent.

RF is a supervised machine learning algorithm involving multiple decision trees on different subspaces of the attribute space. One decision tree connects a decision to a set of descriptive variables or attributes. Each decision tree is formed as a set of variables and conditions, hierarchically structured, and continuously utilized in a dataset. The decision trees are diversified by generating them from several training datasets that are randomly resampled from the original dataset. In financial forecasting, a variety of decision tress offers autonomous numerical estimates of the arbitrage opportunity (i.e., increase in price change) rather than class labels for predictions. The RF algorithm learns the relationships among the following inputs: (a) row data (opening, closing, high and low prices, and the trading volume per day), (b) fundamental analysis information, (c) eight technical indicators, (d) DC price events, and (e) intraday seasonality statistics. The algorithm then generates one of three trading signals (buy, sell, or hold). Fig. 2 depicts the design framework of the forecasting model based on the RF algorithm for stock market prediction.

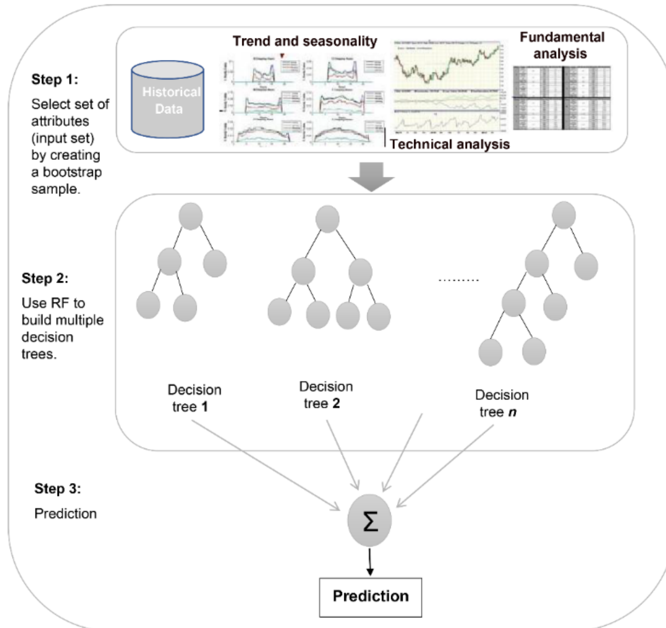

Fig. 2. Design Framework of a Forecasting Model based on the Random Forest (RF) Algorithm for Stock Market Prediction.

To create a single decision tree, we start from the root node and recursively split the data into two child nodes using a set of rules based on the market domain. The tree-building terminates when a definite stop condition is reached. The RF algorithm selects the attributes by a random process rather than employing all attributes. The resampling is performed by a random module and the combinations of attributes for the data-splitting are optimized to acquire more representative nodes. IF–THEN rules are derived from the trained decision trees by tracing the path from the root node toward each leaf node in each decision tree. The obtained rules are merged into a single decision-rule set. Along each path, the attributes and variables of the nodes are determined under the rule conditions, and the class of the leaf node represents the result of the rules (the trading signals). Fig. 3 shows a possible decision tree generated by the RF algorithm, and the following code derives a decision rule from the decision tree.

2) RF algorithm: The RF algorithm constructs an ensemble model of multiple unpruned decisions from random subsets of attributes that do not overfit the data. In this study, we build a RF of decision trees from bootstrapped training data. Therefore, instead of defining the best split among the entire set of input variables, we extract a subset of randomly selected attributes. In Algorithm 1 below, forests of decision trees are constructed using the training dataset D = $\{(x_1, y_1), (x_2, y_2), \cdots, (x_T, y_T)\}$. The number of attributes is A and the number of trading days is T. Algorithm 1 is the core mechanism of the RF algorithm.

Algorithm 1: Random forest (RF) algorithm

```
procedure RF(D)                        D is the training dataset
    f = new Array()                    --> create a new forest
    for do i = 0 to N
     D_i = bootstrapSamples(D) --> randomly select n data from D
    attribute_i = RandomAttributeSelection(D_i)
    DT_i = new DecisionTree()
     DT_i.train(D_i,attribute_i)
    f.add(DT_i)
    end for loop
    return forest f                    --> return the new forest
end procedure RF(D)
```

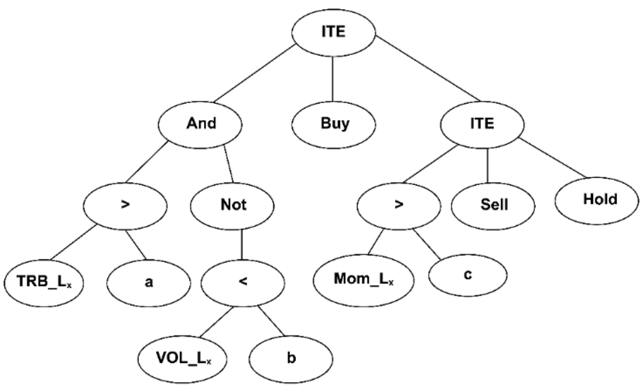


```
If ((TRB_Lx > a) And (Not (VOL_Lx < b))) Then
  Buy
Else
  If (Mom_Lx > c) Then
   Sell
  Else
   Hold
  End if
End if
```

Fig. 3. A Possible Decision Tree Model in an RF (top), and Code Showing how a Decision Rule is Derived from the Decision Tree (Bottom).

The aim is to find a function $f : X \rightarrow Y$, where X is the attribute space and Y is the output trading signal space. The procedure is outlined below.

1. To form a bootstrap sample, randomly select *n* data from *D* drawn with or without replacement from the training dataset.

2. Among the *A* attributes, select $a \epsilon A$ attributes to create a decision tree. Using a subset of data ensures variety and avoids the overfitting problem.

3. At each node, randomly select the attributes and optimize the data split (based on the Gini impurity). Note that the smaller the value of $Gini_D$, the higher is the purity of *D*. The Gini impurity measures a node's splitting quality. At each node *N*, it is defined as

$$Gini(N) = \sum_{i \neq j} p(w_i)p(w_i) \quad (2)$$

4. Grow *n* decision trees to the most considerable extent by reiterating steps 1 to 3 until the maximum number of nodes is reached. The depth of each decision tree is controlled by the allowed maximum depth and the minimum number of required variables and constants at a leaf node. This so-called pruning criterion reduces the underlying complexity of the decision tree.

5. Define the mean prediction of all individual decision trees in the forest. The aggregate prediction represents the output at time *t*.

The examinations and visualizations were implemented in the R programming language [21, 22]. The following libraries and supplementary materials were also used: forecast [68], RF [69], gdata [70], ggplot2 [71], and reshape2 [72].

3) Variable adjustment: After choosing a machine learning technique, the input variables and output signals are adjusted to fit the desired algorithm. In this phase, the input dataset is decomposed for dividing the forecasting model into smaller sub-models. The machine learning technique (RF in this case) models the relationships among the input variables based on their initial definitions, and produces output signals. In the financial literature, machine learning techniques build the forecasting model using different numbers and types of input variables. Fundamental analysis offers numerous candidate attribute variables, such as firm size, cash flow, liquidity, and profitability. In contrast, technical indicators describe technical attributes such as moving averages, volatility, and momentum. In financial forecasting, the set of input variables for building a forecasting model (and thus designing a trading agent) is unlimited.

4) Architecture configuration: The architecture is configured by adjusting the set of input and output variables of the chosen machine learning technique. A practical design for a trading agent requires three main components. The first specifies the trading rules governing the entry and exit times of trades. Exploiting the forecasted output signals, these trading rules discover the optimal time to buy or sell an asset's quantity to maximize the investment profit. The second component evaluates the forecast and operates the risk control system. This component requires a set of rules that evaluate and protect the invested assets. Evaluation and risk control strategies include defining the profit objectives and risk appetites intended for each trade (e.g., maximum loss). The third component is the trading management mechanism, which manages the trading position size, resources, time window, and risk. This component emphasizes the impact of real-world constraints, such as transaction costs, news, transaction volume limits, and volatility [52].

E. *Training*

Once an agent has been developed from a training dataset and its variables have been adjusted on the validation set, the agent-trading strategy must be trained and evaluated on a new subset of the time-series data (namely, the test dataset). Here, a new subgroup is employed because the agent-trading strategy may be influenced by the training dataset. Therefore, it may overfit the data, producing an unrealistically high profitability. The training phase proceeds in three steps: testing the performance of the methods, determining the forecasting horizon, and estimating the retraining period.

1) Training dataset size: Most of the financial forecasting models divide a financial time series into training and testing datasets. This approach is static because the same data are used throughout the complete testing period, with no updates. Splitting the data into training and testing datasets reduces the quantity of data available for learning and the resulting design may exclude various significant price events. Moreover, the forecasting performance sometimes depends on the time-series distribution used in the training and test datasets. This dependence is problematic, as the performance can be driven artificially high. Alternatively, the forecasting model can be trained by dynamic sliding-window cross-validation. In this approach, several evaluations are performed on small amounts of sequentially ordered data. Because the training-time window size may strongly affect the forecasting accuracy, we trialed sliding windows of different sizes.

2) Retraining period: Periodic retraining assesses the trading rules generated by the agent, thereby improving the average forecasting accuracy and accumulated profits. However, increasing the size of the training dataset over time may affect the forecasting performance. The price trends must be forecasted using an up-to-date training dataset representing the current market conditions. When designing the agent, the trading rules should be updated whenever the agent's wealth drops below a defined threshold value. This approach has been practiced in several automated agent-trading strategies [73].

F. Forecasting Evaluation

Among the many performance measures of forecasting models for trading agents, the ROI is probably the most popular choice.

1) Evaluation measure: The ROI represents the realized profits or losses of the trading strategy relative to the amount of money invested in the design. In our analysis, each trading decision was evaluated using the mean absolute percentage error (MAPE), mean absolute error (MAE), relative root mean squared error (rRMSE), and mean squared error, which are respectively calculated as follows:

$$MAPE = \frac{1}{n}\sum_{t=1}^{n}\frac{|R_t - F_t|}{|R_t|} \times 100 \quad (3)$$

$$MAE = \frac{1}{n}\sum_{t=1}^{n}\frac{|R_t - F_t|}{|R_t|} \quad (4)$$

$$rRMSE = \sqrt{\frac{1}{n}\sum_{t=1}^{n}\left(\frac{R_t - F_t}{R_t}\right)^2} \quad (5)$$

$$MSE = \frac{1}{n}\ \sum_{t=1}^{n}(R_t - F_t)^2 \quad (6)$$

Here, R_t and F_t are the actual and forecasted values, respectively.

The investment performance was evaluated with three performance indicators: Rate of correctness (RC), rate of missing chances (RMC), and rate of failure (RoF). These performance measures are calculated by Eqs. 7, 8, and 9, respectively. The four criteria in these equations are defined in the contingency table (Table II).

$$RC = \frac{TP+TN}{TP+FP+FN+TN} \quad (7)$$

$$RMC = \frac{FN}{FN+TP} \quad (8)$$

$$RF = \frac{FP}{FP+TP} \quad (9)$$

TABLE II. CONTINGENCY TABLE OF VARIABLES IN THE INVESTMENT PERFORMANCE INDICATORS

	Forecasted Negative	**Forecasted Positive**
Real negative	# of True Negative (TN)	# of False Positive (FP)
Real positive	# of False Negative (FN)	# of True Positive (TP)

2) Risk control: A successful trading agent requires a risk control mechanism that protects the invested assets by a set of trading rules such as a stop-loss limit order. Risk control strategies must define the profit objectives and risk appetites of each trade. Here we employed the Sharpe ratio (SR), which assesses the investment performance relative to risk. The SR is calculated by Eq. 10. Note that the higher the SR, the better is the risk-adjusted return, and (by inference) the better are the trading rules. According to Eq. 10,

$$SR = \frac{\mu - RF}{\sigma}\sqrt{n} \quad (10)$$

where μ is the mean of the portfolio returns, *RF* is the risk-free rate, σ is the portfolio's standard deviation, and n is the number of observations in the time series.

IV. RESULT

The previous section described the essential features and parameters of an autonomous trading agent. To handle the various possible mixtures of such features and parameters, a systematic design approach is required for an autonomous trading agent. This section details the verification experiments of the proposed approach. The results are expected to assist the design of autonomous trading agents and decision support systems for investment arbitrage in stock markets.

A. Data

The effectiveness of the proposed autonomous trading-agent design was tested on three stock market indices: Yahoo Finance S&P500 (US) [74], Yahoo Finance FTSE100 (UK) [75], and the Yahoo Finance DAX (GER) [76]. For the analysis, we extracted four years of historical data from September 1, 2015 to August 30, 2019. These three market indices were chosen for their popularity and strong liquidity in the global financial market. The study period covers various market conditions and time-series scenarios. The technical indicators were computed from the close, high, low, and opening levels of the three stock indices. All data were obtained from the Yahoo Finance websites.

B. Trading Strategies for Comparison

To verify the efficiency and effectiveness of the autonomous trading agent, we compared its trading performance with those of five well-known trading strategies: Buy and Hold (B&H),

technical analysis (TA), fundamental analysis (FA), zero-intelligence with constraint agents (ZI), and GP. The B&H strategy is a reactive investment strategy that emphasizes buying several stock assets and holding them for an extended period, regardless of fluctuations in the market-price time series. The TA strategy forecasts an asset's price movement using TA indicators (see subsection 3.2.2), and the FA strategy analyzes the potential influencing factors of the asset-price time series (subsection 3.2.3). The ZI randomly places orders under given budget constraints. However, such benchmarking is based only on the architecture of the proposed RF agent. Whether our RF proposal outperforms the existing machine learning and artificial intelligence techniques is an open question. Does the proposed RF-based agent architecture effectively outperform the other architectures based on other forecasting techniques? To answer this question, we added a fifth trading strategy based on GP, an evolutionary approach that extends genetic algorithms. GP evolves the programs of artificial intelligence to generate applicable solutions in a decision tree structure. Decision trees are generated by combining various defined functions and terminals. Both the function and terminal sets are derived from the problem search domain. Here we employed the GP trading agent designed by [29], which searches over the space of TA indicators.

C. *Trading Performance Results*

In the experiments, we varied the time horizon and combination of input attributes (parameters). The reported values were averaged over 30 runs in each trading model. After determining the agent design's most significant attributes based on the forecasting performance, the dataset was divided into two subsets using sliding-window cross-validation. The subsets were used for training and validating the RF algorithm.

After adjusting the model settings, we compared the performances of our RF-based agent design and the five competing trading agents: B&H, TA, FA, ZI, and GP. In the first evaluation, we measured the investment effectiveness of the RF-based agent using the ROI and SR as the investment performance metrics (a higher value indicates better performance). Table III compares the performance data of the six agents for each market index.

TABLE III. COMPARISON OF ANNUALIZED RETURN ON INVESTMENT (ROI) AND SHARPE RATIO (SR) OBTAINED BY VARIOUS TRADING AGENTS FROM SEPTEMBER 1, 2015 TO AUGUST 30, 2019

Stock Index	RF	B&H	TA	FA	ZI	GP
S&P500						
ROI	18.5%	2.4%	11.5%	2.62%	1.6%	11.9%
SR	1.7	0.97	1.2	0.9	0.1	1.1
FTSE100						
ROI	9%	−2.7%	6.6%	−3.6%	−27.6%	7.5%
SR	1.3	−0.2	1.1	−0.5	−0.01	1.03
DAX						
ROI	12.2%	−0.32%	10.2%	0.21%	−11.7%	10.8%
SR	1.4	−0.1	1.3	0.01	−0.6	1.4

[a] RF: random forest; B&H: Buy and Hold; TA: technical analysis; FA: fundamental analysis; ZI: zero-intelligence with constraint agents; GP: genetic programming

The trading agent based on the RF model significantly outperformed the other trading agents over the four-year study period. The RF model achieved an average annualized profit of 13.22%. On the S&P500 data, the SR of the RF-based model was 1.72, followed by 0.97 for the B&H strategy, 1.21 for the TA agent, and 1.12 for the GP agent. The RF strategy also delivered the highest ROI and SR on the FTSE100 and DAX datasets. The results of the B&H and FA agents were comparable, as demonstrated in Table III.

The RF, TA, and GP agents employing the TA indicators significantly outperformed the remaining three trading agents. Therefore, generating the trading rules using TA indicators promises high investment results. However, determining the possibility of future trading achievement based on the ideal combination of TA indicators and its time horizon is a challenging task.

The RF algorithm limits the number of attributes used without compromising the profitability of the trading strategy. In particular, the RF-based trading agent can outperform the B&H approach when the selected attributes (inputs to the machine learning algorithm) are appropriately combined.

In summary, after studying the literature on automated trading agents and testing our RF-based approach, we conclude that a developed level of intelligence and diversity of the chosen attributes is essential for boosting the investment returns of the trading agent. Learning and adaptation intelligence can improve the ability of automated agents to process the market information and dynamics of price time series and thereby adapt to financial market events and different circumstances.

D. *Forecasting Accuracy*

In the second part of the study, we analyzed the forecasting accuracy of the RF and GP agents. As shown in Table IV, the RF- and GP-based forecasting models achieved strong RC, RMC, and RoF. For the RF agents, the RC ranged from 72.08% to 81.92% (average 77.22%), the RMC varied from 17.11% to 24.46% (average 20.90%), and the RoF ranged from 5.84% to 18.45% (average 13.18%). Clearly, the RF agents outperformed the GP agents in forecasting accuracy. We must clarify that the results in Table III influenced the accuracy of the forecasting performance. Moreover, selecting the right set of attributes improved the accuracy of classifying the training dataset, but does not guarantee better trading-strategy performance. Our findings suggest a substantial relationship between the profits generated and the fundamental/technical indicators, which may be important for creating practical trading rules.

The results of the RF algorithm emphasize the importance of attribute selection (data preprocessing, time-series segmentation, dimensionality reduction, and variable adjustments) as a preprocessing stage. The proposed agent design can assist (to some extent) the forecasting of stock prices. Accordingly, we conclude that when designing a trading agent to predict stock prices, we must examine the attribute types used to build the trading strategy and their values.

TABLE IV. SUMMARY OF FORECASTING PERFORMANCES IN 30 RUNS OVER THE TESTING PERIOD, MEASURED BY THE RATE OF CORRECTNESS (RC), RATE OF MISSING CHANCES (RMC), AND RATE OF FAILURE (ROF)

Stock Index	RC	RMC	RoF	MAE	MAPE	RMSE
S&P500						
RF	81.92	21.15	5.84	0.006	0.002	0.006
GP	74.31	28.21	9.52	0.009	0.003	0.009
FTSE100						
RF	77.65	17.11	15.25	0.009	0.007	0.009
GP	71.46	23.12	19.26	0.010	0.006	0.009
DAX						
RF	72.08	24.46	18.45	0.007	0.004	0.008
GP	68.13	28.04	19.64	0.009	0.004	0.009

[a] MAE: mean absolute error; MAPE: mean absolute percentage error; RMSE: root mean squared error

E. Statistical Significance Test

The reliability and precision of the findings were tested in a paired t-test, which contrasts the means of two agents' datasets with variable ROIs. For this purpose, we divided the dataset into two equal subsets. An adequate paired t-test requires a roughly normally distributed variation of the data. Therefore, the normality was checked through a normal probability plot and a Jarque–Bera test.

The paired t-test was applied by specifying two values: the t-statistic value *tsv* and the t-critical value (two-tail variable) *tc* under the 95% confidence level. The first and second datasets were represented by A and B, respectively, where $a \in A$ and b ∈ B. The means of A and B were denoted as m_A and m_B, respectively. Both datasets were of equal size *n*. The numeral *i* indexed the record in both datasets, where $1 \leq i \leq n$. The null hypothesis stated that *B* is pairwise statistically equivalent to *A*, where $m_A - m_B = 0$. We define a new dataset *D* with *n* records, in which each form is specified by $d_i = a_i - b_i$, $d_i \in D$. The mean and standard deviation of this set were denoted by m_D and σ, respectively. The *tsv* was calculated as

$$tsv = \frac{\mu_D}{SE(\mu_D)} \tag{11}$$

where $SE(\mu_D)$ is the standard error of the mean difference, defined as

$$SE(\mu_D) = \frac{\sqrt{\sigma}}{n} \tag{12}$$

The *t*-critical value was determined from the t-distribution table. If $|tsv| < |tc|$, the difference between datasets *A* and *B* is trivial, and we can accept the null hypothesis. Table V shows the t-statistic (*tsv*) and Pearson correlation (*corr*) values of the paired *t*-test at the 95% confidence level. The results of the six trading agents on the first part of the dataset approximated those on the second part of the dataset with 95% confidence. Furthermore, the correlation coefficients demonstrate a high level of dependency between the results of the two datasets.

TABLE V. VALUES OF THE T-STATISTIC VALUE (TSV) AND PEARSON CORRELATION (CORR) OF THE PAIRED T-TEST AT THE 95% CONFIDENCE LEVEL (THE T-CRITICAL TWO-TAILED VALUE = 2.07)

Agent Type	*tsv*	*corr*
RF	3.54E−09	+0.98
B&H	3.01E−10	+0.94
TA	3.61E−09	+0.98
FA	2.82E−09	+0.95
ZI	2.32E−09	+0.97
GP	3.36E−09	+0.97

V. DISCUSSION

This study designed a simple automated intelligence agent for trading in the financial markets. An algorithmic (automated) trading agent is vital for developing trading strategies and forecasting models. This study provides a systematic approach for designing a trading agent using the RF approach. The approach was experimentally tested on four years of historical data of three stock indices: S&P500, FTSE100, and DAX.

The contribution of our work was twofold. First, we presented the main steps of building an intelligent automated trading agent for stock market trading. We categorized the main stages into five essential components: (i) the primary goal of the trading strategy (e.g., short term, long term, and high frequency); (ii) the context of the financial market domain; (iii) the input variables used; (iv) the proposed machine learning technique, and (v) diversity of the data sources.

Our second contribution was the design and implementation of adaptive RF trading agents for financial markets using various parameters (TA indicators and fundamental factors). It was hypothesized that trading agents learn, adapt, and identify periodic patterns in price time series. The RF trading agent evolved the trading rules of financial market trading investment. After the learning process, the RF algorithm achieved higher returns and better forecasting accuracy than the Buy & Hold trading strategy and agents based on technical and FA. We believe that this outperformance was achieved by selecting the right set of attributes (i.e., the inputs to the machine learning algorithm).

In future research, we could adapt machine learning techniques to dynamically select the appropriate set of attributes based on the market conditions. For this purpose, data reduction and segmentation could be combined with the sequential steps of developing an intelligent selection approach, as proposed in this study.

As another research direction, we could systematically test diverse intelligence trading strategies in the automated intelligence-based approach, and hence assess the required level of intelligence for designing autonomous trading agents. Examining and understanding the impact of complexity on a trading strategy might improve the effectiveness of that strategy. Nonetheless, a straightforward trading-strategy design, such as that developed in this study, might be more suitable than a complex one. To conclude, we should explore different artificial intelligence techniques and their effects on the effectiveness and trading rules of the strategy.

ACKNOWLEDGMENT

We would like to thank the anonymous reviewers for their useful comments and suggestions. The authors thank the Deanship of Scientific Research and RSSU at King Saud University for their technical support.

REFERENCES

[1] Malkiel, B., 1973. A. Random Walk Down Wall Street: W. W. Norton, & Company, New York.

[2] Dacorogna, M., R. Gençay, U. Müller, R. Olsen, and O. Pictet, 2001. An introduction to high-frequency finance. San Diego: Academic Press.

[3] LiCalziLicalzi, M., and P. Pellizzari. 2003. Fundamentalists clashing over the book: a study of order-driven stock markets. *Quantitative Finance* 3:470–80. doi: 10.1088/1469-7688/3/6/306.

[4] Menkhoff, L., R. R. Rebitzky, and M. Schröder. 2009. Heterogeneity in exchange rate expectations: evidence on the chartist-fundamentalist approach. *Journal of Economic Behavior & Organization* 70:241–52. doi: 10.1016/j.jebo.2009.01.007.

[5] Dempster, M. H., T. W. Payne, Y. Romahi, and G. P. Thompson. 2001. Computational learning techniques for intraday fx trading using popular technical indicators. *IEEE Transactions on Neural Networks* 12:744–54. doi: 10.1109/72.935088.

[6] Leigh, W., R. Purvis, and J. M. Ragusa. 2002. Forecasting the NYSE composite index with technical analysis, pattern recognizer, neural network, and genetic algorithm: a case study in romantic decision support. *Decision Support Systems* 32:361–77. doi: 10.1016/S0167-9236(01)00121-X.

[7] Murphy, J., 1986. Technical analysis of futures markets. New York Institute of Finance.

[8] Hsu, M. W., S. Lessmann, M. C. Sung, T. Ma, and J. E. V. Johnson. 2016. Bridging the divide in financial market forecasting: machine learners vs. financial economists. *Expert Systems with Applications* 61:215–34.

[9] Lahmiri, S. 2017. Modeling and predicting historical volatility in exchange rate markets. *Physica. Part A* 471:387–95. doi: 10.1016/j.physa.2016.12.061.

[10] Lahmiri, S. 2018. A technical analysis information fusion approach for stock price analysis and modeling. *Fluctuation & Noise Letters* 17. doi: 10.1142/S0219477518500074

[11] Pinto, J. M., R. F. Neves, and N. Horta. November 2015. Boosting trading strategies performance using vix indicator together with a dual-objective evolutionary computation optimizer. *Expert Systems with Applications* 42:6699–716. doi: 10.1016/j.eswa.2015.04.056.

[12] Teixeira, L. A., and A. L. I. de Oliveira. 2010. A method for automatic stock trading combining technical analysis and nearest neighbor classification. *Expert Systems with Applications* 37:6885–90. doi: 10.1016/j.eswa.2010.03.033.

[13] Yao, J., and C. L. Tan. 2000. A case study on using neural networks to perform technical forecasting of forex. *Neurocomputing* 34:79–98. doi: 10.1016/S0925-2312(00)00300-3.

[14] Basak, S., S. Kar, S. Saha, L. Khaidem, and S. R. Dey. 2019. Predicting the direction of stock market prices using tree-based classifiers. *The North American Journal of Economics & Finance* 47:552–67. doi: 10.1016/j.najef.2018.06.013.

[15] Booth, A., E. Gerding, and F. McGroarty. 2014. Automated trading with performance weighted random forests and seasonality. *Expert Systems with Applications* 41:3651–61. doi: 10.1016/j.eswa.2013.12.009.

[16] Chihab, Y., Z. Bousbaa, M. Chihab, O. Bencharef, and S. Ziti. 2019. Algo-trading strategy for intraweek foreign exchange speculation based on random forest and probit regression. *Applied Computational Intelligence & Soft Computing* 2019:1–13. doi: 10.1155/2019/8342461.

[17] Krauss, C., X. A. Do, and N. Huck. 2017. Deep neural networks, gradient-boosted trees, random forests: statistical arbitrage on the S&P 500. *European Journal of Operational Research* 259:689–702. doi: 10.1016/j.ejor.2016.10.031.

[18] Chang, P.-C., C.-H. Liu, J.-L. Lin, C.-Y. Fan, and C. S. P. Ng. 2009. A neural network with a case based dynamic window for stock trading prediction. *Expert Systems with Applications* 36:6889–98. doi: 10.1016/j.eswa.2008.08.077.

[19] Gutjahr, S., M. Riedmiller, and J. Klingemann, 1997. Daily prediction of the foreign exchange rate be- tween the US dollar and the German mark using neural networks. In Joint PACES/SPICES Conference 492–8.

[20] Kamruzzaman, J., and R. Sarker, 2003. Comparing ANN based models with ARIMA for prediction of forex rates. *Asor Bulletin* 22:2-11.

[21] The R Core Team, 2017. *R*: A language and environment for statistical computing. Vienna, Austria: R Foundation for Statistical Computing.

[22] Zimmermann, H. G., R. Neuneier, and R. Grothmann. 2001. Multi-agent modeling of multiple FX-markets by neural networks. *IEEE Transactions on Neural Networks* 12:735–43. doi: 10.1109/72.935087

[23] Aguilar-Rivera, R., M. Valenzuela-Rendón, and J. J. Rodríguez-Ortiz. 2015. Genetic algorithms and Darwinian approaches in financial applications: A survey. *Expert Systems with Applications* 42:7684–97. doi: 10.1016/j.eswa.2015.06.001.

[24] Allen, F., and R. Karjalainen. 1999. Using genetic algorithms to find technical trading rules. *Journal of Financial Economics* 51:245–71. doi: 10.1016/S0304-405X(98)00052-X.

[25] Bauer, R., 1994. Genetic algorithms and investment strategies. New York: John Wiley & Sons.

[26] Mahfoud, S., and G. Mani. 1996. Financial forecasting using genetic algorithms. *Applied Artificial Intelligence* 10:543–66. doi: 10.1080/088395196118425.

[27] Versace, M., R. Bhatt, O. Hinds, and M. Shiffer. 2004. Predicting the exchange traded fund dia with a combination of genetic algorithms and neural networks. *Expert Systems with Applications* 27:417–25. doi: 10.1016/j.eswa.2004.05.018.

[28] Aloud, M. 2017. Adaptive GP agent-based trading system under intraday seasonality model. *Intelligent Decision Technologies*. IOS Press 11:235–51. doi: 10.3233/IDT-170291.

[29] Aloud, M. 2018. Investment opportunities forecasting: a genetic programming-based dynamic portfolio trading system under a directional-change framework. *Journal of Computational Finance* 22:1–35. doi: 10.21314/JCF.2018.346.

[30] Chen, S.-H., and C.-H. Yeh. 2001. Evolving traders and the business school with genetic programming: a new architecture of the agent-based artificial stock market. *Journal of Economic Dynamics & Control*. Elsevier 25:363–93. doi: 10.1016/S0165-1889(00)00030-0.

[31] Dunis, C. L., J. Laws, and A. Karathanasopoulos. 2013. Gp algorithm versus hybrid and mixed neural networks. *The European Journal of Finance* 19:180–205. doi: 10.1080/1351847X.2012.679740.

[32] Kampouridis, M., and E. Tsang, 2010. EDDIE for investment opportunities forecasting: extending the search space of the GP. In Proceedings of the IEEE congress on evolutionary computation. Barcelona, Spain: 2019, 26.

[33] Vasilakis, G. A., K. A. Theofilatos, E. F. Georgopoulos, A. Karathanasopoulos, and S. D. Likothanassis. December 2013. A genetic programming approach for eur/usd exchange rate forecasting and trading. *Computational Economics* 42:415–31. doi: 10.1007/s10614-012-9345-8.

[34] Gandhmal, D. P., and K. Kumar. 2019. Systematic analysis and review of stock market prediction techniques. *Computer Science Review* 34:100190. doi: 10.1016/j.cosrev.2019.08.001

[35] Henrique, B. M., V. A. Sobreiro, and H. Kimura. 2019. Literature review: machine learning techniques applied to financial market prediction. *Expert Systems with Applications* 124:226–51. doi: 10.1016/j.eswa.2019.01.012.

[36] Arthur, W. 1991. Designing economic agents that act like human agents: A behavioral approach to bounded rationality. *American Economic Review* 81:353–9.

[37] Chan, N. T., B. LeBaron, A. W. Lo, and T. Poggio, 1999. Agent-based models of financial markets: A comparison with experimental markets.

[38] Cristelli, M., L. Pietronero, and A. Zaccaria, 2011. Critical overview of agent-based models for economics. Quantitative Finance Papers 1101.1847.

[39] Farmer, J. D., and D. Foley. 2009. The economy needs agent-based modelling. *Nature* 460:685–6. doi: 10.1038/460685a.

[40] Alfi, V., M. Cristelli, L. Pietronero, and A. Zaccaria. 2009. Minimal agent based model for financial markets I: origin and self-organization of stylized facts. *The European Physical Journal. Part B* 67:385–97. doi: 10.1140/epjb/e2009-00028-4.

[41] Alfi, V., M. Cristelli, L. Pietronero, and A. Zaccaria. 2009. Minimal agent based model for financial markets II: Statistical properties of the linear and multiplicative dynamics. *The European Physical Journal. Part B* 67:399–417. doi: 10.1140/epjb/e2009-00029-3.

[42] Aloud, M., M. Fasli, E. Tsang, A. Dupuis, and R. Olsen. 2017. Modeling the high-frequency FX market: an agent-based approach. *Computational Intelligence* 33:771–825. doi: 10.1111/coin.12114.

[43] Aloud, M., and M. Fasli. 2017. Exploring Trading Strategies and Their Effects in the Foreign Exchange Market. *Computational Intelligence* 33:280–307. doi: 10.1111/coin.12085.

[44] Martinez-Jaramillo, S., 2007. *Artificial financial markets: an agent based approach to reproduce stylized facts and to study the Red Queen effect* [PhD thesis]. Martinez: Centre for Computational Finance and Economic Agents (CCFEA), University of Essex, 2007.

[45] Gerlein, E. A., M. McGinnity, A. Belatreche, and S. Coleman. 2016. Evaluating machine learning classification for financial trading: an empirical approach. *Expert Systems with Applications* 54:193–207. doi: 10.1016/j.eswa.2016.01.018.

[46] Kim, K. j. 2003. Financial time series forecasting using support vector machines. *Neurocomputing* 55:307–19. doi: 10.1016/S0925-2312(03)00372-2.

[47] Lu, C.-C., and C.-H. Wu, 2009. Support vector machine combined with garch models for call option price prediction. In *Proceedings of the 2009 international conference on artificial intelligence and computational intelligence* Vol. 01, AICI '09:35–40. Washington, DC, USA, IEEE Computer Society.

[48] Tay, F. E. H., and L. Cao. 2001. Application of support vector machines in financial time series forecasting. *Omega* 29:309–17. doi: 10.1016/S0305-0483(01)00026-3.

[49] Pai, P.-F., K.-P. Lin, C.-S. Lin, and P.-T. Chang. 2010. Time series forecasting by a seasonal support vector regression model. *Expert Systems with Applications* 37:4261–5. doi: 10.1016/j.eswa.2009.11.076.

[50] Pendharkar, P. C., and P. Cusatis. 2018. Trading financial indices with reinforcement learning agents. *Expert Systems with Applications* 103:1–13. doi: 10.1016/j.eswa.2018.02.032.

[51] Patel, J., S. Shah, P. Thakkar, and K. Kotecha. 2015. Predicting stock and stock price index movement using trend deterministic data preparation and machine learning techniques. *Expert Systems with Applications* 42:259–68. doi: 10.1016/j.eswa.2014.07.040.

[52] Cavalcante, R. C., R. C. Brasileiro, V. L. F. Souza, J. P. Nobrega, and A. L. I. Oliveira. 2016. Computational intelligence and financial markets: A survey and future directions. *Expert Systems with Applications* 55(Suppl. c):194–211. doi: 10.1016/j.eswa.2016.02.006.

[53] Palit, A. K., and D. Popovic, 2005. Computational intelligence in Time series forecasting: theory and engineering applications (advances in industrial control). Secaucus, NJ: Springer-Verlag New York, Inc.

[54] Masry, S., M. Aloud, A. Dupuis, R. Olsen, and E. Tsang, 2010. High frequency FOREX market transaction data handling. In 4th CSDA International Conference on Computational and Financial Econometrics, London, UK.

[55] Pyle, D., 1999. Data preparation for data mining. 1st ed. San Francisco, CA: Morgan Kaufmann Publishers, Inc.

[56] Brownlees, C. T., and G. M. Gallo. 2006. Financial econometric analysis at ultra-high frequency: data handling concerns. *Computational Statistics & Data Analysis* 51:2232–45. doi: 10.1016/j.csda.2006.09.030.

[57] Falkenberry, T., 2002. High frequency data filtering. Tick Data, Inc.

[58] Hautsch, N., 2012. Econometrics of financial high-frequency data. Berlin, Heidelberg: Springer-Verlag.

[59] Aloud, M., E. Tsang, R. B. Olsen, and A. Dupuis. 2011. A directional-change events approach for studying financial time series. Economics Discussion Paper 2011:28.

[60] Aloud, M., M. Fasli, E. Tsang, A. Dupuis, and R. Olsen. 2013. Stylized facts of trading activity in the high frequency FX market: an empirical study. *Journal of Finance & Investment Analysis* 2:145–83.

[61] Glattfelder, J. B., A. Dupuis, and R. B. Olsen. 2011. Patterns in high-frequency FX data: discovery of 12 empirical scaling laws. *Quantitative Finance* 11:599–614. doi: 10.1080/14697688.2010.481632.

[62] Müller, U. A., M. M. Dacorogna, R. B. Olsen, O. V. Pictet, M. Schwarz, and C. Morgenegg. 1990. Statistical study of foreign exchange rates, empirical evidence of a price change scaling law, and intraday analysis. *Journal of Banking & Finance* 14:1189–208. doi: 10.1016/0378-4266(90)90009-Q.

[63] Gypteau, J., F. E. B. Otero, and M. Kampouridis, 2015. Generating directional change based trading strategies with genetic programming. In Lecture notes in *Computer Science*, *ed. A. M. Mora, and G. Squillero* 9028:267–78. Springer International Publishing:267–78. doi: 10.1007/978-3-319-16549-3_22.

[64] Aloud, M. 2016. Profitability of directional change based trading strategies: the case of Saudi stock market. *International Journal of Economics & Financial Issues (IJEFI)* 6:87–95.

[65] Ito, T., and Y. Hashimoto. 2006. Intraday seasonality in activities of the foreign exchange markets: evidence from the electronic broking system. *Journal of the Japanese & International Economies*. Elsevier 20:637–64. doi: 10.1016/j.jjie.2006.06.005.

[66] Murphy, J. J., 1999. Technical analysis of financial markets: A comprehensive guide to trading methods and applications. New York Institute of Finance, *New York*.

[67] Farmer, J. D. 2002. Market force, ecology and evolution. *Industrial & Corporate Change* 11:895–953. doi: 10.1093/icc/11.5.895.

[68] Hyndman, R. J., M. O'Hara-Wild, C. Bergmeir, S. Razbash, and E. Wang, 2017. Forecast: forecasting functions for time series and linear models, R package version 8.1. Accessed January 19, 2021. https://rdrr.io/cran/forecast/.

[69] Liaw, A., and M. Wiener, 2002. Classification and regression by randomForest. *R News* 2:18–22.

[70] Warnes, G. R., B. Bolker, G. Gorjanc, G. Grothendieck, A. Korosec, T. Lumley, D. MacQueen, A. Magnusson, and J. Rogers, 2017. Gdata: various R programming tools for data manipulation, R package version 2.18.0. Accessed January 19, 2021. https://cran.r-project.org/web/packages/gdata/index.html.

[71] Wickham, H., 2016. Elegant graphics for data analysis. 2nd ed. Cham, Switzerland: Springer International Publishing:Ggplot2.

[72] Wickham, H. 2007. Reshaping data with the reshape package. *Journal of Statistical Software* 21. doi: 10.18637/jss.v021.i12.

[73] Martinez-Jaramillo, S, and E. P. K. Tsang. 2009. An heterogeneous, endogenous and coevolutionary GP-based financial market. *IEEE Transactions on Evolutionary Computation* 13:33–55. doi: 10.1109/TEVC.2008.2011401.

[74] Yahoo. *Finance* (S&P 500). Accessed February 7, 2021. https://finance.yahoo.com/quote/%5EGSPC/history/.

[75] Yahoo finance (FTSE 100). Accessed February 7, 2021. https://uk.finance.yahoo.com/quote/%5EFTSE/.

[76] Yahoo. *Finance* (DAX). Accessed February 7, 2021. https://finance.yahoo.com/quote/%5EGDAXI/.

Risk Assessment of Attack in Autonomous Vehicle based on a Decision Tree

Sara FTAIMI[1], Tomader MAZRI[2]
Laboratory of Advanced Systems Engineering, Ibn Tofail University, Kenitra, Morocco

***Abstract*—Risk management has become increasingly essential in all areas, and it represents a cornerstone of the Safety Management System. In principle, it brings together all the procedures to identify and evaluate risks to improve systems performance. With the development of the transportation system and the appearance of intelligent ones (ITS) that are changing citizens' mobility nowadays, the risks associated with them have also increased exponentially. In ITS, vehicles can reach 100% autonomy since they are equipped with sensors to move safely. The vehicle's architecture and embedded sensors enfold inherent vulnerabilities that attackers may exploit to craft malicious acts. In addition, vehicles communicate with each other and with the road infrastructure via vehicular adhoc network (VANET) and may use Internet connections, raising the risk that an attacker performs malicious actions and may take control of a vehicle to perform terrorist acts. This paper aims to draw attention to the risks associated with autonomous vehicles (AV) and the interest in evaluating flaws inherent in AV. For this purpose, our paper will extensively detail a new approach to assess the risk of attacks targeting autonomous vehicles. Our proposed approach will use a decision tree model to predict risk criticality based on the probability of attack success and its impact on the targeted system.**

Keywords—Vehicular adhoc network; intelligent transportation system; decision tree; risk assessment; impact; autonomous vehicle; attacks

I. Introduction

The emergence of the smart city concept has brought several sub-concepts to the forefront, like transportation which is very important in smart cities. Making transportation intelligent will facilitate the mobility of citizens, which is a major concern in smart cities. Every second, a citizen uses a mode of transportation to go to work or school or even to travel. Making these systems intelligent will make citizens satisfied and facilitate their travel by enriching users with advanced information on traffic, real-time operating information on local convenience, seats. Resulting in reduced travel time for citizens and improve their safety and comfort and make the experience enjoyable. Therefore, the benefit of ITS is not restricted to control and give information on traffic jams, but also to reduce the rate of accidents because, in several studies, the human factor is the cause of a very high percentage of accidents. In an intelligent transportation system(ITS), we will have autonomous vehicles. These vehicles are based on the information collected by the several sensors installed on-board the vehicles and on machine learning algorithms that analyze this information and make decisions (whether the vehicle should stop or continue its trajectory), besides the infrastructure such as roadside units and base stations, installed all along the road. The vehicle will communicate with each other via vehicle to vehicle communication, and the infrastructure will communicate with the vehicle by sharing with them information about the status of the road via infrastructure to vehicle communication. Nowadays, vehicles are equipped with several ports to connect phones or other devices, and those devices are connected to the Internet, which presents a door for an attacker to conduct their attack. The security of vehicular Adhoc networks (VANET) and the different port of the vehicles besides the sensors installed in the vehicle represent a major challenge for the ITS. The security in ITS is critical because if an attacker could control a vehicle, he could cause an accident or steal the vehicle to cause a terrorist attack, and this will cause dangerous damages such as the loss of life and the perturbation of the whole ITS. Several kinds of research in the field of intelligent transport focus on the security aspect. The importance of this paper resides in the fact that unfortunately in the literature there is no work related to the risk in relation to the field of transport and especially the attacks on autonomous vehicles. In This article, we will study the assessment of risk in the context of an autonomous vehicle. It is very important in an ITS to measure risk, prevent dangerous damages, and make our system more resistant to attacks. This study will focus on the attack on the autonomous vehicle since attacks in ITS cames from the vehicle itself or the network. Therefore to measure the risk of attack, we need to calculate the probability of attack success because an attack that has a probability of attack success equal to zero could not harm our system because it could not happen, while an attack with a high probability of success should be taken into consideration while measuring risk. So we propose to implement a decision tree that will predict the probability of success of an attack.

In this article, we will create a decision tree that will predict the class of probability of attack success. Then we will create a decision tree to predict the risk based on the probability of attack success and the impact of the attack. The paper's structure will be as follows: we will start by presenting risk management and our proposed scheme, which contains two subsections. In the first subsection, we conduct a study on identifying risk threaten an autonomous vehicle, i.e., interfaces that attackers can exploit to produce an attack besides the attack in each interface. In the second subsection, we will assess risk by measuring the probability of attack success using a decision tree, and we will also describe the impact of attacks on an autonomous vehicle (AV). Furthermore, finally, we will present the risk assessment by using a decision tree based on two criteria: the probability of attack success and the impact of attack and conclusion.

II. Risk Management

In our daily lives, we are exposed to risks. The development of technologies made this risk bigger and bigger, especially in the intelligent transport system where we will have a 100% autonomous vehicle (with no driver intervention), which makes any safety violation very dangerous. Therefore, it is essential to start with risk management more than ever to avoid any danger such as death. In this section, we propose to study risk management in the context of the ITS by starting with the identification of all interfaces that can pose a loophole for an attacker to start his attack, and after that, we will analyze risk by using a machine learning algorithm that will predict the probabilities of success of an attack and measure the risk. The measure of risk will be very helpful in preventing attacks that can be very damaging for the citizen and the ITS.

A. Proposed Scheme

We will be based on the risk management scheme to start our proposed algorithm to predict risk in an autonomous vehicle. Risk management identifies the possible risks in advance, analyzes them, and implements safety measures to decrease and reduce the risk. As shown in Fig. 1, risk management starts by identifying risk, assessing the risk, and controlling the risk [1].

1) Risk identification: Attacks on ITS can come from two systems, the vehicle itself and the network. In our study, we focused on attacks against autonomous vehicles(AV). Attacks that can threaten an AV can come from four interfaces described in Fig. 2. In this section, we will present the interfaces that have vulnerabilities and the attacks that have occurred by exploiting these interfaces. Table I summarizes the result found.

a) Buses and ports

i) CAN: The Controller area network (CAN) is an electronic communication bus defined by the ISO 11898 standards, well known for its low cost. It allows communication between the different systems or electronic control units (ECU) of the vehicle. However, the CAN protocol is exposed to several inherent vulnerabilities, such as broadcast transmission. The CAN protocol sends the packet to all the other nodes without exception to transmit the information to a specific node. Therefore, if there is a malicious node, it can easily spoof all transmitted frames from other nodes.

Moreover, since it does not support the identification mechanism [2], each node must decide for itself whether the packet should be rejected or supported. As a result, a receiving node cannot differentiate between valid and false frames. This feature helps a malicious node easily hide its identity and send false frames to other nodes connected to the CAN bus to control the vehicle. Among the problems encountered when using CAN is the ID-Based Priority Scheme. Each packet has a number that indicates the packet's priority when packets sent on the bus are continuously relevant and may delay the delivery of a less urgent packet, which makes the network vulnerable to DOS attacks. Providing the example of a malicious node that streams frames with the smallest identifier to have the highest priority, preventing legitimate nodes from sending their valid frames. Besides, the CAN frame is not encrypted. Therefore, an attacker can rely on the recorded history of the CAN frames to scan the CAN frames. Among the major problems that the CAN network faces is that the attackers can access the network via interfaces such as the OBD port and CD drive, USB port, and telematics systems. Therefore, various attacks can be implemented, including DoS attacks, frame sniffing, and frame injection. As mentioned before, the CAN frame presents several intrinsic vulnerabilities, which may necessitate a switch to a new version of CAN protocol which is the CAN-FD.

- CAN FD offers three main advantages over the traditional CAN.
- It offers a higher data rate of up to 8 Mbit/s.
- It allows data payloads of up to 64 bytes (as opposed to 8 bytes).
- It allows the authentication mechanism.

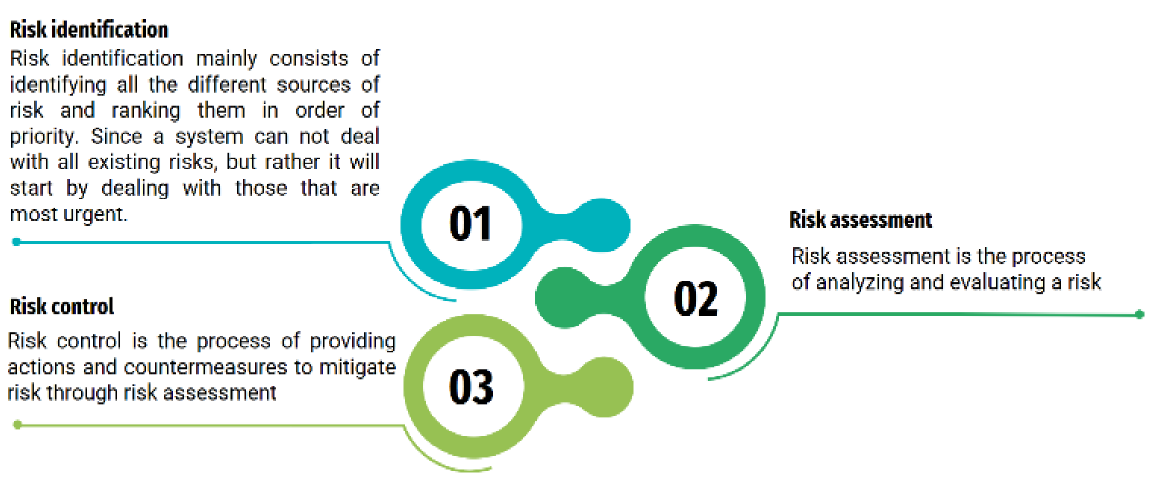

Fig. 1. Risk Management.

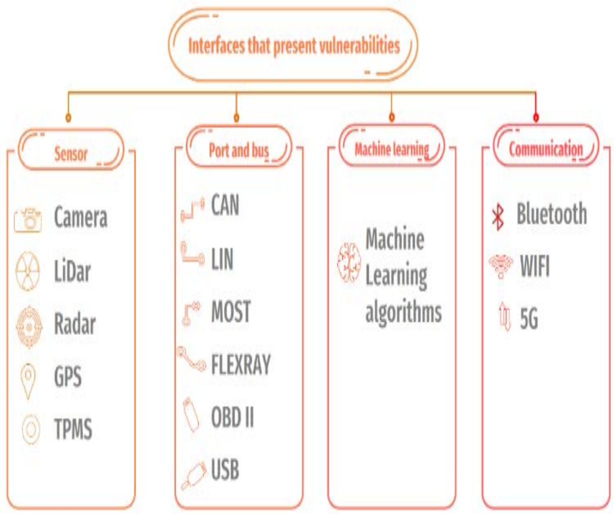

Fig. 2. Taxonomy of Attacks in Autonomous Vehicle.

ii) OBD-II: OBD-I was first introduced in 1987 to give a standardization of on-board diagnostics for vehicles, but the latter encountered many flaws and challenges, which led car manufacturers to migrate to a new version of OBD in 1996 called OBD II as well as all vehicles built after that date was equipped with an OBD II port. On-Board Diagnostics (OBD) is a vehicle self-diagnosis and reporting system that provides access to the status of various vehicle sub-systems, such as airbags, braking, speed control, and is used to monitor the condition of the vehicle's systems. OBD systems use a standardized digital communication port to transfer data in real-time. The OBD system uses the can bus to perform these data transfers. When the vehicle fails, the OBD system uses a standardized set of Diagnostic Trouble Codes (DTCs) to identify the malfunction and remedy the identified problem quickly. However, OBD II exposes the vehicle to several threats because today's vehicles are equipped with wireless communication tools (WIFI, Bluetooth 5G), so attackers can use these communication channels to send malicious programs to the CAN bus via the OBD port in order to control the vehicle. In addition, some scanners may also have a feature that allows them to extract and modify ECU codes. An attacker who uses this type of scanner can easily modify the ECU code for malicious purposes. An adversary can also use the OBD port to connect to the vehicle to listen to unencrypted packets and gather data for a replay attack [3], [4].

iii) LIN: The Local Interconnection Network (LIN) is a low-cost vehicle bus standard, the communication rate used by the LIN does not usually exceed 20kbps [5] therefore, it is only used for data that does not require high transmission rates such as control of lights, engines, air conditioning, steering wheels, seats and doors [5]. LIN is based on a master/slave architecture that consists of a single master node and many slave nodes connected using a single wire. While most research on embedded networks security is focused on CAN, the attacks on Local Area Network (LIN) is also as harmful as they can's attacks since a LIN master serves as a gateway to the CAN bus so the attacks can spread easily to other ECUs and other ECUs as well. The access to the LIN bus can be logical or physical. An attacker can access the LIN via the master node because the master node is always connected to the CAN bus [5]. Among the attacks that LIN buses are exposed we quote header collision, Spoofing, and response collision.

TABLE I. INTERFACES AND ATTACK ON AUTONOMOUS VEHICLE

Interfaces		Attack
Port et bus	CAN	• Replay attack [6], [32], [33]. • DOS [6], [33]–[35]. • Eavesdropping attack [6], [33]. • Injection attack [6], [33].
	OBD II	• Code Modification[4] • Code Injection: [4] • Packet Sniffing [4] • Packet Fuzzing[4]
	LIN	• Header collision [5], [6] • Spoofing [6], [8]. • Response collision [5], [6]
	MOST	• Forged messages [9]. • Jamming attacks[8], [9], [36] . • Synchronization disruption attacks[6], [8].
	Flexray	• Replay attacks[6], [37]. • Spoof attack [7] . • Injection attacks [6], [7], [37]. • The Masquerading [6], [37]. • Eavesdropping attack [6], [7], [37].
	USB	• Injection attacks[6] • Spoof attacks[6]
Short-range Communication	WIFI	• Eavesdropping attack [6], [16]. • Dos [6], [17]. • Jamming attack [6], [15].
	Bluetooth	• Eavesdropping attack [11], • Sniffing [11], • Stealing personal information[11], • Buffer overflow attack.[11]
	RFID	• Eavesdropping [6], [18]. • Brute force [6], [18]. • Replay [6], [18]. • Man-in-the middle [6], [18]. • Synchronization attacks [6], [19].
Sensor	Camera	• Blind camera[4], [20], [21]
	Radar	• Jamming [23], [38], [39]. • Ghost vehicular attack [22]–[24].
	LiDar	• Jamming [4], [20], [21]. • Spoofing [4], [20], [21].
	GPS	• Spoofing [4], [20], [22]. • Jamming [4], [20], [22].
	TPMS	• TPMS based attack [4], [20], [21], [27].
Machine learning		• Adversarial attacks [29], [30] • Black box attack [28].

In a spoofing attack, the master in a LIN network can force a slave to perform tasks including sleep and SYNC field definition. An attacker can exploit these two characteristics of the master to force slaves to fall asleep and cause the network to shut down. In addition, it can spoof messages and modify the SYNC field to distort the synchronization [6]. While The collision attack consists of sending a wrong message simultaneously as a correct message is sent. In the LIN protocol, an attacker exploits the LIN error handling mechanism, which consists of stopping transmission of a slave node when he detects that the value in the bus differs [6]. The Header collision attacks happen when an attacker sends a false header to crash against a legitimate header from the master node. When a response is sent from the new editor node, the attackers can carry out a response collision attack to insert their illegal message. In this way, attackers can distort the sequence of responses sent on the LIN bus and leave the vehicles' automated sliding doors open and lock the steering wheels while the vehicles are on the road[6].

iv) Flexray: Flexray was developed in 2007 by BMW. Flexray is an expensive and complex communication tool. It is used for critical data that requires more security; this is due to the time-division multiplexing of FlexRay, which facilitates the design of modular, distributed, and security-related systems. Flexray is known for its transmission speed which can reach 10Mbps for each channel, and FlexRay offers scalable fault tolerance by allowing one or two-channel communication. Nevertheless, one channel can also be connected when redundancy is not required. However, The bandwidth can be increased by using both channels to transfer non-redundant data. The absence of the confidentiality mechanism in the FlexRay protocol allows an attacker to read all data sent over the bus. In addition, FlexRay does not have an authentication mechanism so an attacker can create and inject data, e.g., an attacker can create and inject a request to switch on the stoplight [7]. Flexray protocol is also vulnerable to attacks that can target the static segment of the FlexRay communication, such as replay attacks, injection attacks, and the Masquerading [6].

v) MOST: MOST (Media Oriented System Transport) is a serial communication system used for audio, video, and control data transmission via fiber optic cables, and it is also used for GPS. MOST (Media Oriented System Transport) is a serial communication system used for audio, video, and control data transmission via fiber optic cables, and it is also used for GPS. This high-performance technology is based on synchronous data communication with a high data rate of up to 150 Mbps and the fact that MOST is not sensitive to electromagnetic interferences since it uses plastic optical fibers instead of traditional copper wire. MOST communication is susceptible to synchronization-disrupting attacks and jamming or denial-of-service attacks [8], [9]. An attacker can perform a jamming attack by prompting a malicious node to continuously send fake messages that continuously block legitimate messages. In addition, an attacker can cause a synchronization interruption by sending fake synchronization frames to disrupt the MOST synchronization [6], [8].

vi) USB: Nowadays, all vehicles have a USB port to connect phones, navigation systems, or any USB devices. However, this port exposes the vehicle to different threats since attackers can access the CAN buses via a USB port and inject malicious code or spoof network cards [6].

b) Short-range communication

i) Bluetooth: Bluetooth is a very well-known communication protocol and is widely used in today's vehicles. Once the phone is connected via Bluetooth to the vehicle, it allows fully wireless access calling functions from the phone via the vehicle's dashboard, control screen, steering wheel buttons, or voice commands, which is very convenient because the driver can keep both hands on the steering wheel. However, this protocol exposes the vehicle to several threats because of the vulnerabilities it faces. The lack of an authentication mechanism before pairing the devices makes it easier for hackers to access the vehicle. Therefore, an attacker can inject viruses or malicious programs to exploit important information (e.g., address book passwords) once the Bluetooth device is paired. In addition, the Bluetooth interface enhances the routes of the cyber-attack as follows: Eavesdropping attack, Sniffing, stealing personal information, Buffer overflow attack [10]–[12].

ii) WIFI: WIFI is a wireless network used to connect multiple devices. The term WIFI is an abbreviation of Wireless Fidelity. The IEEE 802.11 standards govern it. WIFI is similar to Bluetooth in the vehicle except that WIFI has lower latency and higher bandwidth and, of course, a high cost [13]. WIFI remains less used in the vehicle than Bluetooth due to the cost and interference with Bluetooth since the two technologies share an overlapping spectrum[14]. WIFI usage in the vehicle exposes the vehicle to serious threats, namely jamming attacks [15]. In addition, an attacker can also get access to an illegitimate WiFi access point and listen to the vehicle's activity [16]. WiFi protected access can also be threatened by a denial of service attack [17].

iii) RFID: RFID is a radio frequency-based technology to identify tagged objects that pass close to a detector. Thus, contrary to the barcode, we can follow the path of objects and store and retrieve their data. Nowadays, RFID technology is widely applied in several sectors (aeronautics, transport, food industry, health ...), and we can also find this technology in our daily lives, namely transport cards, anti-theft tags, contactless keys, highway badges. However, RFID technology is vulnerable to several threats, namely eavesdropping, brute force, replay, and man-in-the-middle attacks [18] and Synchronization attacks [19] that block the synchronization system.

c) Sensor

i) Camera: The camera is a very important sensor because it allows the vehicle to understand its surroundings. In order to maintain a 360-degree view of its surroundings, the vehicle must be equipped with at least eight cameras installed at several angles. In addition, the camera allows the detection of obstacles and object recognition, but unfortunately, a fast laser burst of 650 nm is capable of completely blinding the camera without ever getting recovered from blindness [4], [20], [21].

ii) Radar: Radar is a system that allows the detection of objects. However, this system is also vulnerable to attacks such as jamming attack and ghost vehicular attack which aims to convert and store the signal using a DRFM (digital radio frequency memory) and use it to deceive the transmitting radar in order not to recognize it from other legal signals and considered as an obstacle [22]–[24].

iii) Lidar: Lidar, is an abbreviation of Light Detection and Ranging, is a method of remote sensing which uses light in the shape of a laser pulse to measure distances (varying distances) to the object. This system is used in autonomous vehicles to detect obstacles. However, liDar is also exposed to attacks such as jamming and spoofing [4], [20], [21]. For example, an attacker deceives the lidar by pretending the existence of an obstacle and forcing the vehicle to stop [25], [26].

iv) GPS: The GPS is a Satellite Geolocation System. It can determine the geographic coordinates of any point on the surface of the globe. The attacker can block a vehicle to receive the GPS signal by performing a jamming attack. In addition, GPS can be easily hacked by an attacker using a radio transmitter that broadcasts a false GPS signal and interferes with nearby GPS receivers in order to perform a spoofing attack and deceive the GPS device by forcing the driver to deem that the vehicle is in an area when it is not [4], [20], [22].

v) TPMS: Indirect TPMS is used to calculate the rotation speed of each wheel. If a wheel rotates faster, it means that its pressure is not correct. The TPMS must send this data to the vehicle control unit (ECU). An attacker can exploit this data and execute a TPMS based attack and modify this data and send erroneous data to the ECU [4], [20], [21], [27].

d) Machine Learning

in adverse attacks, the attack strategy may differ from one attacker to another. This strategy is based on the attacker's capability, the purpose of the attack, and the expertise of the attacker. The concept of a contradictory attack consists of adding noise to the model's input to lead them to produce an erroneous prediction. The author in [28] successfully disrupted a deep neural network model by forcing it to predict wrong classes without prior knowledge of the model or the data used in the learning phase. This type of attack is called a black box attack. Szegedy et al. [29] carried out contradictory example attacks against MNIST, QuocNet [30], AlexNet [31]. They performed perturbations on inputs so that the correct and modified inputs cannot be distinguished from each other. This perturbation led to misleading the model.

2) Risk assessment: In this step, we are interested in measuring risk. We define risk as a relation between two variables: the probability of attack success and the attack's impact on the system. In this section, we will conduct a study to calculate the probability of attack success based on a decision tree then we will conclude the value of the risk.

$$Risk = Probability \times Impact \tag{1}$$

a) Impact of attacks

In the intelligent transport system, we will divide the impact of attacks on the system into four distinct levels levels shown in Fig. 3. The first level is the most important one, the impact on human life when the attacker aims to cause accidents or to hit pedestrians; this attack has to be considered because human life counts the most. The second level involves material damage to the VANET network, which is also dangerous because if an attacker manages to break down a base station, this can cause traffic jams and even accidents. The third level includes material and ecological damage when an attacker crashes into a tree, for example. Finally, the last level is moral damage; we refer to the attack intended to capture the driver's information or hack into the network information. It is important to mention that we may have a mixture of these levels of damage; in fact, we may have both material and physical damage or physical and moral damage, depending on the case.

b) Probability of attack success

The attacker is an essential element in calculating the probability of success of the attack. We will focus on two criteria of the attacker, which are the attacker's capability and his knowledge. These two criteria are very important in the calculation of the probability of success of the attack. For example, suppose an attacker has very high expertise and capability besides having a very high knowledge of the system. He can easily carry out an attack that can be very dangerous, and the probability of the attack being successful will be very high.

Fig. 3. Impact Levels.

On the contrary, if the attacker's capacity is very low and knowledge of the system is also low, then the probability of a successful attack will be very low as he/she does not have the expertise to perform a successful attack. If the attacker has high knowledge but very low capability, the attacker can carry out an attack that is very easy to perform but cannot carry out a very complex and dangerous attack. Therefore, we can conclude that the type of attack is another essential criterion in calculating the probability of success. In order to calculate the probability of success, we will focus on the complexity of the attack because a very complex attack need a that the attacker has a very high knowledge of the system and also very high capacity and expertise on the contrary of an easy attack that does not need attacker to be expert. So to measure the complexity of the attack, we will focus on four criteria.

- The attacks' adaptability is the type of attack that even if the system detects them, they can adapt and find another flaw and access to the system. Therefore, those types of attack require a very high capability of attack and very high knowledge of the system because they are very complex, and the probability of attack success is very high if the attacker has the essential element needed.
- Imperceptibility of the attacks: The degree of imperceptibility has a significant impact in determining the complexity of the attack. Because the system becomes imperceptible to differentiate between malicious nodes and legitimate ones, intrusion detection will be very hard. In this case, the attacker can carry out attacks that will cause accidents or send erroneous messages that will be considered the right messages since the system considers him a legitimate node. He can also carry out any attack, namely, DNS.
- The specificity of the attacks: when the attack has a specific target, and the attack aims to put down a specific functionality of the vehicle or even to change the value of the targeted function. For example, changing the value of the TMPS sensor and providing the wrong value of the wheel pressure.
- Type of attacks: The type of attack means if the attack needs physical access or remote access. The attack with physical access is very damaging since they can access the vehicle ECU and control the vehicle. The physical access means that the attacker can access the car via a port such as OBDII or USB, see Section IIA(1). The attacker can also access the vehicle via remote by using wireless communication. In this case, an attacker can carry out attacks such as jamming or spoofing.
- The probability of attack success is a relation between the complexity of attacks that contain four criteria and the attacker containing two criteria.

$$Probability\ of\ attack\ success = R(complexity, capacity, knowledge) \quad (2)$$

A successful attack has a probability of 1, and a non-successful attack has a probability of 0. In our case, we define the probability of success into six classes, as shown in Fig. 4. An attack that is sure to happen has a probability of success between 90 and 100%, and those attacks are very complex to detect by the system and the capability and knowledge of the attacker are very high the attacker can perform easily an attack that could be specific and target an ECU. As a result, he can control the vehicle and cause dangerous damage. Another type of attack that also presents a very high risk for the system is the attack with a percentage of success between 89% and 70%. In this type of attack, the attacker has a high capability and medium knowledge, and the attacker can perform an attack with a medium level of complexity. The third class is the class that remains dangerous but less than the fourth class. The percentage of probability of success is between 69- 50%. In this type o attack, the capability of the attacker and the knowledge are medium, and the attacker can perform attacks that have a level of complexity low or medium. The second class contains the attacks that might succeed or not; the probability of attack success is between 49% and 30%. In this class, the attacker's capability is low, and the attacker's knowledge is very low, so the attackers cannot perform complex attacks but rather can perform an easy attack such as eavesdropping. The second class contains attacks with a low probability of success between 29% and 10%. The attacker in this class has a very low capability; he cannot perform a complex attack, and he will find difficulty conducting an easy attack. The last class is the attack with a very low probability of success between 9% and 0%. In this class, the attacker's capability is extremely low, and the attacker's knowledge they cannot perform any attack.

c) Decision tree

As described in the previous section, we define six classes of probability, and because the probability of attack success is a relation between three-component, we will not be able to calculate it using a mathematical function. Rather, we will use a machine learning algorithm to predict the probability based on the attack's complexity, capacity, and knowledge. Finally, the decision tree will build a tree that will use our logic described in (Section IIA(2)) to find the probability class.

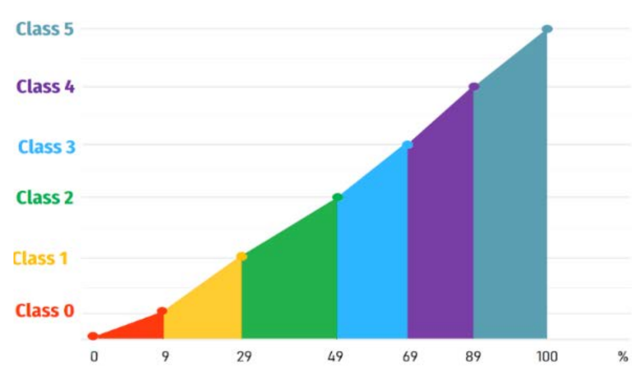

Fig. 4. Probability of Success.

The decision tree algorithm is a supervised algorithm that can be applied to regression and classification tasks [40], [41]. The decision tree is composed of three essential elements, which are:

- The root node: this is the node that represents the top of the tree.
- Intermediate nodes: these are the nodes that are placed between the root and the end nodes.
- Leave nodes: these are the final nodes of the tree, where predictions of a category or numerical value are made.

Decision trees use several algorithms to decide to split a node into two or more sub-nodes. The creation of sub-nodes increases the homogeneity of the resulting sub-nodes. Several decision tree algorithms are used to split the node. In our case study, we will use C4.5, a decision tree algorithm that supports several classes higher than two in its decision node calculation. In order to determine the placement of nodes in the trees, we will use the entropy and information gain principle [40], [41].

The entropy is the order of a data set, and we compute the entropy at each node of the tree then subtract the child's entropy from the parents' entropy. The outcome of this calculation is the information gain [40].

$$E(S) = \sum_{i=1}^{c} p_i \log_2 p_i \quad (3)$$

We choose the decision tree because it is easy to work with and also to interpret. The decision tree(DT) provides a graphical tree that will help understand the result. Besides, DT is tolerant of missing value and simple to implement. In our case study, the decision tree is the wright algorithm since, in each step, the algorithm must ask some questions (for instance, if the attacker has a high capability or not), and based on the result of the question, a decision will be made to find the other feature that may give the right class of probability. The decision tree may present a problem of overfitting, which will be corrected using a post pruning technique. Pruning is a technique used for machine learning algorithms that reduces the size of the trees by deleting segments of the tree. The result is a significant reduction in the complexity of the final classifier and consequently enhanced predictive accuracy by reducing overfitting. Tree pruning can be done in two ways: pre-pruning or post-pruning. In our experiments, we will use post-pruning based on reduced error pruning. The algorithm is very simple and fast. It produces small, compact trees. It will sequentially transform each subtree into one single leaf. It assesses the pattern against a set of test data and then compares the error rate with the original tree. The sub-tree having the highest error reduction would be pruned. This process would be repeated until there is no more error reduction.

III. Experiment Result

A. *Probability of Attack Success*

Before starting the creation of the decision tree, we first prepare the database that will be the input of the machine learning algorithm. Machine learning algorithms are highly data-dependent. Therefore, data preparation is a very important step as it speeds up the learning of the algorithms and gives a correct result. Therefore, the first step in creating the decision tree was the data cleaning or removing any missing data, and then we transform the data using hot encoding as the algorithm does not support categorical data.

TABLE II. ACCURACY VALUE

	Before pruning	After pruning
Training accuracy	90%	90%
Testing accuracy	75%	87%

The database we use in our algorithm is created randomly by giving each criterion, namely attacker capability, attacker knowledge, attack adaptability, attack specificity, attack type, and attack imperceptibility, one of the following values (very low, low, medium, high, or very high). After creating the database and preparing it, we split the data into test and training sets. Then we will create the decision tree and calculate the accuracy of the tests and training to identify whether there is an over-fitting. We start first by creating the decision tree and measuring the accuracy for the training and the test. As mentioned in Table II, the accuracy of the training is 90%, and the test accuracy is 75%, which means that there is an over-fitting. To resolve the overfitting problem, we recreate the decision tree. We use a post pruning technique described in (Section IIA(2)) to correct the overfitting, so as mentioned in Table II, after the post pruning, the accuracy of the training is 90%. The accuracy for the test is 87%, the overfitting is corrected, and the accuracy of the tests was increased by 12%, and the gap between training and testing was reduced to 3%, we can conclude that the algorithm learns well.

The decision tree is constructed through iteration from the root node to the leaves node using the training set. First, the data set is split into two sets: the training set, which the decision tree is using to learn, and the test set, which is used to evaluate predictions to the real values and measure the performance of the decision tree. Next, the tree is built by calculating entropy and the information gain. The node with the highest information gain is eventually placed as the root node in the decision tree. Then we will repeat this process when the subset is split.

Moreover, each time, we will recalculate the remaining values that are in that subset. If two nodes are compared together, and they have the same information again. Then a concept called the gain ratio will determine which of these will be used. The gain ratio is calculated based on the node that has the fewest unique values. This node will become preferred. It can be seen that this tree includes a total of 58 nodes, among which 30 are leaves nodes, including one leave node in class 0, 3 leaves nodes in class 3, five leaves nodes in class 2, 14 leaves node in class 3, 5 leaves nodes in class 4 and 2 leaves nodes in class 5 as shown in Fig. 5. Note that entropy is also calculated and given in each node to characterize the purity of the sub dataset in that node. For every node, there is information about the split/decision. For the top of the tree root node, the tree starts by assessing whether the attacker has a high capability or low capability. The entropy criterion at this point is 2.347. An entropy of 0 represents purity. Therefore the value of the entropy criterion must be lower as we move down the branches. The number of samples at this node is 131.

The class prediction at this point is 3. This prediction will become significantly more accurate as we go down the tree. We will assess the first True of the decision tree, which means that the capability is very low, so the decision node will assess whether the attacker has knowledge about the system. At this node, The entropy criterion is equal to 1.226 as discussed earlier, the entropy criterion is decreasing, and the class prediction here is class 1. For the second true, we get to a leave node with an entropy equal to 0 and a prediction class equal to zero, which means that an attacker with a very low attack's capability and also a very low attacker's knowledge the attack probability will belong to class 0, which means that the attacker could not perform an attack on the system. If we evaluate the second false in the decision tree, the decision node here evaluates the specificity of the attack. The entropy is equal to 0, 455, and the prediction class equals one if the attack is specific. The decision tree arrives at a leave node with an entropy equal to 0 and a prediction class equal to 1. we can explain that by following the decision logic if the attacker's capability was very low. He has a high knowledge. Then the decision tree evaluates whether the attack is complex by first evaluating whether the attack is specific. If the attack is specific, then the probability of attack success will be class 1 because an attacker with high knowledge and very low capability could not perform a complex attack. If the attack was not specific, then the decision tree will look for the other criterion: adaptability and imperceptibility.

B. *Risk Assessment*

To measure the risk, we first started by identifying risk interfaces in the autonomous vehicles, then we calculated the probability of attack success and evaluated the impact and severity of the attack; then, we can conclude the value of the risk. As mentioned in section (b), the risk is a relation between the attack's impact and the probability of success of the attack. There is a set of rules that can be executed to measure the risk. If the probability of attack success is (very high or high) means that the probability belongs to class five or the fourth class and the attack's impact is physical then, the risk will be very high, and we should stop the attack as soon as possible. Besides, if the impact is material, then the risk will be high. While if the impact is not so dangerous, which means that the impact is moral and the attacker is trying to steal information from the network, then the risk is medium, and we should consider this attack, but it is not urgent compared to the first one. If the probability of success is medium, that means that the probability of attacks belong to the third or the second class and the impact is physical or materiel or both then the risk will be medium because the attack may happen or not the priority of those attack is less than the first one but should be taken into consideration. While if the impact is moral, then the risk will be low because there are no damages, and we should increase the mechanism of confidentiality and authenticity to stop the attacker from listening to the network. If the probability of attacks belongs to class zero, then the risk will be low. We will use a decision tree that will predict the class of the risk. We could present these rules in a decision tree that will predict the value of the risk based on the value of the probability of attack success and the impact of the attack.

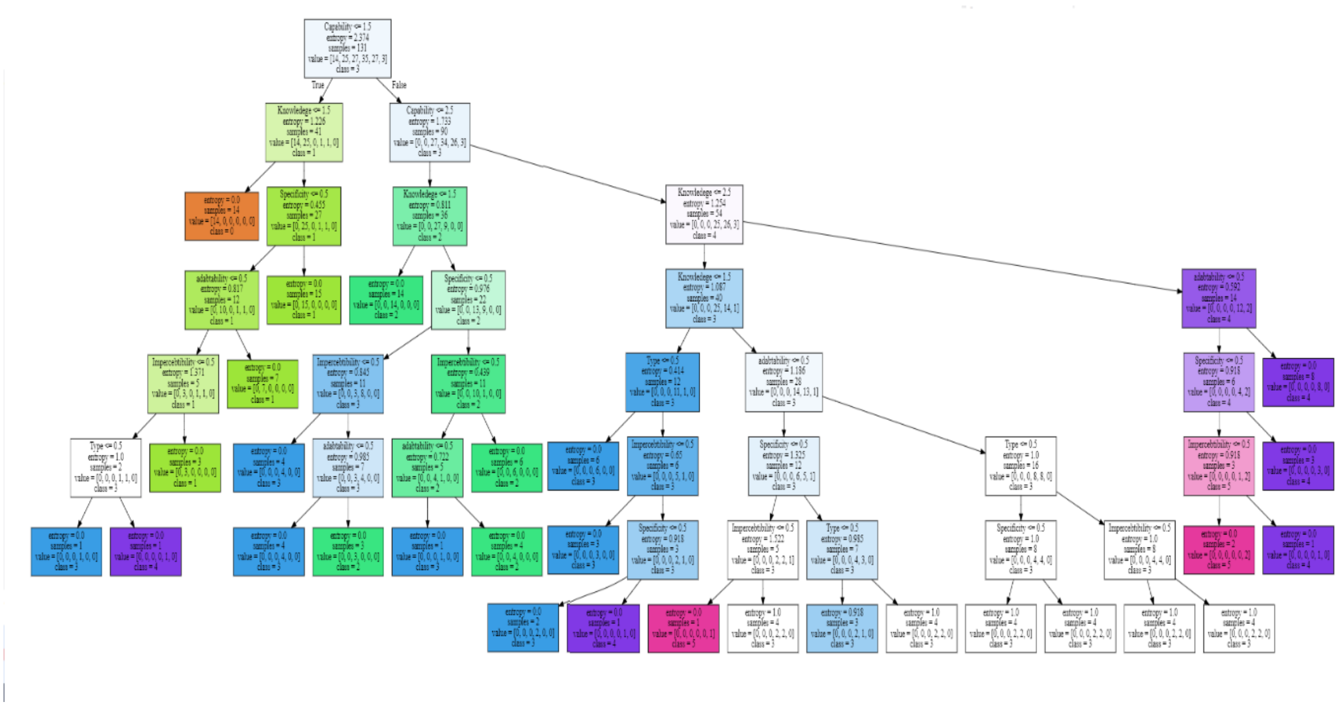

Fig. 5. Decision Tree of the Probability of Attack Success.

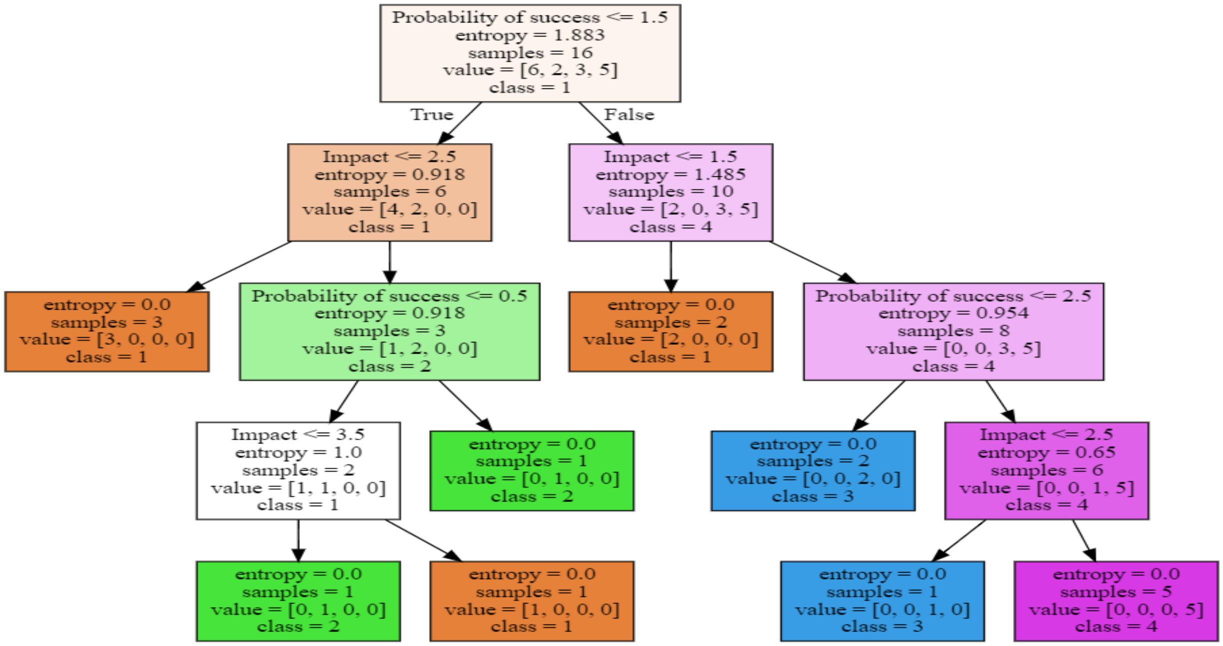

Fig. 6. Decision Tree of Risk Assessment.

It can be seen that in Fig. 6, the tree includes a total of 15 nodes, among which 6 are leaves nodes, including three leave nodes in class 1, 2 leave nodes in class 2, two leaves nodes in class three, and two leave nodes in class four. Note that entropy is also calculated and given in each node to characterize the purity of the sub dataset in that node. The accuracy of the decision tree is 100%, and the max depth of the tree is 4. The tree's leave has an entropy of zero, which means that all leaves are pure, and the tree follows the logic described in the previous paragraph. The tree started with the probability of attack success as a root of the tree because it has the highest entropy, and the entropy criterion decrease while going down the tree.

IV. Conclusion

It is very important to list risks associated with autonomous vehicles to develop defensive mechanisms to enhance security in smart transportation.

The study and the evaluation of risk constitute an essential step in decision-making to opt for a mitigation technique more tailored to the transportation context.

The approach that we have explained in this paper suggests a new technique to evaluate the risks that may be enfolded in an autonomous vehicle based on two criteria: the attack success rate and its impact on the targeted system. To measure attack success probability, we have studied two main variables: the attacker's capabilities and the type of attack they perform. We have used a decision tree algorithm to forecast the risks class. We have derived a graphical tree that we have presented in this paper to help in understanding the proposed results. We will conduct a study on other machine learning classifiers in future work, and we will compare their performance in risk evaluation with the obtained results.

References

[1] H. Fang and M. Duan, ‘Safety System Engineering for Offshore Oil’, in Offshore Operation Facilities, Elsevier, 2014, pp. e183–e347.

[2] O. Avatefipour and H. Malik, ‘State-of-the-Art Survey on In-Vehicle Network Communication (CAN-Bus) Security and Vulnerabilities’, ArXiv180201725 Cs, Feb. 2018, Accessed: Apr. 15, 2021. [Online]. Available: http://arxiv.org/abs/1802.01725.

[3] A. D. Kumar and K. N. R. Chebrolu, ‘A Brief Survey on Autonomous Vehicle Possible Attacks,Exploits and Vulnerabilities’, p. 6.

[4] V. L. L. Thing and J. Wu, ‘Autonomous Vehicle Security: A Taxonomy of Attacks and Defences’, in 2016 IEEE International Conference on Internet of Things (iThings) and IEEE Green Computing and Communications (GreenCom) and IEEE Cyber, Physical and Social Computing (CPSCom) and IEEE Smart Data (SmartData), Chengdu, China, Dec. 2016, pp. 164–170, doi: 10.1109/iThings-GreenCom-CPSCom-SmartData.2016.52.

[5] J. Takahashi et al., ‘Automotive Attacks and Countermeasures on LIN-Bus’, J. Inf. Process., vol. 25, no. 0, pp. 220–228, 2017, doi: 10.2197/ipsjjip.25.220.

[6] Z. El-Rewini, K. Sadatsharan, D. F. Selvaraj, S. J. Plathottam, and P. Ranganathan, ‘Cybersecurity challenges in vehicular communications’, Veh. Commun., vol. 23, p. 100214, Jun. 2020, doi: 10.1016/j.vehcom.2019.100214.

[7] D. K. Nilsson, U. E. Larson, F. Picasso, and E. Jonsson, ‘A First Simulation of Attacks in the Automotive Network Communications Protocol FlexRay’, in Proceedings of the International Workshop on Computational Intelligence in Security for Information Systems CISIS’08, vol. 53, E. Corchado, R. Zunino, P. Gastaldo, and Á. Herrero, Eds. Berlin, Heidelberg: Springer Berlin Heidelberg, 2009, pp. 84–91.

[8] M. A. Chowdhury, A. Apon, and K. Dey, Eds., Data analytics for intelligent transportation systems. Amsterdam: Elsevier, 2017.

[9] M. Wolf, A. Weimerskirch, and C. Paar, ‘Secure In-Vehicle Communication’, in Embedded Security in Cars, K. Lemke, C. Paar, and M. Wolf, Eds. Berlin/Heidelberg: Springer-Verlag, 2006, pp. 95–109.

[10] A. Yadav, G. Bose, R. Bhange, K. Kapoor, N. Ch. S. N. Iyengar, and R. D. Caytiles, ‘Security, Vulnerability and Protection of Vehicular On-board Diagnostics’, Int. J. Secur. Its Appl., vol. 10, no. 4, pp. 405–422, Apr. 2016, doi: 10.14257/ijsia.2016.10.4.36.

[11] H. Onishi, K. Wu, K. Yoshida, and T. Kato, 'Approaches for Vehicle Cyber-Security in the US', Int. J. Automot. Eng., vol. 8, no. 1, pp. 1–6, 2017, doi: 10.20485/jsaeijae.8.1_1.

[12] S. Checkoway et al., 'Comprehensive Experimental Analyses of Automotive Attack Surfaces', p. 17.

[13] R. Friedman, A. Kogan, and Y. Krivolapov, 'On Power and Throughput Tradeoffs of WiFi and Bluetooth in Smartphones', IEEE Trans. Mob. Comput., vol. 12, no. 7, pp. 1363–1376, Jul. 2013, doi: 10.1109/TMC.2012.117.

[14] A. Mourad, S. Muhammad, M. O. Al Kalaa, H. H. Refai, and P. A. Hoeher, 'On the performance of WLAN and Bluetooth for in-car infotainment systems', Veh. Commun., vol. 10, pp. 1–12, Oct. 2017, doi: 10.1016/j.vehcom.2017.08.001.

[15] T. D. Vo-Huu, T. D. Vo-Huu, and G. Noubir, 'Interleaving Jamming in WiFi Networks', in Proceedings of the 9th ACM Conference on Security & Privacy in Wireless and Mobile Networks, Darmstadt Germany, Jul. 2016, pp. 31–42, doi: 10.1145/2939918.2939935.

[16] O. Nakhila, E. Dondyk, M. F. Amjad, and C. Zou, 'User-side WiFi Evil Twin Attack detection using SSL/TCP protocols', in 2015 12th Annual IEEE Consumer Communications and Networking Conference (CCNC), Las Vegas, NV, USA, Jan. 2015, pp. 239–244, doi: 10.1109/CCNC.2015.7157983.

[17] M. Vanhoef and F. Piessens, 'Denial of Service Attacks Against the 4-Way WiFi Handshake', in Computer Science & Information Technology (CS & IT), Nov. 2017, pp. 85–94, doi: 10.5121/csit.2017.71508.

[18] J.-S. Cho, Y.-S. Jeong, and S. O. Park, 'Consideration on the brute-force attack cost and retrieval cost: A hash-based radio-frequency identification (RFID) tag mutual authentication protocol', Comput. Math. Appl., vol. 69, no. 1, pp. 58–65, Jan. 2015, doi: 10.1016/j.camwa.2012.02.025.

[19] C. Zhang, W. Zhang, and H. Mu, 'A Mutual Authentication Security RFID Protocol Based on Time Stamp', in 2015 First International Conference on Computational Intelligence Theory, Systems and Applications (CCITSA), Ilan, Taiwan, Dec. 2015, pp. 166–170, doi: 10.1109/CCITSA.2015.52.

[20] S. Parkinson, P. Ward, K. Wilson, and J. Miller, 'Cyber Threats Facing Autonomous and Connected Vehicles: Future Challenges', IEEE Trans. Intell. Transp. Syst., vol. 18, no. 11, pp. 2898–2915, Nov. 2017, doi: 10.1109/TITS.2017.2665968.

[21] J. Petit and S. E. Shladover, 'Potential Cyberattacks on Automated Vehicles', IEEE Trans. Intell. Transp. Syst., pp. 1–11, 2014, doi: 10.1109/TITS.2014.2342271.

[22] C. Yan, 'Can You Trust Autonomous Vehicles : Contactless Attacks against Sensors of Self-driving Vehicle', 2016.

[23] M. Pham and K. Xiong, 'A Survey on Security Attacks and Defense Techniques for Connected and Autonomous Vehicles', ArXiv200708041 Cs, Jul. 2020, Accessed: Apr. 15, 2021. [Online]. Available: http://arxiv.org/abs/2007.08041.

[24] S. J. Roome, 'Digital radio frequency memory', Electron. Commun. Eng. J., vol. 2, no. 4, p. 147, 1990, doi: 10.1049/ecej:19900035.

[25] B. G. B. Stottelaar, Practical cyber-attacks on autonomous vehicles. 2015.

[26] M. Harris, 'Researcher Hacks Self-driving Car Sensors', 2015.

[27] I. Rouf et al., 'Security and Privacy Vulnerabilities of In-Car Wireless Networks: A Tire Pressure Monitoring System Case Study', p. 17.

[28] N. Papernot, P. McDaniel, I. Goodfellow, S. Jha, Z. B. Celik, and A. Swami, 'Practical Black-Box Attacks against Machine Learning', ArXiv160202697 Cs, Mar. 2017, Accessed: Apr. 15, 2021. [Online]. Available: http://arxiv.org/abs/1602.02697.

[29] C. Szegedy et al., 'Intriguing properties of neural networks', ArXiv13126199 Cs, Feb. 2014, Accessed: Apr. 16, 2021. [Online]. Available: http://arxiv.org/abs/1312.6199.

[30] Q. V. Le et al., 'Building high-level features using large scale unsupervised learning', ArXiv11126209 Cs, Jul. 2012, Accessed: Apr. 15, 2021. [Online]. Available: http://arxiv.org/abs/1112.6209.

[31] A. Krizhevsky, I. Sutskever, and G. E. Hinton, 'ImageNet classification with deep convolutional neural networks, Commun. ACM, vol. 60, no. 6, pp. 84–90, May 2017, doi: 10.1145/3065386.

[32] T. Hoppe and J. Dittman, 'Sniffing/replay attacks on can buses: A simulated attack on the electric window lift classified using an adapted cert taxonomy', Workshop Embed. Syst. Secure., pp. 66–72, 2007.

[33] J. Liu, S. Zhang, W. Sun, and Y. Shi, 'In-Vehicle Network Attacks and Countermeasures: Challenges and Future Directions, IEEE Netw., vol. 31, no. 5, pp. 50–58, 2017, doi: 10.1109/MNET.2017.1600257.

[34] P. Carsten, T. R. Andel, M. Yampolskiy, and J. T. McDonald, 'In-Vehicle Networks: Attacks, Vulnerabilities, and Proposed Solutions', in Proceedings of the 10th Annual Cyber and Information Security Research Conference, Oak Ridge TN USA, Apr. 2015, pp. 1–8, doi: 10.1145/2746266.2746267.

[35] K. Koscher et al., 'Experimental Security Analysis of a Modern Automobile', in 2010 IEEE Symposium on Security and Privacy, Oakland, CA, USA, 2010, pp. 447–462, doi: 10.1109/SP.2010.34.

[36] N. Kalid, A. A. Zaidan, B. B. Zaidan, O. H. Salman, M. Hashim, and H. Muzammil, 'Based Real-Time Remote Health Monitoring Systems: A Review on Patients Prioritization and Related "Big Data" Using Body Sensors information and Communication Technology', J. Med. Syst., vol. 42, no. 2, p. 30, Feb. 2018, doi: 10.1007/s10916-017-0883-4.

[37] R. Zhao, G. H. Qin, H. P. Chen, J. Qin, and J. Yan, 'Security-Aware Scheduling for FlexRay-Based Real-Time Automotive Systems', Math. Probl. Eng., vol. 2019, p. 4130756, Jun. 2019, doi: 10.1155/2019/4130756.

[38] R. M. Whitson and M. J. Lewis, '(75) Inventors: Walter E. Buehler, Issaquah, WA (US)';, p. 16.

[39] R. N. Lothes, M. B. Szymanski, and R. G. Wiley, Radar vulnerability to jamming. Boston: Artech House, 1990.

[40] S. Singh and P. Gupta, 'Comparative Study ID3, Cart and C4.5 Decision Tree Algorithm: A Survey', Int. J. Adv. Inf. Sci. Technol., p. 7, 2014.

[41] A. Priyam, R. Gupta, A. Rathee, and S. Srivastava, 'Comparative Analysis of Decision Tree Classification Algorithms', Int. J. Curr. Eng. Technol., p. 4, 2013.

An Automated Framework for Enterprise Financial Data Pre-processing and Secure Storage

Sirisha Alamanda[1]
Research Scholar, Department of Computer Science
Jawaharlal Nehru Technological University (JNTU-H)
Hyderabad, India

Dr. Suresh Pabboju[2]
Professor, Department of Information Technology
Chaitanya Bharti Institute of Technology
Hyderabad, India

Dr. G. Narasimha[3]
Professor, Department of Computer Science
Jawaharlal Nehru Technological University (JNTU-H)
Hyderabad, India

***Abstract*—The analysis on the financial data is highly crucial and critical as the results or the conclusion communicated based on the analysis can generate a greater impact on the personal and enterprise scale business processes. The primary source of the financial data is the business process and often the data is collected by automation tools deployed at various points of the business process data flow. The data entered in the business process is primary done by the stake holders of the process and at various levels of the process the data is modified, translated and sometimes completed transverter, due to which the impurities or anomalies are introduced in the data. These impurities, such as outliers and missing values, cause a high impact on the final decision after processing these datasets. Hence an appropriate pre-processing for financial data is the demand of the research. A good number of parallel research outcomes can be observed to solve these problems. Nonetheless, majority of the solutions are either highly time complex or not accurate effectively. Thus, this work proposes an automated framework for identification and imputation of the outliers using the iterative clustering method, identification and imputation of the missing values using Differential count based binary iterations method and finally the secure data storage using regression based key generation. The proposed framework has showcased nearly 100% accuracy in detection of outliers and missing values with highly improved time complexity.**

***Keywords*—Financial data pre-processing; outlier treatment; missing value treatment; regression; differential iterations; iterative clustering**

I. Introduction

The financial data is primarily considered to be time series data, which is variant to the time. The major complexity with the time series data analysis is two. Firstly, the speed of data change is very high. Thus, the algorithm designed to analyse the data, must be highly time efficient. Secondly, the time series data is collected from various sources, thus, the format of the data is also highly critical. These problems are well furnished in the work by C. Chatfield et al. [1]. Nonetheless, the time series data sets are the only option for a valid data analysis for making financial decisions as these financial decisions are expected to be highly time dependent [13].

Many of the cases, it is relevant to analyse the data using neural network-based algorithms due to the factor that these algorithms are less time complex and can generate better results with moderate accuracy. The work by L. Montesdeoca et al. [2] establishes significant observations in concluding the benefits of such algorithms on the financial data. Nevertheless, the primary demand of any neural network-based algorithm is highly sanitized dataset. Thus, the pre-processing of any financial data is highly expected. Also, many of the cases, a big enterprise primarily relies on the outcomes from small business units, which demands final data aggregation for the enterprise as showcased in the work by T. Cook et al. [3]. During such aggregation operations, it is highly possible to receive the final dataset with huge impurities, majorly missing values. Henceforth, it is conclusive that, the pre-processing of the financial data [Fig. 1] is a highly expected feature in any framework. Thus, this research focuses on building a framework for data pre-processing and storage security for business-critical data [19].

A. Research Problem

For financial risk analysis, a plethora of techniques has been created. In general, traditional unsupervised methods for clustering and classification do not provide adequate accuracy and semantics, while supervised approaches for classification and clustering depend on a significant quantity of training data.

B. Motivations and Objectives

This article investigates the semi-supervised scheme for financial data prediction, in which accurate predictions may be anticipated with a bit of quantity of labeled data, as shown in the previous paper. Existing semi-supervised methods have difficulty achieving acceptable results with financial data because of a lack of significant distinguishability across variables. Rather than simply propagating the input labeled data, we transform the input labeled hints to the prior global probability and propagate the 'soft' prior probability to learn the posterior probability to enhance performance.

C. Contributions

The purpose of this paper is to present automated framework for identification and imputation of the outliers using the iterative clustering. For low-security applications that only need modest levels of protection, it is necessary to provide sufficient security Secure Storage for Financial Data. The rest of the work is furnished such as, in the Sections II and III, the fundamental concepts of the data pre-processing and encryption methods for data at rest is analyzed and understood, in the Section IV, the parallel research outcomes are critically reviewed, in Sections V and VI, the proposed solutions are proven using mathematical models and the relevant algorithms are designed with desired framework, in Section VII, the obtained results are discussed and further in Section VIII, the results and the frameworks are compared with parallel research outcomes and finally in Section IX, the final research conclusion is presented.

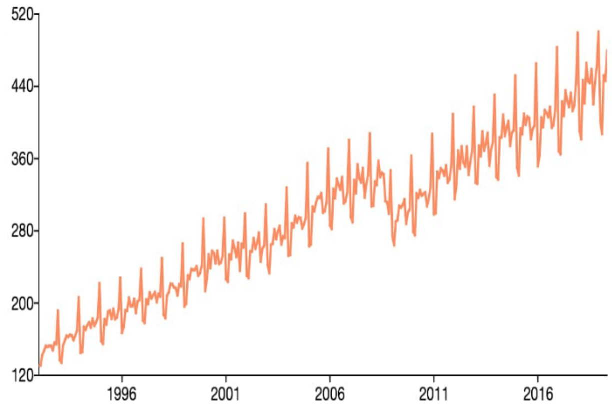

Fig. 1. Financial Data Model – Trend Based Data.

II. Data Pre-processing Fundamentals

After the primary context setting of the research outlines, in this section of the work, the fundamental strategies for data pre-processing are discussed. Due to the nature of the data collections, often the collected data is prune to the impurities which are primarily classified as outliers, missing values or sometimes noises in data analytics terms.

Thus, in this section of the work, the focus is to realize the fundamentals of these above-mentioned data defects in terms of identification and the data imputation or data cleaning.

A. Outlier Detection Fundamentals

Firstly, the outlier detection and removal process are analysed.

Assuming that the total dataset is denoted as D[] and the set of attributes forming the dataset is A[], where each and every attribute can be considered as A_i. Thus, for n number of attributes, the relation can be formulated as,

$$D[] = A[] = \langle A_1, A_2, A_3, ...A_n \rangle \tag{1}$$

Assuming that, each attribute is having the specified domain or the set of values under that attributes, which is denoted as λ. Thus, this relation can be formulated for a total of m number of observations as,

$$A_i = \langle \lambda[1], \lambda[2], ...\lambda[m] \rangle \tag{2}$$

The detection of the outlier is the process, where the values not in the range of valid or acceptable values for any specified attribute shall be identified and further eliminated or replaced with the calculated values. The generic method for identification of the valid value range can be demonstrated in two different ways as.

- Firstly, the calculation of the mean value can be performed for any specified attribute and then each value under the same attribute can be compared with the mean value to identify the deviations. The set of deviations can again be summarized as mean deviation and further be compared with each deviation obtained earlier. Finally, the deviations are above the mean deviation or standard deviation, those connected attributes can be identified as outliers.

Assuming the mean value for the domain λ is M, Thus, this can be formulated as,

$$M = \frac{\sum_{j=1}^{m} \lambda[i]}{m} \tag{3}$$

Further, the deviation set, DS[] can be calculated as,

$$DS[] \leftarrow \bigcup_{j=1}^{m} |\lambda[i] - M| \tag{4}$$

Again, the calculation of the standard deviation, σ, can be formulate as,

$$\sigma = \frac{\sum_{k=1}^{r} DS[k]}{(m)} \tag{5}$$

Here r is the length of the deviation set.

Further, the differences between the deviations from the DS[] set must be calculated and if any deviations are more than the σ, then those connected attribute values shall be identified as outliers, as:

$$Iff \; |DS[i] > \sigma, DS[i] \rightarrow A_X \tag{6}$$

Then, A_X can be identified as outlier for the specified attribute domain.

- Secondly, for every attribute, based on the domain specificity or the nature of the data, a pre-decided valid value range is often assigned to the domain. Any data items violating the range, shall be considered as outliers.

From the Eq. 2, assuming that the limit or the valid value range of the specific attribute is α and β, respectively. This can be formulated as,

$$A_i = \sum_{j=1}^{m} \lambda[j], j_{\min} = \beta, j_{\max} = \alpha \tag{7}$$

Thus, any value beyond these limits must be considered as outliers.

For, either of the cases, the imputation method is fundamentally same. If any of the attributes, $\lambda[]$, are identified as outliers, then the mean deviation must be adjusted to bring to the normal value.

B. Missing Value Detection Fundamentals

Secondly, the missing values are one more type of complications in the datasets for achieving better and accurate results. The values under any specified attribute domain can be seen missing and these missing values can result into errors in the calculations on the same dataset. From Eq. 2, if any of the attribute value is null or empty, denoted as Φ, then this can be presented as,

$$\lambda[j] \to \Phi \tag{8}$$

Thus, $\lambda[j]$ can be identified as missing value and must be imputed in order to pre-process the dataset.

The imputation method for the missing value is fundamentally relies on moving average method for calculating the replacement values. Mathematically, if the $\lambda[j]$, which is j^{th} element in the dataset, then the moving average, Υ, till the $(j-1)^{th}$ element must be calculated as,

$$\Upsilon = \frac{\Upsilon + \sum_{i=1}^{j-1} \lambda[i]}{\langle \lambda[1], \lambda[2], \lambda[3], \ldots, \lambda[i-1] \rangle / i} \tag{9}$$

Once, the moving average is calculated, then the imputation process can be realized as,

$$\lambda[j] \leftarrow \Upsilon \tag{10}$$

C. Noise Detection Fundamentals

Finally, the last type of impurity in the dataset can be identified as noises. It is important to realize that, each data, whether represented in textual format or other formats, must be collected and stored using various devices which are often magnetically operated and during transmission it is possible to have a small amplitude shift in the data signal. Most of the times, the amplitude shift is very minor and can be ignored. However, in case of the financial data, the minor shift in the data signal can result into few decimal points in the data values, which can certainly change the course of the processing and decision-making process.

The fundamental process of detection of the noise in the data is to identify the standard length of the data values and if the data values are identified with added or extra length than the regular or pre-defined, then the extra length of the data must be reduced computationally to remove the noise from the data.

The details of the imputation process are discussed in the further sections of this work.

Henceforth, after the detailed discussion on the data pre-processing fundamentals, which is highly important to identify the gaps in the present research and further helpful in formulating the research problems, in the next section of this work, the secure storage options are identified.

III. Storage Security Fundamentals

The data security for any domain of computing is the integral part of the framework and the need for storage security cannot be ignored. Thus, in this section of the work, the fundamentals of storage security aspects are analyzed mathematically.

The primary concept of the data security at rest or the storage security relies on the concept of encryption and decryption.

From Eq. 2, assuming that any single data item under any specified domain can be considered as $\lambda[x]$. This can be presented as,

$$\lambda[x] \subseteq A[] \subseteq D \tag{11}$$

From the fundamental concepts of the encryption methods, with the two randomly selected prime numbers, as X and Y, and with the random hash e, the encryption key, KP, can be formulated as,

$$KP = \{(X.Y), e\} \tag{12}$$

And the decryption key, KPP, can be formulated as,

$$KPP = e^{-1} \% \left|(X-1).(Y-1)\right| \tag{13}$$

Thus, before storing the data item, $\lambda[x]$, the encryption process is established and the new encrypted data, $\lambda'[x]$ is generated as,

$$\lambda'[x] = \lambda[x]^{e} \%(KP) \tag{14}$$

Further, during the retrieval process, the decryption process must be invoked as,

$$\lambda[x] = \lambda'[x]^{KPP} \% KP \tag{15}$$

Nevertheless, during a financial data processing, the regular encryption and decryption process must be highly time complex and can deteriorate the complete process. Hence, the regular encryption-decryption process is not suitable for financial data storage security. The solution to this problem is formulated in the upcoming sections of this work.

Further, in the next section of the work, the parallel research outcomes on the data pre-processing and security are discussed.

IV. Related Work

After the detailed understanding of the fundamental strategies of the pre-processing techniques and data security at rest, in this section of the work, the parallel research outcomes are analyzed.

The primary method for analyzing the financial data for detection of anomalies or detection of the trends is the method of clustering as discussed in the work by A. Pazienza et al.[4]. However, the generic method of clustering can be sufficient for detection of the groups based on properties, but the detection of outliers or any other anomalies can be highly difficult by the generic clustering methods. Henceforth, this method is criticised by the research community. This method can be further enhanced with the method proposed in the work by S. Squires et al. [5], where the metric ranking system can be deployed to speed-up the process of clustering [12]. Nonetheless, the outcome of such ranking methods will rank the attributes and further, can reduce the number of attributes from the actual datasets. During this process, the attributes with higher number of anomalies can be directed removed by such methods, which leads to information loss [14].

In the other hand, the work formulated by Y. Kawachi et al. [6] demonstrates the use of encoding method, where the actual data items are encoded with differential parameters to identity the anomalies such as missing values or outliers [15]. This existing method is highly effective in terms of identification of anomalies, but due to higher time complexity, the applicability for financial data pre-processing is arguable. Nevertheless, the same approach is widely adopted in managing web application data as showcased by H. Xu et al. [7]. Many of the parallel research attempts have tried to reduce the time complexity of this existing method by introducing the benefits of machine learning driven optimization. One such work is worth the mention is the work by S. Squires et al. [8]. The bottleneck with such solutions is the definitive time complexity and limitations of managing a large search space. Hence, once again this method is also arguable for applicability on financial data [17].

Yet another direction of the research is proposed by A. Prügel-Bennett et al. [9] by combining the features of the encoding method with non-attribute reduction methods. These types of solutions can be applied on the financial datasets conditionally based on the model complexity limits.

Further, in the recent time, a good number of tools can be identified to automate the process of anomaly detection and reduction for the datasets as listed by A. Paszke et al. [10]. Nonetheless, these tools are not specialized for financial data managements.

Henceforth, with the detailed understanding of the parallel research outcomes, in the next section of the work, the identification of the problems and the proposed solutions are furnished.

V. Problem Identifications and Proposed Solutions

After the detailed understanding of the pre-processing fundamentals, storage level security and the outcomes from the parallel researches, in this section of the work, the proposed solutions to the identified problems are discussed.

In the due course of study, this work has identified the following issues in the current parallel research outcomes as,

- The detections of the outliers are primarily focused on the mean deviation, which is a time complex process for higher number of elements in any datasets.
- Secondly, the missing value identification process is also highly vulnerable due to the fact that, any dataset can represent the missing values in any format as #NA or NA or "?" or blank. Thus, the formal process of identification of the missing values must be formulized to detect any of the specified notations. Also, for a large dataset, detection of the missing values after verification of individual elements can be highly time complex. Thus, the time efficient solution must be designed.
- Thirdly, during the analysis of the encryption process for data at rest, the additional time required for encryption and the decryption process is slowing down the process for data analysis, which must be reduced. Thus, a time efficient encryption solution, specified for financial data, must be designed [16].

Further, the proposed solutions are discussed with the mathematical models.

Lemma – I: The time complexity for detection of the outliers can be significantly reduced with the help of proposed deep clustering method.

Proof: The most enhanced method for grouping a set of elements or forming set of groups based on specified (supervised) or un-specified (un-supervised) set of characteristics is clustering. This principle is applied in the proposed method for identification of the outliers.

Firstly, from the Eq. 1 and 2, the total number of attributes are n and each attribute domain have a length of m. Thus, the total number of elements, k, can be formulated as,

$$k \leftarrow n.m \tag{16}$$

Also, from the Eq. 9, it is significant to realize that, for calculating the deviations or difference among m number of elements, a total of (m-1) number of comparisons are needed and for calculating the final standard deviation, one additional step to be performed. Hence, the total time complexity, t_1, to identify the outlier can be formulated as,

$$t_1 = n.(m-1)+1 = O(n^2),\ n \approx m \tag{17}$$

Now, focusing on the proposed method for identification of the outlier, the following formulations can be designed.

Assuming that the complete dataset is denoted as D [] and each attribute in the dataset is assumed to be presented as, A_x for total of n number of attributes. Hence, the following relation can be formed.

$$D[] \rightarrow < A_1, A_2, A_3, ...A_n > \tag{18}$$

Here, each and every attribute is considered to have their own domain with m number of values each and the data elements are denoted as D_i, which can be represented as,

$$A_x[] = \sum_{i=1}^{m} D_i \tag{19}$$

Further, the Euclidian distance between the data points can be considered as the similarity measure and the total distance set is represented as $\lambda[]$, then,

$$\lambda[] = \int_{i=1}^{m-k} \left| D_i - D_{i+1} \right| \tag{20}$$

Further, the Euclidian distance between the elements of $\lambda[]$ are calculated,

$$\overline{\lambda}[] = \int_{i=1}^{m-k-1} \left| \lambda_i - \lambda_{i+1} \right| \tag{21}$$

The new $\overline{\lambda}[]$ set defines the relation between the elements based on their similarities.

Furthermore, the repetitive iteration of the Eq. 20 can measure the similarities with deeper and contextual aspect, which can be represented as,

$$\overline{\lambda}_k[] = \int_{i=1}^{m-k} \left| \overline{\lambda}_i - \overline{\lambda}_{i+1} \right| \tag{22}$$

Thus, based on the similarity measures of Euclidian distance of the elements and the final cluster centroids can be calculated as,

$$C[] = \overline{\overline{\lambda}}_k[] = \frac{\overline{\lambda}_k[]}{\left| \lambda_i - \lambda_{i+1} \right|_{i=0}^{n}} \tag{23}$$

Here, the primary factor to be considered as in every iteration as discussed in the Eq. 20 will continuously reduce the number of data items to be analysed for outlier detections. Hence, the time complexity, t_2, can be formulated as:

$$t_2 = \frac{n.m}{2} + \frac{n.m}{4} + \frac{n.m}{8} + \frac{n.m}{16} = O(\log_2 n.m) \tag{24}$$

Naturally, the proposed method showcases a much lower time complexity, than the regular method and $t_2 << t_1$.

Further, the missing value detection problem is analyzed here.

Lemma 2: The detection of the missing values, using the proposed domain count iterative method, reduces the time complexity.

Proof: The domain count of any dataset shall be realized as the maximum number of elements without the missing or null values. Hence, the maximum count will ensure that the maximum number of elements are considered without the missing values and in case of all missing values, the complete tuple is ignored.

Assuming that, the total dataset, DS[], is a collection of multiple domains, D[], and each domain is again collection of multiple data points, D_i. Thus, for a n number of domains or attributes, the initial relation can be formulated as,

$$DS[] = \langle D[](1), D[](2), D[](3)....D[](n) \rangle \tag{25}$$

Also, assuming that each domain is consisting of m number of data points, thus, this relation can be formulated as,

$$D[](i) = \langle D_1, D_2, D_3, ..., D_m \rangle \tag{26}$$

Further, assuming that, the method Φ, is responsible for identification of the number of data points without the missing or null values. Then, ƛ being the count of data points, this proposed function can be formulated as,

$$\text{ƛ} = \Phi(D[](i)) \tag{27}$$

Subsequently, the count of data points from each domain can be presented as ƛ[] and can be formulated as,

$$\text{ƛ}[] = \forall\left(D[](X)\right) \tag{28}$$

Further, assuming the maximum value from the ƛ[] collection is δ, and then this can be formulated as,

$$\delta =_{MAX} \left(\text{ƛ}[]\right) \tag{29}$$

Further for domain the count of the number of data points, Y, must be compared with the maximum data point count, X, using the divide and conquer method as following:

$$\begin{array}{|l} Iff\ \delta > \text{ƛ}[i], \\ Then, Compare\ \delta/2 > \prod_{j=1}^{i/2}(\text{ƛ}[j]) \end{array}$$
$$Else, Compare\ \delta/2 > \prod_{j=i/2+1}^{i}(\text{ƛ}[j]) \tag{30}$$

Henceforth, if the count of data points is less than the expected count of the data points in first or second half of the domain, then the process must be repeated to identify the missing values only in that half of the domain and the process shall be repeated iteratively to identify all missing values.

Further, the time complexity of this proposed method is analysed against the generic method.

Assuming that, a total of k number of iterations has to be performed for n number of domains, thus the time complexity, T_1, can be formulated as,

$$T_1 = 1 + n/2 + n/4 + ... n/k \tag{31}$$

This can be re-written as,

$$T_1 = O(k \log_2 n) \tag{32}$$

In the other hand, for the similar identification, using the generic methods, thus the time complexity, T_2, can be formulated as,

$$T_2 = k * n \tag{33}$$

It is natural to realize that

$$T_1 << T_2 \tag{34}$$

Hence, the proposed method for outlier detection significantly reduces the time complexity with higher accuracy.

Finally, the solution for the encryption problem is furnished here.

Lemma 3: Generation of the security keys using regression method can be highly time efficient.

Proof: The regression method is primarily used for predictive analysis. Nevertheless, the highly time efficient characteristics of regression method can be utilized to produce random numbers. This solution focuses on the same aspect.

From Eq. 11, the data items to be encrypted are $\lambda[x]$ with the encryption key. The components of the encryption keys can be generated using the regression methods.

The proposed method starts with the selection of the random value, p(t) and the second component q(t) can be generated using the regression method as following with the regression coefficient $\beta_{pq}(t)$,

$$q(t) = \beta_{pq}(t-1).p(t) \tag{35}$$

Here, the regression coefficient can be formulated as,

$$\beta_{pq}(t-1) = \frac{q(t-2)}{p(t-2)} \tag{36}$$

Further, the hash, e, the following formulation can be utilized,

$$e(t) = \beta_{pe}(t).p(t) + \beta_{qe}(t).q(t) \tag{37}$$

And, the regression coefficients can be formulated as,

$$\beta_{pe}(t) = \frac{e(t-1)}{p(t-1)} \tag{38}$$

And,

$$\beta_{qe}(t) = \frac{e(t-1)}{q(t-1)} \tag{39}$$

Further, from the Eq. 12 to Eq. 15 can be replicated with the newly generated components for encryption and decryption.

It is natural to realize that, the time for selection of random numbers as components of the encryption methods, is highly reduced as in the proposed method only one random number must be selected and for only one number the randomness shall be verified. Thus, the overall time complexity reduced to a greater extend.

Further, in the next section of this work, based on the proposed mathematical models, algorithms are designed with the proposed framework.

VI. Proposed Algorithm and Framework

After the detailed discussion on the fundamental processes for pre-processing, storage security, problem identification and proposed mathematical solutions, in this section of the work, the proposed algorithms and the proposed framework is furnished.

Firstly, the outlier removal algorithm is furnished.

Algorithm - I: Iterative Clustering for Outlier Detection & Imputation (**ICOD-DI**) Algorithm

Input:

The initial dataset as DS[]

Output:

The outlier reduced dataset as DS1[]

Process:

Step - 1. Load the initial dataset as DS[]

Step - 2. For each element in the DS[] as DS[i]

- a. List the number of attributes as A[]
- b. For each attribute as A[j]
    - i. List the data items as I[] and for each data item I[k]
        1. Cluster the I[] using K-Means Method and store in cluster set C[]
        2. Calculate the cluster centroids as C1[] and further cluster the centroids and store in cluster set C2[]
        3. Identify the outliers from the second cluster set C2[] as O[]
        4. If O[n] is outlier,
        5. Then,
        6. Check for C1[k] as outlier
            - a. If C1[k] is outlier,
            - b. Then,
            - c. Mark I[k] as outlier
    - ii. Calculate the moving average till I[k] as AVG[k] for O[n]
    - iii. Update the values O[n] = AVG[k]
- c. Else,
- d. DS1[i] = DS[i]

Step - 3. Return the outlier reduced dataset as DS1[]

Oddities, or exceptions, can be a difficult issue when preparing AI calculations or applying measurable strategies. They are regularly the aftereffect of mistakes in estimations or remarkable framework conditions and in this manner don't portray the normal working of the basic framework. In reality, the best practice is to carry out an exception evacuation stage prior to continuing with additional examination.

Sometimes, exceptions can give us data about confined inconsistencies in the entire framework; so, the identification of anomalies is an important interaction on account of the extra data they can give about your dataset.

Secondly, the algorithm for missing value detection is furnished here.

Algorithm - II: Differential Count Based Missing Value Detection & Imputation (**DCB-MVDI**) Algorithm

Input:

Outlier Removed Dataset, DS1[]

Output:

Missing Value reduced dataset, DS2[]

Process:

Step - 1. Load the dataset DS1[]

Step - 2. For each element in DS1[] as DS1[i]

a. List the number of attributes as A[]

b. For each element in A[] as A[i]

   i. Calculate the number of elements as Count(A[i]) => C[j]

c. If C[j] > C[j+1],

d. Then,

   i. Divide A[i+1] as A1[] and A2[]

   ii. Calculate the number of elements as Count(A1[]) = C1 and Count(A2[]) = C2

   iii. If C1 > C2,

   iv. Then,

   v. Divide A2[] as A11[] and A12[] and repeat the process until C1 = C2.

   vi. Mark the missing values as M[] //Using Eq. 6

   vii. Calculate the moving average till A[i] as AVG[k] for M[k]

   viii. Update the values M[k] = AVG[k]

e. Else,

f. DS2[i] = DS1[i]

Step - 3. Return the missing value reduced dataset as DS2[]

Missing information can happen due to nonresponse: no data is accommodated at least one thing or for an entire unit ("subject"). A few things are bound to produce a nonresponse than others: for instance, things about private subjects like pay. Weakening is a sort of missingness that can happen in longitudinal investigations—for example considering advancement where an estimation is rehashed after a specific timeframe. Missingness happens when members drop out before the test closures and at least one estimation are absent.

Thirdly, the algorithm for the data storage security is discussed here.

Algorithm - III: Polynomial Regression-based Encryption and Decryption (**PRR-ED**) Algorithm.

Input:

Missing value reduced dataset DS2[]

Output:

Encrypted dataset as DS3[]

Process:

Step - 1. Load the dataset DS2[]

Step - 2. For each element in DS2[] as DS2[i]

a. List the number of attributes as A[]

b. Select the random number p(t) and calculate q(t) & e(t) //Using Eq. 35 to 39

c. Calculate the Public and Private key //Using Eq. 12 to 15

d. For each element in A[] as A[i]

   i. List the data items as I[] and for each data item I[k]

   ii. Encryption:

      1. II[k] = I[k]%PublicKey

      2. DS3[j] = II[k]

   iii. Decryption:

      1. DS2[j] = POW(DS3[j],PublicKey)%PrivateKey

   iv. Regression:

      1. p(t+1) = p(t)

      2. q(t+1) = {q(t-1)/p(t-1)}.p(t)

      3. e(t+1) = {e(t-1)/p(t-1)}.p(t) + {e(t-1)/q(t-1)}.q(t)

   v. Repeat the process till m = length of A[i]

Relapse investigation is principally utilized for two theoretically particular purposes. In the first place, relapse examination is generally utilized for expectation and anticipating, where its utilization has significant cover with the field of AI. Second, in certain circumstances relapse investigation can be utilized to construe causal connections between the autonomous and ward factors. Critically, relapses without anyone else just uncover connections between a reliant variable and an assortment of autonomous factors in a fixed dataset. To utilize relapses for forecast or to deduce causal connections, separately, an analyst should cautiously legitimize why existing connections have prescient force for another specific situation or why a connection between two factors has a causal understanding. The last is particularly significant when specialists desire to appraise causal connections utilizing observational information [18].

Finally, the proposed framework is furnished here [Fig. 2].

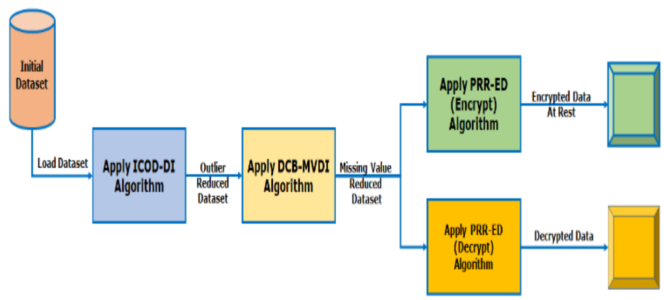

Fig. 2. Proposed Data Pre-Processing and Security Framework.

Further, in the next section of this work, the obtained results from the proposed framework is elaborated and discussed.

VII. Results and Discussions

After the detailed discussions on the problem formulation and solutions with the proposed algorithms and framework, in this section of the work, the obtained results are furnished and discussed.

The results are highly satisfactory and furnished in four phases for detailed understanding.

A. Dataset Information

Firstly, the description about the dataset [11] is furnished here [Table I].

The initial dataset conditions are also visually identified here [Fig. 3].

Here the dataset initially showcases a lot of anomalies in the form of outliers and missing values. In the next part of the results, the outlier treatment outcomes are listed.

TABLE I. Dataset Details

Table Head	Table Column Head
Number of Attributes	8
Number of Instances	2545
Number of Missing Values	2360
Number of Outliers	728

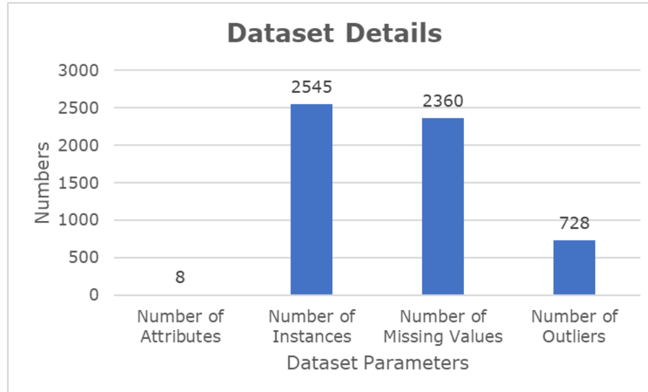

Fig. 3. Initial Dataset.

B. Outlier Treatment Outcomes

Secondly, the outlier detection results are analyzed here [Table II].

TABLE II. Outlier Treatment – Pre-Condition

Parameter Name	Type	Number of Outliers
LTV	Numeric	0
Recovery_rate	Numeric	0
lgd_time	Numeric	0
y_logistic	Numeric	0
lnrr	Numeric	728
Y_probit	Numeric	0
type	Numeric	0
class	Nominal	0

Here is it natural to realize that, the outliers are observed for only one parameter and after applying the proposed algorithm, the following outcomes are received [Table III].

TABLE III. Outlier Treatment – Post-Condition

Parameter Name	Parameter Values
Number of Outliers Present	728
Number of Outliers Detected	728
Number of Outliers Imputed	728
Accuracy (%)	100%
Time to Detect (ms)	11.02

The results are visualized graphically here [Fig. 4].

It is natural to observe that, due to the higher effectiveness of the proposed algorithm, which is proven using the mathematical model, 100% accuracy is obtained.

After the successful removal of the outliers, in order to make the data anomaly fee, in the next part of the results, the missing value treatment outcomes are discussed.

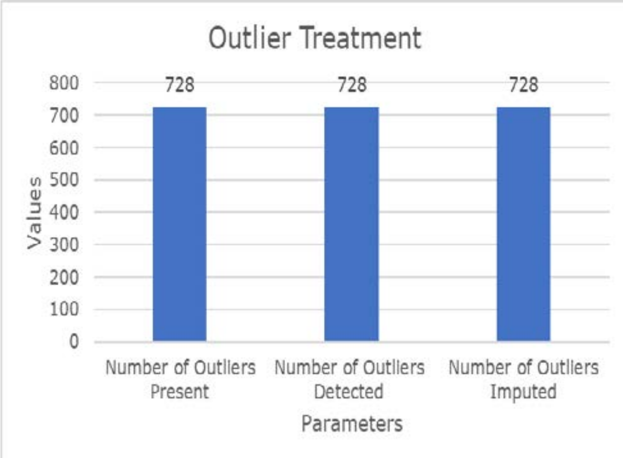

Fig. 4. Outlier Treatment.

C. Missing Value Treatment Outcomes

Thirdly, the missing values detection results are analyzed here [Table IV].

TABLE IV. MISSING VALUE TREATMENT – PRE-CONDITION

Parameter Name	Type	Number of Outliers
LTV	Numeric	0
Recovery_rate	Numeric	0
lgd_time	Numeric	0
y_logistic	Numeric	0
lnrr	Numeric	0
Y_probit	Numeric	0
type	Numeric	2360
class	Nominal	0

Here is it natural to realize that, the missing values are observed for only one parameter and after applying the proposed algorithm, the following outcomes are received [Table V].

The results are visualized graphically here [Fig. 5].

It is natural to observe that, due to the higher effectiveness of the proposed algorithm, which is proven using the mathematical model, 100% accuracy is obtained.

After the successful removal of the missing values from the dataset, in the next part of the results, the encryption and decryption at rests are discussed.

TABLE V. MISSING VALUE TREATMENT – POST-CONDITION

Parameter Name	Parameter Values
Number of Missing Values Present	2360
Number of Missing Values Detected	2360
Number of Missing Values Imputed	2360
Accuracy (%)	100%
Time to Detect (ms)	9.18

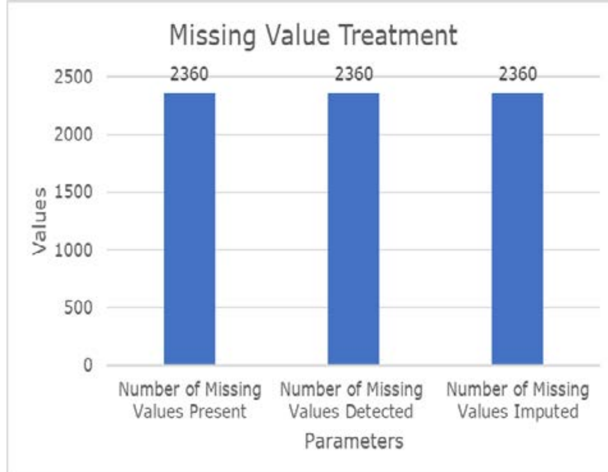

Fig. 5. Missing Value Treatment.

D. Encryption – Decryption at Rest Outcome

Finally, the encryption and decryption time complexity analysis are furnished here [Table VI]. The time complexity is tested for a total of 10 iterations here.

TABLE VI. DATA AT REST ENCRYPTION – DECRYPTION ANALYSIS

Iteration #	Key Generation Time (ms)	Encryption Time (ms)	Decryption Time (ms)
1	9	27.351	36.853
2	2	15.482	25.248
3	1	5.58	13.804
4	2	12.446	18.829
5	6	59.61	67.886
6	3	13.35	22.657
7	3	3.351	9.067
8	3	20.145	28.562
9	8	54.088	59.27
10	8	72.72	77.578

The results are visualized graphically here [Fig. 6].

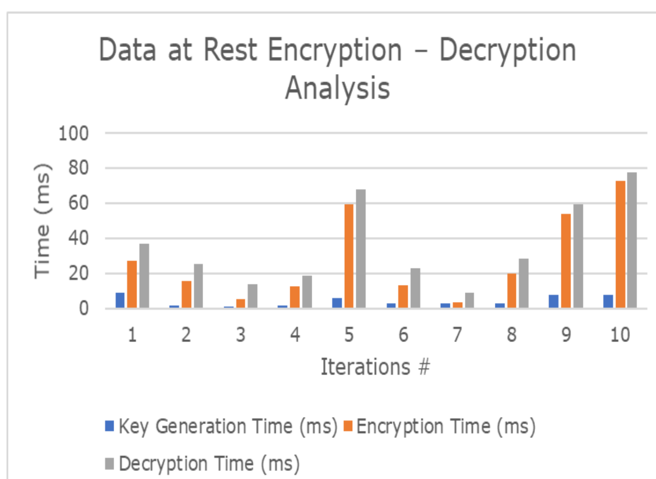

Fig. 6. Data at Rest Encryption – Decryption Analysis.

It is natural to realize that, out of 10 iterations, in 7 iterations the time complexity is reduced to a greater extend.

Further, after the detailed analysis on the obtained results, in the next section of this work, the proposed framework is compared with the parallel research outcomes.

VIII. Comparative Analysis

After the detailed analysis of the obtained results, in this section of the work, the proposed framework is compared with notable significant other parallel research outcomes [Table VII].

TABLE VII. Comparative Analysis

Author, Year	Proposed Method	Pre-Process-ing	Storage Security	Framework Complexity
A. Pazienza et al. [4], 2016	Clustering	No	No	$O(n^n)$
Y. Kawachi et al. [6], 2018	Auto Encoding	Yes	No	$O(n^3)$
S. Squires et al. [8], 2019	Variational Auto Encoder	Yes	No	$O(n^2)$
Proposed Framework, 2021	Iterative Clustering, Differential Algorithms and Regression	Yes	Yes	$O(n^2)$

Henceforth, it is natural to realize that, the proposed framework has outperformed the parallel research outcomes.

Further, in the next section of this work, the final research conclusion is presented.

IX. Conclusion

The financial data analysis is the recent trend in research and many parallel research outcomes are focusing primarily on the aspect of cleaning the data for making the dataset completely anomaly free. In the due course of study, this work identified that, firstly, the detections of the outliers are primarily focused on the mean deviation, which is a time complex process, thus needs to be optimized. Secondly, the missing value identification process is also highly vulnerable due to the fact that, any dataset can represent the missing values in any format, thus, the time efficient solution must be designed. Thirdly, during the analysis of the encryption process for data at rest, the additional time required for encryption and the decryption process is slowing down the process for data analysis, which must be reduced, thus, a time efficient encryption solution, specified for financial data, must be designed. Henceforth, this work proposes an automated framework for identification and imputation of the outliers using the iterative clustering method, identification and imputation of the missing values using Differential count based binary iterations method and finally the secure data storage using regression based key generation. The proposed framework has showcased nearly 100% accuracy in detection of outliers and missing values with highly improved time complexity for making the world of financial data analysis a better place. In future, further step can be taken to make data affinity and labelling structures more consistent by combining similarity matrices from the feature space and label space in an adaptive manner, which may be done using the label diffusion framework. It helps to make the structures of data affinity and labelling more consistent. An iterative optimization technique may be used to solve the energy function in a practical manner. Experimental findings on publicly available datasets show that the suggested approach outperforms the comparable methods in terms of overall performance.

References

[1] C. Chatfield, The analysis of time series: An introduction, Chapman and Hall/CRC, 2016.

[2] L. Montesdeoca, M. Niranjan, "Extending the feature set of a data-driven artificial neural network model of pricing financial options", 2016 IEEE Symposium Series on Computational Intelligence (SSCI), pp. 1-6, Dec 2016.

[3] T. Cook, A. S. Hall, "Macroeconomic indicator forecasting with deep neural networks", Federal Reserve Bank of Kansas City, no. 17-11, 2017.

[4] A. Pazienza, S. F. Pellegrino, S. Ferilli, F. Esposito, "Clustering underlying stock trends via non-negative matrix factorization", Proceedings of the First Workshop on Mining Data for Financial Applications, pp. 5-16, 2016.

[5] S. Squires, L. Montesdeoca, A. Pnigel-Bennett, M. Niranjan, "Non-negative matrix factorization with exogenous inputs for modelling financial data", International Conference on Neural Information Processing, pp. 873-881, 2017.

[6] Y. Kawachi, Y. Koizumi, N. Harada, "Complementary set Variational Autoencoder for supervised anomaly detection", International Conference on Acoustics Speech and Signal Processing (ICASSP). IEEE, pp. 2366-2370, 2018.

[7] H. Xu, W. Chen, N. Zhao, Z. Li, J. Bu, Z. Li, Y. Liu, Y. Zhao, D. Pei, Y. Feng et al., "Unsupervised anomaly detection via Variational Autoencoder for seasonal KPIs in web applications", Proceedings of the 2018 World Wide Web Conference, pp. 187-196, 2018.

[8] S. Squires, A. P. Bennett, M. Niranjan, A Variational Autoen-coder for probabilistic non-negative matrix factorisation, 2019.

[9] S. Squires, A. Prügel-Bennett, M. Niranjan, "Rank selection in nonnegative matrix factorization using minimum description length", Neural computation, vol. 29, no. 8, pp. 2164-2176, 2017.

[10] A. Paszke, S. Gross, S. Chintala, G. Chanan, E. Yang, Z. DeVito, Z. Lin, A. Desmaison, L. Antiga, A. Lerer, "Automatic differentiation in PyTorch", NIPS Autodijf Workshop, 2017.

[11] X. Zhou, Z. Pan, G. Hu, S. Tang, C. Zhao, "Stock market prediction on high-frequency data using generative adversarial nets", Mathematical Problems in Engineering, vol. 11, 2018.

[12] Yeo AC, Smith KA, Willis RJ, Brooks M (2001) Clustering technique for risk classification and prediction of claim costs in the automobile insurance industry. Intell Syst Acc Finance Manage 10(1):39–50.

[13] Kou G, Peng Y, Wang G (2014) Evaluation of clustering algorithms for financial risk analysis using MCDM methods. Inf Sci 275:1–12.

[14] Wang Y, Meng Y, Fu Z et al (2017) Towards safe semi-supervised classification: adjusted cluster assumption via clustering. Neural Process Lett 46(3):1031–1042.

[15] Ma X, Gao L, Yong X, Lidong Fu (2010) Semi-supervised clustering algorithm for community structure detection in complex networks. Physica A 389:187–197.

[16] Zhao Y, Karypis G (2001) Criterion functions for document clustering: experiments and analysis, Technical Report TR 01-40, Department of Computer Science, University of Minnesota.

[17] Tay FEH, Cao LJ (2002) ε-Descending support vector machines for fnancial time series forecasting. Neural Process Lett 15(2):179–195.

[18] Arratia A, Belanche LA, Fábregues L (2019) An evaluation of equity premium prediction using multiple kernel learning with fnancial features. Neural Process Lett 52:117–134.

[19] Ngoc MT, Park DC (2018) Centroid neural network with pairwise constraints for semi-supervised learning. Neural Process Lett 48(3):1721–1747.

System Design and Case Study Reporting on AQASYS: A Web-based Academic Quality Assurance System

Adel Alfozan[1], Mohammad Ali Kadampur[2]
Dean College of Engineering, Imam Mohammad Ibn Saud Islamic University, P.O.Box:5701 Riyadh 11432 KSA[1]
Assistant Professor Department of Electrical Engineering, Imam Mohammad Ibn Saud Islamic University, Riyadh 11432 KSA[2]

***Abstract*—The demands of modern education have evolved from a teacher-centric requirement to a learner-centric requirement. Knowledge, skill, and competence are the most sought-after attributes of a graduate. Features such as the objective focus of learning, curriculum planning, a set of high expectations, and extended opportunities to the learner after completion of education are at the center of all the planning. It is all about skill-oriented, outcome-based standardization that has been infused by the societal stakeholders into the modern global education system to create a work-ready human capital. In this paper, a software product for academic quality assurance is presented. The software provides a generic framework to any educational institution that operates to implement known international standards of education. The software accepts the data and computes the quality parameters as per the selected standards. It has an analytical module that provides summary analytics and generates the course reports in the given format automatically. The software is tested with a case study and results are presented. The paper also presents the system design approach with discussion on the technologies selected for the development.**

Keywords—Outcome-based education; quality standards; automated software; system design; education technology; accreditation

I. Introduction

In the last decade or two, the requirements of higher education particularly in professional education have shifted from a "teacher-centric" approach to a "learner-centric approach" [5]. In the traditional approach whatever teacher knew was used as the content or curriculum of the teaching. However, in the changing societal needs and driving forces of the job market, industry, and global changes, the learner needs to have knowledge, skill, and competence in the chosen areas of learning. The learner selects the domain of learning and sets objectives to achieve them at the end of the learning. This kind of pole shift and paradigm shift in teaching-&-learning has brought the educational institutes to frame new curricula, with defined objectives and clearly stated goals as" what the learner will be able to do" at the end of the learning? The standard educational institutes continuously loop around these parameters and assess the level of achievement through their operational practices. This activity is given the word "Quality" [1][2] in most of the educational institutes that are signatories to the internationally recognized standards organizations [5].

In this work, a web-based academic quality management system is implemented. The paper describes the system design process and reports on the results after specific case study data is input to the system. The system is called AQASYS, an Academic Quality Assurance System.

The research questions on methods of quantifying Course Learning Outcomes (CLO's), Program Learning Outcomes, the Difficulty level of the course, automated feedback assessments, CLO, PLO attainments are addressed. An automated CLO mapping module, design of a text-mining based Bloom's level recommender module are built and integrated into the system. The system generates course-specific and program-specific results providing several summary analytic outputs of business value. The system addresses the issue of "closing the loop" to assess the committed objectives.

The system facilitates the academic quality assessment process with web-interface for the users and a reliable database at the backend. It is a secured, reliable, and all-time available resource for its users. The system provides all inherent advantages of web-based applications.

II. Motivation

Most of the institutes that were visited and the faculty that were consulted, shared their experience of handling "academic quality" matters in their respective institutes and departments. Based on this the following major observations were made:

1) Each faculty was using some kind of excel sheet and running around for the templates and methods of calculations on assessments. There was absolute last-minute chaos, confusion, and lethargy in what they were doing.

2) There was no archive of centralized data repository to click and see the analytics of the past and explore it for future strategies.

3) Lack of sound research-driven statistical and mathematical foundations uniformly applied across the departments for assessment and achievements.

4) Plenty of “number in number out” kind of manipulated data to skew the academic quality for the personal advantage of the faculty or to the advantage of the department. The piety of the information was affected.

5) Irrational ways of mapping CLOs with the question paper text, resulting in the illusion of whole quality exercise. And finally,

6) Very poor regularity and ease of academic data management.

In light of these observations, the paper is presenting a web-based academic quality assurance system that has a centralized repository of academic data, research-driven academic foundation for all quality parameters, and above all ease of access with availability, confidentiality, and integrity.

The paper is organized in the following way: Section III presents a literature review and related work. Section IV lists the contributions of the paper. Section V presents in detail the software architecture used. Section VI addresses system design features. Section VII briefs about the development platform and the associated technologies used in the product development. Section VIII discusses the operational parameters and their formulae of computation. Section IX presents results and selected screenshots. The final section, Section X is the concluding section.

III. Related Work

In the past two decades, there have been several research papers and software products attempting to illustrate and automate the process of academic accreditation [10] in higher education. This section reviews and compares systems like the one presented in this paper.

ABET Course Assessment Tool (ACAT) [4] is one of the earliest (2010) and decent attempts found to be made to automate the accreditation process. It is a web-based application designed to assist in the collecting of data and the generation of standardized reports.

Course and Student Management System (CSMS) [9] is a Web-based system based on the concept of an articulation matrix that maps various course outcomes to ABET program outcomes[6]. The articulation matrix is nothing but the course assessment matrix. It is a 2D table, in which rows represent learning objectives, and columns represent class activities conducted to meet those learning objectives. The articulation matrix is filled when the course learning objectives are achieved.

Program and Courses Outcomes System (PACOS) [13] is an initiation from Hong Kong University [12]. It is an open-source web-application. PACOS has various power levels of access with different user privileges. A user can perform CRUD (Create, Read, Update, Delete) operations on courses, course information, and program outcomes. PACOS manages data with excel files as inputs and displays result in the form of histogram and reports.

Program Outcome Assessment (POA) [3][11] is a web-based program developed using ASP.Net technologies to automate the program assessment. It supports a complete flow from defining the program outcomes [6] to entering all course information in real-time. The program computes on-the-fly performs all the evaluations and presents the output in the form of graphs, color-coded tables, and a year, year to year comparison of various program outcomes for a span of five years.

Apart from the above work in which mainly academicians have demonstrated automated software programs for program assessment and accreditation, there are many software companies offering these services through their proprietary software products.

1) CLOSO: CLOSO [17] is an excellent, sustainable & affordable tool for monitoring the educational process and performance. It is a product from smart-accredit.com. It allows to plan and design assessments, generate course folders, collect and analyze feedbacks, display outcome attainments. It offers a free trial version for individuals for a limited period of testing the product.

2) Contineo: 'Contineo' [18] is a pioneering software platform for the implementation and administration of academic autonomy with the guided philosophy of the Outcome-Based Education System. It mainly focuses on the accreditation standards such as the National Board of Accreditation (NBA) followed in India and the subcontinent. Service is available through contineo.in for personalized customization in the product.

3) Watermark: [19] It is a Cloud-based software that helps higher education institutions manage assessment, accreditation, curriculum, course evaluation, & faculty activity. It is available at (https://www.watermarkinsights.com/)

4) WEAVE: [19] Weave is a cloud-based accreditation and assessment solution designed to help higher education institutions with program review, course planning, and more. The programmatic assessment functionality lets organizations analyze assessments and provide insight into student performance. It is available at (https://weaveeducation.com/).

There is another plethora of companies offering accreditation services spanning industry and academia. To list a few here [19] ARMATURE, Jetpack, Jura, SPOL, powerDMS, qualtrax, compWalk, DocTract, Submittable, WizeHive, and the list grows. It is to be noted that the companies listed in this paragraph however are not focusing on academic accreditation in particular but targeted for commercial business enterprises in general.

IV. Ccontributions of the Paper

Academic quality Assurance System (AQASYS) presented in this paper is different from most of the above products in the following major ways:

1) It has an intelligent box (iBOX) feature which automatically classifies assessment questions and assigns proper CLOs as per Bloom’s taxonomy.

2) It maps back the assessment questions to Program Learning outcomes via the Course Learning Outcomes (CLO).

3) It produces the Course report automatically in each course by collecting relevant grade-book information, student feedback analysis, CLO achievement statistics and intelligent recommendations for course improvement wherever necessary.

4) It produces the summary analytics of the program for all courses of the program in a single view so that executives of the program can easily comprehend the course statistics.

5) It has in-built triggers to remind and notify the user about data entry delays so that the system can track the punctuality of the faculty in pursuing the quality matter in their academic functioning.

6) It has data archiving and data freezing facilities so that the data cannot be modified even by the data owner (faculty) after a specified due date. This helps to keep the sanctity of data and draw a line for "end of a cycle".

7) It is generic in accepting program-dependent PLOs, CLOs, any number of students, any type of assessment, with time stamps and user foot-prints being recorded in the background.

8) It has a file upload facility to store quality files and course portfolios.

9) It provides data-isolation, user authentication, and ease of usage. The user need not bother about the computational details of quality standards.

*10)*Of course it is a web-based product with MVC architecture and accessible on desktop, tablet, and mobile as the design is made self-responsive.

V. The Software Architecture

Considering the existing IT environment, user dynamics, software quality attributes that are required, design structure and business strategy employed in most of the higher education institutes a Model View Controller (MVC) framework was used in a client-server architecture, refer Fig. 1. The open source framework called *Codeigniter* [14] was selected for this purpose. It supports MVC development with PHP [7].

- Model: The Model contains only the pure application data, Model works as back-end. It deals with back-end operations and fetches data from the database and send it to the controller.
- View: A view is simply a web page, or a page fragment, like a header, footer, sidebar, etc The View presents the model's data to the user. It works as front-end. It displays data and captures user actions, sends user actions to the controller.
- Controller: The controller works as an intermediator between model and view and controls the actions between them. It listens to events triggered by the view (or another external source) and executes the appropriate reaction to these events. Controllers decide how the HTTP requests are to be handled.

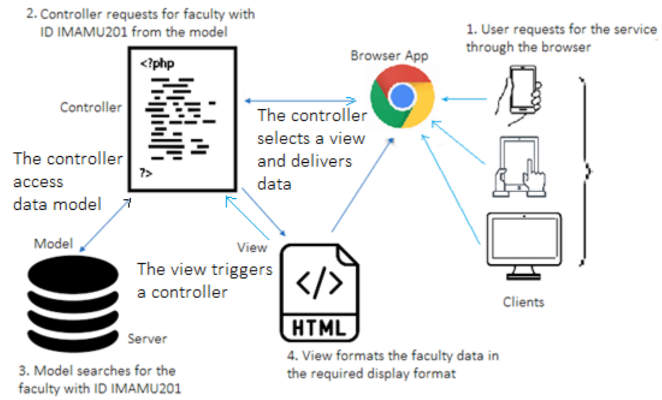

Fig. 1. MVC Client Server Architecture of AQASYS.

A. *The AQASYS Interface*

The AQASYS has five main modules with sub-modules as listed below:

1) Data entry module
   a) Uploading from excel sheets
   b) Enter by using GUI forms
   c) Upload from URLs
2) Assessment Module
   a) CLO Assessment
   b) PLO Assessment
   c) KPI Assessment
   d) SO Assessment
3) Analytics Module
   a) CLO achievement analysis
   b) PLO achievement analysis
   c) Filtered PLO attainment analysis
   d) Feedback Analysis
4) Reporting module
   a) Automatic course report generation
   b) View charts
5) The AI ML module (iBOX)
   a) Bloom's taxonomy tool

Fig. 2 below shows the AQASYS block diagram.

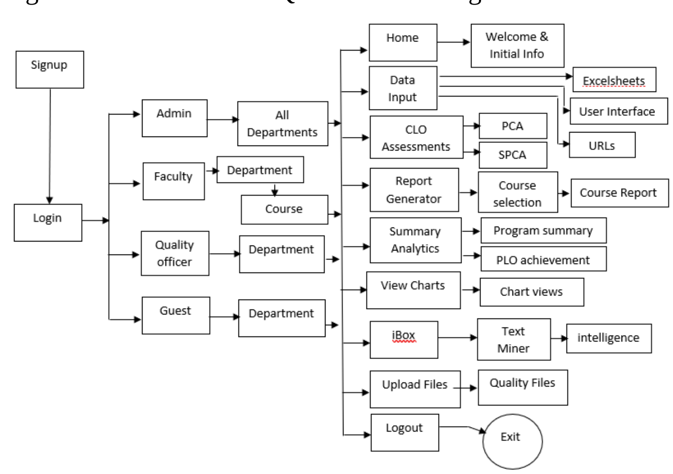

Fig. 2. Block Diagram of AQASYS.

VI. The System Design

This section presents selected system design features of AQASYS.

A. The Use Cases

The use case diagram Fig. 3, describes how the different users interact in the AQASYS. Admin, Faculty, Student are all a type of users with different access privileges. New user is also a type of user who requires signup before getting access to AQASYS services. Each user can avail different services as indicated in the use case boundary.

B. The Class Diagram

The class diagram Fig. 4, describes the structure of AQASYS. The user class is the parent class for many user types such as student, faculty, admin, guest and the NewUser. Every user is associated with a department. A department has PLOs and courses. Each course has CLOs, KPIs and course assessments. CLOs contribute to PLOs of the department and they are associated with PLOs. The CLOs, KPIs and the assessments are mapped while producing the Table of Specifications (ToS) on the course, example refer Table I. In order to perform mapping, AQASYS provides an intelligent auto-mapper class called iBOX. The iBOX is based on the Bloom's taxonomy. The iBOX class is associated with MappingTable class. Most of the operational methods are grouped in AqasysOp class.

C. The Data Model

This section describes the selected listing of databases and the table structures within each database. A sample of the model is shown in Fig. 5. The model has databases for each department and inside each department there are tables such as studentlist, facultylist, courses, courseallotment, plodefintions, clodefintions, kpidefinitions, tostable, etc. refer Fig. 6. There is a separate database for users of AQASYS. The application_users database has tables such as users, userlogs, departments, contactform. The database on Bloom data stores an incrementally growing data as a result of text processing in the AQASYS application. The Bloom data and associated alogorithms add intelligence to the system through iBOX tab.

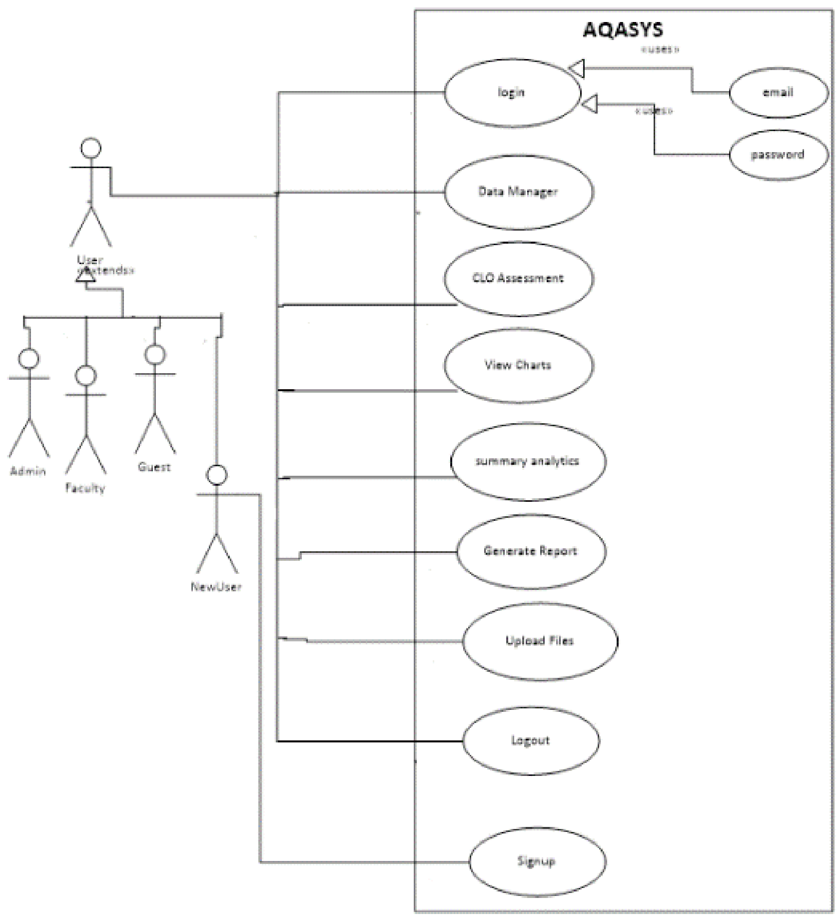

Fig. 3. Use Case Diagram of AQASYS.

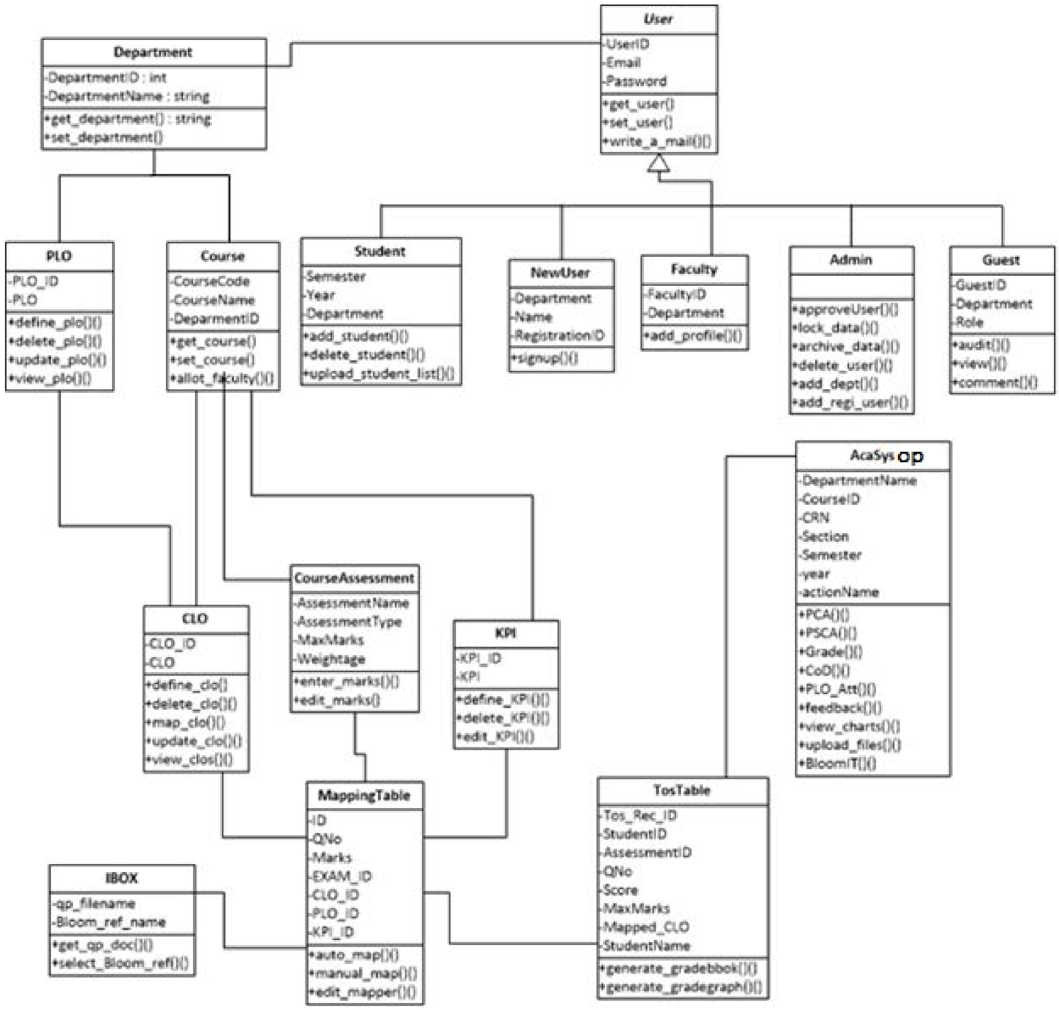

Fig. 4. The Class Diagram.

TABLE I. SELECTED LIST OF MVC METHODS

Table Column Head		
Model	***View***	***Controller***
generate_assessments.php generate_charts.php generate_cr.php get_clo.php get_clomselections.php get_clomselections_student.php get_coursecode.php get_exam.php get_feedbackgraph.php get_gradebookdata.php get_gradegraph.php get_kpi.php get_maxmarks.php get_plo.php get_plo_analytics.php.jsx get_so.php get_so_kpi_data_table.php get_summary_analytics.php get_summary_plo.php get_tostableyear.php get_userinfo.php import_coursedata.php	view_assessments.php view_charts.php form_cl_clo.php form_clo_definitions.php form_clodata.php form_clomdata.php form_clomtable.php form_evaluationschema.php form_exam_table.php form_gradebook.php form_kpi_definitions.php form_plo_definitions.php form_registered_students.php form_so_definitions.php form_so_kpi_data_table.php form_so_kpi_relationship.php	Login_controller.php Access_controller.php Delete_controller.php Update_controller.php Create_controller.php Display_controller.php Print_controller.php Logout_controller.php Signup_controller.php Validation_controller.php Bloom_controller.php Session_controller.php

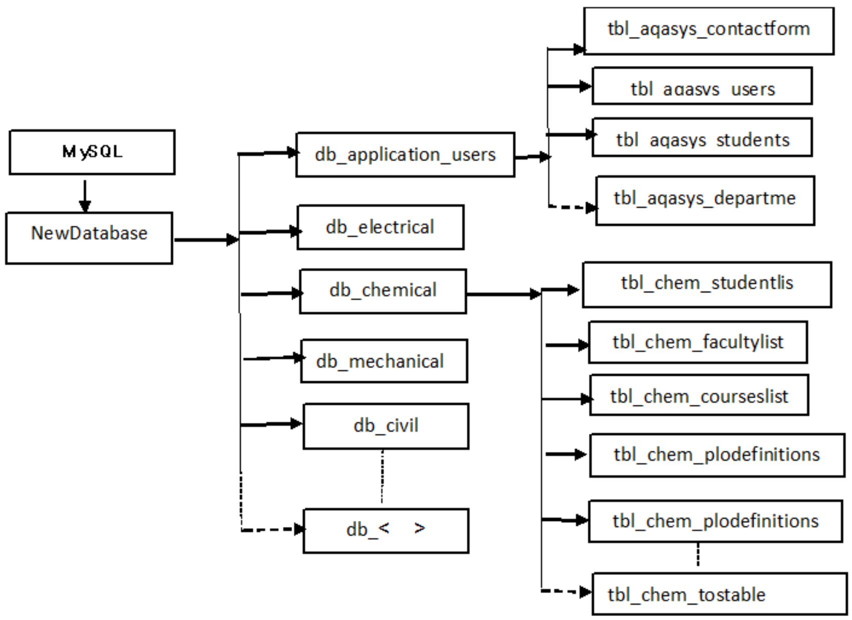

Fig. 5. The Block Diagram of the Data Model.

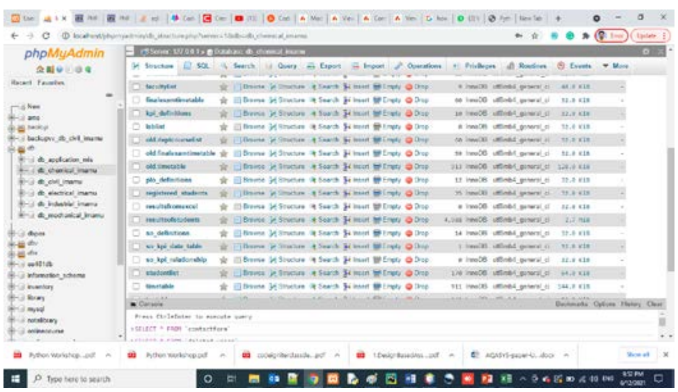

Fig. 6. The MYSQL View of the Data Model, a Sample Table Structure.

VII. The Development Platform

Choosing a development platform and technology is always an intriguing question for the developer. After conducting good research, in this application, Codeigniter MVC framework [14] with PHP was chosen for the reason that the Codeigniter has a light footprint, flexible with MVC and non-MVC applications, supports MYSQL database and the learning curve is not very steep for the developer. Codeigniter has inbuilt security against Cross-Site Request Forgery (CSRF) and Cross-Site Scripting (XSS) attacks and provides content security.Finally, Codeigniter 4.0.3, PHP 7.2, HTML 5, CSS, JavaScript, AJAX, Bootstrap 4.

MYSQL are the combination of technologies used for the development.

VIII. The Operations in AQASYS

This section presents various operations and computations involved in AQASYS. These computational formulae are adopted from the academic quality standards and customized to the institutional requirement. Refer the following Table II, to understand the computations of this section.

1) Percentage CLO Attainment PCA (Pure): This calculation considers all the students who have appeared for the exam and obtained some score including the failure scores if any. This calculation doesn't exclude the failed student while calculating PCA hence the name PCA(Pure). It is basically the percentage of the CLO mark attained by the students as defined below:

$$PCA = \frac{\left\{\dfrac{\sum_0^N MS_{CLO=j}}{N}\right\}}{\sum_0^k MX_{CLO=j}}$$

Where MS is the mark of each student and MX is Maximum marks allotted for that question of the assessment (CLO). N is the total number of students addressed by the j^{th} CLO.

For example consider CLO 2.1:

$$PCA = \frac{\dfrac{\mathbf{2+4+4+4+3+1+0+4+3+4} \atop \underline{\mathbf{+3+2+5+6+6+5+6+4+5+1}}}{(10+10)}}{(4+6)}$$

PCA=0.36 Or 36%

Similarly, for CLO 1.1, 1.2 and 3.1 the % attainment values are

$$PCA = \frac{\dfrac{\mathbf{3+3+3+3+3+2+3+0+3+3}}{(10)}}{(3)}$$

$$= 0.866; 86.6\%$$

$$PCA = \frac{\frac{\mathbf{2+2+1+0+0+2+1+2+2+1}}{(10)}}{(2)}$$
$$= 0.65; 65\%$$

$$PCA = \frac{\frac{\mathbf{1+5+2+5+3+3+5+4+1+2}}{(10)}}{(5)}$$
$$= 0.62;\ 62\%$$

These values can be verified, referring to the Table II.

TABLE II. TABLE OF SPECIFICATIONS (TOS) EXAMPLE

	Q1	**Q2**	**Q3**	**Q4**	**Q5**
MaxMarks	**4**	**5**	**6**	**2**	**3**
CLO	**2.1**	**3.1**	**2.1**	**1.2**	**1.1**
StudentID					
S101	2	1	3	2	3
S102	4	5	2	2	3
S103	4	2	5	1	3
S104	4	5	6	0	3
S105	3	3	6	0	3
S106	1	3	5	2	2
S107	0	5	6	1	3
S108	4	4	4	2	0
S109	3	1	5	2	3
S110	4	2	1	1	3
PCA	36%	62%	36%	65%	86.6%
DL	27.5%	38%	28.3%	35%	13.3%
ODL	=28.43%				

2) Percentage student CLO attainment (PSCA): It is a measure of x% of students who attained y% of CLO mark. As per the user requirements, the PSCA calculation excludes the records of failed students and classifies the graded students into four classes viz. Excellent (E), Adequate (A), Medium (M), Unsatisfactory(U). The target range for classifying into E, A, M, and U are dynamically adjustable with the slider scale Fig. 7. After classifying them into E, A, M, and U percentage numbers of (E+A) students are calculated. If this number is above a certain set target, then the corresponding CLO is declared as "attained". The target selection is also dynamically adjustable as per the policy requirements of the quality committee. The following screenshot of the slider, (Fig. 7) and the specimen calculations make the PSCA calculation clear:

Slider:

Fig. 7. Criteria Setting Slider for CLO Assessments.

As per the above slider, the numbers indicate the upper limits for each range. That means the ranges for each class are as follows (Table III):

TABLE III. TABLE OF SPECIFICATIONS (TOS) EXAMPLE

Unsatisfactory (U)	0-25
Medium (M)	26-60
Adequate (A)	61-75
Excellent (E)	76-100
E+A target criteria	76-100
Target criteria (Unsatisfactory)	0-60

Target criteria: 0-60 unsatisfactory; 61-75 satisfactory; 76-100: Attained.

The following Table IV presents values of different operational parameters for the example data of Table II with E,A,M and U classification. Fig. 8 presents comparison of PSCA(Pure) and PSCA(adjusted). In the "adjusted value computation the records of failed students are not considered. This PSCA(adjusted) parameter, slightly skews the results towards PLO attainment advantage. Fig. 9 shows final values.

3) Grading: Grade Book generation is dependent on the complete marks submission in all assessments as planned for the course. Incomplete submission will not produce the grade book. The mark submission is to be done at each question level at each assessment for all the registered students. Any lapse is considered as incomplete data submission and grade book will not be generated. This strategy is adopted to collect the data from the root of the assessment source alleviating any high-level manipulation or adjustments to alter the grades. The grade ranges used are as below in Table V.

AQASYS generates course specific grade summary charts for the faculty login and grade summary charts for all the courses of the department for the administrator login. The sample grade summary screen shot is as shown in Fig. 10 below:

4) PLO Attainments: Before calculating the PLO attainments, it is important to understand the relation between CLO, PLO and course Assessments of the department. The following Entity-relationship diagram, Fig 11, shows relation between entities: department, course, assessment, PLOs and CLOs.

It means that a department will have many courses, a course will have many assessments. A course will have many defined CLOs. Each assessment will have many CLOs. And finally, many CLOs contribute to many PLOs.

a) PLO Attainment in the course (CPLO): Now it is clear that, the CLOs of a course will contribute to one or more PLOs. There is "many to many " (m:n) relation between CLOs and PLOs of the course. Therefore, while calculating the PLO attainment by a course, the contributions of each CLO to the PLO in question are to be considered. The attainment in i^{th} PLO is given by the average sum of all the contributing CLOs. The general formula used is as given below:

$$CPLO(i) = \frac{\sum_{j=0}^{k} V(i)_{CLO=j}}{k}$$

Where V(i) is the value of j^{th} CLO contributing to i^{th} PLO.

TABLE IV. TABLE OF SPECIFICATIONS (TOS) EXAMPLE

	Q1	Q2	Q3	Q4	Q5
Max Marks	4	5	6	2	3
CLO	2.1	3.1	2.1	1.2	1.1
StudentID					
S101	2=50% (M)	1=20% (U)	3=50% (M)	2=100% (E)	3=100% (E)
S102	4=100% (E)	5=100 % (E)	2=33% (M)	2=100% (E)	3=100% (E)
S103	4=100% (E)	2=40% (M)	5=83% (E)	1=50% (M)	3=100% (E)
S104	4=100% (E)	5=100 % (E)	2=33% (M)	0=0% (U)	3=100% (E)
S105	3=75% (A)	3=60% (M)	6=100% (E)	0=0% (U)	3=100% (E)
S106	1=25% (U)	3=60% (M)	5=83% (E)	2=100% (E)	2=66% (A)
S107	0=0% (U)	5=100 % (E)	6=100% (E)	1=50% (M)	3=100% (E)
S108	4=100% (E)	4=80% (E)	4=60% (A)	2=100% (E)	0=0% (U)
S109	3=75% (A)	1=20% (U)	5=83% (E)	2=100% (E)	3=100% (E)
S110	4=100% (E)	2=40% (E)	1=16% (U)	1=50% (M)	3=100% (E)
Total Students	10	10	10	10	10
PSCA (Pure)	70%	40%	60%	50%	90%
Comments (Pure)	satisfactory	Unsatisfactory	Unsatisfactory	Unsatisfactory	Attained
PSCA (Adjusted)	87.5%	77.7%	85.7%	87.5%	100%
Comments (Adjusted)	Attained	Attained	Attained	Attained	Attained
DL	27.5%	38%	35%	35%	13.3%
ODL	29.76%				
Final CLO Assessment Results and Comments					
	PSCA (Pure)	Comments PSCA (Pure)	PSCA (Adjusted)	Comments PSCA (Adjusted)	
CLO 1.1	90%	Attained	100%	Attained	
CLO 1.2	50%	Unsatisfactory	87.5%	Attained	
CLO 2.1	65%	Satisfactory	86.6%	Attained	
CLO 3.1	40%	Unsatisfactory	77.7%	Attained	

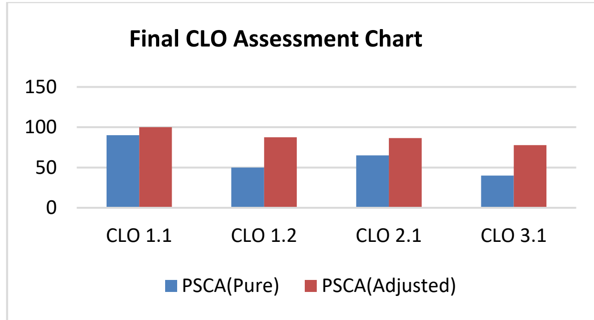

Fig. 8. Final Percentage CLO Attainments PSCA (Pure) and PSCA (Adjusted).

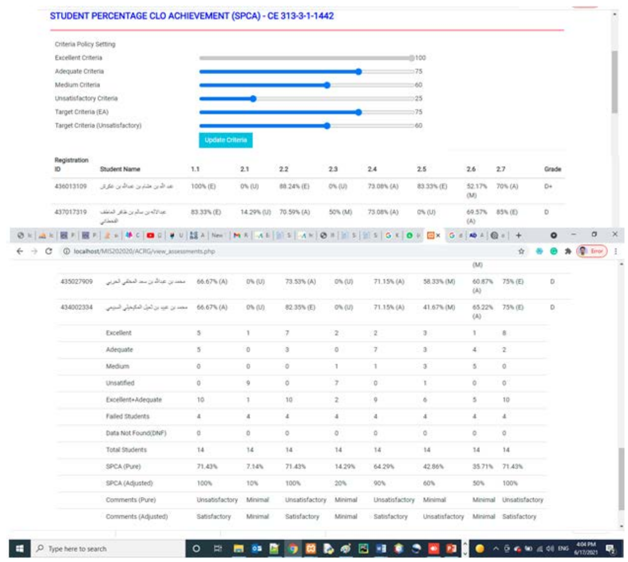

Fig. 9. Screen Shots from AQASYS: Final Percentage CLO Attainments PSCA (Pure) and PSCA (Adjusted).

TABLE V. GRADING POLICY AND RANGES

Range of Marks	Grade Assigned
100>= Marks>= 95	A+
94>=Marks>= 90	A
89>= Marks>= 85	B+
84>= Marks>= 80	B
79>= Marks>= 75	C+
74>= Marks>= 70	C
69>= Marks>= 65	D+
64>= Marks>= 60	D
59>= Marks>= 0	F

b) PLO Attainment in the semester for the program (SPLO): This is the average of i^{th} PLO attainment in all courses in the semester. The generalized formula that is used to calculate this parameter in AQASYS is as below:

$$SPLO(i) = \frac{\sum_{m=0}^{N} CPLO(i)}{N}$$

where, N is the total number of courses.

Fig. 12, Fig. 13, and Fig. 14, show instances of system results for this section.

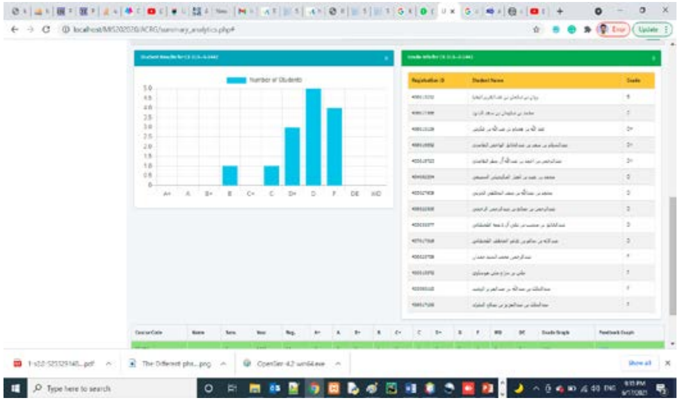

Fig. 10. Sample Grade Summary Chart Generated by AQASYS.

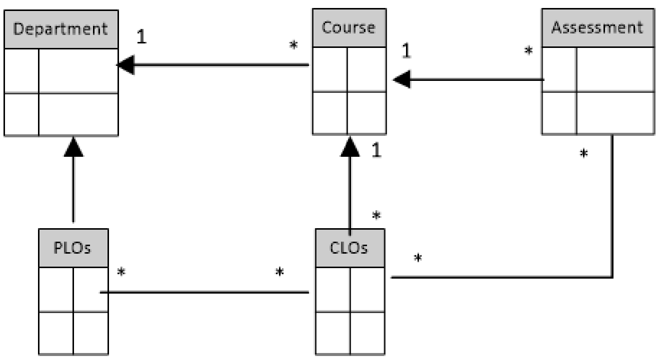

Fig. 11. Entity-Relationships in a PLO Calculation Scenario.

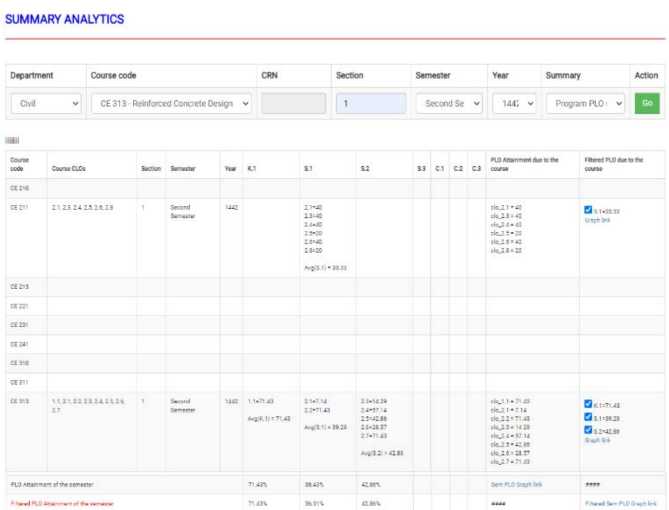

Fig. 12. PLO Attainments (SPLO and CPLO).

Fig. 13. Graph Showing PLO Attainments (CPLO).

Fig. 14. Graph Showing PLO Attainments (SPLO).

5) Difficulty Level(DL): This parameter is captured as Coefficient of Difficulty else-where[], however the parameter is not very convincing as it takes into account the only maximum scores. In this paper a new parameter is defined to capture the difficulty level. In this paper, the difficulty Level (DL) is the degree of difficulty of the assessment as felt by the students (the learner). It is defined as below:

$$DL = 1 - \frac{\sum_{i=0}^{N} M_i}{N * M_X}$$

Where M_i is the mark scored by i^{th} student, M_x is the maximum mark for the question (CLO) and N is the number of students. If all the students secure the allotted maximum mark then, the numerator of the fractional term in the above equation will be equal to its denominator resulting in the final value of DL=0, suggesting that the question paper was easy. If it is extremely difficult then all the students would score zero, resulting in DL=1 suggesting a very difficult question paper. The maximum value of DL is 1 and the minimum value is 0. DL may be expressed in a percentage value. Overall Difficulty Level (ODL) is the average of all the DLs.

6) Survey collection & Analysis: AQASYS collects the different kinds of surveys including course feedback surveys, alumni surveys and any survey as launched by the administrator. The system has two major provisions to upload the survey forms into the database.

- Through the excel sheets.
- Directly from the survey forms (example Google form).

After the due date of collection of survey data, the results are analyzed by the bar charts, pie charts, etc. Fig. 15 shows an instance of such a feedback graph as generated by the system.

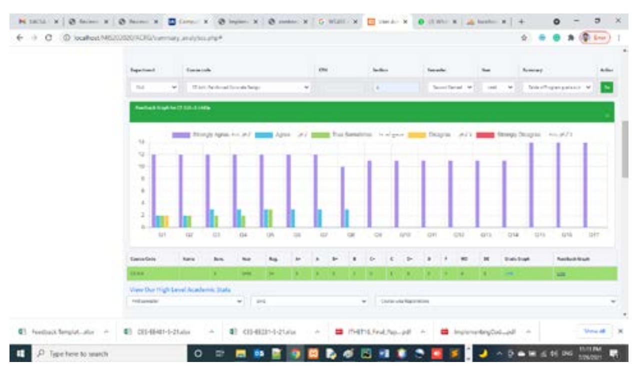

Fig. 15. Screen Shot of a Survey Graph Generated by AQASYS.

7) CLO Mapping (CLOM): CLO mapping is the most important part of the quality assurance system. Generally, it was found that.

- During the curriculum design of most of the programs, the care that is due for defining the CLOs, is not given.
- While mapping the assessment questions to appropriate CLOs, the attitude and approach is very un-scientific to the educational philosophy. Most of the faculty sways hay.

The underpinning point here is that if an academic institution has symptoms as observed above, then the whole exercise of quality evaluation becomes just an exercise of number jargon that would remain far removed from the real state of academics in the organization.

Keeping these observations at the center of the design, AQASYS integrates an intelligent auto-mapping module called iBOX that assigns possible CLOs automatically to the questions of an assessment questionnaire. iBOX works on the text mining algorithms and takes into account Bloom's taxonomy to recognize action verbs.

a) iBOX Design: This section presents the design basics of iBOX (Fig 16). The goal is to first automatically identify the action verbs from the assessment questions and map them to CLOs, later map CLOs to the PLOs.The iBOX design explores Bloom's taxonomy and Action Verbs (refer to Table VI).

The iBOX algorithms, initially extract the action verbs from the given text document after verb extraction, the algorithms search Bloom's database for the matching verbs. If the matching verb is found in the database then, categorizes and label the document as per the scheme shown in Fig. 17, other- wise the algorithm allows human intervention to match the sentence with the action verb and Bloom's level. The algorithm updates Bloom's database with this newly learned action verb. Thus iBOX is incrementally learning while it continues to automatically classify the CLO, PLO, and question sentences into different Bloom's levels. Fig. 16 shows the iBOX as it appears in AQASYS.

iBOX basically processes the input text files to identify the action verbs and match them to the verbs available in the Bloom database. If a proper match is found, it labels the CLO, PLO mapping automatically else it adds the new unmatched verb to the new verb list in the Bloom database. The new verb then becomes part of Bloom's verb list. The user is allowed to manually classify the new verb and insert it into an appropriate Bloom level list as an update. This way the iBOX follows incremental learning.

Three text files containing 1) The question paper 2) CLO definitions 3) PLO definitions are the inputs to a sentence segmentation and verb extraction module of IBOX.

This module uses Stanford parser [16] and wordNet database [8][15] to extract the exact verb from the sentences of the input documents. Table VII shows the decision making process that is inbuilt in the iBOX.

V_q → is a verb in the question paper

V_c → is a verb in the CLO definitions

V_p → is a verb in the PLO definitions

The extracted verbs are searched for their presence in the verb list of Bloom database. If they are present, then each verb (Vq, Vc, Vp) is compared with the members of the other verb lists corresponding to each Bloom's level (Remember, Understanding, Apply, Analyze, Evaluate, Design). If the verb under test is the same as the word in the other group then it is denoted as W_s (similar word), else if it is different, it is denoted as W_d (different word). It is to be noted that each of these verbs is already verified to be present in the Bloom database.

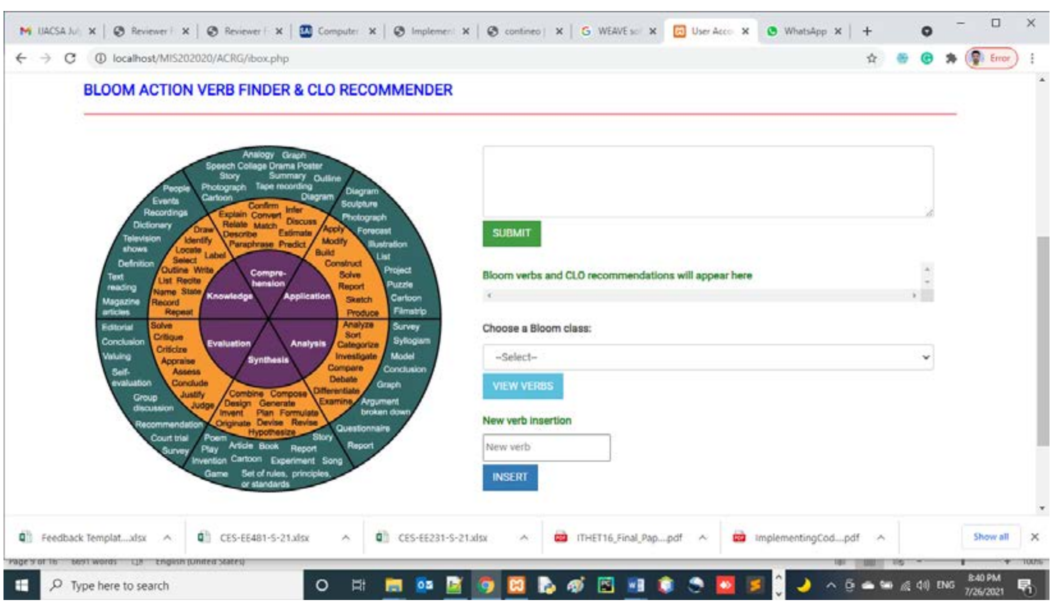

Fig. 16. iBOX-Bloom Level and CLO Recommender System.

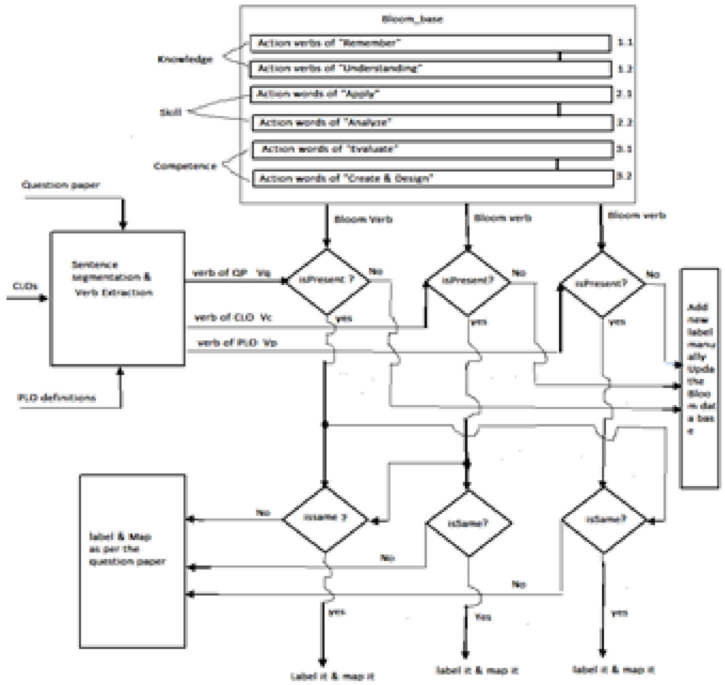

Fig. 17. Block Schematic of Decision making in iBOX Algorithms.

TABLE VI. ANDERSON'S REVISED BLOOM ACTION VERBS

Remember	Understand	Apply	Analysis	Evaluate	Design
Arrange Define Describe Duplicate Identify Label List Match Memorize Name Order Outline Recognize Relate Recall Repeat Reproduce Select State	Classify Convert Defend Describe Discuss Distinguish Estimate Explain Express Extend Generalized Give example(s) Identify Indicate Infer Locate Paraphrase Predict Recognize Rewrite Review Select Summarize Translate	Apply Change Choose Compute Demonstrate Discover Dramatize Employ Illustrate Interpret Manipulate Modify Operate Practice Predict Prepare Produce Relate Schedule Show Sketch Solve Use Write	Analyze Appraise Breakdown Calculate Categorize Compare Contrast Criticize Diagram Differentiate Discriminate Distinguish Examine Experiment Identify Illustrate Infer Model Outline Point out Question Relate Select Separate Subdivide Test	Arrange Assemble Categorize Collect Combine Comply Compose Construct Create Design Develop Devise Explain Formulate Generate Plan Prepare Rearrange Reconstruct Relate Reorganize Revise Rewrite Set up Summarize Synthesize Tell Write	Appraise Argue Assess Attach Choose Compare Conclude Contrast Defend Describe Discriminate Estimate Evaluate Explain Judge Justify Interpret Relate Predict Rate Select Summarize Support Value

TABLE VII. DECISION MAKING IN IBOX

V_q	V_c	V_d	Labeling decision
W_s	W_s	W_s	$L(W_s)$
W_s	W_s	W_d	$L(W_s)$
W_s	W_d	W_s	$L(W_s)$
W_s	W_d	W_d	$L(W_d)$
W_d	W_s	W_s	$L(W_s)$
W_d	W_s	W_d	$L(W_d)$
W_d	W_d	W_s	$L(W_d)$
W_d	W_d	W_d	$L(W_d)$

The decision making uses the highest probability (dominant) principle and labels as per the maximum number of occurrences of the word. If W_s or W_d belongs to a specific Bloom's list then the level of that list is marked and mapped to CLO and PLO along with the designated number labels. Example (Remember:1.1,Understanding:1.2,Apply:2.1, Analyze:2.2,Evaluation:3.1,Design:3.2) If the three verbs (V_q, V_c, V_p) that are present in the Bloom's database with all being different and there is no similarity among them, then decision label will be marked as per the Bloom level of V_q , (refer Fig 17 and Table VII.). Table VIII shows the exact statements of SOs/PLOs and Table IX shows Bloom's classification for those statements after recognizing action verbs and mapping them to the available verbs in the Bloom database.

TABLE VIII. SOs/PLOs:STATEMENTS

	Student Outcome (SO/PLO) Statement
a	An ability to **apply** knowledge of computing and mathematics appropriate to the program's student outcomes and to the discipline
b	An ability to **analyze** a problem, identify and define the computing requirements appropriate to its solution.
c	An ability to **design**, implements, and evaluate a computer-based system, process, component, or program to meet desired needs.
d	An ability to **function** effectively on teams to
e	An **understanding** of professional, ethical, legal, security and social issues and responsibilities
f	An ability to **communicate** effectively with a range of audiences.
g	An ability to **analyze** the local and global impact of computing on individuals, organizations, and society
h	**Recognition** of the need for and an ability to engage in continuing professional development.
i	An ability to **use** current techniques, skills, and tools necessary for computing practice.
J	An ability to **apply** mathematical foundations, algorithmic principles, and computer science theory in the modeling and design of computer based systems in a way that demonstrates comprehension of the tradeoffs involved in design choices
k	An ability to **apply** design and development principles in the construction of software systems of varying complexity

TABLE IX. BLOOM CLASSIFICATION INSTANCES FOR PLOs

SO's	**Dominant action Action word identified**	**CLO Category**	**Recommended CLO Number**	**Member words from Bloom's table**
a	apply	skill	2.1	Apply, Build Choose, Construct Develop Experiment With, Identify Interview Make, use Of, Model Organize Plan, Select Solve, Utilize
b	analyze	skill	2.2	Analyze, Assume Categorize Classify, Compare Conclusion Contrast Discover, Dissect Distinguish Divide, Examine Function, Inference Inspect, List Motive Relationships Simplify, Survey Take part in Test for, Theme
c	Design	competence	3.2	Adapt, Build Change, Choose Combine, Compile Compose, Construct, Create Delete, Design Develop, Discuss Elaborate, Estimate Formulate, Happen Imagine, Improve Invent, Makeup Maximize, Minimize Modify, Original Originate, Plan Predict, Propose Solution, Solve Suppose, Test Theory
d	function	knowledge	1.2	Classify, Compare Contrast Demonstrate Explain, Extend Illustrate Infer, Interpret Outline, Relate Rephrase, Show Summarize, Translate
e	understand	knowledge	1.1	Choose, Define Find, How Label, List Match, Name Omit, Recall Relate, Select Show, Spell Tell, What When, Where Which, Who Why
f	communicate	knowledge	1.1	Choose, Define Find, How Label, List Match, Name Omit, Recall Relate, Select Show, Spell Tell, What When, Where Which, Who Why
g	analyze	skill	2.2	Analyze, Assume Categorize Classify, Compare Conclusion Contrast Discover, Dissect Distinguish Divide, Examine Function, Inference Inspect, List Motive Relationships Simplify, Survey Take part in Test for, Theme
h	Recognize/ engage	competence	3.1	Agree, Appraise Assess, Award Choose, Compare Conclude, Criteria Criticize, Decide Deduct, Defend Determine, Disprove Estimate, Evaluate Explain, Importance Influence, Interpret Judge, Justify Mark, Measure

SO's	Dominant action Action word identified	CLO Category	Recommended CLO Number	Member words from Bloom's table
				Opinion, Perceive Prioritize, Prove Rate, Recommend Rule on, Select Support, Value
i	Use	knowledge	1.2	Classify, Compare Contrast Demonstrate Explain, Extend Illustrate Infer, Interpret Outline, Relate Rephrase, Show Summarize, Translate
j	Apply	skill	3.1	Apply, Build Choose, Construct Develop Experiment With, Identify Interview Make, use Of, Model Organize Plan, Select Solve, Utilize
k	Apply	skill	3.1	Apply, Build Choose, Construct Develop Experiment With, Identify Interview Make, use Of, Model Organize Plan, Select Solve, Utilize

8) Course report generation: Utilizing all the information available about the course in the database AQASYS generates the academic course report in the required format automatically in a single click.

It intelligently inserts recommendations in the report wherever necessary. The automatic course report generation feature makes AQASYS unique from other competitive research in this field. Fig. 18 shows the user interface for course report generation and Fig. 19 shows the instance of the course report being generated.

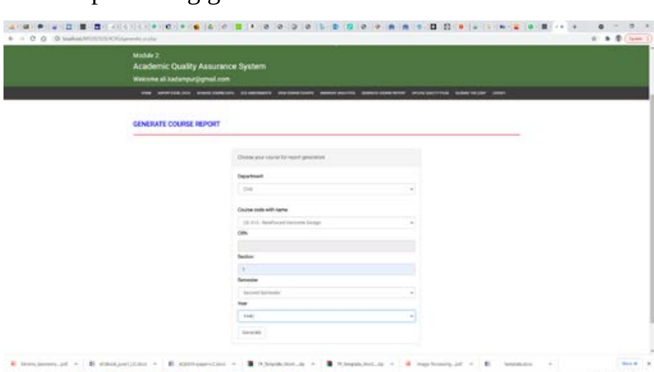

Fig. 18. Interface for Generating Course Report.

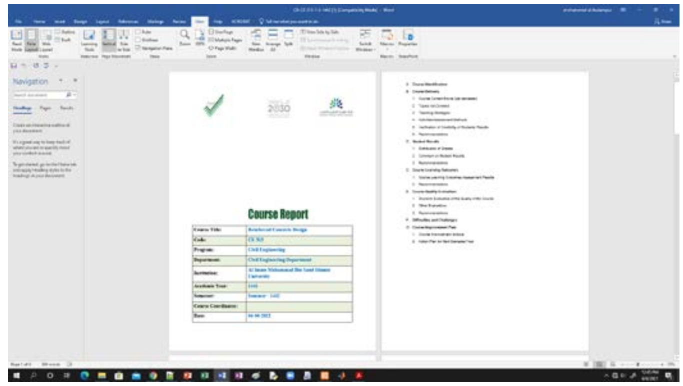

Fig. 19. Instance of System Generated Course Report.

IX. Results and Screenshots

Instances of AQASYS results are already presented in earlier sections wherever the discussion arose. In this section, few computed operational parameters are compared with manually computed values. Table X is the partial data reference table for CLO 1.1. The system computed parameters exactly match the expected values. Refer to results in Table XI.

TABLE X. Example Marks of 14 Students for CLO 1.1

CLO 1.1 Max Marks:3	2	3	2.5	3	2	2	3
	3	3	0	2	3	2	2

TABLE XI. Parameters Compared

SNo	Parameter	Manually computed value	System generated value
1	PCA (Pure); 1.1	**77.4%**	**77.4%**
3	PSCA (Pure)	**92.6%**	**92.6%**
4	PSCA(adjusted)	**100%**	**100%**
5	DL	**22.61%**	**22.61%**
Verified parameters			
7	GRADE summary	✓	✓
8	PLO attainment at courses level	✓	✓
9	PLO attainment at Semester level	✓	✓
10	Filtered PLO attainment at course level	✓	✓
11	Filtered PLO attainment at Semester level	✓	✓

Fig. 20 shows instance of grade results and Fig. 21 shows instance of PLO attainments.

1) AQASYS Performance evaluation: In order to evaluate the performance of the application, the following few application performance metrics were considered. Refer Table XII. The Appdex metric, as defined below:

$$Appdex = \frac{satisfiedcount + \frac{ToleratingCount}{2}}{Totalsamples}$$

was considered to evaluate "user satisfaction".

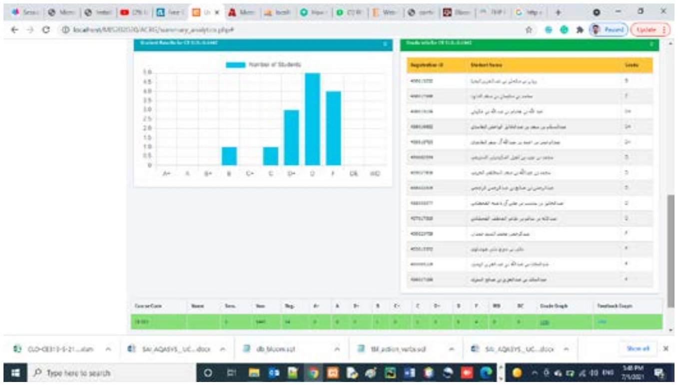

Fig. 20. Instance of Grade Results.

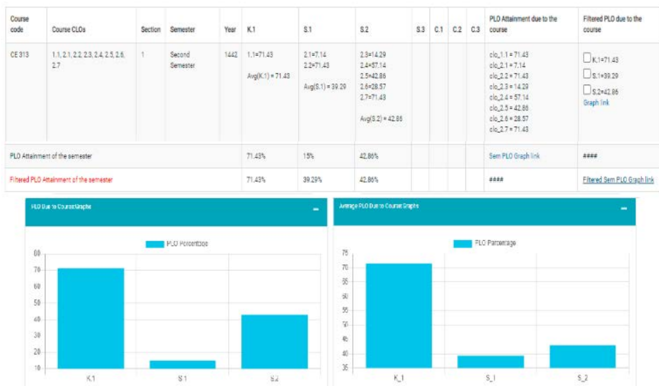

Fig. 21. Instance of PLO Attainments.

TABLE XII. APPLICATION PERFORMANCE METRICS

SNo	Parameter	Value
1	App user total count	**48**
2	App user satisfied count	**41**
3	Tolerating count	**7**
4	Appdex	0.927
5	Observed max number of concurrent users	48
6	Application availability	100% (Pinged all the time in a 72 hours of monitoring)

The count of concurrent users was observed to understand the "request rate" and the load that the application can handle. The application was found to be performing quite satisfactorily. "Availability" of web-application like the one in this paper is very important from the user's perspective. The application was "pinged" at an interval of a minute regularly for a duration of 120 hours. The log results showed successful "ping" all the time. The application was highly available.

2) AQASYS selected screenshots: The following figures, Fig 22 through Fig. 28, show various instances of AQASYS output as depicted against their names.

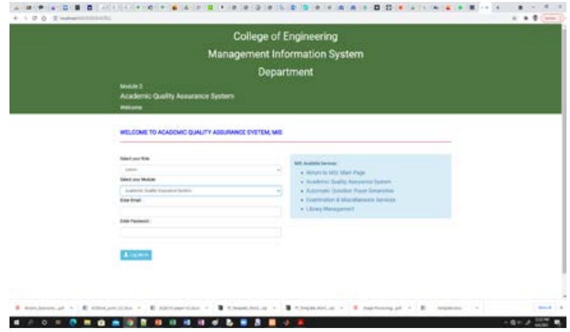

Fig. 22. Instance of Login Page.

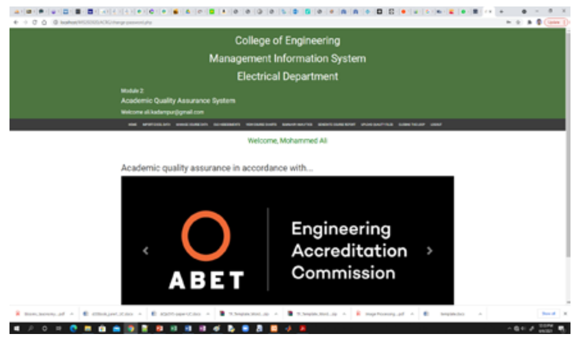

Fig. 23. Instance of Home Page.

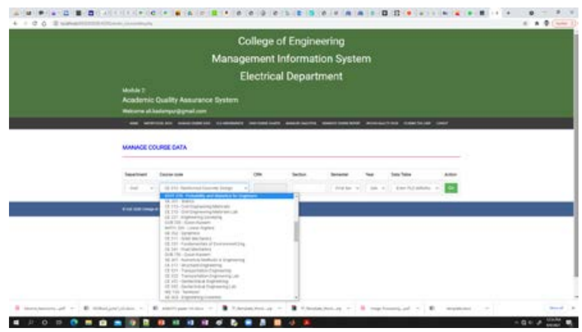

Fig. 24. Instance of Course Selection.

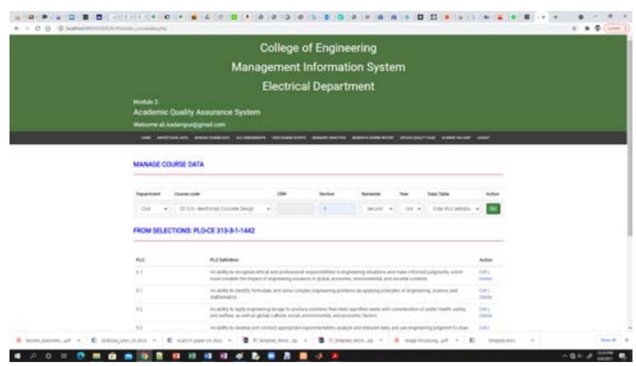

Fig. 25. Instance of CLO Definitions.

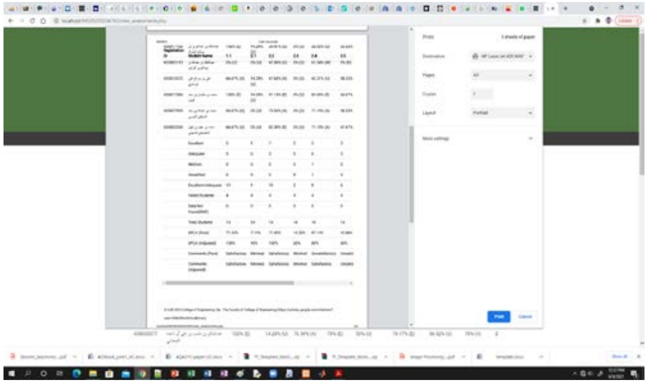

Fig. 26. Instance of PSCA Computations.

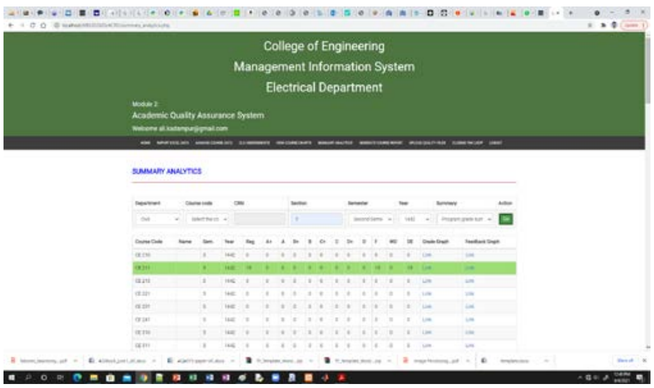

Fig. 27. Instance of Summary Analytics.

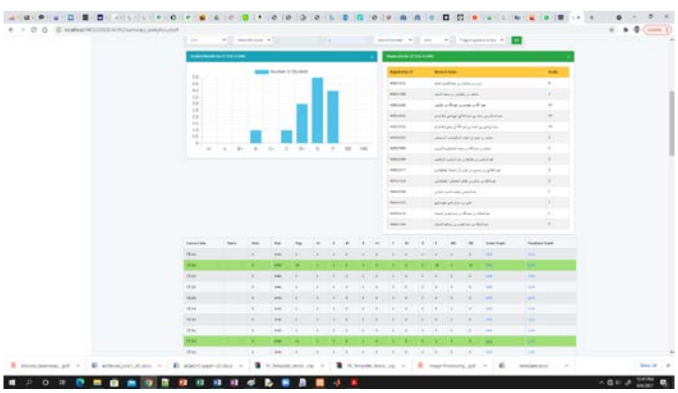

Fig. 28. Instance of Grade Summary Display.

X. CONCLUSION

This paper presented a web-based academic quality assurance system. The unique features of the system included automatic course report generation and intelligent Bloom's level and CLO-PLO mapping module, that automatically assigns appropriate Bloom levels to the text presented to it by matching the action verbs. The paper presented the content from the system designer's perspective as well as from the user's perspective. The system was launched in the institutional LAN on a pilot basis and real-time data was loaded onto the system. Different operational parameters such as PCA, PSCA, DL, Course level PLO attainment (CPLO), Semester PLO attainment (SPLO), course-wise grade details, and other summary analytic were tested. The computed parameters were found to be as expected in the quality standards.

This system would help the faculty, quality committee, and the administration to measure the learning quality in the selected program according to the ABET and NCAAA standards. The faculty need not worry about the clumsy calculation formulae and heaps of excel-sheets and run around seeking last-minute templates to stitch the quality. The faculty now can focus on teaching, followed by assessing and entering the scores of the students. All the calculations related to quality are carried out by the system automatically. The system provides summary charts and tabulates data outputs. As the application uses a client-server architecture, the server database archives the historical data and is available for viewing at any point in time.

The application makes the matters of handling of academic quality, a seamlessly an easy task with features of reliability, security, availability, and privileged access being embedded into the system.

ACKNOWLEDGMENT

The authors acknowledge the support of department heads and colleagues of the college of engineering Imam Mohammad Ibn Saud Islamic University, Riyadh, KSA. Particular thanks are extended to Dr. Aun Bashir, Dr.Farid Fadellah, Dr.Ali Hennache, Dr. Rashid Khan for their support in providing data and testing the application.

REFERENCES

[1] Burge LL, Leach RJ. An advanced assessment tool and process. In Proceedings of the 41st ACM technical symposium on Computer science education 2010 March 10: 451-454. ACM.

[2] Costreie S, Ianole R, Dinescu R. An Evaluation of the Quality (Assurance) Evaluation–Case Study: The University of Bucharest. Quality Assurance.

[3] Khwaja Amir. A Web-Based Program Outcome Assessment Tool. 2018 21st Saudi Computer Society National Computer Conference (Ncc). 345 E 47th St, New York, Ny 10017 Usa: IEEE; 2018.

[4] E. Essa, A. Dittrich, S. Dascalu, and F. C. Harris Jr., "ACAT: A WebBased Software Tool to Facilitate Course Assessment for ABET Accreditation," Proceedings of the 2010 Seventh Intl. Conf. on Info. Tech.: New Generations (ITNG), April 12-14, 2010, pp. 88-93.

[5] ABET (Accreditation Board for Engineering and Technology). (2015). "Criteria for accrediting engineering programs."⟨http://www.abet.org/accreditation/accreditation-criteria/criteria-for-accrediting-engineering-programs-2016-2017⟩ (Nov. 9, 2015).

[6] Ketchman K, Dancz CLA, Burke RD, Parrish K, Landis AE, Bilec MM. Sustainable Engineering Cognitive Outcomes: Examining Different Approaches for Curriculum Integration. J Prof ISSUES Eng Educ Pract. 2017;143. https://doi.org/10.1061/(ASCE)EI.1943-5541.0000324.

[7] Development reference and learning resources from : https://phpgurukul.com/codeigniter-introduction/.

[8] Silveira, N., Dozat, T., Marneffe, M., Bowman, S., Connor, M., Bauer, J., & Maning, C.: A Gold Standard Dependency Corpus for English. Proceedings of the Ninth International Conference on Language Resources and Evaluation (LREC-2014), 2897-2904 (2014).

[9] S. A. ElRahman and S. S. Shabanah, "Course and Student Management System Based on ABET Computing Criteria," I. J. of Info. Engineering and Electronic Business, 3, 2016, pp. 1-10.

[10] Accreditation," Proceedings of the 2010 Seventh Intl. Conf. on Info. Tech.: New Generations (ITNG), April 12-14, 2010, pp. 88-93.

[11] A. Khwaja, B. Alfalah, F. Alharbi, and R. Alarfaj, "WebCOAT: A Web-Based Course Outcome Assessment Tool," Proc. of the 2016

GlobalConf. on Teaching and Learning with Tech. (CTLT 2016), June 16-17, 2016, pp. 215-220.

[12] Center for education innovation Hong Kong: http://cei.hkust.edu.hk/teaching-resources/outcome-based-education/school-resources/school-business-and-management.

[13] Progams and Courses Outcomes System (PACOS). http://pacos.ust.hk/ [Last Retreived: Feb 20, 2018].

[14] Jamie Rumbelow "The codeigniter handbook " Efendi Publishing, Vol-1, ISBN: 978-0-9571791-1-0.

[15] G. Miller, R. Beckwith, +2 authors K. Miller "Introduction to WordNet: An On-line Lexical Database" International Journal of Lexicography 1990, DOI:10.1093/IJL/3.4.235 Corpus ID: 2146137.

[16] Christopher D. Manning, M. Surdeanu, John Bauer, J. Finkel, Steven Bethard, David McClosky " The Stanford CoreNLP Natural Language Processing Toolkit " ACL publisng 2014, DOI:10.3115/v1/P14-5010Corpus ID: 14068874.

[17] Accredidation Support Software https://www.smart-accredit.com/index.php.

[18] Outcome Based Education Software http://www.contineo.in/.

[19] Weave education https://www.capterra.com/accreditation-management-software/.

A Systematic Literature Review of the Types of Authentication Safety Practices among Internet Users

Krishnapriyaa Kovalan[1], Siti Zobidah Omar[2]*, Lian Tang[3], Jusang Bolong[4]
Rusli Abdullah[5], Akmar Hayati Ahmad Ghazali[6], Muhammad Adnan Pitchan[7]
Institute for Social Science Studies (IPSAS), Universiti Putra Malaysia[1, 2, 6]
Department of Communication, Faculty of Modern Languages and Communication, Universiti Putra Malaysia[1, 2, 3, 4]
Baoji University of Arts and Sciences[3]
Department of Software Engineering and Information System[5]
Faculty of Computer Science and Information Technology, Universiti Putra Malaysia[5]
Department of Media and Communication Studies, Faculty of Social Science and Humanities, Universiti Kebangsaan Malaysia[7]

***Abstract*—The authentication system is one of the most important methods for maintaining information security in smart devices. There are many authentication methods, such as password authentication, biometric authentication, signature authentication, and so on, to protect cloud users' data. However, online information is not yet effectively authenticated. The purpose of this systematic literature review is to examine the current types of authentication methods as a safety practices for information security among Internet users. The PRISMA method was adopted to present a systematic literature review of 28 articles from three main databases (20 articles from Scopus, one article from Google Scholar, and seven articles from Dimension). This study used the Prediction Study Risk of Bias Assessment Tool to appraise the quality of the included studies. From the findings of the study, a total of three main themes were identified: password authentication, biometric authentication, and multiple-factor authentication. Multiple-factor authentication was found to be the most secure and most frequently recommended authentication method. It is highly recommended to implement three-factor authentication and multi-biometric model in the future, as it provides a higher surveillance level in terms of information security among cloud computing users.**

Keywords—Password authentication; biometric authentication; multi-factor authentication; information security; safety practices

I. Introduction

Smart telecommunication devices have become a fundamental element in most of our lives, and for many have become a trusted companion. It is where we store almost all our data and information. However, in Malaysia, the statistics for denial of service, malicious attacks, intrusion, and fraud indicated 6898 cases in 2016, 6686 cases in 2017, 7993 cases in 2018, 9890 cases in 2019, and 9646 cases in 2020 respectively [1]. The statistics show that information security incident reports increased from 2017 through 2019 and decreased slightly in 2020. The expanding number of smart devices and increasing availability of Internet access have changed the lives of many individuals. People began to use the Internet for different purposes, such as obtaining information, communicating, banking, entertainment, and many more [2]. The Internet also plays an important role as a teaching aid in universities [3]. Cloud computing allows users to save data online and access it from anywhere at any time via an Internet connection, instead of using a hard drive or other storage devices [4]. The development of cloud storage, however, has its own negative aspects, such as information security attacks. Data transmittal in the cloud environment can require a huge amount of bandwidth, which may allow hackers to retrieve the information [5] and the insufficiency of authentication is the cause of information attacks in cloud computing [6]. Data transparency and unauthorized information usage are the reasons behind these attacks [7]. With safe Internet usage awareness, being vulnerable to cyber threats and becoming a cyber victim can be avoided [8].

Authentication is a method for estimating the level of trust one can have that the source of information is who it is stated to be [9]. The authentication process happens when information is entered into the login system with a database. Then, the system checks whether the information entered matches the database information. If it matches, the user can access the system [10]. Social environment factors such as parents, friends, work colleagues, social media, and government policies play a vital role in educating Internet users about cybersecurity [11]. The public and organizations have to realize that cybercrime is highly risky, and that they have to take safety precautions to protect their information from being shared online [12]. An effective way to protect storage and authorization of data in the cloud environment is by having an appropriate authentication [13]. The general objective of this study is to examine the authentication methods used as a safety-enhancing practice for information security among Internet users. This study will benefit the Internet user society acknowledging that authentication plays an important role in enhancing a greater cloud environment. The higher the demand of Internet of Things (IoT) justifies the usefulness of safe authentication method. Further, research gap was noticed in the types of authentications used in the last five years. Hence, this paper intends to develop a systematic literature review by focusing on the types of authentications used in the last five years.

*Corresponding Author
The authors would like to thank the Ministry of Higher Education (MOHE) Malaysia for Funding this project under Fundamental Research Grants Scheme, Project Code 05-01-18-2036FR and FRGS/1/2018/SS09/UPM/02/1/5540161.

II. METHOD

Using a systematic literature review, an exhaustive exploration of the research topic was made to provide the objective summary of current studies related to the research topic. Systematic literature described as a qualitatively and quantitatively identifying, merging, and assessing all available data to produce results related to a specific research question [14]. It is also a study to analyse research problems by recognizing, evaluating, and integrating results of all related studies acknowledging one or more research objectives [15]. The Preferred Reporting Items for Systematic Reviews and Meta-Analyses (PRISMA) method was used to study authentication method as a safety practice for information security among Internet users. Studies related to the authentication method for the 5 years from 2016 through 2020 were reviewed. Figure 1 displayed the flow diagram of this systematic review process.

A. *Systematic Review Process*

The systematic review process can be classified into three stages which are identification, screening and included [36]. This process is in accordance with PRISMA 2020 Flow Diagram (as shown in Figure 1).

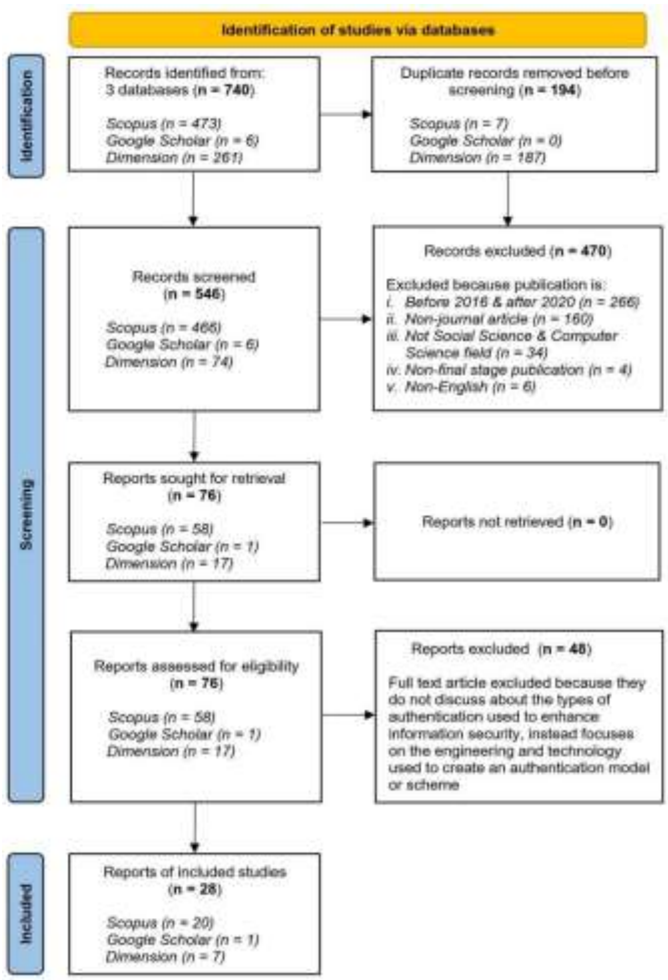

Fig. 1. The Flow Diagram of this Systematic Review Process Source: Page et al. [45].

B. *Identification*

The systematic review process can be categorized into three stages. The first is the identification of keywords of a specific study, a process to enrich keywords in a search string. Keyword searching related to this study was based on synonym searching in thesauruses, dictionaries, and past research. Sa'di et al. [16] found that, in Merriam Webster's dictionary, "authentic" means "original, actual, or truthful" as well as "true" (http://www.merriam-webster.com/dictionary/authentic). However, in this study, the theme was mostly about the types of authentications. "Authentication" is defined as "verification" and "certification" in the thesaurus. The dictionary also defines authentication as verification, certification, and validation.

The terms 'certification' and 'validation' were removed from the search string as use of these terms did not return the expected theme of study from the databases. The search strategy was developed in March 2021, as shown in Table 1. below. This process retrieved a total of 740 papers (473 from Scopus, six from Google Scholar and 261 from Dimension). Before moving to the screening process, 194 duplicate papers obtained from all three main databases were manually removed (as shown in Figure 1).

C. *Screening*

The second stage of the systematic review is screening. From the three main databases, a total of 546 papers were screened based on inclusion and exclusion criteria as determined by the researchers (Scopus = 466 papers; Google Scholar = 6 papers; Dimension = 74 papers; as shown in Table 1). The first criterion was that the timeline of this review was only focused on papers published during a five-year period from 2016 to 2020. Second, only research articles in journals were included. Then, only articles published in the fields of computer science and social science were retrieved. In addition, only articles that had reached final publication stage are reviewed in this study. Last, only English-language articles were included. A total of 470 articles were excluded based on the inclusion and exclusion criteria (as shown in Table 2).

Seventy-six articles were retrieved from the inclusion and exclusion criteria process. All 76 articles were successfully moved into the next stage of the screening process, eligibility. Eligibility is a manual process of document exclusion, the purpose of which is to filter the articles based on their respective abstract, method, results, or findings section to ensure that the articles match the objective of the systematic review. A total of 48 articles were excluded in this process because their contents were mostly about pure engineering and science that did not address the objective of this review.

D. *Inclusion*

A total of 28 articles were eligible for inclusion in this systematic review [17 - 44].

E. *Selection and Data Collection*

The main review process in this paper consisted of coding the themes, known as thematic analysis. A panel of five researchers from the field of cybersecurity, analysed the selected articles one by one. They independently reviewed titles and abstracts of 76 screened articles and discussed all the inconsistencies found. The themes were then generated by the panel for validation, individually and in pairs. This is to ensure that there is no bias toward the themes discussed. The themes were then double-checked and renamed, if necessary, after several discussions among the panel of researchers. The researchers came up with several themes once the article reviewing process was completed. This process was repeated three times before the themes were finalized. The panel later auto generated a standardized data, extraction form to abstract the characteristics of a study, which included type of authentication, research objectives, research design, findings, contribution, and limitation. Reviewers worked independently and simultaneously to extract article data. Data extraction was completed only when conflicts of idea were resolved, and reviewers were assured that their view of the topic was neutral.

TABLE I. KEYWORDS AND SEARCH STRATEGY

Database	Keywords and Search String
Scopus	TITLE-ABS-KEY ((“password authentication” OR “two factor authentication” OR “multi-factor authentication” OR “token authentication” OR “biometric authentication” OR "transaction authentication" OR "computer recognition authentication" OR "single sign-on authentication” OR "email authentication” OR "laptop recognition authentication” OR "gadget recognition authentication" OR “fingerprint authentication” OR "fac* authentication" OR "device authentication" OR “mobile authentication” OR "android authentication" OR “ios authentication” OR “password verification” OR “two-factor verification” OR “multi-factor verification" OR “token verification” OR “biometric verification" OR “transaction verification” OR "computer recognition verification" OR "single sign-on verification” OR "email verification” OR "laptop recognition verification” OR "gadget recognition verification" OR “fingerprint verification” OR "fac* verification" OR "device verification" OR “mobile verification” OR “android verification" OR “ios verification”) AND ("information security" OR " information protection” OR "information safety" OR "data security" OR "data protection" OR "data safety”))
Google Scholar	Phase 1: allintitle: “authentication” OR “verification”, “security” Phase 2: allintitle: “password authentication” OR “two factor authentication” OR “multi-factor authentication” OR “token authentication” OR “biometric authentication” OR "transaction authentication" OR "computer recognition authentication" OR "single sign-on authentication” OR "email authentication” OR "laptop recognition authentication” OR "gadget recognition authentication" OR “fingerprint authentication” OR "facial authentication" OR "device authentication" OR “mobile authentication” OR "android authentication" OR “ios authentication” OR “password verification” OR “two-factor verification” OR “multi-factor verification" OR “token verification” OR “biometric verification" OR “transaction verification” OR "computer recognition verification" OR "single sign-on verification” OR "email verification” OR "laptop recognition verification” OR "gadget recognition verification" OR “fingerprint verification” OR "facial verification" OR "device verification" OR “mobile verification” OR “android verification" OR “ios verification” "information security" OR " information protection” OR "information safety" OR "data security" OR "data protection" OR "data safety”
Dimension	Phase 1: ("authentication" OR "verification") AND (security) Phase 2: (“password authentication” OR “two factor authentication” OR “multi-factor authentication” OR “token authentication” OR “biometric authentication” OR "transaction authentication" OR "computer recognition authentication" OR "single sign-on authentication” OR "email authentication” OR "laptop recognition authentication” OR "gadget recognition authentication" OR “fingerprint authentication” OR "facial authentication" OR "device authentication" OR “mobile authentication” OR "android authentication" OR “ios authentication” OR “password verification” OR “two-factor verification” OR “multi-factor verification" OR “token verification” OR “biometric verification" OR “transaction verification” OR "computer recognition verification" OR "single sign-on verification” OR "email verification” OR "laptop recognition verification” OR "gadget recognition verification" OR “fingerprint verification” OR "facial verification" OR "device verification" OR “mobile verification” OR “android verification") AND ("information security" OR " information protection” OR "information safety" OR "data security" OR "data protection" OR "data safety”)

TABLE II. THE INCLUSION AND EXCLUSION CRITERIA

Criterion	Inclusion	Exclusion
Timeline	From 2016 to 2020	Before 2016 and after 2020
Literature type	Journals (research articles)	Journals (review papers), books, preprints, book chapters, series, conference proceedings, trade journal
Subject area	Computer science and social science	Other than computer science and social science
Publication stage	Final	Other than final
Language	English	Non-English

F. *Quality Appraisal*

This present study used the Prediction Study Risk of Bias Assessment Tool (PROBAST) to appraise the quality of the included articles. Based on PROBAST, five experts in this research group assessed the risk of bias by means of 22 multiple-choice questions with the responses No (N), Yes (Y), Unclear (U), and Not Applicable (X). The answer of “Y” for each signalling question was assigned 1 point, and that of “N,” “U,” or “X” was assigned 0 points. The total score ranged from 0 to 22. The five reviewers gave an overall score for each included study. An average score of 0–7 for each article is considered low quality, 8–14 is considered medium quality, and 15–22 is considered high quality [46][47]. All 28 articles were retained in the final review, as they met the standard of medium quality.

G. *Data Analytic Strategy (Synthesis Methods)*

Twenty-eight articles were reviewed, evaluated, and analysed after the eligibility process in this study. The search was thoroughly done according to the objective of this review, which is to study the current types of authentication methods as safe practice for information security among Internet users. The studies were classified into relevant themes by using qualitative synthesis. This was done by reading the title, abstract, and keywords of each study. Furthermore, a thematic analysis was performed to classify themes related to type of authentication method. Through an article review process, relevant groups were identified. Finally, a total of three main themes including password authentication, biometric authentication, and multifactor authentication methods emerged. Password-based methods were grouped into textual and graphical authentication. Biometric methods were classified into fingerprint, facial, retina or iris, voice, and digital signature authentication. Several review processes were done by the authors to finalize the themes and sub-themes.

III. Results

Seven hundred forty papers were identified based on the search strings. Later, 28 articles were found to be eligible for the review process by using qualitative synthesis. The results of the systematic literature review are further summarized in Table 3. The table shows the title of article, layer(s) of authentication applied, authors and, subject of the study. Of the 28 articles reviewed, 20 were about biometric authentication [18 - 21], [23 - 33], [35], [37], [40], [42], [44]. There were 17 studies about textual password authentication [17], [21], [23], [25 - 27], [30], [32 - 38], [41 - 43] and three studies about graphical password authentication [22], [34], [39]. Seventeen studies discussed multifactor authentication [17], [19], [21], [23 - 28], [30], [32 - 37], [42] (as shown in Figure.2.). The review found that most scholars had chosen to focus on biometric authentication. There were some studies excluded from this review [48 - 52] as they did not focus on types of authentication methods as a safety practice for information security. Of the 28 articles reviewed, 13 were based in India [20 - 26], [30], [34 - 37], [42]; four were from China [32], [33], [38], [44]; two from Saudi Arabia [18], [19] one from Poland [27]; one from the Czech Republic [31]; one from the United Arab Emirates [28]; one from Turkey [43]; one from Ukraine [40]; 1 from Jordan [17]; and one each from Zambia [29]; Philippines [39]; and the United States [41] (as shown in Figure 2).

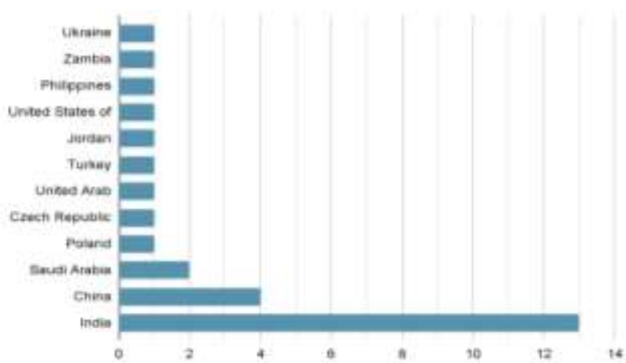

Fig. 2. Countries of Origin.

IV. Discussion

A. Types of Authentication

Based on the analysis, this section discusses types of authentications, such as password authentication (textual and graphical authentication), biometric authentication (fingerprint, facial, retina, voice, and digital signature), and multifactor authentication.

- Password authentication

Password has been used to protect online information since the early existence of the Internet. Passwords often do not expire, and users tend to use the same password for a long period, which leads to cyberattacks [53]. Passwords are one of the most significant risk factors because they are vulnerable to threats and attacks. Thus, a well-formulated and structured password should be “easy to remember but hard to hack” [54]. In this paper, the review has found two sub-themes under password authentication: textual and graphical.

1) Textual password authentication: Textual password authentication is knowledge based. Only four studies have focused on textual authentication [17] [38][41][43], whereas 12 other studies considered textual password as a part of multifactor authentication [23] [25-27] [30] [32-37] [42]. Furthermore, textual password authentication was studied by Akingbade [4]. Their study aimed to construct a protected login interface that could avoid cybersecurity attacks by using the 6 × 6 sized alpha numeric characters. The keyboard used in this experimental study was divided into letters, numbers, and symbols. Besides, users were allowed to select different of password lengths and different characters according to their preference. In fact, textual password method has been used in traditional bank environments, such as keying in the six-digit ATM personal identification number (PIN) [17]. In another experimental study that involved two groups: a control group and an experimental group; aimed to enhance the security of text-based passwords and to examine the effectiveness of creating a text-based password [43]. It was found that the experimental group experienced a more successful method of creating strong passwords that were also easy to remember. Another study, using a qualitative methodology aimed to understand the practice of mobile authentication user’s security awareness [41]. Twenty mobile device users made up the sample study, 19 of whom were aware of risk management in authentication. Additionally, used dynamic password technology, also known as One-Time Password (OTP) [38]. Each password is generated using the current time and can be only used once based on the function of the SM3 Hash Algorithm. This proposed scheme can be further improved to enhance network security. Moreover, applied multifactor authentication by using textual password authentication from server to user, then from user to server [36]. This approach provides users with anonymous identity, mutual authentication, surveillance against cyberattacks, and session key compliance in a multi-server environment.

2) Graphical password authentication: Graphical password authentication is more difficult to circumvent than biometric authentication, is more user-friendly, has easy-to-remember passwords, and provides high-level security [34][55]. The image-based authentication system is the main type of graphical password authentication [56]. This authentication method is based on recognition and recall approaches. Although this authentication method is highly secure, the ability to remember the password plays an important role. Songcuan et al. further mentioned that used graphical password authentication in an experimental study measuring students' memory ability, speed of registration, and speed of authentication [39]. The results recorded 100% successful password memory in the first session and 90.90% in the second session. There is a decrease in memory percentage because the second session took place after two weeks of delay. Hence, these findings prove that memorability plays a huge role in this type of authentication. A survey on graphical password authentication using images as passwords was conducted [22] and found that the memorability of graphical passwords was better than that of textual passwords. The authors noted that graphical password technology was still immature; hence more research is needed to achieve a higher level of usefulness.

- Biometric authentication

The security of biometric identification depends on body patterns such as fingerprints or facial features [57]. This type of authentication has the uniqueness derived from a human body [58]. Biometric authentication has been increasingly used as it provides a more secured process of identifying users [44]. Biometric authentication methods are more likely to be convenient, secure, and strong used compared with traditional authentication methods [59]. This section discusses fingerprint, facial feature, retina/iris, voice, and digital signature authentication.

3) Fingerprint authentication: In the protocol proposed by Zhu et al. [44], the first two modules of this scheme can be classified into enrolment and authentication phases. These two phases enable data to be protected better rather than in a one-step login phase and provides higher resistance against some possible threats. Moreover, ArunPrakash et al. [20] said that personal data stored in cloud computing can be protected because authentication can be completed only when the fingerprint encryption matches the enrolment phase data. This way, it is impossible for any harmful cyber threats to occur. Besides, they proposed a scheme for mobile banking application users to apply an efficient and privacy-preserving biometric identification outsourcing scheme in mobile banking applications [31]. This study suggested using a multibiometric system for a more significant variability.

4) Facial authentication: Musambo and Phiri [29] have proposed a facial authentication scheme for university students. It was found that the system only obtained 66% detection rate. This was due to the lighting conditions when the images are captured and the complexion of students' face. Another researcher also proposed a facial authentication scheme to be used in online banking services [18]. The proposed scheme can deny access for unauthorized usage and determines ways to identify different testing images. Ten different images were taken from the same user. The results of authentication accuracy were 97.50% from the first image. In the second image, a result of 100% successful authentication was achieved.

5) Iris/Retina authentication: Retina authentication provides unique biometric structure, shape, and specified image specification, and it has one of the longest lifespans of biometric data. A user who authenticates by this method even with glasses or contact lens will still be able to effectively use this process. However, this authentication method may not be well received by cloud computing users. This is because this form of authentication has not been widely practiced and expensive [29]. A multifactor authentication combining fingerprint and iris was formulated [24]. They used a qualitative methodology to enhance the authenticating system for cloud computing users by using finger vein and iris authentication. Their results showed that the finger vein's biometric template cannot be duplicated; hence, this methodology can strengthen security systems compared with other authentication methods.

TABLE III. LAYER(S) OF AUTHENTICATION OF THE ARTICLES SELECTED TO BE REVIEWED

No	Title of article	Layer(s) of authentication	References	Subject
1	A Smooth Textual Password Authentication Scheme Against Shoulder Surfing Attack	*Password authentication* Textual-based	[17]	Textual password users
2	Research And Implementation of Time Synchronous Dynamic Password Based on Sm3 Hash Algorithm	*Password authentication* Textual-based	[38]	Internet users
3	An Empirical Study Examining the Perceptions and Behaviours of Security-Conscious Users of Mobile Authentication	*Password authentication* Textual-based	[41]	20 IT mobile users
4	Encouraging Users to Improve Password Security And Memorability	*Password authentication* Textual-based	[43]	Text-based password users
5	Graphical Password Authentication – Survey	*Password authentication* Graphical	[22]	Computer users
6	Towards Usability Evaluation of Jumbled PassSteps	*Password authentication* Graphical	[39]	30 students from Don Mariano Marcos Memorial State University
7	Biometric Encoding and Biometric Authentication (Beba) Protocol For Secure Cloud in M-Commerce Environment	*Biometric authentication* Fingerprint	[20]	Cloud users

8	Hand-Based Biometric Recognition Technique – Survey	*Biometric authentication* Hand-based	[31]	Mobile banking application users
9	An Efficient and Privacy-Preserving Biometric Identification Scheme in Cloud Computing	*Biometric authentication* Fingerprint	[44]	Cloud computing users
10	Edge-Centric Multimodal Authentication System Using Encrypted Biometric Templates	*Biometric authentication* Facial	[18]	Cloud computing users
11	Student Facial Authentication Model Based on Open Cv's Object Detection Method and Qr Code For Zambian Higher Institutions of Learning	*Biometric authentication* Facial	[43]	3000 students in University of Zambia
12	A Method For User Authenticating to Critical infrastructure Objects Based on Voice Message Identification	*Biometric authentication* Voice	[40]	Cloud computing users
13	Multi-Biometric Authentication Using Deep Learning Classifier for Securing of Healthcare Data	*Multifactor authentication* Biometric (digital signature & fingerprint)	[19]	Patients in medical sector
14	Accomplishment of New Protocol for Stupendous Security in Cloud Environment	*Multifactor authentication* Biometric (fingerprint) & password (textual)	[21]	Cloud computing users (30 different fingerprint with eight different repetitive to compare results)
15	Multi-Biometric Authentication System Using Finger Vein and Iris in Cloud Computing	*Multifactor authentication* Biometric (fingerprint & iris)	[24]	Cloud computing users
16	Cloud Service Security Using Two-Factor or Multi Factor Authentication	*Multifactor authentication* Biometric (digital signature) & password)	[25]	Smartphone users
17	Multifactor Authentication Protocol in a Mobile Environment	*Multifactor authentication* Biometric (fingerprint) & password (login key)	[27]	200 Android users
18	Securing Personal Health Records Using Advanced Multi-Factor Authentication in Cloud Computing	*Multifactor authentication* Password (textual) & biometric (digital signature & iris)	[35]	Patients in hospital
19	Multi-Layered Multimodal Biometric Authentication for Smartphone Devices	*Multifactor authentication* Biometric (fingerprint, facial & voice)	[42]	Smartphone users
20	Access Control Framework Using Multi-Factor Authentication in Cloud Computing	*Multifactor authentication* Biometric (fingerprint) & password (textual & login key)	[30]	Cloud computing users
21	New Robust Biometrics-Based Mutual Authentication Scheme With Key Agreement Using Elliptic Curve Cryptography	*Multifactor authentication* Biometric (fingerprint) & password (login key)	[33]	Single-client server application in mobile environment
22	Anonymous Biometrics-Based Authentication With Key Agreement Scheme for Multi-Server Environment Using Ecc	*Multifactor authentication* Biometric (fingerprint) & password (login key)	[32]	Multi-server environment using ECC
23	Research and Development of User Authentication Using Graphical Passwords: A Prospective Methodology	*Multifactor authentication* Password (Textual & graphical)	[34]	Cloud computing users
24	An Improved and Secure Two-Factor Dynamic ID Based Authenticated Key Agreement Scheme for Multiserver Environment	*Multifactor authentication* Password (server to user & user to server)	[36]	Multi-server environment
25	I-Voting on Cloud Framework	*Multifactor authentication* Biometric (fingerprint & facial) & password (login key)	[23]	Internet voting platform users
26	Analysis of information Security Service for Internet Application	*Multifactor authentication* Biometric (fingerprint) & password (login key)	[37]	Internet application users
27	A Highly Secure Multi- Factor Authentication System Using Biometrics to Enhance Privacy in Internet of Things (IoT)	*Multifactor authentication* Password (textual & login key) & biometric (palm print)	[26]	Internet users
28	Privacy Preserving Biometric Authentication and Identification in Cloud Computing	*Multifactor authentication* Password (login key) & biometric (fingerprint)	[42]	Cloud computing users

6) Voice authentication: Voice authentication is a conversion of a human voice into an electrical signal that can be digitally coded to recognize a user from the coded voice data [60]. People usually speak faster than they write; hence, voice authentication can be considered a time-preserving method. Memon [28] proposed a multifactor biometric authentication including fingerprint, face, and voice for smartphone users. He found that this biometric used in smartphones is more robust and secure compared with single-layered biometric. Additionally, Trysnyuk et. al. [40] proposed a voice message identification method to improve the standard password authentication. It was found that the security of this method can be enhanced by applying another layer of password or biometric authentication.

7) Digital signature authentication: Digital signature is a behavioral biometric which has high acceptance rate and ease in data collection [28]. Digital signature is less cumbersome compared with handwritten signature. It was suggested that a multifactor authentication model was used based on digital signature and password [25]. However, this study found the scheme can only be applied for a small proportion of users. In addition, digital signature was also implemented in a health care system with fingerprint verification [19]. As proposed, the signature verification process has several steps. The main purpose of this signature authentication is to protect patients' health record and to avoid misplacing of their personal data. It was found that the patient's information was highly secured as it increases the system performance rate compared to single-factor authentication. Moreover, combined password, iris verification, and digital signature in their authentication scheme is needed to secure health care records [35]. This scheme comprises key generation and signature encryption stage. The key generation stage creates random number combinations to be used as a private key. Iris features are used because of clear-cut texture of the cornea. This study results show that the multifactor authentication method provides security and confidentiality to health care records. The authors suggested the use of hybrid technologies in the future to enhance health care data security.

- Multiple-factor authentication

Multiple-factor authentication involves two or more phases of authentication and is widely used because it increases the mechanism of data protection compared with single factor authentication. The authors in [27] [37] used two-factor authentication in their proposed scheme combining password verification and fingerprint authentication. Password identification comprises of OTP and secret question, whereas fingerprint authentication is required as a second factor to verify the user's identity. The system will accept or reject authentication based on the fingerprint received during each authentication process. Besides, a scheme using two-factor authentication for the password change process is also proposed [36]. This verification process is a two-way; server to user and user to server. This two-way authentication gives a protected multi-server environment. Another researcher proposed a three-factor authentication (3FA) scheme to be used in a mobile banking environment among 200 Android users [37]. The OTP received must be typed correctly in the provided field and biometric authentication is then used to activate the account with fingerprint access. The authors found that two-factor authentication makes a cloud environment more robust. The concept of mutual authentication scheme key agreement in a single-server environment has been implemented to improve the security [33] [61]. Qi and Chen [32] then introduced an approach through implementation of BAN logic. This project aimed to provide a new method based on mutual authentication that allows use of the same session key. Both studies involve multifactor authentication of fingerprint and textual authentication. Furthermore, Reshma and Shivaprasad [34] combined textual and graphical authentication to provide a better authentication system for cloud computing users and to avoid data breaches. Besides, Balaji and Saravanakumar [21] presented a biometric method using thirty different fingerprints with eight different repetitions along with textual authentication. The results show that the scheme reduces false rejection rate and false acceptance rate.

Then, Yellamma et al. [42] proposed a biometric scheme with registration and verification processes by designing a new coding rule to prevent hackers from attacking the cloud environment. The findings show that the scheme provides higher security from malicious attacks. Moreover, Patel et. al. [30] suggested an authentication model consisting of fingerprint, facial, PIN, and OTP. The results of study were disrupted due to the delay in OTP receiving. This study later suggested improving the method of biometric collection for future studies and the availability of mobile network to effectively receive the OTP. Additionally, Sathishkumar et al. [23] designed an authentication model for online voting. The authentication mode involves fingerprint, facial, and OTP. The advantages of using this proposed voting framework are that the frequency of voting is higher but fewer personnel are required. It is hoped to facilitate a fairer voting system that allows more people to practice their voting rights. Besides, Qi and Chen [33] proposed an authentication consisting of palm print, four-digit user password, and OTP. The results show that this method functions well and provides a lower false rejection ratio. The study aims to work more on the combination of multi-biometric scheme.

V. Conclusion

Based on the discussion above, the summary of the types of authentications reviewed in this paper is presented below (as shown in Figure 3.) Previously, much of the authentication was created based on traditional password i.e. using textual. With the advances in technology, a value can be added to the password authentication by using biometric data, which led to multifactor authentication and a more secure cloud environment. Thus, with the multilayer authentication, it is difficult for hackers to attack the system, especially related to the use of passwords. Further, more awareness on authentication is needed among Internet users to help create a secure online environment. In future, different biometric authentication methods can be combined for greater key encryption, which improves information security. Biometric authentication should also be used whenever there is in need for higher security. OTP can be used to increase surveillance and safety templates, as it changes on the device with each use. In addition, information security awareness should be taught to users so that they know how to safely access the Internet. Future research should combine authentication methods in large-scale studies and increase the sample size for better results. It is also recommended that future studies evolve in a multi-server environment. This systematic review also concluded that no study was done to examine the types of authentication methods being used in Malaysia among Internet users. Most of the studies were found to be in India, China, countries from Middle East, and Europe. Research about authentication method used in Malaysia is highly recommended. This is because Malaysia is one of the leading communication technology countries with almost 89% of its population which is equivalent to 25.4 million Internet users. Future research can propose a secure authentication scheme according to the suitability of subjects of study. We hope this study can provide cloud users with increased awareness of the types and importance of authentication.

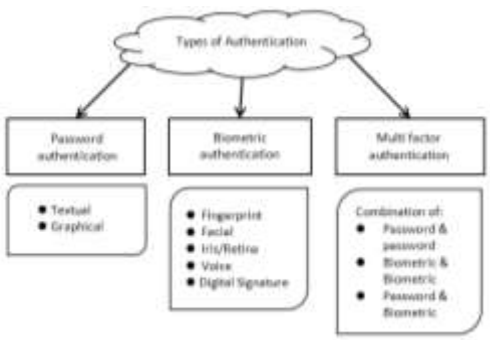

Fig. 3. Summary of Authentication Types.

ACKNOWLEDGMENT

This research was supported by Ministry of Higher Education (MOHE) through Fundamental Research Grant Scheme (FRGS/1/2018/SS09/UPM/02/1/5540161), Project Code 05-01-18-2036FR.

REFERENCES

[1] MyCERT, *Incident Statistics. Reported Incidents Based on General Incident Classification Statistics*, 2021. Available online: https://www.mycert.org.my/portal/statistics-content?menu=b75e037d-6ee3-4d11-8169-66677d694932&id=2650ed29-88be-4cec-86cc-13f8e07ae228 (accessed on 24 March 2021).

[2] Omar, Siti Zobidah, Raidah Mazuki, Jusang Bolong, Jeffrey Lawrence D'Silva, and Hayrol Azril Mohamed Shaffril, "Pattern of Internet Usage at the Rural Library among Rural Youth in Malaysia," *Mediterranean Journal of Social Sciences*, vol. 7, 2016.

[3] Segura-Robles, Adrián, Antonio-José Moreno-Guerrero, María-Elena Parra-González, and Jesús López-Belmonte, "Review of Research Trends in Learning and the Internet in Higher Education," *Social Sciences*, vol. 9, no. 6, pp. 101, 2020.

[4] Akingbade, Luisa, "Cloud storage problems, benefits and solutions provided by data de-duplication," *International Journal of Engineering and Innovative Technology*, vol. 5, no. 6, pp. 70-77, 2016.

[5] Ungurean, Ioan, and Nicoleta Cristina Gaitan, "Software Architecture of a Fog Computing Node for Industrial Internet of Things," *Sensors*, vol. 21, no. 11, pp. 3715, 2021.

[6] Jain, Anil, Arun Ross, and Salil Prabhakar, "An introduction to biometric recognition," *IEEE Transactions on circuits and systems for video technology*, vol. 14, pp. 4-20, 2004.

[7] Kadam, Yashpal, "Security Issues in Cloud Computing A Transparent View," *International Journal of Computer Science Emerging Technology*, vol. 2, pp. 316-322, 2011.

[8] Pitchan, Muhammad Adnan, Siti Zobidah Omar, Jusang Bolong, and Akmar Hayati Ahmad Ghazali, "Amalan Keselamatan Siber Pengguna Internet Terhadap Buli Siber, Pornografi, E-Mel Phishing Dan Pembelian Dalam Talian," *Jurnal Komunikasi: Malaysian Journal of Communication*, vol. 35, pp. 212–227, 2019.

[9] Bishop, Matt, Essay. *In Computer Security: Art and Science*. Boston: Addison-Wesley, 2012.

[10] Lal, Nilesh A, Salendra Prasad, and Mohammed Farik, "A review of authentication methods," *International Journal of Scientific & Technology Research*, vol. 5, pp. 246-249, 2016.

[11] Pitchan, Muhammad Adnan, Siti Zobidah Omar, Jusang Bolong, and Akmar Hayati Ahmad Ghazali, "Analysis of Cyber Security from the Perspective of Social Environment: A Study of Internet Users in Klang Valley," *Journal of Social Sciences and Humanities*, vol. 12, pp. 16-29, 2017.

[12] Brandao, Pedro Ramos, "The Importance of Authentication and Encryption in Cloud Computing Framework Security," *International Journal on Data Science and Technology*, vol. 4, no. 1, pp. 1-5, 2018.

[13] Vouk, Mladen A, "Cloud Computing - Issues, Research and Implementations," *Journal of Computing and Information Technology*, vol. 16, no. 4, pp. 235-246, 2008.

[14] Petrosino, Anthony, Robert F. Boruch, Haluk Soydan, Lorna Duggan, and Julio Sanchez-Meca, "Meeting the Challenges of Evidence-Based Policy: The Campbell Collaboration," *The ANNALS of the American Academy of Political and Social Science*, vol.578, no. 1, pp. 14-34, 2001.

[15] Baumeister, Roy F, "*Writing a Literature Review*," In The portable mentor: Expert guide to a successful career in psychology. Edited by Mitchell J Prinstein. North Carolina, USA: Springer, pp. 119-132, 2013.

[16] Sa'di, Mustapa Mursilalaili, Abdul Rani Kamarudin, Duryana Mohamed, and Zulfakar Ramlee, "Authentication of electronic evidence in cybercrime cases based on Malaysian laws," *Pertanika Journal of Social Science and Humanities*, vol. 23, pp. 153-168, 2015.

[17] Al-Husainy, Mohammed A. Fadhil, and Diaa M. Uliyan, "A Smooth Textual Password Authentication Scheme Against Shoulder Surfing Attack," *Journal of Theoretical & Applied Information Technology*, vol. 96, no. 9, pp. 2546-2556, 2018.

[18] Ali, Zulfiqar, M. Shamim Hossain, Ghulam Muhammad, Ihsan Ullah, Hamid Abachi, and Atif Alamri, "Edge-Centric Multimodal Authentication System Using Encrypted Biometric Templates," *Future Generation Computer Systems*, vol. 85, pp. 76-87, 2018.

[19] Amirthalingam, Gandhimathi, and Harrin Thangavel, "Multi-Biometric Authentication Using Deep Learning Classifier for Securing of Healthcare Data," *International Journal of Advanced Trends in Computer Science and Engineering*, vol. 8, pp. 1340–1347, 2019.

[20] ArunPrakash, R., T. Jayasankar, and K. Vinothkumar, "Biometric Encoding and Biometric Authentication (Beba) Protocol for Secure Cloud in M-Commerce Environment," *Applied Mathematics & Information Sciences*, vol. 12, no. 1, pp. 255-263, 2018.

[21] Balaji, S, and S Saravanakumar, "Accomplishment of New Protocol for Stupendous Security in Cloud Environment," *International Journal of Innovative Technology and Exploring Engineering*, vol. 9, no. 1, pp. 2616-2619, 2019.

[22] Bhootwala, Jasmin P., and Pravin H. Bhathawala, "Graphical Password Authentication - Survey," *Global Journal For Research Analysis*, vol. 9, no. 2, pp. 31-35, 2020.

[23] D, Sathishkumar, SureshAnand M, JeganAmarnath J, SangeeraniDevi A, and Gurusubramani S. "I-Voting on Cloud Framework," *International Journal of Engineering and Advanced Technology*, vol. 9, no. 1S, pp. 61-64, 2019.

[24] Ilankumaran, S., and C. Deisy, "Multi-Biometric Authentication System Using Finger Vein and Iris in Cloud Computing," *Cluster Computing*, vol. 22, no. S1, pp. 103-117, 2018.

[25] Luckose, Jubin, Sameer Chindarkar, and Dhanamma Jagli, "Cloud Service Security using Two-factor or Multi factor Authentication," *International Research Journal of Engineering and Technology*, vol. 4, pp. 2066-2070, 2017.

[26] M, Vijay, and Indumathi G, "A Highly Secure Multi- Factor Authentication System Using Biometrics to Enhance Privacy in Internet of Things (IOT)," *International Research Journal of Multidisciplinary Technovation*, vol. 1, no. 6, pp. 26-34, 2019.

[27] Maciej, Bartlomiejczyk, El Fray Imed, and Miroslaw Kurkowski, "Multifactor Authentication Protocol in a Mobile Environment," *IEEE Access*, vol. 7, pp. 157185–157199, 2019.

[28] Memon, Qurban A, "Multi-Layered Multimodal Biometric Authentication for Smartphone Devices," *International Journal of Interactive Mobile Technologies (iJIM)*, vol. 14, no. 15, pp. 222, 2020.

[29] Musambo, Lubasi Kakwete, and Jackson Phiri, "Student Facial Authentication Model Based on OpenCV's Object Detection Method and QR Code for Zambian Higher Institutions of Learning," *International Journal of Advanced Computer Science and Applications*, vol. 9, no. 5, pp. 88-94, 2018.

[30] Patel, Subhash Chandra, Sumit Jaiswal, Ravi Shankar Singh, and Jyoti Chauhan, "Access Control Framework Using Multi-Factor Authentication in Cloud Computing," *International Journal of Green Computing*, vol. 9, no. 2, pp. 1-15, 2018.

[31] Prihodova, Katerina, and Miloslav Hub, "Hand-Based Biometric Recognition Technique – Survey," *Advances in Science, Technology and Engineering Systems Journal*, vol. 5, no. 6, pp. 689–698, 2020.

[32] Qi, Mingping, and Jianhua Chen, "Anonymous Biometrics-Based Authentication with Key Agreement Scheme for Multi-Server Environment Using ECC," *Multimedia Tools and Applications*, vol. 78, no. 19, pp. 27553–27568, 2019.

[33] Qi, Mingping, and Jianhua Chen, "New Robust Biometrics-Based Mutual Authentication Scheme with Key Agreement Using Elliptic Curve Cryptography," *Multimedia Tools and Applications*, vol. 77, no. 18, pp. 23335–23351, 2018.

[34] Reshma, and Shivaprasad G., "Research and Development of User Authentication Using Graphical Passwords: A Prospective Methodology," *International Journal of Innovative Technology and Exploring Engineering*, vol. 8, no. 9S3, pp. 385–390, 2019.

[35] S, Meena, and Gayathri V., "Securing Personal Health Records Using Advanced Multi-Factor Authentication in Cloud Computing," *International Journal of Recent Technology and Engineering*, vol. 8, no. 6, pp. 5133–5140, 2020.

[36] Sahoo, Shreeya Swagatika, Sujata Mohanty, and Banshidhar Majhi, "An Improved and Secure Two-Factor Dynamic ID Based Authenticated Key Agreement Scheme for Multiserver Environment," *Wireless Personal Communications*, vol. 101, no. 3, pp. 1307–1333, 2018.

[37] Shanker, Ravi, Sahil Verma, and Kavita, "Analysis of Information Security Service for Internet Application," *International Journal of Engineering & Technology*, vol. 7, no. 4, pp. 58-62, 2018.

[38] Silue, Dognery Sinaly, Wanggen Wan, and Muhammad Rizwan, "Research and Implementation of Time Synchronous Dynamic Password Based on SM3 Hash Algorithm," *Open Journal of Applied Sciences*, vol. 6, no. 13, pp. 893–902, 2016.

[39] Songcuan, Jerome P., Ariel M Sison, Ruji Medina, "Towards Usability Evaluation of Jumbled PassSteps," *International Journal of Advanced Trends in Computer Science and Engineering*, vol. 8, pp. 1032–1037, 2019.

[40] Trysnyuk, Vasyl, Yevhen Nagornyi, Kirill Smetanin, Igor Humeniuk, and Tetyana Uvarova, "A Method For User Authenticating To Critical Infrastructure Objects Based On Voice Message Identification," *Advanced Information Systems*, vol. 4, no. 3, pp. 11-16, 2020.

[41] Wolf, Flynn, Ravi Kuber, and Adam J Aviv, "An Empirical Study Examining the Perceptions and Behaviours of Security-Conscious Users of Mobile Authentication," *Behaviour & Information Technology*, vol. 37, no. 4, pp. 320-334, 2018.

[42] Yellamma, Pachipala, Rajesh P.S.S., Pradeep V.V.S.M., Manishankar Y.B., "Privacy Preserving Biometric Authentication and Identification in Cloud Computing," *International Journal of Advanced Science and Technology*, vol. 29, pp. 3087-3096, 2020.

[43] Yildirim, M., and I. Mackie, "Encouraging Users to Improve Password Security and Memorability," *International Journal of Information Security*, vol. 18, no. 6, pp. 741–759, 2019.

[44] Zhu, Liehuang, Chuan Zhang, Chang Xu, Ximeng Liu, and Cheng Huang, "An Efficient and Privacy-Preserving Biometric Identification Scheme in Cloud Computing," *IEEE Access*, vol. 6, pp. 19025–19033, 2018.

[45] Page, Matthew, Joanne McKenzie, Patrick Bossuyt, Isabelle Boutron, Tammy Hoffmann, Cynthia Mulrow, Larissa Shamseer, et al., "The PRISMA 2020 Statement: An Updated Guideline for Reporting Systematic Reviews," *PLOS Medicine*, vol. 18, no. 3, pp. e1003583, 2021.

[46] Meier, Kennedy, Jacqueline Parrish, and Rohan D'Souza, "Prediction Models for Determining the Success of Labor Induction: A Systematic Review," *Acta Obstetricia et Gynecologica Scandinavica*, vol. 98, no. 9, pp. 1100–1112, 2019.

[47] Wolff, Robert F., Karel G.M. Moons, Richard D. Riley, Penny F. Whiting, Marie Westwood, Gary S. Collins, Johannes B. Reitsma, Jos Kleijnen, and Sue Mallett, "PROBAST: A Tool to Assess the Risk of Bias and Applicability of Prediction Model Studies," *Annals of Internal Medicine*, vol. 170, no. 1, pp. 51-58, 2019.

[48] Abuarqoub, Abdelrahman, "D-FAP: Dual-Factor Authentication Protocol for Mobile Cloud Connected Devices," *Journal of Sensor and Actuator Networks*, vol. 9, no. 1, pp. 1-23, 2019.

[49] Lalitha, Krishnan, Subramanian Vaithyasubramanian., K Vengatakrishnan, A Christy, and M Metilda, "A Novel Authentication Procedure for Secured Web Login Using Coloured Petri Net," *International Journal of Simulation: Systems, Science & Technology*, vol. 19, 2019.

[50] Shin, Sanggyu, and Yoichi Seto, "Security improvement of biometric authentication systems at cancelable biometrics," *Information (Japan)*, vol. 19, pp. 505-513, 2016.

[51] Thakur Priyanka, Ravishanker, and Ashish K Luhach, "Personal data access control based on trust and reputation in cloud computing," *International Journal of Control Theory and Applications*, vol. 9, pp. 5263-5270, 2016.

[52] Yoshida, Atsumasa, "The measures applied internally by the NEC Group to forestall and prevent cybersecurity incidents," *NEC Technical Journal*, vol. 12, pp. 29-33, 2018.

[53] Curran, Kevin, Jonathan Doherty, Ayleen McCann, and Gary Turkington, "Good Practice for Strong Passwords," *The EDP Audit, Control, and Security Newsletter*, vol. 44, no. 5, pp. 1-13, 2011.

[54] Wiedenbeck, Susan, Jim Waters, Jean-Camille Birget, Alex Brodskiy, and Nasir Memon, "Authentication Using Graphical Passwords," in *Proceedings of the 2005 symposium on Usable privacy and security - SOUPS '05*, vol. 93, pp. 1-12, 2005.

[55] Fong, Teoh Joo, Azween Abdullah, N. Z. Jhanjhi, and Mahadevan Supramaniam, "The Coin Passcode: A Shoulder-Surfing Proof Graphical Password Authentication Model for Mobile Devices," *International Journal of Advanced Computer Science and Applications (IJACSA)*, vol. 10, no. 1, pp. 302-308, 2019.

[56] Al-Husainy, Mohammed A. Fadhil, and Raghda Ahmed Malih, "Using Emoji Pictures to Strengthen the Immunity of Passwords against attackers," *European Scientific Journal*, vol. 11, no. 30, pp. 153-165, 2015.

[57] Hodge, Edwin, Helga Hallgrimsdottir, and Marianne Much, "Performing Borders: Queer and Trans Experiences at the Canadian Border," *Social Sciences*, vol. 8, no. 7, 2019.

[58] Bharadi, Vinayak Ashok, "Texture Feature Extraction For Biometric Authentication using Partitioned Complex Planes in Transform Domain," *International Journal of Advanced Computer Science and Applications(IJACSA)*, vol. 2, no. 1, pp. 39-46, 2012.

[59] Jain, Anil, Lin Hong, and Sharath Pankanti, "Biometric identification," *Communications of the ACM*, vol. 43, pp. 90-98, 2000.

[60] Tripathi, K P., "A Comparative Study of Biometric Technologies with Reference to Human Interface," *International Journal of Computer Applications*, vol. 14, no. 5, pp. 10-15, 2011.

[61] Chaudhry, Shehzad Ashraf, Husnain Naqvi, and Muhammad Khurram Khan, "An Enhanced Lightweight Anonymous Biometric Based Authentication Scheme for TMIS," *Multimedia Tools and Applications*, vol. 77, no. 5, pp. 5503–5524, 2018.

Development of Learning Analytics Dashboard based on Moodle Learning Management System

Ong Kiat Xin[1], Dalbir Singh[2]
Center for Software Technology and Management (SOFTAM)
Faculty of Information Science and Technology, Universiti Kebangsaan Malaysia
Acronyms Acceptable, Bangi, Malaysia

***Abstract*—Digitalization catalyzes drastic changes to a particular subject or area. Digitalization is an operational structure transformation process, such as in the educational domain. Digitalization in the academic field has brought the classroom to the users' fingertips with the prevalence of e-learning applications, learning management systems, etc. However, with the increasing number of digital learning platform users, educators find it hard to monitor their students' progress. Analytics that analyze data generated from the usage pattern of the users contribute to giving the educators an insight regarding the performance of their students. With that, they can apply early intervention and modification of their delivery method to suit the students' needs and, at the same time, increase the quality of the content. This study illustrates the development of a learning analytics dashboard that can improve learning outcomes for educators and students.**

***Keywords*—Learning analytics; learning management system; moodle**

I. Introduction

Learning Management System (LMS) is a software application developed for the administration, tracking, reporting, and delivery of educational courses and contents [1]. There are various LMS(s) to choose from in the market; for example, Moodle is the most widely used LMS. LMS utilizes the internet as an extension of learning, allowing users to access the content anytime and anywhere. With more learning activities conducted online, obtaining relevant and accurate data from these activities has become more important for educators to monitor their students' performance [2]. However, some existing analytics dashboards available on the market do not present accurate and relevant data for educators to understand their students' performance [3]. Purposely, an analytics dashboard is expected to indicate the attainment of the learning outcomes by the learners and triggers continuous improvement in the delivery and assessment method. Therefore, it is vital to develop a dashboard that displays accurate and relevant data that could provide insight for learners, educators and relevant stakeholders, which could eventually improve the overall learning process.

In this study, the analytics dashboard development approach has been proposed. Firstly, the back-end of the analytics dashboard has been designed and developed so that accurate and relevant data can be displayed on the dashboard. Secondly, a straightforward and easy-to-use interface has been created to allow users to read data easily. The analytics dashboard has been designed to fulfil the need in order to obtain relevant and meaningful data from a data source so that educators can better understand their students' performance [4]. There are three (3) main sections that focus on (a) review relevant studies and related analytics dashboards, (b) analytics dashboard requirement, and (c) proposed analytics dashboard design that constructs the proposed learning analytics dashboard as the contribution of study which outlines relevant data visualization strategy.

II. Review of Relevant Studies and Related Analytics Dashboards

This section discusses relevant previous studies and related analytics dashboards. It comprises the following three (3) sections that focus on Moodle LMS, data analytics, and a review of a corresponding analytics dashboard. It aims to provide a fundamental understanding of the related area and prepares for a review of data visualization and dashboard design in the subsequent section.

A. Moodle LMS

Moodle LMS is a web-based system specifically developed to complement traditional learning methods that allow users to attend courses, submit assignments, and many more online. Moodle LMS is an open-source learning management system developed using PHP programming language and was first released in 2002. With the increasing demand and usage of online learning, Moodle now has more than 278 million registered users in 2021 [5].

Moodle LMS is designed to support teaching and learning with over ten (10) years of development guided by social constructionist pedagogy [6]. Moodle LMS has a simple interface with drag-and-drop features and well-documented resources along with ongoing usability improvements. Moodle LMS has very high flexibility and scalability that can be customized to support the needs of both small classes and large organizations.

B. Data Analytics for Moodle LMS

Data analytics is the process of analyzing raw data to conclude the information contained in them. Valuable insights can be extracted from data analytics to assist users in planning and taking actions [7]. Data analytics can be divided into four categories: descriptive analytics, diagnostic analytics, predictive analytics, and prescriptive analytics [8]. Descriptive analytics contributes to showing the value of measured metrics and what had happened in a specified period. Descriptive analytics process raw data from data sources to give valuable insights into the past. Implementing descriptive analytics in the learning analytics dashboard would allow the educators to understand their students' performance trends and identify any issues. Diagnostic analytics is the next step of complexity in data analytics. While assessing the descriptive data, diagnostic, analytical tools allow the analyst to drill down and isolate the root cause of a problem. Diagnostic analytics gives in-depth insights into a particular problem on why the problem occurred.

Predictive analytics is advanced analytics that brings many advantages, such as sophisticated analysis based on machines or deep learning. It is a proactive approach that enables predictions. Predictive analytics contributes to providing a forecast of what is likely to happen. Predictive analytics utilizes descriptive and diagnostic analytics findings to detect clusters and exceptions and predict future trends. Predictive analytics is a valuable tool for forecasting. Prescriptive analytics is sophisticated analytics that utilizes machine learning and algorithms to prescribe a possible action that can be taken to eliminate a future problem.

Therefore, four types of analytics can be implemented into the analytics dashboard for Moodle LMS. Most commercial solutions available in Moodle LMS are descriptive analytics [6]. Moodle LMS provides various built-in reporting tools based on log data; however, they are primarily illustrative. Third-party developers can develop learning analytics dashboards that emphasize diagnostic and prescriptive analytics to understand the cause of events and figure out solutions to improve learning outcomes.

C. Review of Relevant Analytics Dashboard for Moodle LMS

It has become a challenge for developers to design an analytics dashboard that suits the needs in the educational domain to process the data generated by online learning activities [2]. Each analytics dashboard has features that do not necessarily fulfil every user's requirement [9]. The design of the analytics dashboard can be varied, depending on the implementation of the developer. Providing a simple easy-to-read dashboard is very important.

In our study, three (3) analytics dashboards have been chosen: Piwik Analytics, Blocks: Progress Bar, and Blocks: Analytics Graph. These analytics dashboards were selected to be most actively updated in the Moodle LMS plug-in library [6]. Fig. 1, Fig. 2, and Fig. 3 shows three (3) examples of the analytics dashboard available as Moodle LMS plug-in. As shown in Fig. 1, Piwik Analytics provides reporting in the form of a comparative table. Data such as page views, bounce rate, and average generation time are recording to provide an overview for the user to understand their contents hit rate.

As shown in Fig. 2, Blocks: Progress Bar is a reporting tool that reports on the students' progress. The users can gather information regarding the progression of the students.

As shown in Fig. 3, Blocks: Analytics Graph shows the distribution of the hits of the course content in the form of a line graph. Similar to Piwik Analytics in Fig. 1, the contents accessed rate of the students shown in the chart that allows the user to develop an overview of the course contents access rate.

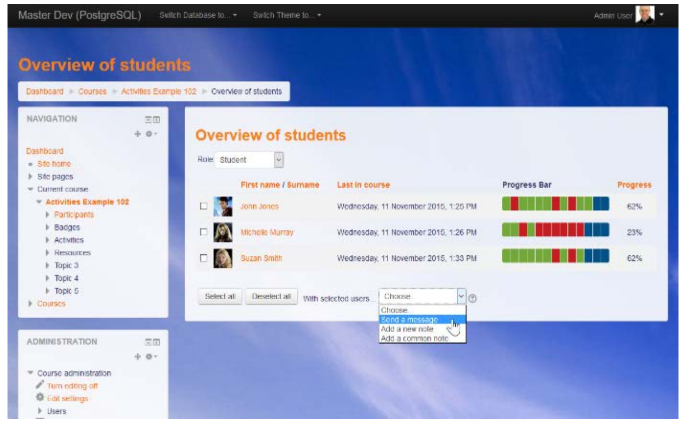

Fig. 1. Piwik Analytics

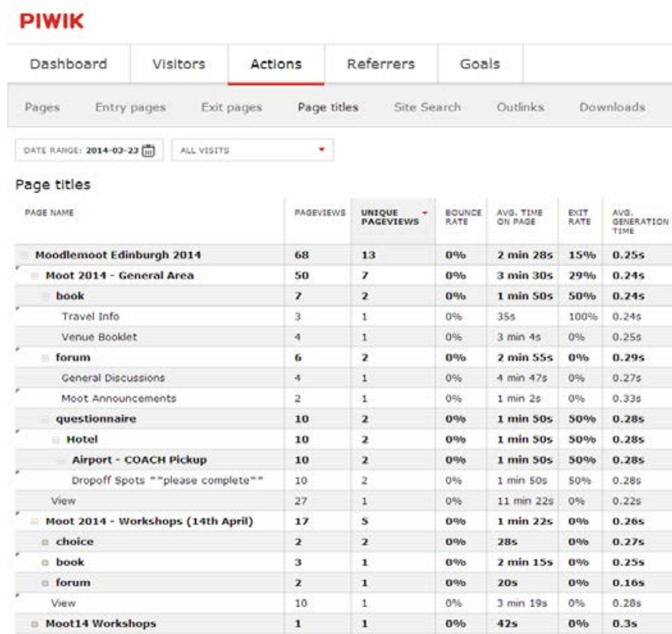

PAGE NAME	PAGEVIEWS	UNIQUE PAGEVIEWS	BOUNCE RATE	AVG. TIME ON PAGE	EXIT RATE	AVG. GENERATION TIME
Moodlemoot Edinburgh 2014	68	13	0%	2 min 28s	15%	0.25s
Moot 2014 - General Area	50	7	0%	3 min 30s	29%	0.24s
book	7	2	0%	1 min 50s	50%	0.24s
Travel Info	3	1	0%	35s	100%	0.24s
Venue Booklet	4	1	0%	3 min 4s	0%	0.25s
forum	6	2	0%	2 min 55s	0%	0.29s
General Discussions	4	1	0%	4 min 47s	0%	0.27s
Moot Announcements	2	1	0%	1 min 2s	0%	0.33s
questionnaire	10	2	0%	1 min 50s	50%	0.28s
Hotel	10	2	0%	1 min 50s	50%	0.28s
Airport - COACH Pickup	10	2	0%	1 min 50s	50%	0.28s
Dropoff Spots ""please complete""	10	2	0%	1 min 50s	50%	0.28s
View	27	1	0%	11 min 22s	0%	0.22s
Moot 2014 - Workshops (14th April)	17	5	0%	1 min 22s	0%	0.26s
choice	2	2	0%	28s	0%	0.27s
book	3	1	0%	2 min 15s	0%	0.25s
forum	2	1	0%	20s	0%	0.16s
View	10	1	0%	3 min 19s	0%	0.28s
Moot14 Workshops	1	1	0%	42s	0%	0.3s

Fig. 2. Blocks: Progress Bar.

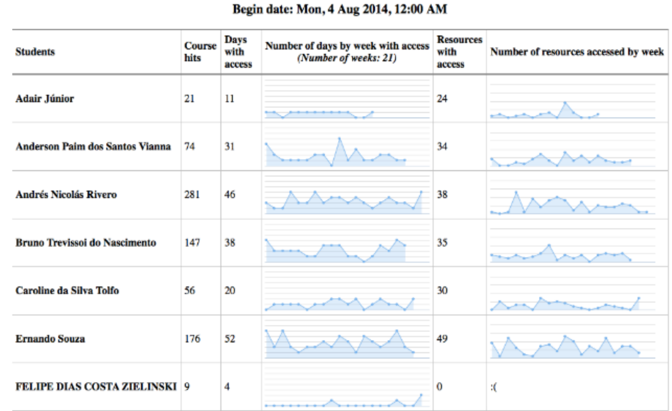

Hits distribution

Course: 2014/2 - Roteamento - Prof. Marcelo

Begin date: Mon, 4 Aug 2014, 12:00 AM

Students	Course hits	Days with access	Number of days by week with access *(Number of weeks: 21)*	Resources with access	Number of resources accessed by week
Adair Júnior	21	11		24	
Anderson Paim dos Santos Vianna	74	31		34	
Andrés Nicolás Rivero	281	46		38	
Bruno Trevissoi do Nascimento	147	38		35	
Caroline da Silva Tolfo	56	20		30	
Ernando Souza	176	52		49	
FELIPE DIAS COSTA ZIELINSKI	9	4		0	:(

Fig. 3. Blocks: Analytics Graph.

Based on the comparative analysis of the common features available in these dashboards, a comparison table is tabulated, as shown in Table I. The finding based on Table I reveals that assignment progress and learning progress can be considered as common features between these analytics dashboards. Indirectly, assignment progress and learning progress are essential features for any learning analytics dashboard [10].

TABLE I. COMPARISON BETWEEN EXISTING DASHBOARDS

Features (Measuring Metrics)	***Piwik Analytics***	***Blocks: Progress Bar***	***Blocks: Analytics Graph***
User active time	Yes	No	Yes
Assignment Progress	No	Yes	Yes
Learning Progress	No	Yes	Yes
Marks	No	No	Yes
Assignments Submission	No	No	Yes
Contents Hit Count	Yes	No	No

III. LEARNING ANALYTICS DASHBOARD REQUIREMENTS

User requirements have to be fulfilled to achieve the objective of developing the analytics dashboard. The primary user base of the analytics dashboard focuses on the educators who use a learning management system such as Moodle as part of their teaching medium. The analytics dashboard will become a tool for them to monitor their student's progress quickly and efficiently.

Various types of assessment can be implemented in LMS [11]. Our study revealed that assignments handouts using LMS are common usages of LMS in modern learning. Tracking a student's assignment has become more important for educators to keep track of their students. Knowing the performance of their students allows educators to decide on how to improve the outcome.

Learning progress reporting is also an essential element in a learning analytics dashboard. A learning analytics dashboard that has both the educator-facing dashboard and student-facing dashboard is an ideal implementation [10]. The educator-facing dashboard allows the educators to understand the progress report of their students and helps the educators develop an overview of their courses and identify students with low performance. On the other hand, the students-facing dashboard allows the students to keep track of their progress, which helps them increase their self-awareness of their performance.

The learning analytics dashboard is designed to extract data from the data source and convert the data into meaningful data visualization. The data visualization allows the users to understand the information that is shown in the analytics better. Key data visualization charts in the analytics dashboard include marks of students' assignments, quizzes, attendance, project marks, and, most importantly, their progress in terms of learning outcomes.

The system model of the analytics dashboard only involved three main entities: Moodle LMS, the analytics dashboard, and the users. Data is generated continuously from online activities held in Moodle LMS, such as online quizzes and online assignments. The information is then stored in the Moodle LMS server. The data is then downloaded and converted into a readable format of the analytics dashboard. Once the data is uploaded to the analytics dashboard, the back-end system of the analytics dashboard will automatically convert the data into data visualization, such as a table, line charts, and bar charts. The users can interact with the dashboard after the data visualization.

IV. PROPOSED LEARNING ANALYTICS DASHBOARD DESIGN

The design specification of the analytics dashboard is influenced by the objective and the current design trend. The design specification of a system that will be developed is important because the users' workflow is affected by design. The analytics dashboard is created as a web application using Python and Dash framework. This approach allows the developer to better focus on data visualization as the Dash framework in Python is specialized in data visualization. Besides, developing the system as a web application is more productive as users do not need to install the software; they can view the dashboard using any web browser. Fig. 4 shows an example of an analytics dashboard design that can be implemented.

The design of the analytics dashboard has to produce data visualization with simplicity so that the users can read the data accordingly when there is a lot of data. Implementing personalized options and interaction in the dashboard is preferable for a better user experience [12]. The back-end of the analytics dashboard is designed so that the data obtained from the data source can be converted into data visualization. One of the approaches our study has revealed is that the analytics dashboard can be developed using the Dash framework in Python. The end product will be a web-based analytics dashboard that can be accessed using any web browser. The main component of the analytics dashboard is the interface. The dashboard will display all the data visualization in a scrollable manner. The users can glance through all of the data quickly. Fig. 5 shows the name list of all the students in a certain course in a table that can be implemented in the dashboard. The table provides a simple overview of the student's performance in a specific course.

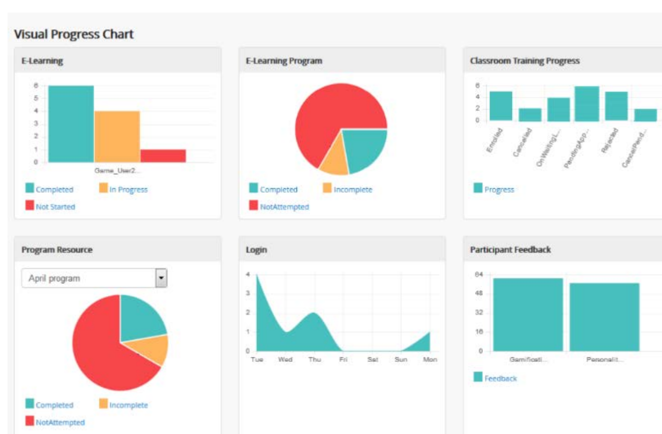

Fig. 4. A Design Example of an Analytics Dashboard.

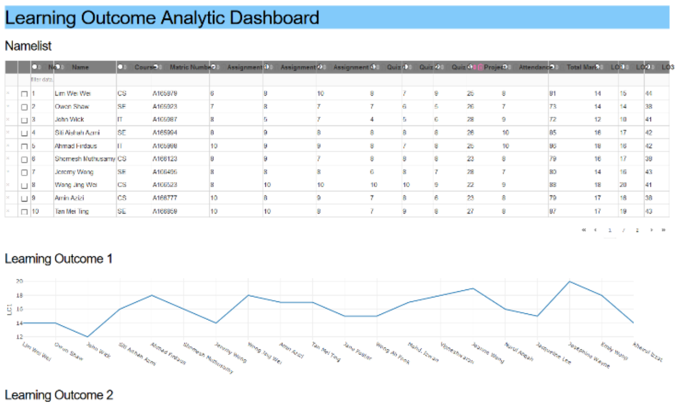

Fig. 5. The Interface of the Analytics Dashboard.

Moreover, the analytics dashboard also shows the students' achievement in terms of learning outcomes in a line graph. This type of data visualization provides a simple explanation of the performance of the student. The users can know the highest performer as well as the lowest. Fig. 6 shows the line graphs shown in the analytics dashboard.

The other data visualization available in the analytics dashboard includes the bar chart. The bar charts show the individual mark of each student in terms of assignments, quizzes, attendance, and their total marks. Fig. 7 and 8 show the bar charts that are shown in the analytics dashboard. The bar charts allow the users to read the progress trend of each student in each measuring metric.

Other than data visualization, analytics dashboards that allow users to interact will provide a better user experience. Fig. 9 shows the selected students in the table. The users can pick whichever student they want in the table on top of the analytics dashboard. The chosen students will be highlighted in Fig. 10, 11 and 12. This provides the users with convenience when reading the data.

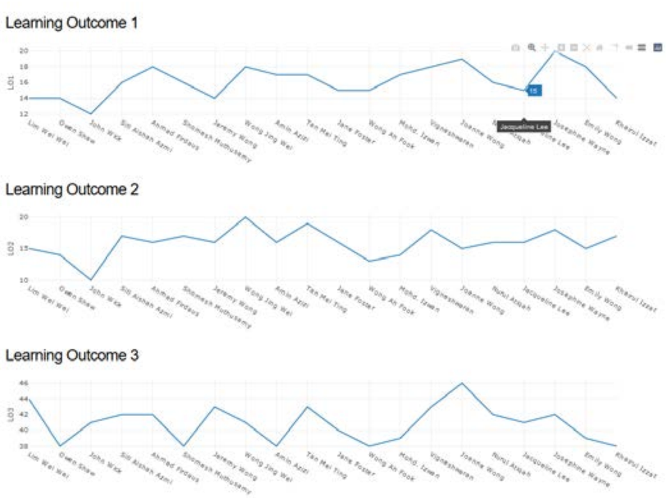

Fig. 6. Example Line Graphs.

Fig. 7. Example Bar Charts 1.

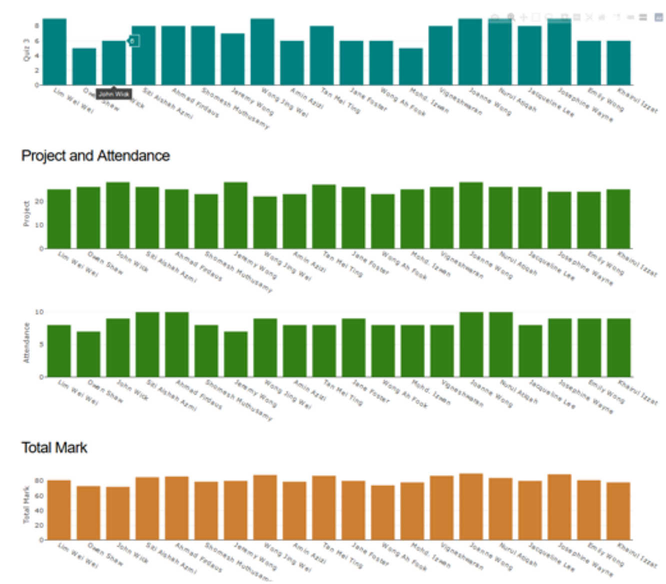

Fig. 8. Example Bar Charts 2.

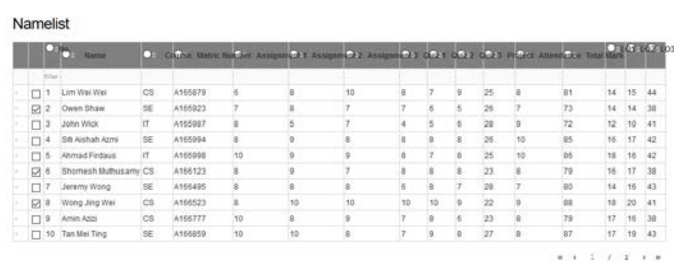

No.	Name	Course	Matric Number	Assignment 1	Assignment 2	Assignment 3	Quiz 1	Quiz 2	Quiz 3	Project	Attendance	Total Mark	LO1	LO2	LO3
1	Lim Wei Wei	CS	A165879	6	8	10	8	7	9	25	8	81	14	15	44
2	Owen Shaw	SE	A165923	7	8	7	7	6	5	26	7	73	14	14	38
3	John Wick	IT	A165987	8	5	7	4	5	6	28	9	72	12	10	41
4	Siti Aishah Azmi	SE	A165994	8	9	8	8	8	8	26	10	85	16	17	42
5	Ahmad Firdaus	IT	A165998	10	9	9	8	7	8	25	10	86	18	16	42
6	Shomesh Muthusamy	CS	A166123	8	9	7	8	8	8	23	8	79	16	17	38
7	Jeremy Wong	SE	A166495	8	8	8	6	8	7	28	7	80	14	16	43
8	Wong Jing Wei	CS	A166523	8	10	10	10	10	9	22	9	88	18	20	41
9	Amin Azizi	CS	A166777	10	8	9	7	8	6	23	8	79	17	16	38
10	Tan Mei Ting	SE	A166859	10	10	8	7	9	8	27	8	87	17	19	43

Fig. 9. Selected Students.

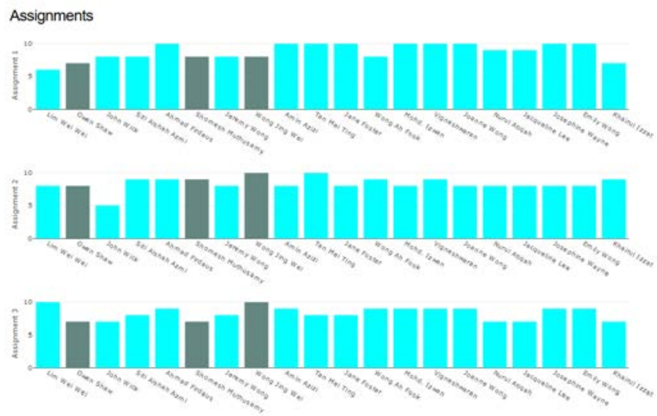

Fig. 10. Highlighted Students in Assignment.

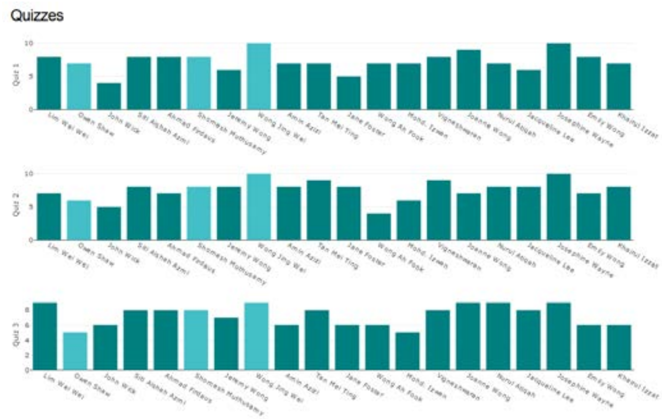

Fig. 11. Highlighted Students in Quizzes.

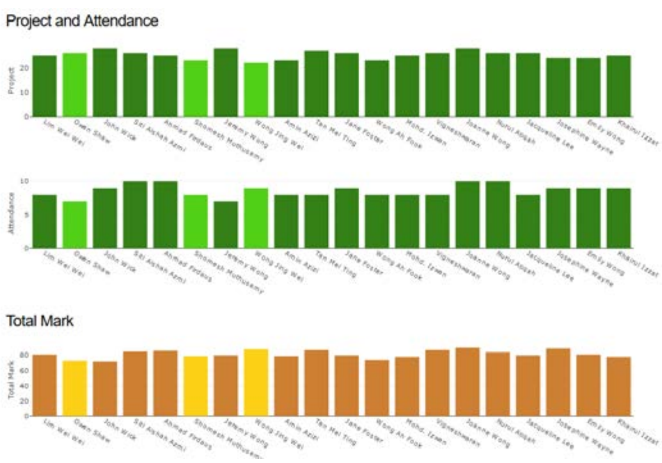

Fig. 12. Highlighted Students in Project and Attendance.

V. Conclusion

In conclusion, the study has provided an extensive view of the approach when developing a learning analytics dashboard that can be implemented within Moodle LMS. A well-designed analytics dashboard will allow educators to understand better the data collected by the LMS through online learning activities [13]. Meaningful insights obtained from the analytics will help educators to understand the performance of their students [14] [15] [16]. Descriptive analytics will allow educators to monitor the performance of their students in a specific period. In contrast, more complex analytics such as diagnostic and prescriptive analytics will explain the cause of events and actions to improve the situations. Thus, such implication has the potential for future research work which could benefit educators and learners [17] [18] [19] [20] [21]. Furthermore, studies investigating novel and innovative methods for measuring learning outcomes attainment, especially for online learning during COVID-19 pandemic era, have caught the attention of various researchers [22] [23]. Thus, this triggers the development of a learning analytics dashboard, particularly for Moodle, as it is the most widely used LMS.

Acknowledgment

The researchers would like to express their highest gratitude towards Universiti Kebangsaan Malaysia's research grant: GGP-2019-026.

References

[1] A. K. Alhazmi and A. A. Rahman, "Why LMS failed to support student learning in higher education institutions," IEEE Symposium. E-Learning, E-Management E-Services, pp. 1–5, October 2012.

[2] H. Aldowah, H. Al-Samarraie, and W. M. Fauzy, "Educational data mining and learning analytics for 21st century higher education: A review and synthesis," Telematics and Informatics, vol. 37, pp. 13–49, April 2019.

[3] O. Viberg, M. Hatakka, O. Bälter, and A. Mavroudi, "The current landscape of learning analytics in higher education," Computers in Human Behavior, vol. 89, pp. 98–110, December 2018.

[4] N.-S. Chen, C. Yin, P. Isaias, and J. Psotka, "Educational big data: extracting meaning from data for smart education," Interactive Learning Environments, vol. 28, no. 2, pp. 142–147, February 2020.

[5] Moodle, "Moodle Statistics," Moodle, 2021. [Online]. Available: https://stats.moodle.org/. [Accessed: 25-July-2021].

[6] Moodle, "Moodle Documentation," Moodle, 2020. [Online]. Available: https://docs.moodle.org/39/en/About_Moodle. [Accessed: 11-Aug-2020].

[7] G. Elia, G. Polimeno, G. Solazzo, and G. Passiante, "A multi-dimension framework for value creation through Big Data," Industrial Marketing Management, vol. 20, pp. 508–522, October 2020.

[8] N. Nistor and Á. Hernández-Garcíac, "What types of data are used in learning analytics? An overview of six cases," Computers in Human Behavior, vol. 89, pp. 335–338, December 2018.

[9] D. Gašević, S. Dawson, T. Rogers, and D. Gasevic, "Learning analytics should not promote one size fits all: The effects of instructional conditions in predicting academic success," The Internet and Higher Education, vol. 28, pp. 68–84, January 2016.

[10] H. Deng et al., "PerformanceVis: Visual analytics of student performance data from an introductory chemistry course," Visual Informatics, vol. 3, no. 4, pp. 166–176, December 2019.

[11] C. Schumacher and D. Ifenthaler, "Features students really expect from learning analytics," Computers in Human Behavior, vol. 78, pp. 397–407, January 2018.

[12] D. Azcona, I. H. Hsiao, and A. F. Smeaton, "Personalizing computer science education by leveraging multimodal learning analytics," IEEE Frontiers in Education Conference (FIE), pp. 1–9, October 2018.

[13] N. R. Aljohani, A. Daud, R. A. Abbasi, J. S. Alowibdi, M. Basheri, and M. A. Aslam, "An integrated framework for course adapted student learning analytics dashboard," Computers in Human Behavior, vol. 92, pp. 679–690, March 2019.

[14] E. A. C. Olga I. Vaganova, Zhanna V. Smirnova, Ekaterina V. Vezetiu, Maxim M. Kutepov, "Assessment tools in e-learning Moodle," International Journal of Advanced Trends in Computer Science and Engineering, vol. 9, pp. 2488–2492, May 2020.

[15] A. J. P. D. and R. N. V. Glendell R. Jadraque, "Algorithmic Analytics for Outcomes-based Tertiary Education Performance Assessment," International Journal of Advanced Trends in Computer Science and Engineering., vol. 9, pp. 766–773, February 2020.

[16] A. M. and H. A. Sami Hachmoud, Adil Hachmoud, "Analysis of Students Online Learning Behavior in a Pedagogical Model combining Blended Learning and Competency Based Approach," International Journal of Advanced Trends in Computer Science and Engineering, vol. 8, pp. 3389–3395, December 2019.

[17] N. Alias, Z. Zakariah, N. Z. Ismail, and M. N. A. Aziz, "E-Learning Successful Elements for Higher Learning Institution in Malaysia," Procedia - Social and Behavioral Sciences, vol. 67, November 2011, pp. 484–489, November 2012.

[18] M. M. Mohd Salihan Ab Rahman, Nazlena Mohamad Ali, "Comelgetz Prototype in Learning Prayers among Children," Asia-Pacific Journal of Information Technology and Multimedia, vol. 6, pp. 115–125, June 2017.

[19] N. A. M. Z. Mercy Trinovianti Mulyadi, "Mmorpg Game Framework based on Learning Style for Learning Computer Netwoking," Asia-Pacific Journal of Information Technology and Multimedia, vol. 8, pp. 63–77, June 2019.

[20] N. A. A. Salyani Osman, Noraidah Sahari@Ashaari, Nor Azan Mat Zin, Ratna Zuarni Ramli, "Courseware using Cognitive Apprenticeship Strategy," Asia-Pacific Journal of Information Technology and Multimedia, vol. 5, pp. 1–18, December 2016.

[21] T. S. M. T. W. Hairulliza Mohd. Judi, Hanimastura Hashim, "Knowledge Sharing Driving Factors in Technical Vocational Education and Training Institute using Content Analysis," Asia-Pacific Journal of Information Technology and Multimedia, vol. 7, pp. 11–28, December 2018.

[22] M. Diena Dwidienawati, Sri Bramatoro Abdinagoro, David Tjahjana, Dyah Gandasari, "Forced Shifting to e-Learning during the COVID-19 Outbreak: Information Quality, System Quality, Service Quality, and Goal Orientation influence to e-Learning Satisfaction and Perceived Performance," International Journal of Advanced Trends in Computer Science and Engineering, vol. 9, pp. 1518–1525, May 2020.

[23] S. N. Wan Hassan, W.A.S., Ariffin, A., Ahmad, F., Sharberi, S.N.M., Nor Azizi, M. I., Zulkiflee, "COVID-19 Pandemic: Langkawi Vocational College Student Challenge in Using Google Classroom for Teaching and Learning (T&L)," International Journal of Advanced Trends in Computer Science and Engineering, vol. 9, pp. 3299–3307, May 2020.

Real-time Driver Drowsiness Detection using Deep Learning

Md. Tanvir Ahammed Dipu[1], Syeda Sumbul Hossain[2], Yeasir Arafat[3], Fatama Binta Rafiq[4]
Department of Software Engineering, Daffodil International University
Dhaka, Bangladesh

Abstract—**Every year thousands of lives pass away worldwide due to vehicle accidents, and the main reason behind this is the drowsiness in drivers. A drowsiness detection system will help to reduce this accident and save many lives around the world. To defend this problem, we propose a methodology based on Convolutional Neural Networks (CNN) that illustrates drowsiness detection as a task to detect an object. It will detect and localize whether the eyes are open or close based on the real-time video stream of drivers. The MobileNet CNN Architecture with Single Shot Multibox Detector is the technology used for this object detection task. A separate algorithm is used based on the output given by the SSD_MobileNet_v1 architecture. A dataset that consists of around 4500 images was labeled with the object's face yawn, no-yawn, open eye, and closed eye to train the SSD_MobileNet_v1 Network. Around 600 randomly selected images are used to test the trained model using the PASCAL VOC metric. The proposed approach is to ensure better accuracy and computational efficiency. It is also affordable as it can process incoming video streams in real-time and does not need any expensive hardware support. There only needs a standalone camera to be implemented using cheap devices in cars using Raspberry Pi 3 or other IP cameras.**

Keywords—Deep learning; drowsiness detection; object detection; MobileNets; Single Shot Multibox Detector

I. Introduction

Drowsiness while driving tends to vehicle crashes and accidents. Many people die in car collisions every year due to fatigued driving that results from sleeping deprivation, intoxication, drug and alcohol abuse, exposure to heat or alcohol. Automobile manufacturers [8] such as Tesla, Mercedes-Benz, and others have various features for driving assistance such as warning of lane deviation, emergency braking systems, variable cruise control, and aid steering. These innovations have assisted drivers in avoiding the incidence of collisions. Samsung has investigated the attention level of a driver by reading facial characteristics and patterns [10]. At the same time, most of these technologies are proprietary and restricted to high-end cars. These drowsiness identification processes can be divided depending on some of the methods like based on the context of vehicle, behavioral & physiological [39]. Multiple methods for the identification of drowsiness have been developed in the past. Based on vehicle-based, drowsiness identification processes are performed for monitoring the lane switches, steering wheel spin, velocity, compressions on the accelerator pedal. These approaches include measurement of driver physiological signals [11], performance assessment based on vehicles [12], and recording behavior [13]. The bio-signal measurement method demonstrated the highest ability to detect driver drowsiness among these techniques: unlike the other two approaches, it relies solely on the state of the driver. Based on behavior like specific eye closure, yawn, and head posture, drowsiness identification processes need a camera. Another step based on physiological drowsiness identification processes works by monitoring the tiredness to relate between their physiological signals like EOG (electrooculogram) and ECG (Electrocardiogram) [14,15]. The limitation of drowsiness identification processes using the physiological method is that the diver needs to contain electrodes on their body [14]. There is a substantial restriction based on vehicle-based drowsiness identification [15], such as they are prone to forces connected to drivers and vehicles, road situations. There are many techniques stated in different literature those has some restrictions and several benefits.

The aim of this research is to propose a cost-effective procedure to identify the drowsiness among divers while driving vehicles. To develop the drowsiness detector application, we have used a CNN architecture. This work can be divided into two parts based on the main contribution: (a) Convolutional neural networks to identify right drowsiness identification processes based on object detection, (b) and drowsy datasets to help the researchers for drowsiness identification method.

The rest of the paper is organized in the following style: Literature Review is portrayed in Section II that followed by Research Methodology and Results & Discussion in Section III and Section IV, respectively. The final section depicts our Contribution and Limitations.

II. Literatue Review

Eyelid closing has been a much more reliable predictor of drowsiness. Many of the systems has built ought to rely on eyelid closing for driver drowsiness detection even though the other behavior is also a predictor like faster blinking time, sneezing, a slow movement of the eyelid, repeated blinking, set eyes, and sagging pose. Many works of literature have been proposed in this field to predict drowsiness using normal cameras, Infrared (IR) cameras, and stereo cameras. A literature review [27] has been performed to summarize the different drowsiness detection systems and tools. Dwivedi et al. [19] was developed a model using CNN to find drowsiness. In this approach, CNN-based representation feature learning was used and achieved 78% accuracy. To reduce the traffic injuries related to driver drowsiness, the Specialized Driver

Submission Date:- June 25, 2021
Acceptance Dtae:- July 14, 2021

Assistance System was proposed by Alshaqaqi et al. [20]. An algorithm was suggested to locate, map, and evaluate face and eyes to test PERCLOS to diagnose driver drowsiness. Said et al. [23] suggested an Eye-tracking-based driver drowsiness system. The method detects the drowsiness of the driver in this task and rings the alarm to warn drivers. Viola Jones's model was used to detect the area of the face and eye in this work. In indoor tests, it provided 82% accuracy and 72.8% accuracy for the outdoor setting.

Mehta et al. [26] have created a mobile app that can detect facial landmarks and then compute the Eye Aspect Ratio (EAR) and Eye Closure Ratio (ECR) to predict driver drowsiness with an accuracy of 84% based on machine learning models. Smart glass has been created by a start-up Ellcie-Healthy [30] that incorporates a somnolence monitoring technology by providing blink detection, Eye recording, and control of vital signs. By beeping and thereby telling the driver to take a break, the smart glass tracks these inputs and offers somnolence interference. Combination strategies involve multiple sensors on a single device, such as infrared, cameras, and heart rate monitors, to produce outstanding performance. These tools are very costly and require the setting up of proprietary solutions.

Mandal et al. [24] have been proposed a vision-based fatigue identification method for bus driver monitoring. In this work, AHOG and SVM are used respectively for head-shoulder detection and driver detection. They used the OpenCV face detector for face detection and the OpenCV eye detector for eye detection. To learn the eye structure, Spectral Regression Embedding was used, and a new approach was introduced for calculating eye openness. Fusion was used to fuse the features created by two I2R-ED and CV-ED eye detectors. For drowsiness identification, PERCLOS was determined. To detect yawning on the YawDD and NTHU-DDD databases, Xie et al. [25] used transfer learning and sequential learning from yawning video clips. This method was more accurate and stable in terms of adjustments in the direction and orientation of the face to the camera. A vision-based MultiTask Driver Control System was suggested by Celona et al. [21] to examine the eyes, mouth, and location of the head simultaneously to predict the degree of drowsiness.

Jabbar et al. [10, 28] introduced a concept for detecting driver drowsiness for android apps focused on deep learning. They developed a model here that is focused on the identification of facial landmark points. The first images are derived from video frames here, and then the Dlib library was used to extract coordinate points for landmarks. These landmark coordinate points are given as input to the multi-layer perceptron classifier. The classifier classifies these points depending on either drowsy or non-drowsy. Shakeel et al. [22] used the MobileNet-SSD architecture to train 350 images for a custom dataset. The model was capable of achieving a 0.84 Mean Average Precision. As the algorithm could be implemented on an Android device, and the camera stream could be classified in real-time, the method was cost-effective and successful. A Long-term Multi-granularity Deep structure was suggested by Jie Lyu et al. [29] to diagnose driver drowsiness with an accuracy of 90.05 %. However, due to its difficulty, the system was not able to be implemented on mobile devices.

III. Methodology

The overall research methodology is undelineated in this section.

A. Algorithm

It perceives that drowsiness detection is an object detection task. We use images from incoming video streams. From several techniques of deep learning, we use MobileNets [32], a lightweight convolutional neural network architecture, along with the Single Shot Multibox Detector (SSD) [33] system that is on top of the MobileNet architecture to experiment.

- Convolutional Neural Network (CNN)

The suggested system for detecting driver drowsiness is used in the Convolutional Neural Network (CNN) [40]. The pre-processing for CNN is much meagerer compared to others classification algorithms. CNN is a mathematical technique that usually consists of three kinds of pooling, convolution, and fully connected layers. The first two pooling layers are convolution handle extraction of features, and the third one is a completely connected layer, maps the characteristics extracted, such as classification, into the final output. In CNN, which consists of a set of logical operations, such as convolution, A technical method of linear motion, the convolution layer plays a key role. In image data, two-dimensional arrays of pixel values are processed, and at each image location, a small parameter grid called the kernel and function extractor for optimization is added, making CNN's highly effective for image processing since a feature can appear anywhere in the image. Extracted functionality will get more complex hierarchically and gradually as one layer feeds the output into the next layer. The way parameters such, as kernels are optimized is called planning. This can be achieved by a back-propagation and gradient descent optimization algorithm to minimize the discrepancy between outputs and ground truth marks. Fig. 1 represents the CNN architecture.

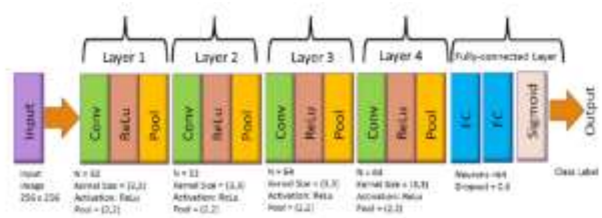

Fig. 1. CNN Architecture.

- Single Shot Multibox Detector (SSD)

For our task, we use MobileNets [32], a lightweight convolutional neural network architecture, along with the Single Shot Multibox Detector (SSD) [33] system that is on top of the MobileNet architecture. There are two types of algorithms used to detect typical objects. To define regions where objects can be found, RCNN [42] and Faster RCNN [43] algorithms use a two-step approach to identify objects only in certain regions. Algorithms such as SSD [33] and YOLO [41] use a completely convolutionary method, on the other hand, through which the network will locate all items in a picture via the ConvNet in one pass. Usually, the algorithms for the region proposal have slightly better precision but are slower to run, whereas single-shot algorithms are more powerful and have satisfying precision. Fig. 2 represents the SSD architecture.

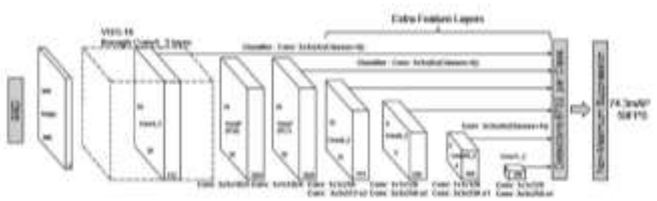

Fig. 2. SSD Architecture.

The SSD has two elements, a backbone model and an SSD head. The Backbone model is usually a pre-trained image classification network as a feature extractor. This network is educated on ImageNet such as ResNet which excludes the entirely connected classification layer. Therefore, we have a deep neural network that can infer semantic meaning from the input image while preserving the spatial structure in the image at a lower resolution. We will clarify the later feature and feature map. The SSD head is only one or more convolutionary layers attached to this backbone, and the outputs are represented as the bounding boxes and object groups in the final layer activation spatial role. There are some important parameters in SSD. The SSD uses a grid (see Fig. 3(a)) to divide the image rather than a sliding window, and each cell of the grid needs to detect the objects in that picture region. Object identification involves simply predicting the class and location of the object within the sector. We admire it as the context class if no object is present, and the location is ignored. Each grid cell is output to the position and the form of the entity it carries.

(a) (b) (c)

Fig. 3. (a) Grid View (b) Anchor Boxes (c) Higher and Lower Anchor Boxes.

If many objects of different shapes exist in one grid cell, the anchor box (see Fig. 3(b)) and the responsive area are considered. There may be separate anchor boxes in the SSD for each grid cell. These anchor boxes are predefined, and each of them is responsible for the size and shape of a grid cell. The face in Fig. 3(c), for example, has the big anchor box while the eyes correspond to the small box. In training, the SSD framework utilizes a mapping step to align the correct anchor box with the bounding box inside an image of each ground truth entity. The anchor boxes with a greater degree of overlap with an object are ultimately responsible for estimating the class of that object and its position. This property is used for preparing the network for detecting objects and their locations. In reality, an aspect ratio and a zoom level describe any anchor box. The objects are not always square those could be narrower, broader, or in varying degrees. With predefined aspect ratios, the SSD architecture requires the anchor boxes to account for this. The parameter ratios are used to determine the various aspect ratios of the anchor boxes at each scale level associated with each grid cell. It is not needed to have the same size as the grid cell for the anchor boxes. Inside the cell, we may select smaller or larger objects. The zoom parameter is used to determine how much for each grid cell the anchor boxes need to be scaled up or down.

The receptive field is defined as the area that a specific CNN function looks at in the input space. We have used "feature" and "activation" here and treat them at the corresponding position as the linear combination of the previous layer. Features on different layers reflect different area sizes in the input picture due to the convolution operation. The scale defined by a function grows bigger while going deeper. We begin with the bottom layer (5x5) in this example below and then add a convolution resulting in the middle layer (3x3), where one attribute represents a 3x3 area of the input layer. And then, add the middle layer convolution and get the upper layer (2x2) where each attribute on the input image corresponds to a 7x7 area. This type of green and orange 2D array is often referred to as feature maps that correspond to a group of features generated in a sliding window fashion by applying the same feature extractor at different input map locations. The features in the same map of characteristics have the same receptive area and aim at different positions with the same pattern.

The core concept of the SSD architecture helps to detect objects at varying scales and output a closer bounding box. As in the ResNet34 backbone outputs an input image function map of 256 7x7. The easiest solution is to define a 4x4 grid to add a convolution to this function map and transform it to 4x4. In reality, this method will function to some degree as the concept of YOLO. The additional step taken by SSD is to attach more convolutional layers to the map of the backbone feature and generate an object detection result for each of these convolution layers. Because earlier layers with a smaller receptive field will reflect smaller objects, earlier layer predictions help with the smaller object. Fig. 4 represents the Convolutional Neural Network feature maps

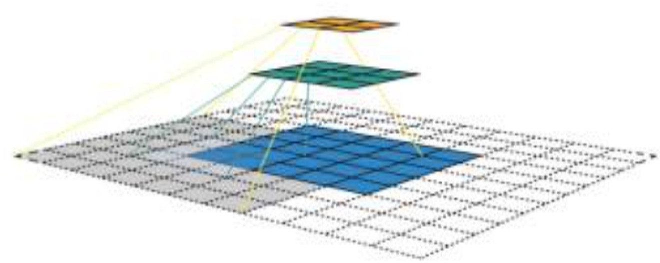

Fig. 4. Convolutional Neural Network Feature Maps.

- MobileNet

The architecture of MobileNets is designed for mobile-based applications, is used for depth-wise separable convolutions, and builds lightweight deep neural networks. Except for the first layer, the MobileNet is a separable convolution [31]. A complete convolutional layer is the first layer. Batch normalization and ReLU non-linearity are accompanied by all the layers. The final layer, however, is a completely related layer without any non-linearity and feeds for classification to the softmax. For downsampling, stridden convolution is used for both deep convolution and the first fully convolutionary layer. The total number of layers for MobileNet is 28, considering convolution as different layers in-depth and stage.

The MobileNet-SSD_v1 [34] framework is capable of detecting multiple objects from an image. We trained it to see a human face for our drowsiness detection task to notice that the diver is yawn or no yawn and the eye open or close. Yawn, no yawn, eye open and close were considering four separate classes. For this experiment, a regular camera is used for the incoming video stream. The technique suggested is exactly presented in Fig. 5.

We observed that the longest length of a blink found equals 7.5 inches from the camera in the training model. From the video stream, we get an image frame, and this function is called image frames processed per second (FPS). The model would declare the driver to be drowsy if any of the driver's eyes are found close for ten consecutive frames in the incoming video stream, and an alarm will raise to wake the driver. The above approach uses only a single convolutional neural network and, thus, the total complexity of the system is much smaller. Now we need to see how well this recommended approach performs under driving environments in real life.

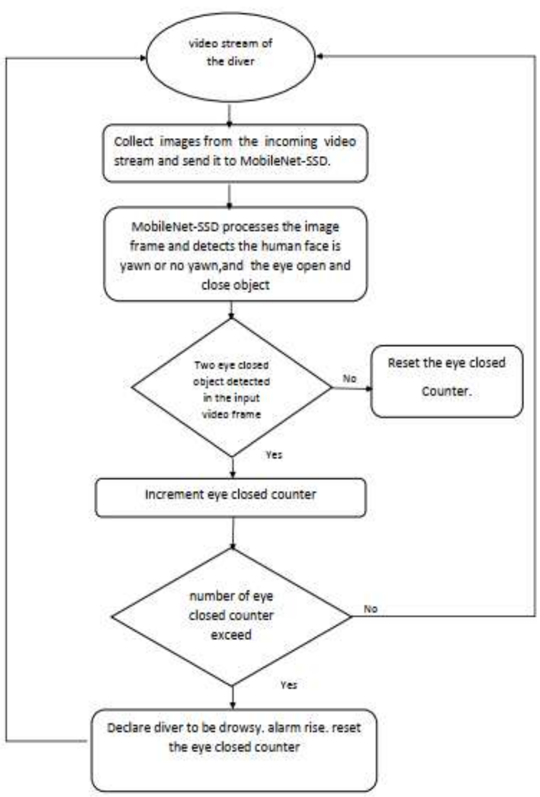

Fig. 5. Drowsiness Detection System Methodology.

B. Data Collection

We have collected and annotated a customized data set to train our model in the MobileNet-SSD system. The annotated image data includes human faces with opened and closed eyes. Our collected data sets consist of images from a few publicly accessible online databases released by reputed users. Fig. 5 represents some dateset.

IV. Open and Close Eyes

The dataset open and closed eyes were collected from the open-source database. This dataset contains all the human eyes that were closed and open. All pictures are available in JPG format. There are 1234 images, which is nearly 10 MB, without annotations. We have annotated all the images in this dataset.

V. Yawning and no Yawn while Driving

The data source of yawning and no-yawning during driving is given by the University of Ottawa, Canada [35]. The data set includes two types of videos that are captured from two separate camera positions inside the vehicle. For the first set of data, the device is installed on the dashboard of the car, and for the second set of data, the device is installed just underneath the front mirror of the car. There are both male and female drivers in these videos. In these videos, the driver is wearing glasses, and some of the drivers are not wearing glasses. There is also an available laughing driver, a yawning driver, a not-yawning driver, and some drivers are looking around. We collected about 1234 frames from all the videos for this dataset. After extracting the frame from the videos, we annotated all the images with labels eyes open, close, yawn, and no-yawn.

VI. Custom used Images

The photos used are freely available and allowed for re-use. The main objective of using these photos is to improve our classification model. This dataset is versatile with different poses and lighting environments. All Pictures are available in JPG format. There are 1900 images, which is nearly 25 MB, are available in this dataset. Although these photos are collected from several online sources, no annotations are available for this dataset. We collected about 250 frames from all the videos for this dataset. After extracting the frame from the videos, we annotated all the images with labels eyes open, close, yawn, and no-yawn.

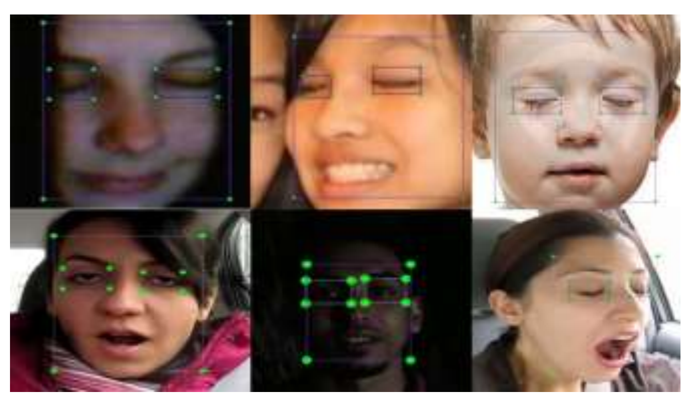

Fig. 6. Dataset Images.

From the image data Fig. 6, one can see that the Drowsy dataset was already collected to combine images from a wide range of positions, perspectives, and lighting conditions to create a balanced dataset to ensure high precision and generalization of the object detection system. Although this dataset contains very few numbers of low-light images, as of now, the objective has been limited to identification drowsiness in daytime conditions.

A. Dataset Training

We have used Tensorflow API to train our model. As TFOD API can read only TFRecord file format, we need to convert our dataset into this format. First, we need an RGB image dataset in jpeg or png format; and create the bounding boxes for the image and mention the classes for those boxes. With LabelImg, we hand-labeled them manually. LabelImg is a Python-written graphical image annotation application with a good user interface. It also supports Python 2 and Python 3. After completing annotation, we convert our dataset XML to CSV to create the TFrecords. We use around 4500 files for training (train.records) and 700 files for testing (test.records). Although the generated dataset did not contain sufficient training images to train the object detection framework, the transfer learning principle has been used [36, 37]. For training our model, we take the TensorFlow Object Detection Model Zoob [38], and the MobileNet_SSD_v1 pre-trained model on the MS COCO dataset [38] to detect a Face. Training can be done on the computer or remotely like AWS, Google Cloud, paperspace, etc. The model was trained until acceptable accuracy.

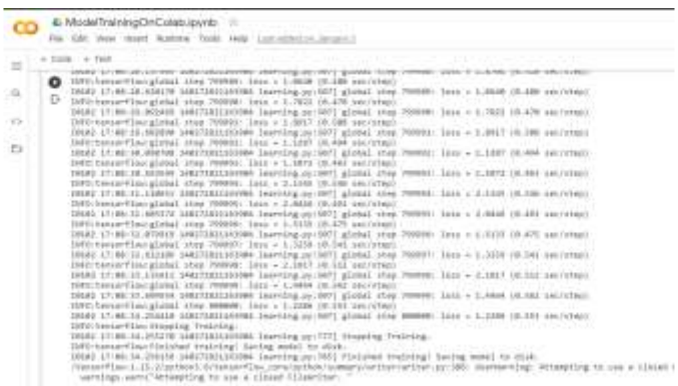

Fig. 7. Dataset Training on Colab.

After finishing with training, we exported the trained model to a single file Tensorflow graph. It is called a frozen inference graph. Fig. 7 presents the dataset training process in colab. All the dataset and the code are available at https://github.com/SshShamma/Drowsiness_Detection_DeepLearning.

VII. Result and Discussion

In this section, the experiment results and associate outcomes have been explained in details.

A. Experiment Results

The experiment is performed in Google cloud using Tensorflow Object Detection API. We train our SSD model with an average step speed of 0.5 s, which means that training one network for 800 k steps takes around six days. After completing our training, we get a frozen inference graph, and then we transform this graph into an inference model. Our inference model was run on a laptop for initial testing and gave 8 frames per second (FPS) for SSD architecture.

PASCAL VOC is a popular dataset and an evaluation tool for object detection and classification. The trained model MobileNet_SSD_v1 is tested using the PASCAL VOC assessment metric on the test dataset. The intersection over Union (IoU) is defined as the area at which the projected bounding box (B) and the ground-truth box (Bgt) are intersected, separated by their union area.

$$IoU=\frac{Area(B\cap Bgt)}{Area(B\cup Bgt)}$$

We consider that, depending on three factors, the detection is a true positive (TP) or false positive (FP). The first one is if the confidence score is higher than 0.5, the second one is the IoU of the predicted bounding box is higher than the ground-truth IoU threshold, and the third one is the predicted class corresponds to the ground truth class. The identification is false positive (FP) if the last two conditions are not fulfilled.

If the same ground-truth applies to multiple forecasts, then the one with the highest confidence score counts as a true positive and the others count as false positives. If the detection confidence level intended to detect a ground-truth is lower than the confidence level, the detection is counted as a false negative (FN). Here are the equations for precision, recall based on assumptions.

$$Precision=\frac{\boldsymbol{TP}}{\boldsymbol{TP+FP}}$$

The number of true positives divided by the sum of true positives and false positives is Precision. Average precision (AP) is used to test the efficiency of the object detectors. For our dataset, AP is calculated based on our four classes. Using the below formula, we get the mean average accuracy (mAP).

$$mAP=\sum_{\boldsymbol{i=1}}^{\boldsymbol{k}}\frac{\boldsymbol{APi}}{\boldsymbol{k}}$$

Here, AP is Average Precision and k is several ground truth boxes.

Table I shows the summary of the result.

TABLE I. RESULT SUMMARY

AP eyes close	**AP eyes open**	**AP No Yawn**	**AP Yawn**	**mAP**
0.962631	0.977191	0.997952	0.983024	0.980199

Fig. 8 shows the Loss function graph from which we can identify minimal losses that occurred.

From Fig. 9, we can see the confidence scores, with bounding boxes representing the object detections produced by the model for a given class at a specific moment in time.

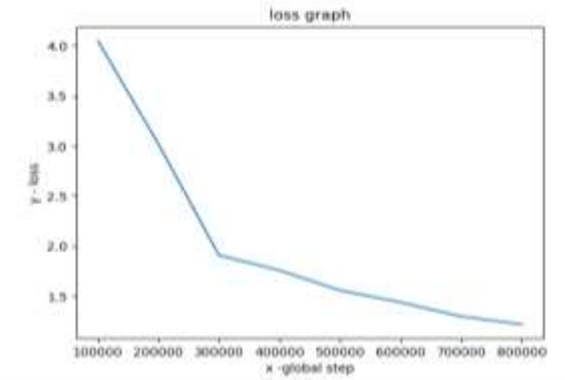

Fig. 8. Loss Function Graph.

Fig. 9. Trained Model in Action.

B. Discussion

In the previous work machine learning algorithm was used for manual feature extraction but nowadays deep learning architectures remove the manual feature extraction. It does automatic learning. Now deep learning architectures extract its feature in an automated process. So, a lot of time is saved here otherwise we have to spend time on determining the feature requirements to improve the classification result.

The dataset of the drowsiness observation model was largely tested with several light conditions, under a broad range of conditions, subjection & obstruction. In normal cases, our model works fine. It gives more than 90% accuracy. We tested the model on different ages and colors of people and get a good result. The success rate while driving in real-world situations was considered flawless. We also found that its efficiency is not much good in some cases. In low-light conditions or when the flashlight is pointed to the camera lens in the background, at that time, the performance of the trained model was not fully satisfied. But when the dataset doesn't accommodate any low light images, it was appropriate. That is why we only require it to function well under this condition.

VIII. Conclusion and Limitations

The paper described an improved drowsiness detection system based on CNN. The key goal is to ensure that a lightweight approach is applied in integrated devices while maintaining and achieving high efficiency. In the trained model, we only use 250 low-light images. The main improvement done in the future is adding more low-light photos to work well in low-light conditions. Further enhancement of the dataset is required using a yawning dataset as we could not use those annotations for detecting drowsiness. Another improvement area is the SSD_MOBILENET architecture for a better suit for drowsiness detection.

References

[1] Amodio,A.,Ermidoro,M.,Maggi,D.,Formentin,S., Savaresi, S.M.(2018). Automatic detection of driver impairment based on pupillary light reflex.IEEE Transactions on Intelligent Transportation Systems, pp. 1-11.

[2] Yang, J.H., Mao, Z.H., Tijerina, L., Pilutti, T., Coughlin, J.F., Feron, E. (2009).Detection of driver fatigue caused by sleep deprivation. IEEE Transactions on Systems, Man, and Cybernetics-Part A: Systems and Humans, 39(4):694-705.

[3] Hu, S., Zheng, G. (2009). Driver drowsiness detection with eyelid related parameters by support vector machine. Expert Systems with Applications, 36(4):7651-7658.

[4] K. Fujiwara, E. Abe, K. Kamata, C. Nakayama, Y. Suzuki, T. Yamakawa, T. Hiraoka, M. Kano, Y. Sumi, F. Masuda, M. Matsuo, and H. Kadotani, ''Heart rate variability-based driver drowsiness detection and its validation with EEG,'' IEEE Trans. Biomed. Eng., vol. 66, no. 6, pp. 1769–1778, Jun. 2019.

[5] C. F. P. George, ''Sleep apnea, alertness, and motor vehicle crashes,'' Amer. J. Respiratory Crit. Care Med., vol. 176, no. 10, pp. 954–956, Nov. 2007.

[6] J. A. Owens, T. Dearth-Wesley, A. N. Herman, and R. C. Whitaker, ''Drowsy driving, sleep duration, and chronotype in adolescents,'' J. Pediatrics, vol. 205, pp. 224–229, Feb. 2019.

[7] Mardi,Z.,Ashtiani,S.N.,Mikaili,M.(2011). EEG-based drowsiness detection for safe driving using chaotic features and statistical tests.Journal of Medical Signals And Sensors,1(2):130-137.

[8] M. Benz, "Mercedes benz safety - s class." [Online]. Available: https://www.mercedes-benz.co.uk/passengercars/mercedes-benz-cars/models/s-class/saloon-w22/safety/intelligent-drive.module.html.

[9] Muze, "Eyesight." [Online]. Available: https://www.eyesight-tech.com/.

[10] Jabbar, R., Shinoy, M., Kharbeche, M., Al-Khalifa, K., Krichen, M., & Barkaoui, K. (2020, February). Driver drowsiness detection model using convolutional neural networks techniques for android application. In *2020 IEEE International Conference on Informatics, IoT, and Enabling Technologies (ICIoT)* (pp. 237-242). IEEE.

[11] Noori,S.M.,Mikaeili,M.(2016).Driving drowsiness detection using a fusion of electroencephalography, electrooculography, and driving quality signals. J Med Signals Sens,6: 39-46.

[12] Using, S., Eog, E.: Development of Vehicle Driver Drowsiness Detection System Using Electrooculogram (EOG). In: 1st International Conference on Computers, Communications, and Signal Processing With Special Track on Biomedical Engineering (CCSP), Kuala Lumpur, Malaysia. pp. 165–168 (2005).

[13] S. K. L. Lal and A. Craig, ''A critical review of the psychophysiology of driver fatigue,'' Biol. Psychol., vol. 55, no. 3, pp. 173–194, Feb. 2001.

[14] C. C. Liu, S. G. Hosking, and M. G. LennØ, ''Predicting driver drowsiness using vehicle measures: Recent insights and future challenges,'' J. Saf. Res., vol. 40, pp. 239–245, Aug. 2009

[15] Q. Ji and X. Yang, ''Real-time eye, gaze, and face pose tracking for monitoring driver vigilance,'' Real-Time Imag., vol. 8, no. 5, pp. 357–377, 2002.

[16] Takei, Y., Furukawa, Y.: Estimate of driver's fatigue through steering motion. 2005 IEEE Int. Conf. Syst. Man Cybern. 2, 1–6 (2005).

[17] Lee, A.: Comparing Deep Neural Networks and Traditional Vision Algorithms in Mobile Robotics. Swart. Coll. (2015).

[18] Lowe, D.G. Distinctive Image Features from Scale-Invariant Keypoints. Int. J.Comput. Vis. (2004).

[19] Lazebnik, S., Schmid, C., Ponce, J.: Beyond bags of features: spatial pyramid matching for recognizing natural scene categories. IEEE Comput. Society.

[20] Dwivedi, K., Biswaranjan, K., Sethi, A (2014). Drowsy driver detection using representation learning.Advance Computing Conference(IACC), IEEE,pp. 995-999.

[21] Alshaquaqi,B.,Baquhaizel,A.S.,AmineOuis,M.E.,Boumehed,M.,Ouamri, A.,Keche,M.(2013).Driver drowsiness detection system. 8th International Workshop on Systems,Signal Processing and Their Applications(WoSSPA).

[22] Shakeel M.F., Bajwa N.A., Anwaar A.M., Sohail A., Khan A., Haroon-ur-Rashid (2019) Detecting Driver Drowsiness in Real Time Through Deep Learning Based Object Detection. In: Rojas I., Joya G., Catala A. (eds) Advances in Computational Intelligence. IWANN 2019. Lecture Notes in Computer Science, vol 11506. Springer, Cham. https://doi.org/10.1007/978-3-030-20521-8_24.

[23] C.-H. Weng, Y.-H. Lai and S.-H. Lai, “Driver drowsiness detection via a hierarchical temporal deep belief network,” in Asian Conference on Computer Vision. Springer, 2016, pp. 117–133.

[24] Said, S., AlKork, S., Beyrouthy, T., Hassan, M., Abdellatif, O., Abdraboo, M.F. (2018). Realtime eye-tracking and detection-a driving assistance system.Advances in Science, Technology and Engineering Systems Journal,3(6):446-454.

[25] Mandal,B.,Li,L.,Wang,G.S.,Lin,J.(2017). Towards detection of bus driver fatigue based on robust visual analysis of eye state. IEEE Transactions on Intelligent Transportation Systems, 18(3):545557.

[26] Y. Xie, K. Chen, and Y. L. Murphey, “Real-time and Robust Driver Yawning Detection with Deep Neural Networks,” Proceedings of the 2018 IEEE Symposium Series on Computational Intelligence, SSCI 2018, pp. 532–538, 2019.

[27] Saini, V., & Saini, R. (2014). Driver drowsiness detection system and techniques: a review. *International Journal of Computer Science and Information Technologies*, *5*(3), 4245-4249.

[28] P. Peyrard, “Personal system for the detection of a risky situation and alert,” Feb. 28, 2019, us Patent App. 16/178,365.

[29] Jabbar, R., Al-Khalifa, K., Kharbeche, M., Alhajyaseen, W., Jafari, M., Jiang, S. (2018). Real-time driver drowsiness detection for an android application using deep neural networks techniques. Procedia Computer Science,130:400-407.

[30] Arcaya-Jordan, A., Pegatoquet, A., & Castagnetti, A. (2019, March). Smart Connected Glasses for Drowsiness Detection: a System-Level Modeling Approach. In *2019 IEEE Sensors Applications Symposium (SAS)* (pp. 1-6). IEEE.

[31] Howard, A.G., Zhu, M., Chen, B., Kalenichenko, D., Wang, W., Weyand, T., Andreetto, M., Adam, H.: MobileNets: Efficient Convolutional Neural Networks for Mobile Vision Applications. (2017).

[32] Liu, W., Anguelov, D., Erhan, D., Szegedy, C., Reed, S., Fu, C., Berg, A.C.:SSD: Single Shot MultiBox Detector. In: European Conference on Computer Vision. pp. 21–37 (2015).

[33] Huang, J., Rathod, V., Sun, C., Zhu, M., Korattikara, A., Fathi, A., Fischer, I., Wojna, Z., Song, Y., Guadarrama, S., Murphy, K.: Speed/accuracy trade-offs for modern convolutional object detectors. Proc. - 30th IEEE Conf. Comput.Vis. Pattern Recognition, CVPR 2017. 2017–Janua, 3296–3305 (2017).

[34] Song, F., Tan, X., Liu, S.: Eyes Closeness Detection from Still Images with Multi-scale Histograms of Principal Oriented Gradients.

[35] Pan, S.J., Fellow, Q.Y.: A Survey on Transfer Learning. IEEE Trans. Knowl. Data Eng. 22, 1345–1359 (2010).

[36] Oquab, M., Bottou, L., Laptev, I., Sivic, J.: Learning and Transferring Mid-Level Image Representations using Convolutional Neural Networks. IEEE Conf. Comput. Vis. Pattern Recognit. 1717–1724 (2014).

[37] Lin, T.Y., Maire, M., Belongie, S., Hays, J., Perona, P., Ramanan, D., Dollár, P., Zitnick, C.L.:Microsoft COCO: Common objects in context. Lect. Notes Comput. Sci. (including Subser. Lect. Notes Artif. Intell. Lect. Notes Bioinformatics). 8693 LNCS, 740–755 (2014).

[38] Huang, J., Rathod, V., Sun, C., Zhu, M., Korattikara, A., Fathi, A., Fischer, I., Wojna, Z., Song, Y., Guadarrama, S., Murphy, K.: Speed/accuracy trade-offs for modern convolutional object detectors. Proc. - 30th IEEE Conf. Comput.Vis. Pattern Recognition, CVPR 2017.2017–Janua, 3296–3305 (2017).

[39] Sahayadhas, A., Sundaraj, K., & Murugappan, M. (2012). Detecting driver drowsiness based on sensors: a review. *Sensors*, *12*(12), 16937-16953.

[40] Albawi, S., Mohammed, T. A., & Al-Zawi, S. (2017, August). Understanding of a convolutional neural network. In *2017 International Conference on Engineering and Technology (ICET)* (pp. 1-6). Ieee.

[41] Jana, A. P., & Biswas, A. (2018, May). YOLO based Detection and Classification of Objects in video records. In *2018 3rd IEEE International Conference on Recent Trends in Electronics, Information & Communication Technology (RTEICT)* (pp. 2448-2452). IEEE.

[42] Chen, C., Liu, M. Y., Tuzel, O., & Xiao, J. (2016, November). R-CNN for small object detection. In *Asian conference on computer vision* (pp. 214-230). Springer, Cham.

[43] Ren, S., He, K., Girshick, R., & Sun, J. (2015). Faster r-cnn: Towards real-time object detection with region proposal networks. *Advances in neural information processing systems*, *28*, 91-99.

Wireless Intrusion and Attack Detection for 5G Networks using Deep Learning Techniques

Bayana alenazi[1], Dr. Hala Eldaw Idris[2]
Collage of Computer and Information Science
Jouf University, Al-Jouf, Saudi Arabia

***Abstract*—A Wireless Intrusion Detection System is an important part of any system or company connected to the internet and has a wireless connection inside it because of the increasing number of internal or external attacks on the network. These WIDS systems are used to predict and detect wireless network attacks such as flooding, DoS attack, and evil- twin that badly affect system availability. Artificial intelligence (Machine Learning, Deep Learning) are popular techniques used as a good solution to build effective network intrusion detection. That's because of the ability of these algorithms to learn complicated behaviors and then use the learned system for discovering and detecting network attacks. In this work, we have performed an autoencoder with a DNN deep algorithm for protecting the companies by detecting intrusion and attacks in 5G wireless networks. We used the Aegean Wi-Fi Intrusion dataset (AWID). Our WIDS resulted in a very good performance with an accuracy of 99% for the dataset attack types: Flooding, Impersonation, and Injection.**

Keywords—Wireless intrusion detection system; 5G; autoencoder; deep learning; attack detection

I. Introduction

Wireless networks are being developed continuously every day due to the wide range of functionalities and capabilities they could provide, which make our lives easier. It is considered an important topic has a lot of research on it.

One of the recent interesting wireless technologies is the 5G (the 5th generation mobile network), which is “a new global wireless standard after 1G, 2G, 3G, and 4G networks that enables a new kind of network designed to virtually connect everyone and everything together including machines, objects, and devices. The 5G wireless technology has many advantages, such as the ability to deliver higher multi-Gbps peak data speeds, ultra-low latency, more reliability, massive network capacity, increased availability, higher performance, and improved efficiency.” (Kei 2015) [1].

As long as 5G wireless technology uses internet protocols and have connectivity features, it means that cyber-attacks could occur on it and cause, and because of the growing number of its functionalities which cause increasing of vulnerabilities on 5G, which resulted increasing in security threats, attacks, and malicious activities on it. This can cause huge damage to devices or lead to data loss.

A lot of cyber-attacks can occur on wireless network technologies like Flooding or packet sniffing, fake authentication, injection, Impersonation, session hijacking, denial of service (DoS), and address spoofing, traffic analysis, and unauthorized access.

The wireless devices relate to each other in one environment, so cyber attackers need to target any software or hardware device or component in this wireless network environment, such as wireless end devices and mobiles, access points, etc. That explains how much necessary to detect these attacks and prevent them from protecting the whole system environment.

The cybersecurity concept, in general, represents techniques and methods that should be used to protect the information system from cyber-attacks, remotely or physically, to avoid destruction and damage that may happen because of it. Several algorithms and technologies have been proposed and used as cybersecurity solutions, but most of these traditional defense solutions fail in detecting or preventing new or zero-day attacks. One of the adaptive and powerful approaches is using machine learning, which is an application of artificial intelligence (AI) that focuses on building applications and systems that can automatically improve themselves from practice and experience by training them on labeled datasets and develop their accuracy over time, in attacks detection, depending on the behavior patterns. And, deep learning, which is “a subset of machine learning, which is essentially a neural network with three or more layers.”(IBM 2021) [2]. Using these techniques results in higher performance and accuracy, reduce the workload on security experts. In the context of research and development for information security Wireless Intrusion systems, numerous machine learning techniques have been widely used: Random Forest,Adaboost [3], Naïve bayes and Random Forest (RF) by Jabbar et al [4], Decision Tree(DT) and k-Nearest Neighbor (KNN) by Yerong et al., 2014 [5].

Few studies have used Deep learning techniques: Artificial Neural Networks (ANN), and Long Short-Term Memory (LSTM) networks and Convolutional Neural Networks (CNN) have been implemented (Raj, Akash, et al., 2018) [6], (Bayan et al., 2019) used Auto-encoder[7], (Riyaz, B., and Sannasi Ganapathy,2020) proposed convolutional neural network CNN[8].

This work suggests a methodology for wireless cyber-attacks detection in 5G networks based on deep hybrid learning that overcomes traditional Machine learning techniques and has shown better performance with high accuracy than prior studies.as shown in Table II.

We have used deep learning algorithms such as Autoencoder, DNN, and others [9]. Then developing a deep learning model that will help detect, defend against cyber-attack, and distinguish between normal and suspicious traffic. The AWID dataset [10] will be used to build this model, which comprises a large set of packets. It contains more than 150 different attributes. And it is available as a CSV format file.

The remaining parts of the research are organized as the Second section shows some of the related papers of cyber-attack on 5G and how to prevent them. Section 3 discusses the methodology we applied and the work details with steps, Section 4 comparison our achievement with other works and the result discussion. The last section is the conclusion and the references of the work.

II. Related Work

Recent years have seen increased use of deep learning, a subdiscipline of machine learning. It has been applied to intrusion detection, where tests showed that deep learning was significantly better than conventional methods. In this section, we present some related works that have been made by prominent researchers that have used Machine learning and deep learning.

In term of network intrusion detection system in general, Dawoud et al. have built multi-layered neural network model that achieved an accuracy of 99%, however, they used KDD99 which is 20 years old and doesn't contain recent or current network attacks. [11].

He Fang et al. proposed modern authentication methodologies that use machine learning algorithms and improve the intelligence in the authentication layer to get more efficient security in 5G wireless networks and they achieve reliable, effective, continuous, and situation-aware authentication approach [12]. Fig. 1 presents their framework diagram of the intelligent authentication design which they proposed.

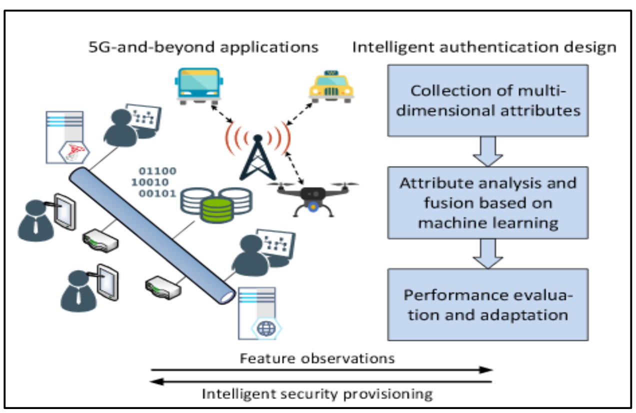

Fig. 1. [12]. Intelligent Authentication Design by (He Fang ,2019).

Jordan Lam et al. have designed an automated end-to-end network defense system that uses CNN machine learning algorithm to design an anomaly detection model for 5G networks, and they have tested the model on a real network environment include malicious and normal traffic flow. The results showed that this system detects the attack with an accuracy of 96% [13]. A high-level view of the End-to-end 5G network threat landscape is shown below in [14]. The idea related to this paper to categorize the threats that could happen on 5G networks.

Lorenzo et al. have developed a novel 5G-oriented cyber defense system to detect cyber threats and attacks in 5G mobile networks fast and efficiently. They used deep learning algorithms for building the model on well-known botnet data set. Good accuracy was achieved in their system. [14].

Jiaqi Li et al. were proposed an intelligent intrusion detection system on Software Defined 5G architecture, taking the advances of artificial intelligence and machine learning, they used the Random Forest technique with the k-mean and Adaboost algorithm. The system was able to detect unknown attacks and the evolution has shown that it has better performance and lower overhead [3].

Fig. 2, [13] End-to-end 5G network threat landscape by (Jordan Lam ,2020) show Core Network Elements" include the following: the Network Function (NF, NFn), the Network Exposure Function (NEF), and the Network Repository Function (NRF).

The approach of this paper tries to solve some issues. That was done by using the AWID dataset that contains real-world wireless network attacks. And, by using deep learning algorithms that give the highest accuracy.

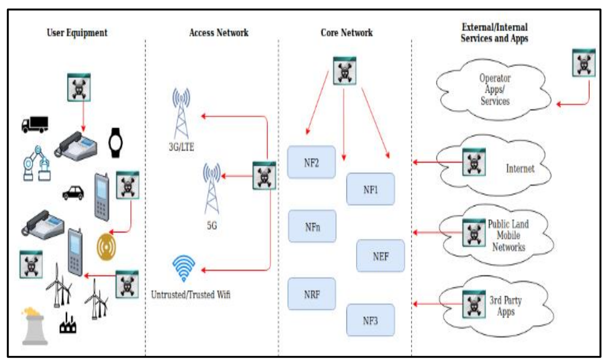

Fig. 2. [13] End-to-end 5G Network Threat Landscape.

III. Methodology

The wireless cyber-attack detection system will start collecting and capturing the traffic inside the wireless network for the database. Then preprocessing and analyzing the collected traffic and log files records. After that, the system applies features (attributes) extraction so that each instance is described by a set of features in an organized way and use an unsupervised learning neural network known as an auto-encoder (AE) with deep neural network DNN attempts to reproduce the input data as much as possible. Two training procedures come into play: the L-BFGS algorithm that sets the network weights before training and fine-tuning, in which the network parameters are fine-tuned. AE can perform dimensionality reduction. We can get more abstract high-level and low-dimensional representations of the original feature data by removing irrelevant and redundant features from the feature vector. The majority of DNNs are Feed-Forward

Networks (FFNNs), in which data flows from the input layer to the output layer without going backward. Fig. 3 showing the steps of model implementation and classification data traffic and identify attacks type.

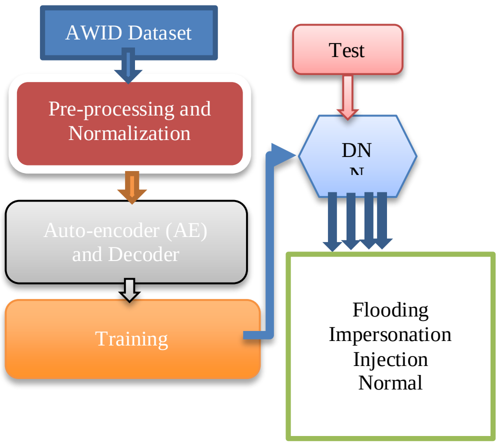

Fig. 3. Model Architecture for our Proposed System.

This model presents the initial design of any 5G network that needs to use for the attack detection system that have been built. However, there are tools that monitor and capture the traffic inside the 5G network such as TCP dump/W Wireshark and CIC Flow meter, then the traffic will be converted as CSV files so that our model could be able to classify it, and will generate a notification when an attack hit the network as shown in Fig. 3.

A. *Aegean Wi-Fi Intrusion Dataset (AWID) Description*

AWID is a public free available dataset[10] that contains Wi-Fi (802.11) network traffic which was captured and collected from physical real-time infrastructure wireless network traffic [15]. The dataset includes about 156 attributes that describe information and data about the MAC layer as numeric or string values. Fig. 4 shows the infrastructure was used to collect the dataset. This dataset is oriented toward being used for IDS especially wireless intrusion detection systems, and it's the first of its type.

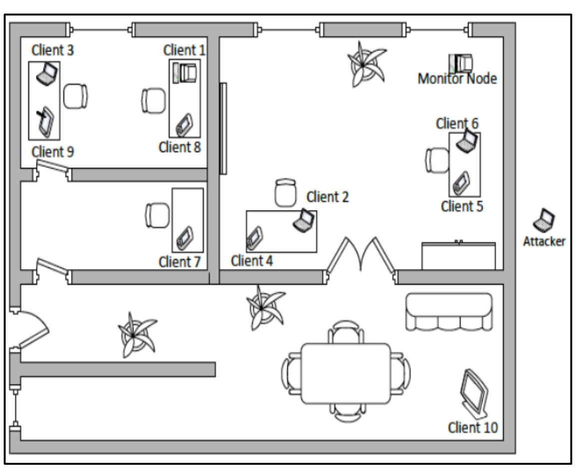

Fig. 4. The Infrastructure used to gather the Dataset [10].

The data collected from network that contains 1 desktop machine, 2 laptops, 2 smartphones, 1 tablet, and 1 smart TV and it was covered by one AP (Netgear N150 WNR1000 v3), protected by the untrusted WEP encryption.

This dataset consists of two types, one of them call "CLS" which contains four labels: Impersonation, Flooding, Injection, and Normal. While the other is called "ATK" that contain 16 classes, which are subcategories of the main four classes exist in "CLS": DE-authentication, disassociation, authentication request, amok, probe request, probe response, beacon, CTS, RTS, power saving, power, evil-twin, caffe-. In this research, we used the "CLS" dataset called (AWID-CLS-R-Trn, AWID-CLS-R-Tst) that contains four labels, three extracted from packets, they can be found in the reference [10] attacks scenario (the dataset contains 155).

TABLE I. SHOW THE REDUCED AND USED FEATURES

NO.	Important Attributes name
1	frame.time_delta_displayed
2	frame.time_relative
3	frame.len
4	radiotap.length
5	radiotap.present.tsft
6	radiotap.present.flags
7	radiotap.present.channel
8	radiotap.present.fhs
9	radiotap.present.dbm_antsignal
10	radiotap.present.antenna
11	radiotap.present.rxflags
12	wlan.fc.type_subtype
13	wlan.fc.version
14	wlan.fc.type
15	wlan.fc.subtype
16	wlan.fc.ds,wlan.fc.frag
17	wlan.fc.retry
18	wlan.fc.pwrmgt
19	wlan.fc.moredata
20	wlan.fc.protected
21	wlan_mgt.fixed.capabilities.cfpoll.ap
22	wlan_mgt.fixed.listen_ival
23	wlan_mgt.fixed.status_code
24	wlan_mgt.fixed.time
25	stamp,wlan_mgt.fixed.aid
26	wlan_mgt.fixed.reason_code
27	wlan_mgt.fixed.auth_seq
28	wlan_mgt.fixed.chanwidth
29	wlan_mgt.tim.bmapctl.offset
30	wlan_mgt.country_infoenvironment
31	wlan_mgt.rsn.capabilities.ptksa_replay_counter
32	wlan_mgt.rsn.capabilities.gtksa_replay_counter
33	wlan.qos.ack
34	wlan_mgt.fixed.timestamp
35	class

B. *Preprocessing the Dataset*

The following steps are adopted to preprocess the Dataset:

- Delete missing value.
- Format data into standard data type.
- To reduce the size of the datasets, reduce the unnecessary accuracy of the float numbers by dropping digits after the decimal point.

- Drop samples with "Infinity" and "NaN" values.
- Parse and remove columns that were repeated in the dataset.
- Reduce the unbalance in the dataset.

After Preprocessing, about 36,366 samples were dropped because of the data cleanup process.

We are going to apply feature selection because the dataset has a huge number of attributes and that would cause failure and affect the accuracy badly.

C. Normalization

Classification performance can be affected by features with different scales.so it is important to normalize the values in each attribute and map features onto a normalized range. So that the minimum value in each attribute is zero and the maximum is one. This provides more homogeneous values to the classier while maintaining relativity among the values of each attribute.

D. Feature Selection

All features with zero amount of variation are removed as those features will not influence the prediction of the target variable. We removed the duplicated features using NetMate and WEKA, as we said and removed all single value features. Then, we dropped unrelated features. In the next step, Features having a high correlation amongst each other are removed. Those features won't bring any additional predictability but may introduce noise.

Finally, the remaining number of features in the dataset after feature engineering is 35 features that we will use in building the model as shown in Table I.

E. Data Splitting

After finishing the feature engineering and preprocessing on the dataset, we split the dataset with (80/20).In the 80/20 method, we split the data into two subsets which take 80% from each label of the dataset for training the model and 20% from each label of the dataset for the test.

F. Model Methodology

In our project model, the essential goal is to get a set of statistics information of traffic flow in the 5G network and identify if this traffic is benign or malicious based on learning a set of already labeled data containing both benign and intrusion traffic.

Training of the Hybrid Deep learning model is two-part, which comprises of forwarding Propagation and Back Propagation. Back Propagation (AE) is responsible for propagating values backward used to give compressed reduced features, and the feed-forward is used for classification data traffic. The first Model is Autoencoder ANN for unsupervised pre-training, which will help in decreasing the rebuilding error. The information we'll get from this step will provide good accuracy to provide an efficient learning system. The autoencoder took all attributes without class attribute (unsupervised) as input, and then it will give compressed reduced features at the end of this phase. The purpose of this stage is to discover the perfect parameters for the next step.

The second Model supervised DNN (dense neural network) classification process, where we applied three Dnn layers that took the first step's output as input here. This stage performs the training process with the label feature as it is a supervised process. The output layer is the layer that compares the actual values (classes) and the predicted values of the test part of the dataset, then calculate the error. We used SoftMax activation for that.

After generating a training and testing dataset, we applied an unsupervised Autoencoder algorithm [16]. We supervised Classification with DNN [17] to get a better classification model with better accuracy that suits any system and to be able to detect any new attack (zero-day) to be effective with the continuous modification and development of wireless technologies. Then we evaluate the results using the criteria of precision, recall, F1 score, and accuracy that we described in the background.

G. Experimental Setup

We used python Keras library with TensorFlow [18] back end on Google colab for implementing the classification model. The colab provides us 12 GB RAM, 68 GB disk space and ability to use GPU hardware accelerator, and the ability to mount Google drive cloud storage to use it.

We used batch normalization that helps make the training process faster. Our model achieved 99.8% accuracy performance, as shown in Table II. The model architecture is shown in Fig. 5.

Layer (type)	Output Shape	Param #
input_5 (InputLayer)	[(None, 34)]	0
model_7 (Functional)	(None, 24)	840
dense_12 (Dense)	(None, 34)	850
dense_13 (Dense)	(None, 24)	840
batch_normalization_2 (Batch	(None, 24)	96
dense_14 (Dense)	(None, 4)	100

Fig. 5. DNN Model Summary.

Fig. 8 shows the confusion Matrix for the four Classes, and the model accuracy is shown in Fig. 9, where it presents the high accuracy of our model during all epochs.

IV. Result and Discussion

Free and Open Datasets: Many public datasets are more attractive to demonstrate and compare productivity and affected Attacks using various detection methods. This section includes two excellent data sets used in many research projects, including AWID and KDDCup datasets; Table II contains the relevant details to see how a certain methodology performs and for comparative purposes.

The performance of ANN, CNN, LSTM, naive Bayesian, random forest, multi-layer perceptron, support vector machine, and other machine learning techniques in the Multi classification are studied in the AWID and KDD datasets. This concludes our analysis of the hybrid deep learning model, which compares favorably to traditional methods. This is evident: the dataset features had an imbalanced distribution. We believe our preprocessing step helped and enabled Autoencoder and DNN on the dataset to achieve high accuracy, as shown in Table II.

TABLE II. COMPARISON OUR MODEL WITH OTHER WORK

Dataset	Number of features used	Technique	Accuracy %
KDD Cup[3]	41	RF	98.5
KDD Cup[4]	15	Naive bayes	82.5
KDD 99 Cup [8]	38	CNN	98.88
AWID[19]	41	RF	94.6
AWID[20]	50	Stacked Autoencoder (SAE)	94.81
AWID[21]	25	Weighted-C4.5	99.72
KDD 99 cup[22]	41	hybrid approach	99
AWID on our model	35	Hybrid Model(HM)	99.8
-	35	HM(Adam optimizer)	99.7

A. Experimental Results

The confusion matrix, Accuracy, Precision, Recall, and F1-Score metrics are being used as evaluation metrics to evaluate the performance of any classifier.

Fig. 6 shows the classification report of our classifier, which explains most of the metrics.

	precision	recall	f1-score	support
flooding	0.98	0.98	0.98	14230
impersonation	0.99	1.00	0.99	17072
injection	1.00	1.00	1.00	20486
Normal	1.00	1.00	1.00	541017
accuracy			1.00	592805
macro avg	0.99	0.99	0.99	592805
weighted avg	1.00	1.00	1.00	592805

Fig. 6. Classification Report for the Model.

The exact accuracy result is shown in Fig. 6 and 7. (WIDS) with Deep learning, this system detects attacks in real-time, the system detects attack by using the model that was trained by different deep learning classification algorithms, the model was applied by using autoencoder and DNN algorithms, then we evaluated it. The model was trained by using the AWID wireless dataset which contains different types of attacks that face the wireless network such as (Flooding, Impersonation, Injection, etc.).

In conclusion, the system ensures the accuracy of the results and the speed of performance, and ease of use.

```
loss: 0.0048 - accuracy: 0.9989
```

Fig. 7. The obtained Accuracy and Loss.

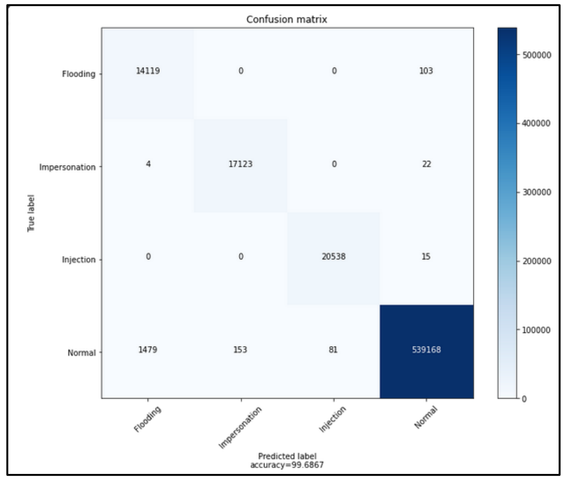

Fig. 8. Confusion Matrix for the 4 Classes.

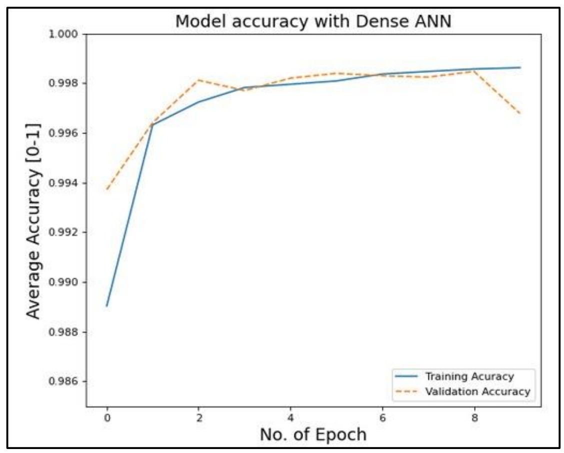

Fig. 9. The overall Accuracy vs Validation.

V. CONCLUSION

Detection Attack facing wireless networks is very important because the network is the main pillar of any 5G wireless network. If this network is compromised, the integrity, safety, and data availability for this architecture do not exist.

Through this project, we implemented a 5G wireless Intrusion Detection System (WIDS) with Deep learning; this system detects attacks in real-time, the system detects attacks by using the model that was trained by different deep learning classification algorithms, the model was applied by using autoencoder and DNN algorithms, then we evaluated it. The model was trained using the AWID wireless dataset, which contains different types of attacks that face the wireless network (Flooding, Impersonation, Injection, etc.). In conclusion, the system ensures the accuracy of the results, speed of performance, and ease of use.

VI. Future Work

Much more can be added to this system. Future work concerns building a complete 5G network in one simulation software to build a complete system that starts with capturing the traffic and classifying it. And make the system easy to use by admin and other users. We can also make the system provides alerts when attacks happen on the 5G network and generate a log for this attack and store it in the database as Archived data.

References

[1] K. Sakaguchi et al., "Millimeter-wave wireless LAN and its extension toward 5G heterogeneous networks," IEICE Trans. Commun., vol. E98B, no. 10, pp. 1932–1948, Oct. 2015, doi: 10.1587/TRANSCOM.E98.B.1932.

[2] "AI vs. Machine Learning vs. Deep Learning vs. Neural Networks: What's the Difference? | IBM." https://www.ibm.com/cloud/blog/ai-vs-machine-learning-vs-deep-learning-vs-neural-networks (accessed Jul. 31, 2021).

[3] J. Li, Z. Zhao, and R. Li, "A Machine Learning Based Intrusion Detection System for Software Defined 5G Network," 2017, Accessed: Jul. 31, 2021. [Online]. Available: www.ietdl.org.

[4] M. A. Jabbar, R. Aluvalu, and S. S. Reddy, "RFAODE: A Novel Ensemble Intrusion Detection System," Procedia Comput. Sci., vol. 115, pp. 226–234, 2017, doi: 10.1016/j.procs.2017.09.129.

[5] Y. Tao, S. Sui, K. Xie, and Z. Liu, "Intrusion detection based on support vector machine using heuristic genetic algorithm," Proc. - 2014 4th Int. Conf. Commun. Syst. Netw. Technol. CSNT 2014, pp. 681–684, 2014, doi: 10.1109/CSNT.2014.143.

[6] A. R. Narayanadoss, T. Truong-Huu, P. M. Mohan, and M. Gurusamy, "Crossfire attack detection using deep learning in software defined its networks," IEEE Veh. Technol. Conf., vol. 2019-April, pp. 1–6, 2019, doi: 10.1109/VTCSpring.2019.8746594.

[7] B. Alsughayyir, A. M. Qamar, and R. Khan, "Developing a network attack detection system using deep learning," 2019 Int. Conf. Comput. Inf. Sci. ICCIS 2019, pp. 1–5, 2019, doi: 10.1109/ICCISci.2019.8716389.

[8] B. Riyaz and S. Ganapathy, "A deep learning approach for effective intrusion detection in wireless networks using CNN," Soft Comput., vol. 24, no. 22, pp. 17265–17278, 2020, doi: 10.1007/s00500-020-05017-0.

[9] A. Di Ciaccio and G. M. Giorgi, "DEEP LEARNING FOR SUPERVISED CLASSIFICATION," 2016.

[10] "AWID - Aegean Wi-Fi Intrusion Dataset." https://icsdweb.aegean.gr/awid/awid2 (accessed Jul. 31, 2021).

[11] A. Dawoud, S. Shahristani, and C. Raun, "Deep learning for network anomalies detection," Proc. - Int. Conf. Mach. Learn. Data Eng. iCMLDE 2018, pp. 117–120, 2019, doi: 10.1109/iCMLDE.2018.00035.

[12] H. Fang, X. Wang, and S. Tomasin, "Machine learning for intelligent authentication in 5G and beyond wireless networks," IEEE Wirel. Commun., vol. 26, no. 5, pp. 55–61, 2019, doi: 10.1109/MWC.001.1900054.

[13] J. Lam, "Machine Learning based Anomaly Detection for 5G Networks."

[14] L. Fernandez Maimo, A. L. Perales Gomez, F. J. Garcia Clemente, M. Gil Perez, and G. Martinez Perez, "A Self-Adaptive Deep Learning-Based System for Anomaly Detection in 5G Networks," IEEE Access, vol. 6, no. February, pp. 7700–7712, 2018, doi: 10.1109/ACCESS.2018.2803446.

[15] C. Kolias, G. Kambourakis, A. Stavrou, and S. Gritzalis, "Intrusion detection in 802.11 networks: Empirical evaluation of threats and a public dataset," IEEE Commun. Surv. Tutorials, vol. 18, no. 1, pp. 184–208, 2016, doi: 10.1109/COMST.2015.2402161.

[16] H. Choi, M. Kim, G. Lee, and W. Kim, "Unsupervised learning approach for network intrusion detection system using autoencoders," J. Supercomput., vol. 75, no. 9, pp. 5597–5621, 2019, doi: 10.1007/s11227-019-02805-w.

[17] Y. Yang, K. Zheng, C. Wu, and Y. Yang, "Improving the classification effectiveness of intrusion detection by using improved conditional variational autoencoder and deep neural network," Sensors (Switzerland), vol. 19, no. 11, 2019, doi: 10.3390/s19112528.

[18] N. K. Manaswi, "Deep Learning with Applications Using Python," Deep Learn. with Appl. Using Python, pp. 31–43, 2018, doi: 10.1007/978-1-4842-3516-4.

[19] U. S. K. P. M. Thanthrige, J. Samarabandu, and X. Wang, "Machine learning techniques for intrusion detection on public dataset," Can. Conf. Electr. Comput. Eng., vol. 2016-Octob, pp. 7–10, 2016, doi: 10.1109/CCECE.2016.7726677.

[20] M. E. Aminanto and K. Kim, Improving Detection of Wi-Fi Impersonation by Fully Unsupervised Deep Learning, vol. 10763 LNCS. Springer International Publishing, 2018.

[21] M. E. Aminanto, H. C. Tanuwidjaja, P. D. Yoo, and K. Kim, "Wi-Fi intrusion detection using weighted-feature selection for neural networks classifier," Proc. - WBIS 2017 2017 Int. Work. Big Data Inf. Secur., vol. 2018-Janua, pp. 99–104, 2018, doi: 10.1109/IWBIS.2017.8275109.

[22] N. Araújo, R. De Oliveira, E. Ferreira, A. A. Shinoda, and B. Bhargava, "Identifying important characteristics in the KDD99 intrusion detection dataset by feature selection using a hybrid approach," ICT 2010 2010 17th Int. Conf. Telecommun., pp. 552–558, 2010, doi: 10.1109/ICTEL.2010.5478852.